19th International Vacuum Congress

1534 abstracts received on 12 September 2013

Breaking News

FPFI-P3-15
DualEEM: a novel surface science technique for simultaneous ultrafast electron spectromicroscopy, nanospectroscopy and diffraction.

Breaking News

#FPFI-P3-15

K. Grzelakowski.

OPTICON Nanotechnology - Wroclaw (Poland).

BREAKING NEWS

We present experimental proof of the novel dual emission electron microscopy (DEEM) technique [1] based on photoemission (PEEM) [2] and low energy electron microscopy (LEEM) [3]. utilizes the idea of the aberration free spherical analyzer α-SDA [4], that assures not only the selection of characteristic energy for imaging, but also an electron optical separation into two imaging channels: energy-selective real image and reciprocal (diffraction) image. Their quasi- simultaneous acquisition in DualEEM offers an unique opportunity to investigate ultrafast dynamic processes on the surface under these two aspects on the sub-femtosecond scale [5]. The idea and its realization is illustrated in Fig.1. An electron gun located inside the immersion objective lens (b) allows a unique electron beam sample illumination and thus, opens a new application field for electron spectromicroscopy under laboratory conditions.

The first test results (<45nm resolution in the spectroscopic modus) obtained from 2μm Pd/Si in ultrahigh vacuum are collected and described in Fig.2. (final res. <10nm, ΔE<100meV)

[1] K.P. Grzelakowski, Ultramicroscopy 130 (2013) 29
[2] E. Brueche, Z.Phys. 86 (1933) 448
[3] E. Bauer, Proc.of the 5thInt. Cong. for Electron Micr.(Academic, N.Y., 1962, p.D-11)
[4] K.P. Grzelakowski, Ultramicroscopy 116 (2012) 95
[5] K.P. Grzelakowski, R. M. Tromp, Ultramicroscopy 130 (2013) 36

Fig. 1. Modus operandi: α-rays (black), γ (blue), p1,p2: real and diffraction plane, respectively: a) E- selective k-projection, upper hemisphere switched off, b) E-selective real image mode, both hemispheres switched on, c) General appearance of the assembled flange-on DualEEM oriented as ‘a’ and ‘b’

Fig.2. Pd/Si, FoV of ‘a’ ~ 7,5μm, pass energy=700eV, top: UV(Hg) illumination, ΔE: 400meV, disp.apt. :~80μm, a) E- selective real image, screen1; b) E-selective K-projection, screen2. bottom: selected area microspectroscopic analysis for two characteristic energy ranges that utlizes a unique method for sample electron beam illumination [1], Fig.1b.

NST/SS-P1-24a
Electronic interaction of silicene with underlying Ag(111) surface

Breaking News

#NST/SS-P1-24a

R. Arafune [1], C.–L. Lin [2], K. Kawahara [2], T. Shirasawa [3], R. Nagao [2], E. Minamitani [4], Y. Kim [4], T. Takahashi [3], M. Kawai [2], N. Takagi [2].

[1]International Center for Materials Nanoarchitectonics (WPI-MANA), National Institute for Materials Science - Ibaraki (Japan), [2]Department of Advanced Materials Science, Graduate School of Frontier Science,The University of Tokyo - Chiba (Japan), [3]Institute for Solid State Physics, The University of Tokyo - Tokyo (Japan), [4]RIKEN - Saitama (Japan).

BREAKING NEWS

Silicene, a 2D honeycomb allotrope by Si, can acquire the Dirac fermion character as graphene [1]. Recently, many works about silicene synthesis on the Ag(111) surface have been reported in rapid succession[2]. As silicene forms into a buckling structure, the interaction with the substrate depends on the site in the unit cell strongly. Thus, silicene on Ag(111) tends to lose its chiral symmetry and thus its Dirac fermion character. We have found that both monolayer and bilayer silicene sheets lose the Dirac fermion character on Ag(111) through the spectroscopy measurement with STM [3,4]. In the spectra of the monolayer silicene on Ag(111), the Landau level related peaks that must appear if system acquires the 2D Dirac fermions were not observed [3]. The STS mapping for the bilayer silicene just showed the usual parabolic band, which should be assigned to the Si-modified silver electronic band. The DFT based calculations, which reproduce the geometric structure determined with the dynamical LEED measurement extremely well [5], have shown strong hybridization between the electronic band of silicene and the underlying Ag(111) substrate. These justify our experimental results showing lack of the Dirac fermion character in silicene on the Ag surfaces.

[1]K. Takeda and K. Shiraishi Phys. Rev. B 50, 14916 (1994).
[2] C. -L. Lin et al., Appl. Phys. Exp. 5 045802 (2012).
[3] C. -L. Lin et al., Phys. Rev. Lett. 110, 076801 (2013).

[4] R. Arafune et al., Phys. Rev. Lett. 110, 229701 (2013).
[5] K. Kawahara et al., Submitted.

SS-P1-07a
Tip suppression of Non-local desorption for Chlorobenzene on Si(111)-7x7 in the STM

Breaking News

#SS-P1-07a

D. Kaya, T. Pan, R.E. Palmer.

Nanoscale Physics Research Laboratory, School of Physics and Astronomy, University of Birmingham - Birmingham (United kingdom).

BREAKING NEWS

The scanning tunneling microscope (STM) is now widely used not only for single atom/molecule imaging in real space, but also for different types of atomic manipulation on the nanoscale. We recently established a surprising non-local mechanism for STM induced molecular desorption in a model system, chlorobenzene (PhCl) chemisorption on Si(111)-7x7 at room temperature [1,2]. Here we focus on the phenomenon of the suppression of the non-local desorption probability in a range of 50 Å from the charge injection site (tip position).

Specifically, we report the effect of the tip-surface electric field on the depth and width (range) of the suppression region. The field was changed by varying the tunneling current between 200 pA and 10 nA where the voltage on the specimen was kept constant (i.e. the tip-surface distance is varied). We find that (i) the decay length of the non-local desorption does not change with increasing current (thus field) while (ii) the same is true for the range of the tip-induced suppression of desorption. These results imply the influence of the field on the dynamic is minor. Instead we propose a mechanism in which desorption proceeds through a physisorbed intermediate state and is hindered by the physical proximity of the STM tip which returns molecules efficiently to the Si surface.

[1] P. A. Sloan, S. Sakulsermsuk and R. E. Palmer, Phys. Rev. Lett. 105, 048301 (2010).
[2] S. Sakulsermsuk, P. A. Sloan and R. E. Palmer, ACS Nano 4, 7344 (2010).

ASS-P1-03a
Realizing a precious metal-free catalyst for purification of combustion exhaust of vehicles through computational materials design

Breaking News

#ASS-P1-03a

H. Kasai [1], J. Moreno [2], A. Padama [2].

[1]Department of Applied Physics & Center for Atomic and Molecular Technologies, Osaka University - Osaka (Japan), [2]Department of Applied Physics, Osaka University - Osaka (Japan).

BREAKING NEWS

Nitrogen oxide (NO_x) is a by-product of fossil fuel combustion and forms nitric acid in the air, which is the main reason for acid rain and smog. Thus, understanding the reduction process of NO_x on surfaces to form less hazardous gases is of utmost importance. It is well known that precious metals (such as Rh, Pd and Pt) work well to reduce the emission of NO_x. However, reducing the cost of environment-friendly vehicles is an important issue for automobile companies and the expensive cost of the precious metals hinders mass production. Therefore, a more readily available and inexpensive material with comparable, if not better, catalytic performance is needed.

In this work, we announce the latest results of our ongoing work on the development of a new catalyst technology without the use of expensive precious metals. Employing computational materials design using density functional theory, we investigated the reduction of NO on Cu-based catalysts [1-3]. Our results show that NO dissociation on Cu-terminated Cu_2O (111) and Cu-terminated CuO (110) surfaces is comparable with its dissociation on Rh (111) [4], which is characterized by a transition state below the reference energy (surface and gas phase NO), as shown in Fig. 1. This is due to the modified electronic and geometric structure of the surface Cu atoms in comparison with that of Cu (111). The density of states (d orbital) of the surface Cu atoms in the oxides are shifted towards the Fermi energy.

We believe this is responsible for their better reactivity. Moreover, in Cu (111), there is a large energy barrier for NO dissociation, thus desorption is more likely.

This ongoing work is made through the initiative of the Ministry of Education, Culture, Sports, Science and Technology (MEXT) of the Japanese government through the Elements Science and Technology (EST) Project, in collaboration with different research groups from the industry and the academe. One aim of the EST Project is to understand the efficient performance of expensive materials used in the energy and automobile industries. Under the EST, we are part of the “Development of Novel Self-Forming Nanoparticle Catalyst without Precious Metals” group that deals with purification of automobile exhausts. Our study on developing these precious metal-free catalysts has also gained recognition as it ranked first in the Technology Trend Survey announced by Nikkei Shinbun. This shows that technologies dealing with alternative materials for scarce resources are of high importance.

[1] A Padama, et al. J Phys.: Condens. Matter. 24 (2012) 175005.
[2] H Kishi, et al. J. Phys.: Condens. Matter. 24 (2012) 262001
[3] H. Kasai, et al. J. Jpn. Petrol. Inst. Accepted. (2013)
[4] S. Gonzalez, et al. J. Catal. 239 (2006) 431.

Fig. 1. Reaction paths for NO dissociation on Rh (111), Cu2O (111) and CuO (110) surfaces.

NST/SS-P1-25
Insight into ridges and wrinkles in multilayers epitaxial graphene on SiC

Breaking News

#NST/SS-P1-25

B. Lalmi [1], J.C. Girard [1], M.G. Silly [2], F. Sirotti [2], A. Ouerghi [1].

[1]CNRS-Laboratoire de Photonique et de Nanostructures (LPN) - Marcoussis (France), [2]Synchrotron-SOLEIL - Gif Sur Yvette Cedex (France).

The two dimensional (2D) honeycomb lattice of carbon atoms, which is widely referred to as graphene, has received great interest during the last years [1-6]. This new most fascinating nano-carbon material has distinctive proprieties; such as very high carrier mobility, efficient heat dissipation, half-integer quantum Hall effect at room temperature and spin transport [5,6], making it a one of the most promising candidate to replace silicon in all kind of devices.

Among the various methods to produce graphene, the graphitization of hexagonal SiC surfaces provides a viable alternative for the synthesis of wafer-sized graphene for mass device production. During later stages of growth, ridges and wrinkles are often observed on the graphene layers (see Fig.1) as a result of bending and buckling to relieve the strain between the graphene and its supporting substrate SiC. Such strain is due to the mismatch of its lattice and thermal coefficient with the SiC substrate.

In the present work, we report a further detailed study of the topological defects (ridges and wrinkles) and their associated effects on the epitaxial multilayers graphene grown on the Si face of 6H-SiC. Using near-field microscopy techniques (AFM/STM), we give insight into the nature and the structural proprieties of such nanostructures. We further show that their structures can be manipulated by the pressure exerted by the STM tip during imaging.

Moreover, combining uniquely spectroscopy tools (STS, XPS, ARPES), the impact of these nanostructures on the electronic properties of epitaxial graphene on SiC(0001) will be presented.

[1] K. S. Novoselov, A. K. Geim, et al , Science 306, 666 (2004).
[2] T. Ohta, A. Bostwick, et al , Science 313, 951 (2006).
[3] A. Ouerghi, et al , ACS Nano 7, 6075 (2012)
[4] A. Ouerghi, et al , PRB 83, 205429 (2011)
[5] Y. Zhang, Y.-W. Tan, H. L. Stormer, P. Kim, Nature 438, 201, (2005).
[6] Dlubak, M.-B. Martin, et al , Nature Phys, 8, 557-561 (2012).

Fig.1 AFM image showing a typical interconnected network ridges in graphene

ASS-P1-03b
Activated carbon behavior upon plasma generated ozone exposure: VOC oxidation and surface poisoning in dry and humid conditions

Breaking News

#ASS-P1-03b

C. Barkat [1], O. Guaitella [1], F. Thevenet [2], A. Rousseau [1].

[1]LPP, Ecole Polytechique, UPMC, Université Paris Sud 11, CNRS - Palaiseau (France), [2]Université Lille Nord-de-France / Mines Douai - Lille / Douai (France).

BREAKING NEWS

With an increasing concern to limit the emissions of volatile organic compounds (VOCs) and odors present in confined environments, established processes such as thermal and thermocatalytical oxidation or actual technologies based on filtration/adsorption are not economically adapted. The treatment of polluted air streams containing VOCs by the coupling of non-thermal plasma (NTP) with an adsorbent bed is an attractive alternative for dilute VOC oxidation and surface regeneration.

A two stage system with the adsorbent bed placed downstream from the NTP reactor is used to investigate i) the surface modification of activated carbon under ozone exposure and ii) the adsorption properties and oxidation of acetone. FTIR spectroscopy is used for the real time analysis of the gas output. The studies are conducted in dry and humid conditions in order to evaluate the influence of humidity in the given processes.

After undergoing a 1h30min pretreatment at 150°C to guarantee surface repeatability amongst the different samples, activated carbon is exposed to approximately 20ppm of ozone for 20 hours. It is shown that in both dry and humid conditions, the surface undergoes irreversible site modification upon prolonged ozone exposure. Figure 1 shows that in the case of air with 50% relative humidity, the surface is no longer able to dissociate ozone after three hours of treatment. An increasing CO_2 and constant

CO productions are also observed and result from the oxidation of the carbon of the material itself. It is shown that the induced surface modification inhibits the subsequent acetone adsorption.

Another study with consecutive adsorption plasma cycles was also performed and showed the same tendency as that observed during prolonged ozone exposure. It was shown that i) the adsorption capacity of acetone gradually decreased after each plasma cycle, ii) carbon is oxidized leading to an increasing CO_2 and constant CO production independently of acetone surface coverage (figure 2) and iii) ozone dissociation decreases after each plasma cycle.

Fig. 1. Ozone concentration at reactor output during non thermal plasma of air with 50% relative humidity (42.57mW, 14ppm O3, 5.1J/L) on activated carbon bed.
Fig. 2. Gas phase products observed upon 5 different plasma cycles of one hour (19mW, 24ppm O3, 2.8J/L) in dry synthetic air.

ASS-P1-20a
Development of technique and mass-spectrum investigation of the phenomena accompanying the field electron emission

Breaking News

#ASS-P1-20a

E. Popov, A.G. Kolosko, S.V. Filippov, P.A. Romanov, A.O. Pozdnyakov.

Ioffe Physical Technical Institute, Russian Academy of Sciences - St. Petersburg (Russian federation).

BREAKING NEWS

Among investigated field emitters - nanocomposite emitters based on the multiwall carbon nanotubes and a polymeric matrix (MWCNT-polymer) are rather promising on the operational properties. For degradation properties examination of the MWCNT-polymer emitters in the large (up to 100 mA) currents modes we suggested to use mass spectrometer methods of main volatile products diagnostics [1].

The further development of our approach consists of the phenomena accompanying FE in various vacuum conditions, current levels and power supply regimes investigation [2]. The examination of the specimens adsorbed on CNT surfaces influence on the FE behavior is of particular interest.

It was offered to use multichannel system of recording current voltage characteristics (IVC) performances and other parameters with simultaneous processing of the incoming information.

The hardware-software complex under control of LabView allows building IVC in Fowler-Nordheim and "slope-intersection" coordinates during FE experiments and also to process spectra TOFMS of reflection type.

The offered technique is universal and can be used not only for MWCNT-polymer, but also for almost any multiple tip field emitters in various longtime FE operating modes for their comparison and certification.

This research is supported by the grant N 12-08-31406 of Russian Foundation for Basic Research and by the grant of “Physics of New Materials and structures” Program of Physics Sciences Department of the Russian Academy of the Sciences.

[1] E. O. Popov, A. A. Pashkevich, A. O. Pozdnyakov and O. F. Pozdnyakov, J. Vac. Sci. Technol. B 26, 2 (2008) 745.
[2] E. O. Popov, A. G. Kolosko, IEEE, 25th IVNC, P2-14 (2012) 308.

TF-P3-16a
Control of microstructure and phase formation in sputtering targets by using rapid hot pressing methods.

Breaking News

#TF-P3-16a

E. Neubauer, M. Kitzmantel, W. Kapaun.

RHP-Technology GmbH & Co KG - Seibersdorf (Austria).

Ti-Al-N films are frequently used as wear resistant coatings, e.g. on cutting tools. For the manufacturing of these thin films either two targets (Al and Ti) or compound Ti-Al targets are used. The thin film processing is taking place under a nitrogen gas flow to form the Ti-Al-N coatings with high hardness and wear resistance. In order to improve further the properties of thin films - especially hot hardness - additional elements are introduced in the Ti-Al target materials. When using compound targets for the thin film manufacturing this can be achieved by admixing of third elements and subsequent consolidation by using powder technological processing such has hot pressing or hot isostatic pressing.

Sputtering targets being composed of two or more metals, which tend to form intermetallic phase during the manufacturing process, show some problems during the subsequent processing such as: difficult to machine as a result of formation of brittle intermetallic phases; lower thermal conductivity of the target as a result of the phase formation and more difficulties to obtain full densification during the powder technological processing.

By using a powder metallurgical process based on a direct hot pressing method it is possible to allow a very fast densification (within minutes) of Ti-Al or other materials with tendency to form intermetallic phases. Starting with an appropriate powder mixture followed by hot consolidation it is possible to obtain target materials with a densification > 99%. The result of fast processing is a control of microstructure and reduction of phase formation and therefore minimization of brittle phase formation. Finally the prepared targets have been analysed with respect to their thermal conductivity. In comparison to the target materials which contain intermetallic phases higher thermal conductivities have been measured on these targets

Figure 1:

Left: Microstructure of Ti-Al target processed by rapid hot pressing showing a minimized intermetallic phase formation between the Al matrix and the Ti powders.

Right: Microstructure of a Ti-Al-X target processed by rapid hot pressing

Plenary

PL-1-PI-1
QUASI-PERIODIC MATERIALS - CRYSTAL REDIFINED

Plenary

#PL-1-PI-1

D. Shechtman [1], D. Shechtman [2].

[1]Technion - Haifa (Israel), [2]Iowa State Univeerity - Ames (United states).

Crystallography has been one of the mature sciences. Over the years, the modern science of crystallography that started by experimenting with x-ray diffraction from crystals in 1912, has developed a major paradigm – that all crystals are ordered and periodic. Indeed, this was the basis for the definition of “crystal” in textbooks of crystallography and x-ray diffraction. Based upon a vast number of experimental data, constantly improving research tools, and deepening theoretical understanding of the structure of crystalline materials no revolution was anticipated in our understanding the atomic order of solids.

However, such revolution did happen with the discovery of the Icosahedral phase, the first quasi-periodic crystal (QC) in 1982, and its announcement in 1984 [1, 2]. QCs are ordered materials, but their atomic order is quasiperiodic rather than periodic, enabling formation of crystal symmetries, such as icosahedral symmetry, which cannot exist in periodic materials. The discovery created deep cracks in this paradigm, but the acceptance by the crystallogra-phers' community of the new class of ordered crystals did not happen in one day. In fact it took almost a decade for QC order to be accepted by most crystallographers. The official stamp of approval came in a form of a new definition of “Crystal” by the International Union of Crystallographers. The paradigm that all crystals are periodic has thus been changed. It is clear now that although most crystals are ordered and periodic, a good number of them are ordered and quasi-periodic.

While believers and nonbelievers were debating, a large volume of experimental and theo-retical studies was published, a result of a relentless effort of many groups

around the world. Quasi-periodic materials have developed into an exciting interdisciplinary science.

This talk will outline the discovery of QCs and describe the important role of electron mi-croscopy as an enabling discovery tool.

[1] D. Shechtman, I. Blech, Met. Trans. 16A (June 1985) 1005-1012.
[2] D. Shechtman, I. Blech, D. Gratias, J.W. Cahn, Phys. Rev. Letters, Vol 53, No. 20 (1984) 1951-1953.

PL-1-PI-2
From a vision to realization

Plenary

#PL-1-PI-2

A. Borschberg.

Solar Impulse (Switzerland).

PL-2-PI-1
TOPOLOGICAL INSULATORS AND THEIR EDGE AND SURFACE STATES

Plenary

#PL-2-PI-1

S. Zhang.

Stanford University (United states).

Recently, a new class of topological states has been proposed and experimentally observed. These topological insulators have an insulating gap in the bulk, but have topologically pro-tected edge or surface states due to the time reversal symmetry. In two dimensions the edge states give rise to the quantum spin Hall (QSH) effect, in the absence of any external magnetic field. I shall review the theoretical prediction[1] of the QSH state in HgTe/CdTe semiconduc-tor quantum wells, and its experimental observation[2]. Bi2Te3, Bi2Se3 and Sb2Te3 are theo-retically predicted to be topological insulators with a single Dirac cone on the surface[3]. I shall discuss experiments which observed these surface states[4,5] and various theoretical proposals for their novel properties. Discovery of topological insulator has the potential to revolutionize surface science, it could also lead to many useful applications.

[1] A. Bernevig, T. Hughes and S. C. Zhang, Science, 314, 1757, (2006)
[2] M. Koenig et al, Science 318, 766, (2007)
[3] Haijun Zhang, Chao-Xing Liu, Xiao-Liang Qi, Xi Dai, Zhong Fang, and Shou-Cheng Zhang, Nature Physics 5, 438 (2009).
[4] Y. Xia, L. Wray, D. Qian, D. Hsieh, A. Pal, H. Lin, A. Bansil, D. Grauer, Y. Hor, R. Cava, et al., Nat. Phys. 5, 398 (2009).
[5] Y. L. Chen, J. G. Analytis, J.-H. Chu, Z. K. Liu, S.-K. Mo, X. L. Qi, H. J. Zhang, D. H. Lu, X. Dai, Z. Fang, et al., Science 325, 178 (2009).

PL-2-PI-2
NANOWIRES – MY “NARROW-MINDED” APPROACH TO MATERIALS, PHYSICS & DEVICES

Plenary

#PL-2-PI-2

L. Samuelson.

Lund University (Sweden).

In the search for new ways to enable the continued trend towards increasingly smaller and more efficient semiconductor devices, as well as the integration of different kinds of materials with mainstream silicon, nanowires have emerged as key candidates. In this talk I will give an update on the general concepts of self-assembly processes that enable the formation of highly ideal nanowires, also such that incorporate advanced axial and radial hetero-structures by which physically interesting three-dimensional semiconductor systems are created. Of special importance have been the technical implementations by which top-down patterning and processing merges with the bottom-up, self-assembly-based methods of nanowire growth. By this approach it has recently been possible to realize advanced nanowire-based systems of importance for ICT- and energy-applications as well as offering interesting interfaces to life-sciences. I will particularly highlight recent progress in research and development of highly efficient nanowire-based solar cells and light-emitting diodes, in both cases with potential to profoundly influence the future of our society.

PL-2-PI-3
APPLICATIONS OF AES AND XPS TO STUDY PRACTICAL TECHNOLOGICAL PROBLEMS

Plenary

#PL-2-PI-3

J. Grant.

University of Dayton (United states).

Several examples will be given where Auger electron spectroscopy (AES) and x-ray photoelectron spectroscopy (XPS/ESCA) have been used to study practical technological problems. I will start with some of my historical studies in AES which were very exciting, and also very challenging due to the lack of desktop computers. The lack of desktop computers made early XPS analysis very challenging as well. I will show how experimental parameters chosen for data acquisition in AES and XPS are very important when analyzing samples. I have found that, even today, many operators do not understand how their instruments work and therefore are not taking data using optimal conditions. Obtaining the required data in the shortest time will also reduce any possible effects of beam damage on the sample. It is also easy to misinterpret spectra. Some issues that will be discussed and illustrated include peak identification, detection limits, and quantification.

ASS-5-Or-6
Ultra fast depth profile measurements of materials: GD OES and Plasma Profiling TOFMS, tools for thin and thick films characterisation

T01 Applied Surface Science

#ASS-5-Or-6

P. Chapon, C. Olivero, A. Tempez, S. Legendre.

Horiba Scientific - Longjumeau (France).

Functional multilayered coatings often feature layers down to the nanometre scale. Reference surface techniques (XPS, AES, SIMS) offer very high surface sensitivity but are limited for depth profiling to thin layers. For embedded nanometre layers or interfaces observation, cross section and SEM EDX or TEM characterisation is generally used.

However there are techniques that could provide a direct measurement of the chemical composition as a function of depth, with a nanometre resolution and the capability to measure both thin and thick layers.

These techniques rely on the fast sputtering of a large area of the material of interest by a high density (1014/cm3) and low energy plasma. The unique characteristics of this plasma allow very fast erosion (2-10nm/s) with minimum surface damage (as the incident particles have an average energy of about 50eV) and it has been shown that this plasma can be used advantageously for sample preparation in SEM.

When coupled to a high resolution optical system, the resulting technique is called RF GDOES and is well established, when coupled to ToF MS detection, it is named Plasma Profiling Time of Flight Ion Mass Spectrometry.
Both instruments feature an advanced pulsed RF source allowing the measurements

of conductive and non conductive layers - the TOFMS offering the additional advantage of isotopic depth profiling.

Various applications taken from different fields from high temperature corrosion in metallurgy to photovoltaic, coatings on glasses to Li batteries will be presented illustrating the capabilities and range of applications of these techniques. A new development will be presented allowing for ultra fast profiling of polymer layers.

[1] R Escobar & al: Towards nanometric resolution in multilayer depth profiling: a comparative study of RBS, SIMS, XPS and GDOES, Anal Bioanal Chem (2010) 396:2725–2740
[2] K. Shimizu &al: New horizons of Applied Scanning Electron Microscopy, Springer 2011

Illustration: GD OES depth profile of a mirror for X ray featuring 60 multilayers [3nmMo/0.3nmB4C/3.7nmSi]. Courtesy of A. Tolstoguzov

ASS-P1-03
Preparation and characterization of supported metal catalysts based on cobalt

T01 Applied Surface Science

#ASS-P1-03

A. Mouna [1], M. Chater [2].

[1]Centre de Recherche Scientifique et Technique en Analyses Physico-Chimiques (C.R.A.P.C), 1Laboratoire d'Etude Physico-Chimique des Matériaux et Application à l'Environnement, USTHB - Alger (Algeria), [2]Laboratoire d'Etude Physico-Chimique des Matériaux et Application à l'Environnement, USTHB - Alger (Algeria).

Heterogeneous catalysts are used for a wide variety of reactions, such as hydrogenations, dehydrogenations and oxidations. Selective hydrogenation of multiple unsaturated molecules towards one particular product is a major challenge. For example, the selective hydrogenation of α,β-unsaturated aldehydes towards unsaturated alcohols is important from an industrial point of view. Moreover, it is an attractive test reaction from a fundamental point of view, since C=C hydrogenation is thermodynamically more favored than C=O hydrogenation.
In this work, we studied the preparation and the characterisation of supported Co catalysts. We examined the effect of metal loading (1, 5 and 10 %) on Co dispersion, on the character of metal-support interactions and on the Co particle size. Catalysts are prepared by impregnation from chlorid precursors and characterised by H2 chemisorption, temperature-programmed reduction (H2-TPR), scanning electron microscopy (SEM), XRD and cyclohexane dehydrogenation. Results obtained showed that the high hydrogen uptake of the catalysts with 1Wt.% Co reflects the high Co dispersion.
However, chemisorption values decrease with increasing Co amount, reflecting a loss in the number of surface sites, suggesting either the development of a SMSI or sintering of the metal particles. This lower ability for H2 chemisorption must be attributed to the larger particle formation.
TPR profils indicate that hydrogen consumption appears from 200 °C. This consommation in attributed to the reduction of Co_3O_4 species. Cyclohexane dehydrogenation results show that the specific activity decreases as the Co content increases. This result indicates that Co dispersion decreases with increasing Co

amount, which is consistent with the formation of large Rh particles as evidenced by H2 chemisorption experiments.

BI/ASS-1-Or-6
Toward a better understanding of the first stages of dairy fouling growth at a stainless steel surface

T01 Applied Surface Science

#BI/ASS-1-Or-6

M. Jimenez [1], G. Delaplace [2], N. Nuns [3], S. Bellayer [4], D. Deresmes [5], G. Ronse [6], G. Alogaili [1], M. Traisnel [1].

[1]UMET/ISP, Lille University - Villeneuve D'ascq (France), [2]INRA - Villeneuve D'ascq (France), [3]IMMCL Chevreul, Lille University - Villeneuve D'ascq (France), [4]ENSCL, Lille University - Villeneuve D'ascq (France), [5]IEMN, Lille University - Villeneuve D'ascq (France), [6]IINRA - Villeneuve D'ascq (France).

Fouling is generally defined as the unwanted formation of thermally insulating materials or deposits from process fluids onto heat transfer surfaces, leading to sanitary risks in food-processing industries [1] and forcing them to take expensive cleaning measures [2]. Research teams are intensively working on antifouling coatings development, which is however an issue, as many parameters are involved; however no fundamental study on the fouling growth mechanism at the interface has been carried out yet. The comprehension of these phenomena might help the development of antifouling coatings in an important manner. In this study, the interfacial behaviour of two different model dairy foulings at a stainless steel surface after different times of exposure to dairy solutions in a heat exchanger were investigated using Electron-Probe Micro Analysis, Time-of-Flight Secondary Ion Mass Spectrometry, X-Ray Photoelectron Spectroscopy and Atomic Force Microscopy. Deposits were formed using two model fouling solutions containing 30 ppm (sol.1) and 120 ppm Calcium (sol.2). After two hours fouling, the fouling layer is thin, smooth and homogeneous when sol.1 is used, whereas it is thick, rough, with a growth in arborescence when sol.2 is used.

To better understand the early stages of the fouling growth, samples were submitted to only one minute fouling in both solutions. Fouling was proven to be initiated by unfolded proteins in the first seconds of exposure to both fouling solutions. When sol.1 is used, a smooth homogeneous surface constituted of small clusters of size 60 nm is observed. 3DToF-SIMS reconstructions evidence that calcium is in low amount

and appears at the same places than the protein. It also confirms that the protein is present both on the steel surface and in the steel defects. When sol.2 is used, 3D ToF-SIMS images evidence that the protein appears at the interface with the steel plate earlier than calcium (Fig. 1a). AFM shows the apparition of particles (Fig. 1 b), corresponding to unstable amorphous calcium carbonate nuclei formed in the sol.2 and stabilized by the protein. These protein-coated nuclei are preferentially trapped in the steel roughnesses. The unfolded protein covers again these calcium particles, etc. This explains the arborescence growth structure observed by EPMA (Fig. 1,c).

[1] Midelet, G.; Kobilinsky, A.; Carpentier, B. Applied and Environmental Microbiology 2006, 72 (4), 2313-2321

[2] Ozden, H. O.; Puri, V. M. Journal of Food Engineering 2010, 99 (3), 250-256

Fig.1: (a) 3D Tof-SIMS image and (b) AFM image after 1 minute fouling with sol.2 (c) EPMA X-Ray mappings in Ca and S after 2 hours fouling with sol.2

ASS-P3-01
ZnO nanocrystals annealed in UHV: Surface chemistry and induced band bending

T01 Applied Surface Science

#ASS-P3-01

L. Ericsson, H. Zhang, K.O. Magnusson.

Karlstad University - Karlstad (Sweden).

ZnO nanocrystals distributed by spin-coating on SiO2/Si surfaces were annealed in UHV and characterized in situ by synchrotron radiation based X-ray Photoelectron Spectroscopy (XPS). Changes in chemical composition and electronic structure on ZnO nanocrystal surfaces were related to increasing annealing temperatures. An annealing temperature of 650 °C drastically reduces the surface contaminant levels without any observed de-composition of ZnO. After annealing at 700 °C an initial de-composition of ZnO together with further reduction of contaminants was observed. As a result, annealing at 650 °C is found to be the optimal temperature for thermal cleaning of ZnO nanocrystals. Chemical changes and induced point defect formation cause changes in the band structure of the ZnO/SiO2/Si system as observed by XPS. An upward band bending of 0.6 eV on the surfaces of the ZnO nanocrystals was observed after annealing at 300 °C. The bands on the surfaces of ZnO nanocrystals gradually bend downwards with increasing annealing temperatures and finally, annealing at 750 °C for 1 h results in a total downward band bending of 1.5 eV. This large downward band bending is explained as due to the balance between oxygen vacancies and zinc vacancies on the surfaces of ZnO nanocrystals.

TF/SE-1-Or-9
Low frictional ZnO thin films synthesized by a combinatorial sputter coating system

T01 Applied Surface Science

#TF/SE-1-Or-9

M. Goto, M. Sasaki, A. Kasahara, M. Tosa.

National Institute for Materials Science - Tsukuba (Japan).

In order to solve the problems of resource depletion and global environment, saving energy have much attention. One of the ways of saving energy is to reduce the friction loss of the moving parts in vehicles and thus save fuel and extend the lifetime of the moving parts. Many low-friction coatings such as transition-metal dichalcogenides, diamond-like carbon, and so forth have been developed so far. However, the friction coefficients of the solid lubricants usually increase upon their reaction with oxygen in air, in oil, in high-temperature and high-humidity, and in space environment. Metal oxide coating is a strong candidate to solve this problem. However, the friction coefficient of the metal oxides known so far is usually too large to be used as low-friction coatings. In this paper, we synthesized the low frictional zinc oxide coating by using a combinatorial sputter coating system.

Cross section TEM image of a low frictional ZnO coating.

SE/ASS-1-Or-9
Interface structure of thin layer joining by gas adsorption

T01 Applied Surface Science

#SE/ASS-1-Or-9

Y. Taga, T. Mashima.

Chubu University - Kasugai, Aichi 487-8501 (Japan).

Interface structure of thin layer joining by gas adsorption
Yasunori Taga* and Takashi Mashima
Thin Film Research Center, Chubu University
Kasugai, Aichi 487-8501, Japan
* y-taga@isc.chubu.ac.jp
Abstract
Attempt has been made to join borosilicate glass and cycloolefin(COP) polymer film by using gas adsorption method. Prior to joining, corona plasma treatment in air atmosphere by changing plasma energy was carried out to control surface functional group on both surfaces. An (3-glycidoxypropyl)trimethoxysilane, GPS was adsorbed on glass and an (3-aminopropyl)triethoxysilane, APS on COP both in air atmosphere, resulting in coadsorption of water vapor and organosilane gases（1）. Surface characterization of plasma treated and gas adsorbed surfaces was carried out by X-ray photoelectron spectroscopy (XPS) using Mg kαX-ray source. Joining was carried out by a roll laminator after contact of both surfaces at room temperature, followed by annealing at 130 ℃ for 10 min. Adhesion strength was evaluated by 180 degree peel test based on ASTM D-903 and durability was examined under the conditions of 60 ℃ and 95 % RH. Surface functional group of OH can be seen on glass surface after plasma treatment. On the other hand, XPS spectra of C1s revealed the existence of complex functional groups of O-H, C-O, C=O, O-C=O and CO3. In addition, plasma treatment energy gives an influence on the concentration of those functional groups on COP surface. At low energy plasma treatment, dominant functional group of COP surface was C-O and O-H and the surface concentration was estimated to be more than 70%. With increase in applied plasma energy, surface concentration C-O and O-H decreased slightly and C=O increased instead, and then O-C=O emerged on the surface as a result of further increase in energy. CO3 carbonate functional group appeared clearly on COP surface after plasma energy over 10 KJ/m2. Thickness of APS gas adsorption layer on COP was

evaluated by the intensity of XPS Si2p peak. It was found that thickness rapidly increased to reach constant value after several minutes, where saturation thickness was estimated to be 1.1 nm by taking inelastic mean free path （2） of Si2p photoelectron into consideration. Adhesion force by pulling test revealed strong adhesion and was found to be more than 5N/25 mm corresponding to almost equal to COP bulk tensile strength. In addition, durability of this adhesion strength remained unchanged over 2000 hrs even after exposure to the durability test conditions of 60 ℃ and 95 % RH. The results can be explained in terms of the formation of H-H hydrogen bond and Si-O covalent bond via silanols at the interface as a result of lamination and annealing processes.
In conclusion, direct joining method using gas adsorption was carried out in the system of glass and cycloolefin polymer film at low temperature. Joining thickness was estimated to be 1-5 nm and joining force more than 5N/5mm and long term durability were also confirmed. The results of ultrathin joining can be explained in terms of formation of hydrogen and covalent bondings at the interface by low temperature reaction process.

References:

（1） H. Shinohara, J. Mizuno and S. Shoji, IEEJ Trans. 2, 301(2007).
（2） M. P. Seah and W. A. Derch, Surf. Interface Analysis 1, 2(1979).

ASS-9-Or-2
Guide on-surface polymerization via metal-directed template towards size-selective and hierarchically-organized macromolecular systems

T01 Applied Surface Science

#ASS-9-Or-2

T. Lin [1], X.S. Shang [2], J. Adisoejoso [1], P.N. Liu [2], N. Lin [1].

[1]Department of Physics, The Hong Kong University of Science and Technology, Clear Water Bay - Hong Kong (China), [2]Shanghai Key Laboratory of Functional Materials Chemistry and Institute of Fine Chemicals, East China University of Science and Technology, Meilong Road 130 - Shanghai (China).

On-surface polymerization represents a novel bottom-up approach for producing macromolecular structures. To date, however, most of the structures formed using this method are lack of long-range ordering, contain structural defects or exhibit a broad size distribution. To overcome these obstacles, here we demonstrate a strategy of using metal-direct template to control the on-surface polymerization processes. Taking advantages of efficient pre-organization provided by flexible pyridyl-Cu-pyridyl coordination, we have synthesized macromolecular porphyrin systems exhibiting a narrow size distribution and hierarchical organization on a Au(111) surface. We use scanning tunneling microscopy and kinetic Monte Carlo simulation to gain single-molecule level insights of the metal-directed polymerization mechanism. The results reveal that the synthesis profits from the rich chemistry of Cu - as catalyst in covalent coupling, as binding motif for topochemical polymerization and as template for size-selective reactions.

ASS-P1-17
EFFECT OF THE BINARY AND TERNARY EXCHANGES ON CRYSTALLYNITY AND TEXTURAL PROPERTIES OF X ZEOLITES

T01 Applied Surface Science

#ASS-P1-17

H. Hammoudi.

FACULTE DES SCIENCES ET TECHNOLOGIE ,UNIVERSITE DE MOSTAGANEM BP227 - Mostaganem (Algeria).

The ionic exchange of the NaX zeolite by Cu2+ and/or Zn2+ cations is progressively driven while following the development of some of its characteristic: crystallinity by XR diffraction, profile of isotherms, RI criterion, isosteric adsorption heat and microporous volume using both the Dubinin–Radushkevich (DR) equation and the t-plot through the Lippens–de Boer method which also makes it possible to determine the external surface area. Results show that the cationic exchange process, in the case of Cu2+ introduced at higher degree, is accompanied by crystalline degradation for Cu(x)X, in contrast to Zn2+-exchanged zeolite X. This degradation occurs without significant presence of mesopores, because the RI criterion values were found to be much lower than 2.2. A comparison between the binary and ternary exchanges shows that the curves of CuZn(x)X are clearly below those of Zn(x)X and Cu(x)X, whatever the examined parameter.
On the other hand, the curves relating to CuZn(x)X tend towards those of Cu(x)X. This would again confirm the sensitivity of the crystalline structure of CuZn(x)X with respect to the introduction of Cu2+ cations. An original result is the distortion of the zeolitic framework of X zeolites at middle exchange degree, when Cu2+ competes with another divalent cation, such as Zn2+, for the occupancy of sites distributed within zeolitic cavities. In other words, the ternary exchange accentuates the crystalline degradation of X zeolites. An unexpected result also is the noncorrelation between crystal damage and the external surface area.

[1] Breck, D.W. Zeolite Molecular Sieves, Wiley-Interscience, New York,1974.
[2] Dyer, A., An Introduction to Zeolite Molecular Sieves, Wiley-Interscience, New York, 1988.
[3] Lippens, B.C., de Boer, J.H. , J. Catal. 4 (1965) 319.
[4] Dubinin, M.M. ,. Radushkevich, L.V, Proc. Akad. Sci. USSR 55 (1947)331.
[5] Ginoux, J.L. Bonnetain ,L., Stud. Surf. Sci. Catal., Vol. 62, Elsevier, Amsterdam, 1991.

BI/ASS/NST-P1-06
Towards Plasmonic Biosensors functionalized by a photo-induced surface reaction

T01 Applied Surface Science

#BI/ASS/NST-P1-06

T. Gschneidter [1], K. Moth-Poulsen [1], S. Chen [2], J. Christensen [3].

[1]Chalmers, Department of Chemical and Biological Engineering - Göteborg (Sweden), [2]Chalmers, Department of Applied Physics - Göteborg (Sweden), [3]University of Copenhagen, Department of Chemistry - Göteborg (Sweden).

We present a method for efficiently coupling of nucleophilic molecules of choice to a nanostructured gold surface via photo-induced surface chemistry. The method is based on photoactive self-assembled monolayers and it is shown how the method can be used to functionalize localized surface plasmon resonance (LSPR) based biosensors with biorecognition motifs while reducing unspecific binding via introduction of hydrophilic units. The photoactive linker molecule, 5-bromo-7-nitroindoline[1] couples nucleophilic molecules such as biotin ethylene diamine to a surface when exposed to 365 nm photons. The specific, non-covalent recognition between biotin and streptavidin is used for demonstration of a simple bio-recognition assay based on the LSPR principle. By doing so, the binding of any streptavidin fusion-proteins attached to specific spots at the gold surface by photochemical reaction can be monitored by a LSPR peak shift (**Figure 1**). Since the surface functionalization is based on a photo-induced reaction, this method can be used to functionalize surface in a local and in a site specific way and biomedical applications such as drug screening platforms, microarrays, solid support protein synthesis, and even single molecule experiments can be envisioned.

[1] K. Moth-Poulsen, V. Kofod-Hansen, F. S. Kamounah, N. S. Hatzakis, D. Stamou, K. Schaumburg, J. B. Christensen, Bioconjugate chemistry 2010, 21, 1056–61.

Figure 1: The photo-induced reaction of nitroindoline (**1**) with biotin (**2**) forming **4** under the release of the indoline moiety **3**. The biotin functionalized surfaces enables specific bio-recognition of streptavidin. This can be monitored as a peak shift of the LSPR of the gold biosensor. The LSPR peak shift can be further enhanced by a enzymatic polymerization of 3,3 diaminobenzidine catalyzed polymerization. The lower pathway visualizes the passivation of the surface due to a light-induced reaction of **1** with ethanol amine.

ASS-P3-02
Surface and thermodynamic characterization of polyaniline complexes by inverse gas chromatography. Relevance to thin films preparation.

T01 Applied Surface Science

#ASS-P3-02

A. Mekki [1], B. Mettai [1], N. Fodil Cherif [1], Z. Ihdene [1], R. Mahmoud [1], Z. Mekhalif [2].

[1]Ecole Militaire Polytechnique, BP 17 Bordj El Bahri - Alger (Algeria), [2]Laboratoire de Chimie et d'Electrochimie des Surfaces, FUNDP, Rue de Bruxelles, 61, B-5000 - Namur (Belgium).

Surface thermodynamic characteristics of polyaniline complexes with two inorganic and organic acids were investigated using inverse gas chromatography. Thirteen solutes were injected into two separate chromatographic columns packed with polyaniline complexes as stationary phases without any chromatographic support. The retention volumes for these solutes were measured to show a strong retention with the both PANI complexes; particularly the three isomers of xylene, i.e. ortho, meta and para. The free energy of adsorption , consisting of dispersive term and the acid-base interaction term was also determined showing that is mainly based on its dispersive contribution. The dispersive surface energy of hydrochloric acid polyaniline complex ranged from 70.39 mJ/m2 at 130°C to 65.75 mJ/m2 at 150°C while the surface energy of dodecylbenzenesulfonic acid polyaniline complex has shown slight upper difference ranging from 70.90 mJ/m2 to 66.23 mJ/m2 in the same temperature's interval, thus reflecting a behavior comparable to that of high surface energy materials. Furhermore, FTIR, Raman spectroscopy, UV-visible XRF, SEM, were used to characterize the PANI complexes powder.
The retention volumes combined with solvation energy relationship (LSER) allowed us to determine the physicochemical parameters describing dispersive, polar and acid-base properties finding out that the surface of both polyaniline complexes is exhibiting a basic nature.

- N.E. Agbor, M.C. Petty, A.P. Monkman, Polyaniline thin films for gas sensing, Sensors and Actuators B 28 (1995) 173-179. Doi: 0925-4005(95)01725-B
- Z. F. Li, F. D. Blum, M. F. Bertino, C. S. Kim, S; K. Pillalamarri, One-step fabrication of a polyaniline nanofiber vapor sensor, Sensors and Actuators B 134 (2008) 31–35. Doi:10.1016/j.snb.2008.04.009
- S. Virji, J. Huang, R. B. Kaner, B. H. Weiller, Polyaniline nanofiber gas sensors:examination of response mechanisms, Nano letters Vol 4, No 3 (2004) 491-496. Doi: 10.1021/nl035122e
- P. P. Sengupta, S. Barik, B. Adhikari, Polyaniline as a gas-sensor material, Materials and Manufacturing Processes 21 (2006) 263–270. Doi: 10.1080/10426910500464602
- Voelkel, B. Strzemiecka, K. Adamska, K. Milczewska, Inverse gas chromatography as a source of physiochemical data, Journal of Chromatography A, 1216 (2009) 1551–1566. Doi: 10.1016/j.chroma.2008.10.096

ESD/ASS-2-Or-1
Application of gold nano-particles for silicon solar cells efficiency increasing

T01 Applied Surface Science

#ESD/ASS-2-Or-1

A. Axelevitch, B. Gorenstein, G. Golan.

Holon Institute of Technology (HIT) - Holon (Israel).

The main problems preventing widespreading of solar cells as alternative energy sources are their high cost and low efficiency. Efficiency of solar cells based on semiconductor materials is limited due to high electrical and optical losses and due to recombination processes. It's known several ways to increase the efficiency of solar cells by using multi-junction devices [1] or various low-dimensional structures [2]. In this paper we present one novel way to increase the efficiency of solar cells by using gold island film imbedded in a semiconductor junction.

Fig. 1 presents a side view of the experimental photovoltaic cell. A conventional p-type silicon wafer with a resistivity of ~ 10 Ω·cm was used as a substrate-base. Series of thin films: gold island film, p-type silicon emitter film, conductive transparent ITO film, Al rear electrode, and Al pass-bar upper electrode were consequently deposited on the substrate, as shown in figure 1. Thin films of Au and Si were deposited using home-made triode sputtering system working at a pressure of 0.5-2.5 mTorr [3] and ITO film was deposited by magnetron sputtering. Al electrodes were deposited by thermal evaporation in vacuum of $3\text{-}5\cdot10^{-5}$ Torr. Prior to the electrode films deposition, the samples were thermally heated in vacuum according to vacuum photothermal process [4].

In order to compare the influence of gold island film on the parameters of the solar cell, we prepared a series of the same pairs samples. In the pair, one of the samples was prepared with the gold island film imbedded between the base and the emitter and the second one was built without a gold film. All the rest parameters of the samples remained the same. Different pairs of samples were varied in thickness of the gold film.

For the made photovoltaic cells, we measured the open circuit voltage and the short circuit current. Measurements were provided in the dark and in the direct sunlight. It was found that imbedded gold film significantly influences on the measured PV cell parameters. The measured open circuit voltage and the short circuit current generated by sunlight in the samples containing the gold island film was higher by about 1.2 and 1.5 times respectively. Also, it was found that the dimensions of gold

islands influence on the current increase value.

1. Sze, S.M. Physics of Semiconductor Devices; John Wiles & Sons: New York, 1981.
2. Green, M.A. Third generation Photovoltaic; Springer: Berlin, 2006.
3. G. Golan, A. Axelevitch, "Novel method of low-vacuum plasma triode sputtering", Microelectronic Journal 33/8 (2002) 651-657.
4. G. Golan, A. Axelevitch, "Progress in vacuum photothermal processing (VPP)", Microelectronics Journal 41/6 (2006) 459-473.

A side view of the experimental photovoltaic cell.

ASS-4-Or-4
Surface and interface studies of metal nanoparticles grown on TiO2 and its oxidation behavior under oxygen environment

T01 Applied Surface Science

#ASS-4-Or-4

J. Pan.

Institute of Materials Research and Engineering, A*Star (Agency for Science, Technology and Research) - Singapore (Singapore).

TiO_2 has attracted remarkable interest as photocatalyst since initial work by Fujishima and Honda on the photolysis of water on TiO_2 electrodes without an external bias. Although TiO_2 itself can be used for the photocatalytic reduction of carbon dioxide, most of time a suitable co-catalyst is needed to obtain a high photocatalytic activity and reasonable reaction rates. In this study, surface science approach was employed to study the growth of Cu, Pt and Co nanoparticles as co-catalysts on rutile TiO_2 (110) single crystal surfaces. Two types of surfaces were used, a sputtered surface and an annealed surface. The co-catalysts were grown through e-beam evaporator in UHV and subsequently characterized by XPS. Only metallic Cu and Pt were observed on TiO_2 surface. Cu and Pt were found to grow in 3D Volmer-Weber growth mode. Interfacial charge transfer on sputtered surface was detected, with electrons transferring from TiO_2 to Cu and Pt resulting in the formation of Shottky interface. Binding energy shift due to cluster effect was observed. Both metallic Co and Co oxides were observed on TiO_2 surface, with more oxide species on sputtered surface as compared to annealed surface. Co was found to grow with higher wetting compared to Pt, with a growth mode that is similar to layer by layer growth. No cluster effect was detected. Co-Ti interactions were found, with electrons transferring from TiO_2 to Co. Oxygen exposure on sputtered TiO_2 surface was found to result in dissociative adsorption that filled oxygen vacancies. The presence of Cu, Pt and Co did not impede this adsorption. Cu and Pt were observed to not be oxidized after exposure to oxygen, while Co was oxidized. The growth of Pt and Co on the same TiO_2 surface was investigated. The initial deposition of Pt followed by the deposition of Co did not alter the growth mode of Co. Nucleation of Co around Pt for 3D growth did not occur. The presence of Pt did not affect the oxidation of Co

when exposed to oxygen. A shift to higher binding energy of Pt was discovered and a possible explanation was put forth involving an induced work function change of Pt due to the oxidation of Co that resulted in the electron transfer of Pt to TiO_2.

ASS-P3-17
AFM/KPFM Investigation of Carborane Cluster Dipoles Chemisorption on Metal Surfaces

T01 Applied Surface Science

#ASS-P3-17

A. Vetushka [1], T. Baše [2], P. Schmutz [1].

[1]Empa - Dübendorf (Switzerland), [2]Institute of Inorganic Chemistry ASCR, v.v.i. - Husinec-Řež (Czech republic).

Clusters of boron hydrides have recently been investigated as new building blocks for self-assembled monolayers on surfaces of gold, silver and copper [1–5]. Twelve-vertex dicarba-closo-dodecaboranes (often referred to only as carboranes) are stable molecules with rigid icosahedral molecular architecture, pseudo-aromatic character and, in case of ortho-carborane (1,2-$C_2B_{10}H_{12}$), also a relatively strong dipole of about 4 Debye. Their thermally robust character and general stability makes them good candidates for effective protection of metal surfaces on a molecular level and their dipolar character can be used to tune the surface potential. In this contribution we will report on a few particular aspects related to: (1) the mechanism and kinetics of formation of SAMs composed of 1,2-dicarba-closo-dodecaborane-1,2-dithiol (A) (the inset of the Figure 1 shows the schematic representation of this isomer on a gold surface) and 1,2-dicarba-closo-dodecaborane-9,12-dithiol (B), (2) the competitive adsorption of both positional isomers A and B, (3) the quantitative analysis of surface potential changes as a result of their immobilization on metal surfaces, and (4) their capacity to protect silver surfaces against corrosive environments. The chemisorption process, electric properties and environmental stability of the SAMs has further been assessed by TOF-SIMS and electrochemical Impedance Spectroscopy. **Acknowledgement:** This work was supported by the SCIEX program (project 11.206) from the Swiss Universities conference within an established cooperation between the Institute of Inorganic Chemistry ASCR, Rez near Prague and EMPA, Dübendorf. We additionally acknowledge the use of facilities of the Laboratory of Nanostructures and Nanomaterials at the Institute of Physics ASCR in Prague.

A. Vetushka is on leave from Institute of Physics, ASCR

[1] J.F. Lübben, T. Baše, P. Rupper, T. Künniger, J. Macháček, and S. Guimond, J COLLOID INTERF SCI 354, 168 (2011)
[2] T. Baše, Z. Bastl, V. Havránek, K. Lang, J. Bould, M.G.S. Londesborough, J. Macháček, and J. Plešek, SURF COAT TECH 204, 2639 (2010)
[3] T. Baše, Z. Bastl, V. Havránek, J. Macháček, J. Langecker, and V. Malina, LANGMUIR 28, 12518 (2012)
[4] T. Baše, Z. Bastl, M. Šlouf, M. Klementová, J. Šubrt, A. Vetushka, M. Ledinský, A. Fejfar, J. Macháček, M.J. Carr, and M.G.S. Londesborough, J PHYS CHEM C 112, 14446 (2008)
[5] T. Baše, Z. Bastl, Z. Plzák, T. Grygar, J. Plešek, M.J. Carr, V. Malina, J. Šubrt, J. Boháček, E. Večerníková, and O. Kříž, LANGMUIR 21, 7776 (2005)

Figure 1. AFM topography image of an atomically flat gold single crystal surface sparsely covered with molecules of isomer A. |Z scale is 2 nm.

ESD/ASS-1-Or-4
Surface Structures and Electrochemical Properties for Platinum-enriched Ni/Pt(111) Bimetallic Surfaces Prepared by MBE

T01 Applied Surface Science

#ESD/ASS-1-Or-4

T. Wadayama, N. Todoroki, R. Takahashi, Y. Asakimori.

Graduate School of Environmental Studies, Tohoku University - Sendai (Japan).

Atomic arrangements or compositions of bimetallic alloy surfaces are expected to affect catalytic properties. As for oxygen reduction (ORR) catalysts of polymer-electrolyte fuel cells (PEFC), numerous studies of the Pt-based alloys's nanoparticles have been conducted. However, discussion of the ORR mechanisms is complicated because of uncertainties in topmost surface structures of the nanoparticles. Our experimental approach is well-defined model-catalyst fabrications in UHV by using MBE. In this study, we discuss the relation between topmost surface structures and ORR activity of the MBE-prepared Pt-enriched topmost surfaces (Ni/Pt(111)-skins). The MBE apparatus and the UHV-EC sample transfer system used in this study has been described earlier [1]. The Ni/Pt(111)-skins were prepared through 0.3nm-thick-Ni deposition onto the clean Pt(111) at 823 K by an electron-beam evaporation method. As-prepared surface structure is observed by using STM and XPS in UHV. Then, the sample was transferred to a rotating disk electrode (RDE) apparatus set in a N_2-purged glove box without being exposed to air. Cyclic voltammetric (CV) curves for the surfaces are recorded in N_2-purged 0.1 M HClO4. After that, linear sweep voltammetry (LSV) measurements were conducted in O_2-saturated 0.1 M $HClO_4$.
A UHV-STM image of the Ni/Pt(111)-skin (Fig. 1) shows 6-fold symmetric honeycomb atomic arrangement that is typical for an fcc(111) topmost surface. However, Atomic-scale disorder with a corrugation of 0.06-0.12nm height is present at the topmost surface. Such corrugations are probably originated from relief of surface-strain derived from lattice mismatch between the topmost Pt layer and subsurface Ni atoms. XPS analysis of the sample showed chemical shift of Pt 4f band (ca. 0.2 eV) relative to clean Pt(111). The LSV curve for the as-prepared Ni/Pt(111)-skin shifts positively relative to the clean Pt(111) and the ORR activity

determined by kinetic controlled current density at 0.9 V was 8 times higher than clean Pt(111). However, the skin surface was degraded rapidly by applying potential cycling between 0.6 V and 1.0 V. The activity enhancement factor estimated after 1000 potential cycles was ca. 2: a UHV-STM image of the sample showed atomically roughened topmost surface caused by dissolution of the under-laid Ni atoms. The results suggest that the ORR activity enhancement of the Pt-skin correlate with surface strains and electronic states of the topmost Pt lattice.

[1] T. Wadayama et al., *Electrochem. Commun.* 2010, **12**, 1112. T. Wadayama et al., *J. Phys. Chem.* C 2011, **115**, 18589. Y. Iijima et al., *J. Electroanal. Chem.* 2012, **685**, 79.

Fig. 1 UHV-STM image of Ni/Pt(111)-skin.

ASS-P3-03
Development of a low energy electron beam source using the photoelectric effect

T01 Applied Surface Science

#ASS-P3-03

T. Hirayama, T. Konishi, T. Tachibana.

Department of Physics, Rikkyo University - Tokyo (Japan).

We have been studying electronic excitation processes in rare gas clusters by electron energy loss spectroscopy. In this study acquisition time for one spectrum was about 50 hours. This is partly due to the low current of incident electron beam (a few nA), which is limited by the use of an electron energy selector. The purpose of this study is to develop an electron beam source which can produce a low energy electron beam of a current ~100 nA with an adequate energy spread (< 0.2 eV) using the photoelectric effect.

Schematic view of the apparatus is shown in fig 1. LaB_6 (100) surface of 1 mm in diameter is used as a photocathode. Visible light from LD (Laser Diode) is focused onto the photocathode surface. A parallel plate electron energy analyzer is used for the measurements of the electron energy distribution. The photocathode is heated to 1800 K for several minutes before the measurements for surface cleaning. Background pressure in the vacuum chamber is about 5×10^{-9} Pa.

Figure 2 shows the results of the electron energy distribution emitted by the irradiation of the photon energy of E_p = 2.79 eV. Solid line represents the result of gauss fitting. FWHM of the peak is 0.34 eV. This yields the photoelectron energy spread to be ~ 0.3 eV, which is estimated considering the energy resolution of the analyzer. From this results it is expected that an electron beam with energy spread less than 0.1 eV can be obtained using a LD of E_p = 2.6 eV. Quantum yield, defined as the number of photoelectrons per photon, is 1×10^{-5} at E_p = 2.79 eV. If we use a LD with a power of about 4 mW, the photoelectron current of 100 nA can be achieved. The lifetime, which is defined as the time when the current of the photoelectrons decreases by half, depends on the pressure of the vacuum chamber.

Lifetimes measured at P = 2 x 10^{-8} and 5 x 10^{-7} Pa were 8000 s and 600 s, respectively, while it is shorter than 10 s when the pressure is in the order of 10^{-6} Pa.

Fig. 1. Schematic view of experimental apparatus.
Fig. 2. Electron energy distribution measured using a LD of E_p= 2.79 eV. Solid circles are measured points and the solid line is the result of Gauss fitting.

ASS-10-Or-11
Atomic dipole moment induced variation of local surface potential on Si(111)-(7×7) surface studied by noncontact scanning nonlinear dielectric microscopy

T01 Applied Surface Science

#ASS-10-Or-11

K. Yamasue, Y. Cho.

Research Institute of Electrical Communication, Tohoku University - 2-1-1, Katahira, Aoba, Sendai 980-8577 (Japan).

Noncontact scanning nonlinear dielectric microscopy (NC-SNDM) can resolve atomic dipole moments on cleaned semiconductor surfaces through the frequency modulation based electrical measurement of tip-sample capacitance. So far, NC-SNDM imaging of a Si(111)-(7 7) surface has revealed that the individual adatoms on the surface have upward (outward-pointing normal to the surface) dipole moments [1]. In addition, the simultaneous measurement of tunneling current, which is induced by ac electric field modulation ( ) in NC-SNDM imaging, has shown that the dipole moment image (image) closely resembles the time-averaged tunneling current ( ) image. A recently proposed explanation attributes this resemblance in the two different images to the existence of a strong electric field localized on the individual adatoms [2]. Since this localized field, which originates from and is proportional to the dipole moment, causes effective shift of the surface potential ( ), it enhances asymmetry of current-voltage ( ) characteristics on the adatoms. The resulting significant rectified current is theoretically derived as and thus proportional to the dipole moments [2]. In order to experimentally

validate the proposed explanation, simultaneous imaging of $\epsilon_3(A\cos\theta)$ and ΔV_d was here performed as shown in Figs. 1 and 2. The images were acquired under $V_p = 1.2$ V at 30kHz and the ΔV_d image was constructed from $I(t)$ and the 3rd harmonic ($I_{3\omega}$) images. As expected, ΔV_d image resembled $\epsilon_3(A\cos\theta)$ one and ΔV_d was spatially maximized on the adatoms. The spatial average of ΔV_d was about +0.2 V and, reasonably, almost equals to the dc bias that was needed to cancel out $\epsilon_3(A\cos\theta)$ in average. These results thus suggest that the local surface potential is governed by the strong electric field from atomic dipole moments, which can be directly imaged through the measurement of the capacitive component at an atomic scale.

[1] Y. Cho and R. Hirose, Phys. Rev. Lett. 99(18), 186101(2007).

[2] K. Yamasue and Y. Cho, J. Appl. Phys. 113(1), 014307(2013).

Fig. 1: NC-SNDM image (a) Topography (b) $\epsilon_3(A\cos\theta)$ (c) ΔV_d.

Fig. 2: Line profiles between A to A' in Fig 1. (a) Topography (b) $\epsilon_3(A\cos\theta)$ (c) ΔV_d.

ASS-8-Or-11
Effect of gamma radiation on low density polyethylene (LDPE) films : FTIR and SEM studies

T01 Applied Surface Science

#ASS-8-Or-11

M. Saad [1], N. Bendjedda [1], I. Toumert [1], B. Touchrift [1], S. Damache [1], M. Salhi [2].

[1]Centre de Recherche Nucléaire d'Alger, 02, Boulevard Frantz Fanon, B.P. 399, Alger RP, Alger - Algiers (Algeria), [2]Centre de Recherche Nucléaire de Birine, B.P 180 Ain Oussera 17200, Djelfa - Algiers (Algeria).

The low density polyethylene (LDPE) films were irradiated with gamma radiation using the 60Co source in the dose range varied from 0 to 500 kGy at dose rate of 24.32 Gy/min in air at room temperature. The induced changes in the chemical structure and morphologic properties were investigated. The structure modifications of the LDPE were recognized using Fourier Transform Infrared Spectroscopy (FTIR). The morphologic properties of the non-irradiated and irradiated LDPE were evaluated by the Scanning Electron Microscopy (SEM). Differences in FTIR spectra were observed. SEM studies showed that the surface morphology of LDPE changed.

[1] J. V. Gulmine, P. R. Janissek, H. M. Heise, L. Akcelrud. Polyethylene characterization by FTIR. Polymer Testing, volume 21, Issue 5, 2002, pages 557-563.
[2] João Carlos Miguez Suarez, Elisabeth Ermel da Costa Monteiro, Eloisa Biasotto Mano. Study of the effect of gamma irradiation on polyolefins-low-density polyethylene. Polymer Degradation and Stability, volume 75, Issue 1, 2002, pages 143-151.
[3] A. Abdel Moez, S.S. Aly, Y.H. Elshaer. Effect of gamma radiation on low density polyethylene (LDPE) films: optical, dielectric and FTIR studies. Spectrochimica Acta Part A: Molecular and Biomolecular Spectroscopy, volume 93, july 2012, Pages 203-207.
[4] L.M. Ferreira, A.N. Falcão, M.H. Gil. Modification of LDPE molecular structure by gamma irradiation for bioapplications. Nuclear Instruments and Methods in Physics

Research Section B: Beam Interactions with Materials and Atoms, volume236, Issue 1-4, July 2005, pages 513-520.
[5] M. Mateev, S. Karageorgiev. Stability of the interphase interaction and changes in the microdestruction mechanisms in low density polyethylene on high energy irradiation. Polymer Degradation and Stability, volume 50, Issue 32, 1995, pages 353-360.

ASS-10-Or-9
New Experiments and Applications Made Possible by a Low Temperature 4-Tip STM with UHV-SEM Navigation

T01 Applied Surface Science

#ASS-10-Or-9

A. Bettac, B. Guenther, J. Chrost, J. Koeble, A. Feltz.

Omicron NanoTechnology GmbH - Taunusstein (Germany).

A major challenge in the development of novel devices in nano- and molecular electronics is their interconnection with larger scale electrical circuits required to control and characterize their functional properties. Local electrical probing by multiple probes with STM precision can significantly improve efficiency in analyzing individual nano-electronic devices without the need of a full electrical integration. Recently we developed a microscope stage that merges the requirements of a SEM navigated 4-probe STM and at the same time satisfy the needs for high performance SPM at low temperatures.
Besides SEM/STM probe fine navigation and imaging with atomic resolution at temperatures of T<5K, the pm-stability of the LT NANOPROBE expands applications to tunneling spectroscopy and even the creation or modification of nanostructures or single atoms by a sharp and precise SPM probe.
A further milestone in the development of the instrument was the implementation of the QPlus- NC-AFM mode [1, 2] for imaging on insulating surfaces. The QPlus mode becomes important if nanowires/nanostructures are deposited on an insulating substrate for a better electrical decoupling of the nanowire from the substrate. In this case the QPlus sensor can be employed to locate the nanostructures and, after finding the structure, to carry out conductance measurements.
In this contribution we will present first QPlus results obtained with the LT Nanoprobe at low temperatures. Furthermore we will focus on measurements that prove the performance level of the instrument as well as on tunneling spectroscopy and atom manipulation experiments on Ag(111) at temperatures of T < 5K.

[1] F. J. Giessibl, Applied Physics Letters 73 (1998) 3956
[2] F. J. Giessibl, Applied Physics Letters 76 (2000) 1470

High resolution NC-AFM QPlus image of a NaCl(001) surface at T=4.4K. Imaging parameters: Δf= - 1.3 Hz, f_{res}= 23.8 kHz, A≈ 0.5 nm, Q ≈20.000, Ugap= -200 mV

ASS-5-Or-7
Cooperative modulation of electronic structures of aromatic molecules coupled to multiple metal contacts

T01 Applied Surface Science

#ASS-5-Or-7

W. Wang [1], X. Shi [2], S. Wang [1], J. Liu [3], M.A. Van Hove [2], P.N. Liu [3], R.Q. Zhang [4], N. Lin [1].

[1]Department of Physics, The Hong Kong University of Science and Technology - Hong Kong (China), [2]Institute of Computational and Theoretical Studies and Department of Physics, Hong Kong Baptist University - Hong Kong (China), [3]Shanghai Key Laboratory of Functional Materials Chemistry and Institute of Fine Chemicals, East China University of Science and Technology - Shanghai (China), [4]Department of Physics and Materials Science, City University of Hong Kong - Hong Kong (China).

We use cryogenic scanning tunneling microscopy/spectroscopy and density-functional theory calculations to inspect the modulation of electronic states of aromatic molecules. The molecules are self-assembled on a Cu(111) surface forming molecular networks in which the molecules are in different contact configurations, including laterally-coupled to different numbers of coordination bonds and vertically-adsorbed at different heights above the substrate. We quantitatively analyze the molecular states and find that a delocalized empty molecular state is modulated by these multiple contacts in a cooperative manner: its energy is down-shifted by ~0.16 eV for each additional lateral contact and by ~0.1 eV as the vertical molecule-surface distance is reduced by 0.1 Å in the physisorption regime. We also report that in a molecule-metal-molecule system the bridging metal can mediate the electronic states of the two molecules.

ASS-10-Or-10
The modification of ultra thin films and in situ electrical conduction measurements using a four-tip STM combined with FIB

T01 Applied Surface Science

#ASS-10-Or-10

N. Fukui, T. Hirahara, S. Hasegawa.

the University of Tokyo - Tokyo (Japan).

The surface conduction becomes more important as the size of electronic devices become smaller. It has been measured by the conventional four-probe method on a planar and uniform surface. In order to unveil further intriguing surface conduction phenomena related to spin transport, one needs a new type of measurement. A promising candidate is surface processing by focused ion beam (FIB), which is an established method for nanoscale fabrication of bulk systems. When FIB process is applied to surface science studies, a problem occurs that the contamination easily destroys the surface states in many cases. Therefore, conductivity measurements and FIB processing should be done in the same ultra high vacuum chamber without exposing the sample surface to air.

In the present work, we performed simultaneous in situ fabrication/conductivity measurement of Bi and Bi_2Se_3 wires. The experiments were performed with our homemade variable temperature four-tip STM equipped with FIB[1]. In the ideal case, the one-dimensional (1D) conductivity of a fabricated wire should be proportional to the wire width and the gradient will be equal to the two-dimensional (2D) conductivity of the original film. The Bi wire, however, had a lower 2D conductivity than that of the original film (Fig. 1 (a)), which is presumably due to the unintended wire destruction. This indicates that even the tail of a FIB beam can change the electrical property of thin film including surface states. Next, a Bi_2Se_3 thin film was capped with Se to keep the film from unintended ion bombardment and then processed by FIB. After that the Se capping layer was lifted off by annealing and its conductivity was measured. Fig. 1 (b) shows the 1D conductivity against the Bi_2Se_3 wire width with and without Se capping process. Without the capping process, the 2D conductivity was lower than the original film like the case of Bi wires. On the other hand, the 2D conductivity of the Bi_2Se_3 wire fabricated with capping layers coincided with that of the original

film. We conclude that FIB processing gives serious damage to the electrical property of an ultrathin film, which can be avoided by capping process. The details will be given in the presentation.

[1] R. Hobara *et al*., Rev. Sci. Instrum. **78**, 053705 (2007)

Fig. 1 (a) The 1D conductivity of Bi wires against the Bi wire width. The red line shows the value estimated from the 2D conductivity which was measured by the four probe method. (b) The 1D conductivity of Bi2Se3 wires against the Bi2Se3 wire width for those with Se capping process (red circles) and without the Se capping process (blue triangles).

ASS-3-Or-6
Effect of yttrium thin layers on the structural and optical properties of Co/Mo2C periodic multilayers

T01 Applied Surface Science

#ASS-3-Or-6

P. Jonnard [1], Y.Y. Yuan [2], K. Le Guen [2], J.M. André [1], C. Meny [3], Z.S. Wang [4], J.T. Zhu [4].

[1]UPMC/CNRS - Paris (France), [2]UPMC - Paris (France), [3]IPCMS - Strasbourg (France), [4]IPOE - Shanghai (China).

Periodic multilayers having layers within the nanometer range can efficiently diffract radiation from the extreme UV (EUV, 30-100 eV) and soft x-ray (100-5000 eV) ranges. Thus this kind of structure is nowadays widely used as optical components on synchrotron beamlines or space telescopes and for applications such as photolithography, x-ray microscopy, x-ray spectroscopy. It is important to develop efficient multilayers in terms of reflectance and bandwidth and for this purpose necessary to control their structure and particularly the quality of their interfaces. The Co/Mo2C periodic multilayer has already been characterized and showed a large difference between the experimental and simulated reflectance values. Moreover, annealing experiments up to 600°C have shown that this multilayer presents a good thermal stability. In this communication, we are interested in investigating the reflectivity changes happening when introducing a third material in the structure. In this case, thin yttrium layers are inserted either at the Co-on-Mo2C or Mo2C-on-Co interfaces to obtain multilayers having three layers in a period. We expect the insertion of the third material to improve the optical path within the structure and then improve the reflectivity and possibly to also act as a diffusion barrier to improve thermal stability.
The Co/Mo2C/Y multilayers are deposited by magnetron sputtering. They are annealed up to 600°C under vacuum. Their reflectance are measured in the hard-ray (8048 eV) and EUV (around 80 eV) ranges and compared to simulations performed for perfect structures, i.e. without roughness or interdiffusion. Preliminary simulations have shown that a reflectance up to 56.5% can be expected for perfect Co/Mo2C/Y multilayers (see figure below). From the fit of the reflectivity curves, the structural parameters of the stacks are determined: density, thickness and roughness of all the

layers including the interfacial ones if any. Nuclear magnetic resonance spectroscopy is also used to know if the cobalt atoms present in the structure interact with the neighbouring Y or Mo2C layers, i.e. are involved in some interlayers.
The influence of the annealing and order of the layers on the optical and structural properties of the Co/Mo2C/Y trilayer system will be presented and discussed in comparison to the results previously obtained on the Co/Mo2C bilayer system.

Acknowledgments: The work is done in the framework of the COBMUL project funded by ANR (#10-INTB-902-01) and NSFC (#11061130549). Colleagues from the BEAR beamline of the Elettra synchrotron facility are thanked for their help during the reflectivity measurements.

SE/ASS-P2-01
Measurement of charge separation by friction between metal and plastic in air and vacuum

T01 Applied Surface Science

#SE/ASS-P2-01

T. Miura, M. Yamaguma.

National Institute of Occupational Safety and Health - Tokyo (Japan).

Electrostatic charges generated by friction between industrial materials induce incendiary electrostatic discharges, such as a spark. In fact, many industrial accidents involving explosions and fires occur due to the electrostatic discharges. In this study, we focus on the elemental process, i.e., charge separation, during friction between metal and plastic. Measurement of the charge separation in a vacuum makes it clear that the real amount of triboelectrification between solid materials because of suppression of charge relaxation through gas discharge in a micro-gap interface of them. In air, we can obtain the relaxation efficiency for the initial charge separation.

Our equipment for measuring the charge separation during friction between metal and plastic, which was constructed on the basis of pin-on-disk technique in a vacuum chamber, is shown in Figure 1. The pin was made of metal and the disk was made of plastic material. Amount of the generated electric charges on the metal pin during friction was measured with an electrometer by connecting to the metal sample electrically.

The experimental results of friction between a stainless steel pin and a poly-ethylene terephthalate (PET) disk in a vacuum and air are shown in Figure 2. It was found that the friction speed were not so significant to the charge separation in a vacuum. The charge density on the rubbed surface of PET was calculated to be about 5×10^{-4} C/m^2 from the generated charge and the width of the friction track. In air, the charge accumulation was, however, one order of magnitude less than the value measured in a vacuum. This should be caused by the charge relaxation as a result of the micro-gap discharge [1].

[1] T. Miura and I. Arakawa, IEEE Transactions on Dielectric and Electrical Insulation, **14**, 560-565 (2007).

Figure 1: Experimental setup

Figure 2: Charge accumulation on the stein-less steel sample as a function of revolution of the PET disk. (a) The normal road of 52 mN, and sliding velocity of 3.02 mm/s in a vacuum (10^{-3} Pa). (b) 170 mN and 1.48 mm/s in a vacuum. (c) 151 mN and 1.50 mm/s in air (temperature 28.1 C degree, humid 71%).

ASS-P1-04
Deuterium retention in W plasma-facing components

T01 Applied Surface Science

#ASS-P1-04

F. Ghezzi [1], R. Caniello [1], D. Giubertoni [2], M. Bersani [2], D. Dellasega [3], A. Hakola [4], M. Anderle [5].

[1]IFP Euratom-ENEA-CNR Association, Via R. Cozzi 53, - Milan (Italy), [2]FBK, Via Sommarive 18, Povo - Trento (Italy), [3]Dipartimento di Energia, Politecnico di Milano, Via Ponzio 34/3 - Milan (Italy), [4]VTT, Association Euratom-Tekes, P. O. Box 1000, 02044 VTT - Helsinky (Finland), [5]Knowledge Department., Autonomous Province of Trento - Trento (Italy).

Results from the JET ITER-like wall, ASDEX Upgrade, and laboratories clearly point to a much lower T retention in metallic (W/Be) plasma facing components (PFC) compared to C-based PFCs. However, ITER metallic walls will face additional effects related to the high particle fluxes, material mixing, and neutron irradiation. For example, polycrystalline self damaged tungsten under 12.3-MeV W^{4+} irradiation has been already observed[1] to show large D retention. D retention in C-Based and metallic PFCs has been extensively studied by post mortem analyses like SIMS, RBS, NRA, and TDS. While TDS can give an absolute integral value, SIMS, RBS, NRA can provide depth information of the retention of D but one needs to combine two techniques to obtain absolute concentrations[2] . In order to use only one technique (SIMS), a common procedure consists of preparing reference standards, of the same matrix to be analyzed, by ion implantation at different doses so that an absolute sensitivity curve can be constructed to calibrate the instrument. However, for the specific case of D in W this is not viable. In fact, in order to get a good signal to noise ratio at 100 nm of Rp, one needs a concentration peak of at least $1x10^{18}$ at/cm^3. SRIM simulation showed that, to reach this value, an implanted fluence of $1x10^{14}$ ions/cm^2 at 20 keV is needed. It was reported that deuterium implantation carried out with energies above 20-25 keV leads to a nuclear reaction generating a non-negligible amount of gamma rays around the implanter[3] . To circumvent the problem, D-W standards have been prepared by co-deposition of W by magnetron sputtering in an Ar-D plasma environment. Various D^+ incident energies ranging from 20 to 200 eVwere used. Since the amount of D retained depend also on the microstructure of the W coating[4] , the microstructure of the standards was varied and

was studied by SEM cross section micrography. The D absolute concentration was determined by NRA. Once the calibration curve has been obtained, the absolute D concentration of W samples coming from the ASDEX-Upgrade divertor will be directly measured by SIMS. A comparison with previous NRA measurements on the above samples is also foreseen.

1 M.H.J. ’t Hoen et al., Nucl. Fusion 52 (2012) 023008.

2 T. Dittmar et al., Phys. Scr. T138 (2009) 014027.

3 K.Saadtman et al. “Radiation Emission from Ion Implanters when Implanting Hydrogen and Deuterium”, Proceeding of 1998 International Conference on Ion Implantation Technology. 1998, Kyoto, Japan, June 22-26, Vol 1 , 292-295.

4 O. V. Ogorodnikova et al. , J. Nucl. Mater. 419 (2011), 194-200.

ASS-P1-05
XPS analysis of nano-structured surfaces with GOSSIP software

T01 Applied Surface Science

#ASS-P1-05

O. Eric.

EADS Innovation Works - Suresnes (France).

The software tool GOSSIP (Generation of Survey Spectra In X-ray Photoelectron Spectroscopy) was developed in 2008 at EADS Innovation Works.
The objective was to develop a simple tool for better comprehension and faster analysis of complex X-ray survey spectra (200-1500 eV) when applying XPS in an industrial context.
It is entirely and only based on S. Tougaard modelling of continuous inelastic background (ref [1]). The main difference with QUASES™ developed and commercialized by S. Tougaard, is that it deals with survey spectra as a whole instead of individual peaks, leading to faster data reduction.
GOSSIP simulates survey spectra of nano-structured surfaces defined by user, that can be compared to experimental data. Principle of GOSSIP and validation of results with simple real nano-structured surfaces have been published in 2009 (ref [2]).
This paper aims at giving a few examples of simple strategies that can be used to "understand" its own XPS data and acquire an expertise at "reading" shapes of XPS survey spectra.
To avoid un-necessary complexities of real XPS spectra, the examples are based on two imaginary pure elements A and B, with very simple survey spectra which have a doublet peak at 1400eV and 1000eV respectively, and identical sensitivity factors. By following an energy dependence law AEp, with p=0.75 and A = 0.01, Effective Attenuation Lengths (EAL) are respectively 2.3 nm and 1.8 nm at these kinetic energies.
It is shown that by using atomic percentages determined on experimental data by the standard method of peak area ratios, models generated by GOSSIP with these atomic percentage values and simple operations (spectra subtraction or division), unknown surface nano-structures can be quickly and easily solved.

[1]: S. Tougaard in Surface Analysis by Auger and X-ray Photoelectron Spectroscopies (Eds D. Briggs, J.T. Grant), IM Publications, Chichester and Surface Spectra Ltd, Manchester, 2003, pp 295, Chapt. 12
[2]: XPS survey spectra simulation of nano-structured surfaces, E. Ollivier, J.P.Langeron, Surf. Interface Anal. 2009, 41, 295-302

imagegossip.jpg

ASS-3-Or-4
GaN surface polarity determination by photoelectron diffraction

T01 Applied Surface Science

#ASS-3-Or-4

O. Romanyuk [1], P. Jiříček [1], T. Paskova [2], I. Bartoš [1].

[1]Institute of Physics, ASCR - Prague (Czech republic), [2]North Carolina State University - Raleigh (United states).

Nitride materials with non-polar and semipolar surface orientations have attracted significant attention because of their importance for optoelectronic device applications. The surface properties of the wurtzite nitrides are strongly influenced by their surface polarities (the topmost atomic layer in the crystal bilayer contains cations or anions). Different methods for polarity determination of the GaN crystals have been reported, but they are either destructive or highly demanding. For example, polarity can easily be determined by surface etching [1] or by nondestructive methods such as photoelectron diffraction (PED) [2,3].

In this work, a nondestructive approach, utilizing PED intensity, is presented for polarity determination of the polar GaN(0001), (000-1), and semipolar GaN(20-21), (20-2-1) crystals. Clean surfaces have been prepared by annealing under NH_3 atmosphere [4]. Angular resolved PED measurements have been performed for a photoelectron kinetic energy of 825 eV (MgKa excitation from the N 1s core level) and of 1234 eV (Ga 3d level). Corresponding angle resolved intensities from the N 1s and Ga 3d levels have been calculated taking multiple electron scatterings into account.

Calculated PED patterns of GaN with both surface polarities (000-1) and (0001) are shown in Fig 1. The peak locations mostly correspond to directions connecting the emitting atoms with their neighbours due to a strong forward scattering of the photoemitted electrons [5]. One can see that while the Ga 3d patterns are quite similar for both polarities, the N 1s patterns are quite different. Much stronger electron scattering cross-sections of Ga atoms, found convincingly during numerical modelling, simplifies the structural interpretation of the photoelectron diffraction patterns. It enables us to suggest a simplified method for polarity determination utilizing photoemitted electron intensities in just a few azimuths of the crystal.

Acknowledgments
Support by the Academy of Sciences of the Czech Republic (project No. M100101201) and by NSF (DMR -1207075) is gratefully acknowledged.

References

1. J.L. Rouviere, J.L. Weyher, M. Seelmann-Eggebert, S. Porowski, Appl. Phys. Lett. 73 (1998) 668.
2. J.R. Williams, M. Kobata, I. Píš, E. Ikenaga, T. Sugiyama, K. Kobayashi, N. Ohashi, Surface Science 605 (2011) 1336.
3. J. L. Rouviere, J. L. Weyher, M. Seelmann-Eggebert, S. Porowski, Appl. Phys. Lett. 73 (1998) 668.
4. O. Romanyuk, P. Jiříček, T. Paskova, Surf. Sci. 606 (2012) 740.
5. P. Alnot, J. Olivier, F. Wyczisk, C.S. Fadley, J. Electron Spectrosc. Relat. Phenom. 43 (1987) 263.

Fig.1 Calculated photoelectron diffraction patterns of the GaN(000-1) a) N 1s, b) Ga 3d, and GaN(0001) c) N 1s, d) Ga 3d. Polar angle theta varies from 0° to 50°.

ASS-P1-09
Analysis of the x-ray fluorescence excited by standing waves in periodic multilayers through the oscillating dipole model

T01 Applied Surface Science

#ASS-P1-09

J. André [1], K. Le Guen [2], Y.Y. Yuan [2], P. Jonnard [3], N. Mahne [4], A. Giglia [5], S. Nannarone [5], Z.S. Wang [6], J.T. Zhu [6].

[1]CNRS - Paris (France), [2]UPMC - Paris (France), [3]CNRS/UPMC - Paris (France), [4]Elettra-Sincrotrone - Trieste (Italy), [5]TASC - Trieste (Italy), [6]IPOE - Shanghai (China).

Periodic multilayers having layers within the nanometer range can efficiently diffract radiation from the extreme UV (EUV) and soft x-ray ranges. Thus this kind of structure is nowadays widely used as optical components on synchrotron beamlines or space telescopes and for applications such as photolithography, x-ray microscopy, x-ray spectroscopy. The reflectance of the multilayer strongly depends on the quality of the interfaces, particularly roughness and interdiffusion.
X-ray standing wave regime enables probing the interfaces of periodic multilayers. Indeed, when the Bragg condition for diffraction of incident radiation is fulfilled, a strong standing wave develops having the periodicity of the multilayer. Then, by slightly changing the incidence angle of the incoming radiation around a Bragg peak, it is possible to move the nodes (maxima) and anti-nodes (minima) of the electric field either at the centre of a layer or at an interface. Upon the excitation by the electric field, secondary processes can take place, such as emission of photoelectrons or of characteristic fluorescence radiation. Fluorescence is interesting to probe multilayers, stacks having a total thickness of a few hundreds nanometers, as the x-ray emission may originate from a great depth whereas the photoelectron escape depth is limited to a few nanometers.
It is also possible to observe the fluorescence, excited or not by standing waves, in a direction close to the Bragg peak for this secondary radiation. Until now, developed models only deal with standing waves of primary radiation. We present a theoretical approach based on the oscillating dipole model and the coupled-wave theory that

can treat both primary and secondary standing wave regimes.
We compare our simulations to experimental data available in the literature and find good agreement. We also present a comparison with some of our experimental results obtained on Co/Mo_2C multilayers having a period of 4.2 nm. The intensity of the Co Lα emission, excited with a radiation having an energy close to the Co L3 photoionization threshold, is observed as a function of the angle scanning the first Bragg peak of the incident radiation. Possible discrepancies between the experiment and the simulation are finally discussed.

Acknowledgments: The work is done in the framework of the COBMUL project funded by ANR (#10-INTB-902-01) and NSFC (#11061130549).

ASS-10-Or-7
Status of scanning Auger microscopy for high spatial chemical resolution

T01 Applied Surface Science

#ASS-10-Or-7

E. Martinez, V. Jousseaume, S. Borel, C. Dieppedale, B. Reig, O. Renault.

CEA, LETI - Grenoble (France).

Auger electron spectroscopy (AES) and microscopy (SAM) are gaining interest to investigate nano-structures or thin multilayers stacks currently developed for nanotechnologies [1]. New generation Auger nanoprobes combine high lateral (<10 nm) and energy (0.1 %) resolutions thus offering the possibility to analyze the chemical composition, as well as the chemical environment, at the deca-nanometer scale. Surface sensitivity (5 nm or less) makes it complementary to electron microscopy techniques such as EDX and EELS.

The performances of these nanoprobes in terms of spatial chemical resolution are illustrated with the analysis of CMOS-compatible Si nanowires [2]. The catalyst (Cu) and growth temperature (< 450°C) are made compatible with the devices fabrication. AES and SAM are potential techniques to bring information about the surface chemical composition, in order to optimize their synthesis and final performances. The chemical nature of both the catalyst and the nanowire can be identified (see figure 1). Restrictions due to backscattered electrons will be discussed.

SAM will be combined with state-of-the-art XPS imaging with photoelectron emission spectromicroscopy (XPEEM). A cluster system enabling UHV transfers between both instruments is used to optimize and preserve the surface preparation. Combined surface analyses are made possible from the micro to the deca-nanometer scale with meaningful complementary information. SAM offers higher lateral resolution in elemental imaging and XPEEM can bring more details about the chemical environment. This is used to investigate surface contamination on µ-switch devices after successive ageing cycles.

This work was performed at the MINATEC Nano-Characterization Centre (NCC) and was partially supported by the French National Reseach Agency (ANR) through the

“Recherche Technologique de Base” (RTB)

[1] S. N. Raman, D. F. Paul, J. S. Hammond and K. D. Bomben, Microscopy Today 19 (2), 12 (2011).
[2] V. T. Renard, M. Jublot, P. Gergaud, P. Cherns, D. Rouchon, A. Chabli and V. Jousseaume, Nature Nanotech. 4, 654 (2009).

Fig. 1 : SEM image of a Si nanowire (NW) and high spatial resolution Auger mapping for Cu.

ASS-10-Or-12
Observation of atomic dipole moment on hydrogen and oxygen adsorbed Si(111)-7×7 surfaces by using noncontact scanning nonlinear dielectric microscopy

T01 Applied Surface Science

#ASS-10-Or-12

Y. Cho, D. Mizuno, K. Yamasue.

Research Institute of Electrical Communication,Tohoku University - Sendai (Japan).

The adsorption on Si surface has been greatly interested in the discipline of surface science [1]. In particular, passivation of Si surfaces by hydrogen or oxygen has been important for semiconductor industry. Scanning probe microscopy (SPM), such as scanning tunnel microscopy (STM) and noncontact atomic force microscopy (NC-AFM), is one of the techniques to observe the passivated surface in atomic level. The images observed by STM and NC-AFM give information on chemical characteristic of the adsorbed surface. For example, in the case of hydrogen adsorption, the dangling bond of Si surfaces forms a chemical bond with atomic hydrogen and then the Si surfaces becomes insensitive to the chemical interaction with reactive molecules and atoms. On the other hand, there have been few studies from the viewpoint of physisorption. Even if a surface is chemically stable, molecular interaction (such as van der Waal's force) is caused by the difference in electronegativity between a Si and hydrogen (or oxygen) atom (Therefore, the surface has dipole moments.). Noncontact scanning nonlinear dielectric microscopy (NC-SNDM) can simultaneously measure the atomic dipole moment and topography by detecting nonlinear dielectric constants ε(3) and ε(4), respectively [2]. In this report, we apply this NC-SNDM to observe atomic dipole moments on the hydrogen and oxygen adsorbed Si(111)-7×7 surfaces in order to investigate the charge distribution around the adatoms. In the case of hydrogen adsorption, it is expected that the atomic dipole moment of the hydrogen-adsorbed adatom becomes weak because the charge distribution around the adatom is nearly central symmetric such as the tetrahedral structure formed by Si atoms in the bulk. Our experimental results are shown in Fig. 1. It was confirmed that

dipole moments on the hydrogen-adsorbed Si adatoms surely became weaker than those on cleaned Si adatoms (shown by black circle in Fig.1(b)). The observed weaken atomic dipole moments suggest that hydrogen-adsorbed surface is passivated physically as well as chemically. Next we observed oxygen adsorbed Si(111)-7×7 surface and found that, in the initial stage of oxidization, the dipole moment at the oxidized adatom (oxygen is inserted into the back-bond of the adatom) becomes weaker. These results can be explained by our model based on the charge distribution around Si adatom [2].

[1] H. Tokumoto et al., J. Vac. Sci.Technol., A 8, 255 (1990).
[2] Y. Cho and R. Hirose, Phys. Rev. Lett., 99, 186101 (2007).

Fig 1. NC-SNDM images of hydrogen- adsorbed Si(111)-7×7 surface. (a) Topography by ε(4) signal, (b) Dipole moment image by ε(3) signal.

ASS-5-Or-1
Electrical phase transition of poly(4,4'-aminotriphenylene hexafluoroisopropylidenediphthalimide) by photogenerated charged carrier injection

T01 Applied Surface Science

#ASS-5-Or-1

K. Lee [1], K. Ihm* [2], T.H. Kang [2], S. Chung [1].

[1]POSTECH - Pohang (Korea, republic of), [2]Pohang Accelerator Laboratory - Pohang (Korea, republic of).

We show a set-up of poly(4,4'-aminotriphenylene hexafluoroisopropylidenediphthalimide) (6F-TPA PI)/Al sample in which holes are injected by photoelectron emission process instead of direct charge carrier injection via metal electrode. In this process, an irreversible electrical phase transition of 6F-TPA PI is found in contrast to the Al/6F-TPA PI/Al structure, leading to a write-once-read-many behavior. The photoelectron spectroscopy results measured before and after the switching process revealed that the irreversible electrical phase transition of 6F-TPA PI is attributed to the chemical modification of the carbonyl group in phthalimide moiety.

Fig. 1 : Novel set-up in which holes are injected by photoemission process

Fig. 2 : The phase change of the PI film at 18.6 V

ASS-2-Or-6
Development of PVD-deposited Pd-Ag functional thin film membranes on ceramic supports for hydrogen purification/separation

T01 Applied Surface Science

#ASS-2-Or-6

C. Tavares [1], A.I. Pereira [1], P. Perez [2], A. Mendes [2], L.M. Madeira [2].

[1]Centre of Physics, University of Minho, Campus Azurém - 4800-058 Guimaraes (Portugal), [2]LEPAE, Chemical Engineering Department, Faculty of Engineering, University of Porto - 4200-465 Porto (Portugal).

Pd-Ag based membranes supported on porous α-Al2O3 (doped with yttria-stabilized zirconia) have been studied for hydrogen selective separation. Magnetron sputtering technique was employed for the synthesis of the thin film membranes. The permeation fluxes can be affected by the membrane columnar structure, which is formed during deposition. From SEM analysis it was observed that different sputtering deposition pressures can lead to distinct columnar structure growth. XRD patterns provided evidence of a Pd-Ag solid solution whose crystalline texture can be altered by the deposition pressure. The average crystallite domain size is 21 nm. The gas-permeation results have shown that the Pd-Ag membrane supported on porous α-Al2O3 is selective towards H2. For optimized conditions, the permeate flow at a pressure feed of 300 kPa of N2 is 73.1 mL/min-1, which shows that the membrane has a reasonable capacity to hinder the permeation of this gas. The selectivity factor α (H2/N2) obtained for the optimized membranes was of the order of 10, revealing its selectivity towards hydrogen.

Figure 1: Membrane co-sputtering deposition from two separate targets: Ag and Pd.

Figure 2: Hydrogen and nitrogen permeance through the PdAg membrane as a function of respective feed pressure.

ESD/ASS-1-Or-8
INTERFACE FORMATION BETWEEN POLYMER-DERIVED CERAMIC SURFACES AND STEEL SUBSTRATES

T01 Applied Surface Science

#ESD/ASS-1-Or-8

A. Schütz, M. Günthner, G. Motz, U. Glatzel.

University - Bayreuth (Germany).

Ceramic coatings synthesised from polysilazane polymers (precursors) are easy to apply and guarantee optimum adhesion even on already oxidised metal surfaces. For some purposes those coatings are too thin or too porous. These shortcomings may be corrected by using filler particles. A coating with excellent surface adhesion to low alloyed steel had to be developed in order to prevent high temperature corrosion in chemically and mechanically agressive environments.
Novel glass particle filled precursor-based coatings were found to offer excellent corrosion protection for steel substrates. The coating systems properties were analysed with different techniques. Adhesion was determined using scratch tests with different loads. The abrasion resistance was tested at a high temperature with large particle freight. Characterisation was done using scanning electron microscopy with energy dispersive X-ray, surface tests as well as thermal conductivity measurements. Micro-structural investigations were conducted using scanning electron microscopy, transmission electron microscopy, and helium ion microscopy.
A specific interface formation was observed in all cases: metal oxide needles grow from the metal substrate surface into the precursor based coating with glass filler particles. In some cases they induce a crystallisation of the coatings glass fillers.

ASS-1-Or-6
Quantitative surface analysis using Low Energy Ion Scattering (LEIS)

T01 Applied Surface Science

#ASS-1-Or-6

T. Grehl [1], P. Bruener [1], M. Fartmann [2], R. Ter Veen [2], H. Brongersma [1], E. Niehuis [1].

[1]ION-TOF GmbH - Muenster (Germany), [2]Tascon GmbH - Muenster (Germany).

Due to its ultimate surface sensitivity and the quantitative elemental information, Low Energy Ion Scattering (LEIS) is a valuable tool for samples from many fields of science and technology [1]. The latest generation of instruments has made these properties available for routine analytical work, leading to a wider use of this technique. This has become possible by high sensitivity and high resolution analyzers in dedicated instruments. Main fields of application are heterogeneous catalysis, fuel cells and related areas, but also in thin film (ALD, PVD, CVD, etc.) research and characterization.

In addition to providing the elemental composition of the outermost atomic layer of a solid, the virtually non-destructive "static" depth profiling yields additional information from the same data. It allows access to the composition of the first few atomic layers below the surface, up to a depth of < 10 nm, without the complication of sputtering artefacts which are present in most other depth profiling techniques. Here, ions scattered in layers below the surface are recorded, which undergo an additional depth-proportional energy loss. Therefore, the signal from deeper layers is spread out on the energy scale, showing the distribution of the elements below the surface.

In this presentation we will demonstrate how LEIS evolved into a practical surface analytical technique. Examples from a variety of samples, including an automotive exhaust catalyst system and thin films, will be shown and discussed. The work on the automotive catalyst material shows how the active phase of the catalyst changes by ageing under working conditions. LEIS is capable of picking up these changes at the outermost layer, where the actual catalytic reaction takes place.

Work on thin film samples demonstrates how the thickness and conformity of the film can be characterized quickly and non-destructively. While for thicker films (> 5 - 10

nm) sputter depth profiling similar to SIMS or XPS is used, static depth profiling is applied to ultra-thin films. The signal from the outer layer can be separated from the in-depth signal, so both the quantification of the surface coverage for all elements as well as the thickness distributions within the film can be derived from a single measurement.

[1] H. Brongersma, Surf. Sci. Reports **62** (2007) 63-109

ASS-2-Or-7
Structure changes of copper in different supported catalysts

T01 Applied Surface Science

#ASS-2-Or-7

A. Oszkó, K. Markó, G. Merza, G. Pótári, A. Erdőhelyi.

University of Szeged - Szeged (Hungary).

Introduction

The surface changes of copper containing catalysts were characterized by XPS. Cu/CeO_2 samples were prepared by different methods and studied in the steam reforming of ethanol. Copper catalysts supported on activated carbon (AC) and MWCNT were tested in the oxidative carbonylation of methanol to produce dimethyl carbonate (DMC).

Experimental

XP spectra were taken with a SPECS instrument. Sample treatments were carried out in a catalysis cell (HPC) in flowing gases at atmospheric pressure. The HPC was directly connected to the analysis chamber of the XP instrument. The samples were treated the same way as usual in other catalytic reactions, e.g. in gas chromatography.

Results and discussion

Cu/CeO_2 prepared by impregnation showed the typical Cu^{2+} 2p doublet in the as received state. On the co-precipitated sample the satellites were less obvious. In this case the oxidation state was determined with the help of the Auger parameter and found that Cu is in the form of Cu^{+} and Cu^{2+}. After oxidation both kinds of samples contained Cu^{2+}. Reduction caused copper to reduce to metal on the impregnated sample, while an additional low binding energy component appeared on the co-precipitated sample. The ceria spectra were deconvoluted in all stages of the treatment. The Ce^{3+}/Ce^{4+} ratio was determined from the Ce(III)/[Ce(III)+Ce(IV)] formula where Ce(III) and Ce(IV) denote the sum of the areas of all synthetic peaks present in the given oxidation state. The reduction degree did not change during

pretreatment. The steam reforming reaction led to the reduction of ceria on the impregnated sample. New peaks on the O 1s and C 1s spectra corresponded to -OH and C-H containing deposits on the catalyst. The reduction degree of ceria was much less on the co-precipitated sample, while an enhanced carbon deposition was observed.

Spectra taken on Cu/MWCNT showed that Cu^{2+} was present on the surface of the starting material. Copper reduced to its metallic state after reduction. The reaction with $MeOH+O_2+CO$ mixture led to the re-oxidation of copper to mostly Cu^{+} with some Cu^{2+}. The amount of the latter increased with reaction time. Only a slight change could be observed on the C 1s spectra. The O 1s spectra showed a complex structure with at least four oxygen components. AC supported copper was also active in DMC production. Several copper forms were identified during the reaction as proved by the Auger parameters and Auger peak positions. Oxygen from X=O, X-OH and -COOR species were present on the catalyst surface. These results contribute to the explanation of the reaction mechanism and to the understanding of the changes in catalytic activity.

Cu LMM Auger spectra taken on Cu/Norit. A.P. means Auger parameter

BI/ASS-1-Or-9
Development and Characterization of MgO/Fluoridated-Hydroxyapatite Composite Coating on Mg-3Zn-0.8Ca Alloy by Micro-Arc Oxidation Coupled with Electrodeposition

T01 Applied Surface Science

#BI/ASS-1-Or-9

I. Ghayad [1], S. Abdel Hallem [2], M. Shoeib [2], M.A. Maamoun [2], N. Nassif [2], H. Soliman [2].

[1]Assoc. Professor (Egypt), [2]Professor (Egypt).

Some unsolved problems, such as poor adhesion of coatings, currently limit the use of Mg alloys for orthopedic application. The present article aims to overcome these obstacles and improves the corrosion resistance of Mg alloys via combination between surface treatment and electrodeposition. The surface of Mg-0.8Ca-3Zn alloy was pretreated using micro-arc oxidation (MAO) to form an oxide layer upon which a top layer of fluoridated-hydroxyapatite (FHA) was electrodeposited. The corrosion behavior of both layers was evaluated in simulated body fluid (SBF) using linear polarization (LP), potentiodynamic polarization and electrochemical impedance techniques. Surface characterization of the untreated, MAO treated and FHA coated alloy was performed.

Scanning electron microscopic (SEM) examination shows that the MAO treated surface is completely covered by FHA layers (Figure 1) because the MAO oxide layer with high porosity offered considerable sites where FHA particles are easily incorporated. Combination between MAO and FHA coatings was also proved by XRD analysis which shows both peaks of MgO and FHA.

Electrochemical tests show that MAO of the Mg-Ca-Zn alloy surface significantly improves its corrosion resistance. The polarization resistance (Rp) of the MAO samples is 12000 ohm which is 5 times more than the untreated alloy (1530 ohm). FHA coat of the MAO treated samples further enhances corrosion resistance of the alloy as shown by the increase of Rp to 59000 ohm which is about 38 times higher than the untreated alloy. Pores blocking at MAO layer via FHA as top coat plays a

key role in obvious corrosion resistance enhancement.

1. X Gu, Y. Zheng, Y Cheng, S. Zhong and T Xi. Biomaterials 30 (2009) 484–98.

2. Y. Shi, M.Qi, Y.Chen and P. Shi, Mater. Letters 65 (2011) 2201-2204.

3. X. N. Gu, N.Li, W. R. Zhou, Y.F.Zheng, X.Zhao, Q.Z. Cai and L.Ruan, Acta Biomaterialia 7 (2011) 1880–1889.

Figure 1: SEM images of FHA coat (a) and FHA - MOA treatment (b) on the Mg-Zn-Ca alloy.

ASS-8-Or-3
Surface Wettability of Macroporous Anodized Aluminum Oxide

T01 Applied Surface Science

#ASS-8-Or-3

I. Buijnsters, R. Zhong, T. Natali, J.P. Celis.

KU Leuven - Leuven (Belgium).

Aluminum and its alloys are important industrial materials due to their low weight and good corrosion resistance. Porous anodized aluminum oxide (AAO) formed by the electrochemical anodization of Al has become a popular and highly versatile material for numerous applications in surface tribology (1), catalysis (2), and template synthesis of 1D nanostructures (3). Aluminum oxide itself is a hydrophilic material, but due to the controllable pore dimension and adjustable surface chemistry the porous AAO structures provide a great potential for producing surfaces with special wettability.

Here, we discuss the correlation between the structural characteristics and the wetting of AAO surfaces with large pore sizes (>100 nm). The roughness-induced wettability is examined for oxide films grown by a 2-step, hard anodization in phosphoric acid of 3 different concentrations using an Al alloy. This is done for as-synthesized AAO layers, after various degrees of pore widening by a wet chemical etching in phosphoric acid solution, and upon surface modification by Lauric acid or a silane. The as-grown AAO films feature structurally disordered pore architectures with average pore openings in the range 140-190 nm but with similar inter-pore distances of about 405 nm. The formation of such AAO structures induces a transition from slightly hydrophilic to moderately hydrophobic surfaces up to film thicknesses of about 5 μm. Increased hydrophobicity is obtained by pore opening and a maximum value of the water contact angle (WCA) of about 128° is measured for AAO arrays with a surface porosity close to 60% (see Figure). Higher surface porosity by prolonged wet chemical etching leads to a rapid decrease in the WCA as a result of the limited pore wall thickness and partial collapse of the dead-end pore structures. Modification of the AAO surfaces by Lauric acid results in 5°-30° higher WCA's, whereas near-superhydrophobicity (WCA~146°) is realized by silane coating. The 'rose petal effect' of strongly hydrophobic wetting with high adhesive force on the produced AAO surfaces is explained by a partial penetration of water through capillary action into the dead-end pore cavities which leads to a wetting state in-between the Wenzel and Cassie states. Moreover, practical guidelines for the

synthesis of rough, highly porous AAO with controlled wettability are provided and the possibility of forming superhydrophobic surfaces is evaluated.

(1) L. Vojkuvka et al., Surf. Coat. Technol. 2012, 206, 2115.
(2) F. Liu et al., Small 2006, 2, 121.
(3) J. Martín et al., Polymer 2012, 53, 1149.

WCA vs. surface porosity of AAO after different anodizing and post-etching treatments. Diamond, circle and square symbols represent data for anodizing in 1, 5, and 10 wt.% phosphoric acid.

SE/ASS-1-Or-2
Structure-function properties of multimeric surfactants on charged surfaces

T01 Applied Surface Science

#SE/ASS-1-Or-2

N. Kampf [1], C. Wu [2], Y. Wang [2], J. Klein [1].

[1]Department of Materials and Interfaces, Weizmann Institute of Science - Rehovot (Israel), [2]Key Laboratory of Colloid and Interface Science, Institute of Chemistry, Chinese Academy of Sciences - Beijing (China).

Surfactants are widely used to modify surfaces and interfaces properties. Unique cationic trimeric and tetrameric surfactants (Fig.1) were found to form liposome-like aggregates in solution (1, 2). Atomic force microscope (AFM) scans under the trimeric surfactant solution demonstrate the presence of large aggregates (ca. 100nm in diameter) surrounded by worm-like micelles on mica surface. We have investigated the normal and shear forces between two atomically smooth mica surfaces across this surfactant using the surface force balance (SFB) technique (Fig.2). Shear forces measured across the trimeric surfactant solution demonstrate ultra-low friction coefficient ($\mu=5x10^{-5}$) under pressure of tens of atmospheres. The contribution of the compressed charged spheres to the ultra-low friction measured can be explained by the efficient hydration lubrication mechanism exist between the hydrated surfactant head-groups and the mica surface. A weak dependence of the friction coefficient to the shear rate or amplitude was observed. When the mica surface withdrawn from the surfactant solution a unique bilayer pattern was formed, covering large macroscopic area. A model for this surface pattern formation will be presented.

(1) Hou et al., Langmuir, 24, 10572 (2008).
(2) Wu et al., Langmuir, 26, 7922 (2010).

(3) Kampf et al., Physical Review Letters, 11;103(11):118304 (2009)

Figure 1:Chemical structure of tri(dodecyldimethylammonioacetoxy)diethyltriamine trichloride (DTAD), left and tetra(dodecyldimethylammonioacetoxy)diethyltriamine trichloride tetrameric) (PATC), right.

Figure 2: Schematically showing the SFB setup of two curved mica surfaces in the SFB, glued on a plano-cylindrical lens and mounted on the sectored piezocrystal (PZT) enabling its lateral (V_S) and normal motion, to measure directly the shear and normal stresses, while the forces are monitored from the bending of a shear (K_S) spring (via capacitance probe) and normal (K_N) recorded real time by white light interferometry manually or by machine vision equipment. This enables to measure changes in the absolute separation (D) and lateral motion at the angstrom level (3).

ASS-8-Or-10
Compositional changes and formation of nanodroplets on GaN epilayer surfaces induced by normally incident 1 keV argon-ion sputtering

T01 Applied Surface Science

#ASS-8-Or-10

V. Venugopal [1], K. Kumar [2], K. Upadhyaya [2], S.M. Shivaprasad [2].

[1]Division of Physics, School of Advanced Sciences, VIT University Chennai Campus - Chennai (India), [2]International Center for Materials Science and Chemistry and Physics of Materials Unit, Jawaharlal Nehru Centre for Advanced Scientific Research - Bangalore (India).

Understanding the effect of low energy Ar^+-ion bombardment on the structural and compositional changes [1] of GaN surfaces is crucial for controlling ion etching process [2] in order to fabricate GaN-based devices. Here we report the surface compositional changes leading to the formation of nanodots on epilayer of GaN on sapphire induced by normally incident 1 keV argon-ion sputtering at an ion flux of ~2.81×10^{14} ions/cm^2/s studied by interrupting sputtering at 400 s, 800 s and 1200 s and *in-situ* characterization of the sputtered surfaces using XPS, under ultrahigh vacuum conditions. The core-level Ga 3d and N 1s spectra indicate dissociation of disordered Ga and N atoms and formation of metallic Ga, and surface re-organization beyond sputtering time of 800 s. The valence band spectra also confirm the formation of metallic gallium and disruption of Ga-N bonds of the GaN epilayer. AFM images of the epilayer surfaces sputtered to 1200 s indicate the formation of nanodroplets [Fig. 1] and EDX measurements indicate that these nanodroplets are Ga-rich. These hemispherical features are mainly located at the ion erosion modified steps on the epilayer. The lateral size and height range of these Ga droplets are 133 ± 16 nm and 15 ± 2 nm respectively, with a density of 1.64 $\times10^8$ cm^{-2}. The results indicate that preferential sputtering, which is not very pronounced due to strong bonding in GaN, is dominant till 800 s and the ion erosion modified steps are mainly responsible for the formation of nanodroplets with the possibility of threading dislocations in the epilayer acting as nucleation centers for the diffusing Ga adatoms. It is shown that the nanodroplets observed here can neither be explained by the continuum theory [3] nor its subsequent modifications that were applied to many III-V

semiconductors [4] to account for normally incident low energy ion induced pattern formation. The compositional changes accounts for the observation of the variation of the sheet resistance of the epilayer as a function of sputtering time. The effect of ion erosion modified surfaces on optical properties of GaN is also discussed.

1. J. Kovac and A. Zalar, Surface and Interface Analysis, **34** (2002) 253.
2. E. D. Pujo and P. Chabert, J. Vac. Sci. Technol. A, **28** (2010) 1105.
3. B. Kahng, H. Jeong, and A.-L. Barabási Appl. Phys. Lett., **78** (2001) 805.
4. S. Fascko, T. Dekorsy, C. Koerdt, C. Trappe, H. Kurz, A. Vogt, and H. Hartnagel, Science, **285** (1999) 1551.

Fig. 1. 10×10 μm^2 atomic force microscopy image of as-received GaN epilayer after sputtering to 1200s.

ASS-P2-05
Three dimensional Monte Carlo study of EBIC at metallic tip

T01 Applied Surface Science

#ASS-P2-05

J. Priesol, A. Šatka.

Institute of Electronics and Photonics, Slovak University of Technology, Ilkovičova 3, 812 19 - Bratislava (Slovakia).

Electron beam induced current (EBIC) as a scanning electron microscopy technique is well known method used in defect and failure analysis of semiconductor devices, for identification of buried junctions and determination of minority charge carrier properties [1]. In this contribution we report on the results of EBIC experiments performed using Schottky contact formed by a tungsten needle set onto the intentionally undoped, planar GaN layer coalesced on an etched nanorod array prepared on insulating sapphire substrate. EBIC line profiles extracted from EBIC maps of the vicinity of the contact area were used to determine the effective diffusion length L_{eff} of minority charge carriers. Furthermore, 3-D Monte Carlo (MC) statistical model has been developed to investigate the effect of various parameters to evaluation of EBIC line profiles at Schottky contact. Spatial distribution of generated charge carriers was calculated using well known models described by Joy [2] and others. Consequently, the diffusion of these carriers was simulated by means of random walk algorithm, whilst the surface recombination velocity was supposed to be $v_S = 0$. Carriers were considered to contribute to the EBIC signal after reaching the circularly shaped area defined onto the sample surface representing Schottky contact. Described MC model was used to investigate the influence of the energy of primary electrons E_{pe}, contact diameter d and bulk diffusion length L_{bulk} of minority carriers to the spatial distribution of recombining carriers and shape of EBIC line profiles. The experimental details, explanation of obtained results and their use in determination of diffusion length of minority carriers and interpretation of EBIC measurements will be discussed.

Acknowledgements
This work was supported by the Slovak Research and Development Agency under the contract APVV-0367-11. The authors gratefully acknowledge the support of the Slovak Grant Agency projects VEGA 1/0921/13 and 1/0866/11.

[1] H. J. Leamy, J. Appl. Phys. 53, R51-R80 (1982)
[2] D. C. Joy, Scanning Microscopy. 5, 329–337 (1991)

ASS-9-Or-5
Isotropic and anisotropic dipeptide films through gas phase deposition

T01 Applied Surface Science

#ASS-9-Or-5

G. Demirel.

Gazi University - Ankara (Turkey).

Vertically aligned nanostructures have recently attracted increasing interest due to their unique properties and they have been exploited for a variety of applications including field emission devices, filter media, superhydrophobic surfaces, synthetic membranes, intracellular gene delivery devices, biosensors, composites, logic and memory devices, and numerous others. We demonstrated the fabrication and application of well-ordered and vertically aligned dipeptide nanostructures based on a simple gas phase deposition. Deposited nanostructures exhibited the superhydrophobic property with a very low sliding angle. Highly reproducible SERS data have also been obtained after combining deposited films with a thin layer of gold. In addition to these, directional peptide films were, for the first time, successfully fabricated based on the oblique angle deposition technique. We believe that such bio-inspired materials would have a great impact in several technological applications involving catalysis, tissue engineering and biosensors.

ESD/ASS-P3-12
Electrochemical Etching of Porous-Pyramids Structure with Low Reflectance

T01 Applied Surface Science

#ESD/ASS-P3-12

A. Lounas.

centre de recherche en technologie des semi-conducteurs pour l'énergétique - Algiers (Algeria).

Electrochemical Etching of Porous-Pyramids Structure with Low Reflectance

A. Lounas[a]*, A. Nait Bouda[b], H. Menari[a] , N. Gabouze[a] CRTSE[a], 02 Bd Frantz Fanon B.P. 140 Alger 7 Merveilles, Alger, Algérie CDTA[b] HaouchOukil B.P.17 Baba-Hassan, Algiers, Algeria

lounasamel@yahoo.fr

By anisotropic etching, pyramids structured silicon can be prepared using sodium hypochlorite for monocrystalline solar cells. Their influence on the reflectance of the silicon surface was studied to optimize the etching and reduce the optical losses of silicon surface more effectively. However, currently the reflectance of the pyramids structured silicon surface can only be reduced to above 10% in the visible range, which is still too high for high efficiency solar cells. Porous pyramids structured silicon is a promising antireflection coating to solve the problem of high surface reflectance in silicon solar cells. In this paper, a promising method for fabricating porous pyramids compound structure on silicon surface was proposed. The silicon surface was first texturized in $NaOCl/C_2H_5OH$ and then electrochemically etched in HF/C_2H_5OH solution. The average reflectance of the surface in the range of 500-900 nm was as low as 5%. The surfaces prepared under optimized condition were investigated by Scanning Electron Microscopy (SEM) and Spectrophotometry (Fig.1).

Fig.1. Comparison of the surface reflectance for: (a) pyramids structure, (b) porous-pyramids structure

ASS-2-Or-1
Methanol adsorption on cerium and tungsten oxide based systems

T01 Applied Surface Science

#ASS-2-Or-1

K. Mašek [1], M. Škoda [1], J. Beran [1], T. Skála [2], N. Tsud [1], P. Blumentrit [1], J. Polášek [1], V. Matolín [1].

[1]Charles University, Faculty of Mathematics and Physics, Department of Surface and Plasma Science, V Holešovičkách 2 - Prague 8 (Czech republic), [2]Sincrotrone Trieste, Strada Statale 14, km 163.5 - Basovizza-Trieste (Italy).

The adsorption and subsequent dissociation reaction of methanol on various model catalyst surfaces have attracted wide-spread attention due to the importance of this reaction used in direct methanol fuel cells (DMFCs), especially due to continuing research of new materials for DMFCs. Cerium oxide and tungsten oxide based systems have been a subject of interest due to their technological importance in a wide field of various electronic, optical, catalytic and gas sensing applications. The reactivity of cerium and tungsten oxide can be influenced by impregnation of the base material by any active metal, for example Pd, Pt, Au etc. The investigation of relations between the chemical and structural properties is often performed on so-called model systems. By deposition of a small amount of active metal on the surface of epitaxial cerium or tungsten oxide thin film we can prepare such well-defined model system.

In this work an adsorption of methanol on the surface of bare and metal doped (Pt, Pd, Au) epitaxial cerium or tungsten oxide layers was studied. The epitaxial cerium and tugsten oxide layers having (111) surface plane were prepared on Cu(111) and W(110) single-crystal surfaces. The crystallographic structure and epitaxial orientation of the layers were determined by reflexion high-energy electron diffraction (RHEED). The chemical state of the film and adsorbed species were investigated by photoelectron spectroscopy induced by X-ray source (XPS) and synchrotron radiation (SRPES).

The 30L adsorption was performed at low temperature of 140 K. The temperature of the sample was increased in several steps up to 600 K. At each step SRPES measurement with high surface sensitivity and energy resolution was performed. At low temperature multilayer adsorption of methanol was observed for all samples. With increasing temperature methanol decomposed and the different species

resulted from the decomposition process were observed. The process of methanol decomposition was investigated by measurement of O1s, C1s and valence band spectra. The changes of the structure as well as of electronic state were deduced from the core level spectra.
The decomposition pathway of methanol can be followed mainly by observation of the C1s spectra (see figure 1). The multilayer adsorption of methanol was observed for all samples at the temperature of 110 K. With increasing temperature methoxy was formed on the surface by OH bond scission (200 K). Dehydrogenation of the bonded methoxy species proceeded via formyl to CO. Carbon formation due to the partial decomposition of CO was found on Pt-CeOx, Pd-CeOx and Pt-WOx systems. All traces of residual carbon dissappeared at high temperatures (500 K for M-CeOx, 400 K for Pt-WOx). Resistence to the carbon poisoning is important for using of these systems in the real catalytic applications. By comparing the results obtained for different substrates we have shown that the clean surface with no adsorbed species was reached at the temperature of 400 K in the case of tungsten oxide based systems and at 600 K for cerium oxide based systems, respectively. Encapsulation of Pt clusters at temperatures above 570 K was deduced from the presence of CO species on the surface. The C 1s spectra from Pd-CeOx have indicated also low amount of formate and formaldehyde species above 300 K.

ASS-P3-04
Determination and Characterization of Edge Flaws in Laser Diced Thin Silicon Wafers

T01 Applied Surface Science

#ASS-P3-04

G. Hayes, H. Fischer, J.E. Bullema.

TNO - Eindhoven (Netherlands).

As silicon dies become thinner to meet current device demands, residual material damage from laser dicing has a large impact on final die strength. These strength limiting flaws in thin dies need to be characterized and quantified in order to utilize laser dicing in industrial practice. Furthermore, an increase in strength could potentially be realized with the removal and repair of the residual edge damage. The edge flaws and residual material damage associated with laser dicing thin (120µm) silicon wafers were characterized via electron backscatter diffraction (EBSD), atomic force microscopy (AFM), scanning thermal microscopy (SThM), and scanning electron microscopy (SEM). Additionally, the hardness and Young's modulus of the damaged edge zone was characterized via nanoindentation. The extent of edge flaws in combination with a damaged edge zone is discussed in relation to the experimentally mechanical properties. The reported mechanical properties, and corresponding damaged zone investigation shows the effectiveness and viability of surface science techniques to industrial laser cutting applications. The edge damage was characterized in terms of crystallinity, composition, and thermal and mechanical properties. Finally, the removal of the damaged edge zone, along with edge flaws via chemical etching is presented.

ASS-7-Or-3
Enhancement of surface properties on commercial polymer packaging films using various surface treatment processes (fluorination and plasma)

T01 Applied Surface Science

#ASS-7-Or-3

J. Peyroux [1], M. Dubois [1], E. Tomasella [1], E. Petit [1], D. Flahaut [2].

[1]Clermont Université, Université Blaise Pascal, Institut de Chimie de Clermont-Ferrand (UMR 6296) - Clermont Ferrand (France), [2]Université de Pau et des Pays de l'Adour, IPREM/ECP (UMR 5254) - Pau (France).

Commonly used polymer packaging films have not only many advantages, such as low cost and processability but exhibit also few drawbacks such as poor adhesion, printability, barrier properties and low chemical resistance. Furthermore, it is also possible to obtain the whole articles from specials polymers or with multilayers packaging films but these kinds of process remain limited due to the high cost and a high complexity of synthesis. The present work focuses on the change of the surface properties by both **fluorination and plasma treatments**; their combinations are also under investigations.

Fluorination treatment process is known to improve polymers surface properties. It is a diffusion-controlled process which may be described as a heterogeneous reaction between a gas (F_2 pure or mixed with other gases) with the polymer surface. This method modifies only the upper surface layer in order to reach a hydrophilic/phobic surface depending on the gaseous mixture. Concerning the bulk properties, they remain unchanged. This process, a safe technology, displays a lot of advantages which allow it to be used for industrials applications. Different fluorination conditions as well as two fluorinating agents, F_2 and atomic fluorine, were investigated with various commercial polymers. Modifications of the surface layer have been characterized using various complementary techniques such as Fourier Transform Infrared spectroscopy, high resolution solid state Nuclear Magnetic Resonance (^{19}F) which are suitable to determine the nature of the C-F bonding and the fluorinated groups. X-ray Photoelectron Spectroscopy was also performed to

extract the surface chemical compositions. The first main objective is to understand the different fluorination mechanisms. The resulting properties were then studied showing that the fluorinated layer reduces the friction coefficient and improves the chemical resistance. To complete our study, measurements of surface energy have been also performed underlining the enhancement of the adhesion and printability properties with a higher polar component.

The second strategy consists in **plasma treatments**. Several experiments were carried out, first, etching treatments using Argon plasma, and then, reactive treatments with gaseous mixture plasma (O_2, N_2). As after fluorination, surface properties of polymer films treated by plasma have been investigated. Composition and morphology of the films were analyzed by contact angle measurements, and XPS. Measurements of surface energy were realized to define the polarity of the polymer films. The main objective is to improve the surface wettability to obtain a better adhesion property. Plasma treatments result in significant changes of the surfaces both in roughness and in composition. Changes of topography and chemical composition convert the polymer surface into highly hydrophilic character, which mainly depends on the roughness state and the contents of oxygenated or nitrogen containing groups at the surface. The O/N ratios were obtained from XPS analysis and have revealed that CO, CN bonds are the key factor for the enhancement of the polymer surface hydrophilicity. The roughness of the surface was also improved at the micrometric scale that influences the surface hydrophilicity.

ASS-P1-14
A study of porous structure of PEG-mediated silica

T01 Applied Surface Science

#ASS-P1-14

O. Gorbunova, O.N. Baklanova, T.I. Gulyaeva.

Institute of hydrocarbon processing, SB RAS - Omsk (Russian federation).

Over the past few decades, many papers devoted to the preparation and application of various colloidal and micro-heterogeneous forms of silica with a developed surface (sols, gels and powders) had been published [1,2]. According to various estimates, from 60 to 80% of the surface-modified materials are made on the basis of silica due to their very considerable merit. First of all, it is possible to vary its structural characteristics (specific surface area, diameter and pore volume, particle size and shape) in a wide range. It is worth to note their availability and relative cheapness. This work is devoted to the synthesis and characterization of porous silica materials based on tetraethoxysilane (TEOS) and polyethylene glycol (PEG) used as the template agent. We studied the effect of PEG macromolecules length and its concentration on the characteristics of the prepared silica porous structure.
The synthesis was performed using the method discussed in detail in [3]. We varied the molecular weight of polyethylene glycol from 1300 to 100000 (at constant polymer concentration 0.005 mol/L) as well as for a fixed PEG molecular weight we changed the concentration from 0.0001 to 0.1 mol/L.
The amount of PEG in the SiO2-PEG composites was determined by thermogravimetric method with STA-449C device (Netzsch). Adsorption-desorption isotherms of nitrogen at 77 K were obtained with the ASAP-2020 device (Micromeritics). Textural characteristics of the calcined silica material (specific surface area, pore volume and pore size) were obtained using different methods: non-local density functional theory (NL DFT), Barrett - Joyner - Halendy method (BJH) and comparative αS - method.
It is shown that using PEG as template agent depending on its molecular weight and concentration it is possible to prepare mesoporous (A_{BET}=620 m^2/g, V_{Σ}=0.43 cm^3/g, $V_{micro}(\alpha_s)$=0.038 cm^3/g) or microporous (A_{BET}=657 m^2/g, V_{Σ}=0.27 cm^3/g, $V_{micro}(\alpha_s)$=0.26 cm^3/g) silica materials.

[1] R.K. Iler, The Chemistry of Silica, John Wiley & Sons, New York, 1979.
[2] M. Pagliaro, Silica-based materials for advanced chemical applications, RSC Publishing, 2009.
[3] O.V. Yatskovskaya, O.N. Baklanova, T.I. Gulyaeva et al., Protection of metals and physical chemistry of surfaces 2 (2013) (to be published).

ASS-9-Or-4
Zigzag interaction lead driving forces for self-assembled structure of S-Proline (4x2) on Cu(110) surface

T01 Applied Surface Science

#ASS-9-Or-4

E. Mateo-Marti [1], G. Biddau [2], C. Rogero [3], C. Sanchez [4], L. Floreano [5], R. Pérez [6], J. Martin Gago [4].

[1]Centro de Astrobiología, INTA-CSIC, Torrejón de Ardoz, 28850, - Madrid (Spain), [2]Departamento de Física Teórica de la Materia Condensada, Universidad Autónoma de Madrid, 28049, - Madrid (Spain), [3]Centro de Física de Materiales CFM - Materials Physics Center MPC (CSIC-UPV/EHU), 20018, - San Sebastian (Spain), [4]Instituto de Ciencia de Materiales de Madrid (CSIC), Cantoblanco, 28049, - Madrid (Spain), [5]Instituto Officina dei Materiali-CNR, Lab. TAS - Trieste (Italy), [6]Departamento de Física Teórica de la Materia Condensada, Universidad Autónoma de Madrid, 28049, - Madrid (Spain).

Self-assembly of organic molecules on surfaces has attracted important attention due to their promising applications in nanotechnology and biotechnology. From these organised molecular units arise the possibility of complex functions like molecular recognition, sensing, electronic properties, conductivity, catalysis, chirality and chemical reactivity that are important in nanoscience.

Amino-acids contain a simple structure and can be used as model to study biomolecule-surface interactions, which can assist in the understanding of more complex systems. Among all the amino-acids, Proline is the only cyclic amino-acid. Therefore, the local adsorption geometry and the two dimensional self-assembly of this molecule is of particular interest because the imino (NH) group is fixed rigidly in the pyrrolidine ring, limiting the conformational mobility of the N–H bond with respect to the COOH group.

Previous studies have been reported by Raval's group on the dense (4×2) overlayer of the amino acid, (S)-proline on Cu(110) surface have proposed one specific structural model in which the juxtaposition of molecules leads to the formation of one-dimensional hydrogen bonded prolate chains directed along the [1-10] direction,

where this (4x2) phase possesses both prolate conformers in a 50:50 distribution [1-3].

Here, We report an original multi-technique experimental approach of (4x2) proline/Cu(110) system based on STM, electron-spectroscopies and diffraction techniques such as XPS, XANES, and XPD [4]. This study includes the first spectroscopy probe for the two different proline conformers orientation on Cu(110) even if the total amount of molecules present the same chemical form, and an accurate molecular model including information of molecular angles respect to the surface. We have confirmed by XPS spectra that S-Proline molecules adsorb on the Cu(110) surface as anionic species, and only one type of chemical species are adsorbed on the surface. Furthermore, this multi-technique study including DFT confirms that prolate anion adsorption adopts two different orientation respects to the surface, nearly flat and upright rings, which flip between the neighbour rows to stabilize molecular network. Two main reasons can drive this unusual adsorption model, first due to steric effect constrains, meaning that the molecules are required to optimize surface space, and second the flat-upright model favours the interaction between molecules by H-bonding which partially drives the self-assembled network of the molecules on the surface. In summary, by the complementary use of several techniques and theoretical calculations we have obtained a molecular-model of (4x2) proline/Cu(110) adsorption, which includes information about self-assembly of biomolecules on surfaces, chemical state of the adsorbates and molecular orientation respect to the surface, meaning models at atomic levels to elucidate the understanding mechanisms for molecular self-organization.

[1] Mateo-Marti, E.; Barlow, S.M.; Haq, S.; Raval, R. Surf. Sci., 501, 191 (2002).
[2] Foster, M.; Dyer, M. S.; Persson, M.; Raval, R. J. Am. Chem. Soc., 131, 10173 (2009).
[3] Foster, M.; Dyer, M. S.; Persson, M.; Raval, R. Angew. Chem., Int. Ed., 49, 2344 (2010).
[4] Mateo-Marti et al. Submitted (2013).

ASS-2-Or-8
Microstructural and photocatalytic properties of nanostructured Au/TiO2 prepared by reactive magnetron sputtering

T01 Applied Surface Science

#ASS-2-Or-8

I. Sayah [1], M. Arab Pour Yazdi [2], F. Schuster [3], A. Aouni [4], A. Billard [5].

[1]IRTES-LERMPS/UTBM - Belfort-Montbéliard (France), [2]IRTES-LERMPS/UTBM - Belfort (France), [3]CEA/ Cross-cutting program on advanced materials - Grenoble (France), [4]ERMMM - Tanger (Morocco), [5]IRTES-LERMPS/LRC+ CEA-IRTES-LERMPS - Belfort (France).

Titanium dioxide is a well-known photocatalytic material with a wide range of applications such as water treatment [1], air purification [2], self-cleaning [3] and anti-microbial hygienic surfaces [4] due to its physical and chemical stability, its ability to degrade a wide range of organic pollutants, low-cost, and non-toxicity [5].
In this study, TiO_2 coatings are deposited by reactive magnetron sputtering on heated quartz glass substrates (1000°C) previously covered by Au thin layer (<100 nm) at different pressures and draw distances. The morphology of the coatings is investigated as a function of deposition parameters in order to increase the film specific area. The obtained coatings were characterized by X-ray diffraction, scanning electron microscopy and by measurement of water angle contact variations. The photocatalytic activity was assessed by using the Orange G decomposition upon the UV illumination.
Finally, microstructural and photocatalytic properties of the obtained coatings are compared with those of the films prepared under the same conditions but without Au thin interface layer.

[1]- Fujishima, A. Hashimoto, K. Watanabe, T., Eds. BKC, Inc.: Tokyo, (2001) 176.
[2]- Pichat, P. Disdier, J. Hoang-Van, C.; Mas, D. Goutailler, G.; Gaysse, C. Catalysis Today, 63(2000) 363.
[3]- R. Wang, K. Hashimoto, A. Fujishima, M. Chikuni, E. Kojima, A. Kitamura,

M.Shimohigoshi and T. Watanabe. Nature; 388 (1997) 431.
[4]- Liang Zhang, Xue Bai, Hua Tian, Lvling Zhong, Cailian Ma, Yuanzhen Zhou, Shuangli Chen, Dongliang Li. Carbohydrate Polym,89 (2012) 1060 .
[5]- K. Nakata, A. Fujishima, J. Photochem. Photobiol C. Photochem 13 (2012) 169.

ASS-2-Or-4
Modification of metal films with the aid of atomically thin oxide layers

T01 Applied Surface Science

#ASS-2-Or-4

L. Deak, L. Óvári, I. Szenti, Z. Kónya.

MTA-SZTE Reaction Kinetics and Surface Chemistry Research Group, Hungarian Academy of Sciences - Szeged (Hungary).

The study of atomically thin metal deposits and metal oxide films is of fundamental interest in relation to heterogeneous catalysis, production of microelectronic devices, corrosion protection of metals, magnetic tunnel junctions, dielectric barriers [1], etc. Although the alteration of electronic properties of metal particles separated from an other metal by atomically thin oxide layer is gaining interest [2], most work apply single crystal for one of the metals. We addressed the modification of rhodium and molybdenum films through formation of ultrathin oxide layers on them in correlation with controlling the work function and catalytic performance of rhodium and preparation of metal-insulator-metal structures. Monometallic and bimetallic layers formed by PVD on moderately O-deficient TiO_2(110) single crystals were characterized by AES, XPS, ISS, TPD and work function (WF) measurements.

Rh deposition led to electron transfer from the metal towards the TiO_2(110) surface below 0.1 monolayer (ML) Rh coverage. Annealing of titania supported Rh multilayers at 950 K in UHV resulted in the surface diffusion of titanium and oxygen ions and formation of a few atomic layer thick titania overlayer in a self-limited way with definite, O-deficient stoichiometry and strongly suppressed capability for CO adsorption. The accompanying 0.3-0.6 eV WF increase at Θ_{Rh}=2-6ML can be attributed to the presence of a TiO_x dipole layer consisting of positive Ti ions at the metal-oxide interface and negative O ions in the topmost position. Deencapsulation, i.e. diffusion of titania overlayer back to the substrate was observed above 800 K on a TiO_2 sample less reduced in its bulk, revealing the role of both the bulk and surface stoichiometry of the substrate in the encapsulation process. Enhancement of the thickness of Rh multilayers supported on the TiO_2(110) single crystal led to an increase in the temperature characteristic for the completion of decoration by TiO_x layer due to hampered ion diffusion from the TiO_2(110) surface.

To prepare a metal-oxide-metal structure, the growth and properties of a second Rh layer has also been studied. The deposition of Rh at 300-500 K on the TiO_x layer, covering Rh multilayer resulted in the growth of particles with similar height up to above one monolayer coverage. At 200 K deposition temperature a 2D Rh layer formed up to 1ML metal coverage, indicating that at this temperature the mixing of second Rh layer with the ultrathin oxide is absent.

Mo deposits displayed high reactivity with the titania substrate and were oxidized even at 300 K accompanied by the reduction of titania as revealed by XPS. Annealing the 2.7 ML thick Mo layer to 1000 K promoted further oxidation and gave a substantially modified surface with WF of 5.7 eV. Deposition of Rh on both clean and oxidized Mo films resulted in 2D film growth up to 1ML coverage, corresponding to a remarkable increase in Rh dispersion due to the presence of Mo, being relevant to the enhancement of catalytic performance of Rh particles.

[1] M. Baumer, H.-J. Freund, Progress in Surface Science 61 (1999) 127.
[2] L. Gavioli, E. Cavaliere, S. Agnoli, G. Barcaro, A. Fortunelli, G. Granozzi, Progress in Surface Science 86 (2011) 59.

ASS-5-Or-4
REDUCED PREFERENTIAL SPUTTERING OF TiO2 AND Ta2O5 USING ARGON CLUSTER ION BOMBARDMENT

T01 Applied Surface Science

#ASS-5-Or-4

M. Baker [1], R. Grilli [1], R. Simpson [2], P. Mack [2], R. White [2].

[1]University of Surrey - Guildford (United kingdom), [2]ThermoFisher Scientific - East Grinstead (United kingdom).

TiO_2 and Ta_2O_5 are technologically important thin film materials for various applications. XPS is a widely used technique to investigate chemical state and surface composition and Ar^+ ion sputtering is employed to remove surface contaminants and to investigate the chemical composition as a function of depth. However, both TiO_2 and Ta_2O_5 are known to suffer from the preferential sputtering of oxygen when etched under typical Ar^+ ion gun conditions for XPS analysis. Hence, sub-stoichiometric metal oxides are formed and the XPS data is no longer representative of the native material.

In this study, TiO_2 and Ta_2O_5 thin films and a TiO_2 single crystal have been exposed to ion bombardment from a 3 keV Ar^+ ion beam, 200 eV Ar^+ ion beam and a novel 4 keV Ar^+ cluster beam. The surfaces have then been analysed by XPS to determine the resulting chemical composition and changes to the metal oxidation state.

The most substantial preferential sputtering takes place for 3 keV Ar^+ bombardment. Lowering the Ar^+ beam voltage to 200 eV slightly reduces the extent of preferential sputtering. However, using the 4 keV Ar^+ cluster beam results in a substantial reduction in preferential sputtering for TiO_2 and no observable preferential sputtering for Ta_2O_5. The reduced damage obtainable with the cluster beam has significant implications in the accurate compositional analysis of many technologically important metal oxide thin films and the potential for widespread use of this novel Ar^+ cluster beam source will be discussed.

ESD/ASS-P3-09
PVdF/HFP membranes with nanostructured titania fillers as a matrix for porous polymer electrolyte

T01 Applied Surface Science

#ESD/ASS-P3-09

P. Polrolniczak, M. Walkowiak, L. Horla.

Institute of Non-Ferrous Metals Branch in Poznan Central Laboratory of Batteries and Cells - Poznan (Poland).

Polymer electrolytes have received considerable attention, because of their potential in solid-state batteries, electrochromic devices and fundamental research of ion transport in disordered phases [1]. The use of polymer electrolytes make batteries safer, lighter and more flexible in shape. Amongs the polymer electrolytes, PVdF-HFP films have received attention as promising host matrix for polymer electrolytes because of its excellent mechanical strength and electrochemical stability [2]. Kim et al. [3] found that the addition of nanoscale inorganic filers, such as alumina (Al_2O_3), silica (SiO_2) or titania (TiO_2) to the polymer electrolyte results in the improvements of ionic conductivity and absorption level of electrolyte solution.

Nanostructured titanium oxide TiO_2 and lithium titanate $Li_4Ti_5O_{12}$ with different morphologies (nanowires, spheres, particles) was obtained using solvothermal synthesis methods. Synthesized nanomaterials were applied as fillers for composite polymer membranes PVdF/HFP. Composite membranes were prepared according to the so-called Bellcore process. By activating in lithium conducting gel electrolytes have been obtained.

Morphology, porosity, thermal stability and electrolyte uptake of prepared composite membranes were evaluated. For determining the electrochemical stability window of the composite polymer electrolytes, a linear sweep voltammetry experiments were performed. Temperature dependence of ionic conductivity by electrochemical impedance spectroscopy was also measured. It was found that when titanium oxide was mixed with PVdF/HFP membrane, the impedance spectroscopy showed that the room temperature conductivity increased from $0{,}54*10^{-3}$ S cm^{-1} to $1{,}43*10^{-3}$ S cm^{-1}.

[1] B. Scrosati, Nature 373 (1995) 557
[2] J.Y. Song, Y.Y. Wang, C.C. Wan, J. Power Sources 77 (1999) 183
[3] K.M. Kim, N. Park, K.S. Ryu, S.H. Chang, Polymer 43 (2002) 3951

The work has been financially supported by the European Regional Development Fund in the frameworks of the Innovative Economy Programme 2007-2013, project No. POIG.01.01.02-00-015/09.

SE/ASS-1-Or-8
The liquid-phase mass transfer of material in the film-substrate irradiated by intense energy streams

T01 Applied Surface Science

#SE/ASS-1-Or-8

A. Leivi.

Yalovets A. - Chelyabinsk (Russian federation).

Now the treatment by intense energy streams (electron or ion beams, plasma) with power density ≥10^6 W/cm^2 is widely used for improvement of material properties. The intense charge particle irradiation of systems like support films is used for material adhesion improvement as a result of layer mixing. The mass transfer in the treated material is very important for material property modification.

The main mixing mechanisms are Richtmyer-Meshkov instability (RMI) on the interface, thermoactivated diffusion and thermocapillary convection.

The quantitative depth estimations for mixing zone caused by thermostimulated diffusion for melting lifetime are about 1 mkm. Experimental mixing depths are considerably greater and approach 10-20 mkm. The role of thermostimulated diffusion is essential in thin layers (tens- hundreds nm) [1].
In ref. [2] it has been shown RMI on the interface can cause near-surface mixing only in case of surface perturbations corresponding to the wave number range which is defined by irradiation regime. Therefore for such mixing the special surface treatment is needed.

The irradiation can cause nonuniform target depth heating. If the target temperature increases with depth there is necessary condition for thermocapillary convection. The target microrelief induces the surface temperature perturbation. For simulation mass transfer the mathematical model including the system of continuum mechanics equations, the kinetic equation for high-speed electron, the wide-range state equation has been developed.

To research roles of thermoactivated diffusion and thermocapillary convection in mixing the mathematical model has been developed. It describes medium flow as a result of irradiation taking into account mentioned mechanisms.

The numerical research reveals the main near-surface mixing mechanism of melted medium is thermocapillary convection. But the pulse duration is necessary to be less than characteristic heat conduction time to arise convective flow. The mixing zone is 1-20 mkm depending on the irradiation regime.

The research was supported by research engineering of FSSFEI HPE “SUSU” (NRU), conducted within the limits of the state assignment of the Ministry of Education and Science of the Russian Federation (№ 2012043-GZ04, № 2012060-GZ21).

1. Rotshtein V.P. and others // Proceedings of the 7th Int. International Conference on Modification of Materials with Particle Beams and Plasma Flows, 2004, p. 258-262.
2. A.Ya.Leyvi and others // Proceedings of the 9-th International Conference on Modification of Materials with Particle Beams and Plasma Flows, 2008, p. 109-112.

ASS-7-Or-6
SiC coating layers of nano sizes.

T01 Applied Surface Science

#ASS-7-Or-6

M. Menyhard, A. Barna, S. Gurban, L. Kotis, J.L. Labar, A. Sulyok, A.L. Tóth, A. Pongracz, E. Vazsonyi.

Research Centre for Natural Sciences, Hungarian Academy of Sciences, Institute for Technical Physics and Materials Science - Budapest (Hungary).

In modern technologies one frequently needs coating of small sizes in all dimensions. We will report on the production of amorphous SiC coating meeting such demand. C/Si multilayer was produced by sputtering. The C layer, 20nm, was amorphous, while the Si layer , 22nm, was polycrystalline. This sample was irradiated by Ga+ applying various fluences (10-120 x 10^{15} ions/cm^2) and projectile energies (10- 30 keV). The irradiation produced a mixed layer the size of which (in the range of 2-8 nm) could be tailored by using appropriate fluence and projectile energy. AES analysis based on the C peak shape could show that some of the mixed Si and C formed silicon carbide. TEM studies proved that the SiC was amorphous. The amount and distribution of of SiC could be altered by changing the irradiation conditions [1].
For checking the chemical resistance of the coating layer 100X100 μm^2 areas were irradiated by various fluences (10, 20, 40, 80 x 10^{15} ions/cm^2) of 30 keV Ga+ ions, creating various thicknesses (3-8 nm) of SiC rich layers. The thickness of the C cover layer varied accordingly. These regions were imbedded in the unaltered layer system. First the carbon layer was removed by oxidation at 500^oC, then the reminder Si or/and SiC covered surface was etched applying various etchants generally used for polysilicon. Because of the lower etching rate of the SiC covered surface, rSiC, columns developed on the surface, Fig.1. Measuring the disappearance of the columns the relative etching rate could be estimated. In the case of a 3 nm thick SiC layer the relative etching rate of r_{SiC} /r_{polySi} < 10^{-3} was found.

1. A. Barna, S. Gurban, L. Kotis, J. Lábár, A. Sulyok, A. L. Tóth, M. Menyhárd, J. Kovac, P. Panjan, Appl. Sur. Sci. 263 (2012) 367.

Figure 1. The SiC covered regions are unaffected by the etching, which removes the polysilicon; columns form.

ASS-10-Or-8
Proximity effect on the superconductor-normal metal hybrid nanostructures: Scanning tunneling microscopy and spectroscopy

T01 Applied Surface Science

#ASS-10-Or-8

H. Kim, Y. Yoshida, Y. Hasegawa.

The Institute for Solid State Physics, The University of Tokyo - Kashiwa (Japan).

A superconductor (SC) in a good metallic contact with a normal metal (NM) induces superconducting properties in NM within a certain distance from their interface, as well as electronic properties, including the local density of states (DOS). Recently, research of the proximity effect has been extensively studied thanks to technological advances in the fabrication of complex mesoscopic structures. Nevertheless, many of these works, mostly characterized via electrical conduectance measurements, addressed macroscopic properties of the samples, thus obtaining average rather than local information.

Here, we investigated proximity effect at the interface between superconducting two-dimensional (2D) Pb islands and a single-atomic-layer surface metal, known as the striped incommensurate (SIC) phase of the Pb formede on Si(111) surfaces by performing local spectroscopy with a low temperature scanning tunneling microscope (STM). We observed tunneling spectra with a fully-developed gap in a normal metal side around superconducting islands and spatial decaying behaviors of the induced gap with the distance from the SC-NM boundary. Additionally, we study influences of the proximity effect by the presence of the external magnetic field, which suppress the superconducting properties in both sides. The experimental results are compared with the predictions of the quasiclassical theory based on the Usadel equation.

SE/ASS-1-Or-4
Investigation of tribochemical interaction between polytetrafluoroethylene and silicon oxide surfaces

T01 Applied Surface Science

#SE/ASS-1-Or-4

M. Copuroglu, A. Ucar, S. Suzer.

Bilkent University - Ankara (Turkey).

Tribochemical interaction between surfaces, and identification of the chemical and physical nature of this interaction are of great academical as well as commercial importance. In addition, hydrophobic surfaces have a wide range of applications in various areas; and therefore there has been a great deal of interest in enhancing the hydrophobicity of surfaces. The aim of this work is thus to investigate the tribochemical interaction between thermally-oxidized silicon and polytetrafluoroethylene (PTFE). A simple rig was designed to actualize a friction motion between the surfaces with an approximate angle of 45° employing also an inclination along the motion in order to bring about a gradual tribochemical interaction. Additionally, some patterns were sketched on the SiOx surface using the PTFE piece to investigate any potential change in the hydrophobicity of the surface. The nature of the interaction was characterized by X-ray photoelectron spectroscopy (XPS) and scanning electron microscopy (SEM). Contact angle measurements were carried out to characterize and monitor the hydrophobicity of the SiOx surface. XPS measurements were performed for the associated elements (C, F, O, and Si) and the relative binding energy peak intensities/areas of these elements were monitored and evaluated in a detailed manner. The results revealed that PTFE could indeed be transferred onto SiOx surfaces even in the case of the application of the friction at relatively small forces. The SEM images taken demonstrated that some morphological changes could be imparted to the SiOx surface. Contact angle measurement results showed that upon PTFE transfer the hydrophobicity of the SiOx surface could be significantly enhanced, which might also depend upon the pattern sketched onto the surface. A contact angle value as high as 101±5° was obtained.

BI/ASS/NST-P1-15
Functionalization of Porous Silicon Surfaces for the Detection of Organophosphorous Compound

T01 Applied Surface Science

#BI/ASS/NST-P1-15

M. Ayat [1], L. Boarino [2], N. Gabouze [1].

[1]Centre de Recherche en Technologie des Semi-conducteurs pour l'Energétique - Algiers (Algeria), [2]Nanofacility Piemonte, Division Electromagnetism, Istituto Nazionale di Ricerca Metrologica INRIM - Torino (Italy).

The field of biosensors is a very attractive field of research. Indeed, biosensors gather the selectivity and sensitivity of a biological compound with power of detection. Porous silicon (PS) appears as the ideal candidate to be linked with biological molecules through its special features such as the high specific surface area and the luminescence property[1,2]. The work we propose is to detect the presence of organophosphates(OP) pesticides and heavy metals traces in the agricultural environment by an ameperometric detection using a PS biosensors based on the immobilization of the Acetylcholoinesterase (AChE) because its catalytic activity is inhibited by the traces of OP pesticides[3]. The surfaces was characterized by SEM (scanning electron microscope) as shown in the pictures below and the FTIR (Fourier Transform Infrared spectroscopy) where we have the appearance of the Si-H bonds at 2085 cm^{-1} (Si-H), 2112 cm-1 (Si-H2) et 2135 cm-1 (Si-H3) which allow to form Si-C bonds and then link the enzyme.

[1] G. Vincent, Appl. Phys. Lett. 64, 2367 (1994)
[2] L.T. Canham, Appl. Phys. Lett. 57, 1046 (1990)
[3] A. Amine, H. Mohammadi, I. Bourais, G. Palleschi, Biosens. Bioelectron. 21 (2006)1405

figure 1: SEM of porous silicon (cleavage view)

figure 2: FTIR Spectrum of silicon surface: (a) before treatment; (b) after treatment

ASS-3-Or-1
In-situ oxidation of Au, Ag and Cu studied with Ambient Pressure Photoelectron Spectroscopy: An attempt to bridge the Pressure-Gap in Heterogeneous Catalysis

T01 Applied Surface Science

#ASS-3-Or-1

K. Roy, C.P. Vinod, C.S. Gopinath.

CSIR-National Chemical Laboratory - Pune (India).

The world of heterogeneous catalysis has been enriched by the development of modern surface science techniques which can actually monitor surface properties under reaction conditions. One of these state-of-the-art *operando* techniques is the Ambient Pressure Photoelectron Spectroscopy (APPES)[1]. We present here the oxidation of coinage metal group (Au, Ag, Cu) elements studied under *in-situ* conditions by a laboratory-APPES commissioned recently at CSIR-NCL, Pune[2]. Interaction of oxygen with polycrystalline foils of Au, Ag and Cu from UHV to 1 mbar pressure and up to 773 K has been studied. Results show Au is inert, Ag and Cu can be totally oxidized. Diffusion of oxygen into subsurfaces of Ag occurs, which is a precursor for oxidation. A pictorial representation of the abstract is shown in Figure 1. No oxide formation could be observed with Au. Ag behaves mildly; formation of subsurface oxide species at 600 K and 1 mbar O_2 pressure demonstrates this fact. However, Cu is prone to react with oxygen and complete surface oxidation to CuO was observed at 1 mbar O_2 and ≥ 600 K. Indeed there is a systematic oxidation of Cu metal to Cu_2O, Cu_2O + CuO and finally to CuO with increasing temperature at 1 mbar O_2 pressure (Figure 2).
This study shows the capability of laboratory-APPES to understand material surfaces under working conditions or closer to that.

1. Salmeron, M.; Schlögl, R.; Surf. Sci. Rep., 2008, 169-199.
2. Design and Performance Aspects of a Custom Built Ambient Pressure

Photoelectron Spectrometer (APPES) Towards Bridging Pressure Gap: Oxidation of Cu, Ag and Au Surfaces, Roy, K; Vinod, C.P; Gopinath, C.S (manuscript submitted)

Figure 1: A cartoon of the APPES approach towards bridging the pressure gap in catalysis and surface science.

Figure 2: Core level spectra of Cu 2p, Cu LMM and O 1s has been showed while exposing O_2 at 1 mbar pressure with various temperatures. A systematic change of Cu metal to CuO through Cu_2O can be seen.

ASS-2-Or-11
Structure and Chemical Activity of Metal Oxides Studied by Vibrational Spectroscopy

T01 Applied Surface Science

#ASS-2-Or-11

H. Noei [1], L. Jin [2], F. Gallino [3], D. Stodt [2], C. Haettig [2], M. Muhler [2], C. Di Valentin [3], Y. Wang [2].

[1]Deutsches Elektronen-Synchrotron (DESY), Notkestraße 85, 22607 Hamburg - Hamburg (Germany), [2]Ruhr-University Bochum - Bochum (Germany), [3]Università di Milano-Bicocca - Milan (Italy).

Metal oxides have recently attracted enormous attention due to their applications in a variety of fields such as catalysis, chemical sensors, solar cells, and electronic devices. Vibrational spectroscopy is among the most powerful analytic techniques for understanding adsorption and reactions on catalyst surfaces. In this contribution, the structure and reactivity of TiO2 and ZnO surfaces are investigated using high-resolution electron energy loss spectroscopy (HREELS) and a novel ultrahigh vacuum (UHV) FTIR spectroscopy.1

One of the important applications of TiO2 is the reduction of NOx released when fossil or other nitrogen containing fuels are burned. We determined the adsorbate structure of NO and its reaction products N2O2, N2O, and NO2 on rutile TiO2 by combining UHV-FTIRS with ab initio periodically embedded cluster calculations.2 These reactions are important for the photo-catalytic reduction of NO in exhaust gas, but yet little is known about the mechanisms or the intermediates involved. Our consistent experimental and theoretical results made it possible to assign the bands observed in the UHV-FTIR spectra to nine species which are formed upon adsorption and reaction of NO on rutile TiO2. After adsorption on the TiO2 surface NO first dimerizes to N2O2 which is decomposed to N2O and an oxygen atom attached to the TiO2 surface, probably bound to a defect or at a (step) edge. The oxygen atom can later react with another NO molecule to form NO2.

Hydrogen transfer on metal oxide surfaces is a fundamental process in heterogeneous catalysis and photocatalysis. In general, oxide surfaces expose

unsaturated sites of oxygen and metal ions where serve as Lewis base and acid sites, respectively. The cooperative interplay between these sites plays a crucial role for the activation of surface reactions involving hydrogen transfer. Here, we present a combined experimental and theoretical study of NH3 adsorption on both ZnO single crystals and powder surfaces. A comprehensive and atomistic picture of the interfacial chemistry of NH3 on ZnO has been established by the surface science study on well-characterized ZnO single-crystal and powder surfaces by HREELS, UHV-FTIR and thermal desorption spectroscopy (TDS) in conjunction with accurate density function theoretical (DFT) calculations and provide consistent evidence for the unusual partial dissociation of chemisorbed NH3 on ZnO(10 0) surface, which occurs only at full monolayer via hydrogen transfer to the neighbouring O2- base sites leading to coexistence of NH3, NH2 and isolated OH groups in a (2x1) superstructure. The unambiguous fingerprint of this hydrogen transfer is an OH band (3607 cm-1) observed for both single crystal and powder samples and fully corroborated by theoretical calculations. The unexpected hydrogen transfer between adsorbed NH3 and surface O is a consequence of the complex interplay of multiple factors including H-bonding, steric repulsion and pKa.3

1. H. Noei, A. Birkner, K. Merz, M. Muhler,Y. Wang, J. Phys. Chem. C 116, 11181 (2012).
2. D. Stodt, H. Noei, C. Hättig, Y. Wang, Phys. Chem. Chem. Phys. 16, 466 (2013).
3. H. Noei, F. Gallino, L. Jin, J. Zhao, C. Di Valentin, Y. Wang, Angew. Chem. Int. Ed. DOI: 10.1002/ange.201207566 (2013).

ASS-10-Or-4
Direct surface-assisted organic synthesis of hyperbenzene nanotroughs

T01 Applied Surface Science

#ASS-10-Or-4

Q. Fan.

University of Science and Technology of China - Hefei City (China).

Direct surface-assisted organic synthesis of hyperbenzene nanotroughs

Qitang Fan[1], Cici Wang[1], Yong Han[1], Junfa Zhu[1*], Wolfgang Hieringer[2], Julian Kuttner[3], Gerhard Hilt[3], J. Michael Gottfried[3]

[1] National Synchrotron Radiation Laboratory, University of Science and Technology of China, Hefei, China
[2] Lehrstuhl für Theoretische Chemie, Friedrich-Alexander-Universität Erlangen-Nürnberg, Egerlandstr. 3, 91058 Erlangen, Germany
[3] Fachbereich Chemie, Philipps-Universität Marburg, 35032 Marburg, Hans-Meerwein-Str., Germany

**Corresponding author*

The surface-assisted synthesis of adsorbed organic nanostructures is a powerful bottom-up approach towards functional surfaces for applications in catalysis, sensor systems, or organic electronics. A major challenge of this approach is that most organic reactions require a solvent and thus cannot be applied to "dry" surfaces in ultra-high vacuum (UHV). An exception is the Ullmann reaction, which achieves C-C coupling between haloarene molecules using metallic Cu and has been employed to prepare one- and two-dimensional (1D/2D) polymers on metal surfaces. Here, we used bromo-terphenyl precursors in a UHV-compatible variant of the Ullmann reaction to synthesize cyclo-octadecaphenylene (hyperbenzene), a novel hexagonal

macrocycle consisting of 18 phenylene units, on a Cu(111) surface. The molecules form close-packed islands with a hexagonal unit cell. Formation and structure of hyperbenzene on Cu(111) were studied with scanning tunneling microscopy, X-ray photoelectron spectroscopy, and first-principles theory.The lack of previous reports on this molecule likely reflects the fact that synthesis in solution, without the stabilizing template effects of the hexagonal Cu(111) substrate, is difficult to achieve.The large inner diameter of the hyperbenzene molecules of 2.13 nm makes them interesting candidates for nanotroughs that can enclose metal particles or organic molecules.Besides these large hydrocarbon molecules, the surface-assisted formation of novel zigzag-shaped 1D organometallic coordination polymers consisting of Cu-bridged terphenylene units will be discussed.

[1] Gourdon, A. Angewandte Chemie-International Edition 2008, 47 (37), 6950-6953.
[2] Ullmann, F.; Bielecki, J., Ueber. Berichte der deutschen chemischen Gesellschaft 1901, 34 (2), 2174-2185.
[3] Franc, G.; Gourdon, A. Physical Chemistry Chemical Physics 2011, 13 (32), 14283-14292.
[4] Lipton-Duffin, J. A.; Ivasenko, O.; Perepichka, D. F.; Rosei, F. Small 2009, 5 (5), 592-597.
[5] Gutzler, R.; Walch, H.; Eder, G.; Kloft, S.; Heckl, W. M.; Lackinger, M.Chemical Communications 2009, (29), 4456-4458.
[6] Wang, W. H.; Shi, X. Q.; Wang, S. Y.; Van Hove, M. A.; Lin, N. Journal of the American Chemical Society 2011, 133 (34), 13264-13267.

Hyper-benzene

ASS-7-Or-2
Cleaning of glass surfaces using diffuse coplanar surface barrier discharge in ambient air

T01 Applied Surface Science

#ASS-7-Or-2

T. Homola [1], J. Matoušek [2], M. Kormunda [2], A. Zahoranová [3], M. Černák [1].

[1]R&D Centre for Low-Cost Plasma and Nanotechnology Surface Modification, Masaryk University, Kotlářská 2 - 611 37 Brno (Czech republic), [2]Department of Physics, Faculty of Science, J.E. Purkinje University, České mládeže 8 - 400 96 Ústí Nad Labem (Czech republic), [3]Department of Experimental Physics, Faculty of Mathematics, Physics and Informatics, Comenius University, Mlynská dolina - 842 48 Bratislava (Slovakia).

We report a study on treatment of flat glass surfaces by ambient air atmospheric pressure plasma generated by a dielectric barrier discharge (DBD) with coplanar arrangement of electrode system – the so called Diffuse Coplanar Surface Barrier Discharge (DCSBD) [1]. The DCSBD atmospheric plasma system (Roplass, Czech Rep.) is made from multiple parallel stripline molybdenum electrodes embedded in 96% alumina. Dimensions of the alumina ceramic of DCSBD system are a = 93 mm in width and b = 230 mm in height and the total plasma area is about 80 mm × 200 mm. The 16 pairs of molybdenum comb-shape electrodes of width and inter-electrode distance c = 1.5 mm and d = 1 mm, respectively, were printed by green-tape technique on a 0.5 mm thick flat ceramic plate. The plasma is generated on the ceramic surface in thin 0.3 mm layer. We observed an influence of a glass on DCSBD plasma in respect to glass-ceramic distance z. The DCSBD plasma consists of two optically different segments: the diffuse plasma and the streamer plasma. We found that the introduction of a glass into DCSBD plasma led to increase of the diffuse plasma width w. This was explained mainly as a consequence of Meek's breakdown criterion [2]. The study of a water contact angle with respect to glass-ceramic distance z showed that water contact angle depends strictly on z in small interval between 0.1 mm < z < 0.6 mm where the most effective treatment occurred. The X-ray Photoelectron Spectroscopy (XPS) technique was used to investigate the changes in surface chemistry before and after the plasma treatment of a glass. The

results are summarized in Table 1. We found that the DCSBD plasma treatment for 3 s led to decrease of carbon concentration and C/Si ratio from 15 at.% to 4 at.% and from 0.69 to 0.15, respectively. The detailed study on high-resolution C1s peak shown that the plasma treatment for 3 s decreased C–C or C–H bonds concentrations while the concentrations of C–O and O–C=O bonds increased. Since the C–C and C–H bonds are related with the initial surface hydrocarbon contaminants this shows that the plasma treatment exhibits the cleaning effect of glass surface. Saturation on total amount of carbon reached after 3 s can be explained by fast accumulation of the carbon contaminants from ambient air during transportation of samples [3].

Table 1 Elemental composition of glass surfaces in atomic concentrations as detected by XPS.

	Concentration [%]							
Sample designation	C1s	O1s	Si2p	Ca2p	F1s	Mg2s	Na1s	Sn3d 5/
Pre-cleaned in 2-propanol	15	50	21	2	2	3	7	0
Cleaned in plasma for 1 s	13	55	19	3	2	4	3	2
Cleaned in plasma for 3 s	4	60	27	2	1	3	2	0
Cleaned in plasma for 6 s	4	58	27	2	2	5	2	1
Cleaned in plasma for 9 s	5	60	26	2	2	4	2	0
Cleaned in plasma for 12 s	4	60	27	2	1	4	2	0
Cleaned in plasma for 15 s	4	61	26	2	1	4	1	0

Acknowledgment
The presented work has been supported by the project R&D centre for low-cost Plasma and nanotechnology surface modifications CZ.1.05/2.1.00/03.0086 funding by European Development Fund.

[1] M. Cernak: Faculty of Mathematics, Physics and Informatics, Mlynska dolina, 842 48 Bratislava, Slovakia: Patent WO 2007/142612 A1 2007.
[2] Y. Raizer, Gas Discharge Physics, Springer (1991) 449 p.
[3] L. So, N. Ng, M. Bilek, P. J. Pigram, N. Brack, Surface and Interface Analysis 38 (2006) 648.

ESD/ASS-P3-13
Raman characterization of aluminium induced crystallization of hydrogenated amorphous silicon (a-Si:H) deposited by PECVD: Effect of aluminum film thickness.

T01 Applied Surface Science

#ESD/ASS-P3-13

F. Kezzoula.

CRTSE - Algers (Algeria).

The crystallization of the amorphous silicon (or formation of polycrystalline silicon) deposited on various and inexpensive substrates (glass, ceramics….) is into full today exploration because it offers the advantages of low costs and a great stability. The crystallization induced by aluminum (AIC) was studied during several decades [1]; it seems that this kind of crystallization technique recently gained an attention increased in the field of the devices in thin layers. The thickness of the aluminum layer can influence various parameters in the AIC process as the grains [2], the temperature of crystallization, the homogeneity of the poly-silicon layer.
In this contribution, we have deposited a 100 nm thickness of hydrogenated amorphous silicon layer by PECVD on a glass (Corning) substrate. A aluminum layer was deposited on the a-Si:H layer with various thicknesses (10 nm, 20 nm and 100 nm) in order to form the Al/a-Si:H/Glass structure. The study of the crystallization of this Al/a-Si:H/Glass structure according to the thickness of the aluminum layer was carried out by using Raman spectroscopy and X-rays diffraction.
The Raman spectra show a crystallization of all the layers of amorphous silicon for the various thicknesses and the durations of annealing. These spectra show the presence of the peaks located around 519 cm-1 and 520.6 cm-1 indiquant thus a crystallization of all the layers, except for the layer of 100nm aluminum thickness annealed during 6 hours (Fig c). Where it is noticed that his spectrum is composed of two distinct peaks, a peak is located at the surrounding of 480 cm-1 which represents amorphous silicon and another to 515 cm-1 which represents the contribution to the crystalline phase. By increasing the thickness of the layer of aluminum one notices a growth of the crystalline fraction. The same behavior was observed par S.Gupta et al

[3].

[1] S. R. Herd, P. Chaudhari, and M. H. Brodsky, J. Non-Crystall. Solids, 7, 309 (1972).
[2] D. A. Porter and K. E. Easterling ” Phase Transformations in Metals and Alloys “2nd ed. (Chapman&Hall, London, (1992).
[3] S.Gupta, H. Chelawat, A.A. Kumbhar, S. Adhikari, R. O. Dusane, Thin Solid Films 516 850–852, (2008).

Fig. 1 Raman Spectra as function of the thickness of aluminum of an amorphous silicon layer deposited by PECVD to and annealing at 500°C: a) 2 hours, b) 4 hours and c) 6 hours.

ESD/ASS-2-Or-2
Al-doped ZnO hierarchical nano- and meso-architectures for highly light scattering transparent conducting electrodes

T01 Applied Surface Science

#ESD/ASS-2-Or-2

C. Casari [1], P. Gondoni [2], V. Russo [2], C.E. Bottani [1], A. Li Bassi [1].

[1]Dept. of Energy, Politecnico di Milano and Center for Nano Science and Technology @PoliMI, Istituto Italiano di Tecnologia - Milan (Italy), [2]Dept. of Energy, Politecnico di Milano - Milan (Italy).

In the field of transparent conducting oxides, in addition to the basic properties of electrical conductivity and optical transparency, the possibility to enhance light trapping and harvesting by means of nanoengineered morphologies would be beneficial for a wide variety of solar cells. In particular, novel 3-D architectures can overpass the limits reached by conventional approaches. Al-doped ZnO (AZO) is getting increasing interest as an alternative to ITO while, in parallel, low deposition temperatures are needed to assure compatibility with plastics and organic materials in view of flexible devices.
By exploiting nanosecond Pulsed Laser Deposition in the presence of a background gas we developed nanostructured AZO architectures constituted by a 3-D hierarchical assembly of atomic clusters which forms a nano-tree forest with multiscale organization from the nano- to the micron-scale. Tuning the gas type (O_2, Ar) and pressure (0.01–500 Pa), room temperature deposition of AZO films with different morphology, structural and electronic properties was obtained and the structure-property relationship investigated [1]. For conventional compact films, performances competitive with AZO films deposited at high temperatures were obtained at 2 Pa O_2 (see fig.1a, resistivity $4x10^{-4}$ ohm cm, carrier density up to $7.5x10^{21}$ cm^{-3}, mobility of 18 cm^2/V s and 86% transmittance in the visible range) even on polymeric substrates [2]. Hierarchical structures are deposited at pressures above 100 Pa O2 and show high light scattering capability (see fig.1b). The mean value of the haze factor in the visible range increases up to 80% while assuring an overall transmittance > 85% [3].
A twofold approach was adopted to address the abrupt conductivity decrease

encountered as a result of the decreased connectivity of such hierarchical architectures. One consists in the use of $Ar:O_2$ gas mixtures to separately control morphology and stoichiometry (i.e. oxygen vacancies). The second is based on a spatial separation of layers with different functionality. By changing the gas pressure during the deposition we realized a graded morphology composed by a hierarchical layer, designed to scatter the light, and a top compact layer designed for electrical conduction. The optimized structure has 80% transparency to the visible light, haze factor higher than 40% and resistivity of $3x10^{-3}$ ohm cm.

[1] P. Gondoni et al. *Thin Solid Films* **520**, 4707 (2012)
[2] P. Gondoni et al. *Nanosci. Nanotechnol. Lett.* (in press)
[3] P. Gondoni et al. *Nanotechnology* **23**, 365706 (2012)

Fig 1. Compact AZO deposited at 2 Pa O_2 (A) and hierarchically organized structures deposited at 100 Pa O_2 (B)

ASS-1-Or-5
In situ GISAXS characterization of metal sputtering on Alq3 thin film

T01 Applied Surface Science

#ASS-1-Or-5

S. Yu [1], G. Santoro [1], K. Sarkar [2], B. Dicke [1], J. Perlich [1], M. Kuhlmann [1], J. Risch [1], M. Schwartzkopf [1], P. Müller-Buschbaum [2], S.V. Roth [1].

[1]DESY - Hamburg (Germany), [2]TUM - Munich (Germany).

Organic light emitting diode (OLED) is an important device as the next generation light source for illumination. Its low cost, easy fabrication and reasonable efficiency have attracted many research interests. The multilayer device structure emphasizes the significance of understanding the interfacial structure and properties. In most OLEDs, Tris(8-hydroxyquinolinato)aluminium (Alq3) is the activating layer and different metals (Al, Au, et al.) are used as the metal electrical contact. Upon sputtering on Alq3, metal atoms can diffuse into the organic layer, modifying the both morphological and electronica structure, which are directly related to the device performance. The interaction between metal and Alq3 has been discussed by different spectroscopic techniques[1,2] and theoretical method[3] at single molecule level. Nevertheless, the growth mechanism of the metal thin film on Alq3 is scarcely studied. For this purpose, in situ grazing incident small angle X-ray scattering (GISAXS) plays a powerful role to characterize the inorganic/organic interfacial structure during the film growth process[4,5]. In this work, we have carried out GISAXS characterization to monitor the entire process of diffusion, coarsening and growth of different metal thin film on top of Alq3 layer during the sputtering process. Considering the elemental chemical reactivity, such as, Al and Au, we elucidate different lateral growth process from the out-of-plane scattering cut. Meanwhile, the sputtered metal/Alq3 films demonstrate good correlation to substrate roughness, illustrated by the in-plane scattering cut. The results benefit the comprehension of the development the general metal/organic semiconductor interfacial structure prepared via sputtering process which is widely used in the industry.

(1) Nguyen, T.; Ip, J.; Jolinat, P.; Destruel, P. Applied Surface Science 2001, 172, 75–83.
(2) Shen, C.; Kahn, A. Organic electronics 2001, 2, 89–95.

(3) Yanagisawa, S.; Lee, K.; Morikawa, Y. The Journal of chemical physics 2008, 128, 244704.
(4) Buffet, A.; Abul Kashem, M. M.; Schlage, K.; Couet, S.; Röhlsberger, R.; Rothkirch, A.; Herzog, G.; Metwalli, E.; Meier, R.; Kaune, G.; Rawolle, M.; Müller-Buschbaum, P.; Gehrke, R.; Roth, S. V Langmuir : the ACS journal of surfaces and colloids 2011, 27, 343–6.
(5) Kaune, G.; Metwalli, E.; Meier, R.; Körstgens, V.; Schlage, K.; Couet, S.; Röhlsberger, R.; Roth, S. V; Müller-Buschbaum, P. ACS applied materials & interfaces 2011, 3, 1055–62.

ASS-P1-06
XPS depth profiling studies of the high-temperature transformation of InGaN/GaN multi-quantum wells

T01 Applied Surface Science

#ASS-P1-06

J. Sobczak, W. Lisowski, A. Jablonski, E. Grzanka, T. Suski.

Institute of Physical Chemistry - Warsaw (Poland).

InGaN quantum-wells (QW) are widely applied in optical and optical devices like blue/green light-emitting diodes and long lifetime violet and blue laser diodes. One of important parameters is thermal stability of the QW at higher temperature. The question arises what the tendency of the changes of QW parameters will be towards high temperature annealing, necessary in technology processes. In this work we present the results of a study dealing with this question, using a XPS depth profiling technique. The results are compared for four InGaN/GaN QW samples, containing two well separated QW, which were annealed at temperatures from 800 °C to 990 °C for 0.5 hour. The InGaN/GaN quantum well (QW) structures were grown on (0001) sapphire substrates by metal-organic chemical vapor deposition (MOCVD) method. Such two InGaN/GaN quantum wells (QWs) are used in light emitting diodes (LEDs) and laser diodes (LDs) emitting at 460nm. All samples, prior to annealing, were prepared at the same experimental conditions. The XPS depth-profiling analysis were carried out using the a PHI 5000 VersaProbeTM (ULVAC-PHI) spectrometer with monochromatic Al Kα radiation. The XPS analysis was combined with Ar+ depth profile sputtering (0.5 keV ions at normal angle of incidence rastered over a 2x2 mm2 surface area) with the Ar+ sputter rate of 0.34 nm min-1.It was found that annealing of the InGaN/GaN QW, performed at temperature range 800-990 °C, leads to distinct QW transformations, which was found to be different at 800 °C, 900 °C and 990 °C, respectively (Fig. 1). After annealing at 800 °C we observed lowering of the QW, which was located close to GaN substrate layer and increase of In concentration in the GaN barrier areas (Fig. 1b). At 900 °C this QW vanished and only one QW, close to surface region, was detected (Fig 1c). Both QW disappeared after annealing at 990 °C and significant increase of In concentration was found at the surface region of annealed QW sample (Fig. 1d). Degradation of both QW is evidently caused by annealing procedure and this process is accompanied by inter-diffusion of In to the surface area of annealed QW samples. The QW remain stable at temperatures lower

than 800 °C.

This research was partially supported by the European Union within European Regional Development Fund, through grant Innovative Economy (POIG.01.01.02-00-008/08), and by the grant no. 2011/01/B/ST4/00959 of the National Science Center of Poland.

Fig. 1. XPS depth profiling of InGaN/GaN quantum well structures annealed at temperatures 800-990 °C.

ASS-1-Or-7
Quantitative ToF-SIMS MCs Dual Beam Depth Profiling with Improved Dynamic Range

T01 Applied Surface Science

#ASS-1-Or-7

S. Kayser, A. Sears, R. Möllers, D. Rading, E. Niehuis.

ION-TOF GmbH - Münster (Germany).

In recent years MCs^+ depth profiling has become increasingly popular for the analysis of thin films using Time-of-Flight SIMS (ToF-SIMS). The MCs^+ mode offers quantitative or semi-quantitative SIMS data and allows for the measurement of electropositive and electronegative elements simultaneously by detecting MCs^+ and MCs_2^+, respectively. In addition, the use of heavy cluster ions like Bi_n^+ or C_{60}^+ allows for a significant increase of the MCs_x^+ yields by a factor of up to 1000 with respect to Ga as primary ion projectile and leads to a remarkable improvement of the achievable detection limits [1].

However, one disadvantage of current TOF-SIMS instruments for the quantification in MCs^+ mode is the limited dynamic range, which restricts the possibility of achieving high sensitivity on the MCs^+ clusters and of using the Cs+ intensity for normalization. The normalization is especially important for the analysis of layer systems where sputter rates or the cesium surface concentration might change from layer to layer. This requires a registration system which is able to detect more than 100 secondary ions of a specific element per primary ion gun pulse with high linearity.

We have developed a new registration system for TOF-SIMS, which increases the useable dynamic range by a factor of 100 i. e. 1E7 counts/sec with an excellent linearity. In this paper we will discuss the characteristics of this new experimental setup. We will present examples of the quantitative depth profiling in the MCs^+ mode to demonstract the benefits of this new detection system.

[1] E. Niehuis, T. Grehl, F. Kollmer, R. Moellers, D. Rading, SIMS Europe, Muenster, 2006

BI/ASS-1-Or-7
Gold nanoparticles-based system for biosensing: surface functionalization and characterization.

T01 Applied Surface Science

#BI/ASS-1-Or-7

V. Spampinato, M.A. Parracino, D. Gilliland, P. Colpo, G. Ceccone, F. Rossi.

JRC-IHCP - Ispra (va) (Italy).

It is well known that gold nanoparticles show extraordinary optical, electronic and molecular-recognition properties, and for this reason they can be very interesting platform for many different applications in various fields as nanotechnology, materials science, life sciences and biosensors.
Gold nanoparticles can be functionalized using different kind of ligands, polymers, biomolecules, etc. depending on the aim for which they are prepared.
In this work, we describe the preparation of a gold nanoparticles-based system for biosensing purposes, and its physico-chemical characterization for each functionalization step.
In particular, we have used a thiolate as nanoparticles stabilizing agent because the bond between gold and sulfur is easy-to-form and quite strong. Since pristine gold nanoparticles (15nm in diameter) were stabilized with citrate ions, the first step of the functionalization process consisted of a dialysis procedure to remove some citrate and then to replace the residual citrate with the thioglucose, forming a self-assembled monolayer on the gold nanoparticles surface. In this way we have a sugar platform that can interact with biological systems like, in our case, the maltose binding protein.
The investigation of the biological behaviour of the glucose-modified particles in presence of the maltose binding protein was performed by surface characterization methods as ToF-SIMS and XPS and confirmed by optical detection method (iSPR). ToF-SIMS and XPS resulted to be very useful tools for monitoring all the functionalization steps and for obtaining information on the effects of dialysis procedures. In particular, by ToF-SIMS spectra, it was possible to identify some characteristic peaks related to the coordination of thio-glucose with gold as well as with the binding pocket of the protein, while XPS provided complementary

quantitative information of surface composition in each functionalization step. Moreover, from the high resolution spectra, additional information about the bonds formed between the different species involved in the functionalization has been obtained.
The same functionalization procedure and characterization was also applied to flat gold substrate for comparison.
The presented method displays a valid approach for surface analyses of functionalized nanoparticles and the results obtained underline the possibility of using the developed system in biodetection field.

ESD/ASS-2-Or-3
Optimization of high efficiency Cu(In,Ga)Se2 solar cells prepared by reactive sputtering

T01 Applied Surface Science

#ESD/ASS-2-Or-3

E. Tomasella [1], J. Posada [2], G. Savidand [2], A. Bousquet [1], A. Tempez [3], J.P. Gaston [3], D. Lincot [2].

[1]ICCF UMR CNRS 6296 – Université Blaise Pascal - Aubière (France), [2]IRDEP-6 Quai Watier, 78401 Chatou - Chatou (France), [3]Horiba Jobin-Yvon, 91120 Palaiseau - Palaiseau (France).

$Cu(In,Ga)Se_2$ (CIGS) thin films solar cells are the most promising technology for high efficiency conversion energy. Several techniques are used to synthesize CIGS absorbers. The record efficiency of 20.3% is obtained by indium, gallium, copper and selenium co-evaporation. This technique is now standard because it leads to the most efficient cells and the consolidation of the 3 stage process, which allows a controlled distribution through the material absorber composition. On the other hand, the reactive sputtering deposition technique is suitable for large surfaces, thus offering the possibility to perform industrial scale-up. This technique also leads to better use of source materials, and its stability is attributed to the control of a single reactive gas (vapor selenium). In this work the absorber is prepared by reactive sputtering. Several samples of Cu (In,Ga) Se_2 deposited on Mo / glass were pulverized at different pressures and powers values. Each one of these samples was analyzed by X-ray fluorescence in order to measure the composition and also the thickness. Raman spectroscopy and X-ray diffraction were used to know the several phases present in the material. To complete the structural analysis a novel depth profiling technique Plasma-Profiling Time-of-Flight Mass Spectrometry (PP-TOFMS) was employed to determine composition distribution, identify contaminants and study the diffusion mechanisms which can occur during the thin film growth. Finally, optical properties were measured by spectroscopic ellipsometry
The optoelectronics properties analysis of each sample was also performed by I(V) under illumination and dark conditions and also by spectral response.

ASS-5-Or-8
Au and Pd nanoparticles supported on CeO2, TiO2, and Mn2O3 oxides

T01 Applied Surface Science

#ASS-5-Or-8

P. Nascente [1], S. Maluf [1], C. Afonso [1], R. Landers [2], A. Pinheiro [1], E. Leite [1].

[1]UFSCar - Sao Carlos (Brazil), [2]Unicamp - Campinas (Brazil).

A new generation of nanoparticle materials has exhibited unique structural, electronic, magnetic, and optical surfaces properties with the potential to develop new technologies in the fields of catalysis, sensors, and devices [1]. In particular, nanoparticles (NPs) of gold and palladium have proved to be effective catalysts for several reactions. In this contribution, we present a study on Au and Pd NPs supported on CeO_2, TiO_2, and Mn_2O_3. The CeO_2, TiO_2, and Mn_2O_3 supports were prepared by a sol-gel method using $Ce(NO_3)_2.6H_2O$, $C_{12}H_{28}O_4Ti$, and $Mn(NO_3)_2.4H_2O$ in order to obtain highly dispersed NPs. Then they are dried and calcined at 250°C for 2 hours. Additions of 0.5 at.% of Au and Pd were incorporated by impregnation using $HAuCl_4.3H_2O$ and $PdCl_2$. The samples were then calcined at 550°C for 4 hours. The synthesized samples were: Au/CeO_2, Au/TiO_2, Au/Mn_2O_3, Pd/CeO_2, Pd/TiO_2, and Pd/Mn_2O_3. The samples were characterized by X-ray diffraction (XRD), X-ray photoelectron spectroscopy (XPS), and high-resolution transmission electron microscopy (HRTEM). The XRD diffractograms presented sharp and intense peaks indicating that the samples are highly crystalline, but no peaks corresponding to Au or Pd phases were detected. This indicates that the Au and Pd NPs were incorporated into the structures of the oxides. It was not possible to obtain an Au 4f spectrum for Au/Mn_2O_3 due to an overlap with the Mn 3p spectrum. The XPS Au 4f spectra for Au/CeO_2 and Au/TiO_2 present negative chemical shifts that could be attributed to strong metal-support interactions [2, 3]. The XPS Pd 3d spectra indicate that for both CeO_2 and TiO_2 substrates, the Pd NPs were in the metallic state, while for the Mn_2O_3 substrate, the Pd NPs were oxidized. The HRTEM results show the formation of nanocrystalline oxides having particles sizes between 50 and 200 nm. TEM micrographs show that the Pd NPs were homogeneously distributed throughout the CeO_2, TiO_2, and Mn_2O_3 supports, while the Au NPs formed nanometric agglomerates.

[1] C.C. Chusuei et al., Top. Catal. 14 (2001) 71.
[2] S. Arrii et al., J. Am. Chem. Soc. 126 (2004) 1199.
[3] Y. Hao et al., J. Mol. Catal. A 335 (2011) 183.

ASS-1-Or-3
Multitechnique electron spectroscopic characterisation of optoelectronic devices

T01 Applied Surface Science

#ASS-1-Or-3

A. Wright, P. Mack, T. Nunney, A. Bushell.

Thermo Fisher Scientific - East Grinstead (United kingdom).

Optoelectronic devices, used for inter-conversion of light and electricity (e.g. photovoltaics and displayes), depend upon careful optimisation of chemical, electronic and structural properties for efficient operation and useful operating lifetime. Characterisation of such a device will typically aim to identify the chemical bonding states, valence band positions, band gap and work function for each component. Lateral and depth resolution may be required to evaluate cell/pixel and multilayer structures.

Electron spectroscopic surface analysis techniques are ideal for the detailed analysis of the electronic structures of optoelectronic devices. Such techniques allow full quantitative characterisation of materials with chemical state and structural information. Surface specificity of spectroscopic information ensures that thin films can be analysed without interference from deeper parts of the sample. Multilayer structures may be studied with depth profiling techniques, and imaging functionality may be used to study cell or pixel structures. Novel cluster ion beam technologies are now available for the profiling of thin, fragile organic layers while preserving chemical state information.

The Thermo Scientific Escalab250Xi offers several such spectroscopic techniques, which have been employed in this study. X-ray Photoelectron Spectroscopy (XPS) offers surface-sensitive, quantified chemical state analysis and imaging capabilities. Ultraviolet Photoelectron Spectroscopy (UPS) allows measurement of valence band positions. Reflected Electron Energy Loss Spectroscopy (REELS) can yield information on the electronic band gap and hydrogen content of a material. In this

study, these techniques are combined for characterisation of the electronic structure of some optoelectronic devices.

ASS-P1-15
Study of structural and electrical properties of nanocomposite films by means of methods of computational physics

T01 Applied Surface Science

#ASS-P1-15

R. Hrach [1], S. Novak [2].

[1]Charles University, Faculty of Mathematics and Physics, Department of Surface and Plasma Science - Prague (Czech republic), [2]J. E. Purkinje University, Faculty of Science, Department of Physics - Usti Nad Labem (Czech republic).

Composite and nanocomposite metal/dielectric structures consist of metal particles embedded into dielectric matrix. The behaviour of the composite films varies with their filling factor, i.e. with an amount of metal component in the film. For small filling factors the structures contain individual metal particles or nanoparticles completely insulated by dielectric or polymer matrix and the films have dielectric properties. With increasing filling factor the conductivity increases and finally the transition into metallic state occurs. Composite films near a percolation threshold, where the change of charge transport mechanism from the thermally-activated tunnelling between individual metal objects into the ohmic conductivity is observed, are especially interesting.

Morphological analysis of the composite and nanocomposite thin films is important both for the characterisation of the films themselves and for the study of their properties. These properties are given not only by the concentration of metal component but also by a spatial distribution of metal objects. An image analysis of their sections and projections is a valuable source of information (e.g. [1]) for the characterisation of composite films structure. However, standard algorithms based on the theory of mathematical morphology [2], typical in thin film physics, lose their sensitivity when applied to composite films. Therefore, in the first part of our contribution an analysis of various morphological methods will be performed.

There exist a close connection between morphological and electrical properties of composite and nanocomposite films [3]. Therefore the charge transport in composite and nanocomposite films is studied by the kinetic Monte Carlo method in the second part of our contribution. Electrical current paths are concentrated into channels creating so-called fuzzy clusters (see Fig. 1) below the percolation threshold. The technology of nanocomposite films can result in both homogeneous and inhomogeneous systems with various distributions of metal objects. The main aim of our study was to find the correlation between the morphological properties of composites and the structures of fuzzy clusters in the dependence on the technology of the composite structures.

[1] Novak S., Hrach R., Morphological study of metal/dielectric composite films with various spatial distributions of metal particles, Vacuum 84 (2010), 174.

[2] Serra J., Image analysis and mathematical morphology, Academic Press, London 1982.

[3] Hrach R., Novak S., Svec M., Correlation between morphology and transport properties of composite films: Charge transport in composites, Applied Surf. Sci. 252 (2006), 5516.

Fig. 1: Conducting paths in the graded nanocomposite structure.

ASS-5-Or-2
Novel Ion Sources for XPS Sputter Depth Profiling Advanced Materials

T01 Applied Surface Science

#ASS-5-Or-2

A. Roberts, W. Boxford, S. Hutton, C. Blomfield, J. Counsell.

Kratos Analytical Ltd - Manchester (United kingdom).

The recent development of polyatomic and argon gas cluster ion sources for surface cleaning and sputter depth profiling materials using x-ray photoelectron spectroscopy (XPS) has greatly increased the types of samples that may be analysed. In particular successful XPS depth profiles of organic polymer materials are now routinely possible where the chemical information of the material is retained during the sputter profile. Whilst polyatomic projectiles such as $C_{24}H_{12}^+$ and C_{60}^+ have been demonstrated to sputter some organic materials with high etch rates, polymers which degrade under irradiation by cross-linking such as polystyrene and polyimide have very low sputter yield with these projectiles. In contrast to the polyatomic ion sources Ar_n^+ cluster ion sources where the number of atoms in the cluster n is typically 500 – 2000 have not demonstrated the limitations of low sputter yields for any class of organic polymers.

Polyatomic ion sources have also been used to profile inorganic materials such as soda lime glass where the concentration depth profile of mobile ions such as sodium have been compromised when profiling with standard monatomic Ar^+ ions. There is also some evidence that sputtering with polyatomic ion sources causes less preferential sputtering of oxygen in inorganic oxide samples relative to monatomic Ar^+ ions.

In this study we contrast the performance of the traditional monatomic Ar^+, novel $C_{24}H_{12}^+$ polyatomic and Ar_n^+ cluster ion sources for sputter depth profiling a range of thin film and multilayer samples. It is known that unlike monatomic Ar^+ ions, large cluster ions do not penetrate deeply into the material with the result that the energy of the impact is deposited within the first few nanometres of the surface. With the larger polyatomic and Ar_n^+ clusters the energy of the ion is shared by all the atoms in the cluster so that the energy per projectile atom or partition energy can be as low as a few electron volts. A poly(lactic-co-glycolic) acid (PLGA) thin film has been used to show that the effect of changing partition energy from 2.5eV to 20eV per Ar atom has

a linear relationship to the yield voume of the material, shown in figure 1. Further characterisation of the different ion sources has been undertaken using samples as diverse as organic and inorganic photovoltaic materials, cross-linked plasma polymers and organic multilayers. Analysis conditions were optimised to maximise retention of chemical functionalities and minimise ion induced interlayer broadening and preferential sputtering.

Figure 1: Yield volume of PLGA as a function partition energy for Arn+ clusters where n=1000.

ASS-8-Or-2
Ru-modified Pt(332) surface studied by STM and XPS

T01 Applied Surface Science

#ASS-8-Or-2

E. Carbonio, M.J. Prieto, A. De Siervo, R. Landers.

Instituto de Física 'Gleb Wataghin',Universidade Estadual de Campinas, 13083-859, SP - Campinas (Brazil).

Ru-modified Pt surfaces are interesting model systems for studying functional properties of the Pt-Ru system, which is extensively used for fuel cells applications[1]. Systematic studies using UHV techniques have been widely reported in the literature for low Miller index Pt single-crystal surfaces, mostly for Ru-modified Pt(111). However, this is not the case for Ru-modified high Miller index Pt surfaces. These model systems are interesting because of the high density of steps, which brings them closer to nanoparticle systems. In this research, Ru-modified Pt (332) surfaces were prepared by evaporation of Ru in UHV conditions over a previously cleaned Pt(332) surface at room temperature. Cleaning procedure is described elsewhere[2]. The prepared surfaces with different coverage were studied by UHV-STM (6×10^{-11} mbar) and XPS (1×10^{-10} mbar).
XPS spectra show that Ru is deposited in metallic form. Figure 1 shows the Pt(332) surface before and after Ru deposition. Due to differences in their electronic properties, Ru atoms appear brighter[3,4]. For low coverage, Ru deposits preferentially on the step edges forming 1D chain structures (step decorating) and some 2D structures. When Ru coverage is increased, STM shows that the formation of 3D structures is favored (islands). The height of the 3D structures was estimated from the STM images to be of two atomic layers.

Differences of surface reactivity may be observed as a consequence of the different structures (1D and 2D, or 3D) formed for the different coverage of Ru.

[1] X. Zaho et. al, Energy Environ. Sci., 4 (2011) 2736.
[2] Z. Zhu et. al, Nano Lett. 12 (2012) 1491.
[3] H.E. Hoster et.al, Phys. Chem. Chem. Phys. 10 (2008) 3812.
[4] A. Berkó et.al, Surface Science 603 (2009) 2556.

Figure 1. STM images of (a) clean Pt(332) surface. U_b = 1.06 V, I_t = 0.4 nA. Inset shows the XPS spectra for the clean surface obtained at an angle of θ = 60 º and using hυ = 1486.6 eV. (b) Ru-modified Pt(332). U_b = 1.10 V, I_t = 0.81 nA. Inset shows the line profile of the resolved 1D chain structure at the step edge.

ESD/ASS-2-Or-4
High-quality detachable CdTe (111) heteroepitaxial films on Al2O3 (0001)

T01 Applied Surface Science

#ESD/ASS-2-Or-4

K. Meinander, G. Devenyi, S. Jovanovic, J. Carvalho, J. Preston.

McMaster University - Hamilton (Canada).

Cadmium telluride is one of the most attractive compound semiconductor materials available for photonics applications. Currently, however, there exist major obstacles limiting its widespread use in new technologies. Most critical among these is the strong tendency for CdTe thin films to grow in multidomain structures, exhibiting both a high defect density and large surface roughness.

Using pulsed laser deposition (PLD) we have developed a novel method for growing nearly single domain CdTe (111) films on sapphire substrates. Through either a modification of the Al_2O_3 (0001) surface prior to deposition, or by an incorporation of impurities, such as Zn, during growth, we can actively control the domain rotation of these single crystal films with respect to the underlying substrate. After growth, using relatively simple lift-off procedures, these films can then be readily detached from their substrates and transferred onto other surfaces without a noticeable degradation of their quality, allowing for both the reuse of the expensive substrates, as well as for the ability to freely choose any desired carrier material.

By combining two-dimensional X-ray diffraction (2D-XRD) and scanning transmission electron microscopy (STEM), together with density functional theory (DFT) structure calculations, we have unraveled the main mechanisms that allow for a controllable alignment of the crystal domains at this unique CdTe-sapphire interface. Additionally, we present an explanation for how these two polar materials can accommodate both the heteroepitaxial growth of CdTe structures, as well as a subsequent easy detachment of the resulting thin films. An in-depth understanding of this complicated interface will also be of great assistance in the future design of similar heteroepitaxial systems for transferable thin film growth.

ASS-2-Or-9
Bismuth Oxide thin films for photocatalytic degradation of textile dyes

T01 Applied Surface Science

#ASS-2-Or-9

S. Rodil, P. Silva-Bermudez, J.C. Medina, M. Bizarro.

Instituto de Investigaciones en Materiales, Universidad Nacional Autonoma de Mexico - Mexico D. F. (Mexico).

Bismuth oxide (Bi_2O_3) thin films were deposited on glass by Magnetron Sputtering technique under different deposition conditions in order to obtain films having different crystalline phases. X-ray diffraction, profilometry, scanning electron microscopy, X-ray photoelectron spectroscopy and optical transmission were used to characterize the films. The results indicated that it was possible to obtain oxide films in the alpha, beta and delta phase or a combination of some phases, depending on the deposition conditions. The photocatalytic activity for each one of the Bi_2O_3 phases was evaluated testing the degradation of methyl orange dye ($C_{14}H_4N_3SO_3Na$) under different light energies (ultraviolet, white and solar light). The photocatalytic activity was measured as a function of the irradiation time, light-energy, concentration and pH of the solution. As comparison, micrometer Bi_2O_3 powders presenting the alpha phase were also tested under similar conditions. The colorant degradation and the kinetic of the reaction were estimated using the variation of the corresponding absorption band. The results pointed out that the photocatalytic effect was only activated under acidic conditions for the thin films, for the other pHs, the activity was negligible. Moreover, it was also found that the delta-phase films presented larger photocatalytic efficiency reaching almost 100% of degradation of the dye solution in only 30 minutes, which was an remarkable result considering the photocatalytic performance of other oxides in similar conditions. The effect of surface roughness was also investigated as a method to enhance the active surface in the thin films. For this, the glass substrates were roughened previously to the oxide deposition, increasing the average roughness from 0.015 to 6.3 μm. However, due to the strong light dispersion caused by the roughness, there was not such increment in the photocatalytic activity as expected.

Acknowledgement: The research leading to these results has received funding from the European Community Seven Framework Programme (FP7-NMP-2010-EU-MEXICO) and CONACYT under grant agreements nº 263878 and 125141, respectively.

Bismuth oxide film deposited on rough glasses

ASS-2-Or-2
Plasma electrolytic oxide coatings on valve metals and their activity in CO oxidation

T01 Applied Surface Science

#ASS-2-Or-2

I. Lukiyanchuk [1], V. Rudnev [2], L.M. Tyrina [1], I.V. Chernykh [1].

[1]Institute of Chemistry FEB RAS - Vladivostok (Russian federation), [2]Institute of Chemistry FEB RAS, Far Eastern Federal University - Vladivostok (Russian federation).

Plasma electrolytic oxidation technique, that is anodization of valve metals under spark and arc discharges, allows one to obtain oxide layers incorporating electrolyte components into coating compositions. So it is perspective for preparing both secondary supports [1] and catalytic oxide layers [2, 3] on metal substrates. The report considers two possibilities of PEO for obtaining catalytically active oxide layers on aluminum and titanium. The first is one-stage PEO technique when precursors of catalytically active compounds are directly involved in forming electrolyte. The second approach is related with modification of PEO coatings (secondary carriers) using other methods such as impregnation in precursor solutions, extraction-pyrolytic method, and template synthesis. Using these approaches we obtained composites including transition (Mn, Fe, Co, Ni, Cu) and noble metals (Pt, Pd) on aluminum and titanium. The composites were tested in CO oxidation into CO_2. It has been shown that Co-, Cu-containing composites have an activity comparable with that for Pt-containing ones. Optimal result is obtained when catalytically active composition is deposited on supports possessing own catalytic activity, Fig 1.

[1] S.F. Tikhov, G.V. Chernykh, V.A. Sadykov, et al. Catal. Today. 53 (1999) 639–646.
[2] F Patcas, W Krysmann, Appl. Catal. A-Gen. 316 (2007) 240-249.
[3] I.V. Lukiyanchuk, L.M. Tyrina, V.S. Rudnev, A.Yu. Ustinov, P.M. Nedozorov, M.S. Vasil'eva, Kinet. Catal. 49 (2008) 439–445.

Temperature dependence of CO conversion over composites formed in PBWNiCu-electrolyte before and after impregnation in H_2PtCl_6 solution.

ASS-2-Or-5
Atomistic Theory of Ostwald Ripening and Disintegration of Supported Metal Particles Under Reaction Conditions

T01 Applied Surface Science

#ASS-2-Or-5

W. Li, R. Ouyang.

Dalian Institute of Chemical Physics, CAS - Dalian (China).

Understanding Ostwald ripening and disintegration of supported metal particles under operating conditions have been of central importance in the study of sintering and dispersion of heterogeneous catalysts for long term industrial implementation. To achieve a quantitative description of these complicated processes, an atomistic and generic theory taking into account of the reaction environment, particle size and morphology, and metal-support interaction is developed [Ref. 1]. The thermodynamic criteria for the reactant assisted Ostwald ripening and induced disintegration are formulated, and the influence of reactants on sintering kinetics and redispersion are mapped out. The theory is applied to TiO2(110) supported Rh particles in the presence of carbon monoxide, and reproduces well the broad temperature, pressure, and particle size range over which the sintering and redispersion occurred in such experiments.

1. R. H. Ouyang, J. X. Liu, W. X. Li, J. Am. Chem. Soc. (2013) DOI: 10.1021/ja3087054

ASS-P3-05
Surface activation bonding of cyclo-olefin polymer to an inorganic substrate: Role of Interfacial Chemistry

T01 Applied Surface Science

#ASS-P3-05

T. Tsukamoto, A. Nakamura, T. Ichii, H. Sugimura.

Department of Materials Science and Engineering, Kyoto University - Kyoto (Japan).

Cyclo-olefin polymer (COP) has been used in a wide variety of applications owing to their excellent transparency, high heat resistance and dimensional stability, and low water absorbency. Extensive studies have been conducted so far to improve adhesivity, dyeability, wettability, etc. of COP. In order to obtain better adhesion of COP, it is necessary to provide adhesive chemical properties on polymer surfaces. We have been reported that the surface modification using vacuum ultra-violet (VUV) light is effective and applicable to the low temperature bonding of COP plates [1]. Here we report on a further extension of this surface activation technique to bonding COP to an inorganic substrate. Materials used in this study were COP sheets (ZF14, Zeon Co.) and Cu substrates covered with a SAM prepared from n-octadecyltrimethoxysilane (CH3(CH2)17Si(OCH3)3, ODS). Prior to forming the ODS-SAM onto Cu substrates, each substrate surface had been irradiated in air with VUV light at 172 nm in wavelength for 20 min in order to form a thin oxide layer. Both a COP sheet and an ODS-Cu substrate were irradiated with VUV (distance 5mm in dry-air). These samples were pressed with facing the VUV-modified surfaces at a temperature 120 °C or lower.Fig.1 shows water contact angles of the COP and ODS-Cu surfaces irradiated with VUV. As the VUV irradiation was prolonged, both the surfaces became hydrophilic. These chemical changes were further studied by XPS as shown in a graph of the O/C atomic ratio (Fig.2). Both the surfaces are confirmed to be oxidized mainly due to atomic oxygen species generated by the dissociative excitation of atmospheric oxygen molecules with VUV. The ODS-Cu substrates show a more marked increase in the O/C ratio because of the smaller carbon amount of ODS than COP. We have confirmed that the VUV-modified COP and ODS-SAM surfaces became adhesive.

[1]Y.-J. Kim, Y. Taniguchi, K. Murase, Y. Taguchi and H. Sugimura, Appl. Surf. Sci. 255 (2009) 364.

Fig.1:Water contact angles of COP and Cu-ODS surfaces with VUV irradiation time

Fig.2: O/C atomic ratio of COP and Cu-ODS surfaces with VUV irradiation time

ASS-P2-4a
Fabrication and Characterization of Distributed Bragg Reflector like Structured Thin Film Passivation Films for Top Emission Flexible OLEDs Display

T01 Applied Surface Science

#ASS-P2-4a

J. An, C. Park, B.H. Choi, J.H. Lee.

Korea Institute of Industrial Technology - Gwangju-Si (Korea, republic of).

One of issue in flexible top emission display is high transmittance in passivation layer. Therefore, optical properties in passivation layer should be considered. In this study, we have studied optical properties of DBR structured multi-layered passivation layer. DBR passivation structure consist of 50 nm thick Al2O3 and 500 nm thick polymer. Al2O3 and polymer layer were prepared by sputtering and evaporation. To prevent water and oxygen permeation into layer, DBR structure was repeated 3 and 5 times, respectively. To enhance passivation effect, the top of layer was capped by 50 nm thick Al2O3 layer. Figure 1 shows FE-SEM images of DBR structure like thin film encapsulation structures of (a) 3.5 and (b) 5.5 dyads. The transmittance spectra of multi-layered passivation layer exhibited periodic interference patterns, which is similar to that of DBR structure. The sharp dips were observed in transmittance spectra in DBR like multi-layered passivation structures due to interference of incident light. It was also observed that interference patterns were sharp and deeper as the number of layer was increased. Furthermore, the number of interference patterns was also increased as the total thickness of passivation layer increased as shown in Fig. 2. It is observed that transmittance dips are appears more within the same wavelength range in thicker thin film passivation layer. Therefore, to increase the transmittance in top layer, the thickness of polymer layer should be reduced in flexible OLEDs devices. By Fig. 1 and 2, it can be concluded that the number of dyads and thickness of each layer should be reduced with comparable passivation properties to obtain high transmittance in top emission flexible OLEDs display.

Figure 1. FE-SEM image of DBR structured passivation films (A) 3.5 dyads, (B) 5.5 dyads

Figure 2. Transmittance of DBR structured TFE films for different numbers of dyads.

SE/ASS-P2-02
Frictional property of BN doped ZnO coating films on 440C stainless steel substrates fabricated by a combinatorial sputter coating method

T01 Applied Surface Science

#SE/ASS-P2-02

M. Sasaki, M. Goto, A. Kasahara, M. Tosa.

National Institute for Materials Science - Tsukuba (Japan).

Zinc oxide sputter coating films are prospected candidate as low friction material for their piezoelectric property [1-3]. The frictional property of ZnO was not satisfied the Amonton-Coulombs' law because of the piezoelectric effect. If the effect will be amplified by changing the coating materials, the friction force can be decreased.
In this paper, in order to change the frictional property of the coating, we fabricated the BN doped ZnO coating films by a combinatorial sputter coating system (COSCOS). It was found that the frictional property was drastically changed by changing the materials of counter balls. <Acknowledgement> The present work was supported by a Grant-in-Aid for Scientific Research (A) (21246030) from the Ministry of Education, Culture, Sports, Science and Technology, Japan. It also was supported by Japan MEXT's GRENE Program.

[1] Masahiro Goto, Akira Kasahara and MasahiroTosa, Tribology Lett., 43 (2) (2011) 155-162.
[2] Masahiro Goto, Akira Kasahara and Masahiro Tosa, Jpn. J. Appl. Phys., 47 (2008) 8914-8916.
[3] M.Goto, A.Kasahara, Y.Konishi, T.Oishi, M.Tosa and K.Yoshihara, Jpn. J. Appl. Phys., 42, 4834-4836 (2003)

Schematic illustration of a combinatorial sputter coating system (COSCOS).

ESD/ASS-P3-11
Pyrite thin films (FeS2) by chemical bath deposition and thermal treatment post-deposit

T01 Applied Surface Science

#ESD/ASS-P3-11

D. Mazon Montijo, M.T.S. Nair, P.K. Nair.

CIE - Temixco (Mexico).

Iron pyrite (FeS_2) thin films, with a band gap of ~ 1 eV, absorption coefficient (α) of ~ 10^5 cm^{-1} in vis-NIR region and *p*-type conductivity have potential for application as solar cell absorbers of abundant elements [1-2]. Methods reported for obtaining these films include spray pyrolysis, molecular beam epitaxy, magnetron sputtering, electrodeposition, and chemical vapor deposition- in most cases accompanied by thermal treatment in sulfur atmosphere [3-5]. This work presents a simple route for obtaining thin films of FeS_2 by chemical bath deposition (CBD) followed by thermal treatment in a sulfur atmosphere under a “sandwich-like configuration”, without the presence of H_2S. First, uniform, homogeneous and yellow-orange colored thin films of amorphous iron sulfur-oxide (*a*-FeO/S) with around 314 nm in thickness were obtained directly from a chemical bath containing $Fe(NO_3)_3$, $Na_2S_2O_3$, $(HOC_2H_4)_3N$ and HCl after 2.5 h of deposition at 40 °C. After heating at 400 °C for different time (from 3 h to 10 h) in N_2/S ambient (~ 10_4 mTorr) in a vacuum oven, the films turned dark-gray, showing X-ray diffraction peaks that match those reported for the cubic phase of the mineral FeS_2 (JCDPS #42-1340). The optical band gap of the films is ~ 0.8 eV due to an indirect transition, and the absorption coefficient of the order of 10^5 cm^{-1} (λ ≤ 1127 nm). The morphological characteristics exhibited by these films are typical for films of iron compounds. Moreover, the effect caused by moisture in the films is also showed. The films are photosensitive, present *p*-type conductivity and electrical conductivity from 0.7 to 1.6 $(\Omega\ cm)^{-1}$, depending on the electrode material.

1. R. Sun et al. Phys Rev. 83 (2011) 235311.
2. Y. H. Liu et al. Thin Solid Films. 479 (2005) 83.
3. J. R. Ares et al. Thin Solid Films. 480-481 (2005) 477.

4. S. Nakamura et al. Sol. Ener. Mat & Sol.Cells. 65 (2001) 79.
5. P. Prabukanthan et al. IEEE (2010) 002965.

ASS-P3-06
Lattice deformation caused by hydrogen- and oxygen- termination of diamond surface

T01 Applied Surface Science

#ASS-P3-06

K. Nose, M. Kamiko, Y. Mitsuda.

The University of Tokyo - Tokyo (Japan).

Attention has been paid to surface termination of diamond because of its unique physical properties. For example, hole conduction on hydrogen-terminated surface[1] has been studied as a potential candidate of electronic devices. In this study, we studied lattice deformation caused by the terminated elements on the surface. Deformed crystal lattice often affects strongly on carrier transport in semiconductor, however, much less is known how termination effects on the surface lattice deformation. Raman spectroscopy with a confocal microscope was performed to analyze the lattice deformation in the vicinity of diamond surface.

(111)-oriented single-crystalline diamond wafers (2.5×2.5×0.5 mm^3, Sumitomo Electrical Hardmetal) were used in this study. Hydrogen termination was achieved by an exposure of the sample to hydrogen plasma at 6 KPa. Wafer temperature was greater than 1070 K, evaluated by a radiation pyrometer. Chemical bonding states of the treated surface was analyzed by X-ray photoelectron spectroscopy (XPS, Quantera, ULVAC-PHI) by analyzing C 1s and O 1s peaks. Horiba T-64000 with a confocal microscope and a green laser (514.5 nm, Ar) was used to obtain Raman spectra. The spot diameter at a focal point was 1 um. The dispersion of the spectrometer was 22 cm^{-1}/mm. The resolution of the wavenumber was around 0.7 cm^{-1}, and the reproducibility of the measured wavenumber of phonon in diamond was enhanced to be 0.01 cm^{-1} on the basis of the reference measurement of a strong Gaussian emission spectrum of Hg.

Surface of as-received diamond wafer was oxygen-terminated. Atomic ratio on the surface was evaluated roughly to be O/C = 10.0 at. % in XPS, suggesting a termination ratio is relatively high if we assume the length of electron penetration and monolayer thickness to be 2 and 0.15 nm, respectively. Confocality of the

spectrometer in the direction normal to the sample surface was evaluated to be 10 μm. Intensity and center wavenumber of Raman spectra of diamond surface are shown in Fig. 1. At the surface of the O-terminated diamond wafer, we detected a negative shift of phonon energy approximately by 0.04 cm^{-1}, indicating a relaxation of lattice at the surface. On the basis of strain parameters of diamond [2], this shift gives us a tensile deformation greater than 2×10^{-5} on the surface compared to the bulk, i.e., inside of the wafer.

[1] F. Maier et. al., Phys .Rev. Lett. 85 3472 (2000).
[2] M. H. Grimsditch et. al., Phys .Rev. B. 18 901 (1978).

Figure 1. Raman shift and intensity of O-terminated diamond plotted against position of the focal point. Surface position is indicated by the red arrow.

ESD/ASS-2-Or-5
Investigation of carrier life time in third generation solar cells by XPS and KFM

T01 Applied Surface Science

#ESD/ASS-2-Or-5

L. Borowik, H. Lepage, N. Chevalier, D. Mariolle, O. Renault.

CEA, LETI, MINATEC Campus - Grenoble (France).

To sustain the progress in photovoltaic field, a development of novel characterization methods field is essential. The most important solar cells parameters which provide good efficiency are: carrier mobility, lifetime of carrier, absorption coefficient, and band gap of the materials. In this paper we are proposing steady method to measure lifetime of carrier by Kelvin force microscopy (KFM) and X-ray photoemission spectroscopy (XPS). Both methods are applicable on the all kind of solar cells (including indirect gap and organic solar cells), additionally KFM method gives possibility to provide a spatially resolved measurement of lifetime.
We will present original method based on modulated illumination, the results are measured on third generation solar cells. Here, we are using hydrogenated and non-hydrogenated bonds Si nanocrystals (NC) [1] (diameter ~5 nm) embedded in 30 nm film of SiO_2. In the case of illuminated solar cell samples, the transfer of charge appears due to the generation of electron hole pairs and followed by electron hole separation in the region of the solar cell junction. This transfer has impact on the sample surface potential and can be measured by KFM [2] or XPS [3] method. We noticed that this phenomenon is reversible in the case of on/off light switching. Moreover, the surface potential can be: measured during modulated illumination and averaged in time. Averaged value of potential is dependent on the modulation frequency. To quantify the carrier lifetime, we calculate potential differences from measured V_{max} (for continuous light) and V_{av} (for modulated light) under the dark and the illuminated conditions. These differences are notified ΔV_{av} and ΔV_{max} and the ratio $\Delta V_{av}/ \Delta V_{max}$ is plotted in the function of the modulated frequency light. Furthermore, experimental points can be fitted by this model (not presented here) where fit parameter is directly lifetime of carrier.
By KFM we find that $\tau = 7\times10\text{-}5$ s and $\tau = 3.5\times10\text{-}5$ s with ±10% accuracy for the hydrogenated and non-hydrogenated NC (Fig. 1), respectively. The longer carrier lifetime for the case of hydrogenated NC, can be explained by the smaller quantity of defaults defects on the NC surface.This work was supported by the French “RTB”

Program. The measurements were performed on the CEA Minatec Nanocharacterization Platform (PFNC).

1 D. Asakura et al., Phys Rev Lett 93 (24) (2004)
2 Ł. Borowik et al. Phys. Rev. B 82 (073302) (2010)
3 K. Surana et al. Nanotechnology 23 (10) (2012)

Fig. 1 $\Delta V_{av}/\Delta V_{max}$ as the function of light modulation frequency. We present XPS and KFM measurements on the hydrogen passivated sample and KFM data from the sample before hydrogen passivation. The fitting curves to KFM data are made by the model.

ASS-P2-06
Low-noise deflection detection system of AFM with quartz tuning fork sensor for imaging in viscous liquid

T01 Applied Surface Science

#ASS-P2-06

H. Shitazaki.

Kyoto Univ - Kyoto (Japan).

Frequency modulation atomic force microscopy (FM-AFM) has been widely used for high-resolution surface structural analysis on various materials such as metals, semiconductors, insulators, and organic materials. It was significantly improved and it is also applicable for investigating liquid/solid interfacial structures. A Si cantilever is mainly used as its force sensor in liquid as well asn in vacuum and in air. However, its quality factor (*Q*) is heavily suppressed in viscous liquid and thus, the force sensitivity and the stability are expected to be decreased. To solve this problem, we have developed an FM-AFM with a quartz tuning fork (QTF) sensor for imaging in viscous liquids. A QTF sensor shows a high *Q* even in the liquid and atomic-resolution imaging was successfully achieved [1]. In that study, the deflection of the QTF sensor was electrically detected by using its piezoelectric effect. The deflection noise density was 125 fm Hz-1/2, which was much larger than that of an improved cantilever-based FM-AFM. The reduction of the deflection noise density would be effective for improvement of force sensitivity, resolution and data acquisition time. Optical beam deflection system, which is commonly used for cantilever-based AFM, is not considered to be suitable for a QTF sensor because a QTF sensor is generally much longer than a Si cantilever. Recently, Morita et al. indicated that the deflection noise density of a QTF sensor was significantly reduced by optical interferometric detection system and atomic-resolution imaging was achieved in ultrahigh vacuum [2]. We considered that this technique is also promising for imaging in viscous liquid using a QTF sensor and developed an optical interferometric detection system for liquid environment as shown in Fig. 1.

[1] T. Ichii, M. Fujimura, M. Negami, K. Murase, H. Sugimura, *Jpn. J. Appl. Phys.* **51** (2012) 08KB08.

[2] K. Morita, Y. Sugimoto, Y. Sasagawa, S. Morita, *Nanotechnology* **21** (2010) 305704.

Fig. 1 Photograph of AFM head with an optical interferometeric detection system for QTF sensor.

SE/ASS-P2-03
Adhesion Promotion in Aluminium Polypropylene Composites Measured by Peel test and Centrifuge technology

T01 Applied Surface Science

#SE/ASS-P2-03

R. Mix, S. Hielscher, J. Friedrich, U. Beck.

Federal Institute of Material Research and Testing - Berlin (Germany).

The measurement of the adhesive strength of coated polymers is an important issue for the evaluation of the quality of surface treatments and performance characteristics of laminated polymer foils. Normally, the peel test is used to retrieve information about the effectiveness of the applied polymer treatment. However, the peel test primarily refers to tear propagation strength (in N/m) with respect to the width of the tape (or sample) and not to the adhesive strength (in N/mm2) of a given polymer-metal system. Problems are associated with well adherent coatings where the delamination may start at the 'wrong' layer or interface which may be the polymer itsself or "undesirable" interfaces in multi-layer composites. For this reason, the practicability of the centrifuge technology [1] was investigated. The determination of adhesive strength between aluminium and surface-treated polypropylene (PP) foils was realized by on-line detection of rupture events of modular Cu-V2A stamps of known mass (glued on the Al layer by means of adhesive) due to the effect of centrifugal force at certain rotational speed (see Fig. 1).

Fig. 1
Principle of the centrifuge technology (TS-test stamp, GS-guiding sleeve of the stamp, S+C-sample with coating, A-adhesive, Fc – centrifugal force, r – radius of the rotational motion)

The surface treatment of the PP was accomplished in two ways: 1) by the introduction of nebulized aqueous solutions (1% w/w) of functionalized monomers (acetic acid) and polymers (vinylalcohol (co)polymers, poly acrylic acid) into a DBD discharge and 2) by deposition of plasma polymers followed by reaction with functionalized substances to create special interface structures concerning the position of the functional group related to the topmost surface. All modified surfaces

were characterized by XPS in dependence on the plasma conditions. The functionality of the surfaces was estimated by derivatization and subsequent XPS characterization.
Adhesive strength of aluminium-coated PP foils was measured for both testing methods. The XPS inspection of the tested samples proved the location of the failure in the PP laminates.

[1] U. Beck, G. Reiners, D. Lerche, U. Rietz, H. Niederwald, Surf. Coat. Technol. 205 (2011) 182.
[2] R. Mix, J. Friedrich, A. Rau, Plasma Proc. Polym., 6 (2009) 566.

Fig. 1

ASS-4-Or-1
Effect of steam treatment on surface morphology of Ni3Al foil catalysts

T01 Applied Surface Science

#ASS-4-Or-1

Y. Xu [1], Y. Ma [2], J. Sakurai [1], Y. Teraoka [3], A. Yoshigoe [3], M. Demura [1], T. Hirano [1].

[1]National Institute for Materials Science - Tsukuba (Japan), [2]North China Electric Powder University - Beijing (China), [3]Japan Atomic Energy Agency - Sayo, Hyogo (Japan).

Ni_3Al intermetallic compound is known as a promising high-temperature structural material because of its excellent high temperature strength and corrosion/oxidation resistance. Recently, we found that Ni_3Al, in the form of both powder and foil, shows high catalytic activity for methanol decomposition [1,2] and methane steam reforming [3,4], indicating a possibility to develop Ni_3Al as catalysts for hydrogen production. More recently, we found that it is possible to enhance catalytic activity by modifying the surface structure of Ni_3Al foil simply by a pre-treatment which includes a steam treatment at proper temperatures followed by a H_2 reduction. In this study, in order to understand the mechanism of the enhancement by the pre-treatment, we investigated the effect of the steam treatment and H_2 reduction on the surface morphology of Ni_3Al foil using a FE-SEM with an EDS system, and synchrotron radiation X-ray photoemission spectroscopy (XPS) at beamline BL23SU of Spring-8. SEM and EDS analysis showed that two surface layers were formed by the steam treatment: the outmost layer consisted of fine particles of Ni oxides, and the layer beneath the outmost layer consisted of Al oxides. The Ni oxides were reduced to metallic Ni by the subsequent hydrogen reduction. XPS analysis revealed the detail chemical state change of Ni and Al in the surface during the pre-treatment process. Figure 1 shows the Ni 2p core level measured before and after the steam treatment and H_2 reduction. Before the steam treatment, the Ni 2p peaks corresponded to the metallic Ni were detected, indicating that the Ni in the surface layer was mainly in the metallic state. After the steam treatment, the relative intensity of the metallic Ni 2p peaks was significantly decreased, and the strong Ni 2p peaks corresponded to NiO appeared, suggesting that most of the metallic Ni in the surface layer were oxidized by the steam treatment. After the H_2 reduction, the relative intensity of the metallic Ni 2p peaks increased again, indicating that NiO was reduced to metallic Ni. These fine

metallic Ni particles formed on the foil surface were considered to enhance the catalytic activity of Ni_3Al foil.

[1] Y. Xu, S. Kameoka, K. Kishida, M. Demura, A.P. Tsai and T. Hirano: Intermetallics 13 (2005) 151.
[2] D.H. Chun, Y. Xu, M. Demura, K. Kishida, D.M. Wee and T. Hirano: J. Catal. 243 (2006) 99.
[3] Y. Ma, Y. Xu, M. Demura, D.H. Chun, G.Q. Xie and T. Hirano: Catal. Lett. 112 (2006) 31.
[4] Y. Ma, Y. Xu, M. Demura, D.H. Chun and T. Hirano: Appl. Catal. B: Enviromental 80 (2008) 15.

Figure 1 Ni 2p core level of Ni_3Al foils before (as-polish) and after steam treatment at 873 K for 1h (H_2O oxi.), H_2 reduction at 873 K for 1h (H_2O oxi. + H_2 red.).

ASS-P3-18
Direct and Fullerene-Templated Photochemical Polymerization of Functionalized Porphyrins on a Silver Substrate

T01 Applied Surface Science

#ASS-P3-18

A. Basagni [1], L. Colazzo [1], M. Di Marino [1], F. Sedona [1], D. Forrer [2], M. Sambi [1].

[1]University of Padua - Padua (Italy), [2]CNR-ISTM - Padua (Italy).

Surface supramolecular chemistry has produced a large variety of atomically controlled systems, but practical applications are seriously restricted by the use of weakly cohesive non-covalent bonds and by the confinement to (mainly) metal surfaces[1]. In order to create systems usable in real devices it is necessary to covalently stabilize the supramolecular structures obtained by molecular self-assembly[2-4]. In this direction we report the formation of a new surface covalent organic framework (SCOF) based on the photo-polymerization reaction of a bi-functional compound. A well-ordered polymeric organic sheet was obtained by depositing 5,15-bis(4-aminophenyl)-10,20-diphenylporphyrin ($TPP(NH_2)_2$) on a Ag(110) surface in ultra-high-vacuum conditions. Covalent stabilization of the units was activated by irradiation of $TPP(NH_2)_2$ at 405 nm for several hours, which resulted in the formation of azo-bridges (RN = NR) between monomers along the è [1-10] direction of the substrate. Two distinct procedures have been optimized for the growth of the polymeric structure. The first one is based on the anisotropy of $TPP(NH_2)_2$ diffusion coefficients along the substrate [1-10] and [001] directions below room temperature (RT). The second method is based on the topological control that C_{60} - co-organized with $TPP(NH_2)_2$ on the substrate surface in a bicomponent supramolecular array[5] - exerts over the $TPP(NH_2)_2$ units by directing and organizing them in an ideal geometry for the photo-assisted reaction at RT. DFT calculations have been used in order to confirm the nature of the chemical bonds within the polymeric chains.

[1] J. Adisoejoso, K. Tahara, S. Lei, P. Szabelski, W. R._Zysko, K. Inukai, M. O. Blunt, Y. Tobe, and S. De Feyter, ACSNANO 2012, 6, 897-903.
[2] D. F. Perepichka, F. Rosei, Science 2009, 323, 216-217.
[3] G. Franc, A. Gourdon, Physical Chemistry Chemical Physics 2011, 13 (32), 14283
[4] L. Lafferentz, V. Eberhardt, C. Dri, C. Africh, G. Comelli, F. Esch, S. Hecht and L. Grill, Nature Chemistry 2012, 4, 215
[5] F. Sedona, M. Di Marino, T. Carofiglio, E. Lubian, M. Casarin and E. Tondello. ACSNANO 2010, 4, 5147-5154.

ASS-P3-07
Modification of c-Si and its oxides using atmospheric-pressure plasma

T01 Applied Surface Science

#ASS-P3-07

D. Skácelová [1], D. Hegemann [2], M. Černák [1].

[1]Department of Physical Electronics, Faculty of Science, Masaryk University, Kotlářská 2, 611 37 - Brno (Czech republic), [2]Swiss Federal Laboratories for Materials Science and Technology, Empa, Lerchenfeldstrasse 5, CH-9014 - St.gallen (Switzerland).

Silicon and silicon dioxide surfaces play an important role in nowadays technologies, especially photovoltaics, integrated circuits and microelectronics. In all these various applications different surface properties are required. Nevertheless, the process of cleaning, oxidating, etching etc. typically includes a complicated wet chemical process or required low pressure systems. Recently it became a tendency to replace such process steps by plasma-based technologies that could provide an environmentally much more friendly alternative.
In this paper we present the surface modification of c-Si by the atmospheric-pressure highly-nonequlibrium plasmas generated using the Diffuse Coplanar Surface Barrier Discharge (DCSBD)
[1-3]. DCSBD generates macroscopically-homogeneous plasma with an extremely high power density of the order of 100 W/cm3 in any working gas including strongly electronegative gases. DCSBD plasma operated in air is able to oxidize c-Si (metalloids) surfaces and creates a distinct silicon dioxide layer with the thickness of several nanometres [4].
In this study c-Si was modified in various working gases (air, oxygen, argon and nitrogen) and optimal conditions of oxidation were specified. In general, oxidation rate depends on the humidity and temperature of the sample. Therefore influence of ambient humidity on the oxidation process was studied and also the effect of the sample temperature was controlled. The influence of native oxide film on Si surface has been investigated. The modification of the surface was studied by various surface analysis including XPS, SIMS, AFM, SEM, UPS and surface energy measurement. Also plasma diagnostics by optical emission spectroscopy during plasma oxidation was studied.
The oxidation by DCSBD seems to be in the future a promising and cheap oxidation process applicable in the field of photovoltaics, microelectronics etc.

[1] M.Šimor, J. Ráhel´, P. Vojtek, M. Černák, Atmospheric-pressure diffuse coplanar surface discharge for surface treatments, Appl.Phys.Lett. 81 (2002) 2716-2718.
[2] M. Černák, L´. Černáková, I. Hudec, D. Kováčik, A. Zahoranová, Diffuse coplanar surface barrier discharge and its applications for in-line processing of low-added-value materials, Eur. Phys. J. Appl. Phys. 47 2 (2009) 1-6.
[3] M. Černák, Method and apparatus for treatment of textile materials, European Patent EP 1387901 B1, 2002.
[4] D. Skácelová, V. Danilov, J. Schäfer, A. Quade, P. Sťahel, M. Černák, J. Meichsner, "Room temperature plasma oxidation in DCSBD: A new method for preparation of silicon dioxide films at atmospheric pressure" Mater.Sci Eng. B. (2012), DOI: 10.1016/j.mseb.2012.10.017, Article in press.

ASS-4-Or-3
SXPS study of photoelectrochemical processes at the GaAs(100)/HCl aqueous solution interface

T01 Applied Surface Science

#ASS-4-Or-3

M. Lebedev [1], W. Calvet [2], T. Mayer [2], W. Jaegermann [2].

[1]Ioffe Physical-Technical Institute, Russian Academy of Sciences - St. Petersburg (Russian federation), [2]Darmstadt University of Technology, Institute of Material Science - Darmstadt (Germany).

Chemical reactions and accompanying charge transfer processes under applied voltages at n-GaAs(100)/1M HCl_{aq} solution interface are analyzed by means of highly surface-sensitive synchrotron-radiation photoemission spectroscopy. Experiments were carried out using a conventional three-electrode scheme in the electrochemistry chamber being part of the integrated system SoLiAS permanently operated at BESSY. This glass chamber is purged with Ar gas and is directly attached to a special buffer chamber to allow for the sample transfer into UHV for subsequent photoemission analysis without contact to ambient air. The GaAs(100) surface composition was analyzed after 30 min contact with the HCl solution under different bias voltages with respect to the Ag/AgCl reference electrode. Results: After contact to the 1M HCl_{aq} solution at zero bias for 3–4 min the native oxide layer is effectively removed from n-GaAs(100) surface. The core-level spectra indicate components assigned to bulk species, elemental arsenic, As–H_2, As–OH, and Ga–Cl bonds, as well as gallium suboxide. Once the anodic bias voltage is applied to n-GaAs(100)/1M HCl_{aq} solution interface the As-to-Ga ratio increases due to enrichment of the elemental arsenic component at the surface (Fig. 1). The elemental As formation is enhanced when the GaAs/solution interface is irradiated by visible light (Fig. 1).
After exposure of the n-GaAs(100) surface to 1M HCl_{aq} solution under cathodic voltage, the chemical composition changes very little. Under these conditions hydrogen is evolved and the As–H_2 component decreases with increasing cathodic voltage. On the other hand, the valence band spectra change strongly (Fig. 2). In particular, the feature with the binding energy of about 5.5 eV increases with cathodic voltage. This feature is related to combinations of the hydrogen orbital with Ga-derived *s*-like states localized in the second atomic plane from the surface.

The paper demonstrates that synchrotron-radiation photoemission spectroscopy can be successfully used for studying the photoelectrochemical processes at semiconductor/electrolyte interfaces in great detail.

2

ASS-5-Or-11
Work function investigation of SiGe heterostructures using Kelvin force microscopy and electron spectroscopy

T01 Applied Surface Science

#ASS-5-Or-11

S. Pouch [1], N. Chevalier [1], D. Mariolle [1], E. Martinez [1], P. Kumar [1], O. Renault [1], J. Morin [1], J.M. Hartmann [1], T. Mélin [2], L. Borowik [3].

[1]CEA, LETI, MINATEC Campus - Grenoble (France), [2]IEMN, CNRS-UMR - Villeneuve D'ascq (France), [3]CEA, LETI, MINATEC - Grenoble (France).

We present here the experimental setup used to perform work function analysis on SiGe/Si heterostructures. These epitaxial heterostructures are consisting in stacks of 500 nm thick SiGe layers with increasing Ge concentration from 6% to 50% [1]. Kelvin force microscopy (KFM) and electronic microscopy like: X-ray photo emission electron microscopy (XPEEM) or scanning Auger microscopy (SAM), provide coupled information on local work function together with surface topography or chemical composition.

The KFM measurements have been performed with Bruker Dimension 3100 and Omicron VT-XA UHV AFM instruments, using a NanoSensors PPP EFM tip (k~2 N/m). KFM is one of the techniques used to detect the contact potential difference (CPD), which is is directly related to work function [2]. The XPEEM measurements were made using an Omicron NanoESCA [3].

The absolute work function map is obtained from spectromicroscopic image series [4] at the photoemission threshold (secondary electrons) recorded with He I or AlKα1 radiations.

Electron spectroscopy analysis has been performed using a PHI-700 Xi Auger nanoprobe system, using an electron beam voltage from 10 to 20 keV and current from 5 to 10 nA [~(8-22) nm spot size]. This technique is based on the acquisition of the emission threshold of secondary electrons which is directly related to the work function [5].

We will present an improved protocol of the former SAM work function measurement [5]. A stack of emission curves is obtained by analyzing each SiGe layer successively. Then, the difference of threshold energy is extracted for each step to obtain the work function difference between these layers.

Furthermore, we will show comparative results of KFM, XPEEM and SAM, and discuss about the capabilities of each technique. Moreover, KFM and XPEEM characterizations (Fig. 1) are combined by using a UHV suitcase to transfer the sample and prevent oxidation and contamination under air exposure.
This work was supported by the French “Recherche Technologique de Base” Program. The measurements were performed on the CEA Minatec Nanocharacterization Platform (PFNC).

1. J-M. Hartmann. et al. ECS Transactions 3 219 (2006).
2. S. Sadewasser et al. Kelvin Probe Force Microscopy (2012).
3. O. Renault et al Surf. and Inter. Anal. 38, 375 (2006).
4. A. Bailly et al. Nanolett., 8, 3709 (2008).
5. G. Baschmann et al. J. Analytic. Chem., 329, 195 (1987).

FIG.1 XPEEM result showing work function difference between each SiGe layer.

ASS-8-Or-5
INFLUENCE OF SURFACE PRETREATMENTS ON THE REACTIVITY OF ALUMINUM ALLOY 6061 TOWARD NITRIC OXIDE: AN in-situ PM-IRRAS STUDY

T01 Applied Surface Science

#ASS-8-Or-5

R. Ngongang [1], C.M. Pradier [2], X. Carrier [2], E. Marceau [2], C. Methivier [2], J.L. Blanc [1], M. Carre [1].

[1]Air Liquide - 1 Chemin De La Porte Des Loges,78350 Jouy En Josas (France), [2]Laboratoire de Réactivité de Surface, UMR CNRS 7197,Pierre and Marie Curie University - 2 Rue Galilée, 94200 Ivry Sur Seine (France).

Aluminum alloys (AA) like AA6061 are widely used in automotive, aircrafts and packaging industries because of their good mechanical properties and their remarkable surface stability due to the presence of native oxide (alumina). However, under common environmental conditions, formation of an uncontrolled oxyhydroxide layer can occur on their surfaces.[1] Yet, for industrial applications like production of exhaust pipe made of aluminum or exposure of aluminum structures to reactive environments containing nitric oxide (NO), the aluminum surface need to be controlled and improved. A common way to improve aluminum surfaces is to deposit self-assembled layers from silane or silicon-based molecules like trichlorosilane ($HSiCl_3$), mainly by immersion in a solution, chemical vapor deposition or plasma techniques.[2] However, to our knowledge, no studies have been conducted to understand the evolution of AA surfaces pretreated with silicon-based molecules; immediately after pretreatment and in presence of reactive molecule like NO. In the present work, we implemented a controlled and reproducible pretreatment procedure consisting in direct exposure of AA 6061 samples to gaseous $HSiCl_3$. We show that $HSiCl_3$ forms discrete nodules (50-500 nm) of silicon oxide on merely polished surfaces, whereas it reacts with OH-rich surface of pseudoboehmite needles formed on hydroxylated (in boiling water) surfaces. We have combined analyses in static (AFM, SEM, XPS) and dynamic (*in-situ* PM-IRRAS) conditions. Then, in line with

former studies on pure aluminum,[3] we put in evidence the poor reactivities of polished metal surfaces toward NO, be they $HSiCl_3$-pretreated or not. In contrast, nitrites, and nitrates are clearly evidenced by *in-situ* PM-IRRAS on hydroxylated AA6061 ($HSiCl_3$-pretreated or not), with the $HSiCl_3$-pretreated hydroxylated AA6061 being less reactive (Fig. 1).

1. Schüth, F., K. S. W. Sing., and Weitkamp, J.; Handbook of Porous Solids. WILEY-VCH: 2002; Vol. 3.
2. Elias B. Wyman and Mathis C. Skief, Organosilanes: Properties, Performance and Applications. Nova Science Pub Inc: 2010.
3. Delebecque A.; Pradier C.M.;Thomas, C.; Methivier C.; Coffre E.; Paoli H.; Carre M., J. Phys. Chem. C 2008, 112 (8), 2964-2971.

Figure 1 : PM-IRRAS difference spectra of hydroxylated AA6061 vs. HSiCl3-pretreated hydroxylated AA6061 upon 15 days NO exposure.

ESD/ASS-P3-05
Synthesis and structural characterization of P-type transparent conducting CuCrO2 thin films deposited by reactive magnetron sputtering

T01 Applied Surface Science

#ESD/ASS-P3-05

H. Sun [1], M. Arab Pour Yazdi [1], F. Sanchette [2], A. Billard [3].

[1]IRTES-LERMPS - Belfort (France), [2]LRC CEA-ICD LASMIS - Nogent (France), [3]IRTES-LERMPS / LRC CEA - Blefort (France).

P-type transparent conducting oxides (p-TCOs) have attracted increasing attention while the photovoltaic industry is being focused upon them [1]. Within the numerous p-TCOs, the delafossite structure ABO_2 is considered to be one of the most potential p-TCOs because of its special layer structure [2]. However, a compromise has to be found between the transparency and the conductivity in all the p-TCOs. Some p-type delafossites have a relative high transmittance, such as $CuAlO_2$, but have a very impractical conductivity [3]. In order to obtain p-TCOs with good optoelectronic properties, the presence of different elements at B sites in ABO_2 delafossite has been studied [4]. It should be noted that, in recent years, the conductivity of $CuCrO_2$ based materials has reached to about 10^2 $S{\cdot}cm^{-1}$, while their transmittance is just under 50% [5].
In this study, we prepare $CuCrO_2$ thin films by reactive magnetron sputtering. Hence, after a short description of the deposition reactor, we present the chemical evolution of the coatings versus deposition parameters. The coatings morphologies and structures will be characterized by scanning electron microscopy and X-ray diffraction and finally the electrical conductivity and the transmittance of the films will be measured.

[1] H. Kawazoe, H. Yanagi, K. Ueda, H. Hosono, Mater. Res. Bull. 25 (2000) 28.
[2] A.N. Banerjee, K.K. Chattopadhyay, Prog. Cryst. Growth Charact. Mater. 50

(2005) 52.
[3] C.F. Windisch Jr., M.H. Engelhard, D.C. Stewart, Thin Solid Films 45 (2001) 398.
[4] M. A. Marquardt, N. A. Ashmore, D. P. Cann, Thin Solid Films 496 (2006) 146.
[5] R. Nagarajan, A.D. Draeseke, A.W. Sleight, J. Tate, J. Appl. Phys. 89 (2001) 8022.

ASS-8-Or-4
Oxide on InSb surfaces

T01 Applied Surface Science

#ASS-8-Or-4

D. Aureau, A. Sthoer, I. Girard, A. Etcheberry.

CNRS-UVSQ - Versailles (France).

For III-V optoelectronic devices, the knowledge and the engineering of the surface oxide layers are often key parameters for the success of a technology. Its instability is related to the high density of states in the band gap generated by the oxide capping and its relevant interface with the compound. The film thickness can vary from ultra thin layer to micron thick. The spatial homogeneity is also a subject of variation. The global properties of the oxide (chemical composition, texture, morphology, etc.) strongly influence the global electrical responses of the structures and particularly the kinetic of the electron transfers through the interface. Among the III-V semiconductors, Indium Antimonide is an important material in infrared photodetectors and light emitters. InSb has the highest electron mobility, the smallest electron effective mass and the largest electron magnetic moment making it a promising candidate for high speed, low power field effect transistors and spintronics. In order to gain control of this material, surface chemistry has to be better understood. For many applications, it is important first to know how the wet etching of the upper layer occurs and how this etching affect the surface chemistry.
In this work, we propose an original and detailed study where the etching is followed by the dosage of metallic ions (In and Sb) released in the aqueous solution and the obtained surface characterized by XPS for its chemical composition and AFM for its morphology. The importance of the work presented in this manuscript is precisely to address the issue of a total overview of the processes involved in the etching bath. The methodology followed suggest that the formulation and the concentrations used in the bath strongly affect the final surface.
Figure 1 shows the 10-41 eV region of the XPS spectrum on a particular InSb surface after HBr/Br2 etching. In this region, both Indium and Antimonide exhibit particular peaks (In4d and Sb4d). A linescan with 5 points has been realized to highlight the utility of local XPS on this non-homogeneous particular oxide. The matrix peaks are seen at the same position when the oxides are shifted. Three different energies, named ox1, ox2,and ox3, are observed for the five points made. This same shift on both elements is associated to a particular charging effect, confirmed by the C1s peaks related to contaminants (inset in figure 1). Two components are seen. At 285 eV, the regular carbon peak is seen when another one

is at higher energy. The shift between the two main carbon peaks is the same than the energy shift between InOx and Inmatrix or SbOx and Sbmatrix confirming a general shift of the peaks related to the oxide. Furthermore, quantitative analysis will be shown and recipes to obtain reproducible low quantity of mixed or Indium-rich oxide will be given.

Figure 1: XPS spectra in the 10-41 eV region (linescan on 5 points) of InSb surfaces after HBr/Br2 etching. Inset: C1s region.

ASS-P2-01
SRSOs grown by PECVD: Controlled structural and optical properties and formation of nanocrystals

T01 Applied Surface Science

#ASS-P2-01

P. Calta, P. Sutta, M. Netrvalová.

University of West Bohemia - Pilsen (Czech republic).

The silicon-rich silicon oxide films (SiO_x, x≤1) were deposited by a rf (13.56 MHz) plasma enhanced chemical vapor deposition on different substrates (Corning glass, Cu and Si(100)) at the low substrate temperature (250°C) in N_2O-SiH_4-Ar discharges. The films obtained at different deposition conditions, varying the gas flow ratio of the precursor gases (R = N_2O/SiH_4), were heat treated to different temperatures up to 1100°C (in air and vacuum). The effect of the gas flow ratio R and thermal annealing on the compositional (EDS), microstructural (XRD), chemical bonding configuration (FT-IR and Raman microscope), optical (spectroscopic ellipsometry and UV-VIS spectrophotometer) and mechanical (by nanoindentation) properties of films and Si nanocrystals formation (TEM) were studied and results are presented and discussed.

Variable elemental composition Si/O, high deposition rate (60 nm/min), good hardness (around 7 GPa), low residual compressive stress (to 0.3 GPa), refractive indices of 1.6-1.8 and optical band-gap values 2 - 3 eV of as-deposited silicon oxide based films were obtained by varying the N_2O/SiH_4 flow ratio. Over 1000°C, annealed SRSO samples showed the c-Si diffraction peaks (Fig. 1), which became narrower with increasing temperature. From the width of the Si (111) peaks, the mean size of Si-ncs and their dependence on temperature was determined and compared to those values from TEM measurements. The size of Si-ncs increases with increasing Si concentration in the films and increasing annealing temperature [1]. FTIR spectroscopy shows the chemical composition of as-deposited films, which was dominated by silicon suboxide containing silicon-nitride and silicon-hydrogen bonds. During annealing, the shift of the Si-O-Si stretching vibration to higher wavenumbers indicates phase separation. The disappearance of the hydrogen related bonds indicates the hydrogen effusion. For the as-deposited films and for the annealed films, Raman spectra show a band approximately at 480 cm^{-1}, related to

amorphous silicon and a band at 517 cm^{-1}, related to nanocrystallite silicon, respectively. The optical band gap and refractive index decreases during annealing.

[1] D. Comedi, O. H. Y. Zalloum, E. A. Irving, J. Wojcik, T. Roschuk, M. J. Flynn, and P. Mascher, J. Appl. Phys. 99, 023518 (2006).

Figure 1. XRD patterns of films deposited at different R (N2O/SiH4 ratio) and annealed at different temperatures.

ASS-P3-08
Nanoscopic Observation of Interface Structure and Chemical States of Beta-FeSi2 Thin Film Fabricated on Si and Silicon-on-Insulator Substrates

T01 Applied Surface Science

#ASS-P3-08

M. Sasase [1], H. Yamamoto [2], K. Shimura [2], K. Yamaguchi [2].

[1]The Wakasa-wan Energy Research Center - Fukui (Japan), [2]Japan Atomic Energy Agency - Ibaraki (Japan).

Beta-iron disilicide (β-$FeSi_2$) is a promising compound semiconductor for application to optoelectronic devices.[1)] For Si-based device fabrication, epitaxial growth of films on Si substrates is one of the techniques employed to achieve better device performance. β-$FeSi_2$ films can be epitaxially grown on Si single crystals, because the lattice mismatch between β-$FeSi_2$ and Si is within ca. 5% for all orientations. Control of the interface structure of the films and substrates is necessary to obtain highly oriented thin β-$FeSi_2$ films that have good optoelectronic properties.

The formation of β-$FeSi_2$ has been achieved using several growth techniques.[2)] In our previous studies, ion beam sputter deposition (IBSD) of β-$FeSi_2$ on Si(100) resulted in the fabrication of highly oriented films.[3, 4)] After subsequent annealing, the obtained films were found to exhibit strong photoluminescence (PL).[5)] In the present study, β-$FeSi_2$ films were deposited on two different substrates, namely, Si(100) and silicon on insulator (SOI). Nanostructural and compositional changes at the interface take place during subsequent annealing and it was expected that these would be dependent on the substrates used. The structural changes at the interface, crystallinity of the β-$FeSi_2$ film and substrates, and the elemental composition, chemical states were investigated using cross-sectional transmission electron microscopy (TEM) and energy dispersive X-ray mapping. The annealed films on these substrates were found to exhibit quite different structures. The β-$FeSi_2$ films on Si(100) were aggregated, forming β-$FeSi_2$ particles with sizes of 20-200 nm. No dislocations or stacking faults were observed in the interface region. Aggregation also occurred to form β-$FeSi_2$ particles with sizes of 20-30 nm on the SOI substrate; however, no β-$FeSi_2$/Si interface was present because the buried SiO_2 layer significantly swelled during annealing and the surface Si layer disappeared. Based

on these observations, the effect of the interface structure and chemical states on the PL properties, which are important for optoelectronic devices, is discussed with atomic scale TEM observation.

1) D. Leong, M.A. Harry, K.J. Reeson, K.P. Homewood: Appl. Phys. Lett. 68 (1996) 1649.
2) M. Takauji, N. Seki, T. Suemasu, F. Hasegawa, M. Ichida: J. Appl. Phys. 96 (2004) 2561.
3) M. Sasase, T. Nakanoya, H. Yamamoto, K. Hojou: Thin Solid Films 401 (2001) 73.
4) H. Yamamoto, K. Yamaguchi, K. Hojou: Thin Solid Films 461 (2004) 99 (and references therein).
5) K. Yamaguchi, K. Shimura, H. Udono, M. Sasase, H. Yamamoto, S. Shamoto, K. Hojou: Thin Solid Films 508 (2006) 367.

ASS-5-Or-3
Surface Spectrometry and Depth Profiling using Argon Cluster Ions

T01 Applied Surface Science

#ASS-5-Or-3

A. Sears, S. Kayser, E. Niehuis, R. Möllers, F. Kollmer, D. Rading.

IONTOF GmbH - Muenster (Germany).

Organic multi-layers have recently become of increasing importance in a number of technological fields. One of these areas is organic electronics which include OLED displays/lighting and power production photovoltaics. The optimization of the performance of these devices in terms of lifetime and efficiency requires a detailed knowledge of layer structure and interface composition.

The depth profiling/3D analysis of organic multi-layers with SIMS is only possible if molecular structural information can be preserved under high dose sputtering conditions. High energy cluster ions such as SF_5 [1] and C_{60} [2] have received interest as their overall energy is large enough to sputter material whilst, at the same time, the energy per atom, of around several hundred eV, is low enough to minimize sample damage. However, there are a variety of organic compounds that cannot be profiled satisfactorily using these ions without the loss of ion signals [3]. Recent studies have shown that massive argon cluster ions have been successfully used for the SIMS depth profiling of a wide range of organic materials without loss of characteristic molecular ion signals [4].

Adequate mass filtering and short pulsing of the argon cluster ions enable them to be used as an analytical beam with high secondary ion yield efficiency on organic materials. In addition, mass spectra generated by these ions exhibit far less fragmentation in characteristic molecular secondary ions in comparison to those obtained using other ion species [5]. This overall simplification of the mass spectrum assists in data interpretation for determining sample composition.

In this paper we shall present the results of dual beam TOF-SIMS depth profiling of bulk and multilayer organic materials using $Ar_{1000\text{-}2500}$ and C_{60} sputtering. The analytical potential of these ions in terms of their influence on mass spectra is also investigated with respect to the dependence of molecular fragment abundance as a function of argon ion energy and cluster size.

[1] C.M. Mahoney, S.V. Roberson, G. Gillen, Anal. Chem. 2004, 76, 3199-3207
[2] N. Winograd, Anal. Chem. 2005, April 1, 143A-149A
[3] M. S. Wagner, Anal. Chem. 2005, 77, 911-922
[4] S. Ninomiya, K. Ichiki, H. Yamada, Y. Nakata, T. Seki, T. Aoki, J. Matsuo, Rapid Communications in Mass Spectrometry 2009, 23, 1601-1606
[5] I. S. Gilmore, M. P. Seah, Applied Surface Science (2000) 161 465-480

ASS-P1-18
Optical characterization of semiconductors: photoluminescence measurements

T01 Applied Surface Science

#ASS-P1-18

M. Berouaken [1], H. Menari [1], N. Gabouze [1], T. Kerdja [2].

[1]CRTSE - Algiers (Algeria), [2]CDTA - Algiers (Algeria).

In this work, we carried out a photoluminescence (PL) test bench for the study of different optical properties of semiconductors. Its operating principle consists to illuminate the sample by means of an intense light beam from a laser. The light emitted by the sample is focused by a collimator on the entrance slit of a monochromator. The optical signal is then detected by means of a webcam and sent to a data acquisition system interfaced to a PC, where it is processed by software. This later allows the control of the monochromator, the acquisition and the processing of image from the webcam for the determination of the light intensity, and the plot of the PL spectrum. The excitation of a porous silicon sample with a laser at 405 nm showed a good correlation with other measurement benches.

ASS-P1-10
Morphological methods suitable for image analysis of thin metal films and composite films: Application of methods of modern computational physics

T01 Applied Surface Science

#ASS-P1-10

D. Novotny [1], R. Hrach [2], M. Maly [1].

[1]J. E. Purkinje University, Faculty of Science, Department of Physics, Ceske mladeze 8, 400 96 Usti nad Labem - Usti Nad Labem (Czech republic), [2]Charles University in Prague, Faculty of Mathematics and Physics, Department of Surface and Plasma Science, V Holesovickach 2, 180 00 Prague 8 - Prague (Czech republic).

In thin film physics as well as in some other fields of science as solid-state physics, astronomy, metallurgy, biology etc. the complex systems consisting of large number of objects are being studied. An important source of information is the image analysis of micrographs of these systems - discontinuous metal films, sections and projections of composite films, surfaces of solids, etc. Image analysis of such structures provides information about both size and spatial distributions of individual objects and these distributions influence fundamentally most of physical properties of the studied films. Standard methods based on the theory of mathematical morphology [1] are often used for a description of the spatial distribution of objects. The recognition ability of these methods for various types of physical systems differs and has some limits. From this point of view it is necessary to analyse existing methods and create new ways for the study of such image structures.
The contribution deals with a new approach to the image analysis of complex systems consisting of a large number of objects based on algorithms of modern computational physics - on neural networks and advanced integral transforms, i.e. Fourier/Hartley transform, Gabor transform and wavelet transform. It was found that both these techniques represent new powerful tools, which allow us to obtain the desired information hidden in the classical morphological characteristics. However, the application areas of both techniques differ, while the neural networks are better

suitable for the analysis of films in the initials stages of growth, the integral transforms bring the best results when analysing semicontinuous films and composite films near the percolation threshold.
The contribution consists of four parts: preparation of simulated structures with given properties (e.g. [2], [3]), detailed analysis of classical morphological algorithms, analysis of novel algorithms based on advanced methods of modern computational physics [4], [5] and application of both types algorithms on simulated structures as well as on selected experimental data. For the preparation of simulated structures various types of models with different complexity were used - ranging from simplified hard-disk and soft-disk models to advanced atomistic models. In atomistic modelling two approaches were combined, the molecular dynamics for the description of nucleation process and the kinetic Monte Carlo method for the simulation of further growth stages. The main source of experimental data used for the comparison with model structures were the TEM micrographs of discontinuous and semicontinuous metal films prepared in our laboratory.

[1] Serra J., Image analysis and mathematical morphology, Academic Press, London 1982.
[2] Hrach R., Novotny D., Hruby V., Vacuum 90 (2013), 121-128.
[3] Novak S., Hrach R., Svec M., Vacuum 85 (2011), 1096-1097.
[4] Novotny D., Hrach R., Kostern M., Vacuum 82 (2008), 282-285.
[5] Maly M., Hrach R., Novotny D., Applied Surf. Sci. 235 (2004), 86-90.

ASS-P1-07
Quantitative Auger analysis of polarity-dependent GaN(0001)/ZnO(0001) wurtzite structures

T01 Applied Surface Science

#ASS-P1-07

C. Su.

Department of Electrophysics, National Chiayi University - Chiayi (Taiwan, republic of china).

Gallium nitride (III-V) and zinc oxide (II-VI) wide band gap semiconductor materials are promising in optoelectronics applications. Due to low lattice mismatch, ZnO substrate is suitable for grow GaN films. In this studies, quantitative Auger analysis of an ideal interface/surface such as Ga/N/ZnO(0001) or N/Ga/ZnO(0001) stacking is simulated. We calculate the Auger emission intensity ratio between interfaces and surfaces by inelastic-mean-free-path and transport-mean-free-path models. Interestingly, recent published report has demonstrated that the surface sensitivity of Auger electron spectroscopy can be effective to recognize the surface polarities such as O-ZnO(0001) or Zn-ZnO(0001) [1]. Thus, we progressively calculate the similar structure GaN(0001) in order to make a P-N junction structure in the further experiment. Different surface treatment, e.g. ion sputtering and annealing, on a clean crystal surface may damage and vary the surface composition. However, through the quantitative analysis the Auger signal measurement can be more effective to predict the surface polarity in the initial growth. Important issues focus on the surface bonding and interface stacking to affect greatly the optoelectronic transport and related physical properties are discussed and presented.

[1] C.W. Su*, M.S. Huang, T.H. Tsai, S.C. Chang, Applied Surface Science 263 (2012) 174–181.

ASS-6-Or-2
Initial oxidation process of hydrogen-terminated Si(110)-(1x1) surface

T01 Applied Surface Science

#ASS-6-Or-2

S. Suto [1], H. Niimura [1], E. Kawamoto [1], S.Y. Matsushita [1], K. Haga [1], T. Yamada [2].

[1]Department of Physics, Graduate School of Science, Tohoku University - Sendai 980-8578 (Japan), [2]RIKEN - 2-1 Hirosawa, Wako, Saitama 351-0198 (Japan).

Recently, hydrogen-terminated Si(110)-(1×1) [H:Si(110)] surfaces are attracted much attention because the two methods using the Si(110) surface have been intensively studied in order to improve the silicon device, in particular the CMOS circuits. One is the 3D device like Tri-Gate FET proposed by the intel company. The other is the attempt to change substrate from standard Si(100) to Si(110) wafers. However, there is almost no investigations on the initial oxidation process of Si(110) surface. We report here the preparation and oxidation processes of an ultraclean and well-ordered Si(110) surface using the high-resolution electron energy-loss spectroscopy(HREELS).

First, we successfully prepared a well-ordered and ultra-clean H:Si(110) surface by etching a Si(110) wafer in 40% aqueous solution of NH_4F [1,2]. The surface order was verified by LEED and the cleanliness was measured by HREELS. Second, we oxidized the Si(110) surface by atomic oxygen produced by a hot tungsten filament, because the surface is too stable to oxidize by oxygen molecules. Third, we observed the HREELS spectra with increasing the time of exposure in atomic oxygen at room temperature. Fourth, the oxygen coverage was estimated from the peak shift of the Si-H stretching mode; the peak energies are 258.5, 266.5, 273.0 and 280.7 meV for clean surface (H-Si), one oxygen atom adsorption (H-SiO), two ($H\text{-}SiO_2$), and three oxygen atoms ($H\text{-}SiO_3$) adsorption at the first layer Si back bond, respectively. Finally, we carried out Monte Carlo simulations to clarify the adsorption processes.

In the HREELS spectra of the clean Si(110) surface, we observed surface phonon mode at 58.7 meV, Si-H bending mode at 77.5 meV and Si-H stretching mode at 258.7 meV. After the oxidation, new peaks of Si-O-Si symmetric and asymmetric stretching modes appeared at 97.3 and 126.9 meV, respectively, and then, the two

peaks shifted higher energy side with increasing the coverage. Furthermore, the peak and the spectral shape of Si-H stretching mode varied with the oxygen coverage depending on how many oxygen atoms exist at the Si back bonds. We determined the relation between the amount of oxygen adsorption and exposure time, and between the amount of oxygen adsorption and the coverage for each oxidation stage, i.e., Si-H, Si-HO, Si-HO_2 and $SiHO_3$.
We successfully simulated above results with Monte Caro method. On the Si(110) surface, first layer Si-Si bonds form the zigzag chain along [1-10] direction (A bond) and there are another Si-Si bonds between first layer and second layer Si bonds (B bond) [2]. At the coverage lower than 1 monolayer (ML), the oxygen atoms prefer to adsorb to form H-SiO3 where two oxygen atoms exist at A bonds and one oxygen atom at B bonds. The full surface coverage is 3 ML. With increasing the coverage, the oxidation proceeds along the zigzag chain. The present understanding may lead to future possibilities of application of Si(110) surface.

[1] H. Kato *et al*., *Jpn. J. Appl. Phys*. **46** (2007) 5701-5705.
[2] S. Suto *et al*., *Appl. Surf. Sci.* in press.

ESD/ASS-P3-10
Morphological and chemico-physical study of dye-sensitized solar cell counter electrode degradation

T01 Applied Surface Science

#ESD/ASS-P3-10

A. Virga [1], M. Castellino [1], A. Sacco [2], A. Lamberti [2], D. Pugliese [2], S. Bianco [2], A. Chiodoni [2], C.F. Pirri [2].

[1]Politecnico di Torino - Torino (Italy), [2]Center for Space Human Robotics - IIT - Torino (Italy).

Due to the high solar energy conversion efficiency, dye-sensitized solar cells (DSCs) represent one of the most promising new generation devices [1]. A DSC consists of 3 main components: (i) photo-anode sensitized with dye molecules, (ii) hole-conducting material and (iii) counter electrode. The whole structure is sealed using hot-melt sealants to avoid electrolyte leakages and protect cell elements from environment. To better understand the behavior of different DSC components, an in-situ analysis should give a help, but it results difficult to be performed without compromising cell integrity. Our novel microfluidic approach for DSCs fabrication [2] is based on a reversible electrodes sealing and allows cell easy assembling and disassembling, making possible a non-destructive components analysis over time [3]. In this study we focused on the counter electrode, which is made by TCO-covered glass coated with a thin (few nm) Pt layer, deposited by 2 different methods: thermal decomposition of a printable transparent Pt catalyst and thermal deposition. Our goal has been to establish which method produces the most reliable Pt film, which can withstand the time-dependent degradation, due to the DSC inner harsh environment. So detailed morphological (FESEM) (fig.1), optical (UV-Visible spectroscopy) (fig. 2), electrical (EIS) and surface (XPS) characterizations [4] have been performed on the counter electrodes over a period longer than 3 months. The obtained results confirmed that degradation has occurred, leading to a strong decrease of the counter electrode photovoltaic performances.

[1] M Grätzel, Nature 414 (2001) 338-344
[2] A Lamberti et al, Microelectron Eng 88 (2011) 2308-2310

[3] A Sacco et al, Appl Phys A 109 (2012) 377–383
[4]G Syrrokostas et al, Sol Energ Mat Sol C 103 (2012) 119–127

Fig 1: FESEM graphs showing top view Pt counter electrodes: fresh assembled cell (a) thermal decomposed and (c) evaporated, and after 2 weeks (b) thermal decomposed and (d) evaporated

Fig 2: Transmittance spectra after 5 weeks (t = 5 w) and 8 weeks (t = 8 w)

ASS-8-Or-1
Structural and electronic characterization of transition metal nanostructures on vicinal Au(332)

T01 Applied Surface Science

#ASS-8-Or-1

M. Prieto, E. Carbonio, R. Landers, A. De Siervo.

Instituto de Física 'Gleb Wataghin',Universidade Estadual de Campinas, 13083-859 - Campinas (Brazil).

Transition metal nanostructures have been extensively studied for several applications in several areas of research [1,2]. Single crystalline surfaces of high Miller index offer the possibility to model materials of technological interest and study the correlations between electronic and geometrical factors with the role of defects. In this presentation we show the results obtained in the study of the morphology of Co and Pt nanostructures deposited on Au(332) surface, as well as their electronic properties.

Figure 1 shows representative STM images of clean and Co-modified Au(332) surface for the lowest θ_{Co}.

From UHV-STM images, θ_{Co} values were estimated as lying in the 0.15-0.6 ML range. In all cases, terraces present on clean Au surface seem to remain unchanged, i.e. do not seem to brake-up due to the presence of Co nanostructures. Additionally, it is determined from image analysis that Co structures have a height of an atomic bilayer.

On the other hand, no reconstruction of the substrate is detected after deposition or even after thermal annealing (TA) of the sample, where a brake up of steps on the substrate due to an apparent diffusion of Co atoms into the Au lattice. XPS measurements reveal that Co deposited is metallic, as suggested by $Co2p_{3/2}$ binding energy (BE = 778 eV) and the absence of the well-known satellites of Co oxides. Additionally, XPS data confirm Co diffusion into Au crystal after thermal treatment and the extent of Co incorporation into Au matrix is expected to be high. Co-Au alloy formation is discarded at all θ_{Co} investigated, since BE of Co core lines remain unchanged as θ increases.

In the case of Pt, XPS reveals the formation of an Au-Pt alloy is detected at all θ_{Pt} explored, even at low values. When Pt/Au(332) surface is investigated by STM, brake up of steps by Pt atom deposition is observed and surface morphology after

deposition is different from that observed in Co/Au(332). XPS data reveals that TA of Pt/Au(332) enhances alloy formation and, in contrast to the Co/Au(332) system, alloing seems to be favored over atom diffusion.

Thus, experimental results obtained indicate that Co and Pt nanostructures have different structure as well as electronic properties, reflecting the chemical differences between both transition metals. Provided that substrate used is the same, potential differences on reactivity could be explained with our results.

[1] D. L. Fedlheim, et al., in "Metal Nanoparticles: Synthesis, Characterization, and Applications". 2001, Marcel & Dekker.
[2] Z. Quan, et al., *Ac. Chem. Res.*, *in press*, **doi**: 10.1021/ar200293n

Figure 1 STM images for clean and Co-modified Au(332) surface. θ_{Co} = 0.17. Typical tunneling conditions are: I_t= 0.15nA; U_{bias}= 1.7 V.

ASS-10-Or-6
Nano-FTIR: infrared spectroscopic chemical identification of materials at the nanoscale.

T01 Applied Surface Science

#ASS-10-Or-6

M. Böhmler [1], F. Huth [1], S. Amarie [1], F. Keilmann [2], R. Hillenbrand [3].

[1]Neaspec GmbH - Munich (Germany), [2]MPQ - Garching (Germany), [3]IKERBASQUE - Bilbao (Spain).

Fourier-transform infrared (FTIR) spectroscopy is an established technique for characterization and recognition of inorganic, organic and biological materials by their far-field absorption spectra in the infrared fingerprint region. However, due to the diffraction limit conventional FTIR spectroscopy is unsuitable for measurements with nanoscale spatial resolution.

We recently applied the principles of FTIR to scattering-type Scanning Near-field Optical Microscopy (s-SNOM) [1-4]. s-SNOM employs an externally illuminated sharp metallic tip to create a nanoscale hot-spot at its apex which greatly enhances the near-field interaction between the probing tip and the sample. The light backscattered from the tip transmits the information about this near-field interaction to the far zone where the FTIR spectra can be recorded. The result is a novel nano-FTIR technique, which is able to perform near-field spectroscopy and imaging with nanoscale resolution.

Here we demonstrate nano-FTIR with a coherent-continuum infrared light source. We show that the method can straightforwardly determine the infrared absorption spectrum of organic samples with a spatial resolution of 20 nm. Corroborated by theory, the nano-FTIR absorption spectra correlate well with conventional FTIR absorption spectra, as experimentally demonstrated with PMMA samples. Nano-FTIR can thus make use of standard infrared databases of molecular vibrations to identify organic materials in ultra-small quantity and at ultra-high spatial resolution.

As an application example we demonstrate the identification of a nanoscale PDMS contamination on a PMMA sample [4]. In figure 1 the topography image (left) reveals a small sample contaminant (B) next to a thin film of PMMA (A) on a Si substrate (dark region). Comparing the nano-FTIR absorption spectra at the positions A and B with standard IR databases reveals the chemical identity of the film and the particle.

We envision that nano-FTIR will become a powerful tool for chemical identification of nanostructures, for investigation of local structural properties (i.e. defects, strain) of crystalline and amorphous nanostructures, as well as for non-invasive measurement of the local free-carrier concentration and mobility in doped nanostructures.

[1] S. Amarie et al, *Opt. Express* **17**, 21794 (2009).
[2] F. Huth, et al, *Nat. Mater.* **10**, 352 (2011).
[3] S. Amarie, et al, *Beilstein J. Nanotechnol.* **3**, 312 (2012).
[4] F. Huth, et al, *Nano Lett.* **12**, 3973 (2012).

Left: AFM topography image of a thin PMMA film (A) on a Si substrate indicates the presence of a 100 nm size contamination B. Right: Nano-FTIR allows for chemical identification of film and particle.

ESD/ASS-P3-06
Properties of nanolaminate structures with granular conductivity and its PV applications

T01 Applied Surface Science

#ESD/ASS-P3-06

A. Harizanova, P. Vitanov, C. Dikov, T. Ivanova.

Central Laboratory of Solar Energy and New Energy Sources, Bulgarian Academy of Sciences - Sofia (Bulgaria).

Properties of nanolaminate structures with granular conductivity and its PV applications
P. Vitanov, Ch. Dikov, A. Harizanova and T. Ivanova
Central Laboratory of Solar Energy and New Energy Sources,
Bulgarian Academy of Sciences, blvd. Tzarigradsko chaussee 72, Sofia, Bulgaria

The rapidly increasing use of transparent and conductive oxide (TCO) films for photovoltaics has promoted the development of inexpensive materials and low cost technological processes. Most of the TCO films are binary or ternary compounds containing one or two metallic elements. The combination of conductivity and transparency is impossible to obtain in intrinsic or undoped stoichiometric oxides. For obtaining high conductivity in these materials, either they have to be nonstoichiometric in composition or should be doped with appropriate element. The aim in this study is formation of a conductive area in nanolaminate dielectric structure. Physical base is the idea is to use an electronic conductivity in granular materials. The granules are arrays of metallic particles of sizes ranging from a few to hundred of nanometers embedded into an insulating matrix.
The nanolayer structure is formed using one or two dielectrics. The electrical conductivity is modified with planar located metal granules. The advantages are reproducibility of technological parameters, effective methods for process control and a selective formation of conductive areas in dielectric structure. It must be noted that the conductivity area of the nanolaminate structure is transparent. The optical transmittance and the sheet resistance are function of the density of the metal nanoparticle in the middle layers.
A transition from an insulating to a metallic conductivity can be explained by the increase in carrier concentration and formation of a degenerate band. Usually TCOs

have semiconductor behaviour as negative temperature coefficient of receptivity (TCR). The nanolaminate structure with metal granulate demonstrate the metallic conductivity as it has a positive TCR. Therefore the carriers are delocalized due to thermal activation and conductivity is dominated by phonon scattering.

The electrical conductivity can be obtained of the nanolaminate structures with dielectrics such as TiO2, Al2O3 and (Al2O3)x(B2O3)1-x, deposited as a first layer on substrate. The electrical conductivity depends on dielectric type and on its thickness. The contact of the nanolaminate structures with p –Si is ohmic.

Surface morphology of nanolaminate structure with (Al2O3)x(B2O3)1-x as “bottom”layer and selective formed conductive area are studied by AFM microscopy. The conductive area is average 5 nm higher than the non conductive one as it can be observed from the section analysis. The reason for this is the effect of the metal granules. The electrical properties of the “conductive” and “dielectric” areas are investigated.

Chemical liquid deposited (Al2O3)x(B2O3)1-x has been included as “bottom”layer of the nanolaminate structure, where selective conductive areas are formed. The good passivation properties of (Al2O3)x(B2O3)1-x can be used and the possibility to form local contacts without etching or laser ablation. The proposed technological approach is perspective for rear passivation and metallization of high efficiency silicon solar cells.

ASS-8-Or-9
Surface characterization of Pt thin films on Si substrates during ion bombardment

T01 Applied Surface Science

#ASS-8-Or-9

A. Hervier, D. Aureau, A. Etcheberry.

Institut Lavoisier de Versailles - Versailles (France).

Ion bombardment techniques have become common tools in a wide variety of applications, from tribology to microelectronics or materials toughening. The common feature of these techniques is that they all produce surface effects, which can be readily characterized.

We present the results of an extensive investigation into the effects of ion bombardment on Pt thin films on Si, at energies high enough to induce phase mixing.

Figure 1 shows the Pt/(Pt+Si) ratio, determined by XPS, of Pt/Si films subjected to different doses of ion bombardment, starting from a fresh, completely covered film, to a mixed surface with no elemental platinum left. A transition is visible at which point the film breaks up and the silicon becomes detectable. AFM measurements show that this transition coincides with a maximum in the roughness of the film and, according to XPS measurements, with the formation of a platinum silicide phase at the surface, as explained in Figure 2.

Features of the platinum film disappear in SEM images with increasing dose. Auger nanoprobe analysis shows that no silicon or silicon oxide is exposed at the surface at the doses used here. Instead, the entire surface consists of platinum silicide.

Previous work has shown that the electronic structure of silicon can vary depending on the type of surface preparation. Effective dopant concentrations, flat-band potentials, or reverse dark currents for example, strongly depend on whether the surface has been mechanically or mechanochemically polished, or chemically etched. Ion bombardment can be thought of as another pre-treatment process, the effects of which can be observed with a combination of surface characterization techniques.

Fig.1 – Pt/(Pt+Si) surface ratio determined by XPS measurements of Pt/Si surfaces subjected to nitrogen ion bombardment

Fig. 2 – XPS Pt4f spectra of samples subjected to increasing doses of helium ion bombardment. The dashed arrow shows the transition from Pt/Si on an as-deposited sample to PtxSi as the ion dose increases. The +1 eV energy shift under ion bombardment is characteristic of the formation of a mixed PtxSi phase.

ASS-2-Or-10
Iron oxide surface engineering: synthesis of magnetically retrievable nano-organocatalysts.

T01 Applied Surface Science

#ASS-2-Or-10

E. Nehlig [1], L. Motte [2], E. Guénin [2].

[1]Université Paris 13, Sorbonne Paris Cité, Laboratoire CSPBAT, - Bobigny (France), [2]Université Paris 13, Sorbonne Paris Cité, Laboratoire CSPBAT - Bobigny (France).

In the past decades, interest for new catalysts and new catalytic reactions increases greatly due to their large applications in several domains such as pharmaceutical and chemical industries. New catalysts were described for an increasing number of organics reactions. Nevertheless, most of the homogenous catalysts are difficult to adapt to industrial process due to separation and regeneration problems. Moreover, though highly efficient, most of the catalysts are containing noble or toxic metals and so new protocols more economically and environmentally friendly need to be developed. The use of magnetic nanoparticles [1] as a catalysts support in organic synthesis has become a subject of intense investigation because they appear as an ideal solution for solving these catalytic problems.
The present project purpose is to mix two new approaches: nano-catalysis and organocatalysis [2] in order to develop new greener nano-organocatalysts. The hybrids are obtained from the grafting of well known organocatalysts (Amino acids, peptides, alkaloids) at the surface of superparamagnetic iron oxide nanoparticles. The 10 nm nanoparticles synthesized by mild conditions [3] in water are stabilized by bidendate coating agent (e.g. bisphosphonates) with a terminal function which enable the post functionalization (grafting from approach) of the particles with organocatalysts. The functionalization is done in aqueous media using microwave-assisted and or click chemistry protocols [4]. A grafting to methodology was also tested in order to modulate the number of catalysts per nanoparticles, using a pre-synthesized organocatalyst bearing a bisphosphonate moiety. These new hybrids are then characterized (TGA, EDX, TEM, IR, UV-visible, MIAplex, MIAtek) and tested for their ability to catalyzed known organic reactions (e.g. enantioselective aldolisation, Michael additions). A Proline loading between 0.12 and 0.15 mM.g-1 was determined

for the different kind of grafting. First results with these new nano-organocatalysts [5] are promising as in some cases yield >95% are obtained with >0.2% mol.

[1]Q. Dai, A. Nelson, Chem. Soc. Rev., 2010, 39, 4057-4066.
[2] P. Melchiorre, M. Marigo, A.Carlone, G. Bartoli, Angew. Chem. Int. Ed. 2008, 47, 6138-6171.
[3] L.Motte, F. Benyettou, C.de Beaucorps, M.Lecouvey, I.Milesovic, Y. Lalatonne, Faraday Discuss. 2010, 149, 211-225.
[4] a) F. Benyettou, E. Guenin, Y. Lalatonne, L. Motte, Nanotechnology. 2011, 22, 055102. b) E. Guénin, J. Hardouin, Y. Lalatonne, L. Motte, J Nanopart. Res. 2012, 14, 7, 965.
[5] E. Nehlig, L. Motte, E. Guénin, Nanocat. Today 2012, accepted DOI: 10.1016/j.cattod.2012.10.027.

BI/ASS/NST-P1-07
Development of Fe3O4-SiO2 films by sol-gel dip-coating method onto pretreated glass surface

T01 Applied Surface Science

#BI/ASS/NST-P1-07

J. Setina, G. Mezinskis, A. Gabrene, A. Pludons, I. Juhnevica.

Riga Technical University - Riga (Latvia).

Obtaining thin films of SiO_2/Fe_3O_4 nanoparticles by sol-gel dip-coating method on the glass involve several stages: preparation of glass surface, preparatory period by creation of substrate for thin films, choice of coating technology.
The soda-lime-silicate glass microscope slides were etched in different solution such as NaOH, H_2SO_4, HF. Etching methods enlarge surface area and generate a new surface by removing material from original glass. Surface property and morphology of glass are changed by all methods of etching. Hydrothermal treatment with NaOH caused hydroxyl ion attack to silica network, converting bridging oxygen into a non-bridging one, thus disrupting the network. Gel-like layer formed during etching by NaOH solution typically provided smoothening effect of surface. Topography and measurements of surface roughness obtained by AFM channel like structure showed. Structured glass surface with holes and cavities could be obtained by combinations of etching media (H_2SO_4 or HF). The atomic percentage of sodium on surface decreases by treatment with H_2SO_4. Morphology of glass surface treated by H_2SO_4 changed dependently on treatment time: R_q-8,558 nm (1h); R_q-3,313 nm (2h); R_q-2,500 nm (20h).
Second step was – preparation of magnetic nanoparticles Fe_3O_4 using coprecipitation method. A coprecipitation in alkaline media starting a mixed $FeSO_4 \cdot 7H_2O/FeCl_3 \cdot 6H_2O$ solution with a molar ratio of Fe^{2+}/Fe^{3+} = 0.5.
Two sol-gel dip-coating methods of production multilayer films of SiO_2/Fe_3O_4 nanoparticles were used: adding of prepared magnetite direct to SiO_2 sol and encapsulation magnetite between two SiO_2 sol-gel layers. Better quality was for sandwich type films obtained by encapsulation magnetite.
The films consisted three layers on a glass substrate. The first and third layers were a SiO_2 prepared by dip-coating from tetraethylortosilicate solutions and subsequent calcination at 500°C temperature in air. The second layer was prepared by dip-coating from the aqueous colloidal dispersion of previously synthesized magnetite.

The average size of synthesized magnetite nanoparticles was estimated to be c.a. 15 nm. The calcined films reported here exhibit crack-free morphology, consisting of aggregated silica/magnetite nanoparticles. Future controlled advancement of this method could provide a low cost solution for mechanically stable composite thin films with various, technologically useful, properties.

Acknowledgment:
This work has received a financial support of the ERDF “Development of solar heat absorbing materials by means of sol-gel and vacuum technologies” (Project No 2DP/2.1.1.1.0/10/APIA/VIAA/156).

ASS-9-Or-1
Templated substrate; New approach to modify self-assembled molecular structures

T01 Applied Surface Science

#ASS-9-Or-1

M. S. Baviloliaei [1], D. Lei [2], N. Lin [2], L. Diekhöner [1].

[1]Department of Physics and Nanotechnology, Aalborg University - Aalborg (Denmark), [2]Department of Physics, Hong Kong University of Science and Technology - Hong Kong (Hong kong).

The design and fabrication of nanostructures at the molecular scale is a key to develop devices with nano-scale precision and ultrahigh efficiency [1]. One of the promising techniques at this point is Self-assembly which gives a very good opportunity to play with molecules and atoms in the bulk and on the surface. By understanding and predicting the possible interactions (molecules-molecule, surface-molecule) existing in the system it is possible to design and create the desired pattern [2]. Molecules with aromatic ring to enhance the interaction with the metal surfaces and functional groups to form multiple H-bondings or metal-organic coordinations are ideal for the supramolecular self-assembly [2,3].
Here we have studied the role of a modulated surface on the self-assembly of organic molecules promoted via either H-bonding or metal-organic coordination. As a substrate we used one monolayer of Ag on Cu(111), which grows in step-flow mode allowing us to fabricate large islands or even cover the entire surface [4,5]. Due to a lattice mismatch, the Ag layer makes a (9x9) reconstruction leading to a Moiré pattern structure with nanometric modulation.
Trimesic acid (TMA) molecule with three functional group for H-bonding, were studied with STM on the Ag/Cu(111) surface and the results were compared with structures formed on flat Ag(111) and Cu(111) surfaces. TMA formed honey-comb pattern on Ag(111) and Cu(111) at room temperature but after annealing to 420K it converted to quartet and close-packed structures, respectively. The experiments on modulated Ag/Cu(111) surface showed an irregular structure at room temperature which indicated that the surface disturbed the self-assembly. Upon annealing it was possible to recover a long range order (quartet structure) on the surface. This quartet structure could be distinguished from the structure formed on Ag(111) by the alignment of the pattern and density of molecules.

We have also studied 1,3,5-trispyridylbenzene (TPyB), which is capable of forming metal-organic network with Cu atoms. The intermolecular interactions are stronger than those of the H-bonded TMA and we therefore expect less influence of the modulated substrate. TPyB/Cu forms a honey-comb structure on Au(111), Cu(111) as well as on the Ag/Cu(111) surfaces. STM images revealed two distinguished phases of honey-comb pattern on the modulated surface. We observed that the molecular structure either undergoes a small structural distortion of the individual hexagons in the honey-comb layer or preserves the undistorted honey-comb shape while rotating slightly from the Moiré pattern alignment.
These experiments indicate that the use of templated substrates like Ag/Cu(111) could be a new approach to manipulate self-assembled structures to modify them for the possible applications.

[1] J. V. Barth, G. Costantini, K. Kern, Nature 437, 671 (2005).
[2] Angelika Kühnle, Current Opinion in Colloid & Interface Science 14, 157 (2009).
[3] N. Lin, S. Stepanow, M. Ruben, J. V. Barth, Top. Curr. Chem. 287, 1 (2009).
[4] A. Bendounan et al, Europhys. Lett. 64, 392 (2003).
[5] E. Bauer, Surface Science 7, 351 (1967).

ESD/ASS-2-Or-6
Multi-technique approach on thin photovoltaic films characterization: demonstration on CIGSe absorbers

T01 Applied Surface Science

#ESD/ASS-2-Or-6

D. Mercier [1], M. Bouttemy [1], J. Vigneron [1], I. Gerard [1], P. Chapon [2], N. Naghavi [3], J.F. Guillemoles [3], J.L. Pelouard [4], D. Lincot [3], A. Etcheberry [1].

[1]Institut Lavoisier de Versailles - Versailles (France), [2]Horiba - Longjumeau (France), [3]Institut de Recherche et Developpement sur l'Energie Photovoltaïque - Chatou (France), [4]Laboratoire de Photonique et de Nanostructure - Marcoussis (France).

Absorbers based on thin films technology and in particular CIGSe (Cu(In,Ga)Se2) are a good alternative to Silicon wafers for highly efficient photovoltaic cells. Currently, CIGSe record efficiencies reach a 20.3% value in laboratory and 13% at the industrial scale. Performances of photovoltaic cells mainly rely on the absorber properties. In the context of understanding and improving cells performances, it is therefore important to control the chemistry (composition, impurities…) in the bulk, at the surface and at the interface of absorbers. This work suggests a multi-technique approach based on ICP-OES (Inductively Coupled Plasma- Optical Emission Spectroscopy), GD-OES (Glow discharge- Optical Emission Spectroscopy) and XPS depth profiling methods to characterize CIGSe absorbers.
The first approach consists in probing the CIGSe absorber depth composition usin real time ICP-OES dosage of the absorber constituents during a chemical etching based on acidic bromide solution (HBr/Br2)... In parallel, XPS analyses are carried out on CIGSe samples having undergone a chemical etching for different durations giving a direct access to the absorber depth composition at specific depth location. A good agreement is found by those both technics indicating the absence of chemical modifications of the absorbers surface.
Secondly, a plasma etching is realized by GD-OES. Chemical composition and impurities are measured. XPS analyses (probe size 400µm) are also performed in the GD crater (2-8 mm) after different etching time in order to calibrate GD-OES depth composition profiles and evaluate surface modifications (roughness effect).

Finally, a direct XPS depth profile using Ar sputtering is carried out on a CIGSe sample for which the thickness has been reduced by chemical treatment from 2.5 µm to 0.5 µm to characterize the Cu/Mo interface. Optimization of the fitting procedure of the main elements Cu, Ga, In and Se permits to precisely determine the chemical environments. . The MoSe2 interface is clearly observed between the CIGSe back-side interface and the molybdenum substrate.
To conclude, a multi-techniques depth profiling approach (ICP-OES/XPS, GD-OES/XPS, XPS) is developed whose aim is to get complementary information on the whole absorber material (surface, bulk and interface) and allow a better understanding of the relation between the absorber composition and photovoltaic cell performances.

XPS depth profile of a CIGSe-Mo interface

ASS-P3-16
Effect of Surface Modification of crystalline and amorphous SiC thin films : optical and structural properties

T01 Applied Surface Science

#ASS-P3-16

A. Keffous.

C.R.T.S.E - Algiers (Algeria).

In this work, we study the effect of surface modification (ESM) on optical and structural properties of porous and unporosified hydrogenated amorphous silicon carbide (PASiC) and porous crystalline silicon carbide (PSiC) thin films deposited onto p-Si(100). The thin films are elaborated by a d.c. magnetron sputtering and laser ablation system and electrochmical etching to perform a porofication, compared to irradiated laser (KrF) of unporosified same thin films forming pillars structure. The porous structure of the SiC layer deposited was developed by an electrochemical (anodization) method.
For unhydrogenated films, an early birth of nano and micro pillars was observed after irradiation with 1 to 80 laser shots. However, a large number of shots is needed, from 2400 to 7200, to form micropillars on 6H-SiC bulk It is showed that the dimension and density of pillars depend on the sample nature, shots number and irradiation energy. Finally, it is demonstrated that the luminescence intensity increases with number of laser shots for the thin films. The films were investigated by UV-visible spectrophotometry, infrared spectroscopy (FTIR), secondary ion mass spectroscopy (SIMS), Scanning electron microscopy (SEM), Raman spectroscopy and photoluminescence spectrophotometry (PL).

ESD/ASS-1-Or-1
Electroless nickel deposition on silicon: nucleation and annealing study

T01 Applied Surface Science

#ESD/ASS-1-Or-1

H. El Belghiti [1], D. Aureau [2], E. Delbos [1], M. Bouttemy [2], A. Etcheberry [2].

[1]Institut Lavoisier de Versailles - OMG UPC - Versailles (France), [2]Institut Lavoisier de Versailles - Versailles (France).

One of the major challenges in the photovoltaic field today, and particularly for the silicon solar cells, is to replace the contact lines made by silver past. Indeed, the contact lines must be optimized in order to both increase the solar cells efficiency and reduce the cost of manufacturing.
Several materials and processes are considered. Electrodeposited copper lines are one of these ways. However, the copper diffusion throughout the silicon substrate, leading to the degradation of the solar cell efficiency, must be avoided. In order to overcome that, one solution is to deposit a nickel layer between the silicon substrate and the copper lines (1,2). In this research works, an electroless nickel process has been chosen.
The main goal is the deposition of a thin, homogeneous, continuous and adherent nickel layer. For that, it is necessary to precisely control the nickel layer growth. Consequently, the first stages of the nickel nucleation on the silicon and the final layer composition, after the annealing, are especially studied.
Therefore, thanks to SEM imaging (figure 1), XPS (figure2) and nano-Auger analyses, a specific work dedicated to the study of the nickel nucleation on silicon substrate is proposed. In a second part, the influence of the annealing temperature on the composition, crystallinity and adhesion of this nickel layer was studied and monitored by EDX, EBSD and XPS analyses.

1- S. Karmalkar, R. Marjorie and V. G. Sumithra, J. Adhesion Sci. Technol. 16 (11) p. 1501 (2002)
2- S. Subir, P. Siddharth, R. B. Tokas, A. K. Poswal and Sangeeta, Bull. Mat. Sci. 31

(5) p. 729 (2008)

Figure 1: SEM analysis of the evolution of the nickel nucleation with the plating time

Figure 2: XPS depth profile: composition of the electroless nickel layer before annealing

ASS-P2-02
Surface Oxidation and Reduction in Titanium Metal Injection Molding

T01 Applied Surface Science

#ASS-P2-02

W. Lee, J.M. Jang, H.J. Lee, S.H. Ko.

Korea Institute of Industrial Technology - Incheon (Korea, republic of).

Metal Injection Molding (MIM) is a near net shape manufacturing method and a cost-effective and flexible manufacturing technique that provides a large innovative potential over existing methods for the industry[1]. Recently, considerable progress in powder injection molding of titanium and its alloys has been accomplished. However, cost of raw materials, especially for gas atomized powders, is still a limiting factor for a number of applications[2-4]. In this work, the formation and dissolution of titanium oxide layer in metal injection molding process were investigated using TiH_2 feedstock (a mixture of about 300 nm-sized TiH_2 powder and binder such as wax and polymer). The TiH_2 powder was produced by ball milling of titanium turning chips in room temperature under hydrogen atmosphere titanium turning chip. After injection molding using the feedstock, subsequent debinding process to remove binder was performed through heating up to 600^oC under flowing high purity hydrogen gas containing 1.8 ppmO_2 and 1.03 ppmH_2O. During debinding, thin Ti_2O and/or Ti_3O oxide layer was formed on surface of the molded part in spite of use of high purity gases and the surface appeared dark-blue. However, after sintering of the debound part at 1250^oC in high vacuum of $6.7x10^{-3}$ Pa, the oxide layer disappeared and any oxide peaks were not observed in XRD analysis, showing bright grey color. The reduction mechanism of the Ti_2O and/or Ti_3O oxide layer is considered as two kinds: one is a reduction due to reaction of titanium oxide and residual carbon after debinding. An amount of residual carbon in samples after debinding was measured to 0.57 wt% and thus, during sintering, titanium oxide is reduced by reaction with residual carbon, releasing CO gas. The other is decomposition of metastable Ti_2O and/or Ti_3O phase. The metastable oxide is decomposed at high temperature in high vacuum and then, oxygen atoms diffuse inside titanium part.

[1] A. Kei, K. Yasunari, I. Hiromichi and T. Masaharu, Adv.Powder Metall. 3, 121 (1989)

[2] F. H. Froes, Metal Powder Report 61, 11 (2006)
[3] T. Ebel, PIM International 2, 2 (2008)
[4] R. Zhang, J. Kruzewski and J. Lo, PIM International 2, 2 (2008)

ESD/ASS-P3-07
Microstructure of µc-Si:H films prepared by PECVD when used different substrates

T01 Applied Surface Science

#ESD/ASS-P3-07

M. Netrvalova [1], P. Sutta [1], P. Calta [1], L. Prusakova [1], V. Vavrunkova [1], I. Novotny [2], V. Tvarozek [2].

[1]University of West Bohemia - Pilsen (Czech republic), [2]Slovak University of Technology - Bratislava (Slovakia).

Tandem solar cell is a one of the concepts well established as a way how to improve solar cell performance beyond that of a single cell. Taking into consideration the thin-film silicon solar cell technology, microcrystalline silicon (µc-Si:H) is very important for this purpose [1]. The µc-Si:H is usually prepared from silane diluted with hydrogen or from silane mixed with argon and diluted with hydrogen by using PECVD [2]. In order to obtain µc-Si:H films of a good quality, their structural and optical properties have to be carefully monitored by X-ray diffraction, Raman and FTIR spectroscopies as well as by UV Vis spectrophotometry and spectroscopic ellipsometry [3]. Developing microcrystalline silicon thin films corning glass is usually used as a substrate for detailed observation its physical properties. Nevertheless, in thin films solar cell configuration the silicon film is deposited on transparent conductive oxide. The aim of this work was to evaluate whether the substrate used influence the microstructure of the film when using the same deposition conditions.
Microcrystalline Si films near the same thicknesses (360 – 410 nm) were deposited on the Corning glass and aluminium doped zinc oxide substrates from silane mixed with argon (90% Ar / 10% SiH4) and diluted with hydrogen using PECVD. Silane diluted with hydrogen (R = H2/SiH4) was applied at levels from R = 20 to 70. In order to ascertain the physical properties of the films the experimental methods mentioned above were used.
X-ray diffraction indicated that regardless of substrate used the films with dilution R = 20 are amorphous, whereas the films with higher dilution R >= 40 are microcrystalline (mixture of amorphous and crystalline phases). Average crystallite size of crystalline phase is in the range of 10 to 20 nm. These results were confirmed also by Raman

and FTIR spectroscopies. Substrates used in this work do not influence too much the microstructure of the films.

The result was developed within the CENTEM project, reg. no. CZ.1.05/2.1.00/03.0088, co-funded by the ERDF as part of the Ministry of Education, Youth and Sports' OP RDI programme.

[1] A. V. Shah, H. Shade, M. Vanecek, J. Meier, E. Vallat-Sauvain, N. Wyrsch, U. Kroll, C. Droz and J. Bailat, "Thin-film Silicon Solar Cell Technology", Progress in Photovoltaics: Research and Applications 2004, 12, 113.
[2] P. Chaudhuri, R. Meaudre, C. Longeaud, "Argon dilution of silane as an alternative to hydrogen dilution for stable and high efficiency silicon thin films solar cells", Journal of Non-Crystalline Solids, 338-340 (2004) 690-693.
[3] P. Sutta, M. Netrvalova, J. Müllerova, L. Prusakova, J. Ocenasek, „Microstructure determination of μc-Si:H analyzing of breadths of diffraction and spectral lines of XRD, Raman and FTIR spectroscopies using the Voigt function", In Proceedings of the 27th EU PVSEC, Sept 24-28, 2012 Frankfurt (Germany).

ESD/ASS-1-Or-5
Non-contact electrical characterization of selected inner domains and interfaces in solar cell devices

T01 Applied Surface Science

#ESD/ASS-1-Or-5

H. Cohen.

Weizmann - Rehovot (Israel).

The inability of existing electrical tools to probe selected inner domains is a critical problem in device characterization and nanoscale fundamental studies. In particular, measuring internal junction fields is essential for realistic construction of band diagrams and device optimization. An answer to this problem is provided by chemically resolved electrical measurements (CREM) [1,2], an essentially non-contact technique that extracts electrical information from x-ray ejected photoelectrons. Applied to multi-interfacial solar cells, key features of the CREM methodology are introduced, including detailed evaluation of the internal fields and band offsets and, furthermore, the quantification of internal dynamic distortions under external stimuli. Problem solving gained by this improved feed-back tool is demonstrated.

1. I. Doron Mor, A. Hatzor, A. Vaskevich, T. van-der Boom-Moav, A. Shanzer, I. Rubinstein, H. Cohen, Nature 406, 382 (2000)
2. H.Cohen, Appl. Phys. Lett. 85, 1271-3 (2004).

SE/ASS-1-Or-1
Interfacial toughness determined from periodic buckling patterns

T01 Applied Surface Science

#SE/ASS-1-Or-1

S. Grachev [1], J.Y. Faou [1], G. Parry [2], E. Barthel [1].

[1]Surface du Verre et Interfaces, UMR 125 CNRS/Saint-Gobain - Paris (France), [2]SIMaP-Laboratoire de Thermodynamique et Physico-Chimie Métallurgiques - Grenoble (France).

Thin films spontaneously buckle under compression forming blisters of various shapes. When attached to a substrate, the buckling phenomenon is restricted by adhesion to the substrate. On one hand, the film buckling is described by the non-linear Föppl–von Kármán equations and has been well reproduced by finite element method (FEM) simulations. On the other hand, the delamination process involves the fracture of the interface under a mixed mode loading (both with normal and shear forces), which influences the energy needed to crack the interface, that is the interfacial toughness. The interplay between the biaxial stress relaxation and the interfacial toughness often results in formation of periodic patterns, as telephone-cord-like blisters. Recently we have shown the importance of taking into account both phenomena [1]. In the current work we make a step further and study the critical conditions for the blisters to branch and to form periodic two-dimensional networks. The parameter's space was thoroughly studied by FEM simulations. We show that the period of a blister rather than its width is defined by the parameters of the system (stress, thickness, materials properties and the interfacial toughness). This relationship provides practical means to estimate the interfacial toughness. Branching and blister networks can form in a certain area of the parameter space, and their period can be predicted. The results of simulations are confirmed by experimental observations of buckling of the sputter-deposited films. In particular, the self-organized hexagonal network was both simulated and observed experimentally with the period of features of ~10 μm.

1. Faou, Parry, Grachev, Barthel, Phys.Rev.Lett. v.108, 2012.

ASS-4-Or-2
From sea urchin to catalyst for CO2 hydration reaction

T01 Applied Surface Science

#ASS-4-Or-2

L. Siller, G. Bhaduri.

Newcastle University - Newcastle Upon Tyne (United kingdom).

The biomineralisation process occurs at room temperature, at atmospheric pressure and is relatively fast. It is commonly accepted that the biomineral growth is assisted by the Carbonic anhydrase (CA) enzyme, however it is also been suggested that the bioaccumulated metal elements may also play some role, perhaps more than just the nucleation sites for calcification. Mimicking the biomineralisation process is important in many areas, such as medical implants or carbon capture. The two major parts in mineralization of carbon dioxide include conversion of carbon dioxide to carbonic acid followed by neutralization of the acid; the rate limiting step being the hydration of carbon dioxide to carbonic acid. The storage of CO2 as a mineral salt has been identified as one of the safest method of carbon capture and storage (CCS).
In this study, we report the use of novel catalyst (discovered from biommicking mineralisation in sea urchins) to catalyse the reversible hydration of CO2 at room temperature and atmospheric pressure [1,2]. We observe that the catalyst increase the CO2 uptake capacity of water. The catalytic activity is pH independent (of the starting value of pH of water 6.2-5.5) and catalysts are water insoluble and can be easily separated from the reaction mixture. The reaction steps are characterised using X-ray photoemission spectroscopy and a possible reaction mechanism has been discussed. We also observe an enhancement in the activity of the catalyst as a function of the increase in temperature.

[1] L. Šiller, G. Bhaduri, ‘Carbon Capture’, Appl. No. P202887GB, 15th May 2012

[2] G. Bhaduri and L. Šiller, Catalysts for reversible hydration of carbon dioxide for mineralization carbon capture and storage, submitted

ASS-10-Or-5
New generation Auger nanoprobes: the challenge of spatial chemical nanometric resolution

T01 Applied Surface Science

#ASS-10-Or-5

M. Bouttemy [1], P. Yadav [1], E. Martinez [2], D. Aureau [1], O. Renault [2], J.M. Hartmann [2], E. Delbos [3], H. El Belghiti [3], A. Etcheberry [1], A. Chabli [2].

[1]Institut Lavoisier de Versailles, UMR CNRS-UVSQ 8180, 45 av. des Etats-Unis - Versailles (France), [2]CEA, LETI, MINATEC Campus, 17 rue des Martyrs - Grenoble (France), [3]OMG Ultra Pure Chemicals, Les Vieilles Hayes - Saint-Fromond (France).

In recent years, Auger spectroscopy has been neglected on benefit of X-Ray photoelectron spectroscopy giving an easier access to the surface composition and chemical shift. Indeed, thanks to new generation electron sources, developed for high resolution microscopy, ultimate probe size of 10 nm are achieved[1,2] with the new generation Auger nano-probes. Such equipments are therefore promising tools to address the need of localized chemical characterization of cutting edge structures whose dimension are reaching the nanometric scale on which “classical” XPS (X-Ray source) is not well adapted. In addition, with energy resolution of 0.1 % (at 2000 eV), nano-Auger electron spectroscopy is not only able to give information about the composition but also, when the chemical shift is high enough, on the chemical environment.

The present work is dedicated to the determination of ultimate performances of nano-Auger spectroscopy. The lateral resolution is evaluated on a certified reference sample, BAM-L200 (« Bundesanstalt für Materialforschung und prüfung »), constituted of a stack of alternated lines of $Al_{0.7}Ga_{0.3}As$/GaAs with variable intervals ranging from 700 to 7 nm. Results obtained with the different acquisition modes (point, line profile or mapping) will be presented (figure 1). Complementary AFM and XPS measurements will permit to extend the discussion about the impact of topography or surface oxidation state on the spatial resolution and on the detection limit. The capabilities of nano-Auger on practical cases are also presented. The question of the origin of the Auger signal with the topography of the sample and the

geometry of electrons collection is approached on a textured Si wafer presenting Ni nuclei. The accuracy of Auger quantification is tested on a SiGe multilayer sample[3] with Ge concentration varying within the cross section from 6 to 30% (X-Ray diffraction calibration) by 300-500 nm steps.

[1] K. Tsutsumi, JEOL news 41(1), 46 (2006).
[2] S. R. Raman, D. F. Paul, J. S. Hammond and K. D. Bomben, Microscopy Today 19(2), 12 (2011).
[3] P. K. Yadav, E. Martinez, F. Bertin, M. Bouttemy, E. De Vito, O. Renault, J. M. Hartmann, A. Etcheberry and A. Chabli, IOP Conf. Series: Materials Science and Engineering 41 (2012) 012020.

Figure 1. Al-LVV et Ga-LMM Auger line profiles and SEM image of the corresponding analysis area on a certified BAM-L200 reference sample (30 kV, 10 nA). The $Al_{0.7}Ga_{0.3}As$/GaAs stack is presented on top.

ASS-2-Or-12
MnCl porphyrins on the Ag(111) surface: axial ligand transformation

T01 Applied Surface Science

#ASS-2-Or-12

B. Murphy [1], S. Krasnikov [2], N.N. Sergeeva [3], A.A. Cafolla [2], A. Preobrajenski [4], O. Lübben [1], A. Chaika [1], M.O. Senge [3], I. Shvets [1].

[1]Centre for Research on Adaptive Nanostructures and Nanodevices (CRANN), Trinity College Dublin - Dublin 2 (Ireland), [2]School of Physical Sciences, Dublin City University, Glasnevin - Dublin 9 (Ireland), [3]SFI Tetrapyrrole Laboratory, School of Chemistry, Trinity College Dublin - Dublin 2 (Ireland), [4]MAX-lab, Lund University, Box 118, S-22100 - Lund (Sweden).

The 3d transition metal porphyrins are very stable planar complexes with extensive applications in catalysis, nonlinear optics, enzyme models, sensors and molecular electronics. Since the practical application of metalloporphyrins is closely related to their underlying unique electronic structures, their investigation has remained a subject of intense research for several decades.

In the present work, scanning tunnelling microscopy (STM), x-ray absorption (XAS) and core-level x-ray photoemission spectroscopy (XPS) were used to study the self-assembly and the central ligand transformation of the surface-supported monolayer of {5,10,15,20-tetraphenylporphyrinato}Mn(III)Cl (MnClTPP).

When deposited onto the Ag(111) surface at room temperature, the MnClTPP molecules self-assemble into large well-ordered molecular domains with a close-packed square structure. In the MnClTPP overlayer, each molecule has a flat orientation on the surface with the molecular plane lying parallel to the substrate. Depending on the applied bias voltage, the axial Cl-ligand can be resolved by STM, and is observed to point out of the plane of the molecule into the vacuum.

Annealing the MnClTPP layer on the Ag(111) surface up to 510 K leads to changes in the molecular structure, keeping the monolayer intact. At this temperature, the chlorine ligand desorbs from the porphyrin, leaving the oxidation state of the central Mn(III) unchanged. The Mn(III)TPP is stabilised through interaction with the substrate, and the Ag(111) surface acts as a fifth ligand for the metal centre.

When the MnTPP molecules are exposed to molecular oxygen, the oxidation state of the central Mn is observed to change from Mn(III) to Mn(IV), as confirmed by XAS, and O_2 is bound to the central Mn ion in peroxide form. The presence of oxygen in the centre of the porphyrins is confirmed by STM, and this oxygen ligand can be manipulated by the STM tip.

This oxidation is reversible. Further annealing at 445 K reduces the O_2-Mn(IV)TPP complex back to Mn(III)TPP/Ag(111), removing the peroxide ligand, and allowing the process to be cycled. However, exposure of the MnClTPP layer to O_2 exhibits no direct substitution of the Cl ligand by O_2.

The activation energies for Cl and O_2 removal, derived from the Arrhenius equation using Cl 2p and O 1s XPS data, were found to be 0.35 eV ± 0.02 eV and 0.26 eV ± 0.03 eV, respectively.

Schematic model of axial ligand transformation. When MnClTPP is annealed to 510 K, the Cl ligand is removed. This MnTPP complex is stabilised by the Ag(111) surface (not shown). Mn(III)TPP can then be oxidised to form O_2-Mn(IV)TPP. Finally, the O_2 ligand can be removed by annealing to 445 K.

ASS-8-Or-7
Secondary electron emission of technical silver plating conditioned by electron irradiation

T01 Applied Surface Science

#ASS-8-Or-7

L. González [1], V.C. Nistor [1], L. Aguilera [2], I. Montero [2], D. Raboso [3], U. Wochner [4], R. Cimino [5], L. Galán [1].

[1]Departamento de Física Aplicada, Universidad Autónoma de Madrid - Madrid (Spain), [2]Instituto de Ciencia de Materiales de Madrid, CSIC - Madrid (Spain), [3]High Power RF Laboratory, ESA - Valencia (Spain), [4]Tesat Spacecom GmbH & Co - Backnang (Germany), [5]CNR-IMIP Istituto Metodologie Inorganiche e Plasmi - Rome (Italy).

The secondary electron emission yield (SEY) of technical materials is of crucial importance in the appearance of impeding effects like multipaction or electron cloud in high-power RF space equipment or in high-energy particle accelerators. The diminishment of electron emission by electron bombardment (electron conditioning or scrubbing) is a known effect and made a good use in technological applications. The growth of a surface carbon layer induced by low-energy electron irradiation on silver has been studied by quantitative X-ray photoelectron spectroscopy (XPS) and SEY measurements. Silver plating on aluminium alloy prepared by a standard technique of space industry was compared to pure silver (Goodfellow); both in technical as-received conditions. 500-eV-electron fluences up to 10^{18} e/cm^2 were used in a vacuum of $5x10^{-9}$ mbar. Quantitative analysis of XPS signals of carbon and oxygen chemical species as well as Ag, allows characterizing the surface contamination over layer along with its growth.

Both total surface carbon, graphitic (sp^2 bonded) carbon, and contamination over layer thickness increases steadily during electron irradiation; while sp^3 carbon, carbon bonded to oxygen species, and total surface oxygen decrease during treatment. Silver plating in as-received conditions has more surface carbon bonded to oxygen species. The treatment produces the reaction of sp^3 bonded carbon into graphitic species but this is not sufficient to explain the growth of this last species. The growth of the surface contamination over layer can amount to a total of about 14

monolayers, thus doubling initial thickness. This is very difficult to understand as having the residual gas interacting with the impacting electrons as the only source of carbon atoms. The grown surface carbon over layer is stable in ultra high vacuum. SEY was measured for normal incidence. First cross-over energy increases from 25-50 to 90-100 eV during electron irradiation; while maximum value decreases from 1.9-2.2 to 1.1.

1. Proceedings of the 6th International Workshop on Multipactor, Corona and Passive Intermodulation in Space RF Hardware (MULCOPIM ’08, and MULCOPIM ’11), Valencia, Spain, and references therein.

2. R. Larciprete, D. R. Grosso, M. Commisso, R. Flammini, and R. Cimino: “Secondary electron yield of Cu technical surfaces: Dependence on electron irradiation”, Physical Review Special Topics - Accelerators and Beams 16, 011002 (2013) and references therein.

3. Valentin C. Nistor, Lydya Aguilera, Isabel Montero, David Raboso, Luis A. González , Leonardo Soriano, Luis Galán, Ulrich Wochner , and Dieter Wolk: “Strategies for Anti-Multipactor Coatings of Suppressed Secondary Emission and Low Insertion Losses for High Power RF Components in Satellite Systems”, in Ref.1.

ASS-7-Or-5
Suppression of secondary electron emission by submicron surface roughness in anti-multipactor coatings for space applications

T01 Applied Surface Science

#ASS-7-Or-5

V. Nistor [1], L. González [1], L. Aguilera [2], I. Montero [2], D. Raboso [3], U. Wochner [4], D. Wolk [4], L. Galán [1].

[1]UAM - Madrid (Spain), [2]ICMM-CSIC - Madrid (Spain), [3]ESA-VSC - Valencia (Spain), [4]TESAT - Backnang (Germany).

The secondary electron emission from materials used in high power RF devices in space is the main trigger and sustaining mechanism of the resonant avalanche electron discharge known as Multipactor effect. It limits the attainable power of these devices and also affects the normal operation of particle accelerators . During decades, research was focused on bulk material properties for obtaining anti-multipactor coatings of low secondary emission yield (SEY). This approach has shown its limitations in space applications where strong requirements on stability in atmospheric environment and surface electrical conductivity are set. ESA is leading technological research on a new approach based on surface roughness which might work as black body or Faraday cup effect. Appropriate surface morphology can reduced effective SEY of any material below one and thus certainly suppress Multipactor effect; however, it might increase RF surface resistance and consequently insertion loss of the device. This can be avoided because of a different dependence on surface morphology.
Anti-multipactor coating are being developed for the 10 GHz range of frequencies by etching submicron high aspect ratio, high density surface roughness of silver standard plating in space industry by the combined effect of a noble gas ion beam and a hard metal atom beam. The resulting surface roughness growth dynamics is complex and different scales of roughness might overlap but appropriate surface morphologies are possible. The deposited amount of the hard metal and its influence on surface resistance are negligible.

That silver rough surface should be further coated for improving intrinsic SEY and stability in air. As long as the last coating is much thinner than RF skin depth, it does not affect either surface morphology or RF surface resistance.

Devices with resulting anti-multipactor coatings are tested for SEY, RF insertion loss, Multipactor power threshold, SEM and AFM microscopies, EDX and XPS analysis.

1. Proceedings of the 6th International Workshop on Multipactor, Corona and Passive Intermodulation in Space RF Hardware (MULCOPIM ’08, and MULCOPIM ’11), Valencia, Spain, and references therein.
2. Valentin C. Nistor, Lydya Aguilera, Isabel Montero, David Raboso, Luis A. González , Leonardo Soriano, Luis Galán, Ulrich Wochner , and Dieter Wolk: “Strategies for Anti-Multipactor Coatings of Suppressed Secondary Emission and Low Insertion Losses for High Power RF Components in Satellite Systems”, in Ref.1.

ASS-P3-15
Characterization of ZnS grown by RF magnetron sputtering

T01 Applied Surface Science

#ASS-P3-15

J. Díaz-Reyes [1], J. Flores-Mena [2], J. Martínez-Juárez [3].

[1]CIBA-IPN - Tepetitla (Mexico), [2]FCE-BUAP - Puebla (Mexico), [3]CIDS-BUAP - Puebla (Mexico).

Zinc sulfide (ZnS) is one of the most important II-VI group semiconductors, with a wide direct band gap of 3.8 eV has been extensively investigated and used in electroluminescent devices, flat panel displays, infrared windows, sensors, and lasers [1]. To explore the possibility of using it in electroluminescent devices, a study of the structural and optical properties of the host material is an important step. Based on the above criterion, the structural and optical properties of ZnS films have been studied in the present work. ZnS thin films were grown on (001) GaAs substrates at different temperatures by RF magnetron sputtering. The x-ray diffraction (XRD) analysis and Raman scattering reveals that deposited films showed hexagonal wurzite phase. The crystallite size range of the films was determined by Scherrer equation, which was from 11.15 to 45.83 nm. The stoichiometry chemical was determined by Energy-dispersive X-ray spectroscopy (EDS). Besides it made an experimental study on first- and second-order Raman scattering of wurtzite. The 300K photoluminescence presents a visible radiative band associates to vacancies of zinc and sulfide [2]. In addition was carried out energy dispersive spectroscopy (EDS) measurements on the films to determine their stoichiometry chemical which allows relating the intensity of radiative bands associated to oxygen and zinc vacancies.

[1] Ming Tan, Weiping Cai, Lide Zhang. Optical absorption of ZnS nanocrystals inside pores of silica. J. Appl. Phys. Lett. 1997;71(25):3697–9.
[2] Fang J, Holloway HP, Yu EJ, Jones SK, Pathangey B, Brettschneider E, et al. MOCVD growth of non-epitaxial and epitaxial ZnS thin films. J Appl Surf Sci 1993;70/71:701–6.

ASS-3-Or-5
Anomalous X-ray Scattering: A Chemically Selective Method To Investigate Supported Nanoalloys

T01 Applied Surface Science

#ASS-3-Or-5

A. Lemoine [1], P. Andreazza [2], Y. Garreau [3], C. Andreazza-Vignolle [2], Z. Kataya [2], A. Coati [4].

[1]CRMD / SOLEIL Synchrotron - Orléans / Saint-Aubin (France), [2]CRMD - Orléans (France), [3]MPQ / SOLEIL Synchrotron - Paris / Saint-Aubin (France), [4]SOLEIL Synchrotron - Saint-Aubin (France).

Amazing nanoparticles properties, as magnetic ones, are mainly governed by their size and structure. Thus, the growing interest of scientists in nanoalloys structural study requires the development of characterization methods providing not only morphology and spatial atomic arrangement, but also chemical order. Therefore, chemical selectivity characterization techniques are essential to determine the nanometric size influence on the alloy state [1,2].

Specially, the anomalous X-ray scattering is promising. This method, based on the atomic scattering factor variations with wavelength next to an X-ray absorption edge, implies to modify one element contribution to the scattering spectrum in function of energy. Thus, the signal obtained is chemically selective. Combining anomalous small [3] and wide angle [4,5] X-ray scattering in grazing incidence (A-GISAXS and A-WAXS), which provides morphological and structural information, the mixing or segregation state of metallic elements in supported nanoalloys is revealed.
Firstly, this experimental work exhibits the anomalous scattering implementation thanks to synchrotron beam (SixS beam line – SOLEIL synchrotron). Then, the chemical order evolution during in-situ annealing of supported AgCo bimetallic nanoparticles smaller than 3nm, elaborated by UHV evaporation on an amorphous substrate, is studied. Finally, the annealing conditions role, and the influence of the deposition mode (sequential deposition and co-deposition) on the nanoalloy state are investigated.

1. C. Langlois, Z.L. Li, J. Yuan, D. Alloyeau, J.Nelayah, D. Bochicchio, R. Ferrando, and C.Ricolleau, Nanoscale, 4, 3381-3388 (2012)
2. P. Andreazza in « Nanoalloys: Synthesis, Structure and Properties », Eds D.Alloyeau et al., p69 (2012) Springer-Verlag, London
3. P. Andreazza, H. Khelfane, O. Lyon, C. Andreazza-Vignolle, A. Ramos, and M. Samah, Eur. Phys. J., 218, 231-244 (2012)
4. T. U. Schülli, et al., Phys. Rev. B, 71, 035326 (2005)
5. Jeng, U.-S., et al., Journal of Applied Crystallography , 40, s418--s422 (2007).

ASS-P3-09
Ultrathin cobalt films studied by angle-resolved XPS

T01 Applied Surface Science

#ASS-P3-09

J. Polcák [1], J. Cechal [2], M. Urbánek [1], T. Šikola [2].

[1]Institute of Physical Engineering, Brno University of Technology, Technická 2, 616 69 - Brno (Czech republic), [2]CEITEC BUT - Brno University of Technology, Technická 10, 616 69 - Brno (Czech republic).

Depth profiling by angle-resolved XPS is a useful method for studying chemical composition of surfaces and ultrathin films. However, the calculation of depth profiles is not an easy task contrary to the theoretical calculations of XPS intensities from the known compositional depth profiles (reversed methods). We have made some improvements in our calculations based on implementation of a genetic algorithm method in finding proper depth profiles. Our calculation algorithm has been successfully tested on modeled samples even when some noise was added to the input data [1]. However, the real samples are influenced by other effects i.e. geometric inaccuracies, real noise, surface contaminations. Another problem is that investigated films are not often sufficiently smooth and the method is very sensitive to the top-most surface composition and morphology. Therefore, we studied ultrathin cobalt films made in situ by UHV atomic-beam evaporation of cobalt on a silicon oxide surface which leads to the formation of smooth uniform layers if deposited under room temperature [2]. To obtain not so smooth films we also deposited cobalt under higher temperatures and made comparison of both cases. In this way, it was possible to observed surface morphology influence to the depth profile calculations and to check the accuracy of the depth profiling method more precisely.

[1] J. Polčák, J. Čechal, P. Bábor, M. Urbánek, S. Průša, T. Šikola, *Surf. Interface Anal*. **2010**, 42, 649
[2] J. Čechal, J. Luksch, K. Koňáková, M. Urbánek, E. Brandejsová, T. Šikola, *Surf. Sci.* **2008**, 602, 2693

ASS-P2-03
Interaction of gold with native SiO2 layers: Au diffusion and SiO2 decomposition

T01 Applied Surface Science

#ASS-P2-03

J. Cechal, J. Polcák, P. Procházka, T. Šikola.

CEITEC BUT, Brno University of Technology - Brno (Czech republic).

The interaction of gold layers prepared by thermal evaporation under UHV conditions was studied in-situ by X-ray photoelectron spectroscopy and ex-situ by scanning electron microscopy and atomic force microscopy. On thermally cleaned silicon sample with a native silicon dioxide layer, gold forms islands above the room temperature. The annealing to higher temperatures leads to diffusion of gold atoms through the oxide layer and subsequent gold silicide formation. The thermal stability of SiO_2 layer is significantly reduced partially due to inducing defect sites during the gold transport though the oxide layer and partially due to a catalytic effect of gold islands. The effects taking place at native oxide layers are compared with samples with thermal oxide layers of various thicknesses and modified samples (e.g. annealed in presence of oxygen or with BN layers on top), and the mechanisms of gold interaction with SiO_2 layers are discussed in detail.

ASS-2-Or-3
Preferential oxidation of CO on Ir(111) and Pt(111) surfaces studied with ambient pressure X-ray photoelectron spectroscopy.

T01 Applied Surface Science

#ASS-2-Or-3

J. Knudsen [1], N. Johansson [2], E. Grånäs [2], M.A. Arman [2], J.N. Andersen [1], J. Schnadt [2].

[1]Division of Synchrotron Radiation Research and the MAX IV Laboratory - Lund (Sweden), [2]Division of Synchrotron Radiation Research - Lund (Sweden).

Preferential oxidation of CO (PROX) is an efficient way to remove CO impurities from hydrogen rich streams used for low temperature fuel cell applications. In contrast to CO oxidation that has been studied extensively on single crystal surfaces [1,2] the amount of published literature reporting PROX-studies on single crystal surfaces is very limited [3]. Here, we used the new ambient pressure X-ray photoelectron spectroscopy (AP-XPS) setup at the MAX IV laboratory to study the PROX reaction over Ir(111) and Pt(111) surfaces at total pressures around 1 mbar. In agreement with ref. [3], that only characterized the reactivity of different metal surfaces, we found that Ir(111) is a better PROX catalyst as compared to Pt(111). In contrast to ref. [3] and since the AP-XPS setup both probe free and adsorbed molecules this talk focus on correlating the atomic scale structure on the surface with the reactivity.
For Pt(111) we find that the surface is blocked by adsorbed CO at sample temperatures below ~ 450 K and no CO_2 or H_2O are, therefore, produced. At higher temperatures, where CO start to desorb from the surface, both CO_2 and H_2O production start and around ~ 550 K the mass transfer limit for CO_2 and H_2O production is reached simultaneously. Thus, the Pt(111) surface is not really able to preferentially oxidize CO at our experimental conditions.
In contrast, we find that Ir(111) is able to selectively oxidize CO at temperatures around ~ 550 K. At this temperature the CO_2 production reached the mass transfer limit, but no water is produced. At higher temperatures (550 – 650 K) we observe an increased water production when the temperature is increased. Similar to our results on Pt(111) we find that both CO_2 and H_2O production are absent below ~ 450 K

because of adsorbed CO that block the surface. By comparing with known structures that is formed in pure oxygen and CO atmospheres we plan to develop atomic models for the inactive phase (< 450 K), the phase present when CO is preferentially oxidized (~ 550 K), and the phase present when both water and CO_2 is produced (550 – 650 K).
Finally, we studied H_2O production on Ir(111) with different amounts CO mixed into the H_2/O_2 feed gas. Interestingly, we found that a small amount of CO promotes the production of H_2O. Too much CO in the feed gas will, however, lead to CO blocking of the entire Ir(111) surface and as a result no CO_2 or H_2O will be produced. Different models explaining CO promoted water production will be discussed at the end of the talk.

[1] R. van Rinj et al., Phys. Chem. Chem. Phys., **13**, 13167 (2011)
[2] G. Feng, Phys. Chem. Chem. Phys., **14**, 6688 (2012)
[2] L. Piccolo et al., Catalysis today, **189**, 42 (2012)

ASS-6-Or-3
Self-organized chromium oxide monolayers on Fe(001)

T01 Applied Surface Science

#ASS-6-Or-3

A. Picone [1], G. Fratesi [2], M. Riva [1], G. Bussetti [1], A. Calloni [1], A. Brambilla [1], M.I. Trioni [3], L. Duò [1], F. Ciccacci [1], M. Finazzi [1].

[1]dipartimento di fisica, politecnico di milano - Milan (Italy), [2]dipartimento di scienza dei materiali, università milano-bicocca - Milan (Italy), [3]CNR - Consiglio Nazionale della Ricerca - Milan (Italy).

The growth of ultrathin epitaxial oxide films on metal supports is attracting considerable scientific interest both
on a fundamental level and for potential technological applications.
Growth techniques such as reactive deposition (i.e., metal deposition in oxygen atmosphere) and/or post-oxidation are typically applied, leading to ordered phases and well defined oxide-metal interfaces on noble metal substrates. On the contrary, when a more reactive metal, such as Fe, is used as a substrate for the nano-oxide growth, these procedures fail to produce sharp metal/oxide interfaces. Indeed, during the metal deposition in oxygen atmosphere, extensive and uncontrolled oxidation of Fe occurs, preventing the stabilization of long-range ordered oxide monolayers.
An alternative route to obtain a sharp interface between a single layer of transition metal oxide and a reactive
substrate may be to exploit the oxygen adsorbed on the surface before metal deposition since, in this case, the
amount of oxygen available is well defined.
The well ordered and defect-free Fe(001)-p(1×1)O surface is an ideal template to implement this strategy.
The surface is characterized by one oxygen atom per surface unit cell, which can be used as a reservoir for
the stabilization of two-dimensional transition metal oxides.
In this contribution, by means of a combination of high resolution Scanning Tunneling Microscopy images, Auger Electron Spectroscopy, and Density Functional Theory calculations, we show how the Fe(001)-p(1 × 1)O surface can be used as a template for the self assembly of two dimensional Cr oxides. Cr deposition on this surface leads to two different phases, depending on the amount of deposited Cr. At 0.75

monolayers coverage a c(4 × 2) overlayer with Cr_3O_4 formal stoichiometry is stabilized, while an overlayer with ($\sqrt{5} \times \sqrt{5}$)R°27 symmetry and Cr_4O_5 stoichiometry is obtained at slightly higher coverages [1].
Furthermore, the magnetic properties of these oxide monolayers are investigated by means of X-ray magnetic circular dichroism.

.

[1] A. Picone, G. Fratesi, M. Riva, G. Bussetti, A. Calloni, A. Brambilla, M. I. Trioni, L. Duò, F. Ciccacci, and M. Finazzi, Self-organized chromium oxide monolayers on Fe(001), submitted to Phys. Rev. B

ASS-10-Or-3
Structure and electronic properties of PTCDI thin film on Au(111).

T01 Applied Surface Science

#ASS-10-Or-3

J. Hieulle, F. Silly.

CEA - Saclay (France).

Controlling the formation of organized structure at the nanometer scale is essential to develop the new generation of electronic components. Perylene imides are promising organic building blocks for photovoltaic application due to there semiconducting nature, and there thermal and photo-stability.
Difficulties associated with organic photovoltaic devices include their low quantum efficiency.
One origin is usually attributed to organic film defects.
Highly ordered organic structure can be tailored taking advantage of molecular self-assembly. To engineer the supramolecular assembly we can use different types of molecular bonds, like covalent bond, hydrogen bond and metal-ligand bond. In our case we selected hydrogen bond, which offer more flexibility for controlling the final arrangement of the supramolecular network, than covalent bond. This enhance flexibility is due to the physical nature of the hydrogen bond. Finally the choice of the hydrogen bond is a good compromise, because it's relatively weak compare to covalent bond but it's really strong compare to Van-der-Waals bond.

We investigated PTCDI [1,2] thin film on a Au(111) surface, using a scanning tunneling microscope in ultrahigh vacuum. We observed the formation of well organized PTCDI monolayer. At room temperature the PTCDI molecule formed a brick-wall structure. By annealing the surface we were able to form a double and triple-row PTCDI structure. We observed that molecular contrast was depending of tunneling parameters in that case.
In addition we used XPS [3] to investigate the PTCDI thin film growth. We observed that PTCDI molecules adopt a flat lying configuration in the monolayer regime as well as in the multilayer regime. We also able to measure the energy of the valance-band and conduction-band states of the PTCDI film depending the film thichness.

1. M. Mura, X. Sun, F. Silly, and L.N, Kantorovich, Phys. Rev. B 2010, 81, 195412, “Experimental and theoretical analysis of H-bonded supramolecular assemblies of PTCDA molecules”.

2. M. Mura, F. Silly, and L.N, Kantorovich, J. Phys. Chem. C, 2009, 113, 21840, “H-Bonding Supramolecular Assemblies of PTCDI molecules on the Au(111) Surface”.

3. Liang Cao, Yu-Zhan Wang, Tie-Xin Chen, Wen-Hua Zhang, Xiao-Jiang Yu, J. Chem. Phys. 2011, 135, 174701, “Charge transfer dynamics of 3, 4, 9, 10 - perylene-tetracaboxilic-dianhydride molecule on Au (111) probed by resonant photoemission spectroscopy”.

ESD/ASS-2-Or-7
Surface analysis of an electrodeposited copper layer on molybdenum substrate for solar applications

T01 Applied Surface Science

#ESD/ASS-2-Or-7

E. Delbos [1], H. El Belghiti [1], D. Mercier [2], M. Bouttemy [2], A. Etcheberry [2].

[1]Institut Lavoisier de Versailles - OMG - Versailles (France), [2]Institut Lavoisier de Versailles - Versailles (France).

Thin films technology is a good alternative to silicon wafers for highly efficient photovoltaic cells. For example, cells based on CIGSe (Cu(In,Ga)Se2) absorbers reach at present about 21% efficiency (in laboratory measurements). To replace indium, a rare and expensive element, CZTS (for Cu2ZnSnSe4) is a promising candidate material for low cost absorber layer.
Electrochemical deposition is an attractive technique for CZTS preparation, one of the possible synthetic paths consists in the precursor layers electrodeposition followed by a thermal annealing. In this synthesis method, the growth of each layer is important and must be absolutely controlled. In this work, we have studied the first growth step of electrodeposited copper on molybdenum substrate by surface analysis (XPS/SEM-FEG and nano-AES). A specific chemistry based on CuSO4 and H2SO4 bath - OMniCu™ High Copper - from OM Group Ultra Pure Chemicals (OMG UPC) enhanced by organic additives - OMniCu™ additives series - has been used. First, SEM-FEG observations have evidenced a three steps copper deposition mechanism: (1) nucleation, (2) coalescence and finally (3) a growing stage. Then, combining XPS and nano-AES (figure 1) surface analyses methods, global (micrometric scale) and localized (nanometric scale) characterizations of the Cu/Mo surface have been jointly performed. More specifically, a thin layer of Cu2O at the surface of copper nuclei has been observed.
To conclude, by combining different characterization methods (XPS, nano-AES and SEM-FEG), complementary information about the different steps of copper electrodeposition on molybdenum substrate have been determined. Using specific chemistry, a dense and thin layer of electrodeposited copper (100 nm) has been

obtained.

Figure 1: Nano-Auger point analysis characterization of Cu nuclei electrodeposited on the Mo substrate (experimental conditions: -0.7V/MSE during 0.7s)

ASS-7-Or-4
Substrate roughness dependence in ion induced spinodal dewetting of thin metal films

T01 Applied Surface Science

#ASS-7-Or-4

L. Repetto [1], B. Šetina Batič [2], G. Firpo [1], U. Valbusa [1].

[1]Dipartimento di fisica, Università di Genova, Via Dodecaneso 33, 16146 - Genova (Italy), [2]Inštitut Za Kovinske Materiale in Tehnologije, Lepi pot 11, 1000 - Ljubljana (Slovenia).

Self organization of thin solid films under an external melting agent has received a great attention both experimentally and theoretically since the work of Bischof et al. [1]. This process indicates a new route for nanofabrication with a strong potentiality for improving the throughput and the resolution capabilities of traditional top down techniques. The pattern characteristics phenomenology has extensively been studied in laser induced melting of thin metal films on substrates like fused silica and a strong analogy with spinodal dewetting of thin liquid films has been found: the concurrent action of surface tension and van der Waals forces can amplify capillary waves in the molten metal film up to its rupture. Recently also ion irradiation has been indicated as a melting agent which can induce spinodal dewetting [2]. However, during ion irradiation, capillary waves of proper wavelength cannot exist due to the reduced size of the molten volume and to its short lifetime which prevents the superposition of molten zones produced by several impacts. In this case initial perturbations for the amplification process are provided by the substrate roughness which produces a background of thickness fluctuations in the film flattened by its surface tension. Here we investigate both experimentally and with simulations the dependence of the spinodal process on the amplitude and on the Fourier spectrum of the roughness with particular attention to the rupture fluence and the possibility to modify the thickness dependence of the characteristic wavelength by modifying the roughness spectrum.

[1] J. Bischof, D. Scherer, S. Herminghaus, and P. Leiderer, Phys. Rev. Lett. 77, 1536 (1996).

[2] L. Repetto, B. Šetina Batič, G. Firpo, E. Piano, and U. Valbusa, Appl. Phys. Lett. 100, 223113 (2012).

SEM image of the experimental (left) and simulated (right) dewetting patterns obtained by 30 keV Ga ion irradiation of a 2.7 nm thick Cr film deposited on a silicon substrate covered by its native oxide. Calibration bar 500 nm. In the inset the Fourier spectrum is reported. The ring shaped spectrum is the typical signature of spinodal dewetting.

ASS-8-Or-6
Interlayer Formation of Diamond-Like Carbon (DLC) Coatings on Plastic Material

T01 Applied Surface Science

#ASS-8-Or-6

C. Fischer [1], M. Rohrbeck [1], S. Wehner [1], M. Richter [2], D. Schmeißer [2].

[1]University Koblenz-Landau, Institute of Integrated Natural Science - Department of Physics - Koblenz (Germany), [2]Brandenburg University of Technology Cottbus, Department of Applied Physics and Sensors - Cottbus (Germany).

The engineering of plastic materials and their popular application in industry and daily life is accompanied by essential requirements. Besides the basic performance of these materials such as flexibility, elasticity, fracture strength and chemical resistance, further determinants are long term stability, durability or biocompatibility. Concerning materials features according to its specified exposure especially the surface is in charge of intensive interaction touching the environment. To avoid incompatibilities in surface characteristics of the optimal parent plastic these materials can be customized for their intended use by coating. The main limiting factor for such modifications is the preservation of basic material performance in addition to benefits like changed adhesive, improved repellent or antibacterial behavior.
Protective coatings with the objective to preserve main characteristics of selected plastic materials have been realized by a few layers of diamond-like carbon (DLC). The assembly of soft plastic material and robust carbon layers is important for the resulting material characteristics. The detailed understanding of the interlayer formation between these unequal materials and the connection of carbon centers in a chemically different neighborhood is the perspective of the presented work.
The composition of DLC layer is a network consisting of sp^2- and sp^3-carbon centers. Depending on the allocation and fraction of each carbon state the material exhibits different properties ranging from medium-hard to stiff. Two types of nanometer-scaled DLC films forming more flexible and hard coatings are investigated. Different DLC compositions and increasing layer thickness have been examined by the use of synchrotron radiation and multiscale microscopic analysis. Results will help to provide an enhanced understanding of layer formation at the interface between the

basic plastic material and the DLC coating and will help to optimize parameters for the surface coating to achieve improved product characteristics. Collected information will be transferable to other plastic materials with diverse needs, e.g. energy storage devices, water treatments and coatings for everyday commodities or industrial parts.

ASS-1-In-2
PROBING ELECTRONIC STRUCTURE IN MATERIALS SCIENCE WITH HARD X-RAY PHOTOELECTRON SPECTROSCOPY

T01 Applied Surface Science

#ASS-1-In-2

W. Drube.

Deutsches Elektronen-Synchrotron DESY - 22607 Hamburg (Germany).

Photoelectron spectroscopy is a well-known, very effective method for electronic structure investigation at solid surfaces. When using hard X-ray excitation in the multi keV range, the energetic photoelectrons emerge from deeper inside the material because their inelastic mean free path significantly increases. It then becomes possible to also study complex bulk materials and/or buried interfaces. Because photoelectric cross sections rapidly decrease with photon energy above ionization thresholds, brilliant undulator radiation at synchrotron sources is generally needed to effectively use the technique which is rapidly emerging at storage ring facilities worldwide.

X-rays in the range 2 to 10 keV are typically used allowing to probe electronic and chemical structure down to a depth of about 10-20 nm. This bulk sensitivity not only is essential in the study of complex correlated materials, which often exhibit a modified surface electronic structure, but also indispensable for technologically relevant multi-layered materials with buried interfaces. Most interesting for materials science applications is the ability to study "as-grown" materials without any need for prior in-situ surface treatment or sensitive structures covered by protective layers. An overview will be given on the current state of the technique at instruments worldwide, highlighting its great potential by recent scientific results.

ASS-P3-10
Raman surface characterization of cadmium telluride using 325 nm and visible laser lines

T01 Applied Surface Science

#ASS-P3-10

M. Soares, A.J. Neves, T. Monteiro.

Department of Physics and I3N, University of Aveiro - Aveiro (Portugal).

Telluride compounds have been extensively studied by micro Raman spectroscopy during the last years. Vibracional modes observed in the range of 90 – 130 cm-1 are associated with tellurium inclusions or aggregates due to the lack of stoichiometry. In previous works we showed Raman peaks of the crystalline tellurium phase and the intensity enhancement behavior with the energy density of the laser spot with energies above the CdTe bandgap. This behavior suggests the formation of crystalline tellurium aggregations on the CdTe surface due to laser irradiation during the acquisition of the spectra.
In this work, the changes on surface morphology and surface composition of Cadmium Telluride (CdTe) single crystals grown by vertical Bridgman process and CdTe thin films surface grown by metalorganic chemical vapor deposition (MOCVD) on GaAs substrate, are studied by Raman Spectroscopy and complemented by Atomic Force Microscopy (AFM) and Energy Dispersive x-ray Spectroscopy (EDS) techniques.
The goal of this work is the study of the appearance of two Raman peaks at around 600-800 cm-1 in CdTe surface when the samples are excited with 325 nm HeCd laser at the room temperature and to clarify the origin of those peaks

ASS-4-Or-5
Interaction of Oxygen with Palladium at O2 Pressures from 10-6 to 105 Pa and temperatures 500 - 1400 K

T01 Applied Surface Science

#ASS-4-Or-5

A. Salanov, E. Suprun, V. Nikulin.

Boreskov Institute of Catalysis SB RAS - Novosibirsk (Russian federation).

Platinum group metals (PGM) are widely used as catalysts in chemical industry and in neutralizers of the automobile exhausts due to their unique properties [1]. Palladium is the most active catalyst for CO and CxHy oxidation with oxygen, and, for this reason, it is most commonly used in the neutralizers and in the catalytic combustion of methane. Therefore, it is necessary to study the interaction of oxygen with palladium in the wide temperature and pressure ranges. In order to understand the mechanism of the interaction of oxygen with palladium, we analyzed the dependences of the amount of oxygen absorbed by polycrystalline palladium foil (Pd(poly)) on exposure to O_2, on oxygen pressure and the surface microstructure and composition of Pd(poly). The samples were treated with O_2 in wide ranges of pressure 10^{-6}–10^5 Pa and temperatures 500–1400 K. The amount of absorbed oxygen by palladium was determined by temperature-programmed desorption (TPD). The surface microstructure was studied using a scanning electron microscope (SEM) JSM-6460 LV (Jeol). The surface chemical composition of the studied samples was determined by Energy Dispersive X-ray Microanalysis (EDS) using INCA Energy-350 instrument (Oxford Inst.).

At low Po_2 values (≤1.3×10^{-5} Pa) and exposure (ε) ≤ 200 L the dissociative chemisorption of oxygen on the Pd(poly) surface is observed. The chemisorbed oxygen coverage of the surface reaches ~0.5 ML. At $Po_2 \geq 10^{-5}$ Pa and ε ≥ 200 L, after the saturation of the O_{ads} layer to θ ≈ 0.5, O_{ads} atoms begin to insert under the surface layer of the metal. This is a consequence of the decrease in the energy of binding of the chemisorbed oxygen atoms to the palladium surface due to the repulsive interactions between O_{ads} atoms. The insertion of O_{ads} atoms under the surface layer of the metal gradually yields surface palladium oxide, and this accompanied by the absorption of up to ~1 ML of oxygen. O_2 chemisorption and the formation of the surface oxide on Pd(poly) are almost temperature-independent at T=500-600 K. At Po_2 = 0.1– 10.0 Pa and $\varepsilon \geq 10^7$ L, oxygen dissolves in the palladium

bulk. The oxygen atoms penetrate deep in the subsurface layers of palladium, diffuse, and accumulate progressively in the metal bulk. Oxygen dissolution in palladium depends strongly on temperature. At $\varepsilon \geq 10^7$ L and T = 500 K, palladium absorbs 1–2 ML of oxygen, while at 600 K it absorbs up to ~20 ML of oxygen. A possible reason why oxygen absorption accelerates with an increasing temperature is that the rate of O atom diffusion in the palladium lattice increases. In addition, at $\varepsilon \geq 10^7$ L an increase in the O_2 pressure (≥0.1 Pa) appreciably accelerates oxygen absorption. As the pressure is raised from 0.1 to 10 Pa, the amount of oxygen absorbed by Pd(poly) at 600 K increases from ~1 to ~20 ML. Detailed analysis of the microstructures observed on the surface of Pd(poly) after treatment in the oxygen atmosphere at $Po_2 = 10^5$ Pa and at temperatures increasing from 500 to 1400 K indicates that the palladium surface microstructure is determined by the formation and decomposition of palladium oxide PdO. At T < 900 K palladium is intensely oxidized to form PdO particles with dimensions 25-50 nm. At 900-1100 K PdO microcrystals with dimensions 250-500 nm are formed.

[1] http://www.platinum.matthey.com/applications

ASS-P1-11
Work Function Measurement of Non-Uniform Surfaces Based on Electron Emission

T01 Applied Surface Science

#ASS-P1-11

J. Trigueiro, N. Bundaleski, A.G. Silva, A.M.C. Moutinho, O. Teodoro.

Departamento de Física da Faculdade de Ciências e Tecnologia Universidade Nova de Lisboa - Caparica (Portugal).

A Work function study based on the onset shift (i.e. following low energy cut-off) of secondary electron spectra has been used for the last four decades to monitor the deposition and adsorption in real time, measure the dipole momentum and polarizability of the surface layer and determine the lateral distribution of the work function [1,2]. Nowadays, it is also known as photoemission measurement of the work function because the secondary electrons are usually produced by photon irradiation (particularly with UV light). In this work we show that the onset shift depends on both, the coverage of species that change the work function and the size of low work function patches. The later dependence on WF using the low energy cut-off, which is due to the so-called patch field effect [3.4], has never been considered in details so far. Neglecting this effect may contribute to different kinds of misinterpretations related to determination of the dipole moment and polarizability of adsorbed dipoles, but also to work function mapping results using a rastered beam to produce secondary electrons.

The influence of the patch size on the onset shift is analyzed in detail. Numerical calculations of the potential distributions above different non-uniform surfaces were performed in order to quantitatively determine this influence. Depending on the patch size, we define three measurement regimes in which the onset position is related to either the surface average of the work function (small patches), the minimum local work function (large patches), or a value in-between (intermediate size patches). It is also shown that the extraction field, which is always present in these measurements due to sample biasing, plays a significant role in these measurements. Therefore, its influence has to be considered for correct interpretation of obtained results.

The conclusions obtained from numerical simulations were tested by performing work

function study of a sample consisting of a low work function material (In) surrounded with a high work function metal (Ni). Experimental data has corroborated the findings of numerical simulations and demonstrated that manipulating with the extraction field intensity enables transition between the measurement regimes. Typical misinterpretations due to the neglecting of the patch size contribution to the onset shift are analyzed.

[1] H. Oechsner, Fresenius J. Anal. Chem. 355, 419 (1996).

[2] O.M.N.D. Teodoro and A.M.C. Moutinho, Key Engineering Materials 230-232, 165 (2002).

[3] C. Herring and M.H. Nichols, Rev. Mod. Phys. 21, 185 (1949).

[4] V. T. Binh, R. Mouton, Ch. Adessi, V. Semet, M. Cahay, and S. Fairchild, J. Appl. Phys. 108, 044311 (2010).

ASS-1-Or-1
Energy loss structures in hard X-ray photoelectron spectra

T01 Applied Surface Science

#ASS-1-Or-1

L. Kövér.

Institute of Nuclear Research of the Hungarian Academy of Sciences - Debrecen (Hungary).

Hard X-ray induced photoelectron spectra of solids are significantly influenced by energy loss processes of the excited high kinetic energy electrons. Obtaining accurate information on electronic structure or chemical composition of surface, subsurface, interface or bulk regions of materials from these spectra assumes the fundamental understanding of the processes leading to electron energy losses in solids. In the first part of the contribution the specific features of interactions yielding energy loss of photoelectrons induced by hard X-rays are discussed. Then the models describing these interactions are compared, including the basic assumptions used by them, their limitations and the areas of applications (e. g. inelastic background correction, concentration depth profiling, extraction of electronic structure information, 3D analysis of surface or - even deeply buried - interface nanostructures). Illustrative examples are presented for the different applications

The described work was carried out as part of the TÁMOP-4.2.2.A-11/1/KONV-2012-0019 project in the framework of the New Széchenyi Plan. The realization of this project is supported by the European Union, co-financed by the European Social Fund.The described work was carried out as part of the TÁMOP-4.2.2.A-11/1/KONV-2012- 0019 project in the framework of the New Széchenyi Plan. The realization of this project is supported by the European Union, co-financed by the European Social Fund.

ASS-1-Or-8
In situ surface analytical characterization of electronic devices: thin film solar cells and lithium ion batteries as examples

T01 Applied Surface Science

#ASS-1-Or-8

T. Kampen, S. Bahr, A. Thissen, M. Meyer.

SPECS Surface Nano Analysis GmbH - Berlin (Germany).

Electronic devices have revolutionized everyday life in industrial countries over the last decades. Especially devices for energy conversion and storage like thin film solar cells and lithium ion batteries are of importance for the future. Recently two main tasks for research and development are dominant: miniaturization for sophisticated applications targetting at the nanoscale, and designing low cost large scale devices. In both fields the device performance is strongly determined by materials quality, composition, combination and last but not least by processes at materials interfaces. Nanostructures, minimization of material consumption and the need to improve device efficiencies consequently leads to the widespread focussing on thin film preparation. For thin film devices surface and interface analysis like photoelectron spectroscopy and surface (spectro-)microscopies are an important tools for material and device characterization. Classical well defined model experiments already reveal important insights using highly integrated vacuum systems for analysis and preparation. But analysis of materials and devices under near ambient conditions and even in situ during operation is an inevitable future development to improve the significance of data for development and quality management. In this respect the application of techniques like Near Ambient Pressure XPS, XPS from liquids and solid liquid interfaces, hard x-ray PES (HAXPS), Near Ambient Pressure SPM on solar cell and lithium ion battery materials is the challenging tasks for manufacturing companies of surface analytical equipment.

ASS-10-Or-2
Versatile Molecular Surface and Interface for High-Performance Organic Electronics

T01 Applied Surface Science

#ASS-10-Or-2

H. Ma.

University of Washington - Seattle (United states).

Versatile surface and interface tailoring has been realized through molecular monolayers. (1) Exquisite control of molecules is reached by monolayer assembly/confinement, and monitored by photon-STM for molecular motions, reactions and conductance in ground state and excited state (Fig. 1).[1] (2) Insulating and semiconducting molecular phosphonic acid (PA) self-assembled monolayers (SAMs) have been developed for applications in organic field-effect transistors (OFETs) for low-power, low-cost flexible electronics. Multifunctional SAMs on ultrathin metal oxides, such as hafnium oxide and aluminum oxide, are shown to enable (a) low-voltage (sub 2V) OFETs through dielectric and interface engineering on rigid and plastic substrates (Fig. 2), (b) simultaneous one-component modification of source/drain and dielectric surfaces in bottom-conatct OFETs, and (c) SAM-FETs based on molecular monolayer semiconductors. (3) High-performance inverted polymer bulk-heterojunction (BHJ) solar cells have been realized by modifying the interface of electron selective ZnO or TiO_2 with a series of fullerene-based SAMs (C_{60}-SAMs) containing different anchoring groups, linkage location, and functionalization. These SAMs serve multiple functions to affect the photoinduced charge transfer at the interface to reduce the recombination of charges, passivate inorganic surface trap states, improve the exciton dissociation efficiency at the polymer/ZnO or TiO_2 interface as well as a template to influence the overlayer BHJ distribution of phases, morphology and crystalline domains leading to better charge selectivity.

1. Kim, M.; Hohman, J. N.; Cao, Y.; Houk, K. N.; Ma, H.; Jen, A. K.-Y.; Weiss, P. S. *Science* **2011**, *331*, 1312-1315.

2. Ma, H.; Acton, O.; Hutchins, D. O.; Cernetic, N.; Jen, A. K.-Y. *Phys. Chem. Chem. Phys.* **2012**, *14*, 14110-14126.

3. Acton, O.; Hutchins, D.; Arnadottir, L.; Weidner, T.; Ting, G. G.; Kim, T. W.; Cernetic, N.; Castner, D. G.; Ma, H.; Jen, A. K.-Y. *Adv. Mater.* **2011**, *23*, 1899-1902.

4. Acton, O.; Dubey, M.; Weidner, T.; O'Malley, K.; Kim, T. W.; Ting, G. G.; Hutchins, D.; Baio, J. E.; Lovejoy T. C.; Gage, A. H.; Castner, D. G.; Ma, H.; Jen, A. K.-Y. *Adv. Func. Mater.* **2011**, *21*, 1476-1488.

5. Ma, H.; Yip, H.-L.; Huang, F.; Jen, A. K.-Y. *Adv. Func. Mater.* **2010**, *20*, 1371-1388.

Fig. 1. Confined Surface for Photoreaction and Molecular Electronics

Fig. 2. Ultrathin SAM/MO Hybrid Dielectrics and Interface for Low-Voltage High-Performance OFETs

ASS-7-Or-7
Synthesis and characterization of chromium carbides

T01 Applied Surface Science

#ASS-7-Or-7

A. Batan [1], M. Detroye [2], J. Vereecken [3], H. Terryn [3], C. Buess-Herman [1], F. Reniers [1].

[1]Université Libre de Bruxelles - Bruxelles (Belgium), [2]MACtac Europe - Soignies (Belgium), [3]Vrije Universiteit Brussel - Bruxelles (Belgium).

Chromium carbides have remarkable properties such as high melting points, good strength and a good corrosion resistance. Therefore, these compounds have been widely used in a variety of industrial applications, such as shaft bearings, seals, high-temperature furnaces, nozzles and metal machining molds.
In this study, we developed an easy and thermodynamically coherent method to synthesize successively the 3 stoichiometrically identified chromium carbides using chromium metal powder and a methane-hydrogen mixture as metal precursor and reactive gases for the carburization reactions. The effects of experimental parameters such as temperature, flow rate of the reactive gas and the methane/hydrogen ratio are investigated and discussed.
Two analysis techniques are used to characterize the products obtained: X-ray diffraction provides structural analysis and Auger electron spectroscopy determines the surface composition.
Depending on the temperature, which is an important parameter in the process of carburization, X-ray diffraction analysis shows the presence of several carbides phases. The sequence of appearance of carbides phases when the temperature increases suggests that the carburization of chromium is progressive. After the reduction of the native chromium oxide layer, chromium is carburized first to the Cr23C6 phase, then to the Cr7C3 phase and finally to the Cr3C2 phase.
The use of a reactive gas mixture of 10% methane in hydrogen shows that, for the same reaction time, the formation of chromium carbides starts at lower temperatures than when a reactive gas mixture of 1% methane in hydrogen is used.
An increase of the reactive gas flow rate results in a decrease of the temperature of appearance of each carbide phase regardless the composition of the reactive gas.

ASS-5-Or-9
Angular Dependent NEXAFS investigation of gold nanoparticles/aromatic thiols hybrids deposited onto inorganic substrates: correlation between molecular orientation behavior, thiol molecular structure and nanoparticles size.

T01 Applied Surface Science

#ASS-5-Or-9

C. Battocchio [1], S. Mukherjee [2], I. Fratoddi [3], M. Quintiliani [3], M.V. Russo [3], G. Polzonetti [1].

[1]"Roma Tre" University, Department of Sciences, via della Vasca Navale 79 00146 - Rome (Italy), [2]Department of Physics North Carolina State University Raleigh, NC 27695 USA - Raleigh (United states), [3]Sapienza Univesrity, Department of Chemistry, P.le A. Moro 5 00185 - Rome (Italy).

Recently, great attention has been devolved to the development of new strategies for the stabilization of metal nanoparticles (MNPs). The chemical stabilization of MNPs by capping metallic clusters with organic ligands has several advantages such as low preparation costs and better NPs size, monodispersity and shape control. The ligands play a double role: they stabilize the MNPs, and, when opportunely selected, they can make the resulting hybrid system better suited for different applications. One of the most interesting properties of MNPs is their Localized Surface Plasmon Resonance (LSPR)[1]. The interaction between MNPs and electromagnetic radiation is constituted by localized surface plasmons, which are coherent oscillations of the metal electrons in resonance with light of a certain frequency (v). The plasmonic properties are strongly dependent on MNPs interactions, since the near-field on one particle interacts with the one on an adjacent particle, coupling together the plasmon oscillations. This interparticle plasmon coupling is responsible for the intense enhancement of spectroscopic signals from molecules adsorbed on MNPs layers,

providing the capability for single-molecule sensing and detection, as in SERS. The coupled-particle LSPR occurs at a v shifted from the single particle one, and the magnitude of the plasmon shift depends on the strength of the interparticle coupling that, in turn, depends on the distance between adjacent MNPs[2]. Since the plasmonic field coupling decays exponentially with inter-particle distance, it is of primary importance, for technological applications, to ensure that the MNPs deposited on an opportune surface are regularly arranged and conveniently spaced. Recently, the ability of angular dependent Near Edge X-ray Absorption Spectroscopy (AD-NEXAFS) to probe that appropriate ligands induce an ordered arrangement of MNPs was assessed[4].
Here we present the AD-NEXAFS investigation carried out on small gold nanoparticles (2-4 nm diameter) capped with trimethylsilyl benzene-thiol (SEB). The hybrid systems molecular structure and organization on a TiO_2 surface was investigated by AD-NEXAFS at C K-edge. To obtain a better insight into the organization of small NPs on the substrate, AD-NEXAFS measurements and calculations were also carried out on a free molecule as well as with a molecule anchored to Au cluster representing the self assembling monolayer. The NPs mean size was tuned by varying the Au/thiol stoichiometry in the synthesis procedure, obtaining samples of different mean diameter, with the aim to find a correlation between nanoparticles sizes and degree of order in their arrangement. It was observed that the smallest NPs are more likely induced to self assemble by the intermolecular interactions arising between the thiols aromatic rings.

[1] M. Rycenga, C.M. Cobley, J. Zeng, W. Li, C.H. Moran, Q. Zhang, D. Qin, Y. Xia, Chem. Rev. 11, (2011), 3669
[2] P.K. Jain, W. Huang, M.A. El-Sayed Nano Lett. 7 (7) (2007) 2080
[3] M. Ranjan, S. Fackso, M. Fritzsche, S. Mukherjee Microel. Eng. 102 (2013) 44
[4] J.H. Kang, Y.C. Kim, K. Cho, C.E. Park, J. Appl. Pol. Sci. 99 (2006) 3433

ASS-1-Or-4
Interface study between Nanostructured TaNx [x=0, 1.8] films and Carbon Nanotubes grown by Chemical Vapor Deposition

T01 Applied Surface Science

#ASS-1-Or-4

B. Bouchet-Fabre [1], M. Pinault [1], C. Jin [2], E. Foy [3], M. Mayne-L'hermite [1], T. Minea [2], M.C. Hugon [2].

[1]Lab. Francis Perrin - Saclay (France), [2]Lab. Physique des gaz et Plasma - Orsay (France), [3]Lab. d'Archéométrie - Saclay (France).

TaNx films were used as buffer layers for the study of the growth of Carbon Nanotubes CNT, by chemical vapor deposition CVD at 850°C, at room pressure, using ferrocene as catalyst source [1,2].
TaNx films 60nm thick, were deposited on Si substrates using High Power Impulse Magnetron Sputtering HIPIMS in reactive gas conditions [3].TaNx film properties were analyzed for various discharge conditions, using Ar/N2 reactive plasmas for Ta target materials. The emission line of metal ionized species Ta+* sputtered from the cathode were detected in HIPIMS discharge, as well as the atomic nitrogen lines [4].
The reactivity of the films was checked in the CVD furnace, used for CNT growth, at 850°C under argon flux in ambient atmosphere [2]. The pristine films, the annealed films and the interface formed by the CNT bottom and the TaNx buffer has been studied, coupling the nuclear analysis for elementary composition NRA, RBS, grazing incidence X-Ray diffraction DRX, X-ray photoelectron spectroscopy XPS, and high resolved Scanning Electron Microscopy SEM-Feg.
The morphology and characteristic of the CNT are presented in relation first with the properties of the pristine TaNx films and their evolution under heat treatment, secondly with the structure of the interface between the CNT and buffer films.

1 B. Bouchet-Fabre, A. Fadjié-Djomkam, R. Fernandez-Pacheco, M. Delmas, M. Pinault, P. Jegou, C. Reynaud, M. Mayne-L'Hermite, O. Stephan, T. Minéa, Diam. &

relat. mat.20, 2011, 999-1004.
2 C. Jin, M. Delmas, P. Aubert, E. Foy, F. Alvarez, T. Minéa, M.C. Hugon, B. Bouchet-Fabre, Thin solid Films 519, 2011, 4097-410
3 D. Benzegoutta, M.C. Hugon, J. Bretagne, M. Ganciu, Plasma Sources Sci. Technol.18, 2009, 045025
4 C. Jin, O. Fromentin, M.C. Hugon, N. Marsot, B. Bouchet-Fabre, R. Sireilles, F. Alvarez and T. Minea, Extended abstract, proceeding of 30th ICPIG, Aug.28th – Sept.2nd 2011, Belfast, Northern Ireland, UK

ASS-1-Or-2
Destructive versus non destructive methods for compositional depth profiles

T01 Applied Surface Science

#ASS-1-Or-2

N. Benito [1], R. Escobar Galindo [2], J. Rubio Zuazo [3], G.R. Castro [3], C. Palacio [1].

[1]Universidad Autónoma de Madrid - Madrid (Spain), [2]ICMM - Madrid (Spain), [3]ESRF - Grenoble (France).

The analysis of the near-surface region of solids can be carried out using either non-destructive or destructive methods depending on the thicknesses to be analyzed. For thin films above 10 nm the method most frequently applied to obtain the concentration depth profiles (CDP), that is, the thin film composition with depth, is ion sputtering in combination with AES, XPS or SIMS [1]. The choice of a specific technique depends on the concrete analytical problem to be solved and the general trend is the simultaneous use of several techniques due to the complementary information provided [1]. The main drawback of this approach is related to the surface modifications produced during ion bombardment since the sputtering process can alter the surface composition, the surface chemistry and morphology [1], etc. Rutherford backscattering spectrometry (RBS) has been also used as a non-destructive method to obtain CDP. However, RBS do not provide chemical information and the depth resolution obtained is rather poor.
Other non- destructive methods to obtain CDP are based on the use of XPS in conjunction with the variation of the information depth. The information depth depends on the kinetic energy of the emitted photoelectrons and on its take off angle [2,3]. Conventional XPS laboratory equipments ordinarily use Mg or Al Kα (1253.6 or 1486.6 eV, respectively for the photon energy) and experimental setup allowing take off angle modifications from 0-70º which limits the information depth to around 10 nm. The variation of take off angle is named Angle-Resolved XPS (ARXPS) and it is useful for analyzing in a non-destructive sense the very near surface of solids and very thin films [3]. The integral equation relating measured intensities as a function of the take off angle and the concentration depth profiles is a prototype of ill-posed problems and different approaches have been proposed to obtain the CDP from

experimental measurements [3,4].
The kinetic energy of emitted photoelectrons and, as a consequence, the information depth can be increased using synchrotron radiation sources. The technique is named Hard X-ray photoelectron Spectroscopy (HAXPES), it is also a non-destructive one and presents some limitations imposed by the high electron energies to be analyzed. Within this work we aim to explore the capabilities of HAXPES to obtain the CDP either of buried interfaces or of thin films that are of interest for optical applications [5], through a comparative study using ARXPS, XPS and simultaneous sputtering, and HAXPES.

[1] Escobar Galindo R, Gago R, Duday D and Palacio C 2010 Anal. Bioanal. Chem. **396** 2725
[2] Zier M, Oswald S, Reiche R and Wetzig K 2007 Michochim. Acta **156** 99
[3] Palacio C, Ocón P, Herrasti P, Díaz D and Arranz A 2003 J. Electroanal. Chem. **545** 53
[4] Paynter R W 2009 J. Electron Spectrosc. Relat. Phenom. **169** 1
[5] Benito N, Díaz D, Vergara L, Escobar Galindo R, Sánchez O and Palacio C 2011 Surf. Coat. Technol. **206** 1484

BI/ASS/NST-P1-08
WETTABILITY OF BIOCOMPATIBLE HYDROXYAPATITE

T01 Applied Surface Science

#BI/ASS/NST-P1-08

M. Mendez-Gonzalez [1], A. Ordoñez-Rodriguez [2], G. Gonzalez M. [3], G. Méndez G. [4].

[1]ESFM-IPN - México (Mexico), [2]UIberoamericana - México (Mexico), [3]UPIBI - México (Mexico), [4]UAQ - Querétaro (Mexico).

Since wettability is a surface characteristic defined by the hydrophilic or hydrophobic behavior of the material, it is determinant for the interaction of biomaterials with biomolecules or for cells adhesion. The present work determinates the wettability of three different liquids that are involved in biological issues that were tested on pills of hydroxyapatyte synthesized by chemical precipitation. This determination was made by the measurement of the contact angle, which gave us the corresponding angles to each solution and pressure of pills. It was concluded that exist a direct relation between the pressures at which the pills were fabricated and the contact angle. Also it was noted that the characteristics of the solutions influence in the calcium phosphates wettability. In the three cases as the pressure increases the contact angles do it to. This behavior due the pressure decreases the space between the calcium phosphates particles. The three liquids tested have the hydrophilic behavior that is desirable for a biomaterial because it is less than 65^0. For further uses is better to used pills of hydroxyapatyte made at 1 Ton due have them a more hydrophilic behavior.

1. R. Aranov, R. Rosenman; Tunable hydroxyapatite wettability: effect on adhesion of biological molecules, Process Biochemistry 41, 2367-2372, **2006**.

2. A. Yamaguchi, T. Komori, T. Suda; Regulation of osteoblast differentiation mediated by bone morphogenetic proteins, hedgehogs, and Cbfa1, Endocr. Rev. 21, 393-411, **2000**.

3. G. Stein, J. Lian; Molecular mechanisms mediating proliferation/differentiation interrelationships during progressive development of the osteoblast phenotype, Endocr. Rev. 14, 424-442, **1993**.

4. B. Heng, T. Cao, L. Stanton, P. Robson, B. Olsen; Strategies for directing the differentiation of stem cells into the osteogenic lineage in vitro, J. Bone Miner. Res. 19, 1379-1394, **2004**.

5. N. Nakamura, O. Sekijima, H. Yamashita; Enhanced osteoblastic adhesion through improved wettability on polarized hydroxyapatite, J. Ceramic Society Japan, 118, 474-478, **2010**.

Figure 1. Contact angle meter screen without drop.
Figure 2. Contact angle meter screen with a drop.

ASS-P2-04
Formation of Local Conduction Path in relation to Electrical Properties of Amorphous IZTO Thin Films

T01 Applied Surface Science

#ASS-P2-04

H. Kang [1], Y.R. Denny [1], K. Lee [1], S. Lee [1], S. Seo [1], D.S. Yang [2], S. Heo [3], J.G. Chung [3], J.C. Lee [3], S. Tougaard [4].

[1]Departement of Physics, Chungbuk National University - Cheongju (Korea, republic of), [2]Departement of Physics Education, Chungbuk National University - Cheongju (Korea, republic of), [3]Analytical Engineering Center, Samsung Advanced Institute of Technology - Suwon (Korea, republic of), [4]Departement of Physics and Chemistry, University of Southern Denmark - Odense M. (Denmark).

The electronic and optical properties of Indium zinc tin oxide (IZTO) films were investigated by X-ray photoelectron spectroscopy (XPS), reflection electron energy loss spectroscopy (REELS), and UV-spectrometer. The EXAFS experiments were carried out to examine the relationship between the local structure and the electrical properties for IZTO thin films, which has not been previously reported. IZTO thin films were grown on glass substrate by RF magnetron sputtering method. The XPS spectra show that all IZTO thin films have mixed metal and oxide phases. REELS spectra revealed that the band gap was increased for IZTO thin films annealed at 350 ^{o}C in air due to Burstein Moss Effect, but decreased with increasing Zn/Sn ratios. The values of the band gaps are consistent with the optical band gaps estimated by UV-spectrometer. The optical parameters were determined from the interference fringes of the transmission spectra for the wavelength ranging from 300 to 3000 nm. Quantitative analysis of the experimental cross sections of REEL spectra was performed using the QUEELS-ε(k,ω)-REELS to determine the dielectric function, refractive index, and transmission of IZTO thin films. The refractive index obtained from the calculated UV-spectrometer is similar to that of the calculated REELS results. Amorphous IZTO films prepared with the zinc content of 48% exhibited high mobility of 30.60 $cm^2V^{-1}s^{-1}$, large on-off current ratio of 10^9, and high transmittance of 85%. The EXAFS and the electrical characteristics indicate that the creation of local conduction paths can result from the nearest neighbors of 4s orbitals of Zn^{2+} ions in

IZTO thin films. Our results can be a guide for device applications for thin-film transistors with high field-effect mobility and good transparency.

ASS-6-Or-5
Corrosion under argon irradiation of titanium and zirconium studied by AFM and Spectroscopic Ellipsometry

T01 Applied Surface Science

#ASS-6-Or-5

D. Gorse-Pomonti [1], E. Garcia-Caurel [2], Y. Serruys [3], N. Bérerd [4], N. Moncoffre [4].

[1]CNRS - Palaiseau (France), [2]Ecole Polytechnique - Palaiseau (France), [3]CEA-DEN - Gif-Sur-Yvette (France), [4]Institut de Physique Nucléaire - Villeurbanne (France).

Until recently the possible existence of damages caused by ion irradiation to metal surfaces in the low MeV range (1 – 10 MeV) was just ignored. This state of the art could be justified by the fact that a simple plot of both nuclear (S_n) and electronic (S_e) energy losses as a function of the projectile energy does not reveal any “accident” which would have justified special attention in this energy range, whatever the target material considered. On the other hand, one should not forget that both S_n and S_e contribute in principle to the overall slowing down process of the projectile in this energy range, complicating the data analysis.

In this paper, we show that, unexpectedly, argon ion irradiation between 1 and 15 MeV produces damages on both titanium and zirconium surfaces, taking the form of accelerated oxidation and/or craterization effects, varying as a function of the projectile energy and the annealing atmosphere (temperature and pressure) [1].

The mirror-polished titanium and zirconium samples are irradiated using the irradiation cell adapted to the extracted beam line of the 4 MV Van de Graaff accelerator of the Nuclear Physics Institute of Lyon. The irradiation conditions are: 1 to 9 MeV Ar^{n+} (n= 1, 3), 3 x 10^{10} ions cm^{-2} s^{-1} up to 5 x 10^{14} ions cm^{-2}.

Using AFM, we show that the titanium and zirconium surfaces are attacked under argon ion bombardment at high temperature (up to 500°C) in weakly oxidizing medium (under rarefied dry air pressure ranging from 5,7 10^{-5} Pa to 5 10^{-3} Pa) for a fixed dose of about 5 10^{14} ions/cm^2. We observe the formation of nanometric craters over the whole titanium surface irradiated between 2 and 9 MeV and the whole zirconium surface irradiated at 4 MeV, the characteristics of which vary depending on the temperature and air pressure. In the case of the Ar/Ti couple, the superficial damage efficiency increases when the projectile energy decreases from 9 to 2 MeV [2]. Moreover, whereas the titanium surface seems to be transparent under the 15 MeV ion beam, the zirconium surface exhibits numerous micrometric craters surrounded by a wide halo.

The crater characteristics (size and superficial density) differ significantly from that observed both in the low energy range (keV) where the energy losses are controlled by ballistic collisions (S_n) and in the high energy range (MeV - GeV) where the energy losses are controlled by electronic excitations (S_e), which was not completely unexpected in this intermediate energy range for which combined S_n - S_e stopping power effects are possibly foreseen.

Using Spectroscopic Ellipsometry, we show that there is an irradiation effect on the thermal oxidation of titanium, enhanced under the argon ion beam, and that there is also an energy effect on the oxide thickness and stoichiometry. More precisely, as seen in Figure 1, we show that there is an oxidation peak as function of the argon ion energy, found maximum at 3 MeV under present experimental conditions [3]. The today available results obtained with zirconium oxidized under irradiation under same conditions strongly suggest the existence of an oxidation peak as function of the argon ion energy, for zirconium as for titanium, in the same projectile energy range.

[1] N.-L. Do, PhD. thesis, Ecole Polytechnique, Palaiseau, November 21 (2012)

[2] N.-L. Do, N. Bererd, N. Moncoffre, F. Yang, P. Trocellier, Y. Serruys, D. Gorse-Pomonti, «Radiation damage induced at the surface of titanium by argon ions of a few MeV», J. Nucl. Mater., 419 (2011) pp.168-176.

[3] D. Gorse-Pomonti, N.-L. Do, N. Bérerd, N. Moncoffre and G. Baldinozzi, «Titanium and zirconium oxidation under argon irradiation in the low MeV range», in proceedings of the MRS fall meeting, Boston (2012).

Figure 1. Oxide thickness determined by SE versus argon ion energy for titanium samples oxidized under irradiation (full line: eye guide). The oxide thickness of the reference oxidized titanium is noted at E = 0.

ASS-10-Or-1
XPS, AFM and TOF-SIMS characterization of silicon surface modified with different aminosilanes

T01 Applied Surface Science

#ASS-10-Or-1

G. Jakša [1], J. Kovač [1], B. Štefane [2].

[1]Jožef Stefan Institute, Jamova 39 - Ljubljana (Slovenia), [2]Faculty of Chemistry and Chemical Technology, Aškerčeva 5 - Ljubljana (Slovenia).

The aim of this work was the preparation and characterization of modified silicon surface, with a purpose for using them in sensor's applications (detection of explosives like TNT, DNT, RDX,…). Single crystal silicon wafers (111) were modified with (3-aminopropyl)-trimethoxysilane (APTMS) and p-aminophenyltrimethoxysilane (APhS). Before the modifications a native oxide layer from the silicon was reduced with HF and then oxidized in a controlled manner by using an oxygen plasma. We deposited the self-assembled layers from a solution of aminosilanes in different solvents under various reaction conditions. The surfaces were characterized using X-ray photoelectron spectroscopy (XPS), atomic force microscopy (AFM) and Time-of-Flight secondary ion mass spectrometry (TOF-SIMS). The surface composition and the chemical bonding were determined by XPS, the surface morphology and roughness by using AFM and the chemical structure with TOF-SIMS. Our results show that increased mobility of molecules at higher temperatures of reaction mixture leads to greater surface coverage and at the same time the formation of thinner layer. At longer deposition times and at higher concentrations of aminosilanes in solvent, polymerization of molecules occurs and the formation of thick layer is observed. Comparison between aliphatic and aromatic aminosilanes will be given.

ESD/ASS-P3-14
Structural properties and radiation resistance of InGaAs solar cells

T01 Applied Surface Science

#ESD/ASS-P3-14

A. Nouri [1], H. Benslimane [1], M. Bouslama [2], M. Ghaffour [2].

[1]université de béchar - Béchar (Algeria), [2]LabMat - Oran (Algeria).

InGaAs semiconductor is an important material due to its high electron mobility of 13000 cm-2V-1S-1 and small energy band gap of 0 .76 eV at 300K [1]. It is widely used for light emission in the range of 1.3–1.5 mm [2] as diode emitter laser radiation and also as detector. Actually it is a very promising material in solar cell fields due to its irradiation resistance [3,4] and the improving overall efficiency of multi-junction based on InGaAs. Its yield can reach 41.3% [5] or 42.3% under a concentration of 500 Suns [6]. In this work we presents results of AFM characterization of the InGaAs/GaAs system, we also study the effect of electron beam irradiation under UHV conditions on InGaAs/GaAs systems using Auger electron spectroscopy (AES) and the electron energy loss spectroscopy (EELS) .

keywords: InGaAs; AES; EELS; AFM, Solar Cell

[1] Pal D, Bose DN. J Appl Phys;77:210 (1995)
[2] Hollinger G, Joseph J, Robach Y, Berngignat E, Commere B, Viktorovitch P, et al. J Vac Sci Technol;B5(4):1108.(1987)
[3] Masafumi Yamaguchi J. Appl. Phys. 78, 1476 (1995)
[4] A. Nouri et al. Vacuum 81 979–984(2007)
[5] Mathews, Ian; O'Mahony, Donagh; Corbett, Brian; et al.optics express, 20; 19, A754 (2012)
[6] R. R. LaPierre, J. Appl. Phys. 110, 014310 (2011)

ASS-3-Or-3
Direct observation of layer-by-layer removal from Si(100) in hydrogen ambient by in situ spectroscopy

T01 Applied Surface Science

#ASS-3-Or-3

P. Kleinschmidt [1], S. Brückner [1], O. Supplie [2], H. Döscher [1], T. Hannappel [1].

[1]TU Ilmenau - Ilmenau (Germany), [2]Helmholtz-Zentrum Berlin - Berlin (Germany).

Good availability, low cost and mature technology has made silicon the material of choice for many semiconductor applications. Most investigations of relevant step structures on Si(100) thus far have been carried out in ultrahigh vacuum (UHV) where standard surface science techniques can be applied. Experimental and theoretical investigations have shown that of the two possible types of single-domain (and hence double-layer stepped) surfaces, the one with surface dimers of the reconstructed surface parallel to the step edges (denoted as D_B) is energetically favorable, while the one with dimers perpendicular to the step edges (D_A) is unfavorable.
Due to adjustable, superior electronic properties of III-V semiconductors, there is a high incentive to combine these advantages with those of silicon using III-V-on-Si heteroepitaxy. Here, the most applicable preparation methods are molecular beam epitaxy (MBE) and metalorganic vapor phase epitaxy (MOVPE), where the latter provides key advantages relating to cost and scalability.
We have studied the surface structure of Si(100) in the H_2-based MOVPE environment using reflection anisotropy spectroscopy (RAS), which measures the normalized difference of the reflected signal in two orthogonal directions of linearly polarized light under normal incidence. In the case of the Si(100) surface, the magnitude and sign of the resulting signal reflects the abundance of the two possible dimer orientations at the surface. We have benchmarked the RAS signals of the surface to scanning tunneling microscopy (STM), low-energy electron diffraction, X-ray photoelectron spectroscopy and Fourier-transform infrared spectroscopy, available via a dedicated MOVPE-to-UHV transfer system showing that our surfaces are H-terminated and contamination-free.

We obtained the energetically unfavorable surface with D_A double-layer steps on the Si(100) surface with 2° misorientation in [011] depending on the sequence of hydrogen pressures and temperatures during the process. We attributed the unfavorable step structure to the interplay of surface vacancy generation, diffusion and annihilation at step edges in a certain temperature range.
Here we subject the Si(100) surface with 0.1° misorientation to the same processing conditions. We observed elongated vacancy islands on the terraces by STM, and by recording RAS transients during annealing in the crucial temperature range, we directly observed an oscillatory behavior of the major dimer orientation at the surface. Hence, under these process conditions, surface atoms are removed in a layer-by-layer fashion, resulting in a surface structure which alternates between predominantly A-type and predominantly B-type. While similar to reflection high energy electron diffraction (RHEED) oscillations, the RAS oscillations do not reflect oscillating surface roughness but the oscillating majority domain, and the technique is applicable under MOVPE conditions where RHEED is not available. Our results provide direct access to the surface layer removal process and enable quantification of the associated removal rate in dependence on process conditions. The surface layer removal process implies the generation of vacancy islands and corroborates our model for D_A step structure generation on 2° Si(100).

ASS-P1-01
Metallic nanoparticles suported on ceria (CeO2) subjected to H2 reduction

T01 Applied Surface Science

#ASS-P1-01

F. Bernardi [1], A.S. Kilian [1], L. Luza [2], M.C.M. Alves [2], J. Morais [1], J. Dupont [2].

[1]Instituto de Física, UFRGS - Porto Alegre (Brazil), [2]Instituto de Química, UFRGS - Porto Alegre (Brazil).

Ceria (CeO_2) is an advanced material used for catalytic applications that has received much attention in the last past years [1]. The main reason is that oxygen vacancies at the surface can be rapidly formed and eliminated which gives to ceria the property of high capacity for oxygen storage. Due to this property, modern catalysts containing ceria are much more effective, for example, in the automotive exhaustion than the previous ones without ceria. Compared to different supports of metallic nanoparticles, ceria also enhances the performance of catalysts constituted of metallic nanoparticles in a variety of reactions such as the water gas-shift and the preferential oxidation of CO [1]. In special, mono and bimetallic Ni and Cu nanoparticles supported on CeO_2 are used in reactions of NO reduction and CO hydrogenation [2-3].
The reduction reaction is a key process employed in catalytic applications. It is very important to understand this process in order to project the final desired properties of the catalysts. For example, when using a reducible support (like ceria) the reduction process can affect the catalytic properties by means of the SMSI effect (geometrical or electronic factor) [4]. The geometrical factor of the SMSI effect can create new catalytic active sites or to block some existing ones, depending on the case studied. In this work it was studied the electronic and structural properties of systems consisting of Ni/CeO_2, Cu/CeO_2 and $Cu_{0.5}Ni_{0.5}/CeO_2$ nanoparticles subjected to H_2 reduction in situ and ex situ. The metallic nanoparticles were synthesized by using the ionic liquid $BMIBF_4$ in a procedure described previoulsy [5]. Thereafter, the nanoparticles were supported on CeO_2 and heated up to 500 ^oC in a H_2 atmosphere. The samples were investigated by means of XPS (X-Ray Photoelectron Spectroscopy), TEM (Transmission Electron Microscopy) and in situ XAS (X-Ray Absorption Spectroscopy) before and after the reduction reaction. In order to obtain kinetic information, in situ DXAS (Dispersive XAS) measurements were employed. All

XAS measurements were performed in the transmission mode at the Ce L_{III} edge, Ni K edge and Cu K edge.
The results show the existence of nanoparticles with ~5 nm diameter. XPS measurements with variable photon incident energy gave us electronic information of the surface of the nanoparticles where Cu and Ni atoms were initially oxidized. The atomic arrangement at the surface of the nanoparticles is discussed based on the XPS results. Structural information was obtained by XAS and DXAS measurements reveal details of the kinetic of H_2 reduction as a function of the reduction temperature and time. The reaction starts at ~285 ^{o}C for Cu/CeO_2, ~160 ^{o}C for Ni/CeO_2, ~190 ^{o}C (Cu) and ~435 ^{o}C (Ni) for $Cu_{0.5}Ni_{0.5}/CeO_2$ nanoparticles. After the beginning of the reduction it takes ~10 min for Cu/CeO_2, ~14 min for Ni/CeO_2, ~12 min (Cu) and ~14 min (Ni) for $Cu_{0.5}Ni_{0.5}/CeO_2$ to reduce completally the nanoparticles supported.

Acknowledgments: The authors thank to CNPq financial support and LNLS.

1. A. Trovarelli, Cat. Rev.: Sci. and Eng. 38 (4), 439, 1996.
2. J. Barrault et al. Appl. Cat. 46 (2), 269, 1989.
3. P. Bera et al. J. Cat. 186 (1), 36, 1999.
4. S. J. Tauster et al. JACS 100 (1), 170, 1978.
5. J. Dupont et al. Chem. Rev. 102 (10), 3667, 2002.

ASS-8-Or-8
XPS, ToF-SIMS and AFM characterization of air-plasma treated substrates and plasma deposited sol-gel siloxane coatings

T01 Applied Surface Science

#ASS-8-Or-8

J. Kovac [1], G. Jakša [1], J. Lahti [2], H. Christophliemk [2], D. Vangeneugden [3], M. Dubreuil [3], K. Rose [4], K. Bokelmann [4].

[1]Jozef Stefan Institute - Ljubljana (Slovenia), [2]Tampere University of Technology - Tampere (Finland), [3]Flemish Institute for Technological Research-VITO - Mol (Belgium), [4]Fraunhofer Institut fur Silicatforschung - Wuerzburg (Germany).

Polymer foils and paper based substrates for packaging applications are often subject of different surface treatments. Advanced analytical techniques are required to understand and control the basic processes during surfaces treatment. In this work we present X-ray photoelectron spectroscopy – XPS, secondary ion mass spectroscopy – SIMS and atomic force microscopy - AFM for characterization of paper and polymer materials modified by air plasma. The combined use of these techniques is demonstrated in the application examples in which a thin air-plasma deposited sol-gel based layer of triethoxysilane was deposited and characterized. The XPS and SIMS techniques were used to follow the surface composition, chemical bonds of surface atoms, molecular structures and spatial distribution of coated material whereas the AFM technique provided the information about the surface morphology. In this presentation the role of surface characterisation will be presented in the frame of the European project PlasmaNice: Atmospheric plasmas for nanoscale industrial surface processing, funded under the FP7 programme (1). The main objective of PlasmaNice was to develop equipment and process for industrial in-line atmospheric plasma deposition of functional nanocoatings on various fibre- and polymer-based substrates. The project aimed at the improvement of recyclability of conventional fossil fuel based plastics and the replacement by renewable bio-based and biodegradable materials for packaging.

(1) http://hlab.ee.tut.fi/plasmanice/home, Funded under the 7th Framework Programme, FP7-NMP-LARGE, Project No. IP 211473

ASS-6-Or-1
A first-principles view of the Cabrera-Mott Model of Metal Oxidation

T01 Applied Surface Science

#ASS-6-Or-1

A. Hellman, J. Baran, H. Grönbeck.

Competence Centre for Catalysis and Department of Applied Physics, Chalmers University of Technology - Göteborg (Sweden).

Oxidation of metals is an every-day phenomenon, which can be an unwanted process, e.g., automotive corrosion. However, under controlled conditions oxidation is of enormous practical importance, both in industry and science. For instance, thin oxides are widely used as catalysts, sensors, dielectrics, and corrosion inhibitors. The work of Cabrera and Mott (CM) in the mid-twenty century still remains the main theoretical model for growth of thin oxides on metals [1]. According to CM, electrons from the Fermi level of the metal substrate traverse the developing oxide film by either tunneling or thermionic emission to acceptor levels of oxygen molecules, thereby forming different anions (O_2^{2-}, O_2^-, O^{2-}, O^-) on the oxide surface depending on the outcome of the charge transfer. The negative anions and their positive counterpart at the metal-oxide interface generate an electric potential, called the Mott potential, which effectively lowers the energy barriers for migration of ions through the oxide. As the oxide thickness increase the additional effect of the Mott potentials to the oxidation rate diminishes and the oxidation process effectively stops at some limiting thickness.
Recently, Zhou et al. [2] have experimentally shown that the limiting thickness of the aluminum oxide on Al(111) can be tuned by the oxygen pressure. They observe that the thickness of the alumina film increases with increasing oxygen pressure up to 1 Torr, beyond which it remains constant at thickness of 12.4 Å.

By means of first-principles we have investigated the thickness of the protective oxide layer on aluminum. Our first-principles calculations [3] support many of the key assumptions of the CM model. For instance, based on our results we estimated the limiting thickness of Al_2O_3 on Al(111) to around 16 Å, which agrees well with the experimental data. Furthermore, the charge transfer to adsorbed oxygen molecules generates a Mott potential which value also agrees well with experimental estimates. However, the underlying reason for observing a limiting thickness of the protective oxide is not the diminishing effect of the Mott potential. Instead we will provide

another underlying reason for the limiting thickness based on our first-principles calculations.

1. Cabrera, N. and N.F. Mott, Reports on Progress in Physics 12 163 (1948).
2. Cai, N., et al., Phys. Rev. Lett. 107 035502 (2011).
3. Baran, J., Grönbeck, H., Hellman, A., submitted

ASS-P1-16
Influence of surface functionalization on metal growth kinetics – an in-situ investigation during sputter deposition

T01 Applied Surface Science

#ASS-P1-16

S. Roth [1], B. Heidmann [1], M. Schwartzkopf [1], A. Buffet [1], G. Herzog [1], R. Mannweiler [1], J. Perlich [1], J. Risch [1], K. Schlage [1], W. Wurth [2], E. Metwalli [3], P. Müller-Buschbaum [3], S. Bommel [1].

[1]DESY - Hamburg (Germany), [2]University of Hamburg - Hamburg (Germany), [3]Technische Universität München - München (Germany).

The interaction of metals with polymeric and functionalized surfaces and interfaces is of utmost importance for tailoring polymer metal nanocomposite materials and devices [1]: This interaction between the metals and the surface/interface [2,3,4] strongly determines the metal layer morphology. The morphology finally governs the layer's physical properties, which are tuned to the desired application in optical technology, sensors, or photovoltaic devices. Sputter deposition on the other hand is one method of choice and widely used in industry to install tailored metal films on surface or in the near surface region. Therefore, it is mandatory to investigate metal layer growth under real processing conditions in-situ and in real-time when tuning the metal-surface interaction.
As is well known, thiol-based surfaces show a strong interaction with gold. In this study we therefore used as a model system gold and the functionalization via different silanization of silicon wafers, allowing for chemi- or physisorption of the deposited gold atoms. The differently functionalized surfaces were investigated prior to and after gold sputter deposition using optical atomic force microscopy, imaging ellipsometry and contact angle measurements. To observe the difference in growth kinetics in-situ, we combined sputter deposition and microbeam grazing incidence small-angle x-ray scattering (µGISAXS) at the synchrotron beamline MiNaXS/P03 of DESY, Hamburg, Germany [5]. The analysis of the gold sputter deposition shows clear changes in cluster growth depending on the differently functionalized surfaces. Depending on predominant chemisorption or physisorption, the gold atoms arrange to well defined clusters or more homogenous layers. As an example, fig. 1 shows the

growth of gold layers on a thiol-based functionalized silicon wafer. The clearly visible maxima indicate cluster growth as a function of deposited gold layer thickness.

[1] F. Faupel et al., Adv. Eng. Mat. 12, 1177 (2010).
[2] A. Buffet et al., Langmuir 27, 343 (2011)
[3] G. Kaune et al., ACS Appl. Mater. Interfaces 1, 353 (2009)
[4] S.V. Roth et al., J. Phys. Cond. Matter 23, 254208 (2011)
[5] A. Buffet, et al., Journal of Synchrotron Radiation 19, 647 (2012).

Fig. 1. Cluster growth on thiol-based surface during sputter deposition. The deposited gold thickness increases from bottom to top. The shift of the maxima indicates a strong cluster growth. Black lines denote data, red lines the analytical fit to the data. The data are shifted for clarity.

ASS-9-Or-3
In situ X-ray photoelectron spectroscopy study of adsorption of (3-aminopropyl) triethoxysilane on rutile TiO2(110)

T01 Applied Surface Science

#ASS-9-Or-3

S. Chaudhary [1], N. Johansson [2], L. Montelius [3], L. Ye [4], J. Schnadt [5].

[1]Division of Synchrotron Radiation Research, Division of Pure & Applied Biochemistry, Lund University, ENI AB, Malmö, - Lund (Sweden), [2]Division of Synchrotron Radiation Research,Lund University - Lund (Sweden), [3]Division of Solid State Physics,Lund University, ENI AB, Malmö, - Lund (Sweden), [4]Division of Pure & Applied Biochemistry,Lund University - Lund (Sweden), [5]Division of Synchrotron Radiation Research, Lund University - Lund (Sweden).

Covalent immobilization and deliberate orientation of molecular sensing materials at surfaces represents an important route towards achieving a more specific response and reducing unspecific binding towards target materials in biosensors. Commonly used for immobilization of biomolecules such as proteins, enzymes, antibodies, and DNA in biomedical sensing applications are self-assembled silane monolayers. Among the potentially useful surfaces is rutile titanium dioxide. Here we have investigated the modification of a TiO_2(110) surface with (3-aminopropyl) triethoxysilane (APTES), which is expected to be a useful coupling layer towards sensing materials.

Our aim is an atomic-scale characterization of the structure and properties of the APTES binding layer, and therefore we have studied the interaction of APTES with a rutile TiO_2(110) surface using synchrotron radiation based x-ray photoelectron spectroscopy. The studies have been performed both in ultrahigh vacuum (UHV) and ambient pressure mode. Prior to the adsorption of APTES, hydroxyl groups (OH) were created on the TiO_2 surface by adsorption of water at room temperature. The x-ray photoelectron spectra confirm the attachment of APTES on TiO_2. The measurements shows that in ultrahigh vacuum APTES reacts with OH groups through its silicon end to form a silanized surface. After the saturation of APTES on TiO_2 in UHV, the deposition of APTES was continued at ambient pressures up to approximately 0.2 mbar. [1] At these pressures we find indications for a reversed

attachment of APTES, i.e. APTES reacts with the surface through the amine group (Fig. 1).[2] This pressure dependence of the adsorption shows that ultrahigh vacuum studies of silanes not always can be extrapolated to the real system, but that investigations at ambient pressure are necessary for the elucidation of silane surface structures. We need to study the system in more detail by variation of deposition parameters such as silane concentration, reaction temperature, and annealing. For the near future we also plan near -edge X-ray absorption fine structure spectroscopy experiments to obtain more information about the APTES adsorption geometry.

[1]. J. Schnadt, J. Knudsen, J. N. Andersen, H. Siegbahn, A. Pietzsch, F. Hennies, N. Johansson, N. Mårtensson, G. Öhrwall, S. Bahr, S. Mähl, O. Schaff, Journal of Synchrotron Radiation, 2012, 19, 701.
[2]. Y.Y. Song, H. Hildebrand, P. Schmuki, Surface Science, 2010, 604, 346–353.

Figure1. Possible adsorption geometries of APTES on TiO_2

ASS-3-Or-2
UV Photoelectron Spectroscopy at Near Ambient Pressure in APPES

T01 Applied Surface Science

#ASS-3-Or-2

C. Gopinath, K. Roy.

National Chemical Laboratory - Pune (India).

Ambient pressure photoelectron spectroscopy (APPES) is becoming increasingly popular to explore the catalysis aspects at near ambient pressure (around 1 mbar) and high temperature conditions. It works fine with x-ray photons, or rather high kinetic energy (KE) electrons, mainly due to relatively lower inelastic scattering and hence good S/N is maintained. However, when the KE of photoelectrons are <100 eV, there are problems in observing decent S/N ratio under near ambient pressure. In the recently installed laboratory APPES system at NCL, Pune, we are able to observe the UVPES with He-II excitation source under near ambient conditions. Figure 1 shows the UVPES spectrum obtained on Ag-surfaces at room temperature and different partial pressure of N_2. Indeed well-defined electronic state of molecular N_2 was also observed between 11 and 15 eV. As a test case we explored the oxidation of polycrystalline copper surfaces under molecular O2 at different partial pressures and temperatures. Changes observed in the valence band spectra were recorded with AlKα and shown in Figure 2 for systematic changes in copper oxidation state. UVPES spectra were also recorded in the above conditions as that of Fig. 2 at near ambient pressure. Indeed both the data are complementary, since the photoionization cross section of Cu 3d and O 2p are high with x-ray and UV photons, respectively. The most important point is the observation of UVPES under high pressure conditions, which demonstrate the possibility of exploring low KE electrons under near ambient conditions. Reasons for the observation of UVPES at near ambient conditions will be presented in detail.

Figure 1: Valence band spectra recorded on Ag foil with He II source at different partial pressure of N_2.
Figure 2: Valence band spectra recorded on Cu foil with monochromatized Al Kα x-

ray source at 1 mbar O_2 pressure. Systematic changes in oxidation of copper is observed.

ASS-P3-11 ELECTROCHEMICAL GRAFTING OF SnO2 THIN FILMS DEPOSITED BY MOCVD FOR SENSOR APPLICATIONS

T01 Applied Surface Science

#ASS-P3-11

R. Drevet [1], N. Prud'homme [1], S. Le Moal [1], C. Legros [1], P. Ribot [1], D. Dragoé [1], M.G. Barthes-Labrousse [1], A. Chaussé [2], M. Andrieux [1].

[1]Univ. Paris Sud 11, LEMHE-ICMMO, CNRS UMR 8182 - Orsay (France), [2]Université d'Evry Val d'Essonne, LAMBE, CNRS-CEA UMR 8587 - Evry (France).

This work aims to synthesize hybrid materials by functionalizing nanostructured tin dioxide (SnO_2) thin films obtained by metal organic chemical vapor deposition technique (MOCVD) [1]. The functionalization of the surface is carried out by electrochemical grafting from the reduction of a diazonium salt [2-3]. This grafted surface is a promising sensor to detect and quantify metallic ions in water samples. The obtained hybrid material (Fig.1) is characterized by several techniques: field emission gun-scanning electron microscopy (FEG-SEM) associated to energy dispersive X-ray spectroscopy (EDS), grazing incidence X-ray diffraction (GIXRD), Fourier transformed infrared spectroscopy (FT-IR) and X-ray photoelectron spectroscopy (XPS).

These characterizations show that MOCVD technique is able to provide a control over the structural properties of the SnO_2 thin film as a function of the experimental parameters used. For example, tetragonal and orthorhombic SnO_2 structures with various nanocrystalline morphologies are obtained in various proportions as a function of the substrate temperature and the deposition frequency used during the process. The modification of the structural properties of the coating is linked to variations of the electrochemical behavior of the surface, which implies various grafting results.

Finally, the sensor properties of the synthesized materials are assessed by electrochemical analytical techniques as cyclic voltammetry (Fig. 2) and reveal that the obtained hybrid material is able to detect, for example, copper ions in water at concentrations lower than 10^{-7} mol.L^{-1}.

[1] M. Andrieux, P. Ribot, C. Gasquères, B. Servet, G. Garry, Applied Surface Science 263, 2012, 284-290.
[2] S. Betelu, C. Vautrin-Ul, A. Chaussé, Electrochemistry Communications 11, 2009, 383-386.
[3] N. Vilà, D. Bélanger, Electrochimica Acta 85, 2012, 538-547.

Figure 1 : Schematic representation of the so obtained hybrid material

Figure 2 : Cyclic voltammetry as a function of graftings amount

ASS-5-Or-10
Spinodal decomposition in Fe-Cr thin films studied by atom probe tomography

T01 Applied Surface Science

#ASS-5-Or-10

Y. Colignon [1], D. Mangelinck [1], K. Hoummada [1], M. Dumont [1], P. Maugis [1], O. Senninger [2], M. Nastar [2], F. Soisson [2].

[1]Aix-Marseille Université, IM2NP-CNRS, Faculté de saint Jérôme, Case 142 - 13397 - Marseille (France), [2]CEA, DEN, Service de Recherches de Métallurgie Physique, F-91191 - Gif-Sur-Yvette (France).

Oxide dispersion strengthened steels (ODS) are used in many areas such as aeronautics and nuclear industry, especially the future fusion nuclear power plant and the fourth generation of fission plants. In fuel cladding of fission reactors, the ODS will be held at temperatures in the range of 350-600°C for many months. In ODS steel based alloys, the aging is accompanied by an embrittlement called 475°C embrittlement. Spinodal decomposition is often cited as the cause of this phenomenon, thus it is important to study spinodal decomposition kinetics in these materials.

In this study, spinodal decomposition has been studied for application as well as from a fundamental point of view, since the Fe-Cr-O system has similarities with complex ODS materials. However the alloy addition elements can modify the decomposition kinetics. We studied spinodal decomposition in thin films and bulk samples. Thin films have been prepared in two ways: (i) homogeneous composition with an average composition in the spinodal domain (Fe50Cr for example) and (ii) a modulated composition in one direction (fig1 and fig2) in order to observe an increase of the modulation amplitude due to spinodal decomposition. This study was based on atom probe tomography which is an ideal technique for spinodal decomposition studies. Several other characterization techniques (XRD, DSC, sheet resistance) were also used. Finally, our results on thin films were compared with experiments on bulk alloys and Kinetic Monte Carlo simulations.

We observed an unexpected damping of the Fe-Cr oscillations even if the average composition is in spinodal domain. This phenomenon may due to the presence of oxygen in the Fe-Cr thin films, of grain boundaries or to the unsuited amplitude and wavelength of the modulation. From the damping kinetics, we have extracted an activation energy for the Fe-Cr interdiffusion. An oxide precipitation has also been observed during aging.

Fig1. Reconstructed volume of a Fe-Cr thin film obtained by atom probe (before ageing)

Fig2. Composition profile along the z direction of reconstructed volume of Fig1

ASS-6-Or-4
In depth characterization of the oxide layers formed on steam generator nickel base alloys

T01 Applied Surface Science

#ASS-6-Or-4

A. Mazenc [1], A. Galtayries [2], A. Seyeux [2], P. Marcus [2], S. Leclercq [3].

[1]EDF R&D and LPCS, UMR 7045 CNRS/ENSCP - Paris (France), [2]LPCS, UMR 7045 CNRS/ENSCP - Paris (France), [3]EDF R&D - Moret Sur Loing (France).

Alloy 690 is a high-chromium nickel alloy widely used in nuclear plants, for steam generator (SG) tubes in Pressurized Water Reactors (PWR). During processing, oxides scales develop on SG tubes: it is composed of a Cr-rich inner layer and a Ni-rich external layer. The release of Ni in primary water leads to the increase of the activity. It is known that the Cr-rich layer, acts as diffusion barrier and limits the nickel release.
This work explores the original use of Time of Flight Secondary Ion Mass Spectrometry (ToF-SIMS), in addition to X-ray Photoemission Spectroscopy (XPS) and m-Raman Spectroscopy to characterize thin oxide films formed on Ni-30Cr, a model of Alloy 690, which has been subjected to different oxidizing conditions: thermal oxidation at 900°C in air for 4 hours or exposed to primary water (liquid water at 325°C) during 4 and 31 days.
According to the published data [1-2], the oxide film formed on Ni-Cr (with a Cr content > 20%) should present a triplex structure: 1) outer nickel oxide layer, 2) intermediate nickel chromite layer, and 3) inner chromium oxide layer.
If XPS does not allow an easy distinction of Cr^{3+} in the intermediate or in the inner layers, ToF-SIMS gives a more molecular determination of the spinel and pure oxide compounds [3]. Using ions markers of mixed or pure compounds, the ToF-SIMS depth profiles confirmed the triplex oxide structure of thermally treated Ni-30Cr.
As regards the oxides formed in primary water: the thickness and composition are different. This approach was also applied to Alloy 690.
The changes in composition, as deduced from the molecular study of the oxide film, are discussed in terms of passivation mechanisms.

[1] G. Calvarin-Amiri, R. Molins, A. M. Huntz,, Materials at high temperatures, 18, 91 (2001)
[2] L. Marchetti, S. Perrin, Y. Wouters, M. Pijolat, Electrochimica Acta, 55, 5384 (2010).
[3] A. Mazenc, A. Galtayries, A. Seyeux, P. Marcus, S. Leclercq, Surface and Interface Analysis, 45, 583 (2013).

ASS-P3-12
A combined in situ study of chlorine adsorption on Cu(110) surface by means of EC-STM, RAS, CV and XPS

T01 Applied Surface Science

#ASS-P3-12

B. Bonanni [1], G. Bussetti [1], M. Di Giovannantonio [1], G. Serrano [1], A. Violante [1], C. Goletti [1], S. Breuer [2], K. Gentz [2], K. Wandelt [2].

[1]Department of Physics, University of Tor Vergata, Via Ricerca Scientifica 1, 00133 - Rome (Italy), [2]Institute for Physical and Theoretical Chemistry, University of Bonn, Wegeler Strasse 12, 53115 - Bonn (Germany).

We have investigated the adsorption of chlorine on the Cu(110) surface in electrochemical (EC) cell by using different techniques, in order to get deeper insight on halide adsorption on this crystal surface. Indeed, the adsorption of chlorine on Cu(100) and Cu(111) from solution is well studied and understood, whereas the situation on Cu(110) is more unclear and different structures have been published for the chlorine layer [1–2].

Our study has been performed by means of in situ electrochemical scanning tunnelling microscopy (EC-STM), in situ reflectance anisotropy spectroscopy (RAS, an optical technique with an enhanced sensitivity for surface optical properties [3]), and cyclic voltammetry (CV) and has been completed by XPS measurements.

The process of chlorine adsorption on a Cu(110) surface has been studied in a EC potential range from hydrogen evolution regime to copper dissolution. The real space structure has been investigated by EC-STM, revealing a strong potential-depending evolution of the surface layer morphology between the bare copper surface and the chlorine covered surface. EC-STM images clearly show the formation of stripes along the [001] direction, as reported in literature, very likely due to Cl- adsorption.

The morphological changes detected at the nanometer scale by EC-STM have been related to the optical properties of the same Cl- covered surface as measured by RAS: the optical anisotropy spectrum has been measured in the range 275-800 nm and exhibits a maximum of intensity when the polarized light is aligned along the

[001] direction. The RAS signal has been monitored also at fixed wavelength of 500 nm, corresponding to RAS maximum, while varying the EC potential in the range of values probed in EC-STM: we have recorded a RAS cycle that we have compared with the CV cycle measured on the same system, obtaining a better comprehension of the effects at the liquid/metal interface during application of varying EC potential.

The in situ studies have been complemented by XPS experiments on a Cu(110) surface prepared in an EC cell with the same procedure followed in EC-STM and RAS experiments. The EC cell was directly connected to the UHV chamber equipped with the XPS facility, so that, after the EC preparation, the Cu(110) has been transferred in the XPS system for chemical analysis. The XPS measurements have confirmed the adsorption and desorption of chlorine ions upon variation of the EC potential in the range of the EC-STM and RAS experiments.

In conclusion, thanks to the employ of different in situ techniques we are able to follow and explain the chlorine adsorption and desorption processes on Cu(110) on the timescale of the potential change.

[1] Li-Jun Wan and Kingo Hitaya, J. Electroanal. Chem. 473,1018 (1999).
[2] W.H. Li et al. J. Phys. Chem. B, 105, 1829 (2001).
[3] See, for instance, C. Goletti et al. Phys. Rev. B 193301 (2001).

BI/ASS-1-Or-4
Electrical behaviour of pyrrolic bio-polymers doped mortars prepared with two types of sand

T01 Applied Surface Science

#BI/ASS-1-Or-4

D. Altamirano-Juarez [1], A. Solís-Herrera [2], G. Ortiz [2], P. Montes-García [3].

[1]Universidad Veracruzana, Research Center in Micro and Nanotechnology - Boce Del Río, Veracruz (Mexico), [2]Centro de Estudios de la Fotosíntesis Humana - Div. de la Energía. independencia 1003 Col. El Plateado - Aguascalientes, Aguascalientes (Mexico), [3]Instituto Politécnico Nacional - CIIDIR-Oaxaca. Hornos 1003 Col. Nochebuena SAnta Cruz Xoxocotlán - Oaxaca, Oaxaca (Mexico).

Mortars were elaborated using a matrix of compositions for two different types of refined sand, and substituting the water of mixed by a dilution of a pyrrolic analogous of melanin (QK) to the 0.4% in water, varying from 0,4 to 1,0 the Water/QK rate. Analysis of surface by Scanning Electron Microscopy reveals a significant diminishing of the porosity as a function of the content of QK, while the diffraction patterns of samples aging the same time, they shows variations in the development of phases, attributed to the presence of the bio-polymer. Likewise, the analysis of the electric measurements on the surface for constant proportions of water or QK show that the pyrrolic analogous induces variations in the relation I-V in all the proportions of liquids tested. The same phenomena were observed into mortars prepared with red or white sand, and they are explained as a capacity of the pyrrolic analogous to produce chelate compounds and to exchange weakly bound water with the cement; regulating so much the formation of hydration products as the particle size [1-4]. All the tests shown correspond to mortars with aging of 180 days.

[1] J. Méndez-Vivar, R. Mendoza-Serna, L. Valdez-Castro. Control of the polymerization process of multicomponent (Si, Ti, Zr) sols using chelating agents. Journal of Non-Crystalline Solids. 228 (2001) pp. 200-209

[2] Houng, Lan-Young et. al. Functional SiO2-TiO2-PEG hybrid resin by direct chelation with cathecolic compound. Journal og Sol-gel Science and Technology. 57 – 3 (2011) pp. 279-286

[3] Patent US6,448,317, B1. Conard E. Kaiser et. al. Dual function gelled mastic adhesive and gelled mastic adhesive mortar. Unit States Patent. 09/10/2012.

[4] Edward M. Petrie. Polymer Modified Cement SpecialChem (2012) www.specialchem4adhesives.com/home/editorial.aspx?id=6223

ASS-P1-02
Effect of the surface of calcium fluoride particles on the non-isothermal crystallization behavior of poly(ethylene terephthalate)

T01 Applied Surface Science

#ASS-P1-02

M. Sánchez Loredo [1], R.J. Sánchez Leija [1], O. Domínguez Espinós [1], D. Cayuela Marín [2].

[1]UASLP - San Luis Potosí (Mexico), [2]UPC - Terrassa (Spain).

The incorporation of inorganic materials in polymer matrices has been an attractive path for improving mechanical, thermal, tribological, electrical, optical, fire resistance, UV resistance and permeability properties. In this work, calcium fluoride particles of different sizes, some of them surface-modified with the organic reagents triethanolamine (TEA) and Cyanex® 921 (tri-n-octylphosphine oxide, TOPO), were incorporated into poly(ethylene terephthalate) (PET) matrices. As far we know, only very few investigations report the addition of inorganic fluorides into polymers [1]. The CaF_2 particles were synthesized by chemical precipitation where the particle size was controlled by addition of different amounts of triethanolamine to the precursors solutions. To modify some of the particles, a heat-treatment with tri-n-octylphosphine oxide in isopropanol, was carried out. The composite materials were prepared by melt-blending PET and particles at different filler loadings.
The influence of the particles surface modification on the non-isothermal crystallization behavior of PET was investigated by using differential scanning calorimetry and field emission scanning electron microscopy. The Jeziorny-modified Avrami equation was applied in order to study the crystallization kinetics and several parameters were calculated (half-crystallization time, Avrami exponent and rate constant). According to the results, the calcium fluoride particles act in general as nucleating agents, accelerating the PET crystallization rate. However, the effect on the polymer crystallization rate was more important with the addition of the non-modified particles, where the surface could play an important role for epitaxial crystallization. Halide crystals were already found to influence the mode of crystallization of various polymers. Their surfaces have the capability to specifically

orient numerous inorganic and organic compounds. Some authors have proposed that epitaxial crystallization between nucleating surfaces and polymer crystals controls nucleation, where the polymer chains align themselves parallel to the substrate [2].
On the contrary, the addition of the particles with an organic coating layer on the surface resulted in a crystallization behavior more similar to the observed for PET. The presence at the surface of adsorbed TOPO, a highly lipophilic long-chain organophosphorous compound, or adsorbed TEA, an organic compound that is both a tertiary amine and a triol, probably alters the chemical nature of the particles; reducing its nucleation ability and perturbing the crystallization temperatures as experimentally detected. Tentatively, the organic coating on the surface of the CaF_2 particles may prevent epitaxial crystallization, giving a hint of the role the surface nature of inorganic fillers play on the epitaxial nucleation of polymers.

[1] S. Sathyamurthy, E. Tuncer, K.L. More, B. Gu, I. Sauers and M.P. Paranthaman, Colloidal synthesis of BaF_2 nanoparticles and their application as fillers in polymer nanocomposites. *Appl. Phys. A.*, 106(3), 661-667 (2012).
[2] J.A. Koutsky, A.G. Walton, E. Baer, Epitaxial crystallization of homopolymers on single crystals of alkali halides, *J. Polym. Sci. A-2 Polym. Phys.*, 4(4), 611-629 (1966).

BI/ASS-1-Or-8
FUNCTIONALIZED CARBON NANOTUBES WITH Phaseolus lunatus LECTIN

T01 Applied Surface Science

#BI/ASS-1-Or-8

A. Perez [1], J. Aguilar [2], A. Salinas [3], S. Lorenzo [3], A. Vázquez [3], E. Pérez-Campos [3], M. Gil [3], Y. Gochi [3].

[1]UNIDAD DE BIOQUIMICA E INMUNOLOGIA, INSTITUTO TECNOLÓGICO DE OAXACA. AV. VICTOR BRAVO AHUJA No. 125, ESQ. CALZ. TECNOLOGICO. CP 68030 - Oaxaca, Oax. (Mexico), [2]UNIDAD DE BIOQUIMICA E INMUNOLOGIA, INSTITUTO TECNOLÓGICO DE OAXACA. AV. VICTOR BRAVO AHUJA NO. 125, ESQ. CALZ TECNOLOGICO. CP 68030 - Oaxaca, Oax. (Mexico), [3]UNIDAD DE BIOQUIMICA E INMUNOLOGIA, INSTITUTO TECNOLÓGICO DE OAXACA - Oaxaca, Oax. (Mexico).

The saccharide biomolecules attached to proteins and lipids, or present on cell surfaces, participate actively in numerous physiological and pathological processes. The structural flexibility of these molecules allows them to function as unique sequences of identity, such as DNA or proteins. Lectins can recognize differences in glycan composition even in its conjugated state, so they are very useful tools in deciphering the "glycocode" associated with a particular physiological or pathological process[1]. These properties are used for analysing lymphoproliferative and cytotoxic functions in mononuclear cells, caused by certain drugs, also for detecting chromosomal abnormalities, for studying the structural changes in glycoconjugates present on cell surfaces, and for detecting malignant cellular transformations[2]. Lectins that join with blood type specificity GalNAc are the most diverse since its taxonomic classification. *Phaseolus lunatus* var. Silvester lectin has a MW of 120 kDa, a content of 4.5% carbohydrate, with higher mannose content, GluNAc, fucose, traces of arabinose and xylose. They are mitogenic for human peripheral T lymphocytes, but no for B lymphocytes. The CNTs are cylinders constructed from a hexagonal array of sp2-hybridized carbon atoms, they are relatively flexible, interact with cell membranes and penetrate several biological surfaces. The objective of CNT functionalization is to increase the tubes affinity and to improve its chemical reactivity with other molecules, as well as to create new structures with improved capabilities

for translocation across cell membranes, and to increased solubilization, stability and bioavailability of the biomolecules. Therefore, the aim of this project was to functionalize multi-walled CNT with *Phaseolus lunatus* lectin var. silvester for biomedical application.
For CNTs preparation and functionalization, they were treated with a mixture of H_2SO_4 and HNO_3, and were subjected to ultrasound for 3 h. The CNTs carboxylated were dispersed in a 1-pirenbutanoico acid solution and were incubated for 1 h under constant stirring. The 1-pirenbutanoico acid residual polymer was removed by centrifugation at 7500 rpm/5 min and the complex formed was washed with pure methanol for obtaining CNT functionalized. A volume of 50 µl of FITC-lectin (20 µg/ml) was added into the CNTs functionalized. It was incubated for 18 h and was washed by centrifugation at 7500 rpm/7 min to remove unbound material. The efficiency of conjugation was visualized with FITC, which had been conjugated lectin previously. The CNT-lectin adhesion was confirmed by agglutination tests, inhibition with specific sugar, by fluorescence microscopy and scanning electron microscopy. The electron microscopy analyses (SEM), fourier transform infrared spectroscopy (FTIR) and Raman showed peaks corresponding to the amino and carboxyl groups, indicating that the CNT-lectin conjugation was performed. The efficiency shown by this type of interaction is high, because once the carbon nanotubes are dispersed by sonication, they can be diluted in a considerable volume.

Work supported by PROMEP (ITOAX-CA-4)

1. Tomáš Bertók & Jaroslav Katrlík & Peter Gemeiner & Jan Tkac. 2013. Microchimica Acta, Volume 180, Issue 1-2, pp 1-13
2. Lis, H.; Sharon, N. Chem. Rev. 1998, 98, 637–674.

ASS-P1-19
Characterization of localized electric fields in InAs/GaAs quantum dots interface by photoreflectance spectroscopy

T01 Applied Surface Science

#ASS-P1-19

J. Kim [1], I.S. Han [1], S.J. Lee [1], S.K. Noh [2].

[1]Department of Physics, Yeungnam University - Gyeongsan (Korea, republic of), [2]Korea Research Institute of Standards and Science - Daejeon (Korea, republic of).

In this work, we have investigated the optical properties of InAs/GaAs quantum dots (QD) by photoreflectance spectroscopy (PR). To investigate the localized electric fields in InAs/GaAs QD interface, we fabricated InAs/GaAs QD by using molecular beam epitaxy. The InAs/GaAs QD samples were grown on GaAs(100) surface. A 500 nm thick GaAs buffer layer was grown on undoped -GaAs substrate at the substrate temperature (Ts) of 580 oC. To form the InAs QD by Stranski-Krastanow mode on GaAs surface, the Ts was decreased 400 oC. Finally, a GaAs capping layer with a thickness of 10 nm was grown at Ts of 400 oC.
For the investigation interface electric fields induced by strain between InAs QD and GaAs interface , PR measurements were carried out at various temperatures (14~300 K). Figure 1 shows (a) the PR spectrum for the InAs/GaAs QD and (b) the selected Franz-Keldysh oscillation (FKO) at different PR measurement temperatures (14, 50, and 77 K). In PR spectra of InAs/GaAs QD, we have observed FKO. In general, at a given localized electric field in GaAs, we expect two components of FKO period in PR spectra due to the heavy-hole (hh) and light-hole (lh) transitions. The localized electric field distributions of InAs/GaAs QDs have been determined from the period of FKO using fast Fourier transform (FFT) method. We also suggested that the localized electric fields are strongly correlated to QDs strain field distribution on GaAs interface.

[1] J. S. Kim et al., Appl. Phys. Lett. 87, 261914(2005)

Fig. 1. (a) Photoreflectance spectrum of InAs/GaAs QD and (b) the selected Franz-Keldysh oscillation (FKO) at different PR measurement temperatures (14, 50, and 77 K).

ASS-6-Or-6
Scanning Auger analysis of pit initiation at MnS nano-inclusions in carbon steel under exposure to sulfate-reducing bacterium D. alkanexedens.

T01 Applied Surface Science

#ASS-6-Or-6

J. Hammond [1], B. Davis [2], I. Beech [3], D. Paul [1], R. Avci [2], K. Bomben [4].

[1]Physical Electronics - Chanhassen, Mn (United states), [2]Montana State University - Bozeman, Mt (United states), [3]Univerisity of Oklahoma - Norman, Oh (United states), [4]Physical Electronics USA - Chanhassen. Mn (United states).

Cold rolled carbon steel (1018) is a commonly used structural material in various applications, including the construction of fuel storage tanks for naval ships. Desulfoglaeba alkanexedens (strain ALDCT) is a known fuel-degrading, anaerobic, sulfate-reducing bacterium (SRB) [1, 2] that thrives at fuel-water interfaces in marine environments and can influence the pitting corrosion of carbon steel. It has long been postulated that MnS inclusions in carbon steel can act as sites of pitting initiation [3]. The propagation of pitting corrosion is relatively well understood; however, the initiation of pits is still a subject of controversy [4, 5]. A careful study of pit initiation and propagation associated with sulfide inclusions, particularly as they relate to microbial influenced corrosion (MIC) under anaerobic conditions, has been lacking, partly because these inclusions are mostly submicron-sized and the evolution of their corrosion is difficult to monitor. The use of nanoprobes instead of microprobes is required to determine the elemental and chemical composition and to map out the elemental distributions at the submicron scale. Quantitative surface sensitive techniques such as Auger electron spectroscopy [4, 5] are essential for monitoring the nanoscale changes associated with surface-related phenomena, including MIC. This presentation will review the results of comprehensive and systematic studies of nano-inclusions on carbon steel surfaces prior to and following exposure of the steel to a solution of a mature ALDCT culture and to abiotic sulfide as a control. The nano-inclusions were carefully characterized using a field emission Auger nanoprobe with a spatial resolution of approximately 10 nm for imaging and spectroscopy and compared with results obtained using X-ray microprobes, which typically have a

spatial resolution of around 1000 nm for spectroscopy and 10 nm for imaging. The study elucidates biologically driven corrosion reactions taking place in and around nano-inclusions. The impact of this fundamental analysis on the understanding of MIC phenomenon will be discussed.

1. Davidova, I.A., et al., *International Journal of Systematic and Evolutionary Microbiology*, 2006. **56**: p. 2737-2742.
2. Morris, B.E.L., J.M. Suflita, and H.H. Richnow, *Geochimica Et Cosmochimica Acta*, 2009. **73**(13): p. A907-A907.
3. G, Waglen. *Corrosion Science*, 1974. **14**: p. 331-349.
4. P. Schmuki, H. Hildebrand, A. Friedrich andS. Virtanen, *Corrosion Science*, 2005. **47**: p. 1239-1250.
5. J.E. Castle and Ruoru Ke, *Corrosion Science*, 1990. **30**(4/5): p. 409-428.

ASS-P3-13
Silicide formation during ion beam depth profiling

T01 Applied Surface Science

#ASS-P3-13

D. Karpuzov.

University of Alberta - Edmonton (Canada).

Silicide Formation in Ion Beam Depth Profiling of Thin Films

Thin films of gold, silver and copper were deposited on silicon and etched with argon ion beam. X-ray photoelectron spectra were followed on each step of the etching. BInding energy changes when the profiling reaches the interface indicate the formation of silicides

ASS-5-Or-5
Development of Ion Mapping for SIMS with an EEM

T01 Applied Surface Science

#ASS-5-Or-5

M. Eller [1], S.V. Verkhoturov [2], S. Della-Negra [1], E.A. Schweikert [2].

[1]Institut de Physique Nucléaire d'Orsay, Université Paris-Sud 11 UMR 8608, CNRS/IN2P3, F-91406 - Orsay (France), [2]Department of Chemistry, Texas A&M University - College Station (United states).

Secondary Ion Mass Spectrometry, SIMS, is a surface analytical technique capable of analyzing myriad of samples including metals, polymers, organic, biological samples, and nano-objects. The surface sensitivity (top 5-10nm) coupled to mass spectrometry makes SIMS a versatile surface analysis tool. The use of SIMS in the event-by-event bombardment detection mode offers several key advantages: investigation of co-localization of molecules within a 100nm^2 area, quantification of surface coverage of molecules and analysis of individual nano-objects.[1,2] However, generating maps or images of the surface with the event by event mode is challenging, as the traditional method of scanning a focused ion beam is time consuming due to low beam fluence. An alternative approach is to localize each projectile impact via the emitted electrons with an electron emission microscope, EEM. In this novel approach, the secondary ions are collected and analyzed with a time of flight mass spectrometer, and the electrons are imaged with an EEM. The result is a mass spectrum with a corresponding impact coordinates. In practice a series of impacts are collected, ~10^5-10^6 individual impacts, and summed to generate a chemical map of the surface (~50x50µm). The instrumentation to couple an EEM to a C_{60} cluster-SIMS instrument is presented (15-75keV total impact energy). The results from a cholesterol pattern are presented to demonstrate molecular ion mapping with ~1µm spatial resolution.

Further improvements using event-by-event mapping are possible by increasing the secondary ion yield. Using 100qkeV Au_{400}^{+4} as a projectile has been shown to increase the yield of molecular ions by ~10X.[3] If the molecular ion yields are increased each pixel will contain more information resulting in more informative maps. Additionally, the success rate for determining the impact coordinates may be improved via enhanced electron emission from a MeV nano-particle projectile. A new

instrument designed to achieve this enhanced secondary ion yield and increased electron emission is under construction at IPN-Orsay, Andromede Project (program for future investment EQUIPEX, ANR-10-EQPX-23). Preliminary results from the new nano-particle ion source are presented: secondary ion yields from lipopolysaccharide samples (analyzed with Au400+4 at 1qMeV) and correlation calculations which demonstrates the power of performing nano-scale mass spectrometry in the event-by-event mode.

[1] Liang, C. K.; Verkhoturov, S. V.; Bisrat, Y.; Dikler, S.; DeBord, J. D.; Fernandez-Lima, F. A.; Schweikert, E. A.; Della-Negra, S. Surface and Interface Analysis 2012, n/a.
[2] Chen, L. J.; Shah, S. S.; Silangcruz, J.; Eller, M. J.; Verkhoturov, S. V.; Revzin, A.; Schweikert, E. A. International Journal of Mass Spectrometry 2011, 303, 97.
[3] Fernandez-Lima, F. A.; Post, J.; DeBord, J. D.; Eller, M. J.; Verkhoturov, S. V.; Della-Negra, S.; Woods, A. S.; Schweikert, E. A. Analytical Chemistry 2011, 83, 8448.

ASS-7-Or-1
Comparison between the surface modification of LDPE induced by atmospheric argon and helium plasma torches

T01 Applied Surface Science

#ASS-7-Or-1

S. Abou Rich [1], T. Dufour [1], P. Leroy [1], L. Nittler [2], J. Hubert [1], J.J. Pireaux [2], F. Reniers [1].

[1]Université Libre de Bruxelles, Bd de triomphe 2 - Brussels (Belgium), [2]PMR, Université of Namur, Rue de Bruxelles 2 - Namur (Belgium).

Polymeric surfaces may be modified by plasma treatment to optimize the adhesion needed for the deposition of subsequent layers with good barrier properties suitable for food packaging. The surface modification of low density polyethylene (LDPE) overcomes several disadvantages such as low surface energy, low roughness, and high chemical inertness.

Two RF atmospheric plasma torches (Ar/O_2 and He/O_2) are mounted onto a robotic arm which can moves in 3D, thus allowing the treatment of large area samples. The surface chemical and physical modifications of LDPE films induced by radiofrequency plasma treatments were correlated with the characteristics of the discharge parameters and the chemical composition of the plasma itself. Water contact angle measurements have been performed, as well as AFM and XPS analyzes, to determine the wettability, the morphology and the chemical composition of the films surfaces respectively.

A comparison was established between both plasma treatments at different source-substrate distances. Figure 1 shows the decreasing roughness and the decreasing weight loss as the surface polymer is away from the plasma source. More material removal is observed in the case of Ar treatment.

Optical emission spectroscopy of the gas phase was performed to determine the role of the plasma species on the surface modifications observed. Altough this has still to be confirmed by other data, it is suggested thatetching could be provoked partly by some noble gas excited or metastable species and/or the ions bombardment, while surface chemical modifications could be due to the action of neutral species on the

plasma-activated polymer surface. A correlation between the etching rate of the ejected material and the abundance of plasma species was established.

Figure 1. Root mean squared (Rrms) roughness values and weight loss observed on the surface of LDPE films treated in Ar or He plasma during 30 s with 60W of power at different source-to-substrate distances (gaps)

ASS-P3-14
Vacuum chamber with in-situ heating and mapping capability for studying wafers up to 300 mm with spectroscopic ellipsometry

T01 Applied Surface Science

#ASS-P3-14

P. Basa, T. Jaszi, D. Selmeczi, C. Defranoux.

Semilab Semiconductor Physics Laboratory Co. Ltd. - Budapest (Hungary).

Determination of film uniformity and mechanical strength are important factors in engineering porous low-k materials in the field of interconnection technology. Such layers, especially in porous form, challenge to be optimized both for low density and mechanically strong structure. Integration in the device preparation process requires the layer to be stable as a function of temperature, ie., no thickness or composition change is allowed during high temperature process steps. Such important factor is the uniaxial CTE (Coefficient of Thermal Expansion) which measures the layer thickness change with temperature. In case of an interconnect multilayer structure, each composing material should be compatible in terms of thermal expansion in order to avoid any mechanical interferences, eg., cracks or delamination.
CTE of low-k materials is reported to be significantly higher than that of other materials in the same structure which leads to mechanism for stress formation in the structure. Thus, lowering of thick porous low-k CTE is essential to reach closer value to that of Cu (50-60 vs. 17 ppm/°C) for high-temperature process.

A unique vacuum chamber tool (PS-2000H) was developed at Semilab Co. Ltd., which enables features of:
- vacuum levels <1 mTorr;
- heating up the 200 or 300 mm wafers up to 350 °C with temperature stability <0.1 °C;
- in-situ spectroscopic ellipsometry measurement for *layer thickness* and *refractive index;*
- measurement of the *uniaxial CTE* by determinig the layer thickness – temperature dependence (see Fig. 1);

- mapping measurement of the wafers with the „Rho-Theta" stage;
- access to conventional organic vapor ellipsometric porosimetry functions *(film porosity, pore size distributions, Young's modulus)* by integrating the solvent capability;
- measurement of the *above quantities* at the same probing area of < 1mm^2

Fig. 1. Typical measurement result of CTE for a thick low-k layer on 300 mm wafer as obtained with Semilab's PS-2000H tool

ASS-6-In-1
ENVIRONMENTAL INTERACTIONS WITH METAL SURFACES : ANALYTICAL APPROACH, MECHANISMS, AND MODELLING

T01 Applied Surface Science

#ASS-6-In-1

P. Marcus.

Laboratory of Physical Chemistry of Surfaces CNRS – Chimie ParisTech (UMR 7045) - Paris (France).

Metal and alloy surfaces interact with their environment (gas or liquid). The understanding and control of the surface interactions is a key factor for the development of metallic materials with extended and predictable life time. Chemical interactions at metal and alloy surfaces (adsorption, oxidation, corrosion) can be studied using advanced surface characterization techniques (surface spectroscopies and microscopies) and modelling and simulation methods.
The aim of this lecture is to review recent results obtained by combining Time-of-Flight Secondary Ions Mass Spectrometry (ToF-SIMS), X-ray Photoelectron Spectroscopy (XPS), Scanning Tunneling Microscopy (STM), Scanning Tunneling Spectroscopy (STS), and Density Functional Theory (DFT). The reviewed data provide a better understanding of metal surfaces, metal-oxide interfaces, and oxide films properties, including corrosion and corrosion resistance mechanisms.
The following issues will be addressed :
- Corrosion at the nanoscale using STM and STS : nanostructure of passive oxide films, local electronic properties
- Formation of vacancies at metal-oxide interfaces
- Early oxidation stages studied by advanced surface analytical techniques (XPS, ToF-SIMS) with applications in the aeronautic and nuclear industries
- DFT modelling of the reactivity of oxide films with corrosive species (Cl-)

The selected examples will cover various metals and alloys (nickel and nickel-base alloys, stainless steels, titanium aluminides).

ASS-4-In-1
COMBINED SURFACE AND REACTOR STUDIES OF INTERMETALLIC COMPOUNDS LEAD TO INNOVATIVE CATALYSTS

T01 Applied Surface Science

#ASS-4-In-1

M. Armbrüster.

Max-Planck-Institut für Chemische Physik fester Stoffe - Dresden (Germany).

Heterogeneous catalysis on intermetallic compounds is an interesting interdisciplinary and fast growing field. Intermetallic compounds combine unique electronic properties and well-ordered crystal structures. Often covalent bonding prevails, resulting in high stability of the intermetallic compounds under catalytic reaction conditions. This enables to pre-select compounds with appropriate electronic and structural properties in order to obtain high catalytic activity and especially selectivity. The approach is applied to develop highly innovative catalysts for the selective hydrogenation of acetylene and the steam reforming of methanol. In this contribution I focus on the benefit of combining in situ surface and reactor studies in the quest of innovative catalytic materials.

ASS-1-In-1
Electron Spectroscopy for Thin Film Devices

T01 Applied Surface Science

#ASS-1-In-1

H. Kang.

Department of Physics, Chungbuk National University - Cheongju (Korea, democratic people's republic of).

X-ray Photoelectron Spectroscopy (XPS) and Reflection Electron Energy Loss Spectroscopy (REELS) analyses provide convenient ways to obtain band alignment and electronic properties for ultrathin high-k dielectric thin films in CMOS. Quantitative analysis of REELS spectra leads us to a straightforward way to determine the dielectric function and the optical properties of transparent conductive oxide thin films in thin film transistors. The band alignment in ultrathin Hf silicate, Zr silicate, and HfZr silicate gate dielectric thin films, grown on Si (100) by atomic layer deposition method, will be presented. The electronic and optical properties of GaInZnO, HfInZnO, and InZnSnO thin films, grown by the RF magnetron sputtering method, will be presented.

ESD/ASS-P3-08
RESEARCHES ON THE STRUCTURE AND PROPERTIES OF MICRO-ALLOYED STEELS OBTAINED IN VIM AND VAR UNITS

T01 Applied Surface Science

#ESD/ASS-P3-08

V. Geanta [1], I. Voiculescu [1], R. Stefanoiu [1], M. Taca [2], D.D. Daisa [2].

[1]POLITEHNICA University of Bucharest - Bucharest (Romania), [2]METAV-CD - Bucharest (Romania).

Micro-alloying of high strength steels with small amounts of elements with very high affinity to carbon and nitrogen, such as Nb, Ti and V contribute to a significant improvement of its mechanical properties. Steel micro-alloying using these elements allows obtaining a mechanical strength and good toughness at low cost as compared with conventional alloy steels.
If the metallurgical processes for obtaining (steelmaking and refining) and thermo-mechanical processing (rolling, forging etc.) are appropriate, precipitates may act within the material by blocking the movement of grain boundaries, which allows the increasing of toughness and thermal stability characteristics at high temperatures.
To study the effects of thermal regime on the microstructure and microhardness of steels micro-alloyed with niobium and vanadium were made several charges, with different chemical composition, using two types of metallurgical units: a Balzers type vacuum induction furnace – VIM and a vacuum arc remelting equipment – VAR.
In order to estimate the effect that the applied thermal regime have on the steel microstructure and hardness characteristics, samples of steel micro-alloyed with Nb and V were normalized at 950 – 970 oC for 20 minutes, after which they were cooled in air. Microstructure analysis by optical and electron microscopy and microhardness measurements were performed. It was found that after applying the normalization treatment, for most analyzed steel samples, the microhardness has decreased with different values, depending on the chemical composition.

Fig. 1: Samples of micro-alloyed steels obtained in VIM
Fig. 2: Samples of micro-alloyed steels obtained in VAR

ASS-2-In-1
DENSITY FUNCTIONAL THEORY CALCULATIONS AS A TOOL FOR UNDERSTANDING/PREDICTING ADSORPTION AND CHEMICAL REACTIONS ON BIMETALLIC AND INTERMETALLIC CATALYSTS

T01 Applied Surface Science

#ASS-2-In-1

A. Juan.

Departamento de Fisica e IFISUR (UNS-CONICET) - Bahia Blanca (Argentina).

Catalysts are complicated materials and there are an enormous number of interesting catalytic processes. About 20% of manufacturing in the industrialized world is dependent on catalysis. Most catalysts used in industry are solids, and the catalysis takes place on the surface of nanoparticles of the active material or in the particle/support interface. Density functional theory (DFT) calculations can provide insight into the atomic-scale reaction mechanisms helping to interpret a large amount of experimental data collected during decades. This presentation shows how DFT and bonding analysis can be used to describe the state of the surface during chemical reactions and the geometrical and electronic changes in both the surface and the adsorbated species. Our research has recently focused on the adsorption of hydrogen, carbon, benzene and CO on bimetallic (FePd, FeNi and PtCo) and intermetallic compounds (PdGa). In our approach the models are build from experimental information. The geometry and surface chemical bonding is described using quantum chemical calculations.

ASS-3-In-1
NEW PEEM (DISPLAY-TYPE ELLIPSOIDAL MESH ANALYZER: DELMA) FOR PHOTOELECTRON HOLOGRAPHY AND STEREO-PHOTOGRAPH

T01 Applied Surface Science

#ASS-3-In-1

H. Daimon [1], H. Matsuda [1], M. Morita [1], S. Kitagawa [1], T. Matsushita [2], F. Matsui [1], L. Toth [3], K. Goto [1].

[1]Nara Institute of Science and Technology (NAIST) - Nara (Japan), [2]Japan Synchrotron Radiation Research Institute (JASRI) - Spring-8 (Japan), [3]University of Debrecen - Debrecen (Hungary).

Usual PEEM cannot measure angular distribution of photoelectrons at above several hundred eV, therefore cannot measure photoelectron holography or stereophotograph [1] of atomic arrangement. We have developed a new PEEM (called DELMA: Display-type Ellipsoidal Mesh Analyzer [2]) using a wide acceptance angle electrostatic lens (WAAEL) [3]. DELMA can display the angular distribution of photoelectrons from the selected small area up to ±60° even at high kinetic energies as well as the magnified image of the sample. DELMA has been successfully installed at BL07LSU in SPring-8, where strong variable-polarization soft x-ray can be used. DELMA is being used to measure (1) photoelectron diffraction from small area such as graphene, (2) band-mapping for several Bullirouin zones, and (3) photoelectron holography or stereophotograph of atomic arrangement.

[1] H. Daimon, Phys. Rev. Lett. 86, 2034 (2001).
[2] L. Toth, et al., Nucl. Inst. Meth. Phys. Research Sec. A 648, S58-S59 (2011).
[3] H. Matsuda et al.: Phys. Rev. E 75, 046402 (2007), and references therein.

ASS-1-Kn-1
LOOKING BENEATH THE SURFACE AT BURIED LAYERS AND INTERFACES WITH STANDING-WAVE AND HARD X-RAY PHOTOEMISSION

T01 Applied Surface Science

#ASS-1-Kn-1

C. Fadley.

Department of Physics, University of California Davis, Materials Sciences Division, Lawrence Berkeley National Laboratory - Davis (United states).

Quantitatively characterizing buried layers and the interfaces between them is one of the great challenges of surface and materials science. I will discuss two recent developments in
photoemission (photoelectron spectroscopy) that have proven capable of providing unique types of information on depth profiles of composition, chemical state, and magnetic order in
multilayer nanostructures, including interface-specific properties. In standing-wave excited photoemission, Bragg reflection of x-rays from a multilayer mirror (either as the sample or on
which the sample is grown) creates a strong reflected wave, which by interference with the incident wave in turn generates a strong sinusoidal standing-wave electric-field profile. This
profile can be scanned vertically through the sample in several ways so as to focus on different depths in the sample and thus much enhance the depth resolution in photoemission.
X-ray energies in both the soft (0.5<hQ<2 keV) and hard (2<hQ<6 keV) regimes have been used for such studies. In hard x-ray photoemission, the energies of excitation are increased to
as high as 10 keV, with the resulting greater inelastic mean free paths of the photoelectrons leading to a measurement that is capable of looking at buried layers and interfaces as deep as
30 nm. After introducing the basic principles of these methods, I will illustrate these new capabilities with several example applications to systems of interest in

spintronics, complex
oxide heterostructures, and semiconductor technology.

ASS-P1-12
LEAD (II) EXTRACTION BY POLYMER INCLUSION MEMBRANE USING ALIQUAT 336 AS MOBILE CARRIER

T01 Applied Surface Science

#ASS-P1-12

N. Sabba [1], O. Arous [1], O. Arous [2], D.E. Akretche [1].

[1]Laboratoire d'Hydrométallurgie et de Chimie Inorganique Moléculaire, U.S.T.H.B, Faculté de Chimie - Alger (Algeria), [2]Centre de Recherche en Ananlyses Physico-chimiques CRAPC - Alger (Algeria).

The polymeric membranes used for the selective transport and separation of metal species have emerged in recent years. In this work, the extraction and transport of Pb(II) in polymeric membranes (PM) using tricapryl chloride ammonium (Aliquat 336) as mobile carrier has been investigated. The optimum conditions of liquid – liquid extraction were determined. The liquid - liquid extraction tests showed a maximum extraction when the agitation time was greater than eight minutes. A good elimination of lead (extraction efficiency 80% to 94%) was observed. The membrane is made up of cellulose triacetate (CTA) modified by Aliquat 336 incorporated into the polymer as carrier and tris- ethyl - hexyl - phosphate (TEHP) as a hydrophobic plasticizer. The membrane polymer + plasticizer + carrier was characterised using chemical techniques as well as Fourier Transform Infra – Red spectroscopy (FTIR). The metal concentrations were determined by sampling at different time intervals aliquots from both the feed and strip solutions analyzed with an atomic absorption spectrophotometer. Thickness (10 to 20 µm) and water content values showed that carrier inclusion in CTA membrane resulted in a homogeneous and hydrophobic polymer inclusion membranes. The CTA polymerization process in presence of carrier and plasticizer should cause changes in intermolecular interaction of CTA chains. However, any sign for new chemical bonds between CTA, Aliquat 336 and TEHP using FTIR spectroscopy were observed. In transport experiments, the trans-membrane flux increased with increasing carrier concentration reaching a limiting value at greater than 10^{-3} M concentration. The optimum of other fundamental parameters (metal concentration and pH) was determined. $1 \leq pH \leq 2$ have been shown to be the best conditions for maximum efficiency of the studied systems. Our results indicate that facilitated transport through plasticized membranes is an

attractive and effective way to solve the enduring problem of membrane stability whilst improving the permeability to metal ions.

KEY WORDS
Extraction, facilitated transport, membrane, tricapryl chloride ammonium, lead.

ASS-P1-13
Synthesis of a biradical ligand by reactivity of diphenylthiocarbazone with Mo(V)

T01 Applied Surface Science

#ASS-P1-13

Z. Izrig, S. Boutamine, H. Slaouti.

Université des Sciences et de la Technologie Houari Boumediène, Laboratoire d'Electrochimie-Corrosion, Métallurgie et Chimie Minérale, Faculté de Chimie - Alger (Algeria).

In this work, we have presented various aspects of the reactivity of diphenylthiocarbazone $C_{13}H_{12}N_4S$ (HL) with molybdenum(V) based on the pH of the aqueous metal solution and the ligand metal ratio. The reaction of an ethanolic solution of diphenylthiocarbazone with an aqueous solution of MoCl5 was investigated at two pH values (2 and 9) for a ligand metal ratio equalling 1. At pH 5 2, purpuse dimeric complex $Mo_2O_3(HL)_2Cl_2$ $1/2H_2O$ was synthesized, whereby HL was the deprotonated species of diphenylthiocarbazone (Complex C1).
A similar reaction was conducted at pH 9, leading to the formation of a biradicalar organic compound, $C_{13}H_{10}N_4S$. The two compounds were characterized by elemental analyses and spectral (IR, UV-Visible, ESR, 1H NMR and 95Mo NMR) data. The biradicallar ligand was also crystallographically characterized and identified by DRX. This technique reveals no existence of molybdenum and the disappearance of the initially-existing N-H groups in free diphenylthiocarbazone. The biradical crystallizes in the monolinic space group C_2/C.

BI/ASS/NST-P1-13
The effect of different surface roughness of austenitic stainless steel on adhesion of bacteria

T01 Applied Surface Science

#BI/ASS/NST-P1-13

M. Hocevar [1], M. Godec [2], M. Jenko [2], D. Drobne [3], N.G. Cimerman [3], S. Novak [3].

[1]Inst.of Metals and Technology - Ljubljana (Slovenia), [2]Inst. of Metals and Technology - Ljubljana (Slovenia), [3]Department of Biology, Biotechnical Faculty, University of Ljubljana - Ljubljana (Slovenia).

Stainless steel is commonly used material for industrial, chemical, medical and food processing applications. The adhesion of bacteria to stainless steel enhances corrosion of material, decreases the performance of processing equipment and presents chronic source of microbial contamination in food and medical industries [1, 2]. The adhesion process is governed by many factors, including environment, bacterial properties and material surface properties, such as surface roughness, topography and chemical composition [1, 3].
Adhesion behaviour of bacteria Escherichia coli DH5 alpha on austenitic stainless steel (AISI 316 L) with different surface roughness and topography was studied, focusing on the number and distribution of adhered cells. Material surface characterization was made by atomic force microscopy (AFM), Auger electron spectroscopy (AES), x-ray photoelectron spectroscopy (XPS) and contact angle goniometer. Samples with various surface roughness (Ra values ranging from 0.002 – 0.4 µm) and topography were exposed to bacterial suspension. The non-adhering bacteria were removed by rinsing the substrate with sterile phosphate buffered saline (PBS). The number and distribution of adhered cells was observed using field emission scanning electron microscopy (FE-SEM).
Escherichia coli was found to adhere to all stainless steel samples, however the number and distribution of the attached bacteria varied. Adhesion level was found to depend on the substrate roughness with minimum at Ra = 0.08 µm. Attachment to both smoother and rougher surfaces was higher. The surface topography influence bacterial adhesion particularly when the surface irregularities (pits, crevices and grooves) are comparable to the size of the bacteria and can provide shelter from

unfavourable environmental factors. The pattern of bacterial adhesion follows these surface irregularities (Figure 1).

1. E. Medilanski, K. Kaufmann, L. Y. Wick, O. Wanner and H Harms. Influence of the Surface Topography of Stainless Steel on Bacterial Adhesion. Biofouling: The Journal of Bioadhesion and Biofilm Research, 18(3):193–203, 2002.
2. H. A. Videla and L. K. Herrera. Microbiologically influenced corrosion: looking to the future. International Microbiology, 8:169-180, 2005.
3. N. Kouider, F. Hamadi, B. Mallouki, J. Bengourram, M. Mabrouki, M. Zekraoui, M. Ellouali and H. Latrache. Effect of stainless steel surface roughness on Staphylococcus aureus adhesion. International Journal of Pure and Applied Science, 4(1):1-7, 2010.

Figure 1. FE-SEM image of attached E. coli to stainless steel sample AIZV (as received).

ASS-P1-08
A study of the properties of the AES inherited noise

T01 Applied Surface Science

#ASS-P1-08

B. Poniku, I. Belic, M. Jenko.

Institute of Metals and Technology - Ljubljana (Slovenia).

Our research work is aiming to fully automate the AES (Auger Electron Spectroscopy) spectral analysis. The task has not been accomplished yet since the AES produces a very complex signal consisting of at least three elements, the characteristic peaks, the spectral background, and the noise. In order to be able to perform the automated analysis, the spectral signal should be as free as possible of the background as well as the noise component. We are not studying the phenomena or physical processes that actually result in producing the noise, our focus is to analyse the already existing noise which gets recorded with the spectra and find the ways to suppress it without the significant distortion of the spectra. This should be done in the processing stage of the spectra, after the measurement has been completed and the data have been gathered. The paper reports on the work done to extract the important properties of the AES inherited noise such as the noise distribution, and the noise amplitude envelope function as the function of the electron energy. Knowing the statistical properties of the noise which is to some extent unique for the used AES equipment enables us to use the statistical methods to suppress the noise to the acceptable level thus improving the signal/noise ratio. On the other hand the gained knowledge enables us to improve the already operational AES simulator which was developed in our laboratory and is in use as the test platform for the different spectra analysis algorithms.
By putting in use the AES simulator just mentioned above we wanted to also reflect upon a common practice in Surface Analysis laboratories. In routine analysis it is common practice to average the spectra for the purpose of increasing the signal to noise ratio by most often averaging three measured Auger spectra in order to obtain spectra with fairly good signal to noise ratio while not spending exceedingly long times for performing one measurement. Even though this practice improves the signal to noise ratio slightly and enables in most cases the identification of the characteristic peaks without too many problems, we wanted to do a quantitative evaluation of the effectivity of this practice by generating simulated spectra with randomly generated noise of a certain profile similar to that which is found in

measured Auger spectra, and then averaging a number of trials. Our findings in this regard will also be reported.

Keywords: Auger Electron Spectroscopy, noise, white noise, spectral distribution, amplitude distribution, amplitude envelope function

BI/ASS/NST-P1-14
Laser Surface Structuring for Anti-biofouling Surfaces

T01 Applied Surface Science

#BI/ASS/NST-P1-14

T. Kokalj [1], D. Kovacic [2], M. Jenko [1].

[1]IMT-Institute of Metals and Technology - Ljubljana (Slovenia), [2]LPKF - Naklo (Slovenia).

The studied biological anti-biofouling surfaces typically consist of hierarchical structure where nanostructure is superimposed on the micro structured pattern. With microstructure the surface gain the resistivity to larger fouling organisms, while the nanostructure combined with the proper surface energy prevents biofouling of smallest microorganisms.
Recently IMT is developing some bio-mimetic micro-/nano- patterns using laser structuring. For the large surfaces we use laser structuring directly on the various metal surfaces. The laser beam in this case has sufficient power to change the metal surface morphology directly. The laser beam diameter is around 15 µm, however the molten metal splashing which is inherent to this kind of laser fabrication creates droplets of sub-micrometer dimensions. This creates a hierarchical micro-/nano-structure as can be seen in Fig. 1a. This surfaces exhibit a huge change in contact angle with water, compared with non-treated surface (Fig. 1b).

The properties of the substrate material and the laser machining parameters define the change of wettablility of the surface. However, the further chemical modification of the surface can additionally change the surface energy and change the contact angle as well as make the surface more resistant to biofouling.
The change of surface properties depending on surface structuring strategies and selection of substrate material will be presented.

Figure 1: Hierarchical micro-/nano-structure on the laser treated copper surface (1a) and high water contact angle on this surface (1b).

ASS-8-In-1
TAILORING THE BIOELECTRONIC INTERFACE

T01 Applied Surface Science

#ASS-8-In-1

J. Vörös.

Laboratory of Biosensors and Bioelectronics, Institute for Biomedical Engineering, ETH - Zurich (Switzerland).

Surface science has achieved a very high level control over the physical and chemical properties of particles and interfaces. A recent trend and some applications desire not only spatial but also temporal control over such properties. Electrodes and electrochemistry provide a convenient mean to switch surface properties on command. Several examples for such concepts will be presented in this talk:
Polyelectrolytes can be removed on command at electrodes using the locally induced pH changes during electrolysis. This effect then can also be used to control the adhesion, growth and migration of cells. [1]
Nanotechnology also provides the possibility to interface cells in their natural environment at the nanometer scale. The FluidFM is a nanosyringe that can be used to inject, patch, or manipulate single cells without compromising their integrity. In addition, biomolecules or nanoobjects can be picked and placed with nanometer precision in liquid environment. [2-5]
Finally, stretchable and biocompatible microelectrode arrays can be used to stimulate intact spinal cord circuits below an injury to control the movement of the limbs aiding rehabilitation and increasing recovery of spinal-cord injured patients.

1. Electrically controlling cell adhesion, growth and migration; M. Gabi, A. Larmagnac, P. Schulte, J. Vörös, Colloids and Surfaces B: Biointerfaces 79(2):365-371, 2010.
2. FluidFM: Combining Atomic Force Microscopy and Nanofluidics in a Universal Liquid Delivery System for Single Cell Applications and Beyond; A. Meister, et al., Nanoletters 9(6), 2501-2507, 2009.
3. Force-controlled spatial manipulation of viable mammalian cells and micro-organisms by means of FluidFM technology, P. Dörig, et al. Appl. Phys. Lett., 97:2, 023701, 2010.

4. FluidFM as lithography tool in liquid: Spatially controlled deposition of nanoparticles; R. Grüter, J. Vörös, T. Zambelli; Nanoscale (2012) DOI:10.1039/C2NR33214K
5. Exchangeable colloidal AFM probes for the quantification of irreversible and long term interactions; P. Dörig et al. Biophysical J., 2013, submitted.

ASS-5-In-1
Measuring molecular attachment to nanoparticles

T01 Applied Surface Science

#ASS-5-In-1

A. Shard.

NATIONAL PHYSICAL LABORATORY - Teddington (United kingdom).

Surfaces exposed to a biological environment will, almost invariably, acquire an adsorbed layer of proteins. For nanoparticles, this process is important both for the designed attachment of proteins for diagnostic and therapeutic applications and for understanding how nanoparticles interact with living systems. Using model systems of poly(ethylene glycol) thiol and immunoglobulin on gold nanoparticles, we compare different techniques which could be used to measure molecular attachment including light scattering, sedimentation, particle tracking and local plasmon resonance. These techniques provide rather different answers unless the data is interpreted correctly, but through a combination of methods it is possible to estimate the average number of molecules attached to each particle and achieve reasonable agreement between the techniques. More information may be obtained by vacuum-based, spectroscopic methods, such as XPS, but in this case, sample preparation and data interpretation are specialised skills. In this talk, accurate and straightforward methods for XPS data interpretation are described and some approaches to sample preparation outlined.

ASS-10-In-1
Scanning Photoemission Microscopy Applications In Surface Chemistry

T01 Applied Surface Science

#ASS-10-In-1

L. Gregoratti.

Elettra Sincrotrone Trieste - Trieste (Italy).

The Scanning Photoemission Microscopes (SPEM) operating at synchrotron radiation sources use the power of the surface sensitive photoelectron spectroscopy to obtain chemical characterization of materials with spatial resolution down to 50 nm and probing depth up to a few tens A°. In the last years this microscopy has been widely used for understanding the most relevant processes and degradation phenomena which characterize the new technologies for the production of energies such as fuel cells. However the application of this technique to the investigation of real devices is strictly linked to its capability to overcome the limits imposed by the so called “pressure gap” which imposes a high vacuum sample environment.
In this respect the SPEM at Elettra offers new and challenging tools for the photoemission spectromicroscopy of the future

ATS-3-Or-6
Spectroscopic Studies of Interstellar Precursor Molecules

T02 Astronomical Frontiers for Surface Science

#ATS-3-Or-6

M. Whelan, N. Panjwani, W. Brown.

UCL - London (United kingdom).

(Abstract for ASTROSURF meeting)

Interstellar dust grains, once thought to be merely an annoyance to astronomers, have been shown to have an active role in the formation of many chemical species observed in the interstellar medium (ISM). Whilst many observed species are produced efficiently in the gas phase, many are also destroyed or consumed upon formation. It was this realisation that prompted scientists to appreciate the importance of dust grain surface reactions. Dust grains provide heterogeneous catalytic sites, which facilitate formation of molecules and ices, and a medium in which the energy released in bond formation can be dissipated.

Formic acid, despite being detected in both the solid and gas phase in a number of different environments, has received relatively little attention from the astrochemistry community. Understanding the formation of formic acid, which is proposed to occur in the gas phase and on the grain surface, is of significant importance for explaining the chemical composition of the ISM. Formic acid is relatively reactive and partakes in the formation of other, larger, organic species. Examples of some of these are the isomers methyl formate, ethanoic acid and glycolaldehyde (GA). Of particular interest is GA, since it has been proposed to have an important role in the formation of amino acids in space and hence may be related to the origins of life.

In addition to its reactive pathways, formic acid is also of interest due to its ability to

hydrogen bond. This is important in the ISM since the most dominant molecule observed in the solid phase is water, which shows a strong propensity for hydrogen bonding.

In light of the importance of formic acid in the ISM, the work presented here focuses on surface science studies of the behaviour of pure formic acid and formic acid in astronomically relevant ices. The studies were conducted using temperature programmed desorption (TPD) and reflection absorption infrared spectroscopy (RAIRS). Investigations of pure formic acid on graphite, an interstellar dust grain analogue, showed a clear phase change of the formic acid and subsequently, a change in its desorption temperature. Studies of coadsorbed layers and mixtures of formic acid and water showed that the two molecules are inextricably linked when both are in a single ice. The significance of these observations with respect to real interstellar ices will be discussed.

ATS-2-Or-7
Accretion Disk Origin of Earth's Water

T02 Astronomical Frontiers for Surface Science

#ATS-2-Or-7

M. Rocca [1], L. Vattuone [1], L. Savio [1], M. Smerieri [1], A. Asaduzzaman [2], K. Muralidharan [2], M.J. Drake [3].

[1]Dept of Physics University of Genoa - Genoa (Italy), [2]Department of Materials Sciences and Engineering, University of Arizona - Tucson (United states), [3]Lunar and Planetary Laboratory, University of Arizona - Tucson (United states).

The presence of water on the Earth is an enigma. It is generally agreed that it was too hot at 1 Astronomical unit (AU) for hydrous minerals to be stable in the accretion disk. Thus, Earth's water is conventionally believed to have been delivered by comets or wet asteroids after Earth formed. However, wet asteroids and comets have elemental and isotopic properties that are inconsistent with those of Earth, limiting the amount of water derived from such objects.

It was thus proposed that water was introduced during planet growth in the accretion disk in a form stable under high temperature conditions. This hypothesis is supported by the presence of water in the disks around young stars and by numerical simulations of water adsorption on silicate grains under conditions corresponding to those in the accretion disk. Such studies, yet to be confirmed experimentally, showed that molecular chemisorption of water on forsterite (Mg-rich end member of olivine, one of the main constituent of the dust grains) might occur and account for the formation of several Earth oceans but neglected water dissociation [1].

Here we apply surface science methods to the study of this astrophysical problem. Water adsorption experiments were performed under ultra high vacuum conditions using a supersonic molecular beam of water and the retarded reflector method to measure the sticking probability. Ab initio, numerical simulations were performed, too, including now also the possibility of dissociation. We find indeed that water adsorbs dissociatively on the olivine {100} surface, implying that this happens also at the temperature (500-1500 K) and water pressure (10^-8 bar) expected for the accretion disk. Water leaves an OH adlayer that is stable at least up to 900 K. This mechanism may result in the formation of many Earth oceans, provided that a viable mechanism to produce water from hydroxyl exists [2].

This adsorption process must occur in all disk environments around young stars. The inevitable conclusion is that water should be prevalent on terrestrial planets in the habitable zone around other stars.

[1] M. Stimpfl, A.M. Walker,M.J. Drake, N.H. de Leeuw, P- Deymier, Journal of Crystal Growth 294, 83-95 (2006)

[2] Luca Vattuone, Marco Smerieri, Letizia Savio, Abu Md. Asaduzzaman, Krishna Muralidharan, Michael J. Drake, and Mario Rocca, Phil Transactions (XX) XX (2013)

ATS-P1-01
Nonlinear surface chemistry analysed with XUV pump - XUV probe at FLASH

T02 Astronomical Frontiers for Surface Science

#ATS-P1-01

B. Siemer [1], R. Frigge [1], H. Zacharias [1], R. Mitzner [2], S. Düsterer [3].

[1]Physikalisches Institut, WWU Münster - Münster (Germany), [2]Helmholtz Zentrum Berlin - Berlin (Germany), [3]Deutsches Elektronen Synchrotron - Hamburg (Germany).

For a better understanding of the formation of interstellar molecules a D_2O ice covered highly-oriented pyrolytic graphite (HOPG) surface is investigated. This analog of interstellar ice covered dust grains, is irradiated with XUV radiation (hv = 38 eV), provided by the free electron laser at Hamburg (FLASH). In a so far unknown reaction cascade O_2^+ ions are formed and emitted with a highly nonlinear dependence on the FLASH intensity proportional to I^3[1]. To investigate the formation process of the desorbing molecular oxygen ions a non-linear XUV pump - XUV probe measurement with a beamsplitter and delay-line device for the energy range of 24 – 200 eV is used. A two-pulse autocorrelation curve of desorbing O_2^+ ions is measured. The time constants for the fitted asymmetric Gaussian points to an electronic process initiating the reaction and long decay time of the O_2^+-signal suggests a motion of molecular constituents during the reaction.

[1] B. Siemer, T. Hoger, M. Rutkowski, R. Treusch and H. Zacharias, J. Phys.: Condens. Matter **22** 084013 (2010)

ATS-2-Or-9
Adsorption-induced nuclear-spin conversion of hydrogen on surfaces

T02 Astronomical Frontiers for Surface Science

#ATS-2-Or-9

K. Fukutani [1], K. Niki [2], T. Okano [1].

[1]University of Tokyo - Tokyo (Japan), [2]Chiba University - Chiba (Japan).

Molecular hydrogen consisting of two identical nuclei exists in nuclear-spin modifications of ortho and para species according to the total nuclear spin (I). Due to the symmetry of the total wave function with respect to the permutation of the two nuclei, ortho-H2 of I=1 is in the rotational state with odd rotational quantum numbers (J), while para-H2 of I=0 has even J. Although the transition between the ortho and para states is slow in gas phase, the conversion is promoted by the interaction with solid surfaces. We have studied H2 ortho-para conversion and D2 para-ortho conversion in physisorption states on Ag [1,2] and ice surfaces [3]. In these studies, we have noticed that the ortho/para ratio right after adsorption on surfaces deviates from the nuclear-spin degeneracy, which suggests ortho-para conversion takes place during the adsorption on surfaces. In the present paper, we have studied possible ortho-para conversion during the adsorption process of H2 on Ag with a use of a pure ortho-H2 source.

The experiments were performed in a UHV chamber. Pure ortho-H2 was prepared by the adsorption separation method on the basis of the difference for the desorption energy between ortho and para H2. The ortho-H2 was admitted to the surface with a pulse valve, and subsequently the surface coverages of ortho and para H2 were monitored by the REMPI technique combined with photostimulated desorption [1]. After the Ag surface was exposed to the pure ortho-H2 at 7 K, the para H2 was found to be on the surface with an intensity of about 20 % of the ortho H2. Since almost no para-H2 was present in the ortho-H2 source, the para-H2 observed on the surface originates from ortho-H2 incident to the surface. It is noted that the time evolution of the ortho-H2 coverage after the adsorption reveals an exponential decay with a time constant of about 600 s [1,2]. When H2 is in the adsorption well, ortho-para conversion proceeds with a conversion time of about 600 s. On the other hand, adsorption of H2 is regarded as vibrational relaxation in the adsorption well. We therefore argue that ortho-para conversion is induced during the vibrational relaxation in the potential well.

[1] K. Fukutani et al., Phys. Rev. Lett. 90 (2003) 096103.
[2] K. Niki et al., Phys. Rev. B 77 (2008) 201403.
[3] T. Sugimoto & K. Fukutani, Nat. Phys. 7 (2011) 307.

ATS-P1-02
Refractive indices of organic thin films simulating Titan aerosols

T02 Astronomical Frontiers for Surface Science

#ATS-P1-02

G. Cernogora, A. Mahjoub, P.R. Dahoo, N. Carrasco, T. Gautier.

UVSQ-LATMOS - Guyancourt (France).

Titan, the biggest Saturn satellite has a dense atmosphere composed of N2 and CH4. In this atmosphere, solid organic aerosols are produced by photochemistry induced by solar photons and by ionic chemistry induced by energetic particles from Saturn's magnetosphere.
In order to simulate in laboratory the formation of these organic aerosols, a low pressure Radio Frequency Capacitively Coupled Plasma discharge is used. The experimental device is described in details in [1]. This discharge can run in N2 CH4 gas mixtures with 1% to 10% of CH4 in order to simulate Titan's conditions. Gas mixture is introduced continuously. Silicon substrates are placed on the grounded electrode. Films of organic material are then produced during 2 or 3 hours in order to obtain film with thickness lower than 1µm. The substrates are at room temperature or can be cooled down to 105 K by a liquid nitrogen flow through the polarised electrode.
Films are observed ex-situ by Spectroscopic Ellipsometry (SE) from 340 to 1000 nm. SE is an optical technique based on the measurement of the change in polarized light upon light reflection on a sample. Two parameters are measured: tan(Ψ), the ratio of the amplitudes and Δ the relative difference in phase for the p- and s-polarized reflected light the film surface. The real and imaginary refractive index (n and k) are deduced from the fit of the ellipsometric parameters Δ and ψ using a physical description, based on a Tauc Lorentz model for the film dielectric constant (correlated with the optical indices). The films thickness and roughness are also deduced from the fit [2].
For films produced at room temperature or at 105 K the imaginary refractive index k decreases when the CH4 amount increases. Then the films are less absorbent for higher CH4 concentrations. From elemental analysis [3] it is shown that this effect is due to a decay of nitrogen incorporation in the films. Moreover, IR absorption measurements [4] confirm the increase of the amine functions with lower amounts of CH4.
It is shown that for the same gas mixture and deposition duration, the thickness of

the films produced at 105 K is smaller than for those produced at room temperature. When the substrate is cooled down to 105 K, for the same gas mixture conditions, the films are less absorbent than films produced at room temperature. The changes in k values at low temperature are attributed to a change in the chemical composition of the gas mixture when the plasma is on, measured in situ by mass spectrometry. Nitrides are condensed on the reactor wall at low temperature. This reduction of nitrogen containing compounds in the gas phase leads to a decay of nitrogen in the films and a decrease of absorption.
These results are compared with the optical properties' of Titan's aerosols deduced from the Cassini Huygens probe measurements.

[1] Alcouffe G., Cavarroc M., Cernogora G., Ouni F., Jolly A., Boufendi L., Szopa C.. Plasma Sources Science and Technology 19, 1 (2010) 015008.
[2] Mahjoub A., Carrasco N., Dahoo P.-R., Gautier T., Szopa C., Cernogora G. Icarus 221, 2 (2012) 670.
[3] Sciamma-O'brien E., Carrasco N., Szopa C., Buch A., Cernogora G. Icarus 209, 2 (2010) 704.
[4] Gautier T., Carrasco N., Mahjoub A., Vinatier S., Giuliani A., Szopa C., Anderson C. M., Correia J.-J., Dumas P., Cernogora G. Icarus 221, 1 (2012) 320.

ATS-1-Or-2
The interaction between atomic hydrogen and PAHs: Implications for molecular hydrogen formation

T02 Astronomical Frontiers for Surface Science

#ATS-1-Or-2

J. Thrower, B. Jørgensen, E. Friis, A. Skov, H. Lemaître, A. Cassidy, R. Balog, M. Andersen, B. Hammer, L. Hornekær.

Department of Physics and Astronomy, Aarhus University - Aarhus (Denmark).

Polycyclic aromatic hydrocarbons (PAHs) account for a significant fraction of the cosmic carbon budget, being observed in a wide range of astrophysical environments. and are thought to play an important part in interstellar chemistry. We have considered the interaction between this important class of interstellar molecule and atomic hydrogen. In addition to forming superhydrogenated PAH species (HPAH) our measurements reveal a previously unexplored route to molecular hydrogen (H_2) formation (See **Fig. 1**). The formation of H_2 is inefficient in the gas phase and requires surface chemistry to be invoked to explain the observed abundance. Numerous investigations have revealed the efficiency of the surface recombination of physisorbed H atoms at the low temperatures found in molecular clouds. At higher temperatures, for example in photodissociation regions (PDRs), reduced residence times mean that alternative mechanisms are required in order to explain the observed H_2 formation rate. The observed correlation between H_2 formation rate and PAH emission in PDRs suggests that PAHs may play a role in H_2 formation in such environments [1]. Density functional theory (DFT) calculations [2] have shown that H-atom addition to PAH molecules can lead to the formation of HPAH species through the addition of H atoms to both the edge and center sites of PAH molecules. They also revealed the presence of energetically favourable abstraction pathways leading to the formation of H_2 molecules. The formation of such HPAH species with additional H atoms is consistent with the observed 3.4 μm band previously attributed to PAH species with additional peripheral H atoms [3,4]. We have confirmed the results of these calculations experimentally using a combination of thermal desorption and scanning tunneling microscopy (STM) measurements. Exposure of a monolayer of coronene ($C_{24}H_{12}$) adsorbed on a graphite substrate to a beam of atomic hydrogen results in the formation of superhydrogenated coronene

molecules [5]. The observed product mass distribution indicates that addition to edge and center sites occurs, along abstraction reactions leading to H_2. The STM measurements provide a direct observation of the adsorbed HPAH species following exposure to the H beam.

[1] E. Habart et al., 2003, *Astron. Astrophys*., **397**, 623.
[5] E. Rauls & L. Hornekær, 2008, *Astrophys. J.*, **679**, 531.
[3] M. P. Bernstein et al., 1996, *Astrophys J.*, **472**, L127.
[4] D. R. Wagner et al., 2000, *Astrophys. J.*, **545**, 854.
[5] J. D. Thrower et al., 2012, *Astrophys. J.*, **752**, 3.

Fig. 1 - Superhydrogenated PAH species formed through H-atom addition provide a route to H_2 formation through H abstraction reactions.

ATS-2-Or-4
RAIRS study of the dipole alignment in spontelectric solid nitrous oxide (N2O) films: Possible astrophysical implications

T02 Astronomical Frontiers for Surface Science

#ATS-2-Or-4

J. Lasne [1], A. Rosu-Finsen [1], M. Collings [1], M. Mccoustra [1], A. Cassidy [2], O. Plekan [3], J.D. Thrower [2], R. Balog [2], D. Field [2], N. Jones [2].

[1]Institute of Chemical Sciences, Heriot-Watt University - Edinburgh (United kingdom), [2]Department of Physics and Astronomy and Institute for Storage Ring Facilities at Aarhus (ISA), Aarhus University, - Aarhus C (Denmark), [3]Sincrotrone Trieste, S.C.p.A. di Interesse Nazionale - Trieste (Italy).

It has recently been discovered at the ASTRID laboratory at Aarhus University that solid cryofilms of simple species such as nitrous oxide (N_2O), propane or toluene spontaneously polarise and give rise to significant surface potentials of typically several volts, corresponding to electric fields in excess of 10^8 V.m^{-1} . It has been suggested that the spontelectric fields form due to the alignment of the permanent dipoles of the molecules in the films. [1-3]

Although the spontelectric effect cannot be directly observed with infrared spectroscopy, this tool can provide information on the degree of dipole alignment in the film. [4] To this aim, we performed reflection-absorption infrared spectroscopy (RAIRS) experiments on pure N_2O films and on dilute N_2O:Xe mixtures, where the spontelectric effect is retained. The influence of deposition temperature on the structure of solid N_2O is discussed in terms of dipole alignment in the film. Segregation of N_2O does not occur in Xe, suggesting that the dipole alignment believed to give rise to the observed spontelectric field is due to an extended network of dipole-dipole interactions within the film.
The spontelectric effect may have important astrophysical implications: in the dense regions of the molecular clouds, dust grains are coated with tens of monolayers of carbon monoxide (CO). CO molecules have a permanent dipole moment; therefore

CO films may exhibit a spontelectric character. This would have consequences for the chemistry of the interstellar medium, which will be discussed in this presentation.

[1] R. Balog, P. Cicman, N.C. Jones, D. Field, Phys. Rev. Lett., 2009, **102**, 073003
[2] O. Plekan, A. Cassidy, R. Balog, N.C. Jones, D. Field, Phys. Chem. Chem. Phys., 2011, **13**, 21035
[3] D. Field, O. Plekan, A. Cassidy, R. Balog, N.C. Jones, J. Dunger. Int. Rev. Phys. Chem. 2013, **32**, 345
[4] B. Rowland, N.S. Kadagathur and J.P. Devlin, J. Chem. Phys., 1995, **102**, 13

ATS-2-Or-8
Spin isomer separation in the lab – principles, performance and potential applications of a high purity ortho-H2O molecular beam source

T02 Astronomical Frontiers for Surface Science

#ATS-2-Or-8

G. Alexandrowicz [1], T. Kravchuk [1], E. Lisitsin [1], P.A. Turgeon [2], P. Ayotte [2].

[1]Technion - Israel Institute of Technology - Haifa (Israel), [2]Université de Sherbrooke - Sherbrooke (Canada).

Astrophysical studies of comets and forming planetary systems have gathered spectroscopic evidence for abnormally low ratios of ortho-H_2O / para-H_2O, reflecting a surprisingly low spin temperature of the gas phase water molecules(e.g. [1]). Suggestions have been made that such low spin temperatures can be related back to the formation conditions of stellar systems due to the extremely slow rate of nuclear spin conversion. While this ability to look into the past is particularly valuable, a fundamental requirement for reliably interpreting these results is a good understanding of nuclear spin conversion mechanisms, both in the gas phase and when interacting with cold solid surfaces. Unfortunately, the current understanding of these conversion mechanisms is rather limited, mostly due to the lack of experimental methods which can separate spin isomers of astrophysically relevant molecules in general and the two spin isomers of H_2O in particular.

A potential breakthrough was reported a decade ago, where selective physical adsorption seemed to enable separation of the H_2O water isomers[2], however, several subsequent attempts to reproduce these results have not been successful. In a recent set of experiments, we have successfully formed a molecular beam of ortho-H_2O by magnetically focusing a slow molecular beam [3]. This unique molecular beam source opens up the possibility of performing highly controlled laboratory studies of nuclear spin conversion of water molecules and other astrophysically relevant molecules. We will present recent infra red spectroscopy measurements

which demonstrate the high H_2O spin isomer purity produced by our molecular beam source and also examine the ability to store the ortho molecules for prolonged times within isolated rare-gas matrices[4].

[1] N. Dello Russo et al., Astrophys. J. 621, 537 (2005) / M. R. Hogerheijde et al. Science, 334, 338 (2011)
[2] V. I. Tikhonov, and A. A. Volkov, Science 296, 5577 (2002)
[3] T. Kravchuk et al., Science, 331, 319 (2011).
[4] P. Turgeon et al. Physical Review A, 86, 062710 (2012).

ATS-1-Or-3
Synthesis of Cosmic Dust Analogues

T02 Astronomical Frontiers for Surface Science

#ATS-1-Or-3

V. Frankland, A. James, J. Plane.

University of Leeds - Leeds (United kingdom).

The harsh conditions of the interstellar medium (ISM) prevent gas-phase chemistry alone from being sufficient to explain the observation of over 150 different molecules [1]. Instead, the dust grains can provide a surface on which the formation of key species, including H_2, can occur.

Sol-gel and microfluidic techniques have been used to synthesize cosmic dust analogues. Particle analysis has revealed that these nanoparticles are highly microporous and provide a suitable surface for ice formation to occur on. Surface chemistry performed in a Knudsen Cell has been used to explore the heterogeneous reactions and adsorption kinetics of a range of gases on the cosmic dust particles mimicking the gas-dust chemistry in the atmospheres of planets and moons and in the ISM.

[1] From "129 reported interstellar and circumstellar molecules" http://www.cv.nrao.edu/%7Eawootten/allmols.html (assessed 15th January 2013)

ATS-3-Or-3
Desorption of O2, CO and N2 from astronomically relevant surfaces

T02 Astronomical Frontiers for Surface Science

#ATS-3-Or-3

A. Rosu-Finsen [1], V. Frankland [2], J. Lasne [1], M. Collings [1], M. Mccoustra [1].

[1]Heriot-Watt University - Edinburgh (United kingdom), [2]Leeds University - Leeds (United kingdom).

In the interstellar medium (ISM), a range of molecules have been observed in the gas phase or condensed onto icy surfaces of dust grains. Oxygen (O_2), carbon monoxide (CO) and nitrogen (N_2) are predicted to be among the most abundant small molecules in dense cores.[1,2,3] Although the concentrations of most species, such as CO, agree well with the observed molecular abundance using gas-phase chemistry, the models are unable to explain the formation and abundance of several molecules, including O_2 and N_2.[1,4] Then, the models need to include the adsorption and desorption processes of these species from the icy grains to match the observed abundances. To this aim, we performed Temperature-Programmed Desorption (TPD) experiments coupled with kinetic modelling to study the desorption kinetics of O_2, CO and N_2 sub-monolayers and multilayers from amorphous silica. Desorption of O_2 from compact and porous amorphous solid water-covered silica is also reported. Our results show that the morphology of the underlying silica surface affects the desorption kinetics of O_2, CO and N_2 and give insights into the understanding of the processes taking place in the ISM.

[1] Liseau R. et al., A&A, 541, A73 (2012)
[2] Chiar J.E., Gerakines P.A., Whittet D.C.B., Pendleton Y.J., Tielens A.G.G.M., Adamson A.J. and Boogert A.C.A., Ap. J., 498, 716 (1998)
[3] Belloche A. and Andre P., A&A, 419, L35 (2004)
[4] Knauth D.C., Andersson B.-G., McCandliss S.R. and Moos H.W., Nature, 429, 636 (2004)

ATS-P1-03
Temperature programmed desorption of small molecules from astrophysical interesting surfaces

T02 Astronomical Frontiers for Surface Science

#ATS-P1-03

T. Suhasaria [1], B. Siemer [2], R. Frigge [2], N. Heming [2], H. Zacharias [2].

[1]Graduate school of chemistry,Physikalisches Institut - Muenster (Germany), [2]Physikalisches Institut - Muenster (Germany).

Chemical surface reactions on dust grains are a possible way of molecule formation in the Interstellar Medium (ISM) [1]. These grains typically consist of graphitic and silicate particles embedded in icy mantels which are formed by molecules like CO, CO_2, H_2O or CH_4. In recent times more than 140 different gases have been reported in the dense regions of interstellar space [2]. Temperature programmed desorption (TPD) is used to investigate the binding energy and reaction order of several interstellar relevant molecules like CO, CO_2, CH_4 and D_2O on different interstellar silicate analogues like Forsterite (Mg_2SiO_4) and Olivine [$(Mg,Fe)_2SiO_4$] shown in the figures below. The experimental set-up consists of a quadruple mass spectrometer, a dosing chamber and a liquid helium cooled sample holder. Due to this set-up it is possible to investigate the behaviour of these molecules at very low temperatures (~ 5 K) comparable to the ISM. Further due to the dosing chamber it is possible to prepare a sample with a precise mixture of different kind of gases and a low coverage. We present desorption spectra, binding energies and their coverage dependence on both Olivine and single crystal Forsterite.

1] D. A. Williams, E. Herbst, Surf. Sci. 500, 823, (2002).
2] D. J. Burkew, W. A. Brown, Phys. Chem. Chem. Phys. 12, 5947-5969, (2010).

fig. 1: Forsterite single crystal

fig. 2: Olivine crystal

ATS-3-Or-4
Sublimation and Irradiation of Glycolaldehdye, Methyl Formate and Acetic Acid Astrophysical Ices

T02 Astronomical Frontiers for Surface Science

#ATS-3-Or-4

D. Burke, F. Puletti, M. Whelan, P. Woods, B. Slater, S. Viti, W. Brown.

UCL - London (United kingdom).

Abstract for ASTROSURF meeting

There is currently great interest among astronomers in the inventory of organic molecules in space. The role surface science plays in astrophysical processes is considerable, ranging from the birth and formation of stars and planets and extending to the origins of life. The importance of surface processes within interstellar ices comes from the observation that the abundance of many molecules detected within interstellar clouds cannot be explained by astrophysical models using only gas-phase processes. These models become more accurate when reactions on the surfaces of dust grains are incorporated, since grains open up reaction pathways to adsorbed atoms/molecules that are not available in the gas-phase. Amongst the most important organic species detected in space is glycolaldehyde (CH_2OHCHO), an isomer of methyl formate ($HCOOCH_3$) and acetic acid (CH_3COOH). It is postulated that glycolaldehyde may have a role in the origins of life in our universe.

We present a detailed investigation of the adsorption and desorption of glycolaldehyde, methyl formate and acetic acid from a model interstellar dust grain using temperature programmed desorption (TPD) and reflection absorption infrared spectroscopy (RAIRS). Primarily we will study the stability of glycolaldehyde/water containing ices to electron/UV irradiation. Electron irradiation (simulating the effect of cosmic ray ionisation) and UV irradiation (over a range of wavelengths) is used to examine competing routes for non-thermal desorption, decomposition and formation. RAIRS and TPD will be used to identify any reaction products and to monitor the desorption/decomposition of glycolaldehyde as a function of irradiation time.

This work forms part of a larger project, incorporating experiment, theory and astrochemical modelling, investigating the formation of glycolaldehyde in space.

ATS-3-Or-5
Electron and Ion Irradiation of Solid Acetonitrile

T02 Astronomical Frontiers for Surface Science

#ATS-3-Or-5

D. Marchione [1], A. Abdulgalil [1], J. Thrower [2], M. Collings [1], M. Mccoustra [1], F. Islam [3], M.E. Palumbo [3], E. Congiu [4], F. Dulieu [4].

[1]Heriot-Watt University - Edinburgh (United kingdom), [2]Aarhus University - Aarhus (Denmark), [3]INAF- Osservatoro Astrofisico di Catania - Catania (Italy), [4]LERMA/LAMAp UMR 8112 du CNRS, de l'Observatoire de Paris et de l'Université de Cergy Pontoise - Cergy-Pontoise (France).

The presence of CH_3CN in the interstellar medium (ISM) is of significance due to its potential as a reactant in the formation of amino acids in astrophysical environments [1]. It has been detected in comets [2], the atmosphere of Titan [3], and as a gas phase molecule in the ISM [4]. CH_3CN is likely to be formed on icy grains from reactions involving CH_3 and CN radicals and injected into the gas phase as the icy grain mantles desorb at temperatures above 90 K [5]. In this study we report on collaborative investigations made as part of the activities of the European network LASSIE, particularly with the Osservatorio Astrofisico di Catania [6] focussing on the investigation of energetic processing of icy mantles where a competition exists between chemical processes and physical processes. To this end the structure and bonding of solid acetonitrile (CH_3CN) films on amorphous silica are studied and chemical and physical processes under irradiation with 200 keV protons and 250 - 400 eV electrons are quantified using transmission infrared spectroscopy (TIRS), reflection absorption infrared spectroscopy (RAIRS), and temperature programmed desorption (TPD), with the assistance of basic computational chemistry and nuclear materials calculations. Astrophysical implications are eventually discussed.

[1] R. L. Hudson, M. H. Moore, J. P. Dworkin, M. P. Martin, and Z. D. Pozun: Astrobiology **8** (2008) 771.

[2] W. B. Huebner, L. E. Snyder, and D. Buhl: Icarus **23** (1974) 580.

[3] L. M. Lara, E. Lellouch, J. J. Lopez-Moreno, and R. Rodrigo: J. Geophys. Res. **101** (1996) 23261.

[4] A. Marten, T. Hidayat, Y. Biraud, and R. Moreno: Icarus **158** (2002) 532.

[5] B. L. Ulich, and E. K. Conkling: Nature **248** (1974) 121

[6] A. G. M. Abdulgalil, D. Marchione, J. D. Thrower, M. P. Collings, M. R. S. McCoustra, F. Islam, M .E. Palumbo, E. Congiu, and F. Dulieu: Phil. Trans. Roy. Soc. London A, in print.

ATS-1-Or-1
Interaction of Benzene with Molecular Solids - The Importance of Hydrogen Bonding

T02 Astronomical Frontiers for Surface Science

#ATS-1-Or-1

M. Mccoustra, D. Marchione, A. Abdulgalil, M. Collings.

Heriot-Watt University - Edinburgh (United kingdom).

Polycyclic aromatic hydrocarbons (PAHs) are large and stable molecules containing about 10-20% of the total available cosmic carbon. While in diffuse cloud environments they are thought to exist in gas phase, in dense clouds IR absorption features attributable to PAHs hints to their presence both in gas and condensed phase. As previous work [1,2] by this group, benzene was conveniently chosen as a prototypical PAH, representing the main building block, but as also because it has been detected around the protoplanery nebula CRL 618 [3]. Therefore there is potential for benzene to be adsorbed on ices of different chemical nature in conditions close to those in the interstellar medium. Reflection-absorption infrared spectroscopy (RAIRS) and a quadrupole mass spectrometry (QMS) have been used to characterise dynamical processes of astrophysical relevance and investigate the role of intramolecular interactions both at the interface and in the bulk ice. Astrophysical implications of our observations will be discussed.

[1] J. D. Thrower, D. J. Burke, M. P. Collings, A. Dawes, P. D. Holtom, F. Jamme, P. Kendall, W. A. Brown, I. P. Clark, H. J. Fraser, M. R. S. McCoustra, N. J. Mason, and A. W. Parker, *Astrophys. J.*, 2008, **673**, 1233.
[2] J. D. Thrower, M. P. Collings, F. J. M. Rutten and M. R. S. McCoustra, *Chem. Phys. Lett.*, 2011, **505**, 106.
[3] J. Cernicharo, A. M. Heras, A. Tielens, J. R. Pardo, F. Herpin, M. Guelin, and L. Waters, *Astrophys. J.*, 2002, **401**, L267.

ATS-3-Or-2
Modelling Non-Thermal Desorption in Interstellar Environments

T02 Astronomical Frontiers for Surface Science

#ATS-3-Or-2

M. Collings, A. Abdulgalil, M. Mccoustra.

Institute of Chemical Sciences, Heriot-Watt University - Edinburgh (United kingdom).

In the coldest, densest regions of molecular clouds, the time-scale for adsorption of molecular species onto dust grains is much shorter than the typical lifetime of such objects [1], therefore, complete freeze-out of molecular species might be expected. However, observations demonstrate that a significant gas-phase population of molecular species is maintained [2]. Therefore, non-thermal desorption mechanisms that enable return of mantle species to the gas phase are required to balance the freeze-out process. Such non-thermal desorption mechanisms remain poorly understood for interstellar ices [3], and are poorly characterised by experimental data.

Here, we present models of desorption in a range of astrophysical environments, in the absence of gas phase chemistry. These models include thermal desorption and various mechanisms of non-thermal desorption, based on recent laboratory results. The relative importance of different desorption mechanisms can thus be tested against the astrophysical conditions.

[1] D. A. Williams, S. D. Taylor, *Quart. J. Roy. Astron. Soc.* (1996), **37**, 565.
[2] V. Wakelam, E. Herbst, F. Selsis, *Astron. Astrophys.* (2006), **451**, 551.
[3] J. F. Roberts, J. M. C. Rawlings, S. Viti, D. A. Williams, *Mon. Not. Roy. Astron. Soc.* (2007), **382**, 733.

ATS-P1-04
Interaction of Oxygen (X,3P) atom with graphenic-like surfaces for astrophysical applications

T02 Astronomical Frontiers for Surface Science

#ATS-P1-04

N. Rougeau [1], S. Morisset [2], D. Teillet-Billy [2].

[1]ISMO, Institut des Sciences Moléculaires d'Orsay, Université Paris Sud CNRS, UMR 8214 - Orsay (France), [2]ISMO, Institut des Sciences Moléculaires d'Orsay, CNRS Université Paris Sud, UMR 8214 - Orsay (France).

In the interstellar medium (ISM), dust grains play a key role in mediating the formation of molecular species. In order to understand and quantitatively describe the related reactive processes, it is of a strong interest to study the interactions (and reactions) of H, C, O atoms present in the interstellar clouds with (and at) grain surfaces.
Many studies have been devoted to the adsorption of hydrogen atoms, the most abundant atomic species in interstellar clouds, and to the formation of H_2 by H recombination/abstraction processes onto the surface of carbonaceous dust grains. We have shown that the atomic adsorption characteristics (physisorption/chemisorption wells, adsorption barrier, defects) play a major role in the molecular formation [1], [2].
In the ISM, the oxygen is the third abundant element after H and He. The atomic oxygen is implied in the formation of heavier molecules such as OH [3], H_2O. In this context, we have studied the adsorption of the atomic oxygen in the fundamental state ^3P on a carbonaceous grain. Indeed previous works have been mainly devoted to the singlet state and only a few to the triplet state [4] [5].
Our theoretical studies have been performed by means of spin polarized DFT/GGA calculations. The grain surface is modeled either as a graphene sheet or as PAH molecules ($C_{24}H_{12}$, $C_{54}H_{18}$). We have considered several adsorption sites: on top of a C atom of the surface, bridged between 2 adjacent C atoms of the surface.
We have obtained adsorption energies and geometries in agreement with previous works [4] [5]. Our main result is the barrierless chemisorption of the atomic oxygen in the ^3P state onto graphenic surfaces. The chemisorption characteristics are site dependent. Regardless of the surface considered, the more stable chemisorption site is the top site.

At larger surface-oxygen distances, the physisorption of the atomic oxygen in the ^3P state onto graphenic surfaces is also obtained. Depending on the surface, the physisortion characteristics are weakly site dependent.
All these electronic/structural studies, including relaxation of surrounding carbon atoms, are the first step needed for the study of the OH/H_2O formation dynamics in order to obtain reaction probabilities, energy sharing between the nascent molecules and the surface.

[1] V. Sidis, F. Aguillon, M. Sizun, N. Rougeau, D. Teillet-Billy, L. Jeloaica, S. Morisset and D. Bachellerie, "Molecules in Space & Laboratory“, Paris, (2007), J.L. Lemaire & F. Combes (editors).
[2] .V. Ivanovskaya, A. Zobelli, D. Teillet-Billy, N. Rougeau, V. Sidis, PR Briddon, Phys. Rev. B 82 (24) 245407(2010).
[3] H. Bergeron, N. Rougeau, V. Sidis, M. Sizun, D. Teillet-Billy, F. Aguillon, J. Phys. Chem. A 1 (2008) 11921.
[4] D.C. Sorescu, K.D. Jordan, P. Avouris, J. Phys. Chem. B 105. (2001) 11227.
[5] V Morón, L. Martin-Gondre, C. Crespos, P. Larregaray, P. Gamallo and R. Sayós, Computational and Theoretical Chemistry, Vol.990, (2012),132.

ATS-1-Or-6
Tracking the thermal desorption of thin water ice films by optical reflection measurements

T02 Astronomical Frontiers for Surface Science

#ATS-1-Or-6

A. Clemens, L. Hellberg, D. Chakarov.

Chalmers University of Technology - Gothenburg (Sweden).

Experimental desorption studies of water ice from surfaces are of high importance to improve astrochemical modeling. Thermal desorption in particular is relevant for modeling of hot core regions where it represents the predominant desorption process of water ice adsorbed on interstellar grains.
In addition to the commonly used methods of temperature programmed desorption (TPD) with mass spectrometry and vibrational spectroscopy methods [1] we present a method of tracking desorption of water ice optically.
Here we address two specific issues of relevance: (i) the role of nanostructured carbon surfaces in the desorption process and (ii) interpretation of the spectral dependence of the reflected light.
The model substrate for water ice desorption consists of truncated cone structures of highly oriented pyrolytic graphite (HOPG), with an upper diameter of 190 nm and a height of 100 nm that cover approximately 30% of the sample surface. The structures are prepared by colloidal lithography and oxygen plasma etching.
Desorption of water ice can be followed by recording the intensity of diffusely reflected light from the surface during a thermal desorption experiment.
The enhanced (resonant) optical absorption in the nanostructured samples (described before by us in [2]) results in a minimum in optical reflection at visible wavelengths. Due to that water ice desorption of initial water coverages as low as two monolayers could be tracked optically with high sensitivity at UV wavelengths.

[1] D. Chakarov, L. Österlund and B. Kasemo, Langmuir 11, 1201-1214 (1995).
[2] H. Fredriksson, T. Pakizeh, M. Käll, B. Kasemo and D. Chakarov, J. Opt. A 11, 114022 (2009).

ATS-2-Or-3
H2 formation and interaction on interstellar silicate analogs via REMPI(2+1) spectroscopy

T02 Astronomical Frontiers for Surface Science

#ATS-2-Or-3

L. Gavilan, J.L. Lemaire, G. Vidali.

Paris Observatory/Univ. Cergy-Pontoise - Paris (France).

Silicate dust surfaces catalyze the formation of molecular hydrogen, the most abundant molecule in the universe. The formation and sticking of this molecule on dust drives the chemical complexity of the ISM. Silicate dust properties depend on their location and lifetime in the ISM, where they can be irradiated by energetic photons and ions. We present this project in collaboration with the Laboratory Astrophysics Group in Jena (Germany), where we produced nanometer sized silicate samples via laser ablation. These are used as surface catalysts in molecular formation experiments within the FORMOLISM setup located in Cergy-Pontoise (France). Silicate samples are prepared according to extreme ISM parameters: structural (fully crystalline or amorphous), and chemical (the forsterite and fayalite endmembers of the olivine family). We present preliminary results on H2 formation on such silicates and the dependance on temperature, possible nuclear spin conversion effects, and rotationally "hot H2".

ATS-2-Or-5
Water formation through O2+D on cold grain surfaces of interstellar interest

T02 Astronomical Frontiers for Surface Science

#ATS-2-Or-5

S. Chaabouni.

Mar o.

Henda Smaoui-Chaabouni[1], Marco Minissale[1], Giulio Manico[2], Emanuele Congiu[1], Jennifer Noble[3], Saoud Baouche[1], Mario Accolla[4], and François Dulieu[1]

[1]LERMA, UMR 8112 du CNRS, de l'Observatoire de Paris et de l'Université de Cergy Pontoise, mail Gay Lussac, 95000 Cergy Pontoise Cedex, France.
[2]Dipartimento di Fisica ed Astronomia Università degli Studi di Catania Via Santa Sofia, 64 95123 Catania, Italy.
[3]Aix-Marseille Université, PIIM UMR 7345, 13397, Marseille, France
[4]Dipartimento di Scienze Applicate-Universita Parthenope di Napoli Centro Direzionale, Isola C4, 80143 Napoli, Italy

Interstellar water formation has been intensively investigated in the past decade. Many studies from different groups have shown an efficient formation through the hydrogenation/deuteration of O, O_2 and O_3 ices [1-4] mostly in the multilayer regime [1,2]. The formation of the first water molecules on bare dust grains (silicates and/or carbonaceous materials) is of primary importance to understand the growth of the icy mantle in dense and cold molecular clouds where the temperature is as low as 10 K. We present the first experimental results of D_2O and D_2O_2 formation through O_2 +D pathway in the sub-and monolayer regimes on bare amorphous silicate grain analogs. For comparison, we also studied the formation of water molecules on porous and non-porous amorphous water ices surfaces held at 10K [5].
The experiments were performed with the FORMOLISM setup located at the university of Cergy Pontoise using atomic deuterium and molecular oxygen triply differential pumping beam lines. The gas surface reactions are analyzed with

Reflection Absorption Infra-Red Spectroscopy (RAIRS) and with Temperature-Programmed Desorption (TPD) techniques.
Results showed that the formation of D_2O water molecules through O_2+D pathway is very efficient (80-90%), but one fraction of the newly formed water stays on the dust grains at 10K, and the other fraction is released into the gas phase. The fraction of water molecules desorbing into the gas phase upon formation depends strongly on the substrate (silicate or water ice). In the case of the silicate substrate, more than 85 % of D_2O water molecules desorb into the gas phase upon formation on the cold surface through the barrierless OD+D->D_2O reaction. The non-thermal desorption, also called the chemical desorption of the newly formed water molecules is induced by the heat released from the exothermic surface reaction between the radicals OD and D atoms [6]. These results are supported by a simple kinetic model taking into account the high desorption rate of water products.

[1] Miyauchi. N, Hidaka. H, Chigai. A, Nagaoka. A, et al., Chem. Phys. Lett , 456, 27 (2008)
[2] Cuppen. H. M, Ioppolo. S, Romanzin. C, Linnartz. H., Phys. Chem. Chem. Phys, 12, 12079 (2010)
[3] Dulieu. F, Amiaud. L et al., Astron. Astrophys. 512, A 30 (2010)
[4] Jing. D, He. J, Brucato. J , Sio. A. D, Tozzetti. L, and Vidali. J., Astrophys. J. Lett, 741, L9 (2011)
[5] Chaabouni. H, Minissale. M, Manicò. G, Congiu.E, et al., J. Chem. Phys. 137, 234706 (2012)
[6] Cazaux. S, Cobut. V, Marseille. M, Spaans. M, and Caselli. P., Astron. Astrophys. 522, A74 (2010).

ATS-2-Or-6
NH2OH formation via barrierless hydrogenation reactions of NO under dark interstellar cloud conditions

T02 Astronomical Frontiers for Surface Science

#ATS-2-Or-6

E. Congiu.

LERMA Univ. Cergy-Pontoise - Obs. de Paris (France).

In surface reactions and solid state chemistry nitric oxide, NO, is thought to be the main precursor species of the NO bonded molecules [1, 2] and one of the precursor molecules of nitrogen-containing organics [3, 4]. Interstellar nitrogen chemistry, however, is rather poorly understood as well as the mechanisms leading to the inclusion of nitrogen into (still) unknown reservoirs of interstellar nitrogen. Charnley et al. [2] proposed that accreted NO might be converted to HNO and hydroxlamyne - NH_2OH- via hydrogenation surface reactions in quiescent dense clouds. In the present laboratory study, temperature-programmed desorption (TPD) and reflection-absorption infrared spectroscopy (RAIRS) techniques are used to investigate hydrogenation reactions of NO molecules under interstellar dark cloud conditions. In this talk, I will focus on the reactivity of NO and H (D-)atoms and present a study of hydroxylamine formation on crystalline H_2O and amorphous silicate – two very realistic analogs of grain surface materials in the interstellar medium – at low temperature (10 K) and in a low-coverage regime (~ 1 monolayer) [5 - 7]. We show that at very low temperatures NH_2OH can be formed efficiently in a series of subsequent H-atom addition reactions of solid NO. The novelty of this reaction scheme is that the whole reaction takes place without adding energy. This adds a new perspective to the way molecules of biological importance may form in space. The model predictions show that hydroxylamine is to be abundant in the solid phase well before a protostar evolves to become a star and should be detectable with ALMA, the new astronomical flagship facility starting up in Chile. The present results add to the discussion whether the seeds of life are disseminated all over the Universe and may have been delivered to planets through impacting celestial bodies [4, 8].

[1] D. T. Halfen, A. J. Apponi, and L. M. Ziurys, Astrophys. J. 561, 244 (2001).
[2] S. B. Charnley, S. D. Rodgers, and P. Ehrenfreund, Astron. Astrophys. 378, 1024 (2001).
[3] R. T. Garrod, S. L. Widicus Weaver, and E. Herbst, Astrophys. J. 682, 283 (2008).
[4] V. Blagojevic, S. Petrie, and D. K. Bohme, Mon. Not. R. Astron. Soc. 339, L7-11 (2003).
[5] E. Congiu, G. Fedoseev, S. Ioppolo, F. Dulieu, H. Chaabouni, S. Baouche, J. L. Lemaire, C. Laffon, P. Parent, T. Lamberts, H. M. Cuppen, and H. Linnartz, Astrophys. J. Lett. 750, L12 (2012).
[6] E. Congiu, H. Chaabouni, C. Laffon, P. Parent, S. Baouche, and F. Dulieu, J. Chem. Phys., 137, 054713 (2012).
[7] G. Fedoseev, S. Ioppolo, T. Lamberts, J. Zhen, H. M. Cuppen, and H. Linnartz, J. Chem. Phys., 137, 054714 (2012).
[8] J. L. Snow, G. Orlova, V. Blagojevic, and D. K. Bohme, J. Am. Chem. Soc. 129, 9910 (2007).

ATS-2-Or-2
Quantum Diffusion and reactivity of Oxygen atoms

T02 Astronomical Frontiers for Surface Science

#ATS-2-Or-2

M. Minissale.

Observatoire de Paris and Université de Cergy Pontoise - Paris (France).

The solid state astrochemistry at low temperature is governed by the possibility of reactants to meet each others. Hydrogenation of numerous species such as H, CO, NO, O_2, O … as been the subject of recent intense experimental investigations. We propose now to focus for the first time on
oxidation.
The experiments presented have been performed with the FORMOLISM device, set in Université de Cergy Pontoise, Observatoire de Paris. Via a triply differentially pumped beam, O atoms (and O_2 molecules) are aimed at a cold (6-25K) sample held in UHV chamber. The products are probed using Thermally Programmed Desorption or Reflexion Absorption Infrared Spectroscopy.
We have varied the following parameters:

1) Substrate morphology (Amorphous water ice, porous and compact, crystalline ice, amorphous silicates, graphite)
2) Coverage, from 0.1 to 1 ML
3) Substrate temperature, from 6.3 to 25 K
4) Dissociation rate (from 35% to 80 %)

From all this set of experimental parameters, we have found that the O+O reaction and the O+O_2 reaction are limited by diffusion of O atoms on the substrate. We derive the diffusion temperature law and observe, like in quantum physics handbooks, the dramatic transition from quantum to classical diffusion. Despite of the high mass of O, quantum tunneling is efficient even at 6K. As a consequence, the solid-state astrochemistry of cold regions should be reconsidered and should include larger organic molecules than previously expected.
The role of the substrate in composition (water ice, silicate or graphite) and morphology (crystalline or amorphous) also reveals some unexpected results.

References

[1] Vidali et al, Faraday discussion, 133, 125, (2006)
[2] Watanabe and Kouchi, PrSS, 83, 439, (2008)
[3] Congiu et al, ApJL, 750, L12, (2012)
[4] Ioppolo et al, PCCP, 12, 12065, (2010)
[5] Mokrane et al, ApJL, 705, L195, (2009)
[6] Matar et al, A&A, 492, 17, (2008)
[7] Watanabe et al, ApJL, 714, L1, (2010)
[8] Karssemeijer et al, PCCP, 14, 10844 (2012)

ATS-1-Or-5
Competing Mechanisms of Catalytic H2 Formation and Dissociation on an Ultrasmall Silicate Nanocluster Dust Precursor

T02 Astronomical Frontiers for Surface Science

#ATS-1-Or-5

B. Kerkeni [1], S. Bromley [2].

[1]Laboratoire Physique de la Matière Condensée (LPMC), Faculté des Sciences de Tunis, Campus Universitaire - Tunis (Tunisia), [2]Departament de Química Física i Institut de Química Teorica i Computational (IQTCUB) Universitat de Barcelona - Barceolona (Spain).

Silicate dust grains adsorb hydrogen atoms and are thought to be essential in catalysing the formation of H_2 (Gould & Salpeter 1963; Kemper et al. 2004; Molster & Kemper 2005); the most abundant molecule in the interstellar medium (ISM). It has been estimated that up to 10 per cent of the mass of interstellar silicates may be in < 1.5 nm sized particles (Draine & Li 2001), these are fundamental intermediates in the formation of silicate dust grains in stellar outflows, and are likely to be ubiquitous in the ISM. In order to investigate the possibility of H_2 catalytic formation and dissociation on such nanosilicates we have conducted *ab initio* quantum chemical calculations to study hydrogen interactions with a stable nanosized silicate dust precursor (see Fig. 1). Specifically, we consider a 1.2 nm diameter nanosilicate composed of 21 atoms having the stoichiometry of forsterite, $(MgO)_6(SiO_2)_3$.

Due to its small size and high percentage of surface atoms our ultrasmall particle inherently does not posses the bulk crystalline structure and offers a number of hydrogen chemisorption and physisorption sites, presumably similar to those that larger amorphous silicates would offer. The best fit by (Katz et al. 1999) to experimental temperature programmed desorption curves for H_2 formation on polycrystalline olivine involved three parameters resulting from solving the rate equations: the barrier for atomic desorption (E_1) is approximately half of our smallest value (E_1=724 K), which corresponds to a H atom physisorbed over the centre of a

(MgOSiOMgO) ring. The experimental value is also a third of that reported on a crystalline forsterite surface (010) (Goumans et al. 2009).

We find a variety of reaction paths for the catalysis of H_2 formation all starting from mechanisms involving a double chemisorption of gas phase H atoms. One striking finding is a H_2 formation route with a barrier of 1515 K and an exothermicity of -7102 K which is energetically more favourable than that predicted previously on a bulk forsterite (010) surface (Goumans et al. 2009). We also find that our nanoparticle allows for many other exothermic H_2 formation routes and also a number of pathways for H_2 catalytic dissociation.

Draine, B. T., and Li, A., **2001**, Astrophys. J., 551, 807
Gould, R. J., and Salpeter, E. E., **1963**, Astrophys. J., 138, 393
Goumans T.P. M., Catlow C.R.A, and Brown W.A., **2009**, Mon. Not. R. Astron. Soc. 393, 1403
Katz N., Furman I., Biham O., Pirronello V., Vidali G., **1999**, Astrophys. J., 522, 305
Kemper F., Vriend W. J., and Tielens A. G. G. M., **2004**, Astrophys. J., 609, 826
Molster, F., and Kemper, C., **2005**, Space. Sci. Rev., 119, 3

Fig. 1: Optimised structure of the $(MgO)_6(SiO_2)_3$ nanocluster

ATS-2-Or-1
Hydrogen atom diffusion on amorphous solid water

T02 Astronomical Frontiers for Surface Science

#ATS-2-Or-1

G. Nyman, B. Senevirathne, S. Andersson.

University of Gothenburg - Gothenburg (Sweden).

H2 is the most abundant molecule in interstellar space. Its formation in gas phase is too slow to explain its abundance. It is believed that formation on grain surfaces is the dominant route. Such surfaces are often covered with a mantle of water ice. If hydrogen atom diffusion is fast on such surfaces this could lead to adsorbed hydrogen atoms moving around to find each other to form hydrogen molecules, which may then desorb from the surface. Experiments have been carried out to investigate how fast hydrogen atom diffusion is on amorphous solid water with apparently conflicting results [1-4]. A recent experiment by N. Watanabe and coworkers [5] sheds light on this and provides an explanation that hinges on the binding energies of the adsorption sites. Here we investigate theoretically the hydrogen atoms diffusion. We are able to verify the interpretation of Watanabe. We calculate barrier heights, see Fig. 1., and rate constants, using harmonic quantum transition state theory to treat tunneling, see Fig. 2, for hopping between local minima on the surface of both crystalline and amorphous ice. We also calculate the diffusion rate constants for hydrogen atom motion on the surfaces, which will be discussed.

[1] G. Manico, G. Ragunı, V. Pirronello, J. E. Roser and G. Vidali; 2001, ApJ, 548, L253.
[2] H. B. Perets, O. Biham, G Manico, V. Pirronello, J. Roser, S Swords and G. Vidali; 2005, ApJ, 627, 850.
[3] L. Hornekær, A. Baurichter, V. V. Petrunin, D. Field and A. C. Luntz; 2003, Science, 302, 1943.
[4] E. Matar, E. Congiu, F. Dulieu, A. Momeni, and J. L. Lemaire; 2008, A&A, 492, L17.
[5] N. Watanabe, Y. Kimura, A. Kouchi, T. Chigai, T. Hama and V. Pirronello; 2010, ApJ, 714, L233.

Fig. 1. Distribution of barrier heights (meV) on amorphous (red) and crystalline ice (blue).

Fig. 2. Arrhenius plot of rate constant with and without tunneling included.

ATS-1-Or-4
“Paris” meteorite analysis using cluster and particle impacts

T02 Astronomical Frontiers for Surface Science

#ATS-1-Or-4

M. Noun [1], D. Baklouti [2], R. Brunetto [2], S. Merouane [2], L. D’hendecourt [2], B. Nsouli [3], M. Roumie [3], F. Jamme [4], C. Sandt [4], P. Dumas [4], T. Calligaro [5], S. Della-Negra [1].

[1]Institut de Physique Nucléaire d’Orsay, Université Paris Sud11, UMR8608. - Orsay (France), [2]Institut d’Astrophysique Spatiale, CNRS, UMR-8617, Université Paris-Sud11 - Orsay (France), [3]Lebanese Atomic Energy Commission, National Council for Scientific Research - Beirut (Lebanon), [4]Synchrotron SOLEIL - Gif-Sur-Yvette-France (France), [5]3Centre de Recherche et de Restauration des musées de France, CNRS UMR171, Palais du Louvre - Paris (France).

“Paris” meteorite is a fragment from a primitive planetesimal, asteroid or comet. A piece of this meteorite is provided by the Museum National d’Histoire Naturelle in Paris and classified as a carbonaceous chondrite CM type belonging to the undifferentiated family [1, 2]. This kind of meteorites keeps the memory of their primary history and contains carbonaceous matter which permits to understand the prebiotic chemistry.

In this paper we present a new analysis approach combining multi complementary techniques elemental and structural ones. This study is performed on a 500*500 μm^2 of the Paris meteorite using mass spectrometry ToF-SIMS coupled to imaging, micro Infra Red, micro Raman and Ion Beam Analysis (Particle Induced X-ray Emission “PIXE”, micro PIXE, Rutherford Backscattering “RBS”).

The ToF-SIMS analyzes are performed using bismuth (Bi^+, Bi_3^+ at 25 keV, 1.3 pA) and argon Ar_{1000} (10keV) beams delivered by an ION-TOFV of the Lebanese Atomic Energy Commission (CNRSL-LAEC). PIXE and RBS are performed using a 3 MeV proton beam delivered by a 1.7 MV tandem accelerator of LAEC while the µ-PIXE (3MeV proton) experiments are performed at the AGLAE (Accelerateur Grand Louvre d’Analyse Elementaire). The micro IR Spectra (1.5-15µm) are registered at the Soleil SMIS (Spectroscopy and Microscopy in the Infrared using Synchrotron) beam line using a NicPlan microscope, coupled to a FTIR spectrometer operating in confocal reflection. Raman micro-spectroscopy uses a DXR Raman spectrometer from Thermo Fisher with a 532 nm exciting laser radiation.

In this paper, we shall discuss the results of the “Paris” fragment analysis obtained by the different complementary techniques. ToF-SIMS permits to identify and localize different elements, minerals and different types of organic compounds (CN-CNO and CxHy). An additional analysis in depth using the argon cluster is done in order to localize, in depth, the different components and especially the organic ones. While micro-IR and micro Raman permit the identification of different mineral compounds (Forsterite, enstatite, calcium sulfate and carbonate) and aromatic carbon ones. Additionally, we used the Ion Beam Analysis (PIXE and RBS) to determine the elemental composition and µ-PIXE to determine the local composition of different minerals like olivine and pyroxene crystal families.

In this presentation, we shall discuss the “Paris” meteorite results obtained with traditional astrophysical methods (µ-IR, µ-Raman) with an emphasis on the ToF-SIMS measurements completed by the IBA results. We conclude the presentation by the advantages and the limitations of these methods.

[1] Bourot-Denise, M., et al.: Paris: the slightly altered, slightly metamorphosed CM that bridges the gap between CMs and COs,41st LPSC, 2010..
[2] M. Noun, M. Roumie, T. Calligaro, B. Nsouli, R. Brunetto, D. Baklouti, L. d’Hendecourt, S. Della-Negra, On the Characterization of the “Paris” Meteorite Using PIXE, RBS and Micro PIXE, accepted in Nucl. Instr.and Meth. in Phys. Res. B (2013)

ATS-3-In-1
UV PHOTODESORPTION OF INTERSTELLAR ICES ANALOGUES: NEW HIGHLIGHTS FOR THE DESORPTION MECHANISMS

T02 Astronomical Frontiers for Surface Science

#ATS-3-In-1

J.H. Fillion [1], M. Bertin [1], E.C. Fayolle [2], C. Romanzin [3], H.A.M. Poderoso [1], K.I. Öberg [4], X. Michaut [1], A. Moudens [1], L. Philippe [1], P. Jeseck [1], H. Linnartz [2].

[1]UPMC, Lab de Physique Moléculaire pour l'Atmosphère et l'Astrophysique (LPMAA) - Paris (France), [2]Leiden Observatory, Sackler Laboratory for Astrophysics - Leiden (Netherlands), [3]Univ Paris Sud 11, Laboratoire de Chimie Physique (LCP) - Orsay (France), [4]Harvard Smithsonian Center for Astrophysics - Cambridge (United states).

Vacuum UV photodesorption of molecular ices is believed to be a major non-thermal process that can explain the presence of gas in various cold interstellar environments (edge of molecular clouds, dense clouds, star-forming regions, protoplanetary disks etc..). Quantitative first estimates of theses photodesorption yields for some major interstellar components could be derived in recent years using broadbands lamps, but the underlying mechanisms responsible for the photodesorption couldn't be constrained. Using the monochromatized vacuum UV output of synchrotron radiation (SOLEIL) we show how, for the first time, energy-resolved desorption spectra has revealed indirect surface mechanism, triggered by the electronic excitation of subsurface molecules, and strongly influenced by the intermolecular interactions in the ice. Typical examples will be presented considering pure and mixed ices samples. Desorption induced after photodissociation and open remaining questions will be also discussed.

ATS-2-Kn-1
TRANSFORMING CARBON ONIONS INTO NANODIAMOND: A NEW PATHWAY WITH ASTROPHYSICAL IMPLICATIONS

T02 Astronomical Frontiers for Surface Science

#ATS-2-Kn-1

N. Marks [1], M. Lattemann [1], D.R. Mckenzie [2].

[1]Physics & Astronomy, Curtin University - Perth (Australia), [2]School of Physics, The University of Sydney - Sydney (Australia).

Nanometre-sized diamond grains are commonly found in primitive chondritic meteorites, but their origin is puzzling [1]. Using evidence from atomistic simulation we establish a mechanism by which nanodiamonds form abundantly in space in a two-stage process involving condensation of vapour to form carbon onions followed by transformation to nanodiamond in an energetic impact [2]. This non-equilibrium process is consistent with common environments in space and invokes the fewest assumptions of any proposed model. Accordingly, the model can explain nanodiamond formation in both presolar and solar environments.

The simulations employ the Environment Dependent Interaction Potential (EDIP) [3] which provides an accurate description of bond formation processes. They reveal that within an optimal energy window of around 1-2 eV/atom carbon onions are efficiently transformed into nanodiamond on the timescale of a picosecond. The process differs substantially from conventional mechanisms for accessing the diamond phase which require high temperature and/or high pressure.

[1] G.R. Huss, Meteoritic Nanodiamonds: Messengers from the Stars, Elements 1, 97-100 (2005).
[2] N. A. Marks, M. Lattemann, D. R. McKenzie, Non-equilibrium route to nanodiamond with astrophysical implications, Phys. Rev. Lett. 108, 075503 (2012).
[3] N. A. Marks, Generalizing the environment-dependent-interaction-potential for carbon, Phys. Rev. B 63, 035401 (2001).

ATS-1-In-1
Atomic hydrogen interaction with polycyclic aromatic carbon systems – the formation of super-hydrogenated PAHs under interstellar conditions.

T02 Astronomical Frontiers for Surface Science

#ATS-1-In-1

L. Hornekær.

Department of Physics and Astronomy, Aarhus University - Aarhus (Denmark).

The interaction of atomic hydrogen with polycyclic aromatic carbon systems such as polycyclic aromatic hydrocarbon (PAH) molecules and graphene and graphite surfaces have been the subject of extensive experimental and theoretical investigations, due to its relevance in fields as diverse as interstellar chemistry, hydrogen storage and fusion reactors, and lately, due to the possibility of using hydrogen to engineer the electronic properties of graphene by chemical functionalization. In my talk I will highlight experimental results on the super-hydrogenation of PAH molecules and discuss the possible catalytic role played by PAHs in interstellar H2 catalysis [1-3].

[1] J. D. Thrower et al. EAS Publications Series, 46, 453 (2011)
[2] V. Menella, L. Hornekaer, J. Thrower, M. Accolla, Astrophysical Journal Letters 745, L2 (2012)
[3] J. D. Thrower et al. Astrophysical Journal 750, 1, (2012

ATS-2-In-1
t.b.a

T02 Astronomical Frontiers for Surface Science

#ATS-2-In-1

T. Loerting.

Institute of Physical Chemistry, University of Innsbruck - Innsbruck (Austria).

BI/ASS/NST-P1-03
Non-label Imaging of Essential Ions in Physiological and Pathological Angiogenesis in the Retina using TOF-SIMS

T03 BioInterphases

#BI/ASS/NST-P1-03

J. Kim [1], T.G. Lee [2], K.W. Kim [3], J.H. Kim [4].

[1]Seoul National Univerisity Hospital - Seoul (Korea, republic of), [2]KRISS - Daejeon (Korea, republic of), [3]Seoul National University - Seoul (Korea, republic of), [4]Seoul National University Hospital - Seoul (Korea, republic of).

Purpose: The pathological angiogenesis in the retina is the major cause of vision loss at all ages. This study was to investigate non-label essential ions imaging in the retinal tissue which would confirm the critical role of ion distribution in physiological and pathological angiogenesis in the retina

Methods: Time-of-flight secondary ion mass spectrometry (TOF-SIMS) was used to obtain non-labeled high-resolution analytic images of ion distribution in the retinas of developing mice and oxygen-induced retinopathy (OIR) mice. To determine the relation of ion distribution with retinal angiogenesis, expression of transient receptor potential (TRP) channels was evaluated by RT-PCR and Western blot analysis in retina and retinal endothelial cells. In addition the role of calcium in retinal angiogenesis was confirmed by anti-angiogenic activity of calcium chelator and calcium channel inhibitor to in vitro angiogenesis asssays (migration and tube formation) and retinal neovascularization of oxygen-induced retinopathy.

Results: Marked changes in Ca2+ distribution, compared with other fundamental ions, such as Na+, K+, and Mg2+, were detected during physiological and pathological angiogenesis in the retina. Most of all, ion mapping of zinc was

successfully obtained, whose distribution was however not significantly changed in retinal angiogenesis. Interestingly, TRP channel 1, 4 and 6 are prominently expressed in the retinal endothelial cell and retina. Blockade of TRP channels in the retina by SKF 96365 and 2-APB significantly inhibited in vitro angiogenesis of migration and tube formation under sub-lethal concentration. Moreover, TRP channels inhibitors effectively suppressed retinal neovascularization in a mouse model of retinopathy of prematurity, and showed no retinal toxicity.

Conclusions: The distribution of essential ions during physiological and pathological angiogenesis in the retina could be simultaneously evaluated without labeling. Interestingly calcium but not zinc would play a critical role in retinal angiogenesis.

BI/ASS/NST-P1-01
Bionanoparticles based chemical sensor

T03 BioInterphases

#BI/ASS/NST-P1-01

M. Wu.

Technical Institute of Physics and Chemistry, CAS - Beijing (China).

Bionanoparticles based chemical sensor

Man Wu and Zhongwei Niu

National Engineering Research Center of Engineering Plastics, Technical Institute of Physics and Chemistry, CAS, Beijing 100190, China Man.wu@mail.ipc.ac.cn

The classical fluorescent chemical sensor has poor water solubility and probably cytotoxic. This could limit its applications in the analysis of biological environment. To overcome this problem, bionanoparticle, especially tobacco mosaic virus (TMV), was used as carrier to prepare a well-structured and size-controlled fluorescent chemical sensor. Tobacco mosaic virus (TMV) is considered biocompatible, biodegradable, non-infectious and non-hazardous in human and mammalian. It has a hollow cylinder structure with a protein coat constructed from 2130 identical protein subunits arranged helically around a single stranded RNA. After removing the genome, TMV coat protein (CP) is capable to self-reassemble in hollow rod-like particle with desired length. Moreover, this rod-like particle has a particular structure of two open-ends. Chemical modifications can be easily realized on either the exterior or interior surface of TMV CP assembly by bioconjugation protocols. This endows assembly with the multifunctional properties by covalent attachment of functional molecule, such as sensor molecules. In other hand, pre-modified and raw CPs could also reassemble into well-structured rod-like structure with defined numbers of sensor molecules grafted either on the outer surface or inside the inner cavity. The influence of the position and ratio of grafted sensor molecule on the protein coat surface and the size of TMV CP-sensor system were systematically studied.

Figure: Schema representation of preparation of TMV CP-sensor system. A). TMV CP; B). well-structured and size-controlled assembly of TMV CP; C). sensor molecules grafted onto surface of TMV CP assembly.

BI/ASS-1-Or-1
SURFACE OXIDATION OF NiTi SHAPE MEMORY ALLOY BY OXYGEN PLASMA

T03 BioInterphases

#BI/ASS-1-Or-1

M. Jenko [1], T. Koklaj [1], M. Mozetič [2], W. Tuckart [3], R. Rudolf [4].

[1]Institute of Metals and Technology - Ljubljana (Slovenia), [2]Jožef Stefan Institute - Ljubljana (Slovenia), [3]Universidad Nacional del Sur - Bahia Blanca (Argentina), [4]Univerza Maribor - Maribor (Slovenia).

Nitinol, a group of nearly equiatomic Ni-Ti alloys, have unique mechanical properties, shape memory effect, superelasticity, and its biocompatibility. A number of useful items have already been produced, such as orthodontic implants, stents orthopaedic staples and even occluding structures to heal congenital heart defects [1,2]. Medical applications are still hindered by the concern for the release of Ni into surrounding tissues. Concerns have been raised about the composition of Nitinol, specifically with the presence of nickel, a known allergenic carcinogen that exhibits one of the highest sensitivities in metallic allergen tests [3]. The patterns of Ni release from Nitinol modify depending on the type of material; NiTi alloys with low or no processing versus commercial sheets[4]. A thick TiO_2 layer is often considered as a reliable barrier against Ni release, but it was shown that Nitinol with the thickest oxide TiO2 showed the highest Ni release [4,5].
Results of our previous research [6,7] showed that the surface of a melt spun NiTi shape memory alloy was covered with a thin oxide film. The thickness of the native oxide film was about 10 nm. After experiments on biocompatibility the oxide film thickness increased to about 20 nm. The oxide film before and after the biocompatibility tests consisted of titanium oxide and near the surface inhomoheniously distributed metallic Ni nano grains.
In order to improve the biocompability and to prevent Ni release, the material has been cleaned by hydrogen plasma and exposed to fully dissociated oxygen plasma. The oxides were characterized by field emission Auger electron spectroscopy (AES) depth profiling and X-ray photoelectron spectroscopy depth profiling (XPS). The AES depth profiling showed that the oxide thickness increased with increasing oxygen plasma treatment time. After treatment from 6 s, to 10 s, the oxide film was estimated from 30 nm to 500 nm. In all cases the oxide film contained TiO_2 and TiO_x, near the surface and no Ni. We have also studied the mechanical properties of oxides.

[1] Machado L, Savi M. Braz J Med Biol Res 2003;36:683–91.
[2] Song HY, Jung HY, Park SI, Kim SB, Lee DH, Kang SG, et al. Radiology 2000;217(2):551–7.
[3] Biesiekierski A, Wang James, Abdel-Hady Gepreel Mohamed, Wena Cuie, Acta Biomaterialia 8 (2012) 1661–1669
[4]Svetlana A Shabalovskaya, He Tian, James W Anderegg, Dominique U Schryvers, William U Carroll, Jan Van Humbeeck, Biomaterials 30(2009) 468-477
[5] He Tian, Dominique U Schryvers,di Liu, Qing Jiang, Jan Van Humbeeck, Acta Biomaterialia (2010)doi 10.1016/j.actbio2010.09.009
[6] Čolić M , Rudolf R , Stamenković D , Anžel, I , Vučević, D, Jenko M , Lazić V , Lojen G . Acta
biomaterialia, Jan. 2010, vol. 6, iss. 1, str. 308-317, doi: 10.1016/j.actbio.2009.06.027.
[7] Jenko M, Grant J T , Rudolf R, Kokalj T, Mandrino Dj., Surf. interface anal., Article first published online:
30 Jan. 2012, doi: 10.1002/sia.4869

BI-2-Or-1
In situ X-ray fluorescence analysis of barnacle larvae and juvenile barnacles

T03 BioInterphases

#BI-2-Or-1

T. Senkbeil [1], T. Mohamed [1], M. Grunze [1], A. Rosenhahn [2].

[1]IFG - Karlsruhe Institute of Technology - Eggenstein-Leopoldshafen (Germany), [2]Analytical Chemistry - Biointerfaces, Ruhr-University Bochum - Bochum (Germany).

Biofouling is the unwanted growth of marine organisms on man-made surfaces with a high ecological and economic impact. Barnacles – as a major macro fouler – contribute substantially to this phenomenon. In order to develop anti-fouling coatings avoiding their settlement on submerged surfaces, it is important to characterize their under-water cement and the mechanism of initial attachment of the motile barnacle larvae. Besides understanding the chemistry side, it is of pivotal importance to decipher the mechanism how the adhesive is able to cure and to adhere to the surface [1]. Here, we are especially interested in the metal distribution in adhesives used by barnacles. In general, studies on underwater cement are hampered by such obstacles as insoluble and/or sticky nature of the sample and poor development of micro-analytical methods for identifying the functions of underwater attachment. While the organic components, namely proteins and polysaccharides are intensively studied [2], inorganic components are barely addressed. Minerals used for calcification are rather obvious (e.g. Ca) and analysis on further metal ions is usually focused on those present in relatively high concentrations (Zn, P) and the accumulation of toxic components in barnacles (Cu, Pb, Cd) [3,4]. While in the adhesive of mussels or algae, iron and vanadium, respectively, play important roles, the function of trace elements in the adhesive of barnacles is not yet clear. Few reports indicate that trace elements, such as iron are present in barnacles [5].
We used X-ray fluorescence at the dedicated X-ray fluorescence end-station FLUO of the synchrotron storage ring ANKA (Karlsruhe Institute of Technology, Germany) to investigate the elemental composition of marine adhesives present in barnacles. The young invertebrates, provided by our biological collaborators (Prof. Clare, Newcastle University) had been settled on an 8 µm Kapton film sealing a small plastic cup filled with artificial seawater to provide a suitable environment for the living marine organisms. Using a focused 17 keV photon beam we were able to obtain elemental distribution maps of the organisms at a spatial resolution of

approximately 15 µm. As the X-ray photons are able to penetrate the whole organism, the images correspond rather to a 2D projection of the elemental distribution, with the depth-visibility of every element depending on the corresponding X-ray fluorescence photon energy. In order to distinguish signals originating from the contact area from those coming from the organism behind, we additionally used a confocal measurement setup providing a depth resolution below 20 µm allowing us to focus on the substances in direct contact with the Kapton substrate.

1. A. M. Smith and J. A. Callow, Biological Adhesives, Springer, Berlin, Germany, 2006.
2. K. Kamino, Barnarcle Underwater Attachment. In Biological Adhesives, Springer Berlin, 2006.
3. A. Viarengo and J. A. Nott, Comparative Biochemistry and Physiology Part C: Comparative Pharmacology, 1993, 104, 355-372.
4. M. I. Powell and K. N. White, Mar. Environ. Res., 1990, 30, 91-118.
5. S. Udaya Bhaskar, A. C. Anil and A. B. Wagh, Marine Pollution Bulletin, 1983, 14, 236-237.

BI-1-Or-1
Nanoparticle click functionalization by photochemical thiol-yne reaction, towards double chemoselective functionalization.

T03 BioInterphases

#BI-1-Or-1

E. Guénin [1], E. Nehlig [1], P. Demay-Drouard [1], J. Hardouin [2], L. Motte [2].

[1]Université Paris 13 - Bobigny (France), [2]Université Rouen - Rouen (France).

In a decade click chemistry has emerged as the method of choice for the coupling of a large panel of molecules (fluorophores, polymers, biomolecules, …) onto various surfaces (SAM, nanoparticles, MOF, …). This chemical development collides with another growing field: the engineering of nanoparticle's surface functionalization[1] for the design of new system at the nanometric level. In the domain of nanobiomedecine the use of click chemistry becomes predominant among the plethora of existing functionalization methodologies due to its versatility, easiness, selectivity and of course biocompatibility. These assets represent some of the criteria proposed by Sharpless and collaborators for a reaction to be designated as "click chemistry". Among all the reactions suitable to be named as click reactions, the Huisgen 1,3 cycloaddition between an azide and an alkyne (Cu-catalysed azide–alkyne cycloaddition: CuAAC) is from far the most popular one. It has been extensively used in nanoscience and was recently thoroughly reviewed.[2] But a variety of other click reactions could and have been used to graft molecules onto nanoparticles: other cycloadditions,thiol-ene reaction, Michael additions, … . Here we want to report the use of a long known reaction recently rediscovered (essentially by polymer scientists) for the functionalization of nanoparticles. Thiol-yne reaction is a water compatible radical reaction that can be done photothermically.[3] Under UV, in presence of a radical initiator two thiol functions are added successively onto an alkyne function. It doesn't require any metal catalysis and while it is described as a little bit slower than thiol-ene it remains fairly quick and more importantly completely irreversible at the difference of thiol-ene. Moreover thiol-yne reaction presents another advantage that makes it really suitable for surface chemistry: since the reaction allows two consecutive additions of thiols onto the alkyne, high surface density of the grafting could be reached quite easily.

So ongoing with our research on the development of multimodal nanoplateform with aim in biomedical and catalysis applications,[4-5] we decided to study the use of thiol-yne reaction for the functionalization of iron oxide superparamagnetic nanoparticles. We used a nanoplateform consisting of g-Fe2O3 nanoparticles coated by a bifunctional molecule from bisphosphonic acid family: (1-hydroxy-1-phosphonohept-6-ynyl)phosphonic Acid (BPheptyne). This nanoplateform so present alkyne functions on its surface on which we evaluated the photochemical coupling of various thiol molecules. We also investigated multiple click chemistry coupling onto this nanoplateform. To our knowledge this work represents the first functionalization of nanoparticles by thiol-yne reaction and the first double click process on the same nanoparticle surface.

1 Perrier, T.; Saulnier, P.; Benoît, J.-P., Chem.Eur. J. 2010, 16, (38), 11516-11529.
2 Li, N.; Binder, W. H., J. Mater. Chem. 2011, 21, (42), 16717-16734.
3 Hoogenboom, R., Angew. Chem. Int. Ed. 2010,49, (20), 3415-3417.
4 Motte, L.; Benyettou, F.; de Beaucorps, C.; Lecouvey, M.; Milesovic, I.; Lalatonne, Y., Faraday Discussions 2010, 149, (0), 211-225.
5 E. Guénin, J. Hardouin, Y. Lalatonne, L. Motte, J Nanopart. Res. 2012, 14, 7, 965.

BI/ASS/NST-P1-02
The effect of hyaluronic acid on the formation of calcium phosphate on CoCrMo alloy

T03 BioInterphases

#BI/ASS/NST-P1-02

I. Milosev [1], J. Hmeljak [2], A. Coer [2].

[1]Jozef Stefan Instutute - Ljubljana (Slovenia), [2]University of Primorska - Izola (Slovenia).

Hyaluronic acid is a component of synovial joint fluid, so the behaviour of orthopaedic alloys in its presence needs to be assessed. HA regulates many important physiological and pathophysiological reactions. It is a glycosaminoglycan (GAG) or mucopolysaccharide, a long, unbranched polysaccharide composed of repeating units of disaccharide N-acetyl-D-glucosamine and D-glucuronic acid (1) – the only non-sulfated GAG and a high molecular mass polymer in excess of 106 Da. It affects cell proliferation and migration and is responsible for the viscosity and resistance to compressive stress of synovial fluid. Electrochemical methods, X-ray photoelectron spectroscopy and scanning electron microscopy have been used to analyse the composition, thickness and morphology of any layers formed on the CoCrMo alloy. The behaviour of CoCrMo alloy has been studied in two simulated physiological solutions – NaCl and Hanks' solutions – each containing the sodium salt of hyaluronic acid. The addition of hyaluronic acid affects the electrochemical parameters of the CoCrMo alloy (2). Further, the presence of hyaluronic acid in simulated Hanks' physiological solution stimulates the formation of a calcium phosphate layer that is homogeneous even at a nano-sized level (Figure). The viability of human osteoblast-like was determined using the Alamar Blue Assay, while the osteogenic activity was evaluated by alkaline phosphatase activity. The presence of hyaluronic acid affects the alkaline phosphatase activity. The obtained results open up the possibility for tailoring the surface properties of CoCrMo alloy.

1. Day AJ, Sheenan JK. Curr Opin Chem Biol 2001;11:617.
2. I. Milošev, J. Hmeljak,A. Cör, J. Mater. Sci. Mater. Med., accepted for publication.

Figure: FE-SEM image recorded at the surface of CoCrMo alloy after 15h immersion in simulated Hanks' physiological solution containing 1 g/L hyaluronic acid. Magnification 50.000×.

BI/ASS-1-Or-2
Chemical and electrical function of diamond in biointerfaces

T03 BioInterphases

#BI/ASS-1-Or-2

B. Rezek.

Institute of Physics ASCR - Prague (Czech republic).

Understanding the interaction between the biological environment (tissues, cells, proteins, electrolytes, etc.) and a solid surface is crucial for biomedical applications such as bio-sensors, bio-electronics, tissue engineering and the optimization of implant materials. Cell adhesion, proliferations, and differentiation are complex processes which strongly depend on the cell cultivation conditions including the type of substrate. Materials which are commonly employed as substrates for in vitro testing are polystyrene and glass. In this context, diamond as a technological material can provide a relatively unique combination of excellent semiconducting, mechanical, chemical as well as biological properties [1].

Here we will present the influence of micro-structuring morphology and atomic termination of diamond thin film surfaces on cell growth and assembly [2-4]. We will investigate the influence of key parameters such as the seeding concentration of cells, the type of the applied cells, the duration of cultivation, the concentration of fetal bovine serum (FBS) in the cultivation medium, the dimensions and shape of microstructures, and surface roughness. We will show that the adsorption of proteins from the FBS serum is the key factor. Atomic force microscopy (AFM) both in solution and in air is applied in order to characterize the morphology of the FBS layers adsorbed on differently terminated diamond substrates. The conformation of proteins and hereby also adhesion and growth of the cells is controlled by the diamond surface atoms, independent of substrate doping. The influence of proteins and cells on the electronic properties of diamond will be demonstrated by employing a field-effect transistor based on nanocrystalline hydrogen-terminated diamond, whose gate is exposed to a solution (SG-FET) [5-6]. These results are discussed from the point of view of fundamental physics and biology as well as the prospects in medicine.

This research was financially supported by the projects P108/12/0996 (GACR), P108/12/G108 (GACR), doctoral project 202/09/H041, and by the Fellowship J.E. Purkyne. This work occurred in frame of the LNSM infrastructure.

1) J. Phys. D: Appl. Phys. 40 (2007) 6443-6466. doi:10.1088/0022-3727/40/20/S21
2) Sensors 9 (2009) 3549-3562, doi:10.3390/s90503549
3) Acta Biomaterialia 5 (2009), 3076-3085, doi: 10.1016/j.actbio.2009.04.020
4) PLoS ONE 6 (2011) e20943, doi:10.1371/journal.pone.0020943
5) Biosens. Bioelectron. 26 (2010) 1307-1312, doi:10.1016/j.bios.2010.07.027
6) Sens. Actuators B 20 (2012) 239–245, doi:10.1016/j.snb.2012.02.049

Schematic model of the interface between surface conductive diamond SGFET channel and the cell medium containing proteins and cells.

BI-1-Or-2
Comparison of thiol/NHS ester bifunctional SAMs on gold formed from symmetric and asymmetric disulfide linkers

T03 BioInterphases

#BI-1-Or-2

C. Ng [1], B. Espiña [1], E. Fernandes [2], V. Martins [1], D. Petrovykh [1].

[1]International Iberian Nanotechnology Laboratory - Braga (Portugal), [2]IBB-Institute for Biotechnology and Bioengineering, Centre of Biological Engineering, University of Minho Campus de Gualtar - Braga (Portugal).

The aim of this work is to analyze the monolayers formed by two different common commercial thiol/NHS ester bifunctional linkers, sulfosuccinimidyl 6-(3'-[2-pyridyldithio]-propionamido)hexanoate (sulfo-LC-SPDP) and 3,3´-dithiobis(sulfo-succinimidylpropionate) (DTSSP), using X-ray photoelectron spectroscopy (XPS). We chose to compare these two molecules, because both are commonly used to link biomolecules to gold, but DTSSP is a symmetric disulfide, while sulfo-LC-SPDP is an asymmetric disulfide, so they may form bifunctional monolayers of different structures. We compared their performance in terms of the attachment chemistry on gold surfaces and the ability to present the reactive NHS ester group post attachment. We find that in most cases, sulfo-LC-SPDP forms a more uniform monolayer than does DTSSP, presumably because the short chain fragment acts as a diluent and reduces steric constraints in the growing monolayer. We observe that sulfo-LC-SPDP produces a monolayer with single-component thiol-gold attachment chemistry, while multiple thiol-gold chemistries are typically present in DTSSP monolayers.

Unexpectedly, in contrast to the common wisdom that NHS esters are easily degraded by reaction with water,[1] we find that during deposition from aqueous solutions, the immobilization time has little effect on the integrity of NHS ester group on the resulting surfaces. However, the NHS ester groups do degrade significantly when exposed to the atmosphere, suggesting that a different degradation mechanism may operate in air and in solution. We quantified the amount of NHS

ester groups available for amine coupling by using a fluorine-labeled amine as a model molecule that produces a distinct XPS signal. Using this method, we compared the efficiency of amine coupling to DTSSP and sulfo-LC-SPDP bifunctional SAMs under different conditions. Without exposure to air, we find that between 50% and 100% of the linkers retain the NHS ester functional group that is available for coupling.

While many different protocols are used for surface attachment of DTSSP and SPDP, there is no previous systematic investigation of how different factors (such as pH, choice of buffer, ionic strength, and reaction time) in the attachment procedure affect the quality of the monolayer. Despite the presence of the charged sulfonate group in both DTSSP and SPDP linkers, we found that in the range of pH 5.7-8.0, the choice of buffer and ionic strength did not have a significant effect on the properties of the bifunctional monolayer.

[1] G. Mattson, E. Conklin, S. Desai, G. Nielander, M. D, Savage, S. Morgensen. *Molecular Biology Reports*, **1993**, 17, 167-183.

BI-1-Or-10
The effect of electrical mode and magnesium addition variations on the characteristics of bioactive calcium phosphate (Ca–P) containing coatings on titanium

T03 BioInterphases

#BI-1-Or-10

O. Terleeva [1], A. Slonova [2], I. Mironov [1], Y. Sharkeev [3], E. Legostaeva [4].

[1]Institute of Inorganic Chemistry of SB RAS - Novisibirsk (Russian federation), [2]Institute of Inorganic Chemistry of SB RAS - Novosibirsk (Russian federation), [3]Institute of Strength Physics and Materials Science of SB RAS - Tomsk (Russian federation), [4]Institute of Strength Physics and Materials Science of SB RAS - Tomsk (Russian federation).

Microplasma processes carried out in homogeneous alkaline electrolytes allow synthesizing bioactive coatings with high Ca/P ratio and satisfactory adhesion on the surface of implants made of valve metals [1]. The paper discusses the effects of the two main factors (electrical mode and electrolyte composition) on synthesis of bioactive calcium phosphate (Ca–P) coatings on nano-structured titanium.

Firstly, the variation of the electrical mode parameters results in a change of the temperature conditions of coating synthesis, which in turn might cause the variability of both coating composition and morphology. It was shown that optimal biocompatible coatings (with thickness 40–45 μm and roughness 4–5 μm) with satisfactory adhesion can be synthesized via successive implementation of the anodic pulse mode with a no-current pause followed by the alternative current mode with a no-current pause.

Secondly, the increase of component concentrations of an electrolyte leads to the formation of more uniform coatings. Additionally, a specific technique allowing to

synthesize calcium phosphate coatings containing prescribed quantity of magnesium was developed.

Furthermore, with the aim of increase of hydroxyapatite content, the possibilities of additional chemical treatment with buffer solutions of calcium phosphate (Ca–P) containing coatings were studied

O.P. Terleeva,Yu.P. Sharkeev,A.I. Slonova, I.V. Mironov, E.V. Legostaeva, I.A. Khlusov , E. Matykina, P. Skeldon, G.E. Thompson. Effect of Parameters of Microplasma modes and Electrolyte Composition on Characteristics of Calcium Phosphate Coatings on titanium for medical Applications, Surface and Coatings Technology 205(2010) 1723-1729

BI/NST-1-Or-1
TOF-SIMS Evaluation of Silica/γ-PGA Hybrids for Bone Regeneration

T03 BioInterphases

#BI/NST-1-Or-1

D. Wang [1], J. Nakamura [2], G. Poologasundarampillai [1], E.M. Valliant [1], J.R. Jones [1], D.S. Mcphail [1].

[1]Imperial College London - London (United kingdom), [2]Nagoya Institute of Technology - Nagoya (Japan).

Hybrids have the potential to have tailored mechanical properties and degradation rates when they are used as scaffolds for tissue engineering. The aim was to apply ToF-SIMS to determine the distribution of critical elements (e.g. silicon and calcium) in sol-gel silica/poly-γ-glutamic acid (γ-PGA) hybrids. Two hybrid systems were studied: i) silica/ γ-PGA where the silica precursor was TEOS with GPTMS employed as a coupling agent; ii) silica/ γ-PGA where the silica source was GPTMS. In i) the use of the free acid form of γ-PGA with $CaCl_2$ as the calcium source was compared to use of the calcium salt form of γ-PGA. In (ii) dimethyl carbonate (DMC) was used to improve the covalent coupling between GPTMS and γ-PGA and its role in the process was examined here.

The data showed that silicon, the network former of the inorganic component in the hybrids, and calcium were unevenly distributed in the silica/γ-PGA (free acid form) hybrids with $CaCl_2$ as the calcium source (Fig. 1a and 2a). A homogenous distribution was obtained when the calcium salt form of the γ-PGA was used (Fig. 1b and 2b). When DMC was added after the formation of the sol, high concentration Si regions were observed while there was no calcium signal in the same areas (Fig. 1c and 2c), implying that silicon-rich particles formed. In contrast, when DMC was added at the start of the sol-gel process, both silicon and calcium were distributed evenly (Fig. 1d and 2d).

The results revealed that the calcium salt form of γ-PGA was promising for calcium incorporation. If DMC is used in hybrid synthesis it should be added at the start of the process to maintain homogeneity. ToF-SIMS can compare inorganic/organic hybrids and can obtain the information throughout the material.

Fig. 1 (left) and 2 (right). Distribution of silicon (Fig. 1) and calcium (Fig. 2) in (a) the free acid form of γ-PGA and $CaCl_2$ as the calcium source; (b-d) the calcium salt form of γ-PGA (b) without DMC, (c) with the addition of DMC after the sol was produced and (d) with the addition of DMC at the start of the sol-gel process.

BI/ASS/NST-P1-04
Characterization of interfaces between polypeptide and DNA layers using X-ray photoelectron spectroscopy

T03 BioInterphases

#BI/ASS/NST-P1-04

S. Reiff, S. Ptasinska.

University of Notre Dame - Notre Dame (United states).

The interaction between proteins and DNA is critical for cells, with DNA binding proteins fulfilling a number of functions including packing DNA into the chromatin structure, assisting with transcription, and the cleaving of DNA molecules. Understanding the interfaces between DNA and protein molecules is of utmost importance for elucidating how these biological processes occur. Of special interest is the role of water in facilitating the interfacial bonding between the two molecules [1,2]. In this study the interface between layers of polypeptides, short chains of amino acids linked by peptide bonds, and DNA were examined using X-ray photoelectron spectroscopy (XPS).

XPS is a powerful surface science technique which can be used to qualitatively and quantitatively characterize the composition of a surface. High resolution spectra of electron core-levels can be obtained to assess chemical bonds present within a sample.

Here, we build upon our previous research of examining a poly-peptide, poly-L-arginine, by constructing bilayer samples of polypeptides and DNA. The bilayer samples were deposited using a layer by layer (LBL) technique, which uses the electrostatic attraction between the positively charged polypeptide and the negatively charged DNA molecule to create layers. We present a study of a number of different peptide-DNA bilayer films (1, 2, 3, 5, and 10 layers) fabricated using either poly-L-arginine or poly-L-lysine and DNA. In addition, single layers of just poly-peptides were measured to examine the interface between the poly-peptide and the silicon substrate.

[1] N. M. Luscombe, R. A. Laskowski, and J. M. Thornton, Nucleic. Acids Res. **29**, 2860 (2001).

[2] J. Janin, Strucutre **7**, R277 (1999).

BI-2-Or-2
Synchrotron radiation as a probe for structural, elemental and chemical properties of melanosomes

T03 BioInterphases

#BI-2-Or-2

T. Gorniak [1], T. Haraszti [2], M. Anderson [3], M. Grunze [2], A. Rosenhahn [1].

[1]KIT, Institute for Functional Interfaces - Eggenstein-Leopoldshafen (Germany), [2]Applied Physical Chemistry, Ruprecht-Karls-University Heidelberg - Heidelberg (Germany), [3]Department of Molecular Physiology and Biophysics, The University of Iowa - Iowa City (United states).

It is of tremendous scientific interest whether the ultrastructure of melanosomes [1], organelles found in the iris cells, is connected with the development of glaucoma, a disease in which the optic nerve suffers damage. The name of these intracellular, membrane bound organelles is derived from the chemical substance they produce and store: melanin [2]. On the one hand, melanosomes are beneficial as they provide photoprotection to the human body and are responsible for the colour of hair, skin and iris. On the other hand a disorder of their functionality is potentially harmful, resulting in an elevated (10 – 50 fold) risk of skin cancer or, in the eye, in the development of glaucoma. The detailed processes and mechanisms of failure are still unknown. However, it is believed that toxic chemical components and proteins, which are part of the organelle's synthesis of melanin [3,4] leach into the surrounding tissue and cause damage to vital cells, when the function of metabolization or containment of the cytotoxic substances is disturbed. We aim to determine if the granularity of the melanosome's internal ultrastructure develops differently for healthy mice and those with a genetic disposition to develop glaucoma. A structural change of the organelles could point towards a disturbed encapsulation of cytotoxic substances and thus play a key role in the development of diseases of pigmented tissue. Since melanin is an exceptionally dense material – making it challenging to probe the melanosomes' ultrastructure with methods like transmission electron microscopy (TEM) – the unperturbed morphology of these organelles is still unknown. In our approach, which relies on hard X-rays with a high penetration depth, melanosomes are characterized by small-angle X-ray scattering (SAXS) and these diffraction fingerprints are correlated with the genetic background to identify possible differences. We supplement the results from these experiments with data from complementary

techniques – namely soft X-ray tomography and NEXAFS spectroscopy [5] – in order to obtain a broader picture allowing for conclusions relevant for an improved treatment of glaucoma

[1] Anderson, M.G. et al., Nature Genetics 30, 81-85 (2001).
[2] Riley, P.A., The International Journal of Biochemistry & Cell Biology 29, 1235–1239 (2003).
[3] Pawelek, J.M. et al., Nature 627–628 (1978).
[4] Creveling, C.R., 266 (F P Graham Company: 2000).
[5] Haraszti, T. et al., Pigment Cell & Melanoma Research 24, 187–196 (2010).

BI-1-Or-3
Functionalization of azide-terminated silicon surfaces with glycans using “click” chemistry for the study of their interaction with proteins

T03 BioInterphases

#BI-1-Or-3

A. Gouget [1], J. Yang [1], F. Ozanam [1], J.N. Chazalviel [2], A. Siriwardena [3], D. Aureau [4], R. Boukherroub [5], S. Szunerits [5].

[1]CNRS-Ecole Polytechnique.fr - Palaiseau (France), [2]CNRS-Ecole Polytechnique - Palaiseau (France), [3]Université Picardie - Amiens (France), [4]Insitut Lavoisier - Versailles (France), [5]IEMN - Villeneuve D'asq (France).

Functionalized organic monolayers covalently anchored to the silicon surface are promising systems for the development of biosensors and microarrays. They can be modified in a controllable way for covalently attaching molecular probes at the surfaces, allowing for specific interactions with biological targets. Among the various strategies for biofunctionalization, the copper-catalyzed azide-alkyne cycloaddition reaction, namely “click” reaction, is widely used due to its specificity and versatility.1

We have developed a new carbohydrate sensor based on silicon using “click chemistry” for the study of glycans/glycan binding proteins such as lectins.2 In this talk, we will present the multi-step modification of crystalline silicon surfaces by azido moieties containing polyoxoethylene groups aimed at avoiding the nonspecific adsorption of proteins. The click reaction was done with a propargyl-terminated mannose or lactose. Each step was carefully analyzed by AFM imaging, XPS and quantitative IR-ATR, allowing us to determine the surface concentration of the immobilized molecules. The specificity of glycans/lectins recognition was demonstrated. The affinity constant for mannose-lectin from lens interaction has been measured, suggesting a multivalency of the binding. The influence of the density of grafted mannoses on the efficiency of the binding will be presented.

1 C. M. Niemeyer et al, Angew. Chem. Int. Ed., 2008, 47, 9618
2 A. C. Gouget-Laemmel et al, J. Phys. Chem C, 2013, 117, 368

BI/ASS-1-Or-3
Optical resonators for biosensing

T03 BioInterphases

#BI/ASS-1-Or-3

L. Pasquardini [1], S. Soria [2], S. Berneschi [3], D. Gandolfi [4], L. Lunelli [1], M. Ghulinyan [5], G. Pucker [5], G. Nunzi Conti [2], L. Pavesi [4], M. Anderle [6], C. Pederzolli [1].

[1]FBK-Laboratory of Biomolecular Sequence and Structure Analysis for Health - Trento (Italy), [2]IFAC-CNR, Istituto di Fisica Applicata "N. Carrara" - Firenze (Italy), [3]Centro Studi e Ricerche "E. Fermi" - Roma (Italy), [4]Nanoscience Laboratory, Dept Physics, University of Trento - Trento (Italy), [5]FBK-Fondazione Bruno Kessler - Trento (Italy), [6]Autonomous Province of Trento, Dept Knowledge - Trento (Italy).

Optical resonators are emerging in the field of biosensors as one of the sensitive technology that does not require amplification or labeling of the analyte [1]. In particular whispering gallery mode (WGM) resonators are receiving a growing interest as optical structures suitable for the realization of miniaturized sensors with high sensitivity [2]. When properly excited, WGM microresonators are able to strongly confine light, through a total internal reflection, along the equatorial plane of the microresonator. The corresponding supported resonances show low losses and a quality factor Q that depends both from the geometrical shape of resonators and from the materials involved. In this work we present two different microresonators: a spherical microcavity with a Q factor value of 10^7, and a planar wedge microdisk [3] with a Q factor value of 10^4. Any minimum change in the surface of the microresonator or in the physical and optical properties of the surrounding environment reduces the Q factor value and modifies the spectral position of the resonances. From a direct measurement of this resonance shift, one can infer the amount of analyte that produces this variation. A crucial step for producing reliable biosensors is their surface functionalization, preserving the starting Q factor values of the resonators. In this work we report a functionalization process based on the use of DNA aptamers, short oligonucleotide sequences that bind to non-nucleic acid targets with high affinity and specificity. Different thrombin and vascular endothelial growth factor (VEGF) specific aptamers are utilized: thrombin belongs to the coagulation cascade and it is involved in many pathological diseases, like atherosclerosis and thromboembolic diseases. VEGF is an important regulator of angiogenesis and it promotes the migration and proliferation of endothelial cells and the formation of new

blood vessels from pre-existing capillaries. The functionalization procedure adopted, preserved the quality factors of both utilized microresonators allowing the target protein recognition in the nM range. Moreover, when using the spherical microcavity, the protein detection is successfully performed in 10% diluted non-filtered human serum sample [4]. In addition, both aptasensors were chemically regenerated by NaOH treatment and then used again. All the regenerated spherical sensors maintained more than 95% of the WGM shift. We have demonstrated that WGM techniques feature low cost, simple detection procedure, rapid response time and high specificity in complex samples.

Financial support by PAT-NAoMI Project is gratefully acknowledged.

[1] Baaske M. and Vollmer F., Chemphyschem, 13 (2), 427-436 (2012).
[2] S. Soria, S. Berneschi, M. Brenci, F. Cosi, G. Nunzi Conti, S. Pelli and G.C. Righini, Sensors 11 (1), 785-805 (2011).
[3] Ramiro-Manzano F., Prtljaga N., Pavesi L., Pucker G., Ghulinyan M., Opt Express, 20 (20), 22934-22942 (2012).
[4] Pasquardini L., Berneschi S., Barucci A., Cosi F., Dallapiccola R., Insinna M., Lunelli L., Nunzi Conti G., Pederzolli C., Salvadori S., Soria S., J Biophotonics, doi: 10.1002/jbio.201200013 (2012).

BI-2-Or-3
Visualization of bacterial biofilms on interfaces with synchrotron hard X-ray microscopy

T03 BioInterphases

#BI-2-Or-3

R. Heine [1], Y. Yang [1], T. Gorniak [2], T. Senkbeil [2], A. Rosenhahn [3], F. Xu [1], H. Suhonen [4], L. Helfen [4], Y.F. Song [5], C.C. Wang [5], T. Baumbach [1], M. Grunze [6], T. Schwartz [2].

[1]ANKA/IPS, Karlsruhe Institute of Technology - Karlsruhe (Germany), [2]IFG, Karlsruhe Institute of Technology - Karlsruhe (Germany), [3]Ruhr-UniversityBochum - Bochum (Germany), [4]ESRF - Grenoble (France), [5]NSRRC - Hsinchu (Taiwan, republic of china), [6]APC, University of Heidelberg - Heidelberg (Germany).

Biofilms are assemblages of bacteria attached to a surface and enclosed in an adhesive matrix of extracellular polymeric substances (EPS) [1]. Biofilms form on most surfaces, e.g., medical devices such as catheters and implants, but also in industrial environments such as food processing plants or in cooling systems. Thus, they are of major concern in medicine and in many commercial enterprises.
Biofilm formation results from a sequence of events: first microbial adherence, then microcolony formation and proliferation, and finally matrix production and biofilm maturation [2]. However the nature of this serial transition is not fully understood. As the morphology and elemental composition of bacterial aggregates on interfaces is of great interest in this topic, synchrotron radiation-based hard X-ray microscopy techniques as a non-destructive approach were applied for investigating biofilms. Microtomography experiments with minimum sample preparation using full-field transmission X-ray microscopy (TXM) [3] with Zernike phase contrast were performed on different biofilm-habitat interfaces. The microbial morphology and distribution can be visualized in three dimensions with tens of nanometers resolution (compare figure 1). Furthermore, we demonstrate the possibility to quantitatively study the elemental content of individual bacteria with sub-cellular spatial resolution by X-ray fluorescence analysis [4].
By correlative measurements at different stages of the biofilm formation on diverse

surfaces, we aim to gain a deeper understanding of the mechanisms involved in this process.

[1] Madigan M.T., Martinko J.M., Stahl D.A., Clark D.P., Brock Biology of Microorganisms, Pearson Press, 2009.
[2] Hetrick E., Schoenfisch M., Reducing implant-related infections: active release strategies, Chem Soc Rev 35, 780-789 (2006).
[3] Yin G.C., Tang M.T., Song Y.F., Chen F.R., Liang K.S., Duewer F.W., Yun W., Ko C.H., Shieh H.P.D., Energy-tunable transmission X-ray microscope for differential contrast imaging with near 60 nm resolution tomography., Appl. Phys. Lett. 88, Issue 24, 241115 (2006).
[4] Ortega R, Cloetens P, Devès G, Carmona A, Bohic S, Iron Storage within Dopamine Neurovesicles Revealed by Chemical Nano-Imaging. PLoS ONE 2(9): e925 (2007).

Figure 1: 3D microtomographic rendering of an unstained bacterial biofilm of *Pseudomonas aeruginosa* on polypropylene investigated by transmission hard X-ray tomography. Field of view is 10 µm (w) x 15 µm (h).

BI-1-Or-4
Adsorption of hemoglobin on silica nanoparticles: an alternative approach to modulate the oxygen affinity of the protein

T03 BioInterphases

#BI-1-Or-4

S. Devineau [1], C. Mathé [1], L. Zargarian [2], J. Bussiere [1], M.H. Mathon [3], J.P. Renault [1], S. Pin [1].

[1]Laboratoire de Radiolyse, UMR 3299 CEA-CNRS - Gif Sur Yvette (France), [2]LBPA, UMR 8113 CNRS-ENS Cachan - Cachan (France), [3]Laboratoire Léon Brillouin, UMR 12 CEA-CNRS - Gif Sur Yvette (France).

The understanding of protein adsorption mechanisms on surfaces is of major interest in both fundamental research and applications such as implants, biosensors and dialysis membranes. Among the applications, development of nanomaterials has created a novel biointerphase with its own specificities, together with enlarged possibilities for experimental studies. To study protein interactions with a mineral surface, we chose silica NP and a model well-known blood protein, pig hemoglobin (Hb). Protein adsorption has been characterized in connection with protein structure and function changes. Indeed protein activity is sensitive to adsorption on mineral surfaces (1) and changes observed on NP can be related both to a surface effect, which is similar to what is observed on plane surfaces, and to a curvature or geometry effect that is specific to NP.

Adsorption of Hb on silica NP has been investigated at the chemical, structural and functional levels by UV-visible spectroscopy, circular dichroïsm and oxygen binding measurements. Hb adsorption is pH dependent and shifts from total adsorption at pH 6 to no adsorption at pH 9. Circular dichroism spectra of adsorbed Hb reveal a partial loss of helix secondary structure. Oxygen affinity of adsorbed Hb increases from 17.1 mmHg to 8.7 mmHg at pH 6 whereas oxygen binding cooperativity decreases from 2.8 to 1.6 (Fig 1A). Binding of inositol hexaphosphate effector (IHP) decreases the oxygen affinity of both free and adsorbed Hb, which suggests that Hb keeps its tetrameric form upon adsorption (Fig 1B). Moreover Hb desorption is achieved in soft

conditions at pH 9 and both Hb structure and activity are recovered after desorption. Thus adsorption of hemoglobin on silica NP represents a new approach to increase the oxygen affinity of the protein in a reversible manner.

1. N. O. Fischer, C. M. McIntosh, J. M. Simard, V. M. Rotello, Proceedings of the National Academy of Sciences of the United States of America 99, 5018 (Apr, 2002).

Figure 1. (A) Hb oxygenation curves before (■) and after (o) adsorption on silica NP, (B) in presence of IHP effector.

BI-1-Or-5
Linking proteins bio-recognition to their orientation on different substrates by means of surface analysis

T03 BioInterphases

#BI-1-Or-5

V. Lebec [1], S. Boujday [2], C. Poleunis [1], C.M. Pradier [2], A. Delcorte [1].

[1]Université catholique de Louvain - Louvain-La-Neuve (Belgium), [2]Université Pierre et Marie Curie - Paris (France).

One key point for applications in the fields of biosensor and biomaterial researches is the preservation or not of the bioactivity of proteins once immobilised on a surface. Using time-of-flight secondary ion mass spectrometry (ToF-SIMS) and principal component analysis (PCA), in combination with a series of complementary techniques (PM-IRRAS, QCM-D and XPS), a methodology was established to explore protein adsorption and orientation on surfaces. Our first results demonstrated the effect of the surface chemistry on the adsorption of β-Lactoglobulin. A model of the protein orientation on gold substrates modified by self-assembled monolayers (SAMs) with different endgroups (-CH_3 and -NH_2) was proposed [1]. In the present study, a similar procedure is used to investigate a more realistic case involving an antibody / antigen couple used in medical tests. For this purpose, Anti-GDH antibodies were adsorbed on bare gold, on -CH_3 and on -COOH terminated SAMs and, finally, they were grafted to the -COOH terminated SAMs activated by NHS-EDC. ToF-SIMS measurements were carried out and PCA performed on the protein peaks of all the samples. PCA couldn't separate samples adsorbed on the bare gold or the -CH_3 terminated SAMs, in contrast, it showed a clear separation between the mass spectra of the Anti-GDH either adsorbed or grafted on –COOH terminated SAMs and also a separation of those from the two first test surfaces. This could indicate that two different preferential orientations are obtained for the -COOH terminated SAMs and a preferential orientation or a random adsorption for bare gold or the -CH_3 terminated SAMs. In addition, the PCA results provide detailed information on the amino-acids that are preferentially displayed at the extreme surface of the samples. Further experiments were carried out to test the biorecognition of the corresponding antigen by the antibodies on the different surfaces. No clear recognition was detected for antibodies adsorbed on bare gold or -CH_3 SAMs when PM-IRRAS and QCM-D data indicate that more antigens are

recognized in the case of the adsorbed antibody than the grafted one on -COOH SAMs. These results suggest that the antibody is in a more favourable orientation for bio-recognition for Anti-GDH simply adsorbed on -COOH terminated surfaces.

[1] V. Lebec, J. Landoulsi, S. Boujday, C. Poleunis, C.-M. Pradier, A. Delcorte, Presentation at the 14th European Conference on Applications of Surface and Interface Analysis (ECASIA'11), 2011, Cardiff, Wales; J. Phys. Chem. C., 2013, Submitted

BI-1-Or-6
Photoactive self-assembled monolayers of functional alkanethiols designed on metal oxides for control of protein-surface interactions

T03 BioInterphases

#BI-1-Or-6

A. Dellinger [1], V. Semetey [2], A. Galtayries [3].

[1]UMR7045 LPCS Chimie Paristech / UMR168 Institut Curie - Paris (France),
[2]UMR168, Laboratoire de Physicochimie, Institut Curie, CNRS - Paris (France),
[3]UMR7045, LPCS Chimie Paristech, CNRS - Paris (France).

The control of biomolecules adsorption (such as proteins) and other microorganisms is of high interest for various fields of biotechnology, such as bioanalytics, cell biology, tissue engineering and biomaterials. An efficient method to control adsorption includes the use of well-defined oligo(ethylene glycol)-terminated self-assembled monolayer (SAM). However, multiple processing steps are often required to prepare SAM onto substrate.

Based on the thiolene reaction process, we developed a two-step method to prepare self-assembled monolayer [1]. This surface modification can either be performed on glass, metal oxides or alloys to control bioadhesion on surfaces starting from commercially available building blocks. By taking advantage of the photoinitiation step, adhesive and anti-adhesive-patterned systems are easily designed.

Such well-controlled grafting strategy has been applied to different metal oxides: from silicon substrates for the methodology set-up to model metal oxides formed on biocompatible metals and alloys. The obtained films are robust; the process is low-cost, simple, and efficient.

Surface characterization as X-ray Photoelectron Spectroscopy (XPS), Time of Flight Secondary Ion Mass Spectrometry (ToF-SIMS) and Infra-Red Surface Spectroscopy

(ATR-IRFT) were used to check the surface composition at different steps of the reactions: the thiolene reaction, the PEG grafting, as well as after interaction with protein solutions: albumin for preliminary tests, and fibronectin, an adhesive protein present in the extra-cellular matrix.

In addition to quantitative information, obtained by XPS, about the oxide composition and thickness at the different steps, and qualitative information, obtained by XPS and ToF-SIMS, surface patterning could be emphasized with ToF-SIMS chemical surface imaging.
The as-proposed grafting method conditions (e.g. poly(ethylene glycol)chain length, chain end functionality, exposure time, or reactive dilution) had been implemented to bind other biomolecules on these chemically patterned surfaces. In that way, peptide sequence or species cell lines were also used to exhibit the site-specific located reaction.

[1] A Facile and Versatile Approach to Design Self-Assembled Monolayers on Glass using Thiol-ene Chemistry', B. Oberleitner, A. Dellinger, M. Déforet, A. Galtayries, A.-S. Castanet, V. Semetey, Chemical Communication, 2013, 49, 1615-1617.

BI/ASS/NST-P1-05
Application of SR-XRF to investigate nanoparticles/cell interactions

T03 BioInterphases

#BI/ASS/NST-P1-05

A. Gianoncelli [1], J. Ponti [2], L. Pascolo [3], M. Salome' [4], G. Ceccone [5], F. Rossi [5], M. Kiskinova [1].

[1]Elettra-Sincrotrone Trieste - Trieste (Italy), [2]European Commission, Joint Research Centre - Ispra (Italy), [3]Institute for Maternal and Child Health, IRCCS Burlo Garofolo - Trieste (Italy), [4]ESRF - Grenoble (France), [5]European Commission, Joint Research Centre - Grenoble (Italy).

Nanotechnology has opened attractive broad application opportunities in various industrial fields from electronics to medical devices. In particular, several nano-sized tools are already employed for diagnostic and therapeutic purpose in medicine (nanomedicine) [1,2,3]. For instance, gold nanoparticles have become popular substrates for a broad range of biomedical applications as well as for chemical, biological and clinical diagnostics [4] Furthermore magnetic NPs such as ferrites (Fe3O4) and cobalt ferrites (CoFe2O4), are also used in biomedicine as drug delivery carriers, hyperthermia treatments in cancer therapy and magnetic resonance imaging (MRI) contrast enhancement [5, 6]. However, the increasing use of nanomaterials and in particular nanoparticles in nanomedicine has raised the growing concern about the health hazards related to their possible toxic effects, not only in the human body, but also in the environment. The lacking information about the NPs impact on environment and on human health, as well as data on risk assessment, requires development of a reliable methodology for control and prediction. Among the promising detection methods, synchrotron radiation X-ray Fluorescence (SRXRF) has already demonstrated its potential in bio-medical research for exploring e.g. neurodegenerative disorders [6, 7]. The application of SRXRF with soft X-rays [7] has also provided access to light elements, which are major constituents of the living matter. In this work, we report examples of SRXRF investigations of the distribution and chemistry of nanoparticles NPs in in different cell lines. In particular, U87 astrocytoma glioblastoma and Balb 3T3 mouse fibroblast cells have been exposed to metal oxides (ferrites, ZnO, Cuo and cobalt ferrites) and SiO2 NPs at different concentrations for 24h. The SRXRF maps show that NPs are accumulating in the cell cytosol near the perinuclear region. However, in the case of

cobalt ferrites, micro-spot spectra indicate that, for concentrations higher than 500 μM, Co and Fe are present also in the nuclear region of the cell, with sensible accumulation of Co[9]. A co-localization of P, Ca and Fe at high concentration has also been observed indicating intracellular sequestration mechanisms as a response or in an attempt to reduce the nanoparticles toxic effects.

[1] R. Duncan, R. Gaspar, Mol. Pharmaceutics, 8, (2011), 2094
[2] L.A. Nagahara, M. Ferrari, T. Groodzinski, MRS bulletin, 34(6), (2009), 406
[3] T. Paunesku at al., Nanoletters, 7(3), (2007), 596.
[4] H. Jans et al., Chem. Soc. Rev., 41, (2012), 2849
[5] D.H. Kim et al, J. Mag.Mag. Mat. 320 (2008), 2390
[6] J.A. Ritter, et al., J. Mag. Mag. Mat., 288, (2005), 403
[7] A. Ide-Ektessabi, Application of Synchrotron Radiation: Microbeams in cell Microbiology and Medicine, Springer, (2007)
[8] R. Ortega et al., Nucl. Inst. Met. B210 (2003), 325
[9] R. Alberti et al., X-ray Spectrometry 38 (2009), 205-209
[10] P. Marmorato, G. Ceccone, A. Gianoncelli, L. Pascolo, J. Ponti, F. Rossi, M. Salomé, B. Kaulich, M. Kiskinova M, Toxicology Letters, 207(2) (2011) 128-136

BI-1-Or-7
Surface immobilised biomolecules quantification and prevention of non-specific biomolecules binding

T03 BioInterphases

#BI-1-Or-7

S. Ray, A. Bella, F. Green, A. Shard.

National Physical Laboratory - London (United kingdom).

In Bioanalytical devices, it is frequently required to control the specific attachment of target biomolecules or protein and to prevent non-specific protein adsorption on surfaces for bio-sensing and diagnostics. To overcome these major challenges, an efficient method for robust chemical modification was developed to achieve excellent specific bio-recognition and stability in complex bio-media supressing non-specific biomolecule adsorption.
In this work, both pure and mixed PEG-Thiol monolayer with carboxylic acid (-COOH) and hydroxyl (-OH) terminal groups on gold coated silicon wafers were prepared. Surfaces were characterized by using spectroscopic ellipsometry, atomic force microscopy and x-ray photoelectron spectroscopy. By varying the surface coverage of mixed PEG thiols and activating available –COOH sites for amide bond formation using uronium/aminium (HBTU) coupling, we have successfully controlled the amount of attached synthetic peptides. Fig.1 shows the variation of atomic percentage of nitrogen by varying the surface fraction of PEG end groups, with higher nitrogen representing higher attachment of peptide. Without the amide coupling activation process, non-specific binding of peptides and proteins were prevented. This method for surfaces modification and controlled attachment of surface bound biomolecules could be used in ultrasensitive bio-sensing and diagnostics in the future.

Figure 1. Atomic percentage variation of nitrogen arising from adsorbed synthetic peptides by varying the surface fraction of carboxylic acid terminated PEG-Thiols. The other fraction of the surface is hydroxyl terminated PEG-thiols.

BI-2-Or-4
Impact of a Model Synovial Fluid on Supported Phospholipid Films

T03 BioInterphases

#BI-2-Or-4

R. Dahint [1], M. Kreuzer [1], T. Hauß [2], R. Steitz [2].

[1]University of Heidelberg - Heidelberg (Germany), [2]Helmholtz-Zentrum Berlin - Berlin (Germany).

The search for biocompatible materials has become one of the key issues in modern medicine. In addition to biocompatibility aspects, the development of artificial joints requires optimization of lubrication under shear forces and pressure. To copy the principles of lubrication observed in natural joints it is important to understand the underlying mechanisms. In natural joints, the opposing bones are coated by cartilage and separated by the synovial fluid which mainly consists of hyaluronic acid (HA) - a high molecular weight, linear polysaccharide. The cartilage, in turn, is covered with phospholipid layers, and it is claimed that in particular the combination of phospholipids and HA plays an import role in lubrication.
In order to elucidate the underlying mechanisms on a molecular scale, we investigated the impact of HA on the structure and stability of supported phospholipid membranes as a function of temperature, pressure and shear by neutron reflectivity and *in situ* infrared spectroscopy. In contact with pure D_2O and below the main phase transition temperature of the system, T_M, a lamellar spacing of 65 Å is observed for the membranes. When temperature is raised above T_M, all lipid bilayers detach except for the innermost lipid lamella directly adsorbed to the silicon support. In contact with a solution of HA in D_2O the oligolamellar lipid system starts swelling. In addition, it is stabilized so that heating above T_M does not result in detachment of the lipid membranes into the liquid phase. The interfacial lipid coating adopts a swollen new lamellar state with an increase in d-spacing by 380% to 247 Å measured after 43 days of incubation with the model synovial fluid. Neutron reflectivity data point to the formation of an interfacial hydrogel layer from phospholipids and interlinked high molecular weight HA, which might exhibit important joint lubrication and protective wear functionalities. Experiments on the shear stability of phospholipid membranes are ongoing.

BI-1-In-1
Spatially and temporally coordinated processes of cells at molecular to cellular scales

T03 BioInterphases

#BI-1-In-1

J. Spatz.

Max Planck Institut for Intelligent Systems & University of Heidelberg - Stuttgart (Germany).

Our approach to engineer cellular environments is based on self-organizing spatial positioning of single signaling molecules attached to synthetic extracellular matrices, which offers the highest spatial resolution with respect to the position of single signaling molecules. This approach allows tuning tissue with respect to its most relevant properties, i.e., viscoelasticity, peptide composition, nanotopography and spatial nanopatterning of signaling molecule. Such materials are defined as “nano-digital materials” since they enable the counting of individual signaling molecules, separated by a biologically inert background. Within these materials, the regulation of cellular responses is based on a biologically inert background which does not initiate any cell activation, which is then patterned with specific signaling molecules such as peptide ligands in well defined nanoscopic geometries. This approach is very powerful, since it enables the testing of cellular responses to individual, specific signaling molecules and their spatial ordering. Detailed consideration is also given to the fact that protein clusters such as those found at focal adhesion sites represent, to a large extent, hierarchically-organized cooperativity among various proteins. We found that integrin cluster have a functional packing density which is defined by an integrin-integrin spacing of approximately 68 nanometers. Such critical spacing values vary as matter of transmembrane receptor choice of interest. We have also developed methods which allows the light initiated activation of adhesion processes by switching the chemical composition of the extracellular matrix. This enabled us to identify the frequency of leader cell formation in collective cell migration as a matter of initial cell cluster pattern size and geometry. Moreover, “nano-digital supports” such as those described herein are clearly capable of involvement in such dynamic cellular processes as protein ordering at the cell’s periphery which in turn leads to programming cell responses.

BI-2-Or-5
Investigating Charge Gradients on Polyelectrolyte brushes

T03 BioInterphases

#BI-2-Or-5

Z. Yenice [1], R. Köhler [2], J. Genzer [3], R. Von Klitzing [1].

[1]Stranski Laboratory, Institute of Chemistry - Berlin (Germany), [2]Stranski Laboratory, Institute of Chemistry & Institute Soft Matter and Functional Materials, Helmholtz-Center Berlin for Materials and Energy - Berlin (Germany), [3]Department of Chemical & Biomolecular Engineering, NCSU - Raligh (United states).

The modification of surfaces with thin polymer films like polymer brushes is widely used to tailor surface properties such as wettability, biocompatibility, corrosion resistance and friction. With further modifications, materials that express specific bio-responsive properties, including antibacterial (biocide) properties can be made. Also nanoparticles can be immobilized on these systems. In this study poly(2-(dimethylamino) ethyl methacrylate) (PDMAEMA), which is a weak polyelectrolyte with pH dependent properties is used and charge gradients were made along the surface-grafted brush resulting on a change in the water contact angle degree. These charges also act as biocides. More investigation was done regarding the charge distribution. Neutron reflectivity is used to detect the change of density and thickness after quaternizing the brush gradually and to see the charge distribution along the brush in both lateral and perpendicular directions. A schematic illustration of the quaternization, of surface-grafted polyelectrolyte brushes is shown below in Figure 1.

BI/NST-1-Or-2
Patterned polymer brushes as a matrix for controlled immobilization of gold nanoparticles

T03 BioInterphases

#BI/NST-1-Or-2

S. Christau, R. Von Klitzing.

Stranski-Laboratorium für Physikalische und Theoretische Chemie, Institute for Chemistry, Technical University Berlin - Berlin (Germany).

In the last years, the modification of surfaces by depositing polymer brushes has become of big interest for nano- and biotechnology applications. The possibility of suppressing or controlling protein or cell adhesion makes them an important tool for the use of otherwise incompatible solids in biological applications [1].

Polymer brushes represent a class of coatings where the polymer chains are tethered to the substrate chemically [2]. Brush systems are promising candidates for the ordering of particles due to their response to external stimuli like pH, temperature, ionic strength or solvent [1]. By adsorbing gold nanoparticles within the polymer brushes, interesting optical properties are induced into the brush system which can be useful for sensor applications. By forming patterns of polymer brushes, the brush system can serve as a matrix for the ordering of immobilized AuNPs *(fig.1).*

Polymer brushes of (N,N-dimethylamino)ethyl methacrylate (DMAEMA) and N-isopropylacrylamide (NIPAM) are grown from a 2-bromo-2-methyl-(3-(triethoxysilyl)propyl
propanamide (BTPAm)-covered silicon surface via surface-initiated atom transfer radical polymerization (SI-ATRP). For the synthesis of both initiator-covered self-assembled monolayer (SAM) and polymer brushes a new type of sealed reactor is used that provides a constant nitrogen flux. The grafted chains are investigated using ellipsometry, atomic force microscopy (AFM), X-ray reflectometry and scanning electron microscopy (SEM).

To study the influence of the polymer's chemical composition and the brush thickness on the particle distribution, patterning of polymer brushes is carried out using UV lithography. Different approaches of patterning are adressed.

[1] Schmelmer, U., Paul, A., Küller, A., Steenackers, M., Ulman, A., Grunze, M., Gölzhäuser, A., et al., *Small* ***2007***, 3(3), 459–65
[2] Bhat, R. R., Tomlinson, M. R., & Genzer, J., *Macromolecular Rapid Communications* ***2004***, 25 (1), 270–274

Figure 1. Distribution of Gold Nanoparticles (AuNPs) within patterns of brushes containing different polymer.

BI/NST-1-Or-3
Mechanical properties of poly-L-lysine (PLL) / hyaluronic acid (HA) multilayer films measured by AFM nano-indentation

T03 BioInterphases

#BI/NST-1-Or-3

J. Hellwig, C. Üzüm, R. Von Klitzing.

Stranski-Laboratorium, Department of Chemistry, TU Berlin - Berlin (Germany).

In recent years smart biomaterials have become a highly developing field of interest for biomedical applications, e.g. drug delivery(1). The layer-by-layer (LbL) technique (2) gives the opportunity to build up self assembled polyelectolyte multilayer films (PEM) with defined architecture, physical and chemical properties. PEM made of poly-L-lysine (PLL) and hyaluronic acid (HA) were produced by using the LbL technique. Potential applications of these PEMs require controlling of the adhesion behaviour by tuning their elastic/viscoelastic properties.

In this study mechanical properties of LbL coated poly(L-lysine)/hyaluronan PLL/HA films were studied by scanning- and colloidal-probe atomic force microscopy as a function of indentation velocity, number of polymer deposition steps and temperature. Film growth was investigated by two independent AFM methods: scratch-and-scan and full-indentation(3). Film thickness increases linearly with polymer deposition steps (Image 1). The Young's modulus ranges between 15 and 40 kPa and does not depend on the film thickness (Image 2). Stress relaxation and creep compliance measurements indicate a viscoelastic film behaviour with multiple relaxation mechanisms.

(1) Volodkin, D. V.; Larionova, N. I.; Sukhorukov, G. B. Biomacromolecules 2004, 5, 1962 – 1972.
(2) Decher, G. Science 1997, 277, 1232 – 1237.
(3) Üzüm, C.; Hellwig, J.; Madaboosi, N.; Volodkin, D.; v. Klitzing, R. Beilstein J. Nanotechnol. **2012**, 3, 778–788.

Image 1: Thickness of $(PLL/HA)_n$ as a function of *n* as measured by scratch-and-scan and full-indentation methods. Error bars indicate the standard deviations.

Image 2: Young's modulus E as a function of $(PLL/HA)_n$ bilayer number *n* for an indenter radius of 2.37 µm (open circles) and 3.35 µm (closed circles).

BI/ASS-1-Or-5
Fabrication and Characterization of Suspended Plasmonic Nanopore Membranes for Biosensing Applications

T03 BioInterphases

#BI/ASS-1-Or-5

J. Junesch [1], T. Sannomiya [2], J. Shi [2], Y. Nakamura [2], J. Vörös [1].

[1]Laboratory of Biosensors and Bioelectronics, Institute for Biomedical Engineering, Swiss Federal Institute of Technology - Zurich (Switzerland), [2]Department of Metallurgy and Ceramics Science, Tokyo Institute of Technology - Tokyo (Japan).

The investigation of biological membrane processes plays an essential role in order to understand cell-cell interaction since cells communicate with their environment via various transport processes through the cell membrane. To mimic these biomembranes, suspended metal membranes with an array of nanoholes, so called nanopores, can be used. These can be optically monitored and by controlling the pore size, single molecules can be flown through the pore in one-by-one manner, and then be captured at the most sensitive position of the sensor where electric field is enhanced [1]. Fabrication of such nanopores are normally expensive and time consuming, as it generally involves the use of focused ion beam (FIB), electron beam (EB), or multiple etching steps. Therefore, we introduce a novel fabrication approach of plasmonic nanopores combining colloidal lithography and a carbon film transfer method for transmission electron microscopy (TEM).

A short-range-ordered nanohole array is fabricated on a solid substrate by colloidal lithography [2]. On top of this colloidal mask a thin film of aluminum (Al), which will serve as sacrificial layer and carbon are deposited. After the mask particles have been removed, the carbon film is separated from the substrate by wet-etching the sacrificial Al layer. The suspended carbon film with the nanopore array can then be re-deposited on a supporting TEM mesh. Through additional sputtering of dielectric materials and gold (Au) layers, the hole size can be further reduced. Finally, the initial carbon film can be removed by plasma or UV ozone etching.

We successfully produced suspended nanopores in carbon films and managed to shrink the initial pore size by additional deposition of aluminum nitride (AlN). In Fig.1 the TEM image of such size reduced nanopores is depicted, where the carbon film was removed by plasma etching. The reduction of the pore size alters the shape of the pore to a funnel (inset SEM image), which is advantageous for molecular filtering or capturing depending on the molecular sizes. Furthermore, we have prepared first AlN/Au nanopores with plasmon resonance and plan to do biosensing experiments by detecting the passing biomolecules optically by plasmon resonance shift and by electrical measurements.

1. Feuz, L., et al., ACS Nano, 2010. 4(4)
2. Storm, A.J., et al., Nat Mater, 2003. 2(8)
3. Junesch, J., et al., ACS Nano, 2012. 6 (11)

Fig.1: TEM image of a suspended nanopore membrane.
The original 100nm nanopores were size-reduced by AlN sputtering, resulting in the funnel shaped pores (inset SEM image).

BI/ASS-1-In-1
DNA Diagnostics – Optical or by Electronics?

T03 BioInterphases

#BI/ASS-1-In-1

W. Knoll.

AIT Austrian Institute of Technology - Vienna (Austria).

The race in DNA diagnostics between optical detection principles (fluorescence, surface plasmons) and electrical/electrochemical/electronic concepts is not decided yet. Both scientific communities continue to offer solutions for fast, multiplexed, simple and cheap detection of oligonucleotides, PCR amplicons, genomic DNA (fragments), etc. Most likely, the competition will never see a single winner that meets all needs because the different practical formats and applicational environments, as well as, market requirements may ask for specific and unique solutions that could be better achieved in one case by optics and in another situation by electronics.

Along these lines, we will briefly review the state of the art in both categories of DNA diagnostics and will then present a number of examples of what has been demonstrated for the sensitive detection of DNA in (from) solution by monitoring surface hybridization reactions of target strands binding from the analyte solution to surface-attached capture oligonucleotides. A particular emphasis will be put on the physico-chemical principles of these surface recognition and binding (or dissociation) reactions in order to be able to develop criteria of how to optimize sensitivity, selectivity, e.g., for the detection of single nucleotide polymorphisms (SNPs), etc., in DNA diagnostics.

The examples given include
• SNP detection in singly and doubly mismatched oligonucleotides and amplicons;
• demonstration of the limit of detection in these surface hybridization reactions;
• multiplexed recording of surface hybridization reactions via quantum dot- labelled targets;
• surface polymerase chain reactions;
• the use of uncharged peptide nucleic acids (PNAs) as capture probes instead of the highly charged DNA;

• label-free detection of DNA by electrochemical techniques, and
• organic field-effect transistor- (OFET-) based monitoring of hybridization reactions.

BI-1-In-2
NONLINEAR OPTICAL SPECTROSCOPY OF INTERFACES

T03 BioInterphases

#BI-1-In-2

H. Arnolds.

UNIVERSITY OF LIVERPOOL - Liverpool (United kingdom).

Vibrational spectroscopy is powerful because intrinsic vibrations of the sample under study provide us with chemical information. Despite the existence of commercial infrared and Raman spectrometers, it is still a challenge to study specifically interfacial molecules, as IR and Raman typically have limited surface sensitivity, and the response of a minor portion of interfacial molecules may be obscured by the bulk response on either side of the interface. The use of even-order nonlinear optical techniques like infrared-visible sum frequency generation, where two incoming photons create a new photon, solves this challenge as their selection rules result in the suppression of the signal from the isotropic bulk, making them inherently sensitive to the region where the bulk structure breaks down, i.e. the interface.

In my talk I will discuss the application of SFG to understand protein adsorption on hydrophobic and hydrophilic self-assembled layers on gold and silicon in comparison to infrared and surface-enhanced Raman spectroscopy, and give a critical overview of the limitations of the technique.

BI/ASS-1-In-2
FABRICATION OF PROTEIN AND SSDNA PATTERNS IN THE PROTEIN-REPELLING MATRIX BY ELECTRON BEAM AND ULTRAVIOLET LITHOGRAPHY

T03 BioInterphases

#BI/ASS-1-In-2

M. Zharnikov.

Angewandte Physikalische Chemie, Universität Heidelberg - Heidelberg (Germany).

Fabrication of well-defined protein patterns on solid substrates is important for cell culture research, proteomics, and biosensors. Frequently, such patterning involves the use of protein-repelling poly(ethylene glycol) (PEG) films or oligo(ethylene glycol) terminated alkanethiolate (OEG-AT) monolayers as a background, which is necessary to prevent the nonspecific adsorption of proteins beyond the preselected areas. Usually, the OEG-AT species are introduced by backfilling process, after patterning protein-binding molecules on the substrate. I present here an alternative, more simple and straightforward approach, viz. the writing of protein-affinity patterns directly in the protein-repelling OEG-AT or PEG matrix by electron beam or ultraviolet lithography (EBL and UVL, respectively). Utilizing the high sensitivity of the OEG and PEG backbones to electrons and UV light, they can be continuously damaged with progressive irradiation, resulting in a gradual and controlled change of the protein-repelling properties. Based on this behaviour, protein affinity patterns can be directly written in a protein-repelling matrix and serve as templates for the subsequent attachment of proteins. Employing this direct writing (DW) approach not only simple “black-white” but also comparably complex “gray-scale” (gradient-like) patterning of proteins was achieved. The only limitation is that the DW procedure relies basically on non-specific adsorption of proteins, which is not always desirable and, in some selected cases, can lead to denaturation of the proteins thereby affecting further their performance and activity. However, a non-specific, OEG-AT based template, generated by EBL or UVL, can be transformed to a specific one by employing irradiation-promoted exchange reaction (IPER). Within this approach, an irradiated

OEG-AT monolayer is subjected to exchange reaction in the course of which the partly damaged OEG-AT moieties in the primary matrix are exchanged for potential molecular substituents bearing a special receptor group for specific binding of the target protein or ssDNA strand. The rate and extent of IPER depend on the density of irradiation-induced defects in the OEG-AT monolayer, which can be precisely controlled by the selection of a suitable dose within a certain dose range. Using the DW and IPER approaches in combination with EBL and UVL, we demonstrated the fabrication of complex non-specific, specific, and multiple protein patterns as well as ssDNA patterns and polymer brushes formed on the ssDNA/OEG-AT templates by surface-initiated enzymatic polymerization.

1. N. Ballav, A. Shaporenko, A. Terfort, and M. Zharnikov, A flexible approach to the fabrication of chemical gradients, Adv. Mat. 19, 998-1000 (2007).
2. N. Ballav, T. Weidner, and M. Zharnikov, UV-promoted exchange reaction as a tool for gradual tuning the composition of binary self-assembled monolayers and chemical lithography, J. Phys. Chem. C 111, 12002-12010 (2007).
3. N. Ballav, S. Schilp, and M. Zharnikov, Electron beam chemical lithography with aliphatic self-assembled monolayers, Ang. Chem. Int. Ed. 47, 1421–1424 (2008).
4. T. Winkler, N. Ballav, H. Thomas, M. Zharnikov, and A. Terfort, Electron-beam writing of protein-resistance gradients on a scale from microns to centimeters, Ang. Chem. Int. Ed. 47, 7238-7241 (2008)

BI/NST-1-Kn-1
BIOMIMETIC NANOPARTICLE FUNCTIONALIZATION AND SMART MEMBRANE ASSEMBLY OF CORE-SHELL NANOPARTICLES FOR TRIGGERED RELEASE APPLICATION

T03 BioInterphases

#BI/NST-1-Kn-1

M. Textor.

ETH ZURICH - Zurich (Switzerland).

The first part of my talk will cover the stabilization and functionalization of ultrasmall, uperparamagnetic iron oxide nanoparticles (SPIONs) by surface self-assembly of linear and dendritic polymers and adhesion chemistry based on substituted catechols. In the second part, I will demonstrate that SPIONs with dedicated, hydrophobic properties can be incorporated into the lipid membrane of liposomes and allow for controlled release triggered by an external (alternating) magnetic field. Potential applications relate to areas such as contrast agents for Magnetic Resonance Imaging (MRI) and triggered/targeted release of nanomedicines, and their combination.

PEG-Stabilized Core–Shell Nanoparticles: Impact of Linear versus Dendritic Polymer Shell Architecture on Colloidal Properties and the Reversibility of Temperature-Induced Aggregation
T. Gillich et al, ACS Nano, Dec. 2012; DOI: 10.1021/nn304045q

Triggered Release from Liposomes through Magnetic Actuation of Iron Oxide Nanoparticle Containing Membranes
E. Amstad et al., Nano Lett. 2011, 11, 1664–1670

Ultrastable Iron Oxide Nanoparticle Colloidal Suspensions Using Dispersants with

Catechol-Derived Anchor Groups
E. Amstad et al., Nano Lett. 2009, 9, 4042-4048

BI/ASS/NST-P1-12
Micro-pattern transfer on metal surface by wet etching

T03 BioInterphases

#BI/ASS/NST-P1-12

K. Zelic, T. Kokalj, M. Jenko.

IMT -Institute of metals and tehnology - Ljubljana (Slovenia).

Surface structuring is one of the major fields of Micro/Nano-technology in recent years. It has been widely investigated due to numerous possible applications. Among the most investigated applications of surface patterning are self cleaning surfaces and anti biofouling surfaces. Especially later is desired on metal surfaces to prevent the adhesion of bio organisms in medicine and ship industry. Preventing of biofilm formation could significantly reduce maintainance and corrosion expenses. There is a lot of different, mainly lithographic methods to structure the metal surface but rare of them are convenient for a large-scale industrial use..
We are testing two newly designed metal surface patterning methods. Both methods are a combination of imprint and wet etching methods. The idea of both methods is to transfer the pattern fabricated by photolithography on a metal surface. Both methods include the pattern transfer from previously designed elastomer stamp to the metal surface by chemical etching. The stamp was made of PDMS polymer patterned with the laser direct imaging lithographic method, with the sub micron resolution (0.8 µm). However, the tested pattern contained the features of a different sizes (from 3µm to 80µm).
The methods were tested on a electropolished(?) copper surface. In the first method the patterned PDMS stamp is covered with etchant and then pressed to the surface. In the regions where stamp features touches the copper surface, the etching does not occur and we obtain direct imprint of a stamp on the surface. The second method includes the use of the ink as a blocker for etchant. The ink is imprinted on the surface by the PDMS stamp. Surface is then exposed to etchant that etch only the regions of surface not covered by ink. Later the ink is removed.
Preliminary experiments show some promising results of micro-pattern transfer from elastomer template to a metalic surface, however further research is needed to optimize the process parameters and improve control over the process.

BI-2-In-1
t.b.a

T03 BioInterphases

#BI-2-In-1

P. Cloetens.

ESRF - Grenoble (France).

BI/ASS-1-In-3
SYNTHETIC PEPTIDES FOR ENZYMATIC SENSING

T03 BioInterphases

#BI/ASS-1-In-3

B. Liedberg.

Center for Biomimetic Sensor Science, Nanyang Technological University - Singapore (Singapore).

Synthetic peptides have become an attractive alternative to antibodies for the development of robust binders for biosensing. This contribution describes how synthetic four-helix bundle motifs can be turned into high-affinity binders for detection of range of biomedically relevant targets. The concept is based on site-selective modification of the four-helix bundle motif by small molecule ligands followed adaptive fitting of the construct to the binding interface of the target molecule. The so-prepared binders are integrated with plasmonic nanoparticles for aggregation-based colorimetric detection of human carbonic anhydrase (HCA) and C-reactive protein (CRP). A few other examples are also described where a set of linear and digestible peptides are utilized for naked-eye detection of environmental toxins, including, Botulinum serotype A, one of the most toxic substances known to man.

T04 Cultural Heritage

CH-1-Or-3
Hydrophobization of marble pores for enhanced stone protection

T04 Cultural Heritage

#CH-1-Or-3

D. Kronlund [1], J.H. Smått [1], A. Bergbreiter [1], M. Lindén [2], P. Miettinen [3].

[1]Åbo Akademi University - Turku (Finland), [2]University of Ulm - Ulm (Germany), [3]Coligro Oy - Helsinki (Finland).

A new treatment method based on total immersion in a fluorosurfactant-containing solution has been developed to hydrophobize marble tiles completely throughout their porous network. The processing parameters like the type of surfactant, concentration, solvent, temperature, and time have been investigated to obtain the optimal hydrophobic treatment. When using the optimized parameters, capillary water absorption measurements (EN 15801) proves that the marble stones are efficiently hydrophobized down to at least 5 mm, which was proven by removing the outer surface through grinding and measuring capillary absorption on the remaining piece. The same treatment method has also been employed to successfully hydrophobize 5x5x5 cm marble cubes and larger marble panels.

Furthermore, a new spectrophotometric assay method is employed to prove that the fluorosurfactant is present in the cores of the marble cubes. The new assay is further used to study the penetration behavior of the fluorosurfactant and the penetration kinetics.

The hydrophobized stones are also subjected to several ageing tests to quantify the stability of the fluorosurfactant as well as the advantages the hydrophobization of the porous network provides. In-house ageing tests include: freeze-thaw cycling, acid rain exposure and UV exposure resistance. The hydrophobization of the porous network within the stone proved to give the stones an extremely good hydrophobic stability, even after the outer surface had dissolved through acid attack.

Even if some of the initial treatment methods gave the stones excellent hydrophobic exterior surfaces (water contact angle > 120°), these samples could fail to prevent water uptake even after short ageing times, e.g. 1 week under a strong UV light. However, for the optimized protocol, the marble stones could withstand water uptake after very harsh ageing tests because of the deep hydrophobization effect.

CH-P1-01
Preparation and characterization of a Keramsit to replace the lightweight concretes in contemporary construction by using different types of organic additions

T04 Cultural Heritage

#CH-P1-01

H. Chemani.

Department of Materials Engineering, Faculty of Engineering Sciences, University M'Hamed Bougara - Boumerdes (Algeria).

Current climate changes call for vigilance and encourage man to develop materials of construction ecological simple and durable. Texture and constitution must meet certain fundamental criteria. The study is carried on the fabrication and characterization of a lightweight granulate type "keramsit" obtained from expanded clay to replace traditional lightweight concrete. Three types of organic named porosants agents: AX, BY and CZ are used in the mixture mass for achieve the best product expansion clay. Chemical analysis, mineralogical and granulometric is performed on the material base. The instruments used are: the fluorescence spectrometer, diffractometer, the Robinson pipette and “Laser granulometer”.The nature of the clay and its capacity to expand is determined from the diagram "Riley». The preparation of samples is carried out on 05 mixtures with proportions of 1 to 3% of additions. Two types of samples were prepared: the form of (aggregates and test pieces). Firing is carried out at the temperatures 1100, 1150, 1200 and 1250°C. The characterization is carried on: the shrinkage, absorption, density, porosity and the mechanical strength. After optimization analysis it was found that (aggregates and test pieces) cooked at 1250°C with 3% of AX give better expansion. Values corresponding bulk densities are respectively: 05,3g/cm3 and 0.54g/cm3.Above the temperature 1150°C the expansion coefficient increases by more than 3 times. The resulting material has properties sufficient to replace the traditional concrete. These products are characterized by good thermal insulation, good resistance to fire, and insensitivity to physical and chemical. They allow advancing towards new horizons of construction as well as in renovation of old buildings, thanks to the great lightness.

Keywords: Expanded clay, Porosants Agent, coefficient of expansion, Lightweight concrete, Preparation, Characterization

Fig (a). Variation of coefficient of expansion as a function of temperature
Fig (b). Variation of bulk density as a function of temperature

CH-1-Or-4
Identification of natural organic dyes used in art works by laser desorption mass spectrometry

T04 Cultural Heritage

#CH-1-Or-4

S. Kuckova [1], M. Styblova [2], I. Krizova [1], R. Hynek [1], T.M. Grygar [3].

[1]Department of Biochemistry and Microbiology, Institute of Chemical Technology - Prague (Czech republic), [2]Department of Chemistry and Chemical Education, Charles University - Prague (Czech republic), [3]Institute of Inorganic Chemistry, Academy of Sciences of the Czech Republic - Rez (Czech republic).

The reliable identification of natural organic dyes that are used in works of art is essential for restorers, conservators and art historians for selection of proper restoration process, improving our knowledge about the painters and for attribution of the artworks.

Identification of the colouring agents in the paint layers of art works is a complex task due to the simultaneous presence of dyes, pigments, inorganic fillers, polysaccharides, proteins, oils, and resins. Pigment identification in paint layers has been relatively well developed for inorganic substances: in restoration practice it is mainly done by optical microscopy in normal and UV light, and by elemental analysis (scanning electron microscopy (SEM-EDX), X-ray diffraction (XRD) or X-ray fluorescence (XRF)) [1-3].

However, the characterization of majority of natural organic dyes has not been satisfactorily solved till now, mainly because of similarity of their elemental composition (C, H, O) and structure, presence in low concentrations, immobilization by chemisorption on inorganic substrates, and difficulty of extractions from complex matrices of the paint layers of the artworks. All these mentioned complications hinder the use of common analytical methods such as liquid chromatography [4], FTIR and Raman spectroscopy [5].

In this work, we apply laser desorption mass spectrometry on the direct identification of the natural dyes in their pure forms, precipitates on inorganic substrates, their mixtures with organic binders, and in real samples of paint layers and textile fibres. The method enables fast and reliable identification without any chemical and time consuming preliminary treatments. Additionally, the method could be considered as a non-destructive because of analysing extremely small amount of samples that is very important in the preservation of cultural heritage objects.

1. Herrera L.K., Montalbani S., Chiavari G., Cotte M., Sole V.A., Bueno J., Duran A., Justo A., Perez-Rodriguez J.L.: Advanced combined application of mu-X-ray diffraction/mu-X-ray fluorescence with conventional techniques for the identification of pictorial materials from Baroque Andalusia paintings. Talanta 80, 71-83 (2009).

2. Romero-Pastor J., Duran A., Rodriguez-Navarro A.B., Van Grieken R., Cardell C.: Compositional and quantitative microtextural characterization of historic paintings by micro-X-ray diffraction and Raman microscopy. Anal. Chem. 83, 8420-8428 (2011).

3. Van der Snickt G., Janssens K., Schalm O., Aibeo C., Kloust H., Alfeld M.: James Ensor's pigment use: artistic and material evolution studied by means of portable X-ray fluorescence spectrometry. X-ray Spectrom. 39, 103-111 (2010).

4. Sanyova J.: Mild extraction of dyes by hydrofluoric acid in routine analysis of historical paint micro-samples. Microchim. Acta 162, 361-370 (2008).

5. Kuckova S., Hynek R., Nemec I., Kodicek M., Jehlicka J.: Critical comparison of spectrometric analyses of non-mineral blue dyes and pigments used in artworks. Surf. Interface Anal. 44, 963-967 (2012).

CH-1-Or-7
Sub micrometer gold leaf for art gilding: how and when was it obtained? A mechanical analysis of gold foil thinning

T04 Cultural Heritage

#CH-1-Or-7

M. Aucouturier [1], E. Felder [2], E. Darque-Ceretti [2].

[1]Centre de Recherche et de Restauration des Musées de France - Paris (France), [2]MINES ParisTech, CEMEF - Sophia-Antipolis (France).

Foil or leaf gilding to decorate artworks or architectural items is used since very ancient antiquity, and still practiced. It has been applied on all kind of supports, wood, Egyptian cartonnage, metal, ceramic, stone, paper.
It is known that gold films used for gilding had very variable thickness [1]. The artisans could use quite thick foils of several micrometers thickness fixed on the artwork by mechanical means or very thin leaves with a thickness down to 0.1 µm (fig. 1). A convention proposed by English speaking scientists [1] is to use the word leaf when the gold foil used for gilding has a thickness so small that it cannot oppose to its own weight, roughly less than 1 or 2 micrometer.
The practice of gold thinning started at a very early period; Egyptian artisans were able to thin gold foils to leaves with a thickness smaller than 1 µm [2]. Pliny the Elder stated that it was possible to reach thinness down to 0.4 micrometer. So the thickness of the gold leaf used for gilding cannot be used as a criterion to propose a dating for objects.
The operation of gold thinning to obtain very thin leaves as observed in modern workshops [3] has been detailed in various encyclopaedias at different periods [4]. Two overall steps are practiced: the first one is a pre-thinning of the gold ingot by hammering (in old times) or rolling (after the invention of the rolling mill). After that, a second series of mechanical operations is performed grouped under the appellation of beating.
The present communication draws a summarised history of gold leaf elaboration and describes a mechanical analysis of the rolling and beating processes. The distribution of deformation and stresses during the steps of rolling and beating is described and quantified to understand the necessity of the beating operation to

obtain sub-micrometer-thick gold leaves. It shows why it is mechanically impossible to reach by simple rolling a thickness smaller than several micrometers. Foil thinning by beating is the result of a biaxial strain effect, due to the elastic deformation of the polymer intermediate and the biaxial stretching of gold.

[1] W.A. Oddy, Gilding of metals in the old world, in : Metal plating and Patination, ed. S. La Niece, P. Craddock, Butterworth, London (1993), 171-181.
[2] G. Nicolini, Techniques des ors antiques, édition Picard, Paris, (1990), 65-96.
[3] B. Dauvet, the last gold leaf beater in France: http://www.dauvet.fr/
[4] D.Diderot, J. le R. d'Alembert, Encyclopédie, ou Dictionnaire Raisonné des Sciences, des Arts et des Métiers, Paris, 1751-1772. Text available on: http://portail.atilf.fr/encyclopedie/index.htm.

Figure 1: Leaf-gilded roof of the Invalides church in Paris

CH-1-Or-5
Presence of nanolayers controlling the corrosion processes on iron based archaeological artefacts, detected by high spatial resolution Raman, TEM, STXM and nanoSIMS analyses.

T04 Cultural Heritage

#CH-1-Or-5

P. Dillmann [1], J.P. Gallien [2], E. Foy [2], D. Neff [2].

[1]CNRS - Gif Sur Yvette (France), [2]CEA - Gif Sur Yvette (France).

The corrosion of low alloy steels in anoxic media during several centuries is a crucial issue in several domains. On the one hand, some archaeological sites are submitted to anoxic conditions and the long term mechanisms must be enlighten for in-situ conservation purposes. On the other hand, in France, nuclear wastes will be submitted to deep geological repository and the overcontainer of low alloy steel will be submitted to anoxic corrosion processes during several centuries.
For that reason, numerous studies focus on understanding the mechanisms controlling the corrosion kinetics. In that frame, both laboratory simulation on short term and specific studies made on archaeological analogues seems to indicate that in addition to a layer of several 100 µm made of iron carbonates (siderite, chukanovite), a sub micrometric layer, located at the metal/corrosion products interface could influence the corrosion processes. Nevertheless, no precise characterisation data has been published on this layer and the way it controls the mechanisms is not unravelled up to now.
This study presents the characterisation results obtained on 400 hundred year old archaeological artefacts corroded in anoxic aqueous media, investigated at the metal/corrosion product interface. Transverse sections and thin films made on these transverse sections were investigated by coupling different structural and chemical methods giving information on the phase nature at the sub micrometric scale. Last developments of High Spatial Resolution Raman allow to investigate a sample with a 500 nm resolution. STXM under synchrotron radiation was used to investigate the iron L edge and to map its variation around the interface with a 25 nm resolution. In a complementary way electron diffraction on TEM was used to investigate the same

zone. The coupling of these methods allowed us to clearly evidence a continuous layer made of a mix of FeII and FeIII species (probably a mix of maghemite and magnetite), separating the metallic substrate from the carbonate (siderite and chukanovite), this latter constituting the main part of the layer. The thickness of this intermediate oxide layer varies on the same artefact from several 10 nm to several 100 nm.
In a complementary way, the investigated archaeological artefacts were put in a D2O desaerated solution, representative of the water of the archaeological site, during several months. After this treatment, nanoSIMS observation of 16O distribution and D/H ratios clearly showed that water (D2O in our case) does not reach the metal by penetrating the pores of the corrosion layer but seems to be stopped by the nanometric interfacial oxide layer that is apparently much less porous than the carbonate corrosion products.
These new data will enlighten the corrosion mechanisms and are an important step for further comprehension and modelling of the long term corrosion processes.

CH-P1-02
Stochastic computer simulation : the prediction of porosity nanostructures into solids surface as a result of ions implantation

T04 Cultural Heritage

#CH-P1-02

G. Zmievskaya, A. Bondareva.

M.V. Keldysh institute of applied mathematics RA - Moscow (Russian federation).

For solution of unstable phase transitions in solid matter problems the numerical method of solving the quasilinear parabolical equations in partial derivatives by replacing them with stochastic analog in form of Ito-Stratonovich differential equations was being developed. The properties of Markovian random processes are used for the creation of the mathematical models of fast-evolving processes of the fluctuative nature in materials under radiation flow treatment. The nucleation of 1st order phase transition (the pore formation in crystal lattice etc.) is investigated on the example of defect formation on the nonlinear stage of phase transition under inert gas flows treatment. The role of fluctuation instability of phase transition in the formation of Si porosity is being investigated (for the the media with a periodical structure of photonic crystals which are usually obtained by crystal etching).The estimate of the momentary elastic deformation of Si crystal lattice with spherical vacancy-gas pore nucleation induced by the pressure contrast on its boundary is conducted with the account for the defect distribution in the sample as the result of Brownian pore movement under the influence of indirect elastic interaction between pores by exciting the acoustic phonons of the lattice and Fridel oscillations of electron density in metal[1].The method of phase transition nucleation simulation [2] is generalized for the formation of elongated radiation-induced linear defects in the form of vacancy discs, dislocations, planar defects (dislocation loops). Methods of stochastic simulation of nonlinear processes arising with defect movement of dislocation type, such as defect immobilization, multiplying and annihilation of dislocations etc., are modified on the models in which Ito-Stratonovich equations by continuous measure (nucleus clusterization and Brownian movement) are complemented by Ito equations by point measure (for the collision processes

description) and their numerical solution algorithms. The kinetic distribution function of stochastic dynamical variables (size and location of defects) are used for calculation porosity, radiation damage principles, which may be used for nondestructive control of defect formation (in the historical heritage objects) and materials of technical purpose, as well as aid the creation of materials with novel properties (porous silicon). Numerical investigation of elastic plastic deformation mechanism on the initial stage of phase transformations induced by implantation with change and distribution of dislocation densities in materials are examined. Authors are thankful prof. Giuseppe Maino (Italy) for new idea in applications of computer simulation models in problems of preservation of cultural heritage and Donatella Biagi Maino (Italy) (prof. of cultural heritage restoration). Work is partially supported by the RFBR grants 11-01-00282-a, 12-01-00490-a and 12-01-00708-a.

[1] Zmievskaya G.I., Bondareva A.L., Savchenko V.V., Levchenko T.V. 2012 Defect and Diffusion Forum 326-328 pp. 243-248
[2] Zmievskaya G.I., Bondareva A.L., Savchenko V.V., Levchenko T.V. 2012 in book Numerical Analysis of Heat and Mass Transfer in Porous Media Springer-Verlag Berlin Heidelberg ISBN: 978-3-642-30531-3 pp. 253-274

CH-1-Or-1
Portuguese ceramics from the 16th century: pigments, glazes and pastes characterization.

T04 Cultural Heritage

#CH-1-Or-1

L. Vieira Ferreira [1], I. Ferreira Machado [1], T. Casimiro [2], P. Colomban [3].

[1]CQFM- Centro de Química-Física Molecular and IN-Institute of Nanoscience and Nanotechnology, Instituto Superior Técnico, Universidade Técnica de Lisboa, Av. Rovisco Pais, 1049-001 - Lisbon (Portugal), [2]Instituto de Arqueologia e Paleociências das Universidades Nova de Lisboa e do Algarve. Departamento de História, Avenida de Berna 26-C, 1069-061 - Lisbon (Portugal), [3]Laboratoire de Dynamique, Interaction et Réactivié, UMR7075 CNRS-Universite´ Pierre-et-Marie-Curie, Paris 6, 4 Place Jussieu, C49 batF, 75252 Paris cedex 05 - Paris (France).

The Portuguese were the first Europeans to send merchant vessels regularly to China, bringing back, since the first half of the 16th century porcelains and other goods highly appreciated in Western Countries. Copies of those porcelains started to be produced in Lisbon, but in the form of faience, trying to imitate Chinese patterns [1]. There is now archaeological evidence that such production started in Lisbon at least in the middle of the 16th century [1 and references therein].
Common earthenware, however, was a much older production in the country, and there is archaeological evidence for its production at “Mata da Machada” and from Santo António da Charneca about 1480 to 1530, both South of Lisbon, and also in Lisbon at Santos o Velho at least from 1561 onwards [2].
In this study our first goal is the spectroscopic characterization of pigments, glazes and pastes of the 16th century Portuguese Faience, which still remains to be done. A comparison with Spanish production of Valencia and Seville was also performed. Raman micro spectroscopy was used as our main tool for such characterization [3 and references therein]. Ground state diffuse reflectance spectra (GSDR), with the use of the Kubelka-Munk treatment for colour evaluation were also obtained [3, 4] as well as FT-IR spectra obtained for the pigment, glaze and paste characterization [3]. A comparison of the spectroscopic data obtained from sherds from Mata da Machada and several other from an archaeological excavation on a small urban site in the city of Aveiro (late 15th century and 16th century) [5] was performed . Also sherds of

imported pottery from Valencia and Seville were studied, since it is well know that Portugal imported significant quantities of those goods from Spain at that time. The obtained results evidence a clear similarity in the micro-Raman spectrum in the white glaze and clays of Portuguese pottery produced at “Mata da Machada” and the sherds found at the medieval house of Aveiro. All these are quite different from the Spanish products under study, pointing to an earlier production of tin glaze earthenware in Portugal than the mid 16th century, commonly assumed.

[1] a) R.S. Calado, ‘‘Portuguese Faiance”, Published by Post and Telecommunications of Portugal (1992). b) T.M. Casimiro, “Portuguese Faience in England and Ireland’’, B.A.R., Oxford, Archaeopress (2011).
[2] a) C. Torres, “Um forno cerâmico dos séculos XV e XVI na Cintura de Lisboa. Mata da Machada – Barreiro" Published by Casa de Velazquez, Archaeologie XIII Madrid (1990) 131-141. b) A.Mangucci, “Olarias de Louça e Azulejo da Freguesia de Santos-o-Velho: dos meados dos séculos XVI aos meados do século XVIII”. Al-Madan. IIª Série. 5 (1996) 155-168.
[3] L.F. Vieira Ferreira* , T. M. Casimiro, Ph. Colomban, “Portuguese tin-glazed earthenware from the 17th century: pigments and glazes characterization”, Spectrochim. Acta, Part A,104 (2013) 437-444.
[4] L.F. Vieira Ferreira, I.L. Ferreira Machado, “Surface Photochemistry: organic molecules within nanocavities of Calixarenes”, Curr. Drug. Discov. Technol., 4 (2007) 229-245.
[5] T. Barbosa, T.M. Casimiro, R. Manaia, “A household pottery group from Aveiro (Portugal)”, Medieval Ceramics, 37 (2009) 119-136.

CH-1-Or-10
Non destructive identification and diagnosis of natural organic substances in cultural heritage: insight from Raman and infrared signatures

T04 Cultural Heritage

#CH-1-Or-10

L. Bellot-Gurlet [1], C. Daher [2], C. Paris [1].

[1]Laboratoire de Dynamique, Interactions et Réactivité (LADIR), UMR 7075 UPMC/CNRS - Paris (France), [2]Centre de Recherche et de Restauration des Musés de France (C2RMF) - Paris (France).

Natural organic substances are wildly used in the history and constitute a precious testimony of human exploitation strategies, exchange networks and techniques for their implementation in numerous ancient objects. These materials have long been neglected because of their poor conservation or small quantities and some limits of analytical approaches. With the re-evaluation of vibrational spectroscopies (Raman and infrared) potentialities through spectral treatment procedures', these could offer alternatives or complements to the current analytical strategies based on separation methods. The use of FT-Raman is needed to avoid fluorescence and infrared measurements are performed using a micro-ATR configuration to eliminate sample preparation.
The identification of a broad range of natural organic substances: proteins (animal glues), triglycerides (oils), polysaccharides (gums) and terpenoids (resins from different geographical provenances), require specific strategies to differentiate vibrational signatures with close features. A methodology is proposed on spectral decomposition of CH stretching massif followed by Principal Component Analyses of extracted parameters. Applying PCA on the raw data, as commonly done, is indiscriminate. However, PCA of the fitting parameters becomes an efficient and powerful tool to cluster the different materials, because it is highly related to their molecular characteristics. This approach proved the possibility of identifying the natural organic substances, sometime at the scale of the tree species, and some alteration or ageing is not an issue to their recognition. This approach could find applications in various contexts (archaeology, museum context, conservation

purpose, but also present industrial application) and for a wide range of natural organic materials as varnishes, binders or adhesives.

Daher C., Paris C., Le Hô A.-S., Bellot-Gurlet L. et Échard J.-P. (2010). A joint use of Raman and infrared spectroscopies for the identification of natural organic media used in ancient varnishes, Journal of Raman Spectroscopy, 41, 1204-1209.

CH-1-Or-8
Colorando Auro: Medieval recipes to colour gilded silver plates studied by SR-XPS and XANES.

T04 Cultural Heritage

#CH-1-Or-8

M. Languille [1], A. Crabbé [2], I. Vandendael [3], J. Hammons [3], M. Silly [4], G. Dewanckel [2], H. Terryn [3], H.J.M. Wouters [2].

[1]CNRS USR3461 IPANEMA - Gif-Sur-Yvette (France), [2]IRPA - Bruxelles (Belgium), [3]VUB - Bruxelles (Belgium), [4]Synchrotron SOLEIL - Gif-Sur-Yvette (France).

The colour of gold and gildings can be influenced in many ways: the composition of the gold alloy or the nature of the substrate on which the gilding is applied [1] are two well known methods to obtain different colours of this metal. Nowadays, we are even able to change the colour of gold by playing with the size of gold nanoparticles or micropatterning pur gold. Several studies have shown an intentional change of the colour of gold over the history. Another less known technique to colour the gildings is the chemical treatment of the gilded surface itself, i.e. after the application and the burnishing of the gilding [2]. This chemical treatment might have been used on goldsmith pieces, such as Our Holy Lady Shrine of Huy (13th c. Mosan art, Belgium [3]) that motivated this study.
Several recipes that were able to give a warmer tone to gilding on a silver plate have been reproduced according to ancient writings. Nevertheless the physical chemistry of this coloration is not fully well understood. That is why we characterized the gilded surfaces before and after application of the re-created recipes. In order to do that, we used the tunability of the synchrotron source to probe the upper surface at two depths by X-ray Photoelectron Spectroscopy (SR-XPS) and we performed X-ray Absorption Near Edge Spectroscopy (XANES) to study elemental markers of the recipes (iron and copper). Thus, we attempted to identify the reagents required for the success of these recipes and to understand the reaction mechanisms occurring on the gilding during the treatment. Finally, we tried to discriminate recipes markers that remain on the coloured gilded surface after the treatment from residues of a modern cleaning product that is commonly used in goldsmith restoration, the « rouge à polir » [4].

1. E. Darque-Ceretti, M. Aucouturier, Dorure : Décor et Sublimation de la Matière (Mines ParisTech, Paris, 2012), 156pp.
2. A. Crabbé, I. Vandendael., H. Wouters, G. Dewanckel, O. Steenhaut, H. Terryn, The Enigma of the Silver Blackening of the 13th Century Notre-Dame Shrine of Huy (Belgium): a surface analysis approach, Surface and Interface Analysis 40 (2008), 469-473.
3. A. Crabbé, G. Dewanckel, in Actes du LVème Congrès de la Fédération des Cercles d'archéologie et d'Histoire de Belgique, vol. 5 (2011), p. 1581.
4. A. Crabbé, M.-A. Languille, I. Vandendael, J. Hammons, M. G. Silly, G. Dewanckel, H. Terryn and H. J. M. Wouters, Colorando Auro: Contribution to the understanding of a medieval recipe to colou gilded silver plates, Applied Physics A, in press.

CH-1-Or-6
Influence of sulfur compounds in iron corrosion: complementary chemical imaging with μ-Raman spectroscopy, FEG-SEM and ToF-SIMS

T04 Cultural Heritage

#CH-1-Or-6

F. Mercier-Bion [1], D. Neff [2], A. Galtayries [3], A. Seyeux [3], A. Verney-Carron [4], P. Dillmann [1].

[1]CNRS (France), [2]CEA (France), [3]Chimie ParisTech (France), [4]Université Paris-Est Créteil (France).

The corrosion of ferrous objects can be influenced by the action of micro-organisms when they lay in a biologically active environment and the understanding of the corrosion mechanisms is important in two scientific domains: (1) the preservation of ferrous archaeological objects; (2) the French concept for geological disposal of nuclear waste based on a multi-barrier system including the metallic containers confined in natural clay. In both fields, the long term behavior of the metal has to be assessed in order to establish conservation treatment or prediction behavior models. One particularly crucial parameter is the influence of the presence of bacteria on the corrosion processes. The presence of iron sulphides and other iron/sulphur-containing compounds in the corrosion layers can be the fingerprint of the role of sulphate-reducing bacteria. Therefore, in this study, complementary imaging techniques were used to characterize the sulphur-bearing compounds in the corrosion products of archeological objects and of ferrous samples corroded in conditions relevant to a future geological disposal of nuclear waste: FEG-SEM for the bacteria images and the elemental mappings, μ-Raman for the identification of sulphur phases and ToF-SIMS for the determination of the 34S/32S ratio (as shown on figure 1). ToF-SIMS is particularly innovative in this scientific research and could permit to identify, from the 34S/32S ratio, how bacteria induce the formation of sulphur-bearing compounds in the iron corrosion process, as it has been reported that the bacterial culture medium shows sulphate aqueous specie depleted in 32S and enriched in 34S.

Figure 1: µRaman image corresponding to iron sulphide border in the corrosion products of an archeological nail of the 16th century (Glinet, Seine-Maritime, France). Laser wavelength: 532 nm.

Figure 2: ToF-SIMS repartition in 32S (left) and 34S (right) of the iron sulphide border (Bi+ ions, negative mode, image size: 242 X 242 µm2).

CH-1-Or-9
Nanoparticles used to darken the patina of antic black bronze: TEM observations on new experimentations

T04 Cultural Heritage

#CH-1-Or-9

F. Mathis [1], S. Tirat [1], E. Grieten [2], D. Robcis [3], M. Aucouturier [3], D. Schryvers [2].

[1]Centre Européen d'Archéométrie - Université de Liège - Liège (Belgium), [2]Electron Microscopy for Materials Science - University of Antwerp - Antwerp (Belgium), [3]Centre de Recherche et de Restauration des Musées de France - Paris (France).

Some studies that started in the nineties [1] proved that some antic artefacts or parts were intentionally patinated using a chemical treatment. In particular one type of patina was characterized on artefacts coming either from Egyptian civilization, Mycenaean period or Roman Empire. This patina has been identified as a precious material mentioned in ancient Egyptian and Roman texts. This particular material is named, depending on the artefacts' origin, black bronze (hmty km), or corinthium aes. This patina is made on copper alloys containing gold and/or silver and is composed mainly of cuprite. It was compared with a Japanese patina which appears in medieval times but which is still in use and known under the name of shakudo. Shakudo are copper gold alloys and they are treated chemically by means of different recipes named nikomi-chakushoku which developed a black layer of cuprite on the surface.
An important study of antic artefacts coming from the collections of French museums has been carried out since the beginning of the 2000's. An experimental protocol based on non-invasive analysis was developed to analyse these very precious objects and to identify and characterize this type of patina in function of the provenance and age of the artefacts [2, 3].
However, some questions about this particular surface layers could not be resolved using this experimental protocol due to the limitation of non-invasive analytical techniques: In particular the question of the formation of the oxide layer, the colouring mechanism of this black cuprite (copper oxide which is red under natural form) and the important adherence properties.

We developed a program of experimentation to make some black patina. These experimentations were based on the utilisation of the Japanese recipes, and we tried to differentiate the effect of the alloying element (Au, Ag, As) and the effects of the chemical treatment.
These patinas were studied by means of various analytical methods and in particular we used TEM to characterize the fine structure of the oxide layer.
The use of transmission electron microscopy (TEM) allows to evidence a hypothesis already mentioned in previous studies [4]: the presence of nanoparticles of gold in the cuprite layers and their role on the coloration of the patina making the black bronze the very first application of nanoparticles in technical history.

1. Craddock, P., Giumlia-Mair, A., 1993. Hsmn-Km, Corinthian bronze, shakudo: black-patinated bronze in the ancient world, in: La Niece, S., Craddock, P. (Eds.), Metal Plating and Patination, Butterworth-Heinemann Ltd, London, pp. 101-127.
2. Aucouturier, M., Mathis, F., Robcis, D., Castaing, J., Salomon, J., Pichon, L., Delange, E., Descamps, S., 2010. Intentional patina of metal archaeological artefacts; a non-destructive investigation of Egyptian and Roman museum treasures, Corrosion Engineering Science and Technology 45, 314-321.
3. Mathis, F., Delange, E., Robcis, D., Aucouturier, M., 2009. HMTY-KM (Black Copper) and the egyptian bronzes collection of the Musee du Louvre, Journal of Cultural Heritage 10, 63-72.
4. Murakami, R., 1993. Japanese traditional alloys, in: La Niece, S., Craddock, P. (Eds.), Metal Plating and Patination, Butterworth-Heinemann Ltd, London, pp. 85-94.

CH-1-Or-2
DiffAbs beamline contribution to the study of ancient materials.

T04 Cultural Heritage

#CH-1-Or-2

S. Reguer [1], C. Mocuta [1], F. Alves [1], D. Thiaudière [1], F. Kergourlay [2], D. Neff [2], E. Foy [2], P. Dillmann [2].

[1]Synchrotron Soleil - Gif Sur Yvette (France), [2]LAPA SIS2M UMR3299 CEA/CNRS and LMC IRAMAT UMR 5060 - Saclay (France).

The DiffAbs beamline, at SOLEIL synchrotron, is located on a bending magnet and provides a monochromatic X-ray beam, tuneable in the 3-23 keV energy range. The multi-scale beam size, “standard” (300 µm) and microbeam (10µm) modes, can be used in conjunction with all the analysis techniques available at the beamline: X-Ray Diffraction, X-Ray Absorption and Fluorescence spectroscopies. The almost simultaneous combination of such techniques offers the possibility of complementing the local structure information by data on the long range order, which is essential for a full characterization of material. All the measurements are performed on the 6/8 circle kappa diffractometer using different well-adapted detectors, ensuring that all experiments are carried out on the same zone of the sample, in absolutely identical physico-chemical conditions (temperature, reactive solution, etc). Since its opening to users in 2008, DiffAbs beamline prove is competitiveness to study ancient materials (see references). Typical experiments will be presented.
For instance, a new specific set-up allowing in situ X-ray diffraction measurements was developed last two years using the XPAD, a new hybrid-pixel detector. The fast and well resolved diagrams acquired using mapping mode on an in-situ cell containing the archaeological sample, allow observing the transformation of the corrosion products of the marine iron artefact during its desalinisation.

1. *Combining XANES, ICP-AES, and SEM/EDS for the study of phytate chelating treatments used on iron gall ink damaged manuscripts.*
Rouchon V., Pellizzi E., Duranton M., Vanmeert F. and Janssens K.
Journal of Analytical Atomic Spectrometry, 26, 2434-2441, 2011

2. *Analyse de la perte de couleur des peintures au smalt par spectroscopie*

d'absorption X.
Robinet L., Trcera N., Pagès-Camagna S., Spring M. and Reguer S.
Techniques de l'Ingénieur, art.n° RE211, 2012

3. *Why Does Prussian Blue Fade? Understanding the Role(s) of the Sub-strate*
Gervais S., Languille M-A., Reguer S., Gillet M., Pelletier S., Garnier C., Vicenzi E.P. and Bertrand L.
Journal of Analytical Atomic Spectrometry, submitted

4. *Structural resolution of the ferrous hydroxychloride β-$Fe_2(OH)_3Cl$ in archaeological context.*
Reguer S., Mirambet F., Rémazeilles C., Vantelon D., Kergourlay F., Neff D. and Dillmann P.

CH-1-Kn-1
BEYOND THE APPEARENCE OF WORKS OF ART

T04 Cultural Heritage

#CH-1-Kn-1

P. Walter.

Laboratoire d'archéologie moléculaire et structurale, CNRS-UMR8220, Université Pierre et Marie Curie (UPMC) - Ivry-Sur-Seine (France).

The study of Cultural Heritage materials requires advanced techniques to shed new lights on ancient technologies and help in their preservation. The implementation of new analytical tools, including mobile laboratories or large/medium scale facilities such as synchrotron radiation, charge particle accelerators, neutron sources allows a deep insight on the archaeological and artistic materials, from the millimeter to the nanometer scales.
During this lecture, current applications and potential needs of multiscale imaging techniques will be presented to show the major role played by analytical techniques to characterize the nature and the mode of preparation of different pigments (origin of the minerals, chemical synthesis of new compounds, crushing of crystals, mixing of matters, etc.). The precious character of the most famous works of art and their uniqueness imply particular cautions and require methods which may give the maximum information with the minimum of sample, if any.

EMP-P3-01
Advanced structural characterisation of micro- and nano-electronics using neutrons and synchrotron X-rays

T05 Electronic Materials and Processes

#EMP-P3-01

E. Mitchell [1], J. Beaucour [2], J.C. Royer [3], P. Bordet [4].

[1]European Synchrotron Radiation Facility and EPSAM, Keele University - Grenoble (France), [2]Institut Laue-Langevin - Grenoble (France), [3]LETI - Grenoble (France), [4]Institut Neel - Grenoble (France).

Large-scale synchrotron and neutron research infrastructures offer unrivalled performance for the advanced characterisation of micro- and nano-electronic devices and systems. Examples include X-ray spectroscopy to study RRAM switching mechanisms, grazing incidence X-ray scattering and neutron reflectivity for structural data on materials for interconnections, hard X-ray PES to understand electronic properties of layered materials, and nano- and micro-X-ray-tomography for unprecedented non-destructive 3D imaging of packaging, vias, etc.

There is an increasing realisation worldwide that large-scale research infrastructures are a key component, not only of academic and fundamental research, but also of the innovation cycle and industrial research and development. However, working with industry has its own special requirements, and can bring to the fore mismatches and clashes between a traditional academic culture and the needs of the market driven commercial world: research infrastructures are often based on an academic modus operandi which can limit their industrial impact.

The IRT Nanoelec, a technological research institute for nanoelectronics, was founded in April 2012 through a joint venture between the French National Research Agency (ANR) and the French Atomic and Alternative Energy Commission (CEA). This public-private partnership comprises 17 public- and private-sector research

partners - including the European research infrastructures European Synchrotron Radiation Facility (ESRF) and Institut Laue Langevin (ILL) which provide world-leading synchrotron light and neutron facilities for both academic and industrial communities. **The IRT NanoElec research will be focused on a core technology programme encompassing 3D assembly integration, nanophotonics on silicon and via technologies, supported by technological infrastructure including a Micro- and Nano-Electronics Characterisation Platform. This platform, being created as a pathfinder project, will largely enhance the effectiveness and attractiveness of the Grenoble-based neutron and synchrotron light source facilities for European micro and nano-technological research.**

The NanoElec funding will provide staff to support electronics research at ESRF and ILL, as well as complementary facilities at the CEA Platform for Nano-Characterisation such as SEM, TEM and FIB. **Off-line sample preparation facilities and complete characterisation processes from industry device to on-line experiment design and performance with data analysis will be made available** as the large-scale facilities and industry learn how to work together. The experience gained and platform facilities will be available for European and international companies, as will opportunities for training in the synchrotron and neutron techniques.

This pathfinder project, together with other initiatives, will serve to highlight the impact that public large-scale facilities can and should have on the economic growth and international competitiveness of companies.

This work is supported by the French government within the Investissements d'Avenir programme with the reference ANR-10-AIRT-05.

EMP-1-Or-1
MULTILAYERD METAL/ POLYPYRROLE ELECTRODES FOR BIOSENSORS

T05 Electronic Materials and Processes

#EMP-1-Or-1

R. Ofek Almog [1], Y. Sverdlov [2], S. Vernick [2], Y. Shacham-Diamand [2].

[1]Department of Advanced Materials Engineering, Azrieli College of Engineering Jerusalem - Ramat Beit Hakerem , Jerusalem (Israel), [2]Department of Physical Electronics, School of Electrical Engineering, Faculty of Engineering, Tel Aviv University - Tel Aviv (Israel).

Multilayer metal/ Polypyyrole /Metal electrodes were fabricated providing better conductivity than that of Polypyrrole (Ppy), and improving the flexibility and sensitivity compared to that of only metal electrodes. We report on the electrical and electrochemical properties of the electrodes, on the Ppy electro-polymerization process integration, and on the gold electroplating on the Ppy.
The Ppy was deposited by electrochemical polymerization using repetitive cyclic voltammetry (CV). The top metal was electrodeposited on the Ppy. The metal nucleation and growth on the Ppy were studied using HRSEM and FIB/SEM. The electrochemical behavior of the metal/Ppy/metal electrodes was tested by CV and impedance spectroscopy. The novel electrode system was tested for their application as whole cell biosensors using substrate - enzyme interaction by product electrochemical activity. We studied the response of the new electrode in biological solutions (PBS). We found that depositing Ppy on thin metal seed layer dramatically increases the measured current of the electrodes, as compared to Au electrode. This effect was also demonstrated by CV measurements as well as in amperometric detection of alkaline-phosphatase enzymatic activity using biological chips. This high current produces noise that interferes with the proper operation. However, when sufficient metal is electrodeposited on the Ppy, the behavior of the electrode becomes similar to that of a metal electrode, as demonstrated by CV and by amperometric detection of enzymatic activity. The CV curve has the same characteristics as that of the planar gold electrode, with a considerably higher current peak (Ip). More important, the new electrode demonstrated an improved ability of enzymatic activity amperometric detection.
The electrodeposition of Ppy followed by Au, on the surface of the biochip's Au seed layer, affected the electrocrystallization of the Au particles on the Ppy (Fig 1) resulting in a high surface area.

This electrode can serve as a highly sensitive, high surface area and flexible sensor for biological species.

HRSEM image of Gold/ Polypyrrole/Gold structure, on Biochip working electrode- Au deposition time- 10 minutes.

EMP-P3-02
Physical and electrical characteristics of Er2O3 and Er2TiO5 InGaZnO thin-film transistors

T05 Electronic Materials and Processes

#EMP-P3-02

T. Pan [1], C.H. Chen [1], F.H. Chen [1], J.L. Her [1], Y.H. Matsuda [2].

[1]Chang Gung University - Taoyuan (Taiwan, republic of china), [2]University of Tokyo - Chiba (Japan).

Amorphous indium-gallium-zinc-oxide (a-IGZO) thin-film transistor (TFT) has been investigated as a replacement for amorphous and polycrystalline silicon TFTs in active-matrix liquid-crystal display devices and active-matrix organic light-emitting displays [1]. In addition, rare-earth (RE) oxide films have been extensively studied to replace a traditional SiO_2 gate dielectric because of their probable thermal, physical, and electrical performance [2]. With its large dielectric constant, wide bandgap energy, and high transparency in the visible range [2], an Er_2O_3 film can be considered as a gate oxide for low-temperature TFT applications. The main issue is that using RE films is moisture absorption to degrade their permittivity due to the formation of low-permittivity hydroxides. To solve this issue, the addition of Ti or TiO_x into the RE dielectric films can cause improved physical and electrical properties [4]. In this study, we compared the physical and electrical properties of Er_2O_3 and Er_2TiO_5 a-IGZO TFT devices.

Fig. 1 displays the XRD patterns of the Er_2O_3 and Er_2TiO_5 thin films deposited on the TaN/SiO_2/Si substrate. A strong Er_2O_3 (400) and weak TaN (101) peaks appeared in the Er_2O_3 film, while only TaN (101) reflection peak was presented in the Er_2TiO_5 film, revealing that Er_2TiO_5 thin film was amorphous. The transfer characteristics of the a-IGZO TFT devices using Er_2O_3 and Er_2TiO_5 gate dielectrics were shown in Fig. 2. The V_{TH} value of the Er_2O_3 and Er_2TiO_5 a-IGZO TFT devices is 1.5 and 0.39 V, whereas the I_{on}/I_{off} ratio is 1.72×10^6 and 4.23×10^7, respectively. Furthermore, the μ_{FE} of the Er_2O_3 and Er_2TiO_5 TFT devices is 6.7 and 8.8 cm^2/V-sec.

[1] L. Y. Su, H. Y. Lin, H. K. Lin, S. L. Wang, L. H. Peng, and J .J. Huang, IEEE Electron Device Lett. 32, 1245 (2011).

[2] M. Fanciulli and G. Scarel, Rare Earth Oxide Thin Film: Growth, Characterization, and Applications, Springer, Berlin, 2007.
[3] R. B. van Dover, Appl. Phys. Lett. 74, 3041 (1999).

Fig. 1. XRD patterns of Er_2O_3 and Er_2TiO_5 dielectric films.

Fig. 2. Transfer characteristics (I_{DS}–V_{GS}) of Er_2O_3 and Er_2TiO_5 a-IGZO TFT devices.

EMP-1-Or-2
Charge transfer in molecules and ultrathin insulating films deposited on metal surfaces

T05 Electronic Materials and Processes

#EMP-1-Or-2

M. Robledo Relaño, S. Díaz-Tendero, F. Martin, M. Alcamí.

Universidad Autónoma de Madrid - Madrid (Spain).

The main feature behind photovoltaic devices, in the framework of organic electronics, is the presence of a stable molecular system in which solar radiation can easily induce electronic transfer. These systems can be constructed by deposition of organic molecules on metal surfaces as well as on metal surfaces covered by insulating layers, thus providing a donor-acceptor set with the possibility of charge transfer between them induced by light. Charge transfer processes lead to level alignment of the frontier orbitals but they may also induce structural transformations. Therefore, a first step towards the design of photovoltaic devices implies an accurate description of the structure and the charge transfer taking place on the ground state. In this communication we present the results obtained in a theoretical study on the interaction between different organic molecules, with potential photovoltaic activity, and clean metal surfaces or metal surfaces covered by ultrathin ionic layers. We have studied a wide range of organic molecules deposited on a metal surface (Cu(100) and Ag(111)). These systems cover from Van der Waals weak interactions (Benzene) to a strong covalent binding (TCNQ, tetracyanoquinodimethane). They also include the well known Fullerene, C_{60}, where not only the study of the system it self is interesting, but also dealing with the size of it is a demanding task. Further, we have chosen NaCl as the insulating film which, placed in between the organic molecules and the metal substrate, will decouple the former and induce changes in the work function of the latter [1].
Thus, we have studied C_6H_6/Cu(100), which is a prime example of the interaction between organic molecules, with π-delocalized electrons, and a metal surface. In order to check the effect of insulating films, we have also studied the following system: C_6H_6/nMLNaCl/Cu(100); (n = 1, 2 and 3), evaluating the geometry, the charge transfer, and the decoupling of the organic molecule. We have as well studied the structural rearrangement and the charge transfer in the system C_{60}/Cu(100) and C_{60}/nML NaCl/Cu(100) obtaining arresting results. Finally, we have studied the

interaction (self-assembled monolayers) of TCNQ on Ag(111) and TCNQ together with TTF on Ag(111). In these systems the geometry is affected after the adsorption on the surface due to the charge transfer. We will give prominence to these results by comparing them with experimental ones [2] and previous works [3]. All calculations have been performed with a plane wave, ultrasoft pseudopotential method as implemented in the VASP code [4]. The projector augmented wave method has been used together with the Perdew-Wang 91 functional. Dispersion forces (van der Waals) have been taken into account with the DFT-D2 Method of Grimme [5].

[1] Jascha Repp and Gerhard Meyer. Phys. Rev. Lett. 94, 026803 (2005)
[2] Koen Lauwaet et al. (Private communication); M.Robledo et al. (To be summitted)
[3] M. Abel et al., Phys.Rev.B67, 245407 (2003); N. Lorente et al. Phys.Rev.B 68, 155401 (2003); Tzu-Chun Tseng et al. Nature Chemistry 2, 374 (2010); G. Schull et al. N.J.Phys. 10, 065012 (2008).
[4] G. Kresse and J. Furthmühller, Comput. Mat. Sci., 1996, 6, 15; G. Kresse and J. Furthmühller, Phys. Rev. B, 1996, 54, 11169
[5] S. Grimme, J. Comp. Chem., 2006, 27, 1787–1799

EMP-P3-18a
New anti-charging method for electron beam observation and lithography of insulating substrates

T05 Electronic Materials and Processes

#EMP-P3-18a

A. Aassime [1], F. Hamouda [2], I. Richardt [3], J. Voillot [4].

[1]Paris-Sud University - Orsay (France), [2]CNRS - Orsay (France), [3]Neyco - Paris (France), [4]Paris-Sud University - Paris (France).

Abstract
Charge accumulation during electron beam exposure of insulating materials is a well-known artifact largely reported in literature [1,2]. To prevent charging effects, a metallic conductive layer is usually deposited either at the top of the resist or between the substrate and the resist [3]. For both methods, an additional etching step of the conductive layer is required giving rise to a complicated pattern transfer to the substrate and contamination issues. Another approach is to replace the metallic layer by a charge polymer dissipator [4]. Some of these dissipators have the advantage of being soluble in water which preserves the resist patterns and structures on the sample. However, these dissipators are generally corrosive and suffer from aging and poor high-resolution capability. The aim of this paper is to highlight a non destructive anti-charging process for electron beam lithography or for electron scanning imaging [5]. It is based on the use of inorganic layer soluble in water and achieves high resolution.

References :
[1] J. Zhang ⇑, M. Fouad, M. Yavuz, and B. Cui, Microelectronic Engineering 88 (2011) 2196–2199.
[2] K. H. Kim, Z. Akase, T. Suzuki and D. Shindo, Materials Transactions, 51 (2010) 1080 - 1083.
[3] D. R. S. Cumming, I.I. Khandaker, S. Thoms, and B.G. Casey, J. Vac. Sci. Technol., B 15 (1997) 2859–2863.
[4] K. Mohamed, M.M. Alkaisi, and R.J. Blaikie, Microelectronic Engineering 86

(2009) 535–538.
[5] A. Aassime and F. Hamouda, patent N° DI-0334

EMP-2-Or-1
Investigation of Ge-Sb-Te and nitrogen doped Ge-Sb-Te thin films by synchrotron-radiation x-ray spectroscopy

T05 Electronic Materials and Processes

#EMP-2-Or-1

H. Shin [1], M.C. Jung [2], Y.M. Lee [1], M.G. Kim [1], K.H. Kim [3], J.G. Chung [3], S.A. Song [3], Y.G. Yoon [4], J.H. Eom [5], J. Ihm [5], Z. Sun [6].

[1]Pohang Light Source, POSTECH - Pohang (Korea, republic of), [2]Okinawa Institute of Science and Technology - Okinawa (Japan), [3]Samsung Advanced Institute of Technology - Yongin (Korea, republic of), [4]Chungang University - Seoul (Korea, republic of), [5]Seoul National University - Seoul (Korea, republic of), [6]Xiamen University - Xiamen (China).

Ge-Sb-Te (GST) and nitrogen doped Ge-Sb-Te (N-GST) thin film layers for phase change random access memory (PRAM) applications were investigated by synchrotron-radiation-based x-ray photoelectron spectroscopy and absorption spectroscopy. The surface is readily oxidized by air exposure.[1] In-situ annealing of amorphous GST thin film resulted in changes in the Sb 3d orbital, indicating that not only Ge but also Sb involved in the phase changes, which was also justified by Stibnite model calculations.[2] Nitrogen doping in GST resulted in more favorable N atoms' bonding with Ge atoms rather than with Sb and Te atoms,[3,4] which explains the higher phase change transition temperature than that of undoped GST thin film. Surprisingly, it was noticed that N atoms also existed in the form of molecular nitrogen, N_2, which is detrimental to the stability of the GST performance.[5] N-doped GST experimental features were also supported by ab-initio molecular dynamic calculations.[4]

[1] M. C. Jung, H. J. Shin, K. Kim, J. S. Noh, and J. Chung, "High-resolution x-ray photoelectron spectroscopy on oxygen-free amorphous $Ge_2Sb_2Te_5$", Appl. Phys. Lett. 89, 043503 (2006).

[2] Min-Cherl Jung, Ki-Hong Kim, Young-Mi Lee, Jae-Hyeon Eom, Jino Im, Young-Gui Yoon, Jisoon Ihm, S. A. Song, Hong-Sik Jeong, and Hyun-Joon Shin, "Chemical state and atomic structure of $Ge_2Sb_2Te_5$ system for nonvolatile phase-change random access memory", J. Appl. Phys. 104, 074911 (2008).
[3] M.-C. Jung, Y. M. Lee, H.-D. Kim, M. G. Kim, and H. J. Shin, K. H. Kim, S. A. Song, H. S. Jeong, C. H. Ko, and M. Han, "Ge nitride formation in N-doped amorphous $Ge_2Sb_2Te_5$", Appl. Phys. Lett. 91, 083514 (2007).
[4] Zhimei Sun, Jian Zhou, Hyun-Joon Shin, Andreas Blomqvist, and Rajeev Ahuja, "Stable nitride complex and molecular nitrogen in N doped amorphous $Ge_2Sb_2Te_5$", Appl. Phys. Lett. 93, 241908 (2008).
[5] Kihong Kim, Ju-Chul Park, Jae-Gwan Chung, and Se Ahn Song, Min-Cherl Jung, Young Mi Lee, Hyun-Joon Shin, Bongjin Kuh, Yongho Ha, Jin-Seo Noh, "Observation of molecular nitrogen in N-doped $Ge_2Sb_2Te_5$", Appl. Phys. Lett. 89, 243520 (2006).

EMP-P3-03
Ultrasound influence on the Si-SiO2 system defects structure

T05 Electronic Materials and Processes

#EMP-P3-03

D. Kropman [1], T. Kärner [2], E. Daukšta [3].

[1]Tallinn University of Technology - Tallinn (Estonia), [2]Tartu University - Tartu (Estonia), [3]Riga Technical University - Riga (Latvia).

The effect of ultrasonic treatment (UST) on the defect structure of the Si–SiO2 system by means of electron spin resonance (ESR), metallography, MOS capacitance technique and secondary ions mass-spectroscopy is presented. The non-monotonous dependence of the point defect densities on the US wave intensity has been observed. The US frequency influence on the ESR signal intensity of the defect centres depended on the defects type and may be caused by vibrational energy dissipation which are a function of defect centre's type. The density of point defects and absorbed impurities at the Si–SiO2 interface can be reduced by appropriate choise of UST.

UST influence on the PD density (Fig. 1) shows the ESR spectra before and after UST. Before UST a signal with g=1.9996 (Pa centers) connected with vacancy complexes is observed. After UST appears another signal with g=2.0055 (broken bonds of Si atoms).

Investigation of the dependence of the spin density on the US frequency of the UST in Si-SiO2 samples with [lll] and [100] crystallographic orientation was carried out. It has been shown that the influence of the US frequency and the sample orientation on the ESR signal intensity varies for different centres. The frequency and orientation dependence of the ESR signal with g=l.9996 and the lack of this dependence for the centres with g=2.0055 show that the vibrational energy dissipation depend on the type of defect centres and their orientation.

Defect density grows with an increase of the US intensity or changes nonmonotonously depending on the oxides thickness (Fig 2.)

In the samples with thick oxide there is a maximum in the dependence of the life time on the US wave amplitude in samples with thick oxides and in the samples with thin oxides-a minimum. This shows that the structural defects form electrically active centres and their density can be varied by UST.

Fig.1. ESR spectra of the Si samples before (1) and after UST treatment (2).

Fig.2. Dependence of the density of sructural defects at the Si-SiO2 interface on the US wave amplitude. SiO2 film thickness 0.4 (1) and 0.7 (2) μm.

EMP-2-Or-2
Soft-X-Ray ARPES at Swiss Light Source: Electronic Structure of 3-Dimensional Systems and Buried Heterostructures

T05 Electronic Materials and Processes

#EMP-2-Or-2

V. Strocov [1], M. Shi [1], M. Kobayashi [2], C. Monney [2], X. Wang [2], J. Krempasky [2], T. Schmitt [2], L. Patthey [2], H. Berger [3], P. Blaha [4].

[1]Swiss Light Source, Paul Scherrer Institute - Villigen (Switzerland), [2]Swiss Light Source, Paul Scherrer Institute; - Villigen (Switzerland), [3]Institut de Physique de la Matière Complexe, EPFL - Lausanne (Switzerland), [4]Institut für Materialchemie, TU Wien - Wien (Austria).

A fundamental benefit of pushing ARPES into the soft-X-ray energy range is the increasing photoelectron escape depth λ. This boosts the bulk sensitivity as well as enables access to buried heterostructures. Furthermore, by the Heisenberg uncertainty principle, the increase of λ improves intrinsic resolution in surface-perpendicular momentum Δk_z. Combined with free-electron final states and atomic-like matrix elements, this enables exploration of the electronic structure 3-dimensional (3D) systems.

The soft-X-ray ARPES (SX-ARPES) facility at Swiss Light Source is installed at the ADRESS beamline [1] which delivers soft-X-ray radiation with variable polarizations in a photon energy range from 300 to 1600 eV. High photon flux topping up 10^{13} photons/s/0.01%BW at 1 keV combined with small spot size and grazing X-ray incidence have allowed breakthrough of the notorious problem of small valence band crossection in the soft-X-ray range. At energies around 900 eV, ARPES images are routinely acquired within 5 min at a combined energy resolution of 110 meV, and within 30 min at resolution of 60 meV.

We unfold on the pilot application of SX-ARPES to explore 3D band structure and Fermi surface (FS) of the paradigm transition metal dichalcogenide VSe_2 [2]. Unprecedented clarity of the experimental electronic structure illustrated in Fig. 1

demonstrates the 3D momentum definition achieved in the soft-X-ray energy range. Investigation of the experimental FS supported by autocorrelation analysis has revealed that the exotic 3D charge density waves in VSe_2 have their precursor in pronounced 3D nesting of the FS due to its out-of-plane warping. Other applications include polarization dependence and alternating FS shapes in pnictide HTSCs, demonstrating intra-cell interference effects; resonant spectroscopy Mn magnetic impurities in GaMnAs, revealing the energy position of the ferromagnetic impurity band and its hybridization with the 3D host GaAs bands, etc. Finally, we flash through the most important results achieved by external users, including topological surface state embedded in 3D valence band of $PbBi_4Te_7$; FS and depth localization of 2D electron gas in $LaAlO_3/SrTiO_3$ hererostructures; standing X-ray waves excited ARPES of multilayer heterostructures; etc. These unfolding results demonstrate an immense potential of SX-ARPES to deliver a clear view of the electronic structure of 3D systems and buried heterostructures.

[1] V.N. Strocov et al, J. Synchrotron Rad. **17**, 631 (2010)
[2] V.N. Strocov et al, Phys. Rev. Lett. **109**, 086401 (2012)

Experimental soft-X-ray ARPES Fermi surface of VSe_2 compared with GGA-DFT calculations.

EMP-P3-04
Air-Stable Organic Solar Cells with Ag/Pentacene Anode Buffer Layer

T05 Electronic Materials and Processes

#EMP-P3-04

K. Harafuji, Y. Omoto.

Department of Electrical and Electronic Engineering, Ritsumeikan University - Kusatsu, Shiga (Japan).

The effect of anode buffer layer on device performances is studied experimentally in small-molecule organic solar cells (OSCs). A proposed OSC (Device A) has the layered structure of indium-tin oxide (ITO, 14.5 nm, anode) on the glass substrate/ thin Ag (0.5 nm)/ pentacene (2 nm)/ copper phthalocyanine (CuPc, 20 nm, donor)/ fullerene (C60, 40 nm, acceptor)/ bathocuproine (BCP, 10 nm, cathode buffer)/ Ag (100 nm, cathode). Here, a combination of thin Ag and pentacene serves as the anode buffer [1, 2]. Following OSCs are also prepared to compare the device performance: (1) Device B with Ag anode buffer, (2) Device C with pentacene anode buffer, and (3) Device D without anode buffer.

Organic materials are evaporated on the ITO substrates at the rate of 0.5 Å/s, under a pressure of less than 1.0×10^{-3} Pa. The deposition rate is monitored by an oscillation quartz microbalance. All the devices are illuminated through the transparent ITO electrode. The photovoltaic current density-voltage (J-V) measurements are carried out in air at room temperature without any encapsulation. Xenon lamp illumination at an intensity of 100 mW/cm^2 is performed, and an air mass 1.5 global (AM1.5G) spectrum is obtained using a solar simulator. Repeated J-V measurement of 30 cycles is made. Here, the one cycle is composed of 3-second illumination and 27-second interval without illumination. The J-V measurement is made during the 3-second illumination.

Figure 1 shows the experimental result of normalized power conversion efficiency η as a function of the illumination cycle. It can be seen that efficiencies for Devices C and D are decreased greatly, whereas those for Devices A and B almost keep their initial values even after the 30th illumination. The S-shaped kink which indicates the device degradation appears in the J-V curves for Devices C and D as the illumination cycle proceeds. The decrease in η is dominated by the decrease in the fill factor of the J-V curve. Initial η for Devices A, B, C and D are 1.03, 0.71, 1.15 and 0.97%, respectively.

In summary, the thin Ag layer as an anode buffer plays an important role to protect

the device degradation. The thin pentacene layer as an anode buffer brings about the slight increase in η. The OSC with the anode buffer composed of the two thin layers is a promising candidate for OSCs with high η and long life time. The improvement is considered to be due to the hole-photocurrent multiplication originated from trapped electrons in the vicinity of the Ag /pentacene interface [2].

[1] T. Oida, T. Naito, Y. Miyagawa, M. Sasaki, and K. Harafuji: Jpn. J. Appl. Phys. **50** (2011) 081601.
[2] T. Oida and K. Harafuji: Jpn. J. Appl. Phys. **52** (2013) 011601.

Fig.1 Normalized power conversion efficiency η as a function of the illumination cycle.

EMP-2-Or-3
UV Raman and Multiwavelength Photoluminescence Characterization of Ultra-Shallow Implanted Junctions

T05 Electronic Materials and Processes

#EMP-2-Or-3

W. Yoo [1], T. Ishigaki [1], T. Ueda [1], K. Kang [1], N. Hasuike [2], H. Harima [2], M. Yoshimoto [2].

[1]WaferMasters, Inc. - San Jose (United states), [2]Kyoto Institute of Technology - Kyoto (Japan).

For monitoring as-implanted dose and depth profiles, Therma-Probe and SIMS have been widely used. Retained dose and dopant depth profiles are routinely monitored after dopant activation anneal. Sheet resistance measurements of activated implant layers are made using four point probes (FPP) to quantify electrical activation. For ultra-shallow junction (USJ) characterization, micro FPP are frequently used for improved spatial resolution and junction punch-through prevention. Rutherford backscattering spectroscopy (RBS) and transmission electron microscopy (TEM) are often used as complementary crystal quality and defect characterization techniques.[1,2]

Conventional characterization techniques require either physical contact or time consuming destructive sample preparation. Development of suitable non-contact, non-destructive, comprehensive subsurface, in-line characterization techniques are strongly desired for fast feedback of implanted USJ characterization results. Preliminary Raman and room temperature photoluminescence (RTPL) characterization of implanted Si has been demonstrated.[3,4]

In this paper, UV Raman spectroscopy and multiwavelength RTPL are used for characterizing B^+ (1 keV $1.0x10^{15}cm^{-2}$) implanted p^+/n USJs, These measurements are then contrasted with sheet resistance (Rs) measurement and SIMS analysis, before and after rapid thermal annealing (RTA) in N_2. The RTA temperature and residence time ranges were 850~1050^oC and 35~140s, respectively. UV Raman characteristics, NIR RTPL intensities and junction depth of USJs showed very strong correlation with Rs. UV Raman and RTPL spectroscopy show promise as non-contact, in-line dopant activation characterization techniques.

1. D.K. Schroder, Semiconductor Material and Device Characterization (John Wiley & Sons, 2006).
2. R.B. Fair, Rapid Thermal Processing Science and Technology (Academic Press, Boston 1993).
3. M. Yoshimoto, H. Nishigaki, H. Harima, T. Isshiki, K. Kang and W.S. Yoo, J. Electrochem. Soc. 153 (2006) G697.
4. S. Takashima, M. Yoshimoto and W.S. Yoo, ECS Transactions, 19 (1) (2009) p. 147.

EMP-1-Or-3
Improvement of device performance by optimizing the Li/F8BT interface structures

T05 Electronic Materials and Processes

#EMP-1-Or-3

X. Feng [1], X. Li [2], H. Ju [1], J. Guo [3], Y. Luo [2], J. Zhu [1].

[1]University of Science and Technology of China - Hefei (China), [2]Department of Theoretical Chemistry and Biology, School of Biotechnology, Royal Institute of Technology - Stockholm (Sweden), [3]Advanced Light Source, Lawrence Berkeley National Laboratory - Berkeley (United states).

Interfaces between metals and conjugated polymers are important for the design of optoelectronic and electronic devices.[1,2] In this study, interface formation between Li and F8BT at 300 K was investigated by XPS, UPS and NEXAFS. With increasing Li thickness, a downward band bending is induced, resulting in a 1.4 eV reduction of electron injection barrier from Li to F8BT. Simultaneously, XPS and DFT calculation results indicate that Li react preferentially with S atoms whereas mildly with N atoms of F8BT. According to the evolution of UPS spectra, a significant decrease of interface work function is observed. Interestingly, after 2 nm Li absorbed on F8BT, an increase of the work function was found, implying the appearance of local electric field at the Li/F8BT interface. From the study on F8BT based light-emitting diode, this upward electric field is considered to improve the efficiency of the devices. Summarizing the XPS, UPS and NEXAFS results, the Li/F8BT interface model at 300 K is derived.

In comparison, the XPS and UPS evolution of Li/F8BT interface at 90 K indicate that the diffusion effects and chemical reactions are reduced. In addition, no S segregation or upward electric field is observed. Moreover, a downward interface dipole and the binding energy shift differences between C 1s, N 1s and S 2p are observed. No gap states appears at Li/F8BT interface, implying the possibility of improving device performance by building a "sharp" interface.

In the other hand, we developed a new method to get clean graphene/polymer interface without using PMMA or thermal release tape. NEXAFS and SRPES results

show that both the diffusion of metal atoms and the chemical reactions between metals and polymers can be reduced by a single layer graphene.

[1] Zhu, J.F., et al., JACS, 2009. 131(37): p. 13498-13507

[2] Feng, X.F., et al., Org. Electron., 2012. 13: p. 1060-1067

Figure 1. Energy level alignment of Li/F8BT interface at 300 K (left) and 90 K (right).

Figure 2. Schematic illustration of the transfer processes for getting graphene/polymer interface

EMP-2-Or-4
SiC Nanophotonic SiC multilayer filters for Bridging the Visible Spectrum to the Telecom Gap

T05 Electronic Materials and Processes

#EMP-2-Or-4

M.A. Vieira [1], V. Silva [1], P. Louro [2], M. Vieira [2].

[1]DEETC-ISEL - Lisbon (Portugal), [2]CTS-UNINOVA - Lisbon (Portugal).

Expanding far beyond traditional applications in optical interconnects at telecommunications wavelengths, the SiC nanophotonic integrated circuit platform has recently proven its merits for working with visible range optical signals. These systems are capable of addressing applications including industrial process, medical diagnostics, and free-space communication. Reconfigurable wavelength selectors that allow for operation on a large number of wavelength channels, with dynamic response, are essential sub-systems for implementing reconfigurable WDM networks and optical signal processing.
In this paper we demonstrate an add/drop filter based on SiC technology. Tailoring of the channel bandwidth and wavelength is experimentally demonstrated. The concept is extended to implement a 1 by 4 wavelength division multiplexer with channel separation in the visible range.
Experimental optoelectronic characterization of the fabricated devices is presented , Fig.1, and shows the feasibility of tailoring channel bandwidth and wavelength. The device consists of a p-i'(a-SiC:H)-n/p-i(a-Si:H)-n heterostructure with low conductivity doped layers [1]. Several monochromatic pulsed lights, separately (input channels) or in a polychromatic mixture (multiplexed signal) at bit rates between 500 bps and 12000 bps illuminated the device. Independent tuning of each channel is performed by steady state violet optical bias superimposed either from the front and back sides of the add/drop filter. Results show that, front background enhance the light-to-dark sensitivity of the long and medium wavelength channels and quench strongly the others. Back violet background has the opposite behavior; it enhances channel magnitude in short wavelength range and reduces it in the long ones. This nonlinearity provides the possibility for selective removal or addition of wavelengths. It provides a low-cost solution to many aspects of optical and optoelectronic interconnection technologies and architectures according to their suitability of use in optical cross connections (OXCs), switches and routers.

Results show that the WDM demonstrated here is ideally suited for inter-chip level communications since it is implemented on a SiC platform. The large interference suppression also ensures minimal crosstalk between adjacent WDM channels. An optoeletronic model gives insight on the system physics. A numerical simulation, having as input parameters the experimental data, is presented and explains the light filtering properties of the add/drop filter, under different electrical and optical bias conditions.

[1] M. Vieira, et all Advances in Photodiodes, InTech, Chap.19, pp:403-425 (2011)

EMP-P3-18
Hydrogen gas sensor based on metal insulator semiconductor fabricated with nanostructured porous silicon.

T05 Electronic Materials and Processes

#EMP-P3-18

H. Seba.

USTHB - Algiers (Algeria).

As a colourless,odourless flammable gas hydrogen cannot be detected by human senses,and other means are therefore required to detect its presence and quantify the concentration.Rapid and accurate hydrogen gas concentration measurement is essential to alert to the formation of potentially explosive mixtures with air.However, there is a continued need for faster, more accurate and more selective detection of hydrogen gas in various areas of industry for monitoring and controlling hydrogen concentration.Alternative hydrogen detection methods employ instruments such as gas chromatographs, mass spectrometers.These instruments are relatively large,expensive, high maintenance and slow in terms of their sampling and reaction times.Hydrogen sensors are transducer devices that detect hydrogen gas molecules and produce an electrical signal with a magnitude proportional to the hydrogen gas concentration.Hydrogen sensors have several advantages over the conventional hydrogen detection methods mentioned above, including their lower cost, smaller size and faster response.These advantages make them more suitable for portable and in situ hydrogen detection in a range of applications.Porous silicon (PS) can be used as an alternative material for hydrogen sensor, operating at relatively lower temperature including the room temperature.The interest in this material is mainly due to its extremely high surface to volume ratio, the ease of its formation and the compatibility with the silicon IC technology.This communication reports on the development of the hydrogen sensor based on the metal oxide semiconductors ($Ag/Sio_2/PSi/c-Si$) structure.The effect of porous silicon porosity on the I-V characteristics and the effect of hydrogen gas on the electrical proprieties (C-V characteristics) of a porous silicon sample are studied.The nano-porous layers for different porosities were prepared from p-type monocrystalline silicon (100) wafer of the resistivity (20–50 ohm.cm) by electrochemical etching in a solution of a hydrofluoric acid HF (48%) ethanol (99.9%) of 1:1 (by volume) and current density are varied from 10 to100 mA/cm2 for 15 minutes.After etching, the samples were

rinsed with deionised water and dried in air at room-temperature.The as prepared samples are annealed at the temperature of 150°C in oxygen atmosphere ender vacuum (10^{-3} torr) in order to replace the unstable Si-H_x by stable Si-O bonds. Silver was thermally evaporated ender vacuum (10^{-5} torr) for ohmic contact at the bottom of p-silicon surface and the metal-insulator-semiconductor MIS structure are formed by evaporation of Ag on the top of samples.Porous silicon layer morphology was observed by a Phillips X 30 scanning electron microscope (SEM).I-V measurements were carried out in a vacuum cryostat using a high precision Keithley 617 programmable electrometer.For C-V measurements the sensor was placed in a stainless-steel vacuum chamber kept at room temperature and connected by a valve gas bottles containing hydrogen this measurements were performed using an Hp 4192A LF impedance analyzer 5HZ-13Mhz. I-V measurements show an increase of the current values when the porosity of the layers increases.The characterisation of the sensor is undertaken at 1 MHz. We have found that the values of capacitance versus bias voltage (C–V) changes proportional to the hydrogen gas concentration.

EMP-P3-15
Nickel nano-particle synthesis by reactive RF thermal plasma

T05 Electronic Materials and Processes

#EMP-P3-15

H. Choi [1], H. Na [1], D. Kim [2], W. Lee [1].

[1]Rare Metal R&D Group, Korea Institute of Industrial Technology (KITECH) - Incheon (Korea, republic of), [2]Green Transformation Technology Center, Korea Institute of Industrial Technology (KITECH) - Daegu (Korea, republic of).

Metallic nano-particles have been extensively studied to utilize their superior electrical/thermal conductivity and size dependent properties for printable electronic components manufacturing. Nickel nano-particle is a representative example for multi-layered ceramic capacitor fabrication or magnetic applications. A complementary synthesis method needs to be developed to be compatible to size reduction and purity of Ni particle though most of Ni nano-particles have been synthesized by liquid base processes. In the present study, RF thermal plasma synthesis of Ni nano-particle was conducted and mass feeding rate of feedstock was considered as regards size manipulation.
Nickel hydroxide micro-powder was chosen for solid feedstock because of its favorable thermo-physical properties. Feedstock powder was fed into argon-hydrogen thermal plasma with mass feeding rate increasing at 1, 5 and 20 g·min-1. After the process, as-synthesized particles were characterized.
As-synthesized nano-particle characteristics are shown in Fig. 1. Through the argon-hydrogen thermal plasma, β-Ni(OH)2 micro-particle is fully transformed to γ-Ni nano-particle via dehydration, vaporization, reduction, and condensation reaction. Considering sluggish heterogeneous reduction and bulk vaporization, vaporization rate may be faster than solid state reduction during the rapid heating reaction. Cooling vapor reaches a critical super-saturation state above which condensing matter is stably growing. Figure 1 (f) shows that mean particle size is increased as feed-rate increases. Within the scope of this study, most feedstock was vaporized regardless of mass feed-rate. Therefore, concentration of Ni gaseous species increases with mass feeding rate increasing. It results in the high temperature shift for starting condensation. Coalescence rate is increased as colliding particle temperature is higher. Accordingly, coarser nano-spheres are frequently observed as mass feeding rate increases.

Acknowledgement
The authors appreciate the financial support from ""ISTK Convergence Research Project" of MKE (Ministry of Knowledge Economy) and ISTK (Korea Research Council for Industrial Science and Technology) of Republic of Korea.

[1] HUANG Guo-yong, et al/Trans. Nonferrous Met. Soc. China 19(2009) 389−393
[2] L. Bai et al. / Journal of Alloys and Compounds 481 (2009) 563–567
[3] Y. Cheng et al. / Chemical Engineering Journal 183 (2012) 483– 491

Figure 1. Characteristics of as-synthesized nickel nano-particles according to mass feeding rate in RF thermal plasma synthesis

EMP-P3-16
W-Cu thick film fabrication for thermal management

T05 Electronic Materials and Processes

#EMP-P3-16

H. Na [1], C. Lim [1], D. Kim [2], Y. Kim [3], W. Lee [4], C. Han [1], H. Choi [1].

[1]Rare Metal R&D Group, Korea Institute of Industrial Technology (KITECH) - Incheon (Korea, republic of), [2]Green Transformation Technology Center, Korea Institute of Industrial Technology (KITECH) - Daegu (Korea, republic of), [3]Advanced Welding & Joining R&D Group, Korea Institute of Industrial Technology (KITECH) - Incheon (Korea, republic of), [4]Advanced Fusion Process R&D Group, Korea Institute of Industrial Technology (KITECH) - Incheon (Korea, republic of).

W and Cu composite materials are used for thermal and electrical managements of electronic components owing to their high thermal/electrical conductivity and compatible thermal expansion coefficient to ceramic materials. While W-Cu composites are generally fabricated as bulk materials, thick film is deposited on alumina substrate by screen printing and sintering process in this study. To do this, W-Cu nano-particle was prepared by feeding a blended feedstock of tungsten trioxide micro-powder and cupric oxide micro-powder into argon-hydrogen thermal plasma. RF thermal plasma synthesis of nano-particle belongs to vapor phase condensation technology. Nano-particle is synthesized by condensation from cooling vaporized species. The weight fraction of cupric oxide is 20 wt.%. Using the synthesized nano-powder, paste for printing was prepared and thick film was deposited as shown in Figure. W-Cu composite nano-particle is composed of α-W, β-W, and Cu phase and nano-cube and nano-sphere are observed. Overall chemical composition was relatively consistent to the target chemistry. As-printed thick film was dried and binder was burned out before sintering. The pre-treated thick film was sintered at 1,000 ℃, 1,200 ℃, 1,300 ℃, and 1,400 ℃ in a reducing environment. According to the sintering temperature, morphological changes and phase evolution were investigated by x-ray diffractometry and scanning electron microscopy. Furthermore, transmission electron microscopy was conducted for specimens that were sampled by focused ion beam method in order to verify interfacial features between tungsten and copper and between film and substrate.

Acknowledgement
The authors appreciate the financial support from ""ISTK Convergence Research Project" of MKE (Ministry of Knowledge Economy) and ISTK (Korea Research Council for Industrial Science and Technology) of Republic of Korea.

[1] D. Gu, Y. Shen / Materials Science and Engineering A 489 (2008) 169–177
[2] Y. Li et al. / International Journal of Refractory Metals & Hard Materials 21 (2003) 259–264
[3] P.K. Sahoo et al. / Int. Journal of Refractory Metals and Hard Materials 29 (2011) 547–554

Figure 1. Characteristics of W-Cu composite nano-particle and as-printed thick film

EMP-1-Or-4
Hybrid inorganic-organic systems: metal nanoparticles (Au, Al and Ag) self-assembled in a wide-gap organic semiconductor matrix

T05 Electronic Materials and Processes

#EMP-1-Or-4

O. Molodtsova [1], I. Aristova [2], O. Vilkov [3], A. Pietzsch [4], M. Tchaplyguine [4], C. Laubschat [5], M. Knupfer [6], V. Kveder [2], V. Aristov [2].

[1]HASYLAB at DESY - D-22607 Hamburg (Germany), [2]Russian Acad. Sci, ISSP - Chernogolovka 142432 (Russian federation), [3]Helmholtz-Zentrum Berlin für Materialien und Energie, BESSY II - D-12489 Berlin (Germany), [4]Lund Univ, MAX-lab - S-22100 Lund (Sweden), [5]IFP, TU Dresden - D-01069 Dresden (Germany), [6]IFW Dresden, Postfach 270116 - D-01171 Dresden (Germany).

Materials with a high on-off resistance ratio could become the basis for resistive random-access memory (RRAM). Such a “storage class memory” would revolutionize the information technology industry as outlined in [1-3]. One type of RRAM can be based on hybrid organic–inorganic systems, mainly consisting of inorganic nanoparticles (NP) blended into an organic matrix. The evolution of the morphology and the electronic properties of the hybrid organic-inorganic systems composed of Al, Ag and Au nanoparticles (NP’s) distributed in an organic matrix, copper phthalocyanine (CuPc), as a function of nominal metal content was studied by transmission electron microscopy and by surface- and bulk sensitive photoelectron spectroscopy. Gold atoms deposited onto the CuPc surface diffuse into the organic matrix and self-assemble to NP’s [4]. There is no formation of a continuous metallic Au film on top of the CuPc film up to large nominal coverages of about 130 Å. Gold atoms are assembled to well defined NP’s with metallic properties. Strong difference in morphology and electronic properties were observed for aluminum nanoparticles formation. E.g., on the very first stage of aluminum deposition, aluminum atoms show strong chemical interaction with substrate atoms. The properties of the nano-composite thin-film are supposed to be significantly dependent on their microstructure, i.e. the size, concentration, bulk- and size-distribution of

nanoparticles.
This work supported by the RFBR grant № 13-02-00818.

[1] J. C. Scott and L.D. Bozano, Adv. Mater. 19, 1452 (2007)
[2] A. C. Dürr, et al, Phys. Rev. B 68, 115428 (2003)
[3] L. Lozzi, S. Santucci, S. La Rosa, J. Vac. Sci. Technol. A 22, 1477 (2004)
[4] V.Yu. Aristov, O.V. Molodtsova, C. Laubschat, V.M. Zhilin, I.M. Aristova , V.V. Kveder, and M. Knupfer, Appl. Phys. Lett. 97, 113103 (2010)

Fig. Microstructure of nanocomposite thin films composed of silver nano-particles embedded in CuPc matrix (HR-TEM). a) -b) nominal Ag deposition 5.7 nm. Magnifications are indicated by insert marks.

EMP-1-Or-5
Study of rectifying mechanism on organic double-layer diode by electric field induced optical second harmonic generation

T05 Electronic Materials and Processes

#EMP-1-Or-5

E. Lim [1], D. Taguchi [2], M. Iwamoto [2].

[1]Dankook University - Yongin-Si (Korea, republic of), [2]Tokyo Institute of Technology - Tokyo (Japan).

By using electric field induced optical second harmonic generation (EFISHG) is a method that allows electric field distributions in organic semiconductor devices to be directly probed. In this study, by using this system, we studied the rectifying property of organic double-layer diodes with a structure of indium-tin-oxide/polyimide/6,13-Bis(triisopropylsilylethynyl)-pentacene/gold (ITO/PI/TIPS-pentacene/Au). Before and after stress biasing the diodes, we measured the current-voltage and capacitance-voltage characteristics, and then the EFISHGs at various pulse voltages. Based on electrical measurements, these are difficult to discuss the physical meaning of these characteristics without knowledge of the electric field distributions in the diodes. However, results of EFISHG measurements probe the change of electric fields in the TIPS-pentacene layer. We can discuss the rectifying mechanism of organic double-layer diodes of electrode charging, carrier injection and carrier transport. These were well traced with time, depending on the d.c. biasing applied to the diodes. Accordingly the electric field distributions in the ITO/PI/TIPS-pentacene/Au diodes with accumulated charges at the PI/TIPS-pentacene interface were allowed to be determined. Analyzing the carrier behavior in ITO/PI/TIPS-pentacene/Au on the basis of the Maxwell-Wagner model, we discussed the rectifying property of the organic-double layer diodes in terms of d.c biasing effect, i.e., threshold voltage shift, and concluded that space charge limited current fllowing across the PI layer governs the rectification of the diodes. Using the EFISHG measurement is an effective way to study the rectifying property of organic double-layer diodes.

EMP-P3-05
Structural and electrical characteristics of Ni/Lu2O3/TaN capacitors for analog IC applications

T05 Electronic Materials and Processes

#EMP-P3-05

C. Chuch, S. Mondal, T.M. Pan.

Chang Gung University - Taoyuan (Taiwan, republic of china).

Following the downscaling of the component size, a high density metal-insulator-metal (MIM) capacitors are needed for analog, radio-frequency, and mixed signal applications [1]. In addition, a small value of voltage coefficient of capacitance (VCC) is also required for this high precision semiconductor microelectronic circuit. Several high-k dielectrics, such as Sm_2O_3 [2], HfO_2 [3], and TiO_2 [4], have already been investigated to serve this goal. Unfortunately, increasing the k value usually decreases the conduction-band offset to the metal electrode, which arises problems of poor thermal leakage current, high VCC, and hence reliability issue. In Fig. 1, no Lu_2O_3 peak was found in the XRD patterns, suggesting that thin Lu_2O_3 film is amorphous. The insets of Figs. 1 show the core level O 1s and Lu $4d_{5/2}$ spectra with their appropriate peak curve-fitting lines of Lu_2O_3 thin film. Fig. 2 shows the capacitance–voltage (C–V) and current density-voltage (J–V) characteristics of the Ni/Lu_2O_3/TaN capacitors for different Lu_2O_3 film thicknesses. The k value of Lu_2O_3 dielectric was estimated to be ~12.8.The Ni/Lu_2O_3/TaN device for a 15 nm Lu_2O_3 film exhibits better electrical characteristics including a high capacitance density of 7.5 fF/μm^2 and a low leakage current density of 5×10^{-8} A/cm^2 at −1 V.

[1] K. C. Chiang, C. H. Cheng, H. C. Pan, C. N. Hsiao, C. P. Chou, A. Chin, H. L. Hwang, IEEE Electron Device Lett. 28 (2007) 235.

[2] J. J. Yang, J. D. Chen, R. Wise, P. Steinmann, Y. C. Yeo, C. Zhu, IEEE Electron Device Lett. 30 (2009)1033.

[3] X. F. Yu, C. X. Zhu, H. Hu, A. Chin, M. F. Li, B. J. Cho, E. L. Kwong, P. D. Foo, M. B. Yu, IEEE Electron Device Lett 24 (2003) 63.

[4] J. H. Lee, Y. C. Lin, B. H. Chen, IEEE Trans. Electron Devices 58 (2011) 672.

Fig. 1. XRD spectra of Lu_2O_3 dielectric on TaN electrode for three different dielectric thicknesses. Insets: XPS spectra of the corresponding (a) O 1s and (b) Lu 4d energy levels of the Lu_2O_3 dielectric annealed at 400 ˚C.

Fig. 2. C-V and J-V characteristics of Ni/Lu_2O_3/TaN capacitors for different Lu_2O_3 film thicknesses. Inset shows schematic of Ni/Lu_2O_3/TaN MIM device.

EMP-P3-06
Annealing of Cr/Au metallizations on p-GaN

T05 Electronic Materials and Processes

#EMP-P3-06

L. Dobos [1], B. Pécz [1], L. Tóth [1], Z.J. Horváth [2], Z.E. Horváth [1], A.L. Tóth [1], M.A. Poisson [3].

[1]Institute for Technical Physics and Materials Science, Research Centre for Natural Sciences, Hungarian Academy of Sciences, H-1525, Budapest, P.O.B. 49 - Budapest (Hungary), [2]Obuda University, Kando Kalman Faculty Electrical Engineering, Institute of Microelectronics and Technology, 1084 Budapest, Tavaszmező u. 15-17. - Budapest (Hungary), [3]Alcatel-Thales III-V lab, Domaine de Corbeville, Orsay, 91404, France - Paris (France).

In this study, we report on the microstructural, morphological and electrical properties of (50 nm)Cr/Au(100 nm) contacts to p-GaN by electron microscopy, X-ray analysis and I-V measurements. Tested contacts were annealed at the temperature of 400, 600, 700 and 900 °C for 10 min in vacuum.
As shown by TEM studies the interface of the as-deposited sample is laterally homogeneous and sharp. 600 °C was the temperature at which we first observed large, but shallow grains grown into the GaN parallel to the interface. EDS analysis confirms the presence of a Cr-rich phase containing also a little amount of Au (twice more Cr than Au) in the ingrowth. Our analysis revealed that Cr and Au diffused into the p-GaN layer. After further annealing at 700 °C numerous grains had grown in the GaN. Crystalline grains developed in the ingrowths, revealed by dark field (DF) images. XTEM investigations of the p-GaN/Cr/Au contact revealed that some new crystalline phases developed in the mixed metal layers at 900 °C.
The surface showed a near featureless morphology up 600 °C, revealed by FESEM. The metal layer began to blister off and ball up during the heat treatment at 600 °C. Tiny grains (AuGa) – contained mainly Au and Ga – have arosen on the surface at 900 °C revealed by FESEM-EDS. Furthermore small metal free holes and voids have formed on the surface as well.
In the XRD plot of the sample annealed at 600 °C in addition to the peaks which were observed in the as-deposited and 400 °C annealed sample, there are little extra peaks which indicate the formation of new interfacial phases. These phases are identified as CrN phases. The first intermetallic phases were observed after

annealing at 600 °C, only. These CrN extra peaks became much bigger at 700 °C. Au7Ga2 phases appeared at 900 °C. The appearance of the Au7Ga2 phase is an indication that Au diffused to the GaN and reacted with it.
The as-deposited and heated up to 700 °C Cr/Au contacts on p-GaN exhibited nonlinear behaviour. Annealing at 900 °C degraded the electrical behaviour. Au metal layer is resistant to oxidation. However, diffusion of Au to the contact/nitride interface resulted in a degraded contact.
Previously examined as-deposited and annealed Cr/Au contacts on n-type GaN are rectifying up to 600 °C. After heat treatment in vacuum at 700 °C and 900 °C the Cr/Au contacts were linear. It is interesting, that in the case of Cr/Au contacts to n-type GaN the formation of CrN phase was not observed upon annealing.
The electrical properties of the contacts can be correlated to the solid phase reactions between the components.
This work was supported by Hungarian National Scientific Foundation (OTKA) through Grants K77331 and K75735.

NST-2-Or-11
Effects of Bi doping on the multi-phase changing properties of InSbTe

T05 Electronic Materials and Processes

#NST-2-Or-11

M. Choi [1], J. Ahn [1], Y.T. Kim [2].

[1]Hanyang University - Seoul (Korea, republic of), [2]Korea Institute of Science and Technology - Seoul (Korea, republic of).

Phase change materials based on chalcogenide such as GST, GeTe, SbTe, and InSbTe have been extensively investigated for phase-change random access memory(PRAM). Among various chalcogenides, we have been investigated the InSbTe alloys as a most promising candidate for multi-level cell (MLC)[1]. According to our previous results, the InSbTe (IST) is more stable than the GST that is known as the best material for PRAM because the IST has high crystallization temperature (Tx) and activation energy (Ea). In this work, we have tried to improve the multi-phase changing properties of IST by doping Bi atom in the IST. The Bi doped IST shows 4 different crystallization temperatures. The Tx on the first crystallization point is lower than the Tx on the same point of the undoped IST, and other phase transformation temperatures become to be lower comparing the undoped IST. With increasing Bi content, the Tx becomes to be more reduced. Moreover, the Ea derived from Kissinger's formula[2] is also reduced along with Tx. We have fabricated PRAM cell devices to confirm the multi-level electrical properties of the Bi-doped IST. The resistance ratio between the amorphous and the crystalline state is more than three orders of magnitude, the Bi doped IST cells perform multi-level operating characteristics and the resistance difference derived from the I-V characteristics seems to be obviously distinguishable owing to the multi-level phase transformations. The threshold voltage (Vth) of the Bi-doped IST cell is clearly lower than that of the undoped IST, which means that the Bi-doped IST PRAM cells might be operated with lower power consumption. To confirm the endurance and reliability of test devices, we have measured the set/reset cycling by nanoscale electrical pulse and the endurance shows more than ~103 cycles. In this work, we will discuss the effects of Bi doping on the atomic structure of IST with high resolution TEM.

[1] Appl. Phys. Lett. 98, 091915 (2011).
[2] H. E. Kissinger, Anal. Chem. 29, 1702 (1957).

<Fig1. DSC measurement of IST>

<Fig2. I-V characteristics of IST>

EMP-P3-07
STRUCTURAL AND ELECTRICAL CHARACTERISATION OF a-Si:H(n)/c-Si(p) HETEROSTRUCTURES PREPARED BY ICP AND PECVD

T05 Electronic Materials and Processes

#EMP-P3-07

J. Kovac [1], M. Mikolášek [1], M. Nemec [1], J. Kovac Jr. [1], A. Vincze [2], S. Lombardo [3], G. Mannino [3], C. Gerardi [4], C. Tringali [4].

[1]Slovak University of Technology - Bratislava (Slovakia), [2]International Laser Centre - Bratislava (Slovakia), [3]CNR-IMM - Catania (Italy), [4]IMS-R&D, ST Microelectronics - Catania (Italy).

The opportunity to achieve high performance has become the motivation for extensive studies of solar cells with amorphous silicon/crystalline silicon (a-Si:H/c-Si) heterojunctions [1]. For outstanding performance, the quality of the a-Si:H/c-Si heterointerface and a-Si:H emitter have to be optimised. This paper focuses on the investigation of a-Si:H(n)/c-Si(p) structures with emitter prepared by ICP and PECVD deposition techniques. Prepared samples were investigated using SIMS, Raman spectroscopy and electrical C-V-F and C–T–ω diagnostic techniques. Results were completed by the dark and light I-V characterization and influence of post-annealing on the solar cell performance. Important information for post-deposition processing and applications in concentrator systems is the influence of the temperature treatment. To inspect this behavior, samples were annealed on the air at various temperatures in the range 160 - 400 °C for 30 minutes for each step and analyzed in term of the structure modification, interface quality and output performances. To get the full profile information about the structures they were analyzed using SIMS instrument (Ion-TOF, SIMS IV) with high-energy Bi+ primary source with combination of low energy Cs+ sputter gun as shown in Fig.1. The capacitance diagnostic results indicated superior heterointerface properties for ICP samples. Measured was also better output performance on these samples. Samples exhibited photovoltaic behavior even after high temperature treatment on the air (Fig. 2).

Acknowledgement
The work have been conducted with the support of the ENIAC JU under grant

agreement n° 270722-2 and from the national programmes/funding authorities of Belgium, Germany, Ireland, Italy, Slovakia, Spain, Netherlands, United Kingdom and Scientific Grant Agency of the Ministry of Education of Slovak Republic VEGA-1/0439/13

[1] M. Zeman, and D. Zhang, Engineering Materials, 0, 13 (2011)

Fig. 1. SIMS profile of AZO/a-Si:H/c-Si structure
Fig.2 Conversion efficiency of annealed solar cell samples.

EMP-1-Or-6
Electronic properties of metal/graphene/n-Silicon interfaces

T05 Electronic Materials and Processes

#EMP-1-Or-6

C. Troadec.

Institute of Materials Research and Engineering - Singapore (Singapore).

Graphene, a zero-band gap semiconductor consisting of a single layer of carbon atoms arranged in a honeycomb lattice, has been described as a “wonder material” for many applications due to its superior electronic properties[1], [2]. Most of the early research on graphene focused on the in-plane properties of graphene and only recently, vertically stacked graphene devices[3] were studied. Electronic properties of graphene are greatly influenced by external contacts and understanding the buried interface of metal/graphene/silicon is essential in the fabrication of graphene devices. We use Ballistic Electron Emission Microscopy (BEEM) [4], a variant of scanning tunnelling microscopy (STM), which is currently the only technique that is capable of measuring the electronic properties of buried interfaces with nanometer spatial resolution [5] to probe and measure the buried interface of metal/multilayer graphene/silicon.

We will present results including current-voltage (I-V) measurements [Fig1] and BEEM measurements of Schottky diodes of the form Metal/n-Si(111) and Metal/multilayer graphene/n-Si(111). By varying the thickness of multilayer graphene, significant differences can be observed in the device characteristics. Dual parameter BEEM[Fig2] measurements [5] is sensitive enough to detect the presence of graphene, unlike I-V. The BEEM spectra and images suggest that although multilayer graphene has a minimal impact on the barrier height, ballistic transmission properties of the device interface was reduced. The effect in the number of graphene layers on the transmission factor will also be presented.

[1] A. K. Geim and K. S. Novoselov, Nature Materials 2007, 6, 183-191
[2] N. O. Weiss, H. Zhou, L. Liao, Y. Liu, S. Jiang, Y. Huang, X. Duan, Advanced Materials 2012, 24, 5782-5825
[3] L. Britnell, R. V. Gorbachev, R. Jalil, B. D. Belle, F. Schedin, A. Mishchenko, T.

Georgiou, M. I. Katsnelson, L. Eaves, S. V. Morozov, N. M. R. Peres, J. Leist, A. K. Geim, K. S. Novoselov, L. A. Ponomarenko, Science 2012, 335, 6071, 947-950
[4] L. D. Bell and W. J. Kaiser, Physical Review Letters 1988, 61, 2368
[5] C. Troadec and K. E. J. Goh, Journal of Vacuum Science and Technology B 2010, 28, C5F1 - C5F4

EMP-P3-17
Impact of Gradual Germanium Profile on Dynamic Characteristics of a SiGe HBT

T05 Electronic Materials and Processes

#EMP-P3-17

M. Lakhdara [1], S. Latreche [1], C. Gontrand [2].

[1]Laboratoire Hyperfréquence & Semi-conducteur (LHS), Département d'Electronique Université,Constantine1, - Constantine (Algeria), [2]INL, Institut des Nanotechnologies de Lyon, INSA- Lyon, - Lyon (France).

In the early 1990s, the use of telecommunication services such as mobile phones and the Internet was marginal. The heterojunction component are well positioned to meet the demand for operating speed and low noise, among these components, the heterojunction bipolar transistor Si/ SiGe/Si [1].
The rate of Ge at the entrance of the base affects the height of the heterojunction, is therefore significantly change the characteristics of static and dynamic component [2]. A high rate of Ge in the base will provide greater value of fT by increasing IC, which in turn helps to increase the base doping to increase fmax[3].
This paper deals the impact of a gradual germanium SiGe HBT in the electrical characteristics of the dynamic characteristics especially the fT and fmax determining the RF performance of the component. The rate of Ge at the entrance of the base has an influence on the bands gap, the intrinsic material density and height of the heterojunction. We present a numerical modeling of an NPN (SiGe) SiGe HBT realized in BiCMOS9G technology industrial: 0.13µm process, taking into account the gradual profile of germanium in the SiGe alloy 10-30%, 15-30%, and 20-30% (figure 1 and 2). We used our device simulator "SIBIDIF ", two dimensional Drift-Diffusion Model (DDM) simulators. It solves the continuity equations for electrons and holes, coupled with the Poisson's equation.

[1] John D. Cressler, Silicon Heterostructure Devices. CRC Press, (2007).
[2] Lacave, and al.« Vertical profile optimization for +400 GHz fMAX Si/SiGe:C HBTs,

Proceedings Bipolar/BiCMOS Circuits and Technology Meeting IEEE, (BCTM), P: 49 - 52, 2010.
[3] S.L. Salmon, J. D. Cressler, R. C. Jaeger, “The Influence of Ge Grading on the Bias and Temperature Characteristics of SiGe HBT’s for Precision Analog Circuits” vol. 47, 2000.

Fig.1 : Evolution of the transition frequency fT (Ge)

Fig.2: Evolution of the maximum oscillation frequency fmax(Ge)

EMP-P3-08
S = 1 and S = 1/2 Kondo effects on atomic chains

T05 Electronic Materials and Processes

#EMP-P3-08

G. Chiappe [1], E.V. Anda [2], L. Costa Ribeiro [3], I. Hamad [2].

[1]Universidad de Alicante - Alicante (Spain), [2]Universidad Catolica do Rio de Janeiro - Rio De Janeiro (Brazil), [3]Centro Federal de Educação Tecnológica Celso Suckow da Fonseca (CEFET-RJ/UnED-NI) - Rio De Janeiro (Brazil).

In this work we investigate the transport and magnetic properties of a system constituted by two quantum dots with a local Coulomb interaction U which are interconnected through a chain of N non-interacting sites and individually coupled to two metallic leads. To perform the task we use two different approaches: the slave boson mean field approximation and a new method which is based on numerical diagonalizations of large clusters, using a multiconfigurational set of states constructed from Hartree Fock orbitals and enlargued properly by iterative application of the full Hamiltonian.

We studied the system in different regions of the parameter space for which we calculate many physical quantities, namely local density of states (LDOS), conductance, total spin and spin correlations.The results reveled a very rich physical scenario which is manifested by at least two types of Kondo regimes, corresponding to s **= 1/2** and s **= 1** respectively. We study the extension of the Kondo cloud in both regimes. Kondo

temperature depends on the parity of N. For odd N it is larger than for an even lenght. We provide an explanation of this fact, observed in recent experiments [1], in terms of a two temperatures Kondo regime.

1] N. Neel, R. Berndt, J. Kroger, T. O. Wehling, A. I. Lichtenstein, M. I. Katsnelson, PRL **107**, 106804 (2011).

EMP-P3-09
Predefined structures in LED surface for modification of radiation characteristics

T05 Electronic Materials and Processes

#EMP-P3-09

J. Skriniarova [1], D. Pudis [2], I. Kubicova [2], A. Kuzma [1], J. Kovac [1], P. Hronec [1], L. Suslik [2].

[1]Inst. of Electronics and Photonics, Slovak University of Technology, Ilkovičova 3 - 812 19 Bratislava (Slovakia), [2]Dept. of Physics, University of Žilina, Univerzitná 1 - 010 08 Zilina (Slovakia).

Effect of periodic structure application on the light emitting diode (LED) surface is well known. Improvement of optical properties of LED such as directionality, far field profile or light extraction efficiency has been already demonstrated by implementation of periodic structures in LED surface [1-4].
The principle of LED light extraction efficiency improvement due to the planar structure introduced in the surface layer is twofold: it is based on the diffraction on the structure roughness [1, 2], or it is due to the photonic band gap effect generated by the structure [3, 4]. Although the effect of periodic structure on the light extraction efficiency is well documented, LEDs with predefined patterning have not been investigated yet. The predefined structure is arbitrary planar pattern prepared in the LED surface; therefore it is not necessarily periodic.
From the diffraction on roughness-based effect it can be suggested, that implementation of predefined planar structure allows local enhancement of light emitting from the LED surface. Application of such structures can be attractive for local enhancement of light from defined areas of the LED surface. Also predefined structure with specific properties is able to modify near- and far-field radiation characteristics [5].
We used optical and ion beam lithography techniques for patterning of the surface of GaAs/AlGaAs based LEDs. The structure was patterned in the upper confinement AlGaAs layer. Surface of the structures was analyzed by employment of scanning electron microscope and atomic force microscope. The overall emission properties of prepared LED with predefined structure in the emitting part were investigated by near- and far-analysis.

Acknowledgments
This work was financially supported by VEGA 1/0439/13.

[1] J. J. Wierer, M. R. Krames, J. E. Epler, N. F. Gardner, M. G. Craford, J. R. Wendt, J. A. Simmons, M. M. Sigalas, InGaN/GaN quantum-well heterostructure light-emitting diodes employing photonic crystal structures, Appl. Phys. Lett. 84 (2004) 3885-3887.
[2] M. L. Hsieh, K. C. Lo, Y. S.Lan, S. Y. Yang, C. H. Lin, H. M. Liu, H. C. Kuo, One-shot exposure for patterning two-dimensional photonic crystals to enhance light extraction of InGaN-based green LEDs, IEEE Photonic. Tech. L. 20 (2008) 141-143.
[3] E. Mattioli, C. Weisbuch, Impact of photonic crystals on LED light extraction efficiency: approaches and limits to vertical structure designs, J. Phys. D: Appl. Phys. 43 (2010) 354005-1 – 354005-22.
[4] M. D. B. Charlton, M. E. Zoorob, T. Lee, Photonic Quasi-Crystal LEDs, Design, modeling, and optimization, Proc. of SPIE6486 (2007) 64860R1-64860R10.
[5] Y. J. Jung, D. Park, S. Koo, S. Yu, N. Park, Metal slit array Fresnel lens for wavelength-scale optical coupling to nanophotonic waveguides, Optics Express 17 (2009) 18852-18857.

EMP-2-Or-6
Elastic and thermodynamics properties of the B2- ErX (X=Cu, Au, Ag, Ir) type rare earth intermetallic compounds from ab-initio calculations.

T05 Electronic Materials and Processes

#EMP-2-Or-6

A. Sekkal [1], A. Benzair [1], G. Merad [1], T. Ouahrani [2].

[1]Laboratoire d'Etude et Prédiction de Matériaux, Unité de Recherche Matériaux et Energies Renouvelables, Département de Physique, faculté des Sciences, Université Abou Bekr Belkaid - Tlemcen (Algeria), [2]Laboratoire de physique théorique Ecole préparatoire sciences et techniques B.P 230, 13000 Tlemcen, Algérie. - Tlemcen (Algeria).

The full-potential linearized augmented plane wave (FLAPW) method were employed within the generalized gradient approximation (GGA) to investigate structural and elastic properties of ErX (X= Cu, Au, Ag, Ir) compounds. The ductility or brittleness of these intermetallic compounds is predicted, through this investigation reveals that the ErAg crystal is more ductile. Moreover, the elastic constants values and the sound velocities were discussed for longitudinal and shear waves. In addition, the chemical bonding of these compounds has been investigated in light of topological analyses approach grounded in the theory of atoms in molecules (AIM). All of the electron density critical points in the unit cell were systematically calculated in order to predict basins interaction of each atom.

Keywords: Rare-earth intermetallic compounds, elastic properties, ab initio method, atoms in molecule formalism
PACS numbers: 71.15.Mb, 71.15.-m., 62.20.de, 31.15.ae

EMP-2-Or-10
Investigation on oxygen diffusion in a high-k metal-gate stack for advanced CMOS Technology by XPS

T05 Electronic Materials and Processes

#EMP-2-Or-10

A. Kechichian [1], P. Barboux [1], M. Gros-Jean [2], F. Martin [3].

[1]École Nationale Supérieure de Chimie de Paris, 11 rue Pierre et Marie Curie - Paris (France), [2]STMicroelectronics, 850 rue Jean-Monnet - Crolles (France), [3]CEA-Leti, 17 rue des Martyrs - Grenoble (France).

In the late 2000s' the 32nm Coupled Metal Oxide Semiconductor (CMOS) technology node required the use of a high-k dielectric with a metal gate instead of the historically used silicon dioxide and polysilicon. The aim was to reduce the leakage current between the gate and the channel which became critical for silicon-based gate stacks [1]. However using a high-k metal-gate architecture makes the control of the electrical properties of the transistor really challenging. Indeed the high-k material strongly interacts with its environment during the manufacturing process, which thoroughly changes the device properties.

Parameters such as the threshold voltage or the Equivalent Oxide Thickness are not only related to a material selection, but are also subject to modification due to the oxygen diffusion throughout the stack [1,2]. The understanding of the oxygen diffusion dynamics hence becomes mandatory.

Our work has been performed inside a cutting-edge STMicroelectronics cleanroom. It focuses on the annealing effects with regard to the oxygen diffusion throughout the stack TiN/HfO2/SiO2/Si. For that purpose, a blank 300mm Si (100) wafer undergoes an oxidizing wet treatment to create an 8Å chemical oxide on its surface. 2nm of HfO2 are deposited onto this wafer by MOCVD with an Applied Material Centura. The annealing processes are made at low pressure (5 torr), with a N2 saturated atmosphere containing 1ppm of O2, at 450°C and 900°C for 60 seconds. The experiment is renewed with 2nm of TiN deposited on the top of the stack by RF-PVD with an Applied Material Endura tool at low temperature (< 50°C), in order to avoid any thermally activated parasitic reactions. All the samples are characterized with a ReVera VeraFlex II XPS tool as fast as possible after the annealing process.

The results show that the annealing without the TiN metal has no noticeable effect with regard to oxygen diffusion, especially at the HfO2-substrate interface. However as soon as TiN is deposited, the Si2p spectra show an increase of the characteristic signature of SiO2 after annealing at any temperature. This clearly indicates the diffusion of some oxygen towards the silicon substrate. Besides, Hf4f spectra show no major changes, but the Ti2p spectra decomposition reveals that the Ti-O component decreases with the annealing process for all the temperatures.

Our hypothesis is that an equilibrium exists between the reduction of the native TiO2 oxide on top of the TiN by the substrate, and the oxidation of the TiN by the ambient O2. The TiN splits up the ambient O2 into a monoatomic oxygen, which will migrate across the HfO2 layer towards the substrate. This effect is discussed as a function of the HfO2 layer thickness.

We finally propose a discussion based on the existence of a battery-like system formed by electrochemical couples separated by a solid electrolyte (HfO2). Electrodes are formed as a gas-metal electrode formed by the TiN-N2-: 1 ppm O2 separated from the Si/SiO2 redox system. This stack accelerates the oxidation of the silicon.

[1] J. Robertson, «Fermi level pinning by defects in HfO2-metal gate stacks», Applied Physics Letters 91 (2007), 132912
[2] K. Kakushima et al. “Origin of flat band voltage shift in HfO2 gate dielectric with La2O3 insertion“, Solid-State Electronics 52 (2008) 1280–1284

EMP-P3-14a
Thin Single-crystalline Silicon Wafer with Thickness of 100 ㎛ for Photovoltaic Applications

T05 Electronic Materials and Processes

#EMP-P3-14a

B. Jang, S. Choi, H. Song.

Korea institute of energy research - Daejeon (Korea, republic of).

Silicon (Si) wafering is one of critical processes that determine production-cost of solar cell. Typically, wafering process accounts for more than 30 % of total production cost of Si solar cell. Thinner wafer results in lower wafering cost because the number of wafers produced from an ingot increases. Therefore, various processes have been developed to decrease a thickness of Si wafer. Multi-wire sawing is widely used process for wafering, but breakage of wafer during the process is serious problem when its thickness was lower than 150 um. Multi-wire sawing system was set up and sawing process was researched to decrease the thickness without serious breakage. Single-crystalline Si wafer with thickness of 100 um was successively sawn by using metal-coated wire (120 um) and SiC abrasives (20 um). Microstructures of sawn wafers were investigated to decrease the breakage. It was noticeable that breakage decreased from 54 % to 26.4 % by modifying the process and polishing ingot's surface, which prevents initial cracks formed on ingot's surface. Si-solar cell was fabricated using this wafer to evaluate the photoelectric conversion efficiency and efficiency of 17.8 % was obtained. Consequently, multi-wire sawing process in this study was effective for the thin single-crystalline Si solar cell with the thickness lower than 120 um.

[1] J.G. Beesley & al., "Slicing 80 Micrometer Wafers Process Parameters in the Lower Dimensions", 22nd European Photovoltaic Solar Energy Conference 2BO.1.5 (2007)
[2] A. Bohne & al., "The Influence of the Wire Sawing Process on Mono- and Multicrystalline Silicon Wafers", Proceeding of the 23rd European Photovoltaic Solar Energy Conference, paper 2CV.5.60 (2008)
[3] A. Bidiville & al., "Towards the Correlation of Mechanical Properties and Sawing

Parameters of Silicon Wafers”, Proceeding of the 22nd European Photovoltaic Solar Energy Conference, paper 2CV.3.19 (2007)

FIg. 1. Photo image of 6-inch thin single-crystalline silicon wafer

Fig. 2. Cross-sectional SEM image of thin single-crystalline silicon wafer

EMP-P3-10
Growth of Carbon Nanotubes inside a Silicon Via to Enable IC Stacking Applications

T05 Electronic Materials and Processes

#EMP-P3-10

S. Burkett [1], M.B. Jordan [1], M. Rao [2], R. Divan [3], A.V. Sumant [3], L. Ladani [1].

[1]The University of Alabama - Tuscaloosa (United states), [2]International Institute of Information Technology - Bangalore (India), [3]Argonne National Laboratory - Argonne (United states).

The growth of carbon nanotubes (CNTs) inside silicon vias has been investigated [1]. This pilot study is part of a larger project to demonstrate the feasibility of filling through silicon vias (TSVs) with a Cu/CNT matrix. The motivation for this work is in improving the electrical and mechanical reliability of TSVs. Currently, Cu filled TSVs have some limitations in terms of electromigration, areas of high stress in the via, and lack of mechanical compliance. The process flow for achieving CNTs in blind vias includes four main steps: 1) patterning the bare Si wafer by photolithography; 2) deep reactive ion etching (DRIE) to form the blind via; 3) depositing the catalyst layer; and 4) growing vertically oriented carbon nanotubes. The via diameter is in the range of 20-25 μm and the vias are etched to a depth of 100 μm resulting in aspect ratios of 4-5. This via diameter is somewhat larger than is currently used in interposer technology; however, these dimensions facilitate experimentation while investigating a new material system. We have used both Bosch DRIE etching and inductively coupled plasma (ICP) cryogenic etching to achieve a via profile which includes a tapered via sidewall. The tapered profile assists in deposition of conformal thin film layers inside the via. For the catalyst layer, 15 nm of Al_2O_3 is deposited by atomic layer deposition (ALD) and 2-4 nm of Fe is deposited by electron beam evaporation. Carbon nanotubes were grown using a thermal chemical vapor deposition (CVD) process at Argonne National Lab with $Ar/H_2/C_2H_4$ gases flowing through the quartz chamber. Previous to growth, annealing in a hydrogen ambient was found to be critical for achieving successful CNT growth. According to transmission electron microscopy (TEM), the CNTs are single walled and have some amorphous or graphitic carbon deposited on their sidewalls. Figure 1 shows CNTs growing out of

the top of a blind via in silicon. Once our process flow is optimized and process repeatability is observed, deposition of a seed layer and electroplating copper inside the via will complete the Cu/CNT matrix. The material system will then be ready for electrical and mechanical characterization.

This research was partially sponsored by ARL (Cooperative Agreement No. W911NF-10-2-0093) and NSF (CMMI-1234652). The Center for Nanoscale Materials at ANL was supported by the U. S. DOE, Office of Science, Office of Basic Energy Sciences, Contract No. DE-AC02-06CH11357.

1. M. B. Jordan, M. Rao, A. V. Sumant, R. Divan, and S. L. Burkett, “Process Flow for Growing Aligned Carbon Nanotubes in Blind TSVs,” 2nd Global Interposer Technology Workshop, Atlanta, GA (2012).

Figure 1. SEM image of CNT grown inside a via formed by ICP Cryogenic Etching.

EMP-P3-11
Dry etching of ZTO Films by using Inductively Coupled Plasma

T05 Electronic Materials and Processes

#EMP-P3-11

H. Kim, Y.H. Joo, J.C. Woo, Y.S. Chun, C.I. Kim.

CHUNG-ANG UNIVERSITY - Seoul (Korea, republic of).

Apart from other transparent conductive oxide (TCO) materials, Zinc Tin Oxide (ZTO) is a very promising candidate among the TCO. ZTO has the advantage of good stability at high temperature and unlike other popular TCOs such as ITO and Cd-Sn-O, ZTO films do not contain expensive or toxic elements. Another advantage of ZTO is its low sensitivity towards visible light. In many organic and hybrid devices ZTO thin films are used as the cathode or electron transport layer. So far, the etching of ZTO thin films is often done through wet chemical etching using hydrochloric acid (HCl). However, the wet etching process causes the problem of isotropy and selective-grain boundary etching [1]. For these reasons, stable dry etching process with high etch rate, selectivity is needed. Therefore, stable dry etching process with high etch rate and selectivity of ZTO thin films in chlorine-based plasma is studied for the organic and hybrid devices. Chemical reaction of the etched ZTO surface has been studied by x-ray photoelectron spectroscopy measurement (XPS). Surface morphology of the etched ZTO thin films was characterized using atomic force microscope(AFM).

[1] M. Takabatake, Y. Wakui, N. Konishi J. Electrochem. Soc. 142 2470 (1995)

3D Atomic Force Microscopy images of the etched ZTO thin films

EMP-2-Or-5
First principle study of structural, electronic and optical properties of InS(1−x)Se(x) alloy

T05 Electronic Materials and Processes

#EMP-2-Or-5

I. Ben Amara, R. Bennaceur.

faculté des sciences Tunis El Manar, Campus universitaire - Tunis (Tunisia).

III-VI compounds become an area of great technological activity, and attracted attention on account of their semiconducting nature and applications in optoelectronic devices, in non linear optic devices such infrared detectors and as electron exchange electrodes in solid-state batteries, and in photovoltaic domain as solar cells compounds. In the recent years, there is strong interest on the III-VI family related to the success of I-III-VI laser semi-conductors which allow the construction a variety of a solar cell used as optic windows. It is known that the major goal in materials engineering is the ability to change artificially the electronic and optical properties of semiconductors and this is assured by forming their alloys. Thus, it appears very interesting to combine two different III-VI compounds with different optical band gaps in the aim to produce novel materials, with intermediate physical properties, used in the future scientific investigations.
Keeping this in mind, we are motivated to study the ground-state properties of the ternary alloy InS(1-x)Sex, for several Selenium compositions. We have investigated their structural, electronic and optical properties within a framework of density functional theory (DFT) [1].We have performed our calculations using Full-Potential linearized augmented plane wave plus local orbital (FP-LAPW+lo)[2] embedded in WIEN2k package .The exchange-correlation potential is treated by generalized gradient approximation (GGA) [3] for the optimized structures. Whereas the Engel-Vosko GGA [4] is applied to approximate the corresponding potential for bands structure calculations. Our investigations on the effect of Se concentration on lattice constants, ionicity factor, band gap, and some optical constants for ternary alloys shows non-linear dependence on the composition x. Deviation of the lattice parameters from Vegard’s law is explained and the microscopic origin of gap bowing are identified and calculated by Zunger approximation [5]. We have also calculated the total and partial densities (DOS and PDOS) for every molar fraction x .The imaginary and real dielectric function are determined and the optical constants such

as refractive index n(ω) , absorption coefficient α (ω) and electron energy-loss function L(ω) are interpreted. Our results are compared with previous works.

[1] P. Hohenberg, W. Kohn, Phys. Rev. 136 (1964) 864
[2] K. Schwarz, P. Blaha, G.K.H. Madsen, Comput. Phys. Commun. 147 (2002) 71
[3] J.P. Perdew, K. Burke, M. Ernzerhof, Phys. Rev. Lett. 77 (1996) 3865
[4] E. Engel, S.H. Vosko, Phys. Rev. B 47 (1993) 13164
[5] J.E. Bernard, A. Zunger, Phys. Rev. B 34 (1986) 5992

Total density of states of ternary compound InS(1-x)Se(x) for: x=0.5

EMP-2-Or-7
Charge Trapping in Perylene Diimide Transistors: A Time- and Wavelength-Resolved Electric Force Microscopy Study

T05 Electronic Materials and Processes

#EMP-2-Or-7

L. Smieska [1], Z. Li [2], A. Braunschweig [3], J. Marohn [1].

[1]Cornell University - Ithaca (United states), [2]New York University - New York City (United states), [3]University of Miami - Coral Gables (United states).

Complementary hole-transporting (p-channel) and electron-transporting (n-channel) materials are both needed to achieve all-organic circuits. Only a few examples of robust n-channel materials are known, and most suffer from threshold voltage shifts due to charge trapping. Unlike hole-transporting materials, for which oxidation of the bulk is key to performance degradation, the concern for electron-transporting materials is the radical anion reactivity.

If the n-channel material's LUMO level is above -4.0 to -4.3 eV, then the radical anion is susceptible to reaction with O2; the long-term stability of the resulting reaction products is still unclear [1]. Similarly, for high-LUMO n-channel materials deposited on untreated silicon dioxide, the radical anion is expected to react with dangling Si-OH groups to yield long-lived traps on the dielectric surface [2]. Other trapping mechanisms, such as traps at chemical impurities or physical defects, are plausible for any LUMO level.

Here we report studies of charge trapping in several perylene diimide derivatives by time- and wavelength-resolved electric force microscopy (EFM). The spatial distribution and kinetics of trapped charge measured by EFM can identify the trapping mechanisms at play. We moreover use EFM coupled with wavelength-resolved illumination to measure the first-ever trap-clearing spectra in perylene diimides (PDIs) (Fig. 1). Such spectra have been shown to offer insight into which chemical species are involved in neutralizing traps [3].

[1] de Leeuw, D.; Simenon, M.; Brown, A.; Einerhand, R. Synth. Met., 1997, 87, 53–59.
[2] Yoon, M.-H.; Kim, C.; Facchetti, A.; Marks, T. J. J. Am. Chem. Soc., 2006, 128, 12851-12869.
[3] Smieska, L. M.; Pozdin, V. A.; Luria, J. L.; Hennig, R. G.; Hines, M. A.; Lewis, C. A.; Marohn, J. A. Adv. Funct. Mater., 2012, 22, 5096-5106.

Figure 1. Trap-clearing (s-1eV-1, dots) and absorption spectra (a.u., solid) for a PDI.

EMP-2-Or-8
Raman Spectroscopy, XPS and XRD of Ferroelectric Domains in Pulsed Laser Deposited Na0.5K0.5NbO3 Films

T05 Electronic Materials and Processes

#EMP-2-Or-8

R. Schwarz [1], M. Leal [2], W. Donner [2], L. Santos [1], N. Bundaleski [3], O. Teodoro [3], R. Ayouchi [1].

[1]Instituto Superior Técnico - Lisbon (Portugal), [2]University of Darmstadt - Darmstadt (Germany), [3]Universidade Nova - Lisbon (Portugal).

Thin films of NKN (Na0.5K0.5NbO3), produced by laser ablation of stoichiometric ceramic targets, have shown an increase of polycrystalline structure and increase in ferroelectric quality, when the substrate temperature is raised from room temperature up to 600 ºC. However, increasing loss of Na and K can occur. Alcali deficiency, a common problem in different deposition methods of NKN thin films, has been quantified by several methods. XPS analysis, using Mg Kα line, confirmed the loss of alcali atoms at deposition temperatures beyond 400 ºC. The analysis takes the intensities of the Na 1s peak at 1071.0 eV, the K 2p doublet with the -2p3/2 peak at 293.4 eV, and the Nd 3d doublet with -3d5/2 peak at 206.0 eV into account. Considering the charge states, we suggest that excess of Nb and O might be present in the form of NbO2.

Detailed information of the morphology and structure of the films was obtained from confocal Raman spectroscopy. The lateral resolution allowed us to scan domains with submicron precision. The change in film structure observed by SEM is accompanied by a shift of the Nb-O-octaeder stretching mode at an energy of 615 cm-1 , suggesting a change in internal stress of the films. Two further strong peaks [1] present in the ceramic NKN targets at 260 cm-1 and 852 cm-1, are either low in intensity in the films or they do not change position. These results are correlated with XRD diffraction data to identify the possible content of non-stoichiometric NKN components.

[1] K. Kakimoto, K. Akao, Y. Guo and H. Ohsato, Raman Scattering Study of Piezoelectric (Na0.5K0.5)NbO3-LiNbO3 Ceramics, Jpn. J. Appl. Phys. 44 (2005) pp. 7064-7067.

EMP-P3-12
Nonlinear charge transport in two-dimensional polymer monolayer

T05 Electronic Materials and Processes

#EMP-P3-12

M. Akai-Kasaya [1], S. Nagano [2], S. Akira [1], Y. Kuwahara [1].

[1]Osaka Univ. - Osaka (Japan), [2]Nagoya Univ. - Nagoya (Japan).

Interface between organic semiconductor and dielectric is an important key requirement to survey the mechanism of carrier transport properties, because only few molecular layers at the interface govern the intrinsic feature in organic field effect transistors (OFETs). In spite of their technological importance, the fundamental questions, which are to be revealed, still remain. We investigated the origin of nonlinear transport in a highly ordered regioregular poly(3-hexylthiophene-2,5-diyl) (P3HT) monolayer.
P3HT monolayer prepared by liquid crystal hybridized Langmuir-Blodgett method [1] was deposited on flattened metal electrodes [2]. Titanium-gold with sub-micro channel width of 0.5-2μm and length of 0.1-0.5 nm was embedded in 100nm thick SiO_2 grown on a highly doped Si substrate. The height difference between the metal and SiO_2, less than 1 nm, minimizes the deformation of deposited molecular layer. The devices work as OFETs with typical mobility of 0.002–0.2$cm^2 V^{-1} s^{-1}$ at 300K. The contact resistance (R_c) of a device at was very small as compared to film resistance.
We investigated the temperature and voltage dependence of the charge transport through the P3HT monolayer. The current decreased as temperature decreases.The mobilities decrease following a straight line with an activation energy of 110 meV in an Arrenius plot. Although,at lower temperatures, 4K-150K, the current characteristics exhibit significant nonlinear response to the voltage increase. What is origin of the nonlinearity? We confirmed that our data never agreed with a conventional exponential expression, which includes "k_BT" in the exponential factor. We founded that the nonlinear currents have voltage threshold (V_t) and obey a power law of $I \propto (V-V_t)^{\xi}$, where typical gradient ξ was 3.9. Respective V_t were in inverse proportion on temperature increase. These characteristics are consistent with a Coulomb-blockade charge transport model in a two-dimensionally (2D) quantum dot array system [3]. We propose an isotropic extended-charged state, which can form a 2D quantum dot array, in P3HT monolayer based on our DFT calculation results.

Estimated self- and mutual-capacitances in the model are roughly but quantitatively consistent with our experimental data.
We conclude and strongly suggest that the Coulomb blockade effect is one of the origins of nonlinear charge transport, which is frequently observed in organic conductors.

[1] S. Nagano, S. Kodama and T. Seki, Langmuir, 24 (2008) 10498.
[2] Y. Higuchi, M. Akai-Kasaya, et al., Jpn. J. Appl. Phys. 45, (2006) L145.
[3] A. Alan Middleton and N. S. Wingreen, Phys. Rev. Lett. 71, (1993) 3198.

Characteristics of current vs. $V-V_t$ of P3HT monolayer observed from 4K to 150K.

EMP-P3-13
Segregation, oxygen vacancies and waterfall behaviour in SrTiO3 : A complete synchrotron radiation study

T05 Electronic Materials and Processes

#EMP-P3-13

A. Levy, J. Avila, E. Frantzeskakis, S. Lorcy, M.C. Asensio.

Synchrotron SOLEIL - Gif Sur Yvette (France).

The development of all-oxide electronic devices presents a quickly advancing technological field were $SrTiO_3$ (STO) plays a key role. An important step for oxide electronics was the discovery of a high mobility 2D electron gas (2DEG) on the $LaAlO_3/SrTiO_3$ interface, two otherwise insulating oxides. On the other hand, a similar 2DEG has been recently reported on the bare STO (001) surface. Among other explanations, the physical origin of the aforementioned confined electron gases has been attributed to surface oxygen vacancies.

In this communication we report on the structural and electronic properties of thermally reduced STO single crystals. We have investigated these systems using a probe with real- and reciprocal-space sensitivity: a synchrotron radiation microsopic setup which offers the possibility of Scanning Photoemission Microscopy and Angle Resolved Photoelectron Spectroscopy (ARPES) down to the nanometric scale. For the first time, we have spectroscopically imaged the chemical composition of samples presenting reproducible and suitable low-energy diffraction patterns after following well-established thermal reduction protocols. At the micrometric scale, Ca-rich areas have been directly imaged using high-energy resolution core level photoemission. Moreover, we have monitored the effect of Ca segregation on different features of the STO (100) electronic band structure, measuring ARPES inside, outside and at the interface of the Ca-rich identified areas. In particular, the interaction of Ca with the well-known intra-gap localized state, previously attributed to oxygen vacancies, has been investigated. Most importantly, the combination of direct imaging and spectroscopic techniques with high spatial resolution has clarified the long-standing dilemma related to the bulk or surface character of Ca segregation in STO. Moreover, new data will be discussed on the light of the calcium segregation, oxygen vacancies and waterfall 2DEG sates.

EMP-2-In-2
VISUALIZATION AND MODELING OF CARRIER MOTION IN ORGANIC DEVICES BY ELECTRIC FIELD INDUCED OPTICAL SECOND HARMONIC GENERATION

T05 Electronic Materials and Processes

#EMP-2-In-2

M. Iwamoto.

Department of Physical Electronics, Tokyo Institute of Technology - Tokyo (Japan).

Probing and modeling of carrier motion in organic materials is a fundamental research subject in science and electronics. By detecting nonlinear dielectric polarization induced in organic materials by moving carriers (electrons and holes), we can visualize and model the carrier motion. The method developed here is a novel optical method based on electric field induced optical second harmonic generation (EFISHG) measurement. In this presentation, basic concept for probing dynamical carrier motions by using EFISHG is discussed briefly, and the visualized carrier motion in organic field transistors, organic ELs, and organic solar cells are presented. After that the carrier motion is discussed based on the Maxwell-Wagener effect model analysis.

EMP-1-In-1
PLASMA ASSISTED MOLECULAR BEAM EPITAXY OF III-NITRIDE SEMICONDUCTOR HETEROSTRUCTURES AND NANOSTRUCTURES

T05 Electronic Materials and Processes

#EMP-1-In-1

A. Georgakilas.

Microelectronics Research Group (MRG), Department of Physics, University of Crete and Institute of Electronic Structure and Laser (IESL), Foundation for Research and Technology-Hellas (FORTH) - Heraklion, Crete (Greece).

Molecular beam epitaxy employing a nitrogen plasma source is successfully used in the research and development of III-nitride semiconductor heterostructures-nanostructures. A significant advantage of the method is the supply of reactive nitrogen species independently of the used substrate temperature, which facilitates the growth of thermally unstable In-containing compounds and of far from equilibrium III-nitride heterostructures. Four important cases which will be discussed concern: (1) the growth of advanced High Electron Mobility Transistor structures, (2) the heteroepitaxy on very dissimilar substrate materials such as single crystal and polycrystalline diamond, (3) the heteroepitaxy of high quality InN layers and InGaN and InAlN alloys spanning the entire composition range, and (4) the catalyst-free spontaneous growth of III-nitride nanopillars as a bottom-up nanofabrication approach.

EMP-2-In-1
Atomic layer etching for next generation nanoscale device processing

T05 Electronic Materials and Processes

#EMP-2-In-1

G.Y. Yeom.

SUNGKYUNKWAN UNIVERSITY - Seoul (Korea, republic of).

Atomic layer etching is a technique that can etch materials layer by layer in an atomic layer scale. It can be applied to various materials not only the crystalline materials such as Si, GaAs, etc. but also amorphous materials such as SiO2, HfO2, etc. In addition, it also can be applied to the removal of 2-D materials such as graphene, etc. layer by layer. It is believed that for the next generation nanoscale device fabrication, the control of the material processing with atomic scale precision without forming any damage to the material is very important. Therefore, in this presentation, the results of atomic layer etching carried out various materials will be reported and the characteristics of the devices fabricated with atomic layer etching will be also reported.

EMP-P3-14
Attempt to manufacture a solar cell by using a simple method of n-type doping of monocrystalline silicon

T05 Electronic Materials and Processes

#EMP-P3-14

R. Ndioukane, M. Biagui, M. Tine, L.G. Ndiaye, K. Kobor.

Laboratoire de Chimie et de Physique des Matériaux (LCPM), Assane Seck University of Ziguinchor (UAS) - Ziguinchor (Senegal).

The electrical behavior of a semiconductor device depends strongly on the dopants distribution within the structure. To make solar cells from monocrystalline silicon, it is necessary to realize a pn junction by implanting phosphorus atoms mainly on a given thickness of the p-type. Different liquid, solid, or gaseous methods are used. These methods often require equipment not available for underdeveloped countries.
In this work, we try to make mono-Si solar cells using an easier doping method. We combined spin-coating thin film deposition method and solid doping technique. This technique can be considered as the SOD method. The difference between these methods is the use of an phosphorus oxide
There are many ways of making thin films that can be classified into physical and chemical ways. The best known methods as regards the physical ways are sputtering, thermal evaporation, etc.. These methods require expensive equipment. In our study, two phosphorous-based gel compounds are prepared and deposited by spin coating. Heat treatment would thus, after deposition of thin layer, diffuse phosphorus atoms into the substrate to obtain a pn diode. I-V measurements characteristics in dark and under illumination of 1000 W give curves close to a pn diode behavior.

Keywords : Monocristalline silicon, doping, spin coating, thin film, solar cell.

Figure 1: The SIMS profile versus time for p-type Si doped by the phosphorus oxide gel.

T06 Energy and Sustainable Development

ESD/ASS-P3-01
Effects of adding silica fume on the properties of high performance concretes subjected to high temperatures

T06 Energy and Sustainable Development

#ESD/ASS-P3-01

B. Chemani.

M'Hamed Bougara University of Boumerdes - Boumerdes (Algeria).

In this study, the compressive strengths and weight losses of the High Performance Concretes (HPC) containing Silica Fume (SF) and superplasticizer (SP) at high temperatures were investigated in comparison to Ordinary Portland Cement (OPC). For many years, the mineral admixtures have been used in Portland cement. As the silica fume is a very reactive pozzolan, it is used in the concrete because of its fine particles, large surface and high percentage SiO2 content.
Its addition to the HPC causes significant effects on the properties of the products obtained. This paper presents the results of experimental work on physical-mechanical behavior of HPC containing different levels of silica fume after being exposed to high temperatures (100, 200, 400, 800, 900° C), without intermediate steps for a ripening cycle of 24 hours.
To achieve these objectives, different types of concrete mixtures were produced. In producing the mixtures, silica fume (SF) was used to replace the Portland cement in the ratios of 0%, 5% and 10% by weight. Half of the mixtures were obtained by adding superplasticizers (SP) to mixtures in the ratio of 1.5 and 2% by weight to OPC.
Weight losses increased from 3% to 12% following exposure to temperatures of 200 ° C and 900 ° C.
A 4% decrease in the compressive strength of concrete was recorded at 200 ° C
At 900 °C it was observed a resistance fall and a concrete spalling with adjuvants

1.5% and 2% respectively
These results show that adding the Silica Fume and the superplastizer to concrete, decreases both unit weight and compressive strength. Additionally, elevating the temperature above 600 °C affects the compressive strength such that the weight loss of concrete is more pronounced for concrete mixtures containing both SP and SF.

ESD/ASS-2-Or-8
The optimization of water flow in the photovoltaic pumping system

T06 Energy and Sustainable Development

#ESD/ASS-2-Or-8

M. Chergui [1], M. Bourahla [2].

[1]University of Mascara-Algeria - Mascara (Algeria), [2]University of Oran-Algeria - Oran (Algeria).

The present work aims to achieve a better strategy for a photovoltaic pumping system using different types of solar cell technology and techniques to control induction motor for maximum optimization of the amount of water pumped operate over the sun that draws water from a well and pumped into a reservoir.
As the rapid development of semiconductor and digital technology, mainly in the control devices and power electronics, slightly improved the performance of photovoltaic systems and reduces its cost. The optimization of our system elements is based on: The design and simulation of a adequate tracking system maximum power point to extract the maximum power irrespective of the generator photovoltaic atmospheric variations (temperature and irradiation); design and simulation of a convenient inverter reliable and high performance by applying the best technique of PWM, the application of the technique uncomplicated and effective control of induction motor coupled to a centrifugal pump.
We present the essential information about solar energy, its current and future use in the world, and its impact on environmental and sustainable development, in particular the strategy photovoltaic pumping in scattered areas. We have developed several methods vector control which optimizes not only the efficiency of the photovoltaic conversion, but also, the losses in the induction motor and the optimization of the quantity of water flow.

[1] Auer.H. Worldwide Emissions of CO2. Durban Conference. November 21, 2011 [2] Parida B, Iniyan S, Goic R. A review of solar photovoltaic technologies. Renew Sust Energy Rev 2011;15(3):1625–36. [3] Adil.N, Cutier. J. C .World Environment Summits: The Role of Energy. Encyclopedia of Energy 2004 ; Vol. 6 :539–548 [4] Belgacem.B. Performance of submersible PV water pumping systems in Tunisia. Energy for Sustainable Development 2012; 16(4):415–420 [5] Sher.H, Addoweesh.

K.E. Micro-inverters-Promising solutions in solar photovoltaics. Energy for Sustainable Development; 2012;16(4) :389–400 [6] Enrique JM, Duran E, Sidrach-de-Cardona M, Andujar JM.Theoretical assessment of the maximum power point tracking efficiency of photovoltaic facilities with different converter topologies.Solar Energy 2007;81:31-8. [7] Mokeddem A, Midoun A, Kadri D, Hiadsi S, Raja Iftikhar A. Performance of a directly-coupled PV water pumping system. Energy Convers Manage 2011;52(10):3089–95. [8] Ilango GS, Rajasekar N. An improved energy saving v/f control technique for solar powered single-phase induction motor. Energy Convers Manage 2009;50(12):2913–8.

ESD/ASS-2-Or-9
Electrochemical performance of pre-lithiated graphite as negative electrode in lithium-ion capacitors

T06 Energy and Sustainable Development

#ESD/ASS-2-Or-9

M. Yuan [1], W. Liu [1], Y. Zhu [2], Y. Xu [1].

[1]Research Institute of Tsinghua University in Shenzhen - Shenzhen (China), [2]Tsinghua University - Beijing (China).

Recently, a relatively new type asymmetric capacitor called lithium-ion capacitor (LIC) was reported , which has storing about 5-10 times more energy than EDLC and having similar levels of high power and long cycle life[1-11]. Electrochemical performance of the pre-lithiated graphite and the as-assembled lithium ion capacitors were investigated within the Li/graphite two-electrode cell. By short circuiting technique, the Li/graphite two-electrode showed a there-stage during the Li-ion intercalation (Fig.1). The EIS spectra included only one semi-cycle and a inconspicuous slash during the Li pre-doping at 1-30 h (Fig.2). The values of the ohmic resistance (Rs) and SEI layer (R1) increased with the increasing doping time (Table 1). The cell of 8 h pre-doping time have the best cycle performance at high C rates compared with that of 1 h, 2 h, 24h and 30 h doping time (Fig.3), which showed the capacity degradation with less than 2% after 600 cycles at 10 C. Within the galvanostatic charging technique, the smaller C rate for Li intercalation gave more discharge capacity (Fig.4), which is favor to improve the electrochemical performance of the as-assembled LICs, the cycle performance of which was slightly inferior to that with 8 h pre-doping time (Fig.5). The present work provided enough information about the pre-lithiated of graphite and the electrochemical performance for the as-assembled LICs.

1.Khomenko V, Piñero ER, Béguin F (2008) J Power Sources 177:643
2.Naoi K, Simon P (2008) Electrochem Soc Interface 17:34
3.Sivakkumar SR, Nerkar JY, Pandolfo AG (2010) Electrochem Acta 55:3330
4.Khomenko V, Pinero ER, Beguin F (2010) J Power Sources 195:4234
5.Burke A (2010) J Energy Res 34:113

6.Böckenfeld N, Kühnel RS, Passerini S, et al (2011) J Power Sources 196:4136
7.Kim JH, Kim JS, Lim YG, et al (2011) J Power Sources 196:10490
8.Krause A, Kosyrev P, Oljaca M, et al (2011) J Power Sources 196:8836
9.Decaux C, Lota G, Pinero ER, et al (2012) Electrochem Acta in press
10.Cao WJ, Zheng JP (2012) J Power Sources 213:180
11.Omar N, Daowd M, Hegazy O, et al (2012) Electrochem Acta in press

ESD/ASS-2-Or-11
BLACK SILICON: MICROFABRICATION TECHNIQUES AND CARACTERIZATION FOR SOLAR CELLS APPLICATIONS

T06 Energy and Sustainable Development

#ESD/ASS-2-Or-11

A. Deraoui.

Université Hassan 1er - Settat (Morocco).

The properties of black silicon are well suited for use in photovoltaics. We plan to use the advantages of black silicon to format new types of solar cells that will be able to capture solar energy across a wider range, thereby realizing greater efficiency in future photovoltaic cells [1–4]. The method of production has brought the use of black silicon in photovoltaic arrays closer to commercial realisation, as it will reduce the cost of black silicon production, minimize reflectivity and maximize the absorbance . The basic objective of this paper is to create black silicon by chemical wet etching techniques using Au nano particles directly formed on silicon substrates. We further decided to try to optimize this material using non-heavily photolithographic methods, such as etching. The morphology of Black Si was characterized by Scanning Electron Microscopy (SEM) and the optical properties were given thanks to Cary Spectrometer.

[1] J.S. Yoo, I.O. Parm, et al., Sol. Energy Mater. Sol. Cells 90 (2006) 3085–3093.
[2] Kensuke Nishioka, Tsuyoshi Sueto, et al., Appl. Surf. Sci. 255 (2009) 9504–9507.
[3] Young Min Song, Eun Sil Choi, Gyeong Cheol Park, Chang Young Park, Sung Jun
Jang, Yong Tak Lee, Appl. Phys. Lett. 97 (2010) 093110.
[4] Yang Xia, Bangwu Liu, Jie Liu, Zenan Shen, Chaobo Li, Sol. Energy 85 (2011) 1574–1578.

ESD/ASS-1-Or-7
Low temperature stable delta Bi2O3 thin films grown by reactive RF sputtering

T06 Energy and Sustainable Development

#ESD/ASS-1-Or-7

P. Lunca Popa [1], S. Sonderby [2], S. Kerdsongpanya [2], J. Lu [2], P. Eklund [2].

[1]ISMO -CNRS, CNRS/Université Paris-Sud Bat.351, Universite Paris-Sud F-91405 Orsay Cedex - Paris (France), [2]Thin Film Division, Department of Physics, IFM, Linköping University, SE-581 83 Linköping, Sweden - Linkoping (Sweden).

In recent years bismuth oxide systems have received an increased attention due to theirs interesting properties, particularly excellent ionic conductivity, an important asset in various technological fields as gas sensors, oxygen pumps, Solid Oxide Fuel Cells (SOFCs) and other applications where conduction by oxygen vacancies is required. SOFCs represents a valuable alternative source of energy providing large fuel adaptability and high efficiency. Current SOFCs operate at high temperatures, (800^{o}C). Current research in the field is focused in decreasing the operating temperature to an intermediate range without affecting the efficiency. Herein we report the synthesis by reactive magnetron sputtering and structural characterization of highly (111)-oriented thin films of δ–Bi_2O_3, the best ionic conductor. Amorphous films, α, β, γ, δ phase films, metallic bismuth films or mixtures of phases were obtained depending on the deposition parameters. For a narrow window in deposition paramaters with respect to deposition temperature (150-200 C) and oxygen flow (15-20% of total gas flow) values the obtained films consist in a highly oriented phase-pure δ-Bi2O3. Small modifications (higher temperature or oxygen flow) on the values of deposition parameters result in α -Bi_2O_3 or phase mixtures formation. Transmission electron microscopy and x-ray diffraction reveal a polycrystalline columnar structure with [111] texture. The delta films are stable from room temperature up to 250° C in vacuum and 350^{o} C in ambient air, when an irreversible transition to monoclinic α-Bi_2O_3 crystal occurs. This low-temperature stability opens new perspectives for use as ionic conductor at low emperature in e.g. SOFCs.

1. *Highly oriented δ-Bi2O3 thin films stable at room temperature synthesized by reactive magnetron sputtering*, P. Lunca Popa, S. Sonderby, S. Kerdsongpanya ,J. Lu and P. Eklund, *Journal of Applied Physics*, **2013**, in press (accepted Jan 11)

fig.1 TEM analysis of α (left) and δ (right) Bi_2O_3 thin films deposited on sapphire

fig.2 *In* and *ex* situ thermal stability of δ-Bi_2O_3 thin films

ESD/ASS-P3-02
Hybrid MnO2 nanowires /Carbon Fiber Paper Electrodes in Urea-Li Salt Molten Complexes: an Outstanding Pseudocapacitive Material

T06 Energy and Sustainable Development

#ESD/ASS-P3-02

J. Chen, M.J. Deng, K.T. Lu.

National Synchrotron Radiation Research Center - Hsinchu (Taiwan, republic of china).

A simple and general approach effected the synthesis of MnO_2 nanowires /carbon-fiber paper (CFP) of Birnessite type as electrodes coupled with a Li-ion melt as electrolytes for supercapacitor applications. A unique mesoporous and nanostructured MNCFP in an urea−$LiPF_6$ ion liquid electrolyte-based EC can be cycled reversibly across voltage 3 V, and exhibits a great energy density 330 W h kg^{-1}. This cell exhibits a greater energy density of 50 W h kg^{-1} even at power density 104 kW kg^{-1}. XPS and in-situ XAS spectra elucidated the mechanism of charge storage in the ion liquid The analytical results indicate that the Mn^{3+}/Mn^{4+} transition during charge and discharge cycling was compensated by the reversible insertion of $Li(urea)_n^+$ cations into, and their withdrawal from, the tunnels between the MnO_6 octahedral units. In contrast, the BMP^+ and Li^+ cations merely adsorbed on the electrode surface, and did not penetrate into the oxide. This work might not only provide an effective method to understand the electrochemical mechanism involving an ion liquid electrolyte but also open a new route for the development of efficient systems to store energy using metal-oxide electrodes deposited on macroporous carbon materials with ion liquid electrolytes.

ESD/ASS-P3-03
Design and Fabrication of Nano-array Architecture for Supercapacitor and Electro-catalytic Reaction

T06 Energy and Sustainable Development

#ESD/ASS-P3-03

Z. Lu, X. Liu, X. Yu, X. Sun.

State Key Laboratory of Chemical Resource Engineering, P.O. Box 98, Beijing University of Chemical Technology - Beijing (China).

Nanostructure arrays, offering uniformed size, ordered structure, lower agglomeration and good connection with the substrate, have been proved as advanced and efficient electrodes in electrochemistry. Through a lot of research, our group has found that the specific capacitance, rate capability and cycling life of the electroactive material could be improved significantly by constructing the materials into nano-array structures.1-2 Hierarchical structure nano-array can provide even higher porosity and loaded mass which lead to the enhencement of areal capacitance (~25 F/cm2) and rate capability, while the specific capacitance and cycling stability can be preserved.3-4

More importantly, nano-array architecture also are effective to gas evolution reaction (e.g. oxygen evolution reaction and hydrogen evolution reaction). Besides the above advantages, nano-array architecture can promote the bubble evolution process because of the low adhesion of the surface to the gas bubbles. This observation should be generally applicable for gas evolution reaction.

(1) Z. Y. Lu, X. M. Sun*, et al. Nano. Res. 2011. 4. 658-665
(2) Z. Y. Lu, X. M. Sun*, et al. Chem. Comm., 2011, 47, 9651-9653
(3) Q. Yang, J. F. Liu*; X. M. Sun*, et al, RSC Adv., 2012, 2, 1663-1668
(4) Z. Y. Lu, X. M. Sun*, et al, Nano. Res. 2012, 5, 369-378

Fig. 1 Schematic Illustration of Nano-arrays for Supercapacitor
Fig. 2 Schematic Illustration of Nano-arrays for Electro-catalytic Reaction

ESD/ASS-2-Or-10
Conductivity Enhancement of Poly(3,4-ethylene dioxythiophene):poly(styrenesulfonate) with spray method

T06 Energy and Sustainable Development

#ESD/ASS-2-Or-10

K. Hwang, S.H. Nam, H.J. Seo, J.H. Boo.

Department of Chemistry and Institute of Basic Science, Sungkyunkwan University - Suwon (Korea, republic of).

Generally PEDOT:PSS conductivity polymers are used as buffer layer for organic based solar cells. It is important that improvement of the PEDOT:PSS electro-properties for high Power Conversion Efficiency(PCE) of solar cells. Furthermore, by getting a high conductivity of PEDOT:PSS films use as electrode for flexible device. In this work, we study on the the morphology and electro-properties of POEDOT:PSS thin films through spray method. PEDOT:PSS thin films are prepared with spin coating method. Then co-solvents are sprayed on the thin-films. To comparatively study the structural effects on the resulted electrical properties, the films are spin-coated on glasses and treated with spry method. At the same time, a contact angle goniometer is used for clarifying a mechanism of wettability of PEDOT (hydrophobic) and PSS (hydrophilic) on the observed conductivity. The structures and electrical properties are investigated by FE-SEM (Field Emission Scanning Electron Microscopy), AFM (Atomic Force Microscopy), and 4-point probe, respectively.

ESD/ASS-1-Or-2
High-resolution imaging of lithium intercalation in graphite particles in a Li-ion battery

T06 Energy and Sustainable Development

#ESD/ASS-1-Or-2

K. Takata.

Kansai university, Faculty of Engnieering Science - Osaka (Japan).

Lithium ion batteries are one of the most interesting power storage devices, and have attracted attentions of many researchers. The main elements to develop are positive electrodes, negative electrodes, separators and electrolytes. Since the report of the electrochemical reactions of lithium intercalation in graphite, the lithium ion batteries have been achieved in great advances though some problems to overcome still exist in the development. The application of the graphite to the anode overcame the dendrite problems, and the lithium ion batteries have been widely used as the most important power storage devices. Intercalation and deintercalation that lithium ions move into and back out the graphite or the layered oxides are interesting phenomena to observe using microscopic techniques. The phenomena are exactly the battery operation, charging and discharging. We focused on the changes in volume due to lithium intercalation. Insertion of lithium ions into graphite leads to expansion, and extraction leads to contraction. We can observe movement of lithium ions by imaging the changes in volume, for example, as follows.
We have studied on imaging of fine strains using SPM since 1993. Basically, SPM is microscopy capable of very high-sensitive detection of changes in the gap between the tip and sample, with high spatial resolutions in the lateral directions. Ordinary topographic SPM images are obtained by detecting the changes in the gap caused by raster scanning of either the tip or the sample, that is, the changes caused by the modulation of the tip position along the sample surface. SPMs can also detect changes in the gap induced by other modulations, with high sensitivities and high spatial resolution. Strain imaging we have proposed is based upon the detection and imaging of changes in the gap caused by surface displacements induced by strains generated by any modulation different from scanning of the tip. Strain imaging was first used for observing piezoelectric/ferroelectric properties. , Subsequently, magnetic strain imaging, thermal strain imaging, and electrochemical imaging have been done.

Variations of the images of volume changes depending on modulation frequencies clearly represented lithium intercalation. A linear relationship between the amplitudes of volume changes and the products of the diffusion elements and the reciprocals of the frequencies has been proven. Thus, the detected signals well quantitatively corresponded to the lithium ion movements.

Keiji Takata, Mitsuhiro Okuda, Nobuki Yura, and Ryota Tamura, Appl. Phys. Express 5 (2012) 047101; DOI: 10.1143/APEX.5.047101.

ESD/ASS-P3-04
Molecular H2 chemisorption by Kubas interaction onto Ti ion coordinated to methyl aluminum oxane/silica

T06 Energy and Sustainable Development

#ESD/ASS-P3-04

J. Lee.

Seoul National University - Seoul (Korea, republic of).

In the last decade, a number of theoretical investigations [1] by DFT calculations have predicted that 3-5 hydrogen molecules chemisorb onto early transition metals such as Sc,Ti, and V atomically decorated onto various substrates by the Kubas interaction with an adsorption energy of 0.25-0.35 eV suitable for reversible hydrogen storge. A new type of hydrogen storage based on this finding may have a great potential but experimental pursuit [3] along this direction is rare so far. We report here the preliminary results of our experimental investigation on the chemisorption of H_2 molecule by the Kubas interaction onto Ti ions coordinated to methyl aluminum oxane (MAO) oligomers attached to the surface of hydroxylated porous silica (3nm pores) powder of 60 μm sise. The coupling reaction of MAO with silica was carried in in pentane as solvent at room temperature and then $TiCl_4$ was added at 150 C under H_2 flow, which we believe to result in $Ti^{+}H_3$ coordinated to the Al^{-} site. Elemental analysis by EDX revealed that Ti of 1.0 wt.% or 4.3 wt. % was coordinated onto the MAO/silica and no Cl was left over. 200 mg of the synthesized sample was loaded in an adsorption cell and throughly evacuated at 150 C with a turbomolecular pump to remove solvent molecules which may remain in the pores of the sample. After D_2 adsorption to saturation at 80 K by filling with 5000 Torr of D_2, the cell was again evatuated to 10^{-8} Torr to pump out all D_2 which is not permanently adsorbed at 80 K. Then, temperature-programmed desorption (TPD) was performed in the closed cell by heating at an average rate of ~ 1K/s while monitoring the pressure increase in the cell. From the total pressure increase we estimate that ~ 0.26 D_2 molecues adsorbed per Ti. Differention of the measured P-T curve yields TPD spectrum showing a sharp peak centered at T_p~110 K with a long tail. The peak temperature corresponds to D_2 adsorption energy of E_{ad}~ 28.3 kJ/mol according to the Redhead relation E_{ad}~ $31kT_p$ [3]. This value is much larger than that of ~10 kJ/mol or less typically measured for H_2 physorbed on various carbonaous materials and molecular organic frames. Thus, one has to attribute the desorption peak to

molecularly chemisorbed D_2 by Kubas interaction onto Ti^+ ions coordinated to Al^- sites. The small amount of D_2 continuously desorbing at T>130 K is due to diffsion-limited desorption from deep in the pores. The same measurement with 4.3 wt.% Ti sample resulted in ~4 times larger amount of D_2 adsorption than that of 1.3 wt.% Ti. Repeated adsorption measurements with the same sample gave almost the same result, indicating that the sample is not degraded. Although the total amount of adsorbed D_2 is very small, the results suggest that hydrogen stroage based on Kubas interaction may provide a viable solution, if a better system can be designed.

[1] Hoonkyung Lee, Woon Ih Choi, and Jisoon Ihm, Phys. Rev. Lett. 97, 056104 (2006)

[2] Tuan K et. al., J. Am Chem. Soc., 2010, 132, 11792–11798 (2010)

[3] P.A.Redhead, Vacuum 12, 203-211 (1962)

ESD/ASS-1-Or-3
Reactive sputter deposition and characterization of K2NiF4 coatings for Intermediate Temperature - Solid Oxide Fuel Cell (IT-SOFC)

T06 Energy and Sustainable Development

#ESD/ASS-1-Or-3

J. Fondard [1], A. Billard [1], G. Bertand [2], P. Bertrand [1], P. Briois [1].

[1]IRTES-LERMPS, UTBM - Belfort (France), [2]CIRIMAT UMR CNRS-INPT-UPS 5085, ENSIACET - Toulouse (France).

Intermediate Temperature-Solid Oxide Fuel Cell (IT-SOFC) produces energy from the reaction between oxygen and hydrogen at 600-800°C. Its core, where the reaction takes place, is composed of three different solid oxide layers, cathode, anode and electrolyte.
One of a major obstacle to the development of IT-SOFC is the large cathode overpotential at these temperatures. One solution is to improve SOFC's electrocatalytic properties by the use of mixed ionic and electronic conductors (MIECs) as cathode material. Rare-earth nickelates with K_2NiF_4 structure, namely Ln_2NiO_4 (Ln= La, Nd, Pr) are assumed to be promising cathode materials for IT-SOFC. Such MIEC materials exhibit both high values of oxygen adsorption and diffusion, and high electronic conductivity. Moreover, their thermal expansion coefficient is close to that of electrolyte materials (CeO_2-Gd_2O_3 (CGO) and ZrO_2-Y_2O_3 (YSZ)). Interesting electrochemical performance of the nickelates have already been demonstrated on $La_2NiO_{4+\delta}$ /YSZ [1], $Nd_2NiO_{4+\delta}$ /YSZ [2] and $Pr_2NiO_{4+\delta}$ /CGO/YSZ [3] symmetric half-cells by Electrochemical Impedance Spectroscopy (EIS). Ni-YSZ /Ni-YSZ /YSZ /CGO /Pr_2NiO_4 [3] and $Nd_{1.95}NiO_{4+\delta}$ /YSZ /Ni–YSZ [4] complete cells were also tested under operating conditions and show promising results.

In this study, we investigate the feasibility of Ni-YSZ /YSZ /Ln_2NiO_4 cells (Ln= La, Nd, Pr) and compare the performance of the different cathode materials. Thin and dense Ln_2NiO_4 coatings were deposited by reactive magnetron sputtering under unstable conditions using Plasma Emission Monitoring (PEM) on an anode/electrolyte half-cell support. This support is composed of dense sputtered YSZ electrolyte layer deposited on porous plasma sprayed anode NiO-YSZ. For cathode deposition, the

discharge current on the Ln target is fixed at 2.5 A and that on the Ni target is adjusted to obtain the convenient composition for nickelate compound. The as-deposited coatings are amorphous and crystallize under K_2NiF_4 structure with appropriate annealing temperature. The structural and chemical features of nickelate coatings and also their compatibility with electrolyte material have been determined by X-Ray Diffraction and Scanning Electron Microscopy. Their electrical properties were evaluated using EIS on YSZ/Ln_2NiO_4 half cells and Ni-YSZ /YSZ /Ln_2NiO_4 complete cells under air and hydrogen.

[1]: F. Mauvy, C. Lalanne, J.M. Bassat, J.C. Grenier, H. Zhao, P. Dordor, Ph. Stevens, Journal of the European Ceramic Society 25 (2005) 2669–2672
[2]: F. Mauvy, J.-M. Bassat, E. Boehm, J.-P. Manaud, P. Dordor, J.-C. Grenier, Solid State Ionics 158 (2003) 17– 28
[3]: C. Ferchaud, J.C. Grenier, Y. Zhang-Steenwinkel, M.M.A. van Tuel, F.P.F. van Berkel, J.M. Bassat, Journal of Power Sources 196 (2011) 1872–1879
[4]: C. Lalanne, G. Prosperi, J.-M. Bassat, F. Mauvy, S. Fourcade, P. Stevens, M. Zahid, S. Diethelm, J. Van herle, J.-C. Grenier, Journal of Power Sources 185 (2008) 1218–1224

ESD/ASS-1-Or-6
Microscopic Measurements of Photovoltaic Energy Conversion

T06 Energy and Sustainable Development

#ESD/ASS-1-Or-6

A. Fejfar, M. Ledinsky, M. Hyvl, A. Vetushka, J. Kocka.

Institute of Physics, Academy of Sciences of the Czech Republic - Prague (Czech republic).

Modern nanostructured solar cells can be described as parallel arrays of random photodiode elements [1]. The elements typicall have mesoscopic size (well below 1 micrometer). Examples of such structures are silicon nanowires, silicon nanodomes and many others. We need to point out that even common thin films based cells using geometric light trapping structures (for example Si thin films folded on ZnO nanorods) will exhibit same features.
Nanostructuring the cells helps to achieve excellent light trapping and enables collection of photogenerated carriers at short distance, providing optically thick and geometrically thin structures.

However, no information is availabe about the distribution of the local efficiencies at different positions of the solar cell. Yet the combination of the diodes may severely limit the open circuit voltage and fill factor of the elements array [1].

We have developed several approaches using the atomic force microscopy with conductive cantilever to measure the local photoresponse (see experimental scheme at Fig. 1) [2]. Measuring local I-V characteristics at each scan point could in principle provide local conversion efficiency, in practice problems with noise, reproducibility and oxidation have to dealt with. Alternatively, Kelvin force microscopy can provide local photovoltage. We shall illustrate the approach by results obtained on solar cells based on microcrystalline grains in mixed phase Si thin films or on Si nanowires obtained by plasma enhanced vapour-liquid-solid growth catalyzed by metal nanoparticles (see Fig. 2).

Finally, we address the reference for the illumination absorbed power which is needed to assess the local photoconversion efficiency.

[1] V.G. Karpov, A.D. Compaan, D. Shvydka, Phys. Rev. B 69 (2004) 045325.
[2] M.Ledinský, A.Fejfar, A.Vetushka, J.Stuchlík, J.Kočka, J. Non-Crystall. Solids 358 (2012) 2082

Fig.1 Scheme of photoresponse measurement using C-AFM

Fig.2 Topography of Si nanowire sample

ESD/ASS-2-In-1
ATOMIC LAYER DEPOSITION FOR PHOTOVOLTAICS

T06 Energy and Sustainable Development

#ESD/ASS-2-In-1

W.M.M. Kessels.

Department of Applied Physics, Eindhoven University of Technology - Eindhoven (Netherlands).

The unique features of atomic layer deposition (ALD) can be employed to face processing challenges for various types of next-generation solar cells. Hence, ALD for photovoltaics (ALD4PV) has attracted great interest in academic and industrial research in recent years. In this presentation, the recent progress of ALD nanolayers applied to various solar cell technologies (c-Si, CIGS, DSSC, and OPV) will be reviewed and their future prospects will be discussed [1]. The presentation will focus particularly on the application of ALD oxides (Al2O3, SiO2, SiO2/Al2O3 stacks, Al2O3/ZnO:Al stacks) for the passivation of surfaces of high-efficiency silicon solar cells [2]. Moreover, the upscaling of ALD to high-throughput solar cell production will be addressed [3].

[1] J.A. van Delft, D. Garcia-Alonso, and W.M.M. Kessels, Semicond. Sci. Technol. 27, 074002 (2012).
[2] G. Dingemans and W.M.M. Kessels, J. Vac. Sci. Technol. A 30, 040802 (2012).
[3] W.M.M. Kessels and M. Putkonen, MRS Bulletin 36, 907 (2011).

ESD/ASS-1-In-1
DYNAMIC ATOMIC SCALE SOLUTIONS TOWARDS SUSTAINABLE ENERGY AND CLEANER ENVIRONMENT: INSIGHTS INTO BIOMASS TRANSFORMATION DYNAMICS USING IN-SITU E(S)TEM AT THE SINGLE ATOM LEVEL

T06 Energy and Sustainable Development

#ESD/ASS-1-In-1

P. Gai, E.D. Boyes.

The York JEOL Nanocentre and Departments of Chemistry, Physics and Electronics, University of York - York (United kingdom).

Considerable efforts are in progress worldwide to secure sustainable energy sources and cleaner environment. Superior catalysts are required for the efficient transformation of biomass and to optimise fuel cells for energy solutions, and for the reduction of emission of pollutants from automobiles. The latter is crucial to minimising the damage to the environment and to improve the air quality. We have directly visualised atomic scale interactions at the environment-catalyst interface in biomass transformation, fuel cells and in environmental control using our novel development of environmental (scanning) transmission electron microscopy (E(S)TEM) at the sub-Angstrom level and have complemented the studies by chemical methods. The studies provide insights into atomic scale active sites for the reactions.

FPFI-1-Or-7
Spectroscopic XPEEM for studying the surface electronics of epitaxial graphene domains

T07 Frontiers in Photoelectron Full-field Imaging and Spectromicroscopy

#FPFI-1-Or-7

H. Kim [1], C. Mathieu [2], N. Barrett [2], J. Coraux [3], O. Renault [1].

[1]CEA, LETI, MINATEC Campus - Grenoble (France), [2]2 CEA-DSM, IRAMIS, SPCSI - Gif-Sur-Yvette (France), [3]Institut Néel, Nanoscience Department - Grenoble (France).

Spectroscopic X-ray Photoelectron Emission Microscopy (XPEEM) has come to maturity over the past ten years with the advent of advanced instruments exploiting both synchrotron and laboratory excitation sources [1-2]. It is a powerful tool for studying the correlations at the microscopic level between electronic and chemical states in epitaxial graphene systems, because it allows to cross-check direct space (work function, core level shifts) and reciprocal space (band structure) information [3]. With laboratory excitation sources, routine analyses at the photoemission threshold can be performed to provide useful information regarding work function heterogeneities, local variations of charge transfer at the graphene/substrate interface (Fig. 1). In the reciprocal space (kPEEM), band structure information is provided at the micron scale, either for providing estimates on the shift of the Dirac point relative to the Fermi level or for fingerprinting graphene after plasma cleaning (Fig. 2). This contribution will provide an overview of XPEEM results regarding graphene/SiC and graphene/metal systems obtained with laboratory excitation sources, with emphasis for the case of growth on metallic substrates and effect of doping/intercalation.

[1] M. Escher et al. , J. Electron. Spectrosc. Relat. Phenom. 178-179 (2010), 303.
[2] A. Locatelli, E. Bauer, J. Phys. Cond. Matter 20 (9) (2009), 093002; C. M. Schneider et al., J. Electron. Spectrosc. Relat. Phenom. 185 (2012), 330.
[3] C. Mathieu et al., AIP Proc. 1395, 95 (2011); Phys. Rev. B. 83, 235436 (2011).

Fig.1- Spectroscopic VUV-PEEM of Graphene on SiC(0001): Work function mapping/distribution (a) and band structure imaging of a 2ML domain (b) with HeI excitation.

Fig.2- Band structure imaging of graphene residues of a structure on SiC(0001).

FPFI-1-Or-1
Direct observation of local redox-processes on resistivly switching SrTiO3 with spatially resolved spectroscopy

T07 Frontiers in Photoelectron Full-field Imaging and Spectromicroscopy

#FPFI-1-Or-1

A. Koehl, C. Lenser, M. Patt, V. Feyer, C.M. Schneider, R. Dittmann, R. Waser.

Research Center Juelich - Juelich (Germany).

The effect of resistive switching in transition metal oxides is a currently very active field due to the possible applications for non-volatile memory applications. In this work we directly monitor the local redox-process during resistive switching in the valence change material $SrTiO_3$. Epitaxial Fe-doped $SrTiO_3$ thin films were grown on conducting, single-crystalline Nb:$SrTiO_3$ substrates by pulsed laser deposition. After an initial forming sweep bipolar resistive switching is enabled and several pads were programmed to different resistive states. After removal of the top electrode spatially resolved X-ray photoelectron spectroscopy (XPS) and X-ray absorption spectroscopy (XAS) are employed in order to investigate the influence of the resistive switching process onto the electronic structure and chemical composition of the sample. The measurements have been performed with the NanoEsca at Elettra, Triest, where spectroscopic information with a lateral resolution down to 100nm can be gained. We compared the Sr-XPS, Ti-XAS and O-XAS signal of a virgin pad with “On” and “Off” pads, which have been set to low and high resistive state respectively. On all electrically treated pads several spots with a Sr-O rich surface component are found, which display a characteristic shift of the Sr 3d spectra to lower binding energies. As this effect is independent of the resistance state the evolution of this new component is assigned to the forming process which involves high voltages and currents. Due to Joule heating during the forming process Sr-diffusion might be enabled allowing the formation of a new Sr phase. Exclusively on the pad in low-resistive state a small feature of 300nm diameter with a Ti^{3+} contribution is found. This is interpreted as a signature of a reduced and therefore conducting filament giving rise to the decreased

resistance. Based on our spectroscopic studies we discuss redox-processes and phase formation on the nanoscale, which are relevant for the resistive switching effect.

Microscopy image at E_{Bind}=132.5eV of formed pad and corresponding Sr 3d spectra.

FPFI-3-Or-9
A new challenge of energy-filtered x-ray photoemmission electron microscopy （EXPEEM）with a Wien filter

T07 Frontiers in Photoelectron Full-field Imaging and Spectromicroscopy

#FPFI-3-Or-9

K. Miyazaki [1], T. Kitayama [1], T. Iwai [2], K. Tsuno [1], M. Kudo [2], H. Hiraiwa [2], K. Asakura [1].

[1]Hokkaido University - Sapporo-Shi (Japan), [2]Suga Co.Ltd - Hokuto-Shi (Japan).

PEEM with an energy analyzer is called as EXPEEM(energy filtered x-ray photoemission electron microscopy) and is a useful tool for chemical mapping of surface with high spatial and energy resolution.[1] The energy selection of photoelectron is usually fulfilled by a hemispherical energy analyzer where an optical axis of photoelectron should be bent and not good for the optical axis adjustment in microscopy.[1,2] We used a Wien filter to keep the straight optical axis even in the energy selection mode. We have developed 12 pole Wien filter to reduce the aberration in the Wien filter and increase the energy resolution and/or sensitivity[1]. The next challenge in this paper is to reduce the cost and increase the maneuverability. One is to decrease the number of poles in Wien filter. We now report a possibility of EXPEEM with 8 pole Wien filter with sufficient energy resolution and sensitivity.[3,4] The other is the perfect alignment of straight optical axis as shown in Fig. 1 by the coincidence of the radii of electrodes and coils.
Figure 1 shows the schematic design of the newly built EXPEEM. The sample is grounded and photoelectron is collected by a combination electrostatic-electromagnetic objective lens (immersion cathode lens). Electrons are running through liner tubes in magnetic lenses. The accelerating voltage of 10kV is retarded to 100V at the Wien filter. The Wien filter consists of 8 poles of air-core coil electromagnets and electrodes, both of which are inside the vacuum. Finally the electron is projected on a screen with a four-stage lens. We can obtain the 100 meV resolution at the slit set after the transfer lens(TL2) followed by the Wien filter at pass

energy =100 eV.
Consequently, we can reduce the cost down to less than half that of the previous EXPEEM and can be improved the maneuverability by using less electric and magnetic poles in the Wien filter and easy alignment of the beam.

[1] D.W. Turner, I.R. Plummer, H.Q. Porter, Rev. Sci. Instrum 59 (1988) 45.
[2] T. Schmidt, U. Groh, R. Fink, E. Umbach, O. Schaff, W. Engel, B. Richter, H. Kuhlenbeck, R. Schlogl, H.J. Freund, A.M. Bradshaw, D. Preikszas, P. Hartel, R. Spehr, H. Rose, G. Lilienkamp, E. Bauer, G. Benner, Surf. Rev. Lett. 9 (2002) 223.
[3] H. Niimi, W.J. Chun, S. Suzuki, K. Asakura, M. Kato, Rev.Sci.Instrum 78 (2007) 063710 .
[4] T. Miyamoto, T. Wada, H. Niimi, S. Suzuki, M. Kato, M. Kudo, K. Asakura, Jpn.J.Appl.Phys. 51 (2012) 046701.

Figure1. The schematic design of the machine. OL is the objective lens, TL1 and TL2 are the transfer lenses and B1 and B2 are the deceleration and acceleration lenses, respectively.

FPFI-1-Or-10
Efficient mapping of the spin resolved bandstructure of cobalt films by spin polarized momentum microscopy

T07 Frontiers in Photoelectron Full-field Imaging and Spectromicroscopy

#FPFI-1-Or-10

C. Tusche [1], M. Ellguth [1], A. Krasyuk [1], C. Wiemann [2], V. Feyer [2], M. Patt [2], C.M. Schneider [2], J. Kirschner [1].

[1]Max-Planck-Institut für Mikrostrukturphysik - 06120 Halle (Germany),
[2]Forschungszentrum Jülich - 52428 Jülich (Germany).

Spin resolved momentum microscopy is an efficient tool to study the band structure of ferromagnets. A spin polarizing electron mirror, i.e. a W(100) crystal, allows the measurement of the spin polarization in the whole momentum image, simultaneously. Thus, spin resolved 3D band structures as function of (k_x,k_y,E) can be measured with unprecedented efficiency, for the first time. We present comprehensive maps of the spin resolved band structure of cobalt grown on Cu(100), measured at the NanoESCA beamline [1] of the Elettra synchrotron. This instrument, consisting of a photoemission electron microscope (PEEM) and an electrostatic energy analyzer directly records the parallel momentum, $k_{||}$, of photoelectrons emitted from the sample. For these measurements, the imaging spin filter [2] was installed temporarily at the exit of the energy analyzer.
A series of momentum images gives direct access to the electronic structure of the Co-film. Using 40eV to 200 eV photons, several constant-energy cuts in the 3D Brillouin zone are selected. Figures 1 and 2 show electronic states in the majority- and minority- spin-channel at the Fermi surface and their dispersion towards larger binding energies. At E_F, intensity is dominated by minority features, while at 300meV below E_F we observe a change of the spin-polarization to positive sign, attributed to the flat dispersing Co d-bands. At larger binding energies sharp bands are only observed in the minority channel. The comprehensive data sets can serve as valuable input for advanced concepts in theory for the refined treatment of spin-dependent electron correlation.

[1] C. Wiemann, M. Patt, I. P. Krug, N. B. Weber, M. Escher, M. Merkel, C. M. Schneider, e-J. Surf. Sci. Nanotech. **9**, 395 (2011)
[2] C. Tusche, M. Ellguth, A. Ünal, C.-T. Chiang, A. Winkelmann, A. Krasyuk, M. Hahn, G. Schönhense and J. Kirschner: Appl. Phys. Lett. **99**, 032505 (2011)

Figure 1: Spin-resolved photoelectron momentum maps for the majority (↑) spin channel measured at four binding energies.

Figure 2: The same for the minority (↓) spin channel.

FPFI-1-Or-3
Nanospectroscopy on FeCu magnetic alloy films: electronic interface effects in organic-metal films

T07 Frontiers in Photoelectron Full-field Imaging and Spectromicroscopy

#FPFI-1-Or-3

M. Niño [1], F.J. Luque [2], I.O. Kowalik [3], P. Perna [1], T.O. Mentes [4], A. Locatelli [4], L. Aballe [5], D. Arvanitis [6], R. Miranda [2], J.J. De Miguel [2].

[1]IMDEA Nanoscience - Madrid (Spain), [2]Universidad Autónoma de Madrid (UAM) - Madrid (Spain), [3]Polish Academy of Sciences - Warsaw (Poland), [4]Elettra Sincrotrone - Trieste (Italy), [5]ALBA Cells - Barcelona (Spain), [6]Uppsala University - Uppsala (Sweden).

Epitaxial, metastable fcc $Fe_{50}Cu_{50}$ alloy films are grown by Fe and Cu codeposition with the aid of a surfactant Pb monolayer pre-deposited on a Cu(111) surface. During codeposition, Pb atoms segregate to the surface and at the same time reduce the lateral mobility of the deposited atoms [1], preventing phase separation of both elements that are inmiscible in bulk. Metastable FeCu alloys are known to display Invar properties as a result of the competition between two structural phases with different atomic volume [2]. Due to the Stranski-Krastanov growth mode of Pb on Cu(111) 3D islands of relaxed Pb are formed for coverages beyond 1 ML. XMCD-PEEM and LEEM experiments allow us to compare the structure and magnetic behavior of the FeCu alloy films grown simultaneously on two different substrates, the Cu(111) crystal and the Pb(111) islands. These measurements reveal a completely different magnetic character for both systems: an 11 ML film of $Fe_{50}Cu_{50}$ (Fig. 1) imaged using circularly polarized x rays at the Fe L_3 absorption edge show that the alloy grown on the Cu(111) substrate is paramagnetic; no dichroic contrast is visible, whereas the same alloy displays an intense in-plane dichroic contrast when lying atop the Pb islands. Micro-LEED measurements demonstrate that all alloy films are fcc with equivalent crystallographic structure and lattice parameter irrespective of the supporting substrate (on the islands and out of the islands), and micro-XPS shows that they also have the same chemical composition and stoichiometry. The origin of the different magnetic behavior it is ascribed to electronic effects at the interface between the alloy and the substrate, as revealed by magnetic circular

dichroism data obtained at synchrotron MAX IV in Lund. These alloy films also constitute a privileged playground to investigate the effect of magnetic order on adsorption phenomena: chiral molecules have recently been proposed as a candidate to spin filter after the observation of intense spin polarization in electron currents transmitted through them. For this purpose we have deposited films of chiral Diphenyl-ethanediol on the alloy and performed a selective dichroic study, exciting electrons from the underlying, ferro- or paramagnetic FeCu film to measure the spin-selective transmission through the molecules.

[1] J. Camarero et al., Surf. Sci. **482-485**, 1077 (2001); J. Ferrón et al., Surf. Sci. 459, 135 (2000).
[2] P. Gorria et al. Phys. Rev. B **69**, 214421 (2004).

Fig. 1. XMCD-PEEM image of 11 ML thick film of $Fe_{50}Cu_{50}$ grown on Cu(111): magnetic contrast can be seen only on top of the Pb islands but not on the surface.

FPFI-2-Or-5
Multiferroic domain imaging by linear and circular dichroism in threshold photoemission microscopy

T07 Frontiers in Photoelectron Full-field Imaging and Spectromicroscopy

#FPFI-2-Or-5

A. Hoefer, W. Widdra.

Institute of Physics, Martin-Luther-Universität Halle-Wittenberg - Halle (Germany).

Threshold photoemission microscopy (PEEM) is an excellent technique to image the ferroelectric domain structure of sample surfaces by using work function differences [1]. For $BaTiO_3$(001) it has been demonstrated that three different ferroelectric domain types are discriminable with significant contrast in Laser-excited PEEM. The observed domain pattern preserves even at temperatures above the Curie point which is explicable by a remaining tetragonal distortion of the topmost unit cells as supported by first principle calculations [2].
So far, the domain patterns of multiferroic surfaces have been imaged by complementary techniques only. Typically, X-ray PEEM has been used to investigate the magnetic and piezoresponse force microscopy the ferroelectric domain structure. Laser-excited threshold PEEM as a lab-based experiment is capable to be sensitive to the ferroelectric as well as the magnetic signal, since also the photoemission from the valence band depends on the magnetization direction.
Here, we demonstrate for magnetoelectric $BiFeO_3$(001) that threshold PEEM allows for the separation of different multiferroic domain structures in a single experiment. There, the imaging is based on work function contrast, linear and circular dichroism. In Laser-PEEM (Fig. 1(a)) two ferroelectric domains can be discriminated by their photoemission yields. Additionally, the contrast observed in PEEM severely depends on the linear or circular polarization of the exciting light, respectively. The normalized difference of two images measured for two different linear polarizations of light or measured with left and right circularly polarized light shows clear domain structures (Fig. 1(b) and (c), respectively). The comparison of these patterns among each other and with the ferroelectric domains reveals in each case additional domain states. With the aid of the ferroelastic domain structure we are able to discriminate all eight

multiferroic domains. The observation of a varying linear dichroism for different ferroelectric domains is explicable by the coupled ferroelectric-antiferromagnetic order in $BiFeO_3$.

We thank Dr. Marin Alexe from the Max Planck Institute of Microstructure Physics Halle for the preparation of the $BiFeO_3$ single crystals. The financial support by the Deutsche Forschungsgemeinschaft through the SFB 762 “Functionality of Oxide Interfaces” is gratefully acknowledged.

[1] A. Höfer et al. IBM Journal of Research and Development 55, 4:1 (2011)
[2] A. Höfer et al., PRL 108, 087602 (2012)

Figure 1 (a) PEEM image (photon energy 4.23 eV), **(b)** linear dichroism pattern and **(c)** circular dichroism pattern in threshold photoemission of a $BiFeO_3$(001) surface (field of view: 150 µm).

FPFI-1-Or-11
Spin-resolved dispersion of unoccupied quantum well states in Co thin films on Cu(001)

T07 Frontiers in Photoelectron Full-field Imaging and Spectromicroscopy

#FPFI-1-Or-11

M. Ellguth [1], C. Tusche [1], C.T. Chiang [1], J. Henk [2], A. Winkelmann [1], J. Kirschner [1].

[1]MPI für Mikrostrukturphysik - Halle (Germany), [2]Institut für Physik, Martin-Luther-Universität - Halle (Germany).

Quantum well states (QWS) can be formed when electrons are confined in ultrathin films due to a projected bulk band gap of the substrate for wavevectors perpendicular to the film surface. In the surface parallel directions, the electron still experiences the periodic potential of an infinite crystal and therefore reflects the bulk band dispersion. In Co thin films on Cu(001) substrate, such QWS are located in the unoccupied part of the band structure. Two-photon photoemission with the second harmonic of a Ti:Sa laser yielding 3.0-eV-photons enables us to observe resonant transitions via the QWS. This approach has been previously employed to study spin-selective electron excitation in normal emission [1].
In this study, we have used an energy-filtered momentum-imaging PEEM [2] that detects photoelectrons of all emission angles in one shot. The $E(k_{||})$-dispersion (Figure 1) of the QWS in 6 ML Co/Cu(001), which is shown in Figure 1, is consistent with the sp-type character of the relevant Co bands.
Using a recently developed 2-dimensional spin filter [3], we have measured momentum maps of the partial intensities for both spin channels (Figure 2). The direct comparison of resonant and non-resonant two-photon transitions reveals that the resonant two-photon excitation via the quantum well leads to nearly 100% spin polarization which mixes with less strongly polarized electrons from non-resonant excitation.

[1] C.-T. Chiang, A. Winkelmann, J. Henk, F. Bisio, J. Kirschner, *Phys Rev B* **85** 165137 (2012)

[2] B. Krömker, M. Escher, D. Funnemann, D. Hartung, H. Engelhard, J. Kirschner, *Rev. Sci. Instrum.* **79**, 053702 (2008)
[3] C. Tusche, M. Ellguth, A. A. Ünal, C.-T. Chiang, A. Winkelmann, A. Krasyuk, M. Hahn, G. Schönhense, J. Kirschner, *Appl. Phys. Lett.* **99**, 032505 (2011)

Figure 1: Two-photon photoemission intensities showing the quantum well state E(k||)-dispersion on a 6 ML Co/Cu(001) thin film
Figure 2: Partial intensities for majority and minority electrons at energies marked by dotted horizontal lines in figure 1.

FPFI-3-Or-4
Using polarized light in PEEM

T07 Frontiers in Photoelectron Full-field Imaging and Spectromicroscopy

#FPFI-3-Or-4

T. Wagner [1], Z. Druckmüllerová [2], D. Huber [1], D.R. Fritz [1], P. Zeppenfeld [1].

[1]Johannes Kepler University - Linz (Austria), [2]Brno University of Technology - Brno (Czech republic).

Photoelectron emission microscopy (PEEM) combines high lateral resolution with the capability to monitor processes on the surface in real-time. For experiments in the lab, unpolarized light of a Hg lamp is commonly used to excite the photoelectrons. In this case, valuable information about the optical anisotropy of the surface under investigation is lost. On the other hand, techniques like reflectance difference spectroscopy (RDS) which are focussed on this anisotropy have proven to be useful tools to study thin adsorbate films of organic molecules. So why not combining both in a single experiment? In this presentation we will show, how polarized light can be used to study the growth of α-sexithiophene on silver and nickel oxide surfaces. As the ionization potential of the molecules is higher than the photon energy, the light of the Hg lamp only excites electrons from the metal-organic interface. In this case, no direct response of the molecules to the polarized light can be expected in the PEEM image. Nevertheless, the molecules are optical anisotropic and act as dichroic filters for the incident light. This effect can actually be used, e.g., to probe the orientation of the molecules even during growth. [1]

[1] Thorsten Wagner, Daniel Roman Fritz, Peter Zeppenfeld: "Probing organic nanostructures by photoelectron-emission microscopy", Applied Surface Science, in press, http://dx.doi.org/10.1016/j.apsusc.2012.04.157

Fig. 1: (a) PEEM image of a Ag(111) surface covered with an α-sexithiophene (α-6T) film deposited at 365 K. The image was acquired with a Hg lamp (4.9 eV). (b) Phase information extracted from a sequence of 361 PEEM images for which a linear polarizer in front of the lamp was rotated in steps of 1°.

FPFI-P3-01
Combined surface-sensitive microscopies for the study of surface modifications of micro-switches upon cycling

T07 Frontiers in Photoelectron Full-field Imaging and Spectromicroscopy

#FPFI-P3-01

O. Renault, E. Martinez, D. Mariolle, B. Reig.

LETI, MINATEC - Grenoble (France).

For the optimization of micro-switching systems with Ru-based active components (Fig.1) , a key parameter to be controlled is the stability of the switching resistance over time upon many cycling processes of the devices. We have implemented in a complementary way different surface-sensitive microscopies to contribute to the understanding of the anomalous cycling effects on such devices. Fig. 2 shows results of core-level spectromicroscopy performed with XPEEM on the gold/ruthenium active part of the switch. It shows that upon cycling, additional core-level components (visible on the micro-spectra of Fig. 1) and shifted to lower binding energies appear on both Ru3d and Au4f images, with a clear localization in the switching region. This cannot be explained by a different surface potential which is shown constant by Kelvin Force Microscopy. This region happens to be over-contaminated in carbon and contains sulphur traces, as shown by scanning Auger nanoprobe. We interpret the spectromicroscopic results in terms of formation of nano-clusters, possibly inducing negative binding energy shift due to final state effects.

Acknowledgement
The work was supported by the French National Research Agency through the Recherche Technologique de Base program and was performed in the Nanocharacterization Centre of MINATEC.

Core-level micro-spectroscopy (middle) and spectromicroscopy after cycling (right) of a Ru-based micro-switch device represented on the left (size of Ru dot is 10µm).

FPFI-2-Or-2
Surface antiferromagnetic domain imaging using low energy unpolarized electrons

T07 Frontiers in Photoelectron Full-field Imaging and Spectromicroscopy

#FPFI-2-Or-2

K. Menon [1], S. Mandal [1], J. Das [1], T.O. Mentes [2], M. Niño [3], A. Locatelli [2], R. Belkhou [4].

[1]Saha Institute of Nuclear Physics, 1/AF Bidhannagar - Kolkata (India), [2]2Sincrotrone Trieste S.C.p.A., Basovizza - Trieste (Italy), [3]Instituto Madrileño de Estudios Avanzados IMDEA Nanociencia - Madrid (Spain), [4]Synchrotron SOLEIL, L'Orme des Merisiers Saint-Aubin - Gif-Sur-Yvette (France).

Surface magnetic domain imaging of antiferromagnetic (AFM) materials has been a challenge to most magnetic microscopies due to the absence of a net magnetic moment. X-ray Magnetic Linear Dichroism (XMLD) based techniques are primarily used nowadays for surface AFM domain imaging, requiring access to dedicated synchrotron beamlines. Thus, there is a strong demand for a laboratory-based imaging technique offering high spatial resolution as well as enhanced sensitivity to surface AFM order enabling routine surface magnetism studies. Here we present an electron microscopic approach for imaging surface AFM domains using coherently exchange-scattered unpolarized electrons in a laboratory-based Low Energy Electron Microscope (LEEM) [1]. Coherent exchange scattering of electrons from AFM surface of NiO(100) are visible at low electron energies (< 100 eV) due to the enhanced exchange scattering cross-section for slow electrons [2]. We employed such exchange-scattered half-order diffraction beams in the dark-field operation mode in LEEM (shortly, AFM-LEEM) to directly image AFM surface domains. Figure 1 sketches the general concept behind this AFM-LEEM experiment; single half-order diffraction beam is selected so that the LEEM image will show only the sample regions that contribute to the selected half-order diffraction spot. The small probing depth (~0.2-0.5 nm) of the low energy electrons enables to explore mostly the top-layer magnetic information. Along with the spatial resolution (~10 nm) this makes AFM-LEEM complementary to XMLD-PEEM techniques. This method has been successfully applied to resolve the surface AFM domains on prototypical systems;

single crystal NiO(100) surface and epitaxial thin films of NiO(100) grown on Ag(100) and are directly compared with XMLD-PEEM experiments demonstrating their complimentary nature. In case of the NiO model system, we have demonstrated that AFM-LEEM provides sufficient intensity to be exploited in realistic imaging experiments, providing valuable information on the AFM state at lateral resolution better than 10 nm with fast acquisition times. High surface sensitivity combined with improved spatial resolution of this technique will open up new route for studying surface magnetism and can grant access to finer details of the AFM domain structures that are still unexplored.

[1] K. S. R. Menon et al., Phys. Rev. B 84, 132402 (2011).

[2] P. W. Palmberg et al., Phys. Rev. Lett. 21, 682 (1968).

Figure 1: AFM surface produces half-order diffraction beams. The dark-field images, formed by the electrons originating from the half-order beams, display contrast due to the surface AFM domains.

FPFI-1-in-1
PIC-mapping of biomineral crystals by PEEM

T07 Frontiers in Photoelectron Full-field Imaging and Spectromicroscopy

#FPFI-1-in-1

P. Gilbert.

University of Wisconsin - Madison (United states).

Biominerals include teeth, bone, mollusk shells and the skeletons of algae, sponges, corals, sea urchins and most other animals. The function of biominerals are diverse: mechanical support, attack, defense, grinding, biting, and chewing, gravitaty and magnetic field sensing, light focusing, and many others. Organisms have evolved to master mineralization, and the nanostructure of their biominerals. We harness x-ray linear dichroism to produce Polarization-dependent Imaging Contrast (PIC) mapping using PEEM (1-10), and reveal the complex architecture of mollusk shell nacre, or mother-of-pearl, and how it is formed by animal-controlled self-assembly (1-3, 9-10).

1. RA Metzler et al. PRL 2007
2. RA Metzler et al. PRB 2008
3. PUPA Gilbert et al. JACS 130, 17519-17527 (2008).
4. Y Ma et al. PNAS 106, 6048-6053 (2009).
5. CE Killian et al. JACS 131, 18404-18409 (2009).
6. RA Metzler et al. JACS 132, 6329-6334 (2010).
7. CE Killian et al. Adv. Funct. Mater. 21, 682-690 (2011).
8. PUPA Gilbert et al. PNAS 108, 11350-11355 (2011).
9. IC Olson et al. JACS 134, 7351-7358 (2012).
10. PUPA Gilbert. J. Electr. Spectrosc. and Rel. Phenom. 185, 395-405 (2012).

FPFI-1-Or-6
Mapping the interplays of organic semiconductor and ferromagnetic layers in vertical organic spin-valve structures

T07 Frontiers in Photoelectron Full-field Imaging and Spectromicroscopy

#FPFI-1-Or-6

D. Wei, Y.L. Chan, Y.J. Hsu.

National Synchrotron Radiation Research Center - Hsinchu (Taiwan, republic of china).

A key issue in constructing layered electronic devices is the control of nanoscale interfaces. This is because the electric current is sensitive to the variation of electric/magnetic field, and interfaces are were the potential energy surfaces experience an abrupt change. For devices aiming to manipulate electrons' spin degree of freedom, the interfaces are even more important - they need to regulate not only the charge flow but also the coherence of spin polarization among carriers. For this regard, the magnetization at interfaces is recognized as a key parameter in GMR showing the GMR effect [1]. In this presentation, I would like to address a concern wondering if the lessons given by inorganic structures can be readily applied to metal-organic hybrid structures [2,3]. I will discuss the magnetic behavior of cobalt-pentacene (Co-Pn) interface from the perspective of X-ray imaging, and its possible correlation with the diminished room temperature magnetoresistance found at hybrid spin-valve structures. In brief, through element-specific X-ray magnetic images acquired from Pn/Co structures, the development of ferromagnetism in Co layer grown on Pn film was found somehow retarded (as shown in figures). X-ray images and micro-spectroscopic evidences indicated that this magnetic retardation is associated with both chemical reaction and metal penetration [4,5]. Our experiments indicate that the magnetism at hybrid structure's interfaces is affected by the order of layer deposition.

[1] S. S. P. Parkin, Phys. Rev. Lett. 71, 1641 (1993).
[2] S. Sanvito, Nat. Phys. 6, 562 (2010).
[3] P. Ruden, Nat. Mater. 10, 8 (2011).
[4] Y.-L. Chan, Y.-J. Hung, C.-H. Wang, Y.-C. Lin, C.-Y. Chiu, Y.-L. Lai, H.-T. Chang, C.-H. Lee, Y. J. Hsu, and D. H. Wei, Phys. Rev. Lett. 104, 177204 (2010).
[5] D. H. Wei, C.-H. Wang, H.-C. Chang,Y.-L. Chan, C.-H. Lee, Y.-J. Hsu, Appl. Phys. Lett. 101, 141605 (2012).

XPEEM images of Pn/Co bilayers recorded with (a) element and (b) magnetic contrast, respectively.

FPFI-1-Or-8
Dark Field Photoelectron Emission Microscopy of Micron Scale Few Layer Graphene

T07 Frontiers in Photoelectron Full-field Imaging and Spectromicroscopy

#FPFI-1-Or-8

K. Winkler [1], B. Krömker [1], N. Barrett [2], E. Conrad [2].

[1]Omicron NanoTechnology GmbH - Taunusstein (Germany), [2]CEA, IRAMIS/SPCSI/LENSIS - Saclay (France).

We present dark field Photoelectron Emission Microscopy and energy filtered electron emission spectromicroscopy with high spatial and wave-vector resolution on few-layer epitaxial graphene on SiC(000-1) grown by furnace annealing.

Conventional electron spectroscopy methods are limited in providing simultaneous real and reciprocal or k-space information from small areas under laboratory conditions. Therefore, the characterization of materials with only micron scale sample homogeneity such as epitaxially grown graphene requires new instrumentation. Recent improvements in aberration compensated energy-filtered photoelectron emission microscopy (PEEM) can overcome the known limitations in both synchrotron and laboratory environments.

Energy-filtered, threshold PEEM is used to locate distinct zones of FLG graphene. In each region, selected by a field aperture, the k-space information is imaged using appropriate transfer optics. By selecting the photoelectron intensity at a given wave vector and using the inverse transfer optics, dark field PEEM gives a spatial distribution of the angular photoelectron emission. Only the combination of high lateral, high energy, high k-resolution and controlled switching between real space and k-space allows detailed understanding of micron size sample sites with 1–3 layers graphene.

N. Barrett, Rev. Sci. Instrum. 83, 083706 (2012), M. Escher, J. El. Spec.Rel. Phen. 178-179 (2010), B. Krömker, Rev. of Sci. Instruments 79 (5) (2008)

Fig. 1 k-PEEM image showing a constant energy cut in the $kx_{||}$, $ky_{||}$ plane at E-EF = 21.0 eV recorded from an area of 73µm on the sample. Bright spots originate from several Graphene sheets (Fig 1 spot a and b) indicated by the differently oriented Dirac points. Fig. 2a, b Dark field images recorded at E-EF = 21.0 eV in real space. The images are obtained by selecting the Dirac cones labeled a-f using a 0.11 $Å^{-1}$ diameter contrast aperture. Each image gives directly the spatial location of a particular commensurate rotation. Fig 3. Colour overlay of all darkfield maps originating from Dirace cones a-f in Fig 1.

FPFI-P3-02
Development of breakthrough stainless steel materials via spectromicroscopy

T07 Frontiers in Photoelectron Full-field Imaging and Spectromicroscopy

#FPFI-P3-02

M. Hannula, K. Lahtonen, M. Valden.

Surface Science Laboratory, Tampere University of Technology - Tampere (Finland).

Stainless steels are versatile materials due to the excellent thermal properties, mechanical strength and corrosion resistance. The enhanced properties of advanced ferritic grades are often achieved through optimization of the alloy composition. Addition of Nb and Ti *e.g.* is used to prevent precipitation of Cr with C or N and induce formation of nanodispersed NbC that enhance the strength of steel.[1] The role of minor alloying elements is crucial at surface and interfaces where the enrichment and segregation of alloy elements under corrosive or high-temperature conditions play an important role.

Our earlier work has focused on the oxidation of stainless steels, segregation phenomena and, in particular, on the role of alloying elements.[2,3] Here we report results obtained from microalloyed ferritic stainless steel with a newly commissioned NanoESCA (Omicron GmbH) spectromicroscopy system. Its sub-micrometer resolution and *in situ* sample preparation facilities allow us to oxidize steel in a controlled fashion and conduct spectromicroscopy experiments to observe segregation phenomena, precipitate formation, surface chemical composition, enrichment phenomena at grain boundaries and passive oxide film formation in general. Figures 1 and 2 present the work function and chemical contrast images of Fe on ferritic stainless steel, demonstrating how the grain structure can be readily correlated with the surface chemical composition. This information is the key to developing new stainless steel materials, since it allows us to understand how alloy constituents, grain boundaries, precipitate formation and segregation phenomena influence surface passivation under oxidative conditions.

[1]Y. Yamamoto, M.P. Brady, Z.P. Lu, P.J. Maziasz, C.T. Liu, B.A. Pint, et al., Science 316, 433 (2007).
[2]H. Ali-Löytty, P. Jussila, T. Juuti, L.P. Karjalainen, A.A. Zakharov, M. Valden, Int. J. Hydrogen Energy 37(19), 14528 (2012).
[3]H. Ali-Löytty, P. Jussila, M. Valden, Int. J. Hydrogen Energy 38(2), 1039 (2013).

Fig. 1. Energy-filtered image of Fe-19Cr-1Mo-(Ti,Nb) at E_k=4.6 eV.

Fig. 2. Imaging XPS of Fe-19Cr-1Mo-(Ti,Nb) at E_b=707 eV (Fe $2p_{3/2}$). Note the same surface region with Fig. 1.

FPFI-3-Or-1
Photoemission electron microscopy using high intensity ultrashort laser pulses

T07 Frontiers in Photoelectron Full-field Imaging and Spectromicroscopy

#FPFI-3-Or-1

E. Mårsell, C.L. Arnold, A. L' Huillier, A. Mikkelsen.

Lund University - Lund (Sweden).

Photoemission electron microscopy (PEEM) together with advanced laser sources has during recent years emerged as a powerful tool to study phenomena such as surface plasmons or magnetization dynamics on surfaces. Most studies have been performed using femtosecond pulses from a Ti:Sapphire oscillator. By instead using intense femtosecond pulses from laser amplifiers, possibilities open up for a variety of non-linear processes. One such process is high-order harmonic generation (HHG), which can produce coherent attosecond extreme ultraviolet (XUV) pulses. The use of such pulses for PEEM studies with unprecedented spatiotemporal resolution was suggested by Stockman et al. in 2007 [1], and some experiments have since then been performed on PEEM imaging using XUV radiation from HHG sources [2-4]. A spectrum of the radiation we have used for the experiments is shown in figure 1. It is, however, a challenging experiment to realize in practice, mainly due to space charge effects and chromatic aberration. We present ways of optimizing imaging conditions, and discuss what improvements are needed to realize PEEM with attosecond temporal resolution.

Multiphoton PEEM using infrared pulses has been shown to be a powerful way of mapping out localized field enhancements at surfaces, and we show results on both semiconductor and metal nanostructures excited by infrared pulses. By optical frequency mixing in non-linear crystals, we can produce femtosecond laser pulses ranging from 400 nm to 2000 nm, and we demonstrate 6-photon PEEM at the important telecommunication wavelength of 1550 nm.

Finally, we present first results from a new HHG setup using femtosecond pulses from a non-collinear optical parametric amplifier (NOPA), which works at repetition rates of hundreds of kHz up to one MHz. Such a high-repetition rate system allows us to decrease the individual pulse energy while keeping high enough average

photoelectron flux for imaging, which will significantly reduce space charge effects. A high enough photoelectron flux also opens up possibilities for energy filtering, thus reducing chromatic aberration.

[1] M. I. Stockman *et al., Nature Photon.* **1,** 539-544 (2007).
[2] A. Mikkelsen *et al., Rev. Sci. Instrum.* **80,** 123703 (2009).
[3] E. Mårsell *et al., Ann. Phys.*, DOI 10.1002/andp.201200269 (2012).
[4] S. H. Chew *et al., Appl. Phys. Lett.* **100,** 051904 (2012).

Figure 1. Typical spectrum of the HHG radiation generated by an 800 nm IR beam in argon. The spectrum, with its discrete peaks every odd harmonic, corresponds to a train of attosecond pulses separated by one half-cycle of the driving field.

FPFI-1-Or-9
Temperature-controlled reversible rippling and bonding of graphene on a square lattice.

T07 Frontiers in Photoelectron Full-field Imaging and Spectromicroscopy

#FPFI-1-Or-9

A. Locatelli [1], C. Wang [2], C. Africh [3], O. Mentes [1], N. Stojic [4], G. Comelli [5], N. Binggeli [4].

[1]Elettra - Sincrotrone Trieste S.C.p.A. - Trieste (Italy), [2]Abdus Salam International Centre for Theoretical Physics - Trieste (Italy), [3]IOM-CNR Laboratorio TASC - Trieste (Italy), [4]Abdus Salam International Centre for Theoretical Physics and IOM-CNR Democritos - Trieste (Italy), [5]Department of Physics, University of Trieste, and IOM-CNR Laboratorio TASC and Elettra - Sincrotrone Trieste S.C.p.A. - Trieste (Italy).

Graphene on metals has evolved into a paradigm for understanding how the substrate interactions influence the electronic properties of two-dimensional sp^2 hybridized atomic networks [1]. Aiming at characterizing its band structure, research has recently focused on high-quality epitaxial films grown on transition metals, investigating a variety of extrinsic, substrate-induced effects. Known since the early days of surface science [2], the growth of few-layer graphene can nowadays be accurately controlled on most fcc(111) or hcp(0001) transition metal surfaces. Epitaxial graphene on metals shows a great variety of rotational structures and moiré patterns originating from the small lattice mismatch with the substrate, often accompanied by the formation of regular corrugations in the film [3]. Despite the huge number of studies that the rise of graphene has triggered, the properties of graphene on crystal faces showing different symmetry than the threefold are still largely unexplored [4,5]. We report here on the structure and electronic properties of graphene grown on Iridium (100), a square symmetry substrate. By combining advanced microscopy methods (spectroscopic photoemission and low energy electron microscopy, microprobe angle-resolved photoelectron spectroscopy, scanning tunneling microscopy) and *ab initio* calculations, we characterize a new commensurate graphene phase that displays exceptionally regular one-dimensional ripples with nm-periodicity and extends over microscopic length scales. A unique

feature of this system is that the buckled graphene phase can be reversibly transformed into flat physisorbed graphene by simple control on the temperature. We demonstrate that this process, which effectively relieves the strain that builds up with temperature variations, involves the formation and rupture of a just few interfacial C-Ir bonds. Our results illustrate how the substrate symmetry can be exploited to control the morphology, bonding and electronic structure of graphene, opening further possibilities for tuning adhesion and charge transport in this material.

[1] A.K. Geim and K.S. Novoselov, Nat. Mat. 6, 183-191 (2007).
[2] H.P. Boehm et al., Z. Naturforsch. B 17, 150-153 (1962).
[3] M. Batzill, Surf. Sci. Rep 67, 83-115 (2012).
[4] J.W Wofford et al., Nano Lett. 10, 4890-4896 (2010).
[5] A.L. Walter et al., Phys. Rev. B 84, 195443 (2011).

Fig 1: Dark-field PEEM has been used to measure the density of states of buckled and flat graphene phases on Ir(100).

FPFI-3-Or-4a
Strain-induced band gap narrowing in Ge-rich SiGe nano-stripes

T07 Frontiers in Photoelectron Full-field Imaging and Spectromicroscopy

#FPFI-3-Or-4a

G. Vanacore [1], M. Chaigneau [2], N. Barrett [3], M. Bollani [4], F. Boioli [5], M. Salvalaglio [5], F. Montalenti [5], N. Manini [6], L. Caramella [6], P. Biagioni [1], D. Chrastina [7], G. Isella [7], O. Renault [8], M. Zani [1], R. Sordan [7], G. Onida [6], R. Ossikovski [2], H.J. Drouhin [9], A. Tagliaferri [1].

[1]CNISM, Dipartimento di Fisica, Politecnico di Milano - Milano (Italy), [2]LPICM, Ecole Polytechnique, CNRS - Palaiseau (France), [3]CEA Saclay, CEA DSM IRAMIS SPCSI - Gif Sur Yvette (France), [4]CNR-IFN e L-NESS - Como (Italy), [5]Dipartimento di Scienza dei Materiali, Università Milano Bicocca - Milano (Italy), [6]Dipartimento di Fisica, Università degli Studi di Milano - Milano (Italy), [7]CNISM e L-NESS, Dipartimento di Fisica, Politecnico di Milano - Como (Italy), [8]CEA, LETI, MINATEC Campus - Grenoble (France), [9]LSI, Ecole Polytechnique, CNRS - Palaiseau (France).

In the last years much work has been devoted to find the best strategy to apply *tensile* strain to Ge structures in order to reduce the energy difference between the direct and indirect band-gaps favoring population inversion and lasing.[1] According to recent k•p calculations,[2] the direct gap condition is dominated by the hydrostatic strain component. Several strained configurations have been explored so far, especially using external stressors.[3] However, high tensile strain has been reached only using thick stressor layers and for large structures (> 1 μm). This reduces their scalability and prevents the applicability of these methods to the design of nanoscale optoelectronic devices.

In this work, we explore a strategy to obtain nanoscale structures with a high gap narrowing, avoiding the use of external stressors. We created Ge-rich SiGe *embedded* nano-stripes (Fig. 1a) with a microscopic strain state maximizing the hydrostatic component. Nanoscale resolved spectroscopies, strain simulations and electronic-structure calculations have been used to map the strain field and the strain-induced band gap variation at the surface of the nano-stripes.

Strain is measured by Tip Enhanced Raman Spectroscopy (TERS) with a lateral resolution of 30 nm (Fig. 1b). A large tensile hydrostatic strain is found in the nano-stripes, as a result of the out-of-plane frustrated relaxation due to the constrained geometry, combined with a plastic relaxation in the (001) plane. The strain-induced variation of the surface electronic structure is studied by valence band and work function mapping using X-Ray Photoelectron Emission Microscopy (X-PEEM) with a resolution better than 100 nm (Fig. 1c-d). A positive work-function shift and a broader dispersion at the valence band edge are found for the nano-stripes with respect to the bulk case. We attribute these findings to the narrowing of the direct band gap induced by the tensile strain. Fitting the experimental results by *ab initio* calculations, the reduction of the energy difference between the direct and indirect band gaps is estimated to be ~ 100-120 meV, larger than that of strained structures reported so far in literature. The present results have a potential impact on the design of optoelectronic devices at nanometer-length scale and on the achievement of the population inversion and lasing by SiGe technology.

[1] D. Liang *et al.*, *Nat. Photonics* **2010**, *4*, 511

[2] O. Aldaghri *et al.*, *J. Appl. Phys.* **2012**, *111*, 053106

[3] D. Nam *et al.*, *Appl. Phys. Lett.* **2012**, *100*, 131112

Figure 1

FPFI-P3-04
The Dreamline at Shanghai Synchrotron Radiation Facility

T07 Frontiers in Photoelectron Full-field Imaging and Spectromicroscopy

#FPFI-P3-04

H. Liu [1], J. Sun [2], J. Dong [1], Y. Shi [1], Q. Wu [1], X. Yang [2], H. Ding [1].

[1]Institute of Physics, Chinese Academy of Sciences - Beijing (China), [2]Dalian Institute of Chemical Physics, Chinese Academy of Sciences - Dalian (China).

Shanghai Synchrotron Radiation Facility (SSRF) is a third-generation of synchrotron radiation light source with an electron energy of 3.5 GeV. An advanced angle-resolved photoemission spectroscopy system (ARPES) and an aberration corrected photoemission microscope (ACPEEM) are installed at a soft X-ray beamline named Shanghai Dreamline. The soft X-ray energy ranges from 20 eV to 2000 eV, covering the K edges of elements C, N, and O, L edges of 3d transition metal elements, and M edges of 4f rare earth elements. The polarization can be set as linear or circular. The focusing beam size is down to 14 μm x 5 μm. The typical photon flux is 4×10^{12} s^{-1}. The ARPES-PEEM facility is designed for a high energy resolution of ~10 meV at a photon energy of 1000 eV for ARPES, and a high lateral spatial resolution of ~10 nm and an energy resolution better than 0.15 eV for PEEM. The current setup is well suited for XMCD-XMLD, nano-XPS, and k-space PEEM studies. The ACPEEM is further improved with a *fs*-laser to study time-resolved dynamics. The Shanghai Dreamline at SSRF is scheduled to be available from July, 2013. More details will be described in this presentation.

FPFI-P3-05
Photoelectron spectromicroscopy using hard x-rays to investigate resistive switching devices

T07 Frontiers in Photoelectron Full-field Imaging and Spectromicroscopy

#FPFI-P3-05

C. Wiemann [1], M. Patt [1], A. Gloskovskii [2], S. Thiess [3], W. Drube [3], M. Merkel [4], M. Escher [4].

[1]Peter-Grünberg-Institut 6, Forschungszentrum Jülich - Jülich (Germany), [2]Deutsches Elektronen-Synchrotron DESY, - Hamburg (Germany), [3]Deutsches Elektronen-Synchrotron DESY - Hamburg (Germany), [4]Focus GmbH - Hünstetten (Germany).

Photoemission electron microscopy (PEEM) is a well-established technique for high-resolution imaging using x-ray excitation. A number of different contrast mechanisms has been exploited to gain valuable insight into electronic and magnetic properties of microstructured systems, among them elemental contrast due to absorption at element-specific absorption edges, magnetic contrast due to magnetic dichroism, and spectroscopic imaging using energy-selected photoelectrons from specific core levels [1]. On the other hand, photoelectron spectroscopy using hard x-rays as excitation (HAXPES) has proven to be a valuable tool to retrieve spectroscopic information from deep bulk regions and from regions buried under surface layers [2]. Recently, we could show that the combination of both methods is feasible using a NanoESCA-type photoemission electron microscope with double hemisphere energy filter [3]. Energy-filtered imaging is possible even at kinetic energies as high as 6.4 keV, where the electron inelastic mean free path reaches values of several 10 Å in most materials. This method is particularly useful to investigate changes in the electronic structure of novel integrated devices. Examples from the class of resistive switching devices (Memristors) will be shown in this contribution (see figure). Here, HAXPES is employed to retrieve spectroscopic information from the active region of the device which is hidden underneath a metal top electrode, while the lateral resolution of PEEM helps to pinpoint changes that occur only in well-defined regions of small extent (like e.g. conductive filaments). In principle, one could even think of observing devices in operando using this method [4].

[1] A. Locatelli, E. Bauer, J. Phys. Condens. Matter 20, 093002 (2008)
[2] K. Kobayashi, Nucl. Instr. Methods A 601, 32 (2009)
[3] C. Wiemann, M. Patt, S. Cramm, et al., Appl. Phys. Lett. 100, 223106 (2012)
[4] T. Bertaud, M. Sowinska, D. Walczyk, et al., Appl. Phys. Lett. 101, 143501 (2012)

Figure 1: Photoemission signal from the Sr 2p3/2 core level in SrTiO3 detected from the bare surface (blue) as well as through a 7nm thick gold top electrode (green). Inset : Sample layer composition. (from [3])

FPFI-1-Or-4
Surface, Interface and Thin Film Processes in Organic Materials Investigated by Photoemission Electron Microscopy and Low Energy Electron Microscopy

T07 Frontiers in Photoelectron Full-field Imaging and Spectromicroscopy

#FPFI-1-Or-4

M. Casu.

Institute of Physical and Theoretical Chemistry University of Tuebingen - Tuebingen (Germany).

By using a combination of microscopic imaging and diffraction techniques with structural and chemical sensitivity, we studied the growth of diindenoperylene (DIP) on gold single crystals. Growth and structure of DIP films of different thickness were monitored in situ including real time PEEM and LEEM performed at the aberration-corrected SMART spectromicroscope, installed at the synchrotron radiation source BESSY (Berlin) and at the SPELEEM, installed at the Nanospectroscopy beamline at Elettra (Trieste). DIP thin films were grown by organic molecular beam deposition at room temperature and at very low evaporation rate. A layer-by-layer mechanism characterizes the initial growth followed by island nucleation, i.e., the growth follows the Stranki-Krastanov mode. The effect of the Ehrlich-Schowebel barrier was also directly observed at the substrate and in the film morphology, in particular inside the islands that show a non-homogenous thickness due to a rough front growth, because of the additional energy required for the diffusing molecules to surmount a downward step [1]. Highly resolved spectromicroscopy reveals that electronic structure, core-hole screening, and molecular orientation depend on the local morphology of thin films. These phenomena, like different screening of the core hole, or different FWHM of the XPS lines, have been previously shown comparing different samples consisting of monolayers and multilayers. In our work we show their occurrence comparing islands versus monolayers in the same film [2]. We also find that island shapes and aggregation in diindenoperylene deposited on Au(100), Au(110), and

Au(111) single crystals are steered by the anisotropy due to the lattice geometry of the substrate [3]. Finally, first preliminary results of our investigations on organic radicals will be shown. This represents the first PEEM/LEEM experiment on this class of materials.

The author thanks the Helmholtz-Zentrum Berlin, Electron storage ring BESSY II, and Elettra for providing beamtime; H. Marchetto, Th. Schmidt, T. O. Menteş, M. A. Niño, A. Locatelli, for taking part in the beamtime and for the helpful and challenging discussions, T. Chassé for constant support and discussions, Wolfgang Neu, Matteo Lucian, and Indro Biswas for technical support. Financial support from the Helmholtz-Zentrum Berlin, the European Commission, BMBF and DFG is gratefully acknowledged.

[1] M. B. Casu, S.-A. Savu, P. Hoffmann, B.-E. Schuster, O. Mentes, M. A. Niño, A. Locatelli, T. Chassé, CrystEngComm, 13 (2011) 4139.
[2] M. B. Casu, B.-E. Schuster, I. Biswas, C. Raisch, H. Marchetto, Th. Schmidt, T. Chassé, Adv. Mater. 22 (2010) 3740.
[3] M. B. Casu, S.-A. Savu, B.-E. Schuster, I. Biswas, C. Raisch, H. Marchetto, Th. Schmidt, T. Chassé, ChemComm 48 (2012) 6957.

FPFI-1-Or-12
Momentum Microscopy with Time-of-Flight Filter and Imaging Spin Detector

T07 Frontiers in Photoelectron Full-field Imaging and Spectromicroscopy

#FPFI-1-Or-12

K. Medjanik [1], S. Chernov [1], H.J. Elmers [1], C. Tusche [2], A. Krasyuk [2], J. Kirschner [2], G. Schönhense [1].

[1]Johannes Gutenberg-Universität, Institut für Physik - Mainz (Germany), [2]Max Planck-Institut für Mikrostrukturphysik - Halle (Germany).

Momentum microscopy [1] is a novel approach to study the electronic structure of surfaces using the cathode-lens technique, well-known from PEEM. Whereas a PEEM is optimized for best resolution in real space, momentum microscopy aims at an ultimate resolution in k-space (reciprocal space). Up to now, dispersive spectrometers have been used as energy filter and an imaging spin filter of W(001) type was employed [2]. In this contribution we present first results using *time-of-flight* (ToF) energy dispersion using a delayline detector, adopting concepts of ToF-PEEM [3]. By setting a ToF condition in the 3D (x,y,t) data sets, we define sections in k-space. In extended simulations we optimized the electron optical design such that for start energies up to 80eV the full half space above the sample surface (more than the first Brillouin zone) is imaged with high k-resolution. Starting from the imaging Ir(001)-type reflection spin filter [4], we were able to extend the lifetime of the surface by orders of magnitude via coating with a thin, pseudomorphic Au(001) overlayer that also stabilizes the surface in the non-reconstructed 1x1 phase. The instrument allows simultaneous spin filtering of many energy sections through momentum space. TOF filtering bears the potential of very high energy resolution. It can be selected via the drift energy and length of drift space. Aberrations are very small because a linear electron-optical column is retained. The instrument is operated using pulsed laser sources and will be installed at BESSY II (beamline RGBL-PGM).

Funded by BMBF (05K12UM2 and 05K12EF1) and COMATT.

[1] B. Krömker, M.Escher, D.Funnemann, D.Hartung, H. Engelhard, and J.Kirschner, *Rev. Sci. Instrum.* **79**, (2008) 053702.
[2] C. Tusche, M. Ellguth, A. Ünal, C.-T. Chiang, A. Winkelmann, A. Krasyuk, M. Hahn, G. Schönhense and J. Kirschner, *Applied Physics Letters* **99**, (2011) 032505.
[3] G. Schönhense, A. Oelsner, O. Schmidt, G. H. Fecher, V. Mergel, O. Jagutzki, H. Schmidt-Böcking, *Surf. Sci.* **480**, (2001) 180.
[4] D. Kutnyakhov, P. Lushchyk, A. Fognini, D. Perriard, M. Kolbe, K. Medjanik, E. Fedchenko, S.A. Nepijko, H.J. Elmers, G. Salvatella, C. Stieger, R. Gort, T. Bähler, T. Michlmayer, Y. Acremann, A. Vaterlaus, F. Giebels, H. Gollisch, R. Feder, C. Tusche, A. Krasyuk, J. Kirschner and G. Schönhense, submitted to *Ultramicroscopy*.

FPFI-P3-06
Twin-Photoemission Electron Microscope

T07 Frontiers in Photoelectron Full-field Imaging and Spectromicroscopy

#FPFI-P3-06

A. Krasyuk [1], C. Tusche [1], G. Schönhense [2], J. Kirschner [1].

[1]Max-Planck-Institut für Mikrostrukturphysik - Halle (Germany), [2]Johannes Gutenberg-Universität Mainz - Mainz (Germany).

We present an innovative twin photoemission electron microscope (Twin-PEEM), which consists of two fully functionally PEEMs crossed in the shared low-energy zone (20-100 eV), see Fig. 1a. The desire to analyze the spin of the photoelectrons forming the image in UV-PEEM experiment bring us about to design this multifunctional Twin-PEEM with high transmission properties. In our design we have used only electrostatic lenses. Due to the combination of a cathode lens and different asymmetric immersion lenses we have achieved performance, which allows to place a single crystalline target directly into the electron optical path after the cathode lens of the microscope (Fig. 1a) and use it as an active electron mirror. In this way it is possible to realize different operating modes of the Twin-PEEM. If the crystal is extracted from the optical axis of microscope (Fig. 1b), then the direct spatial image can be obtained on the multichannel plate of a position sensitive detector (Fig. 1c). If the crystal is inserted into the optical axis of microscope, see Fig. 1(d), then the low energy electrons diffracted from the single crystal can be imaged in a 90° mirror-like geometry (Fig. 1e). As was recently shown [1,2], the W(100) target can be used as a highly efficient spin-filter for 2D PEEM images. In this case Twin-PEEM can be used as Spin Polarised Photoemission Electron Microscope (SP-PEEM) which is able to map magnetic sample by illumination with unpolarised deep ultraviolet light.

[1] C. Tusche, M. Ellguth, A. A. Ünal, C.-T. Chiang, A. Winkelmann, A. Krasyuk, M. Hahn, G. Schönhense, and J. Kirschner, APL99, 032505 (2011).
[2] M. Kolbe, P. Lushchyk, B. Petereit, H.J. Elmers, G. Schönhense, A. Oelsner, C. Tusche, and J. Kirschner. PRL 107, 207601 (2011)

Figure 1. (a) Schematic view of Twin-PEEM. (b) Direct operating mode without single crystal (c) Corresponding UV-PEEM image of gold squares 1 µm x 1 µm on silicon (d) Diffraction mode with single crystal (e) Corresponding UV-PEEM image (Escatt=26 eV).

FPFI-2-Or-3
Strong perpendicular magnetization of [CoNi2] multi-layers with high brightness and high SPLEEM and simulation based on LLG formula

T07 Frontiers in Photoelectron Full-field Imaging and Spectromicroscopy

#FPFI-2-Or-3

M. Suzuki [1], K. Kudo [2], K. Kojima [3], T. Yasue [1], N. Akutsu [1], H. Kasai [3], E. Bauer [4], T. Koshikawa [1].

[1]Osaka Electro-Communication University - Neyagawa Osaka (Japan), [2]Ochanomizu University - Tokyo (Japan), [3]Osaka University - Osaka (Japan), [4]Arizona State University - Tempe (United states).

Current induced domain wall motion is a key phenomenon to realize novel spintronic devices such as a race-track memory (IBM) and a domain wall motion magneto-resistive random access memory (NEC). It has been indicated that domain walls in nanowires with perpendicular magnetic anisotropy can move with lower current density than those with in-plane magnetic anisotropy. Multilayer [$CoNi_2$] multi-layer is known to exhibit perpendicular magnetic anisotropy and is expected as a material for the devices with low operation current [1,2]. We investigated magnetization during growth of the [$CoNi_2$] multi-layer with our high brightness and highly spin-polarized SPLEEM [3-5]. We will also reproduce the magnetic domain pattern formation of the surface of Co/Ni multilayers by numerical simulations, based on the Landau-Lifshitz-Gilbert (LLG) equation, which describes the dynamics of local magnetization. Fig. 1 shows experimental and simulation results of magnetic domain images of multilayers of pairs of [$CoNi_2$] on W(110). The numerical simulations well reproduce the magnetic domain patterns observed in the experiments.

[1] T. Koyama et al., Appl. Phys. Express 1, 101303 (2008).
[2] H. Tanigawa et al., Appl. Phys. Express 2, 053002 (2009).
[3] N. Yamamoto et al., J. Appl. Phys. 103, 064905 (2008).

[4] X.G. Jin et al., Appl. Phys. Express 1, 045602 (2008).
[5] M. Suzuki et al., Appl. Phys. Express 3, 026601 (2010).

Fig.1: Magnetic domain images obtained with experiments (SPLEEM) and simulations (LLG equation)

FPFI-1-Or-5
Signature of silicon doping in Gallium Nitride microwires studied by spectroscopic XPEEM

T07 Frontiers in Photoelectron Full-field Imaging and Spectromicroscopy

#FPFI-1-Or-5

J. Morin [1], O. Renault [1], P. Tchoulfian [1], N. Chevalier [1], V. Feyer [2], M. Patt [2], C.M. Schneider [2].

[1]CEA, LETI, MINATEC Campus - Grenoble (France), [2]Peter Grünberg Institute (PGI-6) - Jülich (Germany).

We investigate by spectroscopic XPEEM the doping signature of intentionally n-doped GaN microwires. We present spectromicroscopic results at threshold and Ga3d core-level emission excited with soft x-ray radiation (Nanospectroscopy Beamline, Sincrotrone Trieste, Italy, NanoESCA MkII instrument [1]). Figure 1 shows the threshold spectra of the Si-doped and non-intentionally doped (NID) regions of the wire. These regions present a 134meV work function difference. The doped region presents the lowest work function, consistent with a n-doping. Moreover, Ga3d binding energy peak maximum presents a shift as a function of its position along the wire. This positive binding energy shift (160 meV) in the doped region is qualitatively and quantitavely in agreement with n-doping and a lower work function. The work function changes are thus, dominated by shift of the Fermi level upon doping. Scanning Auger (SAM) measurements were also performed to confirm the presence of silicon in the wire. Figure 2 highlights the drop of Si concentration along the wire, dropping from 7% to reach a stable 3.5%. This profile is coherent with the growth method, and an expected N.I.D. [2]. Based on complementary laboratory experiments, we will discuss the influence of band bending effect and surface photovoltage [3] on the measured energy level shifts.

The work was supported by the French National Research Agency through the Recherche Technologique de Base program and was performed in the

Nanocharacterization Centre of MINATEC and Sincrotrone Trieste acknowledged for providing beamtime.

[1] C. M. Schneider et al., J. Electron. Spectrosc. Relat. Phenom. 185, 330 (2012).
[2] R. Koester et al., Nanotechnology 21 (1), 015602 (2009).
[3] J.P. Long, V.M. Bermudez , Phys. Rev. B. 66, 121308 (2012).

Figure 1: XPEEM, threshold spectra of doped (blue) and NID (red) region highlighted in the insets: top image taken at 4.88 eV shows the doped region, the bottom inset image (5.02 eV) shows the entire wire.

Figure 2 : SAM measurements performed along the GaN wire. The 0 position represents the base of the wire.

FPFI-3-Or-7
New developments and future trends in high-resolution LEEM and PEEM

T07 Frontiers in Photoelectron Full-field Imaging and Spectromicroscopy

#FPFI-3-Or-7

A. Kaiser, S. Bahr, O. Schaff, A. Pioda.

SPECS Surface Nano Analysis GmbH - Berlin (Germany).

Eighty years ago, Ernst Brüche developed the first photoemission electron microscope (PEEM) in the AEG laboratories in Berlin. Today, the state-of-the-art Low Energy Electron Microscope (LEEM) is produced just a few kilometers away from Brüche's former laboratory carrying forward this groundbreaking developments into the SPECS FE-LEEM P90.

This instrument - based on the sophisticated electron-optical design by Ruud Tromp [1-4] - combines user friendly operation with highest stability and ultimate resolution measurements. For this, the integrated cold field-emission electron gun provides a high-brightness electron beam with low energy spread. Already equipped with an in-line energy filter with high energy resolution [3] it can be upgraded with an optional aberration corrector [3, 4] improving the lateral resolution of the instrument from 5 nm to better than 2 nm by correcting spherical and chromatic aberrations.

For PEEM measurements, various light sources can be employed far beyond the standard of a Mercury discharge source, such as an optional Deuterium source or spectroscopic sources, like Helium discharge lamps, various laser sources or synchrotron sources. For experiments with laser excitation, the excitation source can be fed into the system under different incidence angles ranging between 0° and 90° relative to the sample surface.

Surface preparation techniques, such as ion or evaporation sources can be installed within the sample chamber for in-situ sample preparation or in an additional preparation chamber mounted on the same system frame. For a thorough characterization of the sample surface, the LEEM/PEEM system can be combined with other analysis methods, such as the SPECS Aarhus STM 150 HT for highest stability Scanning Tunneling Microscopy with atomic resolution.

The instrument's development is continuously driven forward. In this presentation, new developments and future trends in LEEM and PEEM will be presented, resulting in new applications of the available operation modes, like NanoARPES. Furthermore, various upgrade capabilities, like the new integrated sample stage will be presented allowing sample positioning with highest precision and stability with up to six computer-controlled degrees of freedom and an optional sample cooling.

[1] Tromp R. M., Mankos, M., Reuter M., C, Ellis A., W, Copel, M., Surf. Rev. Lett. **5**, 1189-1197 (1998).
[2] Tromp R., M, Fujikawa, Y., Hannon J., B, Ellis A., W, Berghaus, A., Schaff, O. , J. Phys. Cond. Mat. **21**, 314007 (2009).
[3] Tromp R., M, Hannon J., B, Ellis A., W, Wan, W., Berghaus, A., Schaff, O., Ultramicroscopy **110**, 852-61 (2010).
[4] Tromp, R.M., Hannon, J.B., Wan, W., Schaff, O., Ultramicroscopy, in press.

LEEM image of monolayer steps of a Graphene/SiC(0001) showing 1.6 nm resolution.

FPFI-3-Or-10
Circular Dichroism of Topological Insulators investigated by momentum microscopy and synchrotron radiation

T07 Frontiers in Photoelectron Full-field Imaging and Spectromicroscopy

#FPFI-3-Or-10

M. Patt, V. Feyer, L. Plucinski, G. Mussler, C. Wiemann, C.M. Schneider.

Peter Grünberg Institute (PGI-6/PGI-9) and JARA-FIT, Research Center Jülich - Jülich (Germany).

Photoelectron Emission Microscopy in combination with high brilliance synchrotron radiation (XPEEM) is known to be an appropriate method for studying surface properties with chemical selectivity. The use of an additional transfer lens in the optical path of such an energy-filtering XPEEM installation allows us to take an angular/momentum resolved image of the excited electrons at a well-defined kinetic energy. Varying this kinetic energy gives access to a robust band structure imaging. With our NanoESCA at the synchrotron Elettra (Italy) [1] in combination with a micro spot refocused synchrotron beam we measure one full momentum distribution with an angular resolution smaller than 0.09 $Å^{-1}$.
We use this method to investigate the topological insulators (TI) Bi_2Te_3 and Sb_2Te_3 grown as epitaxial thin films [2], which are highly interesting future materials regarding their special electronic properties (high mobility and dissipationless spin-locked transport). The excitation of photoelectrons with right and left circular polarized synchrotron light (RCP, LCP) gives access to a strong circular dichroism (CD) contrast [3], which is related to the spin texture of the Dirac state in a TI [4]. We show our CD results for the aforementioned TI's and discuss them with the help of relativistic first-principal photoemission calculations.

[1] C. Wiemann et al., e-J. Surf. Scie. Nanotech. 9, 395 (2011).
[2] L. Plucinski et al., App Phys. Lett. 98, 222503 (2011)
[3] W. Jung et al., Phys. Rev. B 84, 245435 (2011)
[4] H. Mirhosseini et al, PRL 109, 036803 (2012)

Reciprocal space mapping from an epitaxial Bi_2Te_3 (111) film: (a) wide angular range Fermi surface at hv=80 eV at a pass energy of 100 eV; (b) difference of the related photocurrent distribution taken with right and left polarized synchrotron light shows a clear circular dichroism contrast.

FPFI-3-Or-5
Ir(001) Reflection-Type Imaging Spin Filter

T07 Frontiers in Photoelectron Full-field Imaging and Spectromicroscopy

#FPFI-3-Or-5

G. Schönhense [1], D. Kutnyakhov [1], P. Lushchyk [1], K. Medjanik [1], S.A. Nepijko [1], H.J. Elmers [1], F. Giebels [2], H. Gollisch [2], R. Feder [2], C. Tusche [3], A. Krasyuk [3], J. Kirschner [3].

[1]Johannes Gutenberg-Universität, Institut für Physik - Mainz (Germany), [2]Universität Duisburg-Essen, Theoretische Festkörperphysik - Duisburg (Germany), [3]Max Planck-Institut für Mikrostrukturphysik - Halle (Germany).

As Stern-Gerlach type spin filters do not work with electrons, spin analysis of electron beams is accomplished by spin-orbit or exchange scattering processes [1]. Existing single-channel devices are not compatible with parallel imaging microscopes and also not with modern electron spectrometers that simultaneously acquire a certain energy and angular interval. Recently, a novel method was developed that can transport a spin filtered 2D image utilizing k-parallel conservation in LEED [2,3]. In this contribution we present a major enhancement of this imaging spin filter by using an iridium (001) scattering target. The lifetime of this surface in UHV is one day, an order of magnitude higher than for the W(001) target used in our previous work. The inset in Fig. 1 illustrates the operation principle for the ideal case of an incoming parallel beam. The measured spin asymmetry for specular reflection from Ir(001) at 45° impact angle for energies up to 50eV is shown in (b). The experimental curve shows reasonable agreement with a relativistic SPLEED calculation (a), in particular for the leading signal A as well as several characteristic features (B-D). Signal G was not accessible because of too low energy, features E and F are missing in experiment, possibly because the measurement was performed for the 5x1 reconstructed surface, whereas the calculation assumed 1x1.
The imaging spin filter allows to resolve the spatial coordinates (x,y) in *high-contrast spinfiltered PEEM images*, e.g. of ferromagnetic domains [2]. Resolving the energy- and angle-coordinates (E,ϑ) behind an electron spectrometer establishes *multichannel spin polarimetry* [3]. Finally, imaging the transversal components of the momentum vector (k_x,k_y) constitutes *spin-filtered momentum microscopy* [4].

Acknowledgement
We thank Y. Acremann and coworkers (ETH Zurich) for fruitful cooperation. Partly funded by BMBF (05K12UM2) and Stiftung Rheinland Pfalz für Innovation (project 886).

[1] J. Kessler, *Polarized Electrons*, Springer (1976).
[2] C. Tusche, M. Ellguth, A. Ünal, C.-T. Chiang, A. Winkelmann, A. Krasyuk, M. Hahn, G. Schönhense and J. Kirschner, *Appl.Phys.Lett.* **99** (2011) 032505.
[3] M. Kolbe M. Kolbe, P. Lushchyk, B. Petereit, H.J. Elmers, G. Schönhense, A. Oelsner, C. Tusche, J. Kirschner, *Phys.Rev.Lett.* **107** (2011) 207601.
[4] K. Medjanik, S. Chernov, H.-J. Elmers, C. Tusche, A. Krasyuk, J. Kirschner and G. Schönhense, this conference.

Figure 1. (a) Measured spin asymmetry for an Ir (001)-5x1 surface in comparison with (b) a relativistic layer-KKR SPLEED calculation for the unreconstructed 1x1 surface. The inset shows the scheme of the 2D spin filter.

FPFI-P3-07
Cold atom electron sources - a bright future

T07 Frontiers in Photoelectron Full-field Imaging and Spectromicroscopy

#FPFI-P3-07

A. Mcculloch [1], D. Sheludko [2], Y. Bruneau [1], G. Khalili [1], R. Scholten [2], D. Comparat [1].

[1]Laboratoire Aimé Cotton, CNRS, Université Paris-Sud - Orsay (France), [2]ARC Centre of Excellence for Coherent X-ray science, School Of Physics, University Of Melbourne - Melbourne (Australia).

Sources of inherently cold electrons extracted from laser cooled atoms have the potential to transform electron imaging. These new sources promise high current, high coherence electron bunches suitable for both conventional and ultrafast electron imaging. Here, we describe two instances of the cold atom electron source (CAES). Firstly, a source aiming to realise ultrafast di
raction from biological targets with atomic resolution. Secondly, a low energy source capable of triggering targeted surface chemical reactions, whilst simultaneously collecting a high resolution electron energy loss spectrum to identify the reaction pathways.

The cold atom source is a new source of charged particles, based on the extraction of electrons and ions from cold atoms [1]. The produced beam displays high coherence, high brightness and an intrinsically small energy spread. The internal structure of the atoms that form the underlying electron source provides a unique tool for three dimensional control over the density distribution of the electron beam [2]. This shaping provides a method for the realisation of beams which display minimal emittance growth (uniformly distributed ellipsoidal bunches), allows novel methods of beam characterisation and real-time optimisation of the electron beam properties.

Ultrafast electron di
raction (UED) of nanoscale objects such as biological molecules and nanoscale defects in solid state devices provides crucial information of dynamic processes [3]. Progress with UED is currently limited by thebrightness of sources with su

ciently high temporal resolution. Cold Atom Electron Sources have been shown to be bright, but with pulse lengths too long for UED. We demonstrate the production of simultaneously cold and short duration electron pulses from a cold atom electron source by incorporating an ultrafast laser into a two-colour below threshold photoionisation scheme. Counter-intuitively, the large bandwidth of the ultrafast laser pulse does not adversely aff
ect the electron energy spread. Electron bunch shaping is used to characterise the beam and current experiments aim to demonstrate di
raction.

The chemistry of surface compounds can drastically alter the material properties. To probe structure and identify reaction pathways, targeted reactions can be induced with low energy electron beams, usually a few eV. Techniques such as high resolution energy loss spectroscopy (HREELS) allow for the determination of chemical changes, but conventional HREELS sources/detectors require long times to produce high resolution spectra. We report on the assembly and testing of a continuous beam CAES, to be used for both inducing chemical reactions and as the source for producing HREELS spectra. A continuous beam is produced from the fi

eld-ionisation of a transversely cooled ceasium beam, producing a highly monochromatic electron beam. The beam is coupled to a high resolution microscope column and the sample is biased to achieve low electron energies.

[1] BJ Claessens et al., Ultracold electron source. Physical review letters, 95(16):164801, 2005.
[2] AJ McCulloch et al., Arbitrarily shaped high-coherence electron bunches from cold atoms. Nature Physics, 2011.
[3] G. Sciaini et al., Femtosecond electron di
raction: heralding the era of atomically resolved dynamics. Reports on Progress in Physics, 74:096101, 2011.

FPFI-P3-08
PEEM Study of the Near Field of Strongly Coupled Plasmons: Dark Modes and Optical Field Emission

T07 Frontiers in Photoelectron Full-field Imaging and Spectromicroscopy

#FPFI-P3-08

G. Schönhense [1], F. Schertz [1], M. Schmelzeisen [2], R. Mohammadi [2], M. Kreiter [2], H.J. Elmers [1].

[1]Institut fuer Physik, Johannes Gutenberg-Universitaet - Mainz (Germany), [2]Max-Planck-Institut fuer Polymerforschung - Mainz (Germany).

Strongly coupled plasmons are induced in a system of individual gold nanoparticles placed at sub-nanometer distance to a gold film (nanoparticle-on-plane, NPOP) via a monolayer of cysteamine (0.8 nm) as spacer layer. This results in a plasmonic resonator with high quality where two types of modes can be excited: A particle plasmon mode close to the resonance frequency of single, free Au nanoparticles and a so-called gap resonance mode which is strongly red shifted in comparison with the particle plasmon. For the gap resonance our calculations revealed a near-field enhancement in the gap region of 1000.
In the first experiment we investigated the system using two complementary *single-particle spectroscopy techniques.* Optical scattering spectroscopy exclusively detects plasmon modes that couple to the far field via their dipole moment (bright modes). Using photoemission electron microscopy (PEEM), we detected in the identical NPOPs near-field modes that do not couple to the scattered far field. These so-called dark modes are characterized by a strongly enhanced nonlinear electron emission process. This is the first time that both far- and near-field spectroscopy were carried out for identical individual nanostructures interacting via a sub-nanometer gap. Strongly resonant electron emission occurs at excitation wavelengths far off-resonant in the scattering spectra [1].
In a second experiment we performed *electron spectroscopy* using an imaging energy analyzer, in order to elucidate the origin of strongly enhanced emission in the region of the gap resonance. Strongly coupled plasmons are excited in the NPOPs by femtosecond laser pulses. Field-emitted electrons from individual nanoparticles are detected by means of photoelectron emission microscopy and spectroscopy. We

propose optical field emission of electrons as major emission channel [2]. It is generated by the ultra-strong near field of strongly coupled plasmons without the help of a noticeable dc field. The dependence of total electron yield and kinetic energy on the laser power proves that field emission is the underlying emission process. We derived a dynamic version of the Fowler–Nordheim equation that yields perfect agreement with the experiment.

Acknowledgement
We thank Peter Klaer for fruitful cooperation. Project funded by DFG (EL172/16-2) and COMATT.

[1] F. Schertz et al., *Nano Lett.* **12** (2012) 1885−1890.
[2] F. Schertz et al., *Phys. Rev. Lett.* **108** (2012) 237602.

Figure 1. (a) Scheme of the plasmonic resonator; (b) calculated near field; (c) PEEM set-up; (d) PEEM image and (e) SEM image of the same nanoparticle (from [1]).

FPFI-1-Or-2
Spectromicroscopic characterization of thin iron oxide films

T07 Frontiers in Photoelectron Full-field Imaging and Spectromicroscopy

#FPFI-1-Or-2

F. Genuzio, A. Sala, T. Schmidt, H.J. Freund.

Fritz Haber Institute of the Max Planck Society - Berlin (Germany).

Iron oxide, widely used as a catalyst and as a support for catalytically active systems, has been intensively studied with various techniques [1]. However, controversies in the literature regarding the surface termination and structural inhomogeneities hinder the direct linking of surface electronic and structural properties to chemical properties. Our aim is therefore a comprehensive and consistent characterization of the Fe3O4 and Fe2O3 film growth on Pt(111) and Ag(111) substrates by using the SMART instrument [2], operating at BESSY-2, the soft x-ray light source of the Helmholtz Center in Berlin. This energy-filtered LEEM/PEEM instrument is specially designed to obtain chemical and structural information with high lateral resolution in-situ and in real time. It is the first instrument achieving 2.6 nm in LEEM [3] and 18 nm in energy filtered XPEEM [4], which was only possible by simultaneous correction of spherical and chromatic aberrations.

The combined LEEM/LEED and XPEEM study shows that the oxide thin film reveals defects depending on different preparation conditions, for example. a coexistence of different stoichiometric phases (Fe3O4, Fe2O3 and FeO), rotational domains and domains of different surface terminations [5]. We found that the substrate influences the quality of the supported oxide surface and its thermodynamics; e.g. the phase diagram of co-existing Fe3O4 and Fe2O3 phases can differentiate significantly from that calculated for bulk materials. We systematically characterized the conditions to reversibly transform alpha-Fe2O3 to Fe3O4 thin films on Pt(111) and on Ag(111). A comprehensive characterization of oxidation and reduction of mixed-phase films, the various defects in the film, as well as the substrate role in such reactions, will be discussed.

[1] W. Weiss and W. Ranke, Prog. Surf. Sci. 70 (2002) 1-151
[2] R. Fink et al., J. Electr. Spectrosc. Rel. Phen. 84 (1997) 231-250.
[3] Th. Schmidt et al., Ultramicroscopy 110 (2010) 1358–1361
[4] Th. Schmidt, A. Sala, H. Marchetto, E. Umbach, H.-J. Freund, Ultramicroscopy (2012), http://dx.doi.org/10.1016/j.ultramic.2012.11.004
[5] A. Sala, H. Marchetto, Z.-H. Qin, S. Shaikhutdinov, Th. Schmidt, H.-J. Freund, Phys. Rev. B 86 (2012) 155430, 1-10

FPFI-P3-09
Photoelectron microspectroscopy of resistive switching materials using soft x-ray synchrotron radiation

T07 Frontiers in Photoelectron Full-field Imaging and Spectromicroscopy

#FPFI-P3-09

V. Feyer [1], C. Wiemann [1], M. Patt [1], C. Lenser [1], A. Köhl [1], R. Dittmann [1], C.M. Schneider [1], Y. Aoki [2], M. Martin [2], F. Lange [3], M. Wuttig [3].

[1]PGI, Research Center Juelich - D-52425 Jülich (Germany), [2]Institute of Physical Chemistry, RWTH-Aachen - 52056 Aachen (Germany), [3]I. Institute of Physics, RWTH Aachen - 52056 Aachen (Germany).

Typical resistive switching (RS) systems are capacitor-like devices, where the electrode is an ordinary metal and the functional material a dielectric transition metal oxide or a telluride phase change material. Recent studies indicate that a thermal or electrochemical redox reaction in the vicinity of the metal-oxide interface is possibly the mechanism responsible for RS. This results in an altered local electronic structure and local stochiometry during and after switching. These changes are confined to nanoscale areas such as contacts, filaments, grain boundaries, or defects. Synchrotron-based techniques (UPS, XPS and XAS) are sensitive to changes in the electronic structure and chemical states of the studied system. Thus, combining photoemission electron microscopy (PEEM) with synchrotron radiation provides a unique tool to study these phenomena
In the present study, several RS materials have been investigated using PEEM at NanoESCA beamline of Elettra [1]. The observed energy shift of 0.3 eV of the valence band maximum of crystalline AgInSbTe compared to the amorphous phase correlates well with a resistance change during heating to 160°C [2]. The analysis of Te, Sb, In and Ag 3d XPS spectra of bouth phases shows that crystalline AgInSbTe forms, while Ag diffuses into the bulk and the top surface layer is enriched with In and Sb elements. Using micro-probe UPS and XPS we also demonstrate that GaO_x thin films exhibit analog memristive switching based on the bulk diffusion of donor ions (oxide ion vacancies or interstitial gallium ions). The drift of the vacancies creates a nonuniform donor concentration profile across the film and induces a change in the density of states in the valence band top near the Schottky barrier interface between

Pt electrode and GaO_x. In the third case, micro-XAS was used to study a 20nm Fe:SrTiO3 film deposited on the conducting $Nb:SrTiO_3$ substrate. The $Fe:SrTiO_3$ pad was resistively switched by applying bipolar voltage sweeps [3]. The spectra were measured at Ti L-edge (Fig.1a) on areas marked on Fig. 1b. The spectra of resistively switched area “Set” show some difference compared to the spectra measured on the two others. This may indicate a lowering of the symmetry around Ti atom, which is likely related to the creating an oxygen vacancies [3,4].

[1] C. Wiemann,et al, e-J. Surf.Scie.Nanotech. 9, 395 (2011).
[2] W.K. Njoroge and M. Wuttig, J. Appl. Phys. 90, 3816 (2001).
[3] Ch. Lenser, PhD thesis, 2012.; D. Kajewski,et al, Proceed. 21st IEEE 6297843 (2012).
[4] R. Dittmann,et al, Proceed. IEEE PP 1 (2012).

Fig.1.a)Ti L-edge spectra measured on the areas marked on b)

FPFI-P3-10
Time-resolved wave packet observation of surface plasmon polaritons provided by normal incidence photoemission electron microscopy

T07 Frontiers in Photoelectron Full-field Imaging and Spectromicroscopy

#FPFI-P3-10

P. Kahl [1], S. Sindermann [1], C. Schneider [2], A. Fischer [2], M. Aeschlimann [2], M. Horn-Von Hoegen [1], F.J. Meyer Zu Heringdorf [1].

[1]Faculty of Physics and Center for Nanointegration Duisburg-Essen (CeNIDE), Universität Duisburg-Essen - Duisburg (Germany), [2]Department of Physics and Research Center OPTIMAS, University of Kaiserslautern - Kaiserslautern (Germany).

In order to observe surface plasmon polaritons (SPPs) in a photoemission electron microscopy (PEEM) experiment, ultrashort (15 fs) laserpulses of 800nm wavelength are directed onto a surface with plasmonic Ag or Au nanostructures. In the past, non-linear photoemission under grazing incidence was used to obtain a Moiré type contrast of propagating SPPs waves. If the light impinges perpendicular onto the surface (normal incidence) a direct imaging of the plasmon is possible, as the observed fringes resemble the SPP wave fronts. In time-resolved experiments under normal incidence conditions, propagation of isolated SPP wave packets can be observed. In this manner the direct measurement of group velocity and also the in-situ visualization of the propagation length become possible.

Acknowledgement
Financial support by the Deutsche Forschungsgemeinschaft (DFG) through Programs SPP 1391 “Ultrafast Nanooptics” and SFB 616 “Energy Dissipation at Surfaces” is gratefully acknowledged.

Figure 1: *Self-assembled Ag-island in two photon photoemission microscopy under normal incidence illumination with 800 nm laser pulses. The visible fringes represent the phase fronts of the SPP wave and allow a direct measurement of the SPP wavelength.*

FPFI-3-In-1
Normal Incidence 2PPE PEEM

T07 Frontiers in Photoelectron Full-field Imaging and Spectromicroscopy

#FPFI-3-In-1

F.J. Meyer Zu Heringdorf [1], P. Kahl [1], S. Wall [2], C. Witt [1], C. Schneider [3], D. Bayer [3], A. Fischer [3], P. Melchior [3], M. Aeschlimann [3], M. Horn-Von Hoegen [1].

[1]Universität Duisburg-Essen - Duisburg (Germany), [2]present address: MPI für Kohlenforschung - Mülheim A.d. Ruhr (Germany), [3]Universität Kaiserslautern - Kaiserslautern (Germany).

Non-linear photoemission microscopy has in the last years been shown to be a successful method for the imaging of surface plasmon polaritons (SPPs) and for the observation of the time-dependent propagation of SPPs across a surface. Using femtosecond laser pulses of a photon energy that is smaller than the work function of the plasmonic material of interest, SPPs are imaged via a plasmon-enhanced two photon photoemission process in which a part of the laser pulse is used to excite SPPs, while the remaining part of the laser pulse is used to generate photoelectrons and probe the SPP state with spatial resolution. 2PPE PEEM then detects the temporal integral of the fourth power of the superposition of all electric fields at the surface.
So far, almost all experimental 2 PPE PEEM setups have exploited a grazing incidence geometry in which the fs laser pulses impinge on the surface under an angle of ~70° relative to the surface normal. A moiré pattern can then be used to describe the contrast in two-dimensional plasmonic structures. The periodicity of the observed moiré pattern, however, is different from the wavelength of the SPP. For the moiré contrast the projection of the exciting light field into the surface plane is relevant, and accordingly, the spacing of the moiré maxima depends on the angle of incidence of the laser pulses on the surface. In particular, with decreasing incidence angle the moiré pattern is expected to converge into the SPP wavelength until under normal incidence a “direct imaging” of SPP wave packets becomes possible. At the same time the propagation direction of the SPP changes. We present 2PPE PEEM results for Grazing Incidence (GI) and Normal Incidence (NI) 2PPE PEEM and discus the differences between the two situations. The interpretation will be backed up by a simple plane-wave model for the superposition of the plasmon’s electrical field and

the femtosecond laser pulse.

Acknowledgement: Financial support by the Deutsche Forschungsgemeinschaft (DFG) through Programs SPP 1391 “Ultrafast Nanooptics” and SFB 616 “Energy Dissipation at Surfaces” is gratefully acknowledged.

Observation of normal incidence 2PPE patterns of surface plasmon polaritons. (a) LEEM image of a self-organized Ag island. (b)-(d) The top corner of the island as seen in 2PPE PEEM under different polarizations. The direction of the electric field is indicated by the arrows on the upper right in each panel.

FPFI-P3-11
Nucleation and growth of ferromagnetic domains in epitaxial FeRh thin films imaged by PEEM

T07 Frontiers in Photoelectron Full-field Imaging and Spectromicroscopy

#FPFI-P3-11

F. Kronast [1], C. Baldasseroni [2], C. Bordel [2], G. Palsson [3], V. Sergio [1], A.Ü. Ahmet [1], F. Charles [3], H. Frances [2].

[1]Helmholtz-Zentrum - Berlin (Germany), [2]University of California - Berkeley (United states), [3]Lawrence Berkeley National Laboratory - Berkeley (United states).

FeRh is a unique material that undergoes a first order antiferromagnetic (AF) to ferromagnetic (FM) transition above room temperature (near 350 K) [1]. This phase transition, which is coupled to a lattice expansion, can be driven by temperature or magnetic field. FeRh in thin film form is therefore a promising candidate for heat-assisted magnetic recording in an exchange-spring system with a hard magnetic layer (for example FePt) [2,3]. Upon application of heat, FeRh becomes FM and lowers the switching field by a spring exchange mechanism. At room temperature, the AF phase does not alter the coercive field of the hard layer, hence the magnetic information stored in the hard layer is stabilized. Interfacial effects are highly relevant to the understanding of the coupling mechanisms between FeRh and adjacent layers and to the use of FeRh for technological applications.

Here we report on the use of photoemission electron microscopy (PEEM) to investigate the influence of interfaces on nucleation and growth of FM domains in FeRh. Imaging the magnetic contrast at different temperatures via x-ray magnetic circular dichroism (XMCD), we directly observe the nucleation and growth of the FM domains. In epitaxially FeRh thin films (grown on (001) MgO substrates) we find nucleation growth, and coalescence stages of FM domains characteristic for the first order AF to FM phase transition (Fig. 1). Comparing results for samples with different capping layers we find that in some cases an additional capping layer can lead to the formation of interface induced FM domains persisting even at room temperature[4].

1. Fallot, M. & Hocart, R. Sur l’apparition du ferromagnétisme par élévation de température dans des alliages de fer et de rhodium. Rev. Sci. 77, 498-500 (1939)

2. Nam, N. T., Lu, W. & Suzuki, T. Exchange bias of ferromagnetic/antiferromagnetic in FePt/FeRh bilayers. J. Appl. Phys. 105, 07D708 1-3 (2009)

3. Thiele, J.-U., Maat, S. &Fullerton, E. E. FeRh/FePt exchange spring films for thermally assisted magnetic recording media. Appl. Phys. Lett. 82, 2859-2861 (2003)

4. C. Baldasseroni, C. Bordel, A. X. Gray, A. M. Kaiser, F. Kronast, J. Herrero-Albillos, C. M. Schneider, C. S. Fadley, and F. Hellman/ Temperature-driven nucleation of ferromagnetic domains in FeRh thin films. Appl. Phys. Lett. 100, 262401 (2012)

2. Nam, N. T., Lu, W.

Nucleation and growth of ferromagnetic domains in FeRh thin films. PEEM images show the XMCD contrast recorded at the Fe L3 resonance at different temperatures stepping through the phase transition.

FPFI-2-Or-4
Size-dependent investigation on the magnetic properties of Fe, Co, and Ni nanoparticles using X-ray PEEM

T07 Frontiers in Photoelectron Full-field Imaging and Spectromicroscopy

#FPFI-2-Or-4

A. Balan [1], A. Kleibert [1], A. Fraile Rodriguez [2], P.M. Derlet [3], J. Bansmann [4], R. Yanes [5], N. Ulrich [5], F. Nolting [1].

[1]Swiss Light Source, Paul Scherrer Insitut - Villigen (Switzerland), [2]Departament de Fisica Fonamental and Institut de Nanociencia i Nanotecnologia (IN2UB), Universitat de Barcelona - barcelona (Spain), [3]Condensed Matter Theory Group, Paul Scherrer Insitut - Villigen (Switzerland), [4]Institute of Surface Chemistry and Catalysis - Ulm (Germany), [5]Department of Physics - Konstanz (Germany).

Magnetic nanoparticles show a rich variety of new properties when compared to the respective bulk materials, mostly due to the effect of the surface and interface on the magnetic interactions and to critical magnetic length scales such as domain wall width and exchange length .Tuning these properties requires precise control over their size, shape, and composition. For instance the size may determine whether a particle is in a single domain state or whether it will show a non-collinear spin structure [1]. The search for ever smaller nanomagnets being switchable between two states (bistability) at room temperature and sizes which are technologically relevant is a growing area of research due to their potential for applications in fields such as information storage media, biology and medicine. It is therefore important to further develop methods which give insight in the magnetic anisotropy energy and the magnetic reversal of individual nanomagnets [2].

We have used photoemission electron microscopy (PEEM) together with x-ray magnetic circular dichroism (XMCD) to investigate size-dependent magnetic properties of Fe, Co, and Ni nanoparticles.. We observe that a sizeable fraction of Fe and Co nanoparticles with a mean size of about 12 nm is magnetically stable at room temperature. However, Ni particles show no magnetic contrast (cf. Fig. 1). Combining the PEEM data with complementary atomic force microscopy and scanning electron

microscopy data, we will give a detailed comparison of the different systems and discuss the origin of their properties.

[1] A. Fraile-Rodriguez et al., Phys. Rev. Lett. 104, 127201 (2010).
[2] J. Bansmann et al.,Surf. Sci. Rep. 56, 189 (2005).

Fig. 1. a) Elemental contrast image of Fe nanoparticles with a mean size of12 nm. b) Respective magnetic contrast image showing that about one third of the particles reveals magnetic contrast at room temperature. The variation of the magnetic contrast from black to white indicates a random orientation of the magnetic moments. c) Elemental contrast image ofNi particles with similar mean size as the Fe nanoparticles.d) In contrast to the Fe nanoparticles the Ni particles show no magnetic contrast.

FPFI-P3-14
Low work function of oxidised diamond terminated with lithium

T07 Frontiers in Photoelectron Full-field Imaging and Spectromicroscopy

#FPFI-P3-14

N. Fox [1], J. Morin [2], H. Andrade [1], K. Winkler [3], O. Renault [4], K. O'donnell [5].

[1]University of Bristol - Bristol (United kingdom), [2]CEA-LETI - Grenoble (France), [3]Omicron AG - Taunusstein (Germany), [4]CEA-LETI - Grenoble (Germany), [5]Australian Synchrotron - Clayton (Australia).

Low work function surfaces on diamond that are chemically stable and can be operated at elevated temperatures are of great technological interest. Not only do they offer a means to make high brightness, low 'noise' electron sources, but also energy conversion devices and radiation detectors. This is due to the high electron yields often observed when the work function of diamond is significantly lowered. Usually, this is achieved by treating the diamond surface with atomic hydrogen to terminate all the available carbon dangling bonds with hydrogen atoms. Since carbon is more electronegative than hydrogen, each carbon-hydrogen bond is polarised creating a surface dipole with the positive charge on the hydrogen atom. Collectively the dipoles disposed on a diamond surface form a double layer that pulls down the vacuum energy barrier for electron emission (lowering the work function) to such an extent that electrons at the bottom of the diamond conduction band are at a higher potential than the vacuum level. Under these conditions the diamond surface exhibits a Negative Electron Affinity (NEA). For the fully hydrogenated C(100)-(2 x 1):2H surface each surface carbon has two dangling bonds available to bond to hydrogen. The value measured by He I, Ultra violet Photoemission Spectroscopy (UPS) for this NEA on p-type(NA≈1016cm-3), diamond is typically -1.3eV. This compares favourably with the predicted value of -1.95 and gives a minimum work function for this surface of 3.9eV. But recently we have found that for an oxygen-terminated,p-type diamond surface with a single monolayer(1ML) of lithium absorbed on it, the NEA is much larger. Our model calculations suggest that Li adsorption leads to partial delocalization of charges that would otherwise be bound tightly to the surface, leading to a large effective dipole. The predicted value for a energetically stable NEA on the C(100)-(1 x 1):O,Li surface being -3.9eV. The experimental value that we

deduce from UPS measurements is -2.1eV, which is substantially smaller than the theoretical value.Spectroscopic photoelectron emission microscopy provides image contrast influenced by changes in work function induced by crystallinity, crystal orientation, and the nature of atoms absorbed onto a surface. Using this technique, the addition of oxygen and lithium atom layers, and their controlled desorption from polycrystalline diamond surfaces has been studied in order to gain further insight into the distribution and the values of work functions attainable on degenerately doped (NA,ND≈1020cm-3) , p- and n-type diamond films. In this report we demonstrate the use of UHV Scanning Kelvin Probe Microscopy to interpret energy filtered photoemission images of lithiated diamond obtained by NanoESCA.

Fig1(a) Photoemission images obtained from p-type diamond film with oxidised surface and1ML of lithium.

Fig1(b) Photoemission images obtained from p-type diamond film with oxidised surface and variable coverage of lithium due to thermal desorption.

FPFI-2-Or-1
Magnetic domain formation and its dynamics of GdFeCo thin films by laser induced magnetization reversal

T07 Frontiers in Photoelectron Full-field Imaging and Spectromicroscopy

#FPFI-2-Or-1

T. Ohkochi [1], H. Fujiwara [2], M. Kotsugi [1], R. Adam [3], H. Takahashi [4], M. Tsunoda [4], A. Tsukamoto [5], A. Sekiyama [2], T. Nakamura [1], H. Osawa [1], C.M. Schneider [3], T. Kinoshita [1], S. Suga [2].

[1]JASRI/SPring-8 - Sayo, Hyogo (Japan), [2]Osaka Univ. - Toyonaka, Osaka (Japan), [3]Research Centre, Jülich - Jülich (Germany), [4]Tohoku Univ. - Sendai (Japan), [5]Nihon Univ. - Funabashi, Chiba (Japan).

Ultrafast magnetization control by femtosecond laser pulses is an intensively developing technique in recent spintronics researches. In GdFeCo ferrimagnetic thin films having perpendicular magnetizations, unusual phenomena beyond the description of conventional magnetism such as deterministic magnetization reversal which is unable to explain by simple recovery process from heat demagnetization state[1], helicity-dependent magnetization switching[2] and transient breaking of ferrimagnetic coupling state[3] have been reported.

From the viewpoint of practical application, it is also an important issue to optimize the performance of magnetization reversal by controlling compensation of angular momentum and its temperature dependence. Figure 1(a) shows Kerr microscope images of three kinds of [Glass (sub)/Ta(5 nm)/Ru(20 nm)/Si_3N_4(5 nm)/$Gd_xFe_{92-x}Co_8$(20 nm)/Ru(1 nm)/Ta(1 nm)] films (x=22, 24, 26) after applying a circularly polarized laser pulse (λ=800 nm, τ=~120 fs, ~12 mJ/cm^2) at room temperature. By varying only the composition of the GdFeCo alloy layer, the shape of the produced magnetic domains is drastically changed and helicity dependent switching is clearly observed in the sample containing 26% of Gd. It has also been acknowledged that the shape of modified magnetic domain is changed by omitting a Si_3N_4 heat blocking layer or by applying a pulse in different environments (air/vacuum). The results show the importance of controlling the macroscopic heat diffusion by designing optimum multilayer structure as well as the microscopic gyrotropic motion in the process of laser heating. Figure 1(b) shows time-resolved magnetic domain images of

$Gd_{26}Fe_{66}Co_8$ thin film after a laser pulse fluence observed by a photoemission electron microscope (PEEM). In this talk, dynamic behavior of laser induced magnetization reversal and spatial distribution of magnetization in its process will be discussed, showing the results on a variety of GdFeCo films.

[1] T.A. Ostler *et al*.: Nature Communications **3** (2012) 666.
[2] C. D. Stanciu *et al*.: Phys. Rev. Lett. **98** (2007) 207401.
[3] I. Radu *et al*.: Nature (London) **472** (2011) 205.

Fig.1 (a)Status of magnetic domain formation after radiating left (σ^-) or right (σ^+) circularly polarized single laser pulse (~12 mJ/cm^2, φ200 μm) on $Gd_xFe_{92-x}Co_8$ thin films with Si_3N_4 heat blocking layer observed by magneto-optical Kerr microscope. (b) Time resolved XMCD-PEEM images of $Gd_{26}Fe_{66}Co_8$ thin film without Si_3N_4 layer after applying linearly polarized laser pulse.

FPFI-3-Or-8
High resolution band structure imaging with a new photoelectron emission microscope

T07 Frontiers in Photoelectron Full-field Imaging and Spectromicroscopy

#FPFI-3-Or-8

N. Barrett, C. Mathieu.

DSM, IRAMIS, SPCSI, LENSIS - Gif-Sur-Yvette (France).

The analysis of chemical and electronic states in complex and nanostructured material systems requires electron spectroscopy to be carried out with nanometer lateral resolution, i.e. nanospectroscopy. This goal can be achieved by combining a parallel imaging photoelectron emission microscope (PEEM) with a bandpass energy filter. The decisive advantage of energy filtered, photoelectron emission microscopy is the simultaneous combination of high spatial and energy or wave vector resolution. Using an appropriate PEEM system, correlations may be made on the micron or sub-micron scale between chemical and electronic structure. Typical synchrotron beam spots are several tens of microns in width and cannot provide the same spatial resultion unless used in scanning mode with zone plates. On the other hand, their energy resolution is very good, typically better than 50 meV and band structure studies of highly correlated materials require such a spectroscopic resolution. Until now this was not possible in PEEM. Therefore, the challenge for PEEM based chemical and band structure imaging is to approach this figure in order to provide a decisive new tool to study spatially resolved electronic structure.

Here we present some first results using the "MesoXcope", an energy filtered PEEM with target spectroscopic resolution of 50 meV. The initial improvements over existing PEEMs will be discussed in terms of the extra degrees of freedom available for sample alignment, the sample temperature and the use of micro-apertures in an intermediate image plane. Reciprocal space imaging of the band structure with a high intensity, focussed He I/II laboratory source will be shown with a view to its application to graphene and 2D functional oxides.

Top: 3D rendering of the MesoXcope.

Bottom: Wallpaper of the band structure along high symmetry directions of $\vec{k}_{parallel}$ obtained from a 35 micron region using a laboratory He II discharge lamp.

FPFI-3-Or-3
RESONANT 2PPE-PEEM FOR ORGANIC FILMS

T07 Frontiers in Photoelectron Full-field Imaging and Spectromicroscopy

#FPFI-3-Or-3

T. Munakata, C. Udhardt, T. Ueba, R. Terawaki, T. Yamada, H. Kato.

Osaka University - Toyonaka (Japan).

The interplay between the electronic structure and the molecular arrangement is one of the hot topics of surface science. Because the electronic structure of organic films is sensitive to intermolecular interaction as well as to substrate-molecule interaction, the electronic structures are frequently spatially inhomogeneous even on well prepared films. In order to control and improve the functionalities of organic films, the electronic structure should be measured with high lateral resolution. We report lateral distribution of unoccupied electronic states of organic thin films studied by combined use of two-photon photoemission (2PPE) spectroscopy and 2PPE-PEEM.
The light source is the third harmonic output of a titanium sapphire laser operated at the photon energy region between 3.9 and 4.6 eV, a repetition rate of 76 MHz, and a pulse width of 100 fs. The unique feature of our PEEM is the high-precision stage [1]; The step resolution is 10 nm, and the absolute accuracy is better than 100nm. The size of the PEEM image is accurately determined by the translation of the sample. When one-photon photoemission (1PPE) PEEM images are measured for lead phthalocyanine (PbPc) films on HOPG, several islands of different brightness are observed. Photoemission yield curves are obtained for different islands by plotting the brightness as a function of the photon energy. Comparison with the micro-spot photoemission spectroscopy of 0.3 μm resolution clarifies the origin of the islands [2]. 1PPE-PEEM image of sub-ML rubrene on HOPG shows only very weak contrast, because the work function of the film is close to that of HOPG. On the other hand, 2PPE-PEEM images show high-contrast at the pump photon energy of 4.40 eV as shown in Fig.1. The images of the bright islands originate from a resonant excitation to a specific unoccupied molecular orbital (labeled as Ln). Resonant excitation to the Ln level is strongly enhanced by mixing of Ln with the image potential state on HOPG [3]. The bright area is composed of small fine-structures with large boundary. The unoccupied states are more sensitive than occupied ones to the environment around

the molecules [4].

[1] J. Electron Spectrosco. Rel. Phenom. 174, 131-135 (2009), [2] Surf. Sci., 602, 2232-2237 (2008), [3] J. Phys. Chem. C 116, 5821-5826 (2012), [4] Surf. Sci., 605, 982-986 (2011)

Fig1. 2PPE-PEEM images for Rubrene/HOPG (0.8 ML average, 15 μm FOV)

FPFI-2-In-1
Domain wall dynamics in nanostructures studied by time-resolved XMCD-PEEM

T07 Frontiers in Photoelectron Full-field Imaging and Spectromicroscopy

#FPFI-2-In-1

S. Pizzini [1], J. Vogel [1], N. Rougemaille [1], M. Bonfim [1], F. Sirotti [2], O. Boulle [3], T.O. Mentes [4], A. Locatelli [4].

[1]CNRS Institut Néel - Grenoble (France), [2]Synchrotron Soleil - Saint-Aubin (France), [3]CEA and CNRS, SPINTEC - Grenoble (France), [4]Sincrotrone Trieste - Basovizza, Trieste (Italy).

Time resolved XMCD-PEEM measurements have been developed by our group at ESRF, SOLEIL and ELETTRA to allow the direct observation of magnetisation dynamics induced by nanosecond current pulses in magnetic nanostructures.

Manipulation of magnetic domain walls (DW) in these nanostructures, through the spin transfer torque effect, has been extensively studied in the last years [1]. These studies are motivated by potential applications to spintronic devices and memories, but also by the wealth of interesting physical phenomena associated to the interactions between conduction electron spins and local magnetisation. The dynamics of DW under the action of spin polarised current is complex and implies a modification of the internal domain wall structure. A full understanding of it relies on the observation of DW during the application of the current pulse.
We carried out time-resolved XMCD-PEEM measurements for two types of nanostructures: i) trilayers and bilayers containing Py, in which the magnetisation lies in the plane of the layers and DW are relatively wide (a few 100nm); ii) asymmetric structures containing ultrathin Co, where the magnetisation is out of plane and DWs are narrow (some nanometers).

In Py-based trilayers and bilayers, we found that the DW mobility is much larger than in single Py layers, thanks to the action of a non vanishing Oersted field on the Py magnetisation. This field, transverse to the current direction, stabilises the internal DW structure, preventing the periodic transformation that in single Py layers reduces

the average DW speed for large current densities. XMCD-PEEM measurements carried out during the current pulse using our Focus IS-PEEM, allowed us to give clear evidence of the effect of such an Oersted field, which leads to a tilt of the Py magnetisation in the transverse direction [2]. More recent measurements still under development on the Elmitec PEEM in Elettra also show that the DW internal structure is modified during the pulse but that the periodic transformation is suppressed by the presence of the Oersted field.

Time-resolved XMCD-PEEM measurements on Pt/Co/AlOx nanostructures allowed us to study the long distance motion of the DWs during the current pulses, and to show that the domain walls in this system present a very weak inertia. This means that the temporal response of DW to the current pulse is instantaneous: DW start moving as soon as the driving force is applied. This behaviour - different from that found in DW in Py where the inertial effects are very important - is connected with the presence of narrow domain walls (Bloch or possibly Néel) whose internal structure is only weakly modified during the pulse [3]. Our measurements show that these systems are clearly better suited for applications to magnetic memories, where the frequency at which information can be transferred would suffer from the presence of strong inertial effects.

These measurements show that the high spatial and time resolutions obtainable with XMCD-PEEM make this technique a tool of choice for the study of magnetisation dynamics in nanostructures.

[1] O. Boulle, G. Malinowski, and M. Klaui, Mater. Sci. Eng. R-Rep. 72, 159 (2011)

[2] V. Uhlir et al. Phys. Rev. B 83, 020406(R) (2011)

[3] J. Vogel et al. Phys. Rev. Lett. 108, 247202 (2012).

FPFI-3-Or-2
Nanoscale control of plasmon dipolar and quadrupolar resonances in Au triangles using polarization- and energy-dependent light excitation

T07 Frontiers in Photoelectron Full-field Imaging and Spectromicroscopy

#FPFI-3-Or-2

L. Douillard [1], T. Popescu [1], C. Awada [1], F. Charra [1], A. Perron [2], H. Yockell-Lelièvre [2], A.L. Baudrion [2], P.M. Adam [2], R. Bachelot [2].

[1]CEA - Gif Sur Yvette (France), [2]UT Troyes LNIO - Troyes (France).

Localized surface plasmon resonances (LSPR) are coherent charge oscillations within metallic particles offering a way to concentrate and manipulate light on the nanoscale. Aside from size, shape and dielectric environment, the effect of directionality upon the light-plasmon coupling is crucial for applications, including directional nano-antennas, selective control of single molecule fluorescence [1] and surface-enhanced Raman spectroscopy (SERS) [2]. We study this directional aspect here by obtaining qualitative and quantitative measurements of the plasmon resonances in dipolar and quadrupolar modes as a function of the polarization and wavelength of the incident light [3].

We are able to lift the degeneracy between orthogonal plasmonic resonances by varying the linear polarization of the incident light. The experimental results are obtained using photoemission electron microscopy (PEEM), an optical excitation scheme (photon-in, electron out) that allows control over the polarization and energy of the exciting field. We obtain full field images of the plasmon resonance “hot spots” via photoelectrons collected using traditional electron optics. Nanometer scale spatial resolution (20 nm lateral resolution) and a spectral resolution of < 5 meV at 800 nm are achievable.

In the present study, we analyze regular gold triangles with in-plane altitudes spanning the range [100, 300] nm and a thickness of 50 nm, fabricated by electron beam lithography (EBL) and deposited on a 0.5 nm titanium oxide (TiO_2) adhesion

layer and 5 nm of ITO.

According to group theory calculations [4], an isolated triangular prism of group D3h has three dipolar modes that can couple to the linearly-polarized incident field: one inaccessible high-energy out of plane mode, and two degenerate in-plane modes. By varying the polarization between orthogonal p- and s-modes, we are able to excite these two degenerate modes independently. A similar analysis yields the quadrupolar modes, which we observe experimentally. Finally, PEEM results correspond well to simulations using finite difference time domain (FDTD) simulations and the wavelength dependence of the dipolar and quadrupolar modes can be correlated to measurements obtained using extinction spectrometry.

[1] T. Kosako, Y. Kadoya, H.F. Hofmann, *Nat. Photonics* **4** (2010) 312
[2] T. Ming, L. Zhao, H. Chen, K. Choi Woo, H.Q. Lin, *Nano Lett.* **11** (2011) 2296
[3] C. Awada, T. Popescu, L. Douillard et. al., *J. Phys. Chem. C* **116** (2012) 14591
[4] A. Gelessus, W. Thiel, W. Weber, *J. Chem. Educ*. **72** (1995) 505

FPFI-P3-12
Spectroscopic XPEEM at ALBA: first results

T07 Frontiers in Photoelectron Full-field Imaging and Spectromicroscopy

#FPFI-P3-12

L. Aballe [1], M. Foerster [1], J. Fontcuberta [2], C. Ocal [2], E. Barrena [2], S. Matencio [2].

[1]ALBA Synchrotron Light Facility - Barcelona (Spain), [2]Insitut C. Materials Barcelona - Barcelona (Spain).

The spectroscopic XPEEM station at the CIRCE beamline in ALBA started user operation in late 2012. The beamline provides variable polarization photons with high flux and resolution in the energy range 100 – 2000 eV, and the spot at the microscope sample position can be focalized down to a size of ~ 12 x 36 m m 2 VxH. The XPEEM electron optical system including an energy analyzer offers many complementary techniques for the advanced characterization of surfaces, thin films and nanostructures by combining different working modes (spectromicroscopy, microspot, diffraction) with either absorption, dichroic and/or photoemission contrast mechanisms. The experimental station permits in situ sample preparation and fast sample transfer. A brief review of the beamline and microscope performance will be given and first results on self-organized oxide surfaces and thin films will be presented.

FPFI-3-Or-6
PEEM3: An aberration-corrected PEEM at the Advanced Light Source

T07 Frontiers in Photoelectron Full-field Imaging and Spectromicroscopy

#FPFI-3-Or-6

M. Marcus, A. Scholl, A. Doran.

Advanced Light Source, Lawrence Berkeley National Laboratory - Berkeley, Ca (United states).

PEEM3 is a photoemission electron microscope (PEEM) at the Advanced Light Source (Lawrence Berkleley Laboratory). It is fed by an elliptically-polarizing undulator, allowing the use of polarization for imaging of ferroelectric, ferromagnetic and antiferromagnetic domains, as well as crystal orientation. The PEEM also provides the option of using an aberration corrector for high spatial resolution, and a wide-field mode with a 100μm field of view. The sample manipulator provides translation over millimeters and temperatures ranging from 30-800K. This variable-temperature option makes possible a wide range of experiments not possible in most PEEMs. In addition, it is possible to make electrical connections to the sample from electronics on a floating "hot deck", which allows time-resolved measurements using on-sample generation of pulsed electric and/or magnetic fields in a pump-probe mode. An in-situ strain sample holder is also available. The range of incident X-ray energies is 150-1600eV, covering the CNO K-edges, 3d-metal L-edges and lanthanide M-edges. In addition to simple imaging, it is possible to take "stacks" at sequences of energy and, optionally, polarization, thus allowing element specificity. PEEM3 is thus a versatile tool for materials science, especially in the areas of magnetics and multiferroics.

In this presentation, we will show the electron-optical layout of PEEM3, discuss strategies for tuning the instrument, and present examples of a diverse collection of work which has been performed there.

FPFI-P3-14
Soft X-ray Spectromicroscopic Studies of Graphene Nanomaterials by X-ray Photoemission Electron Microscopy (X-PEEM)

T07 Frontiers in Photoelectron Full-field Imaging and Spectromicroscopy

#FPFI-P3-14

J. Wang [1], J. Zhou [1], C. Karunakaran [1], C. Wright [1], S. Urquhart [2].

[1]Canadian Light Source Inc. - Saskatoon (Canada), [2]University of Saskatchewan - Saskatoon (Canada).

Graphene nanomaterials have been attracting enormous attentions in many fields and technological applications for their unique structures and outstanding physicochemical properties. A thorough understanding and analysis of the graphene nanomaterials not only requires nanoscaled spatial resolution for morphology, but also demands the elucidation of the chemical and electronic structure of the systems. The X-ray Photoemission Electron Microscope (X-PEEM) at the Canadian Light Source (covering 130 - 2500 eV) is well suited to these requirements through its powerful spectromicroscopic capabilities. Particularly, X-PEEM provides the X-ray absorption contrast images via total electron yield, the quantitative distributions (maps) of chemical components through spatially-resolved X-ray Absorption Near Edge Structures (XANES) spectroscopy, and the molecular orientation with the help from arbitrarily-controlled polarized X-ray beam, at high spatial resolution (< 50 nm) and high energy resolution (< 0.05 eV). In this poster, selected examples of X-PEEM analysis of graphene nanomaterials, such as reduced graphene oxide (rGO), i.e. graphene, and graphene nanocomposites will be presented. One of the major challenges for X-PEEM measurements of ultra-thin graphene samples is the normalization in the low energy regime, particularly the C and N K-edges, which is due to the incident X-ray beam having significant absorption dips in these energy edges caused by the absorption of the ubiquitous beamline contaminants. To overcome this problem, a few approaches have been explored, such as normalization to clean Si wafer, to Si photodiode and to fresh gold mesh etc. With successful normalization our spectromicroscopic findings reveal the morphological,

chemical and electronic structure information and variations, as well as the defects and contaminants associated with the individual graphene nanomaterials.

FPFI-P3-13
The wide application range of the NanoESCA: From micro-ARPES to HAXPEEM

T07 Frontiers in Photoelectron Full-field Imaging and Spectromicroscopy

#FPFI-P3-13

N. Weber [1], M. Escher [1], T. Kühn [1], M. Merkel [1], C. Wiemann [2], M.C. Patt [2], C.M. Schneider [2].

[1]FOCUS GmbH - Hünstetten (Germany), [2]Peter Grünberg Institute (PGI-6) and JARA-FIT, Research Centre Jülich - Jülich (Germany).

The NanoESCA is a photo electron microscope (PEEM) equipped with a band pass filter. Its capabilities in imaging x-ray photoemission (iXPS) and k-space imaging have been well proven in the past [1, 2]. We now present a modified electron optics, which allows for imaging hard x-ray photoemission spectroscopy (HAXPES) up to 10keV [3]. The newly designed optics simultaneously allows higher transmission and a larger range in imaging k-space.
HAXPES is a well established technique for bulk sensitive photoemission [4]. In order to extend this technique to laterally structured samples, the NanoESCA has been upgraded to be used for hard x-ray photoemission electron microscopy (HAXPEEM). One key feature of this upgrade is the high extraction voltage, which has been raised to 24keV, to enable an easy sample biasing scheme.
HAXPEEM results were obtained at PETRA III [3]. The inset in figure 1 shows the image of a checkerboard-patterned Au/Si sample, using $Au4f_{7/2}$ core level electrons. Bulk sensitivity is demonstrated at the Si2p peak. Whereas the spectrum taken at hv=4.9keV (Fig. 1) shows predominantly the elemental silicon signal, the spectrum at hv=400eV (not shown, Elettra [5]) is dominated by a mixture of different oxidation states of silicon.
The modified electron optics enables the NanoESCA instrument allows to image a larger k-space of 8 $Å^{-1}$. With HeII excitation we can demonstrate a k-space of 6 $Å^{-1}$, limited by the takeoff angle of the photoelectrons (Fig. 2).

[1] M. Escher et al., J. Electron Spectrosc. Relat. Phenom. **178-179**, 303 (2010)
[2] B. Krömker et al., Rev. Sci. Instrum. **79**, 053702 (2008)
[3] C. Wiemann et al., Appl. Phys. Lett. **100**, 223106 (2012)
[4] C. Fadley, J. Electron Spectrosc. Relat. Phenom. **178-179**, 2 (2010)
[5] C. Wiemann et al., e-J. Surf. Sci. Nanotech. **9**, 395-399 (2011)

Figure 1: Si 2p spectra with hard x-rays (hv=4.9keV), the inset shows an image of the Au/Si sample using Au4f7/2 electrons at 6.43keV.

Figure 2: Fermi surface of an Ag(111) single crystal, excited with HeII (hv = 40.8eV). The Brillouin zone has a size of 2.51 $Å^{-1}$, the diameter of the total reachable k-space is 6.0 $Å^{-1}$.

FMMM/NST-P3-01
Functional Proline—Based Chiral Ionic Liquids : Catalysts for Chiral Synthesis

T08 Functional Molecules and Molecular Machines

#FMMM/NST-P3-01

K. Nobuoka [1], S. Kitaoka [2], Y. Yamamoto [1], Y. Ishikawa [1].

[1]Oita University - Oita (Japan), [2]Kinki University - Higashihirosima (Japan).

Ionic liquids have various properties that make them attractive for application. The high designability of the ionic liquids gives various functional possibilities. Among the functional ionic liquids, the chiral ionic liquids have received considerable attention as an enantioselective catalyst and a medium for chiral synthesis or chiral extraction. Therefore, we designed and synthesized novel functional chiral ionic liquids starting from L-proline which is a natural chiral amino acid.

First, we synthesized the chiral ionic liquids which consist of a pyrrolidine ring from L-proline and a bulky quaternized five-membered unsaturated aza-hetero cycle with a simple methyl group (Figure 1(a)). The ionic liquids (a) have low viscosity (124 cP at 25 °C) and very low glass transition temperature (T_g = -73 °C) which are suitable for reactions over a wide temperature range. Thus, we investigated the catalytic ability of the chiral ionic liquids (a) for asymmetric reactions. In Michael reaction of β-nitrostyrene and cyclohexanone, the ionic liquids catalyst (a) gives relatively high stereo- and enantio- selectivities (syn/anti = 92/8, 85% ee(syn)), whereas in moderate yield (52 %). Brønsted acids additives improve the yields without lowering the selectivities (88%: TFA, 93%: salicylic acid). In addition, the chiral ionic liquids (a) could be reused at least three times without significant loss of activity.

The result of Michael reactions revealed that the chiral ionic liquids (a) works well as a chiral catalyst. Subsequently, we designed the ionic liquids (Figure 1(b)) with a hydroxyl ethyl group instead of the methyl group of the ionic liquids (a) in order to improve its reactivity and enable to use the wide range of the asymmetric reactions and the substrates. Its hydroxyl group can form hydrogen bond with the substrates

such as, the nitro group of β-nitrostyrene, in the transition state. Although the presence of a hydroxyl group increases its viscosity somewhat (1024 cP at 25 °C), the glass transition temperature (Tg = -53 °C) is low enough which are suitable for reactions. In the presence of 15 mol % of the ionic liquids (b), the Michael adducts was formed with relatively high yield (76%). Adding *p*-nitrophenol can further improve the yield (86%) and the selectivities (syn/anti = 98/2, 95% ee(syn)). Besides, both chiral ionic liquids could be reused at least three times without significant loss of activity.

These proline-based chiral ionic liquids and their derivatives would be one of the powerful tools for various enantioselective reactions via chiral enamine intermediates. Therefore, we now investigate enantioselective reaction except for Michael reaction.

Fig1. Structures of proline-based chiral ionic liquids

FMMM/NST-P3-02
The Anion effect of Functional Ionic Liquids for Porphyrin Preparation

T08 Functional Molecules and Molecular Machines

#FMMM/NST-P3-02

S. Kitaoka [1], K. Nobuoka [2], T. Matsufuji [2], Y. Ishikawa [2].

[1]Kinki University - Higashi-Hiroshima (Japan), [2]Oita University - Oita (Japan).

Because of their green properties, ionic liquids are widely used for various reactions. We have already reported the porphyrin preparation using acidic ionic liquids as a phase separated catalysis ([1, 2]). The porphyrin preparations in the conventional ionic liquids also have been already reported by us ([2]). However, there is no study about the porphyrin preparation in the functional ionic liquids such as acidic ionic liquids. Herein, we report the tetraphenylporphyrin, TPP preparation in the acidic ionic liquids, $[HC_4im][X]$ (**FIgure 1**).

$[HC_4im][CF_3CO_2]$,$[HC_4im][BF_4]$ and $[HC_4im][Cl]$ produced TPP at 15% , 9% and 5% in yield, respectively (**Table 1**). The yield in $[HC_4im][CF_3CO_2]$ is the same level as the reaction in the propionic acid (15 %). These results suggested that the yields of TPP is affected by the the anion of ionic liquids. The efficacy of the ionic liquids to promote these cyclization reactions was correlated to the basicity of the anions of ionic liquids. It was obserbed that with increasing basicity of the anion (increasing pK_a of the corresponding acid) there is a progressive increase in yield (**Table 1**).

In addition, $[HC_4im][CF_3CO_2]$ could be reused at least 2 times without any loss of its catalytic activity. This porphyrin synthesis in the acidic ionic liquids enabled to suppress the acid waste.

[1] S. Kitaoka, K. Nobuoka, Y. Yuichi, *Chem. Commun*., 1902-1903, (**2004**).
[2] S. Kitaoka, K. Nobuoka, Y. Yuichi, *Tetrahedron*, 61, 7678-7685, (**2005**).

Figure 1 The structure of $[HC_4mim][X]$.

Table 1 The relation of acidity of HX and isolated yield of TPP in $[HC_4mim][X]$.

FMMM/NST-1-Or-1
Observation of Cross-over of Vibration and Kondo Resonance Excitation at Single Molecule Magnet TbPc2 complex

T08 Functional Molecules and Molecular Machines

#FMMM/NST-1-Or-1

T. Komeda, H. Isshiki, J. Liu, K. Katoh, M. Yamashita.

Tohoku University - Sendai (Japan).

There are rising interests of the application of the spin to the quantum information process. Organic molecules have unique capabilities for such applications, and a single-molecule-magnet (SMM) molecule is one of best candidates for them. The analysis of vibrational and spin information are indispensable techniques to characterize a single molecule devices. In addition the interaction of vibrational mode and spin states are of great interest for an advanced control of the molecule conductance.

In this study we want to investigate the interference between the vibrational mode and Kondo resonance in the film of $TbPc_2$ molecule, [1-3] which is a phthalocyanine double decker molecule and shows the SMM property. To obtain higher resolution, we employed low temperature STM in a part of the experiment whose head is cooled by a dilution refrigerator operated at 600 mK, at which temperature we expect the resolution of ~500 μeV.

We show the d^2I/dV^2 spectrum obtained for the centre of the$TbPc_2$ molecule adsorbed on the Au(111) surface in Fig. 1. We can observe peaks at 53, 75 and 95 meV at symmetric positions which are originated from vibrational excitations. Tip position dependence is shown in Fig. 2. At the lobe position we see a derivative like feature at around the Fermi level. This is originated from the Kondo resonance formed by an unpaired π orbital of the Pc ligand. When the tip was moved to the center, only vibrational nature were observed. We confirmed two distinct molecular orbitals on the molecule from DFT calculation. Depending on which orbital the tunneling electron injected, the cross-over between vibration and Kondo excitations occurs.

that the spin and electronic states of the organic molecules are strongly correlated with their structures.[1]R. Robles et al., Nano Lett. 12, 3609 (2012). [2]T. Komeda et al., Nat Commun 2, 217 (2011). [3] K. Katoh et al., Coord. Chem. Rev. 255, 2124 (2011).

Figure 1. d^2I/dV^2 spectra on (a) $TbPc_2$, (b) YPc_2, (c) H_2Pc and (d) second layer H_2Pc.

Figure 2. Site-dependent d^2I/dV^2 spectra measured on a $TbPc^2$ molecule.

FMMM/NST-1-Or-3
Charge-transfer induced rotation of C60 molecules on the WO2/W(110) surface

T08 Functional Molecules and Molecular Machines

#FMMM/NST-1-Or-3

S. Bozhko [1], S. Krasnikov [2], O. Lübben [2], B. Murphy [2], K. Radican [2], V. Semenov [3], E. Levchenko [4], H.C. Wu [2], I. Shvets [2].

[1]Centre for Research on Adaptive Nanostructures and Nanodevices (CRANN), School of Physics, Trinity College Dublin, Institute of Solid State Physics, Russian Academy of Sciences - Chernogolovka (Russian federation), [2]Centre for Research on Adaptive Nanostructures and Nanodevices (CRANN), School of Physics, Trinity College Dublin - Dublin (Ireland), [3]Institute of Solid State Physics, Russian Academy of Sciences - Chernogolovka (Russian federation), [4]Department of Physics, Astrakhan State University - Astrakhan (Russian federation).

Understanding of molecular switching between different charge states is crucial to further progress in molecule-based nano-electronic devices. Scanning tunneling microscopy (STM) is one of the most promising techniques for imaging of prototype molecular devices and testing their properties. We employed scanning tunnelling microscopy to reveal a correlation between charge state of a individual C_{60} molecule and it orientation within a molecular layer grown on the WO_2/W(110) surface. Tunnelling junction based on individual C_{60} molecule is stable below temperature of kinetic rotational transition of 220K [1] when all molecules are static. However, in the temperature range of 220–260 K some isolated molecules switch between high-, and normal- conductance states. At high temperatures the molecules rotate continuously so fast that no “blinking” is observed and all molecules appear as perfect spheres [2]. High- conductance state arises due to charging of the C_{60}, which causes changes in the local density of electron states near Fermi level and consequently a variation in tunnelling current. Using density functional theory calculations, these states were suggested to be: charge-neutral C_{60}; negatively charged C_{60}^{-}, which has accepted an electron. Such molecules appear in STM topography as flashing nano-bulbs on the surface. Switching of the molecule conductance state is accompanied by change of molecule orbital structure detected in STM topography that proves change of

orientation of the molecule during switching. Molecular movement accompanies the molecule's switching between these states; as the molecule rotates, it exchanges charge with the substrate, gaining or loosing an electron.

[1] Sergey I. Bozhko et.al. Phys. Rev. B. 84,195412, (2011)
[2] Sergey A. Krasnikov et.al. Nano Res. 4(2), 194–203, (2011)

FMMM/NST-1-Or-4
Exploring functionality of dual (photochromic and redox) responsive molecular switches for smart monolayer materials

T08 Functional Molecules and Molecular Machines

#FMMM/NST-1-Or-4

O. Ivashenko [1], B.L. Feringa [2], W.R. Browne [2], P. Rudolf [1].

[1]Zernike Institute for Advanced Materials, University of Groningen - Groningen (Netherlands), [2]Stratingh Institute for Chemistry, University of Groningen - Groningen (Netherlands).

Responsive organic monolayers have found application as smart systems – enabling reversible control of surface properties such as wetting, adhesion, catalytic activity, or serve as molecular memory devices or platforms for nano-engineering. In this contribution the functionality of several molecular switches in solution and in monolayers is discussed.
The first example is a remarkably robust self-assembled monolayer (SAM) of a bisthiaxanthylidene redox switch (**1**, Fig. 1) that shows excellent bistability, manifested in reversible changes in spectroscopic and electrochemical properties and in physical properties such as water contact angle (a ca. 30^{o} difference in water contact angle between the two redox states of a bisthiaxanthylidene monolayer) [1]. The effect of surface immobilization of the bisthiaxanthylidene on its photochromic, thermal and electrochemical properties is described. Raman, SERS and XPS spectra provide essential information on molecular transformations in SAMs. As a result, a combination of light and potential allows accessing four distinct conformational and redox states in monolayer.
The second example is a photochromic and redox active spiropyran SAMs (**2**, Fig. 1) that undergo substantial changes in polarity and dipole moment upon switching and have found numerous applications in a wide range of novel smart materials, photonic devices and logic units. Under ambient conditions spiropyrans are in the ring-closed form (SP) and ring-open merocyanine (MC) form can be generated photochemically [2].
We prepared self-assembled monolayers of spiropyran on gold for further utilization of its photochromism and redox activity. Ring open MC form can be successfully

induced in monolayers with UV light, as evidenced with UV/Vis absorption, XPS and SERS spectroscopies. On the other hand, application of electrochemical potential induces oxidation and irreversible chemical reaction in spiropyran. In contrast to earlier reports, we show a spectroscopic evidence for the mechanism of this oxidation in SAMs and identify products of the oxidation cycle in spiropyrans. Thus, the combination of light and redox potential in spiropyrans provides access to six unique states in monolayers of a spiropyran, which represents a versatile system, where it is possible to store information both temporary and permanently.

[1] O. Ivashenko, H. Logtenberg, J. Areephong, A.C. Coleman, P.V. Wesenhagen, E.M. Geertsema, N. Heureux, B.L. Feringa, P. Rudolf, W.R. Browne, *J. Phys. Chem. C* 115, 22965 (**2011**)
[2] Manuscript in preparation, O. Ivashenko, J.T. van Herpt, B.L. Feringa, P. Rudolf , W.R. Browne

Fig. 1 Structure of overcrowded alkene switch **1** and spiropyran **2** self-assembled monolayers on gold

FMMM/NST-1-Or-7
Molecular state imaging, spectroscopy and manipulation on hydrogen passivated semiconductors

T08 Functional Molecules and Molecular Machines

#FMMM/NST-1-Or-7

S. Godlewski [1], M. Kolmer [1], B. Such [1], H. Kawai [2], M. Saeys [3], P. Mcgonigal [4], P. De Mendoza [4], C. De Leon [4], A. Echavarren [4], C. Joachim [5], M. Szymonski [1].

[1]Jagiellonian University - Krakow (Poland), [2]IMRE - Singapore (Singapore), [3]NUS - Singapore (Singapore), [4]ICIQ - Tarragona (Spain), [5]CEMES CNRS - Toulouse (France).

Among several new concepts in electronic technology, the one based on utilization of single organic molecules, acting as active blocks performing logic operations, appears as one of the most appealing and is based on the state-of-the-art use of modern nanotechnology tools, such as scanning tunneling microscopy (STM) and non-contact atomic force microscopy (NC-AFM). In order to facilitate molecular orbital imaging and spectroscopy, electronic decoupling of the molecule in question from the underlying substrate is required. It is expected that proper isolation of such molecular entities could be achieved by application of passivated semiconductor surfaces, e.g., Si(001):H and Ge(001):H.
Following the first experiments with pentacene molecules on the Si(001):H surface we performed measurements of trinaphthylene molecules (Y molecules) on the hydrogenated Ge(001):H substrate with the application of low temperature scanning tunneling microscopy/spectroscopy (STM/STS) supported by the advanced theoretical modeling. In the presentation we will discuss the influence of the substrate on the electronic properties of adsorbed molecules and the role of surface dangling bonds (DBs) on the adsorption, immobilization and molecule imaging. We will show that HOMO states of the molecule physisorbed on the hydrogenated surface are hidden for STM measurements due to filtering by the substrate. These states could be directly accessed only if the molecule is laterally manipulated and connected to surface DBs, that leads to increased coupling. Reversibility of the manipulation processes gives perspectives for practical implementations as molecular switches. Finally, perspectives for tip induced molecule manipulation on passivated

semiconductors leading to further integration of nanoscale circuits based on molecules and DB structures created with atomic precision will be demonstrated.

FMMM/NST-1-Or-5
Controlled release of Au nanoparticles supramolecularly anchored on Si(100): An XPS, AFM and FE-SEM study

T08 Functional Molecules and Molecular Machines

#FMMM/NST-1-Or-5

R. Zanoni [1], A. Boccia [1], F. D'orazi [1], A.G. Marrani [1], A. Arduini [2], A. Secchi [2].

[1]Dipartimento di Chimica, Università La Sapienza - Rome (Italy), [2]Dipartimento di Chimica Organica e Industriale, Università di Parma - Parma (Italy).

Molecular recognition at interfaces is a key aspect in several important present and perspective applications, leading to nanomaterials with new, tunable and improved properties, in the field of sensoring, drug-delivery and molecular electronics.[1] Previous studies have pointed out the importance of calix[4,6]arenes in the production and reactivity of supramolecular architectures based on rotaxanes.[2,3,4] Extending molecular recognition to the surface reactivity of calixarenes may develop additional and more attractive properties, allowing for potential use of the resulting hybrids.
Gold nanoparticles (AuNPs) have been anchored on Si(100) surface through a complex rotaxane-based system, using wet-chemistry procedures and extra-mild Si activation. The resulting samples have been characterized through surface (XPS, AFM and SEM) and electrochemical techniques. Molecular adhesion on the specific binding sites has been demonstrated by the presence and quantitation of XPS signals from specific elements in the molecules. AFM and FESEM measurements have revealed morphology consistent with the presence of AuNPs. Functionalized Si surfaces have been successfully used as electrodes for a controlled release of AuNPs in solution after an electrochemical treatment.

[1] A.B. Descalzo et al., Angew. Chem. Int. Ed. 45 (2006) 5924.
[2] M. Semeraro et al., Chem. Eur. J. 16 (2010) 3467.
[3] A. Boccia et al., Phys. Chem. Chem. Phys. 13 (2011) 4444.
[4] A. Boccia et al., Phys. Chem. Chem. Phys. 13 (2011) 4452.

Figure 1. Schematic representation of the formation of pseudorotaxane complexes with Au nanoparticles, at the interface between a Si(100) surface coated with calix[6]arene-based “wheels” and the viologen-based “axle” present in a CH2Cl2/MeOH solution.

Figure 2. FESEM image of the sample [Si/Calix[6]/bifunctional viologen axle], after its exposure to a solution of 5 nm Au NPs functionalized with calix[4]. The image is a 190nm x 190nm zoomed image from the original frame, taken at 600 KX magnification.

FMMM/NST-1-In-1 FUNCTIONALITIES FROM CORRUGATED SP2-BONDED MONOLAYERS

T08 Functional Molecules and Molecular Machines

#FMMM/NST-1-In-1

J. Osterwalder.

Physik-Institut, Universität Zürich - Zurich (Switzerland).

Single layers of hexagonal boron nitride (h-BN) or graphene exhibit strong corrugations with periodicities in the few nanometer range when grown on transition metal surfaces with a large lattice mismatch. The geometrical corrugation is accompanied by a corrugation of the electrostatic potential, which provides these surfaces with certain functionalities, e.g. for the trapping of molecules. The corrugation can be lifted by the intercalation of hydrogen atoms underneath the monolayer, leading to effects observable also on the macroscopic scale. In my presentation I will give an overview on recent results on these nanomaterials obtained in our research group.

T09 Ionic liquids surfaces and interfaces

ILS-2-Or-4
Identification of macroscopic solid-like correlations from RT-Ionic Liquids to Liquid Water

T09 Ionic liquids surfaces and interfaces

#ILS-2-Or-4

L. Noirez.

Laboratoire Léon Brillouin - Gif-Sur-Yvette (France).

At a macroscopic scale, normal liquids (i.e above the melting temperature of the crystal), are typically and empirically defined by the absence of shear elasticity by opposition to solids or plastic fluids that require a stress threshold for flowing. A novel method optimising the transmission of the shear stress to the sample enables to probe the true mechanical response of liquids. It reveals that glass formers and viscous alkanes exhibit actually finite macroscopic shear elasticity away from any phase transition. This study is for the first time extended to molecular liquids as simple liquids (Heptadecane), room temperature ionic liquids ([emim][Tf2N]) and water, confirming the generic character of the elastic properties governing the sub-millimeter properties of liquids, even away from any phase transition[1,2].

1.Identification of Low Frequency Shear elasticity in Liquids n-Heptadecane, Liquid Water and RT-Ionic Liquids [emim]5Tf2N], L. Noirez, P. Baroni, H. Cao, J. Mol. Liq. **116** (2012) 18990.

2. Identification of a low frequency elastic behavior in Liquid Water", L. Noirez, P. Baroni, J. of Physics: Condensed Matter **24** (2012) 372101.

Highlighting solid-like correlations

ILS-1-Or-5
Surface structure of binary mixtures of ionic liquids using high-resolution Rutherford backscattering spectroscopy

T09 Ionic liquids surfaces and interfaces

#ILS-1-Or-5

K. Kimura, K. Nakajima, S. Oshima, M. Suzuki.

Kyoto University - Kyoto (Japan).

Ionic liquids (ILs) are known as “designer solvents” because their properties can be tuned by appropriate combination of a wide range of anions and cations. The tuning can be also done by mixing different ILs. Recently, surface composition of binary mixtures of ILs was investigated using TOF-SIMS [1]. Although the charge neutrality holds at the surface, remarkable surface segregation of larger cations and/or anions was observed. This suggests the possibility that the bulk and surface properties can be designed separately by mixing appropriate ILs. There are, however, a couple of reports conflicting with the TOF-SIMS result, which shows no surface enrichment of particular molecules in IL mixtures [2, 3]. Thus, the surface segregation of particular molecules in IL mixtures is still the subject of debate. In the present work, the surface structures of equimolar binary mixtures of ILs, which have different anions and a common cation, were systematically studied using HRBS. The chosen substances are imidazolium based ILs, namely [C_6MIM] [TFSI], [C_6MIM] [PF_6], [C_6MIM] Cl, [C_4MIM] [TFSI] and [C_4MIM] [PF_6]. The surface structures of the mixtures of these ILs were observed using HRBSas well as the pure ILs. For pure ILs, the alkyl chains of the cations protrude to the vacuum and the anions are located at almost the same depth as the imidazolium rings of the cations. The [TFSI] anion also shows a preferential orientation at the surface with CF_3 groups pointing toward the vacuum. For the mixtures, the molecules have the same preferential orientations at the surface as in the pure ILs. There is a tendency that larger anions are located at shallower depths than smaller anions in the mixture. In addition, the [TFSI] anion is found to be slightly enriched at the surface relative to [PF_6] with coverage of 60% for [$C_{4(6)}$MIM] $[TFSI]_{0.5}[PF_6]_{0.5}$ although no surface segregation is observed for other mixtures. These results can be roughly explained in terms of the surface tension.

[1] R. Souda, Surf. Sci. **604** (2010) 1694.
[2] K. Nakajima, A. Ohno, H. Hashimoto, M. Suzuki, and K. Kimura, J. Chem. Phys. **133** (2010) 044702.

[3] F. Maier, T. Cremer, C. Kolbeck, K. R. J. Lovelock, N. Paape, P. S. Schulz, P. Wasserscheid, and H.-P. Steinrück, Phys. Chem. Chem. Phys. **12** (2010) 1905.

ILS-1-In-1
IONIC LIQUID SURFACE SCIENCE: INTERFACE PROPERTIES AND CHEMICAL REACTIONS

T09 Ionic liquids surfaces and interfaces

#ILS-1-In-1

H.P. Steinrück.

Physikalische Chemie II, Universität Erlangen-Nürnberg - Erlangen (Germany).

An overview is given on the potential of X-ray photoelectron spectroscopy to investigate ionic liquid (IL) interfaces. The IL/vacuum interface of various imidazolium-based ILs is systematically studied by variation of alkyl chain lengths, by investigation of different anions, and by introduction of functional groups; detailed information on surface orientation, enrichment effects and the correlation to macroscopic surface tension of ILs is derived. The IL/solid interface between ultrathin ionic liquid layers on various substrates is studied with emphasis on the molecular arrangement and growth behaviour. Furthermore, we demonstrate the application of in situ XPS to monitor organic, liquid-phase reactions.

H.-P. Steinrück, Phys. Chem. Chem. Phys. 14 (2012) 2510-2529

ILS-2-Or-3
Metallic nanocolloids prepared by magnetron sputtering on the surface of an ionic liquid

T09 Ionic liquids surfaces and interfaces

#ILS-2-Or-3

P. Lobotka [1], I. Vávra [1], P. Kunzo [1], G. Radnóczi [2], Z. Czigány [2], M. Držík [3].

[1]IEE SAS - Bratislava (Slovakia), [2]MFA KFKI - Budapest (Hungary), [3]ILC - Bratislava (Slovakia).

Similarly to the pioneer work by Torimoto et al. [1], who exploited remarkable property of room temperature ionic liquids (RTILs) – very low vapour pressure of about 10^{-11} mbar – and prepared by sputtering colloids containing Au nanoparticles about 6 nm in size, we used the same procedure in preparation of non-magnetic (Ag-Cu) and magnetic nanoparticles of Ni and Ni-Fe in several RTILs (consisting of EMIM or BMIM cations and BF_4 or PF_6 anions, and BMIM-Tf2N). The main motivation is to prepare colloids with magnetic nanoparticles to be used later in sensorics. A further goal is to deposit proper nanoparticles from the nanocolloid on the surface of planar thin-film gas sensor [2] in order to increase its sensitivity and/or selectivity.

The metals were deposited in UHV sputtering machine from two magnetrons onto RTIL poured in a Petri dish. The nominal composition of Ni-Fe alloy was 80:20 which corresponds to that of permalloy. The presence of the nanoparticles in colloids was revealed by TEM, XRD, and UV-vis spectrometry (using localized surface plasmon resonance effect). We found the size of nanoparticles to be RTIL-dependent. For example, the nanoparticles formed by sputtering of Ni-Fe or Ag-Cu alloys on the surface of the 1-Butyl-3-methylimidazolium bis (trifluoromethylsulfonyl) imide are several times larger than those formed by sputtering on the surface of other RTILs used in the experiments. Even the nanoparticles of the size of ~ 40 nm show facetting which is a property so important for enhanced sensing and catalysis.

In our opinion, this technique provides an elegant way for preparation of nanoparticles with narrow size distribution and of different complex composite materials (metallic, semiconducting or insulating) that cannot be prepared by

chemical means. The nanocolloids are stable for many months; the nanoparticles are protected against oxidation, etc. Recently, we succeeded in deposition of Ni-Fe nanoparticles on a substrate by electrophoresis.

The authors P. L., I. V., and P. K. acknowledge the financial support by the APVV grant agency under the number APVV-0593-11.

[1] T. Torimoto, K. Okazaki, T. Kiyama, K. Hirahara, N. Tanaka, and S. Kuwabata, Appl. Phys Lett. 89 (2006) 243117
[2] P. Kunzo, P. Lobotka, M. Micusik, E. Kovacova, Sensors & Actuators B 171-172 (2012) 838-845.

TEM micrograph of Ni-Fe (80:20) nanoparticles obtained by simultaneous sputtering of Ni and Fe on the surface of the ionic liquid 1-Butyl-3-methylimidazolium bis (trifluoromethylsulfonyl)imide. The average size of facetted nanoparticles is about 12 nm. Please note the self-assembling effect.

ILS-P3-01
Electroplating of Al on Mg alloys in an ionic liquid for corrosion protection

T09 Ionic liquids surfaces and interfaces

#ILS-P3-01

M. Ueda, Y. Tabei, S. Hariyama, T. Ohtsuka.

Hokkaido University - Sapporo (Japan).

Magnesium alloys recently have a great attention and are expected to be future materials due to good mechanical properties and rightness in various fields of auto-mobile, aerospace, and mobile phone etc. These alloys, however, have poor corrosion resistance which restricts the usage of alloys. For the corrosion protection, several surface treatments have been applied such as chemical conversion, anodization, organic coating, metal coating, etc. We aim in this presentation direct electroplating of Al onto Mg alloys in an ionic liquid. The electroplating is one of the simple processes and functional plating is easily produced. In this study, we report the electroplating of Al on Mg alloys from $AlCl_3$-EMIC ionic liquid at the lower temperature of 283 K and 323 K. Observations of surface morphologies of Al deposits and of interfaces between the Al layer and the substrates are also reported.
Aluminum chloride ($AlCl_3$, 99.999% pure) and 1-ethyl-3-methylimidazolium chloride (EMIC, 99.5% pure) were used as received. All chemicals were handled under argon atmosphere in a glove box. A mixture of 67 mol% AlCl3-33 mol% EMIC of 80 ml volume was prepared in the cell. AZ91 and AZ121 magnesium alloy plates with surface area of 3 cm^2 were used as the working electrode. A pure aluminum plate (99.99%) and a pure aluminum wire were used as counter electrode and reference electrode, respectively. Electroplating of Al was done on the Mg alloys electrode under the constant current electrolysis or current pulse electrolysis with current densities of 1.7 $mAcm^{-2}$ and charge density of 7 Ccm^{-2} in the ionic liquid at 323 K and 283 K. The composition analysis and surface observation of electrodeposits were used by EDS and SEM.
In the $AlCl_3$-EMIC ionic liquid, the electrodeposition of Al takes place at the potential lower than 0.0 V v.s. Al/Al(III). Al deposits exhibited silver-gray on AZ91 and AZ121 alloys at 323 K. The appearance of Al deposit on AZ91 and AZ121 alloys were relatively smooth however, the needle-like deposits were observed in edge part of the alloy specimens.
The current pulse electroplating on the Mg alloys at 283K was carried out with applied current density of 1.7 $mAcm^{-2}$, the frequency of 0.67 Hz, and the duty ratio of

67 %. The Al layer on AZ91 and AZ121 were silver-white and some parts of the surface were mirror-like. In the cross-sectional SEM images of Al layers deposited, Al layers on AZ91 and AZ121 were uniformly formed and their average thickness were about 5 μm. Al electroplating on AZ121 reveal a good adherence and no small crevice was observed at the interface.

ILS-1-Or-3
Carbon dioxide capture by a functionalised ionic liquid studied with in-situ high pressure XPS

T09 Ionic liquids surfaces and interfaces

#ILS-1-Or-3

I. Niedermaier [1], W. Wei [2], C. Papp [1], C. Kolbeck [1], S. Krick Calderòn [1], F. Maier [1], P. Schulz [2], P. Wasserscheid [2], H.P. Steinrück [1].

[1]Lehrstuhl für Physikalische Chemie II - 91058 Erlangen (Germany), [2]Lehrstuhl für Chemische Reaktionstechnik - 91058 Erlangen (Germany).

Ionic liquids (ILs) are molten salts composed solely of ions with a melting point below 100 °C and a negligible vapour pressure at room temperature. X-ray photoelectron spectroscopy (XPS) has proven to be a versatile tool for surface investigations of these materials under ultrahigh vacuum conditions (UHV).[1] It even allows to monitor reactions occurring in the near-surface region of ILs.[2] We demonstrate to our knowledge the first gas-liquid reaction studies between an IL and a gaseous species by means of in situ XPS in the mbar pressure regime. The anion of the IL $[Me_2N^+(CH_2CH_2OH)_2][H_2NCH_2CH_2SO_3^-]$ was functionalised with an amine group (H2N−), in analogy to aqueous amine systems for carbon dioxide capture applications. ILs are considered as potential replacements for these aqueous amines due to the extremely low vapour pressure and their typically high thermal stability. Under CO_2 pressures up to 0.9 mbar, in situ XPS reveals reaction schemes involving carbamate and ammonium formation via carbamic acid as an intermediate.
Supported by the Cluster of Excellence - Engineering of Advanced Materials.

1. H. P. Steinrück, Phys Chem Chem Phys, 2012, 14, 5010

2. I. Niedermaier et al., Chemphyschem, 2012, 13, 1725

ILS-1-Or-9
Direct Visualization of Electrochemical Behavior on Ionic-Liquid/Electrode Interfaces by Frequency Modulation Atomic Force Microscopy

T09 Ionic liquids surfaces and interfaces

#ILS-1-Or-9

T. Ichii, M. Negami, K. Murase, H. Sugimura.

Kyoto Univ. - Kyoto (Japan).

Ionic liquids (ILs) are expected to be adopted as new electrolytes in electrochemistry because of their interesting properties. High-resolution structural analysis on IL/electrode interfaces will provide helpful information for IL-based electrochemistry and frequency modulation atomic force microscopy (FM-AFM) would be a promising technique for this purpose. Recently, we have developed an FM-AFM with a quartz tuning fork (QTF) sensor for imaging in viscous ILs and atomic-resolution imaging was successfully achieved [1].
In this study, we newly developed a vacuum electrochemical FM-AFM (EC-FM-AFM) with a QTF sensor and investigated electrochemical behavior on IL/electrode interfaces. Figure 1 shows a two-dimensional frequency shift vs. distance map (2D Δf map) obtained on a interface of 1-butyl-1-methylpyrrolidinium tris(tentafluoroethyl)trifluorophosphate ([$Py_{1,4}$]FAP) and a Au(111) surface. At first, the electrode potential was kept -0.4 V vs. Pt-quasi-ref. (hereafter called “V”) and then it was abruptly shifted to -1.6 V during the imaging. A stripe-like structure with a period of 0.9 nm, which indicates the presence of multiple solvation layers on the interface, was clearly imaged. In addition, the solvation structure was shifted by approximately 0.5 nm to the Au(111) surface when the electrode potential was shifted to -1.6 V. A plateau with a width of 0.35 nm, which corresponds well to the size of the [$Py_{1,4}$] cation, was found near the Au(111) surface on the cross-sectional plots (Fig. 2) at -1.6 V. A likely explanation is that the adsorbed cation layer was formed on the surface. This result indicates that the developed EC-FM-AFM is capable of visualizing electrochemical behavior on IL/electrode interfacial structures.

[1] T. Ichii, M. Fujimura, M. Negami, K. Murase, H. Sugimura, *Jpn. J. Appl. Phys.* **51** (2012) 08KB08.

Fig. 1 2D Δf map obtained on a [$Py_{1,4}$]FAP/Au(111) interface.
Fig. 2 Cross-sectional plots obtained along lines A-B and C-D in Fig. 1.

ILS-1-Or-8
Effect of dissolved LiCl on the Ionic Liquid – Au(111) Interface: in situ STM Study.

T09 Ionic liquids surfaces and interfaces

#ILS-1-Or-8

N. Borisenko, S. Zein El Abedin, F. Endres.

Clausthal University of Technology - Clausthal-Zellerfeld (Germany).

During the recent 5 years it has been found that ionic liquids (ILs) show an interesting interfacial chemistry. Atomic force microscopy (AFM) measurements reveal that ILs display ion layering (multilayers) at solid surfaces causing an oscillating charge (anion + cation) density profile.[1,2] *In situ* scanning tunneling microscopy (STM) studies show the potential dependent long-range restructuring of electrode surfaces as well as the formation of anion/cation adsorption layers.[2,3] For instance, the kinetically hindered formation of the herringbone reconstruction, Au(111)(22 x $\sqrt{3}$), has been imaged at cathodic potentials for a Au(111) surface in contact with neat 1-butyl-1-methylpyrrolidinium tris(pentafluoroethyl)trifluorophosphate ([$Py_{1,4}$]FAP).[2]

In this study *in situ* STM has been employed to elucidate the structure of the charged Au(111)-IL interface in the presence of LiCl. The addition of the Li salt to the ionic liquid has a strong influence on the interfacial structure. For instance, similar to pure [$Py_{1,4}$]FAP (fig. 1), *in situ* STM measurements reveal that the herringbone superstructure can be obtained in the presence of 0.1 M LiCl during cathodic polarization (fig. 2). However, unlike to the pure IL, the reconstruction of the gold surface is not complete. A likely explanation is that either the Li^+ or Cl^- is preferentially adsorbed to the electrode surface (depending on potential), impeding surface-IL contact. This disrupts the templating effect of the surface on the IL, and the strength of interfacial nanostructure is reduced. These results show that the addition of solutes can strongly alter the ILs-electrode interface.

[1] R. Hayes, N. Borisenko, M. K. Tam, P. C. Howlett, F. Endres, R. Atkin, *J. Phys. Chem. C*, 2011, 115, 6855.
[2] R. Atkin, N. Borisenko, M. Druschler, S. Z. El Abedin, F. Endres, R. Hayes, B.

Huber, B. Roling, *Phys. Chem. Chem. Phys.*, 2011, 13, 6849.
[3] N. Borisenko, S. Z. El Abedin, F. Endres, *Chem. Phys. Chem.*, 2012, 13, 1736.

Fig. 1 *In situ* STM image of Au(111) in [$Py_{1,4}$]FAP at -1.2 V, 90 nm x 90 nm.

Fig. 2 *In situ* STM image of Au(111) in [$Py_{1,4}$]FAP + LiCl (0.1 M) at -1.2 V, 90 nm x 90 nm.

ILS-2-Or-2
Molecular Dynamics study of frictional properties of confined ionic liquids

T09 Ionic liquids surfaces and interfaces

#ILS-2-Or-2

F. Federici [1], K. Kurihara [1], A. Shluger [2].

[1]WPI-Advanced Institute for Materials Research, Tohoku University - Sendai (Japan), [2]Department of Physics and Astronomy, University College London - London (United kingdom).

Friction is one of the most fundamental processes in nature, and remains a key design concept in machines and devices at all scales. Globally, thousands of billions are spent annually on expenses attributable to friction and wear [1], and efforts to reduce and control their effects form a massive research area. Moreover, friction and wear effects become even more disrupting in micro-electromechanical systems (MEMS), where even small changes in the device structure can hamper its functionality. In order to counter frictional processes, a lubricant in liquid form, is usually placed between the two sliding surfaces, with the idea of preventing the formation of a contact region where asperities can interlock. In recent years, ionic liquids (IL) have shown great potential as candidates for lubrication [2] because of their excellent stability in a wide range of temperatures and environmental compatibility. The initial experimental success of these systems, triggered the theoretical investigation of the nanoscale mechanisms that makes IL such good lubricants., in order to aid researchers in designing lubricants at the molecular level. We focus our efforts on two IL systems, [C4MIM+][BF4-] and [C4MIM+][NTf2-] confined between two silica plates: their viscous properties were previously studied experimentally [3] with the resonance shear measurement apparatus. In our molecular dynamics (MD) simulations, the organic molecules of the ILs, were treated classically using a coarse-grained model [4], while the silica surfaces are represented by hydroxilated cristobalite (110) surfaces consisting of frozen atoms. Our simulations, carried out both with the HOOMD code, delivering excellent performance on graphics processing units (GPU), and the more conventional and well tested DL_POLY. The results show the formation of three molecular layers in the confined region; in the boundary layers interact strongly with the surfaces, the anion molecules arrange themselves next to the hydroxyl groups while the imidazolium ring of the cation is filling the gaps between H rows. These molecules exhibit very long residence time and effectively behave like a solid. On the other hand, molecules in

the middle layer are more mobile, their time-average density plot does not reveal any dominant structure in the layer plane and they diffuse with the slow dynamics typical of ILs.

[1] R. W. Carpick, Science, 313, 184 (2006)
[2] H. Wang, et al., Wear 256, 44 (2004)
[3] K. Ueno, et al., Phys. Chem. Chem. Phys., 12, 4066 (2010)
[4] X. Zhong, et al., J. Phys. Chem B, 115, 10027 (2011)

Layered structure of [C4MIM][BF4] confined between hydroxilated silica surfaces.

ILS-1-Or-1
Characterization of Ionic Liquid interfaces with Metastable Induced Electron Spectroscopy (MIES) and Photoelectron Spectroscopy (UPS/XPS)

T09 Ionic liquids surfaces and interfaces

#ILS-1-Or-1

S. Krischok [1], A. Ulbrich [1], M. Marschewski [2], O. Höfft [3], W. Maus-Friedrichs [2], V. Kempter [2], F. Endres [3].

[1]Institut für Physik und Institut für Mikro- und Nanotechnologien,Technische Universität Ilmenau - Ilmenau (Germany), [2]Institut für Physik und Physikalische Technologien, Technische Universität Clausthal - Clausthal-Zellerfeld (Germany), [3]Institut für Elektrochemie,Technische Universität Clausthal - Clausthal-Zellerfeld (Germany).

Ionic liquids (IL) are highly interesting solvents for electrochemical processes; mainly due to the combination of their high electrical conductivity, their electrochemical stability and their ability to dissolve a wide range of compounds [1].
It has been shown recently that electrochemical reactions are influenced by solvation layers of ILs on electrodes [2]. Therefore, a detailed knowledge about the structure at the phase boundary between solid interfaces and ionic liquids is important to understand electrochemical processes at electrodes. Furthermore, the molecular composition of the ionic liquid vacuum interface is also of great interest.
Due to the low vapour pressure ionic liquids interfaces can be investigated with electron spectroscopic methods like metastable induced electron spectroscopy (MIES), ultraviolet photoelectron spectroscopy (UPS, HeI/II) and X-Ray photoelectron spectroscopy (XPS) [3]. In this study we use the different surface sensitivity of these methods to investigate liquid solid and liquid vacuum interfaces of ionic liquids with the imidazolium cation in detail.
For the analysis of the solid liquid interface we have prepared monolayers of 1-octyl-3-methyl-imidazolium bis(trifluoromethylsulfonyl)amide ([OMIm]Tf_2N) on Au(111) by vapour deposition at room temperature and at 140K. The obtained data are

compared with results for the thick IL films. At room temperature we find a reorientation of the [OMIm] cation during the growth of the first two layers. In contrast, at 140K an ordered growth of [OMIm]Tf_2N on Au(111) beyond the first monolayer is observed. Heating up the film produced at 140K to room temperature, results in the formation of a disordered film and the data are comparable to those obtained for thick IL layers prepared at room temperature.
The electron spectra of thick [OMIm]Tf_2N films indicate a preferred orientation at the outermost surface. The measurements reveal that the alkyl chain sticks out of the surface. This seems to be a general behavior for [XMIm]Tf_2N (X=Ethyl, Butyl, Hexyl and Octyl) films [4], whereby with increasing alkyl chain length this effect is more pronounced. However, unlike [XMIm]Cl, where no chlorine induced feature is detected in the MIES spectra and the anion seems to be completely buried under the alkyl chain [5], the MIES spectra of [XMIm]Tf_2N show still some features of the [Tf_2N] anion proving that the surface density of states shows still contributions of both, the cation and the anion.

[1] F. Endres, S. Zein El Abedin, Phys. Chem. Chem. Phys., 8 (2006) 2101
[2] F. Endres, O. Höfft, N. Borisenko, L. H. Gasparotto, A. Prowald, R. Al-Salman, T. Carstens, R. Atkin, A. Bund and S. Zein El Abedin Phys. Chem. Chem. Phys. 12 (2010) 1724
[3] H-.P. Steinrück, Surface Science, 604 (2010) 481
[4] K.R.J. Lovelock, C. Kolbeck, T. Cremer, N. Paape, P.S. Schulz, P. Wasserscheid, F. Maier and H.-P. Steinrück, J. Phys. Chem. B, 113 (2009) 2854
[5] A. Ulbrich, M. Reinmöller, W.J.D. Beenken and S. Krischok, ChemPhysChem, 13 (2012) 1718

ILS-1-Or-7
Ion size effect on the structure of quaternary ammonium-based ionic liquids at gold electrode interface studied by SEIRAS

T09 Ionic liquids surfaces and interfaces

#ILS-1-Or-7

K. Motobayashi [1], K. Minami [2], N. Nishi [2], T. Sakka [2], M. Osawa [1].

[1]Hokkaido University - Sapporo (Japan), [2]Kyoto University - Kyoto (Japan).

Ionic liquids (ILs) are promising electrolyte materials for electrochemical reactions or electrochemical devices due to their fascinating properties such as high thermal stability, wide electrochemical window, and high ionic conductivity. Although IL/electrode interfaces must play important roles in such applications, the structures and dynamics of ILs at interfaces are still under debate. The structures of electrode interface of ILs including aromatic cations such as imidazolium or pyridinium ions have been studied by surface-selective spectroscopy techniques. However, the structure of electrode interface of ILs including quaternary ammonium cations have not been studied yet. Here we report in-situ surface enhanced infrared absorption spectroscopy (SEIRAS) studies on the structures of quaternary ammonium based ILs at Au electrode interfaces under electrochemical potential control. We found unique size effect on the interface structure of these ILs.

ILs used in this study (Fig. (a), (b)) are synthesized by the method described in the previous literature[1]. SEIRAS experiments have been performed on an Au thin film electrode deposited on a Si prism. The electrode potential was controlled by a potentiostat and three electrode system (Au film as WE, Pt mesh and wire as CE and RE) introduced in the vacuum glass cell (< 10^{-6} Torr).

SEIRA spectra of [TOMA][C_1C_1N] show four CH stretch modes: symmetric/asymmetric stretch of methyl groups and those of methylene groups (Fig. (c)). Increasing electrode potential leads to smaller band intensities of vibrations of methyl group and larger intensities of methylene groups. Following structure model was proposed from this result. At negative electrode potential, positively charged N

atom of TOMA cations are attracted by the electrode, resulting in methyl groups near the electrode and butyl chains including methylene groups far from the electrode. At positive potential, the electrode is surrounded by C_1C_1N anions and neutral butyl chains of TOMA cations fill the gap in the anion layer without breaking charge compensation.

Alternation of anions showed that the structure of cations at the interface is strongly affected by anions. SEIRA spectra suggested that bulky anions prevent butyl chain from filling the gap in the anion layer. Also shown is that less bulky cations cannot reached to the C_1C_1N layer to fill its gaps. Thus the effect of ion size on IL/electrode interface structure was directly observed.

1. Y. Yasui et al., J. Phys. Chem. B 113 (2009) 3273.

Fig. (a) Chemical structure of TOMA cation and (b) C_1C_1N anion. (c) SEIRA spectrum of [TOMA][C_1C_1N] at Au electrode interface at each electrode potential.

ILS-2-Or-1
Lateral Electrochemistry Without Electrolyte in a Patterned One-Atom-Thick Surface Layer

T09 Ionic liquids surfaces and interfaces

#ILS-2-Or-1

J. Sagiv, R. Maoz, J. Berson, D. Burshtain.

Weizmann Institute of Science - Rehovot (Israel).

We present a generic supramolecular platform that allows deliberate assembly of surface-immobilized one-atom-thick ion fields and ion channels with layout precisely definable over the full range of length scales from nanometer to centimeter. Such single layer ionic entities enable effective spatial confinement of ionic traffic to planned surface paths, thus paving the way to electrochemical surface fabrication without any added electrolyte. This conceptually new electrochemical strategy is based on the use of highly ordered self-assembled organosilane monolayers patterned by a nondestructive electrochemical process (*constructive lithography*) [1-4] carried out with the assistance of a conductive AFM tip (serial patterning) [1,3,4] or stamp (parallel patterning) [2-4] that effects local conversion of the inert, electrically insulating outer surface of the monolayer to a highly efficient solid ionic conductor. Monolayer-supported circuits combining electronic (metal nanowires and contact electrodes) and ion conducting components exhibiting extraordinary lateral ionic conductivities could be successfully fabricated using this novel approach.

1. R. Maoz, E. Frydman, S. R.Cohen, J. Sagiv, *Adv. Mater*. **2000**, *12*, 725-731.
2. A. Zeira, D. Chowdhury, R. Maoz, J. Sagiv, *ACS Nano* **2008**, *2*, 2554-2568.
3. A. Zeira, J. Berson, I. Feldman, R. Maoz, J. Sagiv, *Langmuir* **2011**, *27*, 8562-8575.
4. J. Berson, A. Zeira, R. Maoz, J. Sagiv, *Beilstein J. Nanotechnol*. **2012**, *3*, 134-143.

ILS-1-Or-2
Adsorption, Desorption and Reaction of [C8C1Im][BF4] Ionic Liquid Multilayers on Cu(111)

T09 Ionic liquids surfaces and interfaces

#ILS-1-Or-2

K. Syres, R. Jones.

The University of Nottingham - Nottingham (United kingdom).

Ionic liquids (ILs) are composed of ions held together by a strong Coulomb potential. Their ultra-low vapour pressures allow them to be studied using UHV surface science techniques. In the present study, multilayers of $[C_8C_1Im][BF_4]$ were deposited on a Cu(111) surface by evaporation in UHV and the adsorption and desorption behavior studied.

X-ray photoelectron spectroscopy (XPS) shows that $[C_8C_1Im][BF_4]$ adsorbs without decomposition. The F 1s signal was monitored as the IL was deposited at both room temperature and 120 K (which is below the glass transition temperature of the IL). Despite identical dosing conditions the signal grew much faster when deposited at 120 K. When the F 1s signal was clearly observable on the 120 K surface it was barely visible on the corresponding room temperature surface. This suggests that at 120 K the IL sticks where it lands forming multilayers in a layer by layer process. At room temperature the IL is deposited as islands hence reducing the measured F 1s intensity. With further dosing the F 1s signal does increase as the Cu surface between the islands also becomes covered with IL. XPS shows that multilayers deposited at 120 K melt and convert to the island structure when heated to room temperature.

Further heating causes the IL multilayers to desorb from the surface leaving a monolayer of ≈10 Å thickness at ≈430 K. At higher temperatures the monolayer reacts with the surface. By ~470 K the B 1s signal has completely disappeared, the F 1s signal has nearly disappeared but the C 1s and N 1s signals are still visible and in the same ratio as when deposited. This is consistent with the emission of BF_3 from the surface leaving products containing C, N and some F on the surface.

ILS-1-Or-4
Adsorption, Desorption and Evaporation of [C8C1Im][BF4] on Au(111)

T09 Ionic liquids surfaces and interfaces

#ILS-1-Or-4

M. Buckley, R. Jones.

The University of Nottingham - Nottingham (United kingdom).

Ionic liquids (ILs) possess properties such as low vapour pressure, electrical conductivity, large liquid ranges and chemically tunability which have excited enormous interest over the past decade. Here we investigate the fundamental bonding energetics of ILs on Au(111), and the mode of evaporation of the IL by studying 1-octyl-3-methylimidazolium tetrafluoroborate, $[C_8C_1Im][BF_4]$ and comparing it with previous work1 for 1-ethyl-3-methylimidiazolium bis[(trifluoromethyl)sulfonyl]imide, $[C_2C_1Im][Tf_2N]$.
Using temperature programmed desorption, $[C_8C_1Im][BF4]$ desorbed with first order kinetics (monolayer desorption) followed by zero order desorption (multilayer desorption). The clean surface Au(111) LEED pattern was obscured by monolayer coverage, confirming that the IL wets the surface. The multilayer zero order desorption peak gave an activation energy of 133 kJ mol^{-1} and a pre exponential of 10^{16} s^{-1}, the latter corresponding to an entropy of activation of ≈50 J K^{-1} mol^{-1} that is consistent with an evaporation mechanism involving direct emission of an ion pair from the liquid surface into the gas phase. The activation energy for monolayer desorption (133 kJ mol^{-1}) is the same as for multilayer desorption, in marked contrast to $[C_2C_1Im][Tf_2N]$ on Au(111) where the monolayer value was higher. This is consistent with the small $[BF_4]^-$ sitting on the vacuum side of the imidazolium ring for monolayer and sub-monolayer coverages. This forms dipoles perpendicular to the surface which repel and reduce the chemisorption energy, Fig.1. By contrast, the much larger $[Tf_2N]^-$ ion adsorbs coplanar with $[C_2C_1Im]^+$ at low coverages, forming dipoles parallel to the surface which are arranged laterally in an attractive geometry, hence increasing the adsorption energy.

1. S. G. Hessey and R. G. Jones, *Chemical Science*, 2013, **submitted**.

Figure 1. Left, anion and cation of $[C_2C_1Im][Tf_2N]$ adsorbed coplanar with dipole parallel to surface such that adjacent dipoles can be attractive. Right, anion and cation of $[C_8C_1Im][BF_4]$ with vertical dipoles which are laterally repulsive. Image dipoles are also shown.

ILS-1-Or-6
Activated Absorption of Water, Methanol and Acetone on the Ionic Liquid [C2C1Im][EtSO4]

T09 Ionic liquids surfaces and interfaces

#ILS-1-Or-6

R. Jones, S. Hessey.

School of Chemistry, University of Nottingham - Nottingham (United kingdom).

Ionic Liquids (ILs) are being increasingly used as storage media for gases and supports for catalyst, and have potential as gas capture agents. The kinetics of gas absorption by ILs are dependent upon the interaction of the IL surface with the gas. Here the surface kinetics of three gases on an IL surface are probed using sticking probability measurements (S) and temperature programmed desorption (TPD). The ionic liquid used was 1-ethyl-3-methylimidazolium ethylsulfate, $[C_2C_1Im][EtSO_4]$ Fig.1, and the three gases were water, methanol and acetone. TPD showed that all three vapours physisorb onto the IL surface with adsorption energies, E_{ads} Fig.1, which increase in the sequence acetone (33±1 kJ mol^{-1})< methanol (36±1 kJ mol^{-1})<water (42±1 kJ mol^{-1}). Sticking probability measurements showed that absorption into the bulk of the liquid is an activated process, ΔE Fig.1, and increases in the sequence acetone (8.3±1 kJ mol^{-1})< methanol (9.4±1 kJ mol^{-1})<water (10.7±1 kJ mol^{-1}). Previous kinetic studies of water absorption into $[C_2C_1Im][Tf_2N]$ and $[C_8C_1Im][BF_4]$ IL surfaces[1] and XPS and TPD studies of water trapped within the surfaces of $[C_8C_1Im][BF_4]$[2] and $[C_2C_1Im][Tf_2N]$[3], indicate that ionic liquids are highly structured, comprising a low energy layer at the vacuum interface covering an ionic underlayer where absorbates are strongly absorbed. Using these ideas, we discuss the experimentally observed trends for adsorption onto the low energy outer surface of the ionic liquid, and the barrier height for penetration of the adsorbates into the ionic underlayer.

1. A. Deyko and R. G. Jones, Faraday Discuss., 2012, 154, 265-288.
2. K. R. J. Lovelock, E. F. Smith, A. Deyko, I. J. Villar-Garcia, P. Licence and R. G. Jones, Chem. Commun., 2007, 4866-4868.
3. S. G. Hessey and R. G. Jones, Chemical Science, 2013, submitted.

Figure 1. Diagram of the ionic liquid/vacuum interface indicating potential energy versus distance plots for water, methanol and acetone. The adsorption energy, E_{ads}, and the barrier to absorption, ΔE, are indicated for all three gases. Heavy shading indicates the ionic underlayer.

ILS-P3-02
Electrohydrodynamic simulation of ionic liquid electrosprays

T09 Ionic liquids surfaces and interfaces

#ILS-P3-02

M. Jugroot, M. Forget, C. Malardier-Jugroot.

Royal Military College of Canada - Kingston (Canada).

A precise understanding of electrosprays is highly interesting especially for highly conductive fluids such as ionic liquids used in micro-technology (such as spacecraft propulsion) systems increases. A multi-component CFD-based model coupling fluid dynamics, charged species dynamics and electric field is applied to flows in capillaries and needles. The simulations will describe the charged fluid interface with emphasis on cone-jet transition under the effect of a electric field. The time evolution solutions of the interface will highlight the close interaction among space charge, coulombic forces and the surface tension in the small scale flows. Colloid thrusters in electrospray/droplet mode and ion mode will be fully discussed and compared.

ILS-2-In-1
IONIC LIQUIDS AS SEGREGATED MEDIA: FROM “RED-AND-GREENS” TO CHARGE TEMPLATES.

T09 Ionic liquids surfaces and interfaces

#ILS-2-In-1

J. Canongia Lopez [1], K. Shimizu [2], C.E.S. Bernardes [2], L.P.N. Rebelo [2].

[1]Instituto de Tecnologia Química e Biológica, Universidade Nova de Lisboa - Oeiras (Portugal), [2]Centro de Química Estrutural, Instituto Superior Técnico - Lisboa (Portugal).

Any substance that is composed exclusively of anions and cations (a salt) must possess some kind of short-range organization in order to fulfill local electro-neutrality conditions. In the case of Ionic Liquids (ILs) such imposed short-range ordering does not lead, however, to long-range structures (crystalline forms) at room temperature. This unexpected fact is the defining characteristic of this amazing and complex class of compounds. The difficulty of forming stable crystalline structures in ionic liquids is associated in most cases with the size, asymmetry, charge dispersion, charge segregation and flexibility of the molecular ions that compose the ionic liquids. The presence of low charge density residues such as alkyl-side chains is often a controlling issue.

Taking all these facts into consideration it is not surprising that ionic liquids are presently regarded as meso-structured, nano-segregated fluids: if the ionic liquid has to order its polar parts into local structures that obey electro-neutrality conditions, then its non-polar parts must be segregated elsewhere. It is this interplay between the two types of regions/interactions (polar versus non-polar, long-range versus short-range) that eventually leads to the formation of nano-scale domains and the recognition of ionic liquids as polar networks permeated by non-polar regions.1,2

In this contribution we will show several examples of such interplay and illustrate the enormous variety of structural effects that can emerge when the nature of the ionic liquids or of their mixtures with molecular compounds is changed. We will explore the meso-structures that can be found in ionic liquids ranging from the original “red-and-green” representations, the interactions of ionic liquids with molecular species or solid substrates (ILs as charge templates), or the influence of the ubiquitous alkyl side chains (per-fluorinated, functionalized, symmetrical) in the morphology of the resulting structures.

1. Journal of Molecular Structure: TheoChem 946 (2010) 70–76.
2. Faraday Discussions 154, (2012) 155–169.

T10 Nanoscience and Technology

FMMM/NST-P3-03
Antiangiogenic Effect of Bare Titanium Dioxide Nanoparticles on Retinal Neovascularization without Unbearable Toxicity

T10 Nanoscience and Technology

#FMMM/NST-P3-03

J. Kim [1], D.H. Jo [1], N.W. Song [2], T.G. Lee [2], J.H. Kim [1].

[1]Seoul National University Hospital - Seoul (Korea, republic of), [2]KRISS - Daejeon (Korea, republic of).

To treat vision-threatening complications of diabetic retinopathy, it is important to develop effective and safe therapeutics to suppress retinal neovascularization. In this study, we investigated whether titanium dioxide (TiO2) nanoparticles maintain antiangiogenic effect on retinal neovascularization even at the concentration without definite toxicity. TiO2 nanoparticles do not induce cellular toxicity on 3 different cell lines representing vascular, neuronal, and perineural glial cells even at 100 times the presumptive therapeutic concentration (105 nanoparticles per cell, 130.47 ng/ml). Furthermore, they do not result in histologic abnormalities and significant change in gene expression at the presumptive toxic concentration (10 times the presumptive therapeutic concentration, 106 nanoparticles per cell, 1.30 μg/ml). Interestingly, TiO2 nanoparticles inhibit tube formation and migration of endothelial cells at the presumptive therapeutic concentration. In addition, they suppress ischemia-induced retinal neovascularization in mice model of oxygen-induced retinopathy at the same concentration. In particular, the antiangiogenic effect of TiO2 nanoparticles comes from the suppression of vascular endothelial growth factor receptor-2/mitogen-activated protein kinase pathway, not from toxic effects of them. Taken together, our results demonstrate that TiO2 nanoparticles can exert antiangiogenic effect at the concentration without genetic, cellular, and histologic toxicity on retinal

neovascularization, suggesting possible application in the treatment of diabetic retinopathy.

NST-5-Or-1
Recombination Processes of Photo-carriers in Cu(In,Ga)Se2 Solar Cells Studied by Photo-assisted SPMs

T10 Nanoscience and Technology

#NST-5-Or-1

T. Takahashi [1], Y. Hamamoto [1], H. Yong [1], T. Minemoto [2].

[1]Univeristy of Tokyo - Tokyo (Japan), [2]Ritsumeikan Univeristy - Tokyo (Japan).

A thin film solar cell based on Cu(In,Ga)Se_2 [CIGS] material has attracted growing interests in recent years because of some advantages of CIGS such as band gap tunability and high photon-absorption coefficient. However, material properties of CIGS have not been fully understood yet. In this study, the recombination processes of photo-carriers in the CIGS solar cells were investigated through photovoltaic measurements by photo-assisted Kelvin probe microscopy (P-KFM) [1] and through photothermal spectroscopy by atomic force microscopy (AFM) [2].

In the P-KFM method, the temporally-averaged photovoltage was measured as a function of the modulation frequency of the incident light on some CIGS solar cells with different Ga contents. Then a time constant τ for photovoltage decay, which is considered to represent a time constant required for the carrier movement across the potential barriers at the hetero-interfaces in the cell structure, and a ratio *r* of fast carrier recombination process in the whole recombination process were evaluated. As a result, we have found that the solar cell with high Ga content (50 %) [Sample A] exhibits large *r* and long τ compared with the cell with low Ga content (23 %) [Sample B]. Since large *r* means that the fast carrier recombination in the CIGS layer is enhanced, we can consider that the solar cell performance in Sample A should be degraded compared with Sample B, which is very consistent with a fact that the conversion efficiencies in Samples A and B are 9.1 and 14.7 %, respectively. In order to invesitgate the dependence of r on the Ga content in more detail, the similar measurements were performed on other samples and we have found that the value of *r* gradually increases as an increase of Ga content. These results are attributable to a deduction that the electron-hole separation near a grain boundary is more weakened due to lowering of built-in electric field in the sample with higher Ga content [3]. As for the elongation of τ in Sample A, we interprete it as another

deduction that the electron transport from the surface ZnO layer to the CIGS layer is slightly disturbed due to the broadening of the CIGS band gap.

For the photothermal spectroscopy by AFM, on the other hand, the periodical thermal expansion caused by the non-radiative recombination of the photo-carriers excited by the intermittent light was detected through the dual sampling method in AFM [2], being treated as PT signal. Under the incident light with the photon energy above the band gap of CIGS, an enhancement of the PT signal was observed around the grain boundary in the CIGS material, while the PT signal under the below-gap excitation exhibits relatively uniform distribution over the sample surface except a slight drop around the grain boundary. These results suggest that the distribution of free photo-carriers becomes nonuniform due to the built-in electric field around the grain boundary and that the sub-gap states originating from defects and/or deep level impurities may exist in the CIGS material.

This work was partly supported by JSPS and MEXT.

[1] T. Takahashi, *Jpn. J. Appl. Phys.*, **50**, 08LA05 (2011).
[2] K. Hara et al., *Appl. Phys. Express*, **5**, 022301 (2012).
[3] M. Takihara, et al., *Prog. Photovolt: Res. Appl*. [published online: 16 Nov. (2011)].

NST-12-Or-1
Influence of Organic Modifier Loading on Particle Dispersion of Plasticized Poly(vinyl chloride)/ Natural Montmorillonite Nanocomposites

T10 Nanoscience and Technology

#NST-12-Or-1

O. Dimitry [1], A. Saad [2].

[1]Egyptian Petroleum Research Institute - Cairo (Egypt), [2]National Research Centre - Cairo (Egypt).

Nanostructured polymers have attracted much attention in material sciences because of their unique properties and their applications in nanomaterials and nanodevices. In this study; natural montmorillonite (MMT), Cloisite Na+ was used as nanoclay and two organophilic montmorillonites (OMMTs), Cloisites 20A and 15A (have the same organic modifier with a loading of 90 and 125meq/100g clay, respectively) were used as organoclays. Plasticized poly(vinyl chloride) (PVC)/MMT nanocomposites containing 1,3,5,7 and 10wt% of Cloisite Na+ and PVC/OMMT nanocomposites containing 5 and 10wt% of Cloisites 20A and 15A were prepared via melt compounding using a twin screw extruder to study the influence of organic modifier loading on particle dispersion of PVC/ Cloisite Na+ nanocomposites.

Thermal stabilities of nanocomposites were characterized by TGA analysis which shows that addition of 5wt% of filler to PVC increases its thermal stability1 in the sequence: Cloisite Na+< Cloisite 20A< Cloisite 15A .The interaction between PVC and silicate layer was studied by FTIR spectroscopy which confirms strong interactions between nanometric silicate layers and PVC segments.The electrical conductivity σ which describes the ionic mobility of the systems was studied as a function of temperature and shows that σ of PVC is greatly enhanced on increasing the organic modifier loading at filler content of 5wt% , especially at higher temperatures. The obtained values are situated between the two extremities of those of semiconductors (10-10-10+2 Ω-1cm-1) of which σ of PVC/ 5wt% Cloisite 15A nanocomposite is increased by three orders of magnitude higher than that of pristine

PVC. The activation energy for electrical conductivity was found to be lowest for composite containing 5wt% of Cloisite 15A.The strong interfacial interactions between silicate layers and PVC chains effectively enhance the mechanical properties of PVC nanocomposites on using 5wt% of clay in the sequence: Cloisite Na+< Cloisite 20A< Cloisite 15A.The dispersed behavior of clay in PVC matrix was evaluated by XRD, TEM and SEM analyses2 which reveal intercalated structures in PVC / Cloisite Na+ nanocomposites and exfoliated structures in PVC/OMMT nanocomposites containing 5wt% of organoclay.In conclusion, organophilic treatment improves the thermal stability, electrical conductivity, and mechanical properties of PVC/clay nanocomposite, due to better interactions between PVC matrix and clay in the sequence: Cloisite Na+ < Cloisite 20A< Cloisite 15A.

1. T. Peprnicek et al, Polym. Degrad. Stab. 91,1855 (2006).
2. B. Lepoittevin et al ,Polymer 44,2033 (2003).

Fig 1 . XRD Patterns of Cloisite 15A and Plasticized PVC/5 and 10wt% Cloisite 15A Nanocomposites

NST/SS-3-Or-5
Two-Dimensional Magnetic Field Dependence of Josephson Current and Finite Voltage Steps in Current-Voltage Characteristics of Various Shape Niobium Tunnel Junctions and Superconducting Quantum Interference Devices

T10 Nanoscience and Technology

#NST/SS-3-Or-5

A. Nakayama, S. Abe, N. Watanabe, Y. Nishi.

Kanagawa University - Yokohama (Japan).

Two-dimensional (2-D) magnetic field dependences of zero voltage step (superconducting current I_c) and finite voltage resonant steps in current-voltage (I-V) characteristics of niobium/niobium tunnel junction are measured. Superconducting Josephson current I_c through square-shape niobium tunnel junctions Nb/AlO_x/Nb can be changed by the external magnetic field [1-4]. In this article, thin film Nb/AlO_x/Nb (300/5/200 nm in thickness) tunnel junctions are fabricated by DC-magnetron sputtering apparatus with load-lock chamber. In the case of square shape junction, obtained I_c-H_x-H_y characteristics of zero voltage current I_c are the product of two Fraunhofer diffraction patterns in H_x and H_y directions parallel to the junction edges [5]. Finite voltage resonant steps I_{step} are also modulated by the external magnetic field. From measured I_c-H_x-H_y characteristics (Fig. 1) of 'H' shape junction, the heights of the sub peaks increases in applying external magnetic field parallel to the two vertical strokes of the 'H' shape. If the horizontal stroke is removed from 'H' shape junction, two junction Superconducting Quantum Interference Device (SQUID) is obtained, and capture area of vertical magnetic flux becomes huge. So from measured I_c-H_x-H_y characteristics of SQUID, two modulation periods (200 A/m for junction and 10 A/m for SQUID) of vertical magnetic field can be measured as shown in Fig. 2.

[1]N.Watanabe, A.Nakayama, S.Abe, K.Aizawa, J. Appl. Phys., 97, 10B116 (2005).

[2]N.Watanabe, A.Nakayama, S.Abe, J. Appl. Phys., 101, 09G105 (2007).

[3] N.Watanabe, A.Nakayama, S.Abe, et.al, J. Appl. Phys., 103, 07C707 (2008).

[4] N.Watanabe, A.Nakayama, S.Abe, et.al,, J. Appl. Phys., 105, 07E312 (2009).

[5] A.Nakayama, S.Abe, N.Watanabe, J. Appl. Phys., 111, 113907 (2012).

Fig.1. 2-D Magnetic Field Dependence of Josephson Current in *I-V* Characteristics of 'H' Shape Niobium Tunnel Junctions.

Fig 2. 2-D Magnetic Field Dependence of Josephson Current in *I-V* Characteristics of Superconducting Quantum Interference Devices

NST-10-Or-10
2-D lattice Ni nano-particles self-organized growth on titanium nitride coated Si crystal previously sculpted by low energy ion beam

T10 Nanoscience and Technology

#NST-10-Or-10

M. Morales Corredor [1], B. Bouchet-Fabre [2], T. Minea [3], F. Alvarez [4].

[1]UNICAMP, Instituto de Fisica Gleb Wataghin - 13081-970 Campinas Sp (Brazil), [2]Francis Perrin, Service des Photons Atomes et Molécules, CEA-CNRS, Saclay - 91191 Gif Sur Yvette (France), [3]LPGP, UMR 8578 CNRS-Université Paris-Sud, Bat. 210, 91405 Orsay Cedex - 91405 Orsay (France), [4]Unicamp-Instituto de Fisica, 13083970 Campinas - 13081-970 Campinas Sp (Brazil).

Arrays of metallic nanoparticles are interesting for many applications such as optical, magnetic, and catalytic purposes. In this paper self-organized nickel nano particles were grown on titanium nitride coated crystalline silicon previously sculpted by ion beam bombardment. This study was developed following a sequential in situ routine. First, crystalline Si (100) is bombarded by Xe+ ions at room temperature, generating regular ripples.[1] Afterward, a thin titanium nitride film diffusion barrier is grown by ion beam sputtering (IBS) on the patterned Si substrate conserving the sculpted ripples (500°C, 5 minutes). Immediately, nano-size nickel particles are deposited by IBS at 750°C during 1 minute, forming a well-defined 2-D lattice (left figure). The self-organized Ni 2-D array is explained by a combination of preferential Ni nucleation on the top of sculpted Si groves formed by the ion bombardment and the characteristic surface mean free diffusion length of the metallic particles.[2] The 2-D lattice constants **a** (171 nm) and **b** (184 nm) are indicated (right figure). Each deposition step is analyzed in situ by XPS and ex situ by XRD and AFM. The process of diffusion and ordered nucleation process is presented and discussed.

[1] Bradley and Harper J. Vac. Sci. Technol. A 6 (4), 2390 (1988).
[2] W. L. Chana and E. Chason, J. of Applied Phys. 101, 121301 (2007).

Left Figure: 2-D Ni particles self-organized growth. A missing row defect is indicated. Right Figure: Periodicity in the two preferential directions. Blue: along self-organized Ni particles (**a**). Red: perpendicular to the parallel grooves formed by the ion bombardment (**b**).

NST-12-Or-2
Electron transport through π-stacked system and ionic wires using the single molecule measurement

T10 Nanoscience and Technology

#NST-12-Or-2

M. Kiguchi, Y. Takahashi, I. Junichi.

Tokyo Institute of Technology - Tokyo (Japan).

The single molecular junction has attracted attention due to its potential application in ultrasmall electronic devices [1-3]. In this study, we study the electron transport through π-stacked systems and ionic wires based on the experimental technique of the single molecular junction [4]. Electron transfer in non-covalently bound, π-stacked systems is of particular interest, and plays a vital role in biological systems, organic electronics. However, electron transport through the initial building blocks of π-stacked systems has never been directly examined because creating molecular junctions of stacked π-molecules between nanogapped electrodes is nontrivial. Here, we investigated the conductance of the π-stacked aromatics where the π-stack was sequentially increased from 4 to 6 stacked aromatic molecules.

The single π-stacked aromatics molecular junctions were fabricated by STM break junction technique. The atomic configuration of the single π-stacked systems was characterized by the conductance change during the breaking process of the single molecular junction. The analysis showed that top and bottom triangular aromatic panels of the π-stacked molecules were bound to the Au electrodes. In general, the conductance of a short molecular junction is given by $G = A\exp(-BL)$, where L is the molecular length. The B value for single-molecule π-stacked molecules was 0.1 $Å^{-1}$, derived from the slope of L vs. lnG plots, and was smaller than that of insulating alkane chains, and comparable to that of conductive π-conjugated organic molecules. The small B value for single-molecule π-stacked molecules indicates the efficient electron transport through π stacked system.

We extended our research into the electron transport through the ionic wires. Discrete [mxn] metal ion arrays are readily available as metal ion clusters by stacking cofacial m nuclear metal complexes in n layers within the cages. The number of such assembled metal ions and the whole cluster structure are uniquely determined by the cages, as is the case of the π-stacked system. Using [mxn] metal ion arrays, we demonstrated that electron transport through metal ionic wires with low attenuation

are comparable to that through metal atomic wires and that the absolute conductance value is much larger than that of conventional organic wires containing metal ions.

1. M. Kiguchi et al., Phys. Rev. Lett. 98, 146802 (2007).
2. M. Kiguchi et al., Phys. Rev. Lett. 101, 046801 (2008).
3. T. Konishi, M. Kiguchi et al., J. Am. Chem. Soc., in press.
4. M. Kiguchi et al., Angew. Chem. Int. Ed. 50, 5708-5711 (2011).

Single π-stacked molecule and ionic wire bridging between metal electrodes

NST/SS-5-Or-1
Growth of Centimeter-Scale Single Crystal Graphene on Copper Substrate by Chemical Vapor Deposition

T10 Nanoscience and Technology

#NST/SS-5-Or-1

X. Chen, L. Guo, X. Bai, L. Wang.

Lanzhou Institute of Physics - Lanzhou (China).

Among the intrinsic properties of graphene, the near-perfect 2D lattice is one of the major characteristics of this material. The honeycomb lattice of one atomic layer thick with almost no defects, which has never been achieved before by any other thin film deposition technology, played a major role for the very low scattering and super-high mobility of carriers. Due to the super intrinsic properties and its planar nature, graphene is of great potential for the upcoming nanoelectronics era.
Graphene deposited on substrate by CVD usually comes out as polycrystalline with typical crystal size of microns. Graphene exfoliated from graphite is also in the form of micron-scale flakes. In view of technology, however, large-scale single crystal graphene is essential for nanoelectronics,as single crystal silicon for microelectronics. In the present work, we report our research on large-scale single crystal graphene growth using Chemical Vapor Deposition(CVD) technique. The experimental results have shown that under precise control of deposition parameters and substrate processing procedure, extremely low nucleation density can be achieved and large single crystal graphene domains up to 10mm in size can be grown on cooper substrate in about 10 hours of deposition time. Raman and LEED measurements have confirmed the monocrystalline and monolayer nature of the deposited graphene. The results also revealed that the vapor of cooper might play a key role in suppression of graphene nucleation. Mechanisms of graphene nucleation and growth dynamics are qualitatively discussed.

[1] A. K. Geim, Science 324, 1530 (2009).
[2] Q. Yu, L. A. Jauregui, W. Wu, R. Colby, J. Tian, Z. Su, H. Cao, Z. Liu, D. Pandey, D. Wei, T. F. Chung, P. Peng, N. P. Guisinger, E. A. Stach, J. Bao, S. Pei, Y. P.

Chen, Nature Materials 10, 443 (2011).
[3] Z. Yan , J. Lin, Z. Peng, Z. Sun, Y. Zhu, L. Li, C. Xiang, E. L. Samuel, C. Kittrell, J. M. Tour, ACS Nano, 6, 9110 (2012).
[4] L. Gao, W. Ren, H. Xu, L. Jin, Z. Wang, T. ma, L. P. ma, Z. Zhang, Q. Fu, L. Peng, X. Bao, H. Cheng, Nature Communications 3, 699 (2012).
[5] X. Li, C. W. Magnuson, A. Venugopal, R. M. Tromp, J. B. Hannon, E. M. Vogel, L. Colombo, R. S. Ruo, J. Am. Chem. Soc. 133, 2816 (2011).

NST-P2-06
Template assisted synthesis and characterization of CuSe nanowires

T10 Nanoscience and Technology

#NST-P2-06

H. Kaur, J. Kaur, S. Singh, L. Singh.

Guru Nanak Dev University - Amritsar (India).

In the past few years, research on copper selenide is continuously increasing due to their unique physical and chemical properties and its wide range of applications in the fields such as electronic, optoelectronic and thermo-electronic devices. Copper selenide plays a significant role in the fabrication of solar cells, optical filters, photodetectors, super-ionic conductors and thermoelectric converters.
Copper selenide is that kind of metal-semiconductor material which may possess both stoichiometric (Cu_2Se, Cu_3Se_2, $CuSe_2$, CuSe) and non-stoichiometric compositions ($Cu_{2-x}Se$) with different crystallographic forms (such as cubic, monoclinic and orthorhombic) and each of these compositions are totally depend on the method of preparation. Due to the formation of different stoichiometric compositions, band gap of copper selenide is not well defined.
In the present work, CuSe nanowires were successfully grown electrochemically into the nominal pore diameter (100 nm) of nuclear track etched membranes (Polycarbonate, Whatmann, UK). Morphological characteristics of the so fabricated nanowires were studied by scanning electron microscopy (SEM). Later samples were characterized using X-ray diffraction (XRD) and UV-Visible spectroscopy. XRD result shows the formation of lattice planes confirming the orthorhombic nature of nanowires. The optical properties of these nanowires shows direct band gap at 2.8eV as and indirect band gap at 3eV.

NST-10-Or-4
Formation of metallic glass nanowires

T10 Nanoscience and Technology

#NST-10-Or-4

K. Nakayama, Y. Yokoyama, T. Wada, N. Chen.

Tohoku University - Sendai (Japan).

The gas atomization which is a conventional technique in powder metallurgy is adapted for the formation of metallic glass nanowires. This approach is able to produce a large quantity of the nanowires with the diameters of 50-2000 nm in range, as shown in Fig. 1. Experiments performed with different conditions and alloy compositions confirm that the key mechanism of the nanowire formation is the spinnability which increases exponentially when the melt stream is supercooled from the liquid state. The results follow the spinnability rule where the viscosity below the melting point plays an important role in determining the aspect ratio of the nanostructures [1].

1. K. S. Nakayama et al., " Formation of metallic glass nanowires by gas atomization," Nano Lett. 12, 2404-2407 (2012).

Fig. 1 SEM image shows the high density of Zr-based metallic glass nanowires, forming nanofiber configuration.

NST/SS-3-Or-6
Magnetism of Fe on Pt(111) Revisited by Inelastic Scanning Tunneling Spectroscopy

T10 Nanoscience and Technology

#NST/SS-3-Or-6

J. Wiebe, T. Schlenk, A.A. Khajetoorians, R. Wiesendanger.

Institute of Applied Physics, Hamburg University - Hamburg (Germany).

We revisited the magnetism of single Fe atoms [1] and complexes of Fe atoms with a different number of hydrogen atoms adsorbed on the surface of Pt(111) by means of magnetic field dependent inelastic scanning tunneling spectroscopy [2,3]. We found that the magnetic easy axis is either perpendicular to or within the surface plane, depending on an fcc or hcp adsorption site. Adsorption of hydrogen atoms changes the strength of the magnetic anisotropy and leads to Kondo screening for one of the Fe-hydrogen complexes. For all investigated cases, the magnetic anisotropy energy is almost an order of magnitude lower than recently reported [1].

[1] T. Balashov, T. Schuh, A. F. Takács, A. Ernst, S. Ostanin, J. Henk, I. Mertig, P. Bruno, T. Miyamachi, S. Suga, and W. Wulfhekel, Phys. Rev. Lett. **102**, 257203 (2009).
[2] A. A. Khajetoorians, S. Lounis, B. Chilian, A. T. Costa, L. Zhou, D. L. Mills, J. Wiebe, and R. Wiesendanger, Phys. Rev. Lett. **106**, 037205 (2011).
[3] B. Chilian, A. A. Khajetoorians, S. Lounis, A. T. Costa, D. L. Mills, J. Wiebe, and R. Wiesendanger, Phys. Rev. B **84**, 212401 (2011).

NST-P1-01
Realignment of deposited carbon nanotubes in response to sessile droplets; Marangoni effect or contact line motion?

T10 Nanoscience and Technology

#NST-P1-01

M. Hokkanen* [1], R. Lehto* [1], T. Isojärvi [1], J. Takalo [1], M. Myllys [1], J. Salmela [2], S. Haavisto [2], M. Ahlskog [1], J. Timonen [1].

[1]University of Jyväskylä - Jyväskylä (Finland), [2]VTT Technical Research Centre of Finland - Jyväskylä (Finland).

*These authors contributed equally to this work.

Transport phenomena present in sessile droplets were studied with pre-deposited carbon nanotubes on Si wafers. When a droplet of liquid was allowed to evaporate on such a surface, a distinct ring-shaped imprint could be discerned. Majority of the debris particles became depleted from this region, while most of the CNTs remained. The remaining CNTs appeared to exhibit a radial orientation with respect to the ring geometry. Possible causes for these phenomena include microscopic flows inside the droplet due to the Marangoni effect, a flow arising in response to a surface tension gradient caused by evaporation of the fluid (fig.). Alternatively, the re-positioning may be driven by the contact line motion in response to the broadening of the droplet. We have studied these phenomena by comparing the imprints produced by droplets of different liquids, and analyzing the nature of CNT orientation in more detail.

The Marangoni effect is a well-documented phenomenon known to play a major role in a variety of every-day phenomena, e.g. in the formation of the famous ‘‘tears of wine’’ [1]. While most past work has been focused on the effects of Marangoni flow on the deposition of particles from evaporating colloidal droplets, there exists little information regarding to its influence in repositioning of particles already present on the substrate. Previous work has also been hampered by lack of efficient methods to measure the related flow in situ. The situation has improved with the recent introduction of optical coherence tomography (OCT), by which the flow patterns can

be visualized and measured in three dimensions. In the future, our intent is to apply the OCT technique on CNT-deposited samples to gauge the flows in droplets of different liquids of varying evaporation rate, viscosity and surface tension, so as to help unravel the factors that determine the ring formation and CNT re-orientation.

[1] J. Thomson, Philosophical magazine, 10 (1855) 330-333.

NST/SS-3-Or-7
Correlation-mediated processes for electron-induced switching between Néel states of Fe anti-ferromagnetic chains

T10 Nanoscience and Technology

#NST/SS-3-Or-7

J. Gauyacq [1], S.M. Yaro [2], X. Cartoixa [3], N. Lorente [4].

[1]ISMO, Institut des Sciences Moléculaires d'Orsay - Orsay (France), [2]Escola Tecnica Superior d'Enginyeria, UAB - Barcelona (Spain), [3]Escola Tecnica Superior d'Enginyeria,UAB - Barcelona (Spain), [4]Centre d'Investigacio in Nanociencia y Nanotecnologia, CIN2 - Barcelona (Spain).

A recent experimental study by Loth et al (1) revealed that chains of Fe atoms on a CuN/Cu(100) surface couple anti-ferromagnetically (AFM) to form two Néel states with alterning spin directions on the atoms along the chain. Furthermore, they could show that electrons tunnelling from an STM (Scanning Tunnelling Microscope) tip through one of the Fe atoms can efficiently induce a switch between the two Néel states. A complete view of the electron-induced switching process was missing for this quantal AFM nano-magnet.

We developed a theoretical quantal modelling of the transitions between the two Néel states using a model description of the Fe chain incorporating: magnetic anisotropy terms on each Fe atom (local spin S=2), anti-ferromagnetic coupling between first neighbours, Zeeman energy term. We added a phenomenological Zeeman term on the first atom of the chain to enforce the Néel magnetic structure. The transitions between the various magnetic states of the chain induced by tunnelling electrons were then computed using the strong coupling approach developed to treat magnetic transitions in adsorbates induced by tunnelling currents (2,3). Calculations were performed for chains with up to 10 atoms.

Our study reproduces the experimental findings in a very satisfying way. In addition it allows identifying three different switching processes that dominate the switching in different ranges of the STM voltage:

-at low voltage, a direct transition between Néel states induced by a single electron-chain interaction

-in the intermediate voltage range (6-10 mV), an indirect process in which the

tunnelling electron excites the chain into an intermediate state (quantized spin wave modes) that later decays to the Néel states
-at high voltage (above ~10meV), an indirect process involving domain wall formation as intermediate states
It must be stressed that the above three mechanisms for magnetic excitations are quite different from the more usual local spin-flip mechanism at play e.g. in magnon excitation in ferromagnetic chains. Switching between the two Néel states in a chain requires the flip of all the local spins in the chain and the quantal correlations in the chain (mixing between different configurations of local spins in the chain) yields the driving force of the three above mechanisms for Néel switching.

1. S.Loth, S.Baumann, C.P.Lutz, D.M.Eigler and A.J.Heinrich Science 335 (2012) 196

2. N.Lorente and J.P.Gauyacq Phys.Rev.Lett. 103(2009) 176601

3. J.P.Gauyacq, N.Lorente and F.D.Novaes Prog.Surf.Sci. 87 (2012) 63

NST-9-Or-2
Size control of colloidal particles via mechanistic knowledge: exemplified for silver nanoparticles

T10 Nanoscience and Technology

#NST-9-Or-2

M. Wuithschick, K. Rademann, J. Polte.

Humboldt Univerität - Berlin (Germany).

Metal nanoparticles have attracted much attention due to their specific catalytic, optical and magnetic properties. These properties are dependent on size, composition, crystal structure and morphology.[1] Thus, size control provides one effective key to an accurate adjustment of the colloidal properties. Most of the common synthetic procedures (usually chemical reductions) are relatively simple but do not provide a precise size control. The common approach to size control is testing different sets of parameters via trial and error. The actual particle growth mechanisms and in particular the parameter influences on the growth process remain a black box.[2]

This contribution presents an approach to size control which is based on a profound mechanistic knowledge. It comprises three steps: (i) the investigation of the principle growth mechanism for one set of parameters, (ii) the investigation of parameter influences on the growth mechanism which leads to the identification of size determining parameters and (iii) the well-directed development of synthetic recipes. This approach is exemplified for common silver nanoparticle synthesis (reduction of $AgClO_4$ with an excess of $NaBH_4$).

Recently, we deduced the principle growth mechanism from time-resolved in-situ Small Angle X-Ray Scattering investigations (see Fig. 1).[3] It comprises (1) the rapid reduction of the ionic silver to silver atoms which immediately form dimers, trimers etc., (2) the coalescence of these clusters, (3) an intermediate phase of stability and (4) a second coalescence which is the result of the complete conversion of residual BH_4^- to $B(OH)_4^-$. The final particle mean radius ranges from 4 to 9 nm and is poorly reproducible.

In the next step of the approach, the influences of reaction parameters on the growth mechanisms were elucidated.[4] It was found that reproducibility can be achieved by a controlled aging of the reducing agent. In addition, the decisive size determining parameters could be identified. As a result, synthetic procedures for silver colloids were developed which allow a size control in a wide range without additional steric stabilization.

The presented approach to size control based on mechanistic knowledge is not limited to a certain kind of system. It can also be applied to different nanoparticles (e.g. oxidic, bimetallic particles), matrices (e.g. organic solvents, glass[5]) and methods (e.g. photochemical reduction, thermal decomposition).

[1] Sun and Xia, Y. *Science* **2002**, *298*, 2176–2179.

[2] Xia et al. *Angew. Chem. Int. Ed.* **2009**, *48*, 60–103.

[3] Polte et al. *ACS Nano* **2012**, *6*, 5791–5802.

[4] Wuithschick et al., *submitted*.

[5] Simo et al. *J. Am. Chem. Soc.* **2012**, *134*, 18824–18833.

Fig. 1: Principle nanoparticle growth mechanism

NST-P1-02
INFLUENCE OF SOLUTION TREATMENT PARAMETERS ON MARTENSITE PLATE MORPHOLOGY OF A HOT ROLLED POWDER METALLURGY Fe-14Mn-6Si-9Cr-5Ni (MASS. %) SHAPE MEMORY ALLOY

T10 Nanoscience and Technology

#NST-P1-02

L. Bujoreanu [1], I.P. Spiridon [1], B. Pricop [1], B. Ozkal [2], U. Soyler [2], J. Van Hunbeeck [3], N.M. Lohan [1], A.L. Paraschiv [1], M.G. Suru [1].

[1]Faculty of Materials Science and Engineering, Gheorghe Asachi of Iasi - Iasi (Romania), [2]Particulate Materials Laboratory, Istanbul Technical University - Istanbul (Turkey), [3]Department of Metallurgy and Materials Engineering, Katholieke Universiteit Leuven - Leuven (Belgium).

Fe-14Mn-6Si-9Cr-5Ni (mass. %) shape memory alloy specimens were obtained from powder compacts, with equal amounts of as blended and mechanically alloyed particles, by cold pressing under 400 MPa pressure and sintering for 2 × 3.6 ks, with a rate of 10 K /min, up to 1423 K, [1]. In order to increase the compactness degree, sintered specimens were hot rolled at 1373 K and solution treated at 1473 K [2]. Aiming to emphasize the influence of solution treatment holding time and atmosphere on martensite plate morphology, the treatment was performed using three maintaining periods and environments. The nine solution treated specimens, obtained after 0.6, 2.4 and 4.8 ks holding periods, in vacuum, nitrogen and argon atmospheres, respectively, were analysed by optical, scanning electron and atomic force microscopy. The micrographs revealed that an intensification of chemical segregation was noticeable at the surface of specimens solution treated in inert atmospheres while vacuum enabled a marked reduction of segregated zones which became more uniformly distributed. For instance, after solution treatment for 2.4 ks in nitrogen atmosphere a marked segregation of Silicon and Manganese was noticeable, as illustrated in Fig.1. The detail displays a brown segregated area, with

large crystalline grains, rich in Si and Mn, which coalesced during solution treatment. These results confirm previous observations [3] which reported that protective atmospheres are not always effective in preventing the occurrence of certain chemical reactions, at elevated temperatures. These phenomena were less severe in vacuum.

[1] A. Umut Söyler, Burak Özkal, Leandru G. Bujoreanu, *Sintering Densification and Microstructural Characterization of Mechanical Alloyed Fe-Mn-Si based Powder Metal System*, Supplemental Proceedings: Volume 3 General Paper Selection TMS, 785-792, 2010
[2] B. Pricop, U. Söyler, R. I. Comăneci, B. Özkal, L. G. Bujoreanu, *Mechanical cycling effects at Fe-Mn-Si-Cr-Ni SMAs obtained by powder metallurgy*, Phys Proced 10, 125–131, 2010
[3] B. Pricop, U. Söyler, N.M.Lohan, B.Özkal, L.G.Bujoreanu, D. Chicet, C. Munteanu, *Thermal behavior of mechanically alloyed powders used for producing an Fe-Mn-Si-Cr-Ni shape memory alloy*, J Mater Eng Perform, 21(11), 2407–2416, 2012

Fig.1 Optical micrograph illustrating Si and Mn segregation, caused by nitrogen heat treatment atmosphere at the surface of a Fe-14Mn-6Si-9Cr-5Ni (mass. %) shape memory alloy specimen, held for 2.4 ks at 1473 K. The detail displays a brown area of large segregated Si and Mn-rich coalesced crystalline grains

NST/SS-3-Or-8
Quantitative Ballistic Electron Magnetic Microscopy: magnetic imaging of buried nanostructure with a sub-nanometric lateral resolution

T10 Nanoscience and Technology

#NST/SS-3-Or-8

M. Hervé, S. Tricot, S. Guézo, G. Delhaye, B. Lépine, P. Schieffer, P. Turban.

Institut de Physique de Rennes - Département Matériaux-Nanosciences - Université Rennes I; CNRS, UMR 6251, Campus de Beaulieu, Bât. 11E, 35042 Rennes cedex - Rennes (France).

Ballistic Electron Emission Microscopy (BEEM) is a scanning probe technique derived from STM, which allows characterization of the electronic properties of buried interfaces with a lateral nanometric resolution [1,2]. In the case of a Schottky contact, hot electrons are injected in the metal layer with an energy defined by the STM tip bias voltage. A small part of the injected electrons crosses ballistically the metal layer and reaches the buried interface. If their energy is high enough to overcome the Schottky barrier height, electrons can enter into the conduction band of semiconductor and be detected as a BEEM current.
If the single metallic base layer is replaced by a spin valve, the hot electron current will be modulated by the GMR effect. Thus, we can probe the local magnetoconductance properties of spin valves [3].
We report in this communication the investigation of the local magnetoconductance properties of epitaxial sub-micrometric spin valves Fe/Au/Fe/GaAs with an Fe electrode evaporated through a nanostencil. These sub-micrometric Fe dots can have a circular shape (450nm of diameter) or a rectangular shape (450nm×1700nm). In these structures, the modulation of the collected current by the local magnetic domain structure in the Fe dots allows magnetic imaging of buried nanostructures with strong contrast (500% of relative variation of the BEEM current) and a nanometric lateral resolution. The experimental magnetocontrast observed on these sub-micrometric Fe dots are in excellent agreement with BEEM current maps calculated via micromagnetic simulations [4]. This opens the way to a quantitative

magnetic microscopy technique with a high sensitivity and a nanometric lateral resolution.

[1]L. D. Bell and W. J. Kaiser, Phys. Rev. Lett. 61 (1988) 2368.
[2]S. Guézo, P. Turban, S. Di Matteo, P. Schieffer, S. Le Gall, B. Lépine, C. Lallaizon, and G. Jézéquel, Phys. Rev. B 81 (2010) 085319.
[3] W.H. Rippard and R.A. Buhrman, Appl. Phys. Lett. 75, 1001 (1999)
[4] M. Donahue, D. G. Porter, http://math.nist.gov/oommf/.

NST/SS-P1-01
PREPARATION OF REDUCED GRAPHENE OXIDE BY RADIATION-INDUCED REDUCTION AND ITS APPLITION TO SOLAR CELLS

T10 Nanoscience and Technology

#NST/SS-P1-01

J. Choi [1], Y. Park [2], C. Jung [1], I. Hwang [2], S. Na [3].

[1]Department of Polymer Science and Engineering, Chungnam National University - Yuseong-Gu, Daejeon (Korea, republic of), [2]Research Division for Industry and Environment, Korea Atomic Energy Research Institute - Jeongeup-Si, Jeollabuk-Do (Korea, republic of), [3]Department of Flexible and Printed Electronics, Chonbuk National University - Jeonju-Si, Jeollabuk-Do (Korea, republic of).

Graphene has been attracted a great deal of interest in recent years due to its excellent properties and potential applications [1]. Graphene can be prepared by several methods including the mechanical exfoliation of graphite, chemical vapor deposition, epitaxial growth, and a reduction of graphene oxide (GO). Among these methodologies, the reduction of GO has been regarded as the most convenient route to produce the graphene at a large scale [2]. GO is generally reduced into reduced GO (RGO) using a chemical method with various reducing agents. However, this method has several problems such as the requirement of toxic and explosive chemical reducing agents and high temperature [3].
To overcome these problems, an eco-friendly and simple radiation-induced reduction method of GO is developed in this study. GO prepared by a modified Hummer's method was dispersed in DMF, and then irradiated by γ-rays under various conditions to reduce GO. The analytic results of the resulting radiation-reduced GO (RRGO) revealed that GO in DMF was effectively reduced by γ-ray irradiation-induced deoxygenation, and that its reduction extent was dependant on the absorbed dose. The electrical conductivity of RRGO increased to 12.7 S/cm with increasing the dose, whereas its work function decreased to 4.24 eV. Based on the performance test results of the polymer solar cell devices, the RRGO can be used as a hole transport layer, and the cell device with the RRGO prepared at 50 kGy exhibited the highest performance.

[1] Y. Zhu, S. Murali, W. Cai, X. Li, J. Suk, J. R. Potts, R. Ruoff, Adv. Mater. 22 (2010) 3906.
[2] R. Gengler, K. Spyrou, P. Ruoff, J. Phys. D: Appl. Phys. 43 (2010) 374015.
[3] D. Chen, L. Li, L. Guo, Nanotechnology, 22 (2011) 325601.

NST-P2-07
THE EFFECT OF MULTI-WALLED CARBON NANOTUBES ON RADIATION RESISTANCE OF LOW DENSITY POLYETHYLENE

T10 Nanoscience and Technology

#NST-P2-07

C. Jung, D.H. Lee, J.H. Choi, I.T. Hwang, J.H. Choi.

Korea Atomic Energy Research Institute - Jeongup-Si (Korea, republic of).

Polymers have been widely used in the equipment and components of nuclear power plants, which are generally exposed to high energy radiation. Thus, the physical and mechanical properties of the exposed polymers are deteriorated due to the crosslinking and chain scission reactions caused by high energy radiation, and therefore leading to a considerable reduction in the lifetime of the polymers [1]. To extend the lifetime of the polymers used in the equipment and components of nuclear power plants, the fabrication of polymer composites with various nanofillers such as carbon black, multi-walled carbon nanotubes (MWCNTs), nanoclays, and metal nanoparticles has been recently explored to improve the radiation resistance [2,3]. In this study, MWCNT-reinforced low density polyethylene (LDPE) nanocomposites were fabricated through a melt blending to improve the radiation resistance of LDPE. LDPE nanocomposites prepared through a melt blending at different compositions were exposed to gamma-rays at absorbed doses ranging from 50 to 500 kGy. The exposed nanocomposites were investigated in terms of the tensile properties, activation energy, oxidation stability, thermal stability, and durability. The experimental results revealed that the prepared MWCNT-reinforced LDPE nanocomposites had a higher radiation resistance than the control LDPE. This strategy based on the incorporation of MWCNT into a polymer matrix for the improvement of the radiation resistance can be applicable to the development of new radiation resistant materials.

[1] A. G. A. Lafi, J. N. Hay, D. J. Parker, J. Polym. Sci. Part B: Polym. Phys. 46 (2008) 2212.

[2] G. Markovic, M. Marinovi-Cincovic, V Jovanovic, S. Samarzija-Jovanovic, J. Budinski-Simendic, Composites: Part B 43 (2012) 609.
[3] F. L. Jin, S, J. Park, Carbon Lett. 12 (2011) 57.

NST-P2-08
Investigation of mechanisms of gas-phase atoms adsorption on the boron nitride nanotubes surface

T10 Nanoscience and Technology

#NST-P2-08

I. Zaporotskova, A. Shkodin.

Volgograd State University - Volgograd (Russian federation).

Currently, boron nitride nanotubes [1-2] are the second most sought-after (after carbon nanotubes) for researchers because of their appealing properties, stable conductivity, sufficiently well-tested method of synthesis and their scope for widespread use. However, composites based on BN-tubulenes have been little researched, which can be obtained through different modifications of the surface, including by joining different atoms and molecules, which may lead to changes in their properties.
The possibility of joining gaseous atoms hydrogen, oxygen, fluorine and chlorine to the outer surface of single-walled boron nitride nanotubes (BNNT) was studied, such as "arm-chair" (n, n) and "zig-zag" (n, 0), namely, (6, 6) , (8, 8), (10, 10), (8, 0), (10, 0), (12, 0). Calculations were carried out with a molecular cluster using a semi-empirical method MNDO. A segment of BN-nanotube was selected as the cluster model with three, four or six layers of BN-hexagons. The tube system was circumferentially closed, the cluster boundary closed with hydrogen pseudoatoms. The BN bond length in the nanotube was equal to 1.4 Å.
The adsorption process was modeled using step by step approach (in increments of 0.1 Å) of the adsorbed atoms to the target-atom of the surface along the perpendicular to the longitudinal axis of the tube and passing through the target atom where the adsorption takes place. Four alignments of the adatoms on the surface are considered: I) over the boron atom, II) over the center of BN bond length, III) over the nitrogen atom, IV) over the center of the hexagon BN. Calculations allowed profiles of the potential energy surface of these processes to be drawn.
Analysis of the interaction between the oxygen atom and BN-nanotube leads to the conclusion that, in the case of the option II orientation of the atom relative to the surface BNNT oxygen, the following types are adsorbed on the tubes: (6, 6), (10, 10) and (8, 0), (10, 0), (12, 0), respectively, i.e., for all the candidates, except for (8, 8), for which there is the possibility of a metastable state. The highest adsorption energy

Ea (II) = -2.24 eV is obtained by adsorption of the oxygen atom on the surface of (12, 0) BN-nanotube. The adsorption distance in this case is ra = 1.3 Å, and the height of the energy barrier at a distance rb = 2 Å was Eb = 1 eV (activation energy).
The interaction of the adatoms H, F, Cl with the outer surface of BN-tubulen was explored. Analysis of the energy curves showed that the adsorption of the fluorine atom occurs in positions I, II, IV; the chlorine atom in position II, and the hydrogen atom in position III for the tube (12, 0).
These studies have proved the possibility of adsorption of gaseous molecules on the surface of boron nitride nanotubes, and that the preferred types of adsorption are due to the peculiarities of the adsorbed atoms.
The study was supported by The Ministry of education and science of Russian Federation, project 14.B37.21.0080.

1. Tang C. C., Ding X. X., Huang X. T., Gan Z. W., Qi S. R., Liu W., Fan S. S. // Chem. Phys. Lett. – 2002. – Vol. 356. – P. 254.
2. Golberg D., Bando Y., Eremets M., Takemura K., Kurashima K., Tamiya T., Yusa H. // Appl. Phys. Lett. – 1996. – Vol. 69. – P. 2045.

NST-P1-06
IONIC CONDUCTIVITY OF BC3 BORON-CARBON NANOTUBES

T10 Nanoscience and Technology

#NST-P1-06

P. Zaporotskov, I. Zaporotskova, S. Boroznin.

Volgograd State University - Volgograd (Russian federation).

The ionic conductivity and structure in which it cans be realized research is very important for the development of modern batteries. Using of new materials will enable from such deficiencies as little time of life, small energy, and possibility of leak from battery.
In this paper we present the results of investigation of ionic conductivity process of (6,0) boron-carbon nanotubes BCn, n=3 [1]. Two variants of boron and carbon location on the nanotube surface were modeled. The research was performed using the MNDO method within the framework of a molecular cluster model. For investigation of ionic conductivity process the vacancy formation has been modeled. Energetic and electronic characteristics of these processes have been carried out. The vacancy migration process has been modeled (fig. 1). The energy curves of process were constructed and the activation energies were calculated. Then the conductivity coefficient dependence of temperature has been found.
The study was supported by The Ministry of education and science of Russian Federation, project 14.B37.21.0080.

[1] I.V. Zaporotskova, S.V. Boroznin, E.V. Perevalova. BC3 nanotubes: electronic and structural properties / // Fundamental and Applied NanoElectroMagnetics (FANEM'12). Conference proceedings. – 2012. – P. 43

Fig. 1. Two ways of vacancy migration on nanotube surface.

NST-P2-01
SENSOR ACTIVITY OF CARBON NANOTUBES WITH BOUNDARY MODIFICATION

T10 Nanoscience and Technology

#NST-P2-01

N. Polikarpova, I. Zaporotskova, D. Vil'keeva, P. Zaporotskov.

Volgograd State University - Volgograd (Russian federation).

High sensitivity of electronic characteristics of carbon nanotubes to existence on their border of adsorbed molecules or radicals [1, 2] speaks about creation possibility on this basis of the high-sensitivity super tiny sensor. With its help it will be possible to find availability of the slightest impurity in samples.
We studied the carbon nanotube which border was modified by carboxyl functional group -COOH (fig. 1). This system represents a test probe, capable to react to various chemical elements. For the proof of its sensor activity the theoretical researches of possible interaction of the modified single-walled carbon nanotube type (6,0) with atoms of alkaline metals K, Na, Li, Mg were executed. The quantum-chemical MNDO method within a molecular cluster was used. The process of accession of carboxyl group to the open border of nanotube was simulated and studied. Process of scanning by the test probe of any surface containing subject initialization atoms created thus is investigated, and activity of nanotube with the functional group to K, Na, Li, Mg atoms is defined. Process was modeled by step-by-step approach of metal atoms to hydrogen atom of functional group along the straight line parallel to modified border of the (6, 0) nanotube (fig. 1). Power curves of this process were constructed. The analysis of the constructed power curves found the fact of interaction between the modified nanotube and the chosen atoms (K, Na, Li, Mg). It is illustrated by characteristic minima on curves.
The received results proved possibility of use of the modified carbon nanotube as a sensor for certain elements and radicals.
The study was supported by The Ministry of education and science of Russian Federation, project 14.B37.21.0080.

[1] M.S. Dresselhaus, G. Dresselhaus and P. Avouris. Carbon nanotubes: synthesis, structure, properties, and application. Springer-Verlag. 2000. p. 264.
[2] Zaporotskova I.V. Carbon and non-carbon nanomaterials and composite structures on its base: morphology and electron properties. Volgograd Russia. 2009. 456 p.

Fig. 1. The process of scanning of any surface containing metal atom; points showed a way of moving of atom about (6, 0) nanotube with the -COON functional group.

NST-P2-09
STRUCTURE AND SOME PROPERTIES OF BORON NANOTUBES

T10 Nanoscience and Technology

#NST-P2-09

D. Polikarpov, I. Zaporotskova, E. Boroznina, S. Boroznin.

Volgograd State University - Volgograd (Russian federation).

In 2004 scientists synthesized pure single-walled boron nanotubes [1] which can be considered as a new class of topological structure of boron with the unique physical and chemical properties, opening the widest prospects of its use in nano - and microelectronics. However there is no unequivocal opinion on exact structure of nanotubulary boron, practically it is not known about its electronic and energy structure, physical and chemical properties. In this work results of research of influence of structural modifications of boron nanotubes on electronic structure and conductive characteristics, and also results of calculations of superficial properties single-walled boron nanotubes are presented. The nanotubes with small diameter received by rolling of hexagonal, triangular boron sheets and α-sheet of boron (Fig. 1) are studied. Nanotubes of the arm-chair types (n, n) and zig-zag (n, 0) for each configuration (hexagonal, triangular and α-boron nanotubes) are considered. Features of electronic and energy structure and conductive characteristics of boron nanotubes of various types and configurations are discussed. Calculations are executed within the framework of the ionic-built covalent-cyclic cluster model and the appropriately modified MNDO quantum chemical scheme [2].
The study was supported by The Ministry of education and science of Russian Federation, project 14.B37.21.0080.

[1] Ciuparu, D. Synthesis of Pure Boron Single-Wall Nanotubes / D. Ciuparu [et al.] // J. Phys. Chem. B. – 2004. – V. 108. – P. 3967—3969.
[2] Zaporotskova I.V. Carbon and non-carbon nanomaterials and composite structures on its base: morphology and electron properties. Volgograd Russia. 2009. 456 p.

Fig. 1. Some configurations of boron nanotubes: a – hexagonal (6, 6) type, b - triangular (6, 6) type, c - α-boron (6, 6) nanotubes.

NST-P1-13
Orientation of PCBM in an intermixing overlayer of C60 and PCBM on Au(111) surface

T10 Nanoscience and Technology

#NST-P1-13

H. Suzuki, K. Todaka, H. Sakaue, T. Takahagi.

Hiroshima University - Higashi-Hiroshima (Japan).

Phenyl-C_{61}-Butyric Acid Methyl Ester (PCBM) is one of the promising acceptor materials for organic photovoltaic devices [1]. It is similar structure to C_{60} but it has additional substituent: phenyl-butyric acid methyl ester group. This difference increases solubility of fullerene in a solution and modifies HOMO and LUMO levels. Such differences should change the intermolecular interaction of fullerene derivative, which would result in its different behaviors on a surface from that of C_{60}. In this study, we observed behaviors of PCBM and C_{60} on the same Au(111) surface with UHV-STM. The molecules were deposited on Au (111) surface at room temperature using home-build Ta crucibles. The molecules were observed with variable temperature STM with liquid N2 cryostat at 134 K.

In PCBM overlayer on Au (111) surface at 134K, double row of bright spots decorating the step edges, bright spots at elbows of reconstruction surface, and superstructure with partially hexagonal lattice and irregularities are observed. Characteristic double row of PCBM has been reported to be due to the hydrogen bonding between tail groups (phenyl-butyric acid methyl ester groups) of PCBM [2]. The tail groups also disturb forming a closed packing of PCBM, resulting in irregular regions in the superstructure. These behaviors of PCBM are different from those of C_{60}. C_{60} forms a regular hexagonal lattice superstructure, spreading from the step edges. No C_{60} adsorbs at elbows.

In the case of PCBM and C_{60} on the same Au (111) surface (Fig. 1), some island showing hexagonal lattice are observed as well as the step edge decoration with a double row of bright spots and bright spots at elbows. Though the island must consist of PCBM and C_{60}, the structure of the island is more regular than that of PCBM and similar to that of C_{60}. There are some brighter spots (C in Fig. 1(b)) in the

superstructures, which are not observed in both of the superstructures of PCBM and those of C60. Such brighter ones are higher than both of PCBM adsorbing at elbows and C_{60} around them and do not disturb the hexagonal lattice. Considering the facts that symmetric C_{60} and asymmetric PCBM form the regular hexagonal lattice and the brighter spot is 0.2 nm higher than C_{60}, the brighter one corresponds to the phenyl-butyric acid group facing upward of PCBM. It suggests that the structure of C_{60} has strong mutual attractive interaction with the structure of PCBM.

[1] P. Schilinsky et al., Appl. Phys. Lett. 81 (2002) 3885. X. Yang et al., Nano Lett. 5 (2005) 579.
[2] H. Wang et al.,; J. Phys. Chem. A 116 (2012) 255-262.
[3] C.W. Chu et al. Appl. Phys. Lett. 88 153504 (2006).

STM image of PCBM and C_{60} on Au(111) surface at 134K. Brighter spot (C) is observed in the superstructure.

NST-8-Or-1
Growth control of two-dimensional covalent organic frameworks

T10 Nanoscience and Technology

#NST-8-Or-1

S. Clair [1], M. Abel [2], O. Ourdjini [2], T. Faury [2], L. Porte [2].

[1]CNRS, IM2NP - Marseille (France), [2]Aix-Marseille University, IM2NP - Marseille (France).

Two-dimensional (2D) polymers are expected to have a great impact on many fundamental and applied aspects of science. Some recent demonstrations of covalent polymerization performed directly at surfaces have opened promising perspectives. The polymer formation is usually obtained by deposition of the molecular precursors on the surface followed by thermal activation of the polymerization reaction. The growth process of a covalent network is highly non linear: the formation of a supramolecular phase may compete with the polymerization reaction, and the optimum parameters required at the very early stage of the polymer growth (when individual monomers react with each others) vary generally substantially from those necessary when intermediate oligomers are already formed. In addition, the irreversible character of a covalent bond precludes the formation of the thermodynamically most stable structure through defect self-healing. As a consequence, a large number of defects are usually observed, or the polymer domains are limited in size. The defects can arise from incomplete reaction between the reactants due to steric hindering in 2D-confinment, or from the relative flexibility of the covalent bond that allows easy formation of various geometries with limited stress.
Boronic acids can undergo a self-condensation (dehydration) reaction to create rigid boroxine rings and a planar polymer sheet. By using 1,4-benzenediboronic acid (BDBA) evaporated onto a well-defined metal surface extended nanoporous 2D networks could grow. I will present recent scanning tunneling microscopy (STM) results of our group,[1-5] reflecting various efforts to control the growth process of these two-dimensional covalent organic frameworks (influence of the deposition parameters, local activation of the reaction, coupling with an Ullmann reaction, etc.).

[1] N. A. A. Zwaneveld, R. Pawlak, M. Abel, D. Catalin, D. Gigmes, D. Bertin and L. Porte, Journal of the American Chemical Society 130 (21), 6678-6679 (2008).
[2] O. Ourdjini, R. Pawlak, M. Abel, S. Clair, L. Chen, N. Bergeon, M. Sassi, V. Oison, J.-M. Debierre, R. Coratger and L. Porte, Phys. Rev. B 84, 125421 (2011).
[3] S. Clair, O. Ourdjini, M. Abel and L. Porte, Chemical Communications 47, 8028 (2011).
[4] T. Faury, S. Clair, M. Abel, F. Dumur, D. Gigmes and L. Porte, Journal of Physical Chemistry C 116, 4819 (2012).
[5] S. Clair, O. Ourdjini, M. Abel and L. Porte, Advanced Materials 24, 1252 (2012).

NST-P1-14
Aluminium on the Si(100)2×1 – growth, morphology and different modifications of aluminium dimers studied by STM

T10 Nanoscience and Technology

#NST-P1-14

M. Kucera, F. Rozboril, P. Sobotík, I. Oštádal.

Charles University in Prague - Prague (Czech republic).

At low coverages, group III metals (Al, In, Ga) grow on Si(100) 2×1 surface in a form of single-atom wide chains consisting of dimers. We thoroughly studied growth and morphology of Al chains for coverages from 0.02 ML to 0.09 ML and substrate temperatures from 110 K to 420 K. For all the investigated coverages and temperatures we found significant discrepancies in behaviour and appearance between Al and other group III metals. Indium and gallium atoms assemble into long straight unbroken chains. Additionally there is no difference in appearance of individual dimers. The aluminium atoms, however, form short (several dimers long) chains, which tend to branch and sometimes seems to be broken. Moreover individual Al dimers differ in appearance. We identified three types of the aluminium dimers – “dark”, “faint” and “bright”. They vary in brightness and assemble into distinctive types of chains. Experiments at 115 K showed strong anisotropy of surface migration of single aluminium atoms. The atoms preferably hop in direction parallel to Si dimer rows. We used a statistical analysis of recorded motion of single Al atoms (method used for In in [1]) to estimate heights of diffusion barriers.

[1] M. Setvín, J. Javorský, Z. Majzik, P. Sobotík, P. Kocán, I. Ošťádal, Phys. Rev. B 85, 081403(2012).

NST-P1-15
Growth of Al on Si(100) studied by a kinetic Monte Carlo method

T10 Nanoscience and Technology

#NST-P1-15

F. Rozbořil, M. Kučera, I. Ošťádal.

Charles University in Prague - Prague (Czech republic).

Group III and IV metals deposited on clean Si(100) surface with sub-monolayer coverage form one atom wide chains. These structures have potential applications in various fields of nanotechnology. The process that leads to formation of these structures is called a surface polymerization reaction and its driving force is surface diffusion – thermal motion of adatoms [1]. If the growth occurs far from thermal equilibrium, the kinetics of surface processes plays a significant role.

The growth is affected by temperature, deposition rate and several intrinsic parameters, such as binding energies and diffusion barriers. Kinetic Monte Carlo simulations can be used to study the influence of these parameters on the morphology of metal chains on Si(100). By comparing the simulated structures to relaxed layers observed by scanning tunneling microscope, surface processes in early stages of growth can be studied.

Gallium and indium have already been investigated using this method [2-3]. Theoretical values of diffusion barriers have been calculated for In, Ga and Al [4] and experimentally confirmed for indium [5], but there are no experimental publications about aluminium structures. Our experiments show that Al on Si(100) exhibits a number of interesting properties. We observed that the scaled island size distribution function is monomodal, while the other metals show monotonically decreasing distributions. Aluminium chains grown at room temperature are shorter and create so called "kinks", which are two connected chains separated by one lattice constant on the surface (Fig. 1).

We created a growth model that takes these morphological features into consideration and found the values of the input parameters (especially the activation energies for diffusion) that represent the best agreement with our experimental data.

[1] G. Brocks, P. J. Kelly and R. Car, Phys. Rev. Lett. 70, 2786 (1993)

[2] M. A. Albao, M. M. R. Evans, J. Nogami, D. Zorn, M. S. Gordon, and J. W. Evans, Phys. Rev. B 72, 035426 (2005)

[3] J. Javorský, M. Setvín, I. Ošťádal, P. Sobotík and M. Kotrla, Phys. Rev. B 79, 165424 (2009)

[4] M. A. Albao, Ch.-H. Hsu, D. B. Putungan and F.-Ch. Chuang, Surf. Sci 604 (2010), 396-403

[5] M. Setvín, J. Javorský, Z. Majzik, P. Sobotík, P. Kocán and I. Ošťádal, Phys. Rev. B 85, 081403(R) (2012)

Figure 1: Al chain with a "kink" imaged by STM at tip voltage -2.0 V and tunneling current 300 pA.

NST-P2-02
FEATURES OF BOUNDARY MODIFICATION OF NANOTUBE SYSTEMS WITH CARBOXYL GROUP

T10 Nanoscience and Technology

#NST-P2-02

S. Boroznin, I. Zaporotskova, N. Polikarpova, D. Polikarpov, A. Shkodin, D. Vil'keeva.

Volgograd State University - Volgograd (Russian federation).

Carbon nanotubes can be used to create a unique tip for atomic force microscope. The most interesting possibilities are opened up for use in AFM of chemically modified nanotubes with functional groups at the end of the tip. In this case it is possible to study the chemical composition of the surface. Now carbon nanotubes with the carboxyl -COOH group on open bottom ends were obtained [1]. Theoretically the mechanism of attachment of this group to the boundary carbon atom of the tube was studied [2]. However, at present, much attention is paid to non-carbon boron and boron nitride nanotubes, which has more stable conductive characteristics. That would suggest that the creation of a boundary-modified sensor systems, based on them is possibly and effectively.
We have made calculations of interaction -COOH group with semi-infinite boron nitride tubulenes (8, 8), (10, 10), (10, 0), (12, 0) in the framework of the molecular cluster model, using the semi-empirical scheme MNDO. The process of connecting the -COOH group to the boron atom on the open nanotube boundary was modeled by step approach of carboxyl group along the perpendicular arranged to the tube boundary, and oriented on boron atom. As a result, the curves of the interaction "nanotube - COOH" were built, and their analysis revealed the presence of the energy minimum corresponding to the result of the formation of the chemical bond between the tube and the functional group for each test case. The energy minimum is located at a distance of 1.5Å from the boundary of the tube. Similarly, the analysis of possibility connection of -COOH group to the nitrogen atom on the open boundary of BN-tubule was made. As in the previous case, on the curves of the interaction is clearly visible minimum of energy at a distance of 1.3Å from the tubule – point of formation of chemical bonding to the nitrogen atom and the carboxyl group. Then the simulation of formation of a boundary modification of hexagonal and

triangular boron nanotubes by the carboxyl group was performed. Constructed energy curves were illustrated the possibility of the process creating nanotubular sensor system based on a single-walled boron nanotube, which would be chemically sensitive to the atoms and molecules.
Thus, the use of chemically modified nanotubes in atomic force microscopy is a way to create probes with distinct chemical characteristics.
The study was supported by The Ministry of education and science of Russian Federation, project 14.B37.21.0080.

1. Wong S.S., Josevlevich E., Wooley A.T., Cheung C.L., Lieber C.M. Covalently functionalized nanotubes as nanometer sized probes in chemistry and biology. // Nature. – 1998. - V. 52. – P. 394.
2. Zaporotskova I.V. Carbon and non-carbon nanomaterials and composite structures based on them: the structure and electronic properties. – Volgograd.:Publishing House of the Volgograd State University, 2009. – 490p.

NST-2-Or-6a
Optoelectronic switching and negative differential resistance of molecular self-assembled monolayer junctions

T10 Nanoscience and Technology

#NST-2-Or-6a

D. Ba, X. Gong, J.C. Li.

Vacuum and fluid engineering research center, Northeastern University - Shenyang (China).

Addressable Au/dipyrimidinyl-diphenyl/Au molecular crossbar junctions are fabricated using elastic polymer stamp-printing method. Figure 1 shows the schematic junction and molecular structures. Current-voltage measurements are carried out from 95 up to 295 K in vacuum under both dark and light conditions. Reversible diode, optoelectronic switching and negative differential resistance (NDR) phenomena are observed. The rectification efficiency and the current ratio dramatically decrease with temperature increase or under light irradiation. Data analysis shows that the direct tunneling and the Fowler-Nordheim tunneling act as the main transport mechanism at the low and high bias regions, respectively. The barrier heights is dependent largely on the light irradiation, bias polarity and substrate temperature. The temperature dependence of the charge transport and the NDR phenomena are further investigated using the non-equilibrium Green's function method combined with density functional theory. The NDR mechanism is analyzed in terms of the molecular projected self-consistent Hamiltonian states and transmission spectra. The distinct chemical natures of the top-printed physisorbed Au/molecule interface and the bottom S-Au contact (see Figure 2) may account for the as-observed performances.

Keywords: Metal-molecule-metal junction; Diode rectification; Optoelectronic switching; Charge transport; Negative differential resistance

Figure 1. (a) A geometry optimized schematic depiction of the molecular junction and (b) chemical structure of the dipyrimidinyl–diphenyl molecule.

Figure 2. Calculated I-V curves for the junctions with different contacting geometries, in which the insets show the schematic junctions with (a) flat, (b) triangle and (c) tetrahedron contact interfaces, respectively.

NST-10-Or-5
Gelation of Dilute Suspensions of Spherical and Rod-like Zinc Oxide Nanoparticles by Dye Absorption

T10 Nanoscience and Technology

#NST-10-Or-5

F. Stadler [1], C. Martini [2], F. Fages [2], C. Bailly [3].

[1]Chonbuk National University - Jeonju (Korea, republic of), [2]CNRS, Aix-Marseille Université, Campus de Luminy - Marseilles (France), [3]Université Catholique de Louvain - Louvain-La-Neuve (Belgium).

The adsorption of the amphiphilic Ru^{II} complex Z907 onto the surface of ZnO nanospheres and nanorods causes the gelation of organic solvents, such as THF or acetone. The gels are thermally stable at very low concentration (nanoparticle volume fraction $\varphi = 0.009$), but mechanically fragile, the behavior being dependent on solvent nature, nanoparticle concentration, and Z907-to-ZnO molar:wt. ratio. Rheological experiments confirmed the solid component built up a network to give a viscoelastic gel-phase material with a rather low value of the storage modulus G' around 100 Pa, but all characteristics of a rubbery material (Fig. 1). The brittleness of the manifests itself in a linear-viscoelastic limit around γ_0=0.1%.

However, TEM and SEM experiments did not give evidence that nanoparticle long-range ordering occurred under the experimental conditions investigated. Moreover, time-dependent SAXS measurements pointed to a decrease of the nanoparticles aggregates size upon gelation. All together, the data obtained might be rationalized in terms of aggregate-to-aggregate transition in solution, the primitive large aggregates giving rise to smaller ones upon reaction with Z907. The resulting smaller hybrid aggregates could be the active species that act as self-assembling components in the gelation process.

Given the interesting electronic and photonic properties of zinc oxide nanoparticles, such hybrid organic-inorganic gels could open new directions in materials sciences, low-cost electronics, and photovoltaics.

C. Martini, F. J. Stadler, A. Saïd, V. Heresanu, D. Ferry, C. Bailly, J. Ackermann, F. Fages, Langmuir, **2009**, 25, *15*, 8473–79, DOI: 10.1021/la804280m.

Figure 1: gelation of a mixture of 50 g/l ZnO and 12 g/l Z907 in DEGME

NST-10-Or-6
A general hydrothermal approach to TiO2, TiO2@metal-ions, TiO2@graphene, TiO2@C, and TiO2@CNTs hybrid nanostructures

T10 Nanoscience and Technology

#NST-10-Or-6

G. Cheng, F. Stadler.

Chonbuk National University - Jeonju (Korea, republic of).

TiO_2 has attracted much attention recently due its excellent physicochemical properties and potential applications in environmental remediation as well as energy conversion and storage. The optimization of the structure and composition of TiO_2 for the fabrication of high-performance dye-sensitized solar cells (DSSC), photocatalysts, supercapacitors, and Li-ion batteries still remains a great challenge. Doping TiO_2 with an- or cations, modifying TiO_2 with carbon materials, fabricating TiO_2 with favorable nanostructures have been considered as promising ways to improve the properties Hence, developing an effective approach to TiO_2-based nanocrystals, -hybrids, and -composites is important. Here, we present a general two-step solution-phase reaction to produce TiO_2 with tunable phases, compositions, and structures for exploring the above mentioned properties. Based on the formation mechanism of TiO_2 nanocrystals, we developed this method to form metal ion-doped TiO_2 nanoparticles as well as nanoporous, hybrid TiO_2 (<10 nm) materials on reduced graphene oxide (RGO) sheets, carbon-deposited TiO_2 nanoparticles and nanoporous, and TiO_2 nanodots grown on functionalized carbon nanotubes. TiO_2@graphene hybrid photoanode material exhibited power conversion efficiency η=7.68% in DSSC, significantly better than pure TiO_2 (η=4.78%). In addition, the TiO_2 nanostructures doped with carbon and metal ions indicate potential applications in environmental purification.

Fig.1 Illustration of the formation of TiO_2-based nanocrystals and nanohybrids.

Fig. 2 SEM (a, b and c) and TEM (d, e and f) images of TiO_2 nanocrystals; TEM image (g) of TiO_2@graphene; SEM (h) and TEM (i) images of TiO_2@C; SEM (j) and TEM (k) images of TiO_2@CNTs.

NST-P1-07
Large Magnetoresistance of Self-Assembled Magnetite Type Nanocrystal Films toward Spin Transistor

T10 Nanoscience and Technology

#NST-P1-07

S. Kohiki [1], T. Kinoshita [1], K. Okada [2], M. Mitome [3], A. Kohno [4], H. Deguchi [1].

[1]Kyushu Institute of Technology - Kitakyushu (Japan), [2]Osaka University - Osaka (Japan), [3]National Institute for Materials Science - Tsukuba (Japan), [4]Fukuoka University - Fukuoka (Japan).

Spin diffusion is the real issue for spin transistor. Our idea for the source (S)-drain (D) current switching is employing negative magnetoresistance (MR) of oleic acid coated (OA-) magnetite type $M_{0.5}Fe_{2.5}O_4$ (M:Mn,Fe) nanocrystals (NCs) in the spin-glass (SG) state. When two-dimension hexagonal networks of collinear spins form antiferromagnetic and ferromagnetic spin configuration respectively without and with magnetic field (H), electron tunneling between the NCs is enhanced by $H\neq0$, and tunneling resistivity varies from high to low. In the multiple junctions system, MR is defined as $MR=(R_H-R_0)/R_0$, where R_H and R_0 are the resistances in $H\neq0$ and $H=0$, respectively. MR=50% corresponds to full spin-polarization P=100% [1]. Carriers of Fe_3O_4 with P=100% below 840K is suitable for devices workable above room temperature.

$Mn_{0.5}Fe_{2.5}O_4$, an analogue of Fe_3O_4, is an *n*-type ferromagnetic oxide. In OA-$Mn_{0.5}Fe_{2.5}O_4$ NC film, the NCs self-assembled in hexagonal arrangement (the upper- and lower-left insets of Fig.1), and exhibited SG transition at 150K. At 200K, MR=−38% was achieved in H=0.5T (Fig.1). Spin transport of $P\approx80\%$ was accomplished between the electrodes separated by 1mm (the upper-right inset of Fig.1). Below 250K, self-assembled OA-Fe_3O_4 NC film exhibited bifurcation of field cooled (FC) and zero-field cooled (ZFC) magnetizations (the lower-left inset of Fig.2). At 300K, MR=−46% (Fig.2) was achieved in H=0.2T. Long-range spin transport of $P\approx95\%$ was also accomplished for self-assembled OA-Fe_3O_4 NCs.

In our OA-Fe_3O_4 NCs three terminals device (the upper inset of Fig.2), the S-D current is switched by H, and spin tunneling current is depressed by the gate voltage

(V_G) since the spin polarization is altered by the spin-orbit coupling. Under H=0.2T, MR decreased by application of V_G=4V to a half of that at V_G=0V.

[1] J. Inoue, S. Maekawa, Phys. Rev. B 53, R11927 (1996).

NST-P2-28
Synthesis and Wettability Properties of Silicon Nanowires Arrays

T10 Nanoscience and Technology

#NST-P2-28

S. Naama.

Centre de Recherche en Technologie des Semi-conducteurs pour l'Energétique (CRTSE), 2, Bd. Frantz Fanon, B.P. 140 Alger-7 Merveilles, Alger, Alegria - Alger (Algeria).

Synthesis and Wettability Properties of Silicon Nanowires Arrays

Sabrina Naama [a], Toufik Hadjersi [a], Ghania Nezzal [b]

a Centre de Recherche en Technologie des Semi-conducteurs pour l'Energétique (CRTSE), 2, Bd. Frantz Fanon, B.P. 140 Alger-7 Merveilles, Alger, Alegria

b USTHB, LPT, FGMGP, Département de Génie des Procédés. BP 32, El Alia, Bab Ezzouar, 16111 Alger
*Corresponding author: sabrina_naama@hotmail.fr

ABSTRACT

Currently, semiconducting nanowires are attracting much attention as promising components for future nanoelectronic devices such as: chemical sensors or biological, battery electrode and photovoltaic cells. Several approaches have been successfully developed for the fabrication of the nanowires. These include vapor-liquid-solid (VLS) growth [1], metal catalyzed growth assisted by laser ablation, reactive ion etching combined with lithography technique [2, 3] and metal assisted chemical etching (MACE) technique [4].

The metal-assisted chemical etching (MACE) is a technique novel for fabricating silicon nanowires which no needs of an external bias application. It is a simple, fast, and effective method. In this work, we have studied the effect of the etching

concentration AgNO3 and NH4HF2 on the process of formation of silicon nanowires as function of level doping. The etching is performed in a new chemical solution mixture of NH4HF2 and AgNO3 which has been recently developed.

The morphology of the silicon nanowire layers is investigated by scanning electron microscopy (SEM) and the wettability was investigated measuring the contact angle . It was found that the morphology strongly depends on etching parameters and their wettability change from highly hydrophilic to hydrophobic.

Keywords: nanostructure, metal-assisted chemical etching, silicon nanowires, scanning electron microscopy (SEM), contact angle.

References

[1] Y. W .Wang, V. Schmidt, S. Senz and U. Gosele, Nat.Nanotechnol 1, 186 (2006).
[2] K. J. Morton, G. Nieberg, S. F. Bai and S Y. Chou, Nanotechnology 19, 345301 (2008).
[3] C. M. Hsu, S T. Connor, M. X. Tang and Y. Cui, App. Phys., Lett, 93, 133109 (2008).
[4] X. Li and P. W. Bohn, Appl. Phys., Lett, 77, 2572 (2000).

Figure 1: cross-sectional view SEM images of SiNWs arrays formed in 15NH4HF2/ 0.05 M AgNO3 solution at room temperature for 30 min with resistivity 7.7-8.66Ω.cm.

NST/SS-3-Or-9
Preparation and Evaluation of Shock-compacted Bi-Pb-Sr-Ca-Cu-O Superconductor Including Nano/Micro Seed Crystals

T10 Nanoscience and Technology

#NST/SS-3-Or-9

H. Kezuka [1], T. Kameya [1], H. Matsumoto [2], H. Kishimura [2], S. Arisawa [3].

[1]Tokyo University of Technology - Tokyo (Japan), [2]National Defense Academy of Japan - Kanagawa (Japan), [3]National Institute for Materials Science - Ibaraki (Japan).

Bi-Pb-Sr-Ca-Cu-O oxide superconductors are very attractive material as a highly sensitive magnetic sensor. We tried the technique of adding shock-compacted BPSCCO superconducting crystal grains into the starting materials ($Bi_{1.85}$-$Pb_{0.35}$-$Sr_{1.90}$-$Ca_{2.05}$-$Cu_{3.05}$-O_x calcined powder) as seed crystals in order to obtain larger crystal grain, more dominant Bi-2223 phase and higher T_C. The specimens that contain 5%, 10%, 15%, 20% and 25% of seed crystals were prepared. These specimens were tightly encased in copper containers. The sample chamber of shock compaction gun system was vacuumed to 1.10 Torr, and shock compaction experiments were carried out under the shock pressure of 5-10 GPa.

From scanning electron microscope (SEM) images of the specimens after shock compaction, BPSCCO crystal grains of 1-3 μm were found. Larger crystal grains of 10-30 μm were found from the specimens annealed at 840-860 °C for 48-72 h after shock compaction. The higher content rate of seed crystals, the larger crystal grains were found in average. Figure shows the exceptionally large crystal grains of 95.6 μm found from the specimen content rate of seed crystals 15% - annealed 48 h.

From x-ray diffraction (XRD) analysis, Bi-2223 phase of (0 0 12) and (0 0 24) peaks were found from the specimen seed crystal content rate of 20% before annealing, and then Bi-2223 phase of (0 0 10), (0 0 12), (0 0 14) and (0 0 24) peaks were found from the annealed specimen. Similarly, Bi-2223 phase of (0 0 12) and (0 0 24) peaks were found from the specimen seed crystal content rate of 25% before annealing,

and then Bi-2223 phase of (0 0 10), (0 0 12), (0 0 14), (0 0 16), (0 0 18) and (0 0 24) peaks were found from the annealed specimen. The more peaks of Bi-2223 phase were found from the specimens after annealing. The higher content rate of seed crystals, the more peaks of Bi-2223 phase were found. However, the higher content rate of seed crystals, the lower crystalline were found.

We fabricated a thick film from shock-compacted BPSCCO superconductor. The superconductor bulk was atomized by jet mill. The size of these particles was about 1.8 μm. Particles were dispersed into methyl ethyl ketone, and dropped on the microscope slide. It became a thick film when it dried. From XRD analysis, it became clear not to lose Bi-2223 phase, even if superconductors are atomized and dispersed into solvent.

[1] H. Kezuka, K. Yamagata, M. Itoh, T. Suzuki, M. Kikuchi, T. Atou, M. Kawasaki and K. Fukuoka, J. Vac. Sci. Technol. A, 23, 1010-1012 (2005), DOI:10.1116/1.1897699

[2] H. Kezuka, K. Endo, T. Kameya, M. Itoh, H. Matsumoto, H. Kishimura, T. Endo and S. Arisawa, MRS Proceedings, 1454, 123-127 (2012), DOI:10.1557/opl.2012.1446

NST-12-Or-3
Charge transport and mechanical properties of molecular junctions formed by acetophenone deposited on Si (100) surface

T10 Nanoscience and Technology

#NST-12-Or-3

O. Krejčí, Z. Majzik, M. Setvín, P. Hapala, P. Mutomobo, P. Jelínek.

Institute of Physics ASCR - Prague (Czech republic).

One of the main challenges of Molecular electronics is to understand and control charge transfer through a reproducible single molecule contact between electrodes. Most investigations of electron transport through molecules have been performed in “blind” junction experiments, where the molecular conformation and contact geometry cannot be probed. Therefore large gaps in our knowledge remains since in molecular electronics the atomic-scale structure of the entire junction including the leads is important for its conductance properties.
Our goal is to study electrical transport through well-defined molecular junction on semiconductor surfaces. Formation of molecular junctions using organic molecules on semiconductor surfaces might lead to interesting phenomena such as negative differential resistance [1].
In this contribution, we investigate formation of molecular junction consisting of a single acetophenone molecule deposited on Si (100) surface in upright position by means of simultaneous AFM/STM measurements and DFT calculations. We used a modified UHV VT STM/AFM Omicron machine allowing simultaneous acquisition of the current and forces with atomic resolution using a tuning fork sensor [2]. At first we preformed simultaneous force spectroscopy and current spectroscopy to identify and to determine the position of the molecule. Here in addition we have an idea now how far the tip is located from the molecule and enable us to have precise control of contact formation. All this can be done only with the guide provided by DFT calculations that gives us better insight into interaction mechanism between probe and molecule. Afterwards, we record Kelvin-force spectroscopy, in which the bias voltage is swept and both frequency shift and the current through the junction are monitored as function of tip-sample distance. In addition, we performed DFT-based simulations, which allows us to get more insight into ongoing processes along tip

approach. Our approach combining AFM/STM/KPFM and theoretical simulations provides complex information about the charge states and charge transport through a single acetophenone molecule on Si(100) surface.
In particular, we found strong dependence of transport and mechanical response of single molecule on tip chemical reactivity.

[1] T. Rakshit et al. Nanoletters 4, 1803−1807 (2004).
[2] Z. Majzik et al, Beilstein J. Of Nanotech. 3, 249 (2012).

NST-12-Or-4
Growth and field emission study of NiO nanorods

T10 Nanoscience and Technology

#NST-12-Or-4

A. Moshfegh [1], M. Ebrahimi [1], A. Bayat [1], A.A. Zavarian [2], P. Sangpour [3].

[1]Sharif University of Technology - Tehran (Iran, islamic republic of), [2]Academic Center for Education, Culture &Research (ACECR) Sharif University Branch-High Vacuum Center - Tehran (Iran, islamic republic of), [3]Materials and Energy Research Center - Karaj (Iran, islamic republic of).

Introduction

Recently, extensive investigations have been focused on field emission (FE) property on conducting materials due to their applications in vacuum micro/nanoelectronic such as field emission displays and microwave sources . Among various nanostructures, one-dimensional system such as carbon nanotubes[1] and molybdenum oxide nanostars [2] because of their stability and high aspect ratio have received much attention. In this investigation, we report the result of FE measurements from sputtered nickel oxide nanorods.

Experimental

NiO nanorods have been synthesized in two steps procedure. First, by using DC sputtering method, Ni thin films were deposited on the Si(100) substrate under different growth conditions. The optimized condition for nanorod formation were: Ar discharge power density of 3.60 W/cm2, P~ 4×10-2 Torr, deposition rate 20 nm/min and growth time 30 min. Second, the films were annealed in air at 600˚C for 180 minutes with heating rate of 16˚C/min to obtain crystalline structure with nanorod formation based on SEM observations. Surface chemical composition of the produced layer was examined by XPS. FE measurements were performed under UHV (P ~ 10-8 Torr). Different cathode-anode separation distances (d) were examined to achieve optimum field emission current density (J).

Results and Discussion

Figure 1 shows the XPS spectra of the de-convoluted Ni (2p3/2) core level. It was found four different chemical states of Ni: Ni, NiO, Ni(OH)2 and, Ni2O3. Figure 2

shows typical plots of the measured J, versus the applied electric field (E), at different d values. The inset is Fowler–Nordhiem (FN) linear plot for d=300 μm. Based on our FE measurements, we have found that the turn-on electric field of ~ 3.8 V/μm at d=300 μm and the field enhancement factor of β~ 5913.

[1] Chi Li, Yan Zhang, Matthew T. Cole; ACS Nano 6 (4), 2012, 3236-3242
[2] Khademi A. Azimirad, R., Zavarian, A. A., Moshfegh, A.Z.; Journal of Physical Chemistry C113 (44) , 2009, 19298-19304

Figure 1. XPS core level spectra of the Ni (2p3/2) in the NiO nanorods

Figure 2. Field emission J – E curves measured at different distances. Inset is FN plot for d=300μm .

NST-10-Or-1
Colloidal semiconductor nanosheets as photo-transistors

T10 Nanoscience and Technology

#NST-10-Or-1

C. Klinke.

University of Hamburg - Hamburg (Germany).

Controlled assembly leading to anisotropic nanostructures poses a conceptual challenge in materials research. Oriented attachment of nanocrystal, a self-assembly of particles into larger single crystalline objects, is one of the most promising approaches in nanotechnology to synthesize anisotropic materials. One-dimensional assemblies of oriented attachment have been reported, and in most cases the anisotropy during self-assembly is caused by crystal planes with preferred reactivity and dipole moments in the crystallites. Systems with cubic crystal symmetry, however, like PbS and PbSe, where beautiful one-dimensional oriented attachment occurs, are somewhat more difficult to explain. In a new approach we synthesized truly two-dimensional nanocrystals by oriented attachment with lateral dimensions on the micrometer scale. We show that the formation of ordered and densely packed ligand surface layers of oleic acid on {100} PbS surfaces can drive the normally isotropic crystal growth into a two-dimensional oriented attachment of nanocrystals. Hereby the presence of chlorine containing co-solvents during the initial nucleation and growth process of the nanocrystals plays a prominent role. In the talk the synthesis and the formation mechanism will be discuss and detailed characterizations will be introduced. The obtained two-dimensional structures can be readily integrated into a three-terminal device structure. An analysis of the performance as photo-transistor will be presented.

[1] Schliehe et al., Science 329 (2010) 550.
[2] Dogan et al., Appl. Phys. Lett. 101 (2012) 073102.

TEM image of an ultra–thin single layer PbS nanosheet, and an AFM image of an individual nanosheet contacted with two gold electrodes,

NST/SS-P1-02
Structure and orientation of crystals at metal/graphene interfaces : The effect of van der Waals interactions

T10 Nanoscience and Technology

#NST/SS-P1-02

M. Yeom.

KISTI - Daejeon (Korea, republic of).

Many theoretical and experimental studies have been made on the interfacial interaction of graphene and metal surfaces because metal-graphene interfaces are of critical importance in graphene synthesis, graphene-based device applications, and metal-graphene-metal materials. Molecular dynamics (MD) in conjunction with the semi-experiential many-body potential of the modified embedded-atom method (MEAM) is used to overcome the system size and time limitations of ab initio calculation. The effect of van der Waals interactions on the structure and orientation of metals at metal/grapheme interfaces has been investigated by using Constant temperature and pressure molecular dynamics (NPT) simulations. Face-centered cubic, hexagonal close packed, and body-centered cubic structures were used as the reference structures for Ni, Mg, and Si, respectively.

The initial slab configurations have been consisted of 48 layers which is a 5.5 × 6.5 nm plane. The total number of atoms for each system is about 120,000 atoms. The simulation box was replicated periodically in z dimension. The Nosé-Hoover thermostat and barostat with a time constant of 0.1 ps and 1.0 ps, respectively, were used. The modified embedded-atom-method (EAM) potentials were used to compute pairwise interactions of metals and graphene. In order to investigate the effect of van der Waals interactions on the structure and orientation of metals at metal/grapheme interfaces, we also used corrected pairwise interactions of metals and graphene by the addition of interatomic pair potentials to describe van der Waals (vdW) interactions. Van der Waals (vdW) interaction parameters are obtained from density functional theory (DFT) calculations by using Vienna ab initio simulation package (VASP) with gradient-corrected Perdew-Burke-Ernzerhof (PBE). The NPT dynamics for slabs were run for 5 ns for equilibration with a 1 fs time step. The initial configurations of nanopillars and a graphene inserted nanopillars were then obtained from these equilibrated slab systems. All simulations were performed at 298 K.

Structure of metals at interface, stacking sequence, and the orientation of graphene has been analyzed.

1. Gong et al., ACS Nano. 6,5381 (2012)
2. Mathias batzill, Surface Science Reports, 67, 83 (2012)
3. Xu Z, Buehler MJ. J Phys Condens Matter. 22, 485301 (2010)
4. Xiao et al., Surface Science 603, 1985 (2009)

SS/NST-P1-01
Modeling secondary electron emission in scanning He ion microscope; comparison with scanning Ga ion and electron microscopes

T10 Nanoscience and Technology

#SS/NST-P1-01

K. Ohya, T. Yamanaka.

Institute of Technology and Science, The University of Tokushima - Tokushima (Japan).

Scanning ion microscope (SIM) using gallium (Ga) focused ion beams has been employed as an observation tool in micro-fabrication processes, in a similar way to scanning electron microscope (SEM). Recently, a helium (He) SIM equipped with new high brightness ion source is of current interest for its higher capabilities to produce a sub-nm beam for observation. Although the image formation mechanisms of the SIMs are similar to those in SEM, there are some differences in image properties. We have performed Monte Carlo simulations of secondary electron (SE) emission in He- and Ga-SIMs to compare with those obtained using SEM. The approach has revealed the theoretical spatial resolution and the origin of the image differences [1]. Recent modeling work, including charging of insulating materials and image contrast for nanostructured materials [2], is presented.
When singly charged ions of tens of keV bombard a material surface, kinetic emission mechanism dominates the SE emission, which is similar to SE emission induced by electrons. Irrespective of whether a material is conducting or insulating, the kinetic emission is modeled by a three-stage process. The first stage involves generation of internal SEs by the ions and recoiled material atoms. The second is transport of the SEs to the surface. In the third, the SEs escape over the surface barrier. Trajectories of all the particles are simulated using a Monte Carlo technique [3]. For insulating materials, the model is combined with charge accumulation, electric field formation, and analysis of equation of motion for SEs in the vacuum [2]. The SE emission is simulated also for electron impact.
For He ions, the SE yield increases with increasing the atomic number of metals, in a similar way to that for electrons. However, it shows an opposite dependence for Ga ions, which gives an evidence of the material contrast observed on Ga-SIM, which is

different from He-SIM and SEM. The incident angle dependence of the SE yield for He ions approximately obeys the inverse cosine law even at high angles of 85^{o} and more, whereas for electrons, the dependence is much weaker for high atomic number. This indicates that the topographic contrast on He-SIM is clearer than those of SEM. The spatial image resolution in SIM using zero-diameter He beams is prospected to be smaller or better (<0.1 nm) than for Ga ions and electrons. The SE energy distributions for He ion impact show no high-energy component. This results in higher voltage contrast, down to a nm-sized area, than electron impact.
Since the insulating material is positively charged from arrivals of ions and emissions of SEs, some of emitted SEs are drawn back to the surface and are unable to produce a net emission. The net SE yield decreases as a result of successive positive charging, and finally vanishes. However, thin insulating layers (<250 nm) on a conducting substrate is much less charged for He ions, due to the wide depth and lateral distributions, than for Ga ions and electrons where the distributions are much localized. This is different from the charging of thick materials.

[1] T. Ishitani, T. Yamanaka, K. Inai, K. Ohya, Vacuum 84 (2010) 1018.
[2] K. Ohya, D. Takami, T. Yamanaka, J. Vac. Sci. Technol. B 29 (2011) 06F901.
[3] K. Inai, K. Ohya, T. Ishitani, J. Electron Microsc. 56 (2007) 163.

NST-10-Or-2
From magnetic bimetallic nanoparticles synthesis to their application: advanced antimicrobial treatment and phosphorus removal

T10 Nanoscience and Technology

#NST-10-Or-2

K. Machalova Siskova [1], Z. Markova [1], J. Filip [1], J. Cuda [1], K. Safarova [1], I. Medrik [1], M. Kolar [2], R. Zboril [1].

[1]RCPTM, Faculty of Science, Palacky University in Olomouc - Olomouc (Czech republic), [2]Dept. of Microbiology Faculty of Medicine and Dentistry, Palacky University in Olomouc - Olomouc (Czech republic).

Pollution of the environment is one of the most threatening problems afflicting people. Besides the pollutants such as heavy metals, halogenated organics and pesticides, a large variety of microorganisms including disease causing pathogens as for example bacteria (Salmonella enterica, Staphylococcus aureus, Psedomonas aeruginosa), protozoa (Giardia lambia), fungi (Candida spp.) and viruses (hepatitis A virus) pose a great treat [1]. In order to address this point, we synthesize magnetic bimetallic Fe-Ag nanoparticles which exhibit significant antibacterial and antifungal activities against a variety of microorganisms. Moreover, the bimetallic nanoparticles reveal a prolonged action and high efficiency of phosphorus removal. The preparation of these multifunctional hybrids is fast, simple, feasible in a large scale with a controllable content and size of Ag nanoparticles. We also find out that the air-stability and the efficiency of phosphorus removal are related to the formation of Fe3O4/γ–FeOOH double shell at the interface between iron and silver. As an important environmental aspect, silver nanoparticles are not released from the composite even upon sonication and heating Taking into account the possibility of easy magnetic separation of Fe-Ag nanoparticles, they represent highly promising material for advanced technologies of water treatment including waste and drinking water.

The work is supported by Operational Programs Research and Development for Innovations – European Regional Development Fund (project

775/2887

CZ.1.05/2.1.00/03.0058 of the Ministry of Education,Youth and Sports of the Czech Republic), Technology Agency of the Czech Republic "Competence Centers" (project TE01010218), Integration of Regional Centre of Advanced Technologies and Materials into International Networks of Nanotechnological and Optical Research (project CZ.1.07/2.3.00/20.0058), Education for Competitiveness – European Social Fund (project CZ.1.07/2.3.00/20.0056 of the Ministry of Education, Youth and Sports of the Czech Republic), Unconventional Experimental Techniques in Material and Optical research (project CZ.1.07/2.3.00/20.0155).

[1] Karn B., Kniken T., Otto M. Environ. Health Perspect. 2009, 117, 1813-1831

SE/PST/TF/BI-3-Or-7
How to study changes of proteins structure and stability upon protein-nanoparticle interaction

T10 Nanoscience and Technology

#SE/PST/TF/BI-3-Or-7

L. Calzolai, S. Laera, G. Ceccone, F. Rossi.

European Commission - Ispra (Italy).

The behavior and toxicological properties of nanoparticles (NP) in biological medium depends heavily on their interactions with proteins. In return, the structure, stability and biological properties of the proteins that interact with the nanoparticles are strongly affected by this interaction. Unfortunately, the mechanisms of interaction and their structural consequences are very difficult to analyse. Here we show how biophysical techniques used in structural biology can be adapted to study the changes in structure and stability of proteins upon interaction with nanoparticles. By using synchrotron radiation circular dichroism spectroscopy it is possible to detect changes in the secondary structure and stability of proteins upon interaction with nanoparticles [1]. In some cases it is also possible to identify the protein-nanoparticle interaction domain by using high resolution Nuclear Magnetic Resonance spectroscopy [2].

[1] Laera et al, Nano Lett., Nano Lett 2011, 11:4480
[2] Calzolai et al., Nano Lett. 2010, 10:3101

NST/SS-5-Or-2
Ultrafast charge transfer at graphene surfaces with widely varying coupling to their substrates

T10 Nanoscience and Technology

#NST/SS-5-Or-2

D. Menzel [1], P. Lacovig [2], K. Kostov [3], R. Larciprete [4], S. Lizzit [2].

[1]Physik-Dept., TU Muenchen - Garching (Germany), [2]Elettra, Sincrotrone Trieste - Trieste (Italy), [3]Inst. General and Inorganic Chemistry, Bulgarian Academy of Sciences - Sofia (Bulgaria), [4]CNR Institute for Complex Systems - Roma (Italy).

Ultrafast charge transfer (CT) is decisive for electronic dynamics important for processes involved in photochemistry and electrochemistry at surfaces, and in related devices. A convenient method for investigation of CT at surfaces in the low femtosecond range is the so-called core hole clock method [1,2]. It uses the creation of a localized resonant core excitation of an adsorbate atom, coupled with analysis of the core hole decay spectra; this allows to derive the CT times. With adsorbed Ar as probe, the range between about 1 and 30 fs is accessible, using the $2p_{3/2}$ to 4s excitation [2].

Graphene layers on metallic or insulating substrates show a wide variety of substrate coupling [3] which should have consequences for electron transfer dynamics. So far no such data are available. We have therefore used the core hole clock method with adsorbed argon to measure the transfer rates of a localized electron - the 4s electron on core-excited Ar with an energy of 1 to 2 eV above E_F - to the surface of graphene monolayers (Gr ML) on a wide range of substrates with varied coupling. We have investigated the full range from very strong and locally varying coupling for corrugated Gr ML on Ru(0001) (with "valleys" and "hills"), via still corrugated Gr/Ir(111) and even weaker coupled Gr/Pt(111), to essentially decoupled Gr ML on SiC and on intercalated SiO_2 [4] or O on Ru(0001). Indeed strong variations paralleling the coupling are found. Expressed as charge transfer times (CCT), we find values between ~3 fs (Gr ML strongly coupled to substrate on Gr “valleys”/Ru(0001)) and ~ 16 fs (quasi-free Gr on SiC, and on SiO2, or O/ Ru(0001)). Between the “hills” and “valleys” of the corrugated Gr/Ru layer a CCT ratio of 1.7 is found. The very fast

CT on Gr/Ru is explained as due to hybridized Ru orbitals "reaching through" the Gr layer which change with the relative Gr/Ru alignment and distance, so that three-dimensional final states of CT result. The intermediate CT times for the Gr hills on Ru, for Gr/Ir, and on Gr/Pt show that these regions are far from the "decoupled" condition. On the Gr layers decoupled from their substrates the intrinsic coupling to the two-dimensional Gr empty π* states determines the CT time. Their comparatively large CCTs are partly due to low empty DOS but may also be connected with dynamical Coulomb blockade [5], due to relatively localized empty states in the relevant energy range (around 1.5 to 2 eV above the Dirac point).
The results contribute new information on the influence of substrate coupling on CT which could have importance for the use of Gr as contacts in photo- and electrochemical applications. They also have bearing on the understanding of the (still controversial) states of Gr/Ru.

[1] For an extensive review, see P.A. Brühwiler, O. Karis, and N. Mårtensson, Rev. Mod. Phys. 74, 703 (2002).

[2] For a recent survey, see D. Menzel, Chem. Soc. Rev. 37, 2212 (2008).

[3] M. Batzill, Surf. Sci. Rep. 67, 83 (2012).

[4] S. Lizzit et al., Nano Lett. 12, 4503 (2012).

[5] C. Brun et al., Phys. Rev. Lett. 108, 126802 (2012).

NST-P2-10
High-purity magnetite nanoparticles prepared by co-precipitation via solvent extraction from an iron ore

T10 Nanoscience and Technology

#NST-P2-10

D. Kil, Y.J. Suh, H.D. Jang.

Korea Institute of Geoscience and Mineral Resources - Daejeon (Korea, republic of).

Magnetite nanoparticles are suitable as a heavy metal adsorbent in wastewater treatment due to their high heavy metal adsorption capacity and can be easily recovered after use due to excellent magnetic properties[1]. Also, they can be used as a solute in a purification or desalination plant using osmosis due to water retention properties[2]. In the industrial fields such as wastewater treatment or desalination plants, the amount of water to be treated is huge, and in turn the demand for magnetite nanoparticles is expected to be significant. In the preparation of magnetite nanoparticles in the conventional methods, commercially available high-purity iron salts such as FeCl2, FeCl3, Fe(CH3COO)2, and Fe(CO)5 have been used as starting materials[3]. However, the high-purity iron salts are expensive, which would be problematic in the industrial applications. Therefore, it is necessary to develop a means to reduce the cost of magnetite nanoparticles. Here, we produced high-purity magnetite nanoparticles directly from a low-grade iron ore by a simplified process excluding intermediate steps such as the preparation of an iron salt as a precursor.

After removing the impurities from the leachate of a low-grade magnetite ore by solvent extraction, we prepared magnetite nanoparticles of 10.8 nm in an average size by co-precipitation. Among the major metal components, the weight ratio of Fe increased from 76.9% in the raw iron ore to 99.5% in the magnetite nanoparticles, which is the same level as 99.2% in the nanoparticles prepared from commercially available iron salts. Especially, the contents of Si and Mg that inhibit the formation of magnetite nanoparticles were reduced from 7.26 wt% and 11.49 wt% to 0.18 wt% and 0.02 wt%, respectively. When the Si component is present in an amount of 4.7 wt% or higher in the reactant solution, well-defined magnetite nanoparticles are not

formed. The extractant and stripping agent used were an organic mixture of tri-butyl-phosphate (TBP) and deionized water, respectively. According to X-ray diffraction patterns, the crystal structure of the nanoparticles was identified as magnetite (ICDD 19-0629). The magnetization measurement with a SQUID showed the saturated magnetization of 65.6 emu/g, slightly higher than that of the nanoparticles synthesized with pure reagents, 60.0 emu/g.

In the present study, we have synthesized magnetite nanoparticles with a purity of 99.5% directly from a low-grade iron ore as a starting material by a rather simple hydrometallurgical process. The main impurities of Si and Mg were effectively removed by solvent extraction process. It is possible to reduce the processing cost and the amount of energy used, thus supplying a high-efficiency magnetite nanoparticle adsorbent in large quantities at low cost. This may significantly contribute to the prevention of environmental pollution.

1. de Vicente, I., Merino-Martos, A., Cruz-Pizarro, L., de Vicente, J., J. Hazard. Mater., 181, 375-81 (2010).
2. Ling, M.M., Wang, K.Y., Chung, T.-S., Ind. Eng. Chem. Res., 49, 5869-76 (2010).
3. Lu, A.-H., Salabas, E.L., Schüth, F., Angew. Chem. Int. Ed., 46, 1222-44 (2007).

NST-P2-11
Release of urea from nanofibers of wheat gluten obtained by electrospinning: kinetic studies

T10 Nanoscience and Technology

#NST-P2-11

F. Rodríguez-Félix, B. Ramírez-Wong, P. Torres-Chávez, M. Castillo-Ortega, D. Rodríguez-Félix, L. Armenta-Villegas, D. Castro-Enríquez, R. Dórame-Miranda.

Universidad de Sonora - Hermosillo (Mexico).

Urea is an inexpensive solid nitrogen fertilizer used for agricultural production [1]. However, its use involves the loss of the fertilizer by leaching and volatilization, this due to the techniques of fertilization and irrigation water management [2]. This loss of fertilizer causes poor harvests and great economic loss to farmers, due to the high cost of fertilizers and the low price of the product obtained. Also, creates a potential problem of contamination of groundwater aquifers, therefore, to solve this problem requires seek more efficient techniques of nitrogen fertilization. Recently we reported the preparation and characterization of a prolonged-release material of nitrogen fertilizer (urea, 46-00-00) [3], in order to prevent rapid loss of nitrogen to subsoil and thereby save on this input and simultaneously reduce pollution of the subsoil. This material was obtained from wheat gluten by the method of electrospinning. The wheat gluten was used because it is a material biodegrable, available and inexpensive [4]. The study of release of urea in water at 25 °C showed its potential application as prolonged release system of urea. However, a more detailed study is needed to predict their behavior of release in soils with different pH at water and temperatures different of application. Therefore, in the present work the effects of pH and temperature on the kinetics release of urea from nanofibers of wheat gluten obtained by electrospinning were studied. The release kinetic tests were conducted using a buffer solution as the release medium under pH conditions of 4, 7 and 10, and temperature of 25 and 40 °C. An overall evaluation of the kinetics and mechanism of urea release from nanofibers of wheat gluten was done according to the exponential model developed by Ritger and Peppas. The rate of urea release was increased with increasing temperature in the release medium, and at pH 4 and 10 the rate of urea release was decreased. The results indicate that a slow release is

assumed to obey a mechanism of anomalous transport (Non-Fickian) and a fast release is assumed to obey a Fickian diffusion mechanism. It was concluded that the type of mechanism of release depends on the temperature and pH of the release medium, which affected the release rates.

1. Vashishtha, M.; Dongara, P. and Singh, D. 2010. Improvement in properties of urea by phosphogypsum coating. *Int. J. ChemTech Res*. 2: 36–44.

2. Peña-Cabriales, J.J.; Grageda-Cabrera, O.A. and Vera-Núñez, J.A. 2001. Nitrogen Fertilizer Management in Mexico: Use of Isotopic Techniques (15N). *Terra*. 20: 51-56.

3. Castro-Enríquez, D.D.; Rodríguez-Félix, F.; Ramírez-Wong, B.; Torres-Chávez, P.I.; Castillo-Ortega, M.M.; Rodríguez-Félix, D.E.; Armenta-Villegas, L. and Ledesma-Osuna, A.I. 2012. Preparation, Characterization and Release of Urea from Wheat Gluten Electrospun Membranes. *Materials*. 5: 2903-2916.

4. Reddy, N. and Yang, Y. 2007. Novel Protein Fibers from Wheat Gluten. *Biomacromolecules.* 8: 638-643.

NST-12-Or-5
Energy-dependent Phase-shift of Electrons Scattered in 2D Subband States

T10 Nanoscience and Technology

#NST-12-Or-5

K. Nagaoka [1], S. Yaginuma [2], T. Nakayama [1].

[1]International Center for Materials Nanoarchitectonics (MANA), National Institute for Materials Science (NIMS) - Tsukuba, Ibaraki (Japan), [2]RIKEN - Wako, Saitama (Japan).

As a fundamental step towards a practical use of electron phase-operation via scattering in a solid-state device, we have investigated an atomic-scale scattering phenomenon on a 2D subband state formed in a space charge layer of Si by using STM.

Measurements were performed with Si(111)-β-√3x√3 Bi surface. Particularly, we have noticed a certain point-defect at the surface, around which a standing wave pattern was created by interference of incident and scattered electron wave functions in 2D subband states (Fig. 1). A profile analysis on the dI/dV images provided energy-dependent phase-shift of electrons scattered by the single point-defect potential (Fig. 2).

Consequently, from the dispersion of the scattering phase-shift with respect to the energy, the height and the radius of its induced scattering potential were estimated 0.62 eV and 0.59 nm, respectively, which corresponded to the maximum scattering cross section of 2.2 nm^2. To obtain these numerical values of the detail scattering parameters is a fundamental process toward phase-shift operation by the electron scattering in a solid. Therefore, this result is informative for developments of electronic devices utilizing the wave nature of electron, such as a quantum logic device

FIG.1 dI/dV image around the point defect at Vs=1.4 V; 20 x 20 nm^2

FIG. 2 Experimental scattering phase-shift dispersion as a function of the energy from subband bottom.

BI/ASS/NST-P1-09
Antimicrobial Activity of Electrospun Poly (butylenes succinate) Fiber Mats Containing PVP-Capped Silver Nanoparticles

T10 Nanoscience and Technology

#BI/ASS/NST-P1-09

P. Wang, L. Tian, J. Ji.

Technical Institute of Physics and Chemistry, Chinese Academy of Sciences - Beijing (China).

Electrospinning is recognized as a very simple and highly versatile method that produces polymer fibers with diameters in the range of nanometer to micrometer under the external electric field imposed on polymer solutions or melts. At the same time, poly (butylenes succinate)(PBS) is one of the most commercially available biodegradable polymers with good biocompatibility, biodegradability and excellent mechanical properties. [1-2] In this study, PBS fiber mats were successfully produced by emulsion electrospinning, the ideal of which was mixing a small amount of aqueous solution containing surfactant into PBS chloroform solutions followed by emulsifying. [3] And biodegradable PBS fiber mats containing silver nanoparticles (AgNPs) are successfully prepared via electrospinning using PVP as capping agent as well as reductant for the synthesis of AgNPs and were well characterized by SEM and TEM as showed in figure1. The AgNPs were randomly distributed throughout the PBS fibers and the diameters of AgNPs were several nanometers. Further evaluation of the bactericidal properties of the PBS-AgNPs fiber mat was conducted by checking the number of viable bacteria versus contacting time and the results are displayed in Figure 2.Because AgNPs with small diameter effectively release from the fiber mats in aqueous solutions, the PBS-AgNPs fiber mats exhibited strong bactericidal activity of in a short contacting time with the bacteria. In addition, long-term release performance of Ag from the fiber mats sustained the capacity to inhibit the bacteria growth of the mats over a long period of time.

[1] Coutinho, D. F.; Pashkuleva, I. H.; Alves, C. M. Biomacromolecules 2008, 9, 1139–1145.

[2] Sutthiphong, S.; Pavasant, P.; Supaphol, P. Polymer 2009, 50, 1548-1558.

[3] Sanders EH, Kloefkorn R, Bowlin GL, Simpson DG, Wnek GE. Macromolecules 2003(36): 3803-3805.

Figure 1. The morphology of electrospinning PBS-AgNPs fibre mats.

Figure 2.The plot of colony forming unit versus incubation time for the nanofiber mat PBS/AgNPs and AgNO3 toward E.coil.

NST-P3-16
Fluorescence properties of merocyanine entrapped in titanium dioxide thin film

T10 Nanoscience and Technology

#NST-P3-16

A. Lewkowicz [1], P. Bojarski [1], A. Synak [1], B. Grobelna [2].

[1]Institute of Experimental Physics, University of Gdansk - Gdansk (Poland), [2]Faculty of Chemistry, University of Gdańsk - Gdansk (Poland).

Photophysical properties of thin titanium dioxide films doped with a new type of merocyanine dye are studied. These thin films produced using sol –gel technique occurred highly luminescent and durable materials [1].
The absorption and luminescence properties of the material depend strongly on dye concentration suggesting the formation of fluorescent J aggregates [2]. Time resolved luminescence spectroscopy confirmed the formation of fluorescent J aggregates. The performed measurements and numerical analysis allowed to determine some structural parameters of the aggregates as well as their quantum yield and fluorescence lifetimes.

This research has been partly supported within the International PhD Project "Physics of future quantum-based information technologies" (MPD/2009-3/4) financed by Foundation for Polish Science (A.Lewkowicz) and grant NCN 2011/03/B/ST5/03094 (P.Bojarski, A. Synak, B. Grobelna).

[1] R. Vogel, P. Meredith, M. D. Harvey, H. Rubinsztein-Dunlop, Spectrochim. Acta, Part A 2004, 60, 245−249.

[2] A. Lewkowicz, Bojarski, A. Synak, B. Grobelna, I. Akopova, I. Gryczyński, L. Kułak, J. Phys. Chem. C 2012, 116, 12304−12311.

NST-13-Or-3
Optical response of functionalized gold plasmonic antennas in mid IR

T10 Nanoscience and Technology

#NST-13-Or-3

M. Kvapil [1], R. Měch [1], S. Corvaglia [2], L. Ianeselli [2], L. Vaccari [2], J. Čechal [3], L. Casalis [2], T. Šikola [3].

[1]Institute of Physical Engineering, Brno University of Technology - Brno (Czech republic), [2]Elettra Synchrotrone Light Source - Trieste (Italy), [3]CEITEC, Brno University of Technology - Brno (Czech republic).

We report on the possibility of application of plasmonic antennas for biosensing. The wavelength of localized plasmonic resonance of antennas is dependent on the index of refraction of antenna surrounding. When some molecules are placed on the surface of an antenna or in the close vicinity of it, the resonant frequency shifts due to a resultant change of the effective refraction index. When these molecules are tailored to bond only to a specific molecular group, then the antennas can be used to selectively sense the presence of such group.

In our experiments the samples containing 50 x 50 μm^2 arrays of gold dimer plasmonic antennas on silicon substrates fabricated by electron beam lithography were prepared. The length of antenna rods was in the range from 0.6 to 2.0 μm in order to tune the resonance wavelength of antennas to the middle infrared (MIR). The reflectance spectra of the antenna arrays were taken by FTIR and compared with the results of simulations carried out by the Lumerical FDTD package.

After that the antennas were functionalized. The scheme of functionalization steps is shown in fig. 1. First, a self-assembly monolayer of 24-base single-stranded DNA sequence F5 was bound to the surface of antennas through a thiol group. Then, a complementary single-stranded DNA sequence with biotin molecule was linked to the ss-DNA. Finally, streptavidin which binds strongly to biotin was used. Reflectance spectra were taken by FTIR after each functionalization step. An example of the spectrum is shown in fig. 2.

The spectra taken after each functionalization step show a slight shift of the antenna resonant wavelength (peak maxima) caused by the presence of the DNA monolayer (approx. 3 nm thick) and molecules linked to the DNA.

Fig. 1. Scheme of antenna functionalization steps.

Fig. 2.: FTIR spectra from an array of 1.2 µm-long dimer antennas taken after each functionalization step.

NST-P3-24
Optical properties of nanostructured bioinspired materials

T10 Nanoscience and Technology

#NST-P3-24

A. Deraoui.

UCL - LIn (Belgium).

The nature shows us a great many situations where the optics plays a crucial part, this is particularly the case for birds and insects whose color is usually associated with their behavior as a factor of recognition. This variation of coloration depends on the illumination and depending on the direction of observation: it is the phenomenon of iridescence. The material forming for example the elytra of beetles is the chitin and its refractive index is close to that of ordinary glass. The SEM observation shows that the material is in the form of multilayer separated by layers of air. These layers disturb the refractive index of chitin and cause multiple reflections which interfere and explain the phenomenon of iridescence.
The models clearly confirm this interpretation, but they also show that it is possible to produce structured surfaces in the laboratory with properties similar to natural structures. The project aims to develop methods for producing samples based on natural structures where optical properties can be interesting. These samples will be characterized by various methods and techniques in order to understand its properties. The main goal is to analyze the role of roughness. We determined the optical properties changing of these structured surfaces based on the characteristics of surface roughness and we compared them to those of smooth surfaces.

1] Spectral filtering of visible light by the cuticle of metallic woodboring beetles and microfabrication of a matching bioinspired material.
J.P. Vigneron, M. Rassart, C. Vandenbem, V. Lousse, O. Deparis, L.P. Biro, D. Dedouaire, A. Cornet and P. Defrance, Phys. Rev. E (2006), 73 041905
[2] Structurally tuned iridescent surfaces inspired by nature
O. Deparis, M. Rassart, C. Vandenbem, V. Welch, J.P. Vigneron and S. Lucas New Journal of Physics 10(2008) 013032

NST-1-Or-6
High sensitive biosensor based on the Surface Enhance Raman Scattering (SERS)

T10 Nanoscience and Technology

#NST-1-Or-6

M. Cottat [1], N. Malashikhina [2], A. Sutton [3], N. Charnaux [3], T. Toury [4], V. Pavlov [2], A. Toma [5], E. Di Fabrizio [5], M. Lamy De La Chapelle [1].

[1]Laboratoire CSPBAT-UMR7244, UFR Santé Médecine Biologie Humaine-Université Paris13, 74 rue Marcel Cachin - Bobigny (France), [2]Biofunctional Nanomaterials Department, CIC biomaGUNE, Parque Tecnológico de San Sebastian - San Sebastian (Spain), [3]Laboratoire LI2P, UFR Santé Médecine Biologie Humaine-Université Paris13, 74 rue Marcel Cachin - Bobigny (France), [4]Université de technologie de Troyes, Laboratoire de Nanotechnologie et d'instrumentation Optique, Institut Charles Delaunay, FRE 2848, 12 rue Marie Curie, - Troyes (France), [5]Istituto Italiano di Tecnologia (IIT). Via Morego, 30 - Genova (Italy).

The development of reliable, sensitive and specific biosensors is a very active research field. Among all the technique, the Surface Enhance Raman Scattering (SERS) is one of most sensitive way to detect protein [1,2]. It has been widely used for ultrasensitive chemical analysis down to single molecule detection. Its field of applications now includes chemical-biochemical analysis, nanostructure characterization and biomedical applications. It is also very useful for the detection of conformational changes and structural differences regarding preferred orientations of molecules with respect to a metal surface. In this work, we present the SERS detection of specific protein in the serum, using a functionalizion layer.
To investigate the protein detection, the arrays of metallic nanoparticles were made by electron-beam lithography (EBL) to control the Localized Surface Plasmon Resonance (LSPR) position to be closed to the excitation laser wavelength, in order to obtain the best enhancement [3]. The gold nanoparticles were cylinders and rods.
To be specific and increase the sensitivity, the surface was functionalized with specific aptamer to catch different targets proteins.
In conclusion, we report that we can detect the protein using the LSPR and the SERS. We show that we can characterize the interaction with proteins with the SERS

signal. Moreover, we demonstrate that the functionalization surface assure the specificity of the biosensor and allow to detect the protein at 10-8 M.
The authors want to acknowledge the Nanoantenna collaborative European project (HEALTH-F5-2009-241818) for financial support.

[1] Katrin Kneipp, Yang Wang, Harald Kneipp, Lev T. Perelman, Irving Itzkan, Ramachandra R. Dasari, and Michael S. Feld (1997) Single Molecule Detection Using Surface-Enhanced Raman Scattering (SERS), PHYSI CAL REVIEW LETTERS, V 78, N°9, 1667-1670
[2] Christy L. Haynes, Adam D. McFarland, Richard P. Van Duyne (2005) New substrates and singlemolecule detection are just two of the advances that are fueling interest in SERS, Analytical chemistry, 338A-346A
[3] J. Grand, S. Kostcheev, J.-L. Bijeon, M.Lamy de la Chapelle, P.-M. Adam, A. Rumyantseva, G. Lérondel, P. Royer (2003) Optimization of SERS-active substrates for near-field Raman spectroscopy. Synthetic Metals 139 621–624

NST-P1-04
Improved Hydrophobicity of Tungsten GLAD RF sputtered Nanorods by Poly(tetrafluroethyelne) thin films

T10 Nanoscience and Technology

#NST-P1-04

A. Bayat, M. Ebrahimi, A. Moshfegh.

Sharif University Of Technology - Tehran (Iran, islamic republic of).

Introduction
Hydrophobic and superhydrophobic surface finds many applications in science and technology such as self- cleaning, contamination inhabiting and anti-fogging[1]. Tungsten (W) is well known for itsextreme resistance to corrosion. Surface treatment with low surface energy materials such aspolytetrafluoroethylene(PTFE) is a key process for hydrophobicity [2]. PTFE can be coated on W surface with a suitable method for water repellency property. Glancing Angle Deposition (GLAD) is a method to grow thin films with desired nanostructures such as nanorods and zigzag columns. In this research, we have used GLAD RF sputtering technique to fabricate PTFE on W over glass substrate for obtaining hydrophobic surface.
Experimental
First, the glass substrates mounted on a rotatable substrate holder in a GLAD sputtering chamber with base pressure ~10^{-7} Torr. Dischrge power density and the Ar sputter pressure were 3 W/cm^2 and 10^{-3} Torr, respectively.Tungsten layer was formed in one step by varying the substrate angular speed from 5 to30 RPM. After deposition of W thin films with nanorod structure, a nanometric Teflon layer (~15 nm) was coated by RF sputtering on top of the deposited W layer.
Results and Discussion
According to SEM observations, tungsten nanorods were formed on the substrate with average diameter of ~ 50 nm and length of ~ 300 nm (Fig.1). For the PTFE/W/Glass system, the ratio of F/C was obtained about unity based on XPS analysis. Then, hydrophobic property of systems was investigated by water contact angle measurements and maximum contact angle of~ 121º was obtained at 10 RPM for the PTFE/W/Glass system (Fig. 2). Based on our data analysis, the contact angle varied with substrate angular speed and the results obey Cassie-Baxter model.

[1] W. Liu, Y. Luo, L. Sunb, R.Wub, H.Jiangband Y. Liu, Appl. Surf. Sci. 264 (2013) 872-876.
[2] C. Becker, J. Petersen, G. Mertz, D. Ruch, and A. Dinia, J. Phys. Chem. C 115 (2011) 10675–10681.

Figure1. SEM image ofTungstennanorods on glass substrate

Figure2. Variation of contact angle versus angular speed for theW/Glass and PTFE/W/Glass systems

NST-9-Or-4
Influence of La3+-Nd3+ ions on the growth of hexaferrite nanoparticles

T10 Nanoscience and Technology

#NST-9-Or-4

P. Barman, A. Thakur, R.R. Singh.

JAYPEE UNIVERSITY OF INFORMATION TECHNOLOGY OF INFORMATION TECHNOLOGY - Solan (India).

The hexagonal ferrite $MFe_{12}O_{19}$ (M = Sr, Ba, Pb) is an important materials with magnetoplumbite structure used in various applications such as magnetic recording media, telecommunications equipment and permanent magnets due to appropriate properties including perfect mechanical, chemical and thermal stability [1]. Here, we are presenting some new findings about the substitution of La^{3+}-Nd^{3+} ions in strontium ferrites. The nanocrystalline system $SrNd_xLa_yFe_{12-x-y}O_{19}$: where x = y = 0; y = 0.4, x = 0.0 and 0.2; have been prepared using sol-gel method followed by gel to crystallization technique from high purity nitrates. The influence of the Nd^{3+} and La^{3+} substitution, Fe^{3+}/Sr^{2+} molar ratio and the calcination temperature on the crystallization of ferrite phase have been examined using powder x-ray diffraction (XRD) and Fourier transform infrared spectroscopy (ref: figure 1 and 2). The x-ray diffraction and Mid-IR studies confirmed that the synthesized particles exhibit hexagonal structure [2,3]. The diffraction patterns have been used for the evaluation of crystallite size (30-45 nm), lattice parameter c/a (3.92-3.91), x-ray density (5.11-5.37 g/cm^3) and lattice strain (5.41 $x10^{-3}$-8.11 $x10^{-3}$) of these compounds. Inset of figure 1 representing the micrograph of SEM indicating the formation of nano particles having flake like structure. Infrared spectra of doped ferrite have been analyzed in the frequency range 400-4000 cm^{-1}. The Mid-IR analysis show two fundamental absorption peaks at u_1 = 580–600 cm^{-1} and u_2 = 400–436 cm^{-1}, that corresponds to octahedral and tetrahedral vibrations respectively [4].
Keywords: Hard ferrites, crystallization technique, rare earth, x-ray diffraction

1. T.T.V. Nga, N.P. Duong, T.D. Hien, J. Alloys Compd., 475 (2009) 55–59
2. B. Birsoz, A. Baykala, H. Sozeri, M.S. Toprak, J. Alloys Compd., 493 (2010) 481.
3. X. Shen, M. Liu, F. Song, X. Meng, J. Sol-Gel Sci. Technol. 53 (2010) 448.

4. S. Singhal, T. Namgyal, J. Singh, K. Chandra, S. Bansal, Ceram. Int. 2011; DOI:10.1016/j.ceramint.2011.02.001.

Figure 1: XRD patterns of $SrNd_xLa_yFe_{12-x-y}O_{19}$

Figure 2: IR spectra of a precursor NL-P and $SrNd_xLa_yFe_{12-x-y}O_{19}$

NST-P1-08
The self-breaking mechanism of Au nanocontacts

T10 Nanoscience and Technology

#NST-P1-08

T. Nakazumi [1], Y. Wada [2], M. Kiguchi [1].

[1]Tokyo Institute of Technology - Tokyo (Japan), [2]Keio University - Tokyo (Japan).

Metallic nanocontacts and metal nanogaps have attracted much attention because of their potential applications in ultrasmall electronic devices. The breaking process of the metal nanocontacts is currently a hot topic of great interests. There are several investigations on the breaking process of the metal nanocontacts. The breaking process is affected by many factors, such as the stretching speed, size, and temperature. [1] Whereas most studies on the breaking process were reported for mechanically fabricated metal nanocontacts, self-breaking of the metal nanocontacts has also attracted interest. [2] This is because the self-breaking process can be utilized as a reliable tool to form molecular-sized gap, thereby constituting a useful platform for studying single molecule junction. In the present study, we have investigated the self-breaking process of Au nanocontacts in air at room temperature [3].

Metallic nanocontacts were fabricated using the nano-fabricated mechanically controllable break junction electrodes. Figure (a) shows example of conductance traces during the self-breaking process of the Au contacts. The traces show both 1 G_0 (=$2e^2/h$) and 3 G_0 plateaus or a 2 G_0 plateau. It was suggested that the triple atomic rows preferentially changed into a single row, while the double rows preferentially broke without changing into a single row. This regular self-breaking process was explained by breaking of the thermodynamically stable Au nanocontacts which were formed during the self-breaking of the contacts. Figure (b) shows typical conductance trace of the Au contacts during mechanical stretching of the contact. The conductance decreased in a step wise fashion with each step occurring at integer multiples of G_0. During mechanical breaking process, the Au nanocontact would break before changing into the thermodynamically stable structure. Hence, the regular decrease of the number of atoms in the minimal cross section of the nanocontacts was not observed for the Au nanocontacts.

[1] I. K. Yanson *et al. Phys. Rev. Lett.* **95**, 256806(2005).
[2] M. Tsutsui *et al. J. Appl. Phys.* **108**, 064312(2010).
[3] T. Nakazumi *et al. Nanotechnology* **23**, 405702 (2012).

Figure. Examples of the conductance traces during (a) the self-breaking process of the Au contacts (b). the mechanical breaking process of the Au contact.

NST-P3-01
Low Voltage Electroluminescence from Thin SiO2 Layer Including Ge Nanoparticles at Shallow Depth Formed by Negative Ion Implantation

T10 Nanoscience and Technology

#NST-P3-01

H. Tsuji [1], G. Miyagawa [1], N. Arai [2], Y. Gotoh [1].

[1]Kyoto University - Kyoto (Japan), [2]Sharp Corporation - Tenri (Japan).

Blue-ultraviolet light emission from Ge nanoparticles (NPs) embedded into SiO_2 thin film is expected for application as light emission source in Si semiconductor device. The emission site of blue-UV light is considered to be Ge-related oxygen defect centers (ODCs). The reported electroluminescence (EL) emission needed a relatively high voltage of 380 V[1]. For an application of this EL emission as light source of communication between Si chips and other general ones, the operational voltage of EL applied to such material must be decreased down to a low voltage around 10 V. We considered that the key issues for lowering operational voltage are (1) optical emission site of ODC should be created at shallow depth about 10 nm and (2) the optimization of oxidation for ODC. Si substrates with 50-nm^thik SiO_2 layer were implanted with Ge negative ions three times at 50, 20 and 10 keV with typical each doses of 9.2×10^{15}, 1.2×10^{15}, and 1.1×10^{14} ions/cm^2, respectively. Calculated Ge atomic concentration by TRIM-DYN code was shown in Fig.1. Mainly, Ge concentration between 15 to 40 nm was set to 3 at.%. Samples were subsequently annealed twice: (1) in N_2 at 700^{o}C 1h for NP growth, and (2) in air flow at 600-900^{o}C 1h for oxidation. PL properties were measured with a deuterium ramp for excitation. For EL observation, ITO electrode was deposited on SiO_2 surface and Al elecrode deposited on the rear side of Si. All samples showed PL peaks at 390 nm and 290 nm after annealing at 800^{o}C. Some samples showed EL emission at applied voltage of 15 – 24 V. The EL photograph is shown in Fig. 2. The EL peak wavelength is 390 nm. Thus we achieved the low voltage EL emission at 15 V, where the ODCs was formed at a very shallow depth by implantation of Ge negative ions and by two-stage-annealing method for growth of Ge NP and their oxidation.

[1] L. Rebohle, et al, Appl. Phys. Lett, Vol. 71 (1997) 2089-2811.

Fig 1. Ge depth profiles in SiO_2 calculated by TRIM-DYN at various dose cases; (a) typical dose).

Fig 2. Photograph of EL light from Ge-implanted thin SiO_2 layer at 15 V.

NST-P3-17
Switching of Plasmon Response Function of Au Nanorods on GeSbTe Phase Changing Material

T10 Nanoscience and Technology

#NST-P3-17

F. Kannari, M. Kusaba, K. Hirosawa.

Department of Electronics and Electrical Engineering, Keio University - Yokohama (Japan).

For spatiotemporal control over localized plasmon or surface-plasmon polariton (SPP) in noble metal nanostructures excited by ultrafast lasers, the temporal characterization of femtosecond plasmon field is highly required. We have already developed two methods for characterizing ultrafast plasmon both in temporal amplitude and phase: electrical-field cross-correlation imaging using femtosecond laser dark-field microscopy [1]; and spectral cross-correlation interferometer using scanning near-field optical microscopy [2]. Based on the plasmon response function measured by these methods for noble metal nanostructures such as noble metal nanorods or nano bow-ties, we can deterministically control the plasmon field in both temporal amplitude and phase by shaping femtosecond excitation laser pulses. On the other hand, the plasmon resonance of noble metal nanostructures can be modulated by the change of refractive index of the surrounding medium. When applying materials, of which refractive index can be varied optically or electrically, as a substrate of noble metal nanostructure, we can switch the plasmon response function. For example, phase change materials such as GeSbTe (GST) compounds are commonly used for rewritable memory devices due to high contrast between the amorphous and the crystalline phase in refractive index and resistance, fast write and erase speeds as well as non-volatility, and low energy consumption. Nonthermal amorphization of a GST thin film with femtosecond laser pulse excitation was currently demonstrated [3].

We measured change in the plasmon response function of Au nanorods at change of a GST substrate between the amorphous and the crystalline phase. An ultra-broadband femtosecond laser (750~920 nm) was used to excite the Au nanorods on the GST substrate. The dark-field microscope consists of a parabola mirror (f=1500 mm), an object lens (×10, NA=0.25) and a CCD camera. One laser beam irradiates multi-Au nanostructures and the scattered light is imaged by the object lens, while

the other laser beam directly reaches to the CCD camera with variable optical delay. We obtained a series of image shots by varying the time delay between the pump and the reference pulses, and analyzed the fringe-resolved cross-correlation images for each of the nanostructures. Based on this measurement, we propose metal-dielectric-metal waveguide-resonator systems as a switchable SPP waveguide.

[1] M. Kusaba, J. Oi, S. Onishi, and F. Kannari, “Measurement of femtosecond plasmon response function with cross-correlation dark-field microscopy,” paper presented in Int. Conf. of Nanoscience and Technology, 23-27 July 2012, Paris (PO3.17).
[2] S. Onishi, J. Oi, M. Kusaba, and F. Kannari, “Measurement of plasmon response function by spectral interferometry with NSOM for spatiotemporal plasmon control,” paper presented in Int. Conf. of Nanoscience and Technology, 23-27 July 2012, Paris (NO-5.6).
[3] M. Konishi, H. Santo, Y. Hongo, K. Tajima, M. Hosoi, and T. Saiki: “Ultrafast amorphization in Ge10Sb2Te13 thin film induced by single femtosecond laser pulse”, Appl. Opt. 49, 3470 (2010).

NST-8-Or-2
Gold nanoparticle arrays covalently immobilized on Si

T10 Nanoscience and Technology

#NST-8-Or-2

H. Sugimura, S. Mo, T. Ichii, K. Murase.

Kyoto University - Kyoto (Japan).

Gold nanoparticles (AuNPs) are known to show unique optical properties owing to their localized surface plasmon resonance (LSPR) in the visible range. For practical and advanced applications of AuNP in photonic/electronic devices, AuNPs should be firmly immobilized on a substrate. In order to fulfill the requirement, we have developed a photochemical method by which AuNPs covered with 11-mercaptoudecene (MUD) monolayer are covalently bonded to a hydrogen-terminated Si(111) surface as illustrated in Fig. 1A [1]. Figure 1B shows an FE-SEM image of a 2D array of MUD-AuNPs (diameter = 20 nm) immobilized on a Si(111)-H surface. Hydrogen termination is crucial for this photochemical reaction. Thus, when the surface Si-H groups are replaced with an alkyl monolayer prior to the reaction with MUD-AuNPs, No AuNPs are immobilized on the monolayer-covered region. If we prepare a Si(111)-H surface into a line feature with a width nearly equal to the diameter of the AuNPs, those are aligned into the Si-H nanoline. This strategy is demonstrated in Fig. 2. The Si-H nanoline was fabricated by a scanning probe lithography method [2]. The line width was about 20-30 nm and the remained region was terminated with an alkyl self-assembled monolayer made from 1-hexadecen as a precursor. As shown in an FE-SEM image AuNPs are successfully aligned into the line with forming a 1D AuNP array. In addition, the photochemical reaction between MUD-AuNP and Si(111)-H was confirmed to be assisted LSPR aroused in the AuNPs. Plasmonic enhancement effects in the photochemical process for AuNP assemblies will be presented as well as their optical properties.

1. H. Sugimura, S. Mo, T. Ichii, K. Murase, J. Phys. Chem. C, Articles ASAP DOI: 10.1021/jp306290w

2. H. Sugimura, S. Nanjo, H. Sano and K. Murase, J. Phys. Chem. C. 113(27) (2009) 11643-11646.

Fig. 1: A) Schematic illustration of plasmon-assisted photochemical reaction of MUD-modified AuNP on Si(111)-H. B) FE-SEM image of a 2D-AuNP array.

Fig. 2 Fabrication of a 1D AuNP array. A) A Narrow Si-H line surrounded by an alkyl monolayer. B) FE-SEM image of MUD-AuNPs aligned on the Si-H line.

NST/SS-3-Or-10
Tailoring of the partial band gap in three-dimensional magnetic composites based on magnetoferritin nanoparticles

T10 Nanoscience and Technology

#NST/SS-3-Or-10

S. Mamica, M. Krawczyk.

Faculty of Physics, Adam Mickiewicz University in Poznan - Poznan (Poland).

Biomimetic magnetic nanoparticles (NPs) have been intensively studied because of their unusual physical properties as well as promising applications. The use of protein cages as reaction chambers for the production of NPs has a number of advantages from a high level of homogeneity of the NPs to the possibility of producing highly ordered three-dimensional (3D) structures by self-assembly. E.g. the protein crystallization technique has been successfully used for the production of 3D fcc magnetoferritin (mFT) crystals of highly ordered structure and the external size up to 100 μm. An interesting effect observed in structures produced in this way is a substantial reduction of the lattice constant as a result of dehydration: from 18.5 nm to 14 nm [1].

Magnetic periodic composites, so called magnonic crystals (MCs), the magnetic counterpart of photonic crystals with spin waves acting as information carriers, proved to be promising building-blocks for the construction of new logic systems and improvement of parameters and functionalities of rf devices [2]. The realization of MCs with a lattice constant of tens of nanometers, though technologically possible, remains a challenge. The protein crystallization technique seems to open the prospect of realizing 3D MCs with a lattice constant of ten-odd nanometers. This would be an enormous step forward in magnonics, and would allow shifting the magnonic band gap to the subterahertz frequency range.

In this work we propose an MC based on a 3D mFT crystal with a ferromagnetic material used as a matrix. Our approach is based on Maxwell's equations for magnetostatics, solved by the plane wave method (see [3] for details). In our

previous paper [3] we show that the proper choice of the matrix material can lead to the complete magnonic gap opening. In this work we show that even if there is no *complete* magnonic gap the *partial* gap could exists. Such kind of gap in photonic crystals was proved to leads to many peculiar effects including negative refraction and self-collimation [4].

We study the influence of the mFT NPs total magnetic moment and the lattice constant on the partial magnonic gap for two different directions of the spin wave propagation: parallel and perpendicular the external field. We found that the partial gap width as a function of the lattice constant has a maximum for a lattice constant of approximately 12-13 nm depending on the mFT magnetic moment. The occurrence of this maximum we address to the character of the lattice-constant evolution of the dynamic magnetization profiles for the lowest excitations in the spin-wave spectrum. We also examine influence of the mFT NPs filling material on the width and central frequency of the partial magnonic gap. On the basis of our results we determine the conditions conducive to the occurrence and tailoring of a partial magnonic band gap.

[1] O. Kasyutich et al., J. Appl. Phys. 105, 07B528 (2009).
[2] V.V. Kruglyak et al., "Magnonic Metamaterials", in "Metamaterial", Ed. Dr. Xun-Ya Jiang, ISBN: 978-953-51-0591-6, InTech (2012), Available from: http://www.intechopen.com/books/metamaterial/magnonic-metamaterials
[3] S. Mamica et al., Phys. Rev. B 86, 144402 (2012).
[4] G. Sun and A.G. Kirk, Opt. Express 16, 4330 (2008).

NST-P3-14
Formation of nanoclusters in the magnetic field and the magnetoresistance of magnetoactive elastomers

T10 Nanoscience and Technology

#NST-P3-14

G. Stepanov, V. Bakhtiiarov A.v, A. Semerenko, A. Storozhenko.

State Scientific Research Institute of Chemistry and Technology of Organoelement Compounds (GNIIChTEOC) 105118, Moscow, Russia - Moscow (Russian federation).

Magnetoactive elastomers (MAE) feature a specific type of materials, which exhibit reversible changes of their properties under an external influence.
The MAE are composites prepared on the basis of an elastic polymer matrix impregnated with magnetic micro- and nanoparticles. Placed in the magnetic field, they reversibly change such characteristics as elasticity and viscosity, electroconductivity, dielectric permeability and magnetic susceptibility. These materials also exhibit the shape-memory effect.
In our scientific work the preparation of such materials is conducted by means of the utilization of silicone polymer matrices together with iron and magnetite fillers with particle size in the range 10-1000 nm. Systematic studies of our MAE have demonstrated that the variety of properties and their changes under the influence of the magnetic field is conditioned by the formation of clusters of magnetic particles inside the composite placed in the field. The modelling as well as direct microscopic observations of the material showed that these clusters feature chain-like agglomerates elongated along the force lines of the applied field.
The magnetic field-dependencies of the elasticity and viscosity changes observed in the material have S-shaped curves in the property-field coordinates. The maximal rates of these changes correspond to the beginning of the process of intensive cluster formation observable under the microscope.
The process of the formation of elongated clusters explains the significant magnetoresistive effect exhibited by the MAE. In other words, a change of electroconductivity in fields of up to 400 mT may reach a level of 3-4 orders for a composite having inside its polymer matrix electroconductive particles – such as Fe,

Ni, Co – or particles with an electroconductive coating.
The mechanism of the formation of clusters is based on the dipole interaction of magnetic particles in the magnetic field, whose force lines dictate the direction for the clusters to grow along.

Under the influence of the magnetic field, the magnetic composite material undergoes the formation of clusters and chain-like structures inside its polymer matrix, which results in the appearance of a set of new features including the magnetoresistive effect.

NST/SS-3-Or-11
Spin-dependent friction observed on the atomic scale by using atomic manipulation and spin-polarized scanning tunneling microscopy

T10 Nanoscience and Technology

#NST/SS-3-Or-11

Y. Yoshida [1], B. Wolter [2], A. Kubetzka [2], S.W. Hla [3], K. Von Bergmann [2], R. Wiesendanger [2].

[1]The Institute for solid state physics, The University of Tokyo - Kashiwa (Japan), [2]The institute of Applied Physics and Microstructures, University of Hamburg - Hamburg (Germany), [3]Physics & Astronomy Department, Ohio University - Athens (United states).

Friction is a basic physical phenomenon, which can be found in most general text books of classical mechanics. However, understanding the microscopic origins of friction is no trivial problem. There have been reports about phononic and electronic contributions to friction, which were identified in experiments on the surface of a superconductor at temperatures above and below the superconducting transition temperature [1]. Spin-dependent friction is also theoretically predicted [2], although the experimental observation was not yet achieved. In our study, we used the combination of spin-polarized scanning tunneling microscopy (SP-STM) and single-atom manipulation imaging [3] in order to slide individual magnetic atoms over a magnetic template surface [4]. By monitoring the spin-resolved manipulation traces and comparing them with results of Monte Carlo simulations, we were able to reveal characteristic friction force variations resulting from the occurrence of spin friction on the atomic scale [5]. In the presentation, we will report on details of the experimental results and the numerical analysis.

[1] M. Kisiel, E. Gnecco, U. Gysin, L. Marot, S. Rast, E. Meyer, Nature Materials 10, 119 (2011)

[2] D. Kadau, A. Hucht, D. E. Wolf, Phys. Rev. Lett. 101, 137205 (2008); C. Fusco, D.

E. Wolf, U. Nowawak, Phys. Rev. B 77, 174426 (2008)

[3] J. A. Stroscio and R. J. Celotta, Science 306, 242 (2004)

[4] D. Serrate, P. Ferriani, Y. Yoshida, S.-W. Hla, M. Menzel, K. von Bergmann, S. Heinze, A. Kubetzka, R. Wiesendanger, Nature Nanotechnology 5, 350 (2010)

[5] B. Wolter, Y. Yoshida, A. Kubetzka, S. W. Hla, K. von Bergmann, R. Wiesendanger, Phys. Rev. Lett., 109, 116102 (2012)

NST-12-Or-6
Coulomb blockade in a coupled electron shuttling system

T10 Nanoscience and Technology

#NST-12-Or-6

C. Kim [1], M. Prada [2], J.H. Kim [1], T. Lee [1], S. Lee [1], R. Blick [2].

[1]Sensor System Research Center, Korea Institute of Science and Technology - Seoul (Korea, republic of), [2]Electrical & Computer Engineering, University of Wisconsin-Madison - Madison (United states).

Nanotechnology provides the tools to fabricate nanoscale electro-mechanical systems in which we can push the limits of processing single electrons [1,2]. We present measurements on single electron shuttling through two coupled nanomechanical pendula. The pendula are realized as nanopillars etched out of the silicon-on-insulator (SOI) substrate as shown in Fig. 1(a), where the top crystalline silicon is 190 nm thin and the insulating SiO_2 is about 350 nm. A 50 nm top gold layer serves as the final electrical conduction path. The equivalent circuit diagram is given in Fig. 1(b): the two pillars are individually displaced by x_1 and x_2, which lead to tunable resistances and mutual capacitances. The characteristic current-voltage curve is shown in Fig. 2 where the total Coulomb energy is indicated as E_C [3]. The obtained curve is shown as an overall ohmic response modulated by Coulomb blockade steps at room temperature. From the experimental data we find the charging energy of 40 meV. The observation of Coulomb blockade for a coupled shuttle at room temperature is possible since the cotunneling is effectively suppressed in the coupled shuttles. The application of gate voltages leads to the variation of the charging energy for an additional electron. By controlling the mechanical shuttling frequency we are able to validate the different regimes of electron shuttling.

[1] M. Blencowe, Nanomechanical quantum limits, Science 304, 56-57 (2004).
[2] H. G. Craighead, Nanoelectromechanical systems, Science 290, 1532-1535 (2000).
[3] A. W. Holleitner, R. H. Blick, A. K. H. Hüttel, K. Eberl, and J. P. Kotthaus, Probing and controlling the bonds of an artificial molecule, Science 297, 70-72 (2002).

Figure 1 (a) A scanning electron microscope image of two coupled electron shuttles made of silicon nanopillars and metallic tips on top (b) A circuit diagram of the electron shuttling system. It consists of mechanically tunable tunneling barriers coupling the leads and the shuttles.

Figure 2 Current-voltage response at room temperature. The dashed lines guide the plateaus of the Coulomb staircase. The linear increase on the plateaus is due to the thermal broadening.

NST-3-Or-7
Novel 2.5 D transrotational solid state order revealed by TEM in Crystallizing Amorphous Films

T10 Nanoscience and Technology

#NST-3-Or-7

V. Kolosov.

Ural Federal University - Ekaterinburg (Russian federation).

Novel microstructure with unexpected, dislocation independent, regular internal bending of the crystal lattice planes [1] are revealed by TEM in thin films after amorphous – crystalline transitions. Such **perfect crystals/grains with regularly curved lattice** (built up by simultaneous translation and small regular rotation of the unit cell) **demonstrate a new "transrotational" [2] type of solid state order.** The maximal lattice orientation gradients can reach 300°/ μm (axis of lattice bending ll film plane), Fig.1. TEM studies include primarily bend-contour method [3] supported by *in situ* studies and HREM.

Thin (10 - 100 nm) microcrystals (sizes 0.1 - 100 μm) vary from whiskers (Fig. 1a), belts (Fig. 1b) or spherulites (fig. 2b, c) to polycrystalline areas with a complex texture. They are formed by aging/heating/e-annealing in amorphous films of different chemical nature (i.e. oxides, chalcogen/ides, some metals and alloys) prepared by thermal/laser/e-beam evaporation.

Opposite to other unusual regular nano (*N*-) aggregations of atoms widely recognized in last 30 years (quasi-crystals, fullerenes, *N*-tubes, other *N*- C-derivatives, etc.) our less known "transrotational" crystals/structures are less limited in dimensions. For most simple cylindrical geometry, Fig. 2a, bent atom layers in fine areas resemble that of hypothetical 2.5D halves (180°) of endless (continuous in film plane) multiwall *N*-tubes (Fig.1d). Transrotational nano-scale self-assembly can give even more complicated *N*-structures (e.g., Fig. 2b, c).

[1] I E Bolotov, V Y Kolosov and A V Kozhyn, Phys. Stat. Sol. **72a** (1982) 645.
[2] V Y Kolosov and A R Thölen, Acta Mat. **48** (2000) 1829.
[3] I E Bolotov and V Y Kolosov, Phys. Stat. Sol. **69a** (1982) 85

[4] B J Kooi and J T M De Hosson, J. App. Phys. **95** (2004) 4714.
[5] E Rimini et al, J. App. Phys. **105** (2009) 123502.

Fig.1. TEM of *N*-whisker (a - CuSe) and *N*-belt (b - $Cu_{2-x}Te$) revealing unit cell regular rotation (c) that corresponds to transrotational lattice shown schematically in X-section (d). Bar=1μm

Fig.2. TEM of transrotational crystals (left) of different geometry (right): cylindrical (a – Se), "*N*-onion like" spherulites (b - α-Fe_2O_3, c –Se).

NST-13-Or-5
Local, low energy, electrical excitation of localized and propagating surface plasmons

T10 Nanoscience and Technology

#NST-13-Or-5

E. Le Moal [1], Y. Zhang [1], T. Wang [1], B. Rogez [1], E. Boer-Duchemin [1], G. Comtet [1], G. Dujardin [1], A. Hohenau [2], C. Gruber [2], J. Krenn [2].

[1]Institut des Sciences Moléculaires d'Orsay, Université Paris-Sud - Orsay (France), [2]Institute of Physics, Karl-Franzens-University - Graz (Austria).

Surface plasmons (SP) are associated with highly confined electromagnetic fields, which make them appealing candidates for future nano-optical devices. Most often, photonic excitation is used to excite SP; however local, electrical excitation would be preferable in the view of technological applications. This would allow the development of electrically driven plasmon nanosources that combine nanoelectronics and nanophotonics and could be key components in new communication nano-devices.

The scanning tunnelling microscope (STM) is an ideal, low energy, local source of electrons that can excite both localized and propagating SP through inelastic electron tunnelling effects [1,2]. In contrast to techniques based on high energy electrons, STM excitation of SP is operable in air, with junction biases lower than 3 V, and its spatial selectivity is guaranteed by the strong confinement of the tip-induced gap plasmon mode. Hence this excitation mode is fully compatible with break junctions geometries, in-plane or stacked electrodes.

Our STM is coupled to an inverted optical microscope and the resulting emitted light is collected through the transparent substrate with an objective lens of high numerical aperture (see Fig. 1). In such a setup, both the light emitted from localized SP and the leakage radiation from propagating SP may be recorded. Furthermore the image that forms in the rear focal plane of the objective lens constitutes a direct print of the angular emission pattern, which can be imaged on a CCD camera for accurate analysis. As energy and in-plane momentum component are conserved through SP leakage radiation, this angular emission pattern gives the wavevector distribution of the propagating SP. Remarkably, access to this information was not possible in most of the previous studies because they were based on optical collection from the tip-

side of the sample, which precludes the detection of propagating SP.
We used this setup on thin gold films to demonstrate that both propagating (film eigenmode) SP and confined (tip-induced) gap plasmons could be excited by the STM tip, with relative proportions that depend on the shape and the composition of the STM tip. We also investigated how propagating SP scatter at the edges of gold metal stripes or at gold nanoparticles deposited on a gold thin film.

[1] T. Wang et al., Nanotechnol. 22, 175201 (2011)
[2] P. Bharadwaj et al., Phys. Rev. Lett. 106, 226802 (2011)

Figure 1. Experimental setup: the spatial (real plane), angular (Fourier plane) and spectral distributions of the light from SP excited by STM may be analyzed in this setup.

NST-P3-02
n- and p-type response and NO2 sensing properties of Langmuir-Blodgett Fe2O3 and CoFe2O4 nanoparticle arrays

T10 Nanoscience and Technology

#NST-P3-02

S. Luby [1], P. Siffalovic [1], M. Benkovicova [1], J. Ivanco [1], M. Jergel [1], E. Majkova [1], R. Rella [2], M.G. Manera [2].

[1]Institute of Physics, Slovak Acad. Sci. - Bratislava (Slovakia), [2]IMM-CNR, Unit of Lecce - Lecce (Italy).

Fe_2O_3 and $CoFe_2O_4$ semiconducting oxides were used in gas sensing less frequently than SnO_2 or WO_3, however, their applications increase nowadays. We present nanoparticle (NP) sensors prepared by Langmuir-Blodgett (LB) deposition of colloid γ-Fe_2O_3 or $CoFe_2O_4$ NPs onto alumina substrates. NPs were synthesized from Fe and Co acetylacetonates with oleic acid and oleylamine as surfactant precursors [1]. The thickness of the LB deposit is 1, 2, 4, 7 or 10 NP monolayers (ML). NP arrays were analysed by GIXRD, SEM, GISAXS and XANES. The average NP diameters are 6.4 nm and 7.6 nm for Fe_2O_3 and $CoFe_2O_4$, respectively. The insulating surfactant 1 nm thick was removed by UV irradiation in ozone or by heating in dry air flux which resulted in a discontinuous 1ML (66 % coverage of the substrate) and conductivity dominated by percolation. After formation of continuous structures from 2 or more MLs, the baseline current ≈ 1 μA at 5 V at the working temperature T_W = 400 ^oC was obtained. To avoid NP coalescence $T_W \leq 500\ ^oC$ was used. Measurements were done in the mixtures of dry air with oxidizing NO_2 and, for comparison, with reducing CO gases with concentrations 0.5 – 100 ppm. Besides the standard n-type response of sensors from both oxides (decrease of current at the exposure to NO_2) also p-type response was found in some samples. This transition is ascribed to the NP surface reaction with nitrogen, presumably from oleylamine ($C_{18}H_{37}N$). The inverse response was observed also in reducing CO gas. The devices with 4 or 7 NP MLs showed the best sensitivity. (An equivalent thickness of the deposits after surfactant removal is about 3 and 5 MLs, respectively.) Similar result was obtained with p-type samples, though the response is lower. The sensing

medium is not homogeneous enough for thinner deposit, with thicker one the gas penetration towards the bottom of array is the limiting factor. The response of 38 was found for the most sensitive Fe_2O_3 4ML sample at 0.5 % ppm of NO_2, hence we could move even one order of magnitude down to ppb area. Such devices are conveniet for air quality control and also for the detection of nitrate explosives, approaching the canine detection capabilities. Response to CO was much lower. Sensors showed no hysteresis. Their response and recovery times are 3 – 20 min. Results of NO_2 sensing are compared to those of other oxides - MnO_2, TiO_2, WO_3 and advantage especially of Fe_2O_3 NP sensors is demonstrated. The resistance of NP arrays was studied between 250 and 500 ^oC. We obtained the activation energy of conductivity of NP arrays 0.45-0.87 eV for Fe_2O_3 and 0.56–0.84 eV for $CoFe_2O_4$. High sensitivity of our sensors to electronegative NO_2 matches well the theory of charge self-exhaustion by surface traps in subcritical NPs (size < 100 nm) [2].

S. Luby, I. Chitu, M. Jergel et al., Oxide nanoparticle arrays for sensors of CO and NO_2 gases, Vacuum 86, 2012, 590 - 593.

N. P. Zaretskij, L. I. Menshikov, A. A. Vasiliev, On the origin of sensing properties of the nanostructured layers of semiconducting metal oxide materials, Sensors and Actuators B 170, 2012, 148 - 157.

NST/SS-5-Or-8
Atomically Controlled Heterostructures of 2D Materials

T10 Nanoscience and Technology

#NST/SS-5-Or-8

P. Sutter [1], R. Cortes [1], J. Lahiri [1], P. Zahl [1], B. Wang [2], E. Sutter [1].

[1]Brookhaven National Laboratory - Upton (United states), [2]Vanderbilt University - Nashville (United states).

Heterostructures that integrate different materials to achieve novel properties have been the focus of recent materials research, enabling applications from light-emitting devices to catalysts. The advent of new families of two-dimensional (2D) materials has opened the exciting prospect of exploring novel types of heterostructures designed from atomically thin membranes: Stacks of alternating 2D sheets, reminiscent of conventional quantum wells and superlattices; and in-plane heterostructures, in which a single membrane comprises different, tightly interfaced components. Such engineered materials not only promise new functionality, but also raise fundamental questions on interface formation, intermixing, strain, polarity, etc. in a new context at reduced dimensionality.

The controlled synthesis of 2D heterostructures presents formidable challenges in surface chemistry. We will discuss recent advances toward the synthesis and exploration of the properties of heterostructures of 2D materials on metal substrates. Focusing on graphene [1] and hexagonal boron nitride [2], 2D crystals with similar lattice structure but very different electronic properties, we have identified pathways to the formation of in-plane heterostructures with atomically sharp line boundaries [3]. The controlled synthesis of ‘superlattices’ with arbitrary layer sequences is extremely difficult by conventional methods (e.g., chemical vapor deposition) due to the low reactivity of 2D materials. We have demonstrated alternative processes that can overcome these limitations and provide stacks of 2D materials with atomic-layer control over thickness and stacking sequence [4]. Our combined results establish a powerful toolset for the scalable fabrication of arbitrary heterostructures of 2D materials for fundamental research and novel applications.

[1] P. Sutter, J.I. Flege, and E. Sutter, Nature Materials **7**, 406 (2008).
[2] P. Sutter, P. Albrecht, J. Lahiri, and E. Sutter, ACS Nano **5**, 7303 (2011).
[3] P. Sutter, R. Cortes, J. Lahiri, and E. Sutter, Nano Letters **12**, 4869 (2012).
[4] P. Sutter, J. Lahiri, P. Zahl, B. Wang, and E. Sutter, Nano Letters **13**, 276 (2013).

Fig. 1: Heterostructures of 2D materials: a) Monolayer graphene-boron nitride (MLG/BN) heterostructures with atomically sharp zigzag boundaries. **b)** Atomically precise control over composition and layer stacking sequence in few-layer graphene-boron nitride heterostructures.

NST/SS-4-Or-1
Single molecular spintronics: giant magnetoresistance through a single molecule

T10 Nanoscience and Technology

#NST/SS-4-Or-1

T. Yamada.

Chiba University - Chiba (Japan).

Exploring spin-polarized transport characteristics of single molecules is a promising direction of research with an outlook for potential application in future nano-scale electronic devices the functionality of which will employ not only charge but also the electron's spin.
As the first step towards this goal, we present giant magneto-resistance (GMR) measurements of single hydrogen phthalocyanine (H2Pc) molecules contacted by two ferromagnetic electrodes. Using a spin-polarized scanning tunnelling microscopy (SP-STM) at 4K, single molecules were addressed and their conductance in dependence of the magnetization of the electrodes was measured. Magnetic Co nano-islands on Cu(111) and Co coated W tips were used as ferromagnetic electrodes to make a Co/H2Pc/Co single molecular junction. The different magnetization directions were naturally achieved as the Co nano-islands can either be magnetized into or out of the Cu substrate plane. A GMR of +60% was observed which is significantly larger than the tunnelling magneto resistance of +5% obtained from direct tunnelling measurements between the tip and the nano-islands without the involvement of H2Pc molecules [1].
From the experiments of the Co/H2Pc/Co single molecular junction, the hybridization of LUMO states of H2Pc with Co 3d minority spin states was found to be the key to generate large positive GMR, which indicates different GMR for H2Pc and antiferromagnet Mn as majority spin states dominate around the Fermi energy of Mn. With the spin-polarized STM at 4K we measured magneto-resistance through the Fe/H2Pc/Mn single molecular junction.
H2Pc single molecules were deposited on Mn(001) ultrathin films grown on an Fe(001)-whisker. The bct Mn(001) ultrathin films are known to have layer-wise antiferromagnetic coupling between atomic layers, which was directly observed by SP-STM magnetic images [2]. An Fe-coated W tip was gently approached to the molecule and the conductance in contact was measured. Since the coercive field of

Mn/Fe(001) is much smaller than that of the Fe/W tip, it is possible to switch only the magnetization of the Mn/Fe(001), which was directly confirmed by a reverse of magnetic contrast in STM images. In this way, we succeeded to measure GMR through the same single molecule, and obtained, surprisingly, a negative magneto resistance of -54 % [3], i.e. anti-parallel coupling between Fe and the top most Mn layer has lower resistance, which is comparable to the case of the Co/H2Pc/Co junction. Possible reason of the polarity switch of GMR is that the spin transport through the H2Pc single molecule is dominated by minority and majority spins for Co/H2Pc/Co and Fe/H2Pc/Mn junctions, respectively.
Our experimental results show that the single phthalocyanine molecules can be used for near-future spintronics devices. Hybridization of molecular orbital with spin states of 3d nano metals is the key to obtain large magneto resistance.

[1]S. Schmaus, A. Bagrets, Y. Nahas, T.K. Yamada, A. Bork, F. Evers, and W. Wulfhekel, Nature Nanotechnology 6, 185 (2011).
[2]T.K. Yamada, M.M.J. Bischoff, G.M.M. Heijnen, T. Mizoguchi, and H. van Kempen, Physical Review Letters 90, 056803 (2003).
[3]A. Bagrets, S. Schmaus, A. Jaafar, D. Kramczynski, T.K. Yamada, M. Alouani, W. Wulfhekel, and F. Evers, Nano Letters 12, 5131 (2012).

NST-P2-12
Preparation of Poly(butylene succinate) /Montmorillonite Nanocomposite

T10 Nanoscience and Technology

#NST-P2-12

Y. Xu, J. Ji, J. Wang, C. Zhang.

Technical Institute of chemistry and physics,cas - Beijing (China).

Poly(butylene succinate) is a biodegradable polyester which attracts more and more attention because of its excellent mechanical properties and processability. But its Vicat softening point is only 98℃, and its elasticity module is low too, all these things have limited its application greatly[1]. Poly(butylene succinate)/Montmorillonite nanocomposite was prepared via in-situ polymerization with 1,4-butanediol , succinic acid and OMMT. The kind and content of OMMT, the method of adding OMMT were studied. The best situation of in-situ polymerization was attained . Then a pilot scale experiment was successfully processed in this situation. The composite of the pilot scale is a nanocomposite[2,3], the OMMT is nicely distributed within PBS matrix, the composites has a significantly increased interlayer distance,as seen in fig1, the mechanical properties and Vicat softening point are greatly increased in comparison to the pure PBS,as seen in table 1. With the organically modification of the OMMT becoming better, the intercalation of PBS matrix into the MMT layers increases, but the biodegradability of the composites decreases.

[1]Doi Y, Steinbüchel A. In: Ishioka DR, Kitakuni E, Ichikawa Y, editors. Biopolymers, Vol. 4: Polyesters Ⅲ. Application and commercial products. Weinheim: Wiley-VCH Verlag Gmbh; 2002.

[2]A. Choudhury, A. K. Bhowmick, C. Ong, and M. Soddemann,J. Nanosci. Nanotechnol. 10, 5056 (2010).

[3]S. K. Karna, S. R. Mishra, E. Gunapala, I. Dubenko, V. Malagareddy,G. K. Marasinghe, and N. Ali, J. Nanosci. Nanotechnol. 10, 5879,(2010).

1.Fig1. The XRD spectrum of PBS/MMT nanocomposites prepared in pilot test

2.Table1. The mechanical properties and vicat soften point of PBS and PBS/MMT nanocomposites (PBSCN)

NST-P3-03
Evolution of electronic excitation states in Ar clusters from surface to bulk properties

T10 Nanoscience and Technology

#NST-P3-03

D. Miura, T. Someya, T. Tachibana, T. Hirayama.

Rikkyo University - Tokyo (Japan).

In these 20 years, interesting features of the cluster, such as evolution of bulk property in a cluster, confinement of electronic excitation inside the cluster, etc., has been experimentally studied mainly using a spectroscopic method [1]. Here we report our recent results on the electronic excitation processes in rare gas clusters using electron energy loss spectroscopy (EELS) method.

A pulsed cluster beam is generated by adiabatic expansion through a conical nozzle. A mono-energetic electron beam merges with the cluster beam, and electrons scattered to 0 deg. are energy-analyzed and detected by a CEM.

Figure 1 shows the electron energy loss spectra of Ar clusters at incident electron energy of 100 eV. Cluster size is controlled by changing the stagnation pressure from 2 to 4 atm. The size of the cluster has not been measured in this study, but it is estimated from our previous study [2] to be in the order of 100 - 500 atoms/cluster. Vertical lines indicate the energy positions of the surface and bulk excitons in solid Ar. It is shown that when the stagnation pressure rises, i.e., cluster size increases, the relative intensity of the first order bulk excitation peak (I_B / I) increases, showing that the bulk feature evolves for the cluster with the size of 10^2 atoms/cluster.

[1] for example, R. von Pietrowski, K. von Haeften, T. Laarmann, T. Möller, L. Museur and A. V. Kanaev, Eur. Phys. J. D **38**, 323–336 (2006).
[2] H. Kubotera, T. Sekitsuka, S. Sakai, T. Tachibana and T. Hirayama, Appl. Surf. Sci. **256**, (2009) 1046-9.

Figure 1: Electron energy loss spectra of Ar clusters at incident electron energy of 100 eV. Nozzle temperature is about 300 K, and stagnation pressure is 2 - 4 atm.

NST-8-Or-3
2D Bicomponent Structures Composed of Melamine and Melem at the Solution/Solid Interfaces

T10 Nanoscience and Technology

#NST-8-Or-3

S. Uemura, M. Aono, M. Kunitake.

Kumamoto University - Kumamoto (Japan).

Investigation of 2D self-assembled porous networks composed of organic molecules has been a key issue in nanoscience and nanotechnology. For construction of the 2D porous networks, building blocks with highly symmetrical features and functional groups for multiple intermolecular interactions with neighbour molecules are required because of thermodynamically unstability of such networks with low surface density. Among various building blocks, melamine (Figure 1 left) is often used in supramolecular chemistry, because of its symmetrical shape with three functional groups for hydrogen bonding at the apexes. In this presentation, we report the investigation of 2D self-assembly of melamine and melem (Figure 1 right), which is a similar molecular shape to melamine, at the aqueous solution/Au(111) interfaces by electrochemical (EC) STM.

Previously, the self-assembled structures at the monocomponent solution/Au(111) interfaces have been reported.[1] A melamine honeycomb network was essentially the same structure to that on Au(111) in UHV.[2] Each melamine molecule was connected by “side-by-side” hydrogen bonds. In the case of melem, two kinds of self-assembled structures were revealed. One is the honeycomb network connected by side-by-side hydrogen bonds, and the unit cell parameters were larger than those of melamine depending on the melem molecular size. The other is the closely-packed structure, which was constructed by two hydrogen bonding systems (side-by-side and head-to-tail), and was with the higher surface density than the honeycomb network. Each monoconponent structure was also managed by electrochemical potential control. Especially, the “order-order” transition between the honeycomb and the closely-packed structures of melem was revealed reversibly by EC-STM.

On using the bicomponent solution, several bicomponent self-assembled honeycomb networks of melem and melamine were found at the interfaces. These structures were based on side-by-side hydrogen bonds. Depending on the mixture ratio and the solution concentration, the constructed mono- and bicomponent networks were

different. In the similar way to the monocomponent networks, the “order-order-order” transition of the self-assembled structures was also occurred under the potential control. The appearing order of the structures from the negative to positive potential agrees with the order of the surface density of the observed structures.

1. S. Uemura, M. Aono, T. Komatsu, M. Kunitake, *Langmuir* **2011**, *27*, 1336-1340.
2. F. Silly, A. Q. Shaw, M. R. Castell, G. A. D. Briggs, M. Mura, N. Martsinovich, L. Kantorovich, *J. Phys. Chem. C* **2008**, *112*, 11476-11480.

Figure 1. Chemical structures of melamine (left) and melem (right).

NST-8-Or-4
Programming of Complex 3D-DNA Nanostructures on Chemical Template and Extension by Enzymatic Polymerization.

T10 Nanoscience and Technology

#NST-8-Or-4

M.N. Khan [1], M. Zharnikov [1], V. Tjong [2], A. Chilkoti [2].

[1]Angewandte Physikalische Chemie, Universität Heidelberg. - 69120-Heidelberg (Germany), [2]Department of Biomedical Engineering, Duke University - N C 27708-0300 (United states).

As a holder of genetic information and due to its unique hybridization properties, deoxyribonucleic acid (DNA) represents a key object in modern science and related technology. Self assemble monolayer of single stranded DNA (ssDNA) on coinage metal such as gold can be employed for detection of DNA binding proteins and biosensor applications. A new two-step procedure is developed for fabrication of mixed monolayer of thiolated ssDNA and oligo(ethylene glycole) sub-stituted alkanethiolates (OEG-AT) OEG-AT, which are protein repelling in nature. This approach was combine with surface-initiated enzymatic polymerization (SIEP) for extension in the Z-direction and based on an irradiation-promoted exchange reaction (IPER). This approach allow us to program complex 3D pattern of DNA on surface by electron-beam lithography (EBL). The orientation and ordering of DNA in the one-component A25SH monolayer and mixed ssDNA/OEG-AT monolayers was investigated by near-edge X-ray absorption fine structure (NEXAFS) spectroscopy, which proved a significant control of upright orientation of the DNA strands in both systems. SAMs, homogeneous poly (A) brushes, and poly (A) nanostructures were characterized by laboratory and synchrotron-based PE spectroscopy, ellipsometry and atomic force microscopy (AFM). This system can be widely used as versatile functional moiety and nanoscale building block in such important fields as bio-engineering, bio-sensing, bio-nanotechnology, gene therapy, drug delivery, nanomedicine, and molecular biology.

NST-10-Or-7
Electrophoretic deposition of nanoparticles in ionic liquids

T10 Nanoscience and Technology

#NST-10-Or-7

P. Kunzo [1], P. Lobotka [1], M. Držík [2], E. Kováčová [1], V. Šmatko [1], I. Vávra [1].

[1]Institute of Electrical Engineering SAS - Bratislava (Slovakia), [2]International Laser Centre - Bratislava (Slovakia).

Room temperature Ionic liquids have been recognized as a suitable medium for preparation of colloids by chemical or physical synthesis of nanoparticles [1] with long-term stability. The current problem is how to deposit the nanoparticles on a proper substrate (battery electrode, sensor surface, etc.) and to get rid of the rest of the ionic liquid.
We used the electrophoretic deposition (EPD) to produce a layer of nanoparticles on the surface of chemiresistive gas sensor consisting of interdigitated gold microelectrodes and polyaniline thin film [2]. Colloids containing metallic nanoparticles (Au, Ni, Ag-Cu or Ni-Fe of the size of 12 or 50 nm) were produced by magnetron sputtering of the metals on the surface of imidazolium-based ionic liquids. Although no surfactants were added, the colloid did not show any agglomeration of the nanoparticles (it is believed that the role of surfactant is played by anions attached to the nanoparticle).
The EPD method is based on the application of an electric field between two electrodes immersed in a suspension of charged nanoparticles, which causes their movement toward the oppositely charged electrode [3]. We successfully deposited the nanoparticles from BMIM bis(trifluoromethylsulfonyl)imide ionic liquid onto the surface of thin-film Au electrode. DC voltage of 5 V was applied between the plane electrode and the stainless steel tip used as a counter electrode. The first deposits of nanoparticles were observed after 5 min with anodic polarization of the electrodes. On the other side, no deposits were obtained under the cathodic polarization, neither symmetrical AC voltage. This supports the assumption that the nanoparticles in the ionic liquid are coated by anions. Although the nanoparticles are charged, the EPD is limited by high conductivity of the ionic liquid. Due to the migration of ions, the electrostatic boundary layers are formed at the liquid-electrode interfaces, which cause the shielding of the bias charge of the electrodes. To overcome this problem,

pulsed potential is to be applied.
Nanoparticles adhered on the electrodes and PANI film were studied by the means of SEM, EDS and FTIR. Gas sensing properties of pristine and nanoparticle-decorated thin PANI films exposed to the gaseous ammonia or hydrogen were measured. We found enhanced sensitivity of nanoparticle-decorated PANI film due to the effect of catalytic properties of nanoparticles.
The authors acknowledge the financial support provided by the APVV grant agency under the grant APVV-0593-11.

[1] T. Torimoto, K. Okazaki, T. Kiyama, K. Hirahara, N. Tanaka, and S. Kuwabata, Appl. Phys Lett. 89 (2006) 243117.
[2] P. Kunzo, P. Lobotka, M. Micusik, E. Kovacova, Sensors and Actuators B: Chemical. 171-172 (2012) 838–845.
[3] L. Besra, M. Liu, Progress in Materials Science. 52 (2007) 1–61.

NST/SS-P1-03
Analysis of Monolayer Graphene Nucleation on Polycrystalline Ni Surface

T10 Nanoscience and Technology

#NST/SS-P1-03

Y. Momiuchi [1], K. Yamada [1], H. Kato [1], H. Hibino [2], C. Oshima [3], Y. Homma [1].

[1]Dept. of Phys., Tokyo Univ. of Science - Tokyo (Japan), [2]NTT Basic Research Labos. - Kanagawa (Japan), [3]Dept. of Appl. Phys., Waseda Univ. - Tokyo (Japan).

Graphene growth mechanism during of bulk-dissolved carbon on polycrystalline nickel surface is one of great interest for controlled synthesis of graphene. The growth process has been explored by real time observation using low energy electron microscopy (LEEM) [1]. Although LEEM is a useful method for investigation of graphene growth, the field of view is not large enough to track the nucleation stages and the layer expansion.

Recently, our group reported the capability of imaging monolayer graphene on polycrystalline nickel surface by scanning electron microscopy (SEM), which has a wide field of view and a crystalline orientation effect on the extension of graphene [2]. In the present study, we focused on the graphene nucleation by using in-situ SEM observation and electron backscatter diffraction (EBSD) measurement. We repeated the several cycles of dissolution and segregation carbons on polycrystalline Ni surface. We found that the graphene preferentially nucleates on (111)-oriented grains (Fig. 1). The analysis of the geometric structure using atomic force microscopy (AFM) revealed common morphology characteristic to the nucleation sites. The combination of in-situ SEM observation, AFM and EBSD measurements is useful to gain insights into controlling monolayer graphene growth.

[1] G. Odahara, *et al*. : Appl. Phys. Lett. 5 (2012) 035501.
[2] K. Takahashi, *et al*. : Surf. Sci. 606 (2012) 728.

Fig.1 (a) SEM image of monolayer graphene nucleation on polycrystalline Ni. Graphene-covered area is highlighted with blue in the inset. (b) EBSD mapping on the same area.

NST-5-Or-3
Interaction mechanism for AFM on a H- or O-covered Si(111) surface

T10 Nanoscience and Technology

#NST-5-Or-3

M. Ondracek [1], A. Yurtsever [2], J. Onoda [2], Y. Sugimoto [2], M. Abe [2], S. Morita [2], P. Pou [3], R. Pérez [3], P. Jelínek [1].

[1]Institute of Physics, Academy of Sciences of the Czech Republic - Prague (Czech republic), [2]Graduate School of Engineering, Osaka University - Osaka (Japan), [3]Departamento de Fisica Teorica de la Materia Condensada, Universidad Autonoma de Madrid - Madrid (Spain).

The non-contact atomic force microscope (nc-AFM) allows one to probe forces acting between the apex of the AFM probe and the surface of the sample on the atomic scale. Even chemical identification of atoms can be achieved with this tool [1,2]. However, not only the magnitude of the force but even the mechanism by which the force arises may vary, even for a given surface, depending on the AFM-tip termination and the particular atomic or molecular species directly under the tip. The mechanism of the tip-surface interaction may be, for example, of chemical, electrostatic, or van der Waals origin. Understanding this mechanism is vital for correct interpretation of the experiments, especially when pursuing chemical sensitivity. We have, in particular, explored the interaction of an AFM tip with the Si(111)-7x7 surface partially covered with hydrogen or oxygen. In the experiment with adsorbed hydrogen, two profoundly different types of tip termination could be identified, distinguished by their reactivity. In the same experiment, the hydrogen-free and hydrogen-passivated Si adatoms on the partially passivated surface represented typical reactive and non-reactive surface sites, respectively. Thus, four modes of interaction could be studied on this surface, resulting from either a reactive or a non-reactive tip interacting with either a reactive or non-reactive surface site. We performed first-principles (density functional theory, DFT) simulation, the results of which we compare to the experimental force curves, in order to identify realistic tip models and uncover the mechanism by which the tip interacts with the surface. We propose suitable models for both types of tips, the reactive as well as the non-reactive, and discuss the respective roles of chemical reactivity on the one hand and electrostatic interaction between electrically polarized structures on both the tip and the surface on the other hand. On the partially oxidized silicon surface, the oxygen

atoms form stable structures by incorporating into the backbonds of an Si adatom (see, e.g., [3]). A characteristic pattern arises for maxima of the attractive force when different tips are used to probe this surface. The total force can be expressed as a sum of a component for which the ratio between clean Si and oxidized sites is constant (tip-independent) and an other component, which is almost tip-independent as for its absolute value but which is present only on the oxidized sites. We attribute this observation to simultaneous presence of two distinct mechanisms of interaction. Again, we use DFT calculation to understand the origin of this interactions and we will discuss its implications for the chemical resolution method introduced in [1].

[1] Y. Sugimoto *et al.*, Nature 446, 64-67 (2007). [2] M. Setvin *et al*., ACS Nano **6**, 6969-6976 (2012). [3] Sakamoto *et al.*, Phys. Rev. B **72**, 075346 (2005).

NST-5-Or-4
Imaging the local density of free charge carriers in doped InAs nanowires with infrared near-field microscopy

T10 Nanoscience and Technology

#NST-5-Or-4

B. Hauer [1], K. Sladek [2], F. Haas [2], T. Schäpers [2], H. Hardtdegen [2], T. Taubner [1].

[1]Institute of Physics (IA) and JARA-FIT, RWTH Aachen University - Aachen (Germany), [2]Peter Grünberg Institute (PGI-9), Forschungszentrum Jülich - Jülich (Germany).

For a fundamental understanding of local electrical and chemical processes in electronic materials and composite structures, advanced microscopy tools are indispensable. Chemical and structural properties, as well as free charge carriers can be studied by optical spectroscopy methods. Particularly in the infrared spectral range the identification of characteristic molecular and phononic absorption bands allows for a detailed characterization of materials. Also the Drude contribution of free charges can affect the optical properties in infrared range. However, most established infrared characterization methods lack in spatial resolution due to the diffraction limit of propagating waves.

In scattering-type scanning near-field optical microscopy (s-SNOM) the diffraction limit is circumvented by using a sharp probe as a local scatterer [1]. The evanescent fields at the apex of this tip allow for an optical sample characterization with a wavelength-independent resolution in the order of the tip radius (20 nm). Since the scattering efficiency of the tip–sample system depends on the dielectric function of the involved materials and on their geometric arrangement, regions with different optical properties can be distinguished in s-SNOM.

In this contribution, we demonstrate the capability of s-SNOM to investigate the local density of free electrons in Si-doped InAs nanowires grown by selective-area metalorganic vapor phase epitaxy (SA-MOVPE) [2]. The method of s-SNOM is highly sensitive to variations in the sample permittivity around $\Re(\varepsilon) \approx -2$ [3]. The use of tunable

mid-infrared lasers therefore allows addressing the plasma frequency of free charge carriers in highly doped nanowires [4]. We demonstrate that the sensitivity of s-SNOM is sufficient to detect a slight unintended variation in the carrier concentration during the growth process. In Fig. 1, the optical scattering amplitude is shown in color, together with the topography of a nanowire. The modulation in the scattering intensity reveals an inhomogeneity in the density of free charge carriers. Using model calculations, the actual local density of free electrons can be estimated.

[1] F. Keilmann and R. Hillenbrand, in A. Zayats and D. Richard (eds.) Nano-optics and near-field optical microscopy, 235–265 (Artech House, 2009).
[2] S. Wirths et al., J. Appl. Phys. 110, 053709 (2011).
[3] B. Hauer et al., Opt. Express 20, 13173 (2012).
[4] J. Stiegler et al., Nano Lett. 10, 1387 (2010).

Fig. 1. Topography (relief) and s-SNOM scattering amplitude (color scale) of a doped InAs nanowire.

BI-1-Or-8
Tunable polymeric nanochannel device for single molecules detection

T10 Nanoscience and Technology

#BI-1-Or-8

P. Fanzio [1], C. Manneschi [1], V. Mussi [2], E. Angeli [1], G. Firpo [1], L. Repetto [1], U. Valbusa [1].

[1]Nanomed Labs, Dipartimento di fisica,Università di Genova - Genova (Italy), [2]National Research Council Institute for Complex Systems ISC-CNR - Genova (Italy).

Microarray technology have been developed in order to analyze tens of thousands genes in a single experiment. However, it suffers from various limitations, such as the need for fluorescent labels and optical detection methods, insufficient sensitivity, narrow dynamic range, and non-specific or cross-hybridization. The complete process of sample preparation and measurement is complex and lengthy. Recently, nanopore/nanochannel technology has been proposed for biosensing and genome analysis as a low cost, fast processing and high throughput alternative to microarrays, thanks to the great potentiality of this kind of devices for label-free single molecule analysis and sensing [1]. In this context, we developed a low cost polymeric nanochannel device by using a Focused Ion Beam (FIB) to fabricate a nanometric channel on a pre-patterned silicon master and replicating the structures in a polymeric material by means of soft lithography. The layout of the device is shown in figure 1a: two microchannels are connected by a single nanochannel and two electrodes (yellow) allow applying the voltage and collecting the ionic current. The sensing principle is based on transient interruptions in the ionic current induced by the passage of DNA inside the channel. We show results on single DNA molecule detection [2], demonstrating that, thanks to the elastomeric properties of the used material (PDMS) it is possible to reversibly tune the dimension of the nanochannel by applying a mechanical pressure on the top of the device (figure 1b). This results in the possibility to change in a controlled way the actual detection capabilities of the device [3]. Figure 1c shows a plot of the DNA translocation time across the nanochannel in function of the applied compression of the polymeric device. By increasing the compression, the translocation time increases, demonstrating the possibility to slow down the DNA passage. This simple and low cost method can be coupled with different sensing techniques, is applicable in many research fields (DNA

detection and manipulation) and is promising for further development in sequencing technology. Finally we also show the effects of chemical functionalization of the nanochannel polymer surface, thus opening up a range of possible applications in the fields of bioanalytics and molecular diagnosis.

[1] S. Howorka and Z. Siwy, Chemical Society Reviews, 38, 8, 2360, 2009.
[2] P. Fanzio et al., Lab on a Chip, 11, 17, 2961, 2011.
[3] P. Fanzio et al., Scientific Reports, 2, 791, 2012

Fig 1. a) Sketch of the top view of the device layout b) Sketch of the squeezing setup c) Plot of the translocation time versus the applied compression at 200 mV applied voltage

NST-3-Or-1
Friction : Bridging the Nano-to-Microscale with Microfabricated Plates

T10 Nanoscience and Technology

#NST-3-Or-1

S. O'shea, X. Tang, Y. Loke, P. Lu.

IMRE - Singapore (Singapore).

We show results for the sliding of microfabricated (MEMS) structures called “sleds”. The sleds consist of microfabricated Silicon plates with three sharp tips which rest on a surface to form a 3-point contact (Fig. 1a).

We present a new AFM based approach (Fig. 1b) for measuring the friction of such free standing MEMS structures. An AFM tip is brought into contact with a sled resting on a substrate and then, provided the AFM tip does not slide on the sled, the twisting of the AFM cantilever is used to measure the friction of the underlying sled-substrate interface. The method measures nano-Newton to micro-Newton forces and provides a means to measure friction of macroscopic structures at low load.

Another objective is to make the sleds move under user-controlled friction, similar to electrically actuated superlubricity demonstrated using AFM [1] i.e. to induce mechanical conditions at the point contacts such that sliding occurs. Results showing controllable actuation of the sled motion will be shown. The natural resonance frequencies of a free sled, which are proposed as the driving frequencies for actuation, are modelling and compared to vibrometer data.

Using the MEMS sled approach, we envisage studying macroscopic MEMS devices which are controlled by single asperity, nanoscale phenomena.

[1] A. Socoliuc, et. al. Science 313, 207-210 (2006).

Figure 1 : a) A Silicon microfabricated sled, 300nm thick, 200 micron square, with 3 Si3N4 tips. b) A free standing sled on a surface under an AFM tip for friction measurement.

NST/SS-5-Or-4
Electronic transport in multiwalled carbon nanotubes

T10 Nanoscience and Technology

#NST/SS-5-Or-4

M. Ahlskog [1], D. Mtsuko [1], A. Koshio [2], M. Yudasaka [2], S. Iijima [2].

[1]University of Jyväskylä - Jyväskylä (Finland), [2]NEC Research Center - Tsukuba (Japan).

We have measured the low temperature transport properties of single multiwalled carbon nanotubes (MWNT) of diameters (D) in the range 2-10 nm, see fig. 1. Almost all previous work on MWNT's has been on tubes with diameters above 10 nm. In nearly all samples in this work, with D < 10 nm, the gate dependent conductance (fig. 2) exhibits a gap whose size increases with the inverse tube diameter and increasing electrode separation. This so called transport gap is attributed, based on the experimental findings, on a combination of localization effects and narrow diameter induced gaps in the electronic band structure.

These results have significant similarities to the current research on graphene nanoribbons (GRN). As graphene does not intrinsically possess a bandgap, GNR's are fabricated, where a gap is created via quantum confinement due to the narrow width of the channel/nanoribbon. The size of the gap is then roughly in a similar inverse relation with the width of the constriction as in the case of the diameter dependence of the MWNT's in our work.

The transport gap has not generally been observed in the previous works on MWNT's because of the large diameters of the tubes in these. Our work, of which some early results were published previously [1], complements and bridges previous works on both single walled nanotubes and MWNT's, and also to the field of GNR's.

[1] M. Ahlskog, O. Herranen, A. Johansson, J. Leppäniemi, and D. Mtsuko, Physical Review B, 79, 155408 (2009).

Fig. 1. AFM image of a MWNT contacted with four electrodes.

Fig. 2. Current vs. gate voltage for a MWNT at different temperatures between 270 K and 7 K.

NST-5-Or-5
The Relation between AFM-Tip Water Bridge Dimensions and Pull-off Force Measurements under Ambient Conditions

T10 Nanoscience and Technology

#NST-5-Or-5

M. Bartošík [1], L. Kormoš [2], L. Flajšman [2], Z. Lišková [2], R. Kalousek [1], D. Škoda [1], M. Konečný [2], T. Šikola [1].

[1]CEITEC BUT, Brno University of Technology, Technická 2, 616 69 Brno, Czech Republic - Brno (Czech republic), [2]Institute of Physical Engineering, University of Technology Brno, Faculty of Mechanical Engineering, Technická 2, 616 69 Brno - Brno (Czech republic).

The atomic force microscopy (AFM) is often performed in ambient conditions where the water condenses between a hydrophilic tip and a sample and affects the tip-surface forces and consequently the whole measurement. Moreover, there are a few AFM-lithography techniques utilizing the existence of such a water bridge. The most famous are dip-pen nanolithography (DPN) and local anodic oxidation (LAO). Despite of its relative simplicity, both of these methods are capable of providing features down to 10 nm. Such a high resolution results from the restriction of chemical reactions to an area of tens nanometers determined by the dimensions of the water bridge. Because of these reasons, the information about the amount of water trapped under the tip is very useful for interpretation of topography measurements, improving the mentioned AFM-lithography techniques and determination of local hydrophilicity/hydrophobicity of the sample.

Here we report on the influence of relative humidity on the pull-off force between a silicon AFM tip- and a SiO2 surface under ambient conditions. Furthermore, the influence of the shape, radius and chemical treatment of the tip on this force was studied as well. The pull-off forces are determined from force-distance spectroscopy measurements performed at many sites forming a n-by-n matrix. The humidity was controlled by a home-built computer operated system installed in a glove box. In addition to the experiments on pull-off forces the corresponding numerical simulation

was carried out as well. This simulation was based on the solution of Kelvin's equation for water meniscus at boundary conditions determined by the contact angles (surface-water, tip-water) and provided capillary, tension and van der Waals forces.

In the contribution the experimental and theoretical results will be compared. They will be discussed with respect to those obtained previously [1] and to the calculations of pull-off forces carried out by other groups using both the molecular lattice-gas model in Monte Carlo (MC) simulations and density functional theory (DFT). It has been found that the best agreement between the experiment and simulations has been obtained if the dependence of surface tension on the dimension of the meniscus is assumed. The experimental improvement of reproducibility of pull-off force measurements up to 2% has been achieved and will be discussed as well.

[1] M. Bartošík, D. Škoda, O. Tomanec, R. Kalousek, P. Jánský, J. Zlámal, J. Spousta, P. Dub, T. Šikola, "Role of humidity in local anodic oxidation: A study of water condensation and electric field distribution" Phys. Rev. B 79 (2009) 195406.

NST-P2-13
Growth of Nano sized Bismuth Oxy Chloride on Carbon Nano Tubes.

T10 Nanoscience and Technology

#NST-P2-13

P. Jagdale, I. Shazad, A. Tagliaferro.

Department of Applied Science and Technology (DISAT), Politecnico di Torino, 10129, Italy. - Torino (Italy).

We report for the first time the growth of nano sized Bismuth oxy chloride (BiOCl) platelets on Carbon Nanotubes (CNTs), achieved by Metal Organic Chemical Vapour Deposition (MOCVD) (Figure 1).This method allow the deposition of thin metallic layers with precisely controlled thickness. Nano sized bismuth (NBs) crystals were synthesized from solution containing Bismuth chloride (BiCl3) in Acetone (CH3-CO-CH3). Self assembly of nano bismuth crystals was observed on the CNT surface. Various synthesis parameters were investigated to achieve better depositions, as they significantly affect the formation of nano-crystalline bismuth [1]. Crystalline NBs was characterized by X-ray diffraction (XRD), Field emission scanning electron microscopy (FESEM), Energy-dispersive X-ray spectroscopy (EDS). These analyses confirm the Bismuth nanometer-sized platelets are in the form of tetragonal BiOCl with a mean wall thickness similar to the diameter of CNT i.e 80–90 nm (Figure 2).

[1] Organobismuth Chemistry. Suzuki, H., Matano, Y., Eds.;Elsevier: Amsterdam, 2001.

Figure 1 MOCVD unit diagram Figure 2 Growth of Nano BiOCl on CNTs

Figure 2 Growth of Nano BiOCl on CNTs

NST/SS-4-Or-2
Epitaxial Growth of Rhenium layers for Superconducting Quantum Circuits

T10 Nanoscience and Technology

#NST/SS-4-Or-2

B. Delsol [1], B. Gilles [2], O. Buisson [3], S. Lay [2], H. Courtois [3].

[1]Laboratoire SIMAP / Institut Néel - Grenoble (France), [2]Laboratoire SIMAP - Grenoble (France), [3]Institut Néel - Grenoble (France).

In electronic devices, it is expected that the quantum limit will soon be reached with decreasing system size. Therefore, manipulating quantum information appears as a new challenge. Solid state Qubits based on superconducting Josephson junction (JJ) are promising systems which take advantage of microelectronics technology. However, decoherence time of the quantum states is still a limiting factor. This has been generally ascribed to the poor crystallographic quality of the materials used so far (crystallographic defects, impurities).
We will show that the Molecular Beam Epitaxy (MBE) technique may be used to grow rhenium films of high quality on sapphire substrates. Indeed, alumina-α and rhenium may be in good crystallographic registry when Re is epitaxied on the (0001)-C plane. The growth temperature is the key parameter, as it controls the epitaxial quality. As already shown by Oh [1], a good crystallographic structure is obtained when growth is performed at a temperature above 800°C. We will present how to improve the homogeneity of the film temperature and how to reduce the thickness dependence of the temperature during the deposition.
Also it will be shown that different kinds of surface structures may be observed by Atomic Force Microscopy (AFM) and Scanning Tunneling Microscopy (STM) depending on the temperature and the thickness. For thicknesses ranging from 25 nm to 100 nm and temperatures ranging from 800°C to 1000°C, we observe different growth dynamics, involving nano-grains, single and double spirals (Fig. 1). Theses growth regimes may be explained as an extension of the Burton, Cabrera and Frank theory (BCF) [2], which was developed long time ago for equilibrium growth.
We have also investigated the crystallographic quality of our samples by X-ray diffraction and Electron Back Scattering Diffraction. Our heating optimization has increased the quality of our films that are epitaxied and without any variants.
Preliminary results have shown that single crystal Al_2O_3 barriers and Re layers may subsequently be grown in order to build a complete epitaxial tri-layer JJ.

[1] S. Oh, D.A. Hite, Thin Solid Films, 496, 2, 389-394 (2006).
[2] W.K. Burton, N. Cabrera, F.C. Frank, Phil. Trans. R. Soc. Lond. A, 243, 299-358 (1951).

Fig. 1 : Double spiral on Rhenium thin film (50 nm deposited on Sapphire at 900°C).

NST-10-Or-8
Terahertz vibrations of ZrO2 nanoparticles in a nanopowder under high-pressure

T10 Nanoscience and Technology

#NST-10-Or-8

L. Saviot [1], D. Machon [2], A. Mermet [2], D.B. Murray [3], S.V. Adichtchev [4], J. Margueritat [2], F. Demoisson [1], M. Ariane [1], M.C. Marco De Lucas [1].

[1]Université de Bourgogne - Dijon (France), [2]Université de Lyon - Villeurbanne (France), [3]University of British Columbia - Okanagan (Canada), [4]Institute of Automation and Electrometry - Novosibirsk (Russian federation).

Free several-nanometer-sized nanoparticles are mechanical nanoresonators with frequencies in the terahertz range. They have potential applications in nanoelectromechanical systems provided their quality factor is high enough, *i.e.*, if these vibrations are only lightly-damped by the surrounding medium. In this work, we investigated a powder of ZrO_2 nanoparticles whose diameter is about 5 nm under high pressure up to 20 GPa [1]. The terahertz acoustic vibrations confined within the nanoparticles are observed using low-frequency Raman scattering. The propagation of acoustic waves through the compressed nanopowder (wavelength large compared to the diameter of the nanoparticles) is observed using Brillouin scattering. This study shows that the nanoparticles oscillate almost as if they were free in the highly-compressed nanopowder despite the high applied pressure. This is attributed at least in part to a few monolayers of water molecules adsorbed at the surface of the nanoparticles which act as an isolation layer if the layer thickness is in the right range. To corroborate this, we demonstrate theoretically that lightly-damped acoustic vibrations of nanoparticles are possible in this system. A quasielastic signal is also evidenced from the high-pressure and low-temperature low-frequency Raman spectra. In addition, the two phase transitions of ZrO_2 as pressure is increased result in a modification of the low-frequency spectra which we attribute to the change in the ionicity/covalency of the Zr-O bonds with pressure.

[1] L. Saviot, D. Machon, A. Mermet, D. B. Murray, S. V. Adichtchev, J. Margueritat, F. Demoisson, M. Ariane & M. C. Marco de Lucas, J. Phys. Chem. C 116, 22043 (2012)

Left: Illustration of the vibrations of an ensemble of nanoparticles under an hydrostatic pressure. Right: Evolution of the Raman and low-frequency Raman spectra with pressure.

NST-10-Or-9
New one-pot synthesis of Au or Ag nanoparticles supported on reactive Fe(II)-bearing inorganic particles

T10 Nanoscience and Technology

#NST-10-Or-9

S. Ayadi, L. Legrand.

LAMBE UMR8587 - Evry (France).

Nanoparticles of noble-metals or nanohybrids incorporating nanoparticles exhibit unique optical, chemical and catalytic properties which make them attractive for a wide range of applications in many domains. Nanoparticles are commonly prepared via reducing a soluble metal precursor (Au^{III} or Ag^{I}) by a soluble reducing agent in presence of a stabilizing species to keep them from aggregation [1-2].
In the present communication, we report a new, simple and fast one-pot synthesis of supported Au or Ag nanoparticles by using a reactive inorganic particle (green rust GR = layered Fe^{II}-Fe^{III} HydroxyCarbonate (GRc) or HydroxySulfate (GRs)) as both the reducing agent and the support. The mechanism involves the solid-state oxidation of FeII to FeIII in GR [3] and the reduction-precipitation of soluble metal precursor to metal nanoparticles on the surface (Figure 1). All reactions were proved to be complete and metal load vary between 0 and the maximal theoretical (i.e 25% for Au/exGRs). The resulting nanohybrids were characterized by XRD, FTIR and SEM. The inorganic particles keep the platelet morphology of the GR precursor and they support about 1 to 10 metal nanoparticles with a diameter in the 20-120 nm range (Figure 2).
With only one final separation step, the synthesis of our nanohybrids is very attractive. Their manipulation is easy and relatively safe since mineral-types iron compounds are generally fully biocompatible and metal nanoparticules are well attached to the inorganic matrices. The surface of inorganic and/or metal parts can be functionalized to target specific properties. The nanohybrids can be compacted or cast-deposited to build permeable reactive membranes or modified (bio-) electrodes.

[1] J . Turkevich, P.C. Stevenson, J. Hilier, Discuss. Faraday Soc. 1951, 11, 55.
[2] N. Shirtcliffe, U. Nickel, S. Schneider, J. Colloid Interface Sci. 1999, 211, 122.

[3] L. Legrand, L. Mazerolles, A.Chaussé, Geochim. Cosmochim. Acta 2004, 68, 3497.

Figure 1: Cross-sectional schematic of Au^{III}-GR reaction
Figure 2: Backscattered electron SEM pictures of Au/exGRs nanohybrids. (a) R=50% and (b) R=100%. (c) Size distribution histograms

NST-8-Or-5
Self-assembly of organic molecules and bioinspired nanofabrication based on adhesive effect of climbing plant

T10 Nanoscience and Technology

#NST-8-Or-5

W. Deng.

South China University of Technology - Guangzhou (China).

We synthesized and confirmed a series of fluorenone derivatives and used scanning tunneling microscope (STM) to observe these prepared compounds assembled onto HOPG surfaces to form self-assembly monolayers. We especially investigated that those factors such as molecular structure, van der Waals force, dipole-dipole interaction, hydrogen bond, as well as solvent molecule and concentration how to affect assembled structures [1－3]. Understanding the super adhesion mechanism of biological system is of great scientific interests and a prerequisite for bioinspired design of adhesive systems. We presented strategies to fully study the super adhesive effect of climbing plant ─ Parthenocissus tricuspidata by measuring the mass, attached area, microscopic structure and adhesive strength of single adhesive disc. Microscopic experiments showed some new microstructures which have never been reported and revealed that the adhesive disc has super adhesive property which inspires us to fabricate a lot of mimic adhesives that have potential applications in biomedical science, bioelectronics and space science and technology [4]. We found that there are more than 20 kinds of organic compounds in adhesive disc and we used polystyrene (PS) to fabricate biomimetic surface structure of the adhesive disc and measured its adhesive force using AFM [5,6]. This template-assisted method provides a new means to prepare the macropores of other soluble polymers in future.

[1] Li Xu, Xinrui Miao, Xiao Ying, Wenli Deng, J. Phys. Chem. C 2012, 116: 1061-1069.
[2] Li Xu, Xinrui Miao, Bao Zha, Wenli Deng, J. Phys. Chem. C 2012, 116: 16014-16022.
[3] Xinrui Miao, Li Xu, Zhuomin Li, Wenli Deng, J. Phys. Chem. C 2011, 115: 3358-

3367.
[4] Wenli Deng. Tendril, adhesive disc and super adhesive effect of climbing plant. Nature Precedings 2008, 1, 15 (http://precedings.nature.com/documents/1513/version/1).
[5] Tianxian He, Zhuomin Li, Li Zhang, Wenli Deng, Mat. Letts. 2012, 78: 25-27.
[6] Tianxian He, Li Zhang, Wenli Deng, Mat. Chem. Phys. 2011, 131: 23-26.

NST/SS-5-Or-5
Insights to the interaction between single-stranded DNA and single-walled carbon nanotubes

T10 Nanoscience and Technology

#NST/SS-5-Or-5

S. Srebnik.

Technion - Israel Institute of Technology - Haifa (Israel).

Single-walled carbon nanotubes (SWNTs) have received vast attention over the years due to their unique electronic, mechanical and optical properties. SWNTs are characterized by chiral indices that largely define their geometric and electronic properties (i.e., metallic or semi-conducting). Recent works has focused on single-stranded (ss) DNA-SWNT complexes as a means for separation of SWNTs according to chirality, where outstandingly it was shown that designed ssDNA sequences could be used to separate particular chiral SWNTs. We present small angle neutron scattering (SANS) measurements of some ssDNA-SWNT complexes and use atomistic and coarse-grained simulations to provide insights to this unique registry between the two macromolecules.

NST/SS-4-Or-3
Features of the magnetization reversal mechanisms in the magnetoresistive response of magnetic nanostructures

T10 Nanoscience and Technology

#NST/SS-4-Or-3

P. Perna [1], D. Maccariello [1], C. Rodrigo [1], M. Muñoz [2], J.L. Prieto [3], A. Bollero [1], J.L.F. Cuñado [4], M. Niño [1], C. Navio [1], N. Mikuszeit [1], J. Camarero [1], R. Miranda [1].

[1]IMDEA-NANOSCIENCE - Madrid (Spain), [2]Instituto de Física Aplicada, CSIC - Madrid (Spain), [3]ISOM, Universidad Politécnica de Madrid - Madrid (Spain), [4]DFMC, Universidad Autónoma de Madrid - Madrid (Spain).

Magnetoresistive effects and related phenomena in magnetic nanostructures have found widespread applications in magnetic sensing and recording technologies [1]. Even though it is commonly assumed that the magnetoresistance (MR) depends on the magnetic anisotropy, the direct proof that the magnetoresistive responses are directly related to the magnetization reversal processes is still lacking. In fact, experiments just relies in either magnetization (usually parallel component) or MR curves measured independently for a given applied field angle, normally close to the easy axis (e.a.) direction.
Here, we present a systematic angular-dependent studies on magnetization reversal processes and magnetoresistive responses of nanostructured magnetic systems, including ferromagnetic thin film with well-defined magnetic anisotropy, exchange-biased spin valve [2] and hybrid metal-organic heterostructures.
To do that, we have employed a new experimental set-up that allows us to measure simultaneously magneto-resistance and vectorial-resolved Kerr [3] hysteresis loops, i.e., including in-plane parallel and perpendicular magnetization components [4] and MR, at different applied field angles in the whole angular range. We advance towards a microscopic understanding of the MR properties by showing that their angular dependence leaves distinct fingerprints, which are directly related to their magnetization reversal processes [3].
In the case of FM thin films with defined uniaxial magnetic anisotropy, the dependences with the applied magnetic field and current direction with respect to the anisotropy axis were investigated. The data show that the anisotropic

magnetoresistance (AMR) is dictated by different magnetization reversal processes and provide the direct experimental evidence that the magnetoresistance response depends on the square of the cosine of the angle between the sample magnetization and the direction of the applied current. In the case of spin valve, well-defined MR-plateaus are observed around the e.a. direction whereas just reversible MR transitions are found around the hard axis (h.a.) direction. The MR-plateau value decreases as the magnetic field is misaligned with respect to the e.a. and the maximum of MR decreases approaching the h.a.
The results directly show that the different magneto-resistive behaviors originate from the magnetic anisotropy of the structure, which ultimately depends on the relative magnetization orientation of the FM layers. In particular, the M-H curves give the relevant information about the magnetization reversal processes and lead the direct determination of the magnetization direction during the hysteresis loop. The magnitude and shape of MR(H) are controlled by the orientations of the applied field and current with the magnetic anisotropy axis.

[1] A. Fert, Angew. Chem. Int. Ed. 47, 5956 (2008); C. Chappert, A. Fert and F. N. Van Dau, Nature Mater. 813, 6 (2007); G. A. Prinz, Science 282, 1660 (1998)
[2] B. Dieny, et al., Phys. Rev. B 43, 1297 (1991)
[3] P. Perna, et al., Phys. Rev. B 86, 024421 (2012)
[4] D. Ecija, et al., Phys. Rev. B 77, 024426 (2008)

NST-P1-16
Nanoscale Si/Ge heterostructures prepared by glancing angle deposition

T10 Nanoscience and Technology

#NST-P1-16

C. Grüner, J. Bauer, B. Rauschenbach.

Leibniz Institute of Surface Modification (IOM), Permoserstr. 15, 04318, Leipzig, Germany - Leipzig (Germany).

Free-standing, separated nanoscale structures such as slanted and vertical columns, spirals and zig-zags are of growing interest for many possible applications. In the so-called glancing angle deposition (GLAD) process, contrary to usual PVD thin film deposition, the particle flux reaches the surface under a highly oblique angle. Under these circumstances, self-shadowing processes at the substrate surface lead to the growth of separated needles, inclined towards the particle source. Combined with suitable substrate rotation, this method offers a full three-dimensional control of the nanostructures shape in a bottom-up process with additional capability of self-alignment (details see [1,2]).
For the use of GLAD structures in technical applications, it is necessary to obtain control over the shape of the individual nanostructures, the distribution of the materials inside heterostructures, and the arrangement of the structures on the substrate. Therefore one needs to understand the growth process and the influence of the different process parameters.
Here the GLAD induced growth of Si/Ge hetero nanostructures for different substrate circumstances will be compared, and the influence of pattern periodicity on shape and diameter evolution of the growing structures will be discussed. A fast and geometrically accurate computer simulation is used to support the investigation (see figure).
The growth of the nanostructures is further studied in dependence of substrate temperature, rotation, and deposition rate using scanning electron microscopy, high-resolution transmission electron microscopy, X-ray diffraction and Raman spectroscopy.
Since glancing angle deposition provides a wide nanoscale control over structure, grain orientation and doping characteristics, the mechanical, optical, electrical and magnetic properties of the sculptured thin films may be engineered for various applications.

[1] C. Patzig, B. Fuhrmann, H.S. Leipner, B. Rauschenbach, J. Appl. Phys. 103 (2008) 024313

[2] J. Bauer, M. Weise, B. Rauschenbach, N. Geyer, B. Fuhrmann, J. Appl. Phys. 111 (2012) 104309

Si/Ge heterostructure in a large periodic honeycomb pattern, and a comparable simulated structure.

NST-9-Or-5
Synthesis, Characterization and Anti-bacterial Investigation of Silver-Copper Nanoalloys

T10 Nanoscience and Technology

#NST-9-Or-5

M. Taner Camci, N. Sayar, I. Yulug, S. Suzer.

BILKENT UNIVERSITY - Ankara (Turkey).

Silver and copper nanoalloys have been synthesized and incorporated into ultra-thin layers using the layer-by-layer technique for antibacterial applications. Films with Ag-only and AgCu nanoalloys have been tested against Escherichia coli strains to assess their anti-bacterial behavior. No bacteria colony growth was observed as the evidence for superior anti-microbial characteristics of these films with AgCu nanoalloys.(1) These thin films have been characterized using Optical (UV-visible) and X-ray Photoelectron Spectroscopy (XPS). In order to get further understanding at the molecular level, these films were also analyzed while applying square wave electrical pulses during recording of their XPS data. Our experimental details and results will be presented.

(1) Taner, M. et al. Synthesis, Characterization and Antibacterial Investigation of Silver-Copper nanoalloys.Journal of Materials Chemistry 21,13150-13154 (2011).

NST-2-Or-7
Electric double-layer capacitors having nanostructured electrodes

T10 Nanoscience and Technology

#NST-2-Or-7

K. Fujiwara, M. Omiya.

Keio University - Yokohama (Japan).

Electric double-layer capacitors having ultra capacity are expected to be used instead of secondary batteries. Electric energy storage in electric double-layer capacitors occurs by the formation of electric double-layers on the surfaces of both negative and positive electrodes. In this study, we aimed to increase the capacitance of electric double layer capacitors by increasing the surface area of electrodes and the amount of charge on the surface by fabricating nanostructures on them. Nanostructures are the structures made on a scale of nanometers and prepared by using Dynamic oblique deposition. Dynamic oblique deposition (DOD), in which the deposition angle and in-plane direction of a substrate are varied during deposition, enables us to fabricate nanostructured thin films. This method exploits the atomic self-shadowing effect during physical vapor deposition that arises from deposition at a highly oblique angle.

We fabricated capacitor electrodes which have 200 nm base layer of Au by sputtering and 200 nm nanostructured layer of Cu by using DOD on a glass substrate (20mm × 20mm × 0.7mm). Capacitors were fabricated by laminating polymer electrolyte thin film between electrodes by thermocompression bonding (Temperature:400K, Pressure:0.15MPa, Time:30min). In the same way, capacitors having electrodes without nanostructured layer were fabricated for comparison.

We analyzed the capacitance per unit volume of these capacitors by measuring the Cole-Cole plot using a LCR meter, and fitting equivalent circuit and their results. The electric double layer capacitance of the capacitor having electrodes without nanostructured layer which is measured in 1.5M NaOH solution is C_1=2.2F/cm^3 and C_2=1.4F/cm^3. Furthermore, the electric double layer capacitance of the capacitor having electrodes with nanostructured layer which is measured in 1.5M NaOH Solution is C_1=24F/cm^3 and C_2=6.8F/cm^3. From these results, the capacitance increase 10 times by fabricating nanostructures on the surface of capacitor electrodes.

The capacitor having electrodes with nanostructured layer contains 0.7mm thick glass substrates and 0.5mm thick separator. Therefore, the capacitance of whole of

the capacitor is approximately 30.8F (C_1 + C_2) in size 1cm×1cm×2.19cm. Then, the capacitance per unit volume is 14F/cm^3. This capacitance is 5.8 times that of conventional coin type electric double layer capacitors, which has 2.4 F/cm^3.

NST-P2-14
Electronic Growth, Stratification and Planar Defects in Pb Nanoislands.

T10 Nanoscience and Technology

#NST-P2-14

A. Ionov [1], A. Ksyonz [1], D. Fokin [1], S. Bozhko [1], R. Dimitri [2], F. François [2], C. Tristan [2].

[1]ISSP RAS - Chernogolovka (Russian federation), [2]Institut des Nano-Sciences de Paris - Paris (France).

The electron growth (EG) model based on quantum size effect was proposed to explain the nature of metallic film growth. In a frame of EG model the total energy balance of a thin film also takes into account the energy of the electron gas. The electron gas is considered as confined in a two-dimensional quantum well (QW) its width d being of the film thickness. At small d comparable with electron wavelength the total energy of electron gas oscillates as a function of d. The oscillations period is determined by electron momentum at the Fermi level. Due to a difference between crystal lattice translational vectors of the film and oscillation period, minimum in energy of the electron system can be realized at certain film thicknesses only. The EG model was confirmed in experiments on growth of Pb thin films. Individual Pb islands grow following so-called bi-layer growth: the island height increases by “steps” of 2 mono layers (ML). Statistically, the islands with odd number of MLs are predominant while the islands of 7ML thickness are markedly privileged. Further increase of the island thickness resulted in a stratification of the islands with a slabs of 7ML in thick. DFT simulations argue that the observed growth mode is in good agreement with EG.

NST-1-Or-8
Evolution of MWCNT-polymer composite field emitter characteristics

T10 Nanoscience and Technology

#NST-1-Or-8

A. Kolosko, E.O. Popov, S.V. Filippov, M.V. Ershov.

A.F.Ioffe Physical-Technical Institute of the Russian Academy of Sciences - St.-Petersburg (Russian federation).

Today, recording and processing of current-voltage characteristics (IVC) constitute a basic tool in the study of the materials promising as efficient field emitters. The computerized data acquisition systems used for these purposes are very effective [1]. Application of multichannel recording and computer IVC processing has advantages when studying field emitter operation. This allows better understanding of IVC dynamics and their correlation with the other emission phenomena [2].
We succeeded in developing the technique of multichannel record and on-line data on the field emitter evolution processing. It includes multichannel data acquisition system of current, voltage, vacuum level, temperature and computer on-line processing of these data performed by own LabView program. The program obtains the field enhancement factor (β) and the number of emission sites (N) time dependences and built the slope-interception diagram (in SK-coordinates [3]). The field emission experiments were carried out in standard construction with flat metal electrodes. For obtaining IVC the high-voltage power unit with frequency 50 Hz was used. Electronic rectifier made positive impulses with duration 10 ms and consequently one such half-sinusoidal impulse gave one IVC.
In the present paper some data obtained in the study of nanocomposite field emitters NC-MWCNT (nitrocellulose - multiwall carbon nanotubes) are given. We use certificated Graphistrength nanotubes by Arkema (with diameter 15 nm).
We obtained IVC emitter evolution with a discrete change of interelectrode gap from 450 to 900 um. The maximum current value at impulses (Imax) was supported by a constant ~ 1.5 mA. The IVC curves in Fowler-Nordheim coordinates shifted to high voltages and theirs slope angle increased. The corresponding β and N varied asynchronously: β decreased and N grew up.
A consequent Imax step change at different interelectrode gaps gave a family of almost linear dependences in SK-coordinates (Fig.1). If the interelectrode gap exceeded 500 um, the depen-dences showed the hysteresis. We explained this effect by contribution of thermal field emission from Joule overheated nanotubes

which supported by continuous growth of current loading on one MWCNT (Imax/N).

Work is supported by grant N 12-08-31406 of Russian Foundation for Basic Research.

[1] N.V. Egorov, E.P. Sheshin. Intellect, Dolgoprudniy, 2011, 704 p.
[2] O.F. Pozdnyakov, E.O. Popov, A.O. Pozdnyakov. Tech. Phys. Lett. 37, 3 (2011) 216.
[3] M. Kawasaki, Z. He, Y. Gotoh, H. Tsuji, J. Ishikawa. J. Vac. Sci. Tech. B 28 (2010) C2A77.

Fig.1. Slope-interception diagram for different interelectrode gaps and different emission current amplitudes which increased and then decreased by steps from 1 μA to 3 mA with step 0.5 mA

NST/SS-P2-01
Observation of vortices at the surface of a normal metal coupled by proximity effect to a superconductor by STM/STS.

T10 Nanoscience and Technology

#NST/SS-P2-01

V. Stolyarov [1], C. Brun [2], T. Cren [2], F. Debontridder [2], V. Cerchez [2], I. Khaymovich [3], V. Oboznov [1], O. Skryabina [1], I. Veshchunov [1], V. Ryazanov [1], D. Roditchev [4].

[1]Institut of Solid State Physics, Rassian Academy of science - Chernogolovka (Russian federation), [2]Institute des Nanosciences de Paris, Universit'e Pierre et Marie Curie - Paris (France), [3]Institute for Physics of Microstructures, Russian Academy of Sciences - Nizhny Novgorod (Russian federation), [4]4LPEM-UMR8213/CNRS-ESPCI ParisTech-UPMC - Paris (France).

We report the experimental observation of vortices on the surface of a 50nm-thick layer of Cu in the hybrid structure Cu/Nb with ultra-low temperature Scanning Tunneling Spectroscopy (STS). In the studied samples the non-superconducting Cu-layer acquires superconducting correlations due to the proximity effect with 100nm-thick superconducting Nb. To avoid the oxidation at Cu-surface and allow STS, the samples were ex-situ grown on SiO_2/Si in the inversed order, i.e. Cu was deposited directly on the substrate, Nb was deposited on Cu. The samples were then introduced to the UHV STM chamber and cleaved in-situ. The structural analysis showed that, upon cleavage, the samples break at Cu-SiO_2 interface, thus exposing fresh Cu surface.
The presence of the proximity effect at the surface of Cu was first evidenced by observation of a proximity gap in the tunneling conductance spectra dI(V)/dV, in clear relation to the value of the superconducting gap of bulk Nb. The evolution of the proximity spectra with temperature was also studied in the range (0.3-4.2) K (Fig. e). Upon application of an external magnetic field, spatial variations of the tunneling conductance spectra were observed (see Fig. a,b,c). These variations appear in the detailed STS maps as round nm-size spots, in the centers of which the proximity gap vanishes. The density of spots rises continuously with magnetic field; it corresponds

perfectly to the expected density of Abrikosov vortices in Nb. We identify the observed spots as proximity induced vortices in the normal Cu. On the basis of our STS data, we have determined the size and shape of the proximity vortex cores, and evaluated the coherence length in Cu. Independent numerical calculations of the quasiparticle spectra in S-N hybrids within the Usadel equation formalism were performed and found in agreement with experimental findings.

a-c) STS tunneling conductance maps acquired at 0.3K on Cu-surface of Cu/Nb (50/100nm) at different values of the magnetic field: a) B = 0.005 mT. b) B = 0.05 mT. c) B = 0.1 mT. d) Typical topographic STM image of the sample surface; the green line shows the location where the cross-section plotted on the bottom graph was acquired. e)Temperature dependence of the tunneling conductance spectra at zero-field.

NST-P3-04
XPS study of aqueous oxidation of Ag nanoparticles: a crucial role of oxygen dissolved in silver lattice

T10 Nanoscience and Technology

#NST-P3-04

E. Vishnyakova [1], A. Romanchenko [1], S. Saikova [2], M. Likhatski [1], Y. Mikhlin [1].

[1]Institute of chemistry and chemical technology - Krasnoyarsk (Russian federation), [2]Siberian Federal University - Krasnoyarsk (Russian federation).

The properties of silver nanoparticles, which determine many of their applications and dramatically depend on the synthetic protocols, particle size and shape, stabilizing agents, support, and so on, are widely explored at the solid-gas interface but are poorly understood for the nanoparticles contacting aqueous solution. We have studied the electrochemical reactions and antibacterial activity of “bare” silver nanoparticles (5 nm and 15 nm) obtained via wet chemical reduction with sodium borohydride, and Ag NPs with stabilizing adlayers produced with glucose or sodium borohydride in presence of sodium citrate. It was found using X-ray photoelectron spectroscopy (XPS) and cyclic voltammetry that small “bare” Ag NPs immobilized on highly oriented pyrolytic graphite (HOPG) completely oxidized to silver oxides in the positive-going potential sweep in 1 M NaOH, while only surface layers of the larger particles transformed to oxide phases. Ag NPs prepared with L-glucose and sodium borohydride in presence of sodium citrate were surprisingly resistant to oxidation, including the anodic polarization in alkaline solutions and oxidation in air. We found a direct correlation between affinity of Ag NPs to oxidation and the content of oxygen exhibiting O 1s line at 530.8 eV (Fig.1) that is commonly associated with an oxygen species incorporated in silver lattice (O_β) [1]. There are evidences that the formation of O_β is a necessary stage preceding oxidation of Ag to Ag_2O.

O_β is expected to diffuse over a shell of the big Ag NPs but the whole smaller particles, determining their reactivity. Glucose and citrate ions, however, react with O_β species or their precursors preventing penetration of O_β both into small (~4 nm, according to SAXS and TEM) and large (~9 nm) Ag cores, making them oxidation-

resistive. The effect of oxygen on the antibacterial activity of the Ag NPs is less clear, probably because the organic ligands promote silver dissolution.

[1] T. C. R. Rocha, A. Oestereich, D. V. Demidov, M. Hävecker, S. Zafeiratos, G. Weinberg, V. I. Bukhtiyarov, A. Knop-Gericke, R. Schlögl, Phys. Chem. Chem. Phys., 2012, 14, 4554–4564

Fig. 1. Photoelectron O 1s spectra from silver nanoparticles produced using the molar ratios (a) $Ag^{+}/NaBH_4$ = 10, (b) $Ag^{+}/NaBH_4$/cit = 3:1:3 freshly immobilized on HOPG (1), after 24 h in air (2), and anodized to +0.7 V (vs Ag/AgCl) in 1 M NaOH (3).

NST-P2-15
Core-shell silicon/carbon nanoparticle synthesis by laser pyrolysis, application to anode materials for lithium-ion batteries.

T10 Nanoscience and Technology

#NST-P2-15

J. Sourice [1], A. Quinsac [1], Y. Leconte [1], O. Sublemontier [1], S. Jouanneau [2], N. Herlin [1], W. Porcher [2], C. Reynaud [1].

[1]CEA Saclay DSM/IRAMIS/SPAM/LFP, bât 522 - Gif Sur Yvette (France), [2]CEA Grenoble DRT/LITEN/DEHT/LCPB, bât C2 - Grenoble (France).

Lithium Ion Batteries (LIBs) are now widely used in portable equipments such as cell phones, computers and in recent automotive, including hybrid and electric vehicles, because of their high energy densities and flexible design [1]. However graphite, often used commercial anode, is reaching a limit and cannot meet the increasing energy density requirements due to a limited theoretical capacity (372 $mA.h.^{-1}$) [2]. Nanometric silicon is a promising anode material for LIBs and offers one of the highest theoretical capacity (up to 4200 $mA.h.g^{-1}$) and a low discharge potential relative to Li^+/Li (below 0.5V) [3]. Yet large volume change in silicon (300 %) during lithiation and delithiation process induces poor cycle stability and rapid capacity fading. Moreover, electrical percolation must be ensured into the silicon electrode.

By reducing the particle size to nanometric level, the effect of volume change may be controlled which improves the performance of the electrode in terms of both life and rate capability. Furthermore, silicon materials in a matrix of carbon attract great interest because of the good electrical conductivity and stress-buffer nature of the carbon. The laser pyrolysis appears to be an ideal tool using gaseous precursors as silane and ethylene. A two stages reactor has been developed to allow the one-step production of nanosized core-shell particles: the nanometric silicon is synthetized at the first stage and the carbon coating at the second stage. The process allows a control on the morphology and growth of the silicon core and the carbon shell by adjusting parameters such as the precursors flow, the reactor pressure and the laser

power. The first results show an increase in both life and rate capability of LIBs thanks to the carbon shell (no degradation after 350 cycles at 1000 $mA.h.g^{-1}$).

[1] : J.M. Tarascon et al, Nature 414 (2001)
[2] : Y.P. Wu et al, J. of Power Sources 114 (2003)
[3] : Bruno Scrosati et al, Energy Environ. Sci. 4 (2011)

fig 1 : Double stage reactor

fig 2 : TEM image of a Si@C nanoparticle

NST-P2-16
Characterization and photocatalytic application of TiO2 nanoparticles synthesized by laser pyrolysis

T10 Nanoscience and Technology

#NST-P2-16

S. Bouhadoun [1], N. Herlin-Boime [1], A.M. Jimenez Romero [1], C. Guillard [2], A. Habert [3].

[1]Cea Saclay - Saclay (France), [2]IRCELYON - Lyon (France), [3]Cea Sacaly - Sacaly (France).

Owing to their high stability, nontoxicity and optical properties, titanium dioxide (TiO2) nanoparticles attract a great interest since several years for applications such as self-cleaning windows, anti-bacterial coating and waste water purification[1,2]. These photocatalytic applications require photocatalysts with high efficiency. To enhance it, metallic ions such as Au can be added to TiO2. In fact, gold nanoparticles supported in titania improve photocatalytic electron transfer thanks to their absorption under visible light irradiation. This is attributed to the surface plasmon resonance[3]. Photocatalysis mechanism is the following; under UV-Visible illumination, an electron-hole (e-/h+) pair is created. These electron-hole pairs can then recombine and are lost or be separated which is the efficient way to induce reactions. Holes in the valence band are strong oxidants and the electrons of the conduction band a strong reducing agents. The organic pollutant are oxidized either directly through the holes h+, or indirectly by oxidizing agents (radicals) O2. - / HO2. generated by the oxidation of water.

Laser pyrolysis[4] appear as a convenient way to prepare various nanoparticles (NPs).This versatile method is used for efficient production of nanoparticles with precise chemical composition, size, cristallinity,... It is based on the interaction of an infrared high power (IR) laser beam with precursors. For TiO2 synthesis, titanium tetraisopropoxide (TTIP) is used as precursor. It is decomposed in an incandescent flame observed in the laser-precursor interaction zone where NPs nucleate and grow. Their characteristics are really correlated with experimental parameters; in particular the size of the nanoparticles which depends on the residence time in the laser beam controlled by the gas flow rate of reactants. The cristallinity can be

controlled by the reaction temperature in the reaction zone controlled by the laser power. Their chemical composition also depends on the nature of the different reagent in the precursor mixture. In this context, gold or silver precursors were dissolved in the liquid titanium precursor, and droplets of the mixture were carried to the laser using the pyrosol method. We obtained TiO2 nanocomposite containing gold or silver (Fig.1). They were tested in decomposition of methylene blue, phenol and formic acid. First results are presented there.

1- Fujishima A, Honda K. *Nature* (London) 1972;**238**.
2- Chen X, Mao SS. *Chem Rev* 2007;**107.**
3- Fang. J, Cao. S, Wang. Z. *J of hydrogen energy* 2012;**37**.
4- Maskrot. H, Leconte. Y, Herlin-Boime. N. *Catalysis today;*2006;**116.**

TEM image of Au modified TiO2

NST-13-In-1
Nanotechnologies for high efficiency photovoltaic conversion: visions and realizations

T10 Nanoscience and Technology

#NST-13-In-1

D. Guillemoles.

IRDEP, CNRS-EDF-ENSCP - Paris (France).

NST-9-Or-7
Prediction of dimerization enhancement inside dilute alloy nanoparticles induced by the nano-confinement entropic effect

T10 Nanoscience and Technology

#NST-9-Or-7

L. Rubinovich, M. Polak.

Ben-Gurion University - Beer-Sheva (Israel).

Recently, we predicted a unique nano-confinement effect of entropic origin on the equilibrium state of chemical reactions, NCECE [1]. Thus, when a small number of exothermally reacting molecules is confined to a closed nano-space the extent of the equilibrated reaction can shift significantly towards product formation. The greatly enhanced “equilibrium constant” depends on the number of molecules, and for many reactions also on the nano-space size. Then, we demonstrated qualitatively how the effect is manifested in nucleotide dimerization observed previously within molecular cages, and in the extra deuteration commonly observed for molecules reacting on interstellar dust grain surfaces [2]. In the present work we explore the validity of the NCECE in case of reactions involving alloy nanoparticles (NPs) with separation tendency, especially dilute Pd-Ir cuboctahedra (CO). Due to the Pd strong surface segregation tendency in this alloy, Ir atoms are confined exclusively to the particle core, which thus can serve as a nano-space for their possible dimerization. Employing two models for the system energetics (with and without near-surface bond-energy variations [3]), computations of the exact canonical partition function reveal remarkable nano-confinement induced Ir-Ir dimer stabilization within the NPs, reflected, e.g., by doubling of the *logK* vs. *1/T* slope, as compared to the macroscopic thermodynamic limit (TL, Fig. 1). The presentation will be concluded by a brief discussion of the entropic origin of the NCECE effect and introduction of its first quantitative verification based on new analysis of nanoconfined-DNA dimerization data.

[1] Micha Polak, Leonid Rubinovich, Nano Letters, 8, 3543 (2008).
[2] Micha Polak, Leonid Rubinovich, Phys. Chem. Chem. Phys. 13, 16728 (2011).
[3] Leonid Rubinovich, Micha Polak, Phys. Rev. B 80, 045404 (2009).

Fig.1. The NCECE manifested in Ir dimerization inside various size Pd-Ir CO NPs (55,147, 309,561,923,1415 atoms). The enhancement of K relative to the TL increases for smaller NPs (nanospace effect).

NST-9-Or-8
Prediction of size-dependent intra- and inter-particle separation-like phase transitions in nanoalloys: a basis for nanophase diagrams

T10 Nanoscience and Technology

#NST-9-Or-8

M. Polak, L. Rubinovich.

Ben-Gurion University - Beer-Sheva (Israel).

The temperature dependence of site-specific concentrations in equilibrated Pd-Ir cuboctahedron (CO) and truncated octahedron (TO) nanoparticles (NPs) consisting of up to ~1000 atoms is computed by the recently introduced approach for deriving DFT-based coordination dependence of bond-energy variations (CBEV) [1] combined with the highly efficient statistical-mechanical free-energy concentration expansion method (FCEM) [2]. The results reveal sharp intra-core separation-like nanophase transitions (first reported by us for Pt-Ir [3]) from a core-shell structure at low temperatures to almost solid-solution like “phase” at higher temperatures (Fig.1). The transitions, exhibiting critical temperatures significantly lower than the corresponding alloy bulk ones, depend on the NP size and composition (no sharp intra-core transitions were obtained for 309-atom and smaller NPs). Furthermore, convexities in the low-temperature mixing free-energy curves indicate a tendency for inter-particle separation into two equilibrated systems of NPs having different overall compositions and chemical order, which transform at a critical temperature to a uniform system of solid-solution like NPs. The relationship between the two types of separation transitions as well as the role played by preferential strengthening of surface-subsurface inter-layer elemental bonds are elucidated. As demontrated in Fig.2, the results enabled us to construct for the nanoalloy original intra-particle as well as inter-particle (partial) phase-diagrams.

[1] L. Rubinovich, M. Polak, Phys. Rev. B 80, 045404, (2009).
[2] M. Polak and L. Rubinovich, Surf. Sci. Rep. 38, 127, (2000).
[3] H. Tigger, L. Rubinovich, M. Polak, J. Phys. Chem. C, 116, 26000 (2012).

Fig.1. Phase separation transition inside $Pd_{868}Ir_{55}$ cuboctahedron, as reflected by variations in site-specific inner-core concentrations.

Fig.2. Pd-Ir inter-particle separation-like phase diagram. The miscibility increases with decreased nanoparticle size.

NST-2-Or-8
Surfaces nanostructured locally by atmospheric pressure micro-plasma and micro afterglow

T10 Nanoscience and Technology

#NST-2-Or-8

A. Altaweel [1], D. Kuete Saa1 [1], R. Cardoso [2], T. Gries [1], S. Laminsi [3], T. Belmonte [1].

[1]institut jean lamour - Nancy (France), [2]Universidade Federal do Paraná - Curitiba (Brazil), [3]Université de Yaoundé - Yaoundé (Cameroon).

Recently, atmospheric pressure plasma assisted nanofabrication has shown outstanding capability of promoting self-organization. Plasma-assisted nanofabrication is one of the rapidly emerging methods used for the production of various nanostructured materials and elements of nanodevices. Moreover, nanostructured materials have attracted growing attention due to their unique properties and potential applications.

The possibility to synthesise directly copper oxide nanomaterials with different morphologies has been studied by local oxidation with atmospheric plasma and with atmospheric afterglow. These approaches consist in exposing copper samples in a single treatment step, leading to the synthesis of nanowires, nanowalls, nanoparticles ... with a high level of reproducibility (figure 1).

In this work, we compare results obtained by an Ar – O_2 micro-plasma jet and by an Ar – O_2 micro-afterglow at atmospheric pressure. Their specificities are discussed in detail. This step is followed by a discussion on the role of charge species, temperature and stress on the growth mechanism of nanostructures at atmospheric pressure. Several techniques have been used to analyse the grown structures including Scanning Electron Microscopy, X-Ray Diffraction, Transmission Electron Microscopy and X-ray Photoelectron Spectroscopy.

***Fig. 1**: SEM image of as-synthesized copper oxide nanowires (left) and nanoparticles (right).*

NST-P3-05
Decoration of atomic steps on NaCl(001) cleavage face during deposition of preformed Ag clusters

T10 Nanoscience and Technology

#NST-P3-05

S. Nepijko [1], D. Kostyuk [2], S. Protsenko [2], W. Schulze [3], G. Schönhense [1].

[1]Institute of Physics, University of Mainz - Mainz (Germany), [2]Sumy State University - Sumy (Ukraine), [3]Fritz Haber Institute of the Max Planck Society - Berlin (Germany).

Ag clusters obtained by the gas-aggregation technique were deposited on the cleavage face NaCl(001). The average size of the nanoparticles was varied in the range from 0.2 to 10 nm and the temperature was varied from room temperature to 470 K. Owing to the mobility of the clusters on the substrate, they coalesced with formation of larger particles, decorating atomic cleavage steps on NaCl(001) already at room temperature. It was shown that the step decoration is possible only when the average size of the deposited clusters is commensurate with the height of the cleavage steps.

NST/SS-P1-04
role of carbon nanotubes in AC-driven CNT-OLEDs

T10 Nanoscience and Technology

#NST/SS-P1-04

S. Yu [1], S.Y. Jun [1], B. Won [2].

[1]Hankuk Univ. of Foreign Studies - Yongin (Korea, republic of),
[2]Syungkyunkwan Univ. - Suwon (Korea, republic of).

Organic light emitting devices (OLEDs) have been widely investigated these days. There have been numbersous researches such as, by modifying the structures of devices, synthesizing new organic materials, and combining zero-, one-, and/or two-dimensional nanostructures. [1] Carbnon nanotubes (CNTs), a key material in carbon based nanomaterials, [2] have been examined in organic devices widely. In spite of the fact that the device performaces of CNT-organic composite were improved, there have been few remarks on the current [1]. This was caused by the network formation by CNTs which might easily lead to leakage current. Therefore, controlling the properties of CNTs is an important step to reduce the level of the leakage current.

The devices used in this poster were consisted of four layers--a top metal electrode, a dielectric layer, an emitting layer where CNTs were mixed, and a bottom indium tin oxide (ITO) electrode. Cyanoethyl pullulan (CRS), as a dielectric material, was coated on the ITO-coated glass. poly[2-methoxy-5-(2-ethylhexyloxy)-1,4-phenylenevinylene] (MEH-PPV) was used as an emitting material. CNTs were shortened by the mechanical method. [3] CNTs were mixed with MEH-PPV to be a CNT-polymer composite by varing the CNT concentration (0.03, 0.06, and 0.15wt%). A reference sample (an OLED without CNTs) was fabricated for comparison.

The brightness of the CNT-OLEDs was higher than the reference one. The turn-on of CNT-OLEDs were found to be around 20~30 V, which was obtained by reducting the current roughly 50%, especially for 0.03wt% case. (The data are not shown here.) The enhancement in the brightness of CNT-OLEDs shown in Fig. 1 could be explained by the microcapator effects. [4] This effect might increase the total impedance of devices by addition of capacitivJue reactance originated from numberous CNTs within the emitting layer. Due to AC driving, the capacitive reactance might contribute to the total impedance of the devices. Impedance analysis

was currently under progress and the results will be also presented at the conference.

1. J. Sung, Y. S. Choi, S. J. Kang, S. H. Cho, T.-W. Lee, and C. Park, Nano Lett. 11, 966-972 (2011).
2. S. Iijima, Nature 354, 56-58 (1991).
3. J. H. Lee et al., Carbon 44, 2984-1989 (2006).
4. Z.-M. Dang, L. Wang, Y. Yin, Q. Zhang, and Q.-Q. Lei, Adv. Mater. 19, 852-857 (2007).

Brightness curves for CNT-OLEDs at 10 kHz.

NST-P3-06
Silver and gold nanoparticles for magnetic hyperthermia

T10 Nanoscience and Technology

#NST-P3-06

J. Ghaymouni [1], B. Cagneau [1], S. Topsu [1], L. Chassagne [1], Y. Alayli [1], A.H. Rayas [2], T. Cordova-Fraga [2].

[1]Laboratoire d'Ingénierie des Systèmes de Versailles. Université de Versailles - Saint Quentin (France), [2]División de Ciencias e Ingenierías. Universidad de Guanajuato - Campus León Mexico (Mexico).

Cancer treatments imply the destruction of tumor cells. Traditional methods such as chemotherapy or radiotherapy [1] are actually widely used. However, these methods suffer from several drawbacks. These treatments are usually not specific to tumor cells and may also affect healthy cells. Consequently, they can subsequently increase postoperative delays. Therefore, researchers are working on alternative treatments to improve the patient's recovery.
Magnetic hyperthermia is a biomedical process that relies on external magnetic fields [2]. The aim is to increase the temperature of tumor cells in order to stop their development and to destroy them. In this work, we provide our first in-vitro results with silver nanoparticles. The main objective is the validation of the process (fig. 1) to obtain such nanoparticles (fig. 2) and to measure the thermal effects when particles are exposed to a specific magnetic field. Silver nanoparticles are a good candidate because of their toxicity in regard to the synthesis of ATP [3] of tumor cells. Experimental results are provided to demonstrate that the temperature of the silver nanoparticles reaches 33-35 Celsius degrees, which seems compatible with a biological application. The magnetic field is about 15mT with a frequency of 206kHz.

[1] A.S. Dhadda, P. Dickinson, A.M. Zaitoun, N. Gandhi, E.M. Bessell " Prognostic importance of Mandard tumour regression grade following pre-operative chemo/radiotherapy for locally advanced rectal cancer " European journal of cancer 47 (2011) 1138 –1145.
[2] M. E. Cano, A. Barrera, J. C. Estrada, A. Hernandez, and T. Cordova, An induction heater device for studies of magnetic hyperthermia and specific absorption ratio measurements, Rev. Sci. Instrum. 82, 114904 (2011).

[3] AshaRani PV, Low Kah Mun G, Hande MP and Valiyaveettil S. Cytotoxicity and genotoxicity of silver nanoparticles in human cells. ACS Nano 2009, 3: 279–290.

NST-3-Or-2
Exploring what holds paper together: An AFM based nanomechanical investigation of single cellulose fibers and fiber-fiber bonds

T10 Nanoscience and Technology

#NST-3-Or-2

C. Teichert [1], C. Ganser [1], F.J. Schmied [1], W. Fischer [2], U. Hirn [2], R. Schennach [2].

[1]University of Leoben - Leoben (Austria), [2]Graz University of Technology - Graz (Austria).

Although paper is already known for hundreds of years, the process of bonding two cellulose fibers together is still an open discussion. However, the strength of these bonds is what primarily determines paper strength.
Here, we employ a recently developed method based on conventional atomic force microscopy (AFM) technique to measure the joint strength in z-direction between individaul cellulose fibers [1]. Besides this single quantity, the behavior prior to the failure is analyzed in force vs. distance plots. Further, the fracture surface is recorded by conventional AFM scanning and its morphology is correlated to the breaking behavior. This comprehensive combination reveals new insights into the mechanisms of fiber-fiber bonding and their contribution to the fiber-fiber bond. Clear indications for mechanical interlocks or fibril bridges acting as interlocking elements between the individual fibers are recognized. With this technique the influence of fiber treatment is explored. Fiber-fiber bonds – made from differently beaten pulp - are investigated. Also, fiber-fiber bonds – established from regenerated fibers – are tested to obtain data from more defined surface structures and simpler chemical composition. Dynamically loading of the bond allowed the estimation of elastic energy contributions into the single fiber-fiber bond. Further, statically loading is suitable to study time dependent behavior, such as creep and relaxation in the fiber-fiber bond system as well as the determination of the visco-elastic energy contribution.
Since knowledge on the mechanical properties of pulp fibers in the wet state – when a fiber-fiber bond is formed – is an important factor for understanding the bonding mechanisms in paper, we also employed AFM based nanoindentation to measure

the change in transversal hardness and modulus of pulp fibers under controlled relative humidity as well as in the fully wet state. Hardness and modulus are calculated from the force-vs.-distance curves by employing evaluation procedures developed for classical nanoindentation. We could clearly show a reduction in hardness and modulus with increasing humidity. However, both parameters are reduced even more if the fiber is completely wet. Compared to the dried state (about 5% relative humidity), hardness is decreased almost by a factor of 100 in the wet state. These data serve as important input to simulate the area in molecular contact between two pulp fibers during the drying process [2].

Supported by Mondi and the Christian Doppler Research Society, Vienna, Austria.

[1] F.J. Schmied, C. Teichert, L. Kappel, U. Hirn and R. Schennach, "Joint strength measurements of individual fiber-fiber bonds: An atomic force microscopy based method", Rev. Sci. Instrum. **83**, 073902 (2012).
[2] B.N.J. Persson, C. Ganser, F. Schmied, C. Teichert, R. Schennach, E. Gilli, U. Hirn, "Adhesion of cellulose fibers in paper", J. Phys. Condens. Mat. **25**, 045002(2013).

NST-P3-15
Electronic properties of core shell Ag@Au and Au@Ag nanoparticles

T10 Nanoscience and Technology

#NST-P3-15

A. Ferraz.

IFUSP - São Paulo (Brazil).

Electronic properties of core shell Ag@Au and Au@Ag nanoparticles

A. C. Ferraz1, F. D. Kiss2, and R. Miotto3
1IFUSP, Caixa Postal 66318, CEP 05315-970, São Paulo, SP, Brazil; 2UNILA, Av. Tancredo Neves 6731, CEP 85856-970, Foz do Iguaçu, PR, Brazil; 3CCNH-UFABC, Rua Santa Adélia 166, CEP 09210-170, Santo André,SP, Brazil;

Core shell and alloy bimetallic nanoparticles (NPs) are atracting a great deal of attention, since they provide opportunities to tune the NPs' optical catalytic properties and are potentially useful as taggants for security applications [1]. The AuAg system is of particular interest since the Surface Plasmon Ressonance (SPR) band might be tunable between ~520 nm for Au and ~410 nm for Ag [1]. These interesting physicochemical properties appear because of the combination of two kinds of metals and their fine structures, evolving new surface characteristics. With a view to contribute to a better understanding of the surface properties of these complex systems, in this work we explore the atomic, electronic and dynamical properties of Au@Ag and Ag@Au core shell NPs. Cube-octahedral NPs are modeled in the supercell scheme, following the procedure described in Ref. [2]. In the following, NPs with 147, 309, 561 and 923 atoms, corresponding to 1.7, 2.3, 2.9 and 3.5 nm, are indicated their number of atoms for simplicity. The simulations are carried out using the Vienna Ab-initio Simulation Package (VASP) [3], as previously detailed in Refs. [2,4]. Our total energy calculations suggest that the addition of a single shell layer estabilizes the system, i.e. the formation energy for a core NP with a single shell layer is smaller than the formation energy of the monometalic NP. This estabilization is more pronounced for Ag@Au NPs, where de decreases in the formation energy of almost 10% are obtained. When the shell thickness increases, the electronic properties of the system approaches the electronic properties of the monometalic

NP. It is also observed that a single shell layer is capable to decisevely modify the DOS, as a mixture of both monometallic NPs DOS is seen. In addition, the influence of long range (van der Waals) interactions in the core shell electronic structure and atomic properties is also discussed.

The authors acknowledgement financial support from CNPq and FAPESP (Brazil).
Electronic properties of core shell Ag@Au and Au@Ag nanoparticles

[1] M. S. Shore et al., Small 7, 230 (2011).
[2] F. D. Kiss et al., Nanotec. 22, 275708 (2011).
[3] G. Kresse and J. Furthmüller, Comp. Mat. Science 6, 15 (1996).
[4] R. Miotto et al., Nanotec. 23, 485202 (2012).

NST-P2-17
Influence of electrochemical dissolution valence on silicon nanocrystallite dimensions in anodically prepared p and p++ porous silicon

T10 Nanoscience and Technology

#NST-P2-17

V. Đerek [1], R. Baltić [1], M. Marciuš [2], M. Ivanda [1].

[1]Ruđer Bošković Institute, Division of Materials Physics - Zagreb (Croatia),
[2]Ruđer Bošković Institute, Division of Materials Chemistry - Zagreb (Croatia).

Macro and meso-porous silicon (PSi) samples were prepared by electrochemical anodisation of boron low p-doped (10 Ωcm < ρ < 23 Ωcm) and highly p^{++} -doped (ρ ≤ 0.007 Ωcm) silicon wafers in aqueous/ethanoic 20% w/w HF electrolyte under galvanostatic conditions. Anodistion time and current were varied in order to obtain different PSi morphologies. Electrochemical dissolution valence *n* was calculated from electrical measurements during the anodisation and gravimetric measurements before and after anodisations, indicating whether the sample was prepared in silicon dissolution and PSi-producing regime ($n \approx 2$) or in Si electropolishing regime ($n \approx 4$). Samples were characterized by SEM, photoluminescence (PL) spectroscopy and Raman spectroscopy. Samples prepared on low p-doped substrates were macro-porous (Fig 1), showed visible photoluminescence and no observable phonon confinement in Raman spectrum. Porous silicon prepared on highly-p^{++} doped substrates was mesoporous (Fig 2), showed no observable photoluminescence and intense phonon confinement was observed in Raman spectra. Silicon nanocrystalite dimensions in PSi samples were obtained from photoluminescence [1] and phonon confinement models [2]. Nanocrystalite sizes were correlated with electrochemical dissolution valence *n*, showing decrease in crystallite dimensions for increasing n in highly doped (p^{++}) samples as expected, and increase in crystallite dimensions for increasing *n* in low-doped (p) samples. This seemingly contradictory behavior is discussed, taking into consideration the competing surface effects and quantum-confinement processes responsible for visible s-band photoluminescence from porous silicon.

1.) G. Ledoux , J. Gong, F. Huisken, O. Guillois, C. Reynaud, Appl. Phys. Lett. 90, 4834 (2002).
2.) J. Zi, H. Büscher, C. Falter, W. Ludwig, K. Zhang, X. Xie, Appl. Phys. Lett. 69, 200 (1996).

Fig. 1 – SEM of PSi sample prepared on low p-doped substrate
Fig. 2 – SEM of PSi sample prepared on highy p++-doped substrate

NST-10-Or-3
Solid-state linear visctoelastic properties of a nanocomposite C30B/PA12 and their relations with nanostructure

T10 Nanoscience and Technology

#NST-10-Or-3

H. Hassan [1], N. Aït Hocine [2], P. Médéric [3], M.P. Deffarges [1].

[1]LMR, CERMEL, Université François Rabelais de Tours, 29 rue des Martyres - 37300 Joué-Lès-Tours (France), [2]LMR, CERMEL, Ecole Nationale d'Ingénieurs du Val de Loire, Rue de la chocolaterie - 41034 Blois (France), [3]LLIMATB, Equipe de Rhéologie, Université de Bretagne Occidentale 6 Avenue Le Gorgeu - 29238 Brest (France).

In this study, organically modified montmorillonite (OMMT) / polyamide-12 (PA12) nanocomposites were prepared by melt compounding technique. The PA12 matrix is a commercial product, referenced as Rilsan® AECHVO, supplied by ARKEMA Company (Serquigny, France). The OMMT used as a reinforcement, is referenced as Cloisite® C30B and supplied by Southern Clay Products (Gonzales, Texas, USA).

The composite materials structure was characterized by XRD, TEM and SEM techniques. These structural techniques have clearly revealed a nanocomposite structure, with an exfoliation degree dependent on processing conditions (blade rotational speed). These observations are consistent with melt state rheological measurements highlighting, moreover, that above the OMMT mass fraction threshold of ~2%, the studied nanocomposites present a three-dimensional percolated network structure.

Thermal properties were analyzed by DSC technique and the results showed that the melting point and the crystallinity rate of nanocomposites are not, or slightly, affected by the presence of C30B nanofillers. Consequently, solid state viscoelastic properties were discussed in terms of clay structure.
Dynamical tests were carried out by using a VA4000 Dynamic Mechanical Thermal Analysis (DMTA) machine and the solid state viscoelastic properties of the

nanocomposites were analyzed as a function of clay mass fraction, strain, frequency and temperature. The storage modulus, E', of the different nanocomposites, in glassy state and even in rubbery state, increases with increasing clay mass fraction, independently of strain level and frequency value. The glass transition temperature also increases with increasing clay content, whereas the peak of the loss angle tangent (tan δ) decreases.

Moreover, at room temperature, the reinforcing effect of the structure is showed, i.e. the composite modulus E' increases continuously with increasing frequency. The loss modulus E'' also increases, on the one hand, with adding nanoclay and, on the other hand, with strain increasing. However, this parameter decreases when the frequency growths, whichever clay mass fraction.

Blade rotational speed affects the storage modulus of nanocomposites presenting a three-dimensional percolated network structure: the most exfoliated nanocomposite has the highest storage modulus.

Effect of ageing on solid state properties was also evaluated. Results showed that in the linear behavior region, the aged nanocomposite storage modulus value is less than the unaged one. This degradation seems to be significantly limited with reinforcing clay mass fraction increasing.

NST/SS-P1-05
Computational and Experimental Study of Metal- and Polymer-Few Layer Graphene Composites Induced by Radiation Defects

T10 Nanoscience and Technology

#NST/SS-P1-05

A. Ilyin [1], M. Assubayeva [2].

[1]Nanolab Kazakh National University - Almaty (Kazakhstan), [2]National Nanotechnological Laboratory Open Type - Almaty (Kazakhstan).

Computational and Experimental Study of Metal- and Polymer-Few Layer Graphene Composites Induced by Radiation Defects

A.M.Ilyin, N.R.Guseinov, R.R.Nemkaeva, V.V.Kudrjashov,M.A.Asubaeva
National Nanolab, Kazakh National University, Almaty, Kazakhstan

This work presents some results of computer simulation and experimental study of light metal- and polymer-few layer graphene compositions induced by radiation defects, in particular by bridge-like radiation defects [1]. A possible physical mechanism of modification of carbon nanostructures which are used as reinforcement elements for composite materials is supposed. Results presented show that radiation modification with production of bridge-like defects can become an effective technological tool by production of composite materials, based on light metals or polymers reinforced by carbon nanostructures.

A.M.Ilyin. Computer Simulation of Radiation Defects in Graphene and Relative Structures. In: “Graphene Simulation”; Gong, J.R.;Ed.;InTech: Rijeka , CR, 2011, pp 39-52.

NST/SS-3-Or-1
In Situ Scanning Tunneling Spectroscopy of the Proximity Effect in a Disordered Two-Dimensional Metal

T10 Nanoscience and Technology

#NST/SS-3-Or-1

L. Serrier-Garcia [1], J.C. Cuevas [2], T. Cren [1], C. Brun [1], V. Cerchez [1], F. Debontridder [1], D. Fokin [1], F.S. Bergeret [2], D. Roditchev [1].

[1]Institut des Nanosciences de Paris - Paris (France), [2]Departamento de Fisica Teorica de la Materia Condensada - Madrid (Spain).

The superconducting proximity effect was revealed in a Scanning Tunneling Spectroscopy experiment on in-situ elaborated Pb/undoped Si(111) network, consisting of superconducting single crystalline Pb islands interconnected by a non-superconducting atomically thin disordered Pb wetting layer. In the vicinity of each superconducting island the wetting layer acquires specific tunnelling characteristics which reflect the interplay between the proximity-induced superconductivity and the inherent electron correlations of this ultimate diffusive two-dimensional metal. The observed spatial evolution of the tunneling spectra was accounted for theoretically by combining the Usadel equations with the theory of dynamical Coulomb blockade. The relevant length and energy scales were extracted and found in agreement with independent experimental data.

NST-9-Or-9
Enhanced Oxidation at the Nanoscale – Effects of Particle Size and Interfaces to Other Materials

T10 Nanoscience and Technology

#NST-9-Or-9

E. Sutter, P. Sutter.

Brookhaven National Laboratory - Upton, New York (United states).

When materials are shrunk to the nanoscale they often show behavior and properties that are not simply scaled down bulk properties but are distinctly different. For example, we demonstrated that nanoscale liquid drops crystallize differently from bulk materials [1], and that nanoparticles show dramatically enhanced solute solubility [2,3]. Here, we study oxidation to probe size-effects and the influence of interfaces on the chemical conversion of metal nanoparticles.

Using *in-situ* transmission electron microscopy we investigated the low-temperature growth kinetics during oxidation of In nanoparticles to In_2O_3. Semiconducting In_2O_3 has widespread applications as transparent conductor in solar cells, light emitting diodes, and displays, due to its high optical transparency paired with good electrical conductivity, and is a promising photocatalyst for visible light water splitting.

Our experiments on arrays of In nanoparticles directly demonstrate for the first time the implications of size and curvature on the oxidation process by showing an accelerated oxidation of nanoscale particles with high curvature (Figure 1, [4]). To investigate the effects of nanoscale interfaces on oxidation, we considered In particles at the tips of Si nanowires. This experimental geometry allowed us to evaluate, under identical conditions, both the oxidation of In at the solid-gas interface and the oxidation in the vicinity of a well-defined nanoscale contact to the adjacent Si NW. The direct comparison of the two modes of In oxidation showed a more than tenfold increase of the limiting In_2O_3 thickness at the nanoscale epitaxial interface with Si demonstrating that the limiting thickness in room–temperature oxidation can be overcome by incorporating a nanoscale junction to a different material [5]. Our results demonstrate modifications of oxidation processes at the nanoscale, which need to be taken into account in processes that use oxidation, e.g., in the processing of nano-electronic devices or catalytic reactions.

[1] P. Sutter and E. Sutter, Nature Materials 6, 363 (2007).
[2] E. Sutter and P. Sutter, Nano Lett. 8, 411 (2008).
[3] E. Sutter and P. Sutter, J. Mater. Sci. 46, 7090 (2011).
[4] E. Sutter and P. Sutter, J. Phys. Chem. C 116, 20574 (2012).
[5] E. Sutter and P. Sutter, Appl. Phys. Lett. 100, 231602 (2012).

Figure 1: (a) In-In_2O_3 core-shell particle formed during oxidation of In nanoparticles. (b) Dependence of the In_2O_3 thickness on nanoparticle size for room temperature oxidation determined from TEM measurements (orange squares) and calculated using a modified, size-dependent Mott-Cabrera model (grey line).

NST-P3-18
Determination of local dye concentration in silica and methylated silica nanolayers.

T10 Nanoscience and Technology

#NST-P3-18

P. Bojarski [1], A. Synak [1], B. Grobelna [2], L. Kułak [3].

[1]Institute of Experimental Physics, University of Gdansk - Gdansk (Poland), [2]Faculty of Chemistry, University of Gdansk - Gdansk (Poland), [3]Department of Technical Physics and Applied Mathematics, Technical University of Gdansk - Gdansk (Poland).

Hybrid strongly luminescent materials have been drawing a lot of attention recently due to their numerous applications in multidisciplinary science like physical chemistry, nanomaterials or nanomedicine [1,2]. A common problem which in quantitative description of the properties of such materials is the determination of local mean concentration of fluorophores in the porous inorganic matrix. Concentration is a decisive factor of many physical and chemical processes occurring in various matrices, optical materials and optoelectronic devices.
We propose the method of determination of local dye concentration in nanoporous matrix based on the donor – acceptor energy transfer. The method was tested for Rhodamine 110- Rhodamine 101 system in a silica and methylated silica nanolayers. Evaluation of acceptor (Rhodamine 101) local concentration was carried out by comparing the results of Monte-Carlo simulation of energy transfer from donor (Rhodamine 110) to acceptor (Rhodamine 101) with the experimental data of donor fluorescence decay and other luminescent characteristics in which concentration was treated as a best fit parameter. The obtained values of acceptor local concentration occurred about ten times higher than the mean bulk concentration.

This research has been supported by the grant NCN 2011/03/B/ST5/03094 (P.Bojarski, B.Grobelna) and BW-538-5200-0980-12 (A.Synak).

[1] K. Binnemans, Chemical Reviews 2009, 109, 4283.
[2] R. Gupta, N.K. Chaudhury, Biosensors and Bioelectronics 2007, 22, 2387.

NST-P3-15a
Theoretical Modeling of SiO2:Si Nanostructures for Understanding Luminescence Phenomenon in SRO Films

T10 Nanoscience and Technology

#NST-P3-15a

N. Espinosa Torres [1], J.F.J. Flores Gracia [1], J.A. Luna López [1], M. Aceves Mijares [2].

[1]CIDS-ICUAP - Puebla (Mexico), [2]INAOE - Puebla (Mexico).

Different types of luminescence at room temperature have been found in thin layers of Si:SiOx (SRO) . SRO has generated great interest because their possible applications in optoelectronic devices. Different researchers have reported cathode (CL), electro (EL) and photoluminescence (PL) in these materials off-stoichiometry [1]. A clear understanding of the mechanism of luminescence has not been raised satisfactorily. A large number of investigations have been leaded in order to study the nano-structures and properties of the agglomerates of the silica. Some of the proposed models [2] include structures based on two, three and four members rings (MR) and consist of nanostructures based on 2MR, 3MR, 4MR, hybrid 2MR/3MR and hybrid 3MR/4MR.

In this work, we have calculated the equilibrium energy in the ground and its excited states of this kind of silica molecules with the Density Functional Theory (DFT) to evaluate the contributions to luminescence phenomenon. The computational method employed is an ab initio total energy pseudo-potential technique within DFT, in the Generalized Gradient Approximation (GGA).

Our results include calculated IR and UV-Vis spectra of molecules carefully selected and confirm that the presence of rings of a few members, such as four (4MR), three (3MR) and two members (2MR) show luminescence at room temperature, and Huchino et al [3] have long-established experimentally that those molecules are frequently present in agglomerates of nanometer size silica than in those in which the geometric characteristics of the bulk materials restrict the relaxation of the network.

[1] M. Aceves-Mijares, A. A. González-Fernández, R. López-Estopier, A. Luna, D. Berman-Mendoza, A. Morales. C. Falcony, C. Dominguez, R. Murphy, “On the origin of light emission in Silicon Rich Oxide obtained by Low Pressure Chemical Vapor Deposition”, Hindawi Publishing Corporation, Journal of Nanomaterials, Vol 2012, Art ID 890701, 11 pages, doi:10.1155/2012/890701.
[2] R. Q. Zhang, W. J. Fan, ”Structures and Properties of Silicon Oxide Clusters by Theoretical Investigations”, Journal of Clusters Science, Vol 17, No. 4, Decermber 2006 DOI 10.1007/s10876-006-0087-4
[3]T. Uchino, A. Aboshi, S. Kohara, Y. Ohishi, M.Sakashita, and K. Aoki (2004) Phys. Rev. b 69, 155409.

NST-P1-17
Towards covalently-bonded organic network formation on a semiconductor surface

T10 Nanoscience and Technology

#NST-P1-17

I. Mcgovern [1], N. Berner [1], A. Cafolla [2].

[1]Trinity College - Dublin (Ireland), [2]Dublin City University - Dublin (Ireland).

Covalently-bonded organic network formation in ultra-high vacuum was first demonstrated by Grill et al. via a dehalogenation reaction of bromine-modified porphyrin molecules on the Au(111) surface [1]. The phenomenon was subsequently observed on other coinage metal substrates and using a variety of different organic molecules with bromine or iodine end-groups [2]. This paper reports on recent attempts to reproduce the phenomenon on the technologically more relevant surface of a semiconductor, in this case germanium (100).

The evident objection to this approach is that the latter surface will prove too reactive to the molecules to allow the degree of surface mobility required to form the network; the solution is also evident, namely, to passivate the surface. Initial efforts focused on the simplest passivation, that of atomic hydrogen. However, as discussed elsewhere [3], although this prevents any reaction of the as-deposited molecules with the substrate, this situation is not stable against the moderate annealing necessary for dehalogenation. The current study employs the

more robust passivation of chlorine from a home-made electrochemical source [4].

An Omicron VT STM was employed to image clean, Cl-passivated and molecule-deposited surfaces of Ge(001); in the first instance the molecule was the *free base* 5,10,15,20-tetrakis (4-bromophenyl)porphyrin (TBr4PP).

Upon deposition from a Knudsen-type cell, STM images were noticeably streaky, indicating that the passivation was enabling significant surface mobility. Nevertheless, it was possible to image individual molecules and non-covalent self-assembled islands. Upon annealing at 520 K for 5 min the image changed significantly, with the self-assembled islands of molecules largely transformed into chain-like structures. There is strong evidence for leg-to-leg orientation of adjacent molecules without dark contrast in between, which, in conjunction with a significantly reduced surface mobility, indicates the successful activation of the molecules and subsequent formation of covalent intermolecular bonds. Additionally, the average distance between molecular cores in the dimers, chains and pores observed throughout the STM images has been determined as d=(1.65 +/- 0.12) nm, which is in agreement with the d=1.71 nm measured and calculated by Grill et al. for the distance between to covalently-bonded TPP molecules. However the ease and quality of network formation found on coinage metal surfaces is not replicated to any great degree and possible sources of frustration are further discussed.

[1] Grill, L. et al. Nano-architectures by covalent assembly of molecular building blocks. Nature Nanotechnology 2, 687 (2007).

[2] Mendez, J., Lopez, M. F. & Martin-Gago, J. A. On-surface synthesis of cyclic organic molecules. Chemical Society Reviews 40, 4578 (2011).

[3] N. C. Berner, Y. N. Sergeeva, N. N. Sergeeva, M. O. Senge, A. A. Cafolla, I. T. McGovern, Adsorption of 5,10,15,20-tetrakis (4-bromophenyl)porphyrin on germanium(001), physica status solidi c 9 (2012) 1404

[4] Spencer, N. D., Goddard, P. J., Davies, P. W., Kitson, M. & Lambert, R. M. A simple, controllable source for dosing molecular halogens in UHV. Journal of Vacuum Science Technology A: Vacuum, Surfaces, and Films 1, 1554 (1983).

NST-9-Or-10
Polarity in low dimensions : nano-ribbons and nano-islands

T10 Nanoscience and Technology

#NST-9-Or-10

J. Goniakowski [1], C. Noguera [1], L. Giordano [2], Y. Pan [3], P. Myrach [3], N. Nilius [3], S. Benedetti [4], F. Guller [5], A.M. Llois [5].

[1]Institut des Nanosciences de Paris, CNRS and Université Pierre et Marie Curie - Paris (France), [2]Dipartimento di Scienza dei Materiali, Università di Milano-Bicocca - Milano (Italy), [3]Fritz-Haber-Institut der Max-Planck-Gesellschaft - Berlin (Germany), [4]National Research Center on nanoStructures and bioSystems at Surfaces - Modena (Italy), [5]Centro Atomico Constituyentes - San Martin (Argentina).

Extended polar objects present an electrostatic instability which induces substantial modifications of the surface charge density. Microscopic surface processes related to polarity compensation have been extensively studied in the last decades, also as a potential tool for tuning surface electronic and structural properties [1]. More recently it has become clear that polarity does also concern nano-objects, but that the relevant electrostatic forces and the response they induce may differ from the known ones [2]. In particular, new compensation mechanisms are at work, such as structural transformations of the entire object, resulting in novel structures, with no bulk counterparts, or uncompensated polar states may exist which drive strongly size- and dimensionality- dependent properties [3]. Since oxide nano-objects, such as ultra-thin films and nano-islands, are generally synthesized on metal substrates, their polarity characteristics are additionally modified by the electrostatic coupling between their structure and the interface charge transfer [4].

In this presentation, we will describe how polarity manifests itself in low dimensional objects, such as two-dimensional ribbons or islands [5] and illustrate the theoretical concepts with the recent results on monolayer MgO islands on Au(111), explored with low-temperature scanning tunneling microscopy and density functional theory [6]. We will show that the observed electronic characteristics of the monolayer MgO islands are fully compatible with their predicted induced-polar character, and that their structure and their out-of-plane dipole moment result from a coupling between the film rumpling and the electron exchange at the MgO/Au interface. We will also

identify the in-plane polarity induced by polar edges, and we will analyze its effect on the relative stability of MgO islands of different orientations and under different experimental conditions.

[1] C. Noguera, J. Phys. Cond. Matter. 12, R367 (2000) ; J. Goniakowski, F. Finocchi, C. Noguera, Rep. Prog. Phys. 71, 016501 (2008).
[2] J. Goniakowski, C. Noguera, Phys. Rev. B 83, 115413 (2011) ; C. Noguera and J. Goniakowski, Chem. Rev. DOI: 10.1021/cr3003032.
[3] J. Goniakowski, C. Noguera, L. Giordano, Phys. Rev. Lett 93, 215702 (2004); 98 205701 (2007).
[4] J. Goniakowski, C. Noguera, Phys. Rev. B 79, 155433 (2009); J. Goniakowski, L. Giordano, C. Noguera, Phys. Rev. B 81, 205404 (2010).
[5] J. Goniakowski, L. Giordano, C. Noguera, Phys. Rev. B 87, 035405 (2013); F. Guller, A. M. Llois, J. Goniakowski, C. Noguera, submitted Phys. Rev. B.
[6] Y. Pan et al., J. Phys. Chem. 116, 11126 (2012); N. Nilius et al., Phys. Rev. B 86, 205410 (2012).

NST-1-Or-3
Charge screening at the surface of a topological insulator: Rb adatoms on Bi2Se3(111)

T10 Nanoscience and Technology

#NST-1-Or-3

L. Zhou, P. Löptien, J. Wiebe, A.A. Khajetoorians, R. Wiesendanger.

Institute of Applied Physics, University of Hamburg - Hamburg (Germany).

Adsorption of Rb atoms on Bi_2Se_3(111) leads to the formation of a quantum-confined two-dimensional electron gas (2DEG) in the conduction band at the surface [1]. We investigated the coverage dependent distribution of Rb adatoms with low-temperature scanning tunneling microscopy [2]. By a statistical analysis of the interatomic distances, we quantitatively derived the pair interaction between singly charged Rb adatoms, which fits a screened Coulomb potential. Interestingly, the screening length and the dielectric constant turn out to be very small, which is attributed to the contribution of the 2DEG and the topological surface state.

[1] M. Bianchi, R. C. Hatch, Z. Li, P. Hofmann, F. Song, J. Mi, B. B. Iversen, Z. M. Abd El-Fattah, P. Löptien, L. Zhou, A. A. Khajetoorians, J. Wiebe, R. Wiesendanger, and J. W. Wells, ACS Nano 6, 7009 (2012)
[2] SPECS, Berlin

NST-P2-18
Different morphologies of lanthanides doped GdPO4 nanoscale phosphors obtained by a new hydrothermal process

T10 Nanoscience and Technology

#NST-P2-18

A. Garcia Murillo [1], A. Garrido Hernández [1], A. Potdevin [2], D. Boyer [2], G. Chadeyron [2], R. Mahiou [2].

[1]Instituto Politécnico Nacional - Distrito Federal (Mexico), [2]Institut de Chimie de Clermont-Ferrand - Aubiere (France).

Rare-earth doped lanthanides orthophosphates (LnPO4) represent a class of materials with significant technological importance. Recently, new applications of nanoscale phosphors, including biolabeling, optical imaging or luminescent transparent layers have attracted intensive interests. As a result, several synthesis methods leading to LnPO4 nanocrystals with controlled shape have been developed, based on hydrothermal reactions or high-boiling solvent technique for instance. It is well known that the reduction of particles size or the modification of their shape can dramatically modify their physic-chemical properties.
In this work Eu3+ and Tb3+ doped GdPO4 nanocrystals, with different shapes were successfully synthetized by a new hydrothermal method. The particles morphology was modified changing different parameters like the pH and the synthesis temperature or using the glycerol as surfactant. Depending on the synthesis conditions, TEM analyses have revealed the achievements of hexagonal nanoparticles, nanorods or nanowires with narrow size distributions. Their structural, morphological and photoluminescent properties were investigated and compared. Luminescent films were prepared by dispersing these nanomaterials in a polymer matrix. The influence of the GdPO4 shape on the maximum loading rate and on the mechanical properties of composite films was studied.

NST-2-Or-9
Stability and breakage mechanism of molecular junctions based on different anchoring groups

T10 Nanoscience and Technology

#NST-2-Or-9

T. González [1], E. Leary [1], A. Díaz [2], C. Evangeli [2], G. Rubio-Bollinger [2], N. Agraït [2].

[1]IMDEA-Nanoscience - Madrid (Spain), [2]Universidad Autónoma de Madrid - Madrid (Spain).

The realization and study of molecular junctions formed by a few (down to one) molecules bonded between two metallic electrodes opens the possibility of directly investigating electrical properties of compounds at the ultimate level of a single molecule. Apart from the determination of their electrical conductance, it is important to understand which factors play a role in the formation and breakage of the molecular junctions, and how stable we can expect them to be.
In this work, we present our studies on the stability and breakage mechanism of molecular junctions formed by thiol-, amine-, and C60-terminated molecules. We use a STM (scanning tunneling microscope) break-junction technique to create and characterized single-molecule junctions. We compare thiols and amines on the alkane family [1] and an oligo(phenylenethynylene) (OPE) [2,3]. By studying the molecular-junction stretching length for these compounds, we conclude that, during the junction formation, thiols affect atomic rearrangement at the electrodes significantly more than amines [1].
In addition, by performing stretching experiments at different pulling speeds, we find that junctions of OPE-diamine can be very stable and have adsorption lifetimes well above the time interval explored in the experiment [3]. We identify the breaking of the single-molecule junctions of this compound to be due to simply the elastic limit of the gold-amine bond. On the other hand, multiple-molecule junctions typically break when the inter-electrode gap reaches the molecule length. We find evidence that individual molecules attach and detach during the stretching of a multiple-molecule junction, which warrants the long-life of the molecular junctions in spite of individual molecular desorption. This shows that even using a weak binding group such as

amine, long-lasting junctions can be established in an environment that allows equilibrium between adsorbed and desorbed individual molecules.

[1] C. R. Arroyo, et al., J. Am. Chem Soc, 133, 14313 (2011)
[2] M. T. González et al., J. Phys. Chem. C, 115, 17973 (2011)
[3] M. T. González et al., submitted (2013)

NST-5-Or-6
Thermally-Assisted Electron-Induced Nonlocal Desorption in the STM

T10 Nanoscience and Technology

#NST-5-Or-6

T. Pan [1], S.A. Holmes [1], D. Kaya [1], P.A. Sloan [2], R.E. Palmer [1].

[1]University of Birmingham - Birmingham (United kingdom), [2]University of Bath - Bath (United kingdom).

Atomic manipulation in the scanning tunnelling microscope (STM), provides, at least in principle, a means to create and control nanoscale architectures. A thorough knowledge of the manipulation mechanisms at play is essential to realizing this potential. Here we have investigated the thermally-assisted nonlocal desorption of chlorobenzene molecules on the Si(111)-7x7 surface [1-3] at different temperatures.

In the previous investigation [1], it has been shown that the nonlocal desorption of cholorobenzene can be realized by the electron injected from the STM tip and this process can be affected by different injection sites. Here, we present the effect of temperature to the nonlocal cholorobenzene desorption process. We found that, as the temperature decreased, the range of the non-local effect was reduced from several hundred ångströms down to several tens of ångströms, while the integrated desorption yield also decreased significantly. The difference in yield between 323 K and 77 K, can be as much as one order of magnitude. From the Arrhenius plot, two activation energy regions (~162 meV for the region above 175 K and ~17 meV for the region below 175 K) can be noticed for the nonlocal desorption process. Thus, this one-electron desorption process is thermally-assisted, similarly to the case of C-Cl bond dissociation of chlorobenzene [2-3]. In the lower temperature region, it may be due to the excitation of the surface phonon, while in the higher temperature region, the excitation of the molecule-substrate vibrational mode may come into play.

[1] P. A. Sloan, S. Sakulsermsuk and R. E. Palmer, Phys. Rev. Lett. 105, 048301 (2010).
See also Electron ‘submarines’ help push atoms around, E.S. Reich, New Scientist, 31 July 2010, p. 11.

[2] S. Sakulsermsuk, P. A. Sloan and R. E. Palmer, ACS Nano 4, 7344 (2010).

[3] S. Sakulsermsuk, P. A. Sloan, W. Theis and R. E. Palmer, J. Phys.: Condens. Matter 22, 084002 (2010).

NST-P2-19
EFFECT OF SiO2 ON BaTiO3:Eu3+ CERAMICS OBTAINED BY SOL GEL PROCESS

T10 Nanoscience and Technology

#NST-P2-19

F. Carrillo Romo [1], J. Reyes Miranda [1], M. García Hernández [1], A. Morales Ramírez [1], E. De La Rosa Cruz [2].

[1]INSTITUTO POLITECNICO NACIONAL - Distrito Federal (Mexico), [2]CENTRO DE INVESTIGACIONES EN OPTICA - León Guanajuato (Mexico).

In recent years, lanthanide-doped ultrafine and nanocrystalline barium titanate materials have been widely investigated due to their interesting optical properties, which make them candidates in different advanced fields, such as phosphors for TV screens optical amplifiers and electroceramic applications. Recently there is an interest to produce rare earth ions doped perovskite base materials as barium titanate powders owing to its promising luminescent properties produced by soft chemical routes. The incorporation of a glassy component on the ceramic system has improved the luminescent properties in similar matrix as Y2O3:Eu3+. In this context, the solvothermal route was selected as promising option to prepare BaTiO3:Eu3+ ceramic powders while the sol-gel method was chosen to elaborate the SiO2 matrix. As well as, sol-gel method allow obtaining high purity and homogeneity in the synthetized materials. In the present work, the precursors employed for the synthesis of BaTiO3: Eu3+ ceramic powders, were barium chloride (BaCl2, 99.9%, Aldrich), Europium (III) nitrate pent hydrate (Eu(NO3)3•5H2O, 99.9% Aldrich), titanium butoxide (Ti[O(CH2)3CH3]4, 97%, Fluka). Anhydrous methanol (CH4O, 99.8%, Sigma Aldrich) was used as solvent and metal potassium (K, 98%, Aldrich) as mineraliser. The alcoxyde base precursors used for the elaboration of SiO2 glassy sol, were tetraethyl orthosilicate (CH8H2OO4Si, 98%, Aldrich), ethanol (CH3CH2OH, 99.9% Fermont), hydrochloric acid (HCl, Fermont) and distilled water. In order to improve the luminescent properties of the BaTiO3:Eu3+ ceramic powders, the synthesis of BaTiO3:Eu3+@SiO2 glass ceramic powders are proposed in different Ba:Si molar ratio. The effect of SiO2 (glassy sol-gel matrix) incorporation in BaTiO3:Eu3+ (ceramic hydrothermal matrix) were chemically, structurally and morphologically analyzed by means of FT-IR spectroscopy, X-ray Diffraction and

Scanning Electron Microscopy characterization techniques. Two glass $BaTiO_3:Eu^{3+}$@ SiO_2 ceramic systems: Ba:Si=3:97 and 5:95 presented the major 611 nm red emission intensity as demonstrated by photoluminescent studies.

NST-P2-20
Synthesis of CdS-ZnS nanostructures by microwave radiation

T10 Nanoscience and Technology

#NST-P2-20

I. Gómez, T. Serrano, A. Vázquez, A. Zamora.

UANL - San Nicolas De Los Garza N.l. (Mexico).

Mixed systems of CdS-ZnS nanoparticles were obtained by means of colloidal synthesis assisted by microwave radiation. The optical characteristics obtained in the synthesized samples were compared versus CdS and ZnS separately, these nanoparticles were also synthetized in the current work. Mixed systems were prepared at three different molar relations between cation precursors, 1:1, 2:1 y 1:2, respectively. The samples were prepared from thioacetamide as sulfide source and from CdCl2 or Zn(OAc)2.2H2O for Cd or Zn ions. The experiment obtained with the best optical characteristics such as the bigger photoluminescence in the first part of the work has been chosen to be prepared with different concentrations of stabilizer (sodium citrate), 1.0, 1.5 and 2.0 mM. In both parts of our work the concentration of thioacetamide, pH 8 and a time of 60 seconds under microwave radiation were constant. The mixed systems improve their optical characteristics in comparison to the compound separately; this was determined by UV-Vis and photoluminescence analysis. FESEM analysis let us to observe arrengements of nanoparticles from 20 to 70 nm. The effect over photoluminescence is function of the relation of CdS versus ZnS.

1. Patel J.D., Mighri F., Ajji A. Materials Letters, 2012, 74, 183–186
2. Ratanatawanate C., Xiong C., Balkus,K.J., ACSNano, 2008, 2, 8, 1682–1688 ▪
3. Kumar D. Agarwal G., Tripathi B., Vyas D., Kulshrestha D. 2009,Journal of Alloys and Compounds
484, 463–466
4. Rajamathi M., Seshadri R., Current Opinion in Solid State and Materials Science, 2002, 6, 337–345
5. Neo M., Venkatram N., Li G.S., Chin W.S., Ji W. J. Phys. Chem. C 2010, 114, 18037–18044

NST/SS-5-Or-6
Influence of Randomly Distributed Impurities on Electronic Transport in Carbon Nanotubes: Wave-Packet Dynamics Simulation

T10 Nanoscience and Technology

#NST/SS-5-Or-6

Y. Takada, K. Takashima, T. Yamamoto.

Faculty of Engineering, Tokyo University of Science - Tokyo (Japan).

Carbon nanotubes (CNTs) are quasi-one-dimensional materials, which are attracting much attention for both academic science and practical engineering interests [1, 2]. Semiconducting SWNTs are potential candidates for future ultra-fast switching devices due to their high carrier mobility. However, there are still several serious problems that degrade the transport properties of SWNT devices. To reveal underlying physics behind these problems is a first step to achieve practical SWNT devices.

Recent experiments showed that the impurity and/or defect scattering in a SWNT causes Anderson's localization even at room temperature, originating from its low dimensionality and phase coherency of an electron [3]. In Anderson's localization regime, the typical width of localized wave function is given by the localization length ξ, and therefore the localization can occur when the tube length L is much longer than the localization length ξ. Thus, the localization length ξ is an important quantity charactering the Anderson's localization. However, the relation between the localization length ξ and the strength of impurity potential is not sufficiently clarified yet.

In this study, we numerically investigate the impurity scattering effects on the coherent electronic transport in semiconducting SWNTs with randomly distributed impurities using wave-packet dynamics method [4, 5], focusing particularly on the effects of impurity-potential strength on the localization length ξ. The wave-packet dynamics method is a powerful simulation technique that enables us to simulate transport properties of large systems such as the present disordered system, with low computational cost. Using the wave-packet dynamics method, we estimate the localization length ξ as a function of the strength of impurity potential. Our results show that the system exhibits Anderson's localization due to quasi-one-

dimensionality of nanotubes. Moreover, we reveal the dependence of impurity-potential strength on the localization length ξ, and consequently we show that the localization can occur even at room temperature, which is consistent with the recent experimental results.

[1] R. H. Baughman, A. A. Zakhidov, and W. A. de Heer: Science 297 (2002) 787.
[2] P. L. McEuan, M. S. Fuhrer, and H. Park: IEEE Transaction on Nanotechnology 1 (2002) 78.
[3] C. Gomez-Navarro, P. J. de Pablo, J. Gomez-Herrero, B. Biel, F. J. Garcia-Vidal, A. Rubio, and F. Flores: Nature Mater. 4 (2005) 534.
[4] S. Roche: Phys. Rev. B 59 (1999) 2284.
[5] Y. Takada, and T. Yamamoto: Jpn. J. Appl. Phys. Submitted.

NST-6-Or-1
Formation of one-dimensional ZnS nanostructures and its transformation into ZnS/ZnO heterostructures

T10 Nanoscience and Technology

#NST-6-Or-1

A. Vázquez, Y. Peña, I. Gómez.

Universidad Autónoma de Nuevo León, UANL, Facultad de Ciencias Químicas, Laboratorio de Materiales I - San Nicolás De Los Garza, Nuevo León (Mexico).

One-dimensional ZnS nanostructures were grown through electrophoretic deposition of ZnS nanoparticles prepared by a microwave assisted synthesis by using sodium citrate as stabilizer. HRTEM images show that this synthetic route produces spherical particles with a mean diameter of 20 nm. The one-dimensional ZnS nanostructures were formed without using template membranes after 24 h of electrophoretic deposition on aluminum plates at direct current low voltage. Dimensions of the nanostructures can be varied according to deposition time and electric field. FE-SEM images at different deposition times show that one-dimensional nanostructures are formed by a mechanism of lyosphere distortion and thinning and subsequent dipole-dipole interactions phenomena where the incoming particles are oriented by the particles previously deposited. In this mechanism the first particle/lyosphere deposited act as a dipole and attract the incoming particles to it, creating a polycrystalline one-dimensional nanostructure after some time of electrophoretic deposition. Once the one-dimensional ZnS nanostructures are formed, they were transformed into ZnS/ZnO heterostructures by controlled thermal oxidation at 400º C. FE-SEM images show that the ZnS/ZnO heterostructures can be produced with different ZnS/ZnO ratios by controlling time of heat treatment.

NST-6-Or-2
Density Gradient Ultracentrifugation of Colloidal Nanoparticles

T10 Nanoscience and Technology

#NST-6-Or-2

X. Sun, Y. Kuang, G. Zhang, S. Song.

Beijing University of Chemical Technology - Beijing (China).

High dimensional nanodevice is the ultimate goal for nanoscience and nanotechnology. Bottom up approach, which contains synthesis and assembly of monodisperse nanocomponents, is a general method for the fabrication of high dimensional nanodevices. As an assistance and extension of synthesis optimization, we adopted "density gradient ultracentrifuge separation" (DGUS) method for obtaining more monodisperse or unique colloidal fractions. DGUS method was demonstrated a general method not only for sorting nanoparticles with different size and morphology (Fig. 1 B, C, D) but also applicable for various materials, such as noble metal[1, 2], carbon[3], S-group semiconductor[4], or hydroxide compounds etc. Meanwhile, DGUS separation can be carried out in both aqueous[1] and organic media.[4] Models were set up for typical systems. A series of nano-effects were observed or evidenced on these fractions as property investigations were performed, which provided chance to get deeper view into the structure-property relationship of colloidal nanoparticles. More importantly, nanoseparation demonstrated to us that the formation of nanoparticles with varied size or morphologies in one batch is not a random behavior, in contrast, the size or morphology distribution closely related to synthesis condition, properties of fractions, and composition distribution. The findings provide new inspirations for synthesis optimization.[5]

[1] X.M. Sun, S.M. Tabakman, H.J. Dai* et al, *Angew. Chem. Int. Ed.*, **2009**, 48, 939
[2] L. Bai, X.J. Ma, X.M. Sun* et al, *J. Am. Chem. Soc.*, **2010**, 132, 2333
[3] X.M. Sun*, D.C. Luo, J.F. Liu et al, *ACS Nano*, **2010**, 4,3381–3389
[4] X.J. Ma, Y. Kuang, X.M. Sun* et al, *ACS Nano*, **2011**, 4, 3242
[5] G.X. Zhang, P.L. He, X.J. Ma, X.M. Sun* et al, *Inorg. Chem.*, **2012**, 51, 1302

Fig. 1 (A) Separation mechanism of different-sized colloids in a multilayer step density gradient. DGUS separation of typical (B) 0 dimensional NPs (Au NPs); (C) 1 dimensional NPs (carbon nanotubes) and (D) 2 dimensional NPs (graphene)

Fig. 2 (A) Phase separation and (B) selective synthesis of CdS nanorod with different crystalline structures

NST/SS-P2-02
First-Principles Study on Current-Induced Magnetization Switching in Magnetic Tunnel Junctions

T10 Nanoscience and Technology

#NST/SS-P2-02

M. Araidai [1], T. Yamamoto [2], K. Shiraishi [3].

[1]Center for Computational Sciences, University of Tsukuba - 1-1-1 Tennodai, Tsukuba, Ibaraki 305-8571 (Japan), [2]Faculty of Engineering, Tokyo University of Science - 6-3-1 Niijuku, Katsushika-Ku, Tokyo 125-8585 (Japan), [3]Faculty of Pure and Applied Sciences, University of Tsukuba - 1-1-1 Tennodai, Tsukuba, Ibaraki 305-8571 (Japan).

Investigation of magnetic tunnel junction (MTJ) is a key issue for the development of advanced magnetoresistive random access memories (MRAMs). MTJs consist of two metal ferromagnets, thick spin-fixed and thin spin-free layers, separated by a thin insulator, and they exhibit two resistances, low or high, depending on the relative direction of the magnetizations of the spin-fixed and spin-free layers, parallel (P) or antiparallel (AP) configuration. The simplest way to reverse the magnetization of free layer is switching by external magnetic fields. However, absolute currents required for magnetic-field switching do not scale with reducing the junction size, and it is a major obstacle to promote MRAM devices. At present, current-induced magnetization switching (CIMS) proposed by Slonczewski[1] and Berger[2] is drawing attention as the most promising candidate for a mechanism of magnetization reversal of free layer, owing to the scalability of CIMS[3]. Although CIMS has been successfully applied to the operation of MRAM, the microscopic mechanisms have not been sufficiently understood yet.

In this work, we have theoretically investigated CIMS in MTJs. While many theoretical studies have been devoted to clarify the microscopic mechanisms of CIMS by the phenomenological Landau-Lifshitz-Gilbert equation, we utilize the non-equilibrium Green's function technique coupled with the density-functional theory to reveal the mechanisms together with its device characteristics. We employed a Fe/MgO/Fe model as a typical MTJ. The current-voltage characteristics indicate high tunnel magnetoresistance of the MTJ (about 600% at zero bias) and is highly antisymmetric with respect to the bias voltage, originating from the antisymmetric structure and spin polarization. We found from the current density dependence of

magnetization of free layer that the switching from AP to P configuration could be realized by lower electrical power than P-to-AP case. Through the close examinations on local variation of magnetization at each electric current, we can propose a rational mechanism for magnetization switching in the MTJ within a conventional energy-band picture, i.e., a single-electron picture.

[1] J. C. Slonczewski, J. Magn. Magn. Matter. **159**, L1-L7 (1996).
[2] L. Berger, Phys. Rev. B **54**, 9353 (1996).
[3] Ikeda et al., IEEE TRANSACTIONS ON ELECTRON DEVICES, VOL. **54**, 991 (2007).

NST-2-Or-10
First direct conductivity measurement at a single Si atomic step

T10 Nanoscience and Technology

#NST-2-Or-10

B. Martins [1], M. Salomons [2], R.A. Wolkow [1].

[1]University of Alberta, National Institute for Nanotechnology - Edmonton (Canada), [2]National Institute for Nanotechnology - Edmonton (Canada).

Step edges are a major issue for the implementation of large scale molecular device architecture on silicon surfaces. Electrical resistance associated with this defect imply losses that can prevent efficient signal propagation along the surface. The effect is particularly relevant on Si(111)-7x7 if we consider that its surface is highly conductive as demonstrated by photo-emission experiments [1]. This assumption is quite controversial as evidenced by the large range of surface conductivity values presented in the literature. Wells et al. [2] showed conductivities ranging from 10-4 to 10-8 S. This huge gap is probably due to the problem of separating surface, space-charge layer, surface contamination, contact variability and bulk contributions to the current. At low temperatures, these components could be disentangled and that surface conduction was not as high as expected, clearly not metallic [2]. However, this result did not take into account the important role played by the contacts [3], whose size determines the transport properties of the system. In the case of very small contacts (nanocontacts), most of the conduction is ballistic and propagates through surface states. The use of small, stable contacts allows us to probe surface conductance and therefore the step edge resistance.

In order to properly consider the contact problem, we propose a novel approach for transport measurements on semiconductors. Using a home-built, three-probe, RT STM we measured the surface potential using ZV spectroscopy instead of direct contact. This way we avoid problems related to the non-linear nature of the Schottky barrier due to the contacts which can strongly influence the experimental outcome. We measured potential profiles (Figure 1) along a low-doped surface and across a step edge. The line profiles were used for the calculation of both surface conductivity $\sigma = (1.3 \pm 0.3) \times 10^{-5} S$ and step edge resistance $R = 5.0 \pm 0.5\ k\Omega$. The high conductivity is in full agreement with previous results obtained by Hasegawa et al. [4] using a single STM . The step edge measurement is the first one made. In a last step, we carried out a measurement set

on a dosed surface to remove Si surface states. The dosed line profile, also featured in Figure 1, shows that the step edge potential drop vanishes in this case. This confirms our assumption that the measured signal was due to conduction through surface states.

[1] R.I.G. Uhrberg, T. Kaurila Y.-C. Chao, Phys. Rev. B, 58 (1998) R1730
[2] J.W. Wells, J.F. Kallehauge, Ph. Hofmann, Surf. Sci., 602 (2008) 1742-1749
[3] G.D.J. Smit, S. Rogge, T.M. Klapwijk, Appl. Phys. Lett., 80 (2002) 2568
[4] Y. Hasegawa, I-W Lyo, Ph. Avouris, Surf. Sci., 357-358 (1996) 32

Figure 1: Potential line profiles acquired for clean and dosed surface.

NST/SS-5-Or-10
Graphene-filled syndiotactic polystyrene nanocomposites: microstructure, crystallization and electrical conductivity

T10 Nanoscience and Technology

#NST/SS-5-Or-10

C. Wang, Y.C. Chiu.

Department of Chemical Engineering, National Cheng Kung University - Tainan (Taiwan, republic of china).

Syndiotactic polystyrene (sPS) is a semicrystalline polymer with high melting temperature and good mechanical strength. In this report, sPS nanocomposites filled with different amount of graphenes are prepared by a coagulation method. Two types of graphenes with different thicknesses (denoted to G1 and G10) are studied. Electron microscopy shows that G1 is a wrinkled flake with a thickness less than 2 nm, and G10 is a smooth sheet with a thickness less than 50 nm. The un-modified graphenes are well dispersed in the sPS matrix. After sonication in o-DCB solution, however, the lateral dimensions of G1 and G10 are significantly reduced, and G1 has more defects than G10 as-revealed by Raman spectroscopy. Measurements of electrical conductivity and crystallization of the nanocomposites are carried out to unveil its potential as a conducting material. As expected, at a given graphene content the electrical conductivity is higher for the G1-filled samples than G10-filled ones. Percolation scaling law is applied and the conductivity threshold is determined to be 0.46 vol% for the former and 3.84 vol% for the latter. TEM studies on the melt-quenched nanocomposites reveal that a more uniform dispersion of G1 is developed in the sPS matrix. Striped sPS lamellae are seen in the G10-filled samples with a graphene content higher than 0.5 wt%. Wide-angle X-ray diffraction elucidates the produced sPS crystallites are in the beta form under such a server cooling condition. In contrast, alpha-form sPS crystallites are produced when the melt-quenched samples are cold-crystallized during dynamic heating. With an increase in graphene loading, the isothermal crystallization rate of sPS is increased. Regardless of the graphene content, the glass transition and equilibrium melting temperature of the sPS matrix are unchanged at ~96 and 290 °C, respectively. It is found that G10 is more effective than G1 as a nucleating agent to induce the crystallization of sPS

matrix despite a higher concentration required to form conductive graphene network in the sPS matrix.

NST-6-Or-3
Preparation of sulfonated single-walled carbon nanohorn catalyst and its catalytic activity for biodiesel production by esterification

T10 Nanoscience and Technology

#NST-6-Or-3

C. Poonjarernsilp [1], N. Sano [2], H. Tamon [2].

[1]Department of Chemical Engineering, Kyoto University and Department of Chemical Engineering, Rajamangala University of Technology Krungthep - Kyoto (Japan), [2]Department of Chemical Engineering, Kyoto University - Kyoto (Japan).

An ideal carbon support should have a high specific surface area, good electric conductivity, suitable pore size, favorable surface functional group, good corrosion resistance, and low cost [1]. A lot of work has been done on developing new carbon materials and modifying the carbon materials by treatment with acid, alkali, oxidant, or polymer to meet these requirements. In this work, new carbon nanomaterials that are single-walled carbon nanohorns (SWCNHs) were examined and compared with commercial carbon support such as activated charcoal and carbon black. As-grown SWCNHs were prepared by arc in water with nitrogen gas injection (AIW-GI) method [2]. Acid functional groups were added on the surface of all carbon materials by sulfonation reaction with sulfuric acid at 200^{o}C for 18 hr. Fourier transform infrared spectroscopic results indicated that a sulfonaic acid functional group (SO_3H) was formed on the surface of all carbonaceous catalysts. Additionally from N_2 adsorption analysis for pore size distribution results showed that SO_3-SWCNHs exhibited increasing of BET surface area (418 m^2g^{-1}), porosity (96 cm^3g^{-1}) and higher uniform por size distribution. TEM image of SO3H-SWCNH in Fig.1 shows that the morphology of SWCNHs aggregates have not changed significantly after sulfonation. As an environmentally friendly solid acid catalyst, the catalytic performance of all carbonaceous materials were evaluated by the esterification of palmitic acid for methly palmitate production. Regarding the yield of methyl palmitate, the SO3-SWCNHs showed higher catalytic performace than activated carbon and carbon black. SWCNHs give better performance due to their superior structural features and high acid site density which was proven by ion exchange titration results.

[1] Tang S., Sun G., Qi J., Sun S., Guo J., Xin Q., and Geir MH., “Review of New Carbon Materials as Catalyst Supports in Direct Alcohol Fuel Cells”, Chinese Journal of Catalysis, 2010, 31: 12–17.
[2] Sano N., “Low-cost synthesis of single-walled carbon nanohorns using the arc in water method with gas injection”, Journal of physics D: Applied Physics, 2004, 37: L17–L20.

Figure 1 Typical TEM image of sulfonated single-walled carbon nanohorn

NST/SS-02-Or-10
Intercalation of metals and silicon at the interface of epitaxially grown graphene and Ru(0001) surfaces

T10 Nanoscience and Technology

#NST/SS-02-Or-10

L. Huang, W. Xu.

Institute of Chemistry, Chinese Academy of Sciences - Beijing (China).

Epitaxial graphene on Ru(0001) provides a high quality adlayer, but has a strong interaction with the substrate. This interaction can be effectively weakened via intercalating a layer of Au, Ag, or Cu between epitaxial graphene and its substrate. In this work, we intercalated seven kinds of metals including noble metals Pt, Pd and Au, magnetic metals Ni and Co, a IIIA group metal In and a rare earth metal Ce, at the interface of epitaxially grown graphene and Ru(0001), to show the universality of metal intercalations in this system. Moreover, we intercalated silicon at the interface of graphene/Ru(0001) and demonstrated that silicon-layer intercalation not only weakens the interaction of graphene with the metal substrate but also retains its properties. More importantly, the silicon intercalation process allows for an atomic control of the distance between the graphene and the metal substrate that can be used as a top gate. Our results show potential for the next generation of graphene-based materials with tailored properties.

(1) Y. Pan et al. Adv. Mater. 21 (2009) 2777.
(2) L. Huang et al., Appl. Phys. Lett. 99 (2011) 163107.
(3) J. Mao et al., Appl. Phys. Lett. 100 (2012) 093101.

fig. 1 STM topographic images: Pt (a), Pd (b), Ni (c) and Co (d) intercalation structures in graphene/Ru(0001) after annealing at 800 K. (e) and (f) Atomic resolution images of graphene on a Pd intercalated island and a Co intercalated island, respectively.

fig. 2 Silicon intercalation approach on Ru(0001). (a)-(c) Schematics of the silicon intercalation process: (a) Graphene formation on Ru(0001); (b) Si deposition on Graphene/Ru(0001); (c) Annealing and Si layer intercalation. (d) STM image of graphene on Ru(0001), showing the ordered moiré pattern, 40 nm × 40 nm, 0.1 nA, -3.0 V. (e) Silicon deposition on the graphene, 20 nm × 20 nm, 0.2 nA, -2.0 V. (f) After annealing, the Si intercalation between graphene and Ru(0001), 25 nm × 25 nm, 0.1 nA, -3.0 V. (g) Zoom of the STM image of G/Si/Ru, 6 nm × 6 nm, 0.1 nA, -1.0 V. (h), (i) 3D STM images of the G/Si/Ru surface, 3 nm × 3 nm, 0.2 nA, -1.0 V.

NST/SS-P1-06
Computational Simulation on Electronic Transport in Edge-Disordered Graphene Nanoribbons

T10 Nanoscience and Technology

#NST/SS-P1-06

K. Takashima, Y. Takada, T. Yamamoto.

Faculty of Engineering, Tokyo University of Science - Tokyo (Japan).

Graphene is a potential candidate for channel materials of field effect transistors (FETs) because of their high carrier mobility [1]. However, metallic behavior of graphene is a major hurdle to utilize it to the channel of FETs, because high on-off ratios are not achievable without an energy-band gap. One possible way to overcome the gap-opening problem is to process the graphene in the form of nanoribbon with nanometer width. Graphene nanoribbons has an energy gap and they have been successfully applied to FETs with high on-off ratio [2].
The channel length of cutting-edge GNR-FETs is less than 100nm (the minimum length is ~1nm). Because such channel lengths are shorter than the typical coherent length of GNRs, the GNRs is expected to exhibit remarkable electronic transport properties originating from the wave nature of electrons. A recent experiment reported that the resistance of GNRs increases exponentially with their length even at the room temperature [3]. This non-Ohmic behavior is believed to be due to Anderson's localization caused by the interference between coherent electrons scattered by the disordered edges of GNRs. However, the detail relation between the edge roughness and the coherent length L_φ of GNRs has not been clarified yet.
In this study, we have theoretically investigated the coherent electronic transport in edge-disordered armchair GNRs (AGNRs). The edge disorder has been treated as randomly-distributed carbon-pair vacancies on the edges of AGNRs. We used two simulation methods: (i) the wave-packet diffusion (WPD) method [4] and (ii) the nonequilibrium Green's function method combined with tight-binding (NEGF+TB) method [5]. In the WPD simulation, we have estimated the localization length L_φ of AGNRs from the time-dependent diffusion coefficients. On the other hand, in the NEGF+TB method, we have calculated L_φ of AGNRs from the length dependence of the electronic conductance. From both simulations, we clarified (i) a relation between L_φ and the amount of edge carbon-pair vacancies, (ii) the chemical-potential

dependence of L_φ, and (iii) the ribbon-width dependence of L_φ. We discuss the details of these simulation results in the presentation.

[1] Novoselov, et al., Science **306**, 666 (2004).
[2] Schwierz, Nature Nanotech. **5**, 487 (2010).
[3] Xu et al., Nano Lett. **11**, 1082 (2011).
[4] Roche, Phys. Rev. B **59**, 2284 (1999).
[5] We used a commercially available software ATK-SE (Atomistix ToolKit Semi Empirical); http://www.quantumwise.com/

NST/SS-5-Or-11
Electronic transmission of Graphene with Nano-scale Sharp folds

T10 Nanoscience and Technology

#NST/SS-5-Or-11

X. Li [1], W. Liu [1], X. Wei [2], K. Pang [2], Y. Wu [1], P. Chu [1], X. Wang [1], Q. Li [1], J. Zhang [1], J. Liu [3], K. Tian [1].

[1]Department of Microelectronics, School of Electronics and Information Engineering, Xi'an Jiaotong University - Xi'an (China), [2]School of Science, Xi'an Jiaotong University - Xi'an (China), [3]Xi'an Jiaotong Univ. - Xi'an (China).

Research on machinery strength, photoelectric absorption efficiency and heat transmission response of low dimension material such as graphene and carbon nanowall has draw broad concern1-3. In the course of the experiment, we found an interesting phenomenon. Electrical conductivity in graphene would change as it folded, especially when you fold it up to nano-scale, you will get local high resistance. Here we reported a triode structure of graphene cathode with nano-scale sharp folds. Figure 1 insert picture shows the cross section schematic illustration of graphene with very sharp folds. Taking advantage of photoetching technology, we have obtained triangular prism structure lying on substrate, in which side length is less than 8μm (as shown in Figure 2 insert optical micrograph). We have transferred graphene sheet on one side edge of triangular prism to prepare nano scale graphene folds, and washed off triangular prism afterward as shown in Figure 2. We have measured the triode field emission properties on the setup as shown in Figure 1 insert picture. We found that the current Igc between gate and cathode is decreasing slightly with the voltage Ugc increasing when anode voltage Uac is higher than 1000V (we didn't show the picture). Voltage Ugc has controlled current Iac between anode and cathode a little bit, which could be seen in Figure 1 clearly. The nano scale sharp folds on monolayer graphene could be regarded as bilayer, and the top zone of folds would be high resistance. When voltage Ugc between cathode and gate is applied, the electric field around top zone of folds will be enhanced greatly. The current Iac with Ugc applied would be higher than that of without.

ACKNOWLEDGMENTS
This work was financially supported by the National Natural Science Foundation of China (Grant Nos. 91123018, 50975226, 61172040, ,61172041 and 60801022), the

National 863 Key Project of Panel Displays (Grant No. 2008AA03A314), and the Fundamental Research Funds for the Central Universities.

[1] Hyesung Park , Sehoon Chang , Joel Jean , “Graphene Cathode-Based ZnO Nanowire Hybrid Solar Cells,” Nano Lett., 2013, 13 (1), pp 233–239.

Figure 1. Field emission measurement results and schematic illustration of field emission measurement setup (inset picture). X axis represents the anode voltage.
Figure 2 Top view SEM image of graphene folds that average height is about 20 microns measured from insert optical micrograph.

NST-P3-07
Synthesis and characterization of a new semiconductor nano-particle (Ag2S) in a cage shaped bio-template, apoferritin

T10 Nanoscience and Technology

#NST-P3-07

K. Iwahori [1], K. Naoko [2], Y. Ichiro [2].

[1]Japan Science and Technology Agency, PRESTO - Kawaguchi (Japan), [2]Nara Institute of Science and Technology - Ikoma (Japan).

Various nano paerticles (NPs) are used or expect to be used in many nano-technology applications such as magnetic recording materials, catalytic materials, fluorescent markers, drug delivery systems, or quantum electronics. A lot of methods to produce NPs have been studied. Recently, a biological method using protein cages as the bio-template has become used for the uniform synthesis of metal and semiconductor NPs. We fabricated many kinds of NPs in a bio-template, apoferritin protein from horse spleen (HsAFr)[1)]. HsAFr, the cellular iron-storage protein, is a spherical hollow shell composed of 24 polypeptide subunits. The inner and outer diameters of the HsAFr shell are about 7 nm and 12 nm respectively. Many kinds of metal oxide NP cores (Fe, Co, Ni, In_xO_y) have been efficiently fabricated in the ferritin with small size dispersion. On the other hand, semiconductor NP is also a powerful tool for nano-electric applications, because they exhibit intriguing characters such as a fluorescent, size-effect and quantum effect. We designed a slow chemical reaction system (SCRY) for synthesis of compound semiconductor NPs in the HsAFr. We succeeded in the NPs such as CdSe, ZnSe, Au_2S, CdS, CuS, in the cavity of HsAFr with the narrow size dispersion[1)]. Especially, CdS NPs synthesized in the HsAFr showed the photoluminescence from their NPs and the size effect corresponding to the diameter of CdS NPs [2)]. In addition, the CdS NPs showed the activity of circular polarized luminescent (CPL)[3)].

In this contribution, we report a successful synthesis of new semiconductor NPs, Ag_2S NPs, in HsAFr. An optimization of Ag_2S NPs synthesis was performed and the results suggested that the concentration of ammonia water in the reaction solution is important to the synthesis of Ag_2S NPs. The synthesized Ag_2S NPs showed photoluminescence at 1280 nm by an irradiation of visible light. The analysis of

obtained Ag_2S NPs by X-ray powder diffraction (XRD) indicated that the NPs were Ag_2S cubic crystal. This is a first report of NP with near-IR photoluminescence in the ferritin protein. The obtained Ag_2S NP will be used as quantum dots for nano-electric devises, solar cell, DDS or infrared therapy. The possible biomineralization mechanism of the Ag_2S NP is now under investigation.

1) Ichiro Yamashita, *Biophys.Acta*., **1800**, 846 (2010)
2) Kenji Iwahori, *Nanotechnology*, **19**, 495601 (2008)
3) Naito Masahiro*, Kenji Iwahori*, *Angew.Chem. Int. Ed.*, **49**, 7006 (2010)

The 200eV TEM image of the synthesized Ag_2S NPs in the apoferritin cavity by stain 1% aurothioglucose. The scale bar is 20 nm. The white rings in the figure are ferritin protein shells and the black dots are Ag_2S NPs.

NST-8-Or-6
Tailoring two-dimensional hydrogen-bonded organic nanoarchitectures at the liquid-solid interface: the case of star shaped molecules and salen derivatives

T10 Nanoscience and Technology

#NST-8-Or-6

F. Silly [1], J. Hieulle [1], M. Viciano-Chumillas [2], T. Mallah [2].

[1]CEA - Saclay (France), [2]Université Paris Sud - Orsay (France).

Complex supramolecular two-dimensional (2D) networks are attracting considerable interest as highly ordered functional materials for applications in nanotechnology. The challenge consists in tailoring the ordering of one or more molecular species into specific architectures over an extended length scale with molecular precision. Highly organized supramolecular arrays can be obtained through self-assembly of complementary molecules which can interlock via intermolecular interactions. Molecules forming hydrogen and halogen bonds are especially interesting building blocks for creating sophisticated organic architectures due to high selectivity and directionality of these bindings. Molecular shape, size, structure and nature of molecular substituents as well as their position are key parameters governing the formation of self-assembled nanoarchitectures.

We used scanning tunnelling microscopy to investigate at the atomic scale the formation of hydrogen-bonded organic nanoarchitectures at the liquid-solid interface. We observed in the case of 1,3,5-triphenylbenzene star shaped molecules [1] that changing the nature of peripherical substituent modify the self-assembly of the molecules. Various porous nanoarchitectures having differently-shaped cavities can be engineered. In the case of star-shaped 2,8,14-tripropyloxy-5,11,17-triazatrinaphthylene derivatives, the nature of the bay substituants also plays a key role in the molecular self- assembly process. Porous or compact structure can be selectively created [2].
In comparison nickel salen derivatives with benzoic acid have a rectangular shape. By changing the nature of the substituants close to the metal atom we show that we

can tailor the structure of salen self-assembled nanoarchitectures. Compact and porous two-dimensional salen structures can be formed.

[1] F. Silly, Journal of Physical Chemistry C 116, 10029-10032 (2012).
[2] H. Bertrand, F. Silly, et al., Chemical Communications 47, 10091-10093 (2011).
[3] M. Viciano-Chumillas, J. Hieulle, T. Mallah, F. Silly, Journal of Physical Chemistry C 116, 23404-23407 (2012).

The research leading to these results has received funding from the European Research Council under the European Union's Seventh Framework Programme (FP7/2007-2013) / ERC grant agreement n° 259297.

1,3,5-triphenylbenzene porous structure (left) and salen derivative compact structure (right)

NST-P3-08
EVOLUTION OF THE CATALYTIC PROPERTIES OF DIFFERENT NANO-CRYSTALLINE TITANIUM DIOXIDE POWDERS COATED WITH ULTRATHIN MOLYBDENUM LAYER

T10 Nanoscience and Technology

#NST-P3-08

A. Hemberg [1], X. Noirfalise [2], H. Morgan [3], R. Fabian [1], R. Rony [2].

[1]Materia Nova - Mons (Belgium), [2]Umons - Mons (Belgium), [3]Université de Lille - Lille (Belgium).

Metal oxides represent one of the most important and widely employed categories of solid catalysts, either as active phases or supports. For example, oxygen deficient MoO_x/TiO_2 systems are strongly studied because of their wide applications in catalytic processes.[1] In that context, a lot of effort has been made to improve the surface-to-volume ratio of the system, for example by the generation of MoO_x-based nanostructures.[1] It has already been reported that evaporation of Mo on a (110) rutile TiO_2 surface leads to an interfacial reaction between the deposited metal and the substrate which generates MoO_x nanostructures.[1] Metal-coated particles are a state-of-the-art type of composite materials which present a high specific surface area. Among the potential approach to synthesize this type of composite, magnetron sputtering is a good candidate because it allows minimal impurity, good reproducibility, and flexibility in fabricating a wide variety of materials.[2]

In this work, different amount (0.5; 1; 1.5 and 2 at. %) of metallic molybdenum was deposited by magnetron sputtering on four types of TiO_2 nanoparticles (particle size < 100 nm) differing by their crystalline constitution. Anatase, rutile and two mixtures anatase-rutile (Degussa P25® and Aldrich reference N° 634662) are used. The morphology, the chemical composition and the crystalline properties of the resulting compound were characterized by field transmission electron microscopy (TEM), X-ray photoelectron spectroscopy (XPS) and X-ray diffraction (XRD) analysis. The catalytic properties of the product were evaluated by monitoring the degradation of methanol.

The results indicate that the nano-particles are successfully coated by molybdenum. Wathever the powder used, the XPS results reveal the oxidation of the deposited Mo likely due to oxygen transfer from the TiO_2 substrate. Finally, the catalytic tests show that the decomposition of methanol is dependent on both the amount of Mo and the crystallographic structure of the powders. The anatase powder containing 1 at. % of Mo presents the best conversion rate of ~70%.

[1] X. Noirfalise, F. Renaux, D. Cossement, N. Sebaihi, R. Lazzaroni, R. Snyders, Surface Science 606 (2012) 1680–1684.
[2] X. Yu, Z. Shen, Powder Technology 187 (2008) 239–243.

Figure 1: TEM image of Mo on anatase of titanium oxide powder.

NST-9-Or-11
Controlling structure and chemical order of Co-based supported clusters through thermal activation

T10 Nanoscience and Technology

#NST-9-Or-11

P. Andreazza [1], Z. Kataya [1], A. Lemoine [1], C. Andreazza-Vignolle [1], Y. Garreau [2], H. Khelfane [3], C. Mottet [4], A. Coati [2].

[1]CRMD - Orléans (France), [2]Synchrotron Soleil - Saint Aubin (France), [3]Université de Boumerdes - Boumerdes (Algeria), [4]CINAM - Marseille (France).

Compared to monometallic systems, the addition of one or several metals induces complex behaviors, not always well understood, which give a larger diversity in the structure and morphology of nanoparticles (NPs) and offer an additional degree of freedom to tune their properties for relevant applications - as in magnetic data or energy storage (fuel cell). Besides the composition effect, finite matter quantity effects lead to original variations of atom arrangement, such as disordered/ordered, segregated, core-shell, chemically-induced strained particles. The main challenge is to understand the origin of rearrangements of atomic species in multicomponent nanoparticles, which lead to such structures. The most complete thermodynamic equilibrium description of a nanoalloy is achieved by determining its phase diagram, as a function of size, composition and temperature. However, the kinetic effects which occur during the growth or the evolution of nanoalloys can yield out-of-equilibrium structures, not predicted by thermodynamic considerations alone. In all cases, because of this complexity, the determination of the atom arrangement at the nanoscale in Co-based particles (CoPt and CoAg) is a very difficult task, requiring the synergic efforts of experiment [1,2] and computer modelling [3].
Methods that probe local and average features as well as nanometer to micrometer-sized data, provide highly complementary information about the structure and morphology of nanostructures and are much powerful when used together. For that, we have developed combined X-ray scattering and electron microscopy strategy allowing the determination of the structure at the atomic scale range (small angles) and the morphology at the particle scale range (wide angles), respectively. Because the high reactivity of Co-based particles, x-ray experiments: Grazing Incidence Small-Angle X-ray Scattering (GISAXS) and Grazing Incidence X-ray wide angles

scattering (GIWAXS), are performed in situ in UHV conditions [1,2] during the nanoalloy growth obtained by vapor deposition or during thermal annealing. The quantitative structural analysis have been facilitated and consolidated using Monte Carlo (MC) simulations [2,3] of Co-Pt nanoalloys within a semi-empirical tight-binding potential, to identify the experimental phase transitions (ordered, disordered fcc, multi-twinned decahedra and icosahedra). In addition, the combination of GISAXS and GIWAXS with the anomalous effect (chemical selectivity) have allowed the extraction of scattering data from the two kind of metal atoms to identify core-shell atom arrangement [4].

1. P. Andreazza, in Nanoalloys: Synthesis, Structure and Properties edited by D. Alloyeau, C. Mottet, C. Ricolleau (Springer-Verlag, London, 2012) p69-112.
2. J. Penuelas, P. Andreazza, C. Andreazza-Vignolle, H. C. N. Tolentino, M. De Santis, C. Mottet, Phys. Rev. Lett. 100 (2008) 115502. and, J. Penuelas, et al. Eur. Phys. J., ST 168 (2009) 19.
3. P. Andreazza, C. Mottet, C. Andreazza-Vignolle, J. Penuelas, H.C.N. Tolentino M. De Santis, N. Bouet and R. Felici, Phys. Rev. B 82, (2010) 15.
4. P. Andreazza, H. Khelfane, O. Lyon, C. Andreazza-Vignolle, A. Ramos, M. Samah, Eur. Phys. J., ST 208, 237 (2012)

NST-2-Or-4
Atomic scale study of the first stage of silicide nanocrystals formation on Si(100) for nanoscale molecular contacts

T10 Nanoscience and Technology

#NST-2-Or-4

M. Yengui, D. Riedel.

ISMO, Université Paris Sud, 91405 Cedex - Orsay (France).

Silicides are widely applied in microelectronics devices and have generated substantial research interests due to their electronic structure and metallic properties. In the context of the design of nanometer scale devices, the control of the fabrication of metallic contacts is of crucial importance, particularly when their sizes reach 10 nanometers or below. As a consequence, molecular electronics can take over usual devices. The study of their electronic properties is now possible with scanning tunneling microscopy (STM) techniques bringing new insights to conventional approaches. Earlier experimental study indicate that adsorption of 0.04ML Co on Si(100) surface at room temperature lead to the formation of subsurface site and defect structures [1]. At higher coverage regime (0.1 - 0.8) ML, the formation of conductive pads is shown to be ruled by various parameters such as the surface temperature or the evaporation rate of Co [2, 3, 4]. Within this framework, we have firstly investigated the premises of the silicidation by studying the properties of cobalt atoms adsorbed on the bare silicon Si(100) surface cooled at 12K via at low temperature (9K) STM. We have shown that at 12K, typical Co-Si site can already be observed. Interestingly, the electronically induced reversible manipulation of cobalt adatoms could be performed at 9K. In a second step, we have studied the electronic properties of various cobalt silicide structures on Si(100) fabricated via exposing the hot (500°C ~ 700°C) Si(100) surface to 1ML of Co followed or not by annealing cycles. The various structures observed in each case are compared and their electronic properties are studied. Finally, we have studied the adsorption of Co-TPP molecules on structured silicides pads to potentially create contacts between them enabling new environments for the study of molecular circuits.

[1] J. Choi, Y. Kim, D. K. Lim, D. H. Kim, and S. Kim. J. Phy. Chem. C. 115, 15467-15470 (2011)
[2] I. Goldfarb and G. A. D. Briggs. Phys. Rev B. 60, 4800, (1999)
[3] B. L. Ong , W. Ong , Y. L. Foo , J. Pan , E. S. Tok. Surface Science. 606, 1649-1669 (2012)
[4] J. C. Mahato, D. Das, R. R. Juluri, R. Batabyal, A. Roy, P. V. Satyam and B. N. Dev. App. Phy. L. 100, 263117 (2012)

NST/SS-P1-07
Raman and luminescence properties of single- and few-layer crystals of group VI transition metal dichalcogenides

T10 Nanoscience and Technology

#NST/SS-P1-07

M. Tanaka [1], D. Ogawa [1], S. Okawara [1], S. Ohno [1], T. Suzuki [2].

[1]Yokohama National University - Yokohama (Japan), [2]National Defense Academy - Yokosuka (Japan).

Group VI Transition metal dichalcogenides MX_2 (T=Mo, W, X=S, Se) crystallize in a layered structure and can be easily cleaved in single- or few-layers like graphene which is a strong candidate for the future electronic devices because of high electron mobility. The weak point of graphene transistor is very low on/off ratio because of metallic character. Recently, single-layer MoS_2 transistor was demonstrated to have high mobility comparable to that of graphene nanoribbons and much higher on/off ratios [1]. Since then, physical properties of single- and few-layer MoS_2 have been intensively studied, but those of other WX_2 have not yet been reported except for theoretical calculations. In this study, Raman and luminescence properties of single- and few-layer crystals of WS_2, WSe_2, MoS_2 and $MoSe_2$ are investigated in order not only to explore layered semiconductors more suitable for electronic devices, but also to understand the underlying mechanism of the physical properties.
Typical Raman spectra of A_{1g} and E^1_{2g} modes for single-, few-layers and bulk in WS_2 are shown in Fig. 1. The A_{1g} modes upshift with increasing number of layers in the four MX_2. On the other hand, the E^1_{2g} modes upshift in WS_2 and WSe_2, in contrast, they downshift in MoS_2 [2] and $MoSe_2$. Moreover, the downshift of E^1_{2g} mode with increasing number of layers is apparently correlated with anomalous Davydov splitting between E^1_{2g} and E_{1u} modes in the bulk.The upshift of A_{1g} mode is due to the short-range interlayer interaction, while the metal-dependent frequency trend of E^1_{2g} mode is explained in terms of a stronger dielectric screening of the long range Coulomb interaction between the effective charges, in the same way as in MoS_2 [3]. According to this interpretation, present result indicates that the dielectric screening in MoX_2 is stronger than that in WX_2.
Luminescence spectrum of few-layer MX_2 exhibits two peaks corresponding to direct and indirect transitions. The peak intensity of the direct transition considerably decreases with increasing number of layers as found in MoS_2 [4]. The peak energy of

the indirect transition shifts to lower energies with increasing number of layers. Variation of the Raman intensity ratio $I(E^1_{2g})/I(A_{1g})$ with number of layers, especially apparent in WX_2, may be related to this energy shift through some resonant effect.

[1] B. Radisavljevic *et al*., Nature Nanotech. 6, 147 (2011).
[2] C. Lee *et al*., ACS Nano 4, 2695 (2010).
[3] A. Molina-Sanchez and L. Wirtz, Phys. Rev. B 84, 155413 (2011).
[4] K. F. Mak *et al*., Phys. Rev. Lett. 105, 136805 (2010).

Fig. 1. Raman spectra of the A_{1g} (~420cm^{-1}) and E^1_{2g} (~350cm^{-1}) modes for single-, few-layers and bulk WS_2.

NST-P1-18
A Novel Fabrication Process of Self-organized Epitaxial Ag Nanodods: Ti Seed Layer Mediated Bilayer Agglomeration Phenomenon

T10 Nanoscience and Technology

#NST-P1-18

M. Kamiko [1], R. Suenaga [2], K. Nose [1], J.W. Koo [3], K. Kyuno [2], Y. Mitsuda [1], J.G. Ha [4].

[1]Institute of Industrial Science, The University of Tokyo - Tokyo (Japan), [2]Department of Material Science, Shibaura Institute of Technology - Tokyo (Japan), [3]National Institute for Materials Science - Tsukuba (Japan), [4]Department of Electronic Materials Engineering, Kwangwoon University - Seoul (Korea, republic of).

Methodologies for fabrication of functional nanostructures with specific patterns are in the limelight. Above all, thermal agglomeration phenomenon could be considered as a useful tool for bottom-up materials processing. Recently, we developed a new fabrication process for self-organized nanostructure of metal films by using of a bi-layer agglomeration (BLA) phenomenon [1, 2]. In this study, we report the nano-structural control of epitaxial Ag on MgO substrates via Ti seed layer mediated BLA phenomenon.

Ag/Ti thin films were deposited by RF magnetron sputtering on MgO(100) and (110) substrates. A Ti seed layer (2 nm) and an Ag layer (2 ~ 10 nm) were deposited on the substrates without any heating. Then, the Ag/Ti layer was annealed for 3 ~ 6 hours to promote the agglomeration.

A variety of surface morphologies were obtained by changing the growth conditions, such as annealing temperature, duration of annealing, Ag layer thickness, substrate orientation, etc. Fig. 1 shows the typical AFM image of surfaces of the Ag/Ti films on the MgO(100) substrate after annealing. Self-organized nanodot arrays were formed. The diameter and height of the majority of the nanodots are 120 ~ 160 and 50 ~ 60 nm, respectively. In the case of Ag/Ti on the twofold symmetry MgO(110) substrate,

a relatively large number of rectangular-shaped nanodots (aspect ratio is about 1.4) are confirmed (Fig. 2). XPS and AES results indicated that the fabricated nanodots were mainly covered with Ag. The results of XRD revealed that Ag/Ti films were epitaxially grown on the substrates; the growth orientations of Ag nanodots resulted in a fcc-Ag(100) and (110) structure on the MgO(100) and MgO(110) substrate, respectively. We also observed surface plasmon resonance spectra of the nanostructured Ag/Ti samples.

[1] M. Kamiko et al., J. Vac. Sci. Technol. A30, 031512 (2012).
[2] M. Kamiko et al., Patent Number JP2011137230-A (2011).

Fig. 1 AFM image of Ag(5 nm)/Ti(2 nm)/MgO(100) after annealing at 350 ˚C for 4 hours.
Fig. 2 AFM image of Ag(10 nm)/Ti(2 nm)/MgO(110) after annealing at 350 ˚C for 4 hours.

NST-5-Or-7
Sensitivity in SubSurface-AFM: Tip-Sample Interaction in Heterodyne Force Microscopy

T10 Nanoscience and Technology

#NST-5-Or-7

G. Verbiest, T.H. Oosterkamp, M.J. Rost.

University of Leiden - Leiden (Netherlands).

Experiments in Heterodyne Force Microscopy (HFM) show the possibility to image deeply buried nanoparticles below a surface [1]. In HFM both the tip and the sample are excited at slightly different ultrasonic frequencies in the range of a few MHz such that a difference frequency signal is generated at 1 kHz that contains the subsurface information. However, the contrast mechanism and the motion of the cantilever, which detects the subsurface signal, are not yet understood.

We present both an experimental and a numerical study of the cantilever motion in a HFM mode, where both the ultrasonic frequencies and the difference frequency are far from any resonance of the cantilever [2,3]. The results provide information on the sensitivity to subsurface features.

We calculate and measure the amplitude and phase of the difference frequency generated by the motion of the cantilever. The amplitude shows in both the numerical calculations and the experiments a local maximum in the attractive Van-der-Waals regime and an even higher plateau in the repulsive regime.

Contrarily to what was previously suggested [4], we show how the repulsive part of the tip-sample interaction does generate a signal at the difference frequency.

[1] G.S. Shekhawat and V.P. Dravid, Science 310, 5745 (2005) 89-92
[2] G.J. Verbiest, T.H. Oosterkamp, and M.J. Rost; Ultramicroscopy (submitted)
[3] G.J. Verbiest, T.H. Oosterkamp, and M.J. Rost; Phys. Rev. Lett. (to be published)
[4] L. Tetard, A. Passian, S. Eslami, N. Jalili, R.H. Farahi, and T. Thundat; Phys. Rev. Lett. 106, 18 (2011) 180801

NST/SS-P1-08
Nanopatterning of carbon nanotubes such as single wall and cup-stack carbon nanotubes on nanostructured aluminum surfaces

T10 Nanoscience and Technology

#NST/SS-P1-08

Y. Watanabe, R. Takeuchi, M. Mutoh, H. Kato, S. Takemura, K. Shimada, T. Hiramatsu.

Kanto Gakuin University - Yokohama (Japan).

Development of nano-patternig techniques for the application of carbon nanotubes (CNTs) is an important issue for the production of next-generation devices with CNT.[1] The purpose of the present study is to develop patterning techniques for single wall carbon nanotube (SWNT) and cup-stack carbon nanotube (CSCNT) using nanostructured Al surface as a template. Furthermore the authors intend to investigate the local electronic properties of CNT patterns formed on the nanostructured Al surface. Nanoscale trenches and crater structures were fabricated on an Al surfaces by combined process of chemical treatments and anodization. SWNTs dissolved in catechin containing solution under the ultrasonic wave to separate the bundles of carbon nanotubes. Then droplets of this solution were dropped on the Al template utilizing micropipette and were extended on the surface. Fabricated CNTs patterns were analyzed by Atomic Force Microscopy/Current Imaging Tunneling Spectroscopy (AFM/CITS), Dynamic Force Microscopy (DFM) and Laser Raman Spectroscopy. Figure 1 shows AFM/CITS images of SWNTs on Al line structure. SWNTs were clearly localized in the Al trench and across the line structures as shown in Figs. 1 (a) and 1 (b), respectively. The difference in I-V characteristic was observed on the CNTs as shown in Fig. 1 (c). Next nano-contact transcription was conducted to transfer the CNTs pattern to the Si substrate. Nano-contact transcription was performed according to the following steps. A silicon substrate was attached on a CNT deposited Al template and was removed to transfer the CNTs pattern to the Si substrate. A highly oriented CNTs line pattern was obtained on a Si wafer by nano-contact method using an Al line structure as a template. The line-width of CNTs was less than 100 nm and the height was 3nm. In

the measurement of I-V characteristics by point contact, quantum conductivity such as oscillation-type and staircase-type were observed. On the other hand, in the case of CSCNT deposited on the nanostructured Al surface, the DFM image shows that the CNTs are significantly bending and networking with other tubes. Isolated single CSCNT image was also obtained. Local IV characteristic were also obtained by point-contact indicating that non-linear conductivity associated with negative resistivity. This work was aided by MEXT-supported Program for the Strategic Research Foundation at Private Universities.

1) M. S. Dresselhaus, G. Dresselhaus and R. Saito, Carbon 33, 883 (1995).

Fig. 1. AFM/CITS images of SWNTs on nanostructured Al trenches. (a) AFM image, (b) Current image, and (c) I-V characteristics were obtained.

NST/SS-3-Or-2
Superconducting gap of beta-HfNCl investigated by scanning tunneling microscopy/spectroscopy and break-junction tunneling

T10 Nanoscience and Technology

#NST/SS-3-Or-2

T. Ekino [1], A. Sugimoto [1], A. Gabovich [2], Z. Zheng [1], S. Yamanaka [1].

[1]Hiroshima University - Higashi-Hiroshima (Japan), [2]Institute of Physics - Kiev (Ukraine).

It is well known that electron doping of the layered compounds β -*M*NCl makes them superconducting with the critical temperature T_c = 14 K (*M* = Zr) – 26 K (Hf) [1]. Since Tc is relatively high, a question arises about the relevant superconductivity mechanism.
Our previous experiments using scanning-tunneling microscopy/spectroscopy (STM/STS) and break-junction tunneling spectroscopy (BJTS) clarified unexpectedly large superconducting gap (2Δ) with the ratio $2\Delta/k_BT_c$ up to ~ 10 or more [2, 3]. Such a huge ratio in contrast to the weak-coupling BCS one 3.5 cannot be explained in the framework of the conventional approach. In particular, the density functional theory indicates that the strong-coupling electron-phonon Migdal-Eliashberg theory fails to explain superconductivity of β-MNCl [4]. Therefore, further systematic measurements are necessary to elucidate the nature of superconductivity in β-MNCl.
In this paper, properties of temperature, *T*, evolution of the local gap Δ in β-$HfNCl_x$ (*x* = 0.7) are examined by STM/STS with atomic resolution as well as BJTS measurements.
STM/STS studies were carried out with a micro single crystal and a PtIr tip under ~ 10^{-8} Pa. At the lowest *T* = 4.9 K, the STM image of the *ab* plane shows a triangular lattice of Hf atoms with a period of ~ 0.37 nm, which agrees with the X-ray diffraction measurements. The local STS conductance *G*(*V*) exhibits broadened gap structures, showing rather homogeneous magnitudes within the area of ~100 nm^2 as compared with the results for isostructural $ZrNCl_x$.
A remarkable feature of *G*(*V*) mappings is that the gap distribution systematically varies with *T*. At 5 K, the spatially averaged gap value defined by the peak-to-peak distance of *G*(*V*) is Δ_{ave} ~ 11 – 13 meV. The gap distribution widely spreads up to ~

30 meV, while rather sharp cutoff of the tail occurs at 6 - 8 meV. The upper-boundary of ~ 30 meV in the distribution occupies only a few ~ nm domains. Such features are very similar to the gap distribution of β-$ZrNCl_x$. They are most probably due to the electronic inhomogeneity rather than the bulk crystallographic one, because we observed such an inhomogeneity simultaneously in the regular atomic lattice arrangement on the surface.
At T = 20 K, the distribution profile changes, namely, Δ_{ave} is decreased to ~ 7 meV, showing the spread up to ~ 15 meV along with the gapless tail. It means that the local Cooper pairing in some ~ nm regions is kept almost unchanged upon warming, while superconductivity in other surface areas is reduced much faster than what would be expected from the mean-field thermal behavior. This circumstance may be the origin of the unusual T-dependence of the gap value in this compound previously found by BJTS [2]. Wide gap distributions with large maximum gap features are discussed in more detail for β-$MNCl_x$ (M = Hf, Zr) and α-TiNCl with different crystal structures [3].

[1] S. Yamanaka, K. Kotehama, H. Kawaji, Nature 392 (1998) 580.
[2] T. Takasaki, T. Ekino, A. Sugimoto, K. Shohara, S. Yamanaka, A.M. Gabovich, Eur. Phys. J. B 73 (2010) 471.
[3] A. Sugimoto, K. Shohara, T. Ekino, Z. Zheng, S. Yamanaka, Phys. Rev. B 85 (2012) 144517.
[4] R. Akashi, K. Nakamura, R. Arita, M. Imada, Phys.Rev.B 86 (2012) 054513.

NST/SS-P1-09
Humidity sensing properties of graphene

T10 Nanoscience and Technology

#NST/SS-P1-09

Z. Lišková, M. Bartos, P. Procházka, M. Bartošík, J. Mach, J. Spousta, T. Šikola.

Institute of Physical Engineering, Brno University of Technology and CEITEC BUT - Brno (Czech republic).

Graphene, a very promising material studied extensively in the last decade, is a two dimensional material composed of carbon atoms formed into a honeycomb lattice. It is a building material for other graphitic forms – fullerenes, carbon nanotubes and, of course, graphite. Graphene has extraordinary properties due to its limited dimensions in one direction, primarily low resistance, high mobility and very high transparency for light. Its conductivity can be continuously changed from n-type to p-type due to an ambipolar electric field effect [1].
These properties and also high sensitivity, fast response in electrical properties, and large surface to volume ratio make graphene a very promising candidate for utilization in different types of sensors [2, 3]. As a rule, graphene oxide films are widely used for these purposes.
In our work the humidity sensing properties of pure graphene itself have been studied. Graphene was prepared by two methods – the chemical vapor deposition (CVD) and as a reduced graphene oxide by modified Hummer's method. Both types of graphene were transferred onto a dielectric substrate (280 nm SiO_2/Si). The metal contacts on graphene were prepared by electron beam lithography for the measurement of its electrical properties. The resistivity was measured by the 2-point method and its changes were observed in dependence on relative humidity changes. Relative humidity ranged from 10 to 80 %. It was found that graphene resistivity was growing with relative humidity and the sensing response was very fast.

[1] GEIM, A. K., NOVOSELOV, K. S., Nature Materials, 6 (2007), p. 183

[2] MASSERA, E., at al.: Chemistry Today, 29 (2011), p. 39

[3] YAO, Y., at al., Nanoscale Research Letters, 7 (2012), p. 363

NST-13-Or-9
Growth of Ge thin films on GaAs and In0.53Ga0.47As

T10 Nanoscience and Technology

#NST-13-Or-9

M. Zrir.

CINaM - Marseille (France).

Growth of Ge thin films on GaAs and $In_{0.53}Ga_{0.47}As$

M. Zrir[1],*, M. Petit[1], N. Bertru[2], M. El Kurdi[3], A. Ghrib[3], P. Boucaud[3], V. Le Thanh[1]

[1] CINaM CNRS, Campus de Luminy, Case 913, F - 13288 Marseille Cedex 09
[2] Laboratoire FOTON, INSA, 20 av. des Buttes de Coësmes CS 70839, F – 35708 Rennes Cedex
[3] Institut d'Electronique Fondamentale, Université Paris-Sud, Bât. 220, F - 91405 Orsay
* mzrir@hotmail.com

The semiconductors of the group IV are the basic materials in microelectronics. Because of the indirect nature of there band gap, it was necessary to proceed to researches on the semiconductors of III-V group (GaAs, GaInN …) and II-VI group (CdTe) to use their capability as light emitters in optoelectronics devices. Contrary to Si, germanium presents an interesting optical property, that its gap direct is only at 0.14 eV above the indirect one, while for Si this interval is about 2 eV. Theoretically, it has been demonstrated that the Ge gap could be a direct one under a tensile strain of 1.4%, opening the way towards the realization of optoelectronic devices compatible with the microelectronic technology [1]. One of the experimental approaches to introduce a tensile strain in the film is to deposit Ge on a substrate that has a larger lattice constant. In this context the Ge epitaxy on $In_xGa_{1-x}As$/GaAs substrate has been recently studied, with x ranges between 4.8% and 21% [2, 3]. However, for higher indium content, the use of the substrate $In_xGa_{1-x}As$ on GaAs becomes very difficult due to the surface roughness and the threading dislocations. In order to study the growth of Ge on a substrate with relatively high lattice mismatch (In-content more than 21%), we used $In_{0.53}Ga_{0.47}As$ buffer layers deposited on InP substrates. Taking into account that $In_{0.53}Ga_{0.47}As$ and InP have the same lattice constant, the $In_{0.53}Ga_{0.47}As$ buffer layer does not contain dislocations, and its surface

is atomically flat. The lattice mismatch between Ge and $In_{0.53}Ga_{0.47}As$ is of 3.7%, which presents probably the largest value up to now.
We carried out a preliminary study on growth of Ge on GaAs in order to optimize the Ge growth parameters. We have found that the growth mode is layer-by-layer for the temperature range [RT; 550°C], and films of a good crystalline quality could be made on GaAs As-rich (2x4)-reconstructed substrates. After that, we have studied the growth of Ge on the As-rich (2x4)-reconstructed $In_{0.53}Ga_{0.47}As$ surface as a function of the growth temperature (T_C). The growth on $In_{0.53}Ga_{0.47}As$ follows the Stranski-Krastanov mechanism. The RHEED analysis shows that the critical thickness corresponding to the 2D-3D nucleation decreases when T_C is increased: 3 monolayers for the deposition at RT and 300°C, whereas 1 ML at 450°C. Several types of island morphologies have been observed. Analysis by photoluminescence (PL) spectroscopy will be done in order to estimate the confinement effects as a function of the islands size.

[1]. J. Liu, X. Sun, R. Camacho-Aguilera, L. C. Kimerling, and J. Michel, Opt. Letters **35**, 679 (2010)
[2]. Y. Bai, K. E. Lee, C. Cheng, M. L. Lee, and E. A. Fitzgerald, J. Appl. Phys. **104**, 084518 (2008)
[3]. R. Jakomin, M. de Kersauson, M. El Kurdi, L. Largeau, O. Mauguin, G. Beaudoin, S. Sauvage, R. Ossikovski, G. Ndong, M. Chaigneau, I. Sagnes, and P. Boucaud, Appl. Phys. Letters **98**, 091901 (2011)

NST-P1-03
Electrochemical impedance spectroscopy as a method to control nanowire array quality in porous template

T10 Nanoscience and Technology

#NST-P1-03

G. Kunakova [1], J. Katkevics [2], A. Viksna [2], Z. Alute [1], J.D. Holmes [3], D. Erts [1].

[1]Institute of Chemical Physics, University of Latvia - Riga (Latvia), [2]Department of Analytical Chemistry, University of Latvia - Riga (Latvia), [3]University College Cork - Cork (Ireland).

Nanowires are eligible for application in different electrical devices as functional and constructional elements. To obtain high density architectures for integrated elements, it is convenient to employ nanowire arrays. Although various approaches of nanowires array fabrication have been shown, the template methods present the most advantages, e.g. nanowires are well aligned and mutually isolated [1]. To characterize template grown arrays, it is important to determine nanowire filling quality into a porous template. Conductive AFM measurements can be used for conductance mapping of small areas [2]. However this approach is incapable to do analysis in a range of several square centimeters. In this work we have applied the electrochemical impedance spectroscopy (EIS) as none-destructive method to determine nanowires' filling quality in a porous template combined with electrochemical characterization.

EIS characterization was performed on Bi_2S_3 nanowire arrays grown in anodic aluminum oxide membranes (AAO). Samples ranging in density of nanowire filling from 77% to 99% of nanowires in AAO template as well as an empty AAO reference sample were analyzed. To measure such fragile samples, a specific electrochemical cell with small total volume of electrolyte was fabricated. Measurements were done with a potentiostat "Autolab PGSTA 30" and impedance spectra were analyzed using a program Frequency Response Analysis (FRA) to determine the equivalent electrical circuit and separate impedance element values.

EIS data of empty AAO and Bi_2S_3/AAO samples we interpreted with equivalent circuit model $R_e([R_2(R_3Q_2)]C_1)$, where R_e is electrolyte resistance; R_2 is electrolyte resistance with nanowires in nanopores; R_3 and Q_2 – resistance and capacitance in nanopores; C_1 – capacitance of aluminum oxide nanopores walls. Analysis of the values of individual elements such as R_2, C_1 and impedance modulus for high and low nanowire filling density samples showed a specific correlation between these values and nanowire filling density thus indicating on nanowire array quality in porous template.

1. Xu, J.; Petkov, N.; Wu, X.; Iacopino, D.; Quinn, A. J.; Redmond, G.; Bein, T.; Morris, M. A.; Holmes. J. D. *Chem. Phys. Chem.*, 2007, 8, 235–240.
2. Erts, D.; Polyakov, B.; Daian, B.; Morris, M. A.; Ellingboe. S.; Boland, J.; J. D. Holmes., *J. Phys. Chem. B*, 2006, 110, 820–826.

FMMM/NST-P3-04
Functionalisation and charatcterisation of the Porous Silicon Nanostructure by the peptide Gly-Cys-Gly-Cys

T10 Nanoscience and Technology

#FMMM/NST-P3-04

C. Yaddaden, S. Sam.

CRTSE - Algiers (Algeria).

Hybrid nanomatrials based on organic layer covalently grafted on porous silicon PSi nanostructure appear as promising systems for innovative applications [1]. In this work, we focused on the functionalization of the PSi nanostructure by the peptide Gly-Cys-Gly-Cys, which forms stable complexes with metal ions. This property is exploited to realize toxic metal recognition in water.
The immobilization was achieved using multi-step reactions: Gly-Cys-Gly-Cys was anchored on a previously prepared carboxyl-terminated PSi surface using EDC/NHS coupling agents. This scheme is compatible with the mild conditions required for preserving the probe activity of the peptide. At each step of the functionalization, the surface was monitored by infrared spectroscopy Fourier transform (FTIR) and X-ray photoelectron spectroscopy (XPS).
Electrochemical behaviour of such prepared electrodes was carried out in the presence of copper ions by means of cyclic voltammetry [2]. The recorded cyclic voltammograms showed a quasi-irreversible process corresponding to the Ni2+/Ni0 couple.
These results demonstrate the potential role of peptide-modified PSi nanostrutures in developing strategies for simple and fast detection of metal ions in solution.

[1]. S. SAM, « Complexes bioinorganiques de silicium poreux fonctionnalisé avec des métaux de transition », Thèse d’état, USTHB, Juillet 2010.

[2]. A. Uhlir. "Electrolytic shaping of germanium and silicon". Bell Syst. Tech. J., vol. 35

:page 333, (1956).

NST/SS-P1-10
Carbon drawn graphene films on nanostructured aluminum surfaces

T10 Nanoscience and Technology

#NST/SS-P1-10

S. Takemura, T. Hirakawa, K. Doi, H. Kato, T. Hiramatsu.

Kanto Gakuin University - Yokohama (Japan).

In the present study, the authors focused on fabrication of graphene on nanostructured surfaces by carbon drawing method using HOPG. The carbon drawing method is simpler than the taping method. It is expected that carbon drawing method is also applicable to non-flat surfaces. In the present study, the authors performed carbon drawing method to drag it along nanostructured Al surfaces. Two Al samples were made by immersion in acid solutions. As for the first sample, an Al substrate was immersed in 0.1M H_2SO_4 solution at 35℃ for 24 hours. An Al plate was immersed in 0.1M H_3PO_4 solution at 4℃ for 1 week for the second sample. Then anodization was performed for acquisition of finer nanostructures on the surfaces. Then, carbon drawing was performed on the nanostructured surfaces using HOPG whose surface was renewed by peeling surface layers off with using scotch tape before carbon drawing. Rhombic-shaped craters whose diameters were about 100-200 nm were created on the surface treated with H_2SO_4 [Fig. 1(a)]. After drawing, terrace-like structure was observed whose height was about 20 nm [Fig. 1(b)]. In the Raman spectrum, some characteristic peaks due to carbon such as G, D, and G' bands were observed after drawing. If G/G' is equal to 1.8, the number of graphene layer is 23.[1] In this case, G/G' is about 2.0. This result shows that the number of graphene layer is estimated at over 23. Carbon drawing was performed also on the Al surface treated with H_3PO_4. Rhombic-shaped craters whose diameters were about 600-700 nm were created on the chemically treated Al surface. In this case, a thick film was obtained whose thickness was about 500 nm corresponding to 500 layers. Because the size of craters formed on the Al surface was larger than the former sample, it suggests that graphite layers are more easily peeled off from HOPG. In this case, G/G' is about 2.5 in the Raman spectrum. Both samples have D band, so graphene films in both samples are distorted. Since the intensity of D band in the former sample is less than the latter sample, thin film of former sample is not less distorted than the latter sample. The current image after drawing was obtained by atomic force microscopy/current image tunneling spectroscopy (AFM-CITS)

measurements. Current is not flowing along a cliff formed on the film surface. A characteristic I-V curve was obtained also at the edge of the film, which indicates quantum conduction. This work was aided by MEXT-supported Program for the Strategic Research Foundation at Private Universities.

1) Anindya Das et al, Indian Academy of Sciences, 579 (2008).

Fig.1 DFM images of aluminum surfaces before and after drawing. (a) Before drawing (b) After drawing.

SS/NST-P1-02
Experimental and computional insights at the molecular level of the p-nitroaniline solid-liquid interface

T10 Nanoscience and Technology

#SS/NST-P1-02

P. Spijker [1], T. Hiasa [2], H. Onishi [2], A.S. Foster [1].

[1]Aalto University, Department of Applied Physics, COMP Center of Excellence - Helsinki (Finland), [2]Kobe University, Department of Chemistry - Kobe (Japan).

Solid-liquid interfaces play a fundamental role in many biomolecular and electrochemical applications at the nanoscale. Although spectroscopy and di raction techniques can provide very accurate information about such interfaces, atomic force microscopy (AFM) has the advantage of probing the investigated system locally, thus allowing a deeper understanding of interfaces. Latest developments in frequency modulated AFM (FM-AFM) have opened up a way to observe interfacial liquid structures as a function of the vertical and lateral coordinates [1]. Recently experiments on the p-nitroaniline (101) crystal surfaces in water have been performed in order to better understand the stability and the mechanisms of nucleation or dissolution at crystal surfaces [2]. p-Nitroaniline is an organic compound containing polar NH_2 and NO_2 groups at opposite ends of a benzene ring, and although being a relative simple compound, it gives rise to enough complexity to serve as an excellent experimental test case.

In the experiments clear structuring of the water at the interface is observed. In order to enhance the insight obtained through the FM-AFM experiments on these p-nitroaniline-water interfaces, we performed both DFT and large-scale molecular dynamics simulations of this system. In these simulations we observed that the (101) crystal surface di
ers considerably from the same surface based on existing crystallographic data [3, 4], giving rise to a more elaborate description of the water interface structure observed in the experiments. As such the computer simulations proved to be an important addition for better understanding the AFM experiments.

[1] K. Kimura, S. Ido, N. Oyabu, K. Kobayashi, Y. Hirata, T. Imai, and H. Yamada, Visualizing water molecule distribution by atomic force microscope, J. Chem. Phys., 132:194705 (2010).
[2] R. Nishioka, T. Hiasa, K. Kimura, and H. Onishi, AFMStudy of Specific Hydration on p-Nitroaniline Crystal, submitted (2013).
[3] S.C. Abrahams and J. Monteath Robertson, The Crystal Structure of p-Nitroaniline, NO2.C6H4.NH2, Acta Cryst., 1:252–259 (1948).
[4] K.N. Trueblood, E. Goldish, and J. Donohue, A Three-Dimensional Refinement of the Crystal Structure of 4-Nitroaniline, Acta Cryst., 14:1009–1017 (1961).

NST-P2-03
Effect of focused Ga+ ion beam etching on nanostructured La2Ti2O7 piezoelectric thin films

T10 Nanoscience and Technology

#NST-P2-03

A. Bayart [1], A. Ferri [1], S. Saitzek [1], Z. Shao [1], G. Declercq [1], J. Costecalde [2], D. Rémiens [2], D. Deresmes [3], D. Troadec [3], R. Desfeux [1].

[1]Univ Lille Nord de France, F-59000 Lille, France ; CNRS UMR 8181, Unité de Catalyse et de Chimie du Solide – UCCS ; UArtois, F-62300 Lens - Lens (France), [2]Univ Lille Nord de France, F-59000 Lille, France ; CNRS UMR 8520, Institut d'Electronique, de Microélectronique et de Nanotechnologie – IEMN-DOAE-MIMM ; UVHC, F-59313 Valenciennes - Villeneuve D'ascq (France), [3]Univ Lille Nord de France, F-59000 Lille, France ; CNRS UMR 8520, Institut d'Electronique, de Microélectronique et de Nanotechnologie – IEMN ; F-59652 Villeneuve d'Ascq - Villeneuve D'ascq (France).

Among the ferroelectrics, the layered-perovskite lanthanum dititanate oxide La2Ti2O7 (LTO) is a very promising lead-free ferroelectric material, due to its super-high Curie temperature (TC ~1500°C) and piezoelectric behavior which allow the development of high-temperature devices such as transducers for motor and spatial industry and applications in extreme environments.
In this study, such compounds were grown in thin film form on SrTiO3 substrates by a sol–gel route.[1] At the nanoscale, both poling experiments performed by the tip of atomic force microscope and the existence of local piezoresponse loops within the domains confirm the piezoelectric behavior of the films.[2] Islands in the lateral range 300-500 nm have been successfully fabricated by focused Ga+ ion beam (FIB) etching on platinum top electrode. The impact of Ga+ FIB about functional properties of continuous and nanostructured crystallized piezoelectric thin films of LTO has been investigated on the nanoscale by scanning probe microscopy. Modifications of both surface and electrical behavior for area exposed to ion irradiation are revealed by dynamic force mode and Kelvin force microscopies. Nevertheless, local piezoactivity is still detected confirming the highly resistance of this material to ion-beam.[3] Nanoscale electromechanical response is measured inside these nanostructures by piezoresponse force microscopy. In this case, the local piezosignal

is measured at similar level that the one obtained for the unetched film evidencing no manifest sidewall effect, and this without usual post-annealing treatment for recovering functional properties.[4] Consequently, this study demonstrates that LTO material as well as FIB technique are suitable and promising to pattern such low-dimensional nanostructures, allowing the application of such lead-free piezoelectric thin films in the field of nanoelectromechanical systems.

[1] Z. Shao, S. Saitzek, P. Roussel, M. Huvé, R. Desfeux, O. Mentré, F. Abraham, Journal of Crystal Growth 311 (2009) 4134.
[2] Z. Shao, S. Saitzek, E. Bruyer, A. Sayede, A. Ferri, M. Rguiti, P. Roussel, O. Mentré, R. Desfeux, Advanced Engineering Materials 13 (2011) 961.
[3] K.R. Whittle, G.R. Lumpkin, M. G. Blackford, R.D. Aughterson, K.L. Smith, N.J. Zaluzek, Journal of Solid State Chemistry 183 (2010) 2416.
[4] A. Ferri, S. Saitzek, Z. Shao, G. Declercq, J. Costecalde, D. Rémiens, D. Deresmes, D. Troadec, R. Desfeux, submitted in Journal of Applied Physics.

NST/SS-P1-11
Fabrication and Electrical Transport Measurements of Graphene Devices with End-Contact Geometry

T10 Nanoscience and Technology

#NST/SS-P1-11

Y. Sung, A. Subagyo, K. Sueoka.

Graduate School of Information Science and Technology, Hokkaido University - Sapporo (Japan).

The contact properties between metal electrodes and graphene in graphene devices are crucial to the device performance. Various metals such as Ni, Pd, Au, Pt, Cr, Al and Cu have been applied for fabricating the graphene devices. The device performances have been found to strongly depend on the metal species due to the variation of the contact resistance such as the variation of ON current and carrier mobility in graphene field effect transistors [1-4]. In general, high work function metals such as Pd, Ni and Au provide a low contact resistance and, therefore, are routinely applied for graphene devices. However, the improvement of contact properties is still needed, for example, for high speed electronic application. In this work, we propose a fabrication method for realization graphene devices with end-contact (EC) geometry which has been predicted to form lower contact resistance than the commonly fabricated geometry, i.e. side-contact (SC) [5]. The difference in chemical bonding of end-contact and side-contact geometries is the major key for the improved junction properties. The fabrication of end-contact geometry, however, is much more difficult since metals should be vertically contacted to graphene's edges so that the contact length is limited to the nanometers range. Therefore, the development of a fabrication method of EC geometry is a challenge.

We have fabricated side-contacted devices and end-contacted devices on the same graphene channel for direct comparison. Several devices with channel length between 0.5 and 3 um are fabricated for both SC and EC devices. The transmission line method is used to estimate the contact resistance. The graphene layers were prepared by mechanical exfoliation using a Scotch tape from HOPG and direct transfer into a highly doped Si substrate covered with 285 nm-thick SiO_2. The number of the graphene layer was determined by Raman spectroscopy and atomic force microscopy measurements. The graphene channel with 1 um in width and several tenths um in length is obtained by electron beam lithography patterning and

O_2 plasma etching. Firstly, the SC devices were fabricated by EB patterning and Au-covered Ni electrode deposition. After patterning the electrode areas of EC devices with the same channel length to the SC, the exposed graphene of the patterned areas was removed by Ar^+ ion etching. In this step, several nanometers of SiO_2 under the graphene are removed altogether to allow perpendicular contact between graphene edges and metal electrode. Finally, Au-covered Ni electrodes of similar thickness to SC devices were deposited. The transport properties were evaluated using semiconductor parameter analyzer with the Si substrate as a backgate. The transport characteristics of both SC and EC devices showed field-effect modulation, but had different contact resistance. The comparison with devices using other metals such as Pd and Au is what we are interested in.

[1]. A. Venugopal et al., Appl. Phys. Lett. 96, 013512 (2010).
[2]. S. Russo et al., Physica E 42, 677 (2010).
[3]. J. S. Moon et al., IEEE Electron Device Lett. 31, 260 (2010).
[4]. K. Nagashio et al, Appl. Phys. Lett. 97, 143514 (2010).
[5]. Y. Matsuda et al, J. Phys. Chem. C 114, 17845 (2010).

NST/SS-5-Or-12
STM and LEED studies of continuous graphene monolayer synthesized on cubic-SiC(001)

T10 Nanoscience and Technology

#NST/SS-5-Or-12

A. Chaika [1], O. Molodtsova [2], A. Zakharov [3], D. Marchenko [4], J. Sánchez-Barriga [4], A. Varykhalov [4], M. Portail [5], M. Zielinski [6], I. Shvets [7], V. Aristov [1].

[1]Institute of Solid State Physics RAS - 142432, Chernogolovka, Moscow District (Russian federation), [2]HASYLAB at DESY - D-22607, Hamburg (Germany), [3]MAX-lab, Lund University - Lund (Sweden), [4]Helmholtz-Zentrum Berlin für Materialien und Energie - D-12489, Berlin (Germany), [5]CNRS-CRHEA - Valbonne (France), [6]NOVASiC - Bp267-F73375 Le Bourget Du Lac Cedex (France), [7]CRANN, School of Physics, Trinity College - Dublin (Ireland).

Unique electronic properties make graphene an appealing candidate for novel non-silicon-based electronics. In particular, graphene synthesized on commercially available cubic-SiC(001)/Si(001) wafers could be adapted for graphene-based electronic technologies and directly patterned using Si-electronic lithographic processes. The first reports on graphene growth on the surface of cubic-SiC(001) thin films deposited on Si wafers have been published recently [1,2]. However, they do not provide detailed information on the atomic structure of the graphene overlayer on the SiC(001) surface, its thickness, quality and continuity on a wafer scale. Here we present results of comprehensive atomically resolved scanning tunneling microscopy (STM) and low energy electron diffraction (LEED) studies of graphene layer synthesized on SiC(001). Uniform graphene layers were fabricated on SiC(001)/Si(001) wafers using Si-atom sublimation followed by SiC surface layer graphitization during high-temperature annealing in ultrahigh vacuum. Si-rich 3×2 and 5×2, Si-terminated stoichiometric c(4×2), C-terminated stoichiometric SiC(001)-c(2×2) reconstructions and graphene monolayer on SiC(001) were successively fabricated with increasing annealing temperatures. The atomic structure of the SiC(001) surface on different stages of graphene synthesis and its dependence on the applied sample treatment procedure have been thoroughly studied in-situ by STM and LEED. The results show that graphene monolayer on SiC(001) is continuous

throughout the millimeter-sized samples and consists of rotated nanometer-sized domains with four different lattice orientations connected through the grain boundaries (Fig. 1a). The domains possess atomic and electronic structure typical of single layer graphene. STM image in Fig. 1b demonstrates atomic-scale rippling and asymmetric distributions of carbon-carbon bond lengths typical of free-standing graphene layer [3]. This work was supported by the Russian Academy of Sciences, RFBR grants № 11-02-01253 and 11-02-01256, Marie Curie IIF grant within the 7th European Community Framework Programme and SPP 1459 of the Deutsche Forschungsgemeinschaft.

[1] V. Yu. Aristov *et al*., ***Nano Letters*** 10, 992 (2010).
[2] A. Ouerghi *et al*., ***Phys. Rev. B*** 83, 205429 (2011).
[3] A. Fasolino, J. H. Los, M. I. Katsnelson, ***Nature Mater***. 6, 858 (2007).

Fig. 1. 15 × 15 nm^2 (a) and 3 × 3 nm^2 (b) STM images of graphene layer on SiC(001).

NST/SS-5-Or-9
Controlled plasma modification of mono- and bi-layer graphene

T10 Nanoscience and Technology

#NST/SS-5-Or-9

A. Felten [1], A. Eckmann [2], J.J. Pireaux [1], C. Casiraghi [3].

[1]Research Center in Physics of Matter and Radiation (PMR), University of Namur - Namur (Belgium), [2]of Physics and Astronomy, University of Manchester - Manchester (United kingdom), [3]School of Chemistry and Photon Science Institute, Manchester University - Manchester (United kingdom).

Graphene has recently been proposed as one of the basic building block for nanoelectronics. The ultimate 2D character of the material confers exceptional electronic properties such as outstanding carrier mobility and unusual quantum effect. Unfortunately, the pursuit for applications is impeded by its metallic behavior making it hard to create graphene based transistors. In order to overcome this problem, various approaches to tune and control the electronic properties of graphene have been considered.

In this work, we investigate the controlled modification of mono- and bi-layer graphene using oxygen (O2) [1], hydrogen (H2) and tetrafluoromethane (CF4) plasma treatments. All plasma treatments have been carried out in the same plasma system in order to allow comparison of the results. Chemical functionalization is confirmed by micro-XPS measurements on exfoliated modified graphene. For example, figure 1a shows the C1s spectrum of oxygen plasma modified bilayer and pristine bilayer. The functionalized bilayer presents a shoulder at high binding energy (286-289 eV) corresponding to carbon-oxygen bonds. Structural changes induced on the graphene flakes are monitored using Raman spectroscopy [2]. Figure 1b shows the Raman spectra of pristine and oxygen modified monolayer graphene. After oxygen plasma exposure, new features corresponding to defect activated bands are appearing in the Raman spectra. The most prominent ones are the so called D and D' bands at ~1340 cm-1 and ~1620 cm-1 respectively. Changes in G, D, D' and 2D Raman peaks frequencies and shapes are studied after different plasma treatment conditions.

We show that hydrogen, oxygen and fluorine atoms are grafted on the graphene surface and that a controllable modification can be achieved by varying different

plasma parameters such as plasma power, exposure time, position of the sample inside the chamber and the type of gas. In addition, defect formation kinetics under rf-plasma is found to vary with the number of graphene layers.

[1] A. Felten et al., Small, Single and double-sided chemical functionalization of bilayer graphene, 2012, early view available online
[2] A. Eckmann et al., Nano Letters, Probing the nature of defects in graphene by Raman spectroscopy, 2012, 12, 3925-3930

Figure 1. (a) XPS C1s spectra of oxygen plasma treated bilayer graphene (blue curve). The dotted curve corresponds to the C1s of pristine bilayer. (b) Raman spectra of oxygen plasma treated monolayer graphene The black curve shows Raman spectra of pristine graphene.

NST-2-Or-5
Conductive Atomic Force Microscope Measurements on Large Single Crystals of Conjugated Polymers

T10 Nanoscience and Technology

#NST-2-Or-5

W. Hourani [1], K. Rahimi [2], G. Reiter [2], P. Lienerth [3], T. Heiser [3], J.L. Bubendorff [1], L. Simon [1].

[1]Institut de Science des Matériaux de Mulhouse (IS2M) - Mulhouse (France),
[2]Physikalisches Institut, Universität Freiburg - Freiburg (Germany),
[3]Laboratoire des Sciences de l'Ingénieur, de l'informatique et de l'Imagerie, Université de Strasbourg - Strasbourg (France).

Semiconducting polymers have been widely studied for applications in semiconductor devices such as solar cells, light-emitting diodes and thin film transistors. Usually such studies were performed on amorphous thin molecular films [1]. Here, we explore the possibilities to study single crystals as channels for charge carrier transport in a transistor structure. We used long (up to 50 µm) needle-shaped and well characterized single crystals made of 8-hexyl-thiophene (TH8) molecules, prepared in solution and deposited on a field-effect transistor (FET) structures [2]. The electrical properties of these crystals were measured by conductive atomic force microscope (C-AFM) in air. Moreover, the measured I-V characteristics were fitted with the space charge limited current model and values of charge carrier (hole) mobility have been extracted. As first indicated by Reid et al. [3], we also found that this model overestimates the charge carrier mobility. For C-AFM measurements, the standard Mott-Gurney law cannot be used to fit the measured I-Vs. A semi-empirical model has been proposed which takes into account the ratio of the distance between the macroscopic electrode and the AFM tip to the contact area diameter of the tip. Using the semi-empirical expression of the I-V characteristics proposed in [3], we have extracted values of the mobility of charge carriers. We have studied hole mobility for different crystals and found that current increases with crystal thickness. Knowing the internal structure of the single crystals from selected-area electron diffraction analyses (SAED) [2], we expected an anisotropic charge transport with different mobilities in the direction of π stacking (i.e. along the long axis of the crystal) and along the molecular axis which is oriented in the direction normal to the crystal

surface. The increase of the mobility with crystal thickness is associated to an increased contribution of current in the direction of the molecular axis which suggests a significant conjugation of molecular orbital along this direction.

[1] M. Estrada et al., “MIS polymeric structures and OTFTs using PMMA on P3HT layers,” Solid-State Electronics, vol. 52, no. 1, pp. 53–59, 2008.
[2] K. Rahimi et al., "Controllable processes for generating large single crystals of poly(3-hexylthiophene)", Angewandte Chemie, International Edition, vol. 51, pp. 1 - 6, 2012.
[3] O. G. Reid, K. Munechika, and D. S. Ginger, “Space charge limited current measurements on conjugated polymer films using conductive atomic force microscopy,” Nano letters, vol. 8, no. 6, pp. 1602–1609, 2008.

NST-6-Or-4
Photovoltaic application of titanium oxide nanoparticles synthesized by laser pyrolysis

T10 Nanoscience and Technology

#NST-6-Or-4

J. Wang [1], J. Bouclé [2], Y. Leconte [1], A. Habert [1], C. Di Bin [2], B. Ratier [2], N. Herlin-Boime [1].

[1]IRAMIS/SPAM/LFP, CEA-CNRS URA 2453, CEA de Saclay - 91191 Gif Sur Yvette (France), [2]XLIM UMR 7252, Université de Limoges/CNRS - 87060 Limoges (France).

The titanium dioxide (TiO_2) is widely used as pigment, or in paints, toothpastes, as well as for photo-catalysis. Over the past decades, since the dye sensitized solar cells (DSCs) were introduced by M.Grätzel in 1991 [1] , TiO_2 attracted great interest due to its crucial role as meso-porous electrodes. A very active field of research corresponds to the synthesis of oxide materials absorbing a fraction of the solar spectrum in order to improve the efficiency of solar cells.
In this context, this work deals with the development of solid-state DSCs based on titanium dioxide (TiO_2) nanocrystals synthesized by laser pyrolysis. Compared to conventional sol-gel synthesis procedure, the laser pyrolysis[2, 3] method, based on the interaction of a powerful infrared laser beam with a mixture of gaseous or liquid precursors (titanium tetraisopropoxide in the present study), appears as a versatile and efficient way to produce a large variety of well-controlled titanium oxide based nanopowders as well as “doped” nano-TiO_2 by simple introduction of another reactant in the precursor(i.e. NH_3 for N-TiO_2).
By varying the power of laser and the flow of carrier gas, we obtained titanium dioxide nanoparticles with controlled particle sizes about 20 nm and controlled crystalline phase (anatase).Moreover, nanoparticles “doped” with different Nitrogen contents were obtained by changing the flow of NH_3. Figure 1 presented a significant augmentation in the UV-visible optical absorption spectra as a function of the nitrogen content. XPS was also used to characterize the role of nitrogen in the structure. We observed that the performances of cells elaborated from N-doped or non-doped nanoparticles are comparable, but specific features are revealed in their IPCE (Incident Photon-to-current conversion efficiency) spectra. An increase of

quantum efficiency is observed in the absorption range of the metal oxide, but no clear interpretation on the corresponding charge generation mechanisms are given up to now [4] . By introducing very large flow of NH3, an original titanium oxide TiOx (x = 1-2) material with a low band gap energy (≈2 eV) was synthesized and used in solid-state DSCs. At the same time, we also synthesized TiO2 nanoparticles doped with metallic elements such as gold, the first results of the DSCs with this kind of powder are encouraging.

[1] B. O'Regan and M. Grätzel, Nature 353, 737 (1991).
[2] B. Pignon et al., Eur. J. Inorg. Chem. (2008) 883
[3] P. Simon et al., Chem. Mater. 2010, 22, 3704
[4] H. Melhem et al., Solar Energy Materials and Solar Cells (2012) DOI:10.1016/j.solmat.2012.08.017

Figure 1 UV-Visible absorption spectra of N-TiO2

BI/NST-1-Or-4
Innovative solid-state purification of circulating microRNAs

T10 Nanoscience and Technology

#BI/NST-1-Or-4

C. Potrich [1], G.C. Santini [1], L. Lunelli [1], L. Pasquardini [1], M. Quaglio [2], M. Cocuzza [3], P. Tiberio [4], R. Bertorelli [5], V. De Sanctis [5], C. Pederzolli [1].

[1]FBK-LaBSSAH - Povo (tn) (Italy), [2]CSHR - Center for Human Space Robotics, IIT - Torino (Italy), [3]CNR-IMEM & Chilab - DISMIC - Torino (Italy), [4]Fondazione IRCCS (Istituto Nazionale dei Tumori) - Milano (Italy), [5]University of Trento - LaBSSAH - Povo (tn) (Italy).

MicroRNA are short (20–30 nucleotides) noncoding RNAs which are processed from endogenously expressed pri-miRNAs by enzymes in several steps. Mature miRNAs are found in the cytoplasm as single-stranded molecules loaded in protein complexes whose primary function consists of mRNA silencing. However, there are evidences that miRNAs can be excreted by cells and the level of circulating miRNAs changes under specific conditions such as in the presence of tumor. Circulating miRNAs are therefore promising non-invasive tumor biomarkers whose abnormal expression in body fluids suggests pathological conditions. Current methods for extracellular miRNAs purification are challenging, mainly due to low body fluid concentration, variability, quantification limits.
Here we present the development and functionalization of a silicon-based surface able to selectively bind circulating miRNAs from complex biological samples. Silicon-based surfaces have been functionalized with positive o neutral or mixed molecules in order to have surfaces with different net charge or with different functional moieties. Complementary nucleic acid sequences has also been exploited for the purification of selected miRNAs. Synthetic miRNAs coupled or not with a fluorophore (miR-21 and miR-16, significantly overexpressed in cancer cells) have been incubated on these surfaces and the absorption/release rate has been determined. Different conditions in terms of pH, charge, buffer solutions, mixture of miRNA/total RNA/DNA/proteins have been tested, as well as the purification from cell culture supernatantes (MCF7 and other tumor lines) or patients sera. Moreover, since most of the circulating miRNA are present in exosomes, a functional surface for the purification of miRNA in exosomes has also been developed. Specific

functionalizations have been set up to capture circulating intact exosomes which will be lysed in a second step to release miRNAs.
To verify the efficiency of the new solid-state purification, the obtained miRNAs was both stained with specific dyes (e.g. RiboGreen) and quantified via two-step RT-PCR. The latter method was tested in standard conditions, i.e. commercial kit and thermalcycler, but a dedicated micro-module, consisting of a fluidic chamber where RT-PCR is performed, has also been implemented. In fact, the great potential of the innovative solid-state miRNA purification is the possible inclusion in a lab-on-chip device able to process biological fluids, purifying the included microRNAs and analyze their presence/quantity in order to correlate to tumor diseases with diagnostic purpose.

This work was accomplished in the framework of NEWTON (Advanced nanosystems for a new era in molecular oncology) funded by MIUR (Italian Ministry for Education, University and Research) grants-FIRB 2012-2016-for public/private structures involved in research fields characterized by strategic value.

NST/SS-4-Or-4
Kondo effect in organic radical molecules on gold: theory and experiment

T10 Nanoscience and Technology

#NST/SS-4-Or-4

R. Requist [1], S. Modesti [2], P.P. Baruselli [1], A. Smogunov [3], M. Fabrizio [1], E. Tosatti [1].

[1]Scuola Internazionale Superiore da Studi Avanzati (SISSA) - Trieste (Italy), [2]TASC-INFM - Trieste (Italy), [3]DSM/IRAMIS/SPCSI, CEA Saclay - Gif-Sur-Yvette Cedex (France).

The magnetic moment of an organic radical molecule, if it survives adsorption on a metallic surface, is generally screened at low temperatures by the metal conduction electrons. The resulting Kondo effect causes a characteristic zero bias anomaly in the electron tunneling conductance, similar to that observed for transition metal adatoms. We report joint ab initio theory/scanning tunneling spectroscopy investigations of the Kondo zero bias anomalies in nitric oxide adsorbed on Au(111). Density functional theory calculations predict that NO maintains a S=1/2 and adsorbs N-down at the top site of Au with a tilt angle of approximately 60 degrees, breaking the degeneracy of the singly occupied 2π* orbitals. Subsequent numerical many-body renormalization group calculations based entirely on ab initio input predict a Kondo temperature of 20 K in close agreement with experiment. The calculations find that the Kondo resonance occurs not in the strongly hybridized 2π*-derived orbital but, surprisingly, in the weakly hybridized one. A second case we consider theoretically is the stable α,γ-bisdiphenylene-β-phenylallyl (BDPA) radical, which the Linz group is studying on Au(111) [1], and which also displays a Kondo effect [2]. We attempt to understand the observed anomaly and its evolution from monomers to dimers and trimers through ab initio and numerical renormalization group calculations.

[1] S. Muellegger, M. Rashidi, M. Fattinger and R. Koch, J. Phys. Chem. C, vol. 116, pp. 22587-22594 (2012).

[2] S. Muellegger, M. Rashidi, M. Fattinger and R. Koch, J. Phys. Chem. C, submitted.

NST-P2-04
Influence of the field gradient in force detected spectroscopy

T10 Nanoscience and Technology

#NST-P2-04

S. Won, J. Heo.

Korea Institute of Materials Science - Changwon (Korea, republic of).

We review how a force spectroscopy can be applied to perform magnetic resonance spectroscopy of nanometer scale sample. As a result of mechanical detection of magnetic resonance, the substantial improvement is achieved in both signal sensitivity and spatial resolution. In this technique, one of the most important things to determine the high resolution is the magnetic field gradient apart from the thermal motion of the cantilever. It defines a thin shell on constant field in the sample. We report our experimental results on detecting isolated electron spins in a different field gradient, with an inferred resonance slice thickness. Our results are extracted from the DPPH thin film using force detected ESR microscopy. Such measurements allow reliable prediction of the force signal strength and allow force detected spectroscopy experiments to proceed with confidence. With cylindrical iron magnet, the first harmonic coupling of an amplitude modulated spin polarization is measured as a cantilever frequency shift with theoretical predictions. From these results, we suggest that the experiment can be optimized with selective magnet. A home-built force probe was used to measure the signal and systems are well optimized with our equipment.

[1] J. A. Sidles, Phys. Rev. Lett. 68, 1124 (1992).
[2] S. Lee, S. Won, S. Saun, and S. Lee, Nanotechnology 18, 375505 (2007).
[3] D. Rugar, R. Budakian, H. J. Mamin, and B. W. Chui, Nature 430, 329 (2004).
[4] O. Klein et al., Phys. Rev. B 78, 144410 (2008).
[5] H. J. Mamin, T. H. Oosterkamp, M. Poggio, C. L. Degen, C. T. Rettner, and D. Rugar, Nano Lett. 9, 3020 (2009).

Figure 1: The strength of the z-component of the probe field extracted from the spectrum measurement.

Figure 2: ESR spectrum measured in a DPPH film as a function of the cantilever frequency.

NST/SS-P1-12
Magnetotransport properties of epitaxial graphene grown on (0001) and (000-1) SiC

T10 Nanoscience and Technology

#NST/SS-P1-12

M. Gryglas-Borysiewicz [1], A. Kwiatkowski [1], J. Przybytek [1], S. Butun [2], E. Ozbay [2], W. Strupiński [3], R. Stępniewski [1], M. Baj [1].

[1]Institute of Experimental Physics, Faculty of Physics, University of Warsaw - Warsaw (Poland), [2]Nanotechnology Research Center (NANOTAM), Bilkent University - Ankara (Turkey), [3]Institute of Electronic Materials Technology - Warsaw (Poland).

Magnetotransport studies of few layer graphene (FLG) were performed on samples obtained by chemical vapour deposition on semi-insulating SiC [1]. Two polarities of the substrate were used. FLG was processed by means of optical lithography into relatively large hall bars (526μm x 263μm) with Ti/Au metallization used for ohmic contacts. Transport measurements were performed in an Oxford Instruments VTI system in temperatures ranging from room temperature down to 1.5 K and magnetic fields up to 12T, with additional illumination of the samples at low temperatures. The samples exhibited significant differences in the electrical properties for the two polarities. The samples grown on the silicon (0001) polarity showed quantum oscillations of the resistivity tensor. They had electron conductivity with Hall mobility of the order of 1000 $cm^2/V \cdot s$ and Hall concentration of about $3 \cdot 10^{12}$ cm^{-2}. The samples prepared on carbon–terminated SiC were n-type with significant contribution of holes [2] with Hall concentration of $3 \cdot 10^{13}$ cm^{-2} and Hall mobility few times lower. No oscillations were registered for that group of samples. We have observed that the samples grown on Si-terminated SiC were very sensitive to external environment (making FLG a potentially sensing material), to thermal cycles and exposure to light. In particular, they showed changes of the order of a few % after each thermal cycle while those grown on C-terminated SiC were stable (samples were kept under He atmosphere at all times). Looking for the possible explanation we performed subsequent experiments with illumination of the samples at low temperatures. The behaviour of the samples grown on Si-polarity SiC was influenced by light whereas

the other samples showed no such sensitivity. This diverse response of FLG to thermal cycles and light is discussed in this report.

Acknowledgments:
This work has been partially supported by Polish Ministry of Science and Higher Education projects 670/N- ESF-EPI/2010/0 and 671/N- ESF-EPI/2010/0 within the EuroGRAPHENE programme «EPIGRAT» of the European Science Foundation.

[1] W. Strupiński et al., Nano Lett., 11(4),1786 (2011)

[2] M. Gryglas-Borysiewicz et al., Acta Phys. Pol. A 116, 838 (2009)

NST-P2-21
Electron irradiation effects on atomic scale mechanics of carbon nanotubes: Molecular dynamics study

T10 Nanoscience and Technology

#NST-P2-21

K. Tada [1], Y. Masaaki [2], K. Hiroaki [2], H. Yoshihiko [2].

[1]Toyama National College of Technology - Toyama (Japan), [2]Osaka Prefecture University - Osaka (Japan).

High energy electron irradiation to carbon nanomaterials is expected to become a technique to tailor the structure with desirable properties [1]. However, the mechanical properties of electron-irradiated carbon nanomaterials are not well understood. In our previous study, we developed molecular dynamics (MD) simulation including electron collision effects to study the structural changes of carbon nanotubes (CNTs) under electron beam irradiation [2]. In the present work, electron irradiation effects on atomic stress variation of CNTs are studied with the simulation.

Figure 1 shows the atomic stress distributions of (10, 0) SWNT with no defect during compression ((a) $\varepsilon = 0.00$, (b) $\varepsilon = 0.08$) and stress-strain characteristics of atoms near the center and edge ((c)). During the compression, the stress is uniformly applied to the whole CNT surface and the CNT is elastically deformed to the yielding point. Figure 2 shows the atomic stress distributions of (10, 0) SWNT with 5ns irradiation during compression ((a) $\varepsilon = 0.00$, (b) $\varepsilon = 0.08$) and stress-strain characteristics of atoms near the center and edge ((c)). As shown in Fig. 2(a), residual stress arises due to the defect produced by the electron irradiation. On the other hand, as shown in Fig. 2(b) and (c), the stress concentrates around the defect as the CNT is gradually compressed.

Acknowledgments

This work was supported by the Grants-in-Aid for Scientific Research from the Japan Society for the Promotion of Science.

[1] A. V. Krasheninnikov and F. Banhart, Nat. Mater. 6 (2007) 723-733.
[2] M.Yasuda et al, Phys. Rev. B 75 (2007) 205406.

Fig.1 Atomic stress distributions of (10, 0) SWNT with no defect during compression ((a)ε=0.00, (b)ε=0.08, The region under compression is colored red, and tension blue.) and (c) stress-strain characteristics of atoms near the center and edge.

Fig.2 Atomic stress distributions of (10, 0) SWNT with 5ns irradiation during compression ((a)ε=0.00, (b)ε=0.08, The region under compression is colored red, and tension blue.) and (c) stress-strain characteristics of atoms near the center and edge.

NST-4-Or-1
A novel approach for plasmonic based DNA sensing

T10 Nanoscience and Technology

#NST-4-Or-1

J. Spadavecchia [1], A. Barras [2], C.M. Pradier [3], R. Boukherroub [2], S. Szunerits [2].

[1]Laboratoire de Réactivité de Surface, UMR CNRS 7197, Université Pierre & Marie Curie - Ivry Sur Seine (France), [2]Institut de Recherche Interdisciplinaire (IRI, USR 3078 CNRS), Université Lille 1 - Villeneuve D'ascq (France), [3]Laboratoire de Réactivité de Surface, UMR CNRS 7197, Université Pierre & Marie - Ivry Sur Seine (France).

DNA hybridization assays are of widely employed in molecular biology and for forensic tests. Next to the traditional fluorescent-based DNA assays, biosensors taking advantage of the plasmonic properties of metal films and nanostructures have emerged as alternative methods for detecting DNA hybridization with lower cost and high sensitivity. Localized surface plasmon resonance (LSPR) sensors, employing noble metal nanostructures, have lately attracted considerable attention as a new class of plamsonic nanosensors.8, 9 The detection principle is based on the fact that the position of the nanoparticles extinction maximum is highly dependent on the local refractive index of the nanoparticles and biomolecular binding/unbinding events can be followed in real-time by monitoring the temporal variation in the LSPR signal. However, sensitivity loss can arise when LSPR sensors are functionalized with long surface ligands, as is the case for the linking of oligonucleotides to LSPR interfaces. In an attempt to enhance the sensitivity of LSPR interfaces for the detection of hybridization events, we developed a new detection strategy. .The approach is based on the amplification of the wavelength shift of a multilayered localized surface plasmon resonance (LSPR) sensor interface upon hybridization with gold-nanorods and gold-nanostars labeled DNA (Figure 1) as well as by recording the plasmonic signal of the gold-labeled DNA upon hybridization. The amplification of the wavelength shift, produced by plasmonic coupling between the gold particle label and the gold nanostructures on the LSPR interface, results in a significant decrease of the limit of detection from ≈40 nM as observed for unlabeld DNA to 200 pM for the labeled DNA. The shape of the nanostructures seems not to influence strongly the degree of coupling as seen in a similar shift of the LSPR

sensors wavelength upon DNA hybridization. However, the structure of the labels becomes of interest if its plasmonic characteristics themselves are used for the detection of a successful hybridization event. Both approaches will be compared and discussed.

LSPR based detection of DNA hybridization with and without gold labled DNA.

NST-12-Or-7
EVALUATION OF HEAT CAPACITY OF BENZOXAZINE/CNT NANOCOMPOSITES WITH AEROSPACE APPLICATION

T10 Nanoscience and Technology

#NST-12-Or-7

F. Untem, M. Costa, E. Botelho, M. Rezende.

UNESP - Guaratinguetá (Brazil).

The benzoxaxine resin is a new class of thermoset phenolic resin, which is presenting, in the lasts decades, a great application in the aircraft industry due mainly to its excellent mechanical and thermal properties. This resin associates the mechanical properties of epoxy resin with the thermal and flame retardant properties of phenolic resin. Besides, polybenzoxazines do not need catalyst, they do not generate by products during its curing and they can be stored at ambient conditions. Therefore, they are considered polymers of elevated performance and they are excellent candidates to substitute the current thermoset matrices used in the processing of high performance composites, either reinforced with continuous fibers or nanometric structures. In this study, this matrix was reinforced with multiwalled carbon nanotubes (MWCNT) in different concentrations (0.1%, 0.5% and 1.0% w/w), in order to promote better properties in relation to the neat benzoxazine resin. The main goal of this work is to evaluate the influence of different amount of MWCNT on the heat capacity (Cp) of the Benzoxazine/CNT nanocomposites using differential scanning calorimetry (DSC) and the analysis of the interactions between the composite's matrix and reinforcement, using scanning electron microscopy (SEM).

The determination of nanostructured composites' heat capacity was performed using the Perkin Elmer's equipment, model Pyris 1. There were used samples of 10 mg, with a constant flow of nitrogen (10 $mL.min^{-1}$), at a heating rate of 20°C/min, ranging the temperature from 10°C to 100°C. It was necessary to do the tests at the same conditions for the sample, the standard (sapphire) and the empty container (alumina). The softwares DSC Subtraction and DSC Cp, version 5.7, from EXSTAR6000 System were used to determine the Cp.

The environmental scanning electron microscopy (ESEM) was performed on a Zeiss EVO LS-15, with tungsten hairpin thermionic type electron gun. It was operated at chamber pressures from 10 to 50 Pa with pressure limiting apertures (100 µm and 500 µm with beam sleeve) for in-lens pumping, using nitrogen gas atmosphere to neutralize the electrons charge up effects under Zeiss extended pressure mode, allowing working with samples without metallization process. The analyses were performed with the use of scintillation type variable-pressure secondary electrons (VPSE) detector with accelerating voltage of 5 kV to avoid sample degradation.

Based on the results, it can be infer that the concentration of the CNT influences the values of the Cp of the composites Benzoxazine/CNT. At 25°C, the values obtained were 1.241 J/g°C for the concentration of 0.1% w/w and 1.690 J/g°C for 1.0% w/w, while at 80°C, these values got up to 1.555 J/g°C and 2.341 J/g°C, respectively, indicating that the CNT addition improves significantly this property. The results obtained by SEM's tests better explain the behavior of the material, based on the interactions between matrix and reinforcement, indicating an appropriate dispersion on the CNT inside of benzoxazine resin.

ASTM E1269-05 Standard Test Method for Determining Specific Heat Capacity by Differential Scanning Calorimetry

PEREIRA, A.C. Estudo da cinética de cura e das propriedades térmicas da resina benzoxazina e dos seus compósitos nanoestruturados. Master's Thesis - UNESP, 2011.

NST-9-Or-1
On the Enhancement of Nanoparticle Growth by a Pulsed Plasma

T10 Nanoscience and Technology

#NST-9-Or-1

I. Pilch [1], D. Söderström [1], N. Brenning [2], U. Helmersson [1].

[1]Linköping University, Plasma & Coatings Physics Division, IFM-Materials Physics, SE-581 83 Linköping, Sweden (Sweden), [2]Royal Institute of Technology, School of Electrical Engineering, Division Space & Plasma Physics, SE-10044 Stockholm, Sweden (Sweden).

The growth of copper nanoparticles in a high power pulsed hollow cathode discharge is studied. The material for nanoparticle growth is sputtered from the hollow cathode by applying high power impulses. This technique is known from high power impulse magnetron sputtering where the ionization degree is increased compared to dc magnetron sputtering [1]. The nanoparticles grow in the gas phase and the growth process can be divided into three main stages: nucleation, coagulation, and growth by accretion of atoms and ions [2]. Since nanoparticles above a certain size are negatively charged in the plasma [3], a high ionization degree of the material will be beneficial in the last step of growth (accretion) because the collection cross section for positively charged ions becomes much larger than for atoms. Using the pulsed technique, it has been shown that the nanoparticle size can be altered in a range between 20 and 40 nm by changing the pulse parameters, i.e., frequency, peak current, and pulse width [4]. In this contribution the effect of the plasma on nanoparticle growth is studied by changing the spatial distribution of the plasma, which was controlled by changing the distance between the hollow cathode and the anode ring. It was found that the nanoparticle size increases when the nanoparticles are exposed to the pulsed plasma a longer time. The mechanisms of an enhanced growth of nanoparticles by an exposure of plasma are discussed.

[1] U. Helmersson, M. Lattemann, J. Bohlmark, A.P. Ehiasarian, and J.T. Gudmundsson, “Ionized physical vapor deposition (IPVD): A review of technology and applications,” Thin Solid Films 513, 1 (2006).
[2] M. A. Lieberman and A. J. Lichtenberg, Principles of Plasma Discharges and Materials Processing, 2nd ed. (John Wiley & Sons, Hoboken, New Jersey, 2005),

Chap. 17.4, pp. 662–668
[3] J. Goree, “Charging of particles in a plasma,“ Plasma Sources Sci. and Technol. 3, 400 (1994).
[4] I. Pilch, D. Söderström, N. Brenning, and U. Helmersson,”Size-controlled growth of nanoparticles in a highly ionized pulsed plasma”, Appl. Phys. Lett. (accepted)

NST-4-Or-2
A tailored formation of N-doped fullerene, nanographene or 2D polyaromatic networks by on-surface dehydrogenation of heteroaromatics

T10 Nanoscience and Technology

#NST-4-Or-2

J. Martin Gago [1], A.L. Pinardi [1], G. Otero-Irurueta [1], I. Palacio [1], J.I. Martinez [1], A. Jančařík [2], I. Stará [2], I. Starý [2], M.F. López [1], J. Méndez [1].

[1]ICMM-CSIC - Madrid (Spain), [2]Institute of Organic Chemistry and Biochemistry - Prague (Czech republic).

The controlled on-surface synthesis of intricate π-electron systems may overcome the limits of conventional synthesis, which often faces severe problems if large, fragile or insoluble molecules are to be prepared in solution and subsequently deposited on a solid substrate. Surface-assisted cyclodehydrogenation or dehydrogenative polymerisation of polycyclic heteroaromatic hydrocarbons (PAH) is one of the most important strategies for bottom-up assembly of new nanostructures from their constituent molecular building blocks[1]. Although diverse compounds have been formed in recent years using this methodology,[2,3] limited knowledge on the molecular machinery operating at the nanoscale has so far disallowed to control the reaction outcome.

In this work, we show that the strength of the PAH-substrate interaction rules the reaction pathways (cyclodehydrogenation versus dehydrogenative polymerisation). So, starting from the same precursor and controlling its diffusion by the nature of the supporting surface, temperature-triggered dehydrogenation takes place to provide molecular or polymeric structures of variable dimensionality.

We combined advanced surface techniques (STM and NEXAFS) with theoretical ab-initio calculations to achieve a complete understanding of the self-assembling of molecular precursors on surfaces. Herein, by merging information from these techniques and different single-crystal metal substrates, we report on the diffusion control of competitive intramolecular and intermolecular dehydrogenative processes respectively called cyclodehydrogenation and dehydrogenative polymerisation, which operate in the on-surface synthesis of N-doped fullerene, nanographene,

polyaromatic network or graphene (Fig. 1). By choosing the appropriate N-heteroaromatic precursors and by controlling their diffusion, the on-surface (cyclo)dehydrogenation can either lead to monomolecular triazafullerenes and diazahexabenzocoronenes (N-doped nanographene), or to N-doped polymeric networks.

1. Méndez, J., López, M. F. & Martín-Gago, Chem. Soc. Rev. 40, 4578–90 (2011).
2. Treier, M. et al.Nat. Chem. 3, 61–7 (2011).
3. Bieri, M. et al. JACS 132, 16669–16676 (2010)

Fig. 1: The precursors 1 and 4 are subjected to controlled on-surface dehydrogenation. 1 and 4 may form respectively (i) N-doped triazafullerene 2 or 2,5-diazahexabenzocoronene 5 (through intramolecular cyclodehydrogenation) or (ii) branched 2D polyaromatic architectures 3 or 6 (both through intermolecular dehydrogenative polymerisation and intramolecular cyclodehydrogenation).

NST-9-Or-3
Silver and gold nanoparticles on chitosan

T10 Nanoscience and Technology

#NST-9-Or-3

A.M. Ferraria [1], S. Boufi [2], M. Rei Vilar [3], A.M. Botelho Do Rego [1].

[1]CQFM- Centro de Química-Física Molecular and IN-Institute of Nanoscience and Nanotechnology, Instituto Superior Técnico, Universidade Técnica de Lisboa, Av. Rovisco Pais, 1049-001 - Lisbon (Portugal), [2]Laboratoire des Sciences des Matériaux et Environnement, Faculté des Sciences de Sfax-Université de Sfax - Sfax (Tunisia), [3]ITODYS, UMR7086 CNRS, Université Paris Diderot, Sorbonne Paris Cité - Paris (France).

Silver and gold nanoparticles (NPs) were generated via a mild wet-chemistry process in aqueous chitosan solutions. Gold and silver NPs were created in situ in a chitosan solution through the addition of the corresponding salt and subsequent UV irradiation. Gold and silver NPs were also created by using a sequence of gold and then silver and vice-versa. The amine function existing in the chain monomer operates as the anchoring centre of the metal NP, enabling thus a selective generation of the metal NPs through their nucleation followed by their growth [1,2]. The ensuing hybrid systems were characterized by UV/Vis spectroscopy, X-ray Photoelectron Spectroscopy (XPS), Transmission Electron Microscopy (TEM) and X-ray Diffraction (XRD). The NPs average sizes ranges from 10 to 40 nm for gold and ~20 to ~100 nm for silver. The present approach proved to be efficient in generating bimetallic nanoparticles. The results also suggest that through a sequence of gold followed by silver solutions, gold cores enveloped by silver shells with some discontinuities are created. However, results are unclear when the order of solutions is inverted. The composition of the nanoparticles is explained by the dependence on the standard redox potentials of the system.

[1] A.M. Ferraria, S. Boufi, N. Battaglini, A.M. Botelho do Rego, M. Rei Vilar, Langmuir 26 (2010) 1496.
[2] S. Boufi, A.M. Ferraria, A.M. Botelho do Rego, N. Battaglini, F. Herbst, M. Rei Vilar, Carbohy. Polym. 86 (2011) 1586.

NST-6-Or-5
Understanding the Kirkendall effect at the nanoscale in Cu/CuO system

T10 Nanoscience and Technology

#NST-6-Or-5

A. El Mel [1], M. Buffière [2], L. Molina-Luna [3], S. Konstantinidis [1], C. Bittencourt [1], P.Y. Tessier [4], W. Xu [5], K. Du [5], C.H. Choi [5], H.J. Kleebe [3], R. Snyders [6].

[1]Chimie des Interactions Plasma Surface (ChIPS), CIRMAP, Research Institute for Materials Science and Engineering, University of Mons, 20 Place du Parc, B-7000 Mons, Belgium - Mons (Belgium), [2]Department of Electrical Engineering, KU Leuven, Kastteelpark Arenberg 10, B-3001 Heverlee, Belgium and IMEC, Kapeldreef 75, B-3001 Heverlee, Belgium - Leuven (Belgium), [3]Department of Material- and Geosciences, Technische Universität, Schnittspahnstraße 9, 64287 Darmstadt, Germany - Darmstadt (Germany), [4]Institut des Matériaux Jean Rouxel, IMN, Université de Nantes, CNRS, 2 rue de la Houssinière B.P. 32229 - 44322 Nantes cedex 3 – France - Nantes (France), [5]Department of Mechanical Engineering, Stevens Institute of Technology, Hoboken, NJ 07030, USA - Nj (United states), [6]Chimie des Interactions Plasma Surface (ChIPS), CIRMAP, Research Institute for Materials Science and Engineering, University of Mons, 20 Place du Parc, B-7000 Mons, Belgium and Materia Nova Research Center, Parc Initialis, B-7000 Mons, Belgium - Mons (Belgium).

Huge efforts are nowadays dedicated to the development of relevant methods to fabricate hollow nanostructures of a wide variety of materials [1]. Among hollow nanostructures, oxide nanotubes are considered as potential building blocks for nanoelectronics. Up-to-now, the majority of synthesis method produces oxide nanotubes that suffer from a short length and poor organization. In this contribution, we report for the first time on highly organized ultra-long metal oxide nanotube arrays (length-up to several centimeters) fabricated by thermal oxidation of metal nanowire arrays [2]. The metal nanowires were grown on nanograted surface by the plasma-assisted inverse-template method that we have developed in a recent work [3]. Based on an extensive structural study, performed by transmission electron microscopy, the fundamental mechanisms occurring during the formation of such oxide nanotubes will be discussed and explained according to the nanoscale Kirkendall effect. We further show that such method can be extended for the

fabrication of periodic zero-dimensional hollow nano-objects. This novel fabrication method of oxide nanotubes in a planar configuration opens-up the way to further nanodevice construction and characterization.

[1] Fan, H. J. et al. Monocrystalline spinel nanotube fabrication based on the Kirkendall effect. Nature Mater. 5, 627-631 (2006).
[2] El Mel, A. A. et al. Highly ordered hollow oxide nanostructures: The Kirkendall effect at the nanoscale. Small, in press.
[3] El Mel, A. A. et al. Titanium carbide/carbon composite nanofibers prepared by a plasma process. Nanotechnology, 21, 435603 (2010).

NST-7-Or-5
Fingerprinting Material Interfaces with BEEM

T10 Nanoscience and Technology

#NST-7-Or-5

K. Goh, C. Troadec.

Institute of Materials Research and Engineering (IMRE), Agency for Science, Technology and Research (ASTAR), 3 Research Link, Singapore 117602, Singapore - Singapore (Singapore).

We show how a fingerprint of a material interface may be obtained by Ballistic Electron Emission Microscopy (BEEM).[1] When dissimilar materials come together, the interface thus formed typically creates a barrier for charge transport with certain transmission characteristics. BEEM plays a rather unique role here in that it can extract both the barrier and transmission characteristics with very high lateral resolution (being based on the scanning tunneling microscope) and hence provide localized measurements of buried interfaces.[2,3] This allows the interface of nanoscale or larger devices (e.g. a gate-stack) to be studied with the ability to pin-point with ~nm resolution where the charge barrier or transmission characteristics are different.[2] This is in contrast to conventional techniques such as current-voltage measurements or X-ray diffraction technique which typically averages over much large areas.

A fingerprint defined by the density distribution of the interface barrier and transmission characteristics can be useful for distinguishing between different interfaces and is sensitive even to the presence of a few monolayers of “contaminants” inserted into the interface.[2] We will present the fingerprint for the Au/n-Si interface and show how the insertion of a “contaminant” layer (inorganic and organic) at this interface alters the fingerprint. In addition, we shall present recent results to demonstrate the usefulness of these fingerprints in helping us to understand nanoscale modifications in devices in the context of process optimization, tuning device characteristics and device stressing.

1. L. D. Bell and W. J. Kaiser, Phys. Rev. Lett. 61, 2368 (1988).
2. K. E. J. Goh, A. Bannani, and C. Troadec, Nanotechnology 19, 445718 (2008).

3. Justin C. W. Song, Kuan Eng J. Goh, Natarajan Chandrasekhar, and Cedric Troadec, Phys. Rev. B 79, 165313 (2009).

NST-7-Or-6
Distance Depended Near-filed Optical Microscopy

T10 Nanoscience and Technology

#NST-7-Or-6

U. Schmidt, M. Tchaya, D. Steinmetz, T. Dieing.

WITec GmbH - Ulm (Germany).

Since its invention, Scanning Near-field Optical Microscopy (SNOM) is used for optical imaging where a resolution below the diffraction limit is required [1]. In conventional optical microscopy, using visible light, a lateral resolution of about 200 nm can be achieved, leaving nano-objects outside the detection range.
In SNOM the light propagates through a subwave-length size aperture (50 nm - 100 nm) which is realized in our case using a SNOM cantilever. The SNOM cantilever is brought in close vicinity of the sample using standard AFM feedback technology. The light emitted or collected through the aperture of a SNOM cantilever leads to SNOM images with a resolution in the range of the size of the aperture.
Digital Pulsed Force Mode (DPFM), one of the AFM feedback methods used to study mechanical material properties in AFM [2, 3] allows the fast approach and retraction of the cantilever to and from the sample, thus enables the control of tip sample distance. By combining DPFM technology with SNOM, it is possible to obtain SNOM images as a function of tip sample separation.
The aim of this contribution is to explain the principle of this SNOM method, highlighted with example measurements.

1. D.W. Pohl, W. Denk, and M. Lanz, Appl. Phys. Lett. 44, 651 (1984).
2. A. Rosa-Zeiser, E. Wieland, S. Hild and O. Marti, Meas. Sci. Technol. 8, 1333 (1997).
3. P. Spizig, PhD Thesis, Univ. Ulm (2002).

NST-6-Or-15
Deposition of silver nanoparticles on Graphene nanolayers; an antibacterial nanocomposite

T10 Nanoscience and Technology

#NST-6-Or-15

A. Babapour.

Structural Engineering Institute, College of Civil Engineering and Architecture, Zhejiang University, Hangzhou, 310058, China.

Silver nanoparticle-embedded organic or inorganic matrices show extraordinary physical and chemical properties that are size and shape dependent as well as surrounding medium [1]. Preparing metal nanoparticles into thin films is particularly important for various applications such as optical nanodevices, biocide coating and biological sensing [2]. Graphene-metal nanocomposites potentially provide a new way to develop catalytic, magnetic, optoelectronic and bioactive materials
In this report, we show a facile and fast route to prepare silver nanopartcle decorated graphene oxide sheets and embed them into PVP film.
The UV–Visible spectra of the Ag nanoparticles on GrO in PVP film using different concentrations of AgNO3 indicates the appearance of characteristic surface plasmon band at 420 nm indicates the formation of Ag nanoparticles in the coating. The peaks position of different silver concentration were almost in same range which means the particles are in same sizes. TEM micrograph of silver nanoparticles deposited on grapheme oxide sheets are shown in Figure 1. It shows the wide distribution of particles ranging in the diameter of 5–25 nm (Figure 1a). Figure 1b shows that the smaller particles are hexagonal in shape (marked by black arrows) while the larger nanoparticles are in spherical form. The hexagonal shape could be the result of the deposition of the particles on the graphene sheets. Furthermore, the interface between the sheets and Ag is clearly seen (sheets marked 1 and 2), indicating that Ag nanoparticles are well attached between the surfaces of the two sheets. It also presented that uniform single-entity Ag nanoparticle embedded in the GrO sheets, thus confirming their assembly. The presence of the bigger particles can be due to agglomeration of the smaller particles.

[1] H. Shin, H. Kim, H. Lee, H. Yoo, J. Kim, H. Kim, M. Lee, Adv. Mater. 2008, 20, 3457–3461
[2] Babapour A, Yang B, Bahang S and Cao, Nanotechnology, 2011, 22: 155602

Fig. 1 TEM micrographs of Ag nanoparticles deposited on grapheme oxide sheets. a) GO sheets decorated by nanosilver and b) Ag nanoparticles of hexagonal shapes

NST/SS-1-Or-5
Monitoring the synthesis of nanographene patterned by focused ion beam induced deposition

T10 Nanoscience and Technology

#NST/SS-1-Or-5

M. Castellino [1], G. Rius [2], M. Yoshimura [3], A. Tagliaferro [1].

[1]Politecnico di Torino - Torino (Italy), [2]Nagoya Institute of Technology - Nagoya (Japan), [3]Toyota Technological Institute - Nagoya (Japan).

Today the integration of C nanomaterials, having peculiar determined specifications and properties, presents fabrication and control challenges. The present attention on graphene research, as an effort to enable the full exploitation of its excellent properties, evidences the necessity to find alternative procedures to completely integrate it in the standard semiconductor planar technologies, following the route for a future graphene-based nano-electronics. The bottleneck is clearly identified in the use of metal as a catalyst for the crystallization and the need of transfer to insulating substrates and metal etching, while preserving ideal graphene features. Our present approach is inspired on the planar technology point of view and strategies. Merging the carbon nanomaterial preparation and lithography in a single stage processing by means of focused ion beam induced deposition of carbon (FIBID-C), the aim is to introduce our new concept as an example of a robust and flexible nanofabrication methodology [1]. A multibeam system JIB-4500 from JEOL has been used, with a Ga ion beam operating at 30 kV with a beam current of 300 pA. Square and rectangular patterns have been deposited on a standard substrate of 100-500 um thick SiO_2 (fig.1-a), thermally grown on Si wafer, having thicknesses from 3.5 to 20 nm. The as-deposited processed material characteristics have been studied by TEM (fig.1-b), Raman and XPS [2]. In order to overcome some of the intrinsic issues of FIBID, such as its as-deposited high resistance, we explore how to convert C amorphous film into crystalline materials, namely graphene-like or diamond-like, with thermal treatments. C-film after annealing at 975°C results in no morphological distortions, both in terms of shape and thickness. TEM shows that atomic C arrangement has not suffered significant modification and XPS suggests that the treated film is made by a mixture of C sp2 and sp3 bonds , and a small portion of C-O bonds (fig.1-c) [3]. The best results to obtain the transformation of amorphous C-film into graphene-like patterns were achieved using annealing @ 975°C and 10 um of Ni. TEM confirms the

conversion of as-deposited film into multiple graphene layers. The use of the metal catalyst in the form of foils appears advantageous. In addition to the convenience of allowing the synthesis directly on an insulating substrate, such as SiO_2, spontaneous detachment of metal and C-film patterns after cooling makes unnecessary a metal etching step.

[1] G Rius et al. J Vac Sci Technol B 30 (2012) 03D113-1
[2] AC Ferrari et al. Phy Rev B 61 (2000) 14095-14107
[3] P Merel et al. Appl Sur Sci 136 (1998) 105-110

Fig 1: (a) sample picture (50x), (b) TEM image, (c) C1s peak of C-film ann@ 975°C

BI/ASS/NST-P1-10
Polysomes observed by atomic force microscopy

T10 Nanoscience and Technology

#BI/ASS/NST-P1-10

L. Lunelli [1], G. Viero [2], P. Bernabò [3], C. Pederzolli [1], A. Quattrone [3].

[1]FBK - Laboratory of Biomolecular Sequence and Structure Analysis for Health - Trento (Italy), [2]Institute of Biophysics CNR Unit at Trento and Laboratory of Translational Genomics, Centre for Integrative Biology, University of Trento - Trento (Italy), [3]Laboratory of Translational Genomics, Centre for Integrative Biology, University of Trento - Trento (Italy).

Polyribosomes are clusters of ribosomes held together by messenger RNA that constitute the cellular machinery dedicated to the synthesis of proteins. Using Atomic Force Microscopy (AFM) we have visualized the structure of polyribosomes that have been purified from MCF7 human cell line. Native polyribosomes have been deposited on flat mica after sucrose gradient separation and visualized in liquid and in air environment. The number of ribosomes per polysome increases with the fraction, as expected, ranging from 2-4 in the lightest fraction to few dozens in the heavier ones. While the general shape of the observed polysomes is compatible with cryo-EM results (Brandt 2010), the AFM scans reveals also filaments connecting ribosomes. Two main kind of such objects are detected: filaments with height compatible to that of single strand nucleic acid (Smith 1997), that we found joining clusters of ribosomes, and shorter filaments that often connect a single riboparticle with a larger ribosomal cluster (Fig. 1).
To identify some of the observed structures, we have treated our samples with immuno-gold staining, in order to tag selected proteins with gold nanoparticles, allowing their direct identification in the AFM scans. When using antibodies against a ribosomal protein (RPL26) and against non-polysomal proteins (Ras, Sos) in control samples, we obtain full bead staining and no signal, respectively, confirming the selectivity of the method. When stained against initiation factors (eIF4E, eIF4B, PABP) well separated spots are identified in the images, allowing some insights on their spatial arrangement in the polyribosome.

(Brandt 2010) - F. Brandt, L.A. Carlson, F.U. Hartl, W. Baumeister, K. Grünewald, “The Three-Dimensional Organization of Polyribosomes in Intact Human Cells”, Molecular Cell 39, 560-569, (2010)

(Smith 1997) - Smith, B. L.; Gallie, D. R.; Le, H. & Hansma, P. K. , “Visualization of poly(A)-binding protein complex formation with poly(A) RNA using atomic force microscopy”, J Struct Biol, 119, 109-117, (1997)

Fig. 1 - Three representative AFM scans (400x400 nm^2): top and middle rows are color coded from black to white using two different Z scales to make clear polysomes (top row, Z scale 20 nm) or the connecting strands (middle row, Z scale 2 nm). The 3D representations of the same scans are presented in the row at the bottom. Color scale: grey background, magenta 1.5 nm, yellow 13.5 nm.

NST-P3-09
Imaging and chemical state mapping of zinc oxide nanoparticles combined with gadolinium

T10 Nanoscience and Technology

#NST-P3-09

A. Skallberg, M. Ahrén, L. Selegård, K. Uvdal.

Division of Molecular Surface Physics and Nanoscience, Department of Physics, Chemistry and Biology, Linköping University - Linköping (Sweden).

Zinc oxide nanoparticles combined with gadolinium ions have been synthesized to be used as possible bifunctional probes with tuned properties for increased MR contrast enhancement and fluorescence. Gadolinium based contrast agents have proven to be valuable in magnetic resonance imaging (MRI) by providing high contrast in soft tissues [1]. Zinc oxide nanoparticles have a high stability and inherent photoluminescence properties with a wide band-gap, which has great interest in imaging applications [2]. These probes are promising as contrast agent for in vivo MR studies and as nanoprobes for cell studies and biochip applications. NanoESCA is a powerful tool derived from an electrostatic electron emission microscope for chemical element analysis. In this report, chemical state mapping with energy-filtered photoemission electron microscope has been used to study the zinc oxide gadolinium nanoparticle system. Micro-patterns are formed on silicon surfaces using direct stamping with polydimethylsiloxane (PDMS), which is a simple and reproducible way of producing high resolution structures for a possible biochip application.

[1]. I-Fang Li and Chen-Sheng Yeh, Synthesis of Gd doped CdSe nanoparticles for potential optical and MR imaging applications, J. Mater. Chem., 2010,20, 2079-2081
[2]. John W. Rasmussen et al, Zinc Oxide Nanoparticles for Selective Destruction of Tumor Cells and Potential for Drug Delivery Applications, Expert Opin Drug Deliv. 2010 September, 7(9): 1063–1077

NST-P3-19
IR plasmonic antennas in the vicinity of absorbing silicon-rich oxinitride

T10 Nanoscience and Technology

#NST-P3-19

L. Brínek, É. Zoltán, R. Kalousek, J. Zlámal, V. Krápek, J. Spousta, P. Dub, T. Šikola.

Brno University of Technology , CEITEC - Brno (Czech republic).

The presentation deals with plasmonic antennas in the vicinity of silicon-rich oxinitride (SRON) having a substantial energy absorption in the mid-infrared (around λ^{-1} ~ 1100 cm^{-1}). This work was originally motivated by an effort to exploit electromagnetic energy at antenna resonances for the thermal transformation of SRON into a nanocrystalline Si. Such antennas reveal nonlinear scaling between resonant wavelengths and antenna lengths [1]. The absorption enhancement in SRON is proportional to its absorption coefficient and to an increase of electromagnetic field at the antenna resonance. Hence, the trade-off between the frequencies providing the maximum absorption coefficient on one hand and antenna resonance on the other hand should be found. The optimization of the structure for the maximal electromagnetic field absorption in the SRON is performed via full-electromagnetic field calculations (FDTD). There are two resulting arrangements possessing: a) a SRON layer below a plasmonic antenna and b) antennas with the blocks of SRON in their vicinity (e.g. in the antenna gap). Both types of structures were fabricated by electron beam lithography and their reflectances measured by FTIR microscopy will be shown.

[1] Šikola T., at al.: Mid-IR plasmonic antennas on silicon-rich oxinitride absorbing substrates: Nonlinear scaling of resonance wavelengths with antenna length, Applied Physics Letters **95**, 253109 (2009).

NST-P3-20
Plasmon-enhanced photoluminescence from silicon-rich oxinitride films and Si nanocrystals

T10 Nanoscience and Technology

#NST-P3-20

Z. Edes [1], L. Brínek [2], T. Šamoril [2], T. Neuman [1], M. Hrton [1], V. Krápek [2], P. Dub [2], P. Varga [2], T. Šikola [2].

[1]Institute of Physical Engineering, Brno University of Technology - Brno (Czech republic), [2]CEITEC BUT, Brno University of Technology - Brno (Czech republic).

This presentation deals with the effects of metal nanoparticles on the photoluminescent properties of SRON (silicon-rich oxinitride) films [1] and Si nanocrystals (NCs) in their close proximity. The work was motivated by an effort to enhance the photoluminescence (PL) efficiency of SRON layers and low emitting Si NCs via plasmonic effects. The luminescence of the SRON in the visible region is attributable to the neutral oxygen vacancies [1]. However, annealing to higher temperatures (1100°C) allows the formation of embedded luminescent Si NCs. These NCs contribute to the PL spectrum in the visible-near infrared region (from 600 nm to 900 nm) depending on the size of the NC.
Gold and silver plasmonic nanostructures were fabricated using various preparation techniques (such as EBL, GIS-FIB) on the annealed SRON thin films. Metal nanonstructures were also prepared on bare Si substrates and subsequently Si NCs dissolved in PMMA were deposited using spin coating method. In order to obtain a higher PL signal, the plasmonic structures were arranged in arrays. The PL enhancement was measured for different size and separation of metallic structures and for different excitation wavelengths.
Furthermore, the experimentally observed PL enhancement (or quenching) is compared with the numerical calculations carried out using boundary element method (BEM) and FDTD simulations.

[1] A. Tewary, R. D. Kekatpure, and M. L. Brongersma, Appl. Phys. Lett. **88**, 093114 (2006).

NST-P1-19
Self-Assembling of NiTPP/Cu(111): an XPS and STM study

T10 Nanoscience and Technology

#NST-P1-19

S. Fatayer, M.J. Prieto, A. De Siervo.

Instituto de Física 'Gleb Wataghin',Universidade Estadual de Campinas, 13083-859 - Campinas (Brazil).

Systems of low dimensions, for instance periodic nanostructures at surfaces, are of great technological interest and present exciting scientific challenges. The formation of nanostructured systems, ordered with long range periodicity can be obtained by self-assembling methods. In particular, metallorganic systems in the scale of few nanometers may be efficiently synthesized by the SAM (Self-assembling of Monolayers) method [1].
Organometallic molecules of porphyrinic groups are interesting for technological applications because it is feasible through the SAM method to produce devices in order to act as organic light emitting diodes, optoelectronic systems and sensors for different applications [2].
In the present research we have investigated the electronic and morphological properties of NiTPP (Nickel-Tetraphenyl Porphyrin) self-assembled on Cu(111) surface. The NiTPP films were deposited under UHV on a Cu(111) single crystal at room temperature using a homemade Knudsen cell with a quartz crucible. The main results are based on UHV Scanning Tunneling Microscopy (STM) and X-Ray Photoelectron Spectroscopy (XPS). The STM images showed the coexistence of three distinct domains at the surface as a consequence of the fcc packing of the substrate. NiTPP forms a "nearly-square" lattice with their vectors equal to 1.16 nm and 1.22 nm. Their angle was calculated to be approximately 86.6 degrees. The growth of the NiTPP was found to begin at the step edge of the Cu(111) since it was not observed "free-islands" of the molecules through the images. Using XPS analysis, we explored the chemical stability of NiTPP on Cu(111) upon annealing and the possibilities of molecular demetallization due to Cu-Ni alloy formation.

[1] A. Ulman, Chem. Rev.,1996, 96, 1533

[2] P. Moriarty, Rep. Prog. Phys., 2001, 64, 297.

NST-P3-25
THEORETICAL STUDY OF THE ZnTe QUANTUM DOTS CAPPED WITH ZnSe

T10 Nanoscience and Technology

#NST-P3-25

B. Rerbal, G. Merad.

Laboratoire d'Etude et Prédiction de Matériaux, URMER, Université A. Belkaïd, B.P. 119 - Tlemcen (Algeria).

Self-assembled quantum dots (QDs) are of high interest for optical applications such as low-threshold lasers [1] or single sources for applications in quantum information processing [2,3]. It is well known, as demonstrated by a lot of groups, that the driving force for the islands formation is the strain relaxation between the two materials (Stransky-Krastanov growth mode), but it can be, in some cases, strongly pertubated by surface segregation effect [4]. The competition between the formation of islands and misfit dislocations as strain relaxation mechanisms plays a key role: surface and interface energies, elastic energy and formation energy of misfit dislocations have to be taken into account in the island formation process [5]. This makes the control over the island formation with predictable sizes challenging. A novel method to induce the transition from the 2D strained layer to islands was recently developed [6]. It consists of covering a layer of strained ZnTe on (001) ZnSe with amorphous tellurium at low temperature and of subsequent desorption of this amorphous tellurium at growth temperature [7]. Afterward, the ZnTe islands are capped with ZnSe. The growth of the capping layer was begun at 200°C to avoid interdiffusion and to preserve the islands shape as much as possible [8]. In spite of that, high resolution transmission electron microscopy images showed that the islands were drastically flattened during capping [8]. The tellurium content was found to be much lower than the nominal value: this is caused by the strong segregation of the Te in ZnSe occurring during growth which contributes to both the island flattening and the apparent lost of tellurium [8].
In this work, we attempt to describe these phenomena by calculating the ZnSe/ZnTe interface energy. The calculations are done by performing ab-initio calculations based on the density functional theory (DFT) and using the Vienna ab-initio software package (VASP) [9-12]. We found that the ZnSe/ZnTe interface energy does not change when the Te segregation occurs. Interface change densities are also calculated.

[1] Y. Arakawa, H. Sakaki, Appl. Phys. Lett. 40 (1982) 939.
[2] E. Waks, K. Inoue, C. Santori, D. Fattal and Y. Yamamoto, Nature 420 (2002) 762.
[3]M. Schlz, T. Aichele, S. Ramelow, O. Benson, Phys. Rev. Lett. 96 (2006) 180501.
[4] C. Bougerol, R. André, I.C. Robin, B. Van Daele, G. Van Tendeloo, Phys. Status Solidi (c) 3 (2006) 938.
[5] F. Tinjod, I-C. Robin, R. André, K. Kheng, H. Mariette, J. Alloys. Compd. 371 (2004) 63.
[6] F. Tinjod, B. Gilles, S. Moehl, K. Kheng, H. Mariette, Appl. Phys. Lett. 82, 4340 (2003)
[7] I-C. Robin, R. André, H. Mariette, S. Tatarenko, L.S. Dang, J. Bleuse and J.M. Gérard, Nanotechnology 16 (2005)1116.
[8] R. Najjar, R. André, L. Besombes, C. Bougerol , S. Tatarenko and H. Mariette, Superlattices and Microstructures 46 (2009) 253.
[9] J. Hafner, Acta Materiala, 48 (2000) 71.
[10] G. Kresse and J. Hafner, Phys. Rev. Lett. B, 47 (1993) 558,; 49 (1994) 14251.
[11] G. Kresse and J. Furthmüller, Phys. Rev. Lett. B, 54 (1996) 11169.
[12] G. Kresse and J. Furthmüller, Comput. Mat. Sci., 6 (1996) 15.

NST-P3-10
A new methodology to produce Iron Nanoparticles by Laser Ablation in organic media

T10 Nanoscience and Technology

#NST-P3-10

Y. Vitta Brito, V. Piscitelli Spinielo, A. Fernadez Cuervo, J. Castillo.

Universidad Central de Venezuela - Caracas (Venezuela, bolivarian republic of).

In this work, we present a new methodology of production for iron nanoparticles (iron Np) in organic solvents, by laser ablation. Using an inert gas stream the particles are blowing into solvent (LAiGS). The nanoparticles produced by this method were compared with others produced by direct laser ablation in metal plate immersed in solvent (LAiS). The ablation procedure was performed in 10 minutes steps by triplicate with cooling periods of 5 minutes between ablation. Comparatively particles were obtained under continuous ablation iron plate at different time's ablation, 10, 20 and 30 min. The same procedure was utilized in both cases, LAiS and LAiGS. Optical properties were measured by UV spectroscopy, size distribution were measured by Dinamic Light Scattering and morphological study was performed by atomic force microscope (AFM) to correlate the size and form of the Np whit showed optical properties.

The influence of laser parameters; ablation time, flow gas and employed method on diameter, size distribution and absorption peak intensity of the Np prepared were studied. The absorption peak intensity, number of particles and size distribution of the iron Np obtained in LAiS method are dependent of laser irradiance. This is attributed that at high fluences and long pulse laser, occur re-fractionation laser induced. In LaiGS, the consecutive ablation is the mechanism preferred for particles production; this because the subsequent ablation produces new particles in the same volume of plasma, the concentration increases and this occurs gradually as often repeat the cooling process and the re-ablation. Nps of size ranging between 8 -10 nm and bimodal size distribution were obtained by both methods. Larger particles (micrometers) correspond to aggregates. The particles exhibited Resonance Plasmon Surface, SPR; band between 300 and 380 nm, typical of Fe Np.

LAiSG method was used to prepare Np in organic flammable solvents, obtaining good Np dispersions usefully in experiments wee water presence is regretted.

Fig 1. Nanoparticle Micrographs by AFM.

Fig 2. Size Distribution in Iron Np by LAiGS

NST-4-Or-3
2D assembly of colloidal nanoparticles on semiconductor substrates pre-patterned by charged particle beams

T10 Nanoscience and Technology

#NST-4-Or-3

Z. Druckmüllerová [1], F. Ligmajer [1], M. Kolíbal [2], M. Šimšíková [2], P. Varga [3], T. Šikola [2].

[1]Institute of Physical Engineering, Brno University of Technology, Technická 2, 616 69 Brno - Brno (Czech republic), [2]CEITEC BUT, Brno University of Technology, Technická 10, 61669 Brno - Brno (Czech republic), [3]Institut für Angewandte Physik, Technische Universität Wien, A-1040 - Wiena (Austria).

Colloidal gold nanoparticles represent technological building blocks which are easy to fabricate while keeping full control of their shape and dimensions. Their assembly onto surfaces is required for many applications, including nanowire growth and plasmonics, where the plasmonic resonance can be tuned by the size of nanoparticles and designing nanoparticle clusters, thus forming a new class of colloidal metamaterials [1]. In another example, a metallic nanoparticle placed in a close vicinity of a quantum dot may significantly enhance the luminescence yield [2]. In our contribution we will present a simple two step technique for the assembly and placement of gold and silver colloidal nanoparticles (spheres and rods) on a semiconductor substrate [3]. The exposure of the desired location on such a substrate by the charged particle beam of a very low fluence (electrons or ions in a dual-beam microscope) results in desorption of impurities and, especially, modification of surface chemical groups (Fig. 1a). If such a sample is immersed into a colloidal solution, depending on its pH, the positive (colloidal nanoparticles adhere to the exposed areas only) or negative (colloidal nanoparticles are deposited all over the substrate except the exposed areas) deposition is achieved. We will show our latest data on improved patterning resolution (spherical particle arrays with the pitch below 100 nm) on silicon and GaAs, as well as patterning of rod-like nanoparticles.

[1] Fan A. J. et al., Nanoletters 2012, 12, 5318.
[2] Chen C-T. et al., Applied Physics Letters 2012, 102, 041908.
[3] Kolíbal M. et al., ACS Nano 2012, 6, 10098-10106.

Fig. 1. a) Schematic of a fabrication process leading to a positive or negative colloids deposition. b) Resulting array of 20 nm gold colloidal nanoparticles on a Si substrate.

NST-6-Or-7
Secondary electron emission study of copper oxide nanowires

T10 Nanoscience and Technology

#NST-6-Or-7

L. Aguilera [1], I. Montero [1], M.E. Dávila [1], V. Nistor [2], L. González [2], L. Galán [2], D. Raboso [3].

[1]Instituto de Ciencia de Materiales de Madrid (CSIC) - Madrid (Spain), [2]Universidad Autónoma de Madrid - Madrid (Spain), [3]European Space Agency/ESTEC - Noordwijk (Netherlands).

Nanowires have been shown to provide a promising framework for applying their properties in the design of nanostructures for nanoscience investigations and for potential nanotechnology applications. The smaller length scales are being used in the semiconductor, optoelectronics and magnetics industries, and the intense development of the biotechnology industry where the goals are also at the nanoscale. The sizes of nanowires are usually > 1nm in the quantum confined direction [1].
Low-energy secondary electron emission materials are required for antimultipactor applications in several important technologies and their study and development is also a matter of great scientific interest. Also, electron cloud buildup is a major limitation for high-energy particle accelerators [2]. For this purpose, in this work copper oxide nanowires were grown on Cu substrates by thermal oxidation and the influence of low-energy carbon ion bombardment on the secondary electron emission yield of nanowires was studied. Thus, CuO nanowires were obtained by heating a copper foil in air. The influence of temperature and time on the growth of copper oxide nanowires was investigated. Either a linear or a stepped temperature ramp was applied in this growth procedure. The temperature ramps were at a predefined ramp rate in the range 100-300ºC/h. The growth temperature of CuO nanowires was between 400-800ºC. At each temperature step a different oxidized copper sample was obtained. These synthesis procedures allowed obtaining uniform CuO nanowires with controllable diameters in the range of 20-900 nm and with lengths of up to 30 µm. Structural analysis by electron diffraction and high-resolution SEM were also performed. The composition and chemical bonds formed in the films after low-energy carbon ion bombardment were analyzed by x-ray photoelectron spectroscopy (XPS). XPS revealed the formation of both carbidic and graphitic bonds. Cu-C bonds were

formed up to a limiting value of 0.1 for the carbidic carbon atomic fraction. The secondary electron emission yields for copper oxide nanowires were measured before and after low-energy CHn+ ion bombardment. The experiments have shown that a complete suppression of multipactor can be achieved by coating the nanowires with a thin layer of gold and after carbon ion bombradment, which has a maximum secondary electron yield (SEY) lower than 1. These results lead to a higher threshold of the Multipactor breakdown for high power RF devices in vacuum or a complete suppression of the e-cloud.

[1] M. S. Dresselhaus, Y.M. Lin, O. Rabin, M. R. Black and G. Dresselhaus, “Nanowires", in Springer Handbook of Nanotechnology, edited by Bharat Bhushan, pp. 99-145 (2004).
[2] C. Yin Vallgren, G. Arduini, J. Bauche, S. Calatroni, P. Chiggiato, K. Cornelis, P. Costa Pinto, B. Henrist, E. Me´tral, H. Neupert, G. Rumolo, E. Shaposhnikova, and M. Taborelli, Physical Review Special Topics - Accelerators and Beams 14, 071001 (2011).

NST/SS-4-Or-5
Repeated magnetization reversal in oscillating magnetic nanowires

T10 Nanoscience and Technology

#NST/SS-4-Or-5

T. Muehl, S. Philippi, H. Schlörb, A. Leonhardt, B. Büchner.

IFW Dresden - Dresden (Germany).

The interplay of mechanical and magnetic dynamics at the nanoscale and its potential for fundamental studies and novel applications still need to be fully explored. Here we present an experimental method to repeatedly reverse the magnetization of a single domain ferromagnetic nanowire with no dynamic external fields involved. The magnetization reversal is self-induced by a flexural vibration of a single-side clamped nanowire in a static perpendicular field. The vibration varies the applied field angle with respect to the nanowire axis, and causes the magnetization to reverse whenever the switching condition according to the nanowire's angular dependence of the switching field is fulfilled. Upon magnetization reversal the vibration amplitude is reduced due to the dissipation of energy associated with the magnetization reversal. The periodic driving force leads to an increase of the vibration amplitude until the following switching event occurs. This results in non-trivial sequences of transient vibrational states associated with ever-changing phase relations between the excitation force and the flexural oscillation. In our experiments, individual, freestanding Ni nanowires are used. The presence of the repeated magnetization reversal state is observable in the scanning electron microscope (SEM), as the envelope micrograph of the vibrating nanowire undergoes significant changes as compared to a steady state oscillation (see figure). The time scale between individual reversals has been estimated to several milliseconds both by calculation and SEM-based measurements.

SEM images of a Ni nanowire (a) in the idle state, (b) in a steady flexural vibration state in zero applied field at 279 kHz driving frequency, and (c) vibrating with the same driving frequency in a constant perpendicular field leading to recurring magnetization reversals. The reversals cause amplitude drops.

NST-P3-11
Potential profile of small quantum dots (QD) and the example of GaN-QD imbedded in AlN

T10 Nanoscience and Technology

#NST-P3-11

B. Sanric.

R.Boskovic Institute - Zagreb (Croatia).

It is usually assumed that the quantum well (QW) or quantum dot (QD) have rectangular potential profiles. Here we show that the potential profiles are not rectangular on nano-scale. Instead, the potential step at the interface is a smooth, gradual change of potential over a distance larger than one monolayer.[1] This is important when the size of the quantum structure is around 3-4 nm or smaller. Conclusions are obtained by calculating the electrostatic contribution to the total potential. We examine the dipole layers formed by the ions, at the interfaces in various crystal directions. Although similar to those of the Density Functional Theory, our results are obtained in a simpler and intuitive way. Remarkably, the minimal thickness of the potential barrier is not determined by the distance between the charged planes, but by the lateral spacing between ions of the same polarity. The crossection of the potential of a narrow QW or small QD, do not have the shape of a rectangular well. A more appropriate term is the quantum valley. Due to smooth potential profiles, the energy level positions will be different in comparison to the rectangular QWs. In the example of GaN and AlN, the barrier cannot be thinner than about 3 A. In addition, the 3D profile of a GaN-QD is not spatially uniform since it depends on the crystal orientation at the interfaces, which also effects on the effective depth (or height) of the QD potential.

[1] B. Šantić and N. Šantić, Semicond. Sci. Techn., 27 (2012) 085014 (5pp)

NST-1-Or-4
Epitaxy of Mn-doped ferromagnetic bismuth chalcogenide topological insulators on BaF2 (111) substrates

T10 Nanoscience and Technology

#NST-1-Or-4

H. Steiner [1], R. Kirchschlager [1], G. Bauer [1], O. Caha [2], V. Holy [3], J. Sánchez-Barriga [4], A. Varykhalov [4], E. Schierle [4], E. Weschke [4], O. Rader [4], G. Springholz [1].

[1]Johannes Kepler University - Linz (Austria), [2]Masaryk University - Brno (Czech republic), [3]Charles University Prague - Praha (Czech republic), [4]Helmholtz-Zentrum Berlin - Berlin (Germany).

Topological insulators behave attracted tremendous interest due to their extraordinary physical properties caused by the gapless surface state with linear dispersion that is topologically protected by time-reversal symmetry [1]. Prominent examples are the bismuth chalcogenides such as Bi_2Se_3 and Bi_2Te_3, which exhibit a complicated hexagonal lattice structure consisting of three unit cells of quintuple layers stacked on top of each other. Magnetic impurities like Mn [2-4] in topological insulators are predicted to break time reversal symmetry and lift the degeneracy at the Dirac points, leading to novel phenomena like topological magneto-electric effects, quantum anomalous Hall effect and half-integer charges at magnetic domain boundaries [1].
In this work, epitaxial growth, structural and electronic properties of Mn doped Bi_2Se_3 and Bi_2Te_3 epilayers on BaF_2 (111) substrates was studied as illustrated in Fig. 1. We show that different Bi-Te and Bi-Se phases can be formed in dependence of growth conditions. Incorporation of Mn was achieved up to concentration of a few percent and these layers show ferromagnetic behavior at Tc´s < 10K as revealed by SQUID magnetization and x-ray magnetic dichroism measurements. The effect of Mn on the topological surface state was studied by angular resolved photoemission (ARPES) at BESSY II after desorption of the protective Se capping layer in the ARPES chamber. ARPES spectra of Mn: Bi_2Se_3 layers with Mn content from 0 to 8% are shown in Fig. 1, demonstrating a gap opening that increases with increasing Mn content. The band gap is found to be independent of temperature and persists up to room temperature where the samples are non-magnetic. This indicates that the breaking-up of the

topological surface state is not caused by magnetism and thus, time reversal symmetry breaking but must be of different origin.

[1] X. L. Qi and S. C. Zhang, Rev. Mod. Phys. 83, 1057 (2011).
[2] Y.L. Chen et al., Science 329, 5992 (2010)
[3] Y.S. Hor et al., Phys. Rev. B 81, 195203 (2010).
[4] I. Vobornik et al., Nano Letters 11, 4079 (2011).

Figure 1: ARPES spectra at 7K of $Bi_{2-2x}Mn_{2x}Se_3$ layers with Mn content increasing from 0 up to 8% from (a) to (d), respectivel, showing the Dirac cone of the topological surface state and the opening of a gap with increasing Mn content. The AFM surface image of a Bi_2Te_3 epilayer on BaF_2 (111) is shown in (e).

NST-P1-09
Enhanced Optical Properties of Alkylated Silicon Quantum Dots mixed with Erbium (III) Chloride

T10 Nanoscience and Technology

#NST-P1-09

K. Abualnaja, G. Bhaduri, B. Horrocks, L. Siller.

Newcastle University - Newcastle Upon Tyne (United kingdom).

There has been an increased attention on silicon quantum dots due to their enhanced optical properties. This enhancement is attributing to the quasi- direct band gap within silicon quantum dots which is indirect in bulk silicon. However, the main goal of adding erbium to silicon quantum dots is to observe the energy transfer from the excited state of the silicon quantum dots to the erbium for optical fiber technology applications. In this study, a colloidal suspension of luminescent silicon quantum dots is synthesized when porous silicon prepared at high current densities is refluxed in toluene solutions of 1-undecene under circumstances which allow hydrosilation to occur. The diameter of the Si core of the alkylated-silicon quantum dots is 2.2±0.4 nm was confirmed by scanning transmission electron microscopy (STEM). Mixing alkylated-silicon quantum dots with erbium is achieved by adding aqueous erbium (III) chloride to alkylated silicon quantum dots which enhances the optical properties of silicon quantum dots. The optical luminescent of alkylated silicon quantum dots and alkylated silicon quantum dots mixed with erbium were studied under excitation 400 nm. Orange emission band was observed in the alkylated silicon quantum dots at 590 nm. Alkylated silicon quantum dots mixed with erbium exhibited photoluminescence peak at around 595 nm and 1535 nm which could be assigned to electron-hole recombination in silicon quantum dots and $^4I_{13/2} \rightarrow {}^4I_{15/2}$ intra-4f transition in Er^{3+} respectively. Raman, X-ray photoemission spectroscopic (XPS) and UV-Vis analysis of the alkylated silicon quantum dots and alkylated silicon quantum dots mixed with erbium were carried out to investigate its optical and chemical properties. Raman results indicate that this method increases the Raman signals of alkylated silicon quantum dots mixed with erbium. The XPS results detect the presence of Si-O, Si-Si and Er_2O_3 which confirm the existence of Er within the alkylated silicon quantum dots lattice.

NST-13-Or-7
Deep Ultraviolet plasmonics in Aluminum nanoparticle arrays

T10 Nanoscience and Technology

#NST-13-Or-7

F. Bisio [1], G. Maidecchi [2], G. Gonella [3], R. Moroni [1], A. Giglia [4], S. Nannarone [5], L. Mattera [2], M. Canepa [2].

[1]CNR-SPIN - Genova (Italy), [2]Unige - Genova (Italy), [3]U-Temple - Philadelphia (United states), [4]CNR-IOM - Trieste (Italy), [5]Uni-MoRe - Modena (Italy).

Physical systems based on Aluminum nanoparticles (NPs) have for a long time been strong candidates for extending the plasmonic response of materials towards the deep-ultraviolet (DUV) range, with important fallouts in the fields of non-linear optical spectroscopies and high-sensitivity biosensing. Despite the expectation that Al NPs exhibit a localized surface plasmon resonance (L-SPR) in the DUV range, the metal's reactivity and the synthesis difficulties have strongly hampered the research in this direction.
Employing a strict control of the fabrication process, we realized 2-dimensional Al NPs arrays with DUV-frequency L-SPR supported onto self-organized nanopatterned LiF(110) surfaces. The arrays consist of ensembles of ellipsoidal aluminum nanoparticles, either metalic or in a Al2O3/Al core-shell architecture, aligned along the nanometric grooves of the LiF surface. Atomic-force microscopy showed that the NPs are ordered over large areas and exhibit a coherently-aligned ellipsoidal shape with narrow size distribution in the few tens-of-nm range. High-resolution X-ray photoemission data allowed to assess the metal/oxide fraction in the nanoparticles. Polarized-light absorption measurements in the 3-12 eV range performed by synchrotron light at BEAR beamline at Elettra (Trieste) revealed the presence of the L-SPR at frequencies as high as 6.8 eV, one of the highest LSPR energy ever reported by optical spectroscopy. The experimental data are successfully compared with theoretical calculations for the L-SPR. The results show the suitability of the present method to fabricate DUV-plasmonic Al nanostructures.

Optical absorbance normalized to the substrate reference fo core/shell metal/oxide Aluminum nanoparticles as a function of NP size (green, 17 nm diam, orange 22 nm

diam. and red 28 nm diameter) and excitation geometry (solid markers, short ellipsoid axis, open markers, long ellipsoid axis)

NST/SS-4-Or-6
Magnetism and Electronic Properties of Gold-Supported Stable pi-Radicals

T10 Nanoscience and Technology

#NST/SS-4-Or-6

S. Mullegger, M. Rashidi, M. Fattinger, R. Koch.

Johannes Kepler University - Linz (Austria).

Stable free radicals can be stored and investigated under ambient conditions, which makes them desirable for applications as polarizing agents or novel magnetic materials as well as suitable model systems for investigating sp^2 magnetism in reduced dimensions.
We have studied the stable all-organic spin-1/2 radical, α,γ-bisdiphenylene-β-phenylallyl (BDPA), adsorbed on a weakly interacting metal support by low-temperature scanning tunneling microscopy (LT- STM). We report on the geometric structure, self-assembly, frontier orbital electronic and magnetic properties, Kondo behaviour, radical-radical, and radical-substrate interactions at the atomic-scale. [1,2]

[1] S. Müllegger, M. Rashidi, M. Fattinger, and R. Koch, J. Phys. Chem. C 116, 22587−22594 (2012), DOI: 10.1021/jp3068409.
[2] S. Müllegger, M. Rashidi, M. Fattinger, and R. Koch, J. Phys. Chem. C (submitted).

NST-4-Or-7
Novel strain-free synthesis of epitaxial PbTe/CdTe nanocrystals for mid-infrared devices

T10 Nanoscience and Technology

#NST-4-Or-7

G. Springholz, I. Daruka, H. Groiss, M. Eibelhuber, A. Hochreiner, A. Khiar, F. Schaeffler.

Johannes Kepler University - Linz (Austria).

Semiconductor quantum dots (QDs) have a great potential for optoelectronic devices. The most common synthesis method is based on the Stranski-Krastanow (SK) growth mode of strained-layer heteroepitaxy. The resulting QDs have been widely employed for visible and near-infrared photonics but efficient mid-infrared (MIR) emission has been difficult to achieve. In this work, we present an alternative strain-free synthesis method based on phase separation and nano-precipitation in heterosystems with large miscibility gap. It is shown that under well defined conditions, isolated quantum dots can be produced with strong luminescence emission. With these dots, we demonstrate the first QD lasers emitting in the MIR region.

The investigated PbTe/CdTe model system is a combination of a narrow gap and wide gap semiconductor, featuring identical lattice constants but different lattice structures. Due to phase separation, ultra-thin 2D PbTe/CdTe epilayers grown by molecular beam epitaxy onto GaAs (001) transform into isolated quantum dot nanocrystals during post annealing. As revealed by in situ TEM (see Fig. 1), this process starts with formation of a 1D percolation network, which further splits up into near-spherically symmetric QDs. To reveal the underlying mechanisms, a Monte Carlo model was developed that accounts for the thermodynamics by appropriate choice of the nearest and next-nearest neighboring bond energies. The time evolution is revealed by Monte Carlo snapshots depicted in the lower part of Fig. 1. The MC movies show a remarkable agreement with the TEM images and allow to identify the key parameters for the formatio process. With the obtained QDs, microdisk lasers and light emitting diodes were produced as shown in Fig. 2.

Fig. 1: Formation of epitaxial PbTe/CdTe nanocrystals by nanoprecipitation from 2D PbTe epilayers in CdTe, revealed by plan-view TEM (top) and modeled by Monte Carlo simulations (bottom).

Fig. 2: (a) MIR emission and (b) output versus pump powerof a PbTe/CdTe QD microdisk laser. (c) Cross-sectional TEM and (d) SEM image of the microdisk structure.

NST-6-Or-8
Au-Ag alloy nanoparticles 2D-arrays: fabrication and surface-enhanced Raman spectroscopy application.

T10 Nanoscience and Technology

#NST-6-Or-8

G. Maidecchi [1], A. Toma [2], G. Das [2], C. Vu Duc [3], M. Caminale [4], E. Di Fabrizio [5], F. Bisio [6], M. Canepa [1].

[1]CNISM and Dipartimento di Fisica, Università di Genova, via Dodecaneso 33 - Genova (Italy), [2]Italian Inst Technol, Nanostruct Dept - Genova (Italy), [3]Institute of Materials Science - Hanoi (Viet nam), [4]Dipartimento di Fisica, Università di Genova, via Dodecaneso 33 Science - Genova (Italy), [5]Italian Inst Technol, Nanostruct Dept and Magna Graecia Univ Catanzaro, BioNEM Bio Nano Engn & Technol Med - Genova And Catanzaro (Italy), [6]CNR-SPIN, Corso F.M. Perrone 24 - Genova (Italy).

Alloy nanoparticles (NPs) have attracted much interest because of their unique catalytic, electronic and optical properties. In particular, the NPs localized surface plasmon resonance (L-SPR) can be tuned by controlling the alloy composition. Achieving this goal often requires complex fabrication techniques . Here we propose an extremely easy method, based on a self-organization approach, to fabricate well-ordered 2D arrays of Au-Ag alloy NPs with changing composition across the substrate. This feature makes our arrays very promising for designing surface-enhanced Raman spectroscopy (SERS) substrates, provided a precise control of the nanofabrication process.
The NPs are fabricated by the consecutive deposition of the two metals onto self-organized nanopatterned LiF(110) substrates. The preparation procedure allowed to obtain a linearly varying composition of the NPs on a single LiF substrate. The NPs plasmonic resonance blue-shifts linearly across the substrate with the increase of Ag content, as predicted for homogeneous alloys. The arrays morphology has been studied by scanning electron microscopy and atomic force microscopy. The arrays consist of NPs coherently aligned with a few nanometers interparticle spacing and narrow size distribution in the few tens-of-nm range. The arrays morphology is uniform over a several millimeters area and despite the varying compostion.
These NPs arrays have been employed as SERS substrates after the adsorption of

Rhodamine-6g. The intensity trend of the Raman spectra is directly correlated to the NPs composition, i.e. to the plasmonic resonance wavelength. A strong field enhancement was found, as confirmed also by theoretical simulations, allowing to detect a nanomolar concentration of the test-molecule.

NST-13-Or-8
Improvement of the quality of Probes for Near-Field Scanning Optical Microscopy

T10 Nanoscience and Technology

#NST-13-Or-8

P. Dvorak, T. Šamoril, D. Škoda, M. Urbánek, T. Neumat, J. Spousta, R. Kalousek, T. Šikola.

Institute of Physical Engineering, Brno University of Technology, 682 96 Brno, Czech Republic - Brno (Czech republic).

Quality of probes for near-field scanning optical microscopy plays a crucial role in the efficiency of obtaining the near-field distribution images [1]. Commercially available probes are relatively expensive, technologically inferior and their production is time-consuming. We have improved the fabrication process and, consequently, the resulting quality of those probes. The probes are metal-coated optical fibers with a small aperture (< 100 nm).
The first step of fabrication is etching one end of a fiber in 40% HF acid for 75 min (Turner's method) which creates a tip-shape [2]. Then, the set of fibers (six together) is put in an UHV chamber and their tips sputtered by 400 eV Ar+ ions for 120 s. It removes impurities, provides glazing and modifies tip morphology. Afterwards, 150 nm thick aluminum layer is in situ deposited via Ion Beam Assisted Deposition (IBAD) with an optimized assisting ion beam energy of 100 eV. A 3 nm thick titanium film is used as an adhesive layer between the metal film and the glass substrate We have studied the relation between the size of grains and ion energy. It has been found that the method provides approximately 10 times smaller grains than commercial probes..
The next step is cutting the end of the tip by Focus Ion Beam (FIB). Subsequently, the metal tip is fabricated by ion beam induced deposition (IBID) of Pt . At the end, the aperture of the required geometry is milled by FIB. NSOM experimental images of calibration samples taken by the fabricated probes will by presented and discussed.

[1] Novotny L., Hecht B.: *Principles of Nano-Optics*, Cambridge University Press, (2006).

[2] Turner D. R., *Etch Procedure for Optical Fibers*. United States patent, 4, 469, 554 (1984).

NST-P3-21
Optical scattering by dense ordered metal nanoparticle arrays produced using deposition through ultrathin anodized aluminum oxide masks

T10 Nanoscience and Technology

#NST-P3-21

J. Prikulis, U. Maļinovskis, R. Popļausks, G. Bergs, D. Erts.

Institute of Chemical Physics, University of Latvia - Riga (Latvia).

Metal nanoparticles are interesting for a variety of reasons including applications in catalysis, biosensors, solar cells, electronic devices, or use as model systems for theoretical studies of physical phenomena. Much of attention has been directed towards regular nanoparticle arrays, partly because certain properties can be greatly enhanced due to lattice diffraction effects, and partly because periodicity simplifies calculations, since all elements in an infinitely repeating system are equivalent and the surrounding fields at each site are the same. In this work we address the optical properties of aperiodic arrays, where above simplification is no longer valid and the interaction between nanoparticles results in distinct spectral features.

For array production with minimum particle size of 20 nm, and center separation of 50 nm, we employed the pore self-assembly process in anodized aluminum to produce masks for nanoparticle array deposition. The original method by Masuda and Satoh [1] was modified to use lower voltages and shorten anodization times. which resulted in ultrathin (60-100 nm) layers with high density of pores. After the transfer of the membrane to a glass substrate, a wide selection of materials can be deposited through the porous mask. Using this method we produced arrays of Ag and Au nanoparticles, which are famous for their optical activity due to localized surface plasmon resonances.

The achieved particle sizes are much smaller and packed more densely than what has been reported on similar short range ordered assemblies [2, 3]. In contrast to arrays studied in ref. [4], where disorder is introduced by random displacement of

nanoparticles from their regular grid pattern, our samples preserve no long-range periodicity at distances exceeding the wavelength of incident radiation.

The measured spectra of scattered light show resonances in visible region and vary their peak position and broadening depending on array density and particle shape, which are controllable parameters during sample preparation. We use coupled dipole model [5] to simulate the scattering spectra and obtain results which are consistent with experimental observations. We also find that the dense arrays can be treated as continuous medium with their own propagation parameters.

[1] H. Masuda and M. Satoh, Jpn. J. Appl. Phys. 35, L126 (1996).

[2] P. Hanarp, M. Käll, and D. S. Sutherland, J. Phys. Chem. B 107, 5768 (2003).

[3] K. Nakayama, K. Tanabe, and H. A. Atwater, Appl. Phys. Lett. 93, 121904 (2008).

[4] B. Auguié and W. L. Barnes, Opt. Lett. 34, 401 (2009).

[5] B. T. Draine and P. J. Flatau, J. Opt. Soc. Am. A 11, 1491 (1994).

SEM image of Ag nanoparticle array.

NST-5-Or-8
A high resolution Atomic Force Microscope operated at about 300 mK in up to 10 T under UHV-conditions

T10 Nanoscience and Technology

#NST-5-Or-8

H. Von Allwörden, K. Ruschmeier, A. Schwarz, R. Wiesendanger.

University of Hamburg - Hamburg (Germany).

In atomic force microscopy (AFM) and spectroscopy (AFS) force sensitivity and energy resolution scale with the temperature as √T. To increase the sensitivity or to observe certain phenomena, which occur below a critical temperature only, experiments have to be performed in a cryogenic environment. Up to now low temperature force microscopes are mainly operated with bath cryostats using liquid 4He, whereby temperatures down to 4.2 K can be achieved. Here, a design based on 3He evaporation will be presented that enables AFM experiments at about 300 mK in ultrahigh vacuum (UHV). First results obtained with the instrument demonstrate that (i) clean samples can be prepared, (ii) deposition of single atoms on a cold substrate (T<30 K) is possible and (iii) the microscope is capable of true atomic resolution in the non-contact mode (Fig. 1). Since we are mainly interested in magnetic properties, a magnetic flux density up to 10 T can be applied perpendicular to the sample surface.

The 3He-cryostat from Oxford Instruments uses the evaporation of 3He for cooling to temperatures below 1 K [1] and is similar to an existing set-up in our group [2]. The UHV-compatible insert contains the microscope body, which is surrounded by the 10 T-solenoid. The holding time as well as the minimal base temperature strongly depends on the heat load: First, heat conduction through the electrical wires required for operation, which can be reduced by enhancing the thermal anchoring. Second, since we use a fiber-based optical interferometer, the part of the incoming light, which is not back reflected into the fiber, also contributes to the total heat load. The microscope design is based on the rigid and reliable Hamburg design [3,4]. However, for faster thermalization the body is made from phosphorus bronze instead of the glass-ceramic Macor. To gain access to tip and sample stage the microscope can be lowered from the cryogenic environment into a UHV-chamber at room-temperature. Samples prepared in two additional UHV-chambers attached to the central cryostat

chamber can be transferred and exchanged in-situ. During a typical transfer time of about 15 minutes the microscope temperature stays below 45 K. After moving the microscope back into cryogenic environment, cool down to base temperature by condensation of 3He requires about 2 hours. Realization of the instrument, strategies to minimize the heat load and experimental results will be discussed.

[1] G. Batey *et al.*, J. Low Temp. Phys. **113**, 933 (1998);
[2] J. Wiebe *et al.*, Rev. Sci. Instr. **75**, 4870, (2004).
[3] W. Allers *et al.*, Rev. Sci. Instr. **69**, 221, (1998).
[4] M. Liebmann *et al.*, Rev. Sci. Instr. **73**, 3508, (2002).

Fig.1: atomically resolved NaCl(001)

NST-6-Or-9
Synthesis of Ag@Pt Core-shell Nanowires via Galvanic Replacement

T10 Nanoscience and Technology

#NST-6-Or-9

J. Song [1], S.Y. Chen [2], Y.L. Shen [3], I.G. Chen [4].

[1]Department of Materials Science and Engineering, National Chung Hsing University - Taichung (Taiwan, republic of china), [2]Department of Materials Science and Engineering, National Taiwan University of Science and Technology - Taipei (Taiwan, republic of china), [3]Graduate Institute of Applied Science and Technology, National Taiwan University of Science and Technology - Taipei (Taiwan, republic of china), [4]Department of Materials Science and Engineering, National Cheng Kung University - Tainan (Taiwan, republic of china).

Core-shell structure is an effective way to enhance the efficiency of precious metal electrocatalysts. In combination with the nanostructured core of less expensive or non-precious metals and the shell of Pt, high catalytic activity of core-shell bi-metallic electrocatalysts can be achieved. Previous studies have coated Pt on Pd, Au, Cu and Ag nanowires respectively using PVD (magnetron sputtering) or galvanic deposition. Excellent catalytic activity of those bi-metal NWs has also been demonstrated. Among these cases, the reports related to the synthesis of Ag-Pt core-shell nanowires are rare to our best knowledge. Zamborini et al. converted the surfaces of CTAB-protected Ag NWs into Pt by galvanic exchange reaction as shown below, however, the yield of nanowires thus produced was quite limited [1].

$2Ag^0(s) + PtCl_4^{2-}(aq) \rightarrow Pt^0(s) + 2AgCl(s \text{ or } aq) + 2Cl^-$, Eo cell =0.508V

Without using any templates or surfactants, this study develops a high-yield process to prepare vertical Ag-Pt core shell nanowires by the thermally assisted photoreduction [2,3] of Ag NWs and successive galvanic replacement between Ag and Pt ions. The clean surface of Ag nanowires allows Pt ions to reduce and deposit on it, and forms a compact sheath comprising Pt nanocrystals. The core-shell structural feature of the NWs thus produced has been demonstrated via TEM observation and AES elemental analysis. Kinetic analysis suggests that the deposition of Pt is an interface-controlled reaction and dominated by the oxidative dissolution of Ag atoms. The boundaries in-between Pt nanocrystals may act as microchannels for the transport of Ag ions during galvanic replacement reactions.

1. Grzegorz W. Slawiński, Francis P. Zamborini: Synthesis and alignment of silver nanorods and nanowires and the formation of Pt, Pd, and core/shell structures by galvanic exchange directly on surfaces. Langmuir, 23 (2007) 10357.

2. Y. L. Shen, S. Y. Chen, J. M. Song+, T. K. Chin, C. H. Lin and I. G. Chen, “Direct Growth of Ultra-long Platinum Nanolawns on a Semiconductor Photocatalyst” Nanoscale Research Letters, 6 (2011) 380, 2011.

3. Y. L. Shen, S. Y. Chen, J. M. Song+, and I. G. Chen, “Ultra-long Pt Nanolawns Supported on TiO2 Coated Carbon Fibers as 3D Hybridcatalyst for Methanol Oxidation” Nanoscale Research Letters, 7 (2012) 237.

TEM images showing Pt nanocrystals deposited on the surface of a Ag nanowire, as well as the SAED patterns of Ag core and Pt shell respectively

NST-5-Or-9
Scanning tunneling microscopy of semiconductor nanowires during device operation

T10 Nanoscience and Technology

#NST-5-Or-9

R. Timm, O. Persson, J. Webb, M. Hjort, C. Thelander, L. Samuelson, A. Mikkelsen.

The Nanometer Structure Consortium, Department of Physics, Lund University - Lund (Sweden).

III-V semiconductor nanowires (NWs) offer tremendous possibilities for device application in energy and information technology. It is essential to investigate their atomic surface structure and to correlate this information with electrical measurements on individual NWs. Recently, we have managed to clean InAs NWs from their native oxide and obtained first atomically resolved images of their side surfaces by using scanning tunneling microscopy (STM) [1]. Here, we present STM data covering various NW surfaces of different III-V material systems and different crystal structures, as well as scanning tunneling spectroscopy (STS) results revealing local electronic properties across the interface of NW heterostructures [2].
In order to go further in combining local surface characterization with transport measurements of NW devices, we have developed a novel STM-based setup: We are using combined atomic force microscopy (AFM) and STM/S on individually contacted NWs for mapping the atomic surface structure and the local band alignment along the NW heterostructure under device performance, as sketched in Fig. 1.
We show initial results of this unique approach on InAs-GaSb NW tunnel diodes [3], where we could prove Esaki behavior of a NW (Fig. 2b) while it was investigated by STM/AFM (Fig. 2c). From a set of STS spectra we mapped the band alignment across the broken-gap InAs-GaSb interface, and we determined the position of the Fermi level along the NW for different applied biases, showing an abrupt drop directly at the material interface (Fig. 2d). Results from additional experimental setups like scanning gate microscopy and different NW device systems will underline the versatile potential of this new method.

[1] Hilner et al., Nano Lett. **8**, 3978 (2008)
[2] Hjort et al., ACS Nano **6**, 9679 (2012)
[3] Borg et al., Appl. Phys. Lett. **101**, 043508 (2012)

Figure 1: Sketch of combined AFM/STM/STS measurements on individually contacted NWs.

Figure 2: (a) AFM image of a contacted NW. (b) *I*-*V* curve and (c) AFM image of the same InAs-GaSb NW. (d) Local Fermi level distribution (*V* = 0.3 V applied to the right contact).

NST/SS-5-Or-3
Electron scattering and spin polarization at the graphene/Ni(111) interface

T10 Nanoscience and Technology

#NST/SS-5-Or-3

A. Mugarza [1], A. Garcia-Lekue [2], T. Balashov [1], M. Ollé Soronellas [1], G. Ceballos [1], A. Arnau [3], P. Gambardella [1], D. Sánchez-Portal [3].

[1]ICN - Barcelona (Spain), [2]DIPC - Donostia-San Sebastian (Spain), [3]Centro de Física de Materiales (UPV-CSIC) - Donostia-San Sebastian (Spain).

The interaction of graphene with a metal often perturbs the unique electronic properties of Dirac electrons in graphene. This interaction can be positively exploited to engineer the Dirac bands and obtained graphene interfaces with different functionalities. In this work we study the electronic and magnetic properties of graphene nanoislands grown on Ni(111) [1] by combining scanning tunnelling microscopy and ab-initio calculations. We show that the interaction with the Ni surface opens a gap and spin-polarizes the Dirac bands, which results in a spin filtering effect in the transport across the interface [2]. On the other hand, the standing wave pattern created around the nanoislands reveal an asymmetric potential that depends both on the spin and edge type, suggesting a lateral 2D spin-filter effect similar to that occurring across the interface.

[1] M. Olle et al. Nano Lett. 12, 4431 (2012).
[2] V. M. Karpan et al. Phys. Rev. Lett. 99, 176602 (2007).

NST/SS-6-Or-1
Bias Dependence of Tunnelling Mechanism in CoFeB/MgO/CoFeB Magnetic Tunnel Junction

T10 Nanoscience and Technology

#NST/SS-6-Or-1

R. Oksuzoglu, M. Yildirim.

Department of Materials and Engineering, University Anadolu - Eskisehir (Turkey).

Magnetic tunnel junctions (MTJs) with large tunnel magnetoresistance (TMR) at room temperature are of great importance not only for device application but also for clarifying the physics of tunnelling mechanism. Theoretically, TMR ratios over 1000% were predicted based on the coherent tunnelling of fully spin-polarized Δ_1 electrons [1]. Experimentally, the highest TMR ratio was reported as 604% at room temperature in CoFeB/MgO/CoFeB MTJ [2]. One of the important properties for application is high sensitivity, where the sensitivity generally increases with increasing of TMR ratio. An other point is the bias dependence of TMR ratioand its underlying mechanism is still discussed [3]. In spintronic devices, very thin barriers were grown, on the order of few nm or less, in order to keep the power supply within acceptable limit. Usually, very high intrinsic critical current density (>$5x10^5$ A/cm^2) [4] is passed through the thin barrier by means of large barrier voltage and high electric fields in operations; however, the TMR ratio cannot be easily increased by applying higher barrier voltages. One other point is that, during the read cycles, where the voltage is low, minimum tunnelling is desired to insure good charge retentions [5]. Consequently, an understanding of tunnelling current behaviour over a wide range of applied voltage is essential in MTJ devices with high TMR value. In this contribution, the effect of applied bias on TMR ratio and tunnelling mechanism has been systematically investigated in CoFeB(3nm)/MgO(2nm)/CoFeB(3nm) MTJ, which was deposited using a combination of the pulsed DC magnetron and RF sputtering techniques. While the thickness of junction layers and the interface roughness were determined by X-Ray Reflectometry, the structure properties were investigated by X-Ray Diffraction and Grazing Incidence X-Ray Diffraction techniques. The junction with a 25x25 µm2 area indicates a giant TMR in the order of 506% at room temperature in minimum applied bias, and the TMR ratio decreases with increasing bias voltage. When the applied bias voltage is less than the average barrier height,

direct tunnelling occurs as dominant transport mechanism. In this bias regime, the TMR ratio is almost unaffected by the applied voltage, and Brinkman and Simmon formulas yield reasonable values for barrier thickness and height. If the bias voltage exceeds the average barrier height, Simmon and Brinkman formulas does not lead to correct barrier height and thickness, whereas reasonable barrier parameters could be obtained by Fowler-Nordheim Tunnelling formula, indicating a bias dependent change of the dominant transport mechanism in the investigated MTJs. The structure property correlation was also discussed.

[1] W. H. Butler, X.-G. Zhang, T. C. Schulthess, and J. M. Maclaren, Phys. Rev. B 63, 054416 (2001).
[2] S. Ikeda, J. Hayakawa, Y. Ashizawa, Y. M. Lee, K. Miura, H. Hasegawa, M. Tsunoda, F. Matsukura, and H. Ohno, Appl. Phys. Lett. 93, 082508 (2008)
[3] G. Feng, Sebastiaan van Dijken, J. F. Feng, J. M. D. Coey, T. Leo, and David J. Smith, J. Appl. Phys.105, 033916 (2009).
[4] S. Yuasa and D. D. Djayaprawira J. Phys. D: Appl. Phys. 40, R337-R354 (2007)
[5] Shruti Patil, Andrew Lyle, Jonathan Harms, David J. Lilja and Jian-Ping Wang IEEE International Electron Devices Meeting, Computer Design (ICCD), pp. 125-131 (2010).

NST-9-Or-6
Interfacing quantum dots and graphitic surfaces with Cl-based atomic ligands

T10 Nanoscience and Technology

#NST-9-Or-6

C. Palencia Ramirez [1], F. Iacono [2], L. De La Cueva [3], M. Meyns [1], L. Terracciano [2], A. Vollmer [4], M.J. De La Mata [5], C. Klinke [1], J.M. Gallego [6], B. Hernandez Juarez [7], R. Otero [7].

[1]Hamburg University - Hamburg (Germany), [2]Universidad Autónoma de Madrid - Madrid (Spain), [3]IMDEA Nanoscience - Madrid (Spain), [4]Helmholtz Zentrum Berlin für Materialien und Energie - Berlin (Germany), [5]Servicio Interdepartamental de Investigación. SIdI. Universidad Autónoma de Madrid - Madrid (Spain), [6]ICMM-CSIC - IMDEA Nanoscience - Madrid (Spain), [7]Universidad Autónoma de Madrid - IMDEA Nanoscience - Madrid (Spain).

Semiconductor nanocrystals (NCs) have found application as part of the active material in many optoelectronic and photovoltaic devices, due to their very interesting optical and electronic properties.[1] Usually, the performance of such devices is limited by the reduced charge mobility across the NC-NC and/or NC-electrode interfaces, due to the fact that the surface of the colloidal NCs is stabilized by a shell of organic ligands that are usually long and poor electric conductors. The electronic mobility and thereby the performance of such devices can be enhanced by treatments that substitute the original insulating organic ligands for halides[2,3] or inorganic shells,[4] what improves the electronic NC-NC interface coupling. But not many works have tackled the interface between an NC and a solid surface that might act as an electrode in the device.

In this paper we demonstrate by XPS and solid NMR that Cl is incorporated in the ligand shell of NCs decorating C-sp^2 surfaces; that such incorporation involves the selective substitution of anhydrides of ODPA in the organic capping shell (originally composed of $ODPA^{2-}$ and anhydrides of ODPA); and finally that the structural changes associated with the aforementioned substitution actually strengthen the interaction of the NCs with C-sp^2 surfaces. These investigations have been carried out on Highly-Oriented Pyrolytic Graphite (HOPG), as a model system for general C-sp^2 surfaces such as CNTs or graphene.[5,6] The one-pot sample preparation methodology that we have followed leads to long-range ordered NC monolayers with a close contact between the active NC layer and the C-sp^2 electrode surface. The

possibility to control the coverage degree of hexagonal ordered NCs monolayer on conductive C-sp^2 in one pot opens attractive alternatives to be explored in solution processed optoelectronics.

1 W. U. Huynh, et al. Science 2002, 295 (5564), 2425.
2 J. Tang, et al. Nature Materials 2011, 10, 765
3 B. I. MacDonald, et al. ACS Nano 2012, 6, 5995
4 J. S. Lee, et al. Nature Nanotech. 2011, 6, 348.
5 B. H. Juárez, et al. Nano Lett. 2007, 7, 3564–3568.
6 B. H. Juárez, et al. J. Am. Chem. Soc. 2008, 130, 15282–15284.

Picture 1: The incorporation of chlorine (green dots) in the original $ODPA^-$ related ligand shell promotes the interaction with carbons sp^2 surfaces. (a) The original shell combines $ODPA^{2-}$ and anhydrides (b) the presence of chlorine displaces the anhydrides selectively and (c) promotes the interaction with C-sp^2 surfaces.

NST-7-Or-7
Ultra-High Resolution AM-AFM in Liquids with Small Cantilevers

T10 Nanoscience and Technology

#NST-7-Or-7

I. Revenko [1], J. Cleveland [1], S. Hohlbauch [1], D. Walters [1], M. Viani [1], M. Phillips [2].

[1]Asylum Research, an Oxford Instruments company - Santa Barbara (United states), [2]Asylum Research UK,LTD, an Oxford Instruments company - Bicester (United kingdom).

While the benefits of further miniaturization of cantilevers for AFM have been known for well over a decade, it is only in the last few years that levers as short as 10 µm long and the AFMs capable of using them have become commercially available. This talk will review the benefits of small levers and show some recent results using them.

For imaging in liquids, the biggest benefit is that the thermal noise in a given bandwidth is significantly reduced. The first part of the talk will review the theory behind this and address some common misconceptions involving thermal noise as well as show experimental results. For example, Fig. 1. shows that going from a 200 µm lever to an equivalent stiffness 10 µm lever drops the thermal force noise from 10 pN to about 2 pN. Small levers are also much faster because of the increased resonance frequency and bandwidth.

We have been using small cantilevers in liquids on a variety of sample and have been achieving ultra-high resolution. We will present results including single point defects on calcite crystals, monomer resolution on actin fibers, and resolution of the major and minor groove of the DNA double-helix (see Fig. 2).

Figure 1. Comparison of the thermal noise (left) of three levers (far right) of about the same stiffness and quality factor close to a surface. The equivalent input force noise

in a ±1 kHz bandwidth around resonance is shown.

Figure 2. Consecutive up and down scans of a single DNA molecule in buffer taken with a 30 µm lever at an amplitude of about 8 Å. The major and minor grooves are clearly resolved.

NST-11-Or-1
A new type of super intense cluster beam source based on Matrix Assembly

T10 Nanoscience and Technology

#NST-11-Or-1

W. Terry, L. Cao, F. Yin, R.E. Palmer.

Nanoscale Physics Research Laboratory, School of Physics and Astronomy, University of Birmingham - Birmingham (United kingdom).

Over the last 10-15 years there has been much interest in clusters, due to the highly size dependent properties they exhibit [1]. So far study of the field has been unable to harness the incredible potential of size-selected clusters into viable technologies for research and industry. The low flux of pure size-selected clusters available from current cluster source technology significantly limits the availability of size-selected clusters for test tube scale tests and rules out the use of size-selected clusters in large-scale industrial applications [2,3].

We propose that using the novel method of Matrix Assembly, size selected clusters could be produced in abundance. The Matrix Assembly method pins atoms of desired cluster material (e.g. Au or Ag) within a condensed rare gas matrix (e.g. Ar). Via sputtering the matrix with atomic ions (e.g. Ar+), clusters are produced [4]. Experimental results from our proof of principle testing and further advances are presented here. Our results demonstrate that by carefully selecting generation conditions not only a high flux of clusters, but also a narrow distribution of cluster sizes, can be obtained. Furthermore the average cluster size is governed by the concentration of cluster material atoms in the condensed rare gas matrix.

[1] U. Heiz, A. Sanchez, S. Abbet S and W.-D. Schneider, J. Am. Chem. Soc **121** 3214-3217 (1999).
[2] S. Pratontep, S. J. Carroll, C. Xirouchaki, M. Streun, R. E. Palmer, Rev. Sci. Instrum. **76**, 045103 (2005).
[3] Michael A. Duncan, Rev. Sci. Instrum. **83**, 041101 (2012).

[4] V. Balaji, D.E. David, T.F. Magnera and J. Michl, H.M. Urbassek, Nucl. Instr. and Meth. **B46** 435-440 (1990).

NST-P2-05
Geometric modification of AFM probes by SEM/FIB combination

T10 Nanoscience and Technology

#NST-P2-05

T. Šamoril [1], D. Škoda [2], B. Lencova [3], J. Spousta [1], P. Varga [2], T. Šikola [1].

[1]Institute of Physical Engineering, Brno University of Technology, 682 96 - Brno (Czech republic), [2]CEITEC BUT - Brno University of Technology, Technická 10, 616 69 - Brno (Czech republic), [3]Tescan a.s., Libušina trída 21, 623 00 - Brno (Czech republic).

A typical method of the surface characterization is SPM. As generally known, the resulting image quality of surface structures depends on the quality of SPM probes, especially on their material, geometric shape and the radius of the tip apex curvature. However, the image quality is gradually changing during SPM measurements, due to mechanical wear of the probe tip surface. In our contribution, the modification and repair of standard AFM probes by FIB (Focused Ion Beam) milling and EBID (Electron Beam Induced Deposition), and their combination, is reported. The operation was performed in a dual-beam system TESCAN LYRA3. First, the geometry of the standard AFM tip (NT-MDT CSG 10, NSG 10) was changed using FIB milling as follows: the tip cone angle was decreased to values smaller than 10° (for cone length > 3 μm), the curvature radius was kept constant at 10 nm. To provide it, approximately 10^{10} ions/μm^2 Ga dose was used. Compared to standard Si tips (side angle 36° for tetrahedral part of the tip and 7° - 10° for the last 500 nm from tip apex, the curvature radius 6 nm – 10 nm), a smaller distortion of topography was obtained during measurements of narrow deep structures using these tips. Further, the FIB technique was also used for repairing and sharpening damaged tips and removing impurities from tip surface, additionally. Efficiency of the process depends on the degree of the tip damage. The repaired and modified AFM tips showed the same or lower level of abrasion compared to those unexposed to FIB irradiation. The big advantage of the FIB milling in the dual beam system is the monitoring of the process of tip modification by SEM (Scanning Electron Microscope) simultaneously. Modification of AFM tips was done by EBID as well. The single point-deposition of platinum carried out by decomposition of an organometallic precursor was used. The conical tip with a curvature radius about 5 nm and a small cone angle (6°) was

obtained using this method at a platinum growth rate 100 nm/s, approximately. The prepared AFM tips were successfully used during topography and conductivity (EBID tips) measurement in contact and noncontact mode of AFM.

[1] J.-S. Moon, H. Shin, B. Mizaikoff, C. Kranz: Bitmap-Assisted Focused Ion Beam Fabrication of Combined Atomic Force Scanning Electrochemical Microscopy Probes, Journal of the Korean Physical Society, Vol. 51 (2007)
[2] W. Smirnov, A. Kriele, R. Hoffmann, E. Sillero, J. Hees, O. A. Williams, N. Yang, C. Kranz, C. E. Nebel: Diamond-Modified AFM Probes: From Diamond Nanowires to Atomic Force Microscopy-Integrated Boron-Doped Diamond Electrodes, Analytical Chemistry, Vol. 83 (2011)
[3] Y. H. Kahng, J. Choi, K. Jeong, B. C. Park, D.-H. Kim, J. Lyou, J.-J. Lee, H. Lee, T. Lee, S. J. Ahn: Fabrication of Ball-shaped Atomic Force Microscope Tips by Ion-beam-induced Deposition of Platinum on Multiwall Carbon Nanotubes, Ultramicroscopy, Vol. 110 (2009)

NST/SS-6-Or-2
Site and orbital-dependent charge donation and spin manipulation in electron doped metal-phthalocyanines

T10 Nanoscience and Technology

#NST/SS-6-Or-2

C. Krull [1], R. Robles [2], A. Mugarza [1], P. Gambardella [1].

[1]Catalan Institute of Nanotechnology - Barcelona (Spain), [2]Centre d'Investigació en Nanociència i Nanotecnologia - Barcelona (Spain).

Similar to silicon-based electronics, chemical doping offers a tool for tailoring the electrical characteristics of organic molecular compounds [1]. Contrary to inorganic semiconductors, however, controlling the position of dopants and charge donation in molecular complexes is a complicated task due to the existence of multiple doping sites, electron acceptor levels, and intramolecular correlation effects. Here we use scanning tunneling microscopy to observe the position of single Li dopants within Cu-phthalocyanine and Ni-phthalocyanine molecules in contact with a metal substrate and probe the charge transfer process with unprecedented spatial resolution [2]. We show that individual phthalocyanines can accommodate at least three stable nonequivalent doping sites and up to six dopant atoms. Ligand and metal orbitals can be selectively charged by modifying the configuration of the Li complexes. Because of strong charge-spin correlation in confined molecular orbitals, alkali atoms provide an effective way to tune the molecular spin without introducing magnetic dopants. Controlled manipulation of Li further shows that charge transfer is determined solely by dopants embedded in the molecules, whereas the magnitude of the conductance gap is sensitive to the molecule-dopant separation.

[1] M. F., Craciun, et al. Adv. Mater. 18, 320–324 (2006).
[2] C. Krull, R. Robles, A. Mugarza, P. Gambardella Nat Mat. (Jan 2013) accepted

STM topographic image of CuPc molecules and Li atoms co-deposited on Ag(100). The image size is 19.3 nm x 19.3 nm

NST/SS-7-Or-1
Silicene: First Synthetic Graphenelike Material

T10 Nanoscience and Technology

#NST/SS-7-Or-1

G. Le Lay.

Aix-Marseille University CNRS-CINaM - Marseille (France).

Born In 2012 on a silver plate [1], artificially created since it does not exist in nature [1-6], silicene, graphene's silicon cousin, offers many exciting promises due, typically, to its Dirac fermions, its two-dimensional topological insulator character [7], the hint for high-temperature superconductivity [8], and, last but not least, its direct compatibility with current silicon-based electronics.
In my talk, I will present a state-of the-art review on silicene and draw perspectives for future research and potential applications.

[1] "Silicene: Compelling Experimental Evidence for Graphenelike Two-Dimensional Silicon", P. Vogt, P. De Padova, C. Quaresima, J. Avila, E. Frantzeskakis, M. C. Asensio, A. Resta, B. Ealet, and G. Le Lay, Phys. Rev. Lett. 108, 155501 (2012).

[2] "Structure of Silicene Grown on Ag(111)" C.-L. Lin, R. Arafune, K. Kawahara, N. Tsukahara, E. Minamitani, Y. Kim, N.Takagi, and M. Kawai, Appl. Phys. Express 5, 045802 (2012).

[3] "Experimental Evidence for Epitaxial Silicene on Diboride Thin Films", A. Fleurence, R. Friedlein, T. Ozaki, H. Kawai, Y. Wang, Y. Yamada-Takamura, Phys. Rev. Lett. 108, 245501 (2012).

[4] "Local Electronic Properties of Corrugated Silicene Phases", D. Chiappe, C. Grazianetti, G. Tallarida, M. Fanciulli, and A.Molle, Advanced Materials, 24, 5088 (2012)

[5] "Evidence of Silicene in Honeycomb Structures of Silicon on Ag(111)", Baojie Feng, Zijing Ding, Sheng Meng, Yugui Yao, Xiaoyue He, Peng Cheng, Lan Chen, and Kehui Wu, Nano Lett., 12, 3507 (2012).

[6] "Evidence for Dirac Fermions in a Honeycomb Lattice Based on Silicon", Chen Lan, Liu Cheng-Cheng, Feng Baojie, He Xiaoyue, Cheng Peng, Ding Zijing, Meng Sheng, Yao Yugui, and Wu Kehui, Phys. Rev. Lett. 109, 056804 (2012)

[7] "A topological insulator and helical zero mode in silicene under an inhomogeneous electric field", M. Ezawa, New J. Phys. 14, 033003 (2012).

[8] "Observation of superconductivity in silicene", Lan Chen, Baojie Feng and Kehui Wu, arXiv:1301.1431 [cond-mat.mes-hall]

NST-P3-12
GaN nanocrystalline films and ordered nanostructures prepared by low energy nitrogen ion beam

T10 Nanoscience and Technology

#NST-P3-12

S. Voborný [1], T. Šamoril [1], T. Novak [1], J. Mach [1], L. Dittrichová [2], J. Spousta [2], T. Šikola [2].

[1]CEITEC BUT - Brno (Czech republic), [2]Brno University of Technology - Brno (Czech republic).

The methods of preparation and analysis of nanostructures and thin films based on gallium nitrides have been intensively studied for the last two decades. Within that time many different techniques have been tested for fabrication of nanostructures (nanocrystals, nanopillars, nanowires). Nitride semiconductors still have a great potential in the production of fundamental components of light sources, laser diodes and detectors. However, as for the future nanodevices, the ability to control their exact shape, size and position on the substrate is essential.
In our contribution, we present the results achieved by low-temperature growth of gallium nitride nanostructures on various patterned substrates. In the experiments, the nitrogen ion beam and gallium atomic beam working at the same time under UHV conditions were used.
First, the conductive Si(111) substrate was used. The significant dependence of film morphology and thickness on deposition parameters, especially on substrate temperature and N/Ga flux ratio, was confirmed. Generally, the deposited layer consists of GaN crystals and metallic Ga spherical objects with the size from tens to hundreds nanometers. The size of these objects increases when the temperature of the substrate rises. An excess of gallium under a sufficient nitrogen flux leads to the formation of Ga metallic spherical objects surrounding GaN crystallites. For an increased nitrogen ion flux, the crystalline structure predominates over metallic gallium spheres and separate GaN crystals 200-300 nm in size at 300°C can be observed. Substrate temperature influences Ga diffusion length and, therefore, also promotes the size of GaN crystals. However, above certain substrate temperature, the crystal size does not increase any more due to evaporation, which lowers gallium lifetime on the surface. Further, GaN deposition on non-conductive substrates

(sapphire, quartz) was studied as well. Charging of these substrates was reduced using an electron neutralization filament in the vicinity of the substrate holder. Thereafter, the fabrication of ordered GaN nanostructures on pre-patterned conductive and non-conductive substrates by selective growth was studied. The patterning was done by SEM lithography using standard (organic and inorganic) and carbonized photoresists [1], and FIB.
Chemical composition and morphology of deposited structures will be analysed using XPS and SEM, respectively, the local chemical composition by EDS, which has been proved to be a very useful technique in detection of local composition.

[1] Sang-il Kim, Bumjoon Kim, Samseok Jang, A-young Kim, Jihun Park, Dongjin Byun: Epitaxial lateral overgrowth of GaN on sapphire substrates using in-situ carbonized photoresist mask, Journal of Crystal Growth 326 (2011)

NST-6-Or-10
Dynamic transmission electron microscopy observation of graphitization induced by electron current flow in carbon-based nanofibers

T10 Nanoscience and Technology

#NST-6-Or-10

M. Tanemura [1], Z. Yusop [2], Y. Yaakob [1], G. Kalita [1], P. Ghosh [1], C. Takahashi [1], M. Sasase [3].

[1]Nagoya Institute of Technology - Nagoya (Japan), [2]Universiti Teknologi Malaysia - Johor (Malaysia), [3]Wakasawan Energy Research Center - Fukui (Japan).

Nanocarbon, such as graphene and carbon nanotubes (CNTs), is one of the hottest materials in nanoscience and nanotechnology. To control their growth, their growth process should be well understood. For this purpose, transmission electron microscopy (TEM) observation which provides the detailed structural information in atomic dimension, especially in situ TEM observation, is essential. In this talk, in situ TEM observation of graphene and CNT formation from amorphous carbon-based nanofibers by solid phase reaction will be dealt with.

Metal-included and pristine CNFs were fabricated by Ar ion irradiation of an edge of a graphite foil with and without a supply of metals at room temperature, respectively [1]. The graphite foil thus prepared was cut into small pieces to be mounted directly on a TEM sample holder equipped with a piezo-controlled nanoprobe to verify the current-voltage characteristics of the metal-included and pristine CNFs in direct current and field emission modes. Depending on the included metal element in the CNFs, different type of nanocarbon, such as graphene, ring-shaped graphene, and CNTs, was formed during the electron current flow by solid phase reaction [2]. In the talk, their formation mechanism and current-voltage characteristics will be also dealt with.

[1] M. Tanemura and M. Kitazawa: "Fabrication of Ion-Induced Carbon Nanocomposite Fibers and their Application to Magnetic Force Microscope Probes" in "Advances in Nanocomposites - Synthesis, Characterization and Industrial Applications" Ed. B. Reddy (InTech Publisher) 2011, Ch. 35.
[2] M. Zamri, et al., ASC Nano, 6 (2012) 9567.

NST/SS-7-Or-2
Transfer-Free Electrical Insulation of Epitaxial Graphene from its Metal Substrate

T10 Nanoscience and Technology

#NST/SS-7-Or-2

S. Lizzit [1], R. Larciprete [2], P. Lacovig [1], M. Dalmiglio [1], F. Orlando [3], A. Baraldi [3], L. Gammelgaard [4], L. Barreto [5], M. Bianchi [5], E. Perkins [5], P. Hofmann [5].

[1]Sincrotrone Trieste S.C.p.A. - Trieste (Italy), [2]CNR-Institute for Complex Systems - Rome (Italy), [3]Physics Department and CENMAT, University of Trieste, IOM-CNR Laboratorio TASC - Trieste (Italy), [4]Capres A/S - Lyngby (Denmark), [5]Department of Physics and Astronomy, Interdisciplinary Nanoscience Center, Aarhus University - Aarhus (Denmark).

The remarkable properties of graphene, such as the very high carrier mobility at room temperature, tolerance to high temperature and inertness, make it the most promising candidate for future nanoelectronics. Several methods have been developed to produce graphene layers of various dimensions and quality, which, however, hardly match the requirements for mass production of electronic devices. From one hand, exfoliation-based techniques are time-consuming and produce small flakes or graphene of poor quality; on the other hand large-scale growth on metal substrates is capable of large-area high quality layers, but requires the transfer of graphene on an insulating support in order to guarantee the conduction through graphene.

We have developed a novel transfer-free method to electrically insulate epitaxial graphene from the metal substrate it is grown-on. This is achieved by growing an insulating SiO_2 layer of the desired thickness directly under the epitaxial graphene layer, through a stepwise reaction between intercalated silicon and oxygen [1]. Firstly, epitaxial graphene is grown on a Ru(0001) crystal surface. Subsequent exposure of the sample to a Si flux at 720 K results in Si intercalation and in the formation of Ru silicide below graphene. The final step consists of oxygen intercalation [2] at T=630 K: the Ru silicide is rapidly oxidized producing a thin SiO_2 layer over an oxygen covered Ru surface. By following the entire process by high resolution fast-XPS measurements we establish that graphene does not react with

O_2 and that during the decomposition of the Ru silicide oxygen binds exclusively to Si [3]. At the end of the process, electrical insulation of the graphene layer from the Ru substrate has been demonstrated by performing lateral transport measurements with a microscopic 12 point probe, showing a resistance behaviour characteristic of two-dimensional transport.
The transfer-free method developed in the present work might have wide application in graphene research and in the fabrication of nanotechnology devices.

[1] S. Lizzit *et al*. Nanoletters **12**, 4503 (2012); Research Highlight Nat. Nanotechnol. doi:10.1038/nnano.2012.183
[2] R. Larciprete et al., ACS Nano **6**, 9551 (2012); Research Highlight Nat. Mat. **12**, 3 (2013) doi:10.1038/nmat3536
[3] R. Larciprete et al. J. Am. Chem. Soc. **133**, 17315 (2011)

NST/SS-6-Or-3
Growth and Stress of Epitaxial MgO Films on GaAs(001)

T10 Nanoscience and Technology

#NST/SS-6-Or-3

R. Koch.

Johannes Kepler University - Linz (Austria).

Growth and Stress of Epitaxial MgO Films on GaAs(001)

Shibo Wang, Markus Gruber, Anirban Sarkar, and Reinhold Koch
Johannes Kepler Universität Linz, Institut für Halbleiter- und Festkörperphysik,
Altenbergerstrasse 69, A-4020 Linz, Austria

Integration of ferromagnetic properties into semiconductor devices has become a focus of worldwide research because of the propects for applications in a future spin- and magnetoelectronics. Of particular interest are selected compounds of the Heusler alloys that are half-metallic ferromagnets and may exhibit conduction electrons with 100% spin polarization. Our recent study of the Heusler system Fe1-xSix/GaAs(001) [1] revealed a strong interdiffusion of Fe, Si, Ga, and As at the interface region, creating intermixed layers of 2-3 nm thickness in both, film and substrate. Interdiffusion is dominant already at the moderate growth-temperatures typically required for crystallographic ordering and lithographic processing of the Heusler films, which explains the obtained low spin-injection despite of excellent abrupt interfaces indicated by transmission electron microscopy and x-ray diffraction. In view of our alarming results, the development of appropriate diffusion-barrier layers is essential for ferromagnet/ semiconductor hybrid based devices.

Here we studied the preparation of single crystal MgO films on GaAs(001) as possible diffusion and tunneling barriers. In addition to structural and morphological results we report on in-situ stress measurements that provide direct information on the strain relaxation of the MgO films, which plays a crucial role in the subesequent growth of Heusler films.

[1] C. Gusenbauer, T. Ashraf, J. Stangl, G. Hesser, T. Plach, A. Meingast, G. Kothleitner, and R. Koch, Phys. Rev. B 83, 035319 (2011)

NST-5-Or-2
High-speed imaging in tapping-mode atomic force microscopy

T10 Nanoscience and Technology

#NST-5-Or-2

M. Balantekin.

Izmir Institute of Technology - Izmir (Turkey).

Atomic force microscope (AFM) has become an indispensable tool in the field of nanocale science and technology. Dynamic imaging modes of AFM provide better force sensitivity over contact mode. Hence taping and noncontact modes are the preferred operating modes in air and vacuum environments. However, imaging speeds of conventional tapping-mode AFM systems are not satisfactory for applications such as real-time imaging of biomolecular interactions and industrial scale nanometrology.

The past research on the high-speed AFM imaging has shown that two major factors that limit the scan speed are the bandwidth of the actuator and the transient response of the probe. In the recent studies, sensor and actuator sizes have been minimized to increase the system bandwidth at the expense of increased system complexity. Also, new probe structures with integrated actuators were designed. Despite these efforts, the scan speeds required for the visualization of biomolecules have not been achieved.

In this study, we present a new operating method that we developed to be used in tapping-mode atomic force microscopes. This method is developed to minimize the time spent for tapping-mode AFM imaging experiments. In addition, the real-time imaging without complex AFM systems will be possible with this operating method. We will first describe the method and present our initial simulation results showing that even with a typical tapping-mode cantilever 5 frames/second imaging speed can be easily achieved.

NST/SS-6-Or-4
Synthesis and characterization of carbon-encapsulated ferromagnetic iron nanoparticles

T10 Nanoscience and Technology

#NST/SS-6-Or-4

M. Perez Guzman [1], A.M. Espinoza Rivas [1], R. Ortega Amaya [1], Y. Matsumoto Kuwabara [1], J. Santoyo Salazar [2], M. Ortega Lopez [1].

[1]Departamento de Ingeniería Eléctrica, SEES, Centro de Investigación y de Estudios Avanzados del Instituto Politécnico Nacional - Mexico City (Mexico), [2]Departamento de Física, Centro de Investigación y de Estudios Avanzados del Instituto Politécnico Nacional - Mexico City (Mexico).

Magnetic nanoparticles find a variety of uses, including many devices as motors, sensors, generators, videotapes and hard disks. Iron and the magnetic phases of iron oxide have gained importance in biomedical, environmental remediation, etc[1]. Graphite-coated metal nanoparticles have been prepared by CVD using organic precursors[2].

The present work describes the synthesis and characterization of carbon-encapsulated iron nanoparticles (CEINP´s), which were obtained by CVD starting from previously synthesized magnetite nanoparticles. XRD, TEM, MFM, Raman and VSM were used for characterization.

Magnetite nanoparticles were prepared by co-precipitation using a similar method as that reported in [3]. After being cleaned, they were loaded in a CVD system. The CVD process was carried out at 900 °C under an inert atmosphere comprising argon and hydrogen gas, and methane as the carbon precursor.

The nanoparticles were characterized before and after being coated. Coprecipitation produces the magnetite phase of iron oxide (Fe_3O_4) 5 nm in size nanoparticles. These particles display a superparamagnetic behavior with a 50 emu/g saturation magnetization (M_s), in agreement with values reported by Xianqiao, et al. [4]. After the CVD process, Fe_3O_4 transforms into ferromagnetic iron coated with various graphene sheets, as revealed by XRD (fig. 1). Fig. 2 shows a TEM image of CEINP´s. Magnetic characterization revealed the ferromagnetic character of CEINP´s with a M_s of 165 emu/g and a coercive field of 15 Oe. The MFM measurements

showed that mean size domain distribution varies from 3.5 to 2.5 nm, for magnetite and CEINP´s respectively.

[1]Lu, A., Magnetic Nanoparticles: Synthesis, Protection, Functionalization, and Application. Angewandte Chemie, 2007(46): p. 1222-1244.
[2] Sajitha, E.P., et al., Carbon, 2004. 42(14): p. 2815-2820.
[3] Berger, P. , et al. Journal of Chemical Education, 1999. 76(7): p. 943-948.
[4] Xianqiao, L., et al. Journal of Magnetism and Magnetic Materials, 2006. 304: p. 248-253.

XRD Spectra, TEM Micrograpy

NST/SS-7-Or-3
Electronic Properties of atomically precise Graphene Nanoribbons

T10 Nanoscience and Technology

#NST/SS-7-Or-3

H. Söde [1], L. Talirz [1], C. Pignedoli [1], X. Feng [2], K. Müllen [2], R. Fasel [1], P. Ruffieux [1].

[1]Empa, Swiss Federal Laboratories for Materials Science and Technology - Dübendorf (Switzerland), [2]Max Planck Institute for Polymer Research - Mainz (Germany).

Its remarkable properties make graphene attractive for use in electronic devices. Yet, graphene is semimetallic and thus not directly suitable for most electronic or optoelectronic switching devices, which require a semiconductor with a specific, finite band gap. In armchair graphene nanoribbons (AGNRs), band gaps suitable for room temperature applications open at widths smaller than 3 nm. However, atomically precise control over the edges is crucial to produce AGNRs with reliable electronic transport properties. We recently developed a bottom-up method providing this level of control over the edges [1].

This allows, in particular, to grow atomically precise 7-AGNRs (7 carbon dimers across the width) for which we have determined by scanning tunneling spectroscopy (STS) and angle-resolved photoemission spectroscopy (ARPES) a band gap of 2.3 eV as well as the occupied band structure of the ribbons adsorbed on a gold surface [2].

Here, we present the results of a detailed ARPES and STS of such bottom-up fabricated 7-AGNRs. GNRs of different length have been synthesized in order to explore the length dependence of the electronic band gap. STS data for ribbons of varying length reveals substantially larger band gaps for ribbons shorter than 5 nm. ARPES and Fourier transformed STS were used to determine the band dispersion of occupied and unoccupied bands. Based in these data, we determined the effective masses and energy-dependent charge carrier velocities for the frontier bands of 7-AGNRs. In addition, the experimental results are discussed by a detailed comparison with ab initio simulations of the band structure and the length-dependent band gap.

[1] Cai, J. et al. Nature 2010, 466, 470–3.
[2] Ruffieux, P. et al. ACS Nano 2012, 6, 6930–35.

Figure 1: Chemical structure and STM image of a 7-AGNR on Au(111) and tunneling spectra recorded on the ribbon.
Figure 2: Several dI/dV spectra, taken along the full length of a 7-AGNR, showing charge density waves and the E(k) relation after the Fourier-transform with the indication of the first and second conduction band.

NST-13-Or-6
Comparison of resonant properties of Mid-IR plasmonic antennas fabricated by FIB and EBL

T10 Nanoscience and Technology

#NST-13-Or-6

T. Šikola [1], L. Břínek [1], O. Tomanec [1], M. Kvapil [1], R. Kalousek [1], M. Hrtoň [1], P. Dub [1], T. Hrnčíř [2], P. Varga [1].

[1]BUT - Brno (Czech republic), [2]Tescan - Brno (Czech republic).

Focussed Ga Ion Beam (FIB) is a convenient method for the rapid prototyping of nanostructures in the wide range of applications. Contrary to the multistep procedure of Electron Beam Lithography (EBL), the FIB technique represents a single step mask-less technology.
One of the most straightforward applications of FIB technology is fabrication of plasmonic nanoantennas by milling their shapes out of metallic thin films. However, as the optical properties of antennas fabricated by FIB and EBL and having resonances in the visible range (called “optical antennas”) are considered to be similar, we have found that the Mid-IR Au rectangular antennas (having resonances in the Mid-IR) show different behaviour according to their fabrication origin. The Mid-IR Au antennas prepared by EBL on transparent samples (e.g. Si) possesses linear scaling of resonance frequency with their arm length. Contrary to that, those prepared by FIB revealed more complex behaviour. In principle, the resonant peak of relative reflectance of antennas is split into two sub-peaks separated by a dip at $\lambda \approx 8.2$ μm.. The short-wavelength sub-peak was moving with the antenna arm length towards higher wavelength until its motion almost stopped at higher arm lengths. However, the long-wavelength sub-peak almost did not move with the antenna arm length for shorter arm lengths and then started to move towards higher wavelengths. Comparison with the spectra of antennas prepared by EBL and other techniques revealed that this splitting occurs just at the nanostructures fabricated by Ga FIB. This suggests that the splitting is related to the contamination of the sample by Ga atoms and so most likely to strong damping of electron oscillations [1].

[1] T. Šikola, R. D. Kekatpure, E. S. Barnard, J. S. White, P. Van Dorpe , L. Břínek, O. Tomanec, J. Zlámal, D. Lei, Y. Sonnefraud, S. A. Maier, J. Humlíček, M. L. Brongersma: Mid – IR plasmonic antennas on silicon-rich oxinitride absorbing substrates: nonlinear scaling of resonance wavelengths with antenna length, Appl. Phys. Lett. 95 (2009), 253109.

NST-11-Or-2
Thermal stability of Au nanospheres on different substrates

T10 Nanoscience and Technology

#NST-11-Or-2

P. Bábor [1], R. Duda [1], J. Polčák [1], S. Průša [1], M. Potoček [1], P. Procházka [2], J. Mach [2], P. Varga [1], T. Šikola [2].

[1]CEITEC BUT - Brno University of Technology - Brno (Czech republic), [2]Institute of Physical Engineering, Brno University of Technology - Brno (Czech republic).

The interaction of gold nanospheres with different substrates at elevated temperatures was studied in situ by X-ray photoelectron spectroscopy (XPS) and by time of flight low energy ion scattering (ToF-LEIS). Gold nanospheres were deposited from colloidal solutions on Si (100) substrates covered by native silicon oxide, thermal SiO_2 or graphene. Atomic force microscopy and scanning electron microscopy were used ex situ as complementary methods.
It was found that annealing at high temperatures leads to destruction of Au nanospheres. Au atoms can desorb from the surface or diffuse into and/or on the substrate. Depending on the substrate, chemical reactions can occur at elevated temperatures (e.g. formation of silicides) as well which naturally affects the shape stability of these nanospheres. In the contribution the mechanisms of gold nanospheres interaction with the substrates will be discussed in detail. Especially, the instabilities of the nanospheres at particular temperatures for specific substrates will be explained.

NST-3-Or-3
Nanoscale Mechanical Mapping at a wide range of deformation rates with Atomic Force Microscopy

T10 Nanoscience and Technology

#NST-3-Or-3

S. Minne, B. Pittenger, C. Su.

Bruker - Santa Barbara (United states).

Atomic force microscopes (AFM) can measure and map mechanical properties of materials with very high resolution. Over the years, the methods of mechanical mapping have evolved from slow force volume to multiplefrequency based dynamic measurements using TappingMode and contact resonance. Recently, real-time control of the peak force of the tip-sample interaction has led to a fundamental change in AFM imaging, providing quantitative mapping of mechanical properties at unprecedented resolution. During material property mapping, the time scale of tip-sample interaction now spans from microseconds to seconds, tip sample forces can be controlled from piconewtons to micronewtons, and spatial resolution can reach subnanometer. AFM has become a unique mechanical measurement tool having large dynamic range (1kPa to 100GPa in modulus) with the flexibility to integrate with other physical property characterization techniques in versatile environments. This presentation will review this recent progress, providing examples from a wide range of fields that demonstrate the dynamic range of the measurements, and the speed and resolution with which they were obtained. Additionally, the effect of time dependent material properties on the measurements will be explored.

NST-P1-05
Effects of the sudden electron-hole pair creation on the surface plasmon excitations in cylindrical nanorods

T10 Nanoscience and Technology

#NST-P1-05

J. Gervasoni [1], J. Garcia Gallardo [1], L. Kövér [2].

[1]CNEA - Bariloche (Argentina), [2]Atomki - Debrecen (Hungary).

In this work we study the effect of the excitation of surface plasmons in a metallic cylindrical nanorod by a suddenly created electron-hole pair, using a classical model for the emerging electron and a quantum-mechanical model for the plasmon field in the cylinder [1]. The electron and the hole interact independently with the plasmon field, generating electron density oscillations. Two different trajectories for the emerging electron (parallel to the axis and radial) are studied in an aluminum nanorod. The average number of excited plasmons indicates how important is the role of the hole in the excitation process. We found that the results can be very different according to the trajectory of the emerging electron. We also found that the distinction between intrinsic and extrinsic process is sometimes not applicable.

1. J.A. García Gallardo, J. L. Gervasoni, L. Kövér. Vacuum, 84 (2010) 258.

NST-6-Or-11
Hydrothermal Zinc Oxide Nanowires Growth Using Cooper-Additive Zinc Acetate Solution

T10 Nanoscience and Technology

#NST-6-Or-11

Y. Lai, Y. Wang.

School of Physics and Information Engineering, Fuzhou University - Fuzhou (China).

With a fast write/read speed, a good scaling capability as well as a good compatibility with current fabrication process, resistance random access memory (RRAM) becomes one of promising candidates for next generation non-volatile storage technology. Usually, the defects inside storage medium or on the interface determine the storage performance. As a transparent semiconductor with lots of intrinsic defects, zinc oxide (ZnO) also exhibits resistive storage capability and has potential applications in transparent storage devices. Therefore, doping some elements into ZnO seems to be a feasible way to control the defects and also adjusts its storage properties. Additionally, with the further down-scaling of physical dimension of electronic devices, the conventionally used storage medium in the form of thin film may also be replaced by its nanowire. In this perspective, doped ZnO nanowires are worth synthesis and investigation.

In this work, ZnO nanowries (ZnO_0001) were synthesized on ZnO seed substrates by zinc acetate solution with hydrothermal method. Cooper acetate was also introduced with different cooper concentration (X=Cu/(Cu+Zn), x=1%, 2%, 4%) and the samples (CuZO_001, CuZO_002 and CuZO_003) were respectively obtained. Fig. 1 shows the SEM and HRTEM images of sample ZnO_0001. The pillar nanowires are in vertical alignments with six facets forming hexagonal cross-section, which is a typical characteristic of ZnO. The nanowire is single crystal without any visible defects inside the lattice and it is in a preferential c-axis orientation and exhibits (002) preferential growth. Fig. 2 shows the influence of cooper additive on the properties of 300℃ annealed ZnO nanowires. With the increase of cooper concentration, the UV emission peak in PL spectra becomes broadened and weak,

while the visible peak is enhanced. The cooper additive also produces 581.4cm^{-1} centered E_1(LO) Raman mode, which means the structural defects were introduced.

Figure 1. SEM image (a) and HRTEM image (b) of ZnO nanowire. The inset is the SAED image of single nanowire

Figure 2. Effects of Cu additive on ZnO nanowires: (a) PL spectra of ZnO nanowires; (b) Raman spectra of ZnO nanowires

NST/SS-P2-03
Local barrier height and superconducting gap in Fe(Se,Te) by low-temperature scanning tunneling microscopy/spectroscopy (STM/STS)

T10 Nanoscience and Technology

#NST/SS-P2-03

A. Sugimoto, T. Ekino.

Graduate School of Integrated Arts and Sciences, Hiroshima University - Higashi-Hiroshima (Japan).

Recently discovered iron-based superconductors have been giving a great impact in the related field of research because of its highest critical temperature T_c of ~ 55 K among the non-cuprate superconductors. In the Fe-based superconductors, the iron-chalcogenide Fe(*Ch*) compound (the 11-type, *Ch* = chalcogen) exhibits the simplest crystal structure. Its single crystal is easy to be cleaved and the charge-neutral flat surface can be readily exposed. Therefore, the 11-type is believed to be very suitable for the STM/STS observation. For understanding the superconductivity mechanism, the superconducting gap is a very important quantity. However, the observed signal of the gap in the 11 type by STS measurement has been usually quite weak. Therefore, it is necessary to understand the surface properties such as the distributions of work function (local barrier height, LBH) in order to clarify why the superconducting gap is hardly obtained in this compound.
Here, we examine the spatial distributions of LBH and local density of states (LDOS) by STM/STS using Fe(Se, Te) single crystals, and demonstrate how the surface properties affect the observation of superconducting gap.
The $FeSe_xTe_{1-x}$ single crystals (x ~ 0.3, T_c~15 K) were synthesized by a self-flux method using the double-sealed quartz tubes. The STM equipment used in this experiment is a modified Omicron LT-UHV-STM system. The samples were cleaved *in-situ* at T = 2.5 K in an ultra-high vacuum chamber of ~ 10^{-8} Pa, then it was possible to obtain fresh and unaffected crystal surface. The STM measurements were carried out at T = 4.9 K under the UHV condition of ~ 10^{-8} Pa. The STS conductance dI/dV, which is proportional to the local density of states (LDOS), was obtained by numerical differentiation of the measured tunnel-current (I) – voltage (V) characteristics, $I(V)$, with the spatial interval of ~0.08 nm. The values of LBH were

simultaneously obtained by measuring the dependence of *I* on the tip-sample distance *z*, *I(z)*. The average of LBH values was obtained as φ~4.8 eV, which is turn out to be large enough to provide ideal tunneling conditions.
The STM images show clear regular square arrangements of spots with the lattice spacing ~0.38 nm, together with the randomly-distributed large spots which are considered to be due to the excess Fe atoms. The LDOS maps also show the energy-dependent large spots of the excess Fe. The superconducting gap of the order of Δ~5 meV was observed in the vicinity of excess Fe, which is comparable to the previously obtained maximum values by the break-junction spectroscopy. It is noted that the LBH map clarifies the local area showing the larger φ values in the regular atomic arrangements, which correspond to the position of the excess Fe as seen in the LDOS maps and STM images. Therefore, it is considered that the local area where the gap structure could be observed is probably related to the area of large barrier height which is generated by the excess Fe.

NST-2-Or-1
Charge Transport in Azobenze-Based Single-Molecule Junctions

T10 Nanoscience and Technology

#NST-2-Or-1

A. Garcia-Lekue [1], Y. Kim [2], D. Sysoiev [3], T. Frederiksen [1], U. Groth [3], E. Scheer [4].

[1]Donostia International Physics Center (DIPC); IKERBASQUE - San Sebastian (Spain), [2]Department of Mechanical Engineering, University of Michigan - Michigan (United states), [3]Department of Chemistry, University of Konstanz - Konstanz (Germany), [4]Department of Physics, University of Konstanz - Konstanz (Germany).

Azobenzene molecules have become an archetype of molecular photoswitch research, due to their simple structure and the significant difference of the electronic system between their *cis* and *trans* isomers. However, a detailed understanding of the charge transport for the two isomers, when embedded in a junction with electrodes is still lacking.

With the aim of clarifying this issue, we investigate charge transport properties through single Azobenzene-ThioMethyl (AzoTM) molecules in a mechanically controlled break junction (MCBJ) system at 4.2 K. Single-molecule conductance, *I-V* characteristics, and IETS spectra of molecular junctions are measured and compared with first-principles transport calculations.

Our measured conductance traces clearly show that *cis* isomers have a larger conductance than *trans* isomers. The analysis of our simulations suggests that the difference in conductance of the isomers is due to the difference of their corresponding resonant states.

Experimental IETS spectra of Au-AzoTM-Au junctions exhibit distinct features for *cis* and *trans* isomers. The origin of such features has been elucidated based on simulated IETS spectra, which allows us to conclude that the observed differences in experimental IETS are indeed caused by the *cis-trans* conformation.

In conclusion, our studies elucidate the origin of a slightly higher conductance of

junctions with *cis* isomer and demonstrate that IETS spectra of *cis* and *trans* forms show distinct vibrational fingerprints that can be used for identifying the isomer. [1]

[1] Y. Kim, A. Garcia-Lekue *et al*., Phys. Rev. Lett. **109**, 226801 (2012)

Figure 1: Transmission curves for (a) *cis* and (c) *trans* isomers for different bridging distances. The dashed-dotted lines in (a) and (c) indicate the representative fits for *cis* and *trans*, respectively. The corresponding dominant transmission eigenchannels for (b) *cis* and (d) *trans* isomers are shown.

Figure 2: (a) Experimental and (b) theoretical IETS spectra for *cis* and *trans* isomers (averaged over several configurations).

NST/SS-7-Or-4
Growth of graphene nanoislands on a Ni(111) surface

T10 Nanoscience and Technology

#NST/SS-7-Or-4

M. Ollé Soronellas [1], G. Ceballos [1], D. Serrate [2], A. Mugarza [1], P. Gambardella [1].

[1]ICN, Catalan Institute of Nanotechnology, Campus de la UAB 08193 Bellaterra - Barcelona (Spain), [2]INA-LMA, University of Zaragoza, 50018 - Zaragoza (Spain).

Since they first time a layer of graphene was isolated in 2004 [1], the interest in this material increased exponentially. The main attraction of this material lies in their unusual electronic, mechanical and magnetic properties such as the anomalous quantum Hall effect, the absence of electronic localization, high optical transparency, the high electrical conductivity, flexibility and high mechanical strength. These properties make graphene a very promising material for applications in electronics and spintronics, and therefore it is necessary to control the growth and properties at the nanoscale.

The growth of graphene layers on the nickel surface by decomposition of hydrocarbons is interesting for three main reasons. On the one hand, the lattice constant of the surface of Ni(111) coincides almost perfectly with the lattice constant of graphene, which allows it to grow in a 1×1 structure. Moreover, due to the catalytic effect of nickel surface, it is an autoterminated reaction, the reaction stops once the graphene monolayer is formed avoiding the growth of multilayers [2]. Finally, the Nickel is a ferromagnetic material, which opens the door to applications in spintronics.

Progress in the manufacture of low dimensional structures such as graphene nanoribbons has been reported [3]. It shows that the electronic properties of graphene change in a non-trivial way going to nanoscopic dimensions due to the contribution of edge effects.

In this work we study by STM the growth of graphene on a Ni (111) surface by decomposition of hydrocarbons [4]. By varying parameters such as the dosage of hydrocarbon, reaction time and temperature was possible to obtain in a reproducible manner a wide range of coverages. For low coverages the carbon atoms organize themselves into graphene nanoislands whose size and density are related to the

reaction parameters. These nanoislands, initially with irregular shapes, may, by further thermal treatment selectively acquire a triangular (Fig. 1) or hexagonal shape both with zig-zag edges. In the case of triangular islands all edges have the same packaging with the nickel surface underneath while in the case of hexagonal islands edges change alternatively the packaging. The optimum conditions to obtain nanoislands of particular size and shape are studied by systematic variation of the parameters of the hydrocarbon decomposition reaction and the thermal diffusion of carbon on the surface.

[1]K.S. Novoselov et al, Science, 306, 666 (2004)
[2]J. Wintterlin, M.-L. Bocquet, Surface Science, 603, 1841, (2009)
[3]M.Y. Han et al., Phys. Rev. Lett. 98, 206805 (2007)
[4]M. Ollé, G. Ceballos, D. Serrate and P. Gambardella, Nano Lett. 12, 4431 (2012)

Fig.1 8x8nm STM image of a graphene nanoisland on Ni(111)

NST-1-Or-7
Detection of poly aromatic hydrocarbons with cyclodextrines functionalized nanosensor using Surface Enhanced Raman Spectroscopy

T10 Nanoscience and Technology

#NST-1-Or-7

I. Tijunelyte [1], N. Lidgi-Guigui [1], E. Guenin [1], T. Toury [2], M. Lamy De La Chapelle [1].

[1]Laboratoire CSPBAT-UMR7244, UFR Santé Médecine Biologie Humaine-Université Paris13, 74 rue Marcel Cachin - Bobigny (France), [2]Université de technologie de Troyes, Laboratoire de Nanotechnologie et d'instrumentation Optique, Institut Charles Delaunay, FRE 2848, 12 rue Marie Curie - Troyes (France).

The present situation of environmental water pollution by toxic organic compound is requiring reliable analytical tool that can rapidly screen them with minimal sample handling [1]. The latest European regulations on water quality have aimed to achieve good ecological and chemical status for water bodies by 2015. Our study comes within this scope and is aimed to design a highly sensitive and specific nanosensor which would have the ability to monitor in situ the quality of environmental waters by pre-concentrating and specifically recognizing pollutants.

Surface Enhanced Raman Scattering (SERS) method has been employed to detect trace concentrations of water pollutants. This highly sensitive technique is based on the exploitation of the localized surface plasmon resonance of metallic nanoparticles for Raman scattering enhancement.

In this talk, results obtained with gold nanoparticles made by electron beam lithography [2] will be shown. In order to detect trace concentrations of pollutants, that are small and low soluble molecules, pre-concentrating systems were designed using cyclodextrins. These cyclic oligosaccharides are known to create specific host-

guest complexes with hydrophobic molecules thanks to their hydrophobic cavity. Specifically, alpha, beta and gamma-cyclodextrin, differing by the size of their cavity, were converted to thiol-derivatives and subsequently grafted to gold nanoparticles. Nanosensors with self-assembled cyclodextrins monolayer were then tested for detection of poly aromatic hydrocarbons (PAH) such as naphthalene and fluoranthene and volatile organic compounds: toluene and xylene.

The authors want to acknowledge the ANR REMANTAS project (ANR-11-ECOT-0010) for financial support.

[1] B. Pejcic, P. Eadington, A. Ross, Environmental Science & Technology, 41 (2007) 6333-6342.
[2] M. Lamy de la Chapelle, H. Shen, N. Guillot, B. Frémaux, B. Guelorget, T. Toury, Plasmonics, (2012) 1-5.

NST-P1-10
Efficiency of Graphene-Based Solar Cell as the Number of Graphene Layers

T10 Nanoscience and Technology

#NST-P1-10

K. Ihm, K.J. Lee.

PAL - Pohang (Korea, republic of).

Impressive optical properties of graphene have been attracting the interest of researchers, and, recently, the photovoltaic effects of a heterojunction structure embedded with few layer graphene (FLG) have been demonstrated. Here, we show the direct dependence of open-circuit voltage (Voc) on numbers of graphene layers. After unavoidably adsorbed contaminants were removed from the FLGs, by means of in situ annealing, prepared by layer-by-layer transfer of the chemically grown graphene layer, the work functions of FLGs showed a sequential increase as the graphene layers increase, despite of random interlayer-stacking, resulting in the modulation of photovoltaic behaviors of FLGs/Si interfaces.

NST/SS-6-Or-5
Spin-polarized STM study of Co nano islands on Ag(111) surface

T10 Nanoscience and Technology

#NST/SS-6-Or-5

Y. Hasegawa, K. Doi, S. Yamamoto, H. Kim, Y. Yoshida.

ISSP, Univ. Tokyo - Kashiwa (Japan).

Cobalt is an hcp metal in bulk, but its fcc structure can be formed as a thin film on various substrates. On fcc(111) substrates, an epitaxially grown hcp film has out-of-plane magnetization because of magnetocrystalline anisotropy that favors c-axis magnetization, whereas an fcc film has in-plane magnetization due to the shape anisotropy. Recently, surface-magneto-optical Kerr effect (SMOKE) technique revealed that cobalt thin films on Ag(111) have remnant magnetization in both in-plane and out-of-plane directions indicating the possibility of coexistence of the two structures [1]. To clarify magnetic properties of the system, we have utilized spin-polarized scanning tunneling microscopy and spectroscopy (SP-STM/S) [2], which enables us to characterize magnetization locally with nanometer-scale spatial resolution.
In STM images taken on a Co-deposited Ag(111) surface, we observed island structures with a thickness of 5~6 monolayer having a Moire pattern on their top. These Co islands are categorized into two groups depending on the Moire intensity; strong one and weak one. Using an out-of-plane magnetized tip, we found the strong Moire islands show a hysteretic variation in dI/dV under a sweep of the perpendicular magnetic fields, whereas the weak Moire islands do not. These findings support coexistence of the two structures and suggest that the strong (weak) Moire islands have a hcp (fcc) structure.

[1] Y. Saisyu, *et al.* J. Appl. Phys. 110, 053902 (2011).
[2] R. Wiesendanger, Rev. Mod. Phys. 81, 1495 (2009)

NST-11-Or-3
SELF-ORGANIZED AMPHIPHILIC DI-BLOCK COPOLYMER AS A GOLD NANOREACTOR

T10 Nanoscience and Technology

#NST-11-Or-3

S. Boyer [1], C. Iwamoto [2], R. Nakagawa [2], K. Takahashi [2], T. Yamada [2], H. Yoshida [2].

[1]P PRIME Institute - Futuroscope (France), [2]Tokyo Metropolitan University - Tokyo (Japan).

The design of advanced hybrid ‘‘hard’’ materials (metal or semiconductor nanocrystals) / ‘‘soft’’ materials (copolymers) requires to conduct constant efforts directed to gain exquisite control of the size distribution and shape of various noble metal nanoparticles (NMNPs).
The present work highlights two smart routes to manipulate the structure of hexagonally packed hydrophilic poly(ethylene oxide) (PEO) cylinders as nanoreactors. The objective is to achieve patterning of gold particles (AuPs) in the nanometer scale via a polymer structure-mediated strategy.
Eco-aware treatment dealing with the use of carbon dioxide (CO2) or colloidal aqueous solution is reported as a way for depositing pre-formed AuPs selectivity into the PEO phase-segregated nanodomains of the pre-patterned asymmetric liquid-crystalline (LC) amphiphilic di-block copolymer PEO-b-PMA(Az) scaffold [1]. The pattern deliveries are conducted through rigorous thermodynamic, diffuso-mechanic, geometric, capillary forces and chemical criteria which may be categorized under four main considerations: (i) the specific interactions of LC/solvent (liquid, gaseous and supercritical CO2) systems as a function of pressure, temperature and annealing (time); (ii) the modulation of the surface topology concomitantly with the swelling of the CO2-modified nanophase-separated organization; (iii) the “decorative” AuPs distribution modulation (iv) with the chemical function of the protected AuPs.
The fine thermo-diffuso-chemo-mechanical interactions would provide an essence of a two-dimensional (2D) nanometer crystal growth. Such a nontrivial study is illustrated and discussed on catalyst systems. Interest is to consider gold as a catalyst [2]. The gold ions locate inside PEO, one nucleation site giving rise to one cell growth stage.

The organization of the structure in the nanometer scale was supported by small X-ray scattering (SAXS), Transmission Electron Microscopy (TEM), and grazing incidence small-angle X-ray scattering (GISAXS).

Acknowledgements
The Core Research of Evolutional Science & Technology (CREST) / Japan Science and Technology Agency (JST).

[1] S.A.E. Boyer, J-P.E. Grolier, H. Yoshida, J-M. Haudin, J-L. Chenot, Thermodynamics - Interactions studies - Solids, Liquids and Gases, Chapter 23, 841, J. C. Moreno-Pirajan (Ed.), InTech, Rijeka (2011)
[2] M. Haruta, Studies in Surface Science and Catalysis, 110, 123-134 (1997)

NST-P1-5a
Doping effect of Mg in the catalytic total oxidation of ethanol over copper Ferrite obtained from co-precipitation method

T10 Nanoscience and Technology

#NST-P1-5a

L. Meddour-Boukhobza [1], A. El-Fiad [1], A. Aknoun [2], D. Ammar [3].

[1]LMCCCO, FC, USTHB - Algiers (Algeria), [2]D.P.M - C.R.N.D - Algiers (Algeria), [3]L.GéoPh, FSTGAT, USTHB, - Algiers (Algeria).

Pure and doped copper ferrite with the Mg_xCu_{1-x} Fe_2O_4 (x=0, x=0.02 and x=0.06) structure have been successfully synthesized via co-precipitation method. The obtained precursors were characterized by thermogravimetric TG/DTA to determine the thermal decomposition and they were calcined at 600 and 800°C to obtain the ferrite spinel. The solids obtained were characterized by XRD, and BET isotherm. The TG/DTA thermogravimetric demonstrated the formation of crystalline $CuFe_2O_4$ and the $MgFe_2O_4$ ferrites, as confirmed by XRD.
The X-ray diffraction (XRD) confirmed the formation of spinel structure $CuFe_2O_4$ and mixed oxide (CuO, Fe_2O_3) for all samples also the formation of the $MgFe_2O_4$ specially for the sample doping and calcined at 800°C.
However, the $CuFe_2O_4$ catalysts present low specific surface BET, this last increases progressively by increasing the amounts of dopant added.
The study of effects the magnesium doping in total oxidation (combustion) of ethanol over Mg_xCu_{1-x} Fe_2O_4 (x=0, x=0.02 and x=0.06) prepared by co-precipitation method, is investigated.

Table .1.

catalysts	S_{BET} (m^2/g) Tc= 600°C	S_{BET} (m^2/g) Tc= 800°C
$CuFe_2O_4$	4	0.35
$Mg_{0.02}Cu_{0.98}Fe_2O_4$	6	0.97
$Mg_{0.06}Cu_{0.96}Fe_2O_4$	7	-

[1] J.W. Leff, N. Fierer, Soil Biol. Biochem. 40 (2008) 1629–1636.
[2] D. Delimaris, T. Ioannides, Applied Catalysis B: Environmental 89 (2009)295–302.
[3] D. Mehandjiev, A. Naydenov, G. Ivanov, Appl. Catal. A 206 (2001)13.
[4] M.R. Morales, B.P. Barbero, L.E. Cadus, Applied Catalysis B: Environmental 74 (2007)1–10.
[5] H.G. Lintz, K. Wittstock, Catal Today 29 (1996) 457–61.

Table.1. BET textural properties of catalysts

NST-3-Or-4
The Interaction between Piezo Materials and Microwave Readout of Nanomechanical Resonators

T10 Nanoscience and Technology

#NST-3-Or-4

L. Hao, J. Gallop, J. Wooldridge, K. Lees.

National Physical Laboratory - Teddington (United kingdom).

Nano-electromechanical (NEMS) resonators are an important future technology with wide ranging applications already beginning to appear. As mechanical resonators shrink towards the nanoscale two related problems emerge. The difficulty of excitation of mechanical displacement becomes greater as the length scale reduces and further the ability to detect this displacement also increases. We report on developments to minimise these problems through the use of novel piezo-electric materials for excitation and a near-field microwave resonance technique to excite and readout the mechanical resonator motion. The scale dependent properties of these methods are derived and compared, through both modelling and experiment, with a view to determining which method will be most applicable at the sub-micrometre scale length for NEMS resonators. Piezo materials may be used even at frequencies above 1 MHz, provided care is taken to minimise the high frequency impedance of the structure. But we go on to show that microwave methods are intrinsically more suited to the highest frequencies, even approaching the ability to perform up to 1 GHz.

Early results of microwave readout of the resonance of a composite mechanical resonator consisting of a 1 micron thick PZT layer on a 10 micron Si layer are shown in the figure 1. This shows the mechanical resonance of the membrane as read out by a near-field microwave probe [1] and the shift in resonant frequency from applying a d.c. voltage across the piezo layer. We also report early results on sub-micrometre drum membrane resonators made from graphene, which allow us to deduce mechanical properties of few layer graphene.

[1] L. Hao, J C Gallop and D. C. Cox, ‘Excitation, detection and passive cooling of a micromechanical cantilever using near-field of a Microwave Resonator’ Appl. Phys. Lett. Vol. 95, (2009).

Figure 1. Mechanical resonance of a Si/PZT composite membrane, read-out by a near-field microwave technique. A small voltage (3V) applied to the PZT layer tunes the frequency by as much as 0.4%.

NST-P3-22
Enhancement in light emission efficiency of a Si nanocrystal light-emitting diode by indium tin oxide nanowires

T10 Nanoscience and Technology

#NST-P3-22

C. Huh, T.Y. Kim, B.K. Kim, B.J. Park, E.H. Jang, H.K. Kim.

IT Convergence Technology Research Laboratory, Electronics and Telecommunications Research Institute - Daejeon (Korea, republic of).

In recent years, Si nanocrystals (NCs) has attracted the most attention as a promising light sources for the next generation of Si-based nanophotonics [1]. The optical band gap of Si NCs can be easily tunned by changing the size of NCs due to a quantum confinement effect, meaning that Si NCs are of particular interest as a light-emitting diode (LED) covering whole visible wavelength range. We recently demonstrated a prototype Si NC LED by employing an amorphous SiC(N) film as a suitable electron injection layer [2, 3]. To further improve the light emission efficiency of Si NC LED, a conductive electrode layer that can uniformly deliver the electrons into the Si NCs should be addressed. . In addition, this layer must have a high transparency to increase the probability of photons escaping from the LED device. In this work, a new technique for improving the light emission efficiency of Si NC LEDs by employing indium tin oxide (ITO) nanowires (NWs) was investigated. The ITO NWs were grown by a Q-switched Nd:YAG pulsed laser deposition. The structure of Si NC LED investigated here was ITO NWs/ITO (100 nm)/n-SiC (50 nm)/Si NCs in SiN_x (50 nm)/p^+-Si substrate. The Si NC LED without ITO NWs was also fabricated for comparison. The SEM image of ITO NWs grown at 500 °C is shown in Fig. 1. As the temperature decreased, the ITO NWs were smaller and less uniform in size as compared to those synthesized at 500 °C. The ITO NWs had a tendency to grow perpendicularly above the surface, even though all of them were not perfectly oriented on the surface. The I-V characteristics of Si NC LEDs with ITO NWs was improved as compared to that of Si NC LEDs without ITO NWs. This was attributed to an enhancement in the current spreading property of the ITO layer and a decrease in the dynamic resistance of the whole Si NC LED. Moreover, light output power and wall-plug efficiency of the Si NC LED with ITO NWs were also enhanced. We will

discuss on the electrical and optical properties of Si NC LED with ITO NWs in detail.
Acknowledgements: This work was supported by the Converging Research Center Program through the Converging Research Headquarter for Human, Cognition and Environment funded by the Ministry of Education, Science and Technology (Grant Code: 2011K000655).

[1] L. Pavesi, L. Dal Negro, C. Mazzoleni, G. Franzo, and F. Priolo, Nature 408, 440 (2000).
[2] T. Y. Kim, N. M. Park, K. H. Kim, G. Y. Sung, Y. W. Ok, T. Y. Seong, and C. J. Choi, Appl. Phys. Lett. 85, 5355 (2004).
[3] C. Huh, K. H. Kim, J. Hong, H. Ko, W. Kim, and G. Y. Sung, Electrochem. Solid State Lett. 11, H296 (2008).

Fig. 1. A SEM image of ITO NWs grown at 500 °C.

NST-P2-31
Electrochemical synthesis of CdS/ZnO nanotube arrays with excellent photoelectrochemical properties

T10 Nanoscience and Technology

#NST-P2-31

G. She, X. Qi, L. Mu, W. Shi.

Technical Institute of Physics and Chemistry, Chinese Academy of Sciences - Beijing (China).

Photoelectrochemical cell represents an ingenious approach to directly convert solar energy to electricity or chemical energy such as H_2. The main drawback of ZnO as photoelectrode material is the poor activation in the visible-light region. This issue could be alleviated by decorating ZnO with a narrow band-gap semiconductor, CdS. Meanwhile, the Type-Ⅱ band configuration would reduce the probability of recombination of the photoinduced electron-hole pairs through the spatial charge separation process. In this study, a facile electrochemical method was employed to sensitize the ZnO nanotube (ZNT) arrays with CdS. The ZNT arrays were uniformly sheathed by a compact layer of CdS granular film. CdS films with the optimized thickness (40(±15) nm) can efficiently absorb the incident photons as well as restrain the recombination of the separated electron-hole pairs. Upon illumination, the photocurrent was 7.00 mA/cm^2 for the CdS/ZNR arrays, which is significantly enhanced compared to that of the pure ZNT arrays (0.69 mA/cm^2). Furthermore, the CdS/ZNT arrays exhibited an even higher photocurrent of 10.64 mA/cm^2. We attribute the excellent photoelectrochemical performance to several factors. First, the CdS/ZNT arrays possessed a larger specific area and accordingly offered a larger photoelectrode/electrolyte contact area which is beneficial to the collection of the holes. Second, the nanotube arrays offering a long optical path act like lots of light-trapping wells, leading to a better anti-reflection effect. Third, the configuration of the ZnO nanotubes can result in a highly efficient charge collection. The excellent photoelectrochemical performance of the CdS/ZNT arrays making them of interest as high-performance photoelectrodes in photoelectrochemical cells.

References:

1. X.P. Qi, G.W. She, L.X. Mu, W.S. Shi, Chem. Commun. 2012, 48, 242.
2. G.W. She, X.H. Zhang, W.S. Shi, X.Fan, J.C. Chang, C.S. Lee, S.T. Lee, C.H. Liu, Appl. Phys. Lett. 2008, 92, 053111.

Fig. 1 SEM images of ZnO nanorods (a), ZnO nanotubes (b), CdS/ZnO nanorods (c) and CdS/ZnO nanotubes.
Fig. 2 Photoelectrochemical performance of the photoelectrodes.

NST-7-Or-1
X-ray Photoelectron Spectroscopy on Isolated Nanoparticles

T10 Nanoscience and Technology

#NST-7-Or-1

O. Sublemontier [1], C. Nicolas [2], D. Aureau [3], M.A. Gaveau [1], H. Kintz [1], X. Liu [4], J.L. Legarec [5], J.B.A. Mitchell [5], M. Patanen [6], E. Robert [6], A. Etcheberry [3], C. Reynaud [1], C. Miron [2].

[1]CEA - Saclay (France), [2]Synchrotron SOLEIL - Saint-Aubin (France), [3]Université de Versailles Saint-Quentin - Versailles (France), [4]Synchrotron SOLIEL - Saint-Aubin (France), [5]Université de Rennes - Rennes (France), [6]Synchtrotron SOLEIL - Saint-Aubin (France).

Novel experimental investigations are currently underway to explore fundamental processes involved in the interaction between isolated nano-objects and soft X-ray radiation [1]. This kind of experiment has become possible due to advanced instrumentation that is now available, in particular at the PLEIADES beamline [2] - SOLEIL synchrotron facility.

In this study, we were able to produce a focused beam of silicon nanoparticles in vacuum from a stable suspension in ethanol. The synchrotron radiation crossed the nanoparticle beam at 90° in the focal point of an aerodynamic lens. In the interaction region, the particle beam diameter and the local particle density were estimated to be 300 µm and 10^7 cm^{-3} respectively.

These conditions allowed us to perform X-ray Photoelectron Spectroscopy (XPS) and Near Edge X-ray Absorption Fine Structure (NEXAFS) of isolated surface-oxidized silicon nanoparticles of different sizes and different natural oxidation time. The incident photon energy was 158 eV, and Si 2p photoelectrons were recorded.

The relative chemical shifts for the various oxidation states of Si have been investigated previously for oxidized silicon wafers [3]. As in that experiment, we can observe all the oxidation states of silicon from Si^0 to Si^{4+} on the surface of the nanoparticles. A systematic study of different types of particles suggests that the oxidation process and the oxide-crystal interface structure depend on the oxidation duration and on nanoparticle size.

1. X.J. Liu et al., in manuscript.
2. C. Miron et al., http://www.synchrotron-soleil.fr/Recherche/LignesLumiere/PLEIADES
3. K. Hirose, H. Nohira, K. Azuma and T. Hattori, Prog. Surf. Sci. 82, 3-54 (2007).

NST-2-Or-2
Simulation of synaptic plasticity depending on inorganic/organic interface effects in PEDOT:PSS based memory devices

T10 Nanoscience and Technology

#NST-2-Or-2

F. Zeng.

Department of Materials cience and Engineering, Tsinghua University - Beijing (China).

Simulation of synaptic plasticity depending on inorganic/organic interface effects in PEDOT:PSS based memory devices

Fei Zeng,* Sizhao Li, Jing Yang, and Feng Pan
Laboratory of Advanced Materials (MOE), Department of Materials Science and Engineering, Tsinghua University, Beijing 100084, People's Republic of China
Corresponding Author: zengfei@mail.tsinghua.edu.cn

Abstract:
Interaction in inorganic/organic interface plays decisive role on resistive switching mechanisms when current is injected. It is excited to utilize these interface effects to mimic basic functions of neural systems, one of which is synapse because using a memristor to mimic learning behavior is a very important development of highly efficient and scalable artificial neural networks. Scientists are currently engaged in the search for effective systems to realize synapse plasticity in this emergent field. We have fabricated several artificial synapses using PEDOT:PSS based memory devices. It is found that the synaptic plasticity varies extensively depending on different interface effects. A Ti/PEDOT:PSS/Ti memory device is a combined system of two readily available inorganic and organic memory materials, consisting of Ti compounds near the electrodes and PEDOT:PSS in between. These two mechanisms can be triggered under a bias with the same sign. However, the resistive switching threshold of the Ti compound is lower than that of PEDOT:PSS, higher. Memory mechanism of a Ta/PEDOT:PSS/Ag structure is the migration of Ag ions driven by redox reaction. Both potentiation and depression, in addition to spike time dependent plasticity, have been emulated using these two memory devices. Furthermore, some special features are presented in these two memory devices,

respectively. Complex memory phenomena including nonvolatile and volatile memory behavior are observed in Ti/PEDOT:PSS/Ti system because of the competition between two contrasting memory mechanisms above mentioned. Besides, metaplasticity can be realized in Ti/PEDOT:PSS/Ti system. However, good rectification and high resistivity, which is in favor of integration using crossbar model, are demonstrated in Ta/PEDOT:PSS/Ag structure. These two memory devices are complementary for each other if they are used to mimic different types of synapse in complex neuromorphic circuits. Our devices can provide the basis for Hebbian learning in the brain and facilitates diverse synaptic plasticity mechanisms in large-scale neuromorphic circuits.

Keywords: Memory, Interface effects, PEDOT:PSS, Synapse, Plasticity, Learning

1. Jo SH, Chang T, Ebong I, Bhadviya BB, Mazumder P, Lu W, Nano Lett. 2010, 10, 1297.

2. Alibart F, Pleutin S, Gue´rin D, Novembre C, Lenfant S, Lmimouni, K, Gamrat C, Vuillaume D, Adv. Funct. Mater. 2010, 20, 330.

3. Ohno T, Hasegawa T, Tsuruoka T, Terabe K, Gimzewski JK, Aono M, Nat. Mater. 2011, 10, 591.

4. Carlos Zamarreño-Ramos, et al., On spike-timing-dependent-plasticity, memristive devices,and building a self-learning visual cortex, Fronties in Neuroscience 2011, 5, 1.

5. Song S, Miller KD, Abbott LF, Nat. Neurosci. 2000, 3, 919~926.

NST-7-Or-2
VACUUM RHEOLOGY MANIPULATORS FOR THE MULTICOORDINATE NANOPOSITIONING AND ACTIVE VIBRATION ISOLATION

T10 Nanoscience and Technology

#NST-7-Or-2

V. Mikhailov, A. Basinenkov, I. Zobov, A. Selivanenko.

BMSTU - Moscow (Russian federation).

The advanced vacuum equipment (for surface analysis, for micro lithography and etc.) uses multicoordinate precise positioning manipulators.The new vacuum manipulators on base of magnetic rheology (MR) liquids and MR elastomers are presented. The combination of MR loop control with elastic carriers and thin wall seals ensures small error of linear positioning (< 50 nm), small time of response (< 100 ms), total linear travel on three coordinates X,Y,Z 1 mm and load capacity more then 10 N [1,2].
It was shown, that the error of positioning of the MR manipulators with a loop control system (Fig.1) is determined by static friction force 0,1-1 N, that corresponds to error of positioning 10-100 nm. The response of the manipulators on base of MR elastomer is determined by time of response on a control signal, which value of time should not exceed 100 ms (Fig.2).
The parameters of vibration isolation systems are a cruelty and a viscose friction coefficient. The control system changes the main performances of the manipulator and reduces the oscillation amplitude that helps to move object to the check point. Because of this the MR manipulator can to operate as an active system of vibration isolation. The investigation of parameters: precision of displacement and response time of the vibration isolation system is being carried out. As a result of the work are presented: three coordinate MR hydraulic manipulator and nanopositioning manipulator on base of MR elastomer.

References
1. Mechanics and Physics of Precise Vacuum Mechanisms: FMIA Volume 91/E.A.Deulin, V.P.Mikhailov, Y.V.Panfilov, R.A.Nevshupa/Series Editor R. Moreau, Springer, 2010.–234 p.
2. Positioning magnetorheological actuator/V.Mikhailov, D.Borin, A.Bazinenkov, I.Akimov. Journal of Physics: Conference Series 149 (2009) 01 2075.

Fig.1. Scheme of loop control system of MR manipulator: 1–MR manipulator; 2, 4–digital-analog and analog-digital converters; 3–computer, 5–sensor of transference

Fig.2. The graphs of the transitional process (external load 11 N): 1–position X of MR manipulator, mic; 2–control signal U, V; Δt–time of response 60 ms

BI-1-Or-9
Nanosensors and breathalyzers for personalized diagnostics

T10 Nanoscience and Technology

#BI-1-Or-9

P. Gouma, J. Lee.

State University of New York - Stony Brook (United states).

The work described here involves the development of handheld, portable, inexpensive breath diagnostics

that can detect and monitor specific biomarkers in exhaled breath that signal disease or metabolic malfunction.

These breath diagnostic tools rely on selective chemosensing based on nanostructured metal oxides with controlled polymorphism.

The science and engineering of metal oxide nanowire sensors along with the nature of gas-oxide interactions are discussed

and are correlated to the usefulness of this technology in non-invasive diagnostics and personalized health monitors.

Recent Press reports on our technology:

http://www.nsf.gov/news/special_reports/science_nation/breathprinting.jsp

http://video.foxnews.com/v/1772104500001/bad-breath-a-sign-of-disease

http://www.scientificamerican.com/article.cfm?id=electronic-nose-disease-diagnosis

NST/SS-7-Or-5
One-step fabrication of few-layer graphene pattern on SiO2 without catalyst or lithography

T10 Nanoscience and Technology

#NST/SS-7-Or-5

S. Chun.

Sejong University - Seoul (Korea, republic of).

Any electronic application of graphene needs graphene located at the desired positions on the desired materials. So far, to accomplish this many steps are required, such as graphene growth on a metallic catalyst, etching of the catalyst, transfer to the desired substrate and lithography for pattern formation. Innovative methods have been developed to slim down this process, skipping one or two steps, and these methods can also reduce the complexity and cost.[1,2] Here, we show that direct graphene growth without a catalyst enables the fabrication of arbitrary graphene patterns on SiO2 in a single step. This one-step pattern formation is performed at temperatures as low as 500 °C using plasma enhanced chemical vapor deposition and a shadow mask (Figure 1). The pattern consists mainly of polycrystalline graphene with only a few layers and a small portion of single and double layer graphene (Figure 2). Furthermore, the nucleation of graphene could be prohibited by hydrogen plasma treatment prior to the growth, offering another way of selective growth. This catalyst-free, lithography-free method for graphene patterning, which can be applied to various substrates, would accelerate the use of graphene in processes where simplicity is preferred.

1. Peng, Z. W.; Yan, Z.; Sun, Z. Z.; Tour, J. M. Acs Nano 2011, 5, (10), 8241-8247.
2. Su, C. Y.; Lu, A. Y.; Wu, C. Y.; Li, Y. T.; Liu, K. K.; Zhang, W. J.; Lin, S. Y.; Juang, Z. Y.; Zhong, Y. L.; Chen, F. R.; Li, L. J. Nano Lett 2011, 11, (9), 3612-3616.

Figure 1. Schematic diagram of one-step fabrication method to obtain pre-patterned graphene on dielectric substrates without additional transfer or lithography process.

Figure 2. HRTEM image of a graphene edge on a TEM grid.

NST-P2-22
Sintered TiC-5VC-18NiCr Alloys with Nano Additions of Tungsten Carbide

T10 Nanoscience and Technology

#NST-P2-22

L. Bodrova, H. Kramar, O. Mul, I. Koval.

Ternopil Ivan Pul'uj National Technical University - Ternopil (Ukraine).

At present, it is very actual the problem of creation of new hard alloys and improvement of properties of the existing ones. This problem can be solved both by optimizing the alloys chemical composition and tungsten carbide alloying and by the use of new technological approaches in forming the structure, including nanotechnology elements [1]. In this paper it is investigated the effect of alloying fine-grained and nano additions of tungsten carbide on the microstructure and mechanical properties of the TiC-5VC-18NiCr system alloys. The alloys are obtained by the powder metallurgy method, which includes sintering in a vacuum. It is found that alloying by nano additions of WC (90-200 nm) in the amount of (5-15) % wt. leads to grinding of carbide base grains, retaining the typical core-rim structure (Fig. 1). Here, a change of the dimensional characteristics of the core and the rim of carbide grains occurs as well as a decrease in the tungsten concentration gradient between external and internal zones of the rim and an increase in the number of small homogeneous grains. With the increase of the nano-WC content, microhardness and Rockwell hardness are increasing as well as a slight drop in the crack resistance coefficient is observed. X-ray diffraction investigations of the alloys with nano-WC show that during sintering there is a certain increase in the percentage of the cubic W_2C, which has a higher microhardness in comparison with the hexagonal WC. This effects additively on the alloy hardness in whole. Besides, fine particles of nano-WC dissolve in the binder more easily that leads to the strengthening of carbide-metal bonds and the corresponding increase in hardness and microhardness. With increasing content of nano-WC, the crack resistance decreases. This can be explained by the lack of the binder, by the increase of the number of carbide-carbide contacts and by the decrease of the interphase boundaries strength. When using the nanodispersed additions, the specific surface area of carbides increases and the binder amount, which is optimal for the fine-grained carbide, becomes insufficient to ensure wettability. The values of the crack resistance coefficient for the alloys with WC nano additions (6.2-6.8 $MPa \cdot m^{1/2}$) are

almost 20% higher compared to the fine-grained ones, while preserving the general decreasing trend with a nano-WC growth.

1. Bodrova L., Kramar G., Mul O., Koval I., Sushynskiy V. Effect of Nano WC Alloying Additions on the Structure Formation of TiC-5VC-18NiCr Cermets // World Congress and Exhibition PM 2010 (10-14 October 2010, Florence, Italy) Proceedings, Vol.3, pp. 479-484, EPMA, UK, 2010.

Figure 1. The microstructure of TiC-5VC-18NiCr cermets: with additions of 5 % (wt) of fine-grained WC (left) and nano-WC (right).

NST/SS-6-Or-6
Spin-dependent transport properties in 1D systems: ab-initio studies

T10 Nanoscience and Technology

#NST/SS-6-Or-6

I. Sivkov, V. Stepanyuk.

Max Planck Institute of Microstructure Physics - Halle (Germany).

This contribution presents the results of theoretical *ab-initio* calculation of spin dependent transport properties of one-dimensional systems using Density Functional Theory and Non-Equilibrium Green's Function method.

In experimental works [1,2] authors reported the occurence of spin injection and large magnetoresistance in systems with Co electrodes and Au contacts between them. We perform a theoretical study of conductance and I-V characteristics for Co-Au-Co nanocontacts. Co electrode is constructed as a Co pyramid on hcp Co(0001) surface. Au contact is represented by a Au atomic wire between the electrodes. Calculated conductance and current show quiet high spin polarization due to s-d hybridization of Co electrode states with the states of Au. This effect can explain the experimentally observed high magnetoresistance and spin injection.

Another way to obtain spin polarized currents is to use half-metallic materials. Motivated by results of [3], where a possible half-metallic behavior of GdN-bulk was shown, we investigate conductance and I-V characteristics of GdN atomic zigzag infinite chains. The chain is found to have a half-metallic behavior, which leads to the 100% spin polarization of conductance. Additionally, conductance and current through fcc GdN(001) films with Cu(001) electrodes in the direction perpendicular to the film is studied. It is found that GdN films show strong spin polarization of conductance and current reaching 90%, that can be used as a spin-filter for spintronic devices.

[1] A. Bernand-Mantel, P. Seneor, N. Lidgi at al. APL 89, 062502 (2006)
[2] Stefan Egle, Cecile Bacca, Elke Scheer et al. PRB 81, 134402 (2010)
[3] Chun-gang Duan, R. F. Sabiryanov PRL 94, 237201 (2005)

NST-11-Or-4
Formation of bimetallic Au-Cu nanoparticles on TiO2(110) followed in-situ by STM and GIXD

T10 Nanoscience and Technology

#NST-11-Or-4

G. Prevot [1], A. Wilson [1], R. Bernard [1], Y. Borensztein [1], B. Croset [1], A. Vlad [2], A. Coati [2], Y. Garreau [2].

[1]Institut des Nanosciences de Paris - Paris (France), [2]SOLEIL Synchrotron - Saint Aubin (France).

The fabrication of bimetallic nanoalloys with controlled size, composition and structure attracts a wide interest for magnetic, optical or catalytic applications. The mixing of the two metals can lead to various structures such as alloyed phases, core-shell or janus configurations. In the field of catalysis, Au based nanoalloys are of special interest, due to the specific properties of Au at the nanoscale. Among them, Au-Cu nanoparticles attract a growing interest. Such nanoparticles have been recently shown to be active for various chemical reactions, especially oxidation reactions. Au-Cu nanoparticles supported on oxide substrates have been shown to be active for CO oxidation, preferential oxidation of CO in H_2 environment or propene epoxidation.
Using in-situ scanning tunneling microscopy (STM), we have studied the growth of Au-Cu nanoparticles on TiO_2(110). We show that successive evaporation of Au and Cu leads to the synthesis of alloyed nanoparticles whereas Cu evaporation followed by Au evaporation leads to the renucleation of pure Au nanoparticles. Starting from pure Au NPs of mean size 1.5 nm grown at 300K, we have followed by grazing incidence X-ray diffraction and small angle scattering (GIXD/GISAXS) the change of the NPs during Cu evaporation at room temperature. Alloying occurs instantaneously and the lattice constant of the NPs shifts gradually towards lower values during evaporation. The epitaxial relations with the substrate remain unmodified, with a main relation given by Au(112)//TiO_2(110) and Au[1-10]//TiO_2[001]. After deposition, no chemical ordering could be evidenced in the NPs (of size around 2 nm). However, after annealing at 400°C, AuCu NPs present a L10 chemical ordering, whereas Au_3Cu and $AuCu_3$ NPs remain FCC disordered. No significative variation of the mean size of the NPs is observed. The formation of an ordered phase for such small NPs is

unexpected since it is usually observed for larger NPs (above 10 nm) on amorphous substrates. This specific behaviour could be related to the interaction with the substrate and the specific geometry of the (112) interfacial plane.

STM observation during growth. a) and d) bare TiO2(110) surface. Steps are shown (black lines). Observation of the same area as (a) after 0.01 ML Cu evaporation (b) followed by 0.01 ML Au evaporation. Observation of the same area as (d) after 0.01 ML Au evaporation (e) followed by 0.01 ML Cu evaporation. Size of the images: 88x77 nm^2.

NST-7-Or-3
Fabrication and study of C60-Cox complex using low temperature scanning tunneling microscopy and spectroscopy

T10 Nanoscience and Technology

#NST-7-Or-3

P. Yang, J. Lagoute, V. Repain, C. Chacon-Carillo, Y. Girard, S. Rousset.

MPQ, Université Paris Diderot - Paris (France).

Profound understanding of the electronic process at the metal/molecule interface and the interaction between the organic molecule and metal at atomic scale is critical to fabricate the new generation molecule electronic devices. Moreover, atom manipulation using scanning tunneling microscopy (STM) allows the formation of atomic controlled artificial molecule-metal conjugate [1–3]. As the interface between C_{60} and magnetic material holds promises for molecular spin electronics [4,5], we studied the interaction between C_{60} and Co atoms. Using a low temperature (LT) STM we performed atomic and molecular manipulation to build and study C_{60}-Co_x complex.

The Co atoms and C_{60} molecules are deposited in-situ on a clean Au(111)/mica surface in ultra-high vacuum ($<10^{-10}$mbar) at low temperature (5K). We show that it is possible to move a C_{60} above a Co adatom and then manipulate the molecule-atom ensemble as a single object, suggesting that we formed a Co-C_{60} complex. Moreover C_{60}-Co_x entities with $x>1$ can be formed by a combined lateral manipulation of C_{60} and Co adatoms in two different ways: the molecule is successively moved towards individual adatoms, or a Co_x cluster is built by atomic manipulation and the molecule is moved towards the cluster. We have been able to add up to 9 Co atoms to a C_{60}, which is, to our knowledge, the largest number achieved in such molecule-metal atom complex.

We performed dI/dU spectroscopy using the lock-in technique in order to measure the influence of Co on the molecular spectrum. Although possible doping effect still

need to be clarified, the C_{60}-Co_x spectrum exhibit the main features of the C_{60} single molecule suggesting that the pi states are at most only slightly affected by the interaction between the molecule and the Co atoms.

[1] L. Gross, K.-H. Rieder, F. Moresco, S. M. Stojkovic, A. Gourdon, and C. Joachim, Nat. Mater.2005, 4, 892
[2] J. Repp, G. Meyer, S. Paavilainen, F. E. Olsson, and M. Persson, Science 2006, 312, 1196
[3] R. Yamachika, M. Grobis, A. Wachowiak, and M. F. Crommie, Science 2004, 304, 281
[4] S. L. Kawahara, J. Lagoute, V. Repain, C. Chacon, Y. Girard, S. Rousset, A. Smogunov, and C. Barreteau, Nano Lett.2012, 12, 4558
[5] M. Gobbi, F. Golmar, R. Llopis, F. Casanova, and L. E. Hueso, Adv. Mater. 2011, 23, 1609

NST-6-Or-13
Innovative process for the preparation of lanthanide fluorides nanoparticles: characterizations of the obtained materials and study of their properties

T10 Nanoscience and Technology

#NST-6-Or-13

F. Chaput [1], A.C. Faure [1], A. Chaput [1], F. Lerouge [1], S. Parola [1], F. Mpambani [1], F. Vadcard [1], J. Navarro [1], C. Dujardin [2], G. Ledoux [2], D. Amans [2], A.L. Bulin [2], D. Chateau [1], M. Lecouvey [3], M. Monteil [3].

[1]ENS-CNRS-UCBL - Lyon (France), [2]Institut Lumière Matière - Villeurbanne (France), [3]SMBH-Université Paris13 - Bobigny (France).

Nanoparticles are becoming increasingly important in a wide range of different fields including optics, catalysis, energy, mechanics and biomedical. The exceptional properties of these materials are a direct function of their small size, but also their composition, structures, morphologies and crystallinity. Among all the possible compositions of such materials, lanthanide fluorides receive specific attention. Conventional methods for preparing nanoparticles of lanthanide fluorides are most often difficult to implement (for entire series) for further use on industrial scale. Current processes often lead to compounds with unsatisfactory purity or to nanoobjets with low crystallinity. Additionally, some of these processes use binding temperatures and pressure conditions and/or use expensive raw materials with synthesis routes that are not practical for industrial applications. The present study provides a novel process for a simpler preparation of lanthanide fluoride nanoparticles for all of the lanthanide series, as well as for solid solutions between fluorides. The objects obtained may be isolated as powders or colloidal solutions in a large number of solvents. The method also covers the preparation and shaping of different materials (thin films, monoliths and powders) out of these nanoparticles. The magnetic and emission properties of nano-objects as well as materials obtained will be presented. The figure below shows examples of nanoparticles of lanthanide fluorides prepared using the new process.

NST-3-Or-5
Tuning Surface Stiffness with Thin Oxide Films

T10 Nanoscience and Technology

#NST-3-Or-5

S. Cohen [1], E. Kalfon-Cohen [1], D. Barlam [2], K. Gotlib-Vainshtein [3], O. Girshevitz [3], C. Sukenik [3].

[1]Weizmann Institute of Science - Rehovot (Israel), [2]Ben Gurion University - Beer Sheva (Israel), [3]Bar Ilan University - Ramat Gan (Israel).

Controlling and tuning surface and interfacial mechanical properties is the starting point for many scientific and engineering problems and applications. In this work, surfaces with tunable stiffness have been designed and created by coating a soft polymer (polydimethoxylsilane) by a layer of amorphous titanium oxide with thickness varying between 8 and 70 nm. This protocal allows control of surface stiffness, while preserving the bulk material properties as well as composition and chemical reactivity of the interface. The surfaces were characterized by a variety of techniques, and AFM-based nanoindentation was applied to deduce the mechanical characteristics. Finite element analysis was used to investigate the modes of deformation, as well as respective contribution of substrate and film to the overall mechanical response. It is shown that knowledge of only the film thickness, and elastic modulus of film and substrate allows accurate prediction of the observed load vs. deformation characteristics.[1] These results show promise in design and creation of surfaces with independently customized chemical and mechanical properties.

1. Katya Gotlib-Vainshtein, Olga Girshevitz, Chaim N. Sukenik, David Barlam, Estelle Kalfon-Cohen and Sidney R. Cohen, submitted to J. Phys. Chem C.

Figure 1. FEA simulations (solid lines) fit to experimental data for 3 different titania film thicknesses – 8 (black squares), 14 (red triangles), and 22(blue diamonds) nm deposited on activated PDMS. Figure taken from ref. 1

NST/SS-7-Or-6
Temperature dependence of a graphene growth on a stepped iridium surface

T10 Nanoscience and Technology

#NST/SS-7-Or-6

P. Pervan, I. Šrut, V. Mikšić Trontl, M. Kralj.

Institut za fiziku - Zagreb (Croatia).

Many of the desirable properties of graphene are related to its electronic structure with linearly dispersing pi and pi* bands merging at the Fermi level in a single point. This makes graphene a gapless semiconductor which is a limiting factor for some applications of graphene in electronics where a sizeable band gap at the Fermi energy is required. For that reason, a lot of research effort is directed towards manipulation of the electronic structure of graphene around the Fermi energy. One possible route, which is subject of this work, relies on altering the graphene band structure by means of an additional periodic potential, i.e. graphene superlattice. Calculations indicate that superlattice structures may lead to unexpected and potentially useful charge carrier behavior, e.g. gap openings or Fermi velocity anisotropy [1].
Graphene superlattices have been already realized on well defined monocrystalline substrate surfaces as a consequence of the mismatch of graphene and substrate lattices which leads to the so called moiré superstructures. For graphene on Ir(111) it has been shown that the moiré superstructure adds a long range superperiodic potential to the graphene, which opens minigaps in the Dirac cone [2].

In this work [3] we have used scanning tunneling microscopy to study the growth of graphene on a periodically stepped Ir(332) substrate surface, which is a promising route for modification of graphene properties. We have found that graphene continuously extends over iridium terraces and steps. Moreover, new distinctive mesoscopic features of the underlying surface are formed involving large, flat terraces accompanied by groups of narrower steps. The distribution of the newly formed terraces is sensitive to the preparation temperature and only below 800°C terrace width distribution closer to the intrinsic distribution of clean Ir(332) are found. We propose that the microscopic shape of steps found after graphene formation is

strongly influenced by the orientation of graphene domains, where graphene rotated by 30° with respect to the substrate has a prominent role in surface structuring.

[1] Park CH, Yang L, Son YW, Cohen ML, Louie SG. Anisotropic behaviours of massless Dirac fermions in graphene under periodic potentials. Nature Phys. 2008; 4:213-7.

[2] Pletikosic I, Kralj M, Pervan P, Brako R, Coraux J, N'Diaye AT, et al. Dirac Cones and Minigaps for Graphene on Ir(111). Phys Rev Lett 2009. 2009; 102(5):056808-4.

[3] Iva Šrut, Vesna Mikšić Trontl, Petar Pervan, Marko Kralj, Temperature dependence of a graphene growth on a stepped iridium surface, Carbon 2013, accepted

NST-P2-23
Carbon Nanotubes-Epoxy Resin Composite Synthesis and Mechanical Properties

T10 Nanoscience and Technology

#NST-P2-23

L. Domratcheva Lvova [1], A. Gomez Sanchez [1], L. Garcia Gonzalez [2], P. Gonzalez Garcia [2], E. Huipe Nava [1], N. Flores Ramirez [1], F.G. Granados Martinez [1].

[1]Universidad Michoacana de San Nicolas de Hidalgo - Morelia (Mexico),
[2]Universidad Veracruzana - Boca Del Rio (Mexico).

Since their discovery by Iijima [1] carbon nanotubes (CNTs) attract great interest due to their unique physicochemical, electric and mechanical properties, such as hardness, emission and others, which imply CNTs applications in electronics, and a variety of other properties promising their possible practical applications in other fields.

Carbon nanotubes are produced by chemical vapor deposition (CVD) at 800, 850 and 900 °C from benzene and ferrocene in the flow of argon (50, 80 and 110 ml/min) in the reactor constructed by [2], based on [3]. CVD synthesis proceeds at the atmospheric pressure during one hour. The amounts of CNTs obtained are 0.5-1.7 g. Field Emission Scanning Electron Microscopy, Energy Dispersed Spectroscopy (EDS) and X-Ray Diffraction are used to characterize the obtained CNTs. The observed lengths of the CNTs are 70-412 μm and diameters 15-133 nm. EDS demonstrated about 0.4 of Atomic percentage of Fe in the CNTs. The numbers of CNTs walls are estimated by Scherrer's equation [4]. The different flow of argon produced various numbers of walls: 50 ml/min-41 walls, 80 ml/min-36 walls and 110 ml/min-32 walls average.

The epoxy resin series 2040 with aluminum load by Epolyglas (which is designed to manufacture vacuum molding and structural elements) is used for the preparing of composite. The epoxy resin comes in two components: epoxy aluminum bearing and hardener clear amber liquid. The mixing contained 20 ml of hardener liquid per 0.1 Kg epoxy resin. The obtained nanotubes are dispersed in the epoxy resin using a

solution blending technique to obtain a carbon nanotubes-polymer composite with 3% weight of CNTs. The solidification time was 4 hours. Later the samples were thermally treated in a muffle for 1h, raising the temperature from 30 °C to 150 °C in order to improve the major mechanical resistance.

The obtained composites materials are analyzed with a Micro Vickers Hardness Tester, Mitutoyo 810-129E equipped with Vickers and Knoop indenters. The hardness is evaluated by a force application of 0.05 and 0.1 Kg during 10 s. It can be observed that the higher values of hardness are presented in the composites produced from CNTs with lower number of walls obtained with argon flow of 110 ml/min and temperature 850 °C. The range of Hardness Vickers for obtained composites is 880-1150 Kg/mm^{-2}. It is important to mention that these values exceed more than 4 times the hardness of steel 1018, and far much more the hardness of epoxy resin without CNTs. So the addition of just 3% weight of CNTs allows providing high hardness to CNTs-epoxy resin composite.

[1] Iijima S., Nature, 1991, 354, 56-58

[2] Gómez Sánchez A., Domratcheva Lvova L., López Garza V., Román Doval R. and Mondragón Sánchez Ma. de L., MRS Proceedings, 2012, 1479, imrc12-1479-s1c-o033 doi:10.1557/opl.2012.1607.

[3] Korneeva Yu.V., Novakova A.A., Ob"edkov A.M., Zaitsev A.A., Domrachev G.A., Journal of Surface Investigation. X-ray, Synchrotron and Neutron Techniques, 2007, 1(4), 369-372

[4] Scherrer PH. Göttinger Nachrichten Gesell. 1918, 2, 98-100

NST-6-Or-14
Nano-additives Reinforcing of Binders for Diamond Cutting Tools

T10 Nanoscience and Technology

#NST-6-Or-14

D. Sidorenko.

NUST "MISIS" - Moscow (Russian federation).

Nano-additives Reinforcing of Binders for Diamond Cutting Tools

D. Sidorenko, E. Levashov, V. Kurbatkina, A. Zaitsev, S. Rupasov
National University of Science and Technology “MISIS”

Currently, the diamond cutting tools are becoming more widely used in build industry. Advantages of using it are obvious: low noise and vibration, which can destroy the integrity of building structures; increase in productivity in several times, because this type of cutting tools does not have difficulties with the notch of armature and other metal parts; and after cutting there are clean smooth holes which do not require additional processing. The most important characteristics of cutting tools are the cutting speed and wear resistance, which, in turn, depend on the physical and mechanical properties of a binder.

The incorporation to metal matrix composite (MMC) of even a small amount of reinforcing nanoparticles can significantly increase hardness, bending strength, impact strength, and decrease of friction coefficient, simultaneously, without increasing of the sintering temperature, duration and hot-pressing pressure. This work demonstrates effect of the dispersion strengthening by nanoparticles of tungsten carbide, zirconium dioxide and carbon nanotubes on mechanical and tribological properties of MMC based on iron and copper. Nanoparticles doped conventional MMCs show higher values of hardness and bending strength.

Besides, diamond/binder adhesive force is of great importance for cutting performance. Adhesion between diamond grains and the binder strongly depends on diamond graphitization. Raman spectroscopy studies of WC, ZrO_2 and Mo nanoparticles influence on this process are presented. Mo and ZrO_2 additives accelerate graphitization, while WC nanoparticles decrease graphitization level up to 30%.

Industrial tests of diamond cutting wheels and drills with disperse strengthened by nanoparticles MMC have shown the increase of life time up to 2 times without

reduction of cutting speed.

NST-P2-24
Photoluminescence of YNbO4:Eu phosphor nanoparticles synthesized by mechanochemical method

T10 Nanoscience and Technology

#NST-P2-24

L. Dacanin [1], M. Dramicanin [2], S. Lukic-Petrovic [1], D. Petrovic [1], M. Nikolic [2], T. Ivetic [1].

[1]University of Novi Sad, Faculty of Sciences, Department of Physics - Novi Sad (Serbia), [2]Vinča Institute of Nuclear Sciences, University of Belgrade - Belgrade (Serbia).

Yttrium niobate ($YNbO_4$) phosphor is a perspective efficient material generally used in X-ray intensifying screens. The blue light emission from yttrium niobate phosphors is associated with groups host crystalline lattice [1]. Such luminescent properties can be shifted towards longer wavelengths when doped with other rare-earth ions that partly replace yttrium ions in the host lattice. In the case of Eu^{3+} emission centers red luminescence can be generated.

Yttrium niobate is usually synthesized by solid state reaction method, using a ball mill to grind precursors for tens of hours [2,3], while nanocrystalline yttrium niobate is often obtained by sensitive soft-chemical methods [4]. Here we prepared single-phase Eu^{3+}-doped $YNbO_4$ phosphor nanopowder i.e. nanophosphor, using fast and energetically efficient mechanochemical method followed by annealing. The precursors were mixed in a ball-mill at 100 rpm for 3h, pre-sintered at 800°C for 2h, then ball-milled again and finally annealed at 1200°C for 2h.

The sample crystalline structure is confirmed by XRD measurements. The crystallite size of 42 nm was estimated using Debye Scherrer's equation by determining the line broadening of the main intensity peak. Scanning Electron Microscopy was used to observe microstructure and particle size of the powder. High-resolution photoluminescence measurements were performed at room temperature. The sample exhibits very intense red emission, coming from specific $^5D_0 \rightarrow {}^7F_J$ (J = 1, 2, 3, 4) transitions of the Eu^{3+} ion, with the lifetime around 0.6 ms. Compared to previously reported [5] photoluminescence emission of the microcrystalline $YNbO_4$:Eu phosphor, emission of the nanocrystalline sample is almost twice as strong.

[1] G. Blasse, A Bril, J. Electrochem. Soc. 115, 1067 (1968).
[2] M. Nazarov, Y. J. Kim, E. Y. Lee, K.-I. Min, M. S. Jeong, S. W. Lee, D. Y.Noh, J. App. Phys. 107, 103104 (2010).
[3] E.C. Karsu, E.J. Popovici, A. Ege, M. Morar, E. Indrea, T. Karali, N. Can, J. Lumin. 131, 1052 (2011).
[4] Y. Zhou, Q. Ma, M. Lü, Z. Qiu, A. Zhang, J. Phys. Chem. C 112, 19901 (2008).
[5] Lj.R. Đačanin, M.D. Dramićanin, S.R. Lukić-Petrović, D.M. Petrović, M.G. Nikolić, Rad. Meas. (2013) *in press*

Photoluminescence emission spectrum of YNbO4:Eu nanophosphor

NST-11-Or-7
Nanowires, nanotubes, nanoalloys : a phase diagram story

T10 Nanoscience and Technology

#NST-11-Or-7

I. Braems, F. Berthier.

CNRS - Orsay (France).

The bimetallic submonolayer is the scene of many kinetic processes including deposition, aggregation, surface diffusion and segregation, most of participating in nucleation-growth kinetics whose complete evolution is beyond the capabilities of atomistic-scale simulations. Derived from bulk alloys precipitation, the cluster dynamics is therefore an efficient tool to reach larger time and space scales, at the condition that cluster-scale parameters are consistently derived from atomic-scale quantities measured via Monte Carlo simulations (1).

In this talk we present a comprehensive view of a bimetallic submonolayer described as a collection of bimetallic clusters. For kinetics that tend towards equilibrium such as deposition and ageing, cluster-scale parameters must depend on the thermodynamical equilibrium of the submonolayer in order to satisfy microreversibility. Hence the submonolayer equilibrium first depends on the vacancy mobility and density (2), the latter being here non negligible as compared with 3D bulk counterparts. Second, the atomic phase is to be described as a size distribution of bimetallic finite-size objects, each of them being subjected to edge segregation. We show how segregation in particular affect both morphologies and size distribution of clusters at equilibrium, the thermodynamical properties of each class of clusters depending both on the size to te considered and the average composition of the monolayer (3). We also illustrate the variety of observed configurations within the collection of bimetallic clusters and in particular coexisting configurations with strongly different edge concentrations that can lead to different kinetic routes in modelling surface kinetics.

In the second part of the talk we describe the nucleation kinetics for two codeposited species as a function of their interaction energies and their partial coverage. The key parameters that assess consistency between atomic-scale and cluster-scale simulations are distinguished and the influence of a second species onto atomic

deposition is quantified and illustrated. Extension to size-mismatched systems is discussed.

(1) F. Berthier, E. Maras, I. Braems and B. Legrand, Multiscale Modelling of the Ageing Kinetics of a 2D Deposit, Solid State Phenomena, 172-174, 664 (2011)

(2) K. Yaldram, G.K. Khalil and A. Sadiq, Phase diagram of a dilute binary alloy with annealed vacancies, Solid State Communications 87(11), 1045–1049 (1993)

(3) E. Maras, I. Braems and F. Berthier, Extending cluster description to bimetallic nanowires: The ideal solid solution alloy case, J. Chem. Phys. 135, 224702 (2011)

(4) I. Braems and F. Berthier, Magic Numbers for Bimetallic Clusters, Solid State Phenomena, 172-174, 1038 (2011)

NST-P3-23
Single Molecule Fluorescence from Tetraphenyl-Porphine on GaAs(110) in a STM

T10 Nanoscience and Technology

#NST-P3-23

S. Mühlenberend, N.L. Schneider, R. Berndt.

IEAP, University of Kiel - Kiel (Germany).

The tip of a STM can be used to excite luminescence from atomic scale structures. A major difficulty in STM induced luminescence experiments has been the coupling between molecules and a metallic substrate that largely inhibits molecular fluorescence. Therefore molecules have been decoupled by, e. g., multilayer arrangements. Here we use the semiconductor GaAs(110) as a substrate. Even for very low coverages of Tetraphenyl-Porphine of less than 5% of a monolayer and without injecting electrons into the molecular orbitals, we observe fluorescence. Spectral and polarization analysis show clear evidence of a plasmon at the STM tip inducing intramolecular Q-band transitions. The processes involved in exciting this molecular fluorescence over lateral distances of several nm will be discussed.

NST/SS-6-Or-7
Magnetism and spin transport of molecule/ferromagnet interfaces

T10 Nanoscience and Technology

#NST/SS-6-Or-7

V. Repain [1], L. Kawahara [1], J. Lagoute [1], C. Chacon [1], Y. Girard [1], A. Bellec [1], S. Rousset [1], A. Smogunov [2], C. Barreteau [2], Y.C. Chao [3], Y.C. Hu [3], R. Breitwieser [3], W.W.L. Pai [3].

[1]Matériaux et Phénomènes Quantiques, Univ. Paris Diderot, CNRS - Paris (France), [2]SPCSI, CEA - Saclay (France), [3]National Taiwan University - Taipei (Taiwan, republic of china).

The understanding of the coupling between a molecule and a ferromagnetic electrode is one of the key issues in the promising field of molecular spintronics. Among various molecules, C60 has a particular interest considering its high symmetry and the absence of nuclear spins. In this framework, we have investigated the adsorption of C60 on chromium and cobalt surfaces, studying both the change of magnetism in the magnetic layer and the induced spin polarization on the molecules. The comparison of the experimental data with ab initio calculations allows a good understanding of the specific hybridizations giving rise to a significant molecular spin polarization for certain molecular orbitals.
In a first step, we have measured by in situ magneto-optical Kerr effect how the deposition of a C60 layer can influence the magnetism of underlying Co ultrathin films grown both on Au(111) and Pt(111). For a certain range of thickness, we observe a magnetization reorientation transition, favoring a perpendicular magnetic anisotropy with the organic layer. More interestingly, in a second step, we have performed spin polarized scanning tunneling spectroscopy of individual C60 molecules on a Cr(001) surface (cf. figure) and on Co/Pt(111). On chromium, we have found a tunnel magneto-resistance through single molecules that changes sign depending on the energy, related to the complete spin polarization of the lowest unoccupied molecular orbital of the free C60. These results arise from a statistical analysis over more than 500 molecules and are particularly well reproduced by ab initio calculations, despite of the complexity of the chromium magnetism [1]. On cobalt, the coupling between the molecules and the metal seems to be less important, giving rise to a smaller molecular spin polarization. These results are of particular importance for the future design of organic spintronics devices as they

illuminate the complex interplay between ferromagnetic electrodes and molecular layers on model systems.

[1] “Large Magnetoresistance through a Single Molecule due to a Spin-Split Hybridized Orbital”, S. L. Kawahara, J. Lagoute, V. Repain, C. Chacon, Y. Girard, S. Rousset, A. Smogunov, and C. Barreteau, Nano Letters, 12, 4558 (2012).

Three-dimensional view of the C60 molecules deposited on a Cr(001) surface. The color code indicates the level of local electronic conductance, revealing the local spin polarization at the nanometer scale. A drawing of the magnetic tip and the anti-ferromagnetic substrate have been added for clarity.

NST-2-Or-3
Electrical characterization of free-standing GaAs nanowires by multitip STM

T10 Nanoscience and Technology

#NST-2-Or-3

M. Steidl [1], S. Korte [2], W. Prost [3], W. Zhao [1], P. Kleinschmidt [1], V. Cherepanov [2], B. Voigtländer [2], T. Hannappel [1].

[1]TU Ilmenau, Institut für Physik, Fachgebiet Photovoltaik - 98684 - Ilmenau (Germany), [2]Peter Grünberg Institut (PGI-3), Forschungszentrum Jülich, 52425 Jülich, Germany, and JARA-Fundamentals of Future Information Technology - 52425 - Jülich (Germany), [3]Center for Semiconductor Technology and Optoelectronics (ZHO), University of Duisburg-Essen - 47057 - Duisburg (Germany).

III-V semiconductor nanowires (NWs) are promising candidates as components for future solar cell designs, if a controlled distribution of dopants along NWs can be achieved. To generate a homogeneous axial dopant profile, p-doped GaAs NWs were grown on an n-doped GaP(111)B substrate by Au-assisted metal-organic vapor-phase epitaxy (MOVPE), with Au-particles that had previously been saturated with Zn as dopant.
For electrical characterization these free-standing NWs were contacted using a multitip STM. Four point probe measurements with variation of the probe distances reveal their electrical transport properties. The conductance profile along the NWs and the diode characteristics of the pn-junction to the substrate were measured. We show that the resistivity is constant over most of the NW length of 8 µm, while the base, up to about 1.5µm, has an increased resistivity. The contact between the n-GaAs NW and the p-GaP substrate forms a diode. Using the SEM integrated into the multitip STM setup, an electron beam induced current (EBIC) generated in the pn-junction from substrate to NW can be mapped.
Furthermore, the NWs exhibit high mechanical elasticity. They can be deformed by the STM tips and revert to their original shape when released. Even extreme bending of a NW did not show a significant influence on its conductivity.

SEM scan and schematic diagramm of three STM tips in contact with a free-standing GaAs NW for resistance measurements

NST/SS-P2-04
Magnetic properties of iron nanocrystals

T10 Nanoscience and Technology

#NST/SS-P2-04

D. Li, C. Barreteau, A. Smogunov, F. Silly.

CEA - Gif Sur Yvette (France).

We have investigated the electronic and magnetic properties of iron nanocrystals by means of electronic structure calculations using both the Quantum-espresso package [1] based on density functional theory as well as an efficient tight-binding code [2]. The nanocrystals studied are in shape of truncated square pyramids (see Fig. 1) since it has been shown experimentally that such crystals can be grown on SrTiO3(001) surface[3]. We analyze the atomically resolved magnetization of systems of various sizes. It is found that the spin moments are indeed reinforced on low coordinated (surface, step, edge) sites: (001) facets have larger magnetic moments than (110) facets. We have also performed non-collinear calculations including spin-orbit coupling and determined the magneto-crystalline anisotropies of such objects which is essential to characterize their magnetic stability.

[1] P. Giannozzi et al, J. Phys.: Cond. Matter, 21, 395502 (2009)

[2] C. Barreteau and D. Spanjaard, J. Phys.: Cond. Matter, 24, 406004 (2012)

[3] F. Silly and M. R. Castell, Appl. Phys. Lett. 87, 063106 (2005).

Truncated square pyramid made of 135 Fe atoms. The magnetization (in Bohr magneton) of some relevant surface atoms is indicated.

NST/SS-P1-13
Development of field effet transistors based on graphene using dielectrophoretic deposition and tantalum nitride electrodes

T10 Nanoscience and Technology

#NST/SS-P1-13

A. Pascon De Marque, J. Fernandes De Souza, J.A. Diniz.

Center for Semiconductor Components, State University of Campinas - Campinas (Brazil).

For devices based on graphene, usually, non-refractory metallic electrodes of Ti/Au or Ti/Pd are used. However, to reduce the contact resistance between metal and graphene, an annealing process in vacuum environment at temperature of 700°C is a requirement [1]. Therefore, refractory metallic electrodes, such as tantalum nitride (TaN), must be studied. Graphene in large quantity can be obtained by dielectrophoretic (DEP) assembly [2] of a few layers of insulating graphene oxide, which become metallic after thermal reduction at 450ºC.
In this context, tantalum nitride (TaN) electrodes (deposited by DC reactive sputtering in N_2/Ar environment) are used as metallic contacts with the graphene. In our FET devices, the graphene sheets are deposited between TaN electrodes of source and drain and above the high-k gate dielectric of TaO_x formed on n^+ silicon substrate, which is used as back gate. These sheets were obtained in suspension of DMF (dimethylformamide) with four different graphene concentrations and were deposited using DEP process: ac signals were applied between electrodes with voltage of 3 to 5 V_{pp} and frequencies ranging from 5 to 50 MHz for periods of 25 up to 180 sec. Scanning electronic microscopy (SEM) analyses and current-voltage (I-V) measurements were carried out to get the physical and electrical characteristics of our devices. Our best results, which are presented in Figure1 are for DEP process carried out using frequency of 50 MHz and period of 180 sec. The resistance values measured before and after annealing differ in three orders of magnitude, in agreement with [2]. The Dirac point near V_{BG}=0 results in a low I_{on}/I_{off} ratio (Figure2).

1. Souza J F, Development of Materials and Methods of Fabrication of Chemical/Biochemical Sensors based on Silicion and Carbon Nanostructures (ISFET, CNTFET and GraFET), PhD, FEEC, Unicamp, 2012;
2. Burg B R et al, Appl. Phys, Lett. **94** 053110 (2009);

Figure 1. SEM images with graphene layers deposited between TaN electrodes.

Figura 2. Characteristic I-V and trancondutance, showing the graphene Dirac point.

NST-11-Or-5
Development and investigation of an atmospheric microplasma jet for generation of silicon nanocrystals

T10 Nanoscience and Technology

#NST-11-Or-5

B. Barwe, J. Benedikt.

Group Coupled Plasma-Solid-State Systems, Faculty of Physics and Astronomy, Ruhr-Universität Bochum - Bochum (Germany).

Silicon nanocrystals (SiNC) offer new opportunities in a wide range of electronical and optical devices including solar cells and single-electron transistors. Other fields of applications are nanoelectronic circuit elements, luminescent markers in biomedicine and thermoelectric energy generation because of their spectral tunability and photoluminescence efficiency.
The production of SiNC is connected with several challenges. It is difficult to reach crystalline particles and to avoid particle agglomeration during the generation process. Moreover, it is important to prevent the oxidation of the crystals by providing them a surface passivation. This surface passivation can be performed in a liquid phase, but it is usually a lengthy and demanding process.
We produce SiNC with the help of a dual microplasma jet system, where the SiNC are first synthesized in a DC-microplasma jet using Argon as working gas (as already shown by Sankaran et al. [1]), followed by a passivation step in a second atmospheric pressure plasma to avoid agglomeration, to passivate their surface and to incorporate them in a thin film.
The HRTEM, FTIR, and photoluminescence measurements of SiNC prepared under various experimental conditions and plasma diagnostic results will be presented.

[1] R. Mohan Sankaran, Dean Holunga, Richard C. Flagan, and Konstantinos P. Giapis; Nano Lett., 2005, 5 (3), 537-541

High resolution transmission electron microscope (HRTEM) image of crystalline silicon nanoparticles embedded in an amorphous matrix (gas mixture through plasma: SiH_4ArH)

NST-6-Or-12
Gd decorated ZnO nanoparticles to obtain high fluorescence quantum yield and enhanced MR relaxivity; potential multimodal nanoprobes for bioimaging applications

T10 Nanoscience and Technology

#NST-6-Or-12

L. Selegård, M. Ahrén, A. Skallberg, K. Uvdal.

Molecular Surface Physics and Nanoscience, Linköping University - Linköping (Sweden).

Gd decorated ZnO nanoparticles are potential candidates for future multimodal nanoprobe imaging applications, such as fluorescence imaging and MR signal enhancement. When combining Zn and Gd in this type of nanoparticles, novel properties are obtained, which enable design of nanoprobes for these two complementary imaging techniques. Decoration of ZnO nanoparticles with Gd-acetate enhances both the fluorescence emission and the MR signal, compared to earlier investigations of plain ZnO and Gd alloyed ZnO nanoparticles. In this study, Gd decorated ZnO nanoparticles are synthesized and investigates as a function of Gd/Zn relative ratio, ranging from 1- 0.07. The full set of nanoparticle variations was characterized by means of PEEM, XPS, TEM, Fluorescence spectroscopy and MR, to obtain chemical composition, size, crystallinity, quantum yield and relaxivity values. The results clearly show that presence of Gd acetate surface states induces increased fluorescence emission and MRI signal enhancement.

NST-1-Or-1
Local Probing of Topological Superconductivity in In-doped SnTe

T10 Nanoscience and Technology

#NST-1-Or-1

H. Baek [1], J. Ha [2], N. Levy [2], T. Zhang [2], D. Zhang [2], F. Sharifi [3], J.A. Stroscio [3], Y. Kuk [4], S. Sasaki [5], A.A. Taskin [5], K. Segawa [5], Y. Ando [5], L. Fu [6].

[1]Center for Nanoscale Science and Technology, NIST / Department of Physics and Astronomy, SNU - Gaithersburg (United states), [2]Center for Nanoscale Science and Technology, NIST / Maryland Nanocenter, UMD - Gaithersburg (United states), [3]Center for Nanoscale Science and Technology, NIST - Gaithersburg (United states), [4]Department of Physics and Astronomy, SNU - Seoul (Korea, republic of), [5]Institute of Scientific and Industrial Research, Osaka University - Osaka (Japan), [6]Department of Physics, Massachusetts Institute of Technology - Cambridge (United states).

The discovery of topological insulators has inspired research on a new class of topological materials. Topological crystalline insulators (TCIs) have recently been introduced as new states of quantum matter, with gapless metallic surface states protected by mirror symmetry of the crystal lattice [1]. Tin telluride (SnTe), with a rocksalt structure having four equivalent points in the Brillouin zone, is predicted to be a TCI [2,3]. When indium (In) is doped on the Sn site of SnTe, superconductivity is found with a higher critical temperature and lower carrier concentration relative to pristine SnTe [4].

In this work, we use ultra low temperature scanning tunneling microscopy to investigate the superconducting properties of indium-doped tin telluride ($Sn_{1-x}In_xTe$). In a sample with a critical temperature of ~ 1.6 K, the tunneling spectra show a superconducting gap of 0.2 meV, which is continuous throughout the surface of the cleaved crystal. The superconducting gap is completely suppressed above a critical magnetic field of B=0.50 T, and dI/dV conductance maps reveal a vortex lattice in perpendicular applied magnetic fields. We will discuss the dependence of In concentration on topological superconductivity in this material in relation to previous experiments and predictions [5].

[1] L. Fu, Phys. Rev. Lett. 106, 106802 (2011).
[2] T. H. Hsieh, H. Lin, J. Liu, W. Duan, A. Bansil, and L. Fu, Nature Communications 3, 982 (2012).
[3] Y. Tanaka, Z. Ren, T. Sato, K. Nakayama, S. Souma, T. Takahashi, K. Segawa, and Y. Ando, Nature Physics (2012).
[4] A. S. Erickson, J.-H. Chu, M. F. Toney, T. H. Geballe, and I. R. Fisher, Phys. Rev. B 79, 024520 (2009).
[5] S. Sasaki, Z. Ren, A. A. Taskin, K. Segawa, L. Fu, and Y. Ando, arXiv:1208.0059 (2012).

NST-1-Or-5
Scanning Tunneling Microscopy Study of the Superconducting Pairing Symmetry in CuxBi2Se3

T10 Nanoscience and Technology

#NST-1-Or-5

J. Ha [1], N. Levy [2], T. Zhang [2], F. Sharifi [3], A.A. Talin [3], Y. Kuk [4], J.A. Stroscio [3].

[1]Center for Nanoscale Science and Technology, NIST / Maryland Nanocenter, UMD / Dept. of Physics and Astronomy, SNU - Gaithersburg (United states), [2]Center for Nanoscale Science and Technology, NIST / Maryland Nanocenter, UMD - Gaithersburg (United states), [3]Center for Nanoscale Science and Technology, NIST - Gaithersburg (United states), [4]Dept. of Physics and Astronomy, SNU - Seoul (Korea, republic of).

The discovery of topological insulators has triggered the search for new topological states of matter. A topological superconductor is one such state, characterized by the existence of an unconventional superconducting pairing in the bulk, and gapless Andreev bound states (Majorana fermions) on the surface. Recently, Cu intercalated Bi_2Se_3 ($Cu_xBi_2Se_3$) was found to be superconducting with a $T_C \approx 3.8$ K [1], and is considered a prime candidate for topological superconductivity due to its band structure symmetry properties and strong spin-orbit coupling in this material. Angle resolved photoemission spectroscopy has revealed the preservation of the topological surface states at the Fermi level after Cu intercalation, while recent point contact measurement observed zero-bias conductance peaks, suggesting these as evidence of surface Andreev bound states [2, 3].

In this work, we use an ultra-low temperature scanning tunneling microscope [4] to investigate the superconducting properties of a cleaved $Cu_{0.2}Bi_2Se_3$ bulk crystal. The crystal was synthesized by electrochemical intercalation of Cu atoms into a previously synthesized Bi_2Se_3 bulk crystal. Resistance versus temperature measurements of the bulk crystal show a superconducting transition at 3.65 K, consistent with previous reports. A superconducting gap is observed in scanning tunneling spectroscopy (STS) measurements. The tunneling spectrum shows that the density of states at the Fermi level is fully gapped without any in-gap states. Fitting the spectrum to BCS theory yields a superconducting gap of Δ=0.4 meV. When a

magnetic field is applied, the tunnel spectrum shows a complete suppression of the superconducting gap at a critical field of ≈1.65 T. In addition, spatially resolved measurements of the superconducting gap under an applied magnetic field revealed no bound states in the vortex cores. The spectrum is well described by the BCS theory with a momentum independent order parameter, which suggests that $Cu_{0.2}Bi_2Se_3$ is a s-wave superconductor and not a topological superconductor, contrary to previous expectations and measurements. We will discuss these observations and current work examining the Cu concentration dependence in the context of recent theories of topological superconductors.

[1] Y. S. Hor *et al.*, Phys. Rev. Lett. 104, 057001 (2010)
[2] L. A. Wray *et al.*, Nat. Phys. 6, 855–859 (2010)
[3] S. Sasaki *et al.*, Phys. Rev. Lett. 107, 217001 (2011)
[4] Y. J. Song *et al.*, Rev. Sci. Instrum. 81, 121101 (2010)

NST-8-Or-7
Enantioselective Separation on Chiral Au Nanoparticles Measured by Optical Rotation

T10 Nanoscience and Technology

#NST-8-Or-7

N. Shukla, N. Ondeck, N. Khosla, A. Gellman.

Carnegie Mellon University - Pittsburgh (United states).

The surfaces of chemically synthesized Au nanoparticles have been modified with D- or L-cysteine to render them chiral and enantioselective for adsorption of chiral molecules. Their enantioselective interaction with chiral compounds has been probed by optical rotation measurements when exposed to racemic propylene oxide. The ability of optical rotation to detect enantiospecific adsorption arises from the fact that the specific rotation of polarized light by R- and S-propylene oxide is enhanced by interaction Au nanoparticles. This effect is related to previous observations of enhanced circular dichroism by Au nanoparticles modified by chiral adsorbates. More importantly, chiral Au nanoparticles modified with either D- or L-cysteine selectively adsorb one enantiomer of propylene oxide from a solution of racemic propylene oxide, thus leaving an enantiomeric excess in the solution phase. Au nanoparticles modified with L-cysteine (D-cysteine) selectively adsorb the R-propylene oxide (S-propylene oxide). A simple model has been developed that allows extraction of the enantiospecific equilibrium constants for R- and S-PO adsorption on the chiral Au nanoparticles.

The figure illustrates the reversible equilibrium adsorption of R- and S-PO on Au nanoparticles modified with L- or D-cysteine. The equilibrium constants are enantiospecific.

NST-13-Or-4
Localized light emission and internal electric field screening in GaN Quantum Discs within AlN barriers in Nanowires

T10 Nanoscience and Technology

#NST-13-Or-4

L. Zagonel [1], G. Vitiello [1], L. Tizei [2], M. Tchernycheva [3], L. Rigutti [3], G. Jacopin [3], R. Songmuang [4], M. Kociak [2].

[1]Brazilian Nanotechnology National Laboratory, CNPEM, 13083-970 - Campinas (Brazil), [2]Laboratoire de Physique des Solides, Univ. Paris-Sud XI, 91405 - Orsay (France), [3]Institut d'Electronique Fondamentale, Univ. Paris Sud 11, 91405 - Orsay (France), [4]group «Nanophysique et Semiconducteurs», Institut Néel, 38042 - Grenoble (France).

The presence of internal electric fields in quantum confining structures, like quantum wells and discs (QDiscs), has a major effect on their optical properties.[1] Indeed, upon excitation, additional carriers, in out of equilibrium conditions, will partially screen the electric field within the QDisc. This causes a reduction of the quantum confined Stark effect (QCSE) and shifts energy levels towards higher energies, depending on the carrier concentration.[2] Cathodoluminescence (CL) in a Scanning Transmission Electron Microscope (STEM) allows the deployment of very local excitation probes and the assessment of single QDiscs.[3,4] Here we show a direct observation of very local emission of light from single GaN QDiscs formed between AlN barriers in the growth axis of GaN nanowires. Indeed, due to the height of AlN barrier, the diffusion length of carriers is as short as about 5 nm in this system.[4] Moreover, we show that the internal field can be screened by CL-generated charge carriers inside these QDiscs. CL spectral imaging with nanometre resolution tracks the emission of QDiscs as function of the electron probe position, allowing the creation of different concentrations of carriers in QDiscs. It is then possible to study energy shifts in individual QDiscs by observing different emission rates.

References:
[1] G. Jacopin et al. Applied Physics Express 5 (2012) 014101.
[2] A. Chernikov et a. Phys. Rev. B 87, 035309 (2013).
[3] L. F. Zagonel et al. Nano Lett. 11 (2011) p. 568.
[4] L. F. Zagonel et al. Nanotechnology 23 (2012) 455205.

Figure: (a) HAADF-STEM image of the NW, GaN QDiscs are shown in light gray. (b) On the left: CL map (wavelength from 350 to 450 nm); on the right: the same map with regions of similar luminescence intensity indicated by colors (yellow, orange and red indicate respectively low, middle and high emission rates). (c) Spectra representing different regions in (b) with high, middle and low emission rates. For this QDisc in particular, with a thickness of about 4.8 nm, an energy shift of 0.1 eV is observed.

NST/SS-P1-14
Enabling the study of nanoscale Graphene physics using nanoconfined, large momentum IR light

T10 Nanoscience and Technology

#NST/SS-P1-14

G. Andreev, S. Minne.

Bruker Nano Surfaces - Santa Barbara (United states).

Mid-infrared light confined to nanoscale volumes, as done in the technique of IR-sSNOM, is a powerful and versatile probe of Graphene physics. For instance, recent IR-sSNOM experiments show that one can excite, image, and spectrally characterize Dirac plasmons in Graphene with nanoscale sensitivity[1,2]. Due to the uncertainty principle: $\Delta x \, \Delta k \geq 0.5$, conventional IR microscopy lacks both the spatial momentum and spatial resolution necessary to launch and simultaneously image such surface waves. In the IR-sSNOM technique, nanoconfinement of IR light between a sharp metallic tip (<10nm radius) and the sample surface can reduce Δx to <10nm and consequently increase Δk by as much as 3 orders of magnitude. The IR frequency of the excitation, however, remains unchanged. Beyond the recently demonstrated plasmonic applications, the potential for using IR light with such a large spatial momentum is not yet fully recognized by the Graphene community. We experimentally demonstrate some additional applications that also greatly benefit from the much larger IR momentum. For instance we show a greatly enhanced optical sensitivity to material thickness which enables counting the number of Graphene layers on both suspended and supported regions. We also demonstrate the ability to spectrally determine the carrier density and scattering rate with < 10 x 10 x 1nm spatial resolution. The results of both experiments are confirmed using other techniques such as confocal Raman spectroscopy (layer counting) and Scanning Capacitance Microscopy (conductivity mapping). With these experiments, we hope to raise awareness to previously unattainable characterization capabilities enabled by the use of nanoconfined IR light.

1. Greg Andreev, Z Fei, W Bao, Z Zhao, CN Lau, LM Zhang, M Fogler, G Dominguez, M Thiemens, F Keilmann, D Basov "Extraordinary sensitivity of

nanoscale infrared spectroscopy demonstrated on Graphene and thin SiO2", Bulletin of the American Physical Society, (Oral Presentation on 3/22/2011)

2. Z Fei, AS Rodin, GO Andreev, W Bao, AS McLeod, M Wagner, LM Zhang, Z Zhao, G Dominguez, M Thiemens, MM Fogler, AH Castro- Neto, CN Lau, F Keilmann, and DN Basov. "Gate-tuning of graphene plasmons revealed by infrared nano-imaging". Nature 487, 82-85 (2012)

NST-P3-13
MicroRNA Detection with Double-helix Bio-Barcode Assay

T10 Nanoscience and Technology

#NST-P3-13

J. Park, H. Lee, J.M. Nam.

1 - Seoul (Korea, republic of).

MicroRNAs (miRNAs) are short non-coding RNAs, consisting of very few nucleotides, average of 22. miRNAs bind to target messenger RNA (mRNA), resulting in translational repression or target degradation. Thus, they can act as gene regulators. Most miRNAs have been found to related with various types of diseases, especially cancer. The expression level of miRNAs could be very different from RNA to RNA and disease to disease, and miRNA can be a biomarker for cancer for this reason. Although northern blot, microarray, and qRT-PCR are considered as the standard methods for detecting miRNAs, these protocols require extrinsic labels, complicated procedure and expensive reagents, and show difficulties in probe or primer design.

For theses reasons, we developed double strand (ds) bio-barcode-based miRNA detection method with gel electrophoresis. We demonstrate that this method allows to detect low abundant miRNAs with high sensitivity and selectivity. Furthermore, multiplexed miRNA detection capability is also shown with this approach. This finding could offer a straightforward and inexpensive way of miRNA detection in disease diagnosis on a conventional gel platform.

BI/NST-1-Or-5
Molecular-scale visualization of biomolecules and their biochemical functions by frequency modulation atomic force microscopy

T10 Nanoscience and Technology

#BI/NST-1-Or-5

H. Yamada, I. Shinichiro, U. Kenichi, S. Kazuhiro, K. Kei.

Kyoto University - Kyoto (Japan).

Significant progress has been made in frequency modulation atomic force microscopy (FM-AFM) in liquids over the past several years, which allows us to directly investigate "*in vivo*" molecular-scale biological processes [1-3]. In fact this development has opened the way to high spatial resolution analysis of biomolecules such as membrane proteins and DNA molecules in liquids [4]. In this study, submolecular-resolution imaging of biomolecules has been conducted for the molecular-scale analysis of various biochemical functions. In addition, three-dimensional (3D) hydration structures on the biomolecules have been visualized by 3D force mapping method based on FM-AFM for exploring the roles of water molecules in the biological functions. Furthermore, the molecular-scale distributions of surface charge density on molecular assemblies at solid-liquid interfaces were successfully measured by fitting the force mapping data to a modified DLVO theory. We recently succeeded in FM-AFM imaging of sub-molecular structures of a monoclonal immunoglobulin G (IgG) antibody molecule such as protein domain structures (Ig domains). We newly revealed that the IgG antibodies spontaneously assembled into hexamers and successively formed into a two-dimensional (2D) crystal in an electrolyte solution, as shown in Fig. 1(a). Figure 1(b) shows an FM-AFM image of the 2D antibody crystals interacted with antigenic serum albumin molecules. Although the image shows the surface covered with many irregular structures, we can still see regular crystal pattern in some areas below the irregular adsorbents, directly indicating the specific binding of the antigenic molecules to the antibody crystal.

1. T. Fukuma, K. Kobayashi, K. Matsushige and H. Yamada, Appl. Phys Lett., 2005, 87, 034101.
2. S. Rode, N. Oyabu, K. Kobayashi, H. Yamada and A. Kuhnle, Langmuir, 2009, 25, 2850.
3. K. Kimura, S. Ido, N. Oyabu, K. Kobayashi, Y. Hirata, T. Imai, H. Yamada, J. Chem. Phys., 2010, 132, 194705.
4. S. Ido, K. Kimura, N. Oyabu, K. Kobayashi, M. Tsukada, K. Matsushige, H. Yamada, to be published in ACS Nano, 2013.

Figure 1: FM-AFM images of a 2D crystal of IgG monoclonal antibody (in 50 mM $MgCl_2$) before (a) and after (b-left) the additon of the antigenic selum albumin solution. A crystal regular pattern (surrounded by pink circles) can be seen in the contrast enhanced image (b-right).

FMMM/NST-1-Or-2
Local surface potential measurements of organic field-effect transistors having a submicron crystalline grain channel by Kelvin-probe force microscopy

T10 Nanoscience and Technology

#FMMM/NST-1-Or-2

T. Kimura [1], K. Kobayashi [2], H. Yamada [1].

[1]Department of Electronic Science and Engineering, Kyoto University - Kyoto (Japan), [2]Office of Society-Academia Collaboration for Innovation, Kyoto University - Kyoto (Japan).

The electric characteristics of organic field-effect transistors (OFETs) are governed by not only electrical properties of organic molecules but also those of grain boundaries and organic/metal interfaces. It is difficult to investigate these local effects only by macroscopic electrical measurements. Frequency modulation Kelvin-probe force microscopy (FM-KFM) is a useful technique for the elucidation of these local properties in OFETs, which provides simultaneous imaging of sample topography and surface potential on a nanometer scale without contact damage [1]. In this study, an OFET having submicron-scale electrodes and an alpha-sexithiophene (α-6T) crystalline grain as channel was investigated by FM-KFM in order to reveal the local electronic properties in OFETs.

We first fabricated 10-nm-thick Pt electrodes on a heavily doped n-type Si substrate with a surface oxide layer. α-6T molecules were deposited on it, such that two electrodes were connected with a high-crystalline film (Fig. 1). We applied a drain (V_D) and a gate bias voltage (V_G) to the lower electrode and Si substrate, while upper electrode is grounded as source. Then we performed FM-KFM measurements of this OFET during operation. At V_G = 0 V, we found a large voltage drop at the edge of drain electrode, while potential was linearly changed in grain, which implies pinch-off at reverse-biased drain electrode. On the other hand, no voltage slope in grain was found at V_G = –6 V and source electrode turned to be the main voltage drop site. We measured current-to-voltage characteristics and also found a current increase from around V_G = −6 V. These results suggest that its FET characteristics were limited by

injection barrier at source electrode. We will also discuss the results of the OFET in which the source and the drain electrodes were interchanged.

[1] Y. Miyato, et al.: *Jpn. J. Appl. Phys.* **44** (2005) 1633.

Fig. 1: 3-dimensional topographic image and configuration of α-6T crystalline OFET.
Fig. 2: Surface potential images of α-6T OFET at (a) V_G = 0 V and (b) V_G = –6 V.

SS/NST-1-Or-3
Cantilever effects on the accuracy of surface potential measurements in Kelvin probe force microscopy

T10 Nanoscience and Technology

#SS/NST-1-Or-3

F. Krok [1], K. Szot [2], K. Sajewicz [1], P. Piatkowski [1], J. Konior [1].

[1]Jagiellonian University - Krakow (Poland), [2]Forschungszentrum Julich - Julich (Germany).

We report on studies concerning contribution of the cantilever on the accuracy of surface potential imaging of heterogeneous surfaces in Kelvin probe force microscopy, working in frequency modulation mode (FM-KPFM), performed in ultrahigh vacuum. The system under investigation consisted of a set of electrically isolated Pt nanowires (of 100 nm in width) lithographically deposited on SiO2/Si substrate. The metallic nanowires were externally biased, with respect to the Si substrate, with dc voltage (Vext.dc). Then, with the standard FM-KPFM imaging of the Pt/SiO2/Si system, the spatial distribution of the contact potential difference (VCPD) signal as a function of the dc voltage applied to the Pt nanowires, was measured. A CPD-gradient i.e. (dVCPD/dVext.dc) measured at specific surface location allowed to evaluate the effect of parasitic capacitance between the cantilever and the sample on the accuracy of surface potential imaging. For this case, the experimental findings are compared with the predictions of theoretical calculations based on a realistic model for the cantilever-sample geometry.

NST-P1-11
Conductive PVDF-HFP nanofibers with embedded TTF-TCNQ charge transfer complex

T10 Nanoscience and Technology

#NST-P1-11

R. Khalfin.

Technion - Haifa (Israel).

Conductive PVDF-HFP nanofibers with embedded TTF-TCNQ charge transfer complex

R. Khalfin,[b] R. Gal-Oz, [a] Y. Cohen,[b] and E. Zussman[a],
Departments of Mechanical Engineering,[a] and Chemical Engineering,[b] Technion, Israel

A promising organic conductive system is the Tetrathiafulvalene-Tetracyanoquinodimethane charge-transfer complex (TTF-TCNQ CTC). In this work a conductive organic nanofibers were produced by manufacturing core-shell nanofibers made of poly(vinylidene hexafluoropropene) (PVDF-HFP) with embedded TTF and TCNQ in the shell and in the core respectively, using co-electrospinning process [1] to produce conductive CTC crystals. The fibers diameter was found to be between 100 to 500 nm. X-ray analysis showed strong equatorial reflections (110,200) of oriented copolymer PVDF-HFP crystals (β-form) with copolymer chains oriented along the fiber axis, along with unreacted TCNQ and TTF crystals on surface, and reflection of the CTC (001) indicating that the CTC molecular planes (ab plane of the monoclinic form) are aligned parallel to the nanofiber axis (Fig. 1, 2) [2-5]. The electrospun nanofibers were collected to form a fiber mat which was measured as a working electrode in a three-electrode-cell system, to give differential conductance of 5.23 μ℧.

[1] Z. Sun, E. Zussman, A.L. Yarin, J.H. Wendorff, A. Greiner, Advanced Materials. 2003,15,1929-1936.
[2] Ferraris, J.; Cowan, D. O.; Walatka, V.; Perlstein, J. H., Electron-Transfer in a new highly conducting donor-acceptor complex. Journal of the American Chemical Society 1973, 95, 948-949.
[3] 00-033-1889 card of International centre for Diffracton Data.
[4] Batsanov, A.S., Tetrathiafulvalene revisited. Acta Cryst. 2006, C62, 501-504.
[5] Solovyeva, V.; Huth, M., Defect-induced shift of the Peierls transition in TTF–TCNQ thin films. Synthetic Metals. 2011, 161, 976–983.

Figure 1. SEM image (a) of co-axial electrospun TTF-TCNQ nanofiber free surface showing some crystals of the unreacted reactants (TTF and TCNQ), and (b) TEM image of fiber with CTC crystals.

Figure 2. WAXS pattern of VDF-HFP nanofibers with fillers. Fibers axis placed vertical and parallel to the pattern plane.

NST-13-Or-1
Structural Analysis of Carbon Nanotubes by STM Tip Enhanced Raman Imaging with a few Nanometers Resolution

T10 Nanoscience and Technology

#NST-13-Or-1

C. Chen [1], N. Hayazawa [1], S. Kawata [2].

[1]RIKEN - Wako (Japan), [2]RIKEN; University of Osaka - Suita (Japan).

TERS (tip enhanced Raman spectroscopy) opens a new horizon for nanoscale characterization. Atomic force microscopy (AFM) combined with near field Raman spectroscopy is generally used for hybrid imaging and chemical analysis. However, for higher spatial resolution, we constructed a scanning tunneling microscope (STM) based TERS targeting at Raman spectroscopy of single wall carbon nanotubes (SWNT).

SWNT is selected as our sample for TERS because it exhibits very unique optical properties depending on its clear nanometric morphology/chirality. We simultaneously obtained STM topographic image and TERS spectroscopic images at D-, G- and 2D-bands. Different Raman bands show characteristic distributions with a few nanometers resolution. Local defect is visualized in real space through D band imaging while G band and 2D band provide different structural variations. To the best of our knowledge, our result showed the highest spatial resolution on carbon nanotubes ever that has been obtained by optical spectroscopy.

In summary, TERS is a difficult experiment, which requires sophisticated techniques from both optics and scanning probe microscope. However, now it is possible to make it a more practical research tool for nanoscale chemical analysis. We will show our recent progress and detailed issues in the conference.

NST-7-Or-4
Manufacturing of Cantilever Probes with Sub-100nm Pt-Electrodes Integrated in a Sharp Tip for Scanning Electrochemical Microscopy

T10 Nanoscience and Technology

#NST-7-Or-4

C. Richter [1], P. Weinzierl [1], D. Graf [1], S. Beuer [2], M. Rommel [2].

[1]Nanoworld Services GmbH - Erlangen (Germany), [2]Fraunhofer Institute for Integrated Systems and Device Technology (IISB) - Erlangen (Germany).

Since the introduction of micron-sized ultramicroelectrodes (UMEs) in the early 1980s scanning electrochemical microscopy (SECM) has become a powerful tool for investigating small electrochemically active structures and processes, from characterizing of ion channels in living cells to in situ observation of metal corrosion [1, 2]. Although SECM is a well-known method for years [3], its application is limited by the insufficient availability of sensors which can fulfill the requirements. Commercially available probes for scanning electrochemical microscopy as well as those realized by several scientific groups suffer either from a poor lateral resolution or an inadequate stability under commonly used measurement conditions, i.e. a degradation of the insulating layer can often be observed during probing in liquids. Furthermore the fabrication scheme is generally very complex and, thus, either not applicable for mass production or it is very expensive [4]. Hence we have developed a reliable probe fabrication process suitable for mid-volume production to realize different types of combined atomic force microscopy (AFM) and SECM probes. The probes combine the potential of outstanding lateral resolution and stable ion sensitivity by using an insulated Platinum nanoelectrode on the tip apex which features an exposed area of less than 1µm² (compare Figure.1). The geometry of support chip, cantilever and tip preserve the dimensions of typical AFM-probes. To characterize the functionality and performance of the developed SECM sensors, we have built up a measurement setup for cyclic and differential pulse voltammetry. Corresponding measurements will be presented and critically discussed.

[1] Peng Sun et al., *"Scanning electrochemical microscopy in the 21th century"*, Phys. Chem. Chem. Phys., 9, 802-823, 2007
[2] Angelika Kueng et al., *"AFM-Tip-integrated Amperometric Microbiosensors: High Resolution Imaging of Membran Transport"*, Angew. Chem. 117, 3485-3488, 2005
[3] Johyoun Kwak and Allen J. Bard, *"Scanning Electrochemical Microscopy: Theory of the Feedback Mode"*, Anal. Chem.. 61, 1221-1227, 1989
[4] A. Avdic et al. *"Fabrication of cone-shaped boron doped diamond and gold nanoelectrodes for AFM-SCM"*, Nanotechnology 22, 145306-145311, 2011

Figure. 1: *SEM picture of the tip apex of a SECM probe. The Pt-nanoelectrode is protruding the Si_3N_4 insulation layer at the very end of the tip.*

NST/SS-2-Or-6
The Quadratic Stark Effect In the Fullerene C60

T10 Nanoscience and Technology

#NST/SS-2-Or-6

A. Tuchin, L. Bityutskaya, E. Bormontov.

Voronezh State University - Voronezh (Russian federation).

Fullerenes and their derivatives are promising for applications in the fields of energetics, materials science, nanotechnology, optoelectronics and molecular electronics, memory devices [1-3]. Hybrid structures based on fullerenes are actively studied due to their high hardness, breakdown voltage, the gain on the field, wide band gap, which allow to create devices that emit in the optical range [1].
The field devices based on fullerene and fullerite are of a particular interest due to the possibility of the field doping, metallic conductivity and, in some cases, superconductivity [3]. Therefore, studies of the effect of strong local electric fields on the electronic structure of fullerenes are relevant and allow to identify ways to manage the basic electrical and optical properties of carbon nanomaterials.
The fullerene C_{60} causes huge interest because of the high stability, the mass production and the high symmetry of the truncated icosahedron I_h. A distinctive feature of the molecule of this symmetry, which is not found in other systems of lower symmetry, is the existence of the electron shells gN and hN with degeneracy 4 and 5 at the ground state of the fullerene. The external electric field leads to the polarization and the orientational deformation of fullerenes. Wehrli et al. in [4] showed the splitting of t_{1u} and h_u levels of neutral C_{60} due to the Stark effect. However, the calculations do not take into account the change of the fullerene C_{60} geometry in an electric field. In this paper the density functional theory was used to investigate the splitting of t_{1u} and h_u levels of the neutral C_{60} depending on the magnitude (E= 0…1.2 V/Å) and the direction (**E**||$\mathbf{C_{2v}}$, **E**||$\mathbf{C_{3v}}$, **E**||$\mathbf{C_{5v}}$) of an applied electric field with the consideration of the orientational deformation of the molecule.
It is shown that the σ-electron system of the molecule is stable in the entire range of fields. Notable changes in the electronic structure occurs at the fields of E>0.01 V/Å, which is accompanied by the splitting of the degenerate levels by the quadratic Stark effect. The nature of the splitting of the lowest unoccupied (t_{1u}) orbitals is almost independent of the field direction. The result consists with the calculations conducted by Wehrli [4]. The splitting of the highest occupied molecular orbital (h_u) strongly depends on the direction of the field. At the field of E=1.2 V/Å and **E**||$\mathbf{C_{2v}}$ levels are

shifted up relatively to the ground state by 0.018, 0.065, 0.138, 0.169 and 0.200 eV; at **E||C_{3v}** hu is splits into three levels shifted upward by 0.035, 0.12 and 0.19 eV; for **E||C_{5v}** two closely spaced energy levels are shifted up by 0.142 and 0.150 eV, the stabilization of one of the split levels on the value of 0.022 eV is unexpected. Destabilization of h_u- split levels and a decrease of t_{1u}- split levels lead to the quadratic reduction in the energy gap between the lowest unoccupied (LUMO) and the highest occupied (HOMO) molecular orbitals. The Modulation $E_{LUMO-HOMO}$ by the electric field can be widely used in molecular opto-and nanoelectronics.

1. C.-P. Huang, C.-C. Su, W.C. Su et.al Appl.Phys.Lett. Vol. 97, No 6 (2010) 061908(3).
2. C. Li, Y. Chen, Y. Wang et.al J. of Mat. Chem. Vol. 17 (2007) 2405-2411.
3. L. Forro and L. Mihaly Rep. Prog. Phys. Vol.64 (2001) 649-699.
4. S. Wehrli, E. Koch and M. Sigrist Phys. Rev B. Vol. 68, No 11 (2003) 115412(14).

NST-P2-25
Mechanochemical treatment of layer silicates: preparation of nanostructured materials with enhanced surface properties and reactivity

T10 Nanoscience and Technology

#NST-P2-25

P. Sanchez-Soto [1], M.A. Avilés [1], A. Ruiz-Conde [1], F.J. Gotor [1], E. Garzón [2], J. Pascual [3].

[1]CSIC, Instituto de Ciencia de Materiales de Sevilla (CSIC-US), c/Américo Vespucio 49, 41092 - Sevilla (Spain), [2]Universidad de Almería, Departamento de Ingeniería Rural, La Cañada de San Urbano s/n, 04120 - Almería (Spain), [3]Unidad Asociada al CSIC-Inst. de Ciencia de Materiales de Sevilla, Universidad de Málaga, c/Dr. Ortiz Ramos s/n, 29071 - Málaga (Spain).

There is a general interest in the study of the physical and chemical induced effects by grinding in solids. Dry grinding is most intensive than wet grinding when acting on solids. It originates mechanical stress which are quite diverse, producing important changes such as lattice distortions, amorphization, decrease in particle size, formation of nanostructures and an increase in surface area, besides the formation of new phases by mechanical alloying. Thus, the reactivity of ground solids is enhanced and, therefore, it leads to mechanochemical reactions.The effects of dry grinding on layer silicates have been extensively studied. It is associated to their relevant importance in some industrial applications as ceramic raw materials and processing of advanced ceramics. In the present research, samples of kaolinite (1:1 layer silicate), pyrophyllite and talc (2:1), and vermiculite (1:2:1) have been selected. Dry grinding experiments, using planetary or vibratory milling, have been performed. Several techniques were used to follow the evolution of the layer silicates, mainly XRD, surface area (nitrogen adsorption), SEM, TEM, MAS-NMR, DTA, TGA, FTIR, XPS and particle size analysis.

Modifications of surface area, particle size and shape of short and prolonged grinding

on the crystal structure of the layer silicates have been evaluated. The observed changes have been related to a progressive delamination and structural breakdown during grinding, with final formation of a turbostratic-type structure. However, short grinding times resulted in the breakdown and drastic size reduction of relatively thin particles. On the other hand, it should be noted that the rate of size reduction decreased with time and a limit is reached for each sample producing more rounded particles and aggregates, with a decrease of surface area. These changes also affected the pore size distribution and surface modifications as deduced by XPS. TEM and SEM allow to examine the formation of nanometer size ground powders and further particle agglomeration. It can be also observed an increasing in amorphization as a consequence of the loss of long-range order. It is explained considering that grinding produces a loss of periodicity perpendicular to the layer silicate plane, and the dimensions of the crystallites along the c-direction resulted too small to produce coherent X-ray scattering. On the other hand, it has been found an inverse relationship between coherent X-ray domain and microstrains in the ground powders. Modifications in the coordination of Si and Al nuclei have been also deduced from MAS-NMR spectroscopy, demonstrating a short-range order. The present results are interesting to analyze the formation of nanostructured powders when grinding layer silicates and further to examine the reduction of dehydroxylation temperature when the ground samples are heated.
Acknowledgements: Research supported by Project MAT2011-22981, Group TEP204 and, in part, Project HAR2011-25708/HIST.

NST-2-Or-6
Oscillations of the band gap of single-walled carbon nanotubes depending on their length and diameter

T10 Nanoscience and Technology

#NST-2-Or-6

A. Ganin, A. Tuchin, L. Bityutskaya, E. Bormontov.

Voronezh State University - Voronezh (Russian federation).

Carbon nanotubes and fullerenes can be viewed as ideal quantum wires and dots, having unique optical, electrophysical and chemical properties. However their broad application in nanoelectronics is impeded by difficulties of control of their properties which strongly depend on structure of every particular nanoobject. General classification of single-walled carbon nanotubes (SWCNT) is based on their chirality indices n, m. According to a well known rule infinite SWCNTs of large diameter exhibit metallic properties or zero band gap if |n–m| is a multiple of three (the “3k” rule) and are semiconducting otherwise. Decrease of length and diameter of SWCNTs leads to changes in their electronic structure and violation of the above mentioned rule. Transition from nanowires to quantum dots is insufficiently studied and appears to be interesting both fundamentally and practically [1].
We have theoretically investigated band structure of infinite and finite-length SWCNTs and calculated values of their band gap, ionization energy and work function. A cylindrical unit cell was used. We employed the ab initio method of density functional theory for infinite nanotubes (with periodic boundary conditions) and semiempirical methods for finite-length SWCNTs. Relevance of the method and basis was verified in previous calculations for SWCNTs [2] and also by a direct comparison with experimental and theoretical values. [3]
Electronic structure of finite-length SWCNTs with fullerene caps and chirality indices (5, 5) and (0, 9) was investigated in the length range from 0.7 nm (single fullerene molecule – C_{60}) to 6.1 nm (C_{500}). It was found that the additional confinement of electrons along the axis of the tube leads to a non-zero band gap value. Dependency of the band gap versus number of atoms for SWCNT (0, 9) has monotonic character while for SWCNT (5, 5) this dependency has oscillating character with a consistent pattern. Increase of the length of SWCNT (5, 5) from 0.7 nm to 6.1 nm leads to decrease of the band gap from 4.88 to 1.06 eV.
Electronic structure study was also performed for 30 infinite zigzag and armchair

SWCNTs. The dependency of the band gap versus diameter for semiconducting nanotubes has nonmonotonic oscillating character with a global maximum and a period of $3\sqrt{3}d_0/\pi$ (here d_0 is a distance between two carbon atoms in SWCNT). For tubes (0, 4) and (0, 5) we have obtained zero band gap values (while they are semiconducting according to the “3k” rule). We have also confirmed metallic conductance in armchair SWCNTs.
The results obtained shed light on the intrinsic properties of quantum 0D and 1D systems and open new opportunities for application of SWCNTs in cold cathodes, x-ray machines, photovoltaic panels and elements of electric circuits.

1. Wang, B.-C., Wang, H.-W., Lin, I.-C., Lin, Y.-S., Chou, Y.-M. and Chiu, H.-L., “A semiempirical study of carbon nanotubes with finite tubular length and various tubular diameters,” J. Ch. Chem. Soc. 50, 939-945 (2003).
2. Bormontov, E.N., Ganin, A.A. and Bityutskaya, L.A., “Ionization energy oscillations in metallic and semiconducting nanotubes of ultra small diameters,” Proc. SPIE 8700 (2013).
3. Correa, J.D., Silva, A.J.R. and Pacheco, M., “Tight-binding model for carbon nanotubes from ab initio calculations,” J. Phys.: Cond. Matter. 22, 275503 (2010).

NST/SS-8-Or-1
Oxygen Switching of the Epitaxial Graphene-Metal Interaction

T10 Nanoscience and Technology

#NST/SS-8-Or-1

F. Orlando [1], R. Larciprete [2], S. Ulstrup [3], P. Lacovig [4], M. Dalmiglio [4], M. Bianchi [3], F. Mazzola [3], L. Hornekær [3], A. Baraldi [1], P. Hofmann [3], S. Lizzit [4].

[1]Physics Department and CENMAT, University of Trieste, Via Valerio 2, 34127 Trieste, and IOM-CNR Laboratorio TASC, Area Science Park, S.S. 14 Km 163.5, 34149 - Trieste (Italy), [2]CNR-Institute for Complex Systems, Via Fosso del Cavaliere 100, 00133 - Roma (Italy), [3]Department of Physics and Astronomy, Interdisciplinary Nanoscience Center, Aarhus University, 8000 Aarhus C - Aarhus (Denmark), [4]Elettra-Sincrotrone Trieste, S.S. 14 Km 163.5, 34149 - Trieste (Italy).

The mass production of graphene (GR) based electronic devices requires the synthesis of high quality, i.e. with low defects concentration, and large area layers. This can be achieved by different routes, among which the epitaxial growth on transition metals surfaces is one of the most promising ones. Interaction with the substrate, however, is the major drawback of epitaxial GR [1]. In some cases, e.g. GR layers grown on Ru(0001), Rh(111) or Re(0001), this interaction can be sufficiently strong to prevent the typical electronic properties of GR from being established. On the other hand, a very weak interaction, e.g. GR on Pt(111), leads to the formation of GR domains with different orientations. GR/Ir(111) is a representative example of a weakly bound interface: GR-like electronic properties are observed but the moiré pattern due to the lattice incommensurability between GR and its substrate gives rise to replica bands and minigaps near the Fermi level. It appears thus difficult to achieve a weak interaction with high structural quality at the same time. A possible solution is the epitaxial growth of GR on a sufficiently interacting substrate, such as Ir(111), and the subsequent decoupling by the intercalation of metals, silicon, fluorine or hydrogen in order to restore, at least partly, the pristine linear band dispersion.
Oxygen intercalation appears as a viable route to decouple GR/metal interfaces, but so far intercalation has been demonstrated only for incomplete monolayers or islands [2]. Here, using photoemission spectroscopy with synchrotron radiation, we show that

oxygen intercalation is achieved on an extended layer of epitaxial GR on Ir(111), which results in the “lifting” of the GR layer and in its decoupling from the metal substrate [3]. The oxygen adsorption below GR proceeds as on clean Ir(111), giving only a slightly higher oxygen coverage. Upon lifting, the C 1s signal shows a downshift in binding energy, due to the charge transfer from GR to the electronegative oxygen. Moreover, the characteristic spectral signatures of the GR-substrate interaction in the valence band are removed, and the spectrum of strongly hole-doped, quasi free-standing GR with a linear π-band dispersion is observed. Abrupt oxygen deintercalation with a slight carbon etching occurs around T=600 K. After deintercalation, GR restores its interaction with the Ir(111) substrate. Additional intercalation/deintercalation cycles readily occur at lower oxygen pressure and temperature, consistently with an increasingly defective lattice. Our findings demonstrate that oxygen intercalation is an efficient method for fully decoupling an extended layer of GR from a metal substrate. They pave the way for the fundamental research on GR, where extended, ordered layers of free-standing GR are important and, due to the stability of the intercalated system in a wide temperature range, also for the advancement of next-generation GR-based electronics.

[1] E. Voloshina et al., Phys. Chem. Chem. Phys. 14, 13502 (2012).
[2] P. Sutter et al., J. Am . Chem. Soc. 132, 8175 (2010).
[3] R. Larciprete et al., ACS Nano 6, 9551 (2012). Highlighted in Nat. Mater. 12, 3 (2013)

NST-4-Or-4
Obtainment and properties of self-organized gallium antimonide superclusters

T10 Nanoscience and Technology

#NST-4-Or-4

T. Kutcelyk.

Bityutskaya L.A. - Voronezh (Russian federation).

At the present time structures consisting of semiconductor quantum dots (QD) and nanofibers(nanowires), based on GaSb, which may be used in unique optoelectronic devices applications, are intensively studied. [1,2]. When using the planar technology, concentration of QD on the substrates has physical limitations, and because of this fact this the possibilities of these devices are restricted. Nanostructures with a different way of organization can solve these and many other problems. The current work deals with aspects of the research of the morphology and properties of 3D fractal self-oraganized GaSb structures, obtained by non-equilibrium crystallization from the melt.
A conglomerate of spheroidal globules in size of 0,1-0,001 sm formes in the reaction volume. Microscopic methods, allowing to obtain images in macro-, micro- and nanoscales, were used to investigate the morphology of the surface and the volume of the globules.
Cleaved GaSb globules in size of 0,01 sm were examined by AFM microscopy. To receive AFM topographs of the volume of the GaSb globules the following procedures were done: obtaining of the GaSb cleaves in the liqiud nitrogen, scanning in situ the globules cleaves with increasing resolution: 2*2, 1,6*1,6, 0,8*0,8, 0,4*0,4 um., with the fixed position sonde-substrate. On all scales we observed the self-similarity effect — the system of spheroidal fractally associated particles-modules. This type of structures was predicted by Mackay A.L. in the works and is classified as superclusters [3].
The hierarchy of size scales of spheroidal particles in the volume was defined by the processing of AFM topographs by the method of wavelet analysis [4].
Wavelet-analysis of the AFM topographs was made for following sizes of scans: 0,4*0,4, 0,8*0,8, 1,6*1,6 and 2*2 um with the use of the basic function Gauss8, which provides high resolution in determining the limit of the structural unit. Hierarchical scales of the sizes of the particles amounting to the GaSb supercluster were

specified: 20, 60, 130, 260, 330 and 700 nm. The fractal organization of the GaSb supercluster leads not only to unusual morphology, but to appearance of the new physical and optical properties: the hardness of GaSb nanoparticles is higher, than of crystalline material and it is equal to 105 GPa, density is reduced and it depends nonlinearly on the size of the supercluster, in the visible range at room temperature the cathode luminescence is observed.

[1] N.N. Ledentsov, V.M. Ustinov, A.V. Shchukin, P.S. Kop'ev, Zh.I. Alferov and D. Bimberg, Fiz. I Tekh. Poluprovodn., Vol 32, No.4 (1998) 385-410.

[2] Xiuli Zhou, Wei Guo, Alejandro G Perez-Bergquist, Qiangmin Wei, Yanbin Chen, Kai Sun, Lumin Wang, Nanoscale Res. Lett., Vol 6 (2011) 1-6.

[3] V.Ja. Shevchenko, A.L. Mackay, Glass Physics and Chemistry, Vol 34, No.1 (2008) 3-10.

[4] I. Daubechies, CBMS-NSF Regional Conference Series in Applied Mathematics (1992) 350

ESD/ASS-1-Or-9
Investigations of the effect of CdZnS nano-structures incorporation on performance of P3HT based hybrid solar cell

T10 Nanoscience and Technology

#ESD/ASS-1-Or-9

L. Kumar, R. Sethi, M. Mall.

University of allahabad - Allahabad (India).

Two different nanostructures of cadmium zinc sulphide (CdZnS) viz. nanorods and quantum dots have been synthesized and incorporated in poly(3-hexyl thiophene) (P3HT) to investigate the effect on photovoltaic properties of polymeric solar cell. Different techniques were used for the shape and size controlled synthesis of nanostructures and was confirmed by electron microscopic studies. The device performance were elaborated in terms of the parameters like open-circuit voltage (Voc), short-circuit current density (Jsc), fill factor and power conversion efficiency (PCE). We have further demonstrated the morphological strategy to explain the difference attained in the photovoltaic behavior using two different kinds of nanostructures.

Keywords: P3HT, nanostructures, ternary materials, hybrid solar cell

1. K. Kumari, S. Chand, P. Kumar, S. N. Sharma, V. D. Vankar, Vikram Kumar, Appl. Phys. Lett. 92 (2008) 263504.
2. W.U. Huynh, X. Peng, A.P. Alivisatos, Adv. Mater. 11 (1999) 923.
3. R. Sethi, L. Kumar, P.K. Sharma, A. C. Pandey, Nanoscale Res. Lett. 5 (2010) 96.
4. M. Mall, P. Kumar, S. Chand, L. Kumar, Chem. Phys. Lett. 495 (2010) 236.

Energy level diagram for P3HT:CdZnS nanomaterials based device

NST-4-Or-5
Self-assembly of Molecular Conformational Switches Studied by UHV-STM

T10 Nanoscience and Technology

#NST-4-Or-5

A. Nuermaimaiti, C. Bombis, Y. Ning, J. Cramer, L. Ferrighi, K. Svane, B. Hammer, K. Gothelf, F. Besenbacher, T.R. Linderoth.

iNANO, Aarhus University - Aarhus (Denmark).

Molecular conformational flexibility is widely recognized to be important for molecular self-assembly, but relatively few studies have addressed this explicitly and systematically [1, 2]. Here, we focus on the degrees of freedom introduced by molecular conformational flexibility in a molecular system that displays a number of distinct conformational states after adsorption on the surface (Figure 1). For this purpose we have synthesized a class of rod-shape molecules that consist of two or three naphthalene units connected by ethynylene spokes and functionalized by systematically varied terminal moieties, including bulky tert-butyl and hydrogen bonding carboxyl groups [3]. Using high-resolution STM measurements to identify molecular conformations on the surface (Figure 1c), we investigate adsorption structures formed by UHV thermal deposition on a range of metal surfaces. The structures are systematically compared based on careful statistical analysis, focusing on molecular tiling patterns and the distribution of molecular conformations, allowing us to determine how the conformational degrees of freedom of the single molecules are manifested in the global structures and how intermolecular interactions may lead ordering/selection of molecular conformations. By optimizing the molecular functionality, a highly-ordered lamella-type packing is achieved which is suitable for amplification of molecular conformational information. Differences in the distribution of molecular conformations between molecules individually adsorbed and embedded in the ordered network indicate that the growth of ordered structures may involve dynamic conformational adaptation; to directly elucidate the details of such dynamic processes, we performed time-resolved STM investigations. The STM movies reveal that the evolution of the highly-ordered structures involves propagation of conformational order within the network and dynamic conformational adaptation at the domain boundaries.

1. Weigelt, S., et al. Nature Materials, 2006. 5(2): p. 112-117.
2. Matena, M., et al. Chemical Communications, 2009(24): p. 3525-3527.
3. Cramer, J., et al. European Journal of Organic Chemistry, accepted (2013).

Figure1 [3]: (a) A molecule from the family of Oligo(Naphthylene Ethynylene) Rods. (b) The molecule assumes a number of distinct surface states upon adsorption. (c) STM image of the molecule adsorbed on Au (111), Image size: 100Å×100Å.

FMMM/NST-1-Or-6
On-surface ‘click’-reaction: Azide-Alkyne cycloaddition on Cu(111) in Ultrahigh Vacuum

T10 Nanoscience and Technology

#FMMM/NST-1-Or-6

S. Vadapoo [1], F. Bebensee [1], C. Bombis [1], J.R. Cramer [2], K.V. Gothelf [2], T.R. Linderoth [1].

[1]iNANO-Department of Physics and Astronomy, Aarhus University - Aarhus (Denmark), [2]iNANO-Department of Chemistry, Aarhus University - Aarhus (Denmark).

The on-surface synthesis scheme for forming molecular surface nanostructures where the molecular building blocks are joined by strong covalent bonds has received tremendous recent interest[1]. In this context there is a need to identify suitable chemical reactions that will readily proceed under Ultra High Vacuum conditions. “Click”-chemistry, in particular the 1,3-dipolar Huisgen cycloaddition[2] reaction between azides and terminal alkynes (CuAAC reaction) is a widely used reaction in organic chemistry and is potentially very interesting for on-surface synthesis. However, it remains to be shown, if the CuAAC reaction can be performed in an on-surface synthesis scheme with the reacting groups adsorbed directly on a surface and in the absence of a solvent and the solvated Cu(I) ions normally catalyzing the reaction. Here we study on-surface click chemistry on a Cu(111) surface using scanning tunneling microscopy (STM) and X-ray photoelectron spectroscopy (XPS)[3]. The adsorption structures of the reactants 9-ethynylphenanthrene (alkyne) and 4-azidobiphenyl (azide) were characterized by STM. The alkyne adsorbed individually with distinct orientations believed to result from interaction of the alkyne group with the Cu surface. The azide formed a range of small clusters (involving 2-5 molecules) that express distinct motifs. To perform the on-surface click reaction, the reactants were co-deposited onto the Cu(111) surface held at RT. This procedure led to distinct new features showing an excellent structural correspondence to the expected 1,4- triazole reaction product regarding the bent molecular shape and the positions/appearance of the assumed diphenyl and phenanthrenyl groups. The reaction was confirmed by control experiment using an equivalent ex-situ prepared 1,4-triazole. Quantitative evaluation of the C/N atomic

ratio from XPS measurements showed significant degradation of the azide upon adsorption, which was found to be the limiting factor for the reaction. The apparent yield calculated from the number of reactant and product molecules observed on terraces of the Cu(111) surface is ~2%. The observed click-reaction products must, however, stem from the small fraction of intact azide molecules present on the surface and the reaction yield based solely on intact azides was at least 15% suggesting that the cycloaddtion reaction proceeds quite readily on the surface.

1. Franc, G.; Gourdon, A. Phys Chem Chem Phys 2011, 13, 14283.
2. Tornoe, C. W.; Christensen, C.; Meldal, M. J Org Chem 2002, 67, 3057.
3. Fabian Bebensee et al., J Am Chem Soc, Accepted (2013).

Figure 1: Click Reaction Scheme for CUAAC reaction and STM images of the in-situ click reaction product

NST/SS-8-Or-2
Hetero-epitaxial interfaces of graphene and hexagonal boron nitride on Ir(111)

T10 Nanoscience and Technology

#NST/SS-8-Or-2

F. Schulz, R. Drost, S. Hämäläinen, P. Liljeroth.

Department of Applied Physics, Aalto University - Espoo (Finland).

After almost a decade of intensive research, the interest in graphene is unabated. The material's many exceptional properties make it very attractive as a candidate for industrial and technological applications, while fundamental researchers are especially fascinated by the rich electronic structure of graphene [1]. Hexagonal boron nitride (h-BN), a large bandgap insulator structurally similar to graphite, has emerged as a promising support material for graphene, with electron mobilities of graphene samples on h-BN approaching those measured in suspended graphene [2]. Furthermore, the combination of h-BN and graphene within a single layer, both in the form of domain structures as well as the use of B and N as dopants, offer routes to engineer the graphene band structure [3 - 5]. It is clear that the interface of graphene with h-BN in a hetero-epitaxial monolayer will play an important role in its electronic properties. In order to fully understand the possibilities offered by mixing the two materials, a detailed study of the interface region is necessary.

Both graphene and h-BN samples of high quality can be readily grown by chemical vapour deposition (CVD) on transition metal surfaces under ultra-high vacuum conditions. The growth of graphene has been studied in depth especially on the Ir(111) surface, making it a good testing ground for hetero-epitaxial layers of graphene and h-BN. We grow sub-monolayer coverages of hetero-epitaxial layers of graphene and h-BN on the Ir(111) surface in a two-step process. In a first step, islands of graphene are formed from an ethylene precursor by temperature-controlled growth. Following the deposition of graphene, h-BN is formed in a second step by thermal cracking of borazine on the Ir(111) surface. At the interface between graphene and h-BN islands, the two films hybridize. The resulting hetero-epitaxial interfaces are investigated by tuning-fork-based low temperature scanning probe microscopy. Combining point spectroscopy and high-resolution imaging, we are able to determine structural as well as electronic properties of the interfaces.

[1] A. H. Castro Neto *et al.*, Reviews of Modern Physics **81**(1), 109 (2009).
[2] C. R. Dean *et al.*, Nature Nanotechnology **5**(10), 722 (2010).
[3] L. Ci *et al.*, Nature Materials **9**(5), 430 (2010).
[4] M. P. Levendorf *et al.*, Nature **488**(7413), 627 (2012).
[5] W. H. Brito *et al.*, Physical Review B **85**(3), 035404 (2012).

NST-10-Or-11
Near IR emission properties of colloidal Ag2S quantum dots in water for bio applications.

T10 Nanoscience and Technology

#NST-10-Or-11

I. Hocaoglu [1], H.F. Yagci Acar [1], D. Asik [1], R. Erdem [2], C. Ozen [2], A. Sennaroglu [1], M.N. Cizmeciyan [1], A. Kurt [3].

[1]Koc University - Istanbul (Turkey), [2]Middle East Technical University - Ankara (Turkey), [3]Teknofil. Inc. - Istanbul (Turkey).

Near infrared emiting Quantum dots has gained great interest recently for biotechnology and energy applications[1, 2]. Bulk Ag2S with band gap of 0.9 eV is a best candidate for Near IR emission blend as well as has a great potential for both applications. However, Ag2S QDs are usually synthesized by organic preparation methods. Hence, They are hydrophobic in nature which is not suitable for bio-applications[3]. Those quantum dots are emitting in the range of 700-1100 nm wavelength with the very low quantum yields up to 2%[4]. There are few studies in the literature on aqueous preparation of Ag2S QDs and these are quite complicated[5]. We have synthesized Ag2S NIRQDs in a very simple one step aqueous synthesis with thiolated capping agents. Particles showed near band-edge emission (Figure 1). Those Ag2S NIRQDs are higly luminescent emitting in the range of 800- 900 nm with quantum yield between 7-39%. Thiolate coated Ag2S NIRQDs are cytocompatible. Ag2S-NIR QDs showed almost no toxicity in NIH3T3 and HeLa cell lines. Cellular uptake and intercellular localization of Ag2S-NIRQDs study by a confocal laser scanning microscopy was reported (Figure 2). Besides, The surface of these can be easily functionalized. Hybrid nanoparticles are prepared from these QDs and SPIONs. These particles have both luminescent and magnetic properties, demonstrating a great potential for in vivo bio-applications.

1 Azzazy et al., Clinical Biochemistry, 2007, 40, 917-927.
2. Guchhait, et al., Solar Energy Materials and Solar Cells, 2011, 95, 651-656.
3. Du et al., Journal of the American Chemical Society, 2010, 132, 1470-1471.

4. Jiang et al., Chemistry of Materials, 2011, 24, 3-5.
5. Castañón et al., Materials Letters, 2005, 59, 529-534.

Figure 1: Absorbance and PL emission Spectraof Ag2S QD
Figure 2: Cellular uptake and localization of Ag2S QDs by NIH/3T3 mouse fibroblast cells (200 µg/mL QD, 24 h incubation). (A) Fluorescence, (B) Transmission and (C) Overlay channels of confocal micrograph. The scale bar represents 20 µm.

NST/SS-8-Or-3
Nucleation control of self-organized vertical nano-graphenes using inductively coupled plasma enhanced chemical vapor deposition

T10 Nanoscience and Technology

#NST/SS-8-Or-3

M. Hiramatsu [1], R. Tsukada [1], H. Kondo [2], M. Hori [2].

[1]Meijo University - Nagoya (Japan), [2]Nagoya University - Nagoya (Japan).

Carbon nanowalls (CNWs) are self-organized network of vertical standing few-layer graphenes. The large surface area of vertically standing CNWs is useful as templates for the fabrication of other types of nanostructured materials, electrodes for energy storage devices and biosensors. In view of the practical application using CNWs, further investigations should be performed to clarify their growth mechanism as well as to enable their nucleation control. Here, CNWs were grown by inductively coupled plasma enhanced CVD (ICP-CVD). We have investigated the early growth stage of CNWs on the catalyst-free substrate and the Ti-nanoparticle-catalyzed substrate.

Growth experiments were carried out at substrate temperature of 700˚C, RF power of 500 W, total pressure of 20 mTorr, and flow rates of CH_4/Ar of 50/100 sccm, respectively. Figs. 1(a) and (b) show typical SEM images of CNWs grown on SiO_2 by ICP-CVD employing a mixture of CH_4 and Ar for 30 min. These images show that two-dimensional carbon sheets with a relatively smooth surface were grown vertically on the substrate. A TEM image of CNW shown in Fig. 1(c) reveals that graphene layers are clearly observed at the folded edge of the CNW.

There was an induction period of 1–5 min before the onset of vertical nanographene growth and the height of CNWs almost linearly increased with the increase of growth period in the steady-state condition. An interface layer existed between CNWs and the surface of SiO_2 substrates. The existence of interface layer enables us to grow CNWs on a variety of substrates without a catalyst. Furthermore, ion bombardment on the surface would play an important role in nucleation by creating active sites for neutral radical bonding. By controlling the substrate biasing to decrease the ion flux

incident on the substrate, it became possible to suppress the nucleation of CNWs on the SiO_2 substrates. CNW growth was not observed after 10 min on the substrate biased at +50V. In contrast, nanographene nucleation was enhanced by using Ti nanoparticles. In this case, SiO_2 substrate was coated with Ti nanoparticles 1–2 nm in size using the arc plasma deposition. In the case of growth on Ti nanoparticle-coated SiO_2 substrates, planar nanographenes were directly nucleated from the Ti nanoparticles without forming base layer, even when the substrate was positively biased to suppress the nucleation of CNWs. These results indicate the possibility of area-selective growth of CNWs for the device application such as biosensors or electrochemical sensors in micro-total analysis system (μ-TAS).

Fig.1 SEM images of CNWs grown for 30 min: (a) side view and (b) top view. (c) TEM image of CNW. (d) Raman spectrum for CNWs in (a).

BI/NST-1-Or-6
The potential of magnetic nanoparticles for the use in medicine

T10 Nanoscience and Technology

#BI/NST-1-Or-6

N. Ciobanu.

Technical University of Munich - Munich (Germany).

At present, numerous studies are evidencing the tremendous advantages of magnetic nanoparticles to treat a large class of diseases, from the more simple ones up to complicated forms of cancers. For their use in medicine, magnetic nanoparticles have to prove certain physiological parameters besides their optimal magnetic properties. One class of therapies with magnetic nanoparticles is represented by the magnetic drug targeting. It has novel advantages in the local deposition of chemostatics especially in the cases of cancers that are too critical to be treated by the conventional therapies. The magnetic nanoparticles have to be thoroughly characterized prior to any preclinical and clinical phase tests. Transmission electron microscopy is a convenient tool to image magnetic iron oxide nanoparticles and to inspect their size and morphology (Fig. 1). Large nanoparticles of about 100 nm with a magnetic moment of interest for the medicine are revealed to be formed by subunits of 3 nm single crystals grown together. The magnetic single crystals usually of maghemite γ-Fe2O3 and magnetite Fe3O4. are obtained through the polyol method and are adapted at their surfaces for the in vivo conditions. The optimal saturation magnetic values of such magnetic nanoparticles are situated within the range of 40-65 emu/g (Fig. 2). Physiological suspensions of fluorescently labelled magnetic iron oxide nanoparticles charged with mitoxantrone have been imaged by confocal fluorescence microscopy when submitted to external magnetic fields of 0.5 T. The magnetic nanoparticles show immediate magnetic collection and reversible chain formation which eliminates any danger of embolism.

1. Alexiou, C., Arnold, W., Klein, R.J., Parak, F.G., Hulin, P., Bergemann C., Erhardt, W., Wagenpfeil, S., and Lübbe, A.S.: Locoregional cancer treatment with magnetic drug targeting; Cancer Research 60 (2002) pp.6641-6648

Fig.1: Transmission electron microscopy reveals the morphology of 70 nm selected magnetic iron oxide nanoparticles.

Fig. 2: In external fields of 1.5 T, the magnetic iron oxide obtained in polyol show immediate magnetic collection due to their saturation magnetization of 40-65 emu/g.

NST/SS-P1-15
Development of field effet transistors based on carbon nanotube (CNTFET) using standard lithography, dielectrophoretic deposition and tantalum nitride (TaN) electrodes

T10 Nanoscience and Technology

#NST/SS-P1-15

J. Fernandes De Souza [1], C. De C. C. E Silva [2], J. A. Diniz [3], I. Doi [3], P. J. Tatsch [3].

[1]School of Electrical and Computer Engineering, University of Campinas, Center for Semiconductor Components (CCS), University of Campinas, Center for Information Technology Renato Archer (CTI) - Campinas (Brazil), [2]Center for Semiconductor Components (CCS), University of Campinas - Campinas (Brazil), [3]School of Electrical and Computer Engineering, University of Campinas, Center for Semiconductor Components (CCS), University of Campinas - Campinas (Brazil).

Devices based on carbon nanotube (CNT) are promising candidates for future field-effect transistors (CNTFETs), because of its high carrier mobility, low defect structure and intrinsic nanometer scale. However, on-off current ratio is small owing to the absence of bandgap. A number of approaches have been implemented to create a bandgap, but the mobility is degraded consequently [1]. Current saturation is not observed in devices with high contact resistances of source and drain. The total resistance is a series combination of the channel resistance and the contact resistance [2]. Usually, CNTFETs are fabricated using e-beam lithography to choose the best region with better quality of CNTs on the substrate. Thus, the better characteristics of CNTFETs are obtained, but it cannot be a reproducible method [3]. In this study, we fabricated sets of CNTFETs with sub-micron channel length using standard lithography (a reproducible method), dielectrophoretic deposition (DEP) and TaN electrodes. In a single 3 in. wafer, over 100,000 devices were produced (Figures 1A, B, C, D e E). Random CNT networks were deposited on electrodes by DEP [4] (Figure 1F). Our TaN electrodes are refractory metal structures and present electric

resistance with thermal stability. The physical characteristics of TaN electrodes, such as surface roughness and structural crystallization, were extracted using atomic force microscopy and micro-Raman spectroscopy, respectively. These electrodes present very smooth surfaces (3.0 nm rms roughness), high work function values (~4.4 eV) and low resistivity (~180 μΩ.cm), which allow the low channel and contact resistance values, when it compared with resistance values from Pt, Au and W electrodes, which are often used in CNTFETs. Thermal annealing process was carried out to get the low resistance of CNT/TaN contacts. Also, scanning electron microscopy was carried on the fabricated CNTFETs. The electrical characteristics, such as sub-threshold slope (S=64 mV/dec) and ambipolar characteristics, were extracted.

[1] C. Rutherglen, D. Jain and P. Burke , Nature Nanotechnology, Vol.4, DOI: 10.1038/NNANO.2009.355 (2009). [2] A. D. Franklin and Z. Chen, Nature Nanotechnology, DOI: 10.1038/NNANO.2010.220 (2010). [3] R. Thomas Weitz. et al. Nano Lett., Vol. 9, No. 4, DOI: 10.1021/nl802982m (2009). [4] Martial Duchamp. et al. American Chemical Society Nano, Vol. 4, DOI: 10.1021/nn901559q (2010).

Figure1-(A) Photograph of wafer fabricated, (B) Optical microscopy image of the chip, (C) Photograph of two chips, (D) Magnification image of electrodes, (E) Optical microscopy and (F) SEM image showing the CNTs.

BI/ASS/NST-P1-11
Polysorbate 80 alters the internal structure of phytantriol-based nanocarriers

T10 Nanoscience and Technology

#BI/ASS/NST-P1-11

F. Poletto, W. Loh.

Instituto de Química -Universidade Estadual de Campinas - Campinas (Brazil).

The human brain is affected by many diseases, including cancer and infections. Drugs must pass through the blood brain barrier to achieve therapeutic effect. Permeation of drugs throught it can be increased by Polysorbate 80-coated nanocarriers [1]. Phytantriol-based nanocarriers are receiving increased attention due to their tunable nanoscale internal structure and resistance to esterases [2]. Despite their advantages, there is a lack of studies concerning brain targeting.The liquid crystalline phase behavior of phytantriol could be influenced by Polysorbate 80 due to its hydrophobic anchor and relatively low molecular weight. Determining this influence is a key part of the nanoparticle design using phytantriol for brain targeting because the kind of liquid-crystalline phase can affect drug loading and release kinetics [3].

In this work, the effect of Polysorbate 80 was investigated in bulk and dispersed liquid crystals. Bulk samples were prepared by co-melting (70^{o}C) phytantriol and Polysorbate 80 into glass ampules and then adding water. The ampules were sealed and centrifuged up and down at 5000 x g several times. SAXS curves of phytantriol presented Bragg peaks indexed as a gyroid-type (Ia3d space group) inverted cubic phase. This structure was not altered by adding up to 1 % w/w (Polysorbate 80:phytantriol) of stabilizer. With higher Polysorbate contents (10 to 45 % w/w) SAXS curves displayed a single broad correlation peak centered at *q* ranging from 1.72 nm^{-1} (10 %) to 2.19 nm^{-1} (45 %). The disorganized structure observed for those samples indicated penetration of stabilizer and disorder of the liquid crystalline phase. Correlation distances from 2.77 nm (10 %) to 2.21 nm (45 %) were found and can be related to the flutuations of the phytantriol aggregates. The nanocarrier dispersions were prepared by a fragmentation method where preformed liquid crystals were highly sheared (27700 rpm) into an aqueous phase containing Polysorbate 80. Only

Polysorbate 80 content of 45 % w/w provided monomodal (180 nm) and narrow size distribution (PI < 0.2). SAXS curves of dispersions up to 34 % w/w Polysorbate 80 showed Bragg reflections indexed as double diamond-type (Pn3m space group) inverted cubic phase. A broad peak was also observed in all samples indicating the coexistence of a disordered structure. The highest Polysorbate 80 concentration used (45 %) presented only the broad peak. The stabilizer was probably located at the nanocarrier surface and also penetrated its internal phase.

From these results, we conclude that Polysorbate 80 interacts with phytantriol both in bulk and in the internal phase of the dispersion. A higher concentration of Polysorbate 80 in the dispersions provided monomodal distribution and changed the internal phase of the particles from inverted cubic bicontinuous to a disordered phase, which probably can lead to increased drug loading and faster release.

Work suported by FAPESP processo 2012/12340-8. The authors thank LNLS (Brazil) for the access to D11A-SAXS1 facility.

[1] J. Kreuter, D. Shamenkov, V. Petrov, P. Ramge, K. Cychutek, C. Koch-Brandt, R. Alyautdin. J. Drug Target. 2002, 10, 317-325.

[2] T.-H. Nguyen, T. Hanley, C.J.H. Porter, B. J. Boyd. J. Controlled Rel., 2011, 153, 180-186.

[3] W.K. Fong, T. Hanley, B.J. Boyd. J. Controlled Rel., 2009, 135, 218-226.

NST-11-Or-6
Computational study of adsorbate influence on nanoparticles shape and structure

T10 Nanoscience and Technology

#NST-11-Or-6

P. Stishenko, A. Myshlyavtsev.

Omsk State Technical University - Omsk (Russian federation).

There are experimental evidences of metallic nanoparticles (NP) shape dependence on chemical environment [1-3]. One the other hand, shape and structure of NP are crucial for many applications [2,4]. For a set of metals two significantly different structures with similar potential energies are known – face-centered cubic crystal (fcc) and non-crystalline structure with five-fold symmetry (5fs). To these structures the following shapes respectively correspond: fcc produces octahedral, cuboctahedral, sometimes cubic NPs and 5fs structure produces icosahedral and decahedral shapes. It is known, that for small sizes the most stable structure if 5fs, yet for large NPs and bulk metals the most stable is fcc [5]. In different studies for different metals the crossover size was predicted to vary from hundreds to tenths thousands atoms. Taking into account small energy difference of fcc and 5fs structures in the vicinity of crossover size we suppose that chemical environment significantly affects equilibrium shape and structure of the NP. Therefore we have investigated an influence of adsorbed molecules on relative stability of different NP structures and shapes with Monte Carlo simulations.

Simulations were conducted in a grand canonical ensemble, in a lattice gas model framework. The model we employed considered several possible types of adsorption sites on (111) and (100) faces (e.g. a-top, in-hollow, on-bridge). This approach was previously successfully used for simulation of CO adsorption on supported Pt nanoparticles [6]. Adsorption isotherms and dependency graphs of crossover size on chemical potential were plotted using putative equilibrium shapes and structures obtained in simulations. Example of cuboctahedral Pt NP with adsorbed CO molecules is shown in Figure 1.

1. C. Cui, M. Ahmadi, F. Behafarid, L. Gan, M. Neumann, M. Heggen, B.R. Cuenya and P. Strasser, *Faraday Discuss.*, **2013**, DOI: 10.1039/C3FD20159G.
2. K. An and G. A. Somorjai, *Chem. Cat. Chem.*, **2012**, 4, pp. 1512–1524.
3. H. Yoshida, Y. Kuwauchi, J.R. Jinschek, K. Sun, S. Tanaka, M. Kohyama, S.Shimada, M. Haruta, S. Takeda, *Science*, **2012**, 335, no. 6066, pp 317–319.
4. B. R. Cuenya, *Thin Solid Films*, **2010**, 518, no. 12, pp. 3127–3150.
5. S. Ino, *J. Phys. Soc. Jpn.*, **1969**, 27, pp. 941–953.
6. A.V. Myshlyavtsev, P.V. Stishenko, *Appl. Surf. Sci.*, **2010**, 256, no. 17, pp. 5376–5380.

Figure 1: Pt nanoparticle (light spheres) with adsorbed CO molecules (dark spheres)

NST/SS-8-Or-4
Nitrogen doped carbon nanotubes: an oxygen reduction catalysis route

T10 Nanoscience and Technology

#NST/SS-8-Or-4

A. Etcheberry.

Institut Lavoisier de Versailles - Versailles (France).

Nitrogen doped carbon nanotubes: an oxygen reduction catalysis Route
Xi Cheng1, Mathieu Pinault1, Cecile Reynaud1, Martine Mayne1, Henri Perez1, Muriel Bouttemy2, Jackie Vigneron2, and Arnaud Etcheberry2
1_CEA/IRAMIS/SPAM/Laboratoire Francis Perrin, 91191 Gif/Yvette, F- 91191 Gif - sur-Yvette, France.
2_Institut Lavoisier de Versailles, ILV-UVSQ UMR CNRS 8180, 45 av. des Etats-Unis, F-78035 Versailles Cedex, France.

MWCNTs are prepared by aerosol-assisted catalytic chemical vapor deposition. N precursor are introduced as gazeous NH3 with different experimental conditions. The synthetized nitrogen-doped carbon nanotubes present very reproducible XPS responses with typical multi-contributions N1s core levels and well defined C1s peaks whose FWHM are totally correlated to the N concentration. The XPS responses are compare to sample obtained by other grow methods. The multi-component N1s can be described with different N environments. These environments can be modified more or less by thermal annealing in UHV at different temperatures. Using this opportunity we prepared different sets of MWCNT which are studied about their electrocatalytic oxygen reduction performances. We demonstrated electrochemically that ORR mechanism can be completely modified by the actual N/C ratio. This demonstration about correlation between electrochemistry and photoelectron spectroscopy will be discussed about ORR mechanism understanding at a local level.

NST-6-Or-6
Vertically aligned carbon nanotubes: synthesis by CCVD and applications

T10 Nanoscience and Technology

#NST-6-Or-6

C. Reynaud, C. Castro, L. Belkadi, M. Mille, A. Brouzes, M. Pinault, P. Boulanger, D. Porterat, M. Mayne-L'hermite.

CEA, IRAMIS, SPAM, Laboratoire Francis Perrin (CNRS URA 2453) - Gif Sur Yvette (France).

Vertically Aligned Carbon Nanotube carpets (VACNT) are potential candidates for a large range of applications in nanotechnology. Particularly, they can be considered as building blocks for the design of multifunctional composite materials containing anisotropic nanomaterials [1]. Such an interest absolutely requires the reproducible production of various well controlled VACNT carpets in terms of purity, size and surface chemistry, as well as their controlled processing.
In this communication, we will focus on the Aerosol-Assisted Catalytic Chemical Vapour Deposition (AA-CCVD) method based on a simultaneous feeding of the CVD reactor with both the carbon source and the catalyst metallic source and enabling to produce VACNT carpets (see figure a)) [2, 3]. This one step process is versatile, low cost and easily scalable. However, in order to control this process and to adjust it to different technical requirements for applications, it is necessary to understand nanotube formation and the main parameters controlling CNT growth. The effect of different synthesis parameters such as the nature of the reactive atmosphere, the catalyst source concentration, the reactor location, on catalyst and nanotubes formed will be presented, revealing a gas phase homogeneous nucleation phenomenon for the formation of metal-based catalyst nanoparticles [4] and the importance to adjust the nature and composition of the reactive gas phase in order to control the nanotube diameter. These results have strong impact on the extension of this process to several growth configurations, while controlling the carpet height (e.g. nanotube length) and CNT diameter distributions.
In a second part, our approach of scale-up of VACNT carpet homogeneous growth (see figure b)) will be detailed. In particular, we will emphasize on the reactor configurations, either horizontal or vertical depending mainly on the substrate nature and size. Finally, we will present how to get macroscopic 1D composite sample exhibiting controllable thickness. The properties of such nanomaterials are under

evaluation [5], and a large variety of applications such as space or aerospace materials, filtration or separation, are envisaged.

1 B. L. Wardle et al., Adv. Mater., 20, 2707–2714, (2008)
2 M. Mayne et al., Chem. Phys. Lett., 338, 101-107 (9) (2001)
3 M. Pinault et al., Nano Lett. 5, 2394 (2005)
4 C. Castro et al., Carbon, 48, 3807-3816 (2010)
5 C. Villeneuve et al., J Appl. Phys., 112, 084327-1 084327-6 (2012)

VACNT carpets - a) SEM picture showing the vertical alignement of CNT - b) large CNT carpets deposited on a Si substrate

NST-13-Or-2
Optimized Synthesis and Plasmonic Enhancement of Upconversion NaYF4:Yb,Er Phosphors

T10 Nanoscience and Technology

#NST-13-Or-2

C. Summers [1], H. Menkara [1], L. Brun [1], L. Freund [2], C. Schneller [2], D. Lu [3], S. Cho [3], W. Park [3].

[1]Georgia Institute of Technology - Atlanta (United states), [2]Ecole Nationale d'Ingenieurs de Metz - Metz (France), [3]University of Colorado - Boulder (United states).

$NaYF_4:Yb^{3+},Er^{3+}$ nano upconversion phosphors (NUCPs) are required for biological imaging, security, and manufacturing coupled nanosystems. We report two innovations to improve power conversion efficiency: (1) synthesis of highly efficient NUCPs passivated by undoped or Yb-doped layers; (2) use of surface plasmon enhancement.

Platelets (hexagonal section ~20-35 nm, thickness ~ 10 nm) were synthesized, with X-ray measurements confirming β-phase and TEM core size and layer thickness. The photoluminescence (PL) was excited by 980 nm radiation. To investigate surface passivation undoped and Yb (20%) doped shells[1] were grown on Yb:Er (18%:2%) co-doped cores. Figure 1 shows that the green 546 nm PL from undoped- and Yb-shell coated particles normalized to the core PL, increases as a function of shell synthesis time with both showing an enhancement of ~3.5 after 36 and 10 min, respectively. The undoped shell passivation behaves conventionally; however, for shell doping excited Yb ions transfer energy with equal probability to the surface or Yb + Er doped core to activate PL. Thicker shells progressively lose energy to the surface and the PL decreases enabling a measure of the diffusion length.

To investigate surface plasmon enhancement, silver grating were fabricated tuned to the excitation wavelength. A Si_3N_4 spacer layer alleviates quenching of NUCPs deposited layer-by-layer using amphiphilic polymer coatings. The gratings showed well-defined plasmon absorption and after NUCP deposition, strongly enhanced PL peaks at 546 and 662 nm, Fig. 2(a). PL enhancement varied with Si_3N_4 spacer thickness indicating two effects in play: the spacer layer alleviates quenching but shifts the plasmon resonance. A thickness of 38 nm minimized quenching while maximizing field enhancement. Since up-conversion efficiency depends on excitation power, and absolute up-conversion efficiency decreases with

decreasing power: the enhancement increases. As shown in Fig. 2(b), the enhancement monotonically increases with decreasing power to 30x at 9.4 mW. Even at high power, gains of 10x and 6.3x for red and green emission were observed. Theoretical models will be presented.

F. Vetrone et al, Adv. Func. Mat. 19, (2009)

Figure 1 PL ratio vs. shell synthesis time for undoped and Yb-doped shell samples.

Figure 2 (a) PL spectra of NUCP layers deposited on silver grating and flat film, (b) PL intensity as function of excitation power for NUCP layers deposited on silver grating.

NST-P2-29
Synthesis and magnetic study of some nanocomposites

T10 Nanoscience and Technology

#NST-P2-29

K. Amel [1], B. Bouzabata [1], G. Fillion [2].

[1]Université Badji Mokhtar-Annaba - Annaba (Algeria), [2]LNCMI-G, CNRS-UJF - Grenoble (France).

Synthesis and magnetic study of some nanocomposites

A. Kihal [a], B. Bouzabata [a], G. Fillion [b]
[a] Laboratoire de Magnétisme et Spectroscopie des Solides (LM2S), Université Badji Mokhtar-Annaba, BP-12 Annaba, Algérie
[b] LNCMI-G, CNRS-UJF, 25 Rue des Martyrs, BP-166, 38042 Grenoble-Cedex 9, France
E-mail: amel.kihal@gmail.com

Nanocomposites of metal nanoparticles dispersed by oxide nanoparticles display a variety of interesting chemical and physical properties which can be modified by varying the particle size and metal volume fraction. Mechanical alloying (MA) has been considered as a powerful and practical process for synthesis of compounds and nanocomposites using the mechanochemical reactions.
In the present work, the mixtures of α-Fe_2O_3 and (Cr / Si) powders have been milled for various times up to 15 h, in a planetary ball mill (P7) in air atmosphere. The as-milled powders were structurally and magnetically characterized by X-ray diffraction (using the MAUD program based on the Rietveld method) and magnetic measurements in dc magnetic fields up to 10T at room temperature.
The refinement of the X-ray diffraction patterns (α-Fe_2O_3/Cr) shows that the reduction of hematite by chromium is gradual with the formation of nanoparticles of α-Fe. The final phases α-Fe and Cr_2O_3 are formed, with a nanometric grain size ~ 20 nm and 23 nm at 15 h respectively. The saturation magnetization (Ms) of Fe-Cr_2O_3 nanocomposites jumps from 6 Am^2/kg at 1h to 76 Am^2/kg at 15h. This value of Ms is in relationship with the change in the computed fraction of iron nanoparticles. The value of coercive field (Hc) is about 0.02 T.
In the milled mixture of (Fe_2O_3/Si), there is no change up to 5 h of milling. After 15h of milling, α-Fe nanoparticles are formed in an amorphous SiO_2 phase. All phases have

nanometric size (~ 25 nm, 19 nm at 15 h respectively). The calculated lattice parameter of the iron nanoparticles is a_0 = 2.8687 Å. The magnetic measurements of Fe-SiO_2 nanocomposites show that the (Ms) reaches 70.6 Am^2/kg at 15h. The increase of Ms is expected since this parameter depends on the total mass of material embedded into silica matrix. The values of coercive field (Hc) decreases first then increase reaching a stationary value above 10 h of milling time (about 0.03 T at 15 h).
In addition to the grain size effects, the reduction of the particle size toward the size region of single domain and matrix nature can explain the above structural and magnetic variations.

Keywords: α-Fe_2O_3/Cr mixtures, α-Fe_2O_3/Si mixtures, iron nanoparticles, X-Ray diffraction , magnetic properties.

NST/SS-8-Or-5
Preparation and Characterization of Multi-Walled Carbon Nanotubes networks by ink-jet printing

T10 Nanoscience and Technology

#NST/SS-8-Or-5

I. Oueriemi [1], J.P. Raskin [1], F. Choubani [2], V. Dupont [3], I. Huynen [1].

[1]ICTEAM-ELEN, Université catholique de Louvain Place du Levant 3, - Louvain-La-Neuve (Belgium), [2]Higher school of Communications (Sup'Com), Innov'Com Lab - City-Elgazela (Tunisia), [3]Belgium Ceramics Research Center (BCRC), 4, avenue Gouverneur Cornez - Mons (Belgium).

Since their discovery, carbon nanotubes (CNTs) are emerging as novel nanomaterial for large variety of applications, particularly as electronic material owing to their mechanical, thermal and unique electrical properties [1]. In order to understand the transport phenomenon through CNTs networks, electrical characterization is of key importance. One way to progress in the comprehension of CNTs behaviour is by improving the deposition method.
Inkjet printing is considered as a promising technology, which gives the possibility to readily control the pattern geometry, location, film thickness, and uniformity of the films.In this present study, CNT ink was used to print films on coplanar waveguides (CPWs) lying on Glass substrate. Scanning Electron (SEM) of used Multi-Walled CNTs (MWCNTs) solution and individual CNT features were observed by Transmission Electron microscopy (TEM) Microscopy images are shown in Fig. 1. MWCNT presents 8 walls, a length and a diameter of approximately 10 µm and 15 nm, respectively. Afterwards CNT Ink is prepared using the method described in [2] to correspond to physico-chemical characteristics required for performing printing using inkjet equipment Fujifilm-Dimatix DMP 2831. Four layers of MWCNTs solution, shown in Fig. 2, were successively deposited and followed by a 40°C drying. The diameter and spacing between drops are around 50 µm and 25 µm, respectively.
A stable carbon nanotube (CNT)-based ink has been prepared and printed. Consequently their electrical could be investigated with easy and precise control, which is of great interest for developing accurate models that are required to design new and novel devices based on CNTs.

[1] R. Saito, M. Fujita, G. Dresselhaus, and M. S. Dresselhaus, Appl. Phys. Lett. 60, p. 2204,1992.
[2] A. Denneulin, J. Bras, F. Carcone, Ch. Neuman, and A. Blayo, Carbon, vol. 49, pp. 2603-2614, 2011.

Fig. 1: Scanning Electron (SEM) and Transmission Electron (TEM) Microscopy images of deposited MWCNTs solution.

Fig. 2: Picture of final CPW with Inkjet Printed CNTs network.

NST-10-Or-12
Analytical Study and Comparison of Filamet-like Electron Emitter Behavior with Experiment

T10 Nanoscience and Technology

#NST-10-Or-12

S. Price [1], Y. Mikata [2].

[1]GE GRC - Niskayuna, NY (United states), [2]Bechtel - Niskayuna, NY (United states).

Analytical solutions to a simple 1D model of a nano-scale filament-like field emitter show quite high temperatures can be reached during modest current flow. Current of 1 μA and material properties of CNT show non-linear temperature as a function of length along the emitter. Adsorbed gas species are are bound to the surface of the emitter with a range of energies: 1 - 10s kcal/mole. Desorption of gas during current emission contributes a background gas that can be ionized by the emitter current and contribute to ion backbombardment a life-limiting mechanism. Pressure as a function of time, P(t), can be predicted and is compared to RGA measurements. Spare (low density) emitter densities (1 to 10 μm center-to-center spacing) on a substrate yield modest change in pressure; the decay time of the pressure spike depends on pumping, gas species, and geometrical factors. The high effective pumping speed of nearby solid state getters, surface and bulk, and the like, can reduce the effect of this background and limit the damage to the emitter. Analytical solutions will be presented and a calculation will show the effect of the advantageous changes to pump disposition and geometry. These solutions suggest strategies for longer emitter lifetime. Applications include displays, addressable multi-emitter current sources, and x-ray sources.

NST-3-Or-6
Application of individual free-standing nanowires in bistable multipositional nanoelectromechanical switches.

T10 Nanoscience and Technology

#NST-3-Or-6

D. Erts [1], J. Andzane [2], R. Meija [3], J. Prikulis [2], A. Livshits [2], J.D. Holmes [4].

[1]institute director - Riga (Latvia), [2]senior researcher - Riga (Latvia), [3]PhD student - Riga (Latvia), [4]Professor - Riga (Latvia).

Recently various nanowire/nanotube based two terminal nanoelectromechanical (NEM) switches [1-3] has been reported. The operation of these devices is depending on adhesion forces in nanocontacts. Strong elastic and/or electrostatic forces have to be applied to the active element to surpass adhesion force in the nanocontact. High elastic force causes large distance between elastic active element and contact caused in increase of dimensions of NEM device. To apply strong electrostatic field high voltages has to be applied in system. For two terminal devices high applied voltages causes high currents in nanocontacts after jump in contact leading often to degradation of switches [2,3].

Here we present implementation of DC and AC field to reduce force needed for operation switching *off* events. Experiments were carried out *in situ* by using nanomanipulation systems inside SEM. Ge nanowires were used as active element and etched gold tips was used as contact electrodes.

Switching *off* voltages in NEM switches can be reduced when combined AC+DC electric field is applied. Effect is observed when AC frequency the nanowire resonance frequency.

1. Ke, C., Espinosa, H.D., In Situ electron microscopy electromechanical characterization of a bistable NEMS device, *Small,* 2009, Vol. 2, No. 12, pp. 1484-1489

2. Andzane, J., Petkov, N., Livshits, A., Boland, J.J., Holmes, J.D., Erts, D., Two Terminal Nanoelectromechanical Devices Based on Germanium Nanowires. *Nano Lett*., 2009, Nr. 5, pp. 1824–1829.
3. Andzane, J., Prikulis, J., Dvorzek, D., Mihailovic, D., Erts, D, $Mo_6S_3I_6$ nanowire based two-terminal nano-electro-mechanical switch, *Nanotechnology*, 2010, Nr. 21. pp. 6 (125706).

NST-P2-32
Structure and thermal stability of mechanical properties of Al–TiB2 composites alloyed with Mn and Zr

T10 Nanoscience and Technology

#NST-P2-32

E. Kurbatkina, N. Belov.

National University of Science and Technology “MISiS” - Moscow (Russian federation).

Composite materials based on system aluminum - boron have attracted great attention of scientists and researchers nowadays. They can be widely used in nuclear industry because of good combination of properties, such as low specific density, good thermal conductivity as well as the ability to absorb neutron radiation.
Aim of this work was to obtain aluminum matrix composite material (AMCM) based on Al-B-Ti-Cu-Mn-Zr-Sc system and the study of its structure and properties.
The object of research was an experimental alloy Al-2,5B-1,5Ti-1,5Cu-1Mn-0,2Zr-0,2Sc. AMCM was prepared using liquid-phase technology. Thermo-Calc software was used to calculate the phase composition of this alloy at various temperatures. TiB2 particles formed as endogenous phase during holding at 900°C.
AMCM ingots were rolled at 200°C to the thickness of 3 mm and annealed. Metallographic analysis showed that annealing at temperatures of 300-450°C led to the separation of $Al_{20}Cu_2Mn_3$ and Al_3(Zr,Sc) dispersoids. No secondary Al_2Cu precipitates were detected. Such structure is the most favorable for creep resistance as Mn- and Zr, Sc-containing dispersoids have a higher thermal stability than the Al_2Cu precipitates. We measured mechanical properties, thermal conductivity, corrosion resistance, coefficient of thermal expansion. Analysis of the mechanical properties showed a high thermal stability up to 350°C due to the formation of polygonized structure, which resulted from large amount of $Al_{20}Cu_2Mn_3$ and Al_3(Zr,Sc) dispersoids that effectively pinned down dislocations.
Therefore, replacing the lxxx,5xxx, 6xxx series by Al-Cu-Mn-Zr-Sc alloy as the matrix would be of interest.

NST-P2-30
The preparation and investigation of properties of Dy2O3

T10 Nanoscience and Technology

#NST-P2-30

M. Abdusalyamova.

Professor - Dushanbe (Tajikistan).

The preparation and investigation of properties of Dy2O3
M.N.Abdusalyamova , Kh.Kabgov, F. Machmudov,E.Shaimardanov, Ju.M. Yu..M.Shulga*
Institute of Chemistry of Tajik Academy of Science, Ajni Str.299/2,734063 Dushanbe, Tajikistan, amahsuda@mail.ru
• Institute of Problems of Chemical Physics Russian Academy of Science, Academic N.N.Semenov pr.1, 142432 Chernogolovka of Moscow Region, Russia. shulga@icp.ac.ru

Dysprosium nanooxide has been obtained two methods.
I- method Erbium nanooxide preparation method with chlorides: the corresponding metal amount was dissolved in hydrochloric acid and chloride was obtained. Distilled water +NaOH+NaCl was added to obtained chloride. It was heated at pH=3.6-3.8 and evaporated. Hydrate DyCl3 + H2O= Dy2O3+ 3HCl was prepared. This mixture was roasted at 440°C, washed and filtered using Bruchner filter, the sediment was dried. The second sample was roasted at 540°C, the third one at 640°C. Roasting time for all samples was similar- 1hour.
X-ray phase analysis shown that in the process of roasting the reflex intensity is growing corresponding to cubic Dy2O3 structure. Size value of coherent-scattering region calculated using the Sherrer formula for the samples were 80-120nm.
2- method of preparation of Dy2O3 with use organic compounds, which consisted of several steps:
1step: Synthesis of sodium oleinate.
2step: Synthesis of dysprosium chloride.
3step: Synthesis of dysprosium olenate.
4step: Dyr2O3 nanocrystal preparation.
X-ray phase analysis has shown single phase nanooxide have been obtained with 49nm size.
IR, Raman spectras have been investigated. As it results from IR spectra that there

are groups containing C-O bound (adsorption bands 1530 and 1430 cm-1) in the studied samples. Concentration of these groups can be significant – several percents. Roasting in the air reduces concentration of these groups.
Acknowledgements This work was supported by International Science & technology Center(ISTC), #Project T-1882

NST-P1-12
Multiple Carbon Nanotube Junctions for Stochastic Resonance Devices

T10 Nanoscience and Technology

#NST-P1-12

A. Setiadi, T. Nakanishi, M. Akai-Kasaya, A. Saito, Y. Kuwahara.

Department of Precision Science and Technology, Graduate School of Engineering, Osaka University - Suita (Japan).

Stochastic resonance (SR) is a phenomenon where the noise can enhance the transmission of signal which lied below threshold level. The SR phenomenon can be found in sensory organ of living creatures [1]. This phenomenon also can be reproduced in electronic device [2,3]. According to the previous studies, we need multiple junctions, independent noise, and non-linear response to realize the SR device [2-4]. The large numbers of junction drastically improve the SR effect. However the numbers of junctions in previous electronic device were limited by the fabrication method [2]. To solve this problem, we propose the use of single walled carbon nanotube (SWNT) as we can easily build multiple junctions. The SWNT is a one-dimensional nanomaterial and thus has the possibility to be a source of independent noise due to its Tomonaga-Luttinger liquid behavior [5].

We succeeded to fabricate the device which consist multiple junctions of individual SWNTs. The channel length and width are 0.2 μm and 1 μm, respectively. Our device showed good p-type field effect transistor (FET) behavior since we used semiconducting SWNT. In the SWNT-based FET, the current flows through individual SWNT is strongly affected by the gate voltage. The response of each junction to the external electric field might be different each other. Therefore, we utilized this field effect behavior as a noise generator by applying noise signal to the gate electrode. Increment of the noise signal amplitude yielded different quality of signal transmission. We calculated correlation coefficient of the signal transmission as shown in figure 1. We concluded that this result is the effect of SR phenomenon, though the effects of multiple paths have not been defined yet. In the future, we will vary the channel length and width to increase the number of SWNT junction.

[1] D. F. Russell, L. A. Wilkens, and F. Moss, *Nature* **402**, 291 (1999)
[2] S. Kasai, K. Miura, and Y. Shiratori, *Appl. Phys. Lett.* **96**, 194102 (2010)
[3] T. Kanki, Y. Hotta, N. Asakawa, T. Kawai, and H. Tanaka, *Appl. Phys. Lett.* **96**, 242108 (2010)
[4] J. J. Collins, C. C. Chow, and T. T. Imhoff, *Nature* **376**, 236 (1995)
[5] M. Bockrath, D. H. Cobden, J. Lu, A. G. Rinzler, R. E. Smalley, L. Balents, P. L. McEuen, *Nature* **397**, 598 (1999)

Figure 1. Correlation coefficient of input-output signal as a function of noise voltage. Inset: SR device with SWNT multi junctions.

NST-4-Or-6
Simulation of adsorption of cis-carboxyphenyl substituted porphyrins with directional interactions on square lattice

T10 Nanoscience and Technology

#NST-4-Or-6

S. Akimenko, V. Gorbunov, A. Myshlyavtsev.

Omsk State Technical University - Omsk (Russian federation).

Controlled production of self-assembled nanostructures of complex organic molecules on metallic surfaces is now the constantly growing field of researching and attracts great interest. It has promising potential for electronic and electro-optic devices [1]. Controlled assembly also can be used for creating templates for the accommodation of guest molecules [2, 3]. These systems have potential application in molecular recognition, selective catalysis, and molecular storage.
In this work we have investigated the lattice gas model of 5, 10-bis (4-carboxyphenyl)-15, 20-bis (3,5-di-t-butylphenyl) porphyrin (cis-BCaTBPP) adsorption on a square lattice taking into account the directional interactions between adsorbed molecules. We consider that cis-BCaTBPP molecule occupies only one site of two-dimensional square lattice. The model was studied with transfer-matrix and Monte Carlo techniques in grand canonical ensemble.
In the framework of constructed model we calculated adsorption isotherms, internal energy and phase diagram. All structures of self-assembled adlayer appearing in our model are analogous to real ones.

1. H. Saarenpää, E. Sariola-Leikas, A. P. Perros, J. M. Kontio, A. Efimov, H. Hayashi, H. Lipsanen, H. Imahori, H. Lemmetyinen, N. V. Tkachenko, J. Phys. Chem. C, 2012, 116 (3), pp 2336–2343.
2. J. A. Theobald, N. S. Oxtoby, M. A. Phillips, N. R. Champness, P. H. Beton, Nature, 2003, 424, 1029.
3. H. Spillmann, A. Kiebele, M. Stohr, T. A. Jung, D. Bonifazi, F. Cheng, F. Diederich, Adv. Mater., 2006, 18, 275.

NST-P2-27
Biomimetic Au/TiO2 with hierarchical structures from butterfly wings (Peacock butterfly)

T10 Nanoscience and Technology

#NST-P2-27

S. Mihai [1], A. Dinescu [2].

[1]Petroleum - Gas University of Ploiesti - Ploiesti (Romania), [2]National Institute for Research and Development in Microtechnologies - Bucharest (Romania).

In nature, biologic systems shows a wide variety of structures that can be used in nanotechnology. Peacock butterfly wings have been used as templates for the formation of the Au/TiO_2 inorganic structures. The reticular hierachical structure of butterfly have been synthetized by sol-gel technique by subsequent calcination. The morph - Au/TiO_2 possesses an enhanced light absorption property in visible light region owing to its hierarchical structures, which would be favorable for high photocatalytic activity.

1. Biro LP. Mat. Sci. Eng. B 2010 139: 3-11.

2. Zhang W., Zhang D., Fan T., Ding J., Gu J., Guo Q., Ogawa H. Mat. Sci. Eng. C 2009 29:92-96.

3. Chen J., Su H., Song F., Moon WJ., Kim YS., Zhang D., J. Coloid. Interf. Science 2012 370:117-123.

4. Yao F., Yang Q., Yin C., Zhu S., Zhang D., Moon WJ., Kim YS., Mat. Lett. 2012 77:21-24

FMMM/NST-P3-5
Synthesis of nano-CeO2 and degradation of dye in indoor lighting

T10 Nanoscience and Technology

#FMMM/NST-P3-5

R. Li, B. Zhao, M. Gu, C. Li, X. Song.

Key Laboratory of Aerospace Materials and Performance (Ministry of Education), School of Materials Science and Engineering, Beihang University - Beijing (China).

Azo dyes are an abundant class of synthetic, organic compounds which contain one or more azo bonds (-N=N-). Large amounts of these dyes are produced for use in different applications.

However their complex structure makes them difficult to biologically degrade. We sought to degrade acid orange 7 (AO7) using nitrogen-doped (N-doped) and carbon-nitrogen (C-N) co-doped nano-CeO_2. N-doped monocrystalline CeO_2 nanoparticles was synthesized by solvothermal method using triethanolamine as a nitrogen source at 120 ºC for 24 h. C-N co-doped monocrystalline CeO_2 nanoparticles was synthesized by solvothermal method using hexamethylenetetramine as both nitrogen and carbon source at 140 ºC for 24 h. For purposes of comparison, a sample of undoped CeO_2 was synthesized using the dopant of neither triethanolamine nor hexamethylenetetramine. The doped and undoped CeO_2 monocrystals were all less than 10 nm in diameter. Nitrogen and carbon-nitrogen were shown to be incorporated into CeO_2 lattice from the results of both XRD and X-ray photoelectron spectroscopy analyses.

The degradation of AO7 in water was investigated using a domestic 10 W compact fluorescent lamp. The results showed the degradation ratios of AO7 in the presence of nano-CeO_2 in the sequence of: C-N co-doped CeO_2 > N-doped CeO_2 >> undoped CeO_2, corresponding to magnitudes of 98.8%, 97.6%, and 48.2%, respectively.

NST-12-In-1
THE CHIRALITY INDUCED SPIN SELECTIVITY (CISS) EFFECT- FROM SPINTRONICS TO ELECTRON TRANSFER IN BIOLOGY

T10 Nanoscience and Technology

#NST-12-In-1

R. Naaman.

Department of Chemical Physics, Weizmann Institute - Rehovot (Israel).

Spin based properties, applications, and devices are commonly related to magnetic effects and to magnetic materials. Hence, most of the development in spintronics is currently based on inorganic materials. Despite the fact that the magnetoresistance effect has been observed in organic materials, until now spin selectivity of organic based spintronics devices originated from an inorganic ferromagnetic electrode and was not determined by the organic molecules themselves. In several studies, however, it was found that chiral organic molecules can act as spin filter for photoelectrons transmission, in electron transfer, and in electron transport. Results will be presented from several recent experiments and some implications and applications will be discussed.

NST/SS-4-In-1
SELF-ORGANIZED EPITAXIAL NANO-ALLOYS ON METALLIC SURFACES: GROWTH AND NANOMAGNETISM

T10 Nanoscience and Technology

#NST/SS-4-In-1

S. Rousset.

MPQ, CNRS and University of Paris Diderot - Paris (France).

The use of spontaneously nanostructured substrates as templates allows growing a very high density of ordered nanostructures over macroscopic scales [1]. This opened up studies of both individual and collective physical properties by means of usual spatially averaging techniques.
Taking advantage of our former work on magnetic nanostructures [2, 3, 4], we present here results on more complex systems, namely small magnetic nano-alloys epitaxial dots, which are not yet published. We used the Au(111) surface, since the growth and the characterization of ordered nano-alloys on such a template is still a challenging issue, together with their magnetic properties. The CoPt alloy is one of the most studied bimetallic compounds, due to its potential application for magnetic recording. First we investigate the morphology and the chemical composition of CoPt ordered nano-alloys as a function of the alloy stoichiometry and the size of the dots. Then, their magnetic behavior can be understood by hybridization effects between Co and Pt. We will compare nano-alloys islands with bimetallic core-shell structures [5]. Eventually, we will discuss how to predict the elaboration of 3D magnetic nanostructures stable at room temperature and with a very high density at surfaces, which can have important consequences for magnetic storage.

[1] S. Rousset et al., C. R. Physique 6 – 33-46 (2005)
[2] N. Weiss et al., Phys. Rev. Lett. 95, 157204 (2005)
[3] Y. Nahas et al. Phys. Rev. Lett. 103, 067202 (2009)
[4] S. Rohart et al. Phys. Rev Lett.104, 137202 (2010)
[5] P. Campiglio et al., Phys. Rev. B 84, 235443 (2011)

NST/SS-6-In-2
SPIN LEGOS - BOTTOM-UP FABRICATION OF MODEL MAGNETIC SYSTEMS

T10 Nanoscience and Technology

#NST/SS-6-In-2

A.A. Khajetoorians.

Institute of Applied Physics, Hamburg University - Hamburg (Germany).

With the development of sub-Kelvin high-magnetic field STM, two complementary methods, namely spin-polarized scanning tunneling spectroscopy (SP-STS) [1] and inelastic STS (ISTS) [2-3], can address single spins at the atomic scale. While SP-STS reads out the projection of the impurity magnetization, ISTS detects the excitations of this magnetization as a function of an external magnetic field. They are thus the analogs of magnetometry and spin resonance measurements pushed to the single atom limit. We have recently demonstrated that it is possible to reliably combine single atom magnetometry (SAM) with an atom-by-atom bottom-up fabrication to realize complex atomic-scale magnets with tailored properties [4]. As a first such example of this, we demonstrated that it is possible to realize an all-spin based atomic logic gate comprised of coupled Fe atoms on a metallic surface [5]; a demonstration of a fundamental nano-spintronic concept. In this talk, I will address novel developments illustrating advances in the realization of artificially constructed magnetic nanostructures, like complex two-dimensional indirect-exchange based nanomagnets, as well as investigations of the magnetization dynamics [6] of single and coupled spins as probed with spin-resolved STM techniques.

[1] A.A. Khajetoorians, et al. , PRL, 106, 037205 (2011);
[2] A. J. Heinrich, et al. , Science, 306, 466 (2004);
[3] A.A. Khajetoorians, et al. , Nature, 467, 1084 (2010);
[4] A.A. Khajetoorians, et al., Nature Physics, 8, 497 (2012) [5] A.A. Khajetoorians, et al. , Science, 332, 1062 (2011), [6] A.A. Khajetoorians, et al., Science, in press (2012)

NST-10-In-1
ELECTRON BEAM INDUCED DEPOSITION OF NANOSTRUCTURES: A SURFACE SCIENCE PERSPECTIVE

T10 Nanoscience and Technology

#NST-10-In-1

H. Fairbrother [1], S.G. Rosenberg [1], J.D. Wnuk [1], J.D. Wnuk [2], J.M. Gorham [1], M. Barclay [1], C.W. Hagen [3].

[1]Department of Chemistry, Johns Hopkins University - Baltimore (United states), [2]Intel Cooperation - Hillsboro (United states), [3]Delft University of Technology, Faculty of Applied Sciences - Delft (Netherlands).

Electron beam induced deposition (EBID) is a minimally-invasive, lithographic strategy that uses the electron stimulated decomposition of volatile organometallics under low vacuum conditions to fabricate and prototype three-dimensional metallic nanostructures (Figure 1). One of the limitations of FEBIP lies in the often unacceptably high level of organic contamination in the deposits which adversely affects properties and restricts their value (e.g. as catalysts and biosensors). At the heart of EBID are the electron stimulated reactions of the surface bound organometallic precursors which are responsible for deposition and the ultimate chemical composition of the deposit. In this presentation I will describe the current status of EBID and in particular how surface analytical techniques have been used to provide mechanistic and kinetic insights into the influence that ligand architecture, substrate temperature and electron fluence have on the surface reactions and molecular level processes that underpin EBID.

Figure 1: Electron beam induced deposition of metal nanostructures from organometallic precursors.

SS/NST-1-In-1
ADVANCED CHARACTERIZATION OF SURFACES AND NANOSTRUCTURES BY MEANS OF SIMULTANEOUS AFM/STM WITH ATOMIC RESOLUTION

T10 Nanoscience and Technology

#SS/NST-1-In-1

P. Jelínek.

Institute of Physics of the Academy of Sciences of the Czech Republic - Prague (Czech republic).

Recent progress in simultaneous AFM/STM measurements with atomic resolution opens new possibilities in complex characterization of surfaces and nanostructures. We will discuss both experimental [1] and theoretical [2] aspects and challenges of the technique. Potential of the technique will be demonstrate on (i) understanding of fundamental relation between tunneling current and chemical force at atomic scale [2]; (ii) recognition of single molecules deposited on semiconductor surface and (iii) single-atom chemical resolution of complex 1-D systems [3]. In addition, perspectives of Kelvin force probe microscopy will be briefly discussed [4].

[1] Z. Majzik et al, Beilstein J. Of Nanotech. 3, 249 (2012).
[2] P. Jelinek et al, J. Cond. Mat. Phys. 24, 084001 (2012); M. Ternes et al Phys. Rev. Lett. 106, 016802 (2011).
[3] M. Setvín et al, ACS Nano 6, 6969 (2012).
[4] S. Sadewasser, at el, Phys. Rev. Lett. 103, 266103 (2009).

NST-1-In-2
Epitaxial graphene on Ir(111) – a playground for the fabrication of graphene hybrid materials

T10 Nanoscience and Technology

#NST-1-In-2

T. Michely.

Physikalisches Institut, Universität zu Köln - Koln (Germany).

Highly perfect graphene layers on Ir(111) can be used as a laboratory to construct new types of graphene based compound materials. Due to the inhomogeneous binding of graphene to its substrate a plethora of pattern formation processes is observed: arrays of clusters and molecules, patterned intercalation and the formation of a nanomesh upon ion irradiation. The resulting changes in graphene allow one to tune its properties in a wide range and to locally functionalize it.

NST/SS-3-In-1
SPIN SPIRALS AND MAGNETIC SKYRMIONS STUDIED WITH SPIN-POLARIZED STM

T10 Nanoscience and Technology

#NST/SS-3-In-1

K. Von Bergmann.

Institute of Applied Physics, University of Hamburg - Hamburg (Germany).

Magnetism in low-dimensions is a versatile topic and broken inversion symmetry due to the presence of a surface can induce the formation of non-collinear magnetic states. In such systems the spin rotates from one atom to the next resulting for instance in spin spirals with nanometer sized magnetic periods [1-3]. In the case of the monolayer Fe on Ir(111) competing interaction lead to a lattice of skyrmions on the atomic scale [4,5]. By changing the interface of this system we obtain an ultrathin film system with a spin spiral ground state that can be driven into a skyrmion lattice phase by the application of an external magnetic field. Depending on temperature and measurement parameters we find reversible or hysteretic behavior.

[1] M. Bode et al., Nature 447, 190 (2007).
[2] P. Ferriani et al., Phys. Rev. Lett. 101, 27201 (2008).
[3] M. Menzel et al., Phys. Rev. Lett. 108, 197204 (2012).
[4] K. von Bergmann et al., Phys. Rev. Lett. 96, 167203 (2006).
[5] S. Heinze et al., Nature Phys. 7, 713 (2011).

NST-1-In-1
Electronic properties and electron dynamics in quasi free standing graphene

T10 Nanoscience and Technology

#NST-1-In-1

P. Hofmann.

Aarhus University - Aarhus (Denmark).

Epitaxial graphene grown on SiC as well as on transition metal surfaces has successfully been used as a model system to study the electronic properties and many-body effects in graphene by angle-resolved photoemission spectroscopy and scanning tunnelling spectroscopy. Over the last years, it was shown that the intercalation of hydrogen between graphene and SiC, or oxygen between graphene and a transition metal, can decouple the graphene from its substrate, leading to an electronic structure that resembles that of pristine graphene even more [1-4]. In this talk, I will review the electronic properties and many-body effects in such quasi free-standing graphene. I will also discuss recent results on the ultrafast dynamics of the excited carriers near the Dirac point in quasi free standing graphene, as studied by time and angle-resolved photoemission spectroscopy. Direct access to the Dirac cone in such an experiment is only possible with sufficiently high laser photon energies as provided by the Artemis setup at the Rutherford Appleton Laboratory.

[1] C. Riedl et al., Physical Review Letters, 103, 246804 (2009).
[2] Aaron Bostwick et al. Science, 328, 999 (2010).
[3] Jens Christian Johannsen et al. Journal of Physics: Condensed Matter, 25, 094001 (2013).
[4] Rosanna Larciprete et al. ACS Nano 6, 9551 (2012).

NST-5-In-1
Towards an atomistic understanding of molecule-metal interfaces

T10 Nanoscience and Technology

#NST-5-In-1

F.S. Tautz.

Peter Grünberg Institut, Forschungszentrum Jülich - Jülich (Germany).

Contacts between metals and large π-conjugated molecules are of central importance for organic and molecular electronics. Highly ordered monolayers of electrically active molecules on single-crystal metal surfaces are excellent model systems for metal-molecule contacts. They can be used to study fundamental properties of metal-molecule contacts at the atomistic level. In my talk, I will give examples of our recent work, including precision measurements of adsorbate geometries, comprehensive experiments revealing how observables such as vertical adsorption height, charge reorganization and charge transfer emerge from a complex interplay of different factors, and investigations of the role played by van der Waals interactions at metal-organic interfaces.

NST/SS-3-Kn-1
MOLECULAR QUANTUM SPINTRONICS

T10 Nanoscience and Technology

#NST/SS-3-Kn-1

W. Wernsdorfer.

Institut Néel - Grenoble (France).

A revolution in electronics is in view, with the contemporary evolution of three novel disciplines, spintronics, molecular electronics, and quantum computing. A fundamental link between these fields can be established using molecular magnetic materials and, in particular, single-molecule magnets, which combine the classic macroscale properties of a magnet with the quantum properties of a nanoscale entity. The resulting field, molecular quantum spintronics aims at manipulating spins and charges in electronic devices containing one or more molecules. The objective is to fabricate, characterize and study molecular devices in order to read and manipulate the spin states of one or several molecules and to perform basic quantum operations. The most important results in this new research area will be presented.

NST-9-In-1
CONTROLLED SYNTHESIS OF HETEROSTRUCTURES OF 2D MATERIALS

T10 Nanoscience and Technology

#NST-9-In-1

E. Sutter.

Center for Functional Nanomaterials, Brookhaven National Laboratory - Upton (United states).

The ability to combine materials in heterostructures with controlled interfaces has become one of the foundations of modern materials science. Heterostructures of 2D materials promise tunable properties and new functionality, and raise fundamental questions on interface formation, intermixing, strain, etc., in a new context at reduced dimensionality. I will discuss progress toward meeting key challenges in the controlled formation of 2D heterostructures: atomically precise thickness and stacking control in superlattices, and the creation of atomically sharp line interfaces in heterogeneous monolayer membranes. Our combined findings establish a powerful toolset for the scalable fabrication of 2D heterostructures for research and applications.

NST-P2-26
Viologen-anchored ZnO Electrochromic Nanowires

T10 Nanoscience and Technology

#NST-P2-26

T. Kim, S.M. Cho, S.Y. Kang, C. Seong Ah, J.Y. Kim, H. Ryu.

Electronics and Telecommunications Research Institute, Next Generation Display Research Department - Electronics And Telecommunications Research Institute, Next Generation Display Research Department, (Korea, republic of).

Electrochromic materials can sustain reversible color changes upon the application of a voltage [1], and Viologen is one of the most
important electrochromic materials based on TiO_2 nanoparticle electrode.
However, the white background color of TiO2 nanoparticles are key problems for transparent display applications [2]. The viologen-anchored
ZnO nanowire form is one way to solve these problems because its lower transmittance. In this study, we synthesized viologen-anchored ZnO nanowires and characterized the electrochromic properties of the composite.

Acknowledgements.
This research was supported by the Research & Development Improvement Program for ETRI (project number 10041416) funded by MKE/KEIT in Korea.

[1] C. G. Granqvist, E. Avendaño, A. Azens, Thin Solid Films **2003**, 442, 201.
[2] X. W. Sun and J. X. Wang, Nano Lett. **2008**, 8, 1884.
[3] Lionel Vayssieres, Adv. Mater. **2003**, 15, 464.

Figure 1. Field-emission scanning electron microscopy (FE-SEM) image of threedimensional arrays of ZnO nanowires grown by the aqueous chemical method [2-3].

NST-5-In-2
Scanning probe microscopy characterization and nanopatterning of CVD grapheme

T10 Nanoscience and Technology

#NST-5-In-2

L. Biró [1], L. Tapasztó [1], P. Nemes-Incze [1], G. Dobrik [1], Z. Osváth [1], G.I. Márk [1], P. Vancsó [1], Y.S. Kim [2], X. Jin [2], C. Hwang [2], P. Lambin [3], C. Hwang [3].

[1]Institute of Technical Physics and Materials Science, Centre for Natural Sciences / Korea-Hungary Joint Laboratory for Nanosciences - Budapest (Hungary), [2]Center for Nano-imaging Technology, Division of Industrial Metrology, Korea Research Institute of Standards and Science / Budapest Korea-Hungary Joint Laboratory for Nanosciences - Yuseong (Korea, republic of), [3]Physics Department, University of Namur - Namur (Belgium).

Grain boundaries [1] are a common feature of polycrystalline graphene grown by chemical vapor deposition on transition metal substrates [2, 3]. The simplest model of the boundaries connecting two rotated graphene domains consists of a series of dislocation cores made up of nonhexagonal rings such as pentagons and heptagons. Such grain boundaries have to date been mostly measured by transmission electron microscopy. AFM and STM, being uniquely suited to the study of defects in graphene, have only recently been used to measure grain boundaries in CVD grown graphene [3, 4]. Using scanning tunneling microscopy (STM) and STM spectroscopy (STS), combined with modeling, we present evidence that grain boundaries in graphene grown on copper incorporate a significant amount of disorder and the simplest dislocation core model cannot fully describe these structures.
Beyond characterization, STM in lithographic mode (STL), is a versatile tool for the nanopatterning of graphene [5]. Possibilities of STL [6] and difficulties associated with the nanopatterning of CVD graphene grown on Cu will be discussed.

[1] L. P. Biró & Ph. Lambin, New J. Phys. 15, 035024 (2013).
[2] C. Hwang et al., J. Phys. Chem. C 115 (2011) 22369.
[3] P. Nemes-Incze, et al., Appl. Phys. Lett. 99 (2011) 023104.

[4] L. Tapasztó et al., Appl. Phys. Lett. 100 (2012), 053114.
[5] L. P. Biró et al., Nanoscale, 4 (2012)1824.
[6] L. Tapasztó et al., Nature Nanotech. 3, (2008) 397.

NST-2-In-1
Local investigation of ballistic transport in semiconductor nanostructures

T10 Nanoscience and Technology

#NST-2-In-1

K. Ensslin.

ETH - Zurich (Switzerland).

Electron transport through nanostructures is usually measured by passing current and measuring voltages through macroscopic contacts. Here we show how the biased tip of a scanning force microscope can be used to influence and even control electron transport on a local scale such that the potential landscape in quantum point contacts or confined electron billiards can be mapped out. We demonstrate the measurement of quantized conductance in a tunable network of quantum point contacts. In addition edge states in the integer and fractional quantum Hall regime can be imaged.

NST-2-In-2
Friction, Brownian motion, and energy dissipation mechanisms in adsorbed molecules and molecularly thin films: Heating, Electrostatic and Magnetic Effects*

T10 Nanoscience and Technology

#NST-2-In-2

J. Krim.

North Carolina State University - Raleigh (United states).

In the study of friction at the nanoscale, phononic, electrostatic, conduction electron and magnetic effects all contribute to the dissipation mechanisms [1,2]. Electrostatic and magnetic contributions are increasingly alluded to in the current literature, but remain poorly characterized. I will first overview the nature of these various contributions, and then report on our observations of magnetic and electrostatic contributions to friction for various systems in the presence and absence of external fields. I will also report on the use of a quartz crystal microbalance (QCM) with a graphene/Ni(111) electrode to probe frictional heating effects in Kr monolayers sliding on the microbalance electrode in response to its oscillatory motion. [3]

[1] I. Altfeder and J. Krim, J. Appl. Phys. (2012),
[2] J. Krim, Advances in Physics, Vol. 61, Iss. 3, 155-323 (2012)
[3] M. Walker et al. , J. Phys.: Condensed Matter 24, art# 424201 (2012)

*Work supported by NSF DMR

FMMM/NST-1-In-2
From Molecular Superconductors to Molecular Machines

T10 Nanoscience and Technology

#FMMM/NST-1-In-2

S.W. Hla.

Ohio University - Athens (United states).

Using low temperature scanning tunneling microscopy (STM), spectroscopy, and atom/molecule manipulation schemes, we explore properties of novel molecular materials on surfaces at single atom and molecule level. In this talk, recent results in the area of functional molecules on surfaces studied by STM will be presented. The first part of the talk is focused on molecular superconductors. Below a critical temperature of 10K, (BETS)2-GaCl4 molecular clusters exhibit superconducting properties. In this talk I will present the evolution of electronic structures at the metal-superconductor boundary and the charge transfer processes at the molecule-metal interface. The second part is related to large molecules functioning as molecular motors on surfaces. Here, complex rotation mechanisms of multi-component molecular motors on a Au(111) surface operated by injecting tunneling electrons from an STM tip will be presented.

PST-P3-01
ELECTRIC ARC PLASMA REACTOR FOR FLUID ORGANIC COMPOUNDS DECOMPOSITION

T11 Plasma Science and Technology

#PST-P3-01

L. Szymanski.

Lodz University of Technology - Lodz (Poland).

The aim of the paper is to study a stream rate and quantity of organic fluid waste production by an average analytic chemical laboratory, to find out the required conditions of its thermal treatment in electric arc plasma and to demonstrate a concept of compact system able do utilize from one to a few kilograms of reagent per hour. The main part of the device is the plasma reactor equipped with the electrode spacing adjustment actuator and the power and flow control unit. The collected wasted solvents must be filled in the container feeding the reactor. The gasified waste is heated in the reactor space and must pass across the plasma column going to the compact chlorine absorber and catalytic oxidizer.
In a chemical analytic laboratory practice small amounts of diverse reagents, mostly liquid organic substances are used for many purposes such as chromatography. They are the chlorinated solvents, solvents from the group of alcohols, esters, and aliphatic or aromatic hydrocarbons.
The avoidance of stockpiling and transportation of those waste is the economic challenge in the procedure of utilization of the used reagents. So far any device able to utilize those wastes “in situ” where they are produced had not been offered [1]. Such device had to be placed in/or close to the laboratory and may be working in measure of the need (batch mode) on principle how the office document shredder.
The aim of the paper is to study a stream rate and quantity of organic fluid waste production by an average analytic chemical laboratory, to find out the required conditions of its thermal plasma treatment and to demonstrate a concept of compact device PDUCR - Fig. 1 (Plasma Destructor of Used Chemical Reagents) able do

utilize from one to a few kilograms of reagent per hour. The main part of the device is the plasma treatment reactor equipped with the adjustment actuator and the power and flow control unit. The collected wasted solvents must be filled in the container feeding the reactor. PDUCR will be supplied in the inert gas delivered from the bottle in the slow rate and atmospheric pressure.
To optimize the conditions of the reaction the calculated decomposition of solvents within the range of temperatures from 400 to 3000K using the CHEMSAGE program based on the minimization of Gibb's free energy will be presented.

[1]. K. Cedzynska, Z. Kolacinski: "Plasma Destruction of Toxic Chloroorganic Wastes Towards Zero Residues", Journal of Advanced Oxidation Technologies ISSN 1203-8407 Science & Technology Network, Inc. J. Adv. Oxid. Technol. Vol. 7, No. 1, 2004.

Fig.1. Photo of parts of plasma system (reactor with actuator and catalytic oxidizer).

PST/SE/TF-1-Or-1
Influence of type of gas on the properties of SiOx coatings by cold atmospheric plasma

T11 Plasma Science and Technology

#PST/SE/TF-1-Or-1

H. Hamze [1], M. Jimenez [1], D. Deresmes [2], A. Beaurain [3], N. Nuns [4], M. Traisnel [1].

[1]UMET, ISP-PERF, CNRS 8207, Université Lille Nord de France - Lille (France), [2]IEMN, CNRS 8520, Université Lille Nord de France - Lille (France), [3]UCCS, CNRS 8181, Université Lille Nord de France - Lille (France), [4]Institut Chevreul, Université Lille Nord de France - Lille (France).

In this study, thin layers of SiO_x were applied on glass substrates, using two different gases (air and nitrogen), by a cold atmospheric plasma torch (ULS, AcXys technologies, France). Looking at the literature, the extreme surface of such thin films is usually only analyzed by X-Ray Photoelectron Spectroscopy (XPS) [1-2]. The aim of this work is to investigate on one hand the influence of the gases used during plasma process on the extreme surface composition and morphology of the layer by XPS and Atomic Force Microscopy (AFM) and on the other hand the whole thin film composition, using Time-of-Flight Secondary Ion Mass Spectrometry (ToF-SIMS).

A Hexamethyldisilan (HMDS) precursor was injected in post-discharge in an air or nitrogen plasma, using a carrier gas (air or nitrogen) and applied on the substrate previously pre-treated by an air or nitrogen plasma. The carrier gas and plasma gas flows, the distance between the substrate and the plasma torch, the scanning speed and the precursor flows were held constant during the study.

The gas used during activation pre-treatment shows no further influence on the characteristics of the deposit. When air is used both as plasma and carrier gas, the coating layer is thicker (96 nm) than when nitrogen is used (64 nm). It was also evidenced that the carrier gas precursor has little influence on the hydrophobicity of the coating, on the contrary of the plasma gas. The latter significantly influences the surface characteristics of the coatings. As it can be seen in the figure 1, the layer morphologies are completely different depending on the plasma gas used. Moreover,

the surface contact angles are different: 82° and 100° for the layers respectively obtained with air and nitrogen. This increase of hydrophobicity could be correlated to the increase of Si–O–C bonds in the upper surface layers evidenced by XPS analyzes. This observation was then confirmed by ToF-SIMS analyzes carried out on these thin layers. A uniform distribution of Carbons in the SiO_x coating could also be observed using ToF-SIMS 2D reconstruction images of cross sections of the deposited layers.

Keywords: Cold atmospheric plasma, Gas, SiO_x coatings, Hexamethyldisilan, ToF-SIMS, XPS

1) A. Karakuscu et al., White Luminescence from Sol–Gel-Derived SiOC Thin Films, Journal of the American Ceramic Society, Vol. 92, December 2009, pages 2969–2974

2) R. Navamathavan et al., Deposition and Characterization of Porous Low-Dielectric-Constant SiOC(-H) Thin Films Deposited from TES/O2 precursors by using Plasma-Enhanced Chemical Vapor Deposition, Journal of the Korean Physical Society, Vol. 53, July 2008, pages 351 -356

Figure 1 : AFM 3D Images of SiO_x coatings with Air (a) and N_2 (b)

PST-P2-01
The Effects of Pressure and Boundary Layer on the Propagation of Plasma Jets

T11 Plasma Science and Technology

#PST-P2-01

M. Laroussi, M.A. Akman, S. Mohades.

Old Dominion University - Norfolk, Va (United states).

In this paper we report on the effects of ambient pressure and background gas on the formation and propagation of plasma jets. In the experiments reported in this paper a plasma jet is introduced into a Pyrex chamber where the pressure and gas mixture can be controlled. In this way the plasma plume/jet is launched inside the chamber [1]. The pressure in the chamber is regulated by controlling the gas flow and the rate of evacuation. We discovered that there are three operating phases: A first phase, the stagnant phase, where the plume length remains approximately constant. This is followed by a second phase where the jet inside the chamber rapidly increases in length (up to 28 cm) as the pressure decreases. Then at a pressure around 70 Torr an operational mode transition suddenly occurs where the plume length decreases dramatically. Further lowering the pressure in this third phase, to around 20 Torr, the plasma starts expanding in all directions starting from the point where the plume enters the chamber. At pressures below 2 Torr, the entire volume of the chamber gets filled with homogeneous plasma.
Our most recent studies indicate that the behavior of the plasma jet is not limited to the pressure alone but also to the presence of a physical boundary that confines the gas flow. It is observed that in a chamber filled with only helium, no plasma jet is created and therefore no bullet propagation occurs; however inside the connecting tube in which the helium is flown into the chamber, plasma bullet propagation is visible. This is attributed to the existence of the physical boundary of the wall of the tube. However, we find that this boundary does not need to be an object that surrounds the gas flow. This is evidenced by the introduction of a gas different than helium into the chamber. In this case, the diffuse plasma transitions into a jet as a result of the formation of a helium channel in which the plasma bullets propagate. Therefore, we conclude that in order for plasma bullets to propagate, there needs to be a boundary surrounding the gas channel. In addition to this visual observation, emission profile in VIS range also shows distinct transitions, specifically at 587.4nm.

In this paper, experimental evidence supporting the observations explained above will be presented.

[1] M. Laroussi, M.A. Akman, “Ignition of a large volume plasma with a plasma jet”, AIP Advances, 1, 032138, 2011

PST-P2-02
Generation of Homogeneous Dielectric Barrier Discharge in Atmospheric Air without Preionization

T11 Plasma Science and Technology

#PST-P2-02

E. Shershunova, M. Malashin, S. Moshkunov, V. Khomich.

Institute for Electrophysics and Electric Power RAS - Saint-Petersburg (Russian federation).

Physical properties of dielectric barrier discharge (DBD) and its simple realization make this discharge very attractive to many technological applications: from widely known purifying of gases and liquids to surface treatment, plasma medicine, plasma chemistry and aerodynamics. DBD can exhibit as a filament mode as a uniform one [1, 2]. In 1988 Okazaki and his colleagues realized the homogeneous atmospheric DBD in helium [3]. Later the uniform atmospheric DBD was generated also in other noble gases. But it is a difficult task to get the uniform DBD in air under atmospheric pressure. The nitrogen metastables are considered to play a dominant role in generating the uniform discharge in air, since they create seed electrons due to Penning ionization. However, the activity of the metastables is neutralized in gases, containing oxygen, because the oxygen molecules capture electrons due to their electronegative properties. Therefore, the typical method for generating the uniform DBD in air is use of preionization [4].

According to our experimental results the uniform DBD mode can be realized in atmospheric air without preionization, if the DBD is supplied by voltage pulses with nanosecond rise time.

The experimental setup is shown in figure 1. The discharge was initiated in the discharge gap (DG) between two plane-parallel electrodes in atmospheric air. One of the electrodes was insulated from air by 2 mm alumina ceramic plate. The gap length was fixed to 2 mm. Square unipolar pulses, generated by the solid-state high voltage pulse generator (HVPG) [5], were applied to the DG. The pulse repetition rate was constant during all experiments – 30 Hz. The voltage at the DG was measured by high voltage probe Tektronics P6015A. The discharge current was measured by low inductance resistance detector Rcs. The waveforms of the voltage at the DG and the discharge current were recorded by means of oscilloscope LeCroy WaveRunner 104Xi-A 1 GHz 10 GS/s. The photo registration of the glow in the DG was conducted

by use of photo camera Canon EOS 500D with EFS 18-200 mm objective under the following conditions: exposure time – 2 sec., aperture – 1/5.6, photosensitivity – 3200 ISO. We investigated the dependence of a DBD mode on a value of resistor R, which determined the voltage pulse rise time t.
As a result, we found that at voltage at the DG of 14 kV, the uniform DBD was initiated at pulse rise time of 40 ns and less (R < 100 Ohm) (fig.2). At t = 40 - 70 ns (100 Ohm < R < 4000 Ohm) the uniform DBD turned into a mixed mode, a filamentary discharge with a volume glow around filaments. The filamentary discharge was initiated at pulse rise time of 70 ns and more.
We suppose that the uniformity of the DBD in atmospheric air is attributed to the growth rate of the electric field strength in the DG. The homogeneous volume DBD in atmospheric air exists at the growth rate of the electric field strength of 1.1 kV/cm·ns and more.

1. Kogelschatz U., Eliasson B., Egli W. Pure Appl. Chem. 71, 10, 1819–1828 (1999).
2. F. Massines, N. Gherardi, N. Naudé and P. Ségur. The European Phys. J.: Appl. Phys. 47, 2, 22805-22905 (2009)
3. S. Kanazava, M. Kogoma, T. Moriwaki, S. Okazaki. J. Phys. D: Appl. Phys. 21, 838 (1988)
4. J.R.Roth, j. Rahel, X. Dail, D. M. Shersman. J. Phys. D:Appl. Phys. 38, 555 (2005)
5. Ivanov E.V., Moshkunov S.I., Khomich V.Yu. Instruments and Experimental Technics. 1, 99-90 (2006)

Figure 1. Experimental setup.

Figure 2. Photo image and waveforms of homogeneous DBD in atmospheric air.

PST-P3-02
White Paper for Developing Fast Lithium Pellet Injection System Using High Pressure Gas for Disruption Mitigation on EAST

T11 Plasma Science and Technology

#PST-P3-02

H. Zhuang, X. Zhang.

Institute of plasma physics, Chinese academy of sciences, - Hefei.

In large tokamaks, disruptions of high current plasma would damage PFCs or other inner components due to high heat load, electromagnetic force load and runaway electrons. It would also has influence on the following plasma discharge duo to impurities production during disruptions.[1] So the avoidance and mitigation of disruptions is essential for next generation tokamaks, such as ITER. Massive gas injection and pellet injection are two promising methods for disruption mitigation. Most of the tokamak devices in the world have had research on disruption mitigation by injection massive gas and pellet injection.[2,3] By injecting suitable amount of massive gas or pellet, the harmful effect of disruptions could be mitigated. In the first case(massive gas injection), the high heat load, electromagnetic force and runaway electrons all could be mitigated, but the injected paritcles could only get the boundary of the plasma due to ionized. In the second case(pellet injection), the injected pellet couldn't provided enough particles for RE(runaway electrons)mitigation, but the injected pellets could achieve the core of plasma.

In order to optimizing the methods of disruption mitigation, a new method has been proposed on EAST, and the new system is developing, which will be tested in the next round campaign of EAST. The system consist of two parts, the first part is a fast valve which was driven by eddy current[4], the work chamber was filled with high pressure noble gas, and the pressure in the fast valve could reach 50bar .The second part is the supply system of lithium pellet, the lithium is made into strip shape, the blade which was pushed by cylinder could cut the lithium strip into suitable length that needed which is controled by a stepping motor After a trigger signal, the valve could be opened within 0.5ms, so the high pressure gas in the work chamber could spurt out, and the lithium pellet in the pipeline could be accelerated to a few hundred meters, so both the high pressure gas and lithium pellet could be injected into the

plasma, the injected gas could cooling the edge of plasma ,at the same time the lithium pellet could penetrate into the central area of plasma. So both the boundary and central area of the plasma temperature could be cooling down to a safety level at the same time, which is very important for disruption mitigation.

Lithium is a kind of promising coating material in tokamaks, so the injection of lithium pellet couldn't have bad influence on following discharge. The system will be tested in next round campaign of EAST in 2013. If the project was confirmed feasible, which will be a good news for ITER.

[1] Progress in the ITER Physics Basis 2007, Nucl.Fusion ,47: S128
[2] M.Bakhtiari,M,Y.Kawano,H.Tamai,et al.2002. Nuclear Fusion, 42:1197
[3] P.L.Taylor,A.G.Kellman,B.W.Rice,et al.1996. Physical Review Letters,76:916
[4] S.K.Combs.C.R.Foust,M.J.Gouge.2004,Review Scientific Instuments,75:270

PST-P3-03
Investigation of the plasma density feedback control experiment by gas puff and SMBI on EAST

T11 Plasma Science and Technology

#PST-P3-03

X. Zheng, J. Li, J. Hu, J. Li, B. Cao, J. Wu.

8605515593616 - Hefei.

To achieve stable and desirable plasma density on EAST tokamak, plasma density feedback control was investigated by both of gas puffing and new developed Supersonic Molecular Beam Injection (SMBI) fueling system. And some meaningful results were obtained.
There are two modes using gas puffing for plasma density control. It was found that the pulse width modulation mode [1] seemed much better than voltage modulation mode for plasma density control. If using voltage modulation mode, the plasma density seems difficult to meet the set value due to this mode doesn't meet the fast change of plasma density. However, one disadvantage of gas puffing is its long delay of fueling, the others is that it would lead a high retention on walls, which makes density feedback control difficult.
In 2011, a new core fueling system- SMBI has been also successfully employed as a fast density feedback tool to maintain plasma density for steady-state operations, and it seems much better than gas puffing. SMBI produces a rapid travelling gas jet with a speed exceeding 1 km/s and pulse length ranging from 2 to 20 ms. This leads to a much shorter density response time (2-4 ms) than the conventional gas puffing (16 ms and 77 ms for LHS and HFS, respectively). And SMBI has a higher fueling efficiency of 15~30% with a lower fuel retention on walls [2]. Using SMBI for feedback control, the plasma density is agreed with the set value very well. It is been testified that SMBI is a more feasibility method than gas puffing for plasma density control, especially during performing the discharges with long pulse and high parameters on EAST in the near future.
This research was funded by National Magnetic confinement Fusion Science Program under Contract No.2010GB104002 and No.2013GB114004 and National Nature Science Foundation of China under Contract No.11075185 and No.11021565.

[1] Q. P. Yuan, B. J. Xiao, M. Walker, H. Z Wang, 2009, Plasma Sci. Technol., 11 231
[2] J. S. Hu, X. M. Wang, J. H. Li, et al. Fusion Eng. Des., 84 2167

PST/SE/TF-P1-01
Effect of Heat Exposure Conditions on the APS-W Layer coated on Molybdenum Substrate

T11 Plasma Science and Technology

#PST/SE/TF-P1-01

G. Cho, K. Choe.

Korea Institute of Industrial Technology - Incheon (Korea, republic of).

Pure molybdenum(Mo) possesses a unique combination of physical properties including excellent high-temperature strength, high thermal conductivity, a high elastic modulus and a low thermal-expansion coefficient. Because of these outstanding properties and high melting point (2620°C), technically pure Mo sheet has been used in a wide range of applications, including hot-zone materials such as heating element, heat shield and crucible for high-temperature furnace construction [1]. But, the Mo alloy was vaporized in a vacuum atmosphere and chemically reacted with heating element in a high-temperature furnace. Also, hot-zone Mo alloy degraded on their high-temperature mechanical properties under prolonged exposure to thermal radiation due to the embrittlement of large recrystallized grains [2]. So, plasma sprayed tungsten(PS-W) coatings have been successfully fabricated and studied to protect metallic substrate. It was reported that tungsten seems a promising candidate material for plasma facing components in next fusion experimental devices due to its low sputtering yield and good thermal properties [3]. Vacuum plasma spraying (VPS) process is done in the controlled low pressure of inert gas, which reduces the interaction between plasma jet and oxidative environment. VPS process needs high cost equipment and operation maintenance cost, so a relatively inexpensive air plasma spraying(APS) process has been adopted for limited coating applications. In this work, an effort was made to investigate the influence of heat exposure conditions on the APS-W coating layer on Mo substrate. Thermal exposure experiment was carried out in three atmosphere conditions. After heat exposure, their microstructure and composition changes were characterized by field emission scanning electron microscopy, X-ray diffraction, energy dispersive spectrum. Mo strip of 160mm(L) x 8mm(W) was coated by the air plasma spraying technique. Tungsten coatings were successfully deposited by air plasma spraying technique on Mo substrate. Fig.1 shows the surface photographs of a tungsten thick(775um) coating on 1.0t Mo substrate. The APS-W coating layer was tightly bonded with Mo

substrate. Air plasma spraying W coating layer could be a good thermal radiation protection candidate material for the hot-zone parts application.

1. R.R.Freeman, The Metal Molybdenum, ASM, 1958, 10-30.
2. T.Fujii, R.Watanabe, Y.Hiraoka, M.Okada, J.Less-Common Met. 96 (1984) 297–304.
3. N.Yoshida, J.Nucl.Mater. 266-269 (1999) 197-206.

Fig. 1 Surface photograph of APS-W coating layer on Mo substrate

PST-5-Or-1
Preparation of silica and borosilicate permeation barriers by magnetron sputtering for Laser Megajoule gaseous targets

T11 Plasma Science and Technology

#PST-5-Or-1

P. Rodriguez, S. Le Tacon, C. Chicanne, V. Brunet.

CEA, Valduc - F-21120 Is-Sur-Tille (France).

In order to prepare first fusion experiments performed with the Laser Megajoule (LMJ), some will be realized on a gaseous deuterium – tritium (DT) mixture. The target consists in a doped CH_x microshell containing the gas mixture. Glow discharge polymerization (GDP) is an appropriate technique to produce doped CH_x microshells compatible with LMJ specifications. The capsule has then to be filled with DT mixture of several megapascal and hold for several days at ambient temperature in order to allow laser experiments. However, plasma polymer is highly permeable to light gases in general and DT mixture in particular. We therefore studied the possibility to include a thin film coating as semi-permeable barrier. This functional layer is made of amorphous silica or borosilicate and is obtained by magnetron sputtering onto CH_x microshell. The permeation layer is then buried under a final CH_x layer. A schematic representation of the gaseous target is shown on figure 1.

One of the originality of the present work is the use of magnetron sputtering in order to obtain functional thin layers not on flat substrates but on CH_x capsules with a mean diameter less than 2 mm. We studied the influence of the permeation barrier nature (borosilicate or silica) and the deposition parameters (i.e. pressure, RF power…) on the permeation properties of the targets. These latter are studied by mass spectrometry using deuterium (D_2) as filling gas. The optima thin film coatings exhibit permeable properties at high temperature (e.g. 200 °C) which are useful for the filling step and quasi-blocking properties at ambient temperature with a D_2 permeation coefficients as low as 1.10^{-20} $mol.m^{-1}.s^{-1}.Pa^{-1}$ for silica layers (amorphous silica theoretical limit) and few 10^{-21} $mol.m^{-1}.s^{-1}.Pa^{-1}$ for borosilicate layers. As function of the permeation barrier thickness and the number of barrier layers

incorporated, pressurized targets over 3 MPa with half-life of several weeks are obtained.

Figure 1: Schematic representation of the future LMJ gaseous target.

PST-5-Or-2
Carbon facing plasma in fusion devices: erosion study under argon/hydrogen radiofrequency plasma treatment

T11 Plasma Science and Technology

#PST-5-Or-2

X. Glad, L. De Poucques, J.L. Vasseur, M. Belmahi, R. Hugon, J. Bougdira.

Université de Lorraine, Institut Jean Lamour, CNRS UMR7198 - Vandoeuvre-Lès-Nancy, F-54506 (France).

The new stellarator Wendelstein 7-X, currently under construction in Greifswald, Germany, will include a 10-unit divertor. The plasma-facing material (PFM) selected for this component is grain graphite for the test divertor which, after two-years of operation, will be replaced by a carbon-fiber composite (CFC) high-heat flux divertor[1,2]. These compounds exhibit interesting properties as fusion devices PFMs such as an excellent thermal shock resistance and absence of melting compared to metals. However, carbon raises the critical issue of erosion. This phenomenon generates porous dust polluting the fusion reaction and retaining radioactive elements, leading to efficiency loss and safety concerns. A better understanding of the different erosion processes is thus an essential issue to solve in order to improve the quality of the carbon components. The study presented here focuses on the erosion of flexible graphite, highly ordered pyrolytic graphite (HOPG) and CFC tile samples undergoing plasma treatment under different conditions. The influence of pressure, gas mixture, radiofrequency coupling modes and plasma exposure duration has been investigated in order to characterize etching and re-deposition growth kinetics.

All experiments were conducted in a standard two-chamber helicon reactor[3] allowing four different coupling modes and conditions close to a fusion device scrape-off layer plasma, i.e. electron density and temperature around 10^{11} cm^{-3} and below 5 eV, respectively[4]. Hydrogen/argon discharges are initiated by a new 13.56 MHz RF 2 kW power supply coupled to a Boswell-type antenna surrounding the source chamber. Two sets of copper coils generating a static magnetic field up to 200 G allow the

transition from inductive to wave coupling modes.
Several diagnostics were carried out for the characterization of both the plasma and the carbon samples. Langmuir probe, optical emission spectroscopy and two-photon absorption laser-induced fluorescence were used to evaluate electron and H relative densities. We observed the erosion outcomes with mass loss measurements, Raman spectroscopy, and scanning and transmission electron microscopies in order to estimate the erosion rate and compare structure modifications.
The highest erosion rate obtained is 6 µm/h at a pressure of 10 mTorr in a pure hydrogen inductive discharge. The facts that increasing the pressure limits the plasma transport and that the substrate-holder is at floating potential explain these results. Furthermore, the erosion rate does not seem to be affected by the plasma exposure duration, unlike the re-deposited structures size and porosity, which increase with the latter. Also, the non-increasing re-deposited structure density shows that radicals resulting from the etching tend to be deposited on the already present structures. In fusion devices, such porous structures would allow significant tritium retention. Finally, pure argon discharges, i.e. physical etching, reveal interesting highly-ordered graphite structures that deteriorate with the addition of hydrogen in the gas mixture.

1. A. Peacock et al., Fus. Eng. Des. 84 (2009) :1475.
2. J. Boscary et al., Fus. Eng. Des. 87 (2012) :1453.
3. T. Bieber et al., Surf. Coat. Tech. 205 (2011) :S384.
4. J.P. Sharpe et al., Fus. Eng. Des. 63-64 (2002) :153.

PST-P2-17b
Characterization of discharge in heptane by optical emission spectroscopy

T11 Plasma Science and Technology

#PST-P2-17b

A. Hamdan, C. Noël, G. Henrion, T. Belmonte.

Institut Jean Lamour - Nancy (France).

Electro-discharge machining, treatment of biomaterials, nanoparticles synthesis, plasma electrolytic oxidation, gases production, etc. are some applications of discharges in liquids. Indeed, because of its short lifetime (several hundreds of nanoseconds) and small dimensions (several micrometers), the plasma cannot be characterized easily by conventional techniques. However, radiations emitted during the discharge are very intense. In the present work, nanosecond time-resolved Optical Emission Spectroscopy (OES) is used to characterize the plasma (temperatures, species, densities …) during its expansion and decay phases.
A positive high voltage (+15 kV) is applied to a Pt pin-electrode (anode) located 100 µm above an aluminum plate electrode (cathode), the two electrodes being immerged in heptane (n-C_7H_{16}). Using a Jobin-Yvon TRIAX 550-sprectrometer (gratings: 100, 1200 and 1800 grooves mm^{-1}) coupled with an ICCD detector, spectra averaged from 50 to 1000 discharges are acquired in the range [200-1000] nm. Because of the random nature of discharges in time, we have used a nanosecond-switch with a voltage rise-time of 130 V/ns. Therefore, it is possible to breakdown the plasma with a time-resolution of 50 ns. This time-step is used for this study. Although each discharge event is not perfectly reproducible, the reproducibility of the measurements is very satisfying.
Using a grating with 100 grooves mm^{-1}, global spectra are acquired. Black-body emission is observed with a maximum centered at ~ 400 nm. By fitting the spectrum with a black-body behaviour, one can estimate the temperature of the plasma and its time evolution from 0 to t=1000 ns with a step of 50 ns. An important emission of Balmer-lines (expecially H-alpha, 656.3 nm) is observed. Using the temperature values determined before, we can fit rigorously the H-alpha line (Doppler, van der Waals and Stark broadnings) and then, determine the electronic density and gas temperature.
Gratings with 1200 and 1800 grooves mm^{-1} are used to identify the atomic lines and

rovibronic bands of molecules presents during discharge. Atomic lines start to appear when the intensity of the black-body emission decreases. Auto-absorption is also observed in several lines of Pt atoms. Swan-band of the C_2 molecule is also observed after the decrease in the black-body emission. By modeling the spectra of C_2, we can determine a characteristic temperature and its time evolution. This information is directly related to the synthesis of carbon nanoparticles during the discharge, what opens new perspectives in their control.

PST-1-Or-5
Determination of N, O and N2(A) metastable density in the afterglows of N2 and N2-O2 RF discharges

T11 Plasma Science and Technology

#PST-1-Or-5

A. Ricard [1], S.G. Oh [2].

[1]laplace - Toulouse (France), [2]Ajou Univ - Suwon (Korea, republic of).

Afterglows of N_2 and $N_2 – O_2$ flowing RF discharges are characterized by emission spectroscopy. The N and O atoms and the $N_2(A)$ metastable molecule densities are determined after NO titration for N and measurements of NO and N2 band intensities for O and $N_2(A)$.
The experimental setup showing only the early afterglow, between 32 and 45 cm from the discharge at z=0, is reproduced in Fig.1. The late afterglow appeared after 45 cm. The early and late afterglows have been analysed at z = 37 cm (maximum of the early afterglow) and at z= 55 cm in a dominant late afterglow . At these 2 positions , it has been determined by the method of ref.1 a contribution of the N+N recombination of 10% in the early which is mainly a pink afterglow and 70 % in the late afterglow(still 30% of pink).
The N-atom density is determined by NO titration which allows to calibrate the N_2(580 nm)intensity .
The O-atom density is obtained by comparing the NO(320 nm) intensity resulting from the N+O recombination to the N_2(580 nm) intensity.
The $N_2(A)$ density is deduced from the N_2(316 nm) intensity which mainly comes from the $N_2(A)+N_2(A)$ pooling reaction , also compared to the N_2(580 nm) intensity .

By introducing O_2 into N_2, at 8 Torr , 1 Slm , 100 W, it is found as shown in Fig.2 less N and O atoms in the early (pink) than in the late afterglow with a density slowly decreasing for the N-atoms and inversely increasing for the O-atoms with O_2 into N_2.
The $N_2(A)$ density is higher in the pink afterglow at less than 0.1%O_2 and become important in the late only at more than 0.5 %O_2.

[1]-N Kang, M Lee, A.Ricard and S-G Oh , *Effect of controlled O_2 impurities on N_2 afterglows of RF discharges*, CurrentApplied Physics 12 (2012) 1448-1453

Fig.1- RF capacitive discharge and flowing early afterglow in N_2, at 8 Torr, 1 Slm, 100 W [1].
Small quantities of O_2(10^{-4} – 10^{-2}) are introduced before the N_2 discharge.Ar-1.5 % NO is introduced before the early afterglow.

Fig.2 – Density of N ,O-atoms and N_2(A) metastable molecules versus O_2 percent into the early and late afterglows of N_2 at 8 Torr , 1 Slm , 100 W.

PST-P2-03
Combined gas temperature study in continuous and pulsed He ICP discharges

T11 Plasma Science and Technology

#PST-P2-03

N. Britun [1], N. Kang [2], S.G. Oh [2], R. Snyders [3].

[1]Chimie des Interactions Plasma Surface, Univ. de Mons - Mons (Belgium), [2]Division of Energy Systems Research, Ajou University - Suwon (Korea, republic of), [3]Chimie des Interactions Plasma Surface, Univ. de Mons, Materia Nova Research Center - Mons (Belgium).

Recent results on continuous and time-resolved gas temperature (T_g) diagnostics in He inductively coupled plasma (ICP) discharges are presented. The ICP discharges working at 13.56 MHz in continuous and pulsed mode ignited by a spiral coil in a vacuum chamber have been operating at 100 mTorr of working pressure (with repetition frequency 0.5 and 1 kHz, 50% of duty ratio in the pulsed case). The applied power (P_{RF}) is ranged within 50-400W (continuous) and was about 250W/pulse (pulsed). Fabry-Perot interferometry (FPI), rotational emission spectra analysis, as well as thermocouple measurements are utilized for T_g determination.
The Doppler broadening of one of the component of He 587.56 nm emission line is used for T_g study by FPI. The developed and built interferometer with a typical finesse of ~30 and resolution of ~1 pm is utilized for this purpose. The FPI results show that, in the continuous mode T_g grows linearly with P_{RF} remaining in our case in the range of 300-600 K. In the pulsed mode at P_{RF} = 240W/pulse T_g increases during ~150 μs at the beginning of pulse and later saturates at ~470 K level (see Fig. 1). The obtained FPI results are verified by the time-averaged measurements of N_2^+ rotational temperature (T_{rot}) using the First Negative System of N_2^+ [1]. T_{rot} is determined by the Boltzmann plots drawn for corresponding rotational population in the N_2^+(B) state. A good agreement between the T_{rot} of N_2^+ and the FPI data is obtained within the error of measurements (± ~40 K) in the continuous mode. In the pulsed mode T_{rot} data represents T_g values after saturation in the plasma pulse owing to the fact that the contribution to the rotational spectra coming from the beginning of the plasma pulse is negligible due to the low emission intensity (Fig. 1). The total T_g elevation during the pulse under our conditions is found to be equal to ~150 K.

The time-averaged temperature values measured by a thermocouple attached to a Cu plate located in plasma bulk correlate well with both FPI and T_{rot} results, showing the high level of thermal equilibrium in this type of discharges in the considered pressure range.
The obtained results establish the usability of high-resolution Fabry-Perot spectral analysis for ICP discharges, and can be applied for characterization of the actual ICP plasma processes involving He, as well as the other gases/mixtures, especially where addition of the molecular species for rotational spectral analysis is limited.

Keywords: ICP discharge, Fabry-Perot interferometry, helium, gas temperature

[1] A. Ricard, *Reactive Plasmas*. Paris: SFV Edition, 1996.

Figure 1. Time-resolved gas temperature in a pulsed He ICP discharge measured by FPI. T_{rot} of N_2^+ and thermocouple (T/C) data are given for comparison.

PST-P2-04
Capacitively coupled rf discharges in N2-H2 at low-pressure

T11 Plasma Science and Technology

#PST-P2-04

L. Alves [1], L. Marques [2], A. Mahjoub [3], C. Pintassilgo [4], A. Gouveia [4], N. Carrasco [3], G. Cernogora [3].

[1]Instituto de Plasmas e Fusão Nuclear, Instituto Superior Técnico - Lisbon (Portugal), [2]Instituto de Plasmas e Fusão Nuclear, Instituto Superior Técnico and Centro de Física da Universidade do Minho, Universidade do Minho - Braga (Portugal), [3]Université Versailles St-Quentin, CNRS, LATMOS - Guyancourt (France), [4]Instituto de Plasmas e Fusão Nuclear, Instituto Superior Técnico and Departamento Engenharia Física, Faculdade Engenharia, Universidade do Porto - Porto (Portugal).

Capacitively coupled radio-frequency (ccrf) discharges can be used in planetary studies to simulate, in laboratory environment, the reactivity of ionospheres. The present work is part of a research strategy, involving both simulations and experiment, to analyse the N_2-CH_4 ionospheric chemistry of Titan, the biggest satellite of Saturn. The first step was the study of ccrf discharges in pure N_2 [1], which now pursues with the analysis of N_2-H_2 discharges, considering that the original atmosphere contains hydrogen resulting from the dissociation of methane. N_2-H_2 ccrf discharges are also used for the etching of low-k organic materials and to enhance the plasma-assisted nitriding process.

Simulations use a hybrid code that couples a 2D (*r*,*z*) time-dependent fluid-type module, describing the transport of the charged particles, to a very complete 0D kinetic module, for the nitrogen-hydrogen mixture. The fluid module solves the charged-particle continuity and momentum transfer equations, the electron mean energy transport equations, and Poisson's equation for the rf electric potential. The kinetic module solves the two-term homogeneous and stationary electron Boltzmann equation (accounting for inelastic collisions from ground-state molecules and atoms, and inelastic and superelastic collisions involving vibrationally excited states) and the rate balance equations of the ground-state vibrational excited states and the main electronic excited states with the N_2 and H_2 molecules, the most relevant electronic excited states with the N and H atoms, and the most relevant N_xH_y radicals resulting

from interactions between the two excited systems [2,3]. The space-time map of the electron transport and rate coefficients is obtained from the electron mean energy profile using the local mean energy approximation.

The experimental setup is described in detail in [4]. A system of parallel-plate electrodes (driven at 13.56 MHz frequency) is surrounded by a cylindrical metallic grid, which confines the discharge. The resulting closed reactor acts as a resonant cavity in the microwave range, used to measure the electron density. Optical emission spectroscopy diagnostics are used to study the evolution, with the work conditions, of the First Negative System with N_2^+. The effective rf power coupled to the plasma is determined using the subtractive method [1], hence accounting for the circuitry power losses.

The study analyse the modifications induced in pure N_2 ccrf discharges, running at low-pressure (0.5–1.5 mbar) and low-power (5–20 W, corresponding to 110-220 V applied voltages), by the addition of small amounts of H_2 (up to 5%). The discussion is particularly focused on the evolution of the electron density and the population of N_2^+.

Acknowledgements
Work partially supported by the FCT (Project Pest-OE/SADG/LA0010/2011). A. Mahjoub thanks the ANR program (ANR-09-JCJC-0038 contract) for a post-doctoral position.

[1] L.L. Alves et al, Plasma Sources Sci. Technol. 21 (2012) 045008
[2] L. Marques, J. Jolly and L. L. Alves, J. Appl. Phys. 102 (2007) 063305
[3] E. Tatarova et al, Plasma Sources Sci. Technol. 14 (2005) 19
[4] G. Alcouffe et al, Plasma Sources Sci. Technol. 19 (2010) 015008

PST-4-Or-6
Non-invasive Process Diagnostics of Nanoparticle synthesis in an inductively coupled plasma reactor.

T11 Plasma Science and Technology

#PST-4-Or-6

C. Delval, M. Leparoux.

Empa, Laboratory for Advanced Materials Processing, Feuerwerkerstrasse 39, CH-3602 Thun, Switzerland - Thun (Switzerland).

In the last decades, nanoparticles synthesis using thermal plasma technology has been widely spread [1]. High flexibility of the precursor phase (gas, liquid, solid), high enthalpy of thermal plasmas, and ability to control the chemistry of plasmas (flexible gas mixture), allow the production of almost all materials including those with a high melting point [2] at high production rates (kg/h).
In the process, precursors are vaporized in the thermal plasma leading to a supersaturated gaseous phase with nanoparticles subsequently forming upon cooling. Fine-tuning of targeted stoichiometry is achieved by injecting additional reactive gases.
Among thermal plasmas, Inductively Coupled Plasma (ICP) processing is a powerful technique to produce nanopowders of oxides, metals and hard ceramics such as TiCN or SiC [3].
ICP is a technique of choice to produce nanoparticles with well-defined properties thanks to a longer residence time of the precursor (axial injection), a rapid condensation of the supersaturated gas phase (quenching) and the absence of contamination generated by the electrodes.
In the Laboratory for Advanced Materials Processing of Empa (Thun – CH), the expertise has been focused on the understanding and the precise control of the whole synthesis process which is the key to the development of advanced nanoparticles with tailored and reproducible properties.
In thermal plasma, to obtain high quality nanoparticles with high production yield, the complexity of the subsequent steps of thesynthesis implies a systematic study of the influence of the processing conditions and parameters, and a thorough understanding of the interaction plasma-particle.
At Empa Thun, a RF-ICP setup, based on a Tekna PL-35 torch linked to a 13.56 Mhz generator (Pmax=35 kW), has been dedicated to the investigation of plasma

synthesis and in-flight functionalization of nanoparticles [4] since years. The reactor is equipped with many viewports enabling the observation and characterization of the overall process including plasma properties, gas phase characterization and plasma/particles interactions. Enthalpy probe measurements have been performed to characterize the plasma properties depending on the process parameters. The synthesis chamber is equipped with non-invasive optical diagnostics (FTIR, light extinction spectroscopy, Optical Emission Spectroscopy) to gain insight into the plasma-particles interactions. High speed imaging is assessed to observe the instabilities of the plasma tail and follow the trajectories of the inlet micron-sized precursor particles.
Based on case studies, we will present here the state of the art of the plasma characterization of synthesis of nanoparticles at Empa.

[1] Shigeta M. and Murphy A.B. 2010 Thermal Plasmas for nanofabrication J. Phys. D: Appl. Phys. 44 174025
[2] Ostrikov K., Cvelbar U. and Murphy A.B. 2011 Plasma nanoscience: setting directions, tackling grand challenges J. Phys. D: Appl. Phys. 44 174001
[3] Leparoux M., Schreuders C. and Fauchais P. 2008 Improved Plasma Synthesis of Si-nanopowders by Quenching Adv . Eng. Mat. 10 12 1147-50
[4] Leparoux M., Leconte Y., Wirth A. and Buehler Th. 2010 In Situ Treatment of Thermal RF Plasma Processed Na-nopowders to Control their Agglomeration and Dispersability Plasm. Chem. Plasm. Proc. 30 779-793

PST-3-Or-1
Experimental and theoretical study of the plasma-surface interaction during the growth of ethyl-lactate plasma polymers

T11 Plasma Science and Technology

#PST-3-Or-1

S. Ligot [1], F. Renaux [2], P. Raynaud [3], P. Gerbaux [4], M. Guillaume [5], R. Snyders [1].

[1]Chimie des Interactions Plasma-Surface, University of Mons - Mons (Belgium), [2]Materia Nova - Mons (Belgium), [3]Matériaux et Procédés Plasmas, University Paul Sabatier - Toulouse (France), [4]Groupe de Recherche en Spectrométrie de Masse, University of Mons - Mons (Belgium), [5]Chimie des Matériaux Nouveaux, University of Mons - Mons (Belgium).

Polylactic acid (PLA), derived from renewable resources, is a (bio)degradable polymer accepted as a good alternative to conventional polymers for packaging applications. Nevertheless, as for other polymers, it presents too high water and gas permittivity. In order to improve its barrier properties and, as a consequence, its degradation rate, we are developing a cross-linked ethyl lactate-based plasma polymer film (ELPPF). The control of both chemical composition (hydrolysable ester bonds density) and cross-linking degree would allow tuning the degradation rate of the polymer by ester bond hydrolysis.
In this work, our objective is to correlate the plasma and film chemistries and, ultimately, to propose a clear picture of the plasma-surface interaction during the process.
ELPPF have been synthesized by PECVD using both continuous and pulsed RF power (PRF) through an ICP copper coil (5 W < PRF < 400 W). The ELPPF chemistry, especially the ester function density, has been evaluated by the combination of chemical derivatization and XPS measurements and compared to the plasma phase composition measured by using RGA mass spectrometry and in situ infrared spectroscopy. These plasma diagnostic data are discussed in view of DFT calculations.
Our data reveal that, in the defined experimental window, by increasing PRF, the

ester content in the ELPPF increases from 1.4 at.% to 18 at.% which is perfectly correlated to the in situ FTIR spectroscopy data revealing the loss of the degradation of the ester function in the gas phase with a similar rate. On the other hand, the mass spectrometry data supported by DFT calculations allow proposing a clear fragmentation pattern of the precursor as a function of the experimental conditions. Altogether, this set of data paves the way for a reproducible and controllable synthesis of ELPPF with defined chemical composition.

PST-P2-05
Surface Temperature Measurement using Fraunhofer Diffraction via Photoacoustic Waves for Laser Irradiation Process

T11 Plasma Science and Technology

#PST-P2-05

F. Mitsugi [1], T. Ikegami [1], T. Nakamiya [2], Y. Sonoda [2].

[1]Kumamoto University - Kumamoto (Japan), [2]Tokai University - Kumamoto (Japan).

Pulsed laser irradiation is used for treatment of a solid surface and ablation to fabricate nanoparticles or anneal thin films . When a pulsed laser irradiates a solid surface, photoacoustic waves are caused. For solids, photoacoustic wave generation involve photothermal expansion via thermoelastic expansion, as well as shockwaves induced by ablation plasma. Detection of indirect photoacoustic waves is important because it enables us to obtain maximum surface temperature indirectly. In this research, we introduced an optical wave microphone for detection of indirect photoacoustic waves and shockwaves. The optical wave microphone works based on Fraunhofer diffraction. We reported on waveforms and frequency analysis of photoacoustic waves from Si in air for surface temperature measurement.

Fig.1 shows experimental setup of an optical wave microphone to detect photoacoustic waves. The working region of the microphone is between the diode laser and the lens1. A Si wafer is set within the working region and irradiated by a pulse of YAG laser. The laser energy was varied from 46 to 460 mJ/cm^2. Photoacoustic waves were detected by optical wave microphone even though the energy was as low as 46 mJ/cm^2. It was laser induced ultrasonic waves from Si. The frequency of the obtained waveforms ranged from about 100 to 200 kHz that depended on the detector position. Fig.2 shows intensity and velocity of the obtained signals for pulsed laser irradiation of Si as a function of the energy density of the pulsed laser. The intensity and the velocity increased gradually with the laser energy density when it was less than ablation threshold energy. It showed good agreement with surface temperature calculation of Si. The intensity showed drastic increase and

the velocity obviously exceeded sound speed in air due to the influence of the generation of shockwave when the laser energy density increased and ablation occurred.

[1] F. Mitsugi, R. Ide, T. Ikegami, T. Nakamiya, Y. Sonoda, Thin Solid Films, 521 (2012) 132.
[2] F. Mitsugi, T. Ikegami, T. Nakamiya, Y. Sonoda, Jpn. J. Appl. Phys., 51 (2012) 01AC10.

PST/SE/TF-3-Or-12
Surface patterning of an austenitic stainless steel by different low-temperature thermochemical plasma-assisted treatments

T11 Plasma Science and Technology

#PST/SE/TF-3-Or-12

A. Andrieux, G. Marcos, H. Michel, T. Czerwiec.

Institut Jean Lamour - Nancy (France).

Low-temperature thermochemical plasma-assisted treatments are commonly used on austenitic stainless steel to enhance surface properties by forming an enriched surface layer.
During a nitriding treatment a large amount of nitrogen is introduced in the austenite lattice, inducing high compressive residual stresses. As a result, an expansion of the treated layer from the initial position of the substrate in a direction perpendicular to the surface occurs.
We take advantage of this phenomenon, called uplift, to create a pattern on the surface. The idea is to protect locally the surface by covering it with an appropriate masking technique. By doing so, only the uncovered parts will be exposed to the incident plasma. After nitriding the surface presents a controlled topography, due to the difference of height induced by the spatially restricted uplift. We will show that this uplift phenomenon also happens during carburising treatments, with amplitude comparable to that of nitriding.

It is known [1] that a surface pattern enhanced tribological properties in loaded lubricated contact systems by providing a hydrodynamic pressure that helps separating the mating surfaces. Geometry (holes, grooves, dots, etc) and dimensions (from 1 to several hundred micrometres) strongly depend on the working conditions and the configuration of the contact system. The aim of our study is to develop a patterning process of AISI 316L based on thermochemical treatments. Their parameters will be chosen to insure good surface properties (corrosion and tribological behaviour) while achieving the required patterning.

We use a multi-dipolar plasma, based on the Distributed Electron Cyclotron

Resonance concept, to perform thermochemical treatments on austenitic stainless steel samples recovered by different types of masks: copper TEM grids, especially designed nickel stencils and boron-based layers. We will highlight here the difficulties encountered to achieve an efficient masking.
We conduct SEM, XRD and GD-OES analyses to determine surface layer characteristics and tactile profilometry to measure pattern dimensions. The internal compressive stresses were estimated using the basic elastic model described in ref [2].
We will present results concerning pure nitriding and carburising, nitrocarburising and sequential treatments in different conditions. We investigate their influence on the uplift and on the surface layer depth and concentration in nitrogen and/or carbon.

This work is financially supported by the French National Research Agency (reference ANR 2011 RMNP 008 01).

[1] Etsion, I., Halperin, G., Greenberg, Y.. Increasing mechanical seals life with laser-textured seal faces. In. Proceedings of the fifteenth international conference on fluid sealing. Maastricht: BHR Group; 1997. p. 3–11

[2] Czerwiec,T., He,H., Marcos, G., Thiriet,T., Weber, S., Michel,H.. Fundamental and innovations in plasma assisted diffusion of nitrogen and carbon in austenitic stainless steels and related alloys, Plasma Process. Polym. 6, 401, 2009

PST/SE/TF-P1-12
Effects of transverse magnetic field on cathode spot movement in arc ion plating

T11 Plasma Science and Technology

#PST/SE/TF-P1-12

J. Xiao [1], Y. Zhao [1], W. Lang [2], J. Gong [1], C. Sun [1].

[1]Institute of Metal Research Chinese Academy of Sciences - Shenyang (China), [2]IWenzhou Vocational & Technical College - Wenzhou (China).

Macroparticles (MPs) pollutions severally deteriorate the qualities and mechanical properties of the deposited films by arc ion plating. In order to eliminate them, a transverse magnetic field was provided on the basis of increasing the movement rate of arc. The obtained results showed that with the increase of the rotating transverse magnetic field strength in the low-frequency conditions, the arc spot morphology gradually transformed from the congregation of bright blotches into a straight long thin line. And the greater is the magnetic field strength, the longer and finer the arc spot trajectory line is.
Arc spot trajectory line being long describes the proportional acceleration of the speed of movement of the arc spot; arc spot trajectory line being longer and thinner implied that the arc spot trajectory plaques along a certain direction of the linear movement as a result of ampere force. According to action of the ampere force, the inverse of the arc spot in a transverse magnetic field moved "backwards", in which it possibly verified that the rotating magnetic field means is generated in the target surface with a kind of uniform transverse magnetic field. The MPs on the surface of TiN films were significantly reduced, and the reason lied in the increasing linear movement speed and the shorter residence time in one point at the surface of target.

[1] R. L. Boxman, V. N. Zhitomirsky, Rev. Sci. Instrum. 2006, 77: 6748
[2] I. I. Beilis. Appl. Phys. Lett. 2002, 181: 3936.
[3] A. Anders. Thin Solid Films. 2006, 502: 22.

PST/SE/TF-3-Or-8
Study of O and H atom kinetics in pulsed O2/TTIP/HMDSO low pressure ICP plasmas by time resolved optical emission spectroscopy

T11 Plasma Science and Technology

#PST/SE/TF-3-Or-8

A. Granier [1], S. Elisabeth [2], S. Jacq [2], M. Carette [2], A. Goullet [2].

[1]IMN - Univ Nantes, CNRS - Nantes (France), [2]IMN - Univ Nantes, CNRS - Nantes (France).

Titanium dioxide films (TiO_2) are attractive for a large range of applications including photocatalysis, high-k materials, optical coatings and waveguides. While most studies deal with TiO_2 films deposited by dip coating or magnetron sputtering, much less studies have been devoted to TiO_2 films prepared by plasma enhanced chemical vapor deposition (PECVD) in O_2/TTIP (titanium tetraisoproxide) plasmas. Low pressure high density plasmas, such as microwave electron cyclotron resonance plasmas [1] and inductively coupled RF plasma (ICP) [2] have been shown to allow deposition of amorphous or partially crystallized (anatase and/or rutile phases) films at temperature less than 100°C. Nevertheless, plasma deposited TiO_2 films are columnar, which is detrimental for optical and electrical (high-k material) applications. One way to get free from the columnar structure and obtain an homogeneous film is to add silicon in the TiO_2 film, using O_2/TTIP/HMDSO (hexamethyldisiloxane) plasmas in the case of PECVD.

Here, we investigate RF ICP O_2/TTIP/HMDSO plasmas operated at 4 mTorr , 400 W. The pulsed O_2/TTIP/HMDSO plasmas were analysed by time resolved optical emission spectroscopy (TROES). In order to probe the post-discharge, a second pulse was applied to monitor the active species decay in the post-discharge using the method proposed by Bouchoule et al [3] and previously developed in pulsed O_2/HMDSO plasmas [4].

The TROES measurements carried out in pulsed discharges created in oxygen-rich O_2/TTIP and O_2/HMDSO plasmas allow to determine the recombination probabilities of O and H on SiO_2 and TiO_2 walls, respectively. Therefore, the plasma on time was

varied from 10 to 50 ms at a frequency of 5 Hz. O, H, OH species creation (in the discharge) and loss (in the post-discharge) kinetics were investigated. The time variations of the intensities (I) of the Ar (750.4 nm), O (844.6 nm), Hα (656 nm) lines and OH emission at 310 nm were recorded. The recombination probabilities of O and H derived from the exponential variations of IO/IAr and IH/IAr (using the method detailed in [4]) during the discharge in O_2/HMDSO and O_2/TTIP pulsed plasmas are given hereafter. O and H recombination is shown to be much faster on TiO_2 than on SiO_2 walls.

	O_2/HMDSO plasmas (SiO_2 walls)	O_2/TTIP plasmas (TiO_2 walls)
O atoms	$\gamma_O = 0.03 \pm 0.01$	$\gamma_O = 0.3 \pm 0.1$
H atoms	$\gamma_H = 0.001 \pm 0.0005$	$\gamma_H = 0.014 \pm 0.005$.

Here we will more particularly investigate the decay of O and H density in the post-discharge of O_2/HMDSO and O_2/TTIP pulsed plasmas and compare with the creation kinetics in the discharge period. Then we will investigate the evolution of O, H and OH creation and decay kinetics in O_2/HMDSO/TTIP pulsed plasmas. At last, TROES measurements will be carried out in water vapour and CO_2 plasmas in order to study the effect of H_2O and CO_2 (CO) adsorption on O recombination on TiO_2 based walls.

[1] A. Borras, J. Cotrino, A. R. Gonzalez-Elipe, J. Electrochem. Soc. 154 (2007) 152.
[2] A. Granier, T. Begou, K. Makaoui, A. Soussou, B. Bêche, E. Gaviot, M.P. Besland, A. Goullet, Plasma Process. and Polym. 6 (2009) S741.
[3] A. Bouchoule and P. Ranson, J. Vac. Sci. Technol. A 9 (1991) 317.
[4] A. Bousquet, G. Cartry, A. Granier, Plasma Sources Sci. and Technol. 16 (2007) 597.

PST-2-Or-10
On the Secondary Electron Emission of Metallic Surfaces Exposed to a Plasma

T11 Plasma Science and Technology

#PST-2-Or-10

F. Tabares.

Ciemat - Madrid (Spain).

On the Secondary Electron Emission of Metallic Surfaces Exposed to a Plasma.

Eider Oyarzabal, Ana B. Martin-Rojo and Francisco L Tabarés*

As Euratom-Ciemat, Av Computense 40, 28040 Madrid.Spain

*Corresponding author. Email. tabares@ciemat.es

Samples of lithium, tungsten and stainless steel were exposed to dc Glow Discharges of He, Ar and H_2. Anomalous I-V characteristics for negative biasing (with respect to plasma potential) have been observed in all cases but at different level depending on the kind of surface and the plasma parameters[1]. The parameters for which the anomalous effect was maximized correspond to those allowing for the production and propagation of a high-energy tail in the Electron Energy Distribution Function (EEDF). From the I-V characteristics of the exposed samples, the Secondary Electron Emission (SEE) yield vs. the mean energy of the suprathermal electrons for each value of the applied voltage was calculated for Li, SS and W surfaces. While values in good agreement with previous, plasma-free, reports were deduced for W and SS, the SEE yield for lithium is 2.5 times higher than expected. Although the absolute value of the SEE changed with plasma characteristics (gas, pressure, current, voltage), the deduced yield remained the same for a given element. Experiments to address

the effect of oxygen addition to the lithium surfaces were carried as well in the same set up. A clear decrease of both, Sputtering Yield and SEE Yield of lithium with higher oxygen content was observed, thus precluding a simple surface contamination effect as the driving agent. A possible synergetic effect of the target ion bombardment and the SEE for charge-emitting elements, such as lithium, is suggested.

[1]. E.Oyarzabal et al. Proc. PSI20, Aachen 2012. To appear in J Nucl. Mater.

PST-P2-15
Numerical Simulation of Magnetized Electrostatic Sheath in Presence of Dust Size Distribution

T11 Plasma Science and Technology

#PST-P2-15

S. Chekour, A. Tahraoui, B. Zaham.

Laboratoire d'Electronique Quantique,Faculté de Physique,Université USTHB - Algiers (Algeria).

The sheath formed between plasma and a material boundary has received a lot of attention. The major impetus behind this effort has been an increasing awareness of the importance of the edge plasma in the overall confinement properties of magnetically confined fusion plasmas. Since the sheath represents the outer most layer of the edge plasma, and hence plays an important role in the particle and energy flux to the wall, it is natural that it should attract so much interest. In this work, we have established a three dimensional and stationary theoretical model in presence of oblique magnetic field assuming more realistic plasma where the dust grains are considered with different sizes. For this we have considered a Gaussian law [1]. The positive ions and dust particles are considered as cold fluids. The electron is considered in thermodynamic equilibrium; therefore they obey to Boltzmann's statistic. To describe the dust charge, we have used the orbit motion limited model (OML) [2].

The numerical results show that the presence of magnetic field reduces the sheath thickness but the behavior of the electrostatic potential and the dust grains density is not affected. In addition, the variation the lower value of dust radius has no effect on the sheath structure. However, the increase of the higher value of the dust radius makes the structure of the grain density steeper. The effects of the other parameters are also discussed.

[1] P. Meuris, Planet. Space Sci. 45, 449 (1997); A. Brattli, O. Havres, and F. Melandso, J. Plasma Phys. 58, 691 (1997).

[2] P. K. Shukla and A. A. Mamun, Introduction to Dusty Plasma Physics (Institute of Physics, Bristol, 2001).

PST-P2-18
Nano-porous plasma polymers with stable vertical chemical gradients

T11 Plasma Science and Technology

#PST-P2-18

N. Blanchard, B. Hanselmann, D. Hegemann.

Empa - St.gallen (Switzerland).

Using plasma polymerization, we deposit thin nano-porous films exhibiting a vertical chemical gradient. It has been shown that by varying the gas ratio of polymerizable to non-polymerizable gases during the plasma process a broad range of wetting properties can be achieved [1,2]. We are using this result to generate the vertical gradient structure within the coatings. In addition, to ensure that the plasma polymer coatings simultaneously exhibit a certain porosity and a high stability, a precise control of the plasma polymerization processes by variation of the energy input during film growth (ion bombardment) and into the gas phase (determining the chemical processes in the plasma) is established via the contol of plasma polymerization conditions such as gas ratio, flow rate, pressure and power input. The functional group content within the nano-porous layer can thus be varied by modifying these plasma polymerization conditions. We generate both, hydrophilic-to-hydrophobic (using HMDSO/O_2) and also hydrophobic-to-hydrophilic (using C_2H_4/CO_2 or C_2H_4/NH_3) gradients and show the stability of these coatings as well as the delayed wetting of the “hidden” layer. The intrinsic vertical gradient will allow adsorbing molecules to “sense” both, hydrophilic and hydrophobic components of the layer provided that the gradient structure is of the same size as the adsorbates, which exhibit typical dimensions of a few nanometers. This requires that the deposition rate of the respective plasma polymer coatings is rather low to ensure controllable and reproducible processes. It is expected that amphiphile (bio-) molecules will adsorb in a preferred and oriented way to these gradient layers and that new adsorption/desorption kinetics will arise, which are subject of further studies.

[1] Hegemann, D., Brunner, H., & Oehr, C. (2002). Improving the Adhesion of Siloxane-Based Plasma Coatings on Polymers with Defined Wetting Properties, 174–178.

[2] Körner, E., Fortunato, G., & Hegemann, D. (2009). Influence of RF Plasma Reactor Setup on Carboxylated Hydrocarbon Coatings. Plasma Processes and Polymers, 6(2), 119–125. doi:10.1002/ppap.200800102

PST/SE/TF-P1-02
Investigation of a triode sputter source used for the deposition of the inside wall of narrow hollow cylinders

T11 Plasma Science and Technology

#PST/SE/TF-P1-02

J. Laimer [1], E. Ruppert [1], H. Störi [1], W. Gärtner [2].

[1]TU Wien - Wien (Austria), [2]Miba Gleitlager GmbH - Laakirchen (Austria).

Nowadays, it is common practice to deposit coatings by magnetron sputtering with sufficiently high deposition rate. Even inner walls of hollow cylinders may be coated by this technique. However, due to the space required for magnets in the interior of the cylindrical sputter source there is a limit in down sizing the diameter of the source and hence a limit in the minimal diameter of hollow cylinders to be coated.

Triode sputter deposition, which is known since a long time, does not need the incorporation of magnets as the required higher electron density may be achieved by a hot filament supported auxiliary discharge. By omitting magnets from the interior of cylindrical sputter targets the diameter of the targets can be much smaller and hence the deposition of inner walls of narrower hollow cylinders should be possible.

We present a hot filament supported triode sputter system, optimised for high rate deposition inside narrow spaces. In the present study the sputter target made of $CuSn_8$ had a diameter of 15 mm, whereas the steel sleeve to be coated had an inner diameter of 30 mm in order to prove the principle. This diameters are not the limit of the process, as both diameters could be easily further decreased.

A detailed electrical characterization of the discharge showed a high flexibility and stability of the operation point of the discharge. At filament powers of up to 2600 W and voltages of the auxiliary discharge of up to 65 V discharge currents of up to 20 A were measured. In the present geometry sputter currents of up to 0.75 A for applied sputter voltages of 1000 V were observed leading to deposition rates of up to 1.4 µm/min. The film thickness along the coated sleeve was uniform.

PST-4-Or-7
Deposition of GeTe phase change material by plasma enhanced MOCVD

T11 Plasma Science and Technology

#PST-4-Or-7

M. Aoukar [1], C. Vallée [1], A. Pikon [1], D. Jourde [2], P. Michallon [2], P. Noe [2], S. Maitrejean [2].

[1]Laboratoire des technologies de la microélectronique (LTM) - CNRS/UJF - Grenoble (France), [2]CEA, LETI - Grenoble (France).

The Phase-Change Memory technology is widely recognized as one of the most promising next generation nonvolatile memory solutions, since it offers better scalability, endurance and programming speed compared to standard Flash memories[1]. However this technology presents two major drawbacks: an archival life for high operating temperatures too short and power consumption too high. The binary compound GeTe seems to be a promising candidate; it shows better retention characteristics at high temperature compared to other chalcogenide alloys. Otherwise, it has been demonstrated that energies can be highly decreased by confinement of the material. To achieve the gap filling of the confined structure, conventional sputtering process cannot be used. Hence, more conformal processes as Chemical Vapour Deposition (CVD) or Atomic Layer Deposition (ALD) are required.

Considering the low deposition rate of ALD, we proposed to study the deposition of GeTe in a shower-head type 200 mm plasma-enhanced pulsed liquid injection CVD reactor. Ge and Te liquid precursors are introduced into the deposition chamber as vapours through a pulsed injection system and an evaporating furnace. Capacitively-coupled RF plasma is applied between the shower head and the substrate heater. The role of the plasma in the process is multiple: optimisation of the substrate before deposition, participation to the precursor decomposition, control of carbon concentration. Moreover, thanks to the plasma assistance, homogeneous deposition of the GeTe material on its amorphous phase is obtained[2].

In this work we investigate the influence of many plasma parameters such as the injection frequency of the precursors, RF power, pressure and gas rate on the

decomposition of precursors. Precursor decomposition mechanisms are discussed by analysing optical emission spectra of the plasma. Optical Emission Spectroscopy shows that during deposition, peaks with a frequency equal to the injection frequency can be observed for Te, CN, H and Ar species. As shown in figure 1, the emission of CN* (relative to the decomposition of Ge precursor) and Te* are in antiphase although the synchronised injection of precursors and shows thus a different behaviour of the two precursors in the plasma. Fluctuations of the emission intensities are also observed and are correlated to the in situ XPS depth profiling of the deposited material. The etching capacity of the argon-hydrogen plasma and its influence on the conformity of the films is also discussed.

[1]G. W. Burr et al, J. Vac. Sci. Technol. B 2010, 28 (223)
[2]Gourvest et al, ECS J.Solid State Sci.Technol.1,(6) 2012: Q119-Q22.

Figure1: Evolution of the emission intensity of species during deposition

PST/SE/TF-3-Or-10
Duplex layer structures produced by low temperature Nitrocarburizing and sequential Nitriding/Carburizing treatments of austenitic stainless steel

T11 Plasma Science and Technology

#PST/SE/TF-3-Or-10

G. Marcos, A. Andrieux, Y. Guo, T. Czerwiec.

Institut Jean Lamour - Nancy (France).

In order to improve tribological properties of austenitic stainless steels, low-temperature diffusion treatments as plasma-assisted nitriding (PAN), plasma-assisted carburizing (PAC) or a combination of these two processes, i.e. plasma-assisted nitrocarburizing (PANC), are developed since the 1980s. PAN is a treatment in which nitrogen atoms diffuse in the metallic material producing, below 693 °K, a specific phase usually called expanded austenite or γN phase. Expanded austenite is a metastable nitrogen supersaturated solid solution with a disordered fcc structure and a distorted lattice. Its nitrogen content can reach 35 at% or more, inducing important compressive residual stresses. Replacing nitrogen by hydrocarbon for conducting a low temperature PAC leads to a carburized layer containing the carbon expanded austenite phase (γC). In this case, the maximum carbon content is of 12 at%. This type of treatment has the double advantage of having a good kinetics and limiting plastic deformation of the material. However, the tribological properties of the carburized layers are not as good as those of the nitriding layers. Finally, it is possible to obtain simultaneously these two phases by combining hydrocarbon and nitrogen in the gas phase through a low temperature PANC.

We perform PAN, PAC and PANC treatments by using a multi-dipolar plasma, based on the Distributed Electron Cyclotron Resonance (DECR) concept [1]. The plasma source is a plane-network of eight microwave antennas placed at the top of a cylindrical diffusion chamber. The substrate-holder can be independently heated and biased. The low-pressure plasma phase is a mixture of Ar, N_2, C_3H_8 and H_2, according to the desired treatment. The studies are realized on substrates in austenitic stainless steel AISI 316L, previously polished like a mirror. The main purpose of this work is to compare PANC treatments with sequential ones:

carburizing followed by nitriding or nitriding followed by carburizing. During PANC, it was found that nitrogen and carbon atoms can simultaneously be dissolved into the austenite lattice, forming a dual layer structure with an extremely hard nitrogen-enriched layer near the substrate surface and above a hard carbon-enriched layer. Our aim is to study the role of the repulsive interaction between nitrogen and carbon on the characteristics of this dual layer structure. X-Ray Diffraction is used to identify the presence and structure of the expanded austenite. The layer thickness is observed by optical microscopy and the composition of the layers is determined by GDOES.

During nitriding followed by carburizing treatments we observe that nitrogen pushes the carbon inside the steel inducing the formation of γC phase at the interface with the untreated substrate. During carburizing followed by nitriding treatments carbon diffusion through the nitrided layer is observed to be extraordinary fast due to the repulsive interaction of carbon on nitrogen. The amount of carbon incorporated into the material, determined from the integral of the GDOES signal, is found to be must higher from carburizing followed by nitriding sequential treatments than from nitrocarburizing.

[1] A. Lacoste, T. Lagarde, S. Bechu, Y. Arnal and J. Pelletier, Plasma Sources Sci. Technol. 11, 2002

PST-P3-04
Plasma modification of functionalized, ceramic membranes in composite gel electrolyte

T11 Plasma Science and Technology

#PST-P3-04

M. Pokora, M. Walkowiak, L. Horla, J. Kunicki.

Institute of Non-Ferrous Metals Branch in Poznan Central Laboratory of Batteries and Cells - Poznan (Poland).

Conventional lithium batteries with liquid electrolytes have achieved a tremendous technological and commercial success over the recent two decades, but they are prone to electrolyte leakages and ignition of volatile solvents. One of the most effective ways to prevent these accidents is to entrap conventional liquid electrolyte in a polymeric matrix, thus forming a stable gel. PVdF/HFP copolymer has proved to be one of the most useful polymeric matrices, which can easily be shaped into thin, elastic membranes. By dispersing in such a membrane certain ceramic powders (fillers) it is possible to improve some crucial characteristics of the gel electrolytes, such as mechanical, chemical, thermal and electrochemical stability. Huge amount of scientific reports have been devoted to identification of the most preferable ceramic filler.

In our work we made attempts to synthesize MCM-41 mesoporous silica functionalized with novel fluorine containing silane coupling agent - tridecafluoro-1,1,2,2-tetrahydrooctyldimethylchlorosilane with diffrent amount. The motivation of this approach was to enhance the effect of mesoporous filler by modifying it with functional groups compatible with the polymer matrix, through the existence of fluorine atoms. What is more, fluorine-based functionalization is expected to give rise to an increased chemical, electrochemical and thermal resistance, which is of particular importance for the viable battery technologies.

All membranes were modified by plasma to improve their porosity and increase the electrolyte uptake.

Mesoporous materials and dry membranes have been characterized physicochemically using such techniques as nitrogen adsorption isotherms, XRD, thermal analysis, SEM,TEM and FT-IR. These materials have been examined electrochemically, including the determination of the temperature dependence of specific conductivities (electrochemical impedance spectroscopy), electrochemical

stability window (cyclic voltammetry on platinum electrode) and lithium intercalation ability into graphite. It has been demonstrated that fluorine functionalized mesoporous silica exhibits favorable structural properties, stability and good ionic transport, evidenced by high conductivities.

The work has been financially supported by the European Regional Development Fund in the frameworks of the Innovative Economy Programme 2007-2013, project No. POIG.01.01.02-00-015/09.

PST-4-Or-8
Bistable hybrid memory elements deposited by plasma polymerization

T11 Plasma Science and Technology

#PST-4-Or-8

Y. Busby, J.J. Pireaux.

Centre de Recherche en Physique de la Matière et du Rayonnement (PMR), Laboratoire Interdisciplinaire de Spectroscopie Electronique (LISE), University of Namur, 61 rue de Bruxelles, B-5000 - Namur (Belgium).

Organic memory devices are considered the most promising candidates for a large scale, high density and cost efficient non-volatile memories [1, 2]. The device architecture is very simple, and it is based on an organic layer (which may be evaporated small semiconducting molecules, or a solution processed polymer film), sandwiched between two metal electrodes. The device may include some metal nanoparticles which can be randomly dispersed inside the organic layer or disposed to form an intermediate metal layer.
In this work, the possibility to deposit the organic layer by plasma processing is discussed.

A full polymer memory device based on a polystyrene thin film deposited by plasma polymerization is demonstrated (see J-V curves in *fig.1*). The system shows good switching properties, high On-Off ratio ($>10^4$), and good On-state retention time. The optimized full cycling scheme (which consists in the memory writing, erasing, and rewriting) is achieved by applying short voltage pulses over a certain voltage threshold. The memory elements were successfully cycled over hundreds of cycles without sensibly affecting the device performances.
The results extend the possibilities for organic memory device processing and present some technologically relevant advantages with respect to conventional deposition methods which will be discussed. In particular, the high control over different hybrid device architectures may be useful in studying the switching effect and so improving the future device performances and lowering the production costs. The switching features will be interpreted in terms of the formation and destruction of metallic filamentary paths inside the polymer layer [3].

[1] L. P. Ma, J. Liu, and Y. Yang, Applied Physics Letters **80**, 2997 (2002).
[2] T. W. Kim, Y. Yang, F. Li, and W. L. Kwan, NPG Asia Materials **4**, 1 (2012)
[3] B. Cho, J.-M. Yun, S. Song, Y. Ji, D.-Y. Kim, and T. Lee, Advanced Functional Materials **21**, 3976 (2011).

Fig. 1: Example of a typical J-V scan, obtained in the plasma polymerized styrene memory devices. The scan begins in the low resistance ON-state represented by black full dotted curve; the high resistance (OFF-state) curve,obtained after the [-4; +10] voltage scan, is shown with the dark grey open dots.

SE/PST/TF/BI-2-Or-8
Plasma treatment and cell adhesion experiments of porous 3D PCL scaffolds

T11 Plasma Science and Technology

#SE/PST/TF/BI-2-Or-8

R. Morent, N. De Geyter.

Research Unit Plasma Technology - Department of Applied Physics - Ghent University - Ghent (Belgium).

Poly-ε-caprolactone (PCL) is an aliphatic biodegradable and biocompatible polymer which has gained attention in the past few years due to its potential use in several biomedical applications. Due to the excellent mechanical and structural properties of PCL it can be used for tissue engineering, drug delivery applications and bone repair [1]. It can be used to create different types of scaffolds due to its ability to form the desired 3D shape [2]. In addition, 3D porous structures can be developed that facilitate ingrowth of blood vessels, ultimately leading to a better integration of the implant [3].

However, PCL has a low surface energy and wettability and these surface properties negatively affect cell attachment and proliferation. Therefore, in most cases a surface modification is required. By using plasma treatment, additional functional groups can be introduced on the polymer surface which alter the surface properties to meet the requirements of biomedical applications. Until now, only little work has been done on the plasma treatment of the biodegradable polymer PCL. In most of these studies, the authors have used vacuum (<0.2 kPa) plasma technologies. In this work, a medium pressure dielectric barrier discharge at 5 kPa will be used to activate the PCL samples.

This presentation will give an overview of some recent results on the surface activation of PCL samples. Spincoated PCL layers on glass substrates, small/flat PCL blocks and porous PCL scaffolds are investigated. The plasma is able to enhance the wettability of all sample types and ageing experiments show that at least part of the treatment effect is permanent. X-Ray photo-electron spectroscopy on the treated PCL surface shows an increased oxygen content for all samples; for the porous structures it is shown that also oxygen is incorporated inside the scaffold.

This proves that the plasma is able to penetrate and alter the surface inside the structure. Cell culture tests are done to study the possible beneficial effect of plasma treatment on cell attachment and proliferation. For flat non-porous PCL samples, the plasma effect on cell adhesion and proliferation is still noticeable after 7 days. For the porous 3D PCL scaffolds, the plasma treatment could also increase the cell numbers compared to untreated scaffolds. The promising results obtained in this work demonstrate the advanced possibilities of plasma technology for surface modification. Especially the improved penetration and adherence of cells inside porous PCL scaffolds can be of great importance for sophisticated applications in the field of tissue engineering.

[1] E.D. Yildirim, H. Ayan, V.N. Vasilets, A. Fridman, S. Guceri, and W. Sun; Plasma Processes and Polymers, 5:58–66, 2008.

[2] J. Venugopaland Y. Z. Zhang and S. Ramakrishn; Nanotechnology, 16:2138–2142, 2005.

[3] H. Yoon, S. H. Ahn, and G. H. Kim; Macromolecular Rapid Communication, 30:1632–1637, 2009.

SE/PST/TF/BI-1-Or-2 Atmospheric Plasma Jet for the Regulation of Drug Release from Bone Biomaterials

T11 Plasma Science and Technology

#SE/PST/TF/BI-1-Or-2

C. Canal [1], M. Modic [2], U. Cvelbar [2], M.P. Ginebra [1].

[1]Biomaterials, Biomechanics and Tissue Engineering Group, Dpt. Materials Science and Metallurgy, Technical University of Catalonia - Barcelona (Spain), [2]Jozef Stefan Institute - Ljubljana (Slovenia).

Bones are complex and hierarchical organs consisting of mineralized organic tissue which are exposed to injuries and illnesses that generate the loss of the bone function with consistent human morbidity. With the aim of overturning bone damage, a bone filling material is required in some clinical applications such as nonunion fractures, osteonecrosis, fragility fractures or bone reconstruction after tumor removal, among others [1]. It is estimated that in Europe bone substitutes are annually used in 1 million surgical procedures. The worldwide market of these materials is estimated to be 5 billion Euros, with an annual growth rate of 8-15%. Hydroxyapatite (HA) and beta tricalcium phosphate (b -TCP) are the most clinically used calcium phosphate (CaP) ceramics for bone regeneration. Their main feature is the compositional similarity with natural bone mineral [2] which makes them bioactive and osteoconductive. To further improve their performance, different drugs such as antibiotics or anti-inflammatories have been added to CaPs with the aim of local controlled release [3].

Atmospheric plasmas are of interest with views on different medical applications and in the design of advanced biomaterials with controlled drug release properties [4]. In this work, the effects of low temperature plasma have been evaluated for the first time with regard to CaP ceramics. In particular, a He atmospheric plasma jet was used to treat sintered b -TCP discs at optimized gas flow rate, power and distance to the material. In the first place the surface effects of the atmospheric plasma treatment at different times between 1 and 20 min were characterized by XPS, SEM and AFM. From the chemical point of view the treatment progressively increased the O/C ratio on the surface of b-TCP with time, while interesting modifications were observed on the topography of the surface leading to increased specific surface area.

Doxycycline hyclate – an antibiotic of the tetracycline family often used in periodontal diseases - was used as model drug for its incorporation to the bioceramics. The drug was incorporated to the b -TCP after the atmospheric jet plasma treatment, and its release was studied according to the European Pharmacopoeia standards.
In all conditions evaluated, the plasma jet treatment was effective in slowing down the drug release with respect to the untreated ceramics possibly by increasing the bonding strength between the TCP and the antibiotic studied.

References

1. A.S.Mistry, A.G. Mikos Adv. Biochem Engin/Biotechnol. 94, 1-22 (2005).
2. S.V. Dorozhkin J.Mater.Sci. 42, 1061-1095 (2007).
3. M.P. Ginebra, C. Canal, M. Espanol, D. Pastorino, E.B. Montúfar Adv. Drug Deliv. Rev. 64 (12) 1090-1110 (2012).
4. C. Labay, J.M. Canal, C. Canal, Plasma Proces. Pol., 9 (2) 165-173 (2012).

Acknowledgements

Authors acknowledge the MICINN for the financial support in the MAT 2009-13547 project and the MAT2010-12022-E network, as well as for the Juan de la Cierva Fellowship of CC. Funding through FP7 COST MP1101 Action “BioPlasma” is also acknowledged.

ASS-P1-20
Mass identification of the neutral products generated in the plasma treatment of polluted atmospheres

T11 Plasma Science and Technology

#ASS-P1-20

D. Seymour, A. Rees, S. Davies.

Hiden Analytical - Warrington (United kingdom).

Plasmas produced using Dielectric Barrier Discharge (DBD) devices are very effective in the abatement of air pollution resulting from, for example, the emission of volatile organic compounds (VCOs) by a range of industrial and agricultural processes. The development and monitoring of effective DBD systems can be investigated by advanced mass spectrometric methods specifically configured for analysis at high and atmospheric pressures The present work involves the operation of a small DBD reactor which uses either a helium or nitrogen carrier gas to sustain the plasma to which may be added reactive gases, such as oxygen, as well as samples of pollutants such as chlorinated hydrocarbons, including trichloroethylene. The mass spectrometric analysis was performed using a specially configured system manufactured by Hiden Analytical Ltd. The DBD source may also be combined with a catalyst for plasma-enhanced catalysis. The neutral products of the reactions proceeding in the plasma at atmospheric pressure are sampled through the Hiden capillary sampling system which also reduces the pressure of the gas mixture delivered to the ionisation source of the quadrupole mass spectrometer. The source is designed to generate production of either positive or negative ions from the sampled gas mixture, and also allows optimisation of the source conditions, which depends primarily on the choice of the energy of the electrons used to generate the positive or negative ions. The ions produced are subsequently mass identified. There are clear advantages, when the pollutants of interest are electronegative, in being able to choose the polarity of the ions generated. We describe typical data and comment on the relative advantages of operating the mass spectrometer in the positive and negative ion modes.

PST-P2-16
Nonlinear dust acoustic waves in a dusty plasma with nonthermal ions featuring Tsallis distribution

T11 Plasma Science and Technology

#PST-P2-16

M. Benzekka, M. Tribeche.

Plasma Physics Group, Theoretical Physics Laboratory, Faculty of Sciences-Physics, University of Bab-Ezzouar, USTHB, B.P. 32, El Alia, Algiers 16111, Algeria (Algeria).

From its beginnings with the initial observations of micron-sized particles in astrophysical and processing plasmas, the study of dusty plasmas has rapidly matured as highlighted in recent books and review. Besides affecting the equilibrium quasi-neutrality condition and modifying the existing plasma wave spectra of an electron-ion plasma, charged dust grains also introduce new types of waves in a dusty plasma and are presumed to play an important role in many astrophysical plasmas. Wave propagation in such complex systems is therefore expected to be substantially different from the ordinary two component plasmas. The dust charge may fluctuate becoming a new dynamical variable, and the electron can be strongly modified by the nonlinear plasma potential by generating a population of fast energetic electrons or trapped ones. However, numerous observations clearly indicated the presence of energetic particles (electrons and ions) as ubiquitous in a variety of astrophysical plasma environments and measurements of their distribution functions revealed them to be highly nonthermal. The aim of the present work is therefore to present a theoretical work to investigate nonlinear DA waves in a plasma comprising electrons, positive ions and mobile negatively charged dust grains. The correct nonthermal ion charging current in the Tsallis thermostatistics is based on the orbit motion limited (OML) approach and the variable dust charge is then expressed in terms of the Lambert function. Our results may obtain using a scheme suitable for stiff problems. One can numerically solve Poisson’s equation either as a boundary-value problem or as an initial-value problem. The numerical results reveal that the spatial patterns of the variable charge solitary wave are significantly modified by the nonextensive and the nonthermal ions effects.

PST-P2-17
Dust acoustic dressed solitons in a three component dusty plasma

T11 Plasma Science and Technology

#PST-P2-17

R. Amour, M. Tribeche.

Plasma Physics Group (PPG), Theoretical Physics Laboratory (TPL), Faculty of Sciences-Physics, University of Bab-Ezzouar, USTHB, B.P. 32, El Alia, Algiers 16111, Algeria. (Algeria).

Dust acoustic dressed solitons in a three component plasma consisting of a Boltzmann distributed electrons and ions and dust grains are investigated. Using the expansion of the Sagdeev potential to include fourth-order nonlinearities of electric potential and integrating the resulting energy equation, an exact soliton solution is obtained for our model of plasma. This approach gives soliton solution in terms of coefficients of nonlinearities of second order, third order and fourth order of electric potential in the expansion of the Sagdeev potential. Using the Taylor's series development of Mach number in terms of soliton velocity and keeping the terms up to order of, this exact solution reduces to nonsecular dressed soliton solution. It is found that for a given value of the fractional positrons concentration, the ratio of temperature, and the Mach number, the dressed soliton admits two different structures (compressive and rarefactive) due to the presence of the suprathermal electrons.

SE/PST/TF/BI-P1-04
Development of multi-gas DBD plasma jet source and its applications for medical field

T11 Plasma Science and Technology

#SE/PST/TF/BI-P1-04

K. Uehara [1], T. Oshita [1], T. Toshihiro [1], A. Kawate [1], N. Nakashima [2], H. Miyahara [1], A. Okino [1].

[1]Department of Energy Sciences, Tokyo Institute of Technology - Yokohama (Japan), [2]Plasma Factory, Co. Ltd. - Yokohama (Japan).

In recent years, non-equilibrium atmospheric plasmas have been attracted much attention in medical field such as sterilization or wound healing. These effects are caused by reactive species such as oxygen radical or nitric monoxide generated in plasmas. Amount and kinds of these reactive species depend on the plasma gas species. Therefore, treatment effect varies depending on the plasma gas. For example, oxygen mixed argon plasma was most effective for sterilization of *E. coli* [1].

For application of plasma directly to living body, not only highly effective treatment but also high safety such as no cytotoxicity is important. For instance, plasma sources using Dielectric Barrier Discharge (DBD) is utilized for plasma irradiation to tissue [2]. This plasma source can generate contamination-free plasma that means absence of electrode particle in plasma. However, standard DBD plasma jet sources have limitation in useable plasma gas species such as argon or helium. So, improvement of treatment effect by varying gas species is not expected too much.

In this study, to treat living body with contamination-free and various gas plasma, we developed multi-gas DBD plasma jet source with a new electrode structure and power waveform. The plasma gas flow rate was 3 L/min, copper electrodes spaced 10 mm apart were provided surrounding a glass tube with 1 mm i.d. and 2 mm o.d.. The electrodes were connected to power supply with a frequently of 16 kHz and high voltage of 9 kV. As shown in Fig. 1, the plasma source can generate stable plasma with argon, helium, oxygen, neon, nitrogen, carbon dioxide, air and their mixture gases. And the plasma does not give thermal damage and discharge damage to the target.

To investigate relation between the treatment effect and the plasma characteristics depending on the gas temperature and the excitation temperature was investigated using spectroscopic method. As a result, the helium excitation temperature was 2,700ºC and the gas temperature was 20ºC. The excitation temperature was much higher than the gas temperature so the generated plasma was a kind of non-equilibrium plasma. Besides, *E. coli* in agar medium was irradiated with various gas plasmas by varying irradiation distance, irradiation time and gas flow rate. Influence of plasma gas species on sterilization effect was investigated.

[1] T. Takamatsu, M. Ichikawa, H. Hirai, R. Sasaki, M. Shibata, T. Oshita, H. Miyahara, Y. Matsumoto and
A. Okino, 20th Int. Symp. on Plasma Chemistry, MED09 (2011).
[2] I. G. Koo, C. A. Moore, M. Y. Choi, G. J. Kim, P. Y. Kim, Y. S. Kim, Z. Yu and G. J. Collins, Plasma
Process. Polym., 8 1103 (2011).

Fig.1:The plasma source can generate stable various gas plasmas.

PST-4-Or-9
Plasma electrochemistry in Ionic liquids

T11 Plasma Science and Technology

#PST-4-Or-9

O. Höfft, N. Spitczok V. Brisinski, A. Lahiri, F. Endres.

TU Clausthal, Institute of Electrochemistry - Clausthal-Zelllerfeld (Germany).

Plasma electrochemistry is a powerful tool to generate free nanoparticles in liquids. Because of the high vapour pressure of aqueous solutions nowadays atmospheric-pressure microplasmas or plasma jets are mostly used to generate colloidal metal nanoparticles [1]. However, this method is more or less restricted to the generation of noble metal particles.
Due to their very low vapour pressure ionic liquids can be employed in vacuum experiments as fluid substrates or solvents. Thus, ionic liquids are well suitable electrolytes for plasma electrochemical processes delivering stable and homogeneous plasmas. We have shown that free and isolated copper and germanium nanoparticles can be obtained in ionic liquids (ILs) by applying a plasma as a mechanically contact-free electrode [2,3,4]. In contrast to the classical electrochemistry approach [3], it was not possible with the plasma electrochemistry method to generate silicon nanoparticles in ILs, mainly due to the high vapour pressure of the silicon precursors, like e.g. $SiCl_4$.
Here we report on our new approach to overcome this problem, by using a new plasma setup. With our modified setup it is possible to use the above mentioned high vapour pressure precursors to make Si nanoparticles. We report about the generation of silicon nanoparticles with an argon plasma from $SiCl_4$ in 1-ethyl-3-methylimidazolium bis(trifluoromethylsulfonyl)amide ([EMIm]Tf_2N), and 1-butyl-1-methylpyrrolidinium bis(trifluoromethylsulfonyl)amide ([$Py_{1,4}$]Tf_2N).
We will discuss the plasma electrochemical reactions of SiI_4 in the ILs and compare them with our results for the generation of germanium particles from the solid germanium dichloride-1,4-dioxane complex ($GeCl_2[C_4H_8O_2]$). The analysis of the plasma electrolyte interaction was done with in situ mass spectrometry. The particles were characterized with transmission electron microscopy, dynamic light scattering, UV/VIS spectroscopy and photoluminescence spectroscopy.

[1] C. Richmonds and R. Mohan Sankaran, Appl. Phys. Lett., 2008, 93, 131501.
[2] M. Brettholle, O. Höfft, L. Klarhöfer, S. Mathes, W. Maus-Friedrichs, S. Zein El Abedin, S. Krischok, J. Janek, F. Endres, Phys. Chem. Chem. Phys., 2010, 12 ,1750-1755.
[3] N. Kulbe, O. Höfft, A. Keppler, S. Zein El Abedin, S. Krischok, J. Janek, M. Pölleth, F. Endres, Plasma Processes and Polymers, 2011, 8, 32-37.
[4] A.A. Aal, R. Al Salman, M. Al-Zoubi, N. Borisenko, F. Endres, O. Höfft, A. Prowald, S. Zein El Abedin, Electrochimica Acta, 2011, 56, 10295-10305.

PST-2-Or-5
Anisotropic Shear Melting of a 2D Complex (Dusty) Plasma

T11 Plasma Science and Technology

#PST-2-Or-5

V. Nosenko, A. Ivlev, G. Morfill.

Max-Planck-Institut für extraterrestrische Physik - Garching (Germany).

A complex, or dusty plasma is a suspension of fine solid particles in an ionized gas. Particles get charged by collecting electrons and ions from the ambient plasma and interact with each other via a screened Coulomb pair potential. When these interparticle forces are balanced by other forces (gravity, neutral and ion drag, ambipolar electric fields), the particles can form regular structures called plasma crystals. In the presence of gravity, a single-layer (two-dimensional, 2D) plasma crystal can form [1,2]. The shear modulus of such crystals is on the scale of 10^{-13} N/mm [1], and therefore they can be easily manipulated, e.g. by the radiation pressure force of a focused laser beam [2].

Our experimental setup was a modified GEC (Gaseous Electronics Conference) rf reference cell. Plasma was produced using a capacitively coupled rf discharge in argon at 0.66 Pa [1,2]. A single layer of dust particles was suspended in the plasma sheath of the lower rf electrode. The microspheres made of melamine formaldehyde had a diameter of 9.19 ± 0.09 μm, a mass m = 6.15 × 10^{-13} kg, and acquired an electric charge of Q = -16000 ± 1600e. The suspension included around 9000 particles and had a diameter of approximately 60 mm. In our experimental conditions, the particle suspension self-organized in a highly ordered triangular lattice.

The lattice layer was illuminated by a 660 nm diode laser, with its output expanded into a horizontal sheet by a cylindrical lens. A video camera (Photron FASTCAM 1024 PCI) was mounted above the chamber, capturing a top view of the particle suspension with a size of 42.7 × 42.7 mm^2, resolution 1024 × 1024 $pixel^2$, and recording rate 60 frames per second. The camera lens was equipped with a narrow-band interference filter at the wavelength of the illumination laser. Using Particle Tracking Velocimetry (PTV), we calculated the particle positions and velocities in every frame.

Shear induced melting is a non-equilibrium process where a crystalline lattice is ruptured and eventually melted by an external shearing force. In this work, we

experimentally studied shear induced melting using a 2D plasma crystal as a model system. Shear stress was applied by the radiation pressure force of a focused laser beam that was rastered over a rectangular area in the crystal. A Millennia PRO 15sJ solid-state 532 nm laser with a maximum CW output power of 15 W was used. For the first time, the study was angle-resolved, i.e., the closely packed rows of the crystal were oriented at θ=0° or 30° (two principal orientations) with respect to the shearing force. Shear melting was found to be strongly anisotropic. The transition of a crystal to flowing liquid with increasing shear stress was rather gradual for θ=0° and had a distinctly threshold character for 30°. This is explained by the role of dislocations in the crystal plastic deformation. Their nucleation and motion was facilitated for 0° (dislocations gliding in the direction of the laser beam [1]) and retarded for 30° (dislocations gliding at a certain angle with respect to the laser beam).

1. V. Nosenko, G. E. Morfill, and P. Rosakis, Physical Review Letters **106**, 155002 (2011).
2. V. Nosenko, A. V. Ivlev, and G. E. Morfill, Physical Review Letters **108**, 135005 (2012).

PST-2-Or-6
DEFECT CLUSTERS IN A TWO-DIMENSIONAL COMPLEX (DUSTY) PLASMA

T11 Plasma Science and Technology

#PST-2-Or-6

S. Zhdanov, M. Thoma, G. Morfill.

Max-Planck-Institut fuer extraterrestrische Physik - D-85741 Garching (Germany).

Complex plasmas, i.e. low-temperature plasmas containing micron-sized solid particles [1], allow investigations of many dynamical and self-organizing processes [2]. In the report we address dynamical processes associated with spontaneous disordering and symmetry breaking accompanying nucleation and clustering of defects in highly ordered complex plasmas — so-called *plasma crystals*. The particles, comprising plasma crystals, acquire large negative charges in the plasma. In the size domain of 1-10 μm (normally used in experimental complex plasmas) these particles can be visualized individually, providing hence an atomistic (kinetic) level of investigations. The interparticle spacing can be of the order of 0.1-1 mm and characteristic time-scales are of the order of 0.01-0.1 s. Plasma crystals are perfectly suited to study order-disorder transitions and symmetry alternations, in particular spontaneous disordering that plays an important role in the physics of highly ordered complex plasmas [3-6]. The results of recent simulations and experiments showing such spontaneous disordering are reviewed and interpreted.
The mechanism and physics of defect nucleation are key questions that often remain open irrespective of the suggested melting scenario or the shear instability mechanism. Many important features of the spatial structure of crystals can be modeled with the help of plasma crystals, which are perfectly suited to study the symmetry and multi-scale plasticity of a 2D lattice layer. Complex plasmas can serve as a powerful tool, providing a fundamental insight into the nucleation process generically. Either deformation-induced or thermally initialized nucleation, i.e. the creation of the dislocation pairs, in hexagonal plasma crystals starts with the appearance of compact dislocation clusters having a tetragon in the core. Hence, the competition for the minimal energy configuration between (stable) hexagonal symmetry and (unstable) tetragonal symmetry can be resolved in favour of a (meta-stable) ‘mixed symmetry’ — a cluster of coupled dislocations in a hexagonal

environment. Nucleation of dislocations and symmetry alternation effects are naturally important in complex plasmas where the *particle–plasma* feedback mechanisms underlying many dynamical processes play an important role. Another option, interesting in many applications, is the clustering of a new phase which is asymmetric with regard to a background symmetry. The nontrivial topology of the dislocation clusters is explored in detail, and the results obtained in simulations and theory agree well with experimental observations.

[1] H. M. Thomas and G. Morfill, Nature **379** (1996) 806
[2] G. E. Morfill and A. V. Ivlev, Rev. Mod. Phys. **81** (2009) 1353
[3] C. A. Knapek, D. Samsonov, S. Zhdanov, U. Konopka and G. Morfill, Phys. Rev. Lett. **98** (2007) 015004
[4] V. Nosenko, S. Zhdanov, and G. Morfill, Phil. Mag. **88** (2008) 3747
[5] S.K. Zhdanov, M.H. Thoma, and G.E. Morfill, New J. Phys. **13** (2011) 013039
[6] S.K. Zhdanov, M.H. Thoma, C.A. Knapek, and G.E. Morfill, New J. Phys. **14** (2012) 023030

PST-4-Or-1
Multi-scale approach for simulation of deep silicon etching under SF6/C4F8 Bosch process

T11 Plasma Science and Technology

#PST-4-Or-1

A. Pateau [1], A. Rhallabi [1], M.C. Peignon-Fernandez [1], M. Boufnichel [2], F. Roqueta [2].

[1]Institut des Matériaux Jean Rouxel - Nantes (France), [2]STMicroelectronics TOURS SAS - Tours (France).

Deep etching of silicon represents a new challenge in the silicon semi-conductor manufacturing. Bosch process, one of the most common processes in microelectronics, is used for silicon deep plasma etching. It is based on a cyclic process consisting in alternating etching and deposition.
To better understand the plasma surface interactions for polymer deposition and etching, we have developed a silicon etching simulator under Bosch process using alternating ICP SF_6/O_2 plasma for etching and ICP C_4F_8 plasma for deposition. Such a simulator is composed of three modules permitting to predict the 2D etched silicon morphology versus the operating conditions: plasma kinetic, sheath and etching models. The plasma kinetic model is based on the 0D global approach which allows the calculation of the average densities and fluxes of neutral and ion species as well as the electron density and temperature versus the ICP machine parameters. The sheath model is based on the Monte-Carlo technique. The model allows the calculation of angular and energy ion distribution functions. All these output parameters are introduced as input parameters in the silicon etching model. Cellular Monte-Carlo method is used to describe the plasma surface interactions in a probabilistic way for silicon etching. The reactive species considered are atomic fluorine and CxFy radicals produced in the SF_6 and C_4F_8 discharges respectively as well as positive ions.
Fig 1 shows the fluorine density (nF) evolution versus the $\%O_2$ for different pressure values. The simulation results show that for a low $\%O_2$, nF increases up to a maximum corresponding to about 40% of oxygen. After this value, it decreases with $\%O_2$.
Fig 2 presents the etch profile evolution through the mask. Scalloping effect is

evidenced.
The aim of this work is to validate the set of simulation and show the influence of some input parameters (Rf power, pressure, gas flow rates and bias voltage) on the etching process.

Fig1: F density vs O_2 percentage for p = 10, 20, 30 mtorr, Prf=1000W, Q(SF_6+O_2)=40 sccm

Fig2 : Example of 2D silicon etch profile obtained from Bosch process

PST/SE/TF-P1-03
Superhydrophobicity and self-cleaning by plasma treatments of topographically structured surfaces

T11 Plasma Science and Technology

#PST/SE/TF-P1-03

E. Grimoldi, S. Zanini, C. Riccardi.

Università degli Studi di Milano Bicocca - Milano (Italy).

Superhydrophobicity is a very common phenomenon occurring in nature. The ability of the lotus leaf and other natural materials to promote water repellency and self-cleaning has inspired several research groups. Water drops roll around easily on these surfaces if the substrate is slightly tilted (low roll-off angle). In certain cases, drops rolling off the surface take loosely adherent dirt particles with them, thus giving rise to self-cleaning properties. This effect, called 'Lotus effect', is caused by a combination of chemical (hydrophobic waxes coating) and physical features, i.e. roughness at two or more length scales (hierarchical structures, typically bumps of about 10 µm and submicronic microfibers).
Superhydrophobicity and self cleaning can be achieved onto artificial materials, using appropriate methods of micro/nanostructuring or employing surfaces which possess particular roughness themselves (for example leather or velvet paper).
In this work, hydrophobic and self cleaning surfaces were prepared by means of different plasma treatments. In particular, leather and velvet paper surfaces were modified by low pressure plasma discharges in sulphur hexafluoride (SF_6) and hexamethyldisiloxane (HMDSO) or by atmospheric plasma graft-polymerization of 3,3,4,4,5,5,6,6,7,7,8,8,9,9,10,10,10-Heptadecafluorodecyl acrylate.
Hydrophobic properties were evaluated by means of static and roll-off contact angles measurements, while the morphological characteristics of the surfaces were studied using Scanning Electron Microscopy (SEM) and the surface chemical composition of the treated samples was analyzed with X-rays Photoelectron Spectroscopy (XPS).

Fig. 1. Water drops on untreated (left) and HMDSO plasma treated (right) velvet paper

Fig. 2. Self-cleaning properties of an SF_6 plasma modified leather. White solid particles are titanium dioxide powders, which were removed from the leather surface by a water droplet rolling on it.

PST-2-Or-1
H atom surface loss kinetics in pulsed inductively coupled plasma

T11 Plasma Science and Technology

#PST-2-Or-1

C. Cardinaud, S. Jacq, L. Le Brizoual, A. Granier.

Institut des matériaux de Nantes - CNRS - Nantes (France).

In microelectronics and microtechnology, as the semiconductor feature size decreases and pattern density increases, the industry is facing the challenge of finding new plasma processes to meet the requirement of the next devices generation. Within this scheme pulsed RF plasmas are increasingly being employed for plasma etching or deposition. Besides the interest for potential applications, pulsed plasmas combined to time resolved measurements are known to be powerful tools to study species kinetics.

This study is focused on H atom kinetics in low pressure high density inductively coupled CH_4-H_2 pulsed plasmas. The H density is investigated by time resolved optical emission spectroscopy. Since electron temperature collapses at the end of the ON time, no emission occurs during the OFF time. Hence, plasma induced fluorescence is used to probe the time variation of the H atom density in the afterglow. Ion flux density measurements are done with a planar probe in order to correlate the H atom surface loss probability (β) to the ion flux reaching the wall.

We explore pure H_2, H_2-N_2, CH_4-H_2 and CH_4-N_2 mixtures. These gas mixtures offer very different wall conditions, namely stainless steel for the first two and hydro-carbonated walls for the other two. Results show that β is strongly sensitive to wall conditions. Compared to values of 0.073 (β-on) and 0.065 (β-off) in H_2, β-on increases steadily with the percentage of CH_4 in CH_4-H_2, reaching 0.15 in pure CH_4, while β-off attains 0.4. Adding N_2 to CH_4 leads to β-on values even higher: 0.25 at 75%N2. Results will be discussed considering various surface loss mechanisms. Effect of pressure in stainless steel wall conditions is also investigated. β behaviour shows significant differences between pure H_2 and the H_2-N_2 mixture. E.g. in the latter β-on increases in the whole range of pressure (fig.1), whereas in pure H_2 the evolution of Beta-on with pressure is not monotonic (fig.2).

Acknowledgement
This work is supported by the French ministry of defense (DGA).

Fig. 1 : Evolution of β-on with pressure in 800W H_2-N_2 (75%-25%) plasmas.

Fig. 2 : Evolution of β-on with pressure in 800W H_2 plasmas.

PST/SE/TF-1-Or-2
Study and conception of a DBD (Dielectric Barrier Discharge) process and equipment for the industrial deposition of silica like coatings on continuously running strips

T11 Plasma Science and Technology

#PST/SE/TF-1-Or-2

V. Leclercq.

AC&CS - CRM Group - Liège (Belgium).

As a preliminary work, we studied and tested silica like coatings to improve some of the in use properties of steel (adhesion, corrosion, surface energy, end so on), and we identified the required coating characteristics.

Industrially, these silica layers have to be deposited through a continuous process, on commodity products, which are webs of steel, characterised by their high throughput (thousands of tons per year), their large width (> 1.5m) and their high speed (> 100 m/min).

After considering different technologies, we chose to further look into the DBD (Dielectric Barrier Discharge) technology, especially because of its potential in terms of limited capital expenditures and operating costs.

However, when used in this context, the DBD technology has serious weaknesses, which are:
- too short a distance from substrate to electrode, which prevents the continuous running of many metallic substrates,
- too fast a fouling of the coating equipment, which leads to excessive maintenance and operating costs.

The developments presented permitted the elimination of these weaknesses, via the conception of a maverick process.

Finally, we designed an industrial modular coating equipment, that can be installed on existing conventional production lines, and which takes into account the targeted in use properties, the required product characteristics and the necessary process parameters.

PST/SE/TF-1-Or-6
Atmospheric pressure argon plasma aided nanosecond laser processing

T11 Plasma Science and Technology

#PST/SE/TF-1-Or-6

C. Gerhard [1], S. Roux [2], S. Brückner [3], W. Viöl [1].

[1]University of Applied Sciences and Arts - Göttingen (Germany), [2]Institut d'Optique Graduate School - Palaiseau (France), [3]Clausthal University of Technology - Clausthal-Zellerfeld (Germany).

In this contribution, we present an atmospheric pressure argon plasma aided laser ablation technique for cutting and drilling applications. Here, a cone-shape rotation-symmetric plasma source with an inner hollow-core high-voltage electrode was used. Based on a dielectric barrier discharge, this source provides a slight plasma beam with a diameter of approx. 200 µm. The dielectric separation of the inner high-voltage and outer ground electrode was accomplished by the sample and an additional dielectric, respectively, as the case may be for conductive sample materials such as aluminium. As laser source, a 3rd harmonic Nd:YAG laser with pulse durations in the nanosecond range was applied. As shown in figure 1, both the applied plasma and the laser beam propagate coaxially.
Experiments were performed on barite crown and heavy flint glass, aluminium oxide ceramic and aluminium. In the case of ablation of glasses, an increase in the ablation depth by a factor of 2.1 was achieved by the presented plasma aided technique in comparison to pure laser ablation. Further, the ablated volume was increased by a factor of 1.5 for barite crown glass and 3.7 for heavy flint glass [1]. Regarding aluminium oxide ceramic, it was shown that the presented technique affects a reduction of the laser ablation threshold. The ablation process was additionally enhanced in terms of an increased contour accuracy and ablation rate [2]. Such enhancements were also observed for aluminium, where the ablation rate was significantly increased in comparison to pure laser ablation [3]. The presented plasma aided ablation technique thus allows enhancing laser material processing results and reducing the required laser energy due to energetic synergies that result from de-excitation processes of generated argon metastable species.

[1] C. Gerhard, S. Roux, S. Brückner, S. Wieneke, W. Viöl: Low-temperature atmospheric pressure argon plasma treatment and hybrid laser-plasma ablation of barite crown and heavy flint glass, Applied Optics 51 (2012) 17, 3847-3852

[2] C. Gerhard, S. Roux, F. Peters, S. Brückner, S. Wieneke, W. Viöl: Hybrid laser ablation of Al2O3 applying simultaneous argon plasma treatment at atmospheric pressure, accepted for publication in Journal of Ceramic Science and Technology

[3] C. Gerhard, S. Roux, S. Brückner, S. Wieneke, W. Viöl: Atmospheric pressure argon plasma-assisted enhancement of laser ablation of aluminum, Applied Physics A 108 (2012) 1, 107-112

Fig. 1: Setup for simultaneous atmospheric pressure argon plasma aided laser ablation

PST-P3-15
Acetone and acetone/ethanol removal by air Dielectric Barrier Discharges coupled to catalysis

T11 Plasma Science and Technology

#PST-P3-15

S. Lovascio, N. Blin-Simiand, B. Bournoville, S. Pasquiers.

Laboratory of Plasma and Gases Physics, CNRS (UMR8578) University Paris-Sud - Orsay (France).

Over the last two decades atmospheric pressure non-thermal plasmas coupled to traditional catalysis have received a growing interest as a promising tool for a more efficient VOC removal [1]. The post-plasma catalysis, in particular, can complete the oxidation process started in the plasma phase reducing, at the same time, the reaction temperature at the catalyst surface. In this field the catalytic ozonation of VOCs is particularly advantageous: catalysts based on transition metal oxides are able to decompose the O_3 produced into the discharge thus providing highly active oxygen species which can contribute to oxidation of VOCs at low temperatures [2].
In this work the plasma-catalytic abatement of two target molecules, ethanol and acetone, has been investigated. Air Dielectric Barrier Discharges were carried out in a symmetric pin-to-pin DBD reactor. Due to the high activity of Mn oxides in O_3 decomposition, Al_2O_3 supported MnO_2 (5%) pellets were placed downstream the DBD reactor. The air flow rate was kept constant at 2 l/min, whereas ethanol and acetone concentrations were fixed at 300 ppm. Catalyst temperature was maintained at 60 °C. In line by-products detection and quantification was allowed by a gas chromatograph equipped with a thermal conductivity detector (MicroGC-TCD), a Fourier transform infrared spectrometer (FT-IR), an O_3 UV-absorption based detector and a CO_2-H_2O infrared gas analyzer placed in the exhaust gas line.
A first result, in term of removal efficiency and by-products distribution, for the plasma conversion of the starting pollutants, both alone and in mixture, has already been given [3]. In this work a complete characterization is provided. When singularly considered, the abatement of both pollutants is enhanced by the post-catalytic treatment. As shown in Fig. 1 acetone plasma-catalytic process is quite efficient, as the concentration of all partially oxidized products issued from the plasma phase fall down to zero: both the primary and secondary molecules are converted to CO_2 and CO. Differently, ethanol catalytic conversion, in addition to the CO_2 enhancement,

mainly promotes the acetaldehyde and carboxylic acid production; other species produced in the discharges, as formaldehyde and formic acid, are instead reduced. When 1:1 ethanol-to-acetone mixtures are investigated, competition between the primary VOCs prevents the catalytic acetone abatement.

1. A. M. Vandenbroucke et al., Journal of Hazardous Materials, 195, 30-54, 2011
2. B. Dhandapani et al, Appl. Catal. B 11, 129–166, 1997
3. S. Lovascio et al., IJPEST, 6, 111-118, 2012

Fig. 1: Carbon distribution in plasma and catalytic-plasma treatment of air/acetone mixtures

PST/SE/TF-3-Or-1
Effect of aqueous environment on properties of Ag/a-C:H:O nanocomposite films

T11 Plasma Science and Technology

#PST/SE/TF-3-Or-1

M. Drabik [1], D. Hegemann [1], J. Pesicka [2], H. Biederman [2], N. Blanchard [1].

[1]Empa - St. Gallen (Switzerland), [2]Charles University - Prague (Czech republic).

Metal/plasma polymer nanocomposite coatings have been studied for many decades due to an extraordinary potential in tuning their mechanical, electrical and optical properties in various different directions according to the special requirements of any particular application [1,2]. Several plasma-based vacuum deposition techniques have been utilized in order to incorporate metal nanoparticles into a plasma polymer matrix, e.g. simultaneous magnetron sputtering from metal and polymer targets or metal evaporation during PECVD [3,4,5]. Plasma technology offers a controlled film growth at high surface diffusion and low temperatures.

Filling factor (or volume fraction ratio) is the principal parameter describing structure of a metal/plasma polymer nanocomposite coating. It is defined as the volume of metal inclusions in the total volume of the composite material. Structure of such a nanocomposite film determines also its properties. The filling factor at which the structure of a nanocomposite film switches from an insulating to a conductive nature is called percolation threshold.

For any practical application, a long-term stability and limited aging of such coatings are required for their reliable and repeatable perfomance. In this contribution, we present a study of structure and properties of Ag/a-C:H:O nanocomposite coatings and their changes upon aging in air and influence of an aqueous environment. The characterization of the film microstructure by TEM, optical properties by UV-vis spectroscopy (Figure 1) and electrical properties showed that changes in film properties are much more pronounced upon aging in water than in air.

Acknowledgements
Financial support from the Swiss National Funding (SNF) within the project NanoTera (Tec-in-Tex) and from the Sciex-NMSch programme under project 10.118 – ExTraSens is acknowledged.

[1] Faupel F, Zaporojtchenko V, Strunskus T and Elbahri M 2010 Adv. Eng. Mater. 12 1177-1190
[2] Biederman H, Kylian O, Drabik M, Choukourov A, Polonskyi O and Solar P 2012 Nanocomposite and nanostructured films with plasma polymer matrix Surf. Coat. Tech. 211 127-137
[3] d'Agostino R 1990 Plasma Deposition, Treatment and Etching of Polymers Academic Press New York
[4] Biederman H 2004 Plasma Polymer Films Imperial College Press London
[5] Körner E, Aguirre MH, Fortunato G, Ritter A, Rühe J and Hegemann D 2010 Formation and distribution of silver nanoparticles in a functional plasma polymer matrix and related Ag+ release properties Plasma Process Polym 7 619-625

Figure 1. UV-Vis transmittance spectra of Ag/a-C:H:O film (thickness of 22 nm) as measured right after deposition, 1 month after deposition and after 1 hour in water bath.

SE/PST/TF/BI-1-Or-3
Treatment of Biosystems by Atmospheric Pressure Plasma Jet

T11 Plasma Science and Technology

#SE/PST/TF/BI-1-Or-3

S. Ptasinska [1], X. Han [1], M. Klas [1], Y. Liu [2], S. Stack [2].

[1]Radiation Laboratory and Department of Physics, University of Notre Dame - Notre Dame (United states), [2]Department of Chemistry and Biochemistry, Harper Cancer Research Institute, University of Notre Dame - Notre Dame (United states).

The Atmospheric Pressure Plasma Jet is a unique technique which operates at standard temperature and pressure conditions therefore enables us to explore possibilities of material treatment which cannot be introduced to vacuum system or treated at elevated temperatures. This is especially important for biological systems such as cells and living tissues.
The research conducted on cancer cells irradiated by the APPJ is very new starting just in 2010 [1], where it was hypothesized that the APPJ could initiate the cascade of biochemical processes leading to the death of the cells. It has been also shown that the APPJ offers a complex gas environment consists of reactive oxygen species and reactive nitrogen species, photons, charged particles, which may all contribute to biological effects like cell death [2]. This shows that APPJ treatment can activate cell apoptosis (events which lead to specific changes in morphology of the cell and then death, in contrast to necrosis which happens immediately upon some events). However, a little has been done on understanding of the physical, chemical and biological processes underlying the interaction of APPJ and biological systems. Any data collected on the role of plasma during interaction with the cell or its components is a great concern and helpful in progressing plasma medical technology.
In these studies SCC-25 oral cancer cells were exposed to plasma radiation and cell damage, i.e., DNA double strand breaks in nuclei was analyzed by immunofluorescence microscopy. It has been observed the increase in both effective areas and a number of damaged cells with plasma irradiation time. Such an effect can be due to the fact that the reactive species have been continually accumulating on a surface at the plasma-liquid interface. Optical emission spectra were taken to characterize these reactive species produced in APPJ.

[1] G. Kim, W. Kim, K. Kim, J. Lee, Appl. Phys. Lett., 2010, 96, 021502
[2] K.D. Weltmann, K.D. and Th. von Woedtke, Eur. Phys. J. Appl. Phys., 2011, 55, 13807

PST/SE/TF-2-Or-3
Synthesis of Pt based catalyst for PEM fuel cell by a novel plasma deposition method

T11 Plasma Science and Technology

#PST/SE/TF-2-Or-3

M. Laurent-Brocq [1], N. Job [2], J.J. Pireaux [1].

[1]LISE - Namur university - Namur (Belgium), [2]LGC - Liège university - Liège (Belgium).

Polymer exchange membrane (PEM) fuel cells are promising energy conversion devices [1]. One major challenge for their commercial spreading is to reduce the cost, for example by decreasing Pt loading in the catalytic layers composing the electrodes. To do so while keeping the same catalytic properties, the dispersion of Pt nanoparticles onto the carbon support need to be fine and dense [2].

We propose to apply a novel low temperature plasma method using organometallic precursors [3] to graft Pt nanoparticles on carbon black and to study the influence of synthesis conditions on nanoparticles characteristics. So, catalysts were synthesized under various plasma treatment conditions (gas and power) and then characterized by X-ray diffraction, transmission electron microscopy and X-ray photoelectron spectroscopy. It was deduced that the formation of Pt nanoparticles depends on two phenomena: (i) the functionalization of the carbon black surface which is influenced by the plasma gas nature and (ii) the decomposition of the organometallic precursor which results from a thermal effect and is influenced by the plasma power. Finally, catalysts were annealed and the stability of the nanoparticles was studied.

1. G.W. Crabtree, M.S. Dresselhaus, MRS Bulletin, 33 (2008) 421.
2. H.A. Gasteiger, S.S. Kocha, B. Sompalli, F.T. Wagner, Appl. Catal. B 56 (2005) 9.
3. J.-J. Pireaux, F. Reniers, J. Guillot, M. Gulas , N. Claessens, A. Batan, A. Mansour. Method for depositing nanoparticles on substrates. WO/2012/028695, 2010

PST-P3-05
Acetaldehyde decomposition in atmospheric gases by spatially homogeneous and DBD filamentary plasmas: a comparative study

T11 Plasma Science and Technology

#PST-P3-05

S. Pasquiers [1], W. Faider [1], O. Koeta [2], N. Blin-Simiand [1], P. Jeanney [1], L. Magne [1].

[1]LPGP-CNRS - Orsay (France), [2]LACARE - Ouagadougou (Burkina faso).

Acetaldehyde has long been recognized as a toxic Volatile Organic Compound. This pollutant is found both in indoor air, coming from building materials, and in exhaust gases of ethanol combustion, or coming from incinerators. The reduction of the emissions of dangerous substances like this VOC passes by the development of effective and economically successful processes of clean-up. For this purpose, the use of non-thermal plasma, eventually coupled to catalysis, is under study for many years but works regarding acetaldehyde are rather scarce [1-3].
An important subject to be addressed is the energy needed for a given discharge type in order to convert CH3CHO in other compounds which could be efficiently oxidized by a catalyst placed after the plasma, at low temperature (i.e. as close as possible to the ambient). The specific energy (energy consumed per unit volume of gas processed) should be as low as possible in order to make the process economically attractive. Thus the type of discharge used appears as an important parameter.
In the present work, the conversion of 500 ppm of CH3CHO diluted in N2/O2 mixtures (oxygen up to 20 %) at a total pressure of 0.46 bar (photo-triggered discharge) or 1 bar (dielectric barrier discharges, DBD) are compared. The photo-triggering technique allows one to achieve homogeneous transient high-pressure plasmas in various types of gas mixtures [4]; a detailed description of the UV-preionized reactor used has been previously published [2, 4, 5]. Two kinds of DBD were used also, the first one with a plane-to-plane geometry (a copper plate for HV electrode), and others with a cylindrical geometry (tungsten rods for HV electrode). All DBD reactors were energized using positive pulsed high voltages so that the

generated plasmas were either strongly non-homogeneous (cylindrical reactors) or much less filamentary (flat reactor).
It was found that, at a low percentage of oxygen (less then 2 %), the energetic efficiency of filamentary DBD-plasmas for removing the acetaldehyde is lower than the efficiency for the more homogeneous one. For same gas mixtures, the efficiency for the photo-triggered reactor is even higher than the efficiency for all DBD-reactors. However, the three types of reactors have almost the same energetic performance for an oxygen concentration higher than a few percent. As a result, it seems that the spatial distribution of the deposited electrical energy in the discharge has a strong effect on the energetic efficiency of the plasma reactor when the degradation of acetaldehyde through oxidation reactions by O and by OH (important kinetic for the removal of CH3CHO in a gas mixture with a high oxygen concentration) are counterbalanced by the dissociation of the pollutant molecule through quenching process of the excited (essentially metastable) states of the nitrogen molecule [5] (dominant kinetic in the binary N2/CH3CHO mixture). This will be discussed with the help of a kinetic modeling.

[1] Lee H and Chang M, 2001 Plasma Chem. Plasma Proc. 21 329
[3] Magne L et al., 2005 J. Phys. D: Appl. Phys. 38 3446
[3] Klett C et al., 2012 Plasma Sources Sci. Technol. 21 045001
[4] Lacour B et al., 2003 Recent Res. Dev. Appl. Phys. 6 149
[5] Faider W et al., 2013 J. Phys. D: Appl. Phys. to appear.

PST-2-Or-7
Magnetic field penetration and ion separation in a multy-ion plasma

T11 Plasma Science and Technology

#PST-2-Or-7

A. Fruchtman [1], R. Doron [2], Y. Maron [2].

[1]H.I.T. - Holon Institute of Technology - Holon (Israel), [2]Weizmann Institute of Science - Rehovot (Israel).

A theory is presented that deciphers the puzzle of magnetic field penetration into a multi-ion plasma of an initially uniform electron density observed in recent pulsed plasma experiments.

The Hall electric field has been shown to play a crucial role in the interaction of magnetic field and a plasma, in processes that govern the behavior of plasmas spanning space and laboratory.[1] In all these processes, the role of the Hall electric field becomes dominant only when a relevant charateristic spatial length is smaller than the ion skin depth. For example, the Hall field enhances dramatically the rate of magnetic reconnection when the current layer is narrower than the ion skin depth. An important process in which the Hall electric field has a dramatic effect is the fast magnetic field penetration into a low collisionality plasma. Such a penetration has been measured in detail [2 - 5] and was found to be much faster than expected due to the plasma resistivity. It has been shown theoretically that this fast penetration is induced by the Hall electric field and the characteristic spatial scale that has to be smaller than the ion skin depth was identified in this case to be that of the electron density nonuniformity.[6 - 8] In recent experiments, however, fast magnetic field penetration into multi-ion plasmas was observed even when the initial electron density was approximately uniform.[5] In addition, the magnetic field penetration into the plasma was found to occur simultaneously with ion separation, in which a light-ion plasma is pushed ahead of, while a heavy-ion plasma lags behind the magnetic piston.[4]

In the talk we will present a model that explains these two processes, the fast magnetic field penetration into a plasma of initially uniform density and the ion separation. We will show that if the plasma ion composition is nonuniform, then, even if the total electron density is initially uniform, the different pushing of the different ion

species by the magnetic field generates an electron density nonuniformity which, in turn, induces the field penetration, that increases further the ion separation. Thus, the two processes, magnetic field penetration and ion separation, are closely linked, and occur simultaneously. Since very often plasmas are multi-ions with ion-composition nonuniformity, our analysis shows that magnetic field peneration is a a much more general process that has been previously believed and that ion separation is likely to occur in many cases in which a pulsed current is driven through a multi-ion plasma. The mechanism explained here plays a major role in plasma opening switches, plasma pinches, and other plasma devices. This mechanism is likely to have an important effect also in space and astrophysical plasmas.

1. M. Yamada, R. Kulsrud, and H. Ji, Rev. Mod. Phys. **82**, 603 (2010).

2. M. Sarfaty *et al*., Phys. Plasmas **2** , 2583 (1995).

3. R. Arad, K. Tsigutkin, Y. Maron, A. Fruchtman, and J. D. Huba, Phys. Plasmas **10**, 112 (2003).

4. A. Weingarten, R. Arad, Y. Maron, and A. Fruchtman, Phys. Rev. Lett. **87**, 115004 (2001).

5. B. Rubinstein, R. Doron, Y. Maron, and A. Fruchtman, submitted to Phys. Rev. Lett.

6. A. Fruchtman, Phys. Fluids B3, 1908 (1991).

7. A. V. Gordeev, A. S. Kingsep, and L. I. Rudakov, Phys. Rep. **243**, 215 (1994)

8. A. Fruchtman and L. I. Rudakov, Phys. Rev. Lett. **69**, 2070 (1992).

PST-P2-06
Sheath Potential Measurements in SF6/Xe Plasma

T11 Plasma Science and Technology

#PST-P2-06

Y. Kawai [1], J. Zhang [2], R. Ichiki [3].

[1]Kyushu University - Kasuga (Japan), [2]Dalian University - Dalian (China), [3]Oita University - Oita (Japan).

As well known, there are negative ions in reactive plasmas for such as CVD. Negative ions are confined in plasma without diffusing to discharge electrodes, leading to high negative ion density. Therefore, negative ions may play an important role especially in plasma CVD. However, there are almost no reports on the behaviour of negative ions in plasma CVD because of the difficulty of negative ion measurements in reactive plasma. The simplest method to estimate the negative ion density is to use the Langmuir probe, that is, the negative ion density normalized to the ion density n_-/n_+ is easily estimated from the reduction of the electron saturation current [1]: $n_-/n_+=1-I_{es}/I_{es0}$. Here I_{es} and I_{es0} is the electron saturation current with negative ions and without negative ions, respectively. Furthermore, when there are negative ions in plasma, the sheath potential decreases and Bohm sheath is modified [2]. Thus, the sheath potential that is defined as the difference between the plasma potential and the floating potential provides interesting information about negative ions. In this experiment, we measured the sheath potential in SF_6/Xe DP plasma with the Langmuir probe and compared with the theory [3].

The experiments were performed using a double plasma device. The diameter and length of the stainless vacuum chamber were 500 mm and 1000 mm, respectively. Xe and SF_6 gases were introduced into the chamber with the mass flow controllers separately. The flow rate of Xe gas was kept at 6 sccm ($8x10^{-4}$ Torr) and that of SF_6 gas was regulated from 0 to 0.1 sccm. A 0.6-cm-diam planar Langmuir probe was used to measure the plasma parameters. Mass spectra of positive and negative ion species were analyzed with the QMS.

When $SF_6/(Xe+SF_6)$ was increased, the negative ion concentration increased. Then, we measured the sheath potential as a function of $SF_6/(Xe+SF_6)$ and plotted the sheath potential as a function of negative ion concentration n_-/n_+. The sheath potential is very sensitive to the temperature of ions (T_+) and negative ions (T_-). In this calculation, T_+ ($=T_-$)=0.025 eV and 0.03 eV was assumed. Fig.1 shows the results agree with the theoretical sheath potentials at T_+=0.03 eV except for high

negative concentrations. This deviation is not understood because the sheath potentials in SF_6/Ar plasma agreed with the theoretical ones [1]. In addition, Fig.1 indicates that there are three solutions of the sheath potential at T_+=0.025 eV.

[1] J. Y. Zhang, R. Ichiki and Y. Kawai, Proc.of XXI Europhysics Conference on the Atomic and Molecular Physics of Ionized Gases, P1.5.1(Porto, 2012)
[2] H. Amemiya, J. Phys.D:Appl.Phys.,23, 999 (1990)
[3] H. Shindo and Y. Horiike, Jpn. J. Appl. Phys., 32 5109 (1993)

Fig.1 The observed sheath potential as a function of n_-/n_+.

PST-P3-06
The optimum discharge conditions for the continuous solid-liquid separation of humic acid

T11 Plasma Science and Technology

#PST-P3-06

E. Hong, S. Ryu, S. Yoo, J. Park, T. Lho.

NFRI - Deajeon (Korea, republic of).

Recently, the various treatments processed for removal of non-biodegradable organics have been studied.

High-voltage electrical discharges directly in water are an emerging techniques in environmental pollutant degradation. It can produce hydrogen peroxide, molecular oxygen and hydrogen and hydroxyl, hydroperoxyl, hydrogen, oxygen, ozone and micro bubbles at the high voltage electrode.

The traditional flotation processes have no anti biotic ability. Besides, Dissolved air floatation process(DAF) requires the circulation of compressed water by air, expensive installation and operation cost.

Plasma air flotation can utilize OH radical and micro bubbles generated by plasma. These bubbles and oxidants enhance degradation, separation and inactivation of suspended solids and microorganisms in salt water.

In this study, It is tried to find optimum discharge conditions to remove the non-biodegradable organics. The Fig. 1 is the reactor is divided to 4 regions by 4 walls. 1st region was rapidly mixed for coagulation. 2nd to 4th regions were slowly mixed for flocculation and flotation continuously.

The target material is humic-acids. The selected concentration of humic acid is 100 mg/L. Alum dose for flocculation is 10mL of 1% alum solution in 1L humic salty water (3.5% NaCl).

The flow rate conditions are increased from 1lpm to 3lpm.

The plasma discharge time are 5, 10, 20 seconds. And the plasma discharge cycles are 1,2,4 minutes.

The experimental results, optimal conditions are 4min of discharge cycle, 2lpm of flow rate, 20sec of discharge time.

[1] N Takeuchi, Y Ishii and K Yasuoka "Modelling chemical reactions in dc plasma inside oxygen bubbles in water", Plasma sources science and technology, vol. 21, 2012

[2] S.M. Ryu, E.J. Hong, D.C. Seok, S.Y. Yoo, Y.J. Kim, T.H Lho, B.J. Lee, "Characteristics of discharged sea water generated by underwater plasma system", Current Applied Physics, vol. 11, pp. 87-93, 2011

[3] James K. Edzwald, "Dissolved air flotation and me", Water research. vol. 44, pp. 2077-2106, 2010

Fig. 1. Reactor diagrams for continuous flow type PAF

Fig. 2. Humic acid removal efficiency

PST-5-Or-11
Humic acid separation by plasma aided flotation compared with sedimentation and electrolytic flotation

T11 Plasma Science and Technology

#PST-5-Or-11

S. Ryu, E. Hong, J. Park, S. Yoo, T. Lho.

National Fusion Research Institute - Daejeon (Korea, republic of).

Electrical discharges in water produce lots of oxidants like hydrogen peroxide, hydroxyl radical and hydrogen. In addition, shock waves, UV light and bubbles can be formed. In this experiment, feasibility test of plasma aided bubble flotation for humic acid was conducted compared with sedimentation, heated sedimentation, electrolytic flotation and dissolved air flotation. The humic substance of Aldrich, Inc. was selected as the representative of contaminants. The artificial sea water containing 3.5% concentration of NaCl was used for testing separation efficiency of humic acid. The selected concentration of humic acid is 100 mg/L and UV 254nm absorbance is 2.0~2.3 cm^{-1}. Aluminum sulfate concentration for flocculation is about 100 mg/L. After coagulation and flocculation of salin humic water for 1 and 30 minutes, treated water was moved into batch reactor for separation of humic flocs by sedimentation, heated sedimentation, electrolytic flotation dissolved air flotation and plasma aided flotation. As a results, plasma aided flotation is faster process to remove flocs than others. Therefore PAF process can be an alternative of pretreatment of reverse osmosis

[1] B.R. Locke, M.Sato, P.Sunka, M. R.Hoffmann, J.-S.Chang, “Electrohydraulic Discharge and Nonthermal Plasma for Water Treatment”, Ind. Eng. Chem, vol. 45, pp. 882-905, 2006
[2] N. Li, J.G. Huang, K.Z. Lei, J.F. Chen, Q.F. Zhang, “The characteristics of the bubble generated by underwater high-voltage discharge”, Journal of Electrostatics, vol. 69, pp. 291-295, 2011
[3] S.M. Ryu, E.J. Hong, D.C. Seok, S.Y. Yoo, Y.J. Kim, T.H. Lho, B.J. Lee, “Characteristics of discharged sea water generated by underwater plasma system”, Current Applied Physics, vol. 11, pp. 87-93, 2011

[4] James K. Edzwald, “Dissolved air flotation and me”, Water research. vol. 44, pp. 2077-2106, 2010

Figure 1. Absorbance difference by several separation processes (sedimentation, heated sedimentation, electrolysis, dissolved air flotation, plasma aided flotation)

Figure 2. Trend curvees of humic adid removal efficiency by electrilysis and plasma aided flotation

PST-5-Or-6
Non Thermal Plasma Assisted Catalytic Removal of IPA at ppb level by MnO2 Packed Bed Reactor: Comparison of System Efficiency

T11 Plasma Science and Technology

#PST-5-Or-6

S. Loganathan [1], F. Thevenet [1], P. Gravejat [1], A. Rousseau [2].

[1]École des Mines de Douai - Douai (France), [2]LPP, École Polytechnique - Palaiseau (France).

Volatile organic compound (VOC) removal is becoming more attractive owing to rigorous environmental issues. Moreover, VOCs removal in ppb level is more challenging because of high energy demand. In this regards, Non Thermal Plasma (NTP) coupled with inorganic sorbent (catalyst) system has been widely reported for continuous effluent treatment. This process would be energetically in efficient for ppb level VOC treatment. Therefore, we have suggested that two step process likely Adsorption followed by Plasma treatments would be better method for low level VOC treatment. Hence, this work aims at investigating the energy efficiencies between continuous effluent treatment and Adsorption/Plasma treatment process. MnO_2 coated packed bed reactor has been designed and tested for two step adsorptive removal of VOCs at indoor level (ppb) concentration. Organic products during adsorption and plasma treatment have been monitored by Selective Ion Flow Tube Mass Spectrometry (SIFT-MS); whereas online FT-IR spectroscopy has been used to quantify the COx produced by NTP assisted regeneration step. The system efficiency has been studied by using IPA as a model VOC. In addition to that, IPA removal efficiency have been investigated for two different experimental conditions,
(i), *Continuous plasma treatment:* 300 ppb of IPA were sent to MnO_2 coated reactor, once IPA breakthrough is reached, NTP has been ignited with the fixed power of 0.82 W.
(ii), *IPA adsorption followed by plasma treatment:* After reaching the IPA breakthrough the reactor has been swept with dry air, thereby the reversibly and irreversibly adsorbed IPA has been quantified. Thereafter plasma was ignited under dry air (absence of IPA) with the power of 0.82 W. The removal efficiency of two different conditions has been reported in table 1.

As shown in table 1, Adsorption/Plasma treatment has shown 2 times higher IPA removal efficiency than continuous plasma treatment with same injected power. In addition to that, Adsorption/Plasma treatment has shown 50% less CO selectivity. Moreover, Adsorption/Plasma treatments have been studied for 4 consecutive cycles, and we have found that MnO_2 coated reactor has shown no change in adsorption capacity and product selectivity. In conclusion, Adsorption/Plasma treatment has shown better performance in regards of energy efficiency and product selectivity in comparison with continuous plasma treatment.

Table 1- IPA removal efficiency and product selectivity: comparison between continuous and Adsorption/Plasma treatment.

PST-3-Or-2
Pulsed plasma polymerization of propanethiol: correlation between plasma and film chemistries

T11 Plasma Science and Technology

#PST-3-Or-2

R. Snyders [1], R. Francq [2], M. Guillaume [1], J. Cornil [1], D. Thiry [1].

[1]University of Mons - Mons (Belgium), [2]Materia Nova - Mons (Belgium).

Plasma polymerization of sulfur-based molecules such as propanethiol is a promising approach to grow thiol (-SH) supporting surfaces that can serve as nucleation centers for gold nanoparticles or for the immobilization of DNA molecules. However, despite the potential of such a kind of thin films, it is still necessary to get a deeper understanding of the fundamental mechanism occurring during the plasma polymerization of sulfur-based precursors.
In this work, propanethiol plasma polymers (Pr-PPF) were synthesized using a pulsed ICP plasma varying the mean power dissipated in the discharge (<P>) in the range of 14-100 W. <P> was adjusted by varying toff (0-3.6 ms) while keeping constant ton and the peak power to 0.5 ms and 100 W, respectively. XPS measurements were performed in order to evaluate the chemical composition of the coatings. These data were correlated with the evolution of the plasma chemistry probed by mass spectrometry measurements in Residual Gas Analysis (RGA) mode and understood with the help of DFT calculations.
As a general trend, the sulfur-to-carbon ratio (S/C), measured by XPS, decreases as a function of <P> (From 1 to 0.38). An unexpected observation concerns the Pr-PPF synthesized at low <P> for which the S/C ratio (~1) is much higher than in the precursor (0.33). This behavior is explained by the trapping, in the Pr-PFF, of sulfur-based molecules presenting a high S/C ratio. RGA measurements support this explanation by revealing, at low <P>, a strong production of H2S in the plasma. On the other hand, ageing of these films leads to the “loss” of sulfur which again is consistent with the trapping of stable S-based molecules. For high <P> the plasma is dominated by CS2 molecules illustrating the strong fragmentation degree of the precursor. The modification of the plasma chemistry and the higher interface temperature explain the lower S/C in these conditions.

PST/SE/TF-3-Or-7
Tailoring of the Degradation Processes at Photocatalytically Active Titania Thin Films

T11 Plasma Science and Technology

#PST/SE/TF-3-Or-7

E. Moser [1], K. Ambord [1], S. Chappuis [1], V. Vishnyakov [2].

[1]University of Applied Sciences - Geneva (Switzerland), [2]Dalton Research Institute - Manchester (United kingdom).

The photo induced benefits of titania thin films have been attracting increasing attention during the past years. In particular, the modification of the titania networks has intensely been investigated since it enables to shift the optical energy bandgap to the visible part of the light spectrum.
Recently, the deposition of photocatalytically active titania layers at ambient temperature has been developed using the reactive dc sputtering process and the metal organic chemical vapour deposition (MOCVD) method by increasing the working pressure up to atmospheric pressure for the latter method. [1]
In this work, the wettability and the chemical composition of the titania layers will be modified by adapting the deposition parameters and doping the titania layers using non-metallic elements. The produced titania thin films will be analyzed using AFM, XPS, FTIR, XRD, and Raman spectroscopy. The chemical reactivity and topography of the various titania surfaces will be investiga¬ted in detail. Insight into the incorporation of the doping elements and its consequences onto the photo induced properties will be highlighted.
Preliminary results regarding the mineralization of methylene blue dye and stearic acid by the titania thin films, irradiated under UV light at 365 nm and visible light at 428 nm, will be presented and correlated with the specific functional features of the different surfaces. In this way, the manufacturing of photo active titania layers may be directed towards specific anti-fingerprint and anti-microbial properties.

[1] Sidney Chappuis, Anna Campiche, Damien Gilliéron, Eva Maria Moser, Jukka Lausmaa, Armin Reller, Plasma Process Polym, 6, 440-445 (2008)

Fig.1: Degradation of stearic acid versus time and AFM-images of a 200 nm TiO_2 layer

PST/SE/TF-2-Or-6
High entropy alloys deposited by magnetron sputtering

T11 Plasma Science and Technology

#PST/SE/TF-2-Or-6

P. Dutheil [1], A.L. Thomann [1], H. Hidalgo [1], D. Depla [2], F. Boydens [2], M. Jullien [3].

[1]GREMI - Orleans (France), [2]Research Group DRAFT - Gent (Belgium), [3]Institut Jean Lamour - Nancy (France).

In the 90s Yeh and al. proposed a novel alloy system called “high entropy alloy” (HEA) which contain 5 to 13 major elements (or multi principal elements), with concentrations ranging from 5 at. % to 35 at. %. HEAs exhibit very interesting properties, for examples: hydrophobicity, good temperature stability, high hardness, wear resistance and superplasticity and high corrosion and oxidation resistance. These properties are similar to those of Metallic glasses (MG) but kept at higher temperature. HEA mixing entropy is high, leading to the formation of random solid solutions (FCC or BCC) during solidification, rather than intermetallic compounds or other complex ordered phases [1].
Since 15 years many papers were published on the synthesis of HEA thin films, mainly dealing with the study of the features and properties modification when one of the element concentration is varied. Considering thin films, the challenge is not to stabilize low ordered forms, which is quite easy by working at low temperature, but rather to control the film features. All the reported works point out the complex relationship existing between chemical composition, structure and morphology of the films.
In this work, different studies on HEAs thin films grown by magnetron sputter deposition using powder targets will be presented. In fact, in order to scan a wide range of different compositions of thin films, elements powders were mixed in different quantities to obtain several target compositions. The complex relationships between crystalline structure, thin film composition and experimental parameters will be tackled as well as their influence on the hardness and hydrophobocity properties of HEA thin films.

[1] J-W Yeh, “Recent progress in High entropy alloy”,Ann.Chim. Sci. Mat. 31(6) pp. 633-648 (2006).

PST-5-Or-3
DEVELOPMENT OF AN ICP-RF PLASMA SOURCE FOR THE STUDY OF HELIUM INSERTION IN TUNGSTEN

T11 Plasma Science and Technology

#PST-5-Or-3

L. Pentecoste [1], A. Melhem [1], A.L. Thomann [1], P. Desgardin [2], T. Belhabib [1], M.F. Barthe [2].

[1]Groupe de Recherches sur l'Energétique des Milieux Ionisés, CNRS-Polytech'Orléans, 14 rue d'Issoudun, B.P. 6744, F-45067 Orléans cedex 2, France - Orleans (France), [2]Conditions Extrêmes et Matériaux sous Haute Température et sous Irradiation, CNRS, 3A rue de la Férollerie, F-45071 Orléans, cedex2, France - Orleans (France).

Tungsten has been selected as a potential Plasma Facing Material in the future nuclear fusion reactor such as ITER. It is supposed to become the shield material for the Divertor and will be exposed to the most severe plasma conditions i.e. a bombardment of particles like neutrons, deuterium, tritium and helium. Helium ion flux interaction with a tungsten surface leads to a generation of vacancy defects and eventually larger defects like helium bubbles or vacancy clusters [1]. These defects affect the tungsten mechanical properties and can have an impact on yield and safety of the experimental reactor. The objective of this study is to study the first steps of the implantation process, i.e. at low ion flux and kinetic energy to avoid damaging of the material.

In this study, an ICP-RF plasma source has been built and developed at the GREMI laboratory of Orleans. Both Langmuir probe and Heat Flux Microsensor [2] techniques were used respectively to determine the Helium plasma parameters and to measure the global energy transfer from the plasma to the substrate surface. After helium plasma characterization, the tungsten samples were immersed in the plasma under $^{3}He^{+}$ flux with incident ion energy of the order of 320 eV. The helium behavior in tungsten was studied by using nuclear reaction analysis technique.

The ion flux accessible with the ICP source varies between 10^{11} to 10^{16} at.cm^{-2}.s^{-1}. From plasma characterization optimized implantation conditions were defined for

which ions do not encounter collisions during their acceleration in the sheath (comparing the Debye length to the mean free path of the He^+). The kinetic energy of the ions is thus determined by the substrate bias voltage and can typically be varied between 50 eV to 500 eV. Measurement of the global energy transfer allowed isolating the specific contribution of the incident He^+ ions. At substrate bias voltages lower than –50 V, it seems to be the main part of the global energy flux delivered to the surface. The first surface characterizations with NRA technique showed low He retention rates (below 10^{21} at/m^2) similar to the ones presented by P-E. Lhuillier [3] in a previous study. Positron Annihilation Spectroscopy and Scanning Electronic Microscopy will be used to characterize respectively the vacancy defects induced in the tungsten surface and eventually helium bubbles formation.

[1] H. Iwakiri et al, J. Nuc. Mater 283±287 (2000) 1134±1138
[2] P-A Cormier et al, J. Phys. D: Appl. Phys. 43 (2010) 465201
[3] P.E. Lhuillier et al, J. Nuc. Mater 433 (2013) 305–313

PST-P2-07
Analysis of reaction mechanisms in plasma chemistry

T11 Plasma Science and Technology

#PST-P2-07

V. Hrachova [1], R. Hrach [1], T. Ibehej [1], J.C. Legrand [2], A.M. Diamy [2].

[1]Charles University, Faculty of Mathematics and Physics, Department of Surface and Plasma Science - Prague (Czech republic), [2]Universite Pierre et Marie Curie - Paris (France).

Plasma mixtures containing chemically active species are used in many technologies. When studying processes in such plasmas, a macroscopic kinetic approach is often used. This technique is based on the system of chemical reactions between plasma species, from which the continuity equations for concentrations of individual species can be derived [1]. If the number of species in the model is moderate, the standard numerical methods can be used. However, due to high complexity of processes in many chemically active plasmas, the set of input chemical reactions has to be reduced before the model preparation and solving. In the literature, various techniques of model simplification, e.g. approaches based on the sensitivities of individual reactions, on the corresponding reaction rates or on methods of time-scale separation, can be found. In the present contribution we monitored the speed of every reaction during the kinetic calculation, resulting in weight factors of reactions describing the relative importance of individual reactions in the kinetic scheme. The goal was to preserve only the reactions influencing profoundly the resulting concentrations of main products.

The developed reduction technique was applied to the analysis of two different types of chemically active plasmas. The first system was obtained by the mixing of methane to the nitrogen flowing afterglow discharge [1]. The original kinetic scheme consisted from more than 250 chemical reactions. After the reduction only about 50-60 reactions found to be important. The second studied system was the active discharge in oxygen and argon-oxygen mixtures [2]. The input data for modelling were obtained from the measurements in a DC glow discharge in oxygen containing gas mixtures. The original kinetic scheme was reduced from about 160 reactions to less than 50 chemical reactions between the most important species. After the reduction of model complexity without significant loss of its preciseness, the residual

kinetic schemes of both of methane and oxygen containing mixtures can be solved by standard algorithms for solving stiff sets of differential equations.

In the main part of contribution the role of the most important chemical reactions in the dependence on various plasma parameters was discussed. The obtained results, i.e. the steady-state concentrations of individual species, were used as input data for 2D particle model [3] describing the sheath structure near substrates immersed into chemically active plasma in selected plasma-assisted technologies. Here the main studied question was the determination of the spatial distribution of fluxes of individual charged species to uneven substrates of complicated forms [4].

[1] Legrand J.-C., Diamy A.-M., Hrach R., Hrachova V., Advances in Plasma Physics Research, Vol. I, NOVA Science Publ. Inc., New York, USA (2001).

[2] Ibehej T., Hrach R., Hrachova V.: Modeling of chemical kinetics in plasmas containing oxygen, Proc. XIX GD, Beijing 2012.

[3] Ibehej T., Hrach R.: Computational study of sheath structure for plasma-assisted technologies in the presence of electronegative plasma, Vacuum 86 (2012), 1220.

[4] Hruby V., Hrach R.: Computational simulation of metal ion propagation from plasma to substrates with uneven surfaces, Vacuum 90 (2013), 109.

PST-4-Or-2
Comparison of two hydro-carbonated based plasmas for HgCdTe etching

T11 Plasma Science and Technology

#PST-4-Or-2

A. Pageau [1], C. Cardinaud [1], L. Le Brizoual [1], S. Jacq [1], F. Boulard [2], J. Baylet [2].

[1]Institut des Matériaux Jean Rouxel - Nantes (France), [2]CEA/LETI-DOPT - Nantes (France).

Etching mechanism of mercury cadmium telluride (MCT) has been investigated in hydro-carbonated based mixtures inductively coupled plasma (ICP). According to literature it can be described by the etching of HgTe and CdTe compounds [1][2]. Hg desorbs spontaneously from the surface. Te is etched by the formation of volatile TeH_2. Cd is assumed to form volatile metal organic species with methyl; this latter step limits the etching of MCT.
Methane-based plasma is compared to another methyl precursor gas (labelled B). The plasma phase is characterized thanks to electrostatic probes, optical emission spectroscopy and mass spectrometry. Etched samples are characterized by profilometry, SEM and XPS. Process parameters investigated are source power, pressure and sample bias.
In the same conditions of flow, pressure and source power, the positive ion flow toward the surface and the surface composition are very similar for the two gas precursors (Fig 1), the VI/II ratio is slightly lower in B-based plasma. In this mixture, methyl concentration is typically five times smaller than in the methane-based plasma. However the etch rate does not present such a difference.

On going work concerns quantitative evaluation of the ion and methyl fluxes for a better description of the plasma and the understanding of the etching mechanism. Our experimental results have been compared in the frame of the Mayer and Barker, ion assisted chemical etching mechanism model [3][4] (Eq 1) with a good qualitative agreement (Fig 2).

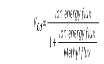

The authors acknowledge the FUI program for financial support within the BIRD project.

[1] R.C. Keller, M. Seelmann-Eggebert and H.J. Richter. J. Electron. Mat., 24, 1155–1160 1995
[2] C.R. Eddy, D. Leonhardt, V.A. Shamamian, J.R. Meyer, C.A. Hoffman and J.E. Butler. J. Electron. Mater., 28, 347–354 1999
[3] T.M. Mayer and R.A. Barker. J. Vac. Sci. Technol., 21, 757–763 1982
[4] R. Gottscho. J. Vac. Sci. Technol. B, 10, 2133–2147 1992

Fig 1 Methyl flow, ion flow, etch rate and surface composition in hydro-carbonated based plasma at constant bias

Fig 2 Etching yield per eV as function of ion energy flow/methyl flow

PST-1-Or-8
Probe Diagnostics of RF Plasmas for Material Processing

T11 Plasma Science and Technology

#PST-1-Or-8

V. Godyak.

RF Plasma Consulting - Brookline, Ma (United states).

During the last decades, plasma processing of materials became a significant component of contemporary industries. Plasma chemistry, manufacturing of semiconductor chips, nanotechnology, and plasma treatment of organic and live tissues are well known examples of plasma processing. To control plasma interaction with materials, the knowledge of plasma parameters and their spatial distribution are vitally important. Typically, processing of low temperature plasma is characterized by a high degree of different kinds of non-equilibrium conditions. The electron temperature in such plasmas exceeds by far the temperatures of ions and neutral species. The electron energy distribution function is non-Maxwellian. The plasma parameters are not in temporal, nor spatial equilibrium with the electromagnetic field that maintains the plasma [1]. Today, numerical modeling is the main method of studying highly non-equilibrium plasma in plasma processing reactors. The validity of those codes for reactive plasmas has never been proved in experiments. The cross section data of some plasma-chemical reactions imbedded in these codes are frequently ambiguous. Moreover, many of these codes are missing effects of non-local electron kinetics and non-local electrodynamics, which both play important roles in rf plasmas at low gas pressure [2]. Most universal and informative diagnostics for low temperature non-Maxwellian plasma at low gas pressure is the Langmuir probe in its Druyvesteyn modification. Contemporary probe diagnostics requires probe measurement of the electron energy distribution function, EEDF, from which the plasma parameters and the rates of plasma-chemical reactions are found as appropriate integral of the measured EEDF [3]. This approach has been successfully implemented for laboratory plasma experiments with noble gases at moderate rf power. However, attempts to implement the same probe diagnostics routine in plasma reactors with chemically active molecular gases have failed due to various kinds of distortions in probe measurement. There are three major problems in implementing meaningful probe diagnostics in rf plasma reactors. They are: 1) a wide frequency spectrum with significant amplitudes of the plasma rf potential corresponding to the rf power and rf bias fundamental frequencies and their

harmonics; 2) contamination of the probe surface with a low conductive layer of the reaction products; and 3) high impedance between the plasma and grounded chamber due to chamber contamination or/and to artificial protective chamber coating. In this presentation, we consider the ways to resolve those issues and illustrate their effectiveness in obtaining undistorted EEDFs with high energy resolution and large dynamic range, in different kinds of rf plasma reactors.

1. V. A. Godyak, Non-Equilibrium EEDF in Gas Discharge Plasmas. (Review), Special Issue of IEEE Trans. Plasma Sci. 34, 755 (2006).
2. V. A. Godyak, Hot Plasma Effects in Gas Discharge Plasma, Phys. Plasmas. (Review), 12, 3553 (2005).
3. V. A. Godyak and V. I. Demidov, Probe Measurements of Electron Energy Distribution in Plasma: What Can We Measure and How Can We Achieve Reliable Results? (Review), J. Phys. D: Appl. Phys. 44, 233001, 2011.

PST-1-Or-9
Ion Temperature Measurement in the Plasma of an ECR Ion Source by Means of Precision X-Ray Spectroscopy

T11 Plasma Science and Technology

#PST-1-Or-9

C. Szabo-Foster [1], P. Amaro [2], M. Guerra [3], A. Gumberidze [4], P. Indelicato [1].

[1]Laboratoire Kastler Brossel - Paris (France), [2]Physikalisches Institut, Heidelberg University - Heidelberg (Germany), [3]Centro de Física Atómica, Departamento de Física, Faculdade de Ciências e Tecnologia, Universidade Nova de Lisboa - Lisboa (Portugal), [4]ExtreMe Matter Institute - Darmstadt (Germany).

In our laboratory we are performing precision x-ray spectroscopy of highly charged ions (HCI) to prove quantum electrodynamics calculations. (QED tests). For these precision measurements down to the ppm level we have developed a double crystal spectrometer (DCS) to allow absolute measurements (without the use of an external reference) and we attached the DCS to an Electron Cyclotron Resonance Ion Source (ECRIS) to directly observe the HCI of the ECR plasma.

Measuring the broadening of transitions in highly charged ions (HCI) in the plasma of an Electron Cyclotron Resonance (ECR) ion source can provide an experimental method for the determination of the natural line widths of these transitions in the x-ray energy range. The energy of the 1s2s 3S1 → 1s2 1S0 “relativistic” M1 line in He-like Ar has been recently measured by our group in the “Source d’Ions Multichargés de Paris” (SIMPA) ECR ion source, at the Laboratoire Kastler Brossel (Ecole Normale Supérieur, Université Pierre and Marie Curie and CNRS), to a 2.5 ppm precision without the use of an external reference [1]. This measurement has been performed directly on the plasma of an ECR ion source with a vacuum double crystal spectrometer [2]. The M1 transition in He-like Ar has a very small (calculated) natural width (~10-7 eV), which can be considered negligible for the purposes of our investigations. By defining the response function of our double crystal spectrometer with the help of a Monte Carlo Simulation code we have obtained ion temperatures inside the ECR plasma from the determined Doppler broadening of the M1 line.

Within our robust analysis, simulations are run for various Doppler and Lorenzian input distributions. An average value of 81±12 meV was found for the Gaussian width of the M1 line in the ECRIS plasma during our measurements, which provides a lower than expected ion temperature for He-like Ar ions inside an ECR ion source. This method can be extended to lines with non-negligible natural line widths and provide experimental values for these widths.

[1] P. Amaro, S. Schlesser, M. Guerra, E.-O. Le Bigot,1 J.-M. Isac, P. Travers, J.-P. Santos, C. I. Szabo, A. Gumberidze, and P. Indelicato; Phys. Rev. Lett. 109, 043005 (2012).

[2] P. Amaro, C. I. Szabo, S. Schlesser, A. Gumberidze, E G. Kessler, Jr, A Henins, E-O Le Bigot, M. Trassinelli, J.-M. Isac, P. Travers, M. Guerra, J. P. Santos and P. Indelicato, arXiv:1205.4520v1 [physics.atom-ph]

PST-2-Or-9
Langmuir-probe analysis of photoemission-assisted Ar plasma for planarization process

T11 Plasma Science and Technology

#PST-2-Or-9

S. Ajia, Y. Ohtomo, S. Ogawa, Y. Takakuwa.

Tohoku University - Sendai (Japan).

A photoemission-assisted (PA) Ar plasma, which is DC discharge plasma triggered by the photoelectrons emitting from the substrate irradiated with UV light as shown in Fig.1, has been developed to make the substrate surface morphology flattened in an atomic scale for applications of surface activated bonding and DNA chips. Hereafter this is called " a dry planarization process". In the previous reports [1], it was demonstrated that the surface roughness is considerably improved for the Al and Cu substrates by this dry process. In this study, we measured the plasma potential distribution of the PA Ar plasma by using a Langmuir probe to estimate the kinetic energy E_k of Ar^+ ions impinging on the substrate.
In the PA Ar plasma apparatus, a Xe excimer lamp with UV light (λ = 172 nm) was employed, leading to the order of 10^{12} photoelectrons/cm^2/s, which enabled us to generate uniformly a glow discharge on a 2-inch Si wafer at bias voltage V_B of 120 V and Ar pressure of 100 Pa, and to increase a discharge current up to 10^{-6}-10^{-4} A at smaller V_B than 120V, which is referred to as Townsend plasma. A Langmuir probe was made of W with 0.8 mm in diameter. Its position was precisely adjusted with a X-Y-Z manipulator between the Si wafer and the Cu electrode with 29 mm in distance. As shown in Fig. 2, the plasma potential distribution is almost flat for the glow discharge at V_B of 150 V, suggesting that an ion sheath is thinner than 1 mm. On the other hand, a plasma potential gradient of the Townsend discharge at V_B of 60 V is almost the same as the calculated electric potential distribution, implying that there is no ion sheath effectively. Taking the energy loss due to elastic collisions between Ar^+ ion and Ar atom into account, we estimate the E_k of Ar ion upon the impingement with the substrate to be 0.23 and 8.9 eV for Townsend and glow discharge, respectively, and a surface flattening model of the dry planarization process is discussed.

[1] Y. Ohtomo et al., Surf. Interface Anal. 44 (2012) 670

Fig.1. Schematic illustration of the the dry planarization process
Fig.2. Plasma potential distributions for the Townsend and glow discharge.

PST-P2-19
Plasma polymerization of allylamine with an atmospheric pressure plasma jet for high-function textile products

T11 Plasma Science and Technology

#PST-P2-19

A. Airoudj [1], A.M. Koenig [2], M. Huet [2], M.F. Vallat [1], Y. Frère [3], V. Roucoules [1].

[1]Institut de Science des Materiaux de Mulhouse, IS2M – UMR 7361 - C.N.R.S. - U.H.A. - Mulhouse (France), [2]Institut Français du Textile et de l'Habillement (IFTH) - Mulhouse (France), [3]Institut Charles Sadron ICS (UPR22-CNRS) - Mulhouse (France).

From an industrial point of view, there is an increasing interest to control the surface functionalities and the surface properties of all kind of materials. In particular, an increasing demand is registered to develop high-function textile products. The new generation of manufacturing processing that includes plasma treatment ensures flexibility of the technology and possibility of easy adaptation for application of different finishing methods to meet variable consumers' requirements [1].

Recent development in the field of atmospheric plasma technology is creating new perspectives for surface treatment of materials [2]. By controlling the atmospheric gas and electrical conditions, one can significantly increase the efficiency of the plasma surface treatment. Besides, by adding reactive chemical precursors to the plasma discharge, the surface chemistry can be controlled and thin functional coatings can be deposited. A wide number of monomers can be used as precursors to incorporate functiononal groups on various surfaces.

In this study, plasma polymers of allylamine were deposited by using an atmospheric pressure plasma jet. Firstly, we have investigated the influence of different external plasma parameters (like deposition time, precursor flow rate, substrate-plasma distance, power frequency...) on the final thin film properties. Physical and chemical properties of the deposited thin films were characterized by several characterization techniques such as ellipsometry, infra-red spectroscopy, SEM or XPS.

Then, examples of potential applications of this amine-containing atmospheric plasma functional coating will be given. First, polyamide microcapsules are immobilized onto plasma treated cotton surfaces via amide linkages which guarantee high durability and accessibility. Secondly, dyeing properties of cotton textile could be enhanced and the dyeing process mainly occurs through the plasma treated regions.

These results show that atmospheric plasma is a promising process for the fabrication of functional coatings on textile substrates and has immense potential for future industrial applications.

[1] A. Grill, Cold Plasmas in Materials Fabrication, IEEE Press,New York, 1994.
[2] U. Lemmatzsch, J. Ihde, Plasma Processes and Polymers 2009, 6(10), 642-648.

PST-P3-07
Optical characterization of a microwave pulsed discharge for optimization of CO2 conversion

T11 Plasma Science and Technology

#PST-P3-07

T. Silva [1], N. Britun [1], T. Godfroid [2], R. Snyders [3].

[1]Chimie des Interactions Plasma Surface (ChIPS), CIRMAP, Université de Mons, 23 Place du Parc, B-7000 Mons, Belgium - Mons (Belgium), [2]Materia Nova Research Center, Parc Initialis, B-7000 Mons, Belgium - Mons (Belgium), [3]Chimie des Interactions Plasma Surface (ChIPS), CIRMAP, Université de Mons, 23 Place du Parc, B-7000 Mons, Belgium / Materia Nova Research Center, Parc Initialis, B-7000 Mons, Belgium - Mons (Belgium).

Keywords: microwave discharge, CO_2 conversion, exhaust gases, optical diagnostics

The recent results on the time-resolved optical diagnostics of CO_2 containing pulsed surface wave-sustained microwave discharges working at 2.45 GHz and operating at moderate pressure (~ 5 Torr) are presented. The plasma was sustained in the flowing CO_2 and CO_2+N_2 gas mixtures in a quartz tube crossing a waveguide [1]. The characteristic plasma temperatures, namely the gas temperature (via the N_2 and CO rotational temperatures), and N_2 vibrational temperature are determined as a function of time at different axial positions along the discharge tube. Besides this, the space-resolved measurements of CO_2 conversion rate through the discharge volume, as well as the measurements of energetic coefficient of plasma efficiency for such a conversion are performed using optical actinometry. For the last purpose, assuming low decomposition rate of molecular nitrogen during the plasma pulse, N_2 molecule is utilized as an actinometer [2,3] to determine the CO density, as one of the products of CO_2 decomposition [4]. The validity of this method has been analysed for the described experimental conditions based on the assumption of a steady state of actinometric signal achieved during the discharge pulse.
The results show a non-uniform dissociation rate of CO_2 that grows from the upper to the bottom part of the discharge tube, where it saturates. The dissociation degree is substantially modified by the variations of the power balance and the composition of the gas mixture.

The results are compared to those obtained by means of the gas chromatography in a 0.9 GHz microwave discharge, showing a good agreement between these two microwave plasma discharges in terms of CO_2 conversion.

References:

1. T. Godfroid, J. P. Dauchot, and M. Hecq, Surf. Coat. Technol. 174–175 (2003) 1276.
2. V. N. Ochkin , Spectrocopy of Low Temperature Plasma, WILEY-VCH Verlag GmbH & Co. KGaA (2009)
3. D. K. Otorbaev, Chemical Physics 196 (1995) 543-550
4. S. N. Andreev, V.V. Zakharov, V. N. Ochkin, S. Yu. Savinov, Spectrochimica A 60 (2004) 3361-3369

SE/PST/TF/BI-2-Or-9
Plasma-assisted deposition of polymethyl methacrylate on titanium substrates

T11 Plasma Science and Technology

#SE/PST/TF/BI-2-Or-9

N. De Geyter, P. Cools, E. Vanderleyden, P. Dubruel, R. Morent.

Ghent University - Ghent (Belgium).

Plasma polymerization is a unique technique to fabricate thin polymer films from a wide variety of organic and organometallic precursors [1]. Plasma polymerized films are pinhole-free and highly cross-linked and therefore insoluble, thermally stable, chemically inert and mechanically tough. Furthermore, such films are often highly adherent to a variety of substrates including conventional polymer, glass and metal surfaces [2]. Due to these excellent characteristics, plasma-polymerized films have been used in a wide variety of applications including barrier coatings, protective coatings, selective permeation membranes and dielectric layers in microelectronics [3]. Besides these well-known examples, state-of-the-art applications are continuously being developed, especially in the biomedical domain. Generally, a large part of research related to plasma-assisted thin film deposition has involved low pressure non-thermal plasma technologies. Although vacuum treatment processes afford good control over gas chemistry and provide the possibility of using high energetic species (in the range of several eV to hundreds of eV) in the deposition process, atmospheric pressure processing techniques are offering specific advantages, such as the elimination of expensive vacuum equipment, easier handling of the samples and scalability for industrial on-line processing [4,5]. Therefore, in recent years, a lot of effort has been put into the development of non-thermal plasma reactors for thin film deposition working at or near atmospheric pressure.

This paper will focus on the formation of coatings in an atmospheric pressure dielectric barrier discharge (DBD) using methyl methacrylate (MMA) as gaseous precursor. Plasma polymerized films will be deposited onto Ti samples, which is a common material used for artificial hips. Depositing a polymethyl methacrylate (PMMA)-like coating onto Ti can improve the fixation of artificial hips, since the bone cement used to fixate the hip into the human body normally consists of MMA or PMMA. In this work, the chemical and physical properties of the obtained PMMA-like

coatings will be discussed in detail using Fourier transform infrared spectroscopy (FTIR), X-ray photoelectron spectroscopy (XPS) and atomic force microscopy (AFM).

[1] F. Benitez, E. Martinez and J. Esteve Thin Solid Films, 2000, 377-378, 109-114

[2] F. Arefi, V. Andre, P. Montazer-Rahmati and J. Amouroux Pure and Applied Chemistry, 1992, 64, 715-723

[3] J. Schwarz, M. Schmidt and A. Ohl Surface and Coatings Technology, 1998, 98, 859-864

[4] G. Kühn, I. Retzko, A. Lippiz, W. Unger and J. Friedrich Surface and Coatings Technology, 2001, 142-144, 494-500

[5] G. Borcia and N.M.D. Brown Journal of Physics D: Applied Physics, 2007, 40, 1927-1936

PST-P3-08
Characterization of Surface Dielectric Barrier Devices for Aerodynamic and Acoustic Applications

T11 Plasma Science and Technology

#PST-P3-08

I. Biganzoli, R. Barni, C. Riccardi.

Dipartimento di Fisica Occhialini, University of Milano-Bicocca - Milan (Italy).

Atmospheric pressure dielectric barrier discharges (DBDs) are widely employed as cold plasma sources for plasma processing and applications [1]. In a Surface Dielectric Barrier Discharge (SDBD) device two electrodes are placed at the opposite sides of an insulating material and a plasma is created by the ionization of a thin air layer just above the dielectric surface.
The non-thermal plasma state allows these devices to be used in presence of thermodegradable materials or living tissues, rendering them suitable for many applications such as surface treatment and sterilization. However, at present SDBDs are mainly known in the field of cold plasma aerodynamic applications, being these discharges particularly suitable in energizing the boundary layer of airflows surrounding a body, and thus in the active flow control field [2]. As a matter of fact, many experimental studies have proved that SDBDs can generate an induced airflow of several m/s. This induced airflow can favourably interact with an external wind and provide, for instance, stall prevention, lift enhancement or drag reduction. It is evident that the aeronautical sector can take many benefits from the application of the so called plasma actuators. However, the growing interest for these devices is also due to the environmental benefits they can deal to. As a matter of fact, apart from the fact that drag reduction can result in fuel and thus pollution reduction, it is known that the problem of acoustic pollution affecting an airport neighbourhood is mainly due to the the airflow detachment occurring in correspondence of an aircraft bluff body (such as a landing gear).
For these kinds of applications, plasma is generally created in correspondence of just one side of the insulating barrier, so one electrode is buried into a dielectric frame whereas the other one is exposed to air. When the device is fed with a sinusoidal high voltage supply some differences in the plasma properties result from this asymmetric configuration. The discharge has been characterized by electrical diagnostics, in particular Rogowski coils have been adopted for measuring the

electrical current flowing into the circuit, which is the superimposition of a low frequency capacitive current, almost independent of the plasma presence, and of a discharge current appearing as a series of fast pulses [3]. A high temporal resolution has been achieved and a statistical analysis has been implemented to evaluate some properties of these current peaks, as well as their distribution in the course of the voltage signal. This allows to evaluate the entity of the asymmetry between the two discharge semi-cycles, which depends on the electric field configuration inside the gap. A change in the dielectric properties and in the electrode configuration influences some plasma properties (such as the intensity of the current pulses or their frequency of appearance) as well as the discharge asymmetry. This electrical characterization is useful not only because the physics of these devices is not completely understood, but also because it allows a better understanding of how aerodynamic effects are correlated to the discharge properties.

[1]U.Kogelschatz, Plasma Chem. Plasma Proc. 23 (2003)
[2]E.Moreau, J. Phys. D: Appl. Phys. 40 (2007)
[3]I.Biganzoli et al., J. Phys. D: Appl. Phys. 46 (2013)

PST-P2-08
Diagnostic of multi-electrode type serpentine plasma discharge process with new ignition system using a high speed camera

T11 Plasma Science and Technology

#PST-P2-08

S. Aoqui [1], F. Mitsugi [2], H. Kawasaki [3], T. Ohshima [3], S. Kinouchi [4], T. Baba [5].

[1]Sojo University - Kumamoto (Japan), [2]Kumamoto University - Kumamoto (Japan), [3]Sasebo National College of Tech. - Sasebo (Japan), [4]DITECT Corporation - Tokyo (Japan), [5]VIC International, Inc. - Tokyo (Japan).

There has been much interest in gliding arc discharge plasma due to its potential for pollution control of exhaust gas decomposition, material processing, surface treatment and biological application such as sanitization, the sterilization. [1,2] It is well known that the gliding arc discharge starts from breakdown of atmospheric gas at the shortest gap between two divergent electrodes under DC or AC power supply and it glides along the same direction as the gas flow. However, our study on simultaneous observation of the dynamic behavior of the plasma path via a high speed camera and the corresponding electrical properties revealed that the plasma path was very complicated due to gas turbulence and reconnections were repeated especially in high gas flow to maintain plasma. Moreover, the plasma impedance was not as low as that of normal arc discharge because plasma length increased with gliding.[3,4] Therefore, we call this plasma as serpentine plasma. A serpentine plasma discharge was nonequilibrium, a kind of the non-steady discharge, and a large number of applied research works has been performed as a gliding arc discharge. Many studies relate to decomposed chemical species, and there are a few papers about the discharge mechanism. We carried out the observation using a high-speed camera (Max flame rate of 1300000 fps) about the discharge mechanism of the serpentine plasma discharge without any kind of pre-ignition system. It was confirmed by using the high speed camera where paths of discharge between electrodes existed temporally. This measurement had been performed in the serpentine plasma discharge system of 2, 3 and 6 electrodes type. However,

discharge voltage rose when a pre-ignition did not exist in comparison with the system which equipped pre-ignition system. In this study, it was proposed a new pre-ignite process which was not based on an electric discharge, and the discharge mechanism with multi electrode (3 and 6) type was confirmed by a high speed camera and I-V characteristics simultaneously.

[1] M. Mlotek, J. Sentek, K. Krawczyk and K. Schmidt-Szalowski, Applied Catalysis A: General 366, 232 (2009)
[2] Z. Bo, J. Yan, X. LI, Y. Chi, K. Cen, Journal of Hazardous Materials 166, 1210 (2009)
[3] F. Mitsugi, T. Ikegami, S. Aoqui, Y. Tashima, H. Kawasaki, T. Nakamiya, Y. Sonoda, H. D. Stryczewska, Przeglad Elektrotechniczny 88 (6), 105 (2012).
[4] F. Mitsugi, J. Furukawa, H. Kawasaki, T. Kawasaki, S. Aoqui, H. D. Stryczewska, The European Physical Journal Applied Physics (2012) inprint.

Fig.1 High speed image (10000 fps) of 6 electrodes type serpentine plasma discharge system

PST-P3-16
Template-free elaboration of polyaniline nanofibers by cold plasma

T11 Plasma Science and Technology

#PST-P3-16

A. Zaitsev [1], A. Lacoste [2], F. Poncin-Epaillard [1], D. Debarnot [1].

[1]LUNAM Université, UMR Université du Maine, CNRS 6283, Institut des Molécules et Matériaux du Mans (IMMM), Département Polymères, Colloïdes et Interfaces (PCI), Avenue Olivier Messiaen - Le Mans (France), [2]Laboratoire de Physique Subatomique et de Cosmologie, Université Joseph Fourier Grenoble 1, CNRS/IN2P3, Institut Polytechnique de Grenoble, 53, Avenue des Martyrs - Grenoble (France).

The interest of one-dimensional materials has been demonstrated in a great number of applications due to their high shape factor and sometimes, new properties.

The objective of this work is to synthesize polyaniline nanofibers thanks to the plasma technique without using any template. To get such architecture, a metallic catalyst (Pd) is used. Two ways of catalyst deposition are considered: by the means of chemical deposition from a colloidal solution and by physical vapor deposition (PEPVD). The catalyst forms a discontinuous layer on the surface of the substrate, in the form of nods with controlled size. This can be done by controlling the size of the colloidal particles and deposition time in the case of chemical deposition and by controlling the plasma conditions (such as target biasing, power supply), and deposition time in the case of sputtering.

The polymerization of polyaniline is conducted by chemical vapor deposition (PECVD) thanks to a reactor that provides the possibility of PEPVD and PECVD. It uses the multi-dipolar microwave-assisted excitation source that offers uniform plasma at low precursor pressures (0.01 Torr) and low energy supply (60W). Also the advantage of this method is that the substrate is situated out of the plasma phase that prevents the polymer from the degradation. The control of the polymer growth consists in the control of process parameters such as the discharge power, the monomer flow, the substrate bias and the deposition time.

The morphology of the catalyst and the polymer is studied by the means of scanning electron microscopy (SEM) and atomic force microscopy (AFM). The chemical

structure of the fibers is studied by Fourier transform infrared spectroscopy (FTIR), X-ray photoelectron spectroscopy and UV-Vis spectroscopy.

This work was supported by Région Pays de la Loire.

SE/PST/TF/BI-1-Or-5
Plasmid DNA degradation induced by atmospheric pressure microplasma jets

T11 Plasma Science and Technology

#SE/PST/TF/BI-1-Or-5

C. Douat [1], J. Santos Sousa [1], L. Tessier [2], G. Bauville [1], M. Fleury [1], P.M. Girard [2], V. Puech [1].

[1]LPGP, CNRS & Univ. Paris-Sud - Orsay (France), [2]Institut Curie - Orsay (France).

In the last few years, atmospheric pressure microplasma jets have sparked considerable interest because of the possibility of propagating non-thermal plasmas in open air. As so, reactive plasma species (viz. radicals, positive or negative ions, electrons, UV radiation), and not only long-lived afterglow species, can be delivered, at ambient pressure and temperature, to targets located some centimeters away from the main discharge zone. This property opens up a host of new and fascinating possibilities including, among others, localized surface treatment in 2D and 3D (for cleaning and thin film deposition), production of nanomaterials, decontamination, and biomedical applications (odontology, dermatology, cancer research,…). To get a better insight into the biomedical effects of plasma jets, fundamental studies on the interaction of the microplasmas with biological structures are essential. In this context, we have exposed plasmid DNA to a plasma jet.
The studied plasma is created by a dielectric barrier discharge (DBD) with an axial symmetry. Indeed, our microjet device consists of concentric tubular electrodes separated by a dielectric cylindrical structure. The dielectric tube is made of quartz, and has inner and outer diameters of 2 and 4 mm, respectively. A grounded electrode is wrapped around the external side of the dielectric, while a high voltage electrode is glued inside the tube. Pure helium is flowing through the inner electrode at a flow rate in the range 100–1000 cm^3/min. High voltage pulses (3–6 kV) are applied between the electrodes at a repetition rate frequency of 20 kHz. The created plasma propagates in surrounding air. Experiments have also been performed with low O_2 admixture (<3%).
The plasma jet is set up vertically with the gas flowing downwards for interaction with plasmid DNA solutions (200 µL of buffer solution with a plasmid DNA concentration

of 20 mg/L) placed inside micro-wells or Eppendorf tubes. The damages to the DNA (oxidized bases, strand breaks, abasic sites) have been analyzed through specific enzymes (Fpg, Nth and Ape1) by agarose gel electrophoresis. Different buffer solutions have been used in order to identify their influence on the DNA degradation. It has been found that most of the damages were direct single and double strand breaks, while the oxidation of the amino-acid bases was of minor importance. The nature of the buffer solution does not change the nature of the DNA damages. However, in order to get a given amount of DNA damages, different exposure times have been required for the several buffer solutions used. It will also be shown that the observed DNA damages result from direct interaction of the plasmid DNA with the plasma jet, e.g., without the participation of by-products from the buffer solution.

PST/SE/TF-3-Or-2
PREPARATION OF DIFFERENT ANTIBACTERIAL POLYETHYLENE TEREPHTALATE BY PLASMA TECHNOLOGY

T11 Plasma Science and Technology

#PST/SE/TF-3-Or-2

F. Poncin-Epaillard [1], D. Debarnot [1], M.J. Perez-Roldan [1], J. Tarrade [2], E. Guittard [2], F. Guittard [2], T. Darmanin [2].

[1]IMMM-PCI - Le Mans (France), [2]LPMC - Nice (France).

The bacterial adhesion and the formation of biofilm are natural and spontaneous processes. These phenomena happen whatever the nature of bacteria, surrounding fluids and receiving substrates (plastics, metals, glasses, ...). The mechanism of biofilm formation proceeds in four steps: transport, adhesion, strengthening and colonization Bacterial adhesion depends on physico-chemical interactions between the bacteria and the receiving substrate. The nature of the substrate and its surface characteristics, such as superhydrophobic or superhydrophilic character, can affect the development of a biofilm. In both cases, the wetting is reduced and associated with the chemical functionality of the coating and its roughness adapted to the size of the bacteria, which is less than 1 micrometer. Therefore, polyethylene terephthalate (PET) foils surfaces were modified by plasma treatment in order to increase or to decrease the surface wetability and to tailor the surface roughness. Nanostructurated and hydrophilic surfaces were obtained with both He and O2 plasma treatments showing features around 45 and 85 nm. A posterior step was carried out by grafting the treated surfaces with polymer solutions in order to modify the surface free energy values. Treated surfaces were grafted with pluronic F108 and F68, polymers well known by their protein repulsive properties and by mixed solutions of pluronic and surfactants. Three different surfactants were selected, nonaethylene glycol monodecyl ether (C12E9), sodium taurodeoxycholate (STDC) and hexadecyltrimethyl ammonium bromide (CTAB) in order to characterize the effect on the surface free energy values of nonionic (C12E9), anionic (STDC) and cationic (CTAB) surfactacts on the grafting with pluronic-surfactant mixed solutions. The grafting homogeneity was studied by pico-contact angle mapping and the ageing

of grafted surfaces was also studied, showing a good adherence of grafted polymers on the hydrophilic surfaces. Besides, remarked variations on the surface free energy parameters were obtained, specially with surfaces grafted with pluronic-CTAB solutions. Besides, the bioadhesive properties of grafted surfaces will be characterized.

Among the methods allowing to structure and functionalize surfaces in order to make them superhydrophobic, plasma is a simple, inexpensive and perfectly manageable method. In order to create the roughness, oxygen plasma is first performed on a PET substrate. Then, the surface is composed of microfibrillars involving a nanostructuration. After, the modified surface is hydrophobized by pyrrole plasma deposition so as to obtain superhydrophobic PET. Each surface-modification was characterized by wettability measurement, AFM and XPS showing the characteristics of superhydrophobic surface whose antibacterial behaviour was tested.

PST/SE/TF-2-Or-5
Study of polymers surfaces metallization by plasma processes

T11 Plasma Science and Technology

#PST/SE/TF-2-Or-5

C. Lambaré [1], P.Y. Tessier [1], F. Poncin-Epaillard [2], D. Debarnot [2].

[1]Institut des Matériaux Jean Rouxel (IMN), Université de Nantes - Nantes (France), [2]Institut des Molécules et Matériaux du Mans (IMMM), Département Polymères, Colloïdes et Interfaces (PCI), Université du Maine - Le Mans (France).

Today, the metallization of plastics materials deals with a lot of industrial applications in the field of automotive, optic, electronic, etc. Nowadays, for industrial applications, the metallization of non conductive substrates (such as polymers) is generally performed by a chemical and/or electrochemical process. These chemical pathways imply the use of hexavalent chromium (CrVI), a molecule which is carcinogenic, mutagenic and toxic for the reproduction, during the surface etching before film deposition.

The aim of this project is to develop one or more innovative processes allowing free of CrVI. To address this problematic the plasma technology considered. The study is focused on: ABS (acrylonitrile butadiene styrene), ABS/PC (acrylonitrile butadiene styrene / poly carbonate) and PEEK (poly ether ether ketone) polymers used by industrial partners of this project. The first metallic layer is a copper layer.
Two pathways are studied to carry out the deposition of the first thin conductive metal layer (so-called primary adhesive layer). This layer is elaborated either by plasma activation of the surface followed by metallic deposition by magnetron sputtering or by plasma enhanced chemical vapor deposition using an organometallic precursor.

The first way consists on a plasma activation of the surface followed by a metallic deposition by magnetron sputtering of a copper target. First of all, surfaces are treated by a radio frequency (13.56 MHz) plasma treatment under argon in order to improve the adhesion of the metallic layer. The characterization by wettability measurements (performed at different scale) highlights that the dependence of the hydrophilic properties of the plasma-treated surface on discharge power, gas flow, gas nature and duration. Plasma parameters were optimized during this study in

order to increase the surface energy. A roughness study has also done before and after the treatment. Then, after the plasma treatment, polymers are coated of a thin copper layer by magnetron sputtering. The copper layer deposition parameters are also studied. The adhesion of the metallic layer is then evaluated with different tests as: pull off test, immersion in industrial partners chemical baths used for the thick deposition of metallic layers. This study shows an improvement of the adhesion of the metallic layer with plasma activated polymers.

The other way consists on a radiofrequency plasma enhanced chemical vapor deposition of a copper layer using an organometallic precursor. The organometallic precursor used is the copper acetylacetonate and depending on plasma parameters, the plasma-deposited metallic layer is characterized by XPS, adhesion tests, SEM, etc.

This work was supported by Région Pays de la Loire within the framework program COMPLIMA.

PST-P3-17
Optical and electrical study of RF plasma for nanotubes film growth and correlation with resulting nanostructures properties

T11 Plasma Science and Technology

#PST-P3-17

M. Gaillard, T. Labbaye, E. Kovacevic, N. Semmar, A. Petit, C. Boulmer-Leborgne.

GREMI - Orleans (France).

The heat transfer study is of prime importance in the microelectronic field because of continuous components size decrease. The heat generated by the active zones reduces systems performance and increases energy consumption. The carbon nanotubes (CNTs) are potential candidates to improve current technology as they behave simultaneously as current and heat conducting material. They are studied in order to be integrated into microelectronics circuits as interconnects between components and support.
Their electrical and thermal properties are function of their microstructure as outer and inner diameter, of their morphology, also function of their surfacic density. The microstructure of CNTs is due to the choice of substrate and catalyst materials [1] and of process parameters chosen.
A low-pressure RF plasma is used to grow densely packed vertically aligned CNTs by plasma enhanced chemical vapor deposition. This study is focused on the influence of the plasma parameters on the morphology of nanotubes and the properties of films. Sets of substrates (TiN, Si3N4, TiNi and TiNiCu) and catalysts (Fe and Ni) systems are chosen in agreement with our partner STMicroelectronics, and remain fixed for the study. The catalyst is deposited by pulsed laser deposition technique with fixed parameters. Then the RF power (from 15 W to 200 W), the polarization of substrate (from 1 W to 100 W), the gas flow (from 15 sccm to 100 sccm), H2/C2H4 gas ratio (from 1 to 4) and finally the pressure (from 0.5 mbar to 10 mbar) are varied.
The CNTs films morphology and microstructure are characterized by SEM and TEM. The electrical properties are checked with the four-probe technique and the thermal

properties are identified with nanosecond pulsed photothermal pyrometry experiments in the IR range [2].

[1] M. Gaillard, C. Boulmer-Leborgne, N. Semmar, É. Millon, A. Petit, Appl. Surf. Scie. 258 (2012) 9237–9241
[2] M. Gaillard, H. Mbitsi, A. Petit, É. Amin-Chalhoub, C. Boulmer-Leborgne, N. Semmar, É. Millon, J. Mathias and S. Kouassi, JVST B 29(4) (2011) 041805-1

PST-P2-20
Surface morphologies of thermo- and water-sensitive ultra-thin nanocomposite films manufactured by plasma polymerization of maleic anhydride and cellulose nanowhiskers

T11 Plasma Science and Technology

#PST-P2-20

M. Brioude [1], H. Haidara [2], V. Roucoules [2], M.P. Laborie [1].

[1]Institute of Forest Utilization and Work Science / Freiburg Material Research Center, University of Freiburg - Freiburg Im Breisgau (Germany), [2]Institut de Science des Matériaux de Mulhouse, Université de Haute-Alsace - Mulhouse (France).

Nowadays, the use of bio-based materials is of great interest and the finding of environmentally-friendly techniques for their processing is of major importance. Plasma polymerization arises as a good alternative for the development of ultra-thin films as this is a non-toxic, solventless and low energy-demanding process. Maleic anhydride (MA) is one of the most studied precursors in plasma polymerization, due to its high reactivity and versatility under pulsed plasma excitation [1-3]. Cellulose nanowhiskers (CNWs) are excellent materials for the development of bio-based nanocomposites. Besides of the intrinsic characteristics of low density and biodegradability of cellulose, CNWs characteristics of high crystallinity and high aspect ratio result in outstanding properties like very high tensile strength and Young's modulus, which are highly demanded in nano-reinforcing fillers for materials [4,5]. In this work, we propose the synthesis of CNWs/plasma polymerized nanocomposite films. The morphology of the obtained ultra-thin film is organized in thermo- and water-sensitive superstructures showing different patterns such as fibrillar superstructures, fractal "trees", and ring structures depending on process parameters and exposure to heat and water. In addition, some fundamental studies were performed in order to investigate the driving forces behind the formation of such structures.

Acknowledgements:

1374/2887

Michel Brioude would like to thank the “Elizabeth and Barbara Grammel Trust” for the stipendium as well as the COST Action FP1006 “Bringing new functions to wood through surface modification” for the support on a short term scientific mission (STSM) at the Institut de Science des Matériaux de Mulhouse, France.

[1] M. E. Ryan, A. M. Hynes, J. P. S. Badyal, *Chem. Mater.* **1996**, 8, 37-42.
[2] S. Schiller, J. Hu, A. T. A. Jenkins, R. B. Timmons, F. S. Sanchez-Estrada, W. Knoll, R. Förch, *Chem. Mater.* **2002**, 14, 235-242.
[3] F. Siffer, A. Ponche, P. Fioux, J. Schultz, V. Roucoules, *Anal. Chi. Acta* **2005**, 539, 289-299.
[4] W. Bai, J. Holbery, K. Li, *Cellulose* **2009**, 16, 455-465.
[5] D. Bondeson, A. Mathew, K. Oksman, *Cellulose* **2006**, 13, 171-180.

PST-3-Or-3
Plasma copolymerization: study of the growth mechanisms and film structuration

T11 Plasma Science and Technology

#PST-3-Or-3

D. Debarnot [1], C. Chahine [1], J.M. Valleton [2], F. Poncin-Epaillard [1].

[1]Institut des Molécules et Matériaux du Mans, UMR CNRS 6283, Université du Mans, Département Polymères, Colloïdes et Interfaces, - Le Mans (France), [2]Laboratoire Polymères, Biopolymères et Surfaces, FRE 3101 CNRS, Université de Rouen, - Mont St Aignan (France).

Plasma copolymerization is nowadays considered as a promising and versatile technique for the deposition of thin films because of its possibility to prepare tailored films with pre-defined surface characteristics. The plasma copolymerization of monomers with different physico-chemical characteristics (eg polar and non-polar) has recently received a lot of attention due to the possibility to combine the properties of each of the monomers which provide a defined surface functionalized and structured.
The present work aims to elaborate thin films of amphiphilic copolymer with chemical and morphological structuration. In this frame, plasma polymerization and copolymerization of 2-(N,N-dimethylamino) ethyl methacrylate (DMAEMA) as polar monomer and heptadecafluoro-1-decene (HDFD) as apolar monomer, under low pressure RF reactor using pulsed mode have been realized. The characterizations of thin layers were done through contact angle goniometry, profilometry, Fourier transform infrared spectroscopy (FTIR), X-ray photoelectron spectroscopy (XPS), atomic force microscopy (AFM) and scanning electron microscopy (SEM). The plasma polymerization study of this couple of monomers showed the catalytic role of fluorine groups leading a more consequent deposition rate for pp-HDFD than for pp-DMAEMA. Even if the growth is significant during the time of discharge, the deposition rate is not negligible during the post-discharge time. The chemical structure of plasma polymers is highly dependent on the plasma parameters and mainly the power and time of discharge. The FTIR spectroscopy has revealed as a powerful tool for evaluating the chemical structure retention of the monomer entity in the plasma polymer. These polymers present a homogenous morphology without roughness.

The plasma copolymerization of these comonomers (p-DMAEMA-co-HDFD) at different ratio showed a kinetic of deposition and surface properties between the two polymers. The different chemical analyses taken at different plasma parameters present a chemical structuration and the formation of a mixture of polymers or a block copolymer but not alternating or random copolymers. The AFM results showed a morphologic structuration and a phase microseparation in the amphiphilic copolymer coating due to the chemical incompatibility between the hydrophilic component (pp-DMAEMA) and the hydrophobic one (pp-HDFD).
Some results on plasma copolymerization using other monomers than DMAEMA and HDFD will also be presented.

PST/SE/TF-1-Or-5
Polymorphism modification of Polyamide6 treated with an atmopsheric pressure plasma jet.

T11 Plasma Science and Technology

#PST/SE/TF-1-Or-5

D. Ben Salem, J. Pulpytel, F. Arefi-Khonsari.

3492 - Paris (France).

Polyamide 6 (PA6) substrates were treated using an atmospheric pressure pulsed-arc plasma jet working with air (fig.1). The samples were treated with a pulse frequency between 21 and 25 kHz for different jet speed ranging from 3 to 30 m/min, enabling very short treatment times around 100 ms. Polyamide 6 has two major crystalline forms, i.e. α and γ which are highly dependent on the cooling speed and thermal treatment [1]. With this fast and innovative process, it was shown that the plasma treatment increased the oxygen concentration of the polymer surface through the formation of carbonyl and carboxylic groups, involving a higher surface energy but also modified the topology of the surface. The latter was mainly due to the thermal component of the plasma jet. [2]. Polymorphism modifications were investigated and linked, along with the other surface properties, to the self-adhesion properties of PA6. Depending on the surface treatments, the relative contents of α and γ PA6 were evaluated using XRD. The results shows that a low jet speed, i.e. long treatment time, corresponding to a more intense heating of the surface, favors the form α. Surface chemistry of the plasma treated polyamide 6 was also studied by XPS and FTIR measurements showing an increase of the hydrophilic groups on the surface.A Gaussian curve fitting method of the infrared spectra has also been investigated to estimate the α/γ crystalline phase ratio. The obtained results were in agreement with the polymorphism modification observed by XRD. Moreover, the surface morphology was also studied by SEM and AFM, and the results showed that low speed and high frequency treatment induced an important increase of the surface roughness, due to the etching of PA6 by the reactive species produced in the plasma.

The self-adhesion properties of the surface were finally linked to the treatment conditions. As expected, adhesion increased with the introduction of chemical polar groups at the surface and with a higher roughness. Moreover, one can suggest that the plasma treatment induces some chain rotation and reorganization of the

hydrogen bonds which can affect the adhesion properties.

[1] H.-X. Huang et al. / Composites: Part B 43 (2012) 972–977

[2] M. Noeske et al. / International Journal of Adhesion & Adhesives 24 (2004) 171–177

Fig 1 : Schematic of the atmospheric pressure plasma system

PST-P3-18
Surface modification of microsized tungsten particles by fluidization with an atmospheric pressure radiofrequency plasma jet

T11 Plasma Science and Technology

#PST-P3-18

G. Dinescu [1], C. Stancu [1], C.F. Florica [2], B. Mitu [1], C. Grisolia [3].

[1]National Institute for Laser, Plasma and Radiation Physics - Magurele-Bucharest (Romania), [2]National Institute for Material Physics - Magurele-Bucharest (Romania), [3]Atomic and Alternative Energies Commission (CEA) - Cadarache (France).

Atmospheric pressure plasma treatment of flat surfaces emerged in the last years as a promising technique for surface modification of organic [1] and inorganic [2] materials, in order to improve their properties and further processability. Nevertheless, the use of cold plasma sources operating at atmospheric pressure for powder functionalization was less investigated. In this context, the present contribution focuses on the modification of micrometric size commercial tungsten powder by using an atmospheric pressure plasma jet working in argon or in admixture with reactive gases.

A fluidized bed reactor was implemented for the tungsten particles treatment. The system consists in a vertically placed cylindrical quartz recipient, used as fluidization chamber, a plasma source based on a radiofrequency discharge with bare electrodes for plasma jet generation [3], an adapting device between them and a separate particle trap on the gas exhaust path. The adaptor was provided with two ports, one for the admission of reactive gases in the chamber, and the other one for the gas exhaust. The vertically plasma jet is directed toward the reactor bottom where the powder is placed, thus providing a drag force adequate to circulate the particles in the jet and expose their surface to plasma species. In order to induce various chemical modifications of the particles surface, discharges were generated in several gases and mixtures, namely argon, argon/nitrogen, and argon/oxygen. Additionally, acetylene was admitted in the fluidization chamber during plasma working in argon and argon/nitrogen, in order to assess the possible carbon deposition process on the particles surface, while preventing the carbon formation inside of plasma source.

The results showed that the fluidization process lead to the transport of small tungsten particles outside the fluidization chamber. Two sets of particles were obtained: one remained in the fluidization chamber and another transported to and collected from the trap. Concluding, the fluidization can be used to separate the particles according to their size. The as received and plasma treated tungsten powders were investigated with respect to the morphology, composition and chemical bonding by means of SEM, EDX and XPS measurements. The compositional characterization evidenced the reduction of oxygen content on the tungsten surface upon argon plasma treatment and respectively their enhanced oxidation when argon/oxygen admixture is used. When acetylene is injected in the fluidization chamber during plasma treatment in argon and argon/nitrogen admixture, the particles are covered with carbon layers.

[1] E.R. Ionita, M.D. Ionita, E.C.Stancu, M. Teodorescu, G. Dinescu, Small size plasma tools for material processing at atmospheric pressure, Appl. Surf. Sci. 2009, 255, 5448-5452
[2] R. P. Cardoso, G. Arnoult, T. Belmonte, G. Henrion, S. Weber, Titanium nitriding by microwave atmospheric pressure plasma: towards single crystal synthesis, Plasma Process. Polym. 2009, 6, S302–S305
[3] M. Teodorescu, M. Bazavan, E.R. Ionita, G. Dinescu, Characterization of an argon radiofrequency plasma jet discharge continuously passing from low to atmospheric pressure, Plasma Sour. Sci Technol. 2012, 21, 5, 055010

PST-5-Or-7
Experimental and modeling study of the simultaneous removal of acetylene and acetaldehyde by a pulsed atmospheric corona discharge

T11 Plasma Science and Technology

#PST-5-Or-7

S. Touchard, Z. Jia, C. Klett, A. Vega-González, K. Hassouni, X. Duten.

LSPM – CNRS UPR 3407 – Université Paris 13, Sorbonne Paris Cité, 99 Avenue J.B. Clément, 93430 - Villetaneuse (France).

Motivation
For the last two decades, atmospheric plasma processes have demonstrated their good efficiency for the removal of a single pollutant [1]. However studies on simultaneous removal of several pollutants by this type of discharge are still scarce. This work proposes to study experimentally and by modeling the degradation of acetaldehyde and acetylene, two representative molecules of volatile organic compounds [2], using an atmospheric pressure pulsed plasma at room temperature.

Experimental and modeling conditions
Generated by a Marx generator, the nano-pulsed atmospheric plasma discharge is occurring in a N_2 gas flow with oxygen (5%) and 1000 ppmC of an equimolar pollutants mixture. The process efficiency is evaluated by measuring pollutants residual concentrations and the end products selectivities as a function of the input energy (expressed in J/L). To improve the description of the chemical phenomena occurring in the plasma, a quasi-homogeneous 0D model taking into account 90 species involved in 460 reactions has been developed [3-5].

Results
As a main result, we observed that the measured residual level, at the reactor exit, of each pollutant individually injected is very close to the rate measured when both pollutants are injected together.
Moreover, we did observe a good agreement between computed and experimental results for pollutants removal as a function of the specific input energy (see figure 1).

Thus, a analysis of the consumption flows of the two pollutants and production of by-products, computed by the model, will be proposed and discussed. One of the main conclusions is that acetaldehyde is mainly decomposed during the pulse period by short life species like N_2 metastable states or electrons, whereas acetylene is mainly consumed during the post discharge phase by long life oxygenated species as O and OH.

[1] A. M. Vandenbroucke, R. Morent, N. De Geyter, C. Leys, Journal of hazardous materials **195** (2011) 30-54
[2] L. A. Graham, S. L. Belisle, C. L. Baas, Atmospheric Environment, **42** (2009) 4498-4516
[3] M. Redolfi, N. Aggadi, X. Duten, S. Touchard, S. Pasquiers, K. Hassouni, Plasma Chemistry and Plasma Processing **29** (2009) 173-195
[4] C. Klett, S. Touchard, A. Vega, M. Redolfi, X. Duten and K. Hassouni, Acta Technica CSAV **56** (2011) 43-55
[5] C Klett, S Touchard, A Vega-Gonzalez, M Redolfi, X Bonnin, K Hassouni and X Duten, Plasma Sources Sci. Technol. **21** (2012) 045001

Figure 1 : Comparison between simulations and experiments for an equimolar mixture containing 1000 ppmC of acetaldehyde and acetylene diluted in a N_2(95%)/O_2 (5%) gas flow

PST-4-Or-5
Electrode surface effect on methane RF dusty plasmas

T11 Plasma Science and Technology

#PST-4-Or-5

J. Lagrange [1], I. Géraud-Grenier [1], F. Faubert [2], V. Massereau-Guilbaud [1].

[1]GREMI, Groupe de Recherche sur l'Energétique des Milieux Ionisés, UMR 7344, CNRS/Université d'Orléans, Site de Bourges, Faculté des Sciences, Rue Gaston Berger, BP 4043 - Bourges (France), [2]IUT de Bourges, Département Mesures Physiques, 63 avenue de Lattre de Tassigny - Bourges (France).

Dust particles are produced by PECVD in a RF capacitive discharge (13.56 MHz) under a pressure of 120 Pa in pure CH_4 injected with a constant total flow rate of 5.6 sccm (9.45×10^{-3} Pa. $m^3.s^{-1}$). Throughout our experiments, the 13.56 MHz RF power is 80 W. The study is based on the discharge duration (2 - 15 min) in order to show the electrode surface effect on the particle formation.
The CH_4 dissociation in the discharge leads to the formation of both particles in the plasma and coating on the powered electrode [1,2]. The surface of the RF electrode modifies the discharge parameters and the particle formation. The time evolution of the electrical characteristics of the discharge is investigated. The plasma is analysed by Optical Emission Spectroscopy (OES). Spectroscopic parameters (such as electron number density and excitation temperature) are determined during discharge processing. Mass Spectrometry of neutral species and ions is used to understand the generation and growth of particles within the plasma [3].
At the end of each experiment, particles and coating are collected. Scanning Electron Microscopy (SEM) analyses are realized on dust particles depending on time. The particles present a spherical shape and a smooth surface, with a diameter range of 0.3 to 2.0 µm (fig. 1). Electrode coating is also observed and shows an unexpected appearance of its surface (fig. 2).

[1] I. Géraud-Grenier, V. Massereau-Guilbaud and A. Plain, Eur. Phys. J. AP **8**, 53-59 (1999)

[2] V. Massereau-Guilbaud, I. Géraud-Grenier, and A. Plain, Eur. Phys. J. AP **11**, 71-76 (2000)

[3] I. Géraud-Grenier, F. Faubert and V. Massereau-Guilbaud, ESCAMPIG, Viana do Castelo, Portugal (2012)

Fig. 1: SEM image of particles (80 W RF discharge, $P(CH_4)$ = 120 Pa)

Fig. 2: SEM image of surface coating (80 W RF discharge, $P(CH_4)$ = 120 Pa)

PST/SE/TF-P1-04
Deposition of thin TiO2 films by atmospheric pressure plasma enhanced chemical vapour deposition (APPECVD) using an Injection Axial Torch

T11 Plasma Science and Technology

#PST/SE/TF-P1-04

Y. Gazal, C. Dublanche-Tixier, A. Roemer, C. Chazelas, P. Tristant, C. Jaoul, C. Le Niniven.

SPCTS (UMR CNRS 7315) - Université de Limoges - Limoges (France).

Plasma enhanced chemical vapour deposition (PECVD) processes are widely used to deposit thin films and particularly thin ceramic films for different applications. Traditionally, PECVD systems operate under controlled pressure (usually from 0.1 Pa to 1 kPa). However, because these processes require expensive vacuum systems and pumps, there has been a growing interest in the last decades to replace them by atmospheric plasma systems [1].
Crystallized titanium oxide films are of great interest both for the photocatalytic activity of this semiconductor and its remarkable electrical and optical properties. Catalytic properties led to interesting industrial applications in water purification, decomposition of organic pollutants, self-cleaning surfaces, hydrogen production, solar cells…
In this context, a deposition system using atmospheric pressure axial injection microwave excited plasma torch (TIA, Torche à Injection Axiale), has been developed to deposit thin films of TiO_2 on silicon (100) substrates. The plasma was ignited with Ar gas. A further quantity of Ar carrier gas saturated with titanium isopropoxide (TTIP, $Ti(OC_3H_7)_4$) by passing through a bubbler, was mixed in the plasma gas before its entrance in the torch. The plasma treatment was carried out in an open-air reactor (fig. 1).
In a previous work, it has been shown that for SiO_x thin films deposition the increase of substrate temperature during the process generates powder formation. Consequently, a substrate temperature controller was installed to keep the substrate

in a suitable domain of temperature [2,3].
For a given deposition time, a parametric study was carried out varying the microwave excitation power, the torch to substrate distance and the precursor mass flow, in order to optimize the film quality by minimising the homogeneous reactions in the plasma phase. These films were characterised in terms of composition and microstructure by X-ray Photoelectron Spectroscopy (XPS), X-ray Diffraction (XRD), Fourier Transformed Infrared Spectroscopy (FTIR) and Scanning Electron Microscopy (SEM). The effects of each parameter were investigated and correlated to the characteristics of the film. Finally, conditions for obtaining crystallized TiO_2 films have been discussed.

[1] L. Bardós, H. Baránkova, Thin Solid Films, 518, 2010, pp. 6705-6713
[2] S.S. Asad et al., Plasma Processes and Polymers, 6, 2009, S508
[3] X. Landreau et al., European Physical Journal D, 2011, DOI : 10.1140/epjd/e2011-20503-7

PST-P2-09
Characterization of a soft atmospheric DBD plasma jet for surface analysis

T11 Plasma Science and Technology

#PST-P2-09

L. Chauvet, C. Muja, B. Caillier, L. Therese, P. Guillot.

Université Jean Fançois Champollion - Albi.

In direct sample analysis domain, atmospheric pressure sources are widely investigated for ambient surface analysis by mass spectrometry [1-3]. In this domain, many plasma sources have been developed from DC to RF excitations. Generated by alternative signals, Dielectric barrier discharge (DBD) can be used as plasma source to generate low temperature plasmas at atmospheric pressure and create soft ionization [4]. The desorption/ionization jet coming out of the discharge cell can be then directed to the contaminated surface to be analyzed. Coupled to mass spectrometry detection, high selectivity and sensitivity can be obtained as a function of the source efficiency and the detector capability.
In this work, a dielectric barrier discharge source has been developed. This source is composed of a large cylindrical dielectric chamber with a capillary termination. One electrode is covering the cylindrical chamber and the second one covering the capillary tube. The source is operating in a flow of rare gases and is powered by a square alternative voltage (tens of kHz). When the plasma is created, a plasma jet is created out of the capillary tube. Then the plasma jet can be directed towards the surface to be characterized during desorption/ionization. This experimental work is based on electrical and optical diagnostics. Electrical measurements are made using a Tektronix TDS7104, 1GHz, 4 channels, 10 GS/s digital phosphor oscilloscope. Optical measurements are achieved using an Ocean Optics spectrometer (USB4000) by an optical fiber. The spatial and temporal characterizations are obtained by a gated ICCD instrument (Princeton PIMAX-1K-RB, 1024x1024 pixels) allowing the observation of the plasma distribution during variation of the power supply signal. The parameters of the study are the maximum voltage, the power and the frequency for the electrical excitation and the flow rate for the operating gas which can be neon, helium or argon. The spatial and temporal distributions and the emission spectra will be presented and discussed according to the previous parameters. The future step will be to couple the dielectric barrier discharge source with Time Of Flight Mass Spectrometer (TOS-MS) and to optimize the plasma conditions for sample surface characterization.

[1] F. J. Andrade, J. T. Shelley, W. C. Wetzel, M. R. Webb, G. Gamez, S. J. Ray, G. M. Hieftje, Atmospheric Pressure Chemical Ionization Source 1-2. , Analytical Chemistry, 80 (2008), 2646-63.
[2] J. T. Shelley and G. M. Hieftje, Ambient mass spectrometry: Approaching the chemical analysis of things as they are, J. Anal. At. Spectrom., 26 (2011), 2153-2159.
[3] J. Orejas, J. Pisonero, N. Bordel, T. Nelis, Ph. Guillot, A. Sanz-Medel, Bidimensional characterization of the emission spectra in a direct current atmospheric pressure glow discharge, Spectrochimica Acta Part B: Atomic Spectroscopy, 76 (2012), 166-174.
[4] S.B. Olenici-Craciunescu, S. Müller, A. Michels, V. Horvatic, C. Vadla, J. Franzke, Spatially resolved spectroscopic measurements of a dielectric barrier discharge plasma jet applicable for soft ionization, Spectrochimica Acta Part B: Atomic Spectroscopy, 66 (2011), 268-273.

PST-4-Or-3
Dry deep etching of GaN wide-bandgap semiconductor

T11 Plasma Science and Technology

#PST-4-Or-3

N. Gosset [1], J. Ladroue [2], T. Tillocher [1], P. Lefaucheux [1], M. Boufnichel [2], R. Dussart [1].

[1]GREMI - Orléans (France), [2]STMicroelectronics - Tours (France).

Gallium Nitride (GaN) is a III-V semiconductor with a large and direct bandgap (3,4 eV). Furthermore GaN has a high electron mobility and strong chemical bonds. These physical properties make GaN very interesting and open new prospects for microelectronics power devices. Indeed, GaN-based devices, compared to silicon devices, can operate under high temperature, high power and high frequency.

For GaN-based power devices, an etched depth as high as 6 to 10 µm is typically required. This is considered as a deep etching, since for light emitter devices the typical etch depth is a few hundred nanometers. It was shown that wet etching of GaN c-plan (plan where etching is generally needed) is limited due to its chemical inertness [1]. Therefore, GaN deep etching is achieved by plasma etching. Generally, chlorine based chemistries are used because $GaCl_3$ is the most volatile Ga etching product.

We studied the etch of GaN (7µm thick epilayer grown on Si) in Cl_2/Ar plasma using two industrial Inductively Coupled Plasma (ICP) reactors (Corial 200-IL and Alcatel A601-E) and with Ar plasma using Ion Beam Etching (IBE) (Plassys MU450). After etching, three types of defects can be observed : columns, pits and "white GaN". It was shown that both first defects are linked to nanopipes and dislocations created during epitaxial growth of GaN [2]. For industrial applications both surface defects and roughness must be limited. Cl_2/Ar plasma investigations using mass spectrometry, optical spectroscopy and Langmuir probe have shown that defects formation closely depends on plasma parameters (RF bias, ICP power,...). Impact of coverplate (silicon or quartz) during etching was also particularly important. Indeed, during etching, coverplate produces oxygen based species which are responsible of columnar defects formation.
In ICP reactors, defects have almost been eliminated by adding $SiCl_4$ to the Cl_2/Ar

chemistry. In the case of IBE, optimisation can also be performed to reduce surface defects.

Finally, impact of adding gas, like $SiCl_4$, BCl_3 or CHF_3, on both the etch rate and selectivity with SiO_2 mask were studied. An etch rate as high as 1µm.min^{-1} and a selectivity of 6 can be obtained.

[1] D. A. Stocker, E. F. Schubert, and J. M. Redwing. Applied Physics Letters, 73 (1998) 2654–2656

[2] J. Ladroue, A. Meritan, M. Boufnichel, P. Lefaucheux, P. Ranson, and R. Dussart, J. Vac. Sci. Technol. A 28, (2010) 1226

PST-2-Or-4
Microwave micro-plasmas continuously sustained in capillary tubes: development, characterization and optimization for chemical species production under microfluidics flow

T11 Plasma Science and Technology

#PST-2-Or-4

S. Dap [1], G.D. Stancu [2], O. Leroy [1], C. Boisse-Laporte [1], P. Leprince [1], C.O. Laux [3].

[1]LPGP - Orsay (France), [2]EM2C/ Ecole centrale Paris - Châtenet-Malabry (France), [3]EM2C/Ecole centrale Paris - Châtenet-Malabry (France).

Micro-plasma sources research and development have known a growing interest over the last years due to their potential applications in various fields. For example they can be used as a powerful UV laser source for waste water decontamination or skin illness treatment [1,2]. Another promising prospect is the use of these plasmas as a source of chemically active species [1], for instance in the field of plasma-medicine or gases treatment, especially when plasma is produced under microfluidics flows conditions.
All the aforementioned potential applications require a compact plasma source. For this purpose a continuous wave electrodeless plasma device was developed at the laboratory using two different microwave applicators: surfatron [3] (surface wave launcher) and microstrip (split ring resonator) [4]. It generates plasmas in a broad range of gas pressure, from mbar up to several bar. Plasmas are initiated in the presence of a gas flow in small capillary tubes with diameters ranging between 180 and 690 microns. Up to now, the elementary processes governing this kind of micrometric scale plasma still remain unknown. Nevertheless, it is of fundamental interest since at this small scale, the sheaths surrounding the bulk plasma represent a significant part of the whole discharge. It could thus significantly modify the energy transfer path to the plasma.
The present work focuses on the plasma properties for various discharge tube diameters, gas mixtures (argon and air), gas flows, and pressures and their

correlations with the production of various chemical species. Several diagnostic tools were employed. Laser based absorption techniques were used to probe key plasma species (e.g. argon metastable, nitric oxide). Spatially resolved optical emission spectroscopy was employed for measurements of species densities, discharge gas temperature and electron density (from Stark broadening). A home-made technique based upon phase measurements of the wave (local wavelength determination) in the case of the surface-wave sustained discharge (surfatron) is also used to provide the electron density. The last diagnostic allows also to assess the electron-neutral collision frequency. This is a key parameter to determine if the behaviour of the microwave discharges in capillary tube is similar to the well-known regime observed for larger tube diameters.
This present characterization of the capillary microwave plasma offers a novel opportunity to understand the mechanisms involved in the chemical species production. The obtained results are useful to design and optimize chemical species sources and are suitable for an extension to other molecular gases.

[1] K. H. Becker et al., J. Phys. D: Appl. Phys. 39 (2006) R55–R70
[2] B. Debord et al., 2011 Conference on Lasers and Electro-Optics: Laser Science to Photonic Applications, CLEO 2011.
[3] M. Moisan et al., Phys. D: Appl. Phys. 24 (1991) 1025-1048
[4] F. Iza et al., Plasma Sources Sci. Technol. 14 (2005) 397–406

PST/SE/TF-1-Or-4
Etching mechanisms of polyethylene and fluoropolymer surfaces treated by an atmospheric He-O2 post-discharge: the role of VUV radiation and O radicals

T11 Plasma Science and Technology

#PST/SE/TF-1-Or-4

T. Dufour, J. Hubert, N. Vandencasteele, F. Reniers.

ULB - Bruxelles (Belgium).

Polyethylene and various fluoropolymer surfaces (PVF, PVDF, PTFE, FEP and PFA) have been exposed to a He and a He-O_2 post-discharge at atmospheric pressure. The plasma source is a radiofrequenced plasma torch from SurfX Technologies, supplied in helium and oxygen gases with powers ranging between 60 and 160 W. Optical emission spectroscopy shows that O radicals and He metastable atoms are produced within the He post-discharge (15 L/min). We also show that the production of excimers (located between the electrodes) is accompanied with the emission of a VUV radiation corresponding to the first He excimer continuum (around 60 nm). When mixing helium gas (15 L/min) with oxygen (200 mL/min), the He metastable species and excimers are consumed while the O radicals (with the O_2^M species) are mostly produced through dissociation reactions. Those two very different post-discharges were therefore investigated on the previously mentioned polymer surfaces. Those ones were characterized by mass losses measurements, dynamic water contact angles, X-ray Photo-electron Spectroscopy (XPS) and Atomic Force Microscopy (AFM). We hence obtain a lot of information on the plasma-treated surfaces in terms of hydrophobicity/hydrophilicity, roughening/smoothing, chemical composition, chemical bonds and the nature of polymeric fragments ejected from the surface during the treatments. For instance, we show that an increase in the O_2 flow rate induced a superhydrophobic state for PTFE, while a dramatic decrease in the water contact angles is obtained in the case of HDPE. We also evidence that an increase in the O_2 flow rate induces a strong mass loss of the sample after its treatment while a tiny mass loss is measured in the case of PTFE. The ejection of carbonated fragments is also evidenced in some cases, depending on the plasma treatment and on the polymer. By correlating all these information with a characterization of the plasma phase, we highlight several etching mechanisms

occurring at the post-discharge/surface interface. We propose a discussion of those mechanisms on the basis of geometrical considerations and on C-C, C-O and C-F bond dissociation energies. We will present how competitive and synergistic effects can result from the oxidation and/or the roughening of the surface but also from the excimer VUV radiation, the He metastable species and the O radicals reaching the polymer surface.

This work was part of the IAP/7 program “PSI - Physical Chemistry of Plasma Surface Interactions” financially supported by the Belgian Federal Office for Science Policy (BELSPO). This work was also financially supported by the FNRS (Belgian National Fund for Scientific Research).

Key-words: etching mechanisms of fluoropolymers, polymer roughening, polymer oxidation, VUV radiation on polymer.

PST-3-Or-4
Impact of the chemical structure of the precursor on the plasma polymer's free radical generation and stabilization

T11 Plasma Science and Technology

#PST-3-Or-4

S. Ershov [1], F. Khelifa [2], P. Dubois [2], R. Snyders [1].

[1](1) Chimie des Interactions Plasma Surfaces, Center of Innovation and Research in Materials and Polymers (CIRMAP), University of Mons UMONS, Place du Parc 23 - Mons (Belgium), [2](2) Laboratory of Polymeric and Composite Materials, Center of Innovation and Research in Materials and Polymers (CIRMAP), University of Mons UMONS, Place du Parc 23 - Mons (Belgium).

Plasma polymerized films (PPF) synthesized by plasma enhanced chemical vapor deposition (PECVD) find increasing applications in biomedicine and microelectronic devices and differ in many ways from conventional polymers. One of the most specific properties of the PPF is the high reactivity of its surface rich in free radicals arising from deposition mechanism. So although generally considered as a disadvantage leading to the ageing of the PPF, reactivity of the plasma treated polymers and PPF surfaces can be beneficially employed, for example, for grafting of a specific chemical functionality. The quantitative evaluation of the surface radical density of the PPF and the mechanisms responsible for their stabilization are thus considered to be the mandatory knowledge for any further grafting reaction.
The aim of this work is to compare the free radicals density in PPF synthesized from a linear precursor and its resonant counterpart in order to evaluate the impact of resonance on the radical's stabilization. In the present study the surface radical density of isopropanol- and benzyl alcohol-based PPF have been quantitatively determined by a combination of NO chemical derivatization and X-ray Photoelectron Spectrosopy (XPS). Once derivatization conditions were optimized, the radical density, derived from at.% N determined by XPS, was evaluated as a function of deposition power.
As an example, for isopropanol it has been found out that the surface density of free radicals presents a maximum for the deposition power of 200 W (~$1.6 \cdot 10^{14}$ spin/cm²) and it stabilizes (~$1.45 \cdot 10^{14}$ spin/cm²) with further power increase. XPS findings were supported by in situ Fourier Transform Infrared Spectroscopy (FTIR) measurements that provided extra information about the degree of plasma

fragmentation yielding fragmentation saturation for a deposition power of 200 W (Figure 1). Finally, some preliminary subsequent chemical grafting experiments with 2-ethylhexyl acrylate (EHA) allowed to cross-check the relevance of derivatization results.

Figure 1. In situ FTIR spectrum of the isopropanol plasma with PRF = 65 W (a) and the surface density of free radicals and the intensity of a C-H stretching band as a function of deposition power (b)

PST-4-Or-4
Improvement of reproducibility in titanium deep etching

T11 Plasma Science and Technology

#PST-4-Or-4

T. Tillocher [1], P. Lefaucheux [1], B. Boutaud [2], R. Dussart [1].

[1]GREMI CNRS/Université d'Orléans - Orléans (France), [2]SORIN CRM - Clamart (France).

Titanium is a biocompatible material which is of great interest in the biomedical field, especially for bioMEMS. Their fabrication is based on micromachining techniques derived from microelectronics technologies. Most of the processes reported in the literature are performed with a Cl_2/Ar chemistry with typical etch rates close to 1 µm/min and provide rather smooth surfaces. A patterned TiO_2, Ni or even thick (40 µm) SU8 layer is often used as a mask.
We report here the performances of deep titanium etching with SF_6 and Cl_2 based chemistries in an Alcatel 601E ICP etching tool. Samples are pieces of a patterned titanium wafer glued on a silicon carrier wafer. The titanium wafer is 300 µm thick and the mask is a 5 µm thick nickel layer. Its backside is coated with a 15 µm thick thermal TiO_2 layer.
Our preliminary results have shown that either a SF_6 plasma or a Cl_2/Ar plasma can be used separately to etch titanium. A SF_6 plasma with a pressure of several Pa helps to reach etch rates as high as 4 µm/min but profiles are isotropic. A Cl_2/Ar chemistry at lower pressure (~1 Pa) is preferred to get vertical sidewalls but the etch rate is reduced. This is why we proposed to mix these two chemistries to obtain anisotropic profiles with an etch rate of almost 1 µm/min. However, these performances were not reproducible since in most cases this process lead to a high roughness, which is not acceptable.
This non-reproducibility may be due to the presence of the silicon carrier wafer: $SiCl_x$ species, coming from the etch by-products of the silicon wafer may redeposit on the surface as well as the chamber walls. It was shown by our group that a SF_6 plasma helps to remove this layer, leading to the formation of SiF_4 and Cl containing volatile species.
Such a result suggests that adding SF_6 in the plasma should make the process more reproducible. But this is not sufficient because non-reproducibility issues can still happen. Process parameters have been further tuned so that the balance between etching and redeposition remains favorable to etching from one process to another.

The resulting profile on one ring is displayed in Figure 1. Titanium has been completely etched down to the backside TiO_2 layer within nearly 3h 30, with an average etch rate of 1.4 µm/min. The profile is not perfectly anisotropic due to the presence of SF_6: the slope is slightly negative on the first half of the ring and tends to be more isotropic on the second half. A significant undercut can also be observed (several 10s of µm). The estimated selectivity to the nickel mask is 35. The process has been repeated many times and the profiles were always reproducible, which is a significant improvement.

Figure 1: Titanium ring fully etched with an optimized $SF_6/Cl_2/Ar$ chemistry.

PST-5-Or-8
Deposition of a metal organic catalytic coating by MO-PECVD for the elaboration of a new microfluidic device

T11 Plasma Science and Technology

#PST-5-Or-8

B. Da Silva [1], C. Guyon [1], S. Guillaume [1], S. Ognier [1], P. Da Costa [2], D. Bonn [1], M. Tatoulian [1].

[1]LGPPTS/ENSCP - Paris (France), [2]UPMC - Paris (France).

A new microfluidic device with a metal-organic catalytic coating was developed using metal-organic plasma enhanced chemical vapor (MO-PECVD) deposition technique. Hot embossing techniques were used to create a microchannel in a COC (Cyclic Olefin Copolymer) surface. The design of the microchannel is a simple 500µm large, 40µm height and 2cm long microchannel. Cobalt oxide-based (CoO and Co3O4) catalysts were chosen for their efficiency during mineralisation of organic pollutants achieved by an Advanced Oxidation Process (AOP) such as catalytic ozonation. Moreover, the antibacterial properties of these oxides are not negligible. Cobalt thin films were deposited using a parallel electrodes RF low-pressure plasma reactor (13.56 MHz, 100 Pa, 200W). Starting from a cobalt carbonyl (Co(CO)8) organo-metallic precursor mixed to argon and oxygen gas carrier, the catalytic coating was directly deposited on the inner surface of the microchannel. Hexamethyldisiloxane (HMDSO) was used to improve the adhesion between the cobalt film and COC substrate. First results showed that the contact angle (CA) of the coated COC decreased from 95º close to 0º. The obtained films were characterized by XPS, XRD, SEM and TEM. SEM micrographs showed that a homogenous 6µm thin cauliflower-shaped layer of cobalt oxides was obtained and XRD proved that nano-clusters of 40nm of cobalt oxides were formed within the film but it wasn't possible to distinguish neither the oxidation degree nor the observed cobalt oxide structure. High resolution XPS analysis allowed excluding the presence of CoO in the deposited layer. The catalytic microsystem was then obtained by sealing the surface with a thin layer of COC under heating and pressure (1 bar, 140°C). Catalytic properties of the

microreactor will be further tested in ozonation of various acids and followed by HPLC as a technique of wastewater treatment.

[1] C. Guyon, A. Barkallah, F. Rousseau, K. Giffard, D. Morvan, M. Tatoulian, “Deposition of Cobalt Oxide thin films by Plasma Enhanced Chemical Vapour Deposition (PECVD) for Catalysis Application”, Surf. Coat. Technol. (2011), doi:10.1016/j.surfcoat.2011.09.060
[2] S. Begolo, G. Colas, J.L Viovy and L. Malaquin, “New family of fluorinated polymer chips for droplet and organic solvent microfluidics”, Lab Chip 11 (2011), 508–512
[3] J. Tyczkowski, R. Kapica, J. Lowewska, Thin Solid Films 515 (2007), 6590-6595

Figure 1. SEM surface view of the cobalt oxide coating in the COC microchannel after MO-PECVD.

PST-1-Or-4
From low to atmospheric pressure plasma diagnostics based on quantum cascade laser absorption spectroscopy

T11 Plasma Science and Technology

#PST-1-Or-4

S. Iseni [1], K.D. Weltmann [2], S. Reuter [1].

[1]Centre for Innovation Competence plasmatis, Leibniz Institute for Plasma Science and Technology (INP) - Greifswald (Germany), [2]Leibniz Institute for Plasma Science and Technology (INP) - Greifswald (Germany).

The interest in plasma jets operating at atmospheric pressure have considerably grown during the last decade. The non-equilibrium properties of the discharge enhances specific and interesting chemistry especially that of reactive nitric-oxide species (RNOS) such as O_3, NO. It is already known that reactive species such as O_3 have biological effects and have been used for sterilization of non-living objects[1]. In the field of plasma medicine, O_3 is investigated as an antibacterial agent to support wound healing. Therefore, we investigate the O_3 and NOx productions of an argon MHz radiofrequency plasma jet operating at atmospheric pressure in order to control the chemistry in the effluent region[2-3]. Moreover, for biomedicine applications, *absolute densities* have to be known in order to identify the biological effects.
For the purpose of our studies, we required a diagnostic technique, which allows a non-disturbing method with a *very high molecular selectivity*. It has to provide accurate and reliable detection and measurements of the selected species. Moreover, it must be able to reach absolute concentration in a sub-ppm range. Such requirement has already been reached at low pressure by using absorption spectroscopy in the mid-infrared (IR) range performed with pulsed quantum cascade laser (QCLAS)[4]. By adapting this diagnostics for the first time from low pressure plasma diagnostic to atmospheric pressure, we were able to reach our goal. The spectral range is restricted to the so-called fingerprint area (500-1500cm^{-1}) which allows a total identification of the species. The mid-IR beam goes through a multipass White type cell in which the plasma jet is operated. Due to an additional air inlet, the inner atmosphere is adjusted to be similar to the application conditions in ambient air. Furthermore, in order to produce species specific detection, the recorded spectra are compared on-line with a spectrum simulation which provides a very good

quality of the measurement. By this technique, a detection limit of 30ppb is reached with an accuracy of 40ppb. Thus, it allows us to measure the *chemical dynamics* of the species production according to the gas admixture such as O_2, N_2 or H_2O.
This talk aims to show the growing interest in this diagnostic technique which evolved from low pressure plasma diagnostics to atmospheric plasma diagnostics. A specific care on O_3 and NO_x production will be presented and the generation dynamics of reactive species regarding different admixtures is discussed.

1. Ehlbeck J, Schnabel U, Polak M, Winter J, von Woedtke T, et al. (2011) Low temperature atmospheric pressure plasma sources for microbial decontamination. Journal of Physics D: Applied Physics 44: 013002
2. Reuter S, Winter J, Iseni S, Peters S, Schmidt-Bleker A, et al. (2012) Detection of ozone in a MHz argon plasma bullet jet. Plasma Sources Science & Technology 21.
3. Reuter S, Winter J, Schmidt-Bleker A, Tresp H, Hammer MU, et al. (2012) Controlling the Ambient Air Affected Reactive Species Composition in the Effluent of an Argon Plasma Jet. Ieee Transactions on Plasma Science 40: 2788-2794
4. Ropcke J, Davies PB, Lang N, Rousseau A, Welzel S (2012) Applications of quantum cascade lasers in plasma diagnostics: a review. Journal of Physics D-Applied Physics 45

PST-5-Or-10
A new microplasma reactor for the decomposition of Volatile Organic Compounds using a combination of dielectric barrier discharges with cobalt based catalyst

T11 Plasma Science and Technology

#PST-5-Or-10

G. Schelcher [1], B. Da Silva [1], C. Guyon [1], S. Cavadias [1], S. Ognier [1], M. Woytasik [2], M. Tatoulian [1].

[1]Laboratoire de Génie des Procédés Plasma et Traitements de Surface, ENSCP - Paris (France), [2]Institut d'Electronique Fondamentale, Uni. Paris Sud - Orsay (France).

Microplasma reactors are very attractive for the decomposition of Volatile Organic Compounds (VOCs) decomposition for indoor air control. By using a dielectric barrier discharge (DBD), a cold microplasma could be generated at ambient temperature and atmospheric pressure leading to the generation of numerous active species such as radicals, electrons, ions, excited species, ... Here, we have developed a miniaturized device combining an atmospheric pressure plasma with a cobalt based catalytic coating for the purpose of VOC decomposition at ppm concentration. The micrometric feature size microchannel (Figure 1) was elaborated by the mean of hot embossing of a Cyclic Olefin Copolymer (COC) substrate. The metallic electrodes were easily patterned on the COC substrate by a combination of photolithography and metallization techniques. Cobalt thin films were deposited using a parallel electrodes RF low-pressure plasma reactor. Starting from a cobalt carbonyl ($Co(CO)_8$) organo-metallic precursor mixed to argon and oxygen gas carrier, the catalytic coating was directly deposited onto the inner surface of the microchannel [1]. Figure 2 exposes an argon discharge under continuous flow performed inside the catalyst coated microreactor. Since the device is fully operational, the challenge will consist in monitoring the mechanisms governing catalytic processes with plasma interactions by using in-situ characterization techniques (OES, ultra-rapid camera, FTIR analysis). Moreover, the electrical performances of the barrier discharge will be

accessed by using the Lissajous method [2]. Finally, VOCs decomposition in the microreactor will be further tested with several model gases and followed by GC-MS.

[1] C. Guyon *et al.*, **Surf. Coat. Technol.**, Vol. 206(7), pp. 1673, 2011
[2] T. C. Manley, **Trans. Electrochem. Soc.**, Vol. 84(1), pp. 83, 1943

Figure 1 : Schematic cross section of our plasma/catalyst device

Figure 2 : An Ar discharge performed in our continuous flow microplasma reactor

PST/SE/TF-3-Or-4
Effect of Plasma Exposure on Unvulcanized Polybutadiene Surfaces

T11 Plasma Science and Technology

#PST/SE/TF-3-Or-4

A. Henry.

IS2M-CNRS-UMR7361 - Mulhouse (France).

Rubbers are polymeric materials with high elasticity and their properties are generally improved by using fillers. Most of the rubbers used are vulcanized and their processing includes also the addition of plasticizers, antioxidants, vulcanizing agent and activator [1].

Adhesive bonding of rubbers presents an especially important problem in diverse branches of industry. [2] The strength and quality of such adhesive-bonded joints depend on important parameters such as compatibility, reactivity and co-crosslinking. In some cases, surface treatment is necessary in order to increase reactivity. Among them, plasma treatments have become a powerful candidate as it combines high chemical reactivity with low operational costs, in environmental friendly processes. Plasma treatment has been extensively studied for surface modification of vulcanized rubbers. [3] The plasma process results in physical or chemical modification of the first few molecular layers of the surface while retaining bulk properties. During plasma exposition, the surface is driven away from its thermodynamic equilibrium and after plasma treatment the modified surface reconstructs (e.g. chain reorgnaization and migration of additives) in order to return to an equilibrium state. [4] These dynamics are strongly dependent on the nature and number of additives in the formulations and the role of each additive during plasma treatments are poorly understood.

To get better understanding the plasma-surface mechanism and to limit the complexity of the study, attention has been paid to unvulcanized filler-free polybutadiene rubber (BR) which can be used as a model rubber.
Low pressure radio-frequencies air plasma was used to modify the surface of unvulcanized BR samples. Plasma processing was carried out in a home-built R.F. plasma reactor. The plasma chamber consists of a glass tube (680 cm3 in volume) coupled with an externally wound copper coil and surmounting with a 20 cm round cylinder glass hall. This design allows to modify the distance between the sample

and the electrodes in a large range. An L-C matching network was used to match the output impedance of a 13,56 MHz R.F. power supply to the partially ionized gas load by minimizing the standing wave ratio of the transmitted power.
The effect of three main parameters which directly influence the amount of energy and the nature of the excited species in the plasma were analyzed: the RF source power, the exposition time, the distance between the rubber samples and the electrodes .
Surface modifications were investigated by wettability measurements. The surface ageing was investigated at different temperatures by comparing the hydrophobic recovery in air and under inert atmosphere at different temperatures. The nature of the surface modifications were characterized by X-Ray Photoelectron Spectroscopy and Electron Spin Resonance. Autohesion properties of assemblies were investigated with tack measurements.

This work puts in light interesting properties of plasma treated unvulcanized rubber surfaces leading to interesting autohesion properties.

1 R. Torregrosa-Coque and al, J. Adhesion Sci. Technol., 26, 813–826, 2012
2 I. Rezaeian, P. Zahedi, A. Rezaeian, J. Adhesion Sci. Technol., 26, 721–744, 2012
3 J. Tyczkowski and al, Eur. Polym. J., 46, 767-773, 2010
4 M. Mortazavi, M. Nosonovsky, Appl. Surf. Sci., 258, 6876-6883, 2012

SE/PST/TF/BI-1-Or-6
Controlled Application of Atmospheric Pressure Plasma Jets Interacting with Biological Liquids

T11 Plasma Science and Technology

#SE/PST/TF/BI-1-Or-6

S. Reuter [1], M. Hammer [1], J. Winter [1], H. Tresp [1], S. Iseni [1], A. Schmidt-Bleker [1], J. Santos Sousa [2], M. Duennbier [1], K. Masur [1], V. Puech [2], K.D. Weltmann [3].

[1]ZIK plasmatis @ INP Greifswald e.V. - Greifswald (Germany), [2]LPGP, CNRS & Univ. Paris-Sud - Orsay (France), [3]INP Greifswald e.V. - Greifswald (Germany).

Only with the recent development of non-thermal atmospheric pressure plasma sources plasmas are broadly studied for application in therapeutic medicine. These plasma sources generate highly reactive plasma components in ambient conditions and their gas temperature is below the destruction threshold of extremely sensitive surfaces such as biomaterials [1].
For an understanding of fundamental processes in plasma surface interaction, a control and detailed diagnostic of the reactive plasma components is vital. To control plasma, three different approaches can be made and will be discussed in the presentation: Control by plasma source design, control of operation parameters, and control of environmental conditions.
In this work we present optical diagnostics on atmospheric pressure plasma jets combined with modeling yielding an understanding of fundamental processes such as air species diffusion into the jet effluent. To gain control over the reactive components, their generation processes need to be controlled [2]. The plasma jet is characterized by laser induced fluorescence spectroscopy, by absorption and emission spectroscopy and by flow simulations [3]. The reactive oxygen and nitrogen output especially O, O_3, $O_2(a^1\Delta_g)$ [4], H_2O_2, NO_2, and OH are investigated. With the gained knowledge, we show that it is possible to tailor the reactive components and to influence plasma jet-liquid interaction. We show that reactive species generation within plasma treated liquids can be controlled and apply the findings to cells and lipids to investigate the effect of reactive oxygen and nitrogen species (RONS) [5].

[1] K.-D. Weltmann, M. Polak, K. Masur, T. v. Woedtke, J. Winter, and S. Reuter, “Plasma Processes and Plasma Sources in Medicine,” Contributions to Plasma Physics, 52 (2012) 644-54.

[2] A. V. Pipa, S. Reuter, R. Foest, and K. D. Weltmann, “Controlling the NO production of an atmospheric pressure plasma jet,” Journal of Physics D: Applied Physics, vol. 45, (2012) 085201

[3] S. Reuter, J. Winter, A. Schmidt-Bleker, D. Schroeder, H. Lange, N. Knake, V. Schulz-von der Gathen, and K. D. Weltmann, “Atomic oxygen in a cold argon plasma jet: TALIF spectroscopy in ambient air with modelling and measurements of ambient species diffusion,” Plasma Sources Science & Technology, 21 (2012) 024005

[4] J. Santos Sousa, G. Bauville, B. Lacour, V. Puech, M. Touzeau, L.C. Pitchford, "$O_2(a^1\Delta_g)$ production at atmospheric pressure by microdischarge" Applied Physics Letters 93 (2008) 011502

[5] S. Reuter, H. Tresp, K. Wende, M. U. Hammer, J. Winter, K. Masur, A. Schmidt-Bleker and K.-D. Weltmann, "From RONS to ROS: Tailoring Plasma Jet Treatment of Skin Cells" IEEE Transaction in Plasma Science, 40 (2012) 2986

PST-4-Or-10
GAD-Precipitation and GAD/TiO2-Precipitation-Adsorption of lead acetate (PbAC) in aqueous solution assisted by a basicity control

T11 Plasma Science and Technology

#PST-4-Or-10

M. Ghezzar [1], N. Haddou [1], F. Abdelmalek [1], M. Martel [2], A. Addou [3].

[1]STEVA Laboratory, Mostaganem University - Mostaganem (Algeria), [2]UFR de chimie, Lille 1 University - Mostaganem (France), [3]STEVA LaboratoryMostaganem University - Mostaganem (Algeria).

Inorganic lead compounds generate liquid wastewaters charged on Pb^{2+} ions. The latter are generally eliminated by precipitation in a basic medium [1]. However, when they are in the organic form, the precipitation technique becomes inappropriate for its elimination such is the case of lead acetate (PbAC). According to Noyes and Withcomb [2], thought this molecule is relatively very soluble in water, it slightly ionises there. The small degree of ionisation appears to be connected with the spontaneous formation of complex anion in aqueous solution.

The Gliding Arc Discharge (GAD) is an efficient non-thermal plasma technique able to degrade organic compounds dispersed in water at atmospheric pressure.

The degradation of the organometallic lead acetate (PbAC) in aqueous solution was realised by two plasmageneous processes GAD and GAD/TiO_2. This degradation was simultaneously followed by the Total Organic Carbon (TOC) and by the Chemical Oxygen Demand (COD). The Pb^{2+} ions released during the degradation process were analysed by Atomic Absorption Spectroscopy (AAS). For 2 hours of GAD/TiO_2 treatment, the degradation rate of PbAC (10 mM) reached 93% with a constant rate of 0.023 min^{-1} in presence of 1 g L^{-1} of TiO_2. For the same duration of treatment and without photo-catalyst (GAD), the degradation reached 83% with a constant rate of 0.014 min^{-1}. The release of Lead II in the solution was of 57% with a constant rate of 6.1 mg L^{-1} min^{-1} for the GAD treatment and was of 95% with a constant rate of 10.2 mg L^{-1} min^{-1} for the GAD/TiO_2 treatment.

The Pb^{2+} release was studied under basic control which was operated at different pH. The results showed that there was a total precipitation of this element at pH = 11.1. Reactional mechanisms were proposed to explain the degradation of PbAC molecule and the Pb^{2+} elimination modes by precipitation.

[1] D. Jiraroja, F. Unoba, , A. Hage`geb, Water Research. 40 (2006) 107 – 112

[2] A. Noyes and W. Withcomb, J.Am.Ch. Soc. 27 (1905) 747.

PST/SE/TF-P1-05
A novel method to control silver doping in TiO2 using TiO2/AgO bi-layer thin film stacks

T11 Plasma Science and Technology

#PST/SE/TF-P1-05

A. Jaiswal.

Ph.D. Student, UPMC - Paris (France).

Multi-layer thin films of TiO_2 and AgO were deposited by RF reactive magnetron sputtering, and their structural, optical, and compositional properties were studied. The total thickness of each film was kept constant. Firstly, the overall composition of the films (AgO to TiO_2 ratio) was kept constant and the number of layers and thickness of each layer was controlled to create bi-layer thin films which were composed of: 2 up to 45 bi-layers. Secondly, different nominal AgO/TiO_2 ratios were attempted within the bilayers. To investigate the benefit of the bilayer coating, we prepared Ag doped TiO_2 by co-sputtering with different percentages of Ag (0 to 10 %, at.) for comparison. The effect of post annealing was investigated on the photocatalytic activity and the photo-electrochemical properties of the different coatings. In addition, bi-layer stacking significantly affected the films optical properties by lowering the band gap into the visible light region, and also showed improvement in the photo activity under UV and visible irradiations due to the formation of Schottky barriers at the interfaces between TiO_2 and AgO layers. Overall, bi-layer stacking of TiO_2/AgO films has shown a unique and highly desirable control over several important physical characteristics which can be beneficial for many optoelectronic and photocatalytic applications due to the good controlled charge separation within the doped TiO_2. Furthermore doping with silver offers bactericidal properties to the TiO_2 coatings.

Key words: TiO_2 thin film, silver doping, photocurrent, bi-layer, RF sputtering, photo catalyze, AgO.

PST/SE/TF-3-Or-5
TiO2/SiO2 mixed layers deposited by PECVD for optical and electrical applications

T11 Plasma Science and Technology

#PST/SE/TF-3-Or-5

M. Carette [1], D. Li [1], S. Elisabeth [1], J.P. Landesman [2], A. Goullet [1], A. Granier [1].

[1]IMN - Nantes (France), [2]IPR - Rennes (France).

Titanium dioxide is an attractive material for electrical (high-k) and optical (high optical index, up to 2.5) applications. However, TiO2 films deposited by plasma processes exhibit a columnar structure [1](figure 1) which is a drawback for MIS (Metal Insulator Semiconductor) and MIM (Metal Insulator Metal) capacitor integration or optical waveguide applications.
One way to get more homogeneous films is to incorporate SiO_2 phase in the TiO_2 network[2].
We study here the deposition of mixed layers of TiO_2/SiO_2 by low pressure ICP plasma enhanced chemical vapour deposition (PECVD) using titanium tetraisopropoxide (TTIP) and hexamethyldisiloxane (HMDSO) mixed with O_2. Plasma is generated by an RF source working at 400 W and 13,56MHz and the working pressure is fixed at 3mTorr.
The resulting composition of the layer depending on the fraction of each precursor injected inside the plasma is determined by X-Ray Photoelectron Spectroscopy and Wavelength-Dispersive X-ray Spectroscopy analyses whereas the distribution of Ti and Si related bonds in the film network is investigated by Fourier Transformed. InfraRed spectroscopy.
The impact of silicon oxide concentration on the layer morphology, roughness, optical refractive index and dielectric permittivity (at 1MHz) are studied by Scanning Electron Microscopy, Atomic Force Microscopy, spectroscopic ellipsometry and C(V) measurements, respectively. In addition the optical gap and leakage currents are also determined.
Preliminary results have already proven the possibility to get rid of the columnar structure of the layers (figure 2) while keeping a rather high optical index (around 1.7 at 1.96 eV).

[1] D. Li, M. Carette, A. Granier, J.P. Landesman, A. Goullet, Thin Solid Films 522, (2012) 366-371
[2] F. Gracia, F. Yubero, J.P. Holgado, J.P. Espinos, A.R. Gonzalez-Elipe, T. Girardeau, Thin Solid Films 500 (2006) 19–26

Figure 1 : SEM picture of TiO_2 layer deposited by PECVD in O_2(16sccm)/TIPT(0,24sccm) plasma
Figure 2 : SEM picture of TiO_2/SiO_2 mixed layer deposited by PECVD in O_2(16sccm)/TIPT(0,24sccm)/HMDSO(0,16sccm) plasma

PST/SE/TF-3-Or-6
Control of nitrogen doping states in N-doped TiO2 by RF reactive sputtering

T11 Plasma Science and Technology

#PST/SE/TF-3-Or-6

H. Fakhouri [1], J. Pulpytel [1], S. Mori [2], A.K. Jaiswal [1], F. Arefi-Khonsari [1].

[1]UPMC - Paris (France), [2]TokyoTech - Tokyo (Japan).

Different structures of N-doped TiO_2 (TiO_xN_y) have been prepared by RF reactive magnetron sputtering with two methods. First, we used dual reactive gas, oxygen and nitrogen, simultaneously in the deposition chamber in order to get homogeneous N–doped TiO_2 with different doping levels. Secondly, we deposited multi-layers of TiO_2 and TiN having different percentages of TiN in the coatings. The multilayers were separated by 1 to 3 nm of Ti in order to get a good Schottky barrier at the interface between TiO_2 and TiN layers (figure 1). The crystalline, optical, and composition properties were analyzed. The behavior of the resulted films was studied by measuring the generated photo-electrochemical current and the photocatalytic activity under both UV and visible light.
The competitive effects of the structure, the chemical composition and nitrogen states on the efficiency of the photo activity of the coatings were investigated. Samples prepared at high pressure gave the best photocatalytic activity due to the high specific surface area, the optimal presence of TiO_xN_y crystals in the lattice and the good charge separation thanks to the interstitial nitrogen sites. However, deposition at low pressure leads to N-doped film with the best photo-electrochemical properties. Under such conditions and in particularly at high nitrogen doping levels (> 6% at.), the formation of TiN crystals became most probable acting as recombination centers between the photo-generated charge carriers. The bilayer morphology gave a good alternative, especially when the films were deposited at lower pressure and higher percentage of nitrogen doping. A good understanding of the complex processes involved in the deposition of the thin coatings by sputtering was achieved. In particularly, the effect of deposition parameters on the photo-activity of the N doped titania, as well as the preferential presence of interstitial and/or substitutional nitrogen sites in the lattice were pointed out.

Figure 1: Electronic band structure of: (a) TiO2 thin film and (b) two bi-layers of TiO2/TiN showing the formation of two Schottky barriers.

PST-2-Or-8
Formation and transport of nanoparticles in magnetically confined acetylene plasmas produced at very low pressure

T11 Plasma Science and Technology

#PST-2-Or-8

G. Al Makdessi [1], J. Margot [1], R. Clergereaux [2].

[1]Université de Montréal - Montréal (Canada), [2]Université Paul Sabatier - Toulouse (France).

Dusty plasmas are plasmas containing charged nano-sized or even charged micro-sized particles. Known for decades, dusty plasmas have attracted the interest of the scientific community in the early 80s, especially in astrophysics when dusty particles were discovered in the rings of Saturn [1]. Comets, planetary rings, interstellar dust and interstellar clouds are some examples of natural objects formed by dusty plasmas [2]. Far from being limited to distant objects, dusty particles are also found in laboratories, in plasmas used for deposition and etching of thin films. In addition, dusty particles are present in different systems such as radio frequency capacitive discharges, inductively coupled discharges and DC discharges when the plasma gas in chemically reactive such as methane or acetylene. Dusty plasmas may behave as weakly coupled environment (such as gases) or strongly coupled environment (like liquids or solids). Therefore, they can form coulomb crystals also called plasma crystals in which aggregates of dust have spontaneously well-organized structure [3,4]. This property can be used to create monolayer crystals and to deposit it on the surface of materials to change their surface properties.
In this presentation, we investigate magnetically confined low pressure dusty plasmas in acetylene. The plasma is created by an electromagnetic surface wave at a frequency of 200 MHz. Our goal is to examine how the use of magnetic confinement allows circumventing the low pressure by enabling the formation of nanoparticles in the plasma volume. By performing a parametric study of the influence of the magnetic field on the formation of these particles, we expect to achieve a good understanding of their creation mechanisms, and, ultimately to control their characteristics.
Our results show that there exist specific conditions in which nanoparticles are

generated. We will present the dependence of characteristics of the deposits as a function of the plasma parameters. In particular, we will examine the influence of the magnetic field intensity (from 0 Gauss to a few hundreds of Gauss) and its spatial distribution on the properties (structure and size) of the nano and micro particles generated in the plasma volume. This will be achieved using various materials characterization techniques, including scanning electron microscopy, X-ray diffraction and Raman scattering. The impact of other parameters on the structure and size of the synthesized particles will also be analysed. These include the degree of dilution of acetylene by a rare gas, the power injected in the plasma and the operating pressure.

1 B.A. Smith et al. Science 215 (4532), 504 (1982)
2 C.K. Goeretz, Rev. Geophys. 27, 271 (1989)
3 H. Thomas, G.E. Morfill, V. Demmel, Phys. Rev. Lett. 73, 652 (1994)
4 H.M. Thomas, G.E. Morfill, Nature 379, 806 (1996)

PST-P2-10
Production of neutral oxygen atoms in low pressure gaseous discharges

T11 Plasma Science and Technology

#PST-P2-10

M. Mozetic.

Jozef Stefan Institute - Ljubljana (Slovenia).

Methods for production of large quantities of neutral oxygen atoms by passing molecular oxygen through a discharge region are presented. Although atmospheric pressure discharges are increasingly popular they do not represent suitable sources of neutral atoms in the ground state due a high probability for gas phase recombination of atoms to parent molecules. Low pressure discharges perform much better for this particular application. A variety of low pressure discharges can be used as sources of neutral atoms and the choice depends on particularity of the required conditions. An important one is optimization of the discharge in order to minimize energy consumption. This requirement dictates application of sources with minimal loss of created atoms. The loss will occur either in the gas phase or on the surfaces. Gas phase loss is effectively reduced if discharges run at low enough pressure to avoid recombination at three body collisions. In many practical cases the maximal allowable pressure is close to 10 mbar. The surface loss is effectively minimized by construction of the system from materials with negligible coefficients for heterogeneous surface recombination of O atoms. The choice of appropriate materials includes many glasses and ceramics as well as some metals which form very stable oxides, such as aluminum. The loss rate depends also on surface morphology so it is recommended to use materials of very small roughness. Since glasses meet these requirements the best discharge chambers are made from these materials. Glasses are electrical insulators so the choice of appropriate electrical discharges is limited to electrode-less high-frequency discharges. Both radiofrequency and microwave discharges are popular for creation of large concentration of neutral oxygen atoms. The microwave discharges often operate with surface waves and are suitable for creation of highly dissociated plasma in rather narrow tubes while radiofrequency discharges are applied in larger volumes. Methods for rather precise determination of the density of O atoms in gasses which have been allowed to pass through a discharge region include the NO titration, optical absorption techniques, actinometry and catalytic probes. These methods were applied to measure the production of O atoms in above mentioned discharges

created at different powers up to 5 kW and in different discharge chambers. The best results in terms of power efficiency are obtained for radiofrequency discharges operating at the pressure of the order of 0.1 mbar. In such systems the efficiency is better than 10%. Atoms are lead to a processing chamber where they are allowed to interact chemically with surfaces of solid materials. The transmission efficiency, i.e. ratio between the atom density in the processing and discharge chambers, depends on the surface finishing of the connection tube as well as vacuum parameters, the main being the conductance of the connecting tube. Several examples will be presented.

PST-P2-11
Spatial distribution of electronic temperature, density and plasma emission in argon inductively coupled plasma for surface treatment

T11 Plasma Science and Technology

#PST-P2-11

C. Laurent, J. Lo, B. Caillier, L. Therese, P. Belenguer, P. Guillot.

DPHE Laboratory, CUFR J.F. Champollion, University of Toulouse - Albi (France).

Inductively coupled plasma (ICP) is currently used in analytical chemistry (e.g. mass and optical spectrometry) and industrial applications. In microelectronic industries, ICP sources associated with a downstream reactor are utilized for layer depositions, surface etching, photoresist stripping and wafer cleaning [1-3]. The advantages of ICP sources are their wide pressure range and high charged species densities obtained even at low pressure [4]. In this work, supported by the French public funding agency OSEO, the aim is to develop and characterize a plasma reactor for surface treatment. Prior to any treatment study, physical and optical diagnostics of the source have been investigated to acquire a better understanding of the plasma properties.

In our experimental setup, the gas is introduced through a cylindrical quartz tube which is connected to a separate process chamber. The discharge is generated within the tube by a 13.56 MHz radiofrequency ICP source including a matching box. Different operating conditions are obtained by regulating independently three parameters: the gas flow (from 10 up to 500 sccm), the chamber pressure (from 5.10^{-3} up to 1 mbar) and the injected power (from 10 up to 1000 W).

A parametric study is conducted on these variables by optical emission spectroscopy and double Langmuir probe diagnostics with respectively a Fully Automated Imaging Spectrometer (iHR320 Horiba Jobin Yvon) with a groove density of 1200 gr/mm (resolution < 0.15 nm) and a linearly driven probe (Impedans ALP Sytem by Impedans Ltd, Ireland). Simultaneous measurements are done through several reactor openings for spatial distribution characterization as a function of the three

mentioned parameters. These measurements will provide us basic plasma characteristics (i.e. plasma optical emission, electron temperature, charged species densities, EEDF and plasma potential) in the entire chamber. They will also supply experimental data necessary for comparison purpose with numerical modelling results.

[1] F. Arefi-Khonsari, J. Kurdi, M. Tatoulian, and J. Amouroux, *Surface and Coatings Technology*, vol. 142-144, p. 437, 2001.
[2] Y.-B. Guo and F. C.-N. Hong, *Diamond and related materials*, vol. 12, p. 946, 2003.
[3] K. Reinhardt et W. Kern, *Handbook of Silicon Wafer Cleaning Technology*. William Andrew, 2008.
[4] J. Hopwood, « Review of inductively coupled plasmas for plasma processing », *Plasma Sources Science and Technology,* vol. 1, no 2, p. 109, 1999.

PST-2-Or-3
Integrated microplasmas on silicon: performances and limitations

T11 Plasma Science and Technology

#PST-2-Or-3

R. Dussart [1], M. Kulsreshath [1], V. Felix [1], L.J. Overzet [2], J. Golda [3], V. Schulz-Von Der Gathen [3], P. Lefaucheux [1], T. Tillocher [1].

[1]GREMI - Orleans (France), [2]UTD - Dallas (United states), [3]RUB - Bochum (Germany).

The potential applications for microdischarges are numerous and span a wide variety of areas such as lighting, detection, local treatments, sensors, lab on a chip, micro-machine processing, instrumentation etc. One of the most important technological and scientific issues of this new research area is the elaboration of the microreactors: They have to be robust enough to sustain power densities as high as a few hundreds of kilowatts per cubic centimeter.
Arrays of microreactors built from silicon wafers in clean room facilities have been recently developed [1, 2]. They consist of Micro Hollow Cathode Discharges (MHCD) operating in parallel in DC. One of the remarkable properties of these MHCDs is that stable DC plasmas can operate at atmospheric pressure without arcing [3]. AC operation is also possible and offers some advantages in terms of homogeneity and life time [4, 5].
We will present recent results obtained in both DC and AC operation. Discharges were formed in both helium and argon gases. While using DC power to ignite large arrays of microdischarges (1024 holes, 100 µm diameter) we observed spiking in the current waveform. This indicates that the microplasmas still have instability. V-I curves were systematically acquired during the experiments. Simultaneous optical characterization was also carried out (both imaging and spectroscopy). The device life time can vary from a few minutes to a few hours in DC operation depending on the injected power level. The failure mechanisms, investigated using different characterization techniques, will also be presented.

RD, PL, VF and MK are supported in part by the ‘Agence Nationale de la Recherche’ contract no ANR-09-JCJC-0007-01 “SIMPAS project”. LJO is supported in part by the European Community 7th Research Program FP7/2007-2013 under grant agreement

no 298741. JG and V. SvdG are supported in part by PROCOPE grant 54366312 of the DAAD.

[1] R. Dussart, et al. r Eur. Phys. J. D , 60, 601-608 (2010)
[2] M.K. Kulsreshath, L. Schwaederle, L.J. Overzet, P. Lefaucheux, J. Ladroue, T. Tillocher, O. Aubry, M. Woytasik, G. Schelcher, R. Dussart, J. Phys. D: Appl. Phys., 45, 285202 (2012)
[3] K. H. Schoenbach et al., Appl. Phys. Lett. 68, 13 (1996)
[4] J G Eden et al. J. Phys. D: Appl. Phys. 36 2869–2877 (2003)
[5] J. Waskoenig et al., Applied Physics Letters, 92, 101503 (2008)

4 subarrays of trench shape microplasmas operating in AC in Argon

PST-P2-14a
RF diagnostics performed on DC Microplasmas

T11 Plasma Science and Technology

#PST-P2-14a

V. Felix [1], R. Dussart [1], M. Kulsreshath [1], P. Lefaucheux [1], J. Golda [2], V. Schulz-Von Der Gathen [2], L.J. Overzet [3].

[1]GREMI - Orleans (France), [2]Ruhr-Universität - Bochum (Germany), [3]University of Texas - Dallas (United states).

Microplasmas were made in DC regime using sandwich type micro-hollow cathode devices.

Plasmas through Ar and He with small admixture of N2 were examined by simultaneously measuring plasma RF impedance and OES of N2 bands as a function of the DC potential between the electrodes and current intensity through the plasma. Since the RF fields are concentrated between the anode and the cathode, these two diagnostics allow us to have an estimate of the electron density inside the hole[1] as a function of DC Current, DC Power, Pressure and Gas Composition.

In addition, time resolved impedance measurements become possible since the RF impedance can be effectively measured during the course of a single RF cycle.

As expected, we found that the plasma resistivity of the Microplasmas decreases monotonically with increasing DC current.

The RF technique will be explained and data from Argon, Helium and Nitrogen containing plasmas will be presented.

JG and V SvdG are supported by PROCOPE grant 54366312 of the DAAD.

LJO was supported in part by a grant from the European Commission Marie Curie Actions : PIIF-GA-2011-298741 and by "le Studium"

VF, RD, MK and PL acknowledge support in part by the French ‘Agence Nationale de la Recherche’ through contract no ANR-09-JCJC-0007-01 under the name SIMPAS project.

[1] L.J. Overzet , D. Jung, M.A. Mandra, M. Goeckner, T. Dufour, R. Dussart, and P. Lefaucheux, Eur. Phys. J. D 60, 449–454 (2010)

Input impedance (Z_{in}) of an argon plasma containing 75mBar of N_2 with respect of the current intensity (I) for various pressure.

Rotationnal temperature (T_{rot}) from a fit of spectroscopic measurements of the second positive system of N_2 of an argon plasma containing 75mBar of N_2 respect of the current intensity (I).

PST-1-Or-10
Atomic processes in laser produced plasmas studied by cavity-ring down spectroscopy

T11 Plasma Science and Technology

#PST-1-Or-10

S. Milosevic, M. Biscan, N. Krstulovic.

Institute of Physics - Zagreb (Croatia).

Plasmas produced by means of small lasers with typically of nanosecond pulse duration (4 ns – 20 ns) and energy up to 300 mJ offers a versatile medium for applications relevant in advanced materials research. The progress in that field depends on a deeper understanding of details of plasma processes by improving plasma diagnostics and theoretical modelling. Cavity ring-down spectroscopy is a versatile absorption method which provides data on the plume and its surroundings, with spatial and temporal resolution [1]. This method of fers advantages compared to classical absorption techniques and can easily reach ppb sensitivity. Recently we have shown that regions around and below the visible plasma plume can be studied, in addition to the plume itself [2]. This opens possibility to study atomic processes important for the small particles formation when pulsed laser deposition technique is employed [3]. We have measured densities of various atomic states within the plume emerging from the target or created in the surrounding gas, and followed their decay [4]. Several examples will be presented discussing advantages and limitations of the CRDS technique applied to laser produced plasma diagnostics.

[1] N. Krstulović, N. Čutić, S. Milošević, Cavity ringdown spectroscopy of collinear dual-pulse laser plasmas in vacuum , Spectrochimica Acta B 64 (2009) 271-277.
[2] M. Bišćan, S. Milošević, Expansion and backscattering of laser produced Fe plasma plume, Spectrochimica Acta Part B: Atomic Spectroscopy (2012) 68 34-39.
[3] P. Dubček, B. Pivac, S. Milošević, N. Krstulović, Z. Kregar, S. Bernstorff, Pulsed laser ablation of GaAs using nano pulse length, Applied Surface Science (2011) 257(12), 5358-5361
[4] M. Bišćan, S. Milošević, Production of metastable 2^3S_1 helium in a laser produced

plasma at low pressures, Spectrochimica Acta Part B: Atomic Spectroscopy (2013) http://dx.doi.org/10.1016/j.sab.2012.12.004, in press

PST-2-Or-2
Energy flux measurements at the substrate position during reactive and non reactive magnetron sputter deposition processes

T11 Plasma Science and Technology

#PST-2-Or-2

P.A. Cormier [1], A. Balhamri [1], A.L. Thomann [2], R. Dussart [2], T. Lecas [2], N. Semmar [2], R. Snyders [1], S. Konstantinidis [1].

[1]ChIPS, UMONS - Mons (Belgium), [2]GREMI, Université Orléans - Orléans (France).

During thin film deposition processes, energetic conditions at the substrate surface influence the thin film characteristics such as density, crystalline structure or roughness. Determining the energy flux at the substrate is therefore of particular relevance for the understanding of thin film growth mechanisms [1]. In this contribution, we have quantified the total energy flux at the substrate position by using heat flux sensor designed for working in PVD processes [2]. The increased sensitivity of the probe allowed differentiating fast energy transfer originating from the bombardment of the plasma species (e.g. ions and electrons) from radiation flux emanating from the heated target surface.
DC magnetron sputtering (DCMS), Pulsed dc magnetron sputtering (pDCMS) and high power impulse magnetron sputtering (HiPIMS) discharges were analyzed. The sputter power delivered to the Ti target, the magnetic field configuration (unabalanced or balanced), the total pressure, and the gas mixture (O_2 in Ar) were systematically varied.
The use of an unbalanced magnetic field is found to significantly increase the energy transferred to the film, whatever the discharge type. Moreover, in situation where the plasma is confined to the target vicinity (balanced field), the target surface heating is enhanced during pulsed processes and large radiative IR fluxes are measured. This contribution is found to be the most significant energy transfer process during the HiPIMS process run with the balanced magnetron target. Finally, when oxygen is added to the gas mixture, the energy flux decreases as the discharge enters the

oxidized regime and it exhibits a hysteresis. Energy flux values are correlated to TiO_2 thin film properties in some particular cases.

[1] I. Petrov et. al, Microstructural evolution during film growth. 21 (2003) S117–S128f
[2] A.-L. Thomann et. al, Diagnostic system for plasma/surface energy transfer characterization, Review of Scientific Instruments, 77(3):033501, (2006)

PST-5-Or-9
Synthesis of electrodes and proton exchange membranes by atmospheric plasma for fuel cells applications

T11 Plasma Science and Technology

#PST-5-Or-9

D. Merche [1], M. Vernaillen [1], M. Laurent-Brocq [2], M. Raes [3], H. Terryn [3], J.J. Pireaux [2], N. Job [4], F. Reniers [1].

[1]ULB - Brussels (Belgium), [2]FUNDP - Namur (Belgium), [3]VUB - Brussels (Belgium), [4]ULg - Liège (Belgium).

Plasma technologies are widely used for a large panel of applications (etching, grafting, thin films deposition, pollutants removal, etc.). They are very advantageous because they are environmental friendly (no release of toxic solvents, process at room temperature), and they present a low energy cost. In this study, (sub)-atmospheric plasmas were used to develop electrodes and proton exchange membranes (on C and on Si substrates) for fuel cells using hydrogen or methanol [1,2]. Plasma processes for the synthesis of electrodes and membranes could be a major asset for the production of the fuel cell elements at lower cost.

An easy-procedure to synthesize half-membrane-electrode assemblies is reported in figure 1:
-Firstly, the catalyst nanoparticles are grafted on carbon powder with high specific surface area (carbon black) by spraying a Pt colloidal solution or by treating a carbon black/Pt acetyl- acetonate mixture in the argon post-discharge of an RF atmospheric plasma torch. The influence of the grafting conditions on the size, dispersion, amount, chemical state of platinum grafted and on the nature of the carbon-metal interface are investigated for both processes by SEM, TEM, XPS and SIMS.

-Secondly, the platinum-loaded carbon is covered in one single-step by plasma synthesized polymeric membrane. The sulfonated polystyrene membranes are synthesized in a DBD by injecting simultaneously styrene and trifluoromethanesulfonic acid monomers, in the presence of a carrier gas (Ar). The trifluoromethane sulfonic acid monomer brings sulfonic acid groups (necessary for the proton conductivity) in the polystyrene matrix. The plasma-membranes are

chemically characterized by XPS, SIMS (static and dynamic), and FTIR (IRRAS). The thickness and the morphology are investigated by SEM. Therefore, it is possible to produce plasma membrane with a good in-depth homogeneity and with a high content of sulfonic acid groups.

This work was financially supported by the Walloon Region (INNOPEM project- grant n° 1117490) and partially by the IAP Physical Chemistry of plasma surface interactions funded by the Belgian Science Policy, and by the FRIA.

[1]D. Merche, et al.,Plasma Processes and Polymers, 2010, 7, (9-10), pg 836
[2]D. Merche,et al., Plasma Processes and Polymers, 2012, 9, (11-12),pg 1144

Figure 1: Procedure to synthesize half membrane electrode by plasma

PST-1-Or-6
Infrared characterization of SiH4 decomposition in a glow dielectric barrier discharge: comparison of continuous and modulated excitation

T11 Plasma Science and Technology

#PST-1-Or-6

J. Vallade [1], F. Massines [2].

[1]CNRS PROMES ADEME - Perpignan (France), [2]CNRS PROMES - Perpignan (France).

The aim of this work is to make in-line SiN_x:H thin films by atmospheric pressure PEVCD. SiN:H is an antireflective and passivating coating for silicon solar cells. The discharge is an $Ar/NH_3/SiH_4$ glow dielectric barrier discharge obtained with a 50kz excitation. The reactor has plane/plane configuration with a 2mm gas gap. Gas is injected on one side of the plasma area, parallel to the substrate displacement. Evolution of gas chemical composition as a function of gas residence time in the plasma induces a gradient of the chemical composition of the thin film which causes problems for the application. Thus, the aim of this work is to reduce this gradient by a better control of SiH_4 decomposition. To reach that goal, FTIR (Fourier Transformed InfraRed) absorption measurements of silane concentration in the gas are made as a function of the gas residence time in the plasma. Continuous and modulated excitations are compared because modulation has proven to reduce the chemical gradient[1]. The infrared beam is a square of $2x2mm^2$. A double pass system allows a total absorption length of 100mm. Space resolution in the direction of the gas flow is $2mm^2$. Gas flow of 3l/min is guided in the plasma zone. Thus, position, d, is related to the mean gas residence time, t, through the relation: t(ms)= (gap x d x plasma length)/(gaz flow)= 2d(mm) .
Figure 1 presents measurements made as a function of the position, the power and the ratio T_{on}/T_{off} of the plasma. These different parameters can be converted in plasma energy a SiH_4 molecule has interacted with E=power $x(T_{on}/T_{off})x$ t. Figure 1 shows silane concentration as a function of energy. All the points are aligned and can be fitted by the exponential law: $[SiH4]=67\ e^{(-524\ E)}$. That means that SiH_4 dissociation depends only on the plasma energy which is defined by T_{on}. Chemistry occurring during the T_{off} is negligible. This result is explained by the nature

of the discharge. GDBD is a pulsed discharge having duration of 2µs. For 50kHz excitation it is on 10% of the time. The fact that the modulation of the excitation at a time scale of ms has no influence shows that SiH_4 dissociation is controlled by mechanisms having a shorter life time. This is in agreement with Ar* excited state life time: 120ns at atmospheric pressure. Modulation allows to maintain the same chemistry for larger t or longer d. SiH_4 decrease is related to the thin film chemical composition and growth rate characterized by IRTF and ellipsometry.

[1]N D Boscher *et al*, Plasma Proc. Polym. 2010 **7** 163

[2]G Laroche *et al*, Rev. Sci. Instrum. 2012 **83** 103508

Figure 1:Silane concentration as a function of the mean plasma energy in a GDBD Ar/NH3/SIH4: Initial concentrations of [SiH4]=67ppm

PST-P2-17a
Kr-Xe excimer lamp excited by Dielectric Barrier Discharge

T11 Plasma Science and Technology

#PST-P2-17a

S. Bendella, B. Larouci, A. Belasri.

USTMB - Oran (Algeria).

Kr-Xe excimer lamp excited by Dielectric Barrier Discharge

S.Bendella, B.Larouci and A.Belasri
Laboratoire de Physique des Plasmas, Matériaux Conducteurs et leurs Applications (LPPMCA),
Université des Sciences et de la Technologie d'Oran, USTO-MB, Oran, Algérie.

This paper presents an electric and kinetic approach to study homogeneous DBD in Kr–Xe plasma. The context of this study, based on a spatially homogenous model including the plasma chemistry module, the circuit module and the Boltzmann equation module is the controlling of the UV emission in Kr–Xe lamp. The model predicts the optimal operating conditions and investigates the electrical and chemical characteristics of high-pressure dielectric barrier discharges. The temporal variations of discharge voltage, dielectric voltage, discharge current, electric field and species concentrations are calculated and the plasma kinetic processes are discussed.

PST-1-Or-7
Study of low pressure plasma decomposition of Zirconium Tetra tert-Butoxide

T11 Plasma Science and Technology

#PST-1-Or-7

R. Verhoef [1], P. Raynaud [2], R. Snyders [3], S. Ligot [3], R. Snyders [4], T. Nelis [5], R. Valledor Gonzalez [5], S. Vitale [5].

[1]Université de Toulouse; UPS, CNRS; LAPLACE (Laboratory on Plasma and Conversion of Energy) - Toulouse (France), [2]CNRS - Toulouse (France), [3]Chimie des Interaction Plasma surface, CIRMAP, UMONS - Mons (Belgium), [4]Materia NOVA Research Center - Mons (Belgium), [5]Institute of Applied Laser, Photonics and Surface Technologies, ALPS. Bern University of Applied Sciences, Berner Fachhochschule (BFH) - Biel-Bienne (Switzerland).

Zirconium containing thin films for optical applications (anti-reflecting systems, high optical index, etc...) are deposited at low temperature with the use of Zirconium Tetra tert-Butoxide (ZTB) as precursor. To understand the reaction mechanisms that lead to the formation of thin films knowledge of the precursor dissociation in the plasma phase is required. Here we monitor a ZTB low pressure (around 0,4 Pa) RF coil plasma at powers ranging from 10 W to 125 W with the help of Fourier Transform Infrared Spectroscopy (FTIR) and Mass Spectrometry (MS).

As we can see on figure 1 and figure 2 the increase in power first decreases specific chemical bond vibrations and then causes the apparition of new bonds. The MS permits the determination of the compounds likely found in the plasma phase. The MS peak attribution is greatly simplified due to the presence of Zirconium and Carbon as there relatively abundant isotopes yield significant signatures. As a result a fragmentation mechanism can be presented, this is strongly supported by the use of Density Functional Theory (DFT) calculations giving the energies of the reactions taking place.

Figure 1: FTIR spectra of pure ZTB, 70W plasma and 125W plasma between 3150 cm-1 and 2800 cm-1

Figure 2: FTIR spectra of pure ZTB, 70W plasma and 125W plasma between 1800 cm-1 and 800 cm-1

SE/PST/TF/BI-P1-05
New sterilization process by non thermal plasma discharge inside disposable bag

T11 Plasma Science and Technology

#SE/PST/TF/BI-P1-05

Z. Ben Belgacem [1], F. Velard [1], D. Laurent-Maquin [1], J.M. Popot [2], B. Cawe [2], M. Boudifa [2], S. Gangloff [1], M.P. Gellé [1].

[1]EA 4691 - Reims (France), [2]CRITT-MDTS - Charleville-Mézières (France).

Steam sterilization (autoclave), ionizing radiation and ethylene oxide are the most commonly methods for medical devices sterilization. However, the sterilization of some new devices presents some difficulties linked to their vulnerability to physical or chemical sterilizing agents. Therefore, new sterilization processes by non thermal plasma have been studied for over 10 years. The idea is to expose a sample to plasma, created in chamber, at atmospheric pressure or in vacuum condition. Many studies have demonstrated the efficacy of plasma on microorganisms inactivation [1, 2, 3]. However, these studies cannot be considered entirely satisfying without generating directly plasma inside the sealed bag containing the medical device and maintaining its sterile state. This is a real challenge which had not been reached up to now. Packaging and storage methods of sterile equipment are an important part of the process leading to obtain sterile conditions [EN ISO 11607, EN 868]. CRITT-MDTS (Charleville-Mézières, France) and EA 4691 “BIOS” (URCA, Reims, France) have developed a process which allows the conservation of the state’s sterilization by a direct plasma treatment inside a sterilization bag. The plasma prototype reactor was manufactured by Sominex (Bayeux, France). The process vacuum was provided by 2 pumps (primary and molecular turbo Agilent Pumps) to obtain a high vacuum (9.10^{-5} mbar). The vessel was equipped in the upper center with a magnetic field coupled with a radio-frequency polarization plate in the lower center to generate hybrid plasma. Samples were packed in a sealed bag that was placed in a chamber and then subjected to vacuum. Different gases were injected into the pouch through a filter and the plasma was raised only in the sterilization bag and not in the chamber.
We evaluated the efficiency of this plasma-sterilization process against Pseudomonas aeruginosa CIP A22 and Staphylococcus aureus CIP 53.154 (Pasteur

Institute, Paris, France). These strains were chosen as they serve as reference in the assays of biocidal activity according to European norms. Bacterial suspensions (10^6cells/mL) were inoculated on glass slides which were placed in a specific sterilization bag and put on the radio-frequency polarization plate in the plasma vessel. The glass slides were exposed to O_2, N_2 or Ar - plasma treatment for various time periods (5, 15 or 30 min). Then bacteria were collected from the slides and the colonies enumeration (CFU) was completed with the standard method agar plate medium. Samples that had not been exposed to plasma were used as controls. The bacterial effect was determined by log N0 –Log Nt, where N0 and Nt are the number of CFUs in control and sterilized respectively. The first microbiological tests with strains of Pseudomonas aeruginosa and Staphylococcus aureus seem promising.

We thank, F. Szynal, D.Boitel and F.Polidor for technical skills.

[1] Moisan M.,Barbeau J., Vrevier MC., Pelletier J., Philip N., Saoudi B., Pure Applied Chemistry (2002) , 74, 3, 349-358.
[2] Rossi F., Kylian O., Rauscher H., Gilliland D., Sirghi L. , Pure and Applied Chemistry (2008), 80, 1939-1951.
[3] Fridman G. and al.., Plasma Processes and Polymers (2007), 4, 370-375.

PST-P3-09
INERTIZATION OF CHROMIUM PRESENT IN GALVANIC SLUDGE BY DIRECT CURRENT THERMAL PLASMA

T11 Plasma Science and Technology

#PST-P3-09

A. Cubas.

UNISUL - Florianópolis (Brazil).

Galvanic sludge results from the treatment of effluents generated by the industrial surface treatment of parts. It is considered to be rich in heavy metals, a material requiring special treatment. The treatment proposed herein is exposure of the galvanic sludge to the high temperatures provided by thermal plasma, a process which aims to vitrify the chromium in the sludge and render this metal inert. Two different reactors were assembled in order to carry out the experiments as follows: with a transferred arc and with a non-transferred arc. In this way it was possible to verify which reactor was more efficient in the inertization of the metals and also to investigate whether the addition of quartzite sand to the sludge influences the vitrification of the material. The chemical composition and the form of the pyrolyzed and vitrified sludge were analyzed by scanning electron microscopy, and the inertization of the sludge was verified in leaching tests, where the leachate was analyzed by flame AAS. The efficiency of the sludge inertization was 100% for chromium. The results also showed that the most efficient reactor was that with the transferred arc and quartzite sand positively influenced the vitrification during the pyrolysis of the galvanic sludge. .

- O. D. Ozdemir, S. Piskin, Characterization and Environment Risk Assessment of Galvanic Sludge. J.Chem.Soc. 34 (2012) 1032-1036.
- Costa, M., & Klein, C. B. Toxicity and carcinogenicity of chromium compounds in humans. Critical Reviews in Toxicology. 36 (2006) 155–163.
- A. L. V. Cubas, ; I. G. Souza, ; N. A. Debacher, ; E. Carasek, . Development of a DC-Plasma Torch Constructed with Graphite Electrodes and an Integrated Nebulization System For Decompositin of CCl4. Journal of the Brasilian Chemical Society. 16 (2005) 531-534.

.

Figure 1 - Chemical composition (a) and image with magnification of 100 times (b) of galvanic raw sludge obtained by SEM.

Figure 2 - Chemical composition (a) and image with magnification of 100 times (b) of galvanic sludge after pyrolysis obtained by SEM.

PST-5-Or-4
Effect of the addition of divinylbenzene on the synthesis of sulfonated polystyrene membranes by dielectric barrier discharge for fuel cells applications

T11 Plasma Science and Technology

#PST-5-Or-4

D. Merche [1], M. Vernaillen [1], M. Laurent-Brocq [2], N. Mine [2], M. Raes [3], H. Terryn [3], J.J. Pireaux [2], N. Job [4], F. Reniers [1].

[1]ULB - Brussels (Belgium), [2]FUNDP - Namur (Belgium), [3]VUB - Brussels (Belgium), [4]ULg - Liège (Belgium).

Plasma processes allow the synthesis of thin ion-exchange membranes in one single step, contrary to the conventional methods such as the “liquid-phase based” methods requiring multiple steps, reactants, solvents and long reaction times.
Plasma polymerized-sulfonated polystyrene membranes deposited by PECVD at (sub)-atmospheric pressure could present interesting properties for applications in fuel cells using polymeric membranes (PEMFC).
The membranes were synthesized from a mixture of styrene and trifluoromethane sulfonic acid (triflic acid) monomers in the discharge of a DBD (cf figure 1). The triflic acid allows the grafting of the proton exchange groups on the polystyrene backbone [1,2]. However, coatings deposited by plasma under atmospheric pressure may suffer from poor mechanical and chemical properties because of a low degree of cross-linking, contrary to their analogous synthesized under low pressure.
Divinylbenzene (DVB) used as a cross-linking agent was added to the liquid styrene vessel to enhance the mechanical and the chemical properties of the membranes.
The effect of the amount of DVB (decreasing the solubility to organic solvents) on the chemical properties and on the elemental composition was studied by XPS, SIMS, and FTIR. XPS measurements confirmed that the elemental composition was not changed in the presence of DVB and all the sulfur was present under the sulfonic acid form. According to the dynamic SIMS results, these groups, necessary for the proton conductivity, were homogeneously grafted on the whole thickness of the

membranes. The influence of the quantity of DVB on the cross-linking was highlighted by solubility tests in methanol. The signal of the substrate was followed by XPS. The cross-linking was also indirectly observed by studying the morphology of the surfaces by SEM.

In addition to the deposition of the membranes on Si for chemical characterizations, the membranes were also deposited on commercial electrodes (gas diffusion layers covered by a catalytic layer) to constitute membranes-electrodes assembly for applications in fuel cells. The various interfaces were characterized by dynamic SIMS and by SEM.

This work was financially supported by the Walloon Region (INNOPEM project- grant n° 1117490) and partially by the IAP Physical Chemistry of plasma surface interactions funded by the Belgian Science Policy, and by the FRIA.

[1]D. Merche, et al.,Plasma Processes and Polymers, 2010, 7, (9-10), pg 836

[2]D. Merche,et al., Plasma Processes and Polymers, 2012, 9, (11-12),pg 1144

Schematic diagram of the experimental process

PST-P3-10
Use of cold plasma treatment to modify the surface of activated carbon as an adsorbent of organochlorinated compounds

T11 Plasma Science and Technology

#PST-P3-10

J. Levalois-Grützmacher, V.K. Rana.

ETH-Zürich - Zürich (Switzerland).

The specific physical characteristics (surface area, pore volume/diameter) and chemical characteristics (pH, ash content, surface functional groups, conductivity) of activated carbon (AC) determine its performance and specific application mode. Because of its high adsorptive porosity, it has been widely used as adsorbent for organochlorinated insecticides and in catalysis or separation processes.
Two organochlorinated insecticides such as chlordecone (CLD) and β-hexachlorocyclohexane (β-HCH) had been intensively used in Guadeloupe and Martinique to control the banana weevil *Cosmopolites sordidus* from 1972 to 1993. Due to their strong persistence in natural environments, high resistance to chemical reactions and microbiological degradation, the intensive use of these compounds resulted to a generalized pollution of the banana producing area. In order to limit the impregnation by this pesticide, in the polluted areas of Guadeloupe and Martinique, drinking water production plants were equipped with commercial activated carbon (AC) filters.
Cold plasma is well known for being used as a surface modifier and surface cleaning technique of various materials, polymers, powders, nanoparticles and so on for the past decade or more. Here in, several Ammonia-, Argon-, Nitrogen-, Carbon dioxide- and their mixture- cold plasma have been used to modify the surface of activated carbon in order to study the influence of new chemical species at its surface for adsorption of organic compound. The textural properties of these samples were probed by adsorption-desorption isotherm of nitrogen at 77K. Fourier Transform Infrared (FT-IR) and X-ray photoelectron spectroscopy (XPS) were further used to investigate the surface chemistry plasma treated activated carbon.

PST-P2-12
A NEW TECHNIQUE FOR DETERMINATION OF THERMAL GRADIENTE IN SOLIDS HEATED BY PLASMA

T11 Plasma Science and Technology

#PST-P2-12

C. Alves Junior [1], E. Aparecido De Deus Leal [2], S.I. Schafer De Souza [2].

[1]Federal University Rural of Semiarid - Mossoró (Brazil), [2]Federal University of Rio Grande do Norte - Natal (Brazil).

When a solid is immersed in plasma, two different types of energy transfer occurs: by radiation and by collision of particles. In the first case the heat is transferred uniformly and parallel to the surface. In the second case, it is transferred to the vicinity of micro regions where the thermal spikes are generated. To investigate these two effects, samples of AISI M35, whose hardness values are strongly temperature sensitive tempering were used as micro thermal sensors. By correlating the hardness values with temperature, it was possible to obtain the thermal profile of the samples of AISI M35 treated by plasma. It was found that plasma treated samples exhibited a surface layer and a lower layer in contact with sample port, which is not present in the samples tempered resistive furnace. Furthermore, it was found that samples with a higher thermal gradient in the lower region, were treated in the hollow cathode planar configuration with a pressure of 2 mbar.

AKAMATSU, H.; YATSUZUKA, M. Simulation of surface temperature of metals irradiated by intense pulsed electron, ion and laser beams. Surface and Coatings Technology, v. 169–170, n. 0, p. 219-222, 2003. ISSN 0257-8972. Source: < http://www.sciencedirect.com/science/article/pii/S0257897203000835 >.

ALVES JR, C.; HAJEK, V.; SANTOS, C. A. Thermal behavior of supersolidus bronze powder compacts during heating by hollow cathode discharge. 2003. Source: < http://www.ingentaconnect.com/content/els/09215093/2003/00000348/00000001/art00640 >.

BARANKOVA, H.; BARDOS, L.; BERG, S. The radio frequency hollow cathode plasma jet arc for the film deposition. Journal of Vacuum Science & Technology a-Vacuum Surfaces and Films, v. 14, n. 6, p. 3033-3038, Nov-Dec 1996. ISSN 0734-2101. Disponível em: < <Go to ISI>://WOS:A1996VV24700007 >.

GALVÃO, N. K. A. M. et al. Structural modifications of M35 steel submitted to thermal gradients in plasma reactor. Journal of Materials Processing Technology, v. 200, n. 1–3, p. 115-119, 2008. ISSN 0924-0136. Disponível em: < http://www.sciencedirect.com/science/article/pii/S0924013607007820 >.

KERSTEN, H. et al. The energy balance at substrate surfaces during plasma processing. Vacuum, v. 63, n. 3, p. 385-431, 2001. ISSN 0042-207X. Source: < http://www.sciencedirect.com/science/article/pii/S0042207X01003505 >.

_____. On the ion energy transfer to the substrate during titanium deposition in a hollow cathode arc discharge. v. 46, n. 3, p. 305–308, March 1995 1995. Disponível em: < http://dx.doi.org/10.1016/0042-207X(94)00068-9 >.

KRAUS, J.; FLEISCH, D. Electromagnetics with applications. 5° ed. Singapore: McGraw Hill, 1999.

KUDRYAVTSEV, B.; PARTON, V.; RUBINSKII, B. Electromagnetic and thermoelastic fields in a conducting plate with a cut of finite length.Solids Mech 1982; 17:110–8.

PARTON, V.; KUDRYAVTSEV, B. Electromagnetoelasticity. New York: Gordon and Breach, 1988.

YAMAZAKI, K. et al. PAS (Plasma activated sintering): Transient sintering process control for rapid consolidation of powders. Journal of Materials Processing Technology, v. 56, n. 1–4, p. 955-965, 1996. ISSN 0924-0136. Source: < http://www.sciencedirect.com/science/article/pii/0924013696851223 >.

PST-P3-19
Deposition of transition-metal nanoparticles by atmospheric plasma for the catalysed growth of carbon nanotubes

T11 Plasma Science and Technology

#PST-P3-19

C. De Vos [1], M. Raes [2], I. Vandendael [2], H. Terryn [2], F. Reniers [1].

[1]Analytical and Interfacial Chemistry (Université Libre de Bruxelles) - Bruxelles (Belgium), [2]Department of Materials and Chemistry (Vrije Universiteit Brussel) - Bruxelles (Belgium).

Carbon nanotubes (CNTs) have generated a growing interest in various multifunctional applications due to their wide-ranging properties such as high electrical and thermal conductivity, good mechanical properties and electron emission properties. More especially, vertically-aligned CNTs are very attractive as they can be readily incorporated into micro- and nanoelectronic devices. The growth of these forests requires a nanoscale transition-metal catalyst (such as cobalt, iron or nickel) homogeneously dispersed on the surface.
It has already been shown that atmospheric plasma is suitable for the deposition of Au, Pt and Rh nanoparticles. A colloidal solution containing metal nanoparticles is nebulized in the afterglow of a RF torch. The present study shows the deposition of monometallic and bimetallic nanoparticles of Fe and Co. Afterwards, the deposited nanoparticles are characterized by XPS and FEG-SEM combined with EDX to determine the sample composition and the nanoparticles dispersion. As seen on the SEM pictures presented in Figure 1, the nanoparticles dispersion strongly depends on the plasma parameters and the injection geometry. The XPS observations show nanoparticles constituted of iron and cobalt. It is seen on Figure 2 that high resolution cobalt spectra can be fitted in four components due to the presence of metallic and oxidized cobalt. The various oxidation states depend on the deposition conditions such as the discharge temperature and the injection geometry. After heating the sample, the oxidation decreases from 32 to 12%. Gases in the discharge and in the post-discharge are analysed by OES to explain the different oxidation percentages of the samples.
In conclusion, transition-metal nanoparticles of iron and cobalt are deposited by an

atmospheric plasma RF torch. The oxidation of these nanomaterials varies with the process conditions and can be controlled to some extent.

Fig 1: FEG-SEM pictures of Fe/Co NPs deposited by atmospheric RF torch a) perpendicular, b) parallel injection
Fig 2: a) XPS components of Co peak, b) Influence of the injection geometry on the oxidation

PST-P3-11
Electron Ionization of RTV Adhesive Outgases inVacuum

T11 Plasma Science and Technology

#PST-P3-11

W. Feng.

Beijing Insitute of Spacecraft Environment Engineering - Beijing (China).

RTV adhesive is widely used in spacecraft such as solar array. It is considered main contamination sources in spacecraft due to outgases of RTV adhesive in orbit. The outgas molecules in orbit might be ionized under space electron environment. Due to spacecraft charging effects in orbit, these contaminant ions will be re-attracted to spacecraft sensitive surfaces and cause severe contamination. In this paper, RTV S691 is used as a contaminant source with heating temperature about 120℃ in vacuum. The outgases are ionized by low energy electrons impact which simulate space electron environment. 500eV of electron energy is found to be optimal for ionization. Ionization properties of outgases are researched experimentally. Magnetic deflection method is used for measuring Q/M of outgassing ions. Q/M of RTV –S691 outgassing ions is about 3×10^{7}C/kg. The results can be used for simulation of charging effect on spacecraft.

PST-1-Or-2
Optical emission spectroscopy and collisional-radiative modeling of He dielectric barrier discharges in presence of wood samples

T11 Plasma Science and Technology

#PST-1-Or-2

L. Stafford [1], R. Gangwar [1], O. Levasseur [1], N. Gherardi [2], N. Naudé [2].

[1]Universite de Montreal - Montreal (Canada), [2]LAPLACE - Toulouse (France).

We have recently extended the range of applications of dielectric barrier discharges (DBD) at atmospheric-pressure to the functionalization of wood with the objective of improving its durability following natural weathering [1]. The physics driving the treatment of such materials is however much more challenging than for conventional substrates. This can be attributed not only to the highly anisotropic nature of this polymer, but also to its highly porous microstructure which can release impurities. The influence of wood outgassing on the plasma characteristics was explored using a combination of optical emission spectroscopy (OES) and plasma modeling. In addition to the expected strong He emission lines between 500 and 750 nm, noticeable emission from N_2 and N_2^+ was observed due to outgassing of air entrapped in wood. OH and O emissions at 309 nm and 777 nm were also present. While the O emission also results from air outgassing, the OH emission is ascribed to etching of the weak boundary layer and humidity desorption from the wood samples and chamber walls. To further analyze the OES spectra and extract the time-evolution of basic plasma parameters we have developed a collisional-radiative (CR) model in which the number density of the emitting n=3 He I states are assumed to be populated according the diagram presented in Fig. 1. Based on this framework, the steady-state rate balance equations for such levels can be written as in Fig. 1, where $[He_i]$ denotes the population of i^{th} state and where 'm' and 'g' refers to metastable and ground state, respectively. A_{ij} is the Einstein coefficient for spontaneous emission. k_1 and k_2 represents the rate coefficients for direct and stepwise electron impact excitation [3]. k_3 , k_4 and k_5 are the rate coefficients for energy transfer reactions between the n=3 levels following their interaction with ground state He atoms [4]. Given the low electron temperature (T_e<1 eV) and the low $[He_m]/[He_g]$ ratio (~10^{-9} [5]), stepwise excitation dominates over excitation from ground state. In such

conditions, the intensity ratios between the various He I lines are only function of T_e. The measured OES spectra were fitted to the prediction of our model using T_e as the only adjustable parameter. T_e was found to decrease from right after ignition of the first discharge when substrate outgassing are important to longer treatment times when “pumping” of the wood samples is nearly complete.

[1] O. Levasseur et al., Plasma Processes and Polymers **9**, (2012) 1168.
[2] T Belmonte et al., J. Phys. D **40** (2007) 7343.
[3] H. F. Wellenstien and W. W. Robertson, J. Chem. Phys. **56**, (1972) 1411.

Fig. 1 : Reaction set used in the C-R model

PST-1-Or-3
CORONA DISCHARGE AS AN ION SOURCE FOR AEROSOL CHARGING: OPTIMISATION OF THE ION PRODUCTION AND EXTRACTION

T11 Plasma Science and Technology

#PST-1-Or-3

N. Jidenko [1], A. Bouarouri [1], D. Boulaud [2], F. Gensdarmes [2], D. Marot [3], J.P. Borra [1].

[1]LPGP (CNRS Univ paris Sud) - Gif Sur Yvette (France), [2]IRSN - Gif Sur Yvette (France), [3]IRSN - Cherbourg (France).

The evaluation of aerosol (solid and liquid particles suspended in gas) dry deposition rate in rural areas is necessary to evaluate impact of pollutants released in the environment. A method based on eddy covariance measurements has recently been developed for this purpose; this method requires aerosol size distribution and wind velocity with a real time measurement (10 Hz)[1]. A device for measuring the aerosol concentration with a response time of 100 ms is to be developed. For such short time measurements, electrical methods based on aerosol charging are promising. Corona discharge is used to produce unipolar ions required for aerosol charging[2]. To limit aerosol losses, charging is carried in the post-discharge zone where the electric field value is lower than 10^5 V.m^{-1}.

For short time charging (<100 ms) a mean ion concentration Ni of 10^{13} m^{-3} is required. Due to electrostatic repulsions, the initial ion concentration is about 10^{16} m^{-3} [2,3].

Tow strategies can be used to increase the ion density extracted from the discharge (i) optimisation of the discharge in order to confine ions produced to the extraction hole and/or (ii) optimisation of the extraction by increasing the proportion of ions extracted. Experimental investigations on different discharge geometries are studied and compared to increase the post discharge ion current and density. This work focuses on the ionic current and density extracted from the discharge. The distribution of ions in the charging zone is the next step.

The transport of ions depends on an electro-hydrodynamic competition. A negative point to plane Corona discharge is first studied in various conditions. Ions are

extracted from the discharge through a hole located in the plane on the axe of the point. The electrical and geometrical parameters are dimensioned to ensure the temporal stability of the ion source. Two methods of ion confinement are than used, convective confinement using a gas flow and electrostatic confinement using an electric field. The effect of the gas flow on the distribution of ionic density of current on the plane for flow range of 5 to 30 L.min-1 and for the hole diameter of 2 mm is studied. The gas flow allows a confinement of the ions to the hole. In fact, the empirical Warburg profile $J(r)=J_0\cos^{4.65}\theta$ given without gas flow4 is modified to $J(r)=J_0\cos^{6}\theta$ (J(r) courant density with radial variation, J_0 current density at r=0, and $tg(\theta)=d/r$; d is the inter-electrode distance). The second method of ion confinement is based on electrostatics, the plane is composed of three layers: a thin metallic layer (<50 µm) on the discharge side superposed with an insulator layer and a metallic layer in the post-discharge side. The electric field generated by the polarization of the sandwich increases ions velocity in the hole. An electric field of 10^5 $V.m^{-1}$ increases by three times the ionic current extracted. Two other arrangements, developed to limit the ion electrostatic losses, are investigated to define the optimal one.

1 P.E Damay et al.(2009) ournal of Aerosol Science 40,1050-1058
2 K.T.Whitby (1961),Rev,Sci,Instrum.32, 1351-1355
3 Marquard, et al.. (2006) Aerosol Science 37 (2006) 1052 – 1068.
4 Goldman, M. et al. (1978) Chapter 4, Volume 1, Electrical discharges in gases.

PST/SE/TF-1-Or-3
Deposition of SiO2/TiO2 nanocomposite thin films by Atmospheric Pressure Townsend Discharge

T11 Plasma Science and Technology

#PST/SE/TF-1-Or-3

J. Profili [1], N. Gherardi [1], L. Stafford [2], O. Levasseur [2], R. Clergereaux [1], N. Naudé [1].

[1]LAPLACE - UPS/INPT/CNRS - Toulouse (France), [2]Université de Montréal, UDEM - Montreal (Canada).

Title : Deposition of SiO2/TiO2 nanocomposite thin films by Atmospheric Pressure Townsend Discharge

Authors : Jacopo Profili[1,2,3], Nicolas Gherardi[1,2], Luc Stafford[3], Olivier Levasseur[3], Richard Clergereaux[1,2], Nicolas Naudé[1,2]

Affiliations :

[1] Université de Toulouse, UPS, INPT, LAPLACE, F-31062 Toulouse Cedex 9, France
[2] CNRS, LAPLACE, F-31062 Toulouse Cedex 9, France
[3] Département de Physique, Université de Montréal, Montréal (Québec) H3C 3J7, Canada

Abstract :

Cold Atmospheric Pressure Plasma Enhanced Chemical Vapour Deposition (AP-PECVD) has already demonstrated its potential for homogeneous thin film deposition. A new challenge is the deposition of nanocomposite thin films in AP discharges in order to obtain multifunctional properties.

This contribution is focused on the study of the growth of nanocomposite coatings

based on titanium oxide (TiO2) nanoparticles embedded in a silica-like (SiO2) matrix, using a parallel plate dielectric barrier discharge (DBD) at atmospheric pressure. The gas mixture is made of nitrogen (N2) as the main gas, a mixture of hexamethyldisiloxane (HMDSO) and nitrous oxide (N2O) for the deposition of the SiO2 matrix, and nanoparticles of TiO2, which are introduced in the gas mixture by nebulizing different stable colloidal solutions.

The discharge works in the homogeneous regime, namely the Atmospheric Pressure Townsend Discharge. The gas mixture is injected longitudinally to the dielectric plates, allowing gas phase and surface analyses as a function of the mean residence time, which gives additional information on the thin film deposition mechanisms. The DBD is characterized through electrical and optical diagnostics and the characterization of the coatings is performed using Fourier transform infrared spectroscopy, X-ray photoelectron spectroscopy, Raman spectroscopy and scanning electron microscopy.

Preliminary results show that TiO2 nanoparticles can be incorporated in the thin film through this process. Moreover, similarly to low-pressure dusty plasmas, the electrostatic forces play a dominant role on the transport of the nanoparticles in the discharge. As a result, an appropriate tuning of the applied voltage waveform (shape, amplitude and frequency) has a direct impact on the distribution of the nanoparticles in the thin film, allowing to elaborate coatings with several potential applications for instance due to the oxygen barrier properties of the SiO2 matrix and the UV-protection properties of TiO2.

PST-P3-12
Modification of Stearic Acid in Inductively Coupled Radio Frequency Plasma

T11 Plasma Science and Technology

#PST-P3-12

C. Farias [1], J.C. Bianchi [1], P.R. Oliveira [1], P.C. Borges [1], E.A. Bernardelli [2], T. Belmonte [3], M. Mafra [1].

[1]UTFPR - Curitiba (Brazil), [2]IFPR - Paranaguá (Brazil), [3]IJL - Nancy (France).

The cleaning processes of metallic surfaces are often expensive and produces high amounts of waste. Plasma cleaning is a alternative process but it's mechanisms are not completely undersood [1,2]. The goal of the present work is to understand how plasma process generates degradation of stearic acid. This material is used as a organic molecule model containing a linear carbonaceous chain and a acid function. The experimental study was made using an inductively coupled RF discharge at 13,56 MHz, with the sample immerse in the discharge. The use of pure Nitrogen as carrier gas is compared with atmospheric air. The mass variation analysis shows that even in long process times it is possible to attain a negative mass variation rate. Atmospheric air plasma showed more efficient cleaning rates than pure N2 as can be seen in Fig. 1. In other hand, a resin like appearance was observed when the air plasma is used. Infrared spectra (FTIR) were performed on both treated and non treated samples, as shown in Fig. 2. New peaks are observed in the air plasma treated sample: the 3400 cm-1 region shows a small and large peak resulting from the O-H stretching from alcohol function. The peak at 1700 cm-1 becomes more intense and large to higher values of wavenumber, meaning that more C=O are formed in new oxygenated functions with the presence of esters between 1735-1750 cm-1. The region 1100-1300 cm-1 become more intense, probably due to the presence of C-O stretching in some of those new oxygenated functions. In pure N2 plasma, none of those modifications were observed, meaning that the SA was degraded, seen by the mass loss, but not functionalized as none N-C, N-H or N-O peaks were found in FTIR spectrum.

[1] Bernardelli, E. A. et al.. Plasma Chemistry and Plasma Processing, v. 31, n. 1, p. 189-203, 2010.
[2] Rabek, J. F.; Lucki, J.; Rånby, B.. European Polymer Journal, v. 15, n. 12, p. 1089-1100, 1979.

Fig.1: Mass variation rate of S.A. in RF plasma with N2 and Dried Atmospheric Air.
Fig.2: Infrared spectrum of the non treated SA and the ones treated in pure N2 and air.

SE/PST/TF/BI-1-Or-7
Applications on bacteria Escherichia coli of reactive gaseous medium formed by atmospheric pressure guided streamers

T11 Plasma Science and Technology

#SE/PST/TF/BI-1-Or-7

S. Cousty [1], A.L. Bulteau [2], L. Chavatte [2], F. Clément [2].

[1]Université Paul Sabatier - Toulouse (France), [2]Université Pau - Pau (France).

In the field of plasma bactericidal effects, role of active species produced by plasma is still discussed. Escherichia coli, a well-known GRAM negative bacterium, is chosen as a model to evaluate biological inactivation induced by Atmospheric Pressure Guided Streamers “APGS”, more often called Plasma Jets [1-2].

In a first part, the description of the reactive gaseous medium used for this study is given. Supplied by a pulsed High Voltage power and based on the formation of Dielectric Barrier Discharges (DBD), the plasma jet reactor is electrically analyzed. Optical emission spectroscopy is used in order to qualify the excited species created. Helium and Argon being used as carrying plasma gas, the air environment around the jet lead to the production of numerous Reactive Oxygen and Nitrogen Species (ROS, RNS, RONS) known for their potential actions on biologic cells [3].

In a second part, bacterial inactivation mechanisms are investigated by two ways. First approach is to realize desiccation of bacteria samples on microscopic glass slides. Under these non-physiological conditions, the bactericidal effect of APGS is estimated by traditional counting: survivor bacteria are incubated, and after an overnight, colonies are numerated on Petri dishes. The second approach is to keep the bacteria in physiological liquid medium and to expose directly the solutions to the APGS. Numeration of survivors allows once again to determine the impact of the plasmas by varying several parameters (gas composition, distance between jet and sample, and exposure times).

Finally and in order to try a better understanding of the interaction mechanisms between APGS and the bacteria, chemical analyses of the liquids exposed using

APOLLO 4000 a free radical analyzer will allow to determine the different Reactive Oxygen and Nitrogen Species in solutions, produced or induced by the excited active gases formed by the “APGS”.

[1] Boeuf J-P, Yang LL and Pitchford LC, 2013 Dynamics of a guided streamer ('plasma bullet') in a helium jet in air at atmospheric pressure, J. Phys D: Appl. Phys. 46 015201
[2] Svarnas P, Matrali SH, Gazeli K, Aleiferis Sp, Clément F and Antimisiaris SG, 2012 Atmospheric-pressure guided streamers for liposomal membrane disruption, Appl. Phys. Lett. 101 264103
[3] Graves DB, 2012 The emerging role of reactive oxygen and nitrogen species in redox biology and some implications for plasma applications to medicine and biology, J. Phys. D: Appl. Phys. 45 263001

PST/SE/TF-P1-06
LOW-TEMPERATURE PLASMA CARBURIZING OF AISI 420 STEEL: MICROSTRUCTURE CHARACTERIZATION OF THE TREATED SURFACES

T11 Plasma Science and Technology

#PST/SE/TF-P1-06

S. Brunatto, C.J. Scheuer, R. Cardoso, S. Henke.

UFPR - Universidade Federal do Paraná - Curitiba (Brazil).

Abstract

Low-temperature plasma carburizing [1] was performed in order to study the effect of treatment temperature and time on the microstructure characteristics of the carburized layer obtained in AISI 420 martensitic stainless steel samples. Plasma carburizing experiments were carried out in DC-pulsed power supply glow discharge, at 700 V voltage, in 99.5% (80% H2+20% Ar) + 0.5% CH_4 gas mixture, 1.66×10^{-6} $Nm^3 s^{-1}$ gas flow rate, and 400 Pa pressure, for temperatures of 623, 673, 723 and 773 K, and times of 8, 12, and 16 h. The carburized layers were characterized by SEM, optical microscopy, XRD analysis for two different geometries, Bragg-Brentano and Glancing Angle, and microhardness measurements. The microstructure of the treated samples was revealed by using different etchants, id. est Nital 2%, Marble, and Acqua Regia. Results are discussed aiming to determine the phase constitution of the carburized layers and the eventual occurrence of precipitation-free diffusion layers obtained for the different studied conditions. According to Fig. 1 results, it is evidenced that treatments performed for high carburizing temperature (773 K) lead to formation of chromium carbide precipitates, being critical for the stainlessness characteristic purpose of the treated steel.

References

[1] C.J. Scheuer, R.P. Cardoso, R. Pereira, M. Mafra, S.F. Brunatto, Materials Science and Engineering A 539 (2012) 369–372.

Acknowledgements
This work was supported by Programa Interdisciplinar de Petróleo e Gás Natural da UFPR (PRH24), CAPES-COFECUB and CNPq. The authors wish to express their thanks to the Laboratory of X-ray Optics and Instrumentation – LORXI, from the Universidade Federal do Paraná (UFPR) by using the X-ray diffraction equipment.

Figure 1 – Microstructure results for sample carburized at 773 K (etchant: Nital 2%).

PST-1-Or-1
Optical emission study of guided streamers at atmospheric pressure

T11 Plasma Science and Technology

#PST-1-Or-1

F. Clément [1], K. Gazeli [2], P. Svarnas [3].

[1]UPPA Université - Pau (France), [2]UPPA - HVL, Université - Pau-Patras (grèce) (France), [3]High Voltage Laboratory, Université Patras - Patras (Greece).

In this work, a DBD-based reactor with coaxial electrode configuration is fed by helium gas (axial flow at 2 slm) and driven by sinusoidal high voltage at 10 kHz. The anode electrode is a microfilament stressed up to 12 kV (peak-to-peak) and housed in a capillary dielectric tube. Thus, apart from the radial DBD due to the coaxial configuration [1], guided streamers (commonly called plasma jets or bullets) are generated [1-3]. The present study, realized by means of spatiotemporally-resolved optical intensity measurements and spatially-resolved optical emission spectroscopy, supports the statement that we deal with classical streamers which are guided by the dielectric. They are propagated in the atmospheric surrounding air and copious excited species are produced along their path. The velocity of those ionizing fronts is found herein to be in the order of magnitude of 106 cm/s. On the other hand, the major reactive species are identified, and the spatial evolution of their intensity and rotational temperature is calculated. The above results contribute to the understanding of the physical mechanisms governing the operation of such systems and as well to their parameterization for different applications.

[1] C. Monge-Dauge, F. Clément, P. Svarnas, J.-F. Loiseau, A. Ricard, B. Held, “Experimental study coupled with electrical modeling for the consideration of DBD-based plasma jet”, IEEE T Plasma Sci 40(9) (2012) 2254-2260
[2] “Dynamics of a guided streamer (‘plasma bullet’) in a helium jet in air at atmospheric pressure”, J.-P. Boeuf, L. L. Yang, and L.C. Pitchford, J Phys D: Appl Phys 46 (2013) 015201
[3] “Atmospheric-pressure guided streamers for liposomal membrane disruption”, P. Svarnas, S.H. Matrali, K. Gazeli, Sp. Aleiferis, F. Clément, Appl Phys Lett 101 (2012) 264103

PST-5-Or-5
Acetaldehyde elimination using a diphasic process combining an atmospheric pressure plasma and a nano-structured catalyst

T11 Plasma Science and Technology

#PST-5-Or-5

A. Vega-González, Z. Jia, K. Hassouni, S. Touchard, A. Kanaev, S. Sauce, X. Duten.

LSPM - CNRS - Villetaneuse (France).

Motivations
Volatile organic compounds (VOCs) are recognized as major contributors to air pollution either, through their toxic nature and/or as participants in atmospheric photochemical reactions. Among VOCs, acetaldehyde (AC) have received great attention. On the one hand, it is an important component of the total VOC reactivity of the atmosphere, providing sources of new radicals that drive ozone formation [1]. On the other hand, it is emitted in high rates from products that are used widely as building materials [2]. Diphasic processes combining an atmospheric pressure plasma at and a catalyst material has gained attention, and several studies reported an enhancement of the VOCs removal efficiency. When using a plasma/catalysis system, the complex nature of the process has to be considered. The VOC removal is obtained through its decomposition in the gas phase as well as on the catalyst surface, and both steps are closely related. This work is an experimental study of AC removal using an atmospheric pressure plasma combined with a nano-structured catalyst. The intermediates of AC adsorption over the catalyst surface were investigated using in situ DRIFTS (Diffuse Reflectance Infrared Fourier Transform Spectroscopy) method.

Experimental procedure
A sinusoidal dielectric barrier discharge is produced in a cylindrical quartz tube filled with the catalyst. Different catalyst/catalyst support were used (SiO_2, TiO_2/SiO_2, $Ag/TiO_2/SiO_2$). The gas mixture is composed by AC (5000 ppm), oxygen (5-20 %) and nitrogen (balance) at a total flow rate of 100 mL/min. Gas chromatography is

used to follow AC concentration at the inlet/exit of the reactor. AC oxidation is evaluated by measuring CO, CO_2, and ozone at the reactor exit. By-products formation is followed by GCMS. The nanoparticles were generated in a sol-gel reactor with rapid (turbulent) micromixting [3].

Results and discussion

The experimental results show that more than 97% of the initial pollutant can be removed at room temperature. The evolution of the CO_2 concentration at the reactor exit show that the type of solid immersed in the plasma discharge had no influence on the CO_2 selectivity. On the contrary, the CO selectivity is strongly affected by the solid particle type. This result indicates a strong interaction between the pollutant and the catalyst (Ag/TiO_2). In order to better understand the role of the catalyst, the interaction of AC with the surface was followed in-situ using the DRIFTS method. The results show that when AC is brought into contact with the Ag/TiO_2 surface, an acetyle intermediate is formed. Based on these results, we propose a two-steps removal process of the pollutant, involving heterogeneous surface and homogeneous plasma chemistry.

[1] Luecken D.J., Hutzell W.T., Strum M.L., Pouliot G.A. Regional sources of atmospheric formaldehyde and acetaldehyde, and implications for atmospheric modelling. Atmos. Environ. 47 (2012) 477 – 490.
[2] Missia D.A., Demetriou E., Michael N., Tolis E.I., Bartzis J.G. Indoor exposure from building materials: A field study. Atmos. Environ. 44 (2010) 4388 – 4395.
[3] R. Azouani, A. Michau, K. Hassouni, K. Chhor, J.-F. Bocquet, J.-L. Vignes, A. Kanaev, Chem. Eng. Res. Design, 88 (2010) 1123-1130

PST/SE/TF-P1-07
Study of the reactivity of water at the interface between an atmospheric argon plasma torch and polyethylene

T11 Plasma Science and Technology

#PST/SE/TF-P1-07

S. Collette [1], V. Cristaudo [2], S. Abou Rich [1], P. Leroy [1], T. Dufour [1], A. Delcorte [2], F. Reniers [1].

[1]Chimie Analytique et Chimie des interfaces (Université Libre de Bruxelles) - Bruxelles (Belgium), [2]Institut de la matière Condensée et des Nanosciences (Université Catholique de Louvain) - Bruxelles (Belgium).

In the literature, few studies focus on the use of water in plasma discharges. Indeed, despite its potential high reactivity, water is also known to destabilize plasmas. In this study, the reactivity of water at the interface between an atmospheric plasma torch and the surface of the low density polyethylene (LDPE) was investigated. The injection of water in the post-discharge avoids the plasma destabilization, while keeping its reactivity. More specifically, the reactivity of the OH radical for surface grafting will be investigated. LDPE was chosen because of its high capacity to be functionalized.

We characterized in parallel the composition of the gaseous post-discharge and the substrate modifications. The water vapor is injected in the post-discharge of a RF torch by an injection system located just under the ground electrode. The post-discharge is characterized by optical emission spectrometry (OES) to determine the different emitting species. The evolution of each species and the impact of the quantity of water are followed by OES. OH, N_2, O_2^+, Ar and atomic oxygen were present in the post discharge and the evolution of their behavior was helpful to understand the reactions in the gas phase. Indeed, as shown in Fig 1, the amount of some species increases with the injection of water (such as OH, O_2^+) whereas it decreases for the other species. The amount of ions can be related to electrical measurements recorded through a copper plate placed downstream of the discharge to determine the ionic current for different plasma conditions and concentrations of water.

The modified LDPE is characterized by static contact angle (WCA), X-ray photoelectron spectroscopy (XPS) and time-of-flight secondary ion mass

spectrometry (ToF-SIMS). The first technique gives access to the surface energy, more specifically its polar component. The functionalization of the surface can be evidenced by the observation of a decreasing WCA. The two others techniques allow to determine the surface chemistry, as well as its in-depth distribution. The use of D_2O for the treatment of the LDPE allows to probe the origin of the functions grafted at the surface of the polymer.
All of these analytical techniques are used to understand mechanisms of the surface functionalization and to predict some reactions in the post discharge and at the surface of the LDPE. This work was supported by IAP – PSI (Physical Chemistry of plasma surface interactions (Belgian Federal Government BELSPO agency)).

Fig 1: a) OES spectrum of the post discharge of a plasma (90W, 30L/min Ar, 27,12 MHz); b) Normalized intensity of species observed in the post discharge (90W, 30L/min Ar, 27,12 MHz)

PST-P3-13
Conversion of CO2 and CH4 mixtures using a dielectric barrier discharge: gas composition and power effect

T11 Plasma Science and Technology

#PST-P3-13

A. Ozkan, G. Arnoult, P. De Keyzer, F. Reniers.

Université Libre de Bruxelles - Bruxelles (Belgium).

Carbon dioxide is usually considered as an end-product in chemistry because of its high stability. Due to the high quantities of CO_2 produced, its conversion received more and more attention in the recent years [1]. The transformation of CO_2, with CH_4 as second reactant and using atmospheric plasma technology shows that, in appropriate conditions, both gases can be converted into valuable products [2-5].
The conversion of CO_2/CH_4 mixtures was performed using a dielectric barrier discharge (DBD) atmospheric plasma using Argon as the plasmagen gas. Gas Chromatography was used to determine the composition of the gas after plasma treatment and this treatment was carried out in a new type of reactor developed in the laboratory. We demonstrate that the synthesis of syngas (CO and H_2), C_2H_6 and C_2H_4 is possible in this type of discharge.
The study is focused on the effect of parameters on the CO_2 and CH_4 conversion rate. The parameters which are evaluated in this work are the ratio of CO_2/CH_4 flow rates and the power supplied.
We show that the ratio of CO_2/CH_4 flow rates in the mixture has a significant impact on the conversion rate. On the other hand, as only small amounts of oxygenated organic compounds have been detected, it is suggested that there are no many interactions between the active species of these two molecules. Moreover, the absence of oxygen after CO_2/CH_4 plasma, suggests that atomic oxygen is consumed by the CH_4 present in the plasma.
On the other hand, the effect of power is clearly visible, showing a linear increase in the CO_2 and the CH_4 conversion rates and of the syngas production with the supplied power [Fig. 1]. Therefore, an electron-driven mechanism is suggested.

[1] T. Sakakura, J-C. Choi and H. Yasuda, Transformation of carbon dioxide, Chem. Rev. 107 (2007) 2365−2387
[2] X. Tao, M. Bai, X. Li, H. Long, S. Shang, Y. Yin and Xiaoyan Dai, CH_4-CO_2 reforming by plasma - challenges and opportunities, Progress in Energy and Combustion Science 37 (2011) 113-124
[3] A-J. Zhang, A-M. Zhu, J. Guo, Y. Xu and C. Shi, Conversion of greenhouse gases into syngas via combined effects of discharge activation and catalysis, Chemical Engineering Journal 156 (2010) 601–606
[4] Istadi, Nor Aishah Saidina Amin, Co-generation of synthesis gas and C_{2+} hydrocarbons from methane and carbon dioxide in a hybrid catalytic-plasma reactor: A review, Fuel 85 (2006) 577–592
[5] Y-P. Zhang, Y. Li, Y. Wang, C-J. Liu and B. Eliasson, Plasma methane conversion in the presence of carbon dioxide using dielectric-barrier discharges, Fuel Processing Technology 83 (2003) 101– 109

Fig. 1: Products percentages with the power

PST-3-Or-5
Deposition of PTFE like film by atmospheric plasma on organic and inorganic substrates

T11 Plasma Science and Technology

#PST-3-Or-5

N. Vandencasteele, J. Hubert, C. Barroo, S. Vranckx, O. Bury, S. Collette, C. De Vos, F. Reniers.

ULB - Brussels (Belgium).

Thanks to its very specific properties (low surface energy, great chemical resistance...) Polytetrafluoroehtylene (PTFE) is a polymer used in a wide range of extreme environment applications. However its high cost and poor recyclability limit its use in more general applications. Atmospheric plasma polymerization enables us to quickly and easily deposit PTFE like films on a wide range of materials. This allows us to modify the surface properties of those materials to obtain properties close to the one of pure PTFE while greatly diminishing the use of expensive and non-environmentally friendly fluorinated compounds. Furthermore we use non toxic liquid precursors. This simplifies their handling and the upscaling of the process for industrial applications.
Several types of fluorinated precursor are compared (C_6F_{14}, $C_{12}F_{27}N$[1]). The influence of the precursor structure on the deposition speed and the film quality is studied. The influence of the plasma gas (Ar or He) is also studied. Surfaces compositions are determined by X-ray photoelectron spectroscopy (XPS) and surface energy by water contact angle (WCA) measurements. Our results shows that the precursor as well as the plasma gas used have little influence on the final composition and surface energy of the coatings. However a strong difference in the deposition rates is observed. Further studies using atomic force microscopy might highlight small differences in the films structure depending on the plasma gas used as already shown in the literature[2].
The coating deposited on various substrates present surface composition (XPS) and surface energies (WCA) similar to the one of pure PTFE regardless of the starting composition and surface energy of the substrate (table 1 and figure 1).
Finally the effect of the plasma source is also studied. Films deposited in the plasma using a dielectric barrier discharge (DBD) are compared to films deposited in the post-discharge of a commercial radio frequency plasma torch.

Substrate	Precursor	Plasma	Post discharge
Glass		35°	
	C_6F_{14}	108°	105°
	$C_{12}F_{27}N$	112°	106°
Steel		74°	
	C_6F_{14}	109°	110°
	$C_{12}F_{27}N$	111°	108°
PE		79°	
	C_6F_{14}	111°	110°
	$C_{12}F_{27}N$	109°	114°
PVC		81°	
	C_6F_{14}	111°	110°
	$C_{12}F_{27}N$	108°	112°

1. RENIERS, F.; VANDENCASTEELE, N.; BURY, O., METHOD FOR DEPOSITING A FLUORINATED LAYER FROM A PRECURSOR MONOMER. WO Patent WO/2009/030,763: 2009.
2. Merche, D.; Poleunis, C.; Bertrand, P.; Sferrazza, M.; Reniers, F., Ieee Transactions on Plasma Science 2009, 37 , 951-960.

Comparison of XPS spectra of steel before and after deposition of PTFE-like film with $C_{12}F_{27}N$ precursor.

PST-05-Or-5a
Dry reforming of CO2 by DBD plasma at atmospheric pressure

T11 Plasma Science and Technology

#PST-05-Or-5a

T. Bieber, G. Arnoult, P. De Keyzer, F. Reniers.

ULB - Bruxelles (Belgium).

Carbon dioxide is usually considered as a waste, unavoidable end-product of many industrial processes. Due to its high chemical stability, carbon dioxide is indeed poorly used as a reactant. It is therefore necessary to develop technologies able to reuse it. In this objective, dry reforming of carbon dioxide by plasma has attracted significant interest to generate carbon monoxide which has an interesting energetic value [1], [2].

We present here a study of the plasma assisted conversion of CO_2 into CO and O_2 in a new Dielectric Barrier Discharge plasma device operating at atmospheric pressure. We focused on determining the influence of several parameters on the conversion efficiency: the input power, the flow rate and finally the presence of oxygen in the input gas mixture. Gas chromatography and mass spectrometry at atmospheric pressure are used to determine the composition of the gas after plasma treatment. Conversion rates for CO_2 can then be extracted.

The conversion rate increases with the power (from 100 W to 300 W), suggesting an effect of the electron density (Fig.1). On the other hand, the conversion rate drops with increasing flow rate, from 1 L/min to 10 L/min. Indeed since the flow rate is inversely proportional to the residence time of the gas in the reactor, increasing it means that the gas spends less time in the plasma. Finally, the presence of oxygen in the input mixture leads to a lower conversion rate, probably due to an increase of the recombination reaction $CO + ½\ O_2 \rightarrow CO_2$.

Optical emission spectroscopy is also performed on the plasma during the

experiment in order to try to understand the physical processes at the origin of these results.

[1] R. Li, Q. Tang, S. Yin, et T. Sato, « Plasma catalysis for CO2 decomposition by using different dielectric materials », Fuel Processing Technology, vol. 87, no 7, p. 617–622, 2006.

[2] S. Paulussen, B. Verheyde, X. Tu, C. De Bie, T. Martens, D. Petrovic, A. Bogaerts, et B. Sels, « Conversion of carbon dioxide to value-added chemicals in atmospheric pressure dielectric barrier discharges », Plasma Sources Science and Technology, vol. 19, p. 034015, 2010.

Fig.1: CO_2 Conversion rate with the power injected in the plasma

PST-P3-14
Spectroscopic investigation of capillary plasmas in the intermediate pressure range

T11 Plasma Science and Technology

#PST-P3-14

J. Barz [1], J. Barz [2], C. Oehr [2], T. Hirth [1], T. Hirth [2].

[1]Institute for Interfacial Engineering and Plasma Technology IGVP, University of Stuttgart - Stuttgart (Germany), [2]Fraunhofer Institute for Interfacial Engineering and Biotechnology IGB - Stuttgart (Germany).

For practical reasons, technical plasmas are commonly in the low-pressure range below 100 Pa or at atmospheric pressures. When considering non-thermal plasmas, low pressure plasmas easily allow for low process temperatures due to the non-equilibrium state between “hot” electrons and “cold” neutral gas. The advantage of these plasmas is the high degree of ionization and high degrees of radical formation which can be achieved. At atmospheric pressure, e.g. dielectric barrier discharges are used for non-thermal processes. The advantage of this pressure regime is that no vacuum pumps are required, however, it is difficult to achieve high radical densities and higher ignition voltages are required.
On the first glance, intermediate pressure between 100 Pa and atmospheric pressure bears mostly disadvantages like elevated ignition voltages when compared to low-pressure plasmas and the necessity of pumps when compared to atmospheric pressure plasmas. However, e.g. in the presence of fluids with a vapor pressure above 100 Pa, this pressure regime is an interesting option.
In our paper, we present first spectroscopic measurements in a capillary plasma in the intermediate pressure range with gas mixtures of nitrogen, oxygen, and water which could occur e.g. during processes for water cleaning by plasmas. The species traced in a variety of gas mixtures are nitric oxide, ozone, atomic oxygen, and OH radicals. These molecules are measured by optical emission spectroscopy [1, 2] and laser-induced fluorescence [3-5]. The study of the pressure dependence allows identifying interesting process windows for future applications.

1. Kuhn, S., et al., Non-thermal atmospheric pressure HF plasma source: generation of nitric oxide and ozone for bio-medical applications. Plasma Sources Science & Technology, 2010. 19(1).
2. Wang, C. and N. Srivastava, OH number densities and plasma jet behavior in atmospheric microwave plasma jets operating with different plasma gases (Ar, Ar/N_2, and Ar/O_2). European Physical Journal D, 2010. 60(3): p. 465-477.
3. Dilecce, G., et al., LIF diagnostics of hydroxyl radical in atmospheric pressure He-H2O dielectric barrier discharges. Chemical Physics, 2012. 398: p. 142-147.
4. Li, L., et al., Measurement of OH radicals at state X(2)Pi in an atmospheric-pressure micro-flow dc plasma with liquid electrodes in He, Ar and N_2 by means of laser-induced fluorescence spectroscopy. Journal of Physics D-Applied Physics, 2012. 45(12).
5. Shen, X., et al., PLIF diagnostics of NO oxidization and OH consumption in pulsed corona discharge. Fuel, 2012. 102: p. 729-736.

PST-P2-13
Abel inversion technique used for radial measurements of the microplasma in Ar-2%H2 flow at open atmosphere

T11 Plasma Science and Technology

#PST-P2-13

B. Sismanoglu, R.F. Caetano.

ITA - São Jose Dos Campos (Brazil).

In this work Abel inversion technique was used for radial measurements of the microplasma in Ar-2%H2 flow at open atmosphere. The gas discharge parameters were investigated using spatially resolved high resolution optical emission spectroscopy (OES) to allow acquisition of OH ($A\ ^2\Sigma+$, v = 0 → $X^2\ \Pi$, v' = 0) rotational bands at 306.357 nm, Ar I 603.213 nm line and N_2 ($C^3\Pi_u$, v = 0 → $B^3\Pi_g$, v' = 0) second positive system with the band head at 337.13 nm. The non-thermal plasma was generated between microhollow anode (~ 500 µm inner diameter) and a cathode copper foil, fed by direct current source. The 1.5 mm length cylindrical-shape plasma has an outspread bright disk (negative glow region) near the cathode surface. Besides the gas temperature, the excitation temperature was measured radially for a current ranging from 20 to 100 mA, either from Boltzmann-plot of Ar I 4p – 4s and 5p – 4s transitions of excited argon or from Cu I two lines method of excited cuprum atoms released from the cathode surface. For the N_2 second positive system with Δv = -2 it was estimated the vibrational temperature for the bright disk (1500 to 5000 K). Hβ line Stark broadening was employed to define the electron number density of the negative glow (10^{15} cm-3). Microplasma are a novel kind of non-thermal, stable and homogeneous glow discharges, operating at moderate to atmospheric pressure [1]. Both direct current (DC) microplasmas (MP) or atmospheric-pressure microplasmas jet (APMJ) are glow plasmas and the latter operates at atmospheric pressure (AP) air. In APMJ the jet is formed by flowing gas (or a mixture of gases) through an open microhollow or microtube (tungsten-carbide, ~ 500 µm inner diameter). Linear Stark splitting of the seven components of Balmer Hβ line and spatially resolved OES (SR-OES) measurements were applied to measure the cathode layer thickness of about dc ~ 70 µm [2]. In the present paper we extended the optical characterizations using SR-OES for the negative glow located next to the cathode foil, from 100 to 500 µm

from the cathode. Through Abel inversion, the radial distribution of T_g could be found for this thin region. OES were carried out with Abel inversion technique aiming to determine the microplasma parameters at the bright region in front of the cathode. Measurentas shows the emission lines from the plasma volume close to the cathode surface, where intense radiation emerge from the negative glow region. One can see in this figure intense Ar I 4p – 4s and5p – 4s lines. The OH, NO, NH and N_2 spectrum commonly appears as well. The bell-shape radial distribution of the gas temperature at the negative glow for different discharge currents was obtained where the maximum of the temperature is about for r = 125 μm and the minimum occurs at r = 300 μm, at the plasma edge. The vibrational temperature (for the plasma disk) was in the range 1500 - 5000 K for a current varying from 20 to 100 mA.

[1] SISMANOGLU, B. N.; AMORIM, J.; SOUZA-CORRÊA, J. A.; OLIVEIRA, C.; GOMES, M. P., Spectroch. Acta Part B 64, (2009), 1287.
[2] SISMANOGLU, B. N.; GRIGOROV, K. G.; SANTOS, R. A., CAETANO, R.; REZENDE, M. V. O.; HOYER, Y. D.; RIBAS, V. W., Eur. Phys. J. D. 60, (2010), 479.

PST-P3-20
MICROWAVE PLASMA SYSTEM FOR THE SYNTHESIS OF CARBON NANOTUBES

T11 Plasma Science and Technology

#PST-P3-20

L. Szymanski, Z. Kolacinski.

Lodz University of Technology - Lodz (Poland).

There is a lot of nanotubes production methods [1-5]. The paper presents the research results of CNTs synthesis in a microwave plasma system in the atmospheric pressure. Synthesis of carbon nanotubes is followed in a steel chamber on a metal substrate. The substrate is a metal strip, which is ideal for this purpose. The paper presents the calculation results of the reactants composition to produce carbon nanotubes. These allow to determine the optimal composition and plasma parameters. Fig.1. shows the photo of the reactor. Fig. 2 shows the CNT forest and nano carpet on metal strip obtain from plasma reactor.

[1] G. Raniszewski: Temperature measurements in arc discharge synthesis of nanomaterials dedicated for medical applications, Eur. Phys. J. Appl. Phys. , Vol. 61, Issue 02, (2013), pp. 24311-p1 - 24311-p6,
[2] M. Keidar, I. Levchenko, T. Arbel, M. Alexander, A. M. Waas, K. Ostrikov, Increasing the length of single-wall carbon nanotubes in a magnetically enhanced arc discharge, Applied Physics Letters 92, 043129 (2008)
[3] A. Thess, R. Lee, P. Nikolaev, H. Dai, P. Petit, J. Robert, C. Xu, Y.H. Lee, S.G. Kim, A.G. Rinzler, D.T. Colbert, G.E. Scuseria, D. Tomanek, J.E. Fischer, R.E. Smalley, Science, 273 (1996) 483
[4] Laplaze, D.; Bernier, P.; Barbedette, L.; Lambert, J.M.; Flamant, G.; Lebrun, M.; Brunelle, A.; Della-Negra, S. Production of fullerenes from solar energy: The Odeillo experiment. C. R. Acad. Sci., Ser. II: Mec., Phys., Chim., Astron. 1994, 318 (6), 733–738.
[5] Hsu, W.K.; Hare, J.P.; Terrones, M.; Kroto, H.W.; Walton, D.R.M.; Harris, P.J.F. Condensed-phase nanotubes. Nature (London) 1995, 377 (6551), 687.

Fig. 1: Photo of plasma system

Fig. 2: CNTs forest SEM photo (left) and CNTs carpet covering both sides on stainless steel # 0.01 mm

PST-2-In-1
THE AFTERGLOW OF SURFACE-WAVE MICROWAVE DISCHARGES IN SERVICE OF BIOMEDICINE AND NANOTECHNOLOGY: SECRETS REVEALED BY MODELLING STUDIES

T11 Plasma Science and Technology

#PST-2-In-1

K. Kutasi.

Research Institute for Solid State Physics and Optics, Wigner Research Center for Physics - Budapest (Hungary).

Low pressure flowing afterglows reach in N and O atoms, as well as in nitrogen and oxygen content metastable and UV radiating species, meet several important applications, such as plasma based medical sterilization, functionalization of polymers, surface treatments, thin film synthesis, with further potentials in nanostructuring and biomedicine. With microwave surface-waves high density discharges can be generated. When the discharge is ignited in flowing gas the species created in the discharge can be transported in different size afterglow reactors. By modelling of an afterglow system the species density distributions at different discharge conditions and system configurations can be determined, as well as the flow of the plasma can be visualized, which make possible the understanding of different application processes and the optimization of the system for given applications. The effect on the active species density distributions of the gas flow, system wall material and configuration of the reactor concerning the position of the gas inlet and outlet are revealed by the modelling results.

PST-5-In-1
PLASMA ENGINES FOR INTERPLANETARY EXPLORATION

T11 Plasma Science and Technology

#PST-5-In-1

C. Charles.

Space Plasma, Power and Propulsion Laboratory Research School of Physics and Engineering, The Australian National University - Canberra (Australia).

Commercial space companies and space agencies are responding to society's growing interest in access to space, i.e. satellites on low or geostationary Earth orbits and long term exploratory missions to moons, planets or asteroids. Plasma engines will play a major role in interplanetary exploration as they are good candidates for providing extended lifetime, power scaling and broad choice of propellant (including use of spacecraft systems's residues and propellant mining from planetary visits). Here the physics behind the development of new-generation low-cost plasma space engines will be presented using the example of the Helicon Double Layer Thruster space qualification. New technological challenges (i.e. design of new electronic modules and new space compliant materials) need to be addressed for safe and successful access to space. Applying these technological advances to plasma based thin film processes will be discussed.

PST-1-In-2
RECENT RESULTS IN EUV AND SOFT X-RAY SOURCE DEVELOPMENT

T11 Plasma Science and Technology

#PST-1-In-2

P. Dunne, G. O'sullivan.

UNIVERSITY COLLEGE DUBLIN - Dublin (Ireland).

Extreme ultraviolet lithography requires the development of highly efficient sources emitting within a 2% bandwidth at 13.5 nm for efficient matching to Mo/Si multilayer mirrors. Recent results in source development at this wavelength reflecting the different needs of metrology and high volume manufacturing will be discussed. Current and recent work on effects of target composition and geometry, laser pulse profile and power density etc will be presented and comparisons will be made between theoretical and experimental results.
In addition, the results of recent work, both experimental and theoretical, on sources for 6.x nm operation for beyond EUV lithography and for ‘water window’ operation in the will be discussed.

PST/SE/TF-1-In-1
COLD ATMOSPHERIC PLASMAS FOR THIN FILM DEPOSITION AND SURFACE TREATMENT

T11 Plasma Science and Technology

#PST/SE/TF-1-In-1

J. Benedikt.

RUHR - Bochum (Germany).

Cold atmospheric plasmas are known for their ability to generate high densities of reactive, excited or ionized species at gas temperature very close to room temperature. It is the result of their non-equilibrium character, where electrons have energies in the range of few electron-volts. We use atmospheric pressure microplasmas to study gas phase reactions (studied for example by molecular beam mass spectrometry) and the interaction of plasma generated species with the substrate. The latter one is achieved in the experiment with several microplasma sources treating rotating substrate. Additionally, a special modification of the jet allows us to separate the effect of plasma-generated photons from the effect of reactive particles. The overview of these experiments and the latest results will be presented.

PST-1-In-1
DIAGNOSTICS OF ACTIVE SPECIES IN ATMOSPHERIC PLESSURE PLASMAS

T11 Plasma Science and Technology

#PST-1-In-1

C. Leys.

GHENT UNIVERSITY - Ghent (Belgium).

Atmospheric pressure plasma jets (APPJs) are being used in a wide range of applications, including (bio)medical. However, the understanding of the underpinning plasma-chemical processes is incomplete. Spatially resolved and quantitative measurements of active species are required to shed some light.
The talk will focus on the application of laser-based diagnostics to atmospheric pressure plasma. The spatial distribution of active species generated in an RF plasma jet in Ar/H_2O and Ar/O_2 mixtures is determined by LIF and TALIF (O_2). Argon metastables produced in the jet afterglow are measured with a diode laser absorption technique. Some problems connected to active and passive laser diagnostics in APPJs will be discussed.

PST-3-In-1
PLASMA PROCESSING OF “SOFT” MATERIALS: REACTIONS BETWEEN ATMOSPHERIC-PRESSURE PLASMAS AND IONIC SUBSTRATES FOR NOVEL MATERIALS APPLICATIONS

T11 Plasma Science and Technology

#PST-3-In-1

M.R. Sankaran.

Department of Chemical Engineering, Case Western Reserve University - Cleveland (United states).

Plasma processing is a well-established technique that typically describes the dry etching and deposition of metallic and semiconducting thin films at low pressures. Plasmas can also be used to modify “soft” materials such as liquids and polymeric films. In this case, the development of atmospheric-pressure plasma tools has facilitated integration with substrates that are often not stable at vacuum conditions. Atmospheric-pressure processing is also compatible with roll-to-roll processing, making it possible to process large areas of polymer films at low cost.

In this talk, I will present our recent investigations of plasmas formed with liquid and polymeric substrates. In particular, I will focus on a specific class of reactions, the reduction of ionic metal precursors by plasma electrons, which can lead to the nucleation of metal nanoparticles either in solution as a colloid, or in films as a nanocomposite. Potential applications of these reactions include the synthesis of metal nanoparticle inks for sensing applications and the direct fabrication of flexible, conductive films for advanced electronics. I will discuss details of our process, hypothesized mechanisms behind the reactions and particle growth, and progress towards applications.

PST-P2-14
LASER MEASUREMENTS OF OH DENSITY AND TEMPERATURE IN AN NRP DISCHARGES IN WATER VAPOR

T11 Plasma Science and Technology

#PST-P2-14

F.P. Sainct [1], D.A. Lacoste [1], D.A. Lacoste [2], C.O. Laux [1], C.O. Laux [2], M.J. Kirkpatrick [3], E. Odic [3].

[1]CNRS, UPR 288, Laboratoire EM2C - Chatenay-Malabry (France), [2]Ecole Centrale Paris - Chatenay-Malabry (France), [3]Department of Power and Energy Systems, E3S, SUPELEC - Gif-Sur-Yvette (France).

Motivation

Previous studies of plasma discharges in liquid water or gaseous mixtures with water [1,2] have demonstrated that non-equilibrium plasma could produce significant active species such as H_2 or H_2O_2. Nevertheless, the fundamental mechanisms of breakdown, as well as the chemistry of water plasmas at atmospheric pressure are not well understood. Our previous studies [3] have shown that H2 production was promising. In this work, we focus on intermediate products of the discharge, in particular the hydroxyl radical.

Results and Discussion

The plasma was generated in water vapor at 450 K and atmospheric pressure by 20-ns duration high-voltage (0-20 kV) pulses, at a repetition frequency of 10 kHz [4]. Between two discharges, the time-resolved density of OH was measured by Planar Laser Induced Fluorescence (Fig. 1a). The temperature during the discharge was determined by optical emission spectroscopy from 0-12 ns, and between two pulses by 2-color OH-PLIF (Fig. 1b).

A 150 K preheating effect from the previous pulses is measured, with a maximum temperature elevation of 950 K during the first 8 µs following each pulse.
The experimental OH density measurements were compared with chemical kinetics simulations. The decay of the OH density depends on the initial OH density. According to Fig. 1c, the numerical simulations obtained show good agreement with

the experimental data with an initial OH density of 500 ppm is assumed, thus providing a quantification of the OH density produced by the pulses.

[1] Fridman A 2008 Plasma Chemistry
[2] Bruggeman P J, Verreycken T, Gonzalez M A, Walsh J L, Kong M G, Leys C and Schram D C 2010 Journal of Physics D: Applied Physics 43 124005
[3] Sainct F P, Lacoste D A and Laux C O AIAA-ASM 2013-1190, Grapevine TX (Dallas Fort Worth Region)
[4] Pai D Z, Lacoste D A and Laux C O 2010 Plasma Sources Science and Technology 19 65015

Fig. 1 (a) – OH PLIF measurement at V = 13 kV. (b) – Time resolved evolution of the temperature. (c) – Estimation of initial OH density from its decay rate.

PST-4-In-1
Strategies for low-damage plasma etching of advanced k=2.0 porous organo-Silicon glass materials

T11 Plasma Science and Technology

#PST-4-In-1

J. De Marneffe.

IMEC - Leuven (Belgium).

VLSI manufacturing beyond the 14nm technology node requires the introduction of interconnect dielectric materials with dielectric constant k of the order of 2.0 or below(Grill, 2009). Up till now, two classes of materials have been investigated, namely organic dielectrics (polymers) and organo-silicate glasses. In all cases, reaching such a low k value requires to introduce porosity (up to 50% with pore radius up to 3nm), which makes the material extremely sensitive to damage during plasma patterning, leading to unwanted change of their dielectric properties. Plasma damage occurs through the diffusion of reactive radicals into the porous structure and/or VUV photo-induced scissioning of Si-CH3 groups, both leading to the formation of silanols and moisture absorption(Baklanov et al., 2013). Conventional approaches to solve this issue can be arranged in three categories: first, the optimization of the low-k dielectric material in order to reduce its sensitivity to plasma damage; second the optimization of the plasma etch process in order to make it less damaging; third the development of repair strategies. A novel solution is the sacrificial pore protection approach, where pores are temporarily filled by a protective agent, avoiding diffusion of radicals. This can take place at room temperature (ex-situ pore protection) and require careful selection of the filling agent and filling conditions(Frot, Volksen, Purushothaman, Bruce, & Dubois, 2011). Another approach (in-situ pore protection) is to perform the plasma etch at cryogenic temperatures (-120 < T < -70°C), where reaction by-products condensate into the pores(Zhang et al., 2012). An overview will be given on the current state of these various concepts, putting the emphasis on innovative solutions to keep sustaining the pace of the ITRS roadmap.

Baklanov, M. R., de Marneffe, J.-F., Shamiryan, D., Urbanowicz, A. M., Shi, H., Rakhimova, T. V, Huang, H., et al. (2013). Plasma processing of low-k dielectrics. Journal of Applied Physics, 113(4), 41101. doi:10.1063/1.4765297
Frot, T., Volksen, W., Purushothaman, S., Bruce, R., & Dubois, G. (2011). Application of the protection/deprotection strategy to the science of porous materials. Advanced materials (Deerfield Beach, Fla.), 23(25), 2828–32. doi:10.1002/adma.201100569
Grill, A. (2009). Porous pSiOCH ultralow-k dielectrics for chip interconnects prepared by PECVD. Annual Review of Materials Research, 39, 49.
Zhang, L., Ljazouli, R., Lefaucheux, P., Tillocher, T., Dussart, R., Mankelevich, Y. a., de Marneffe, J.-F., et al. (2012). Damage Free Cryogenic Etching of a Porous Organosilica Ultralow-k Film. ECS Solid State Letters, 2(2), N5–N7. doi:10.1149/2.007302ssl

SE/TF-2-Or-12
The effect of two step aging on the compressive residual stress and hardness distribution of the shot peened 7075 aluminium alloy with SiCNH coating

T12 Surface Engineering

#SE/TF-2-Or-12

Ł. Kaczmarek [1], K. Kyzioł [2], J. Sawicki [1], M. Stegliński [1], B. Januszewicz [1], H. Radziszewska [1], P. Zawadzki [1], R. Wójcik [1], K. Kubacki [1].

[1]Lodz University of Technology - Lodz (Poland), [2]AGH University of Science and Technology - Cracow (Poland).

This paper describes two stages of optimization of the properties of 7075 aluminium alloys, in particular their resistance to pitting by two-stage artificial aging process (T6I6 or T6I4 treatment) connected with shot peening, of the substrate and SiCNH coating deposition.
After analysis of the measurement of stress gradient one can observe that the relatively high compressive stresses (ca. -170MPa) were present at the depth of approximately 0.15mm. This fact is a consequence of the heat treatment and cold working on surface. The relation between internal stresses and the distance from surface is consistent with the results of studies described in the reference literature [1-3]. On the other hand, the differences in obtained values of internal stresses in analysed samples are influenced by the time of conducting the shot peening process with respect to the two-stage heat treatment. In this case the maximum value of internal stresses on surface layer of analysed samples after T6I6 heat treatment (I stage 393K - II stage 433K) and subsequent shot peening process reached - 280 Mpa ± 5.5MPa. Additionally, the hardness peak reached almost 210 HV. It shows

that there exists a possibility of carrying the aging process of samples formerly subjected to shot peening, by these means virtually eliminating the internal stress relaxation with simultaneous obtainment of the surface hardness of value ≈ 200HV. The obtained results of analysis, related to the attainment of maximum strengthening of surface layer with the highest possible compressive stresses, served as the basis for carriage of precipitation processes in the surface layer, together with simulateous deposition (by radio-frequency chemical vapor deposition method) of low friction (0,05) and low wear gradient layers of SiCNH on 7075 aluminium alloy [4].

In order to check the behavior of obtained materials with coatings in real working conditions a computer simulation with the use of ANSYS software was performed. Numerical simulations were conducted for an existing gear with small module, applied in military spy robot. Analyzing the superposition of stresses it can be observed that the value of compressive stresses in contact point was increased by about 150MPa. Such stress distribution prevents even more the contact fatigue of gear, in such way ensuring the high durability of the discussed system.

This work was supported by the Polish State Committee for Scientific Research under project no. NN 507 269540

[1] M. Benedetti, V. Fontanari, P. Scardi, C. Ricardo and M. Bandini. Reverse bending fatigue of shot peened 7075-T651 aluminium alloy: The role, International Journal of Fatigue 8-9, 1225-1236, 2009.
[2] Y. Gao, Improvement of fatigue property in 7050–T7451 aluminum alloy by laser, Materials Science and Engineering A, 528, 3823-3828, 2011.
[3] M. Mhaede, Y. Sano, I Altenberger, M. Wollmann, L. Wagner:F atigue Performance of Al 7075-T73 and Ti-6Al-V: Comparing Results after Shot Peening, Laser Shock Peening and Ball-Burnishing International Journal of Structural Integrity, volume 2, 2, 2011, 185-199.

[4] Kaczmarek Ł, Stegliński M., Sawicki J, Kula P, Kyzioł K, Batory D, Kottfer D, Klimek L. Method for improving the mechanical properties of aluminium alloys. Patent Application nr P – 398270.

SE/PST/TF/BI-1-Or-8
Strategies to Design Nonleaching Antimicrobial Materials

T12 Surface Engineering

#SE/PST/TF/BI-1-Or-8

E. Taffin De Givenchy, T. Darmanin, S. Amigoni, F. Guittard.

Université de Nice-Sophia Antipolis - Nice (France).

The battle against nosocomial infections such as, among others, surgical infections, remains one of the major actual challenges of the hospital. Today, Health Personnel are extremely cautious to avoid inert surfaces (catheters, implants, therapeutic equipment, floors…) contamination by micro-organisms. However, despite the use of disinfectants, antibiotics, and the setting of strict hygienic conditions, it seems that nosocomial infections control remains one of the major challenges for medicine. If cautions are numerous to avoid any pollution of inert surfaces (catheters, implants, medical equipments, floors, etc.), the phenomena of resistance developed by the most part of pathogenic organisms requires, on one hand, the elaboration of new biocides agents and, on the other hand, completion of long-term bactericidal treatments of surfaces or, in an ideal case, a permanent biocide effect of the surfaces without releasing of the antimicrobial active agents.

In the perspective to elaborate non leaching biocidal materials, our team has undertaken research works in several ways:

• design and evaluation of new low molecular weight fluorinated biocidal agents [1].
• elaboration of biocidal self assembled monolayers on metallic surfaces [2].
• development of biocidal polymers as coatings on various substrates [3].
• and more recently, a novel approach using the repellent properties of super-hydrophobic surfaces has been envisaged [4].

These strategies will be discussed.

[1] M. Massi, F. Guittard, R. Levy, Y. Dussini, S. Geribaldi, S. Eur. J. Med. Chem. 2003, 38, 519-523. M. Massi, F. Guittard, R. Levy, Y. Dussini, S. Geribaldi, S. Int. J. Antimicrob. Agents 2003, 21, 20-26.
[2] P. Thebault, E. Taffin de Givenchy, R. Levy, Y. Vandenberghe, F. Guittard, S. Geribaldi, Eur. J. Med. Chem. 2009, 44, 4227-4234.
[3] L. Caillier, E. Taffin de Givenchy, R. Levy, Y. Vandenberghe, S. Geribaldi, F. Guittard, Eur. J. Med. Chem. 2009, 44, 3201–3208 and ref therein
[4] T. Darmanın, E. Taffın De Gıvenchy, F. Guıttard, Macromolecules, 2010, 43, 9365–9370; T. Darmanin, F. Guittard, J. Am. Chem. Soc., 2011, 133, 15627-15634.

SE/PST/TF/BI-1-Or-9
Highly Functional and Permanent Plasma Polymer Layers Enabling Biomedical Applications

T12 Surface Engineering

#SE/PST/TF/BI-1-Or-9

D. Hegemann, A.G. Guex, A.M. Bühlmann.

Empa - St. Gallen (Switzerland).

Biomedical applications often require stable surface modifications of the used substrates to allow their use in aqueous environments. Electrospun scaffolds for tissue engineering and porous membranes for drug delivery were thus functionalized using plasma polymerization. Nano-scaled plasma polymer layers comprising oxygen or nitrogen functional groups enable the permanent functionalization of the submicron-scaled polymeric substrates without affecting their bulk properties. Hence, the surface chemistry can be modified while maintaining their 3D architecture. For this purpose, however, it is required that both gas phase and surface processes are well controlled during plasma polymerization [1]. While gas phase processes are governed by the energy invested per particle, surface processes also depend on the energy flux during film growth. To enable the modification of structured surfaces with good penetration, however, film growth conditions mainly based on plasma chemical processes have to be explored.

Amino-functionalized plasma polymer layers were investigated for the functionalization of track-etched polyester (PETE) membranes [2]. By varying the NH_3/C_2H_4 gas ratio and the energy input, the amount of incorporated amino groups ($NH_2/C \approx 0.05$) was optimized. These groups were then utilized to chemically attach thermoresponsive poly(oligo(ethylene glycol) methacrylate) (pOEGMA) copolymers forming brushes. The controlled permeation of caffeine through the membrane was demonstrated. Permeation is enabled at 40 °C, while it is blocked at 20 °C.

CO_2/C_2H_4 gas discharges were examined on electrospun poly(ε-caprolactone) (PCL) scaffolds as used for tissue engineering [3]. Gas ratio and energy input into the plasma were found to influence the incorporation of oxygen-containing groups into the plasma polymer layer. Ultrathin layers are required in order not to affect the stiffness and Young's modulus of the substrate. Functionalized scaffolds showed improved proliferation of C2C12 heart muscle cells and the differentiation of myotubes.

All experiments were performed within a capacitively coupled, low pressure plasma set-up in order to make use of large mean free path lengths. A comparison to atmospheric pressure plasmas was performed, as well, showing similarities, but also differences in surface morphology. Highly functional and permanent plasma polymer layers can thus support different biomedical applications by tailored surface engineering.

[1] D. Hegemann, E. Körner, N. Blanchard, M. Drabik, S. Guimond, Appl. Phys. Lett. 101 (2012) 211603.
[2] F. Teixeira Jr., A.M. Popa, S. Guimond, D. Hegemann, R.M. Rossi, J. Appl. Polym. Sci. (2012), DOI: 10.1002/APP.38730.
[3] A.G. Guex, F.M. Kocher, G. Fortunato, E. Körner, D. Hegemann, T.P. Carrel, H.T. Tevaearai, M.N. Giraud, Acta Biomater. 8 (2012) 1481.

SE/TF-P2-01
Influence of 5 eV Collision of O-Atoms on Material Erosions in Low Earth Orbit Space Environment

T12 Surface Engineering

#SE/TF-P2-01

M. Tagawa, K. Yokota.

Kobe University - Kobe (Japan).

Materials used in the exterior surfaces of spacecraft orbiting in the low earth orbit (LEO) experienced severe erosion by the hyperthermal collision with O-atom which is the major atmospheric species in LEO [1]. Due to the high-orbital velocity of spacecraft (8 km/s), the impact energy of O-atom to the spacecraft surface reaches as high as 4.7 electronvolts, which is higher than the interatomic bonding energy of many materials. Thus, the chemical reactions occurred at the spacecraft surfaces are under the effect of high-impact energy. Many flight projects have been conducted to clarify the erosion properties of materials in LEO, for example, Materials International Space Station Experiment (MISSE) [2]. On the other hand, much effort has been paid for simulating the materials degradation in a ground-based facility. A microwave or radio frequency oxygen plasma source has been used for material screening test, however, this type of simulation facility does not simulate the collision energy of atomic oxygen in LEO. In order to simulate the impact energy of O-atom (5 eV), a laser-detonation method has been applied [3]. However, the effect of this impinging energy has not been fully understood.

In this presentation, role of the impact energy on the material degradation is focused. One example of the role of impact energy of O-atom was demonstrated in the temperature dependence of polyimide [4]. It has made clear that the temperature dependence of erosion rate of polyimide showed a discrepancy between ground and space, i.e., no temperature difference was observed in space, in contrast, clear difference was obvious on the ground experiment with thermal O-atom. We have examined the temperature dependence of polyimide erosion by the combination of polyimide-coated quartz crystal microbalance (QCM) and laser detonation hyperthermal O-atom beam source. As a result, a clear difference on the temperature dependence of polyimide erosion was measured depending on the impact energy.

The activation energies of the polyimide erosion were 5.7×10^{-4} eV for the 5.0 eV O-atom beam, whereas 4.5×10^{-2} eV for the 1.1 eV O-atom beam at the temperature range between 253 and 353 K. The effect of impact energy is effective not only in the direct reaction, but also in the trapping desorption. Minton et al. reported that the CO and CO2 signal from the O-atom reaction increased significantly with increasing the impact energy [5]. The similar result was obvious when Ar beam irradiated the oxidized polyimide surface. This experimental result clearly suggests the role of impact energy of incoming atoms on the desorption process of the reaction products in LEO. This is also confirmed from our recent experiment using velocity selector of the neutral beams. The detail of this experiment will be reported in the presentation.

A part of this study was supported by a Grant-in-Aid for Scientific Research from JSPS.

[1] Materials Degradation in Low Earth orbit (LEO), V. Srinivasan and B. A. Banks Eds., TMS (1990).
[2] K. K. de Groh, B. A. Banks e al., High Performance Polymers, 20 (2008) 388.
[3] M. Tagawa, T. K. Minton, MRS Bulletin, 35 (2010) 35.
[4] K. Yokota, M. Tagawa, J. Spacecraft and Rockets, 40 (2003) 143.
[5] T. Minton, J. W. Seale, D. J. Garton, J. Zhang, Proc. 44th Int. SAMPE Symp. (1999) 1051.

SE-2-Or-4
Nanocomposite coatings for improving the corrosion

T12 Surface Engineering

#SE-2-Or-4

L. Benea.

Dunarea de Jos University of Galati - Galati (Romania).

Metal matrix nanocomposites containing dispersed second-phase particulates usually have various special properties such as dispersion hardening, self-lubricity, high temperature inertness, good wear and corrosion resistance, or tribocorosion resistance and chemical compatibility. This accounts for the increased application of metal-based nanocomposites in industry applications and open a way to biocompatible coatings. In order to meet the requirement for developing novel metal-based nanocomposites, many preparation techniques have been investigated. As a technique conducted at a normal pressure and ambient temperature and of low cost and high deposition rate, electrodeposition is considered to be one of the most important techniques for producing nanocomposites and nanostructured surfaces. Electrodeposition is exceptionally versatile, so that new and exciting applications are still being invented. The paper presents some results regarding the co-deposition of nano bio ceramic dispersed phases as ZrO2, CeO2, SiC, or polymeric dispersed phases as UHMWPE (ultra high molecular weight polyethylene) during cobalt or nickel electroplating process in view of obtaining bio composite layers or resistant industrial coating applications. In Figure 1 it is presented a schematic representation of co-electrodeposition process of insoluble CeO_2 bioceramic dispersed phases with metallic matrix of cobalt.

Fig. 1. Schematic electro-co-deposition process of nano-CeO2 dispersed phase to obtain Co/CeO_2 (25 nm) nanocomposite coatings: (a) SEM surface of Co/CeO2 nanocomposite film; (b) Schematic electrochemical process; (c) SEM image of CeO_2 particles.

It is important to adjust the electroplating variables in order to control the properties of the produced nano or micro structured composite coatings that depend on the amount of incorporated particles and their distribution in the metal matrix, as well as, on the micro and nano structural characteristics of the metal matrix. The paper presents challenges and results on ceramic, bioceramic and polymeric dispersed

particles (SiC, ZrO2, CeO2, UHMWPE) into cobalt and nickel matrix as well as the properties investigations and performances of composite coatings obtained. The nanoparticles incorporation into the metal matrix usually causes a noticeable grain refinement and thus an increase to the corrosion and tribocorrosion resistance in aqueous or simulating body fluids (SBF) environments.

[1] Lidia BENEA. Electrochemical Impedance Spectroscopy and Corrosion Behavior of Co/CeO2 Nanocomposite Coatings in Simulating Body Fluid Solution. Metallurgical and Materials Transactions A. Vol 43A, pp 1-9, 2012 (November). ISSN 1073-5623.
DOI: 10.1007/s11661-012-1422-z
[2] Lidia BENEA, Alina CIUBOTARIU, Wolfgang SAND. Biofilm formation and corrosion resistance of Ni/SiC nanocomposite layers. International Journal of Materials Research. 103 (2012) E, November, page 1-9. ISSN: 1862-5282. DOI 10.319/146.110893.
[3] Benea, L; Wenger, F; Ponthiaux, P, Celis J P. Tribocorrosion behaviour of Ni-SiC nano-structured composite coatings obtained by electrodeposition. WEAR , 266 (3-4), 2009, 398-405.
[4]Benea, L; Ponthiaux, P; Wenger, F. Co-ZrO2 electrodeposited composite coatings exhibiting improved micro hardness and corrosion behavior in simulating body fluid solution. Surface and Coatings Technology, 205, (23-24), 2011, 5379-5386.

SE-2-In-1
Self-organized Nanostructuring in Hard Nitride Thin Films

T12 Surface Engineering

#SE-2-In-1

L. Hultman.

Thin Film Physics Division, Department of Physics (IFM) - Linköping (Sweden).

INVITED PRESENTATION

Self-organized Nanostructuring in Hard Nitride Thin Films

Lars Hultman
Thin Film Physics Division, Department of Physics IFM), Linköping University, Linköping, Sweden

Designed nanostructuring is presented for enhancing hardness [1] and fracture toughness [2] in wear-resistant transition metal nitride alloy thin films deposited by cathodic arc, reactive magnetron sputtering, and novel hybrid HIPIMS/DC magnetron sputtering [3]. Model systems for metastable alloy nitrides TiAlN, ZrAlN, HfAlN, TiSiN, MoVN, VWN are analyzed by XRD, HREM, FIB, APT, [4] and phase field modeling [5]. *Ab initio* calculations are employed to assess phase stability and decomposition behavior from lattice mismatch and electronic band structure effects. [6]

Superhardening occurs in TiN/Si3N4 nanocomposites due to Si segregation forming a few-monolayer (ML)-thick SiNx tissue phase [7,8], which can be a vacancy-stabilized cubic-SiNx layer [9]. A hardness maximum at 34 GPa – short of ultrahard - is observed in TiN/SiNx(001) superlattices at the epitaxial break-down limit for the SiNx(001) layers. A method based on focused ion beam milling is described for studying the tool–chip interfaces of the rake face of a TiSiN-coated PCBN insert after turning operation. [10]

The concept of age hardening in transition metal nitride alloys [11] is reviewed for appropriate isotructural model systems. Spinodal decomposition is thus established for TiAlN by the formation of cubic-phase nm-size domains in a checker-board-pattern of TiN and AlN [1] at temperatures corresponding to cutting tool operation. The effects of pressure [12], volume mismatch [13] temperature, composition, disorder [14], and stoichiometry [15] will also be discussed.

1. P. H. Mayrhofer, C. Mitterer, L. Hultman, H. Clemens, Progress in Mater. Sci., 51 (2006) 1033
2. D. Sangiovanni, L. Hultman, V. Chirita, Thin Solid Films 520 (2012) 4080
3. G. Greczynski, J. Lu, M.P. Johansson, J. Jensen, I. Petrov, J.E. Greene, L. Hultman, Vacuum 86 (2012) 1036
4. L. Johnson, M. Thuvander, K. Stiller, M. Odén, L. Hultman, Thin Solid Films 520 (2012) 4362
5. A. Knutsson, J. Ullbrand, L. Rogström, N. Norrby, L.J.S. Johnson, L. Hultman, J. Almer, M. P. Johansson, B. Jansson, M. Odén, in Axel Knutsson, PhD Thesis, Linköping University 2012
6. I. A. Abrikosov, A. Knutsson, B. Alling, F. Tasnadi, H. Lind, L. Hultman, M. Oden, Materials 4 (2011) 1599
7. L. Hultman, J. Bareño, A. Flink, H. Söderberg, K. Larsson, V. Petrova, M. Odén, J. E. Greene, I. Petrov, Phys. Rev. B75 (2007) 155437
8. A. Flink, M. Beckers, J. Sjölén, T. Larsson, S. Braun, L.Karlsson, L. Hultman, J. Mater. Research 24 (2009) 248

9. T. Marten, B, Alling, E. I. Isaev, H. Lind, F. Tasnádi, L. Hultman, I. A. Abrikosov, Phys. Rev. B 85 (2012) 104106

10. A. Flink, R. M'Saoubi, F. Giuliani, J. Sjölén, T. Larsson, P.O.Å. Persson, M.P. Johansson, L. Hultman, Wear 266 (2009) 1237
11. P. H. Mayrhofer, A. Hörling, L. Karlsson, J. Sjölén, C. Mitterer, L. Hultman, Appl. Phys. Lett. 83(10) (2003) 2049
12. B. Alling, M. Odén, L. Hultman, I. A. Abrikosov, Appl. Phys. Lett. 95 (2009) 181906
13. C. Höglund, B. Alling, J. Birch, M. Beckers, P.O.Å.Persson, C. Baehtz, Zs.Czigany, J. Jensen, L. Hultman, Phys. Rev. B 81 (2010) 224101
14. B. Alling, A. V. Ruban, A. Karimi, L. Hultman, I. A. Abrikosov, Phys. Rev. B 83 (2011) 104203
15. B. Alling, et al., Appl. Phys. Lett. 92 (2008) 071903

SE/TF-4-Or-1
High Temperature Friction of CrNV(x) Coatings. Interaction Between Stick-Slip Phenomena and Real Contact Conditions

T12 Surface Engineering

#SE/TF-4-Or-1

L. Rapoport [1], V. Perfilyev [1], A. Moshkovich [1], I. Lapsker [1], T. Hollstein [2], A. Kailer [2].

[1]Holon Institute of Technology - Holon (Israel), [2]Fraunhofer Institute of the Mechanics of Materials - Fraunhofer (Germany).

The CrNV(x) coatings with content of Vanadium (V) in the range of 0.1-32% were obtained using reactive d.c. magnetron sputtering. Two types of the friction tests in wide range of the temperatures (25-700 0C) have been performed: stick-slip and reciprocal ball-on disk experiments. The aim of this work is to study the effect of content of V and the temperature on friction and wear behavior of rubbed surfaces. The interaction between stick-slip phenomena and the friction properties in real (severe) contact conditions will be considered. Amplitude of the friction coefficient and the creep parameter were chosen as the base parameters in the analysis of stick-slip behavior. Spring stiffness, sliding velocity and load were optimized during the preliminary tests. Tribological experiments were also performed using a reciprocating ball-on-flat test machine (SRV-IV, Optimol Instruments). During preliminary tests a frequency of 25 Hz was chosen as the typical frequency. Surfaces at virgin state and after friction were analyzed by XPS, SEM and AFM techniques. The effect of the V content on the fracture toughness was determined. It has been shown that an addition of the V led to decreasing of the grain size and increasing the fracture toughness. With increasing the content of V, the hardness was increased and the trbological properties of coating were improved. The effect of temperature on the friction coefficient and a variation of the structure of surface layers were evaluated. The oxidation of surface layers of coatings with high value of V (25- 32%) led to formation of oxide films of V2O5. These oxide film characterized by Magneli structure provides easy shearing similar to that obtained for self-lubricating materials. The coefficient of correlation between in real contact conditions was estimated. Good

correlation between stick-slip parameters and the values of the friction coefficient was revealed. The presented results demonstrate a possibility to use short stick-slip experiments as express method in the analysis of the effect of content of additive and the temperature of contact on the tribological properties of rubbed surfaces.

SE/TF-P2-02
Synthesis and evaluation of smart self-healing plasma electrolytic oxidation coatings on Mg

T12 Surface Engineering

#SE/TF-P2-02

M. Sun, A. Matthews, A. Yerokhin.

The University of Sheffield - Sheffield (United kingdom).

Owing to low density and high specific strength, magnesium and its alloys have been regarded as ideal materials in a broad range of engineering applications such as aerospace, automotive and electronics [1]. However, these materials are prone to corrosion which dramatically restricts their applications [2-3]. Various surface treatments are therefore being investigated to improve the corrosion resistance of magnesium alloys [4-6]. In this work self-healing capacities of plasma electrolytic oxidation (PEO) coating are investigated, with an outlook of improving the sustainability of Mg alloys. Both hybrid and sequential processing routes are explored to load the formed PEO coatings with inhibitors that would provide a self-healing ability to the surface layer during exploitation. The coating morphology, elemental and phase composition are characterised by SEM, EDX and XRD analyses respectively. Mechanical and tribological and properties are evaluated by nanoindentation and reciprocating sliding wear tests. Both immersion and electrochemical corrosion tests are carried out to evaluate the coating corrosion behavior and self-healing capacity. Electrochemical impedance spectroscopy employed to study the evolution of the coating-electrolyte interface during corrosion process. Mechanisms of corrosion protection and potential of self-healing corrosion resistant PEO coatings on Mg in various applications are discussed.

[1] T. Ishizaki, I. Shigematsu, N. Saito, Surf. Coat. Technol. 203 (2009) 2288.
[2] A.L. Yerokhin, X. Nie, A. Leyand, A. Mattews, S.J. Dowey, Surf. Coat. Technol. 122 (1999) 73.
[3] P. Zhang, X. Nie, D.O. Northwood, Surf. Coat. Technol. 203 (2009) 3271.
[4] Abdel Salam Hamdy, M. Farahat, Surf. Coat. Technol. 204 (2010) 2834.

[5] A. Araghi, M.H. Paydar, Mater. Des. 31 (2010) 3095.
[6] T. Ishizaki, Y. Masuda, M. Sakamoto, Langmuir.27 (2011) 4780.

SE-1-Or-2
Oxide Films Deposited by Reactive Bipolar High Power Impulse Magnetron Sputtering (HIPIMS)

T12 Surface Engineering

#SE-1-Or-2

S. Kadlec [1], J. Čapek [2], J. Kousal [3], J. Vyskočil [1].

[1]HVM Plasma - Praha (Czech republic), [2]University of West Bohemia - Plzeň (Czech republic), [3]Faculty of Mathematics and Physics, Charles University - Praha (Czech republic).

Reactive bipolar pulsed sputtering from a pair of targets can be used for deposition of dielectric films. However, the power balance of both magnetrons can affect film composition and thickness homogeneity, and also lifetimes of used targets.

Recent study of reactive bipolar pulsed sputtering of Al in O_2 [1] has demonstrated that the balance of power delivered to both magnetrons depends on pulse current levels (corresponding to magnetic field strength) and on ON-times of both magnetrons at constant pulse voltage values, and on the oxygen partial pressure. Moreover, operation in the transition mode has resulted in some negative feedback on the power dissipation compensating the tendency for the power unbalancing. However, the behavior of other target materials, such as Ti, can be different as we demonstrate and discuss in this work. Consequently, the stabilization of the working point for both magnetrons can be important.

Oxide films have been deposited by reactive bipolar pulsed sputtering from two metallic targets in Ar + O_2 gas mixture using a MAGPULS unit. A pair of 2-inch round magnetrons were arranged obliquely in load-lock sputtering system, equipped with two Ti targets for TiO_2 deposition and two Al targets for Al_2O_3. The sputtered flux of material from each magnetron was directed mostly to one of two substrates. Power input for each magnetron was evaluated using oscilloscopic data of pulse voltage and current.

The bipolar HIPIMS regime used frequency range 1 to 10 kHz, relatively short on-times and high off-times. The peak magnetron current was up to 10 A, that is about

350 W/cm^2 over the entire target area at typical average power of 250W. The deposition of Al_2O_3 and TiO_2 is compared, when the on-time ratio of both magnetrons has been varied between 75% and 125%. Different magnetic field strengths of magnetrons were also simulated by spacers modifying the magnet-to-target distance. The effects on the power balance of both magnetrons are compared with the deposition rates and properties of films, measured mainly by spectroscopic ellipsometry. Aluminium oxide films have also been deposited by bipolar pulsed reactive sputtering in a larger scale machine for solar applications equipped with two rectangular magnetrons.

[1] S.Kadlec and J. Vyskočil, “Balance of power delivered to magnetrons in bipolar pulsed sputtering of aluminum oxide in high frequency mode and HIPIMS”, International Conference on Reactive Sputtering Deposition (RSD2011) Dec. 8-9,2011 Linköping, Sweden; online: Vacuum Coating Info: http://www.vacuumcoating.info/?p=40010

SE-1-Or-3
Selection of metal ion irradiation for controlling Ti1-xAlxN alloy growth by hybrid HIPIMS/DCMS co-sputtering using synchronized pulsed substrate bias

T12 Surface Engineering

#SE-1-Or-3

I. Petrov [1], G. Greczynski [2], J. Lu [2], J. Jensen [2], J. Greene [1], S. Bolz [3], W. Kölker [3], C. Schiffers [3], O. Lemmer [3], L. Hultman [2].

[1]University of Illinois - Urbana (United states), [2]Linköping University - Linköping (Sweden), [3]CemeCon AG - Wűrselen (Germany).

Metastable NaCl-structure $Ti_{1-x}Al_xN$ is employed as a model system to probe the effects of metal, Al vs Ti, ion irradiation during film growth using a hybrid approach combining high-power pulsed magnetron sputtering (HIPIMS) with dc magnetron sputtering of opposing metal targets and HIPIMS-synchronized pulsed substrate bias Vs. With V_s = 60 V and HIPIMS applied to the Al target, Al^{n+} ion irradiation (dominated by Al^+) of the growing film results in alloys ($0.55 \leq x \leq 0.60$) which exhibit high hardness, H ~ 30 GPa, and low stress, 0.2-0.7 GPa tensile.[1,2] In contrast, films with corresponding AlN concentrations grown with HIPIMS applied to the Ti target, giving rise to Ti^{n+} ion irradiation (with a significant Ti^{2+} component) are two phase (cubic (Ti,Al)N and hexagonal AlN) with low hardness, H = 18-19 GPa, and high compressive stress ranging up to 2.7 GPa.

In another set of experiments we grow $Ti_{1-x}Al_xN$ alloys with x ~ 0.6 and vary the negative bias Vs in the range from 20 to 280 V. The bias is applied to the substrate in synchronous[3] with the metal-ion-rich part of the HIPIMS pulse in order to probe the effects of metal ion momentum. Al-HIPIMS/Ti-DCMS layers deposited under Al^+ (m_{Al} = 26.98 amu) bombardment are single-phase NaCl-structure alloys for $20 \leq V_s < 200$ V, while layers deposited in the Ti-HIPIMS/Al-DCMS configuration with $Ti^+/Ti^{2}+$ (m_{Ti} = 47.88 amu) ion irradiation are two-phase, cubic plus wurtzite, even with V_s = 20 V. We find that precipitation of the wurtzite AlN second phase is primarily determined by the average metal-ion momentum transfer to the growing film rather

than by the deposited metal-ion energy. Moreover, in contrast to rare-gas ion irradiation during film growth, the Al ions are incorporated as a film constituent and do not result in excessive compressive stress. The relatively low mass of the Al ion permits manipulating properties of metastable cubic $Ti_{0.38}Al_{0.62}N$ by tuning V_s to vary, for example, the hardness H from 12 to 31 GPa while minimizing ion-induced compressive stress.

[1] G. Greczynski, J. Lu, M. Johansson, J. Jensen, I. Petrov, J.E. Greene, and L. Hultman, Surf. Coat. Technol. **206** (2012) 4202
[2] G. Greczynski, J. Lu, M. Johansson, J. Jensen, I. Petrov, J.E. Greene, and L. Hultman, Vacuum **86** (2012) 1036.
[3] G. Greczynski, J. Lu, J. Jensen, I. Petrov, J.E. Greene, S. Bolz, W. Kölker, Ch. Schiffers, O. Lemmer and L. Hultman, J. Vac. Sci. .Technol. A **30**, 061504 (2012)

SE/PST/TF/BI-1-Or-10
Synthesis and characterization of silver loaded DLC nanocoatings and their application as tunable, highly stable antibacterial surfaces.

T12 Surface Engineering

#SE/PST/TF/BI-1-Or-10

M. Cloutier [1], S. Turgeon [1], R. Tolouei [1], C. Côté [2], A. Sarkissian [2], M. Tatoulian [3], D. Mantovani [1].

[1]Laboratory of Biomaterials and Bioengineering, Department of Min-Met-Materials Engineering, Laval University & University Hospital Research - Québec (Canada), [2]Plasmionique inc. - Varennes (Canada), [3]Laboratoire de Génie des Procédés Plasma et Traitements de Surface, École Nationale Supérieure de Chimie de Paris - Paris (France).

With the increased concern over pathogenic bacteria in several clinical, industrial and domestic applications, the quest for effective antibacterial surfaces is at the forefront of research in surface engineering. While several existing materials have shown potential to kill bacteria, they are often not suitable as bulk materials due to their inadequate mechanical properties [1]. Hence, the design of antibacterial materials is now increasingly moving towards surface modification and mainly based on three chief strategies: the reduction of bacterial adhesion, the controlled release of biocides and the grafting of contact-killing surface molecules [2]. Still, when exposed to more severe operating conditions, a typical problem arising with most of these engineered materials is their lack of stability (rapid leaching of biocide agent, loss of surface grafted molecules, etc.), which limits their long-term effectiveness. One possibility to overcome these limitations is offered by plasma technologies. Strongly adherent and cohesive coatings with a tunable set of properties can be deposited on various substrates and loaded with the desired biocides, to act as highly stable antimicrobial surfaces.

In this context, a hybrid Plasma Enhanced Chemical Vapor Deposition – Physical Vapor Deposition (PECVD-PVD) system was developed to deposit silver loaded

Diamond-Like Carbon (DLC) nanothin coatings in a one-step process. DLC, an amorphous carbon-based family of materials, is well-known for its excellent mechanical and tribological properties, chemical inertness and nanosmoothness [3]. Moreover, it can be doped with silver nanoparticles, a highly effective broad spectrum antibiotic. The resulting Ag-DLC coatings are expected to provide an interesting solution as antibacterial surfaces in severe environments due to a dual action against bacteria. This presentation will describe the deposition as well as the structural, mechanical and biological characterization of the deposited coatings. The antibacterial properties were studied at different time scales, in order to better assess the stability and long-term effectiveness of the material.

1. Vasilev, K., J. Cook, and H.J. Griesser, Antibacterial surfaces for biomedical devices. Expert Review of Medical Devices, 2009. 6(5): p. 553-567.
2. Lichter, J.A., K.J. Van Vliet, and M.F. Rubner, Design of Antibacterial Surfaces and Interfaces: Polyelectrolyte Multilayers as a Multifunctional Platform. Macromolecules, 2009. 42(22): p. 8573-8586.
3. Hauert, R., A review of modified DLC coatings for biological applications. Diamond and Related Materials, 2003. 12(3–7): p. 583-589.

SE/TF-P2-03
Hipims CrN process as an alternative for hexavalent Cr based electroplating

T12 Surface Engineering

#SE/TF-P2-03

P. Cosemans, I. Truijen.

Sirris - Diepenbeek (Belgium).

Electroplated hard chromium is a well known and widly used coating in many engineering industries due to its high hardness and excellent corrosion resistance. However, environmental and health regulations on chromates drive the exploration of alternative coating methods, among which physical vapor deposition looks very promising.
The recently developed HIgh Power Impulse Magnetron Sputtering (HIPIMS) PVD technique has been investigated as an alternative process for electroplating of hard chromium. In comparison to DC-Magnetron Sputtering (DC-MS), HIPIMS results in denser coatings with superior mechanical, tribological and wear resistant properties .
In this study, CrN coatings are deposited by means of DC-MS, HIPIMS and a combined DC-MS/HIPIMS technique. Mechanical and tribological properties and corrosion resistance of the different coatings is investigated and compared to electroplated hard chromium.

The best alternative HIPIMS-based coating has been tested in an industrial case as an alternative for electroplated hard chrome.

SE-1-Or-11
Time-Resolved Laser Diagnostics in High-Power Impulse Magnetron Sputtering Discharges

T12 Surface Engineering

#SE-1-Or-11

M. Palmucci, N. Britun, S. Konstantinidis, R. Snyders.

Université de Mons - Mons (Belgium).

The results on time-resolved diagnostics of High-Power Impulse Magnetron Sputtering (HiPIMS) discharges by Laser-Induced Fluorescence (LIF) accumulated during recent years are reported. The “short pulse” (5-20 μs) HiPIMS discharges operating in pure Ar gas while sputtering Ti are considered. The LIF measurements were realized using a dye laser pumped by a YAG:Nd 5 ns pulsed laser, with energy of ~10-50 μJ/pulse. The Ar pressure was in the range of 5 - 20 mTorr.

The study is mainly focused on dynamic behaviour of a HiPIMS discharge in terms of relative densities of sputtered particles and their ions, as well as on their velocity distribution function (vdf). The presented laser diagnostics results cover both on- and off- time of HiPIMS plasma.

Among the results we found that the vdf of sputtered species evolves dramatically as a function of time, revealing the abrupt widening during the on-time, changing to a shrinkage in the off-time. The widening happens due to the extensive gas rarefaction at the end of the pulse leading to formation of region with fewer collisions between Ar and the sputtered species. This results in higher measured velocities of sputtered species. On the other hand, the vdf shrinkage in the off-time happens due to gas cooling and refilling effects. These effects are similar for Ti and Ti^+.

The time- and space- resolved study of sputtered species densities agree well with the described vdf results. In particular, the evolution of Ti density represents a wave of sputtered Ti propagating from the target surface with a velocity of ~2 km/s. At higher pressure (20 mTorr), an essential increase of the maximum density is observed for both sputtered Ti and Ti^+. It can be explained by more intensive sputtering due to a higher electron density, and, as a consequence, higher argon ionization. On the other hand, the decays of Ti and Ti^+ densities observed after the pulse are different depending on Ar pressure.

The presented time- and space- resolved results on the vdf and relative densities of sputtered species give an overview of the HiPIMS plasma dynamics, clarifying the

time evolution of these discharges in terms of the basic plasma parameters.

SE-1-Or-1
Structure formation and photocatalytic activity of HiPIMS and pulsed DC reactively sputtered W doped TiO2 coatings

T12 Surface Engineering

#SE-1-Or-1

P. Kelly [1], R. Schmidt [2], M. Ratova [1], M. Wuttig [2], G. West [1].

[1]Manchester Metropolitan University - Manchester (United kingdom), [2]Aachen University - Aachen (Germany).

Photocatalytic titania coatings have many potential applications, including self-cleaning surfaces, antimicrobial/hygienic surfaces, air and water purification, and anti-fogging surfaces for lenses or mirrors. However, despite their great potential and the growing scientific interest in this area, the development and take up of commercialised products is slow. One limitation of these coatings is that photocatalytic activity is dependent on the crystal structure of the coating and it is anatase or anatase/rutile mixed structures that generally show the highest levels of activity. However, photocatalytic activity can be influenced significantly by doping with different metallic or non-metallic elements. One of the most promising candidates for doping is tungsten which has been shown to increase the photocatalytic activity significantly [1]. For reactively sputtered coatings, doping can be achieved by sputtering from a single compound target, co-sputtering from two targets or serial co-sputtering [2,3]. Furthermore, the targets can be driven in HiPIMS, pulsed DC or continuous DC modes. Each process and operating mode has different advantages and disadvantages in terms of flexibility, deposition rate, ease of control, etc. Also, the energy delivered to the growing film will vary, which strongly influences the resulting structure of the coating. For example, coatings deposited by DC processes commonly require post-deposition annealing to develop the required structure, whereas photocatalytic activity has been demonstrated by as-deposited HiPIMS coatings [4]. W-doped titania coatings have therefore been deposited onto a range of substrate materials using the processes and operating modes described above and characterised in terms of their structures and compositions using SEM, EDX, Raman spectroscopy and XRD. Photocatalytic activity has been assessed

under UV radiation (365nm) in terms of the degradation rate of methylene blue dye. The results obtained to date are presented here.

1. M Ratova, PJ Kelly, GT West and I Iordanova, 'Enhanced Properties of Magnetron Sputtered Photocatalytic Coatings via Transition Metal Doping'. Accepted for Surf. Coat. Technol. Doi: 10.1016/j.surfcoat.2012.04.037
2. M. Austgen, D. Koehl, P. Zalden, T. Kubart, T. Nyberg, A. Pflug, M. Siemers, S. Berg, M. Wuttig, J. Phys. D: Appl. Phys. 44, 345501 (2011)
3. T. Kubart, R.M. Schmidt, M. Austgen, T. Nyberg, A. Pflug, M. Siemers, M. Wuttig, S. Berg, Surface and Coatings Technology 206, 5055 (2012)
4. PJ Kelly, PM Barker, S Ostovarpour, M Ratova, I Iordanova and JW Bradley, Rapid Communication 'Deposition of photocatalytic titania coatings on polymeric substrates by HiPIMS,' Vacuum, 86 (2012) 1880-1882.

SE/TF-P2-04
Influence of 9 eV Collision of Chemically Inert Molecules on Fluorinated Polymer Erosion in Sub-Low Earth Orbit Space Environment

T12 Surface Engineering

#SE/TF-P2-04

K. Yokota, M. Tagawa.

Kobe University - Kobe (Japan).

Materials used in an exterior of spacecraft orbiting low earth orbit (LEO) experience hyperthermal collision with O-atom which is the dominant species in the upper thermosphere of the earth. A high-collision energy opens a new reaction path as gas-surface reactions at polymer surfaces. Some polymeric materials including polyimide, which has been widely used as spacecraft thermal control material, do not survive well in the LEO space environment. Much effort has been paid for studying material erosion both by flight and ground-based experiments as reported in the companion presentation [1]. A laser-detonation hyperthermal beam method has been used to simulate the O-atom/surface reactions on many materials. It is basically successful to simulate degradation property for many materials, however, inconsistency of erosion yields between flight- and ground-based experiments were reported [2, 3]. One of the reasons for this consistency is the presence of 9 eV collision of N_2 molecules in LEO which occurs simultaneously with 5 eV O-atom collision. It has been suggested from a computational simulation that N_2 molecules in orbit could erode fluorinated polymers with high collision energies [4]. This computational result suggested the importance of N_2 effect even on the ground-based simulations.
In this study, collision energy dependence on the material degradation under hyperthermal Ar beam exposure was experimentally studied by a laser detonation beam source which can generate intense atomic beam pulses with average energy of approximately 5-15 eV [5]. Note that impact energy of N_2 in LEO was simulated by the 9 eV collision of Ar in the ground-based experiment in order to avoid the unexpected decomposition of N_2 in the laser plasma. It was clearly observed that the polyimide does not show any erosion by Ar beam exposure, in contrast, mass of fluorinated polymer decreased with high-energy collision (>6eV) of Ar bombardment. The threshold energy of Ar-induced erosion of fluorinated polymer is lower than the

collision energy of N_2 in LEO, which is the second major composition in the upper atmosphere of the Earth (9 eV). The N_2-induced erosion, which has been ignored for the last 30 years, was confirmed on the fluorinated polymer erosion in LEO and sub-LEO regions. Detail of the experimental procedure and results will be presented.
A part of this study was supported by the Grant-in-Aid for Scientific Research from Japan Society for Promotion of Science.

[1] M. Tagawa, K. Yokota, IVC-19 (2013) Companion paper.
[2] B. Weihs, M. van Eesbeek, Proc. 6th Int. Symp. Materials in a Space Environment, ESA-SP368 (1994), 277.
[3] M. Tagawa, K. Yokota, Acta Astronautica, 62 (2008) 203.
[4] D. Troya, G. C. Schatz, Protection of Materials and Structures from Space Environment, J. I. Kleiman Ed., Springer, Leiden, The Netherlands, (2006) 365.
[5] M. Tagawa, K. Yokota, K. Kishida, A. Okamoto, T. K. Minton, ACS Advanced Materials and Interfaces, 2 (2010) 1866.

SE-P1-01
Study of Tungsten Erosion in High Power Impulse Magnetron Sputtering Plasma

T12 Surface Engineering

#SE-P1-01

M. Desecures, L. De Poucques, D. Genève, R. Hugon, J.L. Vasseur, J. Bougdira.

Université de Lorraine, Institut Jean Lamour, CNRS-UMR 7198, Faculté des Sciences et Technologies, F-54506 - Nancy (France).

Plasma-wall interactions in fusion devices provide a source of impurities for fusion plasma. In order to diminish the contamination, it is required to use materials with low sputtering yield, such as tungsten (W). The transitory accidental events (such as ELMs-Edge Localized Modes) can generate high fluxes (~$10^{24}m^{-2}s^{-1}$) of charged particles towards the surface, in a typical time scale of 100 µs leading to high sputtering of the walls. W physical erosion results in W atoms and dust particles formation subsequently carried into the plasma core which severely degrades the plasma properties required for the fusion reactions. Dust can also be deposited on other chamber walls or components facing plasma (heating antennas, ELM controllers). The comprehension of the plasma-wall interactions requires a broad knowledge of the influence of plasma ions fluxes on W and W-based materials, responsible for W atoms sputtering, and of the dependency with plasma related properties (particles densities, ion and neutral velocities and temperatures, sputtering rate, re-deposition …). It is possible to use a low pressure magnetron discharge powered by a high power supply which can deliver up to 10 MWm^{-2} during short pulses (~100 µs). Exploiting the capabilities of this type of discharge, known as HiPIMS[1] (High Power Impulse Magnetron Sputtering), it becomes possible to generate high ion fluxes (~$10^{24}m^{-2}s^{-1}$) and to perform a study on W erosion, oriented towards extreme conditions.

The objective of this work is to study the physical etching of W under high fluxes of different types of relevant ions (Ar, He). Moreover this work focuses on the simultaneous characterization of the high density magnetized plasma (HiPIMS) in

terms of ion bombardment of the W target (magnetron cathode) and in terms of the resulting W sputtered vapor behavior when it crosses the plasma. More specifically, it consists in the characterization of the etching rate of W target, transport of W atoms, W dust formation and W deposition. Both spatial and time resolved measurements are performed by means of optical emission spectroscopy, laser absorption spectroscopy, and Langmuir probes. Atoms in gas phase are assessed by tunable diode laser absorption spectroscopy (TD-LAS), W at 407 nm, Ar^+ at 668 nm[2], metastable of He at 1080 nm (no transition can be found for He^+). The time evolution of the temperature and the density of those species are derived from the Doppler profile during the pulse as well as during the plasma decay[3]. Furthermore the modification of the W target composition and structure (ions implantations, bubbles and holes formation by He^+ bombardment) induced by high flux sputtering are performed by surface analysis techniques (MEB, XPS, 2D-profilometry).

1- V. Kouznetsov, K. Macak, J.M. Schneider, U. Helmersson, I. Petrov, Surf. Coat. Technol. 122 (1999) p.290.
2- T Bieber, S Bardin, L de Poucques, F Brochard, R Hugon, J-L Vasseur, J Bougdira, Plasma Sources Science & Technol., vol. 20 (2011) 015023
3- Sushkov, V, H T Do, M Cada, Z Hubicka, and R Hippler. Plasma Sources Science & Technol., no. 1 (2013): 015002.

TF/SE-1-Or-5
Antibacterial Cr-Cu-O thin films prepared by reactive magnetron sputtering

T12 Surface Engineering

#TF/SE-1-Or-5

J. Blazek [1], J. Musil [2], K. Fajfrlik [3], R. Cerstvy [2], S. Proksova [1].

[1]NTIS - European Centre of Excellence, Faculty of Applied Sciences, University of West Bohemia, Univerzitní 22, 306 14 - Plzeň (Czech republic), [2]Department of Physics, Faculty of Applied Sciences, University of West Bohemia, Univerzitní 22, 306 14 - Plzeň (Czech republic), [3]Department of Microbiology, Medical Faculty in Plzeň, Charles University in Praha, E. Beneše 13, 305 99 - Plzeň (Czech republic).

The paper reports on (i) the formation of antibacterial Cr-Cu-O thin films by reactive magnetron sputtering and (ii) the effect of Cu content and thermal annealing on their structure, phase composition, antibacterial activity and mechanical properties. The Cr-Cu-O films were reactively sputtered by a dual magnetron in an $Ar+O_2$ sputtering gas mixture. The dual magnetron was equipped with two identical Cr/Cu targets composed of Cr circular plate fixed by a Cu ring. The inner diameter of the Cu ring was varied from 34 mm to 28 mm with the aim to control the content of Cu in the Cr-Cu-O film. Contact profilometry, X-ray diffraction, X-ray fluorescence, microhardness indentation and optical spectroscopy were used to analyze the thickness and macrostress, structure, elemental composition, mechanical properties and transmittance of the films respectively. Rapid thermal annealing up to 700°C in a rapid thermal processor was used to investigate the changes in structure and phase composition of the Cr-Cu-O films with increasing temperature. The antibacterial efficiency E of killing Escherichia coli bacteria was evaluated using the plate counting method in the daylight and in the dark. It was found that (1) the content of Cu in the Cr-Cu-O film strongly influences its antibacterial activity, (2) 100 % killing of E. Coli bacteria, i. e. E=100 %, is achieved on the surface of Cr-Cu-O film with Cu content ≥ 15 at.% after 3 hours, (3) the Cr-Cu-O films with high (≥ 15 at. %) Cu content are X-ray amorphous and effectively kill E. coli bacteria both in the daylight and in the dark and (4) these X-ray amorphous Cr-Cu-O films exhibit the following mechanical properties: the hardness H≈4 GPa, the effective Young's modulus E*≈80 GPa and elastic recovery W_e≈35%; these mechanical properties are suitable for protective

surfaces.

TF/SE-1-Or-4
High Performance SiO2 Barrier Films Deposited onto Polymer Substrates by RF Reactive Remote Plasma Sputtering

T12 Surface Engineering

#TF/SE-1-Or-4

H. Brown [1], M.J. Thwaites [2], P.J. Hockley [2], R.J. Curry [1], M.A. Baker [1].

[1]University of Surrey - Guildford (United kingdom), [2]Plasma Quest Ltd - Hook (United kingdom).

The use of polymer substrates for organic electronic devices has the potential to enable new applications, such as flexible displays, photovoltaics and organic light emitting diodes (OLEDs) and allow manufacturers to employ cost effective high-volume throughput roll-to-roll fabrication. However, these polymer substrates are susceptible to moisture/oxygen permeation and require encapsulation in the form of a thin film barrier layer. Although much research has been carried out on barrier layers, currently no thin film can be grown completely defect free onto plastics to obtain a water vapour transmission rate (WVTR) low enough for OLED applications.

In this work, SiO_2 barrier layers have been deposited using a novel technique, remote plasma sputtering, in the radio frequency (RF) reactive sputtering mode. Remote plasma sputtering can be used to produce dense films on polymer substrates. For single layer thin films, the sputter deposition parameters (RF power and oxygen flow rate) have been varied. Two further specific methodologies have been employed to improve barrier properties through disrupting the growth of extended defects in the growing film. Firstly, the film growth was interrupted at regular intervals during the deposition and the surface of the film exposed to the plasma for short periods. Secondly, a rotating aperture and a planetary conformal coating system were used to relax the growing film and eliminate columnar growth.

The thin films have been characterised using SEM, GAXRD, AFM, XPS and STEM. SEM cross sections and GAXRD data reveal that single and multilayers of SiO_2 can be deposited using remote plasma sputtering with a dense amorphous structure and without columnar growth. AFM and optical images reveal substrate cleanliness and asperities are crucial in achieving good barrier performance. Two methods have

been explored to minimise these issues and their effect on barrier properties have been studied. Firstly, using the plasma itself to modify the polymer surface and secondly, using a sputtered polytetrafluoroethylene (PTFE) to at act as smoothing interface layer.

A WVTR of $<2x10^{-2}$ g/m^2/day has been achieved for single layer SiO_2 films deposited by remote plasma sputtering. STEM micrographs of SiO_2 with plasma interruptions taken in the secondary electron (SE) mode (shown in Figure 1) clearly display some modification to the film when exposed just to the plasma. Further characterisation results on the barrier film structure and WVTRs for SiO_2 thin films deposited with plasma interruptions, rotating aperture, planetary conformal coating system and PTFE interfacial layer will be presented and discussed.

STEM image in SE mode of SiO_2 with plasma interruptions.

SE/PST/TF/BI-P1-01
Highly controlled system for injecting organic and bio-molecules from solution into ultra high vacuum chambers

T12 Surface Engineering

#SE/PST/TF/BI-P1-01

J. Sobradovj, J. Martin Gago.

CAB (CSIC-INTA) - Torrejon De Ardoz (Spain).

We have designed a new deposition system of organic and bio-molecules from liquid solution into vacuum systems. The solution is injected inside an ultra high vacuum chamber through a valve with a piezoelectric actuator. Argon is used as the carrier gas controlling the injection time and the differential pressure between the solution and the vacuum experimental chamber. The results are analyzed qualitatively and quantitatively by mass spectroscopy and a quartz crystal microbalance .In particular we have used this system to study the deposition of Adenosine triphosphate (ATP), main molecule in the cellular energy exchange processes, on diferent surfaces. We have grown layers of controlled coverage of the intact molecule as depicted by X-Ray Photoemission Spectroscopy (XPS) and Scanning Tunneling Microscopy (STM). We have also used this system to study impurities in salt solutions with different molarities.

1. Preparation of hydrosol suspensions of elemental and core-shell nanoparticles by co-depositio with water vapour from the gas-phase in ultra-high vacuum conditions; J Nanopart Res (2012) 14:1136; Chris Binns, Pilar Prieto, Stephen Baker et all,...

SE/TF-3-Or-5
Super-hydrophobic films synthesis by MOPECVD at Low Temperature

T12 Surface Engineering

#SE/TF-3-Or-5

J. Han [1], S.B. Jin [1], J.S. Lee [1], T. Suzuki [2], Y.S. Choi [1].

[1]NU-SKKU Joint Institute for Plasma-Nano Materials, Sungkyunkwan University, 300 Chunchun-dong Jangan-gu - Suwon (Korea, republic of), [2]Graduate School of Engineering, Nagoya University - Nagoya (Japan).

Super-hydrophobic film have recently attracted great interests for variety of applications such as self-cleaning, anti-fingerprint, prevention of snow sticking, anti-fog, etc.. It has been known that super hydrophobic surfaces of water contact angles (WCA) higher than 150° can be produced only by micro patterning of the surface with hydrocarbon or fluorocarbon containing low energy film materials deposited mostly at elevated temperature. Structuring of micron-sized roughness of the surface combined with control of chemical composition for low surface energy which is called the Casie-Baxter or fakir is not feasible process and often tends to cause degradation of optical transparency and resistance against external agents, and therefore still limited in broad applications, especially plastic based materials and devices. Super-hydrophobic films having nano-sized roughness are synthesized with process and film design based on fundamental understanding of plasmas discharge of precursors and polymerization behaviors at PEMOCVD processes. Duel film processes were performed to synthesize super hydrophobic coatings of various WCA on plastic substrate at room temperature without any heating for suppression of any thermal heating and damage to the substrate and deposited films. SiO_x film was primarily deposited on plastic substrate by PEMOCVD with OMCTS ($(CH_3)_2SiO-)_4$) at O_2 partial pressure and then followed by top coating with HMDS, ($(CH_3)_3$-Si-Si-$(CH_3)_3$) precursor for hydrophobic and super hydrophobic coatings. WCA was controlled by hydrogen addition which play a role to modulate the surface roughness and passivate defects, such as electrically uncovered polar sites rendering non-hydrophobicity. WCA was controlled in the range of 120° to 160° by adjusting process parameters, especially the hydrogen flow rate and discharge power. Surface roughness analysis by AFM showed that the film with a WCA of 145° has 2.5nm roughness in rms value. All the films showed excellent results in resistance tests at salt water and cosmetics owing to super-hydrophobicity and defect passivation. The formation mechanism and synthesis behavior of super hydrophobic films are

discussed with analysis of discharge behavior of precursors with process conditions and film analysis data.

Acknowledgment
The authors are grateful for the financial support provided by the National Research Foundation of Korea (NRF) through the Institute for Plasma-Nano Materials at Sungkyunkwan University

References
[1]Sun, T.; Wang, G.; Feng, L.; Liu, B.; Ma, Y.; Jiang, L.; Zhu, D.Angew Chem Int Ed 43, 357(2004)
[2] O.Takai, A.Hozumi, N.Sugimoto, J. Non-Cryst. Solids 218, 280(1997).
[3] W. Chen, A.Y.Fadeev , M.C.Hsieh, D.Oner , J.Y oungblood, T.J. Mccarthy, Langmuir 15, 3395(1999)

SE/TF-3-Or-1
Selective nitrogen incorporation in the gamma phase of the single crystalline Ni-based superalloy MC2 by low temperature plasma assisted nitriding

T12 Surface Engineering

#SE/TF-3-Or-1

S. Chollet.

Université de Poitiers - Poitiers (France).

MC2, a single crystalline (γ/γ′) Ni-based superalloy, was plasma nitrided at low temperature (400°C) for 1 and 4 hours. The MC2 superalloy is composed by 70 vol.% of γ′ cubical fcc precipitates in coherence with a surrounding γ fcc matrix. Thanks to the monomodal size distribution of the γ′ cube side (~ 400 nm), MC2 was used as a model material in an attempt to investigate the behavior of γ′ precipitates in γ matrix during the nitriding of Ni-based superalloys. The structure and composition of the plasma-nitrided layer were characterized by glow discharge optical emission spectroscopy (GDOES), scanning electron microscopy (SEM), energy and wavelength dispersive spectrometry (EDS/WDS), white-light interferometry (WLI) and X-ray diffraction (XRD). The nitrogen profile obtained in MC2 is significantly different from that obtained in the case of Haynes 230, a Ni-based superalloy without γ′ precipitates: instead of a nitrogen plateau slightly decreasing from 25 to 20 at.% over few microns, nitrided MC2 exhibits a highly nitrided (25 at.%) thin top layer of about 200 nm, followed by a plateau of few micrometers, with nitrogen content of about 10 at.%. This low plateau level can be explained by a γ matrix similarly nitrided than in Haynes 230 (up to ~25at.%), producing an expanded γ_N phase, whereas γ′ precipitates did not incorporate nitrogen. This is confirmed by XRD results, which has revealed a peak located around $2\theta = 46.3°$ that can be attributed to the <002> peak from the expanded γ_N phase. EDX cartography has confirm that the γ′ precipitates in the nitrided plateau accommodate no more than few at.% of nitrogen. Consequently, the γ /γ′ disparity modifies the morphology: the average γ channel width is consequently increased due to the elasto-plastic response to the nitrogen incorporation.

SE/PST/TF/BI-2-Or-1
Biofunctionalization of stainless steel via bifunctional silane monolayers

T12 Surface Engineering

#SE/PST/TF/BI-2-Or-1

L. Vuori [1], M. Hannula [1], K. Lahtonen [1], M. Hirsimäki [1], J. Pärssinen [2], V. Hynninen [2], J. Leppiniemi [2], A. Tõnisoo [3], V. Hytönen [2], E. Nõmmiste [3], M. Valden [1].

[1]Surface Science Laboratory, Tampere University of Technology - Tampere (Finland), [2]Institute of Biomedical Technology, University of Tampere and Tampere University Hospital - Tampere (Finland), [3]Institute of Physics, University of Tartu - Tartu (Estonia).

Stainless steel (SS) is a highly versatile and affordable material which exhibits a self-healing corrosion resistance and a biocompatible surface oxide layer, making it an excellent material for applications in medical industry. However, fabricating SS surfaces with specific biofunctional properties is a challenging task. Here, we propose a scalable bottom-up covalent functionalization of SS which can be used to create surface functionalities that promote or hinder biomolecular adhesion.

The aim of this study was to create an organized bifunctional organic monolayer on SS enabling the coupling of biomolecules on SS surface with controlled spatial distribution. Organofunctional silanes (3-aminopropyl)trimethoxysilane (APS) and (3-mercaptopropyl)trimethoxysilane (MPS) were chosen as they form an overlayer on solid substrates via covalent bonding in lateral and vertical directions. The APS/MPS surface can be biofunctionalized with succinimidyl ester (NHS) and maleimide (MAL) terminated biomolecules, respectively. AISI 316L steel was chosen as substrate as it is widely used in biomedical applications, such as cardiovascular stents and medical instruments.

We have previously reported that an electrochemical treatment of SS can enhance APS monolayer formation [1]. In our earlier studies we have also shown that APS/MPS ratio in the silanization solution does not correlate directly with the silane ratio in the deposited layer on SS surface. Furthermore, the concentration of silanes in the solution, hydrolysis and silanization time affect the formation of the overlayer.

Thus, a careful investigation of the fabricated surface structures is required in order to understand the coverage, orientation, APS/MPS ratio and overlayer thickness of the resulting silane films. In this study synchrotron radiation mediated (MAX IV laboratory, BL D1011, Lund, Sweden) and conventional X-ray photoelectron spectroscopy (XPS) have been employed.

In the present study, we establish the chemical composition of silane layers and show that the majority of functional groups point outwards and remain reactive after deposition. Silane layer morphology is determined by analyzing the inelastic electron energy background of photoelectron spectra [2]. According to our experiments, the silanization process facilitates relatively fast and reproducible fabrication of approximately one monolayer thick functional silane films on SS. In addition, the APS/MPS ratio on surface can be controlled by modifying either the silane concentration in the hydrolysis solution or the silanization time.

We also show that the APS/MPS monolayers can be biofunctionalized with NHS-PEG and MAL-PEG-Biotin molecules creating a SS surface that is receptive for specific adsorption of (strept)avidin. Also, compared to uncoated SS our preliminary experiments on silanized SS indicate an improved resistance towards E. Coli. Finally, the surface reactivity can be easily tailored towards specific applications by modifying the topmost functional layer with the help of numerous, commercially available biotinylated reagents.

[1] P. Jussila, H. Ali-Löytty, K. Lahtonen, M. Hirsimäki, M. Valden, Surf. Interface Anal. 42, 157 (2010).
[2] S. Tougaard, J Electron Spectrosc Relat Phenom 178-179, 128 (2010).

SE/TF-P2-05
Deposition of High-Entropy Alloys by sputtering powder targets: the influence of the composition

T12 Surface Engineering

#SE/TF-P2-05

B. Braeckman, D. Depla.

Ghent University - Gent (Belgium).

Traditional alloy systems are based on one or two principal metallic elements. For example steel is based on iron, intermetallics are based on Ni-Al, Ti-Al compounds, etc. Since the beginning of the 21st century Yeh et al. [1] introduced a novel approach to alloy design with promising properties. High-Entropy Alloys (HEA) are composed of five or more principal elements in equimolar ratios. Due to the high mixing entropy, solid solutions of many elements will tend to form stable phases. In contrary to conventional alloys, the large number of elements will not lead to complex systems but remain fairly simple, essentially amorphous or fcc and/or bcc. HEA's have excellent properties such as high hardness, high strength, high plasticity and extended ductility, even at elevated temperatures, which makes them suitable for a range of applications.

Due to its flexibility, magnetron sputtering is an excellent deposition technique to study the compositional influence on material properties. There are several options available to deposit multi-component thin films. The multiple magnetron method has the benefit that the film composition is easily adapted by changing the discharge power and/or substrate-target distance. However when the number of elements in the film is high, the geometrical setup becomes complex. The preferred method is to sputter from cold isostatically pressed powder targets. In this way the composition of the target and hence the film is easy to control and there is need of only one magnetron.

This work focuses on the deposition of AlCoCrCuFeNi thin films using powder targets. In a first step the targets are sputtered in the metallic regime while the molar ratio of several elements is varied. In a second step the reactive sputtering (addition of oxygen and/or nitrogen) of the multi-component powder targets is considered. The

crystallographic properties were investigated using XRD while the topography and microstructure were studied with (cross-sectional) SEM.

This abstract is submitted to RSD2013.

[1] J.W. Yeh et al., Adv. Eng. Mat. 6, 5 (2004)

SE-2-Or-2
Lattice Ordering Effects on Toughness Enhancement in Transition Metal Nitride Thin Films

T12 Surface Engineering

#SE-2-Or-2

V. Chirita, D.G. Sangiovanni, D. Edström, L. Hultman.

Linköping University - Linköping (Sweden).

Enhanced toughness in hard and superhard thin films is a primary requirement for present day ceramic hard coatings, known to be prone to brittle failure during in-use conditions, in modern applications. In our previous Density Functional Theory (DFT) investigations, we have predicted significant improvements in the hardness/ductility ratio of several pseudobinary B1 NaCl structure transition-metal nitride alloys, obtained by alloying TiN or VN with NbN, TaN, MoN and WN [1, 2]. The initial calculations, which were carried out on model, highly ordered configurations with Cu-Pt ordering on the cation sublattice, reveal that the electronic mechanism responsible for toughness enhancement stems from the high valence electron concentration (VEC) of these alloys, which upon shearing, leads to the formation of alternating layers of high and low charge density oriented orthogonal to the applied stress, and ultimately allows a selective response to tetragonal and trigonal deformations. Recently, these results have been validated experimentally [3]. Single-crystal $V_{0.5}Mo_{0.5}N$/MgO(001) alloys, grown by dual-target reactive magnetron sputtering together with VN/MgO(001) and TiN/MgO(001) reference samples, exhibit hardness >50% higher than that of VN, and while nanoindented VN and TiN reference samples suffer from severe cracking, the $V_{0.5}Mo_{0.5}N$ films do not crack. However, as there is no evidence of Cu-Pt ordering in the synthesized $V_{0.5}Mo_{0.5}N$ films, here we present new DFT results, which address the issue of lattice ordering effects on the mechanical properties of these pseudobinary alloys. Our investigations concentrate on $V_{0.5}Mo_{0.5}N$, $V_{0.5}W_{0.5}N$, $Ti_{0.5}Mo_{0.5}N$ and $Ti_{0.5}W_{0.5}N$ alloys obtained by alloying TiN and VN with WN and MoN, which are all predicted to have significantly enhanced toughness compared to the parent binary compounds. Our calculations, carried out for structures with increasing levels of disorder, reveal that while the degree of electronic structure layering, i.e. the formation of alternating layers of high and low charge density upon shearing, becomes less pronounced in disordered configurations, the overall VEC effect is not affected. The essential feature in the

disordered alloys, as initially predicted for highly ordered configurations, remains the increased occupancy of electronic d-t_{2g} metallic states, which allows the selective response to tensile/shearing stresses, and explains the enhanced toughness confirmed experimentally for $V_{0.5}Mo_{0.5}N$ films.

[1] D. G. Sangiovanni et. al. Phys. Rev. B 81 (2010) 104107.
[2] D. G. Sangiovanni et. al. Acta Mater. 59 (2011) 2121.
[3] H. Kindlund et. al, submitted to Phys. Rev. Lett.

SE/TF-3-Or-2
Transmission electron microscopy of PM S390 MC high-speed steel

T12 Surface Engineering

#SE/TF-3-Or-2

D. Jenko [1], S. Šolić [2], V. Leskovšek [1], F. Cajner [2], M. Jenko [1].

[1]Institute of Metals and Technology - Ljubljana (Slovenia), [2]Faculty of Mechanical Engineering and Naval Architecture - Zagreb (Croatia).

The research deals with the study of the impact of microstructure on the tribological properties of PM S390 MC high-speed steel (Böhler), prepared by powder metallurgy with chemical composition in weight % of 1.64 C, 0.60 Si, 0.30 Mn, 4.80 Cr, 2.00 Mn, 4.80 V, 10.40 W, 8.00 Co and the rest was Fe. Different microstructure conditions of high-speed steel were obtained by heat treatment in two ways: conventional (vacuum hardening, three high-temperature temperings) and deep cooling (vacuum hardening, deep cryogenic treatment, high-temperature tempering). In some experiments, nitriding in plasma of ionising gases was also carried out.

Thin foil specimens for transmission electron microscopy (TEM) were prepared using Jeol EM-09100IS Ion Slicer and further analyzed by TEM (Jeol JEM-2100) using conventional TEM (CTEM) and energy dispersive X-ray spectroscopy (EDS, Jeol JED-2300 Series) at 200 kV electron accelerating voltage. Detailed characterization of the microstructure was performed on thin foil specimens, and electron diffraction method was used as well to carry out the microstructure–crystallographic analysis of the phases. In the martensite microstructure some nanometre sized areas of possible other phase were observed. Further investigation will enable to understand whether these areas are nanometre sized carbide precipitates.

The research showed that the microstructure obtained by deep cooling and nitriding compared to conventional heat treated resulted in an increase of wear resistance of PM S390 MC high-speed steel.

1. A.I. Tyshchenko, W. Theisen, A. Oppenkowski, S. Siebert, O.N. Razumov, A.P. Skoblik, V.A. Sirosh, Yu.N. Petrov, V.G. Gavriljuk, Low-temperature martensitic

transformation and deep cryogenic treatment of a tool steel, Materials Science and Engineering A, Vol. 527, 2010, 7027-7039.

2. B. Nedeljković, V. Lazić, S. Aleksandrović, B. Krstić, M. Mutavdžić, D. Milosavljević, M. Đorđević, Influence of the carbide type tribological properties of the hard Faced layers, MJoM, Vol. 16 (2), 2010, 77-90.

TEM images of specimens prepared by conventional heat treatment (left) and deep cooling (right).

SE/ASS-1-Or-5
Mechanical, Structural and Tribological Characterisation of High Nickel Content Alloys before and after Arc Activated Plasma Nitriding

T12 Surface Engineering

#SE/ASS-1-Or-5

E. Almandoz, J. Fernández De Ara, J.F. Palacio, G.G. Fuentes, J.A. García, R.J. Rodríguez.

AIN - Cordovilla (Spain).

In this study, a full comparison in terms of mechanical, structural and tribological performance of high nickel content alloys (maraging steel grade 300, Inconel 718 and 800 HT nickel alloy) was carried out. These alloys are widely known for their good mechanical properties and good corrosion properties and fairly good temperature resistance. Also, and with the aim of improving their surface properties, two of these alloys - Maraging 300 and Inconel 718 - have been subjected to an arc activated plasma nitriding. The impact of this process on these two materials, with the nitrogen going several micrometers deep in the surface, is shown.

Furthermore, in order to thoroughly characterise these alloys, a myriad of techniques have been employed: Scanning Electron Microscopy coupled with Electron Back Scattered Diffraction and X-Ray diffraction for the study of the microstructure of the samples before and after nitriding; a Nanoindenter, a micro-hardness tester fitted with a Knoop indenter and a Rockwell C for the evaluation of the mechanical properties; and finally, ball on disk tests in dry sliding and with WC-Co as a counterpart, made at room temperature and high temperature (450 ºC- 600 ºC) for the evaluation of the tribological performance of such alloys in these conditions.

SE/TF-3-Or-3
Ion Implantation Based Surface Modifivation of TiAl Materials

T12 Surface Engineering

#SE/TF-3-Or-3

A. Kolitsch, R. Yankov.

Helmholtz-Zentrum Dresden-Rossendorf - Dresden (Germany).

Titanium aluminide (TiAl) alloys are attractive lightweight materials for medium-temperature (500°-750°C) structural applications including components such as jet engine and industrial gas turbine blades, turbocharger rotors and automotive engine valves. However, envisaged service temperatures for future advanced applications will have to be in the range of 750° to 1000°C, over which these alloys suffer from both oxidation and oxygen embrittlement. Therefore, development of surface-engineering techniques for preventing high-temperature environmental damage is critical in exploiting the advantages of TiAl alloys to their fullest extent.

Two efficient approaches to protecting candidate TiAl alloys from high-temperature (>750°C) environmental degradation have been developed at HZDR. The first technique involves a single step, namely treating TiAl alloy components directly by plasma immersion ion implantation (PIII) of fluorine using a mixture of difluoromethane and argon (CH2F2 + 25% Ar) as the precursor gas. The oxidation performance of the fluorine-implanted alloys has been evaluated by thermal gravimetric analysis (TGA) over the temperature range of 750° to 1050°C under conditions of both isothermal and thermal cyclic oxidation in air, and for times as long as 6000 h. This type of surface modification has been shown to produce a stable, adherent and highly protective alumina scale. The second technique involves the fabrication of a durable protective coating in a two-step process, namely formation of a thin aluminum-rich TiAl layer (Ti-60Al) by chemical vapor deposition (CVD) employing a mixture of inorganic precursors, followed by PIII of fluorine. Subsequent long-term oxidation exposures to air at 900°C of a GE 4822 alloy (Ti-48Al-2Cr-2Nb; alloy composition qualified for aerospace applications) have shown that the coating so developed is able to successfully prevent oxidation damage to the base material while maintaining up to 90% of its initial mechanical properties (strength and ductility).

Fluorine ion implanted turbocharger rotors after high temperature treatment air at 1050°C

SE-1-Or-6
A new angle on sputtering magnetrons?

T12 Surface Engineering

#SE-1-Or-6

D. Lundin, C. Huo, M. Raadu, N. Brenning.

Royal Institute of Technology - Stockholm (Sweden).

Sputtering magnetrons are usually described in terms of two aspects. (1) Electrons are trapped close to the cathode by a curved magnetic field, and thus have a long mean free path in the plasma. They can therefore ionize more efficiently than in a usual glow discharge plasma and, as a consequence, the device can be operated at desirably low process gas pressure. (2) The energy input to sustain the discharge is mainly by secondary-emitted electrons that are accelerated across the cathode sheath. However, in this work we present new modeling results on high power impulse magnetron sputtering discharges (HiPIMS) along with experimental data that demonstrate that the second aspect has to be revised: Ohmic heating in the plasma can dominate by up to an order of magnitude over cathode sheath energization. Furthermore, the origin of the Ohmic heating is found to be an extended pre-sheath in the dense plasma region, which has been detected in several HiPIMS experiments, as well as in conventional magnetron devices. This is a new, and physically separate, effect of the magnetic field that needs to be added to the standard understanding of sputtering magnetrons.

SE/ASS-P2-04
Advanced tribological properties of TiC/a-C:H coating sliding against PTFE composite

T12 Surface Engineering

#SE/ASS-P2-04

J. Shen, Y. Pei, J.T.M. De Hosson.

University of Groningen - Groningen (Netherlands).

Previous research has made breakthroughs in the design, deposition and characterization of DLC based nanocomposite coatings on various substrates, with ultra-low friction and wear rate [1]. Since both PTFE composite and DLC coating exhibit self-lubrication effects, it is tempting to investigate the tribological performance of a polytetrafluoroethylene (PTFE) composite/DLC sliding couple. Tribological experiments on PTFE composite reinforced with glass fibers and resin were performed against 100Cr6 steel and TiC/a-C:H thin film coated surfaces. In both cases the coefficient of friction (CoF) increases with increasing sliding distance until a steady-state value is reached. Although the CoFs are very similar, the wear rate of the PTFE composite at a long sliding distance is reduced when the steel ball is coated with TiC/a-C:H coating. This behavior is attributed to the lower surface free energy of TiC/a-C:H coating and its smoother surface after long sliding. The wear mechanism of the PTFE composite is a combination of smearing of PTFE fibers, de-bonding and fragmentation of glass fibers, cracking and fracture of the resin matrix, and generating wear debris and third-body that consists of glass fiber fragments and fractured resin. PTFE transfer films are evident on the surfaces of the hard counterparts, the thickness of which on TiC/a-C:H coated surfaces is measured to be a couple of nanometers by a newly developed method. On the surface of uncoated steel balls, a thicker transfer film is formed and partly covered with thick and scattered polymer flakes.

[1] Y.T. Pei, C.Q. Chen, K.P. Shaha, J.Th.M. De Hosson, J.W. Bradley, S.A. Voronin, M. Čada, Microstructural control of TiC/a-C nanocomposite coatings with pulsed magnetron sputtering, Acta Mater. 56 (2008) 696–709.

SE/ASS-1-Or-6
Wear resistant MoS2/ta-C coatings for applications in various environments

T12 Surface Engineering

#SE/ASS-1-Or-6

T. Gradt [1], G. Theiler [1], A. Brückner [2], V. Weihnacht [2].

[1]BAM - Berlin (Germany), [2]IWS - Dresden (Germany).

For vacuum and inert environments MoS_2 is probably the most suitable solid lubricant. However, pure MoS_2 fails in humid air, which is a problem for applications where contact to the atmosphere cannot be avoided. Graphite and most amorphous carbon coatings show the opposite behaviour: good lubricity in air, but high friction and wear in the absence of humidity.

In order to overcome the low endurance of MoS_2 coatings in normal air, double-layer structures with tetrahedral amorphous carbon (ta-C) were produced and tested. The coatings were deposited on steel substrates by laser-controlled, pulsed vacuum arc process [1]. This method generally produces coatings with high density and good adherence. It combines the advantages of a laser for the precise control of the arc-evaporation spot with the high evaporation rate of vacuum arc and enables film deposition under series production requirements. This type of hydrogen-free diamond-like-coating has a high content of sp^3-type tetragonal bonds and a hardness up to 75 GPa. Highly inert they are excellent wear protective coatings in humid environment, but without further measures the performance of ta-C generally decreases under dry and vacuum conditions [2].

The tribological behaviour of the MoS_2/ta-C double layer coatings was investigated in ball-on-disk tests in air, vacuum, and hydrogen environment. The maximum Hertzian contact pressure was 1.27 GPa and the maximum sliding velocity 0.5 ms^{-1}. In vacuum environment, the friction coefficient against uncoated steel balls varied between 0.005 and 0.02 depending on the contact pressure. At high contact pressures, the friction coefficient was as low as 0.005 and the wear life between 340,000 and 500,000 cycles.

After sliding a highly oriented MoS_2-layer beneath the sliding surface was detected by TEM. Because the initial film was amorphous, the layered structure was not created by orientation of lamellar MoS_2-platelets, but by friction induced

crystallisation.

The coatings showed best performance in hydrogen environment. Tests were run up to 40 h or 650 000 friction cycles without failure. Pure ta-C also showed a good wear resistivity without coating failure during the test duration. However, a distinct running-in occurred with a COF up to 0.5. The double-layer coating showed smooth sliding without a high initial friction state. Because this coating can be deposited by a well proven industrial method, it is a good candidate for tribologically stressed components in hydrogen technology.

[1] B. Schultrich, H.-J. Scheibe, D. Drescher, H. Ziegele, Deposition of superhard amorphous carbon films by pulsed vacuum arc deposition, Surface and Coatings Technology 98 (1998) 1097–1101
[2] C. Donnet, A. Erdemir, Tribology of Diamond Like Carbon Films; Fundamentals And Applications, Springer, New York, 2008

SE/TF-2-Or-9
The deposition of Silicon dioxide films onto Titania substrates from a two step DBD process

T12 Surface Engineering

#SE/TF-2-Or-9

S. Dahle [1], H. Munkert [1], W. Viöl [2], W. Maus-Friedrichs [1].

[1]TU Clausthal - Clausthal-Zellerfeld (Germany), [2]HAWK Göttingen - Göttingen (Germany).

The coating of different substrates with silicon dioxide films is of great interest for a variety of applications ranging from gate oxide layers and anti-reflective glasses to protective coatings against influences as reactive gases, sintering during high temperature processes and many more. The use of plasma-based processes for the film deposition may be advantageous over currently used processes concerning these applications. Unfortunately, most of the approaches employing plasma treatments for the deposition of silicon dioxide films suffer some disadvantages. Using monosilane is difficult because it would instantly react with the oxygen needed for the reaction to form silicon dioxide. Thus, many workgroups use either large organometallic precursors, which tend to leave residual carbon within the produced film or make use of inert oxygen providers such as carbon dioxide or nitrogen oxides, wich also leads to carbon or nitrogen residuals of these molecules within the film. There against, we recently developed a two step approach depositing the metal from a precursor in a first plasma treatment and using a second one to oxidize it. This approach has been proved to work on titanium dioxide nanoparticles before.
The use of the described two step approach on various substrates is currently investigated. In this present contribution, we studied the deposition of silicon dioxide onto metallic titanium as well as titanium dioxide crystals as model substrates for metals and ceramics, as sketched in **Fig. 1**. For both substrates, a strong impact of the process gas pressure is found, leading to the formation of particles at atmospheric pressure but the formation of closed films for low pressure plasma treatments in containing process gases. After the metal deposition onto the substrates we found the depletion of oxygen at the interface of the titanium dioxide substrate with the deposited film. These defects got healed upon the second plasma treatment, indifferent of the used process gas (oxygen or air) or pressure (200 mbar or 1000 mbar). The titanium metal on the other hand revealed an oxidized film at the

interface to the silicon dioxide after complete transformation of the deposited primer film. The investigations were carried out by means of Metastable Induced Electron Spectroscopy (MIES), Ultraviolet Photoelectron Spectroscopy (UPS) and X-ray Photoelectron Spectroscopy (XPS) as well as Atomic Force Microscopy (AFM).

Fig. 1: Schematic representation of the processes found for the two step plasma deposition approach

SE-1-Or-9
Non-uniform mesh modelling of very high density magnetron discharges. Comparison between DC and HiPIMS regimes.

T12 Surface Engineering

#SE-1-Or-9

A. Revel [1], C. Costin [2], T. Minea [1].

[1]LPGP, Université Paris-Sud 11 - Orsay (France), [2]Faculty of physics, A. Cuza University - Iasi (Romania).

The modelling of a magnetron discharge is a delicate issue in DC, but especially in HiPIMS regimes. The high voltage of the cathode (~1 kV) combined with the magnetic field create (~1000 G) a very thin sheath in front of the race-track (where B is parallel to the cathode) and a high plasma density. The Particle In Cell (PIC) method has been chosen because it is able to deal with such complex electro-magnetic fields and compatible with the low working pressures (< 1 Pa). However, to correctly describe the sheath behaviour, the mesh size has to been smaller than the Debye length which increases with the density, typically in HiPIMS $n_e > 10^{18}$ m^{-3}. To better characterize this phenomenon without drastically increasing the computation time, a non-uniform mesh has been implemented. The mesh size has been defined such as it is refined in the cathode layer and rougher far, in the diffusion plasma region. Moreover, in the HiPIMS regime, the time evolution is very fast (> 500 V/microsecond) and the this induces a fast rise of the plasma density.

Because of the high particle density near the cathode, the number of macro-particles required for the modelling is very important. In order to reduce it, a second order charge projection has been implemented. The charge density is consequently better define and so the potential better calculated. This implementation allows us to increase the weight of macro-particles and consequently to decrease their number without lost of accuracy.

This new version of the code has been used to compare the plasma behaviour in both DC and HiPIMS regimes. The two dimensional maps main plasma parameters, electron and ion densities, electrons temperature, ion fluxes to the cathode, etc. will

be presented and discussed. For the HiPIMS case, their evolution in time will be presented.

SE/ASS-P2-05
Flexible diamond-like carbon thin film coated on rubbers

T12 Surface Engineering

#SE/ASS-P2-05

Y. Pei [1], J.T.M. De Hosson [2], J. Shen [2].

[1]Materials innovation institute M2i, University of Groningen - Groningen (Netherlands), [2]University of Groningen - Groningen (Netherlands).

Dynamic rubber seals are major source of friction in lubrication systems and bearings, which may take up to 70% of the total friction. The solution we present is to coat rubbers with diamond-like carbon (DLC) thin film by which the coefficient of friction is reduced to less than one tenth. Coating rubber is very challenging because the film must be flexible and strongly adhered to rubber surface. Here we present and discuss our novel approach by depositing flexible DLC films on various rubbers via self segmentation. By making use of the substantial thermal mismatch between DLC film and rubber substrates a dense crack network forms in DLC films and contributes to flexibility. The size of film micro-segments can be tuned by varying the bias voltage of pulsed DC plasma assisted CVD, which governs the amplitude of the substrate temperature variation during deposition. An analytical model is developed to predict the crack spacing and the result fits well to the measured data. The formation mechanism of crack network and its effect on the flexibility and friction of DLC film coated rubbers are scrutinized. This paper provides generic design rules for the deposition of flexible and ultra low friction DLC films on rubber seals.

Y.T. Pei, X.L. Bui, J.P. van der Pal, D. Martinez-Martinez, J.Th.M. De Hosson. Flexible diamond-like carbon films on rubber: On the origin of self-acting segmentation and film flexibility. Acta Mater., 60 (2012), 5526-5535.
Y.T. Pei, D. Martinez-Martinez, J.P. van der Pal, X.L. Bui, J.Th.M. De Hosson. Flexible diamond-like carbon films on rubber: Friction and the effect of viscoelastic deformation of rubber substrates. Acta Mater., 60 (2012), 7126-7225.

SE/ASS-P2-06
Static and dynamic friction in sliding colloidal monolayers

T12 Surface Engineering

#SE/ASS-P2-06

A. Vanossi [1], N. Manini [2], E. Tosatti [3].

[1]CNR-IOM DEMOCRITOS and SISSA - Trieste (Italy), [2]Dipartimento di Fisica - Università di Milano - Milano (Italy), [3]SISSA, CNR-IOM DEMOCRITOS and ICTP - Trieste (Italy).

In a recent experimental breakthrough, the controlled sliding of two dimensional colloidal crystals over perfectly regular, laser generated periodic or quasi-periodic "corrugation" potentials has been realized in Bechinger's group [1]. Based on realistic molecular dynamics simulations which reproduce the main experimentally observed features, we explore the potential impact of colloid monolayer sliding in nanotribology [2]. The free motion of edge-spawned kinks and antikinks in smooth incommensurate sliding is contrasted with the kink-antikink pair nucleation at the large static friction threshold in the commensurate case. The Aubry pinning/depinning transition is also demonstrated as a function of parameters including the corrugation amplitude. Colloid simulated sliding data allow the extraction of frictional work directly from particles coordinates and velocities as a function of classic friction parameters, primarily speed, and corrugation strength (representing "load"). Analogies with sliding charge-density waves, driven Josephson systems and the sliding of rare gas islands, and other novel features suggest further experiments and insights, which promote colloid sliding to a novel friction study instrument [3].

[1] T. Bohlein et al, “Observation of kinks and antikinks in colloidal monolayers driven across ordered surfaces”, Nat. Mater. 11, 126 (2012).
[2] A. Vanossi, N. Manini, and Erio Tosatti, “Static and dynamic friction in sliding colloidal monolayers”, Proc. Natl. Acad. Sci. USA 109, 16429 (2012).
[3] A. Vanossi, E. Tosatti, “Colloidal friction: kinks in motion”, Nat. Mater. 11, 97 (2012).

SE/ASS-1-Or-7
ION BOMBARDMENT OF DUPLEX COATINGS BY NITROGEN

T12 Surface Engineering

#SE/ASS-1-Or-7

B. Skoric [1], D. Kakas [1], A. Miletic [2].

[1]Professor - Novi Sad (Serbia), [2]Assistent - Novi Sad (Serbia).

In this paper, we present the results of a study of TiN films which are deposited by a Physical Vapor Deposition and Ion Beam Assisted Deposition..The microstructure of obtained nitrided layer showed differences with regard to the presence or absence of a white layer, its thickness and its ε/γ′ phase ratio (XRD) and nitriding depth. In the present investigation the samples with duplex coating was studied, and subsequent ion implantation was provided with N5+ ions. The ion implantation was applied to enhance the mechanical properties of surface. The most successful and widespread model for nanoindentation data analysis is one in which the unloading data are assumed to arise from a purely elastic contact. The form most often used is known as the Oliver and Pharr method. This paper describes the successful use of the nanoindentation technique for determination of hardness and elastic modulus. Therefore, in recent years, a number of measurements have been made in which nanoindentation and AFM have been combined. Indentation was performed with CSM Nanohardness Tester. The results are analyzed in terms of load-displacement curves, hardness, Young's modulus, unloading stiffness and elastic recovery. The nanohardness of coating measured by Berkovich indenter is about 42.6 Gpa. The analysis of the indents was performed by Atomic Force Microscope. The stress determination follows the conventional $\sin 2\psi$ method, using a X-ray diffractometer The analyzed AE signal was obtained by a scratching test designed for adherence evaluation. AE permits an earlier detection, because the shear stress is a maximum at certain depth beneath the surface.
Coating is often in tensile stress with greater microhardness. The film deposition process exerts a number of effects such as crystallographic orientation, morphology, topography, densification of the films.The evolution of the microstructure from porous and columnar grains to densel packed grains is accompanied by changes in mechanical and physical properties. A variety of analytic techniques were used for characterization, such as scratch test, calo test, SEM (Figure 1), AFM, XRD and EDAX. Therefore, by properly selecting the processing parameters, well-adherent

TiN films with high hardness can be obtained on engineering steel substrates. The experimental results indicated that the mechanical hardness is elevated by penetration of nitrogen, whereas the Young's modulus is elevated.

References

1. W. Ensinger, Ion bombardment effects during deposition of nitride and metal films, Surface and Coatings Technology 99,1998,1.
2. J.C.A. Batista, C. Godoy, A. Matthews, A. Leyland,Process Developments Towards Producing Well Adherent Duplex PAPVD Coatings, Surface Engineering, 9, 2003, 37.

Figure 1.Surface morphologies of coating

SE/TF-2-Or-1
Obtaining ferromagnetic Fe-containing Al2O3 or TiO2 layers on aluminum or titanium by plasma electrolytic oxidation

T12 Surface Engineering

#SE/TF-2-Or-1

V. Rudnev [1], I. Lukiyanchuk [2], I.A. Tkachenko [2], A.Y. Ustinov [1], M.V. Adigamova [2], V.P. Morozova [2].

[1]Institute of Chemistry FEB RAS, Far Eastern Federal University - Vladivostok (Russian federation), [2]Institute of Chemistry FEB RAS - Vladivostok (Russian federation).

The essence of the method is electrochemical oxidation of metal surface at voltages of spark and arc electric discharges. Anodic coatings, which are formed by the PEO method, can involve electrolyte components. Coatings were formed for 2-10 min at 10 A/dm^2 in a Na_3PO_4 + $Na_2B_4O_7$ + Na_2WO_4 + $Fe_2(C_2O_4)_3$ aqua electrolyte-suspension. They have a thickness of 3 -33 μm and coercive force about 100 Oe at room temperature, fig. a. There are crystallites of 50 nm - 1 μm in size containing to 70 at% iron in the pores of the coatings, fig. b. We consider that magnetic properties of the coatings are related with these crystallites. The coatings are of interest as protective electromagnetic screens.

SE/TF-P2-06
Thermal and plasma treatment effects of ITO anode layer on performance of OLEDs devices

T12 Surface Engineering

#SE/TF-P2-06

Y. Kim, B.H. Choi, J.H. Lee.

National Center for Nanoprocess and Equipments, Korea Institute of Industrial Technology - Gwangju (Korea, republic of).

We have investigated the effect of surface treatment of indium-tin-oxide (ITO) on electrical and optical characteristics of organic light emitting diode (OLED) lighting devices. 150 nm thick ITO anode layer was patterned directly by using shadow mask during sputtering process without employing conventional photolithography patterning method. The sputtered ITO layer was oxygen plasma and thermally treated to reduce sheet resistance and to improve surface roughness. The thermal treatment was carried out at the temperature of 250 and 380 ^{o}C. The thermal treatment temperature was chosen not to affect the glass substrates and treated for 1 hour. The measured sheet resistance was decreased from 30.86 to 15.42 ohm/square obtained from thermally treated at 380 ^{o}C for 1 hour, followed by oxygen plasma treatment. The surface roughness which was measured in root mean square value was considerably decreased to 3.28 nm by oxygen plasma treatment as shown in Fig. 1. By employing thermal treatment, sheet resistance of shadow mask patterned ITO anode layer was considerably decreased. The spike-like structures formed in shadow mask patterned ITO anode layer were perfectly removed by oxygen plasma treatment. It is worthy while to note that smooth surface and low sheet resistance gives improved electrical and optical characteristics in OLEDs lighting devices. Based on surface treated ITO layer, green phosphorescent emitting OLED devices were fabricated and characterized. Figure 2 shows typical luminance-current density-voltage characteristics of fabricated OLEDs lighting devices fabricated on thermal and plasma treated ITO anode layer. The luminance and current density was the highest from the OLED devices fabricated by using thermally treated at 380 ^{o}C for 1 hour and oxygen plasma treated one. Our study shows that ITO anode layer which has low sheet resistance and surface roughness affected high electrical and optical properties on OLED lighting devices.

Figure 1. AFM image of surface of thermal and plasma treated ITO anode layer.

Figure 2. Luminance characteristics of fabricated OLEDs lighting devices on surface treated ITO anode layer.

SE-1-Or-10
Asymmetric distribution of ion and electron fluxes measured near the target plane in HiPIMS and DCMS discharges

T12 Surface Engineering

#SE-1-Or-10

M. Panjan, R. Franz, A. Anders.

Lawrence Berkeley National Laboratory - Berkeley (United states).

Plasma instabilities in the magnetron discharge play an important role in the transport of charged particles. They have been documented for high power impulse magnetron sputtering (HiPIMS) [1, 2] as well as for well-established direct current magnetron sputtering (DCMS) [3]. Properties of plasma instabilities have been studied by different plasma diagnostic techniques however, only recently the nature of instabilities in the HiPIMS discharge has been revealed by high-speed camera imaging [4, 5]. Images of magnetron discharges revealed dense plasma regions over the racetrack area, which travel in the direction of E × B drift (Fig. 1). These structures, called ionization zones or spokes, have periodic or aperiodic arrangement with an arrowhead shape at lower discharge currents and a more globular shape at higher discharge currents. Side-view imaging revealed that the edge of the ionization zones is accompanied by a dense plasma region expanding normal to the surface of the cathode [4].

This talk will focus on charged particle transfer in the plane of the target of a magnetron operated in HiPIMS or DCMS mode. Previous studies showed that flux and energy of ions in the HiPIMS discharge have strong asymmetric distributions with maxima in the direction of the E × B drift [1, 2]. Based on those studies we performed additional measurements, which show that the transfer of charged particles in HiPIMS is closely related to the occurrence of the ionization zones. Although much weaker, we found evidence that ionization zones also form in DCMS. In the first experiment, two biased collector probes were used to record the evolution of ion and electron fluxes during a HiPIMS pulse. Measurements showed the presence of peaks in the ion and electron fluxes, which correlated with the periodicity

and intensity of the ionization zones. The highest intensity of the particle flux peaks was recorded in the direction of E × B drift. Asymmetric distributions of ion and electron fluxes along the side of the magnetron were measured both in HiPIMS and DCMS. In a second experiment, ion energy distribution functions were recorded in the plane of the magnetron target by mass and energy analyzer. The measurements confirmed the asymmetric ion distributions in HiPIMS and DCMS discharges with the maximum flux in the direction of the E × B drift.

[1] D. Lundin *et al*., *Plasma Sources Sci. Technol*. **17**, 035021 (2008)
[2] P. Poolcharuansin *et al.*, *Plasma Sources Sci. Technol.* **21**, 015001 (2012)
[3] E. Martines *et al.*, *Phys. Plasmas* **11**, 1938 (2004)
[4] A. Anders *et al.*, *J. Appl. Phys.* **111**, 053304 (2012)
[5] A.P. Ehiasarian *et al.*, *Appl. Phys. Lett.* **100**, 114101 (2012)

Fig. 1

SE/TF-P2-07
Studies on the Internal Stress of Electroformed Ni-base Alloy for High Aspect Ratio Micro Parts

T12 Surface Engineering

#SE/TF-P2-07

S. Son, S.C. Park, H.M. Kim, J.H. Kim, W.S. Lee.

Korea Institute of Industrial Technology - Incheon (Korea, republic of).

Recently, Microelectromechanical systems (MEMS) process has been used in fabrication for high aspect ratio of micro parts, gear and molds. Electroforming is the highly specialized used for MEMS application. The internal stress at the interface between electrodeposit and substrate was important for micro electroforming. Internal stress will be affected by current density, temperature, agitation, plating bath, the metal alloy composition, applied power mode of DC or pulse power and the seed layer of the mandrel cathode. Indeed, there is no one special process variable that influences the deposit internal stress, because many variables described above could mutually have an effect on it. In this study, the micro gear and mold for powder injection molding and micro pin-fin heat sink were fabricated by electroforming of Ni-based alloys. The internal stresses in electrodeposited Ni-base alloys were controlled by concentration of organic additives, and various alloying elements. The internal stress was measured by using strain gauge-type stress meter.

The Ni-Fe alloy of electrodeposits was controlled by various organic additives, and it showed the measured internal stress decreased from 446.3 MPa up to 32.8 MPa. Decrease of internal stress is due to introduction of misfit dislocations at interface, when saccharin was added into electrolyte. a uniform and glossy surface and no cracks and delamination was observed in Ni-Fe alloy layer electrodeposited with an addition of organic additives, while many cracks and delamination were observed inside electrodeposition layer and at the interface between electrodeposited Ni-Fe alloy thin film and substrate, respectively, when no additives were added. The electrodeposited layer by pulse current showed lower internal stress than that by direct current, due to leveling effect and homogeneity of grain size. The micro electroformed gear and mold and micro pin-fin heat sink showed the same shape and size as mandrels fabricated by UV lithography and involutes curve of gear teeth was replicated exactly. Micro powder injection molding was performed using the micro electroformed molds. As a result, it is strongly suggested that micro

electroforming is very useful process to manufacture micro mold with high dimensional accuracy for micro PIM.

[1] A. M. El-Sherik, J. Shirokoff, U. Erb, J. Alloys Compunds, Vol 389, No. 1-2 (1995) 140-143.
[2] S.-H. Kim, H.-J. Sohn, Y.-C. Joo, Y.-W. Kim, T.-H. Yim, H.-Y. Lee, T. Kang, Surf. Coat. Tech., Vol 199, No.1 (2005) 43-48.

The photograph and SEM images of SU-8 micro mandrel and electroformed Ni alloy. (micro gear and mold for PIM application and micro pin-fin heat sink)

SE-1-Or-4
Syntheses and characterization of TiC nanocomposite using DC and HiPIMS magnetron sputtering

T12 Surface Engineering

#SE-1-Or-4

A. Patelli [1], M. Colasuonno [1], M. Bazzan [2], G. Mattei [2], V. Rigato [3].

[1]Veneto Nanotech SCpA - Marghera-Venezia (Italy), [2]Universita' di Padova - Padova (Italy), [3]LNL - INFN - Legnaro (pd) (Italy).

The aim of this study is to compare the effect of high power impulse (HiPI) and direct current (DC) power supplies in the deposition via magnetron sputtering (MS) of TiC/a-C nanocomposites on composition, structure and mechanical properties in industrial conditions with no sample biasing.
Titanium Carbide films were deposited in an industrial close field apparatus (target size 12”x4.9”) by HiPIMS and by DC from a titanium target in acetylene (C_2H_2) reactive atmosphere with no substrate bias. Reactive gas flux was changed in order to obtain C/Ti ratios in the coating from 0.8 up to 2. In order to evaluate the differences between the two processes emission spectra were recorded highlighting the presence of Hγ emission line only for the HiPIMS process depending on power and pulsing frequency (fig. 1). The deposition rate scaled linearly with the C_2H_2 flux in the poisoned mode for both DCMS and HiPIMS. Compositional RBS and ERDA characterization also showed lower hydrogen content in HiPIMS coatings than in DC. XRD and TEM characterization showed the presence of TiC nanocrystals with size and spacing dependent on C content surrounded by an amorphous matrix. HiPIMS allows to obtain fine grain TiC nanocrystals at C/Ti ratio closer to 1 than DC allowing for the same carbon content to obtain less amorphous carbon matrix.
The difference between the two deposition techniques were highlighted also by the mechanical properties of the coatings, tested by nanoindentation and microscratch. The deposited coatings showed as a function of the deposition process hardness in the range 10-25 GPa and elastic modulus of about 200 GPa, in particular HiPIMS coatings were characterized by higher hardness values while DC samples were always lower than 15 GPa. An increase of hardness and modulus could be observed for C/Ti content around 1.2-1.3, that was probably related to the nanostructure of the coating. Coefficients of friction showed values lower than 0.2 as a function of carbon coating content and were similar for HiPIMS and DC samples. On the other side

adhesion was improved in HiPIMS samples.
For C/Ti ratios from 1 to 1.4 the resistivity of the HiPIMS samples was around 400 μΩ cm, while DC samples showed a resistivity more than double (> 1000 μΩ cm).

fig. 1: Optical emission spectra of titanium DC and HiPIMS plasma in C_2H_2 atmosphere as a function of reactive gas flux. Hydrogen emission lines are visible in HiPIMS mode and not in DC mode.

SE-2-Or-3
Effect of Si and N on oxidation resistance of magnetron sputtered Zr-Si-B-C-N films

T12 Surface Engineering

#SE-2-Or-3

S. Proksova [1], P. Zeman [1], J. Kohout [1], P. Mares [2], R. Cerstvy [1], J. Vlcek [2].

[1]NTIS - European Centre of Excellence, Faculty of Applied Sciences, University of West Bohemia, Univerzitní 22, 306 14 - Plzeň (Czech republic), [2]Department of Physics, Faculty of Applied Sciences, University of West Bohemia, Univerzitní 22, 306 14 - Plzeň (Czech republic).

The Zr-B-C films prepared in our laboratories by nonreactive magnetron sputtering have showed an enhanced hardness (37 GPa), high electrical conductivity and resistance against oxidation up to 600°C. In the present paper, the effect of Si and N on high temperature behavior of the Zr-Si-B-C-N films is systematically investigated with aim to extend oxidation resistance of the films to higher temperatures while preserving high electrical conductivity and good hardness. The Zr-Si-B-C-(N) films with hardness ranging from 20 to 30 GPa were deposited on Si(100) substrates by dc pulsed magnetron co-sputtering of a single B_4C-Zr-Si target (with a fixed 15% Zr fraction in the target erosion area) in argon or nitrogen-argon gas mixtures. The Si and N content in the as-deposited films was varied in a wide range by the Si fraction in the target erosion area and by the N_2 fraction in the nitrogen-argon gas mixtures, respectively. The oxidation resistance of the Zr-Si-B-C-(N) films was investigated in synthetic air using a symmetrical high-resolution Setaram TAG 2400 thermogravimetric system. Changes in the structure, elemental composition, electrical resistivity and surface morphology of the films subjected to oxidation tests were analysed by X-ray diffraction, Rutherford backscattering spectroscopy, standard four-point method and optical microscopy. Preliminary results show that the addition of Si positively affects the oxidation resistance of the Zr-B-C films resulting in the reduction of mass gains. The Zr-Si-B-C films deposited with the 20% Si fraction in the target erosion area exhibit high hardness (22 GPa), low electrical resistivity (9×10^{-6} Ωm) and good oxidation resistance up to 750°C. The total mass gain detected at 800°C is less than 0.01 mg/cm^2. The addition of N into the Zr-Si-B-C films results in a

further shift of the onset of oxidation to higher temperatures. The films deposited with the 20% Si fraction in the target erosion area and with the 5% N_2 fraction in the gas mixture exhibit high hardness (22 GPa), slightly higher electrical resistivity (4×10^{-5} Ωm) and oxidation resistance up to 1000°C. High hardness and low electrical resistivity are preserved up to 900°C at annealing in air.

SE/TF-P2-08
Effect of air annealing on mechanical properties and structure of SiCxNy magnetron sputtered films

T12 Surface Engineering

#SE/TF-P2-08

V. Kulikovsky [1], R. Ctvrtlik [2], V. Vorlicek [1], P. Bohac [1], L. Jastrabik [1].

[1]Institute of Physics, Academy of Sciences of the Czech Republic - Prague (Czech republic), [2]Joint Laboratory of Optics of Palacky University and Institute of Physics of Academy of Sciences of the Czech Republic - Olomouc (Czech republic).

Ternary silicon carbon nitrides (SiC_xN_y) are considered as a prospective candidate for high temperature wear protective applications due to their high hardness and thermal stability of structure. In contrast to bulk materials these nitrides with variable composition can be relatively easily produced in the form of coatings by PVD and CVD techniques at low or middle temperatures.
Although the understanding the relationship between temperature treatment and mechanical properties is very important for materials exposed to mechanical loading at elevated temperatures there has been no systematic data on composition-related mechanical properties of the SiC_xN_y films after annealing in air.
Amorphous SiC_xN_y films with thickness of 2.2 - 2.7 µm were deposited on Si(111) substrates by reactive DC magnetron sputtering. The $SiC_{1.15}$ target was sputtered at various N_2/Ar gas flow ratios (0, 0.04, 0.08, 0.16, 0.32, 0.48). The as-deposited films were additionally annealed at temperatures of 700, 900 and 1100 °C in the air and at 900 °C in vacuum for 30 min.
Hardness and elastic modulus (nanoindentation), change of the film thickness, film composition (EPMA, GDEOS) and structure (Raman spectroscopy) were investigated in dependence on the annealing temperature.
Increase of N_2/Ar flow ratio results in gradual increase of nitrogen content (up to 40 at.%) in the films at approximately constant C/Si ratio and some reduction of compressive stress.
Air annealing results in slight decrease of film thickness for films sputtered at low N_2/Ar and small increase for films sputtered at high N_2/Ar. The most pronounced change of the relative thickness was observed for the film deposited in pure Ar after annealing at 1100 °C. It did not exceed 4 % that corresponds to ~100 nm.

The hardness of as-deposited films decreases along with the growth of N_2/Ar flow ratio. These films annealed in vacuum at 900 °C exhibit significantly higher values of hardness saving the above-mention trend. Besides their hardness almost do not vary with indentation depth in contrast to air annealed films.
Air annealing at 700 °C leads to the increase of hardness and elastic modulus values regardless of N_2/Ar ratio, while annealing at 900 and 1100 °C reduces them. As the indentation depth increases the hardness of the films annealed at 700 °C remains almost constant. Hardness of the films annealed in the air at 900 and 1100 °C increases accordingly to the structure (composition) changes from the oxidized top-surface (~250 nm) to the annealed non-oxidized subsurface with the improved structure. These results are supported by GDEOS investigation of profile concentration of elements and Raman spectroscopy.
Analysis of Raman spectra of air annealed films clearly points out the effect of nitrogen and oxygen on the facilitation of ordering of the amorphous carbon and onset of graphitization. This together with oxidation is directly reflected by the apparent softening of the films.
The hardness and oxidation resistance of the investigated SiC_xN_y films reduce along with increase of N_2/Ar ratio. The highest values of hardness and elastic modulus before and after air annealing up to 1100 °C exhibit films obtained without nitrogen.

SE/PST/TF/BI-2-Or-2
Enhancing bone ingrowth of titanium dental implants by industrial-scale DC magnetron sputtered Sr-Ti-O coatings

T12 Surface Engineering

#SE/PST/TF/BI-2-Or-2

S. Sørensen [1], K.P. Almtoft [1], I.H. Andersen [1], K. Rechendorff [1], L.P. Nielsen [1], O.Z. Andersen [2], C.S. Jeppesen [1], M.B. Sillassen [2], J. Bøttiger [2], M. Foss [2], C.S. Thomsen [3], H. Andersen [3], V. Offermanns [4], F. Kloss [4].

[1]Danish Technological Institute - Aarhus (Denmark), [2]iNANO Center, Aarhus University - Aarhus (Denmark), [3]Elos Medtech Pinol A/S - Gørløse (Denmark), [4]Medizinische Universität Innsbruck - Innsbruck (Austria).

The benefits of strontium administration on osseointegration of dental and orthopaedic implants are well-known [1,2], but there is at the same time a great interest for developing functionalized implant surfaces for localized delivery and controlled release rates of factors promoting osteointegration (e.g. Sr) at the defect site [3,4]. By tailoring Sr-functionalized thin film coatings improved healing of bone tissue can be achieved, thereby enabling a shorter healing period for patients, which is of great interest both scientifically and commercially.

In the present study, thin film Sr-Ti-O coatings grown by DC magnetron sputtering in an industrial-scale deposition unit are investigated (Figure 1). The deposition technique enables tailoring of the coating properties, e.g. chemical composition and morphology, by varying a number of different parameters such as e.g. sputtering power, deposition temperature, deposition pressure, film thickness and substrate bias voltage, the latter controlling the kinetic energy of the ion flux bombarding the growing film. The thin films have been characterised by XPS, XRD, SEM and RBS. Adhesion of the coatings has been successfully evaluated by bending tests, Daimler-Benz adhesion test and electron microscopy after press fitting a coated cylinder into polyoxymethylene (POM).
Furthermore, the release of Sr from the coatings when immersed in PBS buffer has been investigated by means of ICP-OES. The release of Sr is significantly dependent on the coating microstructure and can be tailored to a specific level. Promising in vivo

studies showing improved bone-to-implant contact and new bone formation will, among other results, be presented from this interdisciplinary project. An in vivo study in osteoporotic rats was initiated in January 2013 and results from this study will also be presented.

[1]: Marie P.J., et al. Calcif. Tissue Int. (2001), 69, 121–129
[2]: Maimoun L., et al. Bone (2010), 46, 1436-1441
[3]: Bosco R., Coatings (2012), 2, 95-119
[4]: Tomsia, A.P., Int. J. Maxillofac. Implants (2011), 26 (Suppl), 25-49

Fig1: Cross-sectional SEM of a Sr-Ti-O film.

SE/TF-P2-09
Real-time measurement of solid surface temperature irradiated by a pulsed laser

T12 Surface Engineering

#SE/TF-P2-09

T. Nakamiya [1], F. Mitsugi [2], Y. Iwasaki [1], T. Ikegami [2], R. Tsuda [1], Y. Sonoda [1].

[1]Tokai University - Kumamoto (Japan), [2]Kumamoto University - Kumamoto (Japan).

Heating with a nanosecond pulsed laser is widely used to the treatment of solid surface and biological applications. However, it is difficult for the real-time measurement of the surface temperature irradiated by a pulsed laser. In order to understand the detailed of surface temperature change, computer models have been developed to simulate the heat-flow conditions during the pulsed laser heating sequence. Kwon et al. refers our simulation result to estimate the surface temperature of carbon nanotube irradiated by a pulsed laser [1,2]. However, detailed physical properties of solid are necessary for computer simulation. The authors have developed the Fraunhofer diffraction method, which could be applied to the measurement of the optical wave diffracted by normal refractive-index waves [3]. This technique has been used to detect the ultrasonic wave generated by the electric discharge [4]. We apply this method to detect the thermal wave and shock wave generated by the irradiation of a pulsed laser to a crystalline silicon surface. Fig. 1 shows the experimental set-up to detect the signal arising from thermal and shock waves produced by a pulsed laser irradiation in air. Si surface was flashed with a single pulse of Nd:YAG laser. The pulsed laser energy density was varied with ND filter until the ablation threshold energy. Diode laser beam was sent towards the free space via a collimator lens 1 through a single mode optical fiber. When a probe laser beam crossed perpendicular to refractive index change with thermal and shock waves, the diffracted waves were generated and propagated to a collimator lens 2. The diffracted waves were then sent to the free space again via a collimator lens 3. The penetrating beam through a Fourier optical lens reached to the observing detector. When Si surface was flashed with a single pulse of Nd:YAG laser, the signals generated by the thermal and shock waves were detected. The intensity of

detected signal and the simulation result of surface temperature were increased with the increase of irradiation energy density. Therefore, we found that surface temperature irradiated by a pulsed laser is possible to estimate from the detected signal.

[1] O. H.Kwon, A. Zewail, Science, 328 (2010) 1668.
[2] T. Nakamiya, T. Ueda, T. Ikegami, F. Mitsugi, K. Ebihara, Y. Sonoda, Y. Iwasaki, R. Tsuda, Thin solid films, 517 (2009) 3854.
[3] Y. Sonoda, M. Akazaki, Jpn. J. Appl. Phys., 33 (1994) 3110.
[4] T. Nakamiya, F. Mitsugi, Y. Iwasaki, T. Ikegami, R. Tsuda, Y. Sonoda, H. D. Stryczewska, Eur. Phys. J. Appl. Phys. (in press).

Fig.1 Experimental set-up to detect the signal arising from thermal and shock waves.

SE/TF-P2-10
Structural Characterization of Advanced AlCrN/CrAlN Superhard Multilayer Coatings Prepared using Lateral Rotating Cathodes Process

T12 Surface Engineering

#SE/TF-P2-10

P. Zacková, Ľ. Čaplovič.

Slovak University of Technology, Faculty of Materials Science and Technology - Trnava (Slovakia).

There is an increasing number of applications for hard coatings in the field of surface engineering where the properties of the single layer coating are not sufficient. One way to solve this problem is to use a multilayer coatings system that combines the properties of several coating materials [1]. One of these types of multilayer is AlCrN/CrAlN coating. This multilayer gives higher cutting speeds, feeds and extended tool life in the case of machining, punching or forming higher strength and abrasion resistive steels or non ferrous metals [2,3]. This paper deals with the structural characterization of AlCrN/CrAlN multilayer coating that was deposited onto AISI M36 tool steel substrate. Multilayer was prepared using Lateral rotating cathodes (LARC®) process that enables to deposition of PVD layers with reduction in macroparticles creation. Scanning electron microscopy fitted with EDX spectroscopy will be used for evaluation of microstructure and surface morphology of multilayer. Laser confocal scanning microscopy will be utilized for determination of AlCrN/CrAlN multilayer surface roughness and morphology as well. Concentration depth profiles through the top of the multilayer surface to the base material will be obtained with Glow discharge optical emission spectroscopy. Both X-Ray diffraction and Electron Backscatter diffraction analysis will be performed for the determination of phases presented in deposited multilayers. Indentation testing, nanohardness measurements, scratch and wear tests will be performed to characterize the mechanical properties of this type of multilayer. The influences of structure and composition of the multilayer coating on the mechanical and tribological behavior will be discussed.

[1] M. Okumyia, M. Griepentrog: Mechanical properties and tribological behavior of TiN–CrAlN and CrN–CrAlN multilayer coatings. Surface and Coatings Technology, Volume 112, Issues 1–3, February 1999, Pages 123–128.

[2] S.H. Tsai, J.G. Duh: Microstructure and mechanical properties of CrAlN/SiNx nanostructure multilayered coatings. Thin Solid Films 518 (2009) 1480–1483.

[3] B. Tlili, C. Nouveau, M.J. Walock, M. Nasri, T. Ghrib: Effect of layer thickness on thermal properties of multilayer thin films produced by PVD. Vacuum 86 (2012) 1048e1056.

SE/TF-4-Or-2
Effect of mild oxidation of carbon/carbon composites on the oxidation protective ability of SiC coating

T12 Surface Engineering

#SE/TF-4-Or-2

Q. Fu, Y.J. Wang.

Northwestern Polytechnical University - Xi'an (China).

In order to improve the oxidation protective ability of SiC coating for C/C composites, the C/C substrate was mild-oxidized before coating. The sample had deeper oxidation thickness at 800℃ than that at 1100℃ after the same time. With the mild oxidation of C/C substrate, large scale gradient transition interface could form at the interface between SiC coating and C/C composites, which is favorable for theinterface bonding. Mass loss of SiC coated C/C sample without mild oxidation quickly reached 1.5 %, after oxidation for 3 h. However, the mild-oxidized composites with SiC coating exhibited better oxidation protective ability. The samples still gained weight 0.3 % after oxidation for 14 h, owing to the release of mismatch of thermal expansion.

[1] J.F. Huang, H.J. Li, X.B. Xiong, et al. progress on the oxidation protective coating of carbon- carbon composites. New Carbon Mater, 20(2005): 373-379.
[2] H.J. Li, H. Xue, Q.G. Fu, Y.L. Zhang, X.H. Shi. Research status and prospect of anti-oxidation coatings for carbon/carbon composites. J. Inorg. Mater.25 (2010): 337-343.
[3] Q.S. Zhu, X.L. Qiu, C.W. Ma. Oxidation resistant SiC coating for graphite materials. Carbon, 37(1999):1475-1484.
[4] L.F. Cheng, Y.D. Xu, L.T. Zhang, X.G. Luan. Oxidation and defect control of CVD coatings on three dimensional C/SiC composites. Carbon, 40(2002): 229-2234.
[5] P. Colombo, T.E. Palson, C.G Pantano. Synthesis of silicon carbide thin films with polycarbosilane (PCS) J. AM. Ceram. Soc., 80(1991): 2333-2340.
[6] J.F. Huang, X.R. Xie, H.J. Li, X.B. Xiong, Y.W. Fu. Influence of preparation

temperature on the phase, microstructure and anti-oxidation property of a SiC coating for C/C composites. Carbon, 42(2004): 1517-1521.
[7] W.G. Zhang, H.J. Hüttinger. Densification of a 2D carbon fiber perform by isothermal, isobaric CVI: kinetics and carbon microstructure. Carbon, 41(2003): 2325-2337.
[8] G.H. Zhou, T.F, Chen, L.L He, H.Q. Ye. In situ observation of fracture interface between an individual fiber and the pyrocarbon matrix in C/C composites. Carbon, 50(2012): 2353-2355
[9] W.M. Guo, H.N. Xiao, E. Yasuda, Y. Cheng. Oxidation kinetics and mechanisms of a 2D-C/C composites. Carbon, 44(2006):3269-3276.

SEM image of C/C composites after mild oxidation at 800℃.

SE/ASS-1-Or-3
Structure characterization and wear performance of nanocomposite MoCN-Ag coatings

T12 Surface Engineering

#SE/ASS-1-Or-3

A. Bondarev.

MISiS - Moscow (Russian federation).

Structure characterization and wear performance of nanocomposite MoCN-Ag coatings

A.V. Bondarev[1], Ph.V. Kiryukhantsev-Korneev[1], K.A. Kuptsov[1], T.C. Rojas[2], V. Godinho[2], A. Fernandez[2], D.V. Shtansky[1]

[1] National University of Science and Technology "MISIS", Leninsky prospect 4 - 164, Moscow, 119049, Russia
[2] Instituto de Ciencia de Materiales de Sevilla CSIC-US, Avda. Americo Vespucio 49, Sevilla, 41092, Spain

PVD coatings are widely used as wear resistant protective layers on bulk materials surface, although development of new coatings generation that combine high hardness and low friction coefficient in a wide temperature range is still the challenge. The ability of coatings to demonstrate low friction coefficient and wear rate in a wide temperature range is of great importance for many tribological applications because friction and wear produce essential energetic losses and decrease efficiency of the mechanical systems. Commonly known lubrication coatings based on pure carbon and transition-metal dichalcogenides have a limited range of operating temperatures. Above 350 – 400 °C such coatings oxidize in air, resulting in increased friction and accelerated wear. To overcome this problem multicomponent nanocomposite coatings, which are known to possess a desired combination of properties, could be employed for operations that require solid lubrication.

The aim of this work was to develop coatings for wide temperature tribological applications up to 700 °C and study their structure and properties.

MoCN-Ag coatings were deposited by pulsed magnetron sputtering of Mo and C (graphite) targets and simultaneous sputtering of Ag target using an additional ion

source. The structure and phase composition of the coatings were investigated by means of X-ray diffraction, transmission and scanning electron microscopy, X-ray photoelectron spectroscopy, and glow discharge optical emission spectroscopy. The elemental and phase composition inside and outside of the wear tracks were examined using Raman spectroscopy and EDX analysis. The MoCN-Ag coatings deposited in a gaseous mixture of Ar + 15 %N_2 had nanocrystalline structure consisted of the cubic Mo(C,N) crystallites and metallic silver particles. When deposition experiments were carried out in nitrogen atmosphere, the MoCN-Ag coatings were consisted of four different phases: c-MoN, h-Mo_2C, a-C, and metallic Ag. The nanocomposite MoCN-Ag coatings demonstrated low friction coefficient in the range of 0.3 - 0.4 both at low (25 – 100 °C) and high (400 – 700 °C) temperatures. This observation can be explained by the presence of amorphous carbon which acted as a solid lubricant at low temperatures and the precipitation of MoO_x and silver molybdate $Ag_2Mo_4O_{13}$ phases which provided low friction above 400 °C. The MoCN-Ag coatings also demonstrated adhesion to cemented carbide substrate above 70 N measured by scratch testing. Fracture toughness and fatigue strength of the coatings were estimated by means of dynamic impact tests. The MoCN-Ag coatings endured the dynamic impact forces of 1300 and 700 N for 10^4 and 10^5 cycles, respectively. The coating failures can be attributed to the adhesion strength limit of the MoCN-Ag coating being exceeded, rather than to low fracture toughness itself.

SE-1-Or-7
Time and spatially resolved ion energy distribution function in reactive HiPIMS

T12 Surface Engineering

#SE-1-Or-7

M. Cada, P. Adamek, J. Olejnícek, Š. Kment, Z. Hubicka.

Institute of Physics ASCR, v.v.i. - Prague 8 (Czech republic).

The High Power Impulse Magnetron Sputtering System (HiPIMS) equipped with 2” in diameter target has been investigated by means of time-resolved mass- and energy-resolved analyser (plasma monitor) from Hiden Ltd., gridded retarding field energy analyser (RFEA) from Impedans Ltd. and so called modified Katsumata probe. All the methods allow to determine ion velocity distribution functions (IVDF) in forward direction to substrate as a function of retarding electric field. However, except plasma monitor latter methods are not able to resolve the mass of particles. The newly developed modified Katsumata probe uses a static magnetic field created by Sm-Co permanent magnets to intercept the most of plasma electron and pull them away back to the plasma bulk. Furthermore, the plasma monitor and the modified Katsumata probe are characterized in very small angular acceptance in comparison with the gridded RFEA. The high power impulse magnetron sputtering system was equipped with pure metallic targets (titanium or iron). As working gas a mixture of Ar and O_2 was used. The working gas pressure ranging between 0.5 Pa to 5 Pa. All the diagnostic instruments were placed at position of substrate. All the measurements were carried out under the same conditions as the thin oxide films TiO_2 and Fe_2O_3 were deposited. A comparative study of all the aforementioned methods has been carried out.
Results clearly demonstrate an influence of angular resolution on measured IVDF. Unlike gridded RFEA the modified Katsumata probe was able to distinguish different groups of ions coming on the substrate in different times of plasma pulse. The gridded RFEA has angular acceptance more than 70° and ions reaching its input orifice originate from different direction unlike the modified Katsumata probe which accepts ions only from cone of a small solid angle. The temporally resolved investigation with plasma monitor revealed that sputtered particles reach a substrate later on. All the plasma diagnostic methods revealed significantly enhanced energy tail in ion velocity distributions measured in HiPIMS in contrast to dc magnetron or mid-frequency pulsed-dc magnetron. An influence of working gas pressure on velocity distributions of argon, metallic and reactive gas ions specifically on presence

of high-energy tail is discussed. The plasma monitor proved that under certain plasma conditions appearance of double ionized sputtered and working gas particles can be observed.

Acknowledgements:
This work was supported by the Ministry of Education, Youth, and Sports of the Czech Republic through project LD120012, by the Czech Science Foundation through projects P205/11/0386, P108/12/2104 and by the COST Action MP0804 through the grant STSM 11182.

SE/ASS-1-Or-10
Preparation and Micro-tribological Behavior of Superhydrophobic Nanofilm on Surface of Ti-6Al-4V Titanium Alloy

T12 Surface Engineering

#SE/ASS-1-Or-10

Z. Kang, G. Fang, Q. Liu, J. Zhang.

South China University of Technology - Guangzhou (China).

A superhydrophobic nanofilm was obtained on Ti-6Al-4V titanium alloy surface through the combination of chemical etching and polymer plating techniques. The hierarchical structured surface was researched by SEM and XRD. The elements, surface topography and wettability of superhydrophobic nanofilm were characterized by XPS, AFM and contact angle meter, respectively. UMT–2 tribometer was utilized to investigate the micro-tribological behavior of the nanofilm. The experimental results show that the surface is coated by organic nanoparticles clusters after polymer plating and the contact angle of distilled water is 155.0°. The friction coefficient of polymer plated surface decreases to 0.21 compared with 0.42 for blank and the wear life is 220 s, therefore the micro-tribological property of Ti-6Al-4V titanium alloy surface is effectively improved.

This work is supported by the National Natural Science Foundation of China (No.51075151) and Key Program of Guangdong Natural Science Foundation (No.10251064101000001).

Keywords: Titanium alloy, Polymer plating, Nanofilm, Superhydrophobic, Micro-tribological property

[1] Romig AD, Dugger MT, McWhorter PJ. Materials issues in microelectromechanical devices: science, engineering, manufacturability and reliability. Acta Materialia, 2003, 51(19): 5837-5866

[2] Song Y, Nair RP, Zou M, Wang YA. Adhesion and friction properties of micro/nano-engineered superhydrophobic/hydrophobic surfaces. Thin Solid Films, 2010, 518(14): 3801-3807
[3] Kang ZX, Lai XM, Sang J, Li YY. Fabrication of hydrophobic/super-hydrophobic nanofilms on magnesium alloys by polymer plating. Thin Solid Films, 2011, 520(2): 800-806
[4] Bhushan B, Her EK. Fabrication of superhydrophobic surfaces with high and low adhesion inspired from rose petal. Langmuir, 2010, 26(11): 8207-8217

Fig. 1 Variation of friction coefficient with reciprocating time for different surfaces

In Fig. 1, it can be concluded that the superhydrophobic nanofilm presents excellent tribological properties, including anti-wear and reducing friction coefficient ability.

TF/SE-1-Or-13
Synthesis and characterisation of Magneli phases of titanium (TinO2n-1) coatings deposited by reactive magnetron sputtering

T12 Surface Engineering

#TF/SE-1-Or-13

Y. Gui [1], M. Arab Pour Yazdi [1], F. Lapostolle [1], A. Besnard [2], A. Billard [3].

[1]IRTES-LERMPS, UTBM, site de Montbéliard - Belfort (France), [2]LaBoMaP, Arts et Métiers ParisTech - Cluny (France), [3]IRTES-LERMPS / LRC CEA - Belfort (France).

Ti_nO_{2n-1}, substoichiometric titanium oxides (Magneli phases) are known to present interesting tribological properties for low wear applications [1, 2]. The existence domain of Magneli phases being limited, it remains difficult to synthesise them. In most published studies, films composed of these phases are obtained either by thermal spraying [3], laser chemical vapour deposition [4], or by sol-gel route [5]. However, few papers deal with the deposition of Magneli phases films by physical vapour deposition through controlling the oxygen content.

In this paper, titanium Magneli phases' coatings were synthesized with different thicknesses at a temperature of 873 K by reactive magnetron sputtering. The substrates are AISI M2 high speed steels previously covered with AlTiN coatings obtained by reactive arc deposition. The chemical, structural and mechanical characteristics of the coatings are presented. In particular, the pin-on-disc tests at ambient and high temperatures are performed to assess the wear resistance of those coatings as a function of their thickness.

In a second part, we investigate the deposition of Ti-O coatings as a function of the oxygen flow rate with the same thickness which presents the best wear resistance at the preceding tests. The pin-on-disc tests at ambient and high temperatures are also performed. We finally present relationships between the oxygen flow rate and the

chemical and structural features of the coatings and their effect on the wear resistance of these coatings.

[1] M.N. Gardos, Tribol. Lett. 8 (2000) 65-78.
[2] M. Woydt, Tribol. Lett. 8 (2000) 117-130.
[3] O. Storz, H. Gasthuber, M. Woydt, Surf. Coat. Technol. 140 (2001) 76-81.
[4] R. Tu, G. Huo, T. Kimura, T. Goto, Thin Solid Films 518 (2010) 6927-6932.
[5] C. Langlade, B. Vannes, T. Sarnet, M. Autric, Appl. Surf. Sci. 186 (2002) 145-149.

TF/SE-1-Or-12
Innovative wear-resistant coating under unlubricated conditions in a wide range of temperature realized by reactive magnetron sputtering

T12 Surface Engineering

#TF/SE-1-Or-12

G. Bouscarrat.

CITRA - Limoges (France).

Nowadays, surface treatments are more and more used in many different industries, especially to enhance wear resistance thanks to better friction coefficient and harder surfaces. Among all technologies, the PVD processes are good solutions for different kind of coatings: TiN, TiC, TiCN, CrN, CrC, TiAlN and DLC mainly, for these applications.
Recently, lots of studies were about tribological issues which represent one of the most important expenses' source for industry. For example, 20 years ago, wear's cost represented in France about 20 billions Euros. In the Unites States of America, American industries estimated the friction loss in the internal-combustion motors to about 0.7% of the global energetic consumption of the USA. Consequently, the realization of highly wear-resistant coatings with low friction coefficient is a point of high interest.
Because of this, an innovative coating was suggested by the Center for Innovative Technology and Research in Advanced coatings (CITRA) in Limoges, France. It was realized by reactive magnetron sputtering using a target mainly made of TiHfCN. Indeed, TiCN coating has a four times higher lifetime than a TiN coating [1] and Hf compounds possess higher melting points than Ti ones [2,3].
Some improvements (i.e. experimental design and parametric study) already lead to the realization of a multilayer coating with enhanced adherence and friction properties. In addition to the advantages of a multilayer-type coating (i.e. multifunctional character, good adherence due to moderate residual stresses, etc.), the increase in nitrogen and carbon concentrations causes a higher wear resistance, low friction coefficient and good substrate adherence. Most of intrinsic characterizations were made using CITRA's equipments and leaded to the properties summarized in table 1 below.

Crystalline phase	Hardness (GPa)	Young's modulus (GPa)	Wear rate ($mm^3/N/m$)	Friction coefficient	Adherence Lc_1 (N)	Thickness (µm)
HfTiCN	32 ± 2	332 ± 13	1.6×10^{-7}	0.05-0.25	18-22	2-4

Table 1 - Coating's properties

Furthermore, some tests confirmed that this coating offers interesting properties until 600°C. Finally, further experimentations will be realized to improve and develop some new layer arrangements adding some metallic elements like chrome and aluminium.
We expect new applications for this multi-purpose coating, especially for extreme temperatures, with or without lubricant.

[1] O. Knotek, F. Löffler, G. Krämer, Vacuum 43 (5–7) (1992) 645–648

[2] R. Keiffer, F. Benesovsky, Hartstoffe, Springer, Vienna, 1963

[3] W. König, Fertigungsverfahren, Band 1, 4. Auflage, VDI, Düsseldorf, 1990

SE/TF-P2-11
Comparative investigation of (TiZr)C and multi-principal-element (TiZrCuSiY)C coatings

T12 Surface Engineering

#SE/TF-P2-11

M. Braic, M. Balaceanu, V. Braic, C.N. Zoita, A. Vladescu, I. Pana.

National Institute for Optoelectronics - Magurele-Bucharest (Romania).

The purpose of the present study was to comparatively investigate the characteristics of (TiZr)C and a novel multi-principal-element (TiZrCuSiY)C coatings, based on high entropy alloy concept [1,2]. The metals in the films are in almost equiatomic concentrations. For (TiZrCuSiY)C films, the metallic constituents were selected taking into account: atomic radius, mixing enthalpy and valence electron concentration. The films were deposited on Si and C45 substrates through co-sputtering of Cu, Si, Ti, Y and Zr targets in an Ar+CH4 reactive atmosphere. The films were analyzed for elemental and phase composition, crystalline structure, mechanical characteristics, tribological and corrosion performance in saline solution (3.5 % NaCl). The influence of carbon concentration on film properties was investigated.
While (TiZr)C films exhibited crystalline structures (fcc), the (TiZrCuSiY)C films were amorphous (Fig.1). Fine grained and smooth surface morphologies were observed by AFM. For the same carbon concentration, the multi-principal-element films exhibited lower wear rates (Fig.2) and friction coefficients, and better corrosion resistance, as compared to the (TiZr)C films.
Considering their fine structures, good wear - corrosion resistance and friction characteristics, the multi-principal-element (TiZrCuSiY)C coatings can represent a valuable alternative in various tribological and anticorrosive applications.

Acknowledgement:This work was supported by a grant of the Romanian NationalAuthority for Scientific Research, CNCS-UEFISCDI, project number PN-II-ID-PCE-2011-3-1016.

[1] J.W. Yeh, S.K. Chen, S.J. Lin, J.Y. Gan, T.S. Chin, T.T. Shun, C.H. Tsau, S.Y. Chang (2004) Adv. Eng. Mater., 6: 299- 303
[2] J.W. Yeh, Ann. Chim. Sci. Mater. (2006) 31: 633–648

Fig. 1 XRD patterns of the deposited coatings (s-substrate)

Fig. 2 Wear rates for the deposited coatings

TF/SE-1-Or-6
BITAVOX.20-based electrochemical sensor built by reactive magnetron sputtering for hydrocarbon detection at moderate temperature.

T12 Surface Engineering

#TF/SE-1-Or-6

E. Dereeper, P. Briois, A. Billard.

IRTES-LERMPS-UTBM - Belfort (France).

As harmful and potentially flammable or explosive compounds, monitoring hydrocarbon vapours atmospheric rates relates to health as well as security issues. Electrochemical sensors are suitable for such an application since they generally exhibit fast response and good sensitivity.

The sensors presented here are built upon thin films of BITAVOX.20 ($Bi_2Ta_{0.2}V_{0.8}O_{5.5}$) electrolyte, chosen for its ability to conduct oxide ions at moderate temperatures (300°C) and platinum and lanthanum perovskites electrodes. They have been deposited on alumina pellets or MSP 769 commercial sensor platform by reactive magnetron co-sputtering. The influence of the deposition parameters on the electrode/electrolyte interface and on the electrodes microstructure has been investigated by X-ray diffraction and SEM observations. The impact of electrode morphological characteristics as well as this of the sensor design and of its ageing on the detection performance in the amperometric mode and in the potentiometric mode has been assessed using a home-made test bench.

SE-2-Or-1
Corrosion Behaviour of Nitrogen-doped Al-Ti-Ni and Al-Cr-Ni Nanostructured PVD Coatings Deposited on Low Alloy Steel

T12 Surface Engineering

#SE-2-Or-1

J. Lawal, O. Fasuba, A. Matthews, A. Leyland.

University of Sheffield - Sheffield (United kingdom).

Low alloy steels (e.g. 4140 and 4145 grades) have found increased application for engineering components as a result of their strength and hardness. They have been used in structural pipe-work and in transport tubing for pressurised fluids (especially in the oil and gas industry). However, such low alloy steel grades have relatively poor corrosion resistance, due mainly to their low chromium content.

Nanostructured PVD coatings comprising a hard nanocrystalline phase embedded in an amorphous matrix have been found to exhibit multifunctional capabilities. These coatings can exhibit unusual combinations of high hardness, long elastic strain to failure, resistance to crack formation – and even exhibit good corrosion resistance (in terms particularly of pitting) [1,2,3,4]. This study investigates the corrosion characteristics of nitrogen-doped Al-(Ti, Cr)-Ni nanostructured coatings prepared by magnetron sputtering. Electrochemical impedance spectroscopy and potentiodynamic polarisation measurements were used to investigate the corrosion behaviour of the coatings in a 3.5 wt. % NaCl environment. This work provides a comprehensive report of the corrosion characteristics of nitrogen-doped Al-Ti-Ni and Al-Cr-Ni nanostructured PVD coatings.

1. Veprek, S., Niederhofer, A., Moto, K., Bolom, T., Mannling, H.-D., Nesladek, P., Dollonger, G., and Bergmaier, A., Composition, nanostruscture and origin of ultrahardness in nc-TiN/a-Si3N4/a- and nc-TiSi2 nanocomposites with Hv = 80 to > 105 GPa. Surface and Coatings Technology, 2000. 133-134: p. 152-159.

2. Voevodin, A.A., Hu, J.J., Jones, J.G., Fitz, T.A., and Zabinski, J.S., Growth and structural characterization of yttria-stabilized zirconia-gold nanocomposite folms with improved toughness. Thin Solid Films, 2001. 401: p. 187-195.

3.Liu, C., Leyland, A., Bi, Q., and Matthews, A., Corrosion resistance of multi-layered plasma-assisted physical vapour deposition TiN and CrN coatings. Surface and Coatings Technology, 2001. 141: p. 164-173.

4. Veprek, S. and Jilek, M., Super- and ultrahard nanocomposite coatings: generic concept for their preparation, properties and industrial applicaion. Vacuum, 2002. 67: p. 443-449.

SE-2-Or-5
Nanostructured tungsten as plasma facing material for nuclear fusion reactor applications

T12 Surface Engineering

#SE-2-Or-5

I. Fernandez [1], N. Gordillo [2], M. Panizo-Laiz [2], E. Tejado [3], A. Rivera [2], F. Briones [4], J.I. Pastor [4], J. Del Río [5], C. Gomez [6], J.M. Perlado [2], R. Gonzalez-Arrabal [2].

[1]Instituto de Energía Solar (IES), Universidad Politécnica de Madrid, Avenida Complutense s/n, E-28040 - Madrid (Spain), [2]Instituto de Fusión Nuclear, ETSI de Industriales, Universidad Politécnica de Madrid, C/ José Gutierrez Abascal, 2, E-28006 - Madrid (Spain), [3]Dept. Ciencia Mat. CISDEM, ETSI de Caminos, Universidad Politécnica de Madrid, E-28040 - Madrid (Spain), [4]Instituto de Microelectrónica de Madrid, IMM-CNM-CSIC, Isaac Newton 8 PTM, E-28760 Tres Cantos - Madrid (Spain), [5]Departamento de Física de Materiales, Facultad de CC. Físicas, Universidad Complutense de Madrid, Ciudad Universitaria s/n, E-28040 - Madrid (Spain), [6]Departamento de Física de Materiales, Facultad de CC. Químicas, Universidad Complutense de Madrid, Ciudad Universitaria s/n, E-28040 - Madrid (Spain).

The constant increase in the world population and in the development degree leads to a high energy consumption. The energy solution is a long standing problem which requires innovative solutions. Nowadays, in combination with other sustainable sources of energy, fusion energy can become within the next two decades a real alternative to fossil fuels. However, the lack of materials able to withstand the severe radiation conditions (high thermal loads and atomistic damage) expected in such reactors is a bottle neck for fusion to become a reality.

The main requisite for plasma facing materials (PFM) is to have excellent structural stability since severe cracking or mass loss would hamper their protection role which turns out to be unacceptable. Additional practical requirements for PFM are among others: (i) high thermal shock resistance, (ii) high thermal conductivity (iii) high melting point (iv) low physical and chemical sputtering, and (v) low tritium retention.

W has been proposed to be one of the best candidates for PFM for both laser (IC) and magnetic (MC) confinement fusion approaches. However, works carried out up to now have identified some limitations for W which have to be defeated in order to fulfill specifications [1,2,3]. Nowadays, the capabilities of ultrafine grain and nanostructured materials for nuclear fusion reactor applications are being investigated [4].

We report on the growth of nanostructured W coatings with a thickness of ~ 2 microns by using DC magnetron sputtering on different kind of substrates (Si, Mo and steel). X-Ray diffraction (XRD) studies show that coatings are pure alfa-phase polycrystalline and present low macro-stress and micro-strain. The influence of substrate on stress is assessed. Scanning electron microscope (SEM) images show that coatings consist of nano-columns with an average diameter of around 100 nm and an inverted pyramidal shape that grows perpendicular to the surface substrate. Nanoindentation tests evidence that the coating hardness is as high as ~14 GPa. The dependence of microstructure, morphology, and mechanical properties on annealing temperature and time ($T \leq 1000$ ºC and $t \leq 240$ min.) will be also reported. No significant change in the studied properties is observed for coatings annealed at 400ºC for 240 min.

[1] Takeshi Hirai, Koichiro Ezato and Patrick Majerus, Materials Transactions, 46, (2005) 412-424

[2] Kajita S., Sakaguchi W., Ohno N., Yoshida N., Saeki T. 2009. Nucl. Fus. 49, 095005

[3] Sharafat S., Takahashi A., Hu Q., Ghoniem N.M. 2009. J. Nucl. Mat. 386-388, 900

[4] M. Rieth et al. private comunication

SE/TF-P2-12
STRUCTURAL CHARACTERISTICS OF PLASMA-NITRIDED LAYERS ON SINTERED IRON SUPERFICIALLY ALLOYING WITH MOLYBDENUM

T12 Surface Engineering

#SE/TF-P2-12

A. Maliska [1], T. Bendo [1], J.J.S. Acuña [2], K.C. Kleinjohann [1].

[1]UFSC - Florianópolis (Brazil), [2]UFABC - São Bernardo Do Campo (Brazil).

During the sintering process using a dc glow discharge, unalloyed iron samples have the surface alloyed with molybdenum (approx. 5 at.%) and after they are nitrided. These samples showed a layer of distinct precipitation between the composite layer and the diffusion layer (Figure 1) with significant increase in the hardness values. The layers characterization was carried out by electron microscopy (SEM and HR-TEM), X-ray diffractometry (XRD) and GDOES (Glow Discharge Optical Emission Spectroscopy). In he XRD analysis was not detected the presence of Mo nitrides or ternary nitrides (Fe-Mo-N) in the nitrided layer, only γ'-Fe_4N and ε-$Fe_{2-3}N$ phases were detected, wich could be attributed to low Mo concentration (3 at 5 at %) [1]. Analysis of the nitrided layers by selected area electron diffraction (SAED) was performed in order to characterize the different regions in nitrided sample. The TEM investigations provided the formation of γ'-Fe_4N and ε-$Fe_{2-3}N$ in white layer. According to [2] in Fe-Mo alloys nitrided between 450-600 oC can be expected compositions γ'-$(Fe,Mo)_4N$ and ε-$(Fe,Mo)_{2-3}N$ with some Fe atoms substituted by Mo atoms. The Figure 2 demonstrated the formation of very small precipitates (20 nm) on the surface sample. In these precipitates was detected the presence of Mo (by nano-EDS) in contrast to the XRD analysis. A high nitrogen concentration was found (by GDOES analysis) in the first 3 μm of surface. The TEM investigations indicate the presence of compounds FexNx-1 with $0,40<x<0,50$ in superficial layer which may have been formed due to the increased solubility of nitrogen on the surface favored by the presence of Mo [3].

[1] M.R. Pinasco, G. Palombarini, M.G. Ienco, G.F. Bocchini, J. Alloys and Comp. 220, 217 (1995).
[2] R. Wagner and S.S. Brenner, Acta Metal. 26, 197-206 (1978).
[3] H. Morita, T. Kaneko, H. Yoshida and H. Fujimori. J. Alloys and Comp. 201, 11-16 (1993).

Figure 1 – Optical cross-sectional micrograph of the sample of iron superficially enriched with Mo and nitride.
Figure 2 – HR-TEM image of Fe-Mo-N precipitates obtained by carbon replica and SAED pattern.

SE/PST/TF/BI-P1-02 Biocompatibilizacion of a porous structure by lipid coverage

T12 Surface Engineering

#SE/PST/TF/BI-P1-02

J. Benavente [1], V. Romero [1], L. Gelde [1], M.I. Vázquez [1], J. Hierrezuelo [2].

[1]Dpto. Física Aplicada I, Facultad de Ciencias. Universidad de Málaga - Málaga (Spain), [2]Dpto. Química Orgánica, Facultad de Ciencias. Universidad de Málaga - Málaga (Spain).

Porous structures are nowadays common systems for applications in water treatment, biomedical applications, microfluidics, dialysis, or tissue engineering … [1]. Particularly, transport through nanoporous supports with well defined structure has received significant attention during the last decade due to their application in processes related with molecular/ion transport control, which is a point of great interest in areas such as biosensors or drug delivery, but requirements on the biocompatibility and the hydrophobic character of the membrane surfaces and their biocompatibility are important factor to be considered, this latter directly related to reduce the membrane fouling, that is, the adsorption or deposition of proteins, macromolecules and colloidal particles on the surfaces of membrane. Surface coverage by lipid compounds can be of significant importance for such applications. This paper presents the surface coverage of a porous polyvinylidenedifluoride (PVDF) membrane by a lipid mixture (glyceryl triestearate (33.5 %), sodium taurocholate (50 %) and L-α-phosphatidylcholine (16.5 %)), and its effect on surface and transport parameters. Membrane surface modification associated to lipid layer was characterized by X-ray photoelectron spectroscopy (XPS) and contact angle (CA) measurements performed with dry samples. However, water and NaCl solutions at different concentrations were used for measurements of transport parameters such as water permeability ($Lp = Jv/\Delta P$), diffusive permeability ($Ps = Js/\Delta C$) and ion transport number (ti, or fraction of the total current carrier by the cation), where Jv and Js represent the water and solute flow, while ΔP and ΔC are the pressure and concentration differences across the membrane. Variations in the characteristic parameter obtained for original and modified membranes give information about changes on membrane pores/porosity. A reduction in the values of both hydraulic permeability (~ 50 %) and NaCl diffusive permeability (~ 30 %) was determined as a result of the lipid coverage of the PVDF membrane, but no permeability dependence on feed solution concentration seems to exist. Moreover, the lipid layer also seems to

modify the electrical character of the membrane surface [2], which affect to both tNa+ values and its dependence with the average concentration of the solutions at both membranes sides. This effect was also supported by the more negative values obtained for zeta potential and surface charge density for the PVDF/lipid modified membrane, which were determined from streaming potential measurements and they also provide us valuable information on the membrane-solution interface [3]. According to these results, the external and internal (pore wall) membrane surfaces of the PVDF/lipid modified samples have been covered by the lipid layer.

We thank to the CICYT for financial support (Project CTQ2011-27770, Spain, FEDER funds) and V. Romero also thanks to MICINN for her FPU scholarship.

References

[1] S.P. Adiga, Ch. Jin, L.A. Curtiss, N.A. Monteiro-Riviere, R.J. Narayan, WIREs Nanomedicine & Nanobiotechnology Advances Review, 1 (2009) 568-581.
[2] V. Romero, V. Vega, J. García, V.M. Prida, B. Hernando, J. Benavente, J. Colloid Interface Sci. 376 (2012) 40-46.
[3] R. de Lara, J. Benavente, Sep. Purif. Technol. 66 (2009) 517-524.

TF/SE-1-Or-3
Deposition of mixed oxide coatings by pulsed reactive co-sputtering

T12 Surface Engineering

#TF/SE-1-Or-3

H. Klostermann, F. Fietzke, B. Krätzschmar.

Fraunhofer Institut fuer Elektronenstrahl- und Plasmatechnik - Dresden (Germany).

Reactive co-sputtering of elemental targets is a versatile technique to deposit ternary coatings of any composition. In the case of oxide coatings, tailored phase formation can be achieved by proper choice of deposition parameters and fine tuning of the composition through variation of pulse lengths (Fig. 1). However, the high affinity of many metals to oxygen requires a rapid feedback control to stabilize the sputtering process in a transition state with non-poisoned target surfaces. In bipolar pulsed sputtering, the coupling of the targets through the common discharge allows establishing long-term stable deposition processes. The composition of the deposited films can be tuned by adjusting pulse lengths and the entire range of mixed oxides is accessible (Fig. 2). The formation of specific crystalline phases for certain compositions will be presented for the ternary system Al-Zr-O, which is especially promising for high temperature protective coatings for different applications.

Fig. 1: Oscilliscope traces of voltage and current in pulsed reactive co-sputtering of aluminium and zirconium in argon-oxygen atmosphere.

Fig. 2: Deposition rates achieved for different coating compositions on rotating substrates.

SE/TF-P2-13
Effects of some electrical parameters on the efficiency of the Plasma Electrolytic Oxidation of aluminium alloys

T12 Surface Engineering

#SE/TF-P2-13

J. Martin [1], A. Nominé [1], I. Shchedrina [1], A.G. Rakoch [2], G. Henrion [1], T. Czerwiec [1], T. Belmonte [1].

[1]Université de Lorraine, UMR CNRS 7198, Institut Jean Lamour - Nancy (France), [2]National University of Science and Technology, Moscou Institut of Steel and Alloys - Moscow (Russian federation).

The Plasma Electrolytic Oxidation (PEO), also known as Micro-Arc Oxidation (MAO) is a particular electrochemical process to produce protective oxide ceramic coatings on light-weight metals (such as Al, Mg, Zr, Ti and their alloys). Growth of the oxide layer takes place at potentials above the dielectric breakdown voltage of the insulating oxide layer leading to the development of numerous short-lived micro-discharges (atmospheric micro-plasma in liquid medium) which move randomly over the processed surface[1-2]. The resulting coating exhibits improved surface performances in terms of hardness, wear protection and corrosion resistance. Associated with the use of environmentally friendly diluted alkaline electrolytes, PEO process gains a growing interest in various industrial domains (transport, energy, medicine) to replace conventional chromic or hard anodizing.

Despite the considerable interest in this process, there is still no clear understanding of the underlying discharge mechanisms that make possible metal oxidation up to hundreds of µm through the ceramic layer. Moreover, no clear relationship has been established between the process parameters and the resulting layer characteristics.

Using an AC pulse bipolar current generator to supply the sample to be processed, the aim of the present communication is to give new insight into the influence of

some electrical parameters on the efficiency of the plasma electrolytic oxidation of aluminum alloys. A particular attention was paid to the current density (from 10 to 80 $A.dm^{-2}$) and the current pulse frequency (from 100 to 900 Hz)[3]. Micro-discharges are characterized during the process by means of optical spectroscopy and fast video imaging (up to 125000 frames/s) with a time and a space resolution of 8 µs and 0.017 mm^2, respectively. Correlations are established between the micro-discharges characteristics (surface density, spatial distribution, lifetime and size) and the elaborated oxide layers (edge effect, morphology, growth rate, roughness).

Results clearly point out the influence of the current density and the current pulse frequency on the process. Coating growth rate is improved with the combination of the highest current density and the highest current pulse frequency. Within these specific electrical conditions it is observed that the detrimental effects of strong (long-duration up to 0.3 ms and large size up to 0.5 mm^2) micro-discharges are minimized.

[1] F. Jaspard-Mécuson, T. Czerwiec, G. Henrion, T. Belmonte, L. Dujardin, A. Viola, J. Beauvir, *Surf. Coat. Technol.* **201** (2007) 8677–8682.

[2] A. Melhem, G. Henrion, T. Czerwiec, J.L. Briançon, T. Duchanoy, F. Brochard, T. Belmonte, *Surf. Coat. Technol.* **205** (2011) S133-S136.

[3] J. Martin, A. Melhem, I. Shchedrina, T. Duchanoy, A. Nominé, G. Henrion, T. Czerwiec, T. Belmonte, *Surf. Coat. Technol.* (2012) Accepted for publication.

SE/TF-2-Or-2
Effect of variation in pulse mode of plasma electrolytic oxidation (PEO) on coating characteristics on an aluminium alloy

T12 Surface Engineering

#SE/TF-2-Or-2

A. Jarvis, A.L. Yerokhin, A. Matthews.

Sheffield University - Sheffield (United kingdom).

Abstract:
A study has been made of the effect on the coating characteristics caused by variation in the pulse mode of the power supply used to produce plasma electrolytic oxidation (PEO) coatings on aluminium alloy. Previous work has shown that the PEO coating deposition process is strongly affected by the characteristics of the power supply, ranging from a simple DC Source, to pulsed DC or pulsed AC and onto more complex hybrid AC/DC pulsed systems. Various electrical parameters can be varied in each case, including: the control mode (constant current or voltage), frequency, pulse characteristics (half-wave or full wave, number per packet, frequency, time on and off) and offset. See the Figure below for a description of these terms for a generic bipolar pulsed source. These factors affect both the coating characteristics as well as the overall energy process efficiency. By varying the power supply characteristics one can aim to optimize the coating's tribological, corrosion resistance, and/or mechanical properties as well as its process energy consumption.

In this work, a specially designed bipolar pulsed power source was used that allowed control of the number and frequency of pulses for both the positive and negative packets of the PEO power source. The number of pulses in both the positive and negative pulse packets (see Figure for explanation) were varied and the subsequent effects on the coating characteristics were observed. The coatings were characterized by measuring their composition (including porosity level and phases present), residual stresses, indentation hardness (micro and nano-indentation) and relative wear resistance.

Figure: Schematic of bipolar pulse output of plasma electrolytic oxidation (PEO) power supply unit: ton: positive pulse on time; toff: positive pulse off time; t'off: negative pulse off time; Tp: working time for positive pulse packet; TN: working time for negative pulse packet; Jm: positive average current density; J'm: negative average current (after Jiang, Wang 2010)

SE/TF-3-Or-6
Corrosion Behaviour of Proprietary EBPVD Aluminium-based Coatings in Neutral Saline Solution

T12 Surface Engineering

#SE/TF-3-Or-6

O. Fasuba [1], S. Banfield [2], A. Yerokhin [1], A. Leyland [1], J. Housden [2], A. Matthews [3].

[1]University of Sheffield - Sheffield (United kingdom), [2]Tecvac Ltd. - Cambridge (United kingdom), [3]University ofSheffield - Sheffield (United kingdom).

Corrosion Behaviour of Proprietary EBPVD Aluminium-based Coatings in Neutral Saline Solution

O.A. Fasuba, S. Banfield, A. Yerokhin, A. Leyland, J. Housden, A. Matthews

Materials Science and Engineering, The University of Sheffield, UK

Abstract

Aluminium coatings are promising candidates for the cathodic protection of construction steels. However, their high sensitivity to localised degradation often limits their applications for corrosion protection. Incorporation of transition metals such as Cr allows for the modification and enhancement of the structural and electrochemical properties of aluminium coatings, such that excellent pitting corrosion resistance is achieved for the coating without compromising its cathodic protection capacity.

In this study, AlCr coatings deposited by Electron Beam Physical Vapour Deposition (EBPVD) in N2 reactive gas of various flow rates were characterised in terms of corrosion behaviour in 3.5 wt. % NaCl solution. The substrate used is 17/4PH precipitation hardening stainless steel. Electrochemical noise and potentiodynamic

polarisation measurements were used to determine the corrosion behaviour of the coatings. Corrosion parameters obtained from the potentiodynamic polarisation tests were compared to the statistical parameters from the signals in time and in the frequency domains of the noise measurements.

Good agreement between data for the different techniques was found. In particular, noise resistance (Rn) values from the noise electrochemical measurements correlate well with corrosion rate (iCorr) values obtained from potentiodynamic polarisation measurements. In terms of pitting corrosion resistance and cathodic protection for the 17/4PH stainless steel substrate, an AlCr PVD coating containing approximately 10 at. % nitrogen proved to be most effective.

SE-1-Or-8
Through-target Study of Plasma Generation and 3-D Analysis of Plasma Transport in High Power Impulse Magnetron Sputtering

T12 Surface Engineering

#SE-1-Or-8

D. Ruzic, L. Meng, H. Yu.

University of Illinois - Urbana (United states).

High power impulse magnetron sputtering (HIPIMS) has distinctive advantages of intense pulse plasma density and high degree of metal ionization suitable for various applications from hard coatings to interconnect metallization in integrated circuits. A fundamental characterization of plasma properties and fluxes of species is critical for the process development. The underlying physics the discharge establishment and plasma transport also need be further explored.

For the first time, the generation of plasma species during the HIPIMS ignition was explicitly measured on the target. To avoid the indirect optical methods or the plasma-disturbing probes, an orifice was created within the target racetrack region, behind which a current-collecting grid and a quartz crystal microbalance (QCM) were placed. The measured ion current didn't show up until a certain delayed point after the pulse beginning. The delay time, ranging from 10 to 40 μs, is a direct supporting evidence for the localization of ionization zone [1] during the HIPIMS ignition. The higher pulse voltage, the shorter was the delay time, suggesting a faster drifting of the localized plasma. Combined with the QCM, high Cu ionization fraction in the vicinity of the target was determined, indicating the self-sputtering effect taking place in HIPIMS.

Triple Langmuir probe was used to measure the time-resolved electron density and electron temperature during HIPIMS. The analysis revealed that it took about 150 μs after the pulse end for the peak of electron density to reach the substrate. Such a plasma expansion was further mapped in three dimensions inside the chamber. The expansion speed was found to depend on pulse parameters as well as the magnetic field configuration. The higher the magnetic field strength, the faster was the

expansion. The plasma potential distribution is believed to be accountable for this effect. A stronger magnetic field (800 Gauss as compared with 200 Gauss) resulted in a larger potential gradient (and thus a stronger electric field) in the bulk plasma region to facilitate the electron diffusion. The Cu ion fractions of up to 60% were measured near the substrate, increased by a higher pulse voltage or a moderate pulse length. A lower magnetic field also gave a higher Cu ion fraction despite a lower plasma density. The relatively flat distribution of plasma potential in the low magnetic field configuration leads to an effective ion release downstream instead of attracting ions back to the cathode.

(This is not part of the abstract, just a note that this paper may also fit into another session T11.01)

[1] A. Anders, P. Ni, and A. Rauch, Journal of Applied Physics 111, 053304 (2012)

SE-P1-02
Optimizing high power impulse magnetron sputtering processes through computational modeling

T12 Surface Engineering

#SE-P1-02

N. Brenning, C. Huo, M. Raadu, D. Lundin.

Royal Institute of Technology - Stockholm (Sweden).

High power impulse magnetron sputtering (HiPIMS) is a successful sputtering technique that has a variety of industrial applications, including protective coatings, optical coatings and functional coatings for electronic applications. The possibility to independently vary the pulse length, shape, peak power, and duty cycle opens up new wide ranges of parameters to explore and tune for discharge optimization. In this contribution, we present an overview of ongoing HiPIMS modeling based on a recently developed time-dependent ionization region model (IRM) [1], which has been used as a flexible tool in the optimization process [2, 3]. The working principle of the IRM is a set of balance equations tracking the production and loss of electrons, ions, excited species, as well as neutrals present in the HiPIMS plasma. As a model system we have here focused on sputtering of Al in an Ar atmosphere, and used it to examine when effects, such as intense gas rarefaction, high degree of ionization of the sputtered species, deposition rate loss, self-sputtering etc. occur. From an end-user point of view, we will also discuss what to include in the IRM based on the objective(s) of the investigation.

[1] M. A. Raadu, I. Axnas, J. T. Gudmundsson, C. Huo, and N. Brenning, Plasma Sources Sci. Technol. 20, 065007 (2011)
[2] N. Brenning, D. Lundin, M. A. Raadu, C. Huo, C. Vitelaru, G. D. Stancu, T. Minea, and U. Helmersson, Plasma Sources Sci. Technol. 21, 025005 (2012)
[3] C. Huo, M. A. Raadu, D. Lundin, J. T. Gudmundsson, A. Anders, and N. Brenning, Plasma Sources Sci. Technol. 21, 045004 (2012)

SE/ASS-1-In-1
Atomic-Scale Friction and Wear of Single Asperities

T12 Surface Engineering

#SE/ASS-1-In-1

R. Carpick.

University of Pennsylvania - Philadephia, Pa (United states).

I will discuss experimental studies of nanoscale single asperity contacts that reveal surprising new insights. First, the behavior of nanoscale contacts with truly 2-dimensional materials including graphene will be discussed. We find that the friction force exhibits a significant dependence on the number of 2-D layers [1]. Surprisingly, adhesion (the pull-off force) does not. However, studies as a function of scanning history reveal further complexities that arise from the combined effects of high flexibility and variable substrate interactions that occur at the limit of atomically-thin sheets.

I will then discuss new insights into nanoscale wear. A better understanding of the physics of wear would allow the development of rational strategies for controlling it at all length scales. As well, wear is a primary limitation of devices such as micro-/nano-electromechanical systems (MEMS/NEMS). We show that ultrastrong materials can be used to be greatly reduce nanoscale wear [2,3]. We have also demonstrated the ability to characterize single-asperity wear with a high degree of precision by performing in-situ wear tests inside of a transmission electron microscope. Silicon probes of different initial radii and shape were slid against a flat diamond substrate. The shape evolution and volume loss due to wear are well described by kinetic model based on stress-assisted bond breaking mechanisms, allowing new insights to be gained about the kinetics of atomic-scale wear [4].

1. Lee, C., Li, Q., Kalb, W., Liu, X.-Z., Berger, H., Carpick, R.W. and Hone, J. Frictional characteristics of atomically-thin sheets. Science 328, 76-80 (2010).
2. Bhaskaran, H., Gotsmann, B., Sebastian, A., Drechsler, U., Lantz, M., Despont, M., Jaroenapibal, P., Carpick, R.W., Chen, Y. and Sridharan, K. Ultra-low nanoscale

wear through atom-by-atom attrition in silicon-containing diamond-like-carbon. Nature Nanotech. 5, 181-185 (2010).
3. Liu, J., Grierson, D.S., Notbohm, J., Li, S., O'Connor, S.D., Turner, K.T., Carpick, R.W., Jaroenapibal, P., Sumant, A.V., Carlisle, J.A., Neelakantan, N. and Moldovan, N. Preventing nanoscale wear of atomic force microscopy through the use of monolithic ultrananocrystalline diamond probes. Small 6, 1140-1149 (2010).
4. Jacobs, T.D.B. and Carpick, R.W. Nanoscale wear as a stress-assisted chemical reaction. Nature Nanotech. in press (2013).

Wear of a silicon asperity imaged in TEM. Color lines: four traces of successive profiles from TEM images of a silicon asperity at 200-nm intervals of sliding distance, along with the TEM image of the asperity just after the final interval shown (background image). The detail view of the traces (inset) demonstrates gradual wear of the silicon, often with less than 1 nm of change in the asperity height per sliding interval. From Ref [4].

SE/TF-2-Or-8
Study on the mechanical and corrosion behavior of ceramic coated 2024-Al alloy produced by plasma electrolytic oxidation

T12 Surface Engineering

#SE/TF-2-Or-8

M. Alizadeh [1], R. Saleh [2], S. Bordbar [1].

[1]Department of Metals, Institute of Materials Science and Engineering, Graduate University of Advanced Technology, PO.BOX: 76315-115, Kerman, Iran - Kerman (Iran, islamic republic of), [2]Department of Plasma Engineering, Graduate University of Advanced Technology, PO.BOX: 76315-115, Kerman, Iran - Kerman (Iran, islamic republic of).

In general, corrosion damages constrain heavy costs to industries due to destructive nature of this phenomenon. Among wide range of engineering metals, aluminum alloys due to favorable properties such as low weight, corrosion resistance and various mechanical behavior are appropriate options for industrial applications. Although, aluminum alloys represent sufficient corrosion resistance in neutral environment but they are sensitive alloys to pitting and crevice corrosion in presence of chloride ions. Coating is the most common technique to improve corrosion behavior of aluminum made constructions.
In this relation, plasma electrolytic oxidation(PEO) is an efficient and modern method. In this technique, micro-arc plasmaappears on the specimen surface due to ionization of the surrounding gaseous in the high voltage. In fact, the electric field of 106to 108 V/m cause ionized gaseous generation. As results of complex chemical and physical reactions, a dense ceramic layer of Al2O3forms on the substrate surface [1].The PEO technique improves corrosion behavior of coated specimens by restrict the access of corrosive species to the Al substrate through the ceramic layer [2].Furthermore, generation of ceramic layer lead to increase the surface hardness. In the present study, the corrosion behavior of coated specimens were investigated by electrochemical impedance spectroscopy (EIS) in 3.5% NaCl solution and generated ceramic layer was analyzed by X-ray diffraction (XRD) method. The main goal of this investigation is to improve corrosion behavior and mechanical properties of 2024-Al alloy by plasma electrolytic oxidationmethod.

[1]A.L.Yerokhin, X. Nie, A.Leyland, A.Matthews and S.J.Dowey, Review: Plasma electrolysis for surface engineering, Surface and Coatings Technology, 122 (1999) 73–93.
[2] K.Wang, Y.J.Kimand Y.Hayashi, Ceramic coatings on 6061 Al alloys by plasma electrolytic oxidation under different AC voltages, Journal of Ceramic Processing Research 10 (2009) 562-566.

SE/TF-2-Or-10
Single Step Process Toward Superhydrophobic Surfaces - Atmospheric Pressure Dielectric Barrier Discharge Deposition Of Hexamethyldisiloxane Coatings

T12 Surface Engineering

#SE/TF-2-Or-10

N. Boscher, D. Duday, P. Choquet.

Centre de Recherche Public - Gabriel Lippmann - Belvaux (Luxembourg).

In the past decade, numerous studies have focused on controlling the surface nano- and microstructure to mimic the dual-scale roughness of superhydrophobic lotus leaves or the high water contact angle (WCA) and large water sliding angle (WSA) of rose petals [1]. Depending on the size of the micro- and nanostructures, which can both be in the Cassie-Baxter [2] or Wenzel state [3], four different wetting states are possible, leading to either “slippy” or “sticky” surfaces with high WCA.

In this work, we present a single step process to the large-scale production of fluorine-free surfaces with high WCA. The surfaces were prepared on various substrates by the atmospheric pressure dielectric barrier discharge (AP-DBD) reaction of hexamethyldisiloxane (HMDSO) in a nitrogen atmosphere. The chemical composition of the coatings was characterised by Fourier-transform infrared spectroscopy (FTIR) and X-ray photoelectron spectroscopy (XPS).The coating nanostructure, greatly impacted by the plasma electrical excitation frequency [4], and the substrate roughness were investigated by scanning electron microscopy (SEM), confocal microscopy and atomic force microscopy (AFM) and were shown to strongly influence the hydrophobic behaviour of the surfaces.

Adjustement of the nano- and microroughnesses allow to produce both “slippy” or “sticky” surfaces with high WCA. Water droplets, which remained on the mixed Cassie-Baxter/Wenzel surface with contact angle of 155°, do not slide even when the surface is tilted vertically or turned upside down. In contrast, water droplets, with

WCA up to 168°, were shown to roll-off easily from the surfaces in the Cassie-Baxter state.

[1] Cho, W. K.; Choi, I. S. *Adv. Funct. Mater.*, 2008, *18*, 1089-1096.
[2] Cassie, A. B. D.; Baxter, S. *Trans. Faraday Soc.*, 1944, *40*, 546-551.
[3] Wenzel, R. N. *Ind. Eng. Chem.*, 1936, *28*, 988-994.
[4] Boscher, N. D.; Choquet, P.; Duday, D.; Verdier, S. *Plasma Process. Polym.*, 2010, *7*, 163-171.

Water droplets on the ppHMDSO thin films deposited by atmospheric pressure dielectric barrier discharge.

SE/PST/TF/BI-2-Or-3
Effects of plasma electrolytic oxidation on corrosion fatigue properties of biodegradable cp-Mg

T12 Surface Engineering

#SE/PST/TF/BI-2-Or-3

Y. Gao, A. Matthews, A. Yerokhin.

The University of Sheffield - Sheffield (United kingdom).

Magnesium alloys have been considered as promising biomaterials; however their application in biological area is limited due to their too high reactivity in the physiological environment. Plasma electrolytic oxidation (PEO) technique is beneficial to improve corrosion performance of magnesium alloys, which enables their application as biodegradable implants. Corrosion fatigue is identified as one of the major problems associated with implant failure. It is therefore of great significance to address this performance aspect of PEO-coated biodegradable Mg materials, which is currently not well understood.
In the present study, PEO coatings are fabricated on cp-Mg, using optimised process parameters, i.e. the current mode, and the composition of a biologically friendly electrolyte. The coating morphology and phase composition are characterised by scanning electron microscopy and x-ray diffraction technique, respectively.The corrosion fatigue tests are performed according to ASTM F1801-97(2009). The specimen is immersed in a simulated body fluid at 37°C during corrosion fatigue test. From the test results, corrosion fatigue strength of PEO coated magnesium is evaluated. Fracture topography analysis is used to identify the effects of PEO coating on the failure mechanisms and kinetics. Finally, the perspectives of using PEO-coated cp-Mg for biodegradable implantapplications are discussed in terms of corrosion fatigue performance.

SE/TF-2-Or-11
Nanocomposite (multi)functional surfaces: various strategies to efficiently incorporate nanoparticles in atmospheric plasma-polymerized thin films

T12 Surface Engineering

#SE/TF-2-Or-11

D. Ruch.

CRP Henri Tudor - Advanced Materials and Structures Department, 5 rue Bommel – ZAE Robert Steichen, - Esch Sur Alzette (Luxembourg).

The success of modern materials is very often (partially or totally) due to the high performances of their functional surfaces. In this frame, the development of high efficient polymer-based coatings and composite thin films is of growing interest when issues linked to flexible microelectronics, adhesion, energy or even healthcare are concerned. The combined recent advances in surface coatings engineering and in polymer science can nowadays lead to the design of increasingly efficient surfaces with functionalities adressing very precise, strict and high level requests depending on the dedicated application.

Atmospheric Plasma polymerization is nowadays considered as a promising and versatile technique allowing to process plasma polymer films with functional properties without affecting the intrinsic properties of the substrate. Usually, the functionality of the plasma deposited layer is mainly determined by the nature of the used vapor precursors or monomers. The molecular structure of the resulting plasma-polymer film can be fine-tuned by a well-advised selection of precursor(s) combined with well adapted plasma parameters. The high performance of thin films grown via atmopheric plasma polymerization lies on very specific appraoches aimed at generating well established and well controled chemical structures and molecular architectures perfectly matching the desired applications. In this frame, Incorporating nanoparticles within plasma polymers could open door for new kind of smart coatings innovative.The present work is mainly focused on the design of nanocomposite functional surfaces. In order to generate this type of hybrid coatings, several

processes will be described: from the direct injection of nanoparticles previously dispersed in the liquid precursor, to the in-situ generation of nanoparticles inside a „reactive“ plasma-polymer thin films used as nanoreactor, or to the use of modified metallic particles as nucleating agent for the growth of the plasma-polymer chains (grafting from).
This contribution will highlight the importance of the control of the chemical structures and molecular architectures at the molecular level in order to reach the expected macroscopic properties and performances and therefore being able to offer new perspectives for atmospheric plasma-polymer coatings, in application domains as varied as corrosion protection, self-healing, or even in the design of alternative electrode materials for PEM fuel-cells...

[1] Michel M., Bour J., Petersen J., Arnoult C., Ettingshausen F., Roth C., Ruch, D., Fuel cell, 2010, (6), 932-937.
[2] Petersen J., Michel M., Toniazzo V., Ruch D., Schmerber G., Ihiawakrim D., Muller D., Dinia A., Ball V., RSC Adv., 2012, Advance Article DOI: 10.1039/C2RA21028B
[3] Bour J., Charles L., Petersen J., Michel M., Bardon J., Ruch, D., Plasma polymer and processes, 2010, (7), 687-694.

SE/PST/TF/BI-2-Or-4
Formation of thin hydroxyapatite-containing titania coatings on cp-Ti for dental implant applications by plasma electrolytic oxidation

T12 Surface Engineering

#SE/PST/TF/BI-2-Or-4

W. Yeung, Y. Gao, A. Yerokhin.

The University of Sheffield - Sheffield (United kingdom).

Due to good osseointegration titanium implants are widely used in orthodontic surgery; however,long healing time is still a problem. The aim of this study is to form a thin (5…10 micron) coating that could help reducing the healing time of Ti dental implants by plasma electrolytic oxidation (PEO) process. This involves improving the surface morphology of the coating and incorporation of osteoconductive calcium phosphate phases, such as hydroxyapatite (HA). Commercially pure Ti was treated in an electrolyte based on an aqueous solution of a sodium phosphate salt with additions of 0.02M…0.4M HA powder. The PEO treatments were carried out for 4 to10 min in a pulsed bipolar current mode with both potentiostatic and galvanostatic controls. The coating thickness and surface morphology were examined by an eddy current thickness gauge and scanning electron microscopy (SEM) respectively. The elemental and phase compositions were studied by energy-dispersive X-ray analysis and X-ray diffraction respectively. Effects of the pulse frequency and the negative current component were discussed. It was found that in the studied range of process parameters, the processing time does not significantly influence the coating thickness; however the introduction of the negative current component appears to improve the coating uniformity and the surface morphology which could be beneficial for osteoconductivity and cell anchorage.

SE/TF-2-Or-4
In-situ impedance spectroscopy based modelling of the plasma electrolytic oxidation process of Al

T12 Surface Engineering

#SE/TF-2-Or-4

C. Liang [1], A. Matthews [1], E. Parfenov [2], A. Yerokhin [1].

[1]The University of Sheffield - Sheffield (United kingdom), [2]Ufa State Aviation Technical University - Ufa (Russian federation).

Plasma electrolytic oxidation (PEO) is a relatively novel surface modification technique that provides excellent wear- and corrosion-resistant coatings on light-weight metals, in particular on aluminium. Formation of PEO coatings involves complex phenomena and mechanisms that are difficult to study. A method of in-situ impedance spectroscopy can be used to provide new insights into fundamental characteristics of PEO processes and coating formation mechanisms as well as to develop new means of the process control. This method is based on application of a variable frequency voltage perturbation signal to obtain impedance characteristics of the electrolyser during the PEO processing. The applied voltage signal and the current response are collected and post-processed to verify the system linearity, refine phase, reduce noise and spline the impedance spectra. The obtained spectra are then fitted with appropriate equivalent circuits to reveal mechanisms underlying the PEO process. Physical meaning of various circuit components is verified using specially designed experiments in which certain system characteristics are set up in such way to obtain controllable processing conditions, such as electric field distribution in the electrolyser, electrolyte resistance or coating thickness. The circuit analysis reveals specific RC and RL loops that can be related to individual processes associated with interfacial charge transfer and transport phenomena. Characteristic time constants corresponding to these processes are evaluated and their evolution with PEO treatment time is considered. Correlations of the process kinetics with phenomena observed during the PEO treatment of Al and coating growth characteristics are discussed.

SE/PST/TF/BI-2-Or-5
Porous Structure Preparation and Wettability Control on Titanium-related Implant

T12 Surface Engineering

#SE/PST/TF/BI-2-Or-5

Z. Lin.

No.11, Lane 3, WenHua Road, HePing District - Shenyang (China).

Titanium (Ti) osseointegration is critical for the success of dental implants. Previous studies have shown that wettability controls are of great importance for their biomedical application. Only relatively recently have the effects of plasma oxidized surface on cell response been considered. The aim of the present study was to develop a simple and scalable surface modification treatment that introduces plasma oxidation method to the surfaces of Ti substrates without changing the original morphology of other surface features. The controlled micro/nano-structures surfaces of Ti substrates are achieved by using sandblast-acid etching (SLA) process. Then, titanium oxide surfaces are achieved on SLA surfaces by using plasma oxidation base on radio frequency plasma enhanced chemical vapor deposition (RF-PECVD) system, while retaining the starting SLA micro/nano-textures topography. The water contact angle (CA) of this surfaces increase and then decrease with the self-bias voltage. Superhydrophilic TiO_2 (anatase) surface can be achieved when the self-bias voltage is 360V. Such plasma oxidized surfaces showed crystal structure of anatase (101) orientation and possessed elemental compositions of TiO_2, Ti_2O_3 and TiO. MG63 cells were seeded on plasma oxidized Ti disks. The results suggested that the introduction of such plasma oxidized surfaces in combination with micro/nano-structures improves osteoblast attaching and spreading, which, in turn, indicates the potential for improved implant osseointegration in vivo.

[1] Lin Z, Liu K, Zhang Y C, Yue X J, Song G Q and Ba D C, 2009 Materials Science and Engineering B 156 79
[2] Lin Z, Lee G H, Liu C M, Lee I S 2010 Surface & Coatings Technology 205 S391
[3]

Figure 1. SEM image (3000×) of the SLA surface with different acid etching time at 75℃: (a) 10min;(b) 20min

SE/TF-2-Or-7
Intumescent coating of (polyallylamine-polyphosphates) deposited on polyamide fabrics via Layer-by-Layer technique

T12 Surface Engineering

#SE/TF-2-Or-7

K. Apaydin [1], A. Laachachi [1], V. Ball [2], M. Jimenez [3], S. Bourbigot [3], V. Toniazzo [1], D. Ruch [1].

[1]Centre de Recherche Public Henri Tudor - 5 Rue Bommel L-4940 Hautcharage (Luxembourg), [2]Faculté de chirurgie dentaire-Universite de Strasbourg - 1 Place De L'hôpital, F-67000 Strasbourg (France), [3]ENSCL-Universite Lille 1 - Bp 90108, F-59652 Villeneuve D'ascq (France).

Nowadays, textile industry represents an important place in the global economy. In fact the market share of textile will reach 120 billion Euros in 2012 [1]. Textile materials are used in many fields such as clothing, transport, packaging, building… Nevertheless, these materials are highly flammable and very often legislation requires low flammability for them. There are two ways to improve the fire performance of these materials: bulk modification and surface treatment [2]. The simplicity and versatility of Layer-by-Layer (LbL) technique (Figure 1) has led numerous scientists to use it as surface treatment technique. In this study, inspired by Li et al. work [3], (polyallylamine-polyphosphates) intumescent coatings were deposited, via LbL technique, in order to improve the reaction to fire of 0.5 mm thick polyamide fabrics. Thermogravimetric analysis (TGA) results indicate that the presence of such assembly catalyzes (for all coated samples) and changes (only for 10, 15 and 40 BL samples) the decomposition of virgin polyamide fabrics. The fire performance was evaluated by Pyrolysis Combustion Flow Calorimeter (PCFC). The fire results exhibit on the one hand a significant decrease of peak of heat release rate (pHRR) and on the other hand a shift to lower temperatures (catalytic effect) as function of the number of bilayers deposited (Figure 2). In this presentation, we will exhibit the growth, morphology, thermal stability and fire performance of this intumescent coating.

1- David Rigby Associates / Techtextil
2- Carosio, F. et al. (2011). "Layer-by-layer assembly of silica-based flame retardant thin film on PET fabric." Polymer Degradation and Stability 96(5): 745-750.
3- Li, Y.-C. et al. (2011). "Intumescent All-Polymer Multilayer Nanocoating Capable of Extinguishing Flame on Fabric." Advanced Materials. 23(34): 3926-3931.

Figure 1 : Schematic representation of Layer-by-layer assembly.

Figure 2 : Heat Release Rate as a function of temperature, evaluated with micro combustion calorimetry, for virgin polyamide fabrics and 5, 10, 15 and 40 BL coated fabrics.

SE/TF-2-Or-5
Data validation for impedance spectroscopy studies of discharge phenomena during plasma electrolytic oxidation of Al

T12 Surface Engineering

#SE/TF-2-Or-5

A. Yerokhin [1], E. Parfenov [2], C. Liang [1], A. Matthews [1].

[1]University of Sheffield - Sheffield (United kingdom), [2]Ufa State Aviation Technical University - Ufa (Russian federation).

Discharge phenomena that occur at the metal anode / electrolyte interface during Plasma Electrolytic Oxidation (PEO) of light alloys play important role in the formation of oxide ceramic surface layers with superior protective and useful functional properties. The mechanisms governing discharge behaviour are not well understood and the major research effort is currently directed towards filling in this knowledge-gap. High speed imaging, optical emission spectroscopy and current probe studies of discharge events have been carried out but so far failed to bring about a suitable model of the process. Impedance spectroscopy could provide be a powerful tool for the development of such a model if the problems of system linearisation and time-variance for the PEO process were solved. In this this work we employed fast (0.5s) frequency sweeps of a pulsed voltage signal which approximates an implied single-sine perturbation to obtain its current response and evaluate instantaneous impedance of the PEO process on Al. We developed an original frequency domain method which utilises linear dependency between the spectrum estimates of voltage and current to evaluate the system linearity. We found that non-linear distortions provide minor contribution to the impedance if the process parameters are carefully selected to ensure that (i) the pulsed voltage waveform provides a good approximation of the implied sine wave; (ii) the pulsed PEO voltammogram is adequately approximated by a linear regression and (iii) discrete voltage and current values are well above the vertical bin size of the probes used. For these process parameters, the noise and nonlinearity distortions do not exceed 15%, indicating that the studied PEO system can be considered as a properly linearised object. This validates the obtained impedance data and justifies the application of *in-situ* impedance spectroscopy approach for modelling the PEO process.

SE/PST/TF/BI-P1-03
On the Effect of Cold Plasma Sterilization on the Surface Properties of Implantable Biomaterials

T12 Surface Engineering

#SE/PST/TF/BI-P1-03

M. Boudifa, F. Lebel, M.P. Gellé, S. Gangloff.

CRITT-MDTS - Charleville-Mézières (France).

Many studies have demonstrated the effectiveness of plasma on microorganism's inactivation with the application of different gas mixtures to various bacteria suspensions.
In a previous work [1], we have shown the efficiency of our innovative low pressure cold plasma sterilization process (Figure 1). Particularly, a specific method has been developed, where the plasmagene elements are only generated in the sterilization pouch. Consequently, the sterile state of the medical device is kept, and makes it ready to use subsequently or in a certain period of time without any additional precautions.
Depending on sterilization process, the surface properties of implant materials can be impacted [2]. Whereas the bacteria inactivation by cold plasma have been well demonstrated, studies about the sterilization effects on their material properties are less well documented, especially, for the plasma sterilization emerging techniques [3].
In this work, the effects cold plasma sterilization on surface characteristics has been studied. The influence of cold plasma treatment on the surface properties of two different materials widely used for prosthetic implant manufacturing was investigated. Ultra High Molecular Weight PolyEthylene (UHWMPE) polymer and TiAl6V4 metallic biomaterials have been subjected to plasma sterilization. Then surface chemical components, hydrophilicity, roughness topology, and morphology have been assessed by mean of X-ray photoelectron spectroscopy (XPS), contact angle measurements, and scanning electron, respectively. The influence of the sterilization pouch has been discussed for samples submitted to the cold plasma sterilization with and without packaging pouch. Thence, the content-containing interactions due to packaging could be taken into account. Preliminary conclusions have been drawn regarding the sterilized biomaterial surfaces.

[1] Marie-Paule Gellé, Zouhaier Ben Belgacem, Mohamed Boudifa, Sophie Gangloff and Dominique Laurent-Maquin. « An innovative method of cold plasma for sterilization of medical devices ». In ICPM4, 4th International Conference on Plasma Medecine, June 17-21, 2012, Orléans, France.
[2] Arciola CR, Alvi FI, An YH, Campoccia D, Montanaro L. « Implant infection and infection resistant materials: a mini review ». Int J Artif Organs 2005;28:1119–25.
[3] Jung Hwa Park, Rene Olivares-Navarrete, Robert E. Baier, Anne E. Meyer, Rina Tannenbaum, Barbara D. Boyan, Zvi Schwartz. « Effect of cleaning and sterilization on titanium implant surface properties and cellular response ». Acta Biomaterialia2012; 8 :1966–1975.

Figure 1 : N2O2 Plasma generated only in the sterilization pouch

SE/TF-2-Or-3
Influence of the electrolyte composition on the oxide layers grown on Mg alloy by the plasma electrolytic oxidation process

T12 Surface Engineering

#SE/TF-2-Or-3

I. Shchedrina, G. Henrion, J. Martin, D. Veys-Renaux, T. Czerwiec, T. Belmonte.

Institut Jean Lamour - Nancy (France).

Nowadays parts made of magnesium alloys find a wide range of applications in many industrial areas such as transportation or building for example.
However because of relatively low corrosion resistance of magnesium alloys in neutral and acid environments, in most of inorganic environments and in the ambient conditions it is necessary to protect it, for example by applying protective coatings on its surface.

Microarc oxidation or plasma electrolytic oxidation (PEO) is a promising process that may advantageously replace conventional anodizing that does no longer comply with the international rules regarding environmental aspects.

Besides the high mechanical and chemical properties (hardness, wear and corrosion resistance, thermal and electrical protection) of oxide layers achieved by PEO, this process has also advantages of requiring single step operation and being environmentally friendly.
However, the PEO coatings generally become protective when their thickness reaches some tens of micrometers, typically greater than 40 µm.

Our work aims at achieving thin (< 15-20 µm) PEO layers on Mg alloy, which would decrease the processing time – and consequently reduce energy consumption – and change the dimensions of the processed parts within acceptable range.

For this purpose, we study the influence of the electrolyte composition on the coating

characteristics.

It can be noted that the addition of potassium fluoride in the electrolyte helps to obtain more coatings with a higher corrosion resistance and with a negligible edge effect – non homogeneity in the layer thickness over the sample surface, with a strong negative gradient from the edge to the centre of the samples. This is due to the strong variation of the electric field in the vicinity of sample edges (edge effect) which results in a much higher number of micro-discharges occurring at these border locations as was shown by high speed video recording of the micro-discharges.

However SEM analyses performed on layer cross sections reveal a high porosity of the layer in all the cases but the addition of sodium silicate helps to achieve less porous coatings in comparison with the others. That also increases the corrosion resistance of the alloy.

SE/TF-3-Or-4
Chromogenic multifunctional coatings of hybrid polymeric/TiO2 by sol-gel

T12 Surface Engineering

#SE/TF-3-Or-4

J. Perez Bueno, L.M. Flores Tandy, Y. Meas Vong.

CIDETEQ - Queretaro (Mexico).

Chromogenic materials have been extensively studied and applied in a variety of fields. There are purely organic, hybrid organic-inorganic, doped inorganics and semiconductors. However, the necessity of chromogenic materials based on compounds of transition metals, for their properties and low costs, makes them a constant interest in materials research. In this work, hybrid and composite organic-inorganic materials based on polyester polymers and titanium hydroxide species had been prepared by sol-gel process. The conjunction of an organic polymeric matrix and hydrolyzed and condensed titanium species resulted in multiple chromogenic materials.
FT-IR, UV-Vis, EPR spectroscopic results show formation of hydrogen bonds between titanium hydroxide and polyester species (Figure 1), n-π* π-π* reversible transitions after light excitation (Figure 2), and formation of permanent complexes after thermal treatments of titanium oxide species into polar solvents [1]. Anticorrosive, antiabrasive, hydrophilic and coloration properties of hybrid coatings were also investigated through electrochemical impedance spectroscopy (EIS), salt spray test, Taber test, scanning electron microscopy (SEM) and contact angle measurements. The results of hybrid coatings show good anticorrosive properties at low sol-gel titania concentrations and high boiling point polymer solvents. High abrasion resistance when reinforced with alumina and zirconia particles, highly hydrophilic coatings when combined with aluminum hydroxide sol-gel particles, high velocity of coloration and low velocity of discoloration at UV and solar light exposition.

Fatma H El-Batal; UV-Visible, infrared, Raman and ESR spectra of gamma-irradiated TiO2-doped soda lime phosphate glasses; Indian Journal of Pure & Applied Physiscs; Vol. 47, (2009), pp. 631-642.

Figure 1. HRTEM image of a photochromic PMMA-TiO2 hybrid.
Figure 2. UV-vis spectra of a hybrid coating reinforced with alumina particles (a) showing a Ti4+ to Ti3+ transition caused by UV exposure (b).

SE/TF-2-Or-6
Temperature effect on wear and oxidation mechanisms of nanostructured AlTiTaN hard coating deposited by magnetron sputtering

T12 Surface Engineering

#SE/TF-2-Or-6

V. Khetan [1], N. Valle [1], D. Duday [1], P. Choquet [1], C. Michotte [2], C. Mitterer [3], M.P. Delplancke [4].

[1]CRP Gabriel Lippmann - Belvaux (Luxembourg), [2]Ceratizit Luxemburg S.à.r.l. - Mamer (Luxembourg), [3]Department of Physical Metallurgy and Materials Testing, Montanuniversität Leoben - Leoben (Austria), [4]4MAT, Universitè Libre de Bruxelles - Bruxelles (Belgium).

Hard nanostructured TiAlN coatings have gained high importance in the field of wear and oxidation resistant coatings. Nevertheless, their use regarding high temperature (>700ºC) applications such as dry high speed machining remains a challenging issue. Additional alloying element such as Ta has shown a beneficial impact on those properties **[1]**. But for better performance of these coatings in such conditions, an in-depth understanding of their oxidation and wear mechanisms over a wider range of temperature is needed which is currently unavailable in literature. This work investigates the wear and oxidation properties of $Al_{0.48}Ti_{0.40}Ta_{0.12}N$ hard coating deposited with a reactive magnetron sputtered at substrate temperature of 250°C. A target with chemical composition $Al_{46}Ti_{42}Ta_{12}$ placed at an angle of 45° with respect to substrate holder was used. The as deposited coatings show a preferential crystallographic orientation of cubic {111} using θ-2θ X-ray diffraction measurements (XRD) with a columnar microstructure. The oxidation kinetics and mechanisms for these coatings were investigated between 700°C and 950°C in air for various durations (1minute - 15 hours). Transmission electron microscopy investigations show retention of the columnar microstructure for the coating after oxidation. For all temperatures and all durations studied, the original nitride layer could be observed after oxidation with a top oxide layer (maximum thickness ~ 800 nm). An oxidation mechanism switch was observed when the temperature was increased from 700°C to 950°C. By combining dynamic secondary ion mass spectrometry and XRD

measurements, it is possible to show that a single amorphous oxide layer comprising of Ti, Al and Ta oxides formed at 700°C become a bilayer comprising of crystalline Al rich layer (protective Al_2O_3) and Ti/Ta rich oxide layer at 900°C as shown in ***fig. 1***. The oxidation mechanism was governed primarily by inward diffusion of O at 700°C while from 800°C onwards outer diffusion of Al and inner diffusion of O controlled the reaction rate.
The wear behaviour was studied by performing wear tests on the coatings deposited on WC substrates at 700°C, 800°C and 900°C. Finally, a correlation was established between the wear behaviour and the oxidation behaviour of the coating at these temperatures.

[1] M. Pfeiler, C. Scheu , H. Hutter, J. Schnöller, C. Michotte , M. Kathrein, “On the effect of Ta on improved oxidation resistance of Ti-Al-Ta-N coatings”, Journal of Vacuum Science and Technology 27 **(2009)**, 554-561.

Fig. 1: SIMS depth profiles of $Al_{0.48}Ti_{0.40}Ta_{0.12}N$ oxidized at 700°C and 900 °C for 6 hours in air.

SE/TF-P2-14
ENHANCED PERFORMANCE OF CERMET COATINGS FOR HIGH TEMPERATURE OXIDATION AND WEAR RESISTANCE DEPOSITED BY FLAME SPRAY TECHNIQUE

T12 Surface Engineering

#SE/TF-P2-14

I. Cervera, K. Razzaq, J. Saura, M. Damra.

University Jaume I - Castellón (Spain).

NiCrAlY alloys are a family of thermal spray coating materials that are known for their excellent resistance to oxidation and hot corrosion. In this paper a new composition coating has been developed, based on an optimized composition of NiCrAlY/Al2O3 cermet.
Both high temperature oxidation and wear resistance were evaluated using a thermobalance and pin-on-disk test. The coatings were applied using an oxifuel gun over a plain carbon steel and studied at three different temperatures.
Oxidation resistance was greatly improved in all the working conditions and so did the wear behaviour of the coatings. A goal of the studied composition is the absence of coupling layers, widely used to avoid thermal mismatches between the substrate and the ceramic layers.
The cermet layers have been examined by a wide range of experimental techniques including SEM, EDS and XRD before and after oxidation process and also a mechanical characterization has been done.

REFERENCES
1. HABIB K.A., DAMRA M.S., SAURA J.J., CERVERA I., BELLES J., Intl. J. of Corrosion (2011) 10 pages
2. HAN Y.F. XING Z.P. et al, Mater. Sci. Eng. A239 (1997) 871-876
3. BRANDL W., TOMA D., GRABKE H.J., Surf. Coat. Technol. 108/109 (1998) 10-15
4. BRANDL W., GRABKE H.J., TOMA D., Surf. Coat. Technol. 86/87 (1996) 41-47

5. CHOI H., YOON B., KIM H., LEE CH., Surf. Coat. Technol. 150 (2002) 297-308
6. RICKERBY D.S., MATHEWS A., “Advanced Surface Coatings: A handbook of Surface Enginneering”, Blackie, London (1992) p.88
7. MOVCHAN B.A., JOM-J. Mine. Met. Mater. Soc. 48 (11) (1996) 40-45
8. ZHAO L., PARCO M., LUGSCHEIDER E., Surf. Coat. Technol. 179 (2004) 272-278
9. YUAN F.H., CHEN Z.X., HUANG Z.W. et al. Corr. Science 50 (2008) 1608-1617
10. ajdelsztajn l., picAS J.A., KIM G.E., et al, Mater. Sci. Eng. A338 (2002) 33-43
11. LI C.L., LI. W.Y., ., Surf. Coat. Technol. 162 (2002) 31-41
12. HABIB K.A., SAURA J.J., FERRER C. et al, Surf. Coat. Technol. 201 (2006) 1436-1443
13. HABIB K.A., SAURA J.J., FERRER C. et al, Rev. Metalurg. 47 (2011) 12 pages
14. HABIB K.A., DAMRA M.S., CARPIO J. J. , CERVERA I. and SAURA J.J., Poster nº 216, 8th International Symposium on High Temperature Corrosion and Protection of Materials, Les embiez, France (2012)

Thermogravimetry

SE-1-Or-5
HIPIMS Process for Sputtering Cu Seed Layer in High Aspect Ratio Via and Trench.

T12 Surface Engineering

#SE-1-Or-5

R. Chistyakov, B. Abraham.

Zpulser LLC - Mansfield (United states).

HIPIMS/HPPMS technology was developed in early 1990s. One of the important features of this technology is the ability to generate IMP (ionized metal plasma). The important applications of HIPIMS/HPPMS could be directional sputtering processes to deposit Cu seed layers into high aspect ratio features (trenches, vias and etc.) for Cu metallization in integrated circuit fabrication process. The experiments were performed with Zpulser Cyprium^{TM} HIPIMS/HPPMS plasma generator that can generate oscillatory voltage pulse shapes (oscillations frequency is about 20-60 kHz) and deliver up to 2-3 MW during the oscillation. It was found that substrate ion current is a function of voltage oscillations frequency in the pulse. The substrates during all these experiments either had floating potential or were connected to the substrate bias power supply. RF power supply was used as a substrate bias power supply. The RF bias is an important feature for the directional sputtering process for nonconductive substrates. The experimental data about field, side and bottom coverage for Cu and Ta for high aspect ratio trenches and vias will be presented.

SE/TF-P2-15
Plasma-coated and microstructured polymer surfaces for reduction of ice formation (Anti-Icing) or for better ice removal (De-Icing)

T12 Surface Engineering

#SE/TF-P2-15

P. Grimmer [1], J. Barz [1], J. Barz [2], M. Haupt [2], C. Oehr [2], T. Hirth [1], T. Hirth [2].

[1]Institute for Interfacial Engineering and Plasma Technology IGVP, University of Stuttgart - Stuttgart (Germany), [2]Fraunhofer Institute for Interfacial Engineering and Biotechnology IGB - Stuttgart (Germany).

The formation of ice on surfaces can lead to several technical problems, e. g. energy losses. An example is ice formation on the wings of wind energy generators, which leads to imbalance and a worse degree of efficiency. For the improvement of energy efficiency surfaces are being developed, that show an improved removal of ice (De-Icing) or can reduce the formation of it (Anti-Icing).
Starting point is the creation of hydrophobic surfaces by plasma coating (PECVD = plasma enhanced chemical vapor deposition). Therefor fluorocarbon or silicone-like films are deposited onto PU-sheets. These surfaces can be further hydrophobied through structuring in the scale of micrometers, which generates so-called superhydrophobic surfaces. With regard to an industrial roll-to-roll process the focus is set to hot stamping of PU sheets.
Analysis of the surface chemistry of the thin films is done by XPS (X-ray photoelectron spectroscopy), the microstructures are examined by digital 3D light microscopy (IGVP) and white light interferometry (HTW Aalen, MPI Stuttgart). The wetting analysis is done by contact angle measurements with water. The contact angle measurements clearly show the water repellency of the plasma coatings (advancing CA = ca. 120°), the hydrophobicity could be further improved by microstructuring (advancing CA = ca. 150°). For determination of the ice adhesion force water droplets are frozen on the produced surfaces in a freezing chamber and the force for removal is then measured by pulling tests. So far the measurement results only show a limited reproducibility.

For reproducible measurement values a new freezing chamber with a more homogeneous temperature distribution is planned. In addition to that it shall be possible to create so-called supercooled large droplets in this chamber, which can lead to ice formation in aviation. Up to date this is not possible with the current freezing chamber. The effects of the impact of these supercooled fluid droplets on the produced surfaces shall be captured optically. First simulations for identifying the proper chamber size and cooling power were done with the software COMSOL Multiphysics.
The effects of hydrophobic coatings and microstructures on ice adhesion have not been fully understood yet. Some simulations on this topic were performed at the Bremen Center for Computational Materials Science (BCCMS) at the University of Bremen, Germany. Complementary simulations of the heat transfer of a water droplet, which is freezing on flat and microstructured surfaces, are planned.

1. Zhang, 2011: Oberflächenfunktionalisierung von Kunststofffolien zur Verminderung der Eisbildung und Eishaftung („Anti-Icing“), Master-Thesis, Fraunhofer IGB, Hochschule Reutlingen
2. Mishchenko, Aizenberg et al., 2010: Design of Ice-free Nanostructured Surfaces Based on Repulsion of Impacting Water Droplets, ACS Nano, Vol. 4, No. 12, 7699–7707
3. Nosonovsky, Bhushan, 2008: Roughness-induced superhydrophobicity: a way to design non-adhesive surfaces, Journal of Physics: Condensed Matter, Vol. 20, 225009

SE-1-In-1
Film deposition from the plasma phase: Origin, management, and use of ion energies

T12 Surface Engineering

#SE-1-In-1

A. Anders.

Lawrence Berkeley National Laboratory - Berkeley (United states).

A scientifically and technologically interesting variant of physical vapor deposition is the deposition from the plasma phase. Instead of depositing films from neutral atoms, film-forming ions are used. They bring very significant kinetic and potential energies to the film growth process, which can be beneficial, for example when films with smooth morphologies are desired. The issue of optimum energy is not trivial because, in a number of cases, excessive ion energy may cause “ion damage,” i.e. various forms of defects, high compressive stress, possibly followed by delamination. In this contribution, a brief overview is given on the history and variety of deposition from the plasma phase, which can be traced back to the 18th century. Modern forms include ion plating, cathodic arc deposition, pulsed laser deposition, sputtering combined with radio-frequency ionization, hollow-cathode gas-flow sputter deposition, and deposition by high power impulse magnetron sputtering. The different origins of ion energies are considered, with options to control and manage those energies for the greatest benefit of applications.

SE/TF-2-In-1
RECENT DEVELOPMENT OF THE SURFACE NANOCRYSTALLIZATION: CONCEPT, PROCESSING AND APPLICATIONS

T12 Surface Engineering

#SE/TF-2-In-1

J. Lu.

CITY UNIVERSITY OF HONG KONG - Hong-Kong (Hong kong).

A significant enhancement of selective surface reaction kinetics in the nanostructured surface layer in iron has been observed after Surface Mechanical Attrition Treatment (SMAT) with significant improvement of mechanical properties (e.g., see our report in Science 299: 686-688, Jan 31, 2003). By combining SMAT and diffusion based treatments, we have created a new category of interface free nanomaterials with a gradient structure of nano-to-micro sized grains, which resulted in remarkable wear, corrosion, mechanical properties, such as high yield strength and good ductility. We also developed SMAT to obtain high strength and high ductility metallic glasses using and developed new methodologies of investigation of mechanical behaviors of ultrahigh strength materials as a function of atomic structural (e.g. see our report in Nature Materials, 619-623, Aug. 2010). We demonstrated that the relationship between the grain boundary and twin boundary for contributing to the strength and the ductility of nanotwinned materials and obtained outstanding high strength and high ductility nanotwinned materials using SMAT. New materials and structures with atomic, nano-, micro- and macro-scale functional gradients for generating different toughening mechanisms using the non-localization approach are developed. The application in biomedical implants, advanced energy systems and light weight transportation systems will be presented.

SE/TF-3-In-1
NANOTRUCTURED PROTECTIVE COATING SYSTEMS FOR AEROSPACE APPLICATIONS: FROM MATERIALS ARCHITECTURE TO COATING REMOVAL

T12 Surface Engineering

#SE/TF-3-In-1

J. Klemberg-Sapieha.

Department of Engineering Physics and Thin Film Research Center, École Polytechnique de Montreal - Montréal (Canada).

Material damage caused by solid particle erosion remains a crucial problem in aeronautical engines. Good understanding of materials deterioration allows one to develop appropriate strategies to protect technologically relevant metal substrate materials. Advanced erosion-resistant coatings, ERC, call for an “ideal” combination of the mechanical elasto-plastic, tribological, corrosion, thermal and other characteristics that can only be satisfied by using specifically tailored coating architectures considering nanocomposite, nanolaminate, multilayer and graded layer systems.
In our presentation, we demonstrate that finite element modeling of the coating architecture, combined with the tailored mechanical properties of individual materials of the coating systems including appropriate stress management, opens new opportunities as a predictive tool for high performance of the ERCs. We introduce and discuss the selection rules describing the overall film behavior with respect to their microstructure and their basic elasto-plastic properties. Finally, we describe the processes and approaches suitable for the coating removal and subsequent repair.

SE/PST/TF/BI-1-Kn-1 BIOACTIVATION OF SURFACES THROUGH LINKER-FREE COVALENT COUPLING OF ORIENTED BIOMOLECULES

T12 Surface Engineering

#SE/PST/TF/BI-1-Kn-1

M.M.M. Bilek [1], A. Kondyurin [2], D.V. Bax [3], Y. Yin [2], S.L. Hirsh [2], E. Kosobrodova [2], N.J. Nosworthy [4], D.R. Mckenzie [2], A.S. Weiss [5].

[1]School of Physics, A28, University of Sydney - Syndney (Australia), [2]School of Physics, A28, University of Sydney - Sydney (Australia), [3]School of Physics, A28 & School of Molecular Biosciences, G08, University of Sydney - Sydney (Australia), [4]School of Physics, A28 & School of Medical Sciences, F13, University of Sydney - Sydney (Australia), [5]Heart Research Institute - Sydney (Australia).

The ability to strongly attach biomolecules to surfaces whilst retaining their biological activity underpins a host of biotechnologies, such as biosensors and diagnostic microarrays for early disease detection. Recent work has revealed that radicals embedded in nanoscale carbon rich surface layers by energetic ion bombardment can covalently immobilize bioactive proteins [Proc. Nat. Acad. Sci 108(35) pp.14405-14410 (2011)]. This new approach delivers the strength and stability of covalent coupling without the need for chemical linker molecules and multi-step wet chemistry. Immobilization occurs in a single step directly from solution and the hydrophilic nature of the surface ensures that the bioactive 3D shapes of the protein molecules are minimally disturbed.

Such energetic ion treatments can be applied to any underlying material making it possible to achieve covalent biomolecule immobilization whilst maintaining the physical properties (including mechanical and electrical) of an underlying material. This opens up the possibility of new applications such as integrated microelectronic or photonic biosensing devices, continuous flow reactors for enzymatic chemical, textile, food or biofuels processing. Implantable biomaterials that interact with their host via an interfacial layer of active biomolecules to direct a desired cellular response to the implant and inhibit undesirable responses are also on the horizon.

This presentation will describe the plasma-based approaches for creating buried radicals through energetic ion impacts that we have developed. A kinetic theory model of the biomolecule immobilization process via reactions with long-lived, mobile, surface-embedded radicals and supporting experimental data will be presented. The roles of surface chemistry and microstructure of the treated layer in simultaneously preventing radical annihilation whilst allowing sufficient radical mobility will be discussed. Preliminary applications of this technology to direct cell growth, create biosensors and diagnostic arrays, and to engineer bioactive surfaces for implantable biomedical devices will be reviewed.

Key Words: biologically functionalized surfaces, covalent immobilization, radicals, energetic ion bombardment, cross-linking, biosensors, protein microarrays, biomaterials

T13 Surface Science

SS-8-Or-1
Atomistic zone-resolved photoelectron spectroscopy (ZPS)

T13 Surface Science

#SS-8-Or-1

C. Sun.

NTU - Singapore (Singapore).

Interatomic bonding and non-bonding and the associated charge distribution dictate the performance of materials. However, correlation, clarification, formulation, and quantification of them remain challenge. Recent progress on the framework of the BOLS-TB theory[1] and the zone-selective photoelectron spectroscopic (ZPS) technology [2] have enabled new knowledge on: i) Pt and Rh adatoms [3], W, Re, and Rh terrace edges, graphite skin and surface vacancies[4]; ii) fcc(Pd, Rh, Pt, Ag), bcc(W, Fe), hcp(Be, Ru, Re, Ti) and Si surfaces; iii) Ag, Ni, Pt, Cu, Au, Pd nanoclusters as a function of size; and, iv) Ag/Pd, Cu/Pd, and Be/W interfaces[5]. Exercises have led to quantitative information of the local bond length, bond energy, binding energy density, atomic cohesive energy, energy levels of an isolated atom and their bulk shifts. We clarified that: i) perturbation to the Hamiltonian by the mis-coordination-induced bond relaxation, the hetero-coordination-induced bond nature alteration, and the polarization of the nonbonding electrons dictates intrinsically the binding energy shift; ii) the local densification and quantum entrapment results in the globally positive core level shift, of which the extent is proportional to the bond energy change; and iii) the polarization of the nonbonding states by the densely-entrapped bonding electrons screens and splits the crystal potential and hence shifts the binding energy negatively. Most strikingly, it has been uncovered that: i) Pt adatoms and CuPd alloy serve as acceptor-type catalysts because of the dominance of entrapment while Rh adatoms and AgPd alloy as donor-type catalysts due to polarization; ii) the graphitic Dirac-Fermi polarons result from the isolation and polarization of the dangling bond electrons by the densely-entrapped local bonding electrons at the graphite surface defects and the graphene zigzag edges. Findings not only demonstrate the power of the BOLS-TB-ZPS approaches in complementing

STM/S and PES but also the essentiality of the perspective of bond and non-bond formation, dissociation, vibration and relaxation and the associated dynamics and energetics of charge repopulation, polarization, densification and localization in engineering bonds and electrons towards devising functional materials at will.

[1] C. Q. Sun, Prog. Solid State Chem. 35, 1 (2007).
[2] C. Q. Sun, edited by WIPOUSA, 2011).
[3] C. Q. Sun et al., J Chem Phys C 113, 21889 (2009).
[4] C. Q. Sun et al., RSC Adv. 2, 2377 (2012).
[5] C. Q. Sun et al., PCCP 12, 3131 (2010).

ZPS of graphite surface and point defects clarifies the undercoordination induced quantum entrapment (T) and polarization (P) as the origin of the Dirac-Fermi polarons associated with defect and z-graphen edges. Z=4 valley corresponds to the surface component.

SS-2-Or-1
STM/STS investigation of Ni-Nb bulk metallic glasses surface near in vicinity of phase transition

T13 Surface Science

#SS-2-Or-1

V. Mantsevich [1], A. Oreshkin [1], S. Savinov [1], S. Oreshkin [1], V. Panov [1], N. Maslova [1], D. Louzguine-Luzgin [2].

[1]Moscow State University - Moscow (Russian federation), [2]Tohoku University - Sendai (Japan).

We investigated the structural evolution and crystallization behavior of the Ni-based bulk metallic glass (Ni63:5Nb36:5) by means of STM/STS technique. The possibility of different surface nanostructures formation in vicinity of phase transition temperature is shown. We demonstrated that atomic locations in these surface nanostructures differs completely from those formed according to Ni-Nb binary phase diagram in the sample bulk area [1].
The obtained clean amorphous surface (samples were heated at 673K) demonstrates the granular structure consisting of many isolated clusters with an average diameter about 5nm. The normalized tunneling conductivity (TC) reveals the energy pseudogap in the vicinity of Fermi level. For energy values above 0.1eV the normalized TC changes linearly with the increasing of applied bias. This results can be understood within suggested theoretical model based on the interplay between electron scattering on random defects and weak intra-cluster Coulomb interaction [2].
The surface crystallization starts to appear when Ni63:5Nb36:5 metallic glass surface was previously annealed at slightly increased temperature (883K), which is still lower than the crystallization temperature. This phenomenon can be connected with surface-induced crystallization. The primary crystallization starts to appear at lower temperatures than eutectic one during step by step metallic glasses heating. According to Ni-Nb binary phase diagram, two phases should coexist in metallic glass Ni63:5Nb36:5 after excess of the crystallization temperature (930K), namely Ni3Nb and Ni6Nb7.
The constant current STM image of the sample annealed at 973K demonstrates a nanostructured eutectic. The analysis of the surface facets structure reveals the presence of three different surface reconstructions: hexagonal, rectangular, and

zigzag. In our opinion, the origin of the hexagonal structure takes place from Ni6Nb7 bulk phase, which is a tetrahedral close-packed structure. This is due to the fact that second possible phase is Ni3Nb which has orthorhombic structure and it is scarcely probable that this kind of structure or its reconstructions can be transformed to new close-packed structure. Rectangular structure most probably corresponds to orthorhombic Ni3Nb surface reconstruction.

We also obtained the normalized tunneling conductivity spectra above amorphous surface and all three structures. We revealed that the position of peaks in the normalized tunneling conductivity curve does not depend on the local point in the range of chosen structure. Consequently, the I(V) spectra contain a mesoscopic information defined by neighborhood environment, chemical bonding, and domain boundaries. Basically we revealed that, two spectrum corresponding to the rectangular and zigzag structures are very similar. Therefore, we suggest that the rectangular and zigzag structures observed in our STM/STS experiments are two possible surface reconstructions of one Ni3Nb phase.

To conclude the obtained results shed a light on the growth of the eutectic structure with nanoscale faceted.

[1] A.I. Oreshkin, V.N. Mantsevich, S.V. Savinov, et.al., Appl. Phys. Lett., 101(18), p. 181601, 2012

[2] A.I. Oreshkin, N.S. Maslova, V.N. Mantsevich, et.al., JETP Letters, 94(1), p.58, 2011

SS-3-Or-11
Curved crystals: the ultimate approach in surface science

T13 Surface Science

#SS-3-Or-11

E. Ortega [1], F. Schiller [2], J. Lobo-Checa [2], A.L. Walter [3], A. Magaña [1], R. Gonzalez-Moreno [3].

[1]University of the Basque Country - San Sebastian (Spain), [2]Centro de Fisica de Materiales CSIC - San Sebastian (Spain), [3]Donostia International Physics Center - San Sebastian (Spain).

Surfaces that are vicinal to high symmetry directions have frequently demonstrated their enormous potential for surface science research and applications. Vicinal surfaces exhibit distinct chemical and physical properties due to the high density of atomic steps, but they are also useful as templates for nanostructure growth, and, more generally, to transmit uniaxial and/or chiral symmetry to epitaxial layers. Moreover, vicinal planes may respond better than high-symmetry surfaces during thin-film growth, e.g., by eliminating azimuthal domains, and hence dislocation boundaries, or by enabling defect-free layer-by-layer growth through “step-flow”.

A curved substrate is an obvious alternative for a fast, thorough surface analysis, i.e., for a rational optimization of physical-chemical and growth properties that are sensitive to atomic steps. Despite the clear advantage of having a tunable surface orientation at hand, the curved crystal approach has barely been used. The reason is mainly the difficulty to fabricate a customized curved surface with high precision, but also the inconveniences that a curved sample imposes, due to its inherent complexity, to surface preparation, data taking, or data analysis. However, the recent evolution of analytical surface science techniques toward laterally-resolved, scan probes at different length scale has brought the curved surface back to the scene in Surface Science.

In the past few years we have used Ag(111), Cu(111) and Au(111) curved noble metal surfaces to test the possibilities of the curved crystal approach to investigate new surface science phenomena[1,2]. In particular, I will discuss with several examples the possibility of tuning the interplay of surface properties, such as electronic, structural and growth phenomena, at critical crystallographic orientations. I

will also show the new ideas that our group is currently exploring around this approach, among them, the use of Ni and Pt curved crystals to tune the growth of graphene.

[1] M. Corso, F. Schiller, L. Fernández, J. Cordón, and J. E. Ortega, J. Phys.: Cond. Matter 21, 353001 (2009).
[2] J. E. Ortega, M. Corso, Z. M. Abd-el-Fattah, E. A. Goiri, and F. Schiller Phys. Rev. B 83, 085411 (2011); J. E. Ortega et al., Phys. Rev. B (submitted).

SS-17-Or-2
Inelastic tunneling spectroscopy for magnetic atoms.

T13 Surface Science

#SS-17-Or-2

E. Goldberg [1], F. Flores [2].

[1]INTEC-CONICET-UNL - Santa Fe (Argentina), [2]Universidad Autonoma de Madrid - Madrid (Spain).

Inelastic tunneling spectroscopy of single magnetic atoms [1-3] and single molecule magnets [4-5] has been recently used to explore the strength, and its anisotropies, of their intrinsic spin. In the single magnetic atom case, Fe or Co have been deposited on a CuN surface, so that the electrons injected with a STM-tip across a single atom interact with the magnetic spin creating spin-flip processes that reveal themselves in the tip-metal tunneling conductance measured as a function of the bias voltage. In this work we address that problem by introducing an ionic Hamiltonian [6] for describing the d-electrons of the magnetic atom, and analyze the tunneling current for a metal/atom/tip configuration using a Green-function Equation of Motion method [7-8]. We analyze in the case of Fe on CuN the possible spin fluctuations between states with S=2 and S=3/2 or 5/2 and conclude, from the found asymmetries and marked structures in the conductance, that the S=2 to S=3/2 fluctuations are dominant and provide a good description of the experimental data. The case of Co is also considered and shown to present, in contrast with Fe, a resonance at the Fermi energy corresponding to a Kondo temperature of 6K. The strong dependence of the spin excitations on magnetic field direction observed experimentally is also well reproduced by our calculations.

[1] C. F. Hirjibehedin et al., Science 317, 1199 (2007).
[2] A.F. Otte et al, Nature Physics 4, 847 (2008)
[3] A.F. Otte et al, Phys Rev Lett 103, 107203 (2009)
[4] J. J. Parks et al., Science 328, 1370 (2010)
[5] A. S. Zyazin et al., Nano Lett. 10, 3307 (2010).
[6] A. C. Hewson, The Kondo Problem to Heavy Fermions, (Cambridge University press, Cambridge, 1993).

[7] E. C. Goldberg and F. Flores, Phys. Rev. B 77, 125121 (2008).
[8] E. C. Goldberg et al., Phys. Rev. B 71, 035112 (2005); R. Monreal et al, Phys. Rev. B 72, 195105 (2005).

SS-16-Or-5
A kinematically driven growth mechanism; AlF3 on Cu(100)

T13 Surface Science

#SS-16-Or-5

J. Ferron [1], L. Gómez [2], V. Martin [3], J. Garces [4].

[1]Surface and interface laboratory, INTEC-FIQ-CONICET, Universidad Nacional del Litoral, 3000 Santa Fe, Argentina. - Santa Fe (Argentina), [2]FCEIA and Instituto de F´ısica Rosario, Universidad Nacional de Rosario, CONICET, 2000 Rosario, Argentina - Santa Fe (Argentina), [3]Centro Atómico Bariloche, CNEA, 8400 Bariloche, R´ıo Negro, Argeíina. - Rio Negro (Argentina), [4]Centro Atómico Bariloche, CNEA, 8400 Bariloche, Río Negro, Argentina. - Rio Negro (Argentina).

The growth of aluminum fluoride (AlF3) on copper single crystal, Cu(100) face, is characterized by several anomalous features. Among them, we have a large diffusion path length at room temperature, nucleation at both sides of steps and island atomistic arrangement along special directions [1, 2]. In this work we introduce a new diffusion model based only on kinematic properties that allows us to explain all the particular properties of this system. The model is based in the rearrangement of a bi-molecules (Al_2F_6) trying to resemble its vacuum behavior. This rearrangement breaks the expected random trajectories of a molecule diffusing over a surface, privileging not only one diffusion direction but also its sense of movement. Additionally, the contact surface is minimized increasing the surface diffusivity. The model is supported by two different calculations, i.e. Monte Carlo simulations based on empirical potentials [3] and Density Functional Theory (DFT) calculations. In the figure we depict the different structures obtained from DFT as well as their corresponding energies. The structure corresponding to the minimum energy is the responsible of the breaking of the random pathway, as well as of the particular features of the AlF_3 growing system.

1. - J.C. Moreno-López, R.A. Vidal, M. Passeggi Jr. and J. Ferrón, Phys. Rev. B 81, 075420 (2010);
2. - J.C. Moreno-López, M.C.G. Passeggi, G. Ruano, R.A. Vidal and J. Ferrón, J. Phys. Stat. Sol. C7, 2712 (2010).

3.- J. Camarero, J. Ferrón, V. Cros, L. Gómez, A.L. Vázquez de Parga, J.M. Gallego, J. E. Prieto, J.J. de Miguel and R. Miranda, Phys. Rev. Lett. 81, 850 (1998).

Different molecule and bi-molecules structures from DFT. A: isolated relaxed bi-molecule (tetrahedron is drawn for clarity).B: relaxed AlF3 molecule on Cu(001). C: unrelaxed bi-molecule plane adsorption along the [100] direction; D: plane relaxed bi-molecule along the[110] direction. E: relaxed bi-molecule along the [010] direction. F: stable minimized energy position of the bi-molecule along the [100] direction. The numbers in the figures are the difference in energy with respect to the ground state, shown in figure F

SS-P3-22
On the origin of Si(110) 16 x 2 single domain surface formation

T13 Surface Science

#SS-P3-22

T. Ichikawa, H. Tamaki, K. Gomaiwa.

Meiji University - Kawasaki (Japan).

When Si(110) surfaces are atomically cleaned by flashing at about 1230 degree C and then annealed at high temperatures, surface reconstruction takes place and 16 x 2 structure forms on the surfaces. Owing to the mirror symmetry of Si(110) 1 x 1 surface, most of the reconstructed surfaces consist of two equivalent domains with the same 16 x 2 structure. However when rectangular strips are cut from Si(110) wafers as specimens whose longer side is oriented in [1 -1 2] or [-1 1 2] direction are flashed and annealed at appropriate temperatures by passing DC current along the longer side, the surfaces are covered with either of the two domains [1]. Such surfaces are named single domain surfaces. Yamada et al. concluded from LEED and STM observations that electromigration during annealing was responsible for the single domain formation [1].

It has generally been accepted that surface stress plays an important role on the formation of surface structure and domain growth. When resistive heating by passing DC current in strip specimens is carried out, both the ends of the specimens are fixed on electrodes, e. g. by using tantalum plate springs. The fixing introduces a compressible surface stress on annealing, though its magnitude depends on details of the fixing. So we have an idea that the surface stress may induce the appearance of the single domain surface rather than the electromigration.

In order to substantiate the idea, we cut rectangular specimens whose longer side was oriented in [1 -1 2] or [-1 1 2] direction. And we placed the specimens on a ceramics heater and annealed the specimens not to pass DC current by using the ceramics heater, fixing both the end. This annealing surely induced the single domain surface as well as the passing of DC current did. Next we laid the same Si(110) specimens across two electrodes and annealed by passing DC current along the longer side, without fixing both the ends. This annealing always grew surfaces composed of the two domains as expected. Therefore it will be reasonable from these evidences to conclude that the appearance of the single domain surface is due to surface stress rather than to electromigration.

The Si(110) 16 x 2 structure has a very complicated atomic geometry. Its major

structural features are (1) periodic up-and-down terraces extending in the [1 -1 2] or [-1 1 2] direction and (2) pairs of pentagons regularly arranged on the terraces [2]. It is worthwhile to note that the direction of the terraces coincides with the direction of the compressible surface stress. We suppose that a compressible surface stress is present along the terrace in the 16 x 2 structure and hence the compressible surface stress on annealing is in favor of the single domain growth.

A further step to understand the effect of the surface stress is to estimate quantitatively the magnitude of the surface stress necessary to grow the single domain surface. Therefore we are now constructing a new measuring apparatus. We will present some results, though preliminary, at the coming conference.

[1] Y. Yamada, et al., Phys. Rev. B76, 153309 (2007)
[2] T. An, et al., Phys. Rev. B61, 3006 (2000)

SS-1-Or-1
Ab initio Modeling of the Hydrogen Adsorption on Pt(111) Surface

T13 Surface Science

#SS-1-Or-1

H. Tran, T. Yoshinari, S. Osamu.

The Institute for Solid State Physics, the University of Tokyo - Kashiwa (Japan).

The hydrogen adsorption on the Pt(111) electrode surface has been intensively investigated. To gain insight into detailed atomistic picture on the equilibrium coverage and structure, we have constructed a lattice gas model by determining the on-site energy and the interaction parameters using the first principles total-energy calculation. Therein atop, fcc, hcp and bridge sites are covered by hydrogen atoms under various coverage conditions ($0ML<\Theta\leq 1ML$) and the total-energy calculations are done for the (1x1), (2x2) and (3x3) cells. The total-energies of (3x3) cell, corrected by the zero-point energy (ZPE), are found well fitted to the lattice gas model. With this model, the Monte Carlo (MC) simulation has been performed. The first-principles calculation combined with MC simulation successfully explains the interaction of H atoms on the Pt(111) surface. The active site of the hydrogen adsorption on the Pt(111) surface, which has been hitherto conceptually discussed but has not been shown by an atomistic simulation, has been identified.

[1] I. Hamada, Y. Morikawa, J. Phys. Chem. C 112 (2008) 10889.

[2] K. Kunimatsu, H. Uchida, M. Osawa, M. Watanabe, J. Electroanal. Chem. 587 (2006) 299.

[3] N.M. Markovic, P.N. Ross, Surf. Sci. Rep. 45 (2002) 117.

[4] A. Lasia, J. Electroanal. Chem. 562 (2004) 23.

Figure 1: The potential dependent surface coverage. The theory (lines points) and the experiment (open marks) [3].

Figure 2: The g-value at 290K is compared with experiment [4].

SS-12-Or-1
Interfacial reaction on the Si-SiO2 system studied by Low Energy Electron Microscopy and Kinetics Monte Carlo

T13 Surface Science

#SS-12-Or-1

P. Müller [1], F. Leroy [1], F. Cheynis [1], Y. Saito [2], E. Bussmann [3].

[1]Aix Marseille University - Marseille (France), [2]Keio University - Yokahama (Japan), [3]Sandia National Labs - Albuquerque (United states).

Precise control of the Si/SiO_2 interface is crucial because of its important role in semiconductor devices. However at high temperature SiO_2 +Si(substrate) → 2 SiO(g) reaction is a dominant process.
We examine the interfacial reaction between Si and SiO_2 during high temperature annealing. For this purpose we study the thermal decomposition of SiO_2 thin film covering a crystalline silicon substrate and the interfacial reaction between Si nanoislands on a SiO_2 substrate.
We use Low Energy Electron Microscope (LEEM) to follow in-situ the void-opening characteristic of the SiO_2 thermal decomposition mechanism due to the reaction SiO_2 +Si(substrate) → 2 SiO(g) . We establish experimental scaling laws of the void-growth versus time under different experimental conditions. The LEEM data are completed by in-situ Atomic Force Microscopy (AFM) and/or Scanning Tunneling Microscopy (STM) measurements to control the front profile, the oxide thickness as well as the roughness of the resulting deoxidized Si surface.
We also use LEEM to show that Si islands on SiO_2, when annealed at very high temperatures, react on the SiO_2 substrate. The reaction Si(3D) + SiO_2(substrate) → 2 SiO(g) is accompanied by a motion of the Si islands from which results a deep depression in the SiO_2 substrate due to the consumption of the SiO_2 substrate. Following the centre of mass of each nanoparticle we put in evidence that the island motion in the small timescale limit is random whereas at late time nanoparticles get trapped inside the hole formed in the SiO_2 substrate induced by the chemical reaction. A complementary Atomic Force Microscopy study of the profile of the depleted zones give information on the chemical process at work (chemical rate, width of the reactive zone…).

From these kinetics studies, effective diffusion coefficient and activation energy barriers are extracted.
Experimental results are supplemented by Kinetic Monte Carlo simulations based on a Solid-On-Solid model including surface diffusion processes and chemical reaction kinetics. The two main ingredients used in simulations are the chemical reaction rate at the interface followed by the gas diffusion towards the triple line (where the SiO gas is expelled).
All the results show that the chemical reaction essentially takes place at the triple line.

SS-3-Or-2
Driving Force of Phase Transition in Indium Nanowires on Si(111)

T13 Surface Science

#SS-3-Or-2

J. Cho, H.J. Kim.

Hanyang University - Seoul (Korea, republic of).

The precise driving force of the phase transition in indium nanowires on Si(111) has been controversial whether it is driven by a Peierls instability or by a simple energy lowering due to a periodic lattice distortion. Unlike local and semi-local density-functional theories, the present van der Waals (vdW) corrected hybrid density functional calculation predicts that the low-temperature 8x2 structure whose building blocks are indium hexagons is energetically favored over the room-temperature 4x1 structure. We show that the correction of self-interaction error and the inclusion of vdW interactions play crucial roles in describing the covalent bonding, band-gap opening, and energetics of hexagon structures. The results manifest that the formation of hexagons occurs by a simple energy lowering due to the lattice distortion, not by a charge density wave formation arising from Fermi surface nesting.

SS-16-Or-1
Medium energy ion scattering investigation of Pt, Pd and Rh deposited onto Cu(110)

T13 Surface Science

#SS-16-Or-1

M. Cropper, T. Fleming.

Loughborough University - Loughborough (United kingdom).

Medium energy ion scattering (MEIS) has been used to investigate the deposition of platinum, palladium and rhodium onto the Cu(110) surface. Sub-monolayer quantities were deposited onto the surface near room temperature using a miniature e-beam evaporation source. The structure of these films was investigated in several shadowing and blocking directions, both as-deposited and following subsequent low-temperature annealing.

MEIS is a real space technique with a high degree of sensitivity to surface structure and composition. The experiments were carried out at the UK National MEIS facility using 100 keV H^+ ions. The films were prepared in an ultra-high vacuum preparation system and transferred under vacuum to the scattering chamber. The ions were aligned parallel to incidence directions giving illumination of one, two and three surface layers; the [-10-1], [-100] and [-2-1-1] directions. Scattered ions were collected across a range of angles that included outgoing blocking dips.

The MEIS data can be presented as energy profiles that give depth profile information and blocking curves that enable the determination of structure. The blocking curves from the two elements present can be separated due to the difference in mass giving different recoil properties. For all three deposited metals the presence of dips in the one-layer blocking curve shows that the deposited metal has occupation of the second layer, indicating either island formation, or of incorporation of the ad-atom into the close packed surface rows followed by decoration by mobile copper atoms from step edges. Quantitative analysis has been carried out by comparison with simulations made by the Monte-Carlo code VEGAS. The relative occupation of different layers has been investigated using reliability factors. For

platinum deposition, the ad-atoms mostly occupy the second layer with a spacing of 123±4 pm.

SS-2-Or-2
On reliability of calculated energies and measured enthalpies of interfacial segregation

T13 Surface Science

#SS-2-Or-2

P. Lejcek [1], M. Sob [2], V. Vitek [3], V. Paidar [1].

[1]Institute of Physics, Academy of Sciences of the Czech Republic - Prague (Czech republic), [2]Central European Institute of Technology, CEITEC MU, Masaryk University - Brno (Czech republic), [3]University of Pennsylvania - Philadelphia (United states).

A very important problem discussed and analyzed extensively for many years until present is the effect of solute segregation on interfacial properties, above all cohesion. Following widespread experimental studies, in particular for grain boundaries (e.g. [1,2]), segregation energies of solutes at interfaces have been calculated in recent years using the density functional theory (DFT). A number of such calculations were published (e.g. [3,4]), which may open new horizons since they can provide not only information on bond strength at grain boundaries as affected by the presence of solutes but also detailed insight into the local charge distribution. Consequently, they can contribute to our understanding of the nature of interfacial cohesion on a qualitatively new level. Unfortunately, when evaluating the energy of segregation an acute problem arises in the case of solutes with low solubility.

Here we demonstrate that the present-day DFT-based calculations of segregation energies are limited to systems with a high solid solubility, provided they employ repeat cells containing about 100 atoms. However, these problems have not been considered in the majority of calculations of segregation energies. Consequently, interfacial segregation energies calculated for systems with low solid solubilities are often dubious. This includes P, C, S and B in α-iron, all of which affect the grain boundary cohesion very significantly and play a major role in steels. On the other hand, even when using repeat cells that are not sufficient for reliable evaluation of the segregation energy the change in the grain boundary cohesion may be inferred with a reasonable accuracy from such calculations [5].

[1] R.H. Jones, Ed., Environmental Effects on Engineered Materials, Marcel Dekker, New York, 2001.
[2] C.J. McMahon, Interface Sci. 12 (2004) 141.
[3] R. Schweinfest, A.T. Paxton, M.W. Finnis, Nature 432 (2004) 1008.
[4] M. Všianská, M. Šob, Prog. Mater. Sci. 56 (2011) 817.
[5] P. Lejček, M. Šob, V. Vitek, V. Paidar, Scripta Mater, in press. http://dx.doi.org/10.1016/j.scriptamat.2012.11.019

NST/SS-6-Or-8
What can we learn about magnetic and nonmagnetic surfaces using spin-polarized single- and two-electron spectroscopy

T13 Surface Science

#NST/SS-6-Or-8

S. Samarin [1], O. Artamonov [2], P. Guagliardo [1], K. Sudarshan [1], A. Suvorova [1], J. Williams [1].

[1]The University of Western Australia - Perth (Australia), [2]St. Petersburg State University - St. Petersburg (Russian federation).

Spin-polarized two-electron spectroscopy, (e,2e) [1], and spin-polarized electron energy loss spectroscopy (SPEELS) provide valuable information on the spin-dependent electronic structure of surfaces and thin films. We applied these spectroscopies to study clean and oxygen covered W(110) surfaces as well as ultrathin layers of Ni, Co, Fe, Au, Ag and bi-layer structures on W(110). Examples of such studies are presented and analysed.
Using (e,2e) spectroscopy one can measure a spin-asymmetry of the Spectral Density Function (SDF) of the sample in the centre of the Brillouin zone [1]. A non-zero value of the spin asymmetry of the SDF indicates an imbalance of spin-up and spin-down states in the valence band of the ferromagnetic metal. If the asymmetries of the (e,2e) spectra measured for non-reversed and reversed target magnetization are denoted AM1 and AM2, then the spin-orbit (ASO) and exchange (Aex) contributions are given to leading order by: A ex = ½ (AM1 – AM2) and ASO = ½ (AM1 + AM2). In such a way the exchange and the spin-orbit interactions in a 3ML Co film on W(110) were identified and located in energy- and momentum- space of the valence band [2].
In contrast to the Co film, a 5 ML Fe film does not show any spin-orbit component in the asymmetry spectrum although a substantial exchange component is observed in the binding energy spectrum and in the energy sharing distribution.
We studied the influence of a thin Au layer on top of the Fe film on the measured asymmetries. The deposition of 1ML of Au on 5 ML of Fe decreases the spin-asymmetry of the SDF from 10% to 7%, still showing a ferromagnetic feature in the

spectrum. At the same time, in the asymmetry of the energy sharing distribution a spin-orbit component of about 2% appeared together with an exchange component of about 7% indicating ferromagnetism in this structure. The ferromagnetic state of the Au/Fe structure is very stable and did not change over a two month period. Since (e,2e) spectroscopy is very surface sensitive this result may indicate a ferromagnetism of the ultrathin Au film on the Fe layer.
A thin Ni buffer layer (1–3 ML) between the 3 ML of Co and the W(110) substrate substantially improves the crystallinity of the Co film and enhances the spin asymmetry of the spectral density function as measured by spin-polarized two-electron spectroscopy.
Spin-orbit splitting of electronic states in W and Au were observed using spin-polarized (e,2e) spectroscopy. The dispersion of these states is measured.
Plasmons in thin Ag films on magnetic and nonmagnetic substrates excited by spin-polarized electrons have been studied using SPEELS.
An asymmetry of Stoner excitations in SPEELS of a thin iron film on a W(110) substrate was used as a measure of the film magnetization to study the influence of the film structure and oxygen adsorption on the magnetic moment of the film.
In addition, the azimuthal dependence of the asymmetry of Stoner excitations can provide information on the magnetic domain structure of a ferromagnetic film.

[1] A. Morozov et al. Phys. Rev. B65 (2002)104425
[2] S. Samarin et al. Phys. Rev. Lett. 97 (2006) 096402

SS-9-Or-1
Self-assembled monolayers of boron cluster molecules on metal surfaces

T13 Surface Science

#SS-9-Or-1

T. Base [1], J. Machácek [1], J. Langecker [1], I. Boldog [1], A. Vetushka [2], P. Schmutz [2], J.C. Thomas [3], H. Auluck [3], P.S. Weiss [3].

[1]Institute of Inorganic Chemistry – Department of Synthesis, Academy of Sciences of the Czech Republic, 250 68 Husinec-Rez, c.p. 1001, Czech Republic - Husinec-Rez (Czech republic), [2]EMPA, Swiss Federal Laboratories for Materials Science and Technology, Department of Corrosion, Übelandstrasse 129, 8600 Dübendorf, Switzerland - Dübendorf (Switzerland), [3]California NanoSystems Institute, University of California, Los Angeles, 570 Westwood Plaza, Los Angeles, CA 90095, United States - Los Angeles (United states).

Clusters of boron hydrides have throughout their history significantly enriched the area of structural inorganic chemistry. These molecules adopt different rigid and robust molecular architectures that make them an interesting, new type of ligands for self-assembled monolayers on metal surfaces. Icosahedral dicarba-*closo*-dodecaborane-thiol derivatives have been introduced and investigated as one of the essential cluster building blocks for SAMs on metal surfaces by our laboratories. Within our research we are concerned with the interactions between these molecules and gold surfaces [1] and also surfaces of silver and copper as substrates with greater commercial potential [2]. Both experimental and computational results covering fundamental characterization of the modified surfaces will be reported. In addition to this we shall present recent results on new, versatile boron cluster molecules from our growing portfolio of cluster modifiers for metal surfaces.
Acknowledgement: This work has been supported by the following grant projects: M200321201 (AS CR), P205100348 (GACR), SCIEX project 11.206, and NSF #CHE-1013042 (JCT, HA, PSW).

1. A) Base T., Bastl Z., Plzak Z., Grygar T., Plesek J., Carr M. J., Malina V., Subrt J., Bohacek J., Vecernikova E., Kriz O. *Langmuir* 2005, 21, 7776-7785. B) Base T., Bastl Z., Slouf M., Klementova M., Subrt J., Vetushka A., Ledinsky M., Fejfar A., Machacek J., Carr M. J., Londesborough, M. G. S. *J. Phys. Chem. C* 2008, 112,

14446-14455. C) Hohman J. N., Zhang P. P., Morin E. I., Han P., Kim M., Kurland A. R., McClanahan P. D., Balema V. P., Weiss P. S. *ACS Nano* 2009, 3 (3), 527-536. D) Hohman J. N., Claridge S. A., Kim M., Weiss P. S. *Mat. Sci. Eng. R.* 2010, 70 (3-6), 188-208.
2. A) Lübben J. F., Base T., Rupper P., Künniger T., Machacek J., Guimond S. *J. Colloid Interface Sci.* 2011, 354, 168-174, B) Base T., Bastl Z., Havránek V., Lang K., Bould J., Londesborough M. G. S., Machacek J., Plesek J. *Surf. Coat. Tech.* 2010, 204, 2639–2646, C) Base T., Bastl Z., Havranek V., Machacek J., Langecker J., Malina V. *Langmuir* 2012, 28, 12518-12526.
3. Thomas J. C., Auluck H., Base T., Weiss P. S. et al Article in preparation 2013.

Cluster analogue of *p*-mercaptobenzoic acid (shown on the right for comparison): 1-SH-12-COOH-1,12-$C_2B_{10}H_{10}$. [3]

SS/NST-P1-03
Edge and Interfacial States of a Two Dimensional Topological Insulator, a Bi(111) Bilayer/Bi2Te2Se

T13 Surface Science

#SS/NST-P1-03

S. Kim [1], K.H. Jin [2], J. Park [2], J.S. Kim [2], S.H. Jhi [2], T.H. Kim [1], H.W. Yeom [1].

[1]Center for Low Dimensional Electronic Symmetry, Pohang University of Science and Technology - Pohang (Korea, republic of), [2]Department of Physics, Pohang University of Science and Technology - Pohang (Korea, republic of).

We successfully identified the edge electronic state of a single Bi(111) bilayer, predicted as a 2D topological Insulator [1, 2], by scanning tunneling spectroscopy and first principles calculations. The zigzag-edged Bi(111) islands are grown in triangular shape on a cleaved Bi_2Te_2Se crystal (BTS). The spectroscopic maps directly show enhanced local density of states near the valence band top of the freestanding Bi(111) bilayer [Fig. 1], which agrees well with the calculation for Bi bilayer nanoribbons on Bi_2Te_2Se. In addition, we observed the interfacial states which have modulations around the edges. Our calculation for a Bi(111) bilayer on Bi_2Te_2Se verifies that the interfacial states originate from the hybridization between the electronic states of Bi(111) and the substrate. According to our results, the previous work [3] interpreted the edge modulation of the interfacial state as the signature of the edge state. This work paves an avenue towards the exploitation of quantum spin Hall states.

[1] M. Wada, S. Murakami, F. Freimuth, and G. Bihlmayer, Phys. Rev. B 83, 121310 (2011).

[2] T. Hirahara et al., Phys. Rev. Lett. 107, 166801 (2011).

[3] F. Yang et al., Phys. Rev. Lett. 109, 016801 (2012).

Fig. 1: a)-d) Normalized spectroscopic maps at -0.5, -0.2, 0.2, and 0.5 V, respectively. The inset in a) shows the topography of a). The edge enhancement of LDOS is observed in a) and b).

SS-4-Or-1
Precipitation of iron and its oxides on titanium dioxide surfaces

T13 Surface Science

#SS-4-Or-1

A. Busiakiewicz, M. Rogala, Z. Klusek.

University of Lodz - Lodz (Poland).

Titanium dioxide (TiO_2) because of its unique physical and chemical properties is one of the most studied metal oxides. Besides the fundamental reasons, the far-flung investigations are motivated by technological applications of TiO_2 including solar cells [1], self-cleaning coatings [2], water decomposition and hydrogen production [3] among others. However, the doped TiO_2 is also technologically promising considering its bulk and surface properties. Recent studies suggest that Fe-doped TiO_2 can be a candidate for a diluted magnetic semiconductor [4] which could be used in spintronics and magneto-optic devices. In turn, the surface of the Fe/TiO_2 system is very interesting mainly because of its catalytic properties [5]. The solubility of Fe in reduced rutile TiO_2 crystal and the followed precipitation on the (001) and (110) surfaces have been studied using X-ray photoelectron spectroscopy (XPS) and scanning tunneling microscopy (STM) in ultra-high vacuum. In the first step Fe is dissolved in reduced TiO_2 at 1073 K by thermal diffusion and the saturated solid state solution is formed. A supersaturated solid state solution is then obtained by fast cooling of the sample. In the next step, when this supersaturated crystal is annealed at low temperatures (about 500 K), Fe starts to precipitate on the surface and spherical Fe-rich nanoparticles are formed. At higher temperatures the size of nanoparticles increases and they are transformed into nanocrystals with clearly visible facets. Simultaneously, the number of nanocrystals substantially decreases. Partial oxidation of Fe is also observed around 900 K which is related to strong metal support interaction between precipitating Fe and reduced TiO_2 surface. The XPS and STM results suggest that nanocrystals are mostly composed of mixed Fe/Ti oxides like $FeTiO_3$ with ilmenite structure (Fig. 1). However, at temperatures close to saturation the nanocrystals disappear which is explained by the restored solubility of Fe cations in reduced TiO_2. The precipitation and disappearance of Fe-rich nanoparticles and nanocrystals on TiO_2 surfaces is a fully reversible process that can be performed many times and easily controlled by annealing temperature.

[1] B. O'Regan, M. Grätzel, Nature 353 (1991) 737.
[2] I.P. Parkin, R.C. Palgrave, J. Mater. Chem. 15 (2005) 1689.
[3] M. Ni, M.K.H. Leung, D.Y.C. Leung, K. Sumathy, Renew. Sust. Energ. Rev. 11 (2007) 401.
[4] G. Mallia, N. M. Harrison, Phys. Rev. B 75 (2007) 165201.
[5] Y. L. Wei , K. W. Chen H. P. Wang, J. Vac. Sci. Technol. B 27 (2009) 1385.

Fig. 1. The STM image of the Fe-rich nanocrystal formed at 973 K on the TiO_2(001) surface.

SS-12-Or-2
Influence of counterions on hectorite swelling properties monitored by NAP-XPS

T13 Surface Science

#SS-12-Or-2

H. Tissot [1], A. Naitabdi [2], F. Bournel [2], J.J. Gallet [2], F. Rochet [2], V. Marry [2], E. Dubois [2], J. Schnadt [3], J. Knudsen [3].

[1]synchrotron soleil - Saint Aubin (France), [2]Université Pierre et Maris Curie - Paris (France), [3]Lund University-MaxLab - Lund (Sweden).

Natural clays are key materials in ecological engineering, from the geological storage of long half-time radioactive waste [1] to CO_2 sequestration [2]. With respect to these issues, it is crucial to establish a bridge between the microscopic scale (ionic exchange, ion solvation, ion and matter transport) and the macroscopic scale (swelling, retention capacities). We are interested in the initial stages of water adsorption on external surfaces and interlayers of synthetic hectorite clays which can be considered as “model clay systems” because of their well defined swelling characteristics (figure 1)[3].
NAP-XPS (Near Ambient Pressure X-ray Photoelectron Spectroscopy) brings a new approach with a surface sensitive technique on the water adsorption by clays. Counterions core-level are sensitive to the hydration state (change in binding energy) due to a screening effect of the negatively charged clay layers by water molecules. In the case of Na-hectorite a shift of -0.9 eV of the Na 2*s* binding energy was observed when relative humidity (RH) was increased to 60% (figure 2). Furthermore, varying the electron mean free path through the excitation energy and analysing the O 1s core level [4] reveal the water thickness in the clay interlayer. These tools help us to understand how the presence of these counterions (of different size and charge as Na^+, Cs^+ and Sr^{2+}) is affecting the swelling pattern.

[1] M. Bradbury, B. Baeyens, *Technical report, Paul Scherrer Institut,* **2003**
[2] I. Gaus, *International Journal of Greenhouse gas control,* **2010,** 4, 73-89
[3] N. Malikova, A. Cadène, E. Dubois, V. Marry, S. Durand-Vidal, P. Turq, J. Breu, S. Longeville, J.M. Zanotti, *J. Phys. Chem. C*, **2007**, 111, 1760

[4] K. Arima, P. Jiang, X. Deng, H. Bluhm, M. Salmeron, *J. Phys. Chem. C,* **2010**, 114, 14900–14906

Figure 1: Water adsorption/desorption isotherms of Na hectorite at room temperature. RH is calculated as the ratio of the water vapor pressure and of the saturated water vapor pressure, P_0 (23.8 mbar at 25 °C).

Figure 2: XPS Na 2*s* spectra evolution with RH (hv = 750 eV)

NST/SS-8-Or-6
Growth of Carbon Nanodiscs through Low Pressure Chemical Vapor Deposition

T13 Surface Science

#NST/SS-8-Or-6

V. Del Campo, R. Henríquez, P. Häberle.

Physics Department, Universidad Técnica Federico Santa María - Valparaiso (Chile).

Carbon nanostructures present important variations in their properties depending on their geometry. Examples of these structures are carbon nanotubes, Buckyballs, graphene and graphene nanoribbons. Here we present the formation of carbon nanodiscs for future characterization of their properties.

We grew carbon nanodiscs on Ru(0001) through Low Pressure Chemical Vapor Deposition (LP-CVD). Then they were characterized with Scanning Tunneling Microscopy (STM). Discs' diameter vary between 20 and 700 nanometers and their height never exceeds 1 nm.

To the best of our knowledge this is the first time carbon nanodiscs are grown by CVD. The most common method for this purpose is hydrocarbon decomposition through pyrolysis. In that case, discs' diameters go from 500 to 4000 nanometers and thicknesses vary between 5 and 70 nm [1]. Growth of carbon nanodiscs through LP-CVD allows the formation of smaller discs and enables the possibility of size control.

[1] T. Garberg, S.N. Naess, G. Helgesenb, K.D. Knudsen, G. Kopstad, A. Elgsaeter; Carbon 46, 1535–1543 (2008).

Acknowledgements to FONDECYT grant # 11121513, FONDECYT grant # 1110935 and USM-DGIP grant # 11.11.62

STM image of carbon nanodiscs on Ru(0001). Image area corresponds to 400 nm x 400 nm (Vsample=0.2 V, It=0.22nA).

SS-P1-16
Surface Electronic Properties on Magnetite Films on MgO(100)

T13 Surface Science

#SS-P1-16

A. Ikeuchi, S. Hiura, A. Subagyo, K. Sueoka.

Graduate School of Information Science and Technology, Hokkaido University - Sapporo (Japan).

Magnetite (Fe_3O_4) is a common magnetic iron oxide that has the advantageous properties such as half-metallicity, high conductivity and high Curie temperature of 858 K. Therefore, The Fe_3O_4 films grown on MgO substrates have been expected to be useful for fabrication spin-sensitive devices. However, epitaxially grown Fe_3O_4 films are well known to contain a high density of antiphase domain boundaries (APBs) as investigated by transmission electron microscopy (TEM)[1]. These APBs make the electrical and magnetic properties of the films complicated. The atomic configurations of the APBs in an epitaxial Fe_3O_4(110) film and their effects on its magnetic properties have been discussed[2]. Meanwhile on surface of Fe_3O_4 films, three types of the APBs have been observed by scanning tunnelling microscopy (STM)[3]. Moreover, it has been reported that APBs could induce inhomogeneous electronic properties[4]. It is also interesting to study the effect of the APBs on the surface electronic in addition to the magnetic properties. In this work, we have applied scanning tunnelling microscopy and spectroscopy (STM/STS) to investigate the local surface electronic properties around the APBs.

The Fe_3O_4(100) films were prepared on MgO(100) substrates by electron beam evaporation of iron in an oxygen atmosphere. The STM image is shown in Fig. 1. The surface of the Fe_3O_4 film was terminated by B-plane, and an APB was clearly observed. Figure 2 is a *dI/dV* conductance map taken simultaneously with the STM image. The *dI/dV* map shows different electronic state distribution on the domains separated by the APB. Our results indicate that the APB could modify the surface electronic property.

[1] S. Celotto, W. Erenstein and T. Hibma, Eur. Phys. J. B **36** (2003) 271.
[2] R. G. S. Sofin, S. K. Arora, and I. V. Shvets, Phys. Rev. B **83** (2011) 134436.

[3] A. Ikeuchi, S. Hiura, T. Mizuno, E. Kaji, A. Subagyo, and K. Sueoka, Jpn. J. Appl. Phys. **51** (2012) 08KB02.
[4] A. Subagyo, Y. Sasaki, H. Oka, and K. Sueoka, Phys. Status Solidi (b) **244** (2007) 4482.

Fig. 1. STM image

Fig. 2. *dI/dV* map

SS-P1-17
STM/STS studies of a modified magnetite thin films surface on MgO(001) substrate

T13 Surface Science

#SS-P1-17

S. Hiura, A. Ikeuchi, A. Subagyo, K. Sueoka.

Graduate School of Information Science and Technology, Hokkaido University - Sapporo (Japan).

Magnetite (Fe_3O_4) is known to have the advantageous properties such as half-metallicity, high conductivity at room temperature and high Curie temperature of 858 K. These properties look appropriate for spintronics, however the surface has unexpected electronic and spin states that differ from bulk. Some adsorption spices affect the surface electronic properties. In some case, surface modification gains spin dependent properties. Recently, it has been verified theoretically and experimentally that hydrogen adsorbed on the clean Fe_3O_4(001) surface largely enhances the spin polarization of the surface[1], [2]. So, we have performed doing scanning tunneling microscopy and spectroscopy (STM/STS) experiments on modified Fe_3O_4(001) surface and investigating the surface crystallographic and electronic structures.

The epitaxial Fe_3O_4(001) films were prepared on MgO substrates by means of electron beam evaporation of iron in an oxygen atmosphere[3], [4]. The films thickness was 20 nm. The surface showed a ($\sqrt{2} \times \sqrt{2}$)R45º reconstructed structure terminated by B-plane. Figure 1 shows STM image acquired at the Fe_3O_4(001) films surface and a superimposed structural model based on Parkinson et al.'s report[5]. We found that bright protrusions in the STM image are attributed to hydroxyl species. They indicate that hydrogen tends to adsorb on O_{NARROW} site and it induces substantial change in electronic states for neighboring surface Fe(B). Moreover, we obtained STS spectra and maps at the surface and observed drastic changes of tunnel current and difference in electronic states between Fe(B) and modified Fe(B) sites (Figure 2).

[1] N. Mulakaluri et al., J. Phys. Chem. C **116**, 16447 (2012).
[2] A. Pratt et al., Phys. Rev. B **85**, 180409 (2012).
[3] A. Subagyo et al., Jpn. J. Appl. Phys. **45**, 2255 (2006).
[4] A. Ikeuchi et al., Jpn. J. Appl. Phys. **51**, 08KB02 (2012).
[5] G. S. Parkinson et al., J. Am. Chem. Soc. **133**, 12650 (2011).

Fig. 1 STM image of the Fe_3O_4(001) film surface and a superimposed structural model

Fig. 2 *dI-dV* spectra taken on the Fe(B) and modified Fe(B) sites

SS-3-Or-12
Lattice dynamics in 2D nanoclusters : a possible way to control the chemical ordering in nanoalloys.

T13 Surface Science

#SS-3-Or-12

H. Bulou [1], F. Scheurer [1], C. Goyhenex [1], N. Moreau [2], V. Repain [2], C. Chacon [2], Y. Girard [2], S. Rousset [2], E. Otero [3], P. Ohresser [3].

[1]IPCMS-CNRS UMR7504-Université de Strasbourg - Strasbourg (France), [2]MPQ-CNRS UMR7162-Université Diderot - Paris (France), [3]Synchrotron SOLEIL - Paris (France).

Since the pioneering work of Faraday on the color of ruby [1], the relationship between morphology and particle properties has been evidenced in many domains, including catalysis [2], magnetism [3] and optics [4]. Nowadays, a major challenge is to shape the particle at a nanoscopic scale to reach specific properties resulting from the combination of reduced dimensionality and controlled morphology, such as the plasmon resonances, the morphological-controlled catalytic or magnetic behavior. A further way to control the physical and chemical properties of nano-clusters is to fabricate alloy clusters. By varying the proportion of the different species in the nanoalloy clusters one can access to new parameters to adjust their properties. Controlling the chemical ordering in nanocluster is however a hard task to achieve due to the large number of intricate phenomena involved during the growth such as segregation or strain for example. During this talk, we will present results concerning the dynamical behavior of nanoclusters supported on a (111) surface of gold[5] and we will conclude by sketching a protocol based on lattice dynamics allowing to induce chemical ordering in the bimetallic nanoclusters (Fig. 1). Pure cobalt, palladium and platinum clusters and some of their alloys will be considered here. We will see that although the thermodynamic equilibrium shape as a function of cluster size is similar for all three pure element clusters and shows a morphology transition from monolayer to bilayer, only Co clusters meet their stable state and undergo a transition. Atomistic simulations on a pico to nanosecond timescale evidence kinetic limitations for Pt and Pd, and allow to understand the experimentally observed morphology for the different species. We will show that stress relaxation, by strongly influencing the energy activation for atom hopping from first to second cluster layer

and the magnitude of vibration of the atoms, is the determinant parameter for the existence or absence of the cluster morphology transition.

[1] M. Faraday, Philos. Trans. R. Soc. London 147, 145 (1857).
[2] J. L. Carter, J. A. Cusumano, and J. H. Sinfelt, J. Phys. Chem. 70, 2257 (1996).
[3] W. A. de Heer, P. Milani, and A. Châtelain, Phys. Rev. Lett. 65, 488 (1990).
[4] W. A. de Heer, K. Selby, V. Kresin, J. Masui, M. Vollmer, A. Châtelain, and W. D. Knight, Phys. Rev. Lett. 59, 1805 (1987).
[5] H. Bulou, F. Scheurer, C. Goyhenex, V. Speisser, M. Romeo, B. Carrière, N. Moreau, V. Repain, C. Chacon, Y. Girard, J. Lagoute, S. Rousset, E. Otero, and P. Ohresser, Phys. Rev. B, in press.

Fig.1: $Co_{25}Pd_{75}$/Au(111) nanoalloy.

SS-8-Or-2
Evolution of Topological Surface States in Sb(111) Ultra-Thin Films

T13 Surface Science

#SS-8-Or-2

X. Wang, G. Yao, Z. Luo, W. Xu, J. Sun.

National University of Singapore - Singapore (Singapore).

Based on an inverted bulk band order, antimony thin films presumably could become topological insulators if quantum confinement effect opens up a gap in the bulk bands. Coupling between topological surface states (TSSs) from nearby surfaces, however, tends to degrade or even destroy their novel characters (e.g., spin polarisation). We investigated the evolution of TSS on Sb(111) thin films and their inter-surface coupling as the thickness is reduced from 30 bilayers (BL, 1 BL = 3.75 Å) to 4 BL using in-situ Fourier-transform scanning tunneling spectroscopy (FT-STS) and density functional theory computations. Due to strong distortion in TSS Dirac cone, rich quasi-particle interference (QPI) patterns have been observed in FT-STS mapping. On a 30-BL sample, these patterns are generated by the scattering of TSS on the top surface only. As the thickness decreases, inter-surface coupling degrades spin polarisation of TSS and opens up new scattering channels which show as additional features in the QPI patterns. The strength of inter-surface coupling is found varying dramatically with the wavevector, resulting in spin degenerate states in a large part of the surface Brillouin zone, whereas the TSS survive near the zone centre without opening a gap at the Dirac point for films thickness > 6 BL. Our results also demonstrate quite different behaviors distinguishing SSs, surface resonances, and bulk states as the film changes from thick to ultrathin category. Based on the understanding of these behaviors, the surface energetic and transport properties of Sb films can be tailored for potential applications.

1. D. Hsieh et al., Observation of unconventional quantum spin textures in topological insulators, Science 323, 919 (2009).
2. K. K. Gomes et al., Quantum imaging of topologically unpaired spin-polarized Dirac fermions, e-print arXiv:0909.0921 (2009).
3 Y. Zhang et al., Crossover of the three-dimensional topological insulator Bi2Se3 to

the two-dimensional limit, Nature Phys. 6, 584 (2010).
4. G. Bian, T. Miller, T.C. Chiang, Passage from Spin-Polarized Surface States to Unpolarized Quantum Well States in Topologically Nontrivial Sb Films. Phys. Rev. Lett. 107, 036802 (2011).

SS/NST-1-Or-4
Microscopic origin of Joule heating studied by SP-STM

T13 Surface Science

#SS/NST-1-Or-4

A. Schlenhoff, S. Krause, R. Wiesendanger.

Institute of Applied Physics, University of Hamburg - Hamburg (Germany).

Heat dissipation in electronic devices influences their performance and reliability. As dimensions approach the nanoscale, sensing and controlling heat flow becomes more and more important. The investigation of basic thermal phenomena on the atomic scale is crucial to understand thermoelectric materials and interfacial transport, providing a way to new miniaturized electronic circuits.
In scanning tunneling microscopy the atom-size probe tip allows for a very local current injection. By changing the tip-sample distance, the tunnel current can be varied by orders of magnitude while keeping the applied sample bias and thus the energy of the charge carriers constant. As shown recently, spin-polarized scanning tunneling microscopy (SP-STM) allows for the direct investigation of current-induced impacts on nanomagnets consisting of only about 50 iron atoms on a W(110) substrate. They frequently invert their magnetic orientation at a temperature of $T \approx 35$ K due to thermal agitation [1], and by observing their current-dependent switching behavior it has been demonstrated that these nanomagnets may serve as local thermometers [2].
In our studies, we utilize an SP-STM setup to position a magnetic tip above the center of such an thermally switching nanomagnet and inject either low-energy tunneling electrons at a sample bias of $U = 200$ mV or higher-energetic field-emitted electrons at $U = 5$ V [3]. In both cases, increasing the current significantly rises the thermal switching frequency of the nanomagnet, indicating considerable Joule heating. However, our experiments reveal that the effective temperature increase of the nanomagnet per electron depends on the electron energy, and an additional dependence of the Joule heating on the temperature is found.
Our results will be presented and discussed within a simple model [4,5] considering temperature-dependent thermal boundary resistance and different phonon excitation probabilities for tunneling and field-emitted electrons. By relating the phenomena of Joule heating to the energy-dependent electron-phonon coupling, our experiments provide insight into the microscopic origin of Joule heating, opening the pathway towards new calorimetric experiments on the atomic scale.

[1] S. Krause, G. Herzog, T. Stapelfeldt, L. Berbil-Bautista, M. Bode, E. Y. Vedmedenko, and R. Wiesendanger, *Magnetization reversal of nanoscale islands: How size and shape affects the arrhenius prefactor*, Phys. Rev. Lett. **103**, 127202 (2009).
[2] S. Krause, G. Herzog, A. Schlenhoff, A. Sonntag, and R. Wiesendanger, *Joule heating and spin-transfer torque investigated on the atomic scale using a spin-polarized scanning tunneling microscope*, Phys. Rev. Lett. **107**, 186601 (2011).
[3] A. Schlenhoff, S. Krause, A. Sonntag, and R. Wiesendanger, *Individual atomic-scale magnets interacting with spin-polarized field-emitted electrons*, Phys. Rev. Lett. **109**, 097602 (2012).
[4] W. A. Little, *The transport of heat between dissimilar solids at low temperatures*, Can. J. Phys. **37**, 334 (1959).
[5] N. Néel, J. Kröger, and R. Berndt, *Local heating at a ferromagnet-metal interface*, Appl. Phys. Lett. **95**, 203103 (2009).

SS-P3-07
The interaction of water vapor with the surface of polycrystalline gadolinium at the temperature range 300-570 K

T13 Surface Science

#SS-P3-07

S. Zalkind [1], S. Cohen [1], A. Abramovich [2], M.H. Mintz [2], I. Jacob [2], R. Akhvlediani [3], A. Hoffman [3], N. Shamir [1].

[1]Nuclear Research Centre-Negev - Beer-Sheva (Israel), [2]Ben-Gurion Univ. of the Negev - Beer-Sheva (Israel), [3]Schulich Faculty of Chemistry, Technion - Haifa (Israel).

The initial Gd hydriding depends strongly on the native oxide condition and hydroxyl groups adsorbed on the surface impede the dissociative chemisorption of hydrogen and inhibit this reaction [1]. Therefore, understanding and manipulating the surface condition is essential in order to understand and control the initial interaction of hydrogen with metals and alloys.
The interaction of water vapor with polycrystalline gadolinium surface, with water vapor pressure from $2x10^{-8}$ and up to 18 Torr, was studied by utilizing Direct-Recoils-Spectrometry (DRS), X-ray Photoelectron Spectroscopy (XPS) and Temperature Programmed Desorption (TPD). It has been found that a native Gd surface compound as well as one that was formed by an exposure to 18 Torr H_2O, for 10 minutes, consists of a multilayer hydroxide phase, Gd(OH)3, transforming into oxide by heating, as depicted by the XPS spectra in Fig. 1, while emitting hydrogen as can be seen from the TPD experiments, presented in Fig. 2. For initial exposures of water vapor on a clean metallic surface, it has was found that initially, full dissociation of the water molecules on the metal surface occurs, for <1 L at 300 K and up to ~3 L at 570 K. On top of the formed oxide there is dissociation to H+OH and hydroxyls are adsorbed, forming, with further exposure, a multilayer hydroxide phase. Dissolution of the oxide/hydroxide layer and enhanced inward diffusion of oxygen into the Gd bulk starts as early as 370 K, similar to results found for oxygen exposures [2].

[1] G. Benamar, D. Schweke, N. Shamir, S. Zalkind, T. Livneh, A. Danon, G. Kimmel and M.H. Mintz, J. Alloys Comp. 498 (2010) 26.
[2] S. Cohen, N. Shamir, M.H. Mintz, I. Jacob and S. Zalkind, Surf. Sci. 605 (2011) 1586.

Fig. 1. O 1s XPS line after exposure of the clean surface to 18 Torr H_2O for 10 min. and heating to elevated temperatures.

Fig. 2. TPD of the Gd surface, following exposures of 200 L and 1000 L H_2O.

NST/SS-8-Or-7
Electron localization on periodically rippled graphene

T13 Surface Science

#NST/SS-8-Or-7

S. Barja [1], B. Borca [1], M. Garnica [1], D. Sánchez-Portal [2], V.M. Silkin [2], E.V. Chulkov [2], D. Stradi [3], C. Díaz [3], M. Alcamí [3], A. L. Vázquez De Parga [1], A. Arnau [2], P.M. Echenique [2], F. Martín [3], R. Miranda [1].

[1]Dep. Física de la Materia Condensada, Universidad Autónoma de Madrid - Madrid (Spain), [2]Materials Physics Center (CSIC-UPV/EHU) - San Sebastián (Spain), [3]Dep. de Química, Universidad Autónoma de Madrid - Madrid (Spain).

Moiré patterns are generated by the superposition of two periodic structures with a lattice mismatch or a rotation between them. They have been observed by means of Scanning Tunneling Microscopy (STM) on different systems and their interpretation, in some cases, is not straightforward. The influence, at the atomic scale, of these patterns in the local density of states of the overlayer is not clear.

The growth of graphene on metallic substrates allow us not only control the periodicity of the moiré pattern but also tailor the interaction strength between the carbon atoms and the metallic substrates. This modulation in the interaction gives rise to regions with larger (H-areas) and shorter (L-areas) height of the graphene layer over the Ru(0001) surface. Field Emission Resonances (FERs), which are detected by STM when applying voltages larger than the work function, can be used to explore with nanometer resolution, the inhomogeneities in the local surface potential landscape. Operating the STM in constant current mode implies a constant electric field between tip and sample and the expected energy position for the FERs is gives information about the surface potential.

The dZ/dV curves measured on graphene/Ru(0001) present three unexpected features: (i) the first graphene image state is localized on the H-areas, while it is more extended on the L-areas, (ii) it does not shift in energy following the 0.25 eV increase of local work function from L- to H-areas, and (iii) a new interfacial state at +3 eV appears in the L-areas. To further investigate and understand the origin of

these features we performed first principle calculations based on density functional theory, which explain the experimental behaviour of the first FER in graphene/Ru(0001) as consequence of the splitting and spatial localization of quasi-two dimensional bands due to the modulation of the strength of the interaction between the graphene layer and the metal surface [1]. The interfacial state, resulting from the hybridization of an unoccupied Ru(0001) surface resonance with the first image state component localized in the low areas of the moiré, was suggested to be responsible for the inversion of contrast observed in graphene/Ru(0001) STM experiments at a bias voltage Vs= +2.6 V [2] [3].

[1] B. Borca et al., Potential Energy Landscape for Hot Electrons in Periodically Nanostructured Graphene, Phys. Rev. Lett. **105**, 036804 (2010)

[2] D. Stradi et al., Role of dispersion forces in the structure of graphene monolayers on Ru surfaces, Phys. Rev. Lett. **106**, 186102 (2011)

[3] D. Stradi et al., Electron localization in epitaxial graphene on Ru(0001) determined by moiré corrugation, Phys. Rev. B **85**, 121404(R) (2012)

SS-P1-08
Atomic orbital character of Cu(111) and Ni(111) surfaces studied by two-dimensional photoelectron spectroscopy

T13 Surface Science

#SS-P1-08

M. Takizawa [1], Y. Fujioka [1], H. Namba [1], F. Matsui [2], H. Daimon [2].

[1]Ritsumeikan University - Kusatsu, Shiga (Japan), [2]Nara Institute of Science and Technology - Ikoma, Nara (Japan).

Stepped surfaces of metals have attracted much attention due to the possible one-dimensional nature. For example, on the Ni stepped surface vicinal to the (111) plane, one-dimensional surface state was found at the step edge [1]. On the Cu stepped surface, on the other hand, two-dimensional surface state was formed, maybe due to the lack of *d* orbital character [2]. In this study, we have focused on the terrace planes, the (111) surfaces of Cu and Ni, to elucidate the atomic orbital character by two-dimensional photoelectron spectroscopy (2D-PES). The experiment was performed at the linearly polarized soft x-ray beamline BL-7 of SR center, Ritsumeikan University [3]. The 2D-PES measurements were performed at room temperature under ~1×10^{-8} Pa using a two-dimensional display-type spherical mirror analyzer [4] with synchrotron radiation (SR) light. Figures 1 and 2 show the symmetrized Fermi surfaces (FS) of Cu(111) and Ni(111) taken with $h\nu$ = 22.5 eV and 45 eV, respectively. As in the case of previous work [5], both the Cu bulk state around $|\mathbf{k}| \sim 1.5$ Å^{-1} and the Schockley surface state around the center were successfully observed (Fig. 1). However, the raw photoelectron intensity angular distributions (PIAD) of both Cu and Ni show the symmetry-lowered patterns due to the relation between the polarization vector of the incident SR and the atomic orbitals constituting the FSs. Compared with the simulated PIADs from the atomic orbitals, it is suggested that the Cu(111) Schockley surface state is composed of *s* orbital and/or *p* orbital normal to the surface and that the Ni(111) FS is constituted by a mixture of d_{xy}, d_{yz}, d_{zx} orbitals.

[1] H. Namba *et al*., J. Electron Spectrosc. Relat. Phenom. **88-91**, 707 (1998). [2] K. Ogawa *et al*., Solid State Commun. **125**, 517 (2003). [3] Y. Hamada *et al*., AIP Conf. Proc. **879**, 547 (2007). [4] H. Daimon, Rev. Sci. Instrum. **59**, 545 (1988). N. Takahashi *et al*., J. Electron Spectrosc. Relat. Phenom. **163**, 45 (2008). [5] F. Reinert and S. Hüfner, New J. Phys. **7**, 97 (2005).

Fig. 1: Symmetrized Fermi surface of Cu(111). Fig. 2: Symmetrized Fermi surface of Ni(111).

SS-P3-36
Two-fold symmetry flattens Dirac cone of surface state with spin polarization at W(110)

T13 Surface Science

#SS-P3-36

K. Miyamoto [1], A. Kimura [2], T. Okuda [1], K. Shimada [1], K. Kuroda [2], H. Iwasawa [1], H. Namatame [1], M. Taniguchi [1], M. Donath [3].

[1]Hiroshima Synchrotron Radiation Center, Hiroshima University - Higashi-Hiroshima (Japan), [2]Graduated School of Science, Hiroshima University - Higashi-Hiroshima (Japan), [3]Muenster University - Muenster (Germany).

Topological insulators and Rashba systems with spin-split energy band structure induced by strong spin-orbit interaction have attracted a great attention for the dissipationless spin current transport. Such spin split energy band structures have been intensively studied by using a spin- and angle-resolved photoemission spectroscopy (ARPES) mainly for the surface of ***sp***-electron systems with C_{3V} symmetry at heavy metals and topological insulators[1]. A material with ***d***-derived spin-splitting band remains yet to be explored. Possible strong correlation effects among ***d***-electrons in topological insulators and Rashba systems could be important scientific targets.

Here, we pay attention to W(110) well known as the prototype material with strong spin-orbit coupling and ***d***-electrons . The surface state on W(110) is formed by ***d***-electrons and the surface structure has C_{2V} symmetry in contrast to the systems described above.

In this work, we have clarified that W(110) possesses the spin-polarized Dirac-cone-like surface state with d_{zx} character using the high-resolution ARPES with tunable polarization and spin-ARPES [2]. The constant-energy cuts are found to be strongly flattened compared with what has been observed in the sp-electron-based surface Dirac cone with C_{3V} symmetry at the (111) surface plane of some Bi-based chalcogenides [Fig.1 (a)]. This characteristic electronic structure is well reproduced by **k•p** perturbation theory taking into account the C_{2V} symmetry. Interestingly, spin simulated by this model Hamiltonian are almost oriented along the $\overline{\Gamma N}$ direction without out-of-plane spin component [Fig.1 (b)]. This situation differs from well-known

Rashba systems and topological insulators with C_{3V} symmetry that would approach surface states with ideal helical spin texture and shorten the spin relaxation time in the presence of disorder at the surface. On the other hand, the spin texture along the $\overline{\Gamma N}$ direction at the surface with C_{2V} symmetry would generate a quasi-one dimensional edge current along the $\overline{\Gamma H}$ direction. This situation would substantially enhance the spin relaxation time through a persistent spin helix mechanism.

[1] K. Kuroda et al., Phys. Rev Lett **105**, 076802 (2010)/ J. H. Dil, J. Phys.: Condens. Matter **21**, 403001 (2009).

[2] K. Miyamoto et al., Phys. Rev. Lett. **108**, 066808 (2012)./ K. Miyamoto et al., Phys. Rev. B **86**, 161411(R) (2012).

Fig. 1 (a) Energy contours of the surface state as function of k_x , k_y for energies around the crossing point (E_D) simulated by the model calculation. (b) Spin texture for the constant-energy surface (solid line) at 20 meV above E_D obtained from the model calculation.

SS-16-Or-2
Discovery of quasicrystalline oxide thin films: A STM and LEED study

T13 Surface Science

#SS-16-Or-2

S. Förster, K. Meinel, W. Widdra.

Institute of Physics, Martin-Luther-Universität Halle-Wittenberg - Halle (Germany).

Quasicrystals represent a fascinating class of materials. In the past thirty years after their discovery by Dan Shechtman they have challenged and changed our fundamental understanding of ordered solids. The extraordinary structure of quasicrystals is accompanied by peculiar properties as for example a reduced wetting, a low friction coefficient, high hardness, and unusual transport properties. The fact that most properties are promoted by the surface demands an understanding of the atomically-clean surfaces which can only be provided by surface science. So far, surface science studies on quasicrystals have been limited to bulk quasicrystalline (QC) material. Surface structural analysis of either bulk crystals or of thin film phases have attracted much attention. The growth of thin films of QC material on periodic substrates has been investigated as well as thin films of crystalline material on QC substrates [1,2].

Here we report on the observation of a two-dimensional QC structure that develops from a classical periodic thin film on a periodic substrate for the case of $BaTiO_3$ on Pt(111). $BaTiO_3$ is the most studied ferroelectric perovskite oxide which has an easily accessible ferroelectric to paraelectric phase transition at 400 K. Due to matching lattice conditions it can be grown epitaxially on other perovskites as well as on selected metal substrates. On Pt(001) and on Pt(111) periodic thin films of either $BaTiO_3$(001) or $BaTiO_3$(111) have been grown [3-5]. As we demonstrate here, alternatively an aperiodic QC structure can be formed by annealing an initially 2.8 nm thick $BaTiO_3$ film on Pt(111). Upon annealing at 1250 K in UHV the material restructures in a QC wetting layer in between a few thicker $BaTiO_3$(111) islands. In LEED the QC structure shows bright and sharp spots with dodecagonal symmetry as shown in Fig. 1. High-resolution STM images reveal that the surface structure is composed by an arrangement of quadratic and triangular building blocks. These are the typical elements of a 2D QC lattice with dodecagonal symmetry. The Fourier

transform of the high-resolution STM data is in excellent agreement with the measured LEED pattern. The analysis as performed here demonstrates once more the power of combining both techniques. The FFT is used as the key for correlating the local structural information of STM with the global structural information as derived from LEED.

[1] E. J Widjaja and L. D Marks, *Phil. Mag. Lett. 83*, 47 **2003**.
[2] V. Fournèe *et al.*, *Isr. J. Chem. 51*, 1314 **2011**.
[3] S. Förster and W. Widdra, *Surf. Sci. 604*, 2163 **2010**.
[4] S. Förster et *al.*, *J. Chem. Phys. 135*, 104701 **2011**.
[5] S. Förster *et al.*, *Surf. Interf. Anal. 44*, 628 **2012**.

LEED pattern of the QC structure derived from $BaTiO_3$ on Pt(111). LEED energy 55 eV.

SS-12-Or-3
Reactivity of ethylene on In and Sn saturated Si(001)2×1 surfaces

T13 Surface Science

#SS-12-Or-3

P. Zimmermann [1], O. Krejcí [2], M. Vorokhta [1], R. Acres [3], I. Oštádal [4], P. Sobotík [4].

[1]Charles University in Prague - Prague (Czech republic), [2]Academy of Sciences of the Czech Republic - Prague (Czech republic), [3]Elettra-Sincrotrone - Trieste (Italy), [4]Charles Univrsity in Prague - Prague (Czech republic).

High reactivity of the bare Si(001)2×1 surface is caused by the presence of one dangling bond per surface atom. Adsorption of conjugated organic molecules proceeds by the creation of covalent bonds between the pi electrons of the molecules and the dangling bond of the surface thus leading to various adsorption configurations and distortion of desired molecular properties [1].

We investigate the possibilities of decoupling the molecules from the Si(001) substrate by saturating the Si dangling bonds by indium (group III) and tin (IV) adatoms. Both elements self-organize into linear dimer chains growing perpendicular to the underlying Si dimer rows [2]. At 0.5 monolayer coverage all Si dangling bonds are saturated.

We examine the reactivity of the decoupling layers by exposing them to ethylene which serves as a simple model for the reactivity of more complex conjugated molecules. Based on STM and PES measurements and DFT calculations we observe that ethylene doesn't chemically interact with the indium decoupling layer whereas it does interact with the tin decoupling layer by chemisorbing on top of Sn dimers. We attribute the inertness (reactivity) of the indium (tin) surface to the the absence (presence) of a pi bond in the In (Sn) dimer respectively.

[1] F. Tao, S. Bernasek, G. Xu, Chem. Rev. 109, 3991 (2009)

[2] M. Setvin, P. Mutombo, M. Ondracek, Z. Majzik, M. Svec, V. Chab, I. Ostadal, P. Sobotik, and P. Jelinek: ACS Nano 8, 6969-6976 (2012)

SS-P3-30
Strain-driven self-assembled CrN nanoislands on Cu(001)

T13 Surface Science

#SS-P3-30

F. Komori, P. Krukowski, T. Iimori, K. Nakatsuji, M. Yamada.

ISSP, Univ. of Tokyo - Kashiwa, Chiba (Japan).

Self-assembly at solid surfaces is a promising way for preparing nanostructures with regular shape and spacing uniformly in a macroscopic scale. For the assembly, long- and short-range lattice strain is one of the important mechanisms. We have studied self-assembled two-dimensional (2D) arrays of CrN square nanoislands on the Cu(001) surface as a system made by a novel short-range mechanism. So far, the short-range mechanism has been adopted only to the assembly of MnN islands on Cu(001).[1]
The CrN assembly was prepared by using a method similar to that for the MnN assembly. Chromium was first deposited on a nitrogen-adsorbed Cu(001) surface, and then the sample was annealed at a temperature between 410 and 430 °C for 15 min. The assembly critically depends on the annealing temperature and Cr coverage. The surface was investigated by STM, XPS, and LEED at RT.
The self-assembled square islands are shown in Figs. 1 and 2. The islands with the edges oriented along the <110> directions locally form a 2D square superstructure as in Fig. 1. The magnified image in Fig. 2 indicates two types of the self-assembled islands with different heights marked as α (0.09 nm) and β (0.18 nm). The substrate in Fig. 2 is predominately covered by α islands while most of the islands in Fig. 1 is β. The stoichiometry of chromium nitride was confirmed to be CrN by XPS. The square lattice image in Fig. 2 suggests a NaCl-type crystal with the lattice constant of 0.39 nm, which is smaller than the value (0.4148 nm) of the bulk CrN crystal.
We propose a model previously applied to the MnN islands on Cu(001) [1] for β CrN islands. The substrate is covered by upper and lower sublayers of the CrN mono-atomic layer. The former forms the square island, while the latter is imaged as a depressed grid. Some properties that are different from those of the MnN assembly are attributed to the differences in the lattice constant of the bulk nitride crystals and thermal stability.

1. X. Liu, *et. al.* Phys. Rev. Lett 98, 066103 (2007).

STM images of CrN islands formed on the Cu(001) surface. The average coverage of the deposited Cr atoms was 3 ML (Fig. 1), or 1.5 ML (Fig. 2).

SS-P3-08
Tritium adsorption and desorption measurements using beta-induced X-ray spectroscopy for KATRIN

T13 Surface Science

#SS-P3-08

M. Babutzka, B. Bornschein, F. Priester, M. Röllig, F. Schneck.

Karlsruhe Institute of Technology - Karlsruhe (Germany).

The aim of the KATRIN experiment is the direct measurement of the electron anti-neutrino with a sensitivity of 200 meV/c2 (90 % C.L.). The working principle bases on the high precision spectroscopy of the tritium beta decay close to its endpoint at 18.6 keV. The experiment uses a windowless gaseous tritium source (WGTS) with pumping systems magnetically guiding the β-decay electrons towards a tandem spectrometer. The spectrometers analyse by combining magnetic-adiabatic collimation with an electrostatic filter. Finally the the decay electrons that passed the spectrometer are counted by a silicon detector.

The WGTS is electrically terminated by the grounded, gold-coated Rear Wall. It is expected that there will evolve a cold plasma in the WGTS with the high energy decay electrons and low energy and mobile ions and secondary electrons. Hence the conducting plasma will carry changes in the Rear Wall surface potential in time or surface area into the source which can produce a shift in the β-electron energy and consequently a systematic error for KATRIN. Therefore a stable surface potential is critical for the KATRIN experiment.

There are different effects that can modify the Rear Wall surface potential but the most risky effects are caused by the exposure of the gold surface to a tritium plasma containing not only the radiochemical tritium but also charged tritium ions. These ions are expected to have a high sticking coefficient to the gold surface (like atomic hydrogen [1]) but this topic was not yet covered in satisfactory detail in literature. This was the reason to set-up the tritium adsorption and desorption experiment (TriADE).

TriADE provides a possibility to solid samples with arbitrary surfaces in tritium atmosphere. The temperature range of operation is -100 °C to +150 °C controlled by

a cold gas machine and the pressure range is 10-8 to 1 mbar with pure tritium, gas mixtures or purge gas. There are two different techniques available to measure the amount of adsorbed tritium: Thermal desorption mass spectroscopy (TDMS) using a quadrupol mass spectrometer (QMS) and beta-induced x-ray spectroscopy (BIXS) with a silicon drift detector (SDD) behind a gold/beryllium window. The later method counts the photons induced by the electrons from the beta-decays of the adsorbed tritium molecules. BIXS as a measurement method to detect small amount of Tritium has been proven by the TriRex Experiment [2]. The geometry suppresses any decay electrons except from the sample surface and the gold surface of the window.

[1] Mildner et al, Electronic excitations induced by surface reactions of H and D on gold
[2] Röllig et al, Activity monitoring of a gaseous tritium source by beta induced X-ray spectrometry

NST/SS-8-Or-8
THEORETICAL CHARACTERIZATION OF CARBONACEOUS SURFACE OXIDATION

T13 Surface Science

#NST/SS-8-Or-8

S. Picaud [1], M. Oubal [1], C. Garcia Fernandez [1], C. Garcia Fernandez [2], M.T. Rayez [3], J.C. Rayez [3].

[1]Institut UTINAM - UMR 6213 CNRS/UFC - Besancon (France), [2]InsTEC - Havana (Cuba), [3]ISM - UMR 5255 CNRS/Univ. Bordeaux1 - Bordeaux (France).

Carbonaceous surfaces have attracted much attention not only because of their technological use but also for their influence on atmospheric chemistry as products of combustion processes. Characterizing the interaction of these surfaces with atmospheric oxidants is thus of great importance because the properties of the resulting oxidized surfaces may differ from those of the bare surface. For instance, the oxidation of soot particles may change their chemical reactivity or their hydrophilic properties, thus modifying their influence on atmospheric chemistry.
In the present work, we make use of DFT calculations to characterize the interaction of graphene sheets and large carbonaceous clusters with atmospheric oxidants such as atomic oxygen, O2, O3, H2O and NO molecules. Both perfect and defective surfaces containing vacancies are studied. In a general way, we show that the oxidation of carbonaceous surfaces occurs more likely at defective sites and depends on the type of site considered in the calculations. For instance, carbon atom vacancies characterized by an odd number of missing carbon atoms are more reactive than those where an even number of atoms is missing and, as a consequence, they can be oxidised more easily.
These results can be used to better understand oxidation processes that likely occur in carbonaceous systems of environmental or technical interest.

[1]. A theoretical characterization of the interaction of water with oxidized carbonaceous clusters.
M. Oubal, S. Picaud, M.T. Rayez, and J.C. Rayez, Carbon 48, 1570-1579 (2010).

[2]. Interaction of water molecules with defective carbonaceous clusters : an ab initio study.
M. Oubal, S. Picaud, M.T. Rayez, and J.C. Rayez, Surf. Sci. 604, 1666-1673 (2010).
[3]. Water adsorption on oxidized single atomic vacancies present at the surface of small carbonaceous nanoparticles modeling soot.
M. Oubal, S. Picaud, M.T. Rayez, and J.C. Rayez, Chem. Phys. Chem. 11, 4088-4096 (2010).
[4]. Structure and reactivity of carbon multivacancies in graphene.
M. Oubal, S. Picaud, M.T. Rayez, and J.C. Rayez, Comput. Theor. Chem. 990, 159-166 (2012).

SS-7-Or-4
Ultrathin Zirconia Films: Growth, Structure and Adsorption Experiments

T13 Surface Science

#SS-7-Or-4

M. Schmid, J.I.J. Choi, W. Mayr-Schmölzer, J. Pavelec, F. Mittendorfer, J. Redinger, P. Varga, U. Diebold.

TU Wien - Vienna (Austria).

Zirconia (ZrO_2), in pure and doped form, is an important material in engineering, dentistry, microelectronics, and catalysis, as well as a solid-state electrolyte for gas sensors, solid-oxide fuel cells and oxygen purification. Nevertheless, its surface properties are poorly understood, which is mainly due to the fact that it is an excellent electronic insulator, which makes it impossible to use techniques like scanning tunneling microscopy (STM). This problem is circumvented by studying ultrathin ZrO_2 films.

Growth of ZrO_2 films by reactive evaporation of Zr [1] is a rather cumbersome approach. We have therefore grown ultrathin zirconia films by oxidation of $Pt_3Zr(0001)$ [2] and $Pd_3Zr(0001)$ substrates and studied them by STM with atomic resolution (Fig. 1), x-ray photoelectron microscopy (XPS), Auger electron microscopy (AES) and density-functional theory (DFT). The films consist of an O-Zr-O trilayer, equivalent to a (111) trilayer of the fluorite structure of cubic ZrO_2, but with contracted in-plane lattice constant and increased layer spacing. DFT shows significant buckling of the Zr layer, nicely explaining the STM data, and also indicates that the oxide weakly binds to the substrate via its Zr atoms. In spite of a formal valency of 4+, in XPS the Zr atoms in the ZrO_2 film show a chemical shift typical for a suboxide, which is explained by the position of the Fermi level in this ultrathin oxide. Depending on sample preparation, the oxide film can sit on either reconstructed Pt_3Zr, presumably with a Pt-terminated surface, or on an alloy surface; this difference of the support also has some influence on the properties of the oxide.

Adsorption experiments indicate that most gases like O_2, CO and H_2 do not stick at the surface at room temperature. We observe adsorption of H_2O with a desorption barrier barely high enough for sticking at room temperature (about 1 eV). We will also present first results of small metal clusters grown on the ultrathin oxide.

[1] K. Meinel, A. Eichler, S. Förster, K.-M. Schindler, H. Neddermeyer, W. Widdra, Phys. Rev. B 74, 235444 (2006) and Refs. therein.

[2] M. Antlanger, W. Mayr-Schmölzer, J. Pavelec, F. Mittendorfer, J. Redinger, P. Varga, U. Diebold, M. Schmid, Phys. Rev. B 86, 035451 (2012).

Fig. 1: STM constant-current image of the trilayer ZrO_2 on $Pt_3Zr(0001)$.

SS-P3-17
Ab initio study of non-polar and semipolar GaN surfaces

T13 Surface Science

#SS-P3-17

P. Mutombo, O. Romanyuk.

Institute of Physics,AVCR,vvi - Prague (Czech republic).

Ab initio study of non-polar and semipolar GaN surfaces

P. Mutombo, O. Romanyuk*

Institute of Physics, ASCR, Cukrovarnicka 10, 162 00, Prague, Czech Republic.

Gallium nitride materials constitute an important group of compounds which have called the attention of scientists because of their application in the optoelectronic industry. It is known that GaN-based devices grown on non-polar and semipolar substrates achieve a greater performance compared to devices grown on conventional c-plane [1, 2]. This is due to the fact that the internal electric field is significantly smaller in the semipolar and non-polar III-nitrides. Thus, the heterostructures formed on these substrates are very promising for the advancement of science and technology.
To understand the non-polar and semipolar surfaces stability, theoretical methods have been used. We have performed Density Functional Theory calculations to determine the atomic and electronic structures of the non-polar GaN(1-100), (11-20), and semipolar GaN(20-21), (20-2-1) surfaces [3]. We have calculated the surface phase diagrams and the relative stability of the (1x1) structures depending on Ga/N stoichiometry on a surface. The results are discussed with respect to previous theoretical findings.

1. P. Waltereit, O. Brandt, A. Trampert, H. T. Grahn, J. Menniger, M. Ramsteiner,M. Reiche, and K. H. Ploog, Nature (London) 406, (2000) 865.
2. F. Bernardini and V. Fiorentini, Phys. Status Solidi B 216 (1999) 391.
3. C.-Y. Huang, M. T. Hardy, K. Fujito, D. F. Feezell, J. S. Speck, S. P. DenBaars, S. Nakamura, Appl. Phys. Lett. 99 (2011) 241115.

Top view of the a) GaN(1-100), b) GaN(11-20) and c) GaN(20-21) surfaces. A (1x1) unit cell is marked by dashed curves. Nonpolar surfaces are terminated by Ga-N dimers, whereas semipolar surface consists of rest-atomic sites and dimer. Large and small spheres correspond to Ga and N atoms respectively.

SS-1-Or-12
Quasiparticle interference at epitaxial Silicene

T13 Surface Science

#SS-1-Or-12

H. Hirayama, Y. Aoki, K. Nakatsuji, A. Ohshiro.

Tokyo Institute of Technology - Yokohama (Japan).

Silicene is a newly emerging two-dimensional material which has a honeycomb lattice made by Si. Because of its specific structure, it has been paid much attention as the Si analog of graphen. However, the first successful synthesis of silicene was reported very recently in 2012. Vogt et. al. firstly reported the epitaxial growth of the silicene which has a honeycomb structure (H) with the 4x4 ordering on the Ag(111)1x1 substrate [1]. Then, the √13x√13-R13.9°honeycomb and 3.5x3.5 closed packed (T) structures were observed as other phases of silicene on the Ag(111) substrates [2]. The √7x√7 and √3x√3 stacking (relative to the silicene 1x1 latice) phases were also reported [3]. But, it is still not conclusive whether all these have the true silicene structure and its intrinsic electonic state. Substantially, two groups proposed the structural models of silicene stacking with the 4x4 and √13x√13 ordering on the Ag(111) [1,2], while one group claimed that only the √3x√3 is the true phase of epitaxial silicene and others do not have the silicene structure [3,4].

This problem can be solved by observing the dispersion relation of these phases, since the silicene should reveal the characteristic Dirac electron-like linear dispersion. However, various phases usually appear to coexist as a patchwork in the epitaxial growth of silicene on the Ag(111) surface. Thus, we investigated the dispersion relation of local domains with different phases by observing the quasiparticle interference pattern (surface electron standing wave pattern) in the dI/dV images of STM. As results, no standing wave pattern was observed on the 4x4 (H), closed packed (T), and √13x√13 phases in the epitaxial growth at relatively low temperatures (c.a. 200-250C). However, the 2nd layer revealed the standing waves in the energy +0.5 to +1.2 eV above the Fermi level. The energy dependence of the standing waves showed a linear dispersion with the Fermi velocity of 1.3×10^6 m/s. We regard that the appearance of the standing wave on the 2nd layer is due to the small influence of the Ag substrate which is weakened by the intermediate the 1st layer.

In the epitaxial growth at higher temperatures, the √3x√3 phase widely covered the Ag substrate. However, the √3x√3 plane bended loosely as to be just put lightly on the Ag substrate, although the √3 lattice was continuous even on the bended region. The standing wave pattern was clearly observed in the full empty state energy from +0.1 to +1.2 eV above the Fermi level on this high temperature √3x√3 phase. Fourier Transformation of the standing waves revealed specific q-vectors which correspond to the intra- and inter-band transition of the Dirac cones at K and K' points in the Brilloiun zone. The energy dependence of the smaller q-vector revealed a perfect Dirac electron's linear dispersion with $v_f = 1.2 \times 10^6$ m/s and $E_D = -0.3$ eV. The larger q-vector connected K and K' valleys. Judging from these results, this √3x√3 phase is regarded as the true silicene.

[1] P. Vogt et. al., PRL108, 155501(2012).
[2] C-L. Lin et. al., Appl.Phys.Exp.5,045802(2012).
[3] B. Feng et. al., Nano Lett. 12,3507(2012).
[4] L. Chen et. al., PRL109,056804(2012).

SS-1-Or-13
Quantum states of proton and positive muon on solid surfaces and in subsurfaces

T13 Surface Science

#SS-1-Or-13

H. Nakanishi, H. Kasai.

Graduate School of Engineering, Osaka University - Suita, Osaka (Japan).

The first principles calculation based on the density functional theory is one of the most successful and powerful methods in the materials physics. And also the first principles molecular dynamics methods have been used for various dynamical behaviors. In the case of small mass atoms like hydrogen atoms, we should treat their nuclei (proton) in a quantum-mechanical manner, in addition to electrons. The quantum behaviors of the nuclei have crucial roles to play in the materials related to today's energy technology: fuel cell and lithium-ion rechargeable battery, and also various catalytic reactions to produce hydrogen fuel, not only from their academic interests [1-4]. Positive muon is also one of our target quantum particles, because it has been used as a magnetic probe particle in materials, mu-SR. The positive muon has the same spin and same charge as a proton and behaves as the very light isotope of hydrogen which has ninth mass of proton. It is important to analyze the quantum behavior of these particles in the materials.
We have been developing the quantum simulation code for the small mass atom nuclei, protons and muons on solid surfaces, in subsurfaces and bulks. These particle-cases are differnet from the situations of electron in the materials:(1) Because of the larger mass, these partciles have the very shorter de Broglie wave length. (2) The potential energy surface for these particle in the materials is normally repulsive around the lattice points. We propose the methods for the quantum state calculation for these particles in materials. In the conference, we will also show our simulation results for muon and hydrogen isotopes on solid surfaces and in subsurfaces, and discuss their quantum mechanical effects [1-5]

1. H. Kasai, et al., Progress in Surface Science, 44 (1993) 101.
2. W. A. Diño, et al., Progress in Surface Science 63 (2000) 63.

3. K. Nobuhara, et al., Surface Science, 507-510, (2002) 82.
4. T. Roman, et al., e-J. Surf. Sci. & Nano., 4 (2006) 619.
5. N. Ozawa, et al., Journal of Physics: Condensed Matter 19 (2007) 365214.

NST/SS-2-Or-5
Band-gap opening of graphene nanoribbons grown on vicinal SiC(0001) substrates

T13 Surface Science

#NST/SS-2-Or-5

K. Nakatsuji [1], T. Iimori [2], S. Kim [2], T. Yoshimura [2], T. Kajiwara [3], A. Visikovsliy [3], Y. Nakamori [3], S. Tanaka [3], F. Komori [2].

[1]Department of Materials Science and Engineering, Tokyo Institute of Technology - Yokohama (Japan), [2]Institute for Solid State Physics, University of Tokyo - Kashiwa (Japan), [3]Department of Applied Quantum Physics and Nuclear Engineering, Kyushu University - Fukuoka (Japan).

Graphene has attracted much interest because of its novel electronic properties due to massless Dirac fermions in the π band states. Modification of its band structure such as carrier doping and band-gap formation is the key for its potential applications. Graphene nanoribbon (GNR) is expected to have a band-gap in the π band due to quasi one-dimensional confinement of the carriers depending on the width and orientations [1]. So far, the band-gap opening and/or the presence of the edge state has been reported only on the GNRs made by lithographic process [2] and CVD growth [3]. In the present study, a high-density array of GNRs with ca. 10 nm width was grown on a vicinal SiC(0001) substrate by molecular beam epitaxy (MBE). The band-gap opening of at least 0.14 eV and its dependence on the GNR width have been confirmed by angle-resolved photoelectron spectroscopy (ARPES) [4].

After high-temperature etching in the H_2 gas, the vicinal SiC substrate 4°-off toward [1-100] direction exhibits periodic arrangement of terrace and step-bunching region with ca. 20 nm period (nanosurface). The C atoms are deposited until the terrace is covered by ($6\sqrt{3}\times6\sqrt{3}$) R30° buffer layer. A periodic arrangement of GNRs with ca. 10 nm width is obtained by hydrogenation of the buffer layer [5] and confirmed by AFM observations. The polarization dependence in the Raman spectra and the line nodes in the STM images in vicinity of the step edges suggest the existence of arm-chair edges. Figure 1 shows the dispersion relation of the π band along Γ-K-M line which is perpendicular to the GNR direction. A single and linear π band confirms the high-

quality single-layer graphene on the terrace. The dots in vicinity of the K point indicate the peaks in the ARPES spectra. There is no states between the valence band maximum and the Fermi level, and the band-gap at least 0.14 eV is opened at the K point assuming the conduction band minimum at the Fermi level. We have also investigated the 5 nm width GNR which shows slightly larger band-gap opening. This is qualitatively consistent with the carrier confinement in the GNR.

[1] K. Nakada et al., Phys. Rev. B 54 (1996) 17954.
[2] M. Y. Han et al., Phys. Rev. Lett. 98 (2007) 206805.
[3] J. Cai et al., Nature 466 (2010) 470.
[4] T. Kajihara et al., submitted.
[5] C. Riedl et al., Phys. Rev. Lett. 103 (2009) 246804.

Figure 1: The band dispersion of GNR near the K point.

SS-P3-23
Potential Sputtering from Rare Gas Solid by Low Energy Multiply-Charged Ion Impact

T13 Surface Science

#SS-P3-23

K. Ban, M. Akiwa, K. Koganei, M. Murakami, T. Tachibana, T. Koizumi, T. Hirayama.

Rikkyo University - Tokyo (Japan).

Potential sputtering is the desorption mechanism which is induced by transfer of the potential energy from incident multiply-charged ions to the solid surface. We have reported previously the *relative* ion yields of potential sputtering from solid Ne [1], and demonstrated that the potential sputtering yield is proportional to the potential energy of the incident ion. Here we report the experimental results of the *absolute* potential sputtering yields using a newly developed simple and precise method.

Ar^{q+} ions (q = 1~6) were produced in an ECR ion source. The ion beam extracted from the ion source was mass-analyzed and introduced into a main chamber. A rare-gas solid was prepared on a Cu substrate which was cooled to 4.9 K at the center of the main chamber.

Absolute sputtering ion yields Y_{ion} were estimated by measuring the incident ion beam current I_{in} and the desorbed ion current. When the sample is irradiated by the ion beam, the current flowing into the Cu substrate I_{Cu} differs from I_{in} because of the desorption of positive ions from the sample. The desorbed ion current can be estimated from (I_{in} - I_{Cu}), and Y_{ion} is then calculated from Y_{ion} = (I_{in} - I_{Cu}) / (I_{in} / q), where q is the incident ion charge.

Fig. 1 shows the absolute sputtering ion yields Y_{ion} from the surface of solid Ne as a function of the incident Ar^{q+} ion energy. To estimate the contribution of potential sputtering, the absolute sputtering ion yields vs. the potential energy of the incident ion are plotted in Fig. 2. It is shown that the potential sputtering ion yields linearly increases with the potential energy of the incident ion, which is consistent with our previous work [1].

[1] K. Fukai et al., J. Phys. Cond. Matt. **22**, (2010) 084007.

Fig. 1. Absolute sputtering ion yields of solid Ne by Ar^{q+} (q = 1 ~ 6) impact as a function of kinetic energy of incident ions. Thickness of the sample film is about 1000 atomic layers.

Fig. 2. The same data as in Fig. 1 plotted as a function of the potential energy of incident ion.

SS-3-Or-1
Specialities of the group III metals mobility on Si(100) surfaces

T13 Surface Science

#SS-3-Or-1

I. Oštádal, M. Kucera, F. Rozboril, K. Majer, P. Sobotík, P. Kocán.

Charles University - Prague (Czech republic).

At low coverage group III metals (Al, In, Ga) form on the Si(100) surface one atom wide chains composed of dimers. The metal chains on the silicon surface attract attention for many reasons. They can be used as model systems for experimental investigation of electron structurte of low dimensional objects, building blocks of more complex surface structures and templates for growing further materials for functionalizing the surface. Mixing with group IV metals results in formation of bimetallic chain structures of interesting properties.

Binding energies together with surface temperature determine mobility of adatoms and stability of grown chains. Deposition rate together with the adatom mobility and chain stability control growth kinetics. Knowledge of intrinsic growth parameters is crucial for growing desirable mono- and bimetallic structures. The binding energies and hopping barriers were theoretically calculated for all three metals [1, 2]. Kinetic Monte Carlo simulations of experimentally obtained growth characteristics provided the barriers for Ga [3] and In [4]. Direct observations of surface hopping by means of scanning tunneling microscopy (STM) resulted in determination of the barriers and frequency prefactors for In [5]. Diffusion parameters obtained by the various methods contain controversy both in the barrier heights and a character of hopping anisotropy.

We present new STM measurements of growth characteristics (Al, In) and observations of adatom hopping at various temperatures. The data are compared with the parameters already reported elsewhere. The existing controversy is discussed with respect to assumptions at theoretical calculations, a role of a surface reconstruction and thermal fluctuations at higher temperatures. An impact of the adatom mobility and hopping anisotropy on growth is estimated for the particular metals.

[1] G. Brocks, P. J. Kelly, R. Car, Phys. Rev. Lett. 70, 2786 (1993).

[2] M. A. Albao, J. W. Evans, F.-Ch. Chuang, J. Phys. Condensed Mat. 21, 502002 (2009); M. A. Albao, Ch.-H. Hsu, D. B. Putungan, F.-Ch. Chuang, Surf. Sci. 604, 396 (2010).

[3] M. A. Albao, M. M. R. Evans, J. Nogami, D. Zorn, M. S. Gordon, J. W. Evans, Phys. Rev. B 72, 035426 (2005).

[4] J. Javorský, M. Setvín, I. Ošťádal, P. Sobotík, M. Kotrla, Phys. Rev. B 79, 165424 (2009).

[5] M. Setvín, J. Javorský, Z. Majzik, P. Sobotík, P. Kocán, I. Ošťádal, Phys. Rev. B 85, 081403(R) (2012).

SS-P1-09
Green's function approach to the dynamics of image potential resonances

T13 Surface Science

#SS-P1-09

S. Tsirkin, E.V. Chulkov.

Donostia International Physics Center - San Sebastian-Donostia (Spain).

The image potential states on metal surfaces form a Rydberg series of states with energies $E_n = -0.85/(n-a)^2$ converging to the vacuum level, where a is the quantum defect. When the vacuum level lies in the continuum of the bulk states of the metal, image-potential resonances (**IPRs**) are formed. Recent advances in time-resolved two-photon photoemission allow to study energies and the lifetimes of IPRs with high quantum numbers [4,5].

In the present work we perform a theoretical study the properties of IPRs on a number of close-packed metallic surfaces, such as Cu(111), Ag(111), Al(001) and many others. The binding energies and lifetimes are calculated from the Green's function (GF), using the fact that the electronic excitation corresponds to a pole of the GF at some complex value ω_n, where $E_n = \mathrm{Re}\,\omega_n$ is the energy, and $\tau_n = 1/(-2\mathrm{Im}\omega_n)$ is the lifetime of the excitation. The electronic structure of the surface is described by a one-dimensional pseudopotential [3], which was slightly modified for some jellium-like surfaces: Al(001), Al(111) and Mg(0001). The GF of the surface is calculated using the Green's function matching method [4].

Previously the theoretical study of surface resonances and image-potential resonances were performed using the wave-packet propagation method (WPP) [5]. The advantage of the GF approach over WPP consists in the principle possibility of including the many-body interactions via solving the Hedin's equations. However, we show that the IPRs practically do not penetrate inside the metal, and hence inelastic scattering into the bulk is unlikely to affect significantly the lifetimes of excitations in IPRs. Thus, we do not include many-body effects in the present calculations. Nevertheless, inelastic scattering is expected to be important for the

dynamics of excitations in surface resonances, and should be accounted for in the future studies.

The calculated lifetimes for some of the studied surfaces are presented in the Figure. It is clearly seen, that the lifetimes obey the scaling law $\tau_n \sim n^3$. The present method gives practically the same results, as the WPP method. Our results are also in agreement with recent experimental results[1,2]. For example, the calculated lifetime of the n=2 IPR on Ag(111) $\tau_{calc} = 19$ fs is close to the experimental value $\tau_{exp} = 23 \pm 2$ fs. [2]

1. M. Winter, E. V. Chulkov, and U. Höfer, Phys. Rev. Lett. **107**, 236801 (2011)

2. M. Marks, C. H. Schwalb, K. Schubert, J. Güdde, and U. Höfer, Phys. Rev. B **84**, 245402 (2011)

3. E. V. Chulkov, V. M. Silkin, P. M. Echenique, Surf. Sci. **437**, 330 (1999)

4. J. E. Inglesfield, J. Phys. C: Solid State Phys. **4,** L14 (1971)

5. A. G. Borisov, E. V. Chulkov, and P. M. Echenique, Phys. Rev. B **73**, 073402 (2006)

Figure: The calculated lifetimes of electrons in the image potential resonances. The line $\tau_n = 1 fs \times n^3$ is a guide to the eye.

SS-5-Or-4
Lying down to standing up transitions in self assembly of butanedithiol monolayers on gold and substitutional assembly by octanethiols

T13 Surface Science

#SS-5-Or-4

J. Jia [1], S. Mukherjee [2], H. Hamoudi [3], S. Nannarone [4], L. Pasquali [4], V. Esaulov [1].

[1]ISMO UNIVERSITE PARIS-SUD - Orsay (France), [2]CNR&ICTP - Trieste (Italy), [3]NIMS - Ibaraki (Japan), [4]CNR&Dipartimento di Ingegneria'Enzo Ferrari', Università di Modena e Reggio Emilia - Modena (Italy).

Self assembly of dithiol molecules has been the object of much interest because of the possibility to link the two thiol ends to different metallic entities. This has been used for instance to measure molecular conductance. Interest in self assembly of these molecules on surfaces has similarly been spurred by their use in making diode structures and in superlattices involving multiple layers of dithiol molecules attached to metal nanoparticles. Howeverproblems have been encountered related to formation of multilayered dithiol structures by molecular interlinking with formation of disulphide bonds, photooxidation processes and formation of lying down phases with both sulphur ends attached to the substrate, on which the SAM assembly was attempted. This has led to interrogations about the possibility of at all forming a standing phase if first a lying down, doubly tethered phase is formed. However work, by some of us [1-5] for some dithiol molecules, shows that quite well ordered SAMs of standing-up molecules with free –SH groups can be produced, although it seemed not in the case of short chain dithiols[1].

The intent of this work was to address the question of transitions from lying down to standing up phase in dithiol self assembly and whether a standing up phase of short chain dithiol can be formed. Self assembly of butanedithiol (C4DT) monolayers (SAMs) on gold and substitutional assembly by octanethiols(C8T) from a lying down doubly tethered phase of butane dithiol, were investigated in a vacuum evaporation experiment by high resolution photoemission. The vacuum evaporative assembly [4] is particularly interesting since it can be used for reactive surfaces.

The lying down dithiol phase, with both sulphur atoms attached to gold, was formed by evaporation and characterized by high resolution XPS at the BEAR beamline (Elettra synchrotron). It was then exposed to C8T molecules. XPS shows formation of a mixed SAM composed of standing up octanethiol and dithiol molecules. The degree of dithiol replacement, as evidenced by the increasing thickness of the SAM is found to augment slowly with increasing exposure to C8T. These results demonstrate that the existence of a lying down dithiol SAM, doubly tethered by sulfur ends, should not be an impediment for producing a standing up dithiol SAM. Furthermore a standing up C4DT phase was found to be formed upon rapid very large exposure to C4DT. Differences in valance band photoemission between the lying down and standing up phases were noted and can be accounted for theoretically. In all cases measurements indicate more than one possible adsorption configuration as evidenced by different sulphur binding energies.

[1] Millone, M. A. D.et.al, Langmuir2009, 25, 12945-12953.
[2] Hamoudi, H.;et.al, Langmuir2010, 26 , 7242–7247.
[3] Hamoudi, H.; Guo, Z. A.; Prato, M.; Dablemont, C.; Zheng, W. Q.; Bourguignon, B.; Canepa, M.; Esaulov, V. A. Phys. Chem. Chem. Phys., 2008, 10, 6836-6841.
[4] Alarcon, L. S.; Chen, L.; Esaulov, V. A.; Gayone, J. E.; Snchez, E. A.; Grizzi, O. J. Phys. Chem. C, 2010, 114, 19993–19999.
[5] Pasquali, L.; Terzi, F.; Seeber, R.; Nannarone, S.; Datta, D.; Dablemont, C.; Hamoudi, H.; Canepa, M.; Esaulov, V.A. Langmuir, 2011, 27, 4713–4720.

SS-P1-01
Selenium adsorption on Au(111) and Ag(111) surfaces: adsorbed selenium and selenide films.

T13 Surface Science

#SS-P1-01

V. Esaulov [1], J. Jia [1], A. Bendounan [2], M.N.K. Harish [3], K. Chaouchi [4], F. Sirotti [4], S. Srinivasan [3].

[1]ISMO, CNRS Universite Paris Sud - Orsay (France), [2]Synchrotron SOLEIL - Gif-Sur-Yvette (France), [3]Department of Physical & Inorganic Chemistry - Bangalore (India), [4]Synchrotron SOLEIL - Gif Sur Yvette (France).

In recent years selenium and tellurium derived self assembled monolayers (SAMs) have attracted much interest as alternatives to thiol-derived SAMs, in e.g. molecular electronics applications, because of different (Se as compared to S) bonding to the substrate. This is a point of key importance for electronic transport. However studies of the headgroup Se atom interaction with metal surfaces are still rare and a thorough spectroscopic characterization of the Se-metal interfaces is still missing. This would be a useful complement to current investigations on self-assembly.
In this work, results of a high resolution photoemission (at Tempo beamline, Soleil synchrotron) and electrochemistry study of Se adsorption on Au(111) and Ag(111) surfaces performed by immersion of pristine samples into an aquous solution of Na2Se are presented. Cyclic voltammetry on Au shows formation of selenium adsorbed species and the structures observed in reductive desorption are related to atomic and polymeric Se species observed. In the case of Au(111) XPS spectra in the Se(3d) region indeed show two main features attributed to Se chemisorbed atomically and polymeric Se_8 features. Smaller structures due to other types of Se conformations were also observed. The Au(4f) peak line shape do not show core level shifts indicative of Au selenide formation. In case of silver on the other hand, XPS spectra for Ag(3d) show a broadening of the peak to lower binding energies and a deconvolution into Ag_B bulk like and Ag_{Se} components shows that the Ag_{Se} is located at a lower binding energy: an effect similar to oxidation and sulphidation of Ag. The Se(3d) XPS spectrum is found to be substantially different from the Au case and dominated by atomic type Se, due to the selenide. A smaller intensity Se

structure at an energy similar to the Se_8 structure for Au is also observed. Changes in the valence band region of gold related to Se adsorption are reported.

SS-11-Or-1
Adsorption, nucleation and desorption of rod-like organic molecules (p-hexaphenyl, pentacene) on inert substrates (mica)

T13 Surface Science

#SS-11-Or-1

A. Winkler, L. Tumbek.

Graz University of Technology - Graz (Austria).

Organic thin films have attracted high interest within the last decade, due to their interesting properties for organic electronics. Although significant progress has been made in the understanding and tailoring of organic film growth, there are still many open questions regarding the initial steps of film formation. Here we present experimental data on the initial film growth of the model systems p-hexaphenyl and pentacene on mica. The films were prepared under UHV conditions by physical vapor deposition. Surface analytical techniques (thermal desorption spectroscopy (TDS), X-ray photoelectron spectroscopy (XPS), atomic force microscopy (AFM)) were applied to study the adsorption and desorption kinetics, as well as the nucleation behavior. Mica was used as a substrate because one can easily change its behavior from reactive (freshly cleaved) to inert (sputtered or contaminated). This leads to films of flat lying molecules in the first case, where long needle-like islands form, or to standing molecules in the second case, where terraced, round shaped islands occur. In both cases a bimodal island size distribution was observed in ex-situ AFM (Figure 1). We could show that this is the result of adsorbate-induced subsequent nucleation when the samples were exposed to air [1]. In case of the freshly cleaved mica, islands grow on a wetting layer in vacuum. This layer dewets and forms the small islands upon venting. In case of the sputtered mica substrate an equilibrium exists between the islands and a 2D gas phase. Again, the latter phase nucleates after venting, forming the small islands. Another important aspect refers to the actual nucleation mechanism. Whereas it is generally assumed that nucleation of organic films can be described by diffusion limited aggregation (DLA) we have demonstrated that under special substrate conditions the nucleation has to be described by attachment limited aggregation (ALA) [2]. We believe that this is a rather generic feature for the nucleation of rod-like organic molecules, because the

incorporation of the monomers at the rim of the islands depends on the orientation of the approaching molecules. Similar arguments hold for the initial sticking coefficient of rod-like organic molecules, which has turned out to be smaller than unity, as unequivocally determined for pentacene on mica by TDS.

[1] L. Tumbek, C. Gleichweit, K. Zojer, A. Winkler, Phys. Rev. B. 86 (2012) 085402.
[2] L. Tumbek, A. Winkler, Surf. Sci. Lett. 606 (2012) L55.

Fig. 1: AFM image of a p-hexaphenyl film with 0.18 ML mean thickness, deposited on a sputtered mica surface at 400 K, demonstrating the bimodal island size distribution. Both, the small and large islands are composed of 1 layer of standing molecules .

SS-P3-01
Using BEEM (Ballistic Electron Emission Microscopy) to probe buried interfaces in metal-organic molecules-semiconductor hybrid heterostructures

T13 Surface Science

#SS-P3-01

A. Junay, S. Guézo, F. Solal, P. Turban, S. Ababou-Girard, G. Delhaye, S. Tricot.

Insitut de Physique de Rennes - Rennes (France).

Ballistic Electron Emission Microscopy (BEEM) is a scanning probe technique derived from STM, which allows characterization of the electronic properties of buried interfaces with a lateral nanometer resolution [1]. In the case of a Schottky contact, hot electrons are injected in the metal layer with an energy defined by the STM tip bias voltage. A small part of the injected electrons crosses ballistically the metal layer and reaches the buried interface. If their energy is high enough to overcome the Schottky barrier height, electrons can enter into the conduction band of semiconductor and be detected as a BEEM current. In molecular electronics, BEEM is an ideal tool to probe local structural and electronic properties of hybrid systems. By using as reference the well-known Schottky contact of Au(110)/GaAs(001) [2], organic molecular layers inserted at metal-semiconductor interfaces [3-5] are here probed by BEEM. The aim of this work is to study organic layers covalently grafted on a single-crystalline substrate of GaAs(001), on which a metal top-contact is deposited. By combining STM/BEEM measurements on these hybrid structures, interface homogeneity, degree of metal penetration through the organic layer and other properties are here discussed.

[1] L. D. Bell and W. J. Kaiser, "Observation of Interface Band Structure by Ballistic-Electron-Emission Microscopy", Physical Review Letters, 61, 2368 (1988)

[2] S. Guézo, P. Turban, S. Di Matteo, P. Schieffer, S. Le Gall, B. Lépine, C.

Lallaizon and G. Jézéquel, "Transverse-momentum selection rules for ballistic electrons at epitaxial metal/GaAs(001) interfaces", Physical Review B, 81, 085319 (2010)

[3] H. Haick, J. P. Pelz, T. Ligonzo, M. Ambrico, D. Cahen, W. Cai, C. Marginean, C. Tivarus and R. T. Tung, "Controlling Au/n-GaAs junctions by partial molecular monolayers", physica status solidi (a), 203, 3438-3451 (2006)

[4] R. T. W. Popoff, A. A. Zavareh, K. L. Kavanagh and H.-Z. Yu, "Reduction of Gold Penetration through Phenyl-Terminated Alkyl Monolayers on Silicon", The Journal of Physical Chemistry C, 116, 17040-17047 (2012)

[5] C. Troadec, L. Kunardi and N. Chandrasekhar, "Ballistic emission spectroscopy and imaging of a buried metal/organic interface", Applied Physics Letters, 86, 072101-3 (2005)

SS-6-Or-1
Spreading of a liquid drop over a plane rigid substrate due to intermolecular forces

T13 Surface Science

#SS-6-Or-1

A. Tyatyushkin.

Institute of Mechanics. Moscow State University - Moscow (Russian federation).

Coating surfaces with monomolecular layers is an important part of many modern technologies. Usually it is preceded by spreading under the action of intermolecular forces. Self-similar solutions of the equation that describes plane spreading due to intermolecular forces represent profiles of drops without contact lines [1]. In the present work, self-similar solutions are found also for axisymmetrical spreading. Both plane and axisymmetrical solutions are matched with the solutions of equations that describe plane or axisymmetrical spreading of monomolecular layers.

A liquid layer spreading over a plane rigid substrate is considered. The equations for its local thickness as function of the distance from the axis or plane of symmetry and time, $\zeta(r,t)$, that describe axisymmetrical and plane spreading due to intermolecular forces and their self-similar solutions are found. For plane spreading, the solutions coincide with those in [1].

When the layer reaches some thickness, h_m, of the order of the molecular size, the liquid forms a monomolecular layer which can be in liquid or gaseous two-dimensional state. The moving boundary between monomolecular and liquid phases is determined by some value, $R_l(t)$, of the variable r for which $\zeta(R_l(t),t) = h_m$.

The liquid monomolecular layer forms a distinct boundary with the uncovered region of the surface of the substrate which is determined by some value, $R_m(t)$, of the variable r. With regarding the surface mass density of the layer, ρ_s, as constant and using the condition of the conservation of the total mass of the spreading liquid, $R_m(t)$ is obtained. At some instant all the liquid is in monomolecular phase and stops spreading.

If the monomolecular layer is gaseous, it has no boundary with the uncovered surface, and the distribution of the surface mass density, $\rho_s(r,t)$, satisfies the differential equation for the surface diffusion with the boundary and initial conditions that follow from continuity of surface mass flux and mass densities on the boundary between the phases and absence of monomolecular phase at $t = 0$. At some instance all the liquid is in monomolecular phase, but continues spreading. The asymptotic behavior of $\rho_s(r,t)$ as t tends to infinity is found.

The functions $R_m(t)$ or $\rho_s(r,t)$ for spreading with formation of liquid or gaseous monomolecular layers can be measured in experiments. In spite of the fact that the proposed models are based on strong simplifying assumptions, one may expect their satisfactory agreement at least with some experiments. In any case, the models allow introducing into consideration various additional physical processes to achieve satisfactory agreement with measured data.

1. Lopez J., Miller C.A., Ruckenstein E., *J. Colloid Interface Sci.*, **53**:460-468, 1976.

SS-3-Or-3
Tiny golden "Eiffel towers" on Si(111)-5x2-Au surface

T13 Surface Science

#SS-3-Or-3

T. Abukawa, Y. Nishigaya.

IMRAM, Tohoku University - Sendai (Japan).

The Si(111)-5x2-Au surface has attracted us because of its strong one-dimensional nature. However, its structure remains as one of the long-standing problems in the surface science. In earlier studies, models with Au coverage of 0.4 ML, were candidates of the structure [1]. Recently, Barke et al. precisely determined the Au coverage on 5x2-Au, and revised the coverage to be 0.6 ML [2]. Then, the model with three gold chains was proposed by a first-principles theory [3]. Here, we have applied Weissenberg reflection high-energy electron diffraction (W-RHEED) [4], and investigated the structure of Si(111)5x2-Au surface [5].
A single-domain 5x2-Au surface was prepared on a Si(111) wafer with an intentional miscut of 1°. A horizontal slice of the three-dimensional (3D) reciprocal map obtained by W-RHEED is shown in Fig.1. 5x1 spots and x2 streaks, which are characteristics of 5x2-Au surface, are clearly visible in Fig.1. Then, a 3D Patterson map was obtained by the Fourier transformation of the 3D reciprocal map. As the conclusion of the structural analysis based on the 3D Patterson map, we propose a new structure model for the Si(111)-5x2-Au. The new model consists of 0.6ML Au, which corresponds to 6 gold atoms in a 5x2 unit as shown in Fig.2. The six gold atoms form a tiny “Eiffel tower” laying on the Si surface. Although the structure of the Si substrate was not optimized in the present study, there is no space for the Si honeycomb chain, which was expected for the 5x2-Au surface [3]. The model is also consistent with the “Y” shape structure commonly observed in STM images [1].

[1] H. Yoon, et al., Phys. Rev. B 72, 3-10 (2005), and references therein.
[2] I. Barke, et. al., Phys. Rev. B 79, 1-9 (2009).
[3] S. Erwin, et al., Phys. Rev. B 80, (2009) 155409.
[4] T. Abukawa, et al., Phys. Rev. Lett. 97, (2006) 245502.
[5] T. Abukawa, et al., Phys. Rev. Lett. 110, (2013), in press.

Fig.1 Horizontal section at s_z=8.5 $Å^{-1}$ of the reciprocal map by W-RHEED.

Fig.2 Ball-and-stick model of the Si(111)-5x2-Au surface proposed in the present study. Large and small spheres represent Au and Si atoms, respectively.

SS-P1-02
Saturation coverage of alkali metal atoms on low-index Si planes evaluated by coverage-dependent SHG signal

T13 Surface Science

#SS-P1-02

T. Suzuki, A. Kokabu, F. Saito.

National Defense Academy - Yokosuka (Japan).

We report the dependence of the alkali metal (AM) densities at the saturation coverage θ_{sat} on the orientation of Si crystal planes by second-harmonic generation (SHG).
AM atoms are known to chemisorb to Si surface up to θ_{sat} at room temperature (RT) with the sticking probability of 1 and physisorption thereafter [1-3]. Desorption is negligible up to θ_{sat}, however desorption was observed from the multilayer Na structures even at RT in a temperature-programmed desorption experiment on Na/Si(111) [2]. To clarify the geometric and electronic structures of the AM-covered silicon surfaces at θ_{sat}, we investigated Rb adsorption by SHG on low-index planes. Clean Si surfaces were obtained by direct resistive heating Si wafers of Si(111), Si(100) and Si(110). Rb was evaporated from well-outgassed dispensers. SHG was obtained by using a Q-switched Nd:YAG laser (pulse energy 1 mJ) at 1064 nm directed at a *p*-polarized incidence angle of 45°. The reflected *p*-polarized SH light was detected using a photomultiplier tube with gated electronics.
Fig. 1 shows the SH intensity for the coverage dependence of Rb/Si under a constant flux. The flux was calibrated by the coverage dependence of Rb/as-received wafer (a). The typical features of SHG reported for AM adsorption are reproduced for all planes including A, the resonance enhancement among AM-derived surface states [3], B, and a dip followed by C, the roughness-induced excitation of surface plasmons [4]. The dip was assigned to θ_{sat} [3], and the adsorption period to the dip was 440 s, 390 s and 320 s for Si(111), Si(100) and Si(110), respectively. Thus, different value of θ_{sat} was obtained depending on the orientation of a crystal plane. The Si atom densities for the corresponding planes are 7.8/nm^2, 6.7/nm^2, 9.7/nm^2, respectively. Thus, the AM density at θ_{sat} for each crystal plane is clearly not correlated with the surface Si density.

In a separate experiment, the SH intensity C for Rb/Si sensitively showed a decrease with increasing sample temperature, and a fast decay after closing the shutter. The decay of the microcrystalline nature of the cold-deposited films by surface diffusion was attributed to the SH decrease. The decay of C fitted by a simple model resulted in the activation energies of ~ 0.2 eV for surface diffusion. The correlation between the AM densities at θ_{sat} and the surface diffusion for each crystal plane will be the next topics to be elucidated.

[1] K. O. Magnusson, B. Reihl, Phys. Rev. B 41 (1990) 12071.
[2] G. Boishin et. al., Surf. Sci. 257 (1991) 190.
[3] K. Fujiwara et. al. Appl. Surf. Sci. 257 (2011) 3758.
[4] T. Suzuki et. al. in press (Appl. Surf. Sci.)

Fig. 1 Coverage dependence of the SH intensity for Rb/Si-surfaces

SS-P3-02
Initial steps of rubicene film growth on silicon dioxide

T13 Surface Science

#SS-P3-02

B. Scherwitzl, W. Lukesch, G. Leising, R. Resel, A. Winkler.

Graz University of Technology - Graz (Austria).

Studies of the initial stages of organic film growth are of great relevance for the use of organic materials in microelectronic devices. This contribution describes the behavior of rubicene ($C_{26}H_{14}$) film growth on silicon dioxide with respect to sample treatment under UHV conditions. Physical vapor deposition from a Knudsen cell was used to create films with varying thickness, from sub-monolayer up to multilayer range. A number of different analytical methods were used to examine film and substrate properties, namely Auger Electron Spectroscopy (AES) for chemical analysis, Thermal Desorption Spectroscopy (TDS) to determine desorption behavior and Atomic Force Microscopy (AFM) for a subsequent ex-situ analysis of the sample surface. It could be shown that the initial film formation of rubicene molecules on SiO_2 exhibits a quite unusual behavior. First a monolayer of flat lying molecules is formed, followed by a second layer. Further deposition of rubicene leads to a destabilization of this bilayer and to a dewetting process with a subsequent formation of bulk-like 3D islands. Different desorption energies suggest that the binding of the organic molecules to the substrate material is not as strong as among the molecules themselves as shown in Figure 1. This is the reason for the strong tendency to dewet. Another reason for a dewetting of the bilayer is the exposure of such a layer to atmospheric conditions. This has been shown by TDS and AFM measurements. Furthermore, for the island-like film under ambient conditions Ostwald ripening was observed, leading to films composed of few, large crystalline islands. In the case of very thin films most of the material in the small islands even disappeared by vaporization within several days. A further peculiarity of the adsorption system rubicene/SiO_2 is related to the sticking coefficient. Contrary to common belief the initial sticking coefficient is not unity, even at low substrate temperatures. We measured an initial sticking coefficient of only 0.2 ± 0.05, depending on the substrate conditions. This low value can be related to the relatively weak interaction energy between the molecules and the substrate, as well as to other reasons such as orientational hindering. Only a weak dependence of the adsorption and desorption behaviour on the substrate chemical composition was observed. Accumulation of

carbon on the surface, due to rubicene dissociation during sample heating, does neither significantly influence the shape of the desorption spectra nor the coverage dependence of the sticking coefficient.

Figure 1. Thermal desorption spectra of rubicene from clean silicon dioxide for different exposures. The exposure is given in Hz, as determined by a quartz microbalance.

SS-P1-03
Oxygen adsorption induced step rearrangement and growth of nano-lattices of Ni-O on Ni(755) and Ni(7911) stepped surfaces studied by STM

T13 Surface Science

#SS-P1-03

H. Namba, K. Yamanaka, N. Fukumoto, Y. Seino.

Ritsumeikan University - Kusatsu (Japan).

On stepped surfaces, a couple of a narrow terrace plane and an atomic step are periodically formed along a specific crystal direction. This step-terrace structure can give one dimensional boundary condition to determine the property of surface electronic states. Indeed, by means of angle-resolved photoelectron spectroscopy, we have found the formation of one dimensional surface states on Ni stepped surfaces. The dispersion relation of the surface states shows strong anisotropy in the direction perpendicular and parallel to step rows[1]. On the other hand, it is well known that steps on surfaces are active to chemisorption of foreign atoms. If foreign atoms are adsorbed selectively at steps or terraces, one dimensional arrays of the adsorbate are formed. So the step-terrace structure on surfaces is a useful template to grow new low dimensional materials in nano-scale. Up to now, many studies of chemisorption and reaction on stepped surfaces have been reported. In those it has been implicitly postulated that the step structure on the clean substrate is maintained through the chemisorption. So stability of the step-terrace structure has been paid little attention. Previously we have reported the first result of step rearrangement on Ni(7911) surfaces induced by atomic hydrogen adsorption[2]. As a function of atomic hydrogen dose, disordering and ordering of the periodic steps are clearly shown in LEED observation. This implies a flexible or soft nature of surface steps in hydrogen chemisorption. Recently we performed a series of oxygen chemisorption studies on Ni stepped surfaces by means of STM, LEED and work function measurements[3]. Two types of the step-terrace structure on stepped surfaces of Ni were chosen as substrate. An ideal model of Ni(7911)[=5(111)x(-101)] surfaces shows repetition of 3- and 4-fold sites at the step edge in [-101]. So the step shape is zigzag. In contrast to Ni(7911), the step on Ni(755)[=6(111)x(100)] has only 4-fold sites. The step along [100] of Ni(755) is smooth. In this conference, we compare the dynamical properties

of surface steps in the process from oxygen chemisorption to formation of low dimensional Ni-O complexes on the surface.

Firstly oxygen selectively adsorbed at step edges on both surfaces. And this induces roughening or disordering of step rows. Further adsorption does not progress step roughening, but recover the step periodicity. Finally, on Ni(7911), nano-lattices with 2x1-like rectangular structure are formed beyond the border due to step edge. On Ni(755), 2x2 hexagonal nano-lattices are formed at each terrace plane, but do not grow beyond the step edge. This forms one-dimensional row of nano-lattices at each terrace plane. The crystal structure of the terrace plane on both stepped surfaces is fcc(111) commonly. Growth of nano-lattices on each surface is clearly different due to the step shape. The present result of roughening or disordering of the step-terrace structure can be very important at growth at elevated temperature. These are key factors to design nano-scale materials.

[1] H. Namba et al. Surf. Sci.242,32(1991).
[2] H. Namba et al. Surf.Sci.357-358,238(1996).
[3] H. Namba et al. ECOSS27, 58(2010).

SS-7-Or-9
Growth and magnetic properties of lowdimensional oxide films on a support: CoO/Ir(100)

T13 Surface Science

#SS-7-Or-9

F. Mittendorfer [1], J. Redinger [1], R. Podloucky [2], M. Weinert [3].

[1]TU Vienna - Vienna (Austria), [2]Univ. Vienna - Vienna (Austria), [3]Univ. Wisconsin-Milwaukee - Milwaukee (United states).

The support of epitaxial films frequently determines their crystallographic orientation, which is of crucial importance for their electronic and magnetic properties. Although the surface stress in the oxide layer is usually seen as the main driving force for its orientation, we could recently show in a combined theoretical and experimental study that the interface chemistry can play a crucial role [1]. This allows for a novel way to alter the film orientation without changing the substrate.
I will present our results for the growth of CoO on the Ir(100) surface, obtained on the basis of DFT calculations with the Vienna Ab-initio Simulations Package (VASP). While the oxide grows in (111) orientation on the bare substrate, the orientation switches to (100) by introducing a single (or a few) monolayer(s) of Co between the oxide and substrate due to the enhances interaction at the interface.

In addition, I will report on the the magnetic ordering in the ultrathin hexagonal c(10x2) CoO(111) film supported on Ir(100). In that case, we find a close relationship between the local structural properties of the oxide film and the induced magnetic order, leading to alternating ferromagnetically and antiferromagnetically ordered segments [2]. While the local magnetic order is directly related to the geometric position of the Co atoms, the mismatch between the CoO film and the Ir substrate leads to a complex long-range order of the oxide.

[1]Phys. Rev. Lett. 108 (2012) 066101
[2]Phys. Rev. Lett. 109 (2012) 015501

SS-11-Or-2
In-situ production, electrical and surface analytical characterization of pentacene thin film transistors

T13 Surface Science

#SS-11-Or-2

R. Lassnig [1], B. Striedinger [2], A. Fian [2], B. Stadlober [2], A. Winkler [1].

[1]Graz University of Technology - Graz (Austria), [2]Joanneum Research Weiz - Weiz (Austria).

Electronic devices based on organic semiconductors are on the verge of taking over large shares of the markets dominated by inorganic systems. While the possibilities to create and optimize organic devices are clearly present, the underlying principles affecting critical parameters such as performance and lifetime are not fully understood to the present date. In order to contribute a new approach to the vast worldwide research on organic semiconductors, we present an analysis on the formation and stability of the semiconducting layer in organic field effect transistors (OFET) through a unique combination of organic layer deposition and in-situ electrical and surface analytical characterization, all performed under ultra-high vacuum conditions. As a well-established model material for organic semiconductors, pentacene was deposited onto pre-contacted SiO2/Si samples through physical vapor deposition (PVD) from a Knudsen cell (bottom gate/bottom contact architecture). The whole sample was clamped onto a stainless steel plate, which allowed cooling and heating in the range from 110 K to 800 K (see Figure 1). The thickness of the deposited pentacene layer could be monitored in the range from sub-monolayer to the multilayer regime by parallel exposure of a quartz microbalance. During and subsequent to deposition the OFET devices were characterized through in-situ electrical characterization, yielding output and transfer characteristics, which were monitored as a function of several factors affecting the semiconducting layer growth and performance, such as layer thickness and device temperature. To reach conclusions about the layer growth and possible growth affecting contaminations, in-situ Auger electron spectroscopy and thermal desorption spectroscopy (TDS) were performed throughout the stages of the device fabrication, parallel to the electrical investigations. Ex-situ atomic force microscopy, in combination with in-situ TDS, enabled the differentiation between layer and island-like growth and the corresponding electrical characteristics of analyzed devices.

While the basic reference for all measurements consisted of well-established bottom gold-contact pentacene organic field effect transistors with highly doped silicon substrates and silicon dioxide as a dielectric, our experimental setup allows a wide range of sample modifications. The simple modification of channel and sample dimensions, as well as changes of the semiconducting organic, contact pad and substrate material enables a wide spectrum of possible test device configurations.

Figure 1: Schematics of the sample holder and model device configuration for in-situ electrical and surface analytical investigations.

SS-8-Or-3
A peculiar non-vortical Rashba spin structure originating from the symmetry of the surface

T13 Surface Science

#SS-8-Or-3

K. Sakamoto [1], M. Ohtaka [1], T. Aoki [1], H. Ishikawa [1], E. Annese [1], T. Kuzumaki [1], B. Mueller [1], Y. Yamamoto [1], J. Osiecki [2], K. Miyamoto [3], Y. Takeichi [4], A. Harasawa [4], K. Yaji [4], K. Miki [5], R. Uhrberg [2], T. Oda [6].

[1]Chiba University - Chiba (Japan), [2]Linkoping University - Linkoping (Sweden), [3]Hiroshima University - Higashi-Hiroshima (Japan), [4]the University of Tokyo - Kashiwa (Japan), [5]National Institute for Materials Science - Tsukuba (Japan), [6]Kanazawa University - Kanazawa (Japan).

In this paper, we present a Rashba system that shows a peculiar non-vortical spin structure around the Γ point. Rashba effect [1] is a novel exotic low-dimensional solid-state property that produces a spin-polarized two-dimensional electron gas from a combined effect of spin-orbit interaction and structural inversion asymmetry even for nonmagnetic materials. In an ordinary Rashba system, the constant energy contour shows isotropic vortical spin structures around the Γ point, with spin polarization vectors lying in the surface plane. Together with its scientific interest, Rashba effect has an interest in the application field since it is the key factor for operating spin field-effect transistor [2] that is one of the most prominent semiconductor spintronics devices. By using spin- and angle-resolved photoelectron spectroscopies, we have measured the Rashba spin bands of a Tl/Si(110)-(1x1) surface, a system with a quasi-one dimensional atomic structure and C1h symmetry. So far, symmetry induced peculiar Rashba effects have been discussed on threefold symmetry systems [3-5]. In these systems, peculiar spins were observed at the boundary of the surface Brillouin zone, and the spin structures around the Γ point were vortical like the ordinary systems. These spin structures observed on threefold symmetry systems are completely different from the present result shown in the figure. Taking the polarization vector of the spins along the Γ-X' direction into account, we obtained peculiar upstanding spins at the apex of the elliptical structure. Furthermore, the spin-polarization vectors along the Γ-X' direction indicate that the probability of inter valley scattering would be negligible. We will also discuss the

origins of the peculiar spin structure based on the symmetry of the surface. Furthermore, since the present system is formed on silicon substrates, the present results would provide a significant step toward the readily realization of silicon spintronics devices with high-efficiency.

1. Y. A. Bychkov and E. I. Rashba, JETP Lett. **39**, 78-81 (1984).
2. S. Datta and B. Das, Appl. Phys. Lett. **56**, 665-667 (1990).
3. K. Sakamoto *et al.,* Phys. Rev. Lett. **102**, 096805-1-4 (2009).
4. K. Sakamoto *et al.,* Phys. Rev. Lett. **103**, 156801-1-4 (2009).
5. K. Sakamoto *et al.*, in preparation.

The constant energy contours around the Γ point at E_B=0.2 eV. X' is the symmetry point of the surface Brillouin zone of Si(110)-(1x1).

SS-14-Or-8
Characterization of catalytically-active Pt-group alloy surfaces and core-shell nanoparticles using atom probe tomography

T13 Surface Science

#SS-14-Or-8

P. Bagot [1], T. Li [1], E. Marquis [2], E. Tsang [1], G. Smith [1].

[1]University of Oxford - Oxford (United kingdom), [2]University of Michigan - Ann Arbor (United states).

Heterogeneous catalysts have proven remarkably successful in catalyzing a wide range of important processes, in fuel-cells, exhaust emission control and in hydrocarbon processing. However, the effects of the operating environment on the surface composition, structure and stability of the noble metal catalysts are poorly understood at the atomic-scale. This knowledge will be required to produce the improved catalysts needed for future energy- and materials-efficient technologies.

Atom probe tomography (APT) offers a unique method for studying these materials, providing atomic-scale chemical characterization of the catalyst surfaces and chemisorbed species. We have used APT to show a rich variety of behavior in an extensive range of Pt-group alloys, investigating the effects of high temperature oxidation exposures on these surfaces. The results reveal pronounced surface segregation behavior, strongly dependent on the treatment conditions, crystallographic planes and alloy compositions [1-3]. Recent work has also shown that trends identified in binary alloys often cannot fully explain those seen in ternary alloys, underlining the need for further atomic-scale investigations. Additionally, while subsequent reduction treatments remove any oxides formed, the marked changes to the metallic surfaces remain. Such results suggest using sequential oxidation and reduction treatments as an alternative synthesis method for designing and preparing nano catalysts with controlled surface compositions. A range of results from these systems will be presented to contrast and highlight the unique behaviors.

In parallel to the fundamental work on catalyst alloy wire samples, we have successfully used APT to characterize core-shell nanoparticles as used in real

catalytic applications, uniquely revealing the core-shell structure clearly in the data [4]. These core-shell materials offer the possibility of finely-tuning the surface activity of bimetallic catalysts to maximize their efficiency. Alongside a description of the sample preparation methods, we will discuss a range of results from these materials, highlighting the correlation between catalytic efficiency and the atomic-scale chemical/structural information uniquely provided by APT.

[1] P. Bagot et al., Surf. Sci. 605 (2011) 1541.
[2] T. Li et al., Catal. Today 175 (2011) 552.
[3] T. Li et al., J. Phys. Chem. C 116 (2012) 4760.
[4] K. Tedsree et al., Nature Nanotech. 6 (2011) 302.

SS-P1-18
Structural and morphological characterization of self-organized nanoporous oxides: TiO2, Al2O3 layers. Potential applications.

T13 Surface Science

#SS-P1-18

M. Pisarek.

Institute of Physical Chemistry PAS - Warsaw (Poland).

Oxides of titanium (TiO_2) and aluminum (Al_2O_3) have been widely studied around the world in recent years. The high level of interest in these materials is due to their wide application in such fields as photovoltaics, catalysis, lithography, optoelectronics, as protective coatings, self-cleaning coatings, bio-sensors and in biomedicine. Moreover, nanoporous layers of aluminum oxide are widely used as “templates/matrices” for creating metallic nanofibres, semi-conductors and conductive polymers. The use of anodic oxidation (anodic polarization) as a method of forming nanostructured oxide layers on metals affords numerous possibilities for controlling their morphology. The anodic oxidation of Ti and Al in neutral or acidic solutions containing fluorides is a typical electrochemical method of surface modification allowing oxide layers of varying thickness, porous morphology in the form of tubes having a diameter of from teens of nm even to several μm. The thickness of such a oxide layer can be controlled through anodization time and applied voltage. Such a wide range of diameters makes it possible to control the porosity and surface properties of the materials under study. The tubes are oriented at ninety degrees to the substrate. The possibility of self-organized oxide layers fabrication (nanotubes) opens a new field of application of such materials, for example: for preparing composites like materials with different amounts of silver deposit for preparation active substrates for SERS investigations of organic adsorbates, which exhibit antibacterial properties and also can be used as a promising substrate for heterogeneous catalysis. In all applications – SERS, biomedical, catalysis – metal particles play an important role which is crucial for these different functionalities.

Acknowledgements
The research was partially supported by the European Union within European Regional Development Fund, through grant Innovative Economy (POIG.01.01.02-00-008/08).

[1] A.Roguska, A.Kudelski, M.Pisarek, M.Opara, M.Janik-Czachor, Vibrational Spectroscopy, 55 (1) (2011) 38-43
[2] A.Roguska, M.Pisarek, M.Andrzejczuk, M.Dolata, M.Lewandowska, M.Janik-Czachor, Materials Science and Engineering C, 31 (2011) 906–914
[3] A.Kudelski, M.Pisarek, A.Roguska, M.Hołdyński, M.Janik-Czachor, Journal of Raman Spectroscopy 43 (2012) 1360-1366
[4] M.Pisarek, A.Roguska, A.Kudelski, M.Andrzejczuk, M.Janik-Czachor, Materials Chemistry and Physics, accepted for publication, http://dx.doi.org/10.1016/j.matchemphys.2012.11.076

Cross section view of the nanoporous layer on Al substrate.

NST/SS-8-Or-9
Nitrogen and Boron doping of Graphene

T13 Surface Science

#NST/SS-8-Or-9

C. Papp [1], R. Koch [2], J. Gebhardt [3], W. Zhao [1], O. Hoefert [1], K. Gotterbarm [1], T. Seyller [2], A. Goerling [3], H.P. Steinrück [1].

[1]Physikalische Chemie II - Uni Erlangen (Germany), [2]Technische Physik - Tu Chemnitz (Germany), [3]Theoretische Chemie - Uni Erlangen (Germany).

The application of graphene in future devices will depend on the possibility to tune its band structure. One desirable way to achieve this is substitutional doping, as this leads to a considerably higher stability than e.g. charge transfer doping by adsorbates. Here we will show different ways to prepare nitrogen- and boron-doped graphene, i.e., via classical CVD approach and in the case of nitrogen doping also via ion implantation. The systems are analyzed with x-ray photoelectron spectroscopy (XPS) and angle resolved photoemission (ARPES). The experimental findings are compared and supported by ab initio density functional calculations. [1] In the case of nitrogen doping we find two chemically different nitrogen species on the surface, namely pyridinic and substitutional nitrogen, whose concentration and relative abundance can be altered by the experimental conditions, see Figure 1. The ARPES measurements show a broadening of the bands and p-doping. In order to decouple the nitrogen-doped graphene from the nickel surface we used gold intercalation, leading to the electronic structure of quasi free standing graphene, while preserving the nitrogen doping. The DFT analysis shows excellent agreement; furthermore, it indicates the possibility to obtain n-doping for substitutionally doped graphene. The introduction of boron in the graphene network leads to solely one chemical species and a strong p-doping. ARPES shows similar effects as for nitrogen, with a broadening of the bands and a retained band structure. From the DFT calculations we find a strong preference of boron-doped graphene for the top-fcc geometry, while in the case of nitrogen doping no preferred site was found. Additionally, we find a buckling of the graphene layer due to the reduced adsorption distance of boron as compared to carbon.

We acknowledge the Cluster of Excellence “Engineering of Advanced Materials” for financial support and BESSY staff for support during beamtime.

[1] R. J. Koch, M. Weser, W. Zhao, F. Vines, K. Gotterbarm, S. M. Kozlov, O. Höfert, M. Ostler, C. Papp, J. Gebhardt, H.-P. Steinrück, A. Görling, T. Seyller, Physical Review B 86 (2012) 75401.

Figure 1: Schematics of the different chemical species occurring in nitrogen doped graphene.

NST/SS-6-Or-9
Tuning non-collinear magnetic states with non-magnetic adlayers

T13 Surface Science

#NST/SS-6-Or-9

N. Romming, M. Menzel, C. Hanneken, J.E. Bickel, B. Wolter, K. Von Bergmann, A. Kubetzka, R. Wiesendanger.

Institute of Applied Physics, University of Hamburg - Hamburg (Germany).

Magnetism in thin films can significantly deviate from commonly known magnetic configurations in bulk systems due to low dimensionality, hybridization effects, a change of the lattice constant, stacking and broken inversion symmetry at interfaces. Both monolayer and double layer systems were recently found to exhibit non-collinear magnetic states such as spin spirals or skyrmion lattices [1-4]. A change on either top or bottom interface may result in different magnetic states. While in the past, magnetism was tuned by the choice of the underlying substrate resulting in various magnetic configurations [1,3,4], here we follow a different approach. We perform spin-polarized STM studies to investigate the influence of non-magnetic adlayers on above mentioned systems. Thus we find interesting magnetic field and temperature dependent behavior.

[1] Y. Yoshida et al., Phys. Rev.Lett. 108, 087205 (2012).

[2] S. Heinze et al., Nature Phys. 7, 713 (2011).

[3] M.Bode et al., Nature 447, 190 (2007).

[4] P. Ferriani et al., Phys. Rev. Lett. 101, 027201 (2008).

SS-12-Or-5
Dehydrogenation of dodecahydro-N-Ethylcarbazole on Pt(111)

T13 Surface Science

#SS-12-Or-5

C. Gleichweit, M. Amende, S. Schernich, W. Zhao, O. Höfert, J. Libuda, H.P. Steinrück, C. Papp.

Lehrstuhl für Physikalische Chemie II, Universität Erlangen-Nürnberg - Erlangen (Germany).

Hydrogen storage in Liquid Organic Hydrogen Carriers (LOHC) is a possible future technology to circumvent the challenges in hydrogen use and storage. [1, 2] The dehydrogenation, i.e. the hydrogen release, of the LOHC dodecahydro-N-ethylcarbazole (H_{12}-NEC) on Pt(111) was studied by high-resolution X-ray photoelectron spectroscopy (HR-XPS) in order to elucidate the relevant elementary steps. H_{12}-NEC was adsorbed under ultra high vacuum (UHV) conditions, and subsequently the reaction was monitored during heating. Although the molecules are quite complex to be studied under surface science conditions, we were able to identify the reaction steps based on a detailed analysis of the C1s and N1s core level spectra. During adsorption at low temperatures the development of monolayer and multilayer peaks was observed. Interestingly, the N1s peak assigned to the multilayer is found at lower binding energy than the monolayer peak. When heating the sample continuously, the multilayer desorbs until temperatures of about 240 K, with the monolayer remaining on the surface. The dehydrogenation of the H_{12}-NEC to NEC occurs between 280 and 500 K. Starting at 390 K, in addition the dealkylation reaction of the NEC to carbazole is observed. Upon further heating to 1000 K decomposition to adsorbed carbon takes place. The reaction scheme, as deduced from the quantitative analysis, is shown in Fig. 1. The dealkylation reaction and the subsequent decomposition of carbazole are detrimental for the concept of using H_{12}-NEC in a regenerable hydrogen storage cycle.

We acknowledge the cluster of excellence “Engineering of Advanced Materials” for financial support and BESSY staff for support during beamtime.

1. Sobota, M.; Nikiforidis, I.; Amende, M.; Zanón, B. S.; Staudt, T.; Höfert, O.; Lykhach, Y.; Papp, C.; Hieringer, W.; Laurin, M.; Assenbaum, D.; Wasserscheid, P.; Steinrück, H.-P.; Görling, A.; Libuda, J., Dehydrogenation of Dodecahydro-N-ethylcarbazole on Pd/Al2O3 Model Catalysts. Chemistry – A European Journal 17, (41), 11542-11552.
2. Teichmann, D.; Arlt, W.; Wasserscheid, P.; Freymann, R., A future energy supply based on Liquid Organic Hydrogen Carriers (LOHC). Energy & Environmental Science 2011, 4, (8), 2767-2773.

Fig.1: Schematics of the reaction of H_{12}-NEC on a Pt(111) surface.

SS-1-Or-8
DFT study of dopamine adsorption on TiO2 surfaces

T13 Surface Science

#SS-1-Or-8

D. Castillo Malla, J.E. Ontaneda Rojas, A. Stashans.

Universidad Técnica Particular de Loja - Loja (Ecuador).

Titanium dioxide, TiO2, is of technological interest in applications including photocatalysis, biomaterials, and novel photovoltaic solar cells [1]. The adsorption of large organic molecules on oxide surfaces is rapidly gaining in technological importance, for example, in dye-sensitization of solar cells.
The present theoretical study is devoted to investigate adsorption of dopamine, C8H11O2N, on rutile (110) and anatase (101) surfaces, respectively. Using density functional theory (DFT) within the generalised gradient approximation as well as DFT+U approach, we study atomic-scale properties of the dye-TiO2 interface, such as the molecular orientation, adsorption geometry, and adsorption sites, which are fundamental parameters in the basic understanding of the electron transfer reaction from any dye molecule to the TiO2 particles.
Geometry of free dopamine molecule consisting of 22 atoms has been successfully reproduced to fit experimental data [2]. In order to study the adsorption phenomenon, a slab of 144 atoms (96 oxygens and 48 titaniums) with eight atomic layers and 12 Å of vacuum space has been used to model the rutile (110) surface. In case of the anatase (101) surface, a supercell of 216 atoms (144 oxygens and 72 titaniums) with 14 Å vacuum space has been exploited.
The first results of our on-going research demonstrate that dopamine molecule is likely to adsorb on the rutile (110) surface by positioning itself vertically, i.e. the plane of the aromatic ring is oriented roughly normal to the surface with the molecule being upright on the surface as shown schematically in Fig. 1. In this particular configuration, each one of the oxygen atoms of the molecule creates a chemical bond with a titanium atom on the surface. While there are several other chemisorption possibilities, we feel that our study illustrates the kind of geometric and electronic effects which are essential to adsorption of large organic molecules on TiO2 surfaces. The computed Ti-O distances are found to be between 2.30 y 2.40 Å, respectively. We expect similar outcome also for the dye adsorption on the anatase (101) surface.
Results obtained from the Bader charge analysis show that there exists electron

transfer from the dye molecule towards the TiO2 surface. Performed density of states calculation implies that the dopamine adsorption leads to reduction of the band-gap width from 2.0 eV (pure rutile-TiO2 crystal) to 1.5 eV (rutile-TiO2 surface with the adsorbed dye). Such a band-gap reduction is favourable for tentative photovoltaic applications.

[1] B. O'Regan, M. Grätzel, Nature 353 (1991) 737.
[2] R. Bergin, D. Carlström, Acta Cryst. B 24 (1968) 1506.

Fig. 1. A schematic diagram of dopamine adsorption on the rutile (110) surface.

SS-2-Or-3
Formation Dynamics SiAu Eutectic Thin Films and Surface Phases

T13 Surface Science

#SS-2-Or-3

D. Ogletree [1], C. Ko [2], T.S. Matthews [2], Z. Lilienthal-Weber [1], D. Chrzan [2], J. Wu [2].

[1]Lawrence Berkeley National Lab - Berkeley Ca (United states), [2]University of California - Berkeley Ca (United states).

Metal-semiconductor eutectics are important for contact formation and control the growth of semiconductor nanowires and related structures through the Vapor-Liquid-Solid process. We have investigated the dynamics of AuSi eutectic formation in non-equilibrium conditions by depositing 12-300 nm Au films on native-oxide passivated Si(100) substrates. When heated to ~ 600° C, the oxide film fails, allowing contact between the Au and Si phases above the 363° C eutectic temperature. Si and Au rapidly interdiffuse, forming a eutectic liquid disk expanding at up to 15 μm/s along with an inverted eutectic pyramid embedded in the Si substrate and bounded by Si {111} planes.[1] Once the liquid disk is larger than ~ 10 μm it becomes unstable and dewets, isolating the bulk Si and Au phases and leaving eutectic droplets on the sample surface and an exposed Si disk with the square surface of the eutectic pyramid in the center. A silicon-rich surface phase also forms on the Au surface around the dewetting disk. (An SEM video is available online [2]). On cooling below the eutecic tempreature the liquid regions phase-sepateate and freeze. We have performed in-situ SEM and high-spatial-resolution Auger experiments to investigate the dynamics of AuSi eutectic phase formation as a function of Au film thickness, the Si-rich Au surface phase, and temperature-dependent surface segregation at the AuSi eutectic-vacuum interface. The eutectic reaction dynamics and the nature of the Si surface phase will be discussed.

[1] Large Reaction Rate Enhancement in Formation of Ultrathin AuSi Eutectic Layers, TS Matthews et al., Phys Rev Lett 108 2012.

[2] "AuSi eutectic" on YouTube from junqiaowu1, http://www.youtube.com/watch?v=PfuMkaWvtyk

SEM image of a growing AuSi eutectic liquid disk at 600° C (grey, at left) surrounded by a Si-rich surface phase (light grey) and a Si disk previously exposed by dewetting (dark, at right).

SS-15-Or-1
Relationship between Strain and Effective Mass in the Metallic Surface State of the √3×√3-Ag Structure on Si(111) epitaxial layer

T13 Surface Science

#SS-15-Or-1

Y. Shigeta, T. Ishii, A. Tosaka.

Yokohama City University - Yokohama (Japan).

Much interest has been attracted on a microscopic lattice strain, because it has a large possibility to design nanoscale properties. The electronic property of the nanostructure depends on its structure including the lattice strain to stabilize the nanostructure. To make clear the relation between electronic states and strain in nanoscale structure, the study in two-dimensional system is very useful and the results will give possibilities for nano-electronics applications.
We have focused on the quasi two-dimensional electron gas (2DEG) state formed on the √3×√3-Ag structure, which is typically reconstructed by Ag adsorption (1 ML) on the Si(111) or the Ge(111), because the dispersion of the 2DEG state could be modified with the lattice strain introduced by heteroepitaxial growth such as the Ge/Si(111) or the Si/Ge(111). The compressive strain is induced to the surface layer by the epitaxial growth of the Ge on the Si (111), and the tensile strain is induced by the growth of the Si on the Ge (111). The relation between the surface electronic state and the lattice strain of the strain-induced √3×√3-Ag structures is investigated by using scanning tunnelling microscopy and angle resolved ultraviolet photoelectron spectroscopy. When the inter-atomic spacing expands (/contracts) about 2.1% (/-2.7%), the values of effective mass of the 2DEG, m^* changes about 30% (/-32%), as shown in Fig. 1 [1,2].
Since the change of m^* is consistent with the view of "*d*-band model" on some metal surfaces, qualitatively [3] , the detailed relation of the m* to the amount of the strain form -3% to +3% is not known but very interesting. To measure the detailed relation, we used SiGe buffer layers, whose lattice spacing depend on the ratio of the composition. The preliminary results show that the relationship between the m* and the strain is not linear relation.
We are grateful to Dr. I. Mochizuki (KEK, Japan) for his support and useful

comments. This work was supported by JSPS KAKENHI Grant Number 1224560031.

[1] I. Mochizuki, R. Negishi, and Y. Shigeta, J. Appl. Phys. 106, 013709 (2009).
[2] I. Mochizuki, R. Negishi, and Y. Shigeta, J. Appl. Phys. 107, 084317 (2010).
[3] D. Sekiba, Y. Yoshimoto, K. Nakatsuji, Y. Takagi, T. Iimori, S. Doi, and F.Komori, Phys. Rev. B 75, 115404 (2007).

Fig. 1 Relative effective mass change, $\Delta m^*/m_0^*$, to the rate of lattice expansion, $\Delta a/a_0$.

SS-9-Or-2
Grafting of Vinylferrocene Molecules onto the Si(111) Surface using Photochemical Preparation

T13 Surface Science

#SS-9-Or-2

M. Herrera, T. Ichii, K. Murase, H. Sugimura.

Kyoto University - Kyoto (Japan).

The Fe atom of ferrocene molecule has two reversible and stable oxidation states. Its oxidation state can increase from + 2 to +3 upon the introduction of potential and can revert back to +2 when grounded. With these characteristics, the ferrocene molecules on semiconductor surfaces are promising materials for the construction of memory storage devices. We are successfully in preparing vinylferrocene-terminated Si(111) using a photochemical preparation technique. The preparation involved illuminating a hydrogen-terminated Si(111), which was immersed in a vinylferrocene-dibutyl ether solution, with visible light. The success of the grafting method was attributed on the presence of photogenerated charges on the silicon surface (Figure 1). The Fe 2p spectra of the samples show that the oxidation state of Fe atoms in the vinylferrocene layer are mainly +2, which are associated with the existence of neutral ferrocene molecules. The AFM images show that the stair-like structure of the hydrogen-terminated Si was preserved even after grafting. This indicates that the vinylferrocene-terminated Si has an atomically flat surface. On the other hand, the sample with n-type substrate has optimum grafting time of 0.5 h while that of p-type substrate is 1 h. At optimum grafting time, both the samples with n-type and p-type substrates have C/Fe ratio of 12.4, which is close to the ideal value of 12. The cyclic voltammograms of the sample show the presence of anodic and cathodic peaks (Figure 2) that signifies that the vinylferrocene molecules are electrically connected with the Si surface. Meanwhile, the separations between the anodic and cathodic peaks are small. This signifies that the redox reaction does not involved diffusion of redox species. In addition, the graphs of peak current density vs. scan rate are linear. This indicates that the oxidation-reduction reaction is confined within the surface of the sample.

SS-3-Or-5
New software tool for I-V LEED analysis being applied to model catalysts

T13 Surface Science

#SS-3-Or-5

J. Lachnitt, D. Mazur.

Faculty of Mathematics and Physics, Charles University - Prague (Czech republic).

I-V LEED is an indirect but powerful technique of crystalline surface structure analysis. The experimental aspect of I-V LEED lies in measuring the dependence of diffraction spot intensities on applied voltage (electron energy). Thus we get intensity-voltage (I-V) curves, one for each inequivalent spot. The theoretical part lies in modelling the I-V curves for given surface structures and searching such a structure, I-V curves of which fit best the experimental ones.

I-V LEED can determine the positions of atoms within several topmost atomic layers with the accuracy of about 0.01 Å but it requires a computational processing which is demanding on both the computer and the researcher. SATLEED software package [1], along with Phase shifts package [1], provides all the necessary tools for the analysis. However, SATLEED is, from the contemporary point of view, very user-unfriendly and it requires a lot of user work that can be automated. The presenter of this contribution has developed a software tool called AutoLEED, which realizes this automation.

AutoLEED is a software overlayer on SATLEED, written in Python. The user still has to design the structural models of the studied surface but the input is much simpler and routine operations are done automatically.

With the help of AutoLEED, we analyze several planar model catalysts. These catalysts are also studied by other experimental techniques in our department. The detailed structure information provided by I-V LEED is crucial for the understanding of the principle of catalysis on given surface. This understanding can help in the development of practical catalysts.

The catalysts studied include a V-Rh(110) surface alloy and a thin cubic Ce_2O_3 film on Cu(111) [2]. The results are not known by the time of abstract submission and other catalysts may be studied in the meantime.

[1] A. Barbieri and M.A. Van Hove: private communication (http://www.ap.cityu.edu.hk/personal-website/Van-Hove.htm).

[2] V. Stetsovych, F. Pagliuca, F. Dvořák, T. Duchoň, M. Vorokhta, M. Aulická, J. Lachnitt, S. Schernich, I. Matolínová, K. Veltruská, T. Skála, D. Mazur, J. Mysliveček, J. Libuda, V. Matolín: *Epitaxial cubic Ce_2O_3 via Ce – ceria alloying*. Not yet published; to be sent to J. Phys. Chem. Letters.

SS-P3-09
The interaction of O2 with the surface of polycrystalline gadolinium at the temperature range 300–670 K

T13 Surface Science

#SS-P3-09

S. Cohen [1], N. Shamir [2], M. Mintz [2], I. Jacob [1], S. Zalkind [2].

[1]Dept. of Nuclear Eng., Ben-Gurion University of the Negev - Beer Sheva (Israel), [2]Nuclear Research Centre-Negev - Beer Sheva (Israel).

Direct-Recoil-Spectrometry (DRS) and Auger-Electron-Spectroscopy (AES) were applied to study the interaction of O_2 with a polycrystalline gadolinium surface, in the temperature range 300–670 K and oxygen pressure up to 2×10^{-6} Torr. It has been found that the initial uptake of oxygen and surface coverage, as measured by DRS and fitted to the clustering (one site) adsorption model, Fig. 1, results in rapid oxide island formation [1]. The subsurface is believed to be a mixture of oxide and oxygen dissolved in the Gd metal, the latter being the mobile species, even at relatively low temperatures.

Enhanced inward diffusion of oxygen into the Gd starts as early as 420 K and dictates the surface oxygen concentration and effective thickness of the forming oxide. The oxygen accumulation rate at the near-surface region, as measured by the O(KLL) AES signal intensity, goes through a maximum as a function of temperature at 420 K. This is a result of the combination of still efficient oxygen chemisorption that increases surface occupation and slow inward diffusion. The thickest oxide, ~1.7 nm, is formed at 300 K and its effective thickness decrease with increasing temperature (due to oxygen dissolution into the metal bulk).

Diffusion coefficients of the oxygen dissolution into the bulk were evaluated from the attenuation of the O (KLL) signal over time, as depicted in Fig. 2. The best fit under our experimental procedure was obtained by the thick layer model [2]. The coefficients that were calculated are $D_0=2.2\times10^{-16}$ m^2s^{-1} and $E_a=46$ kJ/mol [3].

1. M.H. Mintz, J.A. Schultz, J.W. Rabalais, Surf. Sci. 146 (1984) 457.
2. B.J. Flinn, C.-S. Zhang, P.R. Norton, Phys Rev. B 47 (1993) 16499.

3. S. Cohen, N. Shamir, M.H. Mintz, I. Jacob and S. Zalkind, Surf. Sci. 605 (2011) 1586.

Fig. 1. O(DR) intensity vs. O_2 exposure at 300K, fitted to the clustering model. The inset illustrates DRS Spectra of clean and oxidized Gd surfaces.

Fig. 2. The decrease of O(KLL) intensity vs. time at different temperatures due to the dissolution of oxygen into the bulk. The data is fitted to thin (ITOL) and thick (TLM) diffusion models.

NST/SS-8-Or-10
Tailoring the electronic structures of graphene oxides by low-energy N2+ ion sputtering: reduction and N-doping

T13 Surface Science

#NST/SS-8-Or-10

J. Zhu, L. Zhang.

National Synchrotron Radiation Laboratory, University of Science and Technology of China - Hefei (China).

Doping graphene with heteroatoms (such as N, H and B) provides a promising and feasible way to tailor its unique electronic structures, which is of great importance for its potential applications in nanoelectronics, supercapacitors, sensor devices and fuel cells. In this presentation, we report a facile and catalyst-free method to obtain N-doped reduced graphene oxides (N-RGO) through low-energy N_2^+ ion sputtering of graphene oxides (GO). The simultaneous reduction and N-doping of GO during the sputtering process were investigated by the X-ray photoelectron spectroscopy (XPS), near edge X-ray absorption fine structure (NEXAFS) and Raman spectroscopy. The degree of N-doping and GO reduction, which can be respectively determined from the N/C and O/C atomic ratios from the quantitative XPS analysis, can be easily controlled by varying the N_2^+ ion sputtering time. In addition, three different N bonding configurations can be distinguished in N-RGO, namely, the nitrile-like N, the graphitic N and the pyridinic N. This easy and catalyst-free approach offers a great opportunity for fabricating large-area and low-cost N-RGO with controllable N-doping and reduction level for various practical applications in the future.

This work is supported by the National Natural Science Foundation of China (Grant No.21173200) and National Basic Research Program of China (2010CB923302)

SS-8-Or-4
Direct Observation of Topological Solitons in a Quasi-1D Charge-Density Wave

T13 Surface Science

#SS-8-Or-4

T. Kim, H.W. Yeom.

Pohang University of Science and Technology - Pohang (Korea, republic of).

In 1834, a naval engineer John Scott Russell first observed a self-reinforcing and constantly traveling solitary wave in the Union Canal in Scotland. This beautiful phenomenon due to the nonlinearity of wave media is now called a soliton and has important roles in modern technology like optical communication. While macroscopic and classical solitons are easily and ubiquitously observed, from tsunami to blood pressure pulses, those in microscopic and quantum world of atoms and electrons are hard to observe. For example, in conducting polymer chains, solitons are known to exist as topological excitation from the degenerate charge-density wave (CDW) ground states with strange spin and charge relationship. While the existence of such quantum solitons were predicted theoretically and evidenced indirectly by the transport and infrared spectroscopy measurements, the direct observation has been hampered by their high mobility and nanometer dimension. In this talk, we clearly image by scanning tunneling microscopy the quantum soliton in the commensurate (2*a*) CDW ground states of indium atomic wires grown on a silicon surface [1-4]. The solitons exhibit a characteristic spatial variation of the CDW amplitudes with a coherence length of about ~4 nm (see the figure), as expected from the electronic structure of the CDW state. While most of the observed solitons are trapped statically by the defects, moving solitons are also identified when they are trapped transiently. This work paves the avenue toward the microscopic exploitation of the peculiar properties of quantum solitons in solid-state physics.

[1] H. W. Yeom, S. Takeda, E. Rotenberg, I. Matsuda, K. Horikoshi, J. Schaefer, C. M. Lee, S. D. Kevan, T. Ohta, T. Nagao, and S. Hasegawa, *Phys. Rev. Lett.* **82**, 4898 (1999).
[2] S. J. Park, H. W. Yeom, S. H. Min, D. H. Park, and I. -W. Lyo, *Phys. Rev. Lett.* **93**,

106402 (2004).
[3] Han Woong Yeom and Tae-Hwan Kim, *Phys. Rev. Lett*. **107**, 019701 (2011).
[4] Tae-Hwan Kim and Han Woong Yeom, *Phys. Rev. Lett.* **109**, 246802 (2012).

A 3D scanning tunneling microscopy image shows a topological soliton (middle) bridging two degenerate charge-density waves (left and right).

SS-7-In-1
Understanding the nature of TiOx-Graphene interface for a rational design of advanced nanoarchitectures

T13 Surface Science

#SS-7-In-1

G. Granozzi [1], M. Favaro [1], S. Agnoli [1], C. Di Valentin [2], C. Mattevi [3].

[1]University of Padova - Padova (Italy), [2]University of Milano Bicocca - Milano (Italy), [3]Imperial College - London (United kingdom).

Recently, TiO_2/graphene systems have attracted a lot of attention for environmental and energy applications,[1,2] such as photo-catalytic degradation of pollutants,[3] photo-catalytic hydrogen generation,[4] and electrochemical energy storage.[5] However, this field is still denoted by a high level of empiricism and a complete understanding of either the atomic structure of these materials or the reason of their advanced properties is still missing. In the present contribution, we present a detailed investigation of the structural properties of the TiOx/graphene oxide interface based on synchrotron radiation photoemission and *ab initio* calculations. The evolution of the C 1s photoemission spectra during Ti deposition in ultra high vacuum by physical vapour deposition, indicates that carboxyl and carbonyl groups disappear after metal deposition, and similarly epoxy and tertiary alcohol species strongly decrease. On the contrary, the sp^2 C fraction gets more intense indicating the recovery of the honeycomb lattice of graphene. A microscopic view of this process has been determined by density functional calculations: epoxy and hydroxyl groups, the most common surface species present of graphene oxide, interact very strongly with metal Ti leading to the disruption of C-O bond, extraction of the O atom and to the formation of Titanium (hydr)oxide species. Concomitantly C atoms heal the initial defects re-forming perfect graphene.[6] HOwever, when the available oxygen species on graphene oxide surface are consumed by Ti oxidation, metal atoms can react with the carbon backbone, and form carbides as evidenced by the appearance of new components in the C 1s and Ti 2p photoemission spectra. These results can give important indications about the rational for building atomically precise interfaces exhibiting C-O-Ti or C-Ti bonds which is a fundamental parameter for controlling the electronic transfer in nanocomposite. Moreover, this work demonstrates that the evaporation of an easily reduceable metal can be used as a versatile tool for the reduction of graphene oxide: by its nature, this all-solid-state surface reduction does

not lead to the removal of carbon as CO or CO_2 like in the case of thermal reduction or of other chemical methods, allowing obtaining a fully reduced and complete carbon network. If the evaporation of Ti is performed in oxidative conditions keeping the substrate at a certain temperature, different types of composites can be obtained. In particular, by optimizing deposition conditions (T=650°C, PO_2=10^{-6} mar), as determined by a combination of SEM, AFM, XPS, and XAS, it is possible to prepare anatase-graphene systems, where the nanoparticles decorate selectively graphene ripples. This approach paves the way to a new concept in the synthesis of new materials, which consists in the exploitation of the local curvature of graphene as a sophisticated tool for tailoring spatially heterogeneous systems.[7]

1 N. J. Bell, et al, J. Phys. Chem. C, 2011, 115, 6004.
2 X. Y. Zhang, et al J. Mater. Chem., 2010, 20, 2801.
3 J. Du, et al ACS Nano 2011, 5, 590–596.
4 Q. Xiang, at al. Nanoscale 2011, 3, 3670.
5 S. Yang, at al. Adv. Mater. 2011, 23, 3575.
6 M. Favaro, et al. in preparation
7 M. Favaro, at al. submitted

SS-3-Or-8
Characterization of Pd(100) surface under catalitic conditions with High Energy Surface X-Ray Diffraction

T13 Surface Science

#SS-3-Or-8

M. Shipilin [1], J. Gustafson [1], C. Zhang [1], A. Stierle [2], U. Hejral [2], U. Ruett [3], O. Gutowski [3], M. Skoglundh [4], P.A. Carlsson [4], E. Lundgren [1].

[1]Department of Synchrotron Radiation Research, Lund University - Lund (Sweden), [2]University of Hamburg - Hamburg (Germany), [3]Deutsches Elektronen-Synchrotron (DESY) - Hamburg (Germany), [4]Competence Centre for Catalysis, Chalmers University of Technology - Gothenburg (Sweden).

Surface X-ray diffraction (SXRD) is a powerful tool to study surface structures, and has been used for many years to determine the exact atomic positions at surfaces. The technique is particularly useful at conditions not accessible with electron based surface techniques. However it has a major drawback of limited amount of reciprocal space that is observable within a reasonable timeframe.
In this contribution, we present results from using grazing incidence photons of 85 keV to perform High Energy Surface X-Ray Diffraction (HESXRD) combined with a large area X-ray detector. Using high energy photons for diffraction flattens the Ewald sphere to reveal a large part of reciprocal space in a matter of seconds which significantly facilitates the data collection while the small angle of incidence allows to achieve high surface sensitivity.
Experiments were carried out at the beamline P07 of Petra III at Deutsches Elektronen-Synchrotron (DESY) [1]. Specially designed UHV chamber/reactor allowing pressures in the 10^{-10} mbar range was used to prepare the samples and to create the desired environment for catalytic reactions [2].
In SXRD/HESXRD technique the position of surface atoms are probed via so-called crystal truncation rods (CTRs) or in the case of a surface reconstruction or adsorbate surface structure also via superlattice rods. Our study focuses on a Pd(100) single crystal surface under relatively harsh reaction conditions, and in particular on the $(\sqrt{5}\times\sqrt{5})R27^{o}$ surface oxide formed during oxidation. The rotation of the sample in the beam results in a sequence of images covering the significant part of reciprocal lattice and revealing CTRs step by step. By collecting the most intense pixels from

each image, an image representing a comprehensive diffraction pattern from the surface structure can be obtained (fig.).The regular lattice CTRs apparently belong to Pd(100) substrate while the superlattice CTRs represent ($\sqrt{5}\times\sqrt{5}$)R27^{o} surface oxide structure. Analyzing the positions and intensity distribution along the CTRs and the superlattice rods the structure factors can be extracted and the full surface structure can be determined by comparing measured and calculated structure factors. Further, by choosing an appropriate location in reciprocal space and observing the dynamics of diffraction pattern, studies in harsh environments such as catalysis, growth processes, electrochemistry etc can be done with sub-second time resolution.

[1] Deutsches Elektronen-Synchrotron (DESY), http://hasylab.desy.de.
[2] R. van Rijn, M.D. Ackermann, O. Balmes et al., Rewiew Of Scientific Instruments 81 (2010) 014101.

SS-1-Or-2
STM investigation of CO ordering on Pt(111) : from an isolated molecule to high coverage superstructure

T13 Surface Science

#SS-1-Or-2

H. Yang [1], Y. Kim [2], M. Kawai [1].

[1]Univ. of Tokyo - Kashiwa (Japan), [2]RIKEN - Wako (Japan).

We report coverage-dependent observation of CO on Pt(111) using scanning tunneling microscopy (STM) in ultra-high vacuum at cryogenic temperature. From a single CO adsorbed on the atop site and its lateral hopping via 2π* state[1] characterized with action spectroscopy, to gradual development of overlayer structures including atop-dominant $(\sqrt{3}\times\sqrt{3})R30^\circ$ islands, c(4×2) domain, and 1×1 boundary in c(4×2)-2CO domain were visualized as seen in Figure (a)[2,3]. Bridge species start to appear at the edge of (3×3)R30˚ islands, significantly where the edge between edge of $(\sqrt{3}\times\sqrt{3})R30^\circ$ islands forms local c(4×2)-2CO structure. With increasing the coverage, phase transition from $(\sqrt{3}\times\sqrt{3})R30^\circ$ islands to wholly covered c(4×2) domain was observed where the c(4×2) domain including bridge-vacancies aligned to $[1\bar{1}0]$ direction. Where the bridge vacancy exist, the topographic height atop CO in c(4×2) geometry is modulated by the number of adjacent bridge CO (Figure (b)). The origin of height modulation is discussed as the electrostatic interaction between atop and bridge CO due to the opposite direction of dipole.

[1] T. Anazawa, I. Kinoshita, and Y. Matsumoto, J. Electron Spectrosc. Rel. Phenom. 88-91, 585 (1998).

[2] H. Steininger, S. Lehwald, and H. Ibach, Surf. Sci. 123, 264 (1982).

[3] E. Schweizer, B.N.J. Persson, M. Tüshaus, D. Hoge, and A.M. Bradshaw, Surf. Sci. 213, 49 (1989).

(a) STM images with increasing the coverage of CO on Pt(111).

(b) Topographic height of atop CO according to the number of neighboring bridge CO in bridge-vacant c(4×2) domain.

SS-7-Or-3
Interaction of Rh with Rh nanoparticles encapsulated by ordered ultrathin TiOx film on TiO2(110) surface

T13 Surface Science

#SS-7-Or-3

A. Berkó [1], R. Gubó [2], L. Óvári [1], Z. Kónya [1].

[1]MTA-SZTE Reaction Kinetics and Surrface Chemistry Research Group, Hungarian Academy of Sciences - Szeged (Hungary), [2]Department of Applied and Enviromental Chemistry, University of Szeged - Szeged (Hungary).

Deposition and thermal stability of Rh were studied on TiO_2(110) surface covered partially by TiO_x-encapsulated ribbon-like Rh nanoparticles by scanning tunneling microscopy and spectroscopy (STM-STS). These giant Rh particles of approximately 30 x 150 nm^2 lateral size, 20 layer thick and flat top facet of (111) were grown on a clean TiO_2(110) surface by physical vapour deposition (PVD) of Rh (appr. 7 ML - equivalent monolayer) at room temperature (RT) and annealing at 1050 K for a few minutes. The region of the TiO_2(110) surface occupied by Rh was approximately 35 % of the total area and the Rh(111) top facets of the nanoparticles were completely covered by ultrathin (UT) and well ordered hexagonal “wagon-wheel” TiO_x encapsulation film (hUT-TiO_x)[1, 2] (Figure 1). This configuration made it possible to follow paralelly the particle formation both on the encapsulation layer and the atomic terraces of clean TiO_2(110). On the effect of deposition of Rh onto this surface at RT, the oxide encapsulation film becomes strongly disturbed without any sign of ordering at the lowest coverage regime (0.01-0.03 ML) studied. It was found that even at larger coverages (up to 1 ML), one monolayer thick 2D adparticles are formed on the encapsulation film at RT. Their lateral size increases gradually from 1 nm up to 15-20 nm in the temperature range of 500-1000 K, attributable to thermically activated Ostwald-ripening. Below 700 K, the top facet of these 2D particles exhibits unordered chemical contrast suggesting mixed composition, while above this temperature the constant height STM images indicate the development of well ordered hexagonal “wagon-wheel” structure even on the top of the newly formed nanoparticles. The formation of hUT-TiO_x film on the top of the adparticles becomes to be completed at appr. 800 K, where a $Rh_{particle}$-Rh_{ad}-Ti-O layer-sequence can be assumed. These results are in good harmony with those obtained by low energy ion scattering measurements indicating a partial outmost position of Rh up to 700-800 K. The

electronic charaterization of the adparticles by STS was also performed in the different stages of the annealing treatment and will be evaluated in the light of the structural model suggested.

(1) Z. Majzik, N. Balázs, A. Berkó, J. Phys. Chem. C 115 (2012) 9535.
(2) A. Berkó, N. Balázs, G. Kassab, L. Óvári, J. Catal. 289 (2012) 179.

Figure 1: Constant current STM image (400 x 400 nm^2) recorded on Rh/TiO_2(110) surface used as an initial state for the Rh post-deposition. Insert: constant height image (10 x 10 nm^2) showing the structure of the top facets of the encapsulated Rh.

SS-7-Or-10
A full reaction scheme of photocatalytic methanol oxidation to CO on a rutile TiO2(110) surface with solid spectroscopic evidence

T13 Surface Science

#SS-7-Or-10

W. Huang, Q. Yuan.

University of Science and Technology of China, Department of Chemical Physics - Hefei (China).

Photochemistry of methanol acts as a prototype system for the fundamental understanding of complex photocatalytic reactions, but its fundamental understanding is still limited to the photocatalytic oxidation of methanol to formaldehyde on rutile TiO2(110) surface. Here we report the full reaction scheme of photocatalytic methanol oxidation on rutile TiO2(110) to CO acquired by TDS and XPS. Irradiated by UV light, methanol can sequently converted to methoxyl group, formaldehyde and formate; Formate can undego three different reaction pathways: photocatalytic ccross coupling with methocyl to form methyl formate, photooxidation to CO, thermally catalytic self-coupling to form ethylene. The role of oxygen vacancy on rutile TiO2(110), and the difference behaviors of thermally catalytic and photocatalytic oxidation of formaldehyde on rutile TiO2(110) surface will also be discussed.

SS-12-Or-6
The effect of an altered charge state of Pt on methanol decomposition and CO dissociation: studies of Pt nanoclusters supported on a thin film of Al2O3/NiAl(100)

T13 Surface Science

#SS-12-Or-6

M. Luo, C.S. Chao, Y.D. Li, T.C. Hung.

National Central University - Jhongli (Taiwan, republic of china).

Methanol decomposition on oxidized Pt nanoclusters on an ordered Al2O3/NiAl(100) thin film was studied with a variety of surface probe techniques, including STM, IRAS, TPD, RHEED and synchrotron-based PES. The Pt clusters, with a mean diameter 2.3 nm and height 0.4 nm, were grown by vapor deposition onto the thin film Al2O3/NiAl(100) at 300 or 430 K, and oxidized to a state of Pt2+ by annealing the sample to 650 K. The annealed clusters remained structurally ordered but became partially encapsulated by inert alumina; the bare surface Pt remained (30 % of the original) were mostly low-coordinated but reactive. Methanol adsorbed on these oxidized Pt decomposed predominantly through dehydrogenation to CO and secondarily through C-O bond scission, as observed on pristine Pt clusters, whereas the reaction channels were selectively hindered by the altered electronic state of Pt. The produced CO and hydrogen from dehydrogenated methanol per surface Pt on the oxidized clusters amounted to only 50 % of those on pristine Pt clusters; in contrast, the oxidation of Pt has little effect on the C-O bond scission: both temperature of the bond-scission and quantity of the produced methane per surface Pt are similar on the oxidized and pristine clusters. The CO dissociation to elemental carbon was significantly enhanced on the oxidized Pt; the dissociation began at a much lower temperature (200 – 300 K) than that on pristine clusters and thus most molecularly adsorbed CO dissociated, instead of desorbing, with increased temperature.

SS-5-Or-1
From Zero to Two Dimensions: Supra-molecular Nanostructures Formed from PTCDI and Ni on the Au(111) Surface

T13 Surface Science

#SS-5-Or-1

M. Yu [1], W. Xu [2], N. Kalashnyk [2], Y. Benjalal [3], S. Nagarajan [3], F. Masini [4], E. Laegsgaard [4], M. Hliwa [3], X. Bouju [3], A. Gourdon [3], C. Joachim [3], F. Besenbacher [4], T.R. Linderoth [4].

[1]Harbin Institute of Technology - Harbin (China), [2]Aarhus University - Aarhu (Denmark), [3]CEMES-CNRS - Toulouse (France), [4]Aarhus University - Aarhus (Denmark).

Controlled self-assembly of complex supra-molecular surface architectures has considerable potential for application in many fields within the quickly-emerging area of nanoscience and technology, including heterogeneous catalysis, gas storage, chemical sensing, surface-templating, molecular recognition, opto-electronics, guest-host chemistry, and so on. [1-4]
In this study, we investigate metal-organic self-assembly of perylene-3,4,9,10-tetra-carboxylic-diimide (PTCDI) and Ni on the Au(111) surface using high-resolution STM under UHV conditions. The molecule PTCDI and its derivatives are technologically relevant owing to interesting opto-electronic properties,[5,6] and their adsorption properties have been investigated on a wide range of substrates as fundamental model systems understanding the interaction of large aromatic molecules with inorganic surfaces. [eg. 7-8]
We demonstrate that it is possible by delicately tuning the co-adsorption conditions to synthesize three distinct self-assembled Ni-PTCDI nanostructures from zero-dimensional (0-D) nano-dots over one-dimensional (1-D) chains to a two-dimensional (2-D) porous network. In general, the ability to generate a diverse range of nanostructures of different dimensionality from the same elementary building blocks is important since it may help to simplify synthesis of nanostructures for practical applications.
To achieve a full picture of the interactions driving the formation of the observed Ni-PTCDI structures, we have performed molecular mechanics and quantum chemical calculations, as well as STM image calculations. A unifying motif for the 1-D Ni-

PTCDI chains and the 2-D Ni-PTCDI network is found to be double N-H...O hydrogen bonds between PTCDI molecules arranged in staggered rows, similar to the situation found in surface structures formed from pure PTCDI. Most interestingly, we find that while Ni co-deposition with PTCDI is essential to form the observed structures, the role of the Ni ad-atoms is not to participate in metal-organic coordination bonding as cationic centers. Rather, the Ni ad-atoms acquire a negative partial charge through interaction with the substrate and the Ni-PTCDI interaction is entirely electrostatic.

[1] Joachim, C.; Gimzewski, J. K.; Aviram, A. Nature 2000, 408, 541-548.
[2] Davis, M. E. Nature 2002, 417, 813-821.
[3] Schoonveld, W. A.; Wildeman, J.; Fichou, D.; Bobbert, P. A.; van Wees, B. J.; Klapwijk, T. M. Nature 2000, 404, 977-980.
[4] Seo, J. S.; Whang, D.; Lee, H.; Jun, S. I.; Oh, J.; Jeon, Y. J.; Kim, K. Nature 2000, 404, 982-986.
[5] Balakrishnan, K.; Datar, A.; Oitker, R.; Chen, H.; Zuo, J. M.; Zang, L. J. Am. Chem. Soc. 2005, 127, 10496-10497.
[6] Friend, R. H.; Gymer, R. W.; Holmes, A. B.; Burroughes, J. H.; Marks, R. N.; Taliani, C.; Bradley, D. D. C.; Dos Santos, D. A.; Bredas, J. L.; Logdlund, M.; Salaneck, W. R. Nature 1999, 397, 121-128.
[7] Ludwig, C.; Gompf, B.; Petersen, J.; Strohmaier, R.; Eisenmenger, W. Z. Phys. B-Condens. Mat. 1994, 93, 365-373.
[8] O'Shea, J. N.; Saywell, A.; Magnano, G.; Perdigao, L. M. A.; Satterley, C. J.; Beton, P. H.; Dhanak, V. R. Surf. Sci. 2009, 603, 3094-3098.

SS-12-Or-7
Microkinetic Analysis of Ammonia Oxidation on the RuO2(110) Surface

T13 Surface Science

#SS-12-Or-7

J. Jiang, C.C. Wang, J.Y. Wu.

National Taiwan University of Science and Technology - Taipei.

We simulated the ammonia oxidation on the RuO_2(110) by microkinetic analysis, where all the thermodynamic and kinetic parameters were obtained from density functional theory (DFT) calculations. There are 25 elementary steps, including adsorption, surface reaction and desorption processes, adopted in microkinetic models. The rate constants of adsorption and desorption processes were estimated by collision theory, and those in surface reactions were calculated by transition state theory (TST). Recently, the ammonia oxidation on ruthenium dioxide surfaces has been studied by different experimental methods: batch type reaction,[1] and steady-state ammonia oxidation.[1,2] In this microkinetic simulation, we established two models, batch type and continuous type reactions, to investigate the differences between the two experimental methods. In the simulation of batch type ammonia oxidation, the NH_3 and O_2 molecules were pre-adsorbed on the RuO_2(110) surface at 90 K, and then heating up the system under high vacuum environment. In the model of continuous type reaction, the temperature (from 480 K to 670K) and partial pressure of NH_3 and O_2 were set to be constant during the oxidation, and the selectivity of each product were recorded at the steady-state. These two microkinetic models are based on the same elementary reaction steps, but they showed a significant difference in selectivity to oxidation products, which consists with experimental observations. In ammonia oxidation experiments by Wang et al.,[1] there was no N_2O produced during the oxidation; however, in steady-state oxidation by Pérez-Ramírez et al.,[2] N_2O could be one of major oxidation products. According to our simulations, we suggest that N_2O should be produced during the ammonia oxidation, and the partial pressure, O_2/NH_3 ratio and temperature will vary its selectivity from 0% to 30%. By analyzing the microkinetic models, we clarified the mechanical differences between the two methods, and showed how experimental conditions influence the oxidation selectivity.

(1) Wang, Y.; Jacobi, K.; Schöne, W. D.; Ertl, G. *J. Phys. Chem. B* **2005**, *109*, 7883–7893.
(2) Pérez-Ramírez, J.; Lopez, N.; Kondratenko, E. V. *J. Phys. Chem. C* **2010**, *114*, 16660–16668.

SS-12-Or-8
Computer simulation of thermodynamic equilibrium in adsorption monolayer of 1,4-cyclohexadiene on Si(001)-2x1 surface

T13 Surface Science

#SS-12-Or-8

V. Gorbunov, V. Fefelov, A. Myshlyavtsev, M. Myshlyavtseva.

Omsk state technical university - Omsk (Russian federation).

Over the last two decades complex organic molecules such as cyclic unsaturated hydrocarbons have been used for the fabrication of ordered organic adsorption monolayer on Si(001) surface [1]. The organic-semiconductor interface has attracted much attention because it provides the possibility of combining the wide range of functionality of organic molecules with the modern silicon based infrastructure. It is known that such systems have a number of potential applications mostly for various functional coatings, chemical and biological sensors.
Most research efforts in this area are intended to: 1) learn to control an adsorption state of the molecule and the monolayer structure; 2) creation of a stable adsorption monolayer. Theoretical research in this area often limited to quantum chemical calculations and there are no works devoted to the study of phase behavior of the adsorption monolayer as a whole.
In this work we have investigated the formation of equilibrium ordered structures of adsorption monolayer of 1,4-cyclohexadiene on Si(001)-2x1 surface with Monte Carlo method and transfer-matrix technique in the framework of lattice gas model. In the constructed model [2] we took into account the possibility of three adsorption states: π-complex, di-σ complex and double di-σ complex bonded with 1,2 and 4 adsorption sites, respectively.
We have calculated the phase diagram of the adsorption monolayer which reproduces qualitatively the most general features of formation and the phase behavior of real adsorption monolayer of 1,4-cyclohexadiene on Si(001) surface. It is shown that only two ordered structures appear in the adlayer in its pure form: the structure consisted of only π-complexes and the ordered structure consisted of only double di-σ complexes. Additionally, there is nonmonotonous changing of coverage

when increasing of chemical potential (gas phase pressure) in this adsorption system [3].

[1] Kato H.S., Wakatsuchi M., Kawai M., Yoshinobu J., J. Phys. Chem. C 111 (2007) 2557.
[2] Gorbunov V.A., Fefelov V.F, Myshlyavtsev A.V., Myshlyavtseva M.D., Rus. J. Phys. Chem. A 85 (2011) 94.
[3] Fefelov V.F, Gorbunov V.A., Myshlyavtsev A.V., Myshlyavtseva M.D., Chem. Eng. J. 154 (2009) 107.

SS-1-Or-3
Tuning a nanostructure: self-organised growth of oxygen on Cu(110) modified by sulphur co-adsorption

T13 Surface Science

#SS-1-Or-3

F. Wiame, C. Poulain, Z. Budinska, V. Maurice, P. Marcus.

CNRS/Chimie ParisTech - Paris (France).

Self-organised nanostructures grown on surfaces have been the object of much interest in recent years due to their potential applications in the nanotechnology industry as possible alternative to standard lithography techniques. Kern *et al.* [1] demonstrated that a submonolayer coverage of oxygen deposited on Cu(110) may form periodic stripes aligned along the [001] direction and that the periodicity of the system essentially depends on the coverage. However, although this method appears very promising for the growth of nanostructured materials, the applications are limited due to the relatively small domains of periodicity and size as defined by the Marchenko-Vanderbilt model [2] generally admitted for this system. For oxygen coverages θ_O in the range $0.1 < \theta_O < 0.4$ (the fully-covered (2×1) surface corresponding to $\theta_O = 0.5$), the periodicity only varies from 6.5 nm to 11 nm and the oxide band width from 2 nm to 9 nm. We will show that these ranges can be significantly increased by the adsorption of very small amounts of sulphur at the surface. Although surfaces significantly diverging from the Marchenko-Vanderbilt model have been evidenced in the past [3], no systematic method have been reported yet.

The new preparation method presented here, which consists in the partial coverage of the surface by sulphur before annealing of the oxidised surface, enables us to significantly enlarge the domain of accessible periodic structures. Periodicity up to 100 nm and oxide band width up to 30 nm can be reached in a straightforward, reproducible and controlled way. The band width and periodicity dispersions are not modified by the sulphur adsorption. Moreover, while the structure of the O/Cu(110)-(2×1) is fully determined by the surface coverage, our method allows us to define the periodicity independently of the oxygen coverage by adjusting the sulphur amount at the surface. The classical Marchenko-Vanderbilt model, used to explain the common case, has been modified in order to take into account the presence of sulphur at the

surface. It appears that the elastic constant of the system is varying continuously with the amount of sulphur. We attribute this variation to a change in the formation energy of the boundary between the two phases.

This new system may be used for fundamental studies in order to gain information on the elastic and electrostatic properties that are underlying the self-organisation phenomena. Moreover, it represents also an ideal playground to test the change in the reactivity of a surface as a function of its structure as it enables a systematic study of the influence of the periodicity and coverage on the surface reactivity [4].

[1] K. Kern, H. Niehus, A. Schatz, P. Zeppenfeld, J. Goerge, G. Comsa, *Phys. Rev. Lett.* 67, 855 (1991).
[2] V. I. Marchenko, JETP Lett 55, 73 (1992) ; D. Vanderbilt, *Surf. Sci.* 268, L300 (1992).
[3] K Bobrov, L. Guillemot, *Surf. Sci.* 604, 1894 (2010).
[4] C. Poulain, F. Wiame, V. Maurice, P. Marcus, *to be published.*

SS-P3-03
New Topologies in Iron Coordination Networks with Cyano-Containing Organic Linkers

T13 Surface Science

#SS-P3-03

J. Gallego [1], J. Rodríguez-Fernández [2], R. García [3], M.Á. Herranz [3], N. Martín [4], R. Otero [5], R. Miranda [5].

[1]IMDEA Nanociencia - ICMM-CSIC - Madrid (Spain), [2]Universidad Autónoma de Madrid - Madrid (Spain), [3]Universidad Complutense de Madrid - Madrid (Spain), [4]Universidad Complutense de Madrid - IMDEA Nanociencia - Madrid (Spain), [5]Universidad Autónoma de Madrid - IMDEA Nanociencia - Madrid (Spain).

Surface coordination chemistry has been studied intensively over the last few years [1], because traditional bulk coordination compounds have very interesting magnetic, electronic, optical or catalytic properties [2]. Different chemical groups have been used for the formation of the coordination bonding. The most commonly used group is the carboxylic one, which can make coordination bonds with metal ions after deprotonating, changing into a carboxylate group. A few reports have also used nitrogenated moieties (cyano, pyridyl) for the linking to the metal atoms. In particuar, Mn-TCNQ and Ni-TCNQ have been reported [3]. However, in spite of all these previous works, many questions remain open about the nature of such coordination bond when a metal surface is involved.

We have carried out a combined experimental (STM - Scanning Tunneling Microscopy, XPS - X-Ray Photoelectron Spectroscopy) and theoretical (DFT) work to characterize the electronic and structural configuration of an Fe-DCNQI coordination network on a Ag(111) surface. DCNQI (Dicyano-p-quinodiimine) is a strong electron acceptor with two cyano groups that link to the Fe atoms to form two types of coordination networks: the first one (Figure 1b) is formed by an array of 1D parallel chains, while the second one is a surprising new kind of apparently random 2D network, none of which has a counterpart in bulk metal-DCNQI coordination compounds. In addition, both XPS and DFT seem to indicate that the "oxidation state" of the Fe atoms in this system is close to +2 (Figure 2).

[1] Johannes V. Barth, Annu. Rev. Phys. Chem. 58, 375-407 (2007).

[2] See, for example the special issue (No. 5) of Chemical Society Reviews, 2009 (page 1201 to 1508).

[3] T.-C. Tseng et al, J. Phys. Chem. C 115, 10211 (2011).

Figure 1. (65 Å x 80 Å) a) STM images of the Ag(111) surface after depositing an almost complete monolayer of DCNQI; b) STM image taken after depositing Fe on the DCNQI layer and annealing to 400 K.

Figure 2. Fe2p XPS spectra taken a) before and b) after annealing a layer of DCNQI + Fe on Ag(111).

SS-3-Or-10
Thermal behaviors of a metal layer sandwiched by silicon oxide

T13 Surface Science

#SS-3-Or-10

H. Kato, Y. Oizumi, D. Nishimi, K. Yamada, Y. Homma.

Department of Physics, Tokyo University of Science - Tokyo (Japan).

Carbon nanotubes (CNTs) known as a material with incredible electrical, optical, and mechanical properties are synthesized by chemical vapor deposition (CVD) using catalytic nanoparticles on a substrate. Up to now, many efforts have been made to improve CVD process and realize several types of CNT growth. Previously, our group showed thermal embedment of metal nanoparticles into amorphous oxide substrates during the CVD process [1]. Metal particle formation in the subsurface of oxide is considered to play an important role for vertically aligned CNT growth mode [2]. However, the subsurface substrate diffusion mechanism is still not clear due to lack of microscopic knowledge about material transport.

In this study, we observed the thermal behavior of a metal layer sandwiched by silicon oxide (SiO_2) using transmission electron microscopy (TEM). SiO_2/metal (Co or Fe)/SiO_2/Si(100) layers prepared by DC magnetron sputtering were annealed at 670-870°C in Ar/H_2 (100: 3 in volume) atmosphere for 5 min. Figure 1 shows a TEM image of a Co sandwiched layer after annealed at 870°C. The Co layer turns to nanoparticles of uniform size and they line up in original position perfectly. On the other hand, an Fe layer is changed to segregated nanoparticles at both interfaces of SiO_2 after annealing (Fig. 2). The results show that iron atoms tend to diffuse into SiO_2, and they move in the potential which has local minima at the surface and interface of SiO_2.

[1] G.-H. Jeong *et al*., Chem. Phys. Lett. **422**, 83 (2006).
[2] S.-M. Kim *et al*., J. Phys. Chem. Lett. **1**, 918 (2010).

Fig. 1. Cross sectional TEM image of SiO_2/Co/SiO_2/Si(100) annealed at 870°C in Ar/H_2.

Fig. 2. Cross sectional TEM image of SiO_2/Fe/SiO_2/Si(100) annealed at 870°C in Ar/H_2.

SS-9-Or-5
Helim Diffraction Study of Long Chain Thiols and Asymmetric Disulfide SelfAssembled Monolayers on Au(111) Prepared by Supersonic Molecular Beam Deposition

T13 Surface Science

#SS-9-Or-5

M. Danisman [1], G. Bracco [2], E. Albayarak [3], K. Semistan [4].

[1]Middle East Technical University - Ankara (Turkey), [2]University of Cenoa (Italy), [3]Sakarya University (Turkey), [4]Kahramanmaraş Sütçü İmam Üniversitesi (Turkey).

Thiol and asymmetric disulfide self assembled monolayers (SAMs) on gold surfaces have a wide range of applications including surface patterning and metal contact-organic semiconductor interface modification in organic electronic devices. Here we will present our studies about the low coverage phases of long chain alkanethiol SAMs($CH_3(CH_2)_{17}SH$, $CH_3(CH_2)_9SH$ and $HO(CH_2)_{11}SH$) and asymmetric disulfide SAMs ($CH_3(CH_2)_{17}S\text{-}S(CH_2)_{11}OH$ and $CH_3(CH_2)_9S\text{-}S(CH_2)_{11}OH$) on Au(111) surface, grown in vacuum by supersonic molecular beam deposition. Crystal structures, phase behaviors and desorption energies of these films determined by helium atom diffraction technique will be discussed.

E. Albayrak, S. Duman, G. Bracco, M.F. Danışman, "Helium atom diffraction study of low coverage phases of decanethiol self-assembled monolayers prepared by supersonic molecular beam deposition", Applied Surface Science, 2013, DOI:10.1016/j.apsusc.2012.11.174

NST/SS-P1-16
Growth and oxidation of graphene on Rh(111)

T13 Surface Science

#NST/SS-P1-16

K. Gotterbarm, C. Papp, W. Zhao, O. Höfert, H.P. Steinrück.

Friedrich-Alexander Universität - Erlangen (Germany).

Graphene is a 2D material that shows a variety of interesting electronic properties. One important method for the fabrication of graphene is chemical vapor deposition (CVD) of hydrocarbon precursors on transition metal surfaces[1,2].
In our study graphene was grown on a Rh(111) single crystal surface by chemical vapor deposition of propylene at elevated temperatures. The growth process was observed by fast XPS performed at the synchrotron facility BESSY II. The quality of the produced graphene sheets was checked by LEED. Different preparation parameters such as propylene pressure and preparation temperature were varied in order to investigate the influence of these parameters on corrugation and regularity of the produced graphene sheet. The lattice mismatch of graphene on the Rh(111) surface induces corrugation of the graphene sheet leading to two separated signals in the C 1s region.[3] The binding energy separation of the two species becomes more distinct at lower temperatures and varies depending on the preparation parameters mentioned above.

The oxidation of graphene was investigated depending on oxygen pressure, temperature and graphene layer quality. We found sigmoidal reaction kinetics indicating the following reaction mechanism: The oxidation starts at defect sites, inducing a slow induction period. With more free adsorption sites the reaction rate increases until most of the graphene is oxidised. The remaining carbon decays exponentially according to pseudo first order kinetics. The strong influence of the graphene layer quality on the reaction rate supports the assumption that oxidation starts at the defect sites.

[1] J. Wintterlin, M.-L. Bocquet *Surface Science* **603**, 1841 (2009).
[2] W. Zhao, S. M. Kozlov, O. Höfert, K. Gotterbarm, M. P. A. Lorenz, F. Viñes, C. Papp, A. Görling, H.-P. Steinrück *Journal of Physical Chemistry Letters* **2**, 759

(2011).
[3] A. B. Preobrajenski, M. L. Ng, A. S. Vinogradov, N. Mårtensson *Physical Review B* **78**, 073401 (2008).

SS-P3-10
Autocatalytic effect of Cu nano-islands on the reaction of water with the oxygen covered Cu(110) surface.

T13 Surface Science

#SS-P3-10

K. Bobrov, L. Guillemot.

CNRS - Orsay (France).

We present a detailed STM study on the reactivity to water of the oxygen covered Cu(110) surface at 200K. This reactive interaction is known to produce hydroxyls. We found that the hydroxyl chemical state is a key factor regulating further chemical reactions and causing a strong re-structuring of the surface. Parts of the hydroxyls are originally produced on the surface in the form of highly mobile copper-hydroxyl [Cu-OH] complexes. We demonstrate that interaction of the [Cu-OH] complexes with the substrate governs the surface restructuring. The hydroxyl complexes can dissociate either on step sites of the surface, incorporating Cu to the substrate and releasing hydroxyls (OHs) either, remarkably, condensate on the terraces shaping two-dimensional monoatomic height Cu islands possessing under-coordinated sites at their borders. We show that nucleation and growth of these nanometer scaled islands significantly enhance the surface reactivity towards water. Indeed, the Cu islands providing under-coordinated sites enhance water adsorption and furthermore produce a local effect favoring diffusion of the water molecules towards the more reactive sites.

SS-12-Or-9
First oxidation stages of Al-Cu and Al-Co complex metallic alloys

T13 Surface Science

#SS-12-Or-9

S. Le Moal [1], M. Warde [1], J. Ledieu [2], L. Serkovic [2], M. Hérinx [1], M.C. De Weerd [2], V. Fournée [2], M.G. Barthés-Labrousse [1].

[1]Institut de Chimie Moléculaire et des Matériaux d'Orsay - Orsay (France), [2]Institut Jean Lamour - Nancy (France).

Complex metallic alloys (CMAs) are intermetallic compounds whose crystallographic structure differs from that of usual alloys. In particular, their unit cell contains from several tens to a few thousands atoms, which are typically arranged into highly symmetric clusters. They are usually considered as stable approximants of quasicrystals [1]. Al-based CMAs offer great opportunities in the field of catalysis, including flexible chemistry thanks to the huge variety of CMA compositions and tuning of d band centre by selection of CMA composition and structure.
In this work, X-ray Photoelectron Spectroscopy (XPS), Low Energy Electron Diffraction (LEED) and Scanning Tunnelling Microscopy (STM) have been used to investigate under ultrahigh vacuum the first oxidation stages of the γ-Al_4Cu_9(110), Al_9Co_2(001) and o-$Al_{13}Co_4$(100) surfaces.
Whatever the oxidation temperature (from 100 to 923 K) and oxygen partial pressure (from 10^{-8} to 10^{-7} mbar) only aluminium is oxidized, while copper and cobalt remain in the metallic state. We found that the oxidation mechanism of γ-Al_4Cu_9(110) is driven by aluminium segregation at the surface, whereas the oxidation mechanism of Al_9Co_2(001) and o-$Al_{13}Co_4$(100) is related to the amount of oxygen adsorbed on the surface.
For the three CMA surfaces, RT oxidation at saturation in oxygen yields a uniform disordered aluminium oxide film. For γ-Al_4Cu_9(110) surface, subsequent annealing of this disordered oxide layer at 923 K leads to the formation of crystalline aluminium oxide islands which exhibit a peculiar rectangular structure called sixton. This sixton structure is similar to that previously reported for ultrathin alumina films grown on various metallic substrates, as for instance NiAl(110) and Ni(111) [2]. Its unit cell comprises 92 atoms arranged in an interfacial $Al_{24}O_{28}$ plane and a surface $Al_{16}O_{24}$ plane [3-4]. For both Al-Co surfaces, the aluminium oxide film grown at RT dissolved upon subsequent annealing before any ordering occurred, owing to oxygen diffusion

into the bulk.
We found that the sixton structure can occur on Al_9Co_2(001) after oxidation at higher temperature (773 K); however the oxide film is poorly ordered. For the o-$Al_{13}Co_4$(100) surface, no oxidation conditions could be found to form a well-ordered oxide film. The formation of the sixton oxide structure depends on the ability of aluminium to segregate at the surface, which is related to the nature of the intermetallic bonds inside the crystal and, in particular, their covalence degree. Given their strong covalent character, Al_9Co_2(001) and o-$Al_{13}Co_4$(100) exhibit a lower aluminium mobility than γ-Al_4Cu_9(110), which hampers the formation of the sixton structure.

[1] “Complex Metallic Alloys”, edited by J-M. Dubois and E. Belin-Ferré, Wiley-VCH, Weinheim, 2011.
[2] G. Prévot, A. Naitabdi, R. Bernard, Y. Borensztein, Phys. Rev. B 81 (2010) 085405.
[3] A. Stierle, F. Renner, R. Streitel, H. Dosch, W. Drube, B.C. Cowie, Science 303 (2004) 1652.
[4] G. Kresse, M. Schmid, E. Napetschnig, M. Shishkin, L. Kohler, P. Varga, Science 308 (2005) 1440.

SS-7-Or-7
STM and photoemission study of vacancies and hydroxyls at the SrTiO3(110)-(4×1) surface

T13 Surface Science

#SS-7-Or-7

Z. Wang, X. Hao, S. Gerhold, M. Schmid, U. Diebold.

Vienna University of Technology - Vienna (Austria).

The surfaces and interfaces of $SrTiO_3$ have attracted intense interest in diverse fields ranging from solid-state physics to surface chemistry and oxide electronics. In all these applications the structural and electronic surface properties are vital of importance, yet perovskite surfaces are notoriously complex and hard to control.
We report an STM and synchrotron radiation photoemission spectroscopy study of $SrTiO_3$(110) surface. This polar surface tends to form a homologues series of (n×1) (n = 4~6) reconstructions, which can be reversibly tuned by changing surface chemical composition through depositing Sr or Ti metals followed by annealing.[1] The (n×1) reconstructions are well explained by models consisting of tetrahedrally coordinated TiO_4 layers. [2] The commonly observed (4×1) reconstruction is arranged in distorted six- and ten-membered rings. Such an arrangement breaks the mirror symmetry of surface along the [1-10] direction, and two degenerate anti-parallel (4×1) domains are formed. Vacancy clusters of $(Ti_2O_3)^{2-}$ and $(Ti_4O_5)^{6-}$ type are present at domain boundaries. The relative ratio of these domain boundaries can be tuned judiciously by adjusting the oxygen pressure during annealing.
Oxygen vacancies (V_O) can be created by exposure to synchrotron radiation, and are accompanied by the evolution of an in-gap state at a binding energy of 1.3 eV. A similar in-gap state is also observed after exposing the surface to atomic hydrogen. Core-level and valence band photoemission spectroscopy studies of water adsorption on the surface indicate that water doesn't dissociate on the clean surface, while it can dissociate on the surface with V_O. V_O and hydroxyl species (OH) on the surface are identified by STM. OH pairs form on the surface after dosing water at room temperature, indicating water dissociation at the V_O on the surface (see Fig. 1). While water doesn't adsorb and dissociate on the surface upon further dosing water.

Density functional theory calculations are performed on the surfaces with V_O, OH and water. The energy barrier for water dissociation on clean surface and V_O is 0.9 and 1.5 eV, respectively, supporting that V_O boosts water dissociation on the surface.
This work was supported by the Austrian Science Fund (FWF project F45).

[1] Z. Wang et al., Phys. Rev. B 83, 155453 (2011).
[2] J. A. Enterkin et al., Nat. Mater. 9, 245 (2010).

Figure 1 STM images (9×9 nm^2, 2V 0.1nA) of the (a) clean $SrTiO_3$(110)-(4×1) surface and of surfaces with (b) V_O, (c) OH and (d) (18×18 nm2, 2V 0.1nA) the surface exposure to water at RT, respectively. Arrows point to Sr adatoms (red), V_O (blue), OH (white) and OH pairs (white) are indicated with arrows in (a)-(d), respectively.

SS-12-Or-10
Surface Chemistry of Water-Covered Si (001)-2×1: Silicon Radical vs. Silanol Reactivity

T13 Surface Science

#SS-12-Or-10

D. Pierucci [1], H. Tissot [1], A. Naitabdi [2], F. Bournel [2], J.J. Gallet [2], F. Rochet [2], M. Silly [3], F. Sirotti [3], S. Kubsky [3], U. Köhler [4].

[1]LCPMR-UPMC/Synchrotron Soleil - Paris (France), [2]LCPMR-UPMC - Paris (France), [3]Synchroteon Soleil - L'orme Des Merisiers, Saint-Aubain (France), [4]Ruhr-Universität Bochum - Bochum (Germany).

Water reacts dissociatively on the Si (001)-2x1 surface, preserving the dimerization. Monohydrides and silanols are present on the surface, together with a low (10^{-2} ML) surface concentration of isolated dangling bonds (IDBs). Recent STM experiments we have carried out emphasize the impact of Si doping on the areal density and on the charge state of the surface dangling bond (negative on n^+ substrate [1] and neutral on lightly p doped substrate). The charge state of IDBs as a function of the doping found here is similar to that of H-Si (001) terminated surface [2].Therefore by analogy with the case of the H terminated surface, radical chain reactions (via H jumps) between isolated dangling bonds and pi-bonded molecules are expected [3]. However radical reactions via OH jumps, together with direct reactions with silanols and monohydrides must be also envisaged. We present here a study on the chemical reactivity on the water-covered Si (001) surface exposed to alkenes, carboxylic acids and aldehydes, using synchrotron x-ray photoemission. While, alkenes likely react via a radical mechanism (H jump) [4], carboxylic acid grafting consumes surface OH and an ester is formed. The reaction of aldehydes is discussed in terms of the formation of ethers or (hemi-)acetals. Compared with classic organic reactions (esterification, acetal formation) which are slow/reversible, the grafting of aldehydes/carboxylic acids is efficient on the water-covered Si (001)-2x1. This class of high selectivity reactions is an interesting method for the grafting of organic molecules on Si (001), especially for polyfunctional molecules, which generally adopt multiple bonding configurations on the clean Si (001) surface.

[1] Gallet, J.; Bournel, F.; Rochet, F.; Kubsky, S.; Silly, M. G.; Sirotti, F.; Pierucci, D. Journal of Physical Chemistry C 2011,115, 7686–7693.
[2] Liu, F. Y.;Yu, J.; Lyding, J. W. Nanopatterning-From Ultralarge-Scale Integration to Biotechnology, MRS Symposia Procedings 705; Materials Research Society: Pittsurg, 2002: Y6.6.1
[3] Lopinski, G.; Wayner, D.; Wolkow, R. Nature 2000, 406, 48–51.
[4] Bournel, F.; Gallet, J.; Pierucci, D.; Khaliq, A.; Rochet, F.; Pietzsch, A. Journal of Physical Chemistry C 2011,115, 14827–14833.

SS-5-Or-3
Experimental observation of island-type self-assembling of C60F18 polar molecules on Ni(100)

T13 Surface Science

#SS-5-Or-3

V. Stankevich [1], A. Lebedev [1], L. Sukhanov [1], K. Men'shikov [1], N. Svechnikov [1], R. Chumakov [1], M. Brzhezinskaya [2].

[1]NRC Kurchatov Institute - Moscow (Russian federation), [2]Helmholtz-Zentrum Berlin für Materialien und Energie - Berlin (Germany).

Investigation of fluorinated fullerene $C_{60}F_{18}$ sub-monolayer film was carried out by using Near Edge X-ray Absorption Fine Structure (NEXAFS) and X-ray Photoelectron Spectroscopy (XPS) techniques. $C_{60}F_{18}$ molecules having asymmetric type structure and high dipole moment about 10 D (shown by arrow in figure, with F atoms in bottom part of a C_{60}-type cage) were deposited in situ in high vacuum about 10^{-10} mbar by powder evaporation from Knudsen cell at 150ºC on Ni (100) substrate. Angular dependence of NEXAFS spectra obtained for C1s (285 eV) and F1s (690 eV) absorption edges by using synchrotron radiation at RGBL-PGM beamline, BESSY II storage ring, was established. This indicates the presence of an ordered structure of $C_{60}F_{18}$ film on Ni surface. Theoretical calculation by using the Density Functional Theory (DFT) allowed to identify the $1s\rightarrow\pi^*$ and $1s\rightarrow\sigma^*$ spectral peaks, and thus to make conclusion that dipole moment of deposited $C_{60}F_{18}$ molecules is orthogonal to the substrate surface. Moreover, analysis of NEXAFS spectra fine structure shows that molecules are deposited with F atoms touching the substrate. NEXAFS spectra have demonstrated that thermal annealing of $C_{60}F_{18}$ film at 150ºC leads to growth of molecular ordered surface structure. This ordered structure is preserved while heating at least up to 250ºC.
XPS spectra of $C_{60}F_{18}$/Ni(100) system have shown the valence band adsorption state composed from admixture of Ni3d metallic state and F2p band belonging to fluorofullerenes, together with evident Ni2p core levels. This indicates the island-type self-assembling of $C_{60}F_{18}$ film formation on metal substrate. Note that similar island-type structure of $C_{60}F_{18}$ film deposited on graphite HOPG substrate was previously observed by using atomic force microscopy, showing 15-20 nm height islands with mean lateral dimension of 60-80 nm.

Thus, there seems to be outlined a possibility to make island-type nanostructures based on $C_{60}F_{18}$ molecules to obtain nanoscale electric fields.

SS-1-Or-7
Donor-acceptor interactions at solid surfaces controlled by charge transfer

T13 Surface Science

#SS-1-Or-7

K. Lauwaet [1], J. Rodríguez-Fernández [2], R. García Sanz [3], M. Ángeles Herranz [3], N. Martín [3], J.M. Gallego [4], R. Otero [5], R. Miranda [5].

[1]IMDEA-Nanociencia - Madrid (Spain), [2]Departamento de Física de la Materia Condensada, Universidad Autónoma de Madrid - Madrid (Spain), [3]Departamento de Química Orgánica, Universidad Complutense de Madrid - Madrid (Spain), [4]IMDEA-Nanociencia - Instituto de Ciencia de Materiales de Madrid - Madrid (Spain), [5]IMDEA-Nanociencia - Departamento de Física de la Materia Condensada, Universidad Autónoma de Madrid - Madrid (Spain).

Organic charge-transfer (CT) complexes are molecular compounds mixing two species with different electron affinities: an electron donor (D) and an electron acceptor (A). Charge transfer processes between D–A complexes and metallic electrodes are at the heart of novel organic optoelectronic devices such as solar cells [1]. In contrast with the existing exhaustive study of the bulk properties of CT solids, very little is known about the thin-film behaviour. The transition from bulk D-A complexes to ultra-thin films of monolayer thickness deposited on metals introduces a new phenomenology related to the organic–inorganic interface [2]. Effects like hybridization, CT with the surface and molecular level alignment become factors that may govern the electronic transport. Hence, the adsorption of an ultra-thin D–A layer on a metal opens a new field of research for the potential application of CT complexes as devices in the nanoscale.

Simultaneous characterization of the interdependent structural and electronic properties is required for a thorough understanding of the D-A complexes under study [3]. Here, by combining both Scanning Tunnelling Microscopy and X-ray Photoelectron Spectroscopy in situ, we can study the delicate balance that exists between intermolecular and molecule–substrate interactions, as well as the hybridization, and the charge transfer taking place in model D–A assemblies at metal-organic interfaces.

By controlling the stoichiometry between tetrathiafulvalene (TTF, electron-donor) and tetracyanoethylene (TCNE, electron-acceptor), we can tune both the structural and the electronic properties of a donor-acceptor system on Ag(111). We show that this

system exhibits various structural phases two of which are shown in Fig: 1, depending on the stoichiometry. Each phase leads to different levels of charge transfer. Interestingly enough, the charge-transfer does not seem to follow a monotonic behavior with the D:A ratio. These results demonstrate that atomistic studies on the growth of organic thin films under ultrahigh vacuum conditions can lead to the kind of accurate control needed in order to optimize device characteristics.

[1] L. Bartels, Nat. Chem., 2, 87 (2010).
[2] N. Gonzalez-Lakunza *et al.*, Phys. Rev. Lett., 100, 156805 (2008)
[3] D. G. de Oteyza *et al.*, Adv. Funct. Mater., 19, 3567 (2009)

Two 11 nm × 5 nm pseudo 3D STM images of two distinct phases formed by TCNE-TTF on Ag(111). The stripe phase (a) is formed by alternating rows of TTF-molecules (yellow) and TCNE-molecules (pink) (I_t = 0.53 nA; V_t = 423 mV). The snake phase (b) is formed by rows of alternating TTF and TCNE molecules (I_t = 0.43 nA; V_t = -999 mV).

NST/SS-8-Or-11
Termini of bottom-up fabricated graphene nanoribbons

T13 Surface Science

#NST/SS-8-Or-11

L. Talirz [1], H. Söde [1], J. Cai [1], P. Ruffieux [1], S. Blankenburg [1], R. Jafaar [1], R. Berger [2], X. Feng [3], K. Müllen [3], D. Passerone [1], R. Fasel [1], C. Pignedoli [1].

[1]Empa - Dübendorf (Switzerland), [2]University of Mainz - Mainz (Germany), [3]Max Planck Institute of Polymer Research - Mainz (Germany).

One way to introduce a band gap into the electronic structure of graphene is to cut graphene into nanometer-wide ribbons, termed graphene nanoribbons (GNRs). In this top-down approach, however, the lack of control over the edge roughness and edge passivation of the GNRs severely limits the capability to produce GNRs with reliable electronic transport properties. Recently, a bottom-up approach has been developed that enables the fabrication of GNRs with atomically precise edges via thermally induced polymerization and subsequent partial cyclodehydrogenation of suitable precursor molecules on a metal surface[1]. The electronic structure of one specific armchair-type GNR with a width of 7 carbon dimer lines (7-AGNR, Figure 1) has since been studied by scanning tunneling spectroscopy and angle-resolved photoemission spectroscopy and the predicted band gap of 2.3 eV on the metal substrate has been confirmed experimentally[2]. Picking up one terminus of such a GNR with the tip of a scanning tunneling microscope (STM) has further enabled controlled electronic transport measurements on individual GNRs[3].

While the cyclodehydrogenation step of the synthesis has been studied in great detail[4], less is known about the polymerization step, which determines the length of the GNRs. This presentation focusses on the atomic structure found at the termini of 7-AGNRs obtained via the bottom-up approach[1]. The short zigzag edge at the termini of 7-AGNRs gives rise to a localized mid-gap state with a characteristic signature in STM. By combining STM experiments with STM simulations based on large-scale density functional theory calculations (Figure 1), we demonstrate that the termini are passivated by hydrogen[5].

Our findings further suggest that hydrogen may be poisoning the polymerization

reaction. Minimizing premature dehydrogenation during the polymerization step could therefore be a way to grow GNRs with lengths significantly exceeding the 30 nm reported so far. Possible routes will be discussed.

[1] Cai, J. et al. Nature 2010, 466, 470–3.

[2] Ruffieux, P. et al. ACS Nano 2012, 6, 6930–35.

[3] Koch, M. et al. Nat. Nanotechnol. 2012, 7, 713-7.

[4] Blankenburg, S. et al. ACS Nano 2012, 6, 2020–2025.

[5] Talirz, L. et al. Submitted to *JACS* for publication.

Figure 1 STM images of 7-AGNR termini on Au(111). Comparison of STM experiments (U=-0.11 V, I=210 pA) with DFT simulations of possible terminations I-IV (U=-0.3 V).

SS-15-Or-2
Discussion of the density functional theory methods applied for solving complex surface structures based on the example of c(8×2)/(4×2) InAs (001)

T13 Surface Science

#SS-15-Or-2

J. Kolodziej, G. Goryl, D. Toton.

Uniwersytet Jagiellonski - Krakow (Poland).

The surface structure of InAs (001) reconstructed c(8×2)/(4×2) is studied experimentally using scanning probe microscopies (SPM) as well as theoretically by an ab initio density functional theory (DFT) calculations. Based on the experimental results it is found that the structure belongs to a so called ζ-family [1,2] but it fluctuates at room temperature (RT). Because of the fluctuations the surface structure appear regular at RT, while at cryogenic temperatures it freezes to show disorder and a few different local features (Fig. 1a,1b). By DFT calculations many metastable surface structures are identified on the studied surface. Numerical scanning tunneling microscopy (STM) images of these structures are obtained using their DFT density of states and the Tersoff-Hamman approximation (Fig 2). By comparison to the experimental STM images it is found that all features observed on the real surface have their theoretical counterparts. However, certain theoretical structures are not observed in reality even though their energies are the lowest among all the metastable structures found.
Taking into account this as well as the fact that earlier total energy DFT studies [3-5] failed to reach the right solution for the ground state of the structure under study we indicate that the concluding about complex surface structures based on the global DFT energy minimum is rather unsure. On the other hand the mere existence of the DFT energy minima (i.e. local minima) for the structures corresponding to experimentally observed features is usually predicted correctly by the DFT methods.
We acknowledge financial support by Polish NCN under the contract 2011/03/B/ST3/02070.

[1] C. Kumpf et al. Phys. Rev. Lett. 86, 3586 (2001), Phys. Rev. B 64, 075307 (2001).
[2] S.-H. Lee et al. Phys. Rev. Lett. 85, 3890 (2000).
[3] W.G. Schmidt, Appl. Phys. A 75 (2002) 89.
[4] R.H. Miwa, et al. Surf. Sci. 542 (2003) 102.
[5] D.L. Feldwinn, et al., Surf. Sci. 603 (2009) 3321.

Fig. 1: SPM images of the c(8×2)/(4×2) InAs (001) surface; a) at room temperature, b) at 4.2 K.

Fig.2: Examples of the simulated STM images.

SS-12-Or-11
Single molecules in a petri dish: A closer look to dehalogenation on hexagonal boron nitride

T13 Surface Science

#SS-12-Or-11

T. Dienel [1], A.P. Seitsonen [2], M. Iannuzzi [2], R. Widmer [1], J. Hutter [2], O. Gröning [1].

[1]Empa - Dübendorf (Switzerland), [2]University of Zurich - Zurich (Switzerland).

We have studied the adsorption behavior and dehalogenation properties of the hexaiodo-substituted cyclohexa-m-phenylene (CHP) on corrugated hexagonal boron nitride (h-BN) on Rh(111). Well-defined monolayers of h-BN are produced by thermal decomposition of borazine ($(HBNH)_3$) on transition metal surfaces in a self-limiting process. Spatially heterogeneous interaction with the underlying substrate can result in strongly corrugated superstructures, *e.g.* on Rh(111) a regular pattern of depressions with 3.22nm periodicity is formed. Areas of weakly bonded h-BN ("wires") separate strongly bonded “pore” regions that exhibit a diameter of 1.5nm [1]. Single CHP molecules adsorb within those pores and are aligned along the [12] direction of the h-BN lattice (cf. Figure left). The dehalogenation of the CHP is the first step to induce the aryl-aryl coupling leading to the formation of porous graphene [2, 3]. Contrary to the case on metals, where complete thermal dehalogenation can be achieved close to room temperature, the h-BN substrate requires higher temperatures and imposes a distinct abstraction sequence on the molecule. Following the dehalogenation process experimentally by scanning tunneling microscopy and spectroscopy and theoretically by DFT calculations we gain detailed insights to the catalytic properties of h-BN with regard to the site and orientation specific adsorption, the dehalogenation sequence and the CHP radical binding to the h-BN. Thus we can discuss the particular challenges that need to be faced in the *in situ* growth of graphene nanostructures on the insulator h-BN.

[1] M. Corso *et al.*, Science, **303** (2004) 217.
[2] M. Bieri *et al.*, Chem. Commun., **45** (2009) 6919.
[3] M. Bieri *et al.*, JACS , **132** (2010) 16669.

Left: STM overview (-1.85 V, 100 pA) of hexagonal boron nitride on Rh(111) partially covered with CHP molecules. All molecules adsorb in the pores and exhibit the same orientation. Inset: High resolution STM image (-1.2 V, 32 pA). **Right**: STM images (1.5 V, 100 pA) of different stages of the dehalogenation sequence, from the whole molecule (a) to CHP with 3 iodine atoms left (d).

SS-2-Or-4
Structural investigation of the (010) surface of the Al13Fe4 catalyst

T13 Surface Science

#SS-2-Or-4

É. Gaudry [1], J. Ledieu [1], L.N. Serkovic Loli [1], S. Alarcón Villaseca [1], M.C. De Weerd [1], M. Hahne [2], P. Gille [2], Y. Grin [3], J.M. Dubois [1], V. Fournée [1].

[1]Institut Jean Lamour - UMR 7198 CNRS / Université de Lorraine - Nancy (France), [2]Department of Earth and Environmental Sciences, Crystallography Section, Ludwig-Maximilians-Universität - München (Germany), [3]Max-Planck-Institut für Chemische Physik fester Stoffe - Dresden (Germany).

Complex metallic alloys like quasicrystals and approximants are considered as low cost alternative materials for heterogeneous catalysis [1]. The specific reactivity relies on the so-called site isolation concept in which the catalytic performance of a material is determined by small and well separated atomic ensembles containing an active transition metal element at the crystal surface.

The $Al_{13}Fe_4$ intermetallic compound has been identified recently as one such promising candidate for heterogeneous hydrogenation catalysis [2]. In this work, we investigate the structure of the $Al_{13}Fe_4$(010) surface using both experimental methods under ultra-high vacuum (scanning tunneling microscopy, low energy electron diffraction, photoemission) and *ab initio* calculations. The results indicate that the topmost surface layers correspond to incomplete puckered planes present in the bulk crystal structure. The main building block of the corrugated termination consists of two adjacent pentagons of Al atoms, each centered by a protruding Fe atom. These motifs are interconnected via additional Al atoms referred as “glue” atoms which partially desorb above 873 K. The surface structure of lower atomic density compared to the complete bulk puckered plane is explained by a strong Fe-Al-Fe covalent polar interaction that preserves intact at the surface the clusters present in the bulk structure (Fig. 1).

The proposed surface model identifies well separated atomic ensembles in line with the site isolation concept [3]. In conclusion, the surface structure of $Al_{13}Fe_4$(010) is

discussed in relation with that of the structurally close $Al_{13}Co_4$(100) surface [4], both compounds being approximants to the decagonal phase.

Part of this work was carried out within the European Integrated Centre for the Development of New Metallic Alloys and Compounds (European C-MAC, www.eucmac.eu). Part of this work was funded by the "Agence Nationale de la Recherche" (ANR ASURE ANR-08-blan-0041-01 and ANR CAPRICE ANRDFG-2011-INTB-1001-01).

[1] T. Tanabe et al., Catalysis Today, 111 (2006) 153; T. Tanabe et al., Applied Catalysis A: General 384 (2010) 241.
[2] M. Armbrüster et al., Nature Materials, 11 (2012) 690; M. Armbrüster at al., patent EP09157875.7 (2009).
[3] J. Ledieu et al., *Structural investigation of the (010) surface of the $Al_{13}Fe_4$ catalyst*, accepted in Physical Review Letters (2013).
[4] H. Shin et al., Physical Review B, 84 (2011) 085411; R. Addou et al., Physical Review B, 80 (2009) 014203.

Fig.1: Crystal structure of the $Al_{13}Fe_4$ complex metallic alloy.

SS-9-Or-3
Glutamic Acid at Ag surfaces: Self-Assembly in the Non-Zwitterionic Form

T13 Surface Science

#SS-9-Or-3

L. Savio [1], M. Smerieri [2], L. Vattuone [2], M. Rocca [2], I. Tranca [3], D. Costa [4], F. Tielens [3].

[1]IMEM-CNR - Genova (Italy), [2]Università di Genova - Genova (Italy), [3]UPMC Univ Paris 06 - Paris (France), [4]Laboratoire de Physico-Chimie des Surfaces, ENSCP, ParisTech, - Paris (France).

The understanding of the interactions between biomolecules and metal/oxide surfaces is mandatory for all those applications in which this interaction wants to be either exploited (biomaterials, nanoelectronics, hybrid material design) or avoided (fouling, hygiene). The huge experimental effort in this field was however so far insufficient for a complete understanding of the complex bio-molecule/surface interactions at the molecular level. Model experiments and computations are thus mandatory.
Amino acids (AA) are protagonists of fundamental studies, since they are the basic constituents of peptides and proteins and are simple enough to bring information on the chemical interaction of some biological functions with the surface. When deposited from the gas phase, AA self-assemble on metal surfaces most often in the zwitterionic form, while anionic adsorption was sometimes detected.
We report here on the interaction of (S)-Glutamic Acid (Glu) with LMI Ag surfaces at 250 K<T<400 K, investigated by experimental and theoretical methods. Glu molecules self-assemble in different geometries, depending on substrate and deposition temperature, and adsorb always in the non-zwittterionic form [1-4], at variance with what expected for analogy with other AA adsorbed on Ag(111) [5].
On Ag(100) four different structures are identified [2]. For the “squares” and the “flowers” (coexisting at T=350 K – see figure) a carefully combined STM, HREELS, XPS and DFT analysis allowed to unravel the details of the self-assembled layer and the driving mechanisms of the self-assembly process. The “square” geometry consists of neutral Glu molecules, while the “flower” one is made by 50% of neutral units and 50% of anions (forming the tetramers). The Glu-Ag(100) interaction is due to weak van der Waals forces in the former case and to chemisorption when deprotonation occurs. The role of H-bonds, involving mainly carboxyl groups, is

fundamental for both structures. For the “square” geometry the formation of OCOH—OCOH—OCOH—OCOH— cycles at the vertex of the squares is the driving mechanism for self-assembly. This cycle also explains the formation of individual “tetramers”, whereas the whole “flower” structure occurs via a key-slot mechanism between the lateral NH2 moiety and carboxylic groups of the flat molecules.
An empirical model based on statistical analysis of high resolution STM images is proposed for the other layers.

[1] M. Smerieri, L. Vattuone, D. Costa, F. Tielens, L. Savio, Langmuir 26, 7208 (2010).
[2] M. Smerieri, L. Vattuone, T. Kravchuk, D. Costa, L. Savio, Langmuir 27, 2393 (2011).
[3] I. Tranca et al., in preparation.
[4] M. Smerieri et al., in preparation.

[5] J. Reichert et al., ACS Nano 4, 1218 (2010).

SS-P1-10
Cr segregation at the Fe-Cr alloy surface studied by Mössbauer spectroscopy

T13 Surface Science

#SS-P1-10

R. Idczak, R. Konieczny, J. Chojcna.

Institute of Experimental Physics, University of Wrocław, pl. M. Borna 9 - Wrocław (Poland).

In the last few years, there was much interest of mechanical, thermodynamic and magnetic properties of Fe-Cr alloys, in particular many works concerned enthalpy of solution, enthalpy of mixing and short-range order parameter (SRO) of this system at low Cr concentration [1, 2]. Motivation for these studies is fact, that high-chromium ferritic/martensitic steels, containing up to 15 at. % of Cr, are candidate materials for advanced fission reactors (Generation IV), accelerator-driven systems using spallation neutron sources and fusion reactors. These types of steels are able to perform reliably for long time under high irradiation levels (total dose of 50 to 200 displacements per atom (dpa)) and at high temperatures (up to 900 K). Moreover, high-chromium steels are known for their excellent corrosion resistant properties. These properties originate from the formation of a stable surface Cr oxide film, which prevents further oxidation of an alloy deep into the bulk. On the atomic scale, the necessary supply of Cr atoms to the surface should be provided by a segregation of Cr atoms toward the surface. The problem here comes from the existing controversy in both experimental data and theoretical results [3-5]. The disagreement between various studies concern chromium surface segregation remains unresolved. Taking the above into account we decided to measure Cr segregation at the $Fe_{1-x}Cr_x$ alloy surface with x in the range $0.01 \leq x \leq 0.15$ by Mössbauer spectroscopy. This unique experimental technique allows to take data simultaneously from the surface by conversion electron Mössbauer spectroscopy (CEMS) and from the bulk by transmission Mössbauer spectroscopy (TMS). The observed differences between surface and bulk data should give the answer about segregation process in Fe-Cr alloys. Such comparison between obtained from the surface and the bulk Mössbauer spectra for Fe-Cr alloy were presented in Fig. 1. Our results suggest that Cr atoms segregate to the surface of the Fe-Cr alloy.

[1] G. Bonny, D. Terentyev, L. Malerba, J. Phase Equil. Diff. 31, (2010) 439.
[2] R. Idczak, R. Konieczny, J. Chojcan, J. Phys. Chem. Solids 73, (2012) 1095.
[3] S. Suzuki, T. Kosaka, H. Inoue, M. Isshiki, Y. Waseda, Appl. Surf. Sci. 103, (1996) 495.
[4] G. J. Ackland, Phys. Rev. Lett. 97, (2006) 015502.
[5] A. Kiejna, E. Wachowicz, Phys. Rev. B 78, (2008) 113403.

Fig. 1. The room temperature ^{57}Fe Mössbauer spectra for $Fe_{0.95}Cr_{0.05}$ alloy, annealed in the vacuum at 1270 K for 2 h and slowly cooled to room temperature during 6 h.

SS-12-Or-12
Reaction of tetrahydrofuran with a Si(001) surface studied by means of STM and XPS

T13 Surface Science

#SS-12-Or-12

G. Mette [1], M. Dürr [2], M. Reutzel [1], R. Bartholomäus [3], U. Koert [3], U. Höfer [1].

[1]Fachbereich Physik und Zentrum für Materialwissenschaften, Philipps-Universität - Marburg (Germany), [2]Fakultät Angewandte Naturwissenschaften, Hochschule Esslingen - Esslingen (Germany), [3]Fachbereich Chemie, Philipps-Universität - Marburg (Germany).

A promising approach for the further miniaturization in semiconductor device physics is the functionalization of inorganic semiconductor surfaces by organic molecules [1].

In this context, we have investigated the reaction of the common organic solvent tetrahydrofuran (THF) on Si(001) by means of scanning tunneling microscopy (STM) and X-ray photoelectron spectroscopy (XPS). Despite its inert behavior in solvent based organic chemistry, an unexpectedly rich surface chemistry of THF was observed on Si(001). Entirely different adsorption geometries were identified at low temperature and at room temperature. Furthermore, a complex reorganization occurs at elevated surface temperatures.

At low surface temperature of 50 K, the STM measurements indicate an adsorption geometry with the THF molecule localized at the lower Si dimer atom. In the XP spectra an energetic shift of the O(1s) peak to higher binding energies is observed for this configuration when compared with the THF multilayer signal. Thus a dative bonding between a free electron pair of the oxygen atom and the empty dangling bond surface state is suggested. At surface temperatures above 220 K, an irreversible rearrangement of the THF molecules is observed both in the XP spectra and STM images. The resulting configurations bridge two dimers of adjacent dimer rows as clearly indicated in the STM images. For temperatures higher than 700 K, the STM and XPS data point to the decomposition of the molecule into silicon carbide and silicon oxide structures.

In addition to thermal excitation, the conversion between the dative-bonded configuration and the stable room-temperature configuration can also be induced locally by the tunneling tip at low temperature. Based on detailed investigations of the voltage and current dependence, this effect was attributed to a direct electronic excitation induced by electrons which tunnel into an unoccupied molecular orbital.

[1] M. A. Filler and S. F. Bent, Progr. Surf. Sci. **73**, 1 (2003)

SS-12-Or-13
Interaction of water with ZrO2 ultrathin film-from UHV to elevated pressure

T13 Surface Science

#SS-12-Or-13

H. Li, C. Weilach, G. Rupprechter.

Institute of Materials Chemistry, Vienna University of Technology - Vienna (Austria).

Introduction

ZrO_2 is known as an excellent support in the methane steam reforming. Particularly, the interaction of water and ZrO_2 is of great importance, as the hydroxyl group might influence the sintering of supported Ni, or participate in the reforming reaction [1]. In order to conduct fundamental studies on ZrO_2 using a surface science approach, thin film model catalysts have been prepared and their interaction with water have been studied both under UHV and at elevated pressure.

Experimental

The ultrathin ZrO_2 film was prepared following a route proposed by Schmid and coworkers [2]. The structure and the chemical composition of the film were characterized by Low Energy Electron Diffraction (LEED) and high resolution X-ray Photoelectron Spectroscopy (XPS), respectively. Thereafter, the film was exposed to 10 L water at 100 K for monolayer water studies, and to high pressure water in the range from 10^{-6} mbar to 10^{-1} mbar at 300 K for in-situ studies. Temperature Programmed Desorption (TPD) was used to investigate the dissociation of water upon heating, and XPS was used to study the hydroxylation of the film. Besides, defective films prepared by soft sputtering of the pristine film were also studied.

Results

LEED and XPS showed the formation of a well-structured ZrO_2 film. In case of the monolayer water studies, TPD showed a D_2 desorption peak between 200 K and 400 K. And on the defective film, XPS showed the development of a shoulder, as

compared to the single O 1s peak obtained from the pristine film, as shown in Fig.1. For the high pressure studies, TPD gave a broad D_2 desorption peak between 350 K and 650 K. In Fig.2, XPS showed that the above mentioned shoulder developed into a separated peak, which might be attributed to hydroxyl groups.

[1] Y. Matsummura, T. Nakamori, Applied Catalyis A: General 2004, 258, 107-114;
[2] M. Antlanger et.al, Physical Review B 2012, 86, 03451(1)-03451(9).

Figure.1 O1s XP spectra of pristine and defective film, before and after being exposed to 10 L D_2O at 100 K and subsequently annealed to 300 K

Figure.2 O1s XP spectra of the pristine film and the defective film at the indicated pressures at 300 K

SS-1-Or-6
2D lanthanide networks

T13 Surface Science

#SS-1-Or-6

D. Ecija [1], J. Urgel [1], A. Papageorgiou [1], W. Auwärter [1], S. Joshi [1], S. Vijayaraghavan [1], S. Klyatskaya [2], M. Ruben [2], S. Fischer [1], J. Reichert [1], J.V. Barth [1].

[1]Technical University of Munich - Munich (Germany), [2]Karlsruhe Institut für Technologie - Karlsruhe (Germany).

Surface-confined metal organic architectures have recently been studied for alkali and transition metals in 2D.[1] However, the field of lanthanides on surfaces remains largely unexplored. Here we present, via scanning tunneling microscopy (STM), a distinctive supramolecular chemistry coordination between cerium atoms and dicarbonitrile-oligophenyl linkers (p-NC-Phn-CN-p (n=3,4)) on Ag (111).[2,3] Our observations reveal the expression of distinct five-fold coordination nodes, which are flexible and thus useful for intricate periodic surface-confined molecular architectures.

By carefully tuning the concentration and the stoichiometric ratio of rare-earth metal centers and molecular linkers, the peculiar five-fold coordination results in a 2D hierarchic metal-organic assembly based on dodecameric units. For an increase in the cerium supply, a fully reticulated 2D metal-organic network evolves, whereby all linkers are connected to both sides to Ce centers, following a design pattern interpreted as a molecular Archimedean snub square tessellation of the surface.[4]

Thus, our study introduces the first implementation of the f-block elements[5] in a 2D metallosupramolecular assembly, revealing the versatility of surface-confined lanthanide-based chemistry to engineer complex networks and intricate surface tessellations with particular metal-organic motifs.

[1] J. V. Barth. Annu. Rev. Phys. Chem. (2007), vol. 58, 375-407.

[2] U.Schlickum et al. J. Am. Chem. Soc. (2008), vol. 130, issue 35, 11778-11782.

[3] U. Schlickum et al. NanoLett (2007), vol. 7, 3813-3817.

[4] Johannes Kepler. Harmonices Mundi (1619).

[5] J.C. Bünzli. Acc. Chem. Res. (2006), vol. 39, 53-61.

2D surface-confined lanthanide networks on Ag(111). a) Hierarchic metallosupramolecular network from Ce-directed assembly of CN-Ph_3-CN linkers on Ag(111), for a 4:1 (molecule:Ce) stoichiometric ratio. b) Archimedean snub square tessellation of Ag(111) for a CN-Ph_4-CN to Ce stoichiometry of 5 : 2. Image sizes: a) 116 x 116 $Å^2$; b) 85 x 85 $Å^2$. Scanning parameters: a) V_b = -0.1 V, I = 0.1 nA; b) V_b = 0.2 V, I = 0.1 nA

NST/SS-P1-17
Electron spectroscopy of graphene materials

T13 Surface Science

#NST/SS-P1-17

P. Jirícek [1], I. Bieloshapka [1], J. Zemek [1], B. Lesiak [2], L. Stobinski [2].

[1]Institute of Physics, Academy of Sciences of the Czech Republic, Cukrovarnicka 10 - Prague (Czech republic), [2]Institute of Physical Chemistry, Polish Academy of Sciences, Kasprzaka 44/52, 01-224 - Warsaw (Poland).

The direct formic acid fuel cell (DFAFC) [1, 2, 3], operating at temperatures below 90^{o}C, is a promising source of electric power for a range of applications. Catalysts based on metal nanoparticles/conducting polymer/ graphene are important material for using in DFAFC. Because graphene is also applied in many other applications there are manufactures for its preparation now. The graphene materials from different manufactures were subjected to oxidation in ozone, to oxidation in electron pink plasma and to reduction in H_2 atmosphere at higher temperature. Surface properties of these samples were characterized by X-ray photoelectron spectroscopy (XPS) and Reflection Electron Energy Loss Spectroscopy (REELS). The XPS is applied for determination of surface composition and a content of C bonding, whereas REELS, informing on the energy loss processes of the excited electrons during their transport to the surface, for structural characterisation. The REELS spectroscopy provides information from the energy and intensity of the quasi-elastic peak and inelastic π and π+σ energy loss peaks, where the π+σ energy loss peak can be separated into C sp2 and C sp3 surface and bulk components. Obtained experimental data show great influence of surface properties (composition, content of the C sp2 and C sp3 bonds and carbon-oxygen groups) on used chemical processes. Results help to improve preparation procedures of graphene layers.

[1] N. V. Rees, R. G. Compton, J. Solid State Electrochem. 15 (2011) 2095.
[2] K. Brant, M. Steinhausen, K. Wandelt, J. Electroanalytical Chem., 616 (2008) 27.
[3] Y. Zhu, S. Y. Ha, and R. I. Masel, J. Power Sources, 130 (2004) 8.

NST/SS-8-Or-12
Microscopic study of structural and electronic properties of epitaxial silicene on ZrB2(0001)

T13 Surface Science

#NST/SS-8-Or-12

A. Fleurence [1], Y. Yoshida [2], C.C. Lee [1], T. Ozaki [1], Y. Hasegawa [2], Y. Yamada-Takamura [1].

[1]Japan Advanced Institute of Science and Technology - Nomi (Japan), [2]Institute for Solid State Physics, The University of Tokyo - Kashiwa (Japan).

Although the structure of a single atom thick, free-standing honeycomb structure of Si atoms is predicted to be stable in a low-buckled configuration [1] instead of a planar geometry like graphene, their calculated band structures are quite similar, as the linear crossing of π bands at Fermi level gives rise to Dirac cones at the K and K' points of the Brillouin zone [1]. Silicene, the so-called Si-counterpart of graphene, has been recently discovered in epitaxial forms [2-4] and it is now the object of an exponentially increasing interest as an emerging allotrope of Si and for applications in high-speed electronic devices.
We demonstrated that a large scale silicene sheet can form spontaneously on the clean (0001) surface of zirconium diboride (ZrB2) thin films epitaxially grown on Si(111) by ultrahigh vacuum-chemical vapor epitaxy (UHV-CVE). Annealing under UHV condition induces the segregation of Si atoms on the Zr-terminated ZrB2(0001) surface in the form of an uniform epitaxial ($\sqrt{3}\times\sqrt{3}$)-reconstructed silicene sheet [4]. The study by photoelectron spectroscopy using a surface-sensitive radiation pointed out that among the 6 atoms of the unit-cell, two are sitting on hollow sites of the Zr surface, three near bridges sites and one on top of a Zr atom [4]. The silicene nature of this atom-thick silicon sheet is demonstrated by the presence of a parabolic π-electronic band centered at the K point of the Brillouin zone, as resolved by angle-resolved ultraviolet photoelectron spectroscopy. According to our first principles calculations, the band gap opening is primarily a result of the specifically imprinted buckling rather than the electronic coupling with the diboride layer [4].
The silicene sheet is textured into stripe domains regularly separated by linear boundaries. By means of a scanning tunneling microscopy investigation at low temperature (LT), which suppress the thermally-activated hopping of the domain

boundaries, we determined that this large-scale ordering results from repeated rotations of the silicene orientation by 180°. The Si atoms on top of a Zr atom alternate between the two sublattices of silicene. As a consequence of the creation of the domains, the position of the Si atoms at the boundaries deviates from the honeycomb structure of the domain center.
LT-scanning tunneling spectroscopy carried out at the center of the domain evidences the semiconducting nature of the silicene sheet epitaxied on ZrB2(0001). Moreover, the mapping of the local density of states gives precious insights on the microscopic origin of the electronic bands. In particular, it shows that the orbitals of on-top Si atoms contribute predominantly to the π bands in agreement with the sp2-like coordination of those Si atoms, as established by density functional theory calculations. Finally, the consequence of the slightly different coordination of the Si atoms at the boundaries on their electronic properties will be also addressed.

[1] S. Cahangirov, et al., Phys. Rev. Lett. 102, 236804 (2009).
[2] P. Vogt, et al., Phys. Rev. Lett, 108, 155501 (2012).
[3] L. Chen, et al., Phys. Rev. Lett, 109, 056804 (2012).
[4] A. Fleurence, et al., Phys. Rev. Lett, 108, 245501 (2012).

SS-P3-18
Characterization of ZnO polar surfaces irradiated under Ar-ion beam

T13 Surface Science

#SS-P3-18

M. Krawczyk, W. Lisowski, K. Nikiforov, J.W. Sobczak, A. Jablonski.

Institute of Physical Chemistry, Polish Academy of Sciences - 01-224 Warszawa (Poland).

Two polar surfaces of the wurtzite-type ZnO crystal, the Zn-terminated ZnO(0001) and the O-terminated ZnO(000-1) surface planes, have attracted increasing interest. The question arises, how argon ion-beam interaction affects surface morphology and elemental composition in the surface region of both polar ZnO crystals. In order to address this issue, we performed combination of X-ray photoelectron spectroscopy (XPS), scanning electron microscopy (SEM) and atomic force microscopy (AFM) studies. The results were compared for two single-crystalline ZnO with polar (0001) and (000-1) surfaces irradiated with Ar ions of energy 0.5-5 keV at the incidence angle of 55° with respect to the surface normal. XPS spectra were recorded on the PHI 5000 VersaProbe^{TM} scanning ESCA Microprobe using monochromatic Al K_{α} radiation. SEM images were obtained with FEI Nova NanoSEM 450 Scanning Electron Microscope, and AFM images were acquired in non-contact (FM) mode with UHV-350 AFM/STM microscope (RHK Technology). The atomic concentration of zinc and oxygen were evaluated using the multiline program [1], where the integrated area of XPS peaks associated with the Zn 2s, Zn $2p_{3/2}$, Zn $2p_{1/2}$, Zn 3s, Zn 3p, Zn 3d and O1s core levels was used for accurate analysis. Figure 1 displays the ion-energy dependence of the O/Zn at. concentration ratio of the irradiated polar surfaces for the 5 min sputter time. The resulting O/Zn values for the sputter-cleaned Zn-polar and O-polar surfaces were found to be 0.76 and 0.66, respectively, as a result of ion-beam induced loss of oxygen from the surface [2]. SEM and AFM images showed that both ion-irradiated polar surfaces were more defected than the corresponding clean surfaces. The annealing of Ar^{+} ion-beam etched surfaces led to formation of smooth surface with uniform steps [3], and partial removing of surface defects caused by ion-irradiation. In conclusion, our studies on low-energy Ar-ion irradiated polar surfaces of ZnO would be beneficial to use these highly resistive materials under appropriate conditions.

This research was partially supported by the European Union within European Regional Development Fund, through grant Innovative Economy (POIG.01.01.02-00-008/08), and by the grant no. 2011/01/B/ST4/00959 of the National Science Center of Poland.

[1] A. Jablonski, Anal. Sci. 26 (2010) 155.
[2] O. Dulub, L. A. Boatner, U. Diebold, Surf. Sci. 519 (2002) 201.
[3] S. Rohrer, D. A. Bonnel, Surf. Sci. 247 (1991) L195.

Fig. 1. The O/Zn at. concentration ratio of the sputtered polar surfaces of single crystal ZnO, as a function of Ar^+ ion energy for 5 min sputter-time.

SS-4-Or-2
Growth, structure and electronic properties of titanium oxide nanoislands on Au(111)

T13 Surface Science

#SS-4-Or-2

A. Li Bassi [1], P. Carrozzo [2], F. Tumino [2], M. Passoni [2], C.E. Bottani [1], C. Casari [1].

[1]Dipartimento di Energia, Politecnico di Milano; CNST - Center for Nano Science and Technology @PoliMi, Istituto Italiano di Tecnologia - Milano (Italy), [2]Dipartimento di Energia, Politecnico di Milano - Milano (Italy).

We present a scanning tunneling microscopy and spectroscopy (STM-STS) investigation of the structural and electronic properties of titanium oxide nanostructures on Au(111). Gold-supported Ti and TiO_x nanoislands represent both a model system for the investigation of oxide nanostructures and promising systems for applications in catalysis and photocatalysis [1,2]. However detailed STM-STS studies of the morphology, local structure and electronic properties of TiO_x on Au(111) are lacking; only recently Wu et al. [3] have shown, in the regime of partial surface coverage, the presence of atomically ordered structures that differ from typical bulk structures [3].

Ti was deposited by e-beam evaporation, leading to preferential nucleation at the elbows of the herringbone Au reconstruction [4] and, in comparison to other metals, retarded coalescence, out-of-elbow disordered growth, intermixing with Au and interlayer diffusion; the electronic properties of Ti islands have been investigated by STS measurements.

For different Ti initial coverage in the 0.1 ML-1.5 ML range, TiO_x nanostructures were obtained by subsequent exposure to O_2 (~ 500 L) followed by annealing in vacuum at 850 K, leading to a ~ 25% decrease in the equivalent total coverage.

At low coverage (< 0.5 MLeq) the Au(111) reconstruction is distorted and two different phases are observed, named *pinwheel* (constituting the first layer, fig.1) and *triangular*, always observed on top of the pinwheel. We interpret the structure of the pinwheel phase as a Moiré pattern characterized by a $(\sqrt{133} \times \sqrt{133})R17.5°$ reconstruction, which is different from the model discussed in [3].

At higher coverage (0.5-1.5 MLeq) coalescence of pinwheel islands occurs and other

TiO_x phases are observed whose structure and orientation have been identified via atomic resolution STM imaging and LEED: in the first layer the pinwheel and the *honeycomb* phase, characterized by hexagonal symmetry and (2×2) reconstruction; in higher layers the triangular phase and a *row* phase, not reported before, characterized by 20-40 nm wide islands whose surface presents a periodic series of atomic rows with variable apparent height (Fig.1), and which may be related to one of the bulk phase surfaces of TiO_2.
Finally, STS measurements on the different TiO_x nanostructures will be discussed, indicating the presence of a gap in the electron LDOS around Fermi level.

[1] I. Nakamura *et al*., J. Chem. Phys. C **115**, 16074 (2011)
[2] Q. Yi *et al*., Micro. Acta **165**, 381 (2009)
[3] C. Wu *et al*., J. Chem. Phys. C **115**, 8643 (2011)
[4] J. Biener *et al*., J. Chem. Phys.C **123**, 094705 (2005)

Fig.1: atomic resolution images of the TiO_x *pinwheel* (left) and *row* (right) phase.

NST/SS-6-Or-10
Insulating and magnetic ground state of Si(111) 7x7

T13 Surface Science

#NST/SS-6-Or-10

G. Profeta [1], S. Modesti [2], E. Tosatti [3].

[1]University of L'Aquila - L'aquila (Italy), [2]University of Trieste and TASC - Trieste (Italy), [3]SISSA and ICTP Trieste - Trieste (Italy).

The electronic ground state of the Si(111)7x7 surface, many times discussed, is still unclear.
Its room temperature metallic nature, apparently in line with past band structure calculations, has been reported as dwindling upon cooling, but never really investigated down to helium temperatures. Through a careful low temperature STS study, a small but unmistakeable insulating gap is shown to open up below 20 K.

To clarify the nature of that insulating state, we undertook spin-polarized electronic structure calculations which, while density-functional based, are able gauge the strength of electron correlations, including the possibility of Mott type ground states. Results indicate that the ground state of Si(111)7x7 has a multiplicity of competing magnetic phases, including a ferromagnetic state.

By comparing theory and experiment, we discuss possible origins of the observed insulating ground state, especially those involving, along with magnetism, a small symmetry-breaking distortion taking place among the outer Si atoms surrounding the structural DAS vacancy.

SS-9-Or-4
Metalation of H2-tetraphenyl-porphyrins by picking-up a substrate metal atom

T13 Surface Science

#SS-9-Or-4

A. Goldoni.

Elettra - Sincrotrone Trieste - Trieste (Italy).

A. Goldoni(1,2), G. Di Santo(1,2), M. Caputo(1,3), M. Panighel(1,4), C. Castellarin-Cudia(5), A. Verdini(5), L. Floreano(5), F. Bondino(5), E. Magnano(5), C. A. Pignedoli(6), D. Passerone(6)

(1) Elettra - Sincrotrone Trieste, Trieste, Italy
(2) INSTM sezione di Trieste, Trieste, Italy
(3) University of Calabria, Cosenza, Italy
(4) University of Trieste, Trieste, Italy
5) IOM-CNR, Lab. TASC, Trieste, Italy
(6) EMPA, Dübendorf, Switzerland

The possibility to obtain systems where the magnetic or catalytic atoms are well separated and arranged in regular arrays is allowed at the nanoscale by using molecular self assembly of π-conjugated molecules containing metal ions. Porphyrins are a class of such molecules with a planar macrocycle that can accept metal ions of different kind at the center (metalation), thus forming metallo-porphyrins.
There are several ways to metalize porphyrins by wet-chemistry [1]. Even more interesting is the metalation of porphyrins in ultra high vacuum (UHV) by evaporation of metal on H_2-porphyrin self-assembled on surfaces [2-6], since this method allows to obtain metallo-porphyrins that typically are not stable as single-molecules thanks to the action of the support surface, which stabilizes the valence state of the evaporated metal [5,6]. A risk, however, is the formation of metal clusters in addition to metallo-porphyrins due to the reduced mobility of some metals adatoms or to an excessive metal ions deposition.
Here, using synchrotron radiation spectroscopy, we show a new method of porphyrin

metalation in UHV without the metal evaporation. Depositing one monolayer of H_2-tetraphenyl-porphyrins (H_2-TPP) on Fe, Ni and Al substrates, a substrate adatom binds directly to the macrocycle and metalates the porphyrins, forming Fe-TPP, Ni-TPP and Al-TPP, respectively. Metalation in a similar manner was obtained on Cu surfaces by other research groups [7-9]. Energetics obtained by density functional theory calculations confirms the possibility of such a kind of metalation. The redox reaction happens at room temperature for Fe and Ni substrates [10], while it requires heating at 400 K for the Al substrate. Moreover, the interaction with Al is so strong that just above 400 K the molecule starts to decompose forming Al-N alloy.

[1] Buchler, J.W. Synthesis and Properties of Metalloporphyrin, Chapter 10 in Phorphyrins Vol. 1, edited by Dolphin D., Academic Press, New York, 1978

[2] Gottfried, J. M. et al., J. Am. Chem. Soc. 2006, 128, 5644–5645.

[3] Auwärter, W. et al., ChemPhysChem 2007, 8, 250–254

[4] Di Santo, G. et al., J. Phys. Chem. C 2011, 115, 4155–4162.

[5] Weber-Bargioni, A. et al., J. Phys. Chem. C 2008, 112, 3453–3455.

[6] Chen, M. et al., J. Phys. Chem. C 2010, 114, 9908–9916.

[7] Gonzales-Moreno, R. et al., J. Phys. Chem. C 2011, 115, 6849-6854

[8] Dyer, M.S. et al., ACS Nano 2011, 5, 1831-1838

[9] Diller, K. et al., J. Chem. Phys. 2012, 136, 014705

[10] Goldoni, A. et al., ACS Nano 2012, 6, 10800-10807.

SS/NST-1-Or-5
Time domain mapping of short voltage pulses with plasmonic light

T13 Surface Science

#SS/NST-1-Or-5

M. Etzkorn [1], C. Große [1], K. Kuhnke [1], S. Loth [2], K. Kern [1].

[1]Max Planck Institute for Solid State Research - Stuttgart (Germany), [2]Center for Free-Electron Laser Science - Hamburg (Germany).

Time-resolved STM measurements using electronic pulses enable the study of local dynamics in the nanosecond-regime and below [1]. One necessary prerequisite for such measurements are defined pulse profiles of the transient bias voltage V(t) at the tunnel junction. Due to high frequency limitations of the wiring and impedance mismatches in the experiments (in particular for UHV, low temperature set-ups), well defined pulses fed into the STM will deviate from perfectness when they reach the tunnel junction. Here we introduce a new concept that enables a direct, non-invasive, and quantitative mapping of V(t) in the junction using STM-induced light emission via tip-induced plasmons. This method takes advantage of two effects: 1) The number of photons emitted from a tunnel junction is a bijective function of the voltage. 2) Both, plasmon decay and photon detection are fast (< 1 ns) compared to the time scale of the variation of V(t). By redundant measurements of the autocorrelation using an all-electronic pump-probe scheme, we proof that this method indeed measures the correct pulse shapes. Using this new optical read-out we have extracted the transient bias signal in our system for rectangular pulses fed into the bias line of the STM (see Fig. 1). Significant deviations from the feed-in pulses are observed, demonstrating the importance of a possibility to determine V(t). We can assign the deviations to the low-pass filtering and resonances within the cable. Moreover, using this method, we determine the transfer function of our set-up and show, how this function can be used to construct the intended pulse shape in the junction. Fig. 2 shows optimized square pulses which are generated from applied bias time pattern that correct for the imperfections in the bias signal line. This leads for instance to an improvement in the falling edge width from ≈ 50 ns to < 5ns.

[1] S. Loth, M. Etzkorn, C.P. Lutz, D.M. Eigler, A.J. Heinrich, Science 329, 1628 (2010).

Fig.1 Transient bias for rectangular pulses (rise time 10%-90% = 2ns) fed into the STM for different durations of the pulse.

Fig.2 Transient bias for optimized applied voltage signals.

SS/NST-1-Or-8
Bulk Molybdenum Tips for Scanning Tunneling Microscopy and Spectroscopy

T13 Surface Science

#SS/NST-1-Or-8

P. Carrozzo [1], C. Casari [2], M. Passoni [1], C.E. Bottani [2], A. Li Bassi [2].

[1]Dipartimento di Energia, Politecnico di Milano - Milano (Italy), [2]Dipartimento di Energia, Politecnico di Milano; CNST - Center for Nano Science and Technology @PoliMi, Istituto Italiano di Tecnologia - Milano (Italy).

We present a method for the preparation of bulk molybdenum tips for Scanning Tunneling Microscopy and Spectroscopy (STM-STS) and we show their potential in performing high quality and high resolution imaging and local spectroscopic measurements.

STM is a very powerful tool to investigate the morphological, structural and electronic properties of surfaces and nanostructures with extremely high resolution down to the atomic scale. STM-STS measurements in UHV can be performed with mechanically cut Pt/Ir tips or, more commonly, with chemically etched tips, typically made of W, even though other metals are sometimes employed (e.g. Au) [1]. Magnetic tips are instead adopted for spin polarized (SP) measurements, either by fabricating bulk tips (e.g. Cr [2]) or coating W tips. In this framework, thanks to its inertness and ease of handling, Mo represents a good alternative, but up to now Mo tips have not been used for STM measurements.

We have fabricated Mo tips by developing an optimized procedure for electrochemical etching a 99.99% Mo wire in a NaOH solution, exploring conditions such as NaOH concentration and applied bias. Mo tips are characterized by a regular shape at the micron scale and a sharp tip apex with a radius of curvature of about 50 nm, as shown by scanning electron microscopy images (fig.1), and high quality tips can be routinely obtained with a high success rate.

We tested Mo tips by performing atomically resolved STM measurements on single crystal surfaces in UHV. Mo tips permit to obtain very high quality images of the Au(111) superstructure and STS measurements show the Au Shockley peak at -0.47 eV. Imaging and local STS measurements of the Si(111)-7×7 surface were also performed, and atomic resolution was achieved, showing in particular the rest atoms of the Si(111)-7×7 reconstruction at negative bias (below -1.5 V, fig.1), contrary to

what normally happens with conventional W tip [3]. A comparative analysis of STS data acquired with different tips (W, Cr and Mo) can be used to gain information on the dependence on the tip density of states. Finally Mo tips have been successfully employed for original measurements of surface nanostructures, namely structural investigation via atomic resolution imaging of peculiar TiO_x ordered phases grown on Au(111).
The method used for the fabrication of Mo tips is versatile and we show that it can be extended to other metals, e.g. cobalt.

[1] C. Bai, “Scanning Tunneling Microscopy and its applications”, Springer Verlag (2000)
[2] A. Li Bassi et al., Ap. Ph. L. 91, 173120 (2007)
[3] Y. L. Wang et al., Phys. Rev. B 70, 073312 (2004)

Fig.1: (left) SEM image of a Mo tip and (right) Mo tip image of the Si(111), showing the rest atoms (I=0.5 nA; V=-1.5 V).

SS-14-Or-1
Synergistic effect of metal and metal-oxide nanostructures on ethanol reforming over non-noble metal based model catalysts

T13 Surface Science

#SS-14-Or-1

Z. Pászti [1], G. Szijjártó [1], O. Hakkel [1], I. Sajó [1], A. Erdőhelyi [2], G. Radnóczi [1], A. Tompos [1].

[1]Research Centre for Natural Sciences, Hungarian Academy of Sciences - Budapest (Hungary), [2]University of Szeged - Szeged (Hungary).

Widespread utilization of hydrogen as energy carrier requires the solution of issues connected to its sustainable generation and safe distribution. Since our current energy infrastructure is well prepared for handling liquid fuels, a very compelling utilization strategy can be based on on-site hydrogen generation by catalytic conversion of hydrogen-containing compounds such as ethanol. Economically viable approaches, however, require sophisticated yet robust and cheap reforming catalysts. Until recently, noble or near-noble metal-based systems seemed to offer the best choice for ethanol reformers. Apart from efforts for reducing the noble metal content, recent experiments indicate that good results can be obtained on multicomponent catalysts built around the members of the iron group. Ni emerges as a key ingredient for these catalysts, but since a delicate balance between different surface functionalities is needed for suppression of unwanted side reactions, doping with further metal or oxide components is unavoidable. Because of the required complexity, a detailed understanding of the interplay between the constituents of the active surface is a prerequisite for successful design of a noble metal free ethanol reforming catalyst.

Accordingly, a comparative multi-technical study of Ni-based, Co and Ce-containig catalysts on $MgAl_2O_4$ support was carried out. While the Ni- and especially the Ni-Co containing catalysts suffered from extensive coke formation, addition of Ce in the form of a somewhat reduced oxide successfully eliminated this side process. Catalytic tests revealed a strong synergism between Ni and Co, as the desired

conversions, such as water-gas-shift reaction and direct steam reforming of acetaldehyde, are dominating in the bimetallic system leading to high hydrogen yield. Structural and electron spectroscopic studies indicated considerable exchange of Mg cations to Ni or Co, leading to the formation of transition metal doped spinel support. Since Co turned out to preferentially occupy the exchangeable Mg sites, in the bimetallic case considerably larger fraction of Ni could be reduced to metallic state than in the monometallic case. The easier transformation of ethanol to acetaldehyde and the direct steam reforming of acetaldehyde evidenced by catalytic tests and DRIFT measurements were therefore traced to the increased metallic character of Ni, together with charge transfer processes at the interface between the Ni particles and the semiconducting support.

In order to further elucidate the background of the Ni-Co interplay in ethanol steam reforming, model catalysts were developed by depositing mono- and bimetallic layers onto epitaxial CeO_2 films grown on CaF_2-buffered Si(111). In this approach relevant structural parameters such as chemical identity, amount or oxidation state of the active metals can be relatively independently controlled, thus allowing the separation of their influence on the adsorption and initial transformations of ethanol molecules. Results of electron spectroscopic and in situ vibrational spectroscopic measurements emphasized the key role of the finely balanced interaction of the constituents in the working mechanism of noble metal free ethanol reforming catalysts.

SS-11-Or-3
Anisotropic Ultrathin Organic Films studied by Polarized Resonant Soft X-Ray Reflectivity

T13 Surface Science

#SS-11-Or-3

L. Pasquali [1], S. Mukherjee [2], F. Terzi [3], A. Giglia [4], N. Mahne [4], K. Koshmak [5], V. Esaulov [6], C. Toccafondi [7], M. Canepa [7], S. Nannarone [1].

[1]Dipartimento di Ingegneria 'Enzo Ferrari', Università di Modena e Reggio Emilia and IOM-CNR - Modena (Italy), [2]International Centre for Theoretical Physics - Trieste (Italy), [3]Dipartimento di Scienze Chimiche e Geologiche, Università di Modena e Reggio Emilia - Modena (Italy), [4]IOM-CNR - Trieste (Italy), [5]Dipartimento di Ingegneria 'Enzo Ferrari', Università di Modena e Reggio Emilia - Modena (Italy), [6]CNRS, UMR 8214 Institut des Sciences Moléculaires d'Orsay - Paris (France), [7]CNISM and Dipartimento di Fisica, Università di Genova - Genova (Italy).

Resonant soft X-ray reflectivity (RSoXR) is a quantitative tool to study the interplay between electronic properties, geometry and morphology of a wide class of ultrathin films and layered system with sensitivity to the depth distribution of chemical species and buried interfaces. Element- and bond-specific information, beyond the total electron density distributions, can be obtained by scanning the photon energy through specific absorption edges and playing with the polarization and incidence angle of the impinging field.
For the first time to our knowledge, we applied polarized-light resonant soft X-ray reflectivity (P-RSoXR) at the carbon K-edge to study morphology and ordering of an organic anisotropic self-assembled layer on Au(111). In particular, we studied the 1,4 benzenedimethanethiols (BDMT)/Au(111) system. In recent years we gained detailed knowledge on the formation of BDMT SAMs on well-defined gold surfaces, exploiting both in vacuum and in-liquid deposition, thanks to an in-depth investigation by spectroscopic ellipsometry (SE), reflection-absorption IR spectroscopy (RAIRS), electrochemistry, photoemission and X-ray absorption (XAS).(1,2) We were able to elaborate a protocol for obtaining well-organized SAMs of BDMT molecules in a standing up configuration, with a sulfur headgroup bonded to the substrate and the other SH unbound terminal pointing upright. This method was used to prepare the

BDMT films.
P-RSoXR data at the carbon K-edge were taken at the BEAR beamline at ELETTRA in grazing incidence of linear polarized light, from s- to p- scattering geometries.
To interpret the P-RSoXR data we followed an approach based on the calculation from the first principles (through DFT) of the film optical constants. We calculated the anisotropic optical cross sections of the molecule, the corresponding polarizability, we modeled the molecular arrangement and we constructed the corresponding anisotropic dielectric tensor of the film. We finally simulated the propagation of light inside the vacuum/BDMT/Au system as a function of the incidence geometry, obtaining a simulated reflectivity to be fitted to the experiment.
This method permited us to exploit the sensitivity of P-RSoXR to derive quantitative information on the layer anisotropy, molecular orientation and thickness of self-assembled monolayers (SAMs) at surfaces simultaneously.
In the present contribution we demonstrate the validity of this approach which – we believe - opens interesting possibilities in the study of a wide class of organic thin films. The method transfers to soft-X range the knowledge gained in the years in the field of visible (ellipsometry included) and infrared spectroscopy of thin anisotropic films. Moreover, it offers a tool of quantitative investigation in those cases where electron spectroscopy cannot be employed because of the presence of nonconductive materials, poor vacuum or materials buried at distances from surfaces higher than the electron free collision path.

(1) Pasquali, L.; Terzi, F.; Seeber, R.; Nannarone, S.; Datta, D.; Dablemont, C.; Hamoudi, H.; Canepa, M.; Esaulov, V. A. Langmuir 2011, 27, 4713.
(2) Hamoudi, H.; Prato, M.; Dablemont, C.; Cavalleri, O.; Canepa, M.; Esaulov, V. A. Langmuir 2010, 26, 7242.

NST/SS-2-Or-1
Gap opening in an all graphene nanostructure

T13 Surface Science

#NST/SS-2-Or-1

A. Tejeda [1], J. Hicks [2], A. Taleb-Ibrahimi [3], M.S. Nevius [2], F. Wang [2], K. Shepperd [2], J. Palmer [2], F. Bertran [4], P. Le Fèvre [4], J. Kunc [2], W.A. De Heer [2], C. Berger [5], E.W. Conrad [2].

[1]CNRS-IJL and SOLEIL - St Aubin (France), [2]The Georgia Institute of Technology - Atlanta (United states), [3]UR1 CNRS/Synchrotron SOLEIL - St. Aubin (France), [4]Synchrotron SOLEIL - St. Aubin (France), [5]CNRS-Institut Néel and The Georgia Institute of Technology - Grenoble (France).

Scalability and process-induced disorder problems often appear when producing semiconducting–metallic graphene networks. We present here an all graphene nanostructure with a one-dimensional metallic–semiconducting–metallic junction. Our technique relies on graphene grown on patterned SiC steps [1], without chemical functionalization or finite-size patterning.

We have studied these nanostructures by photoemission, that successfully allowed us to observe the ideal dispersion in flat epitaxial graphene on SiC [2,3]. The bottom-up growth procedure promotes graphene strips along the slopes. At the edge of these graphene strips, a semiconductor, is bonded to metallic graphene. This semiconductor is only a few nanometers wide (a few graphene lattice constants), a level of precision beyond modern lithographic limits. Moreover, the properties are preserved across micrometric distances as observed by averaging the properties of the ribbons in the observation area. The band gap is greater than 500 meV in an otherwise metallic graphene ribbon (fig. 1) [4].

[1] M. Sprinkle, M. Ruan, Y. Hu, J. Hankinson, M. Rubio-Roy, B. Zhang, X. Wu, C. Berger, and W.A. de Heer, Nature Nanotechnology **5**, 727 (2010).

[2] M. Sprinkle, D. Siegel, Y. Hu, J. Hicks, A. Tejeda, A. Taleb-Ibrahimi, P. Le Fèvre,

F. Bertran, S. Vizzini, H. Enriquez, S. Chiang, P. Soukiassian, C. Berger, W.A. de Heer, A. Lanzara, and E.H. Conrad, Phys. Rev. Lett. **103**, 226803 (2009).

[3] A. Tejeda, A. Taleb-Ibrahimi, W. de Heer, C. Berger, and E.H. Conrad, New J. Phys. **14**, 125007 (2012).

[4] J. Hicks, A. Tejeda, A. Taleb-Ibrahimi, M. S. Nevius, F. Wang, K. Shepperd, J. Palmer, F. Bertran, P. Le Fèvre, J. Kunc, W. A. de Heer, C. Berger and E. H. Conrad, Nature Phys. **9**, 49 (2012).

Figure 1. Schematic representation of a graphene ribbon on a silicon carbide artificially structured facet. Photoemission measurements on a network of these ribbons show three different regions on the continuous graphene ribbon : two metallic regions with a semiconducting one in between, in the curved region of the ribbon.

SS-5-Or-5
Analysis of organic films deposited by a RF CCP discharge in a N2 CH4 mixture

T13 Surface Science

#SS-5-Or-5

N. Carrasco [1], F. Jomard [2], J. Vigneron [3], A. Etcheberry [3], G. Cernogora [1].

[1]LATMOS - Guyancourt (France), [2]GEMAC - Versailles (France), [3]ILV - Versailles (France).

In Titan's atmosphere, the largest Saturn's satellite, solid organic aerosols are formed by the dissociation of N_2 and CH_4. In order to simulate the chemistry involved in the Titan's atmosphere, a low pressure (0.9mbar) RF CCP discharge is used. The experimental device is described in [1]. Gas mixtures of N_2 and CH_4 mixture (from 1 to 10% of CH_4) are injected continuously. The plasma discharge in N_2-CH_4 gas mixtures leads to the production of analogues of Titan's atmospheric aerosols: both as grains in the volume [2] and as thin films on the surface of the reactor [3]. SiO_2 substrates of 1cm diameter and 1 mm thickness are placed on the grounded electrode of the discharge. Organic films are deposited during 2 hours in order to have films thickness less than 1 µm. After the two hours, samples are recovered at ambient air for ex-situ analysis. Two complementary analyses are performed to analyse the thin film chemical composition: XPS and SIMS.
XPS surface and profile analysis are performed with a high resolution XPS probe. The relative amounts of C, N, O and Si are measured from the first down to the 300 nm along the film depth-profile. It is observed that below 60 nm the amounts of C and N remain constant. No Si is observed in the studied layer, and O is negligible below 60 nm. The relative amount C/N is measured as function of the injected CH_4 amount. It is shown that the ratio C/N decreases from 0.4 to 0.1 when the CH_4 amount increases from1 to 10%. These C/N ratios are lower than those measured in the solid grains produced in the volume of the discharge [2].
In order to check the uniformity of the organic layer, SIMS analysis is performed after XPS studies using an IMS-4F (CAMECA) [4]. The H, C, O and Si secondary ions are measured during the SIMS depth profile . After a few tens of sputtering , the all the ions signals are constant. The organic layer composition is homogeneous. The limit

of the organic film is detected after 600 to 2000 s of etching, by a rapid increase of O and Si signals, corresponding to the SiO_2 substrate. By measuring the depth of the sputtering crater, it is possible to determine the true thickness of the organic film. Absolute elemental analysis measurements are not an easy task with SIMS. However, the evolution of the ratio H/C in arbitrary units is deduced from the ratio of the corresponding ions signals. It is shown that this ratio remains the same, about 0.1, whatever the injected CH_4 amount. For powders, Sciamma O'Brien et al. (2010) have shown that this ratio increases with the amount of injected CH_4.
These results show that important differences exist between the chemical compositions of organic materials produced as powders or films in the same experimental conditions.

[1] Alcouffe G., Cavarroc M., Cernogora G., Ouni F., Jolly A., Boufendi L., Szopa C. Plasma Sources Science and Technology 19, 1 (2010) 015008 (11pp)
[2] Sciamma-O'brien E., Carrasco N., Szopa C., Buch A., Cernogora G. Icarus 209, 2 (2010) 704-714
[3] Mahjoub A., Carrasco N., Dahoo P.-R., Gautier T., Szopa C., Cernogora G. Icarus 221, 2 (2012) 670-677.
[4] R.G. Wilson, F.A. Stevie, C.W. Magee, Secondary Ion Mass Spectrometry: A Practical Handbook for Depth Profiling and Bulk Impurity Analysis, Wiley & Sons, New York, 1989

SS-14-Or-2
Adsorption and self-assembly of functionalized [5]helicene molecules on insulating ionic surfaces

T13 Surface Science

#SS-14-Or-2

B. Hoff [1], M. Gingras [1], R. Peresutti [1], G. Felix [1], C.R. Henry [1], A.S. Foster [2], C. Barth [1].

[1]CINaM-CNRS Campus de Luminy Case 913 13288 Marseille Cedex 9 - Marseille (France), [2]COMP Centre of Excellence, Aalto University School of Science, Department of Applied Physics, Finland - Marseille (France).

In recent years organic thin films on insulating surfaces have become very important since they have the advantage of electronically decoupling molecules from the support, unlike metal surfaces. This leads to new phenomena of adsorption and self-assembly, which detailed mechanisms are studied on the model surfaces of ionic alkali halides by noncontact atomic force microscopy (nc-AFM) and Kelvin probe force microscopy (KPFM) [1].
The current tentative picture for the adsorption of molecules on ionic insulating surfaces in general considers a non-site specific van der Waals interaction between the molecule and the surface, but also an electrostatic interaction between the ionic lattice of the surface and functional groups of the molecule, which contain a partial charge or exhibit a local dipole. Although such two contributions explain to some extent experimental observations, many important questions remain still open – the current tentative model needs urgent further confirmation.
In this contribution we focus on functionalized pentahelicene molecules, which are deposited in ultrahigh vacuum (UHV) onto the (001) surfaces of different pure and Cd2+ doped alkali halide (Suzuki surface) crystals [2]. The local structure of the films and their dipole distribution are studied by UHV nc-AFM and KPFM, respectively, and DFT theory. The helicene molecules carry either one or two bromine atoms (MonoBromo, DiBromo) or one or two cyano groups (MonoCyano, DiCyano) (Figure (a)). We show that the adsorption as well as the self-assembly of the molecules strongly depend on the number of functional groups, the type of group (dipole) and the ionic lattice of the surface. For instance, in Figure (b) the nanostructured (001) Suzuki Surface, which exhibits Suzuki regions (containing all the Cd2+ ions) and

pure NaCl regions, is covered by one monolayer of DiCyano. Self assembly only occurs in the pure NaCl regions, and in the Suzuki regions a rather amorphous structure is found.
We explain that in particular the electrostatic interaction of the functional groups with the ionic lattice plays a major role in the adsorption, where adsorption geometries ('charge matching') and dipole strengths are of key importance. They all may have an impact onto intermolecular interactions determining if self-assembly via π-π stacking of the helicene molecules is possible or not.

[1] C. Barth, A. S. Foster, C. R. Henry and A. L. Shluger, Adv. Mater 23, 477 (2011)
[2] C. Barth, M. Gingras, A. S. Foster, A. Gulans, G. Félix, T. Hynninen, R. Peresutti and C. R. Henry, Adv. Mater. 13, 2061 (2012).

SS-11-Or-4
Electron Spectroscopy Studies of Adsorbed Chiral Molecules on Magnetic and Non-Magnetic Surfaces

T13 Surface Science

#SS-11-Or-4

J. De Miguel [1], F.J. Luque [1], I.A. Kowalik [2], M. Niño [3], R. Miranda [1], D. Arvanitis [4].

[1]Univ. Autónoma - Madrid (Spain), [2]Inst. Physics, Polish Acad. Sci. - Warsaw (Poland), [3]IMDEA-Nanociencia - Madrid (Spain), [4]Uppsala Univ. - Uppsala (Sweden).

Recently, layers of chiral molecules have been shown to scatter electrons differently depending on their spin [1,2]. These experiments prompt questions about the relationship of molecular chirality with spin and the influence that the magnetisation of the substrate can have on the adsorption of chiral molecular films.
Ultra-thin films of the chiral enantiomers (R,R)-(+)- and (S,S)-(–)-1,2-Diphenyl-1,2-ethanediol (DPED, see the inset in Figure 1) have been studied using absorption of circularly polarized x rays (XAS) at the carbon K edge and valence band photoemission. The substrates used were a single-crystal Cu(100) surface and ferromagnetic Co(100) films epitaxially grown on it. The measurements were performed at the I1011 and I3 beamlines of synchrotron MAX IV (Lund, Sweden), as well as in our home lab in Madrid.
Figure 1 shows a representative XAS spectrum acquired on a DPED film grown on Cu(100). The different features in it have been identified and assigned to specific electronic transitions. The sharp peak at ~284 eV corresponds to the π* resonance of the C unsaturated bonds. The set of peaks appearing behind this one between 285 and 290 eV have also π-type character and are assigned to the C–H bonds in the molecules, whereas the broader features at higher energies correspond to σ-type C–C bonds [3].
Pairs of spectra were acquired using circularly polarized radiation with opposite helicity (σ+, σ–) and compared by taking their intensity ratio. The results of these measurements are displayed in Figure 2. Several clearly dichroic features can be observed coincident with the C–C and C–H π orbitals showing opposite signs for the two enantiomers.

The films of chiral DPED have also been grown on ferromagnetic Co(100) films; their effect on the atomic magnetic moments of the Co atoms will also be discussed.

[1] K. Ray et al., Science 283, 814 (1999).
[2] B. Göhler et al., Science 331, 894 (2011).
[3] J. Stöhr, NEXAFS Spectroscopy, Springer Series in Surface Sciences No. 25, Springer (Berlin, 1996).

Figure 1

Figure 2

SS-14-Or-3
Molybdenum Hexacarbonyl Dissociation on Copper (111) and (001) Surfaces

T13 Surface Science

#SS-14-Or-3

M. Petukhov, P. Krüger, W. Xiaowen, C. Dupont, B. Domenichini, S. Bourgeois.

CNRS-Université de Bourgogne - Dijon (France).

The molybdenum hexacarbonyl $Mo(CO)_6$ physisorbs as entire molecules on most noble metals, metal oxides and relatively inert surfaces at liquid-nitrogen temperatures and desorbs upon thermal heating close to 200 K. In the case of copper surface, the temperature programmed desorption measurements established a more complex behaviour [1]. Under heating, decomposition of the adsorbed molecules occurs via several steps over a temperature range from 170 to 480 K. The dissociation channel competes favourably with desorption.

Molybdenum hexacarbonyl has been deposited on copper substrates at low temperature and studied by scanning tunneling microscopy (STM), X-ray photoelectron spectroscopy (XPS) and periodic density functional theory (DFT) calculations. The adsorbed molecules form a dense hexagonal monolayer on both Cu(111) and Cu(100) surfaces [2]. The molecules arrangement and orientation on the surface are confirmed by DFT calculations including van-der-Waals interaction. Under heating, dissociation products adsorb on the surface and generate well-defined monolayers. Dense superstructures with particular domain orientation, depending on the surface symmetry, are observed by STM on Cu(111) and Cu(001). XPS spectra analysis indicates that the superstructures are formed by $Mo(CO)_x$ ($x<6$) fragments, where the number of CO groups depends on the substrate temperature. Experimental results are considered in comparison with theoretical calculations of $Mo(CO)_x$ fragments dissociation on copper surfaces. DFT results confirm the predominance of dissociation channels over desorption: in particular on Cu(001), the first dissociation of $Mo(CO)_6$ is widely favored with an exothermicity close to 2 eV. Following dissociation steps are also preferred compared to desorption with low endothermicities around 1 eV while adsorption energies cost between 3 and 4 eV.

[1] Z.C.Ying and W.Ho, J. Chem. Phys. 93 (1990) 9077.
[2] P.Krüger, M.Petukhov, B.Domenichini, A.Berko, and S.Bourgeois, J Phys Chem. C 116 (2012) 10617.

NST/SS-2-Or-2
Chemical reactions confined under graphene cover

T13 Surface Science

#NST/SS-2-Or-2

Q. Fu, R. Mu, L. Jin, Y. Zhang, X. Bao.

Dalian Institute of Chemical Physics, the Chinese Academy of Sciences - Dalian (China).

We show that an extended two-dimensional (2D) nanospace forms between graphene sheets and solid surfaces, where guest atoms or molecules can be accommodated at the interfaces and chemical reactions may be performed therein (Figure 1). It has been demonstrated that O, Pb, Ni, and Si atoms can diffuse underneath graphene at elevated temperatures, decoupling the graphene layers from the Ru(0001) substrate [1, 2]. Even at room temperature, the intercalation of CO molecules at graphene/Pt(111) interfaces was also observed. The 2D nanospace presents as an extended confined environment, which exhibits nano-confinement effect on the chemical reactions on the solid surface. In-situ low energy electron microscopy (LEEM)/photoemission electron microscopy (PEEM), ambient pressure X-ray photoelectron spectroscopy (AP-XPS), polarization-modulation infrared reflection absorption spectroscopy (PM-IRAS), and density functional theory (DFT) calculations reveal the nano-confinement effect from the graphene cover, which destablizes adsorption of CO on Pt(111) surfaces and promotes the catalytic CO oxidation confined under graphene cover [3]. CO intercalation and CO oxidation under BN cover has also been explored and a similar confinement of the BN cover on surface chemistry was observed.

[1] H. Zhang, Q. Fu, Y. Cui, D.L. Tan, X.H. Bao, J. Phys. Chem. C 2009, 113, 8296; Y. Cui, Q. Fu, H. Zhang, D.L. Tan, X.H. Bao, J. Phys. Chem. C 2009, 113, 20365.
[2] L. Jin, Q. Fu, R.T. Mu, D.L. Tan, X.H. Bao, Phys. Chem. Chem. Phys. 2011, 13, 16655; L. Jin, Q. Fu, H. Zhang, R.T. Mu, Y.H. Zhang, D.L. Tan, X.H. Bao, J. Phys. Chem. C, 2012, 116, 2988; Yi Cui, Junfeng Gao, Li Jin, Jijun Zhao, Dali Tan, Qiang Fu, Xinhe Bao, Nano Research, 2012, 5, 352.
[3] Rentao Mu, Qiang Fu, Li Jin, Liang Yu, Guangzong Fang, Dali Tan, Xinhe Bao, Angew. Chem. Int. Ed. 2012, 51, 4856.

Figure 1 Confined reactions in 2D nanoreators between graphene and metal

NST/SS-P2-05
Structural and Magnetic properties of Cobalt nanoparticles on graphene/SiC(0001)

T13 Surface Science

#NST/SS-P2-05

L. De Lima, A. De Siervo, R. Landers.

State University of Campinas - UNICAMP - Campinas (Brazil).

Fabrication of monodispersed and uniform-sized nanoclusters on substrates is currently a challenging subject that has received great interest. Monodispersed metal nanoclusters on insulating or semiconducting substrates have a wide range of applications in heterogeneous catalysts [1], as well as prototypes for magnetic medias with ultrahigh-density recording [2]. A promising route to fabricate nanostructures arrays is the self-assembly of atoms and molecules induced by surface nanotemplates (atomically well-defined surfaces) that are naturally or artificially patterned at the nanoscale [3]. In this work, cobalt nanoparticles were grown on graphene/SiC(0001). The graphene was obtainned by heating a SiC(0001) surface to temperatures of about 1150°C in ultra-high vacuum and Co was directly deposited on this surface at room temperature by electron-beam evaporation and various sessions of evaporation were done with different deposition rates and times, monitored by X-Ray Photoelectron Spectroscopy (XPS) and Scanning Tunneling Microscopy (STM). Basically, the cobalt clusters prefer to form on the defects sites, in the border between different regions of the substrate. XPS shows that the cobalt peak agrees with metallic cobalt, which indicates that there is no cobalt silicide/carbide formation. The magnetic properties of nanoparticles were investigated with X-Ray Magnetic Circular Dichroism (XMCD) at PGM beamline of Brazilian National Laboratory of Synchrotron Light. The XMCD results (L2,3 edge at 20K) show a enhancement of the orbital moment with a apparent in-plane anisotropy and no contribution of magnetic dipole operator, indicating that the spin density are spherically symmetric. These results were obtainned with the application of sum rules [4].

[1] - C. R. Henry; Surf. Sci. Rep.; 31, 235 (1998).

[2] - S. Sun et al; Science; 287, 1989 (2000).

[3] - W. Chen and A. T. S. Wee; J. Phys. D: Appl. Phys.; 40, 6287 (2007).

[4] - C. T. Chen et al; PRL 75, 152 (1995).

STM image of the g/SiC(0001) template and XMCD spectra of Co nanoparticles.

SS-17-Or-7
Atomic and electronic structure of the InAs (001) surface

T13 Surface Science

#SS-17-Or-7

N. Tomaszewska, J. Kolodziej.

Faculty of Physics, Astronomy, and Applied Computer Science, Jagiellonian University - Kraków (Poland).

The (001) surface of InAs displays multitude of stoichiometry dependent, complex reconstructions. In the present paper we show studies of this surface for two different reconstructions, using angle-resolved photoemision spectroscopy (ARPES), low-energy electron diffraction (LEED), and scanning tunelling microscopy (STM). Standard preparation procedure of the In-rich surface InAs(001) by ion sputtering and heating at 400-550^{o}C is used which leads to the c(8x2)/(4x2) reconstruction. This reconstruction may be transformed to the As-rich (2x4) reconstruction by exposing the surface to As_2 molecular flux and thermal annealing. Prepared surface structures are verified by LEED and their electronic structure is studied along main crystallographic directions, as well as on the Fermi surface, by ARPES. As for today no detailed research of the InAs(001) electronic band structure has been carried out. Atomic structure of InAs(001) c(8x2)/(4x2) was described by Kumpf et al. [1], and recently in detail by G.Goryl et al. [2]. The As-rich (2x4) structure was discussed by W. Barvosa-Carter et al. [3]. Both structures are rather complex, containing many atoms in their unit cells and consequently they support many electronic bands. We give preliminary discussion of these bands and we track the origin of few individual bands. We also discuss the surface electronic state localized near Fermi surface close to *J'* points in the reciprocal space. As we show, this state makes it possible to use STM for imaging of the In sublattice applying extremely low bias voltages. We think that the state arises due to broken translational symmetry at the surface, i.e. it is the Shockley state.

We acknowledge financial support by Polish NCN under the contract 2011/03/B/ST3/02070.

[1] Phys. Rev. Lett. 86 (2001) 3586.

[2] Surf. Sci. 605 (2011) 2073–2081.

[3] Surf. Sci 499 (2002) L129.

Fig. 1. Band structure of InAs(001)-c(8x2)/(4x2) surface with partially identified bands. Electronic band structure measured at 80K along $\overline{\Gamma J'}$.

Fig. 2. Distribution of photoelectron counts depending on binding energy and parallel component momentum of electron near hight symmetry *J'* point.

SS-P3-28
Interfaces of thin film, Studied by SPR Technique

T13 Surface Science

#SS-P3-28

K. Ayadi.

IOMP UFAS - Setif (Algeria).

Abstract: An experimental procedure has been devised to study the diffusion of impurities throughout thin films using the surface plasmon resonance technique. When such a film is in contact with two dielectrics having different indices the surface plasmons, at two interfaces of a metallic film can be optically excited simultaneously, by attenuated total reflection (ATR). The plasmons are totally decoupled..
Experimental results of the diffusion of gold through thin silver films are presented using the experimental procedure outlined above.
Keywords : Surface plasmon, attenuated total reflexion, diffusion

---

Résumé:
Le dispositif expérimental conçu est destiné à exciter optiquement les plasmons de surface aux deux interfaces d'une couche métallique en contact avec deux diélectriques d'indices différents. Les plasmons sont totalement découplés, ce qui nous permet d'accéder séparément aux propriétés de chaque interface. Un tel dispositif peut servir à étudier la diffusion d'une impureté à travers la couche, dans ce travail, nous avons procédé à l'étude de la diffusion entre deux couches d'argent et d'or, cette étude à permit également d'apprécier la vitesse de diffusion a travers la couche d'argent.
Mots clés : Plasmon de surface, diffusion.

INTRODUCTION.

In the visible and near infrared spectrum, materials such as alkyls and noble metals behave as free electron materials. Their electronic optical properties can be particularly reached by exciting the surface plasmons with ATR at the interface of these elements and a dielectric such as vacuum. The surface plasmons are very sensible to the interface properties, as it was reported in several works realised on systems like gold, silver, aluminium and alloys [1-5].

When surface plasmons are decoupled, the properties of the two interfaces become separately accessible and thus the study of the impurities diffusion process is possible. In this paper, the technique is described in details and applied to the diffusion of gold throughout thin silver films.

RESULTS

Fig 2 : Rp(α) at the external interface

Fig 3 : Rp(α) at the internal interface

Figure 2 and 3 : Reflection factor of the system Prism/MgF2/Ag

Serie 1 : λ = 630 nm , Serie 2 : λ = 590 nm , Serie 3 : λ = 550 nm
Serie 4 : λ = 510 nm , Serie 5 : λ = 470 nm

This preliminary study shows that the surface plasmons can be excited separately at two interfaces of a thin metallic film. The resonance curves are completely decoupled due to the judicious experimental set up. This constitutes a powerful and non-destructive probe that may be used to study the diffusion process of impurities through thin films.

REFERENCES.

/1/ A.Tadjeddine, J.Electroanal.Chem., 169, (1984) 129.
/2/ M.Abraham and A.Tadjeddine, J.Phys., 48, (1987) 267.
/3/ A.F.Benhabib and A.Tadjeddine, Solid Stat. Com., 60, (1986) 845.
/4/A.Hadjadj,A.Tadjeddine and G.Hincelin, J.Electroanal.Chem.,228, (1987)251.
/5/ A.F.Benhabib, L.Chahed and A.Tadjeddine, Thin Sol.Films, 202, 11 (1991).
/6/ A.Tadjeddine, S.Chiali and M.Costa, J. Chim. Phys., 80, (1983) 777.
/7/ E. Kretschmann and H.Raether, Z. Naturf. A23. (1968) 2135.
/8/E. Kretschmann, Opt.Commun.,26, (1978) 41.
/9/R. J. Bussjager and H.A. Macleod, Applied Optics, 25, (1996)5044.

Fig 2 : Rp(α) at the external interface

Fig 3 : Rp(α) at the internal interface

NST/SS-2-Or-3
Intercalation of Pb underneath graphene on Ir(111)

T13 Surface Science

#NST/SS-2-Or-3

F. Calleja, S. Barja, M. Garnica, A. Vázquez De Parga, R. Miranda.

IMDEA Nanociencia - Madrid (Spain).

Monolayer graphene (MLG) supported on metallic substrates is a widely studied subject nowadays, among other things because of the interesting moiré patterns arising from the lattice mismatch between graphene and the metal. However, interaction with the metal often leads to the suppression of many interesting effects, like the inter- or intra-valley scattering processes present in the case of non-metallic substrates [1]. A possible way to decouple MLG from the substrate is the intercalation of an atomic layer of a different element between them [2-5], and indeed it has been recently shown that MLG/Si/Ru(0001) do present inter-valley scattering [6]. Here we study the MLG/Pb/Ir(111) system and show that, under certain growth conditions, lead enters through graphene-free patches and intercalates between graphene and iridium preserving the original 9.3 x 9.3 incommensurated moiré structure [7]. As structure for the Pb inter-layer, we propose a rectangular lattice (close to Pb(110)) commensurated with graphene. Our measurements also suggest that lead decouples graphene from the metallic substrate and breaks its sub-lattice symmetry, allowing to observe both inter- and intra-valley scattering processes [8] not present in the absence of Pb.

[1] G.M. Rutter et al, Science 317, 219 (2007)
[2] I. Gierz et al, PRB 81, 235408 (2010)
[3] L. Huang et al, APL 99, 163107 (2011)
[4] M. Gyamfi et al, PRB 85, 205434 (2012)
[5] L. Meng et al, APL 100, 083101 (2012)
[6] J. Mao et al, APL 100, 093101 (2012)
[7] A.T. N'Diaye et al. NJP 10, 043033 (2008)
[8] I. Brihuega et al. PRL 101, 206802 (2008)

Figure 1: FFT map obtained from an STM image acquired on MLG/Pb/Ir(111). The reciprocal lattice vectors of graphene, lead and moiré structure are marked in blue, yellow and red respectively. The green circles mark the corners of the surface Brillouin zone of graphene.

SS-8-Or-5
Visualizing Anderson Localization of Non-Interacting Electrons

T13 Surface Science

#SS-8-Or-5

C. Ast [1], F. Zinser [1], M. Haverkort [1], K. Kern [1], S. Wissing [2], A. Schmidt [2], M. Donath [2].

[1]MPI for Solid State Research - Stuttgart (Germany), [2]Westfälische Wilhelms-Universität - Münster (Germany).

Randomness destroys translational invariance resulting in exponential spatial localization of wave functions through quantum interference. This effect — known as Anderson localization — is a universal property of waves, which has been observed directly in light and matter. In electron systems, Anderson localization has been studied mostly indirectly in transport experiments through metal-insulator transitions or conductance fluctuations. This complicates theoretical descriptions as, e. g., calculating the conductance remains a challenging task despite highly sophisticated models. Using the BiPb/Ag(111) mixed surface alloy, we go beyond averaged quantities both in theory and experiment. We measure simultaneously chemical composition and local electronic structure linking experiment and theory on the most fundamental level: we demonstrate the atomically resolved observation of spatial wave function localization for a mixed surface alloy — a purely two-dimensional electron system in a static disordered potential. We then use the chemical composition as the structural input for the “original” real space Anderson tight-binding model which allows us to directly compare the locally resolved wave functions in experiment and theory with remarkable agreement.

SS-4-Or-3
Interaction of Formic Acid With Anatase TiO2(101)

T13 Surface Science

#SS-4-Or-3

G. Herman [1], H. Nguyen [1], R. Ruther [1], Z. Dohnalek [2].

[1]Oregon State University - Corvallis, Or (United states), [2]Pacific Northwest National Laboratory - Richland, Wa (United states).

The (101) surface is the dominant face exposed on TiO_2 anatase nanoparticles and has been theoretically shown to be the thermodynamically low-energy surface.[1] In spite of the importance of TiO2 catalysis very few studies have been performed on the anatase TiO2(101) single crystal surface.[2-4] Fundamental studies on the role of TiO_2 surface structure on adsorption, dissociation, and desorption of formic acid has been performed on rutile single crystals and it was shown that surface structure plays an important role in observed chemistry.[5] In this investigation we have characterized the interaction of formic acid with anatase TiO_2(101) surfaces using temperature programmed desorption, x-ray photoelectron spectroscopy (XPS), and low energy electron diffraction. Formic acid is found to dissociate on the anatase TiO_2(101) surface on adsorption at low temperature, and undergoes decomposition upon desorption. Using deuterated formic acid and co-dosing with water allows us further elucidate the surface reaction mechanisms. These results will be compared to prior data that has been obtained for rutile single crystal surfaces.

[1]M. Lazzeri, A. Vittadini, A. Selloni, Phys. Rev. B 63, 155409 (2001).
[2]G.S. Herman, Z. Dohnálek, N. Ruzycki, U. Diebold, J. Phys. Chem. B 107, 2788 (2003).
[3]M. Xu, H. Noei, M. Buchholz, M. Muhler, C. Wöll, Y. Wang, Catal. Today 182, 12 (2012).
[4]D.C. Grinter, M. Nicrotra, G. Thornton, J. Phys. Chem. C 116, 11643 (2012).
[5]M.A. Henderson, J. Phys. Chem. B 101, 221 (1997).

NST/SS-1-Or-1
Graphene on cubic-SiC(001): current status and outlook for technology

T13 Surface Science

#NST/SS-1-Or-1

V. Aristov [1], O. Molodtsova [2], A. Zakharov [3], D. Marchenko [4], J. Sánchez-Barriga [4], A. Varykhalov [4], M. Portail [5], M. Zielinski [6], I. Shvets [7], A. Chaika [1].

[1]Institute of Solid State Physics RAS - Chernogolovka, Moscow District 142432 (Russian federation), [2]HASYLAB at DESY - D-22607 Hamburg (Germany), [3]MAX-lab Lund - Lund University, Box 118 - 22100 Lund (Sweden), [4]Helmholtz-Zentrum Berlin für Materialien und Energie, BESSY II - D-12489 Berlin (Germany), [5]CNRS-CRHEA - 06560 Valbonne (France), [6]NOVASiC - Bp267-F73375 Le Bourget Du Lac Cedex (France), [7]CRANN, School of Physics, Trinity College - Dublin 2 (Ireland).

We demonstrate the recent investigations of graphene on cubic SiC(001) substrates. The quality of graphene and number of monolayers on large area of substrate depend on preparation technology, which was proved by a number of experimental techniques (μ-LEED, LEEM, PEEM, ARPES etc). The overlayers show atomic and electronic structure typical for free-standing graphene. We believe, that very soon the method can represents a real step towards graphene-based electronic technologies.

Figure 1. (a) and (b) - micro-diffraction (sampling area 1.5 μm, E=45eV) patterns from different areas (domains) on the surface. (c) – μ-LEED (sampling area 5 μm, E=48eV) from a larger area showing superposition of LEED patterns with different domains. (d-f) The model explaining the origin of 24 diffraction spots and Dirac points in LEED and ARPES data. Insets in (d) and (e) are STM data confirming the model used. (g) and (h) - dark field LEEM (field of view is 20μm, electron energy 52eV) showing the reversed contrast when different domains (A and B) are imaged. (i) μ-LEED pattern from the dark region in panel (h)
Figure 2. Photoemission characterization of graphene grown on cubic-SiC(001). (a) Deconvolution of the C 1s core level spectrum of the graphene grown on cubic-SiC(001) prove major absence of the buffer layer. The experimental curve can be

fitted by only two components corresponding to SiC (green) and graphene monolayer (blue). (b-d) Testing structure of graphene on SiC(001) by angle resolved photoemission. (b) Effective surface Brillouin zone as seen in ARPES due to superposition of signals from various rotational domains. By letters A, B, A', B' different rotated domains are marked, same as at Fig. 3. (c, d) Dispersion of π-band in graphene measured by ARPES along directions 1 and 2 as denoted in (b).

SS-P1-11
Phase Diagram for Chromium-doped FINEMET-type Amorphous Alloys

T13 Surface Science

#SS-P1-11

A. Rosales-Rivera [1], A. Velasquez [1], D. Gomez [1], H. Giraldo [1], F. Saccone [2].

[1]Universidad Nacional de Colombia, Sede Manizales - Manizales (Colombia), [2]Universidad de Buenos Aires - Buenos Aires (Argentina).

A study of the magnetic, magneto-impedance, thermal and structural properties for the amorphous alloys Fe73.5-xCrxNb3Cu1Si13.5B9 with x = 0, 2, 4, 6, 8 and 10 is presented. These alloys were prepared in form of ribbons by a melt spinning technique and their structural state was checked using X-ray diffraction with CuKα radiation. The temperature (T) and the magnetic field (H) dependences of the magnetization were measured using temperature cycling (H fixed) and field cycling (T fixed) with a Vibrating Sample Magnetometer (VSM)-VersaLab Quantum Design, Inc. In the temperature cycling measurements, the sample in its ferromagnetic state is first heated from room temperature to a certain temperature in presence of magnetic field. Then the sample is cooled from the paramagnetic state to room temperature. The temperature and applied field were varied in the ranges 300 ≤ T ≤ 900 K and 0 < H ≤ 1 kOe, respectively. In the heating procedure, the magnetization curves exhibit a Hopkinson-type weak anomaly at a certain temperature T_{Ho} just below the amorphous Curie temperature $T_{Curie,am}$ with increasing temperature and fall basically to zero before that sample reaches its crystallization temperature. It was also found that the magnetization is irreversible below an irreversible temperature $T_i(H)$ with respect to the heating-cooling procedures. The complex impedance in these ribbons was measured for applied dc magnetic fields from - 80 to 80 Oe at room temperature, via the so-called four-probe technique. Here we emphasize the presence of a “three-peak behavior” in magneto-impedance curves. The thermal characterization was carried out using differential scanning calorimetry DSC (TA DSC-Q100) and thermogravimetric analysis TGA (TA TGA-Q500). Particular attention is also given to observation of crystallization kinetics via DSC, TGA, and magnetization. A (H,T) phase diagram that contains T_{Ho}, $T_{Curie,am}$, and Ti(H) for each of the ribbons under study is presented and discussed.

NST/SS-1-Or-2
Elastic Response of Graphene Nanodomes

T13 Surface Science

#NST/SS-1-Or-2

D. Stradi [1], S. Koch [2], E. Gnecco [3], S. Barja [1], S. Kawai [2], C. Díaz [4], M. Alcamí [4], A. Vázquez De Parga [1], T. Glatzel [2], E. Meyer [2], R. Miranda [1], F. Martin [1].

[1]Universidad Autonoma de Madrid & IMDEA Nanociencia - Madrid (Spain), [2]University of Basel - Basel (Switzerland), [3]IMDEA Nanociencia - Madrid (Spain), [4]Universidad Autonoma de Madrid - Madrid (Spain).

The extraordinary electronic properties of graphene makes it one of the most promising candidate materials for future nanoelectronic devices [1]. Additionally, its elastic behavior has recently been determined by indentation experiments on large free-standing monolayer samples and continuum mechanics modelling [2,3]. However, it is unclear up to what extent such features are preserved when the dimensions of the graphene sheet reach the atomic scale. Graphene samples of such dimensions can be produced by growing a graphene monolayer on Ru(0001). In this system, ripples of about a hundred atoms are formed, due to the lattice mismatch between the carbon monolayer and the metallic substrate [4-7]. In this contribution, large scale Density Functional Theory simulations of the indentation of such ripples are used to unravel that Non-Contact Atomic Force Microscopy (NC-AFM) experiments, performed on monolayer graphene/Ru(0001) samples under ultra-high vacuum conditions, are indeed probing the reversible deformation of this corrugated structure. These results prove that the elastic behavior of graphene is preserved at the nanoscale.

[1] A. H. Castro Neto et al., Rev. Mod. Phys. 81, 109 (2009)
[2] C. Lee et al., Science 321, 385 (2008)
[3] C. Gómez-Navarro et al., Nano Lett. 8, 2045 (2008)
[4] A. L. Vázquez de Parga et al., Phys. Rev. Lett. 100, 056807 (2008)
[5] B. Wang et al., Phys. Chem. Chem. Phys. 10, 3530 (2008)
[6] D. Stradi et al., Phys. Rev. Lett. 106, 186102 (2011)
[7] D. Stradi et al., Phys. Rev. B 85, 121404(R) (2012)

SS/NST-P1-04
XANAM measurements with a qplus sensor under X-ray irradiation

T13 Surface Science

#SS/NST-P1-04

S. Suzuki [1], S. Mukai [2], K. Fujikawa [2], C. Wang-Jae [3], M. Nomura [4], K. Asakura [2].

[1]Nagoya University - Nagoya (Japan), [2]Hokkaido University - Sapporo (Japan), [3]International Christian University (ICU) - Tokyo (Japan), [4]The High Energy Accelerator Research Organization (KEK) - Tsukuba (Japan).

Scanning Tunneling Microscopy (STM) and Noncontact Atomic Force Microscopy (NC-AFM) provide atomic-scale information on surface structures and related physical properties in the atomic scale. There has been an excellent study on the classification of atoms through force spectroscopy by Prof. Morita's group [1]. However, it is still difficult to obtain elemental information directly without supports from other surface science techniques. Previously, we reported development of NC-AFM combined with the synchrotron radiation X-ray, named **"X-ray Aided Non-contact Atomic force Microscopy (XANAM)" [2] as a chemically sensitive NC-AFM.** According to the text book on NC-AFM, a chemical bonding arises between a tip-apex and a surface during imaging at the atomic level. Strength of the chemical bonding force may depend on the electron density of bonding and anti-bonding states. Thus, a hypothesis was proposed as follows; if the electron density of states of the chemical bonding was resonant with the inner core level of electrons through X-ray irradiation, changes in the interaction force relevant to chemical information should appear. However, piezo-electric cantilever, a kind of self-detection cantilever, was used in the previous measurements [2]. A sharp tip was difficult to obtain, because the tip was made of piezo thin films fabricated by semiconductor process, though the self-detection cantilever has a merit of reducing complexity for optical beam alignments.

Therefore, **we have modified the cantilever system into a qplus sensor type [3] in order to improve the quality of XANAM measurements.** Adopting the qplus sensor has another merit of adding the functionality for electric current measurement. We carried out simultaneous measurements of dependency of electric current on distance between a W-tip and a gold film, as well as for frequency shift and amplitude

of the qplus sensor (Fig. 1). These measurements were conducted under X-ray irradiation with various energy ranges. In the presentation, we would discuss about data on the dependency of the force spectroscopy and the bias spectroscopy on X-ray energies. This work is majorly supported by several Grants from the JSPS, the MEXT and the NEDO. The experiments were carried out under the approval of Photon Factory Advisory Committee (ex. PAC: Proposal No. 2009G567, 2012G099).

[1] Y. Sugimoto et al, *Nature*, **446**, 64-67, 2007.

[2] Suzuki et al., *Chem. Lett.*, **33**, 636, 2004., Suzuki et al., Suzuki et al., *J. Phys. Conf. Ser.*, **61**, 1171-1121, 2007.

[3] F.J. Giessible et al., *Appl. Phys. Lett.*, **73**, 3956, 1998.

Measurements with a qlus sensor under X-ray irradiation (E=11919 eV): (a) Amplitude, (b) Frequency shift, and (c) Current.

SS-8-Or-6
Exploring Rashba spin-split surface states on semiconductors

T13 Surface Science

#SS-8-Or-6

T. Aruga [1], S. Hatta [1], Y. Otsubo [2], K. Yaji [3].

[1]Kyoto University - Kyoto (Japan), [2]Synchrotron Soleil - Saint Aubin (France), [3]University of Tokyo - Kashiwa (Japan).

Since the Au(111) surface state was found to be spin split to an unexpectedly large extent in 1996, the Rashba spin splitting on the surfaces of heavy elements were studied intensively. In 2007, the Ag surfaces covered with a Bi monolayer [1] or a Ag_2Bi surface alloy [2] were found to exhibit giant Rashba spin splitting, which indicated a possibility of the Rashba effect on light-element semiconductors such as Si and Ge. We have been searching for Rashba spin-split surface states on semiconductors [3-8], which has a lot of implications to semiconductor spintronics. For instance, surface spin accumulation due to the spin Hall effect would be exploited to realize direct spin injection into semiconductors.

Here we discuss on three distinct types of Rashba spin-split surface states. First one is a Rashba spin-split *metallic* surface state that was first identified on a semiconductor surface [5]. The surface state exhibits a free-electron-like dispersion with a spin splitting of 200 meV at E_F. The surface exhibits a high 2D electrical conductivity, implying that the surface can serve as a standard material for surface spin transport studies. Secondly, we show the surface states found at the Γ point on *A*/Ge(111) (A =Bi, Br) [6,7]. These states originate from bulk electronic states but become surface states (resonances) due to the truncation of the crystal at the surface. The surface states are Rashba spin-polarized as evidenced by spin-resolved photoemission. Surprisingly, the first-principles calculation indicates that the spin polarization is induced by the spin-orbit coupling at subsurface Ge atoms. The conclusion is supported by the observation of a significant spin polarization on Ge(111) covered with Br, which has an atomic number very close to Ge. Third example is a surface state on Tl/Ge(111)-(1x1) [8], which has six valley-type electron pockets at K points within the surface Brillouin zone. Due to peculiar symmetrical reasons, the electrons are completely spin-polarized toward the surface normal, with the neigboring electron pockets polarized to the opposite directions (outward/inward).

Thus the surface serves as a unique 2D metal with coupled spin-valley degrees of freedom.

[1] "Transition between tetramer and monomer phases driven by vacancy configuration entropy on Bi/Ag(001)", T. Nakagawa *et al.*, *Phys. Rev.* B **75**, 155409 (2007).

[2] "Giant Spin Splitting through Surface Alloying", C. R. Ast *et al.*, *Phys. Rev. Lett.* **98**, 186807 (2007).

[3] "Band structure of Tl/Ge(111)-(3×1) : Angle-resolved photoemission and first-principles prediction of giant Rashba effect", S. Hatta *et al*., *Phys. Rev.* B **77**, 245436 (2008).

[4] “Large Rashba spin splitting of surface resonance bands on semiconductor surface”, S. Hatta *et al*., *Phys. Rev.* B **80**, 113309 (2009).

[5] "Large Rashba spin splitting of a metallic surface-state band on a semiconductor surface", K. Yaji *et al.*, *Nat. Commun.* **1**, 17 (2010).

[6] "Spin-polarized semiconductor surface states localized in subsurface layers", Y. Ohtsubo *et al.*, *Phys. Rev.* B **82**, 201307(R) (2010).

[7] "Spin-polarized surface states on Br/Ge(111)-(1×1): Surface spin polarization without heavy elements", Y. Ohtsubo et al., *Phys. Rev.* B **86**, 165325 (2012).

[8] “A metallic surface state with uniaxial spin polarization on Tl/Ge(111)-(1x1)”, Y. Ohtsubo et al., *J. Phys.*: *Condens. Matter* **24**, 092001 (2012).

SS-1-Or-9
Scanning Tunneling Microscopy Studies of Orientations and Electronic Structures of C60 Molecules

T13 Surface Science

#SS-1-Or-9

Z. Qin, C. Liu, J. Chen, G. Cao.

Wuhan Institute of Physics and Mathematics, Chinese Academy of Sciences - Wuhan (China).

C_{60}-based compounds and/or assembly have stimulated much physical and technical interest for their unique electronic properties and physical significances in the field of electron amplifiers, molecular sensors, quantum computers, etc [1] , which motivates a considerable amount of studies of the structures and/or self-assembly of C_{60} molecules on various surfaces. The physical behaviors and/or properties of C_{60}-metal system depend on the nature of the chemical bond that is related to the orientations of the C_{60} cage with respect to the substrate, on their geometric adsorption structures, and on the partial filling of the lowest unoccupied molecular orbital (LUMO) which is influenced by the charge transfer from the substrate metal. Here, we present a scanning tunneling microscopy/spectroscopy (STM/STS) study of the molecular orientations and nucleation behaviors of C_{60} molecules on Pt(111) as well as their electronic properties. The chemical bond related molecular orientations as well as the localized geometrical C_{60}/Pt(111) assembled structures and their evolutions are well studied. Moreover, by inserting epitaxial layer between the C_{60} molecules and the metal substrate, the metallic substrate states are effectively decoupled and the interaction of the C_{60} molecules with the epitaxial layer becomes weaker. Due to the inhomogeneous distribution of the work function inside the epitaxial layer the degree of charge transfer between the C_{60} molecules and the Pt(111) is periodically modulated, which results in the formation of the dim-bright STM contrast of C_{60} molecules.

[1] C. Joachim, J. K. Gimzewski, and A. Aviram, Nature 408, 541 (2000).

SS-P3-27
DFT calculation of surfaces of Au(111) and Pd(111) for Pd catalyst on the S-modified Au(111)

T13 Surface Science

#SS-P3-27

M. Yokoyama [1], A. Mitsuhiro [2], S. Satoshi [2], I. Akira [1].

[1]Tottori University - Tottori (Japan), [2]Hokkaido University - Sapporo (Japan).

Transition metal catalyzed reactions have played an important role in synthetic and process chemistry. The homogeneous catalyst surely causes effective reaction; however, a lot of efforts and energy are required for reusing the catalyst. From this viewpoint, development of the easily treatable heterogeneous catalyst is strongly desired for reducing the waste of expensive rare metal. Although the polymer supported catalyst has been developed, it cannot tolerate under severe conditions such as high temperature and it is restricted to use in organic solvents. On the other hand, Pd acetate (Pd(OAc)2) molecules immobilized on the S-terminated GaAs(001) has high catalytic activity and stability for Heck reaction [1]. However, the GaAs substrates including toxic As, it is not suitable for mass productions. To solve this problem, a new type catalyst was reported recently [2], which transition metals were supported on the S-modified Au(111). In order to develop more effective catalysts, it is essential to understand the function of the Pd catalyst of the S-modified Au(111). Therefore, in this study, we tried to find the stable structure of Pd catalyst on the S-modified Au(111) by DFT calculations using the program package VASP [3].
After some experimentation, it showed that the SO4 might be adsorbed to the Au(111) substrate after piranha treatment [2]. Our calculation found that the stable position of SO4 is fcc site on Au(111). The binding energy of SO4 on Au(111) is very strong. After taking a particulate model into consideration, it assumes that the nano cluster surface would be planar in the particulates of about 3-5 nm, and aims at examining the reactivity of the surfaces Pd and SO4. For this reason, we also calculated the stable position of SO4 on Pd(111). Our calculation assumed that there is activity in the portion of the edge of a nanoparticle, and researched the correlation between SO4 and Pd atom on Pd(111) surface. Figure 1 shows the most stable structure of SO4/Pd-Pd(111) in energy. The electric charge of the surface of Pd shifts to +2 direction when SO4 adsorbs.

[1] I. Takamiya, S. Tsukamoto, M. Shimoda, M. Arisawa, A.Nishida and Y.Arakawa, Japanese Journal of Applied Physics.vol.45,No.18, 2006, L475-L477.
[2] Hoshiya N, Shimoda M, Yoshikawa H, Yamashita Y, Shuto S, Arisawa M. J Am Chem Soc. 2010 Jun 2;132(21):7270-2.
[3] G.Kresse and J.Hafner, Phys.Rev.B 47, RC558 (1993).

Figure 1. Schematic illustration of the most stable structure of SO4 on Pd-Pd(111) in energy. The grey, yellow and red sphere corresponding to Pd, S and O atoms, respectivery.

SS-11-Or-5
The Spin interface of Donor-Acceptor Charge-Transfer Complex on Ferromagnetic Surface

T13 Surface Science

#SS-11-Or-5

Y. Hsu [1], Y.L. Lai [1], C.H. Chen [1], J.H. Wang [2], T.N. Lam [3], Y.L. Chan [1], D.H. Wei [1], H.J. Lin [1], C.T. Chen [1].

[1]National Synchrotron Radiation Research Center - Hsinchu (Taiwan, republic of china), [2]Department of Chemistry, National Taiwan Normal University - Taipei (Taiwan, republic of china), [3]Institute of Nano Technology, National Chiao Tung University - Hsinchu (Taiwan, republic of china).

Organic spintronics has attracted growing attention not only because its fundamental interest but also the potential industrial applications. In addition, with organic tailored functionality and enduring spin coherence, organic spintronics offers a new and tantalizing approach toward multifunctional devices. Recently, the interface of ferromagnetic-organic hybrid structures is found to critically influence the efficiency of spin injection and transport in devices. A fundamental understanding of how interfacial properties engineer the surface spin polarization is important to facilitate the spin injection, transport, and the design of the local spin polarization in organic spintronics.

We imitated the interfacial regimes of organic-ferromagnetic heterostructure in a spin-valve structure to investigate how the interfacial hybrid state affects the spin injection/detection. To understand the efficient spin injection at organic-ferromagnetic contact for organic spintronics, we have implemented donor-acceptor pair via a strong organic acceptor on contact with ferromagnetic metal. The electronic structures and magnetic couplings are examined by utilizing various synchrotron-based spectroscopy and microscopy techniques. Our results reveal that the tailored interface by donor-acceptor pair is not only capable of tuning energy levels with a surface dipole layer but also expresses a spin-polarized organic layer and a remarkably enhanced magnetic anisotropy of the ferromagnetic film. The novel magnetic properties are contributed from strong magnetic coupling caused by the molecular restructuring of charge-transfer complex.

1. Y.-L. Chan, Y.-J. Hung, C.-H. Wang, Y.-C. Lin, C.-Y. Chiu, Y.-L. Lai, H.-T. Chang, C.-H. Lee, Y. J. Hsu, and D. H. Wei, Phys. Rev. Lett. 104, 177204 (2010).
2. Y.-J. Hsu, Y.-J. Hung, Y.-C. Lin, Y.-L. Lai, H.-T. Chang, J.-H. Wang, Y. L. Chan, C.-L. Hsia, M.-F. Luo, C.-H. Lee, and D. H. Wei, Synthetic Metals 161, 575-580(2011).
3. Y.-J. Hsu, Y.-L. Lai, C.-H. Chen, Y.-C. Lin, H.-Y. Chien, J.-H. Wang, L. T. Ngoc, Y.-L. Chan, D.-H. Wei, H.-J. Lin, and C.-T. Chen, J. Phys. Chem. Lett., http://dx.doi.org/10.1021/jz301757x (2013).

SS-14-Or-4
Phase Transition of Oxide Growth on Si(111)7×7 Studied by Real-time Photoelectron Spectroscopy and Theoretical Calculations

T13 Surface Science

#SS-14-Or-4

J. Tang [1], K. Nishimoto [1], S. Ogawa [1], A. Yoshigoe [2], S. Ishidzuka [3], D. Watanabe [1], Y. Teraoka [2], Y. Takakuwa [1].

[1]Tohoku University - Sendai (Japan), [2]Japan Atomic Energy Agency - Sayo (Japan), [3]Nagaoka University of Technology - Nagaoka (Japan).

The initial oxidation kinetics on Si(001) with O_2 shows a drastic phase transition from Langmuir-type adsorption to two-dimensional (2D) oxide island growth, where etching of Si surfaces with SiO desorption takes place at the same time of oxide growth, depending on the O_2 pressure and substrate temperature[1-3]. The oxygen uptake curves in the phase transition conditions interpreted by a dual oxide species (DOS) model with movable and steadily bonded oxygen atoms[2]. Although surface migration is negligibly short in Langmuir-type adsorption on Si(001) based on the DOS model, we have recently reported that surface migration of oxygen species, probably metastable oxygen molecule O_2*, affects significantly the oxidation kinetics in Langmuir-type adsorption on Si(111)7×7[4]. In this study, to clarify the influence of O_2* on the phase transition, the initial oxidation kinetics were investigated by real-time photoelectron spectroscopy using He resonance line (21.22 eV) and synchrotron radiation (710 eV) at SPring-8, and theoretical calculations.

In Fig. 1, the O 2p uptakes taken in situ during continuous O_2 supply (solid lines) indicate that Langmuir-type adsorption is in progress due to the curve fitting analysis based on the DOS model. When O_2 gas was stopped at about 50% of the surface oxide coverage θ_{oxide}, however, it is obvious that the O 2p uptakes (broken lines) has almost no decrease and slightly decreased at 590℃ and 610℃, respectively, while it steeply decreased at 640℃ and eventually no oxide remained on Si(111) after 5000 s. The findings suggest that oxide can be decomposed through SiO desorption even at the temperatures in Langmuir-type adsorption region, which is quite different from that on Si(001). Namely it is difficult to define the phase transition of oxide growth on

Si(111) on the basis of the DOS model. Furthermore, O 2p intensities decrease at slower rate when O_2 supply was stopped at the larger θ_{oxide}. The observed changes of decomposition rate are ascribed to those of oxygen adsorption states depending on θ_{oxide} by the curve fitting analysis of O 1s photoelectron spectra and theoretical calculation of O 1s binding energies. Based on the results, a surface reaction model of the phase transition of oxide growth on Si(111)7×7 in which the role of O_2* is taken into account is proposed.

[1] J.R. Engstrom et *al*., Surf. Sci. **256** (1991) 317.
[2] M. Suemitsu et *al*., Phys. Rev. Lett. **82** (1999) 2334.
[3] Y. Enta et *al*., Appl. Surf. Sci. **100/101** (1996) 449.
[4] J. Y. Tang et *al*., e-J. Surf. Sci. Nanothechnol. **10** (2012) 525.

Fig. 1 Time evolution of O 2p intensity during continuous oxidation and with stopping O_2 supply.

NST/SS-1-Or-3
Epitaxial Silicene - tunable hybridization with the substrate and weak interactions with epitaxial organic overlayers

T13 Surface Science

#NST/SS-1-Or-3

R. Friedlein, F. Bussolotti (#), A. Fleurence, Y. Yamada-Takamura.

Japan Advanced Institute of Science and Technology - Nomi, Ishikawa (Japan).

The electronic and structural properties of epitaxial silicene formed on ZrB_2(0001) thin films grown on Si(111) wafers upon adsorption of either potassium atoms and anthracene and pentacene molecules have been studied using photoelectron spectroscopy and electron diffraction. For pristine silicene, a particular, atomic-scale buckling leads to the opening of a direct band gap at the Γ point, while ZrB_2-related surface states are not affected. This is consistent with only a minor degree of hybridization beween Si- and Zr-derived states. The electronic interactions at the interface can be tuned by electron donation from adsorbed potassium atoms, upon which hybridization is progressively switched on.

In oligoacene monolayers, molecules grow with the long molecular axis aligned parallel to the surface. The further growth of pentacene multilayers is strongly temperature-dependent and characterized by a competition of flat and standing configurations. In anthracene films at about 140 K, molecules are found to grow in a point-on-line commensurate relationship between the bulk-like bc-plane of anthracene and silicene. At 293 K, anthracene molecules do still adsorb which indicates that the interactions involved are stronger than those on the graphite (0001) surface and enhanced by the atomic-site specific charge distribution associated with the buckling of silicene.

The results indicate that the charge-density modulation associated with the atomic-scale buckling of silicene render the interactions with organic adsorbates as compared to graphene, which allows for specific epitaxial conditions for the growth of overlayers. On the other hand, the results also confirm that silicene is strikingly

different from other Si surfaces for which the presence of dangling bonds leads to chemisorption of organic adsorbates.

#present address: Graduate School of Advanced Integration Science, Chiba University, Yayoi-cho, Inage-ku, Chiba 263-8522, Japan

[1] A. Fleurence, R. Friedlein, T. Ozaki, H. Kawai, Y. Wang, Y. Yamada-Takamura, Phys. Rev. Lett. **10**8, 245501 (2012).

SS-P3-11
FTIR spectroscopy of water clusters absorbed on solid neon surface

T13 Surface Science

#SS-P3-11

Y. Shimazaki, S. Takekuma, K. Yamakawa, I. Arakawa.

Gakushuin University - Tokyo (Japan).

Water clusters have been investigated for several decades in terms of their structure, dynamics, and interaction between hydrogen bonds in the cluster. Experimentally, water clusters have been generated in the gas phase, on helium droplet, and by matrix isolation mainly with the use of rare gas solids [1, 2, 3]. In addition, there was also a successful investigation to observe the clusters adsorbed directly on Pt(111) surface [4]. In the previous study we investigated the photoinduced desorption of water clusters on solid neon surface [5]. From Photostimulated Desorption Time of Flight Mass Spectrometry (PSD-TOF-MS) we found that the clusters of $(H_2O)_n$ with n=2~12 were generated on the surface. Furthermore, it was revealed that the size distribution of the clusters strongly depends on the coverage in the submonolayer region. In the present study we performed non-destructive measurement of water clusters adsorbed on solid neon surface using the technique of Fourier Transform Infrared Spectroscopy (FTIRS).

The experimental apparatus consists of a vacuum chamber with a liquid helium cryostat, a FTIR spectrometer, and a compartment of a liquid nitrogen cooled MCT detector. After baking at 393K for 24 hours the base pressure of 1×10^{-8}Pa was achieved. The substrate was the gold film which was vacuum-evaporated on the oxygen-free copper holder mechanically fixed on the cryostat. The incident angle of p-polarized infrared light on the substrate was 80°. The solid neon was grown on the substrate at 6 K with the thickness of 300 atomic layers. Then, coverage of water on neon surface was gradually increased from 0.05 to 1.0.

The Infrared spectra of water clusters adsorbed on solid neon surface are shown in Fig. 1. The broad peak from 3000 cm^{-1} to 3700 cm^{-1} was due to the formation of amorphous ice. On the other hand, the adsorption peaks of 3542 cm^{-1}, 3384 cm^{-1}, 3345 cm^{-1}, and 3224 cm^{-1} were attributed to the vibrations of hydrogen bonded OH in the clusters of trimer, tetramer, pentamer, and hexamer, respectively. In the presentation we will discuss the dependency of the cluster size distribution on the amount of adsorption of water, and will compare the result with the one obtained by PSD-TOF-MS.

[1] F. Huisken et al., J. Chem. Phys. **104** (1996) 17.
[2] K. Nauta et al,. Science **287** (2000) 293.
[3] S. Hirabayashi et al., Chem. Phys. Lett. **435** (2007) 74.
[4] M. Nakamura et al., Chem. Phys. Lett. **309** (1999) 123.
[5] I. Arakawa et al., Low Temp. Phys. **38** (2012) 745.

Fig. 1.The Infrared spectra of the water clusters adsorbed on solid neon surface as a function of the coverage from 0.05 to 1.0 at 6 K.

SS-P3-04
Photochemical Assembly of Diazonium Molecular Monolayer on Hydrogen-Terminated Si(111)

T13 Surface Science

#SS-P3-04

K. Shimosaka, T. Ichii, H. Sugimura.

Department of Materials Science and Engineering, Kyoto University - Kyoto (Japan).

[Introduction]
A self-assembled monolayer (SAM) covalently bonded to a Si substrate is promising for molecular electronics. It is well known that organic molecules terminated with a vinyl, hydroxyl or aldehyde group are attached to a hydrogen-terminated Si (Si-H) substrate by replacing its surface H atoms with the organic molecules. Further extension of this process is crucially required in order to modify the bonding structure of SAMs, because it would heavily affect electron-transfer properties between the molecules and the Si substrate. Diazonium molecules, which electrochemically react with Si-H and to form a SAM[1], are candidates. Here we report on a photochemical approach to form a SAM from diazonium molecules without applying an external electrode potential.

[Experimental]
Two types of Si (111) wafer (Phosphorus doped n-type and boron doped p-type) were used for the present experiments. 4-nitrobenzene diazonium tetrafluoroborate (NBD-BF_4) was used as a precursor molecule. 10 mM dimethyl sulfoxide solution of NBD-BF_4 was put in a quartz vessel. Si-H was immersed into the solution and irradiated with visible-light (200 $mWcm^{-2}$) for 4 hours. As schematically illustrated in Fig. 1 NBD molecules photochemically immobilized on the substrate.

[Results and discussion]
X-ray photoelectron spectroscopy (XPS) N 1s spectra of the NBD monolayer on Si (111) was shown in Fig.2. In Fig.2, both spectra have two large peak contributions around 406 eV of binding energy and at about 400 eV, attributed to NO_2 and NH_2 groups, respectively. These results imply that NBD molecules are certainly

immobilized on the Si substrate and a part of the NO_2 group reduced to NH_2 groups. The N 1s peak intensity of the p-type sample is higher than that of the n-type sample. On the p-type Si surface, photo-generated electrons remained more stably than the n-type Si surface. Such electrons more readily reduce NBD molecules to promote the immobilization reaction.

[1] Pinson J and Podvorica F, *Chem. Soc. Rev.*, **34**, 429 (2005)

Fig. 1 NBD molecules immobilization reaction

Fig. 2 XPS spectra of NBD adsorbed Si(111) substrates

SS-8-Or-7
Efficient step-mediated intercalation of silver atoms deposited on the Bi2Se3 surface

T13 Surface Science

#SS-8-Or-7

M. Otrokov [1], S. Borisova [2], V. Chis [3], M. Vergniory [3], S. Eremeev [2], V. Kuznetsov [1], E. Chulkov [3].

[1]Tomsk State University - Tomsk (Russian federation), [2]Institute of Strength Physics and Materials Science - Tomsk (Russian federation), [3]Donostia International Physics Center - San Sebastian (Spain).

The evolution of electronic and structural properties of topological insulator surfaces upon deposition of various adsorbates is of significant interest currently [1-5]. Typically, the Dirac state survives upon such an adsorption, however, additional Rashba-split two-dimensional electron gas states arise at the surface, as was shown for Bi_2Se_3 exposed to molecules [1], alkali [2], noble [3, 4] and magnetic [5] metal atoms. Meanwhile, structural investigations of the impurity deposited Bi_2Se_3 surface revealed partial [2] or almost complete [3, 4] disappearance of adatoms at room and higher temperatures. The authors of these works claimed that majority of the adatoms intercalates below the surface, presumably into the van der Waals gaps of the Bi_2Se_3 crystal, however the mechanism of such an intercalation has not been investigated yet. To study this mechanism we consider the case of the silver atoms deposited on the Bi_2Se_3 surface. Two possible intercalation mechanisms are examined: penetration from the terrace under the step and penetration via interstitials and/or vacancies of the surface quintuple layer block. It is shown that the former mechanism is strongly preferred over the latter one due to significant energy gain appearing at the step. According to performed estimations, the room temperature diffusion length of silver atoms reaches ten microns within a couple of minutes both on the surface and within the van der Waals gap, which essentially exceeds a typical distance between steps. These results shed light on the mechanism of intercalation of metal atoms deposited on the Bi_2Se_3 surface.

[1] H. M. Benia, C. Lin, K. Kern, et al., Phys. Rev. Lett. **107**, 177602 (2011).
[2] M. Bianchi, R. C. Hatch, Z. Li, et al., ACS Nano **6**, 7009 (2012).
[3] Y.-L. Wang, Y. Xu, Y.-P. Jiang, et al., Phys. Rev. B **84**, 075335 (2011).
[4] M. Ye, S. V. Eremeev, K. Kuroda, et al., (2011), arXiv:1112.5869.
[5] J. Honolka, A. A. Khajetoorians, V. Sessi, et al., Phys. Rev. Lett. **108**, 256811 (2012).

NST/SS-1-Or-4
DFT calculation for adatom adsorption on single layer h-BN

T13 Surface Science

#NST/SS-1-Or-4

A. Ishii, T. Torobu, K. Nakada.

Tottori University - Tottori (Japan).

Two-dimensional (2D) materials with a layered structure such as graphene, hexagonal born nitride (h-BN) and molybdenum disulfide (MoS2) have been attracting attention. Similar to graphene, h-BN, MoS2 has a hexagonal crystal structure. h-BN is known as a very good electrical insulator with good thermal conductivity and stability.

Recently, single layer h-BN will be focused attentions to be substrates of new nano structure devices using its two-dimensional feature. It has been widely used in vacuum technology and also been employed in electronics, nuclear energy, x-ray lithography, lubrication, etc [1-2]. As specific device application, the h-BN substrate is used as graphene field-effect transistors (GFETs) [3]. Thus, the single layer h-BN will be focused attentions to be substrates of new nano structure devices using its two-dimensional feature. For functionalizing of single layer h-BN or construction of nano structures on graphene, it is necessary to investigate the binding of materials on single layer h-BN. However, in general, the mechanism of the growth of the three dimensional materials or nano structures on the two-dimensional material is not yet understood.da

For the first step, it is significant to investigate the adsorption of atoms on single layer h-BN. Therefore, in this work, we investigate stabilities and electronic structures of adatom of almost every atomic species to understand the three dimensional material on single layer h-BN which is a typical two-dimensional material. We actually calculated by a method like the calculation of the atomic adsorption on the graphene [4]. The aim of this research discusses with stability of the adatom in h-BN by analysis from the electronic structure using the first-principle calculation technique.

The results will be very helpful to plan the construction of nano structures on single layer h-BN.

[1] V.L. Solozhenko, A.G. Lazarenko, J.-P. Petite, and A.V. Kanaev, J. Phys. Chem. Solids 62, 1331 (2001)

[2] P. Widmayer, H.-G. Boyen, P. Ziemann, P. Reinke, P. Oelhafen, Phys. Rev. B 59, 5233 (1999).

[3] C.R. Dean, A. F. Young, I. Meric, C. Lee, L. Wang, S. Sorgenfrei, K. Watanabe, T. Taniguchi, P. Kim, K. L. Shepard, J. Hone, Nature Nanotech. 5, 722. (2010)

[4] A. Ishii, M. Yamamoto, H. Asano, K. Fujiwara, J. Phys. Conf. Ser. 100 (2008) 052087. ; K. Nakada, A. Ishii, Solid State Commun. 151 (2011) 13 ; K. Nakada, A. Ishii, Jian Ru Gong (Ed.), ISBN: 978-953-307-556-3, InTech

SS-11-Or-6
The properties of organic monolayers on Al(111) enhancing surface inertness

T13 Surface Science

#SS-11-Or-6

T. Yamada, R. Sato, M. Kawai.

RIKEN - Saitama (Japan).

We conducted surface-scientific investigation for a series of organic thiol adsorbates and carboxylic adsorbates on clean surfaces of single-crystalline aluminum (111) for our purpose of passivating metallic Al towards air oxidation. We studied the monolayer structures, thermal and electron-beam alterations, and the ability to block oxidation by ambient O_2, by means of X-ray photoelectron spectroscopy (XPS), X-ray absorption spectroscopy (XAS), vibrational analysis by high-resolution electron energy loss spectroscopy (HREELS), electron diffraction, and scanning probe methods. Clean Al(111) readily accepts alkanethiols, aromatic thiols and fluoroalkane thiols to form stable monolayers at room temperature. The hydrocarbon parts of thiols were proven to be intact after adsorption by the electron spectroscopies for *n*-$C_nH_{2n+1}SH$ adsorbates and 4-biphenylthiol (4BPT). The SH species was not detected vibrationally, indicating that S is anchoring the hydrocarbon part on Al. Irradiation of electron beam (~ 100 eV) introduced a substantial amount of unsaturated C-C bonds with a nearly complete loss of C-H bonds from the monolayer, both from alkane and aromatic thiols. A quasi-graphitic monolayer is anticipated to be formed by electron irradiation. The electron-bombarded monolayers of this type exhibited a substantial robustness towards oxidation in ambient O_2.[1,2] Figure 1 shows the thickness of oxide layer on clean and monolayer-covered, and electron-bombarded Al(111) measured by XPS after an exposure to 0.1 MPa of O_2. Linear fluoroalkanethiols, *n*-$C_nF_{2n+1}C_2H_4SH$ (n=4,8) also form monolayers at room temperature with a full coverage smaller than the alkanethiols. When the adsorption process was made at substrate temperatures higher than 100^oC, the uptake of carbon exceeded the monolayer amount of the precursor molecule, and substantial loss of F from the adlayer was observed. The adlayer seemed to be composed of polymerized fluorohydrocarbon, and exhibited a substantial strength against oxidation. We also tested a series of carboxylic acids ($C_nF_{2n+1}COOH$ (n=1,2,3) and CH_3COOH), referring to preceding researches [3]. Intact monolayers of these compounds exhibited a fair robustness against oxidation.Passivation of metallic Al surface with ultimately thin - monolayer - organic compounds is essential in utilizing the favorable electronic,

thermal and mechanical properties of Al in nanotechnology, in the forms of thin layers and nanoparticles.

[1] S. Nomura, T. Yamada, M. Kawai, *Chem. Lett.* **39** (2010) 1297.
[2] T. Yamada, Japan Patent Application 2011-168725.
[3] V.J.Bellitto, J. N. Russell, Jr., U.S. Patent No. 7,625,600 B1.

Figure 1: The effective Al_2O_3 thickness after exposure to O_2 for 100 sec on the clean, 4BPT adsorbed, and electron-bombarded Al(111)[1].

SS-P3-12
Photochemical reaction of water clusters and methane coadsorbed on solid neon surface

T13 Surface Science

#SS-P3-12

K. Mabuchi [1], S. Takekuma [1], K. Yamakawa [1], I. Arakawa [1], T. Miura [2].

[1]Gakushuin University - Tokyo (Japan), [2]JNIOSH - Tokyo (Japan).

Surface photoreactions of water and hydrocarbons have been investigated for decades because of their importance in the area of planetary physics [1].Although water clusters have drawn much attention in recent years, surface photochemical reaction involving water clusters has not been sufficiently studied yet. In the previous study, we investigated photoreaction of water clusters and methane coadsorbed on rare gas solid. It was revealed from Photostimulated Desorption Time of Flight Mass Spectrometry (PSD-TOF-MS) that the compounds which are not simple combination of water and methane were produced [2]. In the present study, using the technique of Fourier Transform Infrared Spectroscopy (FTIR), we aimed to identify products of photochemical reaction of water and methane, which includes a monomer, clusters, and ice on solid neon surface.

The experimental set up consists of a vacuum chamber with a liquid helium cryostat, a FTIR spectrometer and an external MCT detector cooled by liquid nitrogen. The chamber was evacuated to the ultra high vacuum condition (1×10^{-8} Pa) after baking at 373 K for 24 hours. We adopted the Au film as the substrate, which was vacuum-deposited on the oxygen-free copper holder mechanically connected to the cryostat. The temperature was monitored by a chromel-alumel thermocouple set on the holder. The incident angle of p-polarized infrared light was 80°. Solid neon with 100 atomic layers was prepared on the substrate at 6 K. Then, water vapor was introduced to the chamber from one gas line, followed by the exposure of methane from another gas line. After the coadsorption state of water and methane on solid neon surface was achieved, we irradiated the sample with a laser plasma vacuum-ultraviolet light (the wavelength was ranged from 12 to 108 nm and the photon number was 2×10^{13} per minute). The infrared spectra were measured before and after irradiation.

From the spectrum after irradiation, it was revealed that CO, CO_2, CH_3OH ware generated . The integral intensities of their absorption peaks increased as the

irradiation time became longer. However, increasing rate of the integral intensity of the peak due to CH_3OH was suppressed with time (Fig.1). In the presentation, we will discuss it in terms of the photoreaction mechanism, as well as result of photo reaction of water clusters and methane.

[1] R. Hodyss et al., Icarus **200** (2009) 338.
[2] I. Arakawa et al., Low Temp. Phys. **38** (2012) 745.

Fig.1. The time variation of the integral intensity of the absorption peak due to CH_3OH.

SS-15-In-1
Novel development of very high brightness and highly spin-polarized electron gun with compact 3D spin manipulator for SPLEEM

T13 Surface Science

#SS-15-In-1

T. Koshikawa [1], T. Yasue [1], M. Suzuki [1], K. Tsuno [1], S. Goto [2], X.G. Jin [3], Y. Takeda [4].

[1]Osaka Electro-Communication University - Neyagawa, Osaka (Japan), [2]Sanyu Electron Co., Ltd. - Tokyo (Japan), [3]Nagoya University - Nagoya (Japan), [4]Aichi Synchrotron Radiation Center - Seto, Aichi (Japan).

We have already developed a novel high brightness and high spin-polarized low energy electron microscope (SPLEEM) [1-3]. Our developed SPLEEM can make us the dynamic observation of the magnetic domain images possible. However the size of the spin-polarized electron gun is large and we have started to develop a new compact spin-polarized electron gun with a new idea. Two devices are necessary to operate 3-dimensional spin direction; a spin manipulator which changes the out-of-plane spin direction and a spin rotator which can change the in-plane spin direction. We have proposed a multi-pole Wien filter which enables 3-dimensional spin operation with one device. Fig. 1 shows a drawing of the developing 3D multi-pole spin manipulator which has 8 poles and the magnetic and electric field in the multi-poles Wien filter. Uniform field can be obtained at the center part of the Wien filter with 8 poles and 12 poles, however 4 poles filter gives non-uniform field even at the center. In the present development 8 poles Wien filter has been adopted. The results of magnetic domain images and asymmetries of Co(4ML)/W(110) vs. polar and azimuthal angles with one device have been obtained, which will be shown in the presentation.

1) X.G. Jin et al., Appl. Phys. Express 1, 045002 (2008).
2) N. Yamamoto et al., J. Appl. Phys. 103, 064905 (2008).
3) M.Suzuki et al., Appl. Phys.Express 3, 026601 (2010).

Fig. 1: 3D multi-pole spin manipulator and uniformity of magnetic and electric field.

SS-17-Or-3
Molecular Quantum Mirage via Atomic Surgery

T13 Surface Science

#SS-17-Or-3

S. Du [1], L. Liu [1], B. Song [1], Y. Jiang [1], K. Yang [1], W. Xiao [1], M. Ouyang [2], A.H. Castro Neto [3], H. Gao [1].

[1]Institute of Physics, CAS - Beijing (China), [2]University of Maryland - College Park (United states), [3]National University of Singapore (Singapore).

We report on a quantum mirage formation in molecular systems, manganese-phthalocyanine (MnPc) based organic nanostructures, created by removing H atoms using a low-temperature scanning tunneling microscope. Based on experimental observation and scattering theory, we find out that the observed local density of states (LDOS) around the molecular lobes is a quantum mirage of the Kondo effect at the molecular center. Chemical bonds between unpaired carbon atoms and the Au substrate are selectively formed as scattering centers, by which the two-dimensional electron states on the surface are scattered, and the intervention of electron waves leads to the aforementioned LDOS away from the center. Furthermore, with applying external magnetic field on the artificially-controlled molecular structure, through Zeeman splitting of the Kondo peaks at different atomic sites of a dehydrogenated MnPc molecule, Landé g factors of the molecular structure have been spatially mapped. This finding opens up a new opportunity for controlling quantum scattering and intervention using artificially-controlled molecular structures.

Molecular Quantum Mirage via Atomic Surgery: Hydrogen Detachment from MnPc Molecule

NST/SS-2-Or-9
Template-directed Assembly of Functional Molecules on Epitaxial Graphene on Ru(0001)

T13 Surface Science

#NST/SS-2-Or-9

H. Guo.

Institute of Physics, Chinese academy of Sciences - Beijing (China).

Recently, the graphene monolayers have been found to adopt a superstructure - moiré pattern - on Ru(0001). By using scanning tunneling microscopy/spectroscopy, the selective adsorption and formation of ordered molecular arrays of FePc and pentacene molecules can be realized on the graphene/Ru(0001) templates. With in-depth investigations of the molecular adsorption and assembly processes we reveal the existence lateral electric dipoles in the epitaxial graphene monolayers and the capability of the dipoles in directing and driving the molecular adsorption and assembly. When increasing the molecular coverage, we observed the formation of regular Kagome lattices that duplicate the lattice of the moiré pattern of monolayer graphene. Furthermore, we demonstrate the graphene grown epitaxially on Ru(0001) can be used as a buffer layer to study the intrinsic electronic properties of adsorbed molecules. The intrinsic molecular orbitals of C60, pentacene and perylene-3,4,9,10-tetracarboxylic dianhydride (PTCDA) molecules were imaged by scanning tunneling microscope (STM). High resolution STM images of the molecules reveal that the graphene layer decouples the individual molecules electronically from the metallic substrate, which is also verified by density functional theory calculations. It has great advantages compared to other buffer layers, for instance, thin organic films, NaCl, and oxides. The epitaxial graphene layer on Ru(0001) is of both fundamental and technological importance for investigating molecular interaction and structures on solid surface.

* In collaboration with Haigang Zhang, Jinhai Mao, Haitao Zhou, Lizhi Zhang, Geng Li, Yi Zhang, Yi Pan, Wende Xiao, Yeliang Wang, Shixuan Du, and Hong-Jun Gao et al. Institute of Physics, Chinese Academy of Sciences, Beijing 100190, China.

(1) H, G. Zhang et al, Phys. Rev. B 84, 245436 (2011)
(2) H. T. Zhou et al, Appl. Phys. Lett. 99, 153101 (2011)
(3) L. Z. Zhang et al, J. Phys. Chem. C 115, 10791 (2011)
(4) G. Li et al, Appl. Phys. Lett.100, 013304 (2012).

SS-2-Or-5
Self-Ordered Vicinal-Surface-Like Nanosteps at the Thin Metal-Film/Substrate Interface: new surface structures

T13 Surface Science

#SS-2-Or-5

B. Pokroy, C. Saguy, S. Boroukhin.

Technion - Israel Institute of Technology - Haifa (Israel).

We report on the self-formation of periodic atomic and nano steps at the interface between the metal thin film and the underlying supporting substrate[1] (Figure1), revealed by the template stripping method [2] (Figure 2]. Such vicinal-like and atomic stepped surfaces of metals and semiconductors exhibit well-arranged, periodic atomic steps and have numerous applications in microelectronics, catalysis, direction of nanowire arrays, patterning of quantum dots and magnetic domains, and many more. In contrast to classical vicinal surfaces which are produced by the expensive and tedious procedure in which single crystals of a desired material are cut at a small angle to the low surface energy plane followed by surface sputtering and annealing under ultrahigh vacuum for imaging, our surfaces form on polycrystalline materials, at almost room temperature, and at atmospheric environments and have no need of any other procedure in order to image. We also demonstrate how the step periodicity can be easily controlled and explain the mechanism of formation. We also presnt new atomic structures on these surafces that have never been obsrved previously using standart vicinal suraces.

1. Borukhin S., Sagi C., Koifman M. and Pokroy B. “Self-Ordered Vicinal-Surface-Like Nanosteps at the Thin Metal-Film/Substrate Interface” Journal of Physical Chemistry C. 116. 12149–12155 (2012).

2. Borukhin S. and Pokroy B. “Formation and Elimination of Surface Nanodefects on Ultraflat Metal Surfaces Produced by Template Stripping” Langmuir. 27, 13415–13419 (2011). (Letter).

Figure 1: Schematic presentation the template stripping method of a thin gold surface and the STM image revealing the atomics steps on the stripped surface.
Figure 2: Schematic presentation of the ability to control the atomic step periodicity by different substrates and the corresponding STM images of the stepped surfaces.

NST/SS-1-Or-6
XPS for Characterization of Working Devices

T13 Surface Science

#NST/SS-1-Or-6

S. Suzer.

Bilkent University, Chemistry Department - Ankara (Turkey).

XPS measurements were performed while 3 different devices were under operation. This is achieved by imposing both static and pulsed electrical and optical stresses to devices for their operations:

i- For operating a device, consisting of large area Graphene on a Quartz substrate and between two metal electrodes, a potential was applied to one of the electrodes while the other one was grounded. By following the variations in the binding energy of C1s, the potential drop was monitored, which exhibited a uniform resistive shift for the pristine graphene but was not very uniform after its oxidation, due to formation of cracks and faults. Surprisingly, the O1s peak of the quartz substrate followed the same pattern as the C1s of graphene.

ii- For operating a Si-Diode, both forward and reverse bias were applied across the p-n Junction, and the variations in the position of the Si2p peak were recorded. This enabled us to identify and separate n- and p- domains from each other.

iii- For operating a GaN-Photodiode, the device was subjected to light illumination, in addition to forward and reverse bias applications. This approach enabled us, to detect both dopant dependent (n- or p-) as well as photoresistance changes in the Ga3d peak positions, again reflecting on uniform and defective domains.

Details of the experimental set-up, as well as utilization towards performance measurements and characterization of defects affecting will be presented.

SS-5-Or-2
From achiral molecules to chiral superstructures: an STM study of triphenylamine derivatives on Au(111)

T13 Surface Science

#SS-5-Or-2

S. Gottardi [1], K. Müller [1], J.C.M. Lopez [1], M. Kivala [2], A. Kara [3], H. Yildirim [3], M. Stöhr [1].

[1]Zernike Institute for Advanced Materials - Groningen (Netherlands), [2]Department of Chemistry and Pharmacy,University of Erlangen - Nürnberg (Germany), [3]Department of Physics, University of Central Florida - Orlando (United states).

Supramolecular recognition is a useful tool to realize highly organized and periodic structures at the nanometer scale [1]. Additional spontaneous chiral ordering can be obtained from self-assembly giving rise to new possible applications for these functionalized surfaces [2-3]. However, chiral precursors are not always needed to develop chiral assembled structures on surfaces, as in the case of organizational chirality.
In this work we investigated the self-assembly of achiral triphenylamine derivatives which feature cyano functionalities for the formation of intermolecular non-covalent bonds based on dipolar coupling. As substrate a (111)-oriented Au surface was used and the experiments were carried out with scanning tunneling microscopy (STM) at 77K. We observed the coexistence of two phases, both arranging into chiral porous networks. Homo-chiral domains extend for hundreds of nanometers and, in some cases, even over Au step edges. The structural models, the intermolecular interactions as well as the influence of the substrate on the assembly will be discussed for both two phases. Furthermore, we compare the results with theoretical calculations. Also the effect of post-annealing onto the assembly was investigated: a transformation of one phase into the other occurs together with a global improvement in the quality of the porous network. Such molecular chiral porous networks are of great interest for many applications as in opto-electronic devices, sensors and for catalysis.

[1] S. Stepanow, N. Lin, D. Payer, U. Schlickum, F. Klappenberger, G. Zoppellaro, M. Ruben, H. Brune, J. V. Barth, K. Kern, Angewandte Chemie 2007, 119, 724–727.
[2] J. A. A. W. Elemans, S. Lei, S. De Feyter, Angewandte Chemie International Edition 2009, 48, 7298–7332.
[3] M.-C. Blüm, E. Ćavar, M. Pivetta, F. Patthey, W.-D. Schneider, Angewandte Chemie 2005, 117, 5468–5471.

Chiral porous network

SS-7-Or-5
CeO_{2-x} surfaces as reducible oxide model systems

T13 Surface Science

#SS-7-Or-5

P. Luches [1], F. Pagliuca [2], F. Boscherini [3], V. Grillo [1], S. Valeri [2].

[1]S3, Istituto Nanoscienze, CNR - Modena (Italy), [2]Dip. di Scienze Fisiche, Matematiche e Informatiche, Università di Modena e Reggio Emilia and S3, Istituto Nanoscienze - CNR - Modena (Italy), [3]Dipartimento di Fisica e Astronomia, - Bologna (Italy).

The optimization of materials allowing for an accurate and reliable control of reversible reduction/oxidation processes, i.e. of their reducibility, is a challenging topic for a number of relevant applications of these systems, such as catalysis and energy conversion.
The use of model systems in this context allows for the application of advanced surface science techniques, which can give a detailed atomic scale picture of the investigated process and of the relevant factors which can influence the reducibility of the materials under study.
In this context we present and discuss the results obtained on thin epitaxial films of cerium oxide grown on a Pt(111) substrate. The films grow with a flat surface morphology and a high crystal quality [1]. The epitaxial structure of the layers has been analyzed by X-ray adsorption fine structure measurements on the Ce-L_3 edge [2] and by HR-TEM cross sections. The modifications of the stoichiometry of the films have been studied by angle-resolved X-ray photoemission spectroscopy.
The analysis of the obtained results shows that the concentration of Ce^{3+} ions in the films can be reversibly modified by thermal treatments in UHV and in O_2 atmosphere. The final degree of reduction of the films has been found to depend on several factors, such as annealing time and temperature, and initial degree of oxidation. The effect of the proximity with the Pt surface has also been investigated by comparing films of different thickness. The critical temperature for reversible reduction shows an increase with film thickness. The reduction process is more relevant in the surface layers than in the deeper ones. The film surface shows remarkable changes after a significant reduction, with the appearance of a different contrast in the STM images and of a reconstruction in the LEED patterns (Fig.1). The large scale film morphology instead remains unaltered (Fig.1 c,d). The original stoichiometry, surface morphology

and structure of the films can be reversed back to the original one by heat treatments in O_2.

[1] P. Luches, F. Pagliuca, and S. Valeri, J. Phys. Chem. C 115, 10718 (2011).
[2] P. Luches, F. Pagliuca, S. Valeri, and F. Boscherini, J. Phys. Chem. C, DOI:10.1021/jp310375t.

Fig.1: LEED patterns at E=80 eV of a 2 ML CeO_{2-x} film on Pt(111) (a) before reduction and (b) after reduction. STM images (size 125 nm × 125 nm) of a 10 ML CeO_{2-x} film on Pt(111) (c) before reduction and (d) after reduction.

NST/SS-P1-18
Electronic states of double-layer graphene with various rotated stacking angles

T13 Surface Science

#NST/SS-P1-18

K. Kakitani, H. Kaji.

Department of Electrical and Electronic Engineering, Okayama University of Science - Okayama (Japan).

Graphite or small numbers of layers of graphene with unconventional stacking are expected to show characteristic electronic and optical properties for future electronic devices. Recently experimental results show that one can produce the rotated double-layer graphene with various rotation angles as polycrystalline. For example, Kim et al. perform a Raman spectroscopy study for such double-layer graphene consist with domains having randomly rotated stacking angles. [1] Their experimental results suggest that the two graphene layers keep their electronic structure as a single graphene layer in spite of their unconventional stacking. They succeed to obtain spectra for each single rotation angle double-layer graphene, however, their samples are polycrystalline and consist with small domains. The electronic structure of the whole polycrystalline sample is not clear. In this paper, we investigate the electronic structure of the double-layer graphene with various rotated stacking angles for both the single crystalline and polycrystalline.
We perform the first principles calculation for the rotated double-layer graphene having several rotation angle coexisting with the translational symmetry and construct a tight-binding model. The first principles calculation results shows the rotated double-layer graphenes are insensitive to the displacement parallel to the layers. We also perform the tight-binding model calculations to obtain the electronic states of polycrystalline double layer. For the polycrystalline with random rotation angles, the wave number is not a good quantum number. The superstructures of periodic structures with rotated stacking vary from the rotation angles. We superimpose the density of states projected into the 1x1 reciprocal space (RDOS) for the systems with various rotation angles to obtain the dispersion relation comparable with the angle resolved photoemission measurements. The calculated RDOS shows the similar characteristics of the simple superposition of the graphene layers.

[1] Kwanpyo Kim et al., Phys. Rev. Lett. 108 (2012) 246103.

SS-P3-31
Growth of Thin Zr Films on the GaN Surface

T13 Surface Science

#SS-P3-31

K. Idczak, P. Mazur, S. Zuber, A. Ciszewski, L. Markowski, M. Skiścim, S. Bilińska.

Institute of Experimental Physics, University of Wrocław, pl. M. Borna 9, 50-204 - Wrocław (Poland).

Gallium nitride is a wide band - gap semiconductor. It is characterized by having high thermal stability, large breakdown electric field, good mobility and thermal conductivity. Recently, gallium nitride has attracted interest due to its wide applications for light emitters and detectors, high frequency field effect transistors or high power microwaves devices [1, 2]. One of the important requirement for these systems is more reliable and thermally stable Schottky contacts on n-type GaN. A good example is ZrN/Zr/GaN structure, where the Zr/GaN interface has proper thermal stability [3, 4]. That kind of the nitride - based semiconductor devices consist of many layers of various materials, so it is important to understand the chemical composition and surface reconstruction itself as well as the reconstruction of adsorption layers.

In this work, the result of the growth of Zr on the GaN surface were studied. The samples used were 10 μm thick n-GaN (Si-doped) and p-GaN (Mg-doped) deposited on Al_2O_3 substrates (producer: Technologies and Devices International, An Oxford Instruments Company). Thin Zr layers were deposited at room temperature and subsequent annealed at high temperature between 600 ^oC – 1100 ^oC. Observed changes in the chemical composition, bonding environment and reconstruction of the surface layer, caused by additive Zr adsorption and applied annealing process are presented and discussed. In experiment were used the X-ray photoelectron spectroscopy (XPS), low-energy electron diffraction (LEED) and Auger Electron Spectroscopy (AES). This techniques allowed to investigate the chemical composition, bonding environment and surface reconstruction. All measurement were performed at room temperatures under the pressure below $4x10^{-10}$Tr.

[1] S. Nakamura, T. Mukai, M. Senoh, Appl. Phys. Lett. 64 (1994) 1687
[2] B. F. Chu-Kung, M. Feng, G. Walter, N. Holonyak, T. Chung, D. Yoo, S. Shen, R. D. Dupuis, D. Keogh, P. M. Asbeck, App. Phys. Lett. 89 (2006), 082108-1-3
[3] S. D. Wolter, B.P. Luther, S. E. Mohney, R. Karlicek, R. S. Kern, Electrochem. Solid State Lett. 2 (1999) 151
[4] R. Khanna, K. Ramani, V. Cracium, R. Singh, S. J. Pearton, F. Ren, I. I. Kravchenko, Appl. Surf. Sci. 253 (2006) 2315

SS-3-Or-9
Helium Atom Scattering Measurements of the Surface Structure and Dynamics of Sb(111)

T13 Surface Science

#SS-3-Or-9

M. Mayrhofer-Reinhartshuber, A. Tamtögl, P. Kraus, M. Polanz, W.E. Ernst.

Institute of Experimental Physics, Graz University of Technology - Graz (Austria).

As one of the essential components in the recently discovered group of topological insulators [1], the semimetal antimony (Sb) is an attractive candidate for studying the properties of its surface. Quite recently the surface phonon dispersion curve of Sb(111) as well as the influences of electron-phonon interaction were calculated using density functional perturbation theory [2]. However, there has been a shortage of experimental data for comparison and verification of the models used. Hence, for a comprehensive understanding of topological insulators measurements on antimony are long overdue.
As a surface sensitive technique, Helium Atom Scattering (HAS) allows to investigate elastic as well as inelastic phenomena associated with structure and dynamics of the electronic corrugation slightly above the Sb(111) surface.
Therefore we investigated the surface of an Sb(111) single crystal using HAS measurements. Elastic scans show sharp diffraction peaks which match well with the predicted positions calculated from the already known surface structure. The analysis of resonance features in-between the purely elastic diffraction peaks (see Figure 1) led to three bound states. Based on the bound state energies, a helium-surface interaction potential of pure van der Waals character was determined.
The surface phonon dispersion curve was obtained by analyzing signals from inelastically scattered helium atoms in time-of-flight spectra. The Rayleigh mode is in good agreement with simulations based on ab-initio calculations. Phonon modes localized in the second bilayer result in oscillations of the electronic corrugation at the surface and therefore detectable signals. The possibility to measure these subsurface modes with HAS is a consequence of the electron-phonon coupling. The

phonon dispersion of Bi(111) [3, 4] shows similar modes. Thus, this may be a general property of semimetal surfaces.

[1] H. Zhang et al., Nature Physics 5 (2009) 438-442
[2] D. Campi et al., Phys. Rev. B. 86 (2012) 075446
[3] T. Tamtögl et al., Phys. Rev. B. 87 (2013) 035410
[4] M. Mayrhofer-Reinhartshuber et al., J. Phys.: Condens. Matter 24 (2012) 104008

Figure 1: HAS measurements of Sb(111) along the <10>-direction with the crystal at room temperature: Between the sharp diffraction peaks originating from the surface structure, features from resonance effects could be identified.

SS-2-Or-13
Thermodynamic Criterions of Nanophase Stabilization in Metal Melts

T13 Surface Science

#SS-2-Or-13

Y. Minaev.

Prof.,D.Sci.,Academician - Moscow (Russian federation).

Keywords: Disperse systems. Thin Films. Thermodynamic Criterions. Advanced Alloys
Modification.
Abstract. The thermodynamic analysis of stability conditions was carried out for a disperse
heterophase systems obtained by a method of the nanosize solid phases (NSP) injected into
For a thermodynamic criterion (K) of stability it was selected the specific variation of a free
energy of the process of a disperse system degradation (referred to the unit of a surface of
phases contact change)[1, 2] for three particles in melt; $K_3 = \sigma^2_L - \sigma^{\alpha\gamma}$. The analysis was
carried out in view of formation of thick and thin elastic wetting films of metal with a tension
$\sigma^L = 2\sigma^{\alpha\gamma} + \Pi L$ (here $\sigma^{\alpha\gamma}$ - an interfacial tension on the boundary NSP - metal) and disjoining
pressure Π on the contact boundary of a particles of disperse phase (after Derjaguin
definition). Accepting according Derjaguin the additivity of an operation of surface and
capillary forces[3], those are in equilibrium with a tension $\sigma_2{}^L$ of a thin film in a place of a
tangency between particles and, taking into account equation for σ^L, we obtain:
liquid alloys. The material NSP with higher melting temperature than at an alloy fulfills a role
of a phase for a metal dispersion strengthening. In the present work it was solved the problem

of possibility of evaluation for these purposes of NSP materials.

$$\sigma_2^L = 2\sigma_2^{\alpha\gamma} + \Pi(L)\, L = P_c L_0 + 2\sigma^{\alpha\gamma}\cos\theta^{\alpha\gamma} = 2\sigma^{\gamma}\cos\theta^{\alpha\gamma} + 2\sigma^{\alpha\gamma}\cos\theta^{\alpha\gamma} \quad (1)$$

Known relations $P_c = \sigma^{\gamma}/R_c$, $R_c = L_0/2\cos\theta^{\alpha\gamma}$ for capillary pressure of a meniscus in a narrow clearance L_0 on a perimeter of a tangency of particles here are used. From (Eq.1) the expression Π(L) through experimentally measured parameters was obtained:

$\Pi L = 2\cos\theta^{\alpha\gamma}(\sigma^{\gamma} + \sigma^{\alpha\gamma}) - 2\sigma_2^{\alpha\gamma}$

. For the considered process with substituting σ_2^L from (Eq.1) to K_3, we can write for constant temperature for two and three particles: $K_2 = 2\cos\theta^{\alpha\gamma}(\sigma^{\gamma} + \sigma^{\alpha\gamma}) - (2/3)\sigma^{\alpha\gamma;}$

$K_3 = 2\cos\theta^{\alpha\gamma}(\sigma^{\gamma} + \sigma^{\alpha\gamma}) - \sigma^{\alpha\gamma}$. Here K_2 and K_3 are the new criterions which can be used for performance of equilibrium conditions, stability and direction of the aggregation process. The process of a NSP aggregation (by join of three particles) is impossible, if $K3 \geq 0$. The inequality will be transformed to the thermodynamic conditions of the steady suspension NSP formation in liquid metals with use K_3:

$\cos\theta^{\alpha\gamma} \geq 1/2(1 + \sigma^{\gamma}/\sigma^{\alpha\gamma})$ and if $\sigma^{\gamma} \leq \sigma^{\alpha\gamma}$, $\cos\theta^{\alpha\gamma} \geq ¼$ or $75^0 \geq \theta^{\alpha\gamma} \geq 0$ (2)

In case formation of elastic thin films it is equivalent to a condition of formation of final boundary angles less than 75^0 on a material, prepared from NSP.

On a basis of own experimental data the evaluation of some compounds series of metals IV - VI groups of a periodic system were carried out for justified of possibility of using as exogenous modifiers of a nickel alloys. The example of dispersion hardening was reduced for high-temperature strength nickel alloy for aircraft turbine.

The obtained method evaluation of high temperature disperse systems is accessible for use to wide group of scientists and engineers worked in material science

References

1. Y.A. Minaev, A.I. Rusanov: Izv. Acad.Sci. USSR, Metals, № 5 (1971), p. 59.
2. Y.A. Minaev, M.I.Alymov: Rus. J. Phys.Chem.A, vol.85, №7 (2011), p. 1116.
3. B.V. Derjaguin, N.V. Churaev, V.M. Muller: Surface forces (Science, Moscow, 1987

SS-14-Or-5
On-surface polymerization through covalent coupling of phenyl derivatives

T13 Surface Science

#SS-14-Or-5

T. Pham [1], F. Song [1], M. Mayor [2], M. Stöhr [1].

[1]University of Groningen - Groningen (Netherlands), [2]University of Basel - Basel (Switzerland).

The creation of 1D and 2D polymers directly on a metallic surface from organic monomers is one of the most important topics in molecular nanotechnology [1] because these materials can be seen as a promising alternative to conventional silicon-based materials for a wide range of applications. The rapid progress of the bottom-up approach in nanotechnology has opened up new pathways to build up various 1D and 2D novel architectures on surfaces from starting molecular building blocks. However, the lack of mechanical stability of these nanostructures stabilized by relatively weak and reversible non-covalent interactions can be regarded as a major challenge for implementing such structures in practical applications. In this talk, we introduce an efficient approach to overcome this obstacle.
Herein, organic monomers with different protecting groups were synthesized. They were adsorbed on metallic surfaces under UHV conditions and subsequently, investigations were carried out with STM and XPS before and after annealing the samples [2]. The protecting group can be split off during the annealing step and the de-protected monomers are connected to one another by covalent bonds. By tuning the design of the organic monomers (number of legs, molecular core, controllability over both the reactivity and the size of the polymeric structure are achieved.

1. G. Franc et al., Phys. Chem. Chem. Phys. 13 (2011) 14283
2. S.Boz et al., Angew. Chem. Int. Ed. 48 (2009) 3179

Figure 1. Biphenyl derivatives on Ag(111) for different post-annealing temperatures. (left) Formation of well-ordered structures without annealing. (middle) Formation of

dimers after annealing at 155oC. (right) Formation of polymeric chains after annealing at 200oC.

NST/SS-P2-06
The influence of oxygen and hydrogen adsorption on the magnetic structure of the ultrathin iron film on the Ir(001) surface

T13 Surface Science

#NST/SS-P2-06

F. Maca [1], J. Kudrnovsky [1], V. Drchal [1], J. Redinger [2].

[1]Institute of Physics ASCR - Praha (Czech republic), [2]Institute of Applied Physics TU Vienna - Wien (Austria).

We present a detailed ab initio study of the electronic structure and magnetic order of one Fe monolayer on the Ir(001) surface covered by adsorbed oxygen and hydrogen. Results will be compared with a clean Fe/Ir(001) limit which has been intensively studied recently [1-3] and a strong tendency to the antiferromagnetic order and a complex magnetic structure were indicated. We show that the adsorption of oxygen (and also of the hydrogen) leads to the p(2x1) antiferromagnetic order. This result was obtained by two complementary approaches, namely using the total energy evaluations for limited number of magnetic configurations and by a disordered local moment analysis. Finally, based on the calculated magnetic ground states, we also estimate theoretically the spin-polarized scanning tunneling images using a simple Tersoff-Hamann model.

The following main conclusions can be drawn:
(i) Oxygen adsorbs on the Fe/Ir(001) onto the four-fold hollow sites and influences the atomic geometry of the system more strongly as compared to hydrogen in bridge positions. The interlayer relaxations are presented and compared with clean surface limit.
(ii) The adsorbate-iron hybridizations broaden density of states features as compared to the case without adsorbate. This change of the electronic structure manifests itself in corresponding modifications of exchange interactions and the STM images.
(iii) The magnetic stability is strongly influenced by oxygen adsorption, and we predict the antiferromagnetic p(2x1) state as a magnetic ground state for one monolayer oxygen coverage.

(iv) The p(2x1)-ordering is weakened by decreasing oxygen coverage and changes into complex magnetic ground state for the oxygen free case.
(v) The coverage by one monolayer of hydrogen leads also to a weak stabilization of the antiferromagnetic p(2x1) order.

[1] V. Martin, W. Meyer, C. Giovanardi, L. Hammer, K. Heinz, Z. Tian, D. Sander, and J. Kirschner, Phys. Rev. B **76**, 205418 (2007).
[2] J. Kudrnovsky, F. Maca, I. Turek, and J. Redinger, Phys. Rev. B **80**, 064405 (2009).
[3] L. Deak, L. Szunyogh, and B. Ujfalussy, Phys. Rev. B **84**, 224413 (2011).

SS-11-Or-7
Growth of thin dihydrotetraazapentacene layers on Au(111)

T13 Surface Science

#SS-11-Or-7

C. Becker, T. Léoni, T. Lelaidier, A. Ranguis, O. Siri.

Aix-Marseille Université - CINaM UMR 7325 - Marseille (France).

Dihydrotetraazapentacene (DHTAP, $C_{18}N_4H_{12}$) layers can be used as organic semiconductors with a high potential in electronic and optoelectronic applications such as photovoltaic cells or flexible displays. The charge carrier mobility in these potential devices is of a prime importance in order to realize and optimize them. In crystalline organic materials, this mobility is controlled by the structure of the thin film: the molecular orientation and the electronic coupling between molecules. For this reason the growth of dihydrotetraazapentacene DHTAP on Au(111) at different temperatures has been studied by STM at 77K. DHTAP is a molecule that is nearly planar in gas phase and that can be evaporated in ultrahigh vacuum at temperatures of about 510K. The molecule adopts a lying down adsorption geometry on the Au(111) surface with the molecular plane parallel to the surface. For surface temperatures of about 170K during deposition molecular rows of DHTAP can be found with an intermolecular distance of about 0,75nm. If one increases the temperature of the surface during the deposition above 210K the increased surface mobility of the molecules leads to the formation of distinct ordered regions on the surface. Initially small molecular aggregates can be found on the elbows of the Au(111) herringbone reconstruction and molecular wires form on the fcc domains of the reconstruction. At higher coverage the fcc domains are further decorated and finally a nucleation on the hcp domains can be found. At monolayer coverage both the fcc and the hcp domains are covered with molecular wires formed by the absorbed DHTAP. The intermolecular distance remains at about 0,75nm and the molecules are linked by hydrogen bonds. The noise present in the STM images suggests that even at 77K the molecules rest quite mobile. This fact is corroborated by the evolution of the STM images with time, which clearly show the displacement of the molecules. The second and the third layer grow in perfect registry with the first layer (see fig. 1). Upon annealing of the monolayer or the multilayer at room temperature no evolution of the morphology of the DHTAP layers has been found.

STS measurement have shown that the HOMO-LUMO gap of the molecule, which is 2.93eV in gas phase, is slightly diminished upon adsorption to about 2.6eV for the DHTAP molecules in the second layer.

Figure 1 : A DHATP layer on Au(111). The second layer is in perfect registry with the first layer.

SS-16-Or-4
Low-temperature selective growth of GaN single crystals at nucleation centers induced on a native silicon oxide surface by FIB

T13 Surface Science

#SS-16-Or-4

J. Mach [1], T. Šamořil [2], P. Mareš [3], J. Hulva [3], S. Voborný [1], L. Dittrichová [1], T. Šikola [1].

[1]CEITEC Vysoké učení technické v Brně Středoevropský technologický institut Technická 3058/10 616 00 Brno - Brno (Czech republic), [2]TESCAN, a.s. Libušina tř. 21 623 00 Brno - Kohoutovice - Brno (Czech republic), [3]Institute of Physical Engineering, University of Technology Brno, Faculty of Mechanical Engineering, Technická 2, 616 69 Brno - Brno (Czech republic).

In the first part of our presentation we will report on the low-temperature growth of gallium nitride (GaN) ultrathin films on silicon wafers covered with the native oxide by physical vapour deposition of Ga atoms assisted with a low energy (50 eV) nitrogen ion beam bombardment. This has been carried out using a special atom-ion beam source developed in our group [1]. We have studied the morphology and elemental composition of these layers by atomic force microscopy (AFM) and X-ray photoelectron spectroscopy (XPS) as a function of substrate temperature (RT-300^{o}C). The growth occurred at much lower temperatures than in conventional GaN deposition technologies (e.g. MOCVD, 1000^{o}C). In the second part, we will present the results on a simple hybrid method for the selective growth of GaN nanostructures on a pre-patterned native silicon oxide substrate. The patterning was performed by a Ga focused ion beam (FIB) to create nucleation centers in form of an array of pits and grooves. Using ion –beam assisted physical vapour deposition described above an assembled growth of GaN single crystals at the nucleation sites was achieved at 300^{o}C (Fig. 1). The characterization of these crystals was performed using SEM and AFM related techniques (including EFM and SKFM).

[1] MACH, J.; ŠAMOŘIL, T.; VOBORNÝ, S.; KOLÍBAL, M.; ZLÁMAL, J.; SPOUSTA, J.; DITTRICHOVÁ, L.; ŠIKOLA, T. An ultra-low energy (30–200 eV) ion-atomic beam source for ion-beam- assisted deposition in ultrahigh vacuum. Review of Scientific Instruments, 2011, n 82, Vol. 8, p. 083302

Fig.1 SEM ex-situ analysis of GaN crystals prepared by Ion Beam Assisted Deposition (IBAD) on the pre-patterned native silicon oxide) substrate for diameters of the nucleation centers a) 300 nm and b) 50 nm.

SS-P3-19
Surface treated nano and pigmentary TiO2 for various applications

T13 Surface Science

#SS-P3-19

N. Veronovski, D. Verhovšek, M. Lešnik.

Cinkarna, Metallurgical and Chemical Industry, Celje, Inc. - Celje (Slovenia).

Titanium dioxide (TiO_2) is produced in two major commercial forms worldwide; the pigment and the nano grade. In general, incorporation of UV absorbers like TiO_2 (nano)particles in rutile crystal structure is of potential interest as an ultraviolet (UV) blocking material in personal care products, paints, coatings and plastics because of its excellent UV light absorption properties. Although TiO_2 is an effective UV absorber, it requires special surface treatments to suppress its inherent photoactivity. The most common surface treatments are silica (SiO_2), alumina (Al_2O_3) and zirconia (ZrO_2). The TiO2 final properties can be strongly influenced by the conditions during surface treatment. Thus the aim of this research was to determine optimum treatment conditions, which yield homogeneous coatings of desired morphology, which entirely cover the TiO_2 surface. The structure of the surface treated TiO_2 (nano)particles was characterized using various techniques, such as scanning electron microscopy (SEM), and transmission electron microscopy (TEM). One of the most significant properties of an insoluble oxide like TiO_2 and SiO_2 is the isoelectric point (IET). Surface treatment of TiO_2 resulted in the shift of IET. With intention to determine their applicable value, surface treated TiO_2 (nano)particles were subsequently incorporated into various matrixes.

SS-14-Or-6
The O/Cu(110) nanostructured surface reactivity toward H2S

T13 Surface Science

#SS-14-Or-6

C. Poulain, F. Wiame, V. Maurice, P. Marcus.

LPCS (CNRS and Chimie Paristech) - Paris (France).

Due to the need to find alternative ways to create smaller systems in the microelectronics industry, self-organized growth of nanostructures on metallic surfaces attracts much interest [1]. Among such surfaces, the O/Cu(110) nanostructure consists of O-induced (2x1) reconstructed stripes periodically aligned in the [001] direction and alternating with bare Cu stripes [2]. It is an ideal playground to study the relationship between structure and reactivity at the nanometer scale since periodicity and stripes width are easily tunable by the mean of oxygen exposure [3,4]. Despite an extensive study of the O/Cu(110) nanostructured surface for the last two decades [5], very few is known about its reactivity. It is however a key factor in understanding and controlling its self-organisation by studying the influence of its structural parameters.

After a presentation of the reaction mechanisms occurring on the surface within H_2S exposure, we will present an investigation of the periodicity (L) and oxidized stripes width ($\omega_{Cu\text{-}O}$) roles in the reaction. Four radically different nanostructures have been elaborated to do so. Scanning tunnelling microscopy data showing a critical dependence of the local configuration for the sample reactivity will be presented. Auger electron spectroscopy data will show the role of the structure on the reaction kinetics.

Results show that the reaction leads to the formation of sulphur c-(2x2) islands preferentially on oxidized stripes and that this is favoured on nanostructures with greater $\omega_{Cu\text{-}O}$ (Fig. 1). Sulphur c-(2x2) islands are also found at oxidized stripes edges, at Cu-O rows extremities. The reaction mechanism also involves the detachment of Cu-O row segments from these edges. The segmented rows diffuse on the oxygen-free areas due to short-range repulsion with the oxidized stripes. It is also shown that the periodicity influences the reactivity through the oxidized stripes

edges density (2/L), hence demonstrating the chemical, as well as the physical dependence of the reaction.

[1] J. V. Barth, G. Costantini, K. Kern, Nature 437 (2005) 671.

[2] K. Kern, H. Niehus, A. Schatz, P. Zeppenfeld, J. Goerge, G. Comsa, Phys. Rev. Lett. 67 (1991) 855.

[3] V. Marchenko, JETP Lett. 55 (1992) 73.

[4] D. Vanderbilt, Surf. Sci. 268 (1992) L300.

[5] F. Besenbacher, J. K. Norskov, Prog. Surf. Sci. 44 (1993) 5.

FIG. 1: STM image of S-c(2x2) islands formed on an oxidized stripe and one of its edges. H_2S exposure: 2.70 L. Tunnelling parameters: I = 2.0 nA, V = 0.1 V.

SS-1-Or-10
Sensitivity of calculated electronic and magnetic properties on “molecule-surface” systems with van der Waals corrected Density Functional Theory

T13 Surface Science

#SS-1-Or-10

H. Tang.

CEMES/CNRS - Toulouse (France).

Due to the non local nature of the van der Waals (vdW) force, this dispersive interaction could not to be considered within the local density approximation of classical Density Functional Theory (DFT). Since the mid of 90s, increasing efforts have been put on the vdW correction in the framework of DFT. However, in spite of the improvements recently introduced through different approaches (DFT+D, vdw-DF, TS-vdW, etc ...) [1], the calculated electronic and magnetic properties of a “molecule-surface” system in real case (when the molecule and the substrate are not used to valid a vdW correction method) could be easily affected by the accuracy of vdW correction. In this presentation, a detailed analysis on the variation of the optimized structure, adsorption energy, density of states, work function, partial charge, spin multiplicity and magnetic moment for a couple of molecules (FeTPPCl/FeTPP and “Ru-535” dye on gold, etc ...) will be discussed as a function of vdW interaction description. This comparative analysis will show the importance of preliminary verification of vdW correction as well as experimental results used to validate simulation results.

[1] – Klimes, J.; Michaelides, A. *J. Chem. Phys.* **2012**, 137, 120901.

Electronic configurations of FeTPPCl/Au(111).

SS-P3-24
Faceting of Rh(553) in realistic reaction mixtures of CO and O2

T13 Surface Science

#SS-P3-24

C. Zhang [1], E. Lundgren [1], P.A. Carlsson [2], O. Balmes [3], J. Gustafson [1].

[1]Div. of Synchrotron Radiation Research, Lund University - Lund (Sweden), [2]Competence Centre for Catalysis, Chalmers University of Technology - Gothenburg (Sweden), [3]European Synchrotron Radiation Facility - Grenoble (France).

Defects, such as atomic steps and kinks, play an important role as active sites in many catalytic reactions. One way of studying these defects' role in a catalytic process is by using vicinal surfaces with a high density of periodic steps, and monitor how their surface structures are affected by the reaction conditions. In this contribution we have studied Rh(553) under realistic CO oxidation conditions using in situ surface X-ray diffraction (SXRD) and mass spectrometry.

From a previous study we know that exposure to O_2 leads to major rearrangements of the Rh(553) surface. At intermediate O_2 pressures (about 10^{-5} mbar) the surface facets into (331) and larger (111) facets, while (111) and equivalent (11-1) facets are formed together with the surface oxide at about 10^{-3} mbar [1]. In the present study we show that this faceting behavior applies also in a mixture of CO and O_2 during high catalytic activity. In mixtures that are slightly oxygen rich we find a combination of (331) and (111) facets, and under more oxygen rich conditions we find the surface oxide being formed on the (111) facets. In addition we found faceting into (110) and (111) facets in a CO rich mixture.

It has also been suggested that steps are involved in spontaneous activity oscillations [2]. One of the aims in this study was to find conditions where these oscillations are present and look for changes in the facet structure. Following the recipe from previous experiments, we applied reaction gas mixtures with high O_2 partial pressure and high activity, and then stepped down in O_2 partial pressure to approach the conditions where CO reclaims the surface and kills the reaction. In the beginning of the experiment, this resulted in spontaneous oscillations with a period of about 5 min. After the investigation of the faceting behavior shown above, we were not able to initiate the oscillations again. From the experiments we also found that the

surface is highly active even in CO excess, strongly contradicting our previous results. Our present interpretation is that the steps have become more perfect, due to the extensive exposure to reaction gases, and that the steps are less prone to CO poisoning than a flat surface.

[1]. J.Gustafson, A.Resta, A.Mikkelsen, R.Westerström, J.N.Andersen, E.Lundgren. Phys. Rev. B 74, 035401 (2006)
[2]. B.L. Hendriksen, M.D. Ackermann, R.Van Rijn, D. Stoltz, I. Popa, O. Balmers, A. Resta, D.Wermeille, R. Felici, S. Ferrer, J. W. Frenken, Nat Chem. 2, 730 (2010)

SS-10-Or-4
Surface phonon dispersion and the role of glide symmetry on the hydrogen-terminated Si(110)-(1×1) surface

T13 Surface Science

#SS-10-Or-4

S. Matsushita [1], K. Matsui [1], H. Kato [1], T. Yamada [2], S. Suto [1].

[1]Department of Physics, Graduate School of Science, Tohoku University - Sendai 980-8578 (Japan), [2]RIKEN - Hirosawa, Wako, Saitama 351-0198 (Japan).

We report the surface phonon dispersion curves mapped over the 1st and 2nd surface Brillouin zones (SBZ) of the rectangular unit cell of hydrogen-terminated Si(110)-(1×1) [H:Si(110)] surface by means of high-resolution electron energy loss spectroscopy (HREELS). Generally, it is always possible to select the wave vector of phonons in the 1st Brillouin zone using the reduced zone scheme. In the theory, Prince [1] discussed aspects of band structure, dispersion and degeneracy, as well as selection rules valid in a variety of electron spectroscopies for specific space groups containing the glide symmetry operation as an essential symmetry operation. To confirm the theory, several experiments were performed on the adsorption systems of C/Ni(100), CO/Ni(110) and CO/Pb(110) but, so far, there is no systematic investigation on the role of the glide symmetry operation.
We successfully prepared a well-ordered and ultra-clean H:Si(110) surface by etching a Si(110) wafer in 40% aqueous solution of NH_4F [2,3]. The surface has a two dimensional space group of *p2mg* with two glide planes along the [1-10] direction, i.e., Γ-X direction in reciprocal space. The surface order was verified by LEED. The cleanliness and the phonon dispersion were measured by HREELS [4]. The surface phonon modes were observed exclusively in the 1st and 2nd SBZ, strictly classified into even and odd local modes, respectively. The dipole and impact scattering selection rules on the surface where mirror planes, two-hold rotation axis and glide planes exists, hold quite well and made it possible to assign the phonon modes. For example, when we measured the phonon dispersion curves from 1st to 2nd SBZ along the Γ-X direction, the peak at 25.4 meV suddenly appeared at the X (edge of the 1st SBZ) and existed in the 2nd SBZ. According to the selection rule for the glide symmetry operation, we assigned this peak to C_{t1} mode, which is

exclusively odd-symmetric for the glide plane. We followed the notation of the phonon modes proposed by Gräschus [5], who calculated phonon dispersion curve of H:Si(110) without considering the glide plane. The even modes of RW, C_s, B_0 and S_s modes are observed in only the 1st SBZ, and the odd modes of RW, C_{t1}, B_i and S_a modes are observed only in the 2nd SBZ along the Γ-X direction. On the other hand, along the Γ-X' direction (perpendicular to the Γ-X direction), all the observed phonon modes were mapped in the 1st SBZ, because there is no glide plane.
Furthermore, it is found that the phonon of Si-H bending and stretching mode on H:Si(110) surface was highly anisotropic for the directions of Γ-X and Γ-X'. We observed the two pairs of Davydov splitting peaks of the bending (B_0 and B_i) and stretching (S_s and S_a) modes. We found sizable dispersion of the four modes along the Γ-X direction, but no dispersion along the Γ-X' direction. This indicates that there is no effective physical interaction to pass the vibrational motions in a unit cell to the [001]-neighboring unit cells on the topmost surface.

[1] K.C. Prince, *J. Electron Spectrosc. Relat. Phenom.* **42** (1987) 217.
[2] H. Kato et al., *Jpn. J. Appl. Phys.* **46** (2007) 5701.
[3] S. Suto et al., *Appl. Surf. Sci.* in press.
[4] H. Kato et al., *Phys. Rev.* B **75** (2007) 085319.
[5] V. Gräschus et al., *Phys. Rev.* B **56** (1997) 6482.

SS-15-Or-3
Maximum aspect ratio of a coherent nanowire at equilibrium

T13 Surface Science

#SS-15-Or-3

G. Boussinot.

Max Planck Institut fur Eisenforschung - Duesseldorf (Germany).

Nanostructures elongated perpendicular to their supporting substrate have attracted attention owing to their ability to sustain the coherency at the interface with the misfitting substrate. Although the morphology of nanocrystals can depend on the history of the production process, for example for a catalyst-assisted growth, it may be estimated by an energy minimizing procedure that provides the equilibrium state. Here [1] simple qualitative scaling arguments are used to derive the equilibrium aspect ratio of an elongated coherent cylindrical nanowire depending on its volume V. It is found to scale as $(V/d^3)^{1/4}$ >>1 where d is the elasto-capillary length that arises from the competition between surface energy and bulk elastic energy.

Using the usual law for the critical radius of a nanowire (below which coherency is maintained whatever its height perpendicular to the substrate), the maximum aspect ratio of a coherent nanowire at equilibrium is found to increase linearly with the lattice misfit with the substrate. This demonstrates that coherent nanowires with large aspect ratios exist at equilibrium for large misfits.

In addition, it can be shown that when the height of the coherent crystal is limited to a size L >> d, a possible equilibrium state for V >> L^2d consists of an assembly of non-interacting nanowires.

[1] G. Boussinot, Surface Science 607 (2013) L1-L3

NST/SS-P1-19
Cu intercalation to graphene sheets grown on SiC(0001)

T13 Surface Science

#NST/SS-P1-19

K. Yagyu, H. Tomokage, T. Tajiri, A. Kohno, T. Suzuki.

Fukuoka University - Fukuoka (Japan).

It is well known that graphene sheets are grown above 1200°C on SiC(0001) surface in the consequence of the desorption of Si atoms. A specific linear dispersion at K point is, however, unobserved on the first graphene sheet, “Zero layer”, made by this heating process, because of sp^3-type interactions between the substrate. I. Gierz et al. reported that Au deposition on the zero layer followed by annealing produces a single graphene sheet as a result of Au intercalation under the graphene sheet [1]. In our study, Cu is used instead of Au for a practical electronic device.

First of all, the zero layer was grown on the 4H-SiC(0001) surface after the annealing of the substrate at 1200°C. Cu atom was deposited on the zero layer with the amount of 12 Å at room temperature followed by the annealing, which is called “post-annealing”, at 500-800°C. The obtained surface was analyzed by scanning tunneling microscopy (STM) and x-ray photoemission spectroscopy (XPS).

After the deposition of Cu atoms, the zero layer was covered by three dimensional Cu islands at room temperature. The substrate was unchanged below 500°C of post-annealing. Above 600°C to 700°C, the surface was drastically changed. Cu islands vanished and the graphene lattice was observed by STM, thus the topmost surface is considered to be a single graphene. Moreover the graphene sheet is corrugated with the period of $(6\sqrt{3}\times6\sqrt{3})R30°$(Fig. 1). Low energy electron diffraction pattern of the surface shows 6 satellite spots around a (10) spot, which assists the corrugation found in the STM image. After the post-annealing at 600-700°C, although Cu islands vanished from the surface, Cu was obviously detected by XPS. Therefore Cu is considered to be intercalated under the graphene sheet during the post-annealing, which is similar to the case of Au deposition [1]. C 1*s* core-level spectra were obtained before and after the post-annealing. In the C 1*s* spectra, a signal which shows the 1st layer evolved after the post-annealing. Therefore it is concluded that

the sp^3 interaction between a graphene sheet of zero layer and the substrate disappeared because of the Cu intercalation.

The (6√3×6√3)R30° corrugation disappeared after the post-annealing at 800°C. Instead of the corrugations, zero layer with many defects and triangular structure appeared.

In conclusion, we found that a single graphene sheet is also obtained by the Cu deposition instead of Au; however it was achieved at 600°C, 200°C lower temperature than the Au case of 800°C.

[1] I. Gierz et al.: Phys. Rev. B 81 (2010) 23408

Figure 1. STM image of post-annealed sample shows a lattice of graphene with a (6√3×6√3)R30° corrugation. This sample was annealed at 700°C for 15 min after the Cu deposition.

SS-16-Or-6
Stress evolution during Si surface reconstruction

T13 Surface Science

#SS-16-Or-6

H. Asaoka, Y. Uozumi, Y. Yokoyama, K. Yamaguchi.

JAEA - Tokai, Ibaraki (Japan).

The importance of surface stress as a factor in the surface reconstruction is beginning to be widely recognized in nanotechnology. The Si(111) 7×7 reconstructed surface is well known to be based on dangling bonds reduction and adatom formation. Complex arrangements of the surface atoms, such as adatoms, dimers, and stacking faults are formed on Si(111) 7×7. Calculations by Vanderbilt et al. [1] show that the Si(111) 7×7 surface significantly affects the surface stress by introducing both tensile and compressive stresses depending on the site. Such a surface energy plays a critical role in determining the growth mode of heteroepitaxial layers. For instance, the Ge surface morphology changes from a two-dimensional wetting layer to a three-dimensional nanodot due to trade-off between the surface and the elastic energies. Despite the aforementioned importance of the surface energy of Si, the experimental knowledge on the impacts of reconstruction on the Si surface has been quite limited.

We have focused on measurement of the surface stress during atomic hydrogen exposition on Si(111) 7×7 and Ge(111) 5×5 surfaces, and subsequent Ge deposition on Ge wetting layer growth on H-terminated surfaces. To obtain information on both the surface stress and the surface reconstruction simultaneously, we have combined surface-curvature and RHEED instrumentations in an identical UHV system.

At the beginning of the atomic H exposition on Si(111) 7×7 and Ge(111) 5×5 surfaces, distinct released stresses are observed corresponding to the formation of H-termination. After the above treatment, a complete transformation of the surface structure occurs from each reconstructed surface to the 1×1 one. Furthermore, when the first bilayer growth of Ge on H-terminated Si(111) 1×1, the stress gradient changes drastically with change of the surface structure from 1×1 to 5×5 (Fig.1) resulting from H desorption. The unique stress behavior reveals that the Si(111) 1×1 surface releases 1.6 N/m (=1.3 eV/(1×1 unit cell)), of the surface energy from the strong tensile Si(111)7×7 reconstruction. The released stress matches with the calculated stress [1], which corresponds to the difference of structure between H-terminated Si(111) 1×1 and Si(111) 7×7 surfaces. Simultaneous measurement of the

surface stress and the surface reconstruction reveals the value of the tensile stress in Si(111) 7×7 reconstructed surface comparing to reference H-terminated 1×1 surface.

[1] D. Vanderbilt, Phys. Rev. Lett. 59 (1987) 1456.

Fig. 1. Evolution of RHEED patterns during growth of Ge wetting layer on (a) H-terminated Si(111) 1×1 surface. The coverage of Ge wetting layer is (b) 1.5 BL after deposition.

SS-4-Or-4
Wetting of TiO2(110): influence of temperature and defects

T13 Surface Science

#SS-4-Or-4

A. Sandell [1], M. Amft [2], L.E. Walle [3], D. Ragazzon [1], A. Borg [3], P. Uvdal [4], N.V. Skorodumova [2].

[1]Uppsala University - Uppsala (Sweden), [2]Royal Institute of Technology - Stockholm (Sweden), [3]Norwegian University of Science and Technology - Trondheim (Norway), [4]Lund University - Lund (Sweden).

The formation of the interface between water and a solid is a truly challenging fundamental problem. On many surfaces the formation of this interface or wetting layer is accompanied by water dissociation to hydroxyl (1). The formation of hydroxyl plays an important role in stabilizing the wetting layer but partial water dissociation adds to the complexity of the wetting processes.
We have studied water adsorption on single crystalline rutile TiO2(110) at the Swedish synchrotron radiation facility MAX-lab (2-4). Based on an extensive set of O1s spectra, DFT calculations and Monte Carlo simulations we have been able to derive a mechanism for the adsorption of water and subsequent partitioning into H2O and OH on stoichiometric TiO2(110) at 210K, a temperature at which the uptake is limited to titanium surface sites. When the temperature is decreased, the OH rate of formation decreases leading to an increased H2O/OH ratio. This is discussed in terms of having water stabilized on the oxygen sites, inducing a metastable overlayer structure. A comparison with a previous high pressure XPS study reveals that the wetting layer formed under near-ambient conditions may be a similar, metastable structure (5).
Finally, the issue of surface defects is addressed: Dissociation at bridging O vacancies quenches the dissociation on stoichiometric parts with a correlation close to one. Ti interstitials with a typical density of a few percent have negligible influence on the H2O/OH ratio.

1. P. J. Feibelman, Science 295, 99 (2002).
2. J. Blomquist et al., J. Phys. Chem. C 112, 16616 (2008).
3. L. E. Walle et al., Phys. Rev. B 80, 235436 (2009).

4. L. E. Walle et al., J. Phys. Chem. C 115, 9545 (2011).
5. G. Ketteler et al., J. Phys. Chem. C 111, 8278 (2007).

SS-15-Or-4
Unique surface structure formation on Ge covered Si(110) surface

T13 Surface Science

#SS-15-Or-4

Y. Yokoyama, Y. Uozumi, H. Asaoka.

JAEA - Tokai, Ibaraki (Japan).

The semiconductor devices using SiGe thin film or Ge nano dot structure on a Si surface has the superior features, e.g. high-speed operation, low power consumption and high temperature stability, compared with pure Si semiconductor devices [1]. Therefore, a lot of research and development have been performed toward application in various fields, such as a communication terminal and a semiconductor laser. However, in order to fabricate the high-performance device, well-ordered SiGe thin film and Ge nano dot structure are required. In this study, we aimed for new SiGe nano structure fabrication by using Si(110)-16×2 reconstructed structure.

First of all, to fabricate the single-domain of Si(110)-16×2 structure, dc flowing along the [-11-2] direction is used to heat the surface. The STM image obtained using this procedure is shown in Fig. 1. This image clearly shows that a single-domain structure is formed over the entire specimen with stripes that run along the dc direction. Next, we deposited a Ge by using graphite crucible. In the case of 1 ML Ge deposition at RT, although the surface is covered with small grain of Ge, the striped structure originating from 16×2 single-domain is still maintained. After annealing at 973 K for 240 min, the surface morphology changes from single-domain to double-domain as shown in Fig. 2. The important points here, the direction of these stripes are different from clean 16×2 structure. These stripes directions deviate approximately 7 degrees from <1 1 2> direction, therefore we have determined that the direction of these stripes are <5 5 13>. Since the stable structure of clean Si(110) at 973 K is 16×2 structure that run along the <1 1 2> direction, we have considered that this structure is SiGe surface. Moreover, this structure also differs from the SiGe-Si(110) structure reported by Butz and Lüth [2]. This result suggests that a new SiGe reconstructed structure has been created on the Si(110) surface.

[1] H. Klauk *et. al*., Appl. Phys. Lett. 68, 1975 (1996).
[2] R. Butz, H. Lüth, Surf. Sci. 365, 807 (1996).

Fig. 1. Clean Si(110)-16×2 single domain surface.
Fig. 2. After 1 ML Ge deposition and 240 min heating at 973 K.

SS-P3-32
Pb adsorption on the Si(111)7x7 surface

T13 Surface Science

#SS-P3-32

S. Bilińska, K. Idczak, M. Skiścim, L. Markowski.

Institute of Experimental Physic, University of Wroclaw - Wroclaw (Poland).

Superstructure formation caused by metal films deposition on a semiconductors surface, and in particular metal/Si(111) interface, has been investigated for many years. An example of such a system is the Pb on Si(111). This system has attracted considerable interest, especially due to its properties (its insolubility in the bulk of Si) [1]. It has been studied by many groups using various techniques, in particular at low-temperatures but there are still open questions [2,3]. It is known that the preferred adsorption site of Pb atoms on Si(111) surface is very selective and depends on coverage, temperature and also sample annealing history.

In this work the behaviour of Pb adsorption on the clean Si(111) 7x7 surface and influence of annealing temperature were studied in detail by low energy electron spectroscopy (LEED), Auger emission spectroscopy (AES) and X-ray photoemission spectroscopy (XPS). In the experiment pure Pb (99,999%) was evaporated on the Si substrate at room temperature by the 'one-stage deposition' and subsequent annealed in the temperature range between 300 ˚C - 580 ˚C. For the samples, prepared in such a way, two kind of surface superstructures were observed 3×3 and $\sqrt{3} \times \sqrt{3} R30°$ reconstructions. As an example, LEED images for about 1 ML of Pb coverage, after sample annealing at 300 ˚C ($\sqrt{3} \times \sqrt{3} R30°$ reconstruction) (a) and after further annealing at 480 ˚C (3×3 and $\sqrt{3} \times \sqrt{3} R30°$ reconstructions) (b) are shown in the Fig. 1. The obtained results suggest that the growth of Pb follows the Stranski-Krastanov mode and are consistent with the conclusion that Pb atoms occupy places mainly above the rest atoms and between the Si adatoms [4].

[1] Le Lay G, Abraham M, Kahn A, Hricovini K and Bonnet J E 1991 Phys. Scr. T 35 261;
[2] Estrup P J and Morrison J 1964 Surf. Sci. 2 465;
[3] Saitoh M, Oura K, Asano K, Shoji F and Hanawa T 1985 Surf. Sci. 154 394;
[4] Hwang Ing-Shouh, Martinez R E, Liu Ch and Golovchenko J A 1995 Surf. Sci. 323 241

Fig 1. LEED patterns of Pb/Si(111) surface for 1 ML of Pb on deposited at room-temperature:
a) after annealing at 300 ˚C for 1 minute and b) after annealing at 480 ˚C for 1 minute.

SS/NST-1-Or-6
Nanometer-Range Strain Distribution in Layered Incommensurate Systems

T13 Surface Science

#SS/NST-1-Or-6

F. Dvorák [1], O. Stetsovych [1], L. Szabova [1], S. Fabris [2], J. Myslivecek [1], V. Matolín [1].

[1]Charles University, Faculty of Mathematics and Physics, V Holesovickach 2 - Prague (Czech republic), [2]CNR-IOM DEMOCRITOS, Theory@Elettra Group, Istituto Officina dei Materiali, Strada Statale 14 km 163,5 in AREA Science Park, I-34149 - Trieste (Italy).

We adopt fringe counting from classical moiré interferometry on moiré patterns observed in scanning tunneling microscopy of strained thin films on single crystalline substrates. We analyze inhomogeneous strain distribution in islands of CeO_2(111) on Cu(111) and identify a generic source of strain in heteroepitaxy—a thickness-dependent lattice constant of the growing film. This observation is mediated by the ability of ceria to glide on the Cu substrate. The moiré technique we are describing has a potential of nanometer-scale resolution of inhomogeneous two dimensional strain in incommensurate layered systems, notably in supported graphene. [1]

[1] Stetsovych, O.; Dvorak, F.; Szabova, L.; Fabris, S.; Myslivecek, J.; Matolin, V.; Phys. Rev. Lett. 109, 266102 (2012) [5 pages]

fig. 1: Inhomogeneously strained multilayer island of ceria on Cu(111). 1 ML and 2 ML label the first and second monolayers. Rings are moiré centers of a selected constant fringe order, lines are guides to the eye. Image width 130 nm

fig 2: Simulation of (a) radial displacement and (b) radial strain in a strained 2 ML ceria island. 2 ML area features, intrinsically, a larger lattice constant than 1 ML area. Displacement and strain are evaluated relative to lattice constants of the homogeneous 1 ML or 2 ML, respectively. Image width (a), (b) 65 nm.

NST/SS-1-Or-7
Atomic scale characterization of O and CO intercalation under graphene

T13 Surface Science

#NST/SS-1-Or-7

E. Grånäs [1], J. Knudsen [1], U.A. Schröder [2], T. Gerber [2], M. Andersen [3], M.A. Arman [1], C. Busse [2], K. Schulte [4], B. Hammer [3], J.N. Andersen [4], T. Michely [2].

[1]Division of Synchrotron Radiation Research, Lund University - Lund (Sweden),
[2]II. Physikalisches Institut, University of Cologne - Cologne (Germany),
[3]Department of Physics and Astronomy, Aarhus University - Aarhus (Denmark),
[4]MAX IV Laboratory, Lund University - Lund (Sweden).

Graphene has a large potential for applications within the field of nanotechnology, for example in transparent electrodes and transistors. For many of these applications it is essential to tune the electrical properties of the graphene layer by doping. One very efficient way to dope graphene is by intercalation of atoms or molecules under graphene. Intercalation is also interesting from a chemical point of view, since atoms or molecules confined between the substrate and the graphene layer might exhibit different properties than they would on the bare substrate.
Intercalation of molecules or atoms under graphene has been demonstrated for a number of substrates. The majority of the previous studies prove that intercalation is possible, but lack an atomic level understanding. Here we present atomic scale studies of intercalation of two common gases, oxygen and CO, in the pressure interval from 10^{-8} to 0.1 mbar. Further, we plan to discuss examples of chemistry performed under the graphene layer.
For oxygen exposed graphene we develop a coherent picture of temperature dependent oxygen intercalation.[1] Using X-ray photoemission spectroscopy (XPS) and scanning tunnelling microscopy (STM) we show that a perfect graphene layer forms an impenetrable barrier for the oxygen. In contrast, a partial graphene coverage on Ir(111) enables dissociative oxygen adsorption on the bare Ir and subsequent intercalation underneath graphene flakes at 355 K and above. We determine XPS and STM fingerprints for the intercalated oxygen structure and we unambiguously assign it to a p(2x1)-O structure similar to the one observed on clean Ir(111). The decoupling of the intercalated graphene film from the metal substrate is directly visualized through the inability to form well-ordered Pt cluster arrays on the

O-intercalated areas of graphene on Ir(111). Further, we have identified the rate limiting step for oxygen intercalation to be unlocking of the graphene edge and propose that this takes place through bond breaking between graphene edge bonds and the Ir substrate. We also reveal that oxygen energetically prefers to reside on the bare Ir(111).
Using a combination of high pressure XPS and STM we show that it is possible to intercalate CO under graphene on Ir(111).[2] The ( )R30° structure of the intercalated CO is identical to the structure formed on Ir(111) at high pressures. From DFT calculations the structural and electronic properties of CO-intercalated graphene are found to be similar to p-type doped freestanding graphene. Using STM and Pt-deposition we mark non-intercalated areas and find that they are always present as lines in the CO intercalated areas. They are predominantly formed in HCP and FCC areas due to the formation of weak chemical bonds in these areas upon re-lamination. Similar to wrinkle formation in graphene [3] we suggest that the network of non-intercalated lines is a way of releasing stress in the graphene layer.

[1] E. Grånäs, J. Knudsen, U. A. Schröder,T. Gerber, C. Busse, M. A. Arman, K. Schulte, J. N. Andersen, T. Michely, ACS Nano 6, 9951-9963 (2012)
[2] E. Grånäs, M. A. Arman, T. Gerber, J. Schnadt, J. N. Andersen, T. Michely, J. Knudsen, Submitted
[3] A. T N'Diaye, R. van Gastel, A. J Martínez-Galera, J. Coraux, H. Hattab, D. Wall, F-J. Meyer zu Heringdorf, M. Horn-von-Hoegen, J. M. Gómez-Rodríguez, B. Poelsema, C. Busse, T. Michely, New J. Phys. 11, 113056 (2009)

SS-2-Or-6
Formation of In/Pd(111) surface alloys at low-coverage

T13 Surface Science

#SS-2-Or-6

G. Mcguirk [1], J. Ledieu [1], É. Gaudry [1], M. Armbrüster [2], M.C. De Weerd [1], V. Fournée [1].

[1]Institut Jean Lamour, UMR 7198 CNRS, Université de Lorraine - Ecole Des Mines, Parc De Saurupt, Nancy Cedex (France), [2]Max-Planck-Institut für Chemische Physik fester Stoffe - Nöthnitzer Str. 40, Dresden (dated: October 12, 2012) (Germany).

The high catalytic activity towards methanol steam reforming (MSR) of Pd/ZnO, Pd/In_2O_3 and Pd/Ga_2O_3 has been ascribed to the formation of PdZn, PdIn and PdGa alloys. One way to better understand these systems is to form surface alloys and this has been extensively studied in the case of the Pd-Zn by depositing Zn on Pd(111) under ultra-high vacuum conditions. It has been shown that deposition of 0.5 to 2 ML of Zn on Pd(111) at 300 K leads to the formation of (2 × 1) Pd-Zn domains occurring along three equivalent <110> substrate directions, resulting in an apparent (2 × 2) LEED pattern [1]. In addition to the (2 × 2) phases reported in several other bimetallic systems, a second surface reconstruction of $(\sqrt{3} \times \sqrt{3})R30^{o}$ ordering has been identified in many systems [2]. The In/Pd(111) system exhibits both phases [3], but correlations to surface alloy phases is still lacking.

Here, we report on these different phases obtained after dosing 1 to 2 ML of In on Pd(111) followed by subsequent annealing up to 980 K. While diffuse (2 × 2) LEED patterns are observed at both coverages, the overall quality is slightly improved for 2 ML deposition. Corresponding XPS results suggest a partial coverage of stoichiometric PdIn after RT deposition of both layers. The evidence of PdIn formation is found by comparing Pd *3d* core levels to those obtained for PdIn bulk samples. To analyze the resulting structure, the surface energies of the low index surfaces of PdIn have been evaluated by *ab initio* calculations along with the stabilization of In at the surface or buried in Pd(111) for different atomic concentrations.

Moreover, we have found that annealing the first layer to ~690 K results in a well-ordered $(\sqrt{3} \times \sqrt{3})R30^{o}$ phase with a surface lattice constant of 4.75 Å. This phase shows a slightly rumpled top-layer, characteristic of $(\sqrt{3} \times \sqrt{3})R30^{o}$ substitutional surface alloys found in other systems [2]. Annealing the second layer to the same temperature (±10 K) leads to a surface of higher surface In concentration and a diffuse (1 × 1) LEED pattern. Annealing to higher temperatures (830 K) after 2 ML deposition yields In concentration comparable to those obtained for Pd(111) $(\sqrt{3} \times \sqrt{3})R30^{o}$–In (after annealing ≈ 1 ML). However, the corresponding LEED patterns at this stage show a clear (1 × 1) phase without any indication of $(\sqrt{3} \times \sqrt{3})R30^{o}$ ordering. These results show that the surface reconstructions depend on the In diffusion processes, the latter being dependent on the annealing temperature and coverage.

1. G. Weirum, M. Kratzer, H. P. Koch, A. Tamtoegl, J. Killmann, I. Bako, A. Winkler, S. Surnev, F. P. Netzer, and R. Schennach, *J. of Physical Chemis*try C. **113**, (2009), p. 9788.
2. Ugo Bardi, *Rep. Prog. Phys.* **57** (1994), p. 939.
3. A. Pancotti, A. de Siervo, M. Carazzolle, R. Landers and G. Kleiman, *J. of Electron Spectroscopy and Related Phenomena* **156** (2007), p. 307.

SS-3-Or-4
Ordered H2O structures on a particularly weakly interacting surface - H2O/Au(111).

T13 Surface Science

#SS-3-Or-4

G. Corem [1], N. Avidor [1], T. Kravchuk [1], P.R. Kole [2], J. Zhu [2], J.R. Manson [3], G. Alexandrowicz [1].

[1]Technion - Israel Institute of Technology - Haifa (Israel), [2]Cavendish Laboratory, University of Cambridge - Cambridge (United kingdom), [3]Clemson University - Clemson (United states).

In past decades, numerous experimental and theoretical studies have been devoted to understanding the interaction of H_2O with various metallic surfaces. The interaction between water molecules and the Au(111) surface is weaker than that of all the other close packed noble and transition metals, which could suggest that a wetting layer might not form on this substrate. Nevertheless, scanning probe studies have identified the formation of a first layer which serves as a precursor to the 3D growth of H_2O, a layer which was assumed to be amorphous at the temperature range probed by the experiments[1-2] in apparent contradiction with the sqrt(3)xsqrt(3)R30 ordered pattern obtained in LEED measurements[3].
In this presentation we report helium atom scattering (HAS) measurements of the structure and dynamics of the first H_2O layer on Au(111). HAS is an extremely non-perturbative technique for studying surface structure and dynamics. It is sensitive to light atoms (e.g. the proton order in a water layer) and is capable of measuring the average structure on an atomic scale even in the presence of significant motion. Our measurements, performed at 110K, show a clear sqrt(3)xsqrt(3)R30 helium diffraction pattern which continuously intensifies during the exposure to H_2O, suggesting the gradual formation of highly ordered H_2O islands which are commensurate with the underlying gold surface. Further multilayer growth results in a loss of the diffraction pattern and eventually an angular scattering distribution which is consistent with amorphous solid water phase expected at these temperatures. Additional information about the H_2O surface layer was obtained from inelastic helium-spin-echo measurements on this system[4]. Here we observed the appearance of an energy-loss mode associated with the H_2O surface layer. This

vibrational mode which seems dispersionless near the zone boundary exhibits avoided crossing behavior with the acoustic modes of the gold substrate. Complementary measurements of D_2O provide further insight into the origin of this mode.

[1] N. Ikemiya et al., J. Am. Chem. Soc. 119, 9919 (1997).
[2] D. Stacchiola et al. J. Phys. Chem. C 113, 15102 (2009).
[3] G. Pirug et al., Surf. Sci., 405, 87 (1998).
[4] G. Alexandrowicz et al. J. Phys: Conden. Matter, 19, 305001 (2007).

SS-7-Or-11
Reactions of formate species on metal-deposited TiO2(110) surface; effect of UV illumination

T13 Surface Science

#SS-7-Or-11

A. Farkas, F. Solymosi.

MTA-SZTE Reaction Kinetics and Surface Chemistry Research Group at the University of Szeged - Szeged (Hungary).

The interaction and reactions of formic acid, methanol and their dissociation products were studied on the clean, potassium-deposited and Rh-promoted TiO_2(110) surfaces by high resolution electron energy loss spectroscopy (HREELS), Auger-electron spectroscopy (AES), temperature-programmed desorption (TPD) and work function measurements (WF).
Formic acid adsorbs molecularly on TiO_2(110) at 90K yielding strong losses at 1250, 1395, 1640, 1730 and 2975 cm^{-1}. The weakly adsorbed HCOOH desorbs below 300K, but a small extent of molecule remains on the surface and dissociates to formate and hydrogen. Formate species were identified in HREELS by the symmetric and asymmetric O-C-O stretching mode and C-H stretching mode at 1360, 1590 and 2950 cm^{-1}, respectively. TPD indicated that the main reaction products, CO_2 and H_2, desorbed around 590 K. This reaction very probably occurs on vacancies of the clean TiO_2 surface [1]. Dehydrogenation reaction is the favourable reaction route. Potassium deposition decreases the work function of the TiO_2(110) surface by ~3.3 eV at ΘK ~ 0.9 ML. Potassium as an electropositive additive enhances the rate of the dissociation and thus the concentration of reaction intermediates on the surface. Nevertheless the amount of the reaction products (CO_2, H_2) also increased with the potassium coverage (Td=550-600K).
The dissociation of HCOOH is more pronounced, if we evaporated rhodium onto the TiO_2 surface. We observed a drastic change in the dissociation probability after ~1.5 ML rhodium deposition at RT followed by HCOOH adsorption at 90 K and annealing the surface to 300 K. The vibrations characteristics of formate dominated the HREEL spectra at this temperature; moreover a new adsorption feature appeared in the CO stretching region at ~2050 cm^{-1}. Illumination of the surface layer caused attenuation of the formate bands.
We also followed the effect of illumination on the reaction of methanol adsorbed on

the potassium- and rhodium-deposited TiO_2(110) surface. Majority of the methanol molecules desorbed intact from the clean surface below RT. However a small fraction underwent dissociation to methoxy at and above 200K, as indicated by the appearance of the characteristic vibrations of methoxy at 1050, 1160, 1460, 2850 and 2960 cm^{-1}. On the potassium-covered surface its stability was enhanced and it was detectable by HREELS up to 300K. Interesting feature of the interaction of methanol with the Rh-deposited TiO_2 surface (Θ_{Rh}~1 ML) is that after UV illumination at 300 K we detected the generation of methyl formate. This observation supports our former catalytic results wherein we found that methyl formate is formed in the photoreaction of methanol [2].

[1] Henderson, M. A. *J. Phys. Chem. B* **1997**, 101, 221-229.

[2] Halasi, Gy.; Schubert, G.; Solymosi, F. *J. Catal.* **2012**, 294, 199-206.

SS-P3-13
Dissociation reaction kinetics of metastable oxygen molecule on partially oxidized Si(111) surfaces studied by real-time photoelectron spectroscopy

T13 Surface Science

#SS-P3-13

K. Nishimoto [1], J. Tang [1], S. Ogawa [1], A. Yoshigoe [2], S. Ishizuka [3], D. Watanabe [1], Y. Teraoka [2], Y. Takakuwa [1].

[1]Tohoku University - Sendai (Japan), [2]Japan Atomic Energy Agency - Sayo (Japan), [3]Nagaoka University of Technology - Nagaoka (Japan).

Metastable oxygen molecule O_2*, which appears during the initial oxidation on Si surfaces, has long lifetime of dissociation on Si(111)7×7 surface. Recently, we reported that the number of adsorbed oxygen atoms at the completion of Langmuir-type adsorption on Si(111) increases about three times with increasing temperature from RT to 600℃ and that the strong temperature dependence of the saturation coverage is associated with O_2* [1]. In this study, to clarify the role of O_2* in the initial oxide growth, real-time photoelectron spectroscopy using He resonance line (21.22 eV) and synchrotron radiation (710 eV) at SPring-8 was employed to measure the time evolutions of oxygen uptake, work function φ and oxide adsorption states on partially oxidized Si(111) surface after O_2 supply was stopped.
As observed in Fig. 1,φ increases rapidly upon O_2 supply and then changes suddenly to a decrease, while O 2p uptake changes monotonically in a Langmuir-type adsorption manner. When O_2 supply was stopped at surface oxide coverage θ_{oxide} of 20%, φ does not increase but decreases although θ_{oxide} still continues to increase due to the residual O_2 gas. The observed decrease of φ is ascribed to the dissociation of O_2*. Figure 2 shows the initial θ_{oxide} dependence of the correlations between φ and θ_{oxide}. Over the whole θ_{oxide} region,φ shows a significant decrease, suggesting that O_2* is concerned with the oxide growth until Langmuir-type adsorption is completed. The decay curve of φ is fitted well with two exponential functions. Both of the estimated lifetimes increase with increasing θ_{oxide} up to 15%

and then is considerably shortened. This finding implies that O_2* dissociation is caused more frequently on the Si surface with larger θ_{oxide}. The O_2* dissociation kinetics is discussed based on the changes of the oxygen adsorption states.

[1] J. Y. Tang *et al*., e-J. Surf. Sci. Nanotech. **10** (2012) 525.

Fig. 1. Time evolutions of (a) O 2p intensities and (b) work function.
Fig. 2. Correlations between oxide coverage and work function.

NST/SS-P1-20
Time-Dependent Density Functional Theory Calculation of Dielectric Function of Boron Nitride Nanostructures

T13 Surface Science

#NST/SS-P1-20

K. Watanabe, H. Goto, S. Hagiwara, J. Haruyama, C. Hu.

Tokyo University of Science - Tokyo (Japan).

Hexagonal boron nitride (h-BN), a structural analogue of graphite, has excellent mechanical and chemical stability together with a large electronic energy-band gap, and has been widely used in electronic devices. The BN sheet [1], just the analogue of graphene, has also attracted wide attention due to its useful properties such as a complementary 2D dielectric substrate for graphene electronics. The BN nanoribbons (BNNRs), which were recently produced under unwrapping multiwalled BN nanotubes, show semiconducting properties due to edge states and imperfections, and have width-dependent energy-band gaps [2] that can be tuned by transverse electric fields. Thus, the BN nanostructures are promising materials in optics and opto-electronics as functional semiconductors. However, compared with their carbon analogues, the study on optical properties of BN nanostructures is very few up to now.

The objective of the present study is to understand the dielectric properties of the BN nanostructures (3D h-BN, 2D BN sheet and 1D BNNR) by a first-principles electronic structure calculation, focusing on the dimensional dependence of dielectric functions. We use real-time time-dependent density functional theory (TDDFT) that incorporates vector potential for electric fields in the linear response regime to calculate the dielectric function. [3].

Our results have reproduced plasmon peaks in electron energy loss spectra (EELS) [4] of h-BN and the BN sheet observed in a very recent experiment [5]. We have found that the real part of the dielectric function becomes smooth as a function of energy when decreasing the dimension of the BN nanostructures. It further decreases with reduced ribbon widths and shows a tendency of approaching one. This property indicates that the screening effect of the Coulomb interaction is significantly reduced in low dimensional BN structures. The profiles of EELS spectra

become more similar to those of absorption spectra (imaginary part of dielectric function) for BN structures with lower dimension, especially for BNNRs. This means that the electronic excitations of low dimensional BN structures occur mostly through particle-hole excitations instead of plasmon excitations. We will discuss the above results of BN structures with the comparison of their carbon analogues in the presentation.

[1] H. Zeng, C. Zhi, Z. Zhang, X. Wei, X. Wang, W. Guo, Y. Bando, and D. Golberg, Nano Lett. **10**, 5049 (2010).
[2] C. Hu, R. Ogura, N. Onoda, S. Konabe, and K. Watanabe, Phys. Rev. B **85**, 245420 (2012).
[3] G.F. Bertsch, J.-I. Iwata, A. Rubio, and K. Yabana, Phys. Rev. B **62**, 7998 (2000).
[4] A.G. Marinopoulos, L. Wirtz, A. Marini, V. Olevano, A. Rubio, and L. Reining, Appl. Phys. A **78**, 1157 (2004).
[5] C.T. Pan, R.R. Nair, U. Bangert, Q. Ramasse, R. Jalil, R. Zan, C.R. Seabourne, and A.J. Scott, Phys. Rev. B **85** , 045440 (2012).

SS/NST-P1-05
Electron orbital resolution in distance dependent STM experiments with tungsten tips

T13 Surface Science

#SS/NST-P1-05

O. Luebben [1], A. Chaika [2], S. Nazin [2], V. Semenov [2], N. Orlova [2], E. Postnova [2], S. Bozhko [2], S. Krasnikov [1], B. Murphy [1], K. Radican [1], I. Shvets [1].

[1]CRANN, School of Physics, Trinity College - Dublin (Ireland), [2]Institute of Solid State Physics RAS - 142432, Chernogolovka, Moscow District (Russian federation).

The electron orbital is a fundamental concept of science – it is central to physics, chemistry, and materials science. The possibility of resolving these orbitals directly is highly appealing. This has become possible with the invention of scanning probe microscopy techniques. Direct images of intra-atomic electronic structures have been obtained in recent atomic force microscopy [1,2] and scanning tunnelling microscopy (STM) experiments [3]. Here we present the results of distance dependent STM studies carried out with tungsten tips revealing sub-atomic electron orbital features at small tip-sample separations. The dependence of the STM contrast on the tunneling gap resistance suggests that the relative contribution of particular electron orbitals of the tip and surface atoms involved in tunneling can be controlled during precise distance dependent STM experiments. This is confirmed by STM studies with [001]-oriented single crystalline tungsten tips [4,5]. Electron microscopy images of the W[001] tips prove the formation of atomic scale pyramids at the apex. In our distance dependent STM experiments on a graphite (0001) surface (Fig. 1a,b) the carbon atoms were used to probe different *d*-orbitals of the tip's apex atom. The experimental data and density functional theory (DFT) calculations (Fig. 1c) prove that even localized W 5*d*-orbitals can be controllably probed with sub-Ångström lateral resolution at small bias voltages and tunnelling gaps of 2.0–3.0 Å. The sub-atomic features observed in experiments (Fig. 1b) reproduce the shapes of the $5d_{z^2}$, $5d_{xz}$ and $5d_{xy}$ tungsten atomic orbitals. DFT calculations of both the fully relaxed (Fig. 1c) and constrained W[001] tip – graphite(0001) systems reveal that the transformation of the sub-atomic features is related to a substantial modification of

the orbital structure of the W atom at the tip apex due to a strong tip-surface interaction at small distances. This work was supported by the Russian Academy of Sciences, RFBR grant № 11-02-01256, Marie Curie IIF grant within the 7th European Community Framework Programme and Science Foundation Ireland.

[1] F.J. Giessibl et al., Science 289, 422 (2000).
[2] S. Hembacher et al., Science 305, 380 (2004).
[3] A.N. Chaika et al., Phys. Rev. Lett. 98, 206101 (2007).
[4] A.N. Chaika et al., EPL 92, 46003 (2010).
[5] A.N.Chaika et al., Appl. Surf. Sci., 2012, 10.106/j.apsusc.2012.10.171.

Fig. 1. (a) Model of the tip-surface system showing the orbitals involved in tunneling. (b) 2×2Å^2 STM images measured with the W[001] tip on graphite (0001). (c) PDOS at the W tip atom at different gaps.

SS-11-Or-8
Fluorescence spectroscopy of large π-conjugated molecules on surfaces

T13 Surface Science

#SS-11-Or-8

M. Sokolowski [1], A. Paulheim [1], C. Marquardt [1], M. Müller [1], A. Eisfeld [2].

[1]University of Bonn - Bonn (Germany), [2]Max-Planck-Institut für Physik komplexer Systeme - Dresden (Germany).

Adsorption of large π-conjugated organic molecules on surfaces has become a topic of growing interest during last years under both fundamental and applied aspects, e.g., optoelectronic applications of molecular films. Although fluorescence (FL) spectroscopy of π-conjugated organic molecules is well-established for thin molecular films, for isolated or aggregated molecules on surfaces with coverages in the monolayer regime, this technique is not very common so far [1]. However, as we demonstrate, there are at least two interesting aspects concerning the combination of surface science experiments with FL spectroscopy. The first is related to the high signal-to-noise ratio and the very high spectral resolution of FL spectroscopy which allows performing experiments for ultimate low concentrations of molecules on surfaces down to the 10-5 monolayer range. The second aspect concerns the self-organization of molecules on surfaces. This enables one to prepare well-defined two-dimensional ordered molecular aggregates for which the intermolecular resonance interaction leads to interesting optical phenomena.

We report on these aspects on the basis of experiments performed for the well-studied model molecule PTCDA adsorbed on thin epitaxial films of KCl(100) on Ag(100) [2]. In the first set of experiments we have studied isolated molecules at very low coverages. The FL and FL excitation spectra are highly resolved and allow precise identification of the in-plane vibrational modes of the adsorbed PTCDA on KCl. Interestingly, there are additional low energy vibrational modes which are only explainable under the assumption of a distorted non-planar geometry of the adsorbed molecule, likely related to the electrostatic interaction of the anhydride groups with the surface cations [3]. Hence, information on the molecular geometry can be derived from the FL spectra here. Furthermore, we studied the thermal or optically induced diffusion of the PTCDA molecules from initially occupied terrace sites to energetically

more stable sites at step edges. This site change is visible as a line shift in the spectra [4].

In the second set of experiments, a complete ordered monolayer of PTCDA was prepared. It exhibits an interesting so-called brickwall structure with one molecule per unit cell [2]. As a consequence, the transition dipoles of all molecules are parallel and couple very effectively. This leads to a pronounced enhancement of the vibration-free optical transition (0-0 transition), known as "superradiance". The effect has been observed in self-organized so-called J-aggregates of dyes in solution so far. Here it is demonstrated for a strictly two-dimensional aggregate on a surface. However, the spectral lines shape is found to be broadened with respect that of isolated molecules. From a detailed theoretical modelling, we find that this is related to domain boundaries, possibly due to surface steps or growth defects, which limit the size of the aggregates.

[1] M. Müller, A. Langner, O. Krylova, E. Le Moal and M. Sokolowski, Applied Physics B, *2011*, **105**, 67.
[2] M. Müller, J. Ikonomov and M. Sokolowski, Surface Science, *2011*, **605**, 1090.
[3] M. Müller, A. Paulheim, C. Marquardt and M. Sokolowski, Journal of Chemical Physics, in press.
[4] A. Paulheim, M. Müller, C. Marquardt and M. Sokolowski, PCCP, submitted.

SS-11-Or-9
Resolving the Interfacial Structure of Alkanethiol Self-Assembled Monolayers on Au(111)

T13 Surface Science

#SS-11-Or-9

Q. Guo [1], F. Li [2], J. Gao [1].

[1]University of Birmingham - Birmingham (United kingdom), [2]Tsinghua University - Beijing (China).

We have carried a systematic study of self-assembled monolayers (SAMs) of methyl-, ethyl-, and propyl-thiolate on Au(111) using scanning tunnelling microscopy (STM). High-resolution STM imaging reveals that the SAMs at saturation coverage form a common 3×4 structure at room temperature1. The 3×4 phase consists of zig-zag rows of Au-adatom-dithiolate unit, RS-Au-SR. Moving from propylthiolate to butylthiolate monolayer, transition from 3×4 to (3×2√3)-rect./c(4×2) occurs due to an increasing level of interactions among the alkane chains. 3×4 and (3×2√3)-rect. are two closely-related structures: one with zig-zag rows of RS-Au-SR; and the other with alternating zig-zag and zag-zig rows consisting of the same RS-Au-SR unit.

SAMs of methyl-, ethyl- and propyl-thiolate do not form either the (3×2√3)-rect./ c(4×2) or the √3×√3-R30o structure at any coverage. The well-reported √3×√3-R30o phase for the longer chain alkylthiolate monolayers requires new interpretations. Our analysis shows that there is no pure √3×√3-R30o phase for any alkanethiol SAMs on Au(111) regardless the alkane chain length. The interfacial structure should always be 3×4 or (3×2√3)-rect.. As the chain length increases, the enhanced van der Waals interaction tends to keep the alkane chains at equal distances from each other, leading to the formation of a superficial √3×√3-R30o structure. Due to the flexibility of the alkane chains, a (3×2√3)-rect. structure at the interface is transformed gradually into a √3×√3-R30o-like structure at the surface.

1. L. Tang, F. S. Li, W-C. Zhou, Q. Guo, Surf. Sci. 606 (2012) L31.

Fig.1. STM images showing the 3×4 phase of methylthiolate (c_1), ethylthiolate (c_2) and propylthiolate (c_3) monolayers formed at RT on Au(111).

SS-P3-37
One-dimensional metallic bands of Pt-induced nanowires on Ge(001) observed by angle-resolved photoelectron spectroscopy

T13 Surface Science

#SS-P3-37

K. Yaji [1], I. Mochizuki [2], S. Kim [1], Y. Takeichi [2], Y. Ohtsubo [3], P. Le Fèvre [3], F. Bertran [3], A. Taleb-Ibrahimi [3], A. Kakizaki [1], F. Komori [1].

[1]Institute for Solid State Physics, The university of Tokyo - Kashiwa-Shi, Chiba (Japan), [2]Photon Factory, Institute of Materials Structure Science, KEK - Tsukuba-Shi, Ibaraki (Japan), [3]Synchrotron SOLEIL - Saint-Aubin-Bp, Gif Sur Yvette (France).

One-dimensional (1D) electronic systems are well known as sources of intriguing physical phenomena such as non-Fermi liquid and Peierls type metal-insulator transition. In addition, the surface bands split into two due to the Rashba effect if the 1D systems are including heavy element atoms. For these peculiar phenomena of 1D electronic states, Pt-induced nanowires formed on Ge(001) surface (Pt/Ge(001)-NWs) is remarkable. The defect-less Pt/Ge(001)-NWs was firstly observed by Gürlu et al. with scanning tunneling microscopy (STM) [1]. After that, Houselt et al. reported that the surface periodicity of Pt/Ge(001)-NWs changes from a p(4×2) at room temperature to a p(4×4) below 80 K [2]. Recently, we experimentally proposed the atomic configuration of Pt/Ge(001)-NWs by means of reflection high-energy positron diffraction [3]. In the present study, we have investigated surface and electronic structures of Pt/Ge(001)-NWs by low energy electron diffraction (LEED), STM and angle-resolved photoelectron spectroscopy (ARPES).

The single-domain samples of Pt/Ge(001)-NWs were prepared on a vicinal Ge(001) surface. From LEED and STM, we have found the nanowires that line up parallel to the step edges. The ARPES measurements were performed at BL19A in KEK-PF and Cassiopée beamline in SOLEIL Synchrotron. We have observed four metallic bands associated with Pt/Ge(001)-NWs along the nanowire direction. The ARPES measurements also provide a constant energy map at the Fermi level. We found that the Fermi surface of one band consists of completely straight-line without

two-dimensional undulation. This suggests that the band is an ideal one-dimensional metallic state. On the other hand, the Fermi surfaces of the other bands exhibit weak two-dimensional undulations around the straight lines which a purely 1D Fermi surface would give, meaning some inter-chain interaction. We believe that the 1D metallic bands of Pt/Ge(001)-NWs are very suitable for the study of the peculiar physics in one-dimensional metals.

[1] O. Gürlu *et al*., Appl. Phys. Lett. 83, 4610 (2003).
[2] A. van Houselt *et al*., Surf. Sci. 602, 1731 (2008).
[3] I. Mochizuki *et al*., Phys. Rev. B, 85, 245438 (2012).

SS-18-Or-1
Oligomerization of TCNQ-type Electron Acceptors via Unprecedented Surface-Assisted Decyanation Reaction

T13 Surface Science

#SS-18-Or-1

R. Otero [1], C. Urban [1], Y. Wang [1], J. Rodríguez-Fernández [2], R. García [3], M.Á. Herranz [3], M. Alcamí [2], N. Martín [4], F. Martín [1], J.M. Gallego [5], R. Miranda [1].

[1]Universidad Autonoma de Madrid - IMDEA Nanoscience - Madrid (Spain), [2]Universidad Autonoma de Madrid - Madrid (Spain), [3]Universidad Complutense de Madrid - Madrid (Spain), [4]Universidad Complutense de Madrid - IMDEA Nanoscience - Madrid (Spain), [5]ICMM-CSIC - IMDEA Nanoscience - Madrid (Spain).

The pioneering discovery that brominated porphyrins undergo polymerization reactions upon annealing when adsorbed on a solid surface[1] has motivated extensive investigations over the last few years. The aim of a large part of such investigations has been to exploit other reactions which are known to work well in the solution phase to synthesize 2D polymers[1], graphene nanostructures[2], etc. Alongside these reactions, a number of intriguing reports on surface-based reactions with no solution-phase analog have appeared recently[4, 5]. In these cases, the surface must play a crucial role in the reaction mechanism. However, the atomistic details of how the surface changes the reactivity of the organic adsorbate in such dramatic ways are still not fully understood. Moreover, although purely electronic effects derived from charge-transfer between the adsorbate and the metal surface might be expected to affect the chemical reactivity of the adsorbed organic molecule, no previous study has tackled explicitly this issue.

In this communication we report on the thermally-induced chemical reactions of the organic electron acceptor 15,15,16,16-tetracyano-6,13-pentacene-*p*-quinodimethane (TCPQ) when adsorbed on Cu(100) studied by an in situ combination of Scanning Tunneling Microscopy (STM) and X-ray Photoelectron Spectroscopy (XPS) together with Density Functional Theory (DFT) calculations. We show that charge-transfer from the metal substrate to the organic adsorbate controls the molecular

conformation upon adsorption and, thereby, the strength and geometric avialability of the different chemical groups to undergo chemical reactions. In particular, we will demonstrate that, upon annealing, two cyano groups are selectively eliminated from each molecule, a result that cannot be properly understood unless the role of the surface as a source of electrons is properly accounted for. Subsequent annealing leads to the formation of short oligomeric chains with pentacene and cyano groups in the repeating unit, which might be of interest for applications in organic electronics and photovoltaics.

1 L. Grill, et al. Nat Nano 2007, 2, 687-691. [2] J. Cai, et al. Nature 2010, 466, 470

3 N. A. A. Zwaneveld, et al. J. Am. Chem. Soc. 2008, 130, 6678

4 M. Int'l Veld, et al. Chem. Commun. 2008, 1536

5 D. Zhong, et al. Science 2011, 334, 213

Figure 1. STM images of the morphology of TCPQ molecules adsorbed on Cu(100) before (left) and after (right) annealing to 500 K (left image 6.3 × 4.4 nm^2, V_b = -0.83 V, I = 0.64 nA; right image 23.4 ×19.9 nm^2, inset 11.2 × 9.2 nm^2, V_b = -2 V, I = 0.24 nA).

SS-2-Or-7
Bound-state resonance effects in the mode-selected electron-phonon coupling strengths measured by inelastic He atom scattering

T13 Surface Science

#SS-2-Or-7

P. Kraus [1], A. Tamtögl [1], M. Mayrhofer-Reinhartshuber [1], G. Benedek [2], W.E. Ernst [1].

[1]Graz University of Technology - Graz (Austria), [2]Donostia International Physics Center (DIPC) - San Sebastián (Spain).

Electron-phonon coupling (EPC) determines many relevant materials properties such as the lifetimes of excited electrons, BCS superconductivity, charge density waves, the Kohn anomalies in the phonon dispersion, etc. The information on EPC as currently derived from electron tunneling spectroscopy or heat capacity measurements is restricted to the single parameter λ averaged over all transitions across the Fermi surface and the phonon spectrum. However, a recent inelastic He atom scattering (HAS) analysis on ultrathin Pb films [1] demonstrated the surprising ability of HAS to provide information on the EPC strength for specific surface phonon modes (mode-λ spectroscopy). In this work we show that the extension of this analysis to corrugated semimetal surfaces is not trivial, due to the occurrence of bound-state resonance effects in the inelastic HAS intensities [2]. Unlike low-index metal surfaces which are perfectly flat, the semimetal Bi(111) surface exhibits a large corrugation [3] while supporting conducting electronic states at the surface [4]. Recent iHAS measurements on Bi(111) [5] revealed intense phonon features and comparatively strong EPC for certain modes. Using detailed information on the He-Bi(111) interaction potential obtained from elastic resonances, some of those intense features can be identified as resonantly enhanced. The complete procedure from measuring the relevant bound states to predicting possible resonance positions in the time-of-flight spectra using elastic and inelastic HAS will be presented and thoroughly discussed.

[1] I. Yu. Skyadneva et. al., PRL **107**, (2011) 095502
[2] D. Evans et. al., PRL **50**, (1983) 23
[3] A. Tamtögl et. al., JPCM **22**, (2010) 304019
[4] Yu. M. Koroteev et. al., PRL **93**, (2004) 4
[5] A. Tamtögl et. al., PRB **87**, (2013), 035410

SS-3-Or-6
Grazing Incidence Fast Atom Diffraction: A novel approach to surface structure analysis

T13 Surface Science

#SS-3-Or-6

H. Khemliche [1], A. Momeni [1], M. Debiossac [1], B. Lalmi [1], P. Soulisse [1], M. Mulier [1], P. Roncin [1], P. Atkinson [2], V. Etgens [2], M. Eddrief [2].

[1]ISMO, UMR8214 CNRS-Université Paris-sud Orsay, 91450 France - Orsay (France), [2]INSP, UMR7588 CNRS – Université Pierre et Marie Curie Paris 75005, France - Paris (France).

Surface science is continuously in search of new techniques to characterize the interface between a solid and its environment. During growth, the most refined characterization of the last layers of solid is often required as it sets the actual starting condition, whereas any real time information on the surface morphology and growth dynamics becomes most valuable. In both cases, the main challenge is to gain quantitative information on the terminating atomic layer, its structure, microscopic corrugation, mesoscopic morphology, charge transfer and type of terminating layer in composite materials, mosaicity, etc.
Electron diffraction techniques (LEED and RHEED) are well suited to resolve the lattice parameter of topmost layers, but are usually not sufficient for the unambiguous identification of the microscopic atomic structure. Moreover, the information related to the top layer is often blurred by contributions from undelaying layers. Local description on the last atomic plan is best achieved by near field microscopic techniques (STM, AFM) but these are often too slow to be carried out in real time.
We have developed a new technique based on diffraction of fast atoms at grazing incidence; it is named GIFAD for Grazing Incidence Fast Atom Diffraction.
The main advantages of GIFAD are:
- a superior surface sensitivity, the incident atom probes only the region lying at 2 to 5 Å above the last atomic plan
- the ability to provide simultaneously lattice parameter and microscopic surface corrugation (similar to that measured by AFM) averaged on a macroscopic level [1].
- the high sensitivity to mosaicity [2]
- its geometry being similar to that of RHEED, GIFAD is well suited for real time

monitoring of film growth
- this technique is truly non-invasive
The probing atoms, He with energies in the range 0.2 to 1 keV, are produced by neutralization of ions produced by a bright ion source. The diffraction pattern exhibits Bragg spots whose relative intensities can be analysed to extract the density profile of the valence electrons. Fig. 1 shows an example of such results obtained on a c(2x2) ZnSe(001) surface; the experimentally derived corrugation along the [100] direction points to the fact that maxima in the electron density do not necessarily sit on top of the atoms.
Other analytical properties of GIFAD will be presented and examples given in static as well as dynamical conditions.

[1]. H. Khemliche, P. Rousseau, P. Roncin, V. H. Etgens and F. Finocchi, Appl. Phys. Lett. 95 151901 (2009)
[2]. B. Lalmi, H. Khemliche, A. Momeni, P. Soulisse and P. Roncin, J. Phys.: Condens. Matter 24, 442002 (2012)

Fig.1.

SS-2-Or-8
Core-shell Fe@Au nanoparticles: A DFT study

T13 Surface Science

#SS-2-Or-8

M. Benoit [1], C. Langlois [2], N. Combe [1], H. Tang [1], M.J. Casanove [1].

[1]CEMES/CNRS - Toulouse (France), [2]MATEIS/INSA - Lyon (France).

Magnetic nanoparticles are important in many applications ranging from data storage to ferrofluids and to biomedicine.The ability to control simultaneously the size, shape and composition of the nanoparticles provides a great flexibility to tune their properties for their different bio-medical applications [1]. However, these particles are generally not bio-compatible and can be easily oxidized which alters their magnetic properties.A possible solution is to passivate the surface of magnetic nanoparticles with a chemically inert and biocompatible metal such as gold.The fabrication of cores-shell nanoparticles with a magnetic core and a gold shell has then become a promising route for biomedical applications [2]. Experimentalists of the MC2 group at CEMES (Toulouse) in collaboration with C. Langlois (INSA Lyon) have managed to grow Fe@Au core-shell nanoparticles of ~8-10 nm using phase vapor deposition techniques (Fig. 1). These particles take a very unusual morphology made of an iron nanocube encapsulated by gold truncated pyramids on every cube facet. Composition, size and shape of these nanoparticles show, however, some disparity, the growth mechanisms being difficult to control during growth by physical vapor deposition at high temperature. Furthermore, the influence of the coating on the electronic, structural and magnetic properties of the Fe core is not well known yet, neither its effect on the Fe oxydation properties.In this work, a Fe@Au nanoparticle was modeled by a simplified system in which the Fe core is represented by an infinite substrate, on which several atomic layers of gold are deposited. The Fe/Au interfaces, as they stand on the iron nanocube facets, have been studied using DFT calculations. We present results obtained from the detailed analysis of the structural, magnetic and electronic properties of these interfaces, as a function of the number of gold monolayers deposited on the Fe substrate.

et al., J. Magn. Magn. Mater. **293**, 483 (2005)

[2] S.-L. Cho et al., J. Applied Physics 95, 6804 (2004); M. Chen et al., J. Applied Physics 93, 7551 (2003)
[3] M. Benoit, C. Langlois, N. Combe, H. Tang and M.-J. Casanove, Phys. Rev. B 86, 075460 (2012)

TEM image of two different oriented Fe@Au nanoparticles (left:[110]Fe orientation; right:[001]Fe orientation) grown in Al2O3 by UHV magneton sputtering.

SS-11-Or-10
Adsorption geometry and electronic structure of Zn(II) tetrabromothienylporphyrin on the Ag(111) and Au(111) surfaces.

T13 Surface Science

#SS-11-Or-10

A. Cafolla [1], J.P. Cunniffe [1], T. Carpy [1], J.P. Beggan [1], N. Boyle [1], E. Harvey [1], M. Pryce [1], S. Krasnikov [2], A. Preobrajenski [2].

[1]Dublin City University - Dublin (Ireland), [2]Trinity College Dublin - Dublin (Ireland).

We present a study of the molecular self-assembly of Zn(II) 5,10,15,20-tetra-(5-bromothien-2-yl)-porphyrin (ZnTBrThP) on the Ag(111) and Au(111) surfaces. These surfaces have been characterised by means of scanning tunnelling microscopy (STM), X-ray photoemission spectroscop (XPS), valence band photoemission and x-ray absorption spectroscopy (XAS) from the submonolayer to multilayer regimes, in order to reveal the electronic properties and conformational behaviour of the molecules on these surfaces.
A pronounced substrate dependence is displayed in the self-assembly of the ZnTBrThP molecules on the Ag(111) and Au(111) 22 x √3 surfaces. The molecular assembly on the Ag(111) surface is consistent with metal-directed polymerisation, where linkage of the ZnTBrThP molecules is mediated by coordination to substrate atoms via the bromothienyl groups; the abstraction of Ag atoms is revealed in the formation of substrate vacancy islands. Weaker substrate bonding of the ZnTBrThP molecules on the Au(111) 22 x √3 surface permits a greater influence of direct intermolecular interaction in the self-assembled molecular overlayer. Here attractive dipole-dipole interactions between S and Br moieties of adjacent molecules stabilise the observed face-to-face alignment of the bromothienyl groups. When adsorbed on both surfaces, the ZnTBrThP molecules display a latent thermal lability, which results in the fragmentation of the bromothienyl groups upon annealing [1,2]. The elimination of the bromide moiety is common a feature on both Au(111) 22 x √3 and Ag(111) surfaces, however, in the latter case, the cleavage of the thienyl moiety is also observed.

[1] Grill et al., Nature Nanotechnology 2 (2007) 687.

[2] Krasnikov et al., Nano Research 4 (2011) 376.

Figure 1: Structural model of the ZnTBrThP molecule.

Figure 2: STM image of ZnTBrThP molecules on the Ag(111) surface at a coverage of ~ 0.7 ML.

SS-P3-14
Inhibition of the corrosion of aluminum: DFT studies of the adsorption of 8-hydroxyquinoline on Al(111) and Al2O3 surfaces

T13 Surface Science

#SS-P3-14

F. Chiter [1], C. Lacaze-Dufaure [1], H. Tang [2].

[1]CIRIMAT - Toulouse (France), [2]CEMES - Toulouse (France).

Due to the high toxicity of chromates, the use of classical corrosion inhibitors for aluminum and aluminum alloys has been restricted in industrial applications. As a consequence, intense research efforts are being undertaken to find new environmentally friendly compounds. Experimentally it was shown that nitrogen-containing compounds are the most efficient corrosion inhibitors. Among these molecules, the 8-hydroxyquinoline (8-HQ) (figure-1) is particularly active in the prevention of the corrosion of aluminum and the 2024 alloy [1, 2]. We thus investigate the corrosion inhibition mechanisms of such molecules on pure Al and on Al2O3 surfaces by first principles calculations (periodic computations).

We first present a comparison of the stability of Al(111), γ-Al2O3(111), α-Al2O3(0001) and ultrathin alumina surfaces [3,4]. The interactions between the 8-HQ molecule and these surfaces are thus modeled and discussed, especially in term of adsorption sites and adsorption topology, calculated adsorption energies, stability of complexes formed by 8-HQ molecules with surface Al atoms. A detailed electronic structure analysis (charge transfer, density of states, work function, partial charge, etc …) leads to the determination of the bonding.

References:
[1]-C. Casenave, N. Pébère, F. Dabosi, Materials Science Forum, 192-194 (1995) 599
[2]- L. Guarrigues, N. Pébère, F. Dabosi, Electrochimica Acat, 41 (1996) 1209
[3]- G. Kresse, M. Schmid, E. Napetschnig, M. Shishkin, L. Köhler, P. Varga,

Science, 308 (2005) 1440
[4]- G. Prévot, S. Le Moal, R. Bernard, B. Croset, R. Lazzari, D. Schmaus, Phys. Rev. B, 85 (2012) 205450

SS/NST-P1-06
Secondary electron intensity dependence on the layer structure

T13 Surface Science

#SS/NST-P1-06

A. Sulyok.

MTA TTK - Budapest (Hungary).

Secondary electron intensity dependence on the layer structure

Attila Sulyok[1], Miklós Menyhárd[1] and Ludomir Zommer[2]
1 Research Centre for Natural Sciences, Budapest, Hungary
2 Institute of Physical Chemistry, Warsaw, Poland

The intensity of backscattered current depends on both the layer thickness and the atomic numbers. Thus, the alteration of layer thicknesses may result in a contrast in the secondary electron (SE) image. The old Seiler model described the SE intensity in those situation when a bulk material is covered by a thick layer of another material and an approximating formula was given for the contrast difference as a function of the overlayer thickness. The model cannot be applied to a target of a complex layered structure.
We will present experimental results demonstrating contrast changes because of altering layer thickness. The secondary electron intensity was continuously measured on specimen [3 x (nickel 40 nm / carbon 18 nm) on Si substrate during depth profiling. The actual depth was controlled by AES with simultaneous detection of Auger peaks (Ni and C).
Although there exist computer models for simulating the formation of SE images the reliability of them is not satisfactory. We developed a new Monte Carlo model based on tracking the electron trajectories. It includes the generation of secondary electrons and the main physical effects determining the backscattered SE intensity. BSE at 100 eV are calculated instead of the real SE at its low energies (10eV). Simulated intensity curves over Ni-C layer structure are interpreted and compared to measured results. The backscattering ratios provided by our model are within 10 % to the measured ratios. Both the simulated and the experimental curves demonstrate the complex behavior of SE intensity curves on a multilayer structure.
The backscattering on this Ni-C layer structure was also simulated by CASINO code.

We found higher deviation from the measured backscattering intensity ratios than that of our model.

SS-1-Or-11
Phase behavior of dimer adsorption model on honeycomb lattice at finite temperatures

T13 Surface Science

#SS-1-Or-11

V. Fefelov, S. Akimenko, V. Gorbunov, A. Myshlyavtsev, M. Myshlyavtseva, P. Stishenko.

Omsk state technical university - Omsk (Russian federation).

Dimer adsorption model is a very interesting model, because it allows identifying features of the phase behavior of adsorbed monolayers consisting of molecules with complex shape. Despite its simplicity the model takes into account the multisite adsorption, a different orientation of the molecules as relative to each other and relative to the surface, and also allows us to introduce specific lateral interactions. We have previously studied the phase behavior of the dimer adsorption model on lattices with different coordination numbers (honeycomb, square and triangular [1-3]). These studies have shown a strong dependence of the phase behavior of the adsorption monolayer on the coordination number of the lattice. In the case of square lattice one can observe only two ordered structures, in the case of triangular lattice – already three, but for honeycomb lattice in the ground state one can see devil's staircase of phase transitions (The term «devil's staircase» is usually used to describe the physical systems in which the amount of ordered structures in a finite range of phase space becomes formally infinite). It is interesting that the similar behavior of the adsorption monolayer occurs in real systems – the adsorption of trimesic acid on Au (111) [4].
Commonly, the devil's staircase appears as a result of the competition between long-range repulsive and short-range attractive interactions. Even the simplest models in which devil's staircase takes place include complex sets of interactions between particles. In the case of one-dimensional models it can be variable external field or long-range repulsive interactions, e.g. Frenkel-Kontorova model and one-dimensional Ising model; for three-dimensional models as a rule there are two or more competing interactions, e.g. well-known ANNNI model. However in our model there are only short-range repulsive lateral interactions. The main factor which leads to the appearance of infinite amount of ordered structures in our model is two competing

forms of adsorption.
In [3] we studied the model of dimer adsorption on honeycomb lattice in the ground state. The aim of this work is to investigate of the phase behavior of the model at finite temperatures and answer the question: Is it possible devil's staircase phenomenon of phase transitions at nonzero temperatures?
Model was studied by Monte Carlo method and transfer-matrix.

1. V.F. Fefelov, V.A. Gorbunov, A.V. Myshlyavtsev, M.D. Myshlyavtseva, Model of homonuclear dimer adsorption in terms of two possible molecule orientations with respect to surface. Phys. Rev. E, 82, (2010), 041602.
2. V.A. Gorbunov, A.V. Myshlyavtsev, M.D. Myshlyavtseva, V.F. Fefelov, Simulation of dimers adsorption on triangular lattice. Izvestiya Vysshikh Uchebnykh Zavedenii. Seriya Khimiya i Khimicheskaya Tekhnologiya, 53, (2010), 66-71.
3. V.F. Fefelov, V.A. Gorbunov, A.V. Myshlyavtsev, M.D. Myshlyavtseva, S.S. Akimenko, Devil's staircase behavior of a dimer adsorption model. Adsortion, DOI: 10.1007/s10450-013-9471-1.
4. Ye Y., Sun W., Wang Y., Shao X., Xu X., Cheng F., Li J., Wu K., A Unified Model: Self-Assembly of Trimesic Acid on Gold. J. Phys. Chem. C., 111, (2007), 10138-10141.

SS-P1-12
CORRELATION OF MICROSTRUCTURE AND CHARPY IMPACT TEST PROPERTIES AND THE EFFECTS OF ANNEALING CONDITIONS IN A LOW CARBON STEEL

T13 Surface Science

#SS-P1-12

C. De Carvalho Ares Elisei [1], G. Alves De Souza [1], T. Hashimoto Manabu [2], M. Dos Santos Pereira [2].

[1]CEETEPS - FATEC PINDA - Pindamonhangaba (Brazil), [2]UNESP - FEG - Guaratinguetá (Brazil).

This study correlates the microstructure and Charpy impact test properties of a low carbon steel (0,038%) in different annealing conditions. Three heat treatments were applied. The volumetric fraction was measured and identified with optical microscopy, scanning electron microscopy (SEM) and, atomic force microscopy (AFM). The Charpy impact test results indicated that, when the temperature range was modified, the transition temperature was modified too, and the samples austenitized at 950ºC absorved more energy and the transition temperature decreased.

1 ANDRADE, S.L.; BATISTA, J.F.; TAISS, J.M.; ROSA, L.K.; ULSAB – AVC – O Aço no Automóvel do Futuro. In: 57th Congresso da Associação Brasileira de Metalurgia e Materiais, São Paulo, 2002.
2 YAZICI, M.; DURMUS, A.; BAYRAM, A.; Properties of Dual Phase Steels – Influence of Morphology of Martensite on Tensile and Strain Hardening Properties of Dual Phase Steels. Material Prüfung, v.45, p. 214, 2003.
3 SILVA, F.; LOPES, N. I. A.; SANTOS, D. B.; Microstructural Characterization of the C – Mn Multiphase High Strength Cold Rolled Steel. Materials Characterization, v. 56, p. 3-9, 2005.
6 SHIN, S. Y.; HWANG, B.; KIM, S.; LU, S.; Fracture Toughness analysis in Transition Temperature Region of API X70 Pipeline Steels. Materials Science and

Engineering, A 429, p. 196-204, 2006.
5 LePERA, F. S.; Improved Etching Tecnique to Emphasize Martensite and Bainite in High-Strength Dual-Phase Steel. Journal of Metals. p. 38-39, 1980.
6 FURNÉMONT, Q.; KEMPF, M.; JACQUES, P. J.; GÖKEN, M.; DELANNAY, F.; On the Measurement of the Nanohardness os the Constitutive Phases of TRIP-assisted Multiphase Steels. Material Science and Engineering, A 328, p. 26 – 32, 2002.
7 JEONG, W. C.; Relationship between Mechanical Properties and Microstructure in a 1,5% Mn – 0,3% Mo Ultra-low Carbon Steel with Bake Hardening. Materials Letters, v 61, p. 2579-2583, 2007.
8 SHIN, S.Y.; HWANG, B.; LEE, S.; KIM, N. J.; AHN, S.S.; Correlation of Microstructure and Charpy Impact Properties in API X70 and X80

SS-P1-13
Copper adsorption on Al surfaces: DFT studies

T13 Surface Science

#SS-P1-13

C. Lacaze-Dufaure [1], A. Benali [1], J. Morillo [2], H. Tang [2].

[1]CIRIMAT - Toulouse (France), [2]CEMES - Toulouse (France).

Copper-aluminum alloys are often used for aeronautical applications. In the presence of oxygen, aluminum can form an oxide surface layer, leading to high temperature resistant coatings with good resistance to oxidation and corrosion in aggressive environments. Moreover, copper-aluminum alloys exhibit good mechanical properties. The comprehension of copper deposition on Al and copper segregation in aluminum is thus of prime interest.

We performed periodic calculations in the framework of the density functional theory of copper adsorption on the Al(111) surface. On the perfect surface, several adsorption sites were studied and adsorption pathways normal to the surface for the Cu adsorption in bridge, hcp and fcc hollow sites were determined. An adsorption energy of 3.20 eV is calculated for the three considered sites. There is a large electronic transfer (around 1 electron) from the substrate to the ad-Cu in all cases. The adsorption of copper atoms is thus considered on surface vacancies and on the stepped surface. In both cases, the adsorption energy is increased. The population analysis shows again large charge transfers from the metallic surface to the Cu adatom.

SS-P3-35
Topological Phase, Correlated Electron Spins and Vortex Motion.

T13 Surface Science

#SS-P3-35

J. Williams, S. Samarin, L. Pravica, P. Guagliardo, S. Kathi.

University of Western Australia - Perth (Australia).

Electron spectroscopy enables the investigation of the characteristics of atoms, whether free and single, bound in molecules or in a wide variety of surface and thin films. Inelastic electron scattering offers a way to study momentum and energy transfer with strong correlation effects. Spin-polarised electron scattering opens a fundamental way to study topological effects and topological matter. The basic interactions have many and varied applications such as in magnetism, surface physics, topological insulators, quantum dot resonance fluorescence, cold atoms, the quantum Hall effect and magnon dynamics [1,2].
The present study identifies and expands the discussion of geometric phases from condensed matter to thin films [2], to molecules and to single atom phenomena [3] such as found on surfaces. The geometric phase is discussed from an experimental viewpoint to link concepts of vector potential, gauge transformations, electron correlations and the Pauli exclusion principle with the vector alignment and orientation of angular momentum and its transfer to radiated photons.
For single atoms of zinc and mercury, with two electrons in the outer valence orbits, observations indicate spin-polarized electron exchange excitation from a 1S0 to a 3S1 state [3]. During excitation, the parallel (aligned) electron spin is transported around a closed path to acquire a phase change of π radians which is observed directly as transferred alignment of observed radiated photon angular momentum to confirm coherent transfer in excitation and de-excitation processes.
Two examples of vorticies are observed. (i) Straight vortex lines [4] are inferred for electron scattering (e,2e) momentum distributions from free atoms and surface scattering and are associated with a fixed value of z-component of angular momentum of a wave function and angular momentum conservation. The vortex line signifies a rotational orientation through an angle resembling a gauge degree of freedom and a gauge potential giving rise to a field strength related to a magnetic field with directional orientation of the vortex line. (ii) Vortex rings, formed by the superposition of electric field mixed wave functions with the same energy but different angular momenta, are inferred following the excitation of the electronic

$\Psi(200)$ and $\Psi(210)$ states of hydrogen atoms, with $\pi/2$ phase difference mixed by an external electric field. Coincidence detection of scattered energy-loss electrons with radiated photons shows oscillatory behaviour in the exchange Stokes parameter which changes phase as the electric field reverses and shows different lifetimes of the mixed parity 2S and 2P states.
In conclusion, the geometric phase arises from the breaking of time-reversal symmetry, and has been observed by measurements of the Stokes parameters for sums and differences of photon polarizations through the symmetry requirements of the wave function. The studies are indicating the development of ways to control the behaviour of a geometric phase.

[1] A Shapere and F Wilczek 1989 Eds Geometric Phases in Physics, World Scientific, Singapore
[2] R Resta 2000 J Phys Condens Matter 12 R107–R143
[3] JF Williams, L Pravica and SN Samarin 2012 Phys Rev A 85, 022701
[4] J Feagin 2011 J Phys B 44 01001
[5] I Bialynicki-Birula, Z Bialynicka-Birula and C Sliwa 2000 Phys Rev A 61, 032110

NST/SS-1-Or-8
XPS and STM investigation of the atomic-scale morphology and electronic structure of metals intercaleted on Graphene/SiC(0001)

T13 Surface Science

#NST/SS-1-Or-8

A. De Siervo, L.H. De Lima, R. Landers.

Instituto de Fisica Gleb Wataghin, Universidade Estadual de Campinas - Campinas (Brazil).

Graphene on SiC(0001) is a promising platform for future integration of high performance electronic devices. Despite its fascinating characteristics, graphene has a feature that compromises its potential technological application: it is a zero gap semiconductor. Moreover, graphene on SiC is strongly coupled to Si layer underneath which reduces the electronic properties of graphene. It is then necessary to modify the electronic structure according to the application and this can be done with the functionalization of the graphene with atoms and molecules[1-3]. Using x-ray photoelectron spectroscopy (XPS) and Scanning Tunneling Microscopy (STM) we investigate the intercalation behavior of Co ultrathin films and particles on graphene/SiC. We found that ultrathin films of metallic Co and other metals, for instance W, as well as their oxides can intercalate bellow both, the sp3-hybridized carbon-rich interface layer, the so called buffer layer, and monolayer graphene. XPS shows that after growth, the metal is on the surface of the graphene/SiC and suffer oxidation when exposed to O2. After heating to ~350C in ultra-high vacuum, there is a reduction of cobalt oxide and intercalation between graphene and buffer layer, as indicated by the STM images and XPS. After metal intercalation, graphene acts as a barrier to oxidation, preserving the metallic character of the material. This model was also applied to tungsten and XPS results confirm the hypothesis of intercalation and protection. Based on the experimental results we will also discuss about possible mechanisms of metal intercalation and protection.

[1] T. P. Kaloni, M. Upadhyay kahaly, Y. C. Cheng, and U. Schwingenschlögl, J. Mater. Chem. 22, 23340 (2012).

[2] T. Gao, Y. Gao, C. Chang, Y. Chen, et al., ACS Nano 6, 6562 (2012).

[3] R. Larciprete, S. Ulstrup. P. Lacovig, M. Dalmiglio, et al., ACS Nano 6, 9551 (2012).

SS-18-Or-2
Chemoselectivity in Hydrocarbon Conversion on Pd Model Catalysts

T13 Surface Science

#SS-18-Or-2

K. Dostert, C. O'brien, A.A. Savara, W. Ludwig, S. Schauermann, H.J. Freund.

Fritz Haber Institute of the Max Planck Society - Berlin (Germany).

Recent progress in understanding the kinetics of the hydrogenation of simple unsaturated compounds on Pd [1-3] opened up opportunities to investigate the catalytic conversion of more complex systems. In this study, the kinetics of the hydrogenation of α,β-unsaturated carbonyls, which contain C=C and C=O bonds, on well-defined Pd/Fe_3O_4 model catalysts and Pd(111) is addressed by a combination of surface science techniques and molecular beam experiments.

Insight into the chemoselectivity of π(C=C) vs. π(C=O) hydrogenation were obtained on a microscopic scale by investigating several key step: the adsorption process, the interaction of co-adsorbed reactants, and the kinetics of the conversion were addressed individually. The adsorption of isophorone on Pd(111) was investigated by synchrotron near-edge x-ray absorption fine structure (NEXAFS) and infrared reflection-absorption spectroscopy (IRAS) experiments. The results indicate different geometries of the C=C and C=O bonds with respect to the Pd(111) facet, especially when hydrogen is co-adsorbed. Furthermore, molecular beam experiments on the kinetics of the conversion of acrolein with hydrogen on Pd/Fe3O4 model catalyst show selective hydrogenation of the C=C bond. The activity of the catalyst was found to depend on the cluster size.

The combination of NEXAFS and IRAS experiments is shown to be a powerful tool, not only to obtain detailed information about the adsorption of isophorone on the Pd(111) facet, but also to monitor the interaction between the unsaturated π-bonds and hydrogen. The strong impact of hydrogen on the geometry of the C=C bond is in line with the results of molecular beam experiments, where selective hydrogenation of the C=C bond was observed.

1. M. Wilde, K. Fukutani, W. Ludwig, B. Brandt, J.-H. Fischer, S. Schauermann, H.-J. Freund, Angew. Chem. Int. Ed., 2008, 47(48), 9289-9293
2. K. M. Neyman, S. Schauermann, Angew. Chem. Int. Ed., 2010, 49(28), 4743-4746
3. W. Ludwig, A. Savara, S. Schauermann, H.-J. Freund., et al., ChemPhysChem, 2010, 11(11), 2319-2322

NST/SS-1-Or-9
The interaction of Co oxides with Graphite surfaces

T13 Surface Science

#NST/SS-1-Or-9

L. Soriano, D. Díaz-Fernández, J. Méndez, A. Gutiérrez.

Universidad Autónoma de Madrid - Madrid (Spain).

Since the appearance of the unique Carbon nanostructures like Carbon Nanotubes (CNT's) and Graphene, a lot of attention has been paid to their formation methods. In particular, the use of Co and Mo transition metals as catalysts has been reported in the literature [1]. Also, oxidized Graphene (GO) has been used to obtain Graphene sheets due to its hydrophilic properties which leads to the easy separation of GO [2]. In this work we have studied the interaction of Co with highly pyrolytic graphite (HOPG) surfaces in presence of oxygen.

Firstly, we have studied the growth of cobalt oxides on HOPG by thermal evaporation of metallic Cobalt in oxygen atmosphere ($2x10^{-5}$ mb) at room temperature. A mixed Stransky-Kastanov like way of growth has been detected with the initial formation of a wetting layer 8 Å thick of CoO (Co^{2+}) and accumulation of CoO islands at the HOPG steps. Further deposition produces the formation of dendritic CoO islands on the terraces. These islands keep on growing up to coalescence forming a CoO thin film (Figure 1).

However the most interesting features appear when these films are submitted to thermal annealing at 400 ºC for 1 h in an oxygen atmosphere ($5x10^{-3}$ mb). Firstly, the former Cobalt oxide has been oxidized to Co_3O_4 ($Co^{2+,3+}$) forming islands of about 40 nm size. Attached to this Co_3O_4 islands, multiple concentric nano-rings (30-60 nm diameter) are observed (Figure 2b). Finally, nano-channels associated to the random path of Co_3O_4 islands have been formed due to the oxidation of the graphite surface. As a final result of this process, the graphite surface becomes oxidized with the formation of a buried CoO underlayer.

[1] Y. Murakami, S. Chiashi, Y. Miyauchi, M. Hu, M. Ogura, T. Okubo, S. Maruyama, Chemical Physics Letters 385 (2004) 298–303.
[2] S. Pei, H.M. Cheng, Carbon 50 (2012) 3210–3228

Figure 1: 500x500 nm AFM images of CoO deposited on HOPG as a function of CoO coverage
Figure 2: AFM images of the features observed upon annealing at 400ºC of the CoO/HOPG layers.

SS-2-Or-9
Plasmon resonances on low index flat surfaces of aluminium and silver

T13 Surface Science

#SS-2-Or-9

G. Raseev.

CNRS/Univ. Paris-Sud - Orsay (France).

The UV photoelectron spectra of of plain metals and quantum wells display surface and volume plasmon resonances. For a *p* or transverse magnetic linearly polarized photon a theoretical model should use a transition operator with laser fields calculated for the actual system under study. In the vector potential from electron density-coupled integro-differential equations (VPED-CIDE) model [1] these laser fields are solution of the Ampere-Maxwell classical and material equations in the real space and the temporal gauge (U=0). The present work calculates the electron escaping probability from the power density absorption, the photoionization cross section both directly related to the PES, the reflectance, Feybelman's parameter d(perpendicular) and the induced by the laser electron density.

We study low index surfaces (001) and (111) aluminium [2] in the region 10-30 eV and of silver [3] in the region 3-10 eV. Our calculations favorably compare with the experimental angle and energy resolved photoelectron yield (AERPY) spectrum of Levinson et al. [4] for Al(001) and of Barman et al. [5] for Al(111) surfaces. For Ag(001) and Ag(111) our theoretical spectra are in agreement with the AERPY spectrum of Barman \textit{et al.} [6]. Analysis in terms of the induced by the laser electron density and of the Feibelman's parameter d(perpendicular) permits to identify the nature of the plasmon resonances.

[1] G. Raseev, Laser fields at flat interfaces: I. Vector potential, European Phys. J. D66 (2012) 179.

[2] G. Raseev, Laser fields at flat interfaces: II. Plasmon resonances in aluminium photoelectron spectra, European Phys. J. D66 (2012) 180.

[3] G. Raseev, Plasmon resonances of Ag(001) and Ag(111) in the 2.8-10 eV region, submitted to Surface Science (2013).

[4] H. J. Levinson, E. W. Plummer, The surface photoeffect, Phys.Rev. B24 (1981) 628--638.

[5] S. R. Barman, P. Haberle, K. Horn, Collective and single-particle excitations in the photoyield spectrum of Al, Phys. Rev. B 58 (1998) R4285--R4288.

[6] S. R. Barman, C. Biswas, K. Horn, Collective excitations on silver surfaces studied by photoyield, Surf.Sci. 566-568 (2004) 538--543.

SS-18-Or-3
STM investigation of phenol adsorption on Cu(110)

T13 Surface Science

#SS-18-Or-3

Y. Kitaguchi, S. Habuka, T. Mitsui, S. Hatta, H. Okuyama, T. Aruga.

Department of Chemistry, Graduate School of Science, Kyoto University - Kyoto (Japan).

Phenol (C_6H_5OH) is a relatively simple π-conjugated molecule, and it has been used as a good model of a bifunctional molecule which has both an aromatic ring and an O-H group. We investigated the adsorption of phenol on Cu(110) at a single molecule limit using STM, and the assignments of adsorption states were conducted also using EELS. STM images recorded at 78 K revealed that phenol molecules are stabilized by forming a trimer (fig. 1a). The corresponding EELS showed a broad peak at ~400 meV arising from H-bonded O-H stretch while it showed no signature of free O-H bond, indicating that the trimer is in a cyclic configuration with any O-H bond involved in the H-bond. Such cyclic form of phenol trimer was also proposed to exist in gas phase as well as in the solid. The STM clearly shows four equivalent orientations for the cyclic trimer.

The EELS recorded after annealed to room temperature showed disappearance of the O-H stretch but the vibration modes of the aromatic ring were maintained. We assigned the thermal product as a phenoxy specie (C_6H_5O), as in the previous works [1, 2]. STM images show that the phenoxy species are arranged in one-dimensional chains along the [001] direction with a period of two atomic distance (0.7 nm) (fig. 1b) and form two-dimensional c(2x4) overlayer at saturation coverage [2]. The phenoxy specie is bonded to the short-bridge site via oxygen atom with the phenyl ring nearly parallel to the surface. It is shown that the STM can lift up the phenoxy ring and flip the molecule around the anchoring oxygen atom.

We also investigated the adsorption of benzenethiol (C_6H_5SH) on Cu(110) for the purpose of knowing the role of chalcogen atoms in the adsorption states, and it was revealed that a benzenethiol molecule is adsorbed as benzenethiolate (C_6H_5S) at 78 K and the benzenethiolate species are preferentially arranged along the [1-12] direction. Dipole-dipole interaction is suggested to be responsible for the preferential chain growth, while the chain direction is ruled by the steric repulsion between the chalcogen atom and the phenyl ring.

[1] N. V. Richardson and P. Hoffmann, Vacuum 33 (1983) 793.

[2] X.-C. Guo and R. J. Madix, Surf. Sci. 341 (1995) L1065.

fig.1 A typical STM image of Cu(110) exposed to phenol at 78 K (a) and 300 K (b). (a) V_s = 86 mV, I_t = 0.2 nA, 12×12 nm^2, (b) V_s = 36 mV, I_t = 2.0 nA, 7.9 × 7.9 nm^2.

NST/SS-6-Or-11
Perpendicular magnetic anisotropy of cobalt films in contact with graphene

T13 Surface Science

#NST/SS-6-Or-11

N. Rougemaille [1], A. N'diaye [2], J. Coraux [1], C. Vo-Van [1], O. Fruchart [1], A. Schmid [2].

[1]CNRS - Institut Neel - Grenoble (France), [2]LBNL - NCEM - Berkeley (United states).

Owing to its peculiar electronic band structure, high carrier mobility and long spin diffusion length, graphene is a promising two-dimensional material for microelectronics and spintronics. Graphene also shows interesting magnetic properties when in contact with a ferromagnetic metal (FM). For instance, graphene carries a net magnetic moment when deposited on Fe/Ni(111) [1], and a 13 meV spin splitting can be induced in graphene due to proximity with a heavy element [2].

While these works illustrate potential advantages of integrating graphene within a magnetic stack, the influence of graphene on the magnetic properties of a FM is still largely unexplored. In particular, non-magnetic overlayers generally affect the magnetic anisotropy energy (MAE) of thin layers, where interfaces play an important role. We can then wonder how an interface with graphene would influence the MAE of a thin FM film. However, the fabrication of atomically flat graphene/FM and FM/graphene interfaces is not an easy task (graphene growth on metals is usually conducted at temperatures for which thin film dewetting can occur, and metal evaporation on graphene often yields clustered deposits).

Using spin-polarized low-energy electron microscopy (SPLEEM) and Auger electron spectroscopy, we study the intercalation of cobalt deposited on top of graphene/Ir(111) and find that a graphene top layer affects the magnetic properties of nm-thick Co films on Ir(111) [3,4]. We show that in the intercalated cobalt, perpendicular magnetic anisotropy is favored over an unusually large thickness range. Compared to the vacuum/Co interface, the MAE is significantly larger for a graphene-terminated Co surface. The hybridization of the Co and graphene electron orbitals very likely plays a key role in this unusual MAE. These result open new

perspectives for graphene-based spintronic devices with perpendicular magnetic anisotropy.

[1] M. Weser et al., Phys. Chem. Chem. Phys. 13, 7534 (2011)
[2] A. Varykhalov et al., Phys. Rev. Lett. 101, 157601 (2008)
[3] N. Rougemaille et al., Appl. Phys. Lett. 101, 142403 (2012)
[4] J. Coraux et al., J. Phys. Chem. Lett. 3, 2059 (2012)

10 µm field of view SPLEEM images of 11 ML of Co deposited on Ir(111) (a),(b), and intercalated at the graphene/Ir(111) interface (c),(d). Left and right images show in-plane and out-of-plane components of magnetization, respectively.

SS-2-Or-10
Isolated Pd sites on low indexed surfaces of intermetallic PdGa catalysts

T13 Surface Science

#SS-2-Or-10

R. Widmer.

Empa, Swiss Federal Laboratories for Materials Science and Technology, nanotech@surfaces - Dübendorf (Switzerland).

With its highest technological and economic importance, catalysis is an extremely active research area, which yields in a great impact on the development of new catalyst systems with the aim to produce chemical compounds highly selective and more efficient. To this point the development and optimization of novel catalysts most commonly proceed via the modification of composition and surface treatment in a trial and error fashion. On the other hand, surface science methods offer the possibility to change this paradigm by gaining a fundamental understanding of the chemical reaction on a molecular level and determining the relation between catalytic properties and atomic structure of the surface. The obtained insight can then be applied to a knowledge-based development on novel catalysts showing increased activity and/or selectivity.
In this context, intermetallic compounds have been identified as a promising materials class for novel catalysts with tailored properties [1]. Among these compounds PdGa, with the FeSi type of structure, has attracted considerable attention due to its exceptional selectivity and activity as a heterogeneous catalyst for the semi-hydrogenation of acetylene [2]. These properties were assigned to the separation of catalytic sites on the surface of the intermetallic material [3]. Originating from its structure there are non-equivalent surface terminations of the different low indexed surfaces of PdGa [4, 5]. Special emphasis is put on the intrinsic chirality of the {111} surfaces with regard to enantioselective catalytic reactions.
Here, we present a detailed atomic and electronic structure analysis on low Miller indexed PdGa surfaces based on XPD, LEED-I(V), STM, ARPES and DFT based stability calculations. Additionally, TDS and FT-IR investigations were performed to probe the chemisorption behavior of CO. In particular we will address the very different local arrangement of Pd atoms on the different PdGa surface, which qualifies this intermetallic compound as ideal model system to study the role of site

separation on the catalytic properties. These insights in the surface structure are essential inputs for the determination of catalytic reaction pathways and theoretical calculations of molecular adsorption energies.

[1] J.A. Rodriguez, Surf. Sci. Rep. 24 (7-8), 225 (1996).
[2] M. Armbrüster, K. Kovnir, M. Behrens, D. Teschner, Y. Grin, R. Schlögl, J. Am. Chem. Soc. 132, 14745 (2010).
[3] K. Kovnir, M. Armbrüster, D. Teschner, T. V. Venkov, F. C. Jentoft, A. Knop-Gericke, Y. Grin, R. Schlögl, Sci. Technol. Adv. Mat. 8, 420 (2007).
[4] D. Rosenthal, R. Widmer, R. Wagner, P. Gille, M. Armbrüster, Y. Grin, R. Schlögl, O. Gröning, Langmuir 28, 6848 (2012).
[5] J. Prinz, R. Gaspari, C. Pignedoli, J. Vogt, P. Gille, M. Armbrüster, H. Brune, O. Gröning, D. Passerone, R. Widmer, Angew. Chem. Int. Ed. 51, 9339 (2012).

SS-P3-05
Surface free energy of self-assembled pure and mixed lipid layers

T13 Surface Science

#SS-P3-05

D. Risović, B. Gašparović, A. Penezić.

Rudjer Boskovic Institute - Zagreb (Croatia).

The supported lipid mono and bilayers are widespread tool for mimicking the structure and functions of biomembranes. Lipid layers are also used as sensor element host in development of various novel sensors incorporating membrane based films. The surface free energy (SFE) of lipid films plays a crucial role in physicochemical processes occurring at the interface and its magnitude arises from the kind and strength of involved intermolecular interactions [1, 2].
The surface free energy of solid supported self-assembled pure and mixed lipid layers was studied using contact angle measurements in conjunction with Fowkes and Owens-Wendt-Rabel-Kaelble (OWRK) theories [3]. The measurements of contact angles were conducted using four standard liquids (water, formamide, diiodomethane and ethylene glycol).The investigation comprehended 1,2-dioleoyl-sn-glycero-3-phosphocholine (DOPC) , 1-Palmitoyl-2-oleoylphosphatidylcholine (POPC), and oleic acid triglyceride - triolein (TO). Pure and mixed lipid mono and bi-layers on solid substrates were formed by spontaneous spreading and by transfer of the self assembled monolayer from a subphase of 0.55 M NaCl water solution using the Langmuir–Blodgett / Schaefer techniques. The results of SFE determination of the investigated mixed and single lipid layers on hydrophilic and hydrophobic substrates are presented and discussed in terms of influence of the mixing ratio on the intermolecular interactions and film stability.

[1] C. A. Keller, K. Glasmastar, V. P. Zhdanov, B. Kasemo,. Phys. Rev. Lett. 84 (2000) 5443-5446.
[2]. V. I. Silin et al. J. Am. Chem. Soc. 124, 2002 14676-14683.
[3] D. K. Owens, R. C. Wendt, J. Appl. Polym. Sci., 13 (1969) 1741-1747.

2000/2887

SS-13-Or-1
Plasma Activation of Polymers by Diffuse Coplanar Surface Barrier Discharge and Low Pressure Ion Bombardment

T13 Surface Science

#SS-13-Or-1

M. Kormunda [1], T. Homola [2], J. Matoušek [1], J. Pavlik [1], M. Cernák [2], Z. Kolska [1], P. Hedbavny [3].

[1]J.E. Purkinje University - Usti Nad Labem (Czech republic), [2]Masaryk University - Brno (Czech republic), [3]VAKUUM PRAHA - Praha (Czech republic).

The polymers are important material for many applications from the flexible electronics (displays, solar cells) to biocompatible materials for implants and tissue engineering.
Surface modifications of PET, PEN, PMMA and PEEK polymers by the atmospheric low cost DBD plasma discharge in ambient air and nitrogen at atmospheric pressure were studied. The samples were treated in the 400 W powered DBD plasma discharge. The samples were exposed directly to the plasma. The treating time was from 1 s up to 10 s. A comparison was made to low pressure experiments with oxygen and argon, nitrogen and air ions from MW plasma source (Tectra Sputter Gun) at energies from 100 eV up to 2500 eV.
The surface modifications were investigated by various surface sensitive techniques for example XPS, the contact angle measurement for surface energy evaluations, FTIR, AFM and the electro kinetic potential was also investigated on the modified surfaces over wide range of pH.
For example, the DBD plasma treatment on PEN had no significant influence on the surface morphology. But the water contact angle was reduced by the treatment form initial 79º to 31º (air) and 20º (nitrogen) when after 3 day at normal conditions the contact angles was still about 50º and 40º, respectively.
The oxygen concentration in the PEN foil measured by XPS was increased from an initial 22 at. % up to 45 at. % after first 5s in DBD air plasma. The nitrogen DBD plasma modified surface composition only by implanted nitrogen up to 5 at. %. But the surface modifications in air plasma resulted in the formation of new chemical

bonds between the carbon and the oxygen, e.g., C=O, O–C–O. The O-C bond was reduced significantly on the treated surface.
The physical sputtering process was dominant for the treatment by argon ions at both energies and oxygen ions treatment at higher energy 2.5 kV in low pressure conditions. The O/C ratio evaluated on PEN surface decreased fast from initial value about 0.29 to 0.19 and 0.09 by argon ions treatment with energy 0.2 keV and 2.5 keV, respectively. In contrary the low energy 0.2 keV oxygen ions treatment can increase O/C ratio up to 0.43. The argon ions treatment was the physical sputtering process with the preferential removal of oxygen when the oxygen ions treatment had both physical interactions and chemical reactions. The 2.5 keV oxygen ions treatment modified the PEN surface dominantly by physical interactions therefore the O/C ratio was reduced but certain increase in relative abundance in C-O bonds was observed. The 0.2 keV oxygen ions treatment also faster increases C-O bond then C=O bonds but they are in contrary to other treatments also increased.
The surface modification under various condition evaluated together gives opportunity to compare those techniques under identical conditions.

[1] Kormunda, Pavlik, Polymer Degradation and Stability 95 (2010) 1783-1788
[2] Homola, Matousek, Hergelova, Kormunda, Wu, Cernak, Polymer Degradation and Stability 97 (2012) 2249-2254
[3] Homola, Matousek, Hergelova, Kormunda, Wu, Cernak, Polymer Degradation and Stability 97 (2012) 886-892
[4] Kormunda, Homola, Matousek, Kovacik, Cernak, Pavlik, Polymer Degradation and Stability 97 (2012) 547-553

SS-13-Or-2
Evidence of magnetic order in purely organic 2D layer adsorbed on epitaxial graphene

T13 Surface Science

#SS-13-Or-2

A. Vázquez De Parga [1], M. Garnica [1], D. Stradi [1], S. Barja [1], C. Díaz [1], M. Alcamí [1], N. Martin [2], R. Miranda [3].

[1]Universidad Autonoma de Madrid - Madrid (Spain), [2]Universidad Complutense de Madrid - Madrid (Spain), [3]IMDEA Nanociencia - Madrid (Spain).

In this communication, we show that graphene grown on Ru(0001) electronically decouples 7,7',8,8'-tetracyano-p-quinodimethane (TCNQ) molecules from the Ru(0001) [1]. Graphene on Ru(0001) presents a moiré pattern with a periodic chemical interaction between carbon atoms and the ruthenium, leading to a modulation in the electronic structure and surface potential [2][3][4]. Low Temperature scanning tunneling microscopy/spectroscopy (LT-STM/STS) measurements and Density Functional Theory (DFT) calculations show that isolated TCNQ molecules deposited on a monolayer graphene epitaxially grown on Ru(0001) acquire charge from the substrate and develop a sizeable magnetic moment, which is revealed by a prominent Kondo resonance. The magnetic moment is preserved upon dimer and monolayer formation. The energy position and spatial distribution of the molecular frontier orbitals for a single molecule are measured by STS maps at 4.6K in ultra high vacuum and compare well with the DFT calculations. When the molecular coverage is increased the molecules begin to form chains that finally cover completely the graphene surface. The self-assembled 2D monolayer of magnetic molecules develops spatially extended spin-split electronic bands visualized in the real space by STM (see Figure 1), where only the majority band is filled, thus becoming a 2D, purely organic magnet whose predicted spin alignment in the ground state is visualized by spin-polarized STM at 4.6K.

[1] S. Barja, M. Garnica, J.J. Hinarejos, A.L. Vazquez de Parga, N. Martin, R. Miranda, Chem. Commun. **46**, 8198 (2010)

[2] A.L. Vazquez de Parga, F. Calleja, B. Borca, M.C.G. Passeggi, J.J. Hinarejos, F. Guinea, R. Miranda, Phys. Rev. Lett. **100**, 056807 (2008)

[3] B. Borca, S. Barja, M. Garnica, D. Sanchez-Portal, V.M. Silkin, E.V. Chulkov, C.F. Hermanns, J.J. Hinarejos, A.L. Vazquez de Parga, A. Arnau, P.M. Echenique, R. Miranda, Phys. Rev. Lett. **105**, 036804 (2010)

[4] D. Stradi, S. Barja, C. Diaz, M. Garnica, B. Borca, J.J. Hinarejos, D. Sanchez-Portal, M. Alcami, A. Arnau, A.L. Vazquez de Parga, R. Miranda, F. Martin, Phys. Rev. Lett. **106**, 186102 (2011)

Figure 1: The upper row shows the STM images of the spatially extended electronic bands due to the combination of the Highest Occupied Molecular Orbital (HOMO) (A), the Single Occupied Molecular Orbital (SOMO) (B) and the Single Unoccupied Molecular Orbital (SUMO) (C) of a TCNQ monolayer adsorbed on graphene/Ru(0001). The lower row shows the correspondent simulated topographic image in (D), (E) and (F).

SS-10-Or-2
Influence of the spin-orbit coupling of the BiAg2 surface alloy on electron scattering

T13 Surface Science

#SS-10-Or-2

J. Lobo-Checa [1], F. Schiller [1], P. Gambardella [2], E. Ortega [1], A. Mugarza [2].

[1]Centro de Física de Materiales - San Sebastian (Spain), [2]Catalan Institute of Nanotechnology - Barcelona (Spain).

Transport properties of the solid are interweaved to its electronic wavefunctions. Further inside into them can be achieved through the study of scattering processes at defects, such as adsorbates or steps. The inelastic lifetime and quantum coherence are dependent upon the nature of the system, i.e, the type of defect, the chemistry, and the morphology of the Brillouin zones.

Unraveling the fundamental scattering aspects of electronic states which exhibit no spin degeneracy is nowadays a key goal in the Solid State scientific community. An observation that has fostered this research activity is the lack of back-reflected waves near steps at the surface of topological insulators [1]. The reduction of scattering has been attributed to the topological protection of surface states in the material, which is directly related to the strong spin-orbit interaction.

In order to further understand the effect of spin-orbit coupling on the scattering phenomena, we have investigated by angle resolved photoemission (ARPES) the surface alloy of $BiAg_2$. This system exhibits a giant spin-orbit splitting, that is orders of magnitude larger than, e.g., in semiconductor heterostructures [2]. The spin-splitting is originated from the Rashba-Bychkov effect at the surface-vacuum interface and, in contrast to the topological insulators, the spin-orbit coupling strength can be tuned by alloying [3]. We investigate the $BiAg_2$ surface alloy within the scattering analysis framework previously performed on a Ag(111) curved crystal [4]. The beauty of this substrate is that the density of steps changes progressively as we move along the curvature of the crystal so that the terrace size is continuously tuned from 400 nm to just 10 nm. Our results show unambiguously that the scattering of the surface

electron wavefunctions by the steps is rather weak, much smaller than the underlying substrate of Ag with values of transmission close to the topological insulators. Furthermore, three different type of molecules deposited onto this surface alloy are not observed to interact with the spin-split $BiAg_2$ states. We assign this unexpected behavior to the large spin-orbit coupling that protects these electronic states from impurities, in a similar fashion to the topologically protected surface states in topological insulators [5].

[1] J. Seo, P. Roushan, H. Beidenkopf, Y. S. Hor, R. J. Cava, and A. Yazdani, Nature 466, 343 (2010).
[2] C. R. Ast, J. Henk, A. Ernst, L.Moreschini, M. C. Falub, D. Pacil´e, P. Bruno, K. Kern, and M. Grioni, Phys. Rev. Lett. 98, 186807(2007).
[3] I. Gierz, F. Meier, J. H. Dil, K. Kern, and C. R. Ast, Phys. Rev. B 83, 195122 (2011).
[4] J. E. Ortega, M. Corso, Z. M. Abd-el-Fattah, E. A. Goiri, and F. Schiller, Phys. Rev. B 83, 085411 (2011).
[5] M. C. Cottin, J. Lobo-Checa, J. Schaffert, C. A. Bobisch, R. Möller, J. E. Ortega, and A.L. Walter4. Submitted.

SS-18-Or-4
Unusual two-stage kinetics: unraveling the adsorption of ethylene on Si(100) by real-time optical reflectance measurements and Monte-Carlo approach

T13 Surface Science

#SS-18-Or-4

Y. Borensztein, R. Coustel, O. Pluchery, N. Witkowski.

INSP-CNRS - Paris (France).

As ethylene is the simplest alkene molecule, its adsorption on Si(100)2x1 can be considered as a paradigm for the reactivity of the C=C double bond with the Si dimers at the surface. There is a general agreement concerning the mode of adsorption: it is non-dissociative and almost every ethylene molecule is adsorbed on one Si-dimer by a [2+2] cyclo-addition reaction, the single C-C bond being nearly parallel to the Si-Si bond of the dimer ("di-sigma" on-top configuration) [1].

On the contrary, the kinetics of adsorption has not been understood clearly, and a couple of experiments have shown that, after a fast adsorption until about half monolayer, the sticking coefficient is strongly reduced. Recently, from a Kings-Well-type experiment, it has been proposed that, at room temperature, the adsorption follows a Kisliuk kinetics until about half-monolayer [2]. Unfortunately, so far no complete and detailed investigation of the kinetics has been proposed on the full range of adsorption for RT.

In the present work, we used a real-time and quantitative optical method, the Surface Differential Reflectance Spectroscopy [3], in order to investigate the kinetics of adsorption at room temperature until full saturation. We demonstrate that the adsorption follows a clear two-stage process. An intermediate saturation at 0.45 monolayer is obtained for 1 Langmuir, which corresponds to ethylene molecules adsorbed onto one Si dimer out of two, with a sticking coefficient close to 1, and with some pairs of Si dimers still unreacted. The second stage is shown to be dramatically

slower, yielding the full saturation of 1 monolayer for an exposure of about 400 L. This unusual kinetics for a surface with only one kind of adsorption site is successfully reproduced by a Monte-Carlo calculation taking into account the diffusion of the molecules on the surface, and a decrease by a factor of 400 of the adsorption probability on the Si dimers neighboring already reacted dimers. The Figure gives the full range kinetics in logarithm representation, which shows clearly the two successive stages.

[1] M. Marsili; N. Witkowski; O. Pulci; O. Pluchery; P. L. Silvestrelli; R. Del Sole and Y. Borensztein, "Adsorption of small hydrocarbon molecules on Si surfaces: Ethylene on Si(001)". Phys. Rev. B 77, 125337 (2008)
[2] Lipponer, M. A., Armbrust, N., Durr, M. & Hofer, U. "Adsorption dynamics of ethylene on Si(001)". Journal of Chemical Physics 136 (2012).
[3] Y. Borensztein, O. Pluchery and N. Witkowski, "Probing the Si-Si dimer breaking on Si(100)2x1 surfaces upon molecule adsorption by optical spectroscopy", Phys. Rev. Lett. 95, 117402 (2005)

SS-18-Or-5
On-Surface Polymerization on Rutile Titania Surfaces

T13 Surface Science

#SS-18-Or-5

J. Prauzner-Bechcicki, M. Kolmer, A. Zebari, S. Godlewski, B. Such, M. Szymonski.

Centre for Nanometer-Scale Science and Advanced Materials, NANOSAM, Faculty of Physics, Astronomy and Applied Computer Science, Jagiellonian University - Krakow (Poland).

One of the most intriguing promises of nanotechnology is an ultimate level of control in fabrication of nano-scale structures, machines and devices. To achieve this goal in formation of larger 1D or 2D nanostructures, taking an advantage of thermally induced processes is a very encouraging strategy among others. Recently, there have been interesting reports in the literature on direct, on-surface formation of large covalently bonded molecular structures, both 1D and 2D (see [1] and references therein). Unfortunately, most of them discuss experiments performed on coinage metals with the only exception, i.e. the study of Kittelmann et al. demonstrating the successful covalent linking of four different halide-substituted benzoic acids on calcite [2]. In such a situation the field of on-surface polymerization on semiconducting and insulating surfaces is practically unexplored. Approach that will offer direct formation of a complex molecular structure in predefined form on a desired substrate surface is very attractive from technological point of view. First, functionalizing individual molecular precursors with precisely chosen linking sites should allow for future bottom-up construction of miscellaneous molecular devices [3]. Second, the possibility to induce the covalent linking on desired substrate will allow to choose the substrate best suited for desired application.
In the following, we would like to report on successful realization of on-surface polymerization on metal oxide surface [4]. Molecular precursors (10,10'-dibromo-9,9'-bianthryl, provided by St-Jean Photochemicals Inc.) are deposited on rutile titania surfaces using standard Knudsen cell. Next, the intermolecular colligation is thermally activated, through the sample annealing. The on-surface polymerization reaction can be described as a two-step process [3]: (1) C-Br cleavage resulting in bi-radical formation and (2) followed by bi-radical addition resulting in oligomer formation. The cleavage of carbon-halide bond is possible on TiO_2 surfaces by

thermal activation and the decomposition process is enhanced by the presence of surface hydroxyl groups [5]. The influence of surface reconstruction on polymerization process is discussed through the comparison between two rutile titania surfaces, i.e. (110) and (011) used as a substrate of interests. The fivefold coordinated titania, Ti_{5c}, atoms play an important role in both chemi- and physisorption of organic molecules on the rutile titania surfaces. These Ti_{5c} atoms are present on both discussed surfaces, however, in a very different surroundings that influences their “accessibility”, and thus influences polymerization process.

[1] Franc, G.; Gourdon, A. Physical Chemistry Chemical Physics 2011, 13, (32), 14283-14292.

[2] Kittelmann, M.; Rahe, P.; Nimmrich, M.; Hauke, C. M.; Gourdon, A.; Kuhnle, A. Acs Nano 2011, 5, (10), 8420-8425.

[3] Grill, L.; Dyer, M.; Lafferentz, L.; Persson, M.; Peters, M. V.; Hecht, S. Nature Nanotechnology 2007, 2, (11), 687-691.

[4] Kolmer, M.; Zebari, A.; Prauzner-Bechcicki, J. S.; Polit, A.; Godlewski, S.; Such, B.; Szymonski, M.; in prep.

[5] Wu, W.-C.; Liao, L.-F.; Shiu, J.-S.; Lin, J.-L. Physical Chemistry Chemical Physics 2000, 2, (19), 4441-4446.

SS-18-Or-6
On the mechanism of formic acid decomposition on transition metals

T13 Surface Science

#SS-18-Or-6

M. Mavrikakis, J. Scaranto, S. Singh, L. Roling, S. Li, J. Herron, R. Carrasquillo, B. O'neill, G. Peng, J. Dumesic.

University of Wisconsin - Madison (United states).

Formic acid (HCOOH) is a simple molecule that is an abundant product of biomass processing and can serve as an internal source of hydrogen for oxygen removal and upgrading of biomass to chemicals and fuels. In addition, HCOOH can be used as a fuel for low temperature direct fuel cells. We present a systematic study of the HCOOH decomposition reaction mechanism starting from first-principles and including reactivity experiments and microkinetic modeling. In particular, periodic self-consistent Density Functional Theory (DFT) calculations are performed to determine the stability of reactive intermediates and activation energy barriers of elementary steps. In addition, pre-exponential factors are determined from vibrational frequency calculations. Mean-field microkinetic models are developed and calculated reaction rates, orders, etc are then compared with experimentally measured ones. These comparisons provide useful insights on the nature of the active site, most-abundant surface intermediates as a function of reaction conditions and feed composition. Trends across metals on the fundamental atomic-scale level up to selectivity trends will be discussed. Finally, we identify from first-principles alloy surfaces, which may possess better catalytic properties for selective dehydrogenation of HCOOH than monometallic surfaces, thereby guiding synthesis towards promising novel catalytic materials.

2011/2887

SS-P3-25
Ga surface diffusion simulation - Ising lattice gas model

T13 Surface Science

#SS-P3-25

M. Potoček [1], J. Mach [2], S. Voborný [1], P. Bábor [2], J. Neuman [1], L. Dittrichová [2], T. Šikola [1].

[1]CEITEC BUT - Brno University of Technology, Technická 10, 616 69 - Brno (Czech republic), [2]Institute of Physical Engineering, Brno University of Technology, 616 69 - Brno (Czech republic).

In fabrication of GaN nanocrystals, the surface diffusion of Ga adatoms is one of the key parameters. To study this phenomenon and its influence on island formation, we use the Ising lattice gas model with the Metropolis algorithm [1]. For speeding up the simulations, a graphic card GPU was involved.
This model allows us to simulate the related surface behavior such as Ostwald ripening[2] and TDS measurement which have not a simple character in this case. Using the model we have examined the influence of different temperature, coverage and adatom energy on these surface processes as well.
Further, the influence of nucleation centers on Ga-island formation was simulated and compared to the experimental results on Si samples pre-patterned by e-beam lithography . The simulation for the nucleation sites lattice 5x5 after 1 k MCS and after 50 k MCS is shown in the figure.

[1] N. Metropolis, A. W. Rosenbluth, N. M. Rosenbluth, A. H. Teller and E. Teller, J. Chem. Phys. 21, 1087 (1953).
[2] M. KOLÍBAL, T. ČECHAL, E. BRANDEJSOVÁ, J. ČECHAL, T. ŠIKOLA, Self-limiting cyclic growth of gallium droplets on Si(111) , Nanotechnology 47 Vol.19, 2008, p. 475606.

SS-7-Or-12
Adsorption of isolated Au adatoms on the Fe3O4(001)

T13 Surface Science

#SS-7-Or-12

Z. Novotny, G. Argentero, Z. Wang, M. Schmid, U. Diebold, G.S. Parkinson.

Institute of applied physics, Vienna university of technology - Vienna (Austria).

We present a scanning tunneling microscopy investigation of transition metals deposited at the magnetite $Fe_3O_4(001)$ surface at room temperature (RT). This surface forms a reconstruction with $(\sqrt{2} \times \sqrt{2})R45°$ symmetry [1], where pairs of Fe and neighboring O ions are slightly displaced laterally, forming undulating rows with 'narrow' and 'wide' adsorption sites. At fractional monolayer coverages, Au [2] and other metals (Fe [3], Pd [4]) adsorb as a single adatoms at the 'narrow' sites of the surface unit cell, forming an ordered overlayer on the surface.

Up to coverage of 0.12 ML (1 ML = 1 atom per surface unit cell = 1.42×10^{14} atoms/cm^2), Au adsorbs as isolated adatoms at RT (see Figure 1). With increased Au coverage, the surface contains both Au adatoms and three-dimensional clusters (smallest clusters contain 5 ± 1 atoms), no Au dimers and trimers were observed at RT. For low coverage (only isolated Au adatoms and no clusters) no significant sintering is observed up to annealing temperatures of 400 °C [2], indicating a strong bond of the adatoms to the 'narrow' site of the supporting surface. Mobility of Au adatoms was never observed at RT. However, mobility of Au clusters was regularly observed at RT, and moderate annealing of the surface with higher coverage (adatoms and clusters) causes sintering of the adatoms and growth and merging of the clusters. The Au adatoms stay isolated and do not sinter when exposed to a background pressure of up to 10^{-4} mbar CO. Because of their high thermal stability, the ordered Au adatoms at $Fe_3O_4(001)-(\sqrt{2} \times \sqrt{2})R45°$ should provide useful insights into the chemical reactivity of single atomic species.

This material is based upon work supported as part of the Center for Atomic-Level Catalyst Design, an Energy Frontier Research Center funded by the U.S. Department of Energy, Office of Science, Office of Basic Energy Sciences under Award Number #DE-SC0001058.

[1] Pentcheva, R. et al. Phys. Rev. Lett 94, 126101 (2005).
[2] Novotny, Z. et al., Phys. Rev. Lett 108, 216103 (2012).
[3] Parkinson, G. S. et al., Surf. Sci. Lett. 605, L42 (2011).
[4] Parkinson, G. S. et al. (submitted).

Figure 1: STM image (30 × 30 nm^2, V_{sample} = +1 V, I_{tunnel} = 0.38 nA) of 0.12 ML Au deposited at room temperature. The inset shows two Au adatoms, with a grid showing the (√2 × √2)R45° periodicity.

SS-P3-33
LEED, AES and XPS investigation of the thin indium films on the Si(111) surface

T13 Surface Science

#SS-P3-33

M. Skiscim, K. Idczak, S. Bilinska, L. Markowski.

Institute of Experimental Physics, University of Wroclaw - Wroclaw (Poland).

The growth of indium on the Si(111) surface has been studied over past two decades using various techniques, in many aspects. The deposition of indium on the Si(111) 7×7 surface leads to formation of different one- and two-dimensional ordered structures, depending on the coverage and substrate temperature. In certain conditions Stranski-Krastanov growth occurs [1]. Nowadays In-nanowires formation [2] and electronic properties of In/Si system [3] are of particular interest. While the growth mode is generally accepted, the type of surface structures remains open for discussion. The good example is "$(1 \times 1)R30^{\circ}$" reconstruction, which was later recognized as $\sqrt{7} \times \sqrt{3}$ [4] (LEED image obtained by us is shown in the picture below).

In this work we carried out a detailed study of In/Si(111) 7×7 system for coverage up to few atomic layers in order to systematize and verify the current knowledge. The structural information was provided by Low Energy Electron Diffraction (LEED) and growth behavior and some chemical information by Auger Electron Spectroscopy (AES). Additionally X-ray Photoelectron Spectroscopy (XPS) was used to precisely determine the chemical environment. We propose the phase diagram for a wider range of temperature and coverage than before [5]. We also point to the influence of deposition conditions and subsequent treatment of the sample on the results obtained in the experiment.

[1] H. Ofner, S.L. Sumev, Y. Shapira and F.P. Netzer, Phys. Rev. B 48 (1993) 10940.
[2] J. H. Cho, D. H. Oh, K.S. Kim, L. Kleinman, Phys. Rev. B 64 (2001) 235302.
[3] V.Yu. Aristov, O.V. Molodtsova, D.V. Vyalikh, M. Knupfer, P. De Padova, G. Le

Lay, Journal of Electron Spectroscopy and Related Phenomena 177 (2010) 1-4.
[4] J. Kraft, S.L. Surnev , F.P. Netzer, Surface Science 340 (1995) 36-48.
[5] J. Kraft, M. G. Ramsey, and F. P. Netzer, Phys. Rev. B 55 (1998) 5384.

NST/SS-1-Or-10
Graphene on metal surfaces and the role of the substrate in its hydrogen adsorption

T13 Surface Science

#NST/SS-1-Or-10

M. Andersen [1], R. Balog [1], B. Jørgensen [1], Z. Sljivancanin [2], A. Baraldi [3], R. Larciprete [4], S. Lizzit [5], P. Hofmann [1], L. Hornekær [1], B. Hammer [1].

[1]Interdisciplinary Nanoscience Center (iNANO) and Department of Physics and Astronomy, Aarhus University - Aarhus (Denmark), [2]Vinča Institute of Nuclear Sciences - Belgrade (Serbia), [3]Physics Department and Center of Excellence for Nanostructured Materials, University of Trieste - Trieste (Italy), [4]CNR Instituto dei Sistemi Complessi - Roma (Italy), [5]Sincrotrone Trieste - Trieste (Italy).

Chemical vapor deposition growth of graphene on metal surfaces is an important and efficient synthesis method. Theoretically however, the dispersive metal-graphene interactions are not well understood or easy to describe. Here, we investigate the interaction of graphene with various metal surfaces [1] using density functional theory (DFT) and the meta-generalized gradient approximation M06-L functional [2]. We demonstrate that this method is of comparable accuracy to state-of-the-art calculations using the random phase approximation (RPA) [3].
Hydrogen adsorption on graphene on Ir(111) is studied in detail by combining fast X-ray photoelectron spectroscopy studies with DFT calculated core level shifts [4]. We reveal the presence of two types of hydrogen adsorbate structures at the graphene/Ir(111) interface, namely graphane-like islands and hydrogen dimer structures (see Figure 1a and b). In graphane-like islands every other C atom binds to an H atom above and every other to a metal atom below, thus giving rise to a very stable structure similar to graphane (see Figure 1c). Our data reveal distinctive growth rates and stability of both types of structures, thereby allowing to obtain well defined patterns of hydrogen clusters. Recently it was shown [5], that such graphane-like clusters are responsible for opening a gap in the graphene band structure, which is very desirable for electronic applications. The ability to control and manipulate the formation and size of hydrogen structures on graphene furthermore facilitates tailoring of its properties for a wide range of applications by means of covalent

functionalization.

[1] M. Andersen et al., Physical Review B, 86, 085405 (2012)
[2] Y. Zhao and D. G. Truhlar, The Journal of Chemical Physics, 125, 194101+ (2006)
[3] T. Olsen et al., Physical Review Letters, 107, 156401+ (2011)
[4] R. Balog et al., submitted to ACS Nano
[5] R. Balog et al., Nature Materials, 9, 315 (2010)

Figur 1: a) Graphane-like hydrogen cluster on graphene adsorbed on Ir(111), b) hydrogen dimer and c) graphane. Top view and side view.

SS-P3-38
Spin resolved photo emission of Fe3O4: The effect of surface structure

T13 Surface Science

#SS-P3-38

J. Pavelec, Z. Novotny, M. Setvin, M. Schmid, U. Diebold, G.S. Parkinson.

Institute of Applied Physics, Vienna University of Technology - Vienna (Austria).

Magnetite (Fe_3O_4) is widely considered as an ideal material for future spintronics applications. Density functional theory local spin density approximation (DFT-LSDA) calculations [1] predict half metal magnetite with band gap for the majority spin states, and density of states at the Fermi level for the minority spin states. However, magnetite exhibits strong electron correlation effects, casting doubt on the validity of the DFT-LSDA calculations. Consequently, several groups have attempted to measure the Fermi level spin polarization of magnetite using spin resolved photoemission, with widely varying results (20-80%). One potential problem with such measurements is that photoemission is an inherently surface sensitive technique, and not suited for measuring the bulk properties of materials in which the surface properties differ significantly; a mixture of both regions is probed.

In recent years, the (√2 ×√2) R45°- Fe_3O_4(001) surface has been shown to exhibit a band gap [2], potentially explaining the low spin polarization measured for (001) oriented samples. In prior work [3], we showed that saturation exposure to atomic H lifts the surface reconstruction (by LEED and STM) and metallizes the surface (UPS).

Here, we report spin resolved photoemission spectroscopy (SPES) measurements of two different magnetite samples; thin films [4] of magnetite (001) grown on MgO(001) and a synthetic single crystal. The influence of the surface preparation and termination on the measured spin polarization was investigated for three surfaces: the (√2 ×√2) R45° surface, an Fe-rich terminated surface formed by Fe deposition, and the hydrogenated (metalized) surface [3]. The experiments were performed using synchrotron light with kinetic energies E_k=130 eV and E_k=706.8 eV. Tuning the photo energy with the 2p-3d transition (E_k=706.8 eV) allows enhanced count rate with high bulk sensitivity [5].

Our results show that surface termination has low impact on the measured spin polarization of the state near E_F. The spin polarization value (approx. 25%) is in line with the measurements of ref.[4], suggesting that the magnetite state near E_F is not 100% spin polarized.

[1] Fonin, M., Pentcheva, R., Dedkov, Y. S., Sperlich, M., Vyalikh, D. V., Scheffler, M., Rüdiger, U., Güntherodt, G. (2005). Surface electronic structure of the Fe_3O_4 (100) : Evidence of a half-metal to metal transition. Phys. Rev. B, 72.
[2] Jordan, K., Cazacu, a., Manai, G., Ceballos, S. F., Murphy, S., Shvets, I. V. (2006). Scanning tunneling spectroscopy study of the electronic structure of Fe_3O_4 surfaces. Phys. Rev. B, 74, 085416.
[3] Parkinson, G., Mulakaluri, N., Losovyj, Y., Jacobson, P., Pentcheva, R., Diebold, U. (2010). Semiconductor–half metal transition at the Fe_3O_4 (001) surface upon hydrogen adsorption. Phys. Rev. B, 82, 125413.
[4] Tobin, J. G., Morton, S. a, Yu, S. W., Waddill, G. D., Schuller, I. K., Chambers, S. A. (2007). Spin resolved photoelectron spectroscopy of Fe_3O_4 : the case against half-metallicity. J. Phys. Condensed matter, 19, 315218.
[5] Magnan, H., Le Fèvre, P., Chandesris, D., Krüger, P., Bourgeois, S., Domenichini, B., Verdini, A., Floreano, L., Morgante, A., (2010). Resonant photoelectron and photoelectron diffraction across the Fe L3 edge of Fe_3O_4. Phys. Rev. B, 81, 085121.

SS-18-Or-7
Substrate-mediated interactions between chlorine atoms adsorbed on Au(111), Ag(111) and Cu(111): STM and DFT approach

T13 Surface Science

#SS-18-Or-7

B. Andryushechkin [1], V. Zheltov [1], G. Zhidomirov [1], B. Kierren [2], K. Eltsov [1].

[1]A.M.Prokhorov General Physics Institute of Russian Academy of Sciences - Moscow (Russian federation), [2]Institut Jean Lamour - UMR CNRS 7198 - équipe 102, Université H. Poincaré - Nancy (France).

In this work, we present a combined LT-STM and DFT study of chlorine adsorption on (111) planes of Au, Ag and Cu at low coverage.
According to LT- STM data (Fig.1), chlorine forms chain-like structures at θ<0.1 ML. In the contrast to the case of the (√3×√3)R30° structure (0.33 ML) characterized by the Cl-Cl distance of 5.0 Å for Au and Ag, and 4.4 Å for Cu, we detected noticeably shorter distances within the chains.To find out the driving forces of this unusual coupling of chlorine atoms, we performed the DFT calculations using VASP code.

Different configurations of two chlorine atoms on the Au(111) surface have been tested. As a result, two local minima were found at the distances of 3.83 and 5.02 Å. In the first configuration, one chlorine atom occupies fcc position, while the other one appears to be in the bridge position. In the second case, Cl atoms occupy fcc threefold sites. Adsorption energies per Cl atom calculated for these two configurations appear to be close to each other: 0.961 and 0.964 eV, respectively. This fact is consistent with the experimental STM image in Fig.1 demonstrating the coexistence of the both configurations.
The proximity in the adsorption energy for Cl-Cl distances 3.83 Å and 5.02 Å is surprising, since the bridge position is less energetically favorable than fcc position at the single atom adsorption. To clarify the situation, we calculated the interaction energy between two chlorine adatoms on the relaxed and frozen Au(111) surfaces for different Cl-Cl distances. The calculations for the relaxed substrate shown a

noticeable attraction (-56 meV) at the distance 3.83 Å. In the case of the frozen substrate, no local minimum was found at this distance. However, more weak attraction (-22 meV) was detected at the distance 4.5 Å. These results indicate that there is an attractive interaction between Cl atoms adsorbed on Au(111) which gives rise to the short distance of 3.83 Å and this interaction is mainly mediated by the elastic substrate distortion. The same kind of calculations performed for Cl atoms adsorbed on Ag(111) and Cu(111) shown that, unlike Au(111)/Cl system, the electronic part of the interaction dominates and is responsible for the short fcc-hcp distances.

The formation of chlorine chains has been also tested with DFT. The third chlorine atom was placed at the 12-14 different positions around the pair of chlorine atoms in different fcc and hcp sites. The formation of compact islands was found to be is strongly unfavorable, whereas making the chain is the most energetically favorable scenario for a third atom.

FIG. 1. STM images of Cl-chain structures on Au(111), Ag(111) and Cu(111)

SS-1-Or-5
Water adsorption and clustering on bare and hydroxylated FeO/Pt(111)

T13 Surface Science

#SS-1-Or-5

L. Merte [1], R. Bechstein [2], G. Peng [3], F. Rieboldt [2], C. Farberow [3], H. Zeuthen [2], J. Knudsen [1], E. Laegsgaard [2], M. Mavrikakis [3], F. Besenbacher [2].

[1]Div. of Synchrotron Radiation Research, Lund University - Lund (Sweden), [2]iNANO Center, Aarhus University - Aarhus (Denmark), [3]Dept. of Chemical and Biological Engineering, University of Wisconsin-Madison - Madison (United states).

Using a combination of scanning tunneling microscopy (STM) and temperature-programmed desorption (TPD) measurements and density functional theory (DFT) calculations, we have investigated the effect of surface OH groups on the adsorption and clustering of water on a monolayer FeO film grown on Pt(111). The FeO/Pt(111) oxide thin film has been well-studied with regard to both structure and chemical properties, is easy to prepare in situ, chemically rather inert and electrically conductive and therefore well-suited to fundamental studies by STM. By use of an atomic hydrogen source, we can also create OH groups with a controlled surface concentration (tunable between ~0 and 20%ML) by protonation of the FeO lattice oxygen [1].
STM characterization reveals that the 25 Å moiré structure of the FeO film has a strong impact on the spatial distribution of the OH groups, which prefer FCC-type domains of the surface, causing them to form distinct groups arranged in a hexagonal pattern. The templating effect of the moiré structure on the OH groups is transferred to adsorbed water; although on the bare FeO surface water adsorbs in extended 2D islands whose morphology is only weakly affected by the moiré pattern, the presence of OH causes the water to form small clusters at the FCC domains. TPD measurements of water adsorbed in various coverages and with varying OH concentrations reveal distinct adsorption states associated with binding at OH groups and clustering on the bare FeO surface, respectively. DFT simulations and high-resolution STM measurements suggest that the OH-associated state consists of an ice-like hexagonal structure stabilized by hydrogen bonding to the substrate. The calculations also suggest that the protons involved in hydrogen bonding may be

transferred from the surface to the adsorbed water forming stable, solvated hydronium species, consistent with our previous observations of water-mediated proton hopping at higher temperatures [2].

[1] J. Knudsen, L.R. Merte, L.C. Grabow, F.M. Eichhorn, S. Porsgaard, H. Zeuthen, R.T. Vang, E. Laegsgaard, M. Mavrikakis, and F. Besenbacher, Surf. Sci. 604, 11 (2010).

[2] L.R. Merte, G. Peng, R. Bechstein, F. Rieboldt, C.A. Farberow, L.C. Grabow, W. Kudernatsch, S. Wendt, E. Laegsgaard, M. Mavrikakis, and F. Besenbacher, Science 336, 889 (2012).

Water clusters formed on the hydroxylated, moiré-structured FeO film.

SS-7-Or-14
XPS assessment of the thickness iron oxide nanofilms using a double-Lorentzian asymmetric line-shape

T13 Surface Science

#SS-7-Or-14

M. Bravo-Sanchez [1], A. Herrera-Gomez [1], A. Herrera-Gomez [2], F. Espinosa-Magaña [3].

[1]CINVESTAV-Unidad Queretaro - Queretaro (Mexico), [2]UAM - Azcapotzalco (Mexico), [3]CIMAV-Unidad Chihuahua - Chihuahua (Mexico).

Accurate thickness assessment of metal oxides can be achieved through X-Ray Photoelectron Spectroscopy (XPS) measurements by means of the peak areas of the oxide and the underlying base metal. However, in some cases, determination of these areas has been a major challenge due to difficulties with background removal and line shape representation, the combination of which make up the curve fitting process required to precisely and accurately determine the peak areas. One source of complication arises when the peaks are asymmetrical. As is the case for all metals, the Fe 2p peak and its oxides present this asymmetry. By comparing the results of combinations of the available line shapes and background removal techniques, it was found that the challenges presented by asymmetry, and possibly the entire collection of curve-fitting issues, can be overcome with the use of the double-Lorentzian asymmetric line shape (which is an integrable form), and "Active Shirley" background removal, in which the background intensity is optimized during the peak-fitting process. This method, in comparison with traditional, provides more precise areas for the thickness determination, which has been confirmed with high-resolution transmission electron microscopy.

SS-18-Or-9
Study of Wettability in Solid Iron/Liquid Metals by XPS/nano-Auger spectroscopies

T13 Surface Science

#SS-18-Or-9

T. Auger [1], M. Bouttemy [2], M.L. Giorgi [3], S. Madassamy [1], A. Etcheberry [2].

[1]CNRS/MSSMAT - Chatenay-Malabry (France), [2]UVQ/Institut Lavoisier - Versailles (France), [3]ECP/LGPM - Chatenay-Malabry (France).

A better understanding of the interaction of iron-based materials with liquid metals (Na, Hg, In, Pb, Bi) has important applications in technological areas such as liquid-metal nuclear reactors or spallation sources. The wettability of iron by liquids metals is a fundamental quantity for the evolution of various phenomenons such as grain-boundary grooving, surface faceting, corrosion or liquid-metal embrittlement. This constitutes the driving force for this work as a better knowledge of the wettability for these systems will bring valuable informations of the behavior of iron based materials in liquid metals. This work describes the use of modern surface analysis techniques to analyse wetting experiments performed mainly on the Fe/In system.
We performed an experimental study of the wettability of polycrystalline iron surfaces by In, Pb, Bi using the sessile-drop experiment. After equilibration at 450°C under a protective atmosphere (Ar-5%H2), these systems exhibit partial wettability with maximum wetting angle near 60° (the experiment is carried out such that iron is in its metallic state during the sessile-drop experiment). The wetting angle is found to increase in the following order: In < Pb < Bi. The surface energy of iron is lowered upon adsorption by these low melting point metals. At the triple line, the wetting angle selection requires the equilibrium between 3 energies: the solid-vapor surface energy, the solid-liquid surface energy and the liquid-vapor surface energy. The equilibrium leads to the well-known Young's equation:

Among the 3 surface energies, the solid-vapor one depends on the surface coverage of the adsorbate. While the experimental measurement of the wetting angle is

performed in-situ, one missing experimental quantity is the surface coverage reached on the solid-vapor side. High spatial resolution nano-Auger mapping of the main elements was achieved on polycrystalline substrate and reveals that the surface coverage of adsorbate depends on the orientation of the substrate. To simplify the analysis, iron monocrystal sheets were produced by the critical work hardening technique. Wetting experiments were performed and semi-quantitative XPS and Auger spectroscopy were used to measure at a global (400-50 µm probe size) and a local (12-20 nm probe size) scale the surface coverage using the Seah relation [1]. The detailed quantification procedure to Fe/In will be described. The preliminary results indicate that the coverage ranges from one to two monolayers, in line with studies on other systems [2]. The use of such measurement in models of the triple line will be outlined, particularly how one can hope to obtain a thourough description of wettability by combining experiments with density functional theory.

[1] R. Shimizu, Japonese journal of applied physics, 22, 11 (1983) 1631
[2] Z. Shi, P. Wynblatt, Metallurgical and materials transactions, volume 33A (2002) 2569

SS-P3-34
Interaction of strong acceptor molecules with metal-organic coordination networks on Au(111).

T13 Surface Science

#SS-P3-34

M. Faraggi [1], N. Jiang [2], N. Gonzalez-Lakunza [3], A. Langner [2], S. Stepanow [2], K. Kern [4], A. Arnau [5].

[1]DIPC and Instituto de Astronomia y Física del Espacio-Conicet - Buenos Aires (Argentina), [2]Max-Planck-Institut für Festkörperforschung - Stuttgart (Germany), [3]Donostia International Physics Center (DIPC) - San Sebastian (Spain), [4]Institut de Physique de la Matière Condensée, École Polytechnique Fédérale de Lausanne, CH-1015 Lausanne, (Switzerland) and Max-Planck-Institut für Festkörperforschung - Stuttgart (Germany), [5]Donostia International Physics Center (DIPC) and CFM-MPC, Centro Mixto (CSIC-UPV/EHU) - San Sebastian (Spain).

Within the framework of metal-organic coordination networks, we have studied two different systems on the Au(111) surface (Fig.1). The first one is obtained by evaporation of F4TCNQ ($C_{12}F_4N_4$) molecules onto the metal surface, and the second one consists of TCNQ ($C_{12}H_4N_4$) molecules and co-deposited Mn atoms. In both cases well-ordered quasi-rectangular superstructures are formed. These systems are characterized by scanning tunneling microscopy and dI/dV spectroscopy, combined with density functional theory (DFT) calculations to interpret the observations. F4TCNQ and TCNQ are strong electron acceptors and have been shown to be efficient in controlling the electron charge transfer at the metal-organic interface [1]. The metal centers play an active role in the formation of the two-dimensional arrays by favouring particular coordination numbers, being crucial in the determination of particular stoichiometry, charge transfer and magnetic moment. Additional coordination with transition metal atoms [2], like Mn, that have magnetic moment, is expected to permit the localization of spins in the 2D metal-organic network and, therefore, represent an interesting challenge for the design and fabrication of nano-scale devices.
In this work [3], we find that native Au ad-atoms are segregated from the pristine Au surface at room temperature, and are two-fold coordinated with F4TCNQ. However,

in the Mn-TCNQ case the Mn ad-atom is fourfold coordinated to the TCNQ ligands. In line with this, our DFT calculations show significant differences in the electronic structure close to the Fermi level as a result of the differences in type of bond and degree of charge transfer, this latter being higher from Mn to the TCNQ molecule than from Au-adatoms to F4TCNQ. That result is also in agreement with dI/dV point spectra observations. Finally, we have found a different level of mixing (or hybridization) between Au surface states (SS) and the lowest unoccupied molecular orbital (LUMO) in each system, being higher for Mn-TCNQ/Au(111) as compared with Au-F4TCNQ/Au(111).
Concerning to magnetic moment of Mn atoms in the self-assembled monolayer, we have found almost no variations (4.6 μB) from its atomic value and a weak AFM coupling between Mn centers.

[1] N. Koch et al., Phys. Rev. Lett. 95, 237601 (2005).
[2] T-C. Tseng et al., Phys. Rev. B 80, 155458 (2009).
[3] M. N. Faraggi et al., J. Phys. Chem. C116 (46), 24558 (2012).

Figure 1:[left] STM image (5 nm x 3 nm) and schematic geometry of the Au-F4TCNQ network (I=0.2 nA, U=89 mV) and [right] STM image (8 nm x 8 nm) and schematic geometry of the Mn-TCNQ network (I=0.17 nA, U=1.2 V). Unit cell lattice vectors in red arrows.

NST/SS-2-Or-4
Functionalization of Epitaxial Graphene by gold intercalation

T13 Surface Science

#NST/SS-2-Or-4

M. Narayanan Nair [1], T. Jiang [2], M. Cranney [1], F. Vonau [1], D. Aubel [1], M.L. Bocquet [2], L. Simon [1].

[1]Institut de Sciences des Matériaux de Mulhouse LRC 7228-CNRS, 4, rue des frères Lumière, 68093 Mulhouse, France - Mulhouse (France), [2]ENS Lyon, Laboratoire de Chimie, UMR 5182 CNRS 46, Allée d'Italie 69364 Lyon CEDEX 07, France - Lyon (France).

The epitaxial graphene formed on silicon carbide substrate is obtained by the annealing of the substrate at temperatures up to 1200°C. On the silicon terminated face of the hexagonal SiC(0001), it is formed a graphene layer partially covalently bonded to the substrate called buffer layer (BL) above which the actual graphene layer which shows the expected linear dispersion is formed. Epitaxial Graphene (EG) exhibits n type doping which is induced by the substrate. Inspired by the works of I. Gierz et. al who proposed a simple way to shift Fermi level and induce p type doping by deposition of gold atoms on top of graphene [1], we have performed detailed Scanning Tunneling Microscopy studies of the deposition of gold atoms under ultra_high vacuum conditions and revealed that gold atoms can intercalate between the buffer layer and monolayer graphene in different forms depending on the specific preparation procedure. An inhomogeneous intercalation of gold atoms (DP) or continuous atomic thin film (FP) was first observed [2] then more exotic forms of intercalation such as stripes (SP) as shown in figure below, were also recently observed. Using Fourier transform scanning tunnelling spectroscopy [3], confirmed by Angle-resolved photoemission spectroscopy measurements [4], we have shown that the band structure of the upper monolayer graphene is modified by the inhomogeneous intercalation. Despite the intercalation process, the relativistic character of the quasiparticles is preserved and moreover showed a higher Fermi velocity than that for pristine graphene. The band structure is modified around the Van Hove singularity which shows a large extension [4]. With the help of periodic DFT calculations we discussed the position of the intercalated gold atoms between the ML and BL graphene (or under the BL) and showed the expected STM images and the DOS modifications.

1. I. Gierz et al, Nano Letters 8, 4603, 2008
2. B. Premlal et al, APL, 94, 263115, 2009
3. M. Cranney et al, EPL, 91,66004, 2010
4. M.N.Nair et al, Phys.Rev.B, 85,245421, 2012

SS-3-Or-7
High energy surface X-ray diffraction for in situ surface structure determination - A new view of reciprocal space

T13 Surface Science

#SS-3-Or-7

J. Gustafson [1], M. Shipilin [1], C. Zhang [1], A. Stierle [2], U. Hejral [2], U. Ruett [2], O. Gutowski [2], P.A. Carlsson [3], M. Skoglundh [3], E. Lundgren [1].

[1]Lund University - Lund (Sweden), [2]Deutsches Elektronen-Synchrotron (DESY) - Hamburg (Germany), [3]Chalmers University of Technology - Gothenburgh (Sweden).

In recent years, the aim of bridging the gap towards industrial catalysis has driven surface scientists to develop in situ methods that are able to characterize surfaces in realistic gas pressures during a catalytic reaction. Examples of implemented methods are infrared spectroscopy, scanning tunneling microscopy, high pressure X-ray photoelectron spectroscopy and surface X-ray diffraction. All of these methods have their advantages as well as disadvantages.

Surface X-ray diffraction (SXRD) is a very powerful tool for structure determination, with capability to do detailed quantitative analysis. Since the X-rays interact weakly with gas molecules, it is not affected by a high pressure sample environment and function just as well in realistic reaction gas mixtures. The disadvantage is that the result is given in reciprocal space, which for many is a bit difficult to grasp, especially since one usually only measures a very small part of reciprocal space at the scans the reciprocal space line by line. To produce a two-dimensional map of a certain part of reciprocal space is very time consuming and to map out the three-dimensional space is not to think about. Hence one has to have a good idea about what to look for, and it is very easy to miss an unknown structure. Similarly, producing a proper quantitative data set (of a fairly well known structure) takes in the order of 10 hours.

By using a photon energy of 85 keV at beamline P07 at PETRA III at DESY in Hamburg, we have performed high energy surface X-ray diffraction (HESXRD), which gives a new view of reciprocal space and solves many of the problems. The high energy reduces the diffraction angles, such that a large part of reciprocal space can be caught on a two dimensional detector. By simply rotating the sample, we can then map out the three-dimensional reciprocal lattice in about 10 minutes for qualitative use or about 1-2 hours in order to get a complete data set for quantitative analysis. These data sets include the whole three-dimensional reciprocal space, and we do not risk missing important information just because we do not know where to measure. Furthermore, the measurements enable the presentation of reciprocal space and reciprocal lattices in a much more visual way, which in our view is significantly easier to grasp. Since we get more information into the detector simultaneously, one can also do better time resolved measurements following changes in surface structure for instance as a function of catalytic activity.

In this contribution we present a new view of reciprocal space enabled by HESXRD. We give an introduction to the method and differences to standard SXRD, and show how it can provide visual images of the reciprocal lattice. We also show how to use HESXRD for time resolved measurements of surface structure as a function of catalytic activity and an example of quantitative structure determination.

SS-4-Or-5
Non-contact atomic force microscopy characterization of a crystalline transition alumina surface

T13 Surface Science

#SS-4-Or-5

T. Jensen, K. Meinander, F. Besenbacher, J. Lauritsen.

Aarhus University - Aarhus (Denmark).

Heterogeneous catalysis plays a crucial role in the society today, both as the means for environmental protection and as the backbone technology for most of the chemical industries. The development of new catalysts is given a very high priority since they facilitate a much better utilization of our scarce energy reserves and it can drive the concept of waste-free ‘green’ chemistry and the development of a sustainable energy sector.

Metal oxides like Al_2O_3 play major roles in heterogeneous catalysis as supports for catalytically active nanoclusters because of their excellent mechanical and thermal stability. Of all the transitional aluminas, γ-Al_2O_3 is the most important in catalysis, but so far surface science studies have been unable to address the surface structure of this insulating material in detail. A better understanding of the surface structure of support materials seems to be a prerequisite for the synthesis of more sintering stable catalysts and the realization of nanocatalysts implementing catalyst particles with a tailored size and morphology.

Benefitting from a nearly perfect structural match between the (100) surface of $MgAl_2O_4$ and γ-Al_2O_3, we show that we can use $MgAl_2O_4$(100) as a template to grow thermodynamically stable and crystalline alumina films with γ-Al_2O_3-like properties. Previous atom-resolved nc-AFM studies have shown that the $MgAl_2O_4$(100) surfaces terminates by an Al-O rich termination, which turns out to be ideal for the continuously grown alumina films [1]. Preliminary nc-AFM studies reveals a perfect crystalline film-like growth (see Fig. 1), where up to 4ML thick films of Al_2O_3 were prepared using e-beam evaporation of pure Al onto a $MgAl_2O_4$(100) substrate followed by annealing at 1473 K in an oxygen atmosphere (1×10-7 mbar). Subsequent analysis of atom-resolved NC-AFM images reveals a structure with a

quadratic grid and a high concentration of atomic defects on Mg positions, which is suggesting a surface structure reflecting Al-terminated γ-Al_2O_3.

The stable γ-Al_2O_3(100) films make it possible to open up a whole new range of fundamental studies of the metal/support interaction for catalytic systems based on surfaces with real γ-Al_2O_3 properties. The synthesis of stable well-defined alumina films with transition alumina characteristics will allow us to address important catalytic properties such as acid-based properties, cluster adhesion strength and sintering scenarios for model systems of supported nanoclusters that incorporate the real oxide support structure.

[1] M. Rasmussen, *et al*., *Physical Review Letters* **107** (2011) 036102.

Fig. 1. Large-scale nc-AFM image of γ-Al_2O_3 on $MgAl_2O_4$.

SS-15-Or-5
First stages of 4H-SiC crystal growth: ab initio study

T13 Surface Science

#SS-15-Or-5

E. Wachowicz, A. Kiejna.

Institute of Experimental Physics, University of Wroclaw - Wroclaw (Poland).

The wide band-gap semiconductor silicon carbide has attracted a great interest during the past decades because of number of properties which make it very attractive for many applications in electronic devices. For electronic applications purposes hexagonal 4H-SiC is the preferred polytype. One of the main problems in the development of the SiC-based electronics is still poor quality of the SiC crystals. Therefore, it is necessary to understand the interaction of basic building bricks like Si, C, Si_2C and SiC_2 with the surface. Since hexagonal SiC crystals grow along <0001> direction the interaction of Si, C and Si_2C interaction with Si- and C-terminated {0001} surfaces is examined within DFT framework. The most favourable adsorption sites are identified. Qualitative *ab initio* molecular dynamic simulations show that molecules bind to both examined surfaces without dissociation. It is confirmed by quantitative DFT studies showing that there is no barrier for the molecule adsorption. Moreover, a possible mechanism of Si_2C on-surface dissociation is examined (Figure 1). Our research show that dissociation on C-terminated surface is favourable energetically altough there are two barriers to overcome. On th other hand, Si_2C dissociation on Si-terminated substrate is not favorable energetically.

Figure 1: Adsorption energy E_{ads} changes durong Si_2C molecule dissociation on Si- and C-terminated surfaces 4H-SiC{0001}. *x* indicates the coordiate of the Si atom withdrawn from the molecule.

NST/SS-3-Or-3
Magnetic behavior of Mn-tetraphenyl-porphyrin (TPP) on Fe-TPP/Fe(110) and Cl-Mn-TPP on Fe(110)

T13 Surface Science

#NST/SS-3-Or-3

G. Di Santo [1], A. Goldoni [2], M. Caputo [2], M. Panighel [2], C. Castellarin-Cudia [3], M. Fanetti [2], L. Chhagan Saini [4], B. Taleatu [4], F. Bondino [3], E. Magnano [3], N. Stojic [4], N. Binggeli [4].

[1]Consorzio INSTM UdR Trieste-ST, s.s. 14 Km 163.5 in Area Science Park, 34169 Trieste, Italy - Trieste (Italy), [2]Elettra - Sincrotrone Trieste, s.s. 14 Km 163.5 in Area Science Park, 34149 Trieste, Italy - Trieste (Italy), [3]IOM-CNR, Lab. TASC, s.s. 14 Km 163.5 in Area Science Park, 34149 Trieste, Italy - Trieste (Italy), [4]ICTP - Strada Costiera, 11 I - 34151 Trieste Italy - Trieste (Italy).

Cl-Fe-porphyrins and Cl-Mn-porphyrins monolayers adsorbed on Co and Ni films show a ferromagnetic coupling with the magnetization of the substrates [1-4] while, apparently, there is no evidence for magnetization of the second metallo-porphyrin layer [3]. Moreover, according to DFT calculations [1,4,5], the balance between ferromagnetic vs antiferromagnetic behaviors strongly depends on the presence of Cl attached to Fe and Mn ions: if Cl is desorbed from the molecules, the monolayers behaves as ferromagnetic, while the presence of Cl makes the antiferromagnetic behavior more stable.
Here we analyze the influence of the magnetization at room temperature on the second layer of metallo-TPP by preparing in-situ in ultra high vacuum monolayer (ML) of metalated Mn-TPP (obtained by evaporation of Mn atoms on H2-TPP) deposited on 1 ML of metalated Fe-TPP/Fe(110)/Cu(110) [6]. For this second adsorbed metalated Mn-TPP layer we will study the magnetic properties using NEXAFS and XMCD measurements, in combination with theoretical calculations of the electronic structure. We will demonstrate that the easy axis of magnetization is reversed in the second layer made of Mn-TPP from the in plane Fe magnetization of the first metalated Fe-TPP layer deposited on Fe(110)/Cu(110). We also verified the magnetic behavior of 1 ML of Cl-Mn-TPP deposited on Fe(110)/Cu(110). Surprisingly, contrary to the behavior of Cl-Mn-TPP deposited on Co and Ni films,

also in this case the coupling is antiferromagnetic. The presence of Cl attached to the Mn ions is confirmed by XPS and STM.

[1] A. Scheybal et al., Chem. Phys. Lett. 411, 214 (2005)
[2] H. Wende et al., Nature Mater. 6, 516 (2007)
[3] M. Bernien et al., PRB 76, 214406 (2007); Phys. Rev. Lett. 102, 047202 (2009)
[4] D. Chylarecka et al., J. Phys. Chem. C 115, 1295, (2011)
[5] P.M. Oppeneer et al., Progress in Surface Science 84, 18 (2009)
[6] A. Goldoni et al., ACS Nano 6, 10800 (2012)

SS-14-Or-7
Exploring Click-Chemistry Reaction on Noble Surfaces

T13 Surface Science

#SS-14-Or-7

L. Terracciano [1], R. Otero [2], J.M. Gallego [3], O. Trukhina [1], G. Bottari [1], T. Torres [1], R. Miranda [2].

[1]UAM - Madrid (Spain), [2]UAM/IMDEA - Madrid (Spain), [3]CSIC - Madrid (Spain).

Molecular self-assembly is a well-known strategy for fabrication of devices and systems in the size range of ~0.1-100 nm: organic molecules deposited on surface self-organize into well-defined structures. The process occurs without any external source and is driven by a multitude of atomistic phenomena which determine the shape and the physical properties of these structures[1]. In this sense the ability to control the formation of non-covalent bonds is the key ingredient for the fabrication of supramolecular nanostructures. Recently much effort is being invested in transforming these weakly-bonded supramolecular nanostructures into more robust, covalently linked ones, and the field or organic chemistry on surfaces is starting to develop. One way to create a covalent bond between two molecular subunits is represented by the “click” reactions, in which alkyne groups are made to react with azide-containing molecules (see scheme 1). In bulk the reaction is well studied and use Cu(II) salts as catalyst[2].
We explored this reaction on different metal surfaces using the surface itself like catalyst, thereby eliminating external catalysts. In this study we have characterized each reactant molecule and the final product of the reaction with STM and XPS that give us a complete characterization of the physical-chemical process. Moreover we studied the role of various noble metal surfaces (Au, Ag, and Cu) in promoting or hindering the reaction, comparing their efficiency. In figure 1 we show STM images of the final products of the reaction on Au(111) surface. The potential applications of this bottom-up approach are various. In particular, we will try to use this knowledge to control the formation of new donor-acceptor species directly at metal surfaces. This is a relevant topic for the realization of organic-based optoelectronic and photovoltaic devices

[1] JV Barth et al.;Nature; 437, 671-679 (2005).

[2] H.C. Kolb et al.; Angew. Chemie Int. Ed.; 40(11). 2001-2021 (2001).

Scheme1: scheme of click reaction

Fig.1: Adsorption on Au(111) of the final product of the reaction using the molecules shown up. It=-0.2nA Vt=-1250mV.

SS-2-Or-11
STM Study of Bi/Cu(111): Hard-Hexagon Model and Explosive Etching

T13 Surface Science

#SS-2-Or-11

Y. Girard, C. Chacon, J. Lagoute, V. Repain, S. Rousset.

University Denis Diderot Paris 7 - Paris (France).

The bidimensional $BiCu_2$ alloy belongs to the family of surface alloys with potential applications in spintronics (1). We report the direct observation of a surface alloying and dealloying transition during the submonolayer growth of Bi on the Cu(111) surface. In-situ scanning tunneling microscopy (STM) analysis reveals that at low coverage, embedded Bi atoms are randomly distributed within the first Cu plane, example of a stress driven alloy formation (2). Near the ideal coverage of 1/3, an ordered $BiCu_2$ bidimensional alloy forms, the hard-hexagon-model explains this behavior (3). Between 1/3 and 1/2 monolayer a dealloying process takes place where the surface alloy coexists with a Bi overlayer supported on Cu(111). In order to understand the mechanisms behind this process driven by stress, the ordered alloy has been used as a template for subsequent Bi adsorption. An apparently explosively etched surface develops during deposition and thanks to STM pictures analysis, we propose that this growth mode is caused by subsurface Cu atoms diffusion or equivalently by a surfactant effect of Bi on BiCu2. During annealing, the kinetically limited Ostwald ripening is surpassed and a complete phase separation occurs at local thermodynamic equilibrium.

(1) C. R. Ast et al. Phys. Rev. Lett. 98, 186807 (2007).
(2) C. Goyhenex et al. App. Surf. Sci. 177, 238-242 (2001).
(3) S. A. de Vries et. Al. Surf. Sci. 414, 159-169 (1998).

Fig.1: Bi 0.29 ML (10nmX10nm). Bi has been evaporated at room temperature then annealed at 470 K. Long range order appears only near 0.33 ML.

Fig.2: Dealloying after 0.1 ML overdeposition of Bi on a previous perfect surface alloy of $BiCu_2$ (50nmX50nm). White and brown islands are dense Bi [2012] phase

immersed in a see of $BiCu_2$. This out of equilibrium three phases system (islands of dense Bi on Cu, islands of dense Bi surrounded by surface alloy and surface alloy itself) is obtained after an explosive etching of the surface alloy.

SS-18-Or-10
IONIZATION AND ENHANCED PHOTOCHEMISTRY OF NITRIC ACID ON ICE

T13 Surface Science

#SS-18-Or-10

P. Ayotte [1], G. Marcotte [1], S. Pronovost [1], P. Marchand [1], C. Laffon [2], P. Parent [2].

[1]Université de Sherbrooke - Sherbrooke (Canada), [2]Aix-Marseille Université - Marseille (France).

Nitrates photolysis plays a key role in the chemistry of the polar boundary layer and of the lower troposphere over snow-covered areas (1). Using a combination of vibrational(2) and photoemission spectroscopies, we show that nitric acid is mostly dissociated upon its adsorption onto, and its dissolution in ice at temperatures as low 45K. By irradiation in the environmentally relevant n-π* transition, we also observe that the photolysis rate are significantly higher for surface-bound nitrates compared to that of dissolved nitrates. Surface-enhanced photolysis rates on ice may contribute to the intense photochemical NO_x fluxes observed to emanate from the sunlite snowpack upon polar sunrise.

(1) F. Dominé, P.B. Shepson, Science, 297, 1506-1510 (2002).

(2) P. Marchand, G. Marcotte, and P. Ayotte, Spectroscopic Study of HNO3 Dissociation on Ice, J. Phys. Chem. A 116, 12112-12122 (2012).

SS/NST-1-Or-7 KolibriSensor™, Tyto™ and Nanonis™ Control System: New Milestones in Scanning Probe Microscopy

T13 Surface Science

#SS/NST-1-Or-7

A. Thissen [1], H. Torben [1], D. Yuriy [1], A. Pioda [2].

[1]SPECS Surface Nano Analysis GmbH - Berlin (Germany), [2]SPECS Zurich GmbH - Zurich (Switzerland).

The KolibriSensor™ represents a new quartz sensor on the market that excels in its performance and its reliability. It is based on a symmetrical length extension resonator. The high resonance frequency of 1 MHz and the good signal-to-noise ratio allows for faster data acquisition in scanning microscopy and force spectroscopy. Oscillation amplitudes may be set below 20 pm. High stiffness prevents snap-in and the low noise floor continues to give a good frequency shift signal. The tip of the KolibriSensor™ has a separate contact, guaranteeing clean separation of the signals from the tunneling tip and from the quartz force sensor.

The new TYTO^{TM} scan head is a milestone in the technology of Scanning Probe Microscopy. The modular design allows for various experimental configurations and for the usage of different sensors. A kinematic mount is used for both the sample and sensor. For the first time, this enables different sensors to access identical locations on a sample and to repeat the procedure after successive sample preparation steps. This opens up opportunities for new experiments and will advance the research of surfaces at the nanometer scale. Additional features of the Tyto scan head are: Four openings for in-situ evaporation, two specular ports for simultaneous optical experiments, and large front openings and windows situated on each side of the body and at the back for broad visual inspection of the sample and sensor. Various sample receptors can be installed in the Tyto scan head, with four electrical contacts to the sample. Optional extra features include a calibrated Cernox temperature sensor located directly under the sample plate, and a small heater to control the sample temperature to within 1 mK.

For controlling state-of-the-art SPM experiments a new generation of the leading NANONIS™ Control System is presented.

SS-18-Or-11
Orthogonal interactions of CO molecules on a one-dimensional substrate

T13 Surface Science

#SS-18-Or-11

P. Cabrera-Sanfelix [1], C. Lin [2], H. Petek [3], A. Arnau [4], P.M. Echenique [5], D. Sánchez-Portal [4].

[1]Donostia International Physics Center (DIPC), IKERBASQUE - San Sebastian (Spain), [2]University of Texas at Austin, Department of Physics - Texas (United states), [3]Department of Physics and Astronomy and PINSE, University of Pittsburgh - Pittsburgh (United states), [4]Centro de Física de Materiales (CFM-MPC), CSIC-UPV/EHU, DIPC. - San Sebastian (Spain), [5]Donostia International Physics Center (DIPC) - San Sebastian (Spain).

We investigate the chemisorption structure of CO molecules on the quasi-one-dimensional Cu(110)-(2×1)-O surface by low temperature scanning tunneling microscopy and density functional theory. Contrary to metal surfaces, where CO molecules adsorb in an upright geometry and interact through repulsive intermolecular interactions, we find the most stable CO adsorption structure to be at Cu atoms of substrate Cu-O- chains with the Cu-CO unit bent by ~45º in two equivalent structures at low coverages, and combining in the same structure into highly ordered rows perpendicular to the substrate chains in an approximately 8×1 full monolayer structure. First-principles calculations attribute the unprecedented chemisorption behavior of CO molecules to lifting of the host Cu atoms by 1Å from the surface Cu-O- chains, in order to optimize the bonding and reduce the repulsive interactions with the substrate. This structural distortion enables counter-paradigmatic, short-range intermolecular dipole-dipole attraction and orthogonal long-range surface-mediated repulsion leading to unusual self-assembly of CO molecules into nanograting structures.[1, 2]

[1] Feng M, Cabrera-Sanfelix P, Lin C W, Arnau A, Sanchez-Portal D, Zhao J, Echenique P M and Petek H 2011 ACS NANO 5 8877
[2] Cabrera-Sanfelix P 2013 Submitted

Figure 1. (a) STM topographic images of CO monomers and dimers obtained by dosing 0.01ML of CO onto Cu(110)-O surface at 77K, and recorded at 77K and 4.5K (inset). The change in appearance of CO monomers and dimers at the two temperatures indicates that CO molecules interconvert between two equivalent tilted adsorption structures at 77K, whereas they are frozen in one of the two structures at 4K. The atomic resolution STM image also shows that CO is adsorbed on Cu atoms of -Cu-O- chains. (b) Ball and stick model showing the adsorption structure of CO monomer on -Cu-O- chains obtained by DFT calculation and the total energy surface for the pendular motion of the Cu-CO unit between the equivalent tilted forms. (c) The distribution of CO molecules around CO sampling monomers in the range of 12 lattice sites along the x- and y-directions, showing that the short range repulsion between two CO molecules is strictly along the same -Cu-O- chain, i.e. y direction. (d) STM topographic image showing the propensity for CO self-assembly into 1D linear clusters, indicating attractive interaction along the x-direction. The insert shows the STM image with enhanced contrast showing bias voltage independent, i.e. topographic origin, bright contrast indicative of the lifting of -Cu-O- chains that decays away from adsorbed CO molecules.

SS-6-Or-2
Visualization of hydration structures at the interface between alkali halide crystal surface and aqueous solution.

T13 Surface Science

#SS-6-Or-2

F. Ito [1], K. Suzuki [1], K. Kobayashi [2], H. Yamada [1].

[1]Department of Electronic Science and Engineering, Kyoto University. - Kyoto (Japan), [2]Society-Academia Collaboration for Innovation, Kyoto University. - Kyoto (Japan).

Water molecules form characteristic hydration structures having oscillatory density distributions at solid-liquid interfaces due to their geometrical asymmetry and/or various interfacial interactions. The hydration structures are often strongly related to a wide variety of physical and chemical phenomena including crystal growth/dissolution processes, of which atomic-scale mechanisms have not been fully understood.

Nowadays, three dimensionl (3D) force mapping by frequency-modulation atomic force microscopy (FM-AFM), operationg in liquid environment, allows us to directly visualize local interaction forces at the solid-liquid interface with subnanometer resolution. In fact, a 3D hydration structure at the interface between an electrolyte solution and a muscovite mica surface was revealed by this technique[1]. However, it has been mainly applied to the studies of the hydration structures on insoluble surfaces so far because the measurements of the rapidly changing surfaces in the growth/dissolution processes are difficult. In this study, the hydration structures on alkali halide crystal surfaces in aqueous solution were investigated by FM-AFM.

In this measurement, the concentration of electrolyte solution was kept nearly saturated such that the growth or dissolution rate of the crystal was lowered. It was actually self-controlled by the balance of the solution evaporation and the crystal dissolution in a non-sealed liquid cell. Figure 1(a) and (b) show a NaCl (001) cleaved surface model and the FM-AFM topographic image. A 2-dimensional (2D) frequency shift (Δf) map measured along the line X1-X2 in Fig. 1(b) indicates a molecular-scale hydration structure on the NaCl surface, as shown in Fig. 2(a). A frequency shift curve (Fig. 2(b)) taken along the line Z1-Z2 in 2(a) clearly exhibits an oscillatory feature of the hydration structure.

[1] N. Oyabu et al., The 70th JSAP Autumn Meeting, 2009 (Japan), 9a-L-4

Fig.1 (a) NaCl (001) surface model (b) Topogaphic image.

Fig.2 (a) 2 dimensional frequency shift map (b) Frequency shift curve

SS-7-Or-1
Tuning the electronic properties of MgO/metal buried interfaces by Mg atom intercalation

T13 Surface Science

#SS-7-Or-1

T. Jaouen [1], S. Tricot [2], G. Delhaye [2], B. Lépine [2], D. Sébilleau [2], G. Jézéquel [2], P. Schieffer [2].

[1]Département de Physique and Fribourg Center for Nanomaterials, University of Fribourg - Fribourg (Switzerland), [2]Département Matériaux Nanosciences, Institut de Physique de Rennes UMR UR1-CNRS 6251, Université de Rennes 1 - Rennes (France).

Magnesium oxide ultrathin films grown on metal substrates have received considerable attention because of their technological importance in many research fields, such as spintronics and heterogeneous catalysis [1, 2]. In particular, the artificial manipulation of the local structure at the oxide/metal interface is expected to play a pivotal role in controlling the catalytic activity of oxide films [3]. Interface engineering thus appears as a versatile way to tune the electronic properties of the oxide/metal system without altering the thickness or the structure of the oxide overlayer [4]. However, few experiments concerning the oxide/metal interface, especially involving interface defects, have been performed due to the practical difficulties related to buried systems. In this study, we present combined X-ray excited Auger electron diffraction experiments and multiple scattering calculations and we reveal a layer-resolved shift for the Mg KLL Auger transition in MgO ultrathin films (4-6 Å) on Ag(001). This resolution is further exploited to demonstrate the possibility to control Mg atom intercalation at the MgO/Ag(001) interface and extract the structural parameters of the films. The induced work function changes and the large interlayer relaxation at the metal/oxide interface are evidenced using UV photoelectron spectroscopy and show an excellent agreement with density functional theory calculations [5]. These results are of relevance for the understanding of the relationship between the structural and electronic properties at doped metal-oxide interfaces.

[1] S. Yuasa et *al.*, Nat. Mater. 3, 868 (2004).
[2] H-J. Freund and G. Pacchioni, Chem. Soc. Rev. 37, 2224 (2008).
[3] J. Jung et *al.*, JACS 133, 6142 (2011).
[4] U. Martinez et *al.* , Phys. Rev. Lett. 103, 056801 (2009).
[5] T. Jaouen et *al.*, in preparation.

NST/SS-P1-21
Chemical Reactivity and Confined States of Graphene on Ru(0001) and Ir(111)

T13 Surface Science

#NST/SS-P1-21

S. Altenburg [1], J. Kröger [2], T.O. Wehling [3], B. Sachs [3], B. Wang [4], M.L. Bocquet [4], N. Lorente [5], A.I. Lichtenstein [3], R. Berndt [1].

[1]Institut für Experimentelle und Angewandte Physik, Christian-Albrechts-Universität zu Kiel - Kiel (Germany), [2]Institut für Physik, Technische Universität Ilmenau - Illmenau (Germany), [3]I. Institut für Theoretische Physik, Universität Hamburg - Hamburg (Germany), [4]Université de Lyon, Laboratoire de Chimie, Lyon, CNRS - Lyon (France), [5]Centre d'Investigació en Nanociència i Nanotecnologia, Campus UAB - Bellaterra (Spain).

On a number of metal surfaces single layers of graphene may be grown with a high degree of perfection. The strength of the interaction between graphene and metal substrate may differ between strong chemisorption, e.g. on Ni(111), and weak physisorption, e.g. on Pt(111).
This provides an opportunity to experimentally address a number of intriguing questions: What is the effect of a substrate on the electronic structure of graphene and vice versa? How far does the metal substrate influence, e.g., the adsorption of single atoms or molecules on graphene? To what extent can graphene be used to decouple functional molecules from the metal substrate?

Here we study graphene on Ru(0001) and on Ir(111) as representatives for substrates with strong and weak interactions by low temperature scanning tunneling microscopy (STM) and density functional theory (DFT). We locally probe the chemical reactivity of the graphene C atoms by controllably contacting the graphene sheet with the tip of a cryogenic STM with atomic precision. Comparing with DFT results we find an increased reactivity of specific C atoms of graphene on Ru(0001).

On pristine and graphene-covered Ir(111) surfaces scanning tunneling spectroscopy reveals a hole-like surface resonance which is shifted below graphene, as confirmed by DFT calculations. Nanosized graphene islands confine the resonance and induce

characteristic standing wave patterns. These results invalidate previous reports of confined Dirac states.

Funded by the DFG (SPP 1459, SFB 668, SFB 677), MICINN, MONET, MEST-CT and HLRN.

SS-1-Or-4
The quantum to classical crossover in the diffusion of H and D on Ni(111): a comparison of Helium Spin Echo measurements and diffusion rates derived from DFT potential energy surfaces

T13 Surface Science

#SS-1-Or-4

J. Zhu [1], D. Ward [1], W. Allison [1], J. Ellis [1], M. Sacchi [2], S. Jenkins [2].

[1]Cavendish Laboratory, University of Cambridge - Cambridge (United kingdom), [2]Department of Chemistry, University of Cambridge - Cambridge (United kingdom).

The nature of dynamics of hydrogen and its isotopes on metal surfaces has attracted enormous theoretical and experimental attention in the past decades due to its crucial role in fundamental and important surface processes such as heterogeneous catalysis and hydrogen fuel cells.

In this presentation, we report Helium Spin-Echo (HeSE) measurements [1] of H_2 and D_2 dynamics on Ni(111) surface, which provides terrace, as opposed to over-step, diffusion measurements in equilibrium situations on atomic length scales and ultrafast time scales (pico-seconds) with unparalleled accuracy and reliability. Our experiments show a clear coverage-dependent crossover between classical overbarrier hopping and quantum tunnelling. The temperature dependence of the classical dynamics region follows Arrhenius behaviour with activation energy consistent with previous studies [2], however, the quantum diffusion rates are surprisingly high. We also present first HeSE momentum dependent dynamics data in deep tunnelling regime.

Additionally, we report first principle calculations of hydrogen atom energy states in the atom-surface potential (atomic band structures) based on density functional theory, and extend them to determine the rate of hydrogen diffusion with a formalism

that does not make the arbitrary distinction between ‘overbarrier’ and tunnelling states. We compare HeSE data on the diffusion of H and D on the Ni(111) surface with diffusion rates derived from H and D atom band structures evaluated from DFT calculations of 3D potential energy landscapes of H on Ni(111). We show that the activated diffusion rates predicted from our calculations are in remarkably good agreement with experimental results.

[1] A. P. Jardine *et al. Phys. Chem. Chem. Phys*. **11**, 3355 (2009)
[2] T.-S. Lin and R. Gomer. *Surf. Sci*. **255** 41 (1991)

SS-17-Or-4
Kondo screening of Fe-Porphyrins tuned by on-surface ring-closure reactions

T13 Surface Science

#SS-17-Or-4

B. Heinrich [1], G. Ahmadi [1], V. Müller [1], L.Z. Braun [2], J.I. Pascual [3], K.J. Franke [1].

[1]Institut für Experimentalphysik, Freie Universität Berlin - Berlin (Germany), [2]Fritz-Haber-Institut - Berlin (Germany), [3]CIC nanoGUNE - San Sebastián (Spain).

In metal-organic complexes, it is mainly the structure of the ligand that governs the adsorption on metal surfaces and thereby influences the magnetic interaction between the central ion and the conduction electrons. We use Scanning Tunneling Microscopy and Spectroscopy (STM/STS) at 4.5 K to show for an Fe-Porphyrin on Au(111), how the modification of the ligand structure alters the Kondo screening of of the paramagnetic iron ion.

We anneal Fe(II)-Octaethylporphyrin (FeOEP) on Au(111) to temperatures of 470 K and above. This induces a step-wise electrocyclic ring closure of the ethyl groups and finally produces Fe-Tetrabenzoporphyrin (FeTBP). In STS, complex features at low energies around the Fermi level result from Kondo screening of the iron ion's spin. Changes in width and shape show the tuned interaction of the local spin with the conduction electrons depending on the actual chemical structure of the ligand. These results highlight the importance of chemical engineering for controlling the magnetism of single molecules on surfaces.

STM topography of different Fe-Porphyrins visualizing the step-wise transformation of FeOEP to FeTBP.

SS-18-Or-8
Water adsorption on MOVPE-prepared GaP(100) monitored in-situ with reflection anisotropy spectroscopy

T13 Surface Science

#SS-18-Or-8

M. May [1], O. Supplie [1], W.D. Zabka [1], C. Höhn [1], H.J. Lewerenz [2], T. Hannappel [3].

[1]Helmholtz-Zentrum Berlin - Berlin (Germany), [2]California Institute of Technology - Pasadena (United states), [3]Technische Universität Ilmenau - Ilmenau (Germany).

III-V semiconductors constitute a promising absorber material class for solar-driven water splitting due to their tunable electro-optical properties [1]. For this application, the water-semiconductor interface is of fundamental interest as it impacts corrosion processes as well as the charge-transfer efficiency to the electrolyte [2]. We present model-experiments employing water adsorption in UHV on differently prepared GaP(100) surfaces.

Metal-organic vapour phase epitaxy (MOVPE) is the method of choice for the preparation of III-V semiconductors and features specific surface reconstructions due to process gases such as hydrogen. We prepare atomically well-defined surfaces under in-situ control by reflection anisotropy spectroscopy (RAS) and transfer them contamination-free from the near-ambient pressure MOVPE environment to UHV [3]. After characterisation with LEED and ultraviolet/X-ray photoelectron spectroscopy, the surfaces are exposed to water vapour in UHV, again under RAS in-situ control [4], see Figure 1. The influence of water on the surface is subsequently monitored with photoelectron spectroscopy and LEED. Annealing of the water-covered surfaces in ultra-pure hydrogen or nitrogen atmosphere under RAS control allows further insight into the nature of the water-induced surface changes.

GaP(100) prepared in MOVPE features two surfaces, the Ga-rich, (2x4) mixed-dimer reconstruction and the MOVPE-unique (2x2)-2D-2H P-rich reconstruction [5]. Their identification with highly surface-sensitive RAS is well established and allows for in-situ monitoring of the surfaces on an atomic scale. Upon water exposure, the P-rich

surface is significantly more stable and can be restored more easily than the Ga-rich surface. Stability of the surfaces and their interaction with water will be discussed in the context of RA and PE spectra.

[1] H. Döscher, O. Supplie, M. M. May, P. Sippel, C. Heine, A. G. Muñoz, R. Eichberger, H.-J. Lewerenz, and T. Hannappel, *ChemPhysChem*, 2012, **13**, 2899–2909.

[2] B. C. Wood, T. Ogitsu, and E. Schwegler, *J. Chem. Phys.*, 2012, **136**, 064705.

[3] T. Hannappel, L. Töben, K. Möller, and F. Willig, *J. Electron. Mater.*, 2001, **30**, 1425–1428.

[4] T. Hannappel, M. M. May, and H. J. Lewerenz, in *Photoelectrochemical Water Splitting: Issues and Perspectives*, RSC Publishing, in print.

[5] P. H. Hahn, W. G. Schmidt, F. Bechstedt, O. Pulci, and R. Del Sole, *Phys. Rev. B*, 2003, **68**, 033311.

Figure 1: RA spectra of the P-rich surface after different exposures to H_2O.

NST/SS-P2-07
DFT Studies of the electronic structure and Surface magnetism in desordered binary alloys

T13 Surface Science

#NST/SS-P2-07

M. Solorza Guzmán.

ESCOM-IPN Av. Juan de Dios Bátiz s/n y Av. Miguel Othon de Mendizábal, Lindavista, 07738 - México, D. F. (Mexico).

Ab initio calculations were performed using the methodology based on the quantum version of the Virtual Crystal Approximation (VCA) and the method of density functional theory with generalized gradient approximation (GGA) improved by Wu-Cohen (WC), which methodology is more consistent for calculating lattice constants, crystal structures, the surface energy of metals is improved to functional Perdew-Burke-Ernzerhof (PBE) GGA. The methodology was applied to the case of the binary alloy $Fe_{1-x}Co_x$ disordered. Our results show that the surface magnetic moment is higher than that the bulk to the same concentration *x*, which indicates that the 3*d*-band is narrower in the surface according to the surface magnetic moment is greater than the bulk value.

JA Chemist's Guide to Density Funtional Theory, edited by Wiley-VCH, Wolfram Koch, Max C. Holthausen (Berlin, 2001)

Wu, Z.; Cohen, R. E., Phys. Rev. B, 73, 235116 (2006)

Bellaiche, L; Vanderbilt, D. "Virtual crystal approximation revisited: Application to dielectric and piezoelectric properties of perovskites", Phys. Rev. B, 61, 7877-7782 (2000)

SS-16-Or-7
Interface and surface study of U/Si(111) and U/W(110)

T13 Surface Science

#SS-16-Or-7

C. Qiuyun, W. Feng, X. Lai.

China academy of engineering physics - Mianyang (China).

Our main intention is to study the interface and surface of metal uranium on different substrates. In this paper, uranium thin films were deposited on Si(111)-7×7 and W(110) surface at room temperature. The interface and surface with different annealing temperatures were studied by LT-STM, XPS, LEED and ARPES. STM results showed that the film was disordered as deposited, and ordered crystal structure appeared when annealed at 870 K, see Fig.1. The films were consisted of ordered films and disordered regions, for the ordered films triangle structures were seen very clearly. When annealed at 1200K, the surface of the films turned out to be the same as Si(111) -7×7 reconstruction. And also band structures for the films annealed at different temperatures were obtained and compared with the first-principles calculations, see Fig.2.
Also uranium films were deposited on W(110) substrate, the interaction of uranium with small amount of oxygen was studied. STM results showed that reconstructions were seen when annealed at 1000K and 1200K. Reconstruction structures were studied with STM and LEED, and also band structures were obtained by ARPES.

Fig.1 STM images of U/Si(111) at different annealing temperatures

Fig.2 (a) xps depth profile of U/Si(111) (annealed at 1200K);(b) valence band spectrum; (c) band structure of USi2 (theoretical calculations);(d) band structure of U/Si(111)(as deposited); (e) band structure of U/Si(111)(annealed at 870K); (d) band structure of U/Si(111)(annealed at 1200K);

SS-16-Or-8
The study of ordered cerium metal thin film and CeSix interface on Si(111)

T13 Surface Science

#SS-16-Or-8

W. Feng, Q. Chen, S. Tan, X. Lai.

China Academy Engineer Physics, P.O. Box 919-71, - Mianyang, Sichuan (China).

Combined with the low temperature scanning tunneling microscopy (LT-STM), X-ray photoelectron spectroscopy (XPS) and Angle resolved photoemission spectroscopy (ARPES), we studied the CeSix/Si(111) interface with different coverage and annealing temperature, then we studied the ordered cerium metal thin film obtained by evaporating cerium on CeSix/Si(111) interface and annealing subsequently.

SS-7-Or-6
DFT studies of polaron dynamics for the (110) surface & bulk Ceria

T13 Surface Science

#SS-7-Or-6

A. Green [1], J. Kullgren [2], K. Hermansson [2], C. Castleton [1].

[1]School of Science & Technology,Nottingham Trent University - Nottingham (United kingdom), [2]Department of Chemistry-Ångström, Uppsala University - Uppsala (Sweden).

CeO_2 (Ceria) is an intrinsic n-type fluorite structure semiconductor with numerous applications in gas sensing, car exhaust catalysis and solid oxide fuel cells. When an oxygen vacancy is created at the surface, two extra electrons are left behind from the (mainly) ionic bonding. Each electron enters a Ce4f band-like state and becomes localized in nature, forming a polaron with a single Ce^{3+} ion at the centre, and these can be arranged in various patterns around the vacancy itself [1]. The conductivity in Ceria is mixed ionic-electronic. The ionic conductivity is due to thermally activated hopping of oxygen vacancies (V_o^{2+}), and the electronic conductivity is due to thermally activated hopping of the f-electron polarons through the material. These transport processes of both O vacancies and polarons occur through bulk Ceria, and also across the surfaces. Depending on the dopants added to Ceria and their relative concentrations, the conductivity can vary from mainly ionic to mainly electronic.

We present periodic DFT+U studies of the properties of polarons in bulk Ceria systems, and also across the (110) surface. Previous experimental work [2] for pure CeO_2 finds a polaron activation energy range for polaron hopping in single crystals of CeO_{2-x} of around 0.4–0.52 eV. Results presented are focused on polarons away from the influence of oxygen vacancies or any other defects. For bulk studies, we use the supercell approximation, adding a single localized electron [3]. We examine the critical dependence of results upon various details of calculation methods. A variety of functionals have been tested including LDA+U= 6eV and GGA+U=5 eV, where U is the added on-site coulomb repulsion Hubbard term, as well as popular hybrid functionals. Results include electron localization energy (E_{LOC} = the energy difference between a delocalized and localized f-electron), the level of bond distortion around the polaron site, radial charge distribution of the Ce4f electron and hopping barrier (fig.1).

The LDA+U=6eV functional has been used to study the polaron properties and dynamics at the (110) surface of Ceria. While the (111) surface is more stable, much of the interesting surface chemistry takes place on the (110) surface of Ceria. We will present results for electron localization at the surface and a description of thermally activated polaron hopping across and below the (110) surface. We discuss the various pathways implicated for polaron transport [4].

[1] J. Chem. Phys. 137, 044705 (2012)
[2] J. Phys. Chem. Solids, 1977, Vol 38, pp859-867
[3] Polarons in Ceria, Castleton et al, in preparation
[4] DFT studies of polaron dynamics on the (110) surface of Ceria, Green et al, in preperation

Fig.1 Ce4f polaron transfer energy barrier

SS-2-Or-12
Si interaction on Ni surfaces

T13 Surface Science

#SS-2-Or-12

T. Fukuda [1], I. Kishida [1], K. Umezawa [2].

[1]Osaka City University - Osaka (Japan), [2]Osaka City University - Sakai (Japan).

Metal silicides are the most studied materials and they have been widely utilized in microelectronics. Although thin silicide films have been extensively studied, most silicides were formed on silicon substrates and Si-rich phases were stabilized. By contrast, metal-rich phases formed by Si deposition onto metal substrates have not been drawn attention and scarcely studied so far. Here we address initial reaction of Si and ultrathin silicide film formation on Ni substrates including Ni(111), Ni(100), and Ni(110) surfaces under UHV by employing STM and LEED. We find several superstructures on these surfaces and their STM images were compared with first principles calculations.

Si reacts with Ni(111) substrate beyond 373 K, and when Si is deposited less than 1/3 ML two dimensional silicide with a √3×√3 R30° structure (√3-α) is stabilized. If an initial Si coverage exceeds 1/3 ML, a honeycomb structure with √3×√3 R30° periodicity (√3-β) is formed at 673 K. The surface is very flat and a part of the honeycomb is filled with excess Si adatoms in the image. (Fig.1)

On the Ni(110) surface, deposited Si is embedded into the Ni substrate even at room temperature. For higher temperatures, STM images exhibit irregular defect-like structure with an atomic dimension. (Fig. 2) By increasing the substrate temperature during Si deposition, local order with c(2×2) and p(2×1) reconstructions is stabilized up to 0.5 ML and beyond 373 K. Further increasing Si deposition, unique zigzag islands elongates along [001] direction is seen as the second layer.

We constructed structure models for these structures and calculated their electronic band structures as well as total energy with first-principles local density approximation. STM images were also simulated and they were well reproduced by our models.

Fig. 1:STM images for (a)√3 -α and (b)√3-β structures, resspectively. Scanning areas 2.5 nm×2.5 nm. √3×√3 R30° unit cell is indicated as a solid parallelogram for each image.

Fig. 2:Si deposited Ni(110) surface at 473 K. Scanning area is 10 nm×10 nm.

SS-P1-19
Theoretical simulation of IR spectrometry of SrTiO3 thin layers

T13 Surface Science

#SS-P1-19

E. Amzallag [1], P. Roy [2], R. Tétot [3].

[1]ICMMO/LEMHE - Orsay (France), [2]Synchrotron SOLEIL - Gif-Sur-Yvette (France), [3]robert.tetot@u-psud.fr - Orsay (France).

The demonstration that high quality epitaxial oxides, such as SrTiO3 (STO),VO2 and Gd2O3 can be grown on silicon by Molecular Beam Epitaxy (MBE) was considered as a materials breakthrough and opened the door to a wide variety of new potential applications. Strontium titanate, SrTiO3 (STO), is an incipient ferroelectric very promising for use in high storage capacity devices such as dynamic random access memory (DRAM) capacitors. It features high permittivity and absence of hysteresis loop even at low temperature. Its high dielectric constant (~300) provides an order of magnitude higher capacitance density than the conventional gate dielectrics, such as SiO2 and Ta2O5. The lack of fatigue and ageing (paraelectricity) problems make this material advantageous with respect to other perovskite ferroelectrics for this particular application. Nevertheless, the grain boundaries of polycrystalline films tend to induce high leakage current and amorphous films have low dielectric constant. Heteroepitaxial growth of SrTiO3 on Si is therefore of immense importance.
Since the discovery of its incipient ferroelectricity and first polar soft mode behavior , SrTiO3 has become one of the most studied materials. The optical properties of SrTiO3 bulk material have been extensively analysed experimentally and theoretically. Concerning surface thin layer, we recently measured infrared which presents important differences with bulk material suggesting a different crystallographic structure. The interpretation is hampered by the complicated spectral behaviour which varies with epitaxial conditions and material properties. We have thus performed theoretical calculations using the ab initio periodic LCAO-B3LYP method developed in the CRYSTAL03 code. Relaxed atomic structures of each system (bulk and surface) are carefully analysed and vibrational spectra of SrTiO3 bulk and thin layer are calculated at the Γ point by using the CRYSTAL program. The full set of frequencies is calculated and compared with the experimental ones.
The present work permits to clarify some of the assignment and interpretation problems raised by experiment.

SS-18-Or-13
Formation of a porous network from tetrahydroxybenzene on Cu(111) involving molecular dehydrogenation and coordination to Cu adatom trimers.

T13 Surface Science

#SS-18-Or-13

T.R. Linderoth [1], F. Bebensee [1], K. Svane [1], C. Bombis [1], F. Masini [1], S. Klyatskaya [2], M. Ruben [2], B. Hammer [1], F. Besenbacher [1], T.R. Linderoth [1].

[1]Aarhus University, iNANO - Aarhus (Denmark), [2]Karlsruhe Institite of Technology - Karlsruhe (Germany).

Formation of extended and well-ordered molecular networks on surfaces has received considerable attention recently, not least motivated by potential applications in areas such as functionalized surface coatings, sensors or heterogenous catalysis. Here, we investigate adsorption of the structurally relatively simple molecule tetrahydroxybenzene (THB) on the Cu(111) surface under ultra-high vacuum conditions. High resolution scanning tunneling microscopy (STM) reveals formation of a close-packed molecular overlayer at room temperature. Annealing to 440 K, however, results in extended domains of a porous honeycomb network with a periodicity of 1.75 nm. This network formation is surprising given the molecular structure/symmetry and cannot be explained from a simple hydrogen bonding model. By combining STM with in-situ X-ray photoelectron spectroscopy (XPS) and Density Functional Theory (DFT) modeling, we elucidate factors leading to the observed network formation.
At low temperature (115 K) THB adsorbs essentially intact, but annealing to 370 K induces gradual dehydrogenation of the hydroxyl groups as shown by the O1s XPS signal and confirmed by control experiments using the chemically related compound dihydroxy benzoquinone (DHBQ) where two hydroxyl groups are replaced by carbonyls. The energetics of the dehydrogenation is modeled by DFT, pointing to the importance of the entropic contribution of desorbed hydrogen for the dehydrogenation to occur. Subtle contrast differences between close packed structures formed from THB and DHBQ are explained from DFT-based STM image

calculations. The ensuing network formation observed at 440K involves complete dehydrogenation of the THB hydroxyl groups. The observation of etch pits on the Cu(111) surface upon network formation as well as high-resolution STM images of the network nodes furthermore suggest that Cu adatoms liberated from the substrate participate in the network formation. Based on DFT calculations, we attribute the observed network to an array of Cu adatom trimers each coordinating to three fully dehydrogenated THB molecules, leading to a structure in agreement with STM observations regarding dimensions and symmetry. Overall, the study provides new insights into how on-surface synthesis of a highly reactive coordination ligand in combination with native metal ad-atoms can lead to formation of ordered molecule-metal coordination networks on surfaces.

SS-4-Or-6
Sputtering induced transformation of TiO2 surface to metallic state

T13 Surface Science

#SS-4-Or-6

M. Rogala [1], Z. Klusek [1], C. Rodenbücher [2], K. Szot [2].

[1]Division of Physics and Technology of Nanometre Structures, Faculty of Physics and Applied Informatics, University of Lodz - 90-236 Lodz (Poland), [2]Peter Grünberg Institut & JARA-FIT, Forschungszentrum Jülich - 52425 Jülich (Germany).

Ar^+ ion sputtering is the process which may lead to the creation of quasi 2D metallic layer on the surfaces of primarily insulating materials [1]. Such transformation from band insulator to metallic conductor was previously investigated in binary and ternary transition-metal oxides regarding the changes in oxygen stoichiometry and macroscopic surface conductivity [1,2]. However, the description of the nature of this transition in nanoscale is still insufficient, especially that such processes can be significantly complex and based on serious modifications of both electronic and crystallographic structure [3]. To overcome the existing gap we analyze the sputtering inducted insulator to metal transformation in the surface layer of TiO_2 (110) single crystals with complementary surface sensitive techniques. The scanning probe microscopic techniques (atomic force microscopy (AFM), local conductivity atomic force microscopy (LC-AFM)) both with X-ray/UV photoelectron spectroscopy (XPS/UPS) allow us to understand the complexity of transformations that occur in electronic and crystallographic structure of the surface and in the local conductivity of the surface layer. The latter we analyzed both in- and out-of-plane, which gave the possibility to estimate the depth of the changes introduced to the crystal by the ion sputtering process. We track and analyze the changes that occur on the surface in consequence of selective removing of oxygen (during sputtering process). Our results provide evidence, that from the early beginning of the sputtering process, with increasing sputtering time we deal with a surface structure transformation, which leads to formation of new Ti-O phases. We connect the presence of quasi 2D conducting layer on the TiO_2 with changes of the valence of Ti ions during the formation of clearly visible grain-like surface structures. The phenomena that we analyzed in nanoscale can be essential not only for understanding the transport properties in the surface layer of the investigated material, but are also important for nanoelectronics, optics and catalysis. The changes of the resistivity of the material

described here are specifically related to the mechanisms of resistive switching processes in TiO_2 [3]. The presented investigations shed light on the important aspects of the origin of this phenomena (as in-plane heterogeneity) and can extend the knowledge about this material in the application for redox-based resistive random-access memory (ReRAM) [4].
The project was co-financed by the University of Lodz: Grant supporting young scientists.

[1] Reagor, D. W.; Butko, V. Y. Nat. Mater. 2005, 4, 593–596.
[2] Hashimoto, S.; Tanaka, A.; Murata, A.; Sakurada, T. Surf. Sci. 2004, 556, 22–32.
[3] Szot, K.; Rogala, M.; Speier, W.; Klusek, Z.; Besmehn, A.; Waser, R. Nanotechnology 2011, 22, 254001.
[4] Waser, R.; Dittmann, R.; Staikov, G.; Szot, K. Adv. Mater. 2009, 21, 2632–2663.

SS-P1-04
Self-Assembled Monolayers of Polyhedral Dicarbadodecaborane Dithiols: A Computational Comparison of Bonding through Adatoms and Directly

T13 Surface Science

#SS-P1-04

J. Macháček.

Institute of Inorganic Chemistry AS CR, v. v. i. - Řež (Czech republic).

During the last decade, carborane thiols were introduced as building blocks for self-assembled monolayers on metal surfaces.[1][2][3][4] This work tries to contribute computationally to our understanding of the way the dicarbadodecaborane dithiolate moieties bind to a gold surface. DFT calculations of periodical systems are employed, using the projector-augmented waves method as implemented in the Abinit program.[5]. First, the bonding of the moieties to a flat (111) gold surface was explored, and the geometry of the highest possible coverage, that is one moiety over six surface gold atoms, was optimised. Such a coverage compares well to the experimentally found 6—7 surface atom per molecule on nano-particles and 7—8 on a thin film,[1] especially taking the inevitable imperfection of the samples into account. Then, by simple geometrical considerations, adatom patterns of various density were constructed, and the pattern containing 1 adatom per 7 surface atoms, best matching the experimental data, was selected to study. The geometry was optimised and the adsorption energies calculated for the moieties bound to the surface through the adatom, as well as in the same arrangement with the adatom removed. All the three geometry forms being consistent with the available experimental information, the calculated adsorption energies were used to select the most realistic one; the calculated stabilities of the monolayers formed by 9,12-dithiolate were compared with those of the layers build from 1,2-dithiolate moieties, and related to experimental observations.

The work was supported by the projects M200321201 of the AS CR, and P205100348 of the GACR. Computing and storage facilities provided by National Grid Infrastructure MetaCentrum under the programme LM2010005 were used.

[1] T. Base, Z. Bastl, Z. Plzak, T. Grygar, J. Plesek, M. Carr, V. Malina, J. Subrt, J. Bohacek, E. Vecernikova, O. Kriz, LANGMUIR 21 (2005) 7776–7785.
[2] T. Base, Z. Bastl, V. Havránek, K. Lang, J. Bould, M.G.S. Londesborough, J. Machácek, J. Plesek, Surface and Coatings Technology 204 (2010) 2639–2646.
[3] J.N. Hohman, S.A. Claridge, M. Kim, P.S. Weiss, Materials Science and Engineering: R: Reports 70 (2010) 188–208.
[4] J.F. Lübben, T. Baše, P. Rupper, T. Künniger, J. Macháček, S. Guimond, Journal of Colloid and Interface Science 354 (2011) 168–174.
[5] ABINIT, Université Catholique de Louvain, Corning Incorporated, Université de Liège, Commissariat à l'Energie Atomique, Mitsubishi Chemical Corp., Ecole Polytechnique Palaiseau, and other contributors, n.d.

The geometry of 9,12-S_2-1,2-$C_2B_{10}H_{10}$ moiety forming a high coverage SAM on a (111) gold surface compared to that of the same moiety bound to the surface through an adatom

SS-10-Or-1
Tailoring the electronic texture of a topological insulator via its surface orientation

T13 Surface Science

#SS-10-Or-1

X. Zhu [1], L. Barreto [1], M. Stensgaard [1], W.S.E. Silva [1], S. Ulstrup [1], M. Bianchi [1], M. Dendzik [2], P. Hofmann [1].

[1]Department of Physics and Astronomy, Interdisciplinary Nanoscience Center (iNANO), Aarhus University, 8000 Aarhus C, Denmark - Aarhus (Denmark), [2]Centre for Nanometer-Scale Science and Advanced Materials (NANOSAM), Smoluchowski Institute of Physics, Jagiellonian University, Reymonta 4, 30-059 Kraków, Poland - Kraków (Poland).

Three dimensional topological insulator crystals consist of an insulating bulk enclosed by metallic surfaces, and detailed theoretical predictions about the surface state band topology and spin texture are available. While several topological insulator materials are meanwhile known, the existence and topology of these metallic states was only ever been probed for one particular surface orientation of a given material. For most topological insulators, such as $Bi_{1-x}Sb_x$ and Bi_2Se_3, this surface is the closed-packed (111) surface and it supports one topologically guaranteed surface state Dirac cone. Here we experimentally realize a non closed-packed surface of a topological insulator, $Bi_{1-x}Sb_x$(110), and probe the surface state topology by angle-resolved photoemission. As expected, this surface also supports metallic states but the change in surface orientation drastically modifies the band topology, leading to three Dirac cones instead of one, in excellent agreement with the theoretical predictions but in contrast to any other experimentally studied TI surface. The surface state band structure of $Bi_{1-x}Sb_x$ is calculated by a transfer-matrix technique and Green's function approach. The results confirm the surface state topology of Bi1-xSbx, though the calculated band dispersion dilates from that of experimental results.

Our work illustrates the possibility to tailor the basic topological properties of the surface via its crystallographic direction. Here it introduces a valley degree of freedom not previously achieved for topological insulator systems.

SS/NST-1-Or-2
STM Contrast Mechanisms on a Metal-Oxide Surface: Towards Chemically Selective Imaging by Controlling Tip Apex Chemistry

T13 Surface Science

#SS/NST-1-Or-2

M. Todorovic [1], H. Mönig [2], M.Z. Baykara [3], T.C. Schwendemann [4], L. Rodrigo [1], E.I. Altman [5], U.D. Schwarz [5], R. Pérez [1].

[1]Universidad Autónoma de Madrid - Madrid (Spain), [2]Westfälische Wilhelms-Universität Münster - Münster (Germany), [3]Bilkent University - Istanbul (Turkey), [4]Southern Connecticut State University - New Haven (United states), [5]Yale University - New Haven (United states).

Scanning tunnelling microscopy (STM) has emerged as a multidisciplinary tool in surface characterization. However, the interpretation of atomic scale image contrasts is not straightforward as the structure and chemistry of the probe tip influence the measurements to a large extent. In the present study on a model Cu(100)-O surface, we combine STM experiments with density-functional theory (DFT) and Non-Equilibrium Green's Function (NEGF) calculations [1] to investigate the role of tip apex chemistry in contrast formation mechanisms and understand how it may be exploited to achieve functional imaging.

At the outset, we systematically applied calculations to explore the STM imaging characteristics of Cu-O tips with different chemical terminations as a function of STM tip height and bias voltage. We were able to identify the imaging modes of tips terminating in a metal, non-metal and an intermediate adatom-contamination geometry and interpret them in terms of the contrasting tunnelling properties of Cu and O chemical species for a range of typical experimental parameters. Simulated imaging of a high-symmetry surface with asymmetric tip structures produced insight into asymmetric image features (fig. 1), STM image offsets and the imaging of surface domains on Cu(100)-O.

Based on these results, we conducted an extensive comparison of the computed

STM image database with the bank of experimental image. We found remarkable agreement, which validated the chosen tip models. Our simulations show that dynamic contamination of metallic tips on the Cu(100)-O surface is highly likely, leading to STM image offsets and varied asymmetry effects observed in experiments. O-terminated tips were particularly stable and frequently identified in experimental images: our simulations of their conducting properties show their imaging mode could be manipulated to selectively image metallic or non-metal surface species (fig. 1). By providing a comprehensive understanding of the STM contrast formation mechanisms, we suggest how controlled changes in tip apex chemistry could be employed to enhance the functionality of SPM probes, thus allowing in-depth, species-specific analysis of complex compounds.

[1] J. M. Blanco, F. Flores and R. Pérez, ”STM-theory: Image potential, chemistry and surface relaxation”, Prog. Surf. Sci. 81, 403, (2006).

Figure 1: STM contrast variation with CuO tip approach from 5.5Å to 4.0Å (V=+0.4V), shown alongside the Cu(100)-O surface schematic and the top view of the tip. STM contrast switches from imaging O atoms to asymmetrical imaging of Cu atoms due to tunnelling current contribution from the upper Cu tip atoms.

SS-P3-15
CO oxidation at nanoporous gold: a combined TPD and XPS study

T13 Surface Science

#SS-P3-15

V. Zielasek, S. Röhe, L. Moskaleva, A. Schaefer, A. Wittstock, M. Bäumer.

University of Bremen, Institute of Applied and Physical Chemistry - Bremen (Germany).

More than 25 years ago, the discovery of high catalytic activity of oxide-supported nanosized gold particles for CO oxidation [1] came as a surprise because the noblest of all metals has, above all, a low affinity towards molecular oxygen. The debate on basic mechanisms of oxygen supply in gold-catalyzed gas-phase oxidation reactions received new impetus when, more recently, it turned out that neither any support nor finely dispersed gold particles are required: unsupported nanoporous gold (np-Au) which has a sponge-like morphology consisting of interconnected ligaments with diameters typically on the order of some ten nanometers, is also an efficient catalyst for CO oxidation, even at room temperature and below [2].

In order to gain insight into the mechanisms and surface species relevant for the catalytic performance of np-Au, we employed temperature-programmed desorption (TPD) and x-ray photoemission spectroscopy (XPS) in ultra-high vacuum directly at np-Au samples which were produced by leaching of silver from AgAu alloy and then activated for CO oxidation in a continuous-flow reactor. The experiments, supported by DFT calculations, indicate that the catalytic activity of np-Au for CO oxidation is based on a complex interplay of gold, silver, CO, and several oxygen species on and within the surface.

Residual silver is crucial for the ability of np-Au to dissociate and chemisorb molecular oxygen, resulting in a presumably atomic oxygen species (O_{act}) at the surface available for CO oxidation. The initial activation step at elevated temperatures in the reactor is required to render the np-Au surface capable of O_2 dissociation, probably by uncovering silver sites at the surface. Pronounced CO and CO_2 desorption at temperatures above 200 K observed after exposing np-Au to CO at 105 K indicates an additional, more stable type of CO binding sites on np-Au as

compared to pure gold. Only CO at these binding sites is oxidized by O_{act}. DFT calculations demonstrate that the strong binding of CO to np-Au cannot be explained by the presence of silver residues. It can be conceived, however, that it is induced by the formation of O-Au-CO complexes at low-coordinated surface sites. In fact, besides silver and O_{act}, we find various resident oxygen species on and within the np-Au surface. Strongly bound oxygen, possibly at subsurface sites and stemming from the leaching process, is present as a major species and not consumed by CO oxidation. We propose that the presence of these resident oxygen species stabilizes CO adsorption on np-Au, thereby being as crucial for the observed catalytic activity of np-Au as residual silver.

[1] Haruta, M. K., T.; Sano, H.; Yamada, N. Chemistry Letters 1987, 16, 405.
[2] Zielasek, V.; Jürgens, B.; Schulz, C.; Biener, J.; Biener, M. M.; Hamza, A. V.; Bäumer, M. Angewandte Chemie 2006, 45, 8241.

NST/SS-1-Or-11
NITROGEN DOPING OF CARBON NANOMATERIALS MEASURED BY STM/STS

T13 Surface Science

#NST/SS-1-Or-11

J. Lagoute [1], Y. Tison [1], F. Joucken [2], H. Lin [1], V. Repain [1], C. Chacon [1], Y. Girard [1], H. Amara [3], F. Ducastelle [3], R. Sporken [2], A. Loiseau [3], L. Henrard [2], S. Rousset [1].

[1]MPQ, Université Paris Diderot - Paris (France), [2]PMR, Université de Namur - Namur (Belgium), [3]LEM, ONERA - Chatillon (France).

The tuning the electronic properties of low dimensional carbon materials is a current challenge for the development of carbon based technology. The doping by insertion of foreign atoms in the atomic lattice is a promising strategy to reach the control of the electronic structure of carbon materials. Nitrogen atoms are good candidates for chemical doping due to their suitable atomic radius and the additional electron that they contain as compared to carbon. They can adopt different local environments (graphitic-like, pyridinic-like) which can have various effects on the electronic structure [1].
Experimentally, the link between the local atomic structure and electronic properties can be achieved using scanning tunneling microscopy (STM) and spectroscopy (STS) by combining atomic scale imaging with local spectroscopy.
Using STM/STS operating in ultra high vacuum and at low temperature, we have investigated nitrogen doped graphene grown on SiC(000-1) and nitrogen doped carbon nanotubes. In doped graphene, substitutional nitrogen has been found to be the most common configuration observed characterized by a specific triangular pattern. The spatial distribution of the local density of states in high resolution images indicates a charge transfer between the nitrogen atom and its neighboring carbon atoms. Local spectroscopy reveals that doping induces a shift of the Dirac energy as expected for n-doping together with the formation of an additional localized state in the valence band [2]. This finding is in agreement with Density Functional Theory (DFT) calculations. Beside the observation of single substitutional nitrogen atoms, various other atomic configurations have been observed revealing different electronic properties that will be discussed.

These findings can were compared with nitrogen doped carbon nanotubes where substitutional nitrogen as well as more complex structures was observed. The electronic signature of these doping sites in nanotubes will also be discussed.

[1] B. Zheng, P. Hermet, L Henrard, ACS Nano, 7 4165 (2010)
[2] F. Joucken et al., Phys. Rev. B 85, 161408(R) (2012)

SS-7-Or-13
Photoluminescence of TiO2 - Effect of UV Light and Adsorbed Molecules on Surface Band Structure

T13 Surface Science

#SS-7-Or-13

A. Stevanovic, J.T. Yates, Jr..

University of Virginia - Charlottesville (United states).

The photoluminescence of powdered TiO_2 was found to be a sensitive indicator of the modification of the band structure[1-3]. It was found that upon continuous UV irradiation (3.88 eV) under high vacuum conditions, the degree of upward band bending of a reduced n-type TiO_2 surface gradually diminishes decreasing the depth of the depletion region and leading to more positive surface photovoltage and enhancement of PL intensity[3]. Also, the alteration of the surface potential of TiO_2 by adsorbates (electron acceptor and electron donor molecules) results in a change of the PL intensity as a result of the band bending effects. Reversible band bending, due to the adsorption/desorption of the electron donor NH_3 and CO molecules, has been observed in measurements which combine PL with FTIR surface spectroscopy[4]. In addition, it was found that O_2 acts in two ways- as a reversibly adsorbed electron acceptor molecule and as an irreversibly adsorbed molecule which heals natural oxygen defects in the near surface region[5-6].

(1) Anpo, M.; Chiba, K.; Tomonari, M.; Coluccia, S.; Che, M.; Fox, M. A.,Bulletin of the Chemical Society of Japan 1991, 64, 543.
(2) Patel, M.; Pu, C. J. J.; Sharpe, L. R., Langmuir 1995, 11, 2003.
(3) Stevanovic, A.; Buttner, M.; Zhang, Z.; Yates, J. T., Jr. Journal of the American Chemical Society 2012, 134, 324.
(4) Stevanovic, A.; Yates, J. T., Jr. Langmuir 2012, 28, 5652.
(5) Lira, E.; Hansen, J. O.; Huo, P.; Bechstein, R.; Galliker, P.; Laegsgaard, E.; Hammer, B.; Wendt, S.; Besenbacher, F., Surface Science 2010, 604, 1945.
(6) Scheiber, P.; Riss, A.; Schmid, M.; Varga, P.; Diebold, U., Physical Review Letters 2010, 105.

Work supported by the Army Research Office under grant number 55748CH.

SS-7-Or-8
STM studies of self-assembled C60 and C70 fullerenes on reconstructed SrTiO3 (111) surfaces

T13 Surface Science

#SS-7-Or-8

S. Rahman, C. Wu, M.R. Castell.

University of Oxford - Oxford (United kingdom).

Organic nanomaterials such as fullerenes provide a versatile synthetic base for a variety of applications in (opto)electronics [1]. In order to further exploit their properties there is a desire to arrange these molecules into particular ordered patterns [2, 3]. This is achieved through molecular self-assembly and organisation on surfaces with specific surface periodicities and chemical reactivity that can act as templates. We have used the polar (111) surface of $SrTiO_3$ for this purpose because it shows a variety of surface reconstructions [4]. The work presented here focuses on the self-assembly of C_{60} and C_{70} on the 5×5, 6×6 and 4×4 reconstructions of $SrTiO_3$ (111). We show that fullerenes produce epitaxial hexagonal packed monolayer structures with ordered vacancies on the 5×5 and 4×4 reconstructions. However, disordered islands with random orientations are observed on the 6×6 reconstruction. This demonstrates that the 6×6 reconstruction interacts less strongly with the fullerenes than the other reconstructions and hence indicates that the 6×6 surface is less reactive.

1. Maeyoshi, Y., et al., Fullerene nanowires as a versatile platform for organic electronics. Scientific Reports, 2012. **2**.
2. Li, G., et al., Self-assembly of C60 monolayer on epitaxially grown, nanostructured graphene on Ru(0001) surface. Applied Physics Letters, 2012. **100**(1): p. 013304.
3. Deak, D.S., Silly, F., Porfyrakis, K. and Castell, M.R., Template ordered open-grid arrays of paired endohedral fullerenes. Journal of the American Chemical Society, 2006. **128**(43): p. 13976-13977.
4. Russell, B.C. and Castell, M.R., Surface of sputtered and annealed polar $SrTiO_3$(111): TiO_x-rich (n × n) reconstructions. The Journal of Physical Chemistry C, 2008. **112**(16): p. 6538-6545.

SS-12-Or-4
Enantioselective separations on chiral metal surfaces

T13 Surface Science

#SS-12-Or-4

A. Gellman, Y. Yun.

Carnegie Mellon University - Pittsburgh (United states).

Although the bulk structure of pure metals are highly symmetric and achiral, various high Miller index surfaces of single crystal metals have chiral structures and have been shown to interact enantiospecifically with chiral adsorbates. [1] These surfaces have nanoscaled kinked step edges separating low Miller index terraces. These monoatomic step edges impart chirality to the overall structure of the surface and induce enantiospecific surface chemistry in chiral adsorbates. There are many demonstrations of this phenomenon originating in several laboratories around the world. One example is the enantiospecific adsorption of R-3-methylcyclohexanone on $Cu(hkl)^{R\&S}$ surfaces. [2,3] The adsorption energies of R-3-methylcyclohexanone adsorbed at R- and S-kinks are enantiospecific and the orientations of the molecule at the R and S kinks differ. Recently, we have observed highly enantioselective surface explosion reactions on naturally chiral Cu surfaces. It has been demonstrated that the decomposition of tartaric acid and aspartic acid on Cu surfaces occurs by an explosive mechanism with highly non-linear kinetics. The decomposition of tartaric acid on naturally chiral metals surfaces is more enantioselective than any previously observed process. The extremely high enantioselectivity arises from both the chirality of the substrate and the highly non-linear nature of the decomposition reaction kinetics. The naturally chiral Cu surfaces induce enantioselective separations of racemic mixtures of chiral species, thus enabling enantiomeric purification. The use of ^{13}C isotopic labeling of the L-aspartic acid has made possible to use mass spectrometry to discriminate between the two enantiomers. Exposure of $Cu(3,1,17)^{R\&S}$ surfaces to a racemic mixture of L-^{13}C-1,2-aspartic acid and D-aspartic acid results in establishment of an equilibrium with the surfaces that favors the adsorption of L-aspartic acid on $Cu(3,1,17)^{R}$ and D-aspartic acid on $Cu(3,1,17)^{S}$. This represents the first definitive demonstration of an enantioselective separation on a naturally chiral metal surface. [4]

1. C.F. McFadden, P.S. Cremer, A.J. Gellman, "The Adsorption of Chiral Alcohols on "Chiral" Metal Surfaces" Langmuir, 12(10), (1996), 2483-2487

2. J.D. Horvath, A.J. Gellman “Enantiospecific Desorption of Chiral Compounds from Chiral Cu(643) and Achiral Cu(111) Surfaces” J. Amer. Chem. Soc. 124(10), (2002), 2384-2392

3. J. Horvath, P. Kamakoti, A. Koritnik, D.S. Sholl, A.J. Gellman “Enantioselective Separation on a Naturally Chiral Surface” J. Amer. Chem. Soc. 126(45), (2004), 14988-14994

4. Y. Yun, A.J. Gellman, “Enantioselective separation of DL-aspartic acid on naturally chiral Cu(3,1,17)R&S surfaces” Angewandte Chemie International Edition, in press

SS-P1-14
The photoelectron and phonon interaction at the Cu(110) surface

T13 Surface Science

#SS-P1-14

E. Minamitani [1], R. Arafune [2], N. Takagi [3], M. Kawai [3], Y. Kim [1].

[1]Surface and Interface Science Laboratory, RIKEN - Saitama (Japan), [2]International Center for Materials Nanoarchitectonics, National Institute for Materials Science - Tsukuba (Japan), [3]Department of Advanced Materials Science, The University of Tokyo - Chiba (Japan).

Laser-photoemission spectroscopy (LPES) at metal surface with low-energy photons of ~ 5eV can probe vibrations at surfaces through the observation of photoelectrons inelastically scattered by the vibrations. The inelastic interaction produces a spectral component whose shape is a replica of the elastic one downshifted by the vibrational energy relative to the Fermi level. One of the examples is the observation of vibrational modes of adsorbed CO on Cu(001) [1]. These examples show the rich possibility of LPES as a novel probe of surface vibrations. However, the mechanism of the vibration excitation together with the selection rule is still an open question.

The simplest system in which the characteristic inelastic feature appears in LPES spectra is Cu(110) (Fig. 1 and ref. [2]). In order to gain the insight, we carried out the theoretical calculations for the electronic state and surface phonon modes on Cu(110) based on the density functional theory (DFT) and density functional perturbation theory (DFPT)[3]. From the calculation results of electronic and phonon band structure and electron-phonon coupling, we conclude that the source of inelastic feature on Cu(110) is the photoelectron-phonon interaction at $\bar{Y}$ point of surface Brillion zone. What is more, we found that the phonon modes which strongly coupled to photoelectron at $\bar{Y}$ point are distributed between subsurface and bulk region (Fig. 2). These results indicate the possibility of LPES as a novel technique to detect phonon at subsurface and deeper region.

[1] R. Arafune et al., Phys. Rev. Lett 95, 207601 (2005)
[2] R. Arafune et al., Phys. Rev. B 80, 073407 (2009)
[3] S. Baroni et al., Rev. Mod. Phys 73, 515 (2001)

Fig. 1 LPE spectra of clean Cu(110) surface. The inset shows the atomistic model corresponding to the sample surface.

Fig. 2 The dinsity of phonon for Cu(110) along - Γ direction projected on the first and second layers for share-vertical (SV), shear-horizontal (SH), and longitudinal (L) polarizations.

SS-15-Or-6
Electrical conductance through surface states with large Rashba-type spin splitting

T13 Surface Science

#SS-15-Or-6

S. Hatta, T. Noma, H. Okuyama, T. Aruga.

Department of Chemistry, Kyoto University - Kyoto (Japan).

Strong spin-orbit interaction (SOI) and relevant spin splitting of valence bands have drawn much attention due to its potential application in spintronics. For the Rashba SOI, the coupling of spin polarization and electric field or charge current is one of the most important problems in association with the creation of spin-polarized current. In recent years, large spin splitting (>100 meV, typically) was discovered on several semiconductor surfaces including heavy elements and ascribed to the Rashba-type SOI enhanced by the coupling of atomic SOI and inversion asymmetry at surfaces. Although the Rashba type of spin splitting is also realized in an asymmetric potential well of a semiconductor heterostructure, typical splitting is only about ten meV at the Fermi level (E_F), which would be easily obscured by thermal excitations. From this point of view, surfaces with large spin splitting have an advantageous for studying the effect of Rashba SOI to electron transport properties if one can distinguish the contributions of a surface and a substrate to electrical conductance.

In this work, we performed four-point-probe conductivity measurements of Ge(111) covered with Pb and Bi. The Pb/Ge(111)-β-($\sqrt{3}\times\sqrt{3}$)*R*30° surface (called Pb-$\sqrt{3}$) has a metallic surface state[1]. The surface state displays a nearly parabolic dispersion relation with Rashba-type spin splitting of 200 meV at E_F. The Fermi surfaces are composed of dual closed Fermi surfaces with reversed in-plane spin polarization. On the other hand, the electronic structure of Bi/Ge(111)-($\sqrt{3}\times\sqrt{3}$)*R*30° (called Bi-$\sqrt{3}$) is insulating[2]. The temperature dependence of conductivity on Bi-$\sqrt{3}$ showed two drops at ~300 and ~50 K. This behavior is explained by the decrease of intrinsic carriers and electrons from the donor levels in the Ge substrate (*n*-type). As a result, we found that the conductivity through the substrate is quite small (<0.5 mS/□)

below 50 K. On the other hand, the conductivity of Pb-$\sqrt{3}$ continuously rose with decrease in temperature below 250 K and reached ~10 mS/□ at 9 K. In the temperature range, the linear temperature dependence of resistivity was observed. Assuming that the metallic state is confined between the Pb and the topmost Ge layers, the volume conductivity of the Pb monolayer corresponds to 3 μΩ·cm. Surprisingly, the conductivity is comparable to those of noble metals, indicating that the injection of spin-polarized current to the Rashba system is possible without conductivity mismatch.

[1] K. Yaji et al., Nat. Comm. 1, 17 (2010).

[2] S. Hatta, et al., Phys. Rev. B 80, 113309 (2009).

SS-17-Or-6
Kondo resonance and inelastic tunneling spectroscopy on individual TCNQ molecules deposited on nanostructure graphene

T13 Surface Science

#SS-17-Or-6

M. Garnica [1], D. Stradi [2], F. Calleja [3], S. Barja [1], C. Díaz [4], M. Alcamí [4], N. Martín [5], A. Vázquez De Parga [1], F. Martín [2], R. Miranda [1].

[1]Dep. Física de la Materia Condensada, Universidad Autónoma de Madrid. Instituto Madrileño de Estudios Avanzados en Nanociencia (IMDEA-Nanociencia) - Madrid (Spain), [2]Dep. de Química, Universidad Autónoma de Madrid. Instituto Madrileño de Estudios Avanzados en Nanociencia (IMDEA-Nanociencia) - Madrid (Spain), [3]Instituto Madrileño de Estudios Avanzados en Nanociencia (IMDEA-Nanociencia) - Madrid (Spain), [4]Dep. de Química, Universidad Autónoma de Madrid. - Madrid (Spain), [5]Facultad. de Química, Universidad Complutense de Madrid. Instituto Madrileño de Estudios Avanzados en Nanociencia (IMDEA-Nanociencia) - Madrid (Spain).

The TCNQ molecules are deposited on graphene/Ru(0001) at 300 K and imaged with STM at 4.6 K. The adsorption geometry and the electronic structure of isolated molecules have been calculated from first principles by using density functional theory (DFT) as implemented in the VASP code and accounts for the properties of graphene/Ru(0001)[1,2,3,4]. The lower part of the moiré constitutes a preferential adsorption site for strong acceptors and the topographic images show intramolecular resolution that changes with the bias voltage applied between tip and sample (Fig.1a).
The calculations for individual TCNQ molecules reveal indeed that graphene, which is n-doped from the interaction with the Ru substrate, transfers efficiently electrons to TCNQ, while the Ru substrate is essentially unaffected. Tthe additional electron mainly goes into the LUMO of the neutral molecule, which splits into a Single Occupied Molecular Orbital (SOMO) and a Single Unoccupied Molecular Orbital (SUMO). dI/dV spectroscopy at the level of single molecule allows us to identify the maximum of the HOMO at -2.0 V and provides an unequivocal confirmation of the

existence of an occupied SOMO orbital around -0.8 V. Spatially-resolved dI/dV maps of the HOMO does not show a node in the central plane of the molecules, while both the SOMO and the SUMO are practically identical and display clearly the characteristic central node, indicating that they originate from the same, previously empty LUMO orbital.

The STS spectra measured on top of the TCNQ molecules reveal the existence of a sharp resonance centered at the Fermi level with a width at half maximum of 10 mV, which is absent in the graphene surface. As shown in Fig.1b,c, the Kondo resonance exhibits also a strong dependence of its lineshape on the STM tip location within the TCNQ molecules. Fig.1c shows dI/dV spectra measured on different locations of the TCNQ molecule and on graphene. A sharp peak at zero bias is observed when the STM tip is located on top of the cyano groups (spectra 2) or on top of the carbon atoms a both ends of the central ring connecting the cyano groups (spectra 4). When the tip is moved to the middle of the central ring (spectra 3) the intensity of the Kondo resonance decreases and simultaneously two side peaks appear at ±45 meV attributed to an inelastic Kondo effect mediated by vibron-assisted tunneling.

[1] A.L. Vázquez de Parga et al. Phys. Rev. Lett. 100, 056807 (2008)
[2] B. Borca et al. Phys. Rev. Lett. 105, 036804 (2010)
[3] D. Stradi et al, Phys. Rev. Lett. 106, 186102 (2010)
[4] D. Stradi et al. Phys. Rev. B 85, 121404 (2012)

Figure 1

SS-P3-16
CHARACTERIZATION AND REACTIVITY IN PROPENE OXIDATION OF H3+xPMo12−xVxO40 HETEROPOLYACIDS SUPPORTED ON MESOPOROUS SBA-15

T13 Surface Science

#SS-P3-16

C. Rabia [1], S. Benadji [1], E.M. Gaigneaux [2], P. Eloy [2], A. Leonard [3], B.L. Su [4].

[1]USTHB - Alger (Algeria), [2]UCL - Louvain-La-Neuve (Belgium), [3]ULG - Liège (Belgium), [4]FUNDP - Namur (Belgium).

In Keggin type phosphovanadomolybdate acids (HPAs), vanadium appeared to be the most crucial element for oxidative processes and the strong acidity of HPAs is known to be favourable to functionalization of alkanes [1]. However, the major drawback of this type of materials is their low surface area (< 10 m2/g). This disadvantage can be bypassed by supporting them on suitable materials with large surface area.

The mesoporous silicates such as MCM-41, HMS and SBA-15 are known to have large surface area and high pore volume with uniform mesopores and high thermal stability [2,3]. Among them, the most studied is MCM-41.

In this work, we selected SBA-15 mesoporous silicate, for its larger pore size and its better resistance to acidic media than MCM-41, as support. Thus, a series of Keggin-type heteropolyacids, H3+xPMo12−xVxO40.nH2O where x = 0, 1, 2 or 3 were supported on SBA-15 with HPA loadings of 30 wt.% using the dry impregnation method. All systems were characterized by different techniques (elemental analysis, X-ray diffraction, transmission and diffuse reflectance (DR) FT-IR, Raman and X-ray photoelectron spectroscopies, nitrogen physisorption, thermal analysis (TG−DTA) and scanning electron microscopy (SEM)). The catalytic properties of supported HPAs were compared to those of bulk ones in the propene oxidation by molecular

oxygen at 350 °C.

The obtained results showed that the presence of HPAs modifies the textural properties of mesoporous SBA-15 material (decrease of surface area) without destroying its structure. The interaction support−heteropolyacid leads to the formation of (≡SiOH2+)(H2+xPMo12−xVxO40−) surface species (Scheme 1) more stable than H3+xPMo12−xVxO40 species. These surface species appear to be the active sites in the propene oxidation. The supported HPAs exhibit higher catalytic activity (ca. 21−31% of propene conversion) and favoured the formation of acrolein, acetaldehyde and acetic acid, compared to the bulk catalysts (< 5% of conversion) that lead only to the formation of COx. It is noted that the distribution of products seems to be independent on the vanadium number in the acid.

[1] A. Predoeva, S. Damyanova, E.M. Gaigneaux, L. Petrov, App. Cat. A 319 (2007) 14.
[2] G. Satish Kumar, M. Vishnuvarthan, M. Palanichamy, V. Murugesan, J. Mol. Cat. A 260 (2006) 49.
[3] S. Benadji, P. Eloy, A. Léonard, B.L. Su, K. Bachari, C. Rabia, E.M.Gaigneaux, Micropor. Mesopor. Mat. 130 (2010) 103.

Scheme 1: (≡SiOH2+)(H2+xPMo12−xVxO40−) surface species

SS-6-Or-3
Highly Organized Semifluorinated Alkane Monolayer

T13 Surface Science

#SS-6-Or-3

P. Fontaine [1], M.C. Fauré [2], M. Goldmann [2].

[1]Synchrotron SOLEIL - Saint Aubin (France), [2]INSP - Paris (France).

Semifluorinated alkanes ($C_nF_{2n+1}C_mH_{2m+1}$, FnHm for short) exhibit a lipophobic and an hydrophobic character inducing interesting properties[1]. Despite the lack of polar head group these molecules are able to form Langmuir monolayers ie. monomolecular thick layer at the air-water interface. Due to these antagonist characters the two parts (fluorinated and hydrogenated) tend to avoid each other. Using Grazing Incidence Small Angle X-ray Scattering (GISAXS - see figure 1), we demonstrated that these molecules on liquid surface self assemble to form an hexagonal array of nano-domains with a very large parameter (typ. 30 nm) [2]. This network is observed on water for non zero surface pressure for different hydrocarbon chain length (n=8, 10, m=14, 16, 18, 20)[3].
This structure is in agreement with the domain size observed by Atomic Force Microscopy (AFM) on the same kind of monolayers prepared on silicon substrate [4]. However, the reason of the stability of such domains remains unknown. On high-resolution AFM images, the shape of domains is revealed as facetted domains separated by a hump. Experimentally, macroscopic measurement combined with grazing incidence small (GISAXS) and wide (GIXD) angle x-ray scattering suggest that some molecule within the monolayer do not belong to the domains made of upright molecules. Looking more carefully to the GISAXS off specular (Qxy-Qz) intensity distribution of the diffraction peaks seems to confirm the presence around the upright molecules domains of a corona of lying molecules. Theoretical paper has predicted the possibility of such lying molecules on the surface of water. The presence of molecule in such state could explain the stability of the structure against coalescence of the domains upon compression of the monolayer.

[1] P. Lo Nostro, , Cur. Op. Colloid and Interf. Sci. 8, (2003) 223.
[2] P. Fontaine, M. Goldmann, P. Muller, M.C. Fauré, O. Konovalov, M.P. Krafft, J.

Am. Chem. Soc. 127, (2005) 512.
[3] L. Bardin, M.-C. Fauré, D. Limagne, C. Chevallard, O. Konovalov, E. J. M. Filipe, G. Waton, M.-P. Krafft, M. Goldmann, P. Fontaine, Langmuir, 27, (2011) 13497-13505
[4] L. Bardin, M.-C. Fauré, E. J. M. Filipe, P. Fontaine, M. Goldmann, Thin Solid Films 519 (2010) 414–416
[5] N. Semenov, A. Gonzalez-Perez, M.-P. Krafft, J.F. Legrand, ``Theory of Surface Micelles of Semifluorinated Alkanes'', Langmuir, 22, (2006) 8706.

Qz integrated GISAXS spectra of a F8H18 monolayer measured on the water surface showing 12 diffraction
peaks corresponding to a 2D hexagonal structure of parameter 33.5nm

SS-17-Or-1
Charging and Bond formation of Adsorbates on Ultrathin, Insulating Films Supported by a Metal Substrate : A DFT Study based on a Perfect Conductor Model

T13 Surface Science

#SS-17-Or-1

M. Persson, I. Scivetti.

University of Liverpool - Liverpool (United kingdom).

The ability to characterise and manipulate single atoms and molecules on ultrathin, insulating films by scanning probe techniques has opened up a new frontier in atomic scale science. A most interesting aspect of these systems is the decoupling of the electronic states of the adsorbates from the metal substrate, which still allows for characterisation and manipulation by tunnelling electrons.
The description of the electronic and geometric structure and the dynamics of these systems exhibiting multiple charge states is very challenging for theory [1]. Density functional theory calculations are in many cases prohibitive because of the size of these systems and the delocalization error in current exchange-correlation functionals. In this presentation, we present a new, simplified DFT scheme in which the metallic support is replaced by a perfect conductor. This scheme circumvents these problems and allows us to treat various charge states of adsorbates in a controllable way, together with a considerable reduction of the computational effort. In particular, we are able to carry out ab-initio molecular dynamics on an excited state potential energy surface. We will show some interesting applications of this scheme to different charge states of metal adatoms and the dynamics of reversible bond formation in a metallo-organic molecule [2,3].

[1] J. Repp, et al., Science 305, 493 (2004).

[2] F. Mohn et. al., Phys. Rev. Letter 105, 266102 (2010).

[3] T. Leoni, et al., Phys. Rev. Lett. 106, 216103 (2011).

SS-P3-26
Pure dephasing rate on image state of Cu(001) investigated by high-energy resolution two-photon photoemission

T13 Surface Science

#SS-P3-26

T. Nakazawa [1], R. Arafune [2], N. Takagi [1], M. Kawai [1].

[1]The University of Tokyo - Kashiwa (Japan), [2]National Institute for Materials Sciences - Tsukuba (Japan).

Electron dynamics in the photoexcited states are governed by inelastic scattering and elastic scattering processes. The contribution of the inelastic scattering to the electron lifetime is characterized by the decay rate, and the latter the so-called pure dephasing rate. For complete understanding of the electron dynamics, both of them are needed. As a model system, image potential induced states are intensively studied by two-photon photoemission (2PPE) spectroscopy[1]. Time-resolved 2PPE can evaluate the decay rate and related technique (quautum beat spectroscopy) can evaluate the pure dephasing rate. However, quantum beat spectroscopy is applicable for limited cases. More general way to determine the dephasing rate is linewidth analysis. Since quasielastic scattering alters the relative phase of the wave packets, the decoherence appears as spectral broadening. Spectral linewidth (defined by the full width at half maximum: FWHM) in 2PPE spectra is described as $\Gamma_{total}=\Gamma_{decay\ rate}+2\Gamma_{dephasing\ rate}$[2]. In conventional 2PPE, ultrashort pulse (20-200 fs) lasers are used for the excitation source. Since contribution of quasielastic scattering is small as compared to the inelastic scattering and $\Gamma_{inelastic}$ is comparable with the linewidth of the fs laser pulse, it is difficult to discuss the linewidth from 2PPE spectra excited by the fs laser.

To investigate the effect of the pure dephaing on the electron lifetime in the excited states, we have improved energy-resolution of 2PPE by using relatively narrower band pulse (ΔE~1 meV, Δt~2 ps) laser for the excitation. Figure 1 shows 2PPE spectrum of image potential states of the Cu(001) at normal emission. The energy resolution was set at better than 10 meV. Higher series of image states are well separated up to n=4. Femtosecond 2PPE cannot resolve these peaks spectroscopically. From analytical approach, we reveals that the broad peak near the vacuum level consists of n=5, 6, and 7 at least. From these high-resolution results, we have succeeded in measuring the pure dephasing rate for the n=1 image states.

[1]U. Höfer et al., Science 277, 1480 (1997).
[2] K. Boger et al., New J. Phys. 7, 110 (2005).

Fig.1 2PPE spectra of image potential states of Cu(001).

NST/SS-3-Or-4
Manipulating Magnetism of the Co Ultrathin Films on Epitaxial Graphene by Au Decoration

T13 Surface Science

#NST/SS-3-Or-4

C. Kuo, Y.J. Chan, S.Y. Wu, D.H. Wei.

National Sun Yat-sen University - Kaohsiung (Taiwan, republic of china).

The issue on tailoring magnetism of transition metals on graphene become of the significance in the past years. The perfect spin filtering effect at the interface between magnetic ultrathin film and graphene layers was theoretically predicted. It can be used to optimize the spin injection for the development of spintronics devices. Nevertheless, the suppression of ferromagnetism of the magnetic ultrathin film grown on graphite or graphene surface and lower than expected MR ratio was observed in experiments. These imply that the magnetic films prepared on graphene might not be ideal as expectation, and suppress the spin polarization at the interface. Here we inserted a submonolayer Au on the epitaxial graphene before the film preparation. Integration of experiments were conducted, including X-ray magnetic circular dichroism, X-ray absorption spectroscopy, scanning tunneling microscopy, low energy electron diffraction, and Auger electron spectroscopy, to measure the magnetism, thin films structures and the hybridization of the magnetic thin film and graphene. An enhanced ferromagnetism of Co ultrathin film were observed on the Au/graphene surface as compared to the Co/graphene system. A further discussion will also be addressed in this contribution.

SS-6-Or-4
Investigation of wetting phenomena at the limit of small-scale surface topography in the sub-nanometer regime

T13 Surface Science

#SS-6-Or-4

J. Knauf [1], L. Reddemann [2], A. Böker [3], K. Reihs [4].

[1]Advanced Molecular Films GmbH, DWI an der RWTH Aachen e.V., Lehrstuhl für Makromolekulare Materialien und Oberflächen, RWTH Aachen University - Köln (Germany), [2]Advanced Molecular Films GmbH, Universität zu Köln, II. Physikalisches Institut - Köln (Germany), [3]DWI an der RWTH Aachen e.V., Lehrstuhl für Makromolekulare Materialien und Oberflächen, RWTH Aachen University - Aachen (Germany), [4]Advanced Molecular Films GmbH - Köln (Germany).

Surfaces with defined wetting properties allow for a broad variety of interesting applications in various technical areas. Surface design and manufacture, however, require detailed understanding of fundamental aspects of wetting at the solid/liquid interface which can be strongly affected by topographic features at the surface. We are primarily interested in such effects at the limit of small-scale surface topography with structures in the sub-nanometer range. Such topography shows wetting effects that behave much differently compared to surface topography at longer length-scales.

As a model system we prepare surfaces of hydrophobic monolayers from binary mixtures of *1H,1H,2H,2H*-perfluoroalkyl thiols of different chain lengths on gold. Detailed characterization by static secondary ion mass spectrometry and ellipsometry confirm a binary monolayer of randomly mixed constituents. Owing to their stiff helical conformation such perfluoroalkyl chains create topographic features of well-characterized sub-nanometer dimensions. As a result, we obtain surface topographies of randomly distributed long and short chains of a defined height difference of 1.2 Å per CF_2 group and a next neighbor distance of 5.8 Å.

We present comprehensive investigations of wetting properties of such binary

monolayers of various molar fractions and chain length differences.

As a first example, a binary mixed monolayer from *1H,1H,2H,2H*-perfluorodecyl and *1H,1H,2H,2H*-perfluorododecyl thiols, thus differing by two CF_2 groups, increases the advancing water contact angle from 116.0° for either one of the single component monolayer by about 2° to 117.7° for a surface of an equimolar composition of the two constituents. Such increase is considerably less than expected from simple thermodynamic models. Wenzel´s equation of wetting on rough surfaces predicts an advancing angle difference of 7°. Longer chain length differences thus yielding larger but still sub-nanometer-size features display correspondingly larger deviations from thermodynamic theory. We propose to explain these deviations by an apparent effective reduction of surface energy at short length scales, similar to results obtained from grazing-incidence X-ray scattering experiments [1]. Results of contact angles on various sub-nanometer size topographies will be presented and discussed, using probing liquids with different molecular structures and interactions.

[1] S. Mora et al., Phys. Rev. Lett. **90**, 216101 (2003)

SS-P1-05
Angle-resolved inelastic photoelectron spectroscopy of CO/Cu(001)

T13 Surface Science

#SS-P1-05

K. Morita [1], R. Arafune [2], T. Nakazawa [1], N. Takagi [1], M. Kawai [1].

[1]Department of Advanced Materials Science, The University of Tokyo - Kashiwa (Japan), [2]National Institute for Materials Science - Tsukuba (Japan).

In the conventional photoelectron spectroscopy, the photoelectron emitted from a surface have a spectrum that is the convolution of the density of states with the Fermi-Dirac distribution function. Hence the photoelectron spectra have been assumed to arise exclusively from the photoelectrons emitted elastically. However, if we consider the process of photoemission carefully, it becomes clear that the photoelectrons should excite vibrations at the surface and lose their energy when they go across it. Indeed, we found inelastic components arising from the excitation of the surface adsorbate vibrations and the substrate phonon in the laser photoelectron spectra [1-3]. The inelastic photoemission process produces a spectral component whose shape is a replica of the elastic component down-shifted by the vibration energy.

To develop a novel vibrational spectroscopic technique based on this inelastic phenomena and to gain a deeper understanding of the process, we have measured the inelastic photoemission spectra of the CO covered Cu(001) surface. For this purpose, we have constructed a laser-based photoelectron spectroscopy system equipped with a two-dimensional CCD camera detector. At normal emission (θ=0), the photoelectron spectra excited by the low energy laser photon (hv=4.80 eV, T=7.6 K) contain the inelastic structures arising from the excitation of the frustrated translational (FT) and frustrated rotation (FR) mode. Since the energy shift for the FT mode (i.e. the vibrational energy) is low (~ 5 meV), we cannot measure its angle dependence. On the contrary, the inelastic component for the FR mode shows a very small but systematic dependence on the emission angle (~ -1meV/7 degree). We conclude that this angle dependence of the inelastic component originates from the phonon dispersion of the FR mode. These results demonstrate that the angle resolved inelastic photoemission spectroscopy is a useful tool for measuring the dispersion relation of the low-energy vibrational mode.

[1]R. Arafune et al., Phys. Rev. Lett, 95, 207601 (2005).

[2]R.Arafune et al., Surf. Sci. 600, 3536 (2006).

[3]R. Arafune et al., Phys. Rev. B. 80, 073407 (2009).

SS-13-Or-3
Side-by-side close coupling of Perylene-tetra-carboxylic-di-imide on the rutile TiO2(110) surface.

T13 Surface Science

#SS-13-Or-3

L. Floreano [1], G. Lovat [1], G. Otero [2], V. Lanzilotto [1], G. Bavdek [3], L. Sanchez [2], M.F. López [2], J. Méndez [2], J. Martin Gago [2].

[1]CNR-IOM - Trieste (Italy), [2]ICMM-CSIC - Madrid (Spain), [3]Univ. Ljubljana - Ljubljana (Slovenia).

Perylene di-imides are n-type compounds that recently demonstrated improved charge transport capabilities also in ambient conditions,[1] thus filling the historical gap with the p-type counterparts (e.g. pentacene). We present a detailed structural study on the adsorption of PTCDI on the TiO_2(110)-(1x1) surface revealing how its adorption geometry is quite similar to the planar phases reported for the acenes, [2] notwithstanding a much different mechanism of growth.
PTCDI domain formation proceeds via island growth due to a significant interaction with the substrate, which pins the molecules into a unique structural arrangement that is commensurate with the substrate. By polarization dependent NEXAFS, we observe that molecules adsorb with their long axis parallel to the [001] direction, tilted by an angle of ~35°, and with negligible distortion of the carbon backbone. According to STM measurements, the molecular tilting allows to accomodate side-by-side one molecule atop each O_{br} row, yielding closely coupled molecular domains. From comparison with surface diffraction (He scattering and RHEED), domains are found to display a (1x5) symmetry, which molecular structure (see picture) is much more compact than the (2x6) monolayer phase recently reported for PTCDA.[3] The geometry we found is quite uncommon for perylenes, where the molecular orientation in the surface phases is rather driven by intermolecular H-bonding and leads to the renown canted, domino and brickwall phases.[4] The interaction with the susbstrate is large enough to overcome the intermolecular head-head repulsion and to keep PTCDI straightly parallel to the O_{br} rows. The PTCDI orientation of the (1x5) phase is equivalent to that of pentacene in the monolayer phase [2], which is rather driven by an interplay between side-by-side intermolecular attraction and head-to-head intermolecular repulsion. The resulting close molecular packing (>1 molecule/nm2)

and π-π overlap is expected to enhance the intermolecular transport and to hamper the interdiffusion of atmospheric gases, thus improving the environmental stability of the organic film.[1]

[1] B.A. Jones et al. *Effects of Arylene Diimide Thin Film Growth Conditions on n-Channel OFET Performance*, **Adv. Funct. Mater.** 18, (2008) 1329–1339.

[2] V. Lanzilotto et al. *Planar Growth of Pentacene on the Dielectric TiO2(110) Surface*, **J. Phys. Chem. C**, 115 (2011) 4664

[3] S. Godlewski et al. *Supramolecular Ordering of PTCDA Molecules*, **ACS Nano**, 10 (2012) 8536.

[4] M. Mura et al. *H-Bonding Supramolecular Assemblies of PTCDI Molecules on the Au(111) Surface*, **J. Phys. Chem. C**, 113 (2009) 21840.

SS-P1-15
Measurement of hydrogen permeability of stainless steel membrane by ESD ion mapping

T13 Surface Science

#SS-P1-15

A. Itakura [1], M. Tosa [1], Y. Murase [1], S. Suzuki [2], S. Takagi [2], T. Gotoh [2].

[1]National Institute for Materials Science - Tsukuba (Japan), [2]Toho university - Funabashi (Japan).

We are looking for a new clean energy in Japan such as wind, solar cells, biomass energy, geothermal energy, etc. Hydrogen fuel would be one of the biggest energy resources. Hydrogen in metals causes hydrogen embrittlement, which is the process for various metals to become brittle and crack [1)] . Presently this phenomenon is not completely understood and hydrogen detection, in particular, seems to be one of the most difficult aspects of the problem. In this study we try to investigate hydrogen behavior in metal from observation of two-dimensional hydrogen concentration on metal surface using electron stimulated desorption (ESD) method [2)] . ESD is one of surface analysis technique used an excitation of adsorbed atoms or molecules by electrons. Using a scanning electron beam it is possible to map a two dimensional distribution of adsorbed atom. From the ESD mapping, we can know where the hydrogen comes from, e.g. surface of grains or grain boundaries. The experiment is performed with the good spatial resolution of a scanning electron microscope (SEM). A hydrogen reservoir with a sample and a heater, which is a halogen bulb, is set in the sample chamber of the SEM. Hydrogen gas is supplied to the reservoir up to about 1 atm. Preliminarily SUS304 steel is used as the sample, which thickness of 300μm and diameter of 18mm. The surface has ring shape lines made by lathe when the sample surface was flattened. The sample is welded to a miniature flange in order to suppress to leakage of hydrogen especially under sample heating. The sample can be heated up to 300 C. Hydrogen penetrates from the reservoir side surface of the sample membrane to the UHV side surface through a sample material. The penetrated hydrogen on the surface is detected as an ESD ion by a channel electron multiplier. From comparison of ESD image to the secondary electron image, the position of hydrogen is determined accurately. Since ion yield by the ESD is relative to a hydrogen concentration on the surface, information of diffusion coefficient is estimated from time dependence of ion yield under constant

temperature. In present work each ion image is taken for 400 s to one photograph. Image processing and ion counting are performed by Photoshop.
In ESD image, we detected ring like patterns with the same pitch, 40 micro meters, with lathe made pattern. Consider the lathe moving when it made the pattern on surface, one side of the valley slope has a stress under higher pressure than other slope. Bright ring which is area of higher number of ESD ions were from the area. SUS304 steel is an alloy of Fe, Cr and Ni and formed austenite structure. Under the stress, martensite structure formed in austenite, and which has higher permeability of hydrogen compare with austenite area.

1) T.Tsuchiyama,Hidenori Takebe,Koichi Tuboi and Setsuo Takaki :Scripta Materialia, 62 (2010) 731-734.

2) D.P.Woodruff and T.A. Delchar: "Modern thechniques of surface science" p.299 (Cambridge, 1986)

SS-P3-06
Tetra-aminophenyl porphyrin (TAPP) deposited on Au(111): molecular conformation and electronic properties

T13 Surface Science

#SS-P3-06

L. Giovanelli [1], H.L. Lee [2], C. Lacaze-Dufaure [3], S. Clair [1], M. Koudia [1], M. Abel [1], L. Porte [1], A.A. Cafolla [2], J.M. Themlin [1].

[1]Aix-Marseille Université, IM2NP-CNRS - Marseille (France), [2]School of Physical Sciences, Dublin City University - Dublin (Ireland), [3]Université de Toulouse, INPT, CIRIMAT UMR CNRS 5085, ENSIACET - Tououse (France).

The structure and electronic properties of the contact layer between a π-conjugated organic semiconductor and a metal substrate are of great importance for the performances of opto-electronic devices based on organic thin films. Bonding strength to the substrate as well as the alignment of the electronic levels can be controlled by tuning the interface interaction [1]. Recent studies have shown that the nature of molecule-substrate bonding can influence the growth mode even in the sub-monolayer (ML) regime [2]. Very interestingly the nature of the interface bond does also influence the intra-molecular forces which can have a repulsive term in addition to the usual attractive van-der-Waals interaction [2,3].
The present paper focuses on the effects of molecular conformation on the electronic and supramolecular structures as a function of coverage of the first adsorbed ML. The system under investigation is 5,10,15,20- tetrakis(4 aminophenyl)porphyrin (TAPP) deposited in UHV on Au(111). Employing different techniques such as STM, LEED, UPS and combining the experimental results with theoretical analysis of the molecular orbitals (quantum calculation, Gaussian03 package), the growth of the overlayer was studied from sub-ML coverage to a thick film. The sub-ML coverage is characterized by a 2D gas-phase that condensates close to a ML completion. The features of the UPS spectra of the thick film (4 ML) were interpreted with the help of density of states (DOS) issued from quantum calculations. Two well separated features are present at low binding energy (BE) corresponding to HOMO and HOMO-1. Surprisingly, at sub-ML coverage only one feature is present at low BE. Such spectroscopic feature is related to a conformational change with respect to the relaxed geometry of the free molecule where the phenyl moieties are oriented at 62º

w.r.t. the molecular plane. Indeed, by constraining the four phenyls to lie parallel to the macrocycle plane, the calculated DOS reveals that the HOMO-1 has now shifted towards higher BE. At the completion of the first ML two features become clearly visible at low BE in the UPS spectrum. It is thus clear that a conformational change accompanies the transition to the condensed phase: the phenyls bend back in their relaxed orientation, most probably to accommodate further molecules within the contact layer thereby reducing the total energy. Finally, the behavior of the work function as a function of coverage was also addressed.
In conclusion, these results show that the initial molecular conformation, perturbed by the molecular-substrate interaction, recovers through inter-molecular interactions close to the full-monolayer coverage, allowing a higher stacking density. Furthermore, UPS reveals that such behavior has important consequences on the value of the hole-injection barrier at the metal-molecule interface.

[1] N. Koch, Phys. Status Solidi RRL 6, 277 (2012)
[2] C. Stadler et al. Nature Physics 5,153 (2009)
[3] I. Kröger et al. New J. of Physics 12, 083038 (2010); B. Stadtmüller et al. Phys. Rev. B 83, 85416 (2011); I. Kröger et al. Phys. Rev. B 86, 195412 (2012)

NST/SS-P1-22
Cobalt-Iridium interface - new player in the graphene mediated magnetism

T13 Surface Science

#NST/SS-P1-22

J. Drnec [1], J. Gonzalez [2], H. Isern [1], N. Rougemaille [3], J. Coraux [3], R. Felici [1].

[1]ESRF - Grenoble (France), [2]Universite de Strasbourg - Strasbourg (France), [3]CNRS - Grenoble (France).

Graphene, as the first 2D crystalline material, carries many promises to be the next candidate which could result in a new technical revolution [1]. Literally, every day we see progress in using this new "wonder" material in many applications. A recent interest, amongst others, is in its stabilizing properties of ultra-thin magnetic layers [2]. However, during the preparation process, the sample must be heated to elevated temperatures in order to intercalate Co deposited on top of graphene/Ir surface. The interface between Co and Ir might also change as a result of preparation and induce synergistic effects in the overall behaviour of such a system. In this work, we focus on the Co/Ir interface, rather than the graphene/Co interface, and we study possible effects of elevated temperature on this interface. The studied layers differ in intercalation temperature, the thickness of deposited Co, and the presence of the graphene layer.
The samples are prepared in a UHV environment and studied by LEED, ARXPS and SMOKE techniques. Depending on the Co layer thickness (calibrated by XPS), we find two magnetic transitions. At Co coverage of 4 ML we observe a first transition between no magnetization and vertical magnetic anisotropy. At about 8 ML the layer switches between vertical and horizontal magnetic anisotropy. When the coverage is at the critical value of 4 ML and the layer is heated to 500 °C, the magnetic behavior changes as a result of heating and the magnetization curve corresponding to applied perpendicular magnetic field becomes wider. We hypothesize that this is due to the formation of surface alloy on Co/Ir interface. Angle resolved XPS measurements support this conclusion as the Co/Ir peak intensity ratio decreases when the sample is annealed and the decrease is dependent on the photoelectron exit angle. Two processes can cause this effect: surface roughening or Co/Ir surface alloy formation where Co intermixes with the first few monolayers of Ir substrate. This first option is ruled out by LEED measurement, where we observe clear sharpening of the

diffraction spots, indicating a sign of a smooth surface.
The same set of experiment was repeated with graphene/iridium surface. We observe the same behavior after the Co intercalation at 500 °C: surface alloy formation and changes in magnetic response. However, it is clear that graphene has some further effect on magnetization of the layer, the second transition between in-plane and out-of-plane magnetic anisotropy is less sharp, and both magnetic anisotropies are observed simultaneously within larger Co thicknesses.
Our results show that not only the presence of graphene determines the magnetic properties of ultra-thin Co layers but also that the Co/Ir interface plays an important role. A good knowledge of this interface effects is vital to properly understand the role of the graphene in such magnetic systems.

[1] K.S. Novoselov, *Nature,* 490 (2012) 192

[2] N. Rougemaille, *Applied Physics Letters*, 101 (2012) 142403

SS-18-Or-14
Electron Scattering Study of Dehydrogenation on Platinum Nanoparticles with Oxide Support

T13 Surface Science

#SS-18-Or-14

M. Van Spyk, K. Perrine, J.C. Hemminger.

University of California, Irvine - Irvine (United states).

Catalytic activity can be impacted by nanoparticle morphology and support type, and further studies are required to investigate the role of nanoparticle size in dehydrogenation mechanisms on oxide-supported nanoparticles. High resolution electron energy loss spectroscopy (HREELS) was used in this study to characterize the dehydrogenation of cyclic hydrocarbons on oxide-supported platinum nanoparticles. An Al_2O_3 film was chosen as a support because it is a good representation of the high surface area oxides used as catalyst supports in industry, and the flat surface enables investigation by electron inelastic scattering techniques. The alumina film was grown by oxidation of a NiAl(110) single crystal and platinum nanoparticles were deposited at cryogenic temperatures. Platinum deposition was monitored by the reduction in elastic peak intensity in the HREEL spectra relative to clean Al_2O_3 and also by Auger electron spectroscopy. Cyclohexane was used as a model hydrocarbon because the dehydrogenation on Pt(111) has been studied extensively by vibrational techniques and thus provides a good point of comparison for the nanoparticle studies. The HREELS spectra of cyclohexane on Pt(111) show a distinct low frequency peak at 2600 cm^{-1} which can be monitored to determine the temperature at which dehydrogenation begins.[1,2] The HREELS annealing profile from an alumina film does not exhibit adsorption of cyclohexane or benzene at 170 K, or upon successive annealing. In contrast, the HREEL spectra from platinum nanoparticles on alumina exhibit cyclohexane adsorption at 170 K with the $\nu_{C\text{-}H}$ stretch energy loss peak observed at 2930 cm^{-1}. Interestingly, HREEL spectra from cyclohexane on platinum nanoparticles do not resemble spectra from cyclohexane on Pt(111). Specifically, the additional $\nu_{C\text{-}H}$ energy loss peak observed at 2600 cm^{-1} for cyclohexane adsorbed on Pt(111) is not seen in the case of platinum nanoparticles.[1,2] Our spectra agree more closely with those for cyclohexane adsorbed to a Pt{100}(1×1) surface where a low frequency peak is not observed.[3] In addition, the $\nu_{C\text{-}H}$ energy loss peak from cyclohexane on platinum nanoparticles does

not shift or decrease in intensity until annealed to room temperature. Our results indicate that the platinum nanoparticles may have predominantly Pt{100}(1×1) surfaces.

1. Land, D. P.; Erley, W.; Ibach, H., HREELS Investigation of the Orientation and Dehydrogenation of Cyclohexane on Pt(111). Surface Science 1993, 289 (3), 237-246.

2. Saeys, M.; Reyniers, M. F.; Neurock, M.; Marin, G. B., Adsorption of cyclohexadiene, cyclohexene and cyclohexane on Pt(111). Surface Science 2006, 600 (16), 3121-3134.

3. Lamont, C.L.A.; Borbach, M; Martin, R.; Gardner, P.; Jones, T.S.; Conrad, H.; Bradshaw, A.M., A vibrational specstroscopic study of the adsorption and dehydrogenation of cyclic C_6 hydrocarbons on the (1×1) and (5×20) surfaces of Pt{100}. Surface Science 1997, 374, 215-228.

SS-7-Or-2
Narrowing of band gap in 1D arrays of TiO2 nanoparticles for photocatalysis: studies using x-ray spectroscopies with in situ water exposure and heating

T13 Surface Science

#SS-7-Or-2

Y. Liu [1], J. Taing [1], C.C. Chen [2], A.P. Sorini [3], M.H. Cheng [1], A. Margarella [1], H. Bluhm [4], J.C. Hemminger [1].

[1]University of California, Irvine - Irvine, Ca (United states), [2]Advanced Photon Source, Argonne National Laboratory - Lemont, Il (United states), [3]Stanford Institute for Materials and Energy Science, SLAC National Accelerator Laboratory, - Menlo Park, Ca (United states), [4]Lawrence Berkeley National Laboratory - Berkeley, Ca (United states).

Titanium(IV) oxide (TiO_2) , as a photoactive support for photocatalysts and sensitizers, has applications in catalysis and energy science. Utilizing ambient pressure synchrotron x-ray photoelectron and absorption spectroscopies, we explore the properties of TiO_2 thin films and ordered linear arrays of TiO_2 nanoparticles under in situ water vapor exposure and heating. Our nondestructive depth profiles (obtained by varying the photoelectron kinetic energy) of electronic and surface structures, combined with density-functional theory calculations, indicate an enhancement of the density of states (DOS) near the Fermi level due to surface Ti^{3+} and oxygen vacancies. Introducing water on the interface suppresses this DOS enhancement. Polarized x-ray absorption spectra (Ti L-edge and O K-edge spectra) provide information on the valence electron configuration of the Ti atom and its ligand crystal field environment, helping determine the phases of TiO_2 particles. Our in situ studies suggest that isolated TiO_2 nanoparticles may enhance solar absorption efficiency, and the TiO_2 band gap can be tuned reversibly under water exposure and heating.

1. Taing, J.; Cheng, M. H.; Hemminger, J. C., Photodeposition of Ag or Pt onto TiO_2 Nanoparticles Decorated on Step Edges of HOPG. ACS Nano 2011, 5, 6325-6333.

2. Liu, Y.; Taing, J.; Chen, C.-C.; Sorini, A. P.; Cheng, M. H.; Margarella, A. M.; Bluhm, H.; Devereaux, T. P.; Hemminger, J. C., Narrowing of Band Gap in Thin Films and Linear Arrays of Ordered TiO_2 Nanoparticles, to be submitted to ACS Nano.

NST/SS-5-Or-7
Epitaxial graphene nanoflakes on Au(111): Structure, electronic properties and manipulation

T13 Surface Science

#NST/SS-5-Or-7

P. Leicht [1], L. Zielke [1], S. Bouvron [1], A. Zusan [1], E. Voloshina [2], Y.S. Dedkov [3], M. Fonin [1].

[1]Universität Konstanz - Konstanz (Germany), [2]Humboldt Universität zu Berlin - Berlin (Germany), [3]SPECS Surface Nano Analysis GmbH - Berlin (Germany).

Graphene nanoribbons and graphene nanoflakes (GNFs) have been proposed to exhibit such peculiar phenomena like localized edge states [1] or edge magnetism [2]. Recent attempts of measuring the properties of GNFs on Ir(111) have revealed detrimental edge bonding of graphene to the employed Ir substrate [3,4]. The aim of the present scanning tunneling microscopy (STM) study is the investigation of structural and electronic properties of epitaxial GNFs on the Au(111) surface to further reduce the graphene edge - substrate interaction.
In the present work the preparation of GNFs was performed by a two step process. At the first step, well-shaped GNFs of different sizes down to several nanometers are prepared on the Ir(111) substrate by the temperature programmed growth. At the second step, a thick Au layer was deposited on top of the sample followed by a high temperature annealing, yielding GNFs on a high-quality Au(111) surface. After the preparation two types of GNFs are observed: Whereas embedded GNFs are incorporated in the gold surface, we also observe quasi-freestanding GNFs floating on top of the Au(111) surface.
The structure of both types of GNFs is investigated by STM and shows a moiré contrast depending on the rotation of the flake with respect to the Au lattice, which is additionally modulated by the Au(111) herringbone reconstruction. The hexagonal moiré structure undergoes a switch of the ring-fcc to ring-hcp positions when crossing a Herringbone reconstruction line as a result of the switching of Au positions from fcc to hcp.
We show that quasi-freestanding flakes can be easily manipulated across terraces by the STM tip regardless the size by scanning with appropriate tip parameters.

Furthermore eminent quantum interference patterns at the flake edges are observed which propose very weak coupling of the graphene to the Au(111) surface.

[1] K. Nakada et al.; Phys. Rev. B 54, 17954 (1996)
[2] O. V. Yazyev; Reports on Progress in Physics 73, 056501 (2010)
[3] D. Subramaniam et al.; PRL 108, 046801 (2012)
[4] S. J. Altenburg et al.; PRL 108, 206805 (2012)

Fig. 1: Schematic of graphene nano flake formation on Au(111) (top) and 3D topographic image of a quasi-freestanding graphene flake on Au(111) (bottom). Image shows herringbone reconstruction and moiré as well as quantum interference at the edges.

SS-18-Or-12
Eley-Rideal reactions with N atoms

T13 Surface Science

#SS-18-Or-12

T. Zaharia, M.A. Gleeson, A.W. Kleyn.

FOM Institute DIFFER - Nieuwegein (Netherlands).

Almost all chemical reactions at surfaces proceed via the Langmuir-Hinschelwood mechanism. In environments where hyperthermal reactive atoms are present, also Eley-Rideal type reactions can be expected. However, these have not yet been observed for heavy atoms such as nitrogen. In this work we present results of a systematic study into the importance of such reactions and report the observations thereof.

For this purpose, the interactions of hyperthermal argon (average energy 7.8 eV) and nitrogen (N/N_2; average energies 3.9/4.8 eV, respectively) beams with a Ru (0001) single crystal are discussed. The high energy beams are produced in a cascaded arc plasma source [1] that is coupled to a UHV scattering chamber via a series of differentially pumped stages [2], as illustrated in Figure 1. The chamber has a rotatable mass spectrometer, allowing for detection of scattered particles in a wide angular range.

Studies on bare and adsorbate (N; O) covered surfaces are presented, that focus on the scattering and reaction dynamics of the incident species. Angular and energy distributions of the in-plane scattered species are analyzed and correlated to the incident beam intensity, allowing for direct cross-comparison between different incident species and different surfaces. The effect of adatoms on the physical and chemical nature of the surface and its interaction with incident species is discussed. At the beam energies being utilized the incident particles are sensitive to the atomic structure of the surface. Hence, the measured angular distributions provide information about the ordering of the surface and adsorbate-induced reconstructions.

Additionally, the highly reactive incident N atoms probe the chemical topography of the surface. Evidence for displacement and direct pick-up reactions induced by these

atoms is presented. The likelihood that this represents an Eley-Rideal type reaction in a non-hydrogenic system is discussed.

[1] M.C.M. van de Sanden, G.M. Janssen, J.M. de Regt, D.C. Schram, J.A.M. van der Mullen, B. van der Sijde, Review of Scientific Instruments, **63** (1992) 3369 – 3377.
[2] H. Ueta, M.A. Gleeson, A.W. Kleyn, The Journal of Physical Chemistry A, **113** (2009) 15092 – 15099.

Figure 1: Schematic top-view of the scattering apparatus

SS-P3-21
Organic layers grafted on silicon used to investigate Coulomb blockade in gold nanoparticles

T13 Surface Science

#SS-P3-21

O. Pluchery [1], L. Caillard [1], P. Campbell [2], R. Doherty [1], A.F. Lamic-Humblot [1], P. Dollfus [3], O. Seitz [2], Y.J. Chabal [2].

[1]Universite Pierre et Marie Curie - Paris (France), [2]University of Texas at Dallas - Richardson-Tx (United states), [3]Universite Paris-Sud - Orsay (France).

Coulomb blockade is an electronic phenomenon occurring in ultra-small capacitance such as metallic nanoparticles when their size is about 5nm. A tunnel junction can be fabricated if such a nanoparticle is placed above a conductive substrate with a thin insulating layer junction (thickness ca. 1.5nm). By placing an STM tip above this nanoparticle a **double barrier tunnel junction** (DBTJ) is built. The number of electrons simultaneously trapped in the nanoparticle is controlled by the STM bias (see Figure) and can be adjusted at a single electron level. This phenomenon raised many expectations a couple of years ago. But the lack of reproducibility stopped the enthusiasm of fabricating single electron transistors or single electron memories.

We present a method to prepare highly controlled samples based on an organic layer directly grafted on oxide-free silicon, where **gold nanoparticles** have been deposited through covalent bonding. The organic layer is made by hydrosilylation of alkene molecules of various lengths. Gold nanoparticles are prepared from colloidal solutions and grafted through the amine end of the organic layer [1].

Using STM and STS in UHV we report on the Coulomb blockade of these DBTJ at 25K [2]. We discuss the STS curves as a function of gold nanoparticle diameter, of organic layer thickness. We present an interpretation of our data with a model based on the orthodox theory. Finally the use of a silicon substrate and the fact that it is possible to modulate its doping offers a supplementary handle to adjust the Coulomb blockade effects through band bending at the silicon-organic interface.

[1]. Aureau, D.; Varin, Y.; Roodenko, K.; Seitz, O.; Pluchery, O.; Chabal, Y. J., J. Phys. Chem. C 2010, 114, (33), 14180–14186.

[2]. Caillard, L.; Seitz, O.; Campbell, P.; Doherty, R.; Lamic-Humblot, A.-F.; Chabal, Y. J.; Pluchery, O. Langmuir in revision.

Fig 1. Scheme of the DBTJ made with an STM tip above a gold nanoparticle.

Fig. 2. I(V) curve and its derivative measured in STS where Coulomb oscillations are detected.

SS-17-Or-5
Evidence for single electron tunnel junction using gold nanoparticles

T13 Surface Science

#SS-17-Or-5

L. Caillard [1], O. Seitz [1], P. Campbell [1], R. Doherty [2], A.F. Lamic-Humblot [2], E. Lacaze [2], Y.J. Chabal [1], O. Pluchery [2].

[1]University of Texas at Dallas - Dallas (United states), [2]Université Pierre et Marie Curie - Paris (France).

It has been suggested that the phenomenon of Coulomb blockade could be achieved by placing a metallic nanoparticle between two tunnel junctions. While the Coulomb blockade has been well established theoretically and demonstrated on metal substrates[1], it is more challenging to observe on semiconductor surfaces due in part to the defective nature of the interfaces. We present an experimental study of two ultra small-capacitance normal tunnel junctions connected in series on silicon substrates. To achieve such a structure, we use an amine terminated self assembled monolayer (SAM) grafted on silicon (111) as insulator and linker to attach gold nanoparticles on the surface (fig). The SAM layer is grafted directly on oxide-free silicon through a Si-C bond formation using hydrosilylation reactions and yield to surfaces with low interface state densities[2, 3]. Moreover, this SAM layer provides a long term passivation (weeks) of the interface that prevents oxidation of the substrate. The SAM quality is characterized using an extensive range of characterization techniques, including in-situ IR spectroscopy, spectroscopic ellipsometry, X-ray photoelectron spectroscopy (XPS) and Atomic force microscopy (AFM). The second capacitance is formed by the gap between the gold nanoparticle and the tip of the Scanning tunneling microscope/spectroscope (STM/S). The current-voltage measurements are performed in ultra high vacuum. Several parameters are investigated: silicon doping level, SAM thickness, and size of the gold nanoparticles (AuNps) ranging from 1 to 15 nm. The junction is achieved by grafting synthesized AuNps. Data suggest that coulomb staircases are observed under different conditions[4] (fig): lower temperature is a dominant parameters for a clear observation of the stairs. Steps width and height, which ranges from 100mV to 400mV and 5 to 30pA, respectively, shows a dependence on particle size and SAM thickness. These results are an important step toward future control for single electron transistor applications.

[1] Zhang, H.; Yasutake, Y.; Shichibu, Y.; Teranishi, T.; Majima, Y., Phys. Rev. B, 72, (20) **(2005)**
[2] O. Seitz, P. G. Fernandes, G. A. Mahmud, H.-C. Wen, H. J. Stiegler, R. A. Chapman, E. M. Vogel, and Y. J. Chabal, Langmuir 27, 7337 **(2011)**
[3] D. Aureau, Y. Varin, K. Roodenko, O. Seitz, O. Pluchery and Y. J. Chabal, Phys. Chem. C, 114 (33), pp 14180–14186 **(2010)**
[4] Caillard, L.; Seitz, O.; Campbell, P.; Doherty, R.; Lamic-Humblot, A.-F.; Chabal, Y. J.; Pluchery, O., Langmuir in **revision.**

Fig : System schematic. The derivative of the STS is plotted for two SAM thickness, long (a,b) and short (c) and two doping level, low doping (a) and high doping (b,c).

SS-P1-06
Adsorption of H2 and O2 on the stable and metastable Ir(100) surface studied with X-ray photoelectron spectroscopy

T13 Surface Science

#SS-P1-06

M. Arman [1], K. Jan [1], F. Pascal [2], V. Abhilash [3], M. Florian [3], G. Johan [1], S. Alexander [2], H. Lutz [2], L. Edvin [1].

[1]Division of Synchrotron Radiation Research, Lund University - Lund (Sweden), [2]Lehrstuhl für Festkörperphysik, Universität Erlangen-Nürnberg - Erlangen (Germany), [3]Center for Computational Materials Science, Vienna University of Technology - Vienna (Austria).

Hydrogen and oxygen adsorption structures on metastable Ir(100)-(1×1) and stable Ir(100)-(5×1) have been studied with scanning tunneling microscopy (STM), low energy electron diffraction (LEED), and density functional theory (DFT) in the past, and very detailed structural models exist today [1-3]. In contrast to the detailed structural information, the amount of spectroscopic data is very limited. Such spectroscopic data are important reference data for understanding chemical reactions on Ir(100) surfaces.

Here, we present the first detailed X-ray photoemission spectroscopy (XPS) study of the Ir 4*f* core level binding energies of the stable Ir(100)-(5×1) and meta stable Ir(100)-(1×1) surfaces. Further, we studied the effect of oxygen and hydrogen adsorption on these surfaces.

With XPS we determined the fingerprints of the stable and the metastable Ir(100) surfaces. In addition, we studied hydrogen and oxygen adsorption on both surfaces and observed the following characteristics:

i) For the clean Ir(100)-(1×1) surface we observed two separate components originating from bulk and surface atoms. The Ir $4f_{7/2}$ surface component is shifted by -0.75 eV with respect to the bulk Ir $4f_{7/2}$ component.

ii) For the stable Ir(100)-(5×1) surface we observed four different Ir $4f_{7/2}$ surface

components consistent with the structural model [3].

iii) H_2 adsorption onto the Ir(100)-(1×1) surface leads to Ir1 (Ir-H) and Ir2 (H-Ir-H) components shifted +0.16 eV and +0.31 eV with respect to the surface component.

iv) The presence of hydrogen on the Ir(100)-(5×1) surface lifts the reconstruction, and rows of Ir atoms are formed due to the higher density of atoms in the (5×1) structure. In agreement with this structural model we observe three different Ir $4f_{7/2}$ surface components.

v) After oxygen adsorption onto the Ir(100)-(5×1) surface we observed one Ir1 (Ir-O) component shifted -0.22 eV with respect to the bulk Ir $4f_{7/2}$ component. Simultaneously, the four Ir $4f_{7/2}$ surface components characteristic of the clean Ir(100)-(5×1) surface disappeared. Thus, our measurements very clearly show that the Ir(100)-(5×1) surface reconstruction is lifted upon oxygen adsorption consistent with the literature [4].

vi) Finally, the O 1s binding energy of oxygen adsorbed on Ir(100) reveals one component shifted -0.5 eV as compared to oxygen adsorbed in threefold hollow sites on Ir(111). This observation is fully consistent with O atoms in bridge sites as predicted by the Johnson model [4]; therefore, we have no indications for the model proposed by Sander et al. with bridge and fourfold adsorption sites [5].

Overall, the current status of our analysis demonstrates an excellent agreement between measured and DFT calculated core level shifts, which validates the existing structural models.

[1]K. Heinz et al., Z. Phys. Chem. **218**, 997, (2004)
[2]D. Lerch et al., Phys. Rev. B **73**, 075430 (2006)
[3]A Schmidt et al., J. Phys.: Cond. Matt. **14**, 12353 (2002)
[4]K. Johnson et al., Jour. Chem. Phys., **112**, 10460 (2000)
[5]D. Sander et al., Phys. Rev. B, **81**, 153403 (2010)
[6]C. Giovanardi et al., Phys. Rev. B **74**, 125429 (2006)
[7]K Biedermann et al., J. Phys.: Cond. Matt. **21**, 185003 (2009)

NST/SS-P1-23
Study of Graphene by Low Voltage Scanning Transmission Electron Microscopy and Raman Spectroscopy

T13 Surface Science

#NST/SS-P1-23

E. Mikmekova [1], I. Müllerová [1], L. Frank [1], H. Bouyanfif [2], M. Lejeune [2].

[1]Institute of Scientific Instruments of the ASCR, v.v.i. - Brno (Czech republic), [2]Universite de Picardie Jules Verne - Amiens (France).

The interest in graphene has been growing in recent years since the discovery of a method for easy preparation of this material with high quality and bigger size. Due to interesting properties of graphene, conductivity and transparency together, this material is very attractive for a lot of industry applications. The Raman spectroscopy is usually used for graphene thickness determination [1] but for the study of material quality, the lateral resolution of the device is not sufficient. That is why the electron microscopy is very important for characterization of this material.

The preparation methods can be divided into two groups: exfoliation (preparation from existing graphite crystal) and direct grow on substrates by diverse deposition methods. In this work, the graphene has been prepared by the CVD and after removal of substrates, the various thickness flakes of this material has been put on a copper grid.

The experiments were performed in low voltage scanning transmission electron microscope Magellan 400, which is equipped by cathode lens (CL) system and a multichannel detector of transmitted electrons enabling to acquire the BF, DF and HAADF micrographs. The lower energy of impacted electron caused the higher contrast between graphene frakes of different thickness [2] and the observation by units of eV even enables to determine a single graphene layer.

Raman measurements were performed using the 514.5 nm line from an argon ion laser and analyzed using a Jobin Yvon T64000 spectrometer (triple monochromator, resolution ~ 0.5 cm-1) equipped with a charge coupled device.

[1] A. C. Ferrari, Solid State Communications 143 (2007), 47-57
[2] I. Müllerová, M. Hovorka, L. Frank, Ultramicroscopy 119 (2012), 78-81

Figure 1: Graphene like flakes placed on the holey carbon film are showed at various landing energies of electrons: A. 6000 eV, B. 1000 eV, C. 500 eV, D. 20 eV, E. 5 eV (transmitted signal, BF) and reflected signal F. 6000 eV.

Figure 2: Raman spectra (A, 1 - one layer graphene, 2 - two layer graphene and 3 - multi layer graphene) and TE images observed by 5000 eV (B) and 500 eV (C).

SS-P1-20
Multiphase domain structure in NaNbO3 resolved by energy-filtered PEEM

T13 Surface Science

#SS-P1-20

J. Honolka [1], M. Vondracek [1], K. Horakova [1], Y. Polyak [1], V. Chab [1], J. Lancok [1], A. Dejneka [1], M. Tyunina [2], M. Plekh [2].

[1]FZU, ASCR - Prague (Czech republic), [2]University of Oulu - Oulu (Finland).

The ferroelectric domain structure of epitaxially polished $NaNbO_3$ crystal surfaces is studied by means of energy-filtered PEEM with 100nm lateral spatial resolution. Images were taken at low binding energies of a few eV using a standard Hg lamp as a photon source. In the PEEM images prominent stripe structures are visible, indicative of the complex domain structure in $NaNbO_3$ at room temperature (see Figure). Typically, the width of the stripes ranges from 1µm to 10µm. The absence of ordered domain structures over larger distances suggests a multiphase state with an antiferroelectric phase as the main phase but coexisting ferroelectric inclusions. Different annealing procedures before the experiment as well as the variation of the measuring temperature give further information on domain formation.

Figure: Example of a stripe structure seen in energy-filtered PEEM on a $NaNbO_3$ crystal at room temperature. The total length of the shown stripe is ~ 300µm.

SS-13-Or-4
Study of the substrate influence on the properties of physisorbed self-assembled molecular layers: Azabenzene 1,3,5-Triazine on graphite and graphene on metals

T13 Surface Science

#SS-13-Or-4

L. Rodrigo, P. Pou, A.J. Martínez-Galera, J.M. Gómez-Rodríguez, R. Pérez.

Universidad Autonoma de Madrid - Madrid (Spain).

The properties of molecular overlayers on inorganic substrates depend on a delicate balance between intermolecular and overlayer-substrate interactions [1]. Here we present a combined experimental and theoretical study of azabenzene 1,3,5-Triazine layers grown on both graphite and graphene on Pt(111). VT-STM experiments (see fig. 1) show large overlayer islands with Moiré structures on both substrates [2]. While in both cases the last layer is graphene, the atomic arrangements, the measured molecule diffusion barriers and the growing properties are different [2]. This system is, therefore, a perfect model for the study of the properties of physisorbed self-assembled molecular layers [1]. We have carried out ab initio DFT calculations (using VASP) trying with all the functionals available (LDA, PBE and hybrids) and different approaches for the van der Waals interactions [3] to fully characterize the intermolecular (H bonds and vdW) and molecule-substrate (vdW attraction and Pauli repulsion) interactions (see fig. 2). We have found that the graphene layer, even for these physisorbed molecules, modifies the intermolecular interactions respect to an isolate layer but not significant differences are found between graphite and graphene on Pt substrates. This exhaustive characterization shows the theoretical limitations to describe these weakly interacting systems even with state-of-the-art approaches.

[1] Forrest et al., ChemRev, 97, 1793 (1997); Hooks et al., AdvMat, 13, 227 (2001).
[2] Martinez-Galera et al., JPhysChemC, 115, 11089 (2011); JPhysChemC, 115, 23036 (2011).
[3] S. Grimme et al., J Comp Chem 27 (2006) 1787; Klimes et al, J Phys: Condens Matter, 22, 022201 (2010).

Figure 1. VT-STM experimental image of the graphene + Pt system
Figure 2. Ball-stick scheme of the theoretical simulation for the graphene + Pt system

SS/NST-1-Or-1
When is an STM vacancy, not a vacancy?

T13 Surface Science

#SS/NST-1-Or-1

C. Christopher [1], J. Kullgren [2], A. Hoglund [2], S. Mirbt [2], K. Hermasson [2].

[1]Nottingham Trent University - Nottingham (United kingdom), [2]Uppsala University - Uppsala (Sweden).

One of the most useful tools in surface science is scanning tunnelling microscopy (STM), which can often achieve atomic precision images of surfaces. A great many studies of ionic semiconductors and oxides have relied upon STM to identify surface structures, native defects and impurities. Bright spots in images taken at negative tip bias map out filled valence band states, and hence generally indicate the location of anions. Likewise, bright spots in images taken at positive tip biases map out empty conduction band states, generally indicating the location of cations. Brighter spots or additional spots may then be expected to indicate the location of native adatoms, impurities or antisite defects, and missing spots to indicate the location of surface vacancies. However, we will present density functional theory (DFT) studies indicating that this in not always the case: some impurities look almost exactly like vacancies.

We will show filled and empty state theoretical STM images of vacancies, adsorbed hydrogen and substitutional impurities, and compare them to existing experimental images. We will show that in some cases vacancies and impurities are extremely hard to tell apart, with examples taken from the (110) surfaces of III-V semiconductors and from rare earth oxides. (See Fig.) In the case of many III-Vs, the situation is even more complex, as genuine cation vacancies are not always stable [1], but relax into anion vacancy-anion antisite pairs, leaving no “real” cation vacancies but even more defects that could be taken for anion vacancies in STM.

When preparing materials for applications or for use in surface science investigations, considerable effort goes into avoiding impurities. However, this is not fully possible, and some impurities will remain. Hydrogen, for example, is known to be “ubiquitous” [2], often involved in many stages of material growth and processing,

and extremely difficult to remove without elevated temperatures. We will review evidence that hydrogen and other impurities should indeed be present in the example materials we study, even when if not yet identified in STM images. We propose that this failure to detect hydrogen etc in existing STM studies is due to their similarity to vacancies. In most cases, we propose that both genuine vacancies and fake STM vacancies due to impurities should be present. However, in other cases, stability calculations suggest that the presence of genuine surface layer vacancies is unlikely, so that the apparent vacancies in STM images are probably due mainly to impurities.

1 A.Höglund, S.Mirbt, C.W.M. Castleton, M.Göthelid Phys Rev B 78, 155318 (2008)
2 J. R. Weber, A. Janotti and C. G. Van de Walle App Phys Lett 97, 192106 (2010)

Fig: Simulated filled state STM images.

SS-16-Or-3
Real-Time Characterization of Nucleation and Step-Edge Crossing during the Growth of the Fullerene C60 using X-ray Scattering

T13 Surface Science

#SS-16-Or-3

S. Bommel [1], N. Kleppmann [2], C. Weber [3], H. Spranger [3], P. Schäfer [3], J. Novak [4], S.V. Roth [1], F. Schreiber [4], S.H.L. Klapp [2], S. Kowarik [3].

[1]Deutsches Elektronen-Synchrotron (DESY) - Hamburg (Germany), [2]Institut für Theoretische Physik, Technische Universität Berlin - Berlin (Germany), [3]Institut für Physik, Humboldt-Universität zu Berlin - Berlin (Germany), [4]Institut für Angewandte Physik, Universität Tübingen - Tübingen (Germany).

The popular organic semiconductor C_{60} is a promising material for organic opto-electronic and photovoltaic devices. C_{60} is widely used as a buffer layer in organic light emitting diodes (OLED) and as an acceptor in organic solar cells [1]. The structural order and morphology is crucial for the performance of most organic devices. By the unique combination of X-ray scattering methods and kinetic Monte-Carlo simulations (KMC) we are able to obtain deeper insight into the physical nucleation and growth processes, that is diffusion, lateral binding, and step-edge crossing occurring during the growth of the fullerene C_{60} on the silicate mica.

In this work we characterize the surface morphology and structural order during the growth of C_{60} with simultaneous real-time and in-situ measurements of x-ray diffuse scattering and anti-Bragg growth oscillations during molecular beam deposition of the molecules [2],[3]. The experiments were carried out at the MiNaXS beamline P03, PETRA III (DESY, Hamburg) [4]. For the characterization of the morphology during growth, the island density and island diameter were extracted from the 2D x-ray diffuse scattering pattern as a function of temperature, deposition rate and film thickness. We show that increasing temperature, decreasing deposition rate and a rising film thickness lead to smaller island density and larger island diameters, respectively. Within the growth of one monolayer we quantitatively describe for all temperatures and rates three different growth regimes occurring during 2D island

growth: the nucleation process is followed by the lateral growth of the islands, which again is followed by coalescence. For a more complete understanding not just the in-plane structure, but also the out-of-plane layering was investigated simultaneously by measuring anti-Bragg growth oscillations. High structural order and layer-by-layer growth during molecular beam deposition of multilayer films of C_{60} on mica were found. Additionally we were able to extract the layer coverage and the thin film roughness from the anti-Bragg growth oscillations. From a comparison of the nucleation/ island formation process (island density and island diameter) and the growth oscillations (layer coverages) with kinetic Monte Carlo simulations, we are able to determine the diffusion energy (0.54eV), step-edge barrier (0.11 eV) and binding energy (0.13 eV). This model enables a detailed understanding and predictive simulation of C_{60} growth.

[1] J. Wagner et al., Adv. Func. Mat. **20**, 4295 (2010)
[2] S. Kowarik et al., PRL **96**, 125504 (2006)
[3] C. Weber et al. J. Chem. Phys. **136**, 204709 (2012)
[4] A. Buffet, S.V. Roth et al., J. Synchr. Radiation **19**, 647 (2012)

SS-6-In-1
Photoelectron Spectroscopy of Ammonium-based compounds

T13 Surface Science

#SS-6-In-1

A. Margarella [1], K. Perrine [1], M. Van Spyk [1], B. Winter [2], J. Hemminger [1].

[1]University of California, Irvine - Irvine, Ca (United states), [2]Helmholtz-Zentrum Berlin für Materialien und Energie / Elektronenspeicherring BESSY II - Berline (Germany).

Ammonium –based compounds are very prevalent in the atmosphere and environment. In particular, ammonia is found in atmospheric aerosols and is the primary basic compound that neutralizes acidic compounds. Ammonia (NH_3) can be protonated to ammonium (NH_4^+), and in bulk aqueous solution, this equilibrium is well understood.
In this experimental study, the equilibrium between NH_4^+ and NH_3 for different ammonium compounds is investigated using liquid-jet photoelectron spectroscopy. In this technique, photoelectron spectroscopy is performed on a thin, fast-flowing jet of solution. Utilizing synchrotron light, the surface of the sample is measured, independent from the bulk of the sample. In the N1s photoelectron spectrum, the binding energies of NH_4^+ and NH_3 are separated well enough to deconvolute the spectrum into the different nitrogen containing species. The intensity of the NH_4^+ and NH_3 species qualitatively follow the pH, i.e. at hower pH values (more acidic), there is more NH_4^+. The integrated areas of the photoelectron peaks are used to provide relative ratios of the nitrogen species in solution. The NH_4^+ / NH_3 ratio is presented as a function of bulk solution pH values for both the surface and bulk of the solution.

SS-10-Or-3
Effects of Coulomb interaction on one-dimensional Rashba chain

T13 Surface Science

#SS-10-Or-3

K. Makoshi, T. Mii, N. Shima.

University of Hyogo - Ako-Gun (Japan).

Both the time-reversal and spatial inversion symmetries lead to spin-degenerate electronic states. Rashba and Bychokov proposed a way to get spin-spilling electronic band by breaking the spatial inversion symmetry, so-called Rashba effect [1]. On the other hand, in one-dimensional atomic chains, on-site Coulomb interaction may cause anti-ferromagnetic order and spin-split bands, which sometimes is called Mott physics. Our main interest is crossover physics of these two phenomena.

We discuss effects of Coulomb interaction on one-dimensional Rashba chain based on an extended Hubbard model. The random phase approximation is introduced to analyze the model. The electronic hopping in conventional Hubbard model results in anti-ferromagnetic coupling. In contrast, Rashba type spin-orbit interaction gives rise to ferromagnetic coupling. These competing two couplings lead to several complex phenomena, including spin-splitting electronic states, magnetic order and spin-polarized current. We show “Coulomb energy”-“Rashba parameter” phase diagram in which paramagnetic, ferromagnetic and anti-ferromagnetic states are come out. A helical magnetic order also appears. These magnetic orders spontaneously break the time-reversal symmetry and may allow spin-polarized current.

[1] Y. A. Bychokov and E. I. Rashba, JETP Lett. **39**, 78 (1984)

SS-13-Or-5
Orbital tomography: Deconvoluting photoemission spectra of organic molecules

T13 Surface Science

#SS-13-Or-5

S. Subach [1], M. Willenbockel [1], B. Stadtmüller [1], E.M. Reinisch [2], T. Ules [2], D. Lüftner [2], G. Koller [2], P. Puschnig [2], C. Kumpf [1], M. Ramsey [2], F.S. Tautz [1].

[1]Forschungszentrum Jülich - Jülich (Germany), [2]Karl-Franzens University Graz - Graz (Austria).

Large π-conjugated organic molecules are attracting considerable interest due to their potential applications; however, their valence bands necessarily consist of closely spaced molecular states, which is often challenging for both theory and spectroscopic experiment. We propose a tomographic method that uses the energy and momentum dependence of photoemission from adsorbed molecules to deconvolute the valence band into individual orbitals. The method allows the purely experimental determination of molecule-projected densities of state, to be compared to theoretically calculated. The method further allows the direct observation of the effects of bonding on individual orbitals, and in so doing, provides stringent tests for the development of ab-initio electronic structure theory.

Photoemission experiments on differently ordered phases of perylene-tetracarboxylic-dianhydride (PTCDA) molecule on low index surfaces of silver single crystal were performed at BESSYII using a toroidal electron energy analyzer. The valence band of PTCDA was unambiguously disentangled into contributions from six molecular orbitals within a binding energy range of 4 eV, four of them within an energy range of only 0.4 eV [1]. For the PTCDA phases containing differently oriented molecules in the unit cell, the method grants an access to electronic properties of either molecule separately [2]. This enables detailed description of site- and orientation-specific bonding of organic molecules at metals.

1. P. Puschnig et al., Phys. Rev. B **84**, 235427 (2011).

2. B. Stadtmüller et al., Europhys. Lett. **100**, 26008 (2012).

SS-P3-29
The Effects of Pin Geometry on the Microstructure and Mechanical Properties of Friction Stir Welded AZ31 Joints

T13 Surface Science

#SS-P3-29

H. Torkamani [1], K.H. Darzi [2], T. Saeid [3].

[1]PhD Student, University of Tehran - Tehran (Iran, islamic republic of),
[2]Graduate MSc Student, Sahand University - Tabriz (Iran, islamic republic of),
[3]Associate Professor, Sahand University - Tabriz (Iran, islamic republic of).

Friction stir tool is a feature playing an important role in Friction Stir Welding (FSW) process. it is well known that the heat generation and the material flow are controlled by the pin geometry. Therefore, the pin can affect the soundness, microstructure and mechanical properties of the weld. The main problem in the FSW of AZ31 by using cylindrical pins is the formation of defects, which deteriorate the mechanical properties of the welds. From this, the possibility of obtaining sound welds with proper characteristics was studied by using a taper pin. For this purpose, microstructure and mechanical properties comparisons were made between the AZ31 joints welded by cylindrical and taper pins in same conditions. Microstructure examinations revealed that the microstructure of the joints welded by taper pin shows no defects (figures1 and 2) and consist of finer grain size (table1) compared to those of cylindrical ones. These findings could be discussed in terms of the generated frictional heat, and the amount of material flow. Moreover, using the taper pin resulted in increasing the micro-hardness, tensile strength, as well as elongation significantly (table2) due to different obtained microstructure characterizations.

Table 1.Grain sizes of the joints

Pin geometry	Grain size (µm)
Cylindrical	25.8
Taper	15.7

Table 2. Ultimate tensile strength (UTS), elongation and micro hardness of the joints

Pin Geometry	UTS, MPa	Elongation %	Microhardness, Hv
Cylindrial	162	1.58	60
Taper	223	2.80	73

[1] R.S. Mishra, Friction stir welding and processing, Mater. Sci. Eng, 2005, 1-78.

[2] M.Aydin, R. Bulut, The weldability of AZ31 magnesium alloy by friction stir welding, Kovove Mater, 2010, 97-133.

[3] Y. Zhao, S. Lin, L. Wu, The influence of pin geometry on bonding and mechanical properties in friction stir welding, Mater Lett, 2005.

[4] H.Torkamani, Kh.Darzi,T.Saeid, The Effects of Threading on the Cylindrical Pin in Friction Stir Welding of AZ31 Mg Alloy, AWST, 2011, Turkey.

Figure 1. Microstructure of the joint welded by cylindrical pin showing defects.

Figure 2. Microstructure of the joint welded by taper pin.

SS-P3-39
Chemical imaging and Nano-ARPES at Synchrotron SOLEIL: A new concept in scanning photoelectron microscopy

T13 Surface Science

#SS-P3-39

S. Lorcy, J. Avila, I. Razado-Colambo, M.C. Asensio.

Synchrotron SOLEIL - Gif Sur Yvette (France).

In recent decades we have witnessed exponential advances in new nanotechnologies. Many nano-objects (acting as "building blocks units") have shown remarkable properties in rather different technology areas. However, they had been unexplored if new tools had not been available for viewing and scrutinizing them, at the nanometer scale. In particular, with the latest third generation synchrotron sources, the highly improved photon flux is essentially profited in the area of the X-ray microscopy.

In such a context, a new scanning photoelectron microscope beamline has been constructed at SOLEIL. Contrary to the PEEM microscopy, the imagery in SPEM is generated by a simple nanometric sweeping of the samples and a focusing of the incident light by a set of Fresnel zone plates. Our innovative project is attempting to extend the classical SPEM technique to the domain of low photon energies, for which the states of the valence band have a particularly high cross section. Hence, at the nanoscale, the detection of electronic states close to the Fermi level as well as their dispersions can be guaranteed by Nano angle resolved photoelectron spectroscopy (or Nano-ARPES), with high angular and energy precision. In essence, this new beamline of SOLEIL is fitting the existing emptiness between the atomic electronic information provided by the STM spectroscopy and the low-spatially resolved data supplied by classical ARPES and NEXAFS techniques.

In this presentation, the first results of the ANTARES microscopy beamline will be disclosed. This instrument, with a spatial resolution of several tens of nanometers, is able of carrying out the direct imaging of core levels, their chemical shifts and the band electronic structures of crystalline ordered materials. High precise Chemical images and valence band information of nano-objects like exfoliated grapheme, granular materials and Nanowires will be disclosed

NST/SS-P1-24
Structural determination of a graphene bilayer on SiC(0001) using synchrotron radiation photoelectron diffraction

T13 Surface Science

#NST/SS-P1-24

I. Razado-Colambo [1], J. Avila [1], D. Vignaud [2], S. Godey [2], X. Wallart [2], M.C. Asensio [1].

[1]Synchrotron SOLEIL - Gif Sur Yvette (France), [2]I.E.M.N., UMR CNRS 8520 - Villeneuve D'ascq (France).

Graphene has attracted enormous interest in recent years among the scientific, technological and industrial communities due to its very interesting and novel electronic properties. Graphene is a single sheet sp^2-bonded carbons atoms, which are atomically organized in hexagons. The electronic band structure of graphene shows a linear dispersion at the Fermi energy at the K-point of the surface Brillouin zone instead of a parabolic relation, as it is observed in graphite. However, its electronic band structure is dependent on several factors among others, such as number of layers, symmetry of the lattice, stacking order and interlayer distance. For the 3D graphite, it is known to have the AB stacking structure and an interlayer distance of 3.35 Å, which have been verified in both experiment and theory. However in the case of 2D graphene, the stacking and interlayer spacing between layers are still unclear.
We have investigated the structural properties of bilayer graphene on SiC(0001) using a high-resolution photoemission and a combination of experimental and theoretical photoelectron diffraction. The stacking and in- terlayer distances between graphene layers have been determined with good accuracy. Photoelectron diffraction holograms of the graphene C1s component at two photon energies, 600 and 900 eV, have been measured from which azimuthal curves at specific polar angles have been deduced. Consequently, these sets of experimental data have been utilized in the multiple scattering photoelectron diffraction calculation program developed by Fritzsche to determine the stacking and interlayer distances between graphene layers. Based on the theoretical PED (photoelectron diffraction) calculation performed in this study, it was verified that the bilayer graphene on the Si-terminated SiC(0001) has an AB stacking structure. Furthermore, the distance between the C

buffer layer and the first graphene layer is found to be 3.30 Å and an interlayer distance of 3.50 Å between the first and second graphene layers.

NST/SS-2-Or-7
Electronic band structure of Chemical Vapor Deposition graphene on polycrystalline copper foils by nano-ARPES

T13 Surface Science

#NST/SS-2-Or-7

J. Avila [1], I. Razado-Colambo [1], S. Lorcy [1], R. Fleurier [2], E. Pichonat [2], D. Vignaud [2], X. Wallart [2], M.C. Asensio [1].

[1]Synchrotron SOLEIL - Gif Sur Yvette (France), [2]IEMN, UMR CNRS 8520 - Villeneuve D'ascq (France).

The electronic properties of polycrystalline graphene films are strongly dependent on the size, shape and orientation of their constituent single-crystal grains. Hence, the ability to produce large and free-defects films of graphene is presently a major challenge for multiple graphene applications. Here we report a high angle and lateral resolved photoelectron spectroscopy (nano-ARPES) study of one-atom thick graphene films on thin copper foils synthesized by chemical vapor deposition. In today's state-of-the-art ARPES, probed areas are routinely in the range from tens to hundreds of microns. Notwithstanding in advanced materials, length scales from the nano- to the mesoscopic-cales dictate and characterize the electronic and other relevant properties. Thus it is not possible access relevant length scales for many complex engineered materials using conventional ARPES.

At the Synchrotron SOLEIL, we have recently built a new instrument by combining ARPES principles with scanning microscopy, in which a focused soft x-ray beam is raster-scanned over the samples to create an image one pixel at time while a suitable signal is monitored under computer control. This new nano-probe is capable of investigating innovative materials in their earlier stage of synthesis, which often are initially isolated in small crystalline form or in polycrystals constituted by small grains. With this new instrumentation, we have been able to characterize polycrystalline one-atom-thick graphene films. They were composed by single-crystal grains differently oriented, which appeared patched together like in a quilt. By mapping the electronic dynamics down to single pristine graphene grains, we have shed light on essential

characteristics like doping, gap-size, Fermi velocity and electron-phonon coupling of this unique Dirac system. Randomly-oriented graphene grains showed a giant enhancement of flexural phonon modes, while in highly-oriented grains, they are nearly quenched. These findings provide a new benchmark in our understanding of many-body effects in graphene.

NST/SS-2-Or-8
“More than Moore”: Could silicene be the future of electronics?

T13 Surface Science

#NST/SS-2-Or-8

M.C. Asensio [1], J. Avila [1], G. Le Lay [2], P. De Padova [3], C. Quaresima [3], P. Vogt [4], A. Resta [2].

[1]Synchrotron SOLEIL - Gif Sur Yvette (France), [2]Aix-Marseille University, CNRS-CINaM - Marseille (France), [3]CNR-ISM - Roma (Italy), [4]Technische Universität Berlin, Institut für Festkörperphysik - Berlin (Germany).

Finding novel materials with smart properties is one of the major challenges of material science research activity. In particular, the electronics market demand for increased performance cannot be met anymore with conventional packaging and interconnect technologies. Consequently, the technology roadmap for semiconductors or Moore’s Law, which states that the number of components integrated in a circuit would increase exponentially over time, should be replaced by a more effective approach regarded as “More than Moore” [1]. This new trend adds value to devices by incorporating new functionalities, which do not necessarily scale according to “Moore's Law”.
Graphene is one of such novel materials with Dirac-type electrons near the Fermi level behaving as massless fermions, which give rise to intriguing phenomena such as Klein paradox, anomalous integer quantum Hall effect and appealing properties as strong resistence, stretchable and impermeable attributes. A close relative of graphene, a 2D honeycomb lattice of Si atoms called Silicene has been recently reported as nanoribbons and single layers on silver monocrystals, oriented (111)[2-4]. Silicene has been theoretically predicted as a buckled honeycomb arrangement of Si atoms and having an electronic dispersion resembling that of relativistic Dirac fermions[5]. In this presentation we will provide, (for the first time to our knowledge), compelling evidence, from both structural and electronic properties, for the synthesis of epitaxial silicene sheets on silver single crystals. We have combined scanning tunneling microscopy and synchrotron radiation angle-resolved photoemission spectroscopy to fully characterize this new exciting material.

[1] “More than Moore”, see the Weblink: http://www.itrs.net/news.html
[2] P. Vogt, P. De Padova, C. Quaresima, J. Avila, E. Frantzeskakis, M.C. Asensio, A. Resta, B. Ealet, and G. Le Lay, Phys. Rev. Lett. 108, 155501 (2012)
[3] P. De Padova, C. Quaresima, P. Perfetti, B. Olivieri, B. Léandri, B. Aufray, S. Vizzini, and G. Le Lay, Nano Lett. 8,271 (2008)
[4] P. De Padova et al., Appl. Phys. Lett. 96, 261905 (2010)
[5] S.S. Cahangirov, M. Topsakal, E. Aktürk, H. Sahin and S. Ciraci, Phys. Rev. Lett. 102, 236804 (2009).

SS-13-In-1
VALENCE BAND TOMOGRAPHY AND THE RECONSTRUCTION OF MOLECULAR ORBITALS FROM ANGLE RESOLVED PHOTOEMISSION

T13 Surface Science

#SS-13-In-1

M. Ramsey.

Institute of Physics, Karl-Franzens University Graz - Graz (Austria).

With examples of chain- and plate-like molecules it will be shown that the combination of studies of conjugated molecules with modern electron energy spectrometers has led to advances in understanding valence band photoemission in general and the electronic structure of “organic semiconductors” in particular. Examples of intra- and inter-band dispersion in thick molecular films will demonstrate that a simple Fourier transform of molecular orbitals predicts the, hitherto apparently complex, angular/momentum distribution of emitted photoelectrons. For adsorbate monolayers it will be shown how this orbital tomography can be used to determine molecular geometries, gain insight into the nature of the surface chemical bond, unambiguously determine the orbital energy ordering and reconstruct orbitals in real space.

SS-9-In-1
METAL–ORGANIC INTERACTION PROBED BY FIRST PRINCIPLES STM SIMULATIONS

T13 Surface Science

#SS-9-In-1

M.L. Bocquet.

Ecole Normale Supérieure de Lyon, Laboratoire de Chimie, CNRS UMR 5182 - Lyon (France).

Density Functional Theory (DFT) has now reached the point to mimic in a quantitative way two pillars of the Scanning Tunneling Microscope (STM) probe: the imaging mode convoluting the topographic and electronic properties and the spectroscopy modes comprising of elastic and inelastic detection ways. We present a selection of hybrid interfaces ranging from isolated benzene derivatives, phthalocyanines and porphyrines to thin honeycomb carbon film – a single graphene layer – deposited onto ideal transition metal surfaces. The direct experimental analysis of these interfaces was error-prone, necessitating the confrontation with First Principles atomistic simulations. The few examples thus illustrate the power of different kinds of STM simulations to complement the STM data, in order to unambiguously identify the chemical structure of organic adsorbates.

NST/SS-2-In-1
Growth and Si-Layer Intercalation of Centimeter-scale, Highly-ordered, Continuous Graphene on Metal Surfaces for Future Integrated Electronic Devices*

T13 Surface Science

#NST/SS-2-In-1

H. Gao.

Institute of Physics, Chinese Academy of Sciences - Beijing (China).

Graphene (G) is considered as a serious contender for being the reference material for a post-CMOS technology. Nevertheless, the use of graphene for applications requires mass production of high quality material and also its transfer to insulating substrates. While epitaxial growth in SiC and CVD growth in metal surfaces have seen enormous progress, transfer techniques are still a major challenge and a limiting factor of the material quality. I will present a new strategy for graphene growth on metallic Ru(0001) followed by silicon-layer intercalation that not only weakens the interaction of graphene with the metal substrate but also retains its superlative properties. This G/Si/Ru architecture, produced by silicon-layer intercalation approach (SIA), was characterized by Raman spectroscopy, scanning tunnelling microscopy/spectroscopy, and angle resolved electron photoemission spectroscopy. The SIA eliminates the need for the graphene transfer and also allows for an atomic control of the distance between the graphene and the metal gate, opening doors for a new generation of graphene-based materials with tailored properties.

1. Y. Pan et al., Chinese Physics 16, 3151 (2007).
2. Y. Pan et al., Adv. Mater. 21, 2777 (2009).
3. J.H. Mao et al., Appl. Phys. Lett. 100, 093101 (2012) (Cover story).
* In collaboration with Yi Pan1, Jinhai Mao1, Li Huang1, Junfeng He1, Min Gao1, Lizhi Zhang1, Lida Pan1, Haitao Zhou1, Haiming Guo1, Yuan Tian1, Qiang Zou1,

Haigang Zhang1, Yeliang Wang1, Shixuan Du1, Xingjiang Zhou1, and Antonio H. Castro Neto2. 1 Institute of Physics, Chinese Academy of Sciences, Beijing 100190, China; 2 Physics Department, National University of Singapore

NST/SS-6-In-2
SPIN-POLARIZED LOW-ENERGY ELECTRON MICROSCOPY

T13 Surface Science

#NST/SS-6-In-2

A. Schmid.

National Center for Electron Microscopy, Materials Sciences Division, LBNL - Berkeley (United states).

When a spin-polarized electron beam is scattered on the surface of a magnetic material, reflectivity is a function of the relative alignment between the spin direction of the beam and the magnetization vector in the surface of the sample. The spin-polarized low-energy electron microscope (SPLEEM) uses this effect to resolve the orientation of the magnetization vector at high spatial and angular resolution. This talk highlights capabilities of the technique to reveal in situ and in real time quantitative information on micromagnetic configurations and structure-property relationships in nanomaterials.

SS-4-In-1
SINGLE-ATOM PROCESSES ON METAL OXIDE SURFACES

T13 Surface Science

#SS-4-In-1

U. Diebold.

TU Vienna - Vienna (Austria).

The direct view accessible with STM allows the observation of single atoms at surfaces. This is particularly important for metal oxides, where atomic-size defects act as reactive sites, and where small metal clusters, with sizes down to single atoms, play a key role in catalysis. In the talk I will discuss some results of our recent research on Fe3O4, TiO2, SrTiO3, and other metal oxide materials.

SS-8-In-1
THEORY OF KONDO PHENOMENA IN NANOCONTACTS AND IN STM/AFM SPECTRA OF MAGNETIC ATOMS AND MOLECULES

T13 Surface Science

#SS-8-In-1

E. Tosatti.

SISSA, ICTP, and CNR-IOM Democritos - Trieste (Italy).

The properties of atom and molecule- bridged metallic nanocontacts leading to conductance anomalies at break junctions and in STS spectra and in AFM dissipation are difficult to access, yet very rich of phenomena also in connection with magnetism. Electronically, first principles calculations can account well for the gross features of the ballistic conductance of magnetic metal nanocontacts. [1,2] Magnetic impurities bridging nonmagnetic metal contacts yield subtle zero bias anomalies in STS spectra due to the Kondo effect. Qualitatively similar to those of quantum dots, these anomalies are dominated in this case by the specificities of the atomic and molecular states involved, only accessible through a first principles electronic structure approach. The difficulty to combine the Kondo many body physics with the mean-field ielectronic structure poses a problem. We address this problem by means of a joint density functional plus numerical renormalization group approach recently devised.[3] I will illustrate applications to transition metal impurities on carbon nanotubes,[4] and to magnetic molecules on gold surfaces. The possibility of Kondo-related AFM dissipation will also be discussed. Finally, the circumstances conducive to ferromagnetic Kondo effect, as opposed to ordinary antiferromagnetic Kondo, will be outlined along with possible systems where that unusual situation could be realized.[3,5]

(*) Recent work in collaboration with P.P. Baruselli, M. Fabrizio, R. Requist, A. Smogunov

[1] A. Smogunov et al., Phys.Rev. B 70, 045417 (2004).
[2] A. Smogunov et al, Phys. Rev. B 74, 045429 (2006).

[3] P. Lucignano, et al., Nature Materials 8, 563 (2009).
[4] P. P. Baruselli et al., Phys. Rev. Lett. 108, 206807 (2012).
[5] P. Gentile, et al. EPL, 87 27014 (2009).

SS-11-In-1
MOLECULAR ARCHITECTURES AT SURFACES: EMERGENCE OF COMPLEXITY IN FUNCTION AND STRUCTURE.

T13 Surface Science

#SS-11-In-1

R. Raval.

The Surface Science Research Centre, Department of Chemistry, University of Liverpool - Liverpool (United kingdom).

Molecules represent the most versatile, functional entities available in Nature and are central components in the machinery of life. Recently, the use of powerful microscopes and spectroscopies have revealed the nanoscale details of how molecular entities nucleate, organise and propagate functionality at surfaces. This talk will outline how collections of molecules yield beautiful nanoscale architectures and organised patterns. From these assemblies arise complex functions like molecular recognition, mirror-symmetry breaking, adaptive behaviour and non-linear responses[1-6]. Finally, on-surface synthesis of robust, covalently linked soft-matter using clean, generic connection strategies will be demonstrated, with the direct emergence of structural and topological complexity [7,8].

[1] M.Ortega-Lorenzo, C.J.Baddeley, C.Muryn and R.Raval, 'Extended Surface Chirality from Supramolecular Assemblies of Adsorbed Chiral Molecules', Nature, 404 (2000) 376.
[2] N. Liu, S. Haq, G. R. Darling and R. Raval, 'Direct Visualisation of Enantiospecific Substitution of Chiral Guest Molecules into Heterochiral Molecular Assemblies at Surfaces' Angewandte Chemie Int.Ed., 46 (2007) 7613.
[3] P. Donovan, A. Robin, M. S. Dyer, M. Persson, R. Raval, 'Unexpected Deformations Induced by Surface Interaction and Chiral Self-Assembly of Co(II)-Tetraphenylporphyrin adsorbed on Cu(110): A combined STM and Periodic DFT study'. Chemistry, A European Journal, 16 (2010) 11641.
[4] M. Forster, M. Dyer, M. Persson and R.Raval, 'Probing Conformers and

Adsorption Footprints at the Single-Molecule Level in a Highly Organized Amino Acid Assembly of (S)-Proline on Cu(110)'. J. Am. Chem. Soc., 131 (2009) 10173-10181.
[5] M. Forster, M. Dyer, M. Persson and R.Raval, '2-D Random Organization of Racemic Amino-Acid Monolayers Driven by Nanoscale Adsorption Footprints: Proline on Cu(110)', Angewandte Chemie Int. Ed., 2010 (49), 2344-47.
[6] S.Haq, N. Liu, V.Humblot. A.P.J.Jansen, R.Raval, 'Drastic Symmetry Breaking in Supramolecular Organization of Enantiomerically Unbalanced Monolayers at Surfaces'. Nature Chemistry, 1 (2009) 409-414.
[7] S. Haq, F. Hank, M. S Dyer, M. Persson P. Iavicoli, D. B. Amabilino and R. Raval, 'Clean Coupling of Unfunctionalized Porphyrins at Surfaces To Give Highly Oriented Organometallic Oligomers', J. Am. Chem. Soc. 133 (2011) 12031
[8] M. In't Veld, P. Iavicoli, S.Haq, D. B. Amabilino and R. Raval, "Unique Intermolecular Reaction of Simple Porphyrins at a Metal Surface gives Covalent Nanostructures", Chem. Comm., 2008, 1536.

SS-12-In-1
SITE-SPECIFIC IMAGING OF REACTION STEPS IN CATALYTIC CONVERSION OF DIOLS ON TIO2(110)

T13 Surface Science

#SS-12-In-1

Z. Dohnalek.

Pacific Northwest National Laboratory, Fundamental and Computational Sciences Directorate and Institute for Interfacial Catalysis - Richland (United states).

Variable-temperature scanning tunneling microscopy, temperature programmed desorption and dispersion-corrected density functional theory were employed to study chemistry of diols (ethylene glycol and 1,3-propane diol) on TiO_2(110) surfaces. Atomically resolved imaging reveals information about the preferred adsorption sites, O-H bond cleavage, and formation of high temperature reaction intermediates. Further details are uncovered about the translational and rotation dynamics of surface intermediates. The coverage dependent desorption kinetics of alkene and aldehyde as final gas phase products are determined via temperature programmed desorption. Comprehensive theoretical calculations yield a deep insight into the mechanism and energetics of the observed reaction steps.

SS-17-In-1
ATOMIC FORCE MICROSCOPY OF MOLECULES ON INSULATING FILMS: STRUCTURE DETERMINATION AND IMAGING THE CHARGE DISTRIBUTION WITHIN SINGLE MOLECULES

T13 Surface Science

#SS-17-In-1

G. Meyer.

IBM RESEARCH - Rueschlikon (Switzerland).

Ultrathin insulating films on metal substrates are unique systems to use the scanning tunneling (STM)/ atomic force microscope (AFM) to study the electronic and structural properties of single atoms and molecules, which are electronically decoupled from the metallic substrate. Recent work demonstrates the imaging of molecular orbitals, the molecular structure and the intramolecular charge distribution of single molecules with highest resolution. This opens up the possibility to study molecular processes as bond breaking/formation, conformational switching, charge transfer etc. in utmost detail.

SS-5-Kn-1
SINGLE MOLECULE SPECTROSCOPY AT SURFACES

T13 Surface Science

#SS-5-Kn-1

M. Kawai.

Department of Advanced Materials Science, University of Tokyo - Kashiwa (Japan).

Ultimate spatial resolution of scanning tunneling microscope (STM) enables us to observe the inner electronic, vibrational and spin structures of a molecule adsorbed on solid surfaces. Experimentally defined environment surrounding a molecule such as symmetry of the adsorption site and spatial distribution of electronic structure enables precise theoretical consideration. Examples will be given for spin nature of an iron(II) phthalocyanine (FePc) molecule, electronic structure of which is modified by the interaction with the substrate. With precise determination of the symmetry of the adsorption site, we were able to configure the appearance of novel feature of spin + orbital SU(4) Kondo effect.

SS-P1-07
A magnetically focused source for growth of spin-selected molecules.

T13 Surface Science

#SS-P1-07

T. Kravchuk, G. Alexandrowicz.

Israel Institute of technology TECHNION - Kesalsaba (Israel).

Like hydrogen molecules, many other molecules also exist as spin isomers, with the nuclear magnetic moments of the atoms either parallel or anti-parallel. Unlike hydrogen which can be easily separated to its para and ortho states, separation of the spin-isomers of other molecules is not readily available. The development of spin separation methods is motivated by the currently limited knowledge of the physical properties of spin isomers and their interaction with surfaces as well as by their potential applications in a wide variety of research fields, ranging from astrophysics to hyper sensitive nuclear magnetic resonance (NMR).
In this work we present an experimental setup which has been successfully used to form a focused molecular beam of spin selected molecules and produce thin films with a very high spin-purity[1,2]. The general idea, experimental system, different technical issues and experimental results for both water and methane molecules will be presented.

[1] T. Kravchuk, M. Reznikov, P. Tichonov, N. Avidor, Y. Meir, A. Bekkerman and G. Alexandrowicz, Science, 331, 319 (2011).
[2] P.-A. Turgeon, P. Ayotte, E. Lisitsin, Y. Meir, T. Kravchuk, and G. Alexandrowicz, Phys. Rev. A 86, 062710 (2012)

SS-1-In-1
FIRST-PRINCIPLES TRANSPORT SIMULATIONS OF SINGLE-MOLECULE JUNCTIONS

T13 Surface Science

#SS-1-In-1

T. Frederiksen [1], T. Frederiksen [2].

[1]DONOSTIA INTERNATIONAL PHYSICS CTER - San Sebastián (Spain),
[2]IKERBASQUE, Basque Foundation for Science - Bilbao (Spain).

Electron transport in atomic-scale devices is an important research area where both fundamental physics and technological opportunities are simultaneously addressed. From the theoretical point of view one of the great challenges is to develop general methods for quantitative simulations of real devices taking into account the atomistic details. In this talk I will describe recent developments based on the DFT+NEGF approach and discuss capabilities and limitations to various quantum transport problems. A prototype system is electron transport through single-C60 junctions where a critical comparison with various low-temperature STM experiments can be made and where simulations help to provide insight into the roles of interface geometry, chemical nature of the electrodes, and bond formation/rupture under finite voltages.

SS-8-In-2
EDGE STATES OF 1D AND 2D TOPOLOGICAL INSULATORS

T13 Surface Science

#SS-8-In-2

H.W. Yeom.

Department of Physics, POSTECH (Pohang University of Science and Technology) - Gyungbuk (Korea, republic of).

While 3D topological insulators are attracting huge interests in recent days, we are interested in new low dimensional topological insulators. For example, 1D charge density wave (CDW) systems are 1D topological insulators with solutions as their edge states. 2D topological insulators such as HgTe/CdTe have quantum spin Hall states as their edge states. Since edges states of 1D and 2D topological insulators possess exotic spin-charge characteristics, they can be exploited for unprecedented forms of spin and electronic devices. We have tried to directly observe the edge states of new 1D and 2D topological insulators formed on solid surfaces with scanning tunneling microscopy and spectroscopy. The CDW state of In atomic wires self-assembled on Si(111) was used to observe solitons in real space [1]. The edge electronic states were also clearly resolved for the Bi single bilayer grown on BiTe2Se, which was claimed as a 2D topological insulator. The characteristics of these 1D and 2D edge states are discussed.

[1] T.-H. Kim and H. W. Yeom, Phys. Rev. Lett. 109, 246802 (2012).
[1] S.-H. Kim et al., submitted to Phys. Rev. Lett..

SS-2-In-1
GROWTH OF METALS ON GRAPHENE AND GRAPHITE SURFACES

T13 Surface Science

#SS-2-In-1

P. Thiel.

IOWA STATE UNIVERSITY - Ames (United states).

The formation and thermal stability of metal islands on carbon surfaces is relevant to promising future applications that range from biomass conversion to magnetic storage. In this talk we will discuss metals deposited on flat surfaces of graphene and graphite in ultrahigh vacuum, highlighting both experimental results and theoretical understanding. Energetic values derived from density functional theory show that most transition metals, and noble metals, as well as rare earth metals, should exhibit 3D growth on graphene, and this is confirmed in selected experiments. We describe some specific cases where characteristics of those 3D islands—such as number density and shape—can be related to the energetics of individual processes. Differences and similarities expected for graphene and graphite surfaces are discussed.

SS-3-In-1
First principles simulations of water at interfaces: challenges and opportunities

T13 Surface Science

#SS-3-In-1

A. Michaelides.

LONDON CENTRE FOR NANOTECHNOLOGY - London (United kingdom).

Recent years have seen huge advances in the accuracy and realism of first principles simulations. It is now an exciting time that issues such the role of van der Waals dispersion forces, quantum nuclear effects, and thermal (dynamical) effects can all be explored with first principles approaches. In this talk some of our recent work in this area will be discussed. This includes a discussion on the importance of quantum nuclear effects in hydrogen-bonded clusters, crystals, and overlayers (PRL 104, 066102 (2010); PNAS 106, 6369 (2011)) as well as for H adsorption on graphene. Some of our recent work on the development of improved van der Waals functionals for DFT (JPCM 22, 022201 (2010); PRB 83, 195131(2011)) will be covered as well as the their application to problems relating to water adsorption (PRL 106, 026101 (2011)) and high pressure ice (PRL 107, 185701 (2011)). Time permitting, our suggestion that the surface of crystalline ice has properties resembling that of an amorphous material will also be discussed (Nature Mater. 10, 794 (2011)).

SS-11-In-2
SURFACE-CONFINED MOLECULAR SWITCHES AND ROTORS

T13 Surface Science

#SS-11-In-2

J.V. Barth.

Physik Department E20, Technische Universität München - Garching (Germany).

The confinement of functional molecular species in tailored environments leads to new nanoscale phenomena. Notably the organisation and dynamics of individual molecules were controlled by carefully designed supramolecular host architectures. Here we employ temperature-controlled scanning tunneling microscopy to explore open 2D coordination networks on a smooth metal surface, and to steer the assembly of atomic and molecular guests. We identify caged supramolecules performing concerted rotary motions within the template honeycomb pore, which are monitored and quantitatively analyzed. Following a different route, novel bis(porphyrinato) double-deckers (Ce(TPP)2) and tris(porphyrinato) triple-deckers (Ce2(TPP)3) were synthesized directly on a Ag(111) surface (TPP=tetraphenyl-porphyrin). With such double- and triple-decker moieties the respective top ligands are rotatable by STM manipulation provided spatial constraints do not interfere. Furthermore C60-buckyballs have been selectively positioned and oriented on top of double-decker arrays, which combination represents a donor-acceptor dyad. Finally we use free-base porphyrin modules to realize four-level conductance switches based on single proton transfer as depicted below. The atomically sharp tip of an STM is used to selectively remove one of the two hydrogen atoms from the macrocycle cavity, whence the position of the remaining hydrogen atom can be switched between four equivalent pyrrole moieties giving rise to distinct electric current levels.

Nature Nanotech. 7, 41 (2012); Angew. Chem. Int. Ed. 50, 3872 (2011); Phys. Rev. Lett. 106, 026802 (2011) & 110, 086102 (2013); PNAS 107, 21332 (2010) & 110, 6678 (2013); Nano Lett, 7, 3813 (2007) & 12, 4077 (2012).

SS-10-Kn-1
EXPERIMENTAL REALIZATION OF QUANTUM ANOMALOUS HALL EFFECT IN MAGNETIC TOPOLOGICAL INSULATOR

T13 Surface Science

#SS-10-Kn-1

Q. Xue.

Department of Physics, Tsinghua University - Beijing (China).

Anomalous Hall effect (AHE) was discovered by Edwin Hall in 1880. In this talk, we report the experimental observation of the quantized version of AHE, the quantum anomalous Hall (QAH) effect in thin films of Cr-doped (Bi,Sb)2Te3 magnetic topological insulator. At zero magnetic field, the gate-tuned anomalous Hall resistance exhibits a quantized value of h/e2 accompanied by a significant drop of the longitudinal resistance. The longitudinal resistance vanishes under a strong magnetic field whereas the Hall resistance remains at the quantized value. The realization of the QAH effect paves a way for developing low-power-consumption electronics.

This work was carried out in collaboration with Ke He, Yayu Wang, Xucun Ma, Xi Chen, Jinfeng Jia, Li Lu, Lili Wang, Shuaihua Ji, Zhong Fang, Xi Dai, and Shoucheng Zhang.

T14 Thin Films

SE/TF-P2-22
On the Porosity of Cu Coatings Formed in Earth-Based and Space Conditions

T14 Thin Films

#SE/TF-P2-22

L. Skatkov [1], G. Cheremskoy [2], P. Gomozov [2].

[1]PCB "Argo" - Beer Sheva (Israel), [2]NTU "KhPI" - Kharkov (Ukraine).

Introduction

This work examines issues related to the structure, substructure and submicroporosity of metal coatings with face-centered cubic lattices – Cu following condensation under the conditions of space flight of orbital stations and under Earth-based conditions. As described by Cheremskoy et al [1], one major issue in the development of new materials for aerospace engineering applications is the porosity problem, which has significant effects on the performance properties of these materials. To control the parameters of porous structures and predict their stability during operation in the presence of multifactorial external inputs (for example, in open space),the origin, mechanisms and kinetics of processes used to develop porous materials must be subjected to systematic testing and data analysis. Previously [2], we introduced a theoretical model of pore formation in solids based on thermodynamic considerations. Note that in [4] we conducted an experimental survey of the impact of space on thermostatic metal coatings of black aluminium.

Experimental Section

These experiments were conducted on films of Cu condensed on the OS “SALUT –6” and on board the "MIR" orbital station.Small-angle X-ray scattering (SAXS) was conducted according to the previously described technique [3].

Results and Discussion

After the channels are filled and the entire film has formed a significant amount of macro-, micro- and submicropores (SMP) remain, which form through several mechanisms: diffusion-vacancy, the shadow effect, non-compact coalescence and joining of the structural elements, uneven growth, gas absorption and micro-contraction. Which mechanism predominates is determined by the physical and

chemical conditions of evaporation and condensation processes. This comparison of the porosity features of space and Earth-based samples is extremely important for the analysis of the impact of orbital station flight conditions on the mechanism of porosity formation.

For Cu films of different thicknesses, the total porosity measured based on the absorption of monochromatic radiation reaches several per cent.

Most of the porosity of space and Earth-based samples is constituted of micron-sized macro-pores, which cannot be revealed by SAXS. However, the quantity of SMPs is several times greater than the quantity of macro-pores. The observed small-angle X-ray scattering mostly results from SMP's.

The analysis of SAXS indicatrix asymptotes recorded on an incline reveal that Cu films mostly contain SMPs, the orientation and anisometry of which are mostly determined by aligning the motion of molecular flow during condensation.

The pores of Earth-based samples of Cu films are in prolate form, and due to their large size, are aligned in a direction close to the molecular flow direction. However, in space, SMP samples are almost equiaxial.

References

1. Cheremskoy, P.G.; Slezov V.V.; Betechtin, V.I., Pores in Solid State, Energoatomizdat: Moscow, 1990; p.376.

2. Skatkov, L.; Cheremskoy, P. Phase state and thermodynamical principles in porous systems J Mat. Sci. Eng.2011, 5, (4) 478 – 487.

3. Skatkov, L.; Gomozov, V. About the pore formation in nanocrystal metal films, Proc. Conf. Advanced Processing for Novel Functionasl Materials, Max-Planck Ins., Dresden, Germany, January, 2008; pp.495 – 499.

TF-P3-04
Realization and characterization of thin films of tin oxide and titanium oxide for Application DSSCs

T14 Thin Films

#TF-P3-04

M. Melouki [1], M. Adnane [2], Y. Larbah [3], S. Hamzaoui [2], D. Chaumont [4].

[1]Université des sciences et de la technologie Mohamed BOUDIAF « USTO » - Saida (Algeria), [2]Université des sciences et de la technologie Mohamed BOUDIAF « USTO » - Oran (Algeria), [3]Université des sciences et de la technologie Mohamed BOUDIAF « USTO » - Alger (Algeria), [4]Université des sciences et de la technologie Mohamed BOUDIAF « USTO » - Dijon (France).

The dye-sensitized solar cells or solar cell type called Grätzel offers an alternative concept technically and economically credible today for photovoltaic devices. The aim of this project and realize that cell with a tremendous return. The first steps in this work and to make transparent conductive thin layers with low resistance of SnO2: F and TiO2 layers according to SPRAY method and the method of Dr. BLADE respectively. After that what is the use of organic dye and the preparation of the cathode and against the mounting of the solar cell. The characterizations of thin films and of our cells and organic dye that is optically and electrically, and also spectral. We present the current state of land, new concepts of nanocrystallins dye-sensitized solar cell, and the prospects for the future development of technology.

[01] : Mathieu Urien, cellules photovoltaïques organiques à base copolymères à blocs de type rigide-flexible, Université Bordeaux I, 2008.
[02] : LECHAT Isabelle, Etude expérimentale et développement d'un prototype de caractérisation de cellule solaire à colorant, Université de la Réunion 2007.
[03] : Agence Internationale de l'Energie, World Energy Outlook 2007.
[04] : http://www.iea.org.
[5] : U. Diebold, "The Surface Science of Titanium Dioxide"., Surface science reports. 48
(2003) 53-229.
[6] : T. D. Corner, K. Heerington., Journal of American Chemical Society. 77 (1995)

4708.
[7] : Journal of Photochemistry and Photobiology C: Photochemistry Reviews 4 (2003) 145–153 Dye-sensitized solar cells Michael Grätzel Laboratory for Photonics and Interfaces, Swiss Federal Institute of Technology, CH-1015 Lausanne, Switzerland Received 3 June 2003; received in revised form 1 July 2003; accepted 1 July 2003.
[8]: J. Johnsen et S. Chasteen, Juice from juice Make your own blackberry juice solar cell, Exploratorium Teacher Institute. G. Smestad, Titanium Dioxide Raspberry Solar Cell, MRSEC Interdsciplininary Education Group.
[9] : Dyes and Pigments 81 (2009) 224–230 Triphenylamine-based dyes for dye-sensitized solar cells Fan Zhang a, Yan-hong Luo b, Jin-sheng Song a, Xiao-zhi Guo b, Wei-li Liu a, Chun-ping Maa, Yong Huang a, Mao-fa Ge a, Zhishan Bo a,*, Qing-Bo Meng b,** a Beijing National Laboratory for Molecular Sciences, Institute of Chemistry, Chinese Academy of Sciences, Beijing 100190, China b Beijing National Laboratory for Condensed Matter Physics, Institute of Physics, Chinese Academy of Sciences, P.O. Box 603, Beijing 100190, China.
[10] : D.R. di Valdalbero, 'La Recherche Energétique Européenne: Pont de Coopération sur la Méditerranée', Liaison Energie-Francophonie, N°71, Energie et Développement Durable en Méditerranée, pp. 71 - 76, 2ème Trimestre 2006.
[11] : S. Bentouba, A. Slimani et M.S. Boucherit, 'Les Energies Renouvelables dans le Cadre d'un Développement Durable en Algérie, Wilayas du Grand Sud par Exemple', 8ème Séminaire International sur la Physique Energétique, SIPE'06, Centre Universitaire de Béchar, Algérie, 11 - 12 Novembre 2006.
[12]: A. Ainouche, 'Natural Gas and Algerian Strategy for Renewable Energy', 23rd World Gas Conference, Amsterdam, 2006.

TF-6-Or-4
Structural, Compositional and Electronic Transport Properties of Magnetron Sputtered Hydrogen-Aluminium Co-doped ZnO and ZnMgO Films

T14 Thin Films

#TF-6-Or-4

A. Bikowski, K. Ellmer, D. Zajac.

Helmholtz-Zentrum Berlin für Materialien und Energie GmbH - Berlin (Germany).

ZnO:Al and $Zn_{1-x}Mg_xO$:Al belong to the class of transparent conductive oxides. These materials have a high transparency accompanied by a low resistivity and are used in various fields of application like flat panel displays, thin film solar cells, low emissivity glass, etc. [1]. From experiment and theory, it is known that hydrogen acts as a shallow donor in ZnO [2,3]. Since hydrogen is present in almost all deposition processes, it is vital to understand the influence of hydrogen on the electrical properties of ZnO. However, the electrical properties are strongly determined by structural properties like grain size, density of dopants and defects, inclusion of other phases, etc., which requires a combination of analytical methods to obtain comprehensive information about the relation between doping and electrical and structural properties.

The ZnO:Al and $Zn_{1-x}Mg_xO$:Al ($x \approx 0.12$) films were deposited by magnetron sputtering from ceramic targets at substrate temperatures of 300°C as well as at room temperature (without intentional heating). We studied the influence of adding up to 10% hydrogen to the sputtering gas in comparison to films without (intentional) introduction of hydrogen. Secondary ion mass spectrometry (SIMS), elastic recoil detection analysis (ERDA) and Rutherford backscattering spectrometry (RBS) were used to determine the chemical composition of our samples. X-ray diffraction measurements in the Bragg-Brentano geometry revealed the crystalline quality, while

conductivity and Hall measurements were used to determine the carrier concentration and the Hall mobility as a function of the temperature, respectively.

We found, that the hydrogen in the ZnO films acts as a donor only under certain conditions. The effect of the hydrogen on the electrical properties of the films strongly depends on the deposition temperature. For T_{sub}=300°C, the resistivity of the films increased significantly owing to a decrease of the free carrier concentration and the Hall mobility of the carriers. This effect is attributed to the formation of H_2 molecules in the films [4]. For depositions at room temperature, however, the film resistivity could be reduced by up to 2 orders of magnitude by the addition of hydrogen to the sputtering gas. In this case the hydrogen is incorporated in an electrically active way, most probably in the bond-center configuration [5]. This reduction of the resistivity (caused by increasing mobility and carrier concentration) occurred despite the fact, that the films became X-ray amorphous with increasing amount of hydrogen incorporated. This effect has been further investigated by transmission electron microscopy (TEM) and X-ray absorption spectroscopy (XAS), which allow to obtain a detailed picture of the local atomic structure of the samples. Our investigation showed, that in many ways, these X-ray amorphous ZnO:Al and $Zn_{1-x}Mg_xO$:Al films resemble the amorphous transparent oxides, which are used in transparent thin film transistors.

[1] K. Ellmer, J. Phys. D.: Appl. Phys. **34**, 3097 (2001)
[2] C.G. van de Walle, Phys. Rev. Lett. **85**, 1012 (2000)
[3] Y.-S. Kang, H.-Y. Kim, J.-Y. Lee, J. Electrochem. Soc. **147**, 4625 (2000)
[4] Y.H. Kim, S.Z. Karazhanov, W.M. Kim, Phys. Stat. Sol (b) **248**, 1702 (2011)
[5] A. Janotti, C.G. van de Walle, Rep. Prog. Phys. **72**, 126501 (2009)

SE/TF-1-Or-1
Structure and corrosion properties of TiN films deposited by combined HIPIMS-UBM process

T14 Thin Films

#SE/TF-1-Or-1

P. Hovsepian, A. Sugumaran, P. Mandal, A. Ehiasarian.

Sheffield Hallam University - Sheffield (United kingdom).

TiN films were deposited using four cathode HTC 1000-4 Hauzer coating system equipped with Huettinger Electronic Sp.z.o.o power supplies for High Power Impulse Magnetron Sputtering (HIPIMS) and power supplies for standard Unbalanced Magnetron Sputtering (UBMS). In this study, the coatings were produced using different combinations of HIPIMS and standard magnetron sputtering sources. Increasing the number of HIPIMS sources involved in the combined process proved to be an effective tool to manipulate the ionisation degree in the plasma. Optical emission spectroscopy revealed that the intensity ratio of Ti1+:Ti0 in the plasma increased with increasing the number of HIPIMS sources involved in the process from 0.09 to 1.93 for pure UBMS and pure HIPIMS respectively.
TiN coatings phase composition, microstructure texture as well as residual stress, and corrosion properties were studied by number of surface analyses techniques such as X-Ray Diffraction (XRD), Fracture Cross Sectional Scanning Electron Microscopy, (XSEM), Transmission Electron Microscopy, (TEM) as well as RAMAN spectroscopy.
It was revealed that in mixed HIPIMS - UBMS processes the residual stress can be controlled in vide range from -0.21 GPa to -11.35 GPa by smart selection of the degree of HIPIMS utilisation, strength of the electromagnetic field of the unbalancing coils of the machine as well as the bias voltage applied to the substrate.
XSEM analyses revealed that the fracture morphology changes from open columnar to dense almost glassy morphology when the number of HIPIMS sources in the process increases due to the higher ionisation and therefore higher mobility of the condensing species. Furthermore, higher ionisation with HIPIMS dominated processes leads to change in preferred film orientation from (111) to (200).
Significant improvement in corrosion performance was achieved by increasing the number of the HIPIMS sources involved in the process. Raman spectroscopy was used to analyse the nature of the corrosion products as well as to estimate the extent

of the corrosion damage. When polarised around Ecorr values (-1 V to + 200 mV), pure UBM and 1 HIPIMS + 3 UBMS coatings exhibited iron and chromium oxide (Fe_2O_3, Cr_2O_3) peaks at ~495 cm^{-1} and ~ 550 cm^{-1} in the spectra indicating that the corrosion has reached the substrate. No corrosion products were found in the above potential range for 2 HIPIMS + 2 UBMS and pure HIPIMS coatings demonstrating the advantages of the denser structures.
Mixing HIPIMS with UBMS is also seen as an effective tool for improving the productivity of the deposition process.

TF-P2-22
Hybrid Orientation Structure of CeO₂(100) and (110) Regions on Si(100) Substrates Formed by Orientation Selective Epitaxial Growth

T14 Thin Films

#TF-P2-22

T. Inoue, S. Shida.

Iwaki Meisei University - Iwaki (Japan).

Cerium dioxide (CeO_2) has many advantageous properties for various applications; such as high dielectric constant of 26, chemical stability, transmission in visible and infrared regions and high efficient ultra-violet absorption. For application to silicon technology, especially hybrid orientation technology, we are studying a spatially orientation varied epitaxial growth of thin CeO_2(100) and (110) layers on Si(100) substrates using reactive dc magnetron sputtering. It has been found that the epitaxial CeO_2 layer with (100) or (110) orientation is selectively grown by controlling substrate surface potential, which we call orientation selective epitaxial (OSE) growth. There are two ways for the surface potential control; substrate bias application [1] and charged particle irradiation [2]. The latter gives a way to the spatially controlled OSE growth, which will lead to a hybrid orientation structure (HOS) formation.[3]

This paper describes the experimental results on the HOS formation using electron beam irradiation during reactive sputtering. Fig. 1 shows a schematic diagram of the HOS formation: CeO_2(100) grows in the high potential area due to irradiated electron beams, whereas CeO_2(110) grows in the low potential area. Spatially controlled HOS samples were made on Si substrates with various resistivities. We obtained the lateral orientation profiles within the sample surfaces by X-ray diffraction measurements. It was found that the existence of the transition region containing both (100) and (110) components in between the (100) and (110) areas. It is clarified that the transition region width decreases proportionally with the

logarithm of Si substrate resistivity. This can be explained by a potential model. Here, we propose a new way for perfect separation of the two orientation regions using silicon on insulator (SOI) substrates having lithographically isolated Si islands. Preliminary experiments showed that the orientation components vary stepwise from island to island. In order to realize perfect isolation, we are making efforts to optimize the experimental parameters. This work was supported by KAKENHI (20560024). A part of this work was conducted at the AIST nano-Processing Facility, supported by "Nanotechnology Network Japan" of the MEXT, Japan.

[1] T. Inoue, N. Sakamoto, M. Ohashi, S. Shida and A. Horikawa, J. Vac. Sci. Technol., **A22** (2004) 46.

[2] T. Inoue, T. Saito and S. Shida, J. Cryst. Growth, **304** (2007) 1.

[3] T. Inoue, N. Igarashi, Y. Kanno and S. Shida, Thin Solid Films, **519** (2011) 5775.

A schematic diagram indicating the HOS formation using surface potential modification by electron beam irradiation.

SE/TF-1-Or-2
Stress and structure evolution of nanocomposite TiZrAlN protective coatings under ion irradiation

T14 Thin Films

#SE/TF-1-Or-2

G. Abadias [1], I. Saladukhin [2], V. Uglov [2], A. Michel [1], P. Djemia [3], S. Dub [4], G. Tolmachova [5].

[1]Institut P' - Poitiers (France), [2]Belarusian State University - Minsk (Belarus), [3]LSPM - Paris 13 (France), [4]Institute of Superhard Materials - Kiev (Ukraine), [5]Kharkov Institute of Physics and Technology - Kiev (Ukraine).

Quaternary TiZrAlN coatings, deposited by reactive magnetron co-sputtering, have been shown to possess unique microstructure and mechanical properties when increasing the Al content from 0 to 18 at.%. In particular, the formation of hard (H ~ 24-27 GPa) coatings is revealed for Al content between 4.5 and 8 at.%, corresponding to the formation of a nanocomposite structure consisting of cubic TiZr(Al)N nanosized-grains embedded in a highly disordered matrix [1]. For higher Al content, the films tend to be 'X-ray amorphous'. The typical microstructural evolution with increasing Al content is schematically shown in fig.1

The objective of the present work is to investigate the stability and performance behavior of these nanostructured TiZrAlN films under irradiation, as they constitute potential candidates for **radiation-tolerant nanocomposites** [2]. For this purpose, the phase stability and structural evolution upon ion irradiation (Xe^{2+}, 180 keV) is studied using X-ray Diffraction, while the evolution of hardness and elastic properties is obtained by Nanoindentation and Brillouin Light Scattering experiments. Complementary measurements were obtained by XRD using $\sin^2\Psi$ method to determine the stress state of irradiated films. Interestingly, an amorphous-to-crystalline phase transformation is observed for Al contents close to 10 at.%, as shown in fig.2. Several ion fluences, in the range 1 × 10^{15} to 5 × 10^{17} cm^{-2}, were investigated to obtain insights on the ion irradiation induced crystallization process. The results are discussed based on inverse Kirkendall effect, and related Al redistribution at the grain boundary.

[1] I. A. Saladukhin, G. Abadias, A. Michel, S. V. Zlotski, V. V. Uglov, G. N. Tolmachova, S. N. Dub, Thin Solid Films, in press
[2] M. J. Demkowicz, P. Bellon, B. D. Wirth, MRS Bulletin **35** (2010) 1

Fig.1: Schematic structure zone model of sputter-deposited TiZrAlN films

Fig.2. Evolution of XRD pattern of TiZrAlN film with 12.5 at.% Al before and after ion irradiation.

TF-4-In-1
Thin Film Metallic Glasses: Current Status and Future Trends

T14 Thin Films

#TF-4-In-1

J. Chu.

Department of Materials Science and Engineering, National Taiwan University of Science and Technology - Taipei 10607 (Taiwan, republic of china).

Amorphous alloys, or metallic glasses (MGs), are non-crystalline metals with lack of long-range atomic periodicity because they are generally formed with fast quench rates for the retention of the glassy state from the melt. MGs are considered as non-equilibrium materials with important characteristics of the glass transition and crystallization when heated towards the liquid state. Due to the disordered atomic structure and the absence of grain boundaries, MGs have many excellent properties including good soft magnetic properties and exceptional mechanical properties of high specific strength, large elastic limits (~2%), high resistance to corrosion and wear. Thus, they have been a subject of interest for scientific research and engineering application for decades. The pioneer works by Klement et al., Chen and Turnbull, and Chen in 1960s and 1970s reported the first MG samples based on binary Au-Si and ternary Pd-Si-X (X= Ag, Cu or Au) and Pd-Y-Si (Y= Ni, Co or Fe) systems, using rapid solidification methods such as splat quenching. MGs at that time were limited to relatively small sizes, typically in μm, in order to achieve fast quench rates. The recent advent of MGs with relatively high thermal stability and low critical cooling rates, mainly through multi-component composition design, has led to significant improvements in the characteristic specimen sizes. As a result, many MGs (e.g. Zr-, Cu-, Ti-, Fe-, Pd-, Pt- and Au-based systems) with sizes in excess of 1 mm (or so-called bulk metallic glasses, BMGs) have been reported. These BMG systems in general have good glass-forming ability (GFA) such that rapid solidification is unnecessary and BMGs thus have become obtainable with conventional casting methods.
Increasing interest in developing and understanding this new family of materials has also led to making thin film metallic glass (TFMG) processing possible, which was not readily achieved in the past when MGs were available only as powder or ribbon. To make use of great properties, TFMGs with good GFA are evolving as alternative film materials which are potentially useful for many applications such as micro-electro-mechanical system (MEMS) devices. While MGs and BMGs are considered as

newcomers, there are already many succinct and thorough articles reviewing various topics from the science of glass forming, atomic structure to mechanical properties [1-4]. It is thus important for this presentation [5] to summarize and discuss the progress made in this area of TFMG over the past ten years or so and several challenging subjects will be proposed for future research.

References:
[1] W.H. Wang, C. Dong, C.H. Shek, Materials Science and Engineering: R: Reports 44/2-3 (2004) 45.
[2] C.A. Schuh, T.C. Hufnagel, U. Ramamurty, Acta Materialia 55/12 (2007) 4067.
[3] A. Inoue, A. Takeuchi, Acta Materialia 59/6 (2011) 2243.
[4] Y.Q. Cheng, E. Ma, Progress in Materials Science 56/4 (2011) 379.
[5] Jinn P. Chu, J. S. C. Jang, J. C. Huang, H. S. Chou, Y. Yang, J. C. Ye, Y. C. Wang, J. W. Lee, F. X. Liu, P. K. Liaw, Y. C. Chen, C. M. Lee, C. L. Li, and C. Rullyani, Thin Solid Films, Vol. 520 (2012) 5097.

TF/SE-1-Or-1
Evaluation of time-dependent compound layer formation and removal at target surface by model calculation of mass balance change in reactive sputtering

T14 Thin Films

#TF/SE-1-Or-1

E. Kusano, M. Sakamoto.

Kanazawa Institute of Technology - Hakusan (Japan).

To discuss effects of pumping speed and discharge current on time-dependent mass balance change in Ti-O_2 reactive sputtering, formation and removal of a compound layer on target surface is evaluated by a time-increment model based on a previously proposed dynamic mechanism model on target surface condition change[1)]. In Ti-O_2 reactive sputtering, the following O_2 mass balance change is kept;
$Q_{in}+Q_{sputtered} = P_{O2}(S_{gettering}+S_{oxidization}+S_{pump})+Q_{residing}$,
where Q_{in} is the amount of O_2 gas introduced in the chamber, $Q_{sputtered}$ is the amount of O_2 gas sputtered from the target, P_{O2} is O_2 partial pressure, $S_{gettering}$ is gettering pumping speed for O_2 gas by depositing Ti, $S_{oxidization}$ is O_2 gas consumption speed by target surface oxidization, S_{pump} is vacuum pump pumping speed, and $Q_{residing}$ is the amount of O_2 gas residing in the chamber as an increase in O_2 partial pressure. At a steady state $Q_{in}=Q_{gettered}+Q_{pumped}$, because the compound layer formation and removal at the target are balanced. In the model calculation, mass-balance shown in the equation is calculated for a step of a time-increment and $Q_{residing}$ is given as a result of an increase or decrease in O_2 partial pressure between two sequential time steps. In Fig.1 and 2, results of time-dependent formation and removal of a target surface oxide layer for various Q_{in} are shown as a function of time elapsed after discharge ignition for S_{pump} of 0.20 and 0.40 m^3/s, respectively. The results well show time-dependent oxide formation and removal at the target surface for sequential change in Q_{in}. The changes in coverage θ for S_{pump} of 0.20 m^3/s are faster than those for S_{pump} of 0.40 m^3/s, indicating the difference in process stability for the difference in pumping speed. The model well yields information on time-dependent process change in reactive sputtering.

1. E.Kusano, J.Appl.Phys. 73, pp.8565-8574, 1993.

Fig.1 and 2 Formation and removal of target oxide layer for various O_2 flow rates, Q_{in}, as a function of time elapsed after discharge ignition for vacuum pump pumping speed of 0.20 and 0.40 m^3/s, respectively.

TF-P3-08
Calculating Models for Film Thickness Distribution on Inner Surface of Semispherical Work-pieces by Circular Planar Target Sputtering

T14 Thin Films

#TF-P3-08

S. Zhang, W.H. Zhang, Y.H. Xie.

School of Mechanical Engineering and Automation, Northeastern University - Shenyang (China).

In the vacuum coating production, film coatings on the inner surface of semispherical work-pieces are sometimes in demand. When the sputtering coating method has to be adopted to coat the functional films under certain conditions, obtaining uniform film thickness on the inner surface of semispherical work-pieces has great difficulty due to the limitation of sputtering target shape.

In order to solve this problem, the circular planar magnetron sputtering target is chosen in this paper to coat films on the inner surface of semispherical work-pieces. Three arrangement modes of target-substrate systems are proposed: For the small semispherical work-pieces whose diameters are close to the normal sputtering target – substrate distance, the circular planar target is centrally placed relative to the semispherical work-piece; For the larger size work-pieces, or requiring space to arrange for ion source, the target is eccentrically placed outside, as shown in Fig. 1; For those work-pieces whose diameters are far greater than the normal target-substrate distance, the target is eccentrically and aslant placed in the semispherical work-pieces.

Aiming at above arrangement modes, three models are respectively established and the film thickness distributions are calculated. Based on the assumptions of particle cosine emission and straight line flight as well as simplified circular sputtering line, calculation formulas for film thickness distribution on semispherical work-piece inner surface are deduced and the results are illustrated as shown in Fig. 2. By comparison and analysis of calculation data, the optimal structure parameters are obtained. The optimization result can provide reference for relative engineering and technical personnel in the design of coating equipment structure and evaluation of

film performance.

.

Fig.1 The calculating model for circular planar target eccentrically placing
Fig.2. The optimizing film thickness distribution curves for e=0

TF-P2-12
WATER PURIFICATION USING AN HYBRID SYSTEM MEMBRANES / PHOTO-CATALYSIS

T14 Thin Films

#TF-P2-12

O. Arous.

USTHB / CRAPC - Algiers (Algeria).

Abstract:
In this work, we have developped a novel class of polymeric inclusion membranes (PIMs) for the cations separations. The membrane is made up of cellulose triacetate modified by poly-electrolytes using 2-nitrophenyl-pentyl ether (NPPE) incorporated into the polymer as plasticizer. Different (PIMs) are synthesised and characterised by the Fourier Transform Infra-Red, X-ray diffraction, thermal analysis and scanning electron microscopy. The influence of the membrane nature is studied using supports with different physical characteristics (porosity, thickness, hydrophobia). As application, the transport of Pb^{2+} using PIMs coupled with photo-electrodes is investigated.
The photo-catalytic results indicate that the combined system *p*-$CuCrO_2$/membrane/*n*-$Sr_2Fe_2O_5$ enhances considerably the electrons transfer toward the delafossite $CuCrO_2$.

The position of the conduction band of $CuCrO_2$ is looked to be the key issue for the photo electrochemical Pb^{2+} reduction.

Key words: Membrane; Cellulose; Triacetate; Polyelectrolyte; delafossite $CuCrO_2$; photo electrochemical.

TF-P3-01
Switchable Mirror Device with Adhesive Electrolyte

T14 Thin Films

#TF-P3-01

K. Tajima, M. Shimoike, Y. Yamada, M. Okada, K. Yoshimura.

National Institute of Advanced Industrial Science and Technology - Nagoya (Japan).

In order to reduce the environmental load in houses and buildings, windows having a functional coating on the glass are being developed and becoming widespread as energy-saving windows. Our developed switchable mirror glass will be expected for application in new energy-saving windows since they can reflect solar radiation effectively in the reflective state, which results in a reduction in the cost for air conditioning [1-3].
A typical switchable mirror has a multilayer of Mg-based alloy thin film (40 nm)/Pd/Ta_2O_5/H_XWO_3/indium tin oxide (ITO) on a transparent substrate. The layers act as an optical switching, a proton injector, a solid electrolyte, an ion-storage layer and a transparent conductor, respectively. changes its state followed by electrochromic (EC) principle. When a voltage is applied to the mirror, the protons in the ion-storage layer move to the optical switching layer and the layer is hydrogenated, thus resulting in the transparent state [3, 4].
In our conventional fabrication method, the layers were deposited on the substrate by only magnetron sputtering method. In this method, a long fabrication time might be required and it may be difficult to fabricate a large size sample because our sputtering chambers are small. In this research, we focused on the fabrication method of electrolyte layer, and tried to develop a new fabrication method by using adhesive electrolyte to obtain large sample [5].

A part of this work was supported by Industrial Technology Research Grant Program in 2009 (Project No.09B36002a) from NEDO of Japan.

[1] K. Yoshimura, Y. Yamada, M. Okada, Appl. Phys. Lett. **81** (2002) 4709.
[2] Y. Yamada, K. Tajima, S. Bao, M. Okada, K. Yoshimura, Appl. Phys. Lett. **94** (2009) 191910.

[3] K. Tajima, Y. Yamada, S. Bao, M. Okada, K. Yoshimura, Appl. Phys. Lett. **91** (2007) 051908.
[4] K. Tajima, Y. Yamada, S. Bao, M. Okada, K. Yoshimura, Appl. Phys. Lett. **92** (2008) 041912.
[5] K. Tajima, H. Hotta, Y. Yamada, M. Okada, K. Yoshimura, Appl. Phys. Lett. **101** (2012) 251907.

Fig.1 Picture for transparent state of the developed switchable mirror.

Fig.2 Picture for reflective state of the developed switchable mirror.

TF-3-Or-1
Effects of target grain size and density on properties of rf sputtered aluminium oxide thin film

T14 Thin Films

#TF-3-Or-1

M. Sakamoto, E. Kusano.

Kanazawa Institute of Technology - Hakusan (Japan).

It is well known that impurities in a sputtering chamber and a target affect properties of deposited thin films [1)]. To establish a steady, reproducible deposition process of high-quality aluminium oxide (Al_2O_3) insulating thin film by sputtering, the relationship between thin film properties and target properties were investigated. Al_2O_3 thin films were deposited by rf magnetron sputtering using initial condition or pre-sputtered (discharged for 4.5 kWh) target on borosilicate glass substrate with or without indium-tin-oxide coating. The thin film properties were studied in terms of the target parameters such as target purity, target density and grain size. The surface roughness of the films were analyzed by atomic force microscopy and the refractive index was calculated from UV/Vis/NIR spectra. A precision impedance analyzer was used to measure dielectric constant at 1 MHz. Dielectric breakdown was determined by I-V measurement using an electrochemical analyzer. In Fig. 1, the relationship between dielectric constant of deposited thin films and density and grain size of the targets is shown. The dielectric constant is increased with decreasing grain size of the target. Additionally, the refractive index and the dielectric breakdown show the same trend. Fig. 2 shows the correlation between surface roughness of thin films using initial condition target and that of using pre-sputtered target. The correlation coefficient is 0.95, indicating that the film properties would not be affected by impurities derived from the sputtering chamber, but by target properties. It is concluded that the dielectric constant and other properties of the Al_2O_3 thin films are influenced by grain size and density of the sputtering targets.

1. M. Moriyama et al., Materials Transactions, 46(5), 1036-1041, 2005

Fig. 1 Relationship between dielectric constant of deposited thin films and density and grain size of the targets (using pre-sputtered targets).
Fig. 2 Correlation between surface roughness of thin films using initial condition target and that of using pre-sputtered target .

PST/SE/TF-2-Or-4
Grain Growth of Sputter deposited Gold and Silver Thin Films on Polymer Substrates

T14 Thin Films

#PST/SE/TF-2-Or-4

M. Amberg [1], P. Rupper [1], J. Patscheider [2], A. Ritter [1], M. Drabik [1], D. Hegemann [1].

[1]Empa, Swiss Federal Laboratories for Materials Science and Technology - St. Gallen (Switzerland), [2]Empa, Swiss Federal Laboratories for Materials Science and Technology - Dübendorf (Switzerland).

Metal layers on polymer substrates are used in a wide range of applications, such as micro- and nanoelectromechanical systems (MEMS and NEMS), sensors, catalytic activity, bioengineering, and more recently, new developments emerged in electronic textiles. In all these applications, material properties such as mechanical and electrical resistivity, surface morphology and optical reflectivity are affected by the grain growth of the metal deposit.[1]
Thin gold (Au) and silver (Ag) films in the thickness range of 5 to 200 nm were prepared on Si wafers and polyethylene terephthalate (PET) surfaces by pulsed DC sputtering at different pressure and power levels. The variation of deposition pressure and power influences the directionality and the energy flux onto the deposited film.[2] The grain growth, morphology and film properties of Au and Ag layers were investigated on PET foils and compared to films grown on Si wafers. The grain growth of both metals was identified as a monomodal columnar growth from scanning electron microscopy (SEM) and atomic force microscopy (AFM) investigations. X-ray diffraction and AFM investigations showed on both substrates presence of spherical grains with a preferred (111) orientation almost independent of the metal and film thickness. The number of grains per unit area was extracted from AFM data. In the early stage of film growth a strong decrease of the number of grains per unit area was observed for thickness values between 5 and 100 nm, indicating competitive grain growth. For Au films the steady-state grain density of around 500 grains per µm2 was reached at a film thickness of 60 nm for Au films. In comparison showed Ag coatings larger grain size and lower grain densities due to their higher surface diffusion coefficient.

The optical properties were studied by UV-VIS-NIR spectroscopy as a function of film thickness. Anomalies in optical transmission spectra indicate the conversion from discontinuous to continuous film growth. Optimized optical and adhesive properties can finally be established with films below 100 nm.

[1] V. Kotál, V. Švorčík, P. Slepička, P. Sajdl, O. Bláhov, P. Šutta, V. Hnatowicz, *Plasma Process. Polym.*, **4** (2007) 69.

[2] I. Petrov, F. Adibi, J.E. Greene, L. Hultman, J.E. Sundgreen, *Appl. Phys. Lett.*, **63** (1993) 36.

SE/PST/TF/BI-P1-06
Sensing characteristics of Gd2Ti2O7, Er2TiO5 and Lu2Ti2O7 sensing membrane electrolyte-insulator-semiconductor pH sensors

T14 Thin Films

#SE/PST/TF/BI-P1-06

C. Wang [1], T.M. Pan [1], P.Y. Liao [1], F.C. Chiu [2], L. Chi [3].

[1]Chang Gung University - Taoyuan (Taiwan, republic of china), [2]Ming Chuan University - Taoyuan (Taiwan, republic of china), [3]Westfälische Wilhelms-Universität Münster - Münster (Germany).

Recently, thin films of rare-earth (RE) oxides, including Gd_2O_3, Er_2O_3, and Lu_2O_3 [1], are considered for SiO_2 replacement in ultra-large scale integration technologies due to their high dielectric constants, large bandgap energies, high resistivities, and low interface trap densities. The biggest issue when using RE films is moisture absorption to degrade their permittivity through the formation of low-permittivity hydroxides [2]. To solve this problem, the incorporation of Ti or TiO_2 into the RE dielectric films can cause improved electrical properties [3]. The sensing characteristics of the Gd_2Ti_2O7, Er_2TiO_5 and $Lu_2Ti_2O_7$ sensing films in electrolyte-insulator-semiconductor (EIS) device is not clear to date. In this paper, the sensing properties of the $Gd_2Ti_2O_7$, Er_2TiO_5 and $Lu_2Ti_2O_7$ films deposited on a Si substrate were studied. Fig. 1 shows the sensing characteristics of the EIS devices using different sensing films immersed in different pH solutions. To evaluate the sensing performance, we recorded a set of capacitance–voltage (C–V) curves. In the pH sensing of an EIS device, the change in the pH of the solution caused a shift in the flatband voltage of the C–V curves. The $Lu_2Ti_2O_7$ EIS device exhibited a better sensitivity of 59.32 mV/pH than other EIS devices. This result could be attributed to the higher surface roughness. Fig. 2 revealed the drift characteristics and the stability of the EIS pH sensors with different sensing films. The Er_2TiO_5 EIS device exhibited a better long-term stability (slope = 0.29 mV/hr) in comparison with the other EIS sensors.

[1] M. Fanciulli, G. Scarel, Rare Earth Oxide Thin Film: Growth, Characterization, and Applications, Springer, Berlin, 2007.
[2] Y. Zhao, M. Toyama, K. Kita, K. Kyuno, A. Toriumi, Appl. Phys. Lett. 88 (1999) 072904.
[3] T. Schroeder, G. Lupina, J. Dabrowski, A. Mane, Ch. Wenger, G. Lippert, H.J. Mussig, Appl. Phys. Lett. 87 (2005) 022902.

Fig. 1. Reference voltage of $Gd_2Ti_2O_7$, Er_2TiO_5 and $Lu_2Ti_2O_7$ EIS devices plotted as a function of pH.

Fig. 3. Drift phenomena of $Gd_2Ti_2O_7$, Er_2TiO_5 and $Lu_2Ti_2O_7$ EIS devices in a pH = 7 solution.

TF-3-Or-2
Reactive layer assisted deposition mechanism and properties of silver nano-crystals embedded titanium oxide film as a model photo-catalyst

T14 Thin Films

#TF-3-Or-2

L. Zilberberg, M. Asscher.

The Hebrew University - Jerusalem (Israel).

Titanium oxide (TiO_2) is used for various environmental applications such as solar light harvesting in photovoltaic applications, self-cleaning surfaces and sterilization due to its ability to degrade organic compounds, and become super hydrophilic under UV light illumination. All these applications derive from the unique photo-catalytic activity of TiO_2. However, TiO_2 has a wide band gap which limits its efficiency under solar irradiation, therefore an important challenge is to widen its optical activity into the visible spectrum.
The growth mechanism of TiO_2 films and their morphology are being studied using Reactive Layer Assisted Deposition (RLAD) method under ultra high vacuum conditions. The oxide film formation involves Ti atoms deposition on top of amorphous solid water (ASW) condensed on a SiO_2/Si(100) support at 90K. Subsequent annealing leads to desorption of all non-reacted buffer molecules, and at the same time forming and depositing the titanium oxide film. Employing mass spectrometry and using D_2O as buffer, evolution of deuterium molecules has been detected during titanium atoms deposition. A solid state sol-gel-like formation mechanism of titanium oxide is proposed based on these observations. This is the first demonstration of a cold, solid-state sol-gel like oxide film formation. The morphology of the oxide films has been characterized by ex-situ AFM as a rather uniform amorphous film less than a nanometer thick at room temperature. Upon further vacuum-annealing above 750K, crystallization of the titanium oxide film has set-in coinciding with a dewetting process of the oxide layer, information obtained from similar growth procedure on amorphous carbon and Si_3N_4 covered TEM grids. It was shown that these films are rather insensitive to the under laying substrate at temperature below 500K.
The second part of this work addressed the possibility to improve the photocatalytic

activity of TiO_2, via resonant surface plasmons excitation in the visible by growing Ag nano-particles embedded in the TiO_2 nano-film. The method of growing the silver nanoclusters was, in vacuum, Buffer Layer Assisted Growth (BLAG).
The effect of the silver nanoparticles and the titanium oxide composition on the intensity of surface plasmon resonance was studied. It was found that the optical excitation of the embedded silver nano crystals is significantly more stable over time than the absorption of bare silver particles. Namely, the TiO_2 thin film served as a protection layer against oxidation of the silver particles.
The future research plans include preparation of various composites by using different metal oxides, and different metals and alloys. Eventually, we intend to study the photocatalytic activity of these composites at the gas and at the liquid phases.

L. Zilberberg and M. Asscher, Langmuir, 28(49), 17118-17123 (2012)

TF-P3-05
Facile Preparation and Physical Properties of CdS Thin Films

T14 Thin Films

#TF-P3-05

H. Moualkia, A. Mahdjoub, L. Hadjeris, L. Remache, L. Herissi.

Laboratoire des Matériaux et Structure des Systèmes Electromécaniques et leur Fiabilité, Faculté des Sciences et de la Technologie, Université Larbi Ben M'Hidi, Oum El Bouaghi, Algérie - Oum El Bouaghi (Algeria).

Extensive research has been carried out on the deposition and characterization of cadmium sulfide (CdS) semiconducting thin films because of their potential application in the area of electronic and optoelectronic devices [1-4]. Cadmium sulfide which is a material with a direct and wide band gap (2.42 eV), can provide good matching between the lattice and absorption layer, which favors the stability of copper-indium-galium-diselenide (CIGS) solar cells. The highest conversion efficiency of CIGS solar cells that has been reported to date is 20.3% [5]. Among various techniques for preparing cadmium sulfide, chemical bath deposition (CBD) is a simple and low cost method that produces uniform and adherent thin films for solar related applications. One of the advantages of the CBD CdS layers in photovoltaic devices is deposition of very thin layers (< 50 nm) in a conformal manner on the substrate surface. These characteristics produce an increase in the device photocurrent by enhancing the solar cell absorption spectra in the UV-range. In this work, we report on the preparation of CdS thin films by CBD as a function of deposition time. The influence of deposition time on the optical, morphological and structural properties of chemical bath-deposited CdS thin films has been studied. The optical transmittance is made using Shimadzu 1650 PC UV-visible spectrophotometer in the wavelength range 300–1100 nm. Layers thickness (d) is measured by fitting the transmittance. The photoluminescence measurements are carried out using Perkin-Elmer LS 50B luminescence spectrometer. The photoluminescence (PL) spectra are recorded with the excitation wavelength of 457 nm. Surface morphology is performed by atomic force microscopy (AFM) (Pacific Nanotechnology). The latter technique offers digital images which allow quantitative measurements of surface features, such as root mean square (RMS). The crystalline structure is analysed using a BRUKER D8 Advance X-ray diffractometer with line (wavelength: 1.54Å). The optical measurements show that the elaborated thin films have high optical transmission (85%). The band gap presents a maximum value of

about 2.4 eV at deposition time of 45 minutes corresponding to lower disorder. The deposition rate, deduced from the transmittance spectra, lower than 6.5 nm/min, indicates that ion by ion dominates the deposition process and as a result a much smaller grain size and thinner films are obtain. The AFM images display homogeneous and continuous thin layers with small rounded grains and surface roughness RMS of about 22 nm. X-ray diffraction analysis reveals that the deposition films have a cubic structure and the grain size varies between 13 and 35 nm.

[1] K. Senthil, D. Mangalaraj and S. K. Narayandass: Appl. Suf. Sci. 169-170 (2001) 476
[2] G. Sasikala, P. Thilakan, C. Subramanian, Sol. Energy Mater. Sol. Cells 62 (2000) 275.
[3] T.L. Chu, S.S. Chu, Solid State Electron. 38 (1994) 533.
[4] A. Davis, K. Vaccaro, H. Dauplaise, W. Waters, J. Lorenzo, J. Electrochem. Soc. 146 (1999) 1046.
[5] J. Philips, H. Dimitrios, L. Erwin, P. Stefan, W. Roland, M. Richard, W. Wiltraud, P.
Michael, 2011 New world record efficiency for Cu(In, Ga)Se2 thin film solar cells beyond
20 %. Prog. Photovoltaîcs: Res. Appl. 19. 894-897.

TF-1-Or-10
From nano-layers to large area neutron supermirrors.

T14 Thin Films

#TF-1-Or-10

T. Bigault, V. Gaignon, G. Delphin, A. Vittoz, P. Courtois.

Institut Laue Langevin - Grenoble (France).

Neutron supermirrors are multilayer stacks of two different materials deposited alternatively with varying thicknesses, up to thousands of individual layers. The principle is analogous to interferential optical coatings, or to Bragg diffraction by crystals with a varying inter-atomic distance, with a working range restricted to grazing incidence angles.
These coatings, performed on rather large area substrates (several tens of square centimetres), are used as optical elements on instruments using neutron beams. In particular, when one of the materials is magnetic, these mirrors can reflect or transmit selectively neutrons according to their spin state. Thus neutron beam spin-polarisers and spin-analysers can be produced by using supermirrors [1]. At the world-leading European neutron source ILL, such polarising supermirrors are developed and produced on a large scale by magnetron sputtering, based on Co/Ti and Fe/Si material pairs [2].
A few examples of recent supermirror production projects for ILL instruments will be given.
Optimizing the performance of polarising supermirrors requires tailoring the microstructure and magnetic properties of these complex multilayer stacks [3]. Some challenges linked to this optimization will be presented, together with recent progress in this domain.

[1] O. Schärpf, *Thin-film devices and their role in future neutron spectroscopic investigations*, Phys. B: Cond. Matt. 174, 514-27 (1991).
[2] J. R. Stewart, P. P. Deen, K. H. Andersen, et al., *Disordered materials studied using neutron polarization analysis on the multi-detector spectrometer, D7*, Journ. Appl. Cryst. 42, 69-84 (2009).
[3] P. Hoghoj, I. Anderson, R. Siebrecht, et al., *Neutron polarizing Fe/Si mirrors at ILL*, Phys. B: Cond. Matt. 267-268, 355-9 (1999).

TF-P2-01
Self-organization of nickel nanoparticles in dielectric matrices

T14 Thin Films

#TF-P2-01

M. Jerčinović [1], M. Buljan [1], N. Radić [1], P. Dubček [1], S. Bernstorff [2], G. Dražić [3], D. Pajić [4], K. Zadro [4].

[1]Ruđer Bošković Institute - Zagreb (Croatia), [2]Elettra Sincrotrone - Trieste (Italy), [3]Jožef Stefan Institute - Ljubljana (Slovenia), [4]Faculty of Science - Zagreb (Croatia).

Ni nanoparticles (NPs) attract lot of interest as catalyst for carbon nanotube growth, as particles
forming interacting or noninteracting ensembles, optoelectronic entities, etc. We have produced self-ordered Ni NPs either on surface or embedded into the alumina or silica matrix starting from three types of nickel and alumina multilayered structures prepared
by magnetron sputtering. The structure and morphology of the prepared materials have
been examined by grazing-incidence small-angle scattering (GISAXS), wide-angle X-ray
scattering (WAXS), atomic force microscopy (AFM), and transmission electron microscopy
(TEM), while magnetic properties were measured by SQUID magnetometer.

Thin Ni films deposited onto dielectric's surface exhibit markedly different particle size distribution at room temperature and at elevated temperatures. The effect of temperature on
NP formation has been employed for formation of 3-dim arrays of Ni NPs
in dielectric matrix. Two types of precursor materials have been used: a) multilayers consisting od alternating pure Ni and pure alumina layers, and b) multilayers consisting
od alternating mixed Ni+alumina and pure alumina layers. Both types of precursor material were deposited at room temperature and at elevated temperature, and subsequently
annealed. The size of the Ni NPs and their average lateral distance was controlled

by the amount of Ni in the Ni-containing layer, while their cross-layer interaction was governed by the thickness of intervening dielectric spacer. That way, the magnetic properties
could be controlled, as well.

An example of the effects of alumina dielectric spacer thickness (6 & 2 nm) and annealing
temperature (RT & 500°C) upon Ni NPs sizes and spatial distribution is shown in composite GISAXS Fig. 1.

The size and spatial distributions of Ni NPs govern the supermagnetic properties of such an ensemble. An example of the blocking phenomena of superparamagnets is shown in
Fig. 2 for Ni NP array in silica.

Fig.1. GISAXS maps (first row = as-grown; second row = annealed at 500°C).

Fig.2. Temperature dependence of the zero-field-cooled and field-cooled magnetization.

TF-3-Or-3
Nanopatterned Zinc Titanate Thin Films Prepared by the Evaporation-Induced Self-Assembly Process

T14 Thin Films

#TF-3-Or-3

Q. Xu [1], M. Järn [2], M. Lindén [3], J.H. Smått [1].

[1]Åbo Akademi University - Turku (Finland), [2]YKI, Institute for Surface Chemistry - Stockholm (Sweden), [3]University of Ulm - Ulm (Germany).

Nanopatterned thin films prepared by the evaporation-induced self-assembly (EISA) process have up to now been limited to a few transition metal oxides (i.e. Al_2O_3, TiO_2 and ZrO_2)[1]. Here we describe for the first time the formation of zinc titanate nanoperforated thin films with different Zn/Ti ratios using the dipcoating process. Atomic force microscopy and scanning electron microscopy reveal that the structure consists of well-ordered pseudohexagonal nanoperforations in the range of 30 nm in diameter separated by 25 nm wide metal oxide ridges, while the film thickness is close to 2 nm (Figure 1). For films with a zinc precursor content up to 50 mol-%, the well-organized structure of the thin film can be maintained, while at higher Zn contents the nanostructure is gradually becoming more disordered. Grazing incidence x-ray diffraction measurements on the films calcined at 700 °C indicate that the anatase phase of the pure TiO_2 films is gradually consumed at the expense of a newly formed $Zn_2Ti_3O_8$ phase[2] upon increasing the Zn/Ti ratio in the starting precursor solution (Figure 2). To the best of our knowledge, this is the first demonstration of the preparation of ternary metal oxide nanopatterned thin films using the EISA approach and the unique combination of the nanostructure with the zinc titanate composition grants these films significant application prospects in for instance optics and catalysis.

[1] M.Kuemmel, et al, Chem. Mater. 19 (2007) 3717-3725.

[2] N.T.Nolan, et al, Chem. Mater. 23 (2011) 1496-1504.

Figure 1. AFM images (1*1µm) of metal oxide films with different molar fractions of Zn and in the insets the corresponding FFT images in the range of q = 0-30 μm^{-1}

Figure 2. Thin film XRD patterns of zinc titanate films with different Zn content calcinated at 700°C

PST/SE/TF-2-Or-1
Pt nanoclusters prepared by magnetron sputtering and cluster beam deposition for proton exchange membrane fuel cell

T14 Thin Films

#PST/SE/TF-2-Or-1

A. Caillard [1], S. Cuynet [1], P. Brault [1], T. Lecas [1], S. Baranton [2], C. Coutanceau [2], J. Bigarré [3], P. Buvat [3].

[1]GREMI UMR7344 CNRS-Université d'Orléans - Orléans (France), [2]IC2MP UMR 7285 CNRS-Université de Poitiers - Poitiers (France), [3]CEA DAM, Le Ripault, - Monts (France).

Metallic nanoclusters have found numerous applications in heterogeneous catalysis (effluent treatments, sensors, energy storage and conversion, etc.). Costly and strategic metals from the platinum group are required. There is thus a real interest to obtain the highest catalytic surface area from a low metal weight, in particular for fuel cell electrodes for achieving highest performance.

Here, different techniques of physical vapor deposition have been developed for the synthesis of Pt catalytic nanoclusters. We can distinguish sputtering techniques where the nucleation and the growth clusters occur on the substrate (conventional DC magnetron sputtering – DCMS) from those where the nucleation and the growth happen in the gas phase (low energy cluster beam deposition, LECBD).

In this work, well defined platinum nanoclusters are produced by DCMS/LECBD on perfluoropolymer membranes (Nafion® used as ion conductive electrolyte in fuel cell) and on microporous carbon substrates (Sigracet® carbon used as cathode in fuel cell). Platinum acts as catalyst for oxygen reduction at the cathode-membrane interface. The physical and the electrochemical properties of the Pt nanoclusters have been investigated as a function of the deposition technique and of the deposition parameters. The catalyst coated membrane (CCM) and the catalyst coated backing (CCB) are tested in a proton exchange membrane fuel cell station. The maximum power densities reach 0.7 and 0.50 W cm^{-2}, respectively. The

performance is compared to those obtained with commercial fuel cell where the Pt nanoclusters are grown by chemical routes.

TF-9-Or-6
Uniformity improvements of low-losses mirrors coated by Ion Beam Sputtering on large substrates for future gravitational wave detectors

T14 Thin Films

#TF-9-Or-6

C. Michel [1], L. Pinard [1], B. Sassolas [1], R. Bonnand [2], G. Cagnoli [3], J. Degallaix [1], D. Forest [1], R. Flaminio [1], G. Billingsley [4].

[1]CNRS- Laboratoire des Matériaux Avancés - Villeurbanne (France), [2]CNRS-LAPP - Annecy (France), [3]CNRS- Laboratoire des Matériaux Avancés - Villeurbanne (United states), [4]LIGO-California Intitute of technology - Pasadena (United states).

The second generation of gravitational wave detectors will aim at improving by an order of magnitude their sensitivity versus the present ones (LIGO and VIRGO) [1]. These detectors are based on long-baseline Michelson interferometers @ 1064 nm with high finesse Fabry-Perrot cavity in the arms and have strong requirements on the optics. These large low-losses mirrors (340 mm in diameter, 200 mm thick) must have a near perfect flatness. The coating process shall not add surface figure Zernike terms higher than second order with amplitude >0.5 nm over the central 160 mm diameter. The limits for absorption and scattering losses are respectively 0.5 and 5 ppm. For each optic the maximum loss budget due to the surface figure error should be smaller than 20 ppm. Moreover the transmission matching between the two inputs mirrors must be better than 99%.

Coatings are done using Ion Beam Sputtering (IBS) technique in a large chamber specially developed for this purpose. Low losses optics with very high reflection value (R>99.999%) were obtained by multilayer dielectric coating based on a stack of alternate Titanium doped Tantalum pentoxide (Ti:Ta2O5) layers and silica layers. The total coating thickness is 2.8 µm for the Input mirrors and 5.2 µm for the End Mirrors.

We describe the different configurations that were explored in order to respect all these requirements.

The two first configurations based on a single rotation motion for the substrates combined or not with uniformity masks allow obtaining uniformity around 0.2 % rms on 160 mm diameter [2]. But this is not sufficient to meet all the specifications. A planetary motion completed by masking technique has been studied. With simulated values the loss budget is below 20 ppm, better than the requirements. Experimental results obtained with the planetary system will be presented.

[1] G. M. Harry (for the LIGO Scientific Collaboration), “Advanced LIGO: the next generation of gravitational wave detectors,” Classical and Quantum Gravity 27, 084006 (2010).

[2] B. Sassolas, Q. Benoit, R. Flaminio, D. Forest, J. Franc, M. Galimberti, A. Lacoudre, C. Michel, J.L. Montorio, N. Morgado, L. Pinard- “Twin mirrors for the laser interferometric gravitational-wave detectors” Applied Optics, Vol. 50 n°13 (2011) 1894

TF-9-Or-14
From Surface to Interface Electronic States: In Situ Spectroscopy study of STO and LAO/STO heterostructures

T14 Thin Films

#TF-9-Or-14

M. Radovic [1], N. Plumb [1], E. Razzoli [1], M. Shi [1], M. Kobayashi [1], T. Schmitt [1], V. Strocov [1], L. Patthey [2], J. Mesot [2].

[1]Swiss Light Source, Paul Scherrer Institut - Villigen (Switzerland), [2]Paul Scherrer Institut - Villigen (Switzerland).

The electronic properties of the interfaces between transition metal oxides, and in particular the discovery of 2D conductivity in heterostructures composed of LaAlO3 (LAO) and SrTiO3 (STO) band insulators [1], have generated new paradigms, challenges, and opportunities [2] in condensed matter physics. Recently, a universal surface metallic state was also found on bare STO(001) crystals [3,4,5], raising important questions concerning the role of the LAO overlayer and the effective differences between STO/vacuum and LAO/STO interfaces [6,7]. Here, by using pulsed laser deposition (PLD) coupled in situ with angle-resolved photoemission spectroscopy (ARPES), we show the evolution from the metallic state on STO to the one found in LAO/STO. While the character and size of the Fermi surfaces in all these systems are qualitatively similar, LAO/STO interfaces exhibit a sign of 2×1 reconstruction when the LAO layer matches or exceed the conventional critical thickness of 4 unit cells (uc). In addition, LAO/STO interfaces show a similar response to irradiation as previously reported for bare STO [4]. We interpret these findings within the framework that the low-dimensional metals in STO surfaces and interfaces originate from a polar lattice distortion that can be triggered in multiple ways – e.g., directly by photons, or indirectly through coupling to a secondary deformation driven by polarity, diluted defects and/or strain effects.

1. Ohtomo, A. & Hwang, H. Y., Nature 427, 423-426 (2004).
2. Mannhart, J. & Schlom, D. G., Science 327, 1607-1611 (2010).
3. Santander-Syro, A. F. et al., Nature 469, 189-193 (2011).
4. Meevasana, W. et al., Nature Mater. 10, 114-118 (2011).

5. Di Capua, M. Radovic, G. M. De Luca, I. Maggio-Aprile, F. Miletto Granozio, N. C. Plumb, Z. Ristic, U. Scotti di Uccio, R. Vaglio, and M. Salluzzo, Phys. Rev. B Phys. Rev. B 86, 155425 (2012).
6. Ke-Jin Zhou, Milan Radovic, Justine Schlappa, Vladimir Strocov, Ruggero Frison, Joel Mesot, Luc Patthey, and Thorsten Schmitt, Phys. Rev. B 83, 201402(R) (2011)
7. Z. Salman, O. Ofer, M. Radovic, H. Hao, K. H. Chow, M. D. Hossain, C. D. P. Levy, W. A. MacFarlane, G. M. Morris, L. Patthey, M. R. Pearson, H. Saadaoui, T. Schmitt, D. Wang, and R. F. Kiefl, Physical Review Letter 109, 257207 (2012).

Figure I. Fermi surface maps of STO (001) surfaces and LAO/STO interfaces obtained by ARPES. a, b, c, d panels show evolution of the surface states (obtained with photon energy of 465eV) toward to the interface states after depositing different thicknesses of LAO layer. Fermi surface (with high resolution) of STO surface obtained at 85 eV is presented in subpanel 1.a.

TF/SE-P3-01
Formation of hydrated oxide thin films by reactive sputtering in H2O atmosphere and their electrical properties

T14 Thin Films

#TF/SE-P3-01

Y. Abe, N. Li, K. Nishimoto, M. Kawamura, K.H. Kim, T. Suzuki.

Kitami Institute of Technology - Kitami (Japan).

Proton conducting hydrated oxide thin films have been attracted attentions as a solid electrolyte layer of electrochromic devices and switchable mirrors. (1,2) To prepare hydrated oxide thin films, our group has developed a new reactive sputtering technique using H_2O as a reactive gas. OH radicals and atomic hydrogen formed in the H_2O plasma were incorporated into the growing films and hydrated oxide films were deposited. (3,4)

In this study, metal targets of Ti and Y were reactively sputtered in H_2O atmosphere at substrate temperatures from -30 to +130°C, and hydrated TiO_2, and YOOH thin films were formed. Infrared spectra of all the films indicated that the absorption peak intensity due to OH bonds, which corresponds to the amount of hydrogen in the films, increased with decreasing substrate temperature.

The electrical conductivities of the films were estimated by AC impedance measurements in a frequency range from 10 mHz to 1 MHz at room temperature. The conductivities of the TiO_2 and YOOH films with a thickness of about 1 micrometer are plotted in Fig. 1 as a function of substrate temperature. The conductivities of the Ta_2O_5 and ZrO_2 films (3,4) are also plotted in the figure for comparison. The conductivities of the Ta_2O_5, ZrO_2, and YOOH films increased with decreasing substrate temperature, and maximum conductivities of about 10^{-5} S/m were obtained at the lowest substrate temperature of -30°C. The increase of the conductivity corresponds well with the increase of the absorption peak intensity due to OH bonds. These results suggest strongly that the electrical conductions of the Ta_2O_5, ZrO_2, and YOOH films are caused by proton conduction. In contrast, the conductivity of the TiO_2 films increased with increasing substrate temperature. It is considered that the electrical conduction of the TiO_2 films is caused by electron

transport. N-type semiconducting TiO_2 is though to be formed by the incorporation of hydrogen.

1) F. Z. Tepehan, F. E. Ghodsi, N. Ozer, G. G. Tepehan, Sol. Ener. Mater. Sol. Cells, vol. 59 (1999) p. 265.
2) K. Tajima, Y. Yamada, S. Bao, M. Okada, K. Yoshimura, Solid State Ionics, vol. 180 (2009), p. 654.
3) Y. Abe, F. Peng, Y. Takiguchi, M. Kawamura, K. Sasaki, H. Itoh, T. Suzuki, Jpn. J. Appl. Phys., vol. 47 (2008) p. 7269.
4) N. Li, M. Suzuki, Y. Abe, M. Kawamura, K. Sasaki, H. Itoh, T. Suzuki, Sol. Ener. Mater. Sol. Cells, vol. 99 (2012) p. 160.

Fig. 1 Conductivities of reactively sputtered hydrated oxide thin films as a function of substrate temperature.

TF-2-Or-1
Optical Resonances in Short-range Ordered Nanoholes in Ultrathin Aluminum / Aluminum Nitride Multilayers

T14 Thin Films

#TF-2-Or-1

T. Sannomiya [1], Y. Ikenoya [1], M. Susa [1], A. Dahlin [2], J. Shi [1], Y. Nakamura [1].

[1]Tokyo Institute of Technology - Tokyo (Japan), [2]Chalmers University of Technology - Gothenburg (Sweden).

Introduction

Metallic nanohole arrays have been widely investigated due to their potential application to chemical- and bio-sensing, metamaterials, photovoltaic cells as well as for scientific interests in their unique optical responses. Their useful and also intriguing optical characteristic is the asymmetric resonance originating from the inter-hole coupling through supported bonding- surface plasmons (SPs). In most past research the nanoholes have been fabricated in a single thick layer more than 10 nm using noble metals. In this study, we fabricate nanoholes in ultrathin Al/AlN multilayers with their optical resonance adjusted in the Vis-NIR range. In this system, it is possible to deposit metallic and dielectric films as thin as a few nanometers with atomically smooth interfaces.

Method

100nm colloid particles were deposited on glass substrates and multilayers of Al and AlN were sputter-deposited on the colloid-masked substrates. The colloid particles were then removed to create nanohole arrays. The fabricated samples were evaluated by SEM, AFM and transmission spectroscopy, and analyzed by comparing with the dispersion relation of the multilayer systems. Vacuum annealing up to 400°C was also performed to test the thermal stability.

Results

The created nanoholes, as shown in the AFM image of Fig.1, have a short range order with characteristic spacing. The radial distribution function of the nanoholes exhibits a clear peak around 200 nm corresponding to the characteristic hole-hole

distance. Propagating SPs interfere between nanoholes resulting in the resonance.[1] SP modes can be calculated by solving the dispersion relation. The optical spectra of multilayers, consisting of three 2.3nm AlN and two 5.0/2.5nm Al layers, are shown in Fig.2. The asymmetric resonance shape is characterized by the dip and peak at the higher wavelength, which are here tuned to Vis/NIR.

[1]*Small* 7, 1653-1663, 2011.

Fig.1 : AFM image of nanoholes, Fig.2 : Optical spectra of nanoholes in five layer films

TF-2-Or-2
Molecular dynamics study of the growth of various crystalline phases of TiO2 and Al2O3

T14 Thin Films

#TF-2-Or-2

J. Houska [1], S. Mraz [2], J.M. Schneider [2].

[1]University or West Bohemia - NTIS - Plzen (Czech republic), [2]RWTH Aachen University - Aachen (Germany).

Thin films of crystalline transition metal oxides are of high interest due to a wide range of functional properties. Previously, their preparation has been described in terms of extrinsic process parameters, such as total pressure, oxygen partial pressure or substrate bias potential. We study the growth of individual phases of TiO_2 (rutile x anatase) and Al_2O_3 (α x γ) using a combined approach of magnetron sputtering and atom-by-atom molecular dynamics (MD) simulations (>=3000 deposited atoms per simulation). We focus on the effect of intrinsic process parameters including particle energy, growth temperature and growth template. We report a significant methodological progress: while most of the structures of various materials obtained (predicted) previously by classical MD simulations are amorphous, we study the growth of multiple competing crystalline phases described by a single interaction potential. A particular advantage of these simulations is a disentanglement of the nucleation and the growth. We identify which classes of interaction potentials allow such simulations and which do not.

In the case of TiO_2, experiments indicate that the deposition of rutile requires higher temperatures and/or energies compared to anatase. However, MD simulations [1] show that the growth of (previously nucleated) rutile can take place in a wider range of process parameters (at lower temperatures and especially both at lower and up to higher energies per film-forming atom) compared to anatase. Growth of distorted rutile is observed even on (110) and (111) anatase, in a slightly narrower range of process parameters compared to the undistorted rutile growth.

In the case of Al_2O_3, MD simulations allow us to identify that an energy of 35-50 eV is ideal for the growth of (previously nucleated) α-Al_2O_3. The crystals (i) quickly

amorphize if the energy per film-forming atom is lower and (ii) slowly amorphize if the energy per film-forming atom is higher (especially at small crystal size). The aforementioned ideal energy value slowly decreases with increasing growth temperature. On the contrary, we show that (previously nucleated) γ-Al_2O_3 grows in a very wide range of process parameters.

In all cases, the crystal growth is supported (the amorphization is slowed down) if the crystal (column) is sufficiently wide compared to the thermal spike size. In such a case, the undamaged crystalline cells support "healing" of the damaged neighboring cells.

Phenomena observed experimentally are in agreement with the MD results. Collectively, the results provide an insight into the complex relationships between process parameters and deposited film structures. Consequently, they allow one to tailor the synthesis pathways for the production of TiO_2 and Al_2O_3 thin films, considering conditions for nucleation and different conditions for growth. The phenomena shown (e.g. the fact that the phase which more easily nucleates in not necessarily the same which more easily grows) may be tested for even wider range of materials.

[1] J. Houska, S. Mraz and J.M. Schneider, J. Appl. Phys. 112, 073527 (2012)

TF-P2-02
In-situ time-resolved microGISAXS investigation of the growth kinetics of Ag-PTFE nanocomposites prepared by sputter deposition

T14 Thin Films

#TF-P2-02

G. Santoro, S. Yu, A. Buffet, M. Schwartzkopf, S. Koyiloth Vayalil, S. Bommel, G. Herzog, B. Heidmann, J. Perlich, S. Roth.

HASYLAB at DESY, Notkestr. 85, D-22607 - Hamburg (Germany).

Polymer metal nanocomposites are interesting materials because of the extraordinary physical properties they show. They are used in advanced optical, electrical and medical applications, as well as for data storage and catalytical applications [1]. Among the different methods used to prepare such nanocomposites, sputter deposition is a widely employed technique in industry and research, presenting a major advantage in comparison with wet chemical approaches that is the absence of residual solvents in the prepared thin films. RF sputter deposition allows to extend this technique to depositing insulating materials, such as polymers. Thereby one can especially use the co-sputter deposition of the metal and the organic materials at the same time to create tailored nanostructures.

Ag-polytetrafluoroethylene (Ag-PTFE) nanocomposites prepared by sputter deposition has been shown to exhibit excellent properties that can be exploited for applications such as antibacterial coatings, plasmonic devices or sensors [2]. Nevertheless, in order to fully control the desired final properties of the nanocomposites, that are very sensitive to the size and shape of the nanoparticles as well as to the arrangement of the metal nanoclusters inside the polymeric matrix, it is mandatory to achieve a profound understanding of the growth kinetics of the nanocomposites. In this sense, micro Grazing Incidence Small Angle X-ray Scattering (μGISAXS) [3] is a very powerful and valuable tool for the in-situ characterization of the growth kinetics allowing to extract morphological information of the surfaces that are developing with time resolution on the order of the millisecond [4].

In this work we present important μGISAXS results concerning the time evolution of the structures developed during the RF-sputtering of PTFE/Ag nanocomposites by the co-sputtering of Ag and PTFE. A portable in-situ RF-sputter deposition chamber [5] that can be couple to the P03 beamline (MiNaXS beamline) at the PETRA III storage ring (DESY, Hamburg) has been designed and manufactured (Fig. 1).

[1] J. Perlich, *et al.*, Chemphyschem **10**, 799 (2009).

[2] F. Faupel, *et al.*, Advanced Engineering Materials **12**, 1177 (2010).

[3] P. Müller-Buschbaum, edited by T. Ezquerra, M. Garcia-Gutierrez, A. Nogales and M. Gomez (Springer Berlin / Heidelberg, 2009), Vol. 776, p. 61.

[4] A. Buffet, *et al.*, Journal of Synchrotron Radiation **19**, 647 (2012).

[5] R. Doehrmann *et al.*, Rev. Sci. Instrum. (submitted).

Figure 1. RF sputter deposition experimental set-up at the P03 beamline (MiNaXS beamline) of the PETRA III storage ring (DESY, Hamburg, Germany).

TF-2-Or-3
KMC approach to simulations of mosaic phase formation on the Si(111) surface

T14 Thin Films

#TF-2-Or-3

P. Kocán, P. Sobotík, I. Oštádal, P. Matvija.

Charles University - Prague (Czech republic).

Deposition of metals on the Si(111) surface together with an appropriate thermal activation results in re-organizing of surface atoms to variety of ordered structures, often with interesting properties. A special attention has been paid to mosaic phases of 2D alloys with $(\sqrt{3}\times\sqrt{3})R30^\circ$ symmetry. These structures are usually induced by desorption of metal atoms (Pb, Sn, Tl) together with substitution by Si atoms.

We use configuration-based kinetic Monte Carlo (KMC) model to explain important features related to the mosaic structure formation: 1) the zeroth order of desorption surprisingly observed in the case of Pb/Si(111) system [1-3], 2) mechanism of substitution by Si adatoms and 3) ordering of the 2D metal/Si alloy into the mosaic phase by means of effective repulsive interaction [4].

The zeroth-like order desorption spectra are simulated by means of first-order desorption processes with enhanced desorption from domain boundaries. For the substitution of desorbed metal atoms by Si adatoms, fast diffusion of adatoms on top of 1×1 layer is proposed as the most probable. In the case of the mosaic ordering similar to the 2D antiferromagnetic Ising system on a triangular lattice, a new mechanism of ordering induced by selective desorption is provided and tested.

The model was succesfully applied on the examples of Tl [5] and Pb [1-3] desorption.

[1] M. Saitoh, K. Oura, K. Asano, F. Shoji, and T. Hanawa, Surf. Sci 154, 394 (1985).

[2] E. Ganz, I.-S. Hwang, F. Xiong, S. K. Theis, and J. Golovchenko, Surf. Sci 257, 259 (1991).

[3] J. A. Carlisle, T. Miller, and T.-C. Chiang, Phys. Rev. B 45, 3400 (1992).

[4] M. Svec, P. Jelinek, P. Shukrynau, C. Gonzales, V. Chab, and V. Drchal, Phys. Rev. B 77, 125104 (2008).

[5] P. Kocan, P. Sobotik, P. Matvija, M. Setvin, and I. Ostadal, Surf. Sci.606, 991 (2011).

TF-4-Or-2
Magnetron sputtering of ZrB2 films on 4H-SiC(0001) and Si(100) substrates

T14 Thin Films

#TF-4-Or-2

L. Tengdelius [1], M. Samuelsson [2], J. Jensen [1], J. Lu [1], U. Forsberg [3], L. Hultman [1], E. Janzén [3], H. Högberg [1].

[1]Thin Film Physics Division, Department of Physics, Chemistry, and Biology (IFM), Linköping University, SE-581 83 - Linköping (Sweden), [2]Impact Coatings AB, Westmansgatan 29, SE-582 16 - Linköping (Sweden), [3]Semiconductor Materials Division, Department of Physics, Chemistry, and Biology (IFM), Linköping University, SE-581 83 - Linköping (Sweden).

Zirconium diboride, ZrB_2, combines typical ceramic properties such as high hardness and high melting point with a low resistivity. Moreover, ZrB_2 exhibits a lattice mismatch to 4H-SiC(0001) of only 3.8%, which is favorable for heteroepitaxial growth. This makes ZrB_2 interesting as a thin film contact material in e.g. microelectronics. It is known that the electrical properties of ZrB_2 are influenced by film structure, composition, as well as the level of contaminants. These properties, in turn, can be influenced by process parameters such as growth temperature and bias voltage.

In this study the effect of deposition temperature and applied bias voltage on the electronic properties of ZrB_2 thin films was investigated under industrial conditions. The ZrB_2 films were deposited by direct current magnetron sputtering from a ZrB_2 compound target in an industrial scale high vacuum system on 4H-SiC(0001) and Si(100) substrates. The base pressure of the system was ~0.13 mPa – 1.3 mPa, depending on the growth temperature. A high deposition rate (~30 Å/s), in combination with short deposition times (100 s) minimized the influence of the residual gas. Films were grown at three different temperatures (without intentional heating (RT), 400°C and 550°C), and at a range of substrate bias voltages between -20 V and -80 V. Scanning electron microscopy showed that the films exhibit a columnar appearance. All films showed a B/Zr ratio close to, or slightly below 2 (stoichiometry), and low levels of contaminations (O content < 1 at%), as determined by time-of-flight energy elastic recoil detection analysis. X-ray diffraction and selected area electron diffraction patterns (SAED from TEM, see Fig. 1), showed that with

increasing deposition temperature, the crystallographic structure changed from a (0001) fiber texture to a random orientation. Moreover, increasing the growth temperature in combination with increasing the substrate bias caused the relative metallic content in the films to increase somewhat, yielding B/Zr ratios close to 1.84. Transmission electron microscopy showed an amorphous layer at the interface between the film and substrate for films deposited at RT (see Fig. 1), whereas such a layer was not present in films grown at high temperature. Upon increasing substrate bias voltage as well as the growth temperature, it was found that the electrical resistivity decreased from 200 to ~100 μΩcm. Furthermore, results from ex-situ annealing experiments –an attempt to increase crystallinity and further improve the electrical properties – will be presented.

Fig 1. TEM image and SAED pattern of a film deposited at RT with a substrate bias of -80 V showing an amorphous layer at the substrate interface.

TF-P2-23
Formation and structure of Au and Pt epitaxial clusters supported by tungsten oxide

T14 Thin Films

#TF-P2-23

J. Polášek, K. Mašek, J. Beran, P. Blumentrit, M. Vorokhta, N. Tsud, V. Matolín.

Charles University, Faculty of Mathematics and Physics, Department of Surface and Plasma Sciences - Prague (Czech republic).

Tungsten oxide surface was prepared by radio - frequency (RF) plasma oxidation of (110) tungsten single crystal surface followed by annealing at the high temperature. This process led to the formation of pseudocubic WO3 thin film having (111) surface orientation [1]. Au and Pt were deposited at different substrate temperatures by thermal evaporation. Surface structure, composition and electronic properties were investigated using reflection high energy electron diffraction (RHEED) and synchrotron radiation photoelectron spectroscopy (SRPES).
Deposition of Au or Pt at the substrate temperature of 570 K led to the formation of epitaxial clusters having (111) surface plane. Strong metal - substrate interaction (SMSI) between Pt and tungsten oxide surface was observed leading to the encapsulation of Pt clusters at the temperatures above 570 K. Encapsulation was proven by CO adsorption. Only a weak interaction between Au and substrate was found.
Formation of Au - Pt bimetallic clusters was investigated at the temperature range of 160 K - 870 K. It was found that detailed cluster structure depends on the substrate temperature and order of deposited materials. If Pt is deposited first, Pt particles serve as nucleation sites for the growth of bimetallic clusters. In the case of Pt deposition on Au predeposited surface, bimetallic clusters grows preferentially, but lower Pt mobility leads to formation of pure Pt clusters on the bare tungsten oxide surface [2]. Deposition at low temperature (160 K) and subsequent annealing showed that at the temperatures higher than room temperature, metallic atoms can diffuse on the tungsten oxide surface and pure Pt particles are covered by Au. At the temperature of 500 K, interdifusion of Pt and Au takes place resulting in formation of Pt - Au alloy at the metals interface. At the temperatures around 570 K, the clusters

are composed of Pt core and Pt-Au alloy shell enriched by Au on the surface due to the segregation of Au into the near surface region (fig. 1). Strong interaction between Au and Pt led to the weakening of SMSI of Pt and tungsten oxide, limiting the encapsulation process. Further annealing shoved that temperature above 770 K leads to the reduction of tungsten oxide and strong interaction between metallic W and Pt atoms leads to decomposition of Au - Pt alloy clusters and formation of Pt - W alloy. These findings can explain the physical and chemical properties of Pt/WOx, Au/WOx and Pt - Au/WOx catalysts and gas sensors.

[1] K. Masek, S. Nemsak, V. Matolin, Vacuum 2008, 82, 274.
[2] K. Masek, P. Blumentrit, J. Beran, T. Skala, I. Pis, J. Polasek, V. Matolin, Vacuum 2012, 86, 586

fig. 1: Model of supported Au - Pt bimetallic cluster.

TF-P2-13
The tribological properties of Zr-C:H coatings sliding against various normal loading, wear mode and counterbody

T14 Thin Films

#TF-P2-13

W. Kao.

Professor - Chang Hua.

Diamond-like carbon is an ideal surface coating material since it possesses exceptional properties, including high fatigue life, high hardness, high chemical inertness, low friction and high wear resistance under sliding conditions [1-7]. In this study, Zr-C:H-x coatings are deposited on AISI M2 substrates using a closed field unbalanced magnetron sputtering system with pulsed-direct current (pulsed-DC) power frequencies in the range 30 kHz to 110 kHz (the x in the term Zr-C:H-x is the power frequencies in the deposition process). The study investigates the tribological properties of the coatings under ball-on-disk point and cylinder-on-disk line contact wear modes using an oscillation friction and wear tester. We discuss the tribological behaviour of various wear pairs based on hardness (H), elastic modulus (E), adhesion property, initial Hertzian pressure and transferred layer on various contact surfaces of wear pairs. The experimental results display the Zr-C:H-110 coating with the good adhesion property, the lowest initial Hertzian pressure and the lowest friction coefficient possesses excellent wear resistance under point contact wear mode, while the Zr-C:H-70 coating with the maximum hardness and plastic deformation resistance (H3/E2) displays excellent wear resistance under line contact wear mode.

[1] H. Liu, Y. Jiang, R. Zhou, B. Tang, Wear behaviour and rolling contact fatigue life of Ti/TiN/DLC multilayer filmsfabricated on bearing steel by PIIID Vacuum, 86 (2012) 848-853.
[2] M. Kamiya, H. Tanoue, H. Takikawa, M. Taki, Y. Hasegawa, M. Kumagai, Preparation of various DLC films by T-shaped filtered arc deposition and the effect of heat treatment on film properties, Vacuum 83 (2009) 510-514.
[3] R.P.C.C. Statuti, P.A. Radi, L.V. Santos, V.J. Trava-Airoldi, A tribological study of

the hybrid lubrication of DLC films with oil and water, Wear 267 (2009) 1208-1213.
[4] W. Tillmann, E. Vogli, F. Hoffmann, Low-friction diamond-like carbon (DLC)-layers for humid environment, Thin Solid Films 516 (2007) 262–266.
[5] S. Zhanga, X. L. Buia, X.T. Zengb, X. Lic, Towards high adherent and tough a-C coatings, Thin Solid Films, 482 (2005)138– 144.
[6] C. Charitidis, S. Logothetidis, Nanomechanical and nanotribological properties of carbon based films, Thin Solid Films 482 (2005) 120- 125.
[7] P.W. Shum, Z.F. Zhou, K.Y. Li, Tribological performance of amorphous carbon films prepared on steel substrates with carbon implantation pre-treatment, Wear 256 (2004) 362-373.

SE/PST/TF/BI-2-Or-6
Calcium-phosphate slurry processing: A novel chemical treatment technique to activate osteogenesis on titanium

T14 Thin Films

#SE/PST/TF/BI-2-Or-6

N. Ohtsu, M. Hirano, H. Arai.

Kitami Institute of Technology - Kitami (Japan).

Titanium (Ti) implants have become essential medical products in surgery and dentistry as substitutes for hard tissues. However, it is difficult to achieve a strong mechanical interface between the implant and the surrounding hard tissue because osteogenesis does not progress easily on Ti. This paper presents a novel chemical treatment technique, called calcium-phosphate slurry processing, to activate osteogenesis on Ti substrate, developed by our research group[1-3]. The calcium-phosphate slurry processing is a simple technique, and it involves burying a Ti substrate in calcium phosphate slurry prepared by mixing calcium phosphate powder with distilled water and then heated at 973 K in air. This process induces the substrate to react with the reagent efficiently and crystallizes the surface layer in one step. By treating with the slurry prepared by mixing 1 g of tribasic calcium phosphate ($3Ca_3(PO_4)_2 \cdot Ca(OH)_2$) powder with 1.5 mL of distilled water, a composite coating comprising calcium phosphate and titanium dioxide (TiO_2) was fabricated on a Ti substrate. The thickness of the coating, estimated from a transition electron microscopic (TEM) image, was approximately 300 nm, and the average roughness (Ra) of the treated surface, calculated from the scanning probe microscopic (SPM) image, was slightly increased as compared to that of a non-treated surface. After the sterilization, osteoblast-like MC3T3-E1 cells were seeded on the treated and non-treated Ti substrates and then cultured for 3 d. There was no difference in the attached cell numbers between the non-treated and treated substrates, indicating that the treated Ti surface will not show the cytotoxicity. The cells were thereafter differentiation-induced on the substrates. The calcifications of the cells at 27 d after differentiation-incubation are shown in Fig. 1. The calcified deposits were stained by alizarin red S. The clustered deposits were observed only on the treated Ti substrate. This result indicates that osteogenesis on Ti is activated by treating with calcium-phosphate slurry. On the basis of these experimental results, we propose that

calcium-phosphate slurry processing is one of the hopeful surface treatment techniques to activate osteogenesis of Ti implants.

1) N. Ohtsu, C. Abe, T. Ashino, S. Semboshi, K. Wagatsuma, Surf. Coat. Technol. 202 (2008) 5110-5115.
2) N. Ohtsu, S. Semboshi, C. Abe, S. Tokuda, Surf. Coat. Technol. 205 (2011) 3785-3790.
3) N. Ohtsu, Y. Nakamura, S. Semboshi, Surf. Coat. Technol. 206 (2012) 2616-2621.

Fig. 1. Photograph of calcified deposits in MC3T3-E1 cells stained with a 1% alizarin red S solution . Cells were differentiation-induced on (a) non-treated Ti, and (b) treated Ti for 27 d.

TF-8-Or-1
Perpendicular magnetic anisotropy and perpendicular exchange bias in sputter-deposited CoO/CoPt multilayers

T14 Thin Films

#TF-8-Or-1

J. Shi, J. Wang, T. Sannomiya, Y. Nakamura.

Department of Metallurgy and Ceramics Science, Tokyo Institute of Technology - Tokyo (Japan).

Recently, interests in perpendicular exchange biased (PEB) spin valves for spintronics and magnetoelectronics have been dramatically increased due to their high magnetic stability and low device operating current density.
In this study, the structural and magnetic properties of room temperature sputter deposited CoO/CoPt multilayer were investigated. In Fig.1(a), the as deposited multilayer shows strong perpendicular magnetic anisotropy (PMA) at room temperature. Moreover, after perpendicular field cooling, the multilayer with AF/FM interfaces exhibits a large shift (PEB) as indicated in Fig.1(b). Furthermore, the PMA of the multilayer after field cooling is also enhanced. This is considered due to the strong interfacial exchange coupling between the CoPt and CoO layers. Unlike the CoPt/AlN multilayer we reported before[1], which show PMA after thermal annealing, the multilayers studied here with relatively thick FM layer surprisingly show strong PMA at in the as-deposited state (Fig.1(a)).Therefore, the PMA found in AF/FM multilayer may be partially attributed to the interfacial AF-FM exchange coupling.
On the other hand, XRD result indicates a well-defined layered structure and strong (111) texture for CoPt layers (Fig.2). Lattice fringes in TEM image (Inset of Fig.2) support the results of XRD and confirm that both of the CoPt and CoO layer show (111) texture. It seems that CoO layer here serves as a good seed layer for the growth of textured CoPt layer. As [111] is one of the easy axes for the fcc CoPt, the (111) texture should also benefit the PMA. To our knowledge, this is the first time to prove that PMA can be established with metal/oxide interface. With the remarkable PEB, the CoPt/CoO multilayer show great application potential for magnetoelectronic devices.

[1] Y. Yu, J. Shi, and Y. Nakamura, J. Appl. Phys. 108, 23912 (2010).

Fig. 1. Room temperature (a) and low temperature (80K) (b) hysteresis loops of $[CoPt\ 4nm/CoO\ 4nm/]_5$ multilayer.

Fig. 2. XRD profile of as-deposited $[CoPt\ 4nm/CoO\ 4nm/]_5$ multilayer. (Inset: cross-sectional high resolution TEM image.)

TF-3-Or-14
Structural, optical and electrical properties of Ga-doped ZnO thin films prepared by spray pyrolysis

T14 Thin Films

#TF-3-Or-14

E. Masumdar [1], M. Barote [2].

[1]Rajarshi Shahu Mahavidyalaya, - latur, Maharashtra (India), [2]Rajarshi Shahu Mahavidyalaya, - Lausa,maharashtra (India).

Structural, optical and electrical properties of Ga-doped ZnO thin films prepared by spray pyrolysis

E. U. Masumdar [a] *, M. A. Barote [a]

a: Thin Film Physics Laboratory, Department of Physics, Rajarshi Shahu Mahavidyalaya - Latur-413512, Maharashtra, India.

Abstract:
Gallium doped zinc oxide (GZO) thin films were prepared using the simple spray pyrolysis technique. The molar ratio of Ga in the spray solution was changed in the range of 0–5 at. % in steps of 1 at. %. The films were characterized by various methods to understand their structural, morphological, optical and electrical properties. The X-ray diffraction analysis revealed that the films were polycrystalline in nature having a hexagonal wurtzite type crystal structure with a preferred grain orientation in the (0 0 2) direction [1]. The scanning electron microscopy (SEM) measurements revealed that the surface morphology of the as-deposited ZnO films is greatly affected and a decrease in the grain size [2]with increased doping concentration was observed . The optical band gap was found to increase from 3.25 to 3.58 eV with increase in Ga-doping level [3]. All the films showed good transparency in the entire visible region from 80 to92 %. A blue shift of the optical band gap was observed with an increase in Ga-doping. The electrical characterization was performed using two-probe press contact method. The electrical resistivity was found to vary from 8.02×10^{-4} Ω-cm to 5.43×10^{-4} Ω-cm with increasing doping level [4].
Keywords: Spray pyrolysis; ZnO films; optical properties; electrical properties.

* Corresponding author. Tel.: +91 9421363009.
E-mail address: emasumdar@yahoo.com (E. U. Masumdar)

[1] T. P. Rao, M.C.S. Kumar, J. Alloys and Compd. 506 (2010) 788.
[2] R. A. Smith, Semiconductors, Academic Publishers, Culcutta, 1989, pp-461-463.
[3] U. Pal, S. Saha, A. K. Choudhari, V. V. Rao, H. D. Banarjee, J. Phys. D: Appl. Phys. 22 (1989) 965.
[4] Mujdat Caglar, Yasemim Caglar, Saliha Ilican, Phys. Stat. Sol. 4 (2007) 1118.

Fig. 1. Typical SEM image of 1% GZO film.

Fig. 2 Plot of (αhv)2 vs hv for as deposited GZO thin films.

PST/SE/TF-3-Or-11
Monitoring the exhaust ammonia in conventional plasma nitriding process for closed loop control of compound layer formation

T14 Thin Films

#PST/SE/TF-3-Or-11

H. Klümper-Westkamp.

Stiftung Institut für Werkstofftechnik - Bremen (Germany).

Plasma nitriding and nitrocarburizing has been established in industrial production since many years. This thermochemical surface treatment is applied to various steel components in order to enhance wear resistance, corrosion resistance and fatigue resistance. The process is done at the state of art in a pulsed discharge technique in the region of anomalous glow discharge in a conventional heated furnace. By adjusting the gas composition and plasma parameters different compound layers with different thickness, composition, hardness and morphology can be produced. Up to now applications run under constant gas and plasma parameters, which have to be investigated and evaluated before. A lot of expert knowledge and experience is necessary to get the right parameters for the production of the intended compound layer specification and to secure the reproducibility. Further influencing aspects on the compound layer formation as batch size, batch surface, batch cleanliness, jigging, temperature distribution, cleanliness and leak rate of the plant are difficult to take into account and can cause large deviations.
To overcome these disadvantages a new concept for controlled processing is developed. Investigations in analyzing the exhaust gas of the plasma nitriding process gas showed a significant amount of ammonia, although no ammonia is added to the process. The ammonia is obviously produced in the plasma nitriding process as a reaction product of hydrogen with nitrogen in the glow discharge. Varying the inlet gas ratio of hydrogen to nitrogen, temperature and batch size leads to different ammonia content in the exhaust, as shown in figure 1. Based on this information and further gas measurements a closed loop control is build up to regulate the compound layer formation. First results are shown.
Based on these results as well as results of literature [1, 2, 3, 4], a new and more complete model to describe the mechanisms of plasma nitriding is introduced.

[1] Kölbel, J.: Die Nitridschichtbildung bei der Glimmentladung, Forschungsbericht des Landes NRW Nr. 1555, Westdeutscher Verlag, Köln / Obladen, 1965
[2] Hudis, M.: Study of ion nitriding. J. appl. Phys. 44 (1973) 4, S. 1489
[3] Quast, M.; Stock, R.; Mayr, P.: Plasma assisted nitriding of aluminium-alloy parts. Metals Science and Heat Treatment 46 (2004) 7/8, S. 299
[4] Burlacov, I. et. al.: In situ monitoring of plasma enhanced nitriding process using infrared absorption and mass spectroscopy. Surface & Coatings Technology 206 (2012) S. 3955

fig. 1 Influence of temperature and batch size on the ammonia concentration in an N2-H2 plasma (P=200Pa, U=500V)

SE/PST/TF/BI-2-Or-7
Development of innovative surfaces by plasma technologies on metallic substrates according industrial specifications

T14 Thin Films

#SE/PST/TF/BI-2-Or-7

A. Daniel, C. Archambeau.

CRM Group - AC&CS (Advanced Coatings & Construction Solutions) - Liège (Belgium).

The achievement of functionalized surfaces industrialization relies on various critical parameters that must be considered from the beginning and all along the product developments. Indeed the implementation of a surface functionality generally cannot be only limited to the validation of basic properties at lab scale, but must take into account the use in real conditions according customers' specifications as well as constraints related to associated production technologies, shaping and commercialization.
Taking into account the whole package of requirements we have to study, besides the desired functionality, other aspects such as durability of the function in various environments, aesthetic, forming ability, cost and specific tests if needed.
This approach allows a selection of most promising products and deposition technologies from the first experiments at lab scale.
We propose to illustrate this through a few examples of surface functionalization developed within the CRM Group.
The first example concerns the deposition of an hydrophilic easy-to-clean and anti-staining transparent thin layer on prepainted steel for outdoor building application. Thin films are based on silicon and/or titanium oxides deposited by reactive magnetron sputtering or Plasma Enhanced Chemical Vapor Deposition (PECVD). The end-user specifications are described and some differences in anti-staining and easy-cleaning properties are highlighted between flat substrates and shaped samples showing the importance to study the surface properties as close as possible to the real application. Finally the up-scaling of the functionality is described from lab experiments to industrial production line.
A second example deals with the development of an antibacterial coating on steel.

Thin films based on silver/copper containing oxide matrices are deposited by reactive magnetron sputtering and PECVD. In this case the product requirements are detailed in connection with the associated markets showing that developed antibacterial coating materials have to be adapted depending on the final use.

TF-8-Or-3
Magnetic canting at the interfaces of Fe/ MgO(001) and Fe/Al2O3(0001)

T14 Thin Films

#TF-8-Or-3

T. Kawauchi [1], X. Zhang [2], K. Fukutani [1].

[1]Institute of Industrial Science, The University of Tokyo - Tokyo (Japan), [2]Institute of Materials Structure Science, High Energy Accelerator Research Organization - Ibaraki (Japan).

Magnetization of magnetic films is of considerable interest and importance in recent years. Because of the symmetry breaking at surfaces and interface, ultrathin magnetic films often reveal particular magnetic properties. The magnetization direction of magnetic films has usually been assumed to have a particular direction as an entire film. However, we have recently demonstrated that the magnetization cants only at the surface of Fe films in the surface normal direction [1]. In this paper, we have studied interface magnetization of Fe/MgO(001) and Fe/Al_2O_3(0001) by means of the quantum beat spectroscopy due to nuclear-resonant scattering with synchrotron radiation (SR).

The samples were prepared by evaporating Fe films with the electron bombardment on MgO(001) and Al_2O_3(0001) substrates at room temperature in UHV with a base pressure of $1x10^{-8}$ Pa. As the nuclear-resonant scattering is sensitive to only ^{57}Fe isotope, stacked structures of ^{56}Fe(20nm)/^{57}Fe(1nm)/Substrate and ^{56}Fe(10nm)/^{57}Fe(1nm)/^{56}Fe(10nm)/Substrate were fabricated on MgO(001) and Al_2O_3(0001). From the analysis of the RHEED pattern, we confirmed that Fe(001) was epitaxially grown on MgO(001) with Fe[100]//MgO[110] and Fe[110]//MgO[100]. Although Fe(110) was epitaxially grown on Al_2O_3(0001), on the other hand, the azimuthal direction of the film was found to be random. After transportation of the samples in the air, the nuclear-resonant-scattering experiment was performed in the grazing condition at the PF-AR NE1 beamline of High Energy Accelerator Research Organization.

The time spectra of the nuclear-resonant scattering taken for these samples revealed a clear quantum beat structure reflecting the Zeeman splitting of the ^{57}Fe nuclear level, which definitely showed the films are ferromagnetic. For ^{56}Fe(20nm)/^{57}Fe(1nm)/MgO(001), a quantum beat frequency of only 72 MHz was observed independent of the azimuthal direction of the SR incidence. Considering the polarization direction of SR, the results indicate that the magnetization of ^{57}Fe at

the interface is perpendicular to the interface. On the other hand, the time spectra taken for ^{56}Fe(10nm)/^{57}Fe(1nm)/^{56}Fe(10nm)/MgO(001) showed two beat frequencies of 72 and 124 MHz depending on the azimuthal direction of SR, indicating that the magnetization direction at the middle of the iron film is different from that at the interface. From the analysis of the spectra taking account of the SR polarization, the magnetization has a uniaxially in-plane component in the direction of Fe[100]//MgO[110]. In contrast to Fe/MgO(001), the magnetization direction of Fe/Al_2O_3(0001) was found to be mostly in the parallel direction in the entire film, although the direction of the parallel component is Al_2O_3[11-20] at the interface and Al_2O_3[1-100] in the film. From the temperature dependence of the beat frequency, the internal magnetic field(B_{IN}) was evaluated, which exhibited a gradual decrease with increasing temperature. With a fit of the formula $B_{IN}=B_0(1-T/T_C)^{\beta}$, the critical exponent of $\beta=0.093\pm0.053$ was obtained, which is similar to the value of $\beta=0.125$ expected for the 2-D ising model.

[1] T. Kawauchi et al., PRB 84, 020415 (2011).

TF-3-Or-4
Pulsed Laser Deposition of Sub-Stoichiometric Tungsten Oxide Films: Growth and Structure

T14 Thin Films

#TF-3-Or-4

A. Caruana, M. Cropper.

Loughborough University Physics Department - Loughborough (United kingdom).

Tungsten oxide has attracted vast interest in recent years due to its electrochromic and gas sensing properties (1,2). However, these phenomena tend to occur only in the material in thin film form (2). For example the increased surface area of a thin film greatly enhances the gas sensing properties of tungsten oxide. Reactive pulsed laser deposition (PLD) is being used increasingly in the deposition of oxides, due to the relative ease in which multi component materials can be deposited under relatively high gas process pressures (3). Consequently, work has been done on the influence of deposition pressure (1), and deposition temperature (4) on the film properties and structure, but to our knowledge, very little work has concentrated on the effect of laser fluence on the film structure (5).

In the work reported here, sub stoichiometric films of tungsten oxide deposited by PLD under different laser fluences are investigated. Tungsten oxide films have been deposited onto single crystal Si (100) and $SrTiO_3$ substrates by irradiation of a stoichiometric tungsten oxide target, using a frequency doubled Nd:YAG laser at a repetition rate of 10 Hz. All films were deposited at 500°C under a constant O_2 background pressure of 2.5 x 10^{-2} mbar. The films have been characterised by X-Ray diffraction, X-Ray reflectivity (XRR) and X-Ray photoelectron spectroscopy.

A predominant [001] texture was observed in all films, indicating preferential c-axis orientated growth. Films grown on $SrTiO_3$ exhibited a stronger degree of crystallisation in comparison to those grown on Si. The X-Ray diffraction patterns for the $SrTiO_3$ films showed over an order of magnitude increase in intensity for the [001] texture than was observed at equivalent fluence values on Si substrates. XRR scans revealed that the surface and interface roughness was far greater for films deposited on Si; further indicating that the films grown on $SrTiO_3$ were of better quality. The

deposition rate stayed relatively constant with increasing fluence up until a critical value of 8.9 J cm^{-2}, where the deposition rate approximately doubled. At this critical fluence the FWHM of the [001] texture on the $SrTiO_3$ films reduced significantly, indicating a decreased variation in crystallite orientation and suggesting a greater degree of crystallisation.

1. Nanostructured tungsten oxide thin films by the reactive pulsed laser deposition technique. Lethy, K J, et al., Applied Physics A, Vol. 91, pp. 637–649.
2. Nanostructured Tungsten Oxide – Properties, Synthesis, and Applications. Zheng, Haidong, et al., 2011, Adv. Funct. Mater., Vol. 21, pp. 2175–2196.
3. Spintronic oxides grown by laser-MBE. Opel, Matthias., 2012, Journal of Physics D: Applied Physics, Vol. 45, p. 033001.
4. Structural, optical and morphological studies on laser ablated nanostructured WO3 thin films. Lethy, K J, et al., 2008, Applied Surface Science, Vol. 254, pp. 2369–2376.
5. Morphological and structural studies of WOx thin films deposited by laser ablation. M. Filipescu a, S. Orlando b, V. Russo c, A. Lamperti d, A. Purice a, A. Moldovan a, M. Dinescu a, 2007, Applied Surface Science, Vol. 253, pp. 8258–8262.

TF-4-Or-8
Atomic processes and crystal structures in Cr2AlC films at high temperatures

T14 Thin Films

#TF-4-Or-8

V. Vishnyakov [1], S. Haigh [2], A. Gholinia [2], U. Bangert [2], J. Colligon [1].

[1]Dalton Research Institute, Manchester Metropolitan University - Manchester (United kingdom), [2]Manchester Materials Science Centre, University of Manchester - Manchester (United kingdom).

A Dual Ion Beam deposition system was used to create thin films of Cr_2AlC. The films were deposited onto Silicon, Stainless Steel and Superalloy substrates at substrate temperatures ranging from room temperature to 700 K. Energy Dispersive and Wave Dispersive X-Ray analysis was used to determine the precise film composition, while High Resolution Transmission Electron Microscopy (TEM) coupled with Electron Energy Loss Spectroscopy and Electron Backscatter Diffraction (EBSD-like) mapping in the TEM was used to access for the first time local structural information and phase relationships of crystals on internal and external interfaces in as-deposited and annealed films.

The degree of crystallinity and the size of the crystallites within the film increases with deposition and/or annealing temperature and is also positively linked to the presence of a small surplus of Al above the stoichiometric level. A highly crystalline structure has been observed by EBSD in the TEM after annealing at 973K as shown on Fig.1. The film consists of predominantly the Cr_2AlC MAX phase structure with small traces of other binary phases. The dependence of crystal growth on annealing conditions will be discussed.

From a technical point of view the film's high temperature oxidation behaviour weakly depends on the initial deposition conditions and substrate temperature. We have observed that these films develop a dense protective Cr- and Al-rich surface oxide and that there is also some ingression of oxygen into the film bulk. The overall film oxidation and oxygen uptake appear to be lower for the films with smaller crystals and higher proportion of amorphous phase and we speculate that this can be linked to a slightly higher initial film density

Fig. 1. Electron Backscatter Diffraction-like mapping of a cross section through a Cr_2AlC thin film sample annealed at 973K, showing from left to right, crystal orientation map and structural image.

SE/TF-1-Or-6
Mechanical characterization of AlTiN-coatings processed by different PVD techniques

T14 Thin Films

#SE/TF-1-Or-6

F. Lomello [1], M. Arab Pour Yazdi [2], A. Besnard [3], F. Sanchette [4], F. Schuster [5], A. Billard [2].

[1]LRC CEA-IRTES-LERMPS, site de Montbéliard, UTBM - Belfort (France), [2]IRTES-LERMPS, site de Montbéliard, UTBM - Belfort (France), [3]LaBoMaP (EA 3633) - Equipe MAT, Ecole Nationale Supérieure d'Arts et Métiers - Cluny (France), [4]LRC CEA-ICD LASMIS, Nogent International Center for CVD Innovation (Nicci), UTT Antenne de Nogent, pôle technologique de haute Champagne - Nogent (France), [5]CEA Cross-Cutting program on Advanced Materials - Saclay (France).

In this study, AlTiN coatings were deposited by means of two high energetic deposition techniques such as cathodic-arc deposition and high-power impulse magnetron sputtering (HIPIMS) [1,2].

Recently, the application of single layer AlTiN synthesized by physical vapor deposition (PVD) in cutting applications increased due to their improved tribological and high oxidation temperature (up to 800°C) if compared with a single-phase nitrides [3].

A correlation between these techniques and the resulting morphological-mechanical properties was established. Firstly, a physico-chemical characterization was conducted by means of X-ray diffraction (XRD), transmission electron microscopy (TEM), scanning electron microscopy (SEM), energy dispersive spectroscopy (EDS), glow discharge optical emission spectroscopy (GDOES) techniques.

Subsequently, the mechanical-tribological characterization allowed comparing these properties to the chemical-morphological properties. The resulting properties were strongly depending on the processing routes. For instance, the differences in terms of surface roughness strongly affected the final tribological properties. The

tribological tests were performed at both low- and high-temperature regimes up to 800°C.

Moreover, the higher droplets' density strongly affected the built-up of material at the edge of the wear tracks after ball-on-disc tests. Indeed, the better surface state in the case of HIPIMS leads reducing the coefficient of friction (COF). It is well known that macroparticles emission creates defects (droplets) in non-filtered cathodic-arc evaporation processes.

These droplets act as cutting edges increasing the COF as already reported in the literature [4]. Nowadays, HIPIMS has few industrial applications for this reason a final aspect concerning the industrial up-scaling feasibility was investigated. The developed approach included several aspects such as the deposition parameters and the measured final properties.

[1] F. Sanchette et al. Surf. Coat. Technol. 205 (2011) 5444.
[2] A.P. Ehiasarian et al. Surf.Coat. Technol. 163-164 (2003) 267.
[3] M. Arndt et al. Surf. Coat. Technol. 163-164 (2003) 674.
[4] M. Pfeiler et al. Surf. Coat. Technol. 202 (2007) 1050.

TF-P2-03
MODEL OF RELAXATION AND CRYSTALLIZATION KINETICS OF AMORPHOUS Al-(Mo, W) THIN FILMS UNDER ISOCHRONAL HEATING

T14 Thin Films

#TF-P2-03

T. Car [1], J. Ivkov [2], N. Radic [1], M. Jercinovic [1].

[1]Rudjer Boskovic Institute - Zagreb (Croatia), [2]Institute for Physics - Zagreb (Croatia).

Relaxation processes and crystallization kinetics of Al-(Mo, W) amorphous thin films under isochronal conditions was examined by continuous *in situ* electrical resistance measurements in vacuum. For the isochronal heating, it was observed that the relaxation effects decreased with an increase of the heating rate and decreased with the content of molybdenum and tungsten in the film. The crystallization temperature decreased with an increase of aluminum content. Assuming the linear dependence of resistivity with temperature, the linear ρ (*T*) contribution is extracted from the relaxation effects. Adopted experimental function of ρ (*T*) is fitted to a modified Bloch-Gruneisen formula with excellent agreement of experimental data and fitting function. The adaptation of the JMAK model to the non-isothermal kinetics was used for calculation of crystallization kinetic parameter *n* and activation energy for crystallization E_c. The unified model for both processes is examined and discussed.

TF/SE-1-Or-7
Molecular Dynamics simulations of plasma sputtered ZrxCu1-x amorphous metallic glass thin film growth. Effects of composition and kinetic energy

T14 Thin Films

#TF/SE-1-Or-7

P. Brault, L. Xie, A.L. Thomann.

GREMI UMR7344 CNRS-Université d'Orléans - Orleans (France).

Recently, there has been a huge interest in the atomic-level structure and structure-property relationship in metallic glasses (MGs). These materials have been studied for 40 years because of their promising properties belonging to both metals (electron, heat conductivity, ductility…) and glasses (hardness…). To stabilize an amorphous phase in metallic alloys, atomic diffusion must be prevented. This could be achieved by playing with the chemical composition (mixing of elements with different atomic sizes) or by freezing low ordered phases during the synthesis process. It has been shown that deposition of thin films by condensation onto substrates, even at ambient temperature, allows to synthesize metallic glasses even in binary systems. In this work, we employed classical molecular dynamics simulations model to study Zr_xCu_{100-x} ($3 \leq x \leq 95$) metallic alloy films deposited on a silicon (100) substrate. Input data were chosen to fit with typical experimental operating conditions of magnetron sputter deposition process. The evolution is monitored with variable compositions of deposited atoms. The Zr-Zr, Cu-Cu and Zr-Cu interactions are modelled with the Embedded Atom Method (EAM), the Si-Si interaction with Tersoff potential, the Zr-Si and Cu-Si interactions with Lennard-Jones (12-6) potentials. Snapshots are created for vizualization purposes. X-Ray Diffraction patterns and Radial Distribution Functions are calculated for direct comparison with sputter deposition experiments. Different film morphologies and structures are evidenced when the Zr/Cu composition ratio and the argon sputtering gas pressure are varied. Varying the argon sputtering pressure results in the variation of the Zr and Cu kinetic energies which in turn modifies the input parameters for carrying out the MD simulations. The results are compared with X-Ray Diffraction and Scanning Electron Microscopy analyses of experimentally deposited thin films by magnetron co-sputter deposition. Both simulation and experimental results show that the structure of the Zr_xCu_{100-x} film

varies from crystalline to amorphous depending on the Zr concentration. The kinetic energy affects the layer morphology : below a threshold kinetic energy the film is nanostructured and above it becomes continuous.

Abstract submitted to RSD2013

(a) Experimental XRD patterns of magnetron deposited Zr_xCu_{100-x} films and (b) calculated XRD patterns of MD grown Zr_xCu_{100-x}. x values are the same in (a) and (b)

SE-1-Or-12
Reactive sputtering of transition metal hydride thin films by high power impulse magnetron sputtering and direct current magnetron sputtering

T14 Thin Films

#SE-1-Or-12

H. Högberg [1], M. Samuelsson [2], L. Tengdelius [1], J. Jensen [1], J. Lu [1], E. Broitman [1], F. Eriksson [1], L. Hultman [1].

[1]Linköping University - Linköping (Sweden), [2]Impact Coatings AB - Linköping (Sweden).

Recently, we demonstrated that the group 4 metal Zr can form 111-oriented δ-ZrH_2 films when deposited on Si(100) substrates by reactive high power impulse magnetron sputtering (HiPIMS) and direct current magnetron sputtering (dcMS) [1]. X-ray diffraction (XRD) patterns recorded from films grown in mixed Ar and H_2 plasmas containing: 2.5, 5, 10, 15, and 20% H_2 as seen from the resulting total pressure show that the phase is obtained by both techniques. Time-of-flight energy elastic recoil detection analysis (ToF E ERDA) shows that the films contain up to 61 at.% hydrogen and are very pure with oxygen contents less than 0.2 at.%. Scanning electron microscopy (SEM) images show that the δ-ZrH_2 film deposited by HiPIMS exhibits a glass-like microstructure and a smooth surface structure, while the dcMS film shows a more columnar growth behavior, see Fig. 1; both Zr reference films display a rougher surface and a ductile behavior when fractured for analysis with SEM. Four point probe measurements yield typical resistivity values of about 90-120 μΩcm. Mechanical properties investigations, as obtained by nanoindentation gives hardness values of 6-7 GPa, and reciprocating tribological tests gives a friction coefficient of ~ 0.15 for both deposition methods.
In contrast, for the group 6 metal Cr, we find a different behavior as ToF E ERDA reveals that no hydrogen (< 0.5 at.%) is incorporated into the films even at the highest investigated H_2 partial pressure (20%). However, the resulting film oxygen content is notably low (≤ 0.1 at%), in particular when hydrogen is added to the plasma. XRD shows that all Cr films are 110 oriented, and SEM shows that the films grown by dcMS exhibit a columnar microstructure while those deposited by HiPIMS

display a more glass-like microstructure. Nanoindentation shows hardness values of about 16 to19 GPa for films grown by both techniques irrespectively of hydrogen presence in the plasma. Four-point-probe measurements show resistivity values of ~30 μΩcm for all films, i.e. approximately twice the value for bulk Cr (~13 μΩcm). In addition, results from reactive sputtering of the group 5 element Ta in H_2 will be presented.

[1]. H. Högberg et al., *High Power Impulse Magnetron Sputtering of ZrH_2 and Zr Films*, presented at the 13th International Conference on Plasma Surface Engineering 2012, September 10-14, Garmisch- Partenkirchen, Germany, abstract no. OR1204

Fig. 1: SEM images from δ-ZrH_2 films deposited with 20% H_2 in the plasma and by dcMS, (left) and HiPIMS (right); note the difference in microstructure and thickness

TF-6-Or-1
Columnar microstructure of the ZnO shell in GaP/ZnO nanowires

T14 Thin Films

#TF-6-Or-1

J. Novak [1], I. Vávra [1], P. Elias [1], S. Hasenohrl [1], I. Novotny [2].

[1]IEE SAS - Bratislava (Slovakia), [2]UEF FEI STU - Bratislava (Slovakia).

We report on thin RF-sputtered Ga-doped ZnO layers on gallium phosphide (GaP) substrate and GaP nanowires (NWs); the latter were grown by metal organic vapour phase epitaxy (MOVPE) on the GaP (111)B substrate. The RF-sputtering conditions were adjusted to deposit very thin ZnO layers with defined electrical parameters onto the GaP NWs and substrate, hereby forming a core-shell GaP/ZnO NW surface structure. We studied the properties of planar ZnO layers and core-shell GaP/ZnO NWs using scanning electron microscopy (SEM), transmission electron microscopy (TEM), atomic force microscopy (AFM), and electrical and photocurrent measurement.

Detailed TEM observation showed that ZnO shell consists of multilayered system of ZnO nanocrystallities (grains). This behaviour was observed even the thinnest shell layers (10nm thick) too. Detailed description of the ZnO shell structure is in our previous work [1]. The longitudinal TEM view showed that ZnO deposited on the GaP NWs has a columnar morphology. The columns are inclined at a positive angle close to 70 ^{o} with respect to the GaP core axis; all columns we observed were tilted at this angle to the growth direction. Although we did not observe ZnO columns tilted at 109.5 ^{o} to the growth direction, this possibility cannot be excluded at this stage. One can suppose that ZnO nanocrystallites grew preferentially on the {111}B GaP NW facets.

The polycrystalline character of the ZnO layer, inferred from the TEM images, was confirmed in the XRD pattern. The size of crystallities evaluated from XRD measurements (application of Scherrer´s formula) was in agreement with the size of nanocrystals observed in TEM (an order of nanometers).

It is known that thin ZnO films grow preferentially along the c-axis because of anisotropy in growth rate, as its various crystallographic planes differ in surface energy. In addition, the NWs had defects formed in them during the deposition of ZnO because they were bombarded at high energies by oxygen species from ZnO and Ga_2O_3. The crystallographic quality of the NWs can be improved by thermal annealing [2,3]. Our samples of ZnO:Ga thin films were annealed in vacuum and in

forming gas at temperatures from RT to 500 ºC. The changes of XRD patterns before and after annealing process will be presented. The width of the (002) peak decreased noticeably after annealing. Its full width at the half maximum (FWHM) decreases from 0.795 degrees to 0.57 degrees. Furthermore, the intensity of the peaks increased by a factor of 1.95. Both these observations indicate the increase of the quality of the nanocrystalline ZnO with possible increase of the grain size.

[1] Novák, J., Novotný, I., Kováč, J., Eliáš, P., Hasenöhrl, S., Križanová, Z., Vávra, I., and Stoklas, R.: Preparation of thin Ga-doped ZnO layers for core-shell GaP/ZnO nanowires, Applied Surface Sci 258 (2012) 7607
[2] Ryu Y. R., Zhu S., Budai J.D., Chandrasekhar H.R., Miceli P.F., White H.W., Journal Appl. Phys 88 (2000) 201
[3] Cui M.L.,Wu X.M., Zhuge L.J., Meng Y.D. Vacuum 81 (2007), 899

TF-P2-04
Thermally stable Ag thin films with various surface nanolayers

T14 Thin Films

#TF-P2-04

M. Kawamura, Z. Zhang, Y. Abe, K.H. Kim.

Kitami Institute of Technology - Kitami (Japan).

Silver (Ag) has long been of interest for use as a low-resistivity electrode material, but the problem of agglomeration caused by annealing must be resolved.(1) As a solution, introduction of surface layer and/or interface layer has been reported instead of a solution by alloying Ag.(2-4) In this study, we have investigated usefulness of various metals for surface nanolayers.
60 nm thick films of Ag, Pd, Ni, W, Ti, Nb were deposited on thermally oxidized Si substrate by RF sputtering method. The films were annealed under vacuum at 600 ^{o}C for 1 hour. Figure 1 shows surface morphology of all the samples by SEM observation. The roughness values were obtained by AFM observation. Severe agglomeration is confirmed for Ag film (a) where substrate is largely revealed. Pd film (b) and Ni film (c) show surface roughening with many small voids. On the other hand, W (d), Ti (e) and Nb (f) films have very smooth surface. Thus, we have confirmed that these three metals are hardly agglomerated by annealing under vacuum. W and Nb have high cohesive energy in common.(5) That of Ti is not very high, but fast oxide formation at its surface is considered to be useful for film stability.
Next, we introduced 5 nm thick surface metal (Pd, Ni, W, Ti or Nb) layer on 100 nm thick Ag thin film deposited on thermally oxidized Si substrate, followed by vacuum annealing at 600 ^{o}C. As a result, surface morphology was largely different. Namely, with Pd or Ni surface layer, surface was rough and roughness was over 10 nm. On the other hand, smooth surface with 2 nm of roughness was obtained with W, Ti or Nb surface layer. In conclusion, we have found that W, Ti and Nb, which have high morphological stability on annealing, are appropriate for surface nanolayer to prepare thermally stable Ag thin films.

1)M. Hauder, J. Gstoettner, W. Hansch, and D. Schimitt-Landsiedel:Appl. Phys. Lett. 78 (2001) 838.
2) M. Kawamura, Y. Inami, Y. Abe, and K. Sasaki: Jpn. J. Appl. Phys. 47 (2008)

8917.
3) M. Kawamura, Z. Zhang, R. Kiyono, and Y. Abe: Vacuum 87 (2013) 222.
4) Z. Zhang, M.Kawamura, Y.Abe, and K. H. Kim: Jpn. J. Appl. Phys. 51(2012) 085802.
5) C. Kittel: Introduction to Solid State Physics (Wiley, New Caledonia, 2005) 8th ed., p. 50.

Fig. 1 SEM images and rms surface roughness of the 60-nm-thick (a) Ag, (b) Pd, (c) Ni, (d) W,(e) Ti, and (f) Nb films after annealing at 600 ^{o}C.

TF-P2-24
Growth of Ce2O3 thin layers on preoxidized Cu(110) surface

T14 Thin Films

#TF-P2-24

M. Aulická, K. Veltruská, V. Matolín, T. Duchoň, J. Mysliveček, F. Dvořák, V. Stetsovych.

Charles University in Prague, Mathematics and Physics faculty, Department of Surface and Plasma Science - Prague (Czech republic).

Cerium oxide is very attractive material due to its catalytic activity. It is widely used in catalysts and solid oxide fuel cell nowadays. Its catalytic activity is based on relative easy change of cerium oxidation state via the reversible reaction $2CeO_2 \leftrightarrow Ce_2O_3 + 1/2\ O_2$. Changes from oxidized Ce^{4+} to reduced Ce^{3+} are accompanied by the formation of mobile oxygen vacancies. While ordered stoichiometric layers of model CeO_2 catalyst are commonly prepared, cerium oxide with vacancies is restricted mainly on disordered systems.

In this work, we prepared very thin ordered continuous layer of CeO_x by cerium evaporation onto the oxygen precovered Cu(110) surface. X-ray photoelectron spectroscopy (XPS), low energy electron diffraction (LEED), ion scattering spectroscopy (ISS) and scanning tunneling microscopy (STM) were used for the characterization of prepared systems. The mix of (2x1) and c(6x2) surface reconstruction was formed by oxygen exposure at 300 °C. Cerium was deposited on this surface also at 300 °C. Afterwards temperature stability of this system to 700°C was studied. At first the formation of hexagonal Ce_2O_3(0001) continuous epitaxial film was observed, accompanied by the creation of large hundreds nm long smooth band structures in the [1-10] direction. After annealing to higher temperature the cerium oxide film became gradually discontinuous and oxidation state of cerium significant changed from Ce^{3+} to Ce^{4+}. The formation of CeO_2 regions with saw-tooth relief with the (1,5x1,5) periodicity with respect to the substrate on facets was observed, accompanied by disappearance of Ce_2O_3(0001) areas. Subsequent oxidation caused the change of morphology and formation of CeO_2 regions with the (1,5x2) periodicity with respect to the substrate.

STM picture of the CeO_x/Cu(110) system after annealing to 500 °C

TF-3-Or-5
Tuning the morphology and stoichiometry of ceria catalyst films prepared by magnetron sputtering

T14 Thin Films

#TF-3-Or-5

I. Khalakhan [1], M. Vorokhta [1], M. Dubau [1], J. Lavková [1], M. Chundak [1], S. Haviar [1], I. Matolínová [1], V. Potin [2], V. Matolín [1].

[1]Charles University - Prague (Czech republic), [2]Universite de Bourgogne - Dijon (France).

Cerium oxide thin film catalysts with different thickness were prepared by magnetron sputtering technique on graphite foil. Scanning electron microscopy (SEM), atomic force microscopy (AFM) and transmission electron microscopy (TEM) were used for investigation of surface morphology of the films. Chemical composition of the catalyst was investigated by using photoelectron spectroscopy (XPS) and electron energy loss spectroscopy (EELS).
It was found that magnetron sputtering of ceria led to the formation of nanostructured high surface area catalyst when deposited on carbon substrate. The mechanism of the formation of such structure was explained through simultaneous deposit growth and oxygen plasma etching of carbon substrate. It was also found that thickness had a crucial influence on the structure and morphology of thin films. Hence, we are able to tune the morphology, i.e. active surface area, and stoichiometry of sputtered ceria films by simply changing the deposition time which makes this method promising for production of thin film catalysts. It opened the way to preparation of novel planar catalytic micro-reactors by using planar technology techniques.

TF-1-Or-9
Three steps strategy for thin film growth simulation: example of Cr/CrNx multilayers

T14 Thin Films

#TF-1-Or-9

A. Besnard [1], A. Zairi [1], C. Nouveau [1], N. Martin [2], L. Carpentier [2].

[1]Arts et Metiers ParisTech - LaBoMaP - Cluny (France), [2]Institut FEMTO-ST - Besançon (France).

The growth of thin films depends on the characteristic of the species impinging on the substrate. And these are ruled by the deposition conditions and the process. Taking them into account makes simulated results closer to experimental ones.

In this study, we developed a strategy based on three different tools to simulate the three-dimensional growth of thin films.

- SRIM [1], which takes into account the power applied to the chromium target and simulates the sputtered particles flux.
- SIMTRA [2], which considers the deposition conditions (working pressures, dimensions of the chamber, target-to-substrate distance, target material…) and gives the impinging particles flux on the substrate.
- Simul3D [4], which simulate the growth of the films, taking into account the process conditions and allow obtaining physical information (roughness, density…)

One of the main challenges is to determine the behavior of an atom impinging on the film, in particular sticking and diffusion phenomenon.

This strategy is use in the case of Cr/CrN_x periodic multilayers. They were deposited by reactive magnetron sputtering with a pulsing gas process [4], which alternates reactive and metallic sputtering modes. The duty cycle α between nitrogen injection and non-injection time (t_{on} and t_{off} respectively) was fixed at 50% of the pulsing period T using a square signal. The period T was systematically changed from 10 to 320 s for a same film thickness (± 50 nm).

The deposition conditions and the process are monitored and then used in the simulations tools. The results obtain by simulation are studied at each steps of the strategy. The simulated films are then compared to the experimental characterizations.

[1] J. F. Ziegler, M. D. Ziegler, J. P. Biersack, Nucl. Instrum. Methods. Phys. Res. B 268 (2010) 1818.
[2] K. Van Aeken, S. Mahieu, D. Depla J. Phys D: Appl. Phys. 41 (2008) 205307.
[3] A. Besnard, N. Martin, L. Carpentier, IOP Conf. Series: Mater. Sci. Eng. 12 (2010) 012011.
[4] N. Martin, J. Lintymer, J. Gavoille, J.M. Chappé, F. Sthal, J. Takadoum, F. Vaz, L. Rebouta, Surf. Coat. Technol., 201 (2007) 7720.

TF-4-Or-3
Influence of stoichiometry and microstructural evolution on the electrical and optical responses of AlNxOy films

T14 Thin Films

#TF-4-Or-3

J. Borges [1], N. Martin [2], N.P. Barradas [3], E. Alves [3], J.P. Rivière [4], D. Eyidi [4], M.F. Beaufort [4], T. Girardeau [4], F. Paumier [4], C. Fonseca [5], F. Vaz [1], L. Marques [1].

[1]Centro de Física, Universidade do Minho, 4710-057 - Braga (Portugal), [2]Institut FEMTO-ST, Département MN2S, UMR 6174 (CNRS, UFC, ENSMM, UTBM) 32, Avenue de l'Observatoire 25044 - Besançon (France), [3]Instituto Superior Técnico/ITN, Universidade Técnica de Lisboa, E.N. 10, 2686-953 - Sacavém (Portugal), [4]Institut Pprime - UPR 3346 CNRS-Université de Poitiers-ENSMA, Département de Physique et Mécanique des Matériaux Bât. SP2MI - Téléport 2, BP 30179 F86962 - Futuroscope Chasseneuil (France), [5]Universidade do Porto, Faculdade de Engenharia, Departamento de Engenharia Metalúrgica e de Materiais, Rua Roberto Frias, s/n, 4200-465 - Porto (Portugal).

Metallic (Me) oxynitrides (MeN_xO_y) are an attractive class of materials of emerging interest due to a unique set of versatile properties in different technological domains such as protective applications (wear, diffusion and corrosion-resistance), decorative coatings for high-quality consumer products, gas barriers, microelectronics, optoelectronics, solar cells, etc. Among the group of already studied oxynitrides, aluminium oxynitride (AlN_xO_y) presents some interesting characteristics to be used in different technological fields, since it may combine the behaviour of metallic aluminium, and those of the base binary systems: aluminium nitride, known for its semiconducting and piezoelectric properties and aluminium oxide, for its protective and insulating performance. In this work, thin films of AlN_xO_y were prepared by reactive DC magnetron sputtering, using a pure Al target and an $Ar/(N_2,O_2)$ gas mixture. The particular stoichiometry, structure and morphology of the films leads to the formation of a nanocomposite-like material, with Al nanoparticles randomly dispersed in an AlN_xO_y matrix, forming a percolating network. This fact induced a

wide variation in the electrical properties [1], such as a gradual transition from positive to negative temperature coefficients of resistance (TCR) as the non-metallic/Al atomic ratio increases; as well as distinct optical responses [2], such as an unusual large broadband absorption for some stoichiometries. The nanocomposite films are also very stable in terms of their microstructure and resistance to chemical degradation, even immersed for several weeks in typical solutions such as NaCl. This set of properties opens a wide range of possible applications in the electrical-driven application and in optical coatings such as those used in concentrated solar power systems.

[1] J. Borges, N. Martin, N.P. Barradas, E. Alves, D. Eyidi, M.F. Beaufort, J.P. Riviere, F. Vaz, L. Marques, Thin Solid Films 520 (2012) 6709-6717.
[2] J. Borges, N.P. Barradas, E. Alves, M.F. Beaufort, D. Eyidi, F. Vaz, L. Marques, Journal of Physics D: Applied Physics 46 (2013) 015305.

Fig. 1 - Ternary diagram of the deposited AlN_xO_y films. The films were indexed to three different zones according to their stoichiometry, microstructure and properties: (a) **Zone I**: columnar-like growth, metallic behaviour; (b) **Zone T (Transition)**: nanocomposite films with cauliflower-like growth, high electrical conductivity, evolution from positive to negative TCR values, large broadband absorption; (c) **Zone II**: dense films, insulating behaviour, optical transparency.

TF-P2-25
Cerium oxide thin films supported by sputtered a-C and CNx films on silicon for the use as a catalyst in micro fuel cells

T14 Thin Films

#TF-P2-25

M. Dubau, I. Matolínová.

faculty of mathematics and physics, Charles University Prague - Prague (Czech republic).

Cerium oxide has received much attention due to its promising catalytic properties for a variety of reactions [1-2]. The main goal of our research activity is focused on the fabrication of catalytically active (e. g. for methanol oxidation) cerium oxide based thin films on silicon with large surface for the application as a catalyst for on-chip micro fuel cells. It was shown in an earlier study, that cerium oxide based thin films exhibit a porous structure on glassy carbon [3]. Furthermore, it was shown that partial oxygen plasma etching of the glassy carbon substrate during cerium oxide film deposition is very likely the driving force for the formation of the observed porous structure of cerium oxide. In this contribution we will show to what extend it is possible to achieve similar results on silicon substrates using sputtered amorphous carbon films (a-C) and nitrogenated amorphous carbon films (CNx) as an interlayer. Amorphous carbon and CNx films have been deposited via magnetron sputtering on silicon and studied with respect to their morphological and structural properties. In the second step of this study the behavior of these films in oxygen plasma has been investigated. It was found out, that oxygen plasma treatment leads to a morphological and structural modification of the a-C and CNx film. Besides, CNx films exhibit a significantly lower resistance against oxygen plasma leading to a higher etching rate compared to a-C films. The third part of the study covers the investigation of the morphology and structure of cerium oxide films supported by an a-C or CNx film on silicon depending on cerium oxide film thickness. Investigation with SEM revealed that cerium oxide exhibits a highly porous structure on CNx, while the a-C supported cerium oxide film has a fine grainy surface structure. Investigation with XPS showed that the CNx supported cerium oxide film contains a significantly higher fraction of the Ce3+ oxidation state at the interface compared to the a-C

supported film. Together with the porous surface structure of the CNx supported cerium oxide film these results promise a high catalytic activity of the cerium oxide film.

[1] P. Y. Sheng, W. W. Chiu, A. Yee, S. J. Morrison, H. Idriss; Catalysis Today 129, **2007**, 313-321
[2] Y. Suchorski, R. Wrobel, S. Becker, B. Strzelczyk, W. Drachsel, H. Weiss; Surf. Science **2007**, 601, 4843
[3] I. Khalakhan, M.Dubau, S. Haviar, J. Lavková, I.Matolínová, V. Potin, M. Vorokhta, V. Matolín; Growth of nano-porous Pt-doped cerium oxide thin films on glassy carbon substrate; Ceramics International (2012), article in press, http://dx.doi.org/10.1016/j.ceramint.2012.10.215

fig 1:SEM imges of the 5nm cerium oxide film supported by a 250nm a-C (CNx) film on silicon.

SE/TF-4-Or-6
Effects of pulse bias duty cycle on composition, structure and hardness of Ti-Cu-N nanocomposite films deposited by pulse biased arc ion plating

T14 Thin Films

#SE/TF-4-Or-6

Y. Zhao [1], W. Lang [2], J. Xiao [1], B. Yu [1].

[1]Institute of Metal Research Chinese Academy of Sciences - Shenyang (China), [2]Key Lab of Material Processing and Mould Technology - Wenzhou (China).

Hard nanocomposite Ti-Cu-N films were deposited on high-speed-steel (HSS) substrates by pulse biased arc ion plating with a TiCu (88:12 at. %) single multi-component target. The effects of pulse bias duty cycle of elemental content, structure and mechanical properties of the films were investigated. The Cu atomic content of Ti-Cu-N films was examined by Electron Probe Micro-Analyzer (EPMA). The structure was determined by X-ray diffraction (XRD). Hardness and elastic modulus were determined by nanoindenter. The results showed that the content of Cu appeared to decrease with the duty cycle increasing from 10 to 50 % under the pulse bias voltage of -300 and -600 V. The XPS spectra of Cu 2p of the Ti-Cu-N films showed that there is only pure metallic Cu in the films. The diffraction peak of TiN in preferred orientation (111) was observed when the pulse duty cycle increased to 30 and 50% under the pulse bias voltage of -300V, whereas the corresponding peak changed to preferential orientation (220) when duty cycle increased to 30 and 50% under the pulse bias voltage of -600 V. And no obvious sign of metal copper phase was observed in the XRD patterns. The value of hardness under pulse bias voltage of both -300 and -600 V firstly increased and then decreased with duty cycle increasing from 10 to 50 %. Hardness enhancement was observed, the maximum value of the hardness, 31.5 GPa, was obtained with duty cycle 30 % under -600 V, corresponding to Cu content of 1.75 at.%. The hardness enhancement was discussed.

[1] J. Musil, P. Karvankova, J. Kasl. Surf. Coat. Technol. 139 (2001) 101.
[2] J. Musil, Surf. Coat. Technol. 125 (2000) 323.

[3] Hyun S. Myung, Jeon G. Han, Jin H. Boo, Surf. Coat. Technol. 177-178 (2004) 404.

TF-1-Or-5
Gold/yttria-stabilized zirconia nanocomposite films at the nanoscale

T14 Thin Films

#TF-1-Or-5

D. Horwat, J. Ghanbaja, S. Migot, J.F. Pierson.

Institut Jean Lamour - Nancy (France).

Microstructural and chemical analyses are routine characterizations in materials science. Information at the atomic scale (coordination, oxidation states) is particularly relevant to understand the physical and chemical properties of materials. The local interaction of noble metals and oxides can generate specific local chemical and structural states, which is particularly true when an element can diffuse at the metal/oxide interface [1, 2].
In this communication we treat the case of gold/yttria-stabilized zirconia nanocomposite thin films relevant for the fields of low friction, plasmonics and catalysis. We use local analytical methods available with high resolution transmission electron microscopy (HRTEM) for structural investigation and elemental mapping at the nanometer and atomic scales. X-ray photoelectron spectroscopy (XPS) was used to determine the metal oxidation state. Spectrophotometry has been used for the detection of localized surface plasmon resonance (LSPR), which the results are compared to the literature [3]. Electrical investigations were conducted by "4 point" probe, which are in line with the local chemistry. A special attention was paid to the oxidation state of the metal atoms in relation to the size of the nanoparticles. The size is controlled by the synthesis parameters and the gold content. The influence of the local state on the plasmonic, electrical and catalytic properties is demonstrated.

[1] D. Horwat, M. Dehmas, A. Gutiérrez, J-F. Pierson, A. Anders, F. Soldera, J-L. Endrino. Efficient, Low Cost Synthesis of Sodium Platinum Bronze NaxPt3O4, Chem. Mater. 24 (2012) 2429-2432

[2] G. C. Bond, D.T. Thompson, Gold-Catalysed Oxidation of Carbon Monoxide, Gold Bull. 33 (2000) 41-50

[3] E. Cottancin, G. Celep, J. Lermé, M. Pellarin, J.R. Huntzinger, J.L. Vialle, M. Broyer, Optical properties of noble metal clusters as a function
of the size: comparison between experiments and a semi-quantal theory Theor. Chem. Acc. 116 (2006) 514–523

Fig. 1: Distribution of the diameter of gold nanoparticles in Au/YSZ nanocomposite films

Fig. 2: Evolution of the electrical conductivity of Au/YSZ nanocomposite films.

TF-8-Or-4
Transition of Magnetic Anisotropy in FePt/AlN Layered Structure

T14 Thin Films

#TF-8-Or-4

C. Zhang, J. Shi, Y. Nakamura, S. Muraishi, T. Sannomiya.

Tokyo Institute of Technology - Tokyo (Japan).

Perpendicular magnetic anisotropy (PMA), which can result in preferentially magnetization in the direction perpendicular to the film plane, has long been a research interest. PMA has been found in layered structures consisting of magnetic metals and noble metals, for example Co/Pd, Co/Pt,[1] and CoPt/AlN layered structures.[2] In this work we study the magnetic anisotropy of another metal alloy/nitride layered structure, FePt/AlN layered structure.

The M-H loops of sputter-deposited $[Fe_{0.4}Pt_{0.6}(2\ nm)/AlN(20\ nm)]_5$ layered structures are shown in Fig. 1. It is clear that the as-deposited film (Fig.1a) show in-plane magnetic anisotropy. However, the anisotropy of the layered structures can be altered through annealing. As shown in Figs. 1(b)–1(f), the easy axis of magnetization turn from in-plane to out-of-plane direction with increasing annealing temperature.

In order to understand the change of magnetic property, the structure of the layered structures was characterized by XRD, and the results are shown in Fig. 2. The layered structures show preferred orientations of FePt [111] and AlN [001] parallel to the growth direction. When annealing at temperatures above 500℃, highly symmetrical satellite peaks can been seen clearly superimposing the FePt 111 peak, indicating the sharpness and flatness of interface are enhanced by annealing. Another phenomenon needed to mention is that the peak position of FePt 111 shifts to higher angles with the increasing of annealing temperature. This suggests the change of internal stress inside the FePt layers.

It is considered that transition of the magnetic anisotropy with increasing annealing temperature is due to the improvement of interface quality between FePt and AlN layers and the evolution of internal stress.

1. P. F. Carcia, A. D. Meinhaldt and A. Suna, Appl. Phys. Lett., 47, 178 (1985).
2. Y. Hodumi, J. Shi and Y. Nakamura, Appl. Phys. Lett., 90, 212506 (2007).

FIG. 1. M-H loops of $[Fe_{0.4}Pt_{0.6}(2\ nm)\ /AlN(20\ nm)]_5$ layered structures, as-deposited and annealed.

FIG. 2. X-ray diffraction profiles of $[Fe_{0.4}Pt_{0.6}(2\ nm)\ /AlN(20\ nm)]_5$ layered structures, as-deposited and annealed.

TF-4-Or-10
Structural, optical and electrical properties of chemo-synthesized Cd1-xPbxS thin films

T14 Thin Films

#TF-4-Or-10

M. Barote.

SRTM UNI NANDED - Ausa (India).

M. A. Barote a *, E. U. Masumdar b

a: Department of Physics, Azad college, Ausa-413520, Maharashtra, India.
b: Department of Physics, Rajarshi Shahu Mahavidyalaya - Latur-413512, India.
Abstract:
A simple and inexpensive chemical bath deposition technique is employed for the deposition of Cd1-xPbxS (0 ≤ x ≤ 1) thin films. Cadmium sulphate, lead sulphate and thiourea were used as the basic starting materials. TEA was used as complexing agent. For good quality deposits the various preparative parameters such as deposition temperature, time, speed of substrate rotation and pH of the reaction mixture were optimized to 80 0C, 60 min., 65 rpm and 10.5±0.1 respectively. The 'as-grown' samples were characterized through structural, surface morphological, compositional, optical, electrical and thermoelectric studies. The color of 'as-grown' samples changed from orange yellow to black as x changed from 0 to 1. The X-ray diffractograms of 'as-grown' samples exhibited polycrystalline nature with presence of cubic phases for CdS and PbS and hexagonal phase for CdS alone [1]. The crystal size determined from XRD and SEM micrographs is observed to increase with 'x' up to 0.175 and later on it decreased. The energy dispersive analysis by X-rays (EDAX) revealed that films are cadmium rich. The optical study at room temperature revealed high coefficient of absorption (10^4 cm-1) with a direct allowed type of transition with band gap energy decreasing continuously from 2.47 eV to 0.49 eV with varying composition parameter 'x'. The electrical resistivity measurements revealed semiconducting nature of the film and it is found that the resistivity of the film decreases with increase in 'x' up to 0.175 and further it increases up to x = 1 [2]. The n-type conduction was observed in film from TEP studies [3-4].

Keywords: Chemical bath deposition, Cd1-xPbxS thin films, XRD, EDAX, SEM.

References

[1] A.A. Yadav, M.A. Barote, E.U. Masumdar, J. Alloys Compd. 493 (2010) 179.
[2] D.P. Pandiyan, A. Marikani, K.R. Murali, Mater. Chem. Phys. 88 (2004) 250.
[3] A.E. Rakhshani, Phys. Status Solidi A 169 (1998) 85.
[4] M.A. Barote, A.A. Yadav, E.U. Masumdar, Physica B 406 (2011) 1865.

TF-1-Or-6
Stabilisation of α and β phases of Ta thin films grown by magnetron sputtering

T14 Thin Films

#TF-1-Or-6

A. Michel, J.J. Colin, G. Abadias, C. Jaouen.

Institut Pprime, CNRS- Université de Poitiers- ENSMA, Département de Physique et Mécanique des Matériaux - Poitiers (France).

Considerable research has been carried out in the recent years on the growth of Ta thin films using sputter deposition techniques [1,2]. The technological interest in such films arises from a wide range of potential applications: Ta films can be used in fields spanning from diffusion barriers in micro-electronic devices to protective hard coatings. However, in most of these applications, the physical properties of Ta that are sought are based on the electrical and mechanical properties of the well-known cubic α phase. Therefore, the occurrence of either the α or β-Ta phase plays a key role since, indeed, the metastable β phase, characterised by high electrical resistivity and ill-known mechanical properties, often appears during thin film growth, as dynamic growth processes sometimes oppose thermodynamic equilibrium-based predictions.

In the presented work, Ta thin films were grown using a magnetron sputtering chamber equipped with a multiple beam optical stress sensor (kSA-MOSS system) that allows a real-time *in-situ* monitoring of the stress state of the film. Special attention is given to the control of all parameters during the growth, in order to separate the effects of temperature on the one hand and energy of deposition due to the sputtered species on the other hand. Additionally, the effect of different buffer layers on the film structure was examined. *Ex-situ* investigation techniques (X-Ray diffraction, X-ray reflectivity, electron microscopy, AFM, …), were used in order to obtain as much as possible information on structure, defects and microstructure of the deposited thin films.

It is shown that the β-Ta phase is favoured during RT growth on neutral substrates such as amorphous Si, however the nucleation occurs only after the formation of an

initial amorphous layer (2-3 nm thick). This β-Ta phase formation is extremely stable concerning the energy deposition involved during growth (pressure during deposition ranging from 0.1 to 0.8 Pa, bias voltage applied to the substrate reaching 200 V). However, when the substrate temperature is increased, nucleation of α-Ta phase becomes possible; therefore, a temperature region of coexistence of the two allotropic phases was determined, pure α-Ta films were obtained at higher temperatures (T > 550 K).
An analysis based on the minimisation of the surface/interface energy versus volume energy shows that all results can be interpreted by the nucleation-and-growth approach. The lower surface energy of the (002) textured β-Ta phase then acts as the driving force for low temperature phase stabilisation, whereas at higher temperatures, the increasing difference in Gibbs energy of the respective α and β phases turns, in terms of nucleation, to the advantage of the α-Ta phase.

[1] P. Catania, R. A. Roy, and J. J. Cuomo, Journal of Applied Physics 74, 1008 (1993)
[2] H. Ren, M. Sosnowski, Thin Solid Films 516, 1898 (2008)

PST/SE/TF-P1-08
Study of Sheath in Multicomponent Plasmas

T14 Thin Films

#PST/SE/TF-P1-08

S. Novak, P. Cerny, P. Bruna, R. Hrach.

J. E. Purkinje University - Usti Nad Labem (Czech republic).

A detailed description of physico-chemical processes taking place during an interaction of plasmas with solid surfaces is rather difficult, especially at higher pressures and/or in chemically active plasmas, and thus a combination of experimental and computational approaches is used. Negative ions in such plasmas influence the transport of charged species from the plasma to the immersed solids [1]. First results have been obtained in a 1D approximation [2].

Two different techniques of computational physics were used. First, the particle simulation approach based on the self-consistent PIC-MCC technique was used for study of the interaction between the low-temperature multicomponent plasma and the surface immersed. An effective particle model is used. As input the concentrations of the basic charged species obtained from the following model were used.

The macroscopic kinetic approach was chosen for a study of chemical processes in the chemically active plasma. The kinetic scheme contained more than one hundred reactions between neutral, charged, and excited species in oxygen and argon. The chemical reactions and corresponding rate coefficients were obtained from both the literature and the calculations with help of the ELENDIF program. The time dependencies of concentrations of the neutral, excited, and charged species were obtained for various discharge parameters in a DC glow discharge in Ar/O_2 mixture.

Results of the 2D computer simulations describing the interaction between the low-temperature multicomponent plasma and the immersed metal substrate are presented and compared to the experimental data. The potential distributions in the sheath and presheath were calculated and concentrations of all kinds of charged particles were determined in the dependence on plasma parameters, especially on plasma pressure. The simulations were performed both in the static and dynamic regimes.

For the detailed plasma characterization, the multicomponent plasma consisting of more types of positive and negative species was used. The concentrations of the most important species in oxygen plasma were obtained by the macroscopic kinetic approach [3]. These concentrations were used as input data for the particle simulations. An example of the particle simulation results derived in static case for higher pressure can be found in Fig. 1.

[1] J.I. Fernández Palop, J. Ballesteros, M.A. Hernández, R. Morales Crespo, *Plasma Sources Sci. Technol.* **16** (2007), S76-S86.

[2] P. Cerny, S. Novak, R. Hrach, P. Bruna, *Contrib. Plasma Phys.* **48** (2008) 424-429.

[3] P. Cerny, S. Novak, R. Hrach, *Vacuum* **84** (2010), 97-100.

Fig. 1: Concentrations of charged species in multicomponent Ar/O_2 plasma (plasma composition $Ar:O_2 = 50:50$). Cylindrical probe (radius 1×10^{-4} m), voltage bias +10 volts, pressure 600 Pa.

TF-P2-09
Numerical simulation of porosity development kinetics into multy-layer media

T14 Thin Films

#TF-P2-09

A. Bondareva, G. Zmievskaya.

M.V. Keldysh institute of applied mathematics RA - Moscow (Russian federation).

Numerical simulation of the porosity in the thin layers may be applied to the technological mirror production, EUV-lithograpy applications, plasma engine wall erosion study, semiconductor devices and others. The generalize program system Stosh-An-1 had been developed for simulation of blistering in metals and dielectrics to apply it for models of radiation flow interaction with multilayered media with boundary condition variation between layers by consideration of the crystal lattice vacancies role in the formation of blisters under inert gas flow. The processes of chemically active gases collisions with pore walls are included in the model. Hibbs energy model of pore nucleation is complemented by considering the stress in the crystalline lattice caused by parameter mismatch of layer lattices. The model of Brownian movement of defects based on previously developed methods of accounting the long-range potential of elastic interaction of defects by excitation of acoustic phonons in lattice matrix and Fridel oscillations of electron density is complemented by taking into account the orentation of crystallographic planes of body-centered lattices of sample material relative to the flow. The numerical investigation has been conducted according to the model of blister (vacancy-gas pores) merging into defect structures on the characteristic times of the fluctuation stage of phase transition "vacancy (gas) in lattice - pores". The structure sizes (the number of blisters in the structure) are defined. Using the distribution function of blisters by sizes and placement in the layers the porosity of sample layers and the contribution of pressure contrasts on the bubble boundaries to layer stress are determined. Further stressing of the elongated defect structures may lead to crack formation. The diffuse shuffle of atoms and chemical composure formation on the interlayer surface (in the limits of several monolayers) should be modeled separately. In the current simulations the arising roughness of the layer boundary surface is modeled using the initial fractal distribution of interlayer surface areas and deviations

of their depth relative to the disturbance source. The prospects of the interlayer surface flattening under Xe^{++} radiations are investigated. The method of boundary projection of the elongated defect structures onto the crystallographic planes of layer materials is developed, including the ones perpendicular to the incident flow (crystallographic plane 001) and parallel to it (crystallographic plane (100) and (010)) at bilayer sample temperatures from 0.4 to 0.6 of Molibden melting point, radiation level from 10^{14} to 10^{18} cm^{-2}, ion energy from 1 to 10 keV. Their sizes had been determined. The contribution of radiation defects in Silicon Carbide coating to the stressed layer condition is comparable to the contribution of the lattice parameter mismatch in the "metal-semiconductor" bilayer under the assumption of coherent state of the interlayer boundary. It has been discovered that the average blister sizes in the both layers of the substrate (in both metal and semiconductor) depend nonlinearly on the temperature. Work is partially supported by the RFBR grants 11-01-00282-a, 12-01-00490-a and 12-01-00708-a).

[1] Zmievskaya G.I., Bondareva A.L., Savchenko V.V., Levchenko T.V. 2012 Defect and Diffusion Forum 326-328 pp. 243-248

TF/SE-P3-02
Antireflective SiOxNy layers deposition by reactive gas pulsing process for Si-based thin photovoltaïc films

T14 Thin Films

#TF/SE-P3-02

A. Farhaoui [1], J. Cellier [2], E. Tomasella [3], A. Bousquet [3], A. Moreau [4], R. Smaali [5], E. Centeno [5].

[1]Institut de Chimie de Clermont-Ferrand, Clermont Université, Université Blaise Pascal, BP 10448, F-63000 - Clermont-Ferrand (France), [2]Institut de Chimie de Clermont-Ferrand, Clermont Université, Université Blaise Pascal - Clermont-Ferrand (France), [3]Institut de Chimie de Clermont-Ferrand, Clermont Université, Université Blaise Pascal, - Clermont-Ferrand (France), [4]Institut Pascal, Clermont Université, Université Blaise Pascal, BP 80026, F-63171 AUBIERE - Clermont-Ferrand (France), [5]Institut Pascal, Clermont Université, Université Blaise Pascal, - Clermont-Ferrand (France).

Although the market for photovoltaïc products is evolving rapidly, photovoltaïc developers are concerned about the price. The optimization of the electrical properties of the active layers is progressing. However, the optical properties of the entire device have also to be optimized, especially for thin Si-based film solar cells. In order to capture the maximum of photons, and so to ensure the highest photovoltaïc yield, antireflective layers should be very efficient.

Our challenge is to explore powerful and economical routes using radio-frequency magnetron sputtering, a cheaper and a well-controlled industrial process to develop complex antireflective systems. We are focused on the control of the deposited thin film optical properties through their composition by tuning the deposition parameters (target, gas flows, cathode power, pressure, substrate temperature…). With a refractive index tunable between 1.46 for pure silicon oxide to 2.03 for silicon nitride [1], silicon oxynitrides are interesting candidates for antireflective thin films. Their deposition was carried out using an argon, oxygen and nitrogen gas mixture from a silicon target.
In a first step of our work, Argon and nitrogen were introduced at constant gas flows,

whereas oxygen gas was pulsed in order to adjust films' chemical composition over a large range [2]. For constant Ton and Toff pulse durations, we get a specific composition of SiO_xN_y with a specific refractive index. Then, by changing the O_2 gas flow pulse durations during the deposition steps, we predict a gradient of composition which leads also to a controlled refractive index gradient. It is a way to improve Si thin film photovoltaïc yield with an economical process.
The plasma analysis has been carried on by time-resolved Optical Emission Spectroscopy to identify the generated species in the plasma, and to follow their evolution during the deposition steps. The film composition is investigated by Rutherford Backscattering Spectroscopy, and their structural properties by Fourier Transform Infrared Spectroscopy.
The optical properties have also been studied by spectroscopic ellipsometry and by UV-visible absorption spectroscopy. In addition, to optimize the performance [3] of the realized structures and for a better understanding of their optical properties, an electromagnetic nanostructure model has been established.

[1] [Palik (1985)] E. D. Palik (ed.) Handbook of Optical Constants of Solids, Academic Press, New York, 1985.
[2] E. Aubry, S. Weber, A. Billard, N. Martin, Journal of Applied Surface Science. 257, 2011, 10065.
[3] A. Moreau. R. Smaali, E. Centeno, C. Seassal, Journal of Applied Physics. 111, 2012, 083102.

TF-4-Or-7
The effect of substrate temperature and direct current bias on the properties of titanium oxide thin films elaborated by pulsed filtered cathodic arc technique.

T14 Thin Films

#TF-4-Or-7

F. El Ghoulbzouri, M.P. Delplancke.

Princ - Brussel (Belgium).

Titanium dioxide thin films were deposited on silicon wafer (100) by pulsed cathodic arc technique in an oxygen atmosphere. We studied the effect of substrate temperature and the DC substrate bias on the properties of the elaborated thin films. The crystalline structure, mechanical properties, topography and microstructure were characterized by X-ray diffraction, Raman spectroscopy, nano-indentation, Atomic Force microscopy and Transmission electron microscopy. Without a substrate bias, a transition from amorphous to rutile phase was observed at a temperature of 673 K. The crystalline thin films do not exhibit a preferential orientation. By applying a DC bias of -200 V, we could decrease the temperate at which the crystalline phase occurs to 473 K. In fact, at this temperature, XRD patterns and Raman spectroscopy data showed a formation of Ti_2O_3 thin film. The transition to rutile phase was observed at a substrate temperature of 673 K. All the elaborated crystalline thin films at -200 V DC-bias exhibit a preferential orientation due to the combination effect of substrate heating and bias, allowing to promote the thin film growth according to the lowest energy state. Cross section TEM micrograph (Fig. 1) revealed a columnar growth for the crystalline layer, the grain diameter could be estimated in order of 20 nm. Unfortunately, the application of a DC bias on the substrate over a range of -100 V to -400 V at room temperature was not enough to promote the formation of a crystalline phase. The hardness and the reduced Young modulus of the amorphous/rutile TiO_2 coatings were respectively in order of 8 GPa /19 GPa and 90 GPa/200 GPa. The root mean square roughness measured on a scanned area of 1x1 μm^2 was in the range of 1 nm to 2 nm.

TEM cross section of TiO_2 thin film deposited at a substrate temperature of 873 K and a DC substrate bias of -200 V.

SE/TF-1-Or-4
Performance evaluation of h-BN coatings prepared on titanium via polymer pyrolysis in RTA furnace

T14 Thin Films

#SE/TF-1-Or-4

B. Toury [1], Y. Sheng [2], S. Benyoun [2].

[1]Université de Lyon - Villeurbanne (France), [2]Ecole Centrale de Lyon - Ecully (France).

Today, the aeronautic industry requires the use of titanium alloys-based mechanical tools or components in more and more severe conditions (i.e. high temperature, corrosive and oxidative atmospheres), imposing to coat the solicited piece with a protective coating. Hexagonal boron nitride (h-BN) is known to be eco-friendly, thermally and chemically stable and especially self-lubricant. Thus, shaped as coating, it represents an environmentally acceptable solution to fight against galling and/or wearing solicitations and thus increase the life-time of those metal parts.
h-BN coatings have been prepared through the Polymer Derived Ceramics (PDCs) route and annealed via infra-red irradiation performed by Rapid Thermal Annealing (RTA). Resulting coatings have been demonstrated as crack-free, recovering and homogenous films. Chemical analyses performed on samples annealed at least at 1350 °C under nitrogen or argon; show the presence of a TiN layer recovered by the expected h-BN. Adherence and friction coefficient measurements were carried-out by means of scratch-tests, calo-tests and tribological tests. Results exhibit a weaker friction coefficient for nitrogen-pyrolized samples, which can be explained by a thinner TiN interphase. However, all the samples display a good adhesion between the substrate and the coating, explained by the formation of Ti-B-N bonds at the interface. Hardness was also estimated by micro-indentation, different behaviour was observed between samples annealed under Ar ou N2 probably due to different chemical composition of the coatings. Finally, the effect of ceramic charges and metallic nano-particles loaded in the coating during the synthesis process will also be investigated.

TF/SE-1-Or-8
Structural and dielectric characterization of perovskite oxide and oxynitride lanthanum titanium films deposited by reactive sputtering deposition

T14 Thin Films

#TF/SE-1-Or-8

C. Le Paven [1], Y. Lu [1], H. Nguyen [2], R. Benzerga [1], L. Le Gendre [1], A. Sharaiha [1], C. Delaveaud [3], F. Tessier [4], F. Cheviré [4].

[1]IETR - Saint Brieuc (France), [2]IETR / CEA Leti - Saint Brieuc (France), [3]CEA Leti - Grenoble (France), [4]ISCR - Rennes (France).

In the field of microwaves, the needs of materials with high performances drive the research on perovskite type structure compounds which present attractive dielectric and ferroelectric properties. Our contribution is related to the development of lanthanum titanium perovskite oxide (LTO) and oxynitride films (LTON), for which the substitution between oxygen and nitrogen atoms allows to tune the dielectric properties. Single layers, mixed films and multilayers have been deposited by reactive RF magnetron sputtering using an oxide $La_2Ti_2O_7$ or an oxynitride $LaTiO_2N$ homemade target. Depending on the reactive gas and the nature of substrate, various chemical composition and crystalline textures of films have been evidenced. The dielectric measurements were performed on MIM devices at low and high frequencies. The LTO oxide films present a moderate dielectric constant (epsilon = 60) with very low dielectric loss (tandelta= 0.011) at 10 GHz, with no variation of epsilon under the application of DC electric fields. The dielectric constant of LTON oxynitride films is higher, with values of few hundred but with substantial dielectric loss. The LTON films show a variation of epsilon, but only in low frequency ranges (up to 1 MHZ), for example the tunability is 8 % at 100 kHz with a maximum applied field of 16.7 kV/cm. LTO/LTON bilayers exhibit improved values compared to “pure” oxynitride films, for example a maximum applied field of 44 kV/cm with a tunability of 15 % (Figure 1). The absence of tunability of oxynitride films in high frequencies, as well as the observed dispersed results, suggests that the $LaTiO_2N$ compound does

not behave as a ferroelectric material. In accordance with litterature, its nonlinear dielectric properties may be related to polar nano-regions, coming from a local ordering of oxygen and nitrogen ions in the perovskite structure.

Figure 1. Evolution of the dielectric constant (a) and the dielectric loss (b) depending on a DC bias at 100 kHz of a LTO/LTON bilayer deposited by reactive sputtering with a $La_2Ti_2O_7$ oxide target.

TF-P2-26
Phase transformation of amorphous TiO2 films to anatase / rutile crystalline structure

T14 Thin Films

#TF-P2-26

J. Bruncko [1], M. Netrvalova [2], A. Vincze [1], P. Sutta [2].

[1]International Laser Centre - Bratislava (Slovakia), [2]New Technology Research Centre West Bohemian University - Plzen (Czech republic).

TiO_2 is one of the most studied transition metal oxide that exists at two main polymorphs – anatase and rutile. The increasing application interest (sensor applications, solar cells, photo-catalytic materials, etc.) demands preparation of nanostructured TiO_2 films with controlled phase structure. Phase composition of the functional structures impacts on their performance and efficiency. Both phases crystallises in tetragonal crystal structure but in different space groups which implies that they have different physical properties and chemical behaviour.
The contribution deals with TiO_2 films prepared by pulsed laser deposition (PLD). According to deposition conditions the resulted structure can be amorphous, anatase, rutile or mixed. PLD at room temperature usually lead to amorphous films. We propose an enhanced version of PLD with deposition on substrates cooled below room temperature. Films deposited by such manner exhibited highly porous nature assembled in a very fine hierarchical (like fractal) dendritic arrangement of nanoparticles smaller than 10 nm. Fig. 1 shows a pair of SEM records of TiO_2 films. Fig. 1a represents the sample deposited on cooled Si (100) substrate while the sample shown in Fig. 1b was grown at room temperature. This example shows that despite the same property – both films are amorphous; they differ in porosity and surface morphology.
Phase transformation of amorphous TiO_2 to crystalline permitted controlling of phase composition in dependence on annealing process parameters and initial morphology. The films were investigated by various analytical methods (scanning electron microscopy, X-ray diffraction, optical emission spectroscopy, micro-Raman spectroscopy) and experimental results revealed that transformed films consist of 100% anatase up to 600 °C. They preserved high porosity (typical grain size around 10 - 20 nm) which is desirable property for sensor and photo-catalytic applications.

Fig. 1 The comparison of SEM images of TiO_2 films in as-deposited state prepared at different temperatures on Si (100) substrate (a – substrate temperature near 77 K; b - substrate at RT).

TF/SE-1-Or-11
Yttria-Stabilized Zirconia thin films as oxygen ion conductor for solid oxide fuel cells

T14 Thin Films

#TF/SE-1-Or-11

J. Lamas, W.P. Leroy, D. Depla.

Research group DRAFT - Ghent University - Ghent (Belgium).

Yttria-stabilized zirconia (YSZ) is one of the most popular materials chosen as electrolyte for solid oxide fuel cells. Due to its mechanical strength, chemical stability, high ionic conductivity, low electrical conductivity, good radiation-resistance and low cost, YSZ has also become a popular material in different applications, e.g., as buffer, oxygen sensors, nuclear applications and thermal barriers coatings.
Current studies aim to lower the process temperature of the SOFC by reducing the thickness of the electrolyte. However, reducing the thickness might change the properties of the electrolyte in comparison to the bulk properties of these materials. The fundamental aspects of the oxygen ion conduction, for example, change due to the occurrence of nano-effects. That is why, the good understanding of the microstructure and crystallinity opens the possibility to manipulate the ionic conductivity.
A good approach for understanding the microstructure is the study of YSZ thin films ranging in composition by varying the deposition conditions. The variation of deposition conditions, such as pressure and Y target-substrate distance enables us to modify the film morphology and texture. In this work, YSZ thin films were deposited by the dual reactive magnetron sputtering technique. The analysis of these films were performed in two steps: first, it involves the characterization of the film in a crystallographic way using X-ray diffraction (theta-2theta configuration), pole figures and cross section images via scanning electron microscopy and transmission electron microscopy. The preferential orientation of these films were studied and correlated with an extended structure zone model of the growing material. The columnar microstructure present in those films was fitted in a quantitative model where the columnar angle is related to the variation of composition along the sample and its correspondent grain size. Secondly, it is based on the ionic conductivity of YSZ at different yttrium composition levels using electron impedance spectroscopy. Correlating both approaches allows us to identify the compositional and

crystallographic influences on the ionic conductivity and to unravel the oxygen ion conduction mechanism of the YSZ thin film solid state electrolytes.

This abstract is submitted to RSD2013

TF-9-Or-7
Sputter yield amplification upon reactive serial co-sputtering of doped TiO2

T14 Thin Films

#TF-9-Or-7

R. Schmidt [1], T. Kubart [2], M. Austgen [1], A. Pflug [3], T. Nyberg [2], S. Berg [2], M. Wuttig [1].

[1]I. Institute of Physics, RWTH Aachen University - Aachen (Germany), [2]Solid State Electronics, The Ångström Laboratory, Uppsala University - Uppsala (Sweden), [3]Fraunhofer IST - Braunschweig (Germany).

TiO_2 plays a prominent role in several applications such as anti-reflective coatings [1] or self-cleaning surfaces [2]. Most frequently this material is deposited by reactive magnetron sputtering. Unfortunately TiO_2 suffers from a comparatively low deposition rate. To increase the deposition rate, Sputter Yield Amplification (SYA) can be used through recoil of the sputtering species at implanted heavy dopants below the target surface [3,4,5]. Here we present experimental results for different dopants using a dedicated sputter deposition tool which enables systematic studies of SYA. In this study the rate increase by SYA is investigated for different heavy dopants (e.g. Hf, Ta, W, Bi, etc.). Our experiments show that the rate increase of TiO_2 by some dopants (e.g. Bi) is surprisingly low, whereas other dopants, which are even slightly lighter, result in a large rate increase of up to 250%. This behavior demonstrates that sputter yield amplification does not only require a high mass of recoil atoms but also necessitates high surface binding energies. TRIDYN [6] simulations employing a model optimized for serial co-sputtering [5] confirm and explain the experimentally determined deposition rates.

[1] C. Battaglin, F. Caccavale, A. Menelle, M. Montecchi, E. Nichelatti, F. Nicoletti, P. Polato, Thin Solid Films **351**, 176 (1999)
[2] A. Fujishima, X. Zhang, D. Tryk, Surface Science Reports **63**, 515 (2008)
[3] T. Kubart, T. Nyberg, A. Pflug, M. Siemers, M. Austgen, D. Koehl, M. Wuttig, S. Berg, Surface and Coatings Technology **204**, 3882 (2010)
[4] M. Austgen, D. Koehl, P. Zalden, T. Kubart, T. Nyberg, A. Pflug, M. Siemers, S.

Berg, M. Wuttig, J. Phys. D: Appl. Phys. **44**, 345501 (2011)
[5] T. Kubart, R.M. Schmidt, M. Austgen, T. Nyberg, A. Pflug, M. Siemers, M. Wuttig, S. Berg, Surface and Coatings Technology **206**, 5055 (2012)
[6] W. Moller, W. Eckstein, J.P. Biersack, Comput. Phys. Commun. **51**, 355 (1988)

TF-P1-01
RF magnetron deposition of ZnO thin films on positioned GaP nanowires

T14 Thin Films

#TF-P1-01

D. Buc [1], J. Kovac [1], M. Caplovicova [2], J. Murin [3], V. Kralovic [3], J. Novak [4].

[1]Institute of Elektronics and Photonics, Slovak Technical University in Bratislava - Bratislava (Slovakia), [2]Department of Geology of Mineral Deposits, Comenius University - Bratislava (Slovakia), [3]Institute of Power and Applied Electrical Engineering, Slovak University of Technology in Bratislava - Bratislava (Slovakia), [4]Institute of Electrical Engineering, Slovak Academy of Sciences - Bratislava (Slovakia).

Zinc oxide has been attracting particular interest because of its high optical transparency combined with an excellent electrical conductivity [1]. We incorporate wide band-gap p-GaP/n-ZnO nanowires (NWs) junction to increase solar cell efficiency to shift the absorption edge more to the blue part of the solar spectrum (350-480 nm) for an enhanced photon capture. The GaP NWs were prepared in an AIX 200 MOVPE low-pressure reactor by a vapour-liquid-solid method from 30 nm BBI colloidal Au particles from a water-based colloidal solution [2]. We discuss the deposition of ZnO thin layers on positioned GaP substrate and GaP nanowires by RF magnetron sputtering at different ZnO:Al target-substrate geometry. We selected the tilting angles (0°, 45° and 82°) of substrate normal to the target center-substrate center flow line, see Fig. 1. The surface morphologies of ZnO films and core-shell GaP/ZnO NWs were examined by AFM, SEM and TEM. TEM images of a GaP/ZnO NWs revealed that GaP nanowire has zinc blende crystal structure and growth axis [111], see Fig. 2. ZnO polycrystalline layer formed nano-crystals with wurtzite columnar structure. The positioning of the substrate to the target and its rotating has beneficial influence in the suppression of shadowing effect and provide more homogenized films. We simulated the influence of residual stress on bending of GaP/ZnO NWs using ANSYS software, results of calculations will be compared with experimental observations. The results revealed the ability to utilize p-GaP/n-ZnO NWs in the solar cells development and will be subjected for future electrical and optical properties investigation.

The work is supported by grant of Science and Technology Assistance Agency "GRONA" no. APVV-0301-10, and VEGA projects 1/1106/12, 1/0534 and 1/0439/13.

[1] H. Xu, X. Liu, D. Cui, M. Li, M. Jiang: Sensors and Actuators B, 114, 301 (2006).
[2] S. Hasenöhrl, P. Eliáš, I. Vávra, I. Novotný, J. Kováč, J. Novák, XIV EuropeanWorkshop on Metalorganic Vapor Phase Epitaxy EW-MOVPE 2011, June 5-8, Wrocław, Poland, p.259-262.

Fig.1. Magnetron sputtering geometry
Fig.2. Bright field TEM image of GaP/ZnO NWs

TF-P3-09
Aerosol deposition of size-controlled gold nanoparticles on polymer surfaces.

T14 Thin Films

#TF-P3-09

L. Nittler, Y. Busby, J.J. Pireaux.

University of Namur, Centre de Recherche en Physique de la Matière et du Rayonnement (PMR), Laboratoire Interdisciplinaire de Spectroscopie Electronique (LISE), rue de Bruxelles 61 - Namur (Belgium).

Nanoparticles (NPs) are not only of great scientific interest because they constitute a kind of a link between bulk materials and atomic or molecular structures, but also because they present a wide variety of potential applications in biomedical, optical, and electronic fields, to cite only a few of them. But in order to enhance optical or electronic performance for example, a control of size, shape and spatial distribution of the NPs is required.

Although the chemical synthesis of gold NPs (AuNPs) allows controlling their size and shape, the control of their spatial distribution over a surface or in a bulk is still a challenge. This is especially true for organic material substrates, where the interaction between solvent and the organic surface cannot be neglected.

In this study the deposition of well-defined Au nanoparticles is performed by the aerosol technique, which consists in an injection of a colloidal solution through a high pressure carrier gas pulse into a low pressure plasma reactor. The main advantage of this technique is to control independently the NP size and density for the deposition on nearly all kind of sample substrates under a controlled (eventually reactive) atmosphere.

We study the spatial distribution of AuNPs as a function of the deposition conditions. The main parameters which influence the NP deposition are the pulsing condition of

the aerosol technique, the carrier gas as well as the pretreatment of the polymer surface.

We will compare the deposition and coalescence of AuNPs on different sample surfaces by electron microscopy and AFM. Furthermore we will present preliminary results of the aerosol-AuNPs/polymer chemical interaction by high resolution XPS.

SE/TF-4-Or-5
Annealing effects on Raman spectra of nitrogen doped ZnO thin films produced by N2-reactive sputtering

T14 Thin Films

#SE/TF-4-Or-5

O. Debieu, J. Cellier, A. Bousquet.

Institut de Chimie de Clermont-Ferrand, UMR 6296, Université Blaise Pascal, Campus des Cézeaux, 24 avenue des Landais, BP 80026, 63171 AUBIERE Cedex - Clermont-Ferrand (France).

ZnO has recently received particular attention because of its transparency and electrical conductivity which are interesting for future applications in optoelectronics. However, although n-type semiconductor material is now attainable, the reproducibility and the stability over time of p-type ZnO remain a barrier for the realization of p-n junction diodes. Nitrogen is one of the most promising candidates as acceptor dopants in ZnO since the N-incorporation by substitution of N atoms for O sites is facilitated by the similar atomic radius of N with O. However, the N-content and annealing treatment effects on the mechanisms of the generation of acceptors in ZnO are still unclear and need to be more extensively investigated trough the combined analysis of the structural, optical, and electrical properties of N-doped ZnO. In this work, N-doped ZnO thin layers were produced by N_2-reactive magnetron sputtering. The films were deposited on Si wafer and fused silica substrates at various temperatures ranging from 50 to 400°C using Ar as the main sputtering gas. The doping concentration was set by the N_2 gas flow and monitored through the analysis of the plasma composition by optical emission spectroscopy. The film composition was investigated by Rutherford backscattering spectrometry and by X-ray photon spectroscopy. The optical properties were investigated by means of UV-visible absorption, photoluminescence, and spectroscopic ellipsometry. The carrier density and mobility were determined by Hall effects measurements. The film structure was investigated by X-ray diffraction, by electron paramagnetic resonance, by energy dispersive X-ray analysis, by high resolution transmission electron microscopy, and by Raman spectroscopy.
Raman spectroscopy is particularly suitable for the analysis of the effect of the N content on the ZnO structure because of the coexistence of the anomalous (275 cm^{-1}), E2-high (437 cm^{-1}), and A1-LO (580 cm^{-1}) Raman modes which are related to the

substitution of N for O site, the wurzite crystalline structure quality, and the generation of defects, respectively. Besides, we compared the effect of conventional annealing and laser annealing on the Raman spectra in order to optimize the electrical and optical properties.

TF-4-Or-5
Asymmetrical diffusion at interface of Mg-based multilayer films

T14 Thin Films

#TF-4-Or-5

J. Zhu [1], H. Li [1], Z. Wang [1], K. Guen [2], P. Jonnard [2].

[1]Tongji University - Shanghai (China), [2]Laboratoire de Chimie Physique – Matière et Rayonnement, UPMC Univ Paris 06 - Paris (France).

Multilayer mirrors have been widely used as reflective element in the extreme ultra-violet (EUV) and soft x-ray regions. Interfacial diffusion is one of the most efficient defects that will reduce the reflectance. However interfacial diffusion in these nanoscale multilayers is a phenomenon not as well understood as diffusion in bulk materials. In this report, interface structure of Mg-based multilayer films as EUV reflectors has been studied. We deposited a series of multilayers with the structure of [X1/Mg/X2]×5 (X1,2 = SiC, Si, and C). The nominal thickness of Mg is 5.0 nm and that of X1,2 is 2.5 nm. All multilayers were deposited onto polished Si (001) wafer at ambient temperature by direct current magnetron sputtering. The pressure of residual gas before deposition was 5.0×10-5 Pa and that of sputtering gas Ar was 0.13 Pa. X-ray grazing reflectivity (XRR) measurements were made for each sample using Cu Kα source (λ = 0.154 nm) to determine the multilayer structure (Fig.1). The measured curves were fitted to obtain the interface width. X-ray photoelectron spectroscopy measurements were carried out for the three [X/Mg/X] multilayer samples. Depth-profiles were obtained by Ar etching. Transmission electron microscopy (TEM) measurements were carried out for another three [X/Mg/X] multilayer samples having the same structure with the period repeat number N=80. The cross-section samples for TEM were prepared by focused ion beam etching. X-ray diffraction measurements in the symmetric (θ–2θ) geometry were performed using Cu Kα source (λ = 0.154 nm). The experimental results show that asymmetry is found on the interlayer thickness at all three interfaces. The thickness of the interlayer at Mg-on-Si (>7 nm) and Mg-on-C (>5 nm) is larger than that at Si-on-Mg (3 nm) and C-on-Mg (2.5–3 nm). In the Mg/SiC multilayer, opposite asymmetry is found as the thickness of the interlayer at Mg-on-SiC (1 nm) is smaller than SiC-on-Mg (2.5 nm). Based on XRD, XPS and TEM measurement results, different mechanisms for interfacial diffusion are proposed. These results are not only of fundamental importance in understanding the nanoscale interfacial diffusion but are also beneficial for improving the performance of Mg/SiC multilayers as EUV reflector by means of inserting diffusion barrier layers.

Fig. 1. XRR measured and fitted curves of [X1/Mg/X2]×5 multilayers.

TF-9-Or-9
Growth study: ultra-thin GaN films by ion-beam assisted molecular beam epitaxy

T14 Thin Films

#TF-9-Or-9

J. Gerlach [1], L. Neumann [1], T. Höche [2], B. Rauschenbach [1].

[1]Leibniz-Institut für Oberflächenmodifizierung (IOM) - Leipzig (Germany),
[2]Fraunhofer-Institut für Werkstoffmechanik IWM - Halle (Germany).

The application of energetic nitrogen ions, which possess hyperthermal kinetic energies instead of the thermal atomic nitrogen usually used in conventional molecular beam epitaxy (MBE) of GaN, introduces additional growth parameters to this already complex heteroepitaxial growth system. In analogy to conventional MBE of GaN, the ratio of the impinging hyperthermal nitrogen ion flux to the flux of the incoming Ga atoms (ion to atom ratio I/A) was observed to be one crucial parameter in ion-beam assisted molecular beam epitaxy (IBA-MBE), amongst others like the kinetic energy of the ions [1]. A window of suitable ion energies, where no ion collision induced defects are created below the surface, but instead only at the surface is used (for details see Ref. [2]). This provokes a rearrangement of surface atoms that can be interpreted as ballistically enhanced adatom mobility. Aim of the present study is to determine the influence of the hyperthermal ion irradiation on the nucleation, on the formation and growth of islands, as well as on the structural properties, the morphology and surface topography of the growing ultra-thin GaN films.
Ultra-thin GaN films were grown on 6H-SiC(0001) substrates by deposition of gallium and simultaneous irradiation with low-energy nitrogen ions (energy < 25 eV) delivered by a constricted glow-discharge ion source [3]. The GaN film formation at a constant substrate temperature of 700°C was studied in situ by reflection high energy diffraction (RHEED) during the deposition process and the surface topography of the deposited GaN islands and films on the SiC substrate surfaces was analyzed without interruption of the ultra-high vacuum by scanning tunnelling microscopy (STM). The crystalline structure and quality of the GaN films was studied by x-ray diffraction (XRD). Transmission electron microscopy (TEM) was applied to characterize the film microstructure. The results show that ultra-thin epitaxial GaN films can be obtained by ion-beam assisted molecular beam epitaxy [4]. The I/A ratio at constant nitrogen

ion flux and at constant substrate temperature has a major impact on the properties of the resulting ultra-thin GaN films. The growth mode, the surface roughness, the degree of GaN coverage of the substrate and the polytype mixture depend notably on the I/A ratio. Determined by the I/A ratio, the growth mode changes from three-dimensional (3D) to two-dimensional (2D) growth. At an I/A ratio ≤ 1.6 the formation of islands develops through rapid coalescence into 2D growth. 3D island growth is favoured at an I/A ratio > 1.6. An increase of the island diameter to island height ratio with increasing I/A ratio is observed indicating an enhancement of the lateral growth. In the 2D growth mode, which leads to relatively smooth films of high crystalline quality, the formation of the zincblende polytype of GaN is detected that is absent in 3D grown films. The results are discussed taking into account the influence of the impinging hyperthermal ions on the growing film.

[1] S. Sienz, J.W. Gerlach, T. Höche, A. Sidorenko, B. Rauschenbach, Thin Solid Films 458 (2004) 63.
[2] D.K. Brice, J.Y. Tsao, and S.T. Picraux, Nucl. Instrum. Meth. B 44 (1989) 68.
[3] A. Anders, M. Kühn, Rev. Sci. Instrum. 69 (1998) 1340.
[4] L. Neumann, J.W. Gerlach, B. Rauschenbach, Thin Solid Films 520 (2012) 3936.

TF-P2-05
Optical, structural and microstructural studies of TaON thin films deposited by rf-sputtering

T14 Thin Films

#TF-P2-05

A. Bousquet [1], F. Zoubian [1], C. Taviot-Guého [1], J. Cellier [1], T. Sauvage [2], E. Tomasella [1].

[1]ICCF - Aubière (France), [2]CEMHTI - Orléans (France).

The integration of antireflective coatings in optical applications has made an important improvement in their performance. The simplest antireflective coating consists of a single layer of transparent material with an optimum refractive index. The efficiency is improved by a multilayer structure formed by a succession of layers with graded refractive indices. These films are the essential component of electroluminescent devices used particularly in lighting applications (panel backlighting to liquid crystal displays) providing good illumination by consuming relatively little electric power, and frequently used as protective and antireflection coating in eyeglass lenses and solar panels.
In view of these considerations, we investigated the potential of the use of Tantalum oxynitride thin films in the field of optics. Indeed, Tantalum pentoxide (Ta_2O_5) can used as gate dielectric in electronics, optical devices and in antireflective coatings due to its high transparency, high dielectric constant, large band gap and its large refractive index (~2.3 at 632.8 nm). Tantalum nitride (TaN) is a hard material, resistant to the corrosion and chemically inert. It is used for hard and wear resistant coatings, as diffusion barrier, as well as film resistors since its electrical resistance is very stable and it possesses metallic behaviour. Combining the useful properties of oxide and nitride allows obtaining all the qualities in oxynitride material supervised by controlling the process parameters. That's why, Tantalum oxynitride films are promising candidates for applications in electroluminescent devices and antireflective coatings due to the wide range of variation of their refractive index between 2.3 and 3.8.
In this work we deposited TaOxNy thin films by reactive magnetron sputtering from a pure tantalum target with $Ar/O_2/N_2$ plasma. This process was chosen because of its low working temperatures allowing depositing optical and electrical structures on

sensitive substrates. The possibility of variation of several deposition parameters such as pressure, gas flows, target, power, etc. allows obtaining a wide range of film stoechiometry.
The main goal of this study is about a perfect knowledge of the structure of the deposited films versus the parameters used. From this one, the optical behaviour could be understood.
For that, chemical composition was investigated by ion beam (Rutherford Backscattered Spectroscopy). The structural and microstructural properties of films were investigated using X-ray diffraction technique (Xpert Pro Diffractomer, Cu Kα1,2) in terms of crystal orientation, lattice parameter, and coherent domain size. To estimate the optical band gap and Urbach energy, UV–visible spectrometer was used. The results were completed with phase modulation spectroscopic ellipsometry measurements obtained using a Jobin–Yvon UVISEL instrument in 248-2000 nm (0.6 - 5.0 eV) spectral range.

TF-P2-27
NITROGEN DOPING IN SPUTTERED Ga-DOPED ZINC OXIDE THIN FILMS

T14 Thin Films

#TF-P2-27

K. Shtereva [1], V. Tvarozek [2], I. Novotny [2], S. Flickyngerova [2], A. Vincze [3], M. Vojs [2], C. Jeynes [4], N. Peng [4].

[1]University of Ruse - Ruse (Bulgaria), [2]Slovak University of Technology, Institute of Electronics and Photonics - Bratislava (Slovakia), [3]International Laser Centre - Bratislava (Slovakia), [4]University of Surrey, Ion Beam Centre - Guildford (United kingdom).

We report on the properties of ZnO:Ga thin films deposited on glass and sapphire substrates by rf diode sputtering and then implanted with nitrogen to achieve a p-type semiconductor. After the N implantation, the films were annealed under O_2 and N_2 ambient. The effects of the implantation parameters (energy, dose) and the annealing parameters on the films' properties will be discussed. Ion implantation is an important technique for controllable doping in semiconductors and there have been reports for obtaining a p-type ZnO via N implantation [1]. In our earlier experiments, p-type doping with N_2 was done during sputtering and we reported p-type ZnO:Ga:N films with maximum hole concentration of $2.6x10^{18}$ cm^{-3} [2]. Recently, we have started investigating the p-type doping in ZnO:Ga via N implantation. SIMS measurements showed that the distribution of the complex $^{30}NO^{-}$ ions is Gaussian in the films implanted with 180 keV N^{+} ions (a dose range of $1x10^{15}\div2x10^{16}$ cm-^{2}), and it is uniform when performing two implants at 40 keV and 80 keV with doses of $1x10^{15}$ and $1x10^{16}$ cm^{-2} (Fig. 1). Annealing at temperatures above 400°C resulted in n-type films with electron concentrations 10^{18}-10^{20} cm^{-3}. A conversion of n-type into unstable p-type (hole concentrations 10^{17}-10^{19} cm^{-3}) was observed in some samples after annealing in O_2/200°C and in N_2/400°C. The resistivity of the N_2 annealed films at 200°C is 4.2 Ωcm, almost 2 times lower than that of the O_2 annealed films, and it decreases to 10^{-1} Ωcm with increasing the annealing temperature (Fig. 2). An average transmittance higher than 80 % in the wavelength range of 390-1100 nm proved that N-implanted ZnO:Ga films were highly transparent. Annealing caused the transmittance increase and the band gap widening (3.19-3.3 eV).

[1] Georgobiani A N et al. Nuclear Instr. and Methods in Phys. Research 2003; A 514, 117-121.
[2] Shtereva K et al. Vacuum 2012; 86, 652-656

Fig. 1. SIMS profiles of the negative ^{30}NO complexes in 180 and 40+80 keV N-implanted ZnO:Ga films
Fig. 2. Resistivity versus annealing temperature for 40+80 keV N-implanted ZnO:Ga films annealed in O_2 and N_2

TF-P2-28
Analysis and properties of ZnO layers grown by PLD

T14 Thin Films

#TF-P2-28

A. Vincze [1], J. Bruncko [1], M. Veselý [2], K. Tsutsumi [3], A. Tanaka [3].

[1]International Laser Centre - Bratislava (Slovakia), [2]FEI STU - Bratislava (Slovakia), [3]JEOL Tokyo - Tokyo (Japan).

The ZnO attracts large interest in research activities for its potential application mainly in UV and VIS optoelectronics with native n-type conductivity, excellent electrical, optical, piezoelectric and mechanical properties [1,2]. The pulsed laser deposition (PLD) allows to prepare various kinds of ZnO layers by two different ways, either by sputtering Zn target in O_2 atmosphere or by sputtering ZnO target onto substrate with a high power pulsed laser [3].
The contribution deals with multilayered samples grown by Nd:YAG laser at 355 nm, 5 Pa pressure of ambient O_2, substrate temperature at 400°C and combination of ablating pulses for ZnO target and Al target. Annealing process were done in O_2 ambient at temperature range 400-800°C.
Beside the surface characterisation SIMS and AES depth profiles were done in order to characterize the Al incorporation, Fig 1. After the annealing, the Al level in the SIMS depth profile was changed, Fig 1a. This can be explained by the higher dynamics in Al migration and also by the differences in recrystallization kinetics. The decomposition of the metastable structure to thermodynamically stable wurtzite serves as an efficient diffusion booster supporting the migration of Al atoms. This observation indicates that recrystallization gives a more positive base for the homogenization annealing [4]. The AES depth profile shows similar chemical element's profile, Fig.1b.

This work has been supported by projects from the International Laser Centre VEGA 1/0907/13 and APVV 0424-10.

[1] C. Jagadish, S. J. Pearton, Zinc Oxide Bulk, Thin Films and Nanostructures, Elsevier, 2006
[2] D. C. Look, Recent advances in ZnO materials and devices, Material Science and

Engineering B, Vol. 80, pp. 383-387, 2001.
[3] A. Vincze, J. Bruncko, M. Michalka, D. Figura, Growth and characterization of pulsed laser deposited ZnO thin films, Central European Journal of Physics 5(3), pp. 385–397, 2007.
[4] J. Bruncko, M. Netrvalova, A. Vincze, In-process ZnO thin films doping during pulsed laser deposition, Applied Physics A: Materials Science and Processing, (2012) pp. 1-6. in press.

Fig. 1 a) SIMS and b) AES depth profile of the ZnO:Al structure

TF-7-Or-1
Size control and photoluminescence properties of SiC nanoparticles embedded in a-SiCxNy:H thin film synthesized by N2/H2/Ar/hexamethyldisilazane microwave plasma

T14 Thin Films

#TF-7-Or-1

A. Thouvenin [1], P. Miska [1], L. De Poucques [1], L. Le Brizoual [2], J.L. Vasseur [1], M. Belmahi [1], J. Bougdira [1].

[1]Université de Lorraine (Institut Jean Lamour) - Nancy (France), [2]Université de Nantes (Institut des Matériaux Jean Rouxel) - Nantes (France).

Silicon carbonitride thin films have been drawing a lot of attention in the past 20 years. This stems from their many tunable properties useful in various fields such as microelectronics, solar energy[1] or optoelectronics[2]. Silicon carbonitrides allow different complex compositions and structures. Several synthesis ways exist for SiCN thin films and their characteristics are dependent on the parameters of the chosen elaboration technique. For example, precursor compounds are determinant because of pre-existing bonds in their structure which are likely to end up in the thin films. While silane is a commonly used precursor gas, its manipulation requires a highly secured process as it is explosive and toxic. Hence, using organosilicon compounds is less dangerous and can lead to interesting properties as well as ease the formation of some phase, but can also hinder the versatility of the process.

We worked with a PE-CVD (Plasma Enhanced Chemical Vapor Deposition) method: thin films were synthesized with an H_2/N_2/Ar/hexamethyldisilazane microwave plasma and deposited on Si(100) substrates. Although we have used an organosilicon precursor, our process has been exhibiting significant flexibility. Optical band gap E_g and refractive index n could be tuned with a low addition of N_2 in the gas

mixture ($3,0 < E_g < 5,0$ eV ; $1,8 < n < 2$)[3]. Looking at bonding in the films with XPS measurements, we noticed that a very low N_2 content was necessary to operate a changeover between Si-C and Si-N bond density. In fact, thin films appeared to be a nanocomposite material consisting in 2H-SiC nanocristallites embedded in an amorphous SiCN matrix. The crystallinity of the film was monitored via FTIR measurements and the decomposition of the signal into an amorphous signal and a crystalline signal corresponding to the SiC phase[4]. From XRD measurements, we could deduce that while the substrate temperature increased, so did the nanocristallites size. Substrate temperature and N_2 contents in the gas mixture seem to be crucial parameters. Consequently, the study of the influence of those two parameters enables us to gain more control over SiCN thin films characteristics, especially SiC crystallites size. Besides, controlling film composition, bonding and crystallite sizes is decisive when it comes to photoluminescence properties.

[1] M. Vetter, I. Martin, A. Orpella, J. Puigdollers, C. Voz, and R. Alcubilla. *Thin Solid Films*, 451(2004):340
[2] X. Du, Y. Fu, J. Sun, and P. Yao. *Journal of Applied Physics*, 99(2006):093503
[3] S. Bulou, L. Le Brizoual, P. Miska, L. De Poucques, J. Bougdira, M. Belmahi. *Surface and Coatings Technology*, 208(2012):46
[4] L. Calcagno, P. Musumeci, F. Roccaforte, C. Bongiorno, and G. Foti. *Thin Solid Films*, 411(2002):298

SE/TF-4-Or-4
Studies on composition and optical properties of NbCrON solar selective absorbing coating deposited by magnetron sputtering

T14 Thin Films

#SE/TF-4-Or-4

Y. Na [1], E. Tomasella [1], A. Bousquet [1], C. Wang [2], J. Cellier [1].

[1]Institut de Chimie de Clermont-Ferrand, ICCF UMR CNRS 6296, Université Blaise Pascal, 24 avenue des landais, 63171 Aubière cedex - Aubière (France), [2]Center for Condensed Matter and Materials Physics, Department of Physics, Beihang University - Beijing (China).

Concentrating solar power (CSP) systems use solar absorbers to convert sunlight into electrical power. The direct way to use solar energy is solar thermal conversion method using solar absorbers which are coated with solar selective absorbing coatings. Solar selective absorbing coatings, as a key part in the CSP systems, are used to convert sunlight into thermal energy, so they need to work at high temperature in a vacuum (T≥400℃) for a long time. Consequently, not only an excellent solar spectrally selective absorption property, but also the chemical and thermal stability of film are very important for practical application. The ideal spectrally selective absorbing coating would be cheap, with simple structure and convenient manufacture, require high absorptance (α) in the wavelength range of 300 nm-2500 nm and low emittance (ε) in the infrared region of 2500 nm–30 μm as well. According to the double interference absorptive theory, the film structure of solar selective absorbing coating from substrate to surface consists of an IR-reflective metallic layer, a high metal volume fraction (HMVF) cermet layer and a low metal volume fraction (LMVF) layer (as the double interference absorption layers), and a transparent ceramic antireflection (AR) layer.
Through the previous work it was found that niobium alloys (such as NbTi, NbZr and NbCr etc., their nitride and oxynitride coatings) could have enhanced properties, such as chemical stability and thermal stability. Based on this reason, a new solar selective absorbing coating with the film structure of Al/NbCrN(H)/NbCrON(L)/Si3N4 will be designed and deposited on copper substrate by reactive magnetron

sputtering.
In this study, we present the influence of composition and thickness on the optical properties of the cermet NbCrON coatings. By using Cr-Nb target, the NbCrON thin films were deposited with various Ar-O2-N2 gas atmospheres. The layer composition and morphology were investigated by Rutherford Back Scattering (RBS) and Scanning Electronic Microscopy (SEM), respectively. Moreover, the UV-Vis spectrophotometer and the spectroscopic ellipsometry were used to confirm the optical properties in term of refractive index and optical gap. The spectral properties were also determined to find the highest α and the lowest ε. It is shown that the thickness of HMVF and LMVF cermets for a given composition affects the solar selectivity (α/ε). At the optimum thickness in the range of 100-400 nm, the coating can achieve a high solar selectivity. On the other hand, argon plasma was used to improve the absorptance of the NbCrON cermet films without antireflective coating by significantly changing the roughness of the films. All the results indicate that this material is a promising coating for concentrating solar power systems.

TF-P1-02
Correlation between microstructural and electrical properties of heat treated Ti/Pt layers

T14 Thin Films

#TF-P1-02

D. Resnik.

University of Ljubljana - Ljubljana (Slovenia).

Investigation of DC sputtered Ti/Pt thin film layers on SiO2/n+Si substrate is presented. The main objective of this work was to determine the influence of heat treatment on the morphology and microstructure of Ti (20-50 nm)/Pt (180-250 nm) resistive layers and to correlate them with electrical properties such as Ti/Pt layer resistance and temperature dependency of resistance (TCR) of fabricated temperature sensors. Depth profiles and interdiffusion of individual layers were studied by AES for samples annealed between 300-700 °C.
AES depth profile of the sample annealed between 400-700 °C showed significant diffusion of Ti throughout the Pt layer toward surface, accompanied with oxygen incorporation, keeping rather constant TiOx composition throughout the structure (Fig.1) [1]. AFM surface analyses showed that Pt grain size was almost temperature independent up to 400 °C, while at 500 °C, slightly larger grains were observed. Above this temperature sudden increase of grain size was determined (Fig. 2). At 700 °C, grains have typically diameter of 300-400 nm compared to as-deposited grain diameter which was in the range of 10-30 nm.
Consequently, also electrical properties of the deposited resistive layer change significantly around 400 °C what complies with AES analyses. The correlation of surface roughness and electrical resistance is roughly inversely proportional (Fig. 2). The resistance of the temperature sensors showed linear dependency of R vs. T (±0.5%). The reproducibility of the TCR within the same run was within 10%, mostly due to the nonlinearity of measured resistance at lower temperatures [2]. It was further determined that by increasing the annealing temperature from 300 °C to 700 °C, gradual increase of TCR from 1500 ppm up to 2900 ppm was obtained, respectively, which is a significant value when implementing Ti/Pt layers as a temperature sensing device.

[1] Tiggelaar et al. 2009 Sensors Actuators A 125 39-47.
[2] Mailly et al. 2001 Sensors Actuators. A 94 32-38.

Figure 1. AES depth profile of Ti/Pt annealed at 700 °C.
Figure 2. Dependency of resistance (box plot) and surface roughness (line plot) vs. annealing temperature.

TF-4-Or-6
Nanocomposite TiC/a:C thin films for multifunctional applications: structural, mechanical and tribological properties

T14 Thin Films

#TF-4-Or-6

G. Radnoczi [1], J. Gubicza [2], M. Veres [3], I.E. Lukács [1], M. Menyhárd [1], K. Balázsi [1].

[1]Institute for Technical Physics and Materials Science, Research Centre for Natural Sciences - Budapest (Hungary), [2]Department of Materials Physics, Eötvös Loránd University - Budapest (Hungary), [3]Institute for Solid State Physics and Optics, Wigner Research Centre for Physics - Budapest (Hungary).

Nanocomposite structures composed of crystalline and (or) amorphous phases are of rapidly growing interest. Combination of pure carbon-based thin films with metallic nanoparticles for example will result in a material with enhanced physical properties. Such structures can be obtained by addition of different metals, e.g. Ni, Cu, Ag, Cr, and Ti. Understanding the structural background of mechanical characteristics and atomic mechanism of the development of surface morphology in novel materials is significant because the demands to mechanical and surface properties may be different for different applications.
The main aim of this work is the development of different carbon-metal (Ti) coatings by relatively easy and cheap technology; magnetron sputtering. These films will be applied as self-cleaning protective or hard coatings for multifunctional applications. 500 nm thick films were deposited on oxidized silicon substrates by DC magnetron sputtering of Ti and C targets in argon at 25^{o}C, using different Ti target powers. The structure of the samples was studied by transmission electron microscopy (TEM) and atomic force microscopy (AFM). The layers were found to be consisting TiC nano-crystals of a few nanometres in size embedded in carbon matrix. Auger Electron Spectroscopy (AES) and Raman Spectroscopy were used to characterize the amorphous matrix found to be dependent on the Ti sputtering power. Nano-indentation was used to measure the mechanical properties of the nanocomposites. The measured hardness values were between 35 and 60 GPa, modulus of elasticity between 235–401 GPa depending on Ti content.

Our results show strong relationship between the evolving structure and the mechanical properties of C-Ti films.

Acknowledgements
This work is supported by the János Bolyai Research Scholarship of the Hungarian Academy of Sciences and OTKA Postdoctoral grant Nr. PD 101453, as well as the project OTKA 81360.

TF-P3-10
Large Vertically Aligned Carbon nanotubes films : industrial up-scaling and engineering

T14 Thin Films

#TF-P3-10

P. Boulanger, J. Descarpentries, L. Belkadi, P.M. Nghiem, D. Porterat, M. Pinault, M. Mayne L'hermite.

CEA, IRAMIS, SPAM, Laboratoire Francis Perrin CNRS 2453 - Gif Sur Yvette (France).

While the production capacity of dispersed carbon nanotubes is booming [1], the coming of industrial production of vertically aligned carbon nanotubes carpets/arrays/forests (VACNT) is still at its first stages. but represents the second generation of carbon nanotubes based products. From an industrial point of view, The main challenge is the control of carbon nanotubes characteristics in terms of length, density, cleanness, diameter and structure through a low cost process applicable to large surfaces. In this context, amongst the different methods reported for the growth of aligned CNT [2] Catalytic Chemical Vapour Deposition (CCVD) appears as a versatile process with great potential. CCVD process using catalyst pre-deposition and gaseous precursors, succeeded in controlling CNT morphology and size.

In this paper we focius our work on the co-injection aerosol-assisted Pressure CCVD process [3][4] we developed, that offers a rapid, never-ending and a continuous growth of aligned multiwall CNTs by injecting simultaneously carbon (liquid hydrocarbons) and catalyst precursors (ferrocene). We present the specificity of such a process and its ability to be upscaled for industrial production of VACNT. We demonstrated in small furnace configurations that by adjusting operating conditions nanotubes caracteristics such as length, density, catalyst content or nanotubes diameters can be controlled within a large range [6] an deposited directly on various substrates (flat substrates: silicon, quartz, carbon, metals; porous substrates: fibers [5]). By designing a new furnace, we were able to up-scale the process over large surface while reaching the same versatility process for both flat substrates and especially for fibers where pre-deposition of a protective layer is necessary. This pilot

is seen as a new step towards safer large scale and low cost in-line aligned carbon nanotubes production by aerosol-assisted CCVD.

1. BCC market research Nanotubes 2010

2. Kumar, Nanoscience and Nanotechnology, 10 (2010)

3. M. Mayne et al., Chemical Physics Letters 338, 101-107 (2001)

4. M. Pinault et al, Nano Lett., 5 – 12 (2005)

5. M. Delmas, et al., proceeding euro CVD 2009

6. C. Castro et al., Carbon, (2010)

TF-P3-11
ITO thin films fabricated by a hybrid facing-target sputtering system

T14 Thin Films

#TF-P3-11

S. Morohashi, K. Usui, F. Takaki, T. Murata, K. Kishimoto, N. Harada.

Yamaguchi University - Ube (Japan).

A hybrid facing-target sputtering system has been newly devised. The magnetic field distribution between facing targets can be easily changed by moving a inner rod magnet without breaking the vacuum. By changing the magnetic field distribution between facing targets, Indium-Tin Oxide thin films have been deposited on glass substrates with controlled Ar/O2 gas mixture and with DC power.

Figure 1 shows the schematic diagram of a facing-cathode, with moving rod magnets that change a magnetic field distribution between facing-target in a hybrid facing-target sputtering system and the plasma dischrge state in ITO film deposition. This sputtering system has devised to realize high-speed deposition for improved throughput, while satisfying the requirements for low damage during deposition. The sputtering can be achieved under different magnetic field distribution between facing-target, where the magnetic field distribution is controlled with a moving rod magnet without breaking the vacuum1,2). The polarity of the fixed facing outer cylindrical magnets is opposite. The inner rod magnets are moving magnets. The polarity between the cylindrical magnet and the moving magnet is opposite, and the polarity between the facing inner rod magnets is opposite. With such a magnet arrangement, three magnetic field distributions are created between the facing-targets: (1) a magnetic field distribution due to the facing cylindrical magnets; (2) a magnetic field distribution due to the facing moving rod magnets, which directed oppositely to the magnetic field created by the cylindrical magnets; and (3) a magnetic field distribution created between the stationary cylindrical magnet and the moving rod magnet at the back of each target. The hybrid magnetic field distributions between the facing-target can be controlled by the positions of the moving rod magnets without breaking the vacuum. The magnetic field distribution is shown schematically for the two cases in Figure 1. Figure 1(a) shows the case where the magnetic field distribution of (1) is strong, and Figure 1(b) shows the case where the magnetic field distributions of (2) and (3) are added to the distribution of (1).
Without both substrate heating and post annealing processes, the resistivity of as-

grown ITO film with 200 nm thickness was 7.3 x 10-4 Ω-cm. The deposition rate of ITO films was 142 nm/min and the substrate temperature rise during deposition was 90 ℃ or less.

References :
1) S. Morohashi, J. Vac. Soc. Jpn., 128 (2010) 26.
2) S. Morohashi, et al.: J. Vac. Soc. Jpn., 54 (2011) 181

Fig. 1 Schematic diagram of the magnetic field distribution between facing-cathode in a hybrid facing-target sputtering, (a) in case the moving rod magnet is most close from a target, (b) in case the moving rod magnet most separate to the target. Discharge plasma during ITO deposition using a hybrid facing-target sputtering, (c) in the case of the magnets shown in Fig.1(a), (d) in the case of the magnets shown in Fig.1(b).

TF-8-Or-5
Exploring the effects of Co and (Co,Mo) doping on the properties of TiO2 semiconductor thin films

T14 Thin Films

#TF-8-Or-5

A. Silvestre [1], S. Rout [2], S. Dalui [2], O. Conde [2].

[1]Instituto Superior de Engenharia de Lisboa, Área Departamental de Física and ICEMS, 1959-007 Lisboa, Portugal - Lisboa (Portugal), [2]Universidade de Lisboa, Faculdade de Ciências, Departamento de Física and ICEMS, 1749-016 Lisboa, Portugal - Lisboa (Portugal).

Here we report on the effect of Co and (Co,Mo) doping on the structural, optical and electrical properties of TiO_2 thin films. Undoped TiO_2, Co and (Co,Mo) doped TiO2 films (5 at.% Co, 1 and 3 at.% Mo) were grown by pulsed laser deposition onto Al_2O_3(0001) substrates, using a Ar background pressure of 8×10^{-2} Pa and a substrate temperature of 350 ^{o}C. Films' thicknesses are in the range of 100-140 nm. XRD analyses shows that all films are anatase single phase with (112) orientation. Crystallite sizes in the range of 7-17 nm were inferred depending on the doping. The broad Raman peaks presented by all films are in line with the smallness of the coherent diffraction domains determined by XRD. Optical measurements show that the band gap values of doped films are red shifted when compared to the undoped TiO_2 films. Urbach energies of 784.6, 458.4 and 428.7 meV were estimated for the $Ti_{0.95}Co_{0.05}O_2$, $Ti_{0.94}Co_{0.05}Mo_{0.01}O_2$ and $Ti_{0.93}Co_{0.05}Mo_{0.03}O_2$ films, respectively, which seems to support that Co doping is effective in introducing additional localized states into the band gap whereas Mo doping affects reversely. All the films show weak ferromagnetic semiconductor behavior at room temperature. The nature of the carriers is currently being studied by Hall effect measurements. The role of oxygen vacancies and doping elements on the optical, electrical and magnetic properties of the films are discussed.

Acknowledgement: This work was partially funded by the Portuguese Foundation for Science and Technology (FCT), contract no. PTCD/CTM/101033/2008. S.R. acknowledges FCT for a Post-Doctoral grant, reference SFRH/BPD/64390/2009.

TF-7-Or-5
Cermet coating deposition by DC reactive co-sputtering process controlled by voltage

T14 Thin Films

#TF-7-Or-5

J. Rodrigo [1], B. Navarcorena [1], G. García Fuentes [1], J.A. García [1], R. Escobar [2], C. Prieto [2], J.A. Sánchez [2], E. Céspedes [2], J.M. Albella [2].

[1]AIN - Cordovilla (Spain), [2]ICMM - Madrid (Spain).

Cermet-type coatings are drawing full attention as solar selective coatings for concentrated solar power (CSP) applications [1]. For this application, high melting point transition elements, as for instance Mo, Ni, Pt o Cr, are used as the metallic component of the cermet. This elements are usually inside a dielectrical matrix of SiO_2, Al_2O_3, Si_3N_4 or AlN.

Insulating ceramic compounds deposition by physical vapor deposition (PVD) is typically done by RF assisted sputtering processes. However, due to the low deposition rate achieved by this deposition technique, there is being progressively more used pulsed DC or DC reactive sputtering deposition technique [2].

In DC reactive deposition of insulating ceramic compounds there are two operation modes: metallic mode and reactive mode [3]. The metallic mode is characterized by a low gas partial pressure and a high deposition rate. In the other hand, the reactive mode has a high gas partial pressure and a low deposition rate. The transition between both modes is quite steep with a slight change in the reactive gas. In addition, the transition takes place at different reactive gas rates depending on the direction of the transition, a hysteresis cycle rules the stability of the process.

One of the most important parameters to control in the deposition is the target voltage. Not only for having under control the deposition rate, but also for mandating over the deposited oxide stoichiometry during the reactive sputtering process [4].

In this work the co-deposition of a Mo-SiO_2 coating has been studied. The process was carried out in a DC reactive environment with two targets of silicon and

molybdenum. Process parameters are highly influenced by the deposition strategy. In this case, in one hand we must deposit silicon oxide as matrix and in the other hand we have to deposit metallic molybdenum as dopant in order to achieve LMVF and HMVF required values. Moreover, we should control both cathodes voltage very precisely, managed by a PID controller, in order to avoid undesired transitions between metallic and reactive sputtering modes.

Roughness and thickness of the coatings have been measured, they have been also characterized by GDOES and UV-VIS-nIR and FTIR spectroscopy. The study shows the different absorption and emission coating properties achievable depending on the process parameters. The optical characterization of the coating, with the n and k parameters, allows us to predict the final emission and absorption properties of the complete stack with the help of a coating simulation software.

[1] N. Selvakumar et al., Solar Energy Materials & Solar Cells, 98, 1 (2012).
[2] R. Cremer et al., Surface and Coatings Technology, 120-121, 213 (1999).
[3] I. Safi, Surface and Coatings Technology, 127, 203 (2000).
[4] Kari Koski, Thin solid films 326 189-193 (1998).

TF-6-Or-12
Coloration Mechanism and Optimized Performance of Electrochromic Nickel Oxide

T14 Thin Films

#TF-6-Or-12

Y. Ren [1], S.Y. Chiam [1], J. Liu [2].

[1]Institute of Materials Research and Engineering, A*star - Singapore (Singapore), [2]Department of Chemistry, National University of Singapore - Singapore (Singapore).

Electrochromic (EC) materials are important for enabling technologies such as smart windows and non-volatile displays. The stability of the open-circuit memory can be translated to possible energy savings in integrated windows application for indoor comfort. Nickel oxide (NiO) is a common high-performance anodic EC material. In this presentation, we will introduce solution-based deposition methods of thin film NiO for low-cost and large-scale fabrication, followed by examining the coloration and EC mechanism of NiO. The role of ions is especially important in aqueous electrolyte. Apart from the commonly reported contribution from hydrogen ion (H^+), hydroxyl ions (OH^-) can also play a role. The presence of OH^- ions can lead to existence of different phases for both bleached and colored states and even multiple chemical reactions during the aqueous electrolyte cycling. We show that while H^+ ions are important to give rise to the coloration, initial OH^- ions incorporation in a dehydrated NiO enhance the EC property of the film by increasing inter-layer spacing that allows more H^+ ions movements. Later stages of OH^- ions incorporation results in intercalated H_2O that inhibits further H^+ ions diffusion. This understanding of the role of ions shown in the figure will therefore be crucial in the optimal control of hydroxyl ions for both efficiency and durability of the EC devices. Since one key enabling feature of initial OH^- incorporation is to increase interlayer spacing, a substitution of aqueous electrolyte with non-aqueous electrolyte (Li-PC or solid electrolyte) during cycling will prevent degradation through intercalated water molecules. The optimally hydrated NiO will also need to be well passivated to retain its interlayer spacing. Here, we propose tantalum oxide as a suitable candidate for the solid electrolyte. On the other hand, the coloration mechanism of EC NiO remains controversial and a detailed understanding of the electronic structure evolution has yet to be reported. We show here a detailed study of filled and empty electronic states of the bleach and

color states of NiO thin film. We use X-ray photoelectron spectroscopy (XPS) to show that the removal of H^+ ions give rise to holes that resides in a *p-d* hybridized state of mainly oxygen *p*-character. This can be determined from the slight change in near-valence band edge states from the fitted XPS data. While the valence band edge is not significantly affected, the presence of these ligand holes drastically change the empty state in the conduction band investigated by X-ray absorption spectroscopy. This spectrum weight transfer is believed to be brought by split-off state with primarily *Op*-character and effectively reduces the optical band gap to below 2eV for visible light absorption.

TF-7-Or-6
Low-Cost High-Performance Zinc Antimonide Thin Films for Thermoelectric Applications

T14 Thin Films

#TF-7-Or-6

Y. Sun [1], M. Christensen [2], S. Johnsen [2], B.B. Iversen [2].

[1]School of Science, Harbin Institute of Technology; Center for Materials Crystallography, Department of Chemistry and iNANO, Aarhus University - Harbin (China), [2]Center for Materials Crystallography, Department of Chemistry and iNANO, Aarhus University - Aarhus (Denmark).

Rising demand on energy efficiency and green solutions has made global interest in thermoelectric (TE) devices explode. However, TE power generation still has few commercial applications since no cheap, stable, non-toxic and high performing materials made of abundant elements are known. Recently, low power applications of TE thin films has attracted intense attention. Extremely high TE figures of merit have been reported for superlattices [1,2], yet their complicated and expensive production makes commercialization problematic. Zn_4Sb_3 and ZnSb are cheap, promising p-type TE bulk materials in the intermediate temperature range (473-673 K). Here, we report on the synthesis and characterization of stable, phase pure Zn_4Sb_3 and ZnSb thin films with outstanding TE properties [3]. ZnSb films as well as two completely new meta-stable crystalline phases of zinc antimonide were directly deposited on silica substrates by a co-sputtering method. After post-annealing treatments at 573 K, the two new phases transformed into Zn_4Sb_3+ZnSb and single phase Zn_4Sb_3 films, respectively. Thermoelectric characterization along the in-plane direction revealed that these Zn_4Sb_3 and ZnSb films exhibit very large PF values, which are comparable to the best reported results of the bulk materials [4,5], but unlike the bulk materials, they also have good thermal stability up to 573 K. These thin films fulfill all the key material requirements for commercial TE application, and have significant potential to be used in TE sensors, coolers or self-powered micro-devices.

1. R. Venkatasubramanian, *et al*., Nature 413, 597 (2001).
2. T. C Harman, *et al*., Science 297, 2229 (2002).
3. Y. Sun, *et al*., Adv. Mater. 24, 1693 (2012).
4. G. J. Snyder, *et al*., Nat. Mater. 3 , 458 (2004).
5. E. S. Toberer, *et al*., J. Mater.Chem. 20 , 9877 (2010).

Fig.1. XRD patterns of A) a type A sample (ZnSb), B) a type B sample and an annealed type B sample (Zn_4Sb_3+ZnSb), and C) a type C sample and an annealed type C sample (Zn_4Sb_3).

Fig.2. *zT* of ZnSb and Zn_4Sb_3 films. In order to estimate κ , κ_e was calculated from measured values of ρ , and added to literature values of bulk κ_L .

SE/PST/TF/BI-P1-07
Titanium oxynitride coatings deposited by the reactive magnetron sputtering: structure and physicochemical properties

T14 Thin Films

#SE/PST/TF/BI-P1-07

V. Pichugin, M. Konishchev, N. Morozova, O. Kuzmin, A. Pustovalova.

Tomsk Polytechnic University - Tomsk (Russian federation).

Titanium oxynitride films are perspective materials for different applications. TiNxOy films have been deposited on substrates using reactive magnetron sputtering technique. The deposition process was carried out with pulsing frequencies 60 kHz and duty cycles in the range 50–90%. The method of time-resolved optical emission spectroscopy used to characterize the pulsed magnetron plasma. The experiments were carried out at total pressures in the range 0.1–0.6 Pa in either pure O2 (‘‘oxide’’ mode) or in O2–N2 mixtures. The surface morphology and topography of the films were studied by different techniques (EDX, ESEM, XRD, IR spectroscopy). The results show that deposited coating has character of nanocomposite with two-phase amorphous-crystalline structure with high part of interphase boundary. The adhesion strength of the coatings was in order to 40 MPa. The film has nanocrystalline structure with average grain size equals 13.83 nm. High enough Young’s modulus value (11 GPa) is evidence of high mechanical strength and good elastic properties of coatings. Obtained films possess the properties which allow to use they as coatings for medical grafts applied in implantology.

TF-3-Or-6
Reactive Magnetron Sputtering of AgFeO2 Compounds with the Delafossite Structure

T14 Thin Films

#TF-3-Or-6

F. Mao, T. Nyberg, U. Jansson.

Uppsala University - Uppsala (Sweden).

Delafossites AMO_2 (A=Ag, Cu, Pd, Pt; M=Fe, Co, Ni, Cr, Al, Mn, etc) have received considerable attention due to their potential applications as transparent conducting oxides, photocatalysts, batteries and thermoelectric materials [1]. Recently, high temperature superconductivity was also suggested for doped members of this type of oxide compounds [2]. Many of the interesting properties of delafossites are related to the crystal structure where linear O-A-O bonds connect layers of slightly distorted edge-sharing MO_6 octahedra. Consequently, the delafossites can be described as natural nanolaminates of MO_2 layers separated by A atoms.

Delafossite materials, especially copper compounds, have been studied intensely through synthesis of high temperature solid-state reaction, sol-gel methods, hydrothermal synthesis methods, cation exchange reaction methods and in a few cases reactive sputtering [3]. To our knowledge, however, very few studies have previously been published on silver-based delafossite films deposited by sputtering.

In this work we demonstrated the deposition of single-phase delafossite $AgFeO_2$ thin films using pulsed-dc co-sputtering of silver and iron targets in a reactive Ar-O_2 mixture atmosphere. The effect of O_2 flow rate, substrate temperature, deposition pressure, pulse frequency of sputtering power on the formation of delafossite $AgFeO_2$ were investigated. XPS, XRF, XRD and Raman Spectroscopy were employed to determine the chemical composition and phase structure. Film thickness and morphology were studied by SEM. Optical and electrical properties were also investigated.

Our results showed the possibility of depositing single-phase $AgFeO_2$ films without post-annealing, however, the process window is very narrow and strongly dependent on oxygen flow rate, pulse frequencies, pressure and temperature. In general, high

pulse frequencies above 300 kHz, medium oxygen flow rate (around 15 sccm) and a deposition pressure of 10 mTorr were required. The most critical parameter was the temperature with an optimal deposition temperature at 400 ^{o}C. Typically, less well crystalline films were obtained at lower temperatures while a significant precipitation of metallic Ag was observed at higher temperatures (see Fig.1). This decomposition could be attributed to rather weak O-Ag-O bonds in the structure.

[1] W.C. Sheets, E. S. Stampler, M. I. Bertoni, M. Sasaki, T. J. Marks, T. O. Mason, K. R. Poeppelmeier, Inorg. Chem. 2008, 47, 2696-2705.
[2] A. Nakanishi, H. Katayama-Yoshida, Solid State Communications, 2012, 152 (1) 24-27.
[3] A.N. Banerjee, K.K. Chattopadhyay, “Reactive Sputter Deposition”, Eds. S. Mahieu and D. Depla, Springer , NY, USA; Ch. 12, 2008, 413-484.

Fig.1. XRD of delafossite $AgFeO_2$ deposited at different temperature.

TF-9-Or-8
Irradiation of Ti3SiC2 with 700keV Si

T14 Thin Films

#TF-9-Or-8

B. King [1], C. Liu [2], Q. Qi [2], L. Shi [2], J. O'connor [1].

[1]University of Newcastle - Callaghan (Australia), [2]Fudan University - Shanghai (China).

The interaction of 700keV Si ions, incident at 45 degrees onto a Ti_3SiC_2 surface, has been studied as a function of sample temperature, from 300K to 820K. The samples were irradiated to a dose of $10^{16}cm^{-2}$. SRIM shows that the range of the Si is 300nm at this energy with the ions generating substantial energy deposition from the surface to a depth of 400nm. SEM EDAX analysis of unimplanted material shows a small percentage of alumina grains in the surface. Room temperature irradiation produces a few micron large "dark" and "white" zones on the surface with more C and less Ti in the "white" regions. Glancing incidence synchrotron X-ray diffraction was performed for X-ray incidence angles of 0.2, 0.4, 0.6, 0.8 and 1 degree. For these incidence angles, the X-rays dominantly probe the top 100nm of the surface. Peaks corresponding to the (006), (008), (101), (102), (103), (104), (105),(107), (108), (109), (110) reflections from Ti_3SiC_2 were found, as well as very small peaks from Al_2O_3, $TiSi_2$ and Si_5C_3. In general, all Ti_3SiC_2 peaks broaden under implantation. There is also implantation induced splitting of the Ti_3SiC_2 (104) and (105) peaks for all temperatures other than room temperature, most likely evidence of an expanded Ti_3SiC_2 component. . For RT bombardment, the is growth of a TiC phase with bombardment near the surface, but this is less obvious for higher temeparture bombardments. We have found that the crystallinity of the implanted surface is retained better at an intermediate temperature, 573K, during irradiation compared to higher or lower temperatures.

SE/PST/TF/BI-3-Or-1
Novel detector based on a-SiC:H for FRET analysis

T14 Thin Films

#SE/PST/TF/BI-3-Or-1

P. Louro Antunes, V. Silva, M.A. Vieira, M. Vieira.

ISEL-ADEETC - Lisboa (Portugal).

Glucose sensing is an issue with great interest in medical and biological applications. One possible approach to glucose detection takes advantage of measuring changes in fluorescence resonance energy transfer (FRET) between a fluorescent donor and an acceptor within a protein which undergoes glucose-induced changes in conformation. This demands the detection of fluorescent signals in the visible spectrum. In this paper we analyzed the emission spectrum obtained from fluorescent labels attached to a protein which changes its conformation in the presence of glucose using a commercial spectrofluorometer. Different glucose nanosensors were used to measure the output spectra with fluorescent signals located at the cyan and yellow bands of the spectrum. A new device is presented based on multilayered a-SiC:H heterostructures to detect identical transient visible signals. The transducer consists of a p-i'(a-SiC:H)-n/p-i(a-Si:H)-n heterostructure optimized for the detection of the fluorescence resonance energy transfer between fluorophores with excitation in the violet (400 nm) and emissions in the cyan (470 nm) and yellow (588 nm) range of the spectrum. Results show that the device photocurrent signal measured under reverse bias and using appropriate steady state optical bias, allows the separate detection of the cyan and yellow fluorescence signals.

- M. Vieira, P. Louro, M. A. Vieira, J. Costa, M. Fernandes, A. Fantoni, “Wavelength Selective a-SiC:H p-i-n/p-i-n Heterostructure for Fluorescent Proteins Detection”, Sensor Letters, Vol. 8, 413-418 (2010).
- P. Louro, V. Silva, M. AVieira, M. Vieira, “Detection of Change in Fluorescence Between Reactive Cyan and the Yellow Fluorophores Using a-SiC:H Multilayer Transducers“, Plasmonics, DOI 10.1007/s11468-012-9441-6

Fig. 1 - Device configuration

Fig.2 - Spectral response in dark and using front and back optical bias of different wavelengthsDevice configuration

SE/TF-P2-16
Evaluation of selected nanolayered and nanostructured coatings for cutting applications

T14 Thin Films

#SE/TF-P2-16

M. Cekada [1], G. Geiger [2].

[1]Jozef Stefan Institute - Ljubljana (Slovenia), [2]Vienna University of Technology, Institute of Production Engineering - Vienna (Austria).

PVD hard coatings are nowadays commonly used in protection of cutting tools such as milling tools, cutting inserts, etc. In the development of the coatings, most attention is paid to their structural and mechanical properties. When implemented into selected industrial applications, different objectives become relevant, i.e. the ones related to economical issues. These include increase of tool lifetime, enhanced productivity, workpiece quality, etc.

There are several other issues with a significant influence, yet a relatively small emphasis has been given insofar. In this work we concentrated on two such aspects: (i) evaluation of surface quality of the base material before coating deposition, (ii) testing of the cutting performance on a milling system with in-situ diagnostics of the cutting process.

Cemented carbide mills were used for tests having a diameter of either 6 mm or 10 mm. Two coatings were selected for evaluation: the nanolayer TiAlN/TiN coating and the (Ti,Al,Si)N coating, which consists of a TiAlN base layer, a nanocomposite TiSiN middle layer and a nanolayer/nanocomposite TiAlSiN toplayer. A standard TiAlN coating was used for selected reference tests. They were all deposited by magnetron sputtering in a commercial deposition system CemeCon CC800/9 with a thickness of around 3 µm.

The surface quality was systematically evaluated using a confocal optical microscope. Identical motives were taken on bare tool, after coating deposition, and after cutting tests. We analysed, how do individual failures (both on the bare tool

surface and on the coating alone) influence the cutting performance. Special attention was given to the cutting edge rounding/chipping.

The machining tests were performed on an OPS600 3-axis milling machine equipped with a high-speed spindle. To describe the shifting of the tool behavior during the lifetime several parameters have been measured during every cut of the tests such as cutting forces, tool temperature and tool wear. Afterwards surface quality, chip formation and tool wear analysis have been done. The two coatings have been tested by cutting three different materials: C45E (1.1191), X40CrMoV5-1 (1.2344) and X153CrMoV12 (1.2379) running dry and with minimal quantity lubrication. The tests show that the TiAlN/TiN coating performs best related to the tool wear independent of test material and cooling using the same cutting parameters.

TF-7-Or-8
Optoelectronic Properties of Zinc(II)-Phthalocyanine

T14 Thin Films

#TF-7-Or-8

M. Kozlik, S. Paulke, M. Gruenewald, R. Forker, T. Fritz.

Friedrich Schiller University of Jena - Jena (Germany).

New optoelectronic devices use more frequently organic materials nowadays, e.g. in OLEDs and organic solar cells (OSCs). Zinc(II)-phthalocyanine (ZnPc) is a widely used organic molecule, and the bulk material crystallizes mainly one of the following polymorphs: the metastable α-ZnPc (high conductivity) and the stable β-ZnPc (low conductivity) [1]. In our contribution we will discuss the optical and morphological differences between both phases as well as the critical transformation temperature. Description and simulation of the performance of organic devices require the knowledge of material parameters. We will present the determination of the optical constants (complex index of refraction) and the exciton diffusion length by means of UV-Vis spectroscopy and external quantum efficiency measurements. Based on transmittance and reflactance spectra we extract the real and imaginary part of the refractive index [2]. In combination with the parameters derived we will show the performance of a simplified photovoltaic cell and identify the region of exciton dissociation and the exciton diffusion length.

[1] K. Wihksne et al., J. Chem. Phys. 34 (1961) 2184.
[2] M. Kozlik et al., Org. Electron. 13 (2012) 3291.

Spectra of refractive index n and extinction coffcient k of α- and β-ZnPc.

PST/SE/TF-P1-09
PLASMA POLYMERIZED CITRIC ACID ETHYLENE GLYCOL THIN NANOFILM

T14 Thin Films

#PST/SE/TF-P1-09

R. Mota [1], E. Cavalini [1], E. Campos [1], F. Carvalho [1], J. Bortoleto [2].

[1]UNESP - FEG - Guaratinguetá (Brazil), [2]UNESP - Sorocaba (Brazil).

Thin nanofilms obtained by citric acid ethylene glycol mixture were deposited by 13,56 MHz radio-frequency plasma from 5 to 50W power supply and 10Pa pressure. The results showed that the functional groups of the nanofilms molecular structures were preserved. However, it was observed films modifications by X-ray photoelectron spectroscopy that showed compositional modifications in the samples. It was observed an increasing oxygen-carbon and oxygen-hydrogen bond while carbon-hydrogen decreases as the deposition power increases from 5 to 50W.The films deposition rate increased from 2 to 6nm:min while the power supply increased from 5 to 30W and decreased after this value. This result showed good agreement with the activated growth mechanism that presents competition among polymerization and ablation (1-2). The samples wettability was investigated using goniometric technique and for all depositions conditions the nanofilms presented hydrophilic character. Atomic force microscopy showed that films surface profiles and the glass substrate were similar when the films presented low thickness. The samples refractive index was investigated by UV-Visible spectroscopy presenting values from 1,47 to 1,53.

1- d'Agostino R., Favia.P., Fracassi F.(1997) Plasma Processing of Polymers, NATO ASI SERIES.Dordrecht:Academic Press Publ.
2- Max J.J,Chapados C.(2004) Infrared spectroscopy of aqueous carboxylic acids: comparison between different acids and their salts. Journal Phys.Chem.A,v.108,p.3824

TF-P3-15
Characterization of ZnS thin films grown by SILAR (successive ionic layer adsorption and reaction) Technique

T14 Thin Films

#TF-P3-15

A. Djelloul [1], M. Adnane [2], S. Hamzaoui [2], D. Chaumont [3].

[1]1. Laboratory of Electron Microscopy and Materials Science Department of Physics, Faculty of Science University of Science and Technology of Oran (MB). - Mascara (Algeria), [2]1. Laboratory of Electron Microscopy and Materials Science Department of Physics, Faculty of Science University of Science and Technology of Oran (MB). - Oran (Algeria), [3]2. Department of Computer Science,Bourgogne Dijon France University Laboratory of Electron Microscopy and Materials Science Department of Physics, Faculty of Science University of Science and Technology of Oran (MB). - Bourgogne (France).

Zinc sulfide belongs to group II-VI compound semiconductor materials. ZnS is a very important semiconductor material with a large optical gap (> 3.5 eV), a large utility in thin-filmdevices, such as photoluminescent devices and LEDs. In addition, the ZnS is an important material in solar cells based on thin layers in heterojunctionas buffer layer. In this work, we became interested in the development of thin layers of a semiconductor type II-VI: Zinc sulfide(ZnS), and the study of optical, electrical, structural andmorphological were prepared by the technique SILAR (Successive Ionic layer adsorption and Reaction). Our goal is to provide acomprehensive study on the effect of cycle number on the physical properties of thin films of ZnS. In the first part of this work we havedeveloped deposition techniques, the second part relates to the development of a series of films with different deposition conditionsto optimize the process in order obtain films with good optoelectronic properties for application in photovoltaic eventually. Keywords: ZnS buffer layer, SILAR.

TF-7-Or-4
Application of transition metal nitride thin films as supercapacitors

T14 Thin Films

#TF-7-Or-4

J.F. Pierson [1], S. Bouhtiyya [1], R. Lucio Porto [2], P. Boulet [1], F. Capon [1], T. Brousse [2].

[1]IJL - Nancy (France), [2]IMN - Nantes (France).

During the past decade transition metal oxides were extensively studied as electrode materials for electrochemical capacitors. The semiconductors MnO_2, V_2O_5, Fe_3O_4, among others, were studied due to their several oxidation states of the metal atoms, accessible within a potential window of 1V allowing the surface redox reactions in aqueous electrolytes to take place. Recently, nitrides such as VN, TiN and MoN have been studied, and impressive specific capacitance values up to 1340 F g^{-1} at 2 mV s^{-1} were reported for VN [1]. According to Choi et al., the high specific capacitance of VN results from its high electronic conductivity and from a combination of electrical double layer formation and redox reactions at the surface of the electrode. This presentation aims to compare the properties of various transition metal nitride (TMN) films for application as electrodes in supercapacitors.

TMN films were deposited on glass by reactive sputtering of TM targets. The following TM have been studied: Sc, Ti, V, Cr, Mn, Fe, Co, Ni, Cu and Ru. The deposition conditions were adjusted as a function of the reactivity of transition metal with nitrogen atoms. Whatever TM, the morphology of the films is columnar. Only Cu- and Ni-based films crystallized in a TM_3N-like structure while most of the deposited films exhibit a metal to nitrogen atomic ratio of 1 and. Although the structure of ScN, TiN, VN, CrN and γ'''-FeN is widely described, few information about the structure of MnN and RuN are available in the literature. The synthesis of ruthenium nitride (RuN) was reported for the first time in 2007 [2].The authors suggest that this compound crystallises in a NaCl-like structure. However, ab initio calculations show that this structure is not the most stable [3]. Relative to manganese nitride (MnN), Suzuki and al. have sputter-deposited MnN films that crystallise in a NaCl-type distorted tetragonal structure (fct) [4]. Nevertheless, Miao and al. suggest that the most stable structure is ZnS [5]. Both MnN and RuN films exhibit a strong preferred orientation in the [111] direction and a grain size in the 10 – 25 nm range. X-ray diffraction

analyses and the Rietveld's method evidence that both RuN and MnN thin films crystallize in a ZnS-like structure with lattice constant of 0.451 and 0.428 nm, respectively.

The electrochemical properties of the deposited films were determined by cyclic voltammetry in KOH electrolyte. ScN, Ni_3N, FeN, CrN have shown a poor capacitance suggesting that only double layer is involved in the charge storage mechanism. The large capacitance of MnN, RuN and VN and the waves in the voltammograms suggest a pseudofaradaic process. These nitrides have shown a capacitive behavior at high scan rates due to their high electronic conductivity and fast reversible redox process. The cyclic voltammograms of VN films in KOH 1M at different scan rates evidence a potential window of 1.2 V (from -1.2 to 0 V vs. Hg/HgO). On the other hand, the potential window of RuN thin films is about 0.9 V (from -0.5 to 0.4 V vs. Hg/HgO).

[1] Choi et al., Adv. Mater. 18 (2006) 1178
[2] Moreno-Armenta et al., J. Phys. Chem. Solids 68 (2007) 1989
[3] Bannikov et al., Solid State Comm. 150 (2010) 953
[4] Suzuki et al., J. Alloys Comp. 360 (2003) 34
[5] Miao et al., Phys. Rev. B 71 (2005) 214405

TF-2-Or-5
Synthesis of conductive semi-transparent silver films deposited by a Pneumatically Assisted Ultrasonic Spray Pyrolysis Technique

T14 Thin Films

#TF-2-Or-5

C. Falcony, E. Zaleta-Alejandre, R. Balderas-Xicoténcatl, M.L. Pérez Arrieta, Z. Rivera-Álvarez, A.N. Meza-Rocha.

CINVESTAV-IPN - Mexico Df (Mexico).

The synthesis and characterization of nanostructured silver films deposited on corning glass by a deposition technique called Pneumatically-Assisted Ultrasonic Spray Pyrolysis are reported. Silver nitrate and triethanolamine were used as silver precursor and reducer agent respectively. The substrate temperatures during deposition were in the range of 300 to 450 °C and the deposition times from 30 to 240 sec. The deposited films are polycrystalline with cubic face-centered structure, and crystalline grain size less than 30 nm. Deposition rates up to 600 Å•min-1 were obtained at substrate temperature as low as 300 °C. The electrical, optical, and morphological properties of these films are also reported. Semitransparent conductive silver films were obtained at 350 °C with a deposition time of 45 sec. The preparation and study of metallic silver films have been of interest due to their better electrical and optical performance with respect to other metallic films and to the wide variety of technological applications such as electrical interconnections in microelectronic circuitry, gas sensors, bactericidal coatings, low-emissivity coatings on tempered glass and on bent glass panes for vehicles and recently for electrical contacts in photovoltaic devices on flexible substrates [1]. In this work, the synthesis of conductive silver thin films on corning glass by a pneumatically-assisted ultrasonic spray pyrolysis (PAUSP) technique are reported. This deposition scheme uses a gas jet to assist the ultrasonic spray pyrolysis deposition process of a film by given an additional impulse to the precursors in aerosol drops towards a hot substrate. The structural, electrical and optical properties as a function of the deposition parameters are reported as well. The SEM micrographs for films deposited at 350 °C for two deposition times, 30 and 120 s are shown in fig.1. The micrograph for the film

deposited in 30 sec. (fig. 1a) shows an initial formation of clusters of silver of random sizes with no interconnection, while the film deposited for 240 sec (fig. 1b), shows a totally covered surface by a superposition of small silver grains. This behavior of silver islands formation and later transition to a continuous film has been observed and reported for other deposition techniques.

[1] A. Serra, M. Re, M. Palmisano, M. Vittori Antisari, E. Filippo, A. Buccolieri and D. Manno, Sensors and Actuators B, 145 (2010) 794-799.

Fig. 1. SEM micrographs of surface morphology with deposition time of a) 30 sec and b) 240 sec and substrate temperature of 350 °C.

PST/SE/TF-3-Or-9
IN-SITU OBSERVATION OF MICROCRYSTALLINE SILICON THIN FILM GROWTH USING TAILORED VOLTAGE WAVEFORMS

T14 Thin Films

#PST/SE/TF-3-Or-9

E. Johnson [1], B. Bruneau [1], J.C. Dornstetter [2], J.P. Booth [3].

[1]LPICM-CNRS - Palaiseau (France), [2]Total Energies Nouvelles/LPICM-CNRS - Palaiseau (France), [3]LPP-CNRS - Palaiseau (France).

The industrial use of hydrogenated microcrystalline silicon (µc-Si:H) for photovoltaics requires high-quality thin films deposited at high rates. For radio-frequency plasma enhanced chemical vapour deposition (RF-PECVD) techniques, this implies achieving a high plasma density (and feedgas dissociation) while maintaining a low mean ion-bombardment energy (IBE). The use of Tailored Voltage Waveforms (TVW's) allow one to unequally divide the plasma sheath voltage between the powered and grounded electrode, and thus reduce the mean IBE on the substrate [1], a technique also known as the Electrical Asymmetry Effect [2]. The use of such a TVW to excite a plasma for PECVD has been recently used to deposit the intrinsic microcrystalline layer of µc-Si:H cells using SiH4 diluted in H2 [3].

In addition to being of interest for industrial applications, the ability to decouple plasma density from IBE allows one to perform deeper, direct examination of the importance of IBE for the growth of µc-Si:H, and we do so in this work. This is achieved through the use of both in-situ (spectroscopic ellipsometry, (SE)) and ex-situ (AFM and Raman scattering) techniques. For this study, intrinsic µc-Si:H layers were deposited by PECVD excited with TVWs using both the “Peaks” and the “Valleys” waveforms. In-situ SE was performed during the deposition, and an example of the curves obtained for a high IBE condition is seen in Fig. 2. One can see that such curves result in a constantly changing surface, and given the very low value of the imaginary part of the dielectric function, one that is very rough or porous. To get a complete picture of the process, similar curves were acquired for a variety of process gas mixtures, include the classic SiH4/H2 mixture, but also more exotic SiH4/SiF4/H2 and SiF4/H2/Ar mixtures. This last mixture is of particular interest as

the devices generated from this mixture are of particularly high quality [4]. These in-situ results can be combined with Raman scattering and AFM images to get a coherent picture of the specific role of elevated IBE during µc material growth.

[1] T. Lafleur, J.P. Booth, J. Phys. D : Applied Physics 45 (2012) 395203.
[2] J. Schulze, E. Schüngel, U. Czarnetzki, and Z. Donkó: J. Appl. Phys. 106 (2009) 063307.
[3] E.V. Johnson, P.A. Delattre, J.P. Booth, , Appl. Phys. Lett. 100 (2012) 133504.
[4] J. C. Dornstetter, S. Kasouit, P. Roca i Cabarrocas, , Photovoltaics, IEEE Journal of , 3 (2013) 581.

Figure 1: SE data acquired during growth of µc-Si:H under high IBE conditions.

TF-P3-16
Photoluminescence and infrared of thin films of GaAs and AlGaAs grown by solid-arsenic-based MOCVD

T14 Thin Films

#TF-P3-16

J. Flores-Mena [1], R. Castillo-Ojeda [2], J. Díaz-Reyes [3], M. Galvan-Arellano [4].

[1]BUAP - Puebla (Mexico), [2]UPP - Pachuca (Mexico), [3]CIBA-IPN - Tlaxcala (Mexico), [4]CINVESTAV-IPN - Df (Mexico).

We have studied the optical properties of GaAs and AlGaAs thin films using low-temperature photoluminescence and infrared spectroscopy. The GaAs and its alloys were grown by MOCVD using solid arsenic instead of arsine as the arsenic precursor. The precursors of gallium and aluminum are organometallic compounds, trimethygallium and trimethyaluminum. Some difficulties in the AlGaAs growth by solid-arsenic-based MOCVD are the composition homogeneity of the layers and the oxygen and carbon incorporation during the growth process. The composition homogeneity of the films was demonstrated by low-temperature photoluminescence and Raman espectrocopy. Infrared measurements on the samples allowed to identify the responsible residual impurities, which are carbon-substitutional, Ga_2O_3, molecular oxygen, humidity and, two unidentified impurities. Samples grown at temperatures lower than 750°C were highly resistive, independently of the III/V ratio; the samples grown at higher temperatures were n-type, how it was proved by Hall effect measurements.

SE-1-Or-6a
Plasma potential control for film structure modification in high power pulsed magnetron sputtering

T14 Thin Films

#SE-1-Or-6a

T. Nakano, T. Umahashi, S. Baba.

Seikei Univ. - Tokyo (Japan).

In plasma processes, thin film structure is strongly affected by the substrate temperature (T_s) and energetic particle bombardment onto the growing film surface [1]. With the aid of the latter, fibrous structure with smooth surface can be obtained even at low T_s. To achieve this, it is advantageous to use the ionized physical vapor deposition (IPVD) which is characterized by the high degree of ionization of sputtered atoms. By applying negative substrate bias and attracting the positive ions, the energy flux onto the film surface can be controlled.
High power pulsed magnetron sputtering (HPPMS) is one of the IPVD variant. It applies target power in short pulses with low repetition frequency and very small duty ratio. It can generate high density plasma required for IPVD, while avoiding heavy thermal load to the target. In a previous study [2], we have raised the target voltage during the power-off period of HPPMS and found that the plasma potential V_p of the after-glow plasma was raised. The structure of deposited film was substantially flattened even on the water-cooled and electrically grounded substrate. It was understood that positive ions in the high V_p plasma could bombard the growing film surface.

In this study, we have introduced another electrode to apply positive bias and tried to control V_p for both on and off periods of HPPMS. Figure 1 shows the schematic of this chimney-like electrode above the sputter gun of 2 inch diameter. By applying different electrode potential V_c, Cu films were prepared by HPPMS with 5% of duty ratio and 100 W of average power, in 5 Pa of Ar gas. As shown in Fig. 2, the film surface was greatly flattened at 40 V of V_c. It was also confirmed by the probe measurement that V_p was raised with an increase in V_c. The raise in V_p will be discussed in view of the diode like behavior of the plasma sheath and the current conservation between 3 electrodes.

[1] Anders, Thin Solid Films **518** (2010) 4087.

[2] Nakano, Hirukawa, Sekiya, Baba, Vacuum **87** (2013) 109.

Fig. 1 Magnetron sputter gun and the chimney electrode

Fig. 2 Plan view SEM images of Cu films deposited with different V_c

TF-P2-29
Impedance Measurements in Delta Bismuth Oxide Thin Films

T14 Thin Films

#TF-P2-29

C. Gomez [1], P. Silva-Bermudez [1], S.E. Rodil [1], H. Estrada [2].

[1]Instituto de Investigaciones en Materiales, Universidad Nacional Autonoma de Mexico - Mexico D. F. (Mexico), [2]Centro Nacional de Metrologia - Queretaro (Mexico).

Bismuth oxide Bi_2O_3 has interesting technological applications, which have not been largely used due to the particular polymorphism of the material. Among the interesting properties, it is worth mentioning a large energy gap (from 2 to 3.96 eV depending on the phase) [1], high refractive index, dielectric permittivity, noticeable photoconductivity and photoluminescence. Bismuth Oxide has five polymorphic forms: α, β, γ, δ and ω-Bi_2O_3. Among them, the low-temperature α and the high-temperature δ phases are stable and the others are high temperature metastable [2]. The face-centered cubic δ-Bi_2O_3 is stable over a narrow range 729 - 825 ^oC (melting point) and it is the material that shows one of the highest ionic conductivity. Decreasing the temperature leads to the formation of intermediate metastable phases such as tetragonal β-Bi_2O_3 and/or body-centered cubic γ-Bi_2O_3 before transforming into stable monoclinic α-Bi_2O_3 at room temperature (RT). Remarkably, it has been proved [3-4] that the deposition of nanocrystalline thin films allows the stabilization of the high temperature phase at room temperature. Nevertheless, very few works have tried to measure the ionic conductivity of such thin films. In this work, after studying different deposition conditions: deposition power and substrate temperature, 180 - 430 nm thin films presenting the δ-Bi_2O_3 were consistently obtained. The films were deposited on glass by reactive magnetron sputtering starting from an α-Bi_2O_3 target and using an Ar/O_2 (80:20) atmosphere. The films were characterized by X-ray diffraction, Raman spectroscopy, X-ray photoelectron spectroscopy, as well dc-electrical and optical characterization to ensure the formation of the delta-phase. Finally, ac impedance measurements were done to study the ac conductivity as a function of the temperature. For this, rectangular Pt electrodes were deposited on the surface of the films 0.8 mm apart. The ac impedance was obtained from 0.01 Hz to 100 kHz and the temperature was increased up to 200^oC. The results of the ac conductivity were compared to the dc conductivity.

Acknowledgement: The research leading to these results has received funding from the European Community Seven Framework Programme (FP7-NMP-2010-EU-MEXICO) and CONACYT under grant agreements nº 263878 and 125141, respectively.

[1] L. Leontie et al. Thin Solid Films 473 (2005) 230
[2] C. E. Mohn et al. Physical Review B 80 (2009) 024205

[3] HT Fan et al. Thin Solid Films 513 (2006) 142

[4] Eric W. Bohannan et al. Solid State Ionics 78 (2008) 1735

Fig. 1. XRD patterns of δ-Bi_2O_3 thin films deposited on glass substrates.

SE/PST/TF/BI-3-Or-2
RF-magnetron sputter deposited nanostructured calcium phosphate-based coating containing either silicate or silver ions for implants

T14 Thin Films

#SE/PST/TF/BI-3-Or-2

R. Surmenev [1], M. Surmeneva [1], A. Ivanova [1], V. Pichugin [1], A. Sharonova [1], I. Grubova [1], M. Chaikina [2], A. Kovtun [3], A. Peetsch [3], O. Prymak [3], M. Epple [3].

[1]National Research Tomsk Polytechnic University - Tomsk (Russian federation), [2]Institute of Solid State Chemistry and Mechanochemistry Siberian Branch of the Russian Academy of Sciences - Novosibirsk (Russian federation), [3]University of Duisburg-Essen - Essen (Germany).

INTRODUCTION

This study reports on hydroxyapatite (HA) coatings and HA-based coatings doped with silicate or silver ions. The targets consisted of powders of Si-containing HA (Si-HA) $Ca_{10}(PO_4)_{6-x}(SiO_4)_x(OH)_{2-x}$ (x=0.5 and 1.72) and Ag-containing HA (Ag-HA) $Ca_{10-x}Ag_x(PO_4)_6(OH)_{2-x}$ (x=0.3). Thin nanostructured calcium phosphate-based coatings were deposited by RF-magnetron sputtering (RFMS) at a power level 30-290 W, a negative substrate bias up to 100 V, and a pressure of 0.1 Pa. As-deposited (up to 1 mkm thick) coatings were characterized by EDX, ESEM, XRD, IR spectroscopy, and a pull off test. The cell viability was assessed by the MTT assay with MG-63 osetoblast-like sarcoma cells. In case of Ag-HA coatings, antibacterial tests in vitro using *E. coli* bacteria were performed.

RESULTS AND DISCUSSION

As-deposited calcium phosphate-based coatings are dense, pore-free and their composition resembled that of the precursor target. The chemical, and phase composition as well as thickness and structure can be varied by a particular set of deposition control parameters. A low rf-power density (0.1-0.5 $W \times cm^{-2}$) resulted in amorphous or low crystalline calcium phosphate-coating structure, an increase in rf-power level (>0.5 $W \times cm^{-2}$) induced the coating crystallization. The coatings consisted

of hydroxyapatite as all of the observed X-ray diffraction peaks matched the ICCD 9-432 card. The four strongest peaks were observed at 25.8° (002), 31.7° (211), 32.2° (112), and 32.9° (300). The XRD pattern of the coating at different negative bias showed a halo located at 32° typical for a nanostructured state. A negative substrate bias allowed us to vary the Ca/P ratio between 1.53 and 4 [1]. The adhesion strength of the coatings was higher than 40 MPa. The MTT test showed that the cell viability for the coatings with the different Ca/P ratio was up to 70 percent higher than that in case of the control substrates. Osteoblast-like cells attached and grew well on the surface of the coatings. The experiments with *E. coli* showed that there is no significant influence of the given Ag-content in the Ag-HA films on the vitality of bacteria. No significant antibacterial effect was found in the case of Ti plates with or without Ag-HA coatings. The concentration of Ag was below 0.1 μg L^{-1} after dissolution of the coating by HNO_3 and subsequent Ag determination by atomic absorption spectroscopy, when a coating thickness did not exceed 500 nm. The presence of Ag in HA coating was estimated by EDX to ~1-3 at%. In the case of the Ag-HA target, a clear antibacterial effect was observed. We assume that a higher concentration of Ag in the target or increase in the coating thickness will allow us to prepare a RFMS Ag-containing calcium phosphate coating with antibacterial effect.

CONCLUSIONS

RFMS is well suited to prepare HA-based coatings with different structure and stoichiometry. Based on the obtained results, we suggest that RFMS-deposited coatings are prospective to be used in clinical practice, i.e. in stomatology or craniofacial medicine, where the initial material surface porosity for a further bone in growth should be preserved.

REFERENCES

1. R. Surmenev, Surf. Coat. Technol., 206 (2012) 2035-2056.

TF-P2-44
Growth behavior of cyclic chemical vapor deposited Al2O3 layer for passivation of OLEDs lighting devices

T14 Thin Films

#TF-P2-44

H. Jang, B.H. Choi, J.H. Lee.

Korea Institute of Industrial Technology - Kwangju-Si (Korea, republic of).

One of challenging issue in OLEDs is to prepare high quality passivation layer with high water vapor transmission rate and density. Up to now, alternating structure of sputtered Al2O3 and organic material was used as passivation layer. However, there is an ever increasing interest to form thin film passivation layer with comparable characteristics and thinner thickness. In this study, we have proposed and developed modified deposition technology of Al2O3 layer for the application to passivation layer of OLEDs devices. By modifying ALD into cyclic CVD, very uniform Al2O3 layer was prepared with high density with high deposition rate. TMA and oxygen plasma were used as precursor and reactant, respectively. The precursor injection time and oxygen plasma treatment time was optimized to obtain uniform Al2O3 film with high density. One cycle consist of precursor feeding, reactant feeding followed by plasma treatment and purge. Instead of injecting the precursor and reactant separate cycle, TMA and oxygen was co-fed into the process chamber, followed by plasma treatment like CVD process. Fig.1 shows thickness of Al2O3 as a function of deposition cycles. As deposition cycle increased, the total thickness was increased linearly, which shows typical characteristics of ALD. At low deposition cycles under 50, only Al2O3 islands were observed, which means incubation time is needed. The measured deposition rate was 0.4nm/cycle, which is 3 times higher than normal ALD. The measured density was 3.2 g/cm3, which is a comparable value obtained from bulk Al2O3, and stoichiometry was well matched. Fig.2 shows FE-SEM images of surface and cross-sectional view of prepared Al2O3 layer by cyclic CVD. As shown in Fig. 2, very uniform Al2O3 layer was formed by cyclic CVD technology with high deposition rate and density. Our study shows cyclic CVD grown Al2O3 layer can be used as a passivation layer of OLEDs devices.

Figure 1. Thickness of cyclic CVD grown Al2O3 layer as a function of deposition cycles.

Figure 2. FE-SEM images of (a) surface and (b) cross-sectional view of cyclic CVD grown Al2O3 layer.

TF-P2-30
Optical and structural properties of ITO and ITON thin films

T14 Thin Films

#TF-P2-30

M. Sparvoli, R. Onmori.

Universidade de São Paulo - São Paulo (Brazil).

The oxynitrides of many metals have been investigated during the last decade [1]. Indium tin oxide (ITO) is a n-type degenerate semiconductor with a band gap that varies between 3.2 and 4.0 eV. Recently it was obtained a new oxide type that combines ITO and nitrogen: the indium-tin-oxynitride (ITON). The incorporation of nitrogen into the film could improve further the optical and structural properties of the ITON films and thus making ITON film an ideal transparent and conducting material for opto-electronic applications. The deposition of the oxynitride thin films is generally performed in plasma-containing systems like sputtering and pulsed-laser deposition systems. In this work, ITO and ITON films were fabricated by evaporation and annealing techniques. The substrate was silicon (75 mm, p type, 1-10 W.cm) and optical three-inch glass wafers with 0.5 mm thickness. The thin films were analyzed with UV-Vis-Nir spectra transmittance and absorbance, SEM (Scanning Electron Microscopy) and RBS (Rutherford Back Scattering). The optical band gap was estimated for samples annealed with oxygen and nitrogen; the band gap values obtained were 3.23 eV and 3.05 eV, respectively. RBS spectra showed the presence of nitrogen. These materials are naturally nanostructured (Figure 1) and show amount of optical properties as transparence in visible region.

[1] M. Koufak, M. Sifakis, E. Iliopoulos, N. Pelekanos, M. Modreanu, V. Cimalla, G. Ecke, E. Aperathitis. “Optical emission spectroscopy during fabrication of indium-tin-oxynitride films by RF-sputtering”. Applied Surface Science, p. 405–408, 2006.

Figure 1. ITON thin film Scanning Electron Microscopy

TF-P2-14
A Study on Poly(3,4-ethylenedioxythiophene) Thin Film Vapour Phase-Polymerized with Iron(III) Oxidants on 3-Aminopropyltriethoxysilane Self-Assembled Monolayer

T14 Thin Films

#TF-P2-14

S. Kim, S. Choi, F. Ma, J.W. Lee, B.B. Choi.

Pai Chai University - Daejeon (Korea, republic of).

In this study, Poly(3,4-ethylenedioxythiophene) (PEDOT) thin films polymerized with Iron(III) chloride ($FeCl_3$) and grown on atomically smooth and highly dense 3-aminopropyltriethoxysilane self-assembled monolayer (APS-SAM) surfaces by vapour phase polymerization (VPP) method have been investigated. PEDOT thin films were synthesized on various substrates, i.e., APS self-assembled SiO_2 wafer, glass, and quartz surfaces. Our recent study discovered that electrical conductivity of PEDOT thin film (~100 nm thick) vapour phase-polymerized on SiO_2 surface reaches up to nearly 4,000 S/cm.[1] Such highly conductive polymer film was accomplished via a new combination of a base inhibitor and tri-block copolymer during VPP. In order to explain unusually high conductivity, the films were closely examined by using various analyzing tools such as field emission-scanning electron microscope, atomic force microscope, x-ray reflectivity, grazing angle incidence x-ray diffraction. The close examination is still underway. After careful analyses, it is highly anticipated that how the film conductivity is affected by the additives (base inhibitors and polymers) can be at least in part explained.

1. S. Choi, W. Kim and S. Kim, "Development of highly conductive poly(3,4-ethylenedioxythiophene) thin film using high quality 3-aminopropyltriethoxysilane self-assembled monolayer" J. Chosun Nat. Sci., Vol. 4, page 294-297 (2011).

Fig. 1. FE-SEM image of a 110 nm thick PEDOT nanofilm grown on an oxidant mixture-coated SiO2 surface

Fig. 2. Time dependence of conductivity of PEDOT nanofilm (~100 nm) Conductivity reaches up to nearly 3,700 S/cm

TF/SE-1-Or-10
Advances in Process Technology and Deposition Equipment for HiPIMS Coatings for Cutting Tools

T14 Thin Films

#TF/SE-1-Or-10

C. Schiffers, T. Leyendecker, O. Lemmer, W. Kölker.

CemeCon AG - Würselen (Germany).

Abstract for RSD2013

HiPIMS is characterised by short power pulses with an extremely short signal rise time. The design of the coating equipment need to take this characteristic into account with regard to feeding the electrical energy into the sputtering cathodes and finally into the plasma. This paper will present recent results on the correlation of the hardware design of the machine and the coating process. Fundamental research about the efficiency of the pulse transfer and about methods to transmit an undistorted pulse shape and wave form into the process was done.

The end user of a cutting tool sets its focus to the properties of the coating and, most important, to the machining characteristics of the film. Examples and field data will show how the most up-to-date HiPIMS coatings boost both productivity and quality.

SEM images reveal a dense morphology of HiPIMS coatings. To this feature can be attributed that HiPIMS films combine high hardness and a relatively low Young's modulus indicating a high coating toughness in a way most favourable for metal cutting.
Super smooth coatings, free from any droplets, and low compressive stress are the most beneficial characteristics of sputter coatings for cutting tools. The effective bombardment of the growing film with highly ionized species further improves the surface of HiPIMS coatings.

TF-P3-12
Transparent and conductive amorphous stannic oxide thin films deposited by plasma-enhanced pulsed laser deposition

T14 Thin Films

#TF-P3-12

N. Oda, K. Nose, M. Kamiko, Y. Mitsuda.

Institute of Industrial Science, The Univ. Tokyo - Tokyo (Japan).

Transparent conductive thin films (TCF) have been widely used in optoelectronic devices such as flat panel displays and solar cells. TCF based on SnO_2 are studied extensively because of their high chemical and thermal stability, resource sustainability, and relatively low cost. Fabricating SnO_2 films with high crystallinity is an active area of this material research, since high electron mobility can be obtained in large grains[1]. On the other hand, amorphous SnO_2 films have potential to show high electron mobility due to less scattering at grain boundaries. In this study, we fabricated transparent and conductive amorphous SnO_2 thin films through plasma-enhanced pulsed laser deposition (PE-PLD).

PE-PLD was performed in N_2O gas atmosphere of 5.0×10^{-2} Pa, using pure SnO_2 sintered pellet as targets. Glass substrate was placed at 47 mm distance from the target and set to be 570 K. The energy, wavelength, and repetition frequency of the Q-switched Nd:YAG laser were 30 mJ/pulse, 266 nm, and 10 Hz. Continuous rf power (13.56 MHz) was capacitively supplied during deposition. Deposition rate and time were controlled so that the film thicknesses were constant (around 100 nm). The films were analyzed by XRD, XPS, Hall-effect measurement system, and UV-vis transparent spectrometer.

Figure 1 shows the XRD patterns of the films deposited in pure N_2O atmosphere. Input rf power was (A) 40 W, or (B) 0 W. The film (A) exhibited amorphous structure, while the film (B) was (001)-oriented crystalline SnO. Sn in the film (A) was found to be tetravalent by XPS spectra (not shown). These results indicate that amorphous SnO_2 film on glass substrate was obtained by PE-PLD. The film (A) was highly transparent in visible light (Fig. 2). Resistivity, mobility, and carrier density of the film (A) were 9.6×10^{-3} Ωcm, 13.2 cm, and 4.9×10^{19} /cm3, respectively.

[1] S. Nakao *et al*., Appl. Phys. Express **5**, 061201 (2012).

Figure 1. XRD patterns of the films deposited by (A) PE-PLD and by (B) normal PLD in pure N_2O atmosphere.

Figure 2. Photo images of the films deposited by (A) PE-PLD and by (B) normal PLD in pure N_2O atmosphere.

TF-6-Or-3
Direct evidence of hole states in conducting NiO films observed by X-ray absorption spectroscopy

T14 Thin Films

#TF-6-Or-3

A. Gutiérrez, G. Domínguez-Cañizares, D. Díaz-Fernández, L. Soriano.

Universidad Autonoma de Madrid - Madrid (Spain).

Nickel oxide is an interesting material both from the fundamental and technological point of view [1-3]. Although stoichiometric NiO is a strong insulator, with resistivity values of order of 10^{13} Ω cm, structural disorder and lack of stoichiometry considerably lower these values [4]. Indeed, NiO thin films have been proposed as a p-type semiconducting transparent material [5]. We have grown NiO thin films by RF magnetron sputtering with a mixed O_2-Ar plasma. The oxygen content of the plasma was varied between 0% and 100%, in order to change the structure and stoichiometry of the resulting NiO films. The films were characterized by X-ray diffraction (XRD), and X-ray absorption spectroscopy (XAS), both in XANES and EXAFS mode. The oxygen content of the plasma modifies the structure and properties of the coatings. XRD results reveal a grain refinement and an increased disorder of the lattice when the oxygen content of the plasma is increased. These microstructural effects are confirmed by EXAFS, measured at the Ni-K edge, where an increase of the Debye-Waller factor for higher O_2 content is clearly observed.

The electrical resistivity of the NiO films has been determined by the Van der Pauw method. The resistivity of the samples grown with oxygen in the plasma is lower than that of the sample grown with pure Ar, and decreases as the oxygen content of the plasma increases. Figure 1 shows XANES spectra at the O-K edge of samples grown with different oxygen content in the plasma. The observed peaks are related to empty Ni-3d states hybridized with O-2p states above the Fermi level. The spectrum of the sample with 0% oxygen shows the typical features of standard NiO. For the samples grown with oxygen in the plasma, a peak appears 3 eV below the absorption edge. This peak can be assigned to empty states below the Fermi energy, i.e., to hole states. The intensity of this peak increases with the oxygen content of the plasma, as does the conductivity of the films. Consequently, there is a direct

correlation between the intensity of this peak, associated to hole states, and the conductivity of the NiO films.

[1] J.M. Caruge, J.E. Halpert, V. Bulovic and M.G. Bawendi, Nano Lett. 6, 2991 (2006)
[2] S. Seo, M. Lee, D. Seo, E. Jeoung, D. Suh, Y. Joung and I. Yoo, Appl. Phys. Lett. 85, 5655 (2004)
[3] L. Soriano, I. Preda, A. Gutiérrez, S. Palacín, M. Abbate and A. Vollmer, Phys Rev B 75, 233417 (2007)
[4] D. Adler, J. Feinleib, Phys Rev B 2, 3112 (1970)
[5] H. Sato, T. Minami, S. Takata, T. Yamada, Thin Solid Films 236, 27 (1993)

X-ray absorption spectra at the oxygen K-edge of NiO films grown by magnetron sputtering with different oxygen content in the plasma.

TF-1-Or-2
Production of SiC hollow cylinders starting from CNTs Pillars

T14 Thin Films

#TF-1-Or-2

M. Giorcelli, M. Pavese, M.I. Shahzad, A. Tagliaferro.

Politecnico di Torino - Torino (Italy).

We fabricated Silicon Carbide (SiC) hollow cylinders by reacting silicon monoxide (SiO) powder with Multiwalled Carbon Nanotubes (MWCNTs) pillars. The result was obtained using a multi-step process:
1) a silicon substrate was patterned in order to define the regions where CNTs will grow. In particular, we delimited circular region where to grow CNTs
2) MWCNTs pillars (Fig.1-1) were grown by Chemical Vapour Deposition (CVD) starting from solid precursors, in particular Camphor and Ferrocene [1].
3) CNT pillars were removed from the substrate
4) CNT pillars were heated at high temperature in inert atmosphere in presence of SiO powder. This led to coat (Fig. 1-2) the CNT pillars with a SiC shell
5) Coated pillars were heated at high temperature in presence of oxygen in order to burn carbon material inside SiC Cylinders. SiC hollow cylinders were produced (Fig.1-3)
The SiC nature of the hollow cylinders shell is confirmed by X-ray diffraction (Fig 2), were the characteristic SiC peaks are evidenced.

[1] S. Musso, S. Porro, M. Giorcelli, A. Chiodoni, C. Ricciardi, A. Tagliaferro "Macroscopic growth of carbon nanotube mats and their mechanical properties", Carbon, vol. 45, (2007), pag.1133-1136

Fig.1: 1) MWCNTs pillars, 2) MWCNTs pillars covered by SiC, 3) SiC hollow cylinder.

Fig. 2: XRD pattern of the SiC hallow cylinder. The cristal phases (111), (200), (220), and (311) of SiC are denoted.

TF-7-Or-2
Coating of granulates and powders by magnetron sputtering

T14 Thin Films

#TF-7-Or-2

G. Schmid, C. Eisenmenger-Sittner.

Vienna University of Technology - Vienna (Austria).

This work presents methods of coating granular or powder particles in general, using magnetron sputtering, and more specifically of coating hollow glass microspheres (diameter 5-70 µm, wall thickness approx. 1 µm). Microspheres of this type may serve as efficient system to store hydrogen at high pressures.
Hydrogen is released from previously-filled hollow glass microspheres when they are heated to a temperature of approximately 120 °C. To reach this temperature is the main challenge of this storage system. It is possible to use an exothermal chemical reaction, in this case a NaBH4-water (Venpure™) reaction, which produces hydrogen as a most welcome by-product. This chemical reaction has to be initialized by a catalyst deposited on the hollow glass microspheres. Therefore, it is necessary that every single sphere is coated with the catalyst, which was done by magnetron sputtering.
To generate uniform coatings on the microspheres, an apparatus was designed with a coating vessel of a special shape rotating beneath the sputtering target. As it is known however, in vacuum the particles tend to adhere to one another and to the surfaces of the containing vessel as coating proceeds, especially when the powder is coated with pure metal. This prohibits most of the particles from being coated since they are not exposed to the sputtering beam. To overcome these problems a new concussion mechanism was developed to break up the particle clusters. This concussion mechanism was found to work much more reliable than the mechanism described in an earlier work of the author [1].
It will be shown that powder substrates of different kinds can be coated successfully. In addition results of the catalytic experiments to generate hydrogen and to increase the reaction temperature will be presented.
This work was supported by the Austrian Science Fund (FWF), project "CatSphere", grant number P-22718.

[1] G. Schmid, C. Eisenmenger-Sittner, J. Hell, M. Horkel, M. Keding, H. Mahr, Optimization of a container design for depositing uniform metal coatings on glass microspheres by magnetron sputtering, Surface & Coatings Technology 205 (2010) 1929–1936

TF-9-Or-5
Film thickness measurement with high spatial resolution on granular materials via optical methods

T14 Thin Films

#TF-9-Or-5

H. Mahr, M.T. Smolle, C. Eisenmenger-Sittner.

Vienna University of Technology - Vienna (Austria).

Coatings on powders or granulates may play an important role regarding surface activation, manipulation of sintering properties or in catalysis. The determination of film thickness and thickness uniformity on granular materials can be a difficult and expensive task using commonly available methods. One possible way is film thickness measurement via visible light transmission spectroscopy, which is a viable method as long as substrate material and coating are transparent. To apply this method to granular materials, a way of spatial resolution has to be implemented to distinguish between measurable objects and artefacts.

This can be achieved by using commercially available transmission light scanners as transmission measurement instruments. Thus providing spatial resolutions up to 157 pixels per mm, i.e. below 10 µm, and three distinct wavelengths in the visible range (red, green, blue, depending on the CCD chip used in the given scanner) for wavelength dependant transmission measurement. The viability of this method is shown by the comparison of measurement results for thin planar metallic coatings via the scanning device and established measurement methods, e.g. profilometry or Scanning Electron Microscopy.

For film thickness measurement on granular materials the spatially resolved transmission data has to be processed via particle detection and calculation algorithms. For this purpose each detected particle must be resolved in a minimum number of pixels (approximately 30), which means that particles with minimal diameters of around 200 µm can be measured with common transmission light scanners. Smaller particles, down to diameters of 10 µm need higher spatial resolutions. To achieve that goal a digital transmission measurement workplace supported by an optical microscope was developed.

Both, common scanning devices and the digital transmission measurement workplace were used for film thickness determination of metallic coatings on granular diamond particles (177 - 400 µm) and hollow micro glass spheres (5 - 70 µm). The measurement algorithms were adapted for each case to consider the different morphologies of diamond particles and glass spheres. These results were compared to thickness values obtained from measurements on FIB cross sections of coated particles by Scanning Electron Microscopy and Transmission Electron Microscopy.

This work was supported by the austrian science found project TRP6-N20.

TF-1-Or-4
High-speed deposition of multilayer nanofilms using soap-film coating

T14 Thin Films

#TF-1-Or-4

R. Zhang, H. Andersson, M. Andersson, B. Andres, P. Edström, S. Edvardsson, S. Forsberg, M. Hummelgård, N. Johansson, K. Karlsson, H.E. Nilsson, M. Olsen, T. Uesaka, T. Öhlund, H. Olin.

Mid Sweden University - Sundsvall (Sweden).

Coating [1] of thin films is of importance for making functionalized surfaces with applications in many fields from electronics to consumer packaging. To decrease the cost, large scale roll-to-roll [2] coating techniques are usually done at high speed, for example, ordinary printing paper is coated at a speed of tens of meters per second by depositing micrometer thick layers of clay. However, nanometer thin films are harder to coat at high speed by wet-chemical methods, requiring special roll-to-roll vacuum techniques [3] with the cost of higher complexity.

Here, we report a simple wet chemical method for high-speed coating of films down to molecular thicknesses, called soap-film coating (SFC) [4]. The technique is based on forcing a substrate through a soap film that contains nanomaterials. In the simplest laboratory version, the films can be deposited by a hand-coating procedure set up in a couple of minutes. The method is quite general molecules or nanomaterials or sub-micrometer materials (Figure 1) with thicknesses ranging from less than a monolayer to several layers at speeds up to meters per second. The applications of soap-film coating is quite wide an we will show solar cells, electrochromic devices, optical nanoparticle crystals, and nano-film devices. We believe that the soap-film coating method is potentially important for industrial-scale nanotechnology.

[1]. Tracton, A. A. Coating Technology Handbook (CRC Press, Boca Raton, 2006).
[2]. Ohring, M. Materials science of thin films. (Academic press., 2001).
[3]. Charles, B. Vacuum deposition onto webs, films and foils. (William Andrew, 2011).
[4]. Zhang, R. Y., Andersson, H. A., Andersson, M., Andres, B., Edström, P., Edvardsson, S., Forsberg, S., Hummelgård, M., Johansson, N., Karlsson, K., Nilsson, H.-E., Olsen, M., Uesaka, T., Öhlund, T., Olin H. Soap film coating: High-speed deposition of multilayer nanofilms. Submitted.

Fig. 1. Soap film coating of nanoparticles, layered materials, nanowires, and molecules. a sub-monolayer 240 nm silica nanoparticle (scale bar 2 µm) b monolayer c double layer. d monolayer gold nanoparticles. e single layer TiO2 nanoparticles. f sub-monolayer polystyrene (scale 2 µm), g monolayer of polystyrene. h triple-layer of polystyrene. i monolayer of Ferritin. j AFM image of <1.5 layer GO film (3 µm x 2 µm). k clay on glass (scale 2 µm). l SFC coated nanocellulose. m Absorbance spectra Rhodamine B on a glass slide. AFM of SDS layers n (2 µm x 1.5 µm) and o (20 µm x 15 µm).

TF-1-Or-3
Nanoporous molybdenum films and their application in catalysis

T14 Thin Films

#TF-1-Or-3

I. Vávra [1], B. Horvath [2], M. Hronec [2], Z. Hajovska [1], J. Derer [1], E. Dobrocka [1].

[1]Institute of Electrical Engineering, SAS - Bratislava (Slovakia), [2]Institute of Organic Chemistry, STU - Bratislava (Slovakia).

It is well known that several materials, when are in nano- or well-ordered form, exibit catalytic properties different from those of in bulk phase [1]. Gold nanoparticles [2], thin vanadium oxide layers [3] can be mentioned as examples which later gained industrial importance.
In this contribution we present the preparation of non-continuous MoO_2 films which were created by oxidation of nano-porous pure molybdenum films in a controlled atmosphere. The monoclinic phase MoO_2 particles with mean size lower than 10 nm exhibit 42% selectivity to propylene oxide.
Microstructure of PVD deposited metallic layers is described by Thornton diagram of film growth [4]. Detailed study of Thornton`s model for the deposition at low substrate temperature was published in 2003 by Petrov et al [5]. In this work there was shown the possibility to deposit non-continuous films with various aspect ratios of individual (consisting) metallic particles. By other words there is possibility to prepare non - continuous metallic film consisting of separated metallic needle-shape crystallites. The pores (voids) in such films extend through the entire thickness of the layer. This film morphology is very suitable for the subsequent oxidation needed for the creation of single phase MoO_2 films (Fig. 1).
The dc magnetron sputtering was used for Mo deposition The discontinuity of Mo layers was achieved by the deposition at relatively high Ar pressure (approx. 0,1 Pa) and low substrate temperature (approx. -20 °C).By this procedure we obtain the nano-structured Mo non-continuous films.
The nano-morphology of all prepared films was controlled by in-plane and cross-sectional transmission electron microscopy.

[1] Cavani F. Catal. Today;157(2010) 8.
[2] Gaudet J., et al; J. Catal. 280 (2011) 40.
[3] Bond G.C., Tahir S.F., Appl. Catal. 71 (1991) 1.
[4]Thornton J. A. Rev. Mat. Sci 1977;7;239
[5] Petrov I., BarnaP.B., Hultman L., Greene J.E. J Vac. Sci Technol 2003; A21; S117.

Fig1. Plane view TEM micrograph of MoO_2 non continuous film creating by oxidation of Mo nano-porous film.

TF-2-Or-6
An extremely sensitive and selective NO sensor based on villi-like WO3 thin film nanostructures

T14 Thin Films

#TF-2-Or-6

H. Moon [1], J.S. Kim [1], H.H. Park [2], S.J. Yoon [1], C.Y. Kang [1], H.W. Jang [1].

[1]Korea Institute of Science and Technology - Seoul (Korea, republic of),
[2]Yonsei University - Seoul (Korea, republic of).

Chemoreistive sensors based on semiconducting metal oxides have attracted enormous attention for diverse applications such as environmental monitoring, food processing, semiconductor processing, agriculture, automotive and aerospace industries and medical diagnosis. Among these applications, the detection of human diseases such as lung cancer, asthma and diabetes by analyzing exhaled breath is an emerging field of medical diagnostic, which can be a noninvasive and cost-effective alternative to conventional blood analysis methods. For instance, detecting a NO concentration more than 30 parts per billion (ppb) in exhaled human breath indicates that the human may possess asthma due to inflammatory response in the airways, which is especially serious for young children. However, human breath is a mixture of nitrogen, carbon dioxide, nitric oxide, water vapor (< 80%) and more than 1000 volatile traces with concentrations ranging from several parts per trillion (ppt) to several parts per million (ppm). Due to this complexity of human breath, the selective detection of ppb-level NO using metal oxide-based chemoresistive sensors is very challenging because individual semiconducting metal oxides have in general large responses to both oxidizing or reducing gases such as NO, NO_2, CO, H_2, NH_3, and volatile organic compounds including ethanol and acetone. Herein, we have synthesized the self-assembled villi-like WO_3 thin film nanostructures with large specific surface area which have been achieved using glancing angle deposition. Ultrahigh response, excellent selectivity and a ppt-level detection limit to nitric oxide (NO) in 80% of relative humidity demonstrate the great potential of the porous WO_3 thin film nanostructures for use in high performance breath analyzers.

SE/TF-1-Or-3
Deuterium retention in nanostructured tungsten films exposed to high-flux plasmas

T14 Thin Films

#SE/TF-1-Or-3

M. Passoni [1], D. Dellasega [1], A. Pezzoli [1], M.H.J. 't Hoen [2], P.A. Zeijlmans Van Emmichoven [2].

[1]Dipartimento di Energia, Politecnico di Milano; Istituto di Fisica del Plasma, Consiglio Nazionale delle Ricerche, EURATOM-ENEA-CNR Association - Milano (Italy), [2]FOM Institute DIFFER, Dutch Institute for Fundamental Energy Research, Association EURATOM-FOM, Partner in the Trilateral Euregio Cluster - Nieuwegein (Netherlands).

We present an experimental research aimed at depositing compact nanostructured W films by Pulsed laser Deposition (PLD) and establishing their stability and deuterium (D) retention properties against exposure to high-flux plasmas. W films are extensively studied, thanks to their high thermal stability, hardness and low resistivity. They are used as barrier layer in semiconductor integrated circuits, absorption layers in X-ray lithography and components of X-ray mirrors. W coatings have been recently adopted to cover plasma facing surfaces of first walls in Tokamaks (e.g. JET ITER-like wall) [1]. Neutron, particle, e.m. radiation deeply change first wall material properties during machine operation, inducing modifications at the nanometric level, like vacances, defect formation, nanocrystalline growth [2]. A lot of efforts are currently devoted to the enhancement of non-permeation and resistance properties in hostile environment through suitable control of film nanostructure, but satisfactory results are far from being achieved, mostly because of lack of knowledge in the influence of materials properties at the nanoscale on their macroscopic behavior.
To investigate this issue we deposited by PLD nanostructured W coatings, characterized by high resolution SEM, XRD and EDS [3]. Thanks to the flexibility of PLD it is possible to study a wide range of coating compositions, structures, growths and morphologies, by changing the process parameters. The coatings are dense, non porous and exhibit different crystalline structures, ranging from highly crystallographic oriented with columnar structure to "amorphous like" structure

with high level of nm defects (Fig. 1). Nanocrystalline domain size has been controlled down two less than 2 nm. We exposed the films to high-flux (>10^{24} $m^{-2}s^{-1}$) D plasmas in the divertor simulator Pilot-PSI, to investigate retention and erosion properties varying the crystalline structure. Surface temperatures below 520K and between 600-950K were adopted, to investigate the effect of vacancy migration during D implantation. Thermal Desorption Spectroscopy measurements show that retention properties are highly influenced by nanostructure and disorder. The measured retention levels are similar or even much higher than the highest measured in pre-damaged W. Surface morphology changes, like bubble formation and nano-crystalline structures, were found. An interpretation of this behavior will be given together with possible indications for the surface engineering of Tokamaks divertor/first-wall.

[1] Ruset, C. *et al*., Physica Scripta T128, 171-174 (2007)
[2] M. Victoria, *et al*., J. Nucl. Mat. 276 (2000) 114-122
[3] D. Dellasega *et al.*, J. Appl. Phys. 112, 084328 (2012)

Fig.1

TF-7-Or-12
Electrical characteristics of flexible capacitors using crystallized ferroelectric thin films on polymer substrates by excimer laser annealing technique

T14 Thin Films

#TF-7-Or-12

M. Kang [1], Y.H. Do [1], W.S. Choi [1], H.C. Song [1], W.S. Jung [1], S. Nahm [2], S.J. Yoon [1], C.Y. Kang [1], S.D. Han [1].

[1]Korea Institute of Science and Technology - Seoul (Korea, republic of), [2]Korea University - Seoul (Korea, republic of).

Ceramic thin films are not compatible with flexible electronics, because the crystallization temperature of the ceramic thin films (>600^{o}C) is much higher than melting temperature of flexible polymers (<400^{o}C), although the ceramic thin films have a remarkable functionality such as high dielectric permittivity, ferroelectricity, piezoelectricity, etc. In this works, we used excimer laser annealing (ELA) technique which is attractive heat process for the low-temperature crystallization of the thin films because of its material selectivity, short penetration depth, and the rapid heating time. Amorphous $BaTiO_3$ (BTO) thin films were deposited on the polymer substrates by RF-sputtering at R.T. To determine the ELA condition, COMSOL multi-physic program was used for heat transfer simulation of thermal gradients in the BTO thin films. The ELA was carried out with various conditions as function of the applied laser energy density, the number of pulses, and the repetition rate. The X-ray diffraction (XRD), scanning electron microscopy (SEM), and transmission electron microscopy (TEM) were used to analyze the structural characteristics. The leakage currents, and dielectric constants and dielectric losses were measured by I-V meter and impedance analyzer, respectively. As a result, the crystallized BTO thin films on polymer substrates exhibited significant improvement of crystal quality and electrical performance. We obtained the flexible thin film capacitors with the enhanced dielectric performance by a particular experimental condition on the ELA as the low temperature crystallization process.

SE/TF-4-Or-7
A novel production technique to synthesize of Mg2Si thin films

T14 Thin Films

#SE/TF-4-Or-7

N. Sezgin, E. Kacar, K. Kazmanli, M. Urgen.

Istanbul Technical University, Department of Metallurgical and Materials Engineering, 34469, Maslak - Istanbul (Turkey).

In the present study, to develop a new methodology for production of Mg_2Si thin films, surfaces of silicon substrates were modified with magnesium cathode, by using cathodic arc plasma treatment process. In the literature to form the Mg_2Si thin films, after deposition process of Mg on Si substrates, vacuum annealing heat treatment were applied to the samples. At this study, unlike the literature, to obtain Mg_2Si intermetallic phase, deposition of Mg was achieved under low bias voltages and then to form alloy by enhancing diffusion/mixing high bias voltages were applied to the substrates. Different coating parameters such as; deposition time, bias voltage, duty cycle were investigated. Structural, morphological and elemental properties were determined by SEM, EDS, Thin Film XRD and GDOES analyzing methods.

TF-P2-41A
Electrochromic materials deposited by the magnetron sputtering technique

T14 Thin Films

#TF-P2-41A

T. Venot, S. Dubourg.

CEA - Monts (France).

T. Venot*[1], A.Fabas[2], A.Rougier[2], D. Marteau[1], H. Boquet[1], C. Marcel[1]
[1] CEA le Ripault, BP16 37260 Monts, France
[2] ICMCB-CNRS, UPR 9048 Université de Bordeaux, 87 av. du Dr. Schweitzer, 33 600 Pessac, France
*timothee.venot@cea.fr

In this work, the optimization of an all solid inorganic IR electrochromic device is studied. This electrochromic device works in reflection on absorbing background. Thin layers of amorphous or crystallized WO_3 were deposited on a new, electronically conducting, electrode material based on sub-stoichiometric tungsten oxide "WO_{3-y}" [1]. This stack consists of an IR reflector, crystallized WO_3 in the reduced state, and of an electronic conductor WO_{3-y} which also absorbs IR radiations. This innovative bilayer is deposited on a solid electrolyte composed of tantalum oxide (Ta_2O_5) and a counter electrode serving as a hydrated proton storage layer ($H_xWO_3.nH_2O$).
All these layers are deposited by magnetron sputtering (PVD) in one single run.

The study was focused on optimizing the PVD deposition conditions. The oxygen and water was added to the plasma gas (Argon) to deposit these oxide layers. The stoichiometry of these layers is directly related to the O_2 an H_2O partial pressure, while their morphology depends on the total pressure in the chamber and the substrate temperature.

Then, the in-situ intercalation of structural water in the layer $H_xWO_3.nH_2O$ was addressed. Finally, proton permeability of the solid electrolyte Ta_2O_5 was optimized. All these oxides were characterized by IR spectroscopy, SEM, TEM, X-ray photoelectron spectroscopy (XPS) and ion beam analysis for film composition determination (RBS: Rutherford Backscattering Spectroscopy and NRA: Nuclear

Reaction Analysis). Electrochromic (EC) properties were investigated by cycling the WO_3 based thin films in various electrolytes including ionic liquids. The relationship between the EC performances and the films characteristics will be discussed in details.

[1] CEA patent: All-solid state electrochromic device, bilayer electrode for this device, and preparation process of this device; C.Marcel, F.Sabary, J.Demeaux, D.Marteau (2010)

TF-P2-06
Structural Properties of Ga Doped Zinc Oxide Coatings Formed by RF Sputtering

T14 Thin Films

#TF-P2-06

P. Sutta [1], M. Netrvalova [1], I. Novotny [2], S. Flickyngerova [2], V. Tvarozek [2].

[1]University of West Bohemia - Pilsen (Czech republic), [2]Slovak University of Technology - Bratislava (Slovakia).

One-dimensional nanostructures (such as wires, roads, tubes) have shown wide potential applications in fabricating nanoscale electronics, optoelectronics and sensors. In order to realize various tailor-made functions, nanowires with a core/shell structure have been created by a variety of techniques but there are a few reports on the fabrication of ZnO sheaths by using a sputtering technique [1, 2]. Compared sputtering with other deposition methods, it seems to be more efficient, well-controllable and precise for nano-coatings of three-dimensional samples [3].
The forming of homogenous coatings by transparent/conductive Ga doped zinc oxide (ZnO:Ga) thin films via continual or sequential RF diode sputtering is presented. ZnO:Ga films (thickness of 100 nm) were continually deposited at the nominal rate of 12 nm/min. A sequential sputtering (layer-by-layer, 1 nm–by–1 nm) of films with thicknesses in the range of 10 nm–100 nm was performed at the nominal rate of 8 nm/min. All films deposited by both sputtering modes were preferentially textured in [001] c-axis direction (an inset in figure) and they showed the columnar structure. Nanocrystalline structure of sputtered ZnO:Ga films depended on the mode of sputtering. Continually sputtered films showed higher size of nanocrystals (≈ 40 nm) in comparison with sequentially deposited films (≈ 15 nm). The XRD patterns of ZnO:Ga thin films in-situ annealed in vacuum at temperatures from room temperature to 400 ºC showed that the transition temperature range of structural changes has began at a relatively low temperature about 200ºC (figure). The shift of (002) diffraction lines, improvement of their symmetry and intensity – all demonstrate better texture and more ordered crystalline structure. Presented results confirmed the ability of both sequential and continual modes of RF diode sputtering to prepare ultra-thin

homogenous ZnO:Ga coatings with highly ordered nanocrystaline columnar structure.

[1] H.W. Kim, H.S. Kim, Ch. Lee, M. Kebede, K.Y. Yoo and D.Y. Kim, „MgO-Core/ZnO-shell Nanocables Sheathed by using the Sputtering Technique“, J. of the Korean Phys. Soc., 2009, vol. 55, No. 5, pp. 1887-1891.
[2] H.W. Kim, H.S. Kim, M. Kebede, H.G. Na, J.Ch. Yang and Ch. Lee, „Structural and photoluminescence properties of GaN/ZnO core-shell nanowires with their shells sputtered“, Cryst. Res. Technol, 2009, vol. 44, pp. 636-641.
[3] J. Novak, I. Novotny, J. Kovac, P. Elias, Z. Krizanova, I. Vavra, R. Stoklas, S. Hasenöhrl, “Preparation of thin Ga-doped ZnO layers for core-shell GaP/ZnO nanowires”, Applied Surface Science, 2012, vol. 258(19), pp.7607-7611.

XRD patterns of ZnO (002) line recorded during "in-situ" heat treatment

TF-P2-42
V2O5/Porous Si/Si As structure for CO2 sensing

T14 Thin Films

#TF-P2-42

K. Ayouz [1], N. Gabouze [1], A. Iratni [2], H. Menari [1], A. Keffous [1].

[1]CRTSE(Centre de Recherche en Technologie des Semi-conducteurs pour l'Energétique) - Algers (Algeria), [2]2LMMC , Faculty of engineering sciences. M'HamedBougara University, 35000 -Boumerdès- Algeria. - Algers (Algeria).

ABSTRACT

In the present work, a gas sensing device based on Vanadium oxide thin films (V_2O_5)/ Porous Si (PS) / Si structure has been used to detect CO_2 gas at different concentration. The V_2O_5 thin films were deposited on moncristalline silicon, porous silicon and glass substrates by the sol-gel (Dip-coating) technique. The Vanadium oxide has been produced from vanadium alcoxide precursor. Different structures based on V_2O_5 / Porous Si/Si have been realized and studied. **Figure1** shows a schematic diagram of the V_2O_5/PS/Si sensor, and **Figure 2** shows SEM image of V_2O_5 nanostructures.

Current-voltage characterization shows that the sensor characteristics are modified in the presence of gases. The contribution of each layer (Vanadium oxide and PS) has been established. The mechanisme of CO_2 adsorption in semiconductor is more complex; however the same mechanism in oxide semiconductor is mainly atributed to physical interaction. It is interesting to note that a same shape current variation with CO_2 gas pressure, has been observed for sensors based on CH_x-PS/Si structure in presence of CO_2 and H_2 gas and hydrocarbon gas **[1]**, indicating that the Al/V_2O_5/PS/Si/Al structure behaves like CHx/PS/Si structure. However , for a constant CO_2 gas concentration the current variation ΔI of the sensor based on V_2O_5/PS structure is found lower than tha of the CH_x/PS- based sensor **[2]** probably decause of the presence of the vanadium oxide.

[1] N. Gabouze, S.Belhousse, H.Cheraga, N.Ghellai, Y. Ouadah, Y. Belkacem, A.Keffous, Vacuum 80 (2006) 986-989.
[2] Gabouze N, Belhousse S, Cheraga H. Phys. State Solidi (C) 2005 ; N9 : 3449.

Figure 1: A schematic diagram of the V_2O_5/PS/Si sensor.
Figure 2: Typical morphology of V_2O_5 deposited by dip coating technique on PS substrate

TF-P2-07
Physical Property-Structure Relations in Cu-Mn Alloy Films

T14 Thin Films

#TF-P2-07

F. Misják [1], K. Nagy [1], P. Szommer [2], P. Lobotka [3], Z. Czigány [1], G. Radnóczi [1].

[1]Research Centre for Natural Sciences, Hungarian Academy of Sciences - Budapest (Hungary), [2]Department of Materials Physics, Eötvös Loránd University - Budapest (Hungary), [3]Institute of Electrical Engineering, Slovak Academy of Sciences - Bratislava (Slovakia).

Understanding of Cu-Mn alloy films is of scientific interest because of their possible application as contact or interconnect materials in memory devices or integrated circuits. In this work we aimed to reveal the physical property - structure relations in the system.
Cu-Mn alloy films were co-deposited by DC magnetron sputtering from Cu and Mn targets at room temperature with a thickness of around 1μm. Cross sectional samples for TEM were prepared and HREM investigation was carried out. Electric measurements were made by four probe method and nanoindentation was carried out in a UMIS 2000 nanoindenter using a Bekovich indenter.
Mapping the structure of the Cu-Mn thin film system we found some discrepancies from the equilibrium phase diagram of the bulk system [1]. Beside the pure fcc Cu and pure αMn phases the following structure zones were found. The low Mn content films (up to ~25 at% Mn) have Cu based fcc solid solution structure. Between 40 and 65 at% Mn content a disordered phase region is found, while from ~80 at% Mn content αMn type solid solution forms [2]. Between these one phase regions narrow two-phase regions exist.
Measuring the physical properties can also show correlation with the above phase regions. Deviations from the linear behaviour of electrical resistivity (Fig. 1.) mark the two phase regions of the system. The shape of the curve also suggests that the mutual solubility of components is about 20 at%. The appearance of the clear minimum on the hardness curve points to a structural peculiarity (Fig. 2.). Its position corresponds to the border of the one phase disordered region.

The authors acknowledge the financial support of the Hungarian National Science

Foundation under grant OTKA-K81808. F. Misják and Zs. Czigány also acknowledge the support by the János Bolyai Research Scholarship of the Hungarian Academy of Sciences.

[1] Okamoto HJ. Phase Equilib 1998;19:180.
[2] Zs. Czigány, F. Misják, O. Geszti, G. Radnóczi: Acta Materialia, 2012, 60, 7226-7231.

Fig.1. Electrical resistivity of Cu-Mn alloy films as the function of composition at RT.
Fig.2. Nanohardness of Cu-Mn alloy films as the function of composition.

TF-P2-31
Optical Characterization of Sol-Gel ZnO:Al Thin Films

T14 Thin Films

#TF-P2-31

T. Ivanova [1], A. Harizanova [1], T. Koutzarova [2], B. Vertruyen [3].

[1]Central Laboratory of Solar Energy and New Energy Sources, Bulgarian Academy of Sciences - Sofia (Bulgaria), [2]Institute of Electronics, Bulgarian Academy of Sciences - Sofia (Bulgaria), [3]LCIS/SUPRATECS, Institute of Chemistry B6, University of Liege - Liege (Belgium).

This work presents sol-gel technological process for obtaining thin films of ZnO and ZnO:Al, where the Zn/Al ratio varies. The effect of annealing treatments has been studied on their properties. Structural evolution with temperature is investigated by using X-Ray diffraction (XRD). Fourier Transform Infrared (FTIR) and UV-VIS spectrophotometry are applied for characterization of the vibrational and optical properties.

XRD analysis of ZnO and ZnO:Al films revealed that the main XRD maxima, the strongest lines observed in the spectra, are assigned to wurtzite hexagonal crystal phase of ZnO (JCPDS 01-07-8070). It can be seen that the addition of Al leads to wider lines with considerable lower intensities, which suggests that the crystallization degree is decayed. The average crystallite sizes are estimated from XRD patterns according to Scherrer's formula (from the three XRD peaks attributed to hexagonal ZnO: 100, 002 and 101) and the comparison of the results shows that the average crystallite size of ZnO is 32.3 nm, and the value for ZnO:Al is 20.0 nm.

FTIR analysis reveals that both the metal additive affects the vibrational properties of the studied films. The main absorption bands due to metal-oxide bonds are expected to appear in the spectral range 350-1200 cm-1. For the preheating ZnO:Al films, weak peaks at 665 and 681 cm-1 are observed, which might be assigned to the O-Al-O bonding, they are seen for the highest temperature annealed films. The main IR lines are located in the spectral range 390-425 cm-1. The Al component influences the shapes of the obtained absorption bands, they are broader comparing to pure zinc oxide spectra and their intensity also decreases with increasing the aluminum content.

The optical properties of the sol-gel ZnO and ZnO:Al films reveal very interesting features. The ZnO films possess lower transparency compared to the ZnO:Al films and its transmittance decreases with the annealing temperatures. If the Al

component is increased in the sol solutions, the obtained films possess significantly higher transparency. The experiments with higher Al content manifests transparency as high as 90 %, very close to that of pure Al2O3 films (sol-gel Al2O3 films are prepared for comparison).
The optical band gap values are estimated from the spectrophotometric data. The optical band gap values of pure ZnO show no trend with annealing (Eg=3.28-3.30 eV), for ZnO:Al films the values are slightly decreased with annealing temperature. The ZnO:Al films reveal an increase of the optical band gap values with increasing the Al additions from 3.28 up to 3.44 eV.
Sol-gel technology has been successfully applied for deposition of transparent ZnO and ZnO:Al films by spin coating method. XRD analysis reveals predominantly wurtzite crystal phase with significantly decreasing of the crystallization and crystallite sizes due to Al additive. Optical transmittance improves for ZnO:Al films with increasing the aluminium quantity.

TF-7-Or-11
Measuring the Ductility of Organic Semiconductor Materials

T14 Thin Films

#TF-7-Or-11

T. Kobayashi [1], T. Yokoyama [1], Y. Utsumi [2], H. Kanematsu [3], T. Masuda [4].

[1]Tsuyama National College of Technology - Tuyama, Okayama (Japan), [2]University of Hyogo - Ako, Hyogo (Japan), [3]Suzuka National College of Technolgy - Suzuka,mie (Japan), [4]Q-Light co., Ltd. - Hanamaki, Iwate (Japan).

The evaluation method of the ductility of the materials constituting organic semiconductor was studied, and the relations between applied strain and the fracture of thin films were obtained. The final target of this work is the improvement of flexibility of organic light emitting diode (OLED). The tensile test of the thin films deposited on flexible substrate is conducted, and the vulnerable parts of the constituent material of the OLED is quantitatively understood, further the guideline for designing OLED structure will be obtained. In the present paper, tensile test of aluminum oxide thin films deposited on a polyethylene terephtalate (PET) substrate was carried out under an constant condition, in addition indium zinc oxide (IZO), which is one of a transparent conductive oxide (TCO), and a α-NPD (Bis [N-(1-naphthyl)-N-pheny] benzidine), which is typical organic light emitting material), deposited on polyethylene naphthalate (PEN) substrates prepared by vacuum processes were also examined. Consequently the following results were obtained:(1)Cracking of the aluminum oxide thin films can be observed using an bright field microscopy in more than 40 times the magnification, (2)Cracking initiated at an strain of about 3%, (3)the number of cracking increased proportional to the strain, and saturated at about 9% strain. (4) Organic thin filmα-NPD caused cracking as well as oxide thin films.

[1] Leteir Y., Medico L., Demarco F., Manson. J.A.E., Betz .U., Escola M.E., Olsson M. k., Atamny F., “Mechanical integrity of transparent conductive oxide films for flexible polymer-based display”, Thin Solid Films, vol.460,(2004), pp.156-166.
[2] Kim W.H. and Kafafi Z.H., “Flexible organic light emitting devices using conductive polymeric anodes”, in Soc. Inf. Display. Dig. Tech. Papers, Vol.XXXⅢ,(2002),

pp.1090-1091.

Fig1 An FE-SEM Image of α-NPD film applied around 8% strain

Fig.2 Relation between applied strain and the number of cracks in α-NPD films

TF-P2-15
Deposition and Characterization of Plasma Polymer Nano-Thin Films for Low-k Dielectric Applications

T14 Thin Films

#TF-P2-15

J.H. Boo [1], H.J. Seo [1], S.J. Cho [1], A. Zeng [1], Y. Kim [1], B. Hong [1], S. Kim [2].

[1]Sungkyunkwan University - Suwon (Korea, republic of), [2]Pai Chai University - Daejeon (Korea, republic of).

Organic polymer nano-thin films have been deposited on silicon substrate by using plasma enhanced chemical vapor deposition (PECVD) method (1,2). Ethylcyclohexane (ECH) was utilized as organic precursor, and hydrogen and Ar (argon) were used as a bubbler and carrier gases, respectively. In order to compare the difference of the thermal, electrical, and mechanical properties of the plasma polymerized nano-thin films, the organic polymer nano-thin films with 300 nm thickness were grew up under the conditions of various RF (radio frequency using 13.56 MHz) powers in the range of 20 ~ 60 W and annealed at various temperatures in the range of 200 ~ 500 ℃. The nano-films were in first analyzed by FT-IR, SEM, C-V, and Nano-indentation. The result of FT-IR measurement showed that the plasma polymerized nano-thin films have highly cross-linked density with increasing RF power. However, organic polymerized nano-thin films are thermally unstable because the intensity of -OH peak increased after annealing. SEM data also showed that the nano-films with smooth surface and sharp interface could be grown under various deposition conditions. Impedance analyzer was utilized for the measurements of C-V curves. From the electrical property measurements, the lowest dielectric constant was obtained to be 1.71. While, the values of dielectric constant were increased with increasing annealing temperature due to thermal instability above 300 ℃. The hardness and Young's modulus of the organic thin films increased with increasing RF power, and decreased with increasing annealing temperature, respectively.

(1) I.-S. Bae, S.-J. Cho, W.S. Choi, H.J. Cho, B. Hong, H.-D. Jeong, and J.-H. Boo, Progress in Organic Coatings, 2008, 61(2-4), 245-248.

(2) S.-J. Cho, I.-S. Bae, J.-H. Boo, Y. S. Park, and B. Hong, Journal of the Korean Physical Society, 2008, 53(3), 1634-1637.

TF-7-Or-9
Cu(In,Ga)Se2 solar cell absorber layers prepared by a single-step reactive co-sputtering process in Ar:H2Se

T14 Thin Films

#TF-7-Or-9

J. Schulte, K. Harbauer, K. Ellmer.

Helmholtz-Zentrum Berlin GmbH (HZB) - Berlin (Germany).

Reactive and non-reactive magnetron sputtering is widely used in industry for the deposition of thin films for optical and electronic applications, hard coatings etc.. For thin film solar cells, several layers - mostly the electronically inactive ones (front and back contacts) - are deposited by this plasma-assisted, large area deposition method. Our group is studying the deposition of electronically active chalcopyrite absorber films for thin film solar cells deposited by reactive magnetron sputtering in Ar/H_2S atmospheres. For $CuInS_2$ films we were able to demonstrate the suitability of this process for the deposition of absorber layers by preparing a solar cell with an efficiency of 11.4%, which is comparable with other preparation techniques.
In this work we used reactive magnetron co-sputtering from a CuGa and an In target in an Ar/H_2Se gas mixture. With this one-step process it is possible to prepare single-phase $Cu(In,Ga)Se_2$ thin films with good crystallinity that can be used as absorber layers for thin film solar cells.
One important process parameter is the H_2Se content of the gas that influences not only the incorporation of Se into the film, but also the deposition rates from the metal targets and therefore the thickness, stoichiometry and the crystallinity of the films. The XRD patterns of the H_2Se variation in Fig.1 demonstrate the formation of single phase $Cu(In,Ga)Se_2$ with a preferred (1 1 2) orientation, especially for higher H_2Se contents. For a content of 10% H_2Se in the process gas two additional peaks occur which can be attributed to a metallic Cu phase which indicates, that this reactive gas content is not sufficient for a complete selenization of the metal atoms.
In order to achieve absorber layers with good solar cell quality additional parameters as the specific sequence of process steps (Cu-poor or Cu-rich conditions) and the final film stoichiometry play an important role and are investigated. The influence of Na doping is investigated by comparing standard Mo back contacts to samples which have a Na-doped Mo layer.
The results for the first solar cells processed with absorber layers from these

depositions in Ar:H2Se are promising and demonstrate the opportunities of reactive co-sputtering of electronically active films for thin film solar cells.

[1] S. Seeger, K. Ellmer, Thin Solid Films, (2009) p. 3143

Fig.1: XRD pattern of Cu(In,Ga)Se_2 films prepared with different H_2Se contents in the process gas. In the lower part the nominal positions according to the JCPDS files are shown. The labels mark the diffraction reflexes for Cu(In,Ga)Se_2.

TF-3-Or-10
Duplex FCAD/ALD oxide nanocoatings for corrosion protection of steel

T14 Thin Films

#TF-3-Or-10

V. Maurice [1], B. Díaz [1], E. Härkönen [2], S. Tervakangas [3], J. Światowska [1], L. Tóth [4], G. Radnóczi [4], J. Kohlemainen [3], M. Ritala [2], P. Marcus [1].

[1]CNRS/Chimie ParisTech - Paris (France), [2]University of Helsinki - Helsinki (Finland), [3]DIARC-Technology Inc. - Espoo (Finland), [4]MFA - Budapest (Hungary).

Surface/interface analytical and electrochemical studies have been carried out in order to understand and develop the corrosion protection properties of duplex oxide nanocoatings grown by Atomic layer deposition (ALD) and Filtered Cathodic Arc Deposition (FCAD) on steel (AISI 52100, DIN 100Cr6) substrates. Time-of-Flight Secondary Ion Mass Spectrometry (ToF-SIMS), cross-section Transmission Electron Microscopy (TEM), potentiodynamic polarization and Electrochemical Impedance Spectroscopy (EIS) were used. Immersion tests were performed in corrosive chloride-containing neutral and acidic solutions (0.2 M NaCl, pH 7-7.2 or pH 2) at Open Circuit Potential with in situ monitoring by EIS analysis and post mortem surface and interface analysis mostly by ToF-SIMS. The coating efficiency was derived from the i-V and EIS data.

The results show effective sealing by a thin (typically 50 nm) oxide film deposited by ALD at 150-160°C [1,2]. ALD alumina provides the best sealing properties with a coating efficiency reaching 99.99 % of the substrate surface fraction but dissolves in corrosive environments [3.4]. It is stabilized by introducing tantalum oxide, either forming mixtures or nanolaminates with various architectures. Defects (cracks, pinholes) subsist after deposition due to the use of organic precursors and to organic interfacial residues, requiring to go beyond 10 nm in thickness for sealing of the more defective layers formed in the initial stages of deposition. Fe/Cr oxides poison the interface due to spurious growth prior to actual ALD deposition. In corrosive solutions, the iron-rich interfacial oxide dissolves following the penetration of the corrosive solution to the substrate surface via the coating defects. It creates voids promoting local breakdown and the propagation of localized corrosion.

The key improvement achieved with duplex coated systems is the replacement of the poorly corrosion resistant interfacial iron-rich oxide by a highly resistant interfacial sub-layer. The sub-layer is grown by FCAD that, thanks to sputtering prior to deposition, is able to produce substrate surfaces free of Fe/Cr oxides and organic residues [5]. Ta or Ta/Cr oxide mixtures are then deposited. A 10 nm thickness is enough to produce a continuous interlayer well-adherent to the clean substrate. A conformal 50 nm ALD top layer is then deposited to seal the defects in the FCAD sub-layer. The resulting sealing performance of the duplex system is similar to that of a single ALD layer. As for single systems, defects (cracks, pinholes) subsist after deposition and connect the alloy surface to the environment. In corrosive solutions, the iron-rich interfacial oxide traces also dissolves but only at the substrate surface exposed by the coating defects. There is no propagation of the reaction along the interface due to blocking by the FCAD sub-layer. As a consequence localized corrosion is limited to the bottom of the pre-existing defects and its propagation by coating breakdown is inhibited. The resistance to localized corrosion is thus markedly improved on non passivable substrates.

The research leading to these results has received funding from the European Community's Seventh Framework Programme (FP7/2007-2013) under grant agreement n° CP-FP 213996-1.

SE/TF-P2-17
A novel deposition method for a protective coating for bipolar plates in PEMFC

T14 Thin Films

#SE/TF-P2-17

Y. You, J.S. Choi, J.H. Joo.

Kunsan National University - Kunsan (Korea, republic of).

Protective coatings for bipolar plates in PEMFC (polymer electrolyte membrane fuel cell) should have high anti-corrosion characteristics and electrical conductivity under very aggressive conditions (sulfuric acid). US DOE set threshold corrosion current density as 1 μA/cm^2 as well as contact resistance to 0.02 Ohm*cm^2. Stainless steel sheets are a strong candidate for this purpose which has very stable chromium oxide surface layer. However, the electrical conductivity does not meet DOE specifications. Higher conductive material should be coated on top of SUS sheets. TiN, TaN, CrN and their alloy compounds are considered to meet the standards. Automotive systems must be cost-effective and high rate reactive PVD methods are necessary. Inductively Coupled Plasma (ICP) was proven to be effective in enhancing the film quality (density, microstructure, adhesion) in many material systems. Magnetron sputtering could be a good candidate, but the high cost would be a first barrier for automotive parts business. Evaporation based technique would be more appropriate for this purpose. Thermal evaporation has high deposition rate for most of materials, but reactive process needs secondary plasma to enhancing the surface reactivity and film to substrate adhesion strength. Cr has very high sublimation rate at high temperature before it starts to melt. We adopted inductively coupled plasma as a heating source for Cr rod for film deposition as well as film property enhancing secondary plasma source. 2 MHz driven ICP was used and dc biased Cr rod with Ar + N_2 mixed gas environment was acting as a high rate sputter-sublimation source to give meet DOE specifications: corrosion current density (at 0.6 V) was 2.097E-6 A/cm^2 and contact resistance was 28.8 mOhm*cm^2.

TF-P2-32
Reactive sputter deposited nanocoral ZnO for biosensors

T14 Thin Films

#TF-P2-32

M.A. Borysiewicz [1], A. Baranowska-Korczyc [2], M. Wzorek [1], E. Dynowska [2], T. Wojciechowski [2], E. Kaminska [1], K. Fronc [2], D. Elbaum [2], T. Wojtowicz [2], A. Piotrowska [1].

[1]Institute of Electron Technology - Warsaw (Poland), [2]Institute of Physics, Polish Academy of Sciences - Warsaw (Poland).

Nanocoral ZnO films (see Fig. 1.) are fabricated using a two-step approach including first a deposition of porous Zn through reactive Zn sputtering followed by thermal oxidation. The resulting material exhibits the unique electro-optical ZnO properties (3,4 eV band gap and exciton binding energy of 60 meV) as well as a developed surface enabling absorption-based applications in devices such as gas sensors, biosensors or dye-sensitised solar cells.
The growth mechanism of the films is discussed based on Langmuir probe and optical emission spectroscopy measurements of the plasma during sputtering and their correlation with X-ray diffraction and scanning electron microscopy cross-section image data of the films grown.
The films for biosensing experiments were prepared on highly doped n-silicon (111) substrates through Zn-reactive sputtering in an O2-Ar mixture with subsequent ex-situ annealing at 400oC in an oxygen flow. A Ni back contact to Si was subsequently deposited and annealed at 300oC in a forming gas. Finally, the films were stabilized for applications in the adverse biological environment using gas-phase sulphurisation. The prepared samples were used as gate electrodes in an extended-gate FET configuration with a silicon-based FET transistor.
The films are characterized using X-ray diffraction and scanning electron microscopy (SEM), which evidence their polycrystalline structure with nanocoral morphology. High-resolution transmission electron microscopy is used for the characterization of individual crystallites and energy-dispersive X-ray spectroscopy cross-section scans evidence full sulphur passivation. Stong near-band-edge (NBE) and green deep level (DLE) emission was recorded in the He-Cd excited photoluminescence (PL) spectra of the films. Temperature dependent PL evidenced a splitting of the NBE peak into donor-bound and free exciton peaks with phonon replicas present at 5K. It was also

recorded, that the sulphurisation of the films caused a reduction of the DLE signal and increase in the NBE line.
Using buffer solutions a pH-meter was constructed in the extended-gate configuration, and subsequently bovine serum albumin absorption was detected. Finally, DNA absorption experiments were carried out using complementary DNA strands, one attached to the sample and the other in the detected solution.

This study was partially supported by the European Union within European Regional Development Fund, through grant Innovative Economy (POIG.01.01.02-00-008/08 "Nanobiom") and by the Institute of Electron Technology from Statutory Funds.

Fig. 1. Cross-section SEM image of the nanocoral ZnO film.

TF-8-Or-6
An X-ray photoelectron spectroscopy study of Sn1-x-yCoxMoyO2 semiconductor thin films

T14 Thin Films

#TF-8-Or-6

O. Conde [1], S. Dalui [1], A.M. Ferraria [2], S. Rout [1], A.M. Botelho Do Rego [2], A. Silvestre [3].

[1]Universidade de Lisboa, Faculdade de Ciências, Departamento de Física and ICEMS - 1749-016 Lisboa (Portugal), [2]CQFM- Centro de Química-Física Molecular and IN-Institute of Nanoscience and Nanotechnology, Instituto Superior Técnico, Universidade Técnica de Lisboa - 1049-001 Lisboa (Portugal), [3]Instituto Superior de Engenharia de Lisboa, Área Departamental de Física and ICEMS - 1959-007 Lisboa (Portugal).

Here we present an X-ray photoelectron spectroscopy (XPS) study of undoped, Co and (Co,Mo) codoped SnO_2 films grown by pulsed laser deposition. The thin films were deposited on *r*-cut sapphire substrates, heated at 500 ºC under an ambient argon pressure of 7×10^{-2} Pa, from targets with the following nominal compositions: SnO_2, $Sn_{0.995}Co_{0.005}O_2$, $Sn_{0.97}Co_{0.03}O_2$ and $Sn_{0.96}Co_{0.01}Mo_{0.03}O_2$. In all the films the XPS photoelectrons Sn 3d, Co 2p, Mo 3d and O 1s regions were studied in detail. Both XPS surface analysis and depth profile analysis were carried out in order to identify the oxidation states of Co and Mo ions, their concentration ratio and distribution along film depth. Samples were also studied regarding their structure and microstructure, electrical, optical and magnetic properties.

It is shown that the Co 2p region presents several strong satellites centred around 786.5 eV and 803.0 eV (besides the main peak at ~781.0 eV) which are typical of Co^{2+} species and allow to rule out the presence of Co^{3+} based compounds. The Mo $3d_{5/2}$ region comprises a main peak centred at ~231.1 eV, assigned to Mo^{5+}, and two other less intense peaks at 228.8 and 232.7 eV assigned to Mo^{4+} and Mo^{6+}, respectively. The O 1s peaks clearly show a main component centred at ~530.5 eV, assigned to the oxygen in the lattice, and a shoulder of variable intensity at higher binding energy that can be considered as due to adsorbed oxygen species on the surface of the samples. The intensity ratio for the two oxygen contributions has been

related to the oxygen vacancies in the samples. In all the doped samples the relative amount of cobalt is larger than the expected nominal one.

The overall XPS results are correlated with the electrical conductivity and magnetic properties of the films allowing to understand their non-expected behaviour.

Acknowledgements: This work was partially funded by the Portuguese Foundation for Science and Technology (FCT), grant no. PTCD/CTM/101033/2008. A.M.F. and S.R. acknowledge FCT for Post-Doctoral grants, references SFRH/BPD/26239/2006 and SFRH/BPD/64390/2009, respectively.

TF-P2-16
Characterization of DLC coatings thermal stability by Raman spectroscopy

T14 Thin Films

#TF-P2-16

L. Kilman [1], M. Colas [2], C. Jaoul [2], O. Jarry [3], P. Tristant [2], C. Dublanche-Tixier [2], F. Meunier [4].

[1]Sulzer Sorevi - Sciences des Procédés Céramiques et Traitements de Surfaces, UMR7315 - Limoges (France), [2]Sciences des Procédés Céramiques et Traitements de Surfaces, UMR7315 - Limoges (France), [3]Sulzer Metaplas GmbH - Bergisch Gladbach (Germany), [4]Sulzer Sorevi - Limoges (France).

Hydrogenated amorphous carbon (a-C:H) films show some excellent mechanical and tribological properties due to their high hardness and very low friction coefficient. These properties mostly depend on the ratio of sp^2 to sp^3 hybridized carbon bonds and the hydrogen content of the coating, which can be affected by temperature. When optimized for DLC, Raman spectroscopy is a non-destructive method which allows to obtain details about both sp^2/sp^3 ratio and hydrogen content. The aim of this work was to study the thermal stability of commercial a-C:H films using maximized acquisition parameters.

In this study, in situ heating during Raman analyses were compared with the results obtained for similar samples thermally heated in a vacuum furnace. Raman spectra were performed using a 514.5nm Ar/Kr laser on a Jobin Yvon spectrometer. The choice of parameters such as laser power and acquisition time had to be adapted to the particular temperature conditions of this study, especially for the in situ analyses. Indeed, damaging the samples is more likely due to the combination of laser thermal effect and thermal treatment.

The second part of the work was to analyze spectra acquired in the optimal conditions and to link data to sp^2/sp^3 ratio and hydrogen content. Figure 1 shows spectra obtained for several temperatures during the in situ study. All the spectra

were fitted using two Gaussian peaks corresponding to the features G and D. The G peak (Graphite peak) is associated with all the sp^2 carbon in chains or rings whereas D peak (Disorder peak) is only due to sp^2 carbon in rings. The ratio between the slope of the linear background and the intensity of the G peak is related to the photoluminescence which can be used as a measure of H content. ID/IG ratio, G peak position and full width at half maximum of G peak FWMH(G) have been used to compare the sp^2/sp^3 ratio of our different coatings.

Over a third phase, nanoindentation measurements have been performed before and after heating on each sample in order to compare the influence of the in situ and vacuum furnace heating on the mechanical properties of different coatings.

Finally, a scale up of this method on large real engine parts related to valve train components is presented to illustrate the interest of Raman spectroscopy for wear mechanisms investigation.

Figure 1. Raman raw spectra of samples treated at different temperatures

TF-P2-33
Fabrication and characterization of organic thin-film transistor using antimony-doped tin oxide electrodes

T14 Thin Films

#TF-P2-33

J. Lee [1], S.H. Lee [1], J.H. Boo [1], B. Hong [1], Y.S. Park [2].

[1]Sunkyunkwan University - Suwon (Korea, republic of), [2]Chosun College of Science and Technology - Gwangju (Korea, republic of).

Tin oxide (SnO2) thin films are promising as transparent conducting oxides due to their remarkable physical properties such as high electrical conductivity and high transmittance in the visible part of the spectrum [1-3]. Recently, antimony doped tin dioxide (ATO) thin films have been used in various applications such as transparent electrodes, gas sensors, transparent electric charge shielders, plastic liquidcrystal display devices, touch sensitive overlays, front electrodes of solar cells, and energy efficient windows [4-6].
In this work, the electrical, optical, and structural properties of ATO films prepared on polyethersulphone (PES) by RF sputtering method in the RF power range of 100 W~160 W have been investigated. We investigated the electrical performances of organic thin-film transistor using ATO gate electrodes prepared at various conditions. Antimony-doped tin oxide (ATO) films were deposited on polyethersulphone (PES) substrate by radio frequency (RF) magnetron sputtering method using SnO2 target mixed with Sb of 6 wt% at room temperature with various RF powers for a transparent electrode in the thin film transistor (TFT). We investigated the structural, optical, and electrical properties by using various analysis measurements, such as X-ray diffraction (XRD), UV-visible, and Hall effect measurement. The crystallinity was increased and the conductivity of ATO film was improved with increasing RF power. Based on the data before, we fabricated the organic thin film transistor (OTFT) with ATO electrodes of various conditions. OTFT device is composed of ATO gate electrode, PVP (poly-4-vinyl phenol) gate insulator layer, pentacene active layer, and Au source/drain electrodes. Consequently, the OTFT using ATO electrode fabricated at RF power of 160 Watt as a gate transparent electrode exhibited a good device performance due to the high conductivity and the crystallinity.

[1] Y. K. Fang and J. J. Lee, Thin Solid Films 169 (1989) 52.
[2] E. Shigeno, K. Shimizu, S. Seki, M. Ogawa, A. Shida, M. Ide, and Y. Sawada, Thin Solid Films 411 (2002) 56.
[3] J. L. Huag, Y. Pan, J. Y. Chang, and B. S. Yau, Surface and Coatings Technology 184 (2004) 188.
[4] S. M. Park, K. Ebihara, T. Ikegami, B. J. Lee, K. B. Lim, and P. K. Shin, Curr. Appl. Phys. 7 (2007) 474.
[5] N. S. Murty and S. R. Jawalekar, Thin Solid Films 108 (1983) 277.
[6] A. Chaturvedi, V. N. Mishra, R. Dwivedi, and S. K. Srivastava, Microelectron. J. 31 (2000) 283.

Figure 1. ISD-VSD output and transfer characteristics. Electrical performances for OTFTs with the use of ATO gate electrode prepared at 160 W RF power .

TF-3-Or-11
Growth of an ultrathin FeO2(111) trilayer oxide film followed with ambient pressure X-ray photoelectron spectroscopy

T14 Thin Films

#TF-3-Or-11

N. Johansson [1], E. Grånäs [1], M.A. Arman [1], J.N. Andersen [2], J. Schnadt [1], J. Knudsen [1].

[1]Division of Synchrotron Radiadtion Research, Lund University - Lund (Sweden), [2]MAX IV Laboratory, Lund University - Lund (Sweden).

Many studies of ultrathin oxides for both basic science and future applications have been conducted since Vurens et al. reported a reliable method for ultrathin oxide growth in 1988 [1]. In particular, great interest has been received by trilayer oxide structures due to their catalytic activity; e.g. a trilayer iron oxide grown on Pt(111) has been found active in the low temperature CO oxidation [2].

Here we present results from an x-ray photoelectron spectroscopy (XPS) study of a trilayer iron oxide growth on Pt(111). As a precursor structure ultrathin FeO films are grown on the Pt(111) surface, which are found to form a bilayer with the Fe atoms located between the Pt support and an oxygen layer towards the vacuum. For the creation of the trilayer mbar pressures of O_2 are required, out of reach for standard in situ XPS measurements. Therefore, we have employed the ambient pressure XPS (APXPS) setup at the MAX IV Laboratory [3] to perform an *in situ* study of the trilayer growth.

The formation of the trilayer on Pt(111) could be followed *in situ* from the occurrence of a new peak at higher binding energy in the O 1s spectrum [4]. Further, the main peak that originates from oxygen atoms in FeO(111) before oxidation shifts to lower binding energies upon oxidation to FeO_2(111). The intensity ratio between the new peak at high binding energy and the main peak is found to be 1:3. We also observe a

0.3 eV shift of the Fe 3p core level upon formation of the trilayer film. Additionally, the low energy electron diffraction (LEED) patterns for the bilayer and trilayer are very similar suggesting a similar long range ordering of the two films. Based on our results we will discuss different growth models of the FeO_2(111) film in the talk.

Once the trilayer film is formed in mbar pressures of O_2 we found that it is stable in UHV, which suggest that it is possible to form the trilayer in UHV using strongly oxidizing reagents. To confirm this hypothesis we used NO_2 to oxidize a FeO(111) film at UHV conditions. This study revealed the expected XPS signature of the FeO_2(111) trilayer.

The catalytic activity of trilayer FeO_2(111) was also investigated by gas phase APXPS and simultaneous mass spectrometry measurements. However, no catalytic conversion of CO into CO_2 was observed at the experimental conditions at which the FeO_2(111) film exists. To test that our experimental setup is able to measure catalytic activity, we tested CO oxidation on a clean Pt(111) surface and CO_2 production was clearly observed both with XPS and mass spectrometry.

[1] G. Vurens, M. Salmeron, and G. Somorjai, *Surf. Sci*. **201**, 1988.
[2] M. Lewandowski, I. Groot, S. Shaikhutdinov, and H.-J. Freund, *Catal. Today* **181**, p. 52-55, 2012.
[3] J. Schnadt, J. Knudsen, J. N. Andersen, H. Siegbahn, A. Pietzsch, F. Hennies, N. Johansson, N. Mårtensson, G. Öhrwall, S. Bahr, S. Mähl, O. Schaff, *J. Synchrotron Rad*. **19**, 701, 2012.
[4] N. Johansson, M.Sc. Thesis, Lund University, 2012.

PST/SE/TF-3-Or-3
Plasma polymerisation of aminopropyltriethoxysilane in ECWR plasma: influence of plasma parameters

T14 Thin Films

#PST/SE/TF-3-Or-3

S. Bulou [1], G. Frache [1], P. Choquet [1], T. Belmonte [2].

[1]Centre de Recherche Public Gabriel Lippmann - Belvaux (Luxembourg),
[2]Institut Jean Lamour - Nancy (France).

Amino-functionalised plasma polymers (pp) have gained a high interest in the field of immobilization of bioactive molecules, improvements of implants biocompatibility and adhesion enhancement. For this purpose, alkylamine precursors (allylamine, heptylamine) are widely used. Nevertheless, such plasma polymers commonly exhibit low adhesion on metallic substrates or on specific polymer substrates. A way to overcome this issue is to deposit amino-functionalised siloxane layers that exhibit good adhesion with metallic substrates. Plasma polymerisation of amino-alkylsiloxane is a promising way to deposit such coatings. Nevertheless, it requires a selected activation of the monomer in order to promote the polymerisation of the siloxane network while efficiently incorporating amine functions. Hence, a study of the influence of the plasma parameters on the as-grown thin films and on the plasma phase has to be performed in order to progress in the understanding of the growth mechanisms.

We report here the deposition of pp-aminopropyltriethoxysilane (APTES) in Ar remote ECWR plasma. ECWR plasmas are high density-low pressure plasma sources which have been shown to be well suited for the synthesis of inorganic and hard material. The successful use of ECWR plasma source for plasma polymerisation is reported here for the first time.

The influence of experimental deposition parameters (RF incident power, additional gases, pressure) on the morphology, atomic composition and molecular structure of the synthesised plasma polymers as well as on the plasma phase is studied. The aim is to obtain plasma polymer thin films with a high primary amine function density and to progress in the understanding of the plasma chemical pathways and of the polymerisation mechanisms.

pp-APTES thin films are characterised by means of ToF-SIMS, FTIR, XPS and SEM. The reactor is equipped with a high-vacuum transfer suitcase that is used to transfer the as-grown plasma polymers into ToF-SIMS and XPS instrument, allowing “quasi in-situ” surface analysis, i.e. without exposure to air after deposition. The plasma is analysed by means of Optical Emission Spectroscopy, in order to follow the plasma species (reactive species, radicals, by-products) and progress in the comprehension of the deposition process. Addition of low flow of N_2 and/or O_2 leads to important molecular structure modifications of the deposited films, especially on the primary amine density.
In the light of thin film characterization and plasma diagnostics, plasma polymerisation and thin film growth mechanisms are proposed.

TF-5-Or-1
DIELECTRIC PERFORMANCE IN MWCNTS/EPOXY COMPOSED

T14 Thin Films

#TF-5-Or-1

P. Savi [1], M. Giorcelli [1], A. Naderi [2], A. Tagliaferro [1].

[1]Politecnico di Torino - Torino (Italy), [2]Semnan University - Semnan (Iran, islamic republic of).

Multi Walled Carbon Nanotubes (MWCNTs) have been used as polymer fillers for a number of years . In fact, they can improve, even at low filler contents, the mechanical and electrical performances of the host polymer. Moreover, the higher surface area and large aspect ratios that can be achieved with respect to single wall CNTs lead to superior dielectric properties among nanotubes composites [1;2].
In this work, we tested composites obtained using an Epoxy resin and several types of commercial MWCNTs. Due to the different aspect ratio (length vs diameters ratio) and concentrations used, we have been able to widely tune the dielectric properties of the composites. In particular, we investigated in a wide frequency band (3-16 GHz) the behavior of real and imaginary part of permittivity. Composites samples, moulded in appropriate cylindrical shape, were analyzed using a capacitive sensor (Agilent 85070D) with a Network Analyzer (E8361A) (see Fig.1). A direct correlation between type and density of MWCNTs and the dielectrical properties was observed. The possibility of tuning capacitive and dissipative effect of polymer was also investigated. Finally, all the samples were characterized by SEM in order to investigate the role of dispersion in the polymer matrix in determining the properties (Fig.2).

References:

[1] Dang ZM, Wang L, Yin Y, Zhang Q, Lei QQ. Giant dielectric permittivities in functionalized carbon–nanotube/electro active polymer nanocomposites. Adv Mater 2007;19:852–7.
[2] Wang L, Dang ZM. Carbon nanotube composites with high dielectric constant at low percolation threshold. Appl Phys Lett 2005; 87:042903

Fig. 1 Cole-Cole diagram with 3 different CNTs percentage (0.5, 1 , 3 wt%).

Fig. 2 FeSEM image of MWCNTs at 3wt% dispersed in epoxy matrix.

TF/SE-1-Or-2
How does redeposition influence reactive sputtering?

T14 Thin Films

#TF/SE-1-Or-2

K. Strijckmans, D. Depla.

Ghent University, Research group DRAFT - Ghent (Belgium).

During sputter deposition sputtered atoms can return to the target due to gas scattering, a process entitled redeposition. The key parameter defining the level of redeposition is the working gas pressure. Monte Carlo simulations (SIMTRA [1]) of the sputtering of aluminium in argon, show that at a pressure of 0.4 Pa approximately 4% of the sputtered atoms return to the target. This value increases up to 45% at 5 Pa. Hence, the importance of redeposition can not be neglected during reactive sputtering.
This was previously demonstrated when aiming to model the sputter process of a rotating cylindrical magnetron[2]. In that case, the redeposited material at a given position on the target will rotate into the race track, and will in this way influence directly the poisoning behaviour.
For a planar target, a continuous growth of a layer due to redeposition is expected outside the race track. The inhomogeneous target erosion results in a different level of redeposition over the race track. This complex interplay between sputtering and layer growth will affect the hysteresis behaviour in a non-straightforward manner, which can only be accessed by modelling.
The need for this kind of work is motivated by the industrial relevance of arcing. Indeed, a study by Segers et al. [3] showed that arcing is related to the formation of a porous, non-stoichiometric oxide layer at racetrack rim. Further, this study showed that i) arcing seems to happen only in the narrow transition zone between racetrack and the stable oxide outside the racetrack, ii) for a given set of process parameters the onset of arcing occurs after a fixed time. In our study it will be shown that the time to reach a given number of arcs depends inversely on the argon pressure. According to Segers et al. arcing starts when the layer reaches a given thickness. This seems to confirm the experimental trends. However, the model is lacking from a detailed description of the target condition during reactive sputtering.
In this work, we investigate the effect of redeposition for a planar circular magnetron with a new implementation of the original RSD model in the RSD2012 tool. RSD2012 enables the user to simulate the hysteresis behaviour of a reactive sputtering system.

A graphical user interface (GUI) easily enables to switch on or off the inclusion of redeposition in the model. It also allows us to simulate the time dependency of the compound formation on substrate and target, in a spatial resolved way. This latter option will be used in this work. In particular we are interested in the in-depth oxide formation of an aluminium target sputtering in an Ar/O2 atmosphere. This can give us an idea about the higher observed arcing levels when the process pressure is increased. Combining this model with the work of Segers et al. results in a more complete description of arcing.

ABSTRACT SUBMITTED TO RSD2013

[1] Van Aeken, K.; Mahieu, S.; Depla, D., JOURNAL OF PHYSICS D-APPLIED PHYSICS 41 (2008) 205307
[2] Depla D Li XY Mahieu, S Van Aeken, K, Leroy WP, Haemers J, De Gryse R, Bogaerts A, Journal of Applied Physics, 107 (2010) 113307
[3] Segers A., Depla D, Eufinger K, Haemers J, De Gryse R, SVC 45th Annual Technical Conference Proceedings (2002), 30-35

TF-P2-17
Preparation of hard nc-TiC/a-C:H coatings using hybrid PVD-PECVD process with rotating cylindrical magnetron

T14 Thin Films

#TF-P2-17

P. Vasina [1], R. Zemlicka [1], V. Bursikova [1], P. Soucek [1], P. Vogl [2], M. Jilek [3].

[1]Masaryk University - Brno (Czech republic), [2]Pivot - Sumperk (Czech republic), [3]SHM - Sumperk (Czech republic).

Hybrid PVD-PECVD process of titanium sputtering in a mixture of argon and acetylene combines aspects of both conventional techniques: sputtering of a rotating cylindrical titanium sputtering target (target size: Ø110 x 510 mm) by DC power and deposition from plasma activated acetylene which acts as a source of carbon for polymerization (PECVD). Titanium carbide/carbon nanocomposite hard coatings, which consist of TiC nanocrystallites embedded in amorphous carbon matrix (nc-TiC/a-C:H coating), were deposited on high speed steel and tungsten carbide cermet substrates which were placed on a DC biasable holder performing complex rotation around the Ti cathode. nc-TiC/a-C:H coatings with varying chemical composition prepared at 10 kW DC power (320 °C), 20 kW (450 °C) and 30 kW (450 °C) and bias of -100 V reached maximal hardness of 24 GPa, 37 GPa and 28 GPa respectively. Because it could be expected that the optimal composition of the coating leading to maximal hardness should be reached independently on the applied power a process study was performed. Ti/Ar line intensity and discharge voltage showed sudden drop at the conditions where the maximal hardness was reached. EDX analyses show also sudden drop in Ti atomic concentration at this moment. The maximal hardness of a coating was reached always at conditions preceding the sudden drop which could be used for setting optimal deposition parameters to produce hard, well adherent and thick enough TiC/C coatings with low internal stress using industrially attractive concept of rotating cylindrical magnetron. We acknowledge GACR project 205/12/0407 and CZ.1.05/2.1.00/03.0086 project.

TF-6-Or-13
Structural characterization and evidence of ferroelectricity in metastable Sm2Ti2O7 thin films grown by Pulsed Laser Deposition

T14 Thin Films

#TF-6-Or-13

S. Saitzek [1], A. Bayart [1], M.H. Chambrier [1], A. Ferri [1], M. Huvé [2], P. Roussel [2], R. Desfeux [1].

[1]Univ Lille Nord de France, F-59000 Lille, France ; CNRS UMR 8181, Unité de Catalyse et de Chimie du Solide – UCCS ; UArtois, F-62300 Lens - Lens (France), [2]Univ Lille Nord de France, F-59000 Lille, France ; CNRS UMR 8181, Unité de Catalyse et de Chimie du Solide – UCCS ; ENSCL, F-59652 Villeneuve d'Ascq, France - Villeneuve D'Ascq (France).

Lanthanide dititanate family, Ln2Ti2O7, adopts two types of structure and the stability depends of the ratio between the cations radii Ln3+ and Ti4+. For r(Ln3+)/r(Ti4+) included in the range {1.46-1.78}, the formed compound will privilege a pyrochlore-like structure (cubic) for Ln = Sm to Lu [1]. For ratio higher than 1.78, the layered perovskite type is preferred (monoclinic) for Ln = La to Nd [1]. In recent years, pyrochlore structure compounds have attracted considerable interest due to many potential applications. Indeed, they are used as photocatalyst for the water splitting, they possess a great ability for the realization of immobilization matrices of highly active radionuclides from nuclear wastes and they show photo-luminescent properties when doped with rare earth ions. The layered perovskite structure compounds are known for their ferroelectric [2] and piezoelectric [3] properties mainly used for the elaboration of high temperature devices. In this work, we show it is possible to extend the range of the layered perovskite structure for smaller Ln3+ ionic radii (i.e. Sm, Eu, Gd, ...) through epitaxial strains induced by the substrate in the film. We especially focus on the Sm2Ti2O7 (SmTO) compound. The growth of thin films is achieved by Pulsed Laser Deposition (PLD) on SrTiO3 (STO) and LaAlO3 (LAO) substrates. We present the microstructural characteristics of the films performed by High Resolution X-ray Diffraction on both (100)- and (110)- oriented substrates. Studies performed on (110)-oriented STO or LAO substrates, reveal the

films are (001)-oriented, while considering the (100)-oriented STO or LAO substrates, the films are (012)-oriented, such (012) planes being slightly disoriented with respect to the plane of the substrate. Such crystalline orientations have already been observed and described for La2Ti2O7 thin films in a previous work [4]. Finally, the ferroelectric property, in this metastable Sm2Ti2O7 thin film, is evidenced through measurements performed at the nanoscale level by Piezoresponse Force Microscopy (PFM) [5].

[1] M. A. Subramanian, G. Aravamundan, G. V. Subba Rao, Prog. Solid. State Chem. 15 (1983) 55.
[2] W. S. Kim, S. M. Ha, S. Yun, H. H. Park, Thin Solid Films 420 (2002) 575.
[3] A. Sayir, S.C. Farmer, F. Dynys, Ceramic transactions 179 (2006) 57.
[4] Z. Shao , S. Saitzek , P. Roussel , A. Ferri , O. Mentré and R. Desfeux, CrystEngComm, 14 (20) (2012) 6524.
[5] Z. Shao, S. Saitzek, A. Ferri, M. Rguiti, L. Dupont, P. Roussel and R. Desfeux, J. Mater. Chem., 22 (19) (2012) 9806.

TF-6-Or-9
Atomic interface order in thin LaAlO3/SrTiO3 films

T14 Thin Films

#TF-6-Or-9

X. Torrelles [1], M. Salluzzo [2], S. Gariglio [3], Z. Ristic [4], G. Ghiringhelli [5], J. Drnec [6], M. Moretti [6], R. Felici [6], N. Brookes [6].

[1]Intitut de Ciència de Materials de Barcelona, ICMAB-CSIC - Barcelone (Spain), [2]CNR-SPIN and Department of Physics - Napoly (Italy), [3]Département de Physique de la Matière Condensée, University of Geneva - Geneve (Switzerland), [4]Vinca Institute of Nuclear Sciences - Belgrade (Serbia), [5]CNR-SPIN and Department of Physics Politecnico di Milano - Milano (Italy), [6]ESRF - Grenoble (France).

The physics of transition metal oxide heterostructures is a subject of great interest due to the observations of new interface electronic and magnetic states [1]. The two-dimensional electron gas (2DEG) discovered at the interface between insulating LaAlO3 (LAO) thin films and bulk SrTiO3 (STO) crystals stands as a model and has boosted the great expectations placed in oxide electronics [2,3]. Recently, it has been found that also (001) clean SrTiO3 surfaces [4-6] exhibit two-dimensional electronic states, independent of the bulk doping. From these studies it emerges that, despite possible different doping mechanism, a similar band splitting characterizes the electronic properties of vacuum/STO and LAO/STO [7] interfaces.
As matter of fact, while electron doping is believed to occur by creation of oxygen vacancies in STO surfaces, in LAO/STO interfaces the primary origin of the charge carriers is attributed to an electrostatic instability of the system. In particular, a scenario of electronic reconstruction has been proposed [8] where a Zener breakdown takes place above a LAO thickness of 3 unit cells (uc), as experimentally observed [9]. According to this picture, once the electron transfer occurs, carriers spontaneously occupy bands composed by Ti-3d orbitals, starting with dxy-symmetry bands located within the first adjacent SrTiO3 layers [10]. DFT calculation on LAO/STO bilayers [11] agrees with a distribution of electrons accumulated within the first STO layers that gives rise to an electric field, which in turn induces a rumpling of the SrO and TiO2 interface atomic planes within the same region hosting the 2DEG. Thus, a polar instability scenario predicts for LAO/STO heterostructures structural and electronic modifications of the first SrTiO3 unit cells occurring simultaneously

with the appearance of a 2D-metal. However, not all the experimental results are fully consistent with this picture [12,13]. To clarify these issues, structural synchrotron measurements were performed to study the evolution of the ionic positions at LAO/STO interfaces as a function of the LAO thickness.

[1] P. Zubko, et al, Ann. Rev. Cond Matt 2011, 2, 141
[2] A. Ohtomo & H.Y. Hwang, Nature 2006, 427, 423
[3] J. Mannhart & D.G.Schlom, Science 2010, 327, 1607
[4] A. F. Santander-Syro et al., Nature 2011, 469, 189
[5] W. Meevasana et al, Nature Mater. 2011, 10, 115
[6] R. Di Capua et al., Phys. Rev. B 2012, 86, 155425
[7] M. Salluzzo, et al., Phys. Rev. Lett. 2009, 102, 166804
[8] N. Nakagawa et al., Nature Mater. 2006, 5, 204
[9] S. Thiel S. et al., Science 2006, 313, 1942
[10] P. Delugas et al., Phys. Rev. Lett., 2011, 106, 166807
[11] S. A. Pauli et al., Phys. Rev. Lett. 2011, 106, 036101
[12] A. Savoia et al., Phys. Rev. B 2009, 80, 075110
[13] R. Yamamoto, et al. Phys. Rev. Lett. 2011, 107, 036104

TF-6-Or-8
Single molecule chemistry on an ultrathin MgO film

T14 Thin Films

#TF-6-Or-8

Y. Kim [1], J. Jung [1], H.J. Shin [2], M. Kawai [3].

[1]RIKEN - Wako (Japan), [2]UNIST - Ulsan (Korea, republic of), [3]Tokyo University - Kashiwwa (Japan).

Ultrathin oxide films grown on metal substrate are of great interest not only as supporting materials for chemically active nanoparticles but also as catalysts in the field of heterogeneous catalysis, because they provide an additional dimension, i.e., film thickness, to control the catalytic properties [1]. Using scanning tunneling microscopy (STM) and density functional theory (DFT) calculations, we have demonstrated that the chemical reactivity for water dissociation on an ultrathin MgO film grown on Ag(100) substrate depends greatly on film thickness and is enhanced as compared to that achieved with their bulk counterpart [2]. The artificial manipulation of the local structure at the oxide-metal interface is expected to play a pivotal role in controlling the catalytic activity of oxide film [3]. In this presentation, we show that the chemical reactivity of MgO/Ag(100) for the dissociation of individual water molecules can be systematically controlled by interface dopants over the film thickness [4]. We introduced the 3d transition metal dopants (Sc ~ Zn) into the oxide-metal interface due to the high tunability with a number of d electrons. DFT calculations revealed that the adhesion at the oxide-metal interface can be addressed by the interaction between a dopant and the oxide layer with aid of ligand field theory and is linearly correlated with the chemical reactivity of the oxide film. Controlling the chemical reactivity via the manipulation of oxide-metal interface can be therefore considered the remote tuning of surface property like ‘Marionette’. In addition, our results indicate that the concentration of dopant at the interface can be controlled by tuning the “drawing effect”of oxide film (see figure). Our study provides not only profound insight into the chemical reactivity control of ultrathin oxide film supported by metal substrate but also an impetus for investigating ultrathin oxide films for a wider range of applications.
In addition, a recent result of coupling between molecular vibration and surface phonon in the CO hopping process on MgO/Ag(100) with tunneling electrons will also be introduced [5].

[1] N. Nilius, Surf. Sci. Rep. 64, 595 (2009); H.-J. Freund, Chem. Eur. J. 16, 9384 (2010).
[2] H.-J. Shin, J. Jung, K. Motobayashi, S. Yanagisawa, Y. Morikawa, Y. Kim, and M.Kawai, Nature Mater. 9, 442 (2010); J. Jung, H.-J. Shin, Y. Kim, and M. Kawai, Phys. Rev. B 82, 085413 (2010).
[3] J. Jung, H.-J. Shin, Y. Kim, and M. Kawai, J. Am. Chem. Soc. 133, 6142 (2011).
[4] J. Jung, H.-J. Shin, Y. Kim, and M. Kawai, J. Am. Chem. Soc. 134, 10554 (2012).
[5] H.-J. Shin, J. Jung, M. Kawai, and Y. Kim, submitted

Systematic impurity doping into oxide-metal interface

SE/PST/TF/BI-P1-08
The influence of the bias voltage on the corrosion behavior in artificial saliva of the TiSiON coatings

T14 Thin Films

#SE/PST/TF/BI-P1-08

C. Vitelaru [1], M. Balaceanu [1], A. Vladescu [1], T. Petreus [2], V. Braic [1].

[1]National Institute for Optoelectronics - Bucharest (Romania), [2]University of Medicine and Pharmacy "Gr. T. Popa" - Iasi (Romania).

The low cost fabrication process, combined with good corrosion resistance, make the NiCr alloy one of the most used alloy type for dental applications. In order to reduce the release of Ni and Cr ions in human body, which produce discoloration of soft tissues and allergic reactions, we investigated the role of TiSiON coating on the improvement of corrosion behaviour of this alloy. TiSiON coating was chosen because the oxynitrides are known to possess good biocompatibility and superior corrosion resistance [1, 2].
In this paper, the influence of the bias voltage (ranging from -50 to -200 V) on the corrosion resistance of the TiSiON coatings deposited on NiCr alloy in artificial saliva solution, intended for use in dental applications, was analyzed.The coatings, deposited by cathodic arc method, were characterized in terms of elemental composition (AES), chemical bonds (XPS), crystalline structure and texture (XRD), surface morphology (SEM), and mechanical characteristics. Special attention was devoted to the corrosion tests in artificial saliva (electrochemical tests), quantification of Ni and Cr ion release (atomic absorption spectroscopy), as well as to the investigation of the cell viability.
Coatings with about 4 at.% Si and O/(O+N) ratio of about 0.2 were obtained. The X-ray diffraction patterns indicated the formation of crystalline structure for all the coatings, with a (111) preferred orientation. For coatings of about 3 um thick, hardness values of about 28 GPa and critical loads of 56-58 N at adhesion scratch test were measured. As compared to the uncoated NiCr substrate, all the coated samples exhibited superior corrosion behaviour in saliva solution, and a significant diminution (3-5 times) of Ni and Cr release. The best polarization resistance (243 kΩ), lowest porosity (0.19) and highest protective efficiency (99.1%) were found for the TiSiON films deposited at a bias voltage of -100 V, indicating a good corrosion resistance. All coatings were found to possess good biocompatibility, as compared to

NiCr alloy. The TiSiON films deposited at bias voltage of -100 V exhibited the highest cell viability (98.3%), close to the positive control sample (100%), and the most favourable surface for osteosarcoma cell colonization.

Acknowledgements: The work was supported by the project PN-II-PT-PCCA-2011-3.2-1240 (Coat4Dent).

[1] R.W.Y. Poon, J.P.Y. Ho, Xuanyong Liu, C.Y. Chung, P.K.Chu, K.W.K. Yeung, W.W. Lu and K.M.C. Cheung (2005) Thin Solid Films 488: 20-25.
[2] E.Alves, A.Ramos, N.Barradas, F.Vaz, P.Cerqueira, L.Rebouta and U.Kreissig (2004) Surf. Coat. Technol. 180–181: 372-76.

Fig. 1. Fluorescence microscope images of the bare and coated NiCr alloy, after 5 days of incubation

TF-P2-18
Amorphous Carbon Coatings: Temperature Effect on Secondary Electron Yield (SEY)

T14 Thin Films

#TF-P2-18

A. Silva [1], N. Bundaleski [1], S. Candeias [1], A. Santos [1], P. Pinto [2], M. Taborelli [2], O. Teodoro [1].

[1]Departamento de Física, Faculdade de Ciências e Tecnologia, Universidade Nova de Lisboa - Lisboa (Portugal), [2]CERN - Geneve (Switzerland).

Electron cloud (e-cloud) represents one of the major problems in achieving high quality of the beam in modern particle accelerators [1]. Among several approaches to solve this problem, deposition of low secondary electron yield (SEY) amorphous carbon coatings (a-carbon) onto the inner walls of the accelerator seems to be the most promising solution for suppressing the electron cloud [2]. However, it is known that these coatings change their electron emission properties due to the long-term exposure to air. Carbon coated samples, provided by CERN with initial (as received) SEY of about 0.9, were exposed to different environments and temperatures in order to study the nature and mechanisms of the ageing process.
The a-carbon coatings were deposited on technical stainless steel via magnetron sputtering using Ne as the discharge gas. The samples arrived from CERN Technology Department– Vacuum Surfaces and Coatings group in a UHV container filled with 500 mbar of pure nitrogen.
X-ray Photoelectron Spectroscopy (XPS) has been performed in a multipurpose surface analysis system with a base pressure in the low 10^{-10} mbar range. A homemade apparatus for SEY measurements was mounted to the introduction chamber of the same system providing base pressure in the low 10^{-8} mbar region. Depth profiling of the surface composition has been performed using Time of Flight Secondary Ion Mass Spectroscopy (TOF-SIMS) with a gallium ion gun for the analysis and oxygen ion gun for the sputtering.
Measurements of XPS and sputter depth profiling were systematically carried out in order to follow the changes in the surface composition. SEY measurements are done in parallel with XPS and TOF-SIMS measurements. In our previous work we showed that these samples do not age only in air but also under high vacuum (HV) conditions

[3,4]. The SEY increase can be correlated with the surface concentration of oxygen. In this work, we present and discuss novel and surprising temperature effects on SEY when the samples are annealed in HV and heated in air in a standard furnace. The study of the temperature effects on SEY is done systematically, heating the samples at different temperatures and during different periods.
The results show that heating the samples in air at 100-200 °C reduces the ageing rate and even recovers previously degraded samples. The depth profile results suggest that heating the sample leads to a reduction of the hydrogen content in the coatings. The role played by hydrogen in SEY will be discussed.

ACKNOWLEDGMENTS
Work supported by Fundação para a Ciência e Tecnologia do Ministério da Ciência, Tecnologia e Ensino Superior (FCT/MCTES), through the project CERN/FP/109313/2009. We also acknowledge funding from the Portuguese research grant PEst-OE/FIS/UI0068/2011 (FCT-MEC). We thank Dr. A. Tolstoguzov from Universidade Nova de Lisboa for performing the TOF-SIMS measurements.

[1] J. M. Jimenez et al., “Electron Cloud Studies and Analyses at SPS for LHC-type Beams,” Proceedings of PAC2003 (2007) 307

[2] C. Y. Vallgren et al., Phys. Rev. Spec. Top. Acc. and Beams. 14 (2011) 071001

[3] A. Santos, N. Bundaleski, B.J. Shaw, A.G. Silva, O.M.N.D. Teodoro, Vacuum, submitted.

[4] N. Bundaleski, S. Candeias, A. Santos, O.M.N.D. Teodoro and A.G. Silva, E-Cloud’12 Proceedings, submitted.

PST/SE/TF-2-Or-2
Synthesis of platinum nanoparticles by HiPIMS for fuel cell electrodes

T14 Thin Films

#PST/SE/TF-2-Or-2

S. Cuynet [1], A. Caillard [1], T. Lecas [1], P. Brault [1], J. Bigarré [2], P. Buvat [2], S. Baranton [3], C. Coutanceau [3].

[1]Groupe de Recherches sur l'Energétique des Milieux Ionisés (GREMI) CNRS UMR7344, Université d'Orléans, BP6744, 14 rue d'Issoudun, 45067 - Orléans (France), [2]CEA Centre le Ripault,BP 16, 37 260 - Monts (France), [3]Institut de Chimie des Milieux et Matériaux de Poitier (IC2MP), CNRS UMR7285 Université de Poitier, 86022 - Poitier (France).

Well defined platinum nanoclusters are produced on microporous carbon substrates by conventional Magnetron Sputtering (MS) and High Power Impulse Magnetron Sputtering (HiPIMS) for PEMFC (Proton exchange membrane fuel cell). Magnetron sputtering has already applied to the synthesis of catalyst for fuel cell and gave very good results. Most of Pt atoms are localized in the first 100 nm depth of the porous material (electrode-membrane interface). In the best conditions, MS allows a Pt utilization of 20 kW g_{Pt}^{-1} and a power density of 0.7 W cm^{-2}.

The transport of Pt atoms inside the microporous carbon has been investigated using Rutherford Backscattering Spectroscopy as function of the deposition parameters and as a function of the deposition technique: MS/HiPIMS. The influence of the electrical characteristics of the HiPIMS power source on the deposition parameters is investigated. Different coated microporous carbon substrates are tested for the oxygen reduction in a proton exchange membrane fuel cell station and compared with each other.

TF-P2-10
A comparison of Dielectric properties of TlSbS2, TlSbSe2 and TlSbTe2 Thin Films

T14 Thin Films

#TF-P2-10

K. Ulutas, D. Deger, S. Yakut, M. Parto, H. Kara.

Istanbul University, Science Faculty, Physics Department - Istanbul (Turkey).

A comparison of structures and dielectric properties of $TlSbS_2$, $TlSbSe_2$ and $TlSbTe_2$ thin films deposited in different thicknesses (400-4000 Ao) by thermal evaporation of their crystals grown by Stockbarger-Bridgman technique are presented.

The dielectric constant ε_1 and dielectric loss ε_2 of them have been calculated by measuring capacitance and dielectric loss factor in the frequency range 20 Hz - 10 KHz and in the temperature range 273-433K.

Both of ε_1 and ε_2 of the samples decrease with frequency, but increase with temperature. These behaviors were interpreted depending on polarization mechanisms in the structure. It was observed that the frequency and temperature dependent behaviors of dielectric constant in $TlSbTe_2$ samples were similar with $TlSbSe_2$ and $TlSbS_2$ samples. But, it was shown that the dielectric constant of $TlSbTe_2$ samples increased because of addition of Te, which has upper atomic number.

The temperature variation of ac conductivity of the three sample can be reasonably interpreted in terms of the correlated barrier hopping model since it obeys the ω^s law with a temperature dependent s (s<1) and going down as the temperature is increased.

X-ray analysis showed that the structure of thin films are amorphous.

TF-P2-11
Dielectric Properties of TlSbTe2 thin films

T14 Thin Films

#TF-P2-11

D. Ulutas, K. Ulutas, S. Yakut, H. Kara.

Istanbul University, Science Faculty, Physics Department , Vezneciler - Istanbul (Turkey).

Thin films of the TlSbTe2 on the glass substrates were prepared by thermal evaporation of TlSbTe2 crystals grown by Stockbarger - Bridgman technique. Film thickness is 180- 3300 A. The dielectric properties of the prepared films have been studied in the temperature range 173- 373 K and in the frequency range 20 Hz – 400 KHz. The sturucture of the bulk TlSbTe2 were examined using X-ray diffraction. It was determined that at 1kHz frequency and 293K temperature dielectric constant of TlSbTe2 thin film samples $\varepsilon 1$ changes between 39-740 and dielectric loss $\varepsilon 2$ changes between 51-12000 depending on film thickness. The dielectric constant ε1 and dielectric loss ε2 were found to decrease with increasing frequency and to increase with increasing temperature

TF-7-Or-7
Sputter deposition of AlN and AlScN piezoelectric films for energy harvesting and ultrasonic applications

T14 Thin Films

#TF-7-Or-7

H. Bartzsch [1], S. Barth [2], D. Glöß [1], P. Frach [1], T. Herzog [3], G. Suchaneck [2], J. Juuti [4].

[1]Fraunhofer FEP - Dresden (Germany), [2]Technical University, Institute Solid-State Electronics - Dresden (Germany), [3]Fraunhofer IZFP - Dresden (Germany), [4]University of Oulu - Oulu (Finland).

The paper will report on the deposition and characterization of piezoelectric AlN and AlScN films. Deposition was performed by reactive pulse magnetron sputtering of a metal target in a gas mixture of Argon and Nitrogen. In the case of AlN deposition pure Al targets were used. AlScN was deposited by reactive co-sputtering of Al und Sc targets. Using suitable powering and reactive gas control a deposition rate of up to 200nm/min was achieved by stationary coating on 8" substrates. This very high deposition rate allowed the deposition even of very thick films with up to 50µm thickness.
Films were characterized regarding piezoelectric coefficient, mechanical stress, structure and morphology. Piezoelectric coefficient d_{33} of AlN films was up to 9pC/N on silicon substrates. By scandium doping of the film, d_{33} could be raised up to 29pC/N. Mechanical stress of AlN ranges from -2GPa to +0,5GPa and strongly depends on film thickness, deposition pressure and pulse mode. Precise adaptation of film stress was required to achieve very thick films without film delamination. Potential applications of the films are in ultrasonic microscopy, energy harvesting and SAW/ BAW filters. A pulse echo method was used for characterization in ultrasonic applications. For characterization in energy harvesting, AlN films with electrodes on Si stripes were investigated in bending vibration. In resonance an energy density of 20mW/g•cm^{-3} and a generated power of 270µW were measured. Characterization of AlScN films with respect to energy harvesting will be performed in the near future.

Figure 1: Piezoelectric coefficient d_{33} of AlScN films in dependency on Sc content

TF-4-Or-4
The influence of thermal treatment on the structural and optical properties of amorphous-nano-crystalline thin Si films

T14 Thin Films

#TF-4-Or-4

S. Bernstorff [1], D. Gracin [2], K. Juraić [2], A. Gajović [2], S. Meljanac [2], P. Dubček [2], A. Drašner [2], M. Čeh [3].

[1]Elettra-Sincrotrone Trieste - Basovizza / Trieste (Italy), [2]Ruđer Bošković Institute - Zagreb (Croatia), [3]Jožef Stefan Institute - Ljubljana (Slovenia).

Hydrogenated amorphous-nano-crystalline Si, a-nc-Si:H, is a promising material for high efficiency solar cells. Due to industrial relevance, it is particularly interesting to produce it using standard plasma enhanced chemical vapor deposition (PECVD). In order to test the stability of this kind of material and examine the possibilities of post-deposition treatment, the as deposited samples were exposed to isochronal thermal annealing with a duration of 1 hour at 200, 300 and 400 °C.
The a-nc-Si:H films were deposited by the PECVD method, using a radio frequency discharge in a gas mixture of silane and hydrogen. The hydrogen to silane partial pressure ratio was 20. The structure of as deposited and treated films was studied by high-resolution electron microscopy (HRTEM), Grazing Incidence Small Angle X-ray Scattering (GISAXS), Grazing Incidence Wide Angle X-ray Scattering (GIWAXS) and Raman spectroscopy.
HRTEM micrographs showed that the initial films contained isolated nano-sized ordered domains, nano-crystals, with log-normal size distribution and average size between 5 and 8 nm. The Raman crystal fraction was between 20 and 40%, depending on the preparation parameters. The Raman spectra of as deposited a-nc-Si:H samples showed a crystalline TO peak at frequencies lower than the mono-crystalline Si peak. After thermal treatment, this peak shifts further towards lower frequencies. GISAXS pattern showed that the films contained particles with similar sizes as seen by HRTEM. The analysis of the width of the GIWAXS diffraction lines confirmed that crystals are as small as expected from HRTEM and indicated that strain was present in the samples.

After thermal treatment, the critical angle for total external reflection increased gradually indicating an increase of the mass density, and also the width of the diffraction lines increased indicating an increase of strain. The optical properties of the films were calculated from transmittance measurements in the uv-visible part of the spectrum, and from photo-conductivity. The initial optical gaps of the a-nc-Si:H samples were larger than those from amorphous and crystalline Si, possibly due to two effects: one is quantum size effects, and the other is a consequence of more silicon-hydrogen bonds than in a pure amorphous layer. As a consequence of thermal annealing the optical gap decreases and the absorption coefficient changes. The absorption at energies higher than the optical gap decreases while the absorption at lower energies increases.
The observed changes in the optical and structural properties will be discussed as a consequence of hydrogen effusion and redistribution in the film since the hydrogen concentration gradually decreases during annealing from some 12-15 at% for as deposited samples towards 4-5% in samples annealed at 400 °C.

SE/TF-4-Or-3
Surface and interface properties of TiO2 thin films grown on oxidized Fe(100) substrates

T14 Thin Films

#SE/TF-4-Or-3

A. Brambilla, A. Calloni, G. Berti, L. Duò, F. Ciccacci.

Dipartimento di Fisica, Politecnico di Milano - Milano (Italy).

Titanium dioxide (TiO_2) has been the subject of intense studies in recent years, due to its photoelectric and photochemical properties and its high refractive index and dielectric constant. Thanks to such properties, many applications have highlighted the crucial role played by the TiO_2 surface (see Ref. [1] for a comprehensive review). Many of the fundamental properties that are at the basis of the applications are related to surface and interface properties of TiO_2 coupled to other materials, in particular metals. Such studies would substantially benefit from the use of thin oxide films. For instance, the possibility of synthesizing new titanium oxide phases at low coverages has been demonstrated [2,3]. Additionally, the oxide surface can be electrically and magnetically coupled with the substrate, possibly inducing and stabilizing interesting new phenomena.

We report on the growth of thin TiO_2 layers on pre-oxidized Fe(100) substrates by Ti deposition in a reactive O_2 atmosphere. The experimental approach followed for the growth on Fe(001) is based on our results recently obtained for the growth of thin rutile TiO_2 films on Au(100) [4]. In particular, we have shown in such a case that a crystalline and stoichiometric TiO_2(100) oxide could be produced by Ti reactive deposition with the substrate held at 300 °C, while the growth at room temperature (RT) produced a defective oxide. At variance with the TiO_2/Au case, the growth on Fe(100) was rather difficult to control, due to substrate oxidation and Ti-Fe interdiffusion, activated at high temperature.

In this contribution, we discuss experimental results based on X-ray photoemission spectroscopy (XPS), ultraviolet photoemission spectroscopy (UPS) and low energy electron diffraction (LEED). We observed that growing TiO_2 on Fe(100) at 300 °C produced stoichiometric films but was characterized by a significant chemical mixing at the interface, with part of the oxidized Fe layer segregated to the sample surface. On the other hand, the room temperature growth allowed us to greatly reduce the effects of the interface reactions and to avoid the surface segregation, while the TiO_2

layer was featuring the presence of oxygen vacancies. Finally, we have also investigated the possibility of using a gold buffer layer to obtain better quality TiO_2 films on Fe(001), resulting in crystalline rutile films with a reduced number of oxygen vacancies when compared to room temperature grown samples.

[1] U. Diebold, Surf. Sci. Rep. 48 (2003) 53.
[2] Finetti et al., Surf. Sci. 602 (2008) 1101.
[3] Papageorgiou et al., J.Phys. Chem. C 111 (2007) 7704.
[4] Calloni et al., Thin Solid Films 520 (2012) 3922.

TF/SE-P3-03
Crystallization control of hydrogenated amorphous silicon layers grown on Si(100) and Ge(100) through a glow-discharge of SiH4

T14 Thin Films

#TF/SE-P3-03

L. Hong, G.X. Lee, T.H. Le.

Department of Chemical Engineering, National Taiwan University of Science and Technology - Taipei (Taiwan, republic of china).

We have explored the growth behavior of intrinsic amorphous silicon layers (i a-Si:H) on both Si(100) and Ge(100) wafers in a conventional PECVD reactor through a glow-discharge of silane. The onset of crystallization for the i a-Si:H layers grown on both Si(100) and Ge(100) as functions of deposition temperature and deposition rate was explored and compared. The result showed a critical temperature of 150 °C for a-Si:H grown on Si(100) to phase-transform from amorphous to epitaxial. The critical deposition temperature was extended to over 170 °C when a trace of oxygen was added during a-Si:H growth. Then we achieved a very low surface recombination velocity of 5.9 cm/s for a double-sided intrinsic a-SiOx:H coating on an n-type crystalline Si(100) wafer. The growth behavior of a-Si:H layers on Ge(100) was compared.

1. T. Mishima, M. Taguchi, H. Sakata, E. Maruyama, Solar Energy Materials & Solar Cells, 95, 18 (2011).
2. D. Muñoz, A.S. Ozanne, S. Harrison, A. Danel, F. Souche, C. Denis, A. Favier, T. Desrues, S.M. de Nicolás, N. Nguyen, P.E. Hickel, P. Mur, T. Salvetat , H. Moriceau, Y. Le-Tiec, M.S. Kang, K.M. Kim, R. Janin, C. Pesenti, D. Blin, T. Nolan, I. Kashkoush, P. J. Ribeyron, Proceedings of the 35th IEEE Photovoltaic Specialists Conference, 000039 (2010).
3. S. De Wolf, Y. Andrault, L. Barraud, R. Bartlome , D. Bätzner, P. Bôle, G. Choong, B. Demaurex, A. Descoeudres, C. Guérin, N. Holm, M. Kobas, D. Lachenal, B.

Mendes, B. Strahm, M. Tesfai, G. Wahli, F. Wuensch, F. Zicarelli, A. Buechel, C. Ballif, Proceedings of the 10th IEEE International Conference on Solid-State and Integrated Circuit Technology (2010) 1986.

TF-3-Or-7
Roll-to-roll deposition of optical coatings using magnetized mid-frequency powered plasma processes

T14 Thin Films

#TF-3-Or-7

M. Fahland, T. Vogt, R. Bluethner, T. Preussner.

Fraunhofer FEP - Dresden (Germany).

The topic of the contribution is the roll-to roll deposition technology for a full-dielectric solar control film. Such layers can be incorporated into automotive windshields or architectural glazing, thus reducing the energy consumption for air conditioning. Embedded silver layers can be regarded as the state of the art in this application. However, their performance is limited by the absorption of the metal. Additionally, the low sheet resistance can cause problems with mobile devices inside the car. The layer system presented in this contribution consists of nine transparent non-conductive single layers, creating an adapted transmission spectrum by interference effects. The total thickness of the stack is approximately 1.3 µm. Titania and silica were used for the high index material and for the low index material, respectively. Special emphasis will be put on the plasma processes which were used for the deposition of the single layers.
Titania was produced by reactive sputtering. Two independent closed loop control channels for the oxygen inlet ensured a stable and uniform coating over 600 mm deposition width. The intensity of two spectral lines extracted from the emission spectrum of the plasma served as the indicator for the process working point. A maximum deposition rate of 30 nm*m/min with a refractive index of 2.38 (at 500 nm) could be obtained by this method.
Silica was deposited in a hexamethyldisiloxane (HMDSO) atmosphere using a double-magnetron as the plasma source for the precursor activation. One of the main advantages of this method compared to other PECVD technologies is the low process pressure (approximately 1 Pa), making the process compatible with the reactive sputtering of the high index material.
Maintaining the long term stability is the major challenge for the magnetron-based PECVD process. It generally suffers from instabilities due to target poisoning in reactive gas atmospheres. The paper presents an approach to this problem using a dual rotatable magnetron for the plasma activation of the precursor. There will be a

comparison of the process behavior of rotatable magnetrons to their planar counterparts. It is demonstrated that the oxygen affinity of the target material has a major influence on the process parameters. A maximum dynamic deposition rate of more than 200 nm*m/min was achieved. The mechanical properties of the PECVD layers are superior to those obtained by sputtering. The crack onset strain could be shifted from 1% for sputtering to 5% for PECVD, both measured for 500 nm thick SiOx-single layers. The stack obtained by the combined PVD-PECVD approach is compared to a reference sample with identical layer structure, which was made entirely by sputtering. The optical properties achieved by the combined PVD-PECVD are matching almost exactly those of the fully sputtered reference sample. However, the curling caused by the intrinsic stress of the deposited layers is considerably reduced in case of the combined PVD-PECVD approach.

TF-P2-45
PROPERTIES OF FTO FILMS WITH DIFFERENTS CONCENTRATIONS

T14 Thin Films

#TF-P2-45

J. Luna López, M. Meneses Meneses, J. Carrillo López, F. Flores Gracia, J. Martinez Juárez, J.L. Sosa, E. Gomez Barojas, D. Hernández De La Luz.

BUAP - Puebla (Mexico).

PROPERTIES OF FTO FILMS WITH DIFFERENTS CONCENTRATIONS
J. A. Luna López *, M. Meneses Meneses, J. Carrillo López, F.J. Flores Gracia, J. Martínez-Juárez, J. L. Sosa, E. Gómez Barojas and D. Hernández de la Luz
IC-CIDS Benemérita Universidad Autónoma de Puebla, Ed. 103 C o D, Col. San Manuel, C.P. 72570 Puebla, Pue., México.
Transparent conductive oxides (TCO) have become increasingly important in a large variety of applications due to demands as transparent and conductive materials. Applications of these devices include thin-film solar cells, display devices, optoelectronic devices, polymer-inorganic composite solar cells, gas sensors, and frost-resistant surfaces [1-4]. ITO is an n-type semiconductor where indium oxide (In_2O_3) has been doped with tin oxide in order to improve many of the material's properties, including its electrical conductivity [5]. However, ITO experiences a reduction of electrical conductivity when exposed to oxygen at elevated temperatures (> 300 °C). Therefore, FTO, which is much more thermally stable, is often used as an alternative. FTO is an ideal candidate for applications requiring TCO due to its ability to adhere strongly to glass, resistance to physical abrasion, chemical stability, high optical visible transparency, and electrical conductivity. FTO is more thermally stable because it does not depend on oxygen vacancies to provide charge carriers, when exposed to elevated temperatures, FTO does not experience the characteristic decrease in conductivity seen in the ITO system. In this work, Spray pyrolysis automatized technique was used to deposit FTO films on glass corning. This technique allows us to obtain a better control on thin FTO films, with different properties just by varying the concentration of the fluorine. Figure 1 show the XRD diffractograms of the FTO films. Also, photoluminescence spectra and transmittance spectra were obtained. Structural, optical, and electrical properties of FTO films

prepared by spray pyrolysis and an analysis of the composition, transmittance, nanocrystal size, PL emission, carrier's concentration and conductivity are presented.

[1] T. Fukano, T. Motohiro, Sol. Energ. Mater. Sol. Cells 82, 567 (2004)

[2] N.R. Lynam, in Proceedings of the Symposium on Electrochromic Materials, vol. 90–92, ed. by M.K. Carpenter, D.A. Corrigan. (1990), p. 201
[3] Q. Qiao, J. Beck, R. Lumpkin, J. Pretko, J.T. Mcleskey Jr., Sol. Energ. Mater. Sol. Cells 90, 1034 (2006).
[4] A.N. Banerjee, S. Kundoo, P. Saha, K.K. Chattopadhyay, J. Sol-Gel Sci. Technol. 28, 105 (2003).
[5] H. Fujiwara, S. Otsuka-Yao-Matsuo, N. Ono, Appl. Phys. A 71, 609 (2000).

Figure 1: XRD diffractograms of the FTO films.

TF-P3-13
Adapted tools for accurate deposition of complex optical coatings in an inline sputter-system: computational manufacturing and optical broadband monitoring system

T14 Thin Films

#TF-P3-13

C. Franke, M. Schürmann, S. Wilbrandt, O. Stenzel, N. Kaiser.

Fraunhofer-Institute for Applied Optics and Precision Engineering IOF - Jena (Germany).

The manufacture of complex dielectric optical coatings on curved (e.g. aspheric) substrates requires a high degree of reproducibility and precision of both layer thicknesses and optical constants. Moreover, predicting the suitability of a deposition system with respect to manufacture of different designs that fulfill a given specification on curved substrates requires a reliable knowledge of distribution and variations of physical thickness and optical constants.
It has been proven earlier, that computational manufacturing is a powerful tool to predict the reproducibility of the coating performance as well as the corresponding production yield [1]. To determine the reproducibility in layer thickness and optical constants relevant for the applied coating system, a series of subsequent single layer depositions runs may be used [2]. During the simulation of the production process of complex optical layer systems the impact of different monitoring strategies (termination by optical broadband monitoring or by time) to the yield can be investigated, as well as the dependence of the yield on coating design and specification.

In the present work the approach for computational manufacturing simulations is extended to application in a large inline sputtering system. Numerous series of single layer reproducibility runs have been accumulated to generate relevant input data on optical constants and film thickness for subsequent use in the simulations. As a result

of the simulations it has been shown, that the application of an optical-broadband monitoring can significantly increase the production yield of the system.
In this contribution first results of the outlined computational manufacturing simulations will be presented. Further, a short overview of the current state of adapting and implementing the optical broadband monitoring system OptiMon [3] into the inline sputtering system will be given. Thereby, advantages and disadvantages of different measurement set-ups based on in situ reflectivity- or transmission measurements have been evaluated, and different concepts to integrate optical components of the existing approach (e.g. detector, light source) are compared. Additionally, computational manufacturing simulations have been used to compare different optical monitoring strategies with respect to spectra acquisition and evaluation.

[1] A.V. Tikhonravov; M.K. Trubetskov, “Computational manufacturing as a bridge between design and production”, Appl. Optics 44(32), 6877 (2005).
[2] K. Friedrich; S. Wilbrandt; O. Stenzel; N. Kaiser; K. H. Hoffmann, “Computational manufacturing of optical interference coatings: method, simulation results, and comparison with experiment”, Appl. Optics 49(16), 3150 (2010).
[3] S. Wilbrandt; O.Stenzel; N. Kaiser, “All-optical in-situ analysis of PIAD deposition processes”, Proc. SPIE 7101, 71010D (2008).

PST/SE/TF-P1-10
a-SICN:H MICROWAVE PACVD THIN FILMS FOR SOLAR ENERGY: CORRELATION BETWEEN PLASMA ANALYSIS AND FILMS PROPERTIES

T14 Thin Films

#PST/SE/TF-P1-10

B. Isabelle [1], I. Bousquet [2], A. Soum-Glaude [3], S. Quoizola [1], S. Quoizola [2], E. Hernandez [1], E. Hernandez [2], L. Thomas [1], L. Thomas [2].

[1]Laboratoire PROcédés Matériaux et Energie Solaire (PROMES-CNRS), Tecnosud, F - 66100 Perpignan (France), [2]Université de Perpignan Via Domitia, 52 av. Paul Alduy, F - 66100 Perpignan (France), [3]Laboratoire PROcédés Matériaux et Energie Solaire (PROMES-CNRS), 7 rue du Four Solaire - 66120 Font-Romeu Odeillo (France).

Thin films based on oxides, nitrides or carbides (a-SiC:H), for optics, dielectric properties (SiO, a-SiCO:H) and passivation (a-SiN:H), are used in microelectronics, opto-electronic sensors, therrmechanical applications, photovoltaïcs (PV), and are evaluated as candidates for selective coatings in high temperature solar receivers. From SiN:H to SiC:H, SiCN:H materials can satisfy a large part of those applications. Such deposits are classically grown using low (LF) or radio-frequency (RF) plasma PACVD, and SiH_4/Hydrocarbons/Nitrogen based gases (N_2/NH_3) common mixtures. Our work aims at studying the interest of growing such SiCN:H materials by use of VHF plasmas coupled with liquid organosilicon precursors (tetramethylsilane TMS) to replace dangerous industrial gases such as SiH_4/NH_3 mixtures. The advantage is to possibly manage Si-C, C-C, and Si-N bonding as well as hydrogen content, and attain high growth rates (R_g >1 nm/s) interesting for industry. A PACVD reactor, where the plasma is sustained by microwave applicators (2,45 GHz: Boreal Plasma), is used to grow thin films, that can be DC biased, at a total pressure of 0.15 Torr (250°C < $T_{substrate}$ < 480°C). Studies are focused on the influence of TMS/NH_3 partial pressures ratio ($R_{TMS/NH3}$) and applied DC surface bias, on plasma characteristics, SiCN:H films composition and optical properties. Complex refractive index (n, k) of SiCN:H layers were measured by spectroscopic ellipsometry in the 430-850 nm range. SiCN:H thin films were evaluated as i)

antireflective silicon-PV layers (low n and k) using low TMS/NH_3 ratios (nitride-like films family) and ii) as matrix materials for absorber layers in selective coatings (high n and k) for solar receivers using high precursor ratios (carbide-like layers). FTIR analysis brings out that in SiCN:H materials, 800-900 cm^{-1} FTIR band is complex. It appears that high NHx and SiN contributions occur at low $R_{TMS/NH3}$ (< 0.22), as on the contrary Si-C-C and Si-C bonds are of major prominence (in addition NH_x groups are limited) when $R_{TMS/NH3}$ is increased (> 0.45). DC bias application leads to hydrogenation for nitride-like materials as crosslinking (C-C and Si-C bonding) is observed for carbide-like films.
In Ar/NH_3 Langmuir probe analysis reveals electron densities ne close to $10^{10}cm^{-3}$ (lower than ne=$10^{11}cm^{-3}$ found in pure argon), consequence of electron consumption to dissociate NH_3 molecular and produce NH_x^+, NH_x species. Two electron populations occur, according to DC bias and NH_3 content that enhance hot electron density. Deposits bonds evolutions are finally related to plasma OES measurements performed on CH, C_2, SiH, NH, Si, H, H_2 excited carriers close to the growing surface.

PST/SE/TF-P1-11
Experiences on titanium dioxide deposed films promoted by inductively coupled plasma spputtering

T14 Thin Films

#PST/SE/TF-P1-11

R. Pena-Eguiluz [1], R. Valencia-Alvarado [1], A. De La Piedad-Beneitez [2], R. Lopez-Callejas [3], A. Munoz-Castro [1], A. Mercado-Cabrera [1], B. Rodriguez-Mendez [1], J. De La Rosa-Vazquez [4].

[1]ININ - Mexico (Mexico), [2]ITT - Mexico (Mexico), [3]ININ, ITT - Mexico (Mexico), [4]ESIME-IPN - Mexico (Mexico).

Nowadays, titanium dioxide (TiO_2) thin films in the anatase phase are functional because its photocatalytic characteristics, photoinduced hydrophilicity, self-cleaning and antibacterial properties [1-3]. Meanwhile, those of rutile phase are used as biomaterials for implants and prosthesis [4]. In this work is described an effort to deposit titania film in anatase and rutile phases without any additional annealing over two different substrates glass and silicon. The proposed process has been conducted within a Pyrex-like glass cylindrical vessel used as plasma reactor. A copper solenoidal antenna is placed around this vessel occupying a length equivalent to one quarter of the RF wavelength. The plasma is supplied by a calibrated 70% argon-30% oxygen gas mixture and generated by transferring 500W to the antenna through a coupling network from a 13.56MHz RF generator. The vessel was evacuated at pressures lower than 1×10^{-4} mbar by a mechanical pump. Once the base pressure is attained, the working gas mixture was admitted through a precision leak valve up to $4\text{-}5\times10^{-2}$ mbar pressure at which the highest plasma density is reached. A commercially pure titanium cylindrical target was introduced to the vessel and biased up to -2.0kV and 10mA DC. The colisions of argon and oxygen ions from plasma during 5 hours on the target promoted sputtering on material and its consequent oxidation process due to the presence of several oxygen species. The ion bombardment raised the target temperature around 600°C measured with a K-type thermocouple. Whereas substrate temperature was obtained with a K-type thermocouple in the range of 292 and 387°C in function on the supplied power to the plasma. Electrically floated silicon or glass substrate was placed on the holder 2cm in front of the target. TiO_2 films developed on the substrates were characterized by

several devices. Raman spectroscopy outcomes denote the presence of anatase obtained from deposited film on glass exposed at ~292°C. And rutile phase growth on glass exposed at 387 °C. Chemical composition of deposed coatings were analyzed using SEM/EDS for both substrates. Resulting outcomes give atomic compositions around 75% oxygen/23% titanium. XPS spectrum of Ti_{2p} shows the Ti2p spliting into $Ti_{2p3/2}$ and $Ti_{2p1/2}$ doublet peaks two peaks situated 458eV and 464eV with a splitting (Δ=5.6eV) which corresponds to Ti(IV) in TiO_2. Deposited thickness film was determined by means of a perfilometer. The film presents a maximum value about 1 μm over a semicircular pattern area located just in front of the target. This semicircular deposition behavior decreases until 200 nm as the measured point approaches the border of the substrate. X-ray diffraction spectrum reveals several peaks corresponding with crystalline anatase phase deposited on silicon substrate.

[1] C.K. Jung, I.S. Bae, Y.H. Song, T.K. Kim, J. Vlcek, J. Musil, J.H. Boo, Surf. Coat. Technol. 200 (2005) 534-538.
[2] T. Tölke, A. Kriltz, A. Rechtenbach, Thin Solid Films 518 (2010) 4242-4246.
[3] K. Hashimoto, H. Irie, A. Fujishima, AAPPS Bulletin, 17 (2007) 12-28.
[4] P.K. Chu, IEEE T Plasma Sci. 35 (2007) 181-187.

TF-P2-19
Tailoring of diamond film morphology and electrical properties by CH4/H2/CO2/N2 gas chemistry in large area MWCVD

T14 Thin Films

#TF-P2-19

M. Vojs [1], M. Mikolášek [1], T. Ižák [2], M. Varga [2], O. Babchenko [2], A. Kromka [2].

[1]Institute of Electronics and Photonics, Faculty of Electrical Engineering and Information Technology, Slovak University of Technology, Ilkovičova 3, 812 19 - Bratislava (Slovakia), [2]Institute of Physics, Academy of Sciences of the Czech Republic, v.v.i., Cukrovarnicka 10, 162 53 - Prague (Czech republic).

Diamond film is promising material for a variety of applications. However, its production by standard deposition techniques makes it not attractive for industrial applications (limited deposition area, high temperature of deposition). Recent trends in the deposition techniques, e.g. surface wave plasma [1], linear antenna plasma [2], make diamond growth possible in large areas (up to 1x1m^2) and at lower temperatures [3]. Moreover, addition of oxygen-containing gases leads to enhanced growth rates and film quality.

Yet it is stated, that diamond growth appears only in defined area of C-H-O ternary diagram [4]. However, in our previous study we have shown that diamond growth is possible also out of that area for diamond films deposited in linear antenna plasma [5].

The actual work is a complementary study of our previous results completed by addition of N_2 into $CH_4/H_2/CO_2$ gas chemistry. This unique four-compartment gas system allows controlling of diamond morphology from micro- to nanocrystalline, ballast-like or porous-like character over large areas suitable for destined application. Detailed study was carried out by variation of gas mixture components CH_4, CO_2 and N_2 in hydrogen. The surface morphology of samples was studied by Scanning Electron Microscopy, the character of the films was investigated by Raman Spectroscopy, and growth rates were evaluated by optical methods.

It was found that at the higher oxygen content and no nitrogen in the mixture a

“blockstone-like” structures were formed, while increased N_2 content leads to a “porous-like“ and/or nanowires diamond structures (Fig. 1). At lower oxygen content, increased N_2 led to decreasing of growth rate of (ultra)nanocrystalline diamond. In the article the relation between the diamond film morphology and electrical properties will be pointed out, as well as the early stage of the growth process including plasma chemistry and growth kinetics together with extended region of diamond formation in modified Bachmann ternary diagram will be discussed too.

This work was financially supported by the grants of MS SR No. 1/1103/11 and GACR projects P108/12/G108 and P108/11/0794. This work was carried out in frame of the LNSM infrastructure.

[1] J. Kim et al., Plasma Sources Sci. Technol. 19 (2010) 015003

[2] A. Kromka et al., Vacuum 86 (2012) 776 – 779

[3] T. Izak et al., Phys. Stat. Solid. b 249 (2012) 2600 – 2603

[4] P. K. Bachmann et al., Diam. Rel. Mater. 1 (1991) 1–12

[5] S. Potocky et al., Phys. Stat. Solid. b 249 (2012) 2612-2615

Fig. 1 SEM images of diamond films deposited at 5% CH_4, 30% CO_2 and at various concentration of N_2 in hydrogen rich plasma.

TF-9-Or-2
Generic method for elaboration of nanocomposite films

T14 Thin Films

#TF-9-Or-2

H. Kintz, O. Sublemontier, Y. Leconte, N. Herlin-Boime, C. Reynaud.

Service des Photons Atomes et Molécules, Laboratoire Francis Perrin (CEA-CNRS URA 2453), CEA Saclay - Gif-Sur-Yvette (France).

We present a generic method for elaboration of nanocomposite films by combining the supersonic jet technology and magnetron sputtering. This technique offers the possibility to achieve the nanoparticles synthesis, doped or undoped, and the film growth in a single step process and without any limitation in the respective chemical compositions of the particles [1] and the matrix. The general scheme of the process is presented in Fig. 1. A supersonic expansion is generated by a double stage differential pumping system through an expansion nozzle and a skimmer, so that a supersonic gas beam carrying the nanoparticles is created in an intermediate chamber at low pressure (10-5 mbar). As the speed acquired by the nanoparticles is high [2], their kinetic energy is sufficient to pass through a relatively high pressure (5.10-3 mbar) deposition chamber and get deposited on a substrate. The pressure in this chamber is adequate for running a magnetron sputtering device able to deposit the matrix of the composite film simultaneously to the nanoparticles. A rotary motion of the substrate on its axis ensures the film homogeneity. As an example, in this work, doped silicon nanoparticles (n or p) are synthesized for the first time by laser pyrolysis, and then embedded in a silica matrix produced by magnetron sputtering.

[1] N. Herlin-Boime et al. (2004): Encycl. of Nanoscience and Nanotechnology, Naiwa Ed. Vol. 10, pp.1-26.
[2] M. Ehbrecht et al. Rev. Sci. Instrum. 66 (1995), 3833.
[3] G. Conibeer et al., Thin solid films 511-512 (2006), 654.

Fig. 1: One-step Nanocomposite film elaboration

TF-2-Or-4
Selfcleaning and Antireflective Coatings by Sol-Gel Process on Glass Substrate

T14 Thin Films

#TF-2-Or-4

K. Camargo [1], A.F. Michels [2], F.S. Rodembusch [3], F. Horowitz [3].

[1]LPMCN - Lyon (France), [2]UCS - Caxias Do Sul (Brazil), [3]UFRGS - Porto Alegre (Brazil).

The hydrophobicity of a surface is improved from a chemical modification that lowers the surface energy and also by increasing the surface roughness, and this is due a combination of micro and nano-structures at surface. Superhydrophobic surfaces with low of angular hysteresis allow selfcleaning property[1,2.]
In this work, our proposal was obtain the superhydrophobic coating with anti-reflective properties on glass substrate by sol-gel technique. We used to prepare the first layer a thin film with silica nano-particles coated with dymethylsilane, superhydrophobic nano-particles, and after we prepare the second layer a thin film with silica aerogel to improve optical transmittance and finally recovered with a third thin film of polytetrafluoroethylene (PTFE) by PVD (Physical Vapor Deposition).
Interference coating are the way to many optical devices with anti-reflective properties. The anti-reflective coating consists of a single quarter-wave layer of transparent material whose refractive index is the square root of the substrate's refractive index[3]. In theory this gives zero reflectance at the center wavelength and decreased reflectance for wavelengths in a broad band around the center.
A good technique to obtain the anti-reflective coatings is a combination between refractive indexes, where it is interesting obtain the thin film with highly-index coated under a thin film with low-index, this method makes the contrast between refractive index to coatings two-layer.
Super-hydrophobic thin film was made with super-hydrophobic nano-particles that are hydrophobic fumed silica after treated with dimethyldichlorosilane (Aerosil R972 - Degussa).
Results obtained to this sample were 171º to the contact angle and less than 2º to angle hysteresis[4,5], what meaning in a selfcleaning surface. The optical transmittance was around 97% to visible region and 99%[4,5] to near infrared region, in this case we

get an anti-reflective coating by just three layers on a soda-lime glass substrate by sol-gel technique.

[1] T. Y. Wei, T. F. Chang, et al. J. Am. Ceram. Soc., 90, 2003.
[2] X. T. Zhang, O. Sato, et al. Chem. Mater., 17, 696, 2005.
[3] H. A. Macleod, Thin-Film Optical Filters, New York, 2nd. Ed., 1986.
[4] K. C. Camargo, A. F. Michels, F. S. Rodembusch and F. Horowitz, Chem. Commun., 48 (41), 4992, 2012.
[5] K. C. Camargo, et al.Optical Materials Express Vol. 2, Iss. 7, pp. 969–977, 2012.

TF-9-Or-3
Selective formation of silicon film by chemical transport technique using a high-pressure narrow-gap hydrogen plasma

T14 Thin Films

#TF-9-Or-3

H. Ohmi, H. Kakiuchi, K. Yasutake.

Osaka University - Suita, Osaka (Japan).

Selective growth technique of Si film has become important technology for various device fabrications. Generally selective Si film growth has been demonstrated by CVD method which requires toxic, flammable and halogenated gases, such as SiH_4, SiH_2Cl_2, and etc.
Recently, we have developed a Si film formation method by using a chemical transport in high-pressure, including atmospheric-pressure, hydrogen plasma[1]. This method requires no source gases, because the etching reaction of solid Si by atomic hydrogen (H) behaves as an on-site SiH_4 generator. In this method, H acts as an effective etchant for Si in the same manner as halogen species in selective CVD process. Hence, it is expected that selective deposition of Si film can be achieved by this method. In this study, we have investigated the substrate selectivity of Si film formation and demonstrated selective Si growth.
The apparatus was described in other report[2]. The chamber was filled with H_2/He gas mixture to the total pressure of 400 Torr. The hydrogen compositions of gas mixture and substrate temperature were varied as parameter. The plasma was generated by 150 MHz VHF power. The substrates used for studying substrate selectivity were Si and quartz glass. Furthermore, Si with patterned SiO_2 window was used for selective growth.
Fig.1 shows the temporal evolution of R_d on Si and glass substrates. In case of Si substrates, R_d has no dependence on deposition period (t_d). On the other hand, in the case of glass, R_d gradually increases with t_d and saturates after a certain period of t_d. Fig.1 suggests that Si film is preferentially formed on Si rather than on glass in the initial deposition stage. The selective deposition was demonstrated on patterned SiO_2/Si substrates. Fig.2 shows the surface SEM image. From this image, Si film can

be prepared only on SiO_2 window. Moreover, selectively deposited Si film showed epitaxial growth at T_{sub} of 300^{o}C.

[1] H.Ohmi, et al.,J.Appl.Phys. **102**, (2007) 023302.
[2] H. Ohmi, et al., J. Phys. D：Appl. Phys. **41**, (2008)195208.

Fig.1 Temporal variation of R_d
Fig.2 Surface SEM image of selectively deposited Si film.

TF-7-Or-10
Increasing the solar cells efficiency by charge transfer tuning: comparison of Zn-tetra phenyl poprhyrin / ZnO and TiO2 interfaces

T14 Thin Films

#TF-7-Or-10

M. Caputo [1], P. Vilmercati [2], B. Taletau [3], C. Castellarin-Cudia [4], P. Borghetti [5], G. Di Santo [1], M. Panighel [1], C. Cepek [4], A. Verdini [4], A. Cossaro [4], L. Floreano [4], A. Morgante [4], A. Goldoni [1].

[1]ST-INSTM Lab., Sincrotrone Trieste S.C.p.A. - Trieste (Italy), [2]Department of Physics and Astronomy, University of Tennesse - Knoxville (United states), [3]Department of Physics, Obafemi Awolowo University - Ile-Ife (Nigeria), [4]Lab. TASC, IOM-CNR - Trieste (Italy), [5]Donostia International Physics Center (DIPC) - Donostia-San Sebastiàn (Spain).

In the latest years an increasing environmental sensibility leads the research of more sustainable energy resources. Direct sunlight harvesting obtained by dye sensitized solar cell is a promising technology based on organic materials, extremely cheaper with respect to inorganic based technology. The quantum efficiency for these systems is relatively high, but charge ignition from the chromophore to the electrodes is a key issue that still limits the entire process. Using resonant photoelectron spectroscopy we compare the lifetime of the excited states and the ignition dynamic of a single layer of Zn-tetra phenyl porphyrin (Zn-TPP), a commonly used dye, deposited on a nanostructured ZnO substrate and on a TiO_2 (110)-(1x1) reconstructed surface.
Results show a different dynamic for the excited states localized on phenyl groups and on the macrocycle. While the global quenching of the risonances is more effective for Zn-TPP/TiO_2, the unoccupied states localized on the macrocycle show a faster charge transfer time in Zn-TPP/ZnO with respect to Zn-TPP/TiO_2.

O'Regan, B. & Grätzel, M. A low-cost, high-efficiency solar cell based on dye-sensitized colloidal TiO2 films. Nature 353, 737–740 (1991).

Campbell, W. M., Burrell, A. K., Officer, D. & Jolley, K. W. Porphyrins as light harvesters in the dye-sensitised TiO2 solar cell. Coordination Chemistry Reviews 248, 1363–1379 (2004).

Castellarin-Cudia, C. et al. Substrate influence for the Zn-tetraphenyl-porphyrin adsorption geometry and the interface-induced electron transfer. Chemphyschem A European Journal Of Chemical Physics And Physical Chemistry 11, 2248–2255 (2010).

SE/PST/TF/BI-3-Or-6
Semiconductor thin films for water splitting application prepared by pulsed plasma systems

T14 Thin Films

#SE/PST/TF/BI-3-Or-6

Z. Hubicka, M. Čada, Š. Kment, J. Olejníček.

Institute of Physics ASCR - Prague (Czech republic).

WO_3 and Fe_2O_3 semiconductor structures were recently found very promising as a photoanode material for water splitting applications [1-4]. These materials can absorb a relatively significant portion of the available solar light, due to their lower band-gap energies. The photoelectrochemical characteristics of Fe_2O_3 photoanodes are typically found to have a marked dependence upon the anode preparation conditions and the type of dopant incorporated into the host lattice. Nanocrystalline WO_3 thin films on a conducting glass electrode also provides excellent induced photocurrent efficiency (IPCE) for photoelectrochemical water decomposition under visible light. Semiconductor oxide thin films of Fe_2O_3 and doped Fe_2O_3 by Sn were deposited by reactive sputtering in a pulse magnetron and in a pulsed hollow cathode plasma jet sputtering systems without external heating of the substrate. It was possible to prepare by both methods nanocrystalline or polycrystalline semiconductor thin films with structure of hematite Fe_2O_3. Application of different magnitudes of duty cycle was tested in the range 1% - 50%. Quite different preferred orientation of crystallites relative to the substrate surface was observed in dependence on the duty cycle. This texture was apparent at as deposited films and also at thin films annealed after deposition on 600 ^oC. Nanocrystalline WO_3 thin films were deposited by reactive pulsed magnetron sputtering system. Tungsten target was reactively sputtered in $Ar+O_2$ gas mixture. Deposition experiments were done for different concentration of oxygen in the plasma discharge and different magnitudes of duty cycle. Crystalline structure, optical properties and surface roughness of deposited WO_3 thin films was studied for as deposited films and on annealed films as well. Photoconductivity and photoelectrochemical properties were measured on deposited Fe_2O_3 and WO_3 thin films under 1 AM illumination. IPCE was obtained for these samples.

1. C. J. Sartoretti, M. Ulmann, B. D. Alexander, J. Augustynski and A. Weidenkaff, Chem.
Phys. Lett., 2003, 376, 194.
2. C. J. Sartoretti, B. D. Alexander, R. Solarska, I. A. Rutkowska, J. Augustynski and R.
Cerny, J. Phys. Chem. B, 2005, 109, 13685.
3. A. Kay, I. Cesar and M. Graetzel, J. Am. Chem. Soc., 2006, 128,15714.
4. K. Sivula, F. Formal and M. Grätzel, Chem. Mater., 2009, 21 (13), 2862.

SE/PST/TF/BI-3-Or-3
Performance evaluation of a TiO2 thin films for textile wastewater treatment. Catalytic activity, toxicity assay, deactivation, and regeneration

T14 Thin Films

#SE/PST/TF/BI-3-Or-3

A. Pedroza Rodríguez [1], A. Blanco Vargas [2], C. Campos Pinilla [3], A. Florido Cuellar [4], J. Cardona Bedoya [4].

[1]Grupo de Blotecnología Ambiental e Indsutrial. Pontificia Universidad Javeriana - Bogotá (Colombia), [2]Universidad Javeriana - Bogotá (Colombia), [3]Grupo de Biotecnología Ambiental e Industrial. Pontificia UNiversidad Javeriana - Bogotá (Colombia), [4]Universidad del Tolima - Ibagué (Colombia).

In the present work thin films of titanium dioxide were obtained by sedimentation over borosilicate glass at 50 °C and calcination at 450o C for 1 h. The films were characterized by XRD, UV-Vis scanning and SEM. The XRD of the films showed anatase as the only crystallographic phase with planes (101), (004), (200), (105) and (211). The gap value for control film was 3.25 eV. SEM images showed aggregates and different particle size

The photocatalytic activity of the thin films was evaluated using a cubic reactor and textile wastewater. According to results, the photocatalysis with TiO2/UV was significantly better ($p < 0.0001$) than photolysis, obtaining removals of 83%, 35%, 58% and 53% for discoloration, COD, BOD5 and inactivation of microorganisms at 15 hours of treatment. When performing spectral curves it was seen a decrease in the wavelength of maximum absorption (600 nm) with the appearance of peaks in the ultraviolet spectrum that may be associated qualitatively with chemical transformation process mediated by the action of oxidizing species

Regarding to the toxicity tests to evaluate the wastewater treated by the TiO2 thin films, it was noticed an increase in the percentage of mortality for H. attenuata but in the same concentration than the initial 6.25% v/v. In L. sativa the percentage of inhibition was of 12% to 75% v/v therefore the final toxicity was not increased.

Neither in the curves of photolysis (UV) was evidenced an increase in toxicity for H. attenuate. And in the opposite, in L. sativa it was noticed a slight change obtaining inhibitions of 6 and 10% at the concentration of 50% v/v, lower value than the initial one 75% therefore, it decreased the toxicity.

In order to demonstrate that both TiO2 films as the treated effluent could be reused we performed two experiments. The first one was to reuse the TiO2 films for 4 consecutive cycles of 12 hours each, valuing the effect of the thermal reactivation of the semiconductor oxide and without heat reactivation on the discoloration and inactivation of microorganisms. According to the results obtained in the TiO2 films, they can be reused for 24 hours continuous with discoloration of 53% and 50%, without having significant differences between the thermal reactivation or without reactivation. With regard to the inactivation of microorganisms the inactivation in the 4 cycles ranged between 49 and 33%, respect. No significant differences were observed between cycles and reactivation strategies.

With the second experiment it was demonstrated that the effluent treated by photocatalisys could be used for dyeing of cotton fabrics without having significant differences when comparing with potable water and distilled water. The percentage of adsorption to the fabrics was superior to the 80%, proving that in water on dyeing there was only left the 20% of residual coloring, amount which is lower than reported by the literature for dyeing processes on an industrial scale, which is of the 30%.

Puentes I, Florido A, Cardona J, Campos M, Pedroza A. 2012. Simultaneous decolorization and detoxification of Black Reactive 5 using TiO2 a deposited over borosilicate glass by sedimentation technique. Universitas Scientiarum. 17 (1): 53-63.

TF-5-Or-5
Systematic Study on Vanadium Carbide Thermodiffusion on Steels for CVD Diamond Film Deposition

T14 Thin Films

#TF-5-Or-5

N. Lopes [1], R.A. Campos [2], L.M. Iusuti [1], E.J. Corat [2], D.M. Barquete [1].

[1]Universidade Estadual de Santa Cruz - Ilhéus (Brazil), [2]Instituto Nacional de Pesquisas Espaciais - São José Dos Campos (Brazil).

This work presents an alternative for microcrystalline (MCD) and nanocrystalline (NCD) diamond CVD film deposition on steel using a thermochemical modification in substrate surface. The thermochemical treatment consists in the formation of a thermodiffused layer of vanadium carbide (VC) [1] on steel substrates at 1220 K with. For the thermodiffusion process it was used a salt bath of vanadium pentoxide (V_2O_5), boron carbide (B_4C) e sodium borate decahydrate ($Na_2B_4O_7.10H_2O$). CVD of MCD and NCD diamonds films was realized using HFCVD reactor [2] type in different conditions of steel substrate composition, substrate surface roughness, melting salt composition and thermodiffusion temperature. For the best combination of process parameters the deposited diamond films presented a good adherence to the VC interface, despite the high compressive stress measured. The diamond CVD films and the VC interface were characterized by Scanning Electron Microscopy (SEM) associated with Energy Dispersive X-ray (EDX), X-Ray Diffraction (XRD). The adhesion tests were made with Rockwell C (120°) conical indentor and characterized by Optical Profilometry. The quality of the diamond CVD films on thermodiffused VC coating was evaluated by Raman spectroscopy.

[1] BARQUETE, D. M. ; Corat, E. J. ; CAMPOS, R. A. ; Moura Neto, C. ; Trava-Airoldi, V. J. . Thermodiffused vanadium carbide interface for diamond films on steel and cemented carbides substrates. Surface Engineering, v. 26, p. 506-510, 2010.

[2] CAMPOS, R.A. ; CONTIN, A. ; TRAVA-AIROLDI, VLADIMIR J. ; MORO, J.R. ; BARQUETE, D.M. ; CORAT, EVALDO J. . CVD Diamond Films Growth on Silicon

Nitride Inserts (Si3N4) with High Nucleation Density by Functionalization Seeding. Materials Science Forum (Online), v. 727-728, p. 1433-1438, 2012.

SE/TF-1-Or-5
Corrosion behaviour of organosilicon coatings prepared by cold remote plasma assisted chemical vapour deposition process

T14 Thin Films

#SE/TF-1-Or-5

C. Jama.

ENSCL, UMET CNRS 8207, Equipe ISP, - 59650 Villeneuve D'ascq (France).

Plasma enhanced chemical vapour deposition (PECVD) is known nowadays as a key technology applied in a whole range of industries. It enables deposition of thin films of controlled physico-chemical properties using a variety of different organosilicon precursors. Its advantage over chemical processes is besides being a dry process is the wide range of settings and changeable parameters such as the gas flow rates, the gas ratio, the type of plasma used, which enable to accurately control the growing film characteristic. The organosilicon films formed using PECVD are mostly amorphous in nature and usually associated with a high electrical resistivity (10^9-10^{15} Ω cm). In this work, the barrier properties of organosilicon coatings against corrosion were investigated. The films were deposited on carbon steel using remote microwave nitrogen plasma assisted chemical vapour deposition (MW-PECVD). The monomer precursor used was 1,1,3,3, tetramethyldisiloxane (TMDS, purity 97 %), which was premixed with oxygen (purity ≥99.5 %). Corrosion tests were performed by immersing the uncoated and coated carbon steel samples in aerated 3% NaCl at 30 °C. The evolution of the open circuit potential (E_{OCP}) with time provides information about the corrosion activities of a metal interface. The evolution of E_{OCP} curves when uncoated and coated carbon steel substrates were immersed into saline aqueous solution (NaCl 3 %) were recorded. In the case of unprotected steel, a decrease in E_{OCP} is observed after about 40 h of immersion into NaCl 3 %. This is attributed to the dissolution of iron. The behavior was different for the steel coated with organosilicon films. The E_{OCP} was shifted to more positive potential values and no obvious fluctuation of E_{OCP} was observed in the measurement time frame, indicating that these interfaces seem to have an increased corrosion resistance. Potentiodynamic polarization curves of the different interfaces show clearly that the pre-treatment has a strong influence on the corrosion potential. An increase in the

corrosion resistance behaviour of the organosilicon coated carbon steel specimen was found when the carbon steel interface was pre-treated with an argon plasma. The argon plasma pre-treated samples show the noblest corrosion potential together with decreased corrosion current densities, which are sustained after 30 days immersion into 3 % NaCl.

TF-6-Or-7
Modulation of oxygen flow during deposition of titanium and cobalt oxide films by reactive sputtering

T14 Thin Films

#TF-6-Or-7

J. Dias Da Silva [1], A.L.J. Pereira [2], N.F. Azevedo Neto [1], J. Acuna [3], I.S. Brandt [3], A. Pasa [3], A. Beltran [4], P.N. Lisboa Filho [1].

[1]Unesp University - Bauru Sp (Brazil), [2]Univ Politecnica de Valencia - Valencia (Spain), [3]Federal University of Santa Catarina - Florianopolis Sc (Brazil), [4]University Jaume I - Castelon (Spain).

Most thin film deposition methods rely on substrate thermal energy to provide the atomic arrangement, chemical bonding, film structure and morphology. By contrast, in the glow discharge sputtering processes the primary source of energy is generally the kinetic energy of the species provided by the plasma. In this analysis, the consequences of the energy enhancement and modulations of the oxygen gas flow to the properties of titanium and cobalt oxide films (~500 nm) are investigated. Structural, morphological and electronic aspects are focused in association with the deposition parameters and the corresponding ion/atom collision energetics provided by computer simulations. The films have been deposited using RF and DC plasmas of Ar and O_2 and pure metallic (Ti/Co) targets in a planar diode magnetron configuration. The relatively low total pressure used is compatible with mean free paths bigger than the target to substrate distance, favoring the energetic collisions with the growing film surface. Periodic short term interruptions of the O_2 flow aduring depositions are made in order to produce oxygen depleted thin layers inside the films. Electron and atomic force microscopies, X-ray diffraction, and Raman scattering results, show that the produced films present compact columnar morphology and orientation texture characteristic of the energy enhanced depositions. Concerning the TiO_2 films, modulations of the O_2 flow during reactive sputtering produces a systematic increase of the optical absorption, without significant changes in structure, composition and morphology. In special no evidence for the existence of pure Ti layers are found in the characterizations, particularly on high resolution transmission electron microscopy. Density functional theory calculations and optical absorption results evidence the corresponding changes in

the electronic structure which are associated with oxygen vacancy complexes [1,2]. In cobalt oxide nanostructures the effects of the interruptions to the optical and structural properties are much stronger indicating a better definition of the metallic layers (~2-20 nm). The increase in the optical absorption and electrical conductivity resulting from the oxygen depletion in thin layers of the material are potentially useful for the improvement of the magnetic and photocatalytic properties of the titanium and cobalt oxide films.

[1] A.L.J. Pereira et al. Journal of Applied Physics, Vol. 111, 113513 (2012).
[2] A.L.J. Pereira et al. Journal of Physical Chemistry C. Vol. 116, 8753 (2012).

TF-5-Or-2
Ultra-low density carbon foams produced by pulsed laser deposition

T14 Thin Films

#TF-5-Or-2

V. Russo, D. Dellasega, I. Prencipe, A. Zani, M. Passoni.

Dipartimento di Energia and NEMAS - Politecnico di Milano - Milano (Italy).

We report on the manufacturing by Pulsed Laser Deposition (PLD) of ultra-low density carbon foams, characterized by very low density regimes down to 1 mg/cm^3. Ultra-low density materials (foams) show unique properties, assuming great interest both for fundamental material science and for several applications ([1] and Refs. therein). The density of this kind of material, considered as a mean value over a scale larger than the typical microscopic inhomogeneity scale-length, spans in the range 1-100 mg/cm^3. The possibility to produce foams with controlled and reproducible mean density, area and thickness, with a satisfactory adhesion on a solid substrate is of great importance to achieve desired material properties. Carbon represents a suitable choice to obtain mono-elemental foam, being a light element with volatile oxides. The extension of carbon-based materials to the ultra-low density regime represents a challenging and nearly unexplored topic.
Here we produced carbon foams by PLD with unusual combinations of deposition parameters for the growth of porous carbon, i.e. fluence below 1 J/cm^2, Ar and He ambient gases, pressures in the range 0-1000 Pa, 10 Hz repetition-rate [1]. The film properties have been investigated by means of quartz crystal microbalance (QCM), scanning electron microscopy and Raman spectroscopy as a function of pressure for the two different ambient gases. Areal density has been evaluated with two different methods, the first based on QCM measurements, the second with proper interpretation of Energy Dispersion X Ray Spectroscopy data [3]. Combining such areal density values with an estimate of mean thickness by cross-section SEM analysis, we obtained values of mean density in the range 1-1000 mg/cm^3.
SEM images (fig.1) showed that film morphology was due to the aggregation of nanoparticles in larger particles, which then assembled with each other giving rise to a mesoscale getting opener with increasing pressure. Raman analysis indicated that the deposited material corresponded to a nearly pure sp^2 network of topologically disordered graphitic domains with very low sp^3 content and suggested that a similar nanoparticle structure was achieved for almost all the deposition conditions.
Finally films grown using 100 Pa of fluxing Ar represented an optimal condition to

obtain a very low density foam with satisfactorily homogenous morphology on the mesoscale.
Based on these results, this work showed how pulsed laser deposition can be exploited as a versatile tool for the deposition of carbon foams with tunable and tailored density, thickness and uniformity.

[1] A. Zani et al. Carbon (accepted, 2013)
[2] M.D. Bentzon et al. Diamond & Related Materials 2 (1993) 893

Fig1 He (a) 100 Pa (b) 500 Pa

TF-3-Or-8
Controllable growth of binary copper oxides by reactive direct-current magnetron sputtering

T14 Thin Films

#TF-3-Or-8

Y. Wang, D. Pilloud, J.F. Pierson.

Institut Jean Lamour, UMR 7198-CNRS, Université de Lorraine - Nancy (France).

Binary copper oxides (Cu_2O, Cu_4O_3 and CuO) are the spontaneous p-type semiconductors and have attracted much attention due to the great potential applications in thin film solar cells, transparent thin film transistors, photodiodes, and photocatalyst for solar-driven water splitting. In our work, these three kinds of oxides have been deposited on glass substrates at room temperature by reactive direct-current magnetron sputtering. A process map, which describes the composition as a function of the deposition total pressure and oxygen flow rate, has been depicted. Thin films with different preferred orientations can be attained by varying the total pressure and oxygen flow rate, which can be used to tune the electrical and optical properties of thin films. Taking Cu_2O as an example, thin films deposited at low total pressure (0.5 Pa) has a highly [100] textured orientation, but the highly [111] preferred orientation will appear when the total pressure changing to 1 Pa, as shown in Fig. 1. The [111]-orientated Cu_2O thin film has the room temperature resistivity of 41 Ω cm, which is 10 times lower than that of [100]-orientated film. This low resistivity will be useful to improve the conversion efficiency of Cu_2O-based solar cells. Besides, the optical band gap of Cu_2O can be widened from 2.38 eV to 2.56 eV when the textured orientation changing from [100] to [111], shown in Fig. 2. The Burstein-Moss shift due to the larger carrier concentration is thought to be responsible for this enlargement. Similar behaviors have also been observed in Cu_4O_3 and CuO thin films.

Fig. 1 XRD patterns of Cu_2O thin films deposited at 0.5 Pa and 1 Pa total pressure.

Fig. 2 Plots of $(\alpha E)^2$ vs E of Cu_2O thin films with different textured orientations.

SE/PST/TF/BI-P1-09
Interaction of BSA with the oxidized surfaces of nanostructured Ti, Nb, and Zr thin films

T14 Thin Films

#SE/PST/TF/BI-P1-09

D. Tallarico [1], A. Galtayries [2], A.L. Gobbi [3], P.I. Paulin Filho [1], P. Nascente [1].

[1]Federal University of Sao Carlos - Sao Carlos (Brazil), [2]LPCS (UMR CNRS 7045), Ecole Nationale Supérieure de Chimie de Paris (Chimie ParisTech) - Paris (France), [3]Brazilian Nanotechnology National Laboratory - Campinas (Brazil).

Alloys of titanium, niobium, and zirconium are potential candidates for implant due to the combination of good biocompatibility, high mechanical strength, excellent thermal stability, and optimal corrosion behavior [1-3]. Finding a surface chemical signature of biocompatibility, which is governed, in its first adsorption steps, by the adsorption of proteins, is very important to improve implants [4]. In this work, model titanium, niobium, and zirconium coatings, deposited by DC magnetron sputtering on Si(111) substrates at an elevated oxygen flow, have interacted with bovine serum albumin (BSA) solutions of different concentrations, in physiological-like conditions. The chemical composition and morphological characteristics of the films were analyzed by X-ray photoelectron spectroscopy (XPS) and atomic force microscopy (AFM). The thicknesses of the films were 500 nm. The BSA solutions (pH 7.4, phosphate buffer-saline (PBS)) were deposited at 37 °C for 1h.

The solution concentrations of BSA were 20 and 100 µg/ml. After rinsing with PBS and drying in air, the XPS analyses were performed. The spectra showed that the surfaces were composed by TiO_2, Nb_2O_5, and ZrO_2. AFM images showed that the oxidized films had nanostructured grains and low roughness. After interaction with the BSA solution at 100 µg/ml, the AFM images showed aggregates of adsorbed albumin. The surface morphology of the adsorbed BSA thin films appears different on the three surfaces: the AFM images indicated a monolayer adsorption of BSA onto Nb_2O_5 films, onto TiO_2 surfaces, the adsorption seems to result in two layers of adsorbed protein, and the ZrO_2 surface presented an uncomplete layer of adsorbed

protein. These results are discussed in terms of conformation of the adsorbed protein and tentatively compared to XPS equivalent thickness data and Time of Flight Secondary Ion Mass Spectra (ToF-SIMS) molecular spectra information.

[1] A.E. Aguilar Maya *et al.*, Mat. Sci. Eng. C 32 (2012) 321.
[2] Y. Bai *et al.*, Appl. Surf. Sci., 258 (2012) 4035.
[3] D.A. Tallarico, A.L. Gobbi, P.I. Paulin Filho, A. Galtayries, P.A.P. Nascente, J. Vacuum Sci. & Technol. A, 30 (2012) 051505.
[4] M. S. Wagner, D. G. Castner, Langmuir, 17 (2001) 4649.

TF-P2-34
Characterization and preparation of PbOx thin film by reactive magnetron sputtering

T14 Thin Films

#TF-P2-34

A. Hamzaoui [1], F. Sanchette [2], A. Billard [1], P. Nivet [3].

[1]IRTES-LERMPS-UTBM - Belfort (France), [2]LASMIS-UTT - Troyes (France), [3]SNECMA-SAFRAN - Vernon (France).

Lead oxide (PbO) films are frequently used in various applications due to their excellent semiconducting and photoelectrochemical properties.Indeed the numerous researches show the great potential of photoactivity of lead oxide PbO_x[1][2].In this study, PbO_x coatings are deposited by reactive magnetron sputtering with a metallic target (Pb)on glass slides and alumina (Al_2O_3) substrates.The operating conditions:O_2/Ar flow ratio,current intensity and voltage of target were controlled to study effects of these parameters on thin film deposition.The obtained coatings were crystallized by using a rapid thermal annealer (RTA) and were characterized by X-ray diffraction to analyze the crystallization behavior.The Scanning Electron Microscopy (SEM) was used to examine morphology of PbO_x films.The results obtained will be allowed thereafter to consider evaluate response of coatings films by optical spectrophotometer.

[1] Indrajit Mukhopadhyay, Susanta Ghosh, Maheshwar Sharon. Surface Science 384 (1997).

[2] David O. Scanlon, Aoife B. Kehoe, Graeme W. Watson, Martin O. Jones, William I. F. David, David J. Payne, Russell G. Egdell, Peter P. Edwards, and Aron Walsh. Phys. Rev. Lett. 107, 246402 (2011).

TF-P3-02
Study of InGaAs Alloys Prepared by Magnetron Sputtering

T14 Thin Films

#TF-P3-02

A. Pulzara Mora [1], R. Bernal Correa [1], A. Acevedo Rivas [1], A. Rosales-Rivera [2].

[1]Laboratorio de Nanoestructuras Semiconductoras, Grupo de Investigación en Magnetismo y Materiales Avanzados, Universidad Nacional de Colombia, A.A 127 - Manizales (Colombia), [2]Laboratorio de Magnetismo y Materiales Avanzados. Universidad Nacional de Colombia, A.A 127 - Manizales (Colombia).

In_xGa_{1-x} As (0<x<1) is a semiconductor where the optical and structural properties can be varied by changing the Indium and Gallium ratio [1]. This implies a control of emission and absorption frequencies indispensable to fabricate photonic devices, or efficient solar cells. In this work we have prepared indium gallium arsenide (InGaAs) films on silicon (100) substrate by using R.F. magnetron sputtering, and by varying the power source of In target. Elemental chemical mapping using EDAX in a scale of 20 μm^2, allow us to identify the elements in the alloy, and their spatial distribution. We observed homogeneity in each of the elements, as well as a marked contrast with the In increase. Morphology of InGaAs samples were analyzed using SEM in plain view in a 10 μm scale. These images show several features that depend on the In content. The presence of micro-drops scattered over the surface are likely due to the In segregation. XRD spectra of the as-deposited InGaAs films at different In power source (0< P_{In}<30 W) are shown in Fig.1. In order to avoid the (004) main reflection plane of the Si (001) substrate that is located at 2θ= 65°, all spectra were cut at 2θ= 60°. The InGaAs samples are polycrystalline, but the preferential orientation depends on the In content. In order to identify the vibrational phonon modes relating to GaAs and InAs, a deconvolution of the Raman spectra using Gaussian functions were performed. These results show a strong correlation between the In content and vibrational phonon modes [2].

[1] Gelczuk Lukasz, Dąbrowska-szata M., Modification of energy bandgap in lattice mismatched InGaAs/GaAs heterostructures, Optica Applicata, Vol. XXXIX, No. 4, 2009.

[2] Alexander Milekhin, Alexander Toropov, lexander Bakarov, Steffen Schulze, and Dietrich Zahn. phys. stat. sol. (c) 3, No. 11, 3924–3927 (2006).

Fig. 1. X-rays Diffractograms of the InGaAs films grown on Si (100) with different powers of the In target.

Fig. 2. Raman spectra of the InGaAs films grown on Si (100) with different powers of the In target. The tick solid lines shows the deconvolution of the Raman spectra employing Gaussian functions (dotted lines).

PST/SE/TF-3-Or-13
Multiscale nano-structuring of Si surfaces combining top-down and bottom-up techniques

T14 Thin Films

#PST/SE/TF-3-Or-13

B. Ziberi [1], K. Zimmer [2], F. Frost [2].

[1]State University of Tetova - Tetova (Macedonia, the former yugoslav republic of), [2]Leibniz-Institut für Oberflächenmodifizierung - Leipzig (Germany).

Surface patterning is of tremendous importance in many technological fields with features ranging from nanometers to millimeters. There are different patterning techniques that generally can be assigned to the top-down and bottom-up approaches. One bottom-up method for the generation of self-organized nanostructures is low-energy ion beam erosion. It is an easy one step process for the generation of large scale nanostructures of different materials, usually with a mean size below 100 nm [1, 2]. However due to the stochasticity of the process there is a lack of large scale ordering of nanostructures and of positional control.
In this contribution results on self-organized nanostructuring by ion beam erosion with simultaneous Fe co-deposition of pre-patterned Si surfaces will be presented. This method known as guided self organization has its inspiration in nature and is already successfully applied in heteroepitaxy and in diblock-copolymers. The idea is to combine the top-down technique for pre-patterning of surfaces followed by the ion beam induced self-organization process (bottom-up). Due to the periodicity, shape and lateral ordering of pre-patterns an improved ordering, and an exact positional control of nanostructures is achieved. The method allows also for the formation of new structures not possible on planar surfaces.
The pre-patterned substrates are fabricated by various lithographic techniques in combination with etching techniques for structure transfer. Depending on the shape of the pre-patterned structure (binary gratings with different periods, square arrays of cylinders, gratings with V-grooves) different results are obtained. Some experimental observations are: i) formation of curved ripples on the surface, where the curvature is caused by a continuous change in the local topography within pre-patterned regions; ii) perfectly square ordered dots on exact positions on the surface; iii) enhanced ordering of ripples and the formation of ripples with different orientation due to the local surface orientation; (iv) formation of patterns on curved surfaces.

[1] Ziberi B., Cornejo M., Frost F., and Rauschenbach B., J. Phys.-Condens. Mat., 21 224003, (2009).
[2] Frost F., Fechner R., Ziberi B., Völlner J., Flamm D., and Schindler A., J. Phys.-Condens. Mat., 21 224026, (2009).

TF-6-Or-2
Development of TIO2/WO3 bilayered films for photocatalytic applications

T14 Thin Films

#TF-6-Or-2

S. Sério [1], L.C. Silva [1], B. Barrocas [2], O.C. Monteiro [3], M.E. Melo Jorge [2].

[1]CEFITEC/DF-FCT/UNL - Caparica (Portugal), [2]CCMM/DQB-FCUL - Lisboa (Portugal), [3]CBQ/DQB-FCUL - Lisboa (Portugal).

In recent years, the pollution of the wastewaters with dyes is becoming a major environmental problem due to the growing use of a variety of dyes. Consequently there has been an increasing interest in developing new methods, more effective than the conventional processes, commonly used, to eliminate these environmental contaminants. Advanced oxidation processes (AOP), characterized by the production of hydroxyl radicals ($OH^{\cdot}$) and superoxide anion (O^{2-}), which are generated when a semiconductor catalyst absorbs radiation when it is in contact with H_2O and O_2 are a promising technology. Among various photocatalysts TiO_2 has been intensively studied. Nevertheless two limitations are recognized for a wide practical application, such as the small percentage of the solar radiation, which has the required energy to photogenerate electrons and holes and their high recombination rate. A lot of researches have be done to improve the TiO_2 photocatalyst activity and show that the efficiency of the photocatalytic reaction can be enhanced in heterogeneous semiconductors systems, such as Fe_2O_3-TiO_2, TiO_2-SnO_2, WO_3-TiO_2 etc [1]. Photocatalysts can either be used as powders in a slurry form or as supported films, being this latter configuration advantageous. Among many techniques used to prepare catalytic materials immobilized in film form the sputtering method presents several advantages mainly because the structure, morphology and optical properties of sputtered films can be modified by changing the deposition parameters [2].
This work reports some results of the preparation and characterization of TiO_2/WO_3 nanocomposites films for photocatalytic applications. TiO_2/WO_3 bilayered films were deposited on glass substrates by DC-magnetron sputtering. The crystallographic, optical and morphological properties (figure 1) of WO3 and the TiO_2 layers were studied.
The films photocatalytic activity was tested, under visible irradiation, on the decolorization of Rhodamine 6G aqueous solutions and studied considering the

influence of the crystalline structure and morphology of the prepared films.

[1] C.F. Lin, C.H.Wu, Z.N. Onna, J. Hazard. Mater. 154 (2008)1033–1039.
[2] S. Sério, M. E. Melo Jorge, M. J. P. Maneira, Y. Nunes, Mat. Chem. Phys., 126 (2011) 73-81.

Figure1- FEG-SEM images (surface and cross-sectional image) of TiO_2/WO_3 bilayered films

TF-P3-06
Physical properties of InN nanoparticles prepared by reactive magnetron sputtering

T14 Thin Films

#TF-P3-06

R. Bernal Correa, C. Lopez Velasquez, A. Pulzara Mora.

Laboratorio de Nanoestructuras Semiconductoras, Universidad Nacional de Colombia-sede Manizales - Manizales (Colombia).

Indium Nitride (InN) is a semiconductor material with possible applications in solar cells [1]. In this work we report the formation of micro and nanoparticles of InN on Si (100) substrate obtained by magnetron sputtering in an Ar+N mixture atmosphere. The InN samples were analyzed by scanning electron microscopy (SEM), X-ray diffraction (XRD), UV/Vis absorption and photo-acoustic measurements. The InN layers are policrystalline and exhibit the formation of crystals with a hexagonal structure . SEM images show the formation of micro and nanoparticles (~50 nm diameter and spherical shape) which depend on the substrate temperature (Fig. 1). Bandgap energy (Eg) of InN layers obtained from UV/Vis spectra showed a blue shift [2] as a function of substrate temperature. The thermal diffusivity of each layer was determined by photo acoustic measurements assumed optically and thermally homogeneous slab sample geometry (Fig 2).

[1] Zubrilov A. Properties of Advanced Semiconductor Materials GaN, AlN, InN, BN, SiC, SiGe . Eds. Levinshtein M.E., Rumyantsev S.L., Shur M.S., John Wiley & Sons, Inc., (2001), 49-66.
[2] C. P. Foley, T. L. Tansley, Pseudopotential band structure of indium nitride Phys. Rev. B 33, (1986) 1430–1433.

Fig. 1. SEM micrographs for InN layers prepared at substrate temperatures of: a) 300 ° C, b) 400 ° C , c) 500 ° C (x10000), d) 500 ° C (X80000).

Fig. 2. Photoacoustic signal vs frecuency (Hz) of the InN layers prepared at substrate temperatures of: A1) 300 ° C, A2) 400 ° C , A3) 500 ° C

TF-9-Or-10
Grazing Incidence Fast Atom Diffraction : an alternative to RHEED for in-situ growth monitoring

T14 Thin Films

#TF-9-Or-10

V. Etgens [1], P. Atkinson [2], M. Eddrief [2], H. Khemliche [3], A. Momeni [3], R. Philippe [3], M. Maxime [3].

[1]Université de Versailles Saint-Quentin en Yvelines - Versailles (France), [2]INSP UMR7588 CNRS – Université Pierre et Marie Curie Paris - Paris (France), [3]ISMO UMR8214 CNRS-Université Paris-sud - Orsay (France).

Reflection High Energy Electron Diffraction (RHEED) is perhaps the most commonly used in-situ monitoring method for molecular beam epitaxy, providing quantitative information about surface reconstructions, lattice parameters, growth rates and growth modes, together with semi-quantitative information about surface morphology. The main disadvantages with RHEED are linked to its high energy electron beam, which penetrates several atomic layers of the crystal surface, leading to damage in sensitive materials [1], and making the extraction of information about the reconstruction and morphology of only the topmost atomic layer difficult.

We present here an alternative, recently developed, diffraction technique, which is fully compatible with conventional MBE growth and has the advantage over RHEED in that it is truly surface sensitive. This technique, known as Grazing Incidence Fast Atom Diffraction (GIFAD) [2] uses a beam of neutral atoms such as Helium, with energy of less than 1keV, incident on the surface at a shallow angle. Due to this shallow incidence angle, the energy of the atoms perpendicular to the surface is very small, giving rise to diffraction of the atom beam from the corrugated

surface potential perpendicular to the beam direction. We have mounted a GIFAD system on a commercial MBE machine, and demonstrate the capacity to monitor changes in the surface in real-time during growth (see e.g. Fig. 2). We will discuss the information about surface ordering provided by this technique compared to RHEED.

[1] Y. Horio and S. Satoh, Appl. Surf. Sci. **190** (2002) 80, H. H. Farrell, J. L. deMiguel and M. C. Tamargo, J. Appl. Phys. **65** (1989) 4084

[2] H. Khemliche, P. Rousseau, P. Roncin, V. H. Etgens and F. Finocchi, *Appl. Phys. Lett.* **95** 151901 (2009), H. Winter and A. Schüller, *Progress in Surface Science* **86** (2011) 169

Fig. 1: Change in intensity of the whole GIFAD diffraction during layer-by-layer GaAs growth, and during surface recovery

TF-9-Or-12
Plastic deformation and structural change in the surface layer of metals under the impact with high-speed nanoparticles

T14 Thin Films

#TF-9-Or-12

A. Mayer.

Chelyabinsk State University - Chelyabinsk (Russian federation).

High-power pulsed ion or electron beams are widely used now for surface treatment: they can produce strengthening of the surface layer material [1], smoothing of the surface relief [2], deposition and reinforcement of deferent protective or functional coatings. In this case, microscopic fast particles, accelerated by the electric field, bring their energy to the material and heat it; therefore, the main action of the beam is the material heating. The classical bead-blasting treatment is another limit, in which macroscopic particles strike on the surface and produce its plastic deformation due to the momentum transfer.

The metal surface bombardment by high-speed nanoparticles is an intermediate case, which can be a useful tool for the surface treatment. Previously prepared and charged nanoparticles with diameter of the order of 100 nm can be accelerated by the electric field in vacuum up to velocities of the order of 100 - 1000 m/s. Impact of a high-speed nanoperticle with the metal surface produces a shock wave with amplitude of about several GPa, which is enough for intensive plastic deformation and structural change (change of the dislocation density, et cetera). Each shock wave is spherically diverging, its amplitude decays on the length scale of the nanoparticle diameter; therefore, modification affects only the thin surface layer with the corresponding thickness. Pit impressed on the surface by a nanopaticle is small; therefore, this treatment can be used for processing of the fine-polished surfaces.

In this report, the metal surface layer deformation under the impact with high-speed nanoparticles is numerically investigated on the base of mechanics of continua, supplemented by the dislocation plasticity model [3-5]. Investigation is made from the

viewpoint of potential application of this technology for the surface treatment. Optimal size and velocity of nanoparticles are determined, as well as the features of the obtained structural change in the metal surface layer. Pit impression and the conditions of sticking are analyzed.

The study was supported by The Ministry of education and science of Russian Federation, projects 14.B37.21.0384 and 2.2320.2011.

[1] V.S. Krasnikov and A.E. Mayer, “Numerical investigation of the change of dislocation density and microhardness in surface layer of iron targets under the high power ion- and electron-beam treatment”, Surf. Coat. Techn., 212, 79-87 (2012).
[2] V.S. Krasnikov, A.Ya. Leivy, A.E. Mayer and A.P.Yalovets, “Surface microrelief smoothing mechanisms in a target irradiated by an intense charged particle flux”, Techn. Phys., 52 (4), 41-49 (2007).
[3] V.S. Krasnikov, A.Yu. Kuksin, A.E. Mayer and A.V. Yanilkin, “Plastic deformation under high-rate loading: The multiscale approach”, Phys. Solid State, 52 (7), 1386-1396 (2010).
[4] V.S. Krasnikov, A.E. Mayer and A.P. Yalovets, “Dislocation based high-rate plasticity model and its application to plate-impact and ultra short electron irradiation simulations”, Int. J. Plast., 27 (8), 1294-1308 (2011).
[5] E.N. Borodin, A.E. Mayer and V.S. Krasnikov, “Wave attenuation in microcrystal copper at irradiation by a powerful electron beam”, Current Appl. Phys., 11 (6), 1315-1318 (2011).

SE/TF-1-Or-7
Structural Analysis of Chromium doped TiO2 Thin Film Deposited Using Cathodic Arc Deposition Technique

T14 Thin Films

#SE/TF-1-Or-7

M. Alamgir [1], K. Hameed [2].

[1]NINVAST - Islamabad (Pakistan), [2]NINVAST - Kohat (Pakistan).

Abstract:
Chromium doped TiO2 thin films grown by co-sputtering of titanium and chromium in a Cathodic Arc Plasma evaporation system on various substrates. X-ray diffraction (XRD), Rutherford backscattering spectroscopy (RBS), SEM with EDS used to characterize the films. Deposited pure titanium dioxide thin films possess a mostly anatase structure while Cr-doped TiO2 films are amorphous. Amorphous Cr-doped TiO2 films transformed to a mixed anatase and rutile phase by annealing at various temperatures. Changes in the morphology and composition of the films examined by SEM-EDS. Crystalline Cr-doped TiO2 films became super-hydrophilic which indicate that the absorption edge shifted from an ultraviolet region for TiO2 to a visible region for annealed Cr-doped TiO2 films, which is further confirmed by UV–visible spectroscopy.
Key words: XRD, EDS, RBS, Cathodic Arc Plasma evaporation system, UV–visible spectroscopy.

TF-5-Or-3
Plasma polymerisation of an organophosphorus precursor at atmospheric pressure

T14 Thin Films

#TF-5-Or-3

F. Hilt [1], D. Duday [1], N. Gherardi [2], J. Bardon [3], P. Choquet [1].

[1]CRP Gabriel Lippmann - Belvaux (Luxembourg), [2]Université de Toulouse - Toulouse (France), [3]CRP Henri Tudor - Hautcharage (Luxembourg).

Deposition of dense and adherent polymer coatings containing phosphate groups on thermally sensitive substrates is very interesting for protective or biological applications. Non-equilibrium atmospheric-pressure plasmas have been studied in many processes but phosphorus-containing precursors were never injected into a dielectric barrier discharge (DBD) to deposit organophosphorus coatings on polymer substrates.
In this work, TriEthyl Phosphate (TEP) is injected in a DBD in order to deposit organophosphate coatings at atmospheric pressure. The coating structure (SEM, Ellipsometry) and the coating chemistry are studied (FTIR, XPS, ToF-SIMS, 31P NMR) in order to understand the deposition mechanisms of TriEthyl Phosphate (TEP). FTIR (Figure 1) and XPS indicate a coating containing phosphate, organophosphate and different C-containing groups. N-containing groups are also detected in the coating due to reaction of precursor with reactive nitrogen species coming from process gas N_2. Polyphosphate chains are revealed by ^{31}P NMR (Figure 2) and the polymer structure of the coating is highlighted by SIMS. Electrical and optical (OES) characterizations of the discharge are presented to go further in the understanding of the deposition mechanism.

Figure 1 : ATR-FTIR spectra of the TriEthyl Phosphate monomer (a) and of the plasma-polymerised coating (b)

Figure 2 : ^{31}P NMR spectra of the plasma-polymerised coating

TF-P2-20
Reactive magnetron sputtering of deuterated diamond like carbon films for photocathode application

T14 Thin Films

#TF-P2-20

P. Boháček.

Institute of Electrical Engineering, Slovak Academy of Sciences - Bratislava (Slovakia).

Reactive magnetron sputtering of deuterated diamond like carbon films for photocathode application

J. Huran[1], P. Boháček[1], N.I. Balalykin[2], A.A. Feshchenko[2], A.P. Kobzev[2] , J. Kováč jr.[3], A. Kleinová[4], M. Sekáčová[1], B. Zaťko[1]

[1]Institute of Electrical Engineering, Slovak Academy of Sciences, Dúbravská cesta 9, 84104 Bratislava, Slovakia
[2]Joint Institute for Nuclear Research, Joliot-Curie 6, 141980 Dubna, Moscow Region, Russian Federation
[3]Faculty of Electrical Engineering and Information Technology, Slovak University of Technology, Ilkovičova 3, 81219 Bratislava, Slovakia
[4]Polymer Institute, Slovak Academy of Sciences, Dúbravská cesta 9, 84541 Bratislava, Slovakia

Diamond-like Carbon (DLC) is a disordered carbonaceous material composed of hydrogen and carbon, which is bonded in sp^2 and sp^3 electronic configurations with a significant C-C sp^3 bonds. There are several carbon-based photocathodes, like polycrystalline diamond, hydrogenated amorphous carbon and nanostructured fullerene films.
The influence of diamond like carbon films technology and properties on quantum efficiency of prepared photocathode has been investigated. Diamond-like carbon films were deposited on silicon substrate and stainless steel mesh by reactive magnetron sputtering using carbon target and gas mixture of Ar and reactive gases H_2 and D_2. The concentration of elements in films was determined by RBS and ERD

analytical method simultaneously. Chemical compositions were analyzed by Fourier transform infrared spectroscopy (FT-IR). Raman spectroscopy was used for I(D)/I(G) ratio determination. The quantum efficiency was calculated from the measured laser energy and the measured cathode charge. RBS and ERD analysis indicated that the films contain carbon, hydrogen, deuterium and small amount of oxygen. IR results showed the presence of main C-D, C-H, H-O, D-O bonds. Raman spectra of DLC films show the D and G band conversion which were Gaussian-fitted and identified. The emission process from diamond like carbon films, excited with near-UV radiation, seems to be governed by the intensity ratio I(D)/I(G). Results show, that photocathodes prepared with deuterium as reactive gas have higher quantum efficiency than photocathodes prepared with hydrogen as reactive gas and photocathode quantum efficiency rise up with deuterium and hydrogen flow rate.

This research has been supported by the Slovak Research and Development Agency under the contracts APVV-0713-07, APVV-0321-11 and has been executed in the framework of the Topical Plan for JINR Research and International Cooperation (Project 02-0-1067-2007/2012).

TF-6-Or-10
Surface structures of ultrathin TiOx and BaO films on Au (111)

T14 Thin Films

#TF-6-Or-10

C. Wu, M. Marshall, M.R. Castell.

Department of Oxford, University of Oxford - Oxford (United kingdom).

Following the discovery of enhanced catalytic properties of oxide supported nanoparticles of noble metals, especially Au, interactions between the two have become a focus in research [1-3]. The growth of oxides on Au(111) surfaces serves as an inverse model and provides insights into their interactions. Well-ordered TiO_x and BaO layers were grown on (22 × $\sqrt{3}$)-reconstructed Au(111) surfaces by Ti and Ba deposition and oxidation. Surface structures of these ultrathin oxide films were studied by scanning tunneling microscopy (STM) and auger electron spectroscopy (AES).

In the growth of TiO_x thin films on Au(111), three different structures were observed with increased amounts of Ti deposited [4]. The first structure occurs for Ti surface coverages of <0.5 monolayer (ML), and exhibits a (2 × 2)-reconstructed structure resembling a honeycomb pattern. The second structure arises after depositing 0.5 ML - 1.8 MLs of Ti and exhibits a pinwheel shape. The pinwheel structure forms a $(\sqrt{67} \times \sqrt{67})R12.2^{\circ}$ Moiré pattern. The third structure occurs for >0.5 ML Ti depositions and forms triangular shaped islands. Film growth continues via the coalescence of triangular islands with further increased Ti coverage. Auger electron spectroscopy (AES) indicates that the structures have different chemical compositions.

For BaO ultrathin film growth on Au(111), coexistence of a honeycomb (4 × 4) and a hexagonal $(4\sqrt{3} \times 4\sqrt{3})$ periodicity were observed. Both structures lift the Au herringbone reconstruction [5]. Using the sub-monolayer TiO_x structures on Au(111) as templates, new reconstructions were created following Ba deposition which were not observed when BaO was grown on Au directly. Atomic models are proposed for the observed structures and we demonstrate the possibility of creating novel epitaxial oxide structures on both metal substrates and other oxide templates.

[1] Chen, M.S. and Goodman, D.W. Science, 2004, 306, 252-255.
[2] Overbury, S.H.; Ortiz-Soto, L.; Zhu, H.G.; Lee, B.; Amiridis, M.D.; Dai, S. Catal. Lett., 2004, 95, 99-106.
[3] Zheng, N. and Stucky, G.D. J. Am. Chem. Soc., 2006, 128, 14278-14280.
[4] Wu, C.; Marshall, M.S.J. and Castell, M.R. J. Phys. Chem. C, 2011, 115, 8643-8652.
[5] Wu, C. and Castell, M.R. Surf. Sci. 2012, 606, 181-185.

TF-1-Or-7
Multi-Dye-Molecule-Stacked Structures Grown by Molecular Layer Deposition (LP-MLD) on ZnO

T14 Thin Films

#TF-1-Or-7

T. Yoshimura.

Tokyo University of Technology - Hachioji, Tokyo (Japan).

Molecular Layer Deposition (MLD)[1-3] grows tailored organic thin films with designated molecular arrangements by introducing source molecules sequentially onto substrates. The monomolecular-step growth is achieved by selective chemical reactions or the electrostatic force. Multi-dye-molecule-stacked structures, which will be applied to the dye-sensitized solar cells,[2,3] were grown by the liquid-phase MLD (LP-MLD) on n-type ZnO.

As Fig. 1 shows, a sequence of p-type dye (p1) - n-type dye (n1) - p-type dye (p2) constructs a [ZnO/p1/n1/p2] structure. Here, “p-type dye” and “n-type dye” were defined by Meier.[4] The former tends to have negative charge and the latter tends to have positive charge. Rose bengal (RB) and eosine (EO) were used as p-type source molecules, and crystal violet (CV) as n-type source molecules.

As Fig. 2 shows, in [ZnO/RB] the surface potential becomes negative, which is attributed to electric dipole moments generated by the negative charge in the p-type dye molecules. In [ZnO/RB/CV], the surface potential shifts to the positive side due to the positive charge in CV on the top. When p-type EO molecules are adsorbed on [ZnO/RB/CV] to fabricate [ZnO/RB/CV/EO], the surface potential shifts to negative side.

It was found that photoluminescence spectrum of [ZnO/RB/CV/EO] measured by excitation light of 532 nm in wavelength is a superposition of spectra of [ZnO/RB/CV] and [ZnO/EO], which implies widening of the absorption wavelength range in the multi-dye-molecule-stacked structure.

These results suggest that multi-dye-molecule-stacked structures are definitely constructed on ZnO surfaces with monomolecular steps by LP-MLD.

1. T. Yoshimura, et al., Appl. Phys. Lett. 59, 482 (1991).
2. T. Yoshimura, et al., J. Vac. Sci. Technol. A 29, 051510-1 (2011).
3. T. Yoshimura, et al., J. Electrochem. Soc. 158, 51 (2011)
4.H. J. Meier, Phys. Chem. 69, 719 (1965).

Fig. 1 LP-MLD with molecule switching sequences of p-type dye (p1) - n-type dye (n1) - p-type dye (p2) .

Fig. 2 Surface potential of ZnO layers with dye molecules on the surface.

TF-9-Or-11
Reduction of particle defects on Mo/Si multilayer films for extreme UV mask blank by controlling the surface roughness of chamber shields in ion beam sputtering

T14 Thin Films

#TF-9-Or-11

J. Kageyama [1], M. Yoshimoto [2], A. Matsuda [2], V. Jindal [3], P. Kearney [3], F. Goodwin [3].

[1]Asahi Glass Co., Ltd. and Interdisciplinary Graduate School of Science and Engineering, Tokyo Institute of Technology - Yokohama (Japan), [2]Interdisciplinary Graduate School of Science and Engineering, Tokyo Institute of Technology - Yokohama (Japan), [3]SEMATECH, Inc. - Albany (United states).

Extreme UV lithography using a 13.5 nm light is an emerging technology for the next generation lithography[1]. EUV mask blanks comprise the multilayered Mo/Si film deposited on a glass substrate[2]. The multilayer film is capped with a Ru layer. In fabricating the mask blanks, defects on the film cause the malfunctioning of semiconductor chip. Reducing the defects in the EUV mask blank presents a major challenge to the commercialization of EUV lithography.

In this work, the underlying cause of deposition-derived particle defects in the ion beam sputtering process was investigated with focused on the surface roughness of the chamber shield in order to reduce the defect density on the mask blank film. As a result, it was demonstrated that the shields of roughness exceeding 8 μm greatly reduced the Si-rich particle defects on the mask blank film.

Fig. 1 is a schematic top view of the Ar^+ ion beam sputtering system using rotating targets of Si, Mo, and Ru. The interior walls of the chamber were wholly protected by detachable stainless-steel shields placed in the zones 1 and 2 (zone 1: near the sputtering targets and the substrate, and zone 2: along the chamber interior wall). We prepared shields of different arithmetic average surface roughness *Ra* in the range of 3.1 μm to 19.9 μm. The defect count of each EUV mask blank was inspected across 142 × 142 mm^2 area prior to and following deposition. Particle

composition was analyzed under focused ion beam/SEM, and by EDX spectroscopy. The total defect count of Si and Si/Mo particles (Si-rich particles) having size of several tens of nanometer or more per mask blank was averaged for each experiment. Si-rich particle defect was found to inversely decrease with the square of the surface roughness of the shield, suggesting that Si-rich particles arise from the shield surface.

The obtained results reveal a linear relationship between Si-rich particle defect counts per mask blank and the inverse square of shield surface roughness. To investigate the influence of shield location, we repeated the plot for zone 2 data with Ra_1 (zone 1) maintained approximately constant. These results suggest that Si-rich particle defects coming from the shield surface in zone 2 (the chamber wall shield) similarly affect the defect on the mask blank.

[1] G. Kalkowski, et al., Microelectron. Eng. **88**, 1986 (2011).
[2] P. B. Mirkarimi, et al., Microelectron. Eng. **77**, 369 (2005).

TF-P2-35
Grain Crystallization Control and Large Magnetoresistance Emergence in Fe3O4/a-SiO2 Thin Films Produced by Rapid Thermal Deoxidation Method

T14 Thin Films

#TF-P2-35

H. Kobori [1], T. Murakami [1], A. Yamasaki [1], T. Taniguchi [2], T. Shimizu [3].

[1]Konan University - Kobe (Japan), [2]Osaka University - Osaka (Japan), [3]National Institute of Advanced Industrial Science and Technology - Tsukuba (Japan).

We have observed large magnetoresistance (MR) in Fe_3O_4/a-SiO_2 thin films produced by rapid thermal deoxidation (RTD) method. By use of the RF magnetron sputtering technique, 500nm-thick α-Fe_2O_3 thin films were grown on a-SiO_2 (SiO_2 glass) substrates, through the oxygen reactive process from an Fe (99.99%) target. After that, those films were deoxidized and varied to Fe_3O_4 films by rapid thermal deoxidation (RTD) method. The RTD for α-Fe_2O_3/a-SiO_2 thin films were carried out in the atmosphere of Ar(90%)/H_2(10%) mixture gases by using an infrared image furnace. The heat treatment conditions for the RTD are 430 ºC/20min, 460 ºC/10min, 500 ºC/5min, 550 ºC/2min, and 600 ºC/1min. For comparison, a 500nm-thick Fe_3O_4/a-SiO_2 thin film was also produced by the oxygen reactive process without the RTD. From the X-ray diffraction measurement, it is found that the crystallinity of the α-Fe_2O_3/a-SiO_2 and Fe_3O_4/a-SiO_2 thin films without the RTD are low, whereas that of Fe_3O_4/a-SiO_2 ones with the RTD are highly increased by the heat treatment . In addition, from the atomic force microscope measurement, we find that the Fe_3O_4 nano-particle size in Fe_3O_4/a-SiO_2 thin films with the RTD increases with increasing the heat treatment temperature. Magnetite (Fe_3O_4) is a ferrimagnetic material which has a high Curie temperature (858K) and is also known as a halfmetal. A halfmetal is regarded as one of most promising materials of spintronics devices. The electrical resistivity (ER) and the magnetoresistance (MR) ratios of the Fe_3O_4/a-SiO_2 thin films with and without the RTD were measured between 6 K and 300 K. The ER of the Fe_3O_4/a-SiO_2 thin film without the RTD showed the temperature dependence of the Mott's variable range hopping conduction. This behavior implies that the sample is amorphous-like. On the other hand, the ER of Fe_3O_4/a-SiO_2 thin films with the RTD showed a kink at around the Verwey transition temperature (~120 K), which indicates

that the crystallinity of those is high. Figure 1 shows the temperature dependence of the MR ratios for the Fe_3O_4/a-SiO_2 thin films without and with the RTD. Here ρ(H) is the MR at the magnetic field H and the MR ratio is expressed as Δρ(H)/ρ(0)={ρ(H)-ρ(0)}/ρ(0). The MR ratio of the sample without the RTD is small and monotonically decreases with increasing the temperature. That ratio at 0.7T is 1.8% at 50 K and 1.2% at 300 K. For the samples with the RTD, it is clearly found that the MR ratios are drastically increased as compared with the sample without the RTD. The MR ratio at 0.7T for the sample with the RTD (550 ºC/2min) is 7.6% at 128 K.

Fig. 1

TF-6-Or-11
Adsorption of gold adatoms on ceria thin films

T14 Thin Films

#TF-6-Or-11

Y. Pan [1], J. Paier [2], C. Penschke [2], J. Sauer [2], N. Nilius [1], H.J. Freund [1].

[1]Fritz-Haber-Institut der MPG - Berlin (Germany), [2]Humboldt-Universität zu Berlin, Institut für Chemie - Berlin (Germany).

Low-temperature scanning tunnelling microscopy and spectroscopy have been employed to study the adsorption of individual Au atoms on well-defined CeO_2(111) films grown on Ru(0001). For slightly reduced films, two types of Au species are found on the surface. The first one appears as isolated protrusion, while the second type always forms pairs of 8-10 Å distance and develops distinct Sombrero-shapes. The relative abundance of the two species sensitively depends on the reduction state of the surface, i.e. on the density of oxygen vacancies. According to DFT calculations, we assign the two species to Au atoms in two different charge states. While the simple protrusions correspond to a neutral Au that bind to the ideal, defect-free lattice, the paired species are negatively charged and decorate nearby subsurface oxygen-vacancies. The latter type pairs up, as each O-defect generates two Ce^{3+} cations that are able to transfer one electron each to two surface Au atoms. The presence of Au pairs therefore provides direct evidence for charge-transfer processes between reduced Ce^{3+} ions and electronegative Au species, but also indicates the typical separation of the two Ce^{3+} associated to an O vacancy.

TF-1-Or-8
Delamination and buckling of thin films from an interface step

T14 Thin Films

#TF-1-Or-8

A. Ruffini, J. Durinck, J. Colin, C. Coupeau, J. Grilhé.

P' Institute - Futuroscope (France).

The coatings technology of materials with sub-micron thin films find applications in many industrial fields such as microelectronics or optics. During the deposition process, high stresses reaching sometimes several GPa may develop in the film leading to the interface delamination. The delaminated zone of the film will subsequently buckle if the stress is in compression and its magnitude is beyond a critical value. Understanding the mechanisms responsible for this damaging phenomenon is a major technological challenge in different fields such as materials science, metallurgy and continuum mechanics. Since the early-2000s, the buckling of thin films has been studied in the framework of the continuum theory of elastic thin plates developed by Föppl and von Kármán (FvK). This model has been widely used to describe successfully the elastic behavior of structures such as straight-sided blisters or telephone cord buckles.

More recently, post-mortem AFM observations have evidenced that buckled structures have preferentially grown from nano-steps which have been formed at the interface by the emergence of dislocations coming from the substrate [1]. It is in this context that a twofold study has been set up in order to investigate this phenomenon.

On one hand, atomistic simulations have been performed to understand the elementary mechanisms at the origin of the delamination at the interface between metallic film and substrate. It has been first shown that a delaminated zone extends on both sides of the step as dislocations glide from the substrate to the interface and the step height increases. The buckling of the film has been found to occur for critical step height and applied strain. On the other hand, the expression of the critical strain beyond which the film buckles has been derived, in the framework of the continuum FvK theory, as a function of the step height. The model explains why the buckling of the film is favored above step-like nanostructures.

[1] Foucher F., Coupeau C., Colin J., Cimetière A., and Grilhé J., Phys. Rev. Lett. 97(9), 096101 (2006)

SE/PST/TF/BI-3-Or-4
Polydopmaine Nanoscale Thin Films as Multifunctional Coatings

T14 Thin Films

#SE/PST/TF/BI-3-Or-4

W. Zhang, F. Yang, B. Zhao.

University of Waterloo - Waterloo (Canada).

Dopamine is a “sticky” biomolecule containing the typical functional groups of mussel adhesive proteins. It has a chemical structure of catecholamine (Figure 1a); under alkaline conditions the catechol group can be oxidized to quinine, allowing dopamine to self-polymerize and form a nanoscale thin film on its support surface (Figure 1b). [1] Although the application of polydopamine (PDA) film has been demonstrated as a promising way to functionalize material surfaces, the mechanical and adhesion properties of the PDA film are still largely unexplored. [2] To this end, we recently conducted a systematic study of PDA nanoscale thin filmscoated on both soft (PDMS) and rigid (glass and epoxy) substrates, and investigated the mechanical and interfacial stability of the thin films both in air and under water. [3] It has been found that PDA films were highly hydrated in wet conditions because of their porous membrane-like structures and hydrophilic groups. Upon dehydration, the films form cracks when they were coated on the soft substrate due to internal stresses and the large mismatch in elastic modulus of the film and the substrate (Figure 1c). We also found a significant decrease of friction forces in water on all three PDA-coated surfaces. Thus, we proposed that the PDA film might be able to serve as a water-based lubrication coating. We attributed the different behaviors of PDA film in air and under water to its hydration effects (Figure 2). These research findings provide insights into the stability, mechanical and adhesive properties of the PDA films, which are critical for their effective transfer to practical engineering.

(1) Lee, H.; Lee, B. P.; Messersmith, P. B. *Nature*. **2007**, *448*, 338-341.

(2) Yang, F. K.; Zhang, W.; Han, Y.; Yoffe, S.; Cho, Y.; Zhao, B. *Langmuir*. **2012**, *28*, 9562-9572.

(3) Zhang, W.; Yang, F.; Han, Y.; Gaikwad, R.; Leonenko, Z.; Zhao, B. *Biomacromolecules*. Just accepted and published online.

Figure 1. (a) Dopamine molecule; (b) a digital photo of an apparently homogeneous PDA coated PDMS surface; (c) AFM image of PDA thin film cracks on PDMS substrate. (Adapted from [3])

Figure 2. Mechanical property measurements on hydrated PDA film. (Adapted from [3])

TF-6-Or-6
Determination of the optical properties of ZnOx thin films grown by DC magnetron sputtering

T14 Thin Films

#TF-6-Or-6

W. Chamorro Coral [1], Y. Battie [2], D. Horwat [1], P. Miska [1], A. En Naciri [2].

[1]Institute Jean Lamour, Université de Lorraine, CNRS - Nancy (France), [2]Institut Jean Barriol, Université de Lorraine - Metz (France).

Zinc oxide (ZnO) is a transparent conductive material and a promising candidate for optoelectronic applications. Its optical properties depend on its crystalline quality, microstructure and defect chemistry.
The knowledge of these optical properties is necessary to improve the performance of devices[1]. Nevertheless, there is a large scatter in the data reported in the literature, which can only partially be related to the variation of the intrinsic properties.

ZnO_x thin films were synthesized by DC magnetron sputtering. Different compositions were obtained by varying the oxygen flow rate (OFR). Spectroscopic ellipsometry has been used to determine the optical properties of transparent ZnO_x thin films. The optical constants are extracted using the Forouhi-Bloomer (FB) model [2,3]. The dispersion of the dielectric function, the absorption coefficient and the optical band gap *Eg* are presented and analysed as a function of the OFR and chemical composition. For the sake of comparison, *Eg* was also extracted using the Tauc plot of data obtained by spectroscopic ellipsometry, spectrophotometry in transmission mode and by photoluminescence (Figure 1). We find a significant variation of optical responses with the OFR. More particularly, *Eg* is found to be sensitive to the OFR and to the presence and density of optical defects as detected using photoluminescence measurements. Moreover, this study evidences significant differences in the evolution of *Eg* as evaluated by the different methods, explaining in a large extent the dispersion of data in the literature.

1. Ü. Özgür, Y. I. Alivov, C. Liu, A. Teke, M. A. Reshchikov, S. Doğan, V. Avrutin, S.J. Cho, and H. Morkoç, J. Appl. Phys. 98, 041301 (2005)

2. R. A. Forouhi and I. Bloomer, Phys. Rev. B 34, 7018 (1986)

3. R. A. Forouhi and I. Bloomer, Phys. Rev. B 38, 1865 (1988)

Figure 1. Energy gap of ZnO thin films vs the oxygen flow rate determined by ellipsometry, transmission and photoluminescence measurements.

TF-P2-36
Porous Anodic Alumina as Antireflection Coatings of Thin Film Solar Cells

T14 Thin Films

#TF-P2-36

S. Cheng.

Fuzhou University - Fuzou (China).

Porous anodic alumina (PAA) formed by an electrochemical oxidation method has been investigated for decades. But the potential use of PAA films as antireflection coatings for photovoltaic applications rarely attracted people's attention. In fact PAA films with both antireflection and light scattered properties could help to enhance the light absorption according to the statistical ray optics [1]. Junwu Chen studied PAA films for traditional graded-index antireflection coatings [2], but the light scattered properties of the PAA films were ignored.
Here PAA thin films were also formed by an electrochemical oxidation method. The transmission spectra of the films were measured by a spectrophotometer. The refraction index was characterized by the transmission spectra, using the dielectric model and K-K transformation. The refraction index could be controlled by the time of wet etching, which was the advantage of PAA films as antireflection coatings. We have obtained optimal PAA film sample with the thickness of about 110nm and the refraction index of 1.15, and the transmission of the optimal sample is much better than that of glass substrate in the visible waveband (seen in Fig.1). But the maximum value of transmission at 550nm is about 95% rather than about 100% as theoretical prediction of a thin film with smooth surface. It is perhaps due to the scattered properties of porous structure, which could be used in thin film solar cells to enhance the light absorption. We also formed double layer PAA films on the glass substrates with transmission of 94.56% (91.17% for the glass substrate) in the visible region, which presented better antireflection properties (shown in Fig.2). Therefore, PAA films are suitable for antireflection coatings of thin film solar cells.

[1]. Eli Yablonovitch, Optical Society of America, 1982, Vol.72, No.7, 899-907
[2]. Junwu Chen, Biao Wang, Yi Yang, Yuanyuan Shi, Gaojie Xu, Ping Cui, Optical Society of America, 2012, Vol. 51, No. 28, 6839-6843

Fig.1. The transmission spectra of the PAA films with refraction index of 1.15 and the glass

Fig.2. The transmission spectra of the glass, the PAA films with refraction index of 1.15 and double layer films

TF-6-Or-5
Direct observation of electronic states in gate stack structures: XPS under device operation

T14 Thin Films

#TF-6-Or-5

Y. Yamashita [1], H. Hideki [2], T. Chikyow [2].

[1]National Institute for Materials Science - Sayo (Japan), [2]National Institute for Materials Science - Tsukuba (Japan).

Although gate stack structures with high-k materials have been extensively investigated, there are some issues to be solved for the formation of high quality gate stack structures. In the present study, we employed hard x-ray photoelectron spectroscopy in operating devices(1). This method allows us to investigate bias dependent electronic states while keeping device structures intact. Using this method we have investigated electronic states and potential distribution in gate metal/high-k gate stack structures under device operation. We have found that potential gradient was formed at the metal/HfO_2 interface by analyzing the shifts of the core levels as a function of the applied bias voltage. Angle resolved photoelectron spectroscopy revealed that SiO_2 layer was formed at the metal/HfO_2 interface. The formation of the SiO_2 layer at the interface might concern the Fermi level pinning, which is observed in metal/high-k gate stack structures(2).

(1)T. Nagata, M. Haemori, Y. Yamashita, H. Yoshikawa, Y. Iwashita, K. Kobayashi, T. Chikyo, Appl. Phys. Lett. 99 (2011) 223517

(2)Y. Yamashita, H. Yoshikawa, T. Chikyo, K. Kobayashi, ECS TRANSACTIONS 41 (2011) 331.

Fig. Si 1s substrate peak as a function of bias voltage for a Pt/HfO_2/SiO_2/Si gate stack structure.

TF-9-Or-1
Novel method of reactive magnetron sputtering process control

T14 Thin Films

#TF-9-Or-1

M. Jilek [1], P. Vasina [2], R. Zemlicka [2].

[1]PIVOT a.s. - Sumperk (Czech republic), [2]Masaryk University - Brno (Czech republic).

Novel method of control of reactive magnetron sputtering process is presented. To control reactive magnetron sputtering process the process pressure is regulated by the flow of the reactive gas (nitrogen). Oscillations of the flow of the reactive gas are determined and used as feedback to find the right overall pressure, where stoichiometric coating is deposited. To see typical process behavior, see fig. 1. Proposed method of control was used for deposition of several coatings (TiN, AlTiN, AlCrN, CrTiN, …) on industrial scale central rotating unbalanced magnetron. To achieve superior adhesion of these layers, novel cleaning method called LGD was used. These coatings were used in industrial applications. Applications results in comparison with market standard coatings will be presented along with other measurements of deposited layers (EDX, SIMS, SEM, …).

fig.1: Typical reactive magnetron sputtering process behaviour - searching for the right pressure

TF-9-Or-4
Continuous thin film deposition on cylindrical metallic substrates using a tubular atmospheric pressure dielectric barrier discharge

T14 Thin Films

#TF-9-Or-4

C. Vandenabeele [1], R. Maurau [1], S. Bulou [1], P. Choquet [1], F. Siffer [2], T. Belmonte [3].

[1]CRP-Gabriel Lippmann - Belvaux (Luxembourg), [2]The Goodyear Tire and Rubber Company - Colmar-Berg (Luxembourg), [3]Institut Jean Lamour - Nancy (France).

On-line thin film deposition on cylindrical metallic substrates is of great interest for the development of composite materials, sensors, or for the realization of protective or adhesive layers. Thus, we have built a prototype consisting of a tubular dielectric barrier discharge working at atmospheric pressure. Deposition of organic coatings can be achieved with high deposition rates (up to 50 nm/s when the deposition is performed in static mode) and with a large variety of precursors.

Two examples will be described: organosilicon thin films from octamethylcyclotetrasiloxane (OMCTS or $C_8H_{24}O_4Si_4$) and organochlorinated thin films from methylene chloride (CH_2Cl_2), with or without addition of myrcene ($C_{10}H_{16}$). Precursors are first nebulized in an argon flow before being injected into the reactor.

Influence of experimental parameters (gas flow, dissipated power in the discharge and high voltage frequency) on the morphology and thickness of thin films has been studied by scanning electron microscopy. On the other hand, the discharge has been characterized by electrical measurements and optical emission spectroscopy. By setting ad hoc experimental parameters, dense, smooth, adhesive, stable and homogeneous coatings can be obtained.

In the case of coatings obtained from pure methylene chloride, X-Ray Photoelectron Spectroscopy depth profiling has revealed that the stoichiometry of the film is remarkably constant throughout the layer, indicating a steady thin film growth. Size Exclusion Chromatography has also been performed to determine the chemical structure of the deposited film.

It is worth indicating that with this type of precursors, a 100 nm thick film can be deposited on a wire at a linear speed closed to 1 m/min in a 15 cm long reactor featuring a 2.5 cm long electrode. Therefore, versatility and scalability of the process make it promising and suitable for industrial applications, by simply increasing the electrode length or multiplying the number of reactors, as illustrated in figure 1.

Figure 1: Prototype built for continuous plasma treatments of cylindrical substrates.

TF-P1-03
Electron-phonon interaction in free-standing ultrathin Pb(111) films: the effect of spin-orbit coupling

T14 Thin Films

#TF-P1-03

I. Sklyadneva [1], R. Heid [2], K.P. Bohnen [2], E. Chulkov [3].

[1]Donostia International Physics Center - San Sebastian, [2]Karlsruher Institut fur Technologie - Karlsruhe, [3]Universidad del Pais Vasco - San Sebastian.

The superconductivity of lead films with a thickness of a few monolayers and even of a single Pb layer on silicon has stimulated an active scientific interest in thin Pb films [1-3]. The experimental findings inspired a great amount of theoretical work focused on the thin film properties as well as on the impact of quantum size effect.
We present a theoretical study of the influence of spin-orbit interaction on the electron-phonon (e-ph) coupling strength at the Fermi level as well as on the phonon-induced linewidth of unoccupied and occupied quantum-well states (QWS) in ultrathin Pb(111) films of the thickness ranging from 4 to 10 monolayers. The strength of e-ph interaction as well as the contribution to the QWS linewidth coming from the e-ph scattering were obtained directly using layer-dependent ab initio density functional calculations for free-standing Pb(111) films. The calculations take full account of quantum-size effects on film electron and phonon band structures as well as on the e-ph coupling. It is shown that the spin-orbit interaction produces a large enhancement of the electron-phonon coupling strength regardless of the film thickness. This partly reflects a strong SOC-induced softening of the film phonon spectra, and partly a SOC-mediated increase in electron-phonon coupling matrix elements. For thin films quantum size effects result in pronounced oscillations of the average coupling constant with the number of layers, which become damped for thicker films.

1. Y. Guo, Y.-F. Zhang, X.-Y. Bao, T.-Z. Han, Z. Tang, L.-X. Zhang, W.-G. Zhu, E. Wang, Q. Niu, Z. Qiu, J.-F. Jia, Z.-X. Zhao, and
Q.-K. Xue, Science {\bf 306}, 1915 (2004).

2. X.-Y. Bao, Y.-F. Zhang, Y. Wang, J.-F. Jia, Q.-K. Xue, X. C. Xie, and Z.-X. Zhao, Phys. Rev. Lett. {\bf 95}, 247005 (2005).

3. C. Brun, I.-Po Hong, F. Patthey, I. Y. Sklyadneva, R. Heid, P. M. Echenique, K. P. Bohnen, E. V. Chulkov, and W.-D. Schneider, Phys.
Rev. Lett. {\bf 102}, 207002 (2009).

TF-P2-37
Elaboration of nanocomposite thin films by in-situ reduction during non-reactive sputtering of a ceramic target

T14 Thin Films

#TF-P2-37

L. Presmanes, H. Le Trong, T. Bui, A. Chapelle, I. El Younsi, I. Pasquet, C. Bonningue, A. Barnabé, P. Tailhades.

CIRIMAT / University of Toulouse / CNRS - Toulouse (France).

The preparation of nanocomposite thin films can lead to devices with attractive optical, magnetic, and semiconducting properties. The majority of authors active in the field of oxide thin films, reports the elaboration of oxide thin films by reactive magnetron sputtering from a metallic target using an $Ar–O_2$ gas mixture. The proportion of oxygen present in the plasma then determines the stoichiometry of the oxide. However the control of this chemical reaction is quite difficult. Another method to obtain oxide thin films is by radio frequency (RF) sputtering of an oxide target. During sputtering, the target and the layer growing on the substrate are subjected to continuous bombardment by energetic species. In the case of oxide deposition, oxygen atoms can even be ejected from the target and/or the film when the bombardment becomes stronger. Under-stoichiometric oxides, reduced phases or metallic particles result from such conditions. The amount of reduced phase can then be adjusted by the modification the sputtering conditions. The additional bias polarization of the substrate is a complementary way to increase the bombardment on the growing layer. These extreme conditions of preparation lead to interesting reducing preparation conditions from which metal/oxide or oxide/oxide nanocomposites can result [1, 2].

We present some examples of nanocomposites that have been obtained by direct sputtering from oxide targets in a pure argon gas flow with, or without, additional applied bias power. Especialy we report here the preparation of nanocomposite thin films from various targets:

- Cu/Fe_3O_4, from $CuFeO_2$ target,
- $CuO/CuFe_2O_4$, from $CuFeO_2$ target,
- Fe/FeO, from Fe_3O_4 target,

- FeO/Fe_3O_4, from Fe_3O_4 target,
- $(Zn,Fe)O/ZnFe_2O_4$, from $ZnFe_2O_4$ target,
- $Ni/(Ni,Fe)O/NiFe_2O_4$, from $NiFe_2O_4$ target,
- and $(Co,Fe)O/Co_{1.7}Fe_{1.3}O_4$, from $Co_{1.7}Fe_{1.3}O_4$ target.

These compounds were easily obtained by rf-sputtering of ceramic targets under different in-situ reducing conditions.

Regarding some examples of the properties of such materials, we have shown that these nanoscale composites comprising phases with different magnetic properties (e.g. ferri-, ferro-and antiferro-magnetic) can generate magnetic coupling with strong exchange interactions. In addition, the composite $CuO\text{-}CuFe_2O_4$ showed particularly a very strong increase of the sensitivity for the semiconducting detection of CO_2 gaz [3].

[1] "Nanocomposites of metallic copper and spinel ferrite films: Growth and self-assembly of copper particles". E. Mugnier, I. Pasquet, A. Barnabe, L. Presmanes, C. Bonningue, Ph. Tailhades, Thin Solid Films 493 (2005) 49.

[2] "Nanocomposite $Fe_{1-x}O/Fe_3O_4$, $Fe/Fe_{1-x}O$ thin films prepared by RF sputtering and revealed by magnetic coupling effects". B. Mauvernay, L. Presmanes, C. Bonningue, Ph. Tailhades, J. Magn. & Magn. Mater. 320 (2008) 58.

[3] "CO_2 sensing properties of semiconducting copper oxide and spinel ferrite nanocomposite thin film"
A. Chapelle, F. Oudrhiri-Hassani, L. Presmanes, A. Barnabé, Ph. Tailhades, Applied Surface Science, 256 (2010) 4715.

TF-3-Or-12
STRUCTURAL CHARACTERIZATION AND THERMAL NOISE PERFORMANCE OF TANTALA AND SILICA DEPOSITED WITH IBS

T14 Thin Films

#TF-3-Or-12

G. Cagnoli.

LMA - Villeurbanne (France).

Tantala and Silica deposited by IBS are the constituent materials for the reflecting coatings of the Advanced Gravitational Wave (GW) Detectors core optics, as well as of the ultimate frequency reference standards having line widths of tenths of Hertz. The Laboratoire des Matériaux Avancés (LMA) in collaboration with the Institute Lumière et Matière of the Universitité Claude Bernard Lyon1 has started an investigation on the structural properties of these two materials to detect the centres of relaxations responsible of the thermal noise. This investigation should lead to an amelioration of optical and mechanical characteristics of tantala and silica and, in particular, to a reduction of coating thermal noise that at this moment is the major limit to the performance of GW detectors and frequency standards.
In this presentation, after a brief introduction to the problem of thermal noise in optical coatings, results from the correlation between Raman and Brillouin scattering on one side and mechanical loss measurements on the other will be discussed.

TF-8-Or-2
Growth of FeCo soft magnetic thin films by chemical vapor deposition

T14 Thin Films

#TF-8-Or-2

J. Abelson [1], P. Zhang [1], S. Babar [1], S. Sahoo [2], M. Kautzky [2], L. Davis [1], G. Girolami [1].

[1]Univ. of Illinois - Urbana (United states), [2]Seagate Technology - Bloomington (United states).

FeCo alloys have been widely used in magnetic recording and other industrial applications, due to their excellent soft ferromagnetic properties: high Ms, low Hc and good thermal stability. $Fe_{50-70}Co_{50-30}$ alloys have the highest Ms of 2.4T, which is higher than other soft magnetic alloys such as NiFe and FeSi.
The current methods for FeCo thin film growth are mainly by PVD such as sputtering, MBE or by electrodeposition. It is difficult to coat complex structures conformally using PVD, while chemical vapor deposition (CVD) is known to have better conformality. However, there has been no report of CVD for FeCo alloy thin films yet. Here we demonstrate a process to grow FeCo thin films by low-temperature (< 250 °C) CVD from a gaseous mixture of commercially available Fe and Co carbonyls. The films have high purity and great magnetic properties (Ms = 2.52 T, Hc~ 12 Oe). Film growth is carried out in a UHV chamber. The substrate is planar SiO_2 with 5 nm Ru seed layer. $Fe(CO)_5$ and $Co_2(CO)_8$ precursors are introduced into the chamber by separate gas lines pointing toward the substrate. Precursor fluxes are controlled independently with needle valves. No carrier gas is needed.
Optimized results are obtained at $Fe(CO)_5$ partial pressure of 0.110 mTorr, $Co_2(CO)_8$ partial pressure of 0.060 mTorr and a substrate temperature of 230°C. No additional magnetic field is applied during growth. Films are capped with CVD grown HfB_2 layer to avoid surface oxidation.
Figure 1 shows a cross-sectional TEM image of FeCo film grown for 6 min. It is 336 nm thick with a dense and smooth structure. Auger depth profile shows a constant Fe/Co ratio of 55/45 throughout the film, and the oxygen content is very small. The hysteresis (Fig. 2) shows a perfect soft magnetic film with Hc as low as 12 Oe, which is consistent with its low impurity level. Its Ms is 2.52 T, which is the highest value that an FeCo alloy can reach theroetically.

Fig 1. Cross sectional TEM image of Fe55CO45 film

Fig 2. VSM analysis

TF-1-Or-1
Metastable nanotubular TiO2 and their transformation into anatase nanoparticulate layers on surface of anodized titanium subject to alumina grit blasting

T14 Thin Films

#TF-1-Or-1

M. Mendoza López [1], C.Y. Torres López [2], J. Pérez Bueno [2].

[1]Instituto Tecnológico de Querétaro - Querétaro (Mexico), [2]Centro de Investigación y Desarrollo Tecnológico en Electroquímica - Querétaro (Mexico).

TiO2 nanotubular/Ti electrodes were prepared into organic and aqueous media for photocatalytical decomposition of an azo dye (methyl orange). For this, nanotubes were produced under anodizing process, using two dissolution media: organic medium (98% ethylene glycol, NH4F 0.3 %wt, 60 V) and aqueous medium (1 M Na2SO4, NH4F 0.3 %wt, 20 V) [1]. Considering the attained control with an organic medium, this and its conditions were chosen (Figure 1). Titanium surfaces were pretreated by grit blasting with alumina particles. This was proposed in order to increase adherence by physical anchorage at different topological levels of the modified layer.
The alumina grit blasting technique was applied to titanium plates, prior to anodizing, provided changes beyond increasing adherence. The nanotubes layers were metastable and reactive, if not thermally treated, under exposure to OH media, such as water or alcohol. The dye solutions were decolorized by a new prepared sample only once, without applying UV. Anatase nanocrystallites grow and structure changed completely, as shown at Figure 2. The alumina was crucial for such process. EDS analysis show substantial alumina content increase on surface, from 0.5 % up to 12%, attributed to exposure of remnant grits chucks. Titania underwent restructuring losing tubular shapes and acquiring a nanoparticles coverage. These nanoparticles crystallized as anatase with particle sizes about 4 nm.

[1] C.A. Grimes, O.K. Varghese, S. Ranjan, in: Light, Water, Hydrogen. The Solar Generation of Hydrogen by Water Photoelectrolysis. Springer. New York. 2008. Chapter 5, 257–369.

Figure 1. TiO2 nanotubes obtained by anodizing a titanium plate, which was pretreated with alumina grit blasting.
Figure 2. Modified surface constituted by anatase particles after three days into an azo dye aqueous solution, which was discolored.

TF-P2-38
Near-surface 2D-nanostructures in TiO2-δ and ZnO1–δ meso-structures

T14 Thin Films

#TF-P2-38

A. Lisachenko, L. Basov.

V.A. Fock Institute of Physics, St. Petersburg State University - St. Petersburg (Russian federation).

Previously [1] we proposed a technique for wide-bandgap oxides TiO_2 and ZnO "self-sensitization" in VIS region using the photo-reduction of surface to $TiO_{2-\delta}$ and $ZnO_{1-\delta}$. This creates the coloured electron (F- type) and hole (O^-) V-type centers on the surface and near-surface 2D-nanostructures $TiO_2/TiO_{2-\delta}$ and $ZnO/ZnO_{1-\delta}$. The aim of the present work was to study the nature of VIS-excitations in $TiO_2/TiO_{2-\delta}$ and $ZnO/ZnO_{1-\delta}$.

In situ investigations were performed in gas, adsorbate and solid state [2] using mass-spectrometry, optical UV-VIS-NIR, ESR, UPES spectroscopies. For ZnO we used also the photoluminescence (PL), Kelvin probe (KP) and surface photo-voltage (SPV) measurements. Meso- and nano-structured powders of high-purity TiO_2 and ZnO were used.
Two types of non interacting excited electron subsystems are established: the "fast" one is excited in bulk under UV irradiation and the "slow" one is excited on the surface in VIS region. The energetic levels in the near-surface energy well are discrete, that explains the long lifetimes of excited states, the high efficiency of the VIS-activated reactions and the "memory" effect [3].
The VIS illumination decreases δ, but does not change the values of SPV nor the intensity of UV-excited PL. The UV irradiation decreases the dipole barrier δ and also the barrier V_1 due to the diffusion to the surface of holes generated in the bulk. Oxygen adsorption occurs on electrons, emerging into the surface via V_1 giving O^-_2 species and the green PL quenching.
Hole centers give the adsorption species O^-_3 which is a precursor in POIE and oxidation reactions.
We can expect that "self-sensitization" of $TiO_2/TiO_{2-\delta}$ and $ZnO/ZnO_{1-\delta}$-based photocatalysts and solar photoelectric or photo-electrochemical cells using intrinsic

point defects and near-surface 2D-nanostructures is a real way to optimize the design of efficient VIS photoactive elements for the conversion of sunlight energy.

[1] A.A. Lisachenko, R.V. Mikhailov, L.L. Basov, B.N. Shelimov, M.Che. *J. Phys. Chem. C*. **111** (2007) 14440.
[2]. A.A. Lisachenko. Physica B: Condensed Matter, **404** (2009) 4842.
[3] R.V. Mikhaylov, A.A. Lisachenko, V.V. Titov. *J. Phys. Chem. C.* **116** (2012) 23332.

Electron energy scheme of $ZnO/ZnO_{1-\delta}$, $TiO_2/TiO_{2-\delta}$ 2D near-surface nanostructures. E_F – Fermi level; CB, VB – conduction and valence bands; N(E) – density of occupied surface states (DOS); δ – dipole barrier; V_1 – barrier volume → surface; V_2 – barrier surface → volume; V_{Sch}– Schottky barrier; V_1 and V_2 are the results of superposition of the Schottky barrier in meso-structure and of the near-surface potential of reduced oxide. The latter potential decreases E_g value on the surface.

TF-P2-39
The properties of TiO2 thin films deposited on silicon by Atomic Layer Deposition

T14 Thin Films

#TF-P2-39

R. Mikhaylov, V. Lavrentiev, V. Titov, V. Drozd, L. Basov, A. Lisachenko.

St. Petersburg State University - St. Petersburg (Russian federation).

The sensitization of TiO_2 to VIS region is a key problem for using TiO_2–based convertors of sunlight energy to chemical or electrical one. For this purpose the composites of TiO_2 with narrow-gap semiconductors are designed. Among other an atomic layer deposition (ALD) technique is used. ALD method is promising to create transparent, protective, photoactive layers on the surfaces.

The aim of this work was to investigate a response of thin TiO_2 layers deposited on *p*-Si (100) to VIS light irradiation. TiO_2 layers with various thicknesses (from 2 to 300 nm) were obtained by ALD using $TiCl_4$ and H_2O as precursors. The UV (8.43 eV) PES, mass-spectrometry, SEM, AFM, UV-VIS DRS, hydrophilicity state measurements were used for characterization. SEM and AFM have shown that the films obtained by ALD have a continuous, homogeneous and plane surface.

The comparative photoelectron spectra of TiO_2 films with various thicknesses (from 2 to 300 nm) were obtained. In case of 2 nm TiO_2 films the photoemission current is the sum of the emissions from the film and the substrate. Thicker films partially capture photoelectrons from the substrate, and for the thickness over 25 nm the UV (8.43 eV) photoelectrons generated in the silicon substrate practically do not penetrate through the film.

The changes in the electron structure of TiO_2 films are induced by irradiation in the inter-band as well as in the sub-bandgap region of TiO_2. Not only UV but also VIS irradiation in vacuum reduces the surface because of oxygen losses, that results in a decrease of both thermoelectric workfunction φ_t and contact potential. On the contrary, the irradiation in O_2 leads to oxidizing of TiO_2 surface and to the increase of φ_t. For the thin TiO_2 film (2 nm) the noticeable changes in the electron structure occur even under irradiation with $\lambda > 550$ nm due to light absorption by a silicon substrate with subsequent redistribution of charge between Si and TiO_2.

The photoinduced hydrophilicity of films surface was of special interest. On TiO_2 films the effect of super-hydrophilicity was attained under UV irradiation, as well as under VIS one.

The effects associated with the gas phase are eliminated by the deposition of thin (2 nm) dielectric Al_2O_3 film on TiO_2. A thin layer of Al_2O_3 films was deposited on the TiO_2 film by ALD using trimethylaluminium and water as precursors. Such film protects the structure of TiO_2 film in course of heating and irradiation in vacuum or gas atmosphere. The photoelectrons tunnel through this Al_2O_3 film into the vacuum. Oxygen strongly changes the PES spectra of TiO_2 samples not covered with an Al_2O_3 layer but does not change the PES spectra of protected TiO_2 surface.

The obtained results indicate that the composite TiO_2/*p*-Si can be considered as a perspective photocatalyst for sunlight efficient photocatalytic systems, for a gas sensors and self-cleaning photocatalytic surfaces, in cases when TiO_2 surface contacts with the gas phase. In its turn the active TiO_2 film isolated from gas phase with a thin dielectric Al_2O_3 film may become an effective solar photoelectric or photo-electrochemical cell.

TF-P3-07
Effect of ZnSe quantum dots concentration on optical properties of poly (3-hexylthiophene) thin film by PDS technique

T14 Thin Films

#TF-P3-07

D. Loubiri.

Photothermal laboratory - Nabeul (Tunisia).

Synthesis and incorporation of nanocrystals (NC) offers several opportunities to exploit CNs for the development of next-generation hybrid organic / inorganic solar cells. Among the organic/inorganic hybrids system, the poly(3-hexylthiopene) (P3HT) is one of the most used conjugated polymers (CPs), for inorganic nanocrystals ZnSe quantum dots (QDs) are the most commonly investigated NCs because of their quantum-confined nature and well-matched energy level with P3HT. In this work the Photothermal Deflection Spectroscopy technique (PDS) is used to study the effect of the ZnSe quantum dots concentration in poly(3-hexylthiophene) matrix on optical properties. The optical absorption spectra and the band gap energy are obtained by comparing the experimental curves giving the normalized amplitude variations versus wavelength to the corresponding theoretical ones representing the normalized amplitude variations versus optical absorption coefficient.

TF-3-Or-9
Elaboration of iron cobaltite thin films by RF magnetron sputtering. Study of their spinodal decomposition

T14 Thin Films

#TF-3-Or-9

T. Bui, H. Le Trong, C. Bonningue, L. Presmanes, A. Barnabé, P. Tailhades.

Institut Carnot CIRIMAT CNRS - UPS - INP, Université Paul Sabatier 118 route de Narbonne, 31062 - Toulouse (France).

Iron cobaltite thin films with spinel structure were elaborated by radio frequency (RF) magnetron sputtering from a $Co_{1.73}Fe_{1.27}O_4$ target. The sputtering conditions (argon pressure and RF power) directly govern the reduction of deposited spinel phase. At a moderate fixed power, when argon pressure increases from 0.5 Pa to 1.5 Pa, the dominant deposited phase was changed from spinel phase (Sp) at 0.5 Pa to monoxide phase (MO) at 1.5 Pa (figure 1). At low pressure (0.5 Pa), the minor quantity of monoxide phase is also studied versus the RF power. After optimizing the sputtering conditions to obtain the nearly pure spinel phase, the films of about 300 nm thickness were deposited on Si (100) substrates (figure 2), then post annealed at 600°C to investigate the spinodal decomposition. On XRD spectrum of post annealed films, when processing time grows, the characteristic peaks of the initial spinel phase are progressively split into two peaks, corresponding to two phase (rich in Co phase and rich in Fe phase). This division demonstrates pertinently the spinodal decomposition, which was studied on iron cobaltite powder [1] and iron cobaltite thin films prepared by sol-gel deposition [2]. Changes in structure and microstructure, resulting from this transformation, are confirmed by Raman analysis and TEM images.

[1] H. Le Trong, A. Barnabé, L. Presmanes, P. Tailhades. Solid State Sciences, 10, 550 (2008).
[2] K. J. Kim, J. H. Lee, C. S. Kim. Journal of the Korean Physical Society, 61, 1274-1278 (2012).

Figure 1: XRD pattern of thin films deposited at 0.5 Pa and 1.5 Pa
Figure 2: SEM image of thin film deposited at 0.5 Pa – 20 W

TF-P1-04
Determination of Heavy Metals on a Nanostructured Boron-Doped Diamond Electrode

T14 Thin Films

#TF-P1-04

P. Michniak [1], M. Vojs [1], M. Behúl [1], V. Řeháček [1], M. Veselý [1], V. Tvarožek [1], T. Ižák [2], A. Kromka [2].

[1]Slovak University of Technology, Faculty of Electrical Engineering and Information Technology, Institute of Electronics and Photonics, Ilkovičova 3, 812 19 - Bratislava (Slovakia), [2]Institute of Physics, Academy of Sciences of the Czech Republic, Cukrovarnicka 10, CZ 16253 - Praha (Czech republic).

In recent years, research in carbon films has been focused to diamond thin film synthesis. Low background current and large potential window between oxygen and hydrogen evolution favor to use diamond films for the detection of a variety of analytes, including toxic heavy metals in the environment. Boron-doped diamond (BDD) is a promising material for various applications in electrochemistry. In search for alternative electrode materials, bismuth-film electrodes have been shown to offer comparable performance to mercury-film electrodes for anodic stripping voltammetric measurements of heavy metals. In this contribution, technological steps as a growth of intrinsic nanodiamond (i-NCD)/BDD double layer, electrode fabrication and electrochemical measurements on Zn, Pb and Cd are discussed. Electrochemical measurements were done by square-wave voltammetry (SWASV). During SWASV experiments in Pb(II), Cd(II) and Zn(II) solutions well-shaped stripping peaks were obtained whose heights varied linearly with analyte concentration in the range from 1×10^{-8} M to 3×10^{-7} M and detection limit (3xstandard deviation/slope) and sensitivity for Zn, Cd, Pb with in-situ Bi electrochemical plating were detected. The results show that the nano-structured electrodes exhibit more than two times higher detection limit and sensitivity than non-structured BDD. Under optimal conditions detection limits for nano-structured BDD of 4.8×10^{-9} M, 3.7×10^{-9} M and 5.8×10^{-9} M were achieved for Pb(II), Cd(II) and Zn(II), respectively. Optimal concentration of Bi was 1×10^{-7} M.

Fig.1. SWASV curves for the stripping of 1-100x10^{-9} M Zn, Cd, Pb with 1x10^{-7} M of Bi in solution of 0.1 M acetate buffer for a) None-structured, b) Nano-structured BDD.

TF-4-Or-9
Studies on Transparent Conducting Tin Oxide (SnO2) Films Deposited by Thermal Evaporation

T14 Thin Films

#TF-4-Or-9

B. Beer Pal Singh, R. Rakesh Kumar, J. Jyotshana Gaur, R. Ramesh Chand Tyagi.

CCS University, Meerut - Meeerut (India).

Thin films of metallic oxides like tin oxide, indium tin oxide (ITO), and zinc oxide exhibit electrical conductivity while being transparent in the visible region of the spectrum. Such transparent conductive oxides (TCO) coatings find wide spread use in electro-optical devices such as gas sensors, electroluminescent displays and solar cells etc where the transparency of electrical contacts is a vital requirement for device operation. The surface morphology, structural characteristics and optical properties of the Transparent conducting SnO_2 films deposited by vapor deposition of $SnCl_2.2H_2O$ on heated glass substrate have been evaluated by XRD, SEM, EDAX analysis and spectro-photometric studies. The ‘as deposited’ films of tin oxide were found to be polycrystalline, adhesive and pin hole free. After annealing at a higher temperature these films exhibited an improved crystalline surface morphology and also displayed random perforations having a dendrite structure. It is found that heat treatment of the ‘as deposited’ tin oxide films results in conversion of the SnO component into SnO_2 phase which resulted in a better transparency , larger crystallite size, and reduced film thickness due to diffusion of tin into the matrix of the glass substrate thereby making the film more suitable for device application. The increased porosity of ‘annealed’ films provides more surface area for use as sensors and also makes them less likely to fracture when used as high temperature electrodes.

TF-7-Or-3
Thin-film lithium battery materials

T14 Thin Films

#TF-7-Or-3

J. Ribeiro [1], R. Sousa [1], J.A. Sousa [1], L.M. Goncalves [1], M.M. Silva [2], L. Dupont [3], J.H. Correia [1].

[1]Algoritmi centre, University of Minho - Guimaraes (Portugal), [2]Chemistry centre, University of Minho - Braga (Portugal), [3]LRCS – UMR 6007, Université de Picardie Jules Verne - Amiens (France).

Batteries are crucial for electronic autonomous and portable devices. The size of these devices is a huge challenge, because the miniaturization is increasingly important [1]. The thin-film batteries allow a lighter and small package because no liquids or polymers are used. This technology also increase the safety because no leaking or explosion could occur and the energy density [2]. The thin-film batteries can be fabricated using only physical vapour deposition techniques [3].
A battery is composed by two current collectors, two electrodes and one electrolyte. The electrolyte is an electrical isolator and an ionic conductor to allow the lithium ions pass through it, but not the electrons. The electrolyte selected in this work was lithium phosphorous oxinitride, deposited by RF sputtering, previous reported by our group [4]. The positive electrode selected was lithium cobalt oxide ($LiCoO_2$). The positive electrode (cathode) is where reduction reactions occurs. The $LiCoO_2$ was deposited by RF sputtering with power source of 150 W, deposition pressure of 3×10^{-3} mbar, Ar flow of 40 sccm, a deposition rate of 3,2 Å/s and a thickness of 700 nm. An annealing of 2h at 650 ºC in vacuum was performed for enhance the crystallization and consequently, the capacity of $LiCoO_2$ receive and deliver lithium ions. The oxidation reaction occurs in the negative electrode (anode). The metallic lithium was selected and fabricated by thermal evaporation, with 3 µm thickness. The cathode and anode current collectors were selected to ensure an excellent electrical conduction without reacting with the respective cathode and anode materials selected before. Platinum was selected for $LiCoO_2$ current collector and titanium for metallic Li current collector.
Thin-film lithium battery materials were deposited and characterized in this work. The materials are deposited one after another till the battery is completed. The design for the battery is presented in figure 1 and materials indicated. This design is archived by using shadow masks during depositions.

Supported by FCT with PTDC/EEAELC/114713/2009 and SFRH/BD/78217/2011.

[1]M. Armand, J.-M. Tarascon, “Building better batteries”, Nature, vol.451, pp.652, 2008.
[2]B. Fleutot, *et al.*, “Characterization of all-solid-state Li/LiPONB/TiOS microbatteries produced at the pilot scale”, J. Power Sources, vol.196, pp.10289, 2011.
[3]N. J. Dudney, “Solid-state thin-film rechargeable batteries,” Materials Science and Eng.: B, vol.116, pp.245, 2005.
[4]J. F. Ribeiro, *et al.*, “Enhanced solid-state electrolytes made of lithium phosphorous oxynitride films”, Thin Solid Films, vol.552, pp.85, 2012.

Fig.1: Thin-film lithium battery design with current collectors, cathode, electrolyte and anode indication (not on scale for better visualization).

TF-9-Or-13
Effect of Sputtering Pressure on mechanical properties in sputtered TiNi thin films

T14 Thin Films

#TF-9-Or-13

F. Meng [1], Y. Li [2], F. Lin [1], W. Zheng [1].

[1]Jilin University - Changchun (China), [2]Harbin Engineering University - Harbin (China).

Recently, shape memory alloys have attracted great attention [1]. It is a perfect micro-actuator candidate for the micro-electrical mechanical system, which require actuation and sensing mechanisms with high efficiency, thus the mechanical properties of films are concerned [2]. The TiNi films are deposited onto glass substrates by magnetron sputtering. The sputtering conditions are as follows: base pressure 4.0×10^{-4} Pa; argon pressure 6.0×10^{-2} Pa, 8.0×10^{-2} Pa and 10.0×10^{-2} Pa, respectively; sputtering power, 280 W; sputtering time: 4h; substrate to target distance, 60 mm. The NiTi films thickness is about 6μm. The films composition determined by energy dispersive X-ray spectroscopy is about Ti-51.17at.%Ni. The as-deposited film is treated at 798K for 1h. The microstructures of thin films are studied by the X-ray diffractometer with Cu Kα radiation. The mechanical properties are studied by MTS IIXP Nano-Hardness Tester. From the X-ray diffraction (XRD) profiles of heat-treaded films, it is seen that the peaks of austenite (B2), Ti_3Ni_4 precipitates and martensite (B19') appear in this figure. When the sputtering pressures are 6.0×10^{-2} Pa and 8.0×10^{-2} Pa, there are B2 phase and Ti_3Ni_4 precipitates. There are B2 and B19' phase with the sputtering pressures 10.0×10^{-2} Pa. The result is obtained the indentation hardness of TiNi film versus the displacement into surface under different sputtering pressures. The as-deposited TiNi films is amorphous, Ti_3Ni_4 precipitate appears at heat treatment process. The temperature of martensitic transformation increases with the increase of the sputtering pressure. The mechanical properties are relative to the conditions of the sputtering pressure.

[1] Y. Motemani, M. J. Tan, T.J. White, Materials and Design, 32 (2011) 688.

[2] A. K. Nanda Kumar, C. K. S. Nair, Materials Chemistry and Physics, 97(2006), 308.

TF-P2-21
Synthesis of functionalized graphene-based conductive thin films by microwave plasma-enhanced chemical vapor deposition

T14 Thin Films

#TF-P2-21

S. Mori, S. Kaneda, Y. Anekawa, A. Kameyama, M. Suzuki.

Tokyo Institute of Technology - Tokyo (Japan).

In this study, we synthesized functionalized graphene-based conductive thin films by microwave plasma-enhanced chemical vapor deposition in a $CO/H_2/N_2$ system. In our previous study, we could synthesize carbon nanowalls, which is micrometre-wide freestanding flakes consisting of stacked graphene layers, with very high growth rate. 1) The microwave plasma-enhanced CVD system is a modified ASTeX DPA25 plasma applicator in which the quartz discharge tube of a 15 mm inner diameter is utilized. Silicon single crystal wafers, quartz glass and stainless steel plates were used as substrates with a size of 10×10 mm^2 square. No catalyst materials were used in this study. The parameters of the CNWs deposition process were as follows: CO flow rate, 46 sccm; H_2 flow rate, 4 sccm; N_2 flow rate, 0-20 sccm; total pressure, 250 Pa; microwave power, 60 W. During the deposition, the substrate is placed at the center of the applicator and heated up by the microwave discharge. Substrate temperature was monitored by the radiation thermometer and was about 700 °C during the deposition. The functional groups in CNWs were evaluated by FTIR as shown in Fig. 1. The intensity of the infra-red absorbance peaks around 1000 to 1200 cm^{-1} due to C-N stretching vibrations are gradually increased with an increase in nitrogen feed rates. Figure 2 shows SEM images of the CNWs with different nitrogen feed rates. As shown in Fig. 2, the increase in nitrogen feed rates makes the size of individual CNWs smaller. The spaces between the adjacent walls are diminished with increasing nitrogen partial pressure. The sheet resistance of functionalized CNWs thin films was measured with four-probe method with different N_2 flow rates. The applicability of the functionalized CNWs thin films on the counter electrodes in dye-sensitized solar cells is also discussed.

1) S.Mori, T.Ueno, M.Suzuki, Diamond Relat. Mater. 20 (2011) 1129-1132.

Fig.1 FT-IR spectra of CNWs. N_2 flow rate：(a) 0; (b)4; (c)12; (d)20 sccm.

Fig.2 SEM images of CNWs. N_2 flow rate：(a) 0; (b)4; (c)12; (d)20 sccm.

SE/PST/TF/BI-3-Or-5
Functional polymeric coatings for tissue engineering applications

T14 Thin Films

#SE/PST/TF/BI-3-Or-5

M. Dinescu [1], A.I. Paun [2], A. Matei [1], A. Acasandrei [3], F. Stokker-Cheregi [1], M. Zamfirescu [1], A. Moldovan [1].

[1]NILPRP - Magurele-Bucharest (Romania), [2]Polytechnical University, NILPRP - Bucharest (Romania), [3]IFIN-HH - Magurele-Bucharest (Romania).

Tissue engineering has emerged as a solution in medicine due to the necessity of local rapid intervention with minimum damage for surrounding tissue and absence of organ implants. It consists in producing of biological structures that resemble closely with the in-vivo mechanical and structural properties of the tissues that have to be replaced. Reconstruction of new tissue via tissue engineering involves: (1) cells which are harvested and dissociated from the donor tissue; (2) materials used as scaffold substrates, where the cells are attached and cultured and (3) scaffolds biofunctionalization with growth factors which promote cell adhesion, proliferation, migration and differentiation [Khang G. et al, 2007].
In this paper deposition of biofunctionalized conducting polymeric thin films on tri-dimensional polymeric and metallic scaffolds is reported. For obtaining polymeric layers with controlled properties Matrix Assisted Pulsed Laser Evaporation (MAPLE) was used.
Polymeric tri-dimensional structures (scaffolds) were obtained by Laser Direct Writing via Multiphoton Absorption (LW-2PP) starting from a mixture containing aliphatic hybrid monomers, Tetrahidrofuran and photoinitiator. Metallic scafffolds were produced by laser irradiation of titanium target. For both experiments a Ti: Sapphire laser with 200 fs pulse duration and 2 kHz repetition rate, emitting at 775 nm was used. Then, the obtained structures were used as substrates for biofunctionalized conducting polymeric thin films blends deposition by Matrix Assisted Pulsed Laser Evaporation. In MAPLE the polymer to be deposited is dissolved in an appropriate solvent (0.1-2 wt % concentration) and frozen in a liquid nitrogen-cooled recipient, forming the frozen target. The frozen target is placed in a vacuum chamber and submitted to laser irradiation. During laser irradiation, the solvent vaporize, the polymer is transported by vapors and collected on the substrate in the form of a thin film while the volatile solvent is pumped away by the vacuum pumps. In the present

case, the receiving substrates will consist of the 3D constructs (inorganic hybrid polymers and 3 D patterned titanium. Desired properties of the polymeric coatings can be obtained by selecting laser fluence, number of laser pulses and composition of the frozen target. The conducting polymer chosen for coating the 3D constructs was polypyrrole (PPy). PPy is a suitable substrate for electrical manipulation of cells due to its environmental stability, lack of toxicity, excellent biocompatibility and low costs [Ahmed El-Said A. et al., 2010; Ateh D. D. et al., 2006]. The coating biofunctionalization was achieved by incorporation of biologically active agents within PPy coatings, using the unique capability of MAPLE to deposit in one step blends of polymers, proteins, drugs, etc. while keeping the functionality of each component [Piqué A. et al., 2002, Paun et al., 2010]. The as deposited structures were tested for their biocompatibility and stimulating tissue growth while inhibiting bacterial infections/inflammations.

Ahmed El-Said A. et al. 2010; Ultramicroscopy (110) 676–681
Ateh D. D. et al. 2006; J. R. Soc. Interface (3) 741–752
Piqué A. et al. 2002; Appl. Surf. Sci. (186) 408-415
Paun I. A. et al. 2010; Appl. Phys. Lett. (96) 2

TF-4-Or-1
A microstructural investigation of Zr-Cu thin films metallic glass (TFMG) deposited by magnetron sputtering

T14 Thin Films

#TF-4-Or-1

M. Apreutesei [1], P. Steyer [1], L. Joly-Pottuz [1], A. Billard [2], J. Qiao [1], S. Cardinal [1], F. Sanchette [3], J.M. Pelletier [1], C. Esnouf [1].

[1]INSA de Lyon, MATEIS Laboratory - Villeurbanne (France), [2]LERMPS-UTBM - Montebeliard (France), [3]LASMIS, UTT - Nogent (France).

In the recent years, due to their homogeneity and no structural shape the metallic glasses (MGs) have been extensively studied in the bulk form. Their excellent proprieties at room temperature, especially high yield strength and corrosion/wear resistance together with the lack of grain boundary make them interesting structural materials for several applications [1].
The efforts devoted to the continuous development of such materials promoted the formation of thin films metallic glasses (TFMGs). So far, numerous TFMGs based on multicomponent alloys such as Zr-Cu-Al-Ni, Pd-Cu-Si were reported, while just a few are dealing with simple alloy systems [2].
In this study is attempted to form Zr-Cu (within 13 to 90 at% Cu) thin films metallic glasses (TFMGs) by a PVD magnetron co-sputtering method and to investigate their glass forming ability (GFA). The second objective is to perform a detailed microstructural and chemical investigation at the scale of SEM and TEM with emphasis on thermal and mechanical properties.
SEM images on cross-section revealed shear striations and partially vein pattern, implying the typical characteristic of the BMGs as it is presented in figure 1.
XRD analysis revealed that films are amorphous at room temperature within the (33, 85) at% Cu range detectable by XRD. Yet, after a deeper investigation using TEM for some of the as-deposited Zr-Cu thin films two types of features are observed: films are characterized by a fully amorphous structure, or composed of fine crystalline nanodomains embedded into a Zr-Cu amorphous matrix.
In situ XRD were performed under a helium atmosphere every 30°C from room temperature up to 600 °C in order to study the thermal stability of the disordered structure. The first traces of ZrO2 oxides first appeared from 270°C. Further, the films

crystallize into nanocrystalline Cu10Zr7 and Cu51Zr14 phases upon exposure at temperatures above 350 °C.
The differential scanning calorimetry (DSC) was used to find out the crystallization parameters, namely Tg (glass transition temperature) and Tx (crystallization temperature) of the TFMG. The supercooled region (ΔT) was then found around 75K. The mechanical general mechanism that governs these films is essentially based on the fact that by increasing Cu content a denser atomic packing state is achieved leading to higher Young's modulus values. Young's modulus and hardness values of films, ranging from 100 to 110 GPa and 5 to 8 GPa are better than those of pure metals.

[1] F. Löffler Intermetallics, 11 (6) (2003) 529
[2] J. P. Chu et al., Thin Solid Films (2012) 16

Fig. 1. The cross-sectional SEM micrograph of Zr- 40.1 at %Cu film

SE/PST/TF/BI-P1-10
Titanium dioxide based sputter deposited anti bacterial composite coatings

T14 Thin Films

#SE/PST/TF/BI-P1-10

A. Billard [1], E. Monsifrot [2], M. Arab Pour Yazdi [1], F. Schuster [3].

[1]IRTES-LERMPS - Montbéliard (France), [2]DEPHIS sarl - Etupes (France), [3]CEA - Saclay (France).

Titanium dioxide under anatase form is known to present very high photo active properties which can be exploited in several domains of energy and environment. In particular, anti bacterial surfaces can be obtained by deposited crystallized titanium dioxide. In this case, a UV irradiation is necessary to allow the photocatalytic destruction of bacteries. Another way to produce anti bacterial surfaces is to associate titanium dioxide with a noble metal such as Cu or Ag in a composite metal-oxyde coating. For such coatings, the intrinsic anti bacterial activity of the noble metal dispersed in the ceramic matric of titanium dioxide allows the destruction of bacteries even in absence of UV irradiation.

This paper deals with the deposition of composite TiO2-Cu coatings synthesized by co sputtering of Ti and Cu targets in the presence of reactive Ar-O2 gas mixtures. In order to allow the full oxidation of titanium while limiting that of Cu, the coatings are deposited using plasma emission monitoring (PEM). After a description of the deposition vessel including the closed loop control PEM system, we investigate the setpoint to be monitored to produce stoichiometric titanium dioxide for different Ar pressures. Hence, the Cu enrichment is studied as a function of the discharge current dissipated on the Cu target for two setpoints yielding stoichiometric and slightly sub stoichiometric titanium dioxide and for different pressures. A special attention will be paid to the amount of copper oxide resulting from these different deposition conditions. In all cases, the structural, chemical and morphological characterizations of the coatings are performed. Finally, some specific formulations of composite TiO2-Cu coatings are selected and their performance as anti bacterial coatings are investigated using two model bacteries : Escherichia Coli and Staphylococcus Aureus.

TF-P2-40
ZnO-Ag composite by reactive magnetron co-sputtering: structural and morphological characterisations

T14 Thin Films

#TF-P2-40

R. Francq [1], A. El Mel [2], P.A. Cormier [2], R. Snyders [1].

[1]University of Mons - Materia Nova R&D Center - Mons (Belgium), [2]University of Mons - Mons (Belgium).

Nowadays, zinc oxide (ZnO) is extensively used as a semi-conductor for gas sensor or solar cell applications. It is accepted that doping ZnO films with Ag is a potential strategy to enhance its photocatalytic and antibacterial activities. Therefore, the controlled synthesis of ZnO-Ag thin films is of particular interest for medical use or for waste water purification. Nowadays, ZnO-Ag thin films are generally synthesized by wet chemistry methods (co-precipitation, sol-gel, hydrothermal, flame spray pyrolysis and electro-spinning) often using toxic solvents. Therefore, the development of less pollutant techniques would be of great interest for a large scale development of such a kind of coatings.
In this work, reactive magnetron co-sputtering is chosen as an efficient method to grow ZnO-Ag thin films. This approach allows a fine tuning of the the cristalline structure, morphology and stoichiometry of the films which are the main criteria defining the efficiency of the material in a given application. Our goal is to investigate the correlation between the experimental parameters of our process (applied power, pressure, target to substrate distance, oxygen flow rate) with the composition and the microstructure of the grown films. In addition their photocatalytic activity is evaluated. The deposited films are characterized in terms of phase constitution (X-ray diffraction), microstructure (scanning electron microscopy), and chemistry (X-ray photoelectron spectroscopy).

SE/PST/TF/BI-1-Or-11
Localized functionalization of nanopores for biochemical sensing

T14 Thin Films

#SE/PST/TF/BI-1-Or-11

G. Nonglaton [1], E. Grinenval [1], P. Fürjes [2], R.E. Gyurcsanyi [3].

[1]CEA Leti, MINATEC Campus, Department of microTechnologies for Biology and Healthcare - Grenoble (France), [2]Research Institute for Technical Physics and Materials Science of the Hungarian Academy of Sciences - Budapest (Hungary), [3]Department of Inorganic and Analytical Chemistry, Budapest University of Technology and Economics - Budapest (Hungary).

The label-free detection using chemically modified nanopores is an emerging research field. Nanopore technique is a promising way for very low concentrated molecule sensing. It has a unique property to electrically detect single molecule. Indeed, biological molecules are electrokinetically driven through a nanopore by an externally applied electric field. This results in a characteristic obstruction of the ionic current across the pore. When the nanopore is functionalized with bioreceptors, information on interactions with biomolecules can be extracted. To ensure the most sensitive detection to a biomarker, an anti-fouling layer should coat the outer surface of the nanopore while the coupling chemistry to immobilize bioreceptors is deposited inside the cavity. In this study, different organosilane based coatings were evaluated for antifouling or bioreceptors grafting. Coatings were characterized by static contact angle, streaming-current zeta potential measurements, Surface-Enhanced Ellipsometric Contrast optical technique, and fluorescence imaging. Effects of activation and functionalization processes on SiO2 and SiNx membranes were studied and characterized by Atomic Force Microscopy. As a proof of concept, the surfaces were chemically pattern by lithography technique to demonstrate the compatibility between antifouling chemistry and grafting chemistry. Then a process was developed allowing to sequentially functionalise the outer surface, and then after drilling, the inner surface of nanopores. The antibody immobilization was demonstrated by fluorescence imaging and characterized by Scanning Electronic Microscopy. The preliminary tests are very promising and show that while the control probes practically do not bind cTnI in the nanopores, in the antibody modified nanopores the cTnI binding causes a significant decrease in the trans-pore ion flux. The first results indicate a 10ng/mL cardiac Troponin I detection.

Gyurcsanyi, R. E., Chemically-modified nanopores for sensing. *Trends Anal. Chem.* **2008**, *27* (7), 627-639.

Functionalized nanopores with fluorescent antibodies

TF/SE-P3-04
Physical Properties of Reactive RF Magnetron Sputtered Silicon Dioxide Thin Films

T14 Thin Films

#TF/SE-P3-04

F. Cioldin, I. Doi, M.V.P. Dos Santos, J.A. Diniz, E.A. Zambotti, J. Godoy Filho.

University of Campinas - Campinas (Brazil).

In this work physical properties of silicon dioxide (SiO_2) thin films deposited by reactive RF Magnetron Sputtering were studied using different characterization techniques, such as ellipsometry (refractive index and thickness), scanning profiler (thickness), BHF etching (layer quality), infrared spectra (chemical bonds), and Raman Spectroscopy (composition). MOS capacitors were also fabricated to evaluate defects and dielectric constant of these films. The samples were obtained using silicon target (99.999%) in an Ar/O_2 ambient, at deposition pressure of 4-10 mTorr and 200-300 W of sputtering power. The gas flow ratio was changed in the range of 60-100 sccm (Ar) and 12-20 sccm (O_2). The deposition rate as shown Figure 1a it increases with the discharge power and decreases as the total gas ratio is increased. The refractive index of the samples varied from 1.461 to 1.476. The Infrared spectra, Figure 1b, shows the Si-O-Si vibrational band peak around 1072 $cm^{-1}$and 820 cm^{-1}, corresponding to the stretching and bending mode, which agree well with the band positions of Si-O reported in the literature of the RF sputtered SiO_2 films. No significant changes in IR spectra of the films were observed due to the variations in the deposition pressure. Also no absorption bands in the range of 3300 – 3650 cm^{-1} were observed, corresponding to SiOH group and absorbed water, which indicates low porosity of the obtained SiO_2 films. The Raman spectra showed the SiO_x peak at 193 cm^{-1} and 432 cm^{-1}, for the obtained samples, and that the first band becomes broader with the increase of the Si concentration in the films. Silicon dioxide with thermal grown SiO_2 quality may be obtained by reactive RF sputtering, for instances with 80/16 Ar/O_2 gas ratio, at deposition pressure of 4mTorr and 300 W sputtering power, with relatively high deposition rate of 4.6 nm/min with refractive index and Si/O ratio near to the stoichiometric value.

Figure 1 – (a) Deposition rate and Refractive index x Ar/O_2 Flow. (b) Infrared spectra showing the Si-O bonding.

SE/TF-P2-18
A comparative study of the oxidation behavior of cathodic arc evaporated AlCrN and AlCrYN coatings: A microstructural and physico-chemical investigation

T14 Thin Films

#SE/TF-P2-18

P. Steyer [1], M. Apreutesei [1], L. Joly-Pottuz [1], E. Damond [2], A. Malchere [1], T. Douillard [1], G. Van Der Volk [3], C. Esnouf [1].

[1]INSA de Lyon, MATEIS Laboratory - Villeurbanne (France), [2]Ionbond - Chassieu (France), [3]Ionbond - Venlo (Netherlands).

It yielded that cutting tools are subjected to extreme conditions of temperature, wear, mechanical and friction. Even more, high mechanical stresses are applied on the tools used in aggressive environments and high temperatures. Considering these extreme industrial requirements, alternative solutions had to be developed. Ceramic nitride based coatings could give new functionalities and improve the tools' surface. Their purpose is to increase the lifetime and high oxidation resistance. Recently, new protective materials able to meet these requirements have been proposed, such as Al-Cr-N based coating. A further improvement was obtained by incorporation of yttrium in this system, its beneficial effect being evidenced mainly at high temperature conditions.
This study aims to investigate the oxidation behavior and thermal stability of CrN and AlCrN coatings. Moreover, the effect of yttrium addition on arc evaporated AlCrN coating with emphasis on high temperature behavior is highlighted. Three different coatings of approximately 3 µm thick (CrN, AlCrN and AlCrYN) were deposited on various substrates (M2 steel, Si, glass) in an industrial reactor.
The comparative study of oxidation behavior was performed by thermogravimetric analysis in dry air at selected temperatures from 750 to 950 °C. Thermograms reveal a parabolic evolution of mass gain, suggesting an oxidation process limited by the transport of species. The surface morphology and microstructure of films, oxidized or not, were characterized by means of scanning electron microscopy (SEM), energy

dispersive X-ray analysis (EDX) and transmission electron microscope (TEM). Moreover, films oxidation was observed in real-time at a microscopic scale using a SEM operating in an environmental mode. In situ XRD were performed under protective atmosphere every 30°C from room temperature up to 1000 °C in order to study their thermal stability.
Surface defects density was quantitatively measured by an electrochemical method and was found to be lower than 1% for Y containing films and 0.25 % for Y-free films, respectively.
Films are characterized by a fine grained structure of about 25 nm. Therefore, the aluminum addition into CrN induces a beneficial effect on the thermal stability of the microstructure. At moderate temperature range (800 – 850 °C) oxidation behavior is mainly governed by the intrinsic morphology of the films, while at higher temperatures (950 °C) the beneficial effect of film's composition is emphasized. The oxidation performance of AlCrN films is considerably improved by Y incorporation due to formation of Y_2O_3 phases dispersed into the coating which promote the oxide layer adhesion and hinders grain coarsening.

Key words: AlCrN, AlCrYN, oxidation resistance, thermogravimetric analysis, thermal stability, TEM

SE/TF-P2-19
Mechanical and tribological characterization of TiN, TiAlN and multi-layered TiAlN coatings prepared by different deposition routes: HiPIMS and cathodic arc

T14 Thin Films

#SE/TF-P2-19

A. Quenardel [1], P.Y. Jouan [1], A. Billard [2], F. Lomello [3], F. Schuster [4].

[1]Institut des Matériaux Jean Rouxel - Nantes (France), [2]IRTES-LERMPS, UTBM - Montbéliard (France), [3]DEN/DANS/DPC/SEARS/LISL CEA Saclay - Gif-Sur-Yvette (France), [4]CEA Cross-Cutting program on Advanced Materials Saclay - Gif-Sur-Yvette (France).

TiN is historically one of the most employed coatings in the industry for different applications such as cutting tools, dies, bearings, anti-erosion components, etc.

With the aim of enhancing the mechanical properties of titanium nitride, two main ways can be involved. Firstly, a third chemical element, i.e. aluminum, was added to deposit TiAlN coatings with improved mechanical properties and oxidation resistance. Secondly, nano-layered TiN/TiAlN coatings were synthesized in order to enhance their hardness and their tribological behaviour.

Another way to manage properties of nitride coatings is the control of their intrinsic stress. The possibility of controlling the average energy per impinging atoms is the main way to reach this goal. This can be done using highly ionized discharges.

In this study, a comparison between the emerging HiPIMS (High-Power Impulsed Magnetron Sputtering) and the cathodic arc deposition process was performed owing to the deposition of TiN, TiAlN as TiN/TiAlN nanolayers coatings with different periods.

Structural, chemical and morphological characterization of the coatings was systematically performed using X-Ray Diffraction (XRD), X-Ray Energy Dispersive Spectroscopy (EDS), Glow Discharge Emission Spectroscopy (GDOES) and Scanning Electron Microscopy (SEM). The mechanical (Daimler-Benz Indentation Test, micro and nano-hardness) and tribological (pin on disc) characterizations were also realized on the different architectures obtained with both processes to allow the comparison of these two processing routes owing the performance of TiN based nanostructured coatings.

Keywords : TiN – TiAlN – nanolayer – HiPIMS – Arc Deposition – wear resistance – mechanical properties

TF-P2-41
Structural and optical proprieties of ZnO thin films deposited by Spray Plasma device

T14 Thin Films

#TF-P2-41

K. Baba, C. Lazzaroni, M. Nikravech.

LSPM-CNRS, Laboratoire des Sciences des Procédés et des Materiaux, Université Paris 13, Sornonne Paris Cité - Villetaneuse (France).

Because of its excellent physical properties and potential technological applications, zinc oxide (ZnO) has recently attracted a lot of attention. In this work, we present the characteristics of ZnO thin films deposited by Spray Plasma device [1,2]. In this process, fin droplets of an aqueous solution of zinc nitrate/chloride/acetate produced in an ultrasonic sprayer, are injected in a low pressure RF inductively coupled Argon/Oxygen plasma. The reactivity of non-thermal plasmas permits the transformation of this salts to zinc oxides. The Films were deposited on glass substrate at 200°C. The effect of zinc nitrate and zinc chloride solution, and oxygen ratio in the plasma gas on the structural and optical properties of the deposited films was investigated by X-ray diffraction, atomic force microscopy, transmission electron microscopy and Uv-Vis spectroscopy. Crystallite's size was estimated using Sherrer and Williamson-Hall [3] methods and then compared with MET images. The results show that nanostructured polycrystalline thin layers are formed with the typical wurtzit structure and a preferred c-axis orientation for the tow used solutions (Figure 1). The values of average grain size obtained from the XRD were less similar then those obtained from TEM images, implying the inclusion of strain in the deposited films.The best c-axis orientation and the best transmittance in visible range (80%) were obtained with 5% O_2 in the plasma gas. Radical oxygen emission bands were observed by optical emission spectroscopy indicating that the concentration of oxygen radicals increases first with increasing in O_2 ratio in argon plasma until 10% and then decreases. These results confirme that the O radicals concentrations influences the direction of crystal growth.

[1] M. Nikravech, Journal of Nanoscience and Nanotechnology 10, 1171 (2010).

[2] K. Baba, M. Nikravech, D. Vrel, A. Kanaev, L. Museur, and M. Chehimi, Journal of Nanoscience and Nanotechnology 12, 4744 (2012).

[3] G. K. Williamson and W. H. Hall, Acta Metallurgica 1, 22 (1953).

Figure 1. XRD patterns of ZnO films prepared using two different precursor solution ($ZnCl_2$ and $Zn(NO_3)_2$). In set: Texture coefficient (TC) for the (100),(002),(101) and (103) orientation. C=0.2 M, Plasma: Ar+5%O_2, Power 300W. D: crystallite size.

SE/TF-P2-20
Analysis of residual stresses in thin films Cr, Cr-N, Ti-Al, Cr-Mo-N and Ti-Si-N prepared by PVD

T14 Thin Films

#SE/TF-P2-20

L. Chekour [1], M.A. Djouadi [2], I. Rahil [1], Y. Benlatreche [1], H. Berkane [1], A. Khen [1], D. Derghame [1].

[1]LMDM laboratoire, université Constantine I - Constantine (Algeria), [2]LPCM, Institut des Matériaux UMR 6502 - Nantes (France).

Ceramic coatings are used extensively in industrial applications mostly to reduce wear on engine and machine components. Large residual stresses develop in coating films due to intrinsic stress or thermal stress produced by a mismatch between the thermal contractions of the film and the substrate, or as a result of other reasons. It is important to elucidate the factors that generate residual stresses in the film since residual stresses exert a strong influence on the mechanical properties of the coated material.
The aim of the present work is to investigate the effect of films thickness on residual stress, resistivity and microstructure. Deposits Cr, Ti-N, Cr-N, Ti-Al, Ti-Si-N and Mo-Cr-N are thus produced by PVD on silicon substrates. The determination of residual stresses and resistivity was made using the devices of "Newton Rings" and "four-point probe", respectively. The compressive stress reaches a peak value of about 5GPa. This stress peak appears to thickness ranging from 200 to 300 nm. . The effect of film thickness has also been highlighted on the resistivity of chromium films. There is a correlation between the variation of the stress, the resistivity and the phenomenon of thin film growth. Stress has also been studied for Mo-Cr-N and Ti-Si-N films.

Words - key: *PVD hard coatings, residual stress, resistivity.*

[1] Zhao Z. B., Rek Z. U., Yallisove S. M., Bilello J. C., Thin Solid Films, Volume 415, Issues 1-2, 1 August 2002, Pages 21-31.
[2] N. Marchal, E. Quesnel, Y. Pauleau, J. Mater. Res, 9 (1994) 1820.

[3] W. J. Meng, J. A. Sell, T. A. Perry, L. E. Rehn, P. M. Baldo, J. Appl, Phys. 75 (7) (1994) 3446- 3455.
[4] D. R. Mckenzie, W. D. Mcfall, W. G. Sainty, C. A. Davis, R. E. Collins, Diamand Relat. Mater. 2 (1993) 970.
[5] C. Quaeyhaegens, G. Knyt, J. D'Haen, L. M. Stals, Thin Solid Films 258 (1995) 170-173.
[6] P. Hones, Thèse de doctorat n°2116, Ecole Polytechnique Fédérale de Lausanne, 2000.
[7] Nouveau C., « Etude de revêtements durs (CrxNy) obtenus par méthodes PVD : réalisation et caractérisations, applications à l'usinage du bois », Thèse de doctorat n°21-2001, CER ENSAM Cluny, France.
[8] L. Holland. Vacuum deposited thin films, Champmam et Hall, London (1966).
[9] S.M. Kanga, S.G. Yoona, S.J. Suh, D.H. Yoon, Thin Solid Films 516 (2008) 3568–3571
[10] L. Chekour, C. Nouveau, A. Chala, C. Labidi, N. Rouag and M.A. Djouadi "Growth mechanism for chromium nitride films deposited by magnetron and triode sputtering methods" Surface and Coatings Technology, Volume 200, Issues 1-4, 1 October 2005, Pages 241-244.

TF-5-Or-4
Growth of diamond films and other carbon allotropes by surface wave plasma over large areas

T14 Thin Films

#TF-5-Or-4

A. Kromka, O. Babchenko, S. Potocky, B. Rezek.

Institute of Physics AS CR, v.v.i. - Prague (Czech republic).

Attractiveness of carbon-based allotropes (e.g. graphene, fullerenes, carbon nanotubes – CNT, diamond, etc.) reached extremely large interest in nanotechnologically oriented community due to their wide range of applications as smart-multifunctional materials. At the same time, microwave plasma chemical vapour deposition (CVD) techniques have reached outstanding designs which make the growth of CNTs or diamond thin films realistic for industrial uses. Surface wave plasma in the linear antenna configuration is one of the most attractive solution due to scale up capability to large areas (500x500 cm2 and larger) [1].
Here we will present the influence of process parameters (temperature, gas composition, total pressure, etc.) on the growth of diamond thin films by modified large area linear antenna microwave plasma CVD process from CO2 containing gas mixtures [2]. Adding CO2 facilitates the grain enlargement and improves the film quality as evidenced by electron microscopy and Raman spectroscopy. Next, gas pressure is identified as a crucial process parameter influencing the crystalline character of diamond films. Decrease from 200 to 6 Pa results in enlargement of diamond grains from nanoscale (<20 nm) to polycrystalline character (grain size 500 nm at 570 nm thickness). This result is partially in contrast to other work, where a formation of nano-sized diamond crystals dominated the process due to spontaneous gas phase nucleation [3]. Our growth phenomena are attributed to plasma expansion and change in plasma chemistry (i.e. hydrogen-rich plasma chemistry). The proposed growth model is supported by photographs and optical emission spectra of plasma.
Moreover, we will show that induced surface conductivity of intrinsic diamond thin films due to hydrogen termination can be achieved either by the diamond re-growth in focused plasma or by the CVD growth in linear antenna microwave CVD at lower CO2 (<5%) [4]. A functional solution-gated FET device based on diamond thin films grown by modified large area linear antenna microwave plasma CVD process.

The modified low pressure linear antenna microwave plasma process will be pointed as a challenging technology which expands the family of diamond uses in i) diamond-based optical elements for effective detection of adsorbed or grafted molecules, ii) the low temperature hydrogen termination (250°C) of diamond films and SGFET devices and iii) the growth of carbon nanotubes and/or carbon nano-sheets.
This research was financially supported by the projects P108/12/G108 (GACR), TA01011740 and by the Fellowship J.E. Purkyne. This work occurred in frame of the LNSM infrastructure.

[1] D. Roth, et al., Surface & Coatings Technology 74-75, 637 (1995)
[2] A. Kromka, et al., Vacuum 776-779, 86 (2012)
[3] K. Tsugawa, et al., Physical Review 125460, B 82 (2010)
[4] A. Kromka et al., Advanced Science, Engineering and Medicine (2013), in press.

TF-P3-03
Structural investigation of Si nanoparticles embedded in oxide film

T14 Thin Films

#TF-P3-03

P. Dubcek [1], B. Pivac [1], J. Dasovic [1], R. Slunjski [1], N. Radic [1], H. Zorc [1], S. Bernstorff [2].

[1]Rudjer Boskovic Institute - Zagreb (Croatia), [2]Elettra Sincrotrone Trieste - Trieste (Italy).

Silicon nanoparticle formation from silicon rich SiO2 thin films has been investigated as a function of deposition technique, as well as deposition and annealing temperature. The substrate was monocrystalline silicon and annealing was carried out in forming gas. Rotation of the Si substrate during evaporation ensured homogeneity of the films over the whole substrate. Formation of nanoparticles of different sizes after annealing at various temperatures up to 1100 °C was followed by grazing-incidence small-angle X-ray scattering (GISAXS). We have found that significant concentration of 2-3 nm sized particles is established already at 900 °C. The size distribution is broadening with the increment of the annealing temperatures, while the average sizes do not increase substantially. Photo luminescence measurements confirmed nanoparticle photo activity after passivization in hydrogen.

TF-P2-43
Effect of Bi Doping on Structural, Optical and Photoluminescence Properties of ZnO Thin Films

T14 Thin Films

#TF-P2-43

Y. Beggah [1], F. Chouikh [2], Y. Bouznit [2], N. Ariche [2], M. Birem [2].

[1]LMEPA Laboratory,University of Jijel - Jijel (Algeria), [2]LMEPA Laboratory, University of Jijel - Jijel (Algeria).

The nano-structural Bi-doped ZnO thin films deposited on glass substrate were successfully fabricated at substrate temperature of 350 °C by an inexpensive spray pyrolysis method. The structural, electrical, optical and photoluminescence properties and the morphology of the surface of films were investigated. X-ray diffraction study revealed the crystalline wurtzite (hexagonal) structure of the films and (100) preferential orientation . The spectral transmittance of all films was higher than 80% and so the doping has no effect on this optical property .The optical band gap energy varies between the value 3.19 eV to 3,24Ev. narrow and broad characteristic photoluminescence peaks emerged. The morphology of surface films was thoroughly rough.

[19] M. Krunks, E. Mellikov, Thin Solid Films 270 (1995) 33.
A.Chakrabortya, T. Mondal, S.K. Bera, S.K. Sen, R. Ghosh, G.K. Paul Materials Chemistry and Physics 112 (2008) 162–166
M. Alaoui Lamrani, M. Addou , Z. Sofiani, B. Sahraoui, J. Ebothe ,A. El Hichou , N. Fellahi, J.C. Bernede, R. Dounia Optics Communications 277 (2007) 196–201.
J.J. Tauc, Amorphous and Liquid Semiconductor, Plenum, New York, 1976.
A. Bougrine, A. El Hichou, M. Addou, J. Ebothé, A. Kachouna, M. Troyon, Material Chemistry and Physics (2003) 438-445.
Minhong Jiang and Xinyu Liu , J Mater Sci: Mater Electron (2009) 20:972–976.

TF-P2-08
Morphology and Structure of Sputtered W Thin Films

T14 Thin Films

#TF-P2-08

O. Milat [1], K. Salamon [1], Z. Kovačević [2], P. Dubček [3], M. Jerčinović [3], N. Radić [3].

[1]Institute of Physics - Zagreb (Croatia), [2]Faculty of Textile Technology - Zagreb (Croatia), [3]Rudjer Bošković Institute - Zagreb (Croatia).

Crystal structure and morphology of tungsten (W) thin films, prepared by magnetron sputtering, were studied by grazing incidence x-ray diffraction and small angle x-ray scattering, x-ray reflectivity, and scanning electron microscopy with compositional analysis. Coexistence of two crystalline phases, α-W and β-W, and formation of amorphous phase (a-W) were observed for various Ar pressures (2-20 mTorr), and flow rates controlled by the applied power (10-90 watt)[1]. Depositions at low Ar pressures (< 5 mTorr) and high powers (> 40 watt) result in compact and smooth layers of crystalline α-W phase only. By reducing the sputtering power (20 watt), along with stable α-W, a metastable β-W phase occurs. For even lower power (10 watt), W film becomes amorphous and exhibits a columnar morphology, like in Fig.1, accompanied with a 25% reduced layer's mass density compared to that of the bulk tungsten [2]. A similar columnar morphology was found also for films deposited at higher Ar pressures (> 5 mTorr), and moderate sputtering power of 20 watt; the columns in high pressure films consist of β-W phase. The columns diameter in the amorphous phase was 3 nm, while for β-W phase the average columns size was 4-6 nm[2]. Columnar aggregations were revealed at wide scale of correlation lengths: up to 10^3 nm (Fig.1.). The highest mass density reduction, of up to 50%, was observed for highest pressure of 20 mTorr. Morphology of W films deposited at high Ar pressures was depth dependent with smaller columns (and inter-columnar voids) closer to the Si substrate. In the amorphous film one observed top surface layer of 3.5 nm which could be attributed to the oxygen rich W or WO_3 phase. The appearance of β-W phase is related to the lowered flux of W atoms, increased film porosity, and correspondingly to the higher probability of oxygen incorporation.

[1] N. Radić, A. Tonejc , J. Ivkov, P. Dubček, S. Bernstorff, Z. Medunić Surf. Coat. Technol. **180** (2004) 66

[2] K. Salamon, O. Milat, N. Radić, P. Dubček, M. Jerčinović, accepted J.Phys D (Appl. Phys) **46** (2013)

Fig 1. Plan view of α-W film (SEI) revealing columnar aggregates correlations at: (a) 10^0 μm; (b) 10^2 nm

TF-3-Or-13
Dual Sensor-based Process Control for High Rate Reactive Zirconium and Hafnium Oxide Sputtering

T14 Thin Films

#TF-3-Or-13

M. Audronis [1], K. Juskevicius [2], R. Drazdys [2], A. Matthews [1].

[1]The Univesity of Sheffield - Sheffield (United kingdom), [2]Center for Physical Sciences and Technology - Vilnius (Lithuania).

Zirconia and Hafnia films are often used in multilayer coatings for advanced optical components, such as filters, beam splitters and polarisers. The laser industry has high specification requirements for these components in terms of the laser induced damage threshold. As low extinction as possible in the UV spectral range is highly desirable and significant efforts are spent to advance coating properties on this front. High deposition rate at room temperature (i.e. with no external heating) is also very much sought.
Voltage feedback-based gas flow control is one of the most economical methods to regulate reactive processes and deposit good quality zirconia and hafnia at high rates. It is however very difficult to perform due to multiple transitions in the sensor signal. In this paper we describe a reactive magnetron sputtering technology that exploits the target voltage signal to the full extent yielding a superior deposition process. Zr and Hf oxide films were produced employing a dual sensor-based process control method. We show that the use of this technology can result in improved optical properties, including absorption in the UV spectral range. High quality zirconia and hafnia films at high deposition rates with no external substrate heating were produced. Optical coated sample properties as well as some structural and surface morphology effects were examined and are reported in this paper.

SE-1-Or-13
Influence of nitrogen content on CrSiN thin film properties deposited by reactive HiPIMS

T14 Thin Films

#SE-1-Or-13

A. Ferrec, J. Keraudy, F. Schuster, P.Y. Jouan, M.A. Djouadi.

Institut des Matériaux Jean Rouxel (IMN) - Nantes (France).

Although transitional metal nitride films, such as CrN and TiN, have attracted a lot of interests due to the high hardness, high melting point and high chemical stability, their potential applications are limited, especially at high temperature. Recently, many researchers have focused on the development of complex hard film materials such as TiSiN, CrSiN, ZrSiN, nanocomposite films.
It has been proved that the reactive HiPIMS deposition technique enhance the adhesion, the crystallinity and the hardness of the films.
Here, we have have studied the influence of nitrogen content on the CrSiN thin film charactistics and their oxidation behaviour. The CrSiN were deposited using HiPIMS generator (HIP3 Solvix 5K) at floating potential without heating during deposition. The on-time was set at 30 µs and the frequency was 1000Hz. To obtain films with the same thickness, deposition time was adjusted with nitrogen content injected in the gas mixture. CrSiN thin films have been characterized by XRD, SEM and XPS.

TF-P1-06
CONTAMINATION CONTROL IN ION BEAM SPUTTER DEPOSITED FILMS

T14 Thin Films

#TF-P1-06

D. Pearson.

Oxford Plasma Technology - Bristol (United kingdom).

Ion beam sputter deposition is used in a wide variety of applications where precision film control and high quality, high performance layer materials are required. However, one of the difficulties of sputtering a target material with an ion beam is the control of the beam shape and collimation so as to avoid any energetic ions following trajectories whereby they could sputter other materials than the desired target material (e.g. from the surrounding furniture and fixtures); this results in a potential contamination of the depositing film with impurity material. The effect of this on the performance of the deposited film will depend on the particular application targeted, on the levels of impurities and on the nature of the impurities.
The conventional wisdom to guarantee high purity thin films in IBD has been to use a large vacuum chamber. The chamber size was important to minimise the effect of reflected high energy particles from the target surface sputtering chamber materials onto the substrate and to allow the use of large targets to avoid beam overspill onto chamber furniture: for example, chambers in excess of 1m3 have been used for the deposition of low loss dielectric mirrors. An improved understanding of beam trajectories and re-sputtered material paths has allowed the deposition of thin films with very low metallic impurity content in a chamber volume below 0.5 m^3.
Thus, by optimizing the sputter ion source, target and substrate configuration, and by arranging suitable shielding made of an appropriate material in the process chamber, the levels of contaminants in the deposited films have been reduced to a minimum. With this optimum hardware arrangement, the ion beam process parameters were then optimized with respect to the ppm levels of contaminants measured in the films by SIMS analysis.
Using the deposition of SiO_2 as a standard material for SIMS composition analysis and impurity level determination, it has been shown that our IBS deposition tool is capable of depositing films with contamination levels of <50ppm for the total of all metal impurities in the deposited films.

TF-4-In-2
SELF-ASSEMBLY OF SEMICONDUCTOR QUANTUM DOTS IN AMORPHOUS DIELECTRIC MATRICES

T14 Thin Films

#TF-4-In-2

M. Buljan.

Ruđer Bošković Institute - Zagreb (Croatia).

Three-dimensional semiconductor quantum dot lattices embedded in dielectric amorphous matrices are increasingly important in various nanotechnology applications. Two simple methods based on self-assembly have recently been developed for controlled preparation of such materials: Self-assembled growth of quantum dots during magnetron sputtering codeposition, and ion-beam irradiation of initially amorphous, semiconductor-rich multilayer films.
Both methods yield various three-dimensional quantum dot lattices, differing by the type of spatial ordering, matrix and quantum dots chemical and phase composition, QD's separation, shape, and size distribution. The prepared materials exhibit very interesting size- and ordering- dependent physical properties, with large potential for various applications.

PST/SE/TF-2-In-1
NANOSCIENCE WITH PLASMAS IN LIQUIDS: DIVING INTO THE UNKNOWN

T14 Thin Films

#PST/SE/TF-2-In-1

T. Belmonte.

Institut Jean Lamour - Nancy (France).

Plasmas in liquids are an excellent way to produce large amounts of nanoparticles. Yields are usually expressed in grams per hour. Furthermore, these nanoparticles are trapped in the liquid phase, which makes them innocuous. Many different processes have been developed, showing pros and cons. However, very little is known about the possible mechanisms leading to the synthesis of nanoparticles. Understanding basic mechanisms would help a lot and processes could be controlled much better than they are today. We shall take stock of the current state in the typical example of nanocarbons. While similar energies can be dissipated in different liquids and electrodes arrangements, nanostructures span a wide range of compositions, shapes and sizes. Thus, it is possible to get nanoparticles, nanotubes, nanoonions and even nanohorns. The production of nanodiamonds (sometimes called UDDs for Ultrafine-Dispersed Diamonds) by plasmas in liquids will be evoked specifically. Results of time-resolved optical emission spectroscopy combined with ICCD imaging of nanosecond-pulsed plasmas will be given to describe important physical and chemical features of plasmas in liquids. Finally, we shall show how to organize nanoparticles into larger structures by controlling intense electric fields.

TF/SE-1-In-1
Surface science questions in astrophysics

T14 Thin Films

#TF/SE-1-In-1

R. Baragiola.

University of Virginia - Charlottesville (United states).

I will highlight some surface science questions which are important for the understanding of astronomical bodies such as interstellar grains, icy satellites in the outer solar system, and the rocky surfaces of the Moon, Mercury and asteroids. There will be a special emphasis on opportunities for surface scientists, and the need for special instrumentation for the laboratory and for space landers.

TF-2-In-1
PLASMONICS: SENSORS AND PHOTONICS APPLICATIONS

T14 Thin Films

#TF-2-In-1

R. Lukaszew.

THE COLLEGE OF WILLIAM & MARY - Williamsburg (United states).

We have recently reported on the enhanced magneto-optical activity in plasmonic nanostructures made with gold/silver and magnetic metals. In order to access other areas of interest in the EM spectrum we have expanded our studies to explore other possible plasmonic materials such as conducting oxides as well as highly correlated oxides, for example VO2, which has a metal–insulator transition (MIT) just above ambient temperature at ~340 K. Across the MIT VO2 optical properties are completely modified over a very broad frequency range. I will present our recent investigations on nucleation of the metallic phase, the extreme speed of the light-induced optical switching of VO2 thin films as well as the feasibility of its use to modulate THz radiation.

TF-1-Kn-1
ADVANCED CHARACTERISATION OF MAGNETIC MATERIALS

T14 Thin Films

#TF-1-Kn-1

L. Cohen.

Imperial College London - London (United kingdom).

Magnetic materials play an increasingly important role in our society. Over the last few years the group at Imperial College have built up a suite of novel characterisation tools to study the important physics properties of technologically important magnetic materials. In this talk I will give examples of the use of these tools for the study of spintronic materials, magnetocaloric materials and nanomagnetic artificial spin ice.

TF-1-In-1
GAS PULSING AND OBLIQUE ANGLE DEPOSITION FOR STRUCTURING OF THIN FILMS

T14 Thin Films

#TF-1-In-1

N. Martin.

Institut FEMTO-ST CNRS UMR 6174, Université de Franche-Comté, ENSMM, UTBM - Besancon (France).

Structuring of thin solid films at the micro- and nano-scale is presently one of the most exciting challenges of materials science. I will show various architectures of thin films sputter deposited by RGPP (Reactive Gas Pulsing Process) and oblique angle deposition techniques. The first approach enables an adjustment of the composition and structure (homogeneous or periodic multilayers). The second one plays on the incidence of the particle flux to design the morphology. Both approaches impact on the structuring of the films leading to broaden the range of physical properties compared to the conventional methods. I will present a non-exhaustive analysis of optical, electrical and mechanical characteristics of such films and, in the end, emphasis will be on the RGPP+GLAD combination.

TF-P1-05
Solid state wetting on nano-pillar arrays : dynamics and elasticity effects

T14 Thin Films

#TF-P1-05

M. Ignacio [1], P. Smereka [2], Y. Saito [3], O. Pierre-Louis [1].

[1]Institut Lumiere Matière, Université de Lyon, UMR5306 Université Lyon 1-CNRS - Villeurbanne (France), [2]Univ. Michigan - Ann-Harbor (United states), [3]Keio University - Yokohama (Japan).

A challenging perspective in heteroepitaxial growth is to use nanostructured substrates in order to obtain defect free crystals. Several experimental groups have indeed deposited GaN on Si substrates with nano-pores [1] or nano-pillars [2]. These authors showed that (i) islands can stay at the top of nanostrcutures – with void underneath, and (ii) the density of threading dislocations due to the lattice mismatch can be significantly reduced. These results may have a broad range of applications in optoelectronics.

In this context, we study the morphology and the dynamical evolution of a single crystalline nanoparticle in interaction with an array of nano-pillars [3], using both kinetic Monte Carlo simulations and analytical calculations. Solid islands exhibit several stable or metastable states. Some of these states are already known from the analogy to the literature on liquid-state wetting, such as the Cassie-Baxter (or Lotus) state where the island sits on top of the pillars , the Wenzel state where the island is impaled in the pillars.

We have determined the thresholds of stability of the Cassie-Baxter state depending on the system geometry, and on a parameter called the wettability, which accounts for the wetting properties of the crystal. When the wettability is large enough, the crystal collapses along the pillar until it reaches the base of the pillars. We demonstrate that the collapse dynamics can be decomposed in two phases: a deterministic impalement followed by Brownian motion along the pillar. We show that the dynamics can be controlled either by adatom surface diffusion or by two dimensional nucleation on facets.

Finally, we discuss the consequence of elastic strain induced by a lattice mismatch at

the interface. Elasticity increases the stability of the Cassie-Baxter state. We also find a novel state where the island is partially impaled [4].

[1] K. Zang et al, Appl. Phys. Lett. 88, 141925, (2006)
[2] S. D. Hersee et al, Journal of Applied Physics 97, 124308, (2005)
[3] M. Ignacio and O. Pierre-Louis, Phys. Rev. B 86, 235410, (2012)
[4] Preprint (2013)

Cassie-Baxter to Wenzel transition of a solid island

TF-7-In-1
LICoO2 THIN FILMS: TOWARDS NEW REWRITABLE MEDIA

T14 Thin Films

#TF-7-In-1

I.J. Giapintzakis.

Nanotechnology Research Center and Department of Mechanical & Manufacturing Engineering, University of Cyprus - Nicosia (Cyprus).

Successful integration of oxide thin films in the integrated circuits (ICs) industry could have a major impact in a wide range of applications, such as data storage, spintronics etc. LiCoO2 (LCO) is a two-dimensional layered compound, which is commonly used as a cathode electrode in rechargeable Li-ion batteries. LCO's interesting electrochemical properties are attributed to redox reactions involving the cobalt-oxygen layers and the intercalation and de-intercalation of Li ions. The growth of high quality epitaxial LCO films on technologically important substrates has been scarcely addressed. This presentation will provide an overview of recent studies designed to explore fundamental aspects of LCO thin film growth by pulsed laser deposition (PLD) as well as the suitability of these LCO thin films as a rewritable media in non-volatile memory applications.

TF-6-In-1
THE IMPACT OF DISORDER ON TRANSPORT IN CRYSTALLINE PHASE CHANGE MATERIALS

T14 Thin Films

#TF-6-In-1

M. Wuttig.

RWTH Aachen University of Technology - Aachen (Germany).

Understanding charge transport in phase change materials is crucial to extend the application range of these exciting materials. The reduction of drift, i.e. the increase of the resistivity of the amorphous phase with time, for example, would facilitate the development of multilevel memories. Tailoring the resistance of the crystalline state could help in reducing the power consumption upon amorphization. With this goal in mind we have studied the resistivity of crystalline phase change materials. A pronounced dependence of the room temperature resistivity upon annealing temperature is observed for crystalline phase change materials such as Ge1Sb2Te4 or Ge2Sb2Te5. This finding is corroborated by low temperature measurements as well as FTIR data, which confirm that a metal – insulator transition is observed without a change in crystallographic state. This is indicative for an electronically driven MIT [1].
Such an MIT can be achieved if the electron correlation exceeds a critical value (Mott MIT). A second route to insulating behavior has been identified by Anderson, who showed that increasing disorder turns a metal with delocalized electronic states at the Fermi energy into an insulator with localized states. In this talk, arguments for a disorder induced localization of charge carriers will be presented. The observations are compared with doped semiconductors such as Si:P, where both disorder and correlations are crucial to describe the charge transport. Experimental and theoretical attempts to unravel the origin of disorder induced localization will be presented. These calculations reveal that it is the ordering of vacancies into vacancy layers which drives the transition to the metallic state [2]. The potential of this remarkable impact of disorder for applications as well as our fundamental understanding of solids is discussed.

[1] T. Siegrist et al., Nature Materials 10, 202, (2011)
[2] W. Zhang et al., Nature Materials 11, 952 (2012)

TF-8-In-1
CHALLENGING OF THIN FILM PROPERTIES FOR MAGNETIC RECORDING AT ULTRA-HIGH STORAGE DENSITIES

T14 Thin Films

#TF-8-In-1

D. Suess.

Institute of Solid State Physics, University of Technology - Wien (Austria).

Hard disk media that support high storage densities require small grains in order to obtain high signal to noise ratios. The use of high coercive materials such as alloys in the L10 phase allow for thermally stable grains at grain diameters in the order of 4nm . However state of the art write heads produce too small fields to reverse these extremely hard magnetic grains. Recently composite media and exchange spring media were proposed in order to decrease the write field requirements. In exchange spring media an ultra-hard magnetic storage layer is strongly exchange coupled to softer magnetic layers. It is shown that in exchange spring media the switching field can be completely decoupled from the thermal stability. The high coercive materials can be switched with low fields
Another possibility to write on high coercive materials is to locally heat the media with a laser pulse, known as heat assisted magnetic recording. As a consequence of the heating at temperatures close to the Curie temperature the coercivity significantly decreases and the grain can be reversed. However, errors due to high temperature are introduced. The use of composite media will be presented which allows decreasing these thermal errors.

TF-3-In-1
Transparent electronics: from physical to chemical routes

T14 Thin Films

#TF-3-In-1

E.M.C. Fortunato, P. Barquinha, L. Pereira, R. Martins.

CENIMAT/I3N Departamento de Ciência dos Materiais, Faculdade de Ciências e Tecnologia, FCT, Universidade Nova de Lisboa and CEMOP-UNINOVA - Caparica (Portugal).

Transparent electronics has arrived and is contributing for generating a free real state electronics that is able to add new electronic functionalities onto surfaces, which currently are not used in this manner and where silicon cannot contribute [1,2]. The already high performance developed n- and p-type TFTs have been processed by physical vapour deposition (PVD) techniques like rf magnetron sputtering at room temperature which is already compatible with the use of low cost and flexible substrates (polymers, cellulose paper, among others). Besides that a tremendous development is coming through solution-based technologies very exciting for ink-jet printing, where the theoretical limitations are becoming practical evidences. In this paper we will review some of the most promising new technologies for n- and p-type thin film transistors based on oxide semiconductors and its currently and future applications.

[1] P. Barquinha, R. Martins, L. Pereira and E. Fortunato, Transparent Oxide Electronics: From Materials to Devices. West Sussex: Wiley & Sons (March 2012). ISBN 9780470683736.
[2] E. Fortunato, P. Barquinha, R. Martins, Advanced Materials 2012 (review paper). DOI: 10.1002/adma.201103228

Main landmarks achieved with thin-film transistors (TFTs).

VST-5-Or-14
Outgassing of Materials Stimulated by Mechanical Stress and Rubbing

T15 Vacuum Science and Technology

#VST-5-Or-14

R. Nevshupa [1], E. Roman [2], J.L. De Segovia [2].

[1]IETCC-CSIC - Madrid (Spain), [2]ICMM-CSIC - Madrid (Spain).

Mechanical elements of ultrahigh vacuum technological equipment, drives and manipulators of space systems may produce significant contamination of ultrahigh vacuum due to emission of gases from materials under stress and rubbing. Composition of emitted gases and behaviour of gas emission were studied for various materials including metals (Fe, Ni, steel, Ti, Ta, elastomers) and surface coatings (amorphous carbon, TiN, Mg, MgH_2, etc.). Various behavior scenarios of mechanically stimulated gas emission which can be ascribed to different physico-chemical mechanisms were identified depending on the type of the material subjected to rubbing and the emitted gas. The hypothesis of thermal desorption due to frictional heating was confidently ruled out. Alternative models of mechanically stimulated gas emission were suggested and discussed.

VST-P2-01
The generalized Hobson-Welch model - Calculation of the propagation behavior of leak induced-pressure gradients in cryogenically cooled accelerator beam pipes

T15 Vacuum Science and Technology

#VST-P2-01

S. Wilfert.

GSI Helmholtzzentrum für Schwerionenforschung - Darmstadt (Germany).

The occurrence of He leaks in cryogenically-cooled vacuum systems of accelerators can cause fatal problems. In consequence of the pumping action of the cold walls and due to a lack of suitable pressure measuring instrumentation, local pressure gradients can be built up without being detected for a long time. Such leak-triggered pressure gradients may not only cause premature beam losses, but also even to quenches of superconducting magnets. The currently only method for calculating time-dependent longitudinal pressure profiles in cryogenically cooled accelerator beam pipes with wall-pumping is described in a theory developed by Hobson and Welch [1,2]. This model predicts the built up of a local high pressure gradient and its strongly delayed propagation in a long, cooled tube in the presence of external H_2 or He loads. The experimentally confirmed model is, however, only applicable to cryogenic vacuum tubes with circular cross section.

The poster presents the extension of Hobson-Welch formalism to the application of cryogenic beam tubes with arbitrary cross-sectional shape. Based on experimental study using a cryogenic beam tube with elliptical cross section, the validity of the generalized Hobson-Welch model is demonstrated successfully.

[1] Hobson, J. P.; Welch, K. M.: J. Vac. Sci. Technol. A 11(4) (1993), 1566
[2] Hobson, J. P.; Welch, K. M.: Informal Report, BNL-47434, AD/RHIC-111 (1992)

VST-7-Or-1
Transient thermo-molecular pressure difference in a long tube

T15 Vacuum Science and Technology

#VST-7-Or-1

I. Graur [1], F. Sharipov [2].

[1]Aix Marseille University - Marseille (France), [2]Universidade Federal do Paraná - Curitiba (Brazil).

The thermo-molecular pressure difference (TPD) plays an important role in vacuum systems, e.g. it must be taken into account in calibrations of vacuum gauges [1]. Such a TPD arises because of the thermal creep, i.e rarefied gas flow due to a temperature gradient. Till now, this phenomenon has been studied only in a stationary state. A critical review of works reporting data on the stationary TPD is given in [2]. However, it is not known the time needed to establish the TPD. The aim of the present work is to model a transient TPD in a long tube connecting two containers. A thermal creep flow due to a temperature drop on the tube ends is considered as the initial conditions. It is assumed that the pressure drop is zero at this moment. When the containers are closed, a pressure drop arises between them which establishes after a certain time. Such a situation was experimentally studied in [3]. The modeling of the transient pressure difference is based on the data obtained from the S-model of the Boltzmann equation subject to the Cercignani-Lampis law of gas-surface interaction which are reported in [4]. As a result, a characteristic time needed to establish the stationary TPD was calculated. It is shown that the numerical results are in a good agreement with the experimental data reported in [3].

1. K Jousten, Temperature corrections for the calibration of vacuum gauges, Vacuum/Volume 49, pp. 81 - 87 (1998).
2. F. Sharipov and V. Seleznev, Data on internal rarefied gas flows. J. Phys. Chem. Ref. Data. Volume 27, pp. 657-706 (1998).
3. M. Rojas, I. Graur, P. Perrier, J.G. Méolans, An Experimental and Numerical Study of the
Final Zero-Flow Thermal Transpiration Stage, JTST, Vol.7, No.3, 2012
4. F. Sharipov, Application of the Cercignani-Lampis scattering kernel to calculations

of rarefied gas flows. III. Poiseuille flow and thermal creep through a long tube. Eur.J. Mech. B/Fluids Vol. 22, pp. 145-154 (2003).

VST-3-Or-1
COMMISSIONING OF NSLS-II VACUUM SYSTEMS*

T15 Vacuum Science and Technology

#VST-3-Or-1

H. Hseuh, A. Anderson, W. De Boer, S. Di Stefano, C. Hetzel, S. Leng, K. Wilson, H. Xu, D. Zigrosser.

Brookhaven National Lab - Upton, New York (United states).

The National Synchrotron Light Source II is a state-of-art synchrotron radiation facility designed with ultra-high-flux and -brightness. It consists of a 200-MeV Linac, a 3-GeV Booster and a 3-GeV, 792-meter circumference storage ring. The Booster vacuum system is made of thin-wall stainless steel chambers and is pumped with ion pumps. The Linac and Booster vacuum systems are completed and have reached ultrahigh vacuum. The storage ring vacuum chambers are mainly made of extruded aluminium with ante-chamber. The synchrotron radiation from the bending magnets in the storage ring is intercepted at discrete photon absorbers made of GlidCop. NEG strips in the ante-chamber provide the distributed pumping, while lumped ion pumps and titanium sublimation pumps at photon absorbers remove the desorbed gas. The 200+ long aluminium chambers were manufactured, assembled with pumps, photon absorbers and diagnostic components, integrated into magnet girders and installed in the storage ring tunnel. Most of the 30 DBA cells have been connected with RF bellows, pumped down, in-situ baked and have reached 10-11 mbar. The narrow gap insertion device vacuum chambers are to be coated with NEG and are currently under fabrication. This paper describes conditioning, installation, integrated testing and commissioning of the NSLS-II vacuum systems. Experience from the large scale production, testing, integration and lesson learned will be summarized.

*Work performed under the auspices of U.S. Department of Energy, under contract DE-AC02-98CH10886.

VST-3-Or-13
Development of advanced plasma fueling techniques for EAST tokamak

T15 Vacuum Science and Technology

#VST-3-Or-13

J. Hu, Y. Chen, J. Li, C. Li, X. Zheng, J. Li.

Institute of Plasma Physics, Chinese Academy of Sciences - Hefei (China).

Fuelling system is one of key subsystems of tokamak machine. It is not only providing a fueling source, but also would influence on plasmas performance. The Experimental Advanced Superconducting Tokamak (EAST) is a non-circular advanced steady-state experimental device, which started plasma operation in 2006 in Hefei, China[1]. Long pulse plasmas up to 400s and stationary H-mode plasmas up to 32 seconds have been achieved in 2012 campaign.
Recently, supersonic molecular beam injection (SMBI), and D2 pellet injection at both low field side (LFS) and high field side (HFS) have been successfully developed and applied in EAST for deeper fuelling and fast density feedback control. In the SMBI system, a Laval (0.3mm to 7.5mm in diameter with a taper angle at ±30) was used, and the back pressure for injecting D2 is up to 1.5MPa. In theory, the D2 would be driven to a speed of 2200m/s with a max throughput up to 2.47x1022/s. With the cooperation of PELIN Laboratory in St Petersburg, Russia, a new pellet injection system based on a screw extruder has been successfully installed on EAST in 2011. The pellet is 2 mm in diameter and 2mm in the length, which contents 3.78×10^20 D atoms; it could operated at 10 Hz in 1000s, and pellet velocity could be adjusted from 150 to 300 m /s. The flight tubes which in place to convey the pellets toward the plasma either from low field side or from high field side. And the length of LFS flight tube is nearly 4.5 m while the HFS flight tube is 9.5 m. The injection line is able to pump the propellant gas effectively to make sure no influence to the vacuum of the plasma vessel during the long steady pellet injection.
In the campaign of EAST in 2012, SMBI and PI system has been firstly and successfully tested. And the test showed that both fuelling system have quite high feasibility, stability and reliability. The tested showed that both systems could be used not only for advanced core fueling, but also for ELMs control. SMBI produces a rapid travelling gas jet with a speed exceeding 1 km/s and pulse length ranging from 2 to 20 ms. This leads to a much shorter density response time (2-4 ms) than the conventional gas puffing (16 ms and 77 ms for LHS and HFS, respectively). SMBI has been also successfully employed as a fast density feedback tool to maintain

plasma density for steady-state operations, and it seems much better than gas puffing. The present pellet injection system is mainly used for core plasma fuelling. As expected, pellet injection from HFS exhibits a higher fuelling efficiency with deeper penetration into the core plasma than from LFS, i.e., 18-30% for LFS and 30-60% for HFS, respectively, which much higher than that of SMBI or GP. Both SMBI and pellet injection have also been employed for active control of ELMs.

This research was funded by National Magnetic confinement Fusion Science Program under Contract No.2010GB104002 and No.2013GB114004 and National Nature Science Foundation of China under Contract No.11075185 and No.11021565.

[1] He–ICR cleanings on full metallic walls in EAST full superconducting tokamak, J.S. Hu, at.el., Journal of Nuclear Materials 376 (2008) 207
[2] Vacuum and wall conditioning system on EAST, J.S. Hu, at.el., Fusion Engineering and Design 84 (2009) 2167

VST-7-Or-2
End effect corrections for rarefied gas flows through long capillaries of finite length

T15 Vacuum Science and Technology

#VST-7-Or-2

D. Valougeorgis [1], S. Pantazis [2], F. Sharipov [3].

[1]Department of Mechanical Engineering, University of Thessaly - Volos (Greece), [2]Physikalisch-Technische Bundesanstalt - Berlin (Germany), [3]Universidade Federal do Parana - Curitiba (Brazil).

Fully developed gas flows through long capillaries in the whole range of the Knudsen number have been extensively considered with remarkable success on the basis of linearized kinetic theory. The assumption of the fully developed flow is based on the fact that the capillary is adequately long and that pressure varies only in the flow direction. This assumption permits the simplification of the kinetic formulation leading to precise analysis with very accurate results.

However, the main hypothesis that the capillary is sufficiently long, in order to achieve the fully developed state, is not always true in practical situations, leading to a significant impact on the accuracy of the results because of the capillary inlet/outlet effects. For the case of short capillaries the end effects can be taken into account by including additional regions before and after the capillary. In the case of long capillaries this type of investigation becomes computationally expensive and therefore in most applications only empirical approaches are applied.

The objective of the present investigation is to quantify the influence of the capillary ends by applying the effective length concept in order to extend the applicability of the infinitely long capillary theory to capillaries of moderate length. This concept has been initially applied in slow viscous flows and later on, in rarefied gas flows in an approximate manner. The main idea is to extend the length of the channel by additional length increments for the purpose of calculating the correct pressure profile and flow rate.

Here, the effective length concept has been introduced to investigate the end correction for rarefied gas flows through capillaries of finite length by splitting the flow

domain in the inlet, middle and outlet parts. A kinetic solution of the developing flow in the inlet and outlet parts based on the BGK model equation subject to proper boundary conditions is provided to compute the effective length increment, which depends only on the gas rarefaction parameter (not on the channel length). The kinetic solution is properly combined at the level of the distribution function for the inlet and outlet regions with the typical fully developed solution in the middle part of the capillary. The inlet and outlet length increments are added to the capillary length and then, the well known fully developed approach is applied to compute quantities of practical interest, such as the flow rate. A comparison with the typical (without end correction) fully developed solution as well as with the solution of the complete domain has been performed to demonstrate the superiority of the proposed approach compared to previous ones.

Results for the effective length increment in terms of the Knudsen number are tabulated for flows between parallel plates and through circular tubes. A detailed view of the inlet and outlet flow fields is also provided by plotting the pressure and velocity distributions. The effective length increment values given here can be used in practical applications with minimal computational effort.

ACKNOWLEDGEMENTS
S.P. and D.V. gratefully acknowledge support by the Association Euratom - Hellenic Republic.

VST-7-Or-3
Numerical simulation of rarefied gas flow through a thin orifice based on the ab initio potential.

T15 Vacuum Science and Technology

#VST-7-Or-3

J. Strapasson, F. Sharipov.

UFPR - Curitiba (Brazil).

Rarefied gas flow through a thin orifice is well studied on the basis of the direct simulation Monte Carlo (DSMC) method, see e.g. Ref.[1]. However, all previous calculations are based on molecular models like hard sphere, variable hard sphere etc. Such molecular models contain fitting parameters usually extracted from experimental data. For vacuum metrology, it is important to obtain numerical data without any fitting parameter. Recently, the ab initio potential was implemented into the DSMC method [2]. The aim of the present work is to calculated ab initio the mass flow rate and flow field the whole range of the rarefaction parameter for various values of the pressure ratio. A comparison of the present numerical results with those based on the hard sphere and variable hard sphere models published previously, and also with experimental data available in the open literature is performed.

1. F. Sharipov, Numerical simulation of rarefied gas flow through a thin orifice. J. Fluid Mech. Vol.518, pp. 35-60 (2004).
2. F. Sharipov and J.L. Strapasson, Ab initio simulation of transport phenomena in

rarefied gases.
Phys. Rev. E Vol. 86, paper number 031130 (2012).

VST-P1-16
A profile of the gradational lead rotor with equal axial addendum width in dry twin-screw vacuum pump

T15 Vacuum Science and Technology

#VST-P1-16

S. Zhang, J.L. Zhao, Y.F. Zhang, Z.J. Zhang.

School of Mechanical Engineering and Automation, Northeastern University - Shenyang (China).

The profile design of the screw rotor is one of the most key technologies in dry twin-screw vacuum pumps. The single-thread and variable-pith rotors has won the good graces and much concern of both manufacturers and users in recent years because of its outstanding advantages of energy saving and noise reduction.

All of the previous profiles of the gradational lead screw rotors have the same structural characteristics, i.e., the axial addendum width of the rotor changes to narrow gradually along with the lead becoming narrow gradually from the inlet towards the outlet. This kind of structure leads to the performance of pump descending.

Aiming at the above problems, a new profile of the gradational lead screw rotor with equal axial addendum width is introduced in the article. The end profile of it consists of 4 curves connected in order. As shown in Fig. 1, they are dedendum circle (1), involute (2), addendum circle (3) and a self-meshing transitional curve (4) in turn. When this end profile is expanded by gradational pitch along with the axial, a single-thread and gradational-pith screw rotor is formed which includes 4 tooth surfaces corresponding respectively to 4 curves, as shown in Fig. 2, the dedendum surface (5), the trapezoid surface (6), the addendum surface (7) and the transition tooth surface (8). The main feature of this profile is that the screw lead of the rotor gradually get larger and larger (P1< P2 < P2) along with the rotor axis from inlet towards outlet, the axial length of rapezoid surface also gradually become larger (L1< L2< L3), but the addendum width remains the same (B1= B2 = B3). The entire equations of this profile are presented in the article and its advantages are analyzed in detail. This work can be taken as a useful reference for technical personnel in the design of screw rotors.

Fig.1. The end profile of gradational lead screw rotor

Fig.2. The sketch map of gradational lead screw rotor with equal axial addenaum width

VST-2-Or-4
The non-rotating piston gauge usage in vacuum metrology

T15 Vacuum Science and Technology

#VST-2-Or-4

J. Wang.

National Institute of Metrology - Beijing (China).

The non-rotating piston gauge(FRS5) have been used in vacuum lab of NIM for the calibration service within range 100Pa to 11kPa. The FRS5 is also been used to improve the static expansion primary standard performance both in the volume ratio measurement and the vacuum pressure calibration. The reference gauge method is been used to measure the volume ratio in which the reference gauge would be calibrated immediately by FRS5 after the expansion. The result show that the volume ratio has no relation with the initial pressure which from 10kPa to 130Pa

1. Th Bock, H Ahrendt and K Jousten Reduction of the uncertainty of the PTB vacuum pressure scale by a new large area non-rotating piston gauge Metrologia 46 (2009) 389–396
2. D. Herranz, S. Ruiz, N. Medina, Volume ratio determination in static expansion systems by means of two pressure balances XIX IMEKO World Congress Fundamental and Applied Metrology September 6−11, 2009, Lisbon, Portugal
3. K. W. T. Elliott, P. B. Chapman, “The accurate measurement of the volume ratios of vacuum vessels”, NPL report MOM 28, 1978.

VST-7-Or-4
Time-dependent heat transfer of a gas between two coaxial cylinders

T15 Vacuum Science and Technology

#VST-7-Or-4

M. Ho [1], I. Graur [1], M. Wüest [2].

[1]Aix-Marseille Université, Polytech Marseille, UMR CNRS 7343, 5 rue Enrico Fermi - 13453 Marseille Cedex 13 (France), [2]INFICON Ltd, Alte Landstrasse 6 - Li-9496 Balzers (Liechtenstein).

The evolution of the gas characteristics in time is an important topic from the scientific and practical points of view. In the design and development stages of Pirani gauges [1], the heat flux and the pressure evaluation in time is vital information for adjustment of sensor characteristics.

A Pirani sensor is simulated by two coaxial cylinders. The time-dependent heat transfer of a gas between two coaxial cylinders is studied on the basis of kinetic model equation [2] over a broad range of the gas rarefaction. The response time is determined as a time needed to establish a steady state heat transfer averaged over the distance between the cylinders. As an initial state of the system, a instantaneous increase of the internal cylinder temperature from room temperature to 110 °C is considered. It was found that the response time varies very slightly for the low pressures and increases then drastically when the pressure increases, passing through a minimum between the two regimes. The influence of the gas nature on the response time is analysed.

[1] W Jitschin and S Ludwig. Dynamical behaviour of the Pirani sensor. Vacuum, 75(2):169–176, 2004.
[2] H. Yamaguchi , K. Kanazawa, Y. Matsuda , T. Niimi , A. Polikarpov, I. Graur, Investigation on heat transfer between two coaxial cylinders for measurement of thermal accommodation coefficient, Phys. Fluids 24, 062002 (2012); doi: 10.1063/1.4726059

VST-7-Or-12
Numerical Simulation of Vacuum Spray Jet Atomization For Plain-orifice Nozzle

T15 Vacuum Science and Technology

#VST-7-Or-12

J. Li [1], H.Y. Li [1], J. Chen [2], Y.M. Yang [2].

[1]Vacuum and Fluid Engineering Research Center, Northeastern University - Shenyang (China), [2]Darly Photonics Composite Materials (Shanghai) Corp - Shanghai (China).

Abstract: The vacuum spray jet atomization of plain-orifice nozzle is simulated using the Fluent and Gambit softwares. The influence of spray parameters including chamber pressure, injection pressure and nozzle diameter on the cavitation performances, atomization structure and the Sauter mean diameter (SMD) are systematically investigated. We present the effect of cylindrical, conical and fan-shaped nozzles on the performances such as the jet velocity, initial spray angle, dynamic pressure and TKE. Our results show that high injection pressure ($>$10 MPa) has less effect on the vapor volume inside the nozzle. The TKE outlet the nozzle increases with increasing the injection pressur (see Fig. 1). The spray beam width decreases, while the spray jet penetration distance and the SMD increase with the decrease of the chamber pressure. As the injection pressure increases, the spray beam width increases quickly in the range of 1 to 10 Pa. The SMD changes very little, while the jet penetration distance increases linearly with increasing of the injection pressure. The nozzle with smaller diameter tends to produce longer spray jet penetration distance and smaller SMD. We find that the conical nozzle has a higher dynamic pressure conversion efficiency and larger spray angle than that of the other type of nozzles (see Fig. 2), which is in well agreement with previous experimental observations.

Keywords: Vacuum spray method; Plain-orifice nozzle; Atomization; Cavitation; Sauter mean diameter

Fig. 1 TKE distribution outlet the plain-orifice nozzle under different injection pressures with nozzle diameter of 0.2 mm and chamber pressure of 1 Pa.

Fig.2 Dynamic pressure distribution for different geometric nozzles under injection and back pressures of 0.1 MPa and 10 Pa, respectively.

VST-6-Or-3
On the Joule heat cutting and welding for various metallic nanowires under vacuum environment

T15 Vacuum Science and Technology

#VST-6-Or-3

H. Tohmyoh.

Tohoku University - Sendai (Japan).

To effectively use and create a new function from metallic nanowires (NWs), welding technique for NWs must be vital. Among the reported techniques, the welding technique utilizing Joule heat, where a constant direct current is supplied to a NW system comprising two NWs in contact, is one of the promising ways [1]. The contacting portion of two wires are successfully welded in self-completed manner with Joule heat [2] provided that suitable amount of constant direct current is supplied, see the picture. On the other hand, if the current supplied to the wires is over the upper limit value, the wire is cut out after the welding due to over Joule heating. The lower limit value for welding current was found to be about 70% for the upper limit value, i.e., the current required to cut the wire. Therefore, if the current to cut the wire is identified, the condition for successful Joule heat welding is also know. Generally, the thermal boundary condition around the wire is unknown, and therefore predicting such current is a difficult task.

In this presentation, currents required to cut various mtallic NWs under vacuum environment are estimated from a heat conduction model [3]. Most of the cases to use the NWs, the NWs are need to be observed with high magnification, and such wire is thermally insulated under vacuum. In the experiments for cutting the ultrathin Pt wires with Joule heat in vacuum, only the small region around the middle of the wire was melted and most part of the wire remained solid, see the picture. Thus in the theoretical modeling, we only considered the sensible heat and does not consider the latent heat of melting. The total heat applied to the NW system until the system reaches a steady state is determined. From the theoretical model, we found that the current required to cut the wire depended on the physical properties, i.e., thermal and electrical conductivities, density, specific heat and melting point, and the geometry of the wire, i.e., cross sectional area and length. Moreover, metallic NWs are cut in vacuum with Joule heat and the results are compared with the predicted one.

The author would like to acknowledge Professor M. Saka for valuable discussions. This work was supported by Grant-in-Aid for Young Scientists (A) No. 24686016.

[1] H. Tohmyoh, J. Appl. Phys. 105 (2009) 014907.
[2] H. Tohmyoh and S. Fukui, Phys. Rev. B 80 (2009) 155403.
[3] H. Tohmyoh, (2013) unpublished.

Example of welding two ultrathin Pt wires having the diameter of around 800 nm. (a) Experimental arrangements. (b) Two Pt wires were on thick Ag probes and were successfully welded. (c) The welded Pt wires were cut after the welding due to overheating.

VST-1-Or-7
Survey of primary standards of atmospheric leaks

T15 Vacuum Science and Technology

#VST-1-Or-7

D. Pražák [1], L. Peksa [2], T. Gronych [2], F. Staněk [1], J. Tesař [1].

[1]Czech Metrology Institute - Brno (Czech republic), [2]Charles University - Prague (Czech republic).

The halogenated hydrocarbons were widely used in the last century as volatile cleaning liquid, refrigerant gas and also for leak testing of vacuum systems. Majority of these applications were abandoned due to the environmental reasons but replacing them as refrigerator gas proved to be a difficult and long term task. This is caused not only due to large amount of the devices working with them at present (utilizing mainly R134a, i.e. 1,1,1,2-tetrafluoroethane), but also due to the safety and technological difficulties that are brought by their possible substituents. As the living environment friendly refrigerant media, the most promising are HFO-1234yf (2,3,3,3-tetrafluoropropene) and carbon dioxide. The first is flammable and slightly toxic; the second requires nearly ten times higher pressures during refrigerator cycle than the halogenated hydrocarbons. Hence, even if the halogenated hydrocarbons will be successfully replaced, the need for good leak testing will remain to secure the reliability of the refrigerating and air-conditioning systems.

Thus, the hot topic for metrology will be the measurement of the refrigerant leaks with sufficient accuracy and with traceability to the primary standards. The traceability in the field of leak measurement is performed usually via the secondary standards, so-called calibrated leaks, standard leaks or reference leaks.

Although the regulations of European Union impede the need of the reference leak calibrations, there are only a few national metrology institutes in Europe having a primary standard of this kind and the situation in the World is not much better. This is in contrast with the well established metrology of the helium vacuum leaks.

One reason is the fact that no method of conversion from leak-into-vacuum to leak-into-atmosphere is available, thus, the leaks-into-atmosphere must be determined in these cases which is a more complicated problem then the measurement of leakage into vacuum. At the other hand, the situation is rather simplified by the fact that usually mainly two orders of magnitude of the leak rates have to be covered in contrast to approximately seven orders of magnitude of the leak rates in the case of helium vacuum leaks.

An overview of the primary standard principles applicable for this purpose – used or under consideration – is given in the presentation. They can be classified into two groups: those being sensitive to the leaking gas species and those being insensitive to it. The problem of the first group standards is that they can work with a limited number of the gas species only, the problem of the second group standards is that they measure depleted volume of gas into a space under the atmospheric pressure, i.e. a very small change of a relatively large quantity which brings many experimental obstacles. The solution of CMI will be discussed in detail.

This work benefited from support of the European Metrology Research Programme under Joint Research Project IND 12 – Vacuum metrology for production environments. The EMRP is jointly funded by the EMRP participating countries within EURAMET and the Euopean Union.

VST-6-Or-2
Fabrication and gas permeation properties of ultra-thin PolyDiMethylSiloxane (PDMS) membranes

T15 Vacuum Science and Technology

#VST-6-Or-2

G. Firpo, E. Angeli, L. Repetto, V. Ierardi, F. Buatier De Mongeot, U. Valbusa.

University of Genoa - Physics Department - Genova (Italy).

The polymeric membranes technology is a dynamic growing field, exploited in several areas of application like gas separation,[1] sensors, and vacuum technology.[2] It is based on well-known selective permeation process of gas through a polymer, whose selectivity for two different gas is the ratio of their permeability coefficients P. In the last years have been developed methods to fabricate ultra-thin membrane,[3] but there's no estimation of P. Moreover, even if for thick membrane there is some results, the dependence of P from the thickness is generally poorly investigated.

Here we present a novel method to fabricate stable and resistant ultra thin PDMS membranes, and we show their gas permeation characteristics as function of the membrane thickness and the type of gas: CO_2 and He. The membranes have been fabricated by spin coating with thickness in the range between few micron and 500 nm. Afterwards, in order to guarantee the necessary mechanical stability, they have been transferred on SiN membrane previously drilled by focused ion beam with a number of apertures such that to have an appropriate permeation area (Fig. 1). Permeability measurements have been performed in high vacuum chamber, where the membranes have been exposed to 10^5 Pa of pressure differential without rupturing or stretching, proving their high strength.

The results confirm the higher permeability of the carbon dioxide respect to those of helium, whereas the value of P decreases unexpectedly with the membrane thickness, on the contrary of the CO_2/He selectivity that remains constant. Studies on thickness-dependence of the gas permeability are scarce, but our data (Fig. 2) are in good agreement with a model that considers non-equilibrium reactions at gas-

membrane interface. This make it possible the evaluation of the adsorption and desorption rates, and in conjunction with mechanical properties of the membranes, suggests new technological solutions in the devices miniaturization.

[1] A. Brunetti et. al, J Membr Sci, **359**, 2010.
[2] A. Tison, J Vac Sci Technol A, **14**, n. 3, 1996
[3] A. L. Thangawng et al, Biomed Microdevices, **9**, 2007

VST-3-Or-14
Design and construction of the LCLS-II vacuum system

T15 Vacuum Science and Technology

#VST-3-Or-14

M. Ferreira, D. Gill.

SLAC National Accelerator Laboratory - Menlo Park (United states).

The Linac Coherent Light Source - II (LCLS-II), now under construction at SLAC National Accelerator Laboratory in California, will be an x-ray free electron laser to increase the capacity and capabilities of the operating LCLS. The vacuum system includes a new RF gun and injector, two km of the SLAC linac (sectors 10-20), a new transport line, Undulator hall, X-ray transport optics and diagnostic (XTOD) and end-stations. The vacuum requirements for the different sub-systems need to be addressed taking into account the desired flexibility and technical limitations. We will show the mix of simulations techniques and results used to define the engineering solution for each section of the accelerator including the RF-gun and the injector, representing the most demanding region, and its coupling to the more than 50 years old LINAC section. The system is required to operate with dynamic isolation over a 12 order of magnitude pressure range.

VST-5-Or-2
Physisorption of hydrogen: a mean residence time, an adsorption energy, and a condensation coefficient deduced from the observation of transient states approaching equilibria

T15 Vacuum Science and Technology

#VST-5-Or-2

I. Arakawa, H. Shimizu, N. Inose, W. Kato, K. Yamakawa.

Department of Physics, Gakushuin University - Tokyo (Japan).

Considerable data on the physisorption characteristics of hydrogen on a variety of substrates have been accumulated with the intention of applying them to cryopumping in the various fields of vacuum engineering [1-5]. In the present study, equilibrium and transient properties of hydrogen physisorbed on a cold metal surface were investigated in ultra and extremely high vacuum. Electron stimulated desorption (ESD) technique was applied to measure the adsorption density of hydrogen molecules. Hydrogen was adsorbed on a copper substrate in the temperature range of 3 - 4.2 K and was irradiated with a pulsed electron beam of a few hundreds ns pulse width. ESD ions, H^+, H_2^+, and H_3^+, were mass-separated by a time-of-flight measurement. In submonolayer range, the signal intensity of ESD H^+ was a useful measure for the amount of hydrogen physisorbed. The monolayer completion, which was accompanied by a two dimensional phase condensation, was observed in the rapid rise of H^+ intensity followed by its saturation. An adsorption isotherm was obtained as the ESD signal intensities of H^+ as a function of the hydrogen pressure, which was gradually increased from 10^{-9} to 10^{-4} Pa so as to keep adsorption equilibria. The observable lower ends of the isotherm were $1x10^{-8}$ Pa of the equilibrium pressure and 0.001 of hydrogen coverage, which was limited by back ground signal of H^+ originated from water or hydrocarbons adsorbed on the metal substrate. A transient state measurement was also applied to derive the mean residence time of physisorbed hydrogen. A time development of ESD H^+ intensity was monitored after a stepwise hydrogen pressure rise to a certain value. The time constant of the increase of ESD H^+ intensity is the direct measure of the mean residence time, τ, of hydrogen, which leads to the adsorption energy, E_d, and the

condensation coefficient, α. At 4.2 K of the substrate temperature, τ, E_d, and α were systematically measured as a function of coverage, θ, of hydrogen; 550±50 s, 1.27 kJ, and 0.018, respectively, at θ = 0.18, and 53±2 s, 1.18 kJ, and 0.075, respectively, at θ = 1.0, under the assumptions of τ_0 = $1x10^{-13}$ s and $7.39x10^{18}$ m^{-2} of the monolayer density of hydrogen.

[1] I. Arakawa, J. Vac. Sci. Technol. A **4**, 1459 (1986).

[2] E. Wallen, J. Vac. Sci. Technol. A **15**, 265 (1997).

[3] J. Vorberg, S. Herminghaus, and K. Mecke, Phys. Rev. Lett. **87**,196105 (2001).

[4] G. Moulard, B. Jenninger, and Y. Saito, Vacuum **60**, 43 (2001).

[5] V. Baglin, I. R. Collins, O Gröbner, C. Grünhagel, and B. Jenninger, Vacuum **67**, 421 (2002).

VST-P1-17
Effect of sealing time of anodic aluminum oxide (AAO) film for vacuum parts

T15 Vacuum Science and Technology

#VST-P1-17

J. Kim [1], J.B. Song [2], J.S. Shin [2], J.Y. Yun [1].

[1]KRISS - Daejeon (Korea, republic of), [2]Daejeon Univ. - Daejeon (Korea, republic of).

The damage to the surface structure of Anodic Aluminum Oxide (AAO) caused by plasma and heat is evaluated with respect to the sealing time (0, 10, 30, 60 minutes). With a short period sealing of the oxide layer, the leakage current is abruptly reduced, while the breakdown voltage and permittivity are rapidly improved. Longer sealing becomes less efficient after 10 minutes. An evaluation of resistance to plasma and heat shows that the resistance is best with a sealing time of 10 minutes. In the samples sealed for 30 or 60 minutes, more cracks were formed by plasma and heat treatments, which further reduce the breakdown voltage. In addition, measurement of contamination particles generated in plasma treatment reveals that sealing longer than 10 minutes produces more particles.

[1] Yao Weilian, Mater. Mechanical Eng, 18, 6-14 (1994).
[2] W. J. Yoo and Ch. Steinbruchel, Appl. Phys. Lett. 60, 1073 (1992).
[3] S.-S Kim, H. Lee, J.-W. Choi, B. K. Na, and H. K. Song. J. Ind. Eng. Chem., 9, 787 (2003).
[4] Selwyn G. S. and Patterson E. F. : J. Vac. Sci. Technol. A10, 1053 (1992).
[5] S. K. Kim and J. Y. Chang. Journal of the Korean Vacuum Society. 15, 273-279 (2006).
[6] H. Schmidt, S. Langenfeld, and R. Na. J. Materials Design. 18, 309-313 (1998)
[7] C. D. W Wilkinson and M. Rahman. Phil. Trans. R. Soc. Lond. A 362, 125-138 (2003)

Fig. 1. Dielectric breakdown voltage vs sealing times after the plasma treatment

Fig. 2. Distribution of contamination particles generated during the plasma treatment of 10 min from the samples for different sealing times; (a) unsealed, (b)10min, (c) 30min, (d) 60min

VST-4-Or-2
Monte Carlo simulation of a Vapour Diffusion Pump

T15 Vacuum Science and Technology

#VST-4-Or-2

X. Luo, T. Giegerich, C. Day.

Karlsruhe Institute of Technology - Karlsruhe (Germany).

The vapour diffusion pump was the very first ultrahigh vacuum pump in vacuum history and it is exactly 100 years ago since W. Gaede patented his mercury diffusion pump made of glass in 1913.

Although turbomolecular pumps are the most commonly used high speed UHV pumps nowadays, vapour diffusion pumps do still play a role, especially in harsh applications where a robust and reliable pump is needed. In present applications, mercury has been completely replaced by synthetic oil. However, a new programme is currently underway to develop a mercury diffusion pump for applications in nuclear fusion power plants, because mercury is known to be perfectly tritium compatible. This type of pump would be an ideal alternative for the cryopumps used in present fusion devices, because it is much less demanding in operating cost and complexity and has no need for regeneration. This is the reason why Karlsruhe Institute of Technology (KIT) has started a new effort to develop a vapour diffusion pump using modern molecular modeling efforts.

The code which was correspondingly modified is ProVac3D (Profile of the Vacuum system of 3D complexities), which is a well validated Test Particle Monte Carlo simulation code developed by KIT [1-3]. In this paper, the simulation of a linear mercury diffusion pump will be presented. This also picks up an old pump design formerly used in the 1950s in US.

Diffusion pumps operate by directing a jet of vapour towards the walls of the pump shell where it condenses. On the way, when vapour molecules collide with molecules of incoming gas, the gas molecules are deflected in the direction of the pump exhaust. The vapour stream is created by boiling the pump fluid at the base of the pump and directing the vapour through a series of nozzles which accelerate the vapour molecules.

The modeling approach is as follows. First, we calculate the background density of the mercury molecules established by the mercury jets. Secondly, the gas molecules of the gas load coming from the pump inlet will be simulated. However, the collision between the gas load with the background jet has not been included yet. This step is necessary for checking the influence only from the pump geometry and the backing pump. Thirdly, the collisions between the molecule of the gas load (probe particle A) and the mercury molecule in the background (target particle B) will be considered. This appoach has been newly implemented in ProVac3D. In order to achieve a high simulation precision, the code has been parallelized for optimum use of the powerful supercomputers. Compare the simulation results in the second step and the third step, the pumping effect of the mercury gas jet has been clearly revealed.

[1] X. Luo, Chr. Day, Investigation of a new Monte Carlo method for transitional gas flow, Proc. 27th Int. Symp. on RGD, AIP Conference Proceedings 1333, Melville, W, USA, 2011, pp. 272-276.
[2] X. Luo, Chr. Day, H. Haas, St. Varoutis, Experimental results and numerical modelling of a high-performance large-scale cryopump I, Journal Vac. Sci. Technol. A 29 (2011) 041601/1-7.
[3] X. Luo, Chr. Day, 3D Monte Carlo modeling of the neutral beam injection systems of ITER, Fusion Engineering and Design 85 (2010) 1446-1450.

VST-5-Or-1
Atomic level surface characterization of vacuum fired stainless steel

T15 Vacuum Science and Technology

#VST-5-Or-1

M. Leisch.

Graz University of Technology - Graz (Austria).

Stainless steel (SS) is one of the most commonly used constructional materials for vacuum chambers and components. Special applications like accelerator and storage ring facilities make need for extreme high vacuum (XHV). In the XHV regime a reduction of the outgassing rates of the materials used is essential. Beside surface treatment high temperature vacuum firing became a widely accepted practice of reducing the amount of hydrogen dissolved in SS. For the description of the outgassing rate basically two models common as diffusion limited model (DLM) and recombination limited model (RLM) have been discussed [1,2]. It is well established that the rate of recombination depends strongly on the atomic structure of the surface. In order to gain atomic level information on the real morphology of a surface after common bake-out and vacuum firing SS samples were imaged in the atomic force microscope (AFM) and the scanning tunnelling microscope (STM).
The main experimental work has been carried out on a combined STM – atom probe field ion microscope (AP-FIM) apparatus [3]. A unique feature of the particular instrument is that it allows a fully-predictive preparation of STM probe tips which is important for a reliable imaging of complex surfaces. After the thermal treatment surface inspection by Auger electron spectroscopy (AES) gives reason for a composition change indicated by a reduction of the chromium signal in relation to the iron and nickel. Since the atom probe allows measuring the chemical composition on the surface atomic layer by layer it has been used to study the segregation behaviour on SS samples after bakeout and vacuum firing.
The surface after vacuum firing shows the formation of large flat (111) terraces bounded by bunched steps and facets corresponding in orientation to (110) and (100) planes. The deep grooved grain boundaries and facets represent very active sites for adsorption and recombination. A close up view by STM shows that there are a lot of vacancies too. Theoretical studies on the interaction of hydrogen with lattice imperfections [4] may provide a new insight in hydrogen outgassing. The energy calculations using the ASED method (Atom superposition and Electron Delocalization) result in lower energy levels in Fe vacancies. It supports the picture

that surface and subsurface defects form traps with different energetic levels. From these results a more complete description of the outgassing process may be given. The design of accelerator vacuum chambers requires input from different scientific disciplines such as surface science, material science. Vacuum gas dynamics allows joining them to the vacuum science for particle accelerators. The most time-efficient way of beam vacuum optimization is using a 1D diffusion model where all parameters are defined as a function of a longitudinal coordinate [5]. This theoretical approach corresponds very well with the results of this atomic level surface study.

[1] Redhead PA. Ultrahigh and Extreme High Vacuum Foundations of Vacuum Science and Technology ed Lafferty JM (New York: Wiley) 1998 p 625
[2] Bacher J-P Benvenuti C Chiggiato P Reinert M-P Sgobba S Brass A-M J. Vac. Sci. Technol. A 21(1) (2003) 167
[3] Stupnik A Frank P Leisch M Ultramicroscopy 109 (2009) 563
[4] Rey Saravia D Juan A Brizuela G Simonetti S I J Hydrogen Energy 34 (2009) 830
[5] Maleshev O B, Vacuum 86 (2012) 1669

VST-P2-22
Development of a Gas-sheet Target for Monitoring the High Intensity Proton Beam

T15 Vacuum Science and Technology

#VST-P2-22

N. Ogiwara, Y. Hikichi, J. Kamiya, M. Kinsho.

JAEA - Tokai (Japan).

The 3 GeV Rapid Cycling Synchrotron (RCS) in the Japan Accelerator Research Complex (J-PARC) project accelerates a proton beam up to 3 GeV. At a 25-Hz repetition rate, the RCS is planned to generate a high-power beam of 1 MW. Until now, the beam power of 400 kW has been obtained. In order to supply continuously the beam of 1 MW it is important to reduce the beam loss thoroughly. Thus the non-disruptive and fast-response beam diagnostic tools for extensive researches have been strongly required.
An idea to realize the fast non-disruptive beam profile detection is to introduce a gas target so as to increase the ionization yields with the beam. Luminescence lights (or ions) from the target yielded by the collision with the synchrotron beam are easily observed and utilized to obtain the beam profile. The gas density of about 10^{10} molecules/cm^3 and the thickness of 2-3 mm are required for the measurement in the RCS in the J-PARC.
Therefore, we intended to apply the molecular beam technique for making the compact and large-scale gas-sheet target. First of all, we examined the angular distributions of the outgoing molecules from the exit of the rectangular slits by using the Monte Carlo simulation. The molecules emitted from the slit can be shaped into a sheet. To do so, the following two conditions need to be satisfied: $L >> b$ and $a >> b$. The letters *a, b,* and *L* represent the lengths of the long and short sides, and the length of the slit, respectively. With the parameter set of $L : a : b = 100 : 50 : 0.1$, the fraction of outgoing molecules collimated within the azimuth of 0.01 rad becomes 25% of all molecules[1]. Next simulations demonstrate the generation of large-scale gas-sheet targets in a vacuum by a thin concentric slit with a large aperture. Here gas is introduced from the outside toward the center, leading to the appearance of a large-scale gas sheet around the center. In the case of the circular slit, with inner and outer diameters of 200 and 400, respectively, and a gap of 0.1, the generated gas sheet had a diameter of 130 and thickness of less than 0.4 (half width), where all the

valuables are expressed in ratio. The uniformity of the gas density, which is the ratio of the minimum to the maximum peak value of gas density, was more than 85%. According above results, the experiments have been now under taken. The molecules from the rectangular slit have been found to focus into a sheet. The results for the circular sheet will be presented.

[1] N. Ogiwara and J. Kamiya, J. Vac. Soc. Jpn., **55** (2012) 152.

VST-1-Or-1
Capacitance Diaphragm Gauges for Very Fast Processes

T15 Vacuum Science and Technology

#VST-1-Or-1

M. Wüest [1], F. Mullis [1], K. Jousten [2], J. Buthig [2].

[1]INFICON - Balzers (Liechtenstein), [2]PTB - Berlin (Germany).

Calibration of a vacuum gauge according to ISO 3567 requires stationary conditions in pressure and temperature. In industry however, highly cyclical, non-equilibrium processes with rapid pumping and venting are found. In order to enable the calibration of vacuum gauges for very fast processes, a new calibration system has been developed at PTB. We report on a specially developed fast CDG measuring system that was tested for the fast transient pressures in the new calibration system in the pressure range 10^5 Pa to 10^2 Pa.

Support through the EMRP IND12 project is gratefully acknowledged. The EMRP is jointly funded by the EMRP participating countries within EURAMET and the European Union.

VST-P1-18
Large-scale Hydro-formed Bellows with Inner-surface Polishing, as Flexible as Welded Bellows

T15 Vacuum Science and Technology

#VST-P1-18

O. Koizumi [1], M. Inoue [2], N. Ogiwara [3], J. Kamiya [3], M. Kinsho [3].

[1]Sun-tech limited - Kobe (Japan), [2]Neos Co., Ltd. - Higashimatsuyama (Japan), [3]JAEA - Tokai (Japan).

In the 3 GeV Rapid Cycling Synchrotron (RCS) in the Japan Accelerator Research Complex (J-PARC) project, large-scale bellows were needed to adjust the gap between the ceramic ducts and between the ceramic ducts and the transport ducts. The space for setting the bellows are so narrow that the requirements for the bellows were severe. Typical free length and inner diameter of the bellows were 100 mm and 300-400 mm, respectively; nevertheless, the spring rate of less than 100 N/mm was needed. Then pure Ti and SUS 316L steel were selected as materials for bellows; Ti bellows were set in the high radiation field because of its small residual radioactivity, and the SUS 316L bellows in the other area.

By the way, the formation of oxide scale and surface-roughening are sometimes observed on and/or near the melted parts. As they lead to the increase of outgassing and accumulation of dusts, the long welding trace should be avoided. Furthermore, the long welding trace of Ti is risky for vacuum leak because the penetration of a small amount of oxygen into the melted part under the welding causes the welded part to be brittle. Therefore, we have developed the hydro-formed bellows as flexible as welded bellows. In addition, the technique for polishing inner-surface of hydro-formed bellows has been developed.

In order to make flexible bellows the thin plates and a lot of convolutions are preferred. From this viewpoint, the welded bellows have an ideal structure. Therefore, we have developed the hydro-formed bellows with the almost same structure as the welded bellows. To realize Ti bellows, we had to resolve 2 tasks: 1) Necessary elongation for close contact bending is nearly 100% although the permissive elongation is only 27%; 2) It is difficult to keep the close contact after bending or pressing because of large spring-back effect. The repetition of combination of bending process with annealing enabled us to make sure the close contact of Ti plates.

Then, we have developed the new polishing method “wet mechanical polishing”. Using the fluid containing the minute particles of abrasive we have succeeded to polish the inner-surface of the complicated shape such as corrugation tube. The bellows for the RCS have been polished with this technique after the first bending process, that is, under the ordinary shape of the hydro-formed bellows. Then the bellows have been pressed into the final shape, which are almost the same as the welded bellows. The average roughness factor Ra of 0.02 μm changed to the value of 0.05 μm after the final pressing. The surface flatness just after the polish has been well maintained after the final pressing.

After assembling, mainly to reduce the hydrogen inventory in the bellows, all the bellows have been vacuum-fired for 10h at 650°C for Ti bellows, and at 750°C for SUS316L bellows, respectively.

Thus we have succeeded in developing the large-scale hydro-formed bellows with the inner-surface polishing, as flexible as welded bellows.

VST-P2-23
Transient rarefied gas flow through a slit

T15 Vacuum Science and Technology

#VST-P2-23

A. Polikarpov [1], I. Graur [2].

[1]Ural Federal University - Ekaterinburg (Russian federation), [2]Aix Marseille Université - Polytech Marseille - Marseille (France).

Transient gas flow through a slit into vacuum and at arbitrary pressure ratio was investigated basing on the unsteady S-model kinetic equation. Different gas flow regimes lying from free molecular to continuum regime were considered. The time necessary to reach the steady-state flow conditions was obtained, which varies from 10 to 100 as a function of the pressure ratio between the reservoirs and flow regime. The evolutions of the macroscopic parameters, the number density, the temperature and the bulk velocity in time were analyzed.

VST-P2-02
Vacuum System of the KATRIN Main Spectrometer

T15 Vacuum Science and Technology

#VST-P2-02

J. Wolf [1], S. Görhardt [2], N. Kernert [2], L. La Cascio [2], T. Thümmler [2].

[1]KIT, IEKP - Karlsruhe (Germany), [2]KIT, IKP - Karlsruhe (Germany).

The objective of the Karlsruhe Tritium Neutrino experiment (KATRIN) at the Karlsruhe Institute of Technology (KIT) is to measure the electron neutrino mass from the beta-decay of tritium with an unprecedented sensitivity of 200 meV. A central component is the electro-static main spectrometer (MS), where the energy of the beta-decay electrons at 18.6 keV will be measured with high precision. It consists of a large ultra-high vacuum vessel with a volume of 1240 m^3 and a surface of 690 m^2, which is instrumented with a complex inner wire-based electrode system with more than 120000 individual parts, which almost doubles the inner surface of the MS. The pumping system of the MS consists of 6 turbo-molecular pumps (10000 l/s), a large-scale getter pump (3000 m NEG strips, St707) and three cryo-baffles (6.8 m^2) at LN_2 temperature. It has three major goals: (I) the ultimate pressure, dominated by H_2, has to be kept in the range of 1 $\times$ 10^{-11} mbar in order to maintain a low background rate. (II) In conjunction with a differential pumping section and a cryogenic pumping section of the electron beam line, which connects the gaseous tritium source with the spectrometer, it has to keep the partial pressure of tritium in the MS below 10^{-21} mbar. (III) The NEG strips are known to emanate a small amount of radon atoms, increasing the intrinsic background rate. The cryo-baffles, which have been installed in front of the NEG strips, are expected to capture most of the radon atoms, before they can enter the sensitive volume of the MS. The objective is a reduction of the decay rate in the MS of the order of one decay per day. This paper describes the design of the vacuum system and the properties of its major components.

VST-P1-01
Low negative gauge pressure comparison between CMI and INRIM

T15 Vacuum Science and Technology

#VST-P1-01

Z. Krajíček [1], M. Bergoglio [2].

[1]Czech Metrology Institute - Brno (Czech republic), [2]INRiM - Torino (Italy).

The precise étalonnage of the border areas of vacuum is problematic – both its lower (XHV) and its upper (low negative gauge pressure) ends. The digital non-rotating pressure balance FPG8601 manufactured by Fluke/DH-Instruments is based on a 10 cm2 non-rotating tungsten-carbide piston-cylinder with a conical gap. It is normally used for gauge and absolute pressures in the range from 1 Pa to 15 kPa, but with some modifications it can be used also for the upper vacuum range, i.e. negative gauge pressures down to 15 kPa.
Étalonnage of the negative gauge pressures has been a neglected branch of primary metrology with the lack of international interlaboratory comparisons [1]. Recently an intercomparison (EURAMET.M.P-S8) was performed [2] and two others are in progress (EURAMET.M.P-S9, SIM.M.P-S5). However, none of these covers the negative gauge pressures lower then 10 kPa, and as a consequence an intercomparison confirming its metrological quality was necessary.
During the preparation of the visit of INRIM at CMI for the last comparison within the framework of EURAMET.M.P-K4.2010, it was agreed to perform an additional comparison in the range from 300 Pa to 15 kPa in negative mode. It was registered as a supplementary comparison (EURAMET.M.P-S12) and it is aimed to verify the equivalence of the national low negative gauge pressure standards of Czech Republic and Italy.
In this case a digital pressure controller Fluke/DH-Instruments PPC3-200K was used for pressure regulation of both FPGs instead of Fluke/DH-Instruments Very Low Pressure Controllers (VLPCs) normally utilized. When measuring in negative mode the VLPCs of both FPGs were connected only electrically but pneumatically disconnected. A capacitance diaphragm gauge with a set of valves were used as a zero indicator and separator between both standards. The nominal negative gauge pressure points were 300 Pa, 1 kPa, 3 kPa, 10 kPa and 15 kPa. Measurements were performed in 2 cycles in different days. Nitrogen was used as pressure transmitting medium.

The paper will show the details of the experimental setup, the procedure used and the obtained results of this comparison.

[1] TESAŘ, J., KRAJÍČEK, Z., PRAŽÁK, D., STANĚK, F.: Primary etalonnage of negative gauge pressures using pressure balances at the Czech Metrology Institute. Materiali in Tehnologie. Vol. 43 (2009), No. 3, p. 151 - 156.
[2] RANTANEN, M., SAXHOLM, S., ALTINTAS, A., PAVIS, R., PETERSON, G.: Negative gauge pressure comparison: range -95 kPa to 95 kPa (EURAMET Project 1131). Metrologia. Vol. 47 (2010), Tech. Suppl. 07007.

VST-4-Or-1
Review of 30 years of dry vacuum pumping

T15 Vacuum Science and Technology

#VST-4-Or-1

A. Chew [1], O. Charles [1], R. Coleman [1], A. Mann [1], I. Olsen [1], D. Steele [2], A. Watson [1].

[1]Edwards Vacuum Ltd (United kingdom), [2]Edwards Vacuum Ltd (United states).

Oil-free dry vacuum pumps play a major role in many and varied contemporary vacuum applications. This paper discusses the historical drivers for their introduction and continued developments. Examples are presented for a range of applications including semiconductor and flat-panel production, industrial and chemical processing, scientific instruments and general research. The elements defining the dry pump future road map are also discussed.

VST-3-Or-2
Vacuum Performance of the KATRIN Main Spectrometer

T15 Vacuum Science and Technology

#VST-3-Or-2

S. Görhardt [1], N. Kernert [1], L. La Cascio [1], T. Thümmler [1], J. Wolf [2].

[1]KIT, Institute of Nuclear Physics - 76021 Karlsruhe (Germany), [2]KIT, Institute of Experimental Nuclear Physics - 76131 Karlsruhe (Germany).

The **Ka**rlsruhe **Tri**tium **N**eutrino experiment (KATRIN) at the Karlsruhe Institute of Technology (KIT) has been designed to measure the electron neutrino mass from the β-decay of tritium with an unprecedented sensitivity of 200 meV. A central component is the electro-static main spectrometer, where the energy of the β-decay electrons at 18.6 keV will be filtered with high precision. It consists of a large ultra-high vacuum vessel with a volume of 1240 m^3 and a surface of 690 m^2. After a first successful bake-out of the bare vessel in 2007 a complex wire electrode system with more than 120 000 individual parts has been installed under clean room conditions at KIT, almost doubling the inner surface of the spectrometer.
In order to maintain a low background rate the ultimate pressure has to be kept in the range of $1 \cdot 10^{-11}$ mbar. The pumping system consists of 6 turbo-molecular pumps (10 000 l/s), a large-scale getter pump (3000 m NEG strips) and three cryo-baffles (6.8 m^2) at LN2 temperature. The NEG strips have been found to emanate small amounts of radon atoms, thus increasing the background rate. The cryo-baffles, which have been installed in front of the NEG strips, are expected to capture most of the radon atoms, before they can enter the sensitive volume of the main spectrometer.
This paper reports on the performance of the vacuum system before and after the final bake-out procedure and activation of the NEG pump at 350°C in early 2013.

VST-1-Or-2
Temperature sensing of fast gas expansions

T15 Vacuum Science and Technology

#VST-1-Or-2

J. Buthig, S. Pantazis, K. Jousten.

PTB - Berlin (Germany).

In processes involving fast gas expansions, it is often important to observe the change of temperature. Ongoing experiments in the Physikalisch-Technische Bundesanstalt include a dynamic system, performing an expansion of ratio 1:1800 within 1 s. In this case, a temperature drop of more than 150 K from room temperature may be expected. Assuming room temperature in theoretical calculations of conductance may in this case lead to significant errors. Thus, a temperature sensor should be placed inside the atmospheric pressure vessel. A thermocouple of type T, consisting of copper-constantan wires, has been selected to deal with this low temperature range.
The response time of the sensor is the most important property determining the accuracy of the measurement in fast processes. For this reason, thin wires of 25 µm diameter, which is the smallest possible size commercially available, are used. Several challenges are involved in the process of using a wire of this size, such as the building of a new connection with the 200 µm wires of the vacuum lead through. Various possibilities have been considered, such as laser welding, crimping, bonding and partially modified factory produced connectors. The characterization of the sensor for a rapid temperature change is also discussed. The influence of various factors such as the wire diameter, the gas temperature and velocity on the response time is estimated through simulations. Preliminary results are presented for simplified experiments, as well as the validation of experimental data with simulations.

VST-1-Or-3
Capacitance Diaphragm Gauges with highest measuring rate

T15 Vacuum Science and Technology

#VST-1-Or-3

C. Berg, F. Mullis, H. Hanselmann, M. Wüest.

INFICON AG - Balzers (Liechtenstein).

Capacitance Diaphragm Gauges (CDG) are used in many pressure control applications in industry. In such a typical application the CDG pressure signal is used in the butterfly valve controller to regulate the pressure in a vacuum chamber. The faster the control loop, the quicker the desired pressure value can be achieved. At present, the fastest commercially available CDGs have a time constant of 8 ms, while the majority of the CDGs have time constants of 20 to 30 ms. In this talk we will present CDGs that can deliver a new pressure value at less than 1 ms.

VST-5-Or-3
Comparison of diffusion and recombination limited model of experimental results for outgassing of hydrogen from a stainless steel vacuum chamber

T15 Vacuum Science and Technology

#VST-5-Or-3

S. Avdiaj [1], J. Šetina [2], B. Erjavec [2].

[1]University of Prishtina, Faculty of Natural Sciences and Mathematics - Prishtina (Kosovo), [2]Institute of Metals and Technology - Ljubljana (Slovenia).

Outgassing from the walls of vacuum chambers limits lowest achievable pressure. Austenitic stainless steel is the most common construction material for ultrahigh vacuum (UHV) and extremely high vacuum (XHV) chambers. Hydrogen is the predominant residual gas at very low pressures in stainless steel vacuum systems, i.e., in the UHV and XHV range. Therefore, the reduction of the hydrogen outgassing rate remains a challenging problem in the achieving pressures in those ranges. In this work, a vacuum chamber with a wall thickness of 2.62 mm and made from AISI type 304L stainless steel was examined with the aim of mitigating the outgassing rate. The heat treatments were carried out at 250°C for 380 hours and at 350°C for 140 hours. After baking at 250°C for 380 hours (corresponding to a dimensionless time $F_0 = 3.09$), an outgassing rate was achieved at room temperature. This room temperature outgassing rate was further reduced to after baking for another 140 hours at 350°C ($F_0 = 8.66$, resulting a total dimensionless time $\sum F_0 = 11.75$).

Diffusion limited model governs the initial removal of hydrogen from stainless steel, whereas hydrogen surface recombination plays an important role in the outgassing rate at lower hydrogen concentration. Numerical calculations based on diffusion limited model (DLM) and recombination limited model (RLM) of the same outgassing

data as a function of bake-out time are presented and compared with our measured data.

1. S. Avdiaj, B. Erjavec, Outgassing of hydrogen from a stainless steel vacuum chamber, Materiali in Tehnologije/Materials and Technology 46 (2012) 2, 161-167

2. V. nemanič, T. Bogataj, Outgassing of thin wall stainless steel chamber, Vacuum 50 (1998) 3, 431-437

3. B.C. Moore, Recombination limited outgassing of stainless steel, J. Vac.Sci.Technol. A 13(1995), 545-548

4. Park et.al., Reduction in hydrogen outgassing from stainless steels by a medium temperature heat treatment. J. Vac. Sci. Technol. A 26 (2008), 1166-1171

VST-7-Or-5
Rarefied gas flow between parallel plates of finite length at any pressure ratio

T15 Vacuum Science and Technology

#VST-7-Or-5

S. Misdanitis [1], S. Pantazis [2], D. Valougeorgis [1].

[1]University of Thessaly, Department of Mechanical Engineering - Volos (Greece), [2]Physikalisch-Technische Bundesanstalt - Berlin (Germany).

Due to the enlarged interest in the numerical solution of rarefied gas flows in vacuum applications, it is important to identify the most suitable and computational efficient methods as well as to be able to judge the accuracy to expect from these approaches. In this framework, very recently, in an IUVSTA workshop [1], few benchmark problems have been selected and a comparison between the results obtained by various methodologies has been performed [2]. During this effort it was realized that results for the rarefied gas flow through a channel are very limited and for that reason the comparison for this specific flow configuration has been abandoned.

In the present work, an effort is made to fill this gap by solving the channel flow problem and providing results for the three parameters, namely the reference gas rarefaction parameter δ, the downstream over the upstream pressure ratio Π and the dimensionless channel length L/H, which completely define this problem. This is achieved by numerically solving the nonlinear BGK model equation subject to Maxwell boundary conditions via an upgraded discrete velocity algorithm, which has been optimized by massive parallelization and memory handling techniques [3]. Results are provided for the dimensionless flow rates and the macroscopic distributions of the flow field for $0 \leq \delta \leq 10$, $0 \leq \Pi \leq 1$ and $0 \leq L/H \leq 10$. Furthermore, a comparison is performed with the corresponding linear solution in the case of small pressure differences as well as to the fully developed solution in the case of long channels in order to investigate the extend of validity of these theories. It is hoped that the provided solution will be used for benchmarking purposes as well as for comparison with experimental data.

[1] Workshop website: http://www.itep.kit.edu/VGD-2011
[2] F. Sharipov, Benchmark problems in rarefied gas dynamics, Vacuum 86, 1697-1700, 2012.
[3] S. Pantazis, D. Valougeorgis, Rarefied gas flow through a cylindrical tube due to a small pressure difference, Europ. J. Mech. B/Fluids, 38, 114-127, (2013).

VST-P1-02
A live calibration method of the leak detector of change pressure and experimental research

T15 Vacuum Science and Technology

#VST-P1-02

J. Shi, J. Zhao, L. Sun, F. Qi.

BISEE - Beijing (China).

This paper deals with an easy live calibration method using rise pressure for calibration the leak detector of change pressure. A given model detector is used in the calibration, and five leaks of different leak rate achieved by adjusting a micro-adjustable valve are calibrated. The minimum experiment relative error can arrive at 0.92% using the method in the calibration. The best merit of the method is easy and that the volume of the calibrating container is not introduced into the calculating course. It's needless to found the calibration system of specific size. The effect of the temperature and the leak rate on the result of the test using the leak detector of change pressure is also detailed by calculating. And the calculating result indicates that the biggish error would be introduced into the test result because of lesser change of the temperature if the leak rate and weight of leak are both lesser.

VST-P1-19
Evaluation Design of Reliability Engineering of Vacuum Pumps in the Semi-conductor Industry

T15 Vacuum Science and Technology

#VST-P1-19

J. Lim [1], W.J. Kim [2], S.Y. In [3], D.Y. Koh [4], W. Cheung [1].

[1]KRISS - Daejeon (Korea, republic of), [2]LOT Vacuum - Ansung (Korea, republic of), [3]KAERI - Daejeon (Korea, republic of), [4]KIMM - Daejeon (Korea, republic of).

Methods of the characteristics evaluation of vacuum pumps are well-defined in the international measurement standards such as ISO, PNEUROP, DIN, JIS, and AVS. The Vacuum Center in KRISS has recently designed, constructed, and established the integrated characteristics evaluation system of vacuum pumps based on the international documents by continuously pursuing and acquiring the reliable international credibility through measurement perfection.
Recently advanced industrial processes such as semiconductor and display manufacturing continuously require very precise evaluation of reliability engineering of vacuum pumps including the lab level of characteristics and endurance evaluation via the control of the mass flow of gases. The requirements include very low mass flows of less than 1 sccm or 2 X 10^{-2} mbar·l/s up to 10^{5} mbar·l/s.
Utilizing the combined mass flow systems in KRISS, the measurement of pumping speed has been performed with the throughput and orifice methods dependent on the mass flow regions. However, in the HV range of the molecular flow region, the high uncertainties of the gauges, mass flow rates, and conductance are too critical to precisely accumulate reliable data. In order to solve the uncertainty problems of pumping speeds in the HV range, we introduced an SRG with 1 % accuracy and CVFMs to measure the finite mass flow rates down to 10-3 mbar·l/s with 3 % uncertainty for the throughput method. In this way we have performed the measurement of pumping speed down to less than 10^{-6} mbar with an uncertainty of 6 %.
Based on the measurement of perfection developed we are supposed to develop the evaluation design scheme of reliability engineering of vacuum pumps with mapping the database accumulated in the lab, process, and factory sites. In this article we briefly introduce the current developmental stage of reliability engineering in vacuum

community.

Acknowledgements: Results are partially attributed to two national projects (Contract Nos. 10031858 and 10031836) sponsored by the Korean Ministry of Knowledge Economy, and KRISS main project 13011040.

VST-P1-03
Evaluation of the influence factors on vacuum helium mass spectrum leak detecting system sensitivity

T15 Vacuum Science and Technology

#VST-P1-03

W. Sun, D. Meng, L. Sun, Z. Li, R. Ding.

Beijing institude of spacecraft environment engineering - Beijing (China).

The sensitivity of the existing total leak rate detection methods for the large-scale seal structure was limited at present, and the vacuum helium mass spectrum leak detection system sensitivity is higher, hence evaluating some effect factors of the vacuum helium mass spectrum leak detection system sensitivity was useful for large-scale seal structure total leak rate detection and provided some references for vacuum system design. With large-scale space environment simulator as researching leak detection system, the sensitivity and influence factors of vacuum leak detection method was analyzed by the theory and experimental study. the study conclusions indicate the main influencing factors of vacuum leak detection system include the performancesof leak detector, the vacuum system design, the scheme of leak testing system and the Helium background of the vacuum container.The large-scale seal structure vacuum leak detection sensitivity can achieve $5X10^{-9}Pa{\cdot}m^3/s$. And the molecule pump in series mode can attain alittle large response and sensitivity. Cryopump can effectively improve the degree of vacuum, but it affects the Helium background.The heat sink has little affection for leak detection but is disadvantage for reducing Helium background. These conclusions provide some references and rational advices for improving vacuum leak detecting system.

VST-6-Or-5
Review and measurement of outgassing rates of stainless steel and polymers

T15 Vacuum Science and Technology

#VST-6-Or-5

K. Battes, C. Day, V. Hauer.

Karlsruhe Institute of Technology (KIT) - 76344 Eggenstein-Leopoldshafen (Germany).

The investigation of the outgassing of stainless steel was started a couple of decades ago. Many literature values for different types of steel and polymers are available showing a broad range of outgassing rates depending on pre-treatments and measurement methods even for the same material. The first part of this work is the review of available data and the presentation in a more general way. The Fourier and the Knudsen number are used to decouple temperature dependent from gas specific quantities.

The second part of the work is the experimental investigation of outgassing by using the difference method (a modified throughput method). The Outgassing Measurement Apparatus (OMA, Fig. 1) at KIT was used for the measurement of pre-treated (electro-polished, air-baked) and gel coated stainless steel as well as for different polyimides and Viton®.

The review of literature data including own measurements shows that the hydrogen outgassing from stainless steel can be reduced very effectively by surface treatment whereas the reduction of chemical bound water needs higher efforts especially in polymers and if baking cannot be performed at higher temperatures.

Acknowledgement
Part of this work has been performed under the IND-12 Project within the European Metrology Research Programme.

Fig. 1: Flowchart of the Outgassing Measurement Apparatus (OMA)
1 membrane pump
2 turbomolecular pump
3 conductances
4 sample chamber
5 reference chamber
6 Bayard-Alpert gauges
7 gate valves
8 magnetic feedthroughs
9 quadrupole mass spectrometer
10 lock chamber
11 Pirani vacuum gauges
12 valves (pneumatic)
13 dosing valve

VST-P1-04
A Portable Vacuum Gauge Calibration Apparatus

T15 Vacuum Science and Technology

#VST-P1-04

L. Yaowen [1], C. Xu [1], Q. Jing [2], L. Bo [3], C. Liangzheng [2].

[1](1.Tsinghua University - beijing (China), [2](1.Tsinghua University - Beijing (China), [3](2.Xi'an aerospace Institute of metrology - Xi'an (China).

A portable vacuum gauge calibration apparatus has been developed in order to meet the increasing demands of the on-site vacuum gauge calibration with wider pressure range. Three methods are integrated on this apparatus to expand the calibration pressure range, which are the static comparison method, the static expansion method and the dynamic flow method. The calibration chamber of the apparatus is a spherical container with 200mm diameter, where two capacitance diagram gauges (CDG) with full range of 1.33×10^{5} Pa and 133 Pa are used as the reference standards.

The achieved calibration range of this apparatus is $1\times10^{5}\sim4\times10^{-6}$ Pa, and the combined standard uncertainty is 1.3%～4.7%, which are shown by the experimental results. The size of this apparatus is 450 mm × 400 mm ×750 mm, and its total weight is less than 40 kg. The advantages of this developed apparatus are small volume, light weight, portable and low cost etc, which is suitable to do on-site vacuum gauge calibration with wider pressure range.

VST-P2-03
ARIEL E-linac Vacuum System

T15 Vacuum Science and Technology

#VST-P2-03

D. Yosifov.

TRIUMF - Vancouver (Canada).

The new Advanced Rare Isotope Laboratory (ARIEL) is TRIUMF's flagship facility that will expand Canada's capabilities to produce and study isotopes for physics and medicine. ARIEL Phase I have been funded and include the construction of conventional facilities and the first stage of high-power electron linear accelerator (e-linac) using superconducting radio-frequency niobium cavities. Additional phases of ARIEL will add two full target stations and an additional proton beam line from TRIUMF's main cyclotron.
ARIEL's e-linac will drive photo-fission of actinide target materials to produce exotic isotopes which will be extracted and separated on-line (ISOL) and delivery to TRIUMF's existing ISAC facilities. Employing a 300 keV electron gun (e-gun), the e-linac will deliver 5 mA beams at 25 MeV from an injector cyromodule and 5 mA, ~25 MeV beams at the output of the first accelerator cryomodule by year 2014.
To minimize the collision of electrons with air molecules, the pressure in the e-gun and the section before the injector cryomodule has to be at less than 1E-9mbar, in the accelerators and the section between the accelerators at ~ 1E-7mbar, and in the beam transport lines which deliver beam to the targets or beam dump at level less than 1E-6mbar. To achieve this goal, the e-linac vacuum system has to comply with ultra-high vacuum design, manufacturing and assembly standards.
This document describes the vacuum system of ARIEL E-linac. It identifies all vacuum components as pumps, valves, gauges, and elaborates on the effort spent in finding a cost efficient solution. The document also provides information about the control system and interlocks for the operation of e-linac vacuum system.

VST-P1-20
Study on Diagnostics of Dry Vacuum Pumps Using the Adaptive Parametric Model of State Variables

T15 Vacuum Science and Technology

#VST-P1-20

S. Nam [1], W. Cheung [2], J.Y. Lim [2].

[1]UST - Deajeon (Korea, republic of), [2]KRISS - Deajeon (Korea, republic of).

This paper introduces statistical features extracted from the measured state variables of dry vacuum pumps in the semiconductor processes. They were found to have three distinctive means and overlapped distributions unlike a single normal distribution. Specifically, two distinctive distributions near the upper and lower asymptotic bounds are obviously observed from the gas-loaded states of the vacuum pump and the third one from the idle states. These observations have provided new motivations of not only separating the pump operation state into the gas-loaded and idle states but also modeling the upper and lower bounds as a separated distribution. A linear adaptive parametric model (APM) is addressed to map their linear trends of each state variable onto their corresponding model parameters. Estimated model parameters are used to construct the batch data for each process. The APM-based batches are also exploited to construct the reference batches under the normal operating conditions (NOC) such that the principal components of the NOC (reference) batches are used to diagnose each process batch data in real-time. The APM-based batch is shown to provide a dramatic reduction of memory usage and computation time (1 ~ 2 % memory usage and 10 times faster computation time) in comparison to the conventional dynamic-time wrapping algorithms. Four cases of test results are demonstrated to examine the feasibility of the proposed APM for the diagnostics and predictive maintenance of dry vacuum pumps.

This paper proposes the use of two statistics, the Hotelling's T^2 and the sum of squared residuals, in order to improve the reliability of the self-diagnostics and predictive maintenance of dry vacuum pumps. The first one is exploited to examine what amount of similarity the current process batch has in reference to the normal operation conditions and, furthermore, the second is to examine what contribution the current process batch makes to the noise space. The two proposed statistics are examined to quantitatively analyze the reliability and improvement of the predictive maintenance and self-diagnostics developed in this work.

Gyu-Ho Lee, et. al. “Study on APM-based diagnostic algorithms for predictive maintenance of dry vacuum pumps,” Journal of KSV, 20(3), 2011.

Jong-Yeon Lim, et. al, “Low Vacuum Generation and Control on BIEN Technology; Mass Flow and Dry Pumping Characteristics”, Key Engineering Material, Vols. 277-279, pp. 1000-1015 (2005)

ISO 21360, Vacuum technology – Standard methods for measuring vacuum-pump performances – General description (2007)

APM-based diagnostic algorithm

VST-P1-05
Pumping Speed Measurement Capability of Dry Vacuum Pumps Using a Block of Six Calibrated Sonic Nozzles

T15 Vacuum Science and Technology

#VST-P1-05

W. Cheung [1], S. Nam [2], J.Y. Lim [1].

[1]KRISS - Daejeon (Korea, republic of), [2]UST - Daejeon (Korea, republic of).

This paper addresses the capability of measuring the pumping speed of dry vacuum pumps using a built-up block of multiple calibrated sonic nozzles [1-2]. The first challenging issue comes from the technical limit that their calibration capability of sonic nozzles [3] established by the flow measurement standard laboratories do not fully cover the low vacuum measurement range of 10 through 1000 mbar. In order to tackle the first technical issue, the constant volume flow measurement method [1-3] dedicated for the vacuum range of 10 through 1000 mbar is exploited to calibrate the discharge coefficient multiplied by the cross-section area of each sonic nozzle used in the built-up block of sonic nozzles. On the other hand, the discharge coefficient multiplied by the cross-section area of each sonic nozzle in the upstream pressure range of 2 through 10 bar is calibrated in the gas flow standard laboratory in KTISS. These combined calibration methods are illustrated to enable each sonic nozzle to cover the three decade measureable range of 10 mbar through 10 bar. The second technical issue comes from a logical way of stacking multiple sonic nozzles to expand the capability of measuring the pumping speed of dry vacuum pumps. On the onset of this work, sonic nozzles of 5 mm throat diameter were machined to expand the upper limit pumping speed by stacking three or four nozzles in the built-up block. Of course, small sized nozzles (0.1, 0.16, 0.5, and 1.0 mm throat diameter) were also machined to cover the low and mid range of the throughput of 0.1 through 100 mbar-l/s. A prototype of the built-up block with the capacity of installing six sonic nozzles was tested to investigate its performance. As shown in Figure 1, a maximum pumping speed was realised to be 5,000 m^3/h at the 50 mbar inlet pressure (.equivalent to 67,500 mbar-l/s). This prototype is expected to provide a possible ‘on-line pumping speed tester’ with the capability of 5,000 m3/h or more, applicable to the pumping speed measurement at the on-site flat display and semiconductor processes.

[1] Wan-Sup Cheung, et. al, “Precision vacuum pumping speed measurement using sonic nozzles,” J. Vac. Sci. Technol., A 29(4), 2011.
[2] Wan-Sup Cheung, et. Al, “Expanded Capability of Measuring Pumping Speed of Dry Vacuum Pumps Using Sonic Nozzles,” AVS 59th International Symposium and Exhibition, Tampa: Florida, 2012
[3] ISO 9300, Measurement of gas flow by means of critical flow Venturi nozzles (2005)

Figure 1. Performance test results: Pumping speed and power consumption

VST-P2-16
Simulation study of sensitivity on ionization gauge with carbon nanotube cathode

T15 Vacuum Science and Technology

#VST-P2-16

Y. Xiao [1], D. Li [1], Y. Cheng [1], C. Dong [2], H. Zhang [1].

[1]Science and Technology on Vacuum & Cryogenics Technology and Physics Laboratory, Lanzhou Institute of Physics - Lanzhou, 730000 (China), [2]Institute of Micro-nano Structures & Optoelectronic Devices, Wenzhou University - Wenzhou, 325000 (China).

In this paper, the sensitivity of carbon nanotube (CNT) cathode ionization gauge based Leybold IE514 extractor gauge structure is simulated using SIMION 8.0 [1] software extended by additional code. The simulation and analysis results are as follows:

(1) For the commercial IE514 thermionic cathode ionization gauge, all movement electrons emitted from the heated filament electron source are been restrained inside anode grid, no escape, as shown in Fig.1 (a). However, to the CNT cathode ionization gauge, the area of electron source is larger than thermionic cathode, and requiring high applied gate voltage (V_{gate}>400V) in operation, which results in a few escaped electrons that cannot be collected by anode, as shown in Fig.1 (b). These escaped electrons account for about 4%～10% of total electrons from CNT field emission cathode, and influence the effective electron path length (L_e) in the CNT source ionization gauge. Considering the theory relation between sensitivity and L_e in ionization gauge, the escaped electrons possibly give rise to the unstability of sensitivity. With regard to the sensitivity unstability of CNT source ionization gauge is also discovered in some experimental data reports [2, 3].

(2) As the ratio between anode voltage and gate voltage (V_{anode}/V_{gate}) increases, the L_e increases before, and then almost keeps constant after V_{anode}/V_{gate} >1.6. However, the sensitivity of CNT cathode ionization gauge declines with the anode voltage rising, which is primarily attributed to the decrease on ionization proficiency of gas-phase molecules [4]. Therefore, the reasonable voltage values on the electrodes will be propitious to increase the L_e, and improve the sensitivity, further extending the vacuum measurement lower limit.

As is mentioned above, the simulation results are contributed to penetrate the operation mechanism of CNT source ionization gauge, and provide important theoretical guidance to develop the new-type extreme high vacuum ionization gauge with CNT cathode.

[1] D.A. Dahl. SIMION version 8.0. Idaho National Laboratory, P.O. Box 1625, Idaho Falls, ID 83415.
[2] C. K. Dong, and G. R. Myneni, Appl. Phys. Lett. **84**, 5443 (2004).
[3] W. Knapp, D. Scheleussner, and M. Wüest, J. Phys.: Conf. Ser. **100**, 092007 (2008).
[4] J. T. Tate, and P. T. Smith, Phys. Rev. **39**, 270 (1932).

Fig.1. (Blue lines) Simulation of electrons trajectories
(a) IE514 thermionic cathode ionization gauge, (b) CNT cathode ionization gauge.
(Simulation parameters: $V_{anode}=V_{reflector}=700V$,$V_{gate}=450V$, $V_{collector}= V_{cathode}=0V$)

VST-P2-04
Vacuum acquisition technology applied in artificial climate environmental test facility with diameter of 22m

T15 Vacuum Science and Technology

#VST-P2-04

Q. Li.

18601271729 - Beijing (China).

Vacuum acquisition technology applied in artificial climate environmental test facility with diameter of 22m

Li Qiang Liu Botao Ru Xiaoqin Yang Ruihong Guo Feng
Beijing Institute of Spacecraft Engineering
(101 branch of mailbox 5142, Beijing 100094,China)

Abstract: A super-huge steel artificial climate environmental test facility with diameter of 22m and volume of 12000m^3 is used for the simulation of natural climate at different elevations below 6000m in southwestern China to carry on the characteristic research of the external insulation for ±800kV direct current transmission insulators and provide necessary facility and condition for design specification and technical standard. The key technology of this facility is the acquisition of stable low pressure plateau environment. The facility utilizes three sets of large scale liquid ring pump as prime vacuum pump and one set of lower pumping speed liquid ring pump as holding vacuum pump to evacuate the chamber in steps. Based on the principle of dynamic flow balance, a vacuum regulating valve is used to control the effective pumping speed of holding vacuum pump to achieve a stable experimental vacuum degree. The result of the experiment is as follows : the vacuum degree of 0.05MPa obtained within 15 minutes ,and the control accuracy of vacuum degree at 0.5% .

Key word : Diameter 22m, Artificial climate environmental test, Liquid ring pump, Vacuum degree control, Vacuum regulating valve

[1] Zhang Yichen. Vacuum technology and experimental technology. Beijing: metallurgical industry press, 2006

[2] Yu Yongqing, Li Guangfan, Su Zhiyi, etc. Uhv dc test base construction [J]. China's power, July 2006 (10) :10 - 14

VST-1-Or-6
Capacitance Diaphragm Gauges with very high full scale stability

T15 Vacuum Science and Technology

#VST-1-Or-6

P. Kappenberger, C. Strietzel, M. Wüest.

INFICON AG; Alte Landstrasse 6 - 9496 Balzers (Liechtenstein).

It has been shown that ceramic capacitance diaphragm gauge technology has achieved a great deal of maturity. Long-term stability of those production line gauges with analog electronics have been demonstrated to be within 0.005-0.04% depending on full scale[1] and rivaling the reproducibility of a static-expansion primary standard. Taking advantage of the developments in the electronics industry we have developed a new reference design using digital electronics optimized for high stability. Initial data will be presented.

[1] *Jousten and Naef*: "On the stability of capacitance-diaphragm gauges with ceramic membranes", J. Vac. Sci. Technol. A 29, 011011 (2011) doi:10.1116/1.3529023

VST-P1-06
An Analysis of Gas Flow and Pressure Differences for a High Vacuum Measurement Standard

T15 Vacuum Science and Technology

#VST-P1-06

H. Song, W. Khan, S.S. Hong.

KRISS - Daejeon (Korea, republic of).

A flow-control system has set up at vacuum laboratory, KRISS, which can be used for the calibration of vacuum gauges by comparison method in the pressure range from 0.1 ~ 133 Pa. The system mainly consists of a large vacuum process chamber and a high vacuum pumping system separated by a pneumatically actuated gate valve. To achieve homogeneous pressure inside the chamber, a square-shaped baffle plate of area 289 cm^2 is installed at a distance of 30 mm from the top of the chamber. Two mass flow controllers (MFCs 1 and 2) are installed on top of the chamber with flow controls of 1 slm (1 slm = 1000 sccm = 1.69 Pa m^3 s^{-1}) and 3 sccm (1 sccm = 1.69 × 10^{-3} Pa m^3 s^{-1}) range, respectively. In this work, we studied the following characteristics of the flow-control system; generating stable pressure points in the chamber of the system, the effect of baffle plate on pressure distribution, analysis of gas flow through the conductance-reducer (CR), and measurement of time constant and equilibrium times for various gases. The stable pressures can be generated in the turbo-molecular pump region as well as the scroll pump regions in the range 6.53×10^{-4} Pa ~ 6.27 Pa and 11.2 Pa - 493 Pa, respectively. In order to reduce the pressure non-uniformities, the effect of a baffle plate was investigated by comparison of the pressure ratios in the presence an absence of the plate. The pressure ratios of the four CDGs were close to the mean value of 1.00 in the presence of baffle plate. The gas flow through the conductance-reducer (CR) was analyzed by calculating the Knudsen number K_n for the three gases Ar, N_2 and He. It was observed that initially the flow was molecular which shifted to transitional with rise in pressure across the ends of the CR. The time constant (τ) and 95 % equilibrium time (3τ) we experimentally calculated for Ar, N_2, and He by delivering same flow rates of each gas through the mass flow controller(s). The values of 3τ for Ar, N_2, and He gases were 28 ~ 12, 24 ~ 10, and 10 ~ 6 minutes respectively. It was observed that, equilibrium time for heavy gases were longer and vice versa. From

this we conclude that equilibrium time is dependent on molar mass and size of the gas in the pressure range of nearly 1 Pa ~ 133 Pa.

VST-1-In-1
A dynamic vacuum pressure standard to test the response time of fast vacuum gauges

T15 Vacuum Science and Technology

#VST-1-In-1

K. Jousten [1], S. Pantazis [1], R. Model [1], J. Buthig [1], J. Iwicki [2], M. Wüest [3].

[1]PTB - Berlin (Germany), [2]VACOM GmbH - Jena (Germany), [3]Inficon AG - Balzers (Liechtenstein).

In several industrial applications, such as leak testing, CD metallization or coating processes, fast processes are often involved, requiring rapid changes of pressures in the vacuum regime. Vacuum load locks are typically being used for coating processes, where the pressure changes from atmospheric to medium vacuum within 1 s or less. The control of such vacuum systems is triggered by vacuum gauge readings. Therefore, vacuum gauge manufacturers are interested to know how fast their gauges can follow such rapid changes of pressures.

In order to study the response time of vacuum gauges to rapid pressure changes, the Physikalisch-Technische Bundesanstalt has developed a dynamic vacuum standard where the pressure may change from 100 kPa to 100 Pa within 1 s or less in a predictable manner. This is accomplished by an expansion of gas at 100 kPa from a very small volume of less than 0.1 L into a large volume of 180 L through a well defined orifice. The process is started after the activation of a fast opening gate valve DN40, reaching its final state within less than 6 ms. The flow rate through the orifice needs to be calculated versus time through simulations. Furthermore, the temperature inside the small volume may drop by more than 150 K and therefore needs to be calculated and measured to avoid uncertainties in theoretical calculations. Finally, the pressure in the small chamber found by the simulations will be used as a reference for the indicated pressure of the attached vacuum gauge.

To validate this standard, in a first step, the pressures have only been changed to the extent that the gas flow remains viscous, i.e. the pressure has been decreased from 100 kPa to 1 kPa. Hydrodynamic flow simulations have been carried using the

commercial code ANSYS CFX and compared to experimental results. In a second step, simulations for the case where the pressure changes down to 100 Pa have been performed by a hybrid continuum particle solver. This is a challenging task, due to the fact that the low pressure dictates an approach based on the kinetic theory of gases, but also due to the non-stationary nature and extreme characteristics of the flow, such as the geometrical features and pressure range.

First results of tests regarding the response time of fast vacuum gauges are presented and discussed.

Support through the EMRP IND12 project is gratefully acknowledged. The EMRP is jointly funded by the EMRP participating countries within EURAMET and the European Union.

VST-7-Or-10
FIB nano holes: experimental results and simulation of flow rate

T15 Vacuum Science and Technology

#VST-7-Or-10

V. Ierardi [1], U. Becker [2], J. Buthig [2], S. Pantazis [2], G. Firpo [1], M. Bergoglio [3], U. Valbusa [1], K. Jousten [2].

[1]NanoMed labs, Physics Department, University of Genova - Genova (Italy), [2]Physikalisch-Technische Bundesanstalt - Berlin (Germany), [3]Istituto Nazionale di Ricerca Metrologica - Torino (Italy).

Devices based on permeation leaks and physical leaks are used in order to calibrate leak-detection instruments. For many type of leak devices, the conductance is not predictable based on dimensional, gas species and temperature data, for this reason no estimates or only rough estimates of leak rates are possible for conditions under use where they differ from those of the calibration. Unfortunately, permeation leaks are very sensitive to small temperature fluctuations and can be used only with those gases for which permeating materials are available. While, physical-leaks that overcome these restrictions are susceptible to clogging. Here we present the characterization and the performances of a new kind of physical-leak devices based on nano-holes, namely holes with nanometric size, which overcoming the drawbacks of the physical and permeation leaks [1]. These devices work in the molecular-flow regime up to atmospheric pressure. The nano-holes with diameter of the order of 200 nm are manufactured by milling a silicon nitride membrane 200 nm thick by means of Focused Ion Beam (FIB) [2]. An example of a nano-hole with diameter of 200 nm is shown in figure 1. The geometrical dimensions were determined by Scanning Electron Microscopy (SEM), Scanning Transmission Electron Microscopy (STEM) and Atomic Force Microscopy (AFM) [3]. The performances of the leak devices have been studied using a primary gas flowmeter [4]. The measurements are carried out by a direct comparison of the unknown flow rate from the leak devices based on nano-holes with the known flow rate from the primary gas flowmeter [5]. By direct simulation Monte Carlo method the conductances of these short tubes were calculated from the measured dimensions. The calculated conductances agreed with the values measured by comparison with a primary gas flowmeter within their respective uncertainties.

Acknowledgements-This work is funded by EMRP (European Metrology Research Programme). The EMRP is jointly funded by the EMRP participating countries within EURAMET and European Union.

[1]. G Firpo, et al J. Vac. Sci. Technol. B 27, 2347 (2009).
[2]. L A Giannuzzi, F A Stevie, Introduction to Focused Ion Beam, New York: Springer (2005).
[3]. M Alderighi, et al J. Nanosci. Nanotechnol. 8, 2479(2008)
[4]. K. Jousten, G. Messer, D. Wandrey, Vacuum 44, 135 (1993).
[5]. K. Jousten, H. Menzer, R. Niepraschk, Metrologia 39, 519 (2002).

Figure 1: Nano-hole images: A) SEM Image; B) STEM image; C) lateral view 3D AFM image.

VST-P1-24
Development of new materials and ultra clean processes using the vacuum – plasma – levitation technique

T15 Vacuum Science and Technology

#VST-P1-24

Y. Shin, S. You.

Korea Resear Institute of Standards and Science - Daejeon (Korea, republic of).

It has been known that a lot of new and noble materials which is hard to be synthesized in the earth can be made in the space. We have tried to make space simulated environment system in the laboratory by developing the system conversing the representative elements of the space, such as a vacuum, a plasma and a non-contact status from any other things. The space simulated environment system has been designed and developed. This system was consisted with the precisely controllable vacuum - plasma system, the sample levitation equipment and the temperature control system. Levitation technique can reduce the contamination from the container and the contact effect during the heating process. If we can feed ultra clean material during the well controlled vacuum – plasma – temperature process, we can develop new materials or new processes. In this system, we made the pure particles and tried to use as the evaporating materials immediately without any contact with container. Not only the design and the development processes of the system, but also its application results will be presented. This technique can be expected to be applied in the development of the next generation processing equipment in manufacturing as well as new material synthesis.

Nano particle synthesis and control in the vacuum-plasma-levitation chamber.

VST-1-Or-8
Mass spectrometry residual gas analysis: a key tool to optimize the packaging of MEMS

T15 Vacuum Science and Technology

#VST-1-Or-8

P. Nicolas, P.L. Charvet, D. Bloch, B. Savornin.

CEA, LETI, MINATEC Campus - Grenoble (France).

A vacuum packaging process is required for most of MEMS sensors or actuators such as accelerometers, gyroscopes, resonators, RF switches, micro bolometers. Indeed, the MEMS devices operation and reliability are critically dependent on the vacuum level inside the MEMS cavity after sealing (fig 1). This vacuum level can be improved by using porous absorbing materials, namely getter materials which are deposited inside the MEMS cavities before sealing. Their pumping properties are however gases dependent and it is then important to be able to identify and quantify the different residual gases inside the very small MEMS cavities (~1mm3 or less, at pressure level usually in the 10-2 to 10-3 mbar range. Although different methods have been explored [1], the Residual Gas Analysis (RGA) method -however destructive- reveals to be an interesting one to determine the possible sources of gaseous species present in the MEMS package cavities, in order to assess their reliability.
This paper introduces results recently achieved with a specific RGA test bench, developed at the CEA-LETI (fig 2). This equipment operates with a residual background pressure level in the 10-10 mbar range and uses a quadrupolar mass spectrometer (QMS) for gas analysis.
Experimental results confirm that the RGA technique may be successfully used to identify the nature and proportions of gaseous species [2], trapped in cavities as small as 1 mm3 under a residual pressure lower than 10-2 mbar.

References
[1] I. De Wolf, A. Jourdain, P. De Moor, H. A.C. Tilmans and L. Marchand*, Hermeticity Testing and Failure Analysis of MEMS Packages, Proceedings of 14th

IPFA 2007, Bangalore,India , pp 147-154.
[2] O.B. Malyshev and K.J Middleman, In situ ultrahigh vacuum residual gas analyzer “calibration”, J.Vac.Sci.Technol.A 26(6), Nov/Dec 2008 pp 1474-1479.

Fig. 1: Schematic of a Wafer-Level Package. A getter (in blue color) may be placed inside the cavity to adsorb actively undesired gaseous species generated during the bonding process or outgassed during the lifetime of the device by surrounding materials.

Fig. 2: Ultra High Vacuum (UHV) RGA equipment

VST-P1-25
Effects of the photon stimulated desorption from the surfaces cleaned with ozonized water

T15 Vacuum Science and Technology

#VST-P1-25

G. Hsiung, C.M. Cheng, Y.T. Cheng, C.K. Chan, C.C. Chang, J.R. Chen.

NSRRC - Hsinchu, Taiwan.

The significant pressure burst, typically rising up to more than 3 orders of magnitude, due to the photon stimulated desorption (PSD) from the fresh surface of vacuum beam ducts irradiated by the synchrotron radiation in a large accelerator is a major problem to the beam instability and the limitation of the beam life time. In previous studies [1] in the 1.5 GeV synchrotron accelerator Taiwan Light Source (TLS) the typical outgas molecules of the PSD emitted from the OFHC copper (Cu) or aluminum (Al) alloys contain hydrogen (H_2), carbon monoxide (CO), carbon dioxide (CO_2), methane (CH_4), and water vapor (H_2O). Those outgas molecules comprised of three atoms: H, C, O, were formed on the surface through the complex of recombination or dissociation processes prior to desorption. Any effective surface treatment to reduce the quantity of contamination-atoms in the surface oxide layers will dramatically reduce the rate of PSD-outgas. A cleaning process with ozonized water applied to the pre-cleaned surfaces of Al and Cu has been studied. The Al-chambers were machined with pure alcohol as the coolant and lubricant to protect the surface from oil contamination. A further cleaning with the high purity ozonized water was applied to the machined pieces for thoroughly cleaning of the surface residual contaminants, e.g. C, Cl, Na, F, etc. The thermal outgassing rate of the Al samples after oil-free machining and the ozonized water cleaning (with a concentration of 30 ppm) reaches to a value of ~ 6.4×10^{-12} Pa•m/s after a 24-hours baking at 150 °C.[2] The yield of PSD for Al or Cu samples measured at the 19B(PSD) beam line of the TLS is lower than 5×10^{-5} molecules/photon at the beginning of the photon exposure period which is more than ten times lower than those treated with conventional surface cleaning process. The surface characterization for both Al and Cu samples after the cleaning process presents a lower surface contamination and the consequent lower rate of PSD-outgas. More photon exposure experiments for various materials, e.g. Al, Cu, or stainless steel, are

performed and the effects of the PSD for the samples with or without ozonized water cleaning will be analyzed and described in this paper.

[1] G. Y. Hsiung, K. Y. Young, Y. J. Hsu, and J. R. Chen, J. Vac. Sci. Technol. A19, 1657 (2001).

[2] C. K. Chan, G. Y. Hsiung, C. C. Chang, Rouge Chen, C. Y. Yang, C. L. Chen, H. P. Hsueh, S. N. Hsu, Ivan Liu, and J. R. Chen, Journal of Physics: Conference Series 100 (2008) 092025.

VST-P2-05
Development of a fast mask for Diamond Light Source beamlines

T15 Vacuum Science and Technology

#VST-P2-05

H. Shiers, M. Cox, S. Omolayo, J. Emmins.

Diamond Light Source - Didcot (United kingdom).

Diamond Light Source is the UK's national synchrotron light source. In order to protect the storage ring ultra-high vacuum from a vacuum incident in a beamline, vacuum valves and fast closing valves (10ms) are installed in each of the 22 operating beamlines which close automatically in the case of a vacuum excursion. The main water-cooled photon absorber in each beamline can take several seconds to close and, to avoid photon beam damage to the vacuum valves, it has been necessary up until now to dump the electron beam in the storage ring in case any valve is required to close across the "hot" photon beam. This can result in nuisance x-ray beam trips of the whole facility. A fast mask has recently been developed and tested which is guaranteed to close within 100ms and which can protect downstream vacuum valves by withstanding the "hot" photon beam during the time required to close the main photon absorber in the beamline. This removes the need to dump the stored electron beam in many circumstances with a consequent benefit on facility uptime.

The development and evaluation of the new fast mask, material selection, incorporation into the Diamond Light Source control system and some challenges which had to be overcome will be described.

VST-P2-06
In-house development of PLC controlled vacuum systems for experimental stations at Diamond Light Source

T15 Vacuum Science and Technology

#VST-P2-06

S. Omolayo, P. Amos, H. Shiers, J. Emmins, M. Cox.

Diamond Light Source UK - Didcot (United kingdom).

Diamond Light Source is the UK's national synchrotron light source currently with 22 operating beamlines each with an associated endstation. Some of these endstations are complex ultra-high vacuum systems in their own right, which have to be operated by non-expert users and which have a windowless interface to the x-ray beamline and the electron storage ring. A complex endstation control system with a large number of different dynamic states is therefore required and a PLC-based solution was selected and developed. As well as having an intuitive user interface, the endstation control system has to prevent inappropriate user operations, to provide automated functions for pump down, baking out, venting, sample transfers and valve operation as well as providing interfaces to the main Diamond Light Source EPICS control system. In addition some end stations need complex gas inlet systems for sample dosing combined with regulated pumping speed using PID controlled valves.

The design and development of these end stations, the hardware chosen and its integration into the PLC system as well as into the main EPICS control system will be described. The development and testing of the PLC code for automation of routine operations and for protection against incorrect operation and fault conditions will also be discussed.

VST-P1-22
Absorption of noble gases by sputter-ion pumps: investigating synergetic pumping mechanisms for a better integration with non-evaporable getters

T15 Vacuum Science and Technology

#VST-P1-22

T. Porcelli, A. Bonucci, F. Siviero, A. Conte, L. Caruso, P. Manini.

SAES Getters S.p.A. - Lainate (Italy).

Ultra-high vacuum (UHV) conditions, corresponding to pressures lower than 10^{-9} mbar, are nowadays essential for a large variety of technological applications, ranging from large vacuum systems for particle accelerators to small equipment for portable analysers and devices. The achievement and maintaining of the required vacuum performances, as well as strict constraints in terms of design, size and weight of the vacuum components, led to the development of a novel combination pump, called NEXTorr®, whose functioning is based on the synergetic integration of a non-evaporable getter (NEG) cartridge, representing the main pumping element, and a small sputter-ion pump (SIP) [1]. After having been activated, the NEG cartridge is able to adsorb on its surface all the chemically reactive gases normally present in a vacuum system, i.e. H_2, O_2, N_2, H_2O, CO and CO_2; on the other hand, the SIP is responsible for pumping inert gases and hydrocarbons (especially CH_4), which are not pumped by NEG. The compact and integrated design enhances the synergy between the two pumping elements, providing pumping efficiency for methane and noble gases higher than the one ensured by the sole SIP.
A deeper understanding of the sorption mechanisms of sputter-ion pumps for noble gases is a key factor to further develop the combination pump technology, aiming to enhance its overall pumping efficiency. A series of sorption tests has been conducted for different SIPs; data will be presented with special focus on the pumping of helium, neon, argon and krypton, which are employed in several imaging and analytical instruments. Furthermore, important side effects – such as gas regurgitation during pumping of these species – will be shown and discussed. Lastly, the interactions of certain gases with the inner surfaces of a SIP have been studied and the positive effects of this *purging* mechanism on pumping efficiency will be described.

[1] E. Maccallini, P. Manini, A. Conte, F. Siviero, A. Bonucci, “New Approach to meet vacuum requirements in UHV/XHV systems by Non Evaporable Getter Technology”, Journal of Physics, Conference Series **390** (2012) 012006.

VST-1-Or-4
High-Vacuum Metrology at NIST

T15 Vacuum Science and Technology

#VST-1-Or-4

J. Fedchak.

National Institute of Standards and Technology - Gaithersburg (United states).

The vacuum calibration laboratory at the National Institute of Standards and Technology (NIST; USA) is responsible for realizing and disseminated the SI for pressure covering the range of 10^{-7} Pa to 1 Pa, and for low gas flow from 10^{-6} mol/s to 10^{-13} mol/s, in addition to performing research and development related to metrology in vacuum and low gas-flow. Standard calibration services are offered for ionization gauges, spinning rotor gauges, and He leak artifacts. The heart of the laboratory is the constant pressure flowmeter, which is used as a low gas-flow standard and is also used as a source of a known gas-flow for the dynamic-expansion systems that are the NIST high-vacuum standards. Recent projects include long-term ionization gauge stability studies and developing an orifice flowmeter that can produce low gas-flow based upon a flow calibrated laser-drilled pin-hole orifice. In this talk, an overview of the vacuum lab standards will be given and the results of recent research projects will be presented.

VST-1-Or-11
Comparative RGA measurements in the range from 10^-10 to 10^-5 mbar

T15 Vacuum Science and Technology

#VST-1-Or-11

M. Pendleton.

STFC, ASTeC - Warrington (United kingdom).

Comparative RGA measurements in the range from 10^{-10} to 10^{-5} mbar

Mark D. Pendleton, Joe D. Herbert, Oleg B. Malyshev, Keith J. Middleman.

ASTeC, STFC Daresbury Laboratory, Warrington, WA4 4AD, U.K

Author: mark.pendleton@stfc.ac.uk

The ASTeC Vacuum Science Group, based at the Cockcroft Institute STFC Daresbury Laboratory, primarily focus on the design and operation of large vacuum systems for particle accelerators. One of the main interests is accurate total and partial pressure measurements.

Utilising the existing secondary vacuum gauge comparison facility it has been upgraded to perform accurate RGA comparative measurements in the range between 10^{-10} and 10^{-5} mbar to an extractor gauge calibrated against a primary standard.

In a reported study initial background measurements were taken and recorded for the three instruments which include a Granville Phillips Ion trap 1-145amu, and two standard RGA units from different manufacturers' (Hiden Analytical and MKS) with 1-50amu and 1-200amu respectively. Gas injections at two points per decade are

performed within the pressure range along with separate stage gas mixtures to also study the cross influence of masses, particularly those of interest found within the accelerator.

The presentation will highlight the comparative data obtained using the three instruments which will include the gas species studied over the cited pressure range, calibration coefficients, linearity of the instruments over time and also the influence in which common gases found within the accelerator have upon each other.

VST-4-Or-4
Theoretical and experimental investigation of metal foil vacuum pumps for pumping and separating hydrogen

T15 Vacuum Science and Technology

#VST-4-Or-4

T. Giegerich, C. Day.

1 - Karlsruhe (Germany).

At KIT Karlsruhe, a new vacuum pump based on the physical principle of superpermeation is under development. This ‘metal foil pump’ shall be used in the fuel cycle of fusion power plants. This pump provides two major functions, separating and pumping, simultaneously for hydrogen and its isotopes. It separates a hydrogen and impurities containing gas flow sharply into a pure hydrogen flow that is also being compressed. The remaining impurity (i.e. non-hydrogen gas species) enriched gas flow passes the pump without being pumped.

For superpermeability, a source of molecular hydrogen is needed. This can be achieved by different methods and directly inside the pump. Most important are plasma based or hot rod (atomizer) based methods. For safety reasons (low temperatures in a hydrogen environment) and to be more energy efficient, the plasma method is favored in technical applications though it still needs a high development effort.

An experimental arrangement was set-up to investigate the pumping behavior of metal foils and to produce data for scaling. This asks for an experimental device where atomic hydrogen with clearly defined parameters and at a known flux can be produced and accelerated towards the metal foil. Furthermore, the metal foil has to be heated to investigate it at different temperatures and in a schematic way. It must be easily demountable and withstand the pressure difference during a helium leak test.

In this paper, first results are presented and the physical working principle including modeling of such a metal foil pump is discussed. Furthermore, the development towards a technical-scale pump is shown up.

VST-3-Or-3
Status of the Spiral 2 project - Overview of the vacuum system

T15 Vacuum Science and Technology

#VST-3-Or-3

P. Dolegieviez.

CEA / GANIL - Caen (France).

The Spiral 2 facility is a rare isotope accelerator that will be installed on the GANIL site at Caen (Grand Accélérateur National d'Ions Lourds). This machine is dedicated for the production of high intensity radioactive ion beams using ISOL technique (Isotope Separation On Line). Spiral 2 facility is based on a high power superconducting driver LINAC delivering a deuteron beam (5 mA / 40 MeV) and heavy-ion beams (1mA / 14.5 MeV/u). Radioactive beams are produced by fission reactions of a Uranium target (UCx) maintained at 2000°C and subjected to a high neutron flux. Fission products of different reactions are then scattered out of the target, ionized, separated on line and post-accelerated into the existing CIME cyclotron at GANIL.
The construction of the facility is organized in two phases. First phase including the superconducting driver accelerator and its associated experimental areas, and a second phase including the radioactive ion beams production, the low energy experimental area and the connection to GANIL existing facility. The Spiral 2 facility is now in its construction phase, with the objective of obtaining the first beams with the first phase during 2014.
This paper presents an overview of the project and a status of the construction. A general presentation of the Spiral 2 vacuum system is given, with a focus to the constraints due to the radioactive environment. The specific vacuum systems designed for safety functions are briefly described (storage exhaust gas system, fast valves system and specific trap to limit the radioactive transfer of volatile contamination in the beam lines).

VST-5-Or-11
Penning Gauges Revisited

T15 Vacuum Science and Technology

#VST-5-Or-11

A. Rauch.

graduate of diploma program - Feldkirch (Austria).

Penning Gauges Revisited

Albert Rauch[1,2], Hans K. Pulker[1], Martin Wüest[3]
[1] Institute for Ion Physics and Applied Physics, University of Innsbruck, 6020 Innsbruck, Austria
[2]now at ThyssenKrupp Presta AG, Essanestrasse 10, LI-9492 Eschen, Liechtenstein
[3] INFICON AG, Alte Landstrasse 6, LI-9496 Balzers, Liechtenstein

The plasma in a Penning gauge has been studied in depth with optical emission spectroscopy, Langmuir probes and a retarding field analyzer.
A Langmuir double probe was used to measure the plasma parameters at the center of the discharge. The obtained results are the electron temperature and plasma density. The temperature was found in the range of 1-4.8 eV at a discharge voltage of 1600V. It shows that changing the type of gas has little effect on the electron temperatures. Temperature versus neutral density (pressure) indicates that electron temperature decreases with increasing neutral density, due to the increase of the collision frequency and therefore increases the amount of cooling (electron lose a certain amount of energy through inelastic collisions with neutrals).
Optical Emission Spectroscopy (OES) provides a non-evasive probe to investigate discharge plasma. The optical emission from the Penning gauge was viewed across the anode ring, parallel to the cathode plates. To examine the influence of gas type on the performance of the gauge, different pressures were set and the various spectra were recorded, yielding the dependence of the different emission lines on the discharge current. The observed N_2 rotational temperature is almost the same as the gas temperature.
Retarding field analyzer(RFA) were used to estimate directly the ion energy distribution (IED) of the incident ion flux on the gauge cathode material. The observed mean ion energies have values in the range of 150-525eV and the energy spread is in the range of 5-45eV as the pressure drops from p = 1 10^{-2} mbar to 2 10^{-6}

mbar, while the maximum ion energy is in the range of 300-630eV. It is shown that at constant anode voltage, a decrease in gas pressure is accompanied by a monotonically increase in ion energy.

[1] P. Cruikshank, G. Engelmann, W. Koelemeijer, N. Kos, Vacuum 48 , 759, (1997)
[2] F.M. Penning, Physica 3 and Physica 4 (1936, 1937)

VST-5-Or-9
Novel design for ultralow magnetic stray fields in cold cathode gauges

T15 Vacuum Science and Technology

#VST-5-Or-9

B. Andreaus.

Inficon AG - Balzers (Liechtenstein).

Electromagnetic interference from low-intensity static magnetic fields has been observed to affect the operation of pacemakers and other medical electronic devices. The ICNIRP Guidelines [1] recommend that those devices are not adversely affected by static magnetic fields below 0.5 mT. These recommendation have been incorporated into the Semiconductor Manufacturing Standard SEMI S2-0302 [2] and requires that the magnetic field at exterior surfaces of the equipment (2 to 3 cm from the surface) has to be smaller than 0.5 mT or a pacemaker warning needs to be posted. This is why presently available cold cathode gauges should (but most do not) carry a pacemaker warning label, because they do not fulfill the SEMI S2 standard.

Moreover, from a technical point of view, the presently available cold cathode gauges' magnetic stray fields may impede their usage in applications sensitive to such fields as in the case of analytical instruments.

We have developed an inverted magnetron with a novel magnetic field design, keeping exterior magnetic stray fields below the threshold set by the SEMI norm, and thus extending the usefulness of cold cathode gauges to applications where magnetic stray fields are critical. In this paper, the magnetic design of this inverted magnetron is presented in detail.

[1] Guidelines on Limits of Exposure to Static Magnetic Fields, International Commission on Non-Ionizing Radiation Protection, 2009
[2] Environmental , Health, and Safety Guideline for Semiconductor Manufacturing Equipment, Semi S2-0302, Appendix 5, 2002

VST-P2-07
A simplified vacuum system for the new PC gun in the FERMI@Elettra project.

T15 Vacuum Science and Technology

#VST-P2-07

L. Rumiz, I. Cudin, E. Mazzucco, G. Pangon, M. Trovò, F. Zudini.

ELETTRA Sincrotrone Trieste S.C.p.A. - Trieste (Italy).

The construction of the FERMI@Elettra machine, the single-pass FEL user facility located in Trieste (Italy), started in May 2009. The first installed part was the photoinjector. It was designed to work at a repetition rate of 10 Hz. Its vacuum system is able to keep the pressure lower than $1 \cdot 10^{-9}$ mbar at the photocathode. To reach the 50 Hz rep-rate target, a general upgrade of all the RF plants has been implemented. A new PC-Gun has been also developed with a new and more compact mechanical design that requires a new pumping system. The main challenge was to simplify it, preserving the good vacuum performance of the first gun.
A comparison of the vacuum system designs between the previous and the new gun is discussed.

VST-P2-24
Simulation of electron stimulated desorption ion effect based on Axial-symmetric transmission gauge

T15 Vacuum Science and Technology

#VST-P2-24

D. Li [1], H. Zhang [2], C. Dong [3], Y. Feng [4], Y. Cheng [4], Z. Xi [4], Y. Xiao [4], Y. Wang [4].

[1]Teacher - Lanzhou (China), [2]Student - Lanzhou (China), [3]Teacher - Wenzhou (China), [4]collegue - Lanzhou (China).

The effects of electrode voltages and structure on the collection rate of electron stimulated desorption (ESD) ions in axial-symmetric transmission gauge (ATG) were studied by the theoretical simulation, which was in favor of providing theoretical basis and experimental guidance for analyzing the ESD ion effect, and the study possesses significant meaning to minimize the ESD ion effect and develops new types of extreme high vacuum gauges. Based on Axial-symmetric transmission gauge (ISX2), a physical model was constructed, and the influence of energy analyzer voltage (V_{be}) on ESD ions collection ratio was investigated with the aids of the ion & electron optic simulation software SIMION 3D 8.0. Meanwhile, the experimental study of the ESD ion effect was carried out. Excellent agreements were demonstrated between the theoretical simulations and experimental results. Namely, after crossing the energy analyzer, the energy difference of the ESD and gas phase ions was about 40eV in the ultimate vacuum (1.0×10^{-9}Pa) in both cases. The energy difference between the ESD and gas phase ions would be increased to about 60eV via optimizing the model structure. Consequently, by considering that the effect of gauge structure on the collection ratio of gas phase ions is relatively little, energy difference between two kinds of ions will increase by optimizing the structure reasonably, which was in favor of minimizing the ESD ion effect.

Ions trajectory (Gas phase ions-Black; ESD ions: Green-H+, Red-CO+, Blue-O2+)

VST-P1-07
Comparison of the standards for high and ultrahigh vacuum at LIP laboratory

T15 Vacuum Science and Technology

#VST-P1-07

Y. Cheng, D. Li, Y. Feng, W. Wei, Z. Xi, L. Zhao.

collegue - Lanzhou (China).

A comparison of standards based on different principles for high and ultrahigh vacuum was carried out by the Lanzhou Institute of Physics (LIP) of China. The static expansion standard（SES） [1] and separated flow standard（SFS） [2] were used in the present comparison. Two commercially available gauges, a Bayard-Alpert gauge (BAG) and an extractor gauge (EXG), were chosen as transfer standards. The argon pressures generated by the standards from 4 × 10^{-7} Pa to 1 × 10^{-3} Pa were compared by measuring the sensitivity of the two ionization gauges. The deviation $(S_{SES}-S_{SFS})/S_{SFS}$ was used to describe the agreement of the two standards. The BAG results show an agreement of 0.72% and the EXG results show an agreement of 0.64%. The SES-SFS differences are all within the combined uncertainties of the standards. By this intercomparison, the method to extend the lower limit of the SES by using non-evaporable getter pump to eliminate the outgassing influence has been demonstrated. The SES is to be used in China as a primary standard of ultrahigh vacuum.

[1] Li Detian, Cheng Yongjun. Applications of non evaporable getter pump in vacuum metrology. Vacuum, 2011, 85:739-743.
[2] Li Detian, Guo Meiru, Cheng Yongjun, Feng Yan, Zhang Dixin. Vacuum-calibration apparatus with pressure down to 10-10 Pa, J. Vac. Sci. Technol. A, 2010, 28(5):1099-1104.

VST-P2-17
Electrohydrodynamic microflows in a ring-type mixing chamber

T15 Vacuum Science and Technology

#VST-P2-17

Y. Kim [1], H.S. Seo [2].

[1]School of Mechanical Engineering - Suwon (Korea, republic of), [2]Graduate School of Mechanical Engineering - Suwon (Korea, republic of).

Micro/nano-scale mixing is emphasized in various applications such as homogenization solutions of reagents in chemical and biological reactions, synthesis of nucleic acids and nano drug delivery system, etc. [1]. Especially, electrokinetically driven flow such as electoosmotic flow (EOF) is a highly attractive alternative to pressure-driven flow for fluidic handling and reagents transportation in microfluidics and nanofluidics [2].

In this study, the electrokinetic microchannel with a ring-type mixing chamber was investigated to fast mixing of the species. The three dimensional modeled micromixer that is applied for the electroosmotic effect takes two fluids from different inlets and combines them in a ring-type mixing chamber, and then these are mixed by forming a vortex flow due to applied electric potential at electrodes. The schematic of modeled micromixer applied to this study is shown as Fig. 1. We numerically investigated flow characteristics with electrode dispositions in the ring-type mixing chamber using a commercial code, COMSOL Multiphysics.

Effective mixing basically involves repeated combinations of stretching and folding of fluid elements and small scale diffusion. They were influenced by the electric fields that were produced by each electrode. Also, the vortex flow fields were formed around the electrodes in the mixing chamber and its configurations formed differently caused by electrode dispositions. Through these phenomena, the fluid particles that stayed in the central loop stretched and folded for a long time before they entered the outlet section of the microchannel (see the Fig. 2). In additions, we will discuss the concentration distributions of the dissolved substances in the working fluid and three dimensional flow fields, and compare the mixing performance in the modeled micromixer with various operating conditions.

[1] G. Karniadakis, A. Beskok, N. Aluru, Microflows and Nanoflows, Fundamentals and Simulation (Springer, New York, 2004)

[2] S. Huang, S. Wang, H. Khoo, F. Tseng, Sensors and Actuators B. 125, 326 (2007)

Fig. 1 Schematic of the ring-type micromixer applied to this study

Fig. 2 Stretching and folding behaviors in the modeled mixing chamber

VST-7-Or-8
Time dependent gas mixture flow through a short tube in a wide range of the Knudsen number

T15 Vacuum Science and Technology

#VST-7-Or-8

M. Vargas [1], S. Naris [1], D. Valougeorgis [1], S. Pantazis [2], K. Jousten [2].

[1]University of Thessaly - Volos (Greece), [2]Physikalisch-Technische Bundesanstalt - Berlin (Germany).

Steady-state gas flows through channels of various lengths and cross sections under low, medium and high vacuum conditions have been successfully modeled based on kinetic theory. Reliable results for the conductance, as well as for the flow field have been obtained with moderate computational effort in the whole range of the Knudsen number [1].

In important industrial applications like coating processes, however, fast pressure changes are required and the time response of the vacuum gauge and the vacuum system becomes important. In many of these applications, gas mixtures are involved. In spite of their high practical interest, time dependent flows of gas mixtures have attracted little attention, which is limited so far to unsteady single gas flows [2,3], while the corresponding problems for gas mixtures have not been investigated yet. It is noted that compared to single gases the computational effort for solving gas mixture flows is significantly increased due to the large number of parameters involved in the simulations.

Recently, in order to examine the time response characteristics of gas mixtures compared to single gases, an investigation of rarefied time-dependent binary gas mixture flows through short tubes has been initiated. Within this framework, in the present work the unsteady flow of a gas mixture, namely He-Xe, through a short tube is investigated based on the DSMC method. Preliminary results are provided for one molar fraction of the mixture at typical values of the downstream over the upstream pressure ratio and for some values of the reference Knudsen number covering the free molecular and transition regimes. The critical time needed to reach the steady-state flow conditions is computed and its dependency on the flow parameters

(pressure ratio and Knudsen number) is examined. A detailed view of the flow field is also presented by plotting the transient velocity and density distributions of each species of the mixture. Furthermore, the time dependency of the separation effect, which is always present in gas mixture flows due to the different molecular velocities of the species is considered. A comparison with the corresponding single gas time dependent flow is provided to point out the main differences between the flow conditions in unsteady single and gas mixture flows.

ACKNOWLEDGEMENTS: Support through the EMRP IND12 project is gratefully acknowledged. The EMRP is jointly funded by the EMRP participating countries within EURAMET and the European Union.

1. S. Varoutis, S. Naris, V. Hauer, C. Day, D. Valougeorgis, Experimental and computational investigation of gas flows through long channels of various cross sections in the whole range of the Knudsen number, Journal of Vacuum Science and Technology – A, 27 (1), 89-100, 2009.

2. J. Lihnaropoulos, D. Valougeorgis, Unsteady vacuum gas flow in cylindrical tubes, Fusion Engineering and Design, 86, 2139–2142, 2011.

3. F. Sharipov, Transient flow of rarefied gas through a short tube, Vacuum, 90, 25-30, 2013.

VST-P2-08
Protection of the HIE-Isolde superconducting linac against air inrush

T15 Vacuum Science and Technology

#VST-P2-08

G. Vandoni, M. Hermann.

CERN - Geneva (Switzerland).

The High Intensity and Energy ISOLDE (HIE-ISOLDE) project aims at upgrading CERN present ISOLDE and REX-ISOLDE facilities to increase the energy and intensity of the delivered radioactive ion beams [1]. Energy up to 10 MeV/amu is reached by means of a new post-accelerating, superconducting linac, consisting of quarter wave resonators housed in 6 cryomodules. Three beam drift lines transport the accelerated beam to the three experimental stations. In order to avoid cold-warm vacuum transitions and thus better cope with effective space limitations, the cryomodules feature a common beam and insulation vacuum, imposing the high standards of cavity beam vacuum to the ensemble of the cryostat [2]. Protection against sudden air inrush from the experimental stations is achieved by a fast closing valve, built in the line close to the last cryomodule of the linac, following a scheme generally applied to beam lines in synchrotron light sources [3]. With a short distance between the potential leak source – the experimental station – and the valve, and with particulates swept along the transfer lines at the same speed as the pressure front, even the reported very short reaction time of the valve may not be sufficient to prevent particulate contamination of the cryomodule volume. Delay of the pressure front progression may be achieved naturally by the series of expansion volumes and restrictions naturally embedded in the transfer lines layout in the form of beam transport and diagnostics elements. To evaluate the propagation speed in the real lines, as well as to assess the efficiency of short acoustic delay devices, a Finite-Element simulation of the air inrush dynamics has been performed. A test stand has been set up, with the scope of measuring the valve's reaction time and to experimentally validate the delay effect of a small expansion volume, a stack of diaphragms, a cold section, a deflector.

[1] Status and Future Perspectives of the HIE-Isolde Project at CERN, Y.Kadi et al., 3rd International Particle Accelerator Conference 2012, New Orleans, LA, USA, 20 - 25 May 2012
[2] The high beta cryo-modules and the associated cryogenic system for the HIE-ISOLDE upgrade at CERN, Y.Leclercq et al., CEC-ICMC, June 2013, Anchorage
[3] Measurements on the efficiency of acoustic delay lines in view of beam lines for synchrotron radiation, H.Betz, P.Hofbauer, A.Heuberger, J.Vac.Sci.Technol., 16(3) 1979, 924

VST-P2-25
Numerical analysis of the non-isothermal gas flow through a packed bed of spheres

T15 Vacuum Science and Technology

#VST-P2-25

E. Afrasiabian, L. Marino, C.M. Casciola.

Department of Mechanical and Aerospace Engineering, University "La Sapienza" - Rome (Italy).

The advent of micro-devices with high specific power raises the important challenge of how to dissipate the heat fluxes produced by the active components inside the micro-systems. In this frame, gas flows through porous and/or fibrous media is particular appealing due to their potentially high capability to transfer the heat. While the gas flow through simple micro-devices, like micro channels and micro tubes, has been widely investigated and quite well understood, the physics of rarefied gases through porous matrices is still matter of discussion. Though the literature on transport phenomena through porous media is very large, most of the published papers deal with the flow of an incompressible fluid. Concerning the analysis of the temperature effects in porous media, a great attention has been devoted to convection but, again, in the continuum regime. The influence of the compressibility of a gas flow through a porous matrix can be re-conducted to the prediction of the Klinkeberg law, which actually applies to isothermal flow.
To take into account the effects of a possible rarefaction of a gas flow some investigations have been done. Some efforts have been carried out to establish simple numerical models based on DSMC (Direct Simulation Monte Carlo) simulations, as in Ref. [1]. DSMC shown to be a very efficient method to simulate rarefied gas flows, in particular at high speeds (more generally, at high values of the signal to noise ratio). On the other side its computational cost increases dramatically when the typical values of the molecular velocities are comparable with the thermal speed. As a consequence, simulations of low speed flows, like those at micro and nano scales, can be really expensive from the computational point of view. Although some efforts have been done to reduce the statistical errors for the molecular simulation methods and low-noise Monte Carlo simulations have been presented. Alternative approaches to simulate the gas dynamics near the equilibrium state are based on the solution of the kinetic equations, in particular by means of BGK or S

models, and some results have been preliminary carried out for the analysis of flow through porous medium.
In this paper we present numerical results concerning the gas flow through a porous medium made of a packet bed of spheres. Our approach is based on the Boltzmann equation considering the effect of porous matrix as an additional parameter inside the collisional term proposed by Pavan et al. [2]. This problem, already studied in the isothermal case in [1] by means of DSMC, is here extended to a physical situation where the heat transfer plays an important role, by solving the above mentioned homogenous kinetic equation. We analyzed the case of the gas flow through an annulus between two concentric cylinders filled of porous medium and constant surface temperature or a known heat flux as boundary conditions on the internal cylinder. The corresponding flow is characterized by a Knudsen number (Kn) that spans from the almost continuum flow to nearly free molecular regime.

[1] L.M. De Socio, L. Marino Gas Flow in a Permeable Medium, J. Fluid Mech., Vol. 557, 119-133, 2006.
[2] V. Pavan, L. Oxarango A New Momentum Equation for Gas Flow in Porous Media: The Klinkenberg Effect Seen Through the Kinetic Theory, J. Stat. Phys., Vol. 126, 355-389, 2007.

VST-5-Or-4
Electron Stimulated Desorption from Stainless Steel

T15 Vacuum Science and Technology

#VST-5-Or-4

O. Malyshev [1], B. Hogan [1], R. Jones [2], M. Pendleton [1].

[1]STFC Daresbury Lab - Warrington (United kingdom), [2]University of Bath - Bath (United kingdom).

Stainless steel is one of the main materials used for particle accelerator vacuum chambers and components. The surface preparation, history and condition of use strongly affect the outgassing rate and particle-induced gas desorption. The electron stimulated desorption (ESD) was studied for 316L stainless steel as a function of electron dose, electron energy, and wall temperature. The effect of duration of pumping before the bombardment was also studied. The surface preparation can also affect the results. The ESD yields were compared for polished and TiN coated surfaces. The experimental details and results will be reported.

VST-5-Or-5
Optimisation of Non-Evaporable Getter Coatings for Particle Accelerator Vacuum Chambers

T15 Vacuum Science and Technology

#VST-5-Or-5

R. Valizadeh [1], O. Malyshev [1], B. Hogen [1], A. Hannah [1], R. Jones [2].

[1]STFC Daresbury lab - Warrington (United kingdom), [2]university of Bath - Bath (United kingdom).

The pressure in particle accelerator vacuum chamber bombarded with energetic particles (photons, electrons, ions, etc.) is defined by the desorption induced by these particles and the available pumping speed. When the non-evaporable getter (NEG) coating is applied, the pumping speed is close to ideal for CO and CO2. To reduce the pressure further the main attention was devoted to reducing the particle induces desorption from the NEG coated walls. The dense coating provides lower pumping speed compared to the columnar one but reduction in desorption yields is much more significant, therefore the net effect is a lower pressure in a vacuum chamber. Use of dual layer coating NEG coating allows desorption yields to be reduced with a dense NEG base layer and have increased pumping speed with a columnar NEG as a second layer applied over the base. These results allows reaching the required UHV/XHV conditions at lower cost and, in some cases, is the only solution. In the reported experiments, the samples were 38-mm diameter and 0.5-m long stainless steel tube with the entire internal surface coated. The pumping speed of the sample was measured by H2, CO and CO2 injection. The desorption properties were evaluated by measuring the electron stimulated desorption yield with 500-eV electrons emitted from a filament placed along the tube axis bombarding the tube walls. The experimental details and results will be reported.

VST-2-Or-3
Evaluation of efficient use of molecular drag pumps in vacuum coating systems

T15 Vacuum Science and Technology

#VST-2-Or-3

J. Bhatti, S. Qaiser, K. Chaudhary.

The Islamia University of Bahawalpur - Bahawarlpu (Pakistan).

The beginning of the twentieth century has seen an increasing use of high vacuum in the industrial processes such as thin films, plasma displays, PVD, sputtering, ion etching, simulators and fusion research. These applications greatly depend on the clean environment that requires oil-free pumping. Molecular drag pumping is a rather new and quite good technique for the creating of high vacuum. The present studies represent a real model of a molecular drag pump with an emphasis on its design, theoretical development and vacuum characteristics. Although a complete theory of molecular drag pumps has never been published and theoretical studies are also a few in numbers, yet effort has been made to evaluate a complete theoretical and practical picture of a molecular drag pump. Using a prototype, potential capabilities of a molecular drag pump in vacuum coating processes have been experimentally explored. The results are in quite good conformity to the theoretically computed values.
At the end some applications and use of these pumps in various industrial and technological areas have been high lighted

VST-5-Or-12
Vacuum Lifetime Studies of GaAs Photocathodes

T15 Vacuum Science and Technology

#VST-5-Or-12

K. Middleman [1], N. Chanlek [2], L. Jones [1], B. Militsyn [1].

[1]STFC Daresbury Lab - Warrington (United kingdom), [2]Synchrotron Light Research Institute - Nakhon Ratchasima (Thailand).

Gallium Arsenide (GaAs) photocathodes have in recent years been widely used and have become the focus for use in modern accelerators and light sources such as the Accelerators and Lasers in Combined Experiments (ALICE). Once activated to a Negative Electron Affinity (NEA) state and illuminated by a laser, these materials can be used as a high-brightness source of both polarised and un-polarised electrons. Activated GaAs is extremely sensitive to the vacuum environment and its performance can be compromised if the presence of particular gas species are not minimised. This paper will present the influence of O2, CO2, CO, N2, H2 and CH4 gas injections on the stability of the quantum efficiency (QE) of a negative electron affinity (NEA) gallium arsenide (GaAs) photocathode activated with caesium (Cs) and oxygen (O). This is the first time this has been demonstrated under an extreme high vacuum (XHV) condition, with a base pressure of 6.0 E-12 mbar, where the influence of the background gas is minimised. It was found that exposure of a GaAs photocathode to N2, H2 and CH4 does not affect the QE, whereas exposure to O2, CO2 and CO leads to a substantial reduction in photocathode QE. It was also found that the QE of photocathodes which have been degraded under O2 exposure can be recovered to 95% of their initial QE level by the re-caesiation process, while those which have been degraded under exposure to CO and CO2 can only be partly restored to 60 - 70% of their initial QE levels.

VST-7-Or-9
RAREFIED HELIUM DYNAMICS SIMULATION IN THE “ITER” CRYOSTAT FOR LEAK MAPPING AND DETECTION

T15 Vacuum Science and Technology

#VST-7-Or-9

D. Gordillo [1], A. Kumar [2], A. Kumar [2], S. Claude [1], T. Amita [1], W. Liam [3], P. Robert [3], A. Alexander [3].

[1]FLUIDYN France - Saint-Denis (France), [2]FLUIDYN India - Bangalore (India), [3]ITER Organization - St Paul Lez Durance (France).

Currently under construction in the South of France the ITER project will be, on completion, the largest superconducting fusion device in the world capable of operating with tritium. Key to the success of ITER is the reliable operation of its vacuum systems and it is expected that
Helium leaking from cryogenic components installed in the ITER cryostat will be a cause of significant delays to the ITER program unless the leaks can be localized and repaired in a timely fashion.
It has been proposed that by the use of multiple sensors permanently installed in the cryostat the location of a leaking component can be identified by the creation of a concentration map derived from the sensor signals. In order to the feasibility of this concentration map technique, simulations of gas expanding into cryostat geometries have been performed details of which are described in this paper.
At pressures inside the domain (~10-4 Pa), the mean free path of molecules is larger than the characteristic dimensions of the Cryostat. The equations for continuous media are no longer applicable, and the system behavior is in the molecular regime. Therefore simulations are performed by tracking the molecules inside the domain by Direct Simulation Monte Carlo (DSMC), using the PI-DSMC numerical software.
The Maxwell speed distribution is used for each speed component in the space. The mean thermal velocity is found to be 650 m/s. The global flow is directed outwards from the injection point, the mean flow velocity calculated and added to the thermal speed, in the direction in which the leak is pointing.
It is shown that for leaks with small magnitude (0.01 Pa.m3/s), the steady state distribution in the cryostat is reached in approximately 3 s. The oval shaped gas plume bounded in space by a steep concentration gradient beyond which the

background concentration is continuous reducing the possibility of detecting the leak beyond this space.
The results of simulating small leaks expanding into a “large” open free volume of the cryostat vacuum show that the cryostat vacuum scarcely affected as there are a low number of molecules leaking to occupy the space and therefore, change the background pressure.
For the cases in which the leak expands into a smaller, packed, free volume (full geometry), the number density increases quickly and vacuum is may be perturbed. In this case, the plume may be better detected on surfaces opposite to the leak location, as the molecules near the opposite surface can accumulate over it or may be reflected back towards the leak location. Additionally the plume size will be affected by the surface temperatures surrounding the leak and detection may be further enhanced.
Simulations performed using a cryostat geometry which includes all geometric characteristics at representative temperatures are presented an, based on these results, preliminary design requirements will be drawn for gas detection systems which may be installed in the cryostat.

VST-P2-09
Pumping system of neutral beam injectors.

T15 Vacuum Science and Technology

#VST-P2-09

A. Dranichnikov, V.V. Anashin, A.A. Ivanov, V.S. Khrestolyubov, V.V. Kobets, V.A. Polukhin, D.K. Toporkov.

BINP - Novosibirsk (Russian federation).

A review of different types of vacuum pumping systems for injectors of neutral hydrogen beams is given. The pumping systems based on a cryo condensation allow to obtain the final pressure between the injection better then 10-6 Pa and may to operate under the typical flow rate more then 10 Torr*l/sec with a pumping speed up to 100 m3/sec for hydrogen. Such kind of pumping system is operated in injectors of many plasma systems e.g. in Louzanne (TCV), Boston (ALCATOR), Padova (RFX), Irvain (TAE), Prague (CAMPAS). Another one of injector for tokamak (W-7) for Germany is ready now and will be delivered on site in February this year.

VST-1-Or-9
Calibration of leak artefact for sniffer test by constant volume type flow meter

T15 Vacuum Science and Technology

#VST-1-Or-9

K. Arai, H. Yoshida, T. Kobata.

NMIJ/AIST - Tsukuba (Japan).

A sniffer test, where a leak measurement is performed under atmospheric pressure conditions, is often used for a tightness inspection of objects, for example, air-conditioners. The response of a leak detector against a magnitude of leaks is calibrated by a known-gas flow, which is generated by a leak artefact. To trace the indication of the leak detector to SI-unit, the flow should be calibrated against SI-unit. In this study, a constant volume type flow meter for the measurement of flows into the atmospheric pressure has been designed and fabricated. The calibration system of a leak artefact for a sniffer test was established by using the flow meter.

A measurement principle is based on the pressure rise method. A gas flow rate Q is given by

$$Q = V\frac{\Delta P}{\Delta t}, \quad (1)$$

where ΔP and V are an amount of the pressure change during the time duration of Δt and a volume of a chamber, respectively. A key point of the measurement is the detection of a small pressure increase (about 100 Pa) at the atmospheric pressure (100 kPa). In this flow meter, a pressure change is measured as a differential pressure between two chambers, which are connected by a valve and a differential type diaphragm gauge (FS: 133 Pa) (inset of figure 1).

A change of a differential pressure during a measurement is plotted in figure 1. A leak artefact to be calibrated was a cramped type metal capillary and the test gas is nitrogen. Prior to the measurement, the pressure inside the flow meter was set at 100 kPa and the pressure at the upstream side of the artefact 200 kPa. After the valve was closed at the elapsed time of 0 s, the differential pressure increased with a rate

of 0.22 Pa/s. The volume of the main chamber was 32.33 ml [1]. In case of figure 1, the gas flow from the artefact was calibrated to be 7.1×10^{-6} Pa m^3/s with an uncertainty of 2.0 % (k=2). By changing the pressure in the upstream of the artefact from 110 kPa to 250 kPa, flows into the atmospheric pressure was calibrated ranging from 1×10^{-6} Pa m^3/s to 3×10^{-5} Pa m^3/s.

[1] Kenta ARAI et al., *Proceeding of XX IMEKO world congress,* TC16-O-11, 2012.

Figure 1: Differential pressure profile during the calibration of a leak artefact. Inset of the figure illustrates the flow meter.

VST-3-Or-12
The Vacuum System Design Of A New Electron Beam Test Facility (EBTF) at Daresbury Laboratory

T15 Vacuum Science and Technology

#VST-3-Or-12

J. Herbert, K. Middleman, A. Hannah, O. Malyshev, M. Pendleton, R. Valizadeh.

STFC Daresbury Lab - Warrington (United kingdom).

Recent UK government funding has facilitated the construction of a unique accelerator test facility which can provide enabling infrastructures targeted at the development and testing of novel and compact accelerator technologies, specifically through partnership with industry and aimed at addressing applications in medicine, health, security, energy and industrial processing. The infrastructure provision on the Sci-Tech Daresbury Campus will permit research into areas of accelerator technologies which have the potential to revolutionise the cost, compactness and efficiency of such systems. The main element of the infrastructure will be a high performance and flexible electron beam injector facility using a metal photocathode, feeding customised state-of-the-art testing enclosures, and associated support infrastructure.
This paper will look specifically at the vacuum system design of this unique accelerator detailing the challenging design of the photoinjector, the requirement for shielding of all total pressure gauges and how a differential pumping scheme has been implemented to separate two vacuum systems with 3 orders of magnitude pressure difference over 50 cm. Many other aspects of the accelerator design will be described and data showing the 'real' perfromance of the accelerator presented.

VST-P2-18
MEMS Pirani sensor with increased sensitivity for pressure measurements in the fine and high vacuum

T15 Vacuum Science and Technology

#VST-P2-18

F. Voelklein, M. Grau, A. Meier, G. Hemer, L. Breuer.

University of Applied Sciences Wiesbaden, Institute for Microtechnologies - Rüsselsheim (Germany).

Users require inexpensive, reliable sensors compatible with modern signal processing. One answer to this demand may be provided by microsensors, notably based on silicon by using the integrated circuit (IC) technology. On-chip circuitry, high reliability and low cost batch-process fabrication are the advantages offered by IC technology for the realization of MEMS. This approach has been demonstrated also for MEMS Pirani sensors with resistive or thermoelectric detection principle[1-4]. However, up to now, these sensor chips have not demonstrated an increased sensitivity in comparison to conventional hot wire pirani gauges. We analyse the crucial design parameters which determine the pressure response of MEMS Pirani sensors. Based on this analytical thermal model we have optimized the chip dsign in order to increase the sensor sensitivity, especially in the pressure range between 10-3 to 10-5 mbar. Furthermore, the analytical calculations are compared with Finite Element Methods (FEM) simulations, which support and confirm the analytical results. The calculated thermal conductances of the optimized microchip are in good agreement with the measured parameters. The signal Voltage U(p) as function of pressure p has been calculated for applying the sensor in a Wheastone bridge circuit with constant voltage supply. The theoretical voltage-pressure response is in very good agreement with the measured curves. This response shows a significantly increased pressure sensitivity in the high vacuum range (from 10-3 to 10-5 mbar) compared to conventional Pirani vacuum gauges. Finally, the fabrication steps of the sensors based on batch-process technologies are presented.

1 F. Völklein, W. Schnelle, Sensors and Materials, 3 (1991) 41

2 A.W. van Herwaarden, D.C. van Duyn, J. Groeneweg, Sensors and Actuators A, 25-27 (1991) 565

3 P.K. Weng, J.-S. Shie, Rev. Sci. Instr. 65 (1994) 492

4 Patent CN101256105 (2008)

VST-7-Or-6
MODELLING OF THE RESIDUAL GAS IONIZATION LEADING TO DARK CURRENT CREATION

T15 Vacuum Science and Technology

#VST-7-Or-6

L. Caillault, B. Seznec, T. Minea.

LPGP UMR 8578 CNRS-Université Paris Sud XI, bât. 210, rue Becquerel, 91405 Orsay Cedex - Orsay (France).

In the field of controlled fusion, the high-energy neutral beam injector device which is used as additional heating source to sustain fusion reactions in the tokamak plasma bulk, consists in the acceleration by several electrostatic grids under vacuum of negative ions before their neutralization on a gas target.
The set of grids are connected to high voltage power supplies through an insulating feedthrough - called bushing. Unfortunately, experimental campaigns carried out at IRFM, Cadarache, France have shown that the grid voltage holding was limited by breakdown occurrences (depending on the grid separating distance) and by the creation of an unwanted non negligible electron current (100 mA at 400 kV), usually called dark current. The dark current is the result of electric field emission appearing at the micro-tips at the high voltage electrode surface due to the roughness of the metal (micro-protrusions).
In order to improve the grid voltage holding, a self-consistent modelling of the physical processes occurring in front of micro-protrusions has been developed. This modelling accounts for electron emission as well as heat transfers within micro-protrusions, Joule and Nottingham heating effects and the emitted electron multiplication through ionization collisions with the residual gas, in real three dimension space. Numerical results are presented and discussed.
The present achievement should help designing a new concept for the busing system of the future Neutral injector device useful for the next generation of fusion reactors, like DEMO.

VST-7-Or-11
Experimental and computational investigation of rarefied gas flows through bellows and very short tubes

T15 Vacuum Science and Technology

#VST-7-Or-11

C. Day [1], C. Saglietti [2], S. Varoutis [1], R. Zanino [3].

[1]Karlsruhe Institute of Technology (KIT) - Karlsruhe (Germany), [2]Karlsruhe Institute of Technology / Politecnico di Torino - Karlsruhe (Germany), [3]Politecnico di Torino - Torino (Italy).

Gas flows under vacuum conditions represent one of the main scientific fields in rarefied gas dynamics with many engineering applications, e.g., nuclear fusion. The main characteristic of such flows is that in rough, medium, and high vacuum conditions, the whole range of the Knudsen number (Kn) from the free molecular through the transition and slip regimes up to the hydrodynamic limit may be covered. Typical components of vacuum systems are ducts with various lengths and cross sections, where the estimation of overall macroscopic quantities as mass flow rate, conductance and pressure is of vital importance.

In this context, an experimental investigation of flows through bellows and several very short tubes (with length/diameter ratios in the range from 0.01 to 0.1) in the whole relevant range of Kn (from 0.01 to 50) was performed. The flow is due to a pressure gradient imposed in the longitudinal direction. The experimental work has been performed at the TRANSFLOW experimental facility at KIT [1]. The TRANSFLOW facility represents a reliable tool for measuring the conductance of various geometrical configurations over the whole range of Kn. The main principle of this facility is the dynamic measurement of the pressure difference across the duct by setting a constant mass flow rate through the test channel.

The measured conductance in the aforementioned geometries is compared with available analytical solutions in the free molecular and viscous regimes as boundary cases for validation. Moreover, for the whole range of the Knudsen number, a computational study was conducted based on an open DSMC (Direct Simulation Monte Carlo) code, the results of which are used for additional comparison.

[1] St. Varoutis, Th. Giegerich, V. Hauer, Chr. Day, J. Phys. Conf. Ser. 362 (2012) 012027

VST-P1-15
Detailed investigation of a CNT emitter-based extractor gauge for pressure reading in the cryogenic beam vacuum system of SIS100

T15 Vacuum Science and Technology

#VST-P1-15

M. Lotz, S. Wilfert, A. Krämer, O. Kester.

GSI - Darmstadt (Germany).

The new main accelerator system of the FAIR project, which is built at GSI in Darmstadt (Germany), will be the SIS100 with a circumferential length of about 1.1 km. This heavy ion synchrotron machine uses superconducting magnets to bend and focus the beam. Consequently, about 80% of its beam line vacuum will be operated at cryogenic temperatures between 5 and 15 K. In order to generate sufficiently low UHV conditions in these sections, cryopumping will be used. To guarantee a long beam lifetime, the vacuum pressure during beam operation may not exceed 5×10^{-12} mbar (H2). For this reason the assembly of pressure measuring devices in the cryogenic sections have to be taken into account. However, in consequence of the extreme low-temperature conditions the pressure measurement in cryogenic vacuum systems is not a simple undertaking. With the exception of some very special measuring methods, such as particle life time-based measurements, pressures down to ~10^{-12} mbar can only be measured by ion gauges of extractor type. Commercially available extractor gauges, however, are equipped with a hot-filament cathode whose operation would introduce an immense heat load to the cryogenic system. Although it is known that these gauges can be operated at LHe temperatures [1,2], nevertheless, their use is commonly avoided. To overcome this problem we developed and investigated an extractor gauge whose hot filament was substituted by a CNT field emitter. Compared to a thermionic cathode, this cathode type does not cause a noticeable heat load.
We will present some emission characteristics of the CNT cathode used and results on its long-term emission stability. Further, we investigated theoretically the operating performance of the CNT emitter-based extractor using AMaze simulation calculations. Finally, results on experimental investigations of the measured behavior and characteristics of the modified gauge in both room temperature and cryogenic

vacuum environments are shown. The low emission current yield of the cathode (~150 µAmp) appears to be disadvantageously, since it causes a significant increase of the lower measure limit. Nevertheless, the results clearly imply that CNT emitter-based ion gauges seem to be generally suitable for local pressure measurements in cryogenic vacuum systems.

[1] M. G. Rao and P. Kneisel: The use of extractor gauge at LHe temperatures
CEBAF, Technical Note 93-057 (1993)
[2] V. Baglin, A. Grillot, A. G. Mathewson: Fonctionnement d'une jauge a ionisation a la temperature de l'helium liquide
CERN, Vacuum Technical Note 95-01 (1995)

VST-P2-10
Vacuum Calculations of the FAIR Collector Ring

T15 Vacuum Science and Technology

#VST-P2-10

J. Kurdal.

GSI Helmholtzzentrum für Schwerionenforschung - Darmstadt (Germany).

The Collector Ring (CR) of FAIR (Facility for Ion and Antiproton Research in Europe) is characterised by a circumference of 225m and due to the beam life times a required vacuum pressure in the range of 10-9 mbar. The CR is a dedicated storage ring; its architecture is governed by the stochastic precooling of secondary particles, rare isotopes or antiprotons.
To reach the required beam life times an in-situ bake-out of the ring is not required. Due to space constrains there is no space for large pumping stations, therefore new pumping solutions were studied
The pumping concept is now based on NEG cartridge/ion getter combination pumps. To define the required pumping speed and positions of the pumps vacuum calculations of the CR were carried out by means of three different programs. The analysis of pressure profile of the whole ring was performed with VAKTRAK (a transfer matrices program), which allowed us to optimise the pumps positions. The conductance of every chamber was simulated with Molflow+, a Monte Carlo Simulation program. Additionally, using VAKDYN, which calculates the dynamic pressure, the dynamic pressure profile in the ring was determined.
The results obtained in these calculations will be presented and discussed.

VST-P1-08
A R&D program on Leak localization concepts for actively cooled fusion machines

T15 Vacuum Science and Technology

#VST-P1-08

A. Durocher [1], D. Anthoine [2], V. Bruno [1], M. Chantant [1], L. Gargiulo [1], J.C. Hatchressian [1], M. Houry [1], D. Mouyon [1].

[1]CEA - St Paul Lez Durance (France), [2]Bertin Technologies - Aix-En-Pce (France).

High vacuum conditions are required for the fusion machines operation. Any leak in the vessel, even micrometric (down to 10-6 Pa.m3/s) doesn't allow their operation. The conditions for the leak localization in the next step actively cooled machines like ITER will be more severe and human intervention will no longer be possible. Thus the techniques used in the current actively cooled tokamak like Tore Supra will not be relevant. These techniques consist mainly in pressurization/depressurization cycles of the sub circuits feeding the Plasma Facing Components (PFC). From the Tore Supra experience, some statements can be made. The localization process must be considered in early stage of the cooling circuit design in order to be able to mitigate the leaky PFC. Leak Localization diagnostics which could be quickly deployed as soon as a leak appears are needed.

A R&D program on this last topic has been launched at CEA/IRFM since 2009. Its objective is to define the best experimental conditions and to select the most efficient concepts or diagnostics to localize helium or water leaks quickly maybe by remote operation. Their performances should allow detecting in a few seconds traces of helium or water close to the first wall, corresponding to a micro-leak. Leak sensors would have to be light weight devices in order to be integrated on a carrier or as small as possible to be integrated into the first wall, both of these options should be taken in consideration. The specifications for the Leak Localization concept will depend on the constraints of each machine.

The concepts must be selected among the available technologies and the specific conditions for their implementation. In this framework, a compliance matrix concept

was used. Two test-beds have been erected to validate the concepts in relevant conditions.

The paper will describe some of the most promising concepts and the selection methodology.

VST-P1-09
Development of a low cost, rugged, precision Capacitive Low Pressure Gauge for Cryogenic use.

T15 Vacuum Science and Technology

#VST-P1-09

L. Manceron [1], L. Lago [2], C. Herbeaux [2], P. Roy [2], M. Bol [2].

[1]CNRS - Paris (France), [2]Synchrotron SOLEIL - Saint Aubin (France).

The precise measurement of Infrared absorption cross sections and line profiles of molecules and organic volatile compounds of relevance for atmospheric chemistry in planetary and upper earth atmospheric layers imposes precise pressure measurements between 10^{-3} and a few mbars in the 80 to 300K temperature range. Measurements using room temperature thermostated capacitive gauges outside the cryostatic cell are possible only when thermomolecular effects (which can offset the pressure reading by as much as 90%) have been empirically modeled, which is only the case for a few rare or inert gases [1]. Thus, measurements on various compounds with unknown thermomolecular correction factors have to be made in situ in the operating conditions of temperature. If various prototypes of precision capacitive cryogenic gauges have been built in different laboratories around the world [2, 3], they all rely on high cost, precision capacitive bridges for the read out electronics. A prototype, rugged, precision capacitive pressure gauge for cryogenic use has been designed and built at SOLEIL, and finally tested down to 77K. The design includes corrosion-resistant materials and has been tailored to operate on a differential measurement scheme based on the low cost, high precision AD7747 Σ-Δ capacitance-to-digital converter [4]. The design, realization and performances are presented here, illustrated by a precision better than 1% in the 0.2-40 mbar range with a resolution of 2 10^{-3} mbar. The gauge can be, however, tuned for a higher precision and resolution, at the expense of the maximum high pressure range.

[1] T. Takaishi, Y. Sensui, Farad.Trans. Royal Soc. 2503, 1963.
[2] E.Dwight Adams, Rev. Sci. Inst. 64(3),601, 1993.
[3] P.Thibault, P. Diribarne, T. Fournier, S. Perraud, L. Puech, P.E. Wolf, Rev. Sci.

Inst. 78 (4), 043903, 2007.
[4] Analog Device Inc. (http://www.analog.com/en/analog-to-digital-converters/capacitance-to-digital-converters/ad7747/products/product.html)

VST-2-Or-1
Reinventing Pressure and Vacuum Metrology: Development of an Optical Vacuum Standard

T15 Vacuum Science and Technology

#VST-2-Or-1

J. Hendricks, J. Stone, G. Strouse, D. Olson, P. Egan, J. Ricker, G. Scace.

NIST - Gaithersburg (United states).

We propose to fundamentally change the method for realizing and disseminating the SI unit of pressure. The underlying metrology behind this advance is the ultra-accurate determination of the refractive index of gases by picometer optical interferometry. An optical-based primary pressure standard will improve accuracy and allow the complete replacement of all mercury-based pressure standards which are expensive to operate and have environmental and health hazards. Mercury manometers currently serve as primary standards at 11 National Metrology Institutes (including NIST and PTB). Developing an optical-based pressure and temperature standard is central to the NIST measurement science mission, as it will improve NIST realization and dissemination of important SI units. For pressure and vacuum, the technique will provide a needed improvement in accuracy (3X to 10X) across many industrial sectors in aerospace, energy, advanced manufacturing and government agencies. The primary goal of the ongoing research is to develop a laser-based, SI-traceable pressure standard (1.5 ppm, k=1) along with a transportable version that can be deployed to industry covering a range of 1 Pa (vacuum) to 360 kPa (~4 atmospheres pressure). The two instruments under development are the variable-length optical cavity (VLOC) and a fixed-length optical cavity (FLOC). The primary technical challenge involves building an apparatus to generate and precisely measure equal displacements of Fabry-Perot interferometer mirrors in vacuum and in a helium environment to picometer accuracy, thus determining refractive index in a manner that allows absolute measurement of pressure or temperature if one of these two quantities is known. More specifically, the refractive index, n, is intrinsically related to density such that n-1 depends on P/T, where P is the pressure and T is the temperature. The current state of primary mercury manometers in use at NIST will be

discussed along with technical challenges and recent developments in designing an optical based primary standard.

VST-P2-11
Analysis of a CF500 flange for the Collector Ring of FAIR

T15 Vacuum Science and Technology

#VST-P2-11

L. Urban, A. Krämer, C. Will, I. Schurig.

GSI - Darmstadt (Germany).

The Collector Ring (CR) is a storage ring of the accelerator complex of the Facility for Antiproton and Ion research (FAIR). Its purpose is the stochastic precooling of rare isotope and antiproton beams and the measure of the nuclear masses in an isochronous mode. Following the results of some vacuum simulations the use of DN500CF Flanges are foreseen in some parts of the CR.
In the technical specification ISO/TS 3669-2 are no flanges with a larger dimension then DN400CF.
In order to ensure the tightness of the flange, the idea was to design and construct a CF flange which can be baked or cooled and has a lower leak rate compared to rubber-sealed flanges. Furthermore the dimensions of the CF flange are smaller compared to COF flanges.
To perform leak tests of a DN500CF flange a setup was designed and commissioned at GSI, and it consists of an extractor gauge, a residual mass spectrometer and a pumping station. The flange was mounted in vertical position and screwed with different torques. The final pressure and the leak rate were determined and the corresponding mass spectrum was recorded. Through further measurements, the behavior and the tightness of the flange was detected also during the bakeout.
The results obtained in these measurements will be presented and discussed.

Reference number ISO/TS 3669-2:2007(E)

VST-5-Or-8
Surface and material treatments for XHV vacuum components - An industrial approach for achieving low hydrogen-outgassing rates

T15 Vacuum Science and Technology

#VST-5-Or-8

A. Müller, O. Posth, H. Wunderlich, M. Flämmich, U. Bergner.

VACOM Vakuum Komponenten & Messtechnik GmbH - 07749 Jena (Germany).

Stainless steel has been and still is the most commonly used raw material for ultra-high vacuum (UHV) components. However, the requirement of going beyond the critical total pressure of 10^{-11} mbar has become stronger over the last years, especially driven by research institutions and accelerator facilities. The challenge of suppressing hydrogen outgassing from the bulk material has extensively been discussed in literature resulting in some well-established methods and few new approaches to achieve extremely low hydrogen outgassing rates needed for extremely high vacuum (XHV) applications. Some approaches seem to be promising, but simultaneously they are quite expensive and economically not viable. Industry is always faced with the challenge of producing high quality products for appropriate and affordable costs, often resulting in compromises regarding the applicable processes.

This talk will present an industrial approach to reliably and cost-efficiently manufacture XHV components with hydrogen outgassing rates below 10^{-14} mbar·l/s·cm^2 . An appropriate sequence of cleaning and surface treatment methods is introduced and its correlated effects on surface structure and outgassing behaviour are analysed.

VST-5-Or-10
Improved cold cathode gauge for UHV / XHV

T15 Vacuum Science and Technology

#VST-5-Or-10

J. Iwicki, I. Pongrac, P. Gottschalk, R. Bauer, M. Flämmich, U. Bergner.

VACOM Vakuum Komponenten & Messtechnik GmbH - Jena (Germany).

Ionization vacuum gauges are currently the preferred sensors for total pressure measurements in high-, and ultra-high vacuum (UHV). The two most widely-used types of ionization gauges are hot cathode and cold cathode gauges. While in the first case ionization occurs due to thermionic electrons, in the latter case crossed electromagnetic fields are responsible for the ionization. Such a gauge is mechanically robust, insensitive to accidental venting as well as to vibrations. Mostly cited disadvantages of this sensor type are residual stray magnetic fields and increasing contamination of electrodes after long term operation. Moreover, the plasma discharge is difficult to initiate and maintain at low pressures.
In order to optimize the properties of this gauge type we investigated different penning cell elements, geometries and materials experimentally and by means of theoretical calculations. In this contribution, we present experimental and simulation results and the design of an optimized cold cathode gauge. Major improvements are proven by the experiments. They include enhanced ignition characteristics, a lower magnetic stray field, a better long term operation and a lower pressure limit with pressure readings down to the extremely high vacuum (XHV) region (1E-12 mbar).

VST-4-Or-5
Quantification of IGP pumping speed for different gases

T15 Vacuum Science and Technology

#VST-4-Or-5

A. Schlotter, J. Iwicki, T. Rietmann, O. Posth, A. Müller.

VACOM Vakuum Komponenten & Messtechnik GmbH - Jena (Germany).

Ion getter pumps (IGPs) are well known devices in terms of stability and long term operation. IGPs are preferably used in vibration-free environments and in high and ultra-high vacuum. The pumping mechanism itself is described by ionization of gas particles in a crossed electromagnetic field and the subsequent capture of the particles in terms of implantation, chemisorption, and sputter-induced trapping. Since the quantification of the underlying mechanisms concerning the pumping speed for different gases is not yet fully described by theory, ion getter pumps are predominantly used in air, nitrogen and argon atmospheres.
In order to deepen the understanding of these pumping processes, the pumping speed of several gas species, e.g. CO2, CH4, Ar and He, was systematically investigated conforming to standard DIN 28429. In this contribution we will present and interpret the results of pumping speed measurements for several different gases and the resulting deduction for the quantification of the respective pumping speeds.

VST-6-Or-6
Influence of joining inherent stress birefringence on polarization maintaining capabilities of vacuum optical assemblies

T15 Vacuum Science and Technology

#VST-6-Or-6

T. Rietmann, S. Gottschall, C. Sahib, M. Flämmich, U. Bergner, A. Becker.

VACOM Vakuum Komponeneten & Messtechnik GmbH, Gabelsbergerstraße 9 - 07749 Jena (Germany).

The major challenge in the field of vacuum optics is to balance the diverse product requirements for the two different industries optics and vacuum technology. Tackling this challenge requires identifying parameters of critical importance to the manufacturing process as well as choosing materials that are suitable for both, ultra-high vacuum (UHV) and precision optics. Because the components have to be joined in a manner that ensures UHV compatibility, appropriate jointing technologies have to be identified, developed, optimized and finally applied. Eventually, the component's significant technical parameters are to be characterized and specified for both the user's vacuum and optics requirements.

A significant parameter in optical applications is the polarization of light, which can be affected by a vacuum optical element. In order to evaluate the suitability of the four common joining methods for creating vacuum optical assemblies for optical applications, the joining inherent effect on polarization was investigated by the analysis of stress birefringence. The investigated joining methods are elastomer fitting, bonding, brazing and thermal fusion. In this contribution we will present and interpret the results of stress birefringence measurements and identify high potential joining methods for the two vacuum regimes high vacuum (HV) and ultra-high vacuum (UHV).

VST-5-Or-13
Installation for investigation of low energy electron interaction with surface in the presence of magnetic field

T15 Vacuum Science and Technology

#VST-5-Or-13

A. Krasnov.

BINP - Novosibirsk (Russian federation).

The installation provides time resolved measurements of secondary emission yield and secondary electron velocity/energy distribution in the presence of strong magnetic field. The measurement system is designed to be installed into superconducting solenoid with maximum field of 10T. The experimental data would help to improve computer codes developed for simulation of electron clouds behaviour in a cold beam pipe of particle accelerators. At present time the installation under commissioning at room temperature. The structure and performance capabilities of the setup are described, first experimental results are presented.

VST-3-Or-4
Design Status of the radioactive production area pumping system of SPIRAL2

T15 Vacuum Science and Technology

#VST-3-Or-4

R. Levallois.

GANIL - Caen (France).

SPIRAL2 is a radioactive Ion beam accelerator under construction now at GANIL dedicated to fundamental and applied research in nuclear physics [1]. This machine aims essentially at producing high intensities of exotic nuclei issued from the interaction between a Deuteron beam (E= 40 Mev, I =5 mA) delivered by a superconducting Linac and a carbide uranium target placed in a special zone named production area. Reaction between beam and target in the production area produces a large amount of radioactive gaseous that must be stopped and retained because it may cause a danger for users and also may generate an uncontrollable contamination of machine equipments. That’s why, vacuum pumping system in this special area is considered as a major issue for global machine safety.
In this presentation, we will describe the vacuum system design of the production area in order to obtain a pressure lower than 10-6 hPa and to ensure a strong limitation of radioactive gas transmission.
Firstly, main characteristic of proposed pumping system for which a Monte Carlo Code named MOVAK3D [2] has been used to optimize conductance, will be presented. An additional Cryogenic trap system (named "cryotrap"), handled by robots, will be used if necessary to reinforce pumping capacity.
Secondly, a description of a special experiment using a prototype of Cryotrap, performed recently, will be exposed and the main experimental results with three different gaseous (H2, CO2, N2) will be given. Modelisation with a Monte Carlo Code named Molflow+ [3] with sticking coefficient determined with experimental data will be also showed.
Finally, global status of pumping system will be presented with an illustration of its main specificities in managing radioactive gaseous in the production area where human interventions are forbidden

[1] Status of the Spiral 2 project. Overview of the vacuum system (paper proposed to this conference)

[2] http://www.lv-soft.com/neuheiten/neuentwicklungen/movak.htm

[3] http://test-molflow.web.cern.ch/content/about-molflow

VST-5-Or-6
Quantitative residual gas analysis: industrial methods

T15 Vacuum Science and Technology

#VST-5-Or-6

O. Posth, A. Müller, H. Wunderlich, M. Flämmich, U. Bergner.

VACOM Vakuum Komponenten & Messtechnik GmbH - Jena (Germany).

In both, science and industry, mass spectrometry is a very common tool for the qualitative analysis of the residual gas in vacuum. Main applications are the control of leak tightness of vacuum components and the control of processes where the composition of the residual gas has to be guaranteed because it may interfere with the executed process. Another application is the investigation of desorption behavior of different materials e.g. as the function of temperature or the preceding surface treatment.
Frequently, mass spectroscopy is also utilized for quantitative residual gas analysis of vacuum components after the wet-cleaning or an additional vacuum bake out process in order to estimate the outgassing behavior of the components during the final application. For these investigations there are several different approaches and setups depending on the desorption rate of the components and the dominating gas in vacuum.
In this presentation we will exemplify the necessity of residual gas analysis of vacuum components after surface and cleaning treatments. Three types of methods and measurement setups (the throughput method, the so called box-in-box method and the accumulation method) will be presented with dedicate focus to the advantages and limits of each method and their fundamental reasons. For each method we will compile common applications where the setup fully proves its superiority.

VST-3-Or-5
Large industrial dry vacuum systems for vacuum metallurgy and other applications

T15 Vacuum Science and Technology

#VST-3-Or-5

S. Bruce [1], A. Teeuwsen [2].

[1]Edwards Ltd - Burgess Hill (United kingdom), [2]Edwards GmbH - Munich (Germany).

Very large industrial dry vacuum pumping systems are required for processes ranging from steel degassing in the metallurgy industry, and special vacuum coating systems, to large space simulation chambers used for satellite testing. Possibly the largest current industrial dry vacuum system operating provides a nominal 1 millon cubic metres per hour pumping capacity for a 230 tonne Ruhrstahl-Hereaus steel degasser in Chongqing, China (Figure 1). The assembly of such very large pumping systems requires a combination of large primary dry pump mechanisms with large mechanical vacuum boosters. In such cases multiple parallel sets of these combinations are used. The major challenge is to provide very high pumping capacity in the most compact and energy-efficient way, to minimise space and power consumption, and to create a large vacuum system which is still simple to install, easy to integrate into the process control system, and has low maintenance requirements.

Significant challenges facing global industry are the requirements to increase energy efficiency and to minimise environmental impact. There are also increasing needs to improve productivity and reliability in vacuum processes, to reduce installation and operating costs, and to enable more technological advances to satisfy market demands for increasing functionality and performance. Vacuum pump manufacturers have made significant technological strides in new vacuum pumping mechanisms to provide advanced pumps capable of fulfilling these requirements.
Such developments not only assure the user of excellent vacuum performance and reliability, but also offer significant savings in energy use and a dramatic improvement in ease of integration into vacuum control systems. These advances are typified by new, compact, high capacity, intelligent dry vacuum pumps which are

fitted with on-board controllers to undertake process control functions themselves, and provide easy integration into the vacuum process control system. Large vacuum pumping capacity can be simply provided by mounting such pumps together in a modular fashion, as illustrated by the new steel degassing system (Figure 2) which will be described.

VST-P2-12
Magnetic field shielding by vacuum chambers of soft magnetic materials for beam loss reduction in J-PARC RCS

T15 Vacuum Science and Technology

#VST-P2-12

J. Kamiya, N. Ogiwara, H. Hotchi, M. Nishikawa, Y. Hikichi, T. Yanagibashi, M. Kinsho.

JAEA (Japan).

One of the reasons of beam loss in the 3 GeV synchrotron of J-PARC (Japan Proton Accelerator Research Complex) is unwanted stray magnetic field originating from magnets at the beam extraction line, which distorts the beam orbit so that the beam partially hit a vacuum chamber wall. In this area, the magnetic flux density is about $1 \cdot 10^{-3}$ T along the beam line of 10 m. In such circumstances it is required to shield the unwanted external magnetic field to less than one-tenth. The most effective way to shield such magnetic field is to cover the beam region by magnetic materials. We've developed a vacuum chamber of soft magnetic materials with high permeability [1]. In the previous paper [1], we reported outgassing rate, magnetic shielding characteristics, and heat treatment condition of a vacuum chamber, whose pipe is made of permalloy PC. As a result, such vacuum chamber of soft magnetic materials is applicable to the magnetic shield in 3 GeV synchrotron of J-PARC from the vacuum and magnetic shielding point of view. Considering the read availability of a material and fabrication yield, we decided to make the beam ducts and the bellows by a combination of permalloy PC, SUS430 and SUS316L. The magnetic shielding characteristic of these vacuum equipments is measured by taking the magnetic field mapping inside. As shown in shows a typical result of Fig. 1, the required magnetic shielding performance was achieved. After installing these vacuum equipments in the accelerator, the beam loss measurement was performed. Fig. 2 shows the beam current just after beam injection period before and after magnetic shielding. We achieve the beam loss reduction by the vacuum chambers of magnetic materials.

[1] J. Kamiya, *et al.* Vacuum (2012)

Fig. 1 A typical magnetic shielding characteristic of a beam pipe and a bellows of soft magnetic materials.

Fig.2 Beam current in the 3Gev synchrotron just after injection period before and after magnetic shielding.

VST-P1-10
The Bilateral Comparison of the Helium Leak between Slovene Institute of Metals and Technology and Czech Metrology Institute

T15 Vacuum Science and Technology

#VST-P1-10

M. Vicar [1], J. Šetina [2].

[1]Czech Metrology Institute - Brno (Czech republic), [2]Institute of Metals and Technology - Ljubljana (Slovenia).

The International Key Comparison CCM.P-K12 has been finished in 2011.

After failing in this comparison, CMI located and corrected the source of the systematic error and proposed the Subsequent bilateral comparison CCM.P-K12.1 linked to the finished CCM.P-K12 key comparison.

The helium leak of the similar leak rate as the L1 in the key comparison was used for circulation as the transfer standard.

The Institute of Metals and Technology Laboratory for Pressure and Vacuum has successfully participated in the Key Comparison CCM.P-K12 and agreed to act as pilot laboratory in the bilateral CCM.P-K12.1 comparison.

The comparison was done in 2012 using the procedure close following the K12 protocol. The basic principles and metrological characteristics of the compared primary standards are described together with the comparison procedure.

The CMI laboratory raw measurements results evaluation is explained in details, focusing on the avoidance of the potential systematic deviation sources.

[1] Jousten K., Arai K., Becker U., Bodnar O., Boineau F., Fedchak J. A., Gorobey V., Wu Jian, Mari D., Mohan P., Setina J., Vicar M., Yu Hong Yan: Equivalence of

Standard Leak Calibrations: Results of the First International Comparison, 12th European Vacuum Conference, 3 – 8 June 2012, Dubrovnik.

[2] Vicar, M., Prazak, D., Repa, P., Gronych, T., Peksa, L., Krajicek, Z., Tesar, J., Stanek, F.: The correlations between the mass spectrometer signals for helium and the other gases concentrations in the calibration chamber. In: Book of abstracts of the 10th European Vacuum Conference, 22 – 26 September 2008. Budapest: REPS, 2008, p. 37.

[3] Tesar, J., Prazak, D., Repa, P., Peksa, L., Gronych, T., Vicar, M.: Helium leaks traceability at Czech metrology institute (CMI). In: Abstract book of 6th Iberian Vacuum Meeting. Salamanca: ASEVA, 2006, p. 69.

[4] Prazak, D., Tesar, J., Stanek, F.: The influence of the evaluation model on the resultant uncertainty of the helium leak secondary standards calibration in the Czech Metrology Institute. In: Verhandlungen der DPG. (VI) 37, 1/2002, p. 417.

[5] Tesar, J.: The traceability methods of secondary helium leak standards to primary standard using mass spectrometer technique in CMI (Czech Metrology Institute). In: Abstract proceedings of the 19th Informal meeting on mass spectrometry, Noszvaj, Hungary, 29th April – 3rd May 2001. 2001, p. 100.

VST-P2-13
Surface preparation for the electron beam vacuum system of the European-XFEL

T15 Vacuum Science and Technology

#VST-P2-13

S. Lederer, L. Lilje, T. Wohlenberg.

Deutsches Elektronen-Synchrotron (DESY) - Hamburg (Germany).

The future European X-ray Free Electron Laser, build at DESY, will generate ultra-short pulses of coherent X-rays with wavelengths down to 0.1 nm with extreme brilliance. An electron beam traveling through undulator sections of up to 250 m length produces the light by means of Self-Amplified Spontaneous Emission (SASE). The electron bunches with variable charges between 20 pC and 1 nC are generated in a laser-driven RF-gun, accelerated in superconducting modules and compressed in three bunch compressors to peak currents of several kA. After compression the ultra-short electron bunches are accelerated in a superconducting linac to their final energy of up to 17.5 GeV, transported through a collimation section and distributed to different SASE sections. To preserve the beam quality during transport to the undulators, wake fields, generated by the interaction of the electron bunches and the vacuum system, have to be minimized. To reduce the effects of wake fields to an acceptable level, several countermeasures are applied, e.g. RF-shielding of bellows, pumps and valves but also the oxide layer thickness and roughness of beam pipes have to be in accordance with the impedance budget of the machine.
In this contribution we describe the preparation techniques applied to fulfill the requirements for oxide layer thickness and roughness on standard copper beam pipes as well as for the aluminum undulator vacuum chambers.

VST-5-In-1
Vacuum Improvements for the Jefferson Lab Polarized Electron Source

T15 Vacuum Science and Technology

#VST-5-In-1

M. Stutzman.

Jefferson Lab - Newport News, Va (United states).

Long operational lifetime at the Jefferson Lab high polarization electron source requires vacuum approaching XHV ($1x10^{-10}$ Pa). Electron sources proposed for future efforts will require higher average current, and vacuum improvements are critical for these projects. The work to improve vacuum at Jefferson Lab have focused on three critical aspects: chamber material selection and processing to minimize the outgassing rate, pumping system configuration and protocol for maximizing pump speed at near-XHV pressures, and accurate measurement of pressure through careful understanding of the background factors in gauges. This presentation will include an investigation of the effect of adding a bakeable cryopump to the non-evaporable getter and ion pump system of a test chamber, and a comparison of pressure measurement using three XHV gauges: the Leybold extractor gauge, the Ulvac AxTran gauge, and the Watanabe bent belt beam (3BG) gauge. Finally, progress on reconciling the persistent discrepancies between calculated and measured pressure will be presented.

VST-4-Or-6
Increasing Reliability and Extending Service Intervals of the dry High Vacuum Pump, which Works Against Atmosphere

T15 Vacuum Science and Technology

#VST-4-Or-6

A. Shirinov, S. Oberbeck.

Pfeiffer Vacuum GmbH - Asslar (Germany).

OnTool Booster is a dry high vacuum pump, which works against atmosphere and achieves a final pressure of less than 10E-5 hPa. This pump has a maximal pumping speed of more than 130 m³/h at 0.1 hPa and 20 m³/h at 1000 hPa.
The pump consist of several in series connected side channel stages, which work against atmosphere, and five in series connected holweck stages, which generate a high vacuum.
The rotors of the side channel and holweck stages are placed on one shaft, which rotates with 1000 Hz frequency. The circumferential velocity of side channel and holweck rotors varies from 150 m/s till 310 m/s.
The shaft has two ball bearings on its both sides, which are lubricated with vacuum oil by two pumps. The inlet of the pump is dry and free of hydrocarbons. The lubricating pumps shall be filled with lubricating oil on a regular basis, because it is being used during the operation of the pump. The service interval of the pumps depends strongly on the application in which the vacuum pump works.
The current work describes changed made in the pumping system of the pump and in its lubricating system to increase reliability of the pump, improve its manufacturability and to extend its service intervals.
The results of investigation of the lubricating pumps at different operating pressures, temperatures and with different vacuum oils are demonstrated.

VST-P2-19
Qualification of Liquid Dye Penetrant for use on ITER Vacuum Systems

T15 Vacuum Science and Technology

#VST-P2-19

L. Worth, R.J.H. Pearce, D. Laugier, F. Burdeau.

ITER Organization - St Paul Lez Durance (France).

ITER will comprise one of the largest and most complex vacuum systems yet to be built. Situated in Southern France, the ITER facility covers approximately 190 hectares and is designed to demonstrate the scientific and technological feasibility of magnetic confinement nuclear fusion.
Liquid Penetrant Testing (LPT) is extensively used to find surface defects in welds in the manufacture of pressure vessels; however LPT is not effective in detecting leaks paths which would be considered large for Ultra High Vacuum (UHV) applications but insignificant for pressure applications. Hence in many UHV applications the use of Liquid Dye Penetrant (LDP) has been forbidden due to concerns over potential issues of surface contamination and temporary vacuum leak blocking.
In the ITER vacuum systems, due to the large number of systems components which use high pressure water for cooling there are many cases where vacuum and pressure boundaries are shared. Many boundaries also provide nuclear confinement dictating manufacturing to pressure codes. As an example the design and manufacture of the ITER Vacuum Vessel shall be in accordance with the RCC-MR 2007 code. Among others the code specifies the surface inspection of weld preparations and welded joints either by LPT or by Photo-Thermal Camera (PTC) examination.
In this paper the experimental work to determine the acceptable limits of application of LDP in ITER manufacturing of vacuum components is presented. This includes: the methodology to manufacture samples covering a range of calibrated vacuum leaks with magnitudes representative of potential cracks through ITER welds; the testing of the leak blocking potential of different LDP product families; the cleaning methods applied to determine the unblocking potential of different cleaning techniques.
Finally the policy on the application of LDP product families on ITER vacuum systems as derived from the experimental work is presented.

VST-P2-14
Experience on the vacuum system of SOLEIL synchrotron light source

T15 Vacuum Science and Technology

#VST-P2-14

C. Herbeaux, N. Béchu.

Synchrotron SOLEIL - Gif-Sur-Yvette (France).

The SOLEIL synchrotron light source has been on operation for about six years. SOLEIL was the first storage ring using NEG coating (TiZrV) in an extensive way with about 60 % of the circumference treated [1]. This poster will present the evolution of the storage ring vacuum system. The vacuum conditioning is still improved with the integrated beam dose as for standard stainless steel vacuum chambers. In particular the behavior of the NEG coating will be discussed for cells which have been vented several times in order to install new devices (beam diagnostics, insertion devices…). After intervention for maintenance, the vacuum system presents a fast recovery of the vacuum conditions. Efficiency of NEG coating has been demonstrated at the occasion of activation with an electron beam stored in the storage ring. A beam loss monitor placed in the vicinity of the straight section where the activation was made presented a fast decay of the radiation rate as soon as the minimum activation temperature has been reached. Finally, the comparison of the behavior of a cell pumped only with NEG coating (except in front of primary absorbers) with other cells equipped with standard pumping demonstrated that the quantity of traditional pumps can be reduced.

[1] : Herbeaux, C., Béchu, N., & Filhol, J. M., Vacuum Conditioning of the SOLEIL Storage Ring with Extensive Use of NEG Coating, EPAC-08 European Physical Accelerator Conference 23-27 June 2008, Genova (IT) - THPP142

VST-P1-23
Vacuum performance of glassy carbon

T15 Vacuum Science and Technology

#VST-P1-23

C. Garion, C. Meynier, C. Pasquino, I. Wevers, P. Chiggiato.

CERN - Geneva (Switzerland).

In high-energy particle accelerators, radiation-transparent vacuum chambers are required to maximise particle detection at the collision points and to reduce the material activation and the consequent residual radioactivity. A possible alternative to beryllium, which is the material of choice at present, might be glassy carbon. This material is obtained by high temperature pyrolysis of a highly reticulated resin. In this paper, the compatibility of glassy carbon for UHV applications is addressed. The vacuum performance of two commercial grades is assessed. Thermal outgassing and permeation tests have been carried out and the results are presented.

VST-3-Or-6
Design Principles and Test Results for a Conduction Cooled Beam Pipe for Fast Ramped Accelerator Magnets

T15 Vacuum Science and Technology

#VST-3-Or-6

A. Mierau, E. Fischer, P. Schnizer, S. Wilfert, J. Macavei, F. Walter.

GSI Helmholtzzentrum für Schwerionenforschung GmbH - Darmstadt (Germany).

The heavy ion synchrotron SIS100 of the Facility for Antiproton and Ion Research (FAIR) at GSI Darmstadt will be the world second synchrotron utilising fast ramped superconducting magnets. The high current operation of the machine with heavy ions of intermediate charge state requires maximum vacuum pressures of $5 \cdot 10^{-12}$ mbar under dynamic machine conditions. Such low pressures can be effectively produced when the beam pipes of the sc magnets act as a cryopump. The design of the beam pipe has to fulfill the opposite requirements of safe mechanical stability and low eddy current production despite the fast ramped magnetic field. Beside the minimized field distortion, a sufficient cooling of the beam pipe must be provided to keep its temperature below 15 K in all operation modes. We present possible design versions of the beam pipe for fast ramped superconducting magnets, which were studied using simplified analytical models, FEM calculations and test models.

[1] Mierau A., Schnizer P., Fischer E., Macavei J., Wilfert S., Koch S., Weiland T., Kurnishov R., Shcherbakov P., Main Design Principles of the Cold Beam Pipe in the Fast Ramped Superconducting Accelerator Magnets for Heavy Ion Synchrotron SIS100. Physics Procedia, vol. 36, issue (2012), pp. 1354-1359.
[2] Fischer E. et al., Supercon. SIS100 prototype magnets design, test results. IEEE Trans. On Appl. Supercon. vol. 20, no 3, June 2010, pp. 218-221.
[3] Fischer E. et al., SIS100 Fast ramped magnets and their cryopump functionality for the operation with high intensity intermediate charge state heavy ions. IPAC'10, May 2010.
[4] Fischer E. et al., Numerical Analysis of the Operation Parameters of Fast Cycling Superconducing Magnets. Applied Superconductivity Conference ASC08, IEEE

Trans. On Appl. Supercon. vol. 19, no 3, June 2009, pp. 1266-1267.
[5] Fischer E. et al., Impact of the beam pipe design on the operation parameters of the superconducting magnets for the SIS100 synchrotron of the FAIR project. EUCAS09, September 2009.

VST-1-Or-5
Calibration of reference leaks in a wide pressure range

T15 Vacuum Science and Technology

#VST-1-Or-5

O. Teodoro, A. Fonseca, A. Matos, A. Barreto, A. Moutinho.

METROVAC—CeFITec, Department of Physics, Faculdade de Ciências e Tecnologia, Universidade Nova de Lisboa - Caparica (Portugal).

There are many kinds of reservoirs where tightness has to be checked by sniffer leak detectors. These leak detectors include not only those based on He mass spectrometry but also the refrigerant leak detectors commonly used in the refrigeration and air conditioning industry. In the case of refrigerant circuits, recent requirements as the European Regulation EC 842/2006 (and the subsequent ones) established tightness procedures with a limit of 5g/year of maximum allowable refrigerant fluid loss. Therefore, calibration of reference leaks in this range became mandatory.

In this work we describe a primary standard developed at METROVAC in Lisbon to calibrate leaks of any gas in a typical range of ≈ 4x10-6 mbar.L/s to 4x10-4 mbar.L/s (for R134a ≈0.5 g/year to 50 g/year). The calibration pressure is adjustable by the user in a range defined by the absolute gauge used (in our case 750 mbar to 1300 mbar). With this approach calibration repeatability is increased since the leak delivering pressure may be kept constant, independently of the local atmospheric pressure. Typical calibration pressure is 1013.25 mbar.

The calibration method is based in an expandable volume at constant pressure. As soon as the gas flowing into the closed volume produces a detectable pressure increase (<1 Pa) a gas tight syringe is actuated to keep a quasi-constant pressure. A commercial computer controlled pump controls a 1 mL syringe. The resulting volume step is 28 nL. A typical calibration requires 1000 steps or more, depending on the targeted accuracy. This corresponds to about 10 min calibration time for a 5g/year leak.

The major uncertainty contribution is related with the temperature time stability of the whole system. Since we use an absolute pressure gauge, small temperature drifts produce easily detectable expansions misleading the results. Calibration systems using differential gauges minimize this effect if the reference volume is maintained at the same temperature and has a similar volume. However, in those systems the user cannot select or adjust the calibration pressure as in the one we describe. Moreover, we use a piezoelectric sensor with no heat load for the calibration system, instead of those more common capacitance gauges.

Temperature stability is therefore the main requirement to achieve good uncertainties. The first version of this calibration system showed an overall uncertainty (k=2) of ±3.4% for a leak of 3.5 g/year (R134a) and of 8% for a leak of 7.8 x 10-6 mbar.L/s. The temperature drift was about 0.2 K/hour. A second version has been built with an improved temperature control based in a water bath temperature controlled case. This version is actually being evaluated with an expected improved accuracy.

VST-3-Or-7
VACUUM CHAMBER DESIGN OF THE POLISH SYNCHROTRON FACILITY SOLARIS AND MAXIV – 1.5 GeV

T15 Vacuum Science and Technology

#VST-3-Or-7

L. Walczak [1], E. Al-Dmour [2], J. Alhback [2], M. Grabski [2], M. Quispe Flores [3], M. Berglund [2], M. Eriksson [2], D. Einfeld [2], C.J. Bocchetta [1], M.J. Stankiewicz [1].

[1]National Synchrotron Radiation Centre - SOLARIS - Krakow (Poland), [2]Lund University MAX-lab, Ole Römers väg 1 - Lund (Sweden), [3]CELLS-ALBA Synchrotron, Carretera BP 1413, de Cerdanyola del Vallès a Sant Cugat del Vallès, Km. 3,3, - Cerdanyola Del Valles (Spain).

Synchrotron facility is a one of great laboratories to developing a new technology. Increasing numbers of projects of new facilities gives a signal how it is important for innovations. 3rd generation synchrotron light facility give a wide range to studying discipline like physics, chemistry, medicine, etc. Polish National Synchrotron Radiation Centre - SOLARIS is first unique facility in Poland [1]. Centre will be equipment with a synchrotron machine setup based on the Maxlab technology [2, 3, 4].

The partial pressure in the Solaris storage ring will be lower than 10^{-9} mbar in order to guarantee an overall lifetime of 13 hours (taking into account Touschek events). Synchrotron radiation from both bending magnets and insertion devices will be used. The innovative design of achromat magnets requires precision engineering of the vacuum chamber. Most vacuum chambers will be made of stainless steel with different cross sections inside the magnet section.

In this work we present a common description of the vacuum chamber design of both Solaris and the MAX IV 1.5 GeV storage rings. The conceptual layout of the vacuum chambers in the achromats and straight sections have designed by the CELLS ALBA group (Figure 1) and it has optimized by the finite element analysis. Some details of design of the vacuum chambers including the beam position monitor, discrete absorbers and pumping system (including the Non-Evaporable Getter strips) will be presented. Also, we show predictions for the static and dynamic pressure.

[1] C. J. Bocchetta et al, “Overview of the Solaris Facility”, Proceedings of IPAC2012, New Orleans, USA: TUPPP019; and “Project status of the Polish Synchrotron Radiation facility Solaris”, Proceedings of IPAC2011, San Sebastián, Spain
[2] S. C. Leemann et al, “Beam dynamics and expected performance of Sweden’s new storage-ring light source: MAX IV”, Phys. Rev. ST Accel. Beams 12 (2009) 12071
[3] M. Eriksson et al.,“Challenge of Max IV towards a multi urpose highly brilliant light source”, Proceedings of 2011 Particle Accelerator Conference, New York, NY, USA TUOBS4
[4] M. Eriksson, “The MAX IV synchrotron light source”, Proceedings of IPAC2011, San Sebastián, Spain

Figure 1. *Layout of the vacuum chambers for one section in the Storage Ring.*

VST-P2-26
Windowless Gas Attenuator for LCLS-II SXR (Soft X-ray FEL - Free Electron Laser)

T15 Vacuum Science and Technology

#VST-P2-26

D. Schafer, M. Ferreira, D. Gill.

SLAC National Accelerator Laboratory - Menlo Park (United states).

The principal function of the LCLS-II Gas Attenuator is to provide variable attenuation from 1 (no attenuation) to 10^6 over the operating range of the LCLS-II SXR (Soft X-ray) undulator (250 to 2500[eV]). It is currently proposed to use Argon (Ar) primarily or Nitrogen (N_2), Neon (Ne), or possibly Krypton (Kr) gas (if needed to avoid Ar absorption edges) with the LCLS-II beam passing through to accomplish the attenuation. The absorption and damage thresholds preclude using solid windows to contain the gas at the lower beam energies. On either end of the gas filled cell (upstream and downstream) the gas must be removed with a differential pumping system down to the beamline base pressure of 10^{-7} [Torr].

Differential pumping sections have been designed utilizing adjustable aperture plates and fixed tubes to achieve a pressure drop in the range of ~50[Torr] (2500[eV] X-rays with 4mm diameter aperture) and ~.2[Torr] (250[eV] X-rays with 22mm diameter aperture) in the gas cell to 10^{-7}[Torr] beamline output.

Sharipov, Felix. “VACUUM ANALYSIS OF GAS ATTENUATOR Final report.” (2012): 13 pages. Not published.

Sharipov, Felix. "Numerical simulation of rarefied gas flow through a thin orifice." J. Fluid Mech. (2004), vol 518, pp. 35-60.

Varoutis et al. "Rarefied gas flow through short tubes into vacuum." J. Vac. Sci. Technol. A 26(2), Mar/Apr 2008, pp. 228-238

Chantler, C.T. et al. Detailed Tabulation of Atomic Form Factors, Photoelectric Absorption and Scattering Cross Section, and Mass Attenuation Coefficients for Z = 1-92 from E = 1-10 eV to E = 0.4-1.0 MeV. *X-Ray Form Factor, Attenuation, and Scattering Tables.* Retrieved Aug. 10, 2012 from http://www.nist.gov/pml/data/ffast/index.cfm.

VST-3-Or-8
Numerical simulation of pressure distribution in vacuum chambers for the design of vacuum systems of the DC-280 cyclotron complex

T15 Vacuum Science and Technology

#VST-3-Or-8

A. Tikhomirov, G. Gulbekyan, B. Gikal, I. Kalagin, M. Khabarov.

Joint Institute for Nuclear Research, Flerov Laboratory of Nuclear Reaction - Dubna (Russian federation).

The DC-280 cyclotron complex [1] is presently created at the FLNR, JINR. It is intended to accelerate the wide range of ion beams with ion mass 10 ÷ 238, ion mass to charge ratio 4 ÷ 7, energy 4 ÷ 8 MeV/nucleon and intensity up to 10 pmcA. It will be launched in 2015. The main parameters of vacuum systems for the DC-280 accelerator complex are determined by means of computer programs GENAP and VACLOS. The results of simulation researches are presented. The given modelling programs have been developed and tested on the basis of experiments in four cyclotrons of heavy ions at the FLNR. They have been used for design of the vacuum systems for the number of new cyclotron complexes: the DC-72 cyclotron complex for the Slovak Republic, the DC-60 cyclotron complex for the Republic of Kazakhstan, the DC-110 cyclotron complex for the Dubna Centre of Nano and Nuclear Technology and some others. The given simulation programs estimate ion beam losses based on the numerical simulation of pressure distribution in vacuum chambers practically of any arbitrary geometry as well as on calculation of cross sections for a recharge of ions during acceleration in exchange reactions by electrons with molecules of the residual gas. Simulation results have the good accordance both to experimentally measured pressure distributions and to accelerated ion beam transmission efficiencies.

1. G.G. Gulbekyan, B.N. Gikal, S.N. Dmitriev, S.L. Bogomolov, O.N. Borisov, I.A. Ivanenko, N.Yu. Kazarinov, V.I. Kazacha, I.V. Kalagin, N.F. Osipov, A.V. Tikhomirov, J.Franko. DEVELOPMENT OF FLNR JINR HEAVY ION ACCELERATOR COMPLEX

IN THE NEXT 7 YEARS. NEW DC-280 CYCLOTRON PROJECT. In: Proceedings of IPAC2011, San Sebastián, Spain, 2011, pp. 2700-2702.

VST-6-Or-4
MODELLING OF THE CATHODE PROTRUSION SELF-HEATING IN VACUUM

T15 Vacuum Science and Technology

#VST-6-Or-4

T. Minea [1], L. Caillault [1], G. Maynard [1], P. Zehnter [2].

[1]LPGP - CNRS/University Paris-Sud - Orsay (France), [2]CEA Bruyeres-le-Chatel - Arpajon (France).

Numerous applications such as X-ray tubes, electron microscopes, power vacuum switches, particle accelerators etc., use vacuum for the insulation of high voltages. Their performance reliability is limited by the risk of unpredictable breakdown event between the electrodes. In order to better understand the origin of such phenomena, numerical modeling has been performed to simulate the main elementary mechanisms (e.g. field and thermionic electron emission following the Murphy and Good's theory) occurring before the cathode-initiated breakdown.
The present study focuses on the quasi-two dimensional modeling (1D1/2) of the heat transfer along a micro-protrusion of given axi-symmetrical geometry, accounting for Joule and Nottingham effects. This self-consistent modeling provides temperature profile and voltage breakdown predictions, depending on the macroscopic parameters which are inter-electrodes distance, applied voltage drop, and cathode material properties. Comparison between different micro-protrusion geometries is presented and emphasizes the importance of heat conduction within the cathode material in the voltage breakdown assessment.
The present achievements can take this study towards the development of the macroscopic simulation of a realistic cathode surface roughness using Monte-Carlo approach.

VST-2-Or-2
Long Term Stability of 10 Torr Full Scale Ceramic Capacitance Diaphragm Gauges with 13 mm Diameter

T15 Vacuum Science and Technology

#VST-2-Or-2

C. Strietzel [1], C.H. Wüthrich [2].

[1]INFICON, Product Management - Balzers (Liechtenstein), [2]METAS, section mass, force, pressure - Bern (Switzerland).

Our present 10 Torr full scale capacitance diaphragm gauges (CDG) have a diameter of 38 mm and the membrane is sandwiched between two housing parts. We have now developed a 10 Torr full scale CDG with an asymmetric design, where the membrane is mounted on a base without the use of a cover part. Astonishingly, the asymmetric design is almost as stable in full scale as the traditional design. A full scale stability of 0.03% per year has been demonstrated that compares well with the0.01% that has been achieved with the traditional design [1].

[1] Jousten and Naef, On the stability of capacitance-diaphragm gauges with ceramic membranes, J. Vac. Sci. Technol. A 29, 011011 (2011) doi:10.1116/1.3529023

VST-4-Or-3
Molybdenum Disulfide Coatings for Vacuum Lubrication

T15 Vacuum Science and Technology

#VST-4-Or-3

M. Tosa [1], T. Maruyama [2], J. Nakagawa [2], K. Endo [2], A. Kasahara [1], M. Goto [1].

[1]National Institute for Materials Science - Tsukuba (Japan), [2]Toyama Co., Ltd. - Zama (Japan).

High resolution surface analysis and high quality thin film growth processes have required high quality vacuum environment, where lubricants become an important issue on sliding surfaces in manipulators for smooth motions . Low outgassing grease is generally used as lubricants in a vacuum, but in an ultrahigh vacuum, where pressure is 10^{-6} ~ 10^{-8} Pa, liquid lubricants become an outgassing source and ultrahigh vacuum pressure cannot be maintained stably. In an ultrahigh vacuum manipulation, some solid lubrications have been widely used, especially molybdenum disulfide (MoS_2). Low friction and low outgassing during sliding are also required for a precise and smooth sliding motion without any surafce contamination. Friction characteristics of MoS_2 have been reported to be suitable in a vacuum, but not yet been investigated much in an ultrahigh vacuum region and outgassing characteristics during sliding have not been also known in derail. We therefore investigated the characteristics of MoS_2 sputtering coatings in order to develop high performance ultrahigh vacuum motions. Friction and outgassing characteristics were evaluated of MoS_2 coating films prepared under different sputter coating conditions and we have found out suitable film coating parameters. Friction of the films was measured with a vacuum friction measurement apparatus at an atmospheric pressure and in an ultrahigh vacuum [1]. Outgassing characteristics of the films were evaluated with an outgassing measurement apparatus, which was based on the throughput method [2]. Under ultrahigh vacuum pressure, outgassing rate was measured during a loaded metal indenter was slid on the MoS_2 film.
It was shown that the optimum thickness coating can offer longer lifetime good for ultrahigh vacuum llubricant but film thickness has little effect on the outgassing rate. Large outgassing of argon (Ar), that was used as sputter coating gas, was observed in early stage of sliding. Ar and other adsorption gas (CO and CO_2) can be decreased by annealing during sputter coating process as shown in fig.1.

[1] A. Kasahara, M. Goto, M Tosa and K. Yoshihara, J. Electroanal. Chem. 559, (2003), 45-48.

[2] P. A. Redhead, J. Vac. Sci. Technol. A 20, 1667 (2002).

Figure 1 Change in outgassing after sliding friction of MoS2 coatings with heating during sputter-coating and without heating.

VST-P1-15a
Indigenous development of standard helium permeation leak artifact with different wall thickness and variable filled pressure

T15 Vacuum Science and Technology

#VST-P1-15a

T. Sattar, M. Maqsood, J.A. Bhatti, Z.A. Khan, H.M. Akram.

NINVAST - Islamabad (Pakistan).

With the advancement in nanotechnology, nano-leaks have become very important in high tech research and development. Fabrication and optimization of standard leaks (artifacts) have always been remained a hectic and sensitive issue, such standard leak artifacts are widely used for the calibration of helium leak detectors, residual gas analyzers and mass spectrometers etc.
In the present work, three secondary standard helium leak artifacts are indigenously designed and developed with different wall thicknesses and variable filled pressures at National Institute of Vacuum Science & Technology (NINVAST), Islamabad – Pakistan. These artifacts consist of mainly two parts: Pyrex glass tube as a leak element that restrict the flow of helium through diffusion process and helium reservoir which acts as a constant pressure helium source. Stable and reproducible leak-rates have been achieved at different helium filled pressures at room temperature. A decrease in wall thickness of the leak element gives early and higher leak rate value with less helium filled pressure. The properties and reliability of helium permeation standard leaks, based on approximately two years of accumulated calibration data have also been discussed in detail.

VST-1-Or-10
A New Inverted Magnetron Pirani Combination Gauge

T15 Vacuum Science and Technology

#VST-1-Or-10

J. Marki, B. Andreaus, R. Enderes, M. Wüest.

Inficon - Balzers (Liechtenstein).

One of our latest products is an inverted Magnetron [1] -Pirani [2] combination gauge with a slim footprint design. The new inverted magnetron is equipped with a novel magnet design that allows for a low external magnetic stray field. In addition, the ion chamber or the entire sensor can be replaced separately, facilitating maintenance. The gauge is the shortest conventionally built inverted magnetron gauge which makes it ideal to embed in analytical instrumentation. This new cold cathode gauge generation's control and onboard data pre-processing are performed digitally, enabling customizable functions. In the talk, pertinent sensor characteristics and features will be presented.

[1] J. P. Hobson and P.A. Redhead, Can. J. Physics 36 (1958), 271

[2] M. Pirani, Deutsche Physikalische Gesellschaft, Verh. 8: 24. (1906)

VST-P1-11
Preliminary results of broader campaign of time stability characterization of QMS

T15 Vacuum Science and Technology

#VST-P1-11

R. Kangi [1], J. Šetina [2], A. Elkatmis [1], K. Jousten [3], D. Mari [4], F. Boineau [5], M. Vicar [6], S. Ruiz [7], J. Bdzoch [8].

[1]Ulusal Metroloji Enstitüsü (TUBITAK UME) - Kocaeli (Turkey), [2]Institute of Metals and Technology, (IMT) - Ljubljana (Slovenia), [3]Physikalisch Technische Bundesanstalt (PTB) - Berlin (Germany), [4]Istituto Nazionale di Ricerca Metrologica (INRIM) - Torino (Italy), [5]Laboratoire National de métrologie et d'Essais (LNE) - Paris (France), [6]Czech Metrology Institute (CMI) - Brno (Czech republic), [7]Centro Español de Metrología (CEM) - Madrid (Spain), [8]VACOM – Vakuum Komponenten & Messtechnik GmbH - Jena (Germany).

A group of 7 European national metrology institutes and 5 industrial companies formed a consortium and started a joint project EMRP IND12 "Vacuum metrology for production environments". Project is funded by the European Metrology Research Programme (EMRP). Goals of this project are to open new measurement capabilities for vacuum and to help industry to characterize vacuum in industrial environments. Work package 3 of the project addresses the traceability for partial pressure measurement and outgassing rate measurement for materials characterization in industry. Part of this research focuses on the study of time stability of metrological characteristics of quadrupole mass spectrometers, (QMS) widely used in industry for leak detection and measurements and control of gas composition in vacuum processes, which demands highly stable and well defined low pressure environment. Stability over time of QMS is therefore an important parameter for production stability in industry. There is very limited number of such studies available in the literature. To get information about typical quality of commercial instruments, it was necessary to include in the study several instruments from different manufacturers. This task is jointly performed by seven national metrology institutes: TUBITAK UME, IMT, PTB, INRIM, LNE, CMI and CEM and one industrial partner company VACOM.
To compare results from different participants, a common measurement protocol has been adopted. Selected parameters are measured at regular intervals. The

parameters were chosen from the mandatory parameters of ISO standard 14291 (Definitions and specifications for quadrupole mass spectrometers) to be provided by the manufacturers. Parameters under study include sensitivity, mass resolution, mass number stability and minimum detectable partial pressure. Check intervals are 3 months. In the time between the measurements, the records of usage of the instruments shall be kept.
Study started in the middle of 2012 and the overall duration will be two years. In this contribution we will present the preliminary results obtained during the first year of the study.

VST-3-Or-10
ITER Directly Connected Diagnostic Vacuum Pumping Systems

T15 Vacuum Science and Technology

#VST-3-Or-10

S. Hughes.

ITER - St Paul Lez Durance (France).

S.Hughes1*, S.Bryan1, B Boussier1, R J H Pearce1, R Barnsley1, P Andrew1, K Patel1
ITER Organization,Route de Vinon sur Verdon – 13115 St Paul Lez Durance France

*E-mail address: shaun.hughes@iter.org

ITER is a magnetic confinement fusion device with the purpose of demonstrating the feasibility of fusion as a clean power source. The machine is being constructed to produce 0.5 GW of fusion power from 50 MW of input power and it is expected to be the first fusion device to produce controlled and sustainable net energy. The successful operation of ITER requires the largest, most complex set of vacuum systems yet to be built. The fusion plasma is heated within the main vacuum vessel which has a volume of ~1400 m3 and will achieve a pre-operation base pressure of the order 10-6 Pa.
ITER will be fitted with many diagnostic instruments which provide the means to observe, control and measure plasma conditions. There will be seven Diagnostics which are directly connected to the main tokamak vacuum and incorporate dedicated vacuum pumping systems. The direct connection of these diagnostic to ITER primary vacuum and their need to provide radioactive confinement, dictates novel challenging design and qualification requirements.
In this paper the design of the directly connected diagnostic vacuum pumping systems, which have progressed through their conceptual design phase, is presented. The design and operational features to give high integrity and reliability with minimum maintenance are shown. The validation programs to demonstrate that components forming these pumping systems are compatible with the environmental conditions of high magnetic fields and ionizing radiation are outlined. The applicability of special radiation hard turbo molecular drag pumps with built-in magnetic shielding is discussed.

VST-3-Or-11
LHC Beam Vacuum System 4 TeV Commissioning and Upgrade

T15 Vacuum Science and Technology

#VST-3-Or-11

V. Baglin, G. Bregliozzi, G. Lanza, J.M. Jimenez.

CERN - Geneva (Switzerland).

During commissioning of the Large Hadron Collider (LHC), the 400 mA protons beams collided at 7-8 TeV center of mass before upgrade to nominal intensity and energy after the Long Shutdown 1 (LS1). With high energy circulating beams, synchrotron radiation irradiated the arcs cryogenic vacuum system, held from 5 to 20 K. Moreover, with intense and closely spaced protons bunches, an electron cloud built-up in the cryogenic vacuum system and in the Cu or Non-Evaporable-Getter coated vacuum chambers held at room temperature. During these phases, the beam vacuum system was subjected to stimulated gas desorption induced by photons and electron bombardments. Throughout the years, dynamic pressure rises and conditionings were observed and compared to expectations. Mitigations and innovative solutions were developed and implemented to allow the routine operation or the repair of the machine. This paper discusses the achieved pressure performances with relevant hardware issues and introduces the proposed vacuum upgrade with expected performances following LS1.

VST-3-Or-9
Vacuum system of the large-scale cryogenic gravitational wave telescope, KAGRA

T15 Vacuum Science and Technology

#VST-3-Or-9

Y. Saito [1], R. Takahashi [2].

[1]KEK High Energy Accelerator Research Organization - Tsukuba, Ibaraki (Japan), [2]Institute for Cosmic Ray Research, Univ. of Tokyo - Kashiwa-No-Ha (Japan).

The large-scale cryogenic gravitational wave telescope, KAGRA, is a Fabry-Perot-Michelson interferometer of 3-km long baseline, using a 1064-nm wavelength laser beam. The site is in an underground tunnel of Mt. Ikenoyama in Kamioka town so that ground vibration due to daily traffic and life noise is suppressed. The project was started in 2011 and the tunnel is being excavated. The aimed sensitivity is $3 \cdot 10^{-24}$ $Hz^{-1/2}$ at 100Hz, corresponding to a horizontal mirror displacement of $1 \cdot 10^{-20}$ $m \cdot Hz^{-1/2}$. The predicted noise due to residual gas (water) molecules is $1 \cdot 10^{-21}$ $m \cdot Hz^{-1/2}$, when the pressure in the KAGRA beam tube is kept at $2 \cdot 10^{-7}$ Pa, with a safety margin of 10.

Two of the 3-km long beam tubes consist of 484 of unit tubes of 12 m long and 800 mm in diameter, having a flexible bellows and flanges. Since the tunnel is inconvenient to apply a baking to the entire system, surface passivation is necessary before installing. In order to realize the ultra-high vacuum, the following manufacturing process of the unit tubes is adopted; 1) Before tube forming, the surface of a SS304L sheet of 8 mm thick is ground by abrasive of Grit #150. The surface roughness after grinding is 8 μm. 2) The bellows is made from a SS316L sheet of 0.8 mm thick and formed by hydro pressurizing. Chemical polishing is applied before welding to the unit tube. 3) The unit tube after welding flanges and bellows is processed by electro-polishing so as to remove 30 μm of the surface degraded layer. The surface roughness is reduced to 3 μm (Fig.1). 4) After rinsing by a pure water of 15 MΩ in electrical resistivity, pre-baking process (200°C for 20hours) is finally performed for every unit tube. The result of outgassing rate measurement for

several tubes during production shows a value of the order of 10^{-9} $Pa \cdot m^3 \cdot s^{-1} \cdot m^{-2}$ for 100 hours of pumping.

Other materials to be planned for installing in the KAGRA vacuum systems are also examined. Outgassing rate of aluminum deposited PET films of 12 μm thick, which is to be used as thermal insulation in the cryogenic mirror system, shows drastic decrease after 100 hours pumping, indicating that absorbed water molecules diffuse out of the film. Further, a black-colored plating of NiP compounds for use as optical baffles is found to be available in the ultra-high vacuum when it is pre-baked at 250°C.

Fig. 1. Electro-polished surface of a unit tube for KAGRA.

VST-P2-15
ITER Cryogenic Guard Vacuum System design and performance

T15 Vacuum Science and Technology

#VST-P2-15

J. Bersier, R.J.H. Pearce, B. Boussier, C. Mayaux.

ITER organization - Saint Paul Lez Durance (France).

ITER is a fusion device which will produce 0.5 GW of fusion power from 50 MW of input power and it is expected to be the first fusion device to produce controlled and sustainable net energy. In ITER, the fusion reaction will be achieved in a “Tokamak” device that uses magnetic fields to contain and control the hot plasma.
The successful operation of ITER requires one of the largest, most complex vacuum systems yet to be built.

The design of ITER requires an extensive cryogenic system with more than 3 km of cryolines, feeding components with helium at 4.5K, 80K and at elevated temperatures of up to 470K. To provide the necessary magnetic fields, the ITER machine is designed with 25 main superconducting coils running at 4.5K and housed within the 14000 m3 cryostat. These coils are protected by a 1000 t, 80K, radiation shield. Other systems requiring cryogenic helium are the 22 ITER cryopumps and up to 10 pellet injection systems.

This paper describes the development of the design of the Cryogenic Guard Vacuum System (CGVS) which provides thermal insulation vacuum for all cryogenic distribution systems including cold valve boxes, magnet feeders, cryolines and cryojumpers. The conceptual design phase of the CGVS has been successfully completed.

The CGVS design contains a discrete but modular network of 70 distributed pumping units which serves the cryolines and more than 60 cold valve boxes and magnet feeders. To achieve the overall reliability target for the ITER machine the CGVS will also provide sufficient pumping capacity to allow a tolerance to cryogenic helium leaks within the distribution system; the analysis of this tolerance is presented.

The value engineering exercises and optioneering studies that were performed in the conceptual design phase to reach the current design solutions are discussed. These

resulted in a common design, with modularity on a few options, for all pumping stations even though there is variation in the environmental conditions seen by different units. The pumping unit architecture, including mechanical pumps, instrumentation, and control is described.

VST-P1-12
Study of influence of operating parameters on quadrupole mass spectrometer sensitivity and linearity

T15 Vacuum Science and Technology

#VST-P1-12

B. Erjavec, J. Šetina.

Laboratory for pressure metrology, Institute of metals and technology - Ljubljana (Slovenia).

A computer controlled quadrupole mass spectrometer (QMS) PrismaPlusTM QMG 220 M2 has been selected to study the influence of operating parameters on QMS sensitivity and linearity in a UHV range. The QMS consists of a grid ion source with a dual W filament, a quadrupole mass filter with rods of a 6 mm diameter and 100 mm length, and an ion detector: Faraday cup (FC) and secondary electron multiplier (SEM). The QMS was mounted on a UHV system for material outgassing characterization while QMS performance characteristics were studied by comparison to a BAG which was calibrated at higher pressures by a reference SRG. The QMS sensitivity and linearity depend on the ionization efficiency and ion fragmentation affected by dimensional tolerances of the ion source, and on electron and ion space charge effects dependent on electron emission current and test gas pressure [1,2], respectively. Both characteristics depend on the ion transmission from the ion source through the mass filter to the ion detector influenced by ion extraction and retarding electric fields resulting in a focused ion beam with a narrow angular distribution at the entrance of the mass filter, and ion energy determining the ion velocity to pass the mass filter. Comprehensive measurements are needed to examine the sensitivity K_P^i for a gas species (i) as a function of instrument (ionizer, mass filter and detector) parameters and pressure expressed as:

,

where ΔI_{QMS}^{i} is the change in ion current and ΔP_{ref}^{i} is the change in pressure of gas species (*i*), while electron emission current I^{-}, electron energy E^{-}, ion extraction voltage U_{ex}^{+}, ion energy E^{+}, ratio of the amplitude of RF voltage to the DC voltage *a/d* (defining a constant peak width Δm) and SEM bias voltage U_{SEM} are the instrument parameters [2].
User helpful measurements to determine the sensitivity and linearity for a gas species (*i*) inside the applicable pressure range were arranged in FC mode (U_{SEM}=0) at the default peak width (Δm=1) by varying the remaining instrument parameters (I^{-}, E^{-}, U_{ex}^{+} and E^{+}).
Temporary interesting results and conclusions were:
- The higher electron emission current the higher sensitivity and the lower linearity response range for a particular gas such as Ar (parameters to be considered for a gas species (*i*): ionization cross-section and ion velocity)
- Different power-law dependence of transmission factor on mass for atomic and molecular gases calculated from a relative sensitivity K_r^i, relative ionization probability ε_r^i and ion fragmentation factor F_f^i (measured in FC mode: a detection factor D_f^i=1):

- Similar power-law dependence of the SEM gain on mass of atomic and molecular gases obtained from measurements while operating QMS both in FC and SEM mode
- Deviation of H_2 resolution (Δm<1) depressed the H_2 sensitivity resulting in a deviation from the power-law dependence of transmission factor on mass of molecular gases [1,3].
All measurements presented in this work were taken following a programme of the EMRP IND12 Project: Vacuum metrology for production environments: Partial pressure and outgassing rate measurements (2011-2014).

[1] Rao M.G, Dong C. J. Vac. Sci. Technol. 1997; A 15(3):1312-18
[2] Lieszkovszky L, Filippelli A.R, Tilford C.R. J. Vac. Sci. Technol. 1990; A 8(5):3838-54
[3] Malyshev O.B, Middleman K. J. Vac. Sci. Technol. 2008; A 26(6):1474-79

VST-P1-13
Stationary Coating Materials for Multi-Layered Gas Chromatography Chip Assembly

T15 Vacuum Science and Technology

#VST-P1-13

S. Kim, S. Lim.

Korea Basic Science Institute - Seoul (Korea, republic of).

The microfabrication techniques have advantages in GC column development because it provides better temperature management and better separations that lead to mass spectral deconvolution. Double layered gas chromatography columns in borosilicate wafers have been microfabricated for mass spectrometry. The microfabricated columns were made using a wet chemical etching process that created a 100-μm wide 50-μm deep semi-circular cross section channel. The photoresist SU-8 (for both patterning and etching mask) was applied on a 2000-μm thick 4-inch wafer which was subsequently immersed in a HF etching solution for 3~5 minutes. Using our aligner/exposure, the mirofabrication process was repeated on a single wafer to obtain the gas channel dimension. The inlets of the microfabricated columns were made using the micro electric discharge machining technique.

Wet glass etching was performed because the isotropic degradation results in the semi-circular cross section. In addition to gas channels, efficient inlet structures should be fabricated in the wafer. By manufacturing multi-layered channel structures we were able to provide two types of mobiles phases with different polarities. Because the film materials were also used as coating materials and were applied prior to bonding the etched wafers, the method was effective in controlling the polarity of the column. The thin film of PDMS (polydimethylsiloxane) and PEG (polyethylene glycol) was applied on the etched surface of channel and the bonding surface of the wafers. PDMS and PEG were also placed on the top side of the wafer by spincoating and it was heated on the hot plate at 150 °C for an hour. Three etched wafers were assembled into a double-layered column containing both non-polar (PDMS) and polar (PEG) mobile phases. The three-dimensional etched profile of the microfabricated columns illustrated that they were comparable to fused-silica capillary columns. The substrate was effectively sealed by applying these materials

on the surface of the silicate wafers. The volatile organic compounds including halogenated organic compounds (chloroform and bromofluorobenzenes) were analyzed using the gas chromatography (mass spectrometry) attached with these micro GC column.

Cross-sectional confocal profile for the isotropic HF etching of microfabricated gas chromatographic chips (fig.1)

Gas chromatogram of cholroform and 4-bromoflourobenze analyzed by the chromatographic chip attached with the GC/ECD (fig. 2)

VST-P1-14
The construction of floats for laser interferometric mercury manometer – new primary standard of Russian Federation in the range 0,1 – 130 kPa.

T15 Vacuum Science and Technology

#VST-P1-14

I. Sadkovskaya [1], A. Eichwald [2].

[1]All-Russian D.I. Mendeleyev Research Institute of Metrology - St.petersburg (Russian federation), [2]St. Petersburg State University - St.petersburg (Russian federation).

The Laser Interferometric Mercury Manometer (LIMM) has been constructed in VNIIM (RF) for the new Russian national standard for pressure measurements in the range (0,1 – 130) kPa. In the main its scheme is similar to one developed in [1]. The manometer tubes are made of stainless steel and have an inner diameter 50 mm. The homodyne interferometer with frequency stabilized He-Ne laser, optical scheme and fringe counting device are the same applied earlier to the Laser Interferometric Oil Manometer [2]. The idea to suppress surface waves and to stabilize interference by creating thin layer of mercury and using cat's eye device [1] has been realized now in the original construction of floats as shown on Fig.1. The float stabilizer 1 is a hollow cylinder (49,8 mm in diameter) made of caprolon (polyamide-6). The stainless steel bowl 2 is fixed to it with screws. The gap between it and the wall of the tube 3 is 3 mm. The mercury 4 penetrates into the bowl through the small hole 5 on the bottom and creates a layer with the depth about 2 mm. The lens holder 6 is fixed to the stabilizer with screw- thread to adjust the cat's eye.

The mercury surface tension affects on the float's plunging and depends noticeably on the impurity (mercury oxide). It was found that when the mercury moved down the impurity deposited on the wall of the tube and the surface became cleaner (and vice versa). That could detune the cat's eyes and disturb the fringe counting. To eliminate this effect the fine caprolon guard ring 7 (Fig.2) was placed into the gap between the float and the wall.

1. E.R. Harrison et al., Metrologia, 12, 115-122, 1976
2. I.V. Sadkovskaya, A.I. Eichwald, J. Physics: Conf. Series 100 (2008) 090026, (http://iopscience.iop.org/1742-6596/100/9/092006)

Fig. 1. The construction of the float

Fig. 2. The fragment of the float with the guard ring

VST-5-Or-7
Application of Tungsten Heavy Alloy to Ultra-High Vacuum Chamber for Radiation Shield: Outgassing Properties and Vacuum Performances

T15 Vacuum Science and Technology

#VST-5-Or-7

K. Tamura, M. Oishi, Y. Okayasu, M. Shoji, S. Takano, Y. Taniuchi, M. Masaki, A. Mochihashi, H. Ohkuma.

Japan Synchrotron Radiation Research Institute - 1-1-1 Kouto, Sayo, Hyogo (Japan).

The outgassing properties of tungsten heavy alloy (WHA) and application of it to an ultra-high vacuum (UHV) chamber with an ability of radiation shielding will be presented.

In the synchrotron radiation (SR) beamlines (BLs), radiation shields are necessary to be installed for BL's components, in order to protect BL components and guarantee radiation safety in the downstream of the BLs. To limit the opening against unnecessary radiation and keep the effective aperture for SR as large as possible, development of a new type of radiation shield equipment, which utilizes WHA as an UHV chamber, has been planned. Although WHA blocks have been widely used as safety shutters in BLs at SR facilities, there has been no previous case in which the UHV chamber itself is made of WHA.

The outgassing rate of WHA was measured by the conductance modulation method. Figure 1 shows the temperature change and the outgassing rate of WHA during the baking process. The outgassing rate of stainless steel 304 (SS304) was also plotted. Although the outgassing rate of WHA at the temperature rising phase is greater than that of SS304, both rates become almost the same as the baking process advances. Examination of the vacuum sealing method was performed by using a flange made of WHA. Taking into account the ease of processing and reliability, the sealing with a metallic O-ring has been decided to adopt. The measured helium leak rate of the sealing was confirmed to be less than 10^{-11} Pa・m^3/s.

Figure 2 shows a WHA γ-ray stopper, installed downstream of the double-crystal monochromator of the SPring-8 diagnostics beamline II. The cuboid WHA block with a rectangular through-hole serves as not only a shield of high energy radiation accompanying the incident white X-ray beam to the monochromator, but also a vacuum chamber transporting the monochromatic X-ray. The pressure of the γ-ray stopper successfully reached 10^{-7} Pa in the UHV region after the baking process.

VST-P2-20
LEAK LOCALIZATION: A MAJOR ISSUE FOR NEXT FUSION MACHINES

T15 Vacuum Science and Technology

#VST-P2-20

J.C. Hatchressian [1], A. Durocher [1], M. Chantant [1], M. Houry [1], D. Mouyon [1], D. Anthoine [2].

[1]CEA (France), [2]BERTIN (France).

ITER and future actively cooled fusion devices will very likely be subjected to water or air leaks that will result in high reduction of their availabilities. Due to the complexity and the radioactive environment of these nuclear facilities, manual methods for Plasma Facing Components (PFC) leak localization will no longer be applicable. In this context, remote operations will be mandatory to allow in-vessel interventions in order to limit personal radiation exposures. Hence new methods of leak localization have to be developed to minimize machine down time and operational costs, including R&D and qualification activities.
An attractive option for leak localization process would be to use a device carrying a sensor and allowing a close access to the leak source. Another way could be to instal specific sensors inside the first wall. Consequently CEA has initiated in partnership with industrials a R&D program to define new leak localization concepts, the selection methodology using a compliance matrix and the selected sensor's qualification tests. To perform that under relevant conditions new specific facilities have been built allowing to mesure major criterias such as response time and sensibility.
This paper will present a none exhaustive list of possible concepts, the selection methodology
according the technical and environmental issues, and the first experimental promosing results gained.

Key words: leak localization, fusion, sensor, concept, qualification test

VST-P2-21a
EXPERIMENTAL AND PERFORMANCE ANALYSIS OF A TURBOMOLECULAR VACUUM PUMP ROTOR SYSTEM

T15 Vacuum Science and Technology

#VST-P2-21a

C. Hsu.

National Chin-Yi University of Technology - Taichung City (Taiwan, republic of china).

This study is focused on the experimental and performance analysis of a vertical type turbomolecular vacuum pump (TMVP) rotor system. The research approach can adopt methods are numerical analysis and experimental testing. In numerical analysis, it can use the finite element analysis software ANSYS to construct a three-dimensional model of the rotor system. In this analysis process, it can verify the rotor system finite element models under different boundary conditions by using the pump system testing data. Then, it must calculate the Campbell diagram to study dynamic characteristics of the rotor system, and to compare with the experimental results to verify the models. It can establish the relationship between the rotor critical speed and the bearing stiffness in order to study the design of the turbomolecular pump rotor system. The experimental can adopt the static and dynamic testing. The static modal testing can provide the natural frequencies of the rotor system. The waterfall diagram of the dynamic testing can measure the pump system operating critical speed from zero speed up to the operating speed, and to insure that the pump operating speed is far from the critical speed of at least 10% in the safe margin. Summary, this results can provide the design tool for turbomolecular pump rotor system in order to identify and prevent vibration.The 1st order and the 2nd order critical speed were 110Hz and 490Hz as obtained from the dynamic testing results for the waterfall shown in Fig. 1. Fig. 2 was created ANSYS to simulate the TMVP Campbell diagram for operating speed.

1. Nelson and McVaugh, “The Dynamics of Rotor-Bearing Systems Using Finite Elements,” J. Eng. Ind., Vol.98, pp.593-600, 1976.
2. Nelson, “A Finite Rotating Shaft Element Using Timoshenko Beam Theory,” J.

Mec. Des., Vol.102, pp.793-803, 1980.
3. Chiang, Kuan, and Li, “Turbo Molecular Pump Rotor-Bearing System Analysis and Testing,” J. American Vac. Soc., Vol.27, pp.1196-1203, 2009.
4. Swanson, Powell, and Weissman, “A Practical Review of Rotating Machinery Critical Speeds and Modes,” J. Sou. Vib., Vol. 8, pp.10-17, 2005.

Fig. 1. Dynamic Testing for the Waterfall
Fig. 2. Rotor System Campbell Diagram

VST-6-Or-1
PLA and LDPE barrier properties improvement by the combination of DBD activation and PECVD-based SiNx deposition

T15 Vacuum Science and Technology

#VST-6-Or-1

P. Leroy [1], C. Nouvellon [2], S. Abou Rich [1], A. Roobroeck [2], S. Benali [3], F. Renaux [2], P. Dubois [3], R. Snyders [3], F. Reniers [1].

[1]ULB - Bruxelles (Belgium), [2]Materia Nova - Mons (Belgium), [3]UMons - Mons (Belgium).

Food packaging allows protecting food from the external environment mainly by reducing the diffusion of moisture and oxygen. In this work, we aim to evaluate the barrier properties improvement of LDPE (Low Density PolyEthylene) and PLA (PolyLactic Acid) using a two steps plasma-based treatment in a roll-to-roll system. The first step consists in an activation of the surface in order to promote the adhesion of the subsequently deposited barrier coating.

In a unique treatment chamber consisting in two reactors connected under vacuum, the polymer substrates are first treated by Dielectric Barrier Discharge (DBD) at 100 mbar in order to clean and activate the surface. The second step consists of depositing, at low pressure (7 10-3 mbar), a SiNx like layer by PECVD (Plasma Enhanced Chemical Vapor Deposition) using Ar/SiH4/N2 mixture. The energy, chemistry and topology of the treated surfaces are evaluated by using contact angle measurements, X-ray Photoelectron Spectroscopy (XPS) and Atomic Force Microscopy (AFM), respectively while the permeability of the treated polymers towards oxygen and water vapor are measured for different treatments.

It is shown that a DBD treatment shorter than one second can significantly improve the wettability of polymers (for example the water contact angle of PLA decreases from 77° to 25° after a Helium/Nitrogen plasma treatment).

Oxygen and water vapor permeability studies are carried out on the polymer film /deposited layer samples with and without DBD pretreatment. Without DBD treatment, it is shown that very thin SiNx-like layer (< 20 nm) leads to the best results. In that case, for thicker films, cracks appear in the deposited film, reducing the barrier effect. If the polymer is DBD treated before SiNx-like layer deposition, the experimental windows allowing for good barrier properties is affected demonstrating the positive impact of this step. These results are understood in view of XPS depth profiling allowing characterizing the polymer-thin films interface.

This work is financially supported by FEDER (Everwall project) « Les Fonds Européens de Développement Régional et la Région wallonne investissent dans notre avenir »

VST-2-In-1
PRESSURE MEASUREMENTS AND CALIBRATIONS IN EXTREME HIGH VACUUM (XHV) RANGE

T15 Vacuum Science and Technology

#VST-2-In-1

J. Setina.

Institute of Metals and Technology - Ljubljana (Slovenia).

In demanding vacuum devices, like ultra fast photoemission electron sources for free electron lasers, there is a need for reliable vacuum measurements down to XHV range. Accurate measurements of any physical quantity are possible only if instruments are properly calibrated. Many national metrology institutes (NMIs) around the world maintain primary vacuum calibration systems down to 10^{-8} Pa, but there are only few systems which operate below 10^{-9} Pa. Institute of Metals and Technology (IMT) has recently built an experimental calibration system with a base pressure close to $1x10^{-10}$ Pa. This very low base pressure was achieved by the use of nonevaporable getter (NEG) in the calibration chamber. Calibration pressure is generated by orifice flow method. Because of NEG only inert gases like Ar can be used for calibration. The lowest generated calibration pressure is in the 10^{-11} Pa range. In the talk the XHV calibration system of IMT will be presented and compared with similar systems at other NMIs.

VST-7-Kn-1
VACUUM GAS DYNAMICS: STATE OF ART AND PERSPECTIVES

T15 Vacuum Science and Technology

#VST-7-Kn-1

F. Sharipov.

Departamento de Fisica, Universidade Federal do Parana - Curitiba (Brazil).

Modelling of gas flows under low pressures is an important part of vacuum science. Two main approaches are employed in vacuum gas dynamics, namely, probabilistic and deterministic. The first one is based on the Monte Carlo methods, while the second approach consists of numerical or analytical solution of the kinetic Boltzmann equation. In the lecture, a review of recent results based on both approaches will be given with examples of their applications to practice, i.e. modelling of gas ow in vacuum systems, mathematical models of vacuum pumps, theoretical support of vacuum metrology etc. Directions of further developments of vacuum gas dynamics and its perspectives will be pointed out.

VST-4-In-1
SURFACE TREATMENTS FOR VACUUM SYSTEMS OF PARTICLE ACCELERATORS

T15 Vacuum Science and Technology

#VST-4-In-1

P. Chiggiato.

CERN, European Organization for Nuclear Research - Geneva (Switzerland).

Surface treatments are the last step in the production of all components installed in vacuum systems of particle accelerators. They encompass primarily chemical and electrochemical processes, and coating by both electrolytic and plasma techniques. They have multiple functions that depend on the specific applications. The traditional example is the reduction of surface outgassing both without and with circulating beams, i.e. in presence of particle bombardment onto the beam-pipe walls. Thin film coatings have become a crucial surface treatment in the last two decades. They transform conductance-limited beam pipes into distributed pumps. They decrease the global impedance imposed to beams, modify particle reflectivity and optical emissivity, reduce secondary electron emission, and allow the achievement of very-high accelerating electrical fields. The design of future high-intensity, high-energy and low-emittance accelerators relies on the present surface treatments and trigger challenging developments. The state of art is reviewed, with emphasis on applications for the LHC and new synchrotron light sources. The need for further development is pointed out.

VST-6-In-1
VELOCITY MEASUREMENTS IN LOW PRESSURE CONFINED GAS FLOW BY MOLECULAR TAGGING VELOCIMETRY

T15 Vacuum Science and Technology

#VST-6-In-1

S. Colin.

INSA Toulouse - Toulouse (France).

A significant effort has been recently made to develop accurate models for the low pressure flows of gases in confined situations, covering the different rarefaction regimes. There is currently, however, a crucial lack of experimental local flow data (pressure, concentration, velocity and temperature fields). Molecular Tagging Velocimetry (MTV) is a non-intrusive flow characterization technique, which can avoid some limitations of the particle image velocimetry (PIV) technique. In order to analyze velocity fields in confined internal gas flows, a new experimental setup has been developed. First experimental data obtained in mini channels at atmospheric and low pressures are presented. The ability of the technique to measure local slip at the wall and to perform local temperature measurements is discussed.

VST-P2-21
A high sensitivity neutral atom detector based on electron impact ionisation

T15 Vacuum Science and Technology

#VST-P2-21

D. Ward, D. Chisnall, A.P. Jardine, J. Ellis, W. Allison.

Cavendish Laboratory - Cambridge (United kingdom).

The unrivaled surface sensitivity of neutral atomic and molecular beams has continually driven the development of scattering instrumentation [1] . A major challenge in detection of neutral beams is their high ionisation energies leading to low detector efficiency [2] .
Applications that require time sensitive measurements require a small ionisation volume; however, when high temporal resolution is not required, ionisers having a much larger volume are possible. Here we describe a detector for helium-3 spin-echo experiments [3] , based on principles recently established [4] and having a sensitivity of 0.83Ambar −1 , the highest yet reported for helium atoms. A solenoidal magnetic field is used to confine electrons within an extended ionisation region (~800 mm long), allowing a large proportion of the incident atom beam to be ionised. Careful design of the electric and magnetic fields allow us to utilize electronic space charge to extract ions quickly, without introducing ion trapping, while minimising multiple ionisation. We present experimental results from the detector as well as simulation results and possible improvements for application in a helium atom microscope currently being developed [5] .

[1] Farias, D; Rieder, K.H. Rep. Prog. Phys. (1998), **61**, 1575-1664
[2] Pauly, H. “Atom, molecule and cluster beams”; Springer: Berlin, (2000).
[3] Jardine, A.P., Lee, E.Y.M., Ward, D.J., Alexandrowicz, G., Hedgeland, H., Allison, W., Ellis, J., Pollak, E. (2010) Phys Rev Lett, **105**, 136101,, McIntosh, E.M et al (2013) Phys. Rev. Lett. **110**, 086103; Lechner, B.A.J., et al (2013) Angew. Chemie – Int. Ed., 52 (19), pp. 5085-5088.
[4] A. Alderwick et al. Rev. Sci. Instrum. **79**,123301 (2008).
[5] EC FP7 collaborative project; NEMI

VST-3-In-1
PROGRESS IN THE CONSTRUCTION OF THE ITER VACUUM SYSTEM

T15 Vacuum Science and Technology

#VST-3-In-1

R. Pearce.

ITER Organisation - Saint-Paul-Lez-Durance (France).

The ITER project has the purpose of demonstrating the feasibility of fusion as a clean power source and is being constructed in the south of France. It is one of the world's largest scientific and engineering collaborations. The successful operation of ITER requires some of the largest, complex vacuum systems yet to be built.
ITER will utilise approximately 400 vacuum pumps of 10 different technologies with many pumps and other vacuum technologies being specifically developed to meet operational and environmental challenges of the fusion machine.
In this talk the progress of the project, the progress in construction of the vacuum systems and the new developments in the area of vacuum technology are presented.

Authors index :

,

A

B

C

D

E

F

G

H

I

J

K

L

M

N

O

P

Q

R

S

T

U

V

W

X

Y

Z